HYDRODYNAMICS IN SHIP DESIGN

HYDRODYNAMICS IN SHIP DESIGN

VOLUME TWO

by

HAROLD E. SAUNDERS

Captain, U. S. Navy, (Retired)

Honorary Vice-President, The Society of Naval Architects and Marine Engineers

David W. Taylor Medalist

Published by

THE SOCIETY OF NAVAL ARCHITECTS AND MARINE ENGINEERS
74 Trinity Place, New York 6, N. Y.

1957

If man permits it, the water of the seas does things for him

A surf canoe riding an incoming wave toward Waikiki Beach.

Photograph by courtesy of Photo Hawaii, Honolulu.

Acknowledgements

This section supplements a corresponding section on Acknowledgements in Volume I, to be found on pages vii-xi of that volume.

The author takes this occasion to express his appreciation to a number of his associates and friends who have been most helpful in the preparation of Volume II. Listing their names and accomplishments briefly:

Mrs. Claudette Leveque Horwitz, of the author's staff, especially for her invaluable help in preparing the three sets of indexes for each of Volumes I and II

Mr. W. C. Suthard and the staff members of the Photographic and Reproduction Division of the David Taylor Model Basin for taking the model and flow photographs of TMB models reproduced throughout this volume; Mr. G. R. Stuntz, Jr. and Mr. M. S. Harper of the Ship Powering Division of the TMB Hydromechanics Laboratory for finding them among the vast assortment on hand at Carderock

Mr. Werner B. Hinterthan, of the TMB staff, who translated many of the titles in the German references listed in the present volume, and who helped the author find many German technical references

Miss Margaret M. Montgomery, for her cheerful and ever-ready help in finding books for the author and in guiding him around the TMB library

Mrs. Ruby S. Craven, head of the Aeromechanics Laboratory library at the David Taylor Model Basin, for her assistance in looking up many references in aerodynamics and aeronautical engineering

Mr. C. A. Ryman and other members of the staff of Propellers and Shafting, Bureau of Ships, U. S. Navy Department, for calculating the weight of the screw propeller designed for the ABC ship in Chap. 70 of this volume

Dr. Hans F. Mueller, for his help in furnishing valuable information in the rather limited field of rotating-blade propellers

Mr. William H. Taylor, managing editor of Yachting magazine, who has gone out of his way to render assistance to the author where information from small craft would be of value

Dott. Ing. Emilio Castagneto, Superintendent of the Rome Model Basin (Vasca Navale; Instituto Nazionale per Studi ed Esperienze di Architettura Navale), for assistance in furnishing information concerning models tested in that basin.

In particular, the author wishes to express his appreciation for the useful ideas and information found in a number of Russian technical books written during the past decade. The Russian titles and Russian authors of these books are listed throughout the text wherever direct references are made to them.

In over four decades of experience while working with others, the present author has been blessed with constant and heart-warming cooperation to an unexpected degree. Nevertheless, he is compelled to take this occasion to express his admiration and gratitude for a superlative measure of cooperation in the printing and engraving projects on this book. Mr. Richmond Maury, Mr. W. W. Tompkins, Mr. David G. Wilson, Captain Horace F. Webb, Mrs. Janet Jones, Mr. Orvrille W. Harrell, Mr. Henry F. Drake, Jr., Mr. John L. Moore, Mr. Stuart M. Holmes, Mr. Raymond C. Jones, and other staff members of The William Byrd Press, Inc., of Richmond, Virginia, designers and printers of the book, as well as Mr. Jay R. Golden, of the staff of the Industrial Engraving Company, Easton, Pennsylvania, have contributed with their efforts and their talents a friendship that will always be treasured.

Every reference inserted in the text of the book is intended as a tacit acknowledgement of assistance rendered by the author, book, publisher, or organization mentioned in that reference. The present author and The Society of Naval Architects and Marine Engineers are grateful for permission to make quotations from and adaptations of material developed by others, whether published or unpublished. Specific acknowledgements are made in the cases listed hereunder.

The reproductions in Secs. 18.3 and 18.4 of Chapter 18 in Volume I, of John Scott Russell's admirable drawings of a boat running in confined waters, from the Transactions of the Royal

Society of Edinburgh, as well as the quotation in Sec. 48.12 on page 182 of this volume, are made by permission of the Council of that Society.

Reprints of portions of papers by William Froude and G. H. Bottomley, originally published in the 1870–1871 and 1935 Proceedings, respectively, of the Institution of Civil Engineers in Great Britain and included in Sec. 37.4 of Volume I and Sec. 74.7 of Volume II, are reproduced by courtesy of the Institution.

The adaptation in Fig. 32.D on page 450 of Volume I, and the quotation on page 557 of that volume, are made by permission of E. and F. N. Spon, Limited, publishers of the book "Marine Propellers," by Sydney W. Barnaby, 4th edition, 1900.

The drawings of the magnetic lines of force in Figs. I.B and I.C of the Introduction to Volume I, on page xxvi, are reproduced from the publication "Modern Engineering Practice," edition of 1902, by permission of the American Technical Society of Chicago.

The quotation in Sec. 20.11, on page 299 of Volume I, is from the Proceedings of the Cambridge Philosophical Society.

The quotation from the Reports and Memoranda of the (British) Aeronautical Research Committee, in Sec. 49.8 on page 195 of the present volume, is reproduced by permission of the Controller of Her Britannic Majesty's Stationery Office.

The quotation in Sec. 30.5, on page 427 of Volume I, is reprinted from "Elements of Yacht Design," by Norman L. Skene. Copyright © 1927. Renewal © 1955 by Quentin H. Skene.

The publication rights to the book "Sail and Power," by Uffa Fox, are held by Peter Davies, Limited, of London. The quotation in Sec. 40.3, on page 3 of this volume, is published with their permission. Readers will be interested to know that this firm maintains a stock of the Uffa Fox books on yachting.

The fouling-resistance graphs of E. V. Lewis, adapted from the May 1948 issue of The Log, are embodied in Figs. 45.K and 45.L of this volume by permission of The LOG (now Marine Engineering/Log).

Quotations from the 1950 edition of "Theoretical Hydrodynamics" are by permission of The Macmillan Company of New York, publishers of the American edition, and of Macmillan and Company, Limited, publishers of London, for the British and other world markets.

The quotations and adaptations from the following books, copyrighted on the dates indicated, are by permission of John Wiley and Sons, Inc., of New York:

Durand, W. F., "Resistance and Propulsion of Ships," 1903

Peabody, C. H., "Naval Architecture," 1904

Rouse, H., "Elementary Mechanics of Fluids," 1946

Vennard, J. K., "Elementary Fluid Mechanics," 2nd edition, 1947

Rouse, H., editor, "Engineering Hydraulics," 1950.

The firm of Hutchinson and Company, Publishers, Limited, of 178–202 Great Portland Street, London, W.1, England, in generously granting permission for the use of material from books published by them, advises that the book on motorboats by Juan Baader of Buenos Aires (in Spanish) is to be issued by them in an English edition in 1957. It is to be an improved and enlarged version of "Cruceros y Lanchas Veloces," published in 1951; the English title will be "Cruisers and Speedboats."

Mr. Thomas D. Bowes, consulting naval architect and engineer of Philadelphia, made it possible to embody the photograph of the fireboat in action, reproduced as Fig. 76.H on page 775 of the text.

Table of Contents

CHAPTER 43—DELINEATION OF SOURCE-SINK FLOW DIAGRAMS—Continued

CHAPTER 44—FORCE, MOMENT, AND FLOW DATA FOR HYDROFOILS AND EQUIVALENT FORMS

CHAPTER 45—VISCOUS-FLOW DATA AND FRICTION-RESISTANCE CALCULATIONS

CHAPTER 46—REFERENCE DATA ON SEPARATION, EDDYING, AND VORTEX MOTION

CHAPTER 46—REFERENCE DATA ON SEPARATION, EDDYING, AND VORTEX MOTION—Continued

CHAPTER 47—THE INCEPTION AND EFFECT OF CAVITATION ON SHIPS AND PROPELLERS

CHAPTER 48—DATA ON THEORETICAL SURFACE WAVES AND SHIP WAVES

CHAPTER 49—MATHEMATICAL METHODS FOR DELINEATING BODIES AND SHIP FORMS

CHAPTER 50—MATHEMATICAL METHODS OF CALCULATING THE PRESSURE RESISTANCE OF SHIPS

CHAPTER 51—PROPORTIONS AND SHAPE DATA FOR TYPICAL SHIPS

CHAPTER 52—ANALYSIS OF FLOW DIAGRAMS AND PREDICTION OF SHIP FLOW PATTERNS

CHAPTER 53—QUANTITATIVE DATA ON DYNAMIC LIFT AND PLANING

CHAPTER 54—ESTIMATING THE AIR AND WIND RESISTANCE OF SHIPS

CHAPTER 54—ESTIMATING THE AIR AND WIND RESISTANCE OF SHIPS—Continued

CHAPTER 55—THE CALCULATION OF APPENDAGE RESISTANCE

CHAPTER 56—OBSERVED RESISTANCE DATA FOR MODELS AND SHIPS

CHAPTER 57—ESTIMATE OF TOTAL RESISTANCE FOR SURFACE AND SUBMERGED SHIPS

CHAPTER 58—RUNNING-ATTITUDE AND SHIP-MOTION DIAGRAMS

CHAPTER 58—RUNNING-ATTITUDE AND SHIP-MOTION DIAGRAMS—Continued

CHAPTER 59—PREDICTING THE PERFORMANCE OF PROPULSION DEVICES

CHAPTER 60—SHIP-POWERING DATA FOR STEADY AHEAD MOTION

CHAPTER 61—THE PREDICTION OF SHIP BEHAVIOR IN CONFINED WATERS

CHAPTER 61—THE PREDICTION OF SHIP BEHAVIOR IN CONFINED WATERS—Continued

CHAPTER 62—ESTIMATING THE ADDED MASS OF WATER AROUND A SHIP IN UNSTEADY MOTION

PART 4—HYDRODYNAMICS APPLIED TO THE DESIGN OF A SHIP

CHAPTER 63—BASIC FACTORS IN SHIP DESIGN

CHAPTER 64—FORMULATION OF THE DESIGN SPECIFICATIONS INVOLVING HYDRODYNAMICS

CHAPTER 65—GENERAL PROBLEMS OF THE SHIP DESIGNER

CHAPTER 66—STEPS IN THE PRELIMINARY DESIGN

CHAPTER 66—STEPS IN THE PRELIMINARY DESIGN—Continued

CHAPTER 67—DETAIL DESIGN OF THE UNDERWATER HULL

CHAPTER 68—LAYOUT OF THE ABOVEWATER FORM

CHAPTER 68—LAYOUT OF THE ABOVEWATER FORM—Continued

CHAPTER 69—THE GENERAL DESIGN OF THE PROPULSION DEVICES

CHAPTER 70—SCREW-PROPELLER DESIGN

CHAPTER 71 THE DESIGN OF MISCELLANEOUS PROPULSION DEVICES

CHAPTER 72 DESIGN FEATURES APPLICABLE TO SHALLOW AND RESTRICTED WATERS

CHAPTER 73—THE DESIGN OF THE FIXED APPENDAGES

CHAPTER 74—THE DESIGN OF THE MOVABLE APPENDAGES AND CONTROL SURFACES

CHAPTER 75—THE PROBLEM OF HULL SMOOTHNESS AND FAIRING

CHAPTER 76—THE DESIGN OF SPECIAL HULL FORMS AND SPECIAL-PURPOSE CRAFT

CHAPTER 77 THE PRELIMINARY HYDRODYNAMIC DESIGN OF A MOTORBOAT

CHAPTER 78—MODEL-TESTING PROGRAM FOR A LARGE SHIP

Introduction

Taking for granted a knowledge of the material in Volume I, a reader or user is enabled to lay it aside temporarily and make the estimates or calculations for the preliminary hydrodynamic design of a ship, or the parts thereof, as well as to carry through such a design, solely by reference to Volume II. The latter is to be considered a reference or design volume, containing little or no theory or exposition and only sketchy descriptions of the phenomena or physical laws involved. The publication of these experimental and reference data in a separate volume, in the shape of contours, graphs, diagrams, tables, and other aids, makes it possible to omit from Volume I much of the strictly quantitative data which would have interfered greatly with the continuity of its story.

Many of the aspects of hydrodynamics as applied to ship design have not yet been investigated analytically, or else only the easiest and simplest of the problems have been solved. In these cases it is necessary to fall back upon experimental results and empirical data. It must be admitted that in some respects our knowledge of naval architecture has not expanded greatly from its position of nearly a century ago. At that time the renowned hydrodynamicist, naval architect, and engineer, William John Macquorn Rankine, was moved to observe that:

> "Owing principally to the great antiquity of the art of shipbuilding, and the immense number of practical experiments of which it has been the subject, that part of it which related to the forms of water-lines has in many cases attained a high degree of excellence through purely empirical means. Excellence attained in that manner is of an uncertain and unstable kind; for as it does not spring from a knowledge of general principles, it can be perpetuated by mere imitation only" ["On Plane Water-Lines in Two Dimensions," Phil. Trans., Roy. Soc., London, 1864, Vol. 154, p. 386].

Nevertheless, when necessity demanded, Rankine himself was forced to fall back upon empirical data, as is evidenced in his book "Shipbuilding: Theoretical and Practical," published in 1866. No apologies are therefore offered for following this procedure in the present volume, especially as, in every possible instance, an effort is made to tie in these data with physical laws governing the motion of liquids.

Nor are any apologies offered for following J. Scott Russell, Rankine, and other contemporaries in stretching to the utmost our existing knowledge of hydrodynamics in its application to naval architecture. They made incorrect assumptions in some instances, and arrived at solutions which later had to be corrected, but there is no doubt that in doing so they advanced both the analytical and applied phases of the art.

A good measure of care is called for in the application of data derived from past practice and observations, in both ship operation and model experiment. As Sydney W. Barnaby observed in his book "Marine Propellers," written in 1900, "No table can supply the place of judgment and experience." By a generous insertion of practical examples, in which the use of the formulas, graphs, and procedures is illustrated in the preliminary hydrodynamic design of a hypothetical ship, embodied in Part 4, the reader may see for himself what sort of answers and solutions are derived.

In general, all calculations in examples incorporated in this volume of the book are made with English primary units of pounds, feet, and seconds. Ship speeds may be given in knots in the statement of the problem but are entered as feet per second in the calculations.

Wherever practicable, curves and graphs are supplemented by simple diagrams illustrating the coordinates or parameters.

It is pointed out in the Introduction to Volume I, and repeated here, that the formulas and relationships used in this book for expressing equalities, ratios, and the like are, with very few stated exceptions, in what is known as pure form. That is, they involve only physical concepts and basic relationships between these concepts. The units expressing them are kept entirely separate, to be selected by the one using the relationship. This procedure leaves no uncertainty as to units, physical concepts, and other factors which may be hidden in a mixed equation. A case in point is the former use of 1.00 for 0.5ρ in salt water, in the English pound-foot-second system. The pure form also facilitates checking for dimensionality because all physical quantities stand out clearly. Furthermore, the relationships are dimensionally consistent, so that equalities

have the same physical dimensions, ratios are simple numbers, and so on.

The pure formulas and equations may therefore be employed with any system of measurement or with any combinations of units in a particular system. Brief examples of these applications are as follows:

(a) Effective power = resistance times speed, or $P_E = RV$

(b) Fatness ratio = volume divided by (a constant times length)^3 = $V/(0.10L)^3$

(c) Speed of a shallow-water wave = [(acceleration of gravity) times (water depth)]$^{0.5}$, or $c = \sqrt{gh}$. To indicate that this example is dimensionally consistent

$$c = \text{velocity} = L/t = \sqrt{gh} = [(\text{acceleration}) \text{ times } (\text{distance})]^{0.5} = [(L/t^2)L]^{0.5} = L/t.$$

The elimination of mixed quantities in power formulas represents somewhat of a departure from standard practice. The rate at which work could be done by a horse served conveniently as a point of reference a century ago; it has practically no modern application. It necessitates the use of arbitrary figures such as 33,000 and 550, the use of the term *horse* as a pure unit, and strict conformity of numerical units with those figures. A vastly simpler and much handier unit, for the English system at least, would be 1000 pound-foot-second units, similar in its decimal simplicity to the well-known kilowatt and equivalent to 1.818 horses. A change of this kind may come in the future.

In the meantime, much ambiguity could be saved by the use of a standard large weight unit. The long ton of 2,240 pounds and the metric ton of 2,205 pounds are of the same order of magnitude but are not equal. The short ton of 2,000 pounds is appearing with increasing frequency in naval architecture and shipbuilding on inland lakes and waterways. A simple solution is to use the large weight unit of structural mechanics, the *kip*, or kilopound, equal to 1,000 pounds. It is 0.5 of a short ton, 0.4464 of a long ton of 2,240 pounds, and 0.4535 of a metric ton.

Finally, throughout both volumes the author has introduced some historical highlights where they seemed to be appropriate, and has mentioned the names of pioneers in various lines of endeavor. With many developments now taken for granted, the people responsible for originating them are often forgotten. In the words of an unknown editorial writer of some three decades ago, when discussing an article about the originator of the set of Simpson's rules:

"We wish that our future advanced treatises on naval architecture would follow the theme of Dr. Welch's address and enlighten us, with due proportion, on men as well as on things" [SBSR, 15 Nov 1923, pp. 600-601].

SOURCE ABBREVIATIONS FOR REFERENCES

The source abbreviations employed throughout the text and listed here are formed by combining the first letters of the principal words composing the titles of books, periodicals, and the like, or of the names of organizations and groups which have published transactions, proceedings, and reports of one kind or another.

The resulting abbreviations are set down in alphabetic order, together with sufficient information, as of 1956, to permit the reader to look up the references cited or to get in touch with the organizations concerned.

AD	"Aerodynamic Drag," by S. F. Hoerner, 1951; published by the author, 148 Busteed, Midland Park, N. J.
AEW	Admiralty Experiment Works, Haslar, Gosport, Hampshire, England
AHA	"Applied Hydro- and Aeromechanics," by L. Prandtl and O. G. Tietjens, translated by J. P. Den Hartog (substantially an English translation of HAM), Engineering Societies Monographs, McGraw-Hill, New York, 1934
AM	(American) Motorship, Diesel Publications, Inc., 192 Lexington Avenue, New York 16, N. Y.
ARC	Aeronautical Research Committee, Great Britain
ASCE	American Society of Civil Engineers, 33 West 39th Street, New York 18, N. Y.
ASME	American Society of Mechanical Engineers, 33 West 39th Street, New York 18, N. Y.

ASNE	American Society of Naval Engineers, Inc., Suite 1004, Continental Building, 1012 14th Street, N.W., Washington 5, D.C.
ASTM	American Society for Testing Materials, 1916 Race Street, Philadelphia 3, Pa.
AT	"Aerodynamic Theory," by Dr. W. F. Durand, series of six volumes (in English), Julius Springer, Berlin, 1936
ATMA	Association Technique Maritime et Aéronautique (formerly only ATM), 1, Boulevard Haussmann, Paris, France
ATTC	American Towing Tank Conference
AVA	Aerodynamische Versuchsanstalt, Völkenrode, Germany
BEC	Bassin d'Essais des Carènes, 6, Boulevard Victor, Paris (15me), France
BMF	"Basic Mechanics of Fluids," by Hunter Rouse and J. W. Howe, Wiley, New York, 1953
BNA	"Basic Naval Architecture," by K. C. Barnaby, Hutchinson's Scientific and Technical Publications, London and New York, 1948. A new edition was published in 1954.
BSRA	British Shipbuilding Research Association, 5, Chesterfield Gardens, Curzon Street, London, W.1, England
C and R	Bureau of Construction and Repair, Navy Department, Washington (prior to 1940)
CR	Comptes Rendus, Académie des Sciences, Paris
CIT	California Institute of Technology, Pasadena 4, California
DTMB	David Taylor Model Basin, Washington 7, D. C.
EAAT	"Elements of Aerofoil and Airscrew Theory," by H. Glauert, Cambridge University Press, Cambridge, England, 2nd edition, 1948
EH	"Engineering Hydraulics," edited by Dr. H. Rouse, Wiley, New York, 1950
EMB	Experimental Model Basin, Washington (prior to 1941)
EMF	"Elementary Mechanics of Fluids," by Dr. H. Rouse, Wiley, New York, 1946
ETT	Experimental Towing Tank, Stevens Institute of Technology, 711 Hudson Street, Hoboken, N. J.
FD	"Fluid Dynamics," by Dr. Victor L. Streeter, McGraw-Hill Publications in Aeronautical Science, New York, 1948
FHA	"Fundamentals of Hydro- and Aeromechanics," by L. Prandtl and O. G. Tietjens, (in English), Engineering Societies Monographs, McGraw-Hill, 1934
FMTM	"Fluid Mechanics of Turbomachinery," by Prof. George F. Wislicenus, McGraw-Hill, New York, 1947
HPSA	"Hydromechanische Probleme des Schiffsantriebs," Editors, G. Kempf and E. Foerster, Hamburg, 1932
HAM	"Hydro- und Aeromechanik," Vols. I and II, by L. Prandtl and O. G. Tietjens, (in German), Julius Springer, Vienna, 1934 and 1931
HD	"Hydrodynamics," by Sir Horace Lamb, Dover Publications, New York, 6th edition, 1945
H. O.	Hydrographic Office, U. S. Navy, Washington 25, D. C.
HSVA	Hamburgische Schiffbau Versuchsanstalt (Hamburg Shipbuilding Experimental Establishment), Hamburg, Germany (prior to 1945)
HT	Historical Transactions, SNAME, 1943
1st ICSTS	International Conference of Ship Tank Superintendents held at The Hague, Holland, 1933. This conference was preceded by a preliminary meeting of the superintendents of European model basins in Hamburg in 1932, and followed by a conference in London in 1934.
2nd ICSTS	"Congrès International des Directeurs de Bassins, Paris, Octobre 1935" (Published by the Imprimerie Nationale, Paris, 1935)
3rd ICSTS	"Internationale Tagung der Leiter der Schleppversuchsanstalten," Berlin, 1937

4th ICSTS	(This conference was to have been held in Rome in 1939)
5th ICSTS	"Fifth International Conference of Ship Tank Superintendents," London, 1948 (Published by H. M. Stationery Office, London, 1949)
6th ICSTS	"Sixth International Conference of Ship Tank Superintendents," Washington, 1951 (Published by SNAME, 1953)
7th ICSH	"Seventh International Conference on Ship Hydrodynamics," Scandinavia, 1954 (Published by SSPA, 1955, Rep. 34)
ICT	International Critical Tables, McGraw-Hill, New York, 1926
IME	Institute of Marine Engineers, 85, Minories, London, E.C.3, England
IESS	Institution of Engineers and Shipbuilders in Scotland, 39, Elmbank Crescent, Glasgow, C.2, Scotland The official abbreviation for this Institution in Great Britain is "I.E.S."
IIHR	Iowa Institute of Hydraulic Research, State University of Iowa, Iowa City, Iowa
INA	Institution of Naval Architects, 10, Upper Belgrave Street, London, S.W.1, England
IPT	Instituto de Pesquisas Tecnológicas, Praça Cel. Fernando Prester, 110, São Paulo, Brazil
ITTC	International Towing Tank Conference, formerly ICSTS and ICSH
JAM	Journal of Applied Mechanics, ASME, 33 West 39th Street, New York 18, N. Y.
JR	Journal of Research, National Bureau of Standards, Washington 25, D. C.
KMW	Aktiebolaget Karlstads Mekaniska Werkstad, Kristinehamn, Sweden (sometimes called KaMeWa)
MDFD	"Modern Developments in Fluid Dynamics," Vols. I and II, edited by Dr. S. Goldstein, Oxford University Press, 1938
ME	"Marine Engineering," Vols. I and II, edited by H. L. Seward, SNAME, 1942 and 1944
MENA	Marine Engineer and Naval Architect, Whitehall Technical Press, 9, Catherine Place, S.W.1, London
MESR or MESA	Marine Engineering and Shipping Review, New York, formerly Marine Engineering and Shipping Age, Marine Engineering, and more recently Marine Engineering/Log, 30 Church Street, New York 7, N.Y.
MIT	Massachusetts Institute of Technology, Cambridge 39, Mass.
MNA	"A Manual of Naval Architecture," by Sir William H. White, Van Nostrand, New York, 1900
MSNA	"The Modern System of Naval Architecture," by J. Scott Russell, 3 vols., London, 1865 (out of print)
MU	Naval Tank, Department of Naval Architecture and Marine Engineering, University of Michigan, Ann Arbor, Michigan
NA	"Naval Architecture," by C. H. Peabody, Wiley, New York, 1904
NACA	National Advisory Committee for Aeronautics, 1512 H Street, N. W., Washington 25, D. C. Also model basins at the Langley Aeronautical Laboratories, Langley Air Force Base, Virginia.
NBS	National Bureau of Standards, Washington 25, D. C.
NECI	North-East Coast Institution of Engineers and Shipbuilders, Bolbec Hall, Newcastle-upon-Tyne, England
NN	Towing Tank, Hydraulic Laboratory, Newport News Shipbuilding and Dry Dock Company, Newport News, Virginia
NPL	National Physical Laboratory, Teddington, Middlesex, England
NSP	Nederlandsch Scheepsbouwkundig Proefstation (Netherlands Shipbuilding Experiment Establishment), Wageningen, Holland
NW	Model Basin, The Technological Institute, Northwestern University, Evanston, Illinois
ONR	Office of Naval Research, Navy Department, Washington 25, D. C.
ORL	Ordnance Research Laboratory, Pennsylvania State University, University Park, State College, Pa.
OTT	Hydraulic Laboratory, Division of

	Mechanical Engineering, National Research Council, Ottawa, Canada
PD	Model Propeller Data sheets, SNAME
PNA	"Principles of Naval Architecture," edited by H. E. Rossell and L. B. Chapman, SNAME, 1939, Vols. I and II
R and M	Reports and Memoranda of the ARC, Great Britain
RD	Model Resistance Data and Expanded Resistance Data sheets, SNAME
RPS	"Resistance and Propulsion of Ships," by W. F. Durand, Wiley, New York, 1903
RPSS	"Resistance, Propulsion and Steering of Ships," by W. P. A. van Lammeren, L. Troost, and J. G. Koning, Amsterdam, 1948
RS	Royal Society, London
S and P	"The Speed and Power of Ships," by D. W. Taylor, 3rd edition, U. S. Govt. Printing Office, Washington, D. C., 1943
SBMEB	Shipbuilder and Marine Engine-Builder, Townsville House, 10, Cartington Terrace, Newcastle-on-Tyne, 6, England
SBSR	Shipbuilding and Shipping Record, 33, Tothill Street, Westminster, London, S.W.1, England
	The customary contraction for the name of this periodical in Great Britain is "S. & S. R."
SD	"Ship Design, Resistance, and Screw Propulsion," by G. S. Baker, Vols. I and II, Liverpool, 1933
SEE	"Ship Efficiency and Economy," by G. S. Baker, Liverpool, 1946
SH	Schiff und Hafen, C. D. C. Heydorns Buchdruckerei, Uetersen bei Hamburg, Neuerwall 32, Hamburg 36, Germany
SNAME	Society of Naval Architects and Marine Engineers, 74 Trinity Place, New York 6, N. Y.
SPD	Model Self-Propulsion Data sheets, SNAME
SSBH	"Piloting, Seamanship, and Small-Boat Handling," by C. F. Chapman, Motor Boating, 572 Madison Avenue, New York, 1951 edition
SSPA	Statens Skeppsprovningsanstalt (Swedish State Shipbuilding Experiment Establishment), Göteborg, Sweden
STG	Schiffbautechnischen Gesellschaft, Albert Ballinhaus, Hamburg, Germany
STP	"Shipbuilding: Theoretical and Practical," by W. J. M. Rankine, 1866 (out of print)
TABLAS	"Semejanza Mecanica y Experimentacion con Modelos de Buques, Tablas, Canal de Experiencias Hidrodinámicas, Madrid, Spain, 1943
TH	"Theoretical Hydrodynamics," by L. M. Milne-Thomson, Macmillan, New York, 1950. A third edition was issued in 1955.
TMB	Taylor Model Basin (used as an adjective only)
TNA	"Theory of Naval Architecture," by Prof. A. M. Robb, Charles Griffin and Co., Ltd., London, 1952
TSS	Taylor Standard Series of models
USNI	United States Naval Institute, Annapolis, Maryland
WRH	Werft-Reederei-Hafen; combined with Schiffbau und Schiffahrt into the periodical Schiff und Werft in 1943; see SH, Schiff und Hafen
ZK	Journal of Zōsen Kiōkai, The Society of Naval Architects of Japan.

PART 3

Prediction Procedures and Reference Data

CHAPTER 40

Basic Concepts Underlying All Calculations and Predictions

40.1 The Calculation of Ship-Design and Performance Data. The reader who progresses this far in a consecutive perusal of the book has found a word and a graphic picture of the flow phenomena associated with the motion of a ship. The first part is in general form, considering a simple or schematic ship. The second part is in successively more detailed form, having to do with the behavior and effect of an actual ship and its many components.

To avoid breaking up the story, mathematical derivations, processes, and formulas are purposely omitted from the first two parts, except in a few special cases. The reader has been asked to take the story largely on faith, with copious references if his faith appears to waver at any point.

There is another reason for this procedure, well expressed by R. E. Froude when discussing the second of D. W. Taylor's papers on stream forms in 1895 [INA, Vol. 36, p. 246]:

> ". . . The problems of stream-line motion have hitherto been almost out of the reach of everybody except practical mathematicians; not because all such problems are too abstruse for anyone but a practical mathematician to understand, but rather, because all treatises dealing with those subjects have been condensed and written, so to say, in a language which no one but practised technical mathematicians can understand."

Manifestly, a story alone can not design a ship, nor meet those modern needs which demand answers of how much and how many. Nor will a story alone, no matter how explicit, point the way out of the hydrodynamic tangles that may be expected to confront the naval architect and marine engineer of tomorrow. He must have better and sharper tools with which to face newer and more puzzling problems.

This third part of the book, therefore, is devoted to an exposition of the methods whereby flow and its phenomena may be defined in graphical, mathematical, and numerical terms. It gives a description of the methods, formulas, procedures, and other aids whereby the influences and effects described in Parts 1 and 2 may be predicted or calculated in quantities useful to the ship designer.

Indeed, it is the ultimate aim of all those who take a deep interest in these phases of naval architecture, to develop and to refine methods of computation and calculation by which any aspect of the performance of a ship or any of its parts may be predicted on paper and in the design stage. The modern hydrographer can not afford to wait on the spot to see what the height of the tide and the strength of the tidal current will be at Point X ten years hence; he has designed and built a machine that predicts it for him. The modern owner, operator, and naval architect, by the same token, can not wait, with a ten-million dollar ship at stake, until it runs sea trials to

find out whether it will maintain a reasonable speed in stormy weather.

The modern ship designer, with all the methods and data of the twentieth century at his command, can do wonders in this respect, especially with the help of model tests. However, it is not wise to rely so much on model results that analytic ability and prediction procedure suffer by consequence.

40.2 Useful Formulas Embodied in Theoretical Hydrodynamics. The amazingly large group of naval architects, engineers, scientists, and mathematicians, many of them of great renown, who devoted their thoughts, energies, and talents to a study of the mechanics of fluids, have tackled the problems confronting them along two general lines. Some have conducted experiments, analyzed data, and evolved theories explaining the fluid action observed. Others have started with certain basic assumptions and premises, like the principles of continuity and conservation of energy and the laws of mechanics, and have succeeded, by reasoning and intuitive processes, in deriving fundamental mathematical expressions for the behavior and flow of ideal liquids. By a judicious combination of the results stemming from these two lines of endeavor, there is available a surprising store of mathematical expressions by which data on the flow of real liquids can be derived in numerical terms.

For example, by the application of the well-known kinetic-energy formula for solid bodies, where $E = 0.5mV^2$, and by the theorem which maintains the sum of the potential and kinetic energies constant, it is possible to deduce the ram pressure at the stagnation point in the center of the nose of a body of revolution. Here the liquid-stream velocity is zero, and the ram pressure $q = 0.5\rho U^2$. The modern engineer uses this formula, as he does many others like it, without a moment's hesitation as to its accuracy and certainly without requiring its experimental confirmation.

In this respect, the everyday formulas derived by the mathematics of classical hydrodynamics are to the modern naval architect and marine engineer just so many useful tools. This is the reason why the chapters which follow are given over to a presentation of formulas gathered from many sources, without including the mathematical proofs or derivations among them. The engineer may continue to look upon the mathematics as a means to an end, without rendering himself vulnerable, as long as someone else continues to work out new expressions, like the ram-pressure formula, that help him in his daily work. However, to apply these or other formulas intelligently, the engineer should know what they mean.

Furthermore, as the science of ship propulsion and ship motions progresses, more and more new formulas are needed. Many of them can be derived only through mathematical processes. It is not too much to say that many of them can best be derived by the naval architect himself. The omission of the mathematical derivations in this third part should not be taken, therefore, as an indication that the ability to derive them or to formulate better ones can be omitted from the knowledge of one who aims to specialize in the hydrodynamics of the ship.

The reader who wishes to familiarize himself with the mathematical theory and processes of hydrodynamics is referred to a number of textbooks and other publications. The authors, titles, and other data on these books, listed in Sec. I.3 of the Introduction to Volume I, are repeated here for convenience:

(1) Binder, R. C., "Fluid Mechanics," Prentice-Hall, New York, 1947. A third edition appeared in 1955.
(2) Vennard, J. K., "Elementary Fluid Mechanics," Wiley, New York, 2nd edition, 1947. A third edition appeared in 1954.
(3) Rouse, H., and Howe, J. W., "Basic Mechanics of Fluids," Wiley, New York, 1953
(4) Rouse, H., "Elementary Mechanics of Fluids," Wiley, New York, 1946
(5) Prandtl, L., and Tietjens, O. G., "Applied Hydro- and Aeromechanics," McGraw-Hill, New York, 1934
(6) Rouse, H., Editor, "Engineering Hydraulics," Wiley, New York, 1950
(7) Dryden, H. L., Murnaghan, F. D., Bateman, H., "Hydrodynamics," National Research Council, Washington, 1932
(8) Streeter, V. L., "Fluid Dynamics," McGraw-Hill, New York, 1948
(9) Binder, R. C., "Advanced Fluid Dynamics and Fluid Machinery," Prentice-Hall, New York, 1951
(10) Goldstein, S., "Modern Developments in Fluid Mechanics," Vols. I and II, Oxford Press, 1938
(11) Milne-Thomson, L. M., "Theoretical Hydrodynamics," Macmillan, New York, 2nd edition, 1950
(12) Lamb, Sir Horace, "Hydrodynamics," Dover, New York, 6th revised edition, 1945.

40.3 Present Limitations of Mathematical Methods. Mathematical and analytical methods in their present state, even though stretched to the utmost, can by no means supply all the answers wanted by the modern marine architect. They

can not, in fact, supply any but incomplete answers in cases where the physical phenomena are not as yet fully understood. Friction-drag formulas for ship plating are a case in point. Despite an enormous amount of time and energy expended on the problem of friction flow, both in air and in water, the mechanism of fluid friction is still incompletely understood. Formulas much better than those now in use can not be expected until this knowledge is achieved.

Heretical as it may seem to mathematicians, the use of mathematics, in both science and engineering, must always be tempered by good judgment. In fact, it is a generous gift of this same good judgment that makes a good engineer in any line of work.

It must be recognized that mathematics is always based on some kind of assumptions and conditions, which the mathematician hopes are always complete and correct. They may be neither. This is where judgment enters, in advance as well as in the wake of the mathematics.

It may be interesting to quote here the comments of one well-known designer on this phase of the subject [Fox, Uffa, "Sail and Power," New York, 1937, p. 20]:

"Mathematics are only of value to the person who has the sense to use the right formula and start with the true value. Too many mathematicians today multiply an unknown quantity by an illogical factor, and arrive at proportions that a man with discerning eyes can see are wrong, even though the mathematicians believe the answer to be correct if the mathematics are correctly worked."

It must be said in defense of mathematicians that they are by no means the only people who "multiply an unknown quantity by an illogical factor." This is the reason for inserting some mathematical cautions in a design book for naval architects and marine engineers. Nevertheless, it becomes necessary at times to venture far afield in one's need for arriving at some kind of numerical answer.

A classic example of this kind was well described by William Froude in his reports of the early 1870's to the British Association [Todd, F. H., SNAME, 1951, p. 316], when discussing the means of extrapolating his 50-ft plank friction data to ship lengths of 300 ft or more. The comments in parentheses are those of the present author:

". . . it will make no very great difference in our estimate of the total resistance of a surface 300 feet long, whether we assume such decrease to continue at the same rate (as for the last foot of the 50-foot plank) throughout the last 250 feet of the surface, or to cease entirely after 50 feet; while it is perfectly certain that the truth must lie somewhere between these assumptions."

According to E. V. Telfer and F. H. Todd, as described in the reference cited:

". . . believing the truth to lie between them, but unable to decide on which was nearer to the absolute truth, he (Froude) compromised by taking an exact mean curve."

A more modern example might arise if a marine architect were called upon to estimate the hydrodynamic resistance of the balsa-log raft of South American design, called *Kon-Tiki* and used by Thor Heyerdahl and his companions in their voyage from Peru to the South Pacific Islands in 1947 [Heyerdahl, T., "Kon-Tiki," Rand-McNally, 1950]. Assuming that he could approximate the drag of one log, moving end on, he would with reasonable certainty estimate that the total drag of the nine logs abreast was less than nine times the drag of one log. Similarly, he would know that the drag was more than that of a box-shaped body having the same planform, the same general dimensions, and the same volume displacement. By a series of approximations of this kind he could narrow the probable resistance to within rather close limits.

The diversion in this section is intended partly as a caution, and is in no sense to be looked upon as a discouragement. The fact that considerable space is devoted in the chapters following to means for deriving quantitative data should serve as an indicator of its importance in this line of work.

For an intelligent and proper use of the data, however, a certain amount of preliminary knowledge is necessary, and a few specific rules are to be observed. These are described briefly in the sections following.

40.4 The Principles of Similitude. A knowledge of the theory of similitude, forming the basis of all model-testing procedures, is not necessary for an understanding of the calculation, prediction, and ship-design methods described in Parts 3 and 4 of this book. However, for the marine architect who is interested in knowing the conditions for dynamic similarity of flow and motions, and in utilizing the dimensional-analysis methods expounded by Lord Rayleigh, the Π Theorem of Riabouchinsky, and elaborations upon them by R. C. Tolman, E. Buckingham, P. W. Bridgman, and others, a background of general knowledge of

the theory and principles of similitude is assuredly necessary.

For the reader who wishes to study this method, refresh his memory, or look up doubtful points, a partial list of references is given:

(1) Riabouchinsky, D., "Méthode des Variables de Dimension Zero et son Application en Aérodynamique (Dimensionless Variables and Their Use in Aerodynamics)," Aérophile, 1 Sep 1911
(2) Rayleigh, Lord, Brit. Adv. Comm. Aero., Ann. Rep., 1:38, 1910; 2:26, 1911; 3:30, 1912
(3) Tolman, R. C., "The Principle of Similitude," Phys. Rev., 1914, Vol. III, p. 244
(4) Buckingham, E., "On Physically Similar Systems," Phys. Rev., 1914, Vol. IV, p. 345
(5) Tolman, R. C., "The Principle of Similitude and the Principle of Dimensional Homogeneity," Phys. Rev., 1915, Vol. VI, p. 219
(6) Buckingham, E., "Model Experiments and the Forms of Empirical Equations," Trans. ASME, 1915, Vol. 37, pp. 263–296
(7) Tolman, R. C., "Note on the Homogeneity of Physical Equations," Phys. Rev., 1916, Vol. VIII (Ser. II), p. 8
(8) Bridgman, P. W., "Tolman's Principle of Similitude," Phys. Rev., 1916, Vol. VIII, p. 423
(9) Buckingham, E., "Notes on the Method of Dimensions," Phil. Mag., 1921, Vol. 52, p. 696
(10) Taylor, D. W., "Propeller Design Based upon Model Experiments," SNAME, 1923, pp. 57–109; esp. pp. 99–106, which include the deduction of the Π Theorem on pp. 102–106, from Buckingham's paper, ref. (4) of this series
(11) Slocum, S. E., Discussion of ref. (10) of this series, SNAME, 1923, pp. 80–87
(12) Dryden, H. L., Murnaghan, F. D., Bateman, H., "Hydrodynamics," Nat. Res. Council, Washington, 1932, pp. 4–6
(13) Buckingham, E., "Dimensional Analysis of Model Propeller Tests," ASNE, May 1936, pp. 147–198. Pages 197–198 of this paper list 24 references on the subject.
(14) Bridgman, P. W., "Dimensional Analysis," Yale University Press, rev. edition, 1937
(15) Rouse, H., "Fluid Mechanics for Hydraulic Engineers," McGraw-Hill, 1938, Chap. 1
(16) Davidson, K. S. M., PNA, 1939, Vol. II, pp. 57–58, 60–61
(17) Hankins, G. A., "Experimental Fluid Dynamics Applied to Engineering Practice," NECI, 1943–1944, Vol. 60, pp. 24–25
(18) Rouse, H., EMF, 1946, Appx., pp. 351–354
(19) Van Driest, E. R., "On Dimensional Analysis and Presentation of Data in Fluid Flow Problems," Jour. Appl. Mech., ASME, 1946, Vol. 13, No. 1
(20) Vennard, J. K., "Elementary Fluid Mechanics," Wiley, New York, 2nd edition, 1947, pp. 142–153
(21) Charpentier, H., "Introduction aux Méthodes Dimensionnelles (Introduction to Dimensional Methods)," ATMA, 1947, Vol. 46, p. 156
(22) Rouse, H., EH, 1950, Appx., pp. 995–998, 1001–1004
(23) G. Birkhoff gives a list of eighteen references on this subject, to accompany a chapter on modeling and dimensional analysis in his book "Hydrodynamics" [Princeton Univ. Press, 1950, pp. 182–183]
(24) Langhaar, H. L., "Dimensional Analysis and Theory of Models," Wiley, New York, 1951
(25) Huntley, H. E., "Dimensional Analysis," Macdonald, London, 1952
(26) Duncan, W. J., "Physical Similarity and Dimensional Analysis," St. Martin's Press, New York, 1953.

40.5 Dimensions of Physical Quantities. Whether one is or is not versed in dimensional analysis or the theory of similitude, the concept of the *dimensions* of a physical quantity, in terms of the basic dimensions of length, mass, and time, needs to be clearly visualized. Only in this way can the dimensionless (0-diml) relationships described elsewhere and employed constantly in the book be well understood. The dimensions of the various physical quantities in general use by architects and engineers are derived by relatively simple processes and are tabulated in full in Appendix 2 of Volume I. They may be memorized or a list may be kept handy for ready reference. Better still, they may be derived each time they are needed by the procedure described in Appendix 2.

Natural sines, cosines, and tangents of angles are perhaps the simplest examples of dimensionless ratios. Others are pitch ratio, blade-thickness ratio, and aspect ratio. Unfortunately for the engineer, or so he may think, there are no limits to the complexity or intricacy of other dimensionless combinations. Among the particular 0-diml expressions of interest to the naval architect are the complete set of hull-form and propeller-form coefficients, the Froude number F_n, the Reynolds number R_n, and the cavitation index σ(sigma). All of these are important, and they are in constant use in one form or another.

The opposite sides of all equations involving physical quantities must have the same dimensions [Rouse, H., EH, 1950, pp. 995–998]. A formula for a quantity must have the dimensions of that quantity. Take the familiar $V^2 = 2gh$. Here 2 is 0-diml; g is an acceleration having the dimensions of a length L divided by a time t squared, and the height h has the dimensions of a length L. Hence $V^2 = (L/t^2)(L) = L^2/t^2 = (L/t)^2 = V^2$. Another example is the formula for lift force L, which is $L = C_L(0.5\rho)AU^2$, where A is the projected area of an airfoil or hydrofoil and U is the fluid velocity past it. Since C_L is 0-diml, for the reasons given in the section following, with the dimensions of unity,

$$\text{Force } L = (1)(0.5)\left(\frac{m}{L^3}\right)L^2\left(\frac{L}{t}\right)^2$$

$$= \frac{mL^2(L)^2}{L^3t^2} = \frac{mL}{t^2}$$

The last expression has the dimensions of a force.

40.6 The Derivation and Use of "Specific" Terms. The term "specific" as now applied to ship resistances of various kinds is not a new term to marine architects by any means but it has come into extended use only during recent years. It will surely be encountered more frequently in the years to come. The term expresses, in 0-diml numbers or as a ratio, the relationship between some quantity under consideration and a quantity having the same characteristics which is taken as a standard or reference.

The best-known use of this term is in the expression *specific gravity*, as applied to a liquid. Here the specific gravity of any liquid is represented by the 0-diml ratio of (1) the weight of unit volume of liquid to (2) the weight of unit volume of standard fresh water. In this case, fresh water is taken as a reference because it is readily available, widely used, and its weight per unit volume is easily determined.

Another familiar but unfortunate term is the one known as *specific weight*; unfortunate because it is not truly dimensionless. It signifies the weight of a substance per unit volume and is expressed by the symbol w. While it does have a reference basis of sorts, it has nevertheless the dimensions of a weight divided by a volume. Broken down into its dimensional elements, explained in Appendix 2, and with a weight given the dimensions of a force, $w = \text{Force}/L^3 = (mL/t^2)/L^3 = m/(L^2t^2)$.

Practically all the customary *specific resistance* terms now employed in naval architecture and marine engineering are dimensionless. An example is the specific pressure coefficient, often called simply the pressure coefficient. This expresses the ratio between (1) a pressure difference Δp (or an absolute pressure) at a given point on a body and (2) the ram pressure q developed at the forward stagnation point of that body at the relative speed U. In the form $\Delta p/(0.5\rho U^2)$ the pressure coefficient is also known as the Euler number E_n. In the form $(p_\infty - e)/(0.5\rho U^2)$, where e is the vapor pressure of the liquid, it is the cavitation number σ(sigma).

Another example is the specific drag coefficient C_D, or simply the drag coefficient. This expresses, in simple numerical form, the ratio of (1) the drag force on a given body, moving at a relative speed U, at a certain attitude and under given conditions in a liquid, to (2) the force that would be exerted on the body if the ram pressure q (or $0.5\rho U^2$) acted uniformly over its entire projected area A. Here

$$C_D = \frac{\text{Drag}}{\frac{\rho}{2}AU^2}$$

Still another familiar specific resistance coefficient is that for friction resistance, expressed by C_F. This 0-diml coefficient is again the ratio of (1) the friction resistance R_F to (2) a ram-pressure force, but the reference area in this case is the wetted surface S of the body rather than its projected area. Hence

$$C_F = \frac{R_F}{\frac{\rho}{2}SU^2}$$

Provided the flows around two bodies are in all respects dynamically similar, and the bodies are geosims (geometrically similar), it is possible to determine from model tests and to tabulate for ready reference the drag coefficients of objects having many different forms and running at various attitudes, as in Fig. 55.B. The tests may be made, furthermore, in any convenient medium by using the proper mass-density value in the specific-coefficient formula. Similarly, the coefficients apply to motion in any other medium.

When devising, calculating, and using specific-resistance terms, it is most important that the reference length, area, or volume be carefully understood and defined. For example, in the expression for the lift coefficient of a hydrofoil or a rudder, $C_L = L/(0.5\rho AU^2)$, the area A is that of the *projected* or lift-producing area. In other words, it is the area of the planform or the lateral area of the blade bounded by the profile, as projected on the plane of the base chords. In the expression for hydrofoil drag coefficient, $C_D = D/(0.5\rho AU^2)$, the area A usually remains the projected area as before, notwithstanding that this area is projected on a plane lying generally at right angles to the direction in which the drag force is exerted. In the expression for the specific friction-resistance coefficient of either rudder or hydrofoil, where *tangential* forces are involved, $C_F = R_F/(0.5\rho SU^2)$. Here S is the superficial or *wetted area* of *both* sides of the rudder blade or hydrofoil.

40.7 Double or Multiple Solutions to the Equations of Motion. It is possible for a ship to travel from one port to another by two or more different routes, each of which may be the easiest and best under its own particular combination of circumstances. It is found that nature, in her role as a conserver of energy, causes water and other liquids to flow by different paths from one point to another whenever there is a good reason for doing so. Speaking in terms of mathematics this means that there may be two or more solutions to the equations of motion which govern the action of the liquids or the bodies in question, just as there are two solutions to the ordinary quadratic equations in algebra.

Nature does not select these solutions at random but chooses them in strict accordance with some secondary or lesser cause, which may appear only after the most careful examination or extended study. A case in point, although admittedly not pertaining to liquid flow, is the multiple paths taken by high-voltage discharges and by lightning in darting from one fixed point to another. A shifting flow pattern frequently encountered is that which takes place around and behind a cylindrical stick which is drawn rapidly through the water at right angles to its axis. Fig. 40.A depicts the manner in which a double row of vortexes known as the Bénard or Kármán vortex trail or vortex street is formed in the wake of a 2-diml rod, when drawn through a liquid in a direction normal to its axis. Here large vortexes roll up, first behind one quarter and then behind the other quarter of the rod as it moves along.

The lowest diagram in the figure shows the manner in which a jet of water issuing from a nozzle with a flared exit cone clings to one side or the other of the cone, as the nozzle is flicked quickly from side to side.

Less familiar cases are those encountered by model basins in the transition region between laminar and turbulent flow, where the nature of the flow may and does change with position and time. Similar situations often occur when investigating the flow around ship models. The water passing through a given region on the model at times follows one path and then, apparently without reason, suddenly changes to another path, only to return to the first as unexpectedly as it departed from it. This phenomenon has often been looked upon as a matter of instability in the flow but it can just as well be regarded as a shifting flow condition caused by two solutions to the equations of motion.

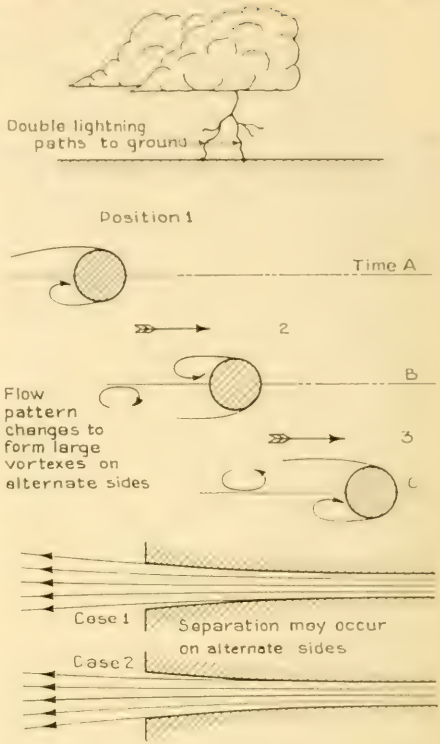

Fig. 40.A Several Examples Taken from Nature Illustrating Double Solutions of the Equations of Flow

In the top diagram electricity flows through the two paths simultaneously. In the middle and bottom diagrams the schematic flow patterns change with time or other circumstances; these illustrations are intended only to indicate that the flow patterns can and do change while the surroundings remain the same.

As a consequence of this situation it may be expected that any of the real solutions to a set of equations of motion may be encountered in actual practice. Considerable study may be necessary to determine which of these solutions will apply under conditions which are apparently identical in every respect. There is on record the case of the fast man-of-war which, at a given speed, rudder setting, and trim, would apparently make its own on-the-spot decision as to whether it would turn in a loose circle or a tight one.

CHAPTER 41

General Formulas Relating to Liquid Flow

41.1 The Use of Pure Formulas. The almost exclusive employment of pure mathematical formulas in this book, described in Sec. I.7 of the Introduction to Volume I, is emphasized here. Unless specific exceptions are mentioned, these formulas contain only symbols representing physical concepts and dimensionless ratios, and they are dimensionally consistent. They may be used as given, with consistent units belonging to any system of measurement.

Examples are $c = \sqrt{gL_W/2\pi}$ for the celerity or velocity of a trochoidal surface wave, and $h = k_W(B_X/L_E)(V^2/2g)$ for the predicted height of the bow-wave crest on a ship. Substituting the dimensions of the physical quantities in the first,

$$\frac{L}{t} = \left[\frac{L}{t^2}\cdot\frac{L}{1}\right]^{0.5} = \frac{L}{t}$$

For the second,

$$L = 1\left(\frac{1}{1}\right)\frac{L^2}{t^2}\left(\frac{t^2}{L}\right) = L$$

There is no restriction whatever upon the units used in these and other formulas like them, *provided they are consistent.* The wave celerity, for example, may be in mi per hr, kt, ft per sec, meters per sec, or what not, so long as g and L_W are in the same units. The examples in the sections following illustrate the use of pure formulas.

41.2 The Quantitative Use of Dimensionless Numbers; The Mach and Cauchy Numbers. The ten dimensionless numbers or relationships of hydrodynamics, previously described in Sec. 2.22 and listed in Table 2.a, are expressed briefly here in quantitative terms to illustrate the manner in which they are generally used. Table 2.a is repeated as Table 41.a in this volume for the convenience of the reader.

The Mach number M_n in liquids is of primary interest in the analysis of underwater-explosion phenomena or high-order impact studies, especially in the immediate vicinity of the impact or explosion. The Cauchy number C_n, related to it, may eventually be found of interest in studies of cavitation erosion on propeller blades and similar objects. Taking account of the elasticity and mass density of the material, it may be useful in analyzing shock-wave erosion on different propeller materials.

As a study of high-order impact and of the details of shock-wave erosion is somewhat beyond the scope of this book, the treatment of the Mach or Cauchy numbers in this section is limited to examples giving the derivation of the shock-wave velocities in salt water and propeller bronze. For the first of these examples it is assumed that salt ocean water at an average temperature of 60 deg F possesses an elastic modulus K at that temperature, from Table X3.m of Sec. X3.7 of Appendix 3, of 340,000 psi, or 144(340,000) lb per ft^2. The mass density of salt ocean water, for the examples quoted here, may be taken as 1.9903 slugs per ft^3. The celerity c of an elastic shock wave in ocean water is then

$$c = \sqrt{\frac{K}{\rho}} = \left[\frac{144(340{,}000)}{1.9903}\right]^{0.5}$$

$$= 4{,}960 \text{ ft per sec, approx.}$$

This is the speed of sound in the ocean water under the conditions described.

For a propeller bronze having a weight density of 519 lb per ft^3, the mass density ρ(rho) at sea level is 519/32.174 = 16.13 slugs per ft^3. Assuming that the elastic modulus E of this bronze is $15(10^6)$ psi, the celerity c of a shock wave in bronze is

$$c_{\text{Bronze}} = \sqrt{\frac{E}{\rho}} = \left[\frac{15(10^6)144}{16.13}\right]^{0.5}$$

$$= 11{,}574 \text{ ft per sec.}$$

The relationship between the two values of celerity, as a matter of interest, is 11,574/4,960 = 2.33: 1.

41.3 The Euler and the Cavitation Numbers. The Euler number E_n, or the pressure coefficient, as it is also known, is a relationship between pressures of the form

$$E_n = \frac{p - p_\infty}{\frac{\rho}{2} U_\infty^2} = \frac{\Delta p}{\frac{\rho}{2} V^2} = \frac{\Delta p}{q} \qquad \text{(2.xviii)}$$

TABLE 41.a—SUMMARY OF DATA ON DIMENSIONLESS RELATIONSHIPS

This table is a duplicate of Table 2.a in Volume I, inserted here for the convenience of the reader.

The ratios of the forces set down in this table follow the listing by J. K. Vennard ["Elementary Fluid Mechanics," Wiley, New York, 1947, pp. 144-145] and by H. Rouse [EMF, 1946, pp. 62, 104, 322, 344]. The forces mentioned are unit forces in each case, and the inertia force is the same as the inertial reaction.

Name of Relationship	Symbol	Mathematical Expression	Relationship between Physical Quantities
Mach	M_n	$\frac{U}{c_E}$	Ratio of $\frac{\text{Velocity of phenomenon}}{\text{Velocity of compression wave}}$ in any medium
Cauchy	C_n	$\frac{U}{\sqrt{\frac{K}{\rho}}}$	Ratio of $\frac{\text{Inertial reaction}}{\text{Elasticity force}}$ in any given medium
Euler	E_n	$\frac{\Delta p}{\frac{\rho}{2} U_\infty^2}$	Ratio of $\frac{\text{Accelerative or pressure force}}{\text{Inertial reaction}}$
Cavitation	σ (sigma)	$\frac{p_\infty - e}{\frac{\rho}{2} U_\infty^2}$	Ratio of $\frac{\text{Accelerative or pressure force}}{\text{Inertial reaction}}$
Froude	F_n	$\frac{U}{\sqrt{gL}}, \frac{V}{\sqrt{gL}}$	Ratio of $\frac{\text{Inertia force}}{\text{Gravity force}}$ in a deep, unlimited body of liquid
Reynolds	R_n	$\frac{UL}{\nu}, \frac{VL}{\nu}, \frac{UD}{\nu}$	Ratio of $\frac{\text{Inertia force}}{\text{Viscosity force}}$
Planing	P_n	$\frac{D_T}{L_D}$	Ratio of $\frac{\text{Drag force or resistance}}{\text{Dynamic-lift force}}$
Strouhal	S_n	$\frac{fD}{U}$	Ratio of $\frac{\text{Longitudinal vortex spacing in a vortex street}}{\text{Body diameter transverse to flow}}$
Weber	W_n	$\frac{U}{\sqrt{\frac{\sigma}{\rho L}}}$	Ratio of $\frac{\text{Inertial reaction to an accelerative force}}{\text{Surface (tension) force}}$
Boussinesq	B_n	$\frac{U}{\sqrt{gR_H}}, \frac{V}{\sqrt{gR_H}}$	Ratio of $\frac{\text{Inertial reaction}}{\text{Gravity force}}$ within boundaries of channel of hydraulic radius R_H

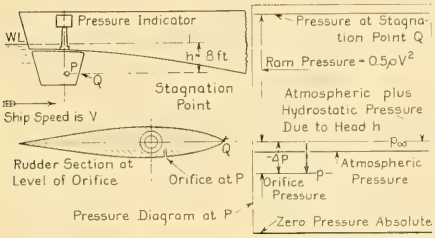

FIG. 41.A SCHEMATIC LAYOUT AND PRESSURE DIAGRAM FOR PRESSURE OBSERVATION ON A SHIP RUDDER

As applied to the rudder section of Fig. 41.A, and specifically to conditions at the orifice P, the measured pressure at that point is p, with the ship underway at the speed V. Assume that, at rest *in fresh water* at a temperature of 59 deg F, the submergence h of the orifice is 8 ft, and that the atmospheric pressure p_A at the time is 14.69 psi absolute.

To find the hydrostatic pressure at the orifice, with the ship at rest, it is noted from Table X3.a of Appendix 3 that the weight density w of the fresh water is 62.366 lb per ft^3, equivalent to a pressure of 62.366/144 = 0.433 psi. At a depth of 8 ft the corresponding hydrostatic pressure p_H is 8(0.433) = 3.464 psi. The ambient pressure $p_A + p_H = p_\infty$ at the orifice is then 14.69 + 3.464 = 18.15 psi absolute.

Assume next that the vessel of Fig. 41.A is underway at a speed of 29 kt, or 48.98 ft per sec. From Table X3.a the mass density ρ of the fresh water is 1.9384 slugs per ft^3. The ram pressure is then

$$q = \frac{\rho}{2} V^2 = \frac{1.9384}{2}(48.98)^2 = 2{,}325 \text{ lb per ft}^2$$

$$= 16.147 \text{ psi}, \quad \text{say } 16.15 \text{ psi.}$$

A small pressure diaphragm back of the orifice P on the rudder, connected to an indicating mechanism at the top of the rudder stock, shows a pressure drop of 2.12 psi *below atmospheric* when running. The negative differential pressure $-\Delta p$ below the ambient pressure p_∞ at rest is then $-3.464 - 2.12 = -5.58$ psi. The absolute pressure at the orifice is $14.69 - 2.12 = 12.57$ psi. These values are shown on the pressure diagram 2 in the middle of Fig. 41.B. The Euler number E_n or the pressure coefficient at the orifice P, when underway, is

$$E_n = \frac{\Delta p}{q} = \frac{-5.58}{16.15} = -0.3455$$

If a model of the ship, with a scale ratio of 25 and a corresponding speed ratio of 5, were being run in an endeavor to obtain dynamically similar flow, the Euler number E_n would be the same but the ram pressure q would be, as indicated in diagram 3 of Fig. 41.B,

$$q_{\text{Model}} = \frac{\rho}{2}\left(\frac{V}{5}\right)^2 = (q_{\text{Ship}})/25$$

$$= \frac{16.15}{25} = 0.646 \text{ psi.}$$

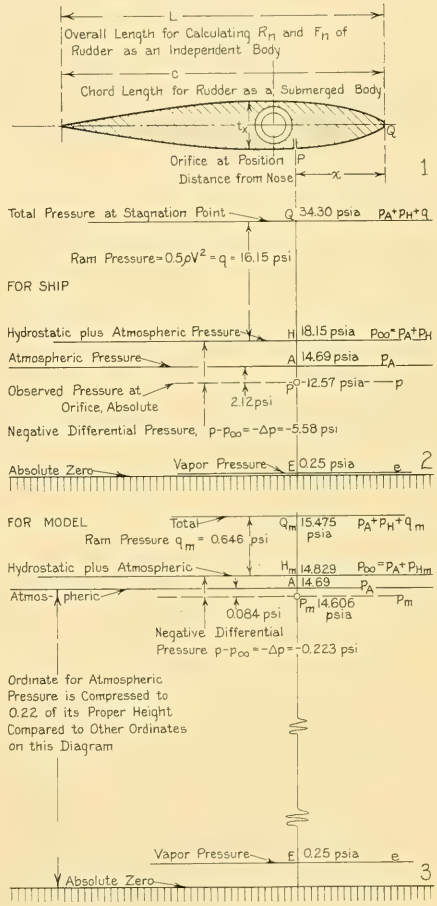

FIG. 41.B DETAILS AND PRESSURE DIAGRAMS FOR A PRESSURE MEASUREMENT ON A RUDDER

Multiplying this by the Euler number $E_n = -0.3455$ gives -0.223 psi as the $-\Delta p$ to be expected at the corresponding orifice position on the model rudder. The submergence of the orifice, with the model at rest, is $S/25 = 0.32$ ft, and the hydrostatic pressure there is $3.464/25 = 0.139$ psi. Hence, from the equality $p - p_\infty = -\Delta p$, $(14.69 - y) - (14.69 + 0.139) = -0.223$, as before, from which $y = (0.223 - 0.139) = 0.084$ psi *below* atmospheric pressure at the orifice. This is the pressure that should be registered by the pressure indicator on the model, on the basis that the flow is dynamically similar.

Another way of expressing the state of pressure at the orifice P on the ship (or on the model) is to say that it is equivalent to $-0.3455q$. Assuming that the test medium is the same, and that the nature of the dynamic flow does not change (it *would* change if cavitation set in on the ship but not on the model), this pressure coefficient is independent of the stream velocity. If a different test medium is used, of a greater mass density in order to obtain greater pressure differences, the value of the pressure coefficient $E_n = -0.3455q$ would still be the same, for dynamically similar flow. In the same way, tests to determine the pressure coefficients over a series of points along the section contour of a model rudder, mounted by itself, could be made in air or they could be run in mercury, whichever was most convenient.

It is customary, when tests are run in a different medium, to set the speed at such a value that the dynamic pressure of the test is the same numerically as the dynamic pressure in the medium in which the full-scale body is to run. As the mass density of mercury is about 13.60 times that of fresh water, the velocity-squared term U_∞^2 would have to be decreased by this ratio to keep the dynamic pressure the same. This would involve a reduction in velocity to a value of $\sqrt{2{,}399/13.60} = \sqrt{176.4} = 13.28$ ft per sec, corresponding to a ship speed of 7.86 kt for mercury instead of 29 kt for water. For a scale ratio of 25, and a corresponding speed ratio of 5, the test speed for the model would be $7.86/5 = 1.57$ kt.

If, as may be expected, the pressure coefficient changes with rudder angle δ(delta) and with the thickness ratio t_X/c of the section, it is convenient for testing and for design purposes to plot the pressure coefficient for any desired point or points on a basis of rudder angle and of thickness ratio. A similar procedure is followed for other variables.

If the liability of cavitation arises in a study of the rudder section at the point P, the cavitation number σ(sigma) for the flow at that level is readily calculated from the expression

$$\sigma = \frac{p_\infty - e}{\frac{\rho}{2} V^2} = \frac{p_\infty - e}{q} \qquad \text{(2.xix)}$$

Here the ambient pressure p_∞ is 3.464 psi gage or $14.69 + 3.464 = 18.15$ psi absolute. The vapor pressure e of fresh water at 59 deg F, with a small amount of dissolved air, may be taken from Table 47.a as about 0.25 psi absolute. The dynamic pressure q is the same as before, 16.15 psi. The cavitation index is now

$$\sigma = \frac{p_\infty - e}{\frac{\rho}{2} V^2} = \frac{18.15 - 0.25}{16.15} = 1.108$$

This index is a measure of the pressure available to create a gradient which will (or will not) cause the water to follow the rudder section. Since it exceeds *numerically* the negative-pressure coefficient $-\Delta p/q = 0.3455$ at the orifice P, there is more than enough pressure available to create a gradient which will turn the water in toward the rudder. No cavitation is taking place therefore at the point P, nor is any to be expected at somewhat higher speeds.

A look at pressure diagram 2 of Fig. 41.B, plotted to scale in psi absolute, explains why this is so. The numerator $p - p_\infty = \Delta p$ in the pressure-coefficient expression is represented by the negative distance from P to H, or $12.57 - 18.15 = -5.58$ psi. The term $p_\infty - e$ in the numerator of the expression for the cavitation number is represented by the distance from H to E. Cavitation is not to be expected until the absolute pressure at P drops to E, at which time both numerators would be equal. Therefore, as long as $p - p_\infty$ is smaller numerically for a given speed than $p_\infty - e$, cavitation does not occur at that speed. This is also evident directly from the fact that the absolute pressure p at the orifice P, $14.69 - 2.12 = 12.57$ psi absolute, is far above the vapor pressure e of the water, taken as 0.25 psi absolute.

Unless one is working constantly in this field, the calculation and use of pressure coefficients and cavitation numbers can become confusing and exasperating. It is recommended that, in these cases, the calculations be supplemented by graphic diagrams drawn approximately to scale, corresponding to those at 2 and 3 in Fig. 41.B.

It is also a help to remember that *the pressure coefficient E_n is a function of body shape,* because it embodies the pressure p which is found or measured on a body under given flow conditions. *The cavitation number is a function of the flow conditions and of the liquid in the stream;* this can be remembered because it embodies the vapor pressure e. The critical cavitation number σ_{CR} occurs when the cavitation number of the flow drops to the same *numerical* value as the pressure coefficient of the body at the point of lowest absolute pressure on the body.

It is customary in some quarters, when convenience dictates the change, to derive the Euler number E_n and the cavitation number σ by using values of head instead of pressure. The expression for the former then becomes

$$E_n = \frac{h - h_\infty}{\dfrac{U_\infty^2}{2g}} \tag{41.i}$$

where $U_\infty^2/(2g)$ is the dynamic or velocity head in the undisturbed liquid. With a vapor-pressure head h_V, the cavitation number is

$$\sigma = \frac{h_\infty - h_V}{\dfrac{U_\infty^2}{2g}} \tag{41.ii}$$

Employing the same data as for the preceding examples, and taking g as 32.174 ft per sec^2, the dynamic or velocity head is

$$h_U = \frac{U_\infty^2}{2g} = \frac{2{,}399}{2(32.174)} = 37.28 \text{ ft.}$$

The measured gage pressure at the orifice P of 2.12 psi *below atmospheric* corresponds to a negative head of $-2.12/0.433 = -4.896$ ft. The pressure coefficient is then:

$$\frac{\Delta p}{q} = \frac{-8.00 - 4.896}{37.28} = -0.346, \text{ as before.}$$

The head corresponding to the atmospheric pressure of 14.69 psi is $14.69/0.433 = 33.93$ ft. The cavitation index σ is based upon a vapor head of 0.25/0.433 or 0.57 ft of water. The index is then

$$\sigma = \frac{h_\infty - h_V}{\dfrac{U_\infty^2}{2g}} = \frac{(33.93 + 8.0) - 0.57}{37.28} = 1.109$$

This is equal to the value previously derived.

41.4 The Froude Number and the Taylor Quotient. If it is assumed that at an excessive trim by the bow, due possibly to damage, the topmost rudder sections in Fig. 41.A lie at the surface of the water instead of below it, then wavemaking and gravity effects come into play and the Froude number is applicable. Here

$$F_n = \frac{V}{\sqrt{gL}}$$

Assuming the length of these rudder sections as 14.6 ft, and the reduced speed as 12 kt, or 20.27 ft per sec, the Froude number *for the rudder only* is

$$F_n = \frac{20.27}{\sqrt{32.174(14.6)}} = 0.935$$

The corresponding Taylor quotient *for the rudder only,* based upon speed in kt and length in ft, is

$$T_q = \frac{V}{\sqrt{L}} = \frac{12}{\sqrt{14.6}} = 3.14$$

The Froude number F_n and the Taylor quotient T_q are related to each other by the constant ratio

$$F_n = \frac{1.6889}{\sqrt{g}}(T_q) \quad \text{and} \quad T_q = \frac{\sqrt{g}}{1.6889}(F_n)$$

where 1 kt is 1.6889 ft per sec. If g is 32.174 ft per sec^2, as in the example given, then $F_n = 0.2978T_q$ and $T_q = 3.358F_n$. For mental calculations or rough approximations, F_n may be taken as $0.3T_q$ and T_q as $(10/3)F_n$.

There are certain applications, such as in planing craft, in which the conventional Froude number is modified by using the beam B as the length dimension rather than the length L, or in which $\forall^{1/3}$ is used for L as the length dimension. The derivation of the numerical values for the modified F_b and $F_\forall$ numbers is obvious from the corresponding expressions

$$F_b = \frac{V}{\sqrt{gB}} \quad \text{and} \quad F_\forall = \frac{V}{\sqrt{g\forall^{1/3}}}$$

There are set down in Table 41.b a series of Froude numbers F_n, covering a range of speed from 2 through 100 ft per sec, equivalent to 1.18 through 59.21 kt, and embracing a range of model and ship lengths from 5 through 1000 ft. A first approximation to the Froude number for a given speed and length, based upon a standard g-value of 32.174 ft per sec^2, is obtained by inspection from this table. More accurate values are calculated by using the formulas in preceding paragraphs of this section.

TABLE 41.b—FROUDE NUMBERS FOR SHIP AND MODEL SPEEDS AND LENGTHS

Velocity		Length of body or ship, ft											
ft per sec	kt	5	10	15	20	25	30	35	40	45	50	60	70
2	1.18	0.158	0.111	0.091	0.079	0.071	0.064	0.060	0.056	0.053	0.050	0.046	0.042
3	1.78	0.237	0.167	0.137	0.118	0.106	0.097	0.089	0.084	0.079	0.075	0.068	0.063
4	2.39	0.315	0.223	0.182	0.158	0.141	0.129	0.119	0.111	0.105	0.100	0.091	0.084
5	2.96	0.394	0.279	0.228	0.197	0.176	0.161	0.149	0.139	0.131	0.125	0.114	0.105
6	3.55	0.473	0.334	0.273	0.237	0.212	0.193	0.179	0.165	0.157	0.150	0.137	0.126
7	4.14	0.552	0.390	0.319	0.276	0.247	0.225	0.209	0.195	0.184	0.175	0.159	0.147
8	4.74	0.631	0.446	0.364	0.315	0.282	0.258	0.238	0.223	0.210	0.199	0.182	0.169
9	5.33	0.710	0.502	0.410	0.355	0.317	0.290	0.268	0.251	0.237	0.224	0.205	0.190
10	5.92	0.788	0.557	0.455	0.394	0.353	0.322	0.298	0.279	0.263	0.249	0.228	0.211
11	6.51	0.867	0.613	0.501	0.434	0.388	0.354	0.328	0.307	0.289	0.274	0.250	0.232
12	7.10	0.946	0.669	0.546	0.473	0.423	0.386	0.357	0.334	0.315	0.299	0.273	0.253
13	7.70	1.025	0.725	0.592	0.512	0.458	0.418	0.387	0.362	0.342	0.324	0.296	0.274
14	8.29	1.104	0.780	0.637	0.552	0.494	0.451	0.417	0.390	0.368	0.349	0.319	0.295
15	8.88	1.183	0.836	0.683	0.591	0.529	0.483	0.447	0.418	0.394	0.374	0.341	0.316
16	9.47	1.261	0.892	0.728	0.631	0.564	0.515	0.477	0.446	0.420	0.399	0.364	0.337
17	10.1	1.340	0.948	0.774	0.670	0.599	0.547	0.506	0.474	0.447	0.424	0.387	0.358
18	10.7	1.419	1.003	0.819	0.710	0.635	0.579	0.536	0.502	0.473	0.449	0.410	0.379
19	11.2	1.498	1.059	0.865	0.749	0.670	0.612	0.566	0.530	0.499	0.474	0.432	0.400
20	11.8	1.577	1.115	0.910	0.788	0.705	0.644	0.596	0.557	0.526	0.499	0.455	0.421
22	13.0	1.735	1.226	1.001	0.867	0.776	0.708	0.655	0.613	0.578	0.548	0.501	0.464
24	14.2	1.892	1.338	1.093	0.946	0.846	0.773	0.715	0.669	0.631	0.598	0.546	0.506
26	15.4	2.050	1.449	1.184	1.025	0.917	0.837	0.775	0.725	0.683	0.648	0.592	0.548
28	16.6	2.208	1.561	1.275	1.104	0.987	0.901	0.834	0.780	0.736	0.698	0.637	0.590
30	17.8	2.365	1.672	1.366	1.183	1.058	0.966	0.894	0.836	0.788	0.748	0.683	0.632
32	18.9	2.523	1.783	1.457	1.261	1.128	1.030	0.953	0.892	0.841	0.798	0.728	0.674
34	20.1	2.681	1.895	1.548	1.340	1.199	1.095	1.013	0.948	0.894	0.848	0.774	0.716
36	21.3	2.838	2.007	1.639	1.419	1.269	1.159	1.072	1.003	0.946	0.897	0.819	0.759
38	22.5	2.996	2.118	1.730	1.498	1.340	1.223	1.132	1.059	0.999	0.947	0.865	0.801
40	23.7	3.154	2.230	1.821	1.577	1.410	1.288	1.192	1.115	1.051	0.997	0.910	0.843
42	24.9	3.311	2.341	1.912	1.656	1.481	1.352	1.251	1.171	1.104	1.047	0.956	0.885
44	26.1	3.469	2.453	2.010	1.735	1.551	1.416	1.311	1.226	1.156	1.097	1.001	0.927
46	27.2	3.627	2.564	2.094	1.813	1.622	1.481	1.370	1.282	1.209	1.147	1.047	0.969
48	28.4	3.784	2.676	2.185	1.892	1.693	1.545	1.430	1.338	1.261	1.197	1.093	1.011
50	29.6	3.942	2.787	2.276	1.971	1.763	1.610	1.490	1.394	1.314	1.247	1.138	1.054
52	30.8	4.100	2.899	2.367	2.050	1.834	1.674	1.594	1.449	1.367	1.296	1.184	1.096
54	32.0	4.257	3.010	2.458	2.129	1.904	1.738	1.609	1.505	1.419	1.346	1.229	1.138
56	33.2	4.415	3.121	2.549	2.208	1.975	1.803	1.668	1.561	1.472	1.396	1.275	1.180
58	34.3	4.573	3.233	2.640	2.286	2.045	1.867	1.728	1.617	1.524	1.446	1.320	1.222
60	35.5	4.730	3.344	2.731	2.365	2.116	1.931	1.787	1.672	1.577	1.496	1.366	1.264
62	36.7	4.888	3.456	2.822	2.444	2.186	1.996	1.847	1.728	1.629	1.546	1.411	1.306
64	37.9	5.046	3.567	2.913	2.523	2.257	2.060	1.907	1.784	1.682	1.596	1.457	1.349
66	39.1	5.203	3.679	3.004	2.602	2.327	2.125	1.966	1.839	1.735	1.645	1.502	1.391
68	40.3	5.361	3.790	3.095	2.681	2.398	2.189	2.026	1.895	1.787	1.695	1.548	1.433
70	41.4	5.519	3.902	3.186	2.759	2.468	2.253	2.085	1.951	1.840	1.745	1.593	1.475
72	42.6	5.677	4.013	3.277	2.838	2.539	2.318	2.145	2.007	1.892	1.795	1.639	1.517
74	43.8	5.834	4.125	3.369	2.917	2.609	2.382	2.205	2.062	1.945	1.845	1.684	1.559
76	45.0	5.992	4.236	3.460	2.996	2.680	2.446	2.264	2.118	1.997	1.895	1.730	1.601
78	46.2	6.150	4.348	3.551	3.075	2.750	2.511	2.324	2.174	2.050	1.945	1.775	1.644
80	47.4	6.307	4.459	3.642	3.154	2.821	2.575	2.383	2.230	2.102	1.994	1.821	1.686
82	48.5	6.465	4.571	3.733	3.232	2.891	2.640	2.443	2.285	2.155	2.044	1.866	1.728
84	49.7	6.623	4.682	3.824	3.311	2.962	2.704	2.502	2.341	2.208	2.094	1.912	1.770
86	50.9	6.780	4.794	3.915	3.390	3.032	2.768	2.562	2.397	2.260	2.144	1.957	1.812
88	52.1	6.938	4.905	4.006	3.469	3.103	2.833	2.622	2.453	2.313	2.194	2.003	1.854
90	53.3	7.096	5.017	4.097	3.548	3.173	2.897	2.681	2.508	2.365	2.244	2.048	1.896
92	54.5	7.253	5.128	4.188	3.627	3.244	2.962	2.741	2.564	2.418	2.294	2.094	1.938
94	55.7	7.411	5.240	4.279	3.706	3.314	3.026	2.800	2.620	2.470	2.343	2.139	1.981
96	56.8	7.569	5.351	4.370	3.784	3.385	3.090	2.860	2.676	2.523	2.393	2.185	2.023
98	58.0	7.726	5.463	4.461	3.863	3.456	3.155	2.919	2.731	2.575	2.443	2.231	2.065
100	59.2	7.884	5.574	4.552	3.942	3.526	3.219	2.979	2.787	2.628	2.493	2.276	2.107

TABLE 41.b—FROUDE NUMBERS FOR SHIP AND MODEL SPEEDS AND LENGTHS—*Continued*

Velocity		Length of body or ship, ft											
ft per sec	kt	80	90	100	120	140	160	180	200	250	300	350	400
2	1.18	0.039	0.037	0.035	0.032	0.030	0.028	0.026	0.025	0.022	0.020	0.019	0.018
3	1.78	0.059	0.056	0.053	0.048	0.045	0.042	0.039	0.037	0.033	0.031	0.028	0.026
4	2.39	0.079	0.074	0.071	0.064	0.060	0.056	0.053	0.050	0.045	0.041	0.038	0.035
5	2.96	0.098	0.093	0.088	0.081	0.075	0.070	0.066	0.062	0.056	0.051	0.047	0.044
6	3.55	0.118	0.111	0.106	0.097	0.089	0.084	0.079	0.075	0.067	0.061	0.056	0.053
7	4.14	0.138	0.130	0.123	0.113	0.104	0.098	0.092	0.087	0.078	0.071	0.066	0.062
8	4.74	0.158	0.149	0.141	0.129	0.119	0.112	0.105	0.100	0.089	0.081	0.075	0.070
9	5.33	0.177	0.167	0.159	0.145	0.134	0.125	0.118	0.112	0.100	0.092	0.085	0.079
10	5.92	0.197	0.186	0.176	0.161	0.149	0.139	0.131	0.125	0.112	0.102	0.094	0.088
11	6.51	0.217	0.204	0.194	0.177	0.164	0.153	0.144	0.137	0.123	0.112	0.104	0.097
12	7.10	0.236	0.223	0.212	0.193	0.179	0.167	0.158	0.150	0.134	0.122	0.113	0.106
13	7.70	0.256	0.242	0.229	0.209	0.194	0.181	0.171	0.162	0.145	0.132	0.122	0.115
14	8.29	0.276	0.260	0.247	0.225	0.209	0.195	0.184	0.174	0.156	0.142	0.132	0.123
15	8.88	0.295	0.279	0.264	0.242	0.224	0.209	0.197	0.187	0.167	0.153	0.141	0.132
16	9.47	0.315	0.297	0.282	0.258	0.238	0.223	0.210	0.199	0.179	0.163	0.151	0.141
17	10.1	0.335	0.316	0.300	0.274	0.253	0.237	0.223	0.212	0.190	0.173	0.160	0.150
18	10.7	0.354	0.334	0.317	0.290	0.268	0.251	0.236	0.224	0.201	0.183	0.169	0.159
19	11.2	0.374	0.353	0.335	0.306	0.283	0.265	0.249	0.237	0.212	0.193	0.179	0.167
20	11.8	0.394	0.372	0.353	0.322	0.298	0.279	0.263	0.249	0.223	0.203	0.188	0.176
22	13.0	0.433	0.409	0.388	0.354	0.328	0.307	0.289	0.274	0.246	0.224	0.207	0.194
24	14.2	0.473	0.446	0.423	0.386	0.358	0.335	0.315	0.299	0.268	0.244	0.226	0.211
26	15.4	0.512	0.483	0.458	0.419	0.387	0.362	0.341	0.324	0.290	0.264	0.245	0.229
28	16.6	0.551	0.520	0.494	0.451	0.417	0.390	0.368	0.349	0.312	0.285	0.263	0.247
30	17.8	0.591	0.557	0.529	0.483	0.447	0.418	0.394	0.374	0.335	0.305	0.282	0.264
32	18.9	0.630	0.595	0.564	0.515	0.477	0.446	0.420	0.399	0.357	0.325	0.301	0.282
34	20.1	0.669	0.632	0.599	0.547	0.507	0.474	0.446	0.424	0.379	0.346	0.320	0.300
36	21.3	0.709	0.669	0.635	0.580	0.536	0.502	0.473	0.449	0.402	0.366	0.339	0.317
38	22.5	0.748	0.706	0.670	0.612	0.566	0.530	0.499	0.473	0.424	0.386	0.358	0.335
40	23.7	0.788	0.743	0.705	0.644	0.596	0.558	0.525	0.498	0.446	0.407	0.376	0.352
42	24.9	0.827	0.780	0.740	0.676	0.626	0.585	0.551	0.523	0.469	0.427	0.395	0.370
44	26.1	0.866	0.818	0.776	0.708	0.656	0.613	0.578	0.548	0.491	0.447	0.414	0.388
46	27.2	0.906	0.855	0.811	0.741	0.685	0.641	0.604	0.573	0.513	0.468	0.433	0.405
48	28.4	0.945	0.892	0.846	0.773	0.715	0.669	0.630	0.598	0.536	0.488	0.452	0.423
50	29.6	0.985	0.929	0.882	0.805	0.745	0.697	0.657	0.623	0.558	0.509	0.471	0.441
52	30.8	1.024	0.966	0.917	0.837	0.775	0.725	0.683	0.648	0.580	0.529	0.489	0.458
54	32.0	1.063	1.003	0.952	0.869	0.805	0.753	0.709	0.673	0.603	0.549	0.500	0.476
56	33.2	1.103	1.041	0.987	0.902	0.834	0.781	0.735	0.698	0.625	0.570	0.527	0.493
58	34.3	1.142	1.078	1.023	0.934	0.864	0.806	0.762	0.723	0.647	0.590	0.546	0.511
60	35.5	1.181	1.115	1.058	0.966	0.894	0.836	0.788	0.748	0.670	0.610	0.565	0.529
62	36.7	1.221	1.152	1.093	0.998	0.924	0.864	0.814	0.773	0.692	0.631	0.583	0.546
64	37.9	1.260	1.189	1.128	1.030	0.954	0.892	0.840	0.797	0.714	0.651	0.602	0.564
66	39.1	1.300	1.226	1.164	1.063	0.983	0.920	0.866	0.822	0.737	0.671	0.621	0.581
68	40.3	1.339	1.263	1.199	1.095	1.013	0.948	0.893	0.847	0.759	0.692	0.640	0.599
70	41.4	1.378	1.301	1.234	1.127	1.043	0.976	0.919	0.872	0.781	0.712	0.659	0.617
72	42.6	1.418	1.338	1.269	1.159	1.073	1.004	0.945	0.971	0.804	0.732	0.678	0.634
74	43.8	1.457	1.375	1.305	1.191	1.103	1.032	0.972	0.922	0.826	0.753	0.696	0.652
76	45.0	1.496	1.412	1.340	1.224	1.132	1.059	0.998	0.947	0.848	0.773	0.715	0.670
78	46.2	1.536	1.449	1.375	1.256	1.162	1.087	1.024	0.972	0.870	0.794	0.734	0.687
80	47.4	1.575	1.486	1.410	1.288	1.192	1.115	1.050	0.997	0.893	0.814	0.753	0.705
82	48.5	1.615	1.524	1.446	1.320	1.222	1.143	1.077	1.022	0.915	0.834	0.772	0.722
84	49.7	1.654	1.561	1.481	1.352	1.252	1.171	1.103	1.047	0.937	0.854	0.790	0.740
86	50.9	1.693	1.598	1.516	1.385	1.281	1.199	1.129	1.072	0.960	0.875	0.809	0.758
88	52.1	1.733	1.635	1.551	1.417	1.311	1.227	1.155	1.097	0.982	0.895	0.828	0.775
90	53.3	1.772	1.672	1.587	1.449	1.341	1.255	1.182	1.121	1.004	0.915	0.847	0.793
92	54.5	1.812	1.709	1.622	1.481	1.371	1.283	1.208	1.146	1.027	0.936	0.866	0.811
94	55.7	1.851	1.747	1.657	1.513	1.401	1.310	1.234	1.171	1.049	0.956	0.885	0.828
96	56.8	1.890	1.784	1.693	1.546	1.430	1.338	1.261	1.196	1.071	0.976	0.903	0.846
98	58.0	1.930	1.821	1.728	1.578	1.460	1.366	1.287	1.221	1.094	0.997	0.922	0.863
100	59.2	1.969	1.858	1.763	1.610	1.490	1.394	1.313	1.246	1.116	1.017	0.941	0.881

TABLE 41.b—FROUDE NUMBERS FOR SHIP AND MODEL SPEEDS AND LENGTHS—*Concluded*

Velocity		Length of body or ship, ft											
ft per sec	kt	450	500	550	600	650	700	750	800	850	900	950	1000
2	1.18	0.017	0.016	0.015	0.014	0.014	0.013	0.013	0.012	0.012	0.012	0.011	0.011
3	1.78	0.025	0.024	0.023	0.022	0.021	0.020	0.019	0.019	0.018	0.018	0.017	0.017
4	2.39	0.033	0.032	0.030	0.029	0.028	0.027	0.026	0.025	0.024	0.023	0.023	0.022
5	2.96	0.042	0.039	0.038	0.036	0.035	0.033	0.032	0.031	0.030	0.029	0.029	0.028
6	3.55	0.050	0.047	0.045	0.043	0.041	0.040	0.039	0.037	0.036	0.035	0.034	0.033
7	4.14	0.058	0.055	0.053	0.050	0.048	0.047	0.045	0.044	0.042	0.041	0.040	0.039
8	4.74	0.066	0.063	0.060	0.058	0.055	0.053	0.051	0.050	0.048	0.047	0.046	0.045
9	5.33	0.075	0.071	0.068	0.065	0.062	0.060	0.058	0.056	0.054	0.053	0.051	0.050
10	5.92	0.083	0.079	0.075	0.072	0.069	0.067	0.064	0.062	0.061	0.059	0.057	0.056
11	6.51	0.091	0.087	0.083	0.079	0.076	0.073	0.071	0.069	0.067	0.065	0.063	0.061
12	7.10	0.100	0.095	0.090	0.086	0.083	0.080	0.077	0.075	0.073	0.070	0.069	0.067
13	7.70	0.108	0.102	0.098	0.093	0.090	0.087	0.084	0.081	0.079	0.076	0.074	0.072
14	8.29	0.116	0.110	0.105	0.101	0.097	0.093	0.090	0.087	0.085	0.082	0.080	0.078
15	8.88	0.125	0.118	0.113	0.108	0.104	0.100	0.096	0.094	0.091	0.088	0.086	0.084
16	9.47	0.133	0.126	0.120	0.115	0.111	0.107	0.103	0.100	0.097	0.094	0.091	0.089
17	10.1	0.141	0.134	0.128	0.122	0.117	0.113	0.109	0.106	0.103	0.100	0.098	0.095
18	10.7	0.149	0.142	0.135	0.129	0.124	0.120	0.116	0.112	0.109	0.106	0.103	0.100
19	11.2	0.158	0.150	0.143	0.137	0.131	0.127	0.122	0.119	0.115	0.112	0.108	0.106
20	11.8	0.166	0.158	0.150	0.144	0.138	0.133	0.129	0.125	0.121	0.117	0.114	0.111
22	13.0	0.183	0.173	0.165	0.158	0.152	0.147	0.141	0.137	0.133	0.129	0.126	0.123
24	14.2	0.199	0.189	0.180	0.173	0.166	0.160	0.154	0.150	0.145	0.141	0.137	0.134
26	15.4	0.216	0.205	0.195	0.187	0.180	0.173	0.167	0.162	0.157	0.153	0.148	0.145
28	16.6	0.232	0.221	0.210	0.201	0.193	0.186	0.180	0.175	0.169	0.164	0.160	0.156
30	17.8	0.249	0.236	0.225	0.216	0.207	0.200	0.193	0.187	0.182	0.176	0.171	0.167
32	18.9	0.266	0.252	0.240	0.230	0.221	0.213	0.206	0.200	0.194	0.188	0.183	0.178
34	20.1	0.282	0.268	0.255	0.244	0.235	0.226	0.219	0.212	0.206	0.200	0.194	0.189
36	21.3	0.299	0.284	0.270	0.259	0.249	0.240	0.231	0.225	0.218	0.211	0.206	0.201
38	22.5	0.315	0.299	0.285	0.273	0.263	0.253	0.244	0.237	0.230	0.223	0.217	0.212
40	23.7	0.332	0.315	0.300	0.288	0.276	0.266	0.257	0.250	0.242	0.235	0.228	0.223
42	24.9	0.349	0.331	0.315	0.302	0.290	0.280	0.270	0.262	0.254	0.247	0.240	0.234
44	26.1	0.365	0.347	0.330	0.316	0.304	0.293	0.283	0.275	0.266	0.258	0.251	0.245
46	27.2	0.382	0.362	0.345	0.331	0.318	0.306	0.296	0.287	0.278	0.270	0.263	0.256
48	28.4	0.398	0.378	0.360	0.345	0.332	0.320	0.309	0.300	0.290	0.282	0.274	0.267
50	29.6	0.415	0.394	0.376	0.360	0.346	0.333	0.322	0.312	0.303	0.294	0.286	0.279
52	30.8	0.432	0.410	0.391	0.374	0.359	0.346	0.334	0.324	0.315	0.305	0.297	0.290
54	32.0	0.448	0.426	0.406	0.388	0.373	0.360	0.347	0.337	0.327	0.317	0.308	0.301
56	33.2	0.465	0.441	0.421	0.403	0.387	0.373	0.360	0.349	0.339	0.329	0.320	0.312
58	34.3	0.481	0.457	0.436	0.417	0.401	0.386	0.373	0.362	0.351	0.340	0.331	0.323
60	35.5	0.498	0.473	0.451	0.431	0.415	0.400	0.386	0.374	0.363	0.352	0.343	0.334
62	36.7	0.515	0.489	0.466	0.446	0.428	0.413	0.399	0.387	0.375	0.364	0.354	0.345
64	37.9	0.531	0.504	0.481	0.460	0.442	0.426	0.412	0.399	0.387	0.376	0.365	0.356
66	39.1	0.548	0.520	0.496	0.475	0.456	0.440	0.424	0.412	0.399	0.387	0.377	0.368
68	40.3	0.564	0.536	0.511	0.489	0.470	0.453	0.437	0.424	0.411	0.399	0.388	0.379
70	41.4	0.581	0.552	0.526	0.503	0.484	0.466	0.450	0.437	0.424	0.411	0.400	0.390
72	42.6	0.598	0.567	0.541	0.518	0.498	0.480	0.463	0.449	0.436	0.423	0.411	0.401
74	43.8	0.614	0.583	0.556	0.532	0.511	0.493	0.476	0.462	0.448	0.434	0.423	0.412
76	45.0	0.631	0.599	0.571	0.546	0.525	0.506	0.489	0.474	0.460	0.446	0.434	0.423
78	46.2	0.647	0.615	0.586	0.561	0.539	0.519	0.502	0.487	0.472	0.458	0.445	0.434
80	47.4	0.664	0.630	0.601	0.575	0.553	0.533	0.514	0.499	0.484	0.470	0.457	0.446
82	48.5	0.681	0.646	0.616	0.590	0.567	0.546	0.527	0.512	0.496	0.481	0.468	0.457
84	49.7	0.697	0.662	0.631	0.604	0.580	0.559	0.540	0.524	0.508	0.493	0.480	0.468
86	50.9	0.714	0.678	0.646	0.618	0.594	0.573	0.553	0.537	0.520	0.505	0.491	0.479
88	52.1	0.730	0.693	0.661	0.633	0.608	0.586	0.566	0.549	0.532	0.517	0.502	0.490
90	53.3	0.747	0.709	0.676	0.647	0.622	0.599	0.579	0.562	0.545	0.528	0.514	0.501
92	54.5	0.764	0.725	0.691	0.661	0.636	0.613	0.592	0.574	0.557	0.540	0.525	0.512
94	55.7	0.780	0.741	0.706	0.676	0.650	0.626	0.604	0.587	0.569	0.552	0.537	0.524
96	56.8	0.797	0.756	0.721	0.690	0.663	0.639	0.617	0.599	0.581	0.564	0.548	0.535
98	58.0	0.813	0.772	0.736	0.705	0.677	0.653	0.630	0.612	0.593	0.575	0.560	0.546
100	59.2	0.830	0.788	0.751	0.719	0.691	0.666	0.643	0.624	0.605	0.587	0.571	0.557

41.5 Calculation of the Reynolds Numbers. Although many rudders lie partly or wholly within the boundary layer of the main hull, it may be assumed in Fig. 41.A that the point P is outside (below) that layer. At the orifice position the boundary layer is assumed to be that due to flow over the rudder alone.

For a ship speed of 29 kt, the velocity U in the Reynolds-number expression UL/ν(nu) for the rudder only is again 48.98 ft per sec and the significant length L of the rudder section, at 8 ft below the at-rest WL, is 10.2 ft. From Table X3.h the kinematic viscosity ν of fresh water at 59 deg F is $1.2285(10^{-5})$ ft^2 per sec. Hence, for the rudder section *as a whole*, sketched in diagram 1 of Fig. 41.B,

$$R_n = \frac{48.98(10.2)}{1.2285(10^{-5})} = 40.66(10^6)$$

As the Reynolds number rarely needs to be expressed in exact terms, its value for a speed of 29 kt, or about 49 ft per sec, and for a length of 10.2 ft, may be taken by inspection from Table 45.a. This gives about $40(10^6)$, almost exactly the same as by computation.

If the flow at the orifice position P is to be studied, the significant Reynolds number is the x-Reynolds number R_x at that point, indicated in Fig. 41.B. It is customary, in asymmetrical as well as symmetrical shapes of this kind, to measure the x-distance from the leading edge along the base chord or other convenient dimension parallel to the direction of flow. In this case it is measured along the meanline. It is customary, also, when the velocity of the liquid along the boundary is not accurately known, to consider it equal to the undisturbed stream velocity. Here $U_\infty = V$.

If the orifice at P lies opposite a point 2.84 ft downstream from the leading edge, then the x-Reynolds number is

$$R_x = \frac{V(x)}{\nu} = \frac{48.98(2.84)}{1.2285(10^{-5})} = 11.32(10^6)$$

by calculation or $11.2(10^6)$ from inspection of Table 45.a. For the 1/25 scale model, run at a speed equal to $48.98/5 = 9.79$ ft per sec with the test point $2.82/25 = 0.113$ ft downstream from the leading edge, the x-Reynolds number is

$$R_x = \frac{9.79(0.113)}{1.2285(10^{-5})} = 0.09(10^6)$$

In the case of flow around a body of short length, broadside to the stream, the body beam B or body diameter D rather than its length L is the determining factor in the type and nature of viscous flow encountered. For this reason, a dimension transverse to the flow rather than one parallel to the flow is used as the space dimension in the numerator of the Reynolds number. For the case of the underwater sound head of Fig. 41.D of Sec. 41.6 it is the diameter D of the head, say 1.72 ft. The relationship so formed is called the d-Reynolds number, represented by

$$R_d = \frac{UD}{\nu} \qquad \text{(2.xxii)}$$

For a ship speed of 14 kt, or 23.64 ft per sec, this is

$$R_d = \frac{UD}{\nu} = \frac{23.64(1.72)}{1.2285(10^{-5})} = 3.3(10^6)$$

There are several other Reynolds numbers in use by hydrodynamicists, such as the δ-Reynolds number R_δ. In this case the thickness δ of the boundary layer replaces L as the space dimension in the expression UL/ν.

One of great importance is the blade-Reynolds number R_b for the blade sections of screw and rotating-blade propellers. This expression is built up in the manner shown by Fig. 41.C. It

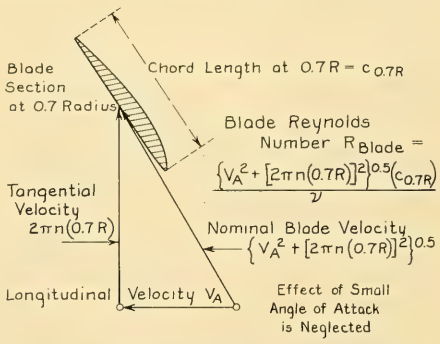

FIG. 41.C DEFINITION SKETCH AND FORMULA FOR BLADE REYNOLDS NUMBER

utilizes as the length dimension the chord length c of a typical blade section, at $0.7R$ on a screw propeller, and a nominal velocity generally parallel to the base chord of the blade. For TMB model propeller 2294 shown in Fig. 78.L, where the chord length c at $0.7R$ is 2.682 inches or 0.2235 ft, the value of $0.7R$ is 3.378 inches or 0.2815 ft, V_A is

assumed as 6.97 ft per sec or 4.13 kt, and n as 650 rpm or 10.83 rps. The blade-Reynolds number for a J-value of $V_A/(nD) = 0.80$ works out as

$$R_b = \frac{[V_A^2 + [2\pi n(0.7R)]^2]^{0.5}(c_{0.7R})}{\nu} \qquad (41.iii)$$

$$= \frac{[(6.97)^2 + [6.2832(10.83)0.2815]^2]^{0.5}(0.2235)}{1.2285(10^{-5})}$$

$$= 0.371(10^6)$$

41.6 Application of the Strouhal Number. For the retractable sound gear shown in Fig. 41.D,

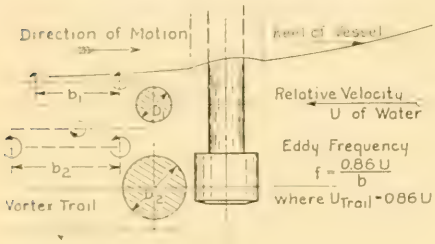

Fig. 41.D Definition Sketch and Formula for Eddy Frequency in a Vortex Trail

having a cylindrical neck of diameter D_1 and a cylindrical head of diameter D_2, separation occurs around the after sides of both the neck and the head. Vortex trails of eddies having fore-and-aft spacings of b_1 and b_2 on each side are left behind the two parts of the device.

Vibration of the neck and head in a transverse plane is certain to be encountered at some speed, and the Strouhal number S_n is of interest in this phenomenon. The situation depicted in Fig. 41.D is complicated by a neck and head of different diameter, so for the purpose of this example it is assumed that the head diameter D_2 is reduced to the neck diameter D_1. This is taken as 0.96 ft.

The value of the d-Reynolds number R_d is then, at say 14 kt or 23.64 ft per sec in standard fresh water,

$$R_d = \frac{UD}{\nu} = \frac{23.64(0.96)}{1.2285(10^{-5})} = 1.85(10^6)$$

It has been found by experiment that there is a relationship between the Reynolds number R_d and the Strouhal number S_n; this is available for a somewhat lower range of R_d in the left-hand diagram of Fig. 46.G [Rouse, H., EH, 1950, Fig. 94, p. 130; Landweber, L., TMB Rep. 485, Jul 1942, Fig. 8, p. 17]. Assuming that the corresponding S_n value is 0.6, and using Eq. (2.xxiii) of Sec. 2.22,

$$S_n = \frac{fD}{U} = 0.6 = \frac{fD}{V}$$

where the eddy frequency

$$f = 0.6\frac{V}{D} = (0.6)\frac{23.64}{0.96} = 14.8 \text{ cycles per sec.}$$

If the frequency of resonant transverse vibration of the cylindrical sound-gear assembly, taking the added mass of the entrained water into account, is close to this value, the vibration caused by the periodic alternating transverse force accompanying the eddy pattern in the vortex trail will be greatly magnified. To avoid resonance without a change in diameter of the sound gear, the extension below the hull may have to be diminished, or the maximum speed reduced.

41.7 The Planing, Boussinesq, and Weber Numbers. The planing number P_n is of limited application. It is expressed, as described in Sec. 2.22, as the ratio between (1) the total drag D_T (or total resistance R_T) of a planing form and (2) the dynamic lift L_D produced by that form. When, as usually occurs at full planing speed, the buoyancy B is zero and the entire displacement Δ(delta) or weight W is supported by the dynamic lift, the expression becomes $P_n = D_T/\Delta = D_T/W$. Expressing the planing number in numerical values for a given case hardly requires an illustrative example here.

The Boussinesq number, similar to the Froude number with the hydraulic radius R_H of a confined waterway as its length dimension, is expressed by

$$B_n = \frac{V}{\sqrt{gR_H}} = \frac{U}{\sqrt{gR_H}} \qquad (2.xxv)$$

The method of calculating the hydraulic radius is described and illustrated in Sec. 61.14.

The Weber number W_n is described in Sec. 2.22. As it is not employed in any of the chapters in this volume, an illustrative example of the method of computing and applying it is omitted.

It is again emphasized that, although normal engineering computations of the various dimensionless numbers would not take account of all the significant figures in the preceding examples,

they are retained here to insure that the same answer is obtained by different methods of calculation.

In view of the dimensionless characters of the parameters described in this section they have the same numerical values when derived by consistent units in the metric or any other system of measurement.

41.8 Derivation of Stream-Function and Velocity-Potential Formulas for Typical Two-Dimensional Flows. The combination of the stream functions ψ(psi) and the velocity potentials ϕ(phi), respectively, of two liquid flows is discussed briefly in Secs. 2.11 and 2.14. To illustrate how this procedure is employed in analytic hydrodynamics a brief outline is given of the formation of the equations for the resultant stream functions and velocity potentials for flow about the following simple forms:

(a) Single-ended 2-diml body with a single source in the nose; body axis parallel to the flow. A partial longitudinal section through this body is shown by the heavy line in Fig. 43.B.
(b) Two-dimensional Rankine stream form developed around a 2-diml source-sink pair whose axis is parallel to the flow. A similar section through such a body is drawn in Fig. 43.D.
(c) Two-dimensional circular cylinder or rod, with its axis normal to the flow, illustrated in diagram 1 of Fig. 41.G
(d) Two-dimensional circular cylinder with its axis normal to the flow, and about which circulation is taking place, corresponding to diagram 3 of Fig. 14.E in Volume I.

The formulas given for the ψ- and ϕ-values of these five classes of bodies enable the coordinates for their potential-flow streamline patterns to be determined and the resultant velocities and pressures at selected points to be calculated. The methods of developing the formulas in the text may be followed for formulas applying to bodies of varied shapes. For all of these bodies, the mathematical expressions characterizing the contours and the flow can be manipulated with mathematical operators to derive other useful data, practical as well as analytical.

The purely mathematic steps in the derivations of this section and the one following are omitted from the text.

I. It is convenient to take first the case of a single 2-diml source of strength m in a uniform

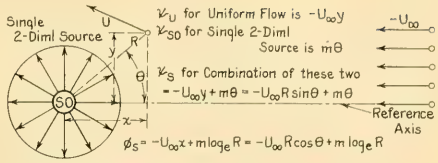

Fig. 41.E Definition Sketch and Formulas for Stream Function and Velocity Potential of Combination of Uniform Flow and Single Source

stream of velocity $-U_\infty$, listed under (a) of the preceding tabulation. The liquid in the stream is moving from right to left, as in Fig. 41.E. Here the 2-diml stream function ψ_{SO} for the single source is $m\theta$(theta), from Eq. (3.xi). The 2-diml stream function ψ_U for the uniform flow is $-U_\infty y$. Adding the two gives the stream function for the combined flow

$$\psi_S = -U_\infty y + m\theta = -U_\infty R \sin\theta + m\theta \quad (41.\text{iv})$$

The 2-diml stream function for $\psi_S = 0$ outlines a single-ended body, of which a portion of one half is pictured in Fig. 43.B. The values of $\psi_S = -1$, -2, -3, and so on, produce resultant streamlines around the body.

The 2-diml velocity potential ϕ_{SO} for the single source is $m \log_e R$, from Eq. (3.xii). That for the uniform flow is $-U_\infty x$. Adding the two gives the velocity potential for the combined flow

$$\begin{aligned}\phi_S &= -U_\infty x + m \log_e R \\ &= -U_\infty R \cos\theta + m \log_e R \qquad (41.\text{v})\end{aligned}$$

II. Take next the case of the 2-diml Rankine stream form, produced by a source-sink pair, lying in a uniform stream having a direction of flow parallel to the stream-form axis, as listed under (b) preceding. It is necessary first to derive the stream function ψ (and the velocity potential ϕ) for the source-sink combination, diagrammed in Fig. 41.F. The stream function is obtained by adding the stream functions of the source and sink. For the source, $\psi_{SO} = m \tan^{-1} [y/(x - s)]$; for the sink, $\psi_{SK} = -m \tan^{-1} [y/(x + s)]$, where the origin of the cartesian coordinates O is at the midlength of the source-sink axis and s is the half-distance between the two. Combining the stream function for the source and sink gives:

$$\begin{aligned}\psi_C &= m\left[\tan^{-1}\left(\frac{y}{x - s}\right) - \tan^{-1}\left(\frac{y}{x + s}\right)\right] \\ &= m \tan^{-1}\left[\frac{2ys}{x^2 + y^2 - s^2}\right] \qquad (41.\text{vi})\end{aligned}$$

$$\text{for Source, } \psi_{SO} = m\tan^{-1}\frac{y}{x-s}$$

$$\text{for Sink, } \psi_{SK} = -m\tan^{-1}\frac{y}{x+s}$$

$$\text{whence } \psi_C = m\left(\tan^{-1}\frac{y}{x-s} - \tan^{-1}\frac{y}{x+s}\right) = m\tan^{-1}\left(\frac{2ys}{x^2+y^2-s^2}\right)$$

Adding the Stream Function $\psi_U = -U_\infty y$ for the Uniform Flow,

$$\psi_S = -U_\infty y + m\tan^{-1}\left(\frac{2ys}{x^2+y^2-s^2}\right)$$

For Source, $\phi_{SO} = m\log_e R_{SO} = 0.5\,m\log_e\left[(x-s)^2+y^2\right]$; see Fig 41 H

For Sink, $\phi_{SK} = -m\log_e R_{SK} = -0.5\,m\log_e\left[(x+s)^2+y^2\right]$

$$\text{For Source-Sink Pair, } \phi_C = \frac{1}{2}m\log_e\left[\frac{(x-s)^2+y^2}{(x+s)^2+y^2}\right]$$

Adding the Velocity Potential $\phi_U = -U_\infty x$ for the Uniform Flow

$$\phi_S = -U_\infty x + \frac{1}{2}m\log_e\left[\frac{(x-s)^2+y^2}{(x+s)^2+y^2}\right]$$

Fig. 41.F Definition Sketch and Formulas for Stream Function and Velocity Potential of Combination of Uniform Flow and Source-Sink Pair

Adding the stream function $\psi_U = -U_\infty y$ of the uniform flow in the direction of the source-sink axis gives for the stream function of the entire 2-diml combination

$$\psi_S = -U_\infty y + m\tan^{-1}\left[\frac{2ys}{x^2+y^2-s^2}\right] \quad (41.\text{vii})$$

The oval body shape for a value of $\psi_S = 0$, and the streamlines for $\psi_S = -2, -4$, and so on, are delineated in Fig. 43.D.

To determine the velocity potential for the 2-diml source-sink pair of Fig. 41.F, that for a source is

$$\phi_{SO} = m\log_e R_{SO} = \tfrac{1}{2}m\log_e\left[(x-s)^2+y^2\right]$$

That for a sink is

$$\phi_{SK} = -m\log_e R_{SK} = -\tfrac{1}{2}m\log_e\left[(x+s)^2+y^2\right]$$

where the relationship of the coordinates is as shown in Fig. 41.H of Sec. 41.9. Adding the two ϕ-values, the velocity potential for the field set up by the source-sink pair is

$$\phi_C = \tfrac{1}{2}m\log_e\left[\frac{(x-s)^2+y^2}{(x+s)^2+y^2}\right] \quad (41.\text{viii})$$

Adding to this the velocity potential $\phi_U = -U_\infty x$ for a uniform stream, the velocity potential for a 2-diml source-sink pair lying in a uniform stream parallel to the source-sink axis is

$$\phi_S = -U_\infty x + \tfrac{1}{2}m\log_e\left[\frac{(x-s)^2+y^2}{(x+s)^2+y^2}\right] \quad (41.\text{ix})$$

III. For the 2-diml circular cylinder diagrammed at 1 in Fig. 41.G and tabulated in (c) preceding, it is shown in Fig. 3.M that this form can be represented by the resultant flow from a 2-diml doublet and from a uniform stream. It is explained in Sec. 3.10 that a doublet is formed by moving the source and sink so close together that they almost coincide, but never do. At the same time the source and sink strength is increased so that the product of the distance $2s$ separating the source and sink times the source strength m remains finite [Glauert, H., EAAT, 1948, p. 29]. Stated mathematically, $\mu(\text{mu}) = 2ms$ as s approaches zero, where μ is finite and is called the doublet strength. The stream function of a doublet is the limit as s diminishes to an infinitesimally small distance in Eq. (41.vi), the stream function of a source-and-sink pair. Expressed in symbols,

$$\psi_D = \lim_{s\to 0} m\tan^{-1}\left[\frac{2ys}{x^2+y^2-s^2}\right] = \frac{2msy}{x^2+y^2}$$

Since $\mu = 2ms$

$$\psi_D = \frac{\mu y}{x^2+y^2} \quad (41.\text{x})$$

Adding to this the uniform-flow stream function $\psi_U = -U_\infty y$, the function of the combined flow becomes

$$\psi_S = -U_\infty y + \frac{\mu y}{x^2+y^2} \quad (41.\text{xi})$$

Setting $\psi_S = 0$, which is its value at the reference surface, in this case that of the solid 2-diml rod,

$$U_\infty y = \frac{\mu y}{x^2+y^2}$$

or

$$U_\infty(x^2+y^2) = \mu = U_\infty R_0^2 \quad (41.\text{xii})$$

Hence the flow takes place around a cylinder of radius R_0 where $R_0 = \sqrt{\mu/U_\infty}$.

The stream function ψ_S of the flow around a 2-diml circular cylinder in a uniform stream normal to its axis can be written in several alternative forms:

$$\psi = -U_\infty y + \frac{\mu y}{R^2} = -U_\infty y\left(1 - \frac{R_0^2}{R^2}\right)$$

$$= -U\left(R - \frac{R_0^2}{R}\right)\sin\theta \quad (41.\text{xiii})$$

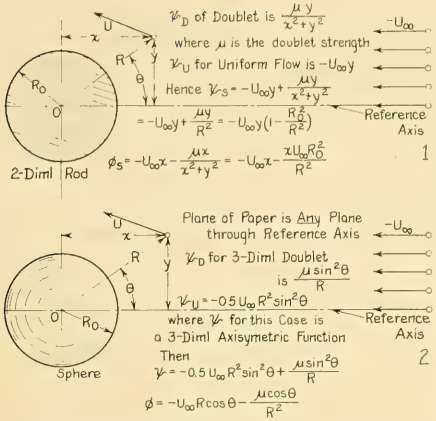

FIG. 41.G DEFINITION SKETCH AND FORMULAS FOR STREAM FUNCTIONS AND VELOCITY POTENTIALS FOR 2-DIML ROD AND 3-DIML SPHERE

The velocity potential ϕ_D of a 2-diml doublet whose strength $\mu = 2ms$ is found by taking the limit of Eq. (41.viii) as s approaches zero. This gives

$$\phi_D = -\frac{\mu \cos\theta}{R} \quad \text{in polar coordinates} \tag{41.xiv}$$

$$\phi_D = -\frac{\mu x}{x^2 + y^2} \quad \text{in cartesian coordinates} \tag{41.xiva}$$

The velocity potential of a uniform flow from right to left in diagram 1 of Fig. 41.G is

$$\phi_U = -U_\infty x$$

Combining the two algebraically gives, for the resultant flow around the rod,

$$\phi_S = -U_\infty x - \frac{\mu \cos\theta}{R} \tag{41.xv}$$

or

$$\phi_S = -U_\infty x - \frac{\mu x}{x^2 + y^2} \tag{41.xva}$$

$$= -U_\infty x - \frac{x U_\infty R_0^2}{x^2 + y^2}$$

$$= -U_\infty x - \frac{x U_\infty R_0^2}{R^2} \tag{41.xvb}$$

In polar coordinates, the tangential velocity at any radius R, $U_\theta = R\, d\theta$, is equal to minus the partial derivative of the stream function with respect to R, or $\partial\psi_S/\partial R = -U_\theta$. From Eq. (41.xiii),

$$\frac{\partial \psi_S}{\partial R} = -U_\infty \sin\theta - \frac{R_0^2}{R^2} U_\infty \sin\theta$$

$$= (-U_\infty \sin\theta)\left(1 + \frac{R_0^2}{R^2}\right) \tag{41.xvia}$$

At any point on the surface of the cylinder, $R = R_0$ and the radial velocity $U_R = 0$. Then the resultant velocity at any point on the surface is the vectorial combination of the tangential and radial velocities, or

$$U = 2U_\infty \sin\theta \tag{41.xvib}$$

It is interesting to note the tangential velocities encountered *abreast* the 2-diml cylinder when $\theta = 90$ deg, at a succession of radii R. Substituting $R = R_0$, $2R_0$, $3R_0$, and so on in Eq. (41.xvia), the local tangential velocities parallel to the uniform stream are:

$R = R_0$	$2R_0$	$3R_0$	$4R_0$	$5R_0$
$U = 2U_\infty$	$1.25U_\infty$	$1.11U_\infty$	$1.06U_\infty$	$1.04U_\infty$

The pressure p at any point on the surface of the cylinder is, by Eqs. (2.xvi) and (41.xvib),

$$p = p_\infty + \tfrac{1}{2}\rho U_\infty^2(1 - 4\sin^2\theta) \tag{41.xvii}$$

or

$$\frac{p - p_\infty}{\frac{\rho}{2} U_\infty^2} = \frac{\Delta p}{q} = 1 - 4\sin^2\theta \tag{41.xviia}$$

IV. For a 2-diml cylinder around which circulation is taking place, depicted in diagram 3 of Fig. 14.E in Volume I and tabulated in (d) preceding, the stream function ψ_H for the hydrofoil flow is formed by combining the function ψ_S for streamline flow with the function ψ_C for circulation. From Sec. 14.3, the circulation strength Γ(capital gamma) $= 2\pi k = 2\pi U_\theta R$, where U_θ is the tangential velocity at the cylinder surface. Then $\psi_C = \int U_R R\, d\theta - \int U_\theta\, dR$. Since the radial velocity $U_R = 0$ at the cylinder surface,

$$\psi_C = -\int U_\theta\, dR = -\frac{\Gamma}{2\pi}\int \frac{dR}{R}$$

$$= -\frac{\Gamma}{2\pi}\log_e R \tag{41.xviii}$$

Adding the stream function for flow around the 2-diml circular cylinder gives, for the hydrofoil flow,

$$\psi_H = -U_\infty\left(R - \frac{R_0^2}{R}\right)\sin\theta - \frac{\Gamma}{2\pi}\log_e R \tag{41.xix}$$

In a similar manner, the velocity potential is obtained by adding the velocity potentials of the separate flows. For circulation alone,

$$\phi_c = \int U_R \, dR + \int U_\theta R \, d\theta = \frac{\Gamma}{2\pi}\theta \qquad (41.xx)$$

For the combined hydrofoil flow,

$$\psi_H = -U_\infty\left(R + \frac{R_0^2}{R}\right)\cos\theta + \frac{\Gamma}{2\pi}\theta \qquad (41.xxi)$$

From either the velocity potential or the stream function, the velocity at the surface of the cylinder is obtained from the relationships

$$\frac{\partial\psi}{\partial R} = -U_\theta\,, \quad \text{or} \quad \frac{1}{R}\frac{\partial\phi}{\partial\theta} = U_\theta$$

$$U_\theta = U_\infty\left(1 + \frac{R_0^2}{R^2}\right)\sin\theta + \frac{\Gamma}{2\pi}$$

Hence, at the surface, where $R = R_0$,

$$U = 2U_\infty \sin\theta + \frac{\Gamma}{2\pi R_0} \qquad (41.xxii)$$

The pressure at any point on the surface of the 2-diml cylinder is, by Eq. (2.xvi),

$$p = p_\infty + \frac{\rho}{2}U_\infty^2\left[1 - \frac{\left(2U_\infty\sin\theta + \dfrac{\Gamma}{2\pi R_0}\right)^2}{U_\infty^2}\right] \qquad (41.xxiii)$$

Upon integration of this pressure over the surface to obtain the resultant force in the y-direction, the lift L is obtained.

$$L = -\int_0^{2\pi} pR_0 \sin\theta \, d\theta = \rho U_\infty \Gamma \qquad (41.xxiv)$$

As a matter of information, the *approximate* value for the stream function in the case of a 2-diml cylinder of radius R_0 in the middle of a 2-diml water passage of width A, as worked out by H. Lamb, is

$$\psi = U_\infty\left[x - \frac{\pi R_0^2}{A}\frac{\sin\dfrac{2\pi x}{A}}{\cosh\dfrac{2\pi y}{A} - \cos\dfrac{2\pi x}{A}}\right]$$

where the origin of cartesian coordinates is apparently taken at the center of the cylinder [Hele-Shaw, H. S., INA, 1898, Vol. XL, p. 28]. A plot of the streamlines for this case is given by Hele-Shaw in Fig. 20 on Plate XI of the reference.

Knowledge of the stream function or velocity potential for the 2-diml circular section is of great value in deriving corresponding data for other section shapes by conformal transformation, described in Sec. 41.11.

41.9 Stream-Function and Velocity-Potential Formulas for Three-Dimensional Flows. Paralleling the exposition of Sec. 41.8, where formulas are derived for the stream function, velocity potential, local velocity, and local pressure in the streamline and hydrofoil flows around a 2-diml rod with its axis normal to a uniform stream of liquid, the present section carries out the same derivation for the flow around:

(a) A 3-diml sphere

(b) A 3-diml body with a head of ovoid shape, formed by placing a single 3-diml source in a uniform stream. A partial longitudinal section of such a body is illustrated in Fig. 67.H. Only that flow is considered which is symmetrical about an assumed x-axis through the center of the sphere and of the body described. By using spherical coordinates, diagrammed in Fig. 41.H,

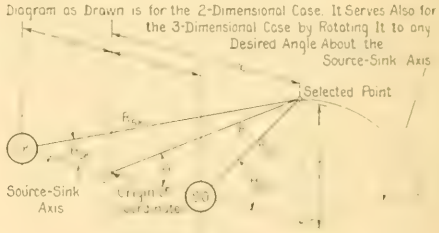

Fig. 41.H Definition Sketch for Cartesian and Spherical Coordinates of Source-Sink Pair

only the coordinates R and θ need be used to define the flow, although the cartesian coordinates for a selected point in any one longitudinal plane through the axis, parallel to the direction of uniform flow, are shown for convenience.

For the purposes of this section, as for use in most text and reference books, the 3-diml stream function ψ is $1/(2\pi)$ times the Stokes stream function described in the concluding paragraphs of Sec. 2.12, on page 32 of Volume I. Hence the quantity rate of flow in a "rod" of radius y, with a uniform velocity of $-U_\infty$, is

$$\psi_{\text{Stokes}} = -U_\infty \pi y^2$$

However, for the 3-diml stream function used here

$$\psi_{\text{3-diml}} = \frac{1}{2\pi}(-U_\infty \pi y^2) = -U_\infty\frac{y^2}{2}$$

I. The first case considered is that of the sphere. The relationships between the stream function, the velocity potential, the radial velocity U_R, and the tangential velocity U_θ are, for the axisymmetric case in spherical coordinates [Milne-Thomson, L. M., TH, 1950, pp. 403–404],

$$\frac{\partial\psi}{\partial R} = -U_\theta R \sin\theta \qquad (41.\text{xxva})$$

$$\frac{\partial\psi}{\partial\theta} = U_R R^2 \sin\theta \qquad (41.\text{xxvb})$$

$$\frac{\partial\phi}{\partial R} = U_R \qquad (41.\text{xxvc})$$

$$\frac{\partial\phi}{\partial\theta} = RU_\theta \qquad (41.\text{xxvd})$$

For the uniform stream of velocity $-U_\infty$, again using spherical coordinates,

$$U_R = -U_\infty \cos\theta$$

$$U_\theta = U_\infty \sin\theta$$

From

$$\frac{\partial\phi}{\partial R} = U_R \quad \text{or} \quad \frac{\partial\phi}{\partial\theta} = RU_\theta,$$

$$\phi_{\text{3-diml}} = -U_\infty R \cos\theta \qquad (41.\text{xxvia})$$

From

$$\frac{\partial\psi}{\partial R} = -U_\theta R \sin\theta \quad \text{or} \quad \frac{\partial\psi}{\partial\theta} = U_R R^2 \sin\theta,$$

$$\psi_{\text{3-diml}} = -\frac{1}{2} U_\infty R^2 \sin^2\theta = -U_\infty \frac{y^2}{2} \qquad (41.\text{xxvib})$$

Considering a 3-diml source having a transverse plane through its center on which $\psi = 0$, and following the notation of Sec. 3.9, where m is the strength of a 3-diml source, $Q = 4\pi R^2 U_R = 4\pi m$, whereupon $m = Q/4\pi$, $U_R = m/R^2$, and $U_\theta = 0$. From Eqs. (41.xxvc) and (41.xxvb), respectively, by integration,

$$\phi_{\text{3-diml}} = -\frac{m}{R} \qquad (41.\text{xxviia})$$

$$\psi_{\text{3-diml}} = -m\cos\theta \qquad (41.\text{xxviib})$$

For a 3-diml sink corresponding to the 3-diml source just mentioned,

$$U_R = -\frac{m}{R^2}$$

$$\phi_{\text{3-diml}} = +\frac{m}{R} \qquad (41.\text{xxviiia})$$

$$\psi_{\text{3-diml}} = +m\cos\theta \qquad (41.\text{xxviiib})$$

It is explained at the end of this section, and illustrated in Fig. 41.I, that for this mathematic representation in spherical coordinates the reference for zero stream function for a source or sink is the transverse plane through the origin, normal to the axis of the system. Referring to the definition sketch of Fig. 41.H, the addition of the values of ϕ and ψ for the sources and the sinks gives

$$\phi = m\left(\frac{1}{R_{SK}} - \frac{1}{R_{SO}}\right) \qquad (41.\text{xxixa})$$

$$\psi = m(\cos\theta_{SK} - \cos\theta_{SO}) \qquad (41.\text{xxixb})$$

where the subscript "SO" applies to the source and "SK" to the sink. For the 3-diml doublet, by the sine rule,

$$\frac{R_{SO}}{\sin\theta_{SK}} = \frac{R_{SK}}{\sin\theta_{SO}} = \frac{2s}{\sin(\theta_{SO} - \theta_{SK})}$$

$$= \frac{s}{\sin\frac{1}{2}(\theta_{SO} - \theta_{SK})\cos\frac{1}{2}(\theta_{SO} - \theta_{SK})}$$

Then

$$R_{SO} - R_{SK} = \frac{s(\sin\theta_{SK} - \sin\theta_{SO})}{\sin\frac{1}{2}(\theta_{SO} - \theta_{SK})\cos\frac{1}{2}(\theta_{SO} - \theta_{SK})}$$

$$= \frac{-2s\cos\frac{1}{2}(\theta_{SO} + \theta_{SK})\sin\frac{1}{2}(\theta_{SO} - \theta_{SK})}{\sin\frac{1}{2}(\theta_{SO} - \theta_{SK})\cos\frac{1}{2}(\theta_{SO} - \theta_{SK})}$$

$$R_{SO} - R_{SK} = \frac{-2s\cos\frac{1}{2}(\theta_{SO} + \theta_{SK})}{\cos\frac{1}{2}(\theta_{SO} - \theta_{SK})}$$

Let $\mu = 2ms$ equal the strength of a 3-diml doublet. Then, from the expression for the velocity potential for a source and sink,

$$\phi = \frac{m}{R_{SK}R_{SO}}(R_{SO} - R_{SK})$$

$$= \frac{-\mu\cos\frac{1}{2}(\theta_{SO} + \theta_{SK})}{R_{SK}R_{SO}\cos\frac{1}{2}(\theta_{SO} - \theta_{SK})}$$

Similarly, for the stream function,

$$\psi = \frac{m(x+s)}{R_{SK}} - \frac{m(x-s)}{R_{SO}}$$

$$= mx\left(\frac{1}{R_{SK}} - \frac{1}{R_{SO}}\right) + ms\left(\frac{1}{R_{SK}} - \frac{1}{R_{SO}}\right)$$

Then

$$\psi = \frac{-\mu x\cos\frac{1}{2}(\theta_{SO} + \theta_{SK})}{R_{SK}R_{SO}\cos\frac{1}{2}(\theta_{SO} - \theta_{SK})} + \frac{\mu}{2}\left(\frac{1}{R_{SK}} + \frac{1}{R_{SO}}\right)$$

To obtain the doublet, $s \to 0$, $\theta_{SO} \to \theta_{SK} \to \theta$, and $R_{SK} \to R_{SO} \to R$. Then, for the 3-diml doublet,

$$\phi = \frac{-\mu \cos \theta}{R^2} \qquad (41.\text{xxxa})$$

$$\psi = \frac{-\mu x \cos \theta}{R} + \frac{\mu}{R}$$

$$= \frac{\mu}{R^3}(R^2 - x^2) = \frac{\mu \sin^2 \theta}{R} \qquad (41.\text{xxxb})$$

Combining the doublet and the uniform-stream velocity potentials and stream functions gives, for the streamline flow around a sphere in a uniform stream of velocity $-U_\infty$, depicted in diagram 2 of Fig. 41.G,

$$\phi_{3\text{-diml}} = -U_\infty R \cos \theta - \frac{\mu \cos \theta}{R^2} \qquad (41.\text{xxxia})$$

$$\psi_{3\text{-diml}} = -\frac{1}{2} U_\infty R^2 \sin^2 \theta + \frac{\mu \sin^2 \theta}{R} \qquad (41.\text{xxxib})$$

Setting $\psi = 0$ at the spherical surface,

$$\frac{1}{2} U_\infty R^2 \sin^2 \theta = \frac{\mu \sin^2 \theta}{R}$$

$$R^3 = \frac{2\mu}{U_\infty} = R_0^3 \quad \text{or} \quad R_0 = \left(\frac{2\mu}{U_\infty}\right)^{1/3}$$

where R_0 is the radius of the sphere about which the flow takes place. Stated in another way, the flow around a sphere of radius R_0 is obtained by adding a uniform stream $-U_\infty$ to a 3-diml doublet of strength $\mu = \frac{1}{2}U_\infty R_0^3$.

Substituting $\mu = \frac{1}{2}U_\infty R_0^3$ into the expressions for ϕ and ψ gives:

$$\phi_{3\text{-diml}} = -U_\infty \cos \theta\left(R + \frac{R_0^3}{2R^2}\right) \qquad (41.\text{xxxiia})$$

$$\psi_{3\text{-diml}} = \frac{U_\infty \sin^2 \theta}{2R}(R_0^3 - R^3) \qquad (41.\text{xxxiib})$$

From Eqs. (41.xxva) and (41.xxvd),

$$U_\theta = -\frac{1}{R \sin \theta}\frac{\partial \psi}{\partial R} \quad \text{or} \quad U_\theta = \frac{1}{R}\frac{\partial \phi}{\partial \theta}$$

$$U_\theta = \frac{1}{2} U_\infty \sin \theta\left(\frac{R_0^3}{R^3} + 2\right)$$

On the surface of the sphere, $R = R_0$, $U_R = 0$, whence the local velocity is

$$U = \tfrac{3}{2}U_\infty \sin \theta \qquad (41.\text{xxxiii})$$

The pressure coefficient at any point on the surface of the sphere is, by Eq. (2.xvi),

$$\frac{p - p_\infty}{\frac{\rho}{2}U_\infty^2} = \frac{\Delta p}{q} = 1 - \frac{U^2}{U_\infty^2}$$

$$= 1 - \frac{9}{4}\sin^2 \theta \qquad (41.\text{xxxiv})$$

II. For the case of the 3-diml body of ovoid shape, formed by placing a 3-diml source of strength m in a uniform stream of velocity $-U_\infty$, as in Fig. 67.II, the 3-diml velocity potential and the 3-diml stream function are obtained as previously explained, by adding the values of ϕ and ψ, respectively, for the two flows. Then, from Eqs. (41.xxvia) and (41.xxviia),

$$\phi = -U_\infty R \cos \theta - \frac{m}{R} \qquad (41.\text{xxxva})$$

From Eqs. (41.xxvib) and (41.xxviib),

$$\psi = -\tfrac{1}{2}U_\infty R^2 \sin^2 \theta - m \cos \theta \qquad (41.\text{xxxvb})$$

whence

$$U_R = \frac{\partial \phi}{\partial R} = \frac{m}{R^2} - U_\infty \cos \theta \qquad (41.\text{xxxvi})$$

$$U_\theta = \frac{1}{R}\frac{\partial \phi}{\partial \theta} = U_\infty \sin \theta \qquad (41.\text{xxxvii})$$

To find the coordinates of the nose of the body, set U_R and U_θ equal to zero since the nose is also the stagnation point. Then

$$\frac{m}{R^2} - U_\infty \cos \theta = 0$$

$$U_\infty \sin \theta = 0$$

Hence the nose is at

$$\theta = 0, \qquad R_Q = \sqrt{\frac{m}{U_\infty}}$$

The 3-diml stream function value which passes through the stagnation point is $\psi = -m$. But this stream function is also the surface of the body. Hence, in axisymmetric spherical coordinates, the equation of the surface is

$$R^2 = \frac{2m(1 - \cos \theta)}{U_\infty \sin^2 \theta} \qquad (41.\text{xxxviii})$$

For the points abreast the source, where $\theta = 90$ deg, $\cos \theta = 0$ and $\sin \theta = 1$, whence

$$R_{90}^2 = \frac{2m}{U_\infty} \quad \text{or} \quad R_{90} = \sqrt{\frac{2m}{U_\infty}}$$

From this it appears that $R_{90} = R_Q\sqrt{2}$.

The transverse radius of a 3-diml ovoid such as

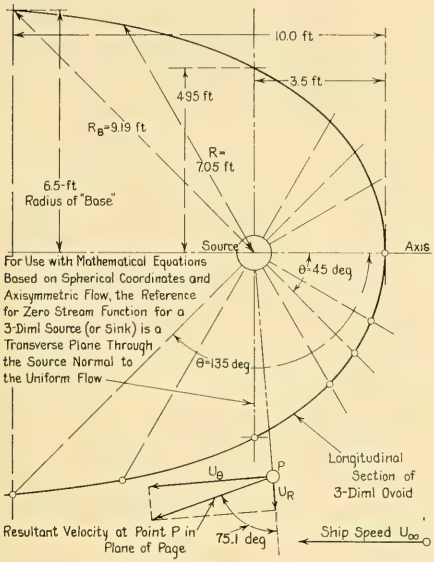

FIG. 41.I CONSTRUCTION OF 3-DIML OVOID BY INSERTING SINGLE 3-DIML SOURCE IN UNIFORM STREAM

that in Fig. 41.I or Fig. 67.H, formed by placing a single 3-diml source in a uniform stream, approaches as an asymptote a limiting value of $2R_Q$ at an infinite distance downstream.

As an example of the use of the formulas, suppose that it is desired to develop the coordinates of an ovoid shape for the bulb bow of the ABC ship of Part 4, resembling the ovoid for which a fore-and-aft section is drawn in Fig. 67.H. Assume that the stream velocity U_∞ is equal to the designed ship speed of 20.5 kt or 34.62 ft per sec, and that at 10 ft abaft the nose it is desired that the ovoid shape have a transverse radius of 6.5 ft.

Fig. 41.I is a longitudinal section through the axisymmetric ovoid of this example, indicating the initial dimensions given and including the ovoid shape derived by the methods described here.

The equation of the ovoid, from Eq. (41.xxxviii), is

$$R^2 = \frac{2m(1 - \cos\theta)}{U_\infty \sin^2\theta}$$

or

$$R = \frac{1}{\sin\theta}\sqrt{\frac{2m(1 - \cos\theta)}{U_\infty}}$$

To satisfy the condition that the ovoid is to have a transverse "base" radius R_B of 6.5 ft, at a distance of 10 ft abaft its nose,

$$\sqrt{\frac{m}{U_\infty}} - R_B \cos\theta_B = 10$$

and

$$R_B \sin\theta_B = 6.5$$

where R_B and θ_B are the coordinates of the rim of the ovoid at its base. Substituting in the foregoing for R_B in terms of θ_B and m, gives

$$\sqrt{\frac{m}{U_\infty}} - \frac{1}{\tan\theta_B}\sqrt{\frac{2m(1 - \cos\theta_B)}{U_\infty}} = 10$$

and

$$\sqrt{\frac{2m(1 - \cos\theta_B)}{U_\infty}} = 6.5$$

From the second equation,

$$m = \frac{42.25U_\infty}{2(1 - \cos\theta_B)}$$

Substituting this expression for m in the first equation gives

$$\frac{4.596}{\sqrt{1 - \cos\theta_B}} - \frac{6.5}{\tan\theta_B} = 10$$

Solving for θ_B by trial and error gives $\theta_B = 135$ deg. Then

$$m = \frac{42.25U_\infty}{2(1 - \cos\theta_B)}$$

$$= \frac{(42.25)(34.62)}{(2)(1.707)} = 428.4 \text{ ft}^3 \text{ per sec.}$$

The equation of the desired ovoid is

$$R^2 = \frac{(2)(428.4)(1 - \cos\theta)}{34.62 \sin^2\theta} = \frac{24.75(1 - \cos\theta)}{\sin^2\theta}$$

The distance of the nose of the ovoid from the coordinate origin is

$$R_Q = \sqrt{\frac{m}{U_\infty}} = \sqrt{\frac{428.4}{34.62}} = 3.52 \text{ ft.}$$

Knowing the value of the 3-diml source strength m, the radial and tangential velocity components for any point P in the field, beyond the ovoid surface, at a radius R from the source and an angle θ from the axis, are found by substituting the proper values of m, R, $\cos\theta$, and $\sin\theta$ in Eqs. (41.xxxvi) and (41.xxxvii), with the fixed value of U_∞. Combining these radial and axial components vectorially gives the velocity and

magnitude of the resultant velocity at the point P.

For example, assume that it is required to find the velocity magnitude and direction for the point P in Fig. 41.I, at a ship speed equal to U_∞, or 34.62 ft per sec. The spherical coordinates of P are $\theta = 85$ deg and $R = 6.0$ ft. Then from Eq. (41.xxxvi) the radial velocity

$$U_R = \frac{m}{R^2} - U_\infty \cos\theta = \frac{428.4}{(6.0)^2} - (34.62)(0.0872)$$

$$= 8.88 \text{ ft per sec.}$$

The tangential velocity U_θ is, from Eq. (41.xxxvii),

$$U_\theta = U_\infty \sin\theta = 34.62(0.9962)$$

$$= 33.49 \text{ ft per sec.}$$

The resultant velocity is $[(33.49)^2 + (8.88)^2]^{0.5} = 34.7$ ft per sec. The value of $\tan^{-1}(8.88/33.49)$ is about 14.9 deg. This means that the direction of the resultant velocity makes an angle of $(90 - 14.9) = 75.1$ deg with the radius R to the point P.

In Fig. 67.H of Sec. 67.7 the 3-diml source used as a means of constructing the ovoid shown there has its 0-valued stream function coinciding with the positive x-axis. If a 3-diml source and sink are both involved, as shown in Fig. 43.J, the stream function of each, and of the combination, has a value of zero at the source-sink axis.

When representing 3-diml sources and sinks mathematically, especially when developing the forms of and the flow around axisymmetric bodies, it is much more convenient to take as the reference for $\psi = 0$ a plane perpendicular to the x-axis (or the source-sink axis) through the center of the source or sink. The sources and sinks are axisymmetric with respect to the x-axis for either method of representation but in the latter case the characteristics of the flow can be represented by the two spherical coordinates R and θ.

As far as the shape of the streamline pattern and the evaluation of liquid velocities at any point are concerned, it makes no difference where the reference line or plane is chosen. But changing the reference of a source or sink changes the stream-function value of a given streamline. This is the reason why the stream-function value which represents the surface of the 3-diml ovoid in Fig. 67.H is zero, while in the mathematical representation of the same flow, Eq. (41.xxxvb), the stream function at the surface of the ovoid has a value of $-m$.

41.10 The Determination of Liquid Velocity Around Any Body. Many of the problems arising from the flow of liquid around a body or ship resolve themselves, directly or indirectly, into the determination of the magnitude and direction of the liquid velocity at any or all points, on the surface and in the vicinity. Once the velocity is known, the pressures, forces, moments, and other factors are derived by relatively simple and expeditious methods. Naval Constructor David W. Taylor, in his paper "On Ship-Shaped Stream Forms," for which he was awarded a gold medal by the Institution of Naval Architects in London in 1894, prefaced his remarks by the following [p. 385]:

> "Doubtless the day will come when the naval architect, given the lines and speed of a ship, will be able to calculate the pressure and velocity of the water at every point of the immersed surface. That day is not yet, but the present state of our knowledge of the mechanics of fluid motion is such that we can determine completely, under certain conditions, the pressure and velocity in a perfect fluid flowing past bodies whose lines closely resemble those of actual ships."

Analytic and design problems concerning ships and their parts involve real liquids, whereas most of the mathematical procedures and formulas apply only to motion in ideal liquids. Fortunately, some adjustment is possible by expanding the body or ship form so that it includes the displacement thickness δ^*(delta star) of the boundary layer around it, explained in Sec. 5.15. Potential flow, as in an ideal liquid, is then assumed to exist around this expanded form, in the manner depicted by Figs. 7.I, 18.A, and 18.G.

The flow net for 2-diml bodies, described in Sec. 2.20 and constructed by graphical, electrical, or other convenient procedure, is one way of finding the velocity. Another method is to shape the body by a combination of radial and uniform flow, employing sources and sinks. Then by calculation or graphic procedures the velocities in the surrounding field are derived. Methods of following the latter procedure are described in Secs. 41.8 and 41.9. The steps for obtaining the desired data by the second method are described in Chap. 43. Both methods give the velocity throughout the field as well as at the body surface.

If a velocity potential ϕ for the field around any body or ship form is assumed or can be set up, by the methods outlined in Secs. 41.8 and 41.9, or by any other methods, expressions for the component velocities u, v, and w are derived by partial differentiation of ϕ with respect to

x, y, and z, respectively. Substituting selected values for the coordinates in the region being investigated, the component velocity values are readily calculated. These comments apply equally to the stream function ψ, and to 3-diml as well as 2-diml forms.

Data on velocity and pressure fields, already calculated or otherwise available for a considerable number of typical body shapes, are referenced in several of the sections of Chap. 42.

G. S. Baker and J. L. Kent give an example of D. W. Taylor's method of using line sources and sinks to delineate a 2-diml ship-shaped body and to determine the magnitude and distribution of pressure around it in an ideal liquid [INA, 1913, Vol. 55, Part II, pp. 50–54]. They describe an adaptation of this method to a determination of the same features around a ship-shaped form in a restricted channel with straight walls parallel to and equidistant from the ship axis.

A. F. Zahm, in NACA Report 253 of 1926, entitled "Flow and Drag Formulas for Simple Quadrics," gives calculated and observed pressures for a series of geometric forms, including a sphere, a circular cylinder, an elliptic cylinder, prolate and oblate spheroids, and a circular disc. He also gives diagrams of isobars and isotachyls about some of these forms, and discusses velocity and pressure in oblique flow.

41.11 Conformal Transformation. An ingenious mathematical process, involving complex variables, was utilized by W. Kutta in the early 1900's to determine the flow characteristics around typical or schematic airfoils [Kutta, W., Ill. Aeronaut. Mitt., 1902; AHA, 1934, p. 173]. Knowing the flow characteristics in the region surrounding some simple geometric form such as a circular rod, by the doublet construction illustrated in Figs. 3.M and 43.J, the circular form and the flow pattern are transformed simultaneously into the form and pattern desired. However, the nature of Kutta's method restricts its use to 2-diml problems.

The transformation is effected by retaining the essential *shape* of the "curvilinear squares" in the flow net around the typical body as the size of these squares is reduced from visible to infinitesimal dimensions. Taking its name from the preservation of angles in each small area as the "mesh" of the flow net is reduced, the process is known as *conformal transformation*. Put in another way, conformal transformation or conformal representation is defined "as a distortion of a geometric figure that preserves geometric similarity of infinitesimal parts of the figure. This means in particular that all angles between corresponding lines are the same in the original figure and in its conformal representation" [Wislicenus, G. F., FMTM, 1947, p. 582].

L. M. Milne-Thomson gives an excellent illustration of conformal transformation, or conformal mapping, as it is sometimes called [TH, 1950, p. 140]. This:

> "... is afforded by an ordinary map on Mercator's projection. It is well known that the angle between two lines as measured on the map is equal to the angle at which the two corresponding lines intersect on the earth's surface; in fact, it is this property which renders the map useful in navigation.
>
> "In particular the lines on the map which represent the meridians and parallels of latitude are at right angles. If we confine our attention to a small portion of the map, we also know that distances measured on the map will represent to scale the corresponding distances on the globe, but that the scale changes as the latitude increases."

By this method of mapping it is possible, starting with a circular rod and the accompanying 2-diml flow pattern of Fig. 3.M, depicting a field in which the velocities and pressures are known, to flatten the rod into a hydrofoil section with a blunt nose and a somewhat pointed tail. The flow pattern is flattened or transformed with the rod so that the velocity and pressure characteristics for the transformed pattern are fully determined.

Stated mathematically, the modified flow picture obeys the same general laws for continuity and for irrotational flow, namely

$$\frac{\partial u}{\partial x} + \frac{\partial v}{\partial y} = 0 \quad \text{and} \quad \frac{\partial v}{\partial x} - \frac{\partial u}{\partial y} = 0$$

as the original flow picture from which it was derived [Wislicenus, G. F., FMTM, 1947, p. 193]. Wislicenus gives a brief discussion of conformal transformation in Sec. 44 of the reference, pages 211–218. H. Rouse gives a more complete treatment in Chap. V of "Fluid Mechanics for Hydraulic Engineers" [McGraw-Hill, New York, 1938, pp. 96–124].

An excellent presentation of this subject is the one by A. Betz, entitled "Konforme Abbildung (Conformal Representation)," published by Julius Springer in Germany.

41.12 Quantitative Relationship Between Velocity and Pressure in Irrotational Potential Flow. Having determined the magnitudes and directions of the velocity at selected (or at all) points in the

field of relative liquid motion around a body, the next practical step is usually to determine the pressures at those points. For irrotational potential flow in an ideal liquid without viscosity, at a depth where the hydrostatic pressure remains sensibly constant, this is a rather simple, straightforward process.

From the basic assumption, explained in Sec. 2.7, that in any stream tube in which the flow is steady and continuous the total pressure remains constant along the tube, the relationship between the dynamic pressure q and the pumping pressure p at two reference points 1 and 2 is expressed by

$$p_1 + \frac{\rho}{2} U_1^2 = p_2 + \frac{\rho}{2} U_2^2 \quad \text{or} \quad p_1 + q_1 = p_2 + q_2$$

If the point 1 is taken at a great distance in the undisturbed liquid from the point 2, say at infinity, then the preceding equation is written as

$$p_\infty + \frac{\rho}{2} U_\infty^2 = p_2 + \frac{\rho}{2} U_2^2$$

Transposing,

$$p_2 - p_\infty = \frac{\rho}{2}(U_\infty^2 - U_2^2) = \frac{\rho}{2}\left(1 - \frac{U_2^2}{U_\infty^2}\right)$$

whence, omitting the subscripts "2,"

$$p - p_\infty = \Delta p = \frac{\rho}{2} U_\infty^2\left(1 - \frac{U^2}{U_\infty^2}\right)$$

This gives the relationship derived in Eq. (2.xvi) of Sec. 2.20, namely

$$\frac{\Delta p}{\frac{\rho}{2} U^2} = \frac{\Delta p}{q} = 1 - \frac{U^2}{U_\infty^2} \qquad \text{(2.xvi)}$$

The equalities expressed in Eq. (2.xvi) are most important and useful. They can with profit be memorized by everyone who works with this subject. The left-hand and middle terms in this equation are expressions for the pressure coefficient or Euler number E_n, expressing the difference in pressures between that at any selected point 2 and that at infinity, as a proportion of the ram pressure $0.5\rho U_\infty^2$ which could be set up in the unlimited, undisturbed stream.

The ratio U/U_∞ is exactly that given by the ratio $\Delta n_\infty/\Delta n$ in the 2-diml flow net described in Sec. 2.20. Hence squaring the fraction $\Delta n_\infty/\Delta n$ and subtracting it from unity gives directly the pressure coefficient for any selected portion of the flow pattern. This ratio is larger than 1.0 when U is larger in magnitude than U_∞. The pressure coefficient $\Delta p/q$ is then negative.

Assume that for the 2-diml flow net around the blunt-ended 2-diml section of Fig. 41.J [adapted from Rouse, H., EMF, 1946, Fig. 26, p. 50], the stream-tube width Δn_∞ is 0.25 in. And that at the point A on the forward shoulder the width Δn is narrowed to 0.20 in. Then $\Delta n_\infty/\Delta n$ is 0.25/0.20 = 1.25, whence $(\Delta n_\infty/\Delta n)^2 = 1.5625$. The pressure coefficient or Euler number E_n at this point is thus 1.000 − 1.5625 or −0.5625.

The values thus derived for any selected number of points are laid down graphically in several ways, depending upon what is to be represented by the plot. If the positive and negative differential pressures $+\Delta p$ and $-\Delta p$ are to be emphasized the scheme followed in diagram 2 of Fig. 41.J is

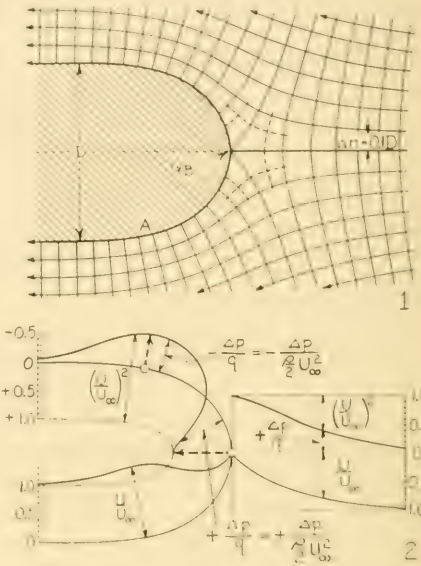

Fig. 41.J Relation Between Velocity and Pressure in Flow of an Ideal Liquid Around a Body

preferable. Here the normal vectors representing the combination of atmospheric and differential pressures are laid off from the solid-surface contour as a reference line, with the $+\Delta p$ vectors directed *toward* the surface and the $-\Delta p$ ones *away* from it. However, the practice of drawing vectors *inside* the solid is not recommended for general usage because they are crowded together in regions of sharp curvature and the solid may be too narrow to lay them down at a conveniently large scale.

If the *total* pressures on the solid surface are to be emphasized the preferred method is to draw a line outside the solid surface, everywhere equidistant from it at a distance which represents conveniently the ambient pressure p_∞, or that of the undisturbed liquid at infinity. A variation of this method is illustrated in diagram 2 of Fig. 2.B, where the atmospheric pressure p_A on the hydrofoil section corresponds to the ambient pressure p_∞ of Fig. 41.J.

In addition, of course, the pressure coefficients may be plotted on the usual x-y coordinates, using the length along the x-axis of the body as the x-coordinate. This method is illustrated in Fig. 2.V, depicting the velocity and pressure variation at a stem section on a ship. A third method is to use the developed distance along the boundary or contour of the body (or an expansion of it) as the distance basis, erecting the velocity and pressure vectors normal to this contour line, as in the right-hand portion of diagram 2 of Fig. 41.J.

The pressure relationships are frequently expressed and plotted as fractions or as multiples of the ram pressure $0.5\rho U_\infty^2 = q$. The dynamic pressure variations caused by body or liquid motion are then referred to as so many "q's," plus or minus. For the previous example the $-\Delta p$ at the point A is $-0.5625q$.

This variation of the customary pressure coefficient or Euler number is sometimes used when investigating the proper location for a pitot-type velocity indicator or a speed meter. As the entire velocity head in the liquid is converted to pressure head at the nose orifice of the pitot tube, this velocity is measured as a pressure when the region under consideration is being surveyed. By relating (1) the pitot pressure observed at any selected point in the field, as registered on an instrument mounted in a fixed

TABLE 41.c—Velocity Ratios and Pressure Coefficients

The data given here are plotted from Eq. (2.xvi),

$$\frac{\Delta p}{\frac{\rho}{2} U_\infty^2} = \frac{\Delta p}{q} = 1 - \left(\frac{U}{U_\infty}\right)^2,$$

for potential flow in an ideal liquid. They apply to a liquid (or a fluid) of any mass density.

$\frac{U}{U_\infty}$	$\left(\frac{U}{U_\infty}\right)^2$	$1 - \left(\frac{U}{U_\infty}\right)^2$	$\frac{U}{U_\infty}$	$\left(\frac{U}{U_\infty}\right)^2$	$1 - \left(\frac{U}{U_\infty}\right)^2$
0.05	0.0025	0.9975	1.25	1.5625	−0.5625
0.10	0.0100	0.9900	1.30	1.6900	−0.6900
0.15	0.0225	0.9775	1.35	1.8225	−0.8225
0.20	0.0400	0.9600	1.40	1.9600	−0.9600
0.25	0.0625	0.9375	1.45	2.1025	−1.1025
0.30	0.0900	0.9100	1.50	2.2500	−1.2500
0.35	0.1225	0.8775	1.55	2.4025	−1.4025
0.40	0.1600	0.8400	1.60	2.5600	−1.5600
0.45	0.2025	0.7975	1.65	2.7225	−1.7225
0.50	0.2500	0.7500	1.70	2.8900	−1.8900
0.55	0.3025	0.6975	1.75	3.0625	−2.0625
0.60	0.3600	0.6400	1.80	3.2400	−2.2400
0.65	0.4225	0.5775	1.85	3.4225	−2.4225
0.70	0.4900	0.5100	1.90	3.6100	−2.6100
0.75	0.5625	0.4375	1.95	3.8025	−2.8025
0.80	0.6400	0.3600	2.00	4.0000	−3.0000
0.85	0.7225	0.2775	2.10	4.4100	−3.4100
0.90	0.8100	0.1900	2.20	4.8400	−3.8400
0.95	0.9025	0.0975	2.30	5.2900	−4.2900
1.00	1.0000	0.0000	2.40	5.7600	−4.7600
1.05	1.1025	−0.1025	2.50	6.2500	−5.2500
1.10	1.2100	−0.2100	2.60	6.7600	−5.7600
1.15	1.3225	−0.3225	2.70	7.2900	−6.2900
1.20	1.4400	−0.4400	2.80	7.8400	−6.8400

TABLE 41.d—RAM PRESSURES AND HEADS FOR STANDARD FRESH WATER

The values listed here are calculated for a temperature of 59 deg F, 15 deg C, for sea level at a latitude of 45 deg.
The value of the mass density ρ is 1.9384 slugs per ft³. The acceleration due to gravity is taken as 32.174 ft per sec².
One (1) psi is taken as equivalent to a head of 2.309 ft. Conversely, one (1) ft head is equivalent to 0.4331 psi.

Velocity		Ram Pressure		Velocity Head, ft	Velocity		Ram Pressure		Velocity Head, ft	Velocity		Ram Pressure		Velocity Head, ft
ft per sec	kt	lb per ft²	lb per in²		ft per sec	kt	lb per ft²	lb per in²		ft per sec	kt	lb per ft²	lb per in²	
2	1.18	3.88	0.027	0.062	42	24.9	1710	11.9	27.4	110	65.1	11727	81.4	188.0
3	1.78	8.72	0.061	0.140	44	26.1	1876	13.0	30.1	120	71.0	13956	96.9	223.8
4	2.37	15.5	0.108	0.249	46	27.2	2051	14.2	32.9	130	77.0	16379	113.7	262.6
5	2.96	24.2	0.168	0.388	48	28.4	2233	15.5	35.8	140	82.9	18996	131.9	304.6
6	3.55	34.9	0.242	0.559	50	29.6	2423	16.8	38.8	150	88.8	21807	151.4	349.7
7	4.14	47.5	0.330	0.761	52	30.8	2621	18.2	42.0	160	94.7	24812	172.3	397.8
8	4.74	62.0	0.431	0.994	54	32.0	2826	19.6	45.3	170	100.7	28010	194.5	449.1
9	5.33	78.5	0.545	1.26	56	33.2	3039	21.1	48.7	180	106.6	31402	218.1	503.5
10	5.92	96.9	0.673	1.55	58	34.3	3260	22.6	52.3	190	112.5	34988	243.0	561.0
11	6.51	117.3	0.814	1.88	60	35.5	3489	24.2	55.9	200	118.4	38768	269.2	621.6
12	7.10	139.6	0.969	2.24	62	36.7	3726	25.9	59.7	210	124.3	42742	296.8	685.5
13	7.70	163.8	1.14	2.63	64	37.9	3970	27.6	63.6	220	130.3	46909	325.8	752.1
14	8.29	190.0	1.32	3.05	66	39.1	4222	29.3	67.7	230	136.2	51271	356.0	822.1
15	8.88	218.1	1.51	3.50	68	40.3	4482	31.1	71.9	240	142.1	55826	387.7	895.1
16	9.47	248.1	1.72	3.98	70	41.4	4749	33.0	76.1	250	148.0	60575	420.7	971.3
17	10.1	280.1	1.95	4.49	72	42.6	5024	34.9	80.6	260	153.9	65518	455.0	1050.5
18	10.7	314.0	2.18	5.03	74	43.8	5307	36.9	85.1	270	159.9	70655	490.7	1132.9
19	11.2	349.9	2.43	5.61	76	45.0	5598	38.9	89.8	280	165.8	75985	527.7	1218.4
20	11.8	387.7	2.69	6.22	78	46.2	5897	40.9	94.5	290	171.7	81510	566.0	1306.9
22	13.0	469.1	3.26	7.52	80	47.4	6203	43.1	99.5	300	177.6	87228	605.8	1398.6
24	14.2	558.3	3.88	8.95	82	48.5	6517	45.3	104.5	310	183.5	93140	646.8	1493.4
26	15.4	655.2	4.55	10.5	84	49.7	6839	47.5	109.7	320	189.5	99246	689.2	1591.3
28	16.6	759.9	5.27	12.2	86	50.9	7168	49.8	114.9	330	195.4	105546	733.0	1692.3
30	17.8	872.3	6.06	14.0	88	52.1	7506	52.1	120.3	340	201.3	112040	778.1	1796.5
32	18.9	992.5	6.89	15.9	90	53.3	7851	54.5	125.9	350	207.2	118727	824.5	1903.7
34	20.1	1120	7.78	18.0	92	54.5	8203	57.0	131.5	360	213.1	125608	872.3	2014.0
36	21.3	1256	8.72	20.1	94	55.7	8564	59.5	137.3	370	219.1	132683	921.4	2127.5
38	22.5	1400	9.72	22.4	96	56.8	8932	62.0	143.2	380	225.0	139952	971.9	2244.0
40	23.7	1551	10.8	24.9	98	58.0	9308	64.6	149.2	390	230.9	147415	1023.7	2363.6
					100	59.2	9692	67.3	155.4	400	236.8	155072	1076.9	2486.4

TABLE 41.e—RAM PRESSURES AND HEADS FOR STANDARD FRESH WATER

The values listed here are calculated for a temperature of 59 deg F, 15 deg C, for sea level at a latitude of 45 deg. The value of the mass density ρ is 1.9905 slugs per ft^3. The acceleration due to gravity is taken as 32.174 ft per sec^2. One (1) psi is taken as equivalent to a head of 2.2485 ft. Conversely, one (1) ft head is equivalent to 0.4447 psi.

Velocity		Ram Pressure		Velocity Head, ft	Velocity		Ram Pressure		Velocity Head, ft	Velocity		Ram Pressure		Velocity Head, ft
ft per sec	kt	lb per ft^2	lb per in^2		ft per sec	kt	lb per ft^2	lb per in^2		ft per sec	kt	lb per ft^2	lb per in^2	
2	1.18	3.98	0.028	0.062	42	24.9	1756	12.2	27.4	110	65.1	12042	83.6	188.0
3	1.78	8.96	0.062	0.140	44	26.1	1927	13.4	30.1	120	71.0	14332	99.5	223.8
4	2.39	15.9	0.111	0.249	46	27.2	2106	14.6	32.9	130	77.0	16820	116.8	262.6
5	2.96	24.9	0.173	0.389	48	28.4	2293	15.9	35.8	140	82.9	19507	135.5	304.6
6	3.55	35.8	0.249	0.559	50	29.6	2488	17.3	38.9	150	88.8	22393	155.5	349.6
7	4.14	48.8	0.339	0.761	52	30.8	2691	18.7	42.0	160	94.7	25478	176.9	397.8
8	4.74	63.7	0.442	0.995	54	32.0	2902	20.2	45.3	170	100.7	28763	199.7	449.1
9	5.33	80.6	0.560	1.26	56	33.2	3121	21.7	48.7	180	106.6	32246	223.9	503.5
10	5.92	99.5	0.691	1.55	58	34.3	3348	23.3	52.3	190	112.5	35929	249.5	561.0
11	6.51	120.4	0.836	1.88	60	35.5	3583	24.9	55.9	200	118.4	39810	276.5	621.6
12	7.10	143.3	0.995	2.24	62	36.7	3826	26.6	59.7	210	124.3	43891	304.8	685.3
13	7.70	168.2	1.17	2.63	64	37.9	4077	28.3	63.7	220	130.3	48170	334.5	752.2
14	8.29	195.1	1.35	3.05	66	39.1	4335	30.1	67.7	230	136.2	52649	365.6	822.1
15	8.88	223.9	1.56	3.50	68	40.3	4602	32.0	71.9	240	142.1	57326	398.1	895.1
16	9.47	254.8	1.77	3.98	70	41.4	4877	33.9	76.1	250	148.0	62203	432.0	971.3
17	10.1	287.6	2.00	4.49	72	42.6	5159	35.8	80.6	260	153.9	67279	467.2	1050.5
18	10.7	322.5	2.24	5.04	74	43.8	5450	37.8	85.1	270	159.9	72554	503.8	1132.9
19	11.2	359.3	2.50	5.61	76	45.0	5749	39.9	89.8	280	165.8	78028	541.9	1218.4
20	11.8	398.1	2.76	6.22	78	46.2	6055	42.0	94.5	290	171.7	83701	581.3	1306.9
22	13.0	481.7	3.35	7.52	80	47.4	6370	44.2	99.5	300	177.6	89573	622.0	1398.6
24	14.2	573.3	3.98	8.95	82	48.5	6692	46.5	104.5	310	183.5	95644	664.2	1493.4
26	15.4	672.8	4.67	10.5	84	49.7	7023	48.8	109.7	320	189.5	101914	707.7	1591.3
28	16.6	780.3	5.42	12.2	86	50.9	7361	51.1	114.9	330	195.4	108383	752.7	1692.3
30	17.8	895.7	6.22	14.0	88	52.1	7707	53.5	120.3	340	201.3	115051	799.0	1796.5
32	18.9	1019	7.08	15.9	90	53.3	8062	56.0	125.9	350	207.2	121918	846.7	1903.7
34	20.1	1151	7.99	18.0	92	43.5	8424	58.5	131.5	360	213.1	128984	895.7	2014.0
36	21.3	1290	8.96	20.1	94	55.7	8794	61.1	137.3	370	219.1	136250	946.2	2127.5
38	22.5	1437	9.98	22.4	96	56.8	9172	63.7	143.2	380	225.0	143714	998.0	2244.0
40	23.7	1592	11.1	24.9	98	58.0	9558	66.4	149.3	390	230.9	151378	1051.2	2363.6
					100	59.2	9953	69.1	155.4	400	236.8	159240	1105.8	2486.4

position and at a fixed attitude on the body or ship, to (2) the ram pressure which would be registered in the direction of motion at an infinite distance, a simple relationship q_r/q is established which greatly facilitates plotting experimental data. Contours of pitot-pressure coefficient of 1.00, with allowable limits on each side, indicate the regions where the pitot orifice of the instrument can be located to give accurate results under the conditions established.

If the flow remains steady and free of rotation, and if viscosity effects are neglected, the pressure and velocity relationships are dimensionless and hold regardless of scale, velocity, liquid density, and overall pressure upon the system.

A pressure determination from known velocity magnitudes and direction is much less determinate when the flow is complicated by viscosity effects.

41.13 Tables of Velocity Ratios, Pressure Coefficients, Ram Pressures and Heads. To facilitate the preparation of diagrams in which the distribution of differential pressure and the variation in velocity are plotted for the potential flow of an ideal liquid around any body, Table 41.e gives the variation of Euler number or pressure coefficient with velocity ratio as determined by the following relationship derived from the Bernoulli Theorem:

$$\frac{\Delta p}{\frac{\rho}{2} U_\infty^2} = \frac{\Delta p}{q} = 1 - \frac{U^2}{U_\infty^2} = 1 - \left(\frac{U}{U_\infty}\right)^2 \qquad \text{(2.xvi)}$$

This relationship applies to liquids of any mass density ρ, provided the values on both sides of the equality sign are for the same liquid.

The ram pressures corresponding to $0.5\rho U_\infty^2 = q$, calculated for both standard fresh water and standard salt water, are set down in Tables 41.d and 41.e, respectively. These are given in both lb per ft^2 and lb per in^2, supplemented by the velocity head in ft. It is to be noted that the *latter* value is the same for water (or other liquid or fluid) of any mass density. The range of velocities covers those normally encountered in model tests and ship design.

CHAPTER 42

Potential-Flow Patterns, Velocity and Pressure Diagrams Around Various Bodies

42.1 Various Methods of Drawing Streamlines Around Bodies. For 2-diml potential flow around a body of any shape, at any orientation with the stream, there are several methods of determining the streamline pattern. Listed briefly, these are:

(a) Constructing a flow net made up of streamlines and equipotential lines
(b) Determining the streamlines mathematically or by graphic construction, if the body shape is one that may be formed by placing one or more sources or sinks, or source-sink pairs, in a uniform stream
(c) Plotting the equipotential-line pattern in an electrolytic tank and constructing the streamline pattern from it
(d) Plotting the streamline pattern as an equipotential-line pattern in an electrolytic tank
(e) Placing the body in a circulating-water channel and observing the streamline pattern by one of several methods
(f) Utilizing conformal transformation.

By following the relatively simple sketching process described in Sec. 2.20, a flow net for continuous, irrotational, potential flow in two dimensions in an ideal liquid can be constructed for a great variety of boundary shapes, channel boundaries, or both. Flow nets are reproduced in Figs. 2.O, 2.P, 2.W; in diagrams 1, 2, 3, and 4 of Fig. 2.X; and in Fig. 41.J. They are to be found frequently in the literature, as listed in Table 42.a.

Despite its limitation to an ideal liquid, the 2-diml flow-net technique has a rather extensive practical usefulness in applied hydrodynamics. There are many instances in the course of ship design or in the analysis of ship behavior where an approximation to the flow pattern by this method is most illuminating. For example, before surface wavemaking has become pronounced, the flow around the uppermost waterlines of a ship is predominantly 2-diml in character, expecially abreast the forward part of the vessel. Several examples are to be found in Figs. 2.S and 4.A. Other examples are the 2-diml flow patterns around a sharp 2-diml bend in a duct, illustrated in diagram 2 of Fig. 2.X, and around the stem bar of a ship, shown without the equipotential lines in diagram 1 of Fig. 2.V.

Three-dimensional flow nets can be constructed [Rouse, H., EH, 1950, Fig. 26 (lower), p. 33] but the technique becomes complicated, as described in Sec. 2.21. Practical methods for constructing them are not considered here.

It is important to note, as mentioned on page 44 of Sec. 2.20, that since the flow in a separation zone is not potential in character, it can not be represented in a flow net. Furthermore, this technique does not take account of centrifugal-force effects as the liquid changes direction around bends and corners in channels and ducts. These forces may be appreciable at high velocities.

42.2 Flow Patterns Around Geometric and

TABLE 42.a—REFERENCE DATA FOR LINE DRAWINGS OF FLOW PATTERNS AROUND GEOMETRIC AND OTHER SIMPLE SHAPES

Type of Body or Shape	Kind of Flow	Kind of Diagram	Reference
Flat plate	Ideal, 2-diml	Streamlines; normal to flow	AHA, 1934, p. 112 and Fig. 131, p. 175 HAM, 1934, Fig. 103, p. 174
Disc, circular	Ideal and real, 2-diml	Streamlines; two flows superposed	BMF, 1953, p. 178 EMF, 1946, p. 236 EH, 1950, Fig. 84, p. 120
Rod, circular	Ideal, 2-diml	Streamlines; steady and unsteady	EH, 1950, p. 18
Rod, circular	Ideal, 2-diml	Streamlines; irrotational flow	BMF, 1953, Fig. 105a, p. 179 TH, 1950, p. 150 EMF, 1946, Fig. 120(a), p. 237; also Fig. 139(a), p. 273 EH, 1950, Fig. 85(a), p. 121; also Fig. 91(a), p. 128 AHA, 1934, pp. 174, 177 HAM, 1934, Fig. 98, p. 167 MDFD, 1938, Vol. I, p. 23
Rod, circular	Real	Streamlines; with separation zones	BMF, 1953, Figs. 105(b), (c), p. 179 EMF, 1946, Figs. 120(b), (c), p. 237 EH, 1950, Fig. 20, p. 23; also Figs. 85(b), (c), p. 121
Strut, in line, streamlined	Ideal, 2-diml	Streamlines	STG, 1924, Vol. 25, Fig. 17, p. 312 BMF, 1953, Fig. 38(b), p. 56 EMF, 1946, pp. 37–38 EH, 1950, p. 7
Strut in line, streamlined	Real, 2-diml	Streamlines; with separation	EH, 1950, Fig. 21, p. 23
Torpedo head	Ideal, 2-diml	Flow net; same as Fig. 41.J	BMF, 1953, p. 64 EMF, 1946, p. 50
Torpedo head	Ideal, 3-diml	Streamlines; partly schematic	TH, 1950, p. 407
Rankine oval, single source	Ideal, 2-diml	Streamlines; stream functions	TH, 1950, p. 196
Rankine oval, source and sink	2-diml	Streamlines; stream functions	STG, 1924, Vol. 25, Fig. 10, p. 305; also TMB Transl. 48, p. 12
Flat plate	Real, 2-diml, discontinuous	Streamlines; schematic	HAM, 1934, p. 186
Rod, elliptic	Ideal, 2-diml	Streamlines; major axis normal to flow	HAM, 1934, Fig. 144, p. 211 and Figs. 146, 147, p. 213
Ship form, lenticular	Ideal, 2-diml	Streamlines; half-body only	Pollard, J., and Dudebout, A., "Théorie du Navire," 1894, Vol. IV, p. 238
Sphere	Ideal, 3-diml	Streamlines; schematic	HAM, 1934, p. 151
Sphere	Real, 3-diml	Streamlines; steady and unsteady cases	EH, 1950, pp. 16–17

TABLE 42.a—(Continued)

Type of Body or Shape	Kind of Flow	Kind of Diagram	Reference
Spheres abreast and in tandem	Ideal, 3-diml	Streamlines; schematic	AHA, 1934, pp. 109–110 HAM, 1934, Fig. 81, p. 151
Torpedo head	Ideal, 3-diml	Streamlines; schematic	AHA, 1934, p. 122
Body with blunt stern	Ideal, 2-diml	Streamlines and equipotential lines; sink in a uniform flow	EH, 1950, p. 344
Source-sink flow	Ideal, 2-diml	Streamlines; equipotential lines	EH, 1950, p. 346
Cylinder near a wall	Ideal, 2-diml	Streamlines	Zeit. für Ang. Math. Mech., Jun 1929, Vol. 9, Fig. 9, p. 209
Cylinders in tandem	Ideal, 2-diml	Streamlines	Zeit. für Ang. Math. Mech., Jun 1929, Vol. 9, Fig. 7, p. 207

Other Shapes; Published Streamline Diagrams. The standard works of reference and the technical literature on hydrodynamics are replete with diagrams of flow nets, flow patterns, streamlines and equipotential lines, photographs, and other graphic representation of liquid flow around a varied assortment of body shapes and through ducts and passages of various kinds. Unfortunately, the diagrams are widely scattered. A large collection of these and other data has been assembled by Dr. E. H. Kennard of the David Taylor Model Basin staff, but efforts to have the data published have so far been unsuccessful.

Space is not available here to reproduce either the photographs or the line drawings that the marine architect might find useful for reference purposes. However, brief descriptions and source information for many of the existing illustrations are assembled in categories and listed in Tables 42.a and 42.b. Table 42.c in Sec. 42.3 lists similar data for ducts and channels, where the water is confined by solid boundaries or air-water interfaces.

Corresponding data on potential-flow patterns around yawed bodies, without circulation, are listed in Table 42.d in Sec. 42.5. For hydrofoils and bodies acting to produce lift, with circulation, lists of references are given in Tables 44.b and 44.c.

The flow directions, magnitudes, and patterns around ships and their models, in a real liquid like water, are depicted and discussed in Chap. 52.

Among the earliest of the flow diagrams published for the benefit of the marine architect, accompanied by descriptions and discussions of flow around floating bodies, are those of David Steel ["The Elements and Practice of Naval Architecture: or, A Treatise on Ship Building," written about 1805 but published in London, 1822, pp. 110–115].

From this early beginning, which appeared to be partly a matter of reasoning and partly of observation, knowledge as to flow patterns expanded along two characteristic lines:

I. The experimental approach, in which various clever methods were employed to generate in the liquid visible streamlines that could be recorded photographically. This was later expanded to the experimental delineation of flow lines by doubly refracting solutions and by electric analogy, described in Secs. 42.12 and 42.13, respectively.

II. The analytic approach, exemplified by the source-sink diagram and the flow net, in which the streamline positions were calculated and drawn, or in which the graphic construction methods were based upon the laws of hydrodynamics. In general, the analytic approach is workable only in liquids without viscosity.

The earliest experiments with liquid streamlines to produce good photographic records appear to have been those of H. S. Hele-Shaw in Great Britain ["Experiments on the Nature of the Surface Resistance in Pipes and on Ships," INA, 1897, Vol. 39, pp. 145–156, also Plates XX

TABLE 42.5—REFERENCE DATA FOR PHOTOGRAPHS OF FLOW PATTERNS AROUND GEOMETRIC AND OTHER SIMPLE SHAPES

Type of Body or Shape	Kind of Flow	Kind of Diagram	Reference
Flat plate, normal to flow	Real, 2-diml	Al. powder; plate stationary	STG, 1905, pp. 68, 70 BMF, 1953, Frontispiece EMF, 1946, Pl. XVIII, p. 248 AHA, 1934, Pl. 25, p. 304
Flat plate, normal	Real, 2-diml	Smoke; plate stationary	MDFD, 1938, Vol. II, Pl. 33, 34, p. 553
Blunt-ended body	Real, 2-diml	Al. powder; body stationary	AHA, 1934, Pls. 12–14, pp. 288–292
Elliptic cylinder, sideways	Real, 2-diml	Al. powder; major axis normal to flow	STG, 1905, Figs. 14, 15, p. 76 AHA, 1934, Pl. 26, p. 305 (3 speeds)
Elliptic cylinder, end-on	Real, 2-diml	Al. powder; streamlines; major axis parallel to flow	STG, 1905, Figs. 17, 18, p. 76 AHA, 1934, Pl. 27, Fig. 67, p. 306 MDFD, 1938, Vol. I, Pl. 11a, p. 75
Rod, normal	Real, 2-diml	Al. powder; rod stationary	BMF, 1953, Frontispiece EMF, 1946, pp. 240, 248 AHA, 1934, Pl. 24, Fig. 59, p. 303
Rod, normal	Real, 2-diml	Rod stationary	STG, 1952, pp. 176–178
Rod, normal	Real, 2-diml	Al. powder; rod stationary; sequence photos	TH, 1950, Frontispiece, Pl. 1 and Pl. 4, Fig. 1 AHA, 1934, Pl. 1, p. 279, and Pl. 2, p. 280 MDFD, 1938, Vol. I, Pls. 7, 8, p. 62; Vol. II, Pl. 31, p. 551
Rod, normal	Real, 2-diml	Al. powder; rod moving, liquid stationary	TH, 1950, Frontispiece, Pl. 4, Fig. 2 AHA, 1934, Pl. 24, Fig. 60, p. 303
Rod, normal	Real, 2-diml	Al. powder; vortex trail	EMF, 1946, p. 241
Strut, in line	Real, 2-diml	Al. powder; strut stationary	STG, Figs. 19, 20, 21, 23, p. 76 BMF, 1953, Frontispiece, 2.5 to 1 proportions EMF, 1946, Pl. IV, p. 39; also Pl. XVIII, p. 248
Thin plate, parallel to flow	Real, 2-diml	Al. powder; body stationary	AHA, 1934, Pl. 27, Fig. 68, p. 306 STG, 1905, pp. 74, 76
Group of thin plates parallel to the flow, abreast	Real, 2-diml	Al. powder; plates stationary and moving	STG, 1934, Figs. 1, 2, p. 162
Airfoil, symmetrical	Real, 2-diml	Smoke; body stationary	MDFD, 1938, Vol. I, Pl. 11b, p. 75
Airfoil, normal form	Real, 2-diml	Al. powder; body stationary	MDFD, 1938, Vol. I, Pl. 12, p. 77 (small and large angles of attack)
Rod, normal, rotating	Real, 2-diml	Al. powder; rod stationary but rotating	MDFD, 1938, Vol. I, Pl. 15, 16, 17, 18, p. 82
House, above flat surface	Real, 2-diml	Al. powder; body stationary	MDFD, 1938, Vol. I, Pls. 20, 21, p. 88

TABLE 42.b—(Continued)

Type of Body or Shape	Kind of Flow	Kind of Diagram	Reference
Vortex street	Real, 2-diml	Al. powder; well abaft a body	MDFD, 1938, Vol. I, Pl. 1, p. 37
Vortex street	Real, 2-diml	Colored liquid	MDFD, 1938, Vol. II, Pl. 32, p. 552
Blunt-ended body, with various stages of separation	Real, 2-diml	Al. powder; body stationary	MDFD, 1938, Vol. I, Pl. 6, p. 60
Sphere, with and without trip wire	Real, 3-diml	Smoke; body stationary	MDFD, 1938, Vol. I, Pl. 10, p. 73
Rectangular-section body	Real, 2-diml	Al. powder; body stationary	STG, 1905, Figs. 12, 22, p. 76
Wedge shape, pointed end forward	Real, 2-diml	Al. powder; body stationary	STG, 1905, Fig. 13, p. 76

through XXIII, Figs. 1 through 23]. These observations, still valid and useful after nearly six decades, were made at relatively low Reynolds numbers, at least at relatively low stream velocities.

In Figs. 8 and 9 on Plate XXI of the Hele-Shaw 1897 reference there is shown the flow past a small 2-diml boat-shaped body with a rectangular projection on one side, like the paddlebox of a sidewheel ship totally immersed in a liquid. In one figure the flow is from forward to aft; in the other figure from aft to forward. The diagrams illustrate remarkably well the type of flow to be expected around small rectangular projections on a rough surface. Fig. 13 on Plate XXII shows the flow around a 2-diml body of lenticular form with a trailing-edge flap set at an angle of about 75 deg. The flow lines in the photograph illustrate clearly the manner in which circulation about the body (a concept unknown at that time) affects the general directions of flow ahead of and abaft the body.

The report of these experiments was followed shortly by a second report [Hele-Shaw, H. S., "Investigation of the Nature of Surface Resistance of Water and of Stream-line Motion under Certain Experimental Conditions: Second Paper," INA, 1898, Vol. 40, pp. 21–46, also Plates VII through XVII, Figs. 1 through 58]. Among the multitude of illustrations in this second report:

(a) Fig. 7 of the reference shows the upstream portion of a vortex street behind a 2-diml bar of rectangular section placed with its long dimension across the flow

(b) The photographs of Fig. 21 of the report, and those following, are beautiful pictures of 2-diml flow patterns around cylinders, semi-cylinders, inclined plates, rectangular bars, and strut sections

(c) Figs. 43 and 44 show the flow around a Taylor ship-shaped stream form

(d) Figs. 45 and 46 show the flow pattern around a 2-diml model with three pairs of saw teeth along its sides

(e) Figs. 24, 29, 30, and 32 are remarkable pictures of flow patterns around and between sources and sinks.

Within the next decade, F. Ahlborn photographed many flow patterns around 2-diml bodies of varied shapes, using sawdust suspended in the water as a motion indicator instead of the aluminum powder later sprinkled on the water surface. From these photographs and from his observations Ahlborn drew sketches and line diagrams illustrating the principal features of the various flow patterns, with their streamlines, path lines, and so on. These photographs and flow diagrams are published in the papers:

(1) "Hydrodynamische Experimentaluntersuchungen (Experimental Researches in Hydrody-

TABLE 42.c—REFERENCE DATA FOR LIQUID-FLOW PATTERNS IN DUCTS AND CHANNELS

Type of Passage	Kind of Flow	Kind of Diagram	Reference
Various	Ideal, 2-diml	Flow net	EMF, 1946, pp. 20–25
Straight channel, contracting	Ideal, 2-diml	Streamlines	EMF, 1946, p. 15
Side jet, filleted	Ideal, 2-diml	Flow net; half-jet only	BMF, 1953, Probl. 83, p. 51
Straight-taper nozzle or slot	Ideal, 2-diml	Flow net; part in duct, part in air	BMF, 1953, p. 49
Straight channel, contracting	Ideal, 2-diml	Flow net	BMF, 1953, p. 46 HAM, 1934, Fig. 88, p. 160
Tapering duct, curved	Ideal, 2-diml	Flow net	BMF, 1953, p. 45
90-deg curved elbow	Ideal, 2-diml	Flow net; including tangent portions	BMF, 1953, Probl. 79, p. 51
Jet from flat orifice	Ideal, 2-diml	Flow net; jet in air	EMF, 1946, Fig. 29, p. 56; also Fig. 44, p. 89 EH, 1950, upper Fig. 26, p. 33; also p. 49
Jet from flat orifice	Real, 2-diml	Al. powder; photograph; inside a channel	EMF, 1946, Pl. XIX, p. 254
Sluice gate in wall	Ideal, 2-diml	Flow net; open jet at bottom	BMF, 1953, p. 96 EMF, 1946, p. 95 EH, 1950, p. 51
Sharp-crested weir	Ideal, 2-diml	Flow net; open jet at top	BMF, 1953, p. 98 EMF, 1946, p. 93 EH, 1950, p. 51 HAM, 1934, Fig. 62, p. 117
Solitary wave on flat bed	Ideal, 2-diml	Streamlines; steady and unsteady flow	BMF, 1953, p. 57 EH, 1950, p. 8
Venturi jet	Real, 2-diml	Al. powder; photograph	EMF, 1946, Pl. XIX, p. 254
Abrupt changes in width	Real, 2-diml	Al. powder; photograph; channel flow	EMF, 1946, Pl. XX, p. 259
Rounded inlet from tank	Ideal, 2-diml	Flow net	EMF, 1946, Fig. 15, p. 25 EH, 1950, p. 22
Jet from flat orifice	Ideal, 3-diml	Flow net	EH, 1950, lower Fig. 26, p. 33
Venturi jet	Ideal, 2-diml	Streamlines	AHA, 1934, Fig. 208, p. 245
Jets and orifices in channels	Real, 2-diml	Streamlines	AHA, 1934, Figs. 209, 210, p. 245
Venturi jet	Real, 2-diml	Photographs; 6 sequences	EMF, 1946, p. 84
Orifice in flat plate	Ideal, 2-diml	Streamlines and equipotential lines, by electric analogy	HAM, 1934, p. 185

TABLE 42.c—(Continued)

Type of Passage	Kind of Flow	Kind of Diagram	Reference
Jet impinging on plate, normally	Ideal, 3-diml (?)	Streamlines, schematic	HAM, 1934, pp. 121, 143
Flow impinging on plate, normally	Ideal, 2-diml	Streamlines	HAM, 1934, p. 142
Flow around corners, inside and outside	Ideal, 2-diml	Streamlines; some with vortexes	HAM, 1934, pp. 164–165, and Figs. 156, 157, p. 218 MDFD, 1938, Pl. 2, p. 40

namics)," STG, 1904, Vol. 5, pp. 417–453. This paper describes and illustrates Ahlborn's apparatus and methods, in most of which the camera (or observer) and the body were stationary while the liquid moved past. As previously mentioned, sawdust was employed as the suspended material to produce the streamlines and path lines. The objects tested in the first experiments were mostly flat, bent, and curved plates, mounted singly and in pairs.

(2) "Die Wirbelbildung im Widerstandsmechanismus des Wassers (The Phenomenon of Eddies and Vortexes in the Mechanism of Resistance in Water)," STG, 1905, Vol. 6, pp. 67–81. This paper describes a continuation of Ahlborn's earlier experiments, discussed and illustrated in the reference preceding. It includes some stereophotographs of surface-flow phenomena, plus the surface-flow and wave patterns about thick plank models, models representing lapped butts (facing forward and aft), lenticular planform and streamlined models, and a rather extensive series of 2-diml geometric models, with vertical axes, projecting through the surface.

(3) "Die Wirkung der Schiffsschraube auf das Wasser (The Working of the Ship Screw Propeller in Water)," STG, 1905, Vol. 6, pp. 82–106. This paper describes studies made by Ahlborn of the 3-diml flow about screw-propeller blades and screw propellers themselves, at low speeds of advance, including zero. Many of the illustrations are stereophotographs in pairs. The data are discussed at some length in Sec. 16.11 of Volume I.

(4) "Die Widerstandsvorgänge im Wasser an Platten und Schiffskörpern. Die Entstehung der Wellen (The Mechanism of Resistance in Water as Affected by Plates and the Ship Hull. The Production of Waves)," STG, 1909, Vol. 10, pp. 370–436. This paper contains many photographs and diagrams made by Ahlborn of streamlines, waves, separation zones, and eddies around flat plates, some normal to the stream and some yawed, some wholly submerged and some partly immersed. In some cases the camera is stationary with respect to the plate; in other cases it is stationary with respect to the main body of liquid. Between pages 408 and 409 of the reference there are many photographs of thin, roughened glass plates moving parallel to their own planes. On pages 412 through 416 there are photographs and diagrams of the liquid-particle motions in gravity surface waves. Between pages 418 and 431 there are many photographs and diagrams of the gravity-wave formation and the streamline flow around small ship models, most of them with blunt sterns. The latter group embodies photographs and diagrams of both streamlines and path lines, depending upon whether the axes of reference are fixed in the model or in the overall body of liquid. These photographs and diagrams warrant more study and analysis than have been given to them in the past.

Some two decades later, G. Flügel published a paper entitled "Ergebnisse aus dem Strömungsinstitut der Technischen Hochschule Danzig (Results of Tests at the Flow Institute of the Technical University, Danzig)" [STG, 1930, Vol. 31, pp. 87–113]. On pages 92 and following there appear many excellent photographs of flow patterns of liquid moving in channels and ducts of varied and unusual shapes and around various objects. O. G. Tietjens followed this with another paper having the English title "Pictures of Flow for Small and Medium Reynolds Numbers" [Proc. 3rd Int. Congr. Appl. Mech., Stockholm,

1931, Vol. I, pp. 331–333]. The latter paper contains excellent photographs of 2-diml objects moving through glycerin with aluminum powder sprinkled on the surface to show the flow patterns. The Reynolds number in Tietjens' experiments varied from 0.25 to 250. The discussion of the paper points out that the double row of vortexes leaving the blunt-ended bodies, now called the vortex trail or street, was noted by Mallock in 1907 and by Bénard in 1908, prior to von Kármán's first paper on this subject in 1911.

The propeller photographs and flow diagrams of Ahlborn were supplemented a few years later by those of R. Wagner, O. Flamm, and F. Gebers, also made in Germany. The results were embodied in the following papers and books:

1. Wagner, R., "Versuche mit Schiffsschrauben und deren praktische Ergebnisse (Tests with Ship Propellers and Their Practical Results)," STG, 1906, pp. 264–366, esp. pp. 293–295, 302, 310–323. This paper embodies many flow diagrams and flow patterns around propeller blades and propellers.
2. Flamm, O., "Beitrag zur Entwicklung der Wirkungsweise der Schiffsschrauben (Contribution to the Development of the Effectiveness of the Ship Propeller)," STG, 1908, pp. 427–438, esp. Figs. 1–12 opp. p. 432
3. Flamm, O., "Die Schiffsschraube und ihre Wirkung auf das Wasser (The Screw Propeller and Its Action in Water)," published by R. Oldenbourg, in Munich and Berlin, 1909. Some of the Flamm photographs are published in STG, 1909, Vol. 10, Figs. 1 through 7, opposite page 346.
4. Gebers, F., "Abwehr der Kempfschen Angriffe und einiges mehr über seine und meine Propellerversuche (Defense of Kempf's Method of Attack and Additional Information on His Propeller Tests and Mine)," Schiffbau, 28 Feb 1912, pp. 388–396. On pp. 390 and 391 there are axial views of model propellers showing some of the flow paths over the widths of the blades, on both faces and backs.
5. Gebers, F., "Neue Propellerversuche (New Propeller Tests)," STG, 1910, pp. 729–784, esp. Fig. 12, opp. p. 758, and Figs. 1, 2, and 3 on p. 782; also INA, 1910, pp. 69–70.

In the course of the last half-century, since most of the foregoing references appeared, a multitude of flow-pattern photographs have been taken, a large number of flowline diagrams have been drawn, and a great many of both have been published. Reference data on some of these are presented in two groups in this section, and in other groups in the sections to follow:

Table 42.a Reference data for line drawings of

TABLE 42.d—Reference Data for Flow Patterns Around Simple Shapes When Yawed

Type of Body or Shape	Kind of Flow	Kind of Diagram	Reference
Flat plate, inclined	Ideal, 2-diml	Streamlines; partly schematic	TH, 1950, p. 162
Flat plate, inclined	Ideal, 2-diml	Streamlines; irrotational flow	BMF, 1953, p. 191 EMF, 1946, Fig. 141(a), p. 279 AHA, 1934, Fig. 107, p. 160 and Fig. 132, p. 175 HAM, 1934, Fig. 104, p. 174
Flat plate, inclined	Real, 2-diml	Streamlines; photographic and schematic	STG, 1904, Figs. 14, 15, 16, 17, pp. 431–434
Elliptic body	Ideal, 3-diml (?)	Streamlines; not consistent	TH, 1950, p. 23
Elliptic body	Ideal, 2-diml	Streamlines; partly schematic	TH, 1950, p. 160 MDFD, 1938, Vol. I, p. 67
Propeller-blade sections, symmetrical	Ideal, 2-diml	Streamlines; some show circulation paths	STG, 1923, pp. 251–254, 257
Elliptic body, thin	Ideal and real, 2-diml	Streamlines, calculated, and filaments, observed	INA, 1900, Pls. XXV, XXXIII. Apparently at very low values of R_n.
Cylinders in echelon	Ideal, 2-diml	Streamlines	Zeit. für Ang. Math. Mech., Jun 1929, Vol. 9 Fig. 10, p. 246

flow patterns around geometric and other simple shapes

Table 42.b Reference data for photographs of flow patterns around geometric and other simple shapes.

To save space in Tables 42.a and 42.b of this section, in Table 42.c of Sec. 42.3, and in Table 42.d of Sec. 42.4, the authors' names in the references are omitted. All photographs which have been made with reflecting particles sprinkled on the liquid surface or suspended within the liquid are marked "Al. Powder," regardless of whether or not aluminum powder was used in every case. "Normal" means that the long dimension of the section or body was across the flow, normal to it. "In line" means that the long dimension was parallel to the flow.

Of the streamline diagrams derived by analytic methods, among the first to be published were those of W. J. M. Rankine, appearing in the literature of the Institution of Naval Architects and of the Royal Society (of Great Britain), in the period 1862–1872. Stemming from the work of Rankine were the analytic streamlines about ship-shaped and other bodies published by D. W. Taylor in the references listed in Secs. 3.8 and 43.6 of the present book, and in Volume II of the 1910 edition of "The Speed and Power of Ships."

Many more streamline diagrams evolved from source-sink combinations have been published since then. Among the references, not well known in America, may be listed:

(i) Legendre, R., "Hydrodynamique Graphique (Graphic Hydrodynamics)," ATMA, 1933, Vol. 37, pp. 395–410. This paper contains a number of flow nets and diagrams giving streamline and equipotential-line patterns for a series of flow conditions.

(ii) Brard, R., "Les Méthodes pour le Trace des Lignes de Courant dans les Écoulements Théoriques ou Réels. Leur Rôle en Hydrodynamique (The Tracing of Streamlines in Theory and Practice. Their Role in Hydrodynamics)," ATMA, 1938, Vol. 42, pp. 65–83. So far as known this paper is not translated into English. A full understanding of it involves a working knowledge of complex variables and conformal transformation.

In the early 1910's, representations of the wake patterns and streamlines alongside and abaft surface-ship and airship models were published in the technical literature. A brief list follows:

a. Eden, C. G., "Apparatus for the Visual and Photographic Study of the Distribution of the Flow Round Plates and Models in a Current of Water," ARC, R and M 31, Mar 1911, pp. 48–49
b. Booth, H., and Eden, C. G., "The Wind Resistance of Some Aeroplane Struts and an Examination of Their Relative Merits," ARC, R and M 49, 1912, pp. 95–96
c. Bairstow, L., and Eden, C. G., "Experiments on Airship Models," ARC, R and M 55, 1912, pp. 48–51
d. Eden, C. G., "Investigation by Visual and Photographic Methods of the Flow Past Plates and Models," ARC, R and M 58, Mar 1912, pp. 97–99
e. Baker, G. S., "Methodical Experiments with Merchant Ship Forms," INA, 1913, Part I, pp. 162–180, esp. pp. 167–168 and Pl. XVIII. This plate shows four photographs made at the stern of totally submerged models, each composed of the underwater body of a ship form with its mirror image superposed, in inverted position.

T. B. Abell published some unusual photographs of the wakes abaft simple ship-shaped bodies, using filaments of colored liquid and air bubbles as indicators ["A Contribution to the Photographic Study of the Mechanism of the Wake," INA, 1933, pp. 145–152 and Pls. XVII, XVIII].

N. W. Akimoff published the results of some flow-pattern and wave studies about vertical circular-section rods and elongated forms suspended in a moving current of water ["Über das Wesen des Mitstroms (On the Behavior of the Wake)," STG, 1934, pp. 149–163].

42.3 Flow Patterns In Ducts and Channels. The naval architect and marine engineer are interested in the details of liquid flow within pipes, ducts, and channels, as well as of the flow outside of bodies and objects of varied shape. Flow-net diagrams for the motion of an ideal liquid within typical open and obstructed passages are shown in Fig. 2.X of Sec. 2.20.

Table 42.c lists reference data for what might be termed "inside" liquid-flow patterns, subject to the notes in Sec. 42.2 applying to Tables 42.a and 42.b.

A paper by H. S. Fowler and V. Walker, entitled "Fluid Flow in Turbo-Machinery" [IESS, 1953–1954, Vol. 97, pp. 113–152], contains many informative diagrams of air flow through ducts, bends, and axial-flow turbine and blower blades.

42.4 Flow Patterns for an Ideal Liquid Around Simple Ship Forms. Available flow diagrams around forms resembling those of ships are relatively scarce. Such as do exist are limited to the more-or-less 2-diml flow about the designed waterline, and that in an ideal liquid only.

Other than those embodied in Figs. 2.S and 4.A

of Volume I of this book there may be listed the following:

(a) Two-dimensional ship having a lenticular form of waterline, for which the flow pattern was derived and published by D. W. Taylor in:

(1) INA, 1894, Vol. 35, Fig. 14, Pl. LXXI

(2) S and P, 1933, Fig. 4, p. 4; practically the same figure as in (1)

(3) S and P, 1943, Fig. 4, p. 6; practically the same figure as in (1).

(b) Bow and forward shoulder waterlines of a 2-diml ship generated by a uniform line source in a uniform stream. Derived and published by H. Föttinger in STG, 1924, Vol. 25, Fig. 11, p. 306; TMB Transl. 48, May 1952, p. 14.

(c) Same as (b) preceding except that the line source increases linearly in strength from the stem. Published in STG, 1924, Fig. 12, p. 307; TMB Transl. 48, May 1952, p. 15.

(d) Complete 2-diml ship with waterlines generated by the combination of a bow line source and a stern line sink, each of constant and equal strength. Generally similar to (c) preceding. Published by F. Horn in "Theorie des Schiffes," Vol. V. Reproduced in RPSS, 1948, Fig. 2, p. 15, including diagrams giving the variation of p and U along and beyond the ship axis.

(e) Three-dimensional ship having a lenticular form of lateral plane, for which a schematic flow pattern was published by D. W. Taylor in:

(i) INA, 1895, Vol. 36, Fig. 6, Pl. XVI. It is to be noted in this figure that the streamlines are not spaced from the body axis at distances corresponding to equidifferent stream functions in tubes about the axis.

(ii) S and P, 1933, Fig. 5, p. 4; practically same figure as in (i)

(iii) S and P, 1943, Fig. 5, p. 6; same comments as for (i) preceding.

(f) Ship-shaped forebody, 2-diml in character, introduced in a uniform stream flowing parallel to the ship axis. G. S. Baker and J. L. Kent give a plot of 2-diml streamlines ahead of and abreast this forebody, when there is no limitation on the extent of the surrounding water ["Effect of Form and Size on the Resistance of Ships," INA, 1913, Part II, pp. 37–60, and Pls. III, IV, especially Fig. 5 on the latter plate]. The lower portion of Fig. 5 gives graphs of pressure variation with distance along the longitudinal axis for two stream surfaces fairly close to the ship.

42.5 Flow Patterns About Yawed Bodies in an Ideal Liquid. The ideal-liquid potential-flow patterns about yawed bodies in a stream, available in the published literature, amount to only a very small fraction of those worked out for axial flow. A partial list of references embodying these patterns is presented in Table 42.d. One such pattern is that around the inclined flat plate in diagram 1 of Fig. 3.B in Volume I.

An excellent source of analytic information in this particular field is the work of A. F. Zahm, embodied in NACA Report 253, 1927, entitled "Flow and Drag Formulas for Simple Quadrics," pages 517–537. Fig. 3.C of Volume I of this book is adapted from Fig. 23 of the Zahm report.

More recent data, applying to pressures rather than streamlines around a yawed body, may be found in Admiralty Research Laboratory (Great Britain) Report ARL/R1/G/HY/19/1 of April 1954 by I. J. Campbell and R. G. Lewis, entitled "Pressure Distributions: Axially Symmetric Bodies in Oblique Flow." A copy of this report is in the TMB library.

42.6 Velocity and Pressure Distribution Around a Body of Revolution. For bodies of revolution having appreciable diameters, the same as for ships with appreciable beams, it is customary to plot velocity and pressure distributions on a basis of body or ship length along the principal or x-axis. This scheme is followed in Figs. 4.C and 4.D of Volume I. However, when the diameter is large in proportion to the length, or when one end or the other is blunt, the velocity and pressure distributions are plotted to much better advantage on a base of length along the section contour, as in diagram 2 of Fig. 2.B of Volume I or in the diagram of Fig. 41.J of this part of the book.

When working with 3-diml rather than 2-diml flow, as with that around a body of revolution, it is important that the nature of the 3-diml flow pattern be clearly understood. In a number of published diagrams in standard works of reference the streamlines approaching and leaving the 3-diml bodies of revolution have, apparently as a matter of convenience in drafting, equidistant radial spacing from the principal body axis. This is equivalent to equidistant transverse spacing when a longitudinal section through the body axis is diagrammed [Prandtl, L., and Tietjens, O. G., AHA, 1934, Fig. 58 on p. 109, Fig. 59 on p. 110, Figs. 63 and 64 on p. 120, and Fig. 65 on p. 122; Taylor, D. W., S and P, 1910, Vol. II, Fig. 20; S and P, 1943, Fig. 5 on p. 6]. The streamlines so depicted do not correspond to equidifferent 3-diml stream functions, as do the traces in diagram 2 of Fig. 2.M of Volume I, and those of Figs. 42.A, 42.B, 43.M, and 43.O.

Consider the symmetrical 3-diml flow of an ideal liquid along a solid rod of circular section of radius R_0, with its axis parallel to the direction of flow, in a stream whose undisturbed uniform

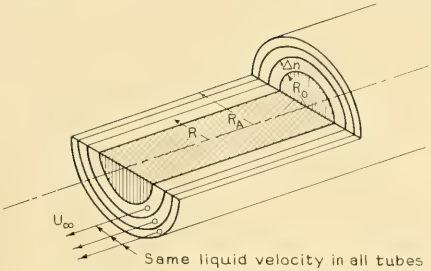

Fig. 42.A Schematic Diagram of Uniform Three-Dimensional Flow Around a Straight Circular Rod With Equidifferent Stream Functions

velocity is U_∞. This situation, pictured in Fig. 42.A, is derived immediately from the 3-diml stream-function ψ(psi) in diagram 2 of Fig. 2.M by freezing the liquid within the central rod, an operation which does not change the flow pattern around it. The immovable quantity of frozen liquid, extending out to radius R_0, is then subtracted from the whole. It is convenient in this process to retain the rod axis as the reference axis for measuring the 3-diml stream functions.

If the thickness of the first, second, or any other tube of liquid is represented by Δn, and its mean radius from the axis by R, then the increment of liquid volume $\Delta \mathcal{V}$ passing through it in the time Δt is represented approximately by

$$\Delta \mathcal{V} = -U_\infty(2\pi R)\Delta n \tag{42.i}$$

where the velocity U_∞ is constant throughout all the tubes. If R_A is the radius to any selected cylindrical stream surface, the 3-diml stream function of that surface is

$$\begin{aligned}\psi_A &= \left(\frac{1}{2\pi}\right)(-U_\infty)\pi(R_A^2 - R_0^2)\\ &= -\frac{U_\infty}{2}(R_A^2 - R_0^2)\end{aligned} \tag{42.ii}$$

At the solid cylindrical surface of radius R_0 the 3-diml stream function is zero.

The subdivision of the uniform liquid flow into stream tubes of equal area means that the normal spacing between the tube-wall traces in any longitudinal plane through the axis is no longer a direct measure of the velocity in each tube, or even of the relative velocity, as it was in the 2-diml case. For equidifferent values of the volume increment per unit time or of the stream function, the tube thickness diminishes inversely in proportion to the increase in its mean radius, to maintain the relationship of Eq. (42.i).

When the flow takes place around some body of revolution which has a varied section along the axis of flow, such as the sphere in Fig. 42.B, the

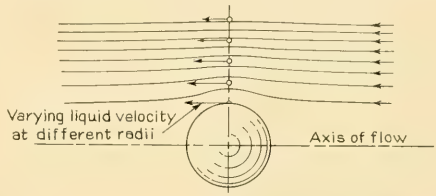

Fig. 42.B Longitudinal Section Through Three-Dimensional Flow Around a Sphere, With Equidifferent Stream Functions

velocity in each stream tube is no longer constant but changes with distance along the x-axis. In fact, there are three variables in the stream-function expression which vary with x, namely R, Δn, and U, where R is measured normal to the axis of the uniform stream flow. It then becomes necessary to make use of some rather involved procedures to delineate the stream surfaces. For two 3-diml bodies of revolution, including the sphere, the stream functions in spherical coordinates are worked out in Sec. 41.9.

A 3-diml stream form, especially one derived from a single source-sink pair, lends itself to graphic construction of the flow pattern around it, as well as to calculation of the elements of this pattern. When so constructed, the radii R_1, R_2, . . . and the stream-tube thicknesses Δn_1, Δn_2, . . . are measured, the local velocities U are determined, and the accompanying pressures p derived from Eq. (2.xvia). The graphic construction is described in Sec. 43.8 and illustrated in Figs. 43.L, 43.M, 43.N, and 43.O. The formulas for a 3-diml sphere are set down in Sec. 41.9 and in diagram 2 of Fig. 41.G.

Fortunately for the physicist, marine architect, and others, certain staff members of the Aerodynamische Versuchsanstalt (AVA) at Göttingen, Germany, have worked out the pressure distributions over 12 forebodies and 59 full bodies of revolution, of a great variety of shapes and proportions. These bodies were created by placing various combinations of point and line sources and sinks along an axis, and then superposing upon this combination a uniform flow of ideal

liquid parallel to the axis. A few of the 3-diml streamlines adjacent to the 12 forebodies are also given in their Report UM 3206, dated 30 December 1944, available in English as TMB Translation 220, issued in April 1947. An English translation of AVA Report UM 3106, by F. Riegels and M. Brand, mentioned on page 1 and listed as Reference 2 on page 7 of TMB Translation 220, is on file in the Aerodynamics Division library at the David Taylor Model Basin.

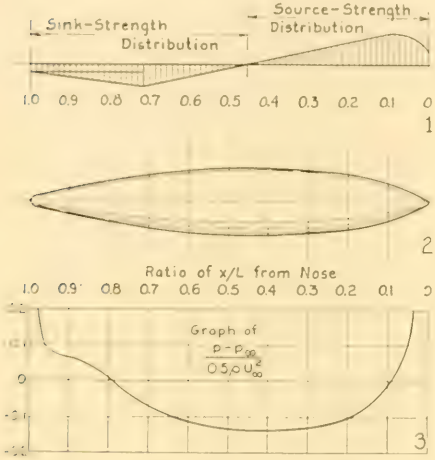

FIG. 42.C SOURCE-SINK STRENGTH DISTRIBUTION, AXISYMMETRIC BODY FORM, AND DISTRIBUTION OF PRESSURE COEFFICIENT AROUND AN AIRCRAFT FUSELAGE

Fig. 42.C gives data pertaining to body A of UM 3206, representing the fuselage of the Russian pursuit plane MIG 1. The plot of pressure coefficient $(p - p_\infty)/(0.5\rho U_\infty^2) = \Delta p/q$ in diagram 3 extends only from $+0.2$ to -0.2; actually this coefficient rises to values of $+1.0$ at the extreme nose and the extreme tail. The source-sink distribution and strength variation are shown by diagram 1 of the figure.

Supplementing the foregoing, there are listed here a few references in the technical literature giving additional velocity and pressure data derived for bodies of revolution. Reference (14) in this series is the same report, authored by I. J. Campbell and R. G. Lewis, as that listed at the end of Sec. 42.5; it appears to have two separate identification numbers. The references are:

(1) Von Kármán, T., "Calculation of Pressure Distribution on Airship Hulls," NACA Tech. Memo 574, Jul 1930; translated from Abhandlungen aus dem Aerodynamische Institut an der Technische Hochschule, Aachen, 1927, No. 6

(2) Upson, R. H., and Klikoff, W. A., "Application of Practical Hydrodynamics to Airship Design," NACA Rep. 405, 1932, pp. 123–140

(3) Kaplan, C., "Potential Flow About Elongated Bodies of Revolution," NACA Rep. 516, 1935, pp. 189–208

(4) Smith, R. H., "Longitudinal Potential Flow About Arbitrary Body of Revolution with Application to Airship *Akron*," Jour. Aero. Sciences, Sep 1935, Vol. 3, No. 1

(5) Kaplan, C., "On a New Method for Calculating the Potential Flow Past a Body of Revolution," NACA Rep. 752, 1943, pp. 7–19

(6) Young, A. D., and Owen, P. R., "A Simplified Theory for Streamline Bodies of Revolution and Its Application to the Development of High-Speed Low-Drag Shapes," ARC, R and M 2071, Jul 1943, pp. 107–127

(7) Young, A. D., and Young, E., "A Family of Bodies of Revolution Suitable for High-Speed or Low-Drag Requirements," ARC, R and M 2204, Aug 1945

(8) Eisenberg, P., "A Cavitation Method for the Development of Forms Having Specified Critical Cavitation Numbers," TMB Rep. 647, Sep 1947

(9) Eisenberg, P., "An Asymptotic Solution for the Flow About an Ellipsoid Near a Plane Wall," Hydrodynamics Lab., CIT, Rep. N-57, Sep 1948

(10) McNown, J. S., and Hsu, E.-Y., "Pressure Distributions from Theoretical Approximations of the Flow Pattern," State Univ. Iowa, Reprints in Eng'g., Bull. 79, 1949

(11) Landweber, L., and Gertler, M., "Mathematical Formulation of Bodies of Revolution," TMB Rep. 719, Sep 1950

(12) McNown, J. S., and Hsu, E.-Y., "Approximation of Axisymmetric Body Forms for Specified Pressure Distributions," Jour. Appl. Phys., Jul 1951, Vol. 22, pp. 864–868. The authors' summary reads as follows:

"The complex relationship between body profile and pressure distribution is important in the design of high-speed undersea bodies. For slender axisymmetric bodies integration of the equations for irrotational flow has been accomplished, the coordinates of the body profile being related to the pressure distribution through coefficients of Legendre polynomials. The limitations and applications of this approximate analysis have been demonstrated through comparisons with preassigned conditions and with the results of experiments. Computed values closely approach those preassigned or measured throughout the central portion of the body if the maximum diameter does not exceed three-tenths of the length. The analysis is accordingly useful in designing bodies with low coefficients of drag and low incipient cavitation numbers."

The problem treated here is essentially the reverse of that forming the subject of the present section.

(13) Landweber, L., "The Axially Symmetric Potential

Flow About Elongated Bodies of Revolution," TMB Rep. 761, Aug 1951. On pp. 59–61 the author lists 28 references, some of which are given here.
(14) Campbell, I. J., and Lewis, R. G., "Pressure Distributions About Axially Symmetric Bodies in Oblique Flow," ARL (Admiralty Research Laboratory) Report (ACSIL/ADM/54/254) of Apr 1954.

42.7 Velocity and Pressure Diagrams for Various Two- and Three-Dimensional Bodies. When the body shape, form, and contour can not be expressed by some type of mathematical equation, or when the liquid flow around a body can not be expressed in the form of a given stream function ψ or velocity potential ϕ, analytic expressions for the velocity and pressure can rarely be established or derived. It becomes necessary, as a rule, to fall back upon experimental observations, or upon data previously derived, assembled, and published by other workers.

Some references containing these data for various 2-diml and 3-diml bodies, usually with graphs of both velocity and pressure, are given under the appropriate categories in Table 42.e. Could this list be made complete, for all published works, the marine architect might find readily at hand a great amount of data that would be directly useful and occasionally most valuable.

42.8 The Distribution of Velocity and Pressure About an Asymmetric Body. Many underwater craft, such as submersibles and submarines, have shapes resembling roughly a body of revolution but they almost invariably possess transverse asymmetry, at least above and below the principal longitudinal axis. Submerged bodies, and craft of the type mentioned, usually possess asymmetry in a fore-and-aft direction as well, reckoned about the midlength.

However, considering first the geometric forms having asymmetry about the principal axis, it so happens that formulas are available for computing the velocity and pressure distribution about what may be termed elliptic ellipsoids. For these bodies, the profiles, planforms, and sections are all of elliptic shape, as in diagram 2 of Fig. 42.D. Indeed, this particular form is special in two respects; first, in that the flow of an ideal fluid around it lends itself to computation, and second, in that, when placed with one axis in the direction of uniform flow, the velocity at the surface is constant everywhere around the girth of the midsection. The latter feature appears to be inherent in these elliptic shapes only.

The flow around an elliptic ellipsoid having axes in the ratio of 6 : 2 : 1, with a uniform flow of velocity U_∞ taking place parallel to the longest axis, has been investigated by H. Chu, P. C. Chu, and V. L. Streeter [Illinois Inst. Tech., Report on Project 4955, sponsored by ONR Contract 47onr-32905, dated 15 Mar 1950]. They found that around the elliptic midsection periphery the surface velocity parallel to the stream axis had a *constant* value of $1.0714U_\infty$. At the quarter-lengths the velocity around the girth of the body varied by only about one per cent from the mean.

The uniformity of tangential surface velocity at the midlength, parallel to the undisturbed stream direction, is a sign that the surface pressure around the midsection girth is likewise everywhere the same. However, at a constant given distance from the body surface, in the plane of the midsection, the velocity and pressure do vary around the girth. This variation has been investigated by R. K. Reber for the elliptic ellipsoid having axes in the ratio of 6 : 2 : 1 [unpubl. memo of 13 Apr 1950 to HES], lying with its

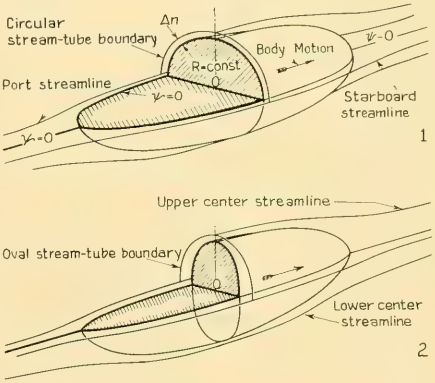

Fig. 42.D Typical Schematic Flow Around Axisymmetric and Elliptic Ellipsoids

longest axis parallel to the uniform stream. The results are shown in Fig. 42.E. Here it is noted that, in the plane of the midsection, the isotachyls or loci of constant velocity (parallel to the body axis and to the stream direction) lie closer than the average distance to those portions of the transverse midsection having the sharpest curvature. Opposite the portions of least curvature they are farther from the body. The transverse velocity gradient is therefore greater in way of

TABLE 42.9—REFERENCES TO PUBLISHED DATA ON VELOCITY AND PRESSURE DISTRIBUTION FOR VARIOUS TWO- AND THREE-DIMENSIONAL BODIES

The 2-diml bodies listed have constant sections along an axis normal to the direction of flow.

Type of Body or Shape	Kind of Flow	Kind of Diagram	Reference
Rod, circular	Ideal, 2-diml, normal to rod axis	Irrotational flow	EH, 1950, Fig. 23, p. 28; Fig. 85(a), p. 121 EMF, 1946, Fig. 120(a), p. 237 BMF, 1953, Fig. 105(a), p. 179 Vennard, J. K., "Elementary Fluid Mechanics," 1947, pp. 134, 136 MDFD, 1938, Vol. I, p. 24
Airfoil	2-diml		BMF, 1953, Fig. 115, p. 192
Rod, circular	Real, 2-diml, normal to rod axis	Tests made in air	EH, 1950, Fig. 89, p. 124; Figs. 85(b), 85(c), p. 121 EMF, 1946, Figs. 120(b), 120(c), p. 237; Fig. 122, p. 239 BMF, 1953, Figs. 105(b), 105(c), p. 179; Fig. 110, p. 187
Flat plate	Ideal, 2-diml		EMF, 1946, Fig. 121, p. 238 EH, 1950, Fig. 88, p. 123
Flat disc, circular	Ideal and real, 2-diml		EH, 1950, Fig. 84, p. 120 EMF, 1946, p. 236 BMF, 1953, p. 178
Strut, streamlined	Ideal and real, 2-diml	$L/D = 2.5$	EH, 1950, Fig. 87, p. 123 BMF, 1953, Fig. 108, p. 186
Building with ridge roof	Real, 3-diml	Tests made in air	EMF, 1953, p. 180
Sphere	Ideal, 3-diml	Irrotational flow	EH, 1950, Fig. 22, p. 28 MDFD, 1938, Vol. I, Fig. 5, p. 25
Balloon model	Ideal and real, 3-diml	Tests made by Fuhrmann	EH, 1950, Fig. 83, p. 120 EMF, 1946, Fig. 118, p. 235 BMF, 1953, p. 177 MDFD, 1938, Vol. I, Fig. 6, p. 25
Flat plate	Real, 2-diml		EH, 1950, Fig. 88, p. 123 EMF, 1946, p. 238 BMF, 1953, Fig. 109, p. 186
Torpedo head	Ideal, 2-diml		EMF, 1946, p. 50 BMF, 1953, p. 64
Elliptic cylinder	Ideal, 2-diml	Pressure coefficient	MDFD, 1938, Vol. I, Fig. 31, p. 75
Airfoil, symmetrical	Ideal, 2-diml	Pressure coefficient	MDFD, 1938, Vol. I, Fig. 31, p. 75; Vol. II, pp. 404–405
Body of revolution, fish-shaped	Ideal and real, 3-diml	Pressure coefficient	STG, 1923, p. 333
Body of revolution, fish-shaped		With propeller at tail	STG, 1923, p. 334

TABLE 42.e—(Continued)

Type of Body or Shape	Kind of Flow	Kind of Diagram	Reference
Simple ship, pointed ends	Ideal, 2-diml	Ordinates of $V^2/2g$	INA, 1913, Vol. 55, Part II, Fig. 5, Pl. IV
Various ship-shaped entrances	Ideal, 2-diml	Ordinates of $V^2/2g$; 6 forms with same L/B ratio	INA, 1913, Vol. 55, Part II, Fig. 1, Pl. III

the region of sharper transverse curvature than alongside the region of lesser transverse curvature. As the transverse distance from the body increases, the isotachyls assume a shape that is more and more nearly circular, exhibiting less and less effect of the transverse body asymmetry. Thus the velocity field at a reasonable distance resembles that of a body of revolution of approximately the same total volume. These features are the same as for the flow around the 3-diml bodies of rectangular and square section, described in Sec. 4.10 of Volume I and illustrated in Figs. 4.M and 4.N.

H. Chu, P. C. Chu, and V. L. Streeter at the Illinois Institute of Technology also investigated the surface flow over an asymmetric body of somewhat irregular transverse section and definite fore-and-aft asymmetry [Illinois Inst. Tech., Report on Project 4955, sponsored by ONR Contract N7onr-32905, dated 15 Jun 1950]. This body was formed by placing a combination of three sources and one sink in a uniform stream, with the sources and the sink symmetrically disposed about a longitudinal body axis parallel to the uniform-stream direction. Fig. 42.F is a fish-eye view of the source-sink arrangement, with enough transverse sections to afford an idea of its shape. Fore-and-aft lines are drawn for the maximum-beam positions along the length, and for the keel line. Since the body is symmetrical about its vertical centerline plane, and about a plane through its midheight, the maximum-beam line and the keel line are also streamlines. Two other streamlines, marked "upper bilge" and "lower bilge," respectively, were drawn as a part of the project. The three component velocities in space, together with their resultants, were calculated for the intersections of the four streamlines with nine of the transverse sections. The table on the figure gives the resultant velocities in terms of the uniform-stream velocity $-U_\infty$, for the thirty-six intersections. A few of these ratios are indicated on the diagram proper.

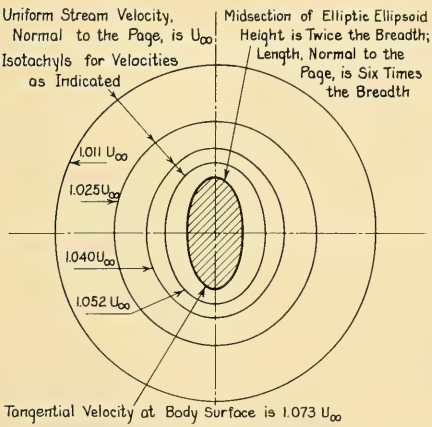

Fig. 42.E Isotachyls in the Transverse Midsection Plane of an Elliptic Ellipsoid Having Axes in the Ratio of 6:2:1

It is rather remarkable that, considering the flow along the maximum-beam streamline, the slight hollowness between Stations −4 and 0 causes a slowing down of the flow to a value at Sta. −1 that is only 0.73 of the uniform-stream velocity. Further that the bulge at Sta. 1 causes a speeding up of the flow to a value of more than $1.25U_\infty$. Considering the girthwise variations around the several sections, the local velocity is greatest at the midheight, where the section lines have the sharpest curvature. It is smallest in way of the bilges, where the section lines have the least curvature.

Unfortunately, the 3-diml stream function of classic hydrodynamics loses its significance in

the case of asymmetric bodies of the kind shown by Fig. 42.F. Nothing has as yet been developed to take its place. For the time being it appears useful to retain the enveloping stream surfaces, such as those of diagrams 1 and 2 of Fig. 42.D, along which the direction of flow is everywhere tangent to the direction of those surfaces. They are qualified, however, as surfaces for which the tangent velocity—not necessarily the axial component of that velocity—is constant around the trace of the stream surface in any transverse plane of the body. For any such section, these traces form what are described in Sec. 1.4 and illustrated in Fig. 1.B of Volume I as isotachyls, or contours of equal velocity. Unfortunately, they do not define the flow completely because the direction of the constant-velocity vector must also be specified for every point around the periphery. This can be done, at the expense of some complication, by adding vectors alongside the contours representing the component in the plane of the contour diagram, as is done in the wake-survey diagrams of Secs. 11.6 and 11.7 of Volume I and Secs. 60.6 and 60.7 of this volume.

42.9 Flow, Velocity, and Pressure Around Special Forms. It is certain that the technical literature contains much more data on the flow patterns and the velocity and pressure distribution around bodies of special shape than are referenced in this book and in others on hydrodynamics and hydraulics. Moreover, it appears reasonable to expect that, in the course of time, data in this field which are now classified will become available for general distribution.

Among the special forms in this category are the planing surfaces on the bottoms of flying-boat hulls and fast motorboats. A considerable amount of experimental work on flow patterns under these surfaces has been carried out by the National Advisory Committee for Aeronautics and the

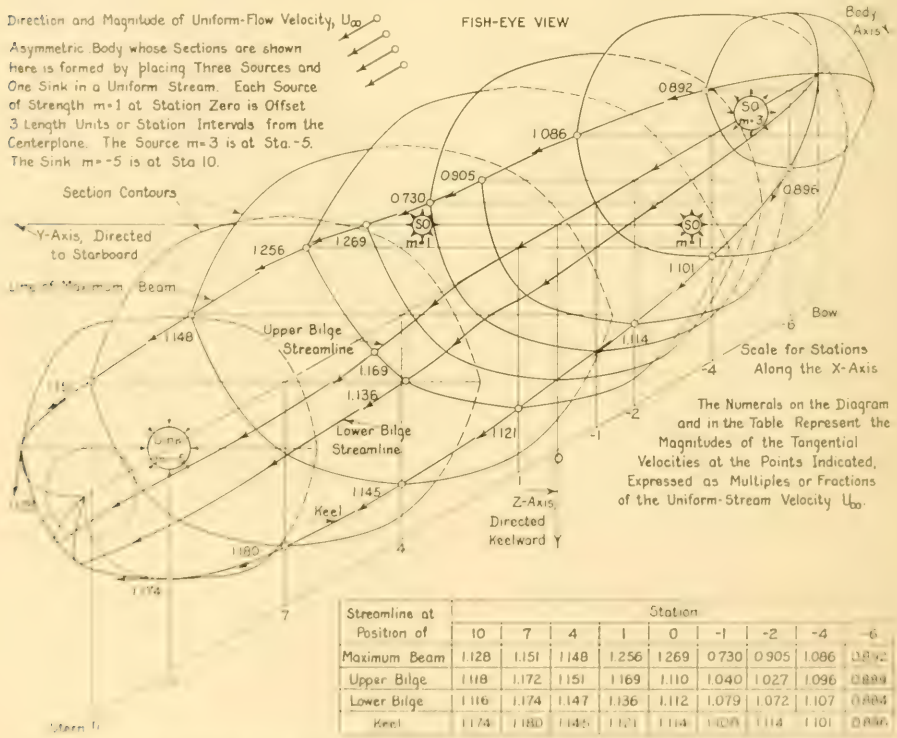

Streamline at Position of	Station								
	10	7	4	1	0	-1	-2	-4	-6
Maximum Beam	1.128	1.151	1.148	1.256	1.269	0.730	0.905	1.086	0.892
Upper Bilge	1.118	1.172	1.151	1.169	1.110	1.040	1.027	1.096	0.899
Lower Bilge	1.116	1.174	1.147	1.136	1.112	1.079	1.072	1.107	0.884
Keel	1.174	1.180	1.145	1.121	1.114	1.009	1.114	1.101	0.896

FIG. 42.F ASYMMETRIC BODY FORMED BY PLACING THREE SOURCES AND ONE SINK IN A UNIFORM STREAM

Experimental Towing Tank at the Stevens Institute of Technology. The following references pertain to this work:

(1) Ward, K. E., "A New Method of Studying the Flow of the Water Along the Bottom of a Flying-Boat Hull," NACA Tech. Note 749, Feb 1940
(2) Sutherland, W. H., "Underwater Photographs of Flow Patterns," ETT Tech. Memo 86, May 1948.

42.10 Velocity and Pressure Distribution Around Schematic Ship Forms. For the determination of velocity and pressure around ship forms whose shapes do not lend themselves to expression in convenient mathematical terms, like those of bodies of revolution or thin, deep planks, theoretical hydrodynamics in its present stage of development offers little that is of practical value to the ship designer or even to the flow analyst. There are definite indications, however, that the theoretical work on wavemaking resistance and on analytic ship-wave relations, described in Chap. 50, may in time lead to reasonable predictions of the characteristics of the flow surrounding a ship, other than its surface configuration and its local direction below the surface. Until that time comes the marine architect has recourse only to non-classified data available at testing establishments and in the technical literature.

Diagrams illustrating, for simple ship forms, the changes in and distribution of velocity or pressure, or both, are to be found in the papers listed hereunder. References which illustrate flow patterns as well as velocity and pressure distribution are duplicated from earlier sections of the present chapter:

(a) Two-dimensional ships having lenticular forms of waterline [Taylor, D. W., INA, 1894, Vol. 35, Figs. 24 and 25 on Pl. LXXV]. Adaptations of these original diagrams are to be found in S and P, 1933, p. 4 and in S and P, 1943, p. 6. In the original diagrams the plots are in terms of pressure heads for fixed speeds, on a basis of distance along and beyond the ship axis.
(b) Five 2-diml forebodies of ship-shaped stream forms, with waterlines delineated by the use of line sources and sinks in a uniform stream, are given by W. McEntee [SNAME, 1909, Vol. 17, pp. 185–187 and Figs. 5 and 6, Pls. 114, 115]. These figures embody curves of velocity ratio $(U_\infty + \Delta U)/U_\infty$ and of pressure head.
(c) A flow diagram for a 2-diml ship-shaped form midway between two walls, with an ideal liquid streaming by, is given by G. S. Baker and J. L. Kent [INA, 1913, Vol. 55, Part II, Fig. 5, Pl. IV]. It is supplemented by curves of pressure coefficients with x-distance from the bow for the streamlines at increasing lateral distance from the form.
(d) Bows and forward shoulders of 2-diml ships generated by line sources (and sinks) in a uniform stream. Curves of velocity and velocity head on a basis of distance along the ship axis are published by H. Föttinger [STG, 1924, Vol. 25, pp. 306–307; TMB Transl. 48, May 1952, pp. 14–15].
(e) Complete 2-diml ship with waterlines generated by bow and stern line sources in a uniform stream. Curves of Δp and ΔU along the ship axis are published by F. Horn ["Theorie des Schiffes," Handbuch der Physikalischen und Technischen Mechanik, Leipzig, 1930, Vol. V; reproduced in RPSS, 1948, p. 15].
(f) Three-dimensional ship having a lenticular form of waterplane, developed by D. W. Taylor [INA, 1895, Vol. 36, Fig. 7, Pl. XVI]. Reproduced later in S and P, 1933, Fig. 7 on p. 4, and S and P, 1943, Fig. 7 on p. 6.
(g) Three-dimensional model of a merchant ship of normal form, on which local pressure measurements were made by W. Laute ["Untersuchungen über Druck- und Strömungsverlauf an einem Schiffsmodell (Investigations of Flow and Pressure on a Ship Model)," STG, 1933, Vol. 34, pp. 402–460; TMB Transl. 53, Mar 1939]. There is a bibliography of 19 items at the end of this paper; some of them are quoted here.
(h) Eggert, E. F., "Form Resistance Experiments," SNAME, 1935, pp. 139–150
(i) Eggert, E. F., "Further Form Resistance Experiments," SNAME, 1939, pp. 303–330; abstracted in SBMEB, Apr 1940, pp. 162–164. Simultaneous pressure measurements were made with a multitude of orifices in the hull of a battleship model having a very large bulb bow.

Methods for determining the velocity at any point in the potential field around a schematic ship form are described by:

(1) Taylor, D. W., INA, 1894, Vol. 35, pp. 396–399
(2) Lerbs, H. W. E., "Die Verteilung der Verdrängungs Strömung neben der Schiffswand (The Distribution of the Displacement (potential) Flow Around the Hull of a Ship)," WRH, 7 Jul 1928, p. 263; TMB Transl. 85, Feb 1944.

Both these methods require rather drastic simplifications of the actual conditions for a ship. Method (1) calls for 2-diml flow throughout. Method (2) requires that the ship form be considered as a body of revolution generated by multiple sources and sinks, having a lateral plane corresponding to the ship waterplane. Neither method takes account of wave formation at the surface, displacement thickness of the boundary layer, possible separation zones, and other factors.

S. Yokota, T. Yamamoto, A. Shigemitsu, and S. Togino describe the "Pressure Distribution over

the Surface of the Ship and its Effect on Resistance" in Paper 789, presented before the World Engineering Congress in Tokyo in 1929. The complete paper is published in the Proceedings of this Congress, Vol. XXIX, Part 1, issued in Tokyo in 1931. The text in question is found on pages 293–318; Figs. 1 through 30, accompanying the paper, are published on pages 319–341.

These experimenters measured the distribution of pressure on the hull and the magnitude of the thrust at the thrust bearing on a self-propelled steel steam launch having a length between perpendiculars of 39.37 ft, an extreme beam of 9.79 ft, and a depth of 5.74 ft. The draft was about 3.99 ft, the trim was zero, and the depth of water for the test with the underwater propeller varied from 12.8 ft to 13.8 ft.

The total number of pressure orifices was 289, well distributed over the entire length of the launch. Each orifice had a diameter of 1 mm (0.04 in), and was connected by flexible tubing to one glass tube of a multiple-tube manometer which was photographed during the tests. However, it was found that those orifices lying above and in the vicinity of the actual wave profile when underway could not be used.

The speed of the launch was measured by a pressure speed log in the form of a standard pitot tube mounted forward of the bow, with its orifice 2.23 ft below the at-rest waterline and about 2.83 ft forward of the stem.

The launch could be driven by its own single, 3-bladed screw propeller or the underwater propeller could be removed and the launch be pushed by an engine-driven airscrew mounted above the deck. A dynamometer served to record the thrust in each case.

Attempts were made to photograph the wave profile from another boat running alongside but the actual wave-surface intersection at the hull was partly obscured by the wave crests beyond the hull. The wave profiles given in the report are those recorded in a model basin on a one-third scale model of the launch.

Tables accompanying the report give the individual pressure readings for a series of several speeds.

42.11 Pressure Distribution Along a Vee Entrance. The pressure coefficients for 2-diml flow along two flat plates, disposed symmetrically in V-fashion in a stream, like those on each side of the stem of a ship, have been calculated and plotted by H. Rouse and J. S. McNown. The results, derived by conformal transformation on the basis that the flow leaves the trailing edges of the plates tangentially, are shown in their paper "Cavitation and Pressure Distribution: Head Forms at Zero Angle of Yaw" [State Univ. of Iowa, Studies in Eng'g., Bull. 32, 1948, pp. 26–28]. These data, supplemented by J. S. McNown for included angles of the order of those encountered on actual ships, are diagrammed in Fig. 42.G.

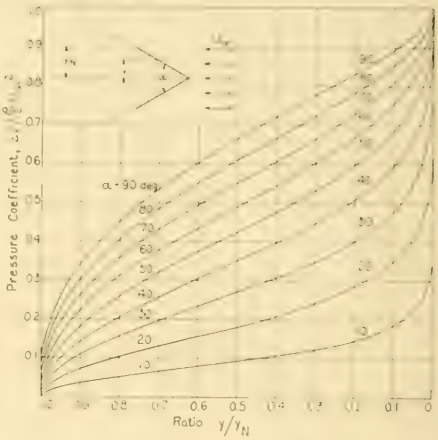

Fig. 42.G Graphs of Pressure Coefficient for Ideal Liquid Flow Along a Two-Dimensional Vee Entrance

The variation of $\Delta p/q$ from the vertex aft serves as an indication of the pressure distribution along the forward portion of the entrance of a simple ship, about as far aft as the forward neutral point. It is expected that these data may eventually be combined with others, possibly those derived from the Guilloton method, for a prediction or determination of the pressure distribution along the 2-diml waterline area of a ship hull of normal design.

This problem is treated by L. M. Milne-Thomson [TH, 1950, pp. 309–310], who obtains an expression for the drag on the pair of plates, with a cavity behind them. H. Lamb [HD, 1945, pp. 104–105] describes the analytic solutions of Rethy and Bobyleff, of 1879–1881, and gives a convenient table of pressure ratios for this system for entrance slopes from 0 to 170 deg.

42.12 Use of Doubly Refracting Solutions for Flow Studies. By a combination of polarized

light and doubly refracting colloidal solutions, mentioned in Sec. 5.6, it is possible to observe certain interesting and useful types of flow phenomena. The solution most commonly used in the past has been water with a finely ground clay called bentonite; the procedure is described briefly by C. H. Hancock [SNAME, 1948, p. 52]. B. Rosenberg, in TMB Report 617, issued in March 1952, goes into the fundamentals as well as the procedure. In this report there are listed 45 references on the subject.

One of these references, plus three others not in the list, are given here:

(1) Dewey, Davis R., II, "Visual Studies of Fluid Flow Patterns Resulting from Streaming Double Refraction," Dr. of Sci. Thesis, Dept. of Chem. Eng'g., MIT, 1941

(2) Takahashi, W. N., and Rawlins, T. E., "The Streaming Double Refraction of Tobacco Mosaic Virus," Science, 1937, Vol. 85, pp. 103–104

(3) Ullyott, Phillip, "Investigation of Flow in Liquids by Use of Birefringent, Colloidal Solutions of Vanadium Pentoxide," Trans. ASME, Apr 1947, pp. 245–251. A list of 23 references is given on pp. 248–249.

(4) Peebles, F. N., Garber, H. J., and Jury, S. H., "Preliminary Studies of Flow Phenomena Utilizing a Doubly Refractive Liquid," [Third Midwestern Conf. on Fluid Mech., Univ. of Minn., Jun 1953, pp. 441–454]. These authors describe similar tests made successfully with an organic dye. On pp. 451–452 they list 26 references on this subject, including the Dewey, Ullyott, and Rosenberg references mentioned previously.

42.13 Delineation of Flow Patterns by Electric Analogy. The story on velocity potential in Sec. 2.13 discusses rather briefly the parallel between velocity potential and electric potential. Diagram 1 of Fig. 2.P illustrates in schematic fashion the use of an electrolytic tank for delineating the equipotential lines around any body or surface in 2-diml streamline flow. Diagram 1 of Fig. 42.H indicates the essentials of the setup for delineating the flow around a 2-diml body of lenticular shape, utilizing a weak liquid electrolyte and direct current passing between the rows of electrodes at the ends of the tank. If the latter is of area sufficiently large compared to that of the body around which the flow is being studied, it is possible to replace the separate electrodes, connected to resistances so as to pass equal amounts of current, by single-plate electrodes. When the equipotential lines are delineated by the probe method it is necessary to sketch in the streamlines by hand, utilizing the principles of the flow net. This means that the streamlines must cross the equipotential lines everywhere at right angles.

Diagram 2 of Fig. 42.H shows how this method is used to trace the streamlines directly. This is accomplished by passing the current across the flow, as it were, and shaping the body out of a conducting rather than a non-conducting material.

Three-dimensional axisymmetric flow is represented by using a tank having a cross section corresponding to one sector of the axisymmetric flow field, like a narrow sector cut out of a log. Diagram 3 of Fig. 42.H illustrates such an arrangement, with the current passed in the direction of flow and the body a nonconductor.

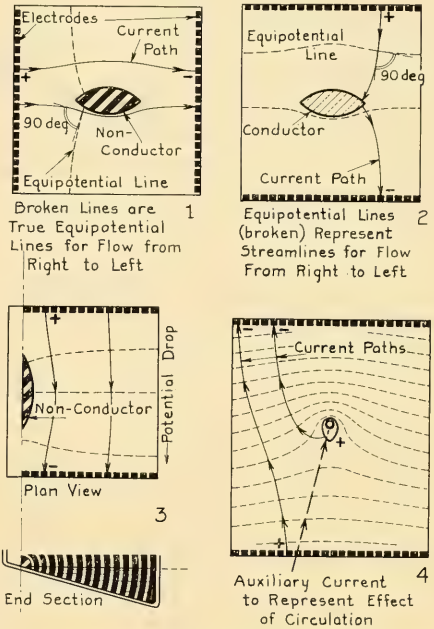

Fig. 42.H Schematic Diagrams of Electrolytic Tank Arrangements to Determine Streamlines and Equipotential Lines Around Bodies

Before 1928, as described in reference (2a) of Sec. 42.14, G. I. Taylor and C. F. Sharman showed that irrotational flow *with circulation* could be represented and delineated in a simple electrolytic setup by feeding some current into the body representing the foil around which circulation is taking place. The current entering one boundary plate is that passing out of the

opposite plate *plus* that being fed into the foil, between the plates. In diagram 4 of Fig. 42.H, traced from one published by H. Föttinger [STG, 1924, Fig. 43, p. 338], the foil is replaced by a small heart-shaped body and the flow resembles that delineated for the Magnus Effect in Fig. 14.E. An auxiliary direct current of the proper amount is fed into the body. This is easily done by connecting it to the source that supplies the row of positive electrodes, and interposing a variable resistance in the circuit of the body. The current from the body flows in the manner shown toward the row of negative electrodes. It pushes aside, as it were, the current paths from the row of positive electrodes. This setup produces equipotential lines which are actually the streamlines of a combination of counter-clockwise circulatory flow around the body and a streamline flow from the right; see Figs. 14.E and 14.F.

The electrolytic-tank technique has now expanded and developed to the point where it needs its own book. All that can be done here is to give a list of the principal references so far unearthed, in generally chronological order, and leave the reader to further study by himself. Comments are appended to some of the references.

42.14 Bibliography on the Electric Analogy for Flow Patterns. In this section there are listed a number of the principal references to the rather extensive literature on the employment of the electric analogy for delineating streamline, equipotential, and other flow patterns.

(1) Relf, E. F., "An Electrical Method of Tracing Streamlines for the Two-Dimensional Motion of a Perfect Fluid," Phil. Mag., Sep 1924, Vol. 48, pp. 535–539; see also ARC, R and M 905, 1924

(2a) Taylor, G. I., and Sharman, C. F., "Problems of Flow in Compressible Fluids," Proc. Roy. Soc., London, Series A, 1928, Vol. 121; also ARC, R and M 1195, Aug 1928

(2b) Taylor, G. I., "The Flow Round a Body Moving in a Compressible Fluid," Proc. Third Int. Cong. Appl. Mech., Stockholm, 1930, Vol. I, pp. 263–275, esp. pp. 265–272

(3) Koch, J. J., "Eine Experimentelle Methode zur Bestimmung der Reduzierten Masse des Mitschwingenden Wassers Bei Schiffsschwingungen (Experimental Method for Determining the Virtual Mass for Oscillations of Ships)," Ing.-Archiv, 1933, Vol. IV, Part 2, pp. 103–109; TMB Transl. 225 of May 1949

(4) Malavard, L., "Application des analogies électriques à la solution de quelques problèmes de l'hydrodynamic (Application of Electrical Analogies to the Solution of Some Hydrodynamic Problems)," Publ. Sci. et Tech., Min. de l'Air, Paris, No. 57, 1934

(5) Salet, G., "Détermination des pointes de tension dans les arbres de révolution soumis à torsion au moyen d'un modèle électrique (Determination of Tensile Stress in Revolving Shafts under a Torsional Load, by Means of an Electric Model)," ATMA, 1936, Vol. 40, pp. 341–351. This paper illustrates and describes an electrolytic tank which is, in effect, a 3-diml affair, inasmuch as the body in the tank has varied depths of electrolyte over it.

(6) Pérès, J., and Malavard, L., "Application du bassin électrique à quelques questions de mecanique des fluides (The Application of Electric Flow in Liquids to Some Questions of the Mechanics of Fluids)," ATMA, 1938, Vol. 42, pp. 529–541. This paper, so far as known, is not translated into English. A number of references are listed on pp. 529, 531, and 534.

The authors go into the question of the use of the electrolytic tank for flow problems involving circulation.

In the same volume, in a paper by Igonet, Plate 3 on p. 551, there is shown a group of equipotential spots for a 3-diml Rankine ellipsoid.

(7) Malavard, L., "Étude de quelque problèmes relévant de la théorie des ailes. Application à leur solution de la methode rhéoélectrique (Study of Problems Relevant to the Theory of Wings. Application of the Rheo-Electric Method to Their Solution)," Publ. Sci. et Tech., Min. de l'Air, Paris, No. 153, 1939

(8) Pérès, J., and Malavard, L., "Rheographic and Rheometric Analog Methods," (in French), Bull. Soc. Fr. Elec., 1939, Vol. 8, pp. 715–744

(9) Malavard, L., and Pérès, J., "Tables numériques pour le calcul de la répartition des charges aérodynamiques sur l'envergure d'une aile (Numerical Tables for the Calculation of the Distribution of Aerodynamic Loads On the Span of a Wing)," Tech. Rep. 9, Group. Français pour les Récherches Aero., 1943

(10) Malavard, L., "Sur la solution rhéoélectrique de questions de representation conforme et application à la théorie des profils d'ailes (On the Rheo-Electric Solution of Questions of Conformal Representation and Application to the Theory of Wing Profiles)," Comptes-Rendus, Acad. Sci., Paris, Jan 1944

(11) Siestrunck, R., "Sur un mode de solution rhéoélectrique des problèmes de l'hélice propulsive (On a Rheo-Electric Method of Solution of Screw-Propeller Problems)," Comptes-Rendus, Acad. Sci., Paris, Sep 1944

(12) Malavard, L., and Siestrunck, R., "Sur une methode d'étude des grilles indéfinies de profils quelconques (On a Method of Study of Undefined Flow Nets Around any Profile)," Cong. Nat. Aviat. Française, Apr 1945

(13) Malavard, L., "Application aérodynamique de calcul expérimental analogique (Aerodynamic Application of Experimental Analogy Calculations)," Cong. Nat. Aviat. Française, Apr 1945

(14) Malavard, L., "Calculateur d'ailes et réseau de

résistances lineaire pouvant remplacer, dans certaines questions, le bassin électrique (Calculations of Linear Wing and Network Resistances which can be Performed, in Certain Cases, in the Electrolytic Tank)," Comptes-Rendus, Acad. Sci., Paris, Jul 1945

(15) Siestrunck, R., "Sur les corrections de parois dans les essais d'hélices (On Wall-Effect Corrections in Screw-Propeller Tests)," Comptes-Rendus, Acad. Sci., Paris, Sep 1945

(16) Siestrunck, R., "Sur le calcul des hélices ventilateurs (On the Calculation of Propeller-Type Fans)," Comptes-Rendus, Acad. Sci., Paris, Sep 1945

(17) Pérès, J., and Malavard, L., "Sur la détermination des corrections de soufflerie (On the Determination of Blowing-Pressure Corrections)," Comptes-Rendus, Acad. Sci., Paris, Sep 1945

(18) Marchet, P., "Détermination des lignes de jet dans les mouvements plans et de révolution (Determination of Streamlines in Two- and Three-Dimensional Flow)," Problème D359A, Travaux du Laboratoire de Calcul Expérimental Analogique, under the direction of L. Malavard

(19) Pérès, J., Malavard, L., and Romani, L., "Problèmes non lineaires de la théorie de l'aile. Application à la détermination du maximum de portance (Non-Linear Problems of the Theory of Wings. Application to the Determination of Maximum Load)," Rep. Tech. Group. Français pour les Récherches Aero.

(20) Malavard, L., "The Use of Rheo-Electrical Analogies in Certain Aerodynamic Problems," Jour. Roy. Aero. Soc., Sep 1947, Vol. 51, No. 441, pp. 739–756. This is an excellent paper, with many photographs and diagrams illustrating the technique and the results.

(21) Hubbard, P. G., "Application of the Electrical Analogy in Fluid Mechanics Research," Rev. Sci. Inst., Nov 1949, Vol. 20, pp. 802–807; also State Univ. Iowa, Reprints in Eng'g., Reprint 82

(22) Surugue, J., "Techniques générales du laboratoire de physique (General Techniques of the Physics Laboratory)," edition of CNRS, Paris, 1950, Vol. II. Chap. 15 contains a discussion by L. Malavard on "Les Techniques des Analogies Électriques (Electric Analogy Technique)."

(23) Rouse, H., EH, 1950, pp. 20–22 and Figs. 17, 18

(24) Markland, E., and Hay, N., "The Potential Flow Tank," Engineering, London, 7 Mar 1952, pp. 292–294

(25) Borden, A., Shelton, G. L., Jr., and Ball, W. E., Jr., "An Electrolytic Tank Developed for Obtaining Velocity and Pressure Distributions About Hydrodynamic Forms," TMB Rep. 824, Apr 1953.

A concise but comprehensive treatment of "Electroanalogic Methods" is given by T. J. Higgins, covering many methods other than the electrical-tank analogue described here [Appl. Mech. Rev., Jan 1956, pp. 1–4]. Part I of this paper, devoted to "Solution of Electrical Problems by Continuous-Type Conductive Procedures," carries at its end a huge array of 111 references, a few of which are to be found in the preceding list. Part II of this paper, entitled "Solution of Continuum-Mechanics Problem by Continuous-Type Conductive Procedures," is supplemented by an even more massive list of 203 references, some of which are also to be found in the preceding list [Appl. Mech. Rev., Feb 1956, pp. 49–55].

CHAPTER 43

Delineation of Source-Sink Flow Diagrams

43.1 General. Secs. 3.8 through 3.13 contain a description and discussion of radial flow and the source and sink, the radial stream function and velocity potential, and other features of source-sink flow. Figs. 3.M through 3.P illustrate a variety of simple stream forms resulting from a graphic combination of the stream functions of uniform and of radial flow. The present chapter contains instructions for drawing many kinds of stream forms and for delineating graphically the flow patterns around them. In Secs. 41.8 and 41.9 there are a few typical formulas for calculating the coordinates of some simple stream forms rather than plotting them graphically. Both sets of sections tell how these constructions and formulas lead to a determination of the velocities and pressures around the forms.

It has been true in the past, and perhaps may be for some time to come, that the stream forms and streamline patterns created in this way have found and will find infrequent use in practical naval architecture, as contrasted to their frequent occurrence in analytic investigations and their use in the development of underwater non-ship forms. Nevertheless, a knowledge of the mechanics of drawing source-sink flow patterns and some experience in drawing them gives one an insight into and a working knowledge of certain phases of hydrodynamics that can not be obtained in any other way. A parallel case is experience in the construction of flow nets. Literally, the marine architect who expects a knowledge of hydrodynamics to serve him should know how to draw source-sink stream forms and flow patterns. Frequent application of this "know how" will greatly expand the usefulness of source-sink or radial-flow knowledge in his work.

43.2 Delineation of Two-Dimensional Stream-Form Contours and Streamlines Around a Single Source in a Stream. Notwithstanding that for every source there must theoretically be a corresponding sink of equal strength, the plotting of the flow around a single 2-diml source in a uniform stream is first described as a preliminary to subsequent operations. For the time being it may be assumed that the companion sink lies at an infinite distance downstream. The plotting method is a single-step combination of the "radial" stream functions for the source and the "parallel" functions for the uniform stream.

Lay down first a set of radial equidifferent stream-function lines for the source. It is convenient, for reasons which appear presently, to have two of these radial lines lie on the customary x- and y-axes, and to place the uniform stream parallel to the x-axis, as in Fig. 43.A. The four quadrants around the source are then each divided into a suitable number of equal arcs by the remaining radial stream-function lines. The stream functions from the source, identified as ψ_{SO}(psi), are then marked with any convenient set of *positive* numbers, in this case 4 through 28,

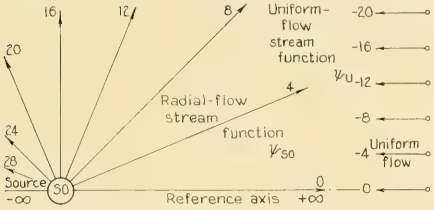

Fig. 43.A Uniform-Flow and Radial-Flow Stream Functions for a 2-Diml Source

starting with 0 at the positive x-axis and going around *both ways* to 32 at the negative x-axis. Only those lines above the x-axis are shown in the figure.

Off to the right draw the stream comb for the uniform flow and assign suitable equidifferent values, marked from $\psi_U = 0$ through $\psi_U = -20$ in Fig. 43.A. The negative signs for the uniform flow signify liquid moving opposite to the positive direction of the x-axis. The stream comb is then extended to the left to form the horizontal *straight-line* portions of Fig. 43.B. In this and succeeding layouts the lower half of the diagram, that is, the mirror image of the upper half, is omitted to save space.

The horizontal line extending from $-\infty$ through the source to $+\infty$, coinciding with the x-axis, represents the trace of the reference plane for the flow diagram to be constructed. If four radial vectors are drawn from SO, between the lines $\psi_{SO} = 0$ and $\psi_{SO} = +4$, they represent schematically the four units of the quantity rate of flow from the source in that sector. If four parallel vectors are drawn between the trace of the reference plane, in the x-axis, and the horizontal line $\psi_U = -4$, they represent in the same manner the quantity rate of flow in that part of the stream. These eight vectors are drawn in broken lines in the figure. The two flows, in which the quantity rates are each numerically equal to 4, buck each other along the region AB in Fig. 43.B. At the intersection B of the radial line $\psi_{SO} = +4$ and the horizontal line $\psi_U = -4$, the resultant stream function value is zero. Assuming for the moment that the reference plane is impenetrable, the uniform flow between the x-axis and $\psi_U = -4$ is deflected upward. There is established a line $\psi_S = 0$ between A and B, across which no liquid passes.

The liquid in the uniform stream ψ_U, in quantity rate equal to -4, turns upward as indicated by the full-line vectors beyond B. It then goes through a gap where the algebraic sum of the radial and uniform-stream functions is equal to -4. Such a gap is that portion of the radial line $\psi_{SO} = +4$ represented by the segment BF, lying between the parallel horizontal lines whose stream functions ψ_U are -4 and -8, respectively. The original four units of liquid in the parallel flow turn up through this gap and cross the line BF. At the point F, therefore, the stream function ψ_S of the combined flow is equal to -4. The four units of liquid in the radial flow turn upward *inside* the point B.

The second four units of uniform flow, between $\psi_U = -4$ and $\psi_U = -8$, now approaching a new barrier at F, turn up between F and J, whereupon the point J lies on the new streamline $\psi_S = -8$.

If the procedure just described is followed for

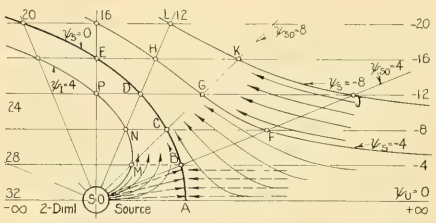

Fig. 43.B Combination of Uniform Flow With Radial Flow From a 2-Diml Source

groups of eight liquid units instead of four, a point C is established at the intersection of $\psi_{SO} = +8$ and $\psi_U = -8$ where the resultant stream function value ψ_S is again zero. There is also found a point G where the stream function of a new series is $\psi_S = -4$ and a point K where $\psi_S = -8$.

A whole pattern of intersections is thus quickly determined, at which the stream functions ψ_S of the third series are equal to the algebraic sums of those of the second and the first series. For example, at E it is found that $\psi_U = -16$ and $\psi_{SO} = +16$, so this point is on the line $\psi_S = 0$. At L, $\psi_U = -20$ and $\psi_{SO} = +12$, so this is a point on the streamline $\psi_S = -8$.

The various points so determined are all intersections of radial stream-function lines having values greater than the uniform stream-function lines by increments equal to the value of the new stream function ψ_S. This means that the parallel stream flow that lay below $\psi_U = -4$ at infinity

now flows across the radial segments BF, CG, DH, and so on. A fair line joining the points B, C, D, and E becomes the streamline or boundary where $\psi_S = 0$. Another line through F, G, H, and corresponding points becomes the streamline where $\psi_S = -4$. A line joining J, K, L becomes the streamline $\psi_S = -8$.

If the same construction is followed *inside* the line BCDE, the radial flow preponderates at the point M, where $\psi_U = -4$ and $\psi_{SO} = +8$, whereupon $\psi_{SO} = +8$ plus $\psi_U = -4$ becomes $\psi_I = +4$. Similarly, at N, $\psi_{SO} = +12$ and $\psi_U = -8$, whence $\psi_I = +4$. A streamline representing $\psi_I = 4$, for *internal* flow, is then drawn from the source through M, N, P, and a corresponding series of intersections. The four radial broken-line vectors, each representing unity quantity rate of liquid, originally lying below the line $\psi_{SO} = +4$, turn upward and to the left as they pass between the boundary BCDE and the inside streamline $\psi_I = 4$.

If all the liquid issuing from the source SO and doubling back inside the boundary BCDE freezes into ice, or is otherwise suddenly solidified, the flow outside that boundary remains exactly the same as defined by the streamlines of the ψ_s-system.

By following this extremely simple and straightforward construction in both quadrants above the reference plane, and then adding its mirror image *below* that plane, the ovoid-shaped bounding surface ABCDE . . . is extended to any desired limit downstream. All the streamlines around it can be sketched through the respective series of intersections by the process of adding the stream functions algebraically and joining the points having equal ψ_S values, as in Fig. 43.B. As few or as many radial and parallel stream function lines are drawn as may be desired. The more are drawn, the more intersections are found and the more accurately is the body defined and the resulting stream pattern delineated. Filling in stream-function lines at intervals of unit quantity rate in Fig. 43.B instead of in increments of four units would give sixteen times as many intersections and four times as many streamlines as are shown there.

The width of the ovoid-shaped boundary opposite the source is equal to the uniform-stream-function position for a value corresponding to the radial-stream-function number at 90 deg from the stream direction. Therefore, to make the solid boundary half as wide as in Fig. 43.B, a source is chosen with a radial stream function $\psi_{SO} = +8$ at 90 deg, instead of $\psi_{SO} = +16$ as shown. Similarly, the uniform-flow stream function ψ_U, if given values twice as great, produces a body only half as wide. It is to be noted particularly, in this and other applications subsequently described, that the velocity of the uniform flow can be increased without changing the shape of the form represented by $\psi_S = 0$ if the radial-flow velocity is increased in the same ratio. This is equivalent to multiplying or dividing all stream functions in Fig. 43.B by the same factor; the form contour and the various streamlines in the diagram remain the same.

The solid boundary around a single source in a uniform stream in 2-diml flow continues to widen with distance downstream so that it is of limited practical application to ship design. However, Secs. 41.9 and 67.7 tell how a 3-diml single source in a uniform stream may be used to delineate an underwater bulb shape for the bow of a ship. The solid boundary around a source *and* adjacent sink in uniform flow is closed and of oval shape, resembling some parts of a ship. Because of the ease with which 2-diml streamlines are constructed around it, this body serves well as a simple ship form, by which to explain and depict many kinds of flow phenomena.

43.3 Graphic Construction of a Two-Dimensional Flow Pattern Around a Source and a Sink. The construction of a solid boundary surface and a streamline diagram for a 2-diml source *and* a 2-diml sink placed in a uniform stream involves one more step than the procedure described for a single source. It is convenient, as before, to take up each of the steps separately. They are simple graphic operations which, when once learned, are easily and rapidly performed.

Let the horizontal line from $-\infty$ to $+\infty$ in Fig. 43.C, passing through the source and the sink and coinciding with the x-axis, represent the trace of the reference plane for the 2-diml uniform-stream flow. The y-axis is midway between the source and the sink. Using separate sheets of tracing cloth, or other suitable transparent material, lay down orthogonal axes in the center of each sheet. In each of the four quadrants draw an equal number of uniformly spaced radial lines, representing equidifferent radial stream functions. Series of numbers differing by 2 or 4 are used generally in the present chapter but any series is permissible.

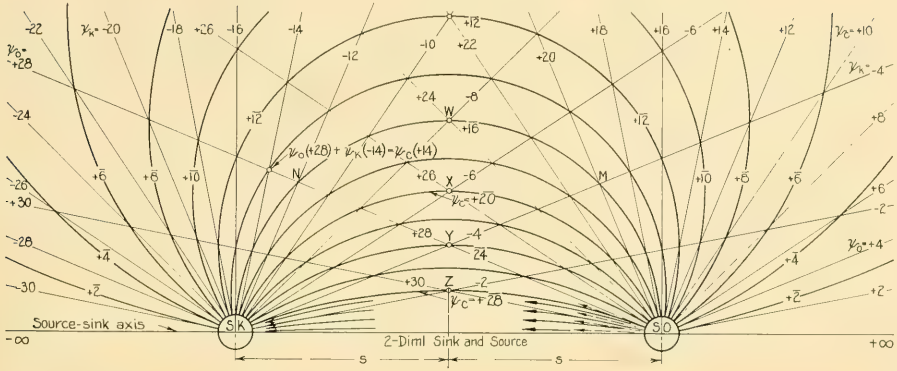

Fig. 43.C Radial Stream Functions for a 2-Diml Source-Sink Pair and the Resultant Stream Functions

Leave a clear space at the center of each sheet where the lines would otherwise be crowded together. One way is to use large circles for the source and sink. Extend the radial lines as far as the drawing area permits or requires. The radial flow from the source is designated as the ψ_{SO}- or ψ_O-system; that from the sink as the ψ_{SK}- or ψ_K-system. Number the radial lines around both source and sink, starting with zero at the reference line in the positive x-axis on the right and increasing numerically *both* ways to the negative x-axis. This applies both to the diagram shown and its mirror image. As previously mentioned, any convenient set of equidifferent numerical values may represent the outflowing and inflowing stream functions, but the sets must be identical. The lines $\psi_O = 0$ and $\psi_K = -0$ both lie over the reference trace and point toward the source of the uniform-stream flow and opposite to its velocity vectors. The lines radiating from the source are marked with positive signs to indicate positive stream functions, while those pointing toward the sink are marked with negative signs.

With the reference-plane trace as a base, superpose these separate radial-flow diagrams with their centers at the selected source and sink positions. Fasten the source and sink sheets in place, then over both diagrams lay a third sheet of tracing paper or cloth, or other transparent material, upon which the straight reference line is drawn and the source-sink positions are marked. The lines visible through the top sheet then appear as the *straight-line* portions of Fig. 43.C.

The next step is the construction of the flow pattern representing the liquid movement from the source to the sink. For this purpose it is more convenient to start from the axis between the source and sink instead of from the axis stretching to the right from the source.

Considering four units of liquid emanating from the source in the sector between the horizontal reference line and the radial-stream-function line $\psi_O = +28$, represented by the four broken-line vectors, these units must enter the sink between the reference line and the radial line $\psi_K = -4$. Where the stream-function line $\psi_O = +28$ crosses the line $\psi_K = -4$, at the point Y, the value of the resultant stream function $\psi_C = +28 + (-4) = +\overline{24}$. The numerical stream-function values of the ψ_C system are distinguished by single bars over the numerals. However, the four liquid units flowing out of the source and into the sink, corresponding to the full-line curved vectors shown, actually pass between the point Z, where $\psi_C = +\overline{28}$, and the reference trace. Whereas the streamline $\psi_C = +\overline{28}$ is tangent to the radial line $\psi_O = +28$ at the source and to $\psi_K = -4$ at the sink, this streamline moves downward or inward, away from those lines, as the distance from the source or sink increases. In other words, instead of passing through Y it passes through Z.

The intersections of other parts of radial lines along a perpendicular to the reference line, midway between the source and sink, occur at the points marked Y, X, and W, where the values of ψ_C are $+\overline{24}$, $+\overline{20}$, and $+\overline{16}$, respectively. Two other points, M and N, on the streamline $\psi_C = +\overline{16}$, are given by the intersection of

$\psi_o = +20$ plus $\psi_K = -4$ equals $\psi_c = +\overline{16}$, as well as by $\psi_o = +28$ plus $\psi_K = -12$ equals $\psi_c = +16$. These permit the streamline $\psi_c = +16$ to be drawn, remembering that, like the first one described, it is tangent to the radial line $\psi_o = +16$ at the source and the line $\psi_K = -16$ at the sink.

Actually, for 2-diml flow between a source-sink pair, all the streamlines of the ψ_c series are *circles* which pass through the source and sink centers. These circles have a radius of s cosec θ(theta), where s is the half-distance between source and sink, and θ is the angle between (1) the radial stream function *at the source* for which the circle is drawn and (2) the reference axis. Considering the radial source streamline $\psi_o = +16$, θ is $\pi/2$ or 90 deg and cosec $\theta = 1$; the radius of the circle for $\psi_c = +\overline{16}$ is therefore s, half the distance from the source to the sink. This particular circle has its center on the reference line and is tangent to the radial streamlines $\psi_o = +16$ and $\psi_K = -16$ at the source-sink axis. When extended below the source-sink axis in the diagram, this circle becomes the stream function $\psi_c = +\overline{16}$ on that side. Similarly, all other circles extended below the axis become what might be termed supplementary streamlines in that region. For example, the streamline for $\psi_c = +\overline{4}$ above the reference line and $\psi_c = +28$ below it are parts of the same circle. Numerically, the stream function for these two parts of any complete circle total 32, the same value as for half of either the source or the sink. The centers of the circular streamlines fall on intersections already given by the radial-flow lines in the diagram, because if the quadrants are divided into a whole number of sectors, there is always a radial stream-function line from the source at right angles to another line from the sink. For example, since the circular streamline $\psi_c = +\overline{12}$ is tangent to $\psi_o = +12$ at the source, its center lies on the line $\psi_o = +28$, where 12 + 16 (for one quadrant) = 28.

On this basis, and with the additional intersections on the diagram, the remainder of the circular streamlines are drawn. Whereas these lines are approximately equidistant from each other at the source and sink centers, they become increasingly farther apart at greater and greater distances from the source and sink, because of the slowing down of the liquid in the widening crescent-shaped sectors. However, once drawn by subdividing each quadrant into a given number of sectors, the circular stream pattern *never* changes for any change in source-sink strength or spacing. Once carefully drawn, it can be enlarged or reduced photographically to suit the source-sink spacing. The numbers on it are altered to suit the source-sink strengths.

This completes the first step in the operation. The second step is the combination of this circular source-to-sink flow pattern with the 2-diml uniform-flow pattern parallel to the reference plane. The uppermost sheet of tracing cloth or paper containing the circular-streamline pattern of the ψ_c system is now transferred and superposed on a sheet which has parallel streamlines of the uniform flow drawn on it. Following this, the ψ_U flow is combined with the ψ_c flow by adding the ψ_c and the ψ_U stream functions algebraically where the streamlines cross each other. For example, in the right-hand portion of Fig. 43.D,

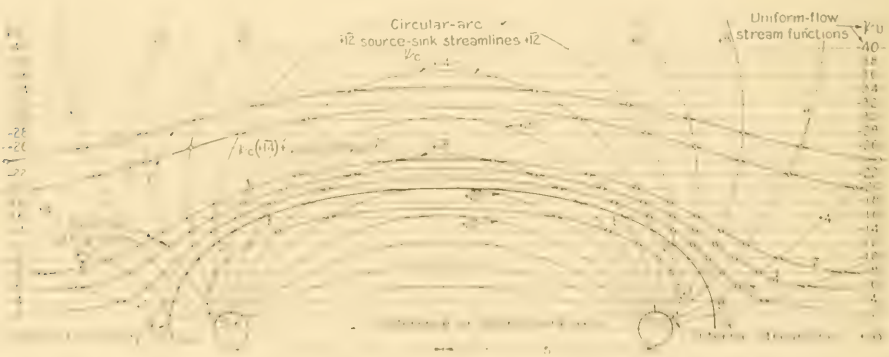

Fig. 43.D Rankine Stream Form and Surrounding Stream Flow Resulting From Insertion of a 2-Diml Source-Sink Pair in a Uniform Stream

at the intersection B of the circular stream-function line $\psi_C = +\overline{4}$ and the uniform-flow stream function line $\psi_U = -4$, the resultant flow is zero. Therefore B is a point on the boundary of the Rankine body to be formed. There is a second, and corresponding point B for $\psi_S = 0$ at the left of the sink. At the intersections of the circles $\psi_C = +\overline{8}$, $+\overline{12}$, and $+\overline{16}$ with the parallel-flow lines $\psi_U = -8$, -12, and -16, respectively, the pairs of points C, D, and E are found, all on the stream-form boundary.

A streamline through the lettered points where $\psi_S = 0$, passing through the stagnation points Q and embracing the lower or mirror image as well as the upper half of the flow diagram, forms an oval-shaped stream form or Rankine body. The flow pattern around this body is constructed by drawing the streamlines for the functions $\psi_S = -\overline{\overline{2}}$, $-\overline{\overline{4}}$, $-\overline{\overline{6}}$, and so on, using the method described for the single source. The resulting body shape and flow patterns are illustrated by the heavy lines of Fig. 43.D. Points near amidships along the body boundary are determined by drawing intermediate streamlines which are radial, circular, and parallel, or they may be determined by calculation, whichever may be found most convenient. The necessary formulas are listed in Sec. 41.8.

Flow from the source to the sink also takes place *within* the boundary of the Rankine body, depicted by the stream-function line $\psi_I = +2$ in the figure. This inside liquid can be considered as solidified and the flow neglected.

The length of the oval-shaped form is partly adjusted but not wholly controlled by the spacing $2s$ between the source and the sink. Its length-beam or fineness ratio is a function of the relative strength of the source-sink flow and the uniform-stream flow. The absolute size of the form is largely a function of the scale upon which the diagram is laid out.

With relatively simple radial- and uniform-flow diagrams made up beforehand on translucent or transparent material, the delineation of a stream form and its surrounding 2-diml flow pattern is a much shorter and easier task than might appear from the detailed description just given. In fact, with a little practice, the freehand sketching of the form and the flow pattern is the work of only an hour or two. Figs. 3.O of Sec. 3.11 in Volume I and 43.G of Sec. 43.5 are examples of this procedure. If the stream-form shape and proportions are not suitable for the work in hand, a new form is as quickly sketched, using different relative strengths for the several flows. The *shape* of the stream form is preserved while changing its velocity relative to the uniform stream by the simple expedient of increasing or decreasing *all* the velocities and stream functions by the same factor. The oval "ship" thus retains its form while changing its speed through the liquid.

43.4 Graphic Determination of Velocity Around Two-Dimensional Stream Forms. The magnitude and direction of the resultant velocity in the streamline field ψ_S is determined in a simple graphic manner, originating with W. J. M. Rankine. By this method the velocity vectors of the separate flows are combined to give a resultant velocity vector of the streamline flow. The interrelation between the composition of stream functions and liquid velocities for 2-diml flow is explained in Secs. 2.11 and 2.14 and illustrated in Figs. 2.L and 2.Q of Volume I. Fig. 43.E diagrams

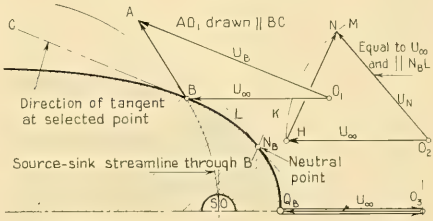

Fig. 43.E Diagram Illustrating Graphic Method of Determining Resultant Velocities for 2-Diml Flow

the graphic method for the example of Fig. 43.D, as applied to several points around the body.

Take first the body point B in Fig. 43.E. A uniform-flow velocity vector $-U_\infty$ is laid off at O_1B, parallel to the reference axis. From B a line is drawn toward A, tangent to the circular or source-sink streamline of the ψ_C system passing through B. The latter is shown by the light circular arc in the diagram. From B a line BC is drawn, tangent to the body surface at B. From O_1 a line O_1A is drawn parallel to the body-surface tangent BC, cutting the line from B which is tangent to the circular-arc streamline. The velocity U_B at the point B is then defined by the vector O_1A. For any point on a streamline in the field *away* from the body, the procedure is exactly the same, considering the streamline as the surface of a new body.

When the resultant velocity U_B is known at a selected point, the corresponding Δp is found by the relationships $\Delta p = 0.5\rho(U_B^2 - U_\infty^2)$ and $\Delta p/q = [1 - (U_B/U_\infty)^2]$, described previously in Sec. 41.12. Values of the pressure coefficient corresponding to various combinations of velocities squared, in English units, for liquids of any mass density ρ(rho), are given in Table 41.c of Sec. 41.13, on page 27.

The forward neutral point N_B occurs at a point in the surface where the streamline velocity U_N, represented by the vector O_2N in Fig. 43.E, equals in magnitude the uniform velocity $-U_\infty$, represented by the vector O_2H. By striking an arc on O_2 as a center, using the radius $O_2H = U_\infty$, it is known that the extremity of the vector O_2N lies somewhere on the arc HM. It is also known that:

(1) The streamline-velocity vector O_2N is parallel to the tangent N_BL at the body surface, at the proper location of the neutral point N_B

(2) The vector HN is parallel to a tangent to the arc N_BK, which represents a portion of the circular-arc source-sink streamline of the ψ_C-system through N_B, where that arc crosses the body boundary.

By a process of trial and error a point N_B on the body surface is found where the necessary conditions are met [Rankine, W. J. M., Phil. Trans. Roy. Soc., 1871, Vol. 161, p. 305, where Rankine calls the neutral point "the point of no disturbance of pressure"].

The use of Rankine's graphic method gives a neat solution for the conditions at the stagnation points Q_B and Q_S, where it is known that the resultant velocity is directed normal to the body surface. At Q_B, for example, the circular-stream-function lines of the ψ_C-system are directed ahead, opposite to the uniform-flow line $\psi_U = 0$. Therefore, at this point the circular-stream velocity vector Q_BO_3 is equal to the vector U_∞ in magnitude but is of opposite sign, hence the resultant velocity at Q_B is zero.

At the midsection of the stream form or Rankine body, and abreast it, the graphic method described in the foregoing breaks down. The circular-flow velocity vectors are parallel to the uniform-flow vectors and the intersection corresponding to A in Fig. 43.E is indeterminate.

43.5 Laying Out the Two-Dimensional Flow Pattern Around Two Pairs of Sources and Sinks in a Uniform Stream. The 2-diml Rankine stream form resulting from the combination of uniform flow with the "circular" flow between one source-sink pair is often too blunt to represent the nose of a body or the bow of a ship, even schematically. This bluntness is modified by the addition of a second source-sink pair on the same axis, placed farther apart than the main pair, and having somewhat less strength [Rankine, W. J. M., INA, 1870, p. 178]. The construction of the body shape and the flow pattern involves four steps as compared to the two of the previous section, but the procedure for each is equally straightforward. An example is worked out here to illustrate the method, using a main source-sink pair, each having a total quantity rate of flow of 128 units, and an auxiliary pair, each having a flow of 32 units.

First, a stream-flow diagram representing the "circular" ψ_{C1}-system flow between the primary source and sink is constructed. When drawn by the method described in Sec. 43.3 and illustrated in Fig. 43.C, one-quarter of it has the appearance of diagram 2 of Fig. 43.F. Second, a stream-flow

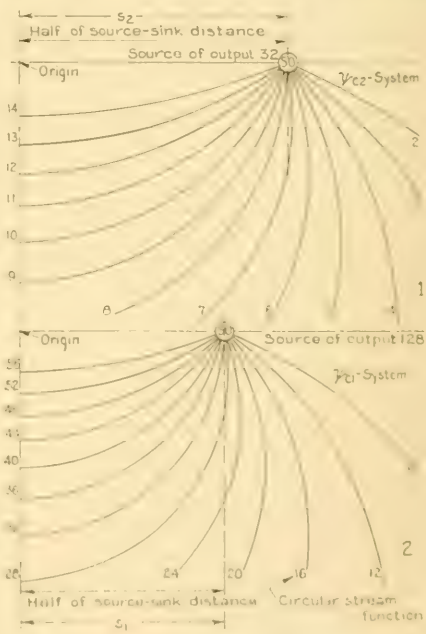

Fig. 43.F Source-Sink Streamlines for Two Source-Sink Pairs of Different Output and Different Axial Spacing

diagram representing the ψ_{C2}-system flow between the secondary source and sink is prepared, by the same method. When completed, one-quarter of it appears like diagram 1 of Fig. 43.F.

It is possible to use the same basic radial diagrams for constructing the circular streamlines associated with the two sets of sources and sinks by assigning to them different radial stream-function values. However, both the ψ_{C1} and ψ_{C2} diagrams must be drawn with lines sufficiently heavy to make them visible through each other and through the sheet carrying the ψ_{C3} diagram, subsequently to be placed on top of them. When the ψ_{C1} and ψ_{C2} diagrams of the primary and secondary source-sink flows are finished and superposed, with the sources and sinks at the distances s_1 and s_2, respectively, from the origin, a third flow diagram is constructed by adding the two sets of "circular" stream functions to form a composite diagram for the two pairs, called for convenience the ψ_{C3} stream-function system. It is shown by the curved broken lines of the freehand sketch of Fig. 43.G, radiating from the two sources.

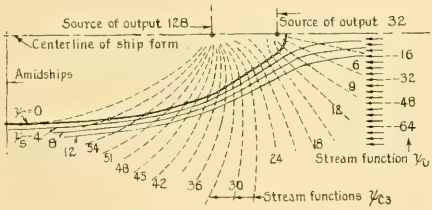

Fig. 43.G Freehand Sketch of Source-Sink Streamlines for Two 2-Diml Source-Sink Pairs, Form of Body When Inserted in Uniform Flow, and Resultant Streamlines

As a fourth and final step, the ψ_{C3}-system is combined with the uniform flow ψ_U-system to produce a stream form $\psi_S = 0$, indicated by the heavy line of Fig. 43.G. This has definitely more pointed ends than the 2-diml body which would be produced by either primary pair alone.

The exact shape of the ends of a body such as that delineated in Fig. 43.G depends upon the strengths of the secondary source and sink and the relative locations selected for them. A great variety of body shapes can be drawn in a surprisingly short time, simply by assigning different stream functions to the radial and parallel flows and changing the source-sink spacing by tacking down the inked radial diagrams in different positions along the source-sink axis.

To make the bow and stern even more pointed a tertiary source-sink system may be added near the extreme ends. The graphic construction of such a form and the streamline pattern around it, involving as it does the six steps listed hereunder, is admittedly tedious but it is readily done for special studies if the results are worth while. These six steps are:

(1) Flow between primary source and sink, ψ_{C1}
(2) Flow between secondary source and sink, ψ_{C2}
(3) Flow between tertiary source and sink, ψ_{C3}
(4) Combination of flows ψ_{C1} and $\psi_{C2} = \psi_{C4}$
(5) Combination of flow ψ_{C4} with flow $\psi_{C3} = \psi_{C5}$
(6) Combination of flow ψ_{C5} with uniform flow $\psi_U = \psi_S$.

Regardless of the combination of stream-function values used in this operation the ends retain some bluntness for any reasonable number of sets or pairs of point sources and sinks. A solution to this problem, developed by D. W. Taylor, is described in the section to follow.

It is pointed out here, as W. J. M. Rankine did in his classic treatise of 1866 on "Shipbuilding: Theoretical and Practical," that it is not strictly necessary to limit a ship curve, for analysis or design, to the contour of the Rankine body or stream form defined by the stream function $\psi_S = 0$. Parts of the lines of ships may be represented by streamlines which lie at some distance from what is considered as the solid boundary of the stream form, described in Sec. 4.2 on page 72 of Volume I. This is in accordance with the principle previously enunciated that any stream surface in an ideal liquid can be replaced by a solid surface without changing the flow pattern on the other side of it.

43.6 The Construction of Two-Dimensional Stream Forms and Stream Patterns from Line Sources and Sinks. It is possible to construct stream forms with the sharp ends customary in ship waterlines, and with practically any desired shape and degree of fineness or fullness, by an ingenious method devised by D. W. Taylor many years ago ["On Ship-Shaped Stream Forms," INA, 1894, pp. 385–406; "On Solid Stream Forms, and the Depth of Water Necessary to Avoid Abnormal Resistance of Ships," INA, 1895, pp. 234–247]. This involves the use of what are called *line sources* and *sinks*.

In its simplest form this procedure embodies the

use of a multitude of minute sources and sinks, not necessarily all of the same strength, with infinitesimal spacing, crowded together along a line representing the longitudinal axis of a body or ship. The sources are grouped along the entrance; the sinks along the run. Despite the minute strength of each source or sink, the combined strength of each group of them along the line is finite.

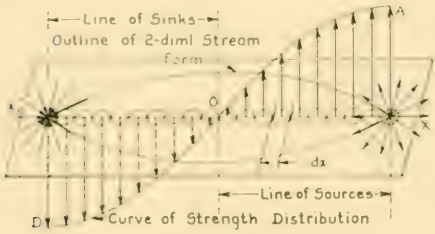

Fig. 43.H Definition Sketch for Line Source and Line Sink

Fig. 43.H depicts schematically such a line, marked X_1OX, with a row of sources from X to O and a row of sinks from O to X_1. The strength of each is represented by the height of a velocity vector perpendicular to the source-sink line. Source strengths are laid off above the line and sink strengths below it. A line joining all the ordinates is the source-sink, strength-distribution curve. If each source or sink occupies a space of dx along the line, then the total strength of all the sources is the length $\overline{OX}$ times the average strength or ordinate. Similarly, the total strength of all the sinks is the length $\overline{OX_1}$ times the average negative ordinate.

The strength of any source or sink along the line XOX_1 may be assigned at will, depending upon the shape of the body or ship which it is desired to form. The only limitation is that the area below the curve of source ordinates, AXO in Fig. 43.H, representing the total source output, *be exactly equal* to the area above the curve of sink ordinates ODX_1, representing the total sink input. Otherwise there will be some liquid lacking or left over, and the resulting stream form will not be bounded by a closed curve.

In practice, when working with line sources and sinks, it is convenient to plot a graph of source and sink strengths as in diagram 1 of Fig. 43.I. The problem then is to find the stream function of the combined flow from the sources distributed along the XO-part of the line to the sinks distributed along the OX_1-part, corresponding to the "circular" stream flow for the simple 2-diml source-sink pair of Sec. 43.3 preceding. When the flow pattern of the resultant source-sink stream function is found, it is combined with the uniform-flow function ψ_U along the reference axis to give the outline of the ship form, defined by the streamline where $\psi_S = 0$. Other values of the stream function ψ_S give the 2-diml flow pattern around the ship form, at a distance from the boundary.

At any selected point G in diagram 1 of Fig. 43.I it is necessary to determine first, the flow from all the dx sources; second, the flow into all the dx sinks; and then to combine them. Taking the line X_1OX as the trace of the reference plane, as before, the stream function at G due to any infinitesimal dx-source, such as at E, is $dx(\overline{BE})\theta_E$, where θ_E is measured counter-clockwise from the reference plane. The stream function at G due to any dx-sink, such as at F, is $-dx(\overline{CF})\theta_F$. Plotting these values as a separate graph, diagram 2 of Fig. 43.I, the source stream function is laid off as the ordinate EH *above* E, and the sink stream function as FJ *below* F. Proceeding in similar fashion for all the dx-sources between X

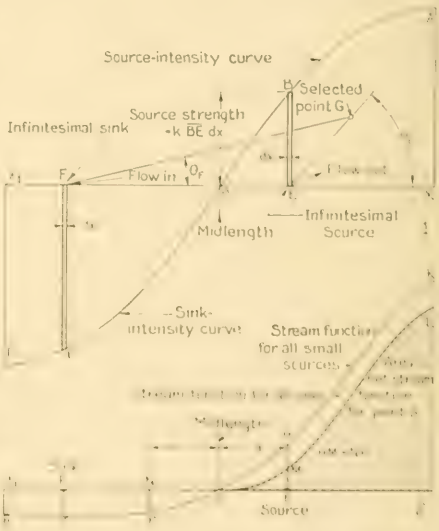

Fig. 43.I Definition Sketch for the Stream Function at a Point in a Line Source-Line Sink Field

and O, and all the dx-sinks between O and X_1, the curves KHO and OJR are produced. Subtracting the area under the first from the area above the second, both measured to the XOX_1 axis, gives the net value of the combined source-sink stream function at the point G. It is represented by the hatched area in diagram 2 of the figure.

Repeating this procedure for all points in the entire field other than G and carrying through the remainder of the operation is a tedious and laborious task, despite the systematic method of calculation outlined and described by D. W. Taylor in the references cited. Nevertheless, it can be and has been done, as witness the works of the AVA, Göttingen, on 3-diml line sources and sinks in their report UM 3206, mentioned in Sec. 42.6. The general problem is simplified immensely by:

(a) Making the source-and-sink lines XO and OX_1 of equal length and the source-and-sink distribution symmetrical about O, as was done by Taylor. The method is explained and used in a practical example by him on pages 392–396 and Plates LXX–LXXIII of his 1894 INA paper.
(b) Shortening the lines of sources and sinks to cover only limited intervals or portions of the length near the bow and stern
(c) Replacing the general source-and-sink strength curves by straight lines; in other words, making the strengths constant along the source-and-sink lines or uniformly varying in those regions. The latter two steps were adopted by H. Föttinger and F. Horn in producing the simple 2-diml ship forms described in Secs. 2.17 and 4.3 and illustrated in Figs. 2.S and 4.C of Volume I. They were also used by Brand and others in producing 3-diml bodies of revolution, one of which is illustrated in Fig. 42.C.
(d) Using a calculating machine developed by H. Föttinger [STG, 1924, pp. 295–344; TMB Transl. 48, May 1952, pp. 14–15].

43.7 Flow Pattern for the Two-Dimensional Doublet and the Circular Stream Form. A source and sink, both 2-diml, when placed infinitely close to each other along a given axis, form a doublet, described in Sec. 3.10 and illustrated in Fig. 3.M of Volume I and in Fig. 43.J of Volume II. The source-sink streamlines retain their circular shape, as in Fig. 43.C. However, the inner streamline circles between the source and the sink diminish in size as the source-sink distance $2s$ along the axis is decreased toward zero. When this distance is reduced to an extremely small value, the only circular streamlines left in sight are the outer ones, *beyond* both the source and the sink. Furthermore, the visible streamlines of the circular pattern now lie tangent to the source-sink axis, regardless of their radius. This is because the line forming the locus of their centers, normal to the axis, now crosses the axis at the doublet position which is, in effect, a common position for both.

When the source and sink are brought together to form a doublet their strengths m are increased to hold the product $m(2s)$ constant. The strength of the doublet is then indicated by μ(mu), where $\mu = 2m(s)$.

When the double-circular flow pattern around a doublet is combined with a uniform flow in the direction of the doublet axis the resulting 2-diml stream form, depicted in half-section in Fig. 43.J, is circular. The derivation of this form is set down in Sec. 41.8. It is convenient, for reasons

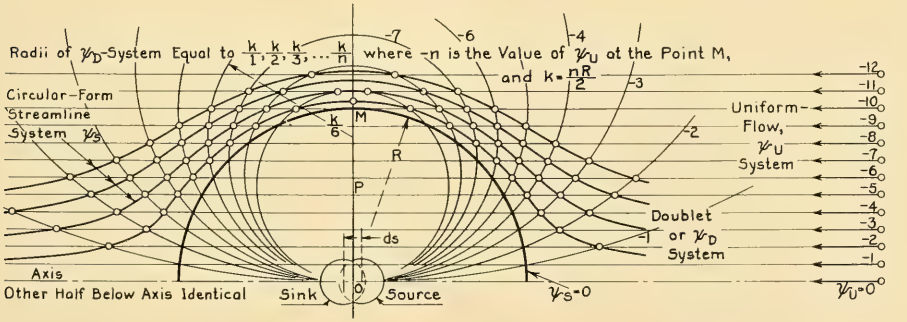

Fig. 43.J Construction Diagram for 2-Diml Doublet

explained presently, to be able to delineate accurately the potential flow of an ideal liquid around this circular form. This is accomplished by combining the circular doublet streamlines of the ψ_D-system with the parallel streamlines of the ψ_U-system, as described for other graphic constructions in the sections preceding. However, the ψ_D-system is constructed in quite different fashion.

Selecting the desired radius R of the circular stream form, the stream functions of the uniform flow are laid off at intervals of say tenths of the radius R on each side of the axis. This is illustrated in Fig. 43.J, drawn for one side only. The innermost circular streamline of the doublet system, not shown in the figure, has a radius of $R/2$. Its geometric center, as for all other centers of the system, lies on a line normal to the doublet axis at the doublet position O. If this innermost circle were drawn from the center P it would be tangent to the doublet axis at O and to the uniform-flow streamline for $\psi_U = -10$ at M. Since M is a point on the stream form where $\psi_S = 0$, this circle has a stream-function value $\psi_D = +10$. The next circle representing a doublet stream function ψ_D is tangent to the axis at O and has a radius $(R/2)(10/9)$. The remaining circles of the ψ_D-system have the radii $(R/2)(10/8)$, $(R/2)(10/7)$, and so on to $(R/2)(10/1)$ for the outermost circle, $\psi_D = +1$. Expressed in another way, at the top of Fig. 43.J, the radii of the ψ_D-system may be taken as $k/1, k/2, k/3, \ldots k/n$, where n has the numerical value of ψ_U at the point M, and $k = nR/2$.

The algebraic addition of the ψ_D and the ψ_U stream functions produces points in the resultant ψ_S-system. The stream function for $\psi_S = 0$ is a circle of radius R. Other stream functions such as $\psi_S = 1, 2$, and so on define the streamlines depicted in Fig. 43.J for the ψ_S-system, covering as large a field as may be desired for analysis.

Both by this graphic construction and by pure calculation, using the formulas of Sec. 41.8 for flow about a 2-diml rod of circular section, it is possible to determine easily the stream function, the velocity potential, the flow pattern, the pressures, the velocities, and other flow characteristics around the circular stream form. By the process of conformal transformation, mentioned in Sec. 41.11, the circular boundary of the 2-diml doublet stream form is transformed into almost any desired shape, taking the flow pattern and the various flow characteristics along with it, so to speak, to suit the new contour. Sections of hydrofoils, propeller blades, rudders and control surfaces, even transverse sections and waterlines of ships, are the end result of this procedure, complete with data for the flow around them. However, because of the discontinuity at the trailing edge of a hydrofoil which is definitely sharp, the method breaks down for the region in this vicinity.

43.8 Graphic Construction of Three-Dimensional Stream Forms and Flow Patterns. The manner in which an oval 2-diml body is formed by inserting a 2-diml source-sink pair into a uniform stream, flowing in a direction parallel to the source-sink axis, is described in Sec. 43.3. It is possible, in much the same way, to form an axisymmetric 3-diml body by inserting a 3-diml source-sink pair into a uniform stream moving parallel to the source-sink axis.

For the mathematical formulations of Sec. 41.8 and the spherical coordinates employed there, it was convenient to use a zero stream-function reference for the 3-diml source (and sink) in the form of a transverse plane through the source center, normal to the source-sink axis. For the graphic construction, however, it is much simpler and more straightforward to use as a zero reference for both source-and-sink flow and uniform-stream flow the source-sink axis itself. The representation of the stream function ψ_U for the 3-diml uniform-stream flow is the same in both cases. It is depicted in diagram 2 of Fig. 2.M of Sec. 2.12, on page 31 of Volume I, where the 3-diml stream function ψ_U corresponds to $-U_\infty y^2/2$, with y measured radially from the source-sink axis.

Using the same zero reference for the 3-diml flow out of the source and into the sink, the radial flow is split up into a cone-and-funnel pattern symmetrical about the source-sink axis rather than into a "pyramidal" pattern uniformly distributed in all directions around the source (or sink) as a center. This means that the innermost subdivision of the radial 3-diml flow takes the form of a cone whose axis is coincident with the source-sink axis, as at B in Fig. 43.K. The radial flow is assumed to pass through the circular-contour spherical base of this cone, notwithstanding that it is shown closed at B in the figure. A similar cone lies diametrically opposite the source or sink, also shown at B.

The next subdivision of the 3-diml radial flow, reckoned outward from the source-sink axis and out of (or into) which a unit quantity rate of

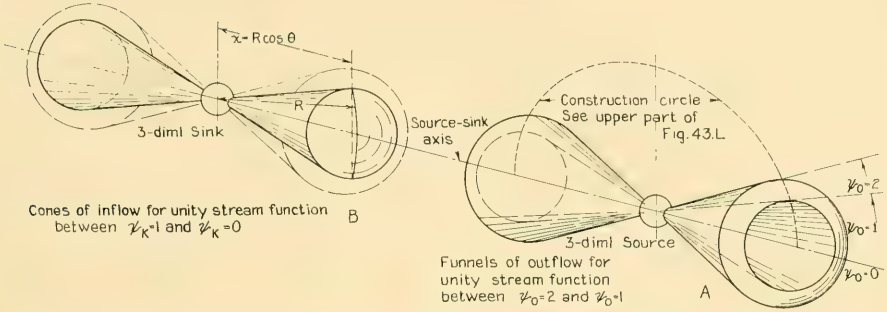

Fig. 43.K Definition Sketch for 3-Diml Source-and-Sink Stream Functions for Graphic Construction of Body Shapes and Flow Patterns

liquid flows, is a conical "funnel," surrounding the cone. The same quantity rate of liquid is assumed to pass through the annular spherical surface at the base of the "funnel." This funnel is diagrammed at A in Fig. 43.K where, to make it stand out more clearly, the cone around the source-sink axis is omitted. Diametrically opposite one funnel is an identical one, drawn at the left side of the 3-diml source in the figure. With a 3-diml stream function $\psi_o = 0$ at the source-sink axis, this stream function has a value of unity (1.0) at the outer surface of the cone and the inner surface of the funnel. It has a value of 2 at the outer surface of the funnel, indicated in the figure. Surrounding the inner funnels are a series of other larger funnels, also concentric with the source-sink axis, terminating in zones of area equal to the first, through which unit quantity rates of liquid flow in and out.

For a given spherical radius and radial velocity at the source and sink, the quantity rates of liquid flowing through the cones and funnels are directly proportional to the areas of their spherical bases and zones, respectively. For the construction of the 3-diml stream forms to be described, the surface of each source or sink "sphere" is divided into an integral number of zones *of equal area,* all symmetrical about the axis.

The area of a spherical segment or zone is expressed by the formula $A_S = 2\pi Rb$, where R is the radius of the sphere and b is the height of the segment or zone in the direction of the polar axis, normal to the planes dividing the zones. In this case the polar axis corresponds to the source-sink axis, and to the direction of flow. Hence a selected or convenient spherical radius along the direction of flow is divided into a number of equal parts corresponding to the selected stream functions for each "hemisphere" of the radial flow, such as $k = 10$. When perpendiculars are erected on this radius at the spacing $b = R/k$, the intersections of these perpendiculars with a circle representing the spherical surface give the limits for the bases of the cones and the funnels through which equal quantities of liquid move out from the source and in toward the sink.

The radial-flow diagram for a 3-diml source (or sink), as projected on a page to represent the traces on any plane passed through the source-sink axis, takes the form indicated in diagram 1 of Fig. 43.L, where only one-quarter of the pattern is shown. That for the sink is the same, with negative signs.

The uniform flow approaching from a distance is assumed to be made up of stream rods and tubes, circular and annular in section and concentric about the extended source-sink axis, as shown in diagram 2 of Fig. 2.M of Volume I and in Fig. 42.A. The inner stream "rod" of Fig. 2.M has the form of a cylinder of any selected radius, depending upon the value of the 3-diml uniform-stream function assigned. The outer stream "tubes" have radial thicknesses such that the quantity rate of flow through each of them equals that through the center "rod." Their divisional surfaces therefore have equidifferent stream functions, based upon their common axis as a reference. The prospective inner and outer radii of the rod and the annular stream tubes are determined graphically by laying down a second-order parabola $y^2 = cx$, with its vertex on the source-sink axis. Perpendiculars are then erected at uniform intervals along the source-sink axis in the manner indicated at 2 in Fig. 43.L [Taylor,

TABLE 43.a—DATA FOR CONSTRUCTING THREE-DIML RADIAL-FLOW DIAGRAMS

This table applies to diagram 1 of Fig. 43.L.

k	Natural cos	Angle θ, deg, min, sec	Angle, deg	Natural sin
0	1.00	0°	0.00	0
1	0.95	18° 11′ 38″	18.19	0.3125
2	0.90	25° 50′ 30″	25.84	0.4359
3	0.85	31° 47′ 19″	31.79	0.5268
4	0.80	36° 52′ 10″	36.87	0.6000
5	0.75	41° 24′ 35″	41.41	0.6614
6	0.70	45° 34′ 22″	45.57	0.7142
7	0.65	49° 27′ 30″	49.46	0.7599
8	0.60	53° 7′ 50″	53.13	0.8000
9	0.55	56° 37′ 58″	50.63	0.8352
10	0.50	60° 00′ 00″	60.00	0.8660
11	0.45	63° 15′ 23″	63.26	0.8930
12	0.40	66° 25′ 18″	66.42	0.9165
13	0.35	69° 30′ 46″	69.51	0.9368
14	0.30	72° 32′ 33″	72.54	0.9539
15	0.25	75° 31′ 21″	75.52	0.9682
16	0.20	78° 27′ 48″	78.46	0.9798
17	0.15	81° 22′ 22″	81.37	0.9887
18	0.10	84° 15′ 40″	84.26	0.9950
19	0.05	87° 08′ 02″	87.13	0.9988
20	0.00	90°	90.00	1.000

D. W., INA, 1895, Pl. XV]. The respective radii y_K may also be calculated by the formula $R_K^2 = y_K^2 = R^2(k/n)$, or $R_K = R\sqrt{(k/n)}$, where n is the number of intervals into which a given radius R is to be divided and k is the identifying number of any cylindrical stream surface, counting outward from the axis. Tables 43.a and 43.b give data for laying down these dimensions directly for $n = 20$ or an integral portion thereof, without the necessity for making a graphic construction similar to Fig. 43.L.

Separate radial diagrams for this 3-diml flow can now be drawn on tracing cloth or other suitable transparent material, corresponding to those described previously in Sec. 43.3 for 2-diml flow. The radial traces on these diagrams are numbered with the selected stream-function values, starting from zero at what is to be the upstream end of the source-sink axis and working both ways, above and below the axis. The radial lines belonging to the sink are numbered in the same way and with the same corresponding numerals, but preceded by negative signs. In other words, the lines for $\psi_O = 2$ and $\psi_K = -2$ are on the upstream sides of the source and sink, respectively.

If it is desired to combine an isolated 3-diml source with a uniform 3-diml flow, the radial source diagram 1 of Fig. 43.L is laid down by itself over the reference line, parallel to the direction of uniform flow. As in the 2-diml case, the companion 3-diml sink is considered to be situated at an infinite distance downstream, to the left in the figure. Over the source diagram is placed the uniform-flow diagram 2 of Fig. 43.L. Over both of them is placed a sheet of tracing paper upon which the 3-diml body and the streamlines around it are to be drawn. The cone-and-funnel flow is now combined with the rod-and-tube uniform stream exactly as was described previously in Sec. 43.2 for the single source and the uniform flow, by adding the 3-diml stream functions algebraically. The trace of the axisymmetric form represented by $\psi_S = 0$ in the 3-diml flow of Fig. 43.M resembles that of the 2-diml flow shown previously in Fig. 43.B except that it is somewhat more blunt.

This construction again finds a practical application in the shaping of a bulb bow, where the forward portion may be built up around a body of revolution having the form shown by the heavy line of Fig. 43.M and the after portion may merge into the lower regions of the entrance, as if directed toward a companion sink of equal

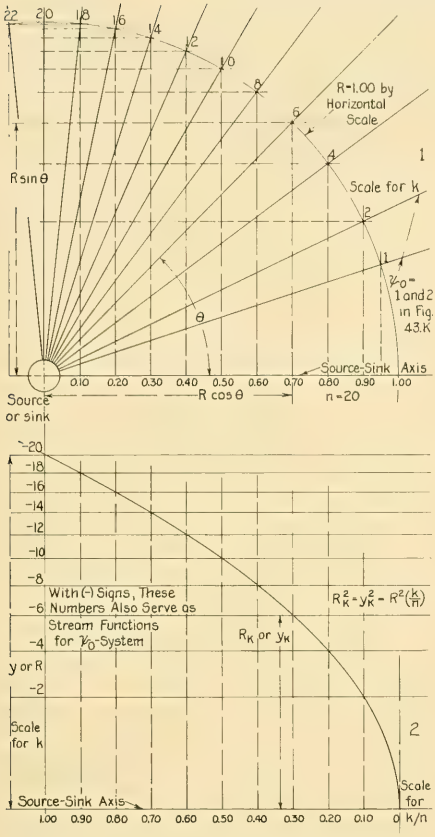

FIG. 43.L DIAGRAM FOR GRAPHIC CONSTRUCTION OF STREAM FUNCTIONS FOR 3-DIML SOURCE OR SINK AND UNIFORM FLOW

strength and great size near the stern. Fig. 67.H in Sec. 67.7 shows the longitudinal half-section of such a 3-diml bulb, extended well abaft the source position.

To construct the longitudinal-plane trace of a complete 3-diml body of revolution with a 3-diml source-sink pair, the transparent radial-flow diagrams of both source and sink are laid down over the reference (source-sink) axis at the selected position of each. A sheet of tracing paper or cloth is superposed on the two. The trace of the resultant 3-diml flow pattern is constructed on the top sheet by marking the intersections of the radial traces with stream-function values ψ_R corresponding to the algebraic sum of the 3-diml source-and-sink functions. Fair curves are next drawn through points of equal value of ψ_R . The surfaces of revolution pertaining to the combined source-and-sink stream functions ψ_R are found, as in Fig. 43.N, to have forms which are generally but not exactly circular where they intersect the plane of the page.

The resultant source-sink stream functions ψ_R are finally combined with the uniform-flow stream functions ψ_U in the same manner as for

TABLE 43.b—DATA FOR CONSTRUCTING THREE-DIMENSIONAL UNIFORM-FLOW DIAGRAMS

This table applies to diagram 2 of Fig. 43.L.

k	k/n for $n = 20$	y_k/y
20	1.00	1.000
19	0.95	0.975
18	0.90	0.949
17	0.85	0.922
16	0.80	0.894
15	0.75	0.866
14	0.70	0.837
13	0.65	0.806
12	0.60	0.775
11	0.55	0.742
10	0.50	0.707
9	0.45	0.671
8	0.40	0.632
7	0.35	0.592
6	0.30	0.548
5	0.25	0.500
4	0.20	0.447
3	0.15	0.387
2	0.10	0.316
1	0.05	0.224
0	0.00	0.000

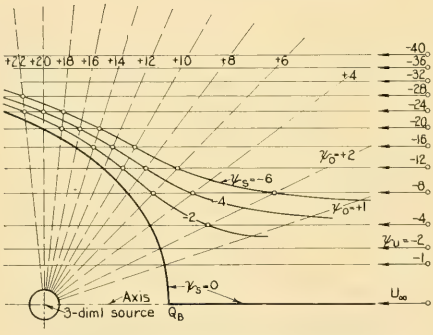

FIG. 43.M COMBINATION OF STREAM FUNCTIONS FOR SINGLE 3-DIML SOURCE AND UNIFORM FLOW

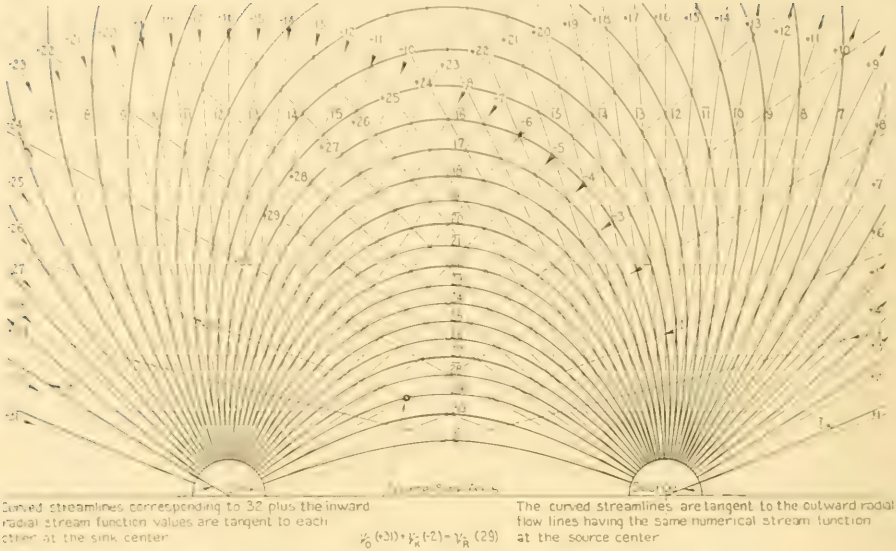

Fig. 43.N Stream-Function Pattern for a 3-Diml Source-Sink Pair

the 3-diml single-source-and-uniform-flow combination described previously in this section and illustrated in Fig. 43.M. The result, indicated in Fig. 43.O, is a plane longitudinal section through the axis of a 3-diml stream form of revolution of oval shape and the 3-diml flow pattern around it. This form may be called, following the lead of D. W. Taylor, a *solid stream form*; it may also be called a *solid Rankine body*. The streamlines lying outside it are the traces of varied-radius stream tubes, formed by the intersection of the circular-section stream surfaces with the plane of the page.

If the solid axisymmetric stream forms resulting from any of these combinations are too blunt, pairs of 3-diml secondary or tertiary sources and sinks may be added, following the scheme described in Sec. 43.5 for 2-diml radial flows of this kind.

The methods of constructing graphically the

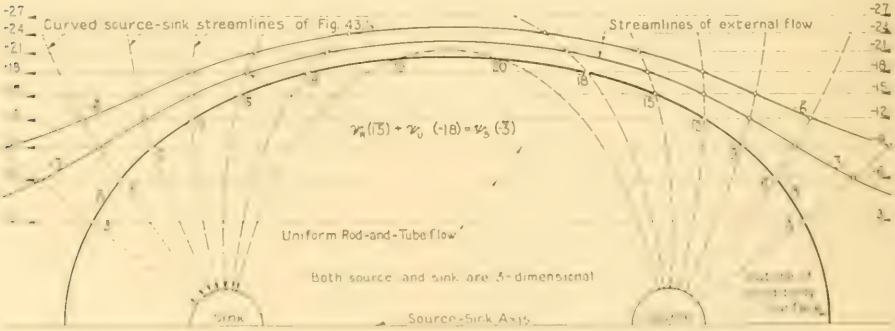

Fig. 43.O Axisymmetric Body Shape for Combination of 3-Diml Source-Sink Pair and 3-Diml Uniform Flow

flow patterns around source-and-sink combinations in uniform flow is described here at some length as an aid in the visualization of this type of flow and in understanding the nature and the combination of stream functions. The more familiar this action becomes to the marine architect, the more frequently is it recognized around a ship form and the more interesting and useful is this knowledge likely to become in practice.

43.9 Variety of Stream Forms Produced by Sources and Sinks. Thanks to Taylor's line sources and sinks, and to mathematical methods which have been developed in the three-quarters of a century since Rankine's time, it is now possible to produce stream functions and velocity potentials for source-sink forms and combinations hitherto undreamed of. This applies not only to the 2-diml source-sink combinations of Secs. 43.2 to 43.7 but to the 3-diml source-sink combinations of Sec. 43.8. Examples of these applications are:

(i) Line sources and sinks along a longitudinal axis parallel to the direction of uniform flow, to form a large number of bodies of revolution, having a great variety of shapes and proportions [AVA, Göttingen, Rep. UM 3206, dated 30 Dec 1944; available in English as TMB Transl. 220, Apr 1947]

(ii) Sources and sinks offset from the longitudinal axis to produce a rather blunt stern on a destroyer form, pictured in Fig. 3.Q on page 69 of Volume I [Lunde, J. K., INA, 1949, Figs. 1 and 2, pp. 186–187]

(iii) Assemblies of doublets introduced in a uniform stream to produce special forms, as has been done by Sir Thomas Havelock

(iv) Ring sources in a plane normal to a uniform stream of relatively high velocity, to form duct or pipe entrances with streamlined outer and inner walls. Longitudinal traces through some of the 3-diml bodies worked out in this fashion by the Illinois Institute of Technology on Project 4955, ONR Contract N7onr-32905, under V. L. Streeter, are illustrated in the First Phase Report of this project, dated 1 February 1949, entitled "Axially Symmetric Flow Through Annular Bodies."

(v) Infinitesimal dA sources spread over the after area of a propeller disc and dA sinks spread over the forward area to reproduce the velocity and pressure effects of a screw propeller, following H. Dickmann. A group of five pairs arranged in this fashion is shown in Fig. 15.F.

The number of forms which can be developed by source-sink combinations is in fact limited only by the ingenuity, imagination, and talent put to work on them. The reward offered by this work is the ability to calculate the characteristics of the flow around these forms, under a great variety of initial conditions. The useful and practical results of these enterprising endeavors are described in somewhat greater detail in Chap. 50, in a discussion of calculated ship resistance.

43.10 Source-Sink Flow Patterns by Colored Liquid and Electric Analogy. In Sec. 2.13, on pages 34 and 35 of Volume I, there are explained, in somewhat general terms, the means by which radial-flow patterns around sources and sinks, singly or in combination, are determined by plotting traces of equal electric potential in a weak electrolyte.

The use of colored liquids, emanating from and flowing into actual holes representing sources and sinks, is mentioned in Sec. 3.8. Excellent source-sink flow patterns for practical use, capable of manual diagramming or photographing, are delineated by this relatively simple, expeditious, and economical technique [Moore, A. D., "Fields from Fluid Flow Mappers," Jour. Appl. Phys., Aug 1949, Vol. 20, pp. 790–804]. Colored liquid moves from the source orifice(s) to the sink orifice(s) through a thin horizontal space between a light-colored slab containing the orifice(s) and a sheet of plate glass just above it. Streamlines of sorts are indicated by colored streaks left on the slab. Motion pictures may be made of the colored liquid while it is flowing.

This method lends itself to the quick solution, not only of 2-diml flow problems but to the delineation of axisymmetric flow in three dimensions. Further, line sources and sinks may be represented, using slots instead of holes. The slot width is varied to correspond to the strength distribution along that axis. Flow from or into relatively large-area sources and sinks is represented by running the colored liquid through small sand beds within the boundaries of the sources and sinks.

Similar representations, employing a liquid flow of constant depth over a broad-crested weir, were utilized by J. F. Harvey to approximate heat-flow patterns in boilers [SNAME, 1950, Vol. 58, pp. 252–257].

43.11 Formulas for the Calculation of Stream-Form Shapes and the Flow Patterns Around Them. The shapes of all the stream forms constructed graphically in the preceding sections of

the present chapter, the traces of the flow patterns around them, and the local stream velocities and pressures, can be calculated by mathematical formulas. This method is often the most convenient and advantageous, depending upon the equipment and facilities available and the use to which the derived data are to be put. Specific formulas for accomplishing this, in a few selected cases, are derived in Secs. 41.8 and 41.9 and are quoted on Figs. 41.E, 41.F, and 41.G accompanying them. These formulas, and others, are found in many modern text and reference books, but more often than not they are without adequate explanation as to the symbols and notation employed.

Some additional formulas were developed by W. J. M. Rankine [Phil. Trans., Roy Soc., 1871], such as those to establish the loci of points of maximum and minimum velocity around stream forms, but the references which contain them are not readily available and the notation in which they were expressed three-quarters of a century ago requires conversion to modern notation.

43.12 The Forces Exerted by or on Bodies Around Sources and Sinks in a Stream; Lagally's Theorem. If a closed body is formed by a stream surface around sources and sinks, as for the bodies around the source-sink pairs described previously in this chapter, there is a resultant hydrodynamic force acting on the stream surface bounding the body. It is explained presently that in a uniform stream the resultant force is zero, conforming to the d'Alembert paradox, but in an unsteady or non-uniform flow the force is finite. It can be evaluated very neatly by the use of what is known as the *Lagally Theorem*. The derivation of Lagally's theorem is beyond the scope of this book, but at the expense of stretching the mathematical truth temporarily, the physical basis for it is rather easily explained.

Consider what happens inside the 2-diml ovoid-shaped boundary which envelops the 2-diml source or upstream singularity in the leading end of such a body, formed around a source and a sink *at a great distance from each other*. In diagram 1 of Fig. 43.P, depicting the nose of this body, lying in a uniform flow of velocity $-U_\infty$, all the liquid emanating from the after part of the source flows more or less directly toward the left, away from the oncoming stream. That from the forward part of the source turns rather sharply and reverses its direction, also to flow downstream toward the left. Regardless of the direction in

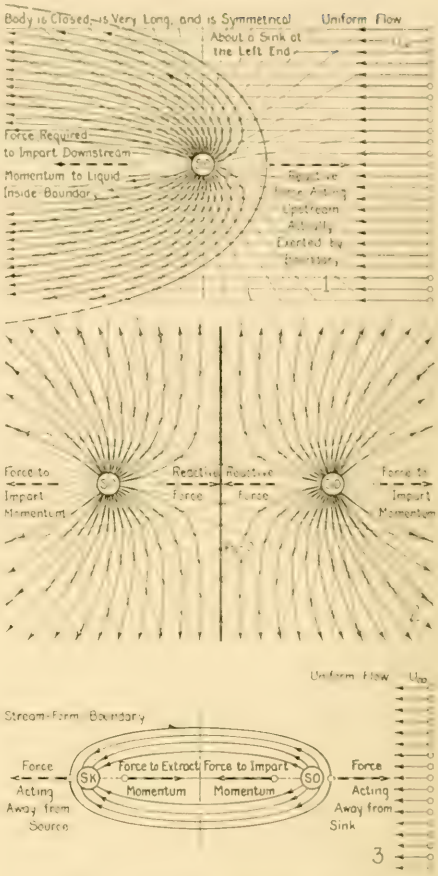

Fig. 43.P Diagrams Illustrating the Factors Involved in the Lagally Theorem

which the liquid emanated from the source, its ultimate direction is downstream.

As the "inside" liquid moves farther and farther from the source the radial component of its velocity progressively diminishes. At a great distance downstream, on its way to the sink, this liquid acquires a velocity $-U$ essentially equal to $-U_\infty$, that of the uniform stream. If a certain volume of liquid issues from the source in unit time, so that Q is the volume or quantity rate of this flow, then the mass of liquid flowing out in unit time is ρQ. Just before the liquid issued from the source it had no component of motion parallel

to the uniform stream. At a large distance downstream, half-way to the sink, it has a velocity approximating $-U_\infty$. Therefore the augment of velocity ΔU imparted to it in the process of flowing around inside the ovoid-shaped stream-form boundary is $-U_\infty$. Its momentum far downstream is its mass times its velocity, or $-\rho Q U_\infty$, assuming that $-U \cong -U_\infty$. This is also its increase in momentum which, by the laws of mechanics, is a measure of the force necessary to impart that increase. The force in question, acting downstream, is balanced by an equal and opposite force acting on the body surrounding the source to shove the body upstream. The latter force may be likened to a thrust which is producing the relative motion depicted between the source boundary and the stream. The different signs for the two terms of the equality $F = -\rho Q U_\infty$ indicate that the direction of F is opposite that of U_∞, indicated in diagram 1 of Fig. 43.P.

At the left or trailing end of the body, an "opposite" situation exists, depicted at the left in diagram 3 of Fig. 43.P. As the velocity in the uniform stream is everywhere $-U_\infty$, the net thrust or drag on the body is obviously zero. When the forces on both source and sink are taken into account, the expression

$$F_{\text{Body}} = -\rho Q_{SO} U_\infty + \rho Q_{SK} U_\infty$$

is a simplified form of the Lagally Theorem, for the special case considered, in which F_{Body} is zero.

The practical and extremely useful applications of the theorem embody situations in which the flow is unsteady and non-uniform and in which the closed body may be 2-diml or 3-diml, formed by any desired number and combination of sources and sinks.

Leaving the schematic physical explanation and turning to one that has hydrodynamic rigor, a simplified form of the theorem is the expression

$$F_{\text{Body}} = -\rho \Sigma (Q_i U_i)$$

where Q_i is the output of the source or sink within the body, expressed as a volume rate of flow, positive for a source and negative for a sink. The symbol U_i represents the velocity of the stream, at the position of the source or sink under consideration, which would occur if the body, and hence all the sources and sinks forming the body, were removed from the stream. For each source or sink the line of action of the individual force is through the singularity under consideration and in the direction opposite to that of U_i. The net hydrodynamic force on the body is the vector summation of the individual forces, evaluated for each source and sink within the body.

If the body is placed in a uniform stream, U_i at each singularity equals the uniform-stream velocity U_∞. And since, for any closed body formed by a stream surface, the source outputs must equal the sink inputs, and the mass density ρ is constant, the net hydrodynamic force acting on the body is zero, which simply confirms d'Alembert's paradox.

The complete theorem developed by M. Lagally ["Berechnung der Kräfte und Momente, die strömende Flüssigkeiten auf ihre Begrenzung ansüben (Calculation of Forces and Moments which Streaming Liquids Exert on Their Boundary)," Zeit. für Ang. Math. Mech., Dec 1922, Vol. 2, pp. 409–422 (in vector notation); Milne-Thomson, L. M., TH, 1950, pp. 208–211] permits the determination of both forces and moments acting on a body in both steady and unsteady flow [Cummins, W. E., "The Forces and Moments Acting on a Body Moving in an Arbitrary Potential Stream," TMB Rep. 780, Sep 1952]. For example, if the uniform flow at the right of diagram 1 of Fig. 43.P is replaced by a single outside source on the x-axis, the flow from the latter is radial rather than parallel and uniform. The velocity U_∞ in the momentum equation is then replaced by an array of radial velocities, varying with distance from the outside source. If the outside source is offset from the x-axis of a source-sink body, there is a moment as well as a force exerted on the ovoid-shaped boundary.

The marine architect who wishes to delve further into this subject may find a paper by A. Betz of Göttingen somewhat more readable than the references cited in the preceding paragraph. This paper is entitled "The Method of Singularities for the Determination of Forces and Moments Acting on a Body in Potential Flow" [TMB Transl. 241, Nov 1950].

In all applications of Lagally's Theorem it is important to remember that, although the line of action of the force on a body, formed by placing a source-sink system in a stream, passes through the source or sink, the force is not to be taken as acting on the source or sink proper but on some type of surface or body boundary surrounding each. However, in the conventionalized diagrams published by Betz in TMB Translation 241, he apparently employed a schematic short-

hand, with no attempt to delineate the surface resulting from the system of sources, sinks, doublets, and vortexes. In his diagrams the resulting forces are shown as emanating directly from the singularities.

There are indications that an important future use of the Lagally Theorem may be in the solution of the problem of determining the forces and the moments exerted on ships when passing or meeting each other in confined waters. This will involve a knowledge of the nature and direction of the forces exerted by the boundaries around nearby sources and sinks, arranged either singly or in groups or arrays, and placed in non-uniform and unsteady flow.

It is interesting in this connection to consider another aspect of the forces involved for one or two simple hypothetical conditions. Assume first that two sources of equal strength, lying opposite each other, are enclosed by two large body surfaces; also that those portions of the body surfaces adjacent to the sources take the form of a pair of parallel but independent flat surfaces placed between them, as at 2 in Fig. 43.P. As there is no superposed stream flow in this case, the liquid flowing from each source toward the adjacent flat portion of body surface is deflected and pushed backward. For the 2-diml case, the flow from each source is pictured graphically by combining the stream functions of the two sources, indicated by the light radial lines in the diagram. Because of the momentum imparted to the surrounding liquid, in a direction opposite to that in which the other source lies, away from the adjacent flat body surface, a reactive force is created on each body, directed *toward* the adjacent body and the other source. While the analogy is by no means a perfect or a valid one, it can be said that, unlike the similar poles of electromagnets, the two adjacent sources give the appearance of attracting each other.

If a source and a sink lie near each other in a uniform stream whose direction of motion is parallel to the source-sink axis, as in diagram 3 of Fig. 43.P, the action of the "inside" liquid is such that equal and opposite reactive forces are directed away from the sink and the source positions, respectively, and act outward on the upstream and the downstream ends of the body. Although the analogy here is perhaps less valid than it was in the case of the adjacent sources, the source and the sink give the appearance of repelling each other. This is again the opposite of the electromagnetic phenomenon, where unlike poles attract each other.

43.13 Partial Bibliography on Sources and Sinks and Their Application. The literature on the application of the radial-flow characteristics of sources and sinks to problems in hydrodynamics is extremely extensive. There are listed here a few of the most important references, with which the marine architect may pursue his studies in this fascinating field:

(1) Rankine, W. J. M., "On Plane Water-lines in Two Dimensions," Phil. Trans., Roy. Soc., 1863

(2) Rankine, W. J. M., "Summary of Properties of Certain Stream-Lines," Phil. Mag., Oct 1864, pp. 282–288

(3) Rankine, W. J. M., "Shipbuilding: Theoretical and Practical," 1866, p. 106

(4) Rankine, W. J. M., "On Stream-Line Surfaces," INA, 1870, Vol. XI, pp. 175–181

(5) Rankine, W. J. M., "On the Mathematical Theory of Streamlines, Especially those with Four Foci and Upwards," Phil. Trans., Roy. Soc., London, 1871, Vol. 161, pp. 267–306; also Pl. XV

(6) Baule, A., "Note sur les Lignes d'eau Proposées par M. le Professeur Rankine (Note on the Waterlines Proposed by Professor Rankine)," Ann. Soc. Sci., Brussels, 1885

(7) Pollard, J., and Dudebout, A., "Théorie du Navire (Theory of the Ship)," 1892, Vol. III, pp. 401–410, 417–418, especially Fig. 135 on p. 408

(8) Taylor, D. W., "On Ship-Shaped Stream Forms," INA, 1894, pp. 385–406

(9) Taylor, D. W., "On Solid Stream Forms and the Depth of Water Necessary to Avoid Abnormal Resistance of Ships," INA, 1895, pp. 234–247 and Pls. XV–XVIII

(10) Fuhrmann, G., "Widerstands- und Druckmessungen an Ballonmodellen (Resistance and Pressure Measurements on Balloon Models)," Zeit. für Flugtechnik und Motorluftschiffahrt, 15 Jul 1911, Vol. II, pp. 165–166

(11) A series of papers in French by van Meerten [ATMA, 1903, pp. 51–60 and Pl. I; 1904, pp. 275–293; 1905, pp. 269–289 and Pls. III–VI]. These discuss the application of hydrodynamic studies of the theory of sources and sinks in both two and three dimensions. They contain diagrams of a variety of source-sink flows, including several involving line sources perpendicular to a uniform flow. A start is made in the 1905 paper to utilize this method of analysis for predicting the resistance of an actual ship.

(12) Föttinger, H., "Fortschritte der Strömungslehre im Maschinenbau und Schiffbau (Advances in the Theory of Flow in Engineering and Shipbuilding)," STG, 1924, Vol. 25, pp. 295–344; English version in TMB Transl. 48, May 1952

(13) Aerodynamische Versuchsanstalt (AVA), Göttingen, Report UM 3206, dated 30 Dec 1944; available in English as TMB Transl. 220, Apr 1947; see also Sec. 42.6

(14) Lamb, H., "Hydrodynamics," 6th ed., Dover, New York, 1945, pp. 57–71
(15) Glauert, H., "The Elements of Aerofoil and Airscrew Theory," 2nd ed., Cambridge, England, 1948, pp. 21–32
(16) Brard, R., "Cas d'Équivalence entre Carènes et Distributions de Sources and de Puits (Similarities Between Ship Hulls and Distributions of Sources and Sinks)," ATMA, 1950, Vol. 49, pp. 189–230 (in vector notation)
(17) Milne-Thomson, L. M., "Theoretical Hydrodynamics," 2nd ed., Macmillan, New York, 1950, pp. 194–223
(18) Cummins, W. E., "The Forces and Moments Acting on a Body Moving in an Arbitrary Potential Stream," TMB Rep. 780, Sep 1952
(19) Hellerman, L., and Van Zandt, T. E., "Rankine Solids," Harbor Protection Project, Edwards Street Lab., Yale Univ., Tech. Memo. 14, 15 Sep 1952.

43.14 Selected References on Lagally's Theorem. For the reader who wishes to investigate further the application of the Lagally Theorem, the following references should prove useful:

(1) Kelvin, Lord, "On the Motion of Rigid Solids in a Liquid Circulating Irrotationally through Perforations in Them or in a Fixed Solid," Phil. Mag., May 1873, Vol. 45
(2) Munk, M., "Some New Aerodynamical Relations," NACA Rep. 114, 1921
(3) Lagally, M., "Berechung der Kräfte und Momente, die strömende Flüssigkeiten auf ihre Begrenzung ausüben (Calculation of Forces and Moments which Streaming Liquids Exert on Their Boundary)," Zeit. für Ang. Math. und Mech., Dec 1922, Vol. 2, pp. 409–422
(4) Taylor, G. I., "The Forces on a Body Placed in a Curved or Converging Stream of Fluid," Proc. Roy. Soc., London, 1928, Series A, Vol. 120
(5) Taylor, G. I., "The Force Acting on a Body Placed in a Curved and Converging Stream of Fluid," ARC, R and M 1166, 1928–1929, Vol. 33, p. 104ff
(6) Glauert, H., "The Effect of the Static Pressure Gradient on the Drag of a Body Tested in a Wind Tunnel," ARC, R and M 1158, 1928–1929, Vol. 33, pp. 81–113
(7) Lamb, H., "Note on the Forces Experienced by Ellipsoidal Bodies Placed Unsymmetrically in a Converging or Diverging Stream," ARC, R and M 1164, May 1928, Vol. 33, pp. 114–117
(8) Mohr, E., "Über die Kräfte und Momente, welche Singularitäten auf eine stationäre Flüssigkeitsströmung übertragen (On the Force and Moment which Singularities Transfer upon Stationary Liquid Flow)," Jour. für die reine und angewandte Mathematik (Crelle's Jour.), 1940, Vol. 182
(9) Pistolesi, E., "Forze e momenti in una corrente leggermente curva convergente (Forces and Moments in a Slowly Coverging Curved Stream)," Commentations, Pont. Acad. Sci., 1944, Vol. 8
(10) Brard, R., "Cas d'Équivalence entre Carènes et Distributions de Sources et de Puits (The Equivalence of Ship Hulls and Distributions of Sources and Sinks)," ATMA, 1950, Vol. 49, pp. 189–230 (in vector notation)
(11) Milne-Thomson, L. M., "Theoretical Hydrodynamics," Macmillan, New York, 2nd ed., 1950, pp. 208–211
(12) Tollmien, W., "Über Kräfte und Momente in schwach gekrümmten oder konvergenten Strömungen (On the Force and Moment in Flows which are Weakly Curved or Convergent)," Ing.-Archiv., 1938, Vol. 9; translated in ETT, Stevens, Rep. 363, Sep 1950
(13) Betz, A., "Singularitätenverfahren zur Ermittlung der Kräfte und Momente auf Körper in Potentialströmungen (The Method of Singularities for the Determination of Forces and Moments Acting on a Body in Potential Flow)," Ing.-Archiv, 1932, Vol. 3, pp. 454–462; TMB Transl. 241, Nov 1950
(14) Weinblum, G. P., MIT Hydrodyn. Symp., 1951, pp. 91–92
(15) Cummins, W. E., "The Forces and Moments Acting on a Body Moving in an Arbitrary Potential Stream," TMB Rep. 780, Sep 1952.

CHAPTER 44

Force, Moment, and Flow Data for Hydrofoils and Equivalent Forms

44.1 General; Scope of Chapter. The hydrofoils and equivalent forms for which performance data are given in this chapter embrace plates and bodies, irrespective of shape or size, which are intended for the production of dynamic lift when submerged in a liquid. The manner of producing this lift, in a direction generally at right angles to the flow or to the direction of body motion, is described in Chap. 14.

Insofar as their behavior is concerned, including test and performance data on them, airfoils may be classed as hydrofoils if it is known that the flow around the two, in air and water, is generally similar. In other words, data from tests in air are perfectly valid for application to the design and performance of hydrofoils in water if it is known that air-water surface effects and cavitation are to be nonexistent. As a rule, separation effects around bodies wholly submerged in air and in water are similar; this applies also to the correlation of these effects between model and full scale.

Since whole books are insufficient to list the airfoil and hydrofoil data presently available (1955) for design purposes, it is manifestly impossible, in this chapter, to do more than to present certain data which the marine architect may find useful in ship and appendage design. These and other data in the technical literature almost invariably apply to steady-state conditions. For control surfaces and other ship parts resembling hydrofoils, the relative speeds and angles of attack may change violently with time.

Nomenclature and symbols for hydrofoils are found in:

(a) Sec. 14.2 and the accompanying Fig. 14.A
(b) Secs. 32.8 and 32.9 and the accompanying Figs. 32.F, 32.G, and 32.H on the geometry of the screw propeller
(c) Secs. 36.2, 37.2, and 37.3 and the accompanying Figs. 37.A, 37.B, 37.C, and 37.D on fixed and movable appendages.

44.2 Formulas for Calculating Circulation, Lift, Drag, and Other Factors. There are no simple formulas which will permit the computation of lift, drag, pitching moment, and other factors on hydrofoils of given shape and on bodies of random shape acting as hydrofoils. There are given here only a few of the basic formulas and procedures for the calculation and prediction of these quantities. In practice it is necessary to rely on experimental data for the determination of design and other factors. The volume of these data is now very large; some of the principal sources are listed in Sec. 44.3 following.

As is customary for groups of formulas relating to other fields, the shape, characteristics, and performance of hydrofoils and equivalent bodies are given in 0-diml ratios, coefficients, and expressions.

The lift force L developed on unit span of a hydrofoil or similar body in a liquid stream, when circulation is set up by an effective angle of attack or other suitable means, is represented by

$$L \text{ per unit span} = \rho U_\infty \Gamma \tag{44.i}$$

where

ρ (rho) is the mass density of the liquid in the stream

U_∞ is the velocity of the uniform stream relative to the hydrofoil

Γ (capital gamma) is the strength of the circulation in a plane parallel to the stream motion and normal to the body axis.

For a hydrofoil of span or breadth b, measured normal to the stream direction and to the plane of circulation, the total lift force

$$L = b\rho U_\infty \Gamma \tag{44.ii}$$

The circulation required to insure that the liquid leaves the hydrofoil tangentially at its trailing edge is approximated by [Rouse, H., EMF, 1946, Eq. (192), p. 279]

$$\Gamma = \pi c U_\infty \sin \alpha \tag{44.iii}$$

where α(alpha) is the geometric angle of attack of an equivalent flat plate and c is the chord.

Expressed in terms of the lift coefficient C_L and the drag coefficient C_D, the overall lift and drag are

$$\text{Lift } L = C_L \frac{\rho}{2} U_\infty^2 bc = C_L \frac{\rho}{2} U_\infty^2 A_H \tag{44.iva}$$

$$\text{Drag } D = C_D \frac{\rho}{2} U_\infty^2 bc = C_D \frac{\rho}{2} U_\infty^2 A_H \tag{44.ivb}$$

For the special case of an infinitely thin flat plate lying at an angle of attack α in a uniform stream, when the plate is also of infinite span, with infinite aspect ratio, the

$$\text{Lift coefficient } C_L = 2\pi \sin \alpha \tag{44.v}$$

[Durand, W. F., "Aerodynamic Theory," 1935, Vol. I, Div. B].

By making an arbitrary assumption as to the distribution of the intensity of lift over a hydrofoil of finite span, an *approximate* induced-drag coefficient is $C_{DI} = C_L^2/[\pi(b^2/A_H)]$, where b^2/A_H is the aspect ratio [Rouse, H., EMF, 1946, p. 285]. By the same reasoning the downwash angle ϵ(epsilon) is *approximately* $C_L/[\pi(b^2/A_H)]$.

The magnitude of the lift by the Magnus Effect on a rotating cylinder in a stream is given by the simple expression $L = \rho U_\infty \Gamma$ for unit length of the cylinder along its axis.

44.3 Test Data from Typical Simple Airfoils and Hydrofoils. There is, in the technical literature, a great wealth of published data on the lift, drag, and moment coefficients and other factors of a great variety of airfoil shapes, when tested in air. Some of these data are in tabular form but most are in graphic form, corresponding somewhat to the information in Figs. 44.A and 44.B. Here,

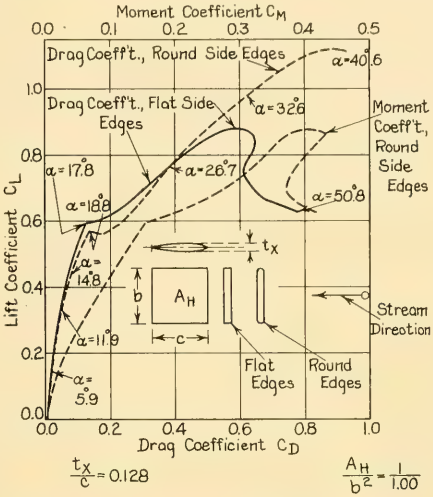

FIG. 44.A LIFT-COEFFICIENT, DRAG-COEFFICIENT, AND MOMENT-COEFFICIENT GRAPHS FOR GÖTTINGEN PROFILE 409 OF ASPECT RATIO 1.00

as in many cases in the literature, the geometric or the nominal angle of attack is the independent variable. For the data in Figs. 44.A and 44.B, adapted from the work of H. Winter at Danzig on Göttingen section 409 ["Flow Phenomena on Plates and Airfoils of Short Span," NACA Tech. Memo 798, Jul 1936, Figs. 16 and 17, respectively], the values of the angle of attack α are spotted along the C_L and C_D curves. To use these graphs, follow along the proper curve until a mark is found for the particular value of the angle of attack that has been selected. Then the abscissa and the ordinate of this mark are the values of drag and lift coefficient, respectively. For example, for the full-line graph of Fig. 44.A, take the point where the angle of attack α is 17.8 deg, at which partial breakdown or preliminary stalling occurs. The corresponding value of C_L is about 0.592 and of C_D about 0.12. The lift-drag ratio at this hydrofoil position is 0.592/0.12 or about 4.93.

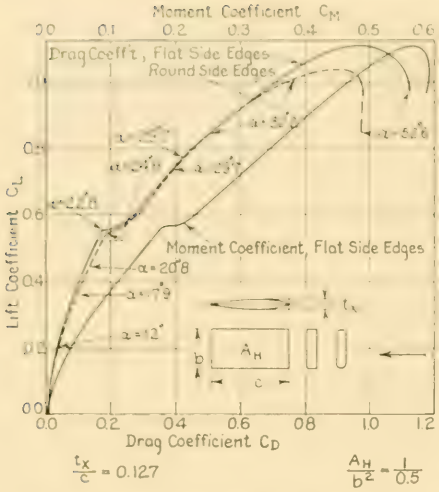

FIG. 44.B LIFT-COEFFICIENT, DRAG-COEFFICIENT, AND MOMENT-COEFFICIENT GRAPHS FOR GÖTTINGEN PROFILE 409 OF ASPECT RATIO 0.5

To prevent confusion, most of the marks for specific angles of attack are omitted from Figs. 44.A and 44.B. In Figs. 16 and 17 of NACA Technical Note 798 there are small circles along the moment-coefficient graphs but no numerals to indicate the numerical values of α.

Tables of coordinates for the symmetric Göttingen section 409, as well as for Göttingen sections 410, 411, 443, 429, 539, 639, and 640, with lift, drag, and moment coefficients, are given by W. P. A. van Lammeren, L. Troost, and J. G. Koning in Tables 3 and 4 on pages 324 and 325 of RPSS, 1948.

It is pointed out here, and it will again be pointed out in later portions of this chapter, that the behavior of a foil in water or in air is often influenced critically by small changes in its section. No performance data are acceptable for design and other purposes in practice, therefore, unless accompanied by a delineation (and preferably also a table of coordinates) of the section, in sufficient detail to permit it to be reproduced to large scale.

For the physicist, engineer, or architect who is looking for a comprehensive compilation of airfoil data in systematic form there is available a summary of airfoil data prepared and published by the National Advisory Committee for Aeronautics in Washington [Abbott, I. H., Von Doenhoff, A. E., and Stivers, L. S., Jr., NACA Rep. 824, 1945]. This report contains, in addition to the usual information on airfoil shape and the customary experimental data, a considerable amount of information on pressure distribution over the airfoils illustrated.

For the specific needs of the marine architect in predicting the behavior of simple movable hydrofoils of the shapes, sections, and proportions required in ship design there are several useful sources of information. These apply principally to hydrofoils of symmetric section and to aspect ratios in the smaller ranges.

I. Data on Thin Rectangular Plates of Aspect Ratio 5.0, 1.0, and 0.20. In PNA, 1939, Vol. II, Fig. 6 on page 204, K. E. Schoenherr gives curves of normal-force coefficient and ratio of (1) distance of center of pressure CP from leading edge to (2) chord length of plate, on a base of nominal angle of attack in degrees, for three flat plates tested at Göttingen [Flachsbart, O., "Messungen an ebenen und gewölbten Platten (Measurements on Flat and Curved Plates)," Ergebnisse der Aerodynamischen Versuchsanstalt zu Göttingen, 1932, Vol. 4, p. 96ff]. Included are graphs for one of the test plates of Joessel, but with no information as to its aspect ratio.

II. Data on NACA Symmetrical Airfoil Sections with t_x/c Ratios of 0.06, 0.12, 0.18, 0.25, and Aspect Ratio 6. In PNA, 1939, Vol. II, pages 205–206, K. E. Schoenherr gives curves of lift coefficient, drag coefficient, and ratio of CP from leading edge to chord length of the hydrofoil. The section ordinates are given, together with a procedure (explained in the text) for converting the given data to that which would be expected for aspect ratios other than 6. The data are taken from a report by E. N. Jacobs and R. E. Anderson ["Large Scale Characteristics of Airfoils as Tested in the Variable Density Wind Tunnel," NACA Rep. 352, 1930].

Additional data are given by E. N. Jacobs, K. E. Ward, and R. M. Pinkerton in NACA Report 460, published in 1933 (pages 299–354 of the volume for that year), entitled "The Characteristics of 78 Related Airfoil Sections from Tests in the Variable-Density Wind Tunnel."

III. Data on Hydrofoils Having Symmetric Sections and Outlines Suitable for Ship Rudders, with Aspect Ratios of 0.5, 1.0, 1.5, and 2.0. In the early 1930's there was tested at the Experimental Model Basin in Washington a series of twelve

hydrofoils of symmetric section, having varied aspect ratios and blade outlines. The results of these tests were reported by R. C. Darnell ["Hydrodynamic Characteristics of Twelve Symmetrical Hydrofoils," EMB Rep. 341, Nov 1932]. The hydrofoils were towed beneath a special flat-bottomed float which carried a dynamometer to measure the lift, the drag, and the torque. The angle of attack was varied from 0 to 45 deg and the gap between the top of the hydrofoil and the bottom of the float was varied from 0 to 2 inches. The report gives the 0-diml lift, drag, and moment coefficients for each hydrofoil in each test condition, together with the positions of the center of pressure with respect to the leading edge. The effect of running the hydrofoils with their trailing edges foremost was also studied.

For hydrofoils having raked or swept-back leading (and trailing) edges and some taper, it is customary to assume a nominal chord length equal to the mean chord length, neglecting local rounding of the outlines at the corners. Although not clearly stated in EMB Report 341, this scheme was followed for the 12 hydrofoils reported upon in that publication.

For fixing the fore-and-aft position of the center of pressure CP or of the point of zero pitching moment, this distance is reckoned along the direction-of-motion chord at midspan. For a blade outline with rake and taper but with straight leading and trailing edges, the chord at midspan is also the mean chord.

In PNA, 1939, Vol. II, Fig. 9 and pages 206–207, K. E. Schoenherr summarized the results of selected tests on five of the twelve symmetrical hydrofoils tested by Darnell, involving those with varied rudder outlines but with the aspect ratio limited to 1.0. In the figure cited he gave graphs of lift coefficient C_L and of the ratio of CP position from the leading edge to the mean chord length of the hydrofoil for the five blade outlines diagrammed in the figure.

IV. Data on Tests of Wageningen Rudders A and B, with Symmetric Sections and Different Outlines. The results of open-water tests on two model spade-type rudders of orthodox shape, outline, and proportions are described by W. P. A. van Lammeren, L. Troost, and J. G. Koning [RPSS, 1948, Figs. 210–214 and pp. 319–322].

44.4 Polar Diagrams for Simple Hydrofoils. A lift-coefficient, drag-coefficient graph such as one of the four in Figs. 44.A and 44.B serves also as a so-called *polar diagram*, which is useful in determining the C_L/C_D ratio at one aspect ratio when the C_L/C_D ratio at another aspect ratio is known [Rouse, H., EMF, 1946, pp. 285–286]. When the ordinate scale of C_L is the same as the abscissa scale of C_D, the slope of a line (with respect to the horizontal) drawn from the origin to any selected value of α along the graph is the value of the lift-drag ratio C_L/C_D. A line from the origin of coordinates, tangent to the graph, represents the maximum lift-drag ratio of the foil; the corresponding angle of attack is indicated at the point of tangency.

Table 44.a lists a number of references to published polar diagrams for representative airfoils. Diagrams of this type are of little use for practical and design purposes, however, unless the section contours of the hydrofoils or airfoils are defined by a rather complete set of coordinates.

44.5 Test Data from Compound Hydrofoils. Figs. 37.A, 37.B, 37.C, and 37.D of Secs. 37.2 and 37.3 indicate that for boats and ships the compound hydrofoil is used as extensively as the simple hydrofoil for movable appendages and control surfaces. Included in this category are hydrofoils with flaps and tabs as well as hydrofoils placed abaft fixed leading-edge portions and abaft fixed horns, fins, and skegs. For steering rudders, diving planes, active roll-resisting fins, and other movable appendages the hydrofoils and hydrofoil

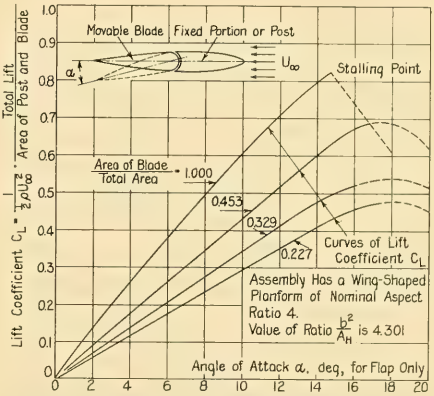

Fig. 44.C Graphs of Lift Coefficient for Compound Hydrofoils Having Varied Proportions and Varied Angles of Attack of the Movable Blade

TABLE 44.a—BRIEF LIST OF REFERENCES ILLUSTRATING POLAR DIAGRAMS AND LIFT/DRAG RATIOS FOR AIRFOILS AND HYDROFOILS

Type of Section	t_X/c Ratio	Remarks	Reference
Airfoil, normal		From Prandtl, with span-chord ratio $b/c = 5$	EMF, 1946, p. 286
Airfoil, typical		No numerical values	Vennard, J. K., "Elementary Fluid Mechanics," Wiley, New York, 1947, p. 314
Airfoil, Clark-Y			Vennard, p. 315 NACA Rep. 502, 1934
Airfoil, normal			AHA, 1934, Fig. 86, p. 148
Airfoil, normal	3 ratios	With camber variations	AHA, 1934, p. 151
Airfoil, normal	6 ratios	Variation of t_X and camber	AHA, 1934, p. 152
Airfoil, normal	2 ratios	Variation of shape	AHA, 1934, p. 153
Airfoils, normal		Aspect ratios 1, 2, 4, 8, ∞	EH, 1950, Fig. 100, p. 133 BMF, 1954, Fig. 118, p. 195
Airfoils, normal		Aspect ratios 1, 2, 3, 4, 5, 6, 7	AHA, 1934, Fig. 172, p. 209
Airfoil, normal		Aspect ratio ∞	BMF, 1953, Fig. 117, p. 195
Airfoil, normal	About 0.122	Göttingen section	STG, 1923, p. 263

Types of Section	L/D Ratio	Remarks	Reference
Airfoil, normal	Lift on a basis of α	Aspect ratios 1, 2, 3, 4, 5, 6, 7	AHA, 1934, Fig. 173, p. 209
Airfoil, Clark-Y		Aspect ratio 6	Vennard, J. K., "Elementary Fluid Mechanics," Wiley, New York, 1947, p. 316 NACA Rep. 502, 1934
Airfoil, Joukowski		C_L and C_D	EH, 1950, p. 132
Airfoil, normal			BMF, 1953, p. 194 MDFD, 1938, Vol. I, p. 35

assemblies are almost always of symmetric section. The data presented or referenced here represent only a small part of those available in the technical literature but they serve to indicate about what may be expected as to the behavior of these assemblies.

Fig. 44.C, adapted from a previous presentation of the same data by K. E. Schoenherr [PNA, 1939, Vol. II, pp. 208–209], gives graphs of lift coefficient C_L for a series of compound hydrofoils with flaps of varying length. The hydrofoil assembly as tested at Göttingen ["Ergebnisse der Aerodynamischen Versuchsanstalt zu Göttingen, III, Lieferung; Messungen an drei Höhenleitwerken (Results of Tests at the Aerodynamic Research Institute, Göttingen, Vol. III; Measurements on Three Flap Assemblies)," Munich and Berlin, 1927, pp. 102–107] had the general planform of an airplane wing, with a nominal aspect ratio of $100/25 = 4.0$ and a ratio $b^2/A_H = 4.301$. The three flaps, measured from the trailing edge to the hinge center, had chord lengths of 0.26, 0.39, and 0.48 times the overall chord. The ratios of the planform areas to the total planform area were

0.227, 0.329, and 0.453, respectively. The variations between the two sets of ratios were due to the rounded ends of the planform of the assembly. For rudders and planes having aspect ratios materially less than 4, stalling should occur at flap angles greater than those shown in Fig. 44.C.

On page 105 of the Göttingen reference there are given some data for a flap-type compound hydrofoil in which the fixed leading portion lies at an angle of attack α to the stream, and flap angle ξ(ksi) is applied to augment the lift, as in diagram 2 of Fig. 14.U.

In the late 1940's the National Advisory Committee for Aeronautics conducted an extensive investigation of control-surface characteristics. Its purpose was to provide experimental data for designers and to determine the section characteristics of various types of fin-and-flap (or airfoil-and-flap) combinations suitable for use as control surfaces.

Two of the reports describing the results of these tests are listed hereunder:

(1) Riebe, J. M., and Church, O., "Medium and Large Aerodynamic Balances of Two Nose Shapes and a Plane Overhang Used with a 0.40-Airfoil-Chord Flap on an NACA 0009 Airfoil," ARR L5 C01, March 1945. This appears to be Part XXI of the report series covering the complete investigation.

(2) Riebe, J. M., and McKinney, E. G., "Medium and Large Aerodynamic Balances of Two Nose Shapes and a Plane Overhang Used with a 0.20-Airfoil-Chord Flap on an NACA 0009 Airfoil," ARR L5 F06 of June 1945. This is Part XXII of the complete series.

As applying to combinations of fixed plates or fins and movable control surfaces abaft them, K. E. Schoenherr gives a graphic summary [PNA, 1939, Vol. II, pp. 207–208] of data derived by experimenters abroad and published in the following references:

(a) Cowley, W. L., Simmons, L. F. G., and Coales, J. D., "The Effect of Balancing a Rudder, by Placing the Rudder Axis Behind the Leading Edge, upon the Controlling Moment of the Motion," Tech. Rep. Adv. Comm. for Aero., R and M 253, 1916–1917, p. 154ff

(b) Munk, M. M., "Systematische Versuche an Leitwerkmodellen (Systematic Tests on Models of Control Surfaces)," Technische Berichte der Flugzeugmeisterei, 1917, p. 168ff.

Fig. 44.D, adapted from Fig. 10 on page 208 of the Schoenherr reference, covers a number of cases of this kind, in sufficient detail to indicate about what may be expected of elementary compound assemblies.

The results of somewhat similar experiments made by T. B. Abell are to be found in his paper "Some Model Experiments on Rudders Placed Behind a Plane Deadwood" [INA, 1936, pp. 137–144]. The results of these experiments are summarized by W. P. A. van Lammeren, L. Troost, and J. G. Koning [RPSS, 1948, pp. 327–328].

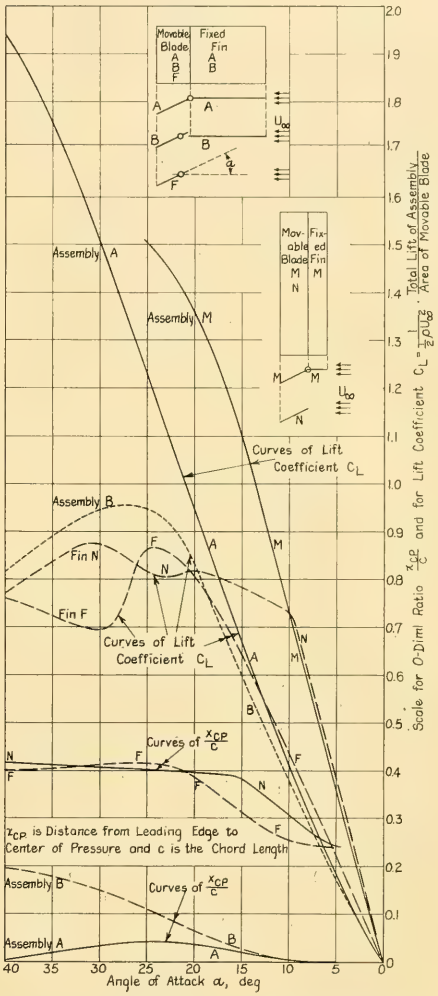

Fig. 44.D Graphs of Lift Coefficient and Center-of-Pressure Position for Several Combinations of Fixed Fins and Movable Blades

TABLE 44.b—LIST OF REFERENCES CONTAINING FLOW DIAGRAMS ABOUT AIRFOILS AND HYDROFOILS

All diagrams represent flow with circulation unless otherwise indicated.

Type or Shape of Hydrofoil	Kind of Flow	Kind of Diagram	Reference
Airfoil, cambered	Ideal, 2-diml	Streamlines; includes separation	BMF, 1953, Fig. 114, p. 192 AHA, 1934, p. 182 MDFD, 1938, Vol. I, p. 77; Vol. II, p. 470
Airfoil, Joukowski	Ideal, 2-diml	Streamlines	EMF, 1946, Fig. 143, p. 281 EH, 1950, Fig. 97, p. 131 HAM, 1934, Fig. 108, p. 176
Airfoil, normal	Ideal, 2-diml	Streamlines; without circulation	MDFD, 1938, Vol. I, Fig. 10(a), p. 34
Curved plate, circular-arc shape	Ideal, 2-diml	Streamlines; without circulation	AHA, Fig. 134, p. 176
Curved plate, circular-arc shape	Ideal, 2-diml	Streamlines; with circulation	AHA, Fig. 140, p. 179 STG, 1923, p. 260 (includes equipotential lines)
Airfoil, cambered	Ideal, 2-diml	Streamlines, with trailing vortexes	HAM, 1934, p. 219
Airfoil, cambered	Ideal, 2-diml	Streamlines only	MDFD, 1938, Vol. I, Fig. 10(c), p. 34
Circular rod, rotating	Ideal, 2-diml	Streamlines	TH, 1950, p. 177 EMF, 1946, Figs. 139(b), 139(c), p. 273 EH, 1950, Figs. 91(b), 91(c), p. 128 AHA, 1934, pp. 83–84 and Fig. 136, p. 178 HAM, 1934, p. 175 MDFD, 1938, Vol. I, p. 33
Flat plate, inclined	Ideal, 2-diml	Streamlines	EMF, 1946, Figs. 141(b), 141(c), p. 279 AHA, 1934, Fig. 106, p. 160 HAM, 1934, Fig. 106, p. 176

These Dutch authors also summarize the results of model experiments by G. Flügel ["Vergleichsversuche an Rudermodellen (Comparative Tests of Model Rudders)," Schiffbau, Schiffahrt und Hafenbau, 15 Jun 1940, pp. 167–169; 8 Jul 1940, pp. 189–194]. Among nine rudder sections tested, Rudder VIII and Rudder IX were of the compound type. Curves of lift coefficient, drag coefficient, moment coefficient on the stock, and ratio of (1) distance of center of pressure CP from the leading edge to (2) chord length of the complete assembly are to be found in Fig. 216 on page 326 of RPSS, 1948.

Data relative to the action of both the control surface and the ship hull in its entirety, in producing a swinging or other moment on the hull, are discussed under control-surface design in Chap. 74.

44.6 Flow Patterns Around Typical Hydrofoils. The published literature on aerodynamics and hydrodynamics contains a considerable number of diagrams depicting the flow about airfoils and hydrofoils of various shapes. There are also a number of published photographs, taken with the aluminum-powder or an equivalent method, which illustrate the nature of the flow around hydrofoils and airfoils throughout rather large ranges of the angle of attack.

Table 44.b lists a number of references where flow diagrams may be found. Table 44.c lists references containing good reproductions of flow photographs.

Fig. 44.E illustrates the typical flow pattern about a symmetrical hydrofoil at a moderate angle of attack, as calculated for an ideal fluid and as determined for a real fluid during a test in a wind tunnel.

TABLE 44.c—List of References Containing Photographs of Flow About Airfoils and Hydrofoils

Type or Shape of Hydrofoil	Kind of Flow	Kind of Diagram	Reference
Airfoil section, stationary	Real, 2-diml	Al. powder; 6 sequence photos	AHA, 1934, Pls. 17–20, pp. 296–299
Airfoil section, moving	Real, 2-diml	Al. powder; 4 sequence photos	TH, 1950, Frontispiece, Pl. 1, 2 AHA, 1934, Pls. 21, 22, pp. 300–301
Airfoil section, moving	Real, 2-diml	Al. powder; 3 sequence photos	EMF, 1946, p. 280
Airfoil section at various angles of attack	Real, 2-diml	Al. powder; 3 photos, 5, 10, 15 deg	EMF, 1946, Pl. XXII, p. 283
Cylinder, rotating	Real, 2-diml	Al. powder; many sequence photos	AHA, 1934, Pls. 5–11, pp. 281–287
Hydrofoil section, stationary	Real, 2-diml	For angles of attack of 0, 10, and 25 deg	ATMA, 1938, Figs. 1–5, pp. 82–83

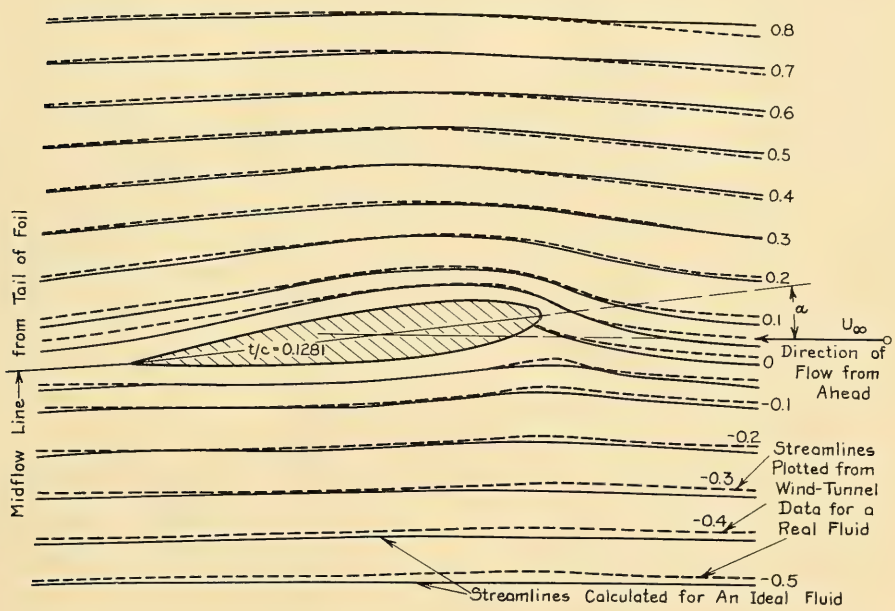

Fig. 44.E Flow Patterns Around a Symmetric Hydrofoil at an Angle of Attack, for Ideal and Real Liquids

This diagram is adapted from one published as Fig. 180 on page 457 of Volume II of the book "Modern Developments in Fluid Dynamics," edited by S. Goldstein and published by the Oxford Press, 1938.

The reader is cautioned to remember that flow patterns made on a plate held firmly against the end of a hydrofoil, normal to its axis, are liable to be misleading. There is a boundary layer of indefinite thickness over this plate, and the pattern depicted on it is affected to some extent by flow at the bottom of this layer ["Photographs of the Flow About an NACA 23015 Airfoil at an Effective Reynolds Number of 480,000," TMB Rep. 557, Apr 1946].

F. Gutsche has published a series of photographs which show the flow traces over hydrofoils which comprise the blades of experimental model screw propellers. These show the paths taken by the surrounding liquid when passing over and between the blades, as viewed generally normal to the projected area of the blade ["Versuche an umlaufenden Flügelschnitten mit abgerissener Strömung (Experiments on Rotating Blade Sections with Breakaway Flow)," Report of the Berlin Model Basin, published in STG, 1940, Vol. 41, pp. 188–226].

44.7 Pitching Moment; Center-of-Pressure Location. As a rule, information as to the pitching-moment coefficient and location of the center of pressure on a hydrofoil to be used on a ship is as important as that relating to the lift and drag coefficients themselves. Indeed, if the hydrofoil can not be rotated in service to change its angle of attack it may be well-nigh useless. The torque applied by hydrodynamic action on the blades of controllable propellers and on rudders is necessary knowledge for their design. The location of the effective center of pressure on the entire underwater body of a turning ship, considered as a hydrofoil, is a major factor in its maneuvering characteristics and in the heel while turning.

Most of the moment (and other) data relating to foils and available for engineering use apply to airfoils. For these a fore-and-aft aerodynamic center is usually assumed, about which the (pitching) moment coefficient for various conditions is relatively constant. This center is sometimes taken on the chord of the meanline, at a distance of $c/4$ from the nose, but usually it lies on the base chord, at the same distance from the nose.

As an indication of what may normally be expected in the way of chordwise shift of the center of pressure CP with varying angle of attack, Fig. 44.F illustrates this feature graphically for a flat, rectangular plate (diagram 1) and for an airfoil section of not-unusual shape (diagram 2).

Some quantitative data on this item, for simple hydrofoils and others suitable for ship rudders, are given in items I. through IV. of Sec. 44.3.

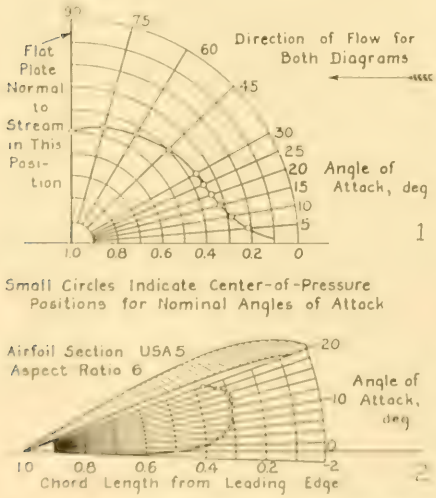

Fig. 44.F Diagrams Illustrating Shift of Center-of-Pressure Position With Angle of Attack, for a Flat Plate and a Hydrofoil

44.8 Distribution of Velocity and Pressure on a Hydrofoil. The distribution of velocity and pressure on an airfoil or hydrofoil, discussed in the present section, is that occurring on and measured directly at its external surface. This is to be distinguished from the velocity and pressure fields around it, described in Sec. 44.9 following, which are those existing outside of and beyond the external foil surface. In general, the pressures occurring on the foil surface determine the lift, drag, and other forces exerted on or by it. The pressures occurring in the adjacent field determine the forces on adjacent objects.

Hydrofoils of symmetric section are widely used in ship design and construction. Figs. 44.G, 44.H, and 44.I, adapted from Volume II of the book "Modern Developments in Fluid Dynamics," edited by S. Goldstein, Oxford Press, 1938 (Fig. 179 on page 455, Fig. 136 on page 402, and Fig. 139 on page 404, respectively), give the chordwise distribution of pressure coefficient on eight typical symmetric sections, covering a wide range of thickness ratios t_x/c. The angle of attack is zero, so the pressures on both sides are the same.

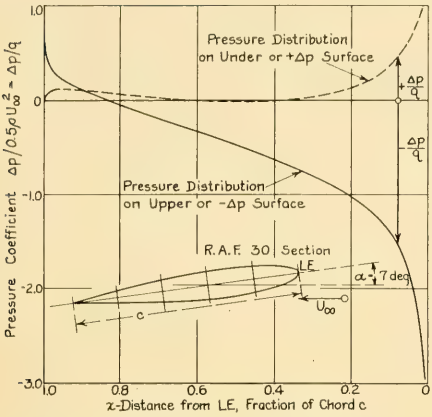

FIG. 44.G TYPICAL CHORDWISE PRESSURE DISTRIBUTION ON FACE AND BACK OF A SYMMETRIC HYDROFOIL AT AN ANGLE OF ATTACK

At the nose the dynamic pressure equals the ram pressure $0.5\rho U_\infty^2$ or $1.00q$. On the back of a symmetric section working at a small angle of attack, the pressure coefficient usually drops very rapidly with distance abaft the nose, to a value of 0.0 at 2 or 3 per cent of the chord. Within from 5 to 20 per cent of the chord length from the leading edge it increases numerically to a large negative value. Then it diminishes with distance abaft the nose, until at about 0.9 or more of the chord length the pressure coefficient may reach zero or have a small positive value. On the face of the section, in a typical case with a small angle of attack, the pressure coefficient drops from its value of 1.00 at the nose to a small positive value, which it holds for most of the chord length from nose to tail.

Pressure-distribution curves for shaft-strut sections in the form of thick symmetric hydrofoils are given by M. S. Macovsky, W. L. Stracke, and J. V. Wehausen in TMB Report 879, issued in January 1948. Two typical sections were tested, having a common thickness ratio of 1/6. One was the Bureau of Ships standard strut section, with a pointed tail, and the other the TMB-EPII (Ellipse-Parabola-Hyperbola) section, with a rounded tail. The pressure distributions were measured for angles of attack of 0, 5, 10, and 15 deg.

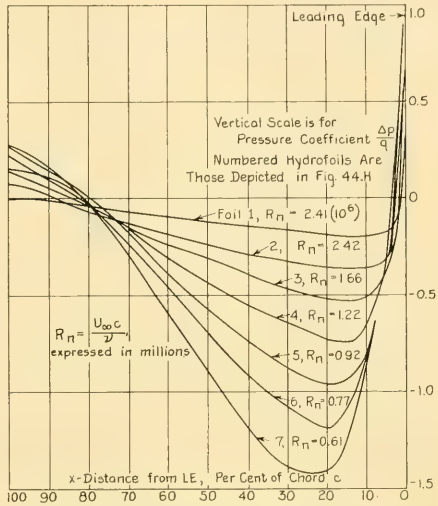

FIG. 44.I CHORDWISE PRESSURE DISTRIBUTION ON THE SURFACES OF THE SEVEN HYDROFOILS OF FIG. 44.H

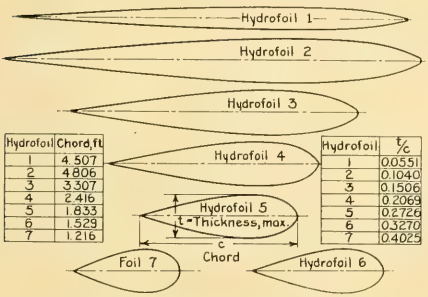

Hydrofoil	Chord, ft
1	4.507
2	4.806
3	3.307
4	2.416
5	1.833
6	1.529
7	1.216

Hydrofoil	t/c
1	0.0551
2	0.1040
3	0.1506
4	0.2069
5	0.2726
6	0.3270
7	0.4029

FIG. 44.H SHAPES AND CHARACTERISTICS OF SEVEN SYMMETRIC HYDROFOILS FOR WHICH THE PRESSURE DISTRIBUTION IS GIVEN IN FIG. 44.I

Many similar diagrams and other data on the distribution of velocity and pressure around airfoils and hydrofoils are published in the technical literature. Among the sources may be mentioned:

(1) Zeitschrift für Flugtechnik und Motorluftschiffahrt, 26 Apr 1913, Vol. IV, No. 8, Fig. 9, p. 92. A series of 56 diagrams show the pressure distribution over the face and back of eight sections of the blade of an airscrew at eight different radii, from 0.25 to 1.00 R_{Max}. The measurements were made at seven values of the real-slip ratio, from +0.11 to +1.00, and from −0.06 to −0.15. As is to be expected, the distribution of pressure over face and

back of the several sections shows wide variations for the extreme values of real-slip ratio represented in the test.

(2) Jones, B. M., and Paterson, C. J., "Investigation of the Distribution of Pressure over the Entire Surface of an Aerofoil," Tech. Rep. Adv. Comm. for Aero for 1912–1913 (England), R and M 73, Mar 1913, pp. 97–108

(3) Norton, F. H., and Bacon, D. L., "Pressure Distribution over Thick Airfoils—Model Tests," NACA Rep. 150, 1922, pp. 451–471. On pp. 451–452 there is a list of a number of prior references on pressure distribution over airfoils.

(4) Fage, A., and Howard, R. G., "A Consideration of Airscrew Theory in the Light of Data Derived from an Experimental Investigation of the Distribution of Pressure over the Entire Surface of an Airscrew Blade, and also Over Aerofoils of Appropriate Shapes," ARC, R and M 681, Mar 1921, pp. 264–357. Pressure measurements were taken on a full-size airscrew, one point at a time.

(5) Briggs, L. J., and Dryden, H. L., "Pressure Distribution Over Airfoils at High Speeds," NACA Rep. 255, 1926

(6) Fage, A., "The Flow of Air and of an Inviscid Fluid Around an Elliptic Cylinder and an Aerofoil of Infinite Span, Especially in the Region of the Forward Stagnation Point," Tech. Rep. Aero. Res. Comm. (England), 1927–1928, Vol. I, R and M 1097, Jul 1926, pp. 61–80

(7) Perring, W. G. A., "The Theoretical Pressure Distribution Around Joukowski Aerofoils," Tech. Rep. Aero. Res. Comm. (England), 1927–1928, Vol. I, R and M 1106, May 1927, pp. 209–221

(8) Perring, W. G. A., Discussion, INA, 1928, Fig. B on p. 253

(9) Knight, M., and Loeser, O., Jr., "Pressure Distribution over a Rectangular Monoplane Wing Model Up to 90 Degrees Angle of Attack," NACA Rep. 288, 1928

(10) Gutsche, F., "Versuche an Propellerblattschnitten (Tests on Propeller Blade Sections)," Schiffbau, 1 Aug 1933, pp. 267–270; 15 Aug 1933, pp. 286–289. The latter group of pages contains many graphs of pressure distribution on airfoil sections.

(11) Schoenherr, K. E., SNAME, 1934, p. 90. Contours for pressure minima in terms of (1) $\Delta p/q$, (2) thickness ratio, and (3) lift coefficient, for ogival and airfoil sections, respectively, are given in Figs. 19 and 20, pp. 109–112.

(12) Winter, H., "Flow Phenomena on Plates and Airfoils of Short Span," NACA Tech. Memo 798, Jul 1936, pp. 7–9 and Figs. 21–24

(13) Shannon, J. F., and Arnold, R. N., "Statistical and Experimental Investigations on the Singing Propeller Problem," IESS, 1938–1939, Vol. 82, pp. 255–374, esp. pp. 270–285, 326

(14) Schoenherr, K. E., PNA, 1939, Vol. II, Fig. 29, p. 176. This diagram gives the pressure distribution along the chord of a hydrofoil (or airfoil) section at an 8.6-degree angle of attack.

(15) Goodall, Sir Stanley V., "Sir Charles Parsons and the Royal Navy," INA, Apr 1942, pp. 1–16, esp. Fig. 5, p. 3; see also SBSR, 23 Apr 1942, p. 451

(16) Van Lammeren, W. P. A., RPSS, 1948, Fig. 104, p. 161

(17) Hill, J. G., "The Design of Propellers," SNAME, 1949, Fig. 11, p. 151. This diagram shows the graphs of pressure coefficient $\Delta p/q$, on a base of per cent of chord from the leading edge, for the backs of two NACA sections with two different camber ratios and two angles of attack.

(18) Reed, T. G., and Ormsby, R. B., Jr., "The AVA Method of Calculating Pressure Distributions Over Profiles of Arbitrary Shape (Including a Translation of 'Über die Berechnung der Druckverteilung von Profilen,' by F. Riegels, Technische Berichte, 1943, Vol. 10)," TMB Aero. Memo 28, Mar 1955.

44.9 Velocity and Pressure Fields Around a Hydrofoil. In Fig. 44.E of Sec. 44.6 there are pictured two flow patterns around a typical symmetric airfoil or hydrofoil, one corresponding to the flow of an ideal liquid and one of a real liquid. Tables 44.b and 44.c of that section list references to diagrams and flow patterns around other airfoils and hydrofoils, made up generally of streamlines. However, the designer can often use to advantage a chart or plot embodying isobars and isotachyls, to show the essential characteristics of the pressure and velocity fields around the foil.

Unfortunately, the published data on this particular item are very meager and there appear to be no distribution plots that can be taken as typical. Most of the data apply to airfoils, of the customary asymmetric sections used for airplane wings. They were taken usually to indicate acceptable positions for the pitot tubes of airspeed meters, and so do not cover the fields surrounding the airfoil as a whole.

A few references indicate sources of some of the published results for projects of this kind:

(1) Piercy, N. A. V., and Richardson, E. G., "On the Flow of Air Adjacent to the Surface of an Aerofoil," ARC, R and M 1224, Dec 1928, pp. 326–348

(2) Tanner, T., "The Two-Dimensional Flow of Air Around an Aerofoil of Symmetrical Section," ARC, R and M 1353, Jul 1930, pp. 106–116

(3) Parsons, J. F., "Full-Scale Wind-Tunnel Tests to Determine a Satisfactory Location for a Service Pitot-Static Tube on a Low-Wing Monoplane," NACA Tech. Note 561, Mar 1936

(4) Gates, S. B., and Cohen, J., "Note on the Standardisation of Pitot-Static Head Position on Monoplanes," ARC, R and M 1778, Jan 1937, pp. 1238–1251

(5) Crabbe, E. R., and Diproso, K. V., "Calculated Pressures Ahead of Struts and Wings," R.A.E., Farnborough (England), Technical Note Aero 1516, Oct 1944

(6) Kuethe, A. M., McKee, P. B., and Curry, W. H., "Measurements in the Boundary Layer of a Yawed Wing," NACA Tech. Note 1946, Sep 1949.

44.10 Spanwise Distribution of Circulation and Lift. Secs. 14.8 and 14.9 and Figs. 14.I and 14.J illustrate the variations that may occur, or that may be planned in the spanwise distribution of circulation and lift across a hydrofoil. These diagrams, plus Figs. 14.L and 14.O, show about where the principal trailing vortexes may be expected for certain circulation distributions. In practice, particular spanwise distributions of circulation and lift are desired for the purpose of:

(a) Reducing the tip-vortex strength and severity, in an effort to reduce the force and energy losses there, as well as the induced drag
(b) Eliminating almost entirely the root vortexes in a cantilevered hydrofoil. This may be done at the roots of screw-propeller blades to reduce the strength and harmful effects of the swirl core.
(c) Applying the greater part of the lift load at a given point or in a given region across the span, because of strength, rigidity, or other requirements
(d) Reducing the magnitude of the $-\Delta p$ values in a region where air is liable to be sucked down from the surface. An example is the top of a rudder which has only a thin layer of water above it.
(e) Distributing the lift load to achieve the greatest efficiency for the hydrofoil as a whole.

The desired circulation distribution is generally obtained by changing the nominal angle of attack across the span, with respect to the probable direction of the inflow velocity. In this connection, it is to be remembered that, as the angle of attack is reduced, the circulation, the lift, *and* the induced velocity diminish with it. A large induced velocity results in a large actual angle of attack, for which compensation must be made when shaping the hydrofoil.

Another method of reducing the circulation and the lift is to diminish the camber of the sections in question. This must usually be done without changing the section thickness, since the latter is required for strength, rigidity, and other considerations.

44.11 Effective Aspect Ratio for Equivalent Ship Hydrofoils. No general procedure is known for determining the effective aspect ratio of a hydrofoil when either or both ends lie close to surfaces which may act as the end plates described in Secs. 14.7 and 14.8 and illustrated in Figs. 14.H, 14.I, and 14.M. Indeed, the effective aspect ratio depends largely on the spanwise distribution of circulation and lift that actually obtains, and is by no means an independent function of the geometric planform shape and proportions. This is because the effectiveness of the end plate depends upon the magnitude of the overall pressure differential between the $+\Delta p$ and the $-\Delta p$ surfaces. If the pressure differential at the tip is zero, and if this differential increases at only a slow rate inboard from the tip, there is no need for an end plate. With a large pressure differential at the tip, an end plate of adequate area (if it were practical) would create an effective aspect ratio roughly twice that of the actual geometric ratio.

At one limit it is probably sufficiently accurate for engineering purposes to say that a gap parallel to the span, equal to the adjacent chord length, has the same effect as one of great width. A tip or an end next to such a gap may be considered free, beyond the influence of the adjacent structure acting as an end plate.

At the other limit the customary working or construction tip clearance used in mechanical design is large enough to prevent the adjacent structure from serving as an end plate, and the hydrofoil from behaving as one of infinite length and aspect ratio. Furthermore, an end plate attached to a tip with zero gap is probably not effective as such unless it extends for at least one chord length *all around* the section. The hub surface of a screw propeller, as one example, is almost never adequate for this purpose, when considered as a combined inner end plate for all the blades.

44.12 Design Notes and Drag Data on Hydrofoil Planforms and Sections. This section is intended to cover hydrofoils designed and fitted for general and special purposes. The design of control-surface hydrofoils is discussed in Chap. 74 and of screw-propeller blades in Chap. 70.

Aside from the influence of planform on the aspect ratio, the principal features in the selection of hydrofoil planforms and section shapes involve:
(a) Increasing the chord length and thickness at points where the foil attaches to some fixed member or structure and where the end-plate effect is sufficient to prevent loss of overall Δp
(b) Diminishing the chord length at the tip because of the low strength needed there and the reduction in tip-vortex loss which normally accompanies the use of a short tip. Values of the taper ratio c_T/c_R may range from 0.3 or less for fixed fins to 1.0 or more for screw-propeller blades.

If rake or sweep-back is necessary or desirable in the leading edge of a hydrofoil, and if the trailing edge is raked in the opposite direction so that the hydrofoil has a taper ratio less than 1.0, the behavior and characteristics may be estimated on the basis of a number of chordwise elements having small spans Δb and varying chord lengths. If the raked or swept-back hydrofoil has approximately constant chord over the span, its performance may be predicted on a basis of (1) a span normal to the relative-flow direction equal to the diagonal length of the hydrofoil, and (2) a relative-flow velocity equal to the direction-of-motion speed times the cosine of the angle of sweep-back. This corresponds to the situation depicted in diagram 1 of Fig. 17.D on page 265 of Volume I.

The appropriate chapters of Part 5 in Volume III describe and illustrate the manner in which ship hulls themselves act as low-aspect-ratio hydrofoils. Of still smaller aspect ratio are the fixed roll-resisting keels whose design is discussed in Secs. 73.15 and 73.16, especially the forward portions which run at varying angles of attack as the ship pitches and rolls.

The maximum section thickness t_x and thickness ratios t_x/c are, more often than not, fixed by requirements for strength and stiffness. Nevertheless, it is well for the designer to know something of the effect of thickness ratio upon hydrofoil drag. Fig. 44.J, adapted from "Modern Developments in Fluid Dynamics," edited by S. Goldstein (Fig. 137 on page 402 of Volume II), indicates the variation in drag coefficient with thickness ratio to be expected on a Joukowski type of airfoil section at low R_n values. Fig. 44.K,

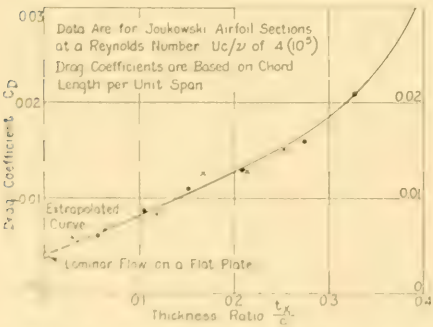

Fig. 44.J Variation in Residuary-Drag Coefficient of Joukowski Airfoil Sections With Thickness Ratio

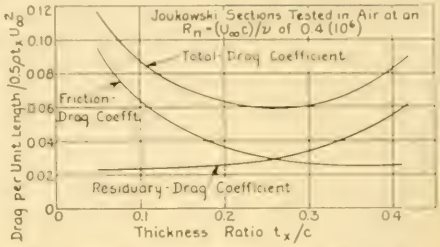

Fig. 44.K Variation of Total-Drag, Friction-Drag, and Residuary-Drag Coefficients of a Joukowski Airfoil With Thickness Ratio

adapted from Fig. 138 on page 138 of Volume II of the referenced book, gives representative values for the total-drag, friction-drag, and residuary-drag coefficients, on a base of thickness ratio, for Joukowski airfoil sections.

44.13 Quantitative Data on Cascade and Interference Effects. On the basis that interference effects do exist between the flows around hydrofoils placed abreast or in cascade, despite the qualifying statement in the last paragraph of Sec. 14.15 on page 228 of Volume I, the matter of allowing for or predicting these effects poses many difficulties. So far as known, there are no reasonably simple or straightforward rules or procedures by which the marine architect may execute a proper new design or even estimate the behavior of an existing design involving two or more hydrofoils approximately abreast each other.

In every screw propeller, even though it has only two blades, there are some small radii where the stagger between blade sections is small with respect to the gap. However, the interference effects here, in the case of an analytic design based upon the circulation or vortex theory, are taken care of by other portions of the design procedure, as described in Chap. 70. It is not easy to transfer the correction procedure to another problem, such as to that of twin or triple steering rudders, side by side.

Problems involving the use of rather closely spaced hydrofoils in cascade are of common occurrence in the design of pumps for handling fluids of all kinds. Although there is an extensive literature in this field, the symbols, methods of analysis, and design procedures for hydraulic machinery are so different from those customary in marine propulsion and related fields that they are not in a form readily usable by naval architects and marine engineers.

Nevertheless, a few of these references are quoted here:

(a) Gutsche, F., "Versuche an Propellerblattschnitten (Tests on Propeller Blade Sections)," Schiffbau, 1 Aug 1933, pp. 267–270; 15 Aug 1933, pp. 286–289; 1 Sep 1933, pp. 303–306. Some of these original data are worked over and adapted by K. E. Schoenherr [SNAME, 1934, pp. 105–107, esp. Fig. 15 on p. 106].

(b) Spannhake, W., "Centrifugal Pumps, Turbines and Propellers," MIT Press, Cambridge (Mass.), 1934

(c) Wislicenus, G. F., FMTM, McGraw-Hill, 1947

(d) Rouse, H., EH, 1950, Chap. XIII, pp. 858–992. A list of 54 references is given on pp. 990–992.

A recent reference, written entirely in readable, straightforward English, is the description of the analytic and experimental work undertaken by Commander W. T. Sawyer, USN, as his doctorate dissertation at the Federal Technical Institute in Zürich, Switzerland. It is entitled "Experimental Investigation of a Stationary Cascade of Aerodynamic Profiles," Mitteilungen aus dem Institut für Aerodynamik, No. 17, an der Eidgenössichen Technischen Hochschule in Zürich, 1949, Verlag Leeman, Zürich (copy in TMB library).

CHAPTER 45

Viscous-Flow Data and Friction-Resistance Calculations

45.1 General. Chaps. 5, 6, and 22 of Volume I give a general physical picture of the viscous flow in a real liquid along flat and curved plate surfaces, and around the external boundaries of an underwater ship hull. The reader who may find useful a somewhat different exposition of friction is referred to a paper by Senor M. L. Acevedo, Superintendent of the Model Basin at El Pardo, near Madrid, Spain, entitled "Ship Friction Resistance." This is an amplified version (in English) of the contribution actually presented by Senor Acevedo at the Fifth International Conference of Ship Tank Superintendents, held in London in September, 1948. It gives a brief resumé of the development of the various friction formulas, a most elaborate comparison of the results obtained from each, and a set of requirements for a satisfactory and acceptable friction formulation. A copy of this paper is available in the TMB library.

There are assembled in the present chapter the formulas, equations, and other quantitative data required for estimating or predicting various features of the viscous flow around bodies and ships, including the friction resistance. Fig. 45.A summarizes these data for convenience and the subsequent sections of this chapter explain how they are used to derive numerical answers for a ship and some of its parts.

The method of calculating and using the Reynolds number and its several variations is described in Sec. 41.5 and in subsequent sections of the present chapter. The Reynolds number serves not only as a flow parameter but as an indicator of the type of viscous flow which may be expected around a body under a given set of conditions. This latter feature is of interest in model rather than in ship work, because most of the Reynolds numbers for models are in the low ranges.

One other feature involving the use of the Reynolds number in practice does require mention. It is customary in many quarters, when considering only the viscous-flow situation for

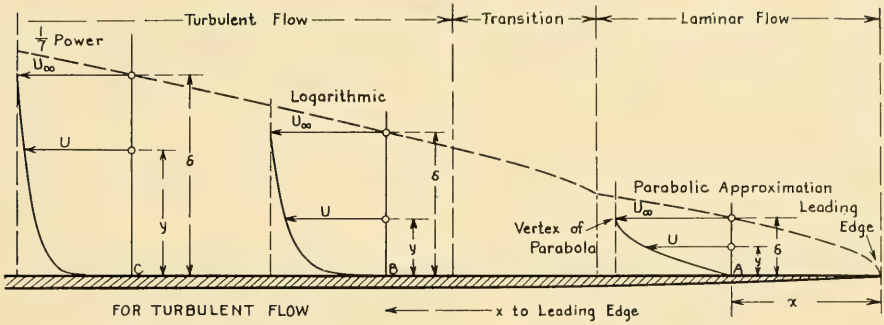

FOR TURBULENT FLOW

Equation of Profile, $U = Cy^{\frac{1}{7}}$ or $U = U_\infty\left(\frac{y}{\delta}\right)^{\frac{1}{7}}$

Equation of Profile, $U = C \log y$ or $U = U_\infty \frac{\log y}{\log \delta}$

Nominal Thickness of Layer at Points B and C, $\delta = 0.38\,x\left(\frac{\nu}{U_\infty x}\right)^{0.2} = 0.38\,x\,R_x^{-0.2}$

Displacement Thickness $\delta^* = 0.14\,\delta$, abt.

Sublayer Thickness $\delta_L = k\frac{\nu}{U_T}$, where $11.6 < k < 12.6$

Momentum Thickness $\theta = 0.097\,\delta$

Shape Factor $H = \frac{\delta^*}{\theta} = 1.3$ to 1.5

Energy Thickness $\theta^* = 0.175\,\delta$, abt.

Shear Stress at Plate $\tau_0 = C_{LF} \cdot q = 0.059 q \cdot R_x^{-0.2}$

Shear Velocity $U_T = \left(\frac{\tau_0}{\rho}\right)^{0.5}$

Shearing-Stress Coefficient $C_T = \frac{\tau}{0.5\rho U_\infty^2} = \frac{\tau}{q}$

Local Frictional-Drag Coefficient at Points B and C, $C_{LF} = 0.059\,R_x^{-0.2}$

Mean Drag Coefficient for x-Distance to B or C, $C_F = 0.074\,R_x^{-0.2}$

FOR LAMINAR FLOW

Equation of Profile, $U_\infty - U = a(\delta - y)^2$ or $U = U_\infty - \frac{U_\infty}{\delta^2}(\delta - y)^2$

Nominal Thickness of Layer at any Point A, $\delta = 5\,x\left(\frac{\nu}{U_\infty x}\right)^{0.5} = 5\,x\,R_x^{-0.5}$

Displacement Thickness $\delta^* = 1.73\,x\,R_x^{-0.5} = 0.35\,\delta$, abt.

Sublayer Thickness δ_L = (Entire Layer is Laminar)

Momentum Thickness $\theta = 0.133\,\delta$, abt.

Shape Factor $H = \frac{\delta^*}{\theta} = 2.6$, abt.

Energy Thickness θ^* = (Not Applicable in This Case)

Shear Stress at Plate $\tau_0 = C_{LF} \cdot q = 0.66 q \cdot R_x^{-0.5}$

Shear Velocity $U_T = \left(\frac{\tau_0}{\rho}\right)^{0.5}$

Shearing-Stress Coefficient $C_T = \frac{\tau}{0.5\rho U_\infty^2} = \frac{\tau}{q}$

Local Frictional-Drag Coefficient at Any Point A, $C_{LF} = 0.66\,R_x^{-0.5}$

Mean Drag Coefficient for x-Distance to A, $C_F = 1.33\,R_x^{-0.5}$

FIG. 45.A SUMMARY OF VISCOUS-FLOW FORMULAS FOR LAMINAR AND TURBULENT FLOW

the entire length L of a body or ship, to use the symbol R_n. When this is done it almost invariably signifies that the space dimension in the Reynolds number is that entire length. However, in many studies of viscous flow and boundary-layer development it becomes necessary to consider the situation at or ahead of a certain point along the body or ship which has an x-distance less than the length L. In these cases the Reynolds number for the situation under study is the x-Reynolds number, expressed as R_x, with the x-distance from the leading edge or stem stated in each case. For example, in the formulas of Figs. 5.R and 45.A, the symbol R_n is used in connection with values averaged for the whole length, while R_x is used for local values, or for situations where the x-distance is itself a factor in the formula.

It seems almost certain that there are factors in viscous flow not taken into account by the Reynolds number, but until more is known of them, they can not well be considered in any quantitative treatment of friction resistance.

Friction-resistance calculations are necessary for the Froude method of predicting ship resistance, in which the residuary resistance derived from tests of a model of the same proportions and shape is added to the friction resistance deduced from resistance tests of flat, smooth surfaces in the form of thin planks or friction planes.

Because of the limitations of model-testing equipment it is still necessary to extrapolate the flat, smooth-plate data well beyond the experimental range, especially for large, fast vessels. It has not been possible to check this extrapolation in the latter range by full-scale ship measurements

TABLE 45.4.—REYNOLDS NUMBERS FOR VARIOUS SHIP LENGTHS AND SPEEDS IN STANDARD FRESH WATER

Velocity		Length of body or ship, ft											
ft per sec	kt	5	10	15	20	25	30	35	40	45	50	60	70
2	1.18	0.814	1.628	2.442	3.256	4.070	4.884	5.698	6.512	7.326	8.140	9.768	11.40
3	1.78	1.221	2.442	3.663	4.884	6.105	7.326	8.447	9.768	10.99	12.21	14.65	17.09
4	2.39	1.628	3.256	4.884	6.512	8.140	9.768	11.40	13.02	14.65	16.28	19.54	22.79
5	2.96	2.035	4.070	6.105	8.140	10.18	12.21	14.25	16.28	18.32	20.35	24.42	28.49
6	3.55	2.442	4.884	7.326	9.768	12.21	14.65	17.09	19.54	21.98	24.42	29.30	34.19
7	4.14	2.849	5.698	8.547	11.40	14.25	17.09	19.94	22.79	25.64	28.49	34.19	39.89
8	4.74	3.256	6.512	9.768	13.02	16.28	19.54	22.79	26.05	29.30	32.56	39.07	45.58
9	5.33	3.663	7.326	10.99	14.65	18.32	21.98	25.64	29.30	32.97	36.63	43.96	51.28
10	5.92	4.070	8.140	12.21	16.28	20.35	24.42	28.49	32.56	36.63	40.70	48.84	56.98
11	6.51	4.477	8.954	13.43	17.91	22.39	26.86	31.34	35.82	40.29	44.77	53.72	62.68
12	7.10	4.884	9.768	14.65	19.54	24.42	29.30	34.19	39.07	43.96	48.84	58.61	68.38
13	7.70	5.291	10.58	15.87	21.16	26.46	31.75	37.04	42.33	47.62	52.91	63.49	74.07
14	8.29	5.698	11.40	17.09	22.79	28.49	34.19	39.89	45.58	51.28	56.98	68.38	79.77
15	8.88	6.105	12.21	18.32	24.42	30.53	36.63	42.74	48.84	54.95	61.05	73.26	85.47
16	9.47	6.512	13.02	19.54	26.05	32.56	39.07	45.58	52.10	58.61	65.12	78.14	91.17
17	10.1	6.919	13.84	20.76	27.68	34.60	41.51	48.43	55.35	62.27	69.19	83.03	96.87
18	10.7	7.326	14.65	21.98	29.30	36.63	43.96	51.28	58.61	65.93	73.26	87.91	102.6
19	11.2	7.733	15.47	23.20	30.93	38.67	46.40	54.13	61.86	69.60	77.33	92.80	108.3
20	11.8	8.140	16.28	24.42	32.56	40.70	48.84	56.98	65.12	73.26	81.40	97.68	114.0
22	13.0	8.954	17.91	26.86	35.82	44.77	53.72	62.68	71.63	80.59	89.54	107.5	125.4
24	14.2	9.768	19.54	29.30	39.07	48.84	58.61	68.38	78.14	87.91	97.68	117.2	136.8
26	15.4	10.58	21.16	31.75	42.33	52.91	63.49	74.07	84.66	95.24	105.8	127.0	148.2
28	16.6	11.40	22.79	34.19	45.58	56.98	68.38	79.77	91.17	102.6	114.0	136.8	159.5
30	17.8	12.21	24.42	36.63	48.84	61.05	73.26	85.47	97.68	109.9	122.1	146.5	170.9
32	18.9	13.02	26.05	39.07	52.10	65.12	78.14	91.17	104.2	117.2	130.2	156.3	182.3
34	20.1	13.84	27.68	41.51	55.35	69.19	83.03	96.87	110.7	124.5	138.4	166.1	193.7
36	21.3	14.65	29.30	43.96	58.61	73.26	87.91	102.6	117.2	131.9	146.5	175.8	205.1
38	22.5	15.47	30.93	46.40	61.86	77.33	92.80	108.3	123.7	139.2	154.7	185.6	216.5
40	23.7	16.28	32.56	48.84	65.12	81.40	97.68	114.0	130.2	146.5	162.8	195.4	227.9
42	24.9	17.09	34.19	51.28	68.38	85.47	102.6	119.7	136.8	153.9	170.9	205.1	239.3
44	26.1	17.91	35.82	53.72	71.63	89.54	107.5	125.4	143.3	161.2	179.1	214.9	250.7
46	27.2	18.72	37.44	56.17	74.89	93.15	111.8	131.1	149.8	168.5	187.2	224.7	262.1
48	28.4	19.54	39.07	58.61	78.14	97.68	117.2	136.8	156.3	175.8	195.4	234.4	273.5
50	29.6	20.35	40.70	61.05	81.40	101.8	122.1	142.5	162.8	183.2	203.5	244.2	284.9
52	30.8	21.16	42.33	63.49	84.66	105.8	127.0	148.2	169.3	190.5	211.6	254.0	296.3
54	32.0	21.98	43.96	65.93	87.91	109.9	131.9	153.9	175.8	197.8	219.8	263.7	307.7
56	33.2	22.79	45.58	68.38	91.17	114.0	136.8	159.5	182.3	205.1	227.9	273.5	319.1
58	34.3	23.61	47.21	70.82	94.42	118.0	141.6	165.2	188.9	212.5	236.1	283.3	330.5
60	35.5	24.42	48.84	73.26	97.68	122.1	146.5	170.9	195.4	219.8	244.2	293.0	341.9
62	36.7	25.23	50.47	75.70	100.9	126.2	151.4	176.6	201.9	227.1	252.3	302.8	353.3
64	37.9	26.05	52.10	78.14	104.2	130.2	156.3	182.3	208.4	234.4	260.5	312.6	364.7
66	39.1	26.86	53.72	80.59	107.5	134.3	161.2	188.0	214.9	241.8	268.6	322.3	376.1
68	40.3	27.68	55.35	83.03	110.7	138.4	166.1	193.7	221.4	249.1	276.8	332.1	387.5
70	41.4	28.49	56.98	85.47	114.0	142.5	170.9	199.4	227.9	256.4	284.9	341.9	398.9
72	42.6	29.30	58.61	87.91	117.2	146.5	175.8	205.1	234.4	263.7	293.0	351.7	410.3
74	43.8	30.12	60.24	90.35	120.5	150.6	180.7	210.8	240.9	271.1	301.2	361.4	421.7
76	45.0	30.93	61.86	92.80	123.7	154.7	185.6	216.5	247.5	278.4	309.3	371.2	433.1
78	46.2	31.75	63.49	95.24	127.0	158.7	190.5	222.2	254.0	285.7	317.5	381.0	444.4
80	47.4	32.56	65.12	97.68	130.2	162.8	195.4	227.9	260.5	293.0	325.6	390.7	455.8
82	48.5	33.37	66.75	100.1	133.5	166.9	200.2	233.6	267.0	300.4	333.7	400.5	467.2
84	49.7	34.19	68.38	102.6	136.8	170.9	205.1	239.3	273.5	307.7	341.9	410.3	478.6
86	50.9	35.00	70.00	105.0	140.0	175.0	210.0	245.0	280.0	315.0	350.0	420.0	490.0
88	52.1	35.82	71.63	107.5	143.3	179.1	214.9	250.7	286.5	322.3	358.2	429.8	501.4
90	53.3	36.63	73.26	109.9	146.5	183.2	219.8	256.4	293.0	329.7	366.3	439.6	512.8
92	54.5	37.44	74.89	112.3	149.8	187.2	224.7	262.1	299.6	337.0	374.4	449.3	524.2
94	55.7	38.26	76.52	114.8	153.0	191.3	229.6	267.8	306.1	344.3	382.6	459.1	535.6
96	56.8	39.07	78.14	117.2	156.3	195.4	234.4	273.5	312.6	351.7	390.7	468.9	547.0
98	58.0	39.89	79.77	119.7	159.5	199.4	239.3	279.2	319.1	359.0	398.9	478.6	558.4
100	59.2	40.70	81.40	122.1	162.8	203.5	244.2	284.9	325.6	366.3	407.0	488.4	569.8

TABLE 45.a—(Continued)

Velocity		Length of body or ship, ft											
ft per sec	kt	80	90	100	120	140	160	180	200	250	300	350	400
2	1.18	13.02	14.65	16.28	19.54	22.79	26.05	29.30	32.56	40.70	48.84	56.98	65.12
3	1.78	19.54	21.98	24.42	29.30	34.19	39.07	43.96	48.84	61.05	73.26	85.47	97.68
4	2.39	26.05	29.30	32.56	39.07	45.58	52.10	58.61	65.12	81.40	97.68	114.0	130.2
5	2.96	32.56	36.63	40.70	48.84	56.98	65.12	73.26	81.40	101.8	122.1	142.5	162.8
6	3.55	39.07	43.96	48.84	56.61	68.38	78.14	87.91	97.68	122.1	146.5	170.9	195.4
7	4.14	45.58	51.28	56.98	68.38	79.77	91.17	102.6	114.0	142.5	170.9	199.4	227.9
8	4.74	52.10	58.61	65.12	78.14	91.17	104.2	117.2	130.2	162.8	195.4	227.9	260.5
9	5.33	58.61	65.93	73.26	87.91	102.6	117.2	131.9	146.5	183.2	219.8	254.0	293.0
10	5.92	65.12	73.26	81.40	97.68	114.0	130.2	146.5	162.8	203.5	244.2	284.9	325.6
11	6.51	71.63	80.59	89.54	107.5	125.4	143.3	161.2	179.1	223.9	268.6	313.4	358.2
12	7.10	78.14	87.91	97.68	117.2	136.8	156.3	175.8	195.4	244.2	293.0	341.9	390.7
13	7.70	84.66	95.24	105.8	127.0	148.2	169.3	190.5	211.6	264.6	317.5	370.4	423.3
14	8.29	91.17	102.6	114.0	136.8	159.5	182.3	205.1	227.9	284.9	341.9	398.9	455.8
15	8.88	97.68	109.9	122.1	146.5	170.9	195.4	219.8	244.2	305.3	366.3	427.4	488.4
16	9.47	104.2	117.2	130.2	156.3	182.3	208.4	234.4	260.5	325.6	390.7	455.8	521.0
17	10.1	110.7	124.5	138.4	166.1	193.7	221.4	249.1	276.8	346.0	415.1	484.3	553.5
18	10.7	117.2	131.9	146.5	175.8	205.1	234.4	263.7	293.0	366.3	439.6	512.8	586.1
19	11.2	123.7	139.2	154.7	185.6	216.5	247.5	278.4	309.3	386.7	464.0	541.3	618.6
20	11.8	130.2	146.5	162.8	195.4	227.9	260.5	293.0	325.6	407.0	488.4	569.8	651.2
22	13.0	143.3	161.2	179.1	214.9	250.7	286.5	322.3	358.2	447.7	537.2	626.8	716.3
24	14.2	156.3	175.8	195.4	234.4	273.5	312.6	351.7	390.7	488.4	586.1	683.8	781.4
26	15.4	169.3	190.5	211.6	254.0	296.3	338.6	381.0	423.3	529.1	634.9	740.7	846.6
28	16.6	182.3	205.1	227.9	273.5	319.1	364.7	410.3	455.8	569.8	683.8	797.8	911.7
30	17.8	195.4	219.8	244.2	293.0	341.9	390.7	439.6	488.4	610.5	732.6	854.7	976.8
32	18.9	208.4	234.4	260.5	312.6	364.7	416.8	468.9	521.0	651.2	781.4	911.7	1042
34	20.1	221.4	249.1	276.8	332.1	387.5	442.8	498.2	553.5	691.9	830.3	968.7	1107
36	21.3	234.4	263.7	293.0	351.7	410.3	468.9	527.5	586.1	732.6	879.1	1026	1172
38	22.5	247.5	278.4	309.3	371.2	433.1	494.9	556.8	618.6	773.3	928.0	1083	1237
40	23.7	260.5	293.0	325.6	390.7	455.8	521.0	586.1	651.2	814.0	976.8	1140	1302
42	24.9	273.5	307.7	341.9	410.3	478.6	547.0	615.4	683.8	854.7	1026	1197	1368
44	26.1	286.5	322.3	358.2	429.8	501.4	573.1	644.7	716.3	895.4	1075	1254	1433
46	27.2	299.6	337.0	374.4	449.3	524.2	599.1	674.0	748.9	936.1	1123	1311	1498
48	28.4	312.6	351.7	390.7	468.9	547.0	625.2	703.3	781.4	976.8	1172	1368	1563
50	29.6	325.6	366.3	407.0	488.4	569.8	651.2	732.6	814.0	1018	1221	1425	1628
52	30.8	338.6	381.0	423.3	507.9	592.6	677.3	761.9	846.6	1058	1270	1482	1693
54	32.0	351.7	395.6	439.6	527.5	615.4	703.3	791.2	879.1	1099	1319	1539	1758
56	33.2	364.7	410.3	455.8	547.0	638.2	729.3	820.5	911.7	1140	1368	1595	1823
58	34.3	377.7	424.9	472.1	566.5	661.0	755.4	849.8	944.2	1180	1416	1652	1889
60	35.5	390.7	439.6	488.4	586.1	683.8	781.4	879.1	976.8	1221	1465	1709	1954
62	36.7	403.7	454.2	504.7	605.6	706.6	807.5	908.4	1009	1262	1514	1766	2019
64	37.9	416.8	468.9	521.0	625.2	729.3	833.5	937.7	1042	1302	1563	1823	2084
66	39.1	429.8	483.5	537.2	644.7	752.1	859.6	967.0	1075	1343	1612	1880	2149
68	40.3	442.8	498.2	553.5	664.2	774.9	885.6	996.3	1107	1384	1661	1937	2214
70	41.4	455.8	512.8	569.8	683.8	797.7	911.7	1026	1140	1425	1709	1994	2279
72	42.6	468.9	527.5	586.1	703.3	820.5	937.7	1055	1172	1465	1758	2051	2344
74	43.8	481.9	542.1	602.4	722.8	843.3	963.8	1084	1205	1506	1807	2108	2409
76	45.0	494.9	556.8	618.6	742.4	866.1	989.8	1114	1237	1547	1856	2165	2475
78	46.2	507.9	571.4	634.9	761.9	888.9	1016	1143	1270	1587	1905	2222	2540
80	47.4	521.0	586.1	651.2	781.4	911.7	1042	1172	1302	1628	1954	2279	2605
82	48.5	534.0	600.7	667.5	801.0	934.5	1068	1202	1335	1669	2002	2336	2670
84	49.7	547.0	615.4	683.8	820.5	957.3	1094	1231	1368	1709	2051	2393	2735
86	50.9	560.0	630.0	700.0	840.1	980.1	1120	1260	1400	1750	2100	2450	2800
88	52.1	573.1	644.7	716.3	859.6	1003	1146	1289	1433	1791	2149	2507	2865
90	53.3	586.1	659.3	732.6	879.1	1026	1172	1319	1465	1832	2198	2564	2930
92	54.5	599.1	674.0	748.9	898.7	1048	1198	1348	1498	1872	2247	2621	2996
94	55.7	612.1	688.6	765.2	918.2	1071	1224	1377	1530	1913	2296	2678	3061
96	56.8	625.2	703.3	781.4	937.7	1094	1250	1407	1563	1954	2344	2735	3126
98	58.0	638.2	718.0	797.7	957.3	1117	1276	1436	1595	1994	2393	2792	3191
100	59.2	651.2	732.6	814.0	976.8	1140	1302	1465	1628	2035	2442	2849	3256

TABLE 45.a—REYNOLDS NUMBERS IN STANDARD FRESH WATER (Continued)

Velocity		Length of body or ship, ft											
ft per sec	kt	450	500	550	600	650	700	750	800	850	900	950	1000
2	1.18	73.26	81.40	89.54	97.68	105.8	114.0	122.1	130.2	138.4	146.5	154.7	162.8
3	1.78	109.9	122.1	134.3	146.5	158.7	170.9	183.2	195.4	207.6	219.8	232.0	244.2
4	2.39	146.5	162.8	179.1	195.4	211.6	227.9	244.2	260.5	276.8	293.0	309.3	325.6
5	2.96	183.2	203.5	223.9	244.2	264.6	284.9	305.3	325.6	346.0	366.3	386.7	407.0
6	3.55	219.8	244.2	268.6	293.0	317.5	341.9	366.3	390.7	415.1	439.6	464.0	488.4
7	4.14	256.4	284.9	313.4	341.9	370.4	398.9	427.4	455.8	484.3	512.8	541.3	569.8
8	4.74	293.0	325.6	358.2	390.7	423.3	455.8	488.4	521.0	553.5	586.1	618.6	651.2
9	5.33	329.7	366.3	402.9	439.6	476.2	512.8	549.5	586.1	622.7	659.3	696.0	732.6
10	5.92	366.3	407.0	447.7	488.4	529.1	569.8	610.5	651.2	691.9	732.6	773.3	814.0
11	6.51	402.9	447.7	492.5	537.2	582.0	626.8	671.6	716.3	761.1	805.9	850.6	895.4
12	7.10	43.96	488.4	537.2	586.1	634.9	683.8	732.6	781.4	830.3	879.1	928.0	976.8
13	7.70	476.2	529.1	582.0	634.9	687.8	740.7	793.7	846.6	899.5	952.4	1005	1058
14	8.29	512.8	569.8	626.8	683.8	740.7	797.7	854.7	911.7	968.7	1026	1083	1140
15	8.88	549.5	610.5	671.6	732.6	793.7	854.7	915.8	976.8	1038	1099	1160	1221
16	9.47	586.1	651.2	716.3	781.4	846.6	911.7	976.8	1042	1107	1172	1237	1302
17	10.1	622.7	691.9	761.1	830.3	899.5	968.7	1038	1107	1176	1245	1315	1384
18	10.7	659.3	732.6	805.9	879.1	952.4	1026	1099	1172	1245	1319	1392	1465
19	11.2	696.0	773.3	850.6	928.0	1005	1083	1160	1237	1315	1392	1469	1547
20	11.8	732.6	814.0	895.4	976.8	1058	1140	1221	1302	1384	1465	1547	1628
22	13.0	805.9	895.4	984.9	1075	1164	1254	1343	1433	1522	1612	1701	1791
24	14.2	879.1	976.8	1075	1172	1270	1368	1465	1563	1661	1758	1856	1954
26	15.4	952.4	1058	1164	1270	1376	1482	1587	1693	1799	1905	2011	2116
28	16.6	1026	1140	1254	1368	1482	1595	1709	1823	1937	2051	2165	2279
30	17.8	1099	1221	1343	1465	1587	1709	1832	1954	2076	2198	2320	2442
32	18.9	1172	1302	1433	1563	1693	1823	1954	2084	2214	2344	2475	2605
34	20.1	1245	1384	1522	1661	1799	1937	2076	2214	2353	2491	2629	2768
36	21.3	1319	1465	1612	1758	1905	2051	2198	2344	2491	2637	2784	2930
38	22.5	1392	1547	1701	1856	2011	2165	2320	2475	2629	2784	2939	3093
40	23.7	1465	1628	1791	1954	2116	2279	2442	2605	2768	2930	3093	3256
42	24.9	1539	1709	1880	2051	2222	2393	2564	2735	2906	3077	3248	3419
44	26.1	1612	1791	1970	2149	2328	2507	2686	2865	3044	3223	3403	3582
46	27.2	1685	1872	2059	2247	2434	2621	2808	2996	3183	3370	3557	3744
48	28.4	1758	1954	2149	2344	2540	2735	2930	3126	3321	3517	3712	3907
50	29.6	1832	2035	2239	2442	2646	2849	3053	3256	3460	3663	3867	4070
52	30.8	1905	2116	2328	2540	2751	2963	3175	3386	3598	3810	4021	4233
54	32.0	1978	2198	2418	2637	2857	3077	3297	3517	3736	3956	4176	4396
56	33.2	2051	2279	2507	2735	2963	3191	3419	3647	3875	4103	4331	4558
58	34.3	2125	2361	2597	2833	3069	3305	3541	3777	4013	4249	4485	4721
60	35.5	2198	2442	2686	2930	3175	3419	3663	3907	4151	4396	4640	4884
62	36.7	2271	2523	2776	3028	3280	3533	3781	4037	4290	4542	4795	5047
64	37.9	2344	2605	2865	3126	3386	3647	3907	4168	4428	4689	4949	5210
66	39.1	2418	2686	2955	3223	3492	3761	4029	4298	4567	4835	5104	5372
68	40.3	2491	2768	3044	3321	3598	3875	4151	4428	4705	4982	5258	5535
70	41.4	2564	2849	3134	3419	3704	3989	4274	4558	4843	5128	5413	5698
72	42.6	2637	2930	3223	3517	3810	4103	4396	4689	4982	5275	5568	5861
74	43.8	2711	3012	3313	3614	3915	4217	4518	4819	5120	5421	5722	6024
76	45.0	2784	3093	3403	3712	4021	4331	4640	4949	5258	5568	5877	6186
78	46.2	2857	3175	3492	3810	4127	4444	4762	5079	5397	5714	6032	6349
80	47.4	2930	3256	3582	3907	4233	4558	4884	5210	5535	5861	6186	6512
82	48.5	3004	3337	3671	4005	4339	4672	5006	5340	5674	6007	6341	6675
84	49.7	3077	3419	3761	4103	4444	4786	5128	5470	5812	6154	6496	6838
86	50.9	3150	3500	3850	4200	4550	4900	5250	5600	5950	6300	6650	7000
88	52.1	3223	3582	3940	4298	4656	5014	5374	5731	6089	6447	6805	7163
90	53.3	3297	3663	4029	4396	4762	5128	5495	5861	6227	6593	6960	7326
92	54.5	3370	3744	4119	4493	4868	5242	5617	5991	6366	6740	7114	7489
94	55.7	3443	3826	4208	4591	4974	5356	5739	6121	6504	6886	7269	7652
96	56.8	3517	3907	4298	4689	5079	5470	5861	6216	6642	7033	7424	7814
98	58.0	3590	3989	4388	4386	5185	5584	5983	6382	6781	7180	7578	7977
100	59.2	3663	4070	4477	4884	5291	5698	6105	6512	6919	7326	7733	8140

TABLE 45.b—REYNOLDS NUMBERS FOR VARIOUS SHIP LENGTHS AND SPEEDS IN STANDARD SALT WATER

Velocity		Length of body or ship, ft											
ft per sec	kt	5	10	15	20	25	30	35	40	45	50	60	70
2	1.18	0.780	1.560	2.341	3.121	3.901	4.681	5.461	6.242	7.022	7.802	9.362	10.92
3	1.78	1.170	2.341	3.511	4.681	5.852	7.022	8.192	9.362	10.53	11.70	14.04	16.38
4	2.39	1.560	3.121	4.681	6.242	7.802	9.362	10.92	12.48	14.04	15.60	18.72	21.85
5	2.96	1.951	3.901	5.852	7.802	9.753	11.70	13.65	15.60	17.55	19.51	23.41	27.31
6	3.55	2.341	4.681	7.022	9.362	11.70	14.04	16.38	18.72	21.07	23.41	28.09	32.77
7	4.14	2.731	5.461	8.192	10.92	13.65	16.38	19.11	21.85	24.58	27.31	32.77	38.23
8	4.74	3.121	6.242	9.362	12.48	15.60	18.72	21.85	24.97	28.09	31.21	37.45	43.69
9	5.33	3.511	7.022	10.53	14.04	17.55	21.07	24.58	28.09	31.60	35.11	42.13	49.15
10	5.92	3.901	7.802	11.70	15.60	19.50	23.41	27.31	31.21	35.11	39.01	46.81	54.61
11	6.51	4.291	8.582	12.87	17.16	21.46	25.75	30.04	34.33	38.62	42.91	51.49	60.08
12	7.10	4.681	9.362	14.04	18.62	23.28	27.94	32.59	37.25	41.91	46.56	55.87	65.19
13	7.70	5.071	10.14	15.21	20.29	25.36	30.43	35.50	40.57	45.64	50.71	60.86	71.00
14	8.29	5.461	10.92	16.38	21.85	27.31	32.77	38.23	43.69	49.15	54.61	65.54	76.46
15	8.88	5.852	11.70	17.55	23.41	29.26	35.11	40.96	46.81	52.66	58.52	70.22	81.92
16	9.47	6.242	12.48	18.72	24.97	31.21	37.45	43.69	49.93	56.17	62.42	74.90	87.38
17	10.1	6.632	13.26	19.90	26.53	33.16	39.79	46.42	53.05	59.69	66.32	79.58	92.84
18	10.7	7.022	14.04	21.07	28.09	35.11	42.13	49.15	56.17	63.20	70.22	84.26	98.31
19	11.2	7.412	14.82	22.24	29.67	37.08	44.50	51.88	59.30	66.71	74.12	88.94	103.8
20	11.8	7.802	15.60	23.41	31.21	39.01	46.81	54.61	62.42	70.22	78.02	93.62	109.2
22	13.0	8.582	17.16	25.75	34.33	42.91	51.49	60.08	68.66	77.24	85.82	103.0	120.2
24	14.2	9.362	18.72	28.09	37.45	46.81	56.17	65.54	74.90	84.26	93.62	112.3	131.1
26	15.4	10.14	20.29	30.43	40.57	50.71	60.86	71.00	81.14	91.28	101.4	121.7	142.0
28	16.6	10.92	21.85	32.77	43.69	54.61	65.54	76.46	87.38	98.31	109.2	131.1	152.9
30	17.8	11.70	23.41	35.11	46.81	58.52	70.22	81.92	93.62	105.3	117.0	140.4	163.8
32	18.9	12.48	24.97	37.45	49.93	62.42	74.90	87.38	99.87	112.3	124.8	149.8	174.8
34	20.1	13.26	26.53	39.79	53.05	66.32	79.58	92.84	106.1	119.4	132.6	159.2	185.7
36	21.3	14.04	28.09	42.13	56.17	70.22	84.26	98.31	112.3	126.4	140.4	168.5	196.6
38	22.5	14.82	29.65	44.47	59.30	74.12	88.94	103.8	118.6	133.4	148.2	177.9	207.5
40	23.7	15.60	31.21	46.81	62.42	78.02	93.62	109.2	124.8	140.4	156.0	187.2	218.5
42	24.9	16.38	32.77	49.15	65.54	81.92	98.31	114.7	131.1	147.5	163.8	196.6	229.4
44	26.1	17.16	34.33	51.49	68.66	85.82	103.0	120.2	137.3	154.5	171.6	206.0	240.3
46	27.2	17.94	35.89	53.83	71.78	89.72	107.7	125.6	143.6	161.5	179.4	215.3	251.2
48	28.4	18.72	37.45	56.17	74.90	93.62	112.3	131.1	149.8	168.5	187.2	224.7	262.1
50	29.6	19.51	39.01	58.52	78.02	97.53	117.0	136.5	156.0	175.5	195.1	234.1	273.1
52	30.8	20.29	40.57	60.86	81.14	101.4	121.7	142.0	162.3	182.6	202.9	243.4	284.0
54	32.0	21.07	42.13	63.20	84.26	105.3	126.4	147.5	168.5	189.6	210.7	252.8	294.9
56	33.2	21.85	43.69	65.54	87.38	109.2	131.1	153.0	174.8	196.6	218.5	262.1	305.8
58	34.3	22.63	45.25	67.88	90.50	113.1	135.8	158.4	181.0	203.6	226.3	271.5	316.8
60	35.5	23.41	46.81	70.22	93.62	117.0	140.4	163.8	187.2	210.7	234.1	280.9	327.7
62	36.7	24.19	48.37	72.56	96.74	120.9	145.1	169.3	193.5	217.7	241.9	290.2	338.6
64	37.9	24.97	49.93	74.90	99.87	124.8	150.0	174.8	199.7	224.7	249.7	299.6	349.5
66	39.1	25.75	51.49	77.24	103.0	128.8	154.5	180.2	206.0	231.7	257.5	309.0	360.5
68	40.3	26.53	53.05	79.58	106.1	132.6	159.2	185.7	212.2	238.7	265.3	318.3	371.4
70	41.4	27.31	54.61	81.92	109.2	136.5	163.8	191.1	218.5	245.8	273.1	327.7	382.3
72	42.6	28.09	56.17	84.26	112.3	140.4	168.5	196.6	225.0	252.8	280.9	337.0	393.2
74	43.8	28.87	57.73	86.60	115.5	144.3	173.2	202.1	231.0	259.8	288.7	346.4	404.1
76	45.0	29.65	59.30	88.94	118.6	148.2	177.9	207.5	237.2	266.8	296.5	355.8	415.1
78	46.2	30.43	60.86	91.28	121.7	152.1	182.6	213.0	243.4	273.9	304.3	365.1	426.0
80	47.4	31.21	62.42	93.62	124.8	156.0	187.2	218.5	249.7	280.9	312.1	374.5	436.9
82	48.5	31.99	63.98	95.96	128.0	159.9	191.9	223.9	255.9	287.9	319.9	383.9	447.8
84	49.7	32.77	65.54	98.31	131.1	163.8	196.6	229.4	262.1	294.9	327.7	393.2	458.8
86	50.9	33.55	67.10	100.6	134.2	167.7	201.3	234.8	268.4	301.9	335.5	402.6	469.7
88	52.1	34.33	68.66	103.0	137.3	171.6	206.0	240.3	274.6	309.0	343.3	411.9	480.6
90	53.3	35.11	70.22	105.3	140.4	175.5	210.7	245.8	280.9	316.0	351.1	421.3	491.5
92	54.5	35.89	71.78	107.7	143.6	179.4	215.3	251.2	287.1	323.0	358.9	430.7	502.4
94	55.7	36.67	73.34	110.0	146.7	183.3	220.0	256.7	293.4	330.0	366.7	440.0	513.4
96	56.8	37.45	74.90	112.3	149.8	187.2	224.7	262.1	299.6	337.0	374.5	449.4	524.3
98	58.0	38.23	76.46	114.7	152.9	191.1	229.4	267.6	305.8	344.1	382.3	458.8	535.2
100	59.2	39.01	78.02	117.0	156.0	195.0	234.1	273.1	312.1	351.1	390.1	468.1	546.1

TABLE 45.b—REYNOLDS NUMBERS IN STANDARD SALT WATER (Continued)

Velocity		Length of body or ship, ft											
ft per sec	kt	80	90	100	120	140	160	180	200	250	300	350	400
2	1.18	12.48	14.04	15.60	18.72	21.85	24.97	28.09	31.21	39.01	46.81	54.61	62.42
3	1.78	18.72	21.07	23.41	28.09	32.77	37.45	42.13	46.81	58.52	70.22	81.92	93.62
4	2.39	24.97	28.09	31.21	37.45	43.69	49.93	56.17	62.42	78.02	93.62	109.2	124.8
5	2.96	31.21	35.11	39.01	46.81	54.61	62.42	70.22	78.02	97.53	117.0	136.5	156.0
6	3.55	37.45	42.13	46.81	56.17	65.54	74.90	84.26	93.62	117.0	140.4	163.8	187.2
7	4.14	43.69	49.15	54.61	65.54	76.46	87.38	98.31	109.2	136.5	163.8	191.1	218.5
8	4.74	49.93	56.17	62.42	74.90	87.38	99.87	112.3	124.8	156.0	187.2	218.5	249.7
9	5.33	56.17	63.20	70.22	84.26	98.31	112.3	126.4	140.4	175.5	210.7	245.8	280.9
10	5.92	62.42	70.22	78.02	93.62	109.2	124.8	140.4	156.0	195.0	234.1	273.1	312.1
11	6.51	68.66	77.24	85.82	103.0	120.2	137.3	154.5	171.6	214.6	257.5	300.4	343.3
12	7.10	74.50	83.81	93.62	112.3	131.1	149.8	168.5	187.2	234.1	280.9	327.7	374.5
13	7.70	81.14	91.28	101.4	121.7	142.0	162.3	182.6	202.9	253.6	304.3	355.0	405.7
14	8.29	87.38	98.31	109.2	131.1	152.9	174.8	196.6	218.5	273.1	327.7	382.3	436.9
15	8.88	93.62	105.3	117.0	140.4	163.8	187.2	210.7	234.1	292.6	351.1	409.6	468.1
16	9.47	99.87	112.3	124.8	149.8	174.8	199.7	224.7	249.7	312.1	374.5	436.9	499.3
17	10.1	106.1	119.4	132.6	159.2	185.7	212.2	238.7	265.3	331.6	397.9	464.2	530.5
18	10.7	112.3	126.4	140.4	168.5	196.6	224.7	252.8	280.9	351.1	421.3	491.5	561.7
19	11.2	118.6	133.4	148.2	177.9	207.5	237.2	266.8	296.5	370.6	444.7	518.8	593.0
20	11.8	124.8	140.4	156.0	187.2	218.5	249.7	280.9	312.1	390.1	468.1	546.1	624.2
22	13.0	137.3	154.5	171.6	206.0	240.3	274.6	309.0	343.3	429.1	514.9	600.8	686.6
24	14.2	149.8	168.5	187.2	224.7	262.1	299.6	337.0	374.5	468.1	561.7	655.4	749.0
26	15.4	162.3	182.6	202.9	243.4	284.0	324.6	365.1	405.7	507.1	608.6	710.0	811.4
28	16.6	174.8	196.6	218.5	262.1	305.8	349.5	393.2	436.9	546.1	655.4	764.6	873.8
30	17.8	187.2	210.7	234.1	280.9	327.7	374.5	421.3	468.1	585.2	702.2	819.2	936.3
32	18.9	199.7	224.7	249.7	299.6	349.5	399.5	449.4	499.3	624.2	749.0	873.8	998.7
34	20.1	212.2	238.7	265.3	318.3	371.4	424.4	477.5	530.5	663.2	795.8	928.4	1061
36	21.3	224.7	252.8	280.9	337.0	393.2	449.4	505.6	561.7	702.2	842.6	983.1	1123
38	22.5	237.2	266.8	296.5	355.8	415.1	474.4	533.7	593.0	741.2	889.4	1038	1186
40	23.7	249.7	280.9	312.1	374.5	436.9	499.3	561.7	624.2	780.2	936.2	1092	1248
42	24.9	262.1	294.9	327.7	393.2	458.8	524.3	589.8	655.4	819.2	983.1	1147	1311
44	26.1	274.6	309.0	343.3	411.9	480.6	549.3	617.9	686.6	858.2	1030	1202	1373
46	27.2	287.1	320.0	358.9	430.7	502.4	574.2	646.0	717.8	897.2	1077	1256	1436
48	28.4	295.6	337.0	374.5	449.4	524.3	599.2	674.1	749.0	936.2	1123	1311	1498
50	29.6	312.1	351.1	390.1	468.1	546.1	624.2	702.2	780.2	975.3	1170	1365	1560
52	30.8	324.6	365.1	405.7	486.8	568.0	649.1	730.3	811.4	1014	1217	1420	1623
54	32.0	337.0	379.2	421.3	505.6	589.8	674.1	758.4	842.6	1053	1264	1475	1685
56	33.2	349.5	393.2	436.9	524.3	611.7	699.1	786.4	873.8	1092	1311	1529	1748
58	34.3	362.0	407.3	452.5	543.0	633.5	724.0	814.5	905.0	1131	1358	1584	1810
60	35.5	374.5	421.3	468.1	561.7	655.4	749.0	842.6	936.2	1170	1404	1638	1872
62	36.7	387.0	435.4	483.7	580.5	677.2	774.0	870.7	967.4	1209	1451	1693	1935
64	37.9	399.5	449.4	499.3	599.2	699.1	798.9	898.8	998.7	1248	1498	1748	1997
66	39.1	411.9	463.4	514.9	617.9	720.9	823.9	926.9	1030	1288	1545	1802	2060
68	40.3	424.4	477.5	530.5	636.6	742.8	848.9	955.0	1061	1326	1592	1857	2122
70	41.4	436.9	491.5	546.1	655.4	764.6	873.8	983.1	1092	1365	1638	1911	2185
72	42.6	449.4	505.6	561.7	674.1	786.4	898.8	1011	1123	1404	1685	1966	2247
74	43.8	461.9	519.6	577.3	692.8	808.3	923.8	1039	1155	1443	1732	2021	2309
76	45.0	474.4	533.7	593.0	711.5	830.1	948.7	1067	1186	1482	1779	2075	2372
78	46.2	486.8	547.7	608.6	730.3	852.0	973.7	1095	1217	1521	1826	2130	2434
80	47.4	499.3	561.7	624.2	749.0	873.8	998.7	1123	1248	1560	1872	2185	2497
82	48.5	511.8	575.8	639.8	767.7	895.7	1024	1152	1280	1599	1919	2239	2559
84	49.7	524.3	589.8	655.4	786.4	917.5	1049	1180	1311	1638	1966	2294	2621
86	50.9	536.8	603.9	671.0	805.2	939.4	1074	1208	1342	1677	2013	2348	2684
88	52.1	549.3	617.9	686.6	823.9	961.2	1099	1236	1374	1716	2060	2403	2746
90	53.3	561.7	632.0	702.2	842.6	983.1	1123	1264	1404	1755	2107	2458	2809
92	54.5	574.2	646.0	717.8	861.3	1005	1148	1292	1436	1794	2153	2512	2871
94	55.7	586.7	660.0	783.4	880.1	1027	1173	1320	1467	1833	2200	2567	2934
96	56.8	599.2	674.1	749.0	898.8	1049	1198	1348	1498	1872	2247	2621	2996
98	58.0	611.7	688.1	764.6	917.5	1070	1223	1376	1529	1911	2294	2676	3058
100	59.2	624.2	702.2	780.2	936.2	1092	1248	1404	1560	1951	2341	2731	3121

TABLE 45.b—(Continued)

Velocity		Length of body or ship, ft											
ft per sec	kt	450	500	550	600	650	700	750	800	850	900	950	1000
2	1.18	70.22	78.02	85.82	93.62	101.4	109.2	117.0	124.8	132.6	140.4	148.2	156.0
3	1.78	105.3	117.0	128.7	140.4	152.1	163.8	175.5	187.2	199.0	210.7	222.4	234.0
4	2.39	140.4	156.0	171.6	187.2	202.9	218.5	234.1	249.7	265.3	280.9	296.5	312.1
5	2.96	175.5	195.1	214.6	234.1	253.6	273.1	292.6	312.1	331.6	351.1	370.6	390.1
6	3.55	210.7	234.1	257.5	280.9	304.3	327.7	351.1	374.5	397.9	421.3	444.7	468.1
7	4.14	245.8	273.1	300.4	327.7	355.0	382.3	409.6	436.9	464.2	491.5	518.8	546.1
8	4.74	280.9	312.1	343.3	374.5	405.7	436.9	468.1	499.3	530.5	561.7	593.0	624.2
9	5.33	316.0	351.1	386.2	421.3	456.4	491.5	526.6	561.7	596.9	632.0	667.1	702.2
10	5.92	351.1	390.1	429.1	468.1	507.1	546.1	585.2	624.2	663.2	702.2	741.2	780.2
11	6.51	386.2	429.1	472.0	514.9	557.8	600.8	643.7	686.6	729.5	772.4	815.3	858.2
12	7.10	421.3	468.1	514.9	561.7	608.6	655.4	702.2	749.0	791.6	838.1	889.4	936.2
13	7.70	456.4	507.1	557.8	608.6	659.3	710.0	760.7	871.4	862.1	912.8	963.5	1014
14	8.29	491.5	546.1	600.8	655.4	710.0	764.6	819.2	873.8	928.4	983.1	1038	1092
15	8.88	526.6	585.2	643.7	702.2	760.7	819.2	877.7	936.2	994.8	1053	1112	1170
16	9.47	561.7	624.2	686.6	749.0	811.4	873.8	936.2	998.7	1061	1123	1186	1248
17	10.1	596.9	663.2	729.5	795.8	862.1	928.4	994.8	1061	1127	1194	1260	1326
18	10.7	632.0	702.2	772.4	842.6	912.8	983.1	1053	1123	1194	1264	1334	1404
19	11.2	667.1	741.2	815.3	889.4	963.5	1038	1112	1260	1260	1334	1408	1482
20	11.8	702.2	780.2	858.2	936.2	1014	1092	1170	1248	1326	1404	1482	1560
22	13.0	772.4	858.2	944.0	1030	1116	1202	1287	1373	1459	1545	1631	1716
24	14.2	842.6	936.2	1030	1123	1217	1311	1404	1498	1592	1685	1779	1872
26	15.4	912.8	1014	1116	1217	1319	1420	1521	1623	1724	1826	1927	2029
28	16.6	983.1	1092	1202	1311	1420	1529	1638	1748	1857	1966	2075	2185
30	17.8	1053	1170	1287	1404	1521	1638	1755	1872	1990	2107	2224	2341
32	18.9	1123	1248	1373	1498	1623	1748	1872	1997	2122	2247	2372	2497
34	20.1	1194	1326	1459	1592	1724	1857	1990	2122	2255	2387	2520	2653
36	21.3	1264	1404	1545	1685	1826	1966	2107	2247	2387	2528	2668	2809
38	22.5	1334	1482	1631	1779	1927	2075	2224	2372	2520	2668	2817	2965
40	23.7	1404	1560	1716	1872	2029	2185	2341	2497	2653	2809	2965	3121
42	24.9	1475	1638	1802	1966	2130	2294	2458	2621	2785	2949	3113	3277
44	26.1	1545	1716	1888	2060	2231	2403	2575	2746	2918	3090	3261	3433
46	27.2	1615	1794	1974	2153	2333	2512	2692	2871	3051	3200	3409	3589
48	28.4	1685	1872	2060	2247	2434	2621	2809	2996	3183	3370	3558	3745
50	29.6	1755	1951	2146	2341	2536	2731	2926	3121	3316	3511	3706	3901
52	30.8	1826	2029	2231	2434	2637	2840	3043	3246	3448	3651	3854	4057
54	32.0	1896	2107	2317	2528	2739	2949	3160	3370	3581	3792	4002	4213
56	33.2	1966	2185	2403	2621	2840	3058	3277	3495	3714	3932	4151	4369
58	34.3	2036	2263	2489	2715	2941	3168	3394	3620	3846	4073	4299	4525
60	35.5	2107	2341	2575	2809	3043	3277	3511	3745	3979	4213	4447	4681
62	36.7	2177	2419	2660	2902	3144	3386	3628	3870	4112	4354	4595	4837
64	37.9	2247	2497	2746	2996	3246	3495	3745	3995	4244	4494	4744	4993
66	39.1	2317	2575	2832	3090	3347	3605	3862	4119	4377	4634	4892	5149
68	40.3	2387	2653	2918	3183	3448	3714	3979	4244	4510	4775	5040	5305
70	41.4	2458	2731	3004	3277	3550	3823	4096	4369	4642	4915	5188	5461
72	42.6	2528	2809	3090	3370	3651	3932	4213	4494	4775	5056	5337	5617
74	43.8	2598	2887	3175	3464	3753	4041	4330	4619	4907	5196	5485	5773
76	45.0	2668	2965	3261	3558	3854	4151	4447	4744	5040	5337	5633	5930
78	46.2	2739	3043	3347	3651	3956	4260	4564	4868	5173	5477	5781	6086
80	47.4	2809	3121	3433	3745	4057	4369	4681	4993	5305	5617	5930	6242
82	48.5	2879	3199	3519	3839	4158	4478	4798	5118	5438	5758	6078	6398
84	49.7	2949	3277	3605	3932	4260	4588	4915	5243	5571	5898	6226	6554
86	50.9	3019	3355	3690	4026	4361	4697	5032	5368	5703	6039	6374	6710
88	52.1	3090	3433	3776	4119	4463	4806	5149	5493	5836	6179	6522	6866
90	53.3	3160	3511	3862	4213	4564	4915	5266	5617	5969	6320	6671	7022
92	54.5	3230	3589	3948	4307	4666	5024	5383	5742	6101	6460	6819	7178
94	55.7	3300	3667	4034	4400	4767	5134	5500	5867	6234	6600	6967	7334
96	56.8	3370	3745	4119	4494	4868	5243	5617	5992	6366	6741	7115	7490
98	58.0	3441	3823	4205	4588	4970	5352	5734	6117	6499	6881	7264	7646
100	59.2	3511	3901	4291	4681	5071	5461	5852	6242	6632	7022	7419	7802

in which the friction resistance can be segregated with reasonable accuracy.

Adequate methods are not yet available for making accurate predictions of the effects of transverse and longitudinal curvature and of pressure gradients, when making the transition from the flat, smooth plate to the model or ship surface.

Limited full-scale data derived from thrust measurements enable a reasonably reliable assessment of combined smooth-plate and rough-ship friction resistances for certain types and conditions of ship-bottom surface.

45.2 Reference Data on Mass Density, Dynamic Viscosity, and Kinematic Viscosity. Tables X3.d through X3.i of Appx. 3 of this volume give values of the mass density ρ(rho) and the kinematic viscosity ν(nu) of "standard" fresh and salt water, the latter of 3.5 per cent salinity, for a range of latitudes and temperatures sufficient to meet the usual needs of the ship designer and marine architect.

Tables X3.j and X3.k of Appx. 3 give values of these characteristics, plus values of the dynamic viscosity μ(mu), over a rather wide range in temperature, for a number of well-known liquids encountered at times in ship-design work. The original data, from which these tables were adapted, are listed somewhat differently in:

(a) Rouse, H., EMF, 1946, Appx., pp. 357–365
(b) Rouse, H., EH, 1950, Appx., pp. 1004–1013, including the references listed
(c) Rouse, H., and Howe, J. W., BMF, 1953, Appx., pp. 231–238.

45.3 Representative Internal Shearing Stresses in Water Alongside Models and Ships. From the relationships given in Chap. 5 of Volume I, particularly in Fig. 5.R, the shearing stress τ(tau) at any point in a liquid undergoing viscous action is $\tau = \mu(dU/dy)$ where y is measured normal to the flow, in the direction in which U is varying. At a solid surface under a viscous liquid flow the shearing stress at the wall is [Rouse, H., EMF, 1946, pp. 185–186]

$$\tau_0 = \mu\left(\frac{dU}{dy}\right)\Big|_{y=0} = C_{LF}\left(\frac{\rho}{2}\right)U_\infty^2 = C_{LF}(q)$$

where τ_0 has the dimensions of a force per unit area or a pressure, namely m/Lt^2. The local specific friction resistance coefficient C_{LF} is as given in the several formulas of Figs. 5.R and 45.A, for the conditions existing or assumed.

A calculated *average* τ_0 for a whole solid surface is found simply by dividing the wetted area S into the calculated friction drag R_F. Its *local value* for any designated point along the solid surface may be found by the formulas of Fig. 45.A and of the preceding paragraph. The numerical examples of Secs. 5.12 and 45.15 give the following representative values for "standard" salt water:

(a) Ship 500 ft long, speed 20.72 kt, S = 45,000 ft^2, τ_0 = 1.797 lb per ft^2 as an average value for the whole ship, calculated at the end of Sec. 5.12
(b) Ship 400 ft long, speed 30 kt, but basing calculations on a point 200 ft abaft the FP, τ_0 = 2.504 lb per ft^2 at that point
(c) Ship 190.5 ft long, speed 12 kt, τ_0 = 0.485 lb per ft^2 for a point at the stern
(d) Ship 510 ft long, speed 20.5 kt, τ_0 = 1.051 lb per ft^2 for a point near the stern, 500 ft from the bow
(e) Model 20 ft long, speed 10 kt, but basing calculations on a point 10 ft abaft the FP, τ_0 = 0.6093 lb per ft^2 at that point.

45.4 Tables of Reynolds Numbers for Various Ship Lengths and Speeds. It is pointed out in Sec. 2.22 of Volume I and in many of the standard reference works on hydrodynamics, that the Reynolds number is a logical and a practical parameter for representing quantitatively the analytical and experimental evidence on viscous flow, involving friction resistance. This is regardless of the type of viscous flow, whether laminar or turbulent, or of the degree to which surface roughness effects enter into the picture. In the latter case there are, however, certain qualifications as to the separate influences of liquid velocity and distance from the leading edge. As such the Reynolds number enters into many of the present-day calculations and predictions, not only with the space dimension x representing length from the leading edge, as in a ship form, but with the space dimension representing the width b or the diameter D of a body.

To facilitate calculations involving its widespread use, Tables 45.a and 45.b give calculated values of $R_n = VL/\nu$ for both "standard" fresh and "standard" salt water, as defined in Appx. 3. The range of lengths L, or x-distances, is large enough to span both model and ship sizes, as is the range of speed, expressed in both ft per sec and kt.

The data in Table 45.a are calculated by the

usual formula $R_n = VL/\nu$, where V is the ship speed in ft per sec, L is the length or space dimension in ft, and ν is the kinematic viscosity for standard fresh water at a temperature of 59 deg F, 15 deg C, namely $1.2285(10^{-5})$ ft^2 per sec.

The data in Table 45.b are calculated in the same way for standard salt water, having a 3.5 per cent salinity and a temperature of 59 deg F, 15 deg C. Under these conditions the kinematic viscosity ν is $1.2817(10^{-5})$ ft^2 per sec.

Values of x- or d-Reynolds numbers are taken from these tables simply by substituting x or D for L.

Values of R_n are in millions, or $R_n(10^{-6})$.

To facilitate calculations of R_n for speeds and lengths not covered by these tables:

(a) Speeds in ft per sec corresponding to integral values of kt, from 1 through 100 kt, are given in Table X4.b
(b) The reciprocal of $1.2285(10^{-5})$ is $0.8140(10^5)$ or $0.08140(10^6)$
(c) The reciprocal of $1.2817(10^{-5})$ is $0.7802(10^5)$ or $0.07802(10^6)$.

G. S. Baker gives a small table of R_n for a ν-value of $1.29(10^{-5})$ for speeds of 2 to 35 kt, and for lengths of 50 to 1000 ft [INA, Apr 1952, p. 61].

45.5 Data on and Prediction of Ship Boundary-Layer Characteristics. A number of detail ship-design problems require, for their proper solution, a good estimate of the boundary-layer thickness δ(delta) at any given point around the underwater hull, long before the ship is in the water. This applies to both clean, new surfaces and those roughened by uneven paint coatings and by fouling in service.

A velocity traverse with a cylindrical pitot tube at a given point on a model of the ship gives some indication of the thickness but this method is tedious and uncertain, at least in the present state of the art. The principal reasons for the uncertainties are:

(a) The boundary-layer thickness at a given point on a model is greater in proportion than at the corresponding point on a *hydrodynamically smooth ship*, for the reasons explained in Sec. 6.8 of Volume I and illustrated in Fig. 6.E of that section
(b) Existing uncertainty (in 1955) as to the effective roughness of the actual ship surface, and its action in thickening the boundary layer, over and above what it would be on a hydrodynamically smooth surface
(c) The difficulties in making accurate velocity traverses in the vicinity of the laminar sublayer on a model, or on a ship, at distances from the surface of the order of a few thousandths of an inch.

F. M. Richardson, J. K. Ferrell, H. A. Lamonds, and K. O. Beatty, Jr., in a paper entitled "How Radiotracers are Used in Measuring Fluid Velocity Profiles" [Nucleonics, Jul 1955, pp. 221–223], describe new tracer techniques by which liquid

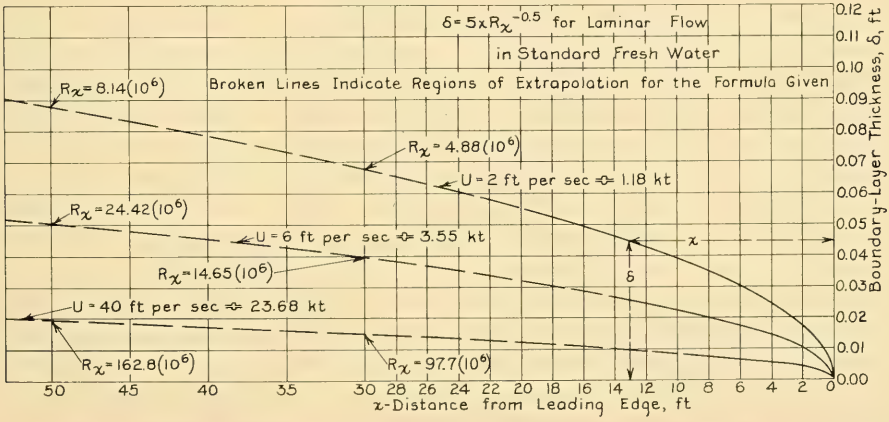

Fig. 45.B Variation of Boundary-Layer Thickness δ with x-Distance from Leading Edge, for Laminar Flow in Fresh Water

velocities may be determined within 0.002 inch of the inner wall of a tube of circular section. Fig. 3 on page 23 of the reference is a plot of local velocity U on distance from the inner wall, embodying observations taken within 0.0006 inch of the solid surface in a regime which is distinctly laminar in character.

Despite the difficulties and drawbacks mentioned, the velocities at a series of normal distances from the hull surface can be and have been measured on both ship and model, and the velocity profiles plotted. Two sets of typical ship profiles are reproduced in Sec. 45.6, and reference data are quoted there on many others. Despite the shortcomings of the observed data, any information at all is considered better than none.

A designer's need for boundary-layer data may be sufficiently pressing—for instance, in selecting propeller-tip clearances alongside the hull on a large and important passenger liner—to justify a rather extensive model- or ship-measurement project. However, it is well for the designer to know beforehand that, no matter how extensive are the measurements projected, they will almost surely be found insufficient when the time comes to plot, analyze, and use the results. This is not intended to discourage the designer before he begins but to broaden the scope of the measurements.

As an illustrative example there may be mentioned the investigation carried out on a cruiser model in the early 1940's, to determine the proper location for a pitot-type speed log. It was necessary to know the position, both fore and aft and relative to the surface of the underwater hull, of the cloak of the boundary layer where, at the designed speed, the relative water velocity was within one per cent plus or minus of the ship speed through undisturbed water. Although it was expected that the log would be installed under the entrance, as is customary for these instruments, an acceptable position was found only after exploring the boundary layer under a model of the ship from the stem to a position far aft, under the after engine room. When the isotachyl representing 100 per cent of ship speed was drawn on the outboard profile it was found that, at the position originally proposed for the log, the isotachyl lay more than 6 ft below the keel. This distance was about twice as great as the contemplated log extension beyond the hull.

On the basis previously mentioned, that some indication of δ-values are better than none, Figs. 45.B and 45.C show plots of boundary-layer thicknesses for laminar and turbulent flow, respectively, derived from the space-velocity relationships of Sec. 5.13 of Volume I and Eqs. (5.vii) and (5.viii) for flat, smooth plates. In plotting these graphs, the data have been extrapolated to ranges far beyond those justified by the manner in which the formulas were derived. The plots are therefore to be considered as indicators of the δ-values, nothing more.

A graph illustrating the values of δ for the

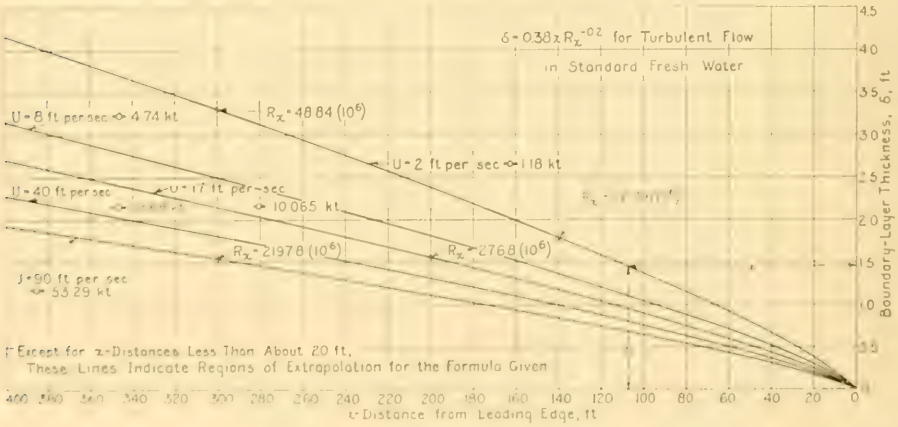

Fig. 45.C Variation of Boundary-Layer Thickness δ with x-Distance from Leading Edge, for Turbulent Flow in Fresh Water

ABC ship designed in Part 4, calculated by this method, is given as Fig. 45.I in Sec. 45.13.

Values of the displacement thickness δ^*(delta star) are even more difficult to predict because they depend upon the shape of the velocity profile within the boundary layer. The ratio $\delta^* = 0.14\delta$ for turbulent flow, given in Fig. 45.A, is an acceptable engineering figure in the absence of more definite data.

45.6 Typical Velocity Profiles in Ship Boundary Layers. It is regrettable that the technical problems involved in the measurement of boundary-layer profiles on ships, or even on models, are of such magnitude that *complete and accurate* observed profiles are almost nonexistent. For an indication of the enormous amount of labor involved in a comprehensive study of this kind the reader has only to study a report by H. B. Freeman entitled "Measurements of Flow in the Boundary Layer of a 1/40-Scale Model of the U. S. Airship *Akron*" [NACA Rep. 430, 1932, pp. 567–579]. This paper contains a considerable number of boundary-layer velocity profiles of the type which should be available to naval architects for typical ship models.

In the cases where ship (or model) profiles are available, described in the references listed hereunder, either:

(a) The velocity traverse was not fine enough, at the small values of y, to follow the velocity variation in the range of U (or V) less than about 0.6 or $0.5U_\infty$ (or V), or

(b) The velocity traverse extended only to a value of y where U (or V) was approximately equal to U_∞ (or V), despite indications that at a greater transverse distance U would exceed U_∞,

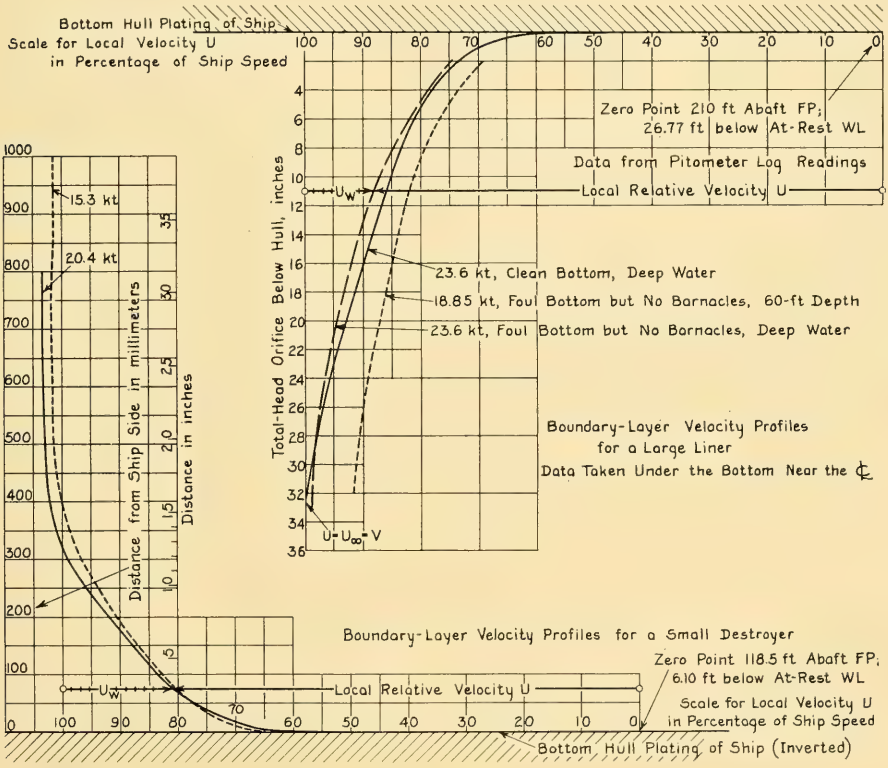

Fig. 45.D Typical Boundary-Layer Velocity Profiles for Several Operating Conditions on Two Ships

because of the augment of velocity $+\Delta U$ to be expected in the potential flow abreast the wide portion of the body or ship.

This lack of essential data makes it impossible, more often than not, to determine the boundary-layer thickness by the delta-velocity method described in Sec. 6.5 of Volume I. An example of this situation is found in the upper right-hand diagram of Fig. 45.D, giving three partial velocity profiles for a large liner, taken from unpublished data kindly furnished by J. P. Comstock and C. H. Hancock of the Newport News Shipbuilding and Dry Dock Company. The data in all cases are from observations with a Pitometer speed log. Unfortunately, the log-tube extension was in this case only sufficient to obtain readings of local relative velocity U equal to the ship speed V at 23.6 kt, with clean bottom and in deep water.

The observations at 23.6 kt, with dirty bottom in deep water, indicate greater local velocities U in the inner portion of the boundary layer and a considerably thicker layer, as diagrammed for a typical foul-bottom boundary-layer velocity profile in Fig. 22.H of Sec. 22.13. Again the full boundary-layer thickness could not be explored because of the limited log-tube extension.

For the test at 18.85 kt, with a dirty bottom and in a depth of water of 2.24 times the draft, the local velocities U are less than for the higher speed with clean bottom in deep water. Consideration of backflow in the shallow water, plus surface roughness, but taking the reduced speed into account, indicates that the local velocities should possibly be higher rather than lower. In any case, the boundary layer is thicker, as it should be.

The boundary-layer velocity profiles for the small destroyer (the Swedish *Wrangel*), shown inverted in Fig. 45.D, are taken from those published by H. F. Nordström [SSPA Rep. 27, 1953, Fig. 39, p. 85], with the horizontal scale modified to suit the features being illustrated. These velocity measurements were, like those on the large liner, made below the ship but fortunately the pitot-tube extension was greatly in excess of the y-distance where $U = U_\infty = V$. With the relatively small submergence of the pitot-tube orifice in the case of the *Wrangel*, it is possible that there is some wave wake being measured with the friction wake. Indeed, it is possible that the wave action in the case of the large liner makes itself felt not only down the side but under the bottom as well.

Both high-speed deep-water profiles on Fig. 45.D show a characteristic flatness—almost a hollowness—at a ratio U/U_∞ of about 0.90. The Laute and Gruschwitz profiles of Fig. 22.C in Sec. 22.6 are actually hollow.

Other ships upon which velocity-profile observations have been made, including the *Wrangel*, are the:

(1) *Hindenburg*, German merchant vessel, early 1920's. The data, as reported by W. Dahlmann, H. Hoppe, and O. Schafer [WRH, 7 Sep 1926, pp. 415–419], were taken with a resistance log towed abeam from a boom, and are rather sketchy.

(2) *Hamilton*, U. S. destroyer (DD 141), 1933–1934. The TMB data are unpublished except for one model-ship velocity profile comparison by E. A. Wright [SNAME, 1916, Fig. 24, p. 393].

(3) *Clairton*, U. S. merchant vessel, 1933–1934. The TMB data are unpublished.

(4) *Tannenberg*, German merchant ship, 1938. Some boundary-layer profiles were measured on this ship but they were not published [WRH, 15 Jun 1939, pp. 167–174].

(5) *Santa Elena*, merchant ship, 1951. Velocity profiles for both rough and smooth hull surfaces were measured amidships, 72 meters (236.2 ft) from the stem and 4 meters (13.1 ft) below the at-rest waterline [Kempf, G., and Karhan, K., HSVA Rep. 260, 1952, Fig. 7A; TMB transl. available; STG, 1951, Vol. 45, pp. 228–243].

(6) *Snaefell* and *Ashworth*, British cross-channel steamers. Observations by G. S. Baker [NECI, 1929–1930, Vol. XLVI, pp. 83–106 and Pls. III-V; also pp. 141–146].

(7) *Wrangel*, Swedish destroyer. Observations by H. F. Nordström and assistants ("Full-Scale Tests with the *Wrangel* and Comparative Model Tests," SSPA Rep. 27, 1953].

(8) Victory ship, *AP3*, *Tervacte*. Observations by G. Aertssen and his assistants [INA, 1953, pp. J21–J56]. Fig. 3 on p. J25 and Fig. 22 on p. J52 (a revision of Fig. 3) show velocity profiles made with a rodmeter speed log under various conditions.

(9) *Lucy Ashton*. Pitot traverses were made by a Pitometer log [INA, 1955, Vol. 97, pp. 543–545 and Figs. 13, 14]. No velocity profiles show $U > U_\infty$.

For the sake of completeness, the references of Sec. 22.6 of Volume I are repeated here, along with a few others. These, however, apply to tests *on models only*:

(a) Laute, W., STG, 1933, pp. 402–460; TMB Transl. 53, Mar 1939. This paper covers flow tests, velocity measurements, and pressure observations on a cargo-ship model.

(b) Hamilton, W. S., "The Velocity Pattern Around a Ship Model Fixed in Moving Water," Doctorate Diss., HHR, Dec 1943. Describes flow measurements made on a model of the German M. S. *San Francisco*.

(c) U. S. S. *Hamilton* (DD 141), destroyer. The TMB data are unpublished except for one model-ship velocity profile comparison by E. A. Wright [SNAME, 1946, Fig. 24, p. 393].

(d) TMB model 3898, representing a proposed twin-skeg *Manhattan*, described by the present author in SNAME, 1947, pp. 112–125. Unpublished data are on file at the David Taylor Model Basin.

(e) Baker, G. S., NECI, 1929–1930, Vol. XLVI, pp. 83–106 and Pls. III, IV, and V; also pp. 141–146 (includes tests on models). On page 86 of this reference, Table I gives other sources of test data on models.

(f) Baker, G. S., NECI, 1934–1935, Vol. LI, pp. 303–320; also SBSR, 28 Mar 1935, Fig. 5, p. 353.

(g) Calvert, G. A., INA, 1893, Vol. XXXIV, pp. 61–77. This reference describes one of the first, if not the first measurement of the velocity profile in the boundary layer of a friction plank, 28 ft long. In Fig. 9 of Pl. III Calvert gives three velocity profiles, for speeds of 2, 3, and 4 kt, for a transverse distance of 0.44 ft from the plank surface.

45.7 The Development of Formulas for Calculating Ship Friction Resistance. Friction resistance was recognized as a sort of separate entity in the ship-resistance picture as far back as the 1790's. Attempts were made then, by Mark Beaufoy and others, to determine its magnitude [INA, 1925, pp. 109, 115]. It remained, however, for the eminent William Froude to conduct the first systematic friction experiments on flat surfaces and to establish the first systematic basis for the calculation of friction drag. Following extensive towing experiments with thin planks having various coatings, he developed the expression

$$R_F = fSV^n \tag{45.i}$$

where f was his own friction-drag coefficient and the exponent n approximated 1.83 for smooth, varnished surfaces. He found a length effect in addition, but this was not reduced to mathematical terms. R. E. Froude, the son of William Froude, after a re-analysis of the observed data, later changed the speed exponent n to 1.825.

Following the elder Froude's work the principal landmarks in the evolution of a suitable formula for calculating ship friction resistance were:

(1) Osborne Reynolds' development in the early 1880's of the dimensionless relationship UL/ν, now named the Reynolds number and expressed as R_n

(2) The development of the boundary-layer theory by Ludwig Prandtl in the early 1900's.

The highlights and details of the last three-quarters of a century of progress on this project have been told many times so that they are not summarized or repeated here. A historical summary was given some time ago by K. S. M. Davidson [PNA, 1939, Vol. II, pp. 76–83] and others more recently by F. H. Todd [SBMEB, Jan 1947, pp. 3–7; SNAME, 1951, pp. 315–317]. A list of the principal references is given in Sec. 45.26 for the benefit of the interested reader.

It has been recognized, practically from the beginning of this development, that a friction formulation which correctly expresses the drag of a thin, flat plank or friction plane by no means applies directly to the prediction of ship friction resistance. There are a number of reasons for this:

(a) The possibility of laminar flow on the plank or plane and on a towing model whose friction drag is calculated from such data, as compared to the fully turbulent flow over practically the entire wetted area of the ship

(b) The effects of transverse curvature on the submerged edge or edges of the plank or friction plane as well as of both transverse and longitudinal curvature on a towing model and on the ship

(c) The effects of various pressure gradients, especially the longitudinal gradients, on the curved surfaces of model and ship

(d) The variation between the calculated at-rest wetted surface of a model or ship and the actual wetted surface when it is moving and making waves, as well as changes in flow caused by orbital wave motion and the like

(e) The smoothness of the plank or friction-plane surface as compared to the relatively rougher ship surface, especially in view of the need for greater absolute smoothness on the ship to insure hydrodynamic smoothness in the larger scale

(f) Other effects of differences in absolute size or scale.

William Froude, B. J. Tideman, and others, working in the 1860's, the 1870's, and later, recognized that no ship is ever as smooth as a friction plane towed in a model basin. They provided in their friction coefficients a series of positive allowances for what they considered to be unavoidable roughnesses in the ships of their day. They did not know, in those years, that the ships had actually to be *smoother*, in an absolute sense, to afford the same degree of hydrodynamic smoothness as obtained on their models. However, the modern friction formulations are all developed for and apply strictly to flat, smooth plates,

because smooth surfaces are reproducible and only in that way can consistent experimental data be assured.

Despite the extensive studies of recent years there is as yet no comprehensive, accurate formula for bridging the gap between an experimental friction plane or model and an actual ship, and for taking account of the effects listed in the second paragraph preceding. In fact, workers in this field are not even agreed on the form which such an expression should take, or whether an attempt should be made to embody all the bridging factors, as it were, into a single formulation.

In the meantime the naval architect must span the gap somehow, and with assurance that his predictions are reasonably correct. The American Towing Tank Conference decided in 1947 that for its work this operation is to be performed by the use of:

(1) The meanline developed by K. E. Schoenherr for expressing the specific friction drag C_F of turbulent flow on a flat, smooth surface as a function of Reynolds number R_n

(2) An additive allowance, in the form of a specific friction resistance and called ΔC_F, for the effect of unavoidable roughness on a clean, new ship.

The Schoenherr meanline, as its generic name implies, was based upon a careful analysis of available experimental results. While these experiments antedate the year 1932, the line can always be shifted to accommodate newer and better data. It does, however, conform to the physical laws for the dependence of friction drag on Reynolds number and it has given satisfactory ship predictions for many years. There is no specific provision in the ATTC 1947 procedure for edge effects, transverse and longitudinal curvature effects, variations in wetted surface and flow patterns due to waves, or any other factors.

The ATTC 1947 (Schoenherr) meanline, depicted graphically by the heavy, solid line in the log-log plot of Fig. 45.E, expresses the relation between C_F and R_n by either of the equations

$$\frac{0.242}{\sqrt{C_F}} = \log_{10}(R_n C_F) \qquad (5.\text{xiva})$$

$$(C_F)^{-0.5} = 4.132 \log_{10}(R_n C_F) \qquad (5.\text{xivb})$$

Since this equation is not readily solved for C_F, sufficient values of C_F and R_n, in the model and ship ranges, have been calculated and tabulated for practical use. The tables are published in SNAME Technical and Research Bulletin 1–2, dated August 1948, for all who need them. Two small portions of these tables, *modified to express all R_n values in millions*, are reproduced in Tables 45.c and 45.d of Sec. 45.9, covering model and ship ranges, respectively.

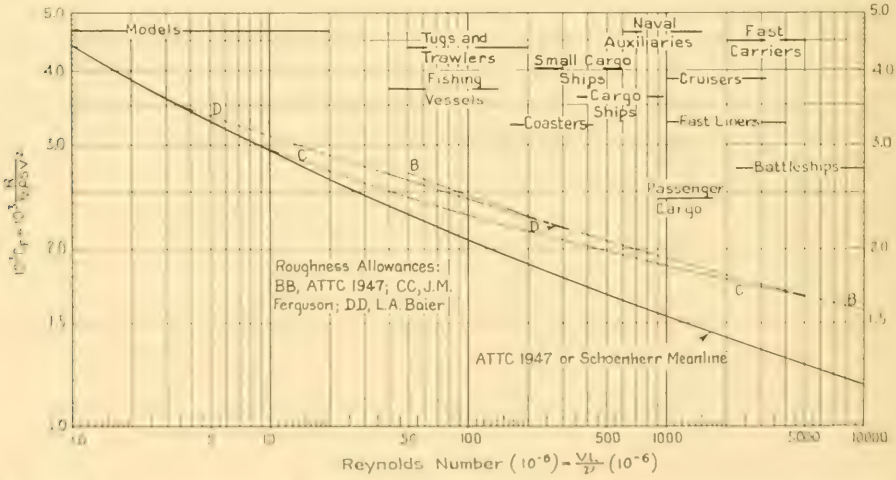

FIG. 45.E PLOT OF THREE TYPES OF ROUGHNESS ALLOWANCE FOR SHIPS, SHOWING VARIATIONS WITH REYNOLDS NUMBER

Using the ATTC procedure, the friction resistance of the wetted area of a ship is calculated by the general formula given as Eq. (22.iv) in Sec. 22.15, based on specific friction-resistance coefficients:

$R_F = qS[C_F$ for fully turbulent flow on a flat, smooth plate having the same S as the ship

$+\Delta_1 C_F$ due to the increment of relative water velocity for longitudinal curvature

$+\Delta_2 C_F$ due to the increment of drag for transverse curvature

$+\Delta_P C_F$ for plate or planking roughness

$+\Delta_S C_F$ for structural roughness

$+\Delta_C C_F$ for coating roughness

$+\Delta_F C_F$ for fouling roughness]

$$= qS(C_F + \Sigma\Delta C_F) \qquad (45.ii)$$

where the ram pressure $q = 0.5\rho V^2$, S is the ship wetted area, and V is the ship speed.

Methods of estimating the curvature allowances are described subsequently in Sec. 45.14. Tentative values for the four listed roughness allowances are given in Secs. 45.18 and 45.20.

In many of the published reports quoting $\Sigma\Delta C_F$ values [Todd, F. H., TMB Rep. 663, 1949; TMB Rep. 729, 1950; SNAME, 1951, pp. 327–345] this term embraces not only all the roughness allowances listed in Eq. (45.ii) preceding but the equivalent resistance of condenser-cooling scoops and discharges and miscellaneous sea chests, as well as the forces involved in driving cooling water through the condensers and in overcoming the effects of forcing water out of and drawing it into certain hull openings.

In towed and self-propelled tests of ship models it is customary to omit the lips, projections, openings, and internal ducts belonging to these systems. Not all ships have them, and in any case they partake of the nature of appendages rather than of structural or other roughnesses. Unfortunately, no suitable procedures have been worked out as yet whereby the true additions to ship resistance occasioned by the devices proper and

TABLE 45.c—SAMPLE TABLE OF R_n AND C_F FOR THE ATTC 1947 MEANLINE IN THE MODEL RANGE

This table is adapted from the upper portion of the table on page 8 of SNAME Technical and Research Bulletin 1–2, published in Aug 1948. The listings of R_n in the extreme left-hand column are in terms of (10^6) or millions. Those in all other columns are $C_F(10^3)$.

Reynolds Number in Millions	0.0	0.1	0.2	0.3	0.4	0.5	0.6	0.7	0.8	0.9	1.0
10	2.934	2.930	2.925	2.920	2.916	2.911	2.907	2.902	2.898	2.893	2.889
11	2.889	2.885	2.881	2.877	2.873	2.868	2.864	2.861	2.857	2.853	2.849
12	2.849	2.845	2.841	2.838	2.834	2.830	2.827	2.823	2.820	2.816	2.813
13	2.813	2.809	2.806	2.802	2.799	2.796	2.792	2.789	2.786	2.783	2.780
14	2.780	2.776	2.773	2.770	2.767	2.764	2.761	2.758	2.755	2.752	2.749
15	2.749	2.746	2.744	2.741	2.738	2.735	2.732	2.730	2.727	2.724	2.721
16	2.721	2.719	2.716	2.713	2.711	2.708	2.706	2.703	2.701	2.698	2.696
17	2.696	2.693	2.691	2.688	2.686	2.683	2.681	2.678	2.676	2.674	2.672
18	2.672	2.669	2.667	2.665	2.662	2.660	2.658	2.656	2.653	2.651	2.649
19	2.649	2.647	2.645	2.642	2.640	2.638	2.636	2.634	2.632	2.630	2.628
20	2.628	2.626	2.624	2.622	2.620	2.618	2.616	2.614	2.612	2.610	2.608
21	2.608	2.606	2.604	2.602	2.600	2.599	2.597	2.595	2.593	2.591	2.589
22	2.589	2.588	2.586	2.584	2.582	2.580	2.579	2.577	2.575	2.573	2.572
23	2.572	2.570	2.568	2.567	2.565	2.563	2.562	2.560	2.558	2.557	2.555
24	2.555	2.553	2.552	2.550	2.549	2.547	2.545	2.544	2.542	2.541	2.539
25	2.539	2.538	2.536	2.534	2.533	2.531	2.530	2.528	2.527	2.525	2.524
26	2.524	2.522	2.521	2.519	2.518	2.516	2.515	2.514	2.512	2.511	2.509
27	2.509	2.508	2.507	2.505	2.504	2.502	2.501	2.500	2.498	2.497	2.496
28	2.496	2.494	2.493	2.491	2.490	2.489	2.488	2.486	2.485	2.484	2.482
29	2.482	2.481	2.480	2.478	2.477	2.476	2.475	2.473	2.472	2.471	2.470

TABLE 45.d—SAMPLE TABLE OF R_n AND C_F FOR THE ATTC 1947 MEANLINE IN THE SHIP RANGE

This table is adapted from the upper portion of the table on page 12 of SNAME Technical and Research Bulletin 1-2, published in Aug 1948. The listings of R_n in the extreme left-hand column are in terms of (10^6) or millions. Those in all other columns are $C_F(10^3)$.

Reynolds Number in Millions	0	10	20	30	40	50	60	70	80	90	100
1,000	1.531	1.529	1.527	1.525	1.524	1.522	1.520	1.518	1.517	1.515	1.513
1,100	1.513	1.512	1.510	1.508	1.507	1.505	1.503	1.502	1.500	1.499	1.497
1,200	1.497	1.496	1.494	1.493	1.491	1.490	1.488	1.487	1.485	1.484	1.482
1,300	1.482	1.481	1.480	1.478	1.477	1.476	1.474	1.473	1.472	1.470	1.469
1,400	1.469	1.468	1.467	1.466	1.464	1.463	1.462	1.461	1.459	1.458	1.457
1,500	1.457	1.456	1.455	1.454	1.452	1.451	1.450	1.449	1.448	1.447	1.446
1,600	1.446	1.445	1.444	1.443	1.442	1.441	1.440	1.438	1.437	1.436	1.435
1,700	1.435	1.434	1.433	1.432	1.431	1.430	1.429	1.428	1.428	1.427	1.426
1/800	1.426	1.425	1.424	1.423	1.422	1.421	1.420	1.419	1.418	1.417	1.416
1,900	1.416	1.416	1.415	1.414	1.413	1.412	1.411	1.410	1.410	1.409	1.408
2,000	2.408	2.407	2.406	2.405	2.405	2.404	1.403	1.402	1.401	1.401	1.400
2,100	1.400	1.399	1.398	1.397	1.397	1.396	1.395	1.394	1.394	1.393	1.392
2,200	1.392	1.391	1.391	1.390	1.389	1.388	1.388	1.387	1.386	1.386	1.385
2,300	1.385	1.384	1.383	1.383	1.382	1.381	1.381	1.380	1.379	1.379	1.378
2,400	1.378	1.377	1.376	1.376	1.375	1.374	1.374	1.373	1.373	1.372	1.371
2,500	1.371	1.371	1.370	1.369	1.369	1.368	1.367	1.367	1.366	1.366	1.365
2,600	1.365	1.364	1.364	1.363	1.363	1.362	1.361	1.361	1.360	1.360	1.359
2,700	1.359	1.358	1.358	1.357	1.357	1.356	1.356	1.355	1.354	1.354	1.353
2,800	1.353	1.353	1.352	1.352	1.351	1.350	1.350	1.349	1.349	1.348	1.348
2,900	1.348	1.347	1.347	1.346	1.346	1.345	1.345	1.344	1.343	1.343	1.342

the pumping of the circulating water can be derived.

45.8 List of Principal Friction-Resistance Formulas for a Flat, Smooth Plate in Turbulent Flow. For convenient reference, there are listed hereunder all friction formulations, including that for the ATTC 1947 (Schoenherr) meanline, which have been used by physicists and naval architects for analysis or calculation purposes for the past eight decades or more:

(1) ATTC 1947 [PNA, 1939, Vol. II, p. 82; SNAME Res. and Tech. Bull. 1–2, Aug 1948, p. 3]

$$(C_F)^{-0.5} = 4.132 \log_{10} (R_n C_F)$$

Alternative forms are

(a) $$0.242(C_F^{-0.5}) = \log_{10} (R_n C_F)$$

(b) $$(C_F)^{0.5} = \frac{0.242}{\log_{10} (R_n C_F)}$$

(c) $$C_F = \left[\frac{0.242}{\log_{10} (R_n C_F)}\right]^2 = 0.0585[\log_{10} (R_n C_F)]^{-2}$$

In this and similar formulas, as $R_n \to \infty$, $C_F \to 0$.

(2) (a) For the local specific friction drag coefficient C_{LF} or the shearing-stress coefficient C_τ, K. E. Schoenherr gives [MIT Hydrodyn. Symp., 1951, p. 109]

$$C_{LF} = \frac{0.279 C_F}{0.279 + C_F}$$

(b) Another expression derived by L. Landweber from the ATTC 1947 formulation is [STG, 1952, p. 137; SNAME, 1953, p. 17]

$$C_{LF} = C_\tau = \frac{0.310}{\log_e^2 (2R_\theta) + 2 \log_e (2R_\theta)}$$

where R_θ is the Reynolds number based upon the momentum thickness θ(theta).

(3) Schultz-Grunow [NACA Tech. Memo 986, Sep 1941]

(a) $$C_F = 0.427(\log_{10} R_n - 0.407)^{-2.64}$$

For all practical purposes this rather cumbersome formula may be replaced by

(b) $C_F = 0.0725(\log_{10} R_n - 2)^{-2}$

(c) $C_{LF} = 0.370(\log_{10} R_x)^{-2.584}$

(4) Prandtl-Schlichting [PNA, 1939, Vol. II, p. 82]

$$C_F = 0.455(\log_{10} R_n)^{-2.58}$$

For the local specific friction drag C_{LF} or shearing-stress coefficient C_τ, H. Schlichting gives [Ing. Archiv, 1936, Vol. 7, p. 29]

$$C_{LF} = C_\tau = (2 \log_{10} R_x - 0.65)^{-2.3}$$

(5) Von Kármán, based on the 1/7-power law of velocity distribution [PNA, 1939, Vol. II, p. 80]; see Sec. 5.10 of Volume I of the present book:

(a) $C_F = 0.072(R_n)^{-0.2}$

This is also given as [Rouse, H., EH, 1950, p. 106]

(b) $C_F = 0.074(R_n)^{-0.2}$

(6) Gebers [INA, 1925, pp. 110–111]

(a) $R_F = k_2 S V^2 (R_n)^{-0.125}$

where k_2 is a rather complicated term defined in the reference.

(b) [PNA, 1939, Vol. II, p. 80]

$$C_F = 0.02058(R_n)^{-0.125}$$

(7) Froude, for salt water:

(a) 300-ft length $C_F = 0.0666 R_n^{-0.175}$

(b) 400-ft length $C_F = 0.0696 R_n^{-0.175}$

(c) 500-ft length $C_F = 0.0722 R_n^{-0.175}$

(d) 600-ft length $C_F = 0.0744 R_n^{-0.175}$

(e) $$R_F = \left[0.00871 + \left(\frac{0.053}{8.8 + L}\right)\right] S V^{1.825}$$

where R_F is in lb for salt water of specific gravity 1.026 at 59 deg F, 15 deg C, L is in ft, S is in ft^2, V is in kt [2nd ICSTS, Paris, 1935; Todd, F. H., SNAME, 1951, pp. 317–318]

(f) For fresh water the formula corresponding to (e) is as follows [Baier, L. A., SNAME, 1951, p. 365]:

$$R_F = \left[0.00846 + \left(\frac{0.0516}{8.8 + L}\right)\right] S V^{1.825}$$

where the units are as given for the preceding formula (e)

(g) The following Froude formula corresponds to (f) preceding, for use with *metric* units and for application to fresh water [SNAME, 1951, pp. 373–374]:

$$R_F = \left[0.1392 + \left(\frac{0.258}{2.68 + L}\right)\right] S V^{1.825}$$

where R_F is in kg S is in square meters
L is in meters V is in meters per sec.

When the temperature differs from 15 deg C, the value of R_F given by (g) preceding is multiplied by the factor $[1 + 0.0043(15 - T)]$, where T is the water temperature in deg C.

(h) As an aid in correlating Froude's "O" friction values with the specific friction resistance coefficients presently used, A. M. Robb has prepared and published tabular and graphic presentations in his paper "An Examination of the Records of the *Greyhound* Experiments" [SBSR, 5 Jun 1947, pp. 568–571]. Page 570 of the reference contains:

(i) A table headed "Association of Froude's 'O' Values and Specific Resistance Coefficients on Basis of Reynolds Number"

(ii) A graph entitled "Froude's 'O' Values in C_F Coefficients." This has ordinates of $C_F = R_F/(0.5\rho S V^2)$ and abscissas of Reynolds number R_n, extending from 1 to 10,000 million (10^6 to 10^{10}).

(8) Tideman

$R_F = k_T S V^n$, where R_F is in lb

k_T is a coefficient given as f in the first two references cited as (a) and (b) hereunder

S is in ft^2

V is in kt.

When, as is the case here, n has a value differing from 2, and ρ is omitted, this formula is dimensional.

The coefficient and exponent values of the Tideman formulation, listed in the following references, are not given here:

(a) Peabody, C. H., NA, 1904, p. 405, for ship lengths of 10 through 500 ft

(b) Taylor, D. W., S and P, 1910,
Vol. I, p. 63; notes only
Vol. II, Table VI, for ship lengths of 10 through 500 ft
1933, Table V, p. 32
1943, Table V, p. 34, with explanatory notes, for ship lengths of 10 through 1,200 ft

(c) PNA, 1939, Vol. II, Table 9, p. 114, for ship lengths of 10 through 500 ft

(d) Pollard, J., and Dudebout, A., "Théorie du Navire," 1892, Vol. III, pp. 374–375, using essentially the dimensional formula given previously but with different symbols and metric units, for ship lengths of 5 through 120 m, 16.4 through 393.7 ft.

(9) Taylor, for 20-ft planks in fresh water at 68 deg F,

(a) $$C_F = 0.0311 R_n^{-0.146}$$

An alternative form is

(b) $R_F = 0.00967\ SV^{1.854}$ for 60 deg F, fresh water, and a 20-ft friction plane.

(10) Lap and Troost [SNAME, North. Calif. Sect., 29 Feb 1952; see SNAME Member's Bull., Jun 1953, pp. 18–22]

$$\frac{K\sqrt{2}}{\sqrt{C_F}} = \log_e\left[\left(\frac{R_n}{A'}\right)\sqrt{C_F}\right] + KC''$$

$$= \log_e\left(\frac{R_n}{A'}\right) + \frac{1}{2}\log_e C_F + KC''$$

or $C_{FD} = 0.133(\log_{10} R_n + 0.724 - \log_{10} A)^{-2.2}$ where the subscript combination "*FD*" signifies friction drag.

(11) G. Hughes' "2-diml" formula is $C_F = 1.328 R_n^{-0.5} + 0.014 R_n^{-0.114}$ [7th ICSH, 1954, SSPA Rep. 34, 1955, p. 76, Eq. (2)].

(12) Telfer, Lackenby, and others,

$$C_F = a + bR_n^{-n}, \text{ so that for } R_n = \infty, \quad C_F = a$$

Here, the lower-case subscript of the Reynolds-number symbol is not to be confused with the exponent n. A table of the specific friction coefficient C_F for "smooth paint surfaces," derived from the Lackenby formula $C_F = 0.0006 + 0.0791 R_n^{-0.21}$ for the Froude-Kempf data, is given by G. S. Baker, over a range of R_n from 1 to 75 million [INA, Apr 1952, p. 62].

(13) Blasius, for laminar flow on a flat, smooth plate,

$$C_F = 1.328 R_n^{-0.5}$$

(14) For a completely rough surface of length L and an equivalent sand-roughness height of K_S, as given by L. A. Baier,

$$C_F = \left[1.89 + 1.62\left(\log_{10}\frac{L}{K_S}\right)\right]^{-2.50}$$

45.9 Specific Friction Coefficients for the Schoenherr or ATTC 1947 Meanline. Tables 45.c and 45.d are small illustrative sections of a group of larger tables, mentioned in Sec. 45.7, calculated in the 1940's by the Experimental Towing Tank of the Stevens Institute of Technology and published in August 1948 as SNAME Technical and Research Bulletin 1–2. These tables give values of the specific friction resistance coefficient C_F as determined by the ATTC 1947 (Schoenherr) meanline, Eqs. (5.xiva) or (5.xivb) and the formulas of item (1) of Sec. 45.8, for fully developed turbulent flow on a flat, smooth plate. The range of the argument R_n for entering the complete set of tables is sufficient to cover both model and ship regions. The entries in Tables 45.c and 45.d are modified so that *all R_n values are in terms of millions* [5th ICSTS, London, 1948, p. 112, item 4, top of page].

The method of picking C_F values by inspection and using them for R_F calculations is illustrated in Sec. 45.22.

45.10 Laminar Sublayer Thicknesses in Turbulent Flow. Some quantitative knowledge of the thickness δ_L of the laminar sublayer next to a solid boundary is of interest in a study of roughness effects, to determine whether these are essentially viscous or primarily pressure phenomena. It has been found [Rouse, H., EMF, 1946, p. 194; Baines, W. D., "A Literature Survey of Boundary-Layer Development on Smooth and Rough Surfaces at Zero Pressure Gradient," IIHR, 1951, p. 25] that the thickness δ_L of the laminar sublayer in turbulent flow over a rough surface can be expressed by

$$\delta_L = (\text{a coefficient})\ \frac{\nu}{\sqrt{\dfrac{\tau_0}{\rho}}} \qquad (5.\text{vi})$$

$$= (\text{a coefficient})\ \frac{\nu}{U_\tau}$$

where values of the coefficient vary from about 11.6 to 12.6, and $U_\tau = \sqrt{\tau_0/\rho}$ is the shear velocity. Using the larger coefficient, a number of δ_L values calculated for a wide range of R_n are plotted in Fig. 45.F. It is to be noted that the *δ_L values increase slowly with length for a given speed, but they decrease rapidly with speed for a given length.* The reasons for this are discussed presently.

It is interesting to note that the permissible average roughness height k_{A_v} for a hydrodynam-

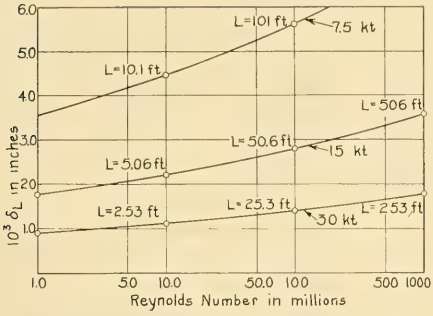

FIG. 45.F VARIATION OF LAMINAR SUBLAYER THICKNESS δ_L WITH x-DISTANCE (L) AND SPEED

ically smooth surface, given by the expression described at greater length in Sec. 45.15 [Goldstein, S., ARC, R and M, 1763, Jul 1936, p. 113], namely

$$k_{Av} < 5\,\frac{\nu}{U_\tau} \qquad (45.\text{iii})$$

indicates that the roughnesses should *average* somewhat less than half the laminar-sublayer thickness δ_L, in the ratio of say 5 to 12.6, if they are to produce no roughness effects.

Granting that the relationship between the height of the roughness on a solid surface and the laminar-sublayer thickness has an important influence on the roughness effects, it is useful to know what factors influence this thickness δ_L. To understand this, Eq. (5.vi) may be written

$$\delta_L = 12.6\nu(\rho)^{0.5}(\tau_0)^{-0.5} \qquad (45.\text{iv})$$

From Eq. (5.iii) of Fig. 5.R or the corresponding equation from the turbulent-flow column in Fig. 45.A, one may also write

$$\begin{aligned}\tau_0 &= 0.059\,\frac{\rho}{2}\,U_\infty^2 R_x^{-0.2}\\ &= 0.059\,\frac{\rho}{2}\,U_\infty^2\left(\frac{U_\infty x}{\nu}\right)^{-0.2}\end{aligned} \qquad (5.\text{iii})$$

Combining these two equations, there is obtained

$$\begin{aligned}\delta_L &= 12.6\nu(\rho)^{0.5}\left(\frac{0.059}{2}\right)^{-0.5}(\rho)^{-0.5}U_\infty^{-1}U_\infty^{0.1}x^{0.1}\nu^{-0.1}\\ &= 12.6(0.0295)^{-0.5}\nu^{0.9}U_\infty^{-0.9}(x)^{0.1}\end{aligned}$$

Dropping out the numerical values for the moment, and assuming that the kinematic viscosity ν is constant for this study,

$$\delta_L \propto \frac{x^{0.1}}{U_\infty^{0.9}} \qquad (45.\text{v})$$

This means that δ_L increases very slowly as x increases and that it decreases rapidly as U_∞ increases. For example, if U_∞ increases from 10 kt to 20 kt and then to 30 kt, δ_L decreases very nearly to $\frac{1}{2}$ and then to $\frac{1}{3}$ of its 10-kt value. If x increases from 5 ft to 15 ft, the increase in δ_L occasioned by it is only in the ratio of 1 to $(3)^{0.1}$ or 1.116.

At the same time, an increase *in either* U_∞ or x to three times its original value multiplies the original Reynolds number by three. It can not be said, therefore, that the change in δ_L, and hence the change in the effect of a given roughness of a certain absolute size and shape, is a function solely of the Reynolds number of the flow, as determined by the product of the relative velocity U_∞ and the distance x from the leading edge (neglecting the kinematic viscosity).

A given barnacle at the bow of a long ship might project through the thin laminar sublayer there but lie just within this layer at the stern. However, as the ship speed increases, the value of δ_L diminishes. A barnacle of the same size at the stern projects more and more through the laminar sublayer and becomes more and more effective as an item of roughness. This is the reason why, in aeronautical circles, it is customary to use a special Reynolds number with the roughness height as a space dimension, instead of the distance x from the nose or leading edge of the body or plate. In fact, if the Goldstein relationship mentioned earlier in this section is rearranged in the manner

$$5 > \frac{k_{Av}U_\tau}{\nu} \qquad (45.\text{vi})$$

it forms a Reynolds number of this kind, where k_{Av} is the space dimension.

This relationship is discussed further in Sec. 45.15.

45.11 Friction Data for Water Flow in Internal Passages. This is not the place for an extended discussion of the friction resistance offered by the internal surfaces, both smooth and rough, of water ducts and passages which are separate from those in the machinery plant. Some reference data on this subject are given by J. K. Salisbury [ME, 1944, Vol. II, Fig. 51 on p. 61 and Art. 12 on pp. 62–63], but it must be noted that the weight density (lb per ft^3) of the liquid is repre-

sented in that reference by the symbol ρ instead of by the ICSTS or ITTC symbol w.

A rather comprehensive discussion of steady flow in pipes and conduits, from the standpoint of hydraulics and hydrodynamics, is given by V. L. Streeter in Chap. VI of "Engineering Hydraulics" [Rouse, H., Editor, 1950, pp. 387–443].

45.12 Computation of the Wetted Surface of a Ship. Although the computation of the wetted surface S of the underwater body of a ship is a problem in solid geometry rather than in hydrodynamics, the flow conditions over different portions of that surface are closely related to the specific friction resistance coefficients. The wetted-surface calculations are therefore made with these conditions clearly in mind. Furthermore, a value of S is required in the early stages of the preliminary design, as described in Sec. 66.9, when the lines may not yet be sketched and there are no girths to measure.

D. W. Taylor solved this problem by the use of a wetted-surface coefficient, now known as C_{WS}, based upon data from a great number of models and many types of lines, not limited to the series bearing his name. When only the displacement Δ (delta; large capital), the maximum-section coefficient C_X, the beam-draft ratio B/H, and the "mean immersed length" L were known, the wetted surface S was determined by $S = C_{WS}\sqrt{\Delta L}$, where Δ was in long tons (2,240 lb) of salt water of sp. gr. 1.024, with a volume density of 35.075 ft^3 per long ton. Since the mean immersed length was usually not known until the form was laid out, the waterline length was often substituted for it.

Contours of C_{WS} on a basis of C_X and B/H were first published by Taylor in the 1910 edition of S and P [Vol. I, p. 47; Vol. II, Fig. 41]. They were repeated in the 1933 edition of S and P, Fig. 20, page 20, and in PNA, 1939, Vol. I, Fig. 33, page 96.

These contours were reworked by M. E. Fowler of the TMB staff in the early 1940's to include data from many additional models of all types. Fig. 20 on page 22 of the 1943 edition of S and P, embodying the revised contours, thus differs slightly from its predecessors.

As C_{WS} is a dimensional quantity, which varies with the system of measurement, D. W. Taylor's formula is for this book converted to the 0-diml form

$$S = C_S\sqrt{\nabla L} = C_S\sqrt{\nabla L} \qquad (45.\text{vii})$$

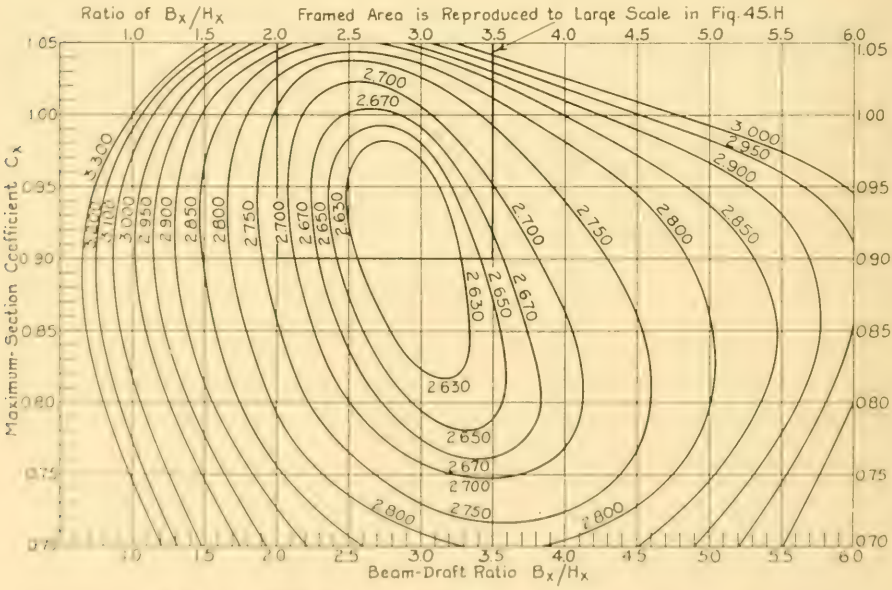

Fig. 45.G Contours of 0-Diml Wetted-Surface Coefficient C_S for Ships

where L is now the waterline length and the conversion from Δ to $\mathbb{F}$ or ∇ is based upon the volume density of salt water previously mentioned. Supplementing this conversion, a further revision of the contours provides new values of C_S which are somewhat more realistic, especially as every ship has to have plating and most of them carry rudders and other simple appendages. The result is a minor increase of about 0.03 over Taylor's revised values of 1943. The new plots are based largely on data taken from SNAME RD sheets 1 through 100, covering modern vessels of many sizes and types and relatively normal form.

Fig. 45.G gives the new contours of C_S, plotted on C_X and B_X/H_X. As the wetted-surface coefficients for the great majority of ships fall in a small area bounded by values of B_X/H_X from 2.0 to 3.5 and C_X from 0.9 to 1.05, expanded contours of this area are shown to a considerably larger scale in Fig. 45.H. A similar plot by M. L. Acevedo [TABLAS, 1943, opp. p. 128] gives values about 4 per cent lower than those in Figs. 45.G and 45.H. The new C_S values have been checked repeatedly since their preparation with all available new data, and the agreement has been found to be within limits of engineering accuracy. The new contours are certainly adequate for use in the early stages of a preliminary design.

However, the C_S contours of Figs. 45.G and 45.H are to be used with caution for vessels of abnormal form, such as those of shallow draft, those with broad, flat sterns, with excessive

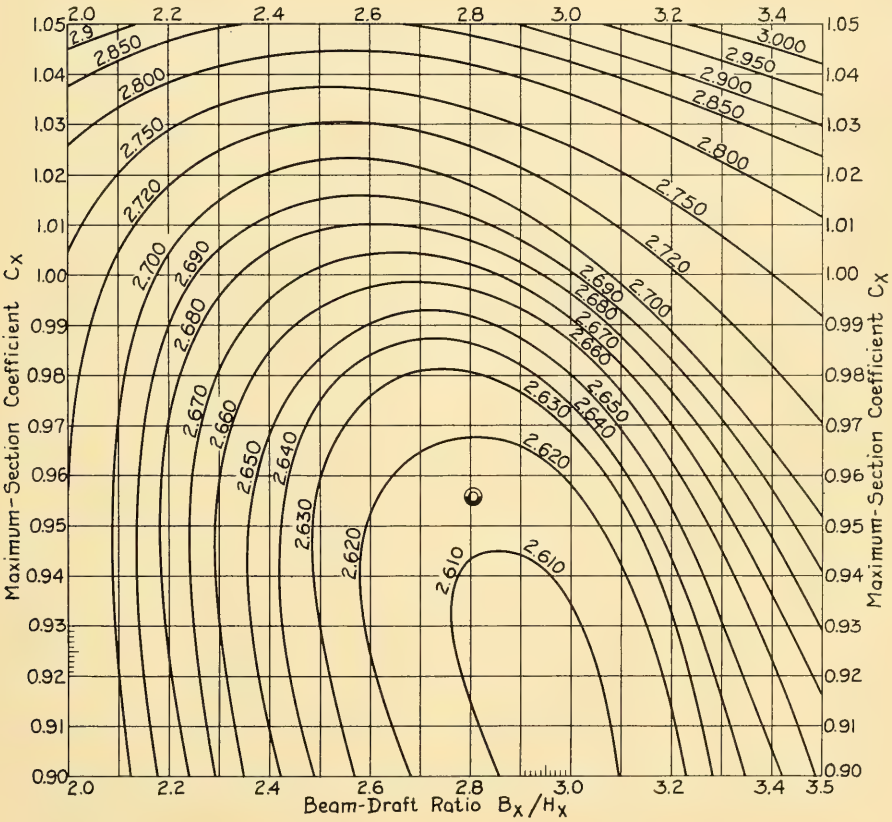

Fig. 45.H Enlarged Plot of 0-Diml Wetted-Surface Coefficient C_S for Usual Ship Ranges

cutaway in the forefoot or aftfoot, and with short, chubby hulls. For these, a value of C_S is determined with reasonable accuracy, provided the correct value of C_S is available for a prototype vessel whose proportions and coefficients do not differ too much from the vessel whose wetted surface is sought. Suppose for example that C_S from Fig. 45.G is small by 0.04 for a craft of abnormal form whose C_S is known. It may be taken as approximately 0.04 small for the same type of hull, even though the proportions and coefficients are changed somewhat from those of the "known" vessel. The C_S derived from Fig. 45.G by using the proportions of the given form, augmented by 0.04, may be relied upon for the abnormal type being developed. If it is known, for instance, that the wetted surface of a twin-skeg stern design is 3.2 per cent greater than that of a normal-form ship, the latter as given by Fig. 45.G, then this allowance may be applied rather generally, for any twin-skeg stern ship, to the predicted result given by the formula.

In any case, because of the present (1955) uncertainty as to the correct roughness allowance for any ship, it seems not necessary, when making preliminary force and power predictions, to calculate the wetted area to a high degree of accuracy.

The procedure currently employed in detail calculations of the friction drag on the doubly curved wetted surface of a ship hull assumes that the surface is flattened into a single thin plate which has a DWL length equal to that of the ship and a width equal to that of the half girth at each station or frame. Such a plate has the general shape indicated by the 0-diml girth curves of Fig. 22.A of Volume I. The two sides of the flat plate correspond to the two sides of the ship. This leads to the general rule that the wetted surface of the main hull, without appendages but with large bossings or skegs, is the product of the waterline length and the mean wetted girth to the waterline. The mean girth may be computed by Simpson's first rule, using 20 equally spaced stations, or by any convenient equivalent method.

The wetted surface of a large appendage, particularly one which is long like a bilge keel, is calculated similarly from its mean wetted girth, to be obtained by any convenient method, and its length as projected on the centerplane of the vessel. The wetted surface of small, short appendages, which are relatively thin and on which the resistance is largely frictional, is calculated by the rules of solid geometry or any convenient method. An appendage is considered small or short when the x-Reynolds number at the trailing edge is less than about 15 million at the given speed. As an example, this occurs for a length of about 7.5 ft at 15 kt, 5.6 ft at 20 kt, and 3.75 ft at 30 kt. If the appendages are very short, like the arms of shaft struts, their wetted surfaces are neglected, and their resistances are computed by the rules of Chap. 55.

The surfaces of exposed rotating shafts, rotating hull plates of cycloidal or rotating-blade propellers, and similar areas not subject to translatory motion only, require to be handled by methods considered appropriate in each case. No logical and systematic procedures have as yet been worked out for these parts. Friction drag on propeller-hub, fairing-cap, and blade surfaces is taken into account in propeller performance.

It has not been practicable, as described in Sec. 12.3 of Volume I, to resolve the tangential forces on each unit of wetted area into components parallel to the direction of ship motion. The summation of the actual friction forces gives therefore a value slightly greater than the sum of the direction-of-motion components; see Fig. 12.A. Effective if not exact compensation for this inequality is achieved by using the mean girth for calculating the wetted surface, without a correction for obliquity, thus giving a wetted-surface area slightly less than the actual area. For those who wish to employ the obliquity correction a diagram giving the necessary factors and instructions for their use is published by D. W. Taylor [S and P, 1943, p. 18]. The obliquity correction is of interest only for full, fat ships. It amounts to about 0.01 for a ship having an L/B ratio of 4 and a B/H ratio of 2.2.

At the design stage where the girths are taken off for the early wetted-surface calculations, usually only the molded lines are available, representing the inside rather than the outside of the plating. A small plus allowance can be made for the surface of the ship to the outside of the plating, or the girths can be measured deliberately a little large.

Unless circumstances indicate that the wave formation along the side may be unusual at the speed for which the R_F calculation is being made, no account is taken of the wave profile in altering the at-rest wetted surface. The wetted surface gained in the crests of waves along the ship's side is probably somewhat less than that lost in the

troughs, but this is largely compensated for by the bodily sinkage of the ship while in motion, described in Sec. 29.2. The reduction in wetted surface becomes appreciable, of course, when a fast or high-speed boat approaches or reaches the planing range.

Often it is *definitely known* that a separation region exists along some part of the wetted surface, such as that behind a transom stern or inside a sizable rudder recess, or the extent of the zone can be estimated *with reasonable certainty*. The wetted area next to the separation zone is then subtracted from that of the rest of the ship, considering the extent of the zone constant at all speeds [Horn, F., 3rd ICSTS, 1937, p. 22; Acevedo, M. L., "Skin Friction Resistance," Madrid, 1948, p. 14].

When a fixed appendage covers a part of the main ship hull, such as a roll-resisting keel of V-section, the area so covered is subtracted from the calculated wetted area of the hull.

Although all hull and appendage wetted areas are frequently lumped together, and although there is some justification for adding an allowance for appendages to the wetted surface S in the early stages of a design, before the appendages are laid out, it is preferable to make separate wetted-surface calculations for the appendages. This gives the designer an idea of what is being added to the S value of the ship.

Summarizing, the calculation of the wetted surface of a ship, when the shape and size of the hull and the underwater appendages are known, takes the following form:

(1) If the lines are not yet drawn, estimate the wetted surface by the use of the wetted-surface coefficient C_S from Fig. 45.H, then combine it with the underwater volume $\forall$ and the waterline length L in the formula $S = C_S\sqrt{\forall L}$. Add a percentage or an area allowance for the contemplated appendages, if it can be estimated at this stage and if it is considered necessary.

(2) With ship lines available, measure the girths from designed waterline to designed waterline at 21 or more equally spaced stations along the waterline length, including the FP. Compute the mean girth from Simpson's first rule [PNA, 1939, Vol. I, p. 16] or the equivalent, and multiply the mean girth by the waterline length. When measuring the girths, include large bossings or skegs and discontinuities in the sections where the ship plating is carried continuously around them. Be generous in measuring girths to include the shell plating outside the molded lines.

(3) For large appendages, especially those long enough to have an x-Reynolds number exceeding 15 million, calculate the wetted girth as for (2) preceding and multiply by the length projected on the centerplane

(4) For small, short appendages, excluding rotating shafts and the like and the propulsion devices proper, if their resistance is primarily frictional, calculate the wetted surface by any convenient method

(5) Make no allowance or correction for *actual* wetted surface between the at-rest WL and the wave profile when the ship is in motion except for $F_n > 0.6$, $T_q > 2.0$, or for unusual cases

(6) Estimate the wetted surfaces of zones of separation, if it is *practically certain* that they will exist at the speeds for which resistance and power estimates are wanted. Otherwise, neglect them.

(7) Calculate the hull area covered by the attachments of fixed appendages of appreciable size

(8) Add the areas of (2), (3), (4), and (5), and subtract the areas (6) and (7). The result is the value of wetted surface S for the design.

45.13 Wetted-Surface and Boundary-Layer Calculations for the Transom-Stern ABC Ship of Part 4. The wetted-surface calculation for the preliminary design of the transom-stern ABC ship designed in Part 4 of this volume is made by using Eq. (45.vii), namely $S = C_S\sqrt{\forall L}$. When the hull lines are available this is checked by a calculation embodying the measured girths at 21 stations, plus those at four half-stations near the ends, namely 0.5, 1.5, 18.5, and 19.5.

At the stage corresponding to the first estimate of wetted surface the pertinent parameters are: $B_X/H_X = 2.808$; $C_X = 0.956$; $\forall = 574{,}000$ ft^3. The latter is derived from an estimated weight displacement of 16,400 t and a round-number volume density of 35 ft^3 per ton. Entering the 0-diml wetted-surface coefficient contours of Fig. 45.H with the first two parameters, the value of C_S by inspection is 2.616. The location of this point is shown on the diagram by the distinctive double circle with its black lower half, used in this volume for the ABC design. Substituting these values in Eq. (45.vii),

$$S = C_S\sqrt{\forall L} = 2.616\sqrt{(574{,}000)510}$$
$$= 44{,}759 \text{ ft}^2.$$

When the exact underwater volume $\mathcal{V}$ is determined by planimeter, using the fair lines of the ship, it is found to be 575,847 ft^3; the corresponding wetted surface S, by Eq. (45.vii), is 44,831 ft^2. This is very close to the value determined by the more precise method described in the next paragraph.

The calculation of wetted surface, using (1) the measured girths at 21 stations, (2) a combination of the Simpson and trapezoidal rules, and (3) no correction for obliquity, gives a value of S for the bare hull, including the cutwater shown on Fig. 67.E, of 44,883 ft^2. It is found, for this ship, that the wetted surface is about 1.2 per cent higher when using two half-stations at each end in addition to the customary 21 stations. However, the precision here is much greater than for the friction-resistance coefficient C_F, especially when roughness is taken into account.

The original estimate of *net* bilge-keel area of Sec. 66.9, assuming a keel length of 200 ft, a width of 3 ft, and a girthwise span at the base of 1 ft, is 2,400 − 400 = 2,000 ft^2. Using the bilge-keel design of Fig. 73.N, with a length of 193.5 ft, a width of 3.5 ft, and a girthwise span of 1.25 ft at the base, the *net* area is calculated to be 2,743 − 489 = 2,254 ft^2. Incidentally, the Reynolds number R_n for a bilge-keel length of 193.5 ft is

$$R_n = \frac{VL}{\nu} = \frac{(20.5)(1.6889)(193.5)}{1.2817(10^{-5})}$$

$$= 522.7 \text{ million.}$$

The wetted surface of the rudder and rudder horn, calculated from the dimensions given in Fig. 74.K, and assuming the wetted area to be twice the projected area, is found to be 748 ft^2.

The only separation zone expected around the underwater hull is that abaft the transom. The area of the after side of the transom is therefore not included in the wetted-surface calculation, using measured girths. No deduction is therefore necessary for it.

No allowance is made in this calculation, nor is any customary, for the change in wetted surface due to substitution of the wave profile at designed speed for the at-rest waterline as an upper boundary of the wetted area.

The hull area covered by the fixed rudder horn is about 10 ft^2.

The actual wetted surface of the transom-stern ABC ship, with all appendages, in ft^2, is:

Bare-hull surface, plus cutwater, from girths	44,883
Bilge keels (2 of), surface exposed to water	2,743
Rudder and fixed rudder horn	748
Deduction for hull area covered by bilge keels	−489
Deduction for hull area covered by rudder horn	−10
Net total, ft^2,	47,875

As an indication of the absolute thickness δ of the boundary layer for the ABC ship, a series of values are calculated by the flat, smooth-plate, turbulent-flow formula $\delta = 0.38(x)(R_x)^{-0.2}$ of Fig. 5.R and plotted in Fig. 45.I. A note on the

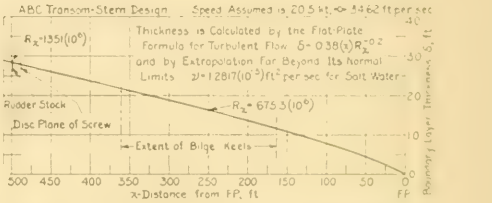

FIG. 45.I VARIATION OF BOUNDARY-LAYER THICKNESS WITH x-DISTANCE FROM STEM FOR ABC SHIP

graph emphasizes that this formula is extrapolated far beyond its usual limits. It should be emphasized further that, since this is a flat-plate formula, the assumption is made that the wetted area on each side of the ship is the same as that on one side of a thin plank of the same length, namely 510 ft. The formula employed takes no account of either longitudinal or transverse curvature in the ship, or of roughness, so that the thickness values for ship ranges indicated on the plot may be altered rather drastically when the ship values are actually known. Even then, they could be considered as only average or typical, because the local boundary-layer thickness, at a given x-distance from the stem, varies with the local radius of curvature, both longitudinal and transverse.

45.14 Estimating the Allowances for Curvature. For estimating the approximate effect of *convex* transverse curvature of a body or ship form, discussed in Sec. 6.8 of Volume I, use is made of Landweber's formula [TMB Rep. 689, Mar 1949, p. 7] for the increase in friction drag of a semi-submerged cylinder over the friction

drag of a flat plate of equal area. This takes the form

$$\frac{R_F}{R_{F0}} = 1 + 0.54\frac{L_1^2}{S_1}C_F \qquad (45.\text{viii})$$

where

R_F is the friction drag of the convex surface
R_{F0} is the friction drag of an equal area of flat plate
L_1 is the length of the convex surface
S_1 is the area of the convex surface
C_F is taken for the whole body or ship.

The sides are vertical at the WL, hence the girth angle from the WL on one side to the WL on the other is 180 deg.

Taking $L_1 = L$ and $S_1 = S$, in other words considering the *whole* ship form, L_1^2/S_1 may be expected to vary from about 10 for a fine form to 4 for a full form. For the ABC ship designed in Part 4 it is 5.8.

Considering only the region of sharp, convex, transverse curvature on a body or ship, the value of L_1^2/S_1 for that region may be considerably higher than the values given; in fact, several times as great. If two relatively sharp bulges are involved, each having a girth angle of 90 deg, as where the bottom joins the two sides, the bulges and the angles may be combined to form a smaller, separate body with a girth angle of 180 deg. Eq. (45.viii) may then be used as given. There is a question as to whether to use a value of the specific resistance coefficient C_F for the ship length L or for only the bulge length L_1. Since the boundary-layer thickness is determined largely by the ship length L it seems reasonable to use the same C_F as is picked from Table 45.d on page 102 for the ship as a whole.

Taking as an example a modern Great Lakes ore carrier about 635 ft long [MESR, Jul 1952, p. 65], the bilge radius is 3 ft and the length L of uniform bulge is 331 ft on each side. L_1^2 is then 109,561 ft^2, and S_1 is $(3)\pi(331)$, or 3,119.6 ft^2, whence $L_1^2/S_1 = 35.12$. The service (sea) speed is 14.15 kt, whence R_n for fresh water from Table 45.a is about 1,242 million and C_F from Table 45.d is $1.491(10^{-3})$. Then

$$\frac{R_F}{R_{F0}} = 1 + 0.54(35.12)(1.491)(10^{-3})$$

$$= 1 + 0.0283$$

whence Δ_2 of Eq. (22.iv), in Sec. 22.15 of Volume I, is 0.0283, or just less than 3 per cent. The value of $\Delta_2 C_F$ is $0.0283(1.491)(10^{-3}) = 0.0422(10^{-3})$.

No procedure has as yet been worked out for making allowances for *concave* transverse curvature. This is seldom of great degree, except for the coves of discontinuous-section hulls, the coves along the inside corners of roll-resisting keels, or the coves along the superstructures of some types of submarines. In these cases, the adjacent convex curvatures on the chines and edges largely neutralize the concave curvatures, so that both may be neglected.

For estimating the effect of longitudinal curvature by Horn's method, described in Sec. 22.5 of Volume I, some knowledge or estimate of the sinkage at given speeds, derived from model tests, may be used. Alternatively, ΔR_F may be calculated from the L/B, B/H, and C_P values by the formula given by F. Horn [3rd ICSTS, Berlin, 1937, Eq. 2, p. 24], as follows:

$$\Delta R_F = 0.01\left[\frac{(11.25 - L/B)^2}{5} + 2.5\right] \cdot (0.35 + C_P)\left(1.3 - \frac{B/H}{10}\right) \qquad (45.\text{ix})$$

This is a good approximation for normal forms of not extreme proportions and for a range of F_n values from 0.0 to 0.35, T_q from 0.0 to 1.18.

For the ore carrier previously referenced, $L/B = 635/70 = 9.07$, $B/H = 70/24.885 = 2.812$, and $C_P = 0.881$, from which ΔR_F (also numerically equal to $\Delta_1 C_F$) is found to be

$$\Delta R_F = 0.01\left[\frac{(11.25 - 9.07)^2}{5} + 2.5\right] \cdot (0.35 + 0.881)\left(1.3 - \frac{2.812}{10}\right)$$

$$= 0.04326$$

For the ABC design, where $L/B = 510/73 = 6.99$, $B/H = 73/26 = 2.81$, and $C_P = 0.62$, substitution in Eq. (45.ix) gives

$$\Delta R_F = 0.01\left[\frac{(11.25 - 6.99)^2}{5} + 2.5\right] \cdot (0.35 + 0.62)\left(1.3 - \frac{2.81}{10}\right)$$

$$= (0.01)(6.13)(0.97)1.019 = 0.0606$$

For the *Lucy Ashton*, a ship of quite different form [INA, Oct 1953, p. 350ff], having an L/B

ratio of 9.07, a B/H ratio of 4.20, and a C_P of 0.705:

$$\Delta R_F = 0.01\left[\frac{(11.25 - 9.07)^2}{5} + 2.5\right] \cdot (0.35 + 0.705)\left[1.3 - \frac{4.20}{10}\right]$$

$$= 0.0320$$

For a paddle steamer like the *Lucy Ashton*, especially of shallow draft, the augment of velocity in the waterline region arising from the induced velocity generated ahead of and abaft the paddles acts to increase the friction drag. This amount is difficult to determine in figures but theoretically it always involves an *increase* in resistance.

Despite the hydrodynamically correct basis for increases in the friction drag due to convex curvature in a ship, both transverse and longitudinal, many cases occur in practice which cast doubt upon the validity of these additions to the friction drag for a smooth, flat plate in turbulent flow. Indeed, there are cases where the entire $\Sigma(\Delta C_F)$ allowance, for all types of roughness as well as for both types of curvature, is practically zero. There are those who say, and with some reason, that results of this kind lead them to question the smooth, flat-plate, turbulent-flow friction formulation itself, which gives higher C_F values than it should in certain ranges of R_n.

In any event, the analyses made to date of existing propeller-thrust data on ships are insufficient to indicate whether the curvature allowances, as estimated by the procedures described, are reasonable or not. All that can be said with certainty is that $\Delta_1 C_F$ and $\Delta_2 C_F$ are probably no larger than indicated, and that they are both positive.

45.15 Criterion for a Hydrodynamically Smooth Surface. As a criterion for hydrodynamic smoothness in turbulent flow S. Goldstein has suggested the expression [R and M 1763, Jul 1936, p. 113]

$$\frac{k_{Av} U_\tau}{\nu} < 5 \qquad (45.\text{vi})$$

where k_{Av} is the *average* height of the hills or roughnesses above the limen, U_τ is the shear velocity $\sqrt{\tau_0/\rho}$, and ν is the kinematic viscosity. As pointed out in Sec. 45.10, the left-hand expression of the inequality has the form of a Reynolds number, so that it can be related to a simple number.

Of interest in this connection is a set of criteria given by J. S. Hay in Porton Technical Paper 428 (unclassified) of 24 June 1954, issued by the Chemical Defense Experimental Establishment of the Ministry of Supply in Great Britain (copy in TMB library). In the symbols of the present volume, and where the factor k_0 is defined solely as a "roughness parameter," these are:

(1) Aerodynamically rough flow,

$$k_0 > 2.5\,\frac{\nu}{U_\tau}$$

(2) Transitional flow,

$$2.5 > \frac{U_\tau k_0}{\nu} > 0.13$$

(3) Aerodynamically smooth flow,

$$k_0 < 0.13\,\frac{\nu}{U_\tau}.$$

To apply Goldstein's criterion to the practical case, it is first necessary to know the local intensity of shear τ_0. For turbulent flow, from Fig. 45.A,

$$\frac{\tau_0}{\frac{\rho}{2} U_\infty^2} = C_{LF} = \frac{0.059}{R_x^{0.2}}$$

whence

$$\tau_0 = 0.059\left(\frac{\rho}{2} U_\infty^2\right)(R_x)^{-0.2} \qquad (5.\text{iii})$$

As an example, assume for a destroyer a point 200 ft abaft the stem and a speed of 30 kt, equivalent to 50.67 fps. The kinematic viscosity ν for salt water is $1.2817(10^{-5})$ ft^2 per sec and $\rho/2$ is 0.995 slugs per ft^3. The value of U_∞^2 is 2,567 fps^2. From Table 45.b R_x is about 790 million, whence $R_x^{0.2} = 60.2$. Then $\tau_0 = 0.059(0.995)(2{,}567)/60.2 = 2.504$ lb per ft^2. The shear velocity $U_\tau = (\tau_0/\rho)^{0.5} = [(2.504)/1.9905]^{0.5} = 1.1215$ ft per sec. From Eq. (45.vi), assuming that $[(k_{Av}U_\tau)/\nu]$ is as large as 5,

$$k_{Av} = (5\nu)/U_\tau = \frac{(5)1.2817(10^{-5})}{1.1215} = 5.714(10^{-5}) \text{ ft},$$

whence $k_{Av} = 0.686(10^{-3})$ in.

This means that the *maximum* permissible roughness heights, for a hydrodynamically smooth surface, would probably be of the order of one-thousandth of an inch. It amounts practically to a laboratory smoothness, exceedingly expensive and laborious if not practically impossible to achieve on a large vessel, even for a special trial.

Assume for the 20-ft towing model of this destroyer a point 10 ft abaft the stem and a speed of 10 kt, equivalent to 16.89 fps. The kinematic viscosity ν for the fresh water of the basin is $1.2285(10^{-5})$. The value of $\rho/2$ is 0.969 slugs per ft^3 for fresh water and U_∞^2 is 285.3 fps^2.

From Table 45.a, R_x is about 13.75 million, whence $R_x^{0.2} = 26.77$. Then

$$\tau_0 = [0.059(0.969)285.3]/26.77$$
$$= 0.6093 \text{ lb per ft}^2$$
$$k_{A\nabla} = [1.2285(10^{-5})5]/0.6093 = 10.08(10^{-5}) \text{ ft},$$

whence

$$k_{A\nabla} = 1.209(10^{-3}) \text{ in.}$$

This value for the model, although not for exactly similar conditions, is about twice the permissible value for the ship.

For the ABC ship, at an x-distance of 500 ft from the FP, and a speed of 20.5 kt, equivalent to 34.625 ft per sec, R_x for standard salt water is, from Table 45.b, about $1{,}350(10^6)$. The shear stress τ_0 at the ship hull is

$$\tau_0 = 0.059 \frac{\rho}{2} U_\infty^2 R_x^{-0.2} \tag{5.iii}$$
$$= 0.059 \frac{1.9905}{2} (34.625)^2[1{,}350(10^6)]^{-0.2}$$
$$= 1.051 \text{ lb per ft}^2.$$

Hence the shear velocity is

$$U_\tau = \sqrt{\frac{\tau_0}{\rho}} = \sqrt{\frac{1.051}{1.9905}} = 0.726 \text{ ft per sec},$$

whence the laminar-sublayer thickness is

$$\delta_L = 12.6 \frac{\nu}{U_\tau} = 12.6 \frac{1.2817(10^{-5})}{0.726}$$
$$= 22.24(10^{-5}) \text{ ft} \quad \text{or} \quad 2.67(10^{-3}) \text{ in},$$

and the permissible average roughness height for a hydrodynamically smooth surface is

$$k_{A\nabla} < 5 \frac{\nu}{U_\tau} < 5 \frac{1.2817(10^{-5})}{0.726} < 8.83(10^{-5}) \text{ ft}$$
$$\text{or} \quad < 1.06(10^{-3}) \text{ in.}$$

For the *Lucy Ashton* [Conn, J. F. C., Lackenby, H., and Walker, W. P., INA, Oct 1953, p. 350ff] the waterline length is 190.5 ft and the speed is 12 kt, or 20.27 fps. The value of U_∞^2 or V^2 is then 410.87 ft^2/sec^2. From Table 45.b, R_n is about 301 million and $R_n^{0.2} = 49.63$. The estimated kinematic viscosity ν (the water temperature is unknown) is $1.42(10^{-5})$ ft^2 per sec and the mass density ρ is 1.985 slugs per ft^3. Then, as a local value at the stern,

$$\tau_0 = 0.059\left(\frac{\rho}{2}\right)U_\infty^2(R_x)^{-0.2}$$
$$= \frac{0.059(0.9925)(411)}{49.63}$$
$$= 0.485 \text{ lb per ft}^2.$$
$$U_\tau = \left(\frac{\tau_0}{\rho}\right)^{0.5} = \left(\frac{0.485}{1.985}\right)^{0.5} = 0.494 \text{ ft per sec.}$$

Then

$$k_{A\nabla} = \frac{5\nu}{U_\tau} = \frac{5(1.42)10^{-5}}{0.494}$$
$$= 14.37(10^{-5}) \text{ ft} \quad \text{or} \quad 1.725(10^{-3}) \text{ in.}$$

45.16 Equivalent Sand Roughness. Although the procedure is admittedly empirical, and is not based upon good roughness criteria, some practical use has been made of a quantitative measure of roughness based upon numerous tests of flat and curved surfaces covered with sand grains of different mean diameters. When a rough surface, of whatever configuration, has a specific friction resistance, either average C_F or local C_{LF}, equal to that of a similar surface completely covered with sand of uniform size, it is said to have an *equivalent sand roughness* equal to the *mean diameter* of the sand grains on the reference surface. This diameter corresponds to the height of the grains as individual protuberances and is represented by the symbol K_S.

With grains completely covering the reference plate surface, the sand-grain density is assumed to be 100 per cent. The actual mean roughness height is then less than the mean grain diameter K_S, indicated in diagram 3 of Fig. 5.O. However, this detail is overlooked when establishing equivalent sand roughness as a practical comparator for surfaces whose irregular roughness can not be measured by any available method.

M. L. Acevedo at the Madrid Model Basin and W. P. A. van Lammeren at the Netherlands Model Basin in Wageningen have published tables [TABLAS, Madrid, 1943, pp. 98–117; van Lammeren, W. P. A., RPSS, 1948, pp. 66–69; 3rd ICSTS, Berlin, 1937, pp. 42–47, 100–101] of roughness allowances based upon the R. E. Froude formulation and the roughness effects developed by H. M. Weitbrecht from the Prandtl

TABLE 45.c—EQUIVALENT SAND ROUGHNESS VALUES K_S OF H. M. WEITBRECHT

The listed values of K_S for "new, painted hull plates, inclusive of butts, seams, and rivet heads . . ." apply to the types of ships indicated.

(a) Sporting and racing craft, torpedo-boats and destroyers	0.10 mm	0.004 in
(b) Cross-channel ships, cruisers, battleships	0.15	0.006
(c) Mail ships, fast liners, carefully built cargo ships	0.20	0.008
(d) Cargo ships of less careful workmanship, tugs	0.25	0.010

theory. In this work Weitbrecht used the values given in Table 45.c.

In a more recent paper H. Sasajima and E. Yoshida pointed out rather convincingly that the type of roughness embodied in the hull coatings of most large ships (not necessarily including fouling roughness), is not the type which produces a constant C_F value at large values of R_n [Int. Shipbldg. Prog., 1955, Vol. 2, No. 13, pp. 441–450]. In other words, since the derived friction-resistance values for full-scale tests appear to involve a *constant increment of* C_F and not a constant total C_F, the effective roughness is of a type different from the sand roughness of Nikuradse's pipes. They reason that the increase in friction drag is due to a waviness in which there is a degree of pressure and separation drag, ahead of and behind the roughnesses, which adds to the normal viscous drag. This means that the dynamic effects on the ship, varying as V^2, form only a part of the friction drag of the rough hull surface, and not all of it.

The feature responsible for this difference in effect is, according to the reasoning of Sasajima and Yoshida, the effective slope of the roughnesses in the direction of the flow. For example, the slope of a wavy surface is less than that of a sand-roughened surface. In fact, according to their findings, the slope or the steepness of the roughness elements is more important than their absolute height. It is interesting in this connection to quote their conclusion "g" on page 450 of the reference: "The roughness effect of paint seems to be almost completely determined by an element of the smallest height but the steepest slope." They derive curves for various roughness effects which appear to conform, reasonably well, to the curves derived from full-scale tests.

45.17 Practical Definitions of Surface Roughness. Sec. 5.21 of Volume I describes some of the known—or suspected—aspects of viscous flow over a rough solid surface and the effect of these features on the friction drag generated at the surface. In particular, it outlines briefly the new approach to the viscous-flow problems presented by rough surfaces on the inside of pipes and conduits, devised by H. N. Morris [ASCE, Hydraulics Div., Jan 1954, Vol. 80, Separate 390]. Fig. 45.J is a diagram prepared by the present

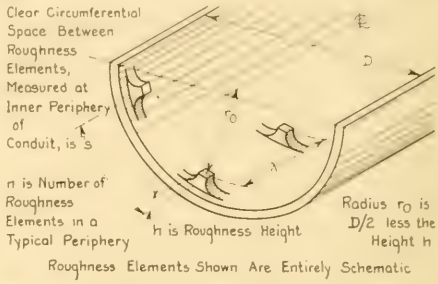

FIG. 45.J DEFINITION SKETCH FOR ROUGHNESS PARAMETERS OF H. N. MORRIS, APPLIED TO THE INSIDE OF A TUBE

author as a definition sketch to illustrate the dimensions used by Morris to represent the roughness characteristics mentioned in his paper. The roughness projections shown in this diagram are purely schematic; Morris gives no dimension for them other than their height h.

It is pointed out in Sec. 22.14 that what might be termed the *roughness index* of a surface, more or less regardless of its shape, must take account of at least seven factors, repeated here for convenient reference. It is possible, in fact probable, that it must take account of others as yet unrecognized or unknown:

(a) Height of roughness peaks above the limen or reference surface, in terms of mean heights (averaged by some suitable method), maximum heights, and a statistical or significant height
(b) Slopes of the roughnesses, on both the upstream and the downstream sides
(c) Orientation of the sloping surfaces with respect to the liquid-flow direction
(d) Spacing of roughnesses in the flow direction, probably with respect to the roughness heights. This corresponds to the distance λ in Fig. 45.J, or to the ratio λ/h.
(e) Type of roughness projections as affecting the

viscous flow, having in mind that sand-coated surfaces give different variations of C_F with R_n than surfaces coated with sprayed plastic paints

(f) General pattern of roughnesses, as viewed normal to the surface, including spacing, density, shadowing or shielding effects, and the like

(g) Finally, it must be possible to ascertain the roughness index easily and quickly in service and to express it (or its results) in quantitative terms.

Further development of the shadowgraph procedure described in Sec. 22.14 and illustrated in Fig. 22.I, or of an equivalent procedure, should give the heights of the roughness peaks above the limen or above the adjacent surface, in terms of the lengths of the shadows for a given inclination of the light rays with reference to the surface as a whole. With an inclination of say 15 deg it could be assumed that any region covered by shadow was in a separation zone and therefore subject to $-\Delta p$'s. It is not known, however, that this is the proper angle or that the angle remains constant. The slopes of the upstream sides of the roughnesses could be determined generally by their relative brightness although it is recognized that the shadowgraph scheme breaks down for an upstream face which lies at a large angle to the limen, say 80 to 90 deg. The orientation of the sloping surfaces with respect to the direction of flow is easily recognized from a photograph taken by this method although it is not so simple to express this orientation in terms of angles or numbers, especially as an average or effective value for a given area. The spacing, density, and general pattern of the roughnesses, as viewed normal to the surface, is perhaps easiest of all to visualize on the shadowgraph, although again not so readily put in terms of numbers or scalar quantities.

It is not improbable that some sort of screen or set of screens may be devised which, when superposed on a shadowgraph, would give a numerical or other roughness index of any given surface.

Whatever may be the method(s) ultimately developed for expressing the physical roughness of a surface, the index derived therefrom must be compared with the hydrodynamic parameters of the viscous flow taking place over that particular surface to determine its roughness effect on friction resistance. These may include the downstream distance x from the leading edge of the body or ship, the speed V of the body or ship or the relative velocity U of the water past it, the thickness δ_L of the laminar sublayer in way of the roughnesses, the thickness δ and characteristics of the boundary layer, and the type of flow existing in the inner regions of that layer.

45.18 Determination of the Allowances for Roughness. It is necessary to estimate the friction resistance and both the effective and the shaft powers early in the design stage. Often it may not be known definitely of what material the shell will be constructed, how smooth the material will be, how the shell plates or planks will be applied, what sort of workmanship is to be expected, or what the eventual external coating will be. If trial predictions only are involved the hull will at least be clean and new, but not necessarily smooth and fair. If an average service performance is wanted, fouling allowances must be estimated and added.

For an intelligent application of the several sets of roughness allowances which have been developed to predict the service performance of a ship, it is necessary to consider the existence of at least six different regimes in the roughness setup. From the knowledge so far gained (1955) it appears that somewhat different physical laws govern the viscous flow in these regimes and that different sets of practical rules apply. The six regimes may be described as:

I. Zero ΔC_F, where, at sufficiently low values of R_n, say up to 4 or 5 million, with a range of C_F above about $3.3(10^{-3})$, roughness effects appear to be small or nonexistent, at least for moderate values of speed compared to length. For example, it has long been known that ship models built for routine resistance and self-propulsion tests required no special finish. It appears that small racing sailboats are in the same category, except at extremely low speeds, say less than 1 kt.

II. Zero ΔC_F, at all values of R_n, where the model, boat, or ship surfaces are hydrodynamically smooth. Secs. 45.10 and 45.15 explain the circumstances under which the laminar sublayer thicknesses exceed the roughness heights by sufficient margins so that this type of smoothness is achieved.

III. Small ΔC_F, at all values of R_n throughout the boat and ship range. In the lower or boat portion of this range the roughness effects appear to be small, especially at low speeds, despite the existence of normal physical roughnesses. In the upper or ship part of the range the use of self-leveling coatings and the existence of certain

roughness configurations, as yet unknown in character, appear to limit the ship roughness effects to subnormal values. The nominal roughness heights in this regime definitely exceed the limiting values for hydrodynamic smoothness.

IV. Large ΔC_F, relatively uniform with speed in the case of any one ship, in the larger ranges of R_n. This situation results largely from the use of rough plastic paints and from fouling. The roughness heights in this regime far exceed those for hydrodynamic smoothness, perhaps by several hundred times, yet the *total* C_F for the ship continues to vary with R_n in a generally normal manner.

V. Very large ΔC_F, with practically constant *total* C_F throughout the speed range. For ships and other large floating craft, this condition probably applies only when the fouling coat is complete and it exceeds 0.4 to 0.5 ft in thickness. In this case the friction resistance is in effect entirely a pressure resistance.

VI. Normal ΔC_F, in which the various roughnesses are normal and the hull of the ship is kept reasonably clean. The ΔC_F values, exclusive of fouling, conform to those represented by the lines C-C or D-D in Fig. 45.E, or to some combination of the two.

To take care of the effects of normal roughness on a clean, new vessel, involving many unknowns, the Froude formulation, listed under item (7) in Sec. 45.8, is still used in many parts of the world. This formulation gives a so-called "Froude Friction Grid," indicated graphically by J. M. Ferguson and others [6th ICSTS, 1951, Fig. 15, p. 68], according to the length of the ship and the speed-length constant Ⓛ. The latter is equal to 3.545 times F_n, as listed at the end of Appx. 1. The lines of this grid lie sufficiently above the ATTC 1947 (Schoenherr) meanline to provide an acceptable roughness allowance for a ship in the "clean, new" category.

A dimensional and carefully systematized attack on the problem of predicting the friction resistance of a full-scale ship, including the effects of roughness, is given by W. W. Smith in his discussion of K. E. Schoenherr's classic SNAME 1932 paper on "Resistance of Flat Surfaces Moving Through a Fluid," pages 305 through 308. Smith's proposed method is too long to be given here, and is likewise somewhat obsolete, but his line of attack is logical and justifies a study of his proposal by anyone working on the problem of roughness friction.

For ship-design purposes in America the American Towing Tank Conference in 1947 adopted an overall tentative roughness allowance ΔC_F of $0.4(10^{-3})$. This is a *constant addition* (not a plus percentage) above the ATTC 1947 meanline for turbulent flow on a flat, smooth plate, regardless of the size or speed of the vessel concerned. As pictured in Fig. 1 on page 2 of SNAME Technical and Research Bulletin 1–2 of March 1952, entitled "Uniform Procedure for the Calculation of Frictional Resistance and the Expansion of Model Test Data to Full Size," it is a compromise between the equivalent plus roughness allowances of the Froude formulation and the tentative ATTC roughness allowances adopted in 1942. The latter increase progressively as the ship length diminishes from 1,000 to 100 ft whereas the former *decrease* slowly as the ship length diminishes from 1,000 to about 300 ft. Below this length the Froude allowances decrease rather rapidly.

There are definite indications, described in Sec. 22.15, that this roughness allowance should diminish with R_n, at least for low values of speed V or relative velocity U. For the lower speeds it appears to diminish toward zero in the region of R_n = 3.5 to 5 million, as does the allowance inherent in the Froude formulation. Fig. 45.E of Sec. 45.7 embodies, in addition to the ATTC 1947 or Schoenherr meanline and the ATTC constant $\Delta C_F = 0.0004$ line, a proposed roughness allowance line C-C proposed by J. M. Ferguson [6th ICSTS, 1951, pp. 67–69], and a line D-D proposed and used by L. A. Baier for some years past. Baier's line leaves the ATTC line at an R_n of about 3 million and reaches the (ATTC + 0.0004) line at an R_n of about 600 million [SNAME, 1951, Fig. 19, p. 365]. Ferguson's line reaches Baier's line at an R_n of about 7,380 million, corresponding to a 1,400-ft ship running at 40 kt in salt water.

Whatever the line or table used to estimate roughness effects in the early stage of a ship design, as soon as more is known about the roughness—or smoothness—to be expected on the hull the tentative value is modified, and the friction resistance is re-calculated.

Assuming that the necessary data are available, the logical method of determining a roughness allowance in the pre-construction stage of a ship design is to select and add together four separate values for the plating, structural, coating, and fouling roughnesses, respectively, as described in Secs. 22.15 and 45.7 and as listed in Eq. (22.iv)

and Eq. (45.ii). Although adequate means do not yet exist for selecting these separate roughness allowances independently and exactly, it is possible to assess reasonable values, within not-too-close limits, to:

(a) A combination of plating and structural roughness
(b) Item (a) plus coating roughness
(c) Item (b) plus fouling roughness.

These serve to subdivide:

(i) The roughnesses built into the ship
(ii) Those inherent in the coating(s) applied after construction or during docking
(iii) Those accumulated in service, after undocking.

TABLE 45.f—TENTATIVE INDIVIDUAL ALLOWANCES FOR ROUGHNESSES OF THREE TYPES

These correspond to three of the types listed at the end of Sec. 45.7. Fouling-roughness predictions are listed in Table 45.g. The present values are intended to apply only to ships of medium and large size, having ship Reynolds numbers at designed speed in excess of about 100 million.

(a) Metal plating, $\Delta_P C_F(10^3)$	
(1) Pickled, sandblasted, or galvanized	0.01 to 0.05
(2) Rusty, pitted, mill scale	0.05 to 0.1
(b) Wooden planking, $\Delta_P C_F(10^3)$	
(1) Plastic, or molded plywood, with few seams or the equivalent, very smooth	0.00
(2) Flush seams, planks in the direction of flow, no open seams, and no calking	0.00 to 0.01
(3) Flush seams, calked, planking not in direction of flow	0.01 to 0.05
(4) Soft planks, slash-grained, rough finish	0.05 to 0.1
(c) Structural roughness, $\Delta_S C_F(10^3)$	
(1) Metal plating, lapped riveted or welded seams, smooth welded butts	0.06 to 0.1
(2) Metal plating, lapped riveted seams and butts	0.08 to 0.15
(3) Wood planking, lapped or clinker style, discontinuities in line of flow	0.12 to 0.18
(d) Coating roughness, $\Delta_C C_F(10^3)$	
(1) Varnish, yacht-racing enamel, polished metal	0.00
(2) Red lead, metallic oxide, zinc chromate	0.05 to 0.18
(3) Self-leveling varnish-type bottom paints	0.02 to 0.12
(4) Vinyl resin	0.05 to 0.3 or 0.4
(5) Cold plastic	0.1 to 0.3
(6) Hot plastic	0.3 to 0.8

The matter of fouling roughness is discussed in Sec. 45.20 following.

Using the best information available in 1955, the plating, structural, and coating allowances may be assigned tentative individual values as listed in Table 45.f, *for values of R_n greater than about 100 million.* For a modern vessel, with clean plates, riveted lapped seams, and flush-welded butts, coated with a self-leveling bottom paint, this gives a $\Sigma\Delta C_F(10^3) = (\Delta_P + \Delta_S + \Delta_C)(10^3)C_F$ (excluding fouling) having a *minimum* value of 0.09 and a *maximum* value of 0.32. For a clean, new steel ship with both flush-welded butts *and* seams, also coated with a self-leveling bottom paint, the value of $\Sigma\Delta C_F(10^3)$ may approach but usually does not exceed 0.2 [Vincent, S. A., unpub. ltr. to HES, 26 Jun 1953]. These values do *not* apply to ships coated with plastic bottom paint of the kinds in use at the time of writing (1955).

Values of $\Sigma\Delta C_F$ for a number of merchant vessels of varied size and type, in the range of R_n from 150 to 1,800 million, are plotted by R. B. Couch on a plate accompanying Appendix XXVIII of the published Minutes of the 1953 ATTC meeting. The ranges of speed for some individual ships are sufficient to show changes in ΔC_F with R_n.

Manifestly, it is seldom logical to predict a roughness allowance by *adding* all the Δ_P, Δ_S, and Δ_C factors. The preservative coating on the bottom may cover up (or even exaggerate) some of the plating (or planking) roughness, just as the fouling may later cover up the plating and coating roughness and perhaps even the structural roughness. A designer may well predict two or more roughness allowances, one for trial and the other(s) for service conditions. The latter should correspond to (1) the ship just out of dock, and (2) the ship with x months in service, following the last docking. In any case, a good prediction of bottom roughness, excluding fouling, requires rather unusual judgment and a better background of reliable roughness and resistance data than are available at present (1955).

45.19 Factors Affecting Fouling Resistance on Ship Surfaces. W. J. M. Rankine, in his 1866 book on "Shipbuilding: Theoretical and Practical," page 5, says of fouling that "It is very common to find the resistance increased by about

a fourth from this cause; and occasionally it is increased more." Unfortunately, Rankine does not say what resistance is involved, whether friction or total. W. F. Durand, in his 1903 book entitled "Resistance and Propulsion of Ships," pages 55 and 56, tabulates *increases* in *total* resistance due to fouling on U. S. Naval vessels of the 1890's as varying from 20 to 200 per cent at speeds of 7 to 11 kt. These are understandable in view of the 12-in barnacles reported to have grown on an old ironclad which spent most of its time at anchor [SBSR, 24 Feb 1938, p. 229]. The reader who may question these data has only to look at the photographs in the book "Marine Fouling and Its Prevention," prepared by the Woods Hole Oceanographic Institution and published by the U. S. Naval Institute in 1952.

The deposits which form on the surface of any ship or ship element, immersed in any type of water, are divided roughly into two classes:

(1) Gelatinous coatings and soft slimes containing no visible solid matter and representing a relatively thin deposit of approximately uniform thickness. These are often a factor in the take-off characteristics of seaplanes and flying boats.
(2) Rough coatings, semi-rigid or rigid, composed of grasses or other marine vegetation, shells, barnacles, and the more-or-less rough and firm growths of all visible types of marine life.

Fouling of the first class usually begins immediately upon immersion, following launching and undocking. It develops its own friction drag from that hour, increasing slowly but progressively until its effect is overtaken by fouling of the second class. A ship resting in warm, quiet water usually acquires a slime coating rather rapidly, whereas one moving continually or resting in cold water may never have more than a thin coating form on it.

Although not to be classed as fouling, in the strict sense, there is mentioned here a deterioration of the bottom paint which occurs at unexpected places and times. The causes of this action seem to be related to the causes of particular kinds of fouling in certain areas at specified times. The deterioration appears to vary by years in the same locality, in somewhat the same way that extra-warm summers or unusually severe winters are encountered. The action is often extremely rapid, especially when a vessel is at anchor. In one short week of immersion a new coat of bottom paint may take on the appearance of having been made up of a mixture of paint and sand.

Also mentioned here is the deterioration of hot-plastic paint coatings due to unfavorable weather conditions, improper application methods, and similar factors. This deterioration sometimes occurs before the ship is waterborne at the end of the docking period. Runs, superposed layers, folds, "icicles," and peeling of the plastic coating involve roughnesses of the magnitude of those encountered in fouling.

Fouling of the second class is accelerated in warm, salt water, especially with slow relative motion of the ship and water. It is augmented by seasonal and other conditions, not too well known, conducive to the rapid growth of marine life, both vegetable and animal. Growth is slower in cold water; much slower when the ship is in almost continual motion. It is practically nonexistent in fresh water, giving trouble only in exceptional cases and then usually along the waterline.

Fouling of both classes may be arrested by the onset of unfavorable conditions for the growing organisms, such as moving a ship from salt water to fresh water. It can not be expected, however, that this will lessen the added friction resistance or that it will eliminate the fouling drag altogether. The firmly fixed barnacle shells on a ship entering the Panama Canal from a long sea voyage will not drop off just because the ship anchors for a few days in the fresh water of Gatun Lake, long enough to kill the barnacles themselves.

The effect of hard, rough fouling is to create a friction drag of the tanqua type, defined in Sec. 5.21 on page 108 of Volume I, varying as the square of the speed. For a ship of medium or large size, this involves a constant ΔC_F allowance above the ATTC 1947 meanline, or above any other modern flat, smooth-plate, turbulent-flow friction line. Whether fouling roughness is a negligible factor at R_n values of 2, 3, or 4 million, as smaller sizes of roughness appear to be, especially at slow speeds, is not yet known. What applies to the latter should, however, also apply to the former.

Numerous rules have been developed from time to time to predict the effect of fouling on the resistance, power, and speed of ships. For any one kind of anti-fouling coating these are based generally upon the time which has elapsed from the application of the last anti-fouling coating, upon the average speed of the ship during certain periods, and upon the kind and the temperature of

the water in which the ship has been floating. Unless an external coating is proof against most types of fouling, an estimate based only on time out of dock is precarious at the best, considering all the variables involved. The basis for fouling effect should be one of *history*, modified in degree to conform to the anti-fouling properties of the outside coatings on the underwater hull. The history embodies a combination of ship location in the navigable waters of the globe, ship operation, elapsed time, the seasons during which the ship is exposed, and the portion of the fouling cycle in each water area which is involved, if this is known.

Assuming that the location, the events, and the time history are fully recorded, it is found that the fouling rates, fouling types, and fouling effects are variable because of seasonal, cyclic, or other factors pertaining to marine life. Furthermore, in making predictions of future fouling effects it is possible only to estimate a probable history for any given period. With our present (1955) knowledge, an average result is the best that can be expected in the prediction of fouling resistance.

It has been the custom in the past to reckon the effect of fouling as a percentage increase in the friction resistance R_F, in the effective power P_E, or in the shaft power P_S. Occasionally it is expressed as a percentage of the total resistance R_T or of the friction power P_F but with the disadvantage that, of the five quantities mentioned, only the shaft power is known with any degree of accuracy on ships in operation. Actually, because the friction resistance of certain not-too-smooth ships of the past—and some of the present—consisted of some tanvis resistance (varying with the Reynolds number), with a large amount of tanqua resistance (varying as V^2), there was some logic in expressing the resistance increase due to fouling as a percentage increase of the total resistance.

Modern knowledge indicates that the average flat, smooth-plate specific friction resistance C_F decreases as the ship size and speed increase. By all indications, the $\Delta_F C_F$ values for fouling as well as for other types of roughness decrease somewhat with the size (length) but they *increase rapidly* with the designed speed of the ship, as described in Sec. 45.10. For a tug or trawler C_F is say $2.3(10^{-3})$ at an R_n of 50 million whereas for a fast liner it is only $1.3(10^{-3})$ at $R_n = 4{,}000$ million. At the same time a "tapering" ΔC_F new-ship allowance for plating, structural, and coating roughness, described in Sec. 45.18 preceding, is of the order of only $0.25(10^{-3})$ for the tug whereas it is about $0.39(10^{-3})$ for the liner.

The roughness drag of fouling is predominantly a tanqua resistance proportional to V^2 and is largely independent of R_n, except possibly at low R_n values. It is *not* a function of the tanvis resistance and should therefore not appear as a percentage of the latter.

The use of a formula with additive specific resistance terms, as in Eq. (45.ii) of Sec. 45.7, requires that the roughness effects of the fouling be considered as a primary function of the size, shape, and distribution of the fouling roughnesses on the hull surface. They may be a secondary function of Reynolds number, at low R_n values, only because of a laminar sublayer which either persists over fouling that is not excessively rough or which is increased in effective thickness by some physical action as yet unknown.

To reduce the observed fouling effects to terms of an additive $\Delta_F C_F$ factor by the older methods is difficult. For most of the cases on record, the propeller thrusts were not measured and the actual ship friction resistances were not known. Furthermore, there is no way to determine how much of these resistances was due to plating, structural, and coating roughnesses, exclusive of fouling. The operation is greatly facilitated by the use of the specific resistances $C_T = C_R + C_F + \Sigma\Delta C_F$, if it is assumed that the specific residuary resistance C_R remains constant regardless of the extent of fouling. The flat, smooth-plate specific friction resistance C_F remains constant by derivation. Therefore any increase in C_T over the clean-bottom value is a *change* due to fouling and may be represented by $\Delta_F C_F$ as a first approximation. This procedure takes no account, for example, of a $\Delta_P C_F$ or a $\Delta_C C_F$ that may be diminished because heavy fouling covers up original plating or coating roughnesses.

It may be presumed that, for a large and a small ship having exactly the same underwater coating, the same exposure position with reference to the adjacent water bodies and currents, and the same fouling history, the fouling will be exactly the same on the underwater surface of each. In other words, the marine growths will be of the same absolute shape and size and will be distributed in the same manner over each unit of area. If each craft has about the same hull shape and a reasonably large draft, there will be

no preponderance of fouling effects along the waterline.

This being the case, the laminar sublayers over the two hulls, *at the same absolute speed* for each hull, will have only a slightly greater thickness δ_L on the large ship than on the small one, indicated in Fig. 45.F of Sec. 45.10. For the higher speed at which it is presumed the larger ship will run, its laminar sublayer will be thinner than on the smaller ship. This means, for example, that a group of barnacles of a given size and distribution will have a greater roughness effect on the large, fast ship than an identical group of identical barnacles on the small, slow ship. If this physical reasoning is correct, the effect of a given amount of fouling in unit surface area of the hull decreases slowly with the increase in ship length but it increases rapidly with the increase in magnitude of the speed term U in the Reynolds number UL/ν.

It can not be said, therefore, that a fouling rate and a fouling effect determined for a small craft will be valid for a large one, and vice versa, any more than the effect of a given roughness is independent of ship size and speed.

Even though all other conditions remain the same, there is almost certainly some non-linearity of the roughness effects with time out of dock. An older curve of several decades ago, given in reference (15) of Sec. 45.21, indicates a moderate rise immediately after undocking, a rate less than the average for the intermediate period, say from 2 to 4 months, and a rapidly increasing rise at the end of the interval, from about 5 months to 9 months. On the other hand, results of experiments by W. McEntee, reported in reference (3) of Sec. 45.21, gave rates that were almost exactly the opposite [Taylor, D. W., S and P, 1943, Fig. 43, p. 38]. Later and possibly more accurate data indicate that the increase in $\Delta_F C_F$ for the first few days and weeks out of dock may be slightly less than the average while the increase under conditions favorable for marine growth, during a later portion of the docking period, may be greater than the average. If the ship is left moored or at anchor to accumulate marine growths having thicknesses of inches or even feet, $\Delta_F C_F$ probably reaches a maximum value by the time the hull surface is *completely* covered with a growth 0.1 or 0.2 ft thick. It may not become larger no matter how dense or thick the growth. However, the weight displacement and the volume displacement both increase perceptibly as the growth thickens. Should the ship have to be propelled or towed while fouled it is effectively larger than when clean and requires additional power in proportion, over and above that due to the fouling roughness. Ships have been known to pick up from 100 to 300 or more tons of marine growth when heavily fouled. The effective, equivalent increase in volume of water displaced is probably still larger.

All additive allowances for fouling effect should constitute increases in the "clean, new" friction drag R_F of a ship. This is not always the case when ship data are reported. In fact, some reports are so ambiguous as not to specify the quantity which increases with the fouling. Strictly speaking, the magnitude of the friction drag is not known for any ship but it can be calculated by the methods described elsewhere in this chapter. It can be estimated as a percentage of the total towrope resistance for the type of ship in question. If corresponding changes in the power and speed are wanted, they may be predicted by the methods described in Chap. 60 for the estimate of power and speed on a new design.

In this connection it must be remembered that an increase in roughness due to fouling increases the thickness of the boundary layer at the propulsion-device positions. This in turn almost invariably increases the average-wake fraction over the thrust-producing area A_0 of the propulsion device. Furthermore, the additional resistance means augmented thrust, higher thrust loading, and undoubtedly a lowered efficiency of propulsion. Estimates of increased shaft power due to fouling are not always accurately predicted, therefore, on a basis of model tests run with an overload allowance only for a clean, new hull surface.

45.20 The Prediction of Fouling Effects on Ship Resistance. Summarizing the effects of fouling on ship resistance, discussed in Sec. 45.19, the principal factors appear to be:

(1) The type and nature of the fouling which adheres to the ship hull

(2) The history of the operation of the ship during any one interval between dockings, taking account of the length of time out of dock, and including the kind and temperature of the water

(3) The fouling rates, cycles, and other features associated with the history of operation. These rates vary widely in the different parts of the

world, from positive heavy fouling to slightly negative scouring.

(4) The size of the vessel, and especially the operating speed for which the fouling prediction is required.

The first three items correspond to those which have been recognized for many years past. The fourth item is, in an analysis of fouling effects, believed to be entirely new.

One may conclude, from the discussion of Sec. 45.19, that the effect of fouling on ship resistance should be expressed as an *additive* rather than as a percentage term, as proposed by G. Kempf in 1936 and 1937. This is on the basis that the fouling creates an increment of resistance depending upon its physical characteristics and the flow around it, without regard to the amount of the friction resistance of a clean, new hull to which the fouling is attached, of the separation drag around the hull, or of the resistance due to wave-making of that hull. A convenient additive form is the use of an increment $\Delta_F C_F$, expressed in units of specific resistance which is to be applied to the sum of the specific pressure (or residuary) resistance and the turbulent-flow specific friction resistance, with or without corrections for curvature.

Considering item (1) at the beginning of this section, it is explained in Sec. 22.11 that relatively little is known about the quantitative effect of surface slime. At the other end of the roughness scale, a very heavy, thick, and rough deposit is necessary to eliminate entirely the effect of viscosity. Such a deposit has the effect of making the sum of the smooth-plate friction resistance and the fouling resistance constant, independent of the Reynolds number. For the normal ship situation, the viscosity effects are retained, so that $\Delta_F C_F$ is roughly constant in the relatively narrow range of speed for any one ship for which fouling effects are to be predicted.

The ultimate solution to this problem, despite the demand for simplicity, seems to call for a subdivision of items (2) and (3) of the summary, to take care of conditions which vary widely in

TABLE 45.g—Proposed Form of Tabulation for Determining the Value of $\Delta_F C_F$ per Day Due to Fouling in an Average Port

FRESH WATER	Warm $T > 77°F$ or $25°C$	Cool $T = 77°$ to $41°F$, $25°C$ to $5°C$	Cold $T < 41°F$, $5°C$
Ship stopped or at anchor at least 10 per cent of the time			
Ship stopped or at anchor at least 50 per cent of the time			
Ship stopped or at anchor at least 95 per cent of the time			
SALT WATER	$T > 77°F$ or $25°C$	$T = 77°$ to $41°F$, $25°C$ to $5°C$	$T < 41°F$, $5°C$
Ship stopped or at anchor at least 10 per cent of the time			
Ship stopped or at anchor at least 50 per cent of the time			
Ship stopped or at anchor at least 95 per cent of the time			

service. Item (2), involving the history of operation, appears to call for about nine groups each, for fresh water and for salt water, respectively. Table 45.g is a proposed framework for carrying the numerical values in these groups, to be determined after further study and investigation. The following notes apply to this table:

I. Fresh water is defined as that which is sufficiently sweet for drinking purposes, even though it may be contaminated by microorganisms. This water should be sufficiently free of salts to kill or prevent the growth of adhering marine life.
II. Salt water is defined as the water found in the oceans and in salt seas, and includes brackish water. It may be expected that the fouling effects in this water will vary approximately in proportion to the salinity or specific gravity, with a specific gravity for average sea water of 1.027, and a corresponding salinity of 3.5 per cent.
III. Warm water is that in which the temperature exceeds 77 deg F or 25 deg C. Cool water has a temperature range of from 77 deg F, or 25 deg C, to 41 deg F, or 5 deg C. Cold water is that in which the temperature is less than 41 deg F or 5 deg C. Seasonal variations, if any, are taken care of by the variations in water temperature.
IV. In the table a ship is assumed to be "stopped" if it is moving at 2 kt or less, relative to the surrounding water, slow enough for marine growths to attach themselves.
V. For the approximate method given, the ship's history need be divided into intervals no smaller than 1 day
VI. All fouling effects reckoned in accordance with the tables are additive.

Concerning item (3) of the summary at the beginning of this section, the information on fouling rates and fouling cycles for specific ports appears limited to that given by G. D. Bengough in reference (22) of Sec. 45.21. These data indicate that certain ports and certain areas appear to be excellent for breeding and attaching marine fouling organisms, and that other ports and areas are relatively free of this nuisance. Based on data in the reference quoted, Table 45.h is a proposed guide for determining the relative fouling rates or the *locality fouling factor* in the ports usually frequented, assuming the ship at anchor (or moving very slowly) and all other conditions the same. This factor is based upon an average rate of fouling in an average port, assumed as unity (1.0).

TABLE 45.h—PROPOSED FORM OF TABULATION TO PERMIT SELECTION OF THE LOCALITY FOULING FACTOR

The list of ports is taken from G. D. Bengough, "Hull Corrosion and Fouling" [NECI, 1942–1943, Vol. 59, Table 5, p. 193], with the two left-hand groups interchanged.

LOCALITY FOULING FACTORS

(Less than 1.0)	(Probably less than 1.0)			(Much greater than 1.0)
I		II	III	IV
Cleaning Ports		Clean Ports	Dirty Ports	Foul Ports (Very Dirty)
Scouring	Non-Scouring			
Calcutta	Bremen	Most British ports	Alexandria	Freetown
Shanghai and Yangtze River ports	Brisbane	Auckland	Bombay	Macassar
	Buenos Aires	Cape Town	Colombo	Mauritius
	E. London (S.A.)	Chittagong	Madras	Rio de Janeiro
	Hamburg	Halifax	Mombasa	Sourabaya
	Hudson River ports	Melbourne	Negapatam	
	La Plata	Valparaiso	Karachi	
	St. Lawrence ports	Wellington	Pernambuco	
	Manchester	Sydney (varies)	Santos	
			Singapore	
			Suez	
			Tuticorin	
			Yokohama	
			Some Norwegian Fjords	

The daily increments, when taken from the proper "box" of Table 45.g, have to be multiplied by the number of days in each operational condition and then added to give the $\Delta_F C_F$ for the effects of items (1) and (2) in the summary. The locality fouling factor is then applied to this sum (by multiplication) to cover the effect of item (3). The upper row of boxes in Table 45.h is left open until such time as data are available to determine values of the locality factor which are reasonably correct, and until such time as additional ports in the Western Hemisphere can be listed.

As for item (4) of the summary, it is perhaps not wise to introduce a set of ship-size and ship-speed parameters into the fouling roughness prediction procedure until the effect of these parameters is fully proved for roughnesses in general. If and when so proved, the variation in $\Delta_F C_F$ with Reynolds number R_n will probably resemble the variations in ΔC_F shown by the lines C-C and D-D of Fig. 45.E.

Judging from the work done recently on this project, it appears hopeless to expect that a single rule, table, graph, or reference, and certainly not a rule of thumb, will furnish adequate prediction data for fouling on ships of all sizes and types, operating in all seasons and in all waters of the world. Nevertheless, there is a definite demand for a simple guide which will give the answer in one operation, as it were.

As an *interim measure* a set of graphs prepared and published by E. V. Lewis [The Log, May 1948, pp. 50–52] serves as a means of determining by inspection a suitable value of $\Delta_F C_F(10^3)$ for any one of three given operating conditions. Lewis' data are reproduced in Fig. 45.K, supplemented by data derived from the trials of three ships, the U. S. destroyer *Putnam* (DD 287), the U. S. battleship *Tennessee* (BB 43), and the Japanese destroyer *Yudachi*. The two former sets of data were used by Lewis; the latter data were not. According to information received subsequent to the date of the reference [unpubl. ltr. of 15 Aug 1955], curve B was actually based on the British Admiralty peace-time standard for ships operating in tropical waters, involving a 0.5 per cent per day increase in friction resistance [INA, 1943, Vol. 85, p. 2]. Curve A was based on the British Admiralty standard for temperate waters, with a rate of 0.25 per cent per day increase in R_F , raised somewhat and given some upward curvature because of the shape of the curve for

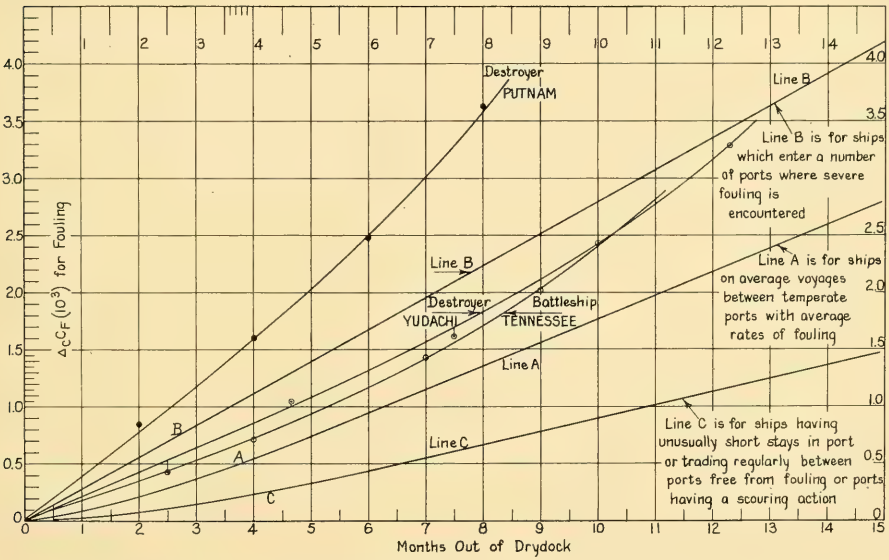

FIG. 45.K GRAPHS OF E. V. LEWIS FOR SPECIFIC FOULING RESISTANCE ALLOWANCES, WITH CURVES FOR THREE SHIPS

the battleship *Tennessee*. Curve C was drawn midway between B and the baseline as a rough guess, with some scattered supporting data. Lewis' graphs A and C indicate a progressive increase in $\Delta_F C_F$ per day for the early months of the period between dockings while graph B, for the heaviest fouling, indicates a linear increase with time. The graphs for the three combatant vessels show a slight increase in rate with elapsed time for the entire interval, and a rate that increases as the next docking time approaches.

Fig. 45.L is a duplicate of the three Lewis graphs with the fouling-effect predictions for the ABC ship of Part 4, under the conditions set fourth in items (18) and (19) of Table 64.c and item (20) of Table 64.d. This ship is expected to have what Lewis terms "average voyages" except that at one end of the route the ship spends an appreciable time in a fresh-water river. The fouling rate may be expected to lie somewhat below that of line A.

The broken line with long dashes of Fig. 45.L, for the ABC ship, involving a fouling rate that increases slowly with time, applies to the hull with a final bottom coating of anti-fouling self-leveling paint (*not* a plastic type).

The dot-dash line of the figure, representing what may be expected of hot plastic paint in the way of fouling roughness only, involves a fouling rate that limits the roughness to a value which, in 4 years, would be equal to that expected of "commercial" anti-fouling paint in only 9 months. However, the *initial* roughness of the hot plastic paint is extremely high, so that this paint is at a disadvantage compared to the "commercial" anti-fouling paint until such time as the latter has acquired considerable roughness due to its increased rate of fouling. It is estimated that, for the average application, and as the ship comes out of dock with a new coat of paint, the $\Delta_C C_F$ of the hot-plastic paint exceeds the $\Delta_C C_F$ of the commercial anti-fouling paint by the order of $0.5(10^{-3})$. For the purpose of this discussion, the augmented $\Delta_C C_F$ for the hot-plastic paint is considered in the nature of a fouling roughness. To make up for this increased resistance of the hot-plastic coating in the first few months out of dock, it must have a much smaller fouling allowance $\Delta_F C_F$ for the remainder of the interval between dockings. Fig. 45.L indicates that the two predicted ABC ship curves cross each other at 5.4 months out of dock. If the hot-plastic paint is to pay its way, so to speak, the interval between dockings must be long enough so that

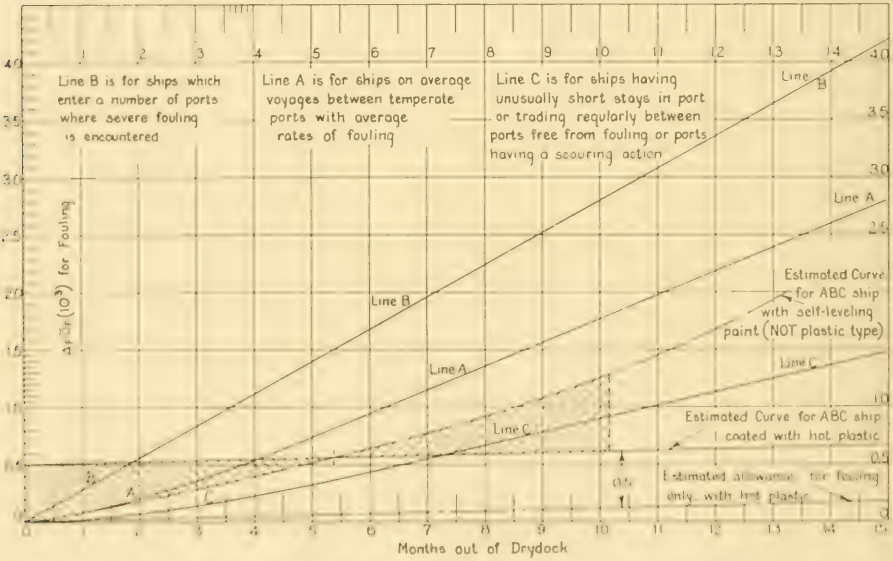

Fig. 45.L Predicted Specific Fouling Resistance Allowances for ABC Ship, with Two Kinds of Paint

the time product of the additional $\Delta_C C_F$ for the first 5.4 months is less than the time product of the additional $\Delta_F C_F$ for the last 4.8 or more months that would have been involved if the hot-plastic coating had not been used. The respective areas on the plot are indicated by different angles of hatching.

Needless to say, what is needed is an anti-fouling paint with the smoothness of a self-leveling coating and the anti-fouling effectiveness of hot plastic. The vinyl resin paints show promise along both these lines.

45.21 References Relating to Fouling as Affecting Ship Propulsion. There are listed hereunder the principal references relating to the fouling of ships as affecting resistance and propulsion. Among these sources from the literature, the reader's attention is called particularly to the pamphlet by Dr. J. Paul Visscher, numbered (9) in the list, and to the book "Marine Fouling and Its Prevention," prepared by the Woods Hole Oceanographic Institution and published by the U. S. Naval Institute in 1952. Each chapter of this book is terminated by a generous list of references, but unfortunately none of these chapters discusses the quantitative effect of fouling on ship resistance.

(1) Young, C. F. T., "The Fouling and Corrosion of Iron Ships: Their Causes and Means of Prevention, with the Mode of Application to Existing Ironclads," (England), 1867

(2) Lewes, V. B., "The Corrosion and Fouling of Steel and Iron Ships," INA, 1889, Vol. XXX, pp. 362–389

(3) McEntee, W., "Variation of Frictional Resistance of Ships with Condition of Wetted Surface," SNAME, 1915, pp. 37–42

(4) McEntee, W., "Notes from the Model Basin," SNAME, 1916, pp. 85–90

(5) Smith, W. W., "The Effect of Wind and Fouling Resistances on U.S.S. *Neptune*," SNAME, 1917, pp. 41–72

(6) Williams, H., "Notes on Fouling of Ship's Bottoms and the Effect on Fuel Consumption," ASNE, May 1923, Vol. XXXV, pp. 357–374. Abstracted in SBSR, 16 Aug 1923, pp. 180–181 and 190–192.

(7) Gardner, H. A., "Toxic Compositions to Prevent the Fouling of Steel Ships and to Preserve Wood Bottoms," Paint Mfrs. Ass'n. of U. S., Sci. Sect. No. 259, Jan 1926, pp. 232–270

(8) Telfer, E. V., "The Practical Analysis of Merchant Ship Trials and Service Performance," NECI, 1926–1927, Vol. XLII, pp. 63–98 and 125–143

(9) Visscher, J. P., "Nature and Extent of Fouling of Ship's Bottoms," Bu. Fisheries, Dept. Commerce, Document 1031, 1927, Vol. XLIII, Part II

(10) Taylor, J. L., "Statistical Analysis of Voyage Abstracts," INA, 1928, pp. 259–269

(11) Roop, W. P., "Frictional Resistance of Ship Models," SNAME, 1929, pp. 45–64

(12) Davis, H. F. D., "The Increase in S.H.P. and R.P.M. due to Fouling," ASNE, Feb 1930, pp. 155–166

(13) Holm, W. J., "Tactical Horsepower of Submarines," USNI, Dec 1931, pp. 1616–1620. Discusses the limitations imposed on speed and rpm (hence speed) of submarines driven by Diesel engines due to restrictions on maximum mean effective pressure developed in the engines. Makes out an argument for reducing the pitch of the propellers to suit a condition of partly foul bottom and shows that a pure electric-drive installation would be superior in point of useful horsepower developed for whole period between dockings. Gives curves of P_S, rpm, and speed of submarines for various months out of dock (in tropical waters).

(14) Smith, W. W., Discussion, SNAME, 1932, p. 305

(15) "Effect of Fouling of a Ship's Bottom Upon Power and Cost of Operation," Nat. Council Am. Shipbldrs., Bull. 246, 23 Aug 1932; also Naut. Gaz., 3 Sep 1932; MESA, Sep 1932

(16) Prandtl, L., and Schlichting, H., "Das Widerstandsgesetz Rauher Platten (The Law of Resistance for Rough Plates)," WRH, 1 Jan 1934, pp. 1–4

(17) Pitre, A. S., and Thews, J. G., "Fouling of Ships' Bottoms; Effect of Physical Character of Surface," EMB Rep. 398, Apr 1935

(18) Kempf, G., "On the Effect of Roughness on the Resistance of Ships," INA, 1937, pp. 109–119, 137–158, esp. pp. 117–119

(19) Stevens, E. A., Jr., "The Increase in Frictional Resistance Due to The Action of Water on Bottom Paint," ASNE, Nov 1937, pp. 585–588

(20) Gawn, R. W. L., "Roughened Hull Surface," NECI, 1941–1942, Vol. LVIII, pp. 245–272 and D143–D152a; "Roughened Hull Surface," SBSR, 11 Jun 1942, p. 608

(21) Baker, G. S., "Ship Efficiency and Economy," Liverpool, 1942, pp. 1–14

(22) Bengough, G. D., "Hull Corrosion and Fouling," NECI, 1942–1943, Vol. 59, pp. 183–206 and D123–D136

(23) Taylor, D. W., "The Speed and Power of Ships," 1943, pp. 37–38

(24) Bengough, G. D., and Shepheard, V. G., "The Corrosion and Fouling of Ships," INA, 1943, pp. 1–34

(25) "Fouling of Ships' Bottoms: Identification of Marine Growths," Jour. Iron and Steel Inst., Great Britain, 1944

(26) "Docking Report Manual: Instructions Regarding the Docking Report and Guide to Fouling Organisms," Bureau of Ships, Navy Dept., Washington, 1944

(27) Harris, J. E., and Forbes, W. A. D., "Under-Water Paints and the Fouling of Ships," INA, 1946, pp. 240–267

(28) Graham, D. P., "Some Factors in the Use of Plastic Ship-Bottom Paints by the U. S. Navy," SNAME, 1947, pp. 202–243

(29) Lewis, E. V., "How to Determine Effects of Ship Bottom Fouling," The Log, May 1948, pp. 50, 52

(30) Barnaby, K. C., "Economic Consequences of Fouling," INA, 1950, p. J15

(31) Todd, F. H., "Skin Friction Resistance and the Effects of Surface Roughness," TMB Rep. 729, Sep 1950. The graph at the end of this report shows that $\Delta_C C_F$ for various coatings is approximately constant over the range of R_n covered by the normal ship speed range. Although not brought out by this report, the $\Delta_F C_F$ for moderate fouling is found to vary in much the same way.

(32) Couch, R. B., "Preliminary Report of Friction Plane Resistance Tests of Anti-Fouling Ship Bottom Paints," TMB Rep. 789, Aug 1951. Figs. 2 and 3 of this report indicate that at some low value of the Reynolds number, probably in the vicinity of 3.5 million, the $\Delta_C C_F$ values for 6 types of bottom coatings for ship hulls, varying from yellow zinc chromate to Norfolk hot plastic, would probably be in the vicinity of zero. At R_n values of from 25 to 30 million the $\Delta_C C_F$ values for each of the 6 coatings become practically constant and remain so up to a Reynolds number of about 40 to 45 million.

(33) Kielhorn, W. V., "Military Biological Oceanography," USNI, Sep 1951, pp. 947–953, esp. pp. 947–948 and 951

(34) "Marine Fouling and Its Prevention," Report 580 of the Woods Hole Oceanographic Institution, published by USNI, Annapolis, 1952

(35) Amtsberg, H., abstract of a report by Prof. Aertssen on the extensive full-scale tests conducted in 1951 and 1952 on the *Tervaete*, formerly the *Pomona Victory*, including the results of fouling on several voyages, Hansa, 9 May 1953, p. 793.

45.22 The Calculation of the Friction Drag of a Ship. The friction resistance of a ship under analysis or design is calculated by the general Eq. (45.ii) of Sec. 45.7, $R_F = qS(C_F + \Sigma\Delta C_F)$. Here C_F is the flat, smooth-plate specific friction resistance at a given R_n, $\Sigma\Delta C_F$ is $(\Delta_1 + \Delta_2 + \Delta_P + \Delta_S + \Delta_C + \Delta_F)C_F$, and Δ_1 and Δ_2 are the allowances for transverse and longitudinal curvature, respectively.

Beginning with the ram pressure q, equal to $0.5\rho V^2$, Tables 41.d and 41.e give values of q in lb per ft^2 for standard fresh and salt water, respectively, at 59 deg F, 15 deg C, over a very large range of ship speeds.

The wetted surface S is determined as described in Sec. 45.12 preceding. If each appendage which had an appreciable wetted area moved through the water by itself, it would theoretically create its own boundary layer, independent of the others and of the hull proper. It would then have its own Reynolds number, based upon its length in the direction of motion. It would also have its own C_F value, depending upon its R_n. The ship friction drag would then be a summation of a bare-hull drag plus a separate friction drag for each appendage. These C_F values would be high because of the short lengths and the small R_n's. Occasionally there may be a special appendage, exposed to undisturbed flow, which extends for a considerable distance from the hull, somewhat like a deep drag pipe on a self-propelled dredge. Such a one may require this treatment. In the main, however, ship appendages lie partly within the hull boundary layer, they do not generate their own layers exclusively, and the average velocities over them are lower than the ship speed.

It is found acceptable, and it is customary, to use the ship value of R_n for all appendages having appreciable lengths and wetted areas, hence the usual summation of all wetted surfaces into a single value of S. The appendages which are short enough to give x-Reynolds numbers less than about 15 million, especially those which are thick in proportion to their length in the direction of flow, are considered to have no separate friction drag. Their pressure drags are predicted as described in Chap. 55.

For the actual friction-drag calculations for a ship, a series of values of ship speed V is selected, extending from the lowest speed of interest to beyond the maximum-speed point. This enables the plotting of curves of R_F and P_F on V. Using the selected speeds and the waterline length of the ship, values of R_n are taken from Tables 45.a or 45.b for either standard fresh or salt water, respectively. If the water is not standard, the R_n's are calculated.

The values of the flat, smooth-plate, turbulent-flow coefficient C_F for the ATTC 1947 (Schoenherr) meanline are picked for the given values of R_n from Table 45.d. In Tables 45.c and 45.d the numerical values of C_F are listed in terms of thousands, called for convenience *thous*. The values of Reynolds number are given in millions. The tabulated values of C_F are therefore to be multiplied by 10^{-3} and those of R_n by 10^6.

For other friction formulations listed in Sec. 45.8 the C_F values are calculated for the desired R_n values or are picked from other tables.

Increases to be made to take care of curvature, either longitudinal or transverse or both, are applied at this stage.

The total roughness allowance $\Sigma\Delta C_F$ is selected on the basis of the general rules laid down in Secs. 45.18 and 45.20.

There follows an example of the procedure described, applicable to the 20.5-kt or trial-speed point for the ABC design of Part 4. The basic data are as follows:

(a) Ship length (wetted length on waterline)	510 ft
(b) Speed (to be achieved with clean bottom)	20.5 kt
equivalent to	34.62 ft/per sec
(c) Wetted surface, with all appendages, from Sec. 45.13	47,875 ft^2
(d) Plating has lapped riveted seams and flush butts	
(e) Coating is "commercial" anti-fouling, with self-leveling properties	
(f) Mass density ρ, for the salt water in the 20-deg latitude of item (16) of Table 64.c, at 68 deg F, from Table X3.e (involves no correction for latitude, as described in Sec. X3.3)	1.9882 slugs per ft^3
(g) Kinematic viscosity ν, for temperature of 68 deg F, from Table X3.h	1.1372(10^{-5}) ft^2 per sec
(h) Time out of dock	12 days
(i) Ocean water	salt
(j) Average sea-water temperature, from item (18) of Table 64.c, 68 deg F.	

The Reynolds number R_n, based on the waterline or wetted length, is

$$R_n = \frac{LV}{\nu} = \frac{(510)(34.62)(10^5)}{1.1372} = 1{,}552.6 \text{ million}$$

From Table 45.d the value of C_F, considering the ship wetted surface as a flat, smooth plate of ship length L in turbulent flow, is 1.451(10^{-3}).

Data are not available (1955) for determining the allowances for longitudinal and transverse curvature in the forms $\Delta_1 C_F$ and $\Delta_2 C_F$, respectively, of Eq. (45.ii) in Sec. 45.7. However, in Sec. 45.14 the value of ΔR_F due to curvature in the hull of the ABC ship has been calculated by F. Horn's method and found to be 0.0606.

Considering the plating roughness $\Delta_P C_F$, a reasonable value for the ship, when new, is 0.02(10^{-3}), from Table 45.f of Sec. 45.18. Similarly, a liberal value of the structural roughness $\Delta_S C_F$ is, from the same table, 0.08(10^{-3}). As the vessel is to be coated with an anti-fouling paint that has self-leveling properties, a conservative value of $\Delta_C C_F$ is the highest one listed in Table 45.f, or 0.12(10^{-3}). For 12 days out of dock, or 0.4 month, the fouling allowance $\Delta_F C_F$ from the dashed-line curve of Fig. 45.L, applying to the ABC ship, is about 0.04(10^{-3}). Adding all these, $\Sigma\Delta C_F$ is (0.02 + 0.08 + 0.12 + 0.04)(10^{-3}) = 0.26(10^{-3}). Then $(C_F + \Sigma\Delta C_F)$ = (1.451 + 0.26)(10^{-3}) = 1.711(10^{-3}).

It will be noted that, in the preliminary-design stage of Sec. 66.9, ΔC_F (actually $\Sigma\Delta C_F$) was taken as 0.4(10^{-3}). When instructions were prepared to test the models of the ABC ship, quoted in Sec. 78.6, the corresponding ΔC_F value was taken as 0.3(10^{-3}). These compare with the final estimate of 0.26(10^{-3}).

The ΔR_F value of F. Horn is equivalent to a C_F addition of 0.0606(1.711)(10^{-3}) = 0.104(10^{-3}). Taking account of this curvature correction, the revised $(C_F + \Sigma\Delta C_F)$ value is (1.711 + 0.104)(10^{-3}) = 1.815(10^{-3}).

Then, by Eq. (45.ii),

$$R_F = qS(C_F + \Delta C_F) = \frac{\rho}{2} V^2 S(C_F + \Delta C_F)$$

$$= \frac{1.9882}{2}(34.62)^2(47{,}875)(1.815)(10^{-3})$$

$$= 103{,}531 \text{ lb.}$$

As a matter of interest the $(C_F + \Sigma\Delta C_F)$ values taken by inspection from Fig. 45.E, using only the R_n value derived here, are:

(1) Taking account of the ATTC 1947 allowance for clean, new vessels, from curve B-B, 1.85(10^{-3})
(2) Considering the roughness allowance proposed by L. A. Baier, from curve D-D, 1.85(10^{-3})
(3) Considering the roughness allowance proposed by J. M. Ferguson, from curve C-C, 1.81(10^{-3}).

These compare with the value 1.815(10^{-3}) derived in the foregoing.

45.23 Allowances for Friction Drag on Straight-Element and Discontinuous-Section Hulls. The transverse curvature at an unrounded chine is always sharp. It may be severe if the chine angle (defined in diagram 3 of Fig. 27.A) is of the order of 80 or 90 deg, as on short sailboats and motorboats, especially those which run at low F_n or T_q values. The Reynolds number is then low, the C_F high, and the added friction due to convex curvature is also relatively large. Coves or regions of concave transverse curvature are rarely to be

found on hulls of this kind, so that there is no compensation for the convex-curvature effects. Landweber's transverse curvature correction, described in Sec. 45.14, becomes rather absurdly large for sharp chines, or even for these chines if they are assumed to be rounded to a small radius. In these cases the increase in R_F is known to be positive, but it is difficult to estimate.

On discontinuous-section forms, coves are generally associated with chines in pairs, so that the increased friction drag caused by the convex chine is partly or wholly offset by the decreased friction in the concave area. For discontinuous sections of not abnormal shape, such as those illustrated in Figs. 76.E and 76.F, it is acceptable to compute the entire wetted surface and to consider that it belongs to a hull of normal form.

45.24 The Friction Resistance of a Planing Hull. A planing hull that benefits by dynamic lift rises out of the water as the F_n increases and loses wetted surface by this process. If friction drag is to be taken into account it is then necessary, either on a model or on the craft itself, to determine the length, shape, and position of the wetted portion of the bottom and to compute the actual wetted area. Only those regions over (or under) which the water moves at the same order of relative speed as the planing craft are included as effective wetted areas. Those wetted by thin spray sheets moving forward or predominantly sideward are excluded. Furthermore, unless the model runs at the same trim as the full-scale craft, either by the action of forces from its own propulsion devices or equivalent forces applied during the test run, the wetted surfaces are not comparable.

It is often feasible to locate, by photographs or visual observation, on either the model or the full-scale craft, the forward end of the wetted surface along the keel. It is usually easy to "spot" the corresponding points along the chines. Having these three points fixed reasonably well, the wetted surface is readily outlined and its area determined.

A length is necessary to fix the approximate values of F_n and R_n in the planing condition. This is usually taken as the *mean wetted length* L_{WS}, the arithmetic mean of the wetted keel and the wetted chine lengths.

These matters, including a method of predicting the wetted length and wetted area, are discussed in detail in Secs. 53.6 and 77.27, to which the reader is referred for specific information on this type of water craft.

45.25 Friction Drag of a Craft Moored in a Stream. A friction-drag problem arises in connection with the mooring of pontoon-bridge floats, barges, lighters, and lightships where swift currents prevail and adequate ground tackle must be provided. In flood conditions this situation is intensified. In these cases the Froude number F_n or Taylor quotient T_e is usually small and most of the drag is due to friction. The friction drag due to current may be a maximum when the wind drag is zero.

The fact that a vessel is anchored or held stationary in a moving stream, rather than pulled or pushed at the same relative speed through stationary water, has no appreciable effect upon its friction resistance. It does not alter the method of calculating the friction drag, provided the flowing water contains no great amount of large-scale turbulence. It is to be remembered, however, that a stationary surface vessel near the center of a fast-moving stream, of not-too-large cross section compared to that of the vessel, has a relative velocity in the center which is *greater* than the *average* velocity of the stream. This is because the velocities in the boundary layer along the banks and over the stream bed are less than the average velocity. The same phenomenon occurs in a pipe where there is a boundary layer all around the inside wall surfaces and the center-line velocity exceeds the average velocity [Rouse, H., EMF, 1946, p. 197]. If the bed clearance under the vessel is small, as for a deep vessel moored in a shallow river, the relative water velocity under the bottom is probably greater than the average current velocity.

Subject to the foregoing, and assuming that the ship axis lies in the direction of stream flow, the computation procedures of Sec. 45.22 suffice for calculating the friction drag.

If the craft is moored at both ends and does not lie in the direction of the stream, friction resistance plays only a small part and the forces on the moorings must be determined by other methods [TMB unclassified Rep. R-332, "Wind Tunnel Tests to Determine Air Load on Multiple-Ship Moorings for Destroyers of the DD 692 Class," by M. E. Long, Dec 1945].

45.26 Selected Bibliography on Friction Resistance. For convenient reference there are listed in this section a moderate number of the multitude of titles in any modern bibliography on friction resistance. Textbooks are listed in the Introduction of Volume I and are not included here.

The reader's attention is invited to the fact that the references listed in this bibliography do not duplicate those listed in Sec. 45.21, relating to fouling as affecting ship propulsion. There is available in the Library of Congress at Washington a long and comprehensive bibliography entitled "Skin Friction and Boundary Flow," prepared by Dr. A. F. Zahm [SNAME, 1932, p. 309].

The titles in the present selected bibliography are divided into three groups, described briefly as:

I. Classical and historical
II. Development of friction-resistance formulations
III. References of modern application.

I. *Classical and Historical*

There are listed in this group a number of the papers which form landmarks, as it were, in the early development of the theory of friction resistance, as applied to bodies and ships moving in both air and water. Included are a number of references which describe the development of the theory, and its practical applications, in much more detail than can be given here.

(1) Stokes, G. G., "On the Steady Motion of an Incompressible Fluid," Trans. Camb. Phil. Soc., 1842

(2) Bazin, H., "Récherches hydrauliques (Research in Hydraulics)," Mem. divers savants, Sci. Math. et Phys., Paris, 1865, Vol. 19

(3a) Froude, W., "On Some Difficulties in the Received View of Fluid Friction," Brit. Assn. Rep. for 1869 (publ. in 1870), pp. 211–214. On pages 212–213 Froude gives an amazingly clear and straightforward exposition of the physical phenomena of fluid friction, as it was known at that time. Much of his statement applies to the knowledge of the physics of fluid friction, as known 85 years later.

(3b) Froude, W., "Experiments on Surface Friction," British Association Reports, 1872 and 1874

(4) Froude, W., "On Experiments with HMS *Greyhound*," INA, 1874, pp. 36–73 and Pls. III through XIII

(5) Tideman, B. J., "Memoriaal van de Marine II. Afdeeling 9e Aflevering," 1876–1880. The paper carries the title "Uitkomsten van proeven op den Wederstand van Scheepsmodellen (Results of Resistance Tests with Ship Models)." There appears to be no English translation of it but a note at the bottom of page 374 of Volume III of Pollard and Dudebout's "Théorie du Navire," 1892, states that Tideman's paper was translated (into French) by M. Dislère, Ingénieur de la Marine, in the Mémoires du Génie Maritime, 6th Book, 1877.

(6) Reynolds, Osborne, "An Experimental Investigation of the Circumstances which Determine whether the Motion of Water Shall be Direct or Sinuous, and of the Law of Resistance in Parallel Channels," Phil. Trans. Roy. Soc., London, 1883, Vol. 174, Part III, pp. 935–982

(7) Prandtl, L., "Über Flussigkeitsbewegung bei sehr kleiner Reibung (On Fluid Motion with Very Small Friction)," Verhandlungen des III Internationalen Mathematiker-Kongresses, Heidelberg, 1904 (Proceedings of the 3rd International Mathematics Congress, Heidelberg, 1904)," Leipzig, 1905, pp. 484–491; reprinted in "Vier Abhandlungen zur Hydrodynamik und Aerodynamik," by L. Prandtl and A. Betz, Göttingen, 1927. These contain Prandtl's original statement of the boundary-layer theory.

(8) Blasius, H., "Grenzschichten in Flüssugkeiten mit kleiner Reibung (Boundary Layers in Liquids of Small Friction)," Zeit. für Math. und Phys., 1908, Vol. 56, p. 1ff

(9) Stanton, T. E., Marshall, D., and Bryant, C. N., "On the Conditions at the Boundary of a Fluid in Turbulent Motion," ARC, R and M 720, 1919–1920, Vol. I, pp. 51–67

(10) Stanton, T. E., "Friction," London, 1923

(11) Bruckhoff, "Reibungskoeffizienten (Friction-Resistance Coefficients)," WRH, 22 Aug 1923, pp. 435–438

(12) Shigemitsu, A., "Skin Friction Resistance and Law of Comparison," INA, 1924; abstracted in SBSR, 17 Apr 1924, pp. 454–455

(13) Burgers, J. M., and van der Hegge Zijnen, B. G., "Preliminary Measurements of the Distribution of the Velocity of a Fluid in the Immediate Neighborhood of a Plane, Smooth Surface," Verh. d. Kon. Akad. v. Wetenschappen, Amsterdam, 1924

(14) "Skin Friction Committee's Report," INA, 1925, pp. 108–123, esp. pp. 115–116

(15) Hansen, M., "Velocity Distribution in the Boundary Layer of a Flat Plate," NACA Tech. Memo 585, Oct 1930

(16) Millikan, C. B., "The Boundary Layer and Skin Friction for a Figure of Revolution," ASME, APM-54-3, 1931, p. 33

(17) "The Prediction of Speed and Power of Ships by Methods in Use at the Experimental Model Basin, Washington," Bu C and R Bull. 7, 1933. Pages 18–20 describe the modified Gebers formula in use at the Experimental Model Basin, Washington, in the period 1923–1947.

(18) Payne, M. P., "Historical Note on the Derivation of Froude's Skin Friction Constants," INA, 1936, pp. 93–109

(19) Lackenby, H., "Re-Analysis of William Froude's Experiments on Surface Friction and Their Extension in the Light of Recent Developments," INA, 1937, pp. 120–158. On pp. 136–137 there is a list of 16 references.

(20) Millikan, C. B., "A Critical Discussion of Turbulent Flows in Channels and Circular Tubes," Proc. Fifth Int. Congr. for Appl. Mech., Sep 1938; published by Wiley, New York, 1939

(21) Davidson, K. S. M., PNA, 1939, Vol. II, pp. 76–82 and Figs. 22–23

(22) Taylor, D. W., S and P, 1943, pp. 31–35

(23) Todd, F. H., "The Fundamentals of Ship Frictional Resistance," IME, 1944

(24) Rouse, H., EMF, 1946, beginning on p. 150. This book traces the technical developments of many friction formulas, although from the point of view of hydraulics rather than naval architecture.

(25) Todd, F. H., "The Determination of Frictional Resistance; A Review of Present Knowledge and Methods," SBMEB, Jan 1947, pp. 15–19

(26) Acevedo, M. L., "Skin Friction Resistance," Spec. Publ., Canal de Experiencias Hidrodinámicas, El Pardo, Madrid, 1948. Only the Conclusions of this paper are published in 5th ICSTS, 1949, pp. 93–98.

(27) Van Lammeren, W. P. A., Troost, L., and Koning, J. G., RPSS, 1948, beginning on p. 32. On pages 111 and 112 there are a number of references additional to those given here.

(28) Rouse, H., EH, 1950, pp. 75–115

(29) Schoenherr, K. E., SNAME, 1932, beginning on p. 279; MIT Symp., 1951, beginning on p. 101.

II. *Development of Friction-Resistance Formulations*

This group comprises references which led to the preparation and use of certain formulations widely used within the last quarter-century for analytic and design work.

(30) Gebers, F., "Das Aehnlichkeitsgesetz für Flächenwiderstand in Wasser geradlinig fortbewegter, politierter Platten (The Law of Similitude for the Surface Resistance of Smooth (Polished) Plates Moving in a Straight Line in Water)," Schiffbau, 1921, Vol. XXII, Nos. 29–33, 35, 37–39. A complete translation is found in NACA Tech. Memo 308 of Apr 1925. This paper gives the results of extended tests on friction planes at the Vienna model basin. It summarizes and compares all previous work on friction resistance of planes, and recommends an expression for friction resistance of the form R_F = (a constant) (wetted surface) V^{2-n}/L^n, where n is 0.125.

(31) Kempf, G., "Flächenwiderstand (Surface Resistance)," WRH, 22 Oct 1924, pp. 521–528. This paper discusses and gives the results of friction tests on long, towed, floating cylinders.

(32) Kempf, G., "New Results Obtained in Measuring Frictional Resistance," INA, 1929, pp. 104–121 and Pls. VI–IX. Describes tests made with "measuring plates" in the side of the steamer *Hamburg* and in the bottom of long, shallow, pontoons towed in the Hamburg Model Basin.

(33) Hoppe, H., "Neue Messungen der Wasserreibung am Schiffskorper (New Measurements of Water Friction on Ship Hulls)," WRH, 7 Mar 1929, pp. 91–93

(34) Kempf, G., "Neue Ergebnisse der Widerstandsforschung (New Results in Resistance Investigations)," WRH, 7 Jun 1929, pp. 234–239 and 22 Jun 1929, pp. 247–252. Figs. 6a and 6b on p. 237 show measured roughness profiles of two typical plate surfaces.

(35) Gruschwitz, E., "Die turbulente Reibungsschicht in ebener Strömung bei Druckabfall und Druckanstieg (The Turbulent Boundary Layer in Plane Flow at Increasing and Decreasing Pressures)," Ingenieur-Archiv, 1931, II, p. 321ff

(36) Bateman, H., "General Physical Properties of a Viscous Fluid," Chap. III of "Hydrodynamics," Bull. 84, Nat. Res. Council, Feb 1932, pp. 89–152. This chapter contains much historical data and an enormous number of references, pertaining to all phases of this subject.

(37) Schoenherr, K. E., "Resistance of Flat Surfaces Moving Through a Fluid," SNAME, 1932, pp. 279–313. On page 297 of this paper there is a list of 30 references, listing certain published papers of the period 1839–1931.

(38) Eisner, F., von Kármán, T., Kempf, G., Schoenherr, K. E., "Reibungswiderstand (Frictional Resistance)," HPSA, 1932, pp. 1–87

(39) Schlichting, H., "Zur Entstehung der Turbulenz bei der Plattenströmung," Nach. Gesell. d. Wis. z. Gött., MPK, 1933

(40) Nikuradse, J., "Strömungsgesetze in rauhen Rohren," VDI-Forschungsheft, 361, 1933. English translation available as NACA Tech. Memo 1292, Nov 1950.

(41) Prandtl, L., and Tietjens, O. G., "Applied Hydro- and Aeromechanics," McGraw-Hill, New York, 1934

(42) Prandtl, L., and Schlichting, H., "Das Widerstandsgesetz rauher Platten (The Resistance Law for Rough Plates)," WRH, Jan 1934, No. 1; English version in TMB Transl. 258, Sep 1955

(43) Hiraga, Y., "Experimental Investigations on the Frictional Resistance of Planks and Ship Models," Zōsen Kiōkai (The Society of Naval Architects of Japan), Dec 1934, Vol. LV

(44) Schlichting, H., "Amplitudenverteilung und Energiebilanz der kleinen Strongen bei der Plattenströmung," Nach. Gesell. d. Wiss. z. Gött., 1935, Vol. I

(45) Lamble, J. H., "On the Effects of Changes in 'Degree of Wetting' and 'Degree of Turbulence' on Skin Friction Resistance and Wake of Models," INA, 1936, p. 125ff

(46) Bakhmeteff, B. A., "The Mechanics of Turbulent Flow," Princeton U. Press, 1936

(47) Schultz-Grunow, F., "Ermittlung des hydraulischen Reibungswiderstandes von Platten mit mässig rauher Oberfläche (The Determination of the Hydraulic Friction Resistance of Plates Having Moderately Rough Surfaces)," Schiffahrtstechnische Forschungshefte, Oct 1936, Heft 7

(48) Schlichting, H., "Experimentelle Untersuchungen zum Rauhigkeitsproblem (Experimental Investigation of the Roughness Problem)," Ing.-Archiv., 1936, Vol. VIII, No. 1

(49) Kempf, G., "Über den Einfluss der Rauhigkeit auf den Widerstand von Schiffen (On the Influence of Roughness on the Resistance of Ships)," STG, 1937, Vol. 38, pp. 159–176; 225–234. In this paper Kempf describes and gives the results of friction tests on long, towed, floating pontoons.

(50) Kempf, G., "On the Effect of Roughness on the Resistance of Ships," INA 1937, pp. 109–119.

Fig. 3 on p. 115 gives friction coefficients of ships and of the HSVA pontoon with different roughnesses (see also RPSS, 1948, pp. 48–49). Fig. 5 on p. 119 gives the effect of density of roughness on resistance.

(51) Schultz-Grunow, F., "Der Hydraulische Reibungswiderstand von Platten mit mässig rauher Oberfläche, insbesondere von Schiffsoberflächen (The Hydraulic Friction Resistance of Plates with Large Roughnesses, such as Those on Ship Surfaces)," STG, 1938, Vol. 39, p. 177ff

(52) Schultz-Grunow, F., "Der Reibungswiderstand mässig rauher Oberflächen, insbesondere von Schiffsoberflächen (The Friction Resistance of Moderately Rough Surfaces, especially Ship's Surfaces)," Zeit. des Ver. Deutsch. Ing., 1938, Vol. 82, pp. 756–758. There is an English translation of this paper in the TMB library.

(53) Homann, F., "Der Überganz zwischen den Strömungsgesetzen für glatte und rauhe Platten (The Correlation Between the Laws of Flow for Smooth and Rough Plates)," Zeit. des Ver. Deutsch. Ing., 2 Apr 1938, pp. 405–406

(54) Schultz-Grunow, F., "Neues Reibungswiderstandgesetz für glatte Platten (New Frictional Resistance Law for Smooth Plates)," Luftfahrtforschung, 20 Aug 1940, Vol. 17, No. 8, pp. 239–246; English translation in NACA Tech. Memo 986, Sep 1941

(55) Sawyer, J. W., "Surface Finish Literature," Machine Design, May and Jun 1955.

III. *References of Modern Application*

The references of this group are selected to describe the extensive research and experimentation conducted since about 1940 on the development of the boundary layer and the characteristics of viscous flow.

(56) Prandtl, L., "The Mechanics of Viscous Fluids," Aerodynamic Theory, Vol. III, Durand Reprinting Comm., Pasadena, 1943

(57) Dryden, H. L., "Some Recent Contributions to the Study of Transition and Turbulent Boundary Layers," Proc. 6th Int. Cong. Appl. Mech., Paris, 1946

(58) Carrier, G. F., "The Boundary Layer in a Corner," Quart. Appl. Math. 1947, Vol. 4, p. 367

(59) Dryden, H. L., "Some Recent Contributions to the Study of Transition and Turbulent Boundary Layers," NACA Tech. Note 1168, 1947

(60) Schubauer, G. B., and Skramstad, H. K., "Laminar Boundary-Layer Oscillations and Transition on a Flat Plate," Nat. Bur. Stds. RP 1722, Feb 1947

(61) Schubauer, G. B., and Skramstad, H. K., "Laminar-Boundary-Layer Oscillations and Stability of Laminar Flow," Jour. Aero. Sci., Feb 1947, Vol. 14, or "Laminar Boundary-Layer Oscillations and Transition on a Flat Plate," NACA Rep. 909, 1950

(62) Wieghardt, K., "Increase in Frictional Resistance due to Turbulence Caused by Surface Irregularities," 1948. The English translation is known as A.C.S.I.L. Translation 380 (ACSIL/ADM/48/85).

(63) "Uniform Procedure for the Calculation of Frictional Resistance and the Expansion of Model Test Data to Full Size," SNAME Tech. and Res. Bull. 1–2, Aug 1948

(64) Todd, F. H., "The Determination of Frictional Resistance," TMB Rep. 663, revised edition, Mar 1949

(65) Landweber, L., "Effect of Transverse Curvature on Frictional Resistance," TMB Rep. 689, Mar 1949

(66) Schlichting, H., "Lecture Series, 'Boundary-Layer Theory,' Part I—Laminar Flows," NACA Tech. Memo 1217, Apr 1949

(67) Schlichting, H., "Lecture Series, 'Boundary-Layer Theory,' Part II—Turbulent Flows," NACA Tech. Memo 1218, Apr 1949

(68) Landweber, L., "A Review of the Theory of the Frictional Resistance of a Smooth Flat Plate with Turbulent Boundary Layers," TMB Rep. 726, Sep 1950

(69) "Progress Report on Research in Frictional Resistance," TMB Rep. 726, Sep 1950

(70) Todd, F. H., "Skin Friction Resistance and the Effects of Surface Roughness," TMB Rep. 729, Sep 1950

(71) Rotta, J., "Beitrag zur Berechnung der Turbulenten Grenzschichten (Contributions to the Calculation of Turbulent Boundary Layers)," Max Planck Institut für Strömungsforchung, Göttingen, 1 Jul 1950; TMB Transl. 242, Nov 1951. Assumes that "the kinematic viscosity and the geometrical configuration of the wall (wall roughness) only influence the velocity profile near the wall in a layer δ_w which is very thin compared with the boundary-layer thickness and that with proper normalization the flow quantities in the remaining zone of the boundary layer appear to be almost independent of viscosity and wall roughness."

(72) Laufer, J., "Investigation of Turbulent Flow in a Two-Dimensional Channel," NACA Tech. Note 2123, Jul 1950 and NACA Rep. 1053, 1951

(73) Todd, F. H., "Skin Friction Resistance and the Effects of Surface Roughness," SNAME, 1951, pp. 315–374

(74) Baines, W. D., "A Literature Survey of Boundary Layer Development on Smooth and Rough Surfaces at Zero Pressure Gradient," Iowa Inst. Hydraul. Res., St. Univ. Iowa, 1951

(75) Schubauer, G. B., and Klebanoff, P. S., "Investigation of Separation of the Turbulent Boundary Layer," NACA Rep. 1030, 1951

(76) Townsend, A. A., "The Structure of the Turbulent Boundary Layer," Proc. Camb. Phil. Soc., Apr 1951, Vol. 47, Part 2, pp. 375–395

(77) Granville, P. S., "A Method for the Calculation of the Turbulent Boundary Layer in a Pressure Gradient," TMB Rep. 752, May 1951

(78) Krzywoblocki, M. Z., "On the Foundations of Certain Theories of Turbulence," Jour. Franklin Inst., 1951, Vol. 252, p. 409ff

(79) Kempf, G., and Karhan, K., "Zur Oberflächenreibung des Schiffes (On the Surface Friction of Ships)," STG, 1951, Vol. 45, pp. 228–243

(80) Allan, J. F., and Cutland, R. S., "Skin Friction

Resistance Derived from Wake Measurement," Proc. Second Int. Conf. Naval Engrs., Ostend, 1951

(81) Hughes, G., "Frictional Resistance of Smooth Plane Surfaces in Turbulent Flow—New Data and a Survey of Existing Data," INA, 1952, pp. 1–20

(82) Karhan, K., "Der Einflus von Sandrauhigkeit auf den Reibungswiderstand (The Influence of Sand Roughness on Friction Resistance)," Schiff und Hafen, Jan 1952, pp. 8–10

(83) Lap, A. J. W., and Troost, L., "Frictional Drag of Ship Forms," SNAME, North. Calif. Sect., 29 Feb 1952; also SNAME Member's Bull., Jun 1953, pp. 18–22

(84) Baker, G. S., "Scale Effect on Ship and Model Resistance and Its Estimation," INA, Apr 1952, pp. 41–63

(85) Locke, F. W. S., "Recommended Definition of Turbulent Friction in Incompressible Liquids," BuAer (Navy Dept.) Research Div. Rep. DR-1415, Jun 1952

(86) Laufer, J., "The Structure of Turbulence in Fully Developed Pipe Flow," NBS Rep. 1974, Sep 1952

(87) Krzywoblocki, M. Z., "On the Fundamentals of the Boundary Layer Theory," Jour. Franklin Inst., Apr 1953, Vol. 255, p. 289ff

(88) Allan, J. F., and Cutland, R. S., "Wake Studies of Plane Surfaces," NECI, 1952–1953, Vol. 69, pp. 245–266, D65–D78

(89) Minutes of the American Towing Tank Conference, MIT, Cambridge, (Mass.), 4–6 May 1953, pp. 9–14 and Appx. XX

(90) Landweber, L., "The Frictional Resistance of Flat Plates in Zero Pressure Gradient," SNAME, 1953, pp. 5–32. On page 20 this paper lists 25 references, of which a number are given here.

(91) Morris, H. N., "A New Concept of Flow in Rough Conduits," ASCE, Hydraulics Div., Jan 1954, Vol. 80, Separate 390. A list of 20 references on friction flow in conduits, pipes, and channels is found on p. 390–423.

(92) Gertler, M., "An Analysis of the Original Test Data for the Taylor Standard Series," TMB Rep. 806, Mar 1954, Gov't. Print. Off., Washington, D. C.

(93) Hughes, G., "Friction and Form Resistance in Turbulent Flow, and a Proposed Formulation for Use in Model and Ship Correlation," INA, 9 Apr 1954

(94) Hama, F. R., "Boundary-Layer Characteristics for Smooth and Rough Surfaces," SNAME, 1954, pp. 333–358. There is a list of 41 references on pp. 349–351.

(95) Schubauer, G. B., "Turbulent Processes as Observed in Boundary Layer and Pipe," Jour. Appl. Phys., Feb 1954, Vol. 25, pp. 188–196

(96) Talen, H. W., "Collective Research on Paints for Ships' Hulls," Int. Shipbldg. Prog., 1955, Vol. 2, No. 13, pp. 401–409

(97) Sasajima, H., and Yoshida, E., "Frictional Resistance of Wavy Roughened Surfaces," Int. Shipbldg. Prog., 1955, Vol. 2, No. 13, pp. 441–450

(98) Hogner, E., "Influence of Edges on the Boundary Layer," Mémoires sur la Mécanique des Fluides," Publ. Sci. Tech. Min. Air, Paris, 1954, pp. 129–134. The paper is in French but there is an English summary in Appl. Mech. Rev., Nov 1955, number 3444, p. 480. This states that "Near the longitudinal edges (of a thin friction plane) the viscous stress is approximately double that in the central region."

(99) Schlichting, H., "Boundary Layer Theory," McGraw-Hill, New York, 1955 (in English). This is the English-language edition of the German book entitled "Grenzschicht-Theorie," by H. Schlichting on the same subject, published in 1951. See Appl. Mech. Rev., Jan 1956, p. 33.

(100) Schubauer, G. B., and Klebanoff, P. S., "Contributions on the Mechanics of Boundary-Layer Transition," NACA Tech. Note 3489, Sep 1955

(101) Allan, J. F., and Cutland, R. S., "Investigation of the Resistance on an 18-Foot Plank," IESS, 1955–1956, Vol. 99, Part 1, pp. 9–56. This paper describes a series of investigations carried out with an 18-ft plank in order to determine its resistance with a smooth surface, with a rough surface, and with a surface arranged to represent a ship hull with plate edges, rivets, welds, etc. The results of an examination of the surface finish of the smooth plank and a description of the instrument used are given. Tests to obtain an exact measure of the roughness of the rough plank are also described and the results presented. On page 56 there is a bibliography of 11 items. A summary of this paper is found in SBSR, 27 Oct 1955, pp. 541–542.

CHAPTER 46

Reference Data on Separation, Eddying, and Vortex Motion

46.1 General. Summarizing from Secs. 7.4 and 7.19 of Volume I, it appears that the following factors are involved in a prediction of separation:

(a) Longitudinal surface slope with reference to the relative direction of motion of water and ship at a distance, in both horizontal and vertical planes
(b) Rising-pressure gradient in the direction of motion of the water past the body or ship surface
(c) Nature of flow in the boundary layer ahead of the separation zone, whether laminar or turbulent; particularly, the magnitude of the transverse velocity gradient dU/dy just forward of the separation point
(d) Roughness of the solid surface ahead of the separation zone
(e) Relative velocity of ship and water, at least insofar as the size and shape of the separation zone and the media which fill it (water or air or both) are concerned
(f) Hydrostatic pressure at the point or in the region under consideration. It seems that atmospheric pressure can be neglected.
(g) Projections, recesses, and discontinuities in the ship surface.

Not too much is known quantitatively about the individual effects of the items listed. However, by taking the fragments of knowledge in combination it is possible to make estimates of probable performance in ship scale and to formulate certain rough design rules.

Caution is necessary when interpreting or making use of published data on separation which have been derived from tests on models, objects, or bodies in air. Here the medium under pressure surrounds the body on all sides, and the undisturbed pressure is very nearly the same in all directions and at all points around the body. For a body operating at or near the surface of the water, where the separation phenomena appear to be governed largely by the hydrostatic pressure and the transverse pressure gradient dp/dy, both the pressure and the gradient are nominally zero at the air-water interface and they increase linearly with depth. Many aspects of separation appear to vary in the same way.

46.2 Separation Criteria. Despite the numerous factors involved, listed in Sec. 46.1, separation appears to be the result, principally, of inadequate lateral pressure, inadequate transverse pressure gradient, and inadequate normal force to accelerate the surrounding liquid inward toward the surface of a body which has a local slope greater than a certain amount in any given plane. This critical slope may and usually does vary with the plane or stream surface in or along which the flow occurs. For the transom stern shown at 1 in Fig. 46.A, there is a determining slope for flow along the waterline and another for flow under the bottom, the latter generally paralleling the buttocks.

It is probable, although not certain, that the critical slopes should be measured along stream or other surfaces of equal ambient or hydrostatic pressure. Knowing the position of these surfaces, and the critical slopes, the naval architect might then predict the locus of the points marking the forward or upstream edges of a separation zone.

Around the stern of a ship, for example, at

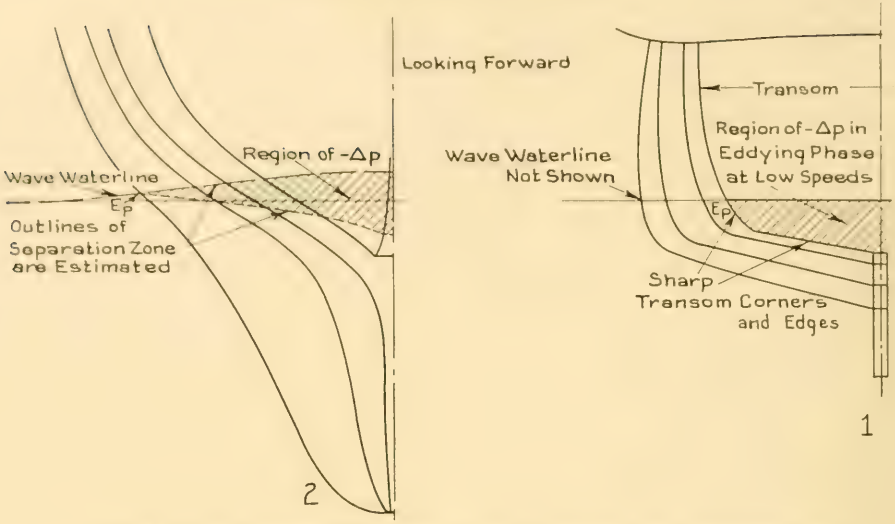

FIG. 46.A TYPICAL SEPARATION-ZONE AREAS ON SHIPS, AS PROJECTED ON A TRANSVERSE PLANE

small distances below the air-water interface, the equal-pressure surfaces would lie generally parallel to the free-water surface, as at 2 in Fig. 46.A. This would be true whether the air-water interface is essentially flat at low speeds or is deformed by waves at higher speeds.

This is a strong probability that other factors enter into the formation of a shallow separation zone abaft the stern. If so, these factors will have to be determined and studied before reliable predictions can be made. G. Birkhoff offers the suggestion that:

"Perhaps, the reason why a free surface affects flow separation at the stern is, that it inhibits vertical turbulence at the surface. Such a reduction in turbulence is known to affect flow separation in other cases" [SNAME, 1954, p. 396].

It might be added that the presence of the ship hull also suppresses those velocity components of turbulence which are normal or nearly normal to the solid surface.

It may be for one or both of the reasons outlined in the preceding paragraphs that separation occurs in the upper surface layers under and behind the run of a sailing yacht. Such a craft, having what is considered a fine, fair form and favored with a perfectly normal curve of section areas, may have a buttock slope i_B of only a few degrees, yet the waterline slope i_W near the surface may be ten or more times that amount. Despite the gently sloping buttocks, separation of the layers close under the water surface occurs at extremely low speeds. This separation is, furthermore, marked by a large number of vertical-axis vortexes, easily visible when the water surface is almost glassy smooth.

For reference purposes a separation zone in the run starts at separation points E_P and E_S along the surface waterline, on the port and starboard sides, respectively. If the wave profile in way of the run is known, it is more accurate to position these points along the waveline. The separation zone is usually bounded by reasonably fair streamlines and stream surfaces, leaving the ship hull at the locus of the separation points. The zone extends far enough astern so that all the hull and the customary appendages abaft the separation-point locus lie within them. On a moving boat or ship the extent of the separation zone on the water surface is readily indicated by sprinkling the water in the vicinity with wood chips. Those in the separation zone swirl around and follow the ship while those outside the zone are rapidly carried astern.

Generally, as plotted on a body plan and as indicated in diagram 2 of Fig. 46.A, the width of the separation zone for a ship with a pointed run is considerably greater than its depth. The

zone is deepest at the centerline and it diminishes in depth toward E_P and E_S . The transverse extent of the zone is rather easily determined by attaching tufts to that portion of the model and watching the behavior of these flexible indicators in the moving water of a circulating-water channel.

A considerable amount of non-systematic but reasonably reliable modern data indicates that the slope of a ship waterline at which separation begins, at the air-water interface, is of the order of 13 to 15 deg. This is reckoned with respect to the relative direction of motion of the ship and the water and is based upon a surface along the ship's side that is more vertical than horizontal. The critical slope given here is somewhat lower than the values of 18 or 20 deg previously quoted in the literature but it has been well checked on ship models. It may be assumed that a separation-free horizontal slope *in the run*, at the water surface, is in the range of 11 to 12.5 deg, as shown in diagram 1 of Fig. 46.B.

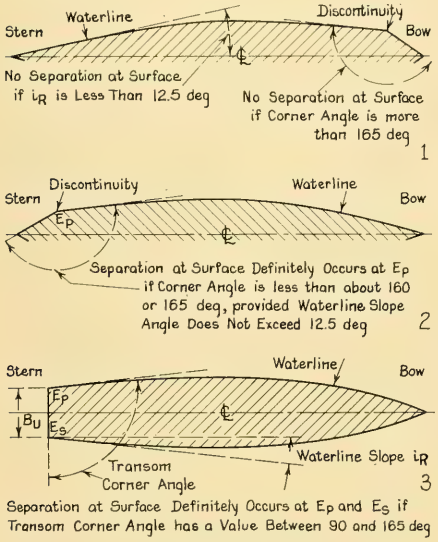

Fig. 46.B Sketch Indicating Typical Separation Criteria for Waterlines

Regardless of the waterline slope with reference to the longitudinal ship axis or direction of motion, separation is almost certain to occur at any discontinuity along that line, where a sharp knuckle exists with a horizontal obtuse angle less than 165 deg. This may be either at the after end of a blunt entrance, indicated at the right in diagram 1 of Fig. 46.B, or at a discontinuity in the run, pictured at the left in diagram 2. Considering the pointed stern of diagram 2 as a form of transom stern, separation is definitely to be expected at the corners E_P and E_S in diagram 3 of Fig. 46.B if the values of the corner angles lie between the limits of 90 deg and about 165 deg.

There is, unfortunately, a serious lack of information upon which to base an estimate of the rate at which the critical slope in a flowplane that is generally horizontal increases with hydrostatic pressure, at levels below the free surface. In the absence of analytic studies or systematic experimental data it may be said tentatively that the separation-free slope increases at the rate of 0.6 deg per ft submergence, on a full-size displacement-type vessel, up to an estimated critical slope of about 36 deg at a depth of 40 ft. The limiting waterline slope for freedom from eddying abaft a skeg, placed ahead of a single propeller, is given by W. P. A. van Lammeren as 20 deg [RPSS, 1948, p. 94]. The corresponding depth is not stated but it is at least as far below the surface as the tip submergence.

The indications are that there is a corresponding variation on the model of such a ship, so that the separation zones and their boundaries are geometrically similar. This is to be expected of a pressure phenomenon which is a function of V^2, when the model is run at corresponding speed.

Fining the trailing edges of sternposts, skegs, and rudders to conform to these critical or limiting horizontal slopes is not always achieved, hence separation abaft them is by no means unusual. In some ships with full runs, like the *Magunkook* of Sec. 23.1 of Volume I, separation has been known to occur abaft the whole underwater hull. In many of these cases there is not only a greatly increased drag but a seriously diminished rudder effect.

On the stern contour or profile, the separation zone begins at the point E_K , marked on diagrams 1 and 2 of Fig. 46.C. When the flow is predominantly in the vertical plane, as it is under the run of the wide, flat barge of diagram 1 of that figure, the maximum separation-free slope appears to be of the order of 14 to 15 deg [Dawson, A. J., SNAME, 1950, p. 9]. This is for a region not more than 2 or 3 ft below the waveline on a ship-size craft. When the flow is both inward and upward, as under the canoe or whaleboat or "cruiser"

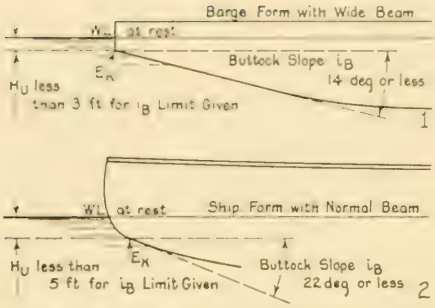

FIG. 46.C TYPICAL SEPARATION CRITERIA FOR BUTTOCKS

stern of diagram 2 of Fig. 46.C, the separation-free buttock or profile slope near the surface may be as great as 25 deg with the horizontal. However, separation may normally be expected beyond the range of 22 to 25 deg, assuming a full-scale depth not more than 5 or 6 ft below the waveline.

A special case is presented by the immersed-transom stern described and illustrated in Sec. 25.14 of Volume I, where separation is known to exist in the region abaft the transom. The quantitative information usually desired is the speed at which the transom will clear in service; in other words, the speed at which the transom surface is entirely free of water contact. This depends upon a number of factors, not yet evaluated in adequate fashion:

(a) The transom corner angle, illustrated and defined in Fig. 25.I on page 379 of Volume I and in Fig. 46.B. The sharp corners define the transverse extent of the stern separation zone, regardless of the speed at which the craft is running.
(b) The transom edge angle, at the lower edge of the transom. This is a measure of the discontinuity in a buttock line in the *vertical* plane. As illustrated in Fig. 25.I, the edge angle defines the lower edge of the separation zone if it has a value of about 160 deg or less, if the lower edge is not rounded, and if the buttock slope ahead of the transom is not too large.
(c) The submergence H_U of the deepest portion of the transom. By one line of reasoning this should be reckoned below the waveline at the outer transom corners, but for wide transoms, where $B_U = 0.5B$ or more, the pressures and flow conditions are certainly not the same all the way across the stern. For design purposes it is almost necessary to use H_U, the maximum immersion below the at-rest WL.
(d) The slope of the flowlines, with reference to the horizontal, for a considerable distance below the lower edge of the transom, say at least 1.0 and possibly 2.0 times the transom immersion H_U. If the buttock slopes are nearly constant for a considerable portion of the length, say $0.3L$, ahead of the transom, it may be assumed that the flowline slope equals the buttock slope. If this is not the case, as on the transom-stern ABC ship hull of Part 4, the actual flowline slopes at the transom edge may be appreciably larger than the buttock slopes.

Further information as to the application of these criteria to a transom-stern design are included in Sec. 67.20.

Notwithstanding the long and extensive use of tunnel sterns for shallow-water craft, and the fitting of twin skegs with tunnels between them on large vessels, there is little systematic quantitative information about the tunnel-roof slopes at which separation would occur under the conditions represented by these various designs. Secs. 67.16 and 67.17 describe the design of the tunnel roof for the alternative arch-type stern of the ABC ship of Part 4, and Fig. 78.F reveals that, at a nominal submergence of about 12 ft in the steepest region, there was no separation for a maximum tunnel-roof slope of about 18.5 deg.

In those tunnel-stern craft having tunnel roofs above the at-rest WL, the nominal submergence and the hydrostatic pressure at the top are negative. Only rarely do tunnel-roof slopes exceed 20 deg, at or near the at-rest WL, but it is doubtful that the critical slope for separation is as large as this. So far as known, at the time of writing (1955), very few craft of this type have been tested in model scale in a circulating-water channel.

It is realized that the slopes mentioned in the preceding paragraphs are not always taken along lines or surfaces of constant pressure, as was pointed out at the beginning of this section. However, no better method of defining possible separation zones appears to be available at this time.

46.3 Detection of Separation; Extent of the Zone. In smooth water and at close range, such as abaft the square stern of a punt or skiff, separation can be "spotted" with a little practice by noting the vertical-axis vortexes or whirls at and near the surface. At longer range, and on larger craft, the separation zone is made clearly

visible by larger eddies, by chips, boxes, or blocks of wood thrown into the zone, or by floating refuse caught in it. As mentioned previously, these are whirled around in the eddies or drawn back toward the hull, and dragged along with the ship. The floating objects outside the separation zone disappear rapidly astern. Special vantage points are necessary in many ships from which to make these observations, because the entire waterline or waveline in the run is not visible from the topside.

Under water, where the eddies can not be seen, separation zones are often detected by the marine growths which flourish in these areas of low relative velocity. When the separation zone is free of large air bubbles, paint surfaces that show little signs of wear may be indicators of stagnant regions. If there are, in an area suspected of being in a separation zone, any sea connections which can be shut off from a system and used as pressure orifices, an observed head at or close to the sea connection which is less than the actual hydrostatic head is an indication that a $-\Delta p$ exists there. Regardless of the exact nature of the water flow outside, this $-\Delta p$ indicates the presence of separation drag if it is on a portion of the hull which faces aft. The $-\Delta p$'s mentioned here are not to be confused with those which may be developed because of potential flow around certain portions of the ship, described in Chap. 4.

By far the most satisfactory method of detecting separation, determining the extent of the zone, and observing the nature of the flow is to test a model. This can be towed in a basin, using a water box and mirrors for viewing the underwater portion, or it can be run in a circulating-water channel and viewed through large observation windows. Colored threads, strings, and tufts are attached directly to the model surface or to slender pins driven into the model so as to lie at a distance from that surface. The tufts may be attached to appendages, or mounted ahead of and abaft propellers on wire frames which will not affect the flow appreciably. Tufts which wave, which curl this way and that, or which actually point forward are unmistakable evidence of unsteady flow, of approaching separation, or of

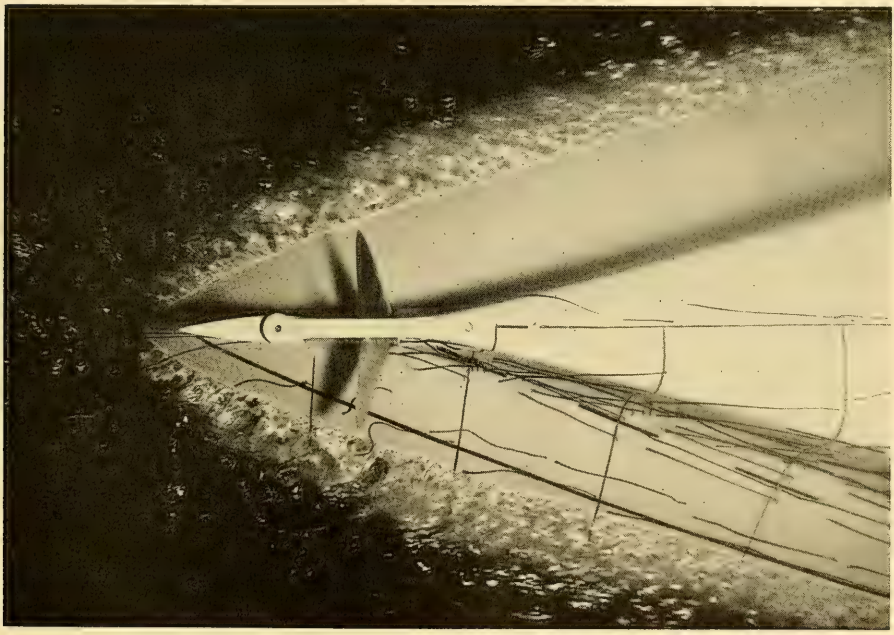

Fig. 46.D Fish-Eye View of a Ship Model with Some Partly Reversed Tufts

the reversed flow of fully developed separation, respectively.

The fish-eye view of Fig. 46.D, taken in the TMB circulating-water channel, shows partially reversed tufts in a separation zone at about the designed waterline (marked by the heavy black stripe) and abreast the propeller. The disturbed under surface of the water in this region also indicates the presence of eddying flow in the separation zone.

Strings or tufts are attached to thin wands like fishing rods, and colored dyes are ejected from long, thin tubes, both moved by hand to any position desired around the model. Fig. 46.E pictures the trail of india ink flowing from such a tube (visible at the extreme right). Part of the flow from the orifice position passes outboard of the offset rudder while a small part of it unexpectedly swings inboard of the rudder.

The predominant characteristic of the flow revealed by the ink in Fig. 46.F is its slowness and what might be called its uncertainty. The tufts reveal the presence of a very large longitudinal-axis vortex, giving the flow alongside the hull a definite upward component of velocity to the left of the ink tube and a marked downward component to the right of it. The flow picture in Fig. 46.F is not clear and complete because the forward ends of some of the tufts shown are attached directly to the model and others are fixed to the outer ends of pins projecting from its surface.

High-speed flash (and motion-picture) photographs, of which Figs. 78.E, 78.F, and those reproduced in TMB Report 810 are further examples, provide a permanent record of the steady continuous flow hoped for over all parts of a ship or of the reversed- and varying-flow characteristics of separation zones. If minute air bubbles are injected into the water, it is possible to detect swirling bubbles in a separation zone formed by a projecting strut-arm pad as small as 0.3 inch wide and projecting only about 0.06 inch from the fair surface of a model.

Vortexes which are not steady or stationary are detected by dye injected in the vicinity, are

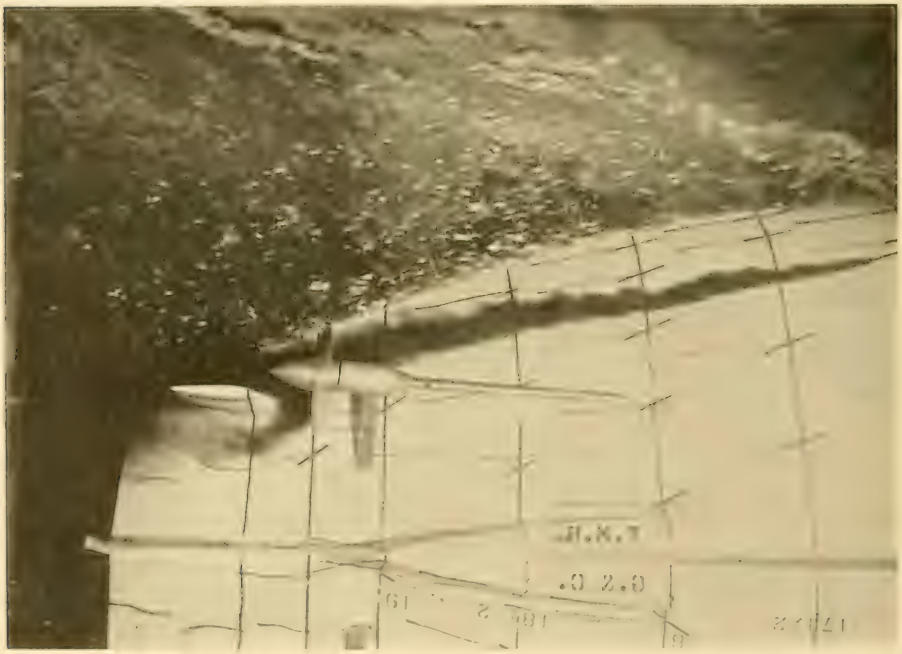

Fig. 46.E Fish-Eye View of a Ship Model With Trail of India Ink to Reveal Flow Pattern

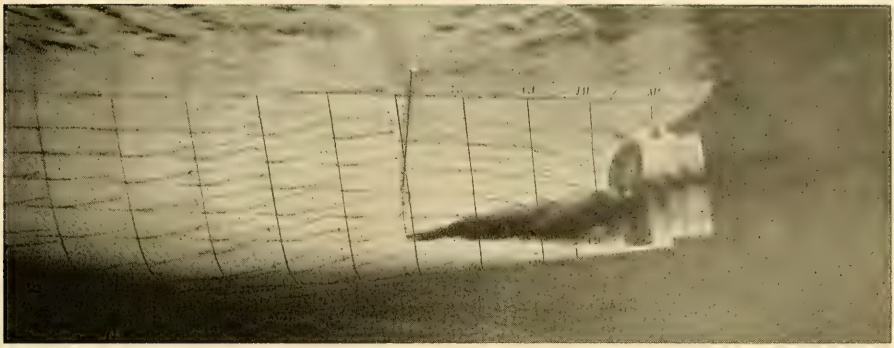

FIG. 46.F ELEVATION OF SHIP MODEL AFTERBODY IN CIRCULATING-WATER CHANNEL WITH INK TRAIL, TUFTS ON SURFACE, AND TUFTS ON PINS PROJECTING FROM SURFACE

observed by eye, or are recorded by high-speed motion photographs. Aggravated air-leakage situations reveal themselves in the channel by air bubbles drawn into the $-\Delta p$ regions around a model, its propulsion devices, or its appendages.

The circulating-water channel lends itself to the simultaneous recording of pressures at many small orifices in a model surface, so that pressure contours may be plotted for any given conditions and the areas of $-\Delta p$ may be definitely traced.

46.4 Predicting Apparent Flow Deflection Around Separation Zones. The detection methods described in the preceding section are most useful in studying the apparent deflection or diversion of flow around separation zones, discussed in Sec. 7.10 on page 134 of Volume I. Prediction of this deflection is, in the present state of the art, based largely upon a background of experience, built up by watching flow tests, studying and analyzing the photographic records, and thinking about the problem.

Since pressures from external regions are not, as a rule, transmitted through separation zones to the ship hull, there may be little information of direct value to resistance studies in a knowledge of the potential-flow pattern, with its changing velocities and pressures, outside the separation zones. However, for the prediction of flow into propulsion devices, and for special appendages and attachments to be carried by a ship at some distance from the side, knowledge of these "outside" flow patterns is a must if the special design is to be logical and the service performance is to be predicted.

For example, in the case of the ten tanker models for which resistance and propulsion data were presented by R. B. Couch and M. St. Denis [SNAME, 1948, pp. 360–379], the flow close to the hull and into the propeller disc was in many cases very nearly horizontal, if not actually downward in some regions. Fig. 46.F shows exactly this type of flow, above the ink "trail." The downward flow was unexpected because the general buttock slope in these regions was distinctly upward, at an appreciable angle to the horizontal. The phenomenon may be explained, at least in one way, by the presence of separation zones abaft the DWL and the near-surface WL's, and by downward deflection of the water passing under the stern. Normally, this water keeps on rising, all the way to the stern, but with a separation zone extending nearly to the top of the propeller aperture, as in Fig. 46.F, the under-the-bottom water and the eddying water obviously can not both occupy the same space.

Another explanation of the downward flow is that it is due to the presence of a large vortex rotating about a longitudinal axis, streaming off the region of the bilge at about the after quarter-point in the manner outlined by the sketch of Fig. 25.F in Sec. 25.6 of Volume I.

46.5 Estimate of Separation Drag Around a Ship. Sec. 7.8, supplemented by Fig. 7.H on page 130 of Volume I, explains how the specific separation-drag coefficient may be approximated by noting the sensibly constant specific pressure-resistance coefficient derived from model tests at low Froude numbers, below the limit at which wavemaking resistance manifests itself [Davidson, K. S. M., PNA, 1939, Vol. II, p. 76; SNAME,

New York Sect., 26 Apr 1951, p. 7, Fig. 1]. This constant specific resistance is reckoned above all allowances for both transverse and longitudinal curvature and for plating, structural, and coating roughnesses which are applied to the flat, smooth-plate, turbulent-flow friction line.

In the usual case the $+\Delta p$'s and $-\Delta p$'s caused by outward deflection of the water at the bow, by speeding up between the forward and after neutral points, and by closing in astern, are not of such sign and magnitude as to balance each other, when integrated over the transverse maximum-area section. This is especially true if the vessel has a bulb of appreciable size at the bow, or if the separation zone at the stern is large enough to interfere with the closing in of the potential flow along the run. Some of the low-speed specific pressure resistance is probably always the result of this action. The remainder, and greater part, is chargeable to separation at the stern, especially if the criteria of Sec. 46.2 indicate a sizable zone of $-\Delta p$, when projected on a transverse plane. Areas of this kind are illustrated by the hatched portions of diagrams 1 and 2 of Fig. 46.A.

There are insufficient data from model tests, and practically none from ship trials, to afford an indication of the numerical values of $-\Delta p$ or of the pressure coefficient $-\Delta p/q$ to be found in ship separation zones. Tests in air on geometric forms indicate separation-zone pressures varying from $-1.4q$ behind a 2-diml flat plate to $-1.15q$ behind a 2-diml circular cylinder, with its axis normal to the stream, to $-0.4q$ or less for a sphere and a circular flat plate, depending upon the R_n of the test. There is little doubt that these values are much too high for separation zones at the stern of a ship. In fact, it is not yet known whether the $-\Delta p$ in those zones is a function of q or perhaps of the hydrostatic pressure p_H.

It is pointed out in Sec. 7.3 of Volume I that aeration, defined as the natural or deliberate admission of air to a separation zone where the $-\Delta p$'s cause added drag, acts to diminish that drag. When discussing separation drag, therefore, it is most necessary to know the extent to which atmospheric air has been admitted to or has found its way into a $-\Delta p$ region that is under a pressure less than atmospheric. In certain regions $-\Delta p$'s are set up deliberately, for propulsion purposes, as on the backs of the blades of screw propellers. It is important to know to what extent, if any, air has leaked into these regions and diminished the useful $-\Delta p$'s. For example, air drawn down to fill the separation zones behind the arms, legs, and feet of swimmers, as revealed by special high-speed photography, may be helpful or detrimental, depending upon whether drag or propelling forces are involved.

B. Perry reports the results of drag measurements on surface-piercing bars of rectangular and circular section, and gives excellent photographs of the air-filled holes alongside of and abaft these bars [Hydrodyn. Lab., CIT, Rep. E-55.1, Dec 1954]. He reports an effect of surface tension in the formation and behavior of the spray roots at the water surface. Sometimes these roots form a sort of closure over the separation zone which prevents the admission of air to it.

Neglecting the free-surface and lower-end effects, Perry reports that the drag of the vertical bars per unit depth, at a submergence h, may be derived from the drag of similar bodies well submerged and trailing water-vapor cavities abaft them. The referenced report gives drag coefficients for bars of circular section, for rectangular bars with one flat edge leading, for wedge-shaped bars with the apex leading (and for various included angles), and for all three kinds when placed at an angle to the flow.

46.6 Separation Phenomena Around Geometric and Non-Ship Forms. It is often useful, in the design of box-type or non-ship-shaped water craft, and in the design and application of appendages, to have information as to the nature of the separation to be expected around them. Some of these data are given in the illustrations on Chap. 7, and references to other data are furnished in certain sections of Chap. 42.

Research on this phenomenon has been underway for many years but the data have not yet been collected and presented in systematic fashion. Over three-quarters of a century ago the following quantitative data were given by W. Froude as the result of towing tests on a cylindrical pitot tube 0.125 ft in diameter and projecting 1.75 ft below the free-water surface. The test was made at a speed of 15 ft per sec, corresponding to about 9 kt. An air-filled hole, called by Froude a "gash," extended for about 3 ft abaft the tube, at which point the gash closed by the gradual meeting of the side streams which bounded it.

". . . from this point to about 7 or 8 feet further sternwards there rose vertically a central wall of water, the crest of which, in its side elevation, had a parabolic form (as far

as could be estimated by the eye), the highest part of the ridge being certainly over 2 feet above the natural water-level . . ." [Brit. Assn. Rep., 1874 (dated 1875), pp. 255–264].

Two references on this subject, listed in Sec. 7.2 of Volume I, are repeated here for the convenience of the reader. These embody a multitude of photographs taken through the water of a basin, showing the air-filled separation zones abaft towed vertical rods of finite lengths. They were made by A. D. Hay and published in "Flow About Semi-Submerged Cylinders of Finite Length," Bureau of Ships, Navy Department, Contract NObs-34006, dated 1 October 1947. Many other photographs of separation zones abaft box-shaped forms, made by A. D. Hay and J. P. Runyon, are embodied in "Photographs and Resistance Measurements of Semi-Submerged Right Parallelepipedons," Contract NObs-34006, dated 1 May 1947. Copies of these reports are in the TMB library.

46.7 Vortex Streets and Related Phenomena. Large vortexes, in pairs or in echelon, may be and usually are shed from non-faired appendages or blunt-ended objects, such as submarine periscopes or thick propeller-blade sections. Similar vortexes may be shed abaft faired appendages such as struts which are yawed slightly with respect to the flow. The vortexes in pairs appear at very low speeds and those in echelon at the higher speeds. Schematic diagrams of these vortex groups are given in Figs. 7.M, 14.W, 14.X and 23.E of Volume I, and in Figs. 40.A and 41.D of the present volume.

The mechanism by which, at certain combinations of forward speed and appendage diameter or thickness, the alternating circulation associated with the shedding of these eddies produces alternating transverse lift forces of considerable magnitude on the moving body, is explained in Sec. 14.22.

For other treatments the reader is referred to the following:

(1) Ahlborn, F., "Über der Mechanismus des hydrodynamischen Widerstandes (On the Mechanism of Hydrodynamic Resistance)," Hamburg, 1902
(2) Bénard, H., Comptes Rendus (in French), 1908:2, Vol. 147, pp. 839–842 and 970–972; 1913, Vol. 156, p. 1225; 1926, Vol. 182, p. 1523; 1926, Vol. 183
(3) Von Kármán, T., Nachr. Ges. Wiss., Göttingen (in German), 1911, p. 509; 1912, p. 547
(4) Von Kármán, T., and Rubach, H., "Über den Mechanismus des Flussigkeits- und Luftwiderstandes (On the Mechanism of Resistance in Liquids and in Air)," Physikalische Zeitschrift, 15 Jan 1912. An English translation of this paper, with some additional material worked up by T. von Kármán, is given by G. de Bothezat in NACA Rep. 28, 1918, Note IV, pp. 149–158.
(5) Relf, E. F., and Simmons, L. F. G., "The Frequency of the Eddies Generated by the Motion of Circular Cylinders through a Fluid," ARC, R and M 917, 1924
(6) Zahm, A. F., "Flow and Drag Formulas for Simple Quadrics," NACA Rep. 253, 1927
(7) Lagally, M., "Die reibungslose Strömung in Aussengebiet zweier Kreise (The Frictionless Flow About Two Circles)," Zeit. für Ang. Math. und Mech., Aug 1929
(8) Rosenhead, L., Proc. Roy. Soc., A, 1930, Vol. 129, p. 115ff
(9) Rosenhead, L., and Schwabe, M., "An Experimental Investigation of the Flow Behind Circular Cylinders in Channels of Different Depths," Proc. Roy. Soc., 1930
(10) Biermann, D., and Herrnstein, W. H., Jr., "The Interference Between Struts in Various Combinations," NACA Rep. 468, 1933
(11) Richards, G. J., "An Experimental Investigation of the Wake Behind an Elliptic Cylinder," ARC, R and M 1590, 1934–1935, Vol. I, pp. 387–392
(12) Prandtl, L., and Tietjens, O. G., AHA, 1934, text on pp. 130–136, diagram on p. 132, photos in Pls. 24, 25, 26
(13) Tietjens, O. G., and Prandtl, L., HAM, 1944, Vol. I, diagram only on p. 225
(14) Lamb, H., HD, 1945, pp. 680–681
(15) Rouse, H., EMF, 1946, pp. 239–241
(16) Wright, E. A., SNAME, 1946, Fig. 3, p. 377
(17) Rouse, H., EH, 1950, pp. 129–130
(18) Rouse, H., and Howe, J. W., BMF, 1953, frontispiece and Fig. 111 on p. 187.

The reader who wishes to delve more deeply into the analytic aspects of this matter is referred to L. Landweber's treatment of this phenomenon on TMB Report 485, dated July 1942.

46.8 Vortex Streets and Vibrating Bodies. The right-hand diagram of Fig. 46.G, adapted from H. Rouse [EH, 1950, Fig. 93 and pp. 129–130], gives quantitative data concerning the vortex trail generated abaft a stationary 2-diml circular cylinder in a uniform stream of velocity U_∞. It indicates that the whole system of alternate vortexes left behind by a moving body in a flowing stream, corresponding to this cylinder, follows it with what may be termed a wake velocity. For the cylinder shown the value of this velocity is about 0.14 of the body speed, so that the absolute downstream velocity of the system of vortexes is about $0.86U_\infty$. The transverse spacing a between the rows of alternate vortexes, for the case of the cylinder illustrated, is about $1.3D$. The longitudinal spacing b between vortexes in either row is about $4.3D$.

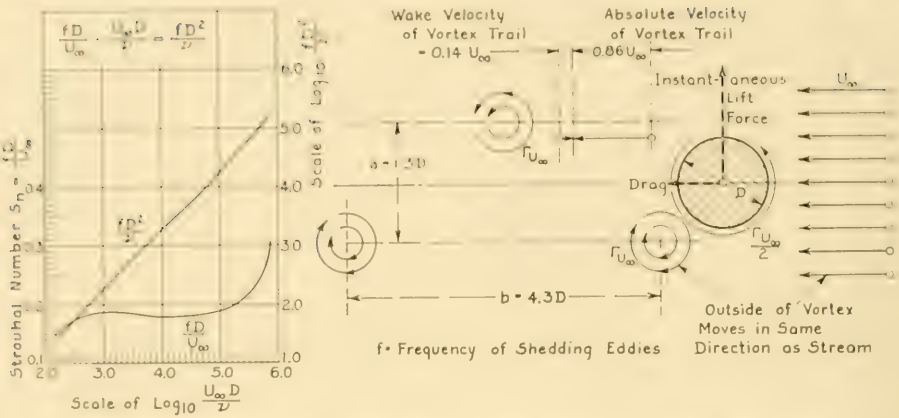

Fig. 46.G Guidance Sketch and Eddy-Frequency Relations for Vortex-Trail Problems

If the vortex trail is being generated by a blunt-ended body instead of a 2-diml circular cylinder normal to the flow, the dimension D corresponds to the effective diameter or width of the trailing edge. Unfortunately, there is no known rule by which this effective diameter may be determined for a trailing edge of any shape.

Because of the basic theorem of hydrodynamics which requires that the circulation around any closed curve within a fluid must remain constant with time [FHA, 1934, pp. 192–193], the circulation Γ(capital gamma) at any instant about the 2-diml cylinder in Fig. 46.G must be equal to, and must be of opposite sign to the *net* circulation of all the vortexes previously formed [Rouse, H., EH, 1950, p. 129]. At time zero, assume that there is no circulation anywhere in the system and that the uniform-stream velocity is zero. This velocity may then be assumed to rise from zero to U_∞. At the same time, the vortex circulation approaches a steady value of $\pm\Gamma_U$, likewise increasing from zero. This increase in vortex circulation takes place in such manner that the algebraic sum of all the vortex circulation from time zero equals $\pm\Gamma_U/2$ after the stream velocity has reached a steady value of U_∞. Since the circulation around the cylinder must be equal to and of opposite sign to the *net* circulation of all the vortexes, the circulation around the cylinder varies from $+\Gamma_U/2$ to $-\Gamma_U/2$.

The approximate magnitude of the lift force per unit span of the 2-diml body, acting in either direction, is, by Eq. (44.i), $L = \rho U_\infty\Gamma$ for the general case. For this particular case, $L = \rho U_\infty\Gamma_U/2$. The absolute downstream velocity of the vortexes as a group is about $0.86U_\infty$. The strength of the vortex circulation Γ_U is about $2.8b(0.14U_\infty) = 2.8(4.3D)(0.14U_\infty)$ or about $1.7U_\infty D$.

The graphs in the left-hand diagram of Fig. 46.G give values of the relationships fD^2/ν and fD/U_∞ in terms of the Strouhal number fD/U_∞ and the applicable Reynolds number $U_\infty D/\nu$. The example of Sec. 41.6 explains the method of using this graph to predict the eddy frequency for a 2-diml rod of diameter D or for a blunt-ended body of effective diameter D. As another example, assume that a cylindrical rod having a diameter of 0.1 ft forms part of an experimental speed log on the ABC ship of Part 4, projecting 2 ft vertically below the bottom of the ship. Assume also that the average velocity U in the boundary layer in way of this rod is $0.95V$ or $0.95U_\infty$. At 20.5 kt, U_∞ is 34.62 ft per sec, whence $U = 0.95(34.62) = 32.89$ ft per sec.

The vortex circulation Γ_U is about $1.7(U)D = 1.7(32.89)(0.1) = 5.59$ ft^2 per sec. The cylinder circulation $\Gamma_U/2$ is 2.8 ft^2 per sec, whence the maximum transverse lift force is $\rho U\Gamma_U/2$ or $1.9905(32.89)(2.8) = 183.3$ lb per ft length of span.

The d-Reynolds number is UD/ν or $(32.89)(0.1)(10^5)/1.2817$ or about 0.257 million, whence from the left-hand diagram of Fig. 46.G the Strouhal number fD/U = about 0.215, from which $f = (0.215)(32.89)/(0.1) = 71$ hertz or 71 cycles per sec. If the virtual mass of the rod, including the added mass of the entrained water, is such that it vibrates transversely as a cantilever at a frequency

approximating this figure, resonant vibration will ensue, with a magnification of vibration amplitude and possible damage to the rod.

The use of deflectors or longitudinal-vortex generators, to serve as an auxiliary transfer mechanism to get fast-moving water from the outer portions of the boundary layers into the inner portions and thus to provide the kinetic energy in the inner portion necessary to defer separation, is discussed in Sec. 36.27 of Volume I. However, the necessary quantitative data for calculating the effect of these generators are not available at the present time (1955).

46.9 Practical Applications of the Strouhal Number to Singing and Resonant Vibration. As an illustration of the application of the knowledge presently available (1955) to the prediction of possible singing of a propeller blade, take the case of the propeller designed for the transom-stern ABC ship in Secs. 70.21 through 70.38 of Part 4.

Assume that this propeller, originally manufactured with the relatively fine trailing edges depicted in Fig. 70.O, has had its edges damaged by curling and nicking so that, as a temporary measure, the trailing edge from about $0.50R_{\text{Max}}$ to $0.78R_{\text{Max}}$ has been chipped away and rounded off as shown by the broken line of diagram 1 of Fig. 70.P. It is estimated that the effective thickness t at this edge is about 0.75 in or 0.0625 ft; see the discussion of this matter in Sec. 70.46. In other words, the vortex trail expected to be shed by the trailing edge corresponds to that which would be shed by a non-vibrating 2-diml circular-section rod 0.0625 ft in diameter, moving through the water at the same speed and occupying the same position as the trimmed-off trailing edge of the damaged blade.

The basic data, for a designed ship speed of 20.5 kt, are, from Sec. 70.26:

Diameter, maximum, of propeller, 20 ft
Speed of advance V_A, 27.87 ft per sec
Speed of rotation of propeller, 1.62 rps
Kinematic viscosity of salt water, $1.2817(10^{-5})$ ft^2 per sec
Mass density of salt water, 1.9905 slugs per ft^3.

The rotational speed of the propeller at the 0.64 radius, halfway between 0.50 and $0.78R_{\text{Max}}$, is $2\pi(20/2)(0.64)1.62 = 65.15$ ft per sec. The blade-section speed at that radius is the combination of the rotational speed and the speed of advance, or $V_{\text{Blade}} = [(65.15)^2 + (27.87)^2]^{0.5} = 70.86$ ft per sec.

The d- or diameter Reynolds number R_d for the effective diameter of the damaged trailing edge is $(V_{\text{Blade}})(t)/\nu = (70.86)(0.0625)(10^5)/1.2817 = 0.3455$ million. From the left-hand diagram of Fig. 46.G the corresponding Strouhal number S_n is about 0.21. Then since $S_n = fD/U_\infty$ or, in this case, $(f)(t)/V_{\text{Blade}}$, the predicted frequency is $f = S_n(V_{\text{Blade}})/t = 0.21(70.86)/0.0625 = 238$ hertz or 238 cycles per sec. This is well above the low limit of 10 cycles per sec and well below the upper limit of 700 cycles per sec for audible singing, given in Sec. 70.46. Singing on the damaged (and temporarily repaired) blade of the ABC ship is liable to occur unless a chisel edge is left when the damaged parts are chipped away, as diagrammed in Fig. 70.P.

Two illustrative examples of the method of calculating the eddy frequency for 2-diml circular-section rods that may be subject to resonant vibration are worked out in Secs. 41.6 and 46.8, respectively. As an indication of the range of frequencies which may be encountered on high-speed vessels where these hydroelastic interactions are liable to pose troublesome problems, take the case of the very wide strut arms, with a chord length of 3.75 ft, mentioned by P. Mandel [SNAME, 1953, p. 514].

Assume that the proposed strut section is used on a large ship, with a thickness-chord ratio of 4.35. As indicated in Fig. 3 on page 408 of the reference, the effective t (or D) along the trailing edge is 2.5 in or 0.21 ft. Assume further a ship speed of 25 kt, equivalent to 42.22 ft per sec, since at higher speeds the vortex trail might be replaced by a vapor cavity. As in Sec. 46.8, the kinematic viscosity is taken as $1.2817(10^{-5})$ ft^2 per sec and the mass density as 1.9905 slugs per ft^3.

The d-Reynolds number is then VD/ν or $(42.22)0.21(10^5)/1.2817 = 0.6917$ million. From the graph of Fig. 46.G the Strouhal number S_n is 0.292. Then $f = S_nV/D = (42.22)0.292/0.21 = 58.7$ hertz or 58.7 cycles per sec.

In practice the strut problem is further complicated by the fact that the strut-arm section may not lie with its meanline exactly in the line of flow. Or if properly aligned for straight-ahead running, even taking account of the twist in the inflow jet which is induced *ahead* of the propeller position, the strut-arm section may run at an appreciable yaw angle when the ship makes a turn. It is probable that, if the yaw angle becomes large enough so that the separation point on that side of the trailing edge which is yawed outward moves aft and becomes essentially fixed at the

trailing edge, the vortex street is no longer formed. The alternating circulation ceases, as does the alternating transverse lift forces on the section. Further research and experiment are needed along these lines.

The hydroelastic interactions in the case of the strut, involving the added mass of the entrained water for transverse or flatwise vibration of the strut arm, the damping effects of the strut section, when moving laterally, the mode of motion of the whole strut assembly, including the strut hub and all the arms, and the elastic characteristics of these parts, are not considered here.

46.10 References on Eddy Systems, Vortex Trails, and Singing. There is given in Sec. 46.7 a short list of references relating directly to the vortex-trail or eddy systems abaft the trailing edges of bodies of varied type and shape. The list in the present section covers a somewhat broader field. It is by no means complete but it is adequate for the beginning of an extended study of the subject. References to photographs of flow patterns involving eddies and vortexes are listed in the text of Sec. 42.2 and in Table 42.b of that section. These are in addition to the references listed in Secs. 7.11 and 14.22 of Volume I.

(a) Helmholtz, H., "Über Integrale der Hydrodynamischen Gleichungen welche den Wirbelwegungen Entsprechen (On Integrals of the Hydrodynamical Equations which Express Vortex Motion)," Crelle's Jour., 1858, Vol. 55; English transl. by P. G. Tait in London, Edin., and Dublin, Phil. Mag., Jan-Jun 1867, Vol. 33 (4th series), pp. 485–511

(b) Ahlborn, F., "Die Wirbelbildung im Widerstandsmechanismus des Wassers (Eddies in the Mechanism of Ship Resistance in Water)," STG, 1905, pp. 67–81. Eddies abaft the forward outboard corners and the after face of a 2-diml rod of rectangular section are shown in Fig. 22 of the reference. A large separation zone abaft a similar section at higher speed is shown in Fig. 12.

(c) Stanton, T. E., and Marshall, D., "Eddy Systems in the Wake of Flat Circular Plates in Three Dimensional Flow," ARC, R and M 1358, 1931–1932, Vol. I; pp. 202–211

(d) Steinman, D. B., "Problems of Aerodynamic and Hydrodynamic Stability," Proc. Third Hydr. Conf., State Univ. Iowa, Studies in Eng'g., Bull. 31, 1947, pp. 136–164. The author lists 19 references on pages 163–164.

(e) Steinman, D. B., "Aerodynamic Theory of Bridge Oscillations," Trans. ASCE, 1950, Vol. 115, pp. 1246–1247, 1254–1255

(f) Den Hartog, J. P., "Recent Technical Manifestations of von Kármán's Wake," Proc. Nat. Acad. Sci., Wash., Mar 1954, Vol. 40, pp. 155–157

(g) Roshko, A., "On the Wake and Drag of Bluff Bodies," Jour. Aero. Sci., Feb 1955, pp. 2, 124–132

(h) Cooper, R. D., and Lutzky, M., "Exploratory Investigation of the Turbulent Wakes Behind Bluff Bodies," TMB Rep. 963, Oct 1955.

The references which follow apply particularly to the singing of the blades of screw propellers:

(1) Richardson, E. G., Proc. Phys. Soc., 1924, Vol. 36, p. 153ff; also 1925, Vol. 37, p. 178ff

(2) Gutsche, F., "Das Singen von Schiffsschrauben (The Singing of Ship's Propellers)," Zeit. des Ver. Deutsch. Ing., 3 Jul 1937, Vol. 81, pp. 882–883. There is available in the TMB library an unpublished English translation of this paper, marked TMB Transl. 123.

(3) Hunter, H., "Singing Propellers," NECI, 1936–1937, Vol. LIII, pp. 189–222, D73–D120

(4) "The Problem of the Singing Propeller," SBSR, 12 Aug 1937, pp. 205–207; 2 Sep 1937, pp. 298–300; 7 Oct 1937, pp. 450–452

(5) Hunter, H., "Singing Propellers," E. and F. N. Spon, London, 1937

(6) Hayes, H. C., and Klein, E., "Methods and Means for Determining the Natural Modes of Vibration of Mechanical Structures," ASNE, 1938, Vol. 50, pp. 519–526. The paper is devoted to a study of the vibrating modes and frequencies of screw-propeller blades.

(7) Conn, J. F. C., "Marine Propeller Blade Vibration," IESS, 1938–1939, Vol. 82, pp. 225–255, 292–374

(8) Shannon, J. F., and Arnold, R. N., "Statistical and Experimental Investigation of the Singing Propeller Problem," IESS, 1938–1939, Vol. 82, pp. 256–291, 292–374. On pp. 289–291 the authors list 35 references.

(9) Kerr, W., Shannon, J. F., and Arnold, R. N., "The Problems of the Singing Propeller," Inst. Mech. Engrs., London, Dec 1940, Vol. 144, pp. 54–90. Abstracted on p. 409 of SBSR, 25 Apr 1940; also SBMEB, Apr 1940, pp. 180–181.

(10) Davis, A. W., "Characteristics of Silent Propellers," IESS, 1939–1940, Vol. 83, pp. 29–102. Abstracted in SBMEB, Apr 1940, pp. 165–169.

(11) Baker, G. S., "Vibration Patterns of Propeller Blades," NECI, 1940–1941, Vol. 57, pp. 43–66, D1–D12

(12) Work, C. E., "Review of Marine Propeller Noise and Vibration Studies," U. S. Nav. Ord. Test Sta. Propulsion Memo 74, 7 Sep 1940

(13) Hughes, G., "Influence of Shape of Blade Section on Singing Propellers," IESS, 1941–1942, Vol. 85, pp. 55–168. On page 130 the author lists 10 references.

(14) Hughes, G., "On Singing Propellers," INA, 1945, pp. 185–216

(15) Lewis, F. M., ME, Vol. II, 1946, p. 131

(16) Hughes, W. L., "Propeller Blade Vibrations," NECI, 1948–1949, pp. 273–300, D51–D70

(17) Burrill, L. C., "Underwater Propeller Vibration Tests," NECI, 1948–1949, pp. 301–314, D50–D70

(18) Work, C. E., "Singing Propellers," ASNE, May 1951, pp. 319–331

(19) Lankester, S. G., and Wallace, W. D., "Some Investigations into Singing Propellers," NECI, 7 Jun 1955, pp. 293–318.

CHAPTER 47

The Inception and Effect of Cavitation on Ships and Propellers

47.1 Scope of This Chapter. The phenomena and mechanism of cavitation in its various forms, and the factors associated with it, are described in Chap. 7, Secs. 7.12 through 7.19, of Volume I. The occurrence of cavitation on ships and propellers, as well as many of its practical features, are discussed in Chap. 23, Secs. 23.9 through 23.16, of that volume. Practical examples illustrating the calculation of the cavitation number are found in Secs. 41.3, 47.4, and 47.5.

Treatment of cavitation in the present chapter, as associated with ships, propellers, and appendages, is limited to data of a quantitative nature, of general interest to the naval architect and marine engineer. A selected cavitation bibliography, containing many recent papers on the subject, concludes the chapter as Sec. 47.13.

47.2 General Rules for the Occurrence of Cavitation on Ships and Appendages. Cavitation occurs when, for any one of several reasons, the pressure in a particular region in the water drops to that of the water vapor, or to that of a combination of water vapor and dissolved air or gas. As the purpose of practically all moving ship appendages, as well as propulsion devices, is to create useful forces by the development of positive and negative differential pressures, it is natural that the $+\Delta p$'s should be made as high, and the $-\Delta p$'s as low as can be accomplished without setting up harmful cavitation. Most such parts of a surface ship operate within a depth of about 37 ft below the free surface. This hydrostatic head, when added to the atmospheric-pressure head of 33 ft, gives an effective head of less than 70 ft before cavitating conditions are reached.

To demonstrate this, set down the pressure equation for steady irrotational flow of an ideal liquid, Eq. (7.i) of Sec. 7.12. Transposing p_∞,

$$p = p_\infty + \frac{\rho}{2}(U_\infty^2 - U^2) \qquad (47.i)$$

For the condition described the critical minimum pressure p is equal to the absolute vapor pressure e, say 0.4 psia. The ambient pressure p_∞ is that corresponding to the full absolute head of 70 ft, or 31.13 psi for standard salt water. The value of the term 0.5ρ(rho) for standard salt water is 0.99525 slugs per ft^3. Introducing the factor 144 to transform psi to psf, then substituting and solving,

$$0.4(144) = 31.13(144) + (0.99525)(U_\infty^2 - U^2)$$

whence

$$(U_\infty^2 - U^2) = -\frac{(31.13 - 0.4)(144)}{0.99525}$$

$$= -4{,}446.2 \text{ ft}^2 \text{ per sec}^2$$

If $V = U_\infty$ is 30 kt, equivalent to 50.67 ft per sec, so that U_∞^2 is 2,567.4 ft^2 per sec^2, then

$U^2 = U_\infty^2 - (-4{,}446.2) = 2{,}567.4 + 4{,}446.2 =$ 7,013.6 ft^2 per sec^2, and

$U = 83.75$ ft per sec.

This means that to keep clear of cavitating conditions the relative velocity of the water

moving aft past a deep part of the 30-kt ship, expressed as $U_\infty + \Delta U$, can not exceed 83.75 ft per sec. Since the ship speed V equals the velocity U_∞, the augment ΔU can not exceed 83.75 − 50.67 = 33.08 ft per sec without the onset of cavitation. For the equator of a 3-diml sphere the augment ΔU is $0.5U_\infty$; if U_∞ is 50.67 ft per sec, ΔU is 25.34 ft per sec. This is less than the limiting value of 33.08 ft per sec, so cavitation would not occur *at the equator* of the sphere at a depth of 37 ft. For the maximum diameter of a 2-diml rod, normal to its direction of motion, the augment ΔU is $1.0U_\infty$ or 50.67 ft per sec. This exceeds the critical velocity, so at the given depth cavitation would begin ahead of the midsection of the rod.

Aeration of the salt water raises its vapor pressure. This has the effect of diminishing numerically the augment of velocity ΔU at which some form of cavitation takes place. At shallower depths on a large ship, or at the shallower drafts and greater speeds customary on high-speed vessels, cavitating conditions are readily encountered on the hull, the appendages, and the propulsion devices.

Bubble cavitation is hastened by the presence of microscopic or submicroscopic pockets of vapor or air or air and gas bubbles, and of cavitation nuclei in the form of impurities, animal or vegetable matter, or entities as yet unknown. The water nearest the surface of the sea carries the most air in solution; this amount is augmented if the surface is disturbed, as during a storm. There are more minute impurities carried in suspension in waters close to the land but there may be more nuclei of other kinds in waters far from the land.

From the manner in which either bubble or sheet cavitation appears to form in the water in which ships operate, a cavitation criterion must take account of at least six factors:

(a) The ambient pressure p_∞ in the water
(b) The vapor, or the gas-air pressure of the water at the temperature concerned
(c) The relative speed U_∞ of the undisturbed water and the body or ship
(d) The shape and proportions of the body or ship
(e) The augment of velocity ΔU due to potential and other flow over and around a body, a ship, or any of its parts
(f) The effective angle of attack α, if the part under consideration resembles a hydrofoil.

Concerning the ambient-pressure factor, it is not sufficient to consider the mean depth at which a hydrofoil section or other movable body operates, such as the depth to the axis of a screw propeller. It is entirely possible for a blade element, at the top of its path, to cavitate through an arc or region of low hydrostatic pressure and to set up objectionable vibration or other conditions from this cause. At the depth of the shaft axis, or at the bottom of its path, it might not cavitate at all.

In real, viscous liquids like water, the over-the-surface liquid velocities at the inner edge of the boundary layer are less than the ship speed V or the velocity U_∞ relative to the undisturbed water. The potential-flow velocities are different than they would be over the same body surface in an ideal liquid, because of the displacement thickness of the boundary layer, so that accurate prediction of cavitation is difficult. Fortunately, most appendages liable to cavitation are short, with boundary layers of insignificant thickness. In any case a prediction disregarding the boundary layer is usually on the safe side, if the prediction is to foretell the worst that may be expected.

47.3 Vapor-Pressure Data for Water. The vapor pressure e of water drops rather rapidly with temperature, so much so that appendages and propulsion devices which cavitate in the tropics under a given set of conditions may not do so in the polar regions under the same conditions.

Values of e for fresh water, over a temperature range from freezing to boiling at sea level, are graphed in Fig. 47.A. They are listed in Table

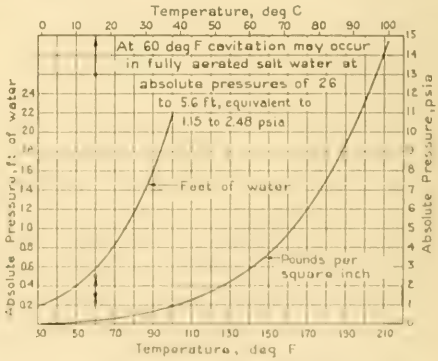

Fig. 47.A Graphs of Vapor-Pressure Data for Fresh Water

TABLE 47.a—VAPOR PRESSURE OF FRESH WATER FOR VARIOUS TEMPERATURES

Degrees		Absolute Pressure		Degrees		Absolute Pressure	
F	C	psia	ft of water	F	C	psia	ft of water
32	0	0.0887	0.2048	120	48.9	1.692	3.9067
35	1.7	0.1000	0.2309	125	51.7	1.941	4.4815
40	4.4	0.1217	0.2810	130	54.4	2.221	5.1281
45	7.2	0.1475	0.3406	135	57.2	2.536	5.8554
50	10.0	0.1780	0.4110	140	60.0	2.887	6.6658
55	12.8	0.2140	0.4941	145	62.8	3.280	7.5732
59	15.0	0.2471	0.5705	150	65.6	3.716	8.5799
60	15.6	0.2561	0.5913	155	68.3	4.201	9.6997
65	18.3	0.3054	0.7051	160	71.1	4.739	10.942
68	20.0	0.3388	0.7823	165	73.9	5.334	12.316
70	21.1	0.3628	0.8377	170	76.7	5.990	13.830
75	23.9	0.4295	0.9917	175	79.4	6.716	15.507
80	26.7	0.5067	1.1699	180	82.2	7.510	17.340
85	29.4	0.5960	1.3761	185	85.0	8.382	19.353
90	32.2	0.6980	1.6116	190	87.8	9.336	21.556
95	35.0	0.8149	1.8815	195	90.6	10.385	23.978
100	37.8	0.9487	2.1905	200	93.3	11.525	26.610
105	40.5	1.1009	2.5419	205	96.1	12.772	29.489
110	43.3	1.274	2.9415	210	98.9	14.123	32.609
115	46.1	1.470	3.3941	212	100.0	14.696	33.932

47.a with corresponding values of deg F, deg C, psia, and absolute head in ft of water.

The vapor pressure of the salt water of the seas of the world is, as mentioned in Sec. 47.2, a function of many variables other than temperature. The effect of these variables is not yet isolated and only somewhat random data are available for calculation purposes. The best of these data are given by S. F. Crump in TMB Report 575, issued in October 1949. Some data are abstracted by P. Eisenberg in TMB Report 712, dated July 1950, pages 18 through 20. A general statement about the range of vapor pressure for salt water is added at the top of Fig. 47.A. Supplementary data are given in Table X3.1 of Sec. X3.6 of Appendix 3 at the end of this volume.

47.4 Tables of and Nomogram for Cavitation Numbers. For convenience in making rapid predictions there have been calculated the values of the cavitation index or number σ(sigma) for standard salt water, covering a rather wide range of velocity and a reasonable range of net head $[(h_A + h_H) - h_V]$, where h_V is the vapor-pressure head. These data, computed for standard conditions and in accordance with the formula $\sigma = (h_A + h_H - h_V)/(\text{Velocity head } h_U)$, are set down in Table 47.b.

Fig. 47.B is a nomogram by which the speed of incipient cavitation may be determined by inspection from a knowledge of the depth of the object below the water surface and the critical cavitation index σ_{CR} for the body shape [Macovsky, M. S., Stracke, W. L., and Wehausen, J. V., TMB Rep. 879, Jan 1948, Fig. 4; Mandel, P., SNAME, 1953, Fig. 8, p. 472]. For example, assume that a speed log of some kind is projected 4 ft below the bottom of the ABC ship of Part 4, and that it is desired to have the log free of cavitation at the clean-bottom trial speed of 20.5 kt. With a ship draft of 26 ft, the nominal submergence of the log is 30 ft, neglecting the effect of sinkage, trim, and ship-wave profiles. To have a suitable margin for an increased vapor pressure due to aeration and similar factors, the speed of incipient cavitation should be at least 24 kt. Then applying a straight edge across the nomogram from $h = 30$ ft to $V = 24$ kt it is found that the critical cavitation index σ_{CR} for the portion of the log in question is 2.48. This means that the pressure coefficient E_n at the point of minimum absolute pressure on the exposed portion of the log cannot exceed -2.48.

To make the situation perfectly clear to the prospective designer, a portion of the discussion of Sec. 41.3 on the Euler and cavitation numbers

TABLE 47.b—CAVITATION NUMBERS FOR A SERIES OF SPEEDS IN STANDARD SALT WATER

Velocity, ft per sec	Speed in kt	Velocity head, ft	Net head, $(h_A + h_H - h_V)$, ft										
			30	32	34	36	38	40	42	44	46	48	50
2	1.18	0.06216	482.6	514.8	547.0	579.2	611.3	643.5	675.7	707.9	740.0	772.2	804.4
3	1.78	0.13985	214.5	228.8	243.1	257.4	271.7	286.0	300.3	314.6	328.9	343.2	357.5
4	2.37	0.24862	120.7	128.7	136.7	144.8	152.8	160.9	168.9	177.0	185.0	193.1	201.1
5	2.96	0.38847	77.22	82.37	87.52	92.64	97.81	103.0	108.1	113.3	118.4	123.6	128.7
6	3.55	0.55940	53.63	57.20	60.78	64.35	67.93	71.50	75.08	78.65	82.23	85.80	89.38
7	4.14	0.76140	39.40	42.02	44.65	47.28	49.90	52.53	55.15	57.78	60.41	63.03	65.66
8	4.74	0.99458	30.16	32.17	34.18	36.19	38.21	40.22	42.23	44.24	46.25	48.26	50.27
9	5.33	1.2587	23.83	25.42	27.01	28.60	30.19	31.78	33.37	34.95	36.54	38.13	39.72
10	5.92	1.5539	19.31	20.59	21.88	23.17	24.45	25.74	27.03	28.31	29.60	30.89	32.18
11	6.51	1.8802	15.95	17.02	18.08	19.15	20.21	21.27	22.34	23.40	24.46	25.53	26.59
12	7.10	2.2376	13.41	14.30	15.19	16.09	16.98	17.88	18.77	19.66	20.56	21.45	22.34
13	7.70	2.6261	11.42	12.18	12.95	13.71	14.47	15.23	15.99	16.75	17.52	18.28	19.04
14	8.29	3.0457	9.849	10.51	11.16	11.82	12.48	13.13	13.79	14.45	15.10	15.76	16.42
15	8.88	3.4963	8.580	9.152	9.724	10.30	10.87	11.44	12.01	12.58	13.16	13.73	14.30
16	9.47	3.9780	7.541	8.044	8.546	9.049	9.552	10.05	10.56	11.06	11.56	12.07	12.57
17	10.1	4.4908	6.680	7.125	7.570	8.016	8.461	8.906	9.352	9.797	10.24	10.69	11.13
18	10.7	5.0347	5.958	6.356	6.753	7.150	7.547	7.944	8.342	8.739	9.136	9.533	9.931
19	11.2	5.6096	5.348	5.704	6.061	6.417	6.774	7.130	7.487	7.843	8.200	8.556	8.913
20	11.8	6.2157	4.826	5.148	5.470	5.791	6.113	6.435	6.757	7.078	7.400	7.722	8.044
22	13.0	7.5210	3.989	4.254	4.520	4.786	5.052	5.318	5.584	5.850	6.116	6.352	6.648
24	14.2	8.9506	3.352	3.575	3.799	4.022	4.245	4.469	4.692	4.916	5.139	5.363	5.586
26	15.4	10.504	2.856	3.046	3.237	3.427	3.617	3.808	3.998	4.189	4.379	4.569	4.760
28	16.6	12.178	2.483	2.648	2.814	2.979	3.145	3.310	3.476	3.641	3.807	3.972	4.138
30	17.8	13.985	2.145	2.288	2.431	2.574	2.717	2.860	3.003	3.146	3.289	3.432	3.575
32	18.9	15.912	1.885	2.011	2.137	2.262	2.388	2.514	2.639	2.765	2.891	3.016	3.142
34	20.1	17.963	1.670	1.781	1.893	2.004	2.115	2.227	2.338	2.449	2.561	2.672	2.783
36	21.3	20.139	1.490	1.589	1.688	1.788	1.887	1.986	2.085	2.185	2.284	2.383	2.483
38	22.5	22.439	1.337	1.426	1.515	1.604	1.693	1.783	1.872	1.961	2.050	2.139	2.228
40	23.7	24.863	1.207	1.287	1.368	1.448	1.528	1.609	1.689	1.770	1.850	1.931	2.011
42	24.9	27.411	1.094	1.167	1.240	1.313	1.386	1.459	1.532	1.605	1.678	1.751	1.824
44	26.1	30.084	.9971	1.064	1.130	1.197	1.263	1.330	1.396	1.463	1.529	1.595	1.662
46	27.2	32.881	.9123	.9732	1.034	1.095	1.156	1.216	1.277	1.338	1.399	1.460	1.521
48	28.4	35.802	.8379	.8937	.9496	1.005	1.061	1.117	1.173	1.229	1.285	1.341	1.397
50	29.6	38.848	.7722	.8237	.8751	.9266	.9781	1.030	1.081	1.133	1.184	1.236	1.287
52	30.8	42.018	.7139	.7615	.8091	.8567	.9043	.9519	.9995	1.047	1.095	1.142	1.190
54	32.0	45.312	.6620	.7061	.7503	.7944	.8385	.8827	.9268	.9710	1.015	1.059	1.103
56	33.2	48.731	.6156	.6636	.6977	.7387	.7798	.8208	.8618	.9029	.9439	.9850	1.026
58	34.3	52.274	.5738	.6121	.6504	.6886	.7269	.7651	.8034	.8416	.8799	.9181	.9564
60	35.5	55.941	.5363	.5720	.6076	.6435	.6793	.7150	.7508	.7865	.8223	.8580	.8938
62	36.7	59.733	.5022	.5357	.5692	.6026	.6361	.6696	.7031	.7366	.7700	.8035	.8370
64	37.9	63.648	.4713	.5027	.5341	.5656	.5970	.6284	.6598	.6912	.7227	.7541	.7855
66	39.1	67.689	.4432	.4727	.5023	.5318	.5613	.5909	.6204	.6500	.6795	.7091	.7386
68	40.3	71.853	.4175	.4453	.4731	.5010	.5288	.5566	.5845	.6123	.6401	.6680	.6958
70	41.4	76.142	.3940	.4202	.4465	.4728	.4990	.5253	.5515	.5778	.6041	.6303	.6566
72	42.6	80.555	.3724	.3972	.4220	.4469	.4717	.4965	.5214	.5462	.5710	.5958	.6207
74	43.8	85.093	.3525	.3760	.3995	.4230	.4465	.4700	.4935	.5170	.5406	.5641	.5876
76	45.0	89.754	.3342	.3565	.3788	.4011	.4234	.4456	.4679	.4902	.5125	.5348	.5571
78	46.2	94.540	.3173	.3385	.3596	.3808	.4019	.4231	.4442	.4654	.4865	.5077	.5289
80	47.4	99.451	.3016	.3217	.3418	.3619	.3821	.4022	.4223	.4424	.4625	.4826	.5027
82	48.5	104.49	.2874	.3066	.3258	.3449	.3641	.3832	.4024	.4216	.4407	.4599	.4791
84	49.7	109.64	.2736	.2918	.3101	.3283	.3466	.3648	.3830	.4013	.4195	.4378	.4560
86	50.9	114.93	.2610	.2784	.2958	.3132	.3306	.3480	.3654	.3828	.4002	.4176	.4350
88	52.1	120.34	.2493	.2659	.2825	.2991	.3158	.3324	.3490	.3656	.3822	.3989	.4155
90	53.3	125.87	.2383	.2542	.2701	.2860	.3019	.3178	.3336	.3495	.3654	.3813	.3972
92	54.5	131.52	.2281	.2433	.2585	.2737	.2889	.3041	.3193	.3345	.3497	.3649	.3801
94	55.7	137.30	.2185	.2330	.2476	.2622	.2767	.2913	.3059	.3204	.3350	.3496	.3641
96	56.8	143.21	.2095	.2234	.2374	.2514	.2653	.2793	.2933	.3072	.3212	.3352	.3491
98	58.0	149.24	.2010	.2144	.2278	.2412	.2546	.2680	.2814	.2948	.3082	.3216	.3350
100	59.2	155.39	.1931	.2059	.2188	.2317	.2445	.2574	.2703	.2831	.2960	.3089	.3218

TABLE 47.b—(Continued)

Velocity, ft per sec	Speed in kt	Velocity head, ft	Net head, $(h_A + h_H - h_V)$, ft										
			30	32	34	36	38	40	42	44	46	48	50
110	65.1	188.02	.1596	.1702	.1808	.1915	.2021	.2127	.2234	.2340	.2447	.2553	.2659
120	71.0	223.79	.1341	.1430	.1519	.1608	.1698	.1787	.1877	.1966	.2056	.2145	.2234
130	77.0	262.62	.1142	.1219	.1295	.1371	.1447	.1523	.1599	.1675	.1752	.1828	.1904
140	82.9	304.58	.0985	.1051	.1116	.1182	.1248	.1313	.1379	.1445	.1510	.1576	.1642
150	88.8	349.64	.0858	.0915	.0972	.1030	.1087	.1144	.1201	.1258	.1316	.1373	.1430
160	94.7	397.83	.0754	.8004	.0855	.0905	.0955	.1005	.1056	.1106	.1156	.1207	.1257
170	100.7	449.12	.0668	.0713	.0757	.0802	.0846	.0891	.0935	.0980	.1024	.1069	.1113
180	106.6	503.51	.0596	.0636	.0675	.0715	.0755	.0794	.0834	.0874	.0914	.0953	.0993
190	112.5	561.00	.0535	.0570	.0606	.0642	.0677	.0713	.0749	.0784	.0820	.0856	.0891
200	118.4	621.62	.0483	.0515	.0547	.0579	.0611	.0644	.0676	.0708	.0740	.0772	.0804
210	124.3	685.34	.0438	.0467	.0496	.0525	.0554	.0584	.0613	.0642	.0671	.0700	.0730
220	130.3	752.12	.0399	.0425	.0452	.0479	.0505	.0532	.0558	.0585	.0612	.0638	.0665
230	136.2	822.10	.0365	.0389	.0414	.0438	.0462	.0487	.0511	.0535	.0560	.0584	.0608
240	142.1	895.10	.0335	.0358	.0380	.0402	.0425	.0447	.0469	.0492	.0514	.0536	.0559
250	148.0	971.26	.0309	.0330	.0350	.0371	.0391	.0412	.0432	.0453	.0474	.0494	.0515
260	153.9	1050.5	.0286	.0305	.0324	.0344	.0362	.0381	.0400	.0419	.0438	.0457	.0476
270	159.9	1132.9	.0265	.0283	.0300	.0318	.0336	.0353	.0371	.0388	.0406	.0424	.0441
280	165.8	1218.4	.0246	.0263	.0279	.0296	.0312	.0328	.0345	.0361	.0378	.0394	.0410
290	171.7	1306.9	.0230	.0245	.0260	.0276	.0291	.0306	.0321	.0337	.0352	.0367	.0383
300	177.6	1398.6	.0215	.0229	.0243	.0257	.0272	.0286	.0300	.0315	.0329	.0343	.0358
310	183.5	1493.4	.0201	.0214	.0228	.0241	.0254	.0268	.0281	.0295	.0308	.0321	.0335
320	189.5	1591.3	.0189	.0201	.0214	.0226	.0239	.0251	.0264	.0277	.0289	.0302	.0314
330	195.4	1692.3	.0177	.0189	.0201	.0213	.0225	.0236	.0248	.0260	.0272	.0284	.0295
340	201.3	1796.5	.0167	.0178	.0189	.0200	.0212	.0223	.0234	.0245	.0256	.0267	.0278
350	207.2	1903.7	.0158	.0168	.0179	.0189	.0200	.0210	.0221	.0231	.0242	.0252	.0263
360	213.1	2014.0	.0149	.0159	.0169	.0179	.0189	.0199	.0209	.0219	.0228	.0238	.0248
370	219.1	2127.5	.0141	.0150	.0160	.0169	.0179	.0188	.0197	.0207	.0216	.0226	.0235
380	225.0	2244.0	.0134	.0143	.0152	.0160	.0169	.0178	.0187	.0196	.0205	.0214	.0223
390	230.9	2363.6	.0127	.0135	.0144	.0152	.0161	.0169	.0178	.0186	.0195	.0203	.0212
400	236.8	2486.4	.0121	.0129	.0137	.0145	.0153	.0161	.0169	.0177	.0185	.0191	.0201

is repeated here. This derived cavitation index 2.48 is a measure of the pressure which must be available at the log position to create a transverse pressure gradient which will cause the water to close in about the nose and follow the shape of the log, with no cavities. It must exceed *numerically* the negative-pressure coefficient $-\Delta p/q$ at any point along the sides of the log, to insure that there is more than enough pressure gradient to turn the water inward abaft the nose of the log and keep it there. As long as $(p - p_\infty)$ at any point is smaller numerically than $p_\infty - e$, or that $(h - h_A - h_H)$ is smaller numerically than $(h_A + h_H - h_V)$, cavitation will not occur at that depth and speed.

There are now (1955) in existence a considerable amount of data, and in time there will be more, which give by inspection the critical cavitation numbers σ_{CR} for the onset of cavitation on a variety of body forms, as well as the shapes and positions of the cavities to be expected at different cavitation numbers. A set of the first, applying to symmetrical hydrofoils, is given in Fig. 47.D of Sec. 47.5; a few of the second are shown in Fig. 47.E of Sec. 47.6.

47.5 The Prediction of Cavitation on Hydrofoils and Blades. Using the procedure described in the preceding section, it is possible to determine, from a knowledge of the cavitation number for a certain set of operating conditions and an inspection of the pressure-coefficient curves for any body, such as those illustrated and referenced in Sec. 44.8, whether or not cavitation is liable to occur, and where it will be found along the body surface. One has only to look for locations on the body where the pressure coefficient $-\Delta p/q$ is greater numerically than the cavitation number $\sigma = (p_\infty - e)/q$. For example, if the R.A.F. 30 section of Fig. 44.G, running at an angle of attack of 7 deg, is placed in a region where the cavitation number is only 2.0, it may be expected to cavitate on the upper or $-\Delta p$ surface directly abaft the nose.

For certain symmetrical or asymmetrical hydro-

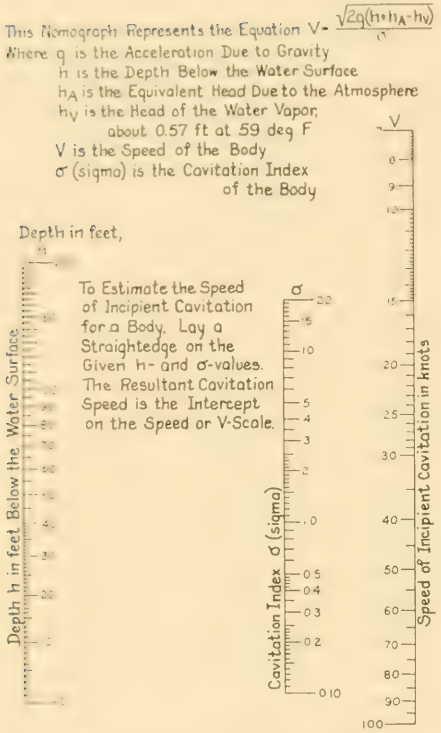

FIG. 47.B NOMOGRAM FOR RELATING SUBMERGENCE DEPTH, CAVITATION INDEX, AND WATER SPEED FOR INCIPIENT CAVITATION

Since incipient cavitation is involved, the cavitation index indicated here is the critical value. From the relation $\sigma = (p_\infty - e)/(0.5\rho V^2)$, the critical value diminishes as the water speed increases. From Sec. 47.5 and Fig. 47.D, the pressure coefficient E_n must diminish numerically with σ_{cR} to avoid cavitation.

foil sections, including many of those used for propeller blades, and for an infinite span, it is possible to calculate the ratio U/U_∞ for all parts of the surface. From this ratio it is possible to determine the pressure coefficient or Euler number E_n at any point, and hence the absolute pressures at all points for any given set of undisturbed-velocity and initial-pressure conditions. Absolute pressures approaching the vapor pressure e of the liquid are indications of incipient cavitation.

Calculations for a great number and a wide variety of hydrofoil sections, already made, are listed in NACA Report 824, referenced in Sec. 44.3.

Any hydrofoil section, no matter how well shaped it may be for straight-ahead flow, cavitates when it makes too great an angle with the incident flow. The excessive angle of attack for a lifting foil may be either positive or negative.

In general it may be said that for any hydrofoil section designed to produce lift, the best shape is one which, under the angle of attack to be expected in service, produces a distribution curve of $-\Delta p$ on the back that has the maximum spread of the greatest reduced pressure across the chord, without an excessively low depression.

The technical literature contains data derived from a limited number of cavitation tests made on hydrofoils under 2-diml flow conditions. A typical result, set down graphically in Fig. 47.C

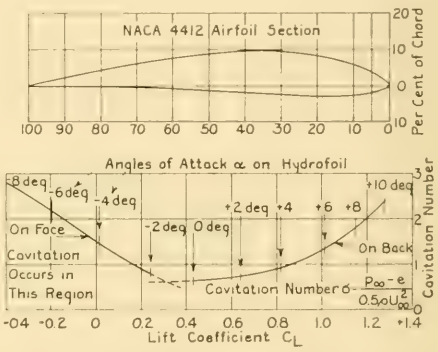

FIG. 47.C CAVITATION LIMITS FOR LIFT COEFFICIENT AND ANGLE OF ATTACK ON A TYPICAL HYDROFOIL

[Daily, J. W., ASME, Jour. Appl. Mech., 1949, Vol. 71, p. 269], shows that at negative angles of attack cavitation generally occurs on the face and at positive angles of attack on the back. There is usually a single angle of attack at which cavitation occurs simultaneously on both surfaces if the cavitation index is reduced to a sufficiently low number. A diagram similar to that referenced, except that it is derived by an analytic procedure for a whole screw propeller, is given by J. F. Shannon and R. N. Arnold [IESS, 1938–1939, Vol. 82, Fig. 18, p. 285].

As is the case for the lift, drag, and moment data on hydrofoils, described and presented in Sec. 44.3, the cavitation test data are of limited design application unless accompanied by section drawings or tables of coordinates of the foil. If it is possible to know also the chordwise pressure

distribution across the $-\Delta p$ side for some representative angle of attack, so much the better.

Taking a representative case, assume a hydrofoil similar to that diagrammed in Fig. 47.C to be running in salt water at a depth of 8 ft below the surface and at a speed of advance of 30 kt, or 50.67 ft per sec. The hydrostatic pressure is, from Tables 41.e or X3.a, 8(0.4447) = 3.56 psi. Assuming a value of p_A of 14.7 lb per in^2, a vapor pressure of 0.4 lb per in^2 and a mass density ρ of 1.9905 slugs per ft^3, the cavitation index works out as

$$\sigma = \frac{p_\infty - e}{q} = \frac{[(3.56 + 14.7) - 0.4]144}{0.99525(50.67)^2} = 1.006.$$

From the lower diagram of Fig. 47.C it is to be noted that at this cavitation parameter the hydrofoil will cavitate on the face or on the back at angles of attack greater numerically than -2.7 or $+4.5$ deg, respectively.

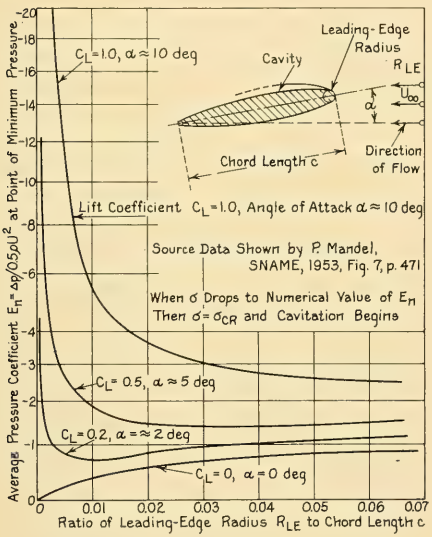

Fig. 47.D Cavitation, Lift-Coefficient, and Angle-of-Attack Data for a Symmetrical Hydrofoil

Fig. 47.D, adapted from a set of graphs given by P. Mandel [SNAME, 1953, Fig. 7, p. 471], gives the average pressure coefficient E_n, at the point of minimum absolute pressure, for a large number of 2-diml symmetrical hydrofoils at four different angles of attack. The E_n-values are plotted on a basis of the 0-diml ratio of the nose radius R_{LE} to the chord length c.

If the cavitation number σ in the adjacent liquid is smaller numerically than the pressure coefficient E_n at the point of minimum absolute pressure on the hydrofoil, cavitation occurs there, hence the pressure coefficient at the lowest-pressure point equals numerically the critical cavitation number σ_{CR}.

As an example of the manner in which the diagrams of Fig. 47.D may be used, consider the situation at the leading edge of a symmetrical streamlined balanced rudder with an all-movable blade. The rudder lies abaft a portion of the upper blade of a screw propeller where the rotational- or tangential-flow component is such as to cause the water in the inflow jet to meet the leading edge of the rudder at a given waterline at an angle of 10 deg. Assume a nose radius of 0.25 ft, a chord length of 10 ft, a nominal depth of submergence h of 15 ft, and a ship speed of 18 kt (actually, the local velocity in the outflow jet may be greater than this). Then from the nomogram of Fig. 47.B the cavitation number σ is about 3.3 if cavitation is to begin at 18 kt. The ratio of nose radius R_{LE} to chord length c is $0.25/10 = 0.025$. From the curve for a 10-deg angle of attack in Fig. 47.D the pressure coefficient E_n at the point of lowest absolute pressure, where cavitation will first appear, is about -3.2. Then σ_{CR} is 3.2, and the differential pressure available to create a gradient which will cause the water to follow the rudder section closely is represented by a cavitation number of only 3.3. The "lee" or $-\Delta p$ side of the rudder section in question is, therefore, just on the verge of cavitation at the given speed.

Contours for pressure minima in terms of (1) $\Delta p/q$, (2) thickness ratio, and (3) lift coefficient, for ogival and airfoil sections, respectively, are given by K. E. Schoenherr [SNAME, 1934, Figs. 19–20, pp. 109–112]. These sections are suitable for use on propeller blades.

47.6 Cavitation Data for Bodies of Revolution and Other Bodies. Cavitation may take place on many parts of a ship and its appendages which do not even remotely resemble the hydrofoils discussed in the preceding section. A considerable number of these parts have the forms of bodies of revolution, or they can be simulated by 3-diml axisymmetric forms, such as certain types of bulbs incorporated into the forefoot.

Cavitation data are available for a great

variety of leading ends of cylindrical bodies, tested in a variable-pressure water tunnel at zero yaw angle. The principal source of these data, "Cavitation and Pressure Distribution: Head Forms at Zero Angle of Yaw," by H. Rouse and J. S. McNown [State Univ. Iowa Studies in Eng'g., Bull. 32, 1948], gives the magnitude and the meridional-distance distribution of pressure coefficient about a series of fourteen head shapes, covering most practical applications. In addition there are recorded the shapes, axial positions, and dimensions of the cavities or of the envelopes ("pockets") of the regions in which vapor bubbles were formed around the bodies carrying these heads.

Diagrams 1, 2, and 3 of Fig. 47.E give the cavitation "pocket" data for a hemispherical head, a 1-caliber ogival head, and an ellipsoidal head having a major-axis to minor-axis ratio of 2, adapted from the referenced report. The several curved lines represent the boundaries of axial sections through the cavitation regions on one side of the head and body, for each of a series of cavitation numbers σ. The meridional positions of these "pockets" and the cavitation numbers belonging to them correspond to the horizontal lower flat portions or "bottoms" of the pressure-distribution curves drawn on pages 49 through 64 of the reference, for the given cavitation numbers. A regular pressure-distribution curve or, more exactly, a curve of pressure coefficient on meridional distance with no flat bottom, indicates no visible cavitation for that condition. Broken lines at the trailing ends of the cavity regions of Fig. 47.E indicate indefinite "pocket" outlines.

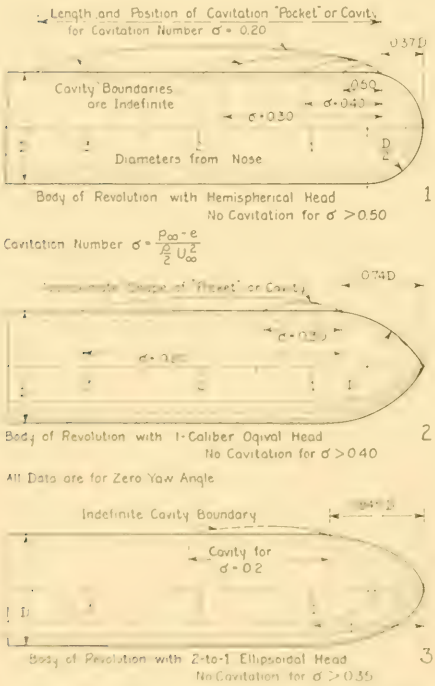

Fig. 47.E Cavitation Indexes for Three Types of Axisymmetric Heads

The calculated and observed speeds for the onset of cavitation around a rather wide variety of 2-diml and 3-diml bodies when submerged in water are given by H. B. Freeman in TMB Report 495, November 1942. A few of these are pure bodies of revolution, others are 2-diml cylinders having a wide variety of section shape, while still others are combinations of the two, with the axisymmetric body attached to the lower end of a streamlined strut.

47.7 The Effect of Cavitation on Screw-Propeller Performance. The typical characteristic curves of a model screw propeller, derived from tests under cavitating conditions in a variable-pressure water tunnel, exhibit a pronounced falling off of thrust coefficient K_T and torque coefficient K_Q as the values of the advance coefficient J decrease and as the cavitation becomes more severe. This is equivalent to saying that the thrust and torque of a cavitating propeller drop with increase in real-slip ratio, slowly at first and then more and more rapidly. This situation applies to the range of advance coefficient in which a normal ship or motorboat propeller operates. It does not necessarily apply to operation in the supercavitating range, mentioned in Sec. 47.12. The decrease in K_T is greater than in K_Q, so the efficiency η(eta) likewise diminishes.

As the cavitation number is reduced, there is a progressive reduction in the numerical values of all three 0-diml characteristics, exhibited in the typical cavitation characteristic curves of Fig. 47.F. The manner in which cavitation enlarges in extent and spreads over a screw-propeller blade as the advance coefficient J is reduced, or as the real-slip ratio s_R is increased, is shown by L. P. Smith in his paper "Cavitation on Marine Propellers" [ASME, Jul 1937, Vol. 59, pp. 409–431;

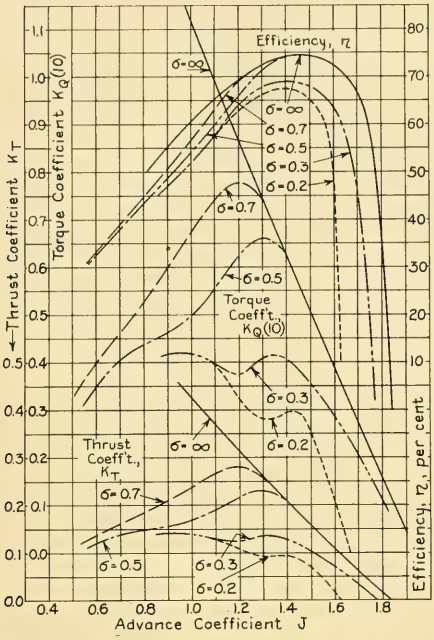

Fig. 47.F Typical Open-Water Test Data For a Model Propeller, Carried into the Cavitating Range

also Vol. 60, pp. 448–452], and by L. C. Burrill and A. Emerson on pages 140–147 of reference (7) following.

The technical literature contains a considerable number of cavitation characteristic curves for screw propellers, among which may be listed the following:

(1) Schoenherr, K. E., PNA, 1939, Vol. II, Fig. 32, p. 182
(2) Taylor, D. W., S and P, 1943, Fig. 143, p. 116
(3) Edstrand, H., "The Effect of the Air Content of Water on the Cavitation Point and Upon the Characteristics of Ships' Propellers," SSPA Rep. 6, 1946
(4) Rouse, H., EH, 1950, Fig. 63, p. 930. These are typical curves only, for which no hydrofoil data or test conditions are given.
(5) "Comparative Cavitation Tests of Propellers," 6th ICSTS, 1951, published by SNAME, 1953, Figs. 16–19 on pp. 78–81; Figs. 23 and 24 on pp. 85–86
(6) Gawn, R. W. L., "Results to Date of Comparative Cavitation Tests of Propellers," SNAME, 1951, pp. 172–213. These give the results of "international" tests of selected model propellers in a number of variable-pressure water tunnels.
(7) Burrill, L. C., and Emerson, A., "Propeller Cavitation: Some Observations from 16 in. Propeller Tests in the New King's College Cavitation Tunnel," NECI, 1953–1954, Vol. 70, pp. 121–150, D185–D188; SBMEB, Apr 1954, Fig. 4, p. 284
(8) "Comparative Propeller Tests," 7th ICSH, SSPA Rep. 34, 1955, Figs. 1–7 on pp. 170–176 and Figs. 11–14 on pp. 180–183.

Although it is not yet (1955) standard practice, the characteristic curves of η, K_T, and K_Q of diagrams similar to that of Fig. 47.F should be accompanied by drawings or sketches showing the location of the cavitating regions on the blades (face or back or both), the type of cavitation encountered (bubble or sheet), and other features visible in a variable-pressure water tunnel, for each value of the cavitation index or for each set of test conditions. This is done for the 1937 ASME paper of L. P. Smith, referenced in Sec. 70.40; for the discussion by F. H. Todd of the V. L. Posdunine paper in INA, 1944; for the SSPA Report 6 by H. Edstrand; and for the L. C. Burrill and A. Emerson paper referenced in the preceding paragraph.

47.8 Photographing the Cavitation on Model and Full-Scale Propellers. The visual observation of cavitation on screw propellers when mounted by themselves in variable-pressure water tunnels, initiated by C. A. Parsons in the early 1900's and carried on extensively since the late 1920's, has now reached the stage where excellent instantaneous photographs can be taken and later reproduced in the technical literature. Many of these photographs are to be found in the more recent cavitation references listed in Sec. 47.13 at the end of this chapter.

Fortunately for the marine architect there are techniques and procedures, developed in the early 1950's, by which still and motion-picture photographs may also be made of full-scale ship screw propellers under operating conditions. These photographs are made through a transparent window in the shell near the propeller. The present availability and use of powerful artificial lighting dispenses with the former necessity of running the vessel in the sunshine and in the clear water which is usually found only in the open sea. The motion pictures are stroboscopic in nature so that they give the impression of a particular propeller blade standing still or moving slowly in the ahead or astern direction.

To facilitate subsequent analysis and for information during the observing periods the screw-propeller blades may be marked in advance with suitable identifying letters, numerals, and signs.

Examples of photographs of this kind are published by J. W. Fisher ["Photography at Sea of Ship Propeller Cavitation," NECI, 1951–1952, Vol. 68, pp. 19–30 and D-1 through D-8]. Other examples are embodied in a paper by A. F. Weeks, entitled "Ship Propeller Cavitation Patterns," presented at the NPL Symposium on Cavitation in September 1955 [SBSR, 3 Nov 1955, pp. 569–570].

It is to be expected that the instrumentation and procedures for making shipboard cavitation photographs on screw propellers will improve rapidly. This will provide the naval architect with extremely valuable data which may be studied and analyzed at leisure.

47.9 Propeller Cavitation Criteria. An analysis of the loss of thrust due to cavitation on ship propellers, when it first occurred on fast naval vessels some sixty or more years ago, led to the establishment of a criterion proposed by S. W. Barnaby, involving a maximum average unit loading on the propeller-blade area. The original figure employed was 11.25 lb per sq in, corresponding to a pressure coefficient (based upon atmospheric pressure) of 11.25 divided by 14.7, or approximately 0.765. This unit loading was subsequently raised by Barnaby to 13.0 lb per sq in, corresponding to a pressure coefficient based on atmospheric pressure of 0.884. In neither case was there any allowance made for the depth of submergence of the propellers. Subsequently, different criteria were proposed by D. W. Taylor, J. M. Irish, and others, based upon a limiting tip speed for any propeller, independent of- or related to the propeller loading but, as before, not a function of the depth of submergence or the associated speed of advance [Schoenherr, K. E., PNA, 1939, Vol. II, pp. 175–176].

In 1932 E. F. Eggert developed a set of relationships which enabled the propeller user or designer to predict, with reasonable accuracy, the rate of rotation or the blade-section velocity at which the propeller thrust would begin to fall off from cavitation effects ["Propeller Cavitation," SNAME, 1932, pp. 58–74]. Discussions of this relationship, embodying somewhat different combinations of variables, are found in:

(1) Schoenherr, K. E., PNA, 1939, Vol. II, p. 178
(2) Taylor, D. W., S and P, 1943, pp. 116–117
(3) Van Lammeren, W. P. A., RPSS, 1948, pp. 180–182.

Still later W. P. A. van Lammeren worked out a relationship between the two 0-diml ratios [$J/(\text{virtual } P/D)$] and [$\sigma_V(A_D/A_0)(\text{virtual } P/D)$] which is an excellent indicator of the point where the thrust breaks down on a screw propeller [De Groot, D., NSP Rep. 89; Schip en Werf; 6th ICSTS, 1951, published by SNAME, 1953, Fig. 30 and pp. 93–95]. When plotted in graph form this appears as the simple curve of Fig. 47.G. The graph is based on the tests of many model propellers, all of which give results remarkably close to the line, independent of the type of blade section. It is thus possible to predict, before carrying out cavitation tests on model propellers, the rate of rotation at which thrust breakdown will take place.

The indications given by the graph of Fig. 47.G are still sufficiently precise for engineering purposes if the actual or average P/D ratio is

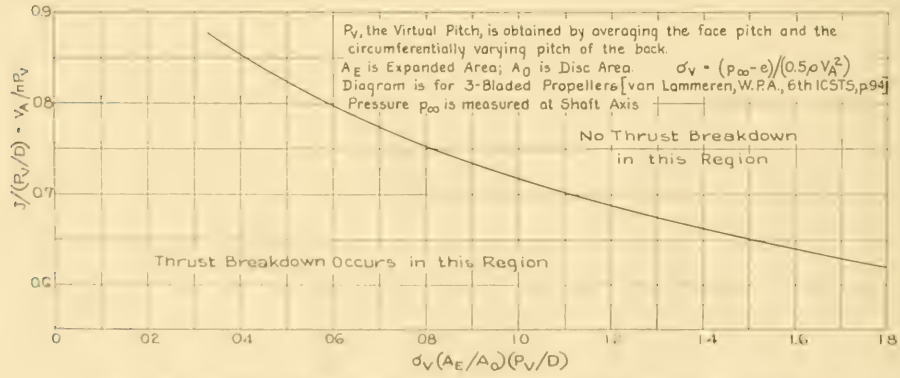

Fig. 47.G Netherlands Model Basin Cavitation Criteria for 3-Bladed Propellers

used in place of the virtual P/D, and if the expanded area A_E replaces the developed area A_D.

W. H. Bowers, of the TMB staff, devised a number of formulations whereby a quick approximation could be made by a ship designer of the rate of propeller rotation beyond which the thrust is affected by blade cavitation. One method of rapidly solving the equation given hereunder was a circular slide rule devised by Bowers and L. W. Sprinkle in 1947. It is not possible to describe the exact method here but the criterion employed by Bowers took the form, expressed in the symbols of this book:

$$n^2 = \frac{37{,}500(1 - s_R)^{2s_R}(h_A + h_H - h_V)\dfrac{\dfrac{c_M}{D}}{\dfrac{t_0}{D}}}{PD} \qquad (47.\text{ii})$$

where n is in rpm and all other linear dimensions are in ft.

To illustrate the application of this formula, take the case of the propeller designed for the ABC ship in Chap. 70 of Part 4, and shown in Fig. 78.L. The necessary basic data for the trial speed of 20.5 kt and for an assumed typical blade section at $0.8R_{\text{Max}}$ are as follows:

Real-slip ratio, s_R (actually s_{RT}), from Fig. 78.Nb	0.238	
Atmospheric-pressure head h_A, assumed	33.0	ft
Hydrostatic head at 12 o'clock blade position, h_H, equal to [26 − 10.5 − (0.8)10], for $0.8R_{\text{Max}}$	7.5	ft
Vapor-pressure head h_V, assumed	0.8	ft
Value of $(h_A + h_H - h_V)$ = (33.0 + 7.5 − 0.8)	39.7	
Mean-width ratio, c_M/D	0.211	
Blade-thickness fraction t_0/D, from Fig. 78.L	0.049	ft
Pitch P, assumed as $0.982D$ at $0.8R_{\text{Max}}$, from Fig. 78.L	19.64	ft
Diameter D	20.0	ft

Substituting in Eq. (47.ii)

$$n^2 = \frac{37{,}500(1 - 0.238)^{2(0.238)}(39.7)\left(\dfrac{0.211}{0.049}\right)}{(19.64)20}$$

$$= 14{,}399$$

whereupon n in rpm is 119.7. This is well above the expected rate of rotation of 97.2 rpm from Sec. 70.26.

47.10 Predicting Hub Cavitation and Hub Vortexes or Swirl Cores. The phenomenon of cavitation abaft a rotating screw-propeller hub, and the production of hub vortexes or swirl cores, are discussed and illustrated in Sec. 23.14 on pages 337–339 of Volume I. This is an important feature of the behavior of high-speed vessels because of the damaging effect of this cavitation upon appendages which lie in its path.

Within the period 1945–1955 it has been possible to produce and to photograph cavitation of this type in variable-pressure water tunnels, circulating-water channels, and model basins. It appears from observation of model propellers at atmospheric pressure in the latter two types of facility that the hub vortex is a rather unstable affair, appearing and disappearing with apparently no change in test conditions. There is reason to believe that it is far more stable in the full scale.

On the basis of the swirl-core theory of Višković it should eventually be possible to predict the presence of a swirl core and its approximate diameter behind the taper end of the hub fairing of a screw propeller. Assuming that it is possible to impart to the water in contact with the outside of the hub, in way of the blade, a tangential velocity equal to that of the hub surface, the resulting centrifugal force at a smaller radius R may be balanced against the probable vapor and gas pressure in the water. For propeller hubs not deeply submerged in sea water this lower limit may be taken as somewhere between 0.5 and 1.0 lb per sq in. The ambient pressure p_∞ is the atmospheric pressure p_A existing at the time plus the hydrostatic pressure p_H to the shaft axis, measured to the *actual* water (wave) surface over the wheel.

The equation of motion of a water particle in a vortex coil, whirling around a vortex core, is

$$\frac{1}{\rho}\frac{\partial p}{\partial R} = \frac{U^2}{R}$$

where U is the local velocity and R is the local radius [Eisenberg, P., TMB Rep. 712, Jul 1950, pp. 4–5; FHA, 1934, pp. 213–214]. From this there may be derived the relationship

$$p \text{ at center of vortex core} = p_\infty - \frac{\rho\Gamma^2}{4\pi^2 R_0^2} \qquad (47.\text{iii})$$

where Γ(capital gamma) is the circulation in the vortex coil, surrounding the core, p_∞ is the ambient pressure in the undisturbed liquid at the same depth as the center of the core, and R_0 is the

outer radius of the vortex core and the inner radius of the vortex coil.

Prediction of the existence of a hub cavity or swirl core and its size by the root-vortex method may be found considerably more difficult. It involves a knowledge—or an estimate—of the circulation at the root sections or of the pressure differences between the face and back of a blade. It should include any additional effect of interference between adjacent blades.

Although the data on the longitudinal extent of a swirl core are somewhat meager it may be assumed from past observations on models and ships that the core persists for at least several propeller diameters. This means that it will be present in the vicinity of any other part of the ship likely to be placed abaft the shaft axis and the propeller.

The swirl core usually comes off the hub fairing in line with the propeller axis but it is often offset from the trailing end of a blunt hub. Whatever may be its exact position, it swings rapidly into the line of the adjacent flow when this is not parallel in direction to the shaft axis. The diameter of the swirl core is increased if air gets into it.

47.11 Prediction of Cavitation Erosion. The results of metallurgical investigations and tests to date indicate that the materials which are most resistant to cavitation erosion are solid-solution alloys which have, in metallurgical parlance, only a single phase. Single-phase alloys have much narrower grain boundaries than polyphase alloys. Many corrosion-resisting steels are austenitic alloys of this type; among them the 13Cr-87Fe alloy is a good example.

A metal intended to resist erosion by cavitation should have high resistance to liquid corrosion, under the conditions in which it is to be used, as well as high fatigue strength [Boetcher, H. N., "Failure of Metals Due to Cavitation Under Experimental Conditions," Trans. ASME, HYE-58-1, Vol. 58, Jul 1936, pp. 355–360].

Numerous tests of a wide variety of materials have indicated a definite superiority in resistance to cavitation erosion on the part of certain alloys. A brief list of these alloys, with references to the published test data, is given in Sec. 70.45. In one series of tests [Stewart, W. C., and Williams, W. L., "Investigation of Materials for Marine Propellers," ASTM, 1946, Vol. 46, pp. 836–845] the best all-around material was found to be a 66.14 nickel- 28.10 copper- 3.65 silicon alloy.

There has recently been issued a paper entitled "A Review of Published Information on Cavitation Erosion," [Admiralty Corrosion Committee Rep. ACC/26/54, N151/54, N316/54 (C.M.L. Report RBS)], stamped 8 October 1954. On pages 25–27 there are listed 56 references in the technical literature. The report is in five parts:

I Historical Introduction
II Theories of Cavitation Erosion
III Factors Affecting Cavitation Erosion Intensity
IV Methods of Testing
V Erosion Resistances of Various Materials.

Tables VIII and IX list many alloys in a scale of relative resistance to cavitation erosion in fresh and sea water, respectively.

Cast-steel blades with corrosion-resisting steel cladding have been used with success in propeller-type turbines of water-power plants [ASNE, Nov 1946, pp. 547–549] but this type of construction has been found not too successful on ship appendages, perhaps because of inadequate attachment to the ferrous material underneath, and perhaps because of harmful galvanic action between the steel cladding and adjacent bronze propellers.

Good design and construction requires the greatest practicable initial smoothness of all surfaces likely to be exposed to cavitation attack. Any projecting irregularity, including definite waviness of a surface, may be expected to initiate cavitation if the pressures in the region approach the vapor pressure of water. This is one important reason why the curved backs of propeller blades and hydrofoil surfaces should, if anything, be more regular and more smooth than the faces. Erosion of the surface may be expected to occur well downstream from a pronounced change in shape of the solid surface. Nicks and turned-over regions along a leading edge are notorious offenders in this respect. A sharp, deep nick in the leading edge may leave a trail of erosion at the radius of the nick, extending irregularly all the way across the blade.

Pits and depressions in a surface, not forming a part of the waviness previously mentioned, appear to have much less initial effect than corresponding projections. However, holes through the blades, such as are sometimes drilled for handling purposes, permit jets of water to squirt through from the face to the back. The discontinuities thus formed in the flow may often be as damaging as a solid projection in place of the hole.

47.12 Propeller Performance Under Supercavitation. The general aspects of the perform-

ance of screw propellers in the supercavitating range are described in Sec. 70.40 of Part 4. The design comments given there are likewise general in nature.

While the references of that section contain data relative to the variation in propeller thrust at high rates of rotation, there are no systematic data which permit the ship or propeller designer to make reliable predictions of supercavitation performance for high-power and high-speed craft.

47.13 Selected Cavitation Bibliography. The published literature on all phases of cavitation in liquids, including cavitation erosion, is almost staggering in its immensity. In December 1947 the David Taylor Model Basin prepared and issued, as TMB Report R-81, "An Annotated Bibliography of Cavitation." This contains references to most of the material published up to that time, especially that relating directly to work in the marine field. Some important papers not listed, and some published since 1947 have either been referenced previously in this chapter or are set down here. These apply to material in Chaps. 7 and 23 as well as to that in this chapter and in Chap. 70 of Part 4.

The first three references help to fill out the historical picture:

(1) Reynolds, Osborne, "On the Causes of the Racing of the Engines of Screw Steamers," INA, 1873, pp. 59–60

(2) Normand, J.-A., "Note sur l'Influence de l'Immersion de l'Hélice et de la Vitesse sur la Rupture du Cylindre d' Eau Actionné (Note on the Influence of Propeller Immersion and Speed on the Rupture of Water in the Propeller Stream)," ATMA, 1893, Vol. 4, pp. 68–73

(3) Thornycroft, J. I., and Barnaby, J. W., "Torpedo Boat Destroyers," ICE, Vol. CXXII, Part IV, 1894–1895, p. 51ff

(4) Wood, R. McK., and Harris, R. G., "Some Notes on the Theory of an Airscrew Working in a Wind Channel," ARC, R and M 662, 1920

(5) Brodetsky, S., "Discontinuous Fluid Motion Past Circular and Elliptic Cylinders," Proc. Roy. Soc., London, Ser. A, Feb 1923, Vol. 102, No. A718, pp. 542–553

(6) Mueller, J., "Über den gegenwartigen Stand der Kavitationsforschung (On the Present Status of Cavitation Research)," Die Naturwissenschaften, Jun 1928, Vol. 22, pp. 423–426

(7) Taylor, G. I., "The Mean Value of the Fluctuations in Pressure and Pressure Gradient in a Turbulent Fluid," Proc. Camb. Phil. Soc., 1936, Vol. 32, pp. 380–384

(8) Van Iterson, F. K. T., "Cavitation et Tension Superficielle (Cavitation and Surface Tension)," Proc. Roy. Acad., Amsterdam, 1936. Abstracted in Engineering (London), 1936, Vol. 142, p. 95ff. Translated by E. F. Wilsey, U. S. Bureau of Reclamation, Nov 1936.

(9) Bottomley, W. T., "Flow of Boiling Water Through Orifices and Pipes," NECI, 1936–1937, Vol. 53, p. 65ff

(10) Green, A. E., "The Mean Value of the Fluctuations in Pressure and Pressure Gradient in a Turbulent Fluid," Proc. Camb. Phil. Soc., 1938, pp. 534–539

(11) Višković, I., "Rotation Losses at the Rear of Turbo-Machine Runner Wheels," Escher Wyss News, 1941, Vol. XIV, pp. 14–19

(12) Freeman, H. B., "Calculated and Observed Speeds of Cavitation About Two- and Three-Dimensional Bodies in Water," TMB Rep. 495, Nov 1942

(13) Edstrand, H., "The Effect of the Air Content of Water on the Cavitation Point and upon the Characteristics of Ships' Propellers," SSPA, Rep. 6, 1946

(14) Harvey, E., McElroy, W. D., and Whiteley, A. H., "On Cavity Formation in Water," Jour. Appl. Phys., Feb 1947, Vol. 18, pp. 162–172

(15) Briggs, H. B., Johnson, J. B., and Mason, W. P., "Properties of Liquids at High Sound Pressures," Bell Tel. Lab. Monograph B-1507, publ. in Jour. Acoust. Soc. America, Jul 1947, Vol. 19, pp. 664–677

(16) Dieudonné, J., "Résultats Obtenus à la Mer avec des Hélices en Régime de Cavitation (Results from Sea Trials with Propellers Operating in the Cavitating Region)," ATMA, 1947, Vol. 46, pp. 253–270. The data were taken on various torpedoboats and destroyers at high speed.

(17) Walchner, O., "Contribution to the Design of Ship Propellers without Cavitation," AVA, 1947

(18) Vennard, J. K., "Elementary Fluid Mechanics," 1947, pp. 329–332

(19) Bell, L. G., "Some Model Experiments on the Effect of Blade Area on Propeller Cavitation," INA, 1948, Vol. 90, pp. 79–91. There are some good cavitation photographs opp. pp. 86–87.

(20) Eisenberg, P., "A Cavitation Method for the Development of Forms Having Specified Critical Cavitation Numbers," TMB Rep. 647, Sep 1947

(21) Macovsky, M. S., Stracke, W. L., and Wehausen, J. V., "Predicted Cavitation Characteristics for the TMB-EPH Strut Section Compared with Those for the Bureau of Ships Standard Strut Section," TMB Rep. 879, Jan 1948

(22) Plesset, M. S., and Shaffer, P. A., "Drag in Cavitating Flow," Rev. Mod. Phys., Jan 1948, Vol. 20, pp. 228–231

(23) Rouse, H., and McNown, J. S., "Cavitation and Pressure Distribution; Head Forms at Zero Angle of Yaw," IIHR, Studies in Eng'g., Bull. 32, 1948

(24) Knapp, R. T., and Hollander, A., "Laboratory Investigations of the Mechanism of Cavitation," Trans. ASME, Jul 1948, Vol. 70, pp. 419–435

(25) Gawn, R. W. L., "Cavitation of Screw Propellers," NECI, 1948–1949, Vol. 65, pp. 339–373, D105–D124

(26) Eisenberg, P., and Pond, H. L., "Water Tunnel Investigations of Steady State Cavities," TMB Rep. 668, Oct 1948

(27) Blake, F. G., Jr., "The Onset of Cavitation in Liquids," Acoustics Res. Lab., Harvard Univ., Tech. Rep. 12, Sep 1949

(28) Crump, S. F., "Determination of Critical Pressures for the Inception of Cavitation in Fresh and Sea Water as Influenced by Air Content in the Water," TMB Rep. 575, Oct 1949

(29) Schneider, A. J. R., "Some Compressible Effects in Cavitation Bubble Dynamics," Doctoral dissertation, Cal. Inst. Tech., 1949

(30) Eisenberg, P., "On the Mechanism and Prevention of Cavitation," TMB Rep. 712, Jul 1950. This report contains, on pp. 63–70, a list of about one hundred of the principal references on the subject.

(31) Rouse, H., "Engineering Hydraulics," 1950, pp. 29–31

(32) Birkhoff, G., "Hydrodynamics," Princeton Univ. Press, 1950

(33) Konstantinov, W. A., "Influence of the Reynolds Number on the Separation (Cavitation) Flow," TMB Transl. 233, Nov 1950

(34) Birkhoff, G., Plesset, M., and Simmons, N., "Wall Effects in Cavity Flow—I and II," Quart. Jour. Math., Part I, Jul 1950, Vol. VIII, pp. 151–168; Jan 1952, Vol. IX, pp. 413–421

(35) Rattray, M., Jr., "Perturbation Effects in Bubble Dynamics," CIT Doctoral dissertation, issued as a CIT Hydrodyn. Lab. report under ONR Contract N6onr-24420 (NR-062-059), (undated but issued in 1951)

(36) Crump, S. F., "Critical Pressures for the Inception of Cavitation in a Large-Scale Numachi Nozzle as Influenced by the Air Content of the Water," TMB Rep. 770, Jul 1951

(37) 6th Int. Conf. Ship Tank Supts., Washington, 1951, published by SNAME, 1953, Subject 3, "Comparative Cavitation Tests of Propellers," pp. 75–97

(38) Gawn, R. W. L., "Results to Date of Comparative Cavitation Tests of Propellers," SNAME, 1951, pp. 168–216

(39) Shalnev, K. E., "Cavitation of Surface Roughnesses," Jour. Theor. Physics, U.S.S.R., 1951, Vol. 21, pp. 206–220 (in Russian)

(40) Trilling, L., "The Collapse and Rebound of a Gas Bubble," Jour. Appl. Phys., Jan 1952, Vol. 23, pp. 14–17

(41) Gilmore, F. R., "The Growth or Collapse of a Spherical Bubble in a Viscous Compressible Liquid," CIT Hydr. Lab. Rep. 26–4, 1 Apr 1952

(42) Kermeen, R. W., "Some Observations of Cavitation on Hemispherical Head Models," CIT Hydro. Lab. Rep. E-35.1, Jun 1952

(43) Waeselynck, R., "Calcul de la Poussée de l'hélice en régime Cavitant (Calculation of the Thrust of Cavitating Propellers)," ATMA, 1952, Vol. 51, pp. 365–388. On page 382 there is a list of 10 references, some of them not given here.

(44) Garabedian, P. R., Lewy, H., and Schiffer, M., "Axially Symmetric Cavitational Flow," Appl. Math. and Statistics Lab., Tech. Rep. 10, Stanford Univ., 25 Apr 1952

(45) Parkin, B. R., "Scale Effects in Cavitating Flow," CIT Hydro. Lab. Rep. 21–8, 31 Jul 1952

(46) Gilbarg, D., "Uniqueness of Axially Symmetric Flows with Free Boundaries," Jour. Rational Mech. and Analysis, Apr 1952, Vol. 1, No. 2

(47) Serrin, J. B., Jr., "Existence Theorems for Some Hydrodynamical Free Boundary Problems," Jour. Rational Mech. and Analysis, Jan 1952, Vol. 1, No. 1

(48) Harrison, M., "An Experimental Study of Single Bubble Cavitation Noise," TMB Rep. 815, Nov 1952, revised edition

(49) Knapp, R. T., "Cavitation Mechanics and its Relation to the Design of Hydraulic Equipment," IME, James Clayton Lecture, 1952, Vol. 166, pp. 150–163

(50) Olson, R. M., "Cavitation Testing in Water Tunnels," St. Anthony Falls Hydr. Lab. Project Rep. 42, Dec 1954. There is a bibliography of 16 items on pp. 31–32.

(51) Burrill, L. C., and Emerson, A., "Propeller Cavitation: Some Observations from 16 in. Propeller Tests in the New King's College Cavitation Tunnel," NECI, 1953–1954, Vol. 70, Part 2, pp. 121–150, D185–D188. There are photographs of hub vortexes or swirl cores abaft model propeller hubs in Figs. 17(a) and 17(b) on p. 149; also cavitation photographs of model propellers on pp. 149–150.

(52) Tulin, M. P., "Steady Two Dimensional Cavity Flows About Slender Bodies," TMB Rep. 834, May 1953

(53) Eisenberg, P., "A Brief Survey of Progress on the Mechanics of Cavitation," TMB Rep. 842, Jun 1953, revised edition; pp. 21–24 contain a list of 44 references

(54) Numachi, F., "Cavitation Tests on Hydrofoils in Cascade," ASME, Oct 1953, Vol. 75, pp. 1257–1269

(55) Knapp, R. T., "Present Status of Cavitation Research," Mech. Eng'g., Sep 1954, Vol. 76, pp. 731–734; ASME, Feb 1955, pp. 44–50. On p. 50 of the latter reference there is a bibliography of six items.

(56) Knapp, R. T., "Recent Investigations of the Mechanics of Cavitation and Cavitation Damage," ASME paper 54-A-106, presented in November-December 1954 (copy in TMB library). The paper describes experiments in a variable-pressure water tunnel in which a torpedo-shaped model, run under cavitating conditions, was surrounded by a rather large annular cavity just abaft the forward shoulder. At water speeds above a certain minimum this cavity was filled (or partly filled) periodically with a reversed or reentrant flow rushing forward as a thin sheet next to the model surface. In other words, the cavity accompanying the normal form of sheet cavitation was not a steady-state affair, even in its forward and middle portions, because of the water which alternately rushed forward into it from the downstream end of the cavity and was then swept away. Cavitation erosion on the aluminum model occurred under the region covered by the periodically advancing and retreating reentrant flow. The author lists 15 references on p. 12.

(57) Kermeen, R. W., McGraw, J. T., and Parkin, B. R., "Mechanism of Cavitation Inception and the Re-

lated Scale-Effects Problem," Trans. ASME, May 1955, Vol. 77, pp. 533–541; a review of this paper is to be found in Appl. Mech. Rev., Jan 1956, p. 29

(58) Daily, J. W., and Johnson, V. E., Jr., "Turbulence and Boundary Layer Effects on the Inception of Cavitation from Gas Nuclei," MIT Hydro. Lab. Techn. Rep. 21, Jul 1955. On pp. 63–65 there is a bibliography of 38 items; most of those relating directly to cavitation are included in the list of the present section.

(59) On 14–17 September 1955 there was held at the National Physical Laboratory, Teddington, England, a symposium on cavitation in hydrodynamics. The authors and titles of the twenty-one papers presented during this symposium are given in SBSR, 25 Aug 1955, pp. 255–256. The subjects considered were:

(1) Factors governing cavitation inception
(2) Experiment techniques
(3) Scale-effect factors
(4) Effects on hydrodynamic performance
(5) Cavitation damage.

The complete proceedings are to be found in a volume issued by the NPL, Teddington, entitled "Cavitation in Hydrodynamics," H. M. Stationery Office, London, 1956.

(60) Tulin, M. P., "Supercavitating Flow Past Foils and Struts," NPL, Teddington, Symp. on Cavitation in Hydrodynamics, Sep 1955; abstracted in SBSR, 3 Nov 1955, pp. 570–571

(61) Burrill, L. C., "The Phenomenon of Cavitation," Second Nav. Arch. Congr., Trieste, 14–16 May 1955; published in Int. Shipbldg. Prog., 1955, Vol. 2, No. 15, pp. 503–511. This paper contains some excellent photographs of cavitating model propellers, including one (Fig. 13) showing eddies leaving a blade trailing edge.

CHAPTER 48

Data on Theoretical Surface Waves and Ship Waves

48.1 Purpose of This Chapter. A brief description of surface and subsurface waves in liquids, illustrated with a number of diagrams, is given in Chap. 9 of Volume I. Chap. 10 discusses waves and wavemaking around schematic ship forms.

Although the general and detailed discussion of wavegoing is embodied in Part 6 of Volume III of the book, it is convenient for a reader who uses the present volume for reference purposes to have available here certain theoretical and observed data on natural and ship waves.

48.2 Theoretical Wave Patterns on a Water Surface. The horizontal pattern of gravity waves, both divergent and transverse, set up abaft a pressure point moving at steady speed in a straight line over the surface of the water, is known as the Kelvin wave system. It is diagrammed in Fig. 10.B of Sec. 10.5 of Volume I. Many similar figures are published in standard reference works and textbooks [S and P, 1943, Figs. 36 and 37, p. 27]. The manner in which this geometric pattern is built up analytically and graphically is explained in Sec. 10.5 and illustrated in Figs. 10.C and 10.D. A. M. Robb shows part of this construction [TNA, 1952, Figs. 3.24, 3.25, and 3.26, pp. 58–59]. However, it has developed, as part of the analytic work on the calculation of the wavemaking resistance of ships, described in Chap. 50, that there is a definite phase difference between the divergent and the transverse waves of the system developed by a traveling pressure point. The transverse waves are shifted ahead of the positions previously predicted for them, so that a plan view of the crests in the revised schematic system has the appearance of the intersecting arcs of Fig. 48.A of Sec. 48.3, where this matter is discussed in greater detail. Actually, as indicated by Fig. 10.E of Sec. 10.6, the transverse wave crests in nature appear to be more nearly straight than curved. Further, the crest pattern for a given moving disturbance changes with water depth and other factors.

A ship represents a traveling group of many pressure disturbances. It has an entrance waterline slope i_E of sensible amount and a finite beam. It often has reverse curvature in the waterlines, either forward or aft, or both, and some shoulders forward of and abaft amidships.

Considerable interference may be expected between the diverging waves of the original or the revised Kelvin point-pressure system and a ship with its stem at the same point. Indeed, W. Hovgaard, D. W. Taylor, and others have noted wide, and as yet unexplained variations in the cusp-line angles with the theoretical value

of 19.47 deg for a traveling pressure point, as described in Sec. 10.6 on page 174 of Volume I [Hovgaard, W., INA, 1909, Vol. 51, table facing p. 260 and Pl. XXIV; Taylor, D. W., S and P, 1943, pp. 27–28].

48.3 Hogner's Contribution to the Kelvin Wave System. Owing to an apparent misunderstanding of the exact nature of a wave-pattern diagram which was published by Lord Kelvin in the papers referenced in Sec. 10.5 on page 170 of Volume I, the planform illustrated in Fig. 10.B of that section has for the past half-century been described in many text and reference books as the exact crest pattern developed by him. E. Hogner brought out, in the 1920's, the fact that the figure given by Kelvin showed only "the envelope curves of the crests of the two-dimensional waves from which he has constructed his three-dimensional waves" ["A Contribution to the Theory of Ship Waves," Arkiv för Matematik, Astronomi och Fysik, Stockholm, 1922–1923, Vol. 17, paper 12, footnote on p. 42]. Kelvin's mathematical formulas actually showed a phase difference at the boundary planes (marked "Line of Crest Intersections" in Fig. 10.B of Volume I) but this was apparently overlooked by most of those who worked in this field in the 1900's and 1910's, until Hogner brought it to light.

Depending upon the assumptions made and the approximations employed, Kelvin's earlier theory gives a phase difference, at the boundary planes lying at angles of 19.47 deg to the direction of motion of the traveling pressure point, of

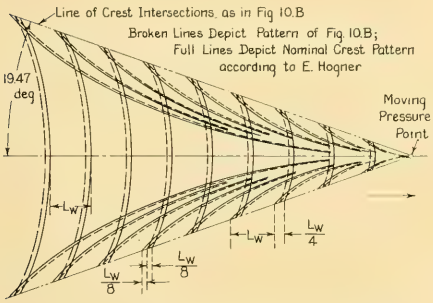

FIG. 48.A MODIFICATION OF KELVIN WAVE SYSTEM ACCORDING TO E. HOGNER

The Kelvin system, corresponding to that in Fig. 10.B of Volume I, is shown in broken lines. The modification according to Hogner, with the transverse waves ahead of the diverging waves, is indicated in solid lines.

$L_W/4$ between the crests of the transverse waves and those of the divergent waves. The crests of the former system lead the others, just as if there were a first transverse crest formed at a position $L_W/4$ ahead of the pressure point. A planform diagram of such a pattern, showing the variations from the Kelvin wave system of Fig. 10.B of this book, is given by Hogner, from which Fig. 48.A is adapted [Proc. First Int. Congr. Appl. Mech., Delft, 1924, Fig. 5, p. 149]. In a reworking of the entire analytic procedure, described by Hogner in the paper listed as the first reference in this section, he shows that the phase difference at the boundary planes is actually $L_W/3$, indicated in detail by his diagram in Fig. 17 on page 46 of that reference.

These same phase differences, although expressed as $2\pi/4$ and $2\pi/3$, are derived by J. K. Lunde [SNAME, 1951, p. 71]. In Fig. 6 of that reference he gives a diagram corresponding to the solid lines of Fig. 48.A.

E. Hogner carries his analytic procedure to the point where he predicts the nature of waves formed in the area beyond the boundary planes. He also substantiates his analytic derivation by photographs which reveal the patterns actually formed on the surface of the water.

48.4 Summary of the Trochoidal-Wave Theory. The notes which follow, adapted from G. C. Manning [PNA, 1939, Vol. II, pp. 6–7], summarize the relationships described and presented in Chap. 9. They are illustrated, as far as practicable, in the definition sketch of Fig. 48.B, which is the elevation of a wave having a steepness ratio h_W/L_W of 1:7.

The principal assumptions of the trochoidal-wave theory, satisfying the requirements of equilibrium, continuity, and uniformity of pressure, are:

(a) The motion is 2-diml, around circular orbits in a vertical plane

(b) The liquid particles revolve in circular orbits with uniform angular velocity ω(omega)

(c) The liquid particles at the crest move in the same direction as the wave is advancing

(d) There are equidifferent phase angles $d\theta$(theta) $= \omega\, dt$ between successive particles whose orbit centers lie at equidifferent distances dL_W along a given horizontal line

(e) Liquid particles whose orbit centers lie in the same vertical line rotate about those centers in the same phase

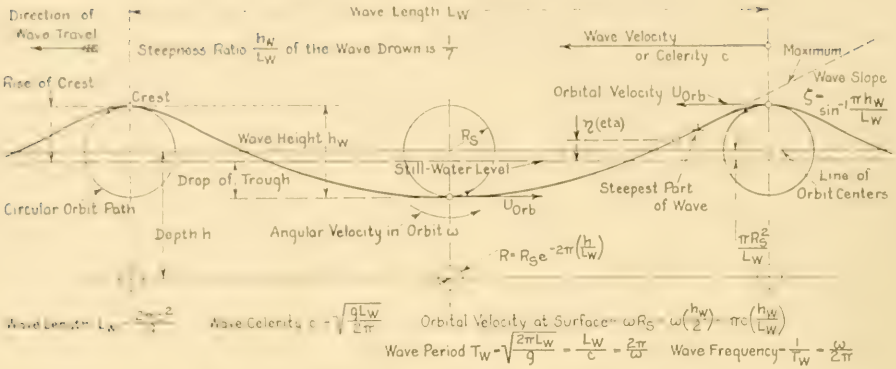

FIG. 48.B DEFINITION DRAWING FOR A TROCHOIDAL WAVE

(f) The depth of the liquid body is unlimited
(g) The liquid is ideal, without viscosity.

The results of principal interest are, based upon a wave length L_W, a wave celerity (velocity) c, a wave period T_W, a wave height h_W, a surface-particle orbit radius R_S, and an acceleration of gravity g for sea level at 45 deg latitude of 32.174 ft per sec^2 or 9.80665 m per sec^2:

(1) $L_W = 2\pi R_{RC}$, where R_{RC} is the radius of the rolling circle for the graphic trochoidal construction

(2) $$c = \sqrt{gL_W/2\pi}$$
$$= 2.263\sqrt{L_W}, \text{ in fps when } L_W \text{ is in ft}$$
$$= 1.249\sqrt{L_W}, \text{ in mps when } L_W \text{ is in m}$$
$$= 1.340\sqrt{L_W}, \text{ in kt when } L_W \text{ is in ft}$$
$$= 2.427\sqrt{L_W}, \text{ in kt when } L_W \text{ is in m.}$$
$$c = \frac{g}{2\pi}T_W$$
$$= 5.121T_W \text{ in fps}$$
$$= 3.032T_W \text{ in kt}$$
$$= 1.561T_W \text{ in m per sec.}$$

(3) $$T_W = \sqrt{2\pi L_W/g}$$
$$= 0.4419\sqrt{L_W}, \text{ in sec when } L_W \text{ is in ft}$$
$$= 0.8005\sqrt{L_W}, \text{ in sec when } L_W \text{ is in m.}$$
$$T_W = \frac{L_W}{c} = \frac{2\pi}{\omega}$$

(4) $$f = \text{Frequency} = \frac{1}{T_W} = \frac{\omega}{2\pi}$$

(5) $$L_W = 2\pi c^2/g$$
$$= 0.1953c^2, \text{ in ft when } c \text{ is in fps}$$
$$= 0.5571c^2, \text{ in ft when } c \text{ is in kt}$$
$$= 0.6407c^2, \text{ in m when } c \text{ is in mps}$$
$$= 0.1697c^2, \text{ in m when } c \text{ is in kt.}$$
$$L_W = gT_W^2/(2\pi)$$
$$= 5.121T_W^2, \text{ in ft when } T_W \text{ is in sec}$$
$$= 1.561T_W^2, \text{ in m when } T_W \text{ is in sec.}$$

(6) $$h_W = 2R_S \quad \text{and} \quad R_S = h_W/2$$

(7) The orbital velocity, as derived in Sec. 48.7, is

$$U_{Orb} = \pi h_W/(0.4419\sqrt{L_W}) = 7.109h_W/\sqrt{L_W}$$
$$= \pi c(h_W/L_W),$$

where U_{Orb} is in fps when h_W and L_W are in ft and c is in fps.

(8) The angular orbital velocity ω is, from (3) and (4) preceding, $2\pi/T_W$, or

$$\omega = \frac{2\pi}{\sqrt{\frac{2\pi L_W}{g}}} = \sqrt{\frac{2\pi g}{L_W}}$$

(9) The line of orbit centers of the surface particles is at the distance $\pi(h_W)^2/(4L_W) = \pi R_S^2/L_W = 0.7854(h_W)^2/L_W$ above the still-water level. At any depth h, where the orbit radius is R, the corresponding distance is

$$\frac{\pi R^2}{L_W} = \frac{R^2}{2R_{RC}}$$

(10) At a depth h below the surface, the radius R of the orbit centers at that depth is given by

$$R = R_S e^{-2\pi(h/L_W)}$$

By substituting $L_W = 2\pi R_{RC}$ this becomes

$$R = R_S e^{-h/R_{RC}}$$

When $h = L_W$, $R = R_S e^{-2\pi} = 0.0019 R_S$. Thus the orbital motion is virtually zero in water as deep as the wave is long, and for practical purposes the assumed unlimited depth is not necessary; see Table 48.f of Sec. 48.7.

(11) The total energy in the wave per unit breadth is approximately $0.125w(h_W)^2 L_W$. By this formula, a salt-water wave 600 ft long and 30 ft high has about 2,000 ft-tons of energy per ft of breadth.

(12) Of the total energy in the wave, half of it is potential energy and half kinetic energy.

(13) From the relationship

$$\text{Steepness ratio } \frac{h_W}{L_W} = \frac{2R_S}{2\pi R_{RC}} = \frac{h_W}{2\pi R_{RC}}$$

the rolling-circle radius $R_{RC} = h_W/[2\pi(\text{steepness ratio})]$. For a limiting steepness ratio of 1/7, as depicted in the diagram of Fig. 48.B,

$$R_{RC} = h_W/0.8976 = 1.114 h_W = 2.228 R_S.$$

(14) The value of the virtual acceleration of gravity is,

At the crest, $(R_{RC} - R_S)g/R_{RC}$
At any intermediate point, $R_I g/R_{RC}$
At the trough, $(R_{RC} + R_S)g/R_{RC}$.

For a limiting steepness ratio $h_W/L_W = 1/7$, the value of the first is $1.228g/2.228 = 0.55g$; of the last, $3.228g/2.228 = 1.45g$.

(15) The maximum slope of the wave surface is $\sin^{-1}(R_S/R_{RC})$ or, in radians, $\pi h_W/L_W$. It occurs at the point where the orbit radius R_S is normal to the radius R_I. For the same limiting steepness ratio of 1/7, where $R_{RC} = 2.228 R_S$, the sine in question is $1/2.228 = 0.4488$, whence the slope angle ζ(zeta) is about 26.7 deg, as compared to 30 deg for the highest possible Stokes irrotational wave of approximately the same steepness ratio.

As an example of the use of the data in the foregoing, an estimate is made of the characteristics of a trochoidal wave within the range of size and proportions listed for the operation of the ABC ship in item (24) of Table 64.d.

Assume that the ship would give its least comfortable performance when steaming nearly ahead into a regular train of waves having a length L_W of 1.2 times the length of the ship. Then $L_W = 1.2(L) = 1.2(510) = 612$ ft; $\sqrt{L_W} = 24.75$ ft.

The celerity c of this wave, reckoned with respect to the undisturbed water, is equal to $\sqrt{gL_W/2\pi} = 2.263\sqrt{L_W} = 2.263(24.75) = 56.01$ ft per sec. This is equivalent to 33.16 kt. For an angle of encounter α(alpha) of about 180 deg, representing a head sea, the speed of encountering the waves is this wave speed plus the speed of the ship, reckoned with respect to the undisturbed water.

The period T_W of this wave is $\sqrt{2\pi L_W/g} = 0.4419\sqrt{L_W}$ or $0.4419(24.75) = 10.94$ sec. The frequency f, corresponding to the number of wave crests which would pass a given point in space in 1 sec, is the reciprocal of the period or 0.0914 wave per sec.

The height h_W of the wave is fixed by the assumption made in item (24) of Table 64.d, which stated that the height would not exceed $0.55\sqrt{L_W}$. For the wave in question this is $0.55(24.75) = 13.61$ ft. The steepness ratio h_W/L_W is then $13.61/612 = 0.0222$ or 1: 45.

The velocity and period of this wave, as taken from the tables of Sec. 48.6, are listed in that section. Its maximum slope and orbital velocity are found in Secs. 48.5 and 48.7, respectively.

48.5 Elevations and Slopes of the Trochoidal Wave. Table 48.a gives the ordinates of a trochoidal wave surface in terms of the wave height h_W. The ordinates are spaced at equidistant

TABLE 48.a—ORDINATES FOR CONSTRUCTION OF A TROCHOIDAL WAVE PROFILE

The data listed here are from PNA, 1939, Vol. I, p. 207. The stations are spaced equally along the horizontal plane from crest to trough. The base line for ordinates is at the bottom of the wave trough.

Station Number	Ordinate, fractions of wave height h_W
0, Crest	1.000
1	0.982
2	0.927
3	0.839
4	0.720
5	0.577
6	0.421
7	0.266
8	0.128
9	0.034
10, Trough	0.000

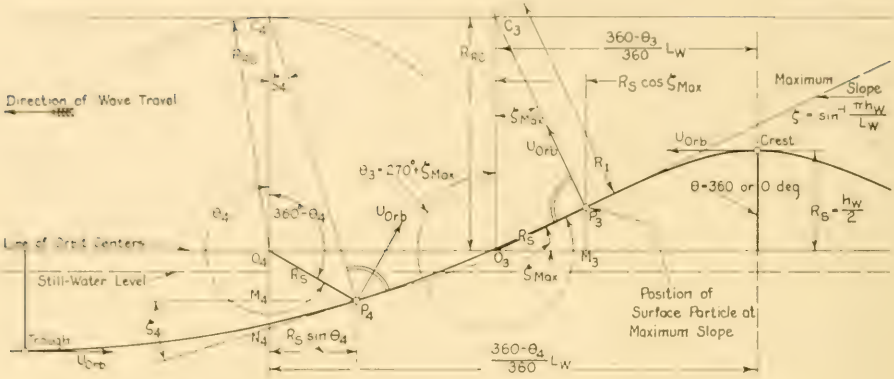

FIG. 48.C EXPLANATORY SKETCH FOR SURFACE SLOPES OF A TROCHOIDAL WAVE

intervals along the horizontal plane between the crest and the trough, in a direction normal to the crest and trough lines.

The expression for the wave slope ζ(zeta) is based upon the fact that a normal to the wave surface at any surface-particle point passes through a point at a distance R_{RC} above the instantaneous orbit center of the particle. In diagram 1 of Fig. 9.G on page 163 of Volume I, the line P_1C_1 is normal to the wave surface at P_1, whence the wave slope ζ equals the angle $P_1C_1O_1$. In the diagram of Fig. 48.C the line P_4C_4 is normal to the wave surface at P_4, and the wave slope ζ_4 is represented by either the angle $P_4C_4O_4$ or the angle $M_4P_4N_4$. By simple geometry, indicated in Fig. 48.C,

$$\tan \zeta_4 = \frac{P_4M_4}{C_4O_4 + O_4M_4} = \frac{R_S \sin \theta_4}{R_{RC} - R_S \cos \theta_4} \qquad (48.i)$$

where θ is measured from the top center of the orbit and $\cos \theta$ in the lower quadrants is negative.

The maximum wave slope occurs when the surface-particle orbit radius P_3O_3 or R_S in the diagram of Fig. 48.C lies normal to the line P_3C_3, whence

$$\zeta_{Max} = \sin^{-1}\left(\frac{P_3O_3}{C_3O_3}\right) = \sin^{-1}\left(\frac{R_S}{R_{RC}}\right) \qquad (48.ii)$$

Since R_S is $h_W/2$ and $R_{RC} = L_W/2\pi$,

$$\zeta_{Max} = \sin^{-1}\frac{\frac{h_W}{2}}{\frac{L_W}{2\pi}} = \sin^{-1}\frac{\pi h_W}{L_W} \qquad (48.iia)$$

as indicated at the right on Figs. 48.B and 48.C.

It is to be noted particularly that the slope indicated by Eq. (48.i) is that at the position of a surface particle lying at the extremity of a radius R_S which lies at the angular orbit position θ. For a wave traveling to the left, as in Figs. 48.B and 48.C, this angle is reckoned counter-clockwise from the top center, starting at a crest at the left or advancing end of a wave. The *horizontal* distance from the crest to the position of the particle is therefore the offset distance of the orbit center from the crest, namely $(360 - \theta/360)(L_W)$, modified by the offset position in the orbit, namely $R_S \sin \theta$.

Thus for $\theta_4 = 2\pi/3$ or 120 deg, with the surface particle lying at P_4,

$$\tan \zeta = \frac{P_4M_4}{C_4O_4 + O_4M_4} = \frac{R_S \sin \theta_4}{R_{RC} - R_S \cos \theta_4}$$

$$= \frac{R_S(0.866)}{R_{RC} - R_S(-0.5)} = \frac{0.866R_S}{R_{RC} + 0.5R_S}$$

The value of $(360 - \theta_4/360)L_W$ is $L_W/3$ and that of $R_S \sin \theta_4 = 0.866R_S$. The latter is measured toward the crest, so the particle position desired, reckoned from the crest in the direction of advance of the wave, is

$$\frac{L_W}{3} - 0.866R_S$$

To determine the maximum slope of the 612-ft wave of Sec. 48.4, for the ABC ship of Part 4, it is necessary to know the orbital radius R_S of a surface particle and the radius of the rolling circle R_{RC} by which the trochoidal surface is

TABLE 48.b—Lengths, Velocities, and Periods of Trochoidal Deep-Water Waves

Length, ft	Velocity		Period, sec	Angular Particle Velocity in Circular Orbits, radians per sec	Frequency, cycles per sec
	kt	ft per sec			
5	2.996	5.060	0.9881	6.359	1.012
10	4.237	7.156	1.397	4.498	0.7158
15	5.190	8.765	1.711	3.672	0.5845
20	5.993	10.12	1.976	3.180	0.5061
25	6.700	11.32	2.200	2.856	0.4545
30	7.339	12.39	2.420	2.596	0.4132
35	7.928	13.39	2.614	2.404	0.3826
40	8.475	14.31	2.795	2.248	0.3578
45	8.989	15.18	2.964	2.120	0.3374
50	9.475	16.00	3.125	2.011	0.3200
60	10.38	17.53	3.423	1.836	0.2921
70	11.21	18.93	3.697	1.700	0.2705
80	11.99	20.24	3.952	1.590	0.2530
90	12.71	21.47	4.192	1.499	0.2385
100	13.40	22.63	4.419	1.422	0.2263
150	16.41	27.71	5.412	1.161	0.1848
200	18.95	32.00	6.249	1.005	0.1600
250	21.19	35.78	6.987	0.8993	0.1431
300	23.21	39.20	7.654	0.8209	0.1307
350	25.07	42.34	8.267	0.7600	0.1210
400	26.80	45.26	8.838	0.7109	0.1131
450	28.43	48.01	9.374	0.6703	0.1067
500	29.96	50.60	9.881	0.6359	0.1012
550	31.43	53.07	10.36	0.6065	0.09653
600	32.82	55.43	10.82	0.5807	0.09242
650	34.16	57.70	11.27	0.5575	0.08873
700	35.45	59.87	11.69	0.5375	0.08554
750	36.70	61.97	12.10	0.5193	0.08264
800	37.90	64.01	12.50	0.5027	0.08000
850	39.07	65.98	12.88	0.4878	0.07764
900	40.20	67.89	13.26	0.4738	0.07541
950	41.30	69.75	13.62	0.4613	0.07342
1000	42.37	71.56	13.97	0.4498	0.07158
1100	44.44	75.05	14.66	0.4286	0.06821
1200	46.42	78.39	15.31	0.4104	0.06532
1300	48.32	81.59	15.93	0.3944	0.06277
1400	50.14	84.67	16.53	0.3801	0.06050
1500	51.90	87.65	17.11	0.3672	0.05845
1600	53.60	90.52	17.68	0.3554	0.05656
1700	55.25	93.31	18.22	0.3449	0.05488
1800	56.85	96.01	18.75	0.3351	0.05333
1900	58.41	98.64	19.26	0.3262	0.05192
2000	59.93	101.2	19.76	0.3180	0.05061

TABLE 48.c—PERIOD, LENGTH, AND VELOCITY OF TROCHOIDAL DEEP-WATER WAVES

This table is indexed by integral values of the wave period T_W in sec. The table includes also the angular orbital velocities and the frequencies with which various waves pass a point in space.

Period, sec	Angular Particle Velocity in Circular Orbits, radians per sec	Frequency, cycles per sec	Length, ft	Velocity	
				kt	ft per sec
1	6.283	1.000	5.121	5.121	3.032
2	3.142	0.5000	20.48	10.24	6.064
3	2.094	0.3333	46.09	15.36	9.096
4	1.571	0.2500	81.94	20.48	12.13
5	1.257	0.2000	128.0	25.61	15.16
6	1.047	0.1667	184.4	30.73	18.19
7	0.8976	0.1429	250.9	35.85	21.22
8	0.7854	0.1250	327.7	40.97	24.26
9	0.6981	0.1111	414.8	46.09	27.29
10	0.6283	0.1000	512.1	51.21	30.32
11	0.5712	.09091	619.6	56.33	33.35
12	0.5236	.08333	737.4	61.45	36.38
13	0.4833	.07692	865.4	66.57	39.42
14	0.4488	.07143	1004	71.69	42.45
15	0.4189	.06667	1152	76.82	45.48
16	0.3927	.06250	1311	81.94	48.51
17	0.3696	.05882	1480	87.06	51.54
18	0.3491	.05556	1659	92.18	54.58
19	0.3307	.05263	1849	97.30	57.61
20	0.3142	.05000	2048	102.4	60.64

generated. From Fig. 48.B and the foregoing summary, R_S is half of the wave height h_W or 13.61/2 = 6.85 ft. The value of R_{RC} is $L_W/2\pi$ = 612/6.28 = 97.5 ft. The maximum wave slope $\zeta_{Max} = \sin^{-1}(R_S/R_{RC}) = \sin^{-1}(6.85/97.5)$ = about 4.03 deg.

48.6 Tabulated Data on Length, Period, Velocity, and Frequency of Deep-Water Trochoidal Waves. It is useful to know the combinations of wave length, wave velocity, and period for any one of a large range of trochoidal waves, corresponding generally to the range of natural waves to be found in the oceans. Small and large tables of this kind have been embodied in many standard works on naval architecture and shipbuilding, at least since the publication of W. J. M. Rankine's "Shipbuilding: Theoretical and Practical," in 1866, with some small variations in numerical values.

Tables 48.b, 48.c, and 48.d give related numerical values of length, period, and velocity, the latter in both fps and kt, for a series of deep-water trochoidal waves varying in length from less than 1 ft to 2,000 ft. They are indexed by integral values of length in ft, period in sec, and velocity in kt, respectively. The calculated values are theoretical, derived from the relationships set down in Sec. 48.4. All values are carried out, wherever applicable, to the nearest fourth significant figure.

These tables include also the angular orbital velocities and the frequencies with which the various waves pass a point in space.

For the assumed wave of Sec. 48.4, in which the ABC ship of Part 4 is to run, the length L_W is 612 ft. Then by interpolation from Table 48.b, the following characteristics are found: Celerity c = 55.99 ft per sec, equivalent to 33.15 kt; period T_W = 10.93 sec; frequency = 0.0915 wave per sec. These agree with the values calculated by the formulas within 2 units in the fourth significant place.

48.7 Orbital Velocities for Trochoidal Deep-Water Waves. Any water particle makes one complete revolution in its orbit in one wave period T_W. For a particle lying in the surface, the orbital distance traveled during this period is πh_W and the (tangential) orbital velocity is $U_{Orb} = \pi h_W/T_W$. The wave velocity c is the length of a complete wave L_W divided by the period T_W, whence $T_W = L_W/c$. Substituting, $U_{Orb} = \pi(c)h_W/L_W = \pi c$ times the steepness

TABLE 48.d—VELOCITY, LENGTH, AND PERIOD OF TROCHOIDAL DEEP-WATER WAVES

This table is indexed by integral values of the wave velocity or celerity c in kt.

Velocity, kt	Velocity, ft per sec	Length, ft	Period, sec	Angular Velocity, radians per sec	Frequency, cycles per sec
1	1.689	0.5571	0.3298	19.05	3.032
2	3.378	2.228	0.6596	9.526	1.516
3	5.067	5.014	0.9894	6.351	1.017
4	6.756	8.914	1.319	4.764	0.7582
5	8.445	13.93	1.649	3.810	0.6064
6	10.13	20.06	1.979	3.175	0.5053
7	11.82	27.30	2.309	2.721	0.4331
8	13.51	35.65	2.639	2.381	0.3789
9	15.20	45.13	2.968	2.117	0.3369
10	16.89	55.71	3.298	1.905	0.3032
11	18.58	67.41	3.628	1.732	0.2756
12	20.27	80.22	3.958	1.587	0.2527
13	21.96	94.15	4.287	1.466	0.2333
14	23.65	109.2	4.617	1.361	0.2166
15	25.34	125.3	4.947	1.270	0.2021
16	27.02	142.6	5.277	1.191	0.1895
17	28.71	161.0	5.607	1.121	0.1783
18	30.40	180.5	5.936	1.058	0.1685
19	32.09	201.1	6.266	1.003	0.1596
20	33.78	222.8	6.596	0.9526	0.1516
21	35.47	245.7	6.926	0.9072	0.1444
22	37.16	269.6	7.256	0.8659	0.1378
23	38.85	294.7	7.585	0.8284	0.1318
24	40.54	320.9	7.915	0.7938	0.1263
25	42.22	348.2	8.245	0.7621	0.1213
26	43.91	376.6	8.575	0.7327	0.1166
27	45.60	406.1	8.905	0.7056	0.1123
28	47.29	436.8	9.234	0.6804	0.1083
29	48.98	468.5	9.564	0.6570	0.1046
30	50.67	501.4	9.894	0.6351	0.1011
31	52.36	535.4	10.22	0.6148	0.09785
32	54.05	570.5	10.55	0.5956	0.09479
33	55.74	606.7	10.88	0.5775	0.09191
34	57.43	644.0	11.21	0.5605	0.08921
35	59.12	682.4	11.54	0.5445	0.08666
36	60.80	722.0	11.87	0.5293	0.08425
37	62.49	762.7	12.20	0.5150	0.08197
38	64.18	804.5	12.53	0.5015	0.07981
39	65.87	847.3	12.86	0.4886	0.07776
40	67.56	891.4	13.19	0.4764	0.07582
41	69.25	936.5	13.52	0.4647	0.07396
42	70.94	982.7	13.85	0.4537	0.07220
43	72.63	1030	14.18	0.4431	0.07052
44	74.32	1079	14.51	0.4330	0.06892
45	76.00	1128	14.84	0.4234	0.06739
46	77.69	1179	15.17	0.4142	0.06592
47	79.38	1231	15.50	0.4054	0.06452
48	81.07	1284	15.83	0.3969	0.06317

TABLE 48.d—(Continued)

Velocity, kt	Velocity, ft per sec	Length, ft	Period, sec	Angular Velocity, radians per sec	Frequency, cycles per sec
49	82.76	1338	16.16	0.3881	0.06188
50	84.45	1393	16.49	0.3810	0.06064
51	86.14	1449	16.82	0.3736	0.05945
52	87.83	1506	17.15	0.3664	0.05831
53	89.52	1565	17.48	0.3595	0.05721
54	91.21	1622	17.81	0.3528	0.05615
55	92.90	1685	18.14	0.3464	0.05513
56	94.58	1747	18.47	0.3402	0.05414
57	96.27	1810	18.80	0.3342	0.05319
58	97.96	1874	19.13	0.3284	0.05227
59	99.65	1939	19.46	0.3229	0.05139
60	101.34	2005	19.79	0.3175	0.05053

ratio. Also, since the surface particle travels in an orbit of radius R_S,

$$U_{\text{Orb}} = R_S\omega$$

whence, by substitution,

$$U_{\text{Orb}} = \frac{h_W}{2}\sqrt{\frac{2\pi g}{L_W}} = 7.111\left(\frac{h_W}{\sqrt{L_W}}\right)$$

Assuming a steepness ratio of 1/12 = 0.083 and a wave velocity c of 36 kt, or 60.8 ft per sec, corresponding to a wave 61.5 ft high and 738 ft long, the orbital velocity U_{Orb} of a surface particle is $\pi(c)h_W/L_W = 3.14(60.8)(0.083) = 15.85$ ft per sec, $\approx$ about 9.4 kt. This means that a small, shallow-draft boat traveling along the surface at a constant speed of 20 kt over the ground, in a direction normal to the crest lines, would have a relative speed through the water of 29.4 kt on the crest and 20 − 9.4 = 11.6 kt in the trough.

For a maximum steepness ratio of 1/7, $U_{\text{Orb}} = \pi(h_W/L_W)c$ = about 0.45c, also for a surface particle.

Table 48.e lists the orbital velocities of the surface particles in a series of trochoidal waves having lengths and steepness ratios covering those normally encountered in service.

Fig. 48.D gives plots of orbital velocities for a range of wave lengths, wave velocities, and steepness ratios likely to be encountered during heavy-weather and emergency conditions at sea. These velocities are important when pounding

TABLE 48.e—ORBITAL VELOCITIES OF SURFACE PARTICLES IN A DEEP-WATER TROCHOIDAL WAVE
The values of velocity listed are in ft per sec.

Wave Length L_W, ft	Steepness Ratio 1/7 or 0.14286	1/10 or 0.1000	1/15 or 0.06667	1/20 or 0.0500	1/25 or 0.0400
50	7.181	5.027	3.351	2.514	2.011
100	10.157	7.109	4.739	3.555	2.844
200	14.363	10.054	6.7027	5.0270	4.0216
400	20.312	14.218	9.4787	7.1090	5.6872
600	24.876	17.413	11.609	8.7065	6.9652
800	28.725	20.107	13.405	10.054	8.0428
1000	32.116	22.481	14.987	11.240	8.9924
1200	35.181	24.626	16.417	12.313	9.8504
1400	38.001	26.600	17.733	13.300	10.640
1600	40.624	28.436	18.957	14.218	11.374
1800	43.088	30.161	20.107	15.080	12.064
2000	45.418	31.792	21.195	15.896	12.717

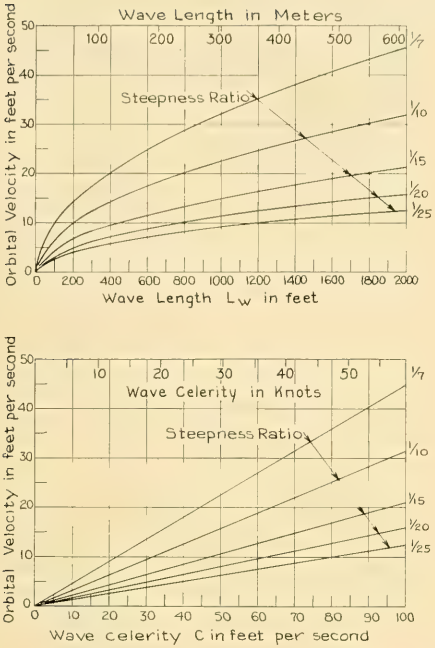

FIG. 48.D GRAPHS INDICATING ORBITAL VELOCITIES IN TROCHOIDAL WAVES OF VARIED STEEPNESS RATIO

and slamming, accompanied by high water-impact velocities, become factors in the design or performance problem.

For the 612-ft Wheelock wave of Sec. 48.4, in which the ABC ship of Part 4 is to travel, the wave height h_W is 13.61 ft. The orbital velocity U_{Orb} is $7.111h_W/\sqrt{L_W}$. Substituting the foregoing values for the given wave, $U_{\text{Orb}} = 7.111(13.61)/24.75 = 3.91$ ft per sec, for a surface particle. Since the steepness ratio of the wave is only 13.61/612 or 1/45, the orbital-velocity value is beyond the ranges of Table 48.e and Fig. 48.D.

Table 48.f lists values of the ratio of the orbit radius R, at any depth h, to the orbit radius R_S at the surface. Beyond a value of h/L_W greater than 1.0, the ratio R/R_S is practically zero.

48.8 Data on Steepness Ratios and Wave Heights for Design Purposes. The steepness ratios of the highest sea waves of different lengths, as observed, estimated, and reported by various investigators, are found to vary rather widely. This is partly because of recognized difficulties in making wave observations from a ship and partly because the average steepness ratios actually vary. They are reported, for example, to be of the order of 1/22 to 1/30 for storm waves in the Atlantic and 1/16 to 1/18 for similar waves in the Indian Ocean.

Maximum steepness ratios on a base of wave length, from a great number of records, have been analyzed by J. Turnbull in connection with a recent study of the longitudinal strength of ships [Engineering (London), 3 Oct 1952, p. 449; SBSR, 2 Oct 1952, p. 441]. Turnbull gives a graph envelope covering the heights of some unusually steep waves which had been encountered and reliably reported over a period of 50 or 60 years. The data exhibit a rather wide range for the highest waves of the size commonly encountered, in some cases about 2 to 1. Further data along the same line are to be found in The Admiralty Ship Welding Committee Report R.8, describing the "S. S. *Ocean Vulcan* Sea Trials: The Forces Acting on the Ship at Sea" [ACSIL/ADM/53/387 of 1953, pp. 8–11, esp. Fig. 9].

TABLE 48.f—DECREASE OF ORBIT RADII WITH DEPTH IN A TROCHOIDAL DEEP-WATER WAVE

The orbit radius is assumed to vary with depth h in accordance with the relationship $R = R_S e^{-2\pi(h/L_W)}$ where R_S is the orbit radius of a surface particle. The data listed here are taken from W. F. Durand, RPS, 1903, p. 75, and C. H. Peabody, NA, 1904, p. 262.

Ratio of Depth of Water h to Wave length L_W, h/L_W	Ratio of Orbit Radii of Particles at depth h and at surface, R/R_S
0.01	0.9391
0.02	0.8819
0.03	0.8283
0.04	0.7778
0.05	0.7304
0.1	0.5335
0.15	0.3897
0.2	0.2846
0.25	0.2079
0.3	0.1518
0.35	0.1109
0.4	0.0810
0.45	0.0592
0.5	0.0432
0.6	0.0231
0.7	0.0123
0.8	0.0066
0.9	0.0035
1.0	0.0019
2.0	0.0000035

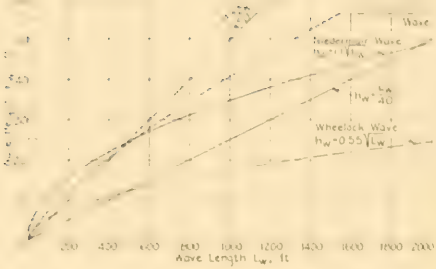

FIG. 48.E RATIOS OF WAVE HEIGHT TO WAVE LENGTH FOR CHARACTERISTIC WAVES USED IN SHIP DESIGN

It has been the practice for many years to base ship-strength calculations on a wave having a steepness ratio of 1/20. This is often referred to as a "static" wave but it may be considered as a following wave that has exactly the same speed as the ship, and is not distorted by the presence of the ship.

Because this wave is not as steep as the storm waves which make trouble for small ships, and is steeper than those which make wavegoing difficult for large ones, J. C. Niedermair recommends a "design" steepness ratio varying with wave length, represented by $h_W = 1.1\sqrt{L_W}$ ["Ship Motions," INA, Int. Conf. Nav. Arch. and Mar. Engrs., 1951, pp. 137–152; ASNE, Feb 1952, pp. 11–34]. A graph giving the variation of wave height h_W with wave length L_W for this "Niedermair" wave is shown in Fig. 48.E. For tests of models in regular wave trains, a steepness ratio of half this amount, namely $h_W = 0.55\sqrt{L_W}$, is proposed by C. D. Wheelock. It appears to give waves as high as those in which ships can be expected to make reasonable headway at sea. All three steepness ratios are plotted in Fig. 48.E, together with a line for waves having a steepness ratio of 1/40.

For convenience, Table 48.g gives the wave heights of both the Niedermair and Wheelock waves for a range of wave lengths sufficient to cover most practical needs.

TABLE 48.g—NIEDERMAIR AND WHEELOCK WAVE-HEIGHT DESIGN VALUES

Wave length L_W, ft	$\sqrt{L_W}$, $ft^{0.5}$	Wave height for $0.55\sqrt{L_W}$, ft	Wave height for $1.1\sqrt{L_W}$, ft
50	7.071	3.89	7.78
100	10.000	5.5	11.00
200	14.142	7.78	15.56
300	17.320	9.53	19.05
400	20.000	11.00	22.00
500	22.361	12.30	24.60
600	24.495	13.47	26.94
700	26.458	14.55	29.10
800	28.284	15.56	31.11
900	30.000	16.50	33.00
1000	31.623	17.39	34.79
1100	33.166	18.24	36.48
1200	34.641	19.05	38.11
1300	36.056	19.83	39.66
1400	37.417	20.58	41.16
1500	38.730	21.30	42.60
1600	40.000	22.00	44.00
1700	41.231	22.68	45.35
1800	42.426	23.33	46.67
1900	43.589	23.97	47.95
2000	44.721	24.60	49.19

TABLE 48.h—ORDINATES FOR A SINE-WAVE PROFILE

The table gives 17 ordinates for the half-length of a sinusoidal wave, distributed at 16 equal intervals between crest and trough, as projected on a horizontal plane.

Station	Ordinate
0, Crest	1.0000
1	0.9904
2	0.9619
3	0.9157
4	0.8536
5	0.7778
6	0.6913
7	0.5976
8	0.5000
9	0.4025
10	0.3087
11	0.2222
12	0.1464
13	0.0843
14	0.0381
15	0.0096
16, Trough	0.0000

48.9 Formulas for Sinusoidal Waves. The profile of a sinusoidal wave, described in Sec. 9.6 of Volume I and illustrated in Fig. 9.E, is an extremely simple geometric construction, pictured in diagram 1 of Fig. 48.F, using 10 stations along the half-length of the wave. The ordinate heights for each station are indicated. Table 48.h gives the ordinate heights along the half-length for 16 station intervals.

For the convenience of workers plotting com-

plex waves with sinusoidal components, such as those forming the basis of Figs. 48.G and 48.H of Sec. 48.11, diagrams 2 through 5 of Fig. 48.F give the spacing in the direction of wave motion of ordinates which differ by successive even fractions of the wave height h_W, such as 1/4, 1/6, 1/8, and 1/10.

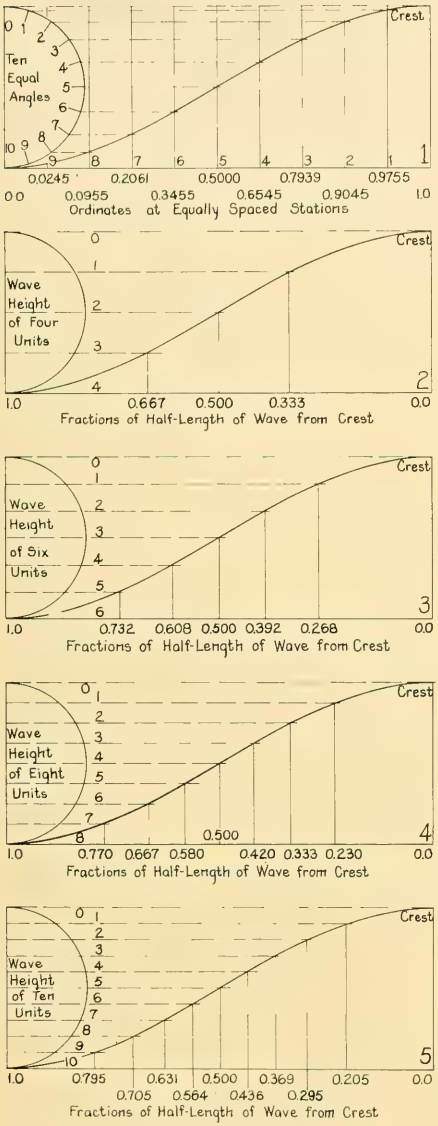

Fig. 48.F Abscissa and Ordinate Data for Sinusoidal Waves

48.10 Standard Simple and Complex Waves for Design Purposes. There are clear indications that the use of the "static" $L/20$ wave or of the Niedermair wave for the structural design of a ship hull will shortly be paralleled by the use of dynamic waves for what might be termed the wavegoing design of the hull. Although the classification societies rather than the owners and operators usually specify the limiting stresses in a ship girder, it may be expected that those who run the ship will have a far greater interest in its wavegoing performance at sea in heavy weather. They may be expected to stipulate that under certain wave conditions its augment of resistance at reduced speeds, its wave-induced motions, and its wavegoing behavior shall be limited to specified values.

Two problems arise here, possibly more. The first is the manner in which the wavegoing performance is to be predicted in the paper stage of the design. This is discussed in Part 6 of Volume III. The second is the establishment of standard dynamic waves in which the ship is to give the wavegoing performance stipulated. These must be of such nature that the principal features of ship behavior in them can be calculated, just as the girder stresses are now calculated for the "static" wave.

The question as to whether these waves are to be statistical, embodying averages and functions for a great mass of data, or whether they are to be geometrical (or mathematical) is not yet decided (1955) and is not discussed here. It is assumed for the time being that the effects of the waves of nature can be produced by profiles that are of sinusoidal, trochoidal, or some other shape lending itself to graphic construction or to calculation.

It seems clear that the standard dynamic waves embodied in the wavegoing specifications of the future will be both (1) single regular trains and (2) complex seas made up of specified combinations of single trains. It is shown in Sec. 48.11 that a combination of three such trains produces an irregular wave system which possesses many of the characteristics of the natural waves of the sea. A single train suitable for the testing of models at angles of encounter α(alpha) of 180 deg (head sea) and 0 deg (following sea) is com-

posed of the Wheelock waves of Fig. 48.E, having a height $h_W = 0.55\sqrt{L_W}$.

A set of tentative standard wave conditions for the determination of the wavegoing performance of ships in the design stage, adapted from an initial proposal by the author in November 1950, is given in Table 48.i.

TABLE 48.i—TENTATIVE STANDARD WAVE CONDITIONS FOR DETERMINATION OF THE WAVEGOING PERFORMANCE OF SHIPS IN THE DESIGN STAGE

(1) Wind and wind effects on the ship are not considered here. The waves described are assumed to be produced by some wind of undefined nature.

> "In short, the old rule still holds, and always will, that it is the waves of a storm, not its winds, that the mariner has to fear; . . ." [Bigelow, H. B., and Edmonson, W. T., "Wind Waves at Sea; Breakers and Surf," U. S. Navy Hydrographic Office publication H. O. 602, Washington, 1947, p. 46].

(2) Unless otherwise stated, the sizes and proportions of the swells and waves are averages or significant values for the water areas of the world, rather than uncommon maxima of one kind or another. They may be local averages if the principal conditions are such that the ship can travel *only* in that area.

(3) The lengths of regular or uniform swells and waves in deep water may in general be taken as a function of their velocities and vice versa.

CASE I. This is intended to represent the conditions obtaining in the general but not immediate vicinity of an area where a wind has been blowing for some time in a nearly constant direction. The result is a simple, regular train of swells, in which the wave velocities may vary from 0.4 to 1.2 or more times the maximum speed of the ship under consideration. This range is intended to be large enough to cover the region of resonant pitching. The steepness ratios of these swells, expressed as wave height h_W to wave length L_W, may vary from 0.083(1/12) to 0.04(1/25) or less. The angle of encounter α of the ship with the direction of travel of the wave train may vary from 0 (following sea) to 180 deg (head sea). The water depth is 600 ft (100 fathoms) or more.

CASE II. This is intended to represent the conditions obtaining in the general vicinity of one strong wind or storm area and in the immediate vicinity of another. Due to a shift in storm center or other causes, the wind in the latter area is blowing in a direction different from that in which it blew in the former area. The result is one or possibly two secondary wave trains imposed upon a selected primary train of swells of CASE I. When the swells are of simple geometric form, this is known as a complex synthetic two-component (or three-component) sea. The secondary wave velocities may vary from 0.4 to 0.8 of the maximum speed of the ship under consideration. In other words, they may exceed the primary swell velocity. The direction of the secondary train (or trains) may lie within 60 deg of the direction of the primary train. This means that both trains are moving in the same general direction. The water depth is 600 ft (100 fathoms) or more.

CASE III. This is intended to represent the conditions obtaining in shallow water within a strong wind or storm region, where relatively large and steep waves are produced by winds of short duration. The result is a single, regular train of waves, in which the wave velocities may vary from 0.4 to 1.2 or more times the maximum speed of the ship under consideration. The steepness ratio may vary from 0.125(1/8) to 0.0625(1/16) or less. The angle of encounter of the wave train may vary from 0 to 180 deg. The depth of water may diminish to 2.5 times the maximum draft, possibly to 2.0 times that draft.

With the three variables listed in CASE I of Table 48.i, namely the ratio L_W/L, the steepness ratio h_W/L_W, and the angle of encounter α, and even with the intervals deliberately made large, the number of possible combinations is almost prohibitive. Undoubtedly certain combinations of variables, especially those producing resonant motion, are critical. Study of those combinations only may ultimately be found sufficient. The wave velocities are extended to a low range because it is possible for a ship with its forefoot nearly out of the water, as in the ballast condition, to encounter short, steep waves whose impact coincides with the natural 2-noded vibration of the ship structure.

48.11 Delineation of a Synthetic Three-Component Complex Sea. As an indication of the appearance and the characteristics of a synthetic complex sea, a graphic example is worked out in which three components or trains of regular sinusoidal waves are superposed. The primary train is assumed to travel in the direction of 90 deg true (east), while the secondary trains travel

TABLE 48.j—CHARACTERISTICS OF THREE COMPONENTS OF A COMPLEX SYNTHETIC SEA

The data listed here apply to the superpositions of Figs. 48.G and 48.H. All the wave components are sinusoidal in form but their velocities of translation and periods are calculated from the formulas for trochoidal waves. For a wave length L_W in ft, these are $c = 2.263\sqrt{L_W}$ in ft per sec; $T_W = 0.4419\sqrt{L_W}$ in sec.

Direction of translation, true	90 deg	75 deg	135 deg
Wave length, ft	400	240	120
Wave height, ft	8	6	4
Steepness ratio	1/50	1/40	1/30
Wave celerity, ft per sec	45.26	35.06	24.79
kt	26.79	20.75	14.67
Wave period, sec	8.840	6.847	4.842
Distance traveled by wave in 3 sec, ft	135.78	105.17	74.373

at 75 deg and 135 deg true. Their wave lengths are 400 ft, 240 ft, and 120 ft, respectively, with rather moderate steepness ratios of 1/50, 1/40, and 1/30, in the order given. The corresponding wave heights h_W are 8, 6, and 4 ft. Other characteristics of these waves are given in Table 48.j.

All components have sinusoidal wave profiles. Their elevations (or depressions) above the assumed quiet water plane may therefore be added algebraically to produce the elevations (considered as a + distance) or depressions (considered as a − distance) of the resultant, above or below the reference plane.

The first step in the graphic superposition is to draw, to a convenient scale, three transparent contour patterns for the three sinusoidal waves, having straight, parallel lines laid off normal to the direction of travel at elevations to represent 1-ft contours, including the crests and troughs. The data for positioning the contour lines between successive wave crests, for various equal subdivisions of the wave height, are given in Fig. 48.F.

The three patterns are laid down over each other in the desired positions. The resultant pattern is built up on a fourth transparent sheet, superposed on the other three, by adding the elevations algebraically at a multitude of points throughout the field.

To show how much of an "îlot" (French for "islet") [Pommellet, A., ATMA, 1949, Vol. 48, pp. 589–608] would be formed by three wave crests piled on top of each other, it is assumed as a starter that all three crest lines intersect at the time t_0 . This intersection is the reference point or origin O, taken to be fixed in space. The three contour patterns, when laid down at the proper angles, are so placed that their crest lines cross the origin. Contours of the composite pattern are then sketched at 1-ft intervals, with the result shown in Fig. 48.G. Those portions of the composite waves whose surfaces slope downward and to the right have the contours indicated by *heavy* broken lines, as though in shadow when illuminated by a low sun at about 270 deg true (in the west).

The validity of this method of superposition

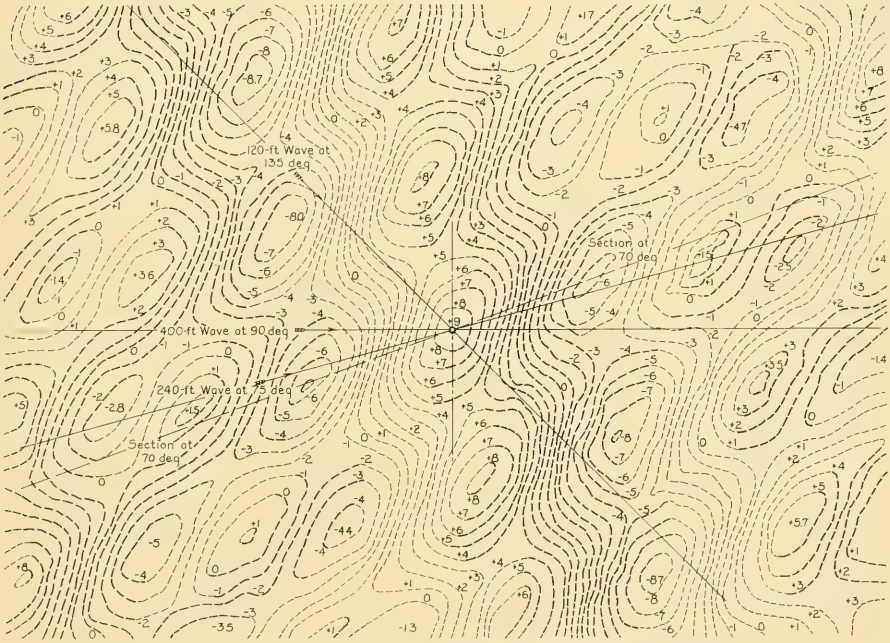

Fig. 48.G Contour Diagram for Three Superposed Sinusoidal Waves

was pointed out many years ago by Franz Gerstner, in his classic paper of 1802 on the trochoidal wave, referenced in Sec. 48.18:

"Since this theory of waves is based upon the equality of hydrostatic pressure, it follows that all motions of the water which do not change this uniformity of pressure, neither disturb the wave motion. This makes it possible for several waves of various sizes to cross in different directions, and continue their motion undisturbed. Again general experience supplies ample verification. At the same time it explains the numerous elevations which frequently appear at the surface of the water" [English translation, Univ. of Cal., 1952, par. 16, p. 14].

Assuming that a ship is traveling through this synthetic complex sea on a course of 70 deg true, there results the profile in diagram 1 of Fig. 48.I. To emphasize the irregularities in surface elevation, the profile ordinates above and below the undisturbed or quiet water level are magnified 6.308 times.

At the origin, the height of the water "islet" above the undisturbed level is $4 + 3 + 2 = 9$ ft. Close to this islet, toward the WSW, is a deep hole, extending 6.4 ft below the undisturbed water level. Within 145 ft of the origin, therefore, one finds a difference in elevation of 15.4 ft. The steepness ratio of the wave near the origin is of the order of 1/18.7, as compared to steepness ratios of 1/30, 1/40, and 1/50 for the components. The maximum wave slope near the origin is about 10 deg.

On either side of this group of one high crest and two deep troughs, within 300 or 400 ft, the waver level is relatively flat, with crests and troughs less than 1.5 ft in magnitude.

Following the composition of the synthetic three-component wave at t_0, each wave is then shifted to the position it would occupy at the time $t_0 + 3$ sec, by the distance indicated in Table 48.j. A new composite pattern is sketched,

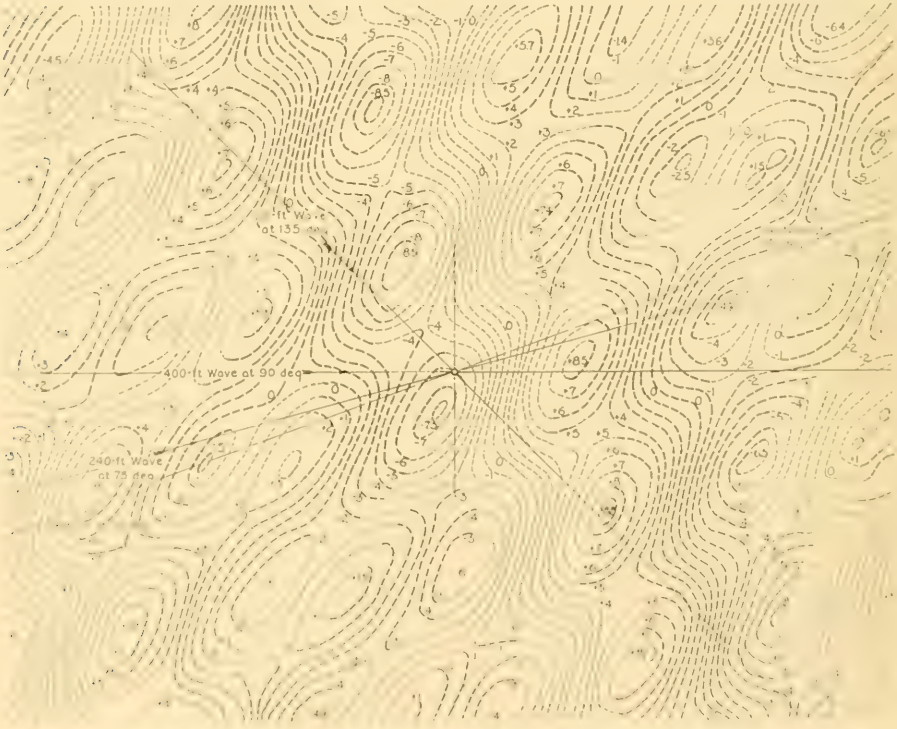

Fig. 48.H Contour Diagram for Three Superposed Sinusoidal Waves, 3 Seconds Later Than Fig. 48.G

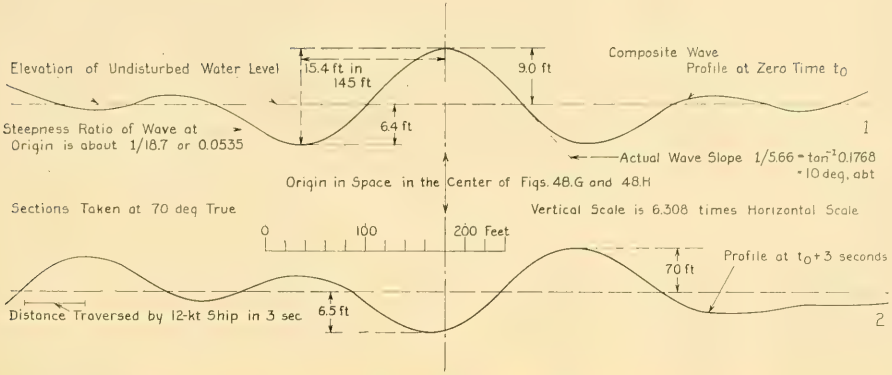

Fig. 48.I Profiles at 70 Deg True for the Wave Patterns of Figs. 48.G and 48.H

indicated in Fig. 48.H for a time 3 sec later. The point of origin in space remains at the center of the figure, as before.

A vertical section through the origin at a direction of 70 deg true is drawn in diagram 2 of Fig. 48.I, again with the vertical scale multiplied 6.308 times. The "islet" which was in the center has moved toward the ENE, but it is now only 7 ft high. The trough at the origin is slightly deeper than before, 6.5 ft. To the east, the surface is depressed but flatter than before, while to the west a large wave is building up.

The area depicted is not large enough to give a reasonable indication of the variations to be expected in resultant wave lengths and wave periods, but within the confines of Figs. 48.G and 48.H the lengths vary from 210 to 220 ft in one group, 270 to 280 ft in another group, and over 400 ft in a third.

While the horizontal patterns of the waves in these diagrams exhibit some systematic regularities, a close examination of the contours reveals that the surface is almost as irregular as one expects the ocean to be.

In fact, C. O'D. Iselin points out that wind waves in nature are not symmetrical, and that their dominant characteristic is the short length of the crests of the individual waves, shown by the plots of Figs. 48.G and 48.H ["Oceanography and Naval Architecture," SNAME, New Engl. Sect., Jun 1954]. The plots could be made more irregular, if desired, by adding two more trains to build up a five-component sea. Graphically, only three components need be combined at once, since the three-component synthetic may be used as the base and the two secondary trains added to it. However, the three-component sea appears at this time (1955) to be sufficiently irregular to serve for ship-design purposes, as indicating the kind of waves in which a ship is expected to travel.

48.12 Tabulated Data for Actual Wind Waves. A table embodying average relationships between natural waves in deep water and the wind causing them is given by Vaughan Cornish in his book "Waves of the Sea and Other Water Waves" [F. T. Unwin, London, 1910]. Additional data are given in his Cantor lecture before the Royal Society of Arts, London, 1914. Cornish's table is quoted by E. L. Attwood, H. S. Pengelly, and A. J. Sims on page 202 of their handbook "Theoretical Naval Architecture," 1953. It is repeated, with some adaptations, in Table 48.k.

It is noted from this table that as the length of wave increases the steepness ratio h_W/L_W decreases. According to the figures given, the standard structural-design ratio of $h_W/L_W = 20$ still used in many quarters can not fairly be applied to ships longer than about 470 ft.

More comprehensive and more modern data on the relationships between the winds and waves of nature are given in the tables of U. S. Navy Hydrographic Office publication H.O. 602, 1947, especially Table 4 on page 18 and Table 15 on page 32. The latter embodies a third and necessary variable in this relationship, namely the duration of the wind which is generating the waves. Both these tables appear to take it for granted that the wind is blowing steadily in one

TABLE 48.k—AVERAGE RELATIONSHIP BETWEEN NATURAL WINDS AND WAVES

For the source of these data, see the accompanying text. The Beaufort scale numbers and wind velocities do not conform to the latest U. S. Navy values as given along the top edge of Fig. 48.J. For this table it is assumed that the waves travel at the same speed as the wind.

Description of wind	Wind force, Beaufort scale	Velocity of wind and velocity of waves, kt	Wave period in sec, $\frac{V(\text{kt})}{3.032}$	Wave length, ft	Greatest average wave height, ft	Steepness ratio, h_W/L_W
Strong breeze	6	21.7	7.2	262	17.5	1/15.0
Moderate gale	7	26.9	8.9	404	21.7	1/18.6
Fresh gale	8	32.1	10.6	575	25.9	1/22.2
Strong gale	9	38.2	12.6	813	30.8	1/26.4
Whole gale	10	46.0	15.2	1180	37.1	1/31.8
Storm	11	55.6	18.3	1720	44.8	1/38.4
Hurricane	12	66.9	22.0	2489		

direction for the duration specified, and that the fetch is long enough to eliminate the effect of nearby land.

Data relating to statistical methods for characterizing the pattern of natural waves in a seaway and for forecasting waves on a basis of known meteorological data are given by W. J. Pierson, Jr., G. Neumann, and R. W. James in a publication entitled "Practical Methods for Observing and Forecasting Ocean Waves by Means of Wave Spectra and Statistics," prepared as Technical Report 1 under Contract N189s-86743, BuAer Project AROWA, July 1953. On pages 320 and 321 there is a bibliography of 39 items. These methods are described in some detail in Part 6 of Volume III.

48.13 The Zimmermann Wave. In the early 1920's Erich Zimmermann published the results of an extensive analysis made by him on the natural waves previously reported by many observers ["Aufsuchung von Mittelwerten für die Formen ausgewachsener Meereswellen auf Grund alter und neuer Beobachtungen (Search for Average Values for the Form of Fully Developed Ocean Waves, Based on Old and New Observations)," Schiffbau, 28 Apr 1920, pp. 633–640; 5 May 1920, pp. 663–670]. On pages 668, 669, and 670 of this paper there are given 72 references from a wide variety of sources, covering the period from 1779 to 1914.

While recognizing the relationship between length, period, and wave velocity in the trochoidal-wave system, Zimmermann set out to find the best possible empirical relationships of the natural waves of the sea between:

Length	Celerity
Height	Period
Breadth (length of crest)	Wind velocity.

He succeeded in developing what he felt was a good average relationship between these values for a wide range of variables. He published a single curve, reproduced with some adaptations in Fig. 48.J, which gives two sets of relationships between three variables in each set. This he did on the basis, admittedly arbitrary, that there is a unique combination in nature between these variables throughout this large range. Nevertheless, Zimmermann's wave can be taken as a sort of statistical average for any point on the range. It does at least give the marine architect an idea of the combinations of variables to be expected at any selected point of the range. The graph of Fig. 48.J contains a worked-out example of its use.

Incidentally, Fig. 1 on page 634 of the 28 April 1920 Schiffbau reference gives a plot made by Zimmermann of thirteen sets of wind-velocity values corresponding to the wind-force numbers of the Beaufort scale; every set is different from every other. The authorities quoted in the reference published their data over the period 1866–1911. To the Zimmermann plot was appended a set of values by Koeppen, Shaw, and Palazzo, from the International Meteorological Conference at Rome in 1913.

After considering them all it was finally decided to adopt for the top-edge scale of Fig. 48.J the values given in "Instructions for Keeping Ship's Deck Log," NavPers 15876 of July 1955, issued by the Bureau of Naval Personnel of the Navy

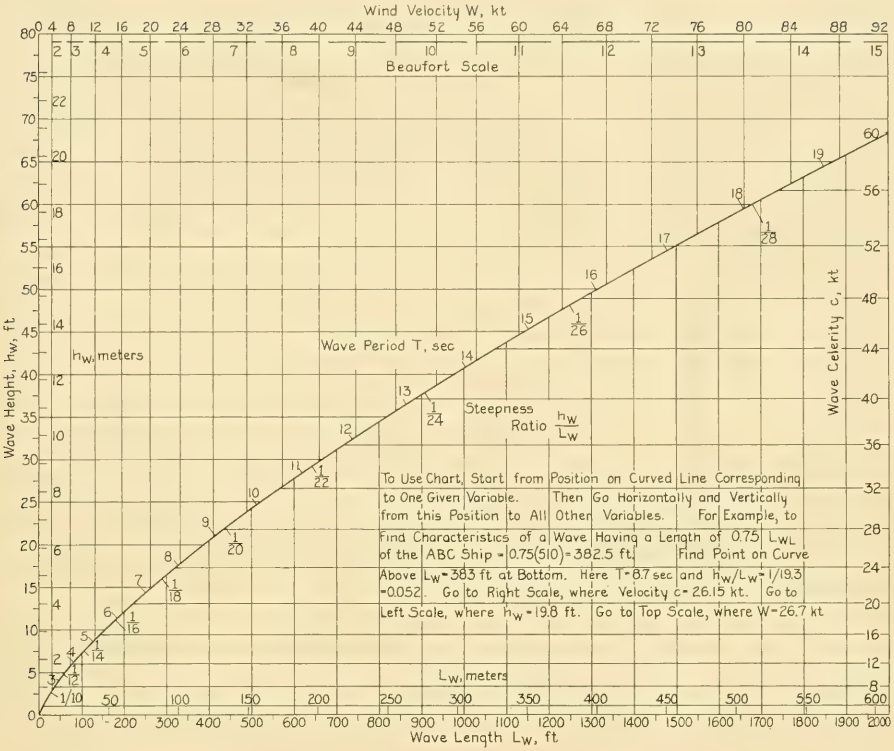

FIG. 48.J GRAPH INDICATING CHARACTERISTICS OF THE ZIMMERMANN WAVE

Department in Washington. Incidentally, these instructions extend the Beaufort scale numbers through 17, as follows:

Wind Force 15,	Velocity	90 through 99 kt
16		100 through 108 kt
17		109 through 118 kt.

A most useful supplementary table, partly pictorial, is published in "All Hands," Bureau of Naval Personnel Information Bulletin, July 1954, pp. 32–33. However, the wind-velocity values for Beaufort-scale numbers do not correspond with those mentioned in the preceding paragraph.

48.14 Wind-Wave Patterns and Profiles by Modern Methods. Modern techniques of photogrammetry render the plotting and sectioning of wave contours and profiles a vastly less laborious and much quicker process than was the case two decades ago, when the stereoscopic wave photographs taken on the German M.S. *San Francisco* were analyzed [Weinblum, G., and Block, W., "Stereophotogrammetrische Wellenaufnahmen (Stereophotogrammetric Wave Photographs)," STG, 1936, Vol. 37, pp. 214–250 and 259–276; TMB Transl. 204, Nov 1949]. For information, Fig. 48.K shows profiles through waves that were photographed and analyzed as a part of the open-sea test project on this vessel.

One modern method involves two synchronized cameras which are mounted on a large ship with their optical axes in transverse planes parallel to each other and parallel to the baseplane of the ship. Their lenses are equidistant from the plane of symmetry so that their negatives lie in a given plane parallel to the ship centerplane. The camera axes are far enough apart, in a fore-and-aft direction, so that good stereoscopic vision is obtained

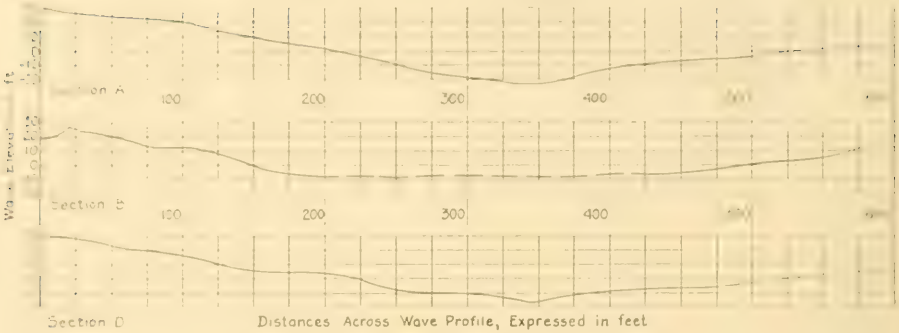

Fig. 48.K Three Profiles Through an Ocean Wave as Determined by G. P. Weinblum and W. Block on the M. S. *San Francisco*

for a considerable transverse distance from the ship, say 1,500 ft.

Short-duration simultaneous exposures are made at the midpoint of a roll; for this instant the planes of the two negatives are vertical. The pairs of stereoscopic photographs thus obtained are placed in a photogrammetric machine and the wave section quickly traced for any plane lying at a selected distance parallel to the ship centerplane. Fig. 48.L is one such photograph taken by C. G. Moody of the TMB staff on the aircraft carrier *Oriskany* (CVA 34), during a storm west of Cape Horn in June 1952.

Fig. 48.M shows nine straight or plane sections through the waves recorded by this pair of photographs, at offset or transverse distances in ft, from the plane of the camera lenses, indicated by the numerals at the left of the diagram. Because of the greater distance from the camera for a wave in the background than for one in the foreground, a unit linear width across the diagram indicates a greater distance along the wave section, parallel to the ship axis, as the transverse distance increases. Scales are given at the right of two of the wave profiles in Fig. 48.M.

Knowing the focal length of the cameras and the distance of the cameras above the mean water level or above the at-rest waterline, it is possible to plot sections along a vertical transverse plane extending outward from the midposition between the camera lenses. The trace of such a plane is shown by the vertical line O-O on the diagram of Fig. 48.M. Similarly, it is possible to plot a section along a diagonal plane extending outward from the point midway between the lenses. The trace of such a plane is the vertical line A-B on Fig. 48.M, drawn on the original at a distance 4 inches to the left of O-O. At 500 ft distance this offset plane intersects the nearest crest at a point 4(23) = 92 ft to the left of the plane through O-O. At 1,500 ft distance the diagonal plane intersects the farthest crest at a point 4(70) = 280 ft to the left of O-O.

Obviously, profiles of wave faces behind crests or otherwise hidden from the cameras are not determined.

Pitching of the ship tilts both cameras, as indicated by the small counter-clockwise rotation of the principal axes of Fig. 48.L, with reference to the apparent horizon. This tilt may be corrected if desired in the photogrammetric analysis procedure. It does not, however, change the wave profile in the particular vertical plane considered.

A further discussion of photographic and plotting methods for sea surfaces is not warranted here. However, as the references on this subject contain many sets of wave contours and profiles of interest to the marine architect the principal papers and books are listed:

(1) Laas, W., "Photographische Messung der Meereswellen (Photographic Observations and Measurement of Sea Waves)," Zeit. d. Ver. Deutsch. Ing., 25 Nov 1905, pp. 1889–1895; 2 Dec 1905, pp. 1937–1942; 9 Dec 1905, pp. 1976–1981. The last of these pages carries a list of 13 references.

The observations described in this series of papers were made from the five-masted sailing ship *Preussen* on a voyage from Hamburg around the Horn to Iquique, Ecuador, and return, during the period 6 Sep 1904 to 3 Feb 1905. The photographs were apparently made with the optical axis of the

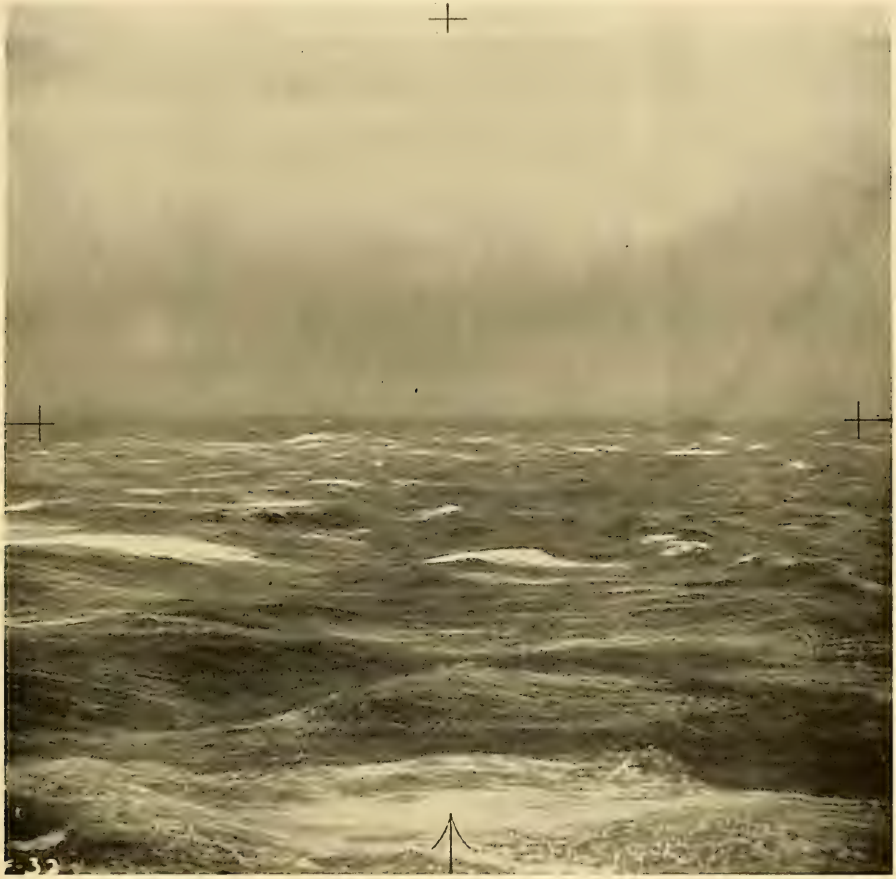

FIG. 48.L ONE OF A PAIR OF STEREOSCOPIC PHOTOGRAPHS TAKEN ABEAM ON THE AIRCRAFT CARRIER *Oriskany*, WEST OF CAPE HORN

camera horizontal, as was the case with the *Oriskany* photographs of 1952. As many as three photographs were made simultaneously at times. The reduction was accomplished by the use of a Zeiss stereocomparator. A contour diagram of one pair of exposures, together with a considerable number of sections through the diagrammed wave, are reproduced on page 1980 of the reference. Photographs are to be found on three plates bound in a separate volume of tables accompanying the text.

(2) Laas, W., "Die Messung der Meereswellen und ihre Bedeutung für den Schiffbau (Measurement of Sea Waves and Its Influence in Naval Architecture)," STG, 1906, Vol. 7, pp. 391–407

(3) Laas, W., "Die Photographische Messung der Meereswellen (The Photographic Measurement of Ocean Waves)," Institut für Meereskunde (Institute of Oceanography), 1921; published by Mitler and Son, Berlin. This report is mentioned in TMB Transl. 204, Nov 1949, p. 72.

(4) Weinblum, G., and Block, W., "Stereophotogrammetrische Wellenaufnahmen (Stereophotogrammetric Wave Photographs)," STG, 1936, Vol. 37, pp. 214–250 and 259–276; TMB Transl. 204, Nov 1949

(5) Schumacher, A., "Ozeanographische Sonderuntersuchungen (Special Oceanographic Examinations)," Erste Lieferung, Stereophotogrammetrische Wellenaufnahmen, Vol. VII, No. 2 of the Scientific Results of the German Atlantic Expedition with the research and experimental ship *Meteor*, Berlin, 1939

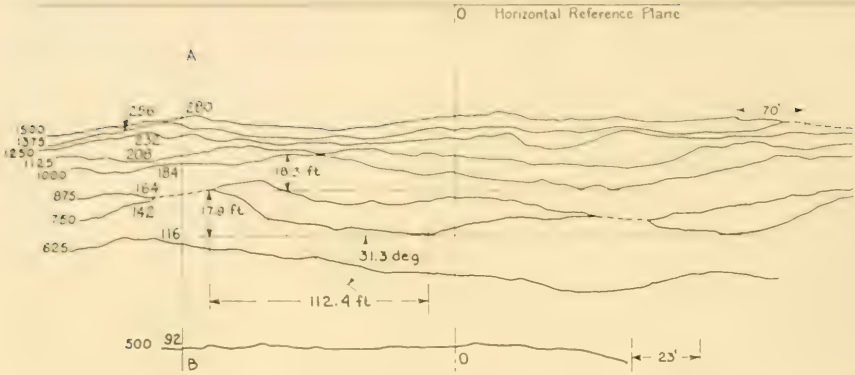

Fig. 48.M Nine Wave Profiles Determined from a Pair of Stereoscopic Photographs Taken from the U. S. S. *Oriskany*

(6) Hidaka, K., "Stereophotogrammetric Survey of Waves and Swells in the Ocean," Memoirs, Marine Observatory, Kobe, Japan, 1941, Vol. 7, pp. 231–368

(7) Marussi, A., "Stereophotogrammetric Apparatus for the Study of Waves Generated by Ship Models," Inter. Shpbldg. Prog., 1955, Vol. 2, No. 15, pp. 537–538. On page 538 there is a list of 6 references.

48.15 Comparison Between Waves in Shallow Water and in Deep Water. Sec. 9.10 describes how, when a deep-water wave moves into shallow water (not necessarily up a sloping beach), its celerity decreases for a given wave length L_W, it becomes steeper, and its crests take on a more peaked profile. Table 29 on page 104 of U. S. Navy Hydrographic Office publication H.O. 602 gives the decrease in lengths and velocities of waves of different dimensions as they advance over a shoaling bottom.

The steady translational speed c_h of a wave in shallow water of constant depth h is, from Sec. 9.10 of Volume I,

$$c_h = c_\infty \left\{\tanh\left(\frac{gh}{c_\infty^2}\right)\right\}^{0.5} \qquad (9.\text{iv})$$

where c_∞ is the deep-water wave speed.

The shallow-water wave velocity in a depth of water h may also be expressed as

$$c_h = \left\{\left(\frac{gL_W}{2\pi}\right)\tanh\left(\frac{2\pi h}{L_W}\right)\right\}^{0.5} \qquad (48.\text{iii})$$

The period of a shallow-water wave is, from Sec. 18.10,

$$\tau = \frac{L_W}{c_h} = \left[\frac{2\pi L_W(e^{4\pi h/L_W} + 1)}{g(e^{4\pi h/L_W} - 1)}\right]^{0.5}$$

The relation between c_h and c_∞ is shown graphically in Fig. 48.N, adapted from D. W. Taylor [S and P, 1943, Fig. 10, p. 12]. Other relationships between shallow-water waves and deep-water waves, taken from W. F. Durand [RPS, 1903, Table V, p. 77], are given in Table 48.I.

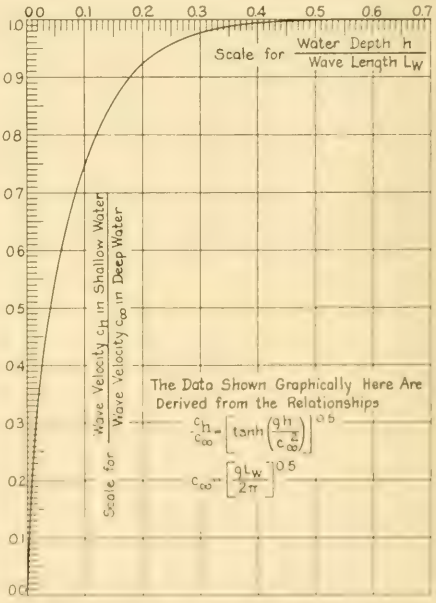

Fig. 48.N Graph Showing Ratio Between Wave Velocities in Shallow and in Deep Water

TABLE 48.l—COMPARISON BETWEEN CHARACTERISTICS OF SHALLOW-WATER AND DEEP-WATER WAVES

Depth of Water as a Fraction of the Wave Length	Ratio between Quantities for Shallow Water and Corresponding Quantities for Deep Water		
	Ratio of Axes of Surface Orbits	Length for Given Velocity	Velocity for Given Length
0.01	0.063	15.90	0.251
0.02	0.124	8.08	0.352
0.03	0.186	5.376	0.431
0.04	0.246	4.065	0.496
0.05	0.304	3.289	0.552
0.075	0.439	2.277	0.663
0.10	0.557	1.796	0.746
0.15	0.736	1.358	0.858
0.20	0.847	1.180	0.920
0.25	0.917	1.091	0.958
0.30	0.955	1.047	0.977
0.35	0.975	1.026	0.987
0.40	0.987	1.013	0.993
0.45	0.993	1.007	0.996
0.50	0.996	1.004	0.998
0.60	0.999	1.001	0.999
0.75	0.9999	1.0001	0.9999
1.00	0.9999	1.00001	0.9999

48.16 Shallow-Water Data. The relationship between the velocity or celerity c and the wave length L_W for various uniform depths h of shallow water of unlimited horizontal area is given in Figs. 48.O and 48.P, adapted from D. W. Taylor [S and P, 1943, Figs. 11 and 12, p. 12]. Somewhat the same data are given in graphic form, but in metric units, by O. Schlichting [STG, 1934, Vol. 35, Fig. 3, p. 130; EMB Transl. 56, Jan 1940, p. 4].

Sir Horace Lamb gives a table relating the wave length L_W, the wave period T_W, the celerity c, and the shallow-water depth h, for lengths of 1, 10, 100, 1,000, and 10,000 ft, and for depths of the same amounts [HD, 1945, p. 369].

For information, Table 72.a in Sec. 72.3 presents a list of speeds for a solitary wave or a wave of translation in shallow water of uniform depth. The range of water depth is from 2 through 40 ft and the celerities are given in both ft per sec and kt.

48.17 General Data for Miscellaneous Waves; The Tsunami or Earthquake Wave. Scientists, mariners, and others have from time to time studied the behavior of waves other than those caused by natural wind. Among these is the *tsunami*, or earthquake wave, generated by a sudden vertical displacement in the earth's crust, usually under the ocean or close to the coast. A gigantic earthquake wave would probably pass unnoticed by a ship in the deep, open sea but over a shoal bank or near the shore it might spell disaster to any vessel.

It is reported that some earthquake waves have traveled at speeds of 600 miles per hr [Votaw, H. C., "Our Navy and South America's Greatest Earthquake," USNI, Mar 1948, p. 345]. It is reported also that an earthquake wave can have

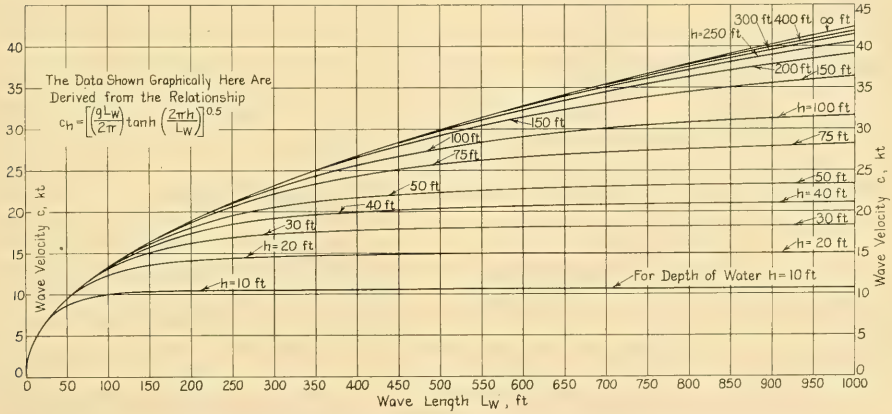

FIG. 48.O RELATION BETWEEN WAVE LENGTH AND WAVE VELOCITY IN VARIOUS DEPTHS OF WATER

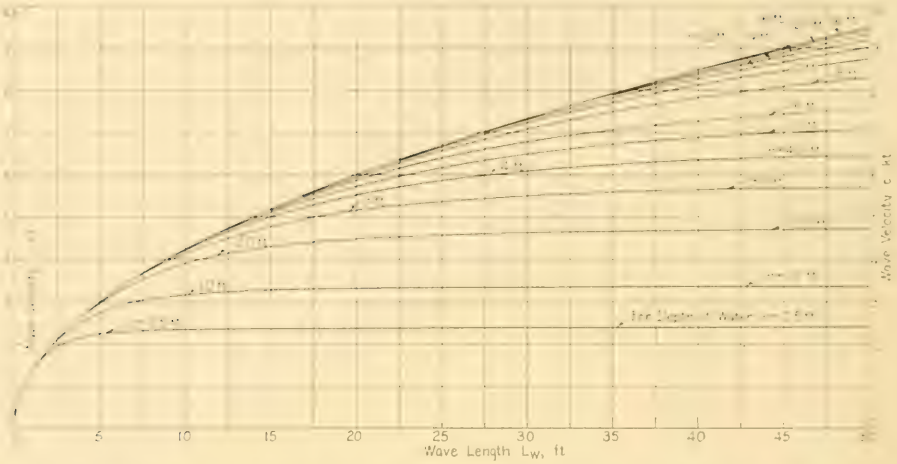

Fig. 48.P Relation Between Wave Length and Wave Velocity in Very Shallow Water

a height of 8 ft at 12,000 miles from its origin. If the relationship $c = \sqrt{gh}$ held at sea, as in shallow water, a celerity of this magnitude (600 mph) would require a water depth h of the order of 24,000 ft.

For earthquake waves traveling across continental shelves of lesser depth the wave velocity appears to be less, but the wave heights are probably greater. David Milne, in a paper entitled "On a Remarkable Oscillation of the Sea, observed at Various Places on the Coasts of Great Britain in the First Week of July 1843" [Trans. Roy. Soc. Edinburgh, 1842–1844, Vol. XV, pp. 609–638, reproduced by permission of that Society], writes as follows on page 633:

"(4) The circumstance that the oscillation of the sea on the Cornish and Devonshire coast preceded the arrival of the storm by some hours, so far from being an objection to the view above suggested, is rather a confirmation of it; as it is well known, from the researches of Mr. Scott Russell, that a wave, when generated by a moving force, will acquire a velocity greater than that of the force producing it, if the depth of water be sufficient. I have elsewhere shewn, that the waves produced by the Lisbon earthquakes came to the English and Irish coasts, with a velocity of from 120 to 160 miles an hour. It is therefore probable, that if a wave were generated by the storm in question, it would move forward with about double the rapidity of the storm itself, which, I have shewn, travelled at a rate of only 70 or 80 miles an hour."

W. Thomson (later Lord Kelvin), writing in a paper "On the Rigidity of the Earth" [Phil. Trans. Roy. Soc., 1863, Vol. 153], states on page 581 that the velocity of long free waves, such as those encountered in mid-ocean, in depths of 10,000 ft or so, is 567 ft per sec. This celerity corresponds to 386.6 mi per hr or 335.7 kt.

The data collected by J. Turnbull and mentioned in Sec. 48.8, plus the data published by H. Keeton in The Marine Observer [1930, Vol. VII, pp. 106–113, esp. pp. 109–110], indicate that single abnormal seas, like onrushing walls of water, are not infrequently encountered in the oceans of the world. No one seems to know their exact cause, nor are there many quantitative data for the more disastrous of them. It is probable that many ships which have been lost without trace have been the victims of these huge waves.

48.18 Bibliography of Historic Items and References on Geometric Waves. Of the extensive bibliography on water waves in general, including sea and wind waves, it is possible only to mention a few of the principal references. The first part of the appended list covers the historical references, prior to 1900. Unfortunately, the reference data on some of the early papers are incomplete.

The references quoted in this section may be supplemented by those of G. C. Manning on pages 48 and 49 of PNA, 1939, Vol. II.

(1) Gerstner, Franz Joseph, "Theorie der Wellen (Theory of Waves)," orig. publ. in Abhandlungen der koenigl. boehmischen Gesellschaft der Wissenschaften zu Prag (Trans. Roy. Bohem. Soc., Prague),

1802. Transl. by R. M. Kay and edited by Oswald Sibul, from an article in German edited by Gilbert, Annalen der Physik, Vol. 32, 1809. Inst. Eng'g. Res., Univ. Cal., Waves Research Lab., Tech. Rep. Ser. 3, Issue 339, TIP U-24940, Sep 1952. The figures from Gilbert's paper of 1809 are reproduced in this translation.

(2) Cauchy, A. L., "Mémoire sur la Théorie des Ondes (Memoir on the Theory of Waves)," 1815. Publ. in Mém. de l'Acad. Roy. des Sciences, 1827; also in "Oeuvres Complètes . . . ," Paris, 1882, Vol. I, 1st series.

(3) Poisson, S. D., "Mémoire sur la Théorie des Ondes (Memoir on the Theory of Waves)," Mém. de l'Acad. Roy. des Sciences, 1816.

(4) Weber, Ernst Heinrich, and Weber, Wilhelm, "Wellentheorie auf Experimente gegründet, oder über die Wellen tropfbarer Flüssigkeiten mit Anwendung auf die Schall- und Licht-wellen (Wave Theory Based upon Experiments, or Concerning the Waves of Non-Viscous Liquids with Application to Sound and Light Waves)," Leipzig, Gerhard Fleischer, 1825. The experiments of the Weber brothers are described briefly and illustrated by H. Rouse and S. Ince in their "History of Hydraulics," Chap. 7, Supplement to "La Houille Blanche," 1955, No. 3, pp. 145–146.

In the words of J. Scott Russell [Brit. Assn. Rep. 1844, p. 332], "The work is distinguished by more than the usual characteristics of German industry in the collection of materials, and contains nearly all that has ever been written on waves since the time of Newton, and as a book of reference alone is a valuable history of wave research."

(5) Young, Dr. Thomas, "Natural Philosophy," (prior to 1833), Vol. II, p. 64ff. The matter of wave reflection is considered in this paper.

(6) Robison, J., and Russell, J. Scott, "Report of the Committee on Waves," British Association Report, 1837. Presented at Liverpool in 1838.

(7) Russell, J. Scott, "Supplementary Report on Waves," British Association Report, 1841

(8) Russell, J. Scott, "Results of Investigations on Waves," British Association Report, 1842

(9) Russell, J. Scott, "Report of Committee on Waves," British Association Report, 1844, pp. 311–390 and Pls. 47–57

(10) Airy, Sir George B., "On Tides and Waves," Encycl. Metropolitana, London, 1845 (reprinted in a separate form)

(11) Stokes, Sir George G., "On the Theory of Oscillatory Waves," Trans. Cambridge Phil. Soc., 1847, Vol. VIII, p. 441ff

(12) Froude, W., "On the Rolling of Ships," Appendix 2 entitled "On the Dynamical Structure of Oscillating Waves," INA, 1862, pp. 48–62 and Pl. III

(13) Rankine, W. J. M., "On the Exact Form of Waves Near the Surface of Deep Water," Phil. Trans. Roy. Soc., 1863, Vol. 153, pp. 127–138

(14a) Rankine, W. J. M., "On the Action of Waves Upon a Ship's Keel," INA, 1864, pp. 20–34

(14b) Rankine, W. J. M., "On Waves Which Travel Along with Ships," INA, 1868, Vol. IX, pp. 275–281.

(15) The Report of the British Association for the Advancement of Science, 1869, embodies the report of a Committee consisting of Mr. C. W. Merrifield, F.R.S., Mr. G. P. Bidder, Captain Douglas Galton, F.R.S., Mr. F. Galton, F.R.S., Professor Rankine, F.R.S., and Mr. W. Froude. This Committee was appointed to report on the state of existing knowledge of the Stability, Propulsion, and Sea-going Qualities of Ships, and as to the application which it may be desirable to make to Her Majesty's Government on these subjects. The findings of this Committee, on page 38, listed as sources of information on waves the references numbered (5) through (12) of this bibliography plus a paper by Cialdi entitled "Sul Moto ondoso del Mare" and some papers in Liouville's Journal of 1866 by Caligny.

(16) Bertin, L. E., "Memoir on the Experimental Study of Waves," INA, 1873, Vol. 14, pp. 155–169. A considerable number of references appear in the footnotes of this paper.

(17) Rankine, W. J. M., "Waves in Liquids," INA, 1873, Vol. 14, pp. 170–178

(18) Bertin, L. E., "Nouvelle note sur les vagues de hauteur et de vitesse variables (New Note on Waves of Variable Height and Velocity)," Comptes Rendus, Acad. Sci., Paris, 9 Mar 1874, Vol. LXXVIII, p. 676ff

(19) Rayleigh, Lord, "On Waves," Phil. Mag., Roy. Soc., 1876, Vol. 5, p. 257ff

(20) Bertin, L. E., "Les vagues et le roulis, les qualités nautiques des navires (Waves and Rolling; The Wavegoing Qualities of Ships)," Paris, 1877, p. 37ff

(21) Woolley, J., "On the Theory of Deep-Sea or Oscillating Waves," INA, 1878, Vol. 19, pp. 66–79

(22) Gatewood, R., "The Theory of the Deep-Sea Wave," USNI, 1883, Vol. 9, pp. 223–254

(23) de Saint-Venant, J.-C. B., "Histoire succinct des récherches sur les ondes (Concise History of Research on Waves)," Annales des Ponts et Chaussées, 1888, Vol. XV, 6th Série, 1st semestre, p. 710ff

(24) Flamant, G., "Exposé sommaire de la théorie actuelle des ondes liquides périodiques (Summary of the Theory of Periodic Waves in a Liquid)," Annales des Ponts et Chaussées, 1888, Vol. XV, 1st semestre

(25) Gaillard, D., "Wave Action in Relation to Engineering Structures," Corps of Engineers, U. S. Army, Prof. Paper 31, 1904. This paper was reprinted in 1935 by the Engineer School, Fort Belvoir, Virginia.

(26) Cornish, V., "Waves of the Sea, and Other Water Waves," F. T. Unwin, London, 1910

(27) Krümmel, O., "Handbuch der Ozeanographie (Handbook for Oceanography)," J. Engelhorn, Stuttgart, 1911, especially "Der Bewegungsformen des Meeres (The Motion Forms of the Ocean) in Vol. II

(28) Cornish, V., Cantor lecture, Royal Soc. Arts (London), 1914

(29) Zimmermann, E., "Aufsuchung von Mittelwerten für die Formen ausgewachsener Meereswellen auf Grund alter und neuer Beobachtungen (Search for Average Values for the Form of Fully Developed Ocean Waves, Based on Old and New Observations)," Schiffbau, 28 Apr 1920, pp. 633–640; 5 May 1920, pp. 663–670

(30) Hogner, E., "A Contribution to the Theory of Ship Waves," (in English), Arkiv för Matematik, Astronomi och Fysik, Stockholm, 1922–1923, Vol. 17, Paper 12

(31) Hogner, E., "Notes on Some New Contributions to the Theory of Ship Waves" (in English), Arkiv för Matematik, Astronomi och Fysik, Stockholm, 1924–1925, Vol. 18, Paper 10

(32) Hogner, E., "Ueber die Theorie der von einem Schiff erzeugten Wellen und des Wellenwiderstandes (On the Theory of Waves and Wave Resistance Caused by a Ship)," Proc. 1st Int. Cong. for Appl. Mech., Delft, 1924, pp. 147–160

(33) Levi-Civita, T., "Détermination rigoureuse des ondes permanentes d'ampleur finie (Rigorous Determination of Permanent Waves of Finite Amplitude)," Math. Ann., 1925, Vol. 93, p. 264ff

(34) Von Larisch, Graf, "Sturmsee und Brandung (Storm Seas and Breakers or Surf)," Bielefeld und Leipzig, 1925. This book contains many excellent wave photographs.

(35) Jeffreys, H., "On the Formation of Water Waves by Wind," Proc. Roy. Soc., Series A, 1925, Vol. 107, pp. 189–206

(36) Thorade, H. F., "Probleme der Wasserwellen (Problems of Water Waves)," published in Probleme der Kosmischen Physik, Vols. 13, 14, H. Grand, Hamburg, 1931

(37) Patton, R. S., and Marmer, H. A., "The Waves of the Sea; Physics of the Earth," 1932. This is Vol. 5 of a work on Oceanography published in Bull. 85 of the National Research Council, Washington, pp. 207–228

(38) Cornish, V., "Ocean Waves and Kindred Geophysical Phenomena," Cambridge Univ. Press (England), 1934

(39) Lavrent'ev, M. A., "Sur la Théorie Exact des Ondes Longues (On the Exact Theory of Long Waves)," translation from Recueil des Travaux de l'Institut Mathématique de l'Académie des Sciences de la RSS d'Ukraine, 1946, No. 8, pp. 13–69. Also, by the same author, "A Contribution to the Theory of Long Waves," translation from C. R. (Doklady) Acad. Sci. UR SSS (N.S.), 1943, Vol. 41, pp. 275–277. Both translations are available in the library of the Bureau of Ships of the Navy Department, library numbers 50655 and 50656, respectively.

(40) Lamb, Sir Horace, "Hydrodynamics," Dover Publications, New York, 6th ed., 1945, Chap. IX on "Surface Waves," pp. 363–475. This book contains many references in the footnotes.

(41) Deacon, G. E. R., "Ocean Waves and Swell," The Occasional Papers of the *Challenger* Society, 1946

(42) Bigelow, H. B., and Edmondson, W. T., "Wind Waves at Sea; Breakers and Surf," U. S. Navy Hydrographic Office publ. H.O. 602, 1947. On page 177 there is a list of 17 selected references, some of which are given here.

(43) "Ocean Surface Waves," Annals N. Y. Acad. Sci., May 1949, Vol. 51, pp. 343–572. This is a collection of fifteen papers by eighteen authors, reporting on a Conference on Ocean Surface Waves held by the Section of Oceanography and Meteorology of the New York Academy of Sciences on 18–19 March 1948. Separate bibliographies are to be found at the end of most of the papers, particularly on pp. 350, 375, 401, 441, 462, 474, 482, 500, 510, 521, and 544.

(44) "Gravity Waves: Proceedings of the NBS Semicentennial Symposium on Gravity Waves, 18–20 June 1951," NBS Circular 521, 28 Nov 1952, Govt. Print. Off., Washington. Contains thirty-three papers by various authors; each paper with its own list of references. Of particular interest are:

1. Neumann, G., "On the Complex Nature of Ocean Waves and the Growth of the Sea Under the Action of Wind," Paper 10, pp. 61–68
2. Deacon, G. E. R., "Analysis of Sea Waves," Paper 23, pp. 209–214.

(45) Keulegan, G. H., "Wave Motion," Chap. XI of "Engineering Hydraulics," 1950, pp. 711–768. On pp. 766–768 the author lists 31 references on waves and wave motion. Some of them apply primarily to hydraulics but there are a considerable number of general interest to the naval architect and to the physicist.

(46) Munk, W. H., and Arthur, R. S., "Forecasting Ocean Waves," Compendium of Meteorology, American Meteorological Society, Boston, 1951, pp. 1082–1089. This paper lists 25 references.

(47) Munk, W. H., "Ocean Waves as a Meteorological Tool," Compendium of Meteorology, American Meteorological Society, Boston, 1951, pp. 1090–1100. There are 16 references with this paper.

(48) Mason, M. A., "Surface Water Wave Theories," ASCE, Hydraulics Div., Mar 1952, Vol. 78, Separate 120. An excellent, readable, well-illustrated, non-mathematic summary of the subject. There is a list of 68 references, of which the first dozen or so give the principal historic papers.

(49) Sverdrup, H. U., Johnson, M. W., and Fleming, R. H., "The Oceans: Their Physics, Chemistry, and General Biology," Prentice-Hall, New York, 1952, Chap. XIV, pp. 516–537

(50) Pierson, W. J., Jr., Neumann, G., and James, R. W., "Practical Methods for Observing and Forecasting Ocean Waves by Means of Wave Spectra and Statistics," prepared as Technical Report 1 under Contract N189s-86743, BuAer Project AROWA, July 1953. On pages 320 and 321 there is a bibliography of 39 items.

(51) Eckart, C., "The Generation of Wind Waves on a Water Surface," Jour. Appl. Phys., Dec 1953, Vol. 24, No. 12, pp. 1485–1494. Review by W. H. Munk in Appl. Mech. Rev., Jun 1954, p. 279.

(52) Proudman, J., "Dynamical Oceanography," Methuen and Company, London; Wiley, New York, 1953

(53) "Waves, Tides, Currents and Beaches: Glossary of Terms and List of Standard Symbols," 1953, Council on Wave Research, Eng'g. Found'n., Univ. Calif., Berkeley

(54) "Gravity Waves: Tables of Functions," 1954, Council on Wave Research, Eng'g. Found'n., Univ. Calif., Berkeley

(55) Deacon, G. E. R., "Response of the Sea Surface to Winds," Jour. Inst. Navigation (United Kingdom), Jul 1954, Vol. 7, pp. 252–261

(56) "Ships and Waves," Proc. First Conf. on Ships and Waves, Oct 1954, publ. by Council on Wave Research and SNAME, 1955.

48.19 Bibliography on Subsurface Waves. For the reader who wishes to pursue the study of surface waves and the Hall Effect beyond the brief discussion of Sec. 10.20, the following references are available:

(1) Lamb, H., HD, 1945, pp. 370–375; "On Waves due to a Travelling Disturbance, with an Application to Waves in Superposed Fluids," Phil. Mag. (6), 1916, Vol. 31, p. 386ff

(2) Froude, W., "Remarks on the Differential Wave in a Stratified Fluid," INA, 1863, Vol. 4, pp. 216–218

(3) Stokes, G. G., Trans. Cambr. Phil. Soc., 1842–1849, Vol. 8, pp. 451–452

(4) "The Mariner's Mirror," Apr 1943, Vol. 29, pp. 73–74

(5) Eckman, V. W., "On Dead-Water," Norweg. North Pole Exp., 1893–1896, Sci. Results, Vol. V, Part XV, Christiania (Oslo), 1906

(6) Bjerknes, V., Solberg, H., Bjerknes, J., and Bergeron, T., "Physikalische Hydrodynamik mit Anwendung auf die dynamische Meteorologie (Physical Hydrodynamics as Applied to Dynamic Meteorology)," Springer, Berlin, 1933, and Edwards Bros., Ann Arbor, 1943, pp. 387–391. This reference gives a table of the maximum velocity of subsurface waves, depending upon the thickness of the upper (lighter-density) layer, and its salinity content.

(7) Milne-Thomson, L. M., TH, 1950, Art. 14.42, pp. 367–368, entitled "Waves at an Interface"

(8) Ippen, A. T., and Harlemen, D. R. F., "Steady-State Characteristics of Subsurface Flow," NBS Circ. 521, June 1951

(9) Sverdrup, H. U., Johnson, M. W., and Fleming, R. H., "The Oceans: Their Physics, Chemistry and General Biology," Prentice-Hall, New York, 1952, pp. 585–602, on "Internal Waves."

CHAPTER 49

Mathematical Methods for Delineating Bodies and Ship Forms

49.1 Scope of This Chapter; Definitions. Mathematical methods for delineating the forms of bodies and ships are those by which the shape of the outer surface, adjacent to the liquid, may be defined wholly or in part by mathematical formulas and equations which express the coordinates in terms of given reference axes. These may be the rectangular (x, y, z) or Cartesian coordinates in one, two, or three dimensions, the cylindrical coordinates about an axis, the polar or spherical coordinates about a point, or whatever may be convenient for the purpose. With a selected set of numerical values assigned to the symbols of these equations, all or part of the surface coordinates or offsets may be calculated.

Part of a body surface may be geometric, such as a nose of hemispherical or ellipsoidal shape of a body of revolution, attached to a cylindrical middlebody or circular section. Some other part of the surface, such as the tail, may be highly irregular, impractical for mathematic representation with any set of reference axes.

Instead of covering a whole 3-diml body surface, the mathematical formulas may be limited to those required for the delineation of 2-diml features. A typical case is the formula for the intersection of a plane with the 3-diml surface, such as the designed waterline on a ship. Here the reference axis almost invariably lies in the intersecting plane.

Even for the 2-diml case it may be convenient to divide the intersection or outline into two or more parts, with a separate origin or set of coordinates for each part, positioned to suit the mathematical formulas employed.

The term *geometric shape* defines a body whose outline or surface is represented by some *simple* mathematical formula. Examples are a cube, a sphere, a circular-section cylinder, a right circular cone, a symmetrical pyramid, a parallelepiped, or an ellipsoid. To achieve simplicity it may be necessary to use a particular system of coordinates and to establish limits in one or several dimensions, as for the cube in cartesian coordinates. For any geometric shape one such simple expression is usually sufficient.

49.2 The Usefulness of Mathematical Ship Lines. Before embarking on a discussion of the mathematical delineation of the lines or surfaces of bodies and ships, it is well to answer the question that arises immediately in the mind of the practical naval architect and shipbuilder: Why bother with mathematical lines when faired lines can be drawn so quickly by experienced personnel?

It is easy to give two answers to this question. In the first place, analysis of the lines of many actual ships, in the form available to the naval architect at large, indicates that they are not strictly fair by any criteria, graphical or mathematical. In the second place, experienced person-

nel are by no means available in sufficient numbers, especially in a national emergency, to draw all the ship lines that need to be laid down.

There are several other good reasons, both practical and scientific. For a ship of a new type, or of a novel shape, it is still a draw-and-erase process, even for an experienced hand, to lay down the lines of a 3-diml ship surface that will have the proportion and shape characteristics selected by the designer. When these characteristics are achieved, the fairing process remains, or the curvatures require to be checked, as described subsequently in this chapter. Assuming a perfect drawing, its dimensions, coordinates, and offsets still require conversion to numbers, so that artisans with rules and scales can build the full-size ship. These numbers have to be "lifted" from the graphic drawing but they are a natural product of the mathematic method.

The numerical values of those hull coefficients and form parameters which are not used to set up the mathematical equations may be calculated before any mathematical lines are laid down on paper. The designer may likewise calculate the positions of the various centers of area and of volume in which he is interested, to insure that they fall in the proper places. Actually, the hull parameters are selected by the hull designer while the subsequent calculations and the drafting work are performed by computing-machine operators and draftsmen.

As an example of what can be done with mathematical lines in an intensely practical case, the shape of the large blisters added to the U. S. battleships of the *New Mexico* class in the early 1930's was delineated by D. W. Taylor's mathematical method, to be discussed presently. In some respects this was a more difficult job than laying down the lines of the whole ship in the first place.

Entirely apart from the shipbuilding aspect, mathematic delineation is invaluable when preparing the lines of a series of models in which some parameter is to be varied systematically from model to model.

The development of mathematical formulas and methods for representing the principal lines or the surfaces of ships has been somewhat spasmodic and is still far from a logical or practical conclusion. A brief history is given here of the outstanding events in the development, together with a summary of the results achieved to date (1955).

49.3 Existing Mathematical Formulas for Delineating Ship Lines. The use of mathematical formulas for calculating the offsets of ship lines, or better, for delineating what may be called mathematical ship surfaces, is not necessarily tied to the mathematical calculation of resistance due to wavemaking and other causes, discussed in Chap. 50. To be sure, many of the calculations for pressure resistance due to wavemaking have been carried out for ship forms whose waterlines and transverse sections could be expressed by mathematical equations. These equations may, however, be used for establishing the lines without a subsequent attempt to calculate any element of the ship resistance.

It appears to have been in the minds of the earliest workers in this field that the use of mathematical equations to derive the usual offsets would also serve to achieve the hull proportions and parameters desired by the designer and to tell him whether his volume and area centers would be where he wanted them.

"The oldest writer on forms of ships who has given any well-defined system of laying down lines was probably the distinguished (Swedish) naval architect Chapman, who proposed to use a system of lines composed of parabolic curves adapted to the intended size and proportions of the vessel" [Thurston, R. H., "Forms of Fish and of Ships," INA, 1887, Vol. 28, p. 418].

Chapman's work in the 1760's or 1770's was followed in the early 1790's by the first recorded systematic tests on models, conducted by Mark Beaufoy and others. These models were geometric shapes and could be said to have had geometric or mathematical lines. From the 1830's to the 1870's mathematical curves such as the versed-sine curve of diagram A of Fig. 24.G, the cycloid, the trochoid, and the streamlines around a Rankine stream form were proposed and actually worked into the lines of ships of that day by J. Scott Russell, James R. Napier, W. J. M. Rankine, and others. Arcs of circles and possibly of ellipses as well have been worked into ship lines since time immemorial [Narbeth, J. H., INA, 1940, p. 147].

John W. Nystrom, in the 1860's, expanded Chapman's use of the parabolic trace and developed what he called the "Parabolic Shipbuilding Construction." He utilized parabolas of varied order, with fractional as well as integral exponents, to make up both waterlines and sections. His method, described in the Journal of The Franklin Institute [Jul-Dec 1863, Third

Series, Vol. XLVI, pp. 355–359 and 389–396, with Pls. II and III], enabled him to calculate the complete set of offsets for a ship body plan representing an underwater form with a numerical value of block coefficient C_B selected in advance. He describes, on page 358 of the reference:

"... a vessel constructed wholly by the parabolic method; every cross section or frame is a parabola; the frame drawing or body plan is laid down direct from calculation without reference to water-lines or diagonals and without exercise of taste."

He was able, with this mathematic method, to use reversed parabolas for hollow waterlines, to calculate both the horizontal and the vertical position of the center of buoyancy CB, and to draw a curve of displacement volume on a basis of draft. His methods are explained in detail in the reference cited and are illustrated by examples.

Nystrom even goes so far as to tell, on page 358 of the reference, how:

"... to form the displacement so as to present the least possible resistance when forced through water. The immersed area of each frame (station) should increase or diminish in a certain series, found theoretically to be that the square root of the sections (areas) should be ordinates in a parabola, the exponent of which depends on the desired fulness of the displacement (block coefficient)."

The words in parentheses are those of the present author.

Subsequent papers by Nystrom, all on the same general subject, appear in references (3) and (4) listed in Sec. 49.17.

Shortly after the Washington Model Basin was put in operation in 1900 D. W. Taylor developed a mathematic "method of deriving quickly the lines of a model possessing certain desired characteristics, and ... practicable and easy methods of systematically varying characteristics of models ..." [SNAME, 1903, pp. 243–267]. This method covered the delineation of waterlines, section lines, and section-area curves. A somewhat different mathematic method of producing waterlines, section-area curves, and body plans, closely resembling those of actual ships, was proposed by J. N. Warrington shortly thereafter [SNAME, 1909, pp. 441–452].

Another decade of development by Taylor, following his original concepts, produced the paper entitled "Calculations for Ships' Forms and the Light Thrown by Model Experiments upon Resistance, Propulsion and Rolling of Ships" [Trans. Int. Eng'g. Cong., Nav. Arch. and Mar. Eng., San Francisco, 1915]. In this revised and amplified procedure, separate formulas are used for waterlines and sections. The curve families for fine sections are 4th-degree parabolas; those for full sections are hyperbolas. The entrance and the run, extending from the bow and stern, respectively, to the section of maximum area, are treated separately, because the origins of the mathematical curves are taken at the bow and at the stern. The families of curves representing waterlines and section-area curves are given by 5th-degree polynomials with five arbitrary parameters, of the type $y = tx + ax^2 + bx^3 + cx^4 + dx^5$. It was apparently Taylor's intention to give a shape to the waterline curves that would impart a predetermined amount of lateral or normal acceleration to the water flowing around them.

No parallel body is mentioned in Taylor's paper although there is of course no difficulty in separating the hull at the section of maximum area and inserting any desired length of cylindrical prism having the maximum-section shape.

Taylor's method is entirely suitable for practical and shipyard use; in fact, it has been used off and on for drawing model and ship lines at Washington for the past 50 years. A number of U. S. naval vessels have been constructed to these lines. The body plan of a modern design, most of which was delineated by Taylor's method, is reproduced in Fig. 49.C of Sec. 49.7.

Elaborating upon the quotation in a preceding paragraph from D. W. Taylor's 1903 SNAME paper, his method makes it possible, by the use of equidifferent or progressive values for the parameters, to develop any desired number of ship forms in a series. This was of inestimable value in the preparation of lines for large groups of models such as the Taylor Standard Series. Using this method the series became scientifically systematic, with the minimum of effort on the part not only of those who planned it but those who had to draw the lines for each model.

An excellent supplementary statement by G. P. Weinblum [TMB Rep. 710, Sep 1950, p. 7], from which the following is paraphrased, says that Taylor developed mathematical formulas, not with the idea that they gave the lines of a ship of minimum resistance but simply to obtain lines possessing desired shapes. This statement is important. Contrary to some attempts to ascribe magic properties to certain analytically defined curves like trochoids and sine curves, the principle of systematization was the decisive argument for their adoption.

Unfortunately, Taylor's method was described in a publication not conveniently available to the average naval architect. There are reprints of this paper but they have been given only limited circulation. Since the equations of waterlines and sections are not linked together into equations of surfaces in which the hull is treated as a whole, it is considered preferable by those who have studied this problem to develop a broader system of ship-hull equations than to make Taylor's work of 1915 available to a more extended group of readers.

The broader purpose envisaged by Weinblum some fifteen years later, explained in references (8) and (9) of Sec. 49.17, of representing the whole ship surface by single equations, was followed by his more recent work at the David Taylor Model Basin, published in the following TMB reports:

710 "Analysis of Wave Resistance," written jointly with J. Blum, Sep 1950. This report is in the category of *must* reading for anyone studying the subject of mathematical ship lines.
758 "The Wave Resistance of Bodies of Revolution," May 1951
840 "Investigations of Wave Effects Produced by a Thin Body—TMB model 4125," Nov 1952. Written jointly with J. J. Kendrick and M. A. Todd.
886 "A Systematic Evaluation of Michell's Integral," Jun 1955, especially those portions having to do with ship lines.

Weinblum has developed mathematical expressions, to be described presently, which:

(a) Are suitable for delineating an entire ship form of given characteristics, based upon an origin amidships. This improves upon the Taylor procedure of treating the forebody and afterbody separately, with origins at the two ends.
(b) Will produce a series of forms with scientific systematic variations in these characteristics
(c) Will provide a basis for the systematic investigation of wave-resistance characteristics of ships. This will, it is hoped, lead eventually to forms of low if not least resistance.
(d) Will provide a basis for the calculation and prediction of the flow pattern and the pressure distribution around a ship
(e) Will form a more general foundation for research on other problems of naval architecture involving maneuvering, wavegoing, and behavior in shallow water and restricted channels.

49.4 Mathematical and Dimensionless Representation of a Ship Surface. In the Weinblum references of Sec. 49.3 the problem of the dimensionless delineation of a ship hull is generalized:

First, by considering the entire underwater boundary as a surface, rather than as a series of intersections of that surface by three sets of parallel planes at right angles to each other, long customary in naval architecture. In other words, instead of defining the shape by offsets of waterlines, of bowlines and buttocks, and of section lines, usually at equidifferent intervals from three given planes of reference, it is defined for the normal case by the y-offsets from the centerplane or the plane of symmetry for *any point* on the hull surface having the coordinates x and z.
Second, by expressing the y-offsets and the x- and z-coordinates not as dimensions in well-known length units but as non-dimensional ratios of the respective offsets and coordinates to the length, breadth, and draft dimensions. These 0-diml ratios are given presently.
Third, by placing the origin O of the coordinate system in the surface waterplane, in the plane of symmetry, and at midlength of the immersed form or underwater hull. The length of this hull is L, the waterline length. While the vertical measurements on an actual ship are usually made upward from the baseplane, in the mathematical system they are made downward because this is the positive direction of the z-axis of the ship, described in Sec. 1.6 and indicated in Fig. 1.K.

In the discussion which follows it is assumed that:

(a) The ship is a simple one which may be considered symmetrical forward of and abaft the midlength station
(b) The ship is symmetrical with respect to the centerplane, as is customary for real ships. The definition sketch of Fig. 49.A is an isometric diagram of the outline of such a ship, correspond-

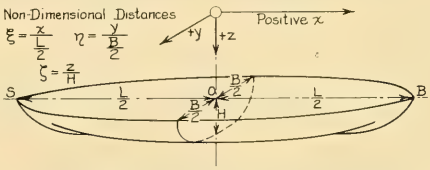

Fig. 49.A Definition Sketch of a Simple Ship Surface with a Single Origin

ing somewhat to the underwater body of a North American Indian canoe.

The general *dimensional* equation of the hull surface is then

$$y = \pm y(x, z) \qquad (49.\text{i})$$

where the plus and minus signs represent identical transverse offsets to starboard and port, respectively, and the expression $y(x, z)$ signifies a transverse y-function for the hull. In this case it is a function of both x and z. For example, if x were 215 ft forward of the amidships origin on a certain vessel, and z were 20 ft below the origin (the latter in the plane of the designed waterline), y would be some value such as ± 14.2 ft, measured to starboard and to port, by virtue of the function $\pm y(x, z)$. If the y-function were 1.0 for any combination of absolute values of x and z, then the starboard and port y-offsets would be equal throughout. When defined by suitable x- and z-limits the craft would have the form of a wall-sided box or parallelepiped.

If the craft were unsymmetrical fore and aft about the midlength it would be necessary normally to use two surface equations:

$$y_F = \pm y_F(x, z) \text{ for the forebody} \qquad (49.\text{iia})$$

$$y_A = \pm y_A(x, z) \text{ for the afterbody} \qquad (49.\text{iib})$$

This procedure has the effect, however, of destroying the ship as an entity, with a single origin and a single surface equation. Carried to its logical conclusion it would break up the ship into two dissimilar half-bodies, one comprising the entrance and the other the run, each with its own set of surface, area, volume, and moment equations. To avoid losing the single ship equation, which may later be introduced into operations involving wavemaking, maneuvering, and wavegoing, Weinblum has developed a special procedure for asymmetry, to be described presently.

Returning to the simple ship, symmetrical fore and aft, the next step is to convert the x-, y-, and z-offsets and coordinates to 0-diml form. When this is done they become

$$\xi(\text{ksi}) = \frac{x}{\frac{L}{2}}, \ \eta(\text{eta}) = \frac{y}{\frac{B}{2}}, \ \zeta(\text{zeta}) = \frac{z}{H} \qquad (49.\text{iii})$$

The 0-diml form of the general equation (49.i) becomes, adopting Weinblum's notation,

$$\eta = \pm \eta(\xi, \zeta) \qquad (49.\text{iv})$$

where $\eta(\xi, \zeta)$ is a transverse 0-diml η-function of the hull. In this case it is a function of both ξ and ζ.

The general surface equations serve equally well as equations of the usual ship lines when one of the set of coordinates is given a fixed value. For the surface waterline, where z or ζ is zero, the equations become

$$y = \pm y(x, 0) \quad \text{and} \quad \eta = \pm \eta(\xi, 0) \qquad (49.\text{v})$$

For the midsection, where x and ξ are zero,

$$y = \pm y(0, z) \quad \text{and} \quad \eta = \pm \eta(0, \zeta) \qquad (49.\text{vi})$$

For a submarine hull which is not a body of revolution and is not symmetrical above and below any horizontal reference plane, there would be required two sets of surface equations, one for the upper and one for the lower portion. The common origin for the two would lie in some convenient horizontal axis or dividing plane. Again, however, this would break up the vessel as an entity by splitting it horizontally. A procedure would have to be devised which would retain a single ship equation for use in analytic studies, say of underwater maneuvering.

Weinblum's general or basic procedure for hulls that are asymmetric with respect to the midlength section is to split up the surface equation into a main part that is symmetric fore and aft and an "asymmetric (skew) deviation" represented by a secondary equation [TMB Rep. 886, Jun 1955, p. 10]. Procedures and equations for the situation where the section of maximum area is not at midlength, with unequal entrance and run lengths, and for other asymmetric variations, become somewhat involved. One such case is that in which the maximum waterline beam does not occur at midlength. The procedures involved are not discussed here but the reader who wishes to study them may consult page 9 and following of Weinblum's TMB Report 886, issued in June 1955, as well as his earlier paper [STG, 1953, pp. 186–215].

Weinblum has pointed out that as more and more mathematical lines and mathematical expressions for ship form come into use, whether analytical or general, it becomes necessary to use ratios or new symbols for quantities formerly expressed by abbreviations [SNAME, 1948, p. 413]. A case in point is the use of the ratio LCB, with a reference point at the FP. Using the ship axes of Fig. 1.K, the distance of the CB from the

origin O at midlength is expressed as the linear distance x_B or as the 0-diml ratio $x_B/(L/2)$, plus if forward and minus aft.

49.5 Application of the Dimensionless Surface Equation to Ship-Shaped Forms. The 0-diml shape or surface function $\eta(\xi, \zeta)$ of the hull may take a great variety of forms, even for boat- or ship-shaped underwater bodies. The simplest are the binomial forms

$$\eta(\xi, 0) = 1 - \xi^n \qquad (49.\text{vii})$$

or

$$\eta(0, \zeta) = 1 - \zeta^m \qquad (49.\text{viii})$$

These produce what are called Chapman parabolas [Weinblum, G. P., TMB Rep. 886, pp. 13–14]. With different numerical values of the exponent n other than 1.0, but not necessarily whole numbers, the shape function of Eq. (49.vii) gives parabolic waterlines of varying curvature and fullness, much like those described and discussed by J. W. Nystrom in the 1863 and 1864 Franklin Institute references quoted in Secs. 49.3 and 49.17.

The shape selected for the designed waterline, in the simplest case, determines the function of the 0-diml fore-and-aft distance ξ from the origin. The shape selected for the midsection determines the function of 0-diml keelward distance ζ from the origin. Thus the shape defined by the expression $\eta = 1 - \xi^n$ of Eq. (49.vii) has an nth-order parabolic waterline and wall sides. That defined by $\eta = 1 - \zeta^m$ has mth-order parabolic sections and square (plumb) ends.

It is possible to shape the waterlines and sections independently by using a surface equation in the form of the binomial product

$$\eta(\xi, \zeta) = (1 - \xi^n)(1 - \zeta^m) \qquad (49.\text{ix})$$

A half-body plan of a hull developed by putting $n = 2$ and $m = 2$ is published by Weinblum [TMB Rep. 886, Fig. 3, p. 20].

Introducing what he calls a *fining function* into the first binomial of the product [TMB Rep. 886, p. 21], Weinblum produces a 0-diml equation of the form

$$\eta(\xi, \zeta) = [1 - \xi^n - (\text{a coefficient})(\xi^m - \xi^p)\zeta](1 - \zeta^q) \qquad (49.\text{x})$$

When given a specific set of values, for example by using a selected coefficient and putting $n = 2$, $m = 2$, $p = 4$, and $q = 9$, Eq. (49.x) becomes

$$\eta = [1 - \xi^2 - (0.5757)(\xi^2 - \xi^4)\zeta](1 - \zeta^9) \qquad (49.\text{xa})$$

With this surface function Weinblum produces the half-body plan of Fig. 49.B, adapted from Fig. 4 on page 21 of TMB Report 886. This has a marked resemblance to some actual ship forms.

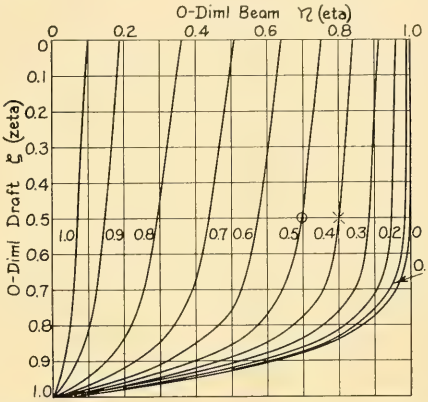

Fig. 49.B Body Plan of a Schematic Ship with Mathematical Sections Developed by Weinblum

Evaluation of the 0-diml transverse offsets from Eq. (49.xa) is fairly simple for a computer with a desk calculating machine. For example, setting the value of ξ as 0.4, for a section just abaft the forward quarter point, and the value of ζ as 0.5, for the half-draft waterline, Eq. (49.xa) becomes

$$\eta = \{1 - (0.4)^2 - (0.5757) \cdot [(0.4)^2 - (0.4)^4](0.5)\}[1 - (0.5)^9] \qquad (49.\text{xb})$$

The 0-diml value of η for the point marked with a diagonal cross in Fig. 49.B is found to be 0.79975. For a value of ξ equal to 0.5 and the same 0-diml waterline at $\zeta = 0.5$, the 0-diml value of η for the point marked with a small circle is 0.6947.

If, in the hull-surface equation (49.xa), ζ is put equal to zero, the result is a 0-diml equation for the surface waterline, namely $\eta = (1 - \xi^2)$. If this equation is differentiated with respect to ξ, the $d\eta/d\xi$ equation resulting gives the 0-diml slope of the surface waterline at any selected value of ξ. If a second differentiation with respect to ξ is made, there is obtained an equation for $d^2\eta/d\xi^2$ which gives the rate of change of 0-diml waterline slope for any value of ξ. These are converted into ship values in terms of x and y

by Eq. (49.iii). The formula for this operation is

$$\frac{dy}{dx} = \frac{B}{L}\frac{d\eta}{d\xi} \qquad (49.\text{xi})$$

It corresponds to Weinblum's Eq. (26) on page 84 of TMB Report 710.

Somewhat unfortunately, in Appendix I of his 1915 paper, D. W. Taylor gave the name of "acceleration" to the second derivative d^2y/dx^2. It might well have resulted in some further development in the field of ship form, in the four decades following that paper, had he combined the first and second derivatives to obtain the well-known radius-of-curvature equation, given in Sec. 49.9 as Eq. (49.xxi). Much more might now be known of the hydrodynamic effects of surface curvature and the best way of working curvature into a hull.

49.6 Summary of Dimensionless General Equations for Ship Forms. In TMB Report 886, issued in June 1955, Weinblum derived and set down for convenience a number of general 0-diml equations not mentioned in the foregoing. These are listed hereunder for convenience, as adapted from pages 8 and 9 of the referenced report, accompanied by some explanatory notes. Weinblum's notation is modified slightly in some places, to bring it more nearly into agreement with the ATTC and ITTC standards, but this should not inconvenience the reader.

All equations listed are developed from the basic hull equation (49.i), namely $y = \pm y(x, z)$, and *all are dimensionless*. It is assumed that the maximum section area occurs at midlength.

Coordinates and offsets

$$\xi(\text{ksi}) = \frac{x}{\frac{L}{2}}, \ \eta(\text{eta}) = \frac{y}{\frac{B}{2}}, \ \zeta(\text{zeta}) = \frac{z}{H} \qquad (49.\text{iii})$$

Hull equation

$$\eta = \pm\eta(\xi, \zeta) \qquad (49.\text{iv})$$

Waterplane equation

$$\eta = \pm(\xi, 0) \qquad (49.\text{v})$$

Midlength section equation

$$\eta = \pm\eta(0, \zeta) \qquad (49.\text{vi})$$

Centerplane or profile equation

$$0 = \pm\eta(\xi, \zeta); \qquad \zeta = \zeta(\xi, 0) \qquad (49.\text{xii})$$

Area-of-section equation

$$A(\xi) = 2\int_0^{\zeta(\xi,0)} \eta(\xi, \zeta)\, d\zeta \qquad (49.\text{xiii})$$

Section-area curve equation with unit ordinate at midlength

$$\frac{A}{A_X} = \frac{1}{C_X}\int_0^{\zeta(\xi,0)} \eta(\xi, \zeta)\, d\zeta \qquad (49.\text{xiv})$$

Midlength section-area coefficient

$$C_X = \frac{A_X}{B_X(H_X)} = \int_0^1 \eta(0, \zeta)\, d\zeta \qquad (49.\text{xv})$$

Load waterplane coefficient

$$C_W = \frac{A_W}{L(B_X)} = \frac{1}{2}\int_{-1}^{+1} \eta(\xi, 0)\, d\xi \qquad (49.\text{xvi})$$

Prismatic coefficient

$$C_P = \frac{\forall}{L(A_X)} = \frac{1}{2}\int_{-1}^{+1} \left(\frac{A}{A_X}\right) d\xi \qquad (49.\text{xvii})$$

Block coefficient

$$C_B = \frac{\forall}{L(B_X)H_X} = \frac{1}{4}\int_{-1}^{+1} A(\xi)\, d\xi. \qquad (49.\text{xviii})$$

49.7 Limitations of Mathematical Lines. It is possible to make excellent and profitable use of geometric shapes and mathematical equations for small "pieces" of ship surfaces. Examples are portions of cones for the local enlargements around single shafts emerging from the trailing ends of skegs, the elongated barrels of bossings, where the conical axis need not coincide with the shaft axis, and the basic portions of bulb bows, such as the one illustrated in Fig. 67.H. There is a limit, however, where the expenditure of time and labor in this process is not justified by the hydrodynamic improvement in the ship or by other advantages enumerated previously. In general, the field of usefulness of the mathematical line, as it is with the accurately faired line to be described presently, centers principally around those traces of the hull which are parallel to the direction of water flow. The statements in Chaps. 24, 25, 27, and 28 indicate that neither unfairnesses in the transverse sections, nor fore-and-aft corners and discontinuities, have too great a detrimental effect upon resistance. It is unnecessary and futile as well as impossible, to try to make a hyperbola of the 200th or the 300th order fit a perfectly acceptable midsection composed of a vertical side line, a horizontal bottom line, and a circular-arc bilge corner. Where the mathematical lines offer an advantage, use them. Where they do not, forget them.

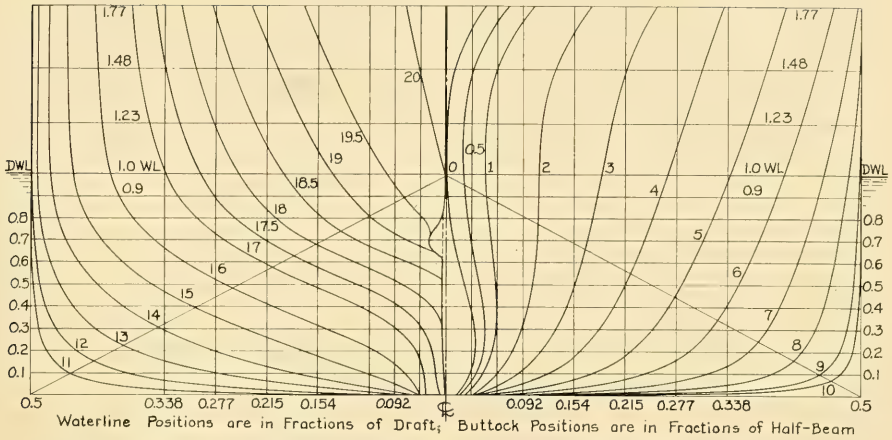

Fig. 49.C Body Plan of Ship with Mathematical Lines Following the Taylor Method
From Sta. 2 through Sta. 14, both inclusive, the lines of the hull represented here are entirely of mathematical derivation.

The body plan of Fig. 49.C, illustrating a tentative form for a multiple-screw vessel of modern (1954) design, is a good illustration of what can be done with D. W. Taylor's system of mathematical lines. From Sta. 2 to Sta. 14, both inclusive, the hull form is entirely of mathematical derivation. Beyond those stations the reverse curves and changes in curvature call for the customary graphic layout and fairing procedure.

For information, the principal 0-diml form coefficients of the hull of Fig. 49.C are:

$$C_P = 0.560 \qquad L/B = 8.31$$

$$C_X = 0.976 \qquad B/H = 3.77$$

$$C_W = 0.684 \qquad \frac{\Delta}{\left(\frac{L}{100}\right)^3} = 60.5$$

$$C_B = 0.547$$

$$\overline{LCB} = 0.5051L \qquad \frac{\forall}{(0.10L)^3} = 2.123.$$

In common with many other tools of the marine architect, mathematical lines are specialized rather than all-purpose affairs. In this respect, however, they may often do well what the others can not do at all. For example:

(1) Mathematical methods lend themselves to working in 0-diml terms

(2) The formulas lend themselves to machine calculations, enabling many ordinates—or abscissas—to be calculated in a given time, and making any subsequent curve drawing more precise. The computing, laying off, and drawing may be performed by not-too-skilled operators, and by those not fully indoctrinated in naval architecture.

(3) It is possible, as explained in Secs. 49.13 and 49.14, to fair the principal ship lines of a set by mathematical methods, and to produce fair full-scale offsets for those principal lines in the design stage. Further, it is possible, by desk-machine calculation, to shift from fair station offsets to fair frame offsets, greatly facilitating the laying down of the full-scale lines.

(4) A mathematical curve is more readily and accurately transferred from small scale on a drawing to full scale in the loft than is a graphical curve

(5) It is possible, for analytical projects, to work on the mathematical formulas with a number of mathematical (not human) operators, such as those which give slopes, rate of change of slopes, and moments.

In general it may be said that graphic representations are unsuitable for analytic investigations, in which modern hydrodynamic parameters are used, general laws are to be established, and predictions of performance are to be made [Weinblum, G. P., TMB Rep. 710, Sep 1950, p. 5]. Formulas and equations are needed for this work.

49.8 Value and Relationship of Fairness and Curvature. There has been an inherent realization among ship designers and shipbuilders since

time immemorial that the underwater surface of a ship hull should be fair in the direction of water flow along it. This was achieved by eye in the hewing process or by bending fore-and-aft structural members such as planks into reasonably fair elastic curves. It is entirely possible, indeed probable, that the hewer of old used flexible wooden strips or battens bent around the hull to check his fairing, as does the wooden-model maker of today. If so, these were the forerunners of the flexible strips or splines later employed for drawing fair lines to which the shipwrights and shipfitters were to work.

It is often taken for granted that because a heavy spline can not have an abrupt kink put into it without splitting or breaking, it must automatically produce a fair or smooth ship line. Whether carried to this extreme or not it is still necessary, in order to achieve the maximum degree of what G. P. Weinblum calls "geometrical smoothness of the ship surface," to use the stiffest spline which can be bent into the desired curve, and to supplement the elastic uniformity of the spline by sighting along it before drawing the line.

In the discussion which follows, adapted largely from the work of Weinblum, his term "smoothness" is eliminated. This makes it synonymous with his term "fairness" and avoids confusion with the use of "smoothness" to describe the condition of a solid surface along which viscous flow takes place in a real liquid.

It is difficult to describe or to specify fairness, especially in a quantitative sense. Following Weinblum, a curve may be called *fair* when its first derivative with respect to a selected ship axis, say dy/dx, is continuous. The *order of fairness* of such a curve may be further defined as the order of the highest derivative which is still continuous. Thus a curve in which there is a continuous second derivative d^2y/dx^2 and continuous curvature is fair to the second order [Weinblum, G. P., and Kendrick, J., "On the Geometry of the Ship, Part I," unpubl. TMB rep.]. The following is quoted from pages 16 and 17 of the referenced report, with "smoothness" replaced by "fairness" and some minor editing:

"Spline curves drawn in the proper way should be at least fair to the second order or have continuous curvature. This follows immediately from the proportionality of the curvature of the elastic axis of a spline to the bending moment on the spline. The graph of the bending moment and therefore the curvature remain continuous even though horizontal concentrated loads are exerted by weights on the spline. Since the draftsman endeavors to avoid these concentrated loads in the process of fairing, the order of fairness will generally be higher than 2."

Weinblum gives several additional criteria for fairness, among which may be mentioned:

(a) A small number of points of inflection in any quadrant between two ship axes normal to each other, preferably only one such point
(b) Freedom from flat regions
(c) Moderate changes in the first and second derivatives. Weinblum goes on to point out that the foregoing concepts of fairness, although derived from experience and found useful in practice, may fail completely to give indications as to ship resistance, especially that due to wave-making.

The uncertainties associated with the fairing of ship lines and the lack of fairness found in the shapes of well-known ships were two reasons which led to the study of longitudinal curvature described in Chap. 4 of Volume I. Others were the comments of W. J. M. Rankine in the 1860's and 1870's relative to the curvature of stream forms developed by the source-and-sink process, the procedures used to shape airship hulls, and the findings of aeronautical engineers in the shaping of strut and similar sections.

Rankine chose, for the waterline of a ship, a streamline somewhat removed from the boundary of a source-sink stream form. Here, along the chosen streamline or lissoneoid, as he called it, the curvature was such as to produce only three changes in differential pressure as liquid flowed along it, from well ahead to well astern. Around the stream form itself there were five changes in pressure undergone by a particle of liquid in moving from a great distance ahead to a great distance astern ["An Investigation on Plane Water-lines," Brit. Assn. Rep., 1863, pp. 180–182, under Mechanical Science; Jour. Franklin Inst., Jan-Jun 1864, Vol. XLVII, Third Series, pp. 24–26]; see Sec. 50.2 and Fig. 50.A.

For the nose or entrance portions of the hulls of the U. S. Naval airships *Akron* and *Macon* of the 1930's, which were joined to parallel middle-bodies, an ellipsoid of revolution of the third order was employed. Based upon a length of entrance a and a radius of middlebody b, the equation of the forebody outline in a longitudinal plane passing through the axis was

$$\frac{x^3}{a^3} + \frac{y^3}{b^3} = 1 \qquad (49.\text{xix})$$

where x was the distance of any point on the forebody surface reckoned forward of the forward end of the middlebody, and y was the radius from the airship axis to that point. When x equaled zero, at the junction point of the entrance and the middlebody, the second derivative d^2y/dx^2 for the outline equaled zero, which meant that the curvature was also zero. Since the straight contours in the middlebody had zero curvature, those of the entrance joined them in what might be called a continuous transition. A 0-diml curvature plot of the outline of a longitudinal axial section would show no break at that point.

In Reports and Memoranda 256 of the (British) Aeronautical Research Committee, dated June 1916, W. L. Cowley, L. F. G. Simmons, and J. D. Coales report as follows:

P. 167. "Previous reports and preliminary experiments for the present report all showed that the air resistance of a strut was extremely sensitive to slight changes in the form and radius of curvature, especially in the neighborhood of the maximum ordinate. For this reason each strut, of a series in which one proportion only is to be varied, must be made with fair accuracy in those dimensions which are to be kept constant."

P. 170. "The results of the investigation appear to show that the air resistance of a strut depends very greatly upon the shape of the fairing in the region in front of the maximum ordinate. In a round-nosed strut the change of curvature and slope in passing from the nose to the fairing piece should not be too rapid, a condition which causes the maximum width to be some distance behind the center of curvature of the nose."

49.9 Notes on Longitudinal Curvature Analysis. For determining and analyzing the curvature of any fore-and-aft ship line, such as the designed waterlines discussed in Secs. 4.4, 4.5, 4.7, and 24.13, there are several methods besides the semi-graphic one described in those references.

Assuming an origin of coordinates at any convenient point along the ship centerplane, with abscissas x parallel to the x-axis and ordinates y measured transversely in the plane of the selected line, the slope of that line with reference to the x-axis is dy/dx. This may be measured as a natural tangent or as a function of an angle, where $dy/dx = \tan\theta$.

The rate of change of slope, called by D. W. Taylor the "acceleration" α(alpha) in his 1915 mathematical-lines paper referenced in Sec. 49.3, is

$$\frac{d^2y}{dx^2} = \frac{1}{R_C}\,[1 + \tan^2\theta]^{3/2} = \frac{1}{R_C}\sec^3\theta \qquad (49.\text{xx})$$

The radius of curvature R_C of any curved line, from standard reference works on this subject, is expressed as

$$R_C = \frac{\left[1 + \left(\dfrac{dy}{dx}\right)^2\right]^{3/2}}{\dfrac{d^2y}{dx^2}} \qquad (49.\text{xxi})$$

The absolute curvature is $1/R_C$; this is dimensional because R_C is dimensional. Strictly speaking, an irregular curved line has no definite radius of curvature. However, at any selected point it has an effective R_C equal to that of a circle, called a *circle of curvature*, which coincides very nearly with the given curved line at the given point. It is possible to plot the dimensional curvature of ship waterlines on a basis of length along the fore-and-aft axis by using the reciprocal values $1/R_C$. A. Emerson has done this by employing the first and second differences of the waterline offsets at 40-station intervals, each equal to $0.025L$ [INA, 1937, Fig. 6, p. 178; unpubl. ltr. of 11 Jan 1952 to HES]. Plotting 0-diml longitudinal curvature is described in Sec. 49.10.

Any of the foregoing methods involving dy/dx or d^2y/dx^2 is satisfactory only if offsets, slopes, and rates of change of slope are taken for at least 40 equally spaced stations along the length of a ship. No method is satisfactory unless the waterline itself is carefully and accurately drawn.

From Eq. (49.xxi) preceding it is apparent by inspection that R_C approaches infinity as the second derivative d^2y/dx^2 approaches zero. This is equivalent to saying that the absolute curvature $1/R_C$ approaches zero with the second derivative. Since the curvature of a straight line is zero, a suitable transition from a curved ship line to a straight one, such as the parallel portion of a waterline, is marked by a diminution of d^2y/dx^2 toward zero at the junction with the straight line.

Proper transition is an acute problem in the laying of tracks for railway cars and trains. If a straight section of track, called in railway parlance a tangent, were joined directly to a curved section of track having a constant radius, the transverse acceleration at the junction would be so great on a high-speed train passing from the straight to the curved section that the train would leave the rails or the track would be torn up. Railway surveyors have developed several acceptable methods for making this transition between straight and curved portions of track. One of them involves the use of a second- or third-order parab-

ola, $x^2 = ay$ or $x^3 = by$, with its vertex at the end of the straight section of track. For a ship, it involves a similar curve with its vertex at the end of the straight or parallel portion of the ship line.

For a 3-diml form, particularly a body of revolution, perfect transition of this kind is achieved by joining a parallel cylindrical portion with half of an ellipsoid of revolution defined by the relationship given in Eq. (49.xix) of Sec. 49.8 or by the identical relationship

$$\frac{x}{L_E} + \frac{y}{R_B} = 1 \qquad \text{(49.xxii)}$$

This is the equation of the 2-diml intersection of the outer skin with a plane passing through the axis, sketched in Fig. 49.D, and not of the 3-diml

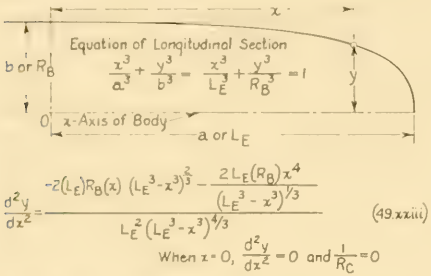

FIG. 49.D SKETCH OF AIRSHIP NOSE OUTLINE OF THIRD-DEGREE ELLIPTIC SHAPE

body surface. The origin of coordinates is on the axis at the junction of the two portions; L_E is the half-length of the ellipsoid, and R_B is its maximum transverse radius, equal to the radius of the parallel portion. This corresponds to the combination of nose and middlebody portions of the hulls of the airships *Akron* and *Macon*, mentioned in the section preceding. The longitudinal section drawn on Fig. 49.D indicates the extremely gradual transition from the parallel middlebody to the after portion of the entrance or nose.

Upon double differentiation with respect to x, Eq. (49.xxii) reduces to the value of d^2y/dx^2 indicated on Fig. 49.D as Eq. 49.xxiii). In this case, as shown on the figure, when $x = 0$, $d^2y/dx^2 = 0$ and $1/R_C$ is 0. The combination of third-order ellipsoid and cylinder described in the foregoing gave most gratifying resistance and propulsion results when used on the large rigid airships mentioned.

Modern hull-design procedure requires that equally good transitions be made, if practicable, between the parts of fore-and-aft ship lines. Further, the finished lines should be as fair as modern technology can make them. This calls for the use of some method for guaranteeing a longitudinal curvature that will eliminate Δp disturbances along these lines or that will indicate the presence of localized pressure disturbances if they can not be avoided. Unfortunately, it is not easy for a human being to realize how sharp this transition may be along the side of a ship, certainly not as easily as it would be if he were in a train, going around a geometrically similar curve.

The aerial view of Fig. 49.E, taken of a modern (1955) merchant ship and reproduced with the permission of the Kockums Mekaniska Aktiebolag, Malmö, Sweden, illustrates this feature in a rather extraordinary manner. It is almost possible to discern the Velox waves generated by the forward-shoulder pressure disturbance, where the hollow in the entrance waterline shifts rather abruptly to the parallel waterline amidships through a convex transition region of rather sharp curvature. Methods of taking care of this situation, for cases where there is no limitation on the extreme beam and no parallel waterline is necessary, are described in Secs. 67.2 and 67.3.

49.10 Graphic Determination of the Dimensionless Longitudinal Curvature of any Ship Line. Details of the graphic procedure mentioned in Secs. 4.4, 4.5, and 4.7, for determining 0-diml longitudinal curvature in waterlines, buttocks, and diagonals, are given here.

Briefly, the 0-diml curvature of a designed waterline of a ship is determined for any selected point along the length by the ratio

$$\frac{\text{Beam } B_X \text{ at the section of maximum area}}{\text{Length of 1-deg arc of the circle of curvature}}$$

where both linear dimensions are given in the same unit of measurement.

The value of B_X is taken directly from the ship lines; it is the magnitude of the beam *on the drawing being analyzed*, not that of the ship itself. Determining the value of the denominator in the ratio given is facilitated by drawing on transparent film, by photographic reproduction or the equivalent, a series of arcs of circles of varied radii, comprising the range of curvature to be expected in any body or ship lines to be analyzed. Opposite each such arc is marked, in

Fig. 49.E Aerial View of a Ship, Showing Relatively Sharp Transition between Hollow Entrance Waterline and Parallel Waterline Amidships

the same units as are to be used for measuring the beam on the drawing, the length of a 1-deg arc *on the transparency*, calculated from the relationship: Length $= 0.017453R_C$.

Three such series of arcs, on two separate sheets of film, have been prepared by the Society of Naval Architects and Marine Engineers, which can furnish film positives for the use of naval architects. The radii of the circles of curvature vary from 0.2865 to 28.65 inches on one sheet and from 25 inches to 500 inches on the other sheet. A small section of the first sheet is reproduced, *but not to full size*, in the upper LH corner of Fig. 49.F. The lengths of the 1-deg arcs on these sheets are given in inches. The waterline beams on the drawings to be analyzed are therefore also measured in inches.

The transparent sheet is placed over the ship line and moved around until some circle of curvature on it fits the waterline at a selected station, indicated in the lower diagram of Fig. 49.F. The number or location of the station is then tabulated and with it the dimension found opposite that circle of curvature. The process is repeated along the length until all stations or selected points are covered. When working from large-scale ship lines it is often difficult to determine just which circle of curvature makes the best fit. The solution is to determine which circle is obviously too slack, then which is definitely too sharp, and select the mean between the two.

The 1-deg arc length found for each station or point is then divided into B_X and the quotient is tabulated. The 0-diml curvatures are plotted on length, following the method of Figs. 4.H, 24.F, and 67.C. They are reckoned as positive and laid off above the axis for lines convex to the water; negative and below the axis for lines concave to it. The method falls down for sharp corners and discontinuities, as where an entrance (or a run) waterline with finite slope meets the imaginary prolongations of the ship along the centerplane,

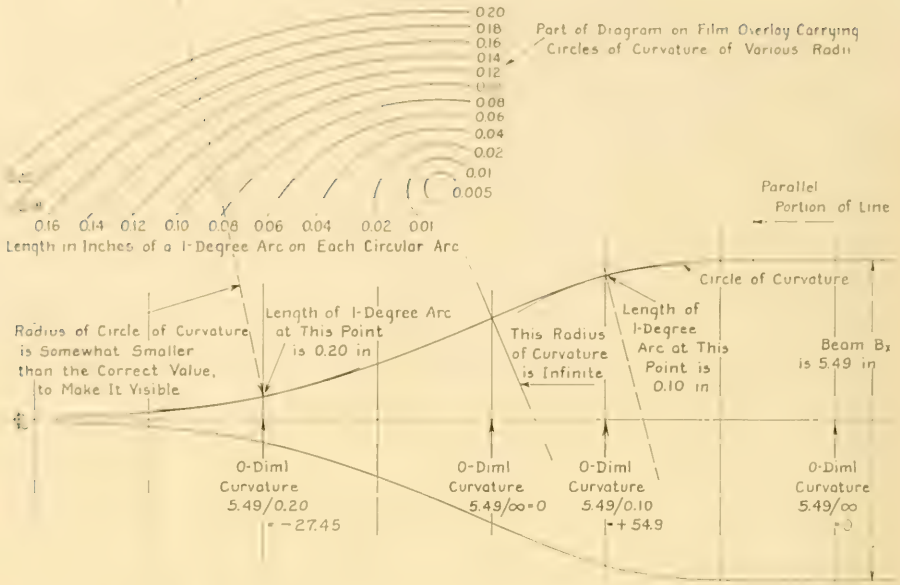

Fig. 49.F Instruction Plan for Determining 0-Diml Curvature of any Ship Line

beyond the bow (or stern). It appears advisable in this case to terminate the plot at a point where the circles of curvature no longer fit, say at about $0.025B_X$ on each side of the centerline.

A legible waterline drawing of any scale may be analyzed, *provided* the longitudinal and transverse scales are identical. Although the circles of curvature are fitted by eye to the curve underneath, this graphic method is extremely sensitive to sudden changes in curvature, unfairness, and inaccuracies in the ship line being analyzed.

For determining the 0-diml longitudinal curvature of a bow line or buttock the procedure is exactly the same as described for the waterline. However, instead of the maximum beam B_X, the transverse linear dimension in the numerator is *twice* the maximum depth from the DWL to the lowest point of the buttock measured on the drawing. This corresponds to the existence of a mirror image of the ship above the DWL, and to measuring the transverse dimension from the highest to the lowest points of the image-and-ship combination.

For any diagonal on the ship lines the transverse linear dimension in the numerator is taken as *twice* the maximum diagonal offset *on the drawing*, measured along the diagonal trace from its intersection with the plane of symmetry. This is equivalent to the waterline-analysis procedure if both port and starboard diagonal planes are swung upward about the centerplane intersection so as to coincide at the plane of the waterline at that intersection.

49.11 Mathematic Delineation and Fairing of a Section-Area Curve. Those working on the analytic phase of wavemaking resistance, developing methods whereby this resistance may be calculated for certain ship forms, have endeavored to determine the effect on ship resistance of the distribution of volume along the length. This distribution is shown by the orthodox section-area or A-curve, described in Sec. 24.12 and illustrated in Fig. 24.F. Indeed, the optimum form of A-curve, for minimum resistance, has been found for a sort of geometric ship having rectangular sections throughout and moving in a non-viscous liquid [SNAME, 1953, Fig. 38, p. 582].

Supplementing this work, P. C. Pien has developed mathematic section-area curves which

approximate very closely the A-curves of actual ships and models [SNAME, 1953, pp. 580–582]. Having the equations of these curves, a further development along the lines proposed by R. Taggart, using methods similar to those described in Secs. 49.13 and 49.14, should serve for the mathematic fairing of the curves in question.

As a check on the fairing of any section-area curve, whether represented by a mathematical equation or not, the dimensionless curvature may be determined as described for a waterline in Sec. 49.10. For the A/A_X curve, the transverse, linear dimension in the numerator of the 0-diml curvature ratio is taken arbitrarily as the height of the maximum ordinate on this curve. It is measured on the plot, and is expressed in the *same units* of measurement as the lengths of the 1-deg arcs on the circle-of-curvature transparencies. Assuming that the height/length ratio of the section-area curve is 1/4, following the convention of Sec. 24.12, plots of 0-diml longitudinal curvature of all such curves are comparable *provided* the stations on the section-area curve are spaced along its length exactly the same as are the ship stations along the ship line. A 0-diml curvature plot of the A/A_X curve for the transom-stern design of the ABC ship, for the Taylor Standard Series parent form, and for a merchant ship of good design are given in Fig. 67.X.

49.12 Longitudinal Flowplane Curvature. A longitudinal flowplane around a ship hull is defined in Sec. 4.11 and illustrated in Figs. 4.P, 4.Q, and 24.L. This plane is admittedly arbitrary, principally because it is assumed to stand normal to every section line from bow to stern as it crosses that line. It is likewise somewhat arbitrary to represent a square stream tube along the flowline at the hull as twisting so that one side of the tube, and the same side, lies always in the flowplane.

As the flowplane is almost never a flat one, in a strict geometric sense, it has to be untwisted and straightened into the flat before its 0-diml longitudinal curvature may be measured. This operation involves laying out, on paper, what would be the shape taken by the inner edge of a piece of sheet metal if twisted into the flowplane shape, trimmed to fit the side of a model at the flowline, and then untwisted into the flat. It is a somewhat tedious piece of 3-diml geometry, involving the slightly expanded station lengths as ordinate spacing and the developed lengths of the flowline between stations, measured on the body plan, as ordinate increments. Drawing the unrolled and untwisted flowline is followed by a measurement of its 0-diml curvature.

The process is not described in detail or illustrated here because it does not take account of the untwisting necessary to get the actual model flowplane into the single plane of the paper on which it is laid down. There can be a large curvature without twist, in the buttocks of a short barge with steeply raked ends, or there can be large twist with small longitudinal curvature, when water flows up and around the bossings on a twin-screw ship.

Undoubtedly a graphic method could be developed for taking account of both twist and curvature but this should await more definite knowledge as to the hydrodynamic effects of each of these features in creating differential pressures on the underwater hull.

49.13 Checking and Establishing Fairness of Lines by Mathematical Methods. The measurement and plotting of the 0-diml curvature of a selected ship's line, described in Sec. 49.10, serve as a graphic fairness indicator for any line drawn in the customary way with a ship's curve, spline, or batten. R. Taggart has devised a mathematical method of checking and establishing fairness, entirely independent of any graphic procedure [ASNE, May 1955, pp. 337–357]. Instead of D. W. Taylor's fifth-order polynomial $y = a + bx + cx^2 + dx^3 + ex^4 + fx^5$ he found it necessary to employ a sixth-order expression of the following form:

$$y = ax + bx^2 + cx^3 + dx^4 + ex^5 + fx^6 \quad \text{(49.xxiv)}$$

Furthermore, Taggart uses integrated relationships instead of the differential relationships of Taylor to determine the unknown constants.

The constant first term of the Taylor expression is eliminated if an origin be selected along a continuous part of the ship line where y and x are simultaneously zero. For the customary waterline this calls for:

(1) Separate origins at the bow and at the stern
(2) A maximum value of x where the entrance or run encounters the middlebody
(3) A slope of zero in the ship line at this maximum value of x
(4) Offsetting the origin from the plane of symmetry in the event the half-siding at the bow or stern has a finite value. For convenience the maximum value of x and the half-beam value of

y are both placed equal to 1.0. This places the data in 0-diml form.

Taggart's integrated relationships are:

$$C_1 = \int_0^1 y\,dx \qquad \text{(49.xxv)}$$

$$C_2 = \int_0^1 xy\,dx \qquad \text{(49.xxvi)}$$

$$C_3 = \int_0^1 x^2y\,dx \qquad \text{(49.xxvii)}$$

$$C_4 = \int_0^1 x^3y\,dx \qquad \text{(49.xxviii)}$$

These may be determined from any curve by the application of Simpson's rule. The relationship between the constants and the coefficients a, b, c, d, e, and f are given in Taggart's Fig. 3, corresponding to Fig. 49.H of Sec. 49.14. His explanation of the mathematical procedure is detailed and complete, hence it is not repeated here. His worked-out example is supplemented by a second example in Sec. 49.14, covering the fairing of the designed entrance waterline of the transom-stern ABC ship, described in Part 4 of this volume.

49.14 Illustrative Example for Fairing the Designed Waterline of the ABC Ship. To illustrate Taggart's method, a sample calculation for fairing the designed (26.163-ft) waterline abreast the entrance of the ABC ship is carried out according to the steps listed hereunder. Actually, the fairing is accomplished on that portion of the DWL from the FP back to the position of maximum waterline beam B_{WX}. From Fig. 67.A in Part 4 this is at Sta. 11. It is not to be confused with the fore-and-aft position of the section of maximum area, which is at Sta. 10.6. The successive steps are described in some detail:

I. Draw the designed waterline from the FP to Sta. 11 as accurately as possible, considering the stage of the hull design, or use a waterline drawing already made. It is helpful to continue the waterline for at least two stations abaft the position of B_{WX}, as is done in Fig. 49.G. Actually, the DWL in this figure is drawn with a vertical scale much larger than the horizontal scale, to show the various features to better advantage. Drawing this or any other ship line to a fairly large scale will produce the accurate offsets needed to take full advantage of the mathematical method. It is preferable to make the scale large enough so that the derived 0-diml values of B/B_X (or actual offsets divided by the half-beam) are accurate to 4 significant figures following the decimal point. In the SNAME RD sheets the 0-diml values are given to only three significant decimal places. For the ABC ship example worked out here, the 0-diml B/B_X coordinates are those listed in the SNAME RD sheet for the transom-stern design, TMB model 4505, reproduced as Fig. 78.Ja in Part 4. They are listed in Col. B of Table 49.a.

TABLE 49.a—MODIFICATIONS OF OFFSETS FOR DESIGNED WATERLINE OF ABC SHIP TO SUIT LIMITING CONDITIONS FOR MATHEMATICAL FAIRING PROCESS

Col. F lists the 0-diml offsets used in this calculation.

Col. A Original ship stations	Col. B B/B_X from RD sheet	Col. C $B/B_X - (B/B_X)_0$	Col. D New "prime" stations	Col. E Offsets from Fig. 49.G	Col. F Col. E times 1/0.990
0	0.013	0	0′	0	0
1	0.121	0.108	1′	0.1205	0.1217
2	0.252	0.239	2′	0.2665	0.2692
3	0.396	0.383	3′	0.4265	0.4308
4	0.542	0.529	4′	0.5850	0.5909
5	0.679	0.666	5′	0.7280	0.7354
6	0.794	0.781	6′	0.8370	0.8455
7	0.882	0.869	7′	0.9153	0.9245
8	0.943	0.930	8′	0.9610	0.9707
9	0.980	0.967	9′	0.9835	0.9934
10	9.997	0.984	10′	0.9900	1.0000
11	1.003	0.990			
12	0.999				
13	0.983				

II. Locate on the waterline drawing the origin O of the 0-diml waterline which is to be used in the mathematical analysis. This waterline is to have a length corresponding to 11 station intervals on the ship, from the FP back to the position of B_{WX}, and it is to pass through the point where $y = 0$ when $x = 0$. Fig. 67.E of Part 4 shows that the DWL offset at the FP is 0.5 ft, when continued forward as indicated by the diagonal broken line in the upper right-hand corner of Fig. 49.G. However, it is assumed here, to keep the numerical figures consistent, that the molded offset at the FP on the ship corresponds *exactly* to 0.013 times the half-beam, tabulated on Fig. 78.Ja. In absolute dimensions on the ship this is 0.013(73.08/2) = 0.475 ft. A stem of semicircular section, lying inside the cutwater shown in Fig. 73.B, would then have a molded radius of 0.545 ft, from the large-scale diagram of Fig.

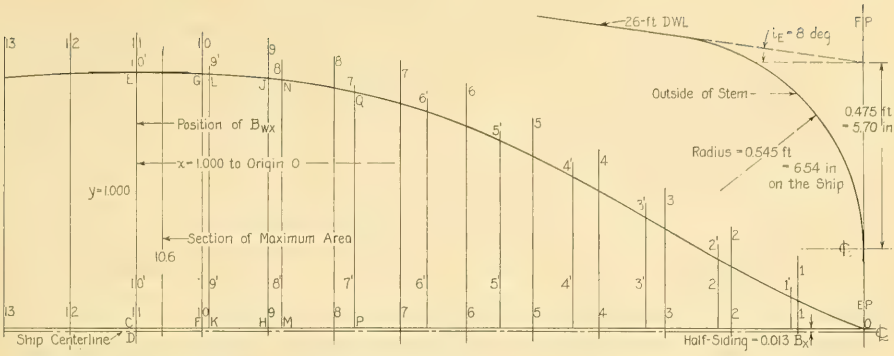

FIG. 49.G DEFINITION SKETCH FOR MATHEMATICAL FAIRING OF DESIGNED WATERLINE ENTRANCE OF ABC SHIP

49.G. The origin O is accordingly fixed at the FP at a distance of $0.013(B_{WX}/2)$ from the ship centerline. A line OC, drawn through O parallel to the ship centerline, then forms the basis for measuring the y-coordinates of the 0-diml DWL which are to be introduced into the mathematical formulas.

III. The length of the 0-diml waterline diagram to be analyzed is the distance OC in Fig. 49.G, corresponding to the length of 11 station intervals on the ship. This distance is divided into 10 equal lengths and new ordinates are erected, marked on Fig. 49.G as 1′ through 9′. The ship station 11 is at the "prime" station 10′. The distance OC is then the 0-diml x-distance of 1.000.

IV. The 0-diml value of B/B_X from D to E is, from the referenced RD sheet, equal to 1.003. The 0-diml value of CE, equal to DE − DC, is 1.003 − 0.013 = 0.990. The values of the 0-diml ordinates FG, HJ, and so on, at the ship stations, are then found by subtracting the constant value 0.013 from the RD sheet values. They are listed in Col. C of Table 49.a.

V. The offsets of the DWL curve at the 10 "prime" stations are then taken off the diagram of Fig. 49.G for the distances marked KL, MN, PQ, and so forth. They are converted into 0-diml values by dividing the half-value of B_{WX} into them, following which they are listed in Col. E of the table. Since the 0-diml y-ordinate at Sta. 11 must equal 1.000 for the mathematical computation, when the 0-diml x-abscissa also equals 1.000, it is made so by dividing the 0-diml ordinate at station 10′ by itself. For this station, 0.9900/0.9900 = 1.000. All other 0-diml ordinates at the prime stations are divided by the same factor 0.9900, producing the final 0-diml computation ordinates in Col. F of Table 49.a.

VI. If the 0-diml B/B_X values are already available for a given designed waterline, as they were for the ABC ship, it is somewhat simpler to plot a diagram like Fig. 49.G, embodying 0-diml B/B_X ordinates on a base of ship length, rather than ordinates of ship beam to some selected scale. The diagram then becomes simply a graphic means of picking off the 0-diml ordinates

x/L_E	Ordinate	M_1	M_2	M_3	M_4
0	0	—	—	—	—
0.1	0.1217	2	1	1	1
0.2	0.2692	1	1	2	4
0.3	0.4308	2	3	9	27
0.4	0.5909	1	2	8	32
0.5	0.7354	2	5	25	125
0.6	0.8455	1	3	18	108
0.7	0.9245	2	7	49	343
0.8	0.9707	1	4	32	256
0.9	0.9934	2	9	81	729
1.00	0.500	1	5	50	500
ΣM (Ordinate)		9.5879	30.8735	224.697	1754.769

$$C_1 = \Sigma M_1 \cdot (\text{Ordinate}) \div 15 = 9.5879 \div 15 = 0.639193$$

$$C_2 = \Sigma M_2 \cdot (\text{Ordinate}) \div 75 = 30.8735 \div 75 = 0.411647$$

$$C_3 = \Sigma M_3 \cdot (\text{Ordinate}) \div 750 = 224.697 \div 750 = 0.299596$$

$$C_4 = \Sigma M_4 \cdot (\text{Ordinate}) \div 7500 = 1754.769 \div 7500 = 0.233969$$

FIG. 49.H CALCULATION OF CURVE COEFFICIENTS FOR ABC SHIP

for the prime stations. This is facilitated, for the ABC ship, by making the ordinate DE equal to 100.3 units to a convenient scale, namely 100 times the 0-diml value. The ordinate DC is made equal to 1.3 units, and CE then equals 99.0 units. In the original drawing for Fig. 49.G one such ordinate unit represented 1 ft length in the horizontal scale.

VII. The final 0-diml computation ordinates in Col. F of Table 49.a are then entered as ordinates in the second column of Taggart's form for Calculation of Curve Coefficients in Fig. 49.H, following which the computation outlined in that form is carried through to obtain the numerical values of the coefficients C_1, C_2, C_3, and C_4.

Entering these coefficients in the form for Calculation of Constant Terms, at the top of Fig. 49.I, produces the numerical values of the constant terms a, b, c, d, e, and f. Carrying through the Check Calculation of Original Curve at the bottom of Fig. 49.I produces a series of cumulative products, which are the mathematically faired 0-diml values of y for the "prime" stations 1′ through 10′ on Fig. 49.G. These are to be compared with the unfaired 0-diml values for the same prime stations in Col. F of Table 49.a for an indication of the modifications that were made in the fairing process. The faired values are laid down at the prime stations and the entrance portion of the designed waterline in Fig. 49.G is redrawn through them.

The procedure described in steps I. through VI. is then worked backward to find the 0-diml y-ordinates at the ship stations, the B/B_X values

CALCULATION OF CONSTANT TERMS

For Designed 26.163-ft Waterline of Entrance of ABC Ship

Multipliers Constant	C_1 = 0.639193	C_2 = 0.411647	C_3 = 0.299596	C_4 = 0.233969	Summation
	$42.0\,C_1$ =	$3360\,C_2$ =	$7560\,C_3$ =	$5040\,C_4$ =	a =
+30.000 000	+268.461060	−1383.133920	+2264.945760	−1179.203760	+1.06914
	$42.00\,C_1$ =	$37800\,C_2$ =	$90720\,C_3$ =	$63000\,C_4$ =	b =
−435.000 000	−2684.610600	+15560.256600	−27179.349120	+14740.047000	+1.34388
	$14700\,C_1$ =	$141120\,C_2$ =	$352800\,C_3$ =	$252000\,C_4$ =	c =
+1960.000 000	+9396.137100	−58091.624640	+105697.468800	−58960.188000	+1.79326
	$23520\,C_1$ =	$235200\,C_2$ =	$604800\,C_3$ =	$441000\,C_4$ =	d =
−3780.000 000	−15033.819360	+96819.374400	−181195.660800	+103180.329000	−9.77676
	$17640\,C_1$ =	$181440\,C_2$ =	$476280\,C_3$ =	$352800\,C_4$ =	e =
+3276.000 000	+11275.364520	−74689.231680	+142691.582880	−82544.263200	+9.45252
	$5040\,C_1$ =	$52920\,C_2$ =	$141120\,C_3$ =	$105840\,C_4$ =	f =
−1050.000 000	−3221.532720	+21784.359240	−42278.987520	+24763.278960	−2.88204

CHECK CALCULATION OF ORIGINAL CURVE

Constants		Multipliers									
a =	+1.06914	0.100 000	0.200000	0.300000	0.400000	0.500000	0.600000	0.700000	0.800000	0.900000	1.000 000
b =	+1.34388	0.010000	0.040000	0.090000	0.160000	0.250000	0.360000	0.490000	0.640000	0.810000	1.000000
c =	+1.79326	0.001000	0.008000	0.027000	0.064000	0.125000	0.216000	0.343000	0.512000	0.729000	1.000000
d =	−9.77676	0.000100	0.001600	0.008100	0.025600	0.062500	0.129600	0.240100	0.409600	0.656100	1.000000
e =	+9.45252	0.000010	0.000320	0.002430	0.010240	0.031250	0.077760	0.168070	0.327680	0.590490	1.000000
f =	−2.88204	0.000001	0.000064	0.000729	0.004096	0.015625	0.046656	0.117649	0.262144	0.531441	1.000000
Cumulative Products	y =	0.21266	0.269127	0.431786	0.592149	0.734009	0.846120	0.924203	0.970870	0.993507	1.000000
	$\frac{x}{L_E}$	0.1	0.2	0.3	0.4	0.5	0.6	0.7	0.8	0.9	1.0

FIG. 49.I CALCULATION OF CONSTANT TERMS; CHECK CALCULATION OF ORIGINAL CURVE

CALCULATION OF MOLD-LOFT OFFSETS

For Two Frame Positions Along Designed 26.163-ft Waterline of Entrance of ABC Ship

Baseline Intercept at Station 0 — Maximum-Ordinate Tangency at Station 11.0

Maximum Ordinate 36.175 ft — Half-Siding 0.475 ft — Length of Curve, x_1, 11.0 Stations

Frame	Feet from Sta. 0	Ship Station Number at 25.5 ft per Station	a = +1.06914 $\left(\frac{x}{x_1}\right)$	b = +1.34388 $\left(\frac{x}{x_1}\right)^2$	c = +1.79326 $\left(\frac{x}{x_1}\right)^3$	d = −9.77676 $\left(\frac{x}{x_1}\right)^4$	e = +9.45252 $\left(\frac{x}{x_1}\right)^5$	f = −2.88204 $\left(\frac{x}{x_1}\right)^6$	Cumulative Product* y	Offset = y (Max. Ord) plus Half-Sid'g.
	128	5.0196	0.456327	0.208234	0.095023	0.043362	0.019787	0.009029	0.675195	24.900 ft
	178	6.9804	0.634582	0.402694	0.255542	0.162162	0.102905	0.065302	0.876972	32.199 ft

$$* \text{ Cumulative Product} = a\left(\frac{x}{x_1}\right) + b\left(\frac{x}{x_1}\right)^2 + c\left(\frac{x}{x_1}\right)^3 + d\left(\frac{x}{x_1}\right)^4 + e\left(\frac{x}{x_1}\right)^5 + f\left(\frac{x}{x_1}\right)^6$$

Fig. 49.J Calculation of Mold-Loft Offsets for Designed Waterline of ABC Ship at Two Frames

at those stations, and finally the designed waterline offsets B.

49.15 Practical Use of Mathematical Formulas for Faired Principal Lines. There is no reason why, if the lines of a vessel can be laid down on a drafting table from offsets produced by working out mathematical formulas, the full-scale lines can not similarly be laid down in a mold loft in such manner that much of the loft fairing now found necessary will be eliminated.

The mathematical procedure which determines the offsets of a faired ship line, described in Sec. 49.13 and illustrated in Sec. 49.14, is extended by R. Taggart to calculate the offsets of that fair line at any or all frame stations along the length for the actual ship. This means, for example, that the mold loft can be supplied with *calculated* offsets for a faired designed waterline, accurate to as many significant figures as desired. Furthermore, if five shipyards are to build five sets of sister vessels, each of the five is furnished with exactly the same faired WL offsets, accurate to say a thousandth of a foot, or 0.012 inch.

An example of this procedure is worked out in Fig. 49.J for the designed waterline entrance of the ABC ship, using the waterline portion already faired mathematically. The offsets are calculated for two selected frames at 128 ft and 178 ft, respectively, from the FP. These correspond to Stas. 5.0196 and 6.9804 in the ship series, where the station length is 25.5 ft. In this case the 0-diml diagram is exactly 11 ship-station intervals long; Taggart has worked out other examples [ASNE, May 1955, p. 354] where the "prime" stations and the ship stations do not coincide, and where the 0-diml curve is from 7.00 to 9.33 ship-station intervals in length.

For the ABC ship the ordinates of the *faired* designed waterline curve at the selected frame locations are found to be 24.900 and 32.199 ft, respectively.

The examples given by Taggart on page 350 and following of his paper for calculating frame offsets (not station offsets) [ASNE, May 1955], cover only three principal fore-and-aft ship lines:

(1) The designed waterline
(2) A higher waterline in the abovewater body, at about $1.47H$
(3) The bilge diagonal.

A fourth set is established, without benefit of

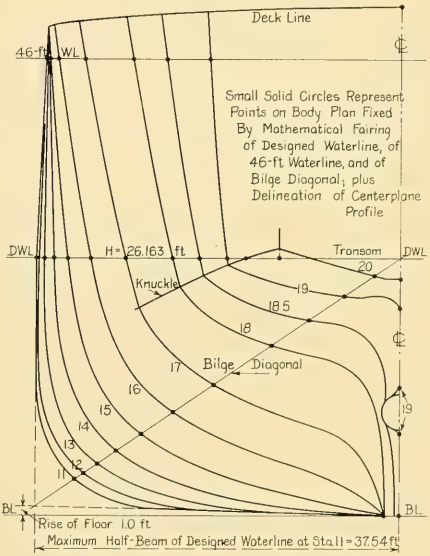

Fig. 49.K Schematic Body Plan Showing Four Sets of Proposed Points to be Determined by Mathematical Methods

mathematics, by the contour or profile drawing of the hull in the plane of symmetry. This involves (usually) a straight keel, a stem profile of the selected type, and a stern profile to suit the propeller and rudder.

Restricting the calculations to these four lines is on the basis that if four sets of points are established on selected frames in accordance with the foregoing, they should be sufficient to insure that the principal dimensions and shape, as laid down in any mold loft, will be as contemplated by the designer. Fig. 49.K illustrates the location of these four sets of points on a schematic body plan. Calculation of offsets for ships of special form may be made, of course, for as many additional lines as are desired.

49.16 The Geometric Variation of Ship Forms. Somewhat related to the use of mathematical equations for ship lines is a combination of mathematics and geometry for effecting a variation of hull parameters and coefficients in a given ship form. Perhaps the simplest procedure of this kind is that in which the fore-and-aft position of the maximum-area section is shifted along the x-axis. Here, by holding the same sections and section areas, the stations in the entrance are closed up and those in the run are opened out, or vice versa. Or, by closing up the sections in both forebody and afterbody, a portion of parallel middlebody is inserted between them. The ship length remains the same in both cases.

A variation is that in which a ship is lengthened by the addition of a middlebody. Usually the cut is made at the maximum-section-area position but this is by no means mandatory. If the lengthening is accompanied by a repowering and a speed increase, the new portion inserted may not be of uniform section. It may well have a maximum-section area A_x greater than that of the original ship.

Geometric variations are almost unavoidable when laying out model series in which one parameter is systematically varied, described by D. W. Taylor [S and P, 1943, p. 55] and others. More elaborate procedures are explained and illustrated in detail by H. Lackenby in his paper "On the Systematic Geometrical Variation of Ship Forms" [INA, Jul 1950, pp. 289–316].

When a geometric-variation procedure is applied to a given ship form to produce a new one there is serious question whether the water will take kindly to the change. In other words, what appears to be a good geometric or parametric variation may not work out so well hydrodynamically. This situation was pointed out by J. L. Kent in his discussion of the Lackenby paper [p. 310].

One may visualize a ship form of low total resistance for its displacement, despite an LMA position that appears by Fig. 66.L to be too far forward for its speed-length quotient and prismatic coefficient. Stretching the entrance and contracting the run may be an easy way to achieve what appears to be a better LMA position and what should give a slight but definite improvement in performance. There is no assurance, however, in the present state of the art, that because of the geometric variation alone the modified section-area curve, the modified designed waterline, and other altered features will produce better hydrodynamic behavior.

49.17 Selected References Relating to Mathematical Lines for Ships. Certain references which describe methods developed in the past for delineating the forms of bodies and ships are listed here for convenience. They begin with the work of F. H. de Chapman in the 1760's, although his efforts may not have been the first along these lines:

(1) Chapman, F. H. de, "A Treatise on Ship-Building," translated into English by the Rev. James Inman, Cambridge and London, 1820

(2) Nystrom, J. W., Jour. Franklin Inst., Jul-Dec 1863, Third Series, Vol. XLVI, pp. 355–359 and 389–396, with Pls. II and III

(3) Jour. Franklin Inst., Jan-Jun 1864, Vol. XLVII, Third Series, pp. 46–51, accompanied by Plate I of the Nystrom series of papers; also pp. 241–244 in the same volume

(4) Jour. Franklin Inst., Jul-Dec 1864, Vol. XLVIII, Third Series, pp. 261–264. This paper contains some historical data on Chapman's previous work on mathematical lines (principally parabolas) in Sweden. Plate IV of the series, mentioned here, is bound out of place (opp. p. 236) in the volume consulted.

(5) Taylor, D. W., "On Ships' Forms Derived by Formulae," SNAME, 1903, pp. 243–267

(6) Warrington, J. N., "System of Mathematical Lines for Ships," SNAME, 1909, pp. 441–452

(7) Taylor, D. W., "Calculations for Ships' Forms and the Light Thrown by Model Experiments upon Resistance, Propulsion and Rolling of Ships," Trans. Int. Eng'g. Cong., 1915, Naval Architecture and Marine Engineering, San Francisco, 1915

(8) Weinblum, G., "Beiträge zur Theorie der Schiffsoberfläche (Contribution to the Theory of the Ship Boundary)," WRH, 22 Nov 1929, pp. 462–466; 7 Dec 1929, pp. 489–493; 7 Jan 1930, pp. 12–14. This paper illustrates a number of ship forms whose lines were derived mathematically.

(9) Weinblum, G. P., "Exakte Wasserlinien und Spant-

flächencurven (Exact Waterlines and Transverse-Section Curves)," Schiffbau, 15 Apr 1934, pp. 120–121; 1 May 1934, pp. 135–142

(10) Benson, F. W., "Mathematical Ship's Lines," INA, 1940, pp. 129–151

(11) Sparks, W. J. C., "A New Method of Approximate Quadrature," INA, 1943, pp. 104–117. This paper gives approximate methods for calculating the following from the values of a few ordinates taken from a ship curve, based upon fitting a 5th-order parabola to that curve:
(a) Area or fullness coefficient
(b) Center of area
(c) Square moment of area about a longitudinal axis
(d) Square moment of area about a transverse axis.

(12) Lackenby, H., "On the Systematic Geometrical Variation of Ship Forms," INA, Jul 1950, pp. 289–316

(13) Thieme, H., "Systematische Entwicklung von Schifflinien (Systematic Development of Ship Lines)," Schiff und Hafen, Jul 1952, pp. 241–245. On page 245 there is a list of 31 references.

(14) Taggart, R., "Mathematical Fairing of Ships' Lines for Mold Loft Layout," ASNE, May 1955, pp. 337–357.

CHAPTER 50

Mathematical Methods of Calculating the Pressure Resistance of Ships

50.1 General. The inquiring and enterprising marine architect has long felt a need for a story on the theoretical calculation of the *wavemaking resistance* of a ship. He has known that mathematicians, physicists, and even some naval architects have been engaged on this project for nearly a century but that their work was on a plane "sky-high" compared to his own. He has realized, from looking at some of their simpler graphs, that their results compared rather well with experimental data from model basins, well enough to sustain a keen interest among workers of their caliber. The forward-looking ship architect and designer, unfamiliar with higher mathematics, has wanted to know about these things but could not understand the papers that were being written. He has felt, and justifiably so, that if the story relating to the calculation of wave resistance could not be made simple, it should at least be made readable to him. Someone should take the trouble to make it understandable to those who had to spend their days fashioning and building ships rather than covering sheets of paper with mathematical equations.

Beginning in about 1950, several workers prominent in the mathematical field set out to do just this. Among their efforts may be mentioned:

(a) The early paper of T. H. Havelock entitled "Wave Patterns and Wave Resistance" [INA, 1931, Vol. 76, pp. 430–446] which, in the words of W. C. S. Wigley, describes the theory "without mathematical complications"

(b) The somewhat mathematical but nevertheless very readable paper presented by Professor Sir Thomas H. Havelock on two occasions in 1950 in the United States, entitled "Wave Resistance Theory and Its Application to Ship Problems" [SNAME, 1951, pp. 13–24]

(c) The rather brief but more general (and less mathematical) account written by G. P. Weinblum and entitled "The Practical Use of Theoretical Studies in Wave Resistance" [MESR, Oct 1951, pp. 49–52]

(d) Weinblum's paper entitled "Analysis of Wave Resistance," published as TMB Report 710 in September 1950. On page 2 he states that the purpose of the paper:

> ". . . is to show to what extent theory has succeeded in furnishing valuable practical results and how the scope of its applications can be extended . . .
>
> "There is common agreement that theory has furnished a valuable description of general phenomena; it is less well known that it also has given us the proof of considerable practical value of how sensitive wave resistance can be to changes, even small changes, in ship form."

(e) The most interesting account presented by the mathematician-physicist-naval architect team of G. Birkhoff, B. V. Korvin-Kroukovsky, and J. Kotik in their "Theory of the Wave Resistance of Ships," especially Part 1 [SNAME, 1954, pp. 359–396].

The present chapter, prepared by one definitely

not in the mathematical part of the field, is an endeavor to present a somewhat different version of the story for the benefit of the practising marine architect. It places emphasis on certain features important in ship design. For the architect and engineer who have progressed this far in a consecutive reading of the preceding chapters of Volumes I and II, it is possible to discuss the calculation of the pressure resistance of a ship in rather specific terms, eliminating the terms involving viscosity effects as found in the Weinblum presentation listed in (c) preceding.

For the period from about 1950 to 1956 the matters discussed here have been under intensive study by the Panel on Analytical Ship-Wave Relations, under Project H-5 of the SNAME Hydrodynamics Committee.

The present author takes the liberty of quoting directly from the first paragraph of Sir Thomas Havelock's 1950 paper, found on page 13 of the SNAME 1951 reference previously cited:

> "It is impossible to give any adequate survey of this work here, and fortunately it is not necessary to make the attempt; there are excellent summaries which have been published from time to time, and in particular I would refer, for a comprehensive account with references, to Wigley's recent paper, "L'État Actuel des Calculs de Resistance de Vagues (The Present Position of the Calculation of Wave Resistance)," ATMA, Paris, 1949, Vol. 48, pages 553–587."

So far as known, the Wigley paper referenced here has not been translated into English.

For the benefit of the naval architect who is giving this matter serious attention for the first time, two features should be pointed out in advance:

(1) Regardless of what he may have thought of their work in the past, he should realize that practically all the analysts who have been engaged on this problem, for the period 1925–1955, have followed up their theoretical work with model experiments, in an effort to prove—or to disprove—their theories

(2) They have strived to make it clear that they are engaged in a calculation of *wavemaking resistance only*. Other phases of pressure resistance have been considered, but not included in their predictions.

50.2 Early Efforts to Analyze and Calculate Ship Resistance. Until the period 1840–1860 the aim of ship designers and builders was to crowd the maximum of carrying capacity into merchant vessels and to fire the heaviest weight of broadside from war vessels. With some few exceptions, they left to nature the composition of the propelling power of the sails and the resistance of the ship into a speed through the water that would meet the service requirements of those days.

The designers who first put their minds to a technical analysis of the ship-propulsion problem appeared to have an instinctive feeling, as did those who labored at the task until about the period 1850-1870, that there was a ship form of minimum resistance waiting to be discovered. The fact that speed was a dominating factor in this quest for the most easily propelled ship form seems to have been overlooked, because the range of speeds at that time was still small. However, those seeking this form of least resistance appeared to have a definite thought that, somehow or other, they could calculate or derive its shape by analytic methods. Calculating its resistance was a thought and a task for the future.

Nevertheless, surface waves were recognized as having an appreciable, if not a major effect on ship resistance, so much so that J. Scott Russell, W. J. M. Rankine, J. R. Napier, and others of their times made use of certain properties (principally the profiles) of trochoidal surface waves in laying out the waterlines of their ships. They evidently hoped that a useful degree of wave-resistance compensation could be achieved by plotting the profile of a trochoidal wave accompanying the afterbody, turning this profile over on its side, and then making the waterline of the ship's run a sort of complement to the wave profile. This was done, in the words of J. Scott Russell, to use "the lateral displacements of wavy water to correct the effects of its undulating surface, . . ." [INA, 1863, p. 226].

It is to be remembered that the developments outlined in this section all took place before the first model basin was commissioned by William Froude in 1872. It is apparent, further, from the fact that proposals such as those in the preceding paragraph were made by eminent men of the period, that their reasoning was not equaled by their observation of ship phenomena. It is a sign of real progress that the testing of ship models, subsequent to this time, has been accompanied by a greatly increased attention to and observation of hydrodynamic phenomena on ships, in the full scale.

Rankine, in the early 1860's, tackled the problem of the flow of water around a ship from a

purely analytic point of view. He started with a two-dimensional body in an unlimited liquid and then brought it to the surface, so to speak. When he did so he realized that surface waves would be formed but of these "principal vertical disturbances" he assumed them "to be so small, compared with the dimensions of the body, as not to produce any appreciable error in the consequences of the supposition of (liquid) motion in plane layers" [Phil. Trans., Roy. Soc., London, 1864, pp. 383–384].

Whatever may be said of Rankine's sense of values and of physical laws in this matter, he did succeed in deriving mathematically an infinite series of 2-diml and 3-diml shapes for which not only the boundary coordinates but the velocity and pressure distribution could be calculated. It seems reasonable to suppose that eventually he hoped to be able to calculate their resistances to motion in a liquid. With the assistance of Clerk Maxwell, as related previously in Sec. 2.11, he devised graphic and geometric methods of drawing the outlines of these oval forms, called here Rankine stream forms, as well as the procedures for constructing the streamlines around them. Rankine's endeavors [Phil. Trans., Roy. Soc., 1864 and 1871] constitute, so far as known, the first scientific attempt to take into account the prime factors of velocity and pressure around a ship hull. This important scientific contribution embodied Rankine's invention of the concept of radial flow, later to be known in some quarters as source-sink flow, and subsequently to be utilized to some extent in practically all attacks on the wave-resistance problem from 1890 to the present. While it is reported that G. R. Kirchhoff employed the artifice of sources and sinks in analytic hydrodynamics as early as 1845 [Rouse, H., and Ince, S., "History of Hydraulics," La Houille Blanche, B/1955, Chap. 9, p. 201], Rankine's search for the fundamental velocity and pressure relationships in the surrounding flow laid the groundwork for the useful features of this concept today.

One interesting feature of Rankine's work, seldom brought to mind in these years, is that while he considered the oval shapes resulting from his new procedure to be general forms of waterlines, it was not at all his intention that the blunt-ended "neoids" or stream-form outlines generated by placing a source-sink pair in a uniform stream be incorporated as waterlines in actual ships. He proposed instead that one of the stream surfaces lying in the liquid *outboard* of the oval form, comprising both hollow regions and convex shoulders, be used as the hull surface at the ship waterline. To this shape of boundary, represented by the trace $L_S - L_B$ in diagram 1 of Fig. 50.A, or by any streamline farther removed from the stream form, he gave the name "lissone-

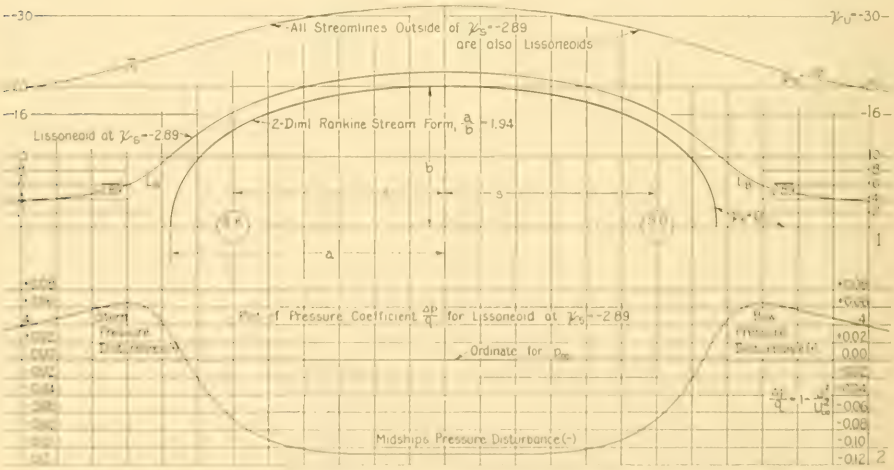

Fig. 50.A Diagram of Streamlines in 2-Diml Flow, Illustrating Rankine's Lissoneoid, with Longitudinal Pressure Variations

oid," signifying a ship surface over which the water might glide easily [INA, 1864, pp. 327–328].

Of these surfaces he said:

> "The co-efficients of those Lissoneoids which are of proportions available for practical use (the length being four times the breadth, and upwards) range from three-fifths to two-thirds, and differ but little in any case from 0.637, which is also the co-efficient of fineness for a curve of sines" [INA, 1864, p. 327].

The latter corresponded to J. Scott Russell's waterline curve of versed sines, reproduced in diagram A of Fig. 24.G in Volume I. It seems clear that Rankine, as a ship designer of that day as well as a mathematician and scientist of considerable renown, did use shapes resembling lissoneoids for the waterlines of some ships.

Rankine points out, in his 1864 paper, cited earlier in this section, that along a lissoneoid, clear of the stream form, there is a region of maximum positive differential pressure $+\Delta p$ abreast the leading edge and another abreast the trailing edge, with *only one* region of maximum negative differential pressure $-\Delta p$ abreast the middle of the body. Around the neoid or stream form proper there are two points, one on each shoulder, where the Δp drops to its maximum negative numerical value, while at amidships it rises to a somewhat lesser negative numerical value. This means that, around and along a neoid, the pressure *changes* the sign of its longitudinal gradient (rises and falls) six times, whereas along a lissoneoid it changes only four times. This situation is shown schematically in diagram 2 of Fig. 50.A. The significance of these changes was appreciated by Rankine, who felt that the fewer the pressure changes along the side of a ship the better.

With this background, and some previous work on waves [Phil. Trans., Roy. Soc., 1863], Rankine developed two formulas, essentially similar, for calculating the resistance of a ship having a certain shape of waterline. They are described here at some length, not so much because of their interesting historic value, or of their practical and physical worth, but because of the lines of reasoning by which they were derived. It is of little present importance that the hydrodynamics was faulty or that they proved inadequate for design purposes but it is important that the derivation was based on considerations of hydrodynamics rather than on the intensely practical nautical knowledge of that day.

Rankine considered, first, that the length L of the ship was matched by the length L_W of a trochoidal wave traveling at the same speed, with two adjacent crests opposite the bow and stern, and with its trough amidships. Second, he assumed a hypothetical barge-shaped ship with a given constant beam and a vertically curved bottom, shaped to a nicety so that it fitted exactly into the trough of the trochoidal wave and rested everywhere upon the wave surface, like a sailor relaxing in a hammock. He took for granted, as did everyone else at that time, that the friction resistance along the ship's side varied as the square of the speed. Further, that the friction resistance along the under side of the barge-shaped ship was balanced by a forward thrust or propelling force which, exerted by the water under the run, just counteracted the friction effects upon the whole barge. This procedure appeared to be exceedingly clever, because it obviated the necessity of estimating or computing those effects.

Rankine then transformed the curved-bottom barge into a ship with a mean girth equal to the barge's beam, and with a run which was characterized by a waterline having the shape of a trochoid. Utilizing a few more transformations that read like a story of alchemy, Rankine evolved a formula for the *total* resistance of the ship. Rewritten in the notation of this book, his formula states that the total ship

$$\begin{aligned}\text{Resistance} &= C_F \frac{w}{2g} V^2 L\begin{pmatrix}\text{mean}\\ \text{girth}\end{pmatrix} \cdot [1 + 4\sin^2 i_R + \sin^4 i_R] \\ &= C_F \frac{\rho}{2} V^2 L\begin{pmatrix}\text{mean}\\ \text{girth}\end{pmatrix} \cdot [1 + 4\sin^2 i_R + \sin^4 i_R]\end{aligned} \tag{50.i}$$

where i_R is the maximum slope of the trochoidal waterline in the run and V is the ship speed. The third term in the brackets, $\sin^4 i_R$, may become small enough to be neglected in comparison with the others. Based on the use of English units of measurement, the friction coefficient C_F, according to the knowledge of that time, was about 0.0036 for the clean, painted surfaces of iron ships ["On the Computation of the Probable Engine-Power and Speed of Proposed Ships," INA, 1864, pp. 316–333].

The terms to the left of the brackets, combined with the first term within them, namely unity, gave the friction resistance only. The pressure resistance was added by taking account of the

second and third terms in the brackets, but in such a manner that it formed a quantity calculated in the same way as the friction resistance and added to it. More is said of this unusual feature later. Rankine called the combination of the product of the length L, the mean girth, and the terms within the brackets "the augmented surface."

The year following the publication of this first formula, and after developing his neoids and lissoneoids, Rankine derived from them a similar formula but by a quite different approach, taking "into account not only the direct resistance caused by the *longitudinal* component of the friction, but the resistance caused indirectly through the decrease of pressure at the bow, and diminution of pressure at the stern, assuming the vertical disturbance (of the water surface) to be unimportant" (italics and comments in brackets are those of the present author) [Phil. Trans., 1864, p. 384]. Rankine's reasoning here is not too clear, especially as to the source of the reduced pressure at the stern in a region of potential flow, but there is no doubt that he was thinking intensely on the subject.

The second formula, given "as a probable approximation for lissoneoids" [Phil. Trans., 1864, p. 390], takes the following form when put in the notation of this book:

$$R = C_F \frac{\rho}{2} SV^2\left[1 + 4\left(\frac{\Delta V}{V}\right)^2\right] \qquad (50.\text{ii})$$

where S is the wetted surface with *no* obliquity correction and ΔV, measured abreast the middle of the body, is the increase in the "velocity of gliding" over the speed of the vessel, due to the potential flow around the ship.

If the $\sin^4 i_R$ term of Eq. (50.i) is neglected, the expressions within the brackets in these two equations become essentially similar in that both are indirectly functions of the beam. Increasing the beam increases both $\sin^2 i_R$ and $(\Delta V/V)^2$ and at the same time increases the resistance. In fact, the inclusion of these terms to the second power may not be too distantly related to the conclusions derived many decades later, to the effect that under similar circumstances the calculated resistance due to wavemaking increases as a function of the square of the beam [Havelock, T. H., INA, 1948, p. 261].

Despite the incomplete knowledge of physical phenomena upon which they were based, Eqs. (50.i) and (50.ii) bear a striking likeness to those in use in many quarters today, as may be noted from Sec. 50.7 of this part of the book and from SNAME Technical and Research Bulletin 1-2, March 1952, page 3. If Rankine did not choose to emphasize those factors which have since become important, he must at least be given credit for outspoken discussion of the subject and professional honesty, still highly prized. In the referenced 1864 paper, on page 390, he headed the section containing his expression for Eq. (50.ii) with the frank statement "Provisional Formula for Resistance." On page 296 of his later 1871 paper a similar heading reflected his increased confidence in the formula by reading "Probable Law of Resistance."

Despite his lack of knowledge of the laws of friction resistance Rankine brought out the following important points:

(a) The use of the longitudinal instead of the tangential components of the friction drag in the direction of motion

(b) The use of the velocity with which the water actually moved over the surface of the ship, as contrasted to the overall speed of the ship.

During the period from 1858 to 1863, and probably at other times, Rankine (with J. R. Napier) used the formulas of Eqs. (50.i) and (50.ii) "with complete success in practice, to calculate beforehand the engine-power required to propel proposed vessels at given speeds" [Phil. Trans., 1863, p. 136].

Other engineers and scientists, working independently on the problem in Great Britain, endeavored to find formulas for calculating both the friction and the pressure resistance [Phipps, G. H., Inst. Civ. Engrs., London, 8 and 15 Mar 1864; Jour. Franklin Inst., Jan-Jun 1864, Vol. XLVII, Third Series, pp. 308–312].

As with many other things of that period the ship-resistance formulas have long since been forgotten, at least in their original form, but their purpose remains as valid as when it was expressed nearly a century ago.

50.3 Modern Developments in the Calculation of Pressure Resistance Due to Wavemaking. The early history of the analytic attack on the problem of ship resistance, sketched in Sec. 50.2, shows first some groping and spasmodic efforts, then the beginnings of an active campaign that in the period 1920-1955 has become systematic and has shown increasing promise of practical results.

This campaign was initiated by J. H. Michell in 1898 [Phil. Mag., London, 1898, Vol. 45, pp. 106–123] and carried on by T. H. Havelock, W. C. S. Wigley, E. Hogner, G. P. Weinblum, R. S. Guilloton, J. K. Lunde, and others, along somewhat varied and independent lines. It is based generally upon one or more of the following:

(1) Utilization of the slopes of the ship surfaces with respect to the direction of motion
(2) Utilization of source-sink combinations and distributions to represent the disturbance produced by a moving ship
(3) Calculation of the wavemaking resistance from the velocity potential derived for the flow around the ship form.

This procedure involves considerable modifications of Rankine's original work on point sources and sinks and the later development of line sources and sinks by D. W. Taylor. The stream-form ship is not only brought to the surface from a region of unlimited liquid all around it, but the surface waves are now so large that the wavemaking effects enter as a major factor in the resistance.

A distribution of radial flow from one or more sources and sinks which, in a uniform stream of unlimited extent, produces a given body form, requires extensive modification to produce the same form at and near a free surface. Furthermore, the secondary surface waves set up by the moving pressure disturbances incident to this radial flow do not form a pattern which is symmetrical forward and aft with relation to the ship. Hence, although the schematic ship moves in an ideal liquid, it does possess a pressure drag due to wavemaking. D'Alembert's paradox no longer holds here, where the body is so close to the surface that its motion produces surface waves containing an appreciable amount of energy.

The calculation of this pressure drag, along theoretical and analytical lines, has been the primary aim of those who have done the recent work on this problem. However, it became evident at a rather early stage that these methods pointed the way to other achievements in calculation and prediction procedures. Some of them are described by F. H. Todd [SNAME, 1951, pp. 78–79], among them the analytic work of W. C. S. Wigley on the bulb bow, described in Sec. 67.6. Before proceeding to discuss the modern lines of attack in somewhat more detail, it may be well to emphasize this fact, because it is often lost sight of in discussions of theoretical amd mathematical methods. The fact that it is invariably necessary to establish the velocity potential of the flow around the ship means that there is concurrently available a powerful tool for deriving most of the flow characteristics and hence many useful features of ship performance.

For example, if the expression for the velocity potential can be modified to take account of boundary-layer, propeller-suction, and other effects, if should be possible to determine from it any one or all of the following:

(a) The direction of flow over the underwater hull surface at selected points [Guilloton, R. S., INA, 1948, Vol. 90, pp. 48–63]
(b) The stream function, which in turn should enable a 3-diml plotting of the stream surfaces in the surrounding field. This takes for granted the ultimate practicability (not now achieved) of expressing the stream function for the flow around a 3-diml body which is not a body of revolution.
(c) The complete pressure distribution over the hull form
(d) The points in the field surrounding the hull where the local velocity is equal to the ship speed, such as are required for many types of instrumentation
(e) The effect of changes in the ship size, proportions, and shape.

An example showing the effect of changing the distribution of section area in the forebody is given by J. V. Wehausen [SNAME, 1951, Fig. B and p. 26]. The general subject of wavemaking resistance as a function of the ship form, proportions, and dimensions is discussed by G. P. Weinblum in TMB Report 710, dated September 1950, pages 25–61. Embodied in this is the discussion of a considerable number of detail features.

In connection with (e) preceding, it may often be simpler and quicker, especially with modern computing machines, to introduce special conditions into an equation and solve for the answer than it is to endeavor to obtain the answer experimentally.

Regardless of the line of attack employed for deriving the wavemaking resistance, it forms one of the three (or more) principal components of the total resistance, following the W. Froude subdivision of the early 1870's. The others are friction resistance, eddy-making or separation resistance, and the interactions listed in Sec. 12.1 of Volume I, if they are taken into account.

To be sure, as is explained shortly, the current (1955) mathematical theory does not recognize the fact that the actual ship moves in a real liquid, that it is surrounded by a boundary layer of varying thickness and velocity, that it is generally accompanied by a separation zone at the stern, or that it is driven by propellers with velocity and pressure fields of their own. No more does the simple beam theory take account of the complexities in the structure of a modern ship, yet it is continually employed to predict the stresses and strains in this structure. If corresponding complications do not prevent everyday use of the simple beam theory, the assumptions implicit in the present-day applications of theoretical hydrodynamics to a prediction of ship behavior should not hinder its use wherever applicable. Continuation of the theoretical and analytical development of the past 50 years for another half-century into the future, corresponding to the full century that the beam theory has been in use for ship structures, may well bring to the hands of naval architects a flow theory equally simple in application if not in character or expression.

50.4 Assumptions and Limitations Inherent in Present-Day Calculations. The assumptions which must be made to obtain a solution of the theoretical wave resistance of a ship by the most modern mathematical methods (1955) will, it is believed, appear in a clearer light if the analytic procedure is first explained. Paraphrasing T. H. Havelock, to whom we are principally indebted for it, this procedure is described as follows [Lunde, J. K., "On the Theory of Wave Resistance and Wave Profile," Norwegian Model Basin Rep. 10, Apr 1952, p. 2]:

(1) The first step is to neglect any wave motion produced on the free surface, as if the latter were covered with a sheet of ice which moves aside to permit passage of the ship, and to consider only the liquid motion produced by the ship

(2) The second step is to obtain the wave disturbance produced by this motion while ignoring the presence of the ship in its effect upon these waves

(3) The third step, not yet possible with existing theory, is to evaluate the influence of the ship on the waves so calculated

(4) Finally, by a series of successive approximations which remain to be worked out, to determine the actual wave disturbance around the ship. From the pressures developed on the ship surface, or from the energy in the wave system, to calculate the ship resistance due to wavemaking.

The actual assumptions made, as embodied in the Lunde 1952 reference, are quite definite and straightforward:

(a) The liquid is homogeneous, it retains its continuity, and it is incompressible; that is, it is not subjected to elastic deformation

(b) The liquid is ideal in that it is without viscosity

(c) The action has continued for a sufficiently long time so that steady motion is established everywhere

(d) The wave height is small in comparison to the wave length, with a wave slope and a wave steepness that are likewise relatively small

(e) The velocities due to wave motion are small compared to the ship speed

(f) Outside of the displacement thickness δ^*(delta star) of the boundary layer, which is relatively thin compared to the beam or draft of the ship, the liquid motion is irrotational and can be characterized by a velocity potential ϕ(phi) which, when differentiated partially, produces the three component velocities along the body axes:

$$u = \frac{\partial \phi}{\partial x} \qquad v = \frac{\partial \phi}{\partial y} \qquad w = \frac{\partial \phi}{\partial z}$$

These velocities are assumed to be so small in comparison with the ship's velocity that their squares and higher powers can be neglected.

(g) The liquid motion around the ship can be represented by the combination of a uniform-stream flow parallel to the ship axis and a radial flow associated with the desired or necessary combination of sources, sinks, and doublets, placed anywhere within or on the hull boundary

(h) For reasons largely mathematical, to keep certain integrals determinate, it is assumed that the ideal liquid does exert a *small* friction force proportional to the liquid velocity. The damping coefficient thus arbitrarily introduced is diminished to zero in the analysis as soon as it has served its purpose. Actually, this procedure insures that the surface waves always trail the ship.

(i) Other than as listed in (h) preceding, the effects of viscosity in the liquid are neglected and the boundary layer as such is considered absent

(j) The pressure resistance due to wavemaking, under the foregoing conditions, can be considered

equivalent to that encountered when viscous flow is present, as on an actual ship. In other words, the friction resistance and the resistance due to wavemaking do not influence each other, at least as a first approximation, and may therefore be calculated separately.

(k) The ship form possesses easy waterlines and buttocks (with small slopes), so that separation does not occur in any region around its boundary

(l) The length-beam ratio is large and the beam-draft ratio moderately small

(m) Change of trim and sinkage due to the ship motion do not affect the pressure resistance. This is a simplifying but not a necessary assumption.

The wave height, the particle velocity in the wave, and the slopes of the ship waterlines and buttocks are limited in magnitude only by the necessity of keeping the general expressions for velocity potential and wave resistance in linear form [Lunde, J. K., SNAME, 1951, p. 83]. Actually, the ship forms to which the analytic procedure can be and has been applied are by no means excessively thin and fine, as witness the forms depicted in SNAME, 1951, Fig. 6 on page 18, Fig. 8 on page 20, Fig. 9 on page 21, Fig. 7 on page 72, and Fig. 3.Q in Sec. 3.13 of Volume I of this book.

Change of trim, involving slope drag in addition to hydrodynamic resistance, is not a sizable factor except in vessels intended to run at high speed-length quotients. The pressure resistance due to wavemaking, in the usual model-testing and ship-powering technique, is considered to be independent of the friction resistance, although there are known to be interactions between the two, discussed in (d) of Sec. 12.1.

This leaves but two limitations of consequence. The fact that the run of the ship must be sufficiently tapering, both horizontally and vertically, to avoid all separation means that the analytic method as now developed is limited definitely to pressure resistance due to wavemaking. Pressure resistances due to separation and other factors have to be calculated separately. It is effective, therefore, in determining only a part of what is generally classed as residuary resistance.

The major limitation of the analytic procedure is that it fails to take account of the effective change in form of the run, especially near and at the stern, caused by the displacement thickness of the boundary layer and by whatever separation zones exist there. While the displacement thickness

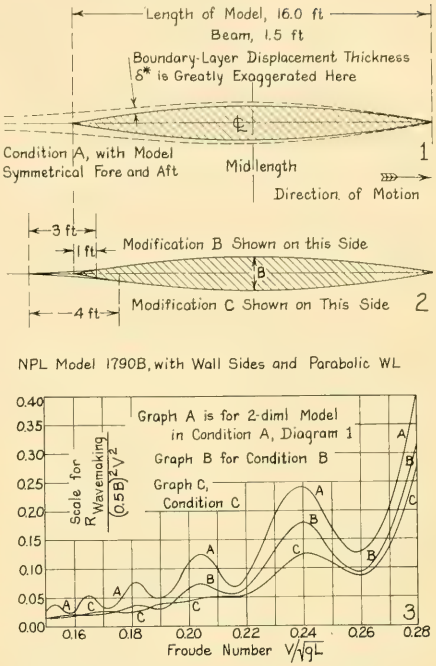

FIG. 50.B CALCULATED RESISTANCE DATA FOR SLENDER 2-DIML SHIP FORMS WITH AND WITHOUT ALLOWANCES FOR BOUNDARY-LAYER THICKNESS AND SEPARATION

is small in proportion to the ship's transverse dimensions, indicated at 1 in Fig. 50.B, this is true only from the stem to that region along the run where the boundary layer thickens perceptibly as the ship surface recedes from the water flowing past it. When it recedes at too rapid a rate separation occurs in a form such as to fill out or fair out the blunt endings.

The separation-zone effect can be allowed for after a fashion by a method developed by T. H. Havelock and illustrated schematically at 2 in Fig. 50.B, adapted from Fig. 1 on page 262 of INA, 1948. Here the ship form is enlarged by the addition of an "appendage" at the stern which is estimated to be of the proper size and shape to produce a potential flow (and a surface-wave system) about the idealized ship that is found around the actual ship. Unfortunately, this estimate involves a knowledge of and an ability to predict separation which is greater than that

reflected in Chap. 46 of this part of the book, but it is certainly a step in the right direction.

Curve A in diagram 3 of Fig. 50.B gives values of the expression $R_W/[(0.5B)^2V^2]$, on a basis of Froude number $F_n = V/\sqrt{gL}$, for the calculated wavemaking resistance of the 2-diml model in diagram 1 of the figure, when moving ahead in an ideal liquid, with no boundary layer. Curve B in diagram 3 represents the calculated wavemaking resistance R_W divided by $[(0.5B)^2V^2]$, for a symmetrical stern appendage corresponding to Modification B in diagram 2 of Fig. 50.B. Curve C gives similar data for Modification C. The effect of easing the waterline slopes in the run appears to be very large compared to the small size of the appendages added.

Allowing for the boundary-layer effect is discussed briefly by J. K. Lunde [SNAME, 1951, p. 83].

50.5 Formulation of the Velocity-Potential Expression. Given the assumptions listed in Sec. 50.4 preceding and accepting the limitations stated there, one analytic procedure may be outlined briefly as follows. Granting that the shape of the underwater ship hull, as well as the motion of the water around it, is defined by a given combination of sources and sinks and a superposed uniform flow, the internal sources and sinks, balancing each other in strength, can determine the hull shape but they have no effect upon the external resistance. This is caused solely by the image source(s) used to produce the surface boundary condition; that is, to keep the free surface sensibly flat. By starting with the force produced on a typical internal source by the fluid velocity at that point resulting from the image source, it is possible to arrive at an expression for the surface wave resistance.

Expressed in more specific terms, one may start with a 3-diml source placed at some point inside the bow of the schematic ship, below the waterline. This source is so placed that, in combination with others to be added later, and when superposed on a uniform-stream flow, it produces an entrance for the ship of the desired size and shape.

Moving by itself at a steady speed close under the free liquid surface, the low source, called A for convenience, not only diverts the liquid flowing toward it at its own level but also produces a surface wave above it. Following the procedure described at the beginning of Sec. 50.4, step (1) is to flatten out the bow wave above source A, bringing the free surface back to its original at-rest condition. For this purpose a second 3-diml or image source B, with a velocity potential of opposite sign, is added at a distance above the free-surface plane equal to the submergence of source A below it.

The velocity potentials of the two 3-diml sources, taken from Eq. (3.xiii) of Sec. 3.9 of Volume I, are expressed as

$$\phi_A = \frac{m}{R_A} \quad \text{and} \quad \phi_B = -\frac{m}{R_B}$$

They are added to form the velocity potential of the source moving under the flat free surface. A general term

$$\phi_S = \Sigma_S \frac{m_S}{R_S}$$

is then added to produce the effect of all other supplementary sources, whether they are "body" sources below the liquid surface or image sources in the air above it. Hence the velocity potential for a moving source may, to the first approximation, be written

$$\phi = \phi_A + \phi_B + \phi_S = -\frac{m}{R_A} - \frac{m}{R_B} + \Sigma_S \frac{-m_S}{R_S}$$

In many of the references of Sec. 50.13 it will be found that these expressions are modified by having 4π in the denominator. This is solely because the 3-diml source strength m is defined as equal to the quantity rate of flow Q, instead of as $Q/4\pi$. The latter corresponds to the notation in this book.

Making use of the Bernoulli Theorem, and passing through a long series of mathematic transformations, much too complicated and involved to be given here, an expression is derived for the velocity potential which permits almost any finite number of sources and sinks to be used to represent the underwater form of the ship. This velocity potential may, in fact, be expressed in a number of different forms, depending upon the phenomena which are to be predicted or calculated from it. In any of its forms, however, it must first satisfy the continuity conditions. Second, it must satisfy the various boundary conditions corresponding to the shape of the underwater form and the shape of the free surface around the moving ship (this surface need not necessarily be flat in the final form of the velocity potential; indeed it is not flat).

In the words of M. M. Munk, when speaking of

vortex theory, one might say that any method actually used:

"... seems not to appeal readily to minds not thoroughly trained mathematically, and gives rise to confusion among practical men rather than serving to enlighten them" [Proc. First Int. Cong. Appl. Mech., Delft, 1924, p. 435].

50.6 The Calculation of Wavemaking Resistance. Having achieved a suitable expression for the velocity potential ϕ which meets the continuity and boundary conditions, much easier said than done, there are several ways of using it to obtain the answers desired. In the case of the resistance due to wavemaking, at least six lines of approach are open, defined briefly as follows:

(a) The most direct and obvious method, considering that the pressure drag due to wavemaking is indeed developed as a pressure directly on the ship, is to integrate the longitudinal component of the resultant liquid pressure over the hull. This is equivalent, as T. H. Havelock says [INA, 1934, p. 439], to obtaining "the combined backward resultant of the fluid pressures taken over the hull of the ship; but this is by no means the simplest method for purposes of calculation."

(b) Introducing artificial viscosity as a damping effect, listed in assumption (h) of Sec. 50.4, or in fact employing any artificial kind of liquid resistance, means that the energy put into the wave system has to be derived from the rate of dissipation of energy in the liquid around the body. This method, in the words of J. K. Lunde, "... has certain important analytical advantages; nevertheless, it is highly artificial ..."

(c) By a direct application of the method of energy and work, it is possible to calculate the pressure drag due to wavemaking if the wave pattern at a great distance to the rear of the ship is known. As the liquid has no viscosity, all the energy put into the wave system remains there, and the wave pattern at that distance is free of all the local disturbances produced by the ship. This is, according to Havelock [INA, 1934, p. 440], the "most natural method" under the circumstances.

(d) By utilization of the Lagally Theorem and the forces exerted between the boundaries of bodies enclosing pairs of sources (or sinks) of equal strength. J. K. Lunde explains this method as follows ["On the Theory of Wave Resistance and Wave Profile," Norwegian Model Basin Rep. 10, Apr 1952, p. 17]:

"It is known that the total force between two sources and two sinks of strengths m and m', respectively, is given by $4\pi\rho mm'/r^2$ where r is the distance between them [Lamb, H., "Hydrodynamics," 5th ed., Art. 144, p. 138. This result is not given in the later edition]. This force is an attraction if m and m' are of the same sign, and a repulsion when of opposite sign, that is, if one is a source and one a sink. If we suppose a body to be at rest in a uniform stream, we know that the resultant motion is due to the stream itself together with the given sources and sinks in the region outside the body whilst the effect of the body is equivalent to an internal distribution of sources and sinks.

"Now Havelock has shown that the resultant forces and couples on the body may be calculated from the forces on the internal sources and sinks due to attraction and repulsion between external and internal sources and sinks taken in pairs" [Havelock, T. H., "The Vertical Force on a Cylinder Submerged in a Uniform Stream," Proc. Roy. Soc., Series A, 1928, Vol. 122, p. 387ff].

G. P. Weinblum adds the following comment:

"When the velocity potential corresponding to a source-sink distribution is known, the horizontal velocity is also known, and the resistance X (the total resistance R_T in standard notation) can be written down as the integral of the product of the distribution and the horizontal velocity over the region of the distribution" [TMB Rep. 710, Sep 1950, p. 16].

(e) By the method of G. P. Weinblum, in which the shape of the hull is expressed mathematically, as described in Secs. 49.4 and 49.5. In general, Weinblum's method differs from the others mentioned here in that the velocity potential is developed on the basis of equations expressing the hull shape in mathematic terms, rather than upon an array of sources and sinks, or upon the slope of the hull surface with respect to the direction of motion.

(f) By the method of R. Guilloton, in which the hull is represented as a summation of simple geometric bodies, in the form of wedges, and the Michell velocity potential is used to calculate the pressure disturbance of an elementary wedge. The total velocity potential, obtained as the sum of the component potentials, is then expressed directly as a function of the hull shape as defined by a table of offsets [Guilloton, R., INA, 1940, Vol. 82, p. 69ff; 1946, Vol. 88, p. 308ff; 1948, Vol. 90, p. 48ff; SNAME, 1951, Vol. 59, pp. 86–128; Korvin-Kroukovsky, B. V., and Jacobs, W. R., ETT Stevens Rep. 541, Aug 1954, p. 4].

(g) More recently, Guilloton has developed a new approach to the calculation of wavemaking resistance utilizing the measurements of wave profiles taken on towing models [Guilloton, R., SNAME, Tech. and Res. Bull. 1–15, Dec 1953;

INA, 1952, Vol. 94, p. 343ff; Birkhoff, G., Korvin-Kroukovsky, B. V., and Kotik, J., SNAME, 1954, pp. 359–396]. This method has the disadvantage that it is difficult to measure or record the profile positions accurately. The profile appears to shift in any one run, even when the model is moving at nominally constant speed. Further, the differences in profile positions for successive speeds are small.

G. P. Weinblum gives a summary of most of these methods, in more mathematical terms, in Appendix 2 of TMB Report 710, September 1950, pages 89–94.

It has been shown by Lunde that all six methods lead to exactly the same result if carried out correctly. Further, that for a thin ship the methods of Havelock and Guilloton give identical results.

The derivation of the resistance equations by any of these six methods, as well as the calculation of the resistance for a range of speed, is exceedingly involved. No attempt is made to give it here but those who wish to pursue this matter further may find the work carried out in several ways in the references quoted in Sec. 50.13.

One could wish that the ingenuity of the workers in the analytic field had been matched by those in the experimental field, and that there were an equal number of methods by which the resistance and other characteristics of a towing model could be determined. Further, that when so determined, the values would all be equal!

50.7 Components of the Calculated Wavemaking Resistance. The mathematic expressions for resistance derived by the processes mentioned, for shapes which lend themselves to this operation, can sometimes be broken down into four or more parts. These represent the components due to separate wave systems formed at the bow and stern and along the sides, plus the interference effects between these components. Exactly the same unraveling process may be applied to the expressions for the surface elevation (or depression) of the combined gravity-wave system.

As an example, Fig. 50.C gives the formula derived by T. H. Havelock for the wavemaking resistance of the essentially 2-diml and symmetrical form shown there, made up of two parabolic waterlines having their vertexes at midlength [INA, 1934, Eq. (28), pp. 441–442]. This formula consists of a constant factor times a V^2 term times the *sum* of five terms whose significance is described in the diagram. It is to be noted that the fourth and fifth terms of the series are negative, indicating an overpresent benefit from the interferences of all except the bow and stern wave patterns. The general and physical reasons for this are explained in Sec. 10.14 and other sections of that chapter.

Furthermore, the last three terms contain a sine and two cosines which vary with κ(kappa) $= g/V^2$, hence these terms have values which are said to oscillate with speed. The oscillations give rise to the well-known humps and hollows in the curves of resistance due to wavemaking, illustrated in diagram 3 of Fig. 50.B.

50.8 Comparison of Calculated and Experimental Resistances. As an indication of the correlation obtained between the calculated and experimental values of resistance derived from a model which resembles an actual ship, Fig. 50.D gives the ©-curves, based on *total* resistance, for the destroyer model devised by J. K. Lunde and

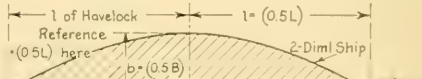

PRESSURE RESISTANCE DUE TO WAVEMAKING

$$= \frac{32\rho(0.5B)^2V^2}{\pi}\left(\mathrm{I}+\mathrm{II}+\mathrm{III}+\mathrm{IV}+\mathrm{V}\right), \text{ where}$$

Term I is $\frac{2}{3}\left(\frac{V^2}{g(0.5L)}\right)^2$, the Resistance Due to the Bow and the Stern Wave Patterns, Assumed to Exist Independently

Term II is $\frac{8}{15}\left(\frac{V^2}{g(0.5L)}\right)^4$, the Resistance Due to the Wave Patterns from the Two Curved Sides, Existing Independently

Term III is $\left(\frac{V^2}{g(0.5L)}\right)^2\int_0^{\frac{\pi}{2}} \cos^3\theta \cos\left[2\kappa(0.5L)\sec\theta\right]d\theta$, the Resistance Due to the Interference of the Bow and the Stern Wave Patterns

Term IV, $(-)2\left(\frac{V^2}{g(0.5L)}\right)^3\int_0^{\frac{\pi}{2}} \cos^4\theta \sin\left[2\kappa(0.5L)\sec\theta\right]d\theta$, the Resistance Due to the Interference of Bow or Stern Wave Patterns with Entrance or Run Patterns

Term V, $(-)\left(\frac{V^2}{g(0.5L)}\right)^4\int_0^{\frac{\pi}{2}} \cos^5\theta \sin\left[2\kappa(0.5L)\sec\theta\right]d\theta$, the Resistance Due to Mutual Interference of the Wave Patterns of the Entrance and the Run

FIG. 50.C TABULATION OF TYPICAL COMPONENTS OF WAVEMAKING RESISTANCE

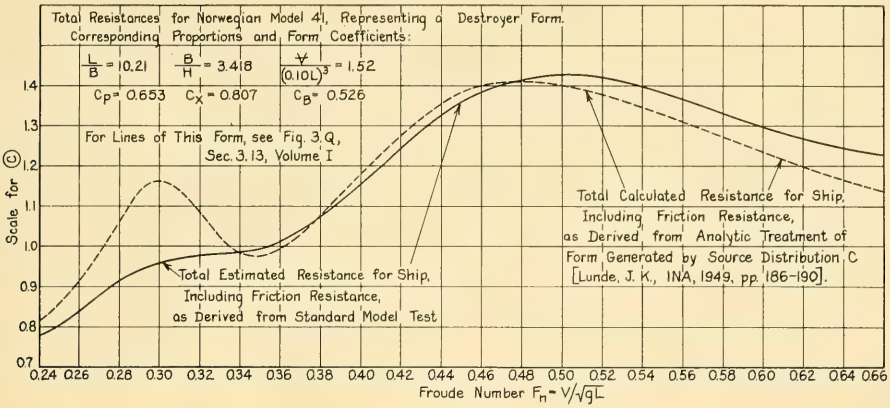

FIG. 50.D COMPARISON OF TOTAL RESISTANCES FOR LUNDE'S DESTROYER MODEL, AS CALCULATED AND AS DETERMINED FROM MODEL TESTS

depicted in Fig. 3.Q of Sec. 3.13 of Volume I [INA, 1949, Fig. 3, p. 188]. Except for the hump in the curve of calculated resistance at a Froude number F_n of about 0.30, much more pronounced in the calculated data than in the experimental data from a routine towing-model test, the agreement is considered to be remarkably good. The shift in the hump of the ©-curve at an F_n of about 0.48, from its position on the theoretical graph to that on the experimental curve, is considered due to the fact that the displacement thickness of the boundary layer around the towed model gives it a greater effective length than its actual physical length. At least, its effective length appears to be greater than that of its counterpart in the real liquid.

Other comparisons are given by the following, some of them original and some taken from the technical literature:

(1) Weinblum, G. P., TMB Rep. 710, Sep 1950, Fig. 6 on p. 22 and Fig. 7 on p. 24
(2) Shearer, J. R., "A Preliminary Investigation of the Discrepancies Between the Calculated and Measured Wavemaking of Hull Forms," NECI, 1950–1951, Vol. 67, pp. 43–68 and D21–D34
(3) Havelock, T. H., "Wave Resistance Theory and Its Application," SNAME, 1951, Fig. 6 on p. 18; Fig. 7 on p. 19
(4) Birkhoff, G., Korvin-Kroukovsky, B. V., and Kotik, J., SNAME, 1954, Fig. 5 on p. 366. This is the first diagram mentioned in item (3) preceding.

50.9 Other Features Derived from Analytic Ship-Wave Relations. Of great interest to the naval architect are the features, other than the wavemaking resistance of a ship in deep water, which the workers in this field have been able to derive by the use of analytic methods and mathematics. Among these may be mentioned (with the source references):

(1) Wavemaking resistance in deep water in accelerated rather than steady motion. This is of fundamental importance in the design and operation of model testing basins and in the conduct of ship trials over measured-mile courses.

Wigley, W. C. S., "Ship Wave Resistance," Proc. Third Int. Congr. Appl. Mech., Stockholm, 1930, Vol. I, pp. 58–73, esp. Figs. 6–9 on pp. 68–70
Havelock, T. H., Quart. Jour. Mech. and Appl. Math., (Oxford), 1949, Vol. 2, p. 325ff and p. 419ff
Havelock, T. H., Proc. Roy. Soc., 1950, Series A, Vol. 201, p. 297ff.
Lunde, J. K., SNAME, 1951, pp. 40–44

(2) Wavemaking resistance in steady motion in an infinitely deep canal with vertical walls.

Sretensky, L. N., Phil. Mag., 1936, Vol. 22, p. 1005ff
Lunde, J. K., SNAME, 1951, pp. 44–50.

(3) Wavemaking resistance in steady motion in restricted waters.

Havelock, T. H., Proc. Roy. Soc., 1921, Series A, Vol. 100, p. 499ff
Havelock, T. H., Proc. Roy. Soc., 1928, Series A, Vol. 118, p. 30ff
Weinblum, G. P., Schiffbau, 1934, Vol. 35, p. 83ff
Sretensky, L. N., Phil. Mag., 1936, Vol. 22, p. 1005ff
Weinblum, G. P., STG, 1938, Vol. 39, p. 166ff.

(4) Wavemaking resistance in steady motion in shallow water of uniform depth and unlimited horizontal extent.

Weinblum, G. P., TMB Rep. 710, Sep 1950, pp. 94–95
Lunde, J. K., SNAME, 1951, pp. 50–55
Kinoshita, M., "Wave Resistance of a Sphere in a Shallow Sea," Jour. Zōsen Kiōkai (Society of Naval Architects, Japan) 1951, Vol. 73.
Lunde, J. K., Norwegian Model Basin Rep. 10, Apr. 1952, pp. 46–59

(5) Wavemaking resistance in accelerated motion in shallow water of uniform depth.

Lunde, J. K., SNAME, 1951, pp. 55–57 (considers linear acceleration).

(6) Wavemaking resistance for steady motion in a shallow canal of rectangular section.

Weinblum, G. P., TMB Rep. 710, Sep 1950, p. 95
Lunde, J. K., SNAME, 1951, pp. 57–59.

(7) Wavemaking resistance for accelerated motion in a shallow canal of rectangular section.

Lunde, J. K., SNAME, 1951, pp. 59–60 (considers linear acceleration).

(8) Wave profiles along the side of and abaft a moving ship.

Wigley, W. C. S., "Ship Waves," NECI, 1930–1931, Vol. 47, pp. 153–196
Havelock, T. H., "Ship Waves," Proc. Roy. Soc., 1932, Series A, Vol. 135, p. 1ff; also Vol. 136, p. 465ff
Wigley, W. C. S., "A Comparison of Experiment and Calculated Wave-Profiles and Wave-Resistance . . .," Proc. Roy. Soc., 1934, Series A, Vol. 144, p. 144ff
Wigley, W. C. S., "The Analysis of Ship Wave Resistance into Components Depending on Features of the Form," Trans. Liverpool Eng'g. Soc., 1940, Vol. LXI, pp. 2–35 (NBS library number TA1.L7)
Havelock, T. H., SNAME, 1951, Fig. 8 on p. 20, from the works of R. Guilloton
Lunde, J. K., Norwegian Model Basin Rep. 10, Apr 1952, pp. 60–84.

(9) Resistance of a ship moving among waves.

Lunde, J. K., Norwegian Model Basin Rep. 10, Apr 1952, pp. 84–97. Considers first-order effects only, neglecting reflection or scattering of waves by the ship itself, as well as heaving and pitching motion.
Havelock, T. H., "The Resistance of a Ship Among Waves," Proc. Roy. Soc., 1937, Series A, Vol. 161, p. 299ff
Havelock, T. H., "The Drifting Force on a Ship Among Waves," Phil. Mag., 1942, Vol. 33, p. 467ff and p. 665ff
Havelock, T. H., Phil. Mag., Series 7, 1940, Vol. 29, p. 407ff
Havelock, T. H., INA, 1945, Vol. 87, p. 109ff
Weinblum, G. P., and St. Denis, M., SNAME, 1950, pp. 184–218.

(10) Streamlines or lines of flow along the hull surfaces of ships in steady motion and quiet water.

Guilloton, R., "Stream Lines on Fine Hulls," INA, 1948, Vol. 90, pp. 48–63. Diagram 1 of Fig. 50.E, adapted from Fig. 2 on p. 52 of the reference, indicates what had been achieved by Guilloton as of the date of this paper.

(11) Lines of equal pressure [$\zeta = (-v/g)\ (\partial\phi/\partial x)$ corresponding to each waterline] around the hull of a ship in steady motion in quiet water.

Guilloton, R., "Stream Lines on Fine Hulls," INA, 1948, Vol. 90, pp. 48–63. Diagram 2 of Fig. 50.E, adapted from Fig. 3 on p. 54 of the reference, depicts some of these lines on a so-called mathematical model.

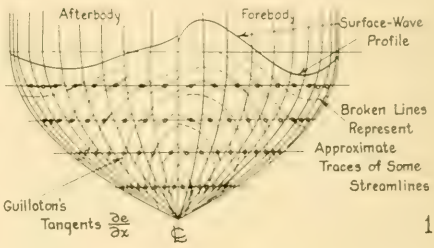

Both Body Plans Represent W.C.S. Wigley's Model 755, when Run at a Froude Number of 0.274

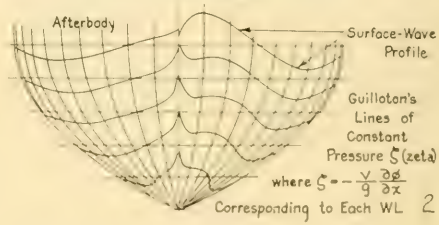

Fig. 50.E Streamlines and Lines of Constant Pressure as Derived Analytically by R. Guilloton

(12) Effect of longitudinal distribution of displacement and shape of the section-area curve.

Weinblum, G. P., TMB Rep. 710, Sep 1950, pp. 38–50. In Fig. 31 on p. 58, the author gives some forebody section-area curves for ships of least resistance at various Froude numbers. In Fig. 32 on p. 60 he reproduces some similar full-length A-curves from G. Pavlenko.
Pien, P. C., SNAME, 1953, pp. 580–582.

(13) Effect of vertical distribution of displacement.

Weinblum, G. P., TMB Rep. 710, Sep 1950, pp. 50–56. Covers influence of the midship-section coefficient, shape of sections, shape of waterlines, section-area curve, bulb bows, and cruiser sterns.

50.10 Ship Forms Suitable for Wave-Resistance Calculations. The simplified ship of J. H. Michell's 1898 paper was little more than a friction form with somewhat convex sides. Many of the forms subsequently used resembled deep canoes more than real ships. This was largely because the slopes of the fore-and-aft lines of these "ships" were small, and because the source-sink distribution, when employed, was for many years limited to positions on the centerplane. Possibly the greater part of the forms were selected because their boundaries could be defined by mathematical formulas based upon the ship axes. If the expressions were not to become too involved, appreciable limitations were imposed on the shapes represented by them. Body plans and other lines drawings of these forms are illustrated by:

(1) Wigley, W. C. S., and Lunde, J. K., INA, 1948, Vol. 90, Fig. 1, p. 97; also Havelock, T. H., SNAME, 1951, Fig. 6, p. 18, and Birkhoff, G., SNAME, 1954, Fig. 5, p. 366
(2) Guilloton, R., INA, 1948, Vol. 90, Fig. 2, p. 52 and Fig. 3, p. 54.

While they are not to be classed as ships, the thin friction forms and thick planes used in friction-resistance tests in model basins lend themselves admirably to the calculation of their wavemaking resistance. No matter how thin they may be constructed they are rarely free of wavemaking at the higher speeds.

Of late years, the calculation technique has progressed to the point where combined radial and uniform flow can be utilized to produce hull shapes not unlike those of actual ships. Fig. 3.Q of Sec. 3.13 of Volume I illustrates such a form designed by J. K. Lunde and made the subject of rather extensive studies [INA, 1949, Vol. 91, Figs. 1 and 2, pp. 186–187].

To produce a 3-diml ship of this type, simple enough from the naval architect's viewpoint but extremely complex when translated into radial-flow and uniform-flow stream functions, may require as many as 30 pairs of sources and 20 pairs of sinks. The sources of each pair are disposed symmetrically about but offset from the centerplane, as are the sinks, with offset distances which vary from pair to pair.

While the labor involved in the numerical calculations increases with the number of radial-flow points or singularities, it is diminished appreciably by the use of certain tables now in existence. It can possibly be reduced further in the future by the generous use of computing machines.

A remark made by W. J. M. Rankine on page 83 of his 1866 book entitled "Shipbuilding: Theoretical and Practical" applies to many phases of predicting ship performance other than the one discussed in this chapter:

". . . as for misshapen and ill-proportioned vessels, there does not exist any theory capable of giving their resistance by previous computation."

50.11 Necessary Improvements in Analytical and Mathematical Methods. All workers in the field of theoretical and analytical wave-resistance calculations now (1956) agree that there are appreciable discrepancies between the derived and observed resistance data for most of the forms concerned. While these are hardly first-order differences, and while the wavemaking resistances of models can not be measured independently, the variations are large enough to indicate that all the hydrodynamic actions have probably not been taken into account. One of these is the slope drag (or thrust), due to the position of the vessel on the back (or front) of a wave of its own Velox system. This may be the reason for the increased resistance of the destroyer model of Fig. 50.D at Froude numbers above about 0.48, $T_q = 1.61$.

Moreover, it is recognized at the outset that the major viscous effects are neglected, as are all the interactions listed as (d), (e), and (f) in Sec. 12.1. It is entirely possible that the hydrodynamic actions mentioned previously are not recognized in routine analytic and experimental studies of resistance and propulsion, let alone in calculations of wavemaking resistance.

Because of the severe limitations imposed by many analytical methods, such as the necessity for retaining the same type of transverse section from stem to stern of the ship being worked upon, the use of radically different procedures is being studied. One of these is the slender-body theory, widely employed by aerodynamicists but hitherto not applied to surface-ship forms. Without going into details, this method is based upon the assumptions that:

(a) All transverse dimensions are assumed to be small in comparison with the length
(b) The elevations of the Velox wave system, caused by the passage of the slender body through the water, are assumed to be concentrated along the x-axis, as if the wave system were shifted inward due to a transverse collapse of the body to zero beam.

Notwithstanding the modifications to simplify the problem, the mathematical equations are still formidable, the procedure has not yet (1956) been refined, nor have the results received more than preliminary experimental verification. However, the method has the great advantage of lending itself to performance predictions on ship forms with *any type or shape of transverse section*, and with radical changes in transverse section along the length, such as that which occurs at a transom stern. Furthermore, preliminary indications are that a great many actual ship forms fall within the "slender-body" category.

50.12 Practical Benefits of Calculating Ship Performance. Viewed from that point in the progress curve which has been reached to date (1956), the most valuable promise which the analytical and mathematical method now offers to the practical designer is its indication of the relative influence of various shape parameters on the behavior of ship hulls. When the progress is such that adequate mathematical expressions can be set up for ship and liquid motions, the influence of these shape parameters and of particular assumptions and conditions will be made readily apparent and be expressed quickly in numerical or engineering terms. This is exactly the function of the tide-predicting machine which, when it is supplied with the basic information and its wheels are set going, rolls out the data for tide tables with effortless ease.

If the model-testing technique is advantageous because of its relatively low cost, quick answers, and ability to take all physical actions into account, the machine-calculating method promises a saving in time and labor and a greater degree of freedom in setting up the basic conditions. The factors in a mathematical expression can be given any reasonable values, they can be given greater or less weight, as appears to be called for, or they can be omitted entirely.

As to the indication of the influence of various shape parameters of a ship hull, the analytic attack has already to its credit a considerable number of important and useful conclusions and contributions. Whether these could have been achieved by other methods or whether they had already been discovered by observation, deduction, intuition, or experimentation is somewhat beside the point. The fact is that they came out of the analytic "machine" with negligible assistance from other sources.

Among the conclusions and contributions may be listed:

(a) The combination divergent- and transverse-wave pattern due to a moving pressure disturbance, as developed by Lord Kelvin and as worked on by E. Hogner, T. H. Havelock, and others
(b) Extensive knowledge of the physical reasons for the oscillatory variations in the pressure resistance due to wavemaking, resulting in the well-known humps and hollows of residuary-resistance and wavemaking-resistance curves
(c) The reduction in pressure resistance due to wavemaking as the displacement volume is taken away from the vicinity of the surface waterline and moved farther down
(d) A greater appreciation of the necessity for fairness in all ship lines, principally those paralleling the water flow
(e) The physical and theoretical explanation for the beneficial action of the bulb bow in the reduction of pressure resistance due to wavemaking
(f) Knowledge as to separate contributions to the wavemaking resistance made by the diverging and the transverse waves of the Velox system. Fig. 50.F, adapted from J. K. Lunde [SNAME, 1951, Fig. 7, p. 72], indicates this feature most vividly for a rather wide range of Froude numbers.

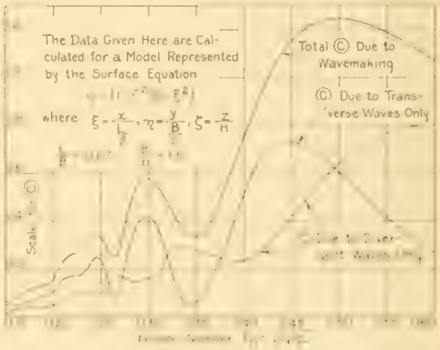

Fig. 50.F Graphs Indicating Separate Contributions Made by the Diverging and the Transverse Waves to the Total Wavemaking Resistance

(g) The definite knowledge that, *under certain conditions*, which are as yet unfortunately not too well defined, small changes in the longitudinal distribution of displacement, indicated by the customary section-area curve, produce relatively large changes in wavemaking resistance. Similarly, that small variations in surface-waterline shape may produce unexpectedly large changes in this resistance.

The work done along these lines during the period 1945–1955, at least in the United States, has given a new impetus to the mathematical delineation of ship lines, described in Chap. 49. In particular, it has initiated studies of the problems of fairing the lines of ships, so that this may be done impersonally—automatically, if need be—in a manner which will benefit the overall hydrodynamic performance of the ship.

The discussion of this chapter may well be concluded by some comments of G. P. Weinblum, to be found on pages 2 and 3 of TMB Report 710, published in September 1950:

"Experienced experimenters are often somewhat bewildered by the fact that the wave resistance may vary appreciably for different but reasonable types of lines, although all the form parameters generally considered as decisive are identical. From a theoretical viewpoint this appears to be quite natural, since the wave resistance depends to a first approximation upon a complicated function of the surface slope in the longitudinal direction, i.e., on derivatives. On the other hand, the most commonly used (hull) coefficients are integrals, which even when kept constant still admit of very wide variations of the slopes. We realize now why the solution of the basic problem of the model basins mentioned above—to establish the resistance as a function of the form—remains almost hopeless as long as the ship surfaces (or at least their most important features) are not defined in a rigorous way by mathematical expressions. Hence, our first task must be to find equations for the ship surface, continuing the work of D. W. Taylor."

50.13 Reference Material on Theoretical Resistance Calculations. Supplementing the remarks in Sec. 50.2 concerning early efforts to analyze and to calculate ship resistance, there are given here a few of the references which contain interesting accounts of this work. They do not include the Rankine references mentioned in the text of Sec. 50.2:

(1) An excellent and most readable summary of the work done prior to 1869 relative to the *calculation* of ship resistance by formula is to be found in the report of the Committee of the British Association headed by C. W. Merrifield and counting among its members Professor W. J. M. Rankine and Mr. William Froude, Brit. Assn. Rep., 1869, pp. 11–21.

(2) Of the work (and workers) which followed that of Rankine, an excellent summary is to be found in a paper by A. W. Johns entitled "Approximate Formulae for Determining the Resistance of Ships" [INA, 1907, pp. 181–197]. In this paper Johns mentions the formulas of:

(a) Middendorf, published in 1879 and given by Wilda in "Marine Engineering," 1906

(b) Admiral Fournier of France. His formula is published in English, with comments, in INA, 1907, page 190.

(c) D. W. Taylor, quoted and commented upon briefly in SNAME, 1894, Vol. 2, page 143.

(3) Lorenz, H., "Beitrag zur Theorie des Schiffswiderstandes (Contribution to the Theory of Ship Resistance)," Zeit. des Ver. Deutsch. Ing., 16 Nov 1907, No. 46

(4) Rothe, "Bemerkungen zur Schiffswiderstandstheorie von H. Lorenz (Note on the Theory of Ship Resistance of H. Lorenz)," Schiffbau, 8 Jan 1909, Vol. 9, pp. 253–354; 2 Jan 1909, pp. 289–290.

The technical literature covering the modern (20th century) analytic attempts to calculate the resistance of ships and to predict other aspects of their performance, as set forth in this chapter, is amazingly extensive. There are listed here only a few of the references which contain large bibliographies:

(5) Weinblum, G. P., TMB Rep. 710, Sep 1950. Pages 98–102 list 116 items, principally by authors. The individual references are extremely sketchy.

(6) Williamson, R. R., "Bibliography on Theoretical Calculation of Wave Resistance," ETT, Stevens (unpublished and undated). This contains 62 items, listed by authors.

(7) Lunde, J. K., "On the Linearized Theory of Wave Resistance for Displacement Ships in Steady and Accelerated Motion," SNAME, 1951, pp. 25–85. Pages 75–76 list 55 items.

(8) Guilloton, R., "Potential Theory of Wave Resistance of Ships, with Tables for its Calculation," SNAME, 1951, pp. 86–128. On pages 120–123 there is a section entitled "Bibliography," listing 91 items in seven different categories. In spite of the completeness of this list it does not give the subjects or titles of the papers.

(9) Korvin-Kroukovsky, B. V., and Jacobs, W. R., "Calculation of the Wavemaking Resistance of Ships of Normal Commercial Form by Guilloton's Method and Comparison with Experimental Data," ETT, Stevens, Rep. 541, Aug 1954. Pages 51–53 list 29 items.

(10) Birkhoff, G., Korvin-Kroukovsky, B. V., and Kotik, J., "Theory of the Wave Resistance of Ships," SNAME, 1954, pp. 359–396. Pages 384 and 385 list 47 items. This list brings the bibliography on the subject practically up to date (1955), except for the items to follow.

(11) Sezawa, K., "Wave Resistance of a Submerged Body in a Shallow Sea," Paper 610, Proceedings, World

Engineering Congress, Tokyo, 1929, Vol. XXIX, Part 1, pages 179–190. This paper comprises a mathematical treatment, largely to the exclusion of a physical discussion. The "body" is apparently a 2-dim'l cylinder with its axis parallel to the surface (and to the bed). There is some discussion of the resistance of a moving underwater sphere.

(12) Lunde, J. K., "On the Linearized Theory of Wave Resistance for a Pressure Distribution Moving at Constant Speed of Advance on the Surface of Deep or Shallow Water," Skipsmodelltankens Meddelse, Trondheim, No. 8, Jun 1951

(13) Lavrent'ev, V. M., "The Effect of the Boundary Layer on the Wave-Making Resistance of Ships," Section on Hydromechanics, Doklady of the Academy of Sciences, USSR, 1951, Vol. LXXX, No. 6

(14) Lunde, J. K., "On the Theory of Wave Resistance and Wave Profile," Norges Tekniske Høgskole, Trondheim, Skipsmodelltankens Meddelse No. 10, Apr 1952. This is the printed version (in English) of Lunde's M. S. Thesis at King's College, Newcastle, finished in May 1945. There are copies in the TMB library.

(15) Lunde, J. K., "The Linearized Theory of Wave Resistance and Its Application to Ship-Shaped Bodies Moving in Deep Water," Norwegian Ship Model Basin Report 23, Mar 1953. This is in Norwegian, with an English summary, but it is being published as an SNAME Technical and Research Bulletin. On pages 110–124 of the Norwegian version there is a very comprehensive list of 185 references on this subject.

(16) G. E. Pavlenko, in his "Soprotivleniye Vody Dvizheniyu Sudov (The Resistance of Water to the Movement of Ships)" [Moscow, 1953], devotes Sec. 13 of Chap. IV, pages 183–186, to a "Method of Calculating (mathematically) the Resistance of an Actual Ship," but he includes no example, and it is doubted whether this method is used in practice in Russia.

(17) Inui, Takao, "Japanese Developments on the Theory of Wave-Making and Wave Resistance," 7th ICSH, Oslo, 20 Aug 1954. This paper, with its illustrations and with many additional enclosures, was published as Skipsmodelltankens Meddelelse Nr. 34 (Norwegian Model Basin Report 34), Apr 1954. In the Bibliography of this report, covering "Japanese papers on Ship Wave Motion and Kindred Subjects from 1929 to 1953," there are listed 75 additional Japanese papers. Of this group, 48 have been translated into English in Japan and are to be published as TMB translations.

(18) Weinblum, G. P., "Problems in Ship Theory," Inst. Eng'g. Res., Univ. of Calif., 1 Nov 1955, Series 82, Issue 1, pp. 11–13.

CHAPTER 51

Proportions and Shape Data for Typical Ships

51.1 General Comments. The ship-design procedures of Part 4 are based on the development of each new design as a separate project, to meet the particular requirements set up for it, rather than upon copying or modifying existing designs, no matter how good the latter may be. Nevertheless, new design requirements often call for a ship hull that resembles one which exists and for which there are proved performance data. It is useful to the designer, therefore, to have proportions and shape data which may be consulted for reference and guidance purposes.

The SNAME Resistance Data sheets were developed, prepared, and issued to fill part of this need, especially for architects and engineers who did not have access to the funds of information available in large ship-design and shipbuilding organizations. Samples of these sheets, filled out with test data for two models of the ABC ship designed in Part 4, are embodied in Figs. 78.Ja, 78.Jb, 78.Jc, 78.Ka, 78.Kb, and 78.Kc. The body plans on SNAME RD sheets 1 through 100 are rather small, so that the shape data are meager with respect to the data on proportions and model performance. Those on RD sheets 101 through 160 are much larger.

While limitations on space preclude the reproduction of many large-scale lines drawings in the present chapter, there are given in subsequent sections a considerable number of references to source material embodying such drawings.

51.2 Parent Form of the Taylor Standard Series. In view of the recent reworking by M. Gertler of the Taylor Standard Series data, embodied in TMB Report 806 and described in Sec. 56.5, the resistance data from this series are likely to be used long after the 1943 edition of D. W. Taylor's book "The Speed and Power of Ships" is out of print. Although the body plan and profile of the parent form, and the section-area curves for the series are given in Fig. 28 on page 92 of PNA, 1939, Vol. II, and in the two references mentioned, the complete data from the 1943 edition of S and P are reproduced here. Some editing has been done on the drawing but the model and curve shapes and the numerical data remain unchanged.

Fig. 51.A embodies the lines of EMB model 632 (modified) and the original group of section-area curves, together with the principal proportions and form coefficients. Table 51.a lists the *original* 0-diml offsets for the parent form of Fig. 51.A, in an arrangement somewhat more convenient than those of the references cited in the preceding paragraph, although not as complete as those given by Gertler in TMB Report 806. Table 51.b lists the 0-diml ordinates for the complete series of A-curves in the figure.

51.3 References to Tabulated Data on Principal Dimensions, Proportions, Coefficients, and Performance of Ships. From time to time there have been published tables of dimensions, characteristics, and performance data on ships of many types and sizes. Rarely do these data correspond, for any two tables listing the same ship(s), and often they omit the very information which the inquiring marine architect desires. Taken by themselves, the data are insufficient for design purposes, and perhaps too meager for statistical studies, but taken together they frequently permit analyses of performance that are extremely useful.

For example, many of the ships of the period from 1850 to 1900 and later were extremely narrow by modern standards, having L/B ratios of 10, 11, or more. Their B/H ratios were also

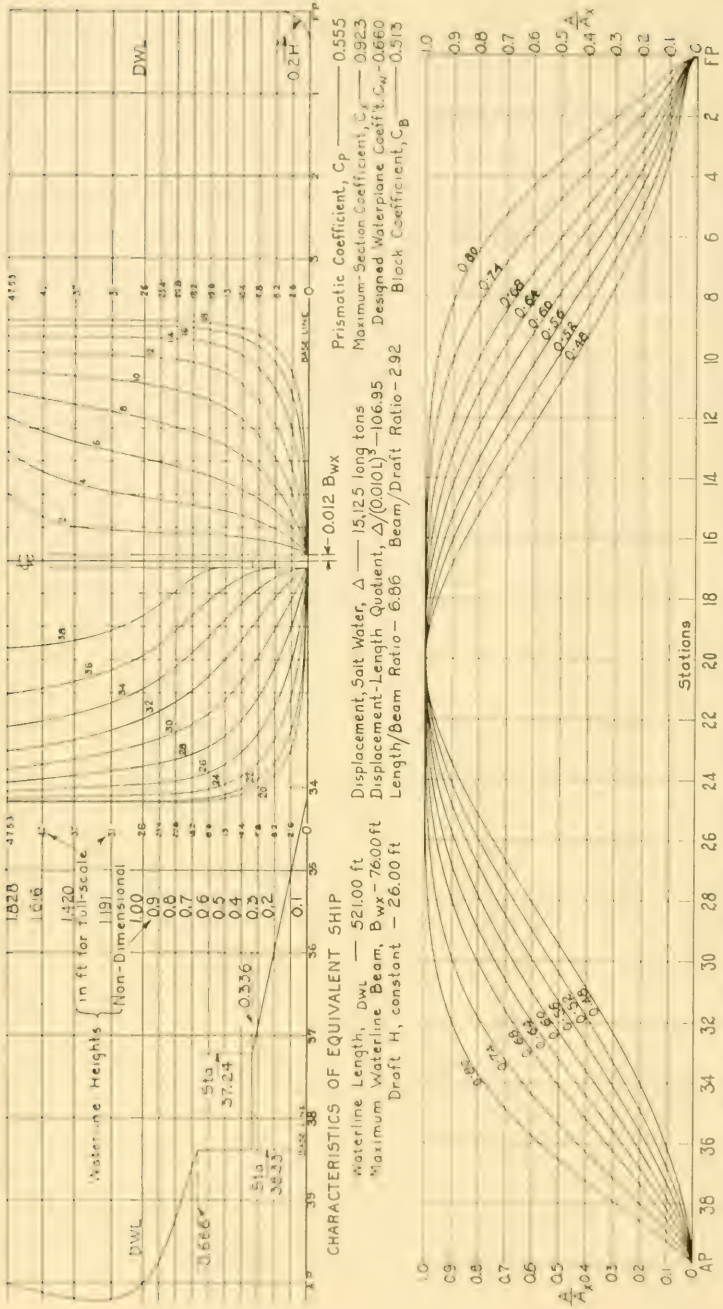

Fig. 51.A Lines and Section-Area Curves of the Taylor Standard Series Parent Form, EMB Model 682 (Modified)

less than is now customary (1955). There is reason to believe that certain of these ships, if not the group as a class, had some wavegoing characteristics superior to those of modern vessels. Despite the augmented safety standards of the 1950's, it is possible that studies of a new and improved hull form could be furthered by data from these old vessels.

It is true that many if not most of the ships listed in the tables referenced in the present section are old, even ancient, and are no longer in commission or in existence. The data are, nevertheless, of far more than historical value because they apply to ships that were actually built, and that gave satisfactory service in eras when it was perhaps more difficult than at present to achieve the performance expected of them. Finally, one may hope that listing these tabulated data may bring forth corresponding information on modern ships.

In the early 1850's a project was initiated in Great Britain which had as its aim the collection

TABLE 51.a—Non-Dimensional Offsets for Parent Form of Taylor Standard Series, EMB Model 632 (Modified)

Stations in Forebody

Waterlines	Max	18	16	14	12	10	8	6	4	2	1	0.5	FP
1.828	1.000	0.987	0.966	0.921	0.861	0.789	0.697	0.587	0.452	0.274	0.166	0.090	
1.616	1.000	0.987	0.966	0.921	0.857	0.774	0.667	0.531	0.362	0.178	0.089	0.043	
1.420	1.000	0.987	0.966	0.921	0.853	0.763	0.642	0.490	0.318	0.142	0.065	0.031	
1.191	1.000	0.987	0.966	0.920	0.846	0.747	0.614	0.452	0.285	0.126	0.062	0.029	
DWL	1.000	0.987	0.966	0.917	0.839	0.728	0.586	0.423	0.260	0.118	0.060	0.030	
0.9	0.999	0.987	0.964	0.915	0.835	0.717	0.570	0.406	0.253	0.117	0.060	0.033	
0.8	0.997	0.986	0.963	0.914	0.828	0.704	0.552	0.389	0.243	0.115	0.062	0.036	
0.7	0.993	0.983	0.960	0.909	0.817	0.685	0.531	0.370	0.232	0.111	0.065	0.042	
0.6	0.984	0.979	0.954	0.897	0.800	0.662	0.506	0.349	0.217	0.109	0.067	0.047	
0.5	0.975	0.970	0.941	0.877	0.772	0.630	0.473	0.324	0.203	0.103	0.066	0.050	
0.4	0.960	0.955	0.920	0.846	0.730	0.584	0.434	0.295	0.184	0.098	0.064	0.051	
0.3	0.940	0.929	0.885	0.794	0.665	0.522	0.381	0.259	0.162	0.088	0.063	0.050	
0.2	0.896	0.880	0.821	0.708	0.568	0.430	0.310	0.211	0.131	0.075	0.056	0.047	
0.1	0.793	0.781	0.694	0.551	0.405	0.292	0.209	0.143	0.089	0.056	0.044	0.040	
0.05	0.685	0.674	0.554	0.408	0.276	0.195	0.139	0.098	0.064	0.041	0.036	0.034	
Baseplane													

Stations in Afterbody

Waterlines	AP	39	38	37	36	34	32	30	28	26	24	22	20
1.828		0.246	0.360	0.460	0.548	0.684	0.784	0.859	0.911	0.949	0.975	0.987	1.000
1.616		0.239	0.350	0.441	0.525	0.661	0.762	0.837	0.897	0.941	0.972	0.987	1.000
1.420		0.226	0.332	0.416	0.496	0.633	0.737	0.817	0.882	0.935	0.970	0.987	1.000
1.191		0.183	0.286	0.371	0.449	0.583	0.696	0.788	0.866	0.927	0.966	0.987	0.996
DWL		0.126	0.227	0.314	0.389	0.527	0.647	0.754	0.849	0.918	0.964	0.987	0.996
0.9		0.084	0.179	0.265	0.342	0.486	0.615	0.732	0.836	0.913	0.963	0.987	0.995
0.8		0.036	0.123	0.207	0.286	0.437	0.578	0.707	0.820	0.905	0.960	0.986	0.994
0.7			0.070	0.146	0.222	0.379	0.534	0.674	0.797	0.892	0.953	0.984	0.992
0.6			0.037	0.092	0.162	0.314	0.476	0.632	0.766	0.871	0.941	0.978	0.986
0.5				0.054	0.108	0.243	0.405	0.574	0.722	0.837	0.921	0.964	0.978
0.4				0.033	0.065	0.177	0.326	0.496	0.659	0.790	0.887	0.941	0.960
0.3					0.037	0.116	0.241	0.399	0.570	0.717	0.833	0.903	0.933
0.2						0.066	0.154	0.288	0.447	0.602	0.739	0.838	0.884
0.1						0.036	0.079	0.163	0.278	0.423	0.570	0.705	0.780
0.05						0.030	0.051	0.096	0.167	0.288	0.420	0.573	0.658
Baseplane													

TABLE 51.b—NON-DIMENSIONAL ORDINATES OF SECTION-AREA CURVES FOR TAYLOR STANDARD SERIES

These data are copied directly from S and P, 1943, Table XXXVI, p. 184.

FOREBODY

Stations	20	18	16	14	12	10	8	6	4	2	1	0.6	0.4	0.2	FP
C_P = 0.48	1.000	0.955	0.853	0.724	0.586	0.450	0.323	0.211	0.126	0.066	0.042	0.037	0.031	0.021	0.000
0.52	1.000	0.971	0.893	1.784	0.655	0.517	0.382	0.257	0.152	0.078	0.046	0.040	0.034	0.022	0.000
0.56	1.000	0.983	0.929	0.838	0.722	0.587	0.446	0.307	0.184	0.092	0.051	0.044	0.036	0.023	0.000
0.60	1.000	0.992	0.955	0.886	0.786	0.658	0.514	0.364	0.221	0.107	0.056	0.048	0.038	0.026	0.000
0.64	1.000	0.997	0.976	0.928	0.846	0.731	0.587	0.426	0.264	0.128	0.063	0.053	0.043	0.029	0.000
0.68	1.000	0.999	0.990	0.961	0.901	0.803	0.668	0.499	0.316	0.152	0.073	0.061	0.049	0.032	0.000
0.74	1.000	1.000	0.998	0.987	0.957	0.893	0.784	0.625	0.423	0.206	0.093	0.078	0.063	0.041	0.000
0.80	1.000	1.000	1.000	0.998	0.988	0.959	0.892	0.766	0.564	0.298	0.133	0.107	0.082	0.054	0.000
0.86	1.000	1.000	1.000	1.000	0.999	0.995	0.977	0.913	0.751	0.423	0.190	0.152	0.113	0.071	0.000

AFTERBODY

Stations	AP	39	38	37	36	34	32	30	28	26	24	22	Terminal values t AP	Terminal values t FP
C_P = 0.48	0.000	0.012	0.034	0.065	0.103	0.200	0.322	0.460	0.604	0.745	0.870	0.964		
0.52	0.000	0.018	0.050	0.090	0.136	0.251	0.385	0.528	0.669	0.797	0.903	0.974	0.270	0.240
0.56	0.000	0.027	0.066	0.115	0.173	0.304	0.450	0.596	0.731	0.846	0.932	0.984	0.430	0.350
0.60	0.000	0.037	0.087	0.149	0.217	0.368	0.522	0.667	0.793	0.891	0.957	0.991	0.600	0.470
0.64	0.000	0.048	0.112	0.185	0.265	0.433	0.595	0.737	0.848	0.928	0.976	0.996	0.815	0.605
0.68	0.000	0.060	0.142	0.231	0.322	0.506	0.671	0.804	0.898	0.958	0.988	0.999	1.075	0.775
0.74	0.000	0.092	0.201	0.315	0.428	0.631	0.789	0.895	0.957	0.987	0.998	1.000	1.640	1.320
0.80	0.000	0.140	0.290	0.436	0.567	0.773	0.898	0.963	0.992	0.998	1.000	1.000	2.500	2.340
0.86	0.000	0.208	0.414	0.599	0.745	0.920	0.987	0.999	1.000	1.000	1.000	1.000	——	——

and analysis of characteristics and performance data for many if not all of the steamships then in operation in the United Kingdom and Western Europe. In 1866 a committee of the British Association (for the Advancement of Science) was formed to condense and to analyze the numerous data. It was composed of some of the leading engineers and scientists of the country, among them:

John Scott Russell, naval architect and ship designer

William Fairbairn, a distinguished engineer versed in structural mechanics

Thomas Hawksley, a civil engineer

James R. Napier, a distinguished engineer

W. J. M. Rankine, a teacher, scientist, hydrodynamicist, and naval architect.

The British Association Report for 1868 (published in 1869), pages 114–139, entitled "Second Report of the Committee on the Condensation and Analysis of Tables of Steamship Performance," contains some two dozen pages of tabulated data for a great many steamers driven by paddlewheels and screw propellers. It embodies information on the ships, their machinery, and propulsion devices. What is more, it contains data worked up by Scott Russell and Professor Rankine in an effort to find, by analysis, some formulation which would serve as an indicator of good or superior ship performance.

Incidentally, several pages of the British Association Report of 1868 are taken up with recitals of the difficulties encountered in obtaining accurate and correct factual data on the many ships studied. The problems of the present day, in this respect, are by no means new.

A two-page "Revised Table of Analysis, According to Mr. Scott Russell's Method," is given on pages 332–333 of the British Association Report for 1869 (published in 1870). This is embodied in a "Supplement to the Second Report of the Committee on the Condensation and Analysis of Tables of Steamship Performance," to be found on pages 330–333 of the reference cited. The table lists 14 ships of the time, 4 driven by paddlewheels and 10 by screw propellers, with 29 entries for each.

In the years following the 1870's, many tabulations similar to the foregoing were published, with accent on the dimensions, proportions, and other characteristics rather than on the vessel's performance. References to a number of these tables are listed here for the convenience of those who wish to consult the data:

(1) John, W., "Atlantic Steamers," INA, 1887, Vol. 28; Table III on p. 164 gives hull data for 17 large ships of that day, 14 entries for each

(2) Wilson, T. D., "Steel Ships of the United States Navy," SNAME, 1893, Vol. I, pp. 116–139. The data in this paper cover vessels in two categories:

(a) Data on early unarmored steel vessels of the U. S. Navy for the period 1883–1893. The principal dimensions and general information for 25 vessels, isting 21 entries per vessel, are found on pp. 128–131.

(b) Data on early armored vessels of the U. S. Navy, 1874–1893. Similar data are given for 14 ships, with 24 entries per ship, on pp. 132–135.

(c) Data on early special-service vessels and torpedoboats, 1883–1892, 6 vessels, 21 entries per vessel, pp. 136–137

(d) Additional data on dimensions, form coefficients, propellers, and machinery of 14 of the vessels in the foregoing three groups are to be found in the folded tables opposite p. 162 of the reference, 64 entries per vessel

(e) Outboard profiles and main deck plans, midship sections, machinery, shafting, and propeller arrangements of certain of the vessels in these three groups are to be found in the same reference, Pls. 6 through 41.

(3) White, Sir W. H., MNA, 1900, tables as follows:

(a) Pages 100–101, 23 merchant steamships, 9 entries per ship, with emphasis on inclining-experiment data

(b) Pages 104–105, 19 different warships, merchant ships, and yachts, 9 entries per ship, with emphasis on inclining-experiment data

(c) Page 136, 9 different ships, including the dispatch vessel *Iris*, 6 entries per ship, with emphasis on metacentric stability data

(d) Page 138, 10 ships, all sailing vessels and yachts, 6 entries per ship, with accent on metacentric stability

(e) Page 642, 4 warships, 5 entries per ship, giving L, B, H, W, and P_I

(f) Page 649, 7 ships, 5 entries per ship, with accent on indicated power P_I .

(4) Durand, W. F., RPS, 1903, pp. 415–425; hull data for 78 ships, 8 entries for each; propeller and trial data for 84 ships, 12 entries for each

(5) Biles, J. H., "Cross-Channel Steamers," INA, 1903, pp. 243–253. Pl. XXXII lists hull and machinery data for 45 vessels of this type, built in the era 1886–1903, with 24 entries for each. Pls. XXXIV-L give arrangement sketches of many of these vessels.

(6) Peabody, C. H., NA, 1904, pp. 522–553; 45 ships of 10 types, 13 entries for each

(7) Speakman, E. M., "Marine Steam Turbine Development and Design," SNAME, 1905, pp. 247–286. This paper describes vessels driven by steam turbines in the era 1894–1905. It gives, on Pl. 139, principal dimensions and general information for 50 vessels with 18 entries per vessel.

(8) Stevens, E. A., Jr., "A Substitute for the Admiralty Formula," SNAME, 1913, Vol. 21, pp. 49–54. In the text, and especially in Pls. 35–46, the author gives a considerable amount of tabulated data on a large number of naval and merchant vessels, ranging from the battleships of that time to fast motor launches and navy launches intended to be carried aboard ship.

(9) Peskett, L., "On the Design of Steamships from the Owner's Point of View," INA, 1914, pp. 173–192. The author presents, in Table I opposite p. 182, some particulars of 28 vessels of the Cunard fleet, from the *Britannia* of 1840 to the *Aquilania* of 1915, with 7 entries of hydrodynamic interest per vessel. These data are also quoted in The Shipbuilder (now SBMEB), Jan-Jun 1914, Vol. X, pp. 274–275.

(10) Owen, W. S., PNA, 1939, Vol. I, Table 4, p. 53; 13 types of vessels, 22 entries for each

(11) Pluymert, N. J., "Modern Tanker Design," SNAME, 1939, pp. 168–188; also SBMEB, Apr 1940, pp. 134–137. This paper lists the hull and machinery data for 5 steam-driven and 7 diesel-driven tankers, of the era 1930–1939, with 32 entries for each.

(12) Bates, J. L., and Wanless, I. J., "Aspects of Large Passenger Liner Design," SNAME, 1946, pp. 317–373. Tables 1, 2, and 3 on pp. 318–319 give the general dimensions, form coefficients, and machinery characteristics, respectively, of six recent Atlantic liners (1930 to 1940), plus the U. S. Maritime Commission projected design *P3-S2-DA1* of 1949, with a total of some 25 entries per vessel. On p. 369 are given some additional data on the proposed Ferris superliner of 1931 and the *Queen Mary*.

(13) Robinson, H. F., Roeske, J. F., and Thaeler, A. S., SNAME, 1948, pp. 432–443. This paper contains tabulated data for thirteen 13,000-t tankers, twelve 16,000-t tankers, and twelve tankers of 18,000 t and larger, with about 70 entries for each.

(14) Lavrent'ev, V. M., "Marine Propulsion," Moscow, 1949, p. 96. A translation of this table, with both metric and English units, appears as Table 51.c.

(15) Todd, F. H., "Some Further Experiments on Single-Screw Merchant Ship Forms—Series 60," SNAME, 1953, Table 1, p. 518. Principal dimensions and some hull coefficients are given for the *Mariner*, the *Schuyler Otis Bland*, the U. S. Mar. Comm. *C-2* class, the tanker *Pennsylvania*, and a Bethlehem 400-ft design, in comparison with TMB Series 57 models. There are about 10 entries per vessel. Other data on these vessels are given throughout the paper.

(16) De Rooij, G., "Practical Shipbuilding," published by H. Stam, Haarlem, Holland, 1953. On pp. 13–29 and 336–382 there are given the principal dimensions and characteristics, plus the general arrangement drawings, of a large number and variety of ship types. The smaller sketches in the book proper are supplemented by a considerable number of large folded plates in the back of the book.

(17) Henry, J. J., "Modern Ore Carriers," SNAME, 1955, pp. 57–111. The bibliography with this paper lists 24 references. Table 1 gives the characteristics of 12 ocean iron-ore carriers, with about 100 entries per vessel, while Table 2 gives similar data for 9 Great Lakes iron-ore carriers, with about 92 entries per vessel. Table 3 gives data on 100 or more features for each of 6 oceangoing general bulk cargo carriers.

(18) There is given, in Table 76.d of Sec. 76.4, a presentation of the principal characteristics of 14 Great Lakes bulk carriers of recent design

(19) Table 76.f lists the principal dimensions and other data for 10 icebreakers of recent design and construction.

51.4 References to Tabulated Data on Yachts and Small Craft. Dixon Kemp gives a "Table of Elements of Steam Yachts" comprising 22 vessels, with from 25 to 26 items per vessel ["Yacht Architecture," Cox, London, 1897, 3rd ed., pp. 317–318]. On page 319 of the reference he includes a table of "Steam Yacht Performance" for 13 vessels, with 39 items per vessel. On page 525 he presents a table listing 29 sailing yachts with their displacement in tons, the total weight of ballast in tons, the weight of this ballast in the keel, and the ballast ratio. The amount of ballast as compared to the displacement varied from a minimum of 0.361 to a maximum of 0.681.

In the appendix of the book cited, on page 532, Kemp gives the names and 10 design elements of 35 sailing yachts of that day.

W. P. Stephens, in a paper entitled "Yacht Measurement: Origin and Development" [SNAME, 1935, pp. 7–41], includes lines drawings and other design data on American and British yachts of the 1870's to the 1890's.

In his paper "The 'America's' Cup Defenders," C. P. Burgess gave a great deal of design information, including lines drawings of the large J-class yachts of that period [SNAME, 1935, pp. 43–87]. No tabulated data are included in the paper.

Principal dimensions and form coefficients for 7 fishing vessels, 2 small freighters, 3 ferryboats, 1 fireboat, and 1 tug, 24 entries per vessel, are given by D. S. Simpson [SNAME, 1951, Table 5, p. 563]. The first entry gives the actual length of each craft; all the others give converted data, referred to a standard length of 100 ft.

51.5 Designed Waterline Shapes and Coefficients. The designed waterlines for the paddle steamer *Mary Powell* (afterbody only) and for the Taylor Standard Series parent form (EMB model 632, modified) are shown to small scale in Fig. 24.G on page 355 of Volume I. The half-waterline of Donald McKay's clipper ship *Flying Cloud*, described in Sec. 24.13 on pages

TABLE 51.c—Russian Tabulation of Ship Data

Translated and adapted from "Marine Propulsion" by V. M. Lavrent'ev, Moscow, 1949, Table 8, page 96. Supplementary columns at the right give the length and volume in ft and ft³ units, respectively.

Type of Ship	L, meters	∇, meters³	Speed, kt	Power, horses (metric)	Power / ∇	Adm'ty. Coeff.	L, ft	∇, ft³
Fast steamers	280.0	57,700	23.2	61,800	1.07	302	918.7	2,037,964
	202.0	22,900	23.5	37,800	1.65	298	662.8	808,828
	190.5	21,385	22.0	27,000	1.26	327	625.03	755,318
Large passenger ships	194.0	22,100	18.0	17,200	0.78	287	636.5	780,572
	193.0	23,200	15.0	9,800	0.40	315	633.2	819,424
	170.0	17,250	16.5	10,600	0.61	305	557.8	609,270
	136.5	13,170	13.5	4,800	0.36	308	447.9	465,164
	121.4	10,340	11.5	2,500	0.24	322	398.3	365,209
Small passenger ship	69.5	2,200	10.0	1,050	0.48	190	228.02	77,704
Canal (river?) boats	92.0	1,915	20.0	5,600	2.92	220	301.9	67,638
	83.8	1,695	20.0	5,400	3.19	211	275.0	59,867
Steam yachts	121.9	5,710	15.0	3,700	0.65	307	400.0	201,677
	116.6	4,260	21.5	9,650	2.27	291	382.6	150,463
Large cargo steamers	170.7	24,800	13.5	5,460	0.22	418	560	875,936
	152.4	21,115	12.0	4,000	0.19	359	500	745,782
	131.1	12,400	11.0	2,500	0.20	316	430.1	437,968
	105.2	7,985	11.0	1,700	0.21	357	345.1	282,030
Small cargo steamers	88.1	4,580	10.5	1,225	0.27	305	289.1	161,766
	79.8	3,400	9.0	700	0.21	288	261.9	120,088
	62.1	1,760	9.0	440	0.25	307	203.8	62,163
	47.3	940	8.0	350	0.37	181	155.1	33,200
	37.8	320	9.0	260	0.81	173	124.0	11,302
Small river steamers	32.0	130	12.0	225	1.73	263	105	4,592
	26.0	66	12.0	220	3.33	172	85.3	2,331
Fishing boat	41.0	445	10.9	490	1.10	194	134.5	15,717
Towboats	40.0	390	11.0	350	0.90	262	131.2	13,775
	35.0	340	12.1	520	1.53	203	114.9	12,009
	15.2	48	9.1	150	3.13	91	49.9	1,695
Icebreaker	47.2	890	9.5	500	0.56	200	154.9	31,435
River freight str. with prop.	60.0	481	7.3	205	0.43	156	196.9	16,989
River passenger boats	62.0	325	9.9	503	1.55	114	203.4	11,479
	40.5	100	11.1	250	2.50	157	132.9	3,532
River freight	67.0	550	7.2	382	0.69	85	219.9	19,426
Paddlewheel drive	50.0	300	10.3	620	2.07	98	164.1	10,596
	40.0	212	10.5	300	1.42	179	131.2	7,488
Sternwheel drive	46.8	144	9.0	210	1.46	128	153.6	5,086
	22.8	43	8.0	80	1.86	125	74.9	1,519
Bark (barca)	15.0	23	8.0	65	2.83	107	49.2	812

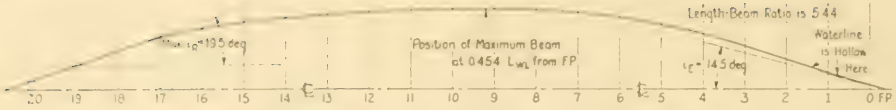

Fig. 51.B Designed Half-Waterline of the Clipper Ship *Flying Cloud*

356–357 of Volume I, is depicted in Fig. 51.B.

In Fig. 51.C there are drawn the half-DWL's of six vessels typical of those for five different ship types, operating at the speed-length or Taylor quotient T_q values indicated on the diagram. The SNAME RD sheet numbers are given for four of the waterlines.

One feature of designed waterlines to which insufficient attention has been devoted in the past is the length and position of the *parallel portion of the waterline.* This is not to be confused with the amount and position of the parallel middlebody, indicated for three of the DWL's on Fig. 51.C. Table 51.d lists the parallel waterline data for over thirty ships and ship designs of various types. The lengths and positions tabulated are not necessarily the optimum. Fig. 66.J of Sec. 66.15 of Part 4 shows a range of optimum length of parallel waterline while Fig. 66.K gives the optimum fore-and-aft position of the midpoint of this length, for use in design.

51.6 Reference Data for Drawing Section-Area Curves. Supplementing the lines, section-area curves, and offsets of the Taylor Standard Series models, reproduced in Fig. 51.A and in Tables 51.a and 51.b, there are listed hereunder

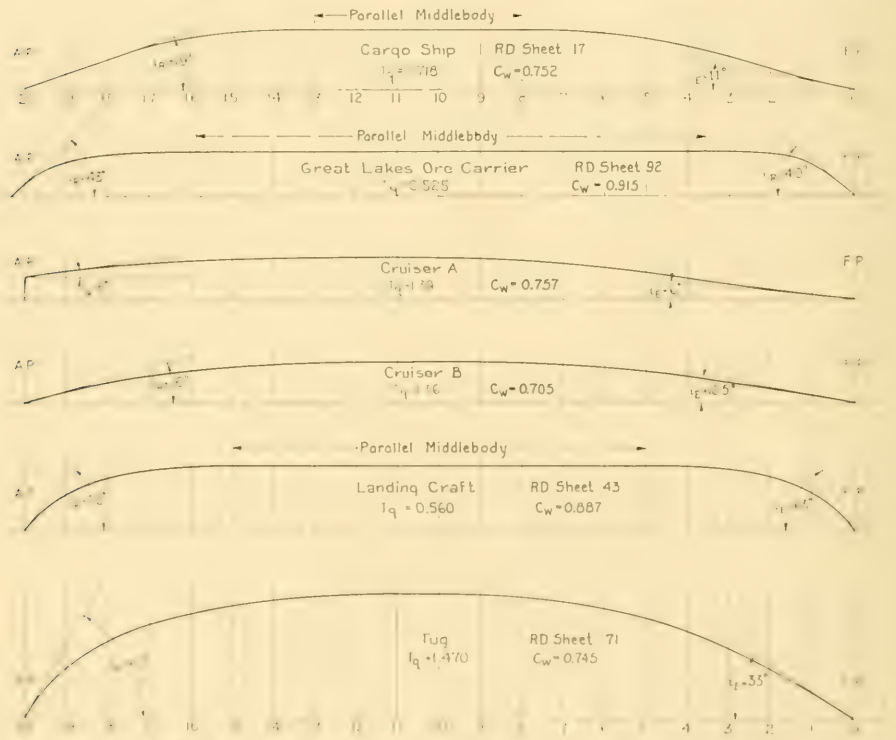

Fig. 51.C Designed Half-Waterlines of Six Vessels of Five Types or Classes

several references to diagrams by which section-area curves for new ship designs can be drawn, corresponding to selected form coefficients or parameters:

(1) Gertler, M., "A Reanalysis of the Original Test Data for the Taylor Standard Series," TMB Rep. 806, Mar 1954, Gov't. Print. Off., Washington. The data mentioned in the preceding paragraph are found on pp. 2–6 of this report. In addition, on pp. 6–8 there are graphs, tables, and instructions by which any section-area curve belonging to the family of the Taylor Standard Series can be reproduced mathematically.
(2) Bates, J. L., "Shipbuilding Encyclopedia," 1920, Figs. 26, 27
(3) Vincent, S. A., "Merchant Vessel Lines," MESA, Mar 1930, p. 138. These have since been improved upon but no published or unpublished revision is available.
(4) Schiffbau Kalender, 1935, p. 160
(5) Van Lammeren, W. P. A., Troost, L., and Koning, J. G., "Resistance, Propulsion, and Steering of Ships," 1948, pp. 92–93.

The SNAME Resistance Data sheets, one of which is illustrated in Fig. 78.Ja of Sec. 78.16 of Part 4, contain section-area curves, area ratios A/A_X , and values of dA/dL for the models of some 160 typical ships of many classes.

51.7 "Standard" Body Plans. At various times so-called "standard" body plans have been used for reference and comparison purposes. Some of these were drawn with fixed proportions, in which the maximum (or midsection) waterline beam was always twice the draft. All underwater and abovewater sections were distorted to comply with this proportion. Each half-beam and the whole draft were divided into ten equal spaces. Thus the "standard" offsets or heights for a given position on one ship could be compared with

TABLE 51.d—Reference Data on Amount and Position of Parallel Designed Waterline

Reference Number	Ship Type or Name	Prismatic Coefficient, C_P	Per Cent of Parallel Designed WL	Position of Midlength of Parallel DWL in Per Cent of L_{WL}
1	Tanker	0.746	0.40	0.50
2	Fast tanker, *Altmark*	0.624	0.125	0.488
3	*America*	0.600	0.18	0.525
5	U. S. Mar. Comm. *C1-A*	0.712	0.35	0.475
8	*C-2* Cargo	0.695	0.35	0.501
10	U. S. Mar. Comm. *C2-SU*	0.702	0.325	0.488
13	*C2-S1-A1*	0.605	0.175	0.523
14	*C-3* Cargo	0.667	0.325	0.523
15	*C3-S-A3*	0.643	0.19	0.48
16	*C4-S-A1*	0.657	0.25	0.525
17	*City of Paris*	0.625	0.075	0.513
18	*Conte di Savoia*	0.618	0.15	0.525
19	*DD 364*	0.591	0.05	0.575
20	*EC2-S-C1*	0.745	0.45	0.475
21	*Great Northern*	0.559	0.04	0.505
23	*Manhattan*	0.659	0.20	0.50
24	*Mariposa*	0.654	0.20	0.55
25	*Mauretania* (old)	0.623	0.05	0.525
28	*P1-S2-L2*	0.600	0.125	0.538
32	Passenger liner	0.617	0.150	0.523
35	*Panama* (1939)	0.630	0.250	0.525
36	*Pasteur*	0.599	0	0.500
37	*President Coolidge* (1931)	0.675	0.25	0.525
38	*President Taft*	0.633	0.20	0.55
39	*Prinz Eugen*	0.639	0	0.50
42	*Rex*	0.628	0.075	0.538
43	*S4-S2-BB3*	0.581	0.20	0.575
44	*S4-SE2-BD1*	0.668	0.30	0.525
47	*T1-M-BT1*	0.735	0.35	0.475
48	*Corsicana*	0.734	0.375	0.488
50	*T-2* tanker	0.740	0.375	0.488
54	Proposed German liner	0.554	0	0.50

TABLE 51.[illegible] LIST OF "STANDARD" BODY PLANS AVAILABLE FOR REFERENCE AT THE DEPARTMENT OF NAVAL ARCHITECTURE AND MARINE ENGINEERING, MASSACHUSETTS INSTITUTE OF TECHNOLOGY

Ship or Design	Principal Dimensions, ft					Block Coeff.	Displ., tons	Remarks
	L_{wl}	L_{pp}	Beam, B	Depth, D	Draft, H			
[illegible]: Pacific Mail Liner; EMB model 1349	681	660	75		30.0		29,730	
Cramp Hulls 427, 438, and 439, Oct 1920	420.5	404	53.75		25.9	0.749		Grace Line steamer *Santa Barbara*, with counter stern
U. S. Scout Cruisers 9-13, *Omaha* Class	555.5	550	54.8	25.9	13.5	0.605	7,130	Hulls 448–449, 501, 502, 503. Cramp lines drawing GH-5015.
Cramp Hulls 434 and 435; tested in model scale	443.3	424.5	60	35	24.5		11,290	Twin-screw steamers *Siboney* and *Orizaba*
U. S. Navy Collier *Cyclops*, Cramp Hull 355	542	520	65	39.5	27.5		19,118	
Passenger Steamer [illegible], Cramp Hull 348	455.7	437.8	55	22	13		5,422	EMB model 696
Battle Cruiser; EMB model 1936		850	89.7		30		33,000	
Cargo Ship; EMB model 2023	416.8	400	57.3	33	26	0.7744		
500-ft Collier, 15 Dec 1913	521.6	502.1	62	39.8	27.94		19,300	Proposal 638 for twin-screw colliers
Motorships *Californian* and *Missourian*	461.6	445	59.7	39	28.5		16,420	Twin-screw vessels
Massachusetts, *Bunker Hill*, and *Old Colony*	392.8	375	52	22.5	14.5		3,800	Fast passenger and freight steamers, Boston-New York service
Leviathan	949.8	929	100	61.5	37.0	0.607		
Steamer *Standard Arrow*	484.8	468	62.5	39.5	26.3		17,850	EHP curves from model test at Ann Arbor
Yarmouth and *Evangeline*, Eastern S. S. Co.; Cramp Hull 518; EMB model 2642	378*	365	55.5	29.5	18.0	0.542	5,880	Cramp drawing GH-5054; Ferris drawing 518 GH 129-2
Proposal for Hull 505		325	29		16.0		3,920	Proposed Lines for 505-GH-500, Str. *Cuba*
Matson Liner *Malolo*, Hull 509; EMB model 2598	577*	554	83	44.5	26	0.543	19,300	Proposed Matson Nav. Co. twin-screw liner, as drawn by Gibbs Bros., 1925. See also SNAME RD sheet 34.
U. S. Shipping Board 10,000-ton, Type B; EMB model 2218	440	425**	56	38	27.75		14,108	
Similar to Steamer *Tyler*	320.5	308.6	47		20	0.66		Reference is to S. S. *Tyler* of Old Dominion Line; single-screw ship with large propeller aperture
Standard Body Plan, Tankers		430	58	33.3	25.5		14,481	Cramp Hulls 428; etc.; name not legible. EHP estimated from EMB model 2288, tested in Sep 1920

TABLE 51.e—(Continued)

Ship or Design	Principal Dimensions, ft					Block Coeff.	Displ., tons	Remarks
	L_{OA}	L_{PP}	Beam, B	Depth, D	Draft, H			
American International Corpn.; Type "B" Steamer	448	435	58	40	28		13,340	
Allegheny and proposed *Berkshire*	368	350	52	35	19.0		6,922	For Merchants' and Miners' line; vessels actually built by Federal Shipbuilding and Dry Dock Company
Hull 505, as built	340 on 16-ft WL	325	47		16	0.537	3,915	Pass. Str. *Cuba*; load displ., 3,923 t
Santa Ana, Santa Luisa, Santa Teresa	373.8	360	51.5	33.5 to shelter deck	24.0		8,933	
Matson Liner Study	578	552	73.5 (Max.)		26.5		16,940	Lines drawing 829-GH-110
Matson Liner Study		577	79		26		18,736	As drawn by Gibbs Bros. for 79-ft beam design
U. S. Navy Destroyers, original numbers (DD450-455) (old 4-stackers)	314	310	30.95		9		1,157	Similar to USN DD113-118 class
Cramp Hulls 434-435	443	424.5	59	36.0	24.5		11,205	Preliminary; see previous entry for 4th item
G. S. Baker Model 56C		400	52.2		23.2		9,108	
U. S. Shipping Board Model, 10,000-ton Dwt. "A"	440	425	56	38 to upper deck	27.8		14,168	
Moosehead	194.9	185.2	30.5 at WL		10.5		710	Passenger ferry, sponsoned to 36.7-ft beam over guards
U. S. Naval Transport		460	60.9		19.4		9,702	Lines drawing H.15278-1
Matson Liner, 1924	578	552	73.5		26		17,380	
Mathematical Lines, Proposal 829 for Matson Navigation Company	578	552	73.5		26		17,380	EMB model 2532, tested in Dec 1923. Note says 72.5-ft beam at 26-ft WL. Lines drawing P829GH-105
Mathematical Lines, Proposal for Matson	578	552	73.5		26.5		16,830	
S. S. *Mt. Clinton* and *Mt. Carol*		440	57		28.8		15,175	EMB model 2272; mathematical lines number 1
U. S. Navy, BB49-54 Class	684	660	104.6		32.8		42,953	
H. Proposal; *Great Northern* and *Northern Pacific*; EMB model 1560	513.4, on 20.6-ft WL	500	63	50.5 to "A" dk	20.6	0.507	9,625	Lines drawing H-12103-5; does not include bossings.
U. S. S. *Delaware* (BB28)		510	85		27		20,000	

*Length on designed waterline
**Length on waterline 433 ft

those for the corresponding position on another ship. Tracings of the "standard" body plans could be superposed against a window or over a light table to compare the section shapes, section-line slopes, offsets at given stations, and other features.

However, for hydrodynamic analysis, and for ship-design purposes as well, these "2 to 1" body plans do not show the section shapes in their true form nor the section-line slopes at their proper value. It is not possible to compare flow patterns by this method since on vessels of the same type the beam-draft ratios may vary from 2 to 4, or from 6 to 10, by ratios that approximate 2 to 1 or more.

Propeller tip clearances, bossing termination angles, and similar features can not be judged or compared easily on these "2 to 1" body plans. Most of the tip circles would be ellipses if drawn properly, and the slopes of bossings and struts would be the same as their true values only if the B/H ratio of the ship were 2.00.

A more rational and useful scheme is to draw all the "standard" body plans to the same absolute width, using as a reference the waterline beam at the midsection or at the section of maximum area. When tracings of these body plans are superposed, the waterline offsets for a series of 10, 20, or 40 stations are directly comparable, as are the drafts and the underwater shapes when referred to the beam.

The staff of the old Cramp shipyard at Philadelphia prepared and kept on file a set of three dozen or more of these "standard-width" body plans. Table 51.e lists these plans, with the names and principal dimensions or characteristics of the proposals, designs, and ships involved. All were drawn on tracing cloth, with a standard waterline beam of 10 inches. The body plans, both underwater and abovewater, were supplemented (on the same drawing) by tables of principal ship dimensions, non-dimensional coefficients and parameters, and large-scale layouts of the section-area ratios A/A_X and the half-beams of the designed (or load) waterlines. When available, data on model resistances and ship effective powers were added to the sheets.

Fortunately, although the Cramp shipyard is no more, the Cramp standard body plan tracings are preserved in the files of the Department of Naval Architecture and Marine Engineering at the Massachusetts Institute of Technology in Cambridge, Mass. There they may be consulted by all who are interested in them.

51.8 Single-Screw Body Plans. There are available in the technical literature a few large-scale body plans of models and ships which have acquired prominence in one way or another, either because many tests and trials have been made on them, or because of outstanding good performance. Among these may be mentioned:

(1) G. S. Baker's model 56C, of which a body plan is reproduced in SBSR, 3 Aug 1916, Fig. 13, p. 107; also in SNAME, 1930, Pl. 108. EMB model 2933 was built to these lines and tested at Washington. The data are available in SNAME RD sheet 160.

(2) German motorship *San Francisco* of the 1930's, owned and operated by the Hamburg-American Line, on which a German scientific party made many measurements and observations at sea in 1934.

A body plan of this vessel, with no appendages shown, is published by G. Kempf [SNAME, 1936, Fig. 1, p. 197]. On pages 197 through 199 of this paper there are to be found the original observed data from ship and model tests, including open-water tests of the model propeller. Dimensions and other data of ship and model are given in Table 1 on page 196 of the reference.

(3) Passenger and cargo vessel *Panama* of 1939, designed by George G. Sharp, for which a body plan was published by Marine Engineering and Shipping Age [May 1939, p. 206].

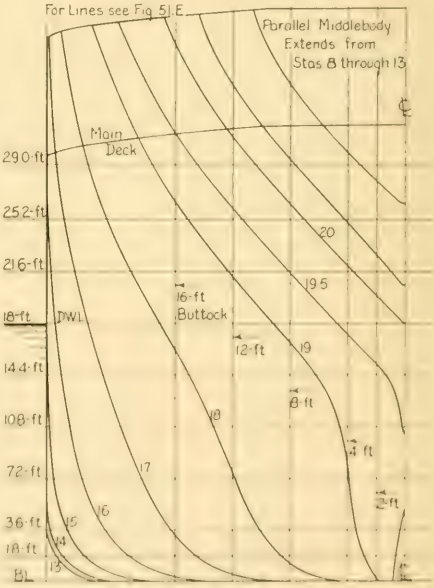

Fig. 51.D Body Plan for Run of U. S. Maritime Commission *C1-M-AV1* Class of Cargo Vessel

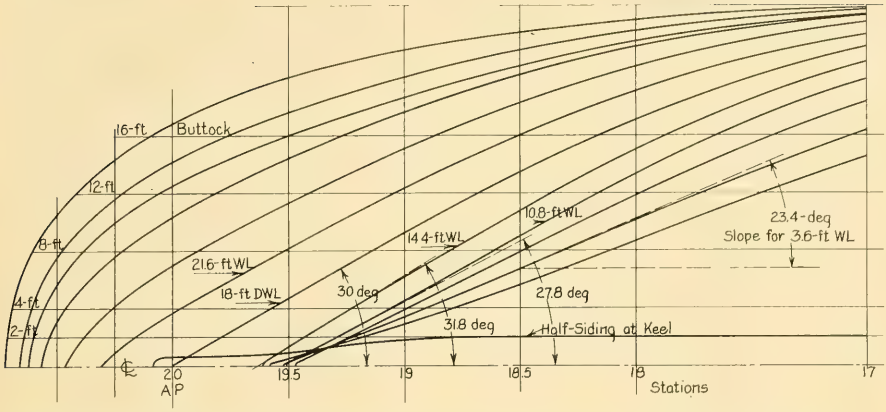

Slopes of Designed and Other Waterlines for This Form are Excessive; Separation is Certain to Occur Abaft Them. If Length is Limited, It is Better to Adopt a Different Type of Stern, to Insure Proper Flow of Water to the Propeller and Rudder.

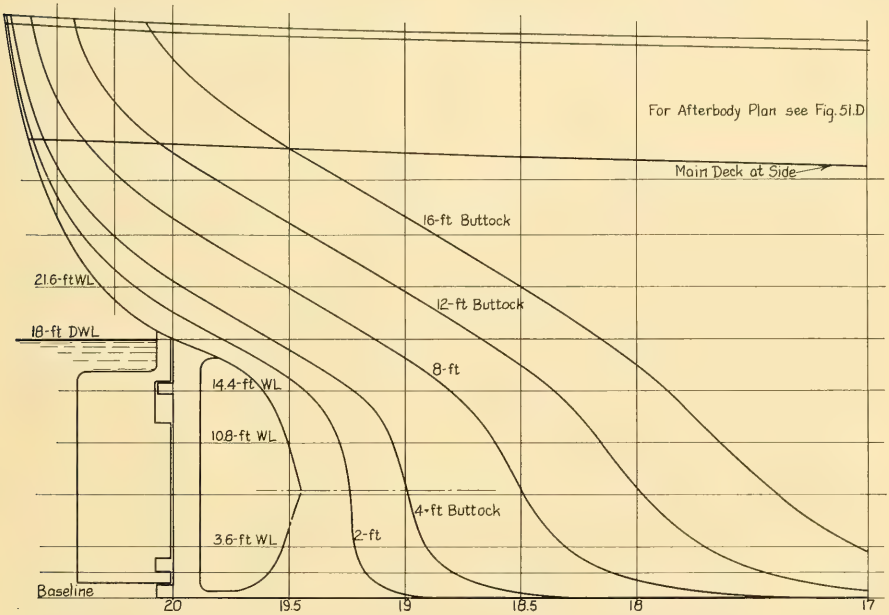

FIG. 51.E WATERLINES AND BUTTOCKS IN THE RUN OF THE U. S. MARITIME COMMISSION *C1-M-AV1* CLASS OF CARGO VESSEL

(4) U. S. Maritime Commission *C1-M-AV1* class of the 1940's. The plan of the afterbody and of the waterlines and run of this vessel are illustrated in Figs. 51.D and 51.E, respectively. These lines are included as an example of a stern that is definitely too blunt, with slopes that are excessive for good flow to the propeller. This class was tested as TMB model 3839, and the complete model results are given in SNAME RD sheet 19.

(5) U. S. Maritime Commission *C-3* type cargo vessel, for which a body plan is to be found in SNAME, 1950, Fig. 77 on p. 563. This class was tested as TMB model 3534, but at the time of writing (1955) the complete results had not yet been embodied in an SNAME RD sheet.

(6) Todd, F. H., and Forest, F. X., "A Proposed New Basis for the Design of Single-Screw Merchant Ship Forms and Standard Series Lines," SNAME, 1951, pp. 642–744. This paper covers the TMB Series 57 forms.

(7) Todd, F. H., "Some Further Experiments on Single-Screw Merchant Ship Forms—Series 60," SNAME, 1953, pp. 516–589. This paper gives all the data in sufficient detail to indicate the exact forms of the various models, their hull coefficients, and their distribution of section area along the length. It also gives corresponding data for the U. S. Maritime Commission *C-2* class of cargo ship, for the *Mariner* class, for the modified *C-3* vessel *Schuyler Otis Bland*, for a Bethlehem design of cargo vessel, and for the tanker *Pennsylvania*.

(8) Russo, V. L., and Sullivan, E. K., give a body plan of the *Mariner* class, including a wave profile at a speed of 20 kt and a T_q of 0.877 (SNAME, 1953, p. 115 and Fig. 12 on p. 122]. This design was tested as TMB model 4358W-3. The stern profiles, both closed (as tested in model scale) and open, as built into the ships, are shown in Figs. 13 and 14, pages 123 and 125, respectively, of the reference.

(9) A small-scale body plan of the *Gopher Mariner* is published by V. L. Russo and R. T. McGoldrick in SNAME, 1955, Fig. 9 on p. 449

(10) H. De Luce and W. I. H. Budd give a body plan, wave profile, and some lines of flow around the tanker *Pennsylvania* [SNAME, 1950, Fig. 7, p. 430]

(11) Body plans, and in many cases lines drawings, are published by J. Baader for a great variety of large and small single-screw vessels in his book "Cruceros y Lanchas Veloces (Cruisers and Fast Launches)," published in Buenos Aires in 1951, Figs. 225–239, pp. 287–301.

Typical body plans for shallow-water paddle-driven vessels are given in Figs. 72.A, 72.B, and 72.D.

Limitations of space preclude the reproduction of lines drawings, body plans, or even tabulated data on other interesting and instructive designs. Indeed, in view of the availability (in 1956) of some 160 SNAME Resistance Data sheets, with their wealth of quantitative data, and with the prospect of additional sheets year by year, the marine architect has ready at hand a very considerable amount of reference data.

The Index sheets and Summary sheets accompanying RD sheets 1 through 150 (and later) add to the store of information and present it in a slightly different fashion.

51.9 Twin-Screw Body Plans. The general comments of Sec. 51.8 relative to single-screw ships, including the notes on the SNAME RD sheets, Index sheets, and Summary sheets, apply to twin-screw vessels as well. Among the ships (or designs) for which body plans are available in the literature there may be mentioned:

(1) Atlantic liner *Manhattan*, represented by TMB model 3041. Fig. 17 on p. 111 of SNAME, 1947. General characteristics of the hull are given in Table 3 on p. 113 of the reference.

(2) Twin-skeg *Manhattan* design, tested in small scale as TMB model 3898 but never worked up as a ship design or built as a ship. Body plans are shown in Figs. 18 and 24 on pp. 112 and 116, respectively, of SNAME, 1947. General characteristics of this design are given in Table 3 on p. 113 of the reference.

(3) Proposed design of a large tanker of extremely wide beam, developed by the Sun Shipbuilding and Dry Dock Company, tested in small scale as TMB models 3817 and 3821. The lines are shown in Fig. 11 on p. 107 and Fig. 13 on p. 108 of SNAME, 1947. Table 1 on p. 109 gives the general characteristics of the proposed ship.

(4) TMB model 3930, representing a twin-screw liner, 745 ft long on the waterline, with a normal form of stern [Bates, J. L., SNAME, 1947, Fig. 41, p. 137]. The body plan is accompanied by a table of general characteristics.

(5) Bates, J. L., "Large Passenger-Carrying Ships for Certain Essential Trade Routes," SNAME, 1945, pp. 290–334. Table 1 on page 296 lists the principal dimensions and characteristics of the five designs described in the paper.

(6) TMB model 3917, representing a twin-screw liner, 745 ft long on the waterline, with a twin-skeg stern [Bates, J. L., SNAME, 1947, Fig. 42, p. 137]. The body plan is accompanied by a table of general characteristics.

51.10 Multiple-Screw Sterns. A great number of quadruple-screw vessels have been built in the period 1900–1955, yet the published data on lines, form coefficients, hull parameters, and other hydrodynamic features are surprisingly meager. In fact, data on the shape of the runs, the propeller positions and diameters, hull (tip) clearances, and shape of appendages carrying the propeller shafts are limited largely to stern photographs of these vessels on the launching ways or in dock.

In the late 1920's and early 1930's, T. E. Ferris made many studies of a large, high-speed trans-

atlantic passenger vessel. He reported upon these studies in the paper "Design of American Superliners" [SNAME, 1931, pp. 303–350 and Pls. 1–13]. Table 1 on page 318 of this reference gives the ship dimensions and hull coefficients corresponding to three of the fourteen models tested at the Experimental Model Basin, Washington. All these designs embodied 4 propellers. This paper was published, practically in full, in Marine Engineering and Shipping Age, December 1931 and January through April 1932.

E. P. Trask discussed this design problem further in his paper "A Proposed 800-ft Atlantic Liner" [MESA, Jul 1932, pp. 268–275]. This vessel was designed for an operating speed of 28.5 kt.

At the conclusion of World War II, J. L. Bates and I. J. Wanless made an analysis of existing passenger liners and worked up a new design, which they reported upon in their paper "Aspects of Large Passenger Liner Design" [SNAME, 1946, pp. 317–373]. This paper tabulates many dimensions and characteristics of the *Europa*, *Manhattan*, *Conte di Savoia*, *Rex*, *Normandie*, and a projected U. S. Maritime Commission design *P3-S2-DA1* for trans-ocean service. One of the ships analyzed, the *Manhattan*, is a twin-screw vessel but all the others are quadruple-screw ships.

Corresponding information on triple-screw vessels, with sterns which are the most difficult of any to design, is very scarce. This is partial justification for referring to a paper, now almost historic, by G. W. Melville entitled "Notes on the Machinery of the New Vessels of the United States Navy" [SNAME, 1893, pp. 140–175]. Plate 41 of this paper illustrates the triple-screw arrangement of the U.S.S. *Columbia* (old) of 1890.

Fig. 51.F is a body plan resembling those of the coastwise triple-screw passenger steamers *Yale* and *Harvard*, designed in the early 1900's, and reported upon by C. H. Peabody, W. S. Leland, and H. A. Everett in a paper "Service Test of the Steamship *Harvard*" [SNAME, 1908, pp. 167–186]. These vessels gave long and distinguished service on many difficult routes, so much so that their designs would warrant further analysis if accurate and reliable data and drawings could be found.

Fig. 51.G is a body plan of the high-speed, triple-screw passenger and cargo vessel *Great Northern* (and sister vessel *Northern Pacific*), designed in about 1914 and famous for outstanding performance in heavy weather. Unfortunately, it is not possible to add propeller-disc positions and appendage data to either of these drawings.

German naval architects have probably had more experience than all others combined in the design of triple-screw vessels. However, as almost all of these were combatant craft, their lines and the design rules pertaining to them appear not to have been published. What might be considered an exception to this is the study for a medium-size fast liner published by E. Foerster [SNAME,

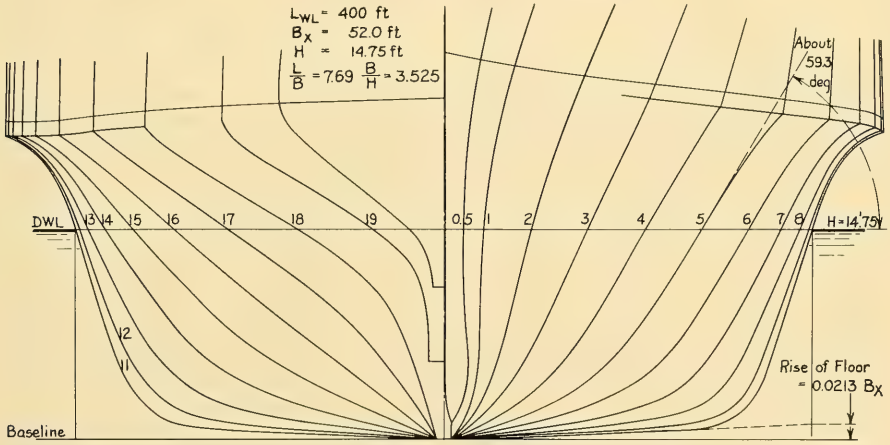

Fig. 51.F Body Plan Resembling Those of the Triple-Screw Coastal Passenger Vessels *Yale* and *Harvard*

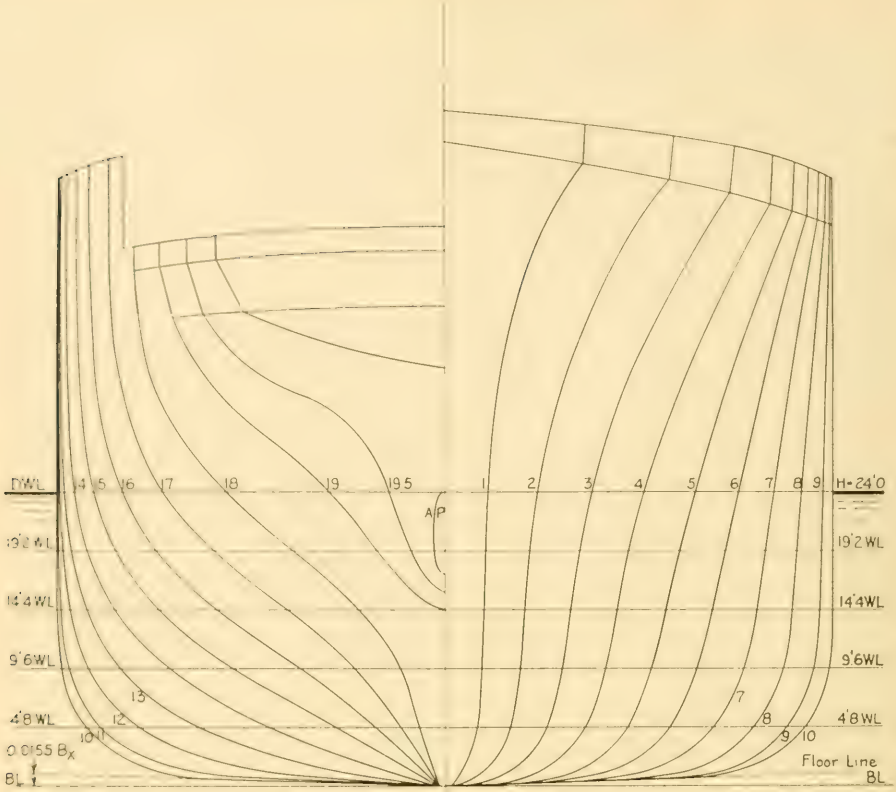

Fig. 51.G Body Plan of the Triple-Screw Passenger and Cargo Vessel *Great Northern*

1936, pp. 228–287]. This unusual vessel, for which some section- and hull-shape data are given, was to have had twin propellers carried by orthodox bossings, plus a centerline Voith-Schneider propeller which was to have been used for steering as well as propulsion. Resistance and power data, derived from model tests, are given for various combinations.

Fig. 51.H Sketch of One Section of the Triple-Screw German Cruiser *Prinz Eugen*

One of the most modern of the German combatant vessels, the World War II cruiser *Prinz Eugen*, was taken over by the United States. Some data on this vessel are in the files of the U. S. Navy Department. Fig. 51.H gives the general features of one of its transverse sections.

Vessels with five screw propellers have been considered in the design stage but so far as known no data on these studies have been published (SBSR, 17 Oct 1946, p. 439].

Further reference data on vessels driven by multiple propellers are given in Secs. 67.14 and 67.15.

CHAPTER 52

Analysis of Flow Diagrams and Prediction of Ship Flow Patterns

52.1 Scope of Chapter. Supplementing the potential-flow, ideal-liquid data on streamline patterns around bodies and the discussion on distribution of velocity and pressure in Chap. 42, there is given here some representative information on flow and on velocity-and-pressure distribution in the water around ship models. There are very few full-scale data on ships, either in the technical literature or in form available for publication, with which to confirm the model data.

Space limitations prevent the inclusion of the vast amount of model data available in America, mostly at the David Taylor Model Basin, on the flow around ship models, representing many ship types. Indeed, these data comprise sufficient material for an entirely separate study and analysis.

52.2 Typical Ship-Wave Profiles. An analysis of the flow patterns around a body or ship, at least for a craft running on the surface, begins properly with the surface-wave profile. This is the outstanding feature of the 3-diml flow around a 2-diml simple ship form, when the latter is brought up from a deeply submerged position and run at the air-water interface. This feature has perhaps more importance for 3-diml forms and actual ships because, at the speeds where surface wavemaking is prominent, the wave pattern there influences the flow over a considerable extent of the ship's side, often down to and including the bilge-keel positions.

Fortunately, it is not too difficult to obtain the wave profile on a ship because this region is available for observation or photographic recording. A number of ships in the past have had painted on one side a grid pattern of some sort for the builder's or the acceptance trials. By looking over the side, the intersections of the actual wave profile could be observed and marked on an outboard-profile drawing carrying the same grid. The two full-scale profiles of Fig. 52.A, for the U. S. battleship *Maine* (new), were ob-

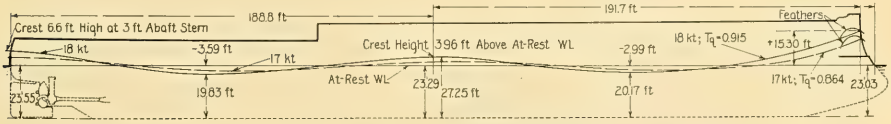

Fig. 52.A Observed Wave Profiles at Two Speeds on a Battleship

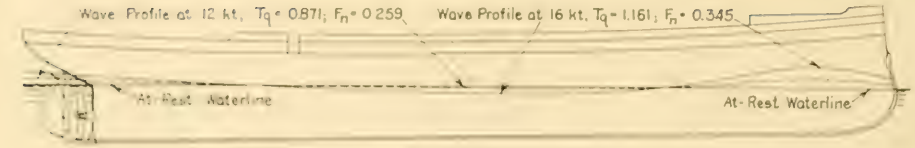

Fig. 52.B Observed Wave Profiles at Two Speeds on a Gunboat

served in this manner [Powell, J. W., SNAME, 1902, p. 49 and Pl. 14]. Wave profiles observed at two speeds during the trials of the U. S. Coast Guard cutter *Manning* of the late 1890's are drawn over an outboard profile of the ship in Fig. 52.B [Peabody, C. H., SNAME, 1899, Pl. 93; NA, 1904, Fig. 208, p. 543].

There are in the literature literally thousands of photographs of ships underway, surrounded (on the near side at least) by the waves of the ship's Velox system. Almost never are these photographs of more than pictorial value because either:

(1) They do not show the wave profile directly against the ship's side, or
(2) They do not state the exact speed at which the ship is traveling.

Nevertheless, they are better than no data at all, especially because systematic procedures are lacking for the prediction of wave profiles alongside models or ships in advance of tests or trials.

One interesting photograph of this kind shows a small battleship of the German *Deutschland* class at full speed [STG, 1940, p. 341]. Another, equally interesting because of two very large wave crests that appear in the photograph, shows the German World War I battle cruiser *Goeben* at what appears to be full speed [USNI, 1912, Vol. 38, p. 1668]. A third shows wave profiles alongside the German battle cruiser *Moltke* of the World War I period [Schiffbau, 22 May 1912, p. 649]. These indicate in a general way that the first Velox wave is something less than one ship length long, because of the lag of the first wave crest abaft the bow, but otherwise they are useless for analysis by any known method.

Some data are listed here relative to excellent photographs of certain French men-of-war of a half-century ago, when underway at what appear to be full speed and full power. The photographs in question are reproduced in the July 1954 issue of the U. S. Naval Institute Proceedings, pages 796 to 799. The numerical data appended here are taken from contemporary issues of "Jane's Fighting Ships":

(a) French cruiser *Condé* of about 1904, making about 22 kt. The photograph shows that the Velox wave length is about $L/2$. For this vessel, L = 452.75 ft, B = 65.33 ft, H = 24.5 ft, Δ = 10,000 t, P_S = 20,500 horses, V = 21 kt (nominal); for 22 kt, T_q = 1.034.

(b) French cruiser *Chateaurenault* of about 1898. The photograph reveals a considerable trim by the stern and a Velox wave length of well over L. Here L = 443 ft, B = 56 ft, H = 22.5 ft, Δ = 8,018 t; P_S = 23,000 horses, V = 23 kt (estimated); for 23 kt, T_q = 1.093. For a speed-length quotient only slightly greater than that of the *Condé*, the Velox wave length appears to be much greater.

(c) French battleship *Magenta* of 1890. The photograph gives the distinct impression that the ship is down by the head. The Velox wave length appears to be about $L/2$. Here L = 330 ft, B = 65.5 ft, H = 28.5 ft, Δ = 10,850 t, P_S = 12,000 horses, V = 16 kt; T_q = 0.881 at this speed.

(d) The *Voltaire* shows a Velox wave length of about $L/2$. For this ship, L_{WL} = 475.75 ft, B = 84.75 ft, H = 27.5 ft, Δ = 18,400 t, P_S = 22,500 horses, V = 19.4 kt; T_q = 0.889 at this speed.

(e) A photographic wave profile of the U. S. battleship *Iowa* (old), presumably made at or near full speed, shows one crest at the bow, one amidships, and one at the stern [ASNE, Aug 1897, p. 454]. A similar photograph appears in "Jane's Fighting Ships," 1910, p. 192. The wave length at this speed, assumed to be 17.087 kt, is thus about half the length of the ship. For a waterline length of 360 ft, T_q = 0.9005, F_n = 0.2682. For a trochoidal wave in deep water, the wave length L_W for 17 kt is about 162 ft, something less than half the ship length. Data for the old *Iowa*, corresponding to those for the French ships, are: L_{WL} = 360 ft, B = 72.0 ft, H = 24.02 ft, Δ = 11,363 t, P_S = 11,835 horses, C_P = 0.668, C_X = 0.944, S = 31,110 ft², C_W = 0.733, A_X = 1,635 ft².

(f) Wave profiles at two speeds for the Italian cruiser *Piemonte* are published in INA, 1889, Plate XXVII. The ship is 325 ft long, and for the higher speed the wave length is about equal to the ship length, minus the lag in the bow-wave crest. At 20 kt the value of T_q is 1.11, F_n = 0.331; at 21.5 kt, T_q is 1.193 and F_n = 0.355.

(g) The Danish ship *Tjaldur* is shown running at 18 kt, revealing a deep trough at an estimated position of $0.45L$ from the bow and a second crest (following

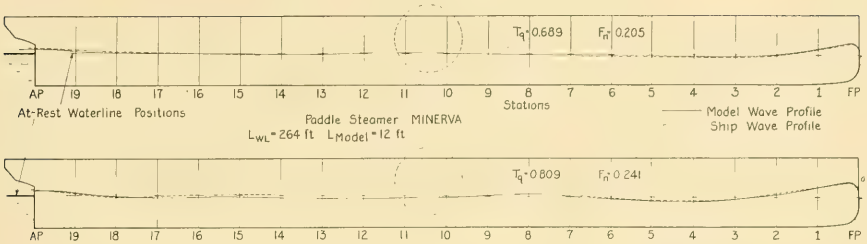

Fig. 52.C Observed Wave Profiles on Ship and Model for Paddle Steamer *Minerva*

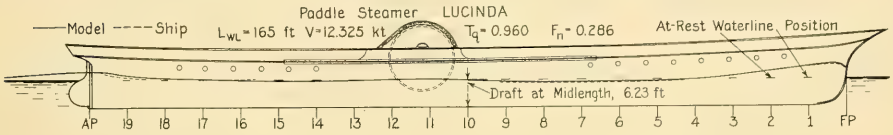

Fig. 52.D Observed Wave Profiles on Ship and Model for Paddle Steamer *Lucinda*

the bow-wave crest) at about 0.93L [SBMEB, Mar 1953, p. 159]. The T_q value at this speed, for an estimated length of 280 ft, is 1.077; F_n is 0.321.

In the discussion of an old paper by Professor J. H. Cotterill entitled "On the Changes of Level in the Surface of the Water Surrounding a Vessel Produced by the Action of a Propeller and by Skin Friction" [INA, 1887, Vol. 28, p. 298], there is some comment by Mr. F. P. Purvis concerning the profiles of the waves alongside both models and ships driven by paddlewheels. He mentions an IESS paper for 1884–1885, having to do with the paddle steamer *Lucinda*. Messrs. William Denny and Brothers, Ltd., of Dumbarton, Scotland, kindly furnished the author with drawings showing wave profiles of the paddle steamer *Minerva* as well as of the *Lucinda*. Figs. 52.C and 52.D were prepared from these drawings.

E. P. Panagopulos and A. M. Nickerson, Jr., give a partial wave profile (at the stern) as observed on the large tanker *Chryssi* [SNAME, 1954, Fig. 13, p. 217].

52.3 Wave Profiles Alongside Models. It has been customary, since the early days of model testing in basins, to record the shape and position of the wave profile along the model at selected speeds. Typical modern photographs showing this feature are reproduced in Figs. 78.A and 78.B. Projections of the wave profiles on a transverse plane are shown on the body plans for a number of models on SNAME RD sheets 15, 16, 17, 18, 20, 95, 96, 97, and 98. RD sheet 144 shows a wave profile projected on the centerplane.

A rather familiar, but not often remembered model wave profile is that first published by W. Froude in 1877, in his first paper on parallel middlebody [INA, 1877, Vol. XVIII, Pl. VI]. It was reproduced by R. E. Froude four years later [INA, 1881, Vol. XXII, Fig. 1b, Pl. XVI]. The model represented a ship having a length of 500 ft, a beam of 38.4 ft, a draft of 14.4 ft, and a length of parallel middlebody of 340 ft, or 0.68L. It was run at a T_q of 0.645, F_n = 0.192.

Wave profiles of three models tested in the Michigan basin at Ann Arbor are given by H. C. Sadler [SNAME, 1907, Vol. 15, Pl. 10]. The published data are among the few which state the speed-length quotient at which the ship or model was run. However, the values of T_q were so low that the profiles do not have prominent crests and troughs.

Wave profiles alongside a 39.37-ft self-propelled steel launch (considered here as a large model) are given by S. Yokota, T. Yamamoto, A. Shigemitsu, and S. Togino in Fig. 18 on page 328 of a paper entitled "Pressure Distribution over the Surface of a Ship and its Effects on Resistance" [World Eng'g. Congr., Tokyo, 1929, Proc., Vol. XXIX, Part 1, publ. in Tokyo, 1931]. Attention is invited to the comments on pages 297 and 298 concerning difficulties encountered in recording these profiles. Nevertheless, the published data include profiles for two conditions, (1) with the launch driven by its underwater propeller and (2) with it driven by an abovewater airscrew.

Three sets of wave profiles around models with

bulbs, $f_B = 0.08$, 0.04, and 0.00, with the vertical scales exaggerated about 7 times, are given by E. M. Bragg in SNAME, 1930, Pl. 51:

$T_q = V/\sqrt{L}$	Station for first bow-wave crest abaft FP, on a basis of 20 stations
1.2	About 1.7, approx. $0.085L$ from FP. Varied from Sta. 1.6 to Sta. 1.9 for the three models referenced
1.0	About 1.2, approx. $0.06L$ from FP. Varied from Sta. 1.0 to Stas. 1.6 or 1.7 for the three models
0.8	About 0.8, approx. $0.04L$ from FP. Varied from Sta. 0.7 to Sta. 1.0 for the three models.

The author of this paper comments on the fact, still unexplained, that despite the amazing similarity of the wave profiles for all three models at a T_q of 1.2, the model with the largest bulb had 15 per cent less resistance than the one with no bulb. The present author makes the further comment that, at all three T_q values, the model with the largest bulb had the highest bow-wave crest! This feature likewise remains unexplained.

O. Schlichting, in his 1934 STG paper on tests of models in shallow and restricted waters, referenced in Sec. 61.3, gives in Figs. 13a and 13b the wave profiles alongside models of a heavy cruiser and a light cruiser, respectively, for values of F_n varying from 0.21 to 0.38, T_q of from 0.71 to 1.28.

The wave profile for a double-ended model having mathematical lines is given on Plate 1, page 545 of a paper on wake by C. Igonet [ATMA, 1938, Vol. 42, pp. 543–569]. This plate shows not only a body plan of the model but a *transverse* profile of the water surface abreast the model at Stas. 1 and 19, corresponding to 0.05 and $0.95L$ from the FP.

E. Heckscher published a series of wave profiles alongside a given model, for F_n values of 0.19, 0.23, 0.25, 0.295, and 0.325, T_q of 0.64, 0.775, 0.842, 0.991, and 1.091, corresponding to five hump-and-hollow positions along the curve of resistance with speed [WRH, 15 Aug 1939, Fig. 4, p. 262].

In the Annual Report of the Rome Model Basin for the year 1941, Vol. X, there are shown two wave profiles for Rome model C.295, at two speeds. The corresponding T_q values are 1.082 and 1.204. These profiles, with the body plan of the model, as published in Table XII of the referenced report, are reproduced here in Fig. 52.E.

D. W. Taylor shows the wave profiles for two models at various speed-length quotients [S and P, 1943, Figs. 21–25, p. 24]. Wave profiles are also traced on the body plans of two series of models with widely varying midsection coefficients in Figs. 26–35 on page 25 of the reference. This set of body plans is reproduced as Fig. 52.Q in Sec. 52.7 of the present chapter.

G. de Verdière and J. Gautier give a series of

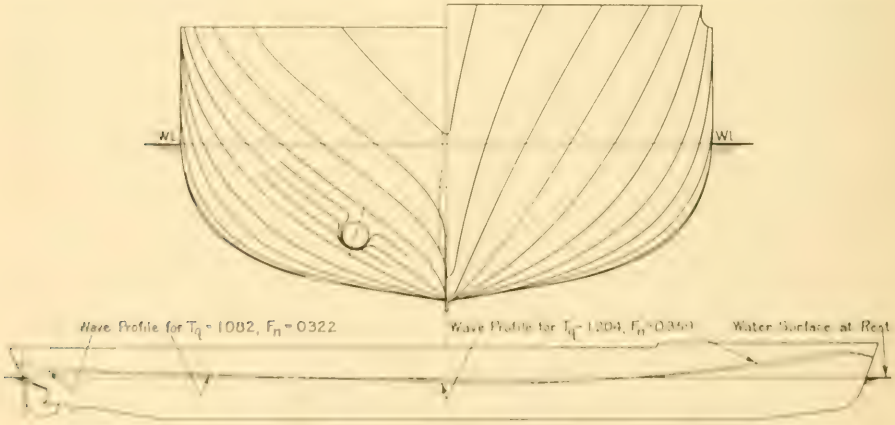

Fig. 52.E Observed Wave Profiles on Rome Model Basin Model C.295

wave profiles as determined from tests of four models of ships having waterline lengths L of from 459.3 ft to 448.2 ft [ATMA, 1948, p. 490]. The ordinates are in meters for the full-scale ships and the abscissas in 0-diml length ratios x/L, with Sta. 0 at the AP and Sta. 20 at the FP. The profiles in diagram **a** of Fig. 8 on page 490 of the reference are plotted with respect to the undisturbed water surface at infinity. Those in diagram **b** are plotted with respect to the at-rest ship waterplane, so that they differ by the amounts of the sinkage at each station. The T_q values for these plots range from 0.747 for the short ship to 0.756 for the long ship; corresponding F_n values are 0.222 and 0.225.

Wave profiles are shown for the ten tanker models reported upon by R. B. Couch and M. St. Denis [SNAME, 1948, Figs. 2(a)-10(a), pp. 360–378]. A single wave profile is reproduced by W. P. A. van Lammeren in RPSS, 1948, Fig. 38, on page 88, for a T_q of 0.64, without the body plan of the ship in question.

Six sets of wave profiles for two self-propelled models, showing the changes in profile over a wide range of speed, are given by S. A. Harvald in SSPA Report 13, published in 1949, entitled "Medstrømskoefficientens Afhaengighed af Rorform, Trim og Haekbølge (The Dependence of Wake Fraction on Shape of Rudder, Trim, and Stern Wave)." The profiles appear on pages 13, 14, 34, 35, 36, and 40. On the last-named page there is a set of profiles for the model running astern. On pages 56–60 there is a summary in English.

Wave profiles at three speeds for seventeen models of coasters are given by A. O. Warholm in SSPA Report 24, published in 1953, entitled "Några Systematiska Försök med Modeller av Mindre Kustfartyg (Systematic Tests with Models of Coasters)." The profiles, apparently taken during resistance (and not self-propelled) tests, are printed on pages 85–90. On pages 48–50 there is a summary in English.

Provision is made, on SNAME RD sheets having numbers in excess of 100, to depict the wave profiles at designed speed in either or both of two locations. Examples of these are sheets 114, 115, and 144.

52.4 General Rules for Wave Interference Alongside a Ship. For a ship form having abrupt and localized changes in waterline curvature, resulting in what may be considered as point-pressure disturbances, it is possible to approximate analytically the resultant wave profile, taking account of wave-interference effects. Fig. 10.F in Volume I, adapted from W. C. S. Wigley, does this for a 2-diml ship having a parallel middlebody and triangular ends. Many barges have nearly square-cornered rectangular waterlines but on most ships the pressure disturbances are regions rather than points. This renders it extremely difficult to predict the shape and fore-and-aft position of the wave form generated by each such disturbance.

Several further complications in working out wave interferences and their effects along the waterline of a ship of normal form are:

(1) Lack of information as to the variation of level along the ship of the crests and trough of the Bernoulli contour system, described in Sec. 10.3. This is undoubtedly a function of the surface-waterline shape and it may also be a function of the section-area curve.

(2) Lack of a precise determination of the effect of the presence of the ship entrance abaft a point-pressure disturbance such as a stem

(3) Inadequate knowledge as to the effect of variations in the waterline slopes in such an entrance, discussed briefly in Sec. 10.6 on page 174 of Volume I and in Sec. 48.2

(4) Uncertainty as to the amount of crest lag (and trough lag) in the Velox wave systems generated by pressure disturbances abaft the bow

(5) Uncertainty as to the factors determining the fore-and-aft position and shape of a stern-wave crest on an actual ship, in the presence of a separation zone, of boundary layers, and of water coming up from under the ship

(6) Lack of knowledge as to the lengths of actual (or trochoidal) waves for a given celerity, when occurring abreast a ship instead of in the open, unobstructed sea.

In the absence of these data it is difficult to set down specific rules for wave interferences and their effects alongside a moving ship. If the individual profiles could be determined and positioned longitudinally, there is every reason to believe that in most cases the interference effects could be determined by simple superposition of the heights of the transverse waves in each system at any selected station.

K. S. M. Davidson gives a few diagrams [PNA, 1939, Vol. II, pp. 66–67] in which this superposition is indicated, in addition to the schematic

diagrams in Figs. 10.G, 10.J, and 10.K of Chap. 10 of Volume I.

W. P. A. van Lammeren, L. Troost, and J. G. Koning discuss the features and effects of wave interference along somewhat different lines [RPSS, 1948, pp. 54–55].

52.5 Estimate of Bow-Wave and Stern-Wave Heights and Positions. Prediction of the surface-wave profile, outlined in Sec. 52.6, requires in particular an estimate of the heights and positions of the bow-wave and stern-wave crests. There is an appreciable space lag in the bow-wave crest position abaft the stem, described in Sec. 10.15 on page 180 of Volume I, especially if the speed is high. This lag is particularly noticeable in Fig. 52.B of Sec. 52.2 and in Figs. 52.I and 52.J of Sec. 52.6.

J. Scott Russell, in Plate 118 of MSNA, 1865, Vol. II, Fig. 31, shows a vessel being driven so fast that the bow-wave crest lags back to a point abreast midships. He explains this feature in Vol. I of the reference, page 636. A situation almost exactly similar is reproduced in the familiar photograph of Parsons' *Turbinia* at full speed [SNAME, HT, 1943, p. 439].

An empirical formula for estimating "good average values" of the height of the bow-wave crest is given by J. L. Kent [NECI, 1949–1950, Vol. 66, p. 435]. This is in the dimensional form $h = k(B/L_E)V^2$, where h, B, and L_E are in ft, V is in kt, and $k = 0.083$. It resembles a formula given by Laubeuf many years ago [ATMA, 1897, p. 211].

Kent's k-value is for "ordinary merchant ships," derived from wave profiles observed when towing a number of ship models at the NPL, Teddington. Presumably it applies to ships without bulb bows. Furthermore, it takes no account of angle of entrance at the stem, hollowness or fullness in the entrance waterlines, flare of bow sections, rake of the stem profile, or of any other feature which might reduce or augment the bow-wave crest height. Preliminary plots indicate that the value of k varies rather widely, from the order of 0.015 to 0.13 or more.

Transformed into a dimensionally consistent equality for any units of measurement, Kent's formula becomes, for the height h of the bow-wave crest above the at-rest WL:

$$h = k_w\left(\frac{B_x}{L_E}\right)\frac{1}{w}\left(\frac{\rho}{2}\right)V^2 = k_w\left(\frac{B_x}{L_E}\right)\frac{V^2}{2g} \qquad (52.i)$$

For the range of form of displacement-type ships, k_w for the 0-diml Eq. (52.i), as indicated by the wave profiles observed on their models, varies from 0.3 to nearly 3.0, indicated graphically in Fig. 52.F. This extreme variation is undoubtedly

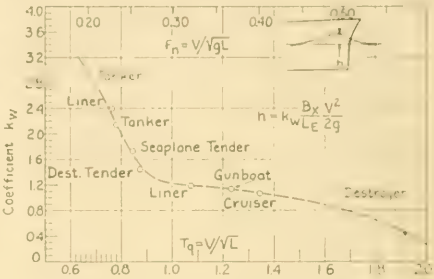

Fig. 52.F Graph for Estimating Bow-Wave Crest Height

The spot applying to each vessel is calculated for the designed speed of that vessel

due to the fact that the ratio B_x/L_E does not take adequate account of the WL slopes at and just abaft the stem. A large waterline slope not only produces a high value of pressure coefficient close behind the stem, but the large slope throws the projection of the crest on the centerplane farther forward, toward the stem.

The models on which pressure distributions were observed by E. F. Eggert, EMB 2861 and 3383 [SNAME, 1935, pp. 129–150; 1939, pp. 303–330], show bow-wave crests considerably higher than those given by either formula, in the T_q range of 0.76 through 1.2. On the other hand, the bow-wave crest heights measured on two narrow models by W. C. S. Wigley, in the same speed range, are lower than the formula values [NECI, 1930–1931, Vol. 47, pp. 153–196; INA, 1935, Fig. 6, Pl. XXVI]. It is possible that on some towed models it is difficult to tell where the wave profile ends and the spray root begins; also that factors additional to those in the formulas affect this phenomenon. For either or both of these regions Eq. (52.i) and the k_w-curve of Fig. 52.F are considered as preliminary only.

The estimated bow-wave crest height for the ABC ship of Part 4 at 20.5 kt (34.62 ft per sec), using a k_w of 1.385 from Fig. 52.F and employing Eq. (52.i), is

$$h = k_w\left(\frac{B_x}{L_E}\right)\frac{V^2}{2g} = 1.385\frac{73(1{,}198.5)}{(262.65)64.348} = 7.17 \text{ ft.}$$

It appears proper that this height be measured from the undisturbed water level rather than from the at-rest WL of the ship, as might be painted on its hull, because of the drop (or rise) of the bow due to the combined effects of the Bernoulli contour system and the Velox wave system at the ship speed in question. Adding to the calculated h the value of this drop for the ABC ship, -2.35 ft, as measured during the model resistance test, and allowing for the lag in the bow-wave crest, to be determined presently, gives a value of 9.47 ft for the bow-wave crest height, measured above the 26-ft DWL. The full details of this calculation are given in Sec. 66.28.

Based upon observations of EMB model 2861 E. F. Eggert evolved a rule for estimating the bow-wave crest lag, defined as the fore-and-aft distance of that crest abaft the intersection of the stem and the at-rest WL, when projected on the centerplane [EMB Rep. 392, Nov 1934, p. 1]. The $+\Delta p$ peak may not always lie exactly at the intersection just mentioned, but it is near enough for all practical purposes. Eggert's formula, in dimensional form, says that the crest lies at a distance $x = 0.033V^2$ abaft this intersection, where the x-distance is in ft and V is in kt. In 0-diml form this becomes, for the distance abaft the stem at the WL at rest,

$$x = 0.372\,\frac{V^2}{g} \qquad (52.\text{ii})$$

This equation is plotted in Fig. 52.G to give values of the crest lag x in fractions of the waterline length L_{WL}, on a basis of both Taylor quotient

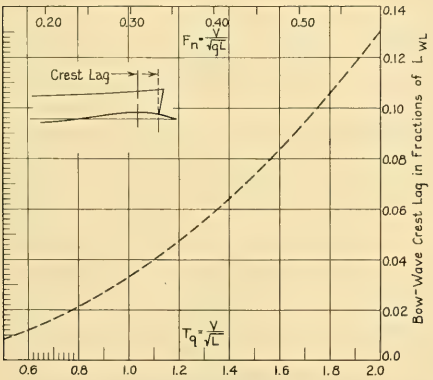

Fig. 52.G Graph for Estimating Bow-Wave Crest Lag Abaft Stem

T_q and Froude number F_n. For the ABC ship at 20.5 kt, or 34.62 ft per sec, this crest lag works out as $0.372(34.62)^2/32.174 = 13.86$ ft. From Fig. 52.G the value of the crest lag for a T_q of 0.908 is $0.0272L_{WL}$. The value observed on TMB model 4505 of the ABC ship and indicated on Fig. 66.R, where the crest occurs at about Sta. 0.7, is 17.85 ft or $0.035L_{WL}$.

Model data for a variety of ship forms, from which the graph of Fig. 52.G was derived, show rather wide variations from the value predicted by Eq. (52.ii) in some cases and exact agreement in others. Thus this equation and the broken-line curve of Fig. 52.G are both to be considered as preliminary.

S. A. Harvald, in his "Wake of Merchant Ships" [Danish Tech. Press, 1950, pp. 81–84], gives a diagram by which the stern-wave height may be estimated, as a means of predicting the amount of wave wake in any particular case. Fig. 52.H, adapted from Harvald's Fig. 41 on

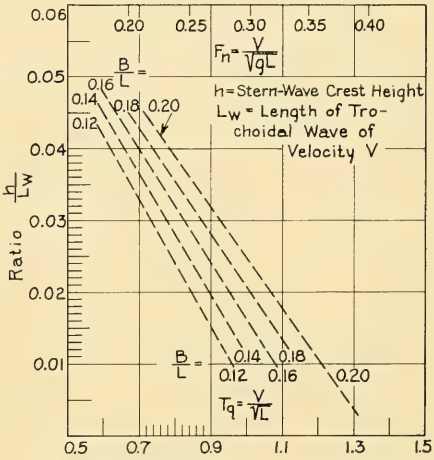

Fig. 52.H Graphs for Estimating Stern-Wave Crest Height

page 83 of the reference cited, indicates the parameters employed, B/L, h/L_W, and T_q. Harvald admits that a number of apparently important factors are not taken account of in his diagram but, like the other diagrams of this section, it will serve until something better is developed.

For the ABC ship, or one of its proportions, $B = 73$ ft and $L = 510$ ft, whence $B/L = 0.143$. At a T_q of 0.908, Harvald's diagram gives a value

for h/L_W of about 0.0195. From Table 48.d the length L_W of a trochoidal wave having a velocity equal to the ship speed of 20.5 kt is 234.3 ft. Then, for the estimated height of the stern wave,

$$h = 0.0195L_W = 0.0195(234.3) = 4.57 \text{ ft.}$$

If this height is reckoned above the undisturbed water level, the height above the 26-ft DWL is 4.57 ft plus the sinkage (about 0.75 ft), or 5.32 ft.

Although Harvald's data are not intended to take care of transom-stern ships, the height of the observed stern-wave crest just forward of the transom, as measured from the profiles on TMB model 4505, reproduced in Fig. 66.R, is about 4.1 ft, reckoned above the 26-ft DWL.

52.6 Prediction of the Surface-Wave Profile. There is a definite lack of accurate, comprehensive, and reliable information in Secs. 52.2 and 52.3, and in the literature in general, upon which to develop a wave-profile prediction method by the analysis of systematic data. This applies not only to elevations in the wave profile but to the exact speeds corresponding to the profiles, and to the shapes and proportions of the ships making the waves. Nevertheless, it is possible to sketch an approximation of the surface-wave profile for a ship design by using the empirical data of Secs. 52.2 and 52.3, plus some additional experimental data relative to the number of wave lengths to be expected between the bow-wave crest and the stern.

The latter data are based preferably upon the

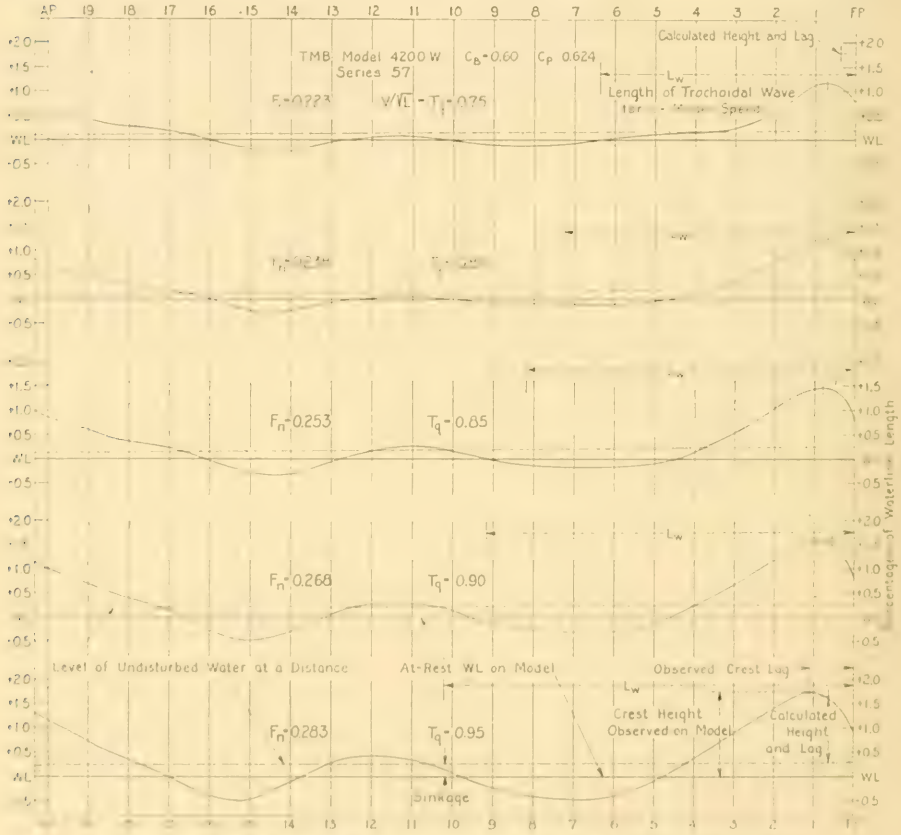

FIG. 52.I WAVE PROFILES FOR TMB SERIES 57, MODEL 4200W, AT VARIOUS SPEEDS

speed-length or Taylor quotient T_q or the Froude number F_n. It is known that, in general, when the crest of a transverse wave of the Velox system generated by the bow coincides with the first wave crest of the stern Velox system, there is a drop in total resistance. When a trough of the bow system coincides with a crest at the stern, there is a rise in resistance. When these effects are plotted on a base of speed-length quotient T_q or F_n, the humps and hollows in the curve of total (or wavemaking) resistance are found to fall in the positions indicated along the lower edge of Fig. 66.A.

It is also known, for ships of normal form, that certain T_q values correspond to ship lengths that are multiples of the transverse-wave lengths in whole numbers. Roughly:

(1) For $T_q = 0.63$, the ship is 4 wave lengths long
(2) For $T_q = 0.72$ to 0.73, the ship is 3 wave lengths long
(3) For $T_q = 0.88$, the ship is 2 wave lengths long

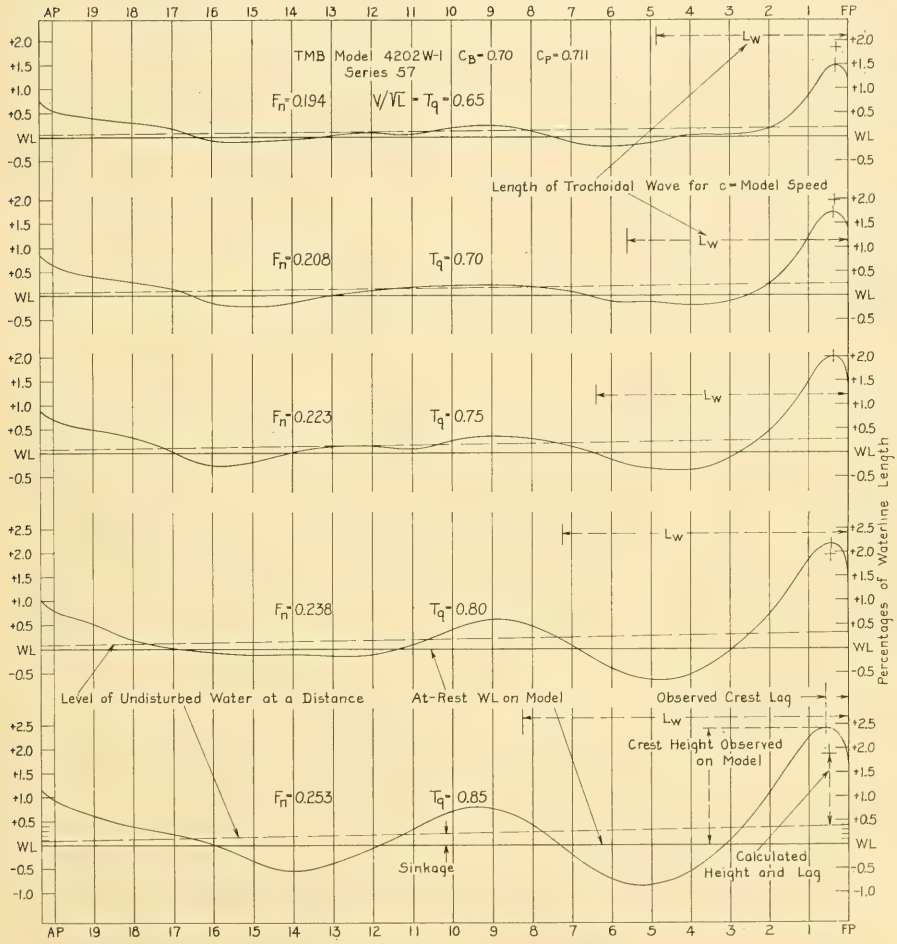

FIG. 52.J WAVE PROFILES FOR TMB SERIES 57, MODEL 4202W-1, AT VARIOUS SPEEDS

(4) For $T_q = 1.15$, the ship is about 1 wave length long. This is the case for some large, fast combatant vessels and for most tugs and sailing yachts at full or designed speed.

By the same reasoning, the humps in the resistance curves occur when the ship length corresponds approximately to half-lengths of the transverse wave system. Again roughly:

(5) For $T_q = 0.67$, the ship is $3\frac{1}{2}$ wave lengths long
(6) For $T_q = 0.80$, the ship is $2\frac{1}{2}$ wave lengths long
(7) For $T_q = 0.99$ to 1.02, the ship is $1\frac{1}{2}$ wave length long
(8) For $T_q = 1.5$ to 1.7, the ship is about $\frac{1}{2}$ wave length long. For most destroyers at full speed, running at a T_q of about 2.00, the ship is somewhat less than half a wave length long.

The values given in the foregoing are derived from preliminary examination of published and available wave profiles, without a careful study of the effects of bow-wave crest lag. For this purpose, a wave profile shown broadside, for the full model or ship length, is much more useful and valuable than a wave profile shown in its projected position on a body plan. When there is a parallel waterline portion of considerable length, the positions of the crests and troughs abreast it are not readily apparent in an end view of the hull.

Figs. 52.I and 52.J show the wave profiles for five speed-length quotients on each of two models of TMB Series 57, having block coefficients C_B of 0.60 and 0.70, respectively. The body plans and other data for these models are given by F. H. Todd and F. X. Forest [SNAME, 1951, pp. 642–691].

General rules and procedures for predicting the wave profile along a ship of normal form, in the usual range of speeds, are described in Sec. 66.28, using the ABC ship of Part 4 as the example.

52.7 Typical Lines-of-Flow Diagrams for Ship Models. Thanks to the work of D. W. Taylor and his associates at the Experimental Model Basin at Washington in the period 1900–1910 there appears in the technical literature a number of lines-of-flow diagrams. These are body plans upon which the projected flowline positions are

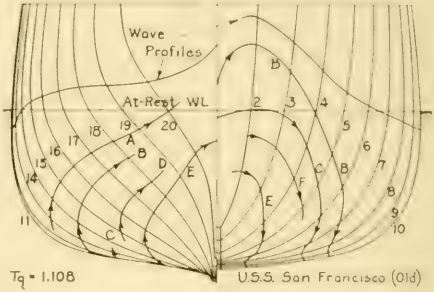

Fig. 52.Ka Lines of Flow for Old Cruiser Model

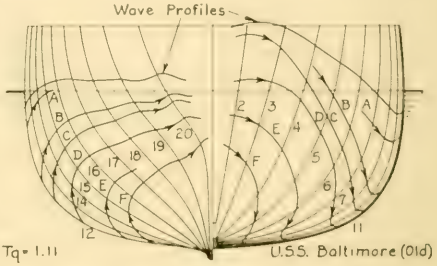

Fig. 52.Kb Lines of Flow for Old Cruiser Model

TABLE 52.a—Ship Data for Models with Observed Lines of Flow

The ship lengths and speeds, except for the *Pensacola*, are from D. W. Taylor [SNAME, 1907, p. 4], as are the body plans carrying the lines of flow.

Fig. No.	Name or type of vessel	L_{WL}, ft	Speed, kt	$T_q = V/\sqrt{L}$
52.Ka	*San Francisco* (old)	310.0	19.52	1.108
52.Kb	*Baltimore* (old)	327.5	20.10	1.11
52.Kc	*Pensacola*	570.0	32.70	1.370
52.L	Great Lakes ore steamer	540.0	10.42	0.448
52.M	Collier	460.0	15.00	0.699
52.Na	*Sotoyomo*, full speed	94.64	10.31	1.06
52.Nb	*Sotoyomo*, slow speed	94.64	5.50	0.565
52.O	Shallow-draft river steamer	257.0	19.00	1.18
52.P	Special type with bulges	490.25	19.00	0.858

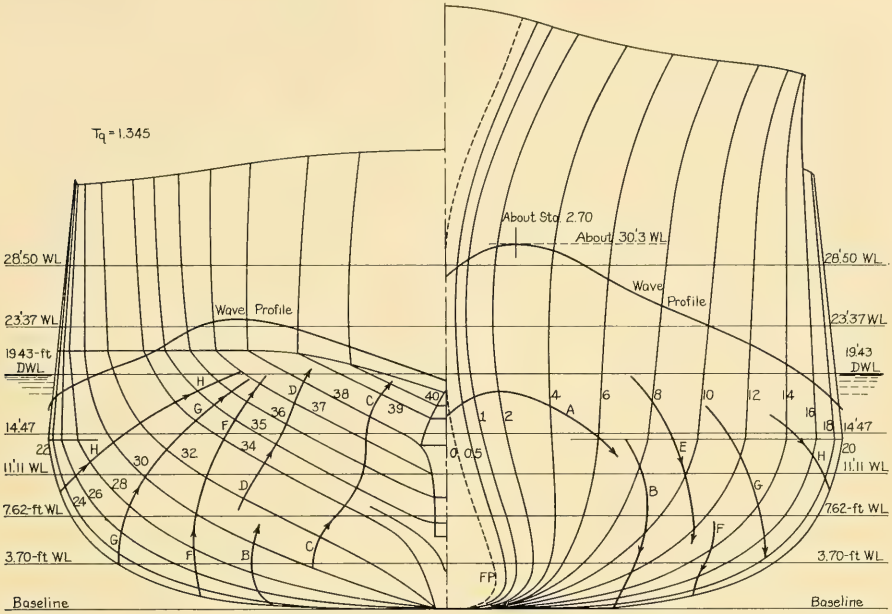

Fig. 52.Kc Lines of Flow for New Cruiser Model

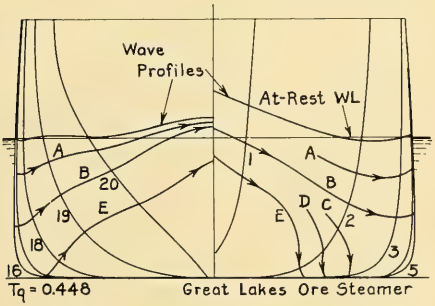

Fig. 52.L Lines of Flow for Old Great Lakes Bulk Carrier

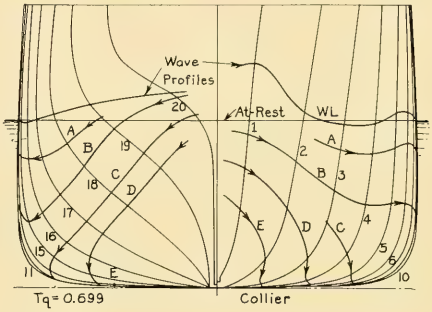

Fig. 52.M Lines of Flow for Old Cargo-Ship Model

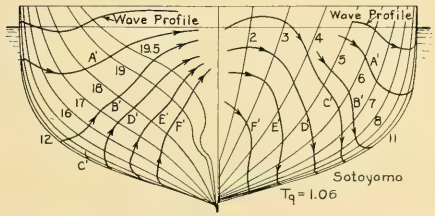

Fig. 52.Na Lines for Flow for Tug Model, Full Speed

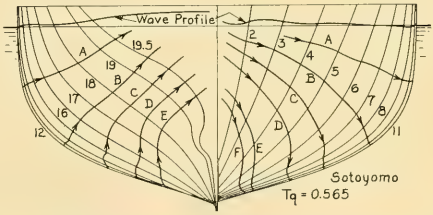

Fig. 52.Nb Lines of Flow for Tug Model, Slow Speed

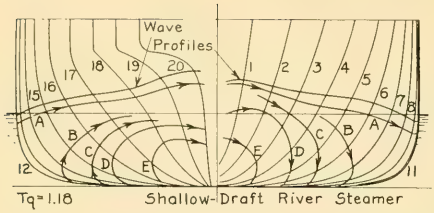

FIG. 52.O LINES OF FLOW FOR SHALLOW-DRAFT STEAMER

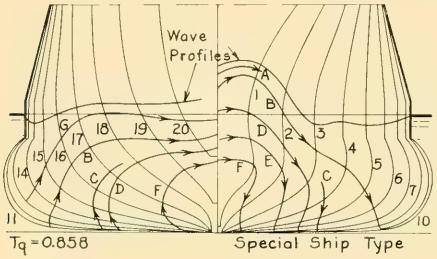

FIG. 52.P LINES OF FLOW FOR SHIP WITH UNDERWATER BULGES

drawn. A considerable number of ship types are represented [SNAME, 1907, pp. 1–12, Plates 1–7]. Figs. 52.K through 52.Q are adapted from the diagrams in the reference cited, with the proper T_q values shown on each. Table 52.a gives the information presently available on the ships represented by seven models of this group.

In 1910 Taylor published the lines-of-flow diagrams for two model series, one apparently for a battleship and the other for a light cruiser of that day, in which the maximum-section coefficient C_X was varied from 0.70 through 1.10 for each group of five [S and P, 1943, Figs. 26–35, p. 25]. Fig. 52.Q is adapted from the Taylor reference by adding the principal hull parameters and coefficients, as well as the speed-length ratios.

Despite the major differences in form between the two parent models the flow patterns are remarkably similar.

Since 1910 a great many flow tests have been run on ship models at the Experimental Model Basin and the David Taylor Model Basin but unfortunately only a few of the lines-of-flow diagrams have been published in unclassified EMB and TMB reports and the technical literature. Figs. 52.R and 52.S are copied from two unpublished diagrams. Fig. 52.T is a reproduction, for ready reference, of one such diagram previously published.

The Swedish State Shipbuilding Experimental Tank makes use of the wet-paint technique for depicting flowlines around selected portions of ship models [SSPA Rep. 32, 1954, Figs. 18 and 19, pp. 26–27]. For the local areas covered they are excellent. A. F. Lindblad includes photographs of flowlines around the bulb bow of a model made with this technique [SSPA, Rep. 8, 1948, Figs. 15 and 17, pp. 18–19]. Published with them is a model body plan upon which a number of flowlines are indicated.

In 1947 R. Brard and J. Bleuzen published photographs of models in which flowlines were determined during steering tests [ATMA, 1947, Figs. 10, 11, 12, and 13, between pp. 332–335; TMB Transl. 248]. H. F. Nordström published similar photographs of the flow near the bow-propeller position on an icebreaker model [SSPA, Rep. 20, 1952].

In his book "Marine Propulsion Devices," published at Leningrad and Moscow in 1949, V. M. Lavrent'ev shows body plans on pages 65 and 66 with lines of flow drawn over them.

A multitude of photographs have likewise been made of EMB and TMB models with the flow traces marked on them, but only a few are available for study by marine architects [SNAME, 1947, Fig. 9 on p. 104; Figs. 25, 26, and 27 on pp. 116–117]. Lines-of-flow traces for a few selected locations appear on SNAME RD sheets 114 and 115. It is hoped that, in the future, these can be shown on all such sheets when the data are available.

Fig. 52.U gives a rather comprehensive flow pattern for the transom-stern ABC ship hull worked out in Chap. 66. Figs. 78.C and 78.D are photographs of the model showing the nature and positions of some of the flow traces.

52.8 Analysis of Model Surface-Flow Diagrams. The method of analyzing photographs and diagrams of flow lines and flow patterns taken directly on the surface of a model depends upon the technique employed in tracing the flow. Wet-paint streaks are usually short but if the paint lines are closely spaced in a fore-and-aft direction they may be combined like the short vectors that form path lines, described in Sec. 1.4 of Volume I. The traces left by chemicals ejected from orifices in the hull are much longer, sometimes half the length of the model. They may be assumed to give a better representation

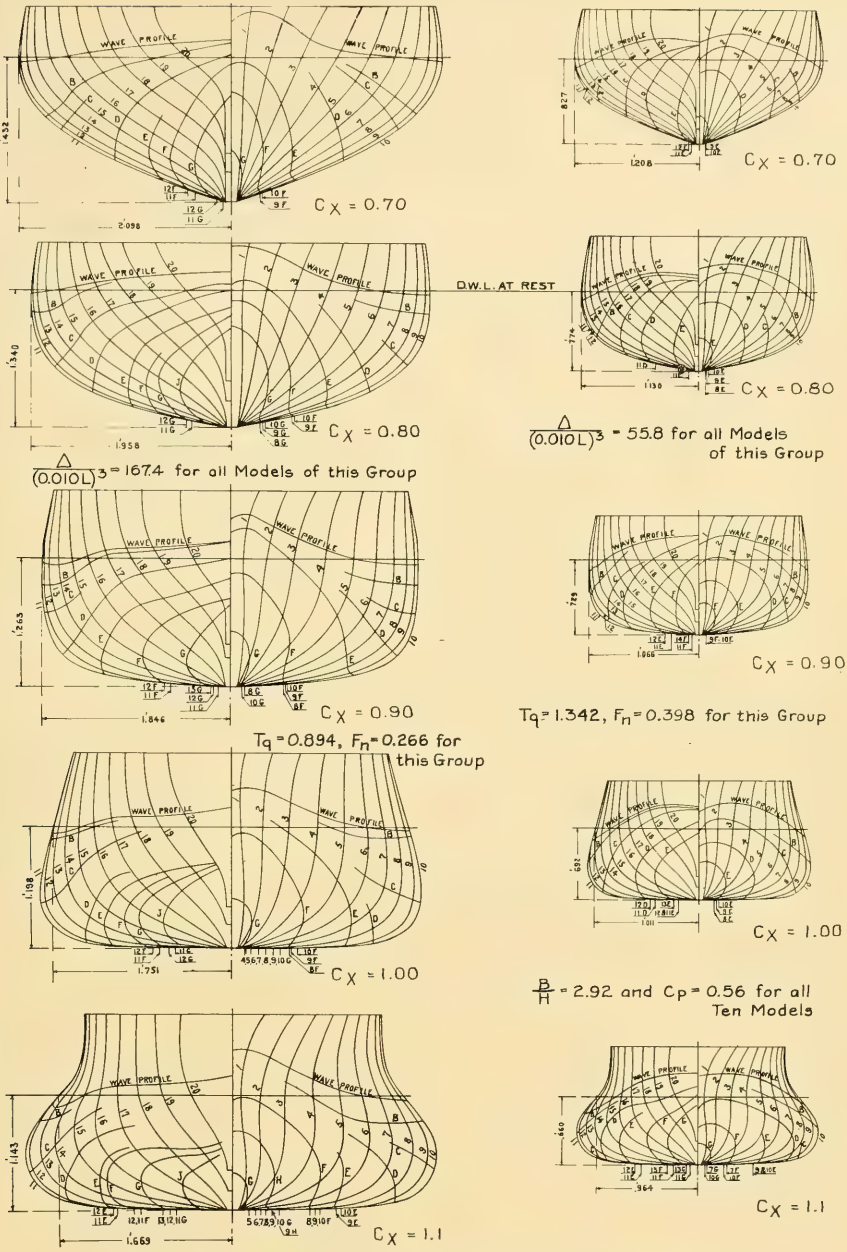

FIG. 52.Q VARIATION OF FLOW PATTERN WITH MAXIMUM-SECTION COEFFICIENT C_X

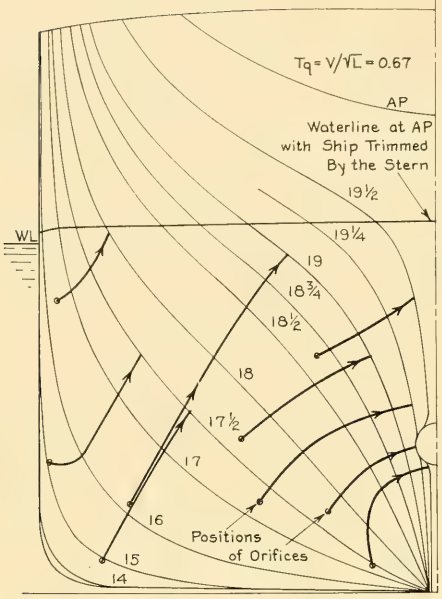

Fig. 52.R Lines of Flow for Run of Model of S. S. *Clairton*

of the surface flow. The details of the chemical methods, some representative results, and instructions for interpreting the traces are described by J. F. Hutchinson in TMB Report 535, of May 1944, entitled "The Delineation of Surface Lines of Flow and Wave Profiles at the David Taylor Model Basin." Two body plans showing lines of flow are reproduced on pages 6 and 7 of this report.

Several flowlines are likely to come together as they approach the surface, usually between the after quarterpoint and the stern. A case in point is that of the flow along lines E and F on TMB model 3898, representing the twin-skeg *Manhattan* design, depicted in Fig. 52.T [SNAME, 1947, Fig. 24 on p. 116 and Fig. 26 on p. 117]. Here, at Sta. 18.5, the two lines of flow not only join but appear to be about ready to project themselves up through the water surface, just above the junction point. Apparently the two large-size stream tubes along E and F change shape rapidly between Stas. 16, 17, and 18.5, so that opposite the latter point they are both very thin in a girthwise direction and very thick in a direction normal to the hull. The junction point is apparently close to the separation point at that girthwise position, so that abaft Sta. 18.5 the stream tubes in question have gone off and left the hull.

The following is copied from page 7 of TMB Report 535, referenced earlier in the section:

> "A careful study of the streamlines on the model will afford a fund of information not only as to the direction of flow, but concerning the nature of the flow. A long, narrow line indicates high velocity; a short, wide and smeary line indicates low velocity; a sudden breaking off of the line indicates separation from the surface of the model; and an irregular line or an area with diagonal tails indicates eddying along the model."

The orthodox lines-of-flow diagrams, such as those in Figs. 52.R, 52.T, and 52.U, show only very indirectly the direction taken by the water when flowing aft *under* a ship model, especially if the bottom is flat. Fig. 52.V is a fish-eye view,

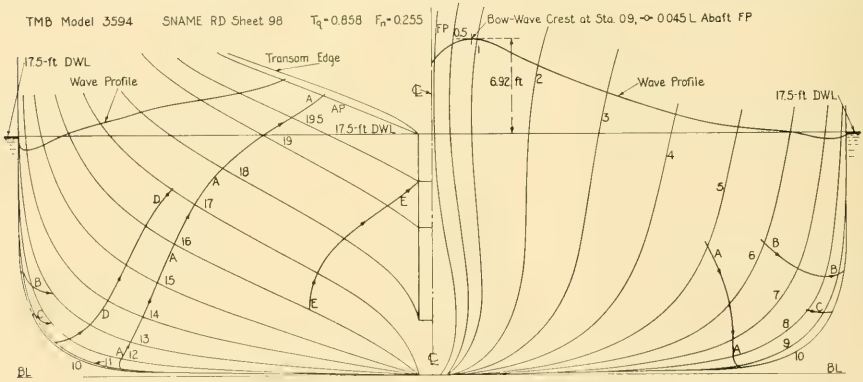

Fig. 52.S Lines of Flow for TMB Model 3594, Representing Minelayer U. S. S. *Terror*

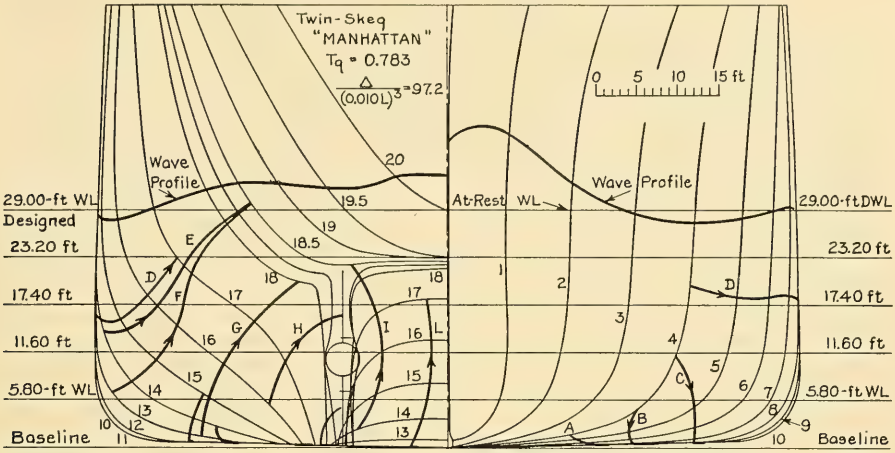

Fig. 52.T Lines of Flow of TMB Model 3898, Representing Twin-Skeg *Manhattan*

greatly contracted longitudinally, of the flowlines under TMB model 3898, representing the twin-skeg *Manhattan* design developed by the U. S. Maritime Commission [SNAME, 1947, pp. 112–125]. The projection is made *upward* on the plane of the designed waterline; all flowlines are shown on the same side of the centerplane. Three photographs are available showing the original lines of flow on the model [SNAME, 1947, Fig. 25 on p. 116 and Figs. 26 and 27 on p. 118].

The transverse spreading of the flow shown by

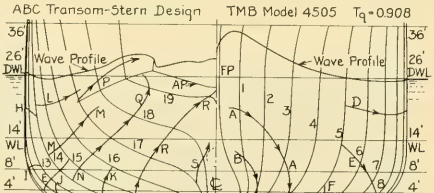

Fig. 52.U Lines of Flow Around Model of Transom-Stern ABC Ship

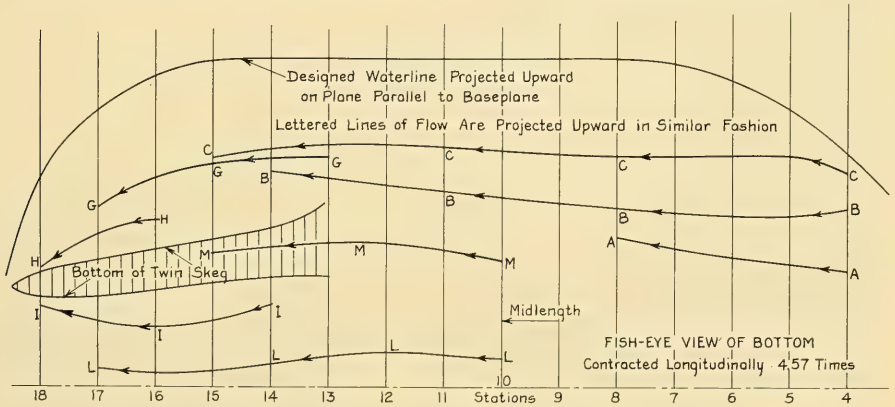

Fig. 52.V Fish-Eye View of Lines of Flow Under Bottom of TMB Model 3898

The transverse scale here is 4.57 times the longitudinal scale, to permit showing the flowlines to better advantage

traces A, B, and C, and by the forward portions of traces L and M, is typical of the flow under models in general. It is possible that it indicates a slowing down in the next-to-the-hull water layers because of the thickening of the boundary layer under the hull. The increase in x-distance from the stem is one cause of thickening; another is the increase in width of the flat portion, with its small (or zero) transverse curvature.

52.9 Observation and Interpretation of Off-the-Surface Flow Data on Models. It is customary in circulating-water channels and wind tunnels to observe the nature and direction of the flow over a body or ship surface by watching the behavior of short strings or tufts of yarn. These may be attached not only to the surface directly but to slender pins projecting any required distance from the surface, indicated in Fig. 52.W. Different tuft colors may be used to represent different normal distances from the hull. Indeed, the tufts may be attached to the ends of long, thin wands, moved about by hand to the desired positions.

Tufts have the disadvantage of shortness, like the streaks from a transverse line of wet paint. However, there is no limit to the number of them that can be used over the surface of a ship model. They are extremely valuable as nature-of-flow indicators, streaming straight out in a fast, regular (or uniform) flow and waving gently or lazily in a slow flow that is irregular and uncertain.

Off-the-surface vane and rigid-flag indicators require little in the way of interpretation since they reveal velocity direction only. This is usually sufficient when they are employed to determine a single line of flow such as a bilge-keel trace.

Colored inks and dyes may be ejected from the ends of long, thin tubes, moved to any desired position in the water around the model. Figs. 46.E and 46.F show ink trails along a model.

To permit subsequent study at leisure, after completion of the test, flash photographs are made of the tuft positions, like those reproduced in Fig. 52.W, as well as in Figs. 36.F, 36.G, 46.D, 46.E, 46.F, 78.E, and 78.F. Similar still photographs have been made at the Experimental

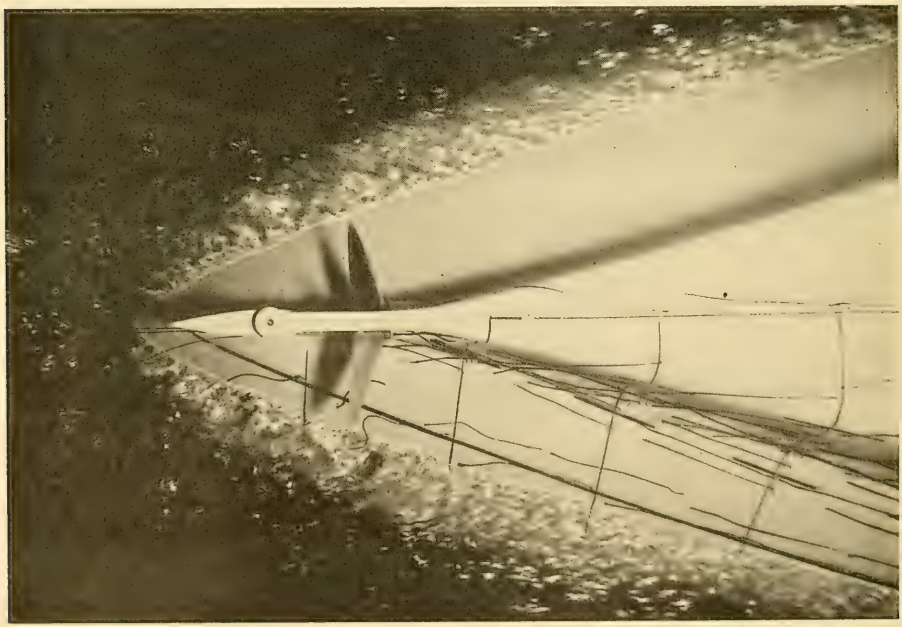

Fig. 52.W Fish-Eye View of Self-Propelled Model in Circulating-Water Channel, Showing Tufts Carried by Pins and Tufts on Model Surface

Towing Tank, Stevens Institute of Technology, and published in:

(a) Sutherland, W. H., "Underwater Photographs of Flow Patterns," ETT, Stevens, Note 75, May 1948. This includes some observations made from underneath a model during a turn.
(b) Ashton, R., "An Underwater-Photographic Method for Determining Flow Lines of Ship Models," ETT Tech. Memo 101, Feb 1949.

Other published flow-test photographs showing tufts attached to the model surface and ink or dye injected into the water through small tubes are found in:

(c) Baier, L. A., "Trouble-Shooting the *Martha E. Allen*," Mar. Eng'g., Sep 1955, p. 54
(d) Baier, L. A., and Ormondroyd, J., "Suppression of Ship Vibration by Flow Control," Proc. Third Midwestern Conf. on Fluid Mech., Univ. of Minn., Jun 1953, pp. 397–411
(e) Harper, M. S., and Weaver, A. H., Jr., "Model Flow Studies Around Stern of U. S. Navy Fleet Tug *ATF-163*, TMB model 3531," TMB Rep. 810, issued in Jan 1952. This report contains 10 photographs, showing both tuft positions and ink trails.

If the flow contains eddies, vortexes, and counter-currents, or otherwise varies with time, motion-picture photographs are taken. However, neither type of photographic record can compare in vividness and reality with direct visual observation. Fortunately, this can include study and interpretation also by continuing any given set of test conditions in the circulating-water channel for as long as may be desired, or until the observer understands what is going on.

References to the studies of various experimenters, relating to the off-the-surface flow on models, are listed in Sec. 52.12 and in Sec. 22.6 on page 311 of Volume I.

52.10 Estimating the Ship Flow Pattern on the Body Plan. It will some day be considered as important, and as necessary, to *estimate* the flow pattern around a newly shaped hull, in advance of model tests, as it is to predict its resistance or the effective (and shaft) power required to drive it.

Based upon the physical aspects of flow around a ship form, described in Chap. 4 of Volume I, with emphasis on the flow around surface-ship forms in Secs. 4.10 and 4.11, an attempt is made in Sec. 66.28 to formulate a few preliminary instructions for guidance in predicting the flowline and wave-profile positions. Following these instructions, a flow pattern is sketched for the transom-stern ABC hull designed in Chaps. 66 and 67; in fact, it was drawn out in ink *before* the flow tests on the ABC ship model were made. The rather large variations between prediction and observations revealed in Fig. 66.R, especially in the forebody, show that the tentative instructions of Sec. 66.28 require further attention and study.

In this connection the comments made by H. C. Sadler, W. Hovgaard, D. W. Taylor, and others, in the discussion and closure of D. W. Taylor's paper "An Experimental Investigation of Stream Lines Around Ship Models" [SNAME, 1907, pp. 1–12], will be found most helpful.

52.11 Prediction of the Ship Flow Pattern at the Bilges. The portion of the hull flow pattern of the most immediate and practical interest is that in way of the propulsion devices, discussed in Sec. 17.2, in Chap. 33, and in Secs. 52.16 and 59.12. The next in importance is that in way of the bilge or roll-resisting keels, especially if these keels extend beyond any parallel middlebody that may be worked into the hull.

In some quarters it is considered sufficiently accurate to place the bilge-keel trace, as projected on the body plan, along a line bisecting the angle at the bilge between the side and the bottom at the section of maximum area. This neglects the effect of B/H ratio and similar factors. In other quarters it is assumed that the flow must certainly follow the bilge diagonal, at least close enough for all practical purposes. Both rules of thumb ignore the effect of the surface-wave pattern as far down as the bilge.

For slow ships, with low T_q values, the surface-wave effect probably is small but for fast ships, with medium or high T_q values, the prediction must be based on knowledge of the flow to be expected in this region. There is ample evidence that for ships operating at T_q values in excess of 0.85 or 0.90, $F_n > 0.253$ or 0.268, the crests and troughs in the surface-wave system are reproduced to a lesser degree at the bilge-keel level. The bilge-keel traces of the *Mariner* class, shown by V. L. Russo and E. K. Sullivan [SNAME, 1953, Fig. 18, p. 127], determined by both the chemical method and the vane or flag method, are excellent examples of this situation. Unfortunately, the wave profile (Fig. 12 of the reference) does not appear on the same drawing as the bilge-keel traces, so as to make the surface-wave effect readily apparent.

For ships with a considerable extent of parallel side at the waterline, the surface-wave profile is not outlined well enough on a body plan to permit predicting its effect on a bilge-keel trace. The

wave profile in side elevation should be used for this purpose.

A prediction of flow in way of the bilge keels should cover the light-load or ballast condition as well as that for the designed load, using the appropriate speed-length quotients in each case. Almost certainly the traces will be different, unless the speeds are low, although the differences may be small. A decision is called for in the design stage to determine which load and speed condition is to be favored in positioning the bilge keels on the ship.

52.12 Probable Flow at a Distance From the Ship Surface. At normal or lateral distances from the 3-diml ship form greater than those involved in placing the roll-resisting keels, available data for predicting flow conditions become rather rare. A few sources giving data on tests of ship models, which may or may not cover the distances with which a ship designer is concerned, are mentioned:

(a) Laute, W., "Untersuchungen über Druck- und Strömungsverlauf an einem Schiffsmodell (Investigations of Pressure and Flow on a Ship Model)," STG, 1933, Vol. 34, pp. 402–460; English version in TMB Transl. 53, Mar 1939. See also Figs. 22.D and 22.E in Sec. 22.8 of Volume I.

(b) Lamble, J. H., "An Experimental Examination of the Distribution of Velocity Around a Ship's Model Placed in a Turbulent Stream," INA, 1934, pp. 136–143 and Pls. XV, XVI

(c) Hamilton, W. S., "The Velocity Pattern Around a Ship Model Fixed in Moving Water," Doctorate Diss., IIHR, Dec 1943. Available in TMB library, number VM298.H11.

In the present state of the art, the prediction of flow conditions from available reference data only, for an important part of a ship or an important region near the ship, is uncertain at the best. Reliance upon flow tests with a model is definitely indicated.

52.13 Estimating the Change in Flow Pattern for Light or Ballast Conditions. Predicting the flow pattern—and wave profile—for a ship design when the vessel is assumed to be in a light or ballast condition requires modifications of the rules in Sec. 66.28. In the first place, the forefoot is usually well out of water, so that whether it is cut away or is occupied by a bulb, the section lines are by no means vertical in that region. In the second place, the free surface, disturbed by Velox waves, is much closer to the bottom of the ship than at normal draft. The surface-wave pattern may be expected, therefore, to have a considerable influence on the flow pattern, at least as far down as the flat floor under the ship.

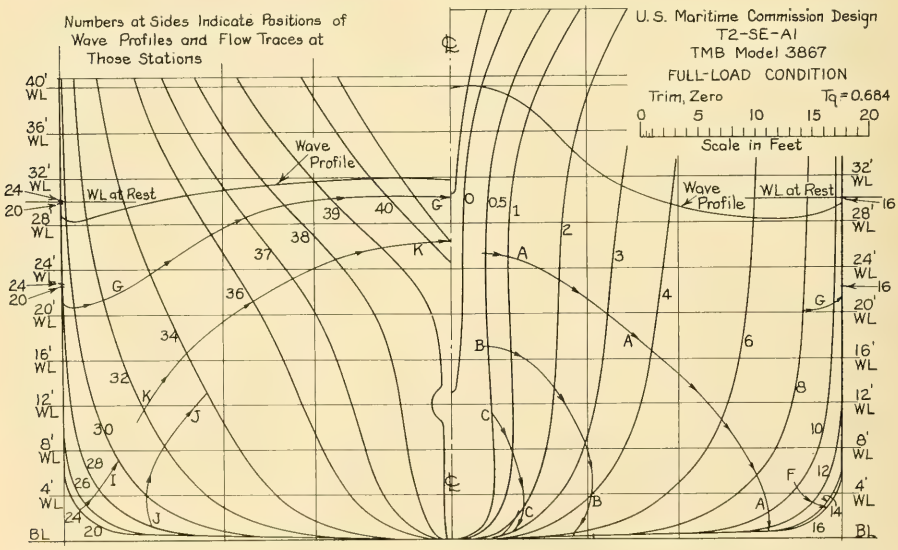

Fig. 52.Xa Lines of Flow in Full-Load Condition for U. S. Maritime Commission Design *T2-SE-A1*

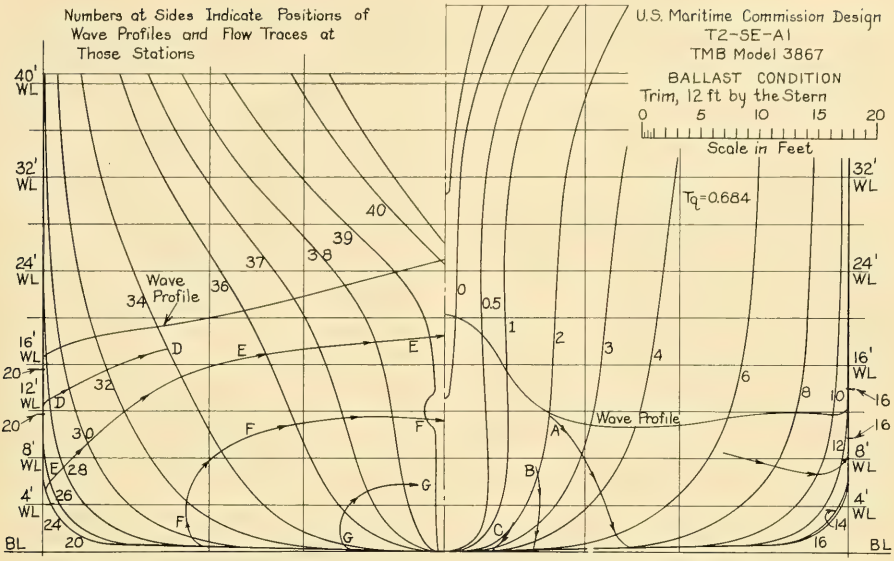

Fig. 52.Xb Lines of Flow in Ballast Condition for U. S. Maritime Commission Design *T2-SE-A1*

With a broad, blunt bulb as a waterline beginning, at light draft, the bow-wave crest may be surprisingly high, although the upper portion of the crest is more apparent than real, in the form of a bow feather.

Whether the sections at the forward end of the entrance are sharply flared outward or are of the bulb type, the flowlines will undoubtedly curve and pass under the ship very close abaft the stem. This means, for one thing, that air entrained in the bow-wave crest may be expected to flow along under the bottom at transverse distances rather close to the centerline.

Figs. 52.Xa and 52.Xb indicate the differences in wave profile and flow pattern found on two model tests of a tanker. In the light condition the displacement is less than half the full-load displacement, and the trim by the stern is very large.

52.14 Predicting Velocity and Pressure Distribution Around Ship Forms. If the magnitudes, direction, and distribution of velocity and pressure are to be calculated by the methods discussed in Chap. 50, this prediction will be for a hull form which has the shape of the physical ship plus the displacement thickness of the boundary layer, as nearly as the latter can be determined. If the velocity and pressure factors are to be predicted on the basis of empirical data, the fund of information presently available must be greatly expanded. It now comprises the references listed in Sec. 52.12 plus the following:

(1) Eggert, E. F., "Form Resistance Experiments," SNAME, 1935, pp. 139–150
(2) Eggert, E. F., "Further Form Resistance Experiments," SNAME, 1939, pp. 303–330
(3) Yokota, S., Yamamoto, T., Shigemitsu, A., and Togino, S.; see Sec. 52.3 for the complete listing
(4) Izubuchi, T., full-scale experiments on the Japanese destroyer *Yudachi*, Zōsen Kiōkai, December 1934, Vol. 55; English translation available in Research and Development Division, Bureau of Ships, U. S. Navy Department
(5) Hiraga, Y., "Experimental Investigations on the Resistance of Long Planks and Ships," Soc. Nav. Arch., Japan, 1934.

Fig. 52.Y is a reproduction of one of the afterbody plans of EMB model 3383 from (2) preceding [SNAME, 1939, Fig. 30 on p. 314]. It carries the isobars for a multitude of Δp values, as indicated in the diagram.

A comprehensive measurement of pressure around the surface of a ship or model is a prodigious undertaking, yet anything less than comprehensive is not worth the effort, from the

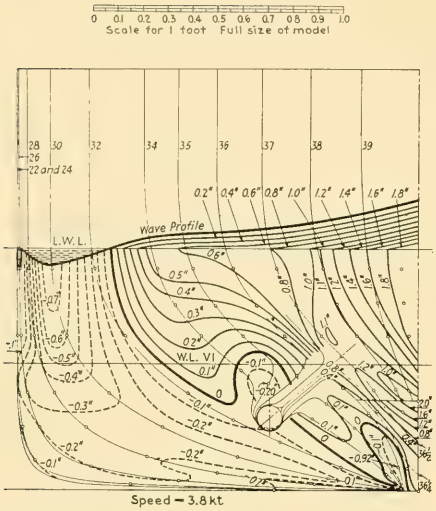

Fig. 52.Y Pressure Distribution on Afterbody of EMB Model 3383 at a Speed of 3.8 kt, $T_q = 0.844$

The numerals on the isobars indicate differential pressures in inches of water of the same mass density as that in which the model was towed

standpoint either of hydrodynamic research or of ship design.

52.15 Use of Flow Diagrams for Positioning Appendages. The comments of Sec. 52.12 apply generally to the proper positioning of appendages such as bossings, shaft struts, small skegs, and rudders, as well as to the outer portions of roll-resisting keels.

Special model-basin techniques are available to determine the proper strut-section angles for shaft struts. Since the variation from straight-ahead positioning of these parts seldom exceeds 7 or 8 deg, and almost never is greater than 10 deg, a prediction without model-test confirmation would have to be extremely precise, relative to present (1955) standards.

When rudders (and diving planes) are of the spade or horn-supported type they are necessarily rather thick to achieve strength and rigidity. Extended observation of flow around model appendages in the circulating-water channel indicates that their presence affects the flow to considerable distances on either side. The ink trail in Fig. 46.E shows this feature clearly. It is not adequate, therefore, when making flow predictions, to suppose that the object for which the flow directions are desired is always of the thin-plate variety. Its position, shape, and bulk, as affecting the flow, all must be taken into account.

52.16 Estimated Flow at Propulsion-Device Positions. Extended discussion of the flow to the propulsion-device positions, amounting almost to duplication (it appears in Sec. 17.2, in Chap. 33, and in Secs. 59.12 and 60.7), is considered justified in view of the importance of this feature and the insufficient attention it has received in many quarters in the past. However, the extensive model-basin instrumentation now available (1955) is still inadequate to give the ship and the propulsion-device designers all the advance information they should have in the design stage.

The hull-surface traces of the flow just ahead of a propeller position, particularly those on a centerline skeg in front of a single screw, are usually good indicators of the type of inflow into the wheel positions close to the centerplane. For example, in Fig. 52.R it appears that the flow just ahead of the single propeller, at least into the 11 o'clock to 1 o'clock and 5 o'clock to 7 o'clock positions, may be expected to have only a slight upward component of velocity. For each offset propeller position of Fig. 52.T, it is expected that the flow outboard of the skeg ahead will have a small upward component but that inboard of the skeg it will have a large one.

Nevertheless, in the absence of any proved general rules for interpreting them, it can not be said that the surface traces are completely reliable indicators in this respect. Before an acceptable procedure for estimating the flow at propdev positions can be formulated, it will be necessary to make, and to analyze, companion off-the-surface flow traces such as those described and illustrated in Sec. 52.9 and 3-diml wake-survey diagrams of the type diagrammed in Sec. 60.6. Until that time the surest and most reliable prediction method is actually to observe the flow in the vicinity of the propulsion device(s) on a model of the vessel in a circulating-water channel. If the propdev characteristics are approximately known, a stock model of the device can be added to the ship model and observations made under thrust-producing conditions. In most cases these tests can be made and this study completed at a sufficiently early stage in the design to permit changing the hull or appendages (or both), to correct or to improve the flow.

A situation somewhat out of the ordinary is

encountered on certain not-too-large vessels where a relatively high power is delivered to a single screw propeller on a vessel having a small displacement-length quotient or fatness ratio $\nabla/(0.10L)^3$ and a large keel drag. Examples are river and bay passenger steamers, tugs, trawlers, and whale catchers. Because of the projection of the propeller below what might be called the main body of the hull it could be expected that the flow would have only a small degree of non-axiality. However, a considerable declivity in the shaft, downward and aft, is sometimes necessary to accommodate the machinery position inside the hull.

It is to be expected that, on single-screw ships, much of the water moving toward the blades of the propeller, in their lower positions, will be unaffected by the presence of the hull, lying mostly at an upper level. The present trend (in the 1950's) of eliminating the rudder shoe and cutting away the aftfoot on vessels of this type, means that the flow to the lower blades is almost entirely free of hull influence. Although uniform and regular, it may be expected to have little or no positive wake velocity unless the vessel "pulls" a large stern-wave crest above it.

52.17 Analysis of the Observed Flow at a Screw-Propeller Position. Although not a part of the estimating or predicting procedure, strictly speaking, it is still necessary to analyze graphic, tabulated, and other records from flow-indicating devices at screw-propeller positions to determine the principal characteristics of the flow. Simply making a flow record does not tell whether the nature of the flow is acceptable or not. In fact, there are at least four reasons for analyzing the observed flow at a screw-propeller position, when determined by suitable instrumentation on a model, *before* the model is fitted with or driven by its model propeller(s). The record in this case is assumed to be a 3-diml wake-survey diagram similar to Figs. 11.F and 60.D:

(1) To determine, by visual inspection, whether there are any longitudinal eddies passing through the disc, whether there are obvious differences in flow direction at two or more points near each other, and whether there are obvious large differences in the longitudinal or transverse components of flow for two or more such points
(2) To estimate the probable magnitude of the wake fraction for a screw propeller occupying a disc region of given size (diameter) and position
(3) To determine a systematic wake-fraction variation with radius if one exists, and to embody it, if desired, in the design of a wake-adapted propeller (or selection of such a propeller from stock)
(4) To ascertain, at an early stage in the design, the liability and the magnitude of objectionable variations in thrust and torque, per blade and per wheel, for all angular positions in one revolution. This latter feature is discussed further in Sec. 59.17.

It is assumed, in the foregoing, that the advance-velocity vectors for the proposed propeller-disc position are 3-diml in nature and are determined by the method described and illustrated in Secs. 11.6 and 11.7 and Figs. 11.E and 11.F of Volume I. This method is, by the instrumentation such as that currently (1955) in use at the David Taylor Model Basin [Janes, C. E., "Instruments and Methods for Measuring the Flow of Water Around Ships and Models," TMB Rep. 487, Mar 1948], somewhat artificial. For example, the additional velocity induced by the action of the propeller when it exerts thrust is not represented, nor is the straightening effect of the propeller jet acting upon the water flowing into the propeller position. However, a wake determination of this kind is most revealing, and many features of the propeller action can be predicted from a careful study of it. Instructions for conducting such a study, and for determining quantitative values from it, are found in Secs. 60.6, 60.7, and 60.8.

52.18 Flow Abaft a Screw Propeller. The water in the outflow jet of a screw propeller producing thrust is known to be contracting at the point where it leaves the propeller disc, illustrated by Fig. 16.E in Sec. 16.6 of Volume I. It is known to be increasing in velocity at that point, and there are rotational or tangential velocity components in it, additional to the axial component of induced velocity. The brief discussion of Sec. 17.17 reveals that the screw-propeller outflow is unusual among submerged liquid jets in that it maintains its identity as a jet for many propeller diameters astern of the disc position.

The first quantitative observations on the nature of the actual flow abaft a screw propeller, in and around an outflow jet, appear to have been made in about 1865 by Arthur Rigg of Chester, England, in connection with his development of the first contra-rudder [Inst. Engrs.

Scot. and Scot. Shipbldrs. Assoc., 1865–1866, Vol. IX, pp. 52–64]. By suspending over the stern of a small screw-propelled vessel a flat swinging vane with an indicator he measured "the angle of the water driven off from the screw" with reference to the centerplane. The vane was raised and lowered to cover a range of positions from $0.285R$ to $0.8R$ below the axis. The data given below are for a propeller radius of approximately $0.8R$. By turning the vane in a direction *normal* to the current at its axis and measuring the moment on the vane Rigg was also able to obtain a rough idea of the actual velocity at each of the measuring stations. For three conditions of operation he recorded the following data:

(1) The vessel propelling itself only, at 144 rpm; 35 deg, 2.1 psi
(2) Towing a large "flat," with cargo, at 160 rpm; 45 deg, 1.0 psi
(3) While moored to a post at 136 rpm; 72.5 deg, 0.4 psi.

Other published data on the distinctive features of the outflow jets of marine propellers have so far not been discovered. Some unpublished data from the tests of two model propellers at the

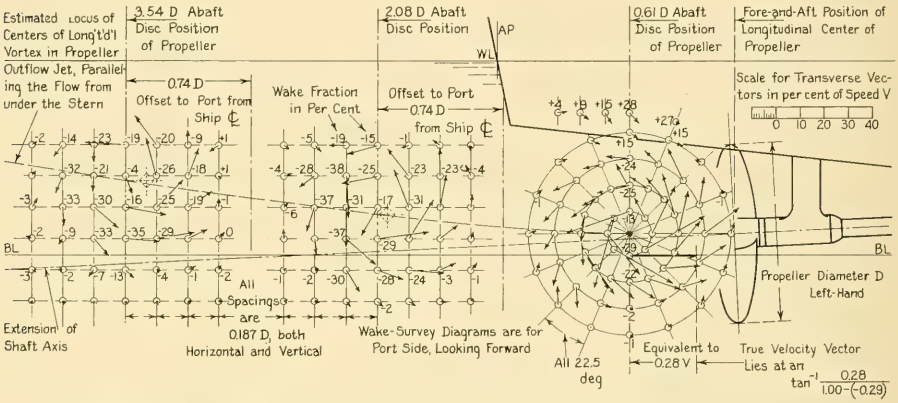

FIG. 52.Za DIAGRAMS INDICATING COMPONENTS OF NET AUGMENTED AXIAL AND ROTATIONAL VELOCITIES IN OUTFLOW JET OF PORT PROPELLER ON TMB MODEL 3613

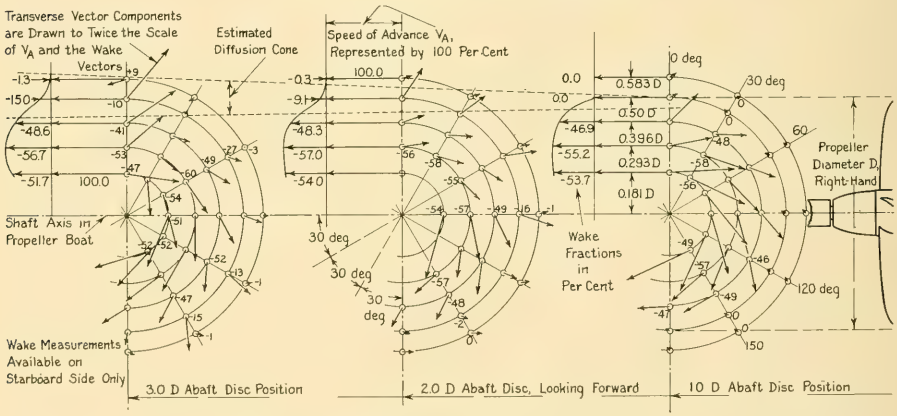

FIG. 52.Zb DIAGRAMS INDICATING AXIAL AND ROTATIONAL COMPONENTS OF VELOCITY IN THE OUTFLOW JET OF EMB PROPELLER 857, RUNNING IN OPEN WATER

David Taylor Model Basin, partially analyzed, are presented in Figs. 52.Za and 52.Zb. Summarizing these tests briefly:

I. A model of a destroyer, TMB 3613, was towed and a 3-diml wake survey was made at the propeller-disc position. It was then self-propelled by its own model propellers, TMB numbers 2170 and 2171. While self-propelled, at a simulated ship speed of 28.6 kt, three additional wake surveys were made, at positions corresponding to 0.607, 2.075, and 3.543 propeller diameters abaft the disc position. The *net* axial and tangential components of velocity (by vectorial subtraction), due to the action of the propeller, as averaged for several radii, are indicated by vectors in the several diagrams of Fig. 52.Za. The thrust-load coefficient C_{TL} for the conditions given was 0.907. Other pertinent data applying to this test are added to the diagram.

II. A model propeller, EMB 857, of 9 inches diameter, was mounted at the end of the long shaft ahead of the propeller boat [Bu C and R Bulletin 7, 1933, Fig. 5 on p. 24] and the assembly run at a speed of advance of 3.26 kt. Wake surveys were made at 1, 2, and 3 propeller diameters abaft the disc position. The available records do not indicate the thrust-load coefficient at which the propeller was working but it was apparently very high. The axial and tangential components of velocity, due to the action of the propeller in producing thrust in open water, as averaged for several radii, are indicated by vectors in the three diagrams of Fig. 52.Zb.

III. A series model, EMB 3424, was towed and a wake survey was made at the propeller-disc position. It was then self-propelled by its own propeller, EMB 1884. While self-propelled, at a model speed of 3.00 kt, four additional wake surveys were made, at positions corresponding to 1, 5, 15, and 24 propeller diameters abaft the disc. These data are available at the David Taylor Model Basin but have not been reproduced here.

Abaft the destroyer model, it is obvious that the longitudinal centerline of the outflow jet does not lie along an extension to the propeller shaft axis but rises rather abruptly. This rise begins at the disc position, increases rapidly, and then coincides more or less with the rise in the water which has flowed under the stern, generally parallel to the buttock lines on the model. This change in vertical position with distance abaft the disc is confirmed by noting the upward curve in the swirl core or hub vortex trailing a screw propeller on a destroyer model in the circulating-water channel.

It is difficult, because of the lack of observations in the upper portions of the propeller outflow jet abaft the stern of the destroyer model, to estimate the limits and shape of the cone of diffusion between the outflow jet and the surrounding water. With a net augmented axial velocity in the outflow jet which is roughly 20 to 25 per cent greater than the ship speed, the cone of diffusion is rather thick. Its inner surface, as well as can be determined, is of such slope that the jet core will persist to a distance of 5 or 6 diameters abaft the disc.

For the model mounted on the propeller boat, the net augmented axial velocity in the outflow jet is about 55 per cent greater than the ship speed. The cone of diffusion is relatively thin, with an inner-surface slope small enough to indicate that the jet will preserve some measure of its identity to a distance of perhaps 15 diameters abaft the disc position.

For EMB model propeller 1884 on EMB model 3424, for which no graphic data are given, there are definite signs of augmented axial velocity and rotational velocity in the outflow jet at 15 propeller diameters astern of the disc. There are traces of the rotational velocity at 24 diameters astern.

52.19 Persistence of Wake Behind a Ship. It is often useful to know the characteristics of the wake left in the path of a body or ship, mentioned in Sec. 11.11, even though the ship propulsion device(s), like those of the sailboat or the flying boat, may be entirely clear of the water. The wake may involve only the mean residual velocity along the ship track, over a section taken across the body or ship path. It may involve effects of another order such as variations from the mean velocity, the scale and intensity of the residual turbulence, the presence of entrained air, or some other characteristics of interest. As a rule, the transverse surface waves of the Velox system are dissipated, by spreading transversely and by internal viscous damping, long before the disturbances *within* the water disappear.

Quantitative data on the persistence of wake, applying to the mean velocity only, are almost nonexistent. Perhaps the most extensive and reliable are derived from model-testing techniques, but the validity of stepping these data up to ship size is still uncertain. It is known that the

wake from a vertical turbulence-stimulating strut having a diameter of say 0.01 the model beam and a submergence equal to the model draft, when towed a short distance ahead of a small model, causes a measurable change in its resistance. It is often necessary to wait from 10 to 20 minutes between runs in the basin, when towing a large, heavy model, to insure that the residual currents left in its wake have diminished to the order of 0.01 kt or less. On the basis of a 20-ft model running at 4 kt, this means that if the model kept on going it would be 200 lengths away from the finishing point of the run in the course of 10 min. For a 500-ft ship traveling at 20 kt in a channel of comparable relative size, this is the equivalent of over 3.3 nautical miles. It is one reason why a ship has to make a long approach run before entering a measured mile [SNAME "Standardization Trials Code," 1949, p. 7; van Lammeren, W. P. A., RPSS, 1948, p. 352] to insure that it does not meet, as a counter-current, its own wake from the preceding run.

Model-basin experience indicates that the presence of the walls and bottom, not too far from the model track, damps out the residual currents due to towing and self-propelling. Since the basin depth is of the order of 20 times the model draft and its width the order of 20 times the beam, the corresponding dimensions for a ship like the ABC design of Part 4 would be 520 ft depth and 1,460 ft width—hardly a restricted channel!

It is reported, from not-too-precise observations, that at 8 to 10 lengths abaft the stern of a high-speed towing vessel of form similar to a destroyer, at a T_a of about 1.4 or 1.5, the effect of the towing-vessel disturbance on a towed vessel of similar type is practically negligible.

52.20 Bibliography on Wake. Considering how little was known or understood about wake conditions abaft a ship a century ago (about 1855), the literature which has accumulated on the subject since that time is little short of tremendous. S. A. Harvald has recently (1950) made a valiant endeavor to systematize the available data, and to arrive at a logical and reliable method of predicting wake conditions from a design, but he has found the answer most elusive, as indicated in Sec. 60.8. It appears certain that the problem will have to be studied analytically, beginning at its fundamentals. Fortunately for the profession at large, this work is now (1955) in progress in the United States.

In view of the inclusion in Harvald's study of a practically complete bibliography on wake, there are mentioned here only a few special papers and others which have appeared since 1950:

(1) Dahlmann, W., Hoppe, H., and Schäfer, O., "Messung der Wassergeschwindigkeiten neben der Schiffswand (Measurement of Water Speeds near a Ship Hull)," WRH, 7 Sep 1926, pp. 415–419

(2) Baker, G. S., "Ship Wake and the Frictional Belt," NECI, 1929–1930, Vol. XLVI, pp. 83–106 and Pls. III, IV; discussion on pp. 141–146. Describes results of tests on planks and ship models, and on the fast channel steamer *Snaefell* and the single-screw merchant ship *Ashworth*.

(3) Baker, G. S., "Wake," NECI, 1934–1935, Vol. LI, pp. 303–320 and D137-D146. Describes results of tests on two models, and full-scale observations on the *Ashworth* and on the *Pacific Trader*.

(4) Igonet, C., "Note on Wake," ATMA, 1938, Vol. 42, pp. 543–569. This paper has apparently not been translated into English.

(5) Schoenherr, K. E., and Aquino, A. Q., "Interaction Between Propeller and Hull," TMB Rep. 470, Mar 1940

(6) Harvald, S. A., "Wake of Merchant Ships," Danish Tech. Press, Copenhagen, 1950; copy in TMB library

(7) Harvald, S. A., "Three-Dimensional Potential Flow and Potential Wake," Trans. Danish Acad. Sci., 1954

(8) Korvin-Kroukovsky, B. V., "On the Numerical Calculation of Wake Fraction and Thrust Deduction in a Propeller and Hull Interaction," Int. Shipbldg. Prog., 1954, Vol. 1, No. 4, pp. 170–178.

CHAPTER 53

Quantitative Data on Dynamic Lift and Planing

53.1 Relationship to Other Chapters. The basic phenomenon of planing is described in Chap. 13, and the behavior of planing craft in general is discussed in Chap. 30. Rules and procedures for the hydrodynamic design of a full-planing type of motorboat are to be found in Chap. 77, with a preliminary design worked out for one boat.

The basic data for predicting the behavior of simple planing surfaces are rather voluminous, when the test results on flying-boat and seaplane-float models are included. Several workers in the field, as related in the sections following, have succeeded rather well in their efforts to assemble, analyze, correlate, and systematize the available planing-surface data, so as to make them directly applicable to and useful for new designs. It is not possible, within the scope of this chapter, to do much more than reference a few of the sources which contain quantitative data in a form to be readily usable to the designer of planing craft.

In addition to the selected bibliography on planing in Sec. 53.8, a partial bibliography on hydrofoil-supported craft is included as Sec. 53.9.

53.2 Principal Quantitative Factors Involved in Planing. The magnitude of the dynamic pressure intensity and the dynamic lift under a planing surface inclined at a small angle of attack α(alpha), or under a V-bottom boat running at a trim θ(theta) by the stern, is a function of a considerable number of factors. Further, the center CP of this pressure system, or the point where the resultant dynamic lift is exerted, and its location with respect to the center of gravity CG, is as important for the proper design of a planing craft as it is for the design of an airplane.

Among these factors may be mentioned:

(1) Length, breadth, and planform shape of the planing surface actually in contact with the water in any given running condition, with respect to an axis parallel or nearly so to the direction of motion. At running attitude and position, the length dimension becomes the mean wetted length L_{WS} and the breadth dimension becomes the mean chine beam B_C .
(2) Wetted area of the planing surface. This is the actual and not the nominal area.
(3) Forward speed V with respect to the water underneath the bottom of the planing craft, neglecting the cosine of the angle of trim
(4) Mass density ρ(rho) and weight density w of the water
(5) Trim angle θ with reference to the horizontal
(6) Rise-of-floor angle β(beta), for a planing surface that is V-shaped in transverse section
(7) Distance of the CP from the after termination, usually a sharp edge of the planing surface, in any given running condition.

Related to these features are the:

(8) Dynamic lift L
(9) Total resistance or drag R_T , in the direction of motion
(10) Friction resistance R_F , exerted parallel to the wetted bottom surface
(11) Residuary resistance R_R , as for any other surface craft
(12) Total weight W(or Δ) of the craft
(13) Buoyancy B, due to partial immersion of the hull at some speeds
(14) Acceleration of gravity g.

There are a number of dimensionless ratios and coefficients utilized in planing-surface and planing-craft design:

(15) Ratio of the chine beam B_C to the mean wetted length L_{WS}, or the aspect ratio

(16) Planing number R_T/W. Its reciprocal may be used if it is an advantage to do so.

(17) Ratio of the distance designated as [CP from trailing edge of planing surface] to the mean chine beam B_C

(18) Speed coefficient C_V or beam-Froude number, where $C_V = V/\sqrt{gB_C}$

(19) Load coefficient, where C_Δ or C_W, symbolized preferably as C_{LD}, $= W/(wB_C^3)$

(20) Dynamic-lift coefficient, $C_{DL} = W/(qB_C^2) = 2(C_{LD})/C_V^2$

(21) Resistance or drag coefficient $C_{\text{Planing } R} = R_T/(wB_C^3)$.

The marine architect, seeing this list for the first time, is amazed at its length and complexity, as compared to that for a surface ship of the displacement type. It is perhaps satisfying, but not always comforting for this architect to realize that his amazement is fully justified. The problem of estimating and predicting planing-craft performance is indeed more intricate and involved than that for a normal type of surface ship.

53.3 Principal Forces and Moments on a Planing Craft. As an aid in presenting, in systematic fashion, the quantitative data relating to prediction of planing-craft performance, Fig. 53.A is drawn to supplement Fig. 13.C in Sec. 13.3 on page 206 of Volume I. The accompanying figure shows the principal forces acting on a craft during planing. The propulsive force and its component, not shown in Fig. 13.C, are indicated here, as are the buoyancy force (assumed finite and not negligible), the relative-wind forces, and the drag of the appendages. The relative-wind drag is in this case assumed equal to the still-air resistance. The thrust-deduction force is assumed as zero, although in practice this is probably never the case. In the diagram of Fig. 53.A there would be a thrust-deduction force exerted on the strut and rudder assembly abaft the propeller and on the exposed shaft ahead of it, if not on the hull proper.

There are forces due to the formation of spray roots and the generation of spray, indicated on the diagrams of Figs. 13.B and 13.D, but their positions and vector directions are not well known.

53.4 Determination of Dynamic Lift. There is no liquid circulation as such about an inclined flat plate skimming along the water surface, or about any planing craft in the manner described for the hydrofoils of Chap. 14 of Volume I. It is found possible, nevertheless, to estimate the dynamic lift of such a plate reasonably well by calculating the lift due to circulation, as if the

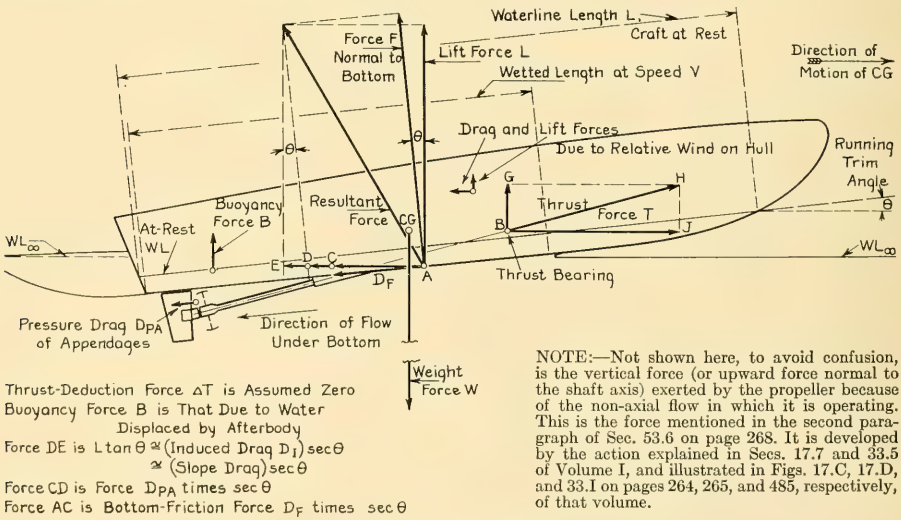

NOTE:—Not shown here, to avoid confusion, is the vertical force (or upward force normal to the shaft axis) exerted by the propeller because of the non-axial flow in which it is operating. This is the force mentioned in the second paragraph of Sec. 53.6 on page 268. It is developed by the action explained in Secs. 17.7 and 33.5 of Volume I, and illustrated in Figs. 17.C, 17.D, and 33.I on pages 264, 265, and 485, respectively, of that volume.

FIG. 53.A DEFINITION DIAGRAM OF FORCES ON A PLANING BOAT

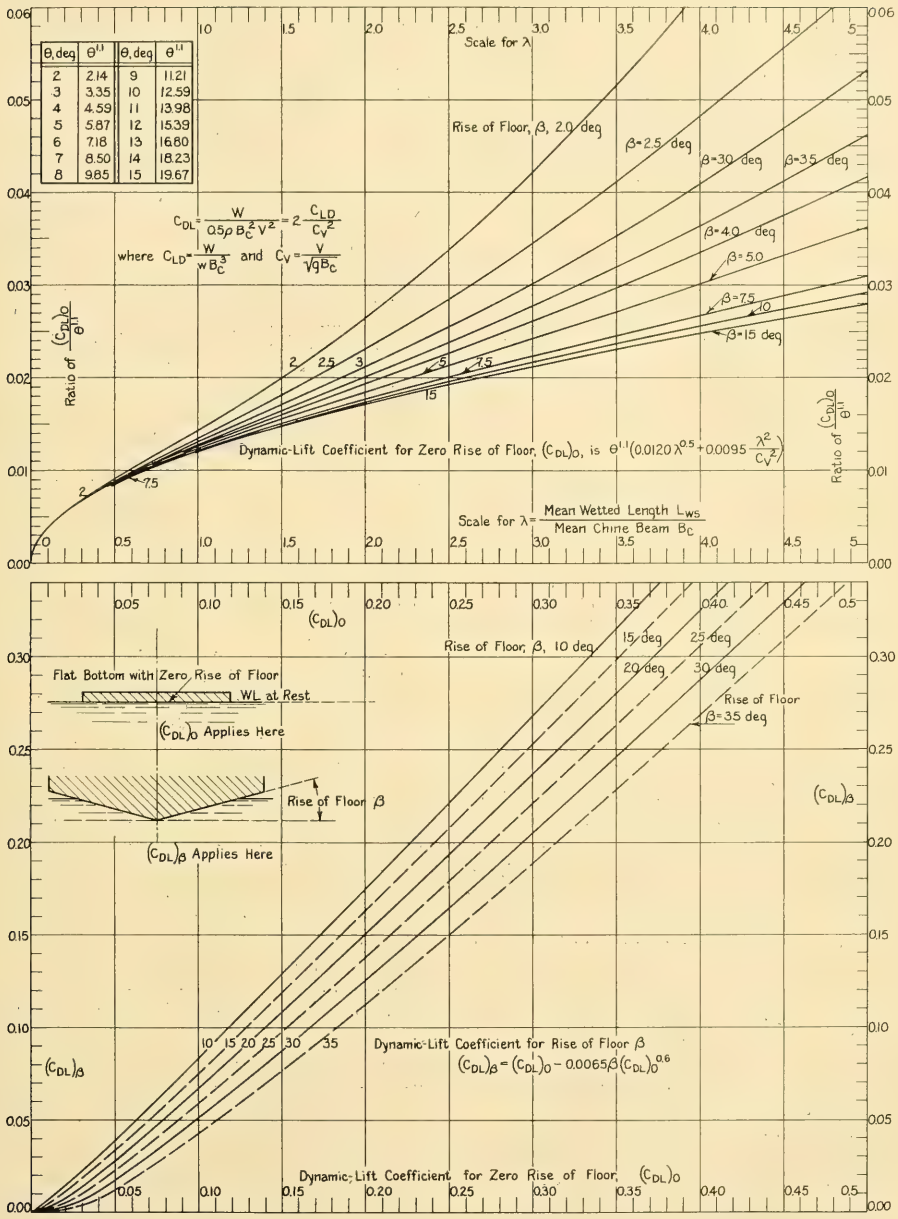

θ, deg	$\theta^{1.1}$	θ, deg	$\theta^{1.1}$
2	2.14	9	11.21
3	3.35	10	12.59
4	4.59	11	13.98
5	5.87	12	15.39
6	7.18	13	16.80
7	8.50	14	18.23
8	9.85	15	19.67

FIG. 53.B GRAPHS FOR RELATING THE DYNAMIC-LIFT COEFFICIENT TO OTHER FEATURES OF A PLANING FORM

plate were completely submerged, and then halving this value.

Without going further into the analytic hydrodynamics of planing, set forth in detail in many of the references listed in Sec. 53.8, it is stated simply that the dynamic lift exerted normal to a flat inclined plate of length L and breadth B, in contact with a liquid surface on its under side only, is expressed by

$$L_D \text{ normal to plate} = \frac{\pi}{8}\rho B^2 V^2 \alpha \qquad (53.\text{i})$$

where α is the angle of attack or trim by the stern and L_D is not, as customary, measured normal to the direction of motion.

The dynamic lift to be expected from a simple planing surface, defined as one with straight buttocks and keel and a constant rise-of-floor angle β, running at a trim angle θ, may be derived more precisely in terms of equations set up by B. V. Korvin-Kroukovsky, D. Savitsky, and W. F. Lehman [ETT Rep. 360, Aug 1949]. These equations, with their representation in graph form, are used by A. B. Murray in his paper "The Hydrodynamics of Planing Hulls" [SNAME, 1950, Fig. 11, p. 666].

The dynamic lift is expressed in terms of 0-diml dynamic-lift coefficients C_{DL} , using $(C_{DL})_0$ for a planing surface with zero rise of floor and $(C_{DL})_\beta$ for one with a rise-of-floor angle β. The equations for these coefficients are, strictly speaking, dimensionless in that all the factors composing them have dimensions of zero. Nevertheless, the fact that the trim angle θ, expressed as τ(tau) in the references, appears to the 1.1 power and the term $(C_{DL})_0$ to the 0.6 power seems to indicate that other terms as yet unknown should eventually be embodied in the equations.

Expressed in standard and ATTC notation these equations are:

(1) $$C_{DL} = \frac{W \text{ (or } \Delta)}{\frac{\rho}{2} B_C^2 V^2} = 2\frac{C_{LD}}{C_V^2} \qquad (53.\text{ii})$$

where B_C is the mean chine beam, C_{LD} is the load coefficient, and C_V is the speed coefficient, previously defined

(2) For a flat, inclined plate, having a rise-of-floor angle β of zero and a trim of θ deg,

$$(C_{DL})_0 = \theta^{1.1}\left(0.0120\lambda^{0.5} + \frac{0.0095\lambda^2}{C_V^2}\right) \qquad (53.\text{iii})$$

where $(C_{DL})_0$ is the lift coefficient for a zero rise of floor and λ(lambda) is the ratio of the mean wetted length L_{WS} to the mean chine beam B_C

(3) For a V-surface having a constant rise-of-floor angle of β deg,

$$(C_{DL})_\beta = (C_{DL})_0 - 0.0065\beta[(C_{DL})_0]^{0.6} \qquad (53.\text{iv})$$

Graphs giving the relationships between these variables, convenient for the use of a planing-craft designer, are drawn in Fig. 53.B, adapted from diagrams previously published in the references listed earlier in this section.

The method of using the equations listed and the accompanying graphs is described by A. B. Murray [SNAME, 1950, pp. 669–670] and is illustrated for a specific design of planing-type motorboat in Sec. 77.26.

53.5 Typical Pressure Distribution and Magnitude on Planing-Craft Bottoms. Diagrams showing typical transverse and longitudinal pressure distributions on the wetted bottoms of planing forms, similar to those reproduced in Figs. 13.B and 13.D on pages 205 and 207 of Volume I, are rather plentiful in the technical literature. They are to be found in many of the references of Chaps. 13 and 30 and of Sec. 53.8 of the present chapter. For example, the graphs of longitudinal $+\Delta p$ distribution published by A. B. Murray [SNAME, 1950, Fig. 19 on p. 675] are taken from data developed by W. Sottorf, in a paper listed as reference (21) of Sec. 53.8.

Assuming a V-bottom craft, the transverse pressure distribution is characterized by peak pressures over the regions of origin of the port and starboard spray roots, along the diagonal stagnation loci depicted in Fig. 13.D. At small immersions of the keel, all the pressure is concentrated near the centerplane. At greater immersions the two pressure concentrations move outward toward the chines.

Reliable specific data on the distribution of pressure and the magnitude of the pressure intensities on the bottoms of planing craft having given characteristics, especially when subjected to heavy impact in waves, are relatively meager. Much of the available information is in a classified status, so that the naval architect is forced to fall back upon the results of theoretical analysis or upon published data concerning measurements on the hulls of seaplanes and flying boats.

For the determination of CP positions in specific cases the equations and graphs set up by B. V. Korvin-Kroukovsky, D. Savitsky, and W. F. Lehman are useful [ETT Rep. 360, Aug

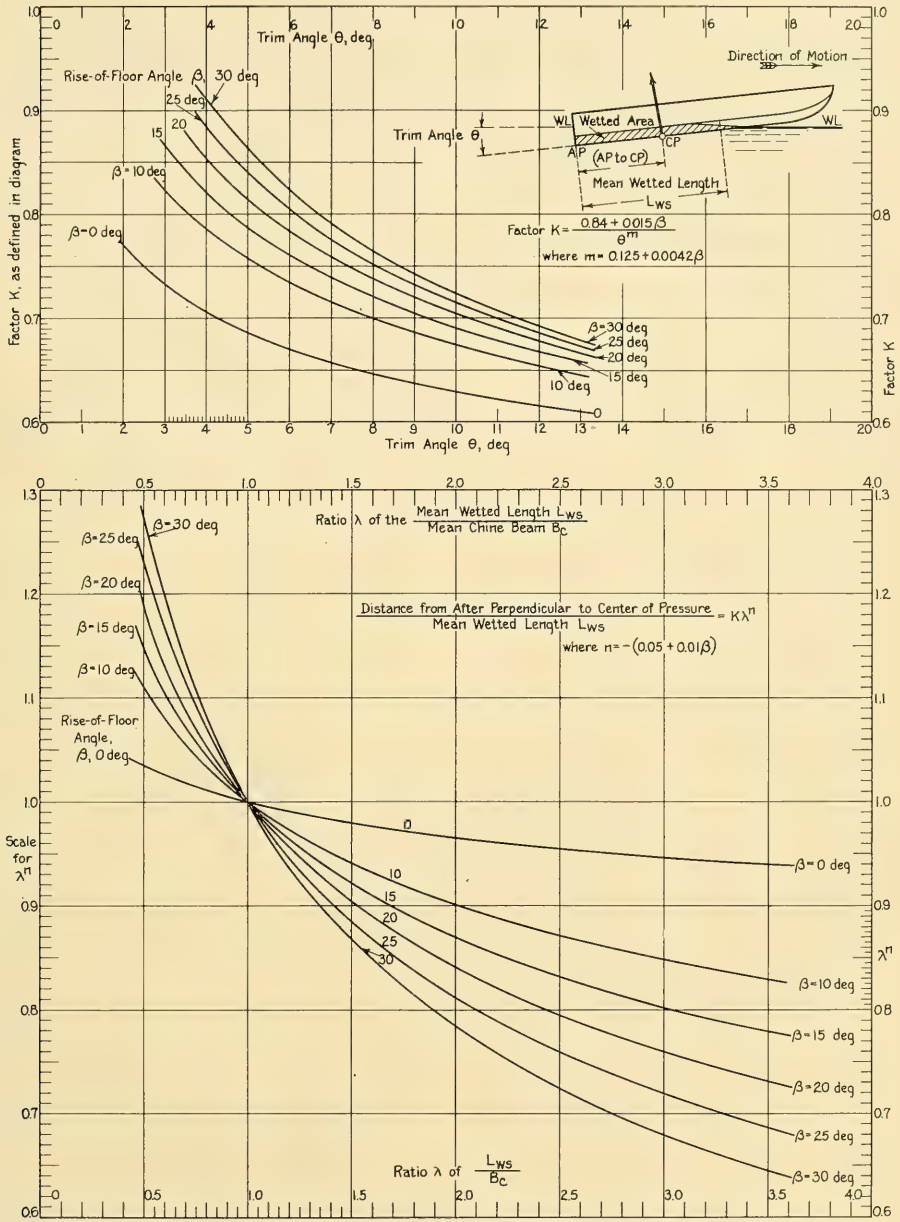

FIG. 53.C GRAPHS FOR DETERMINING THE FORE-AND-AFT CENTER-OF-PRESSURE LOCATION UNDER A PLANING FORM

1949]. Both equations and graphs are reproduced by A. B. Murray [SNAME, 1950, Fig. 10, p. 665]. The distance of the center of pressure CP from the trailing edge of the planing surface, assumed at the after perpendicular AP, is expressed as

$$\text{The } x\text{-distance [CP to AP]} = K(L_{WS})\lambda^n \quad (53.\text{v})$$

where L_{WS} is the mean wetted length, λ is the ratio L_{WS}/B_C, and K is a function of the angle of trim θ and of the rise-of-floor angle β. This relation is

$$K = \frac{0.84 + 0.015\beta}{\theta^m} \quad (53.\text{vi})$$

where β and θ are both expressed in degrees.

The exponents n and m are derived from

$$n = -(0.05 + 0.01\beta) \quad (53.\text{vii})$$

$$m = 0.125 + 0.0042\beta \quad (53.\text{viii})$$

where β is again expressed in degrees.

Graphs giving the relationships between these variables, in convenient form, are drawn in Fig. 53.C, adapted from diagrams previously published in the references quoted.

The method of using the equations listed and the accompanying graphs is described by A. B. Murray [SNAME, 1950, pp. 670–671] and is illustrated for a specific design of full-planing motorboat in Sec. 77.26.

53.6 Wetted Length, Wetted Surface, and Friction Resistance. Diagrams indicating the general position and shape of the wetted area under a planing craft when running at or near its designed speed are found in Chaps. 13 and 30. The changes in wetted surface and wetted length at speed are discussed briefly in Sec. 30.8. Since these features are important factors in predicting performance, the method of estimating or determining them, in a running rather than an at-rest condition, requires further explanation.

The shape and extent of the wetted area of the bottom or dynamic-support surface of a planing craft is rather easily determined by running a model under a given set of conditions. This method is, however, open to the objection that a model which is towed and not self-propelled may not run at the proper trim for the prototype because the vertical forces exerted by the propeller(s) are missing. A change in trim almost always means a change in both wetted length and wetted area, possibly a change in the center-of-pressure position as well.

A. B. Murray illustrates the ETT method of determining wetted chine and keel lengths for a towed model [SNAME, 1950, Figs. 14 and 15, pp. 672–673]. Both wetted length and wetted area may be determined by fish-eye views made photographically, using a painted grid on the under surface of the model and a water box, underwater mirror, or other suitable setup [ETT, Stevens, Rep. 378, Sep 1951, pp. 46–47]. The general shape of the wetted area for a V-bottom craft is the same, illustrated by Figs. 13.D, 30.A, 30.C, 30.F, and 77.P. Small-size photographs and diagrams, in the form of fish-eye views published by A. G. Smith, show the general shapes of the wetted area and of the spray roots under V-bottom planing forms with a 25-deg rise of floor and a 6-deg trim by the stern [5th ICSTS, 1949, pp. 70–73 and Figs. 1–5].

C. W. Spooner, in his unpublished report "Speed and Power of Motorboats up to a Speed-Length Ratio of 3," dated October 1950, gives a table listing the principal characteristics and wetted-surface area of a considerable number of motorboat designs. In his Fig. 13 he includes tentative graphs for estimating the wetted surface of craft of this type, based on a coefficient $S/(LB)$, which increases slowly with fatness ratio $\nabla/(0.10L)^3$. For a motorboat with a single centerline skeg the coefficient is:

0.950 at a fatness ratio of 4.0
0.984 at a fatness ratio of 6.0
1.01 at a fatness ratio of 8.0,

where L and B are presumably in ft, and S is in ft^2. For a bare hull the corresponding coefficient values are 0.860, 0.889, and 0.911, respectively.

J. P. Latimer gives the layouts, lines, principal characteristics, and wetted surface for a USCG 40-ft utility boat ["Characteristics of Coast Guard Powered Boats," SNAME, Ches. Sect., 13 Oct 1951].

Contour charts for determining wetted areas of the EMB Series 50 models, applicable as first approximations of the wetted areas of other V-bottom planing craft having speed-length T_q values of from 2.0 to 6.0, are described and published on pages 6 and 85–94 of TMB Report R-47, revised edition, March 1949.

Further data may be found in a paper by B. V. Korvin-Kroukovsky, D. Savitsky, and W. F. Lehman, entitled "Wetted Area and Center of Pressure of Planing Surfaces" [ETT, Stevens, Rep. 360, Aug 1949].

The method of computing the friction resistance is essentially the same as for any other type of surface craft, described in Sec. 45.22. The mean wetted length L_{WS} is used as the length dimension to determine the Reynolds number R_n for the craft in any specified running condition. Throughout the whole speed range the wetted length, Reynolds number, and wetted area all change with speed but at and near the designed speed they are practically constant.

Sec. 77.26 embodies an example in which the wetted area and the friction resistance of a full-planing type of motorboat are calculated, following the methods described by A. B. Murray in a reference cited earlier in this section.

If there is wetting of the sides as well as the bottom at full speed it can be taken care of as an augment of the wetted area. Normally, however, consistent wetting of the sides of a full-planing craft is evidence of poor design somewhere. Rather than to calculate the effect, the cause should be eliminated.

A few words are in order here relative to roughness of the bottom surface. Although the mean wetted length of modern (1955) planing craft is usually low, well under 100 ft or say 30 meters, the rubbing speed of the water is high. By the reasoning of Sec. 45.10, this means a very thin laminar sublayer under the boat and a large increase in drag if the bottom surface is rough. The permissible roughness height is small, even though the overall R_n may likewise be small.

53.7 Variation of Total and Residuary Resistances with Speed. It is most interesting to note, from the diagrams in Figs. 20 and 21 on pages 676 and 677, respectively, of A. B. Murray's paper [SNAME, 1950], that the total-resistance-to-weight ratios of many planing craft, when plotted on a base of speed-length quotient T_q, lie remarkably close to a meanline for a rather wide range of speed. The corresponding values for both V-bottom and round-bottom motorboats and sailing craft given by H. M. Barkla exhibit the same characteristic [INA, 1951, Vol. 93, p. 237], as do the data for many types of large vessels plotted in Fig. 56.M of Sec. 56.10. However, the ordinates of Fig. 56.M have values that are 2,240 times the ordinate values of the Murray and Barkla graphs.

Murray's planing-craft data cover ranges of displacement-length quotient $\Delta/(0.010L)^3$ of from 100 to 180, yet it is only above a T_q of about 3.5 to 4.0 that much dispersion is found. These data are, as stated by Murray, most useful for preliminary resistance estimates, when the shape and proportions of a new design of hull have not yet been determined.

Considering only residuary resistances R_R, the few available data indicate a greater degree of irregularity than that described in the foregoing. Fig. 53.D illustrates variations in the

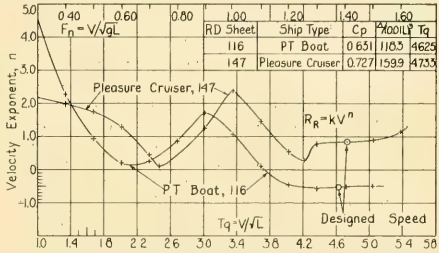

FIG. 53.D VARIATION OF SPEED EXPONENT FOR THE DERIVED RESIDUARY RESISTANCES OF TWO PLANING CRAFT

To keep the presentation simple the T_q values for the two planing vessels were calculated on the basis of the waterline length at rest

exponent n of the expression $R_R = kV^n$, for two typical planing craft, over a considerable range of speed-length quotient. However, despite the large variation in $\Delta/(0.010L)^3$, the two graphs resemble each other closely. Of great interest here are the low values of n for the designed-speed points, actually negative for the PT boat.

53.8 Selected Bibliography on Planing Surfaces, Dynamic Lift, and Planing Craft. There is given here a rather full but by no means complete list of references for the reader who wishes to delve further into the matters presented in this chapter on planing phenomena. Included in the list are pertinent references on seaplanes and flying boats. For references on planing-craft design the reader is referred to the partial bibliography on motorboats in Sec. 77.41.

(1) Greer, J. F., "First Flight of an American Aeroplane from the Water," Scientific American, 11 Feb 1911, p. 132. Gives a drawing and some illustrations of the tandem planing-float scheme once used by Glenn H. Curtiss.

(2) Fauber, W. H., U. S. Patent 1,024,682 of 30 Apr 1912 for boats or ships with planing steps

(3) Baker, G. S., and Millar, G. H., "Some Experiments in Connection with the Design of Floats for Hydro-Aeroplanes," Adv. Comm. Aero. (England), 1912–1913, R and M 70, pp. 239–245

(4) Steele, J. E., "The Longitudinal Stability of Skimmers and Hydro-Aeroplanes," INA, 1913, Part 1, pp. 136–147 and Pl. XIII

(5) Richardson, H. C., "Hydromechanic Experiments with Flying Boat Hulls," US Navy-Smithsonian Misc. Collections, 20 Apr 1914, Vol. 62

(6) Millar, G. H., "Some Notes on the Design of Floats for Hydro-Aeroplanes," INA, 1914, pp. 313–328

(7) Richardson, H. C., "Aeronautics in Relation to Naval Architecture," SNAME, 1916, pp. 43–51

(8) Crowley, J. W., and Ronan, K. M., "Characteristics of the Boat Type Seaplane during Take-Off," NACA Rep. 226; 1925 reports, pp. 393–401

(9) Richardson, H. C., "Naval Development of Floats for Aircraft," SNAME, 1926, pp. 15–28

(10) Diehl, W. S., "Tests on Aeronautical Fuselages and Hulls," NACA Rep. 236, 1926 reports, pp. 131–150. This paper gives drag and moment data on a great variety of airplane fuselages, seaplane and flying-boat hulls, airship cabins, nacelles, and the like.

(11) Richardson, H. C., "The Trend of Flying Boat Development," ASNE, May 1926, Vol. XXXVIII, pp. 231–253. Contains a great deal of information which still remains of value (1955) in studying and predicting the behavior of planing craft.

(12) Richardson, H. C., "Design of a Large Flying Boat," SNAME, 1928, pp. 77–88

(13) In Vol. 32 of the Bulletin d'Association Maritime Technique et Aéronautique (ATMA), Paris, 1928, on pp. 319–324, there appears a long list of references on planing forms. The titles are in both French and the original language and the references extend back to the year 1914.

(14) Sottorf, W., "Versuche mit Gleitflächen (Tests with Gliding Surfaces)," Part I, WRH, 7 Nov 1929, pp. 425–432; English transl. in NACA Tech. Memo 661, Mar 1932

(15) Schröder, P., "Über die Bestimmung von Widerstand und Trimmoment bei gleitenden Wasserfahrzeugen (Determination of Resistance and Trimming Moment of Planing Water Craft)," Zeit. für Flugtechnik und Motorluftschiffahrt, 28 Nov 1930, Vol. 21, No. 22; English transl. in NACA Tech. Memo 619, May 1931

(16) Pavlenko, G., "On the Theory of Gliding; The Motion of a Plank at a Small Angle of Inclination to the Water Surface," Proc. Third Int. Congr. Appl. Mech., Stockholm, 1930, Vol. I, pp. 179–183. For a Froude number F_n of 4 and above, Pavlenko gives the resistance formula $R = \rho V^4 \tan^2 \alpha/(4g)$, where ρ is the mass density of the water and α is the trim angle or nominal angle of attack.

(17) Wagner, H., "Über den Aufschlag gekielter Flächen auf Wasser (Concerning the Impact of V-Bottom Planing Surfaces on the Water)," Proc. Third Int. Conf. Appl. Mech., Stockholm, 1930, Vol. I, pp. 215–219

(18) Wagner, H., "Über die Landung von Seeflugzeugen (Landing of Seaplanes)," Zeit. für Flugtechnik und Motorluftschiffahrt, 14 Jan 1931, Vol. 22, pp. 1–8. English transl. in NACA Tech. Memo 622, May 1931.

(19) Wagner, H., "Über Stoss- und Gleitvorgänge an der Oberfläche von Flüssigkeiten (Concerning Impact and Gliding Phenomena near or at the Surface of Liquids)," Zeit. für Ang. Math. Mech., Aug 1932, Vol. 12, pp. 193–215. A number of additional references are given in the footnotes. There is an informal translation of this paper in the TMB library.

(20) Diehl, W. S., "The Establishment of Maximum Load Capacity of Seaplanes and Flying Boats," NACA Rep. 453, Sep 1932; 1933 reports, pp. 211–213

(21) Sottorf, W., "Versuche mit Gleitflächen (Experiments with Planing Surfaces)," Part II, WRH, 1 Oct 1932, pp. 286–290; 15 Feb 1933, pp. 43–47; 1 Mar 1933, pp. 61–66. English transl. in NACA Tech. Memo 739, Mar 1934.

(22) Perring, W. G. A., "Porpoising of High Speed Motor Boats," INA, 1933, Vol. 75, pp. 268–296

(23) Wagner, H., "Über das Gleiten von Wasserfahrzeugen (On the Planing of Watercraft)," STG, 1933, Vol. 34, pp. 205–227; English transl. in NACA Tech. Memo 1139, Apr 1948

(24) Wagner, H., "Über das Gleiten von Körpen auf der Wasseroberfläche (Concerning the Gliding of Bodies on the Water Surface)," Proc. Fourth Int. Cong. Appl. Mech., Cambridge (England), 1934, pp. 126–147. On pp. 146–147 there are listed 27 references.

(25) Shoemaker, J. M., "Tank Tests of Flat and V-Bottom Planing Surfaces," NACA Tech. Note 509, Nov 1934

(26) Perring, W. G. A., and Johnston, L., "The Hydrodynamic Forces and Moments on Simple Planing Surfaces and An Analysis of the Hydrodynamic Forces and Moments on a Flying Boat Hull," ARC, 1934–1935, Vol. II, R and M 1646, pp. 553–575

(27) Eshbach, O. W., "Handbook of Engineering Fundamentals," 1st ed., 1936, pp. 6–50, 6–51

(28) Allison, J. M., and Ward, K. E., "Tank Tests of Models of Flying-Boat Hulls Having Longitudinal Steps," NACA Tech. Note 574, May 1936

(29) Sottorf, W., "Gestaltung von Schwimmwerken (The Design of (Planing) Floats)," Luftfahrtforschung, 20 Apr 1937, Vol. 14, pp. 157–167; English transl. in NACA Tech. Memo 860, Apr 1938

(30) Weinig, F., "Zur Theorie des Unterwassertragflugels und der Gleitfläche (On the Theory of Hydrofoils and Planing Surfaces)," Luftfahrtforschung, 20 Jun 1937, pp. 314–324; English transl. in NACA Tech. Memo 845, Jan 1938. On pp. 26–27 there are 11 references listed.

(31) Sottorf, W., "Analyse Experimenteller Untersuchungen über Gleitvorgang an der Wasseroberfläche (Analysis of Experimental Investigation of the Planing Process on the Surface of Water)," Jahrbuch der Deutschen Luftfahrtforschung, 1937, pp. 320–339; English transl. in NACA Tech. Memo 1061, Mar 1944

(32) Diehl, W. S., "A Discussion of Certain Problems Connected with the Design of Hulls of Flying Boats and the Use of General Test Data," NACA Rep. 625, Nov 1937; 1938 reports, pp. 253–260. Page 260 lists 24 references.

(33) Bollay, W., "A Contribution to the Theory of Planing Surfaces," Proc. Fifth Int. Congr. Appl. Mech., 1938, pp. 474–477; published by Wiley, New York, 1939

(34) Sambraus, A., "Planing-Surface Tests at Large Froude Numbers—Airfoil Comparisons," NACA Tech. Memo 848, Feb 1938. Originally published in Luftfahrtforschung, 20 Jun 1936, Vol. 13, pp. 190–198.

(35) Sottorf, W., "Versuche mit Gleitflächen, Part IV, (Tests with Planing Surfaces, Part IV)," WRH, 1 Mar 1938, Vol. 19, pp. 51–56; 15 Mar 1938, pp. 65–70

(36) Coombes, L. P., "Scale Effect in Tank Tests of Seaplane Models," Proc. Fifth Int. Cong. Appl. Mech., 1939, pp. 513–519

(37) Truscott, S., "The Enlarged NACA Tank, and Some of its Work," NACA Tech. Memo 918, 1939

(38) Diehl, W. S., "The Application of Basic Data on Planing Surfaces to the Design of Flying-Boat Hulls," NACA Rep. 694, 16 Dec 1939; 1940 reports, pp. 287–293.

(39) Sedov, L. I., "Planing on a Water Surface," RTP Transl. 2506, Brit. Min. Aircraft Prod. (from Tech. Vosdushnogo Flota, No. 4–5, 1940). Also Durand Reprinting Committee, Calif. Inst. Tech., Pasadena 4, Calif.

(40) Adamson, G., and Van Patten, D., "Motor Torpedo Boats: A Technical Study," USNI, Jul 1940, Vol. 66, pp. 976–996

(41) Schubert, R., and Thieme, H., "Klärende Darstellung der Hydrodynamischen Erscheinungen beim Start von Seefluzeugen (Explanatory Representation of the Hydrodynamic Phenomena Occurring at the Takeoff of Seaplanes)," Bericht S110, Hamburg, 5 Jul 1946

(42) Sedov, L. I., "Scale Effect and Optimum Relations for Sea Surface Planing," NACA Tech. Memo 1097, Feb 1947

(43) Locke, F. W. S., Jr., "Tests of a Flat Bottom Planing Surface to Determine the Inception of Planing," NAVAER DR Rep. 1096, Bur. Aero., Navy Dept., Dec 1948

(44) Locke, F. W. S., Jr., "An Empirical Study of Low Aspect Ratio Lifting Surfaces with Particular Regard to Planing Craft," Jour. Aero. Sci., Mar. 1949, pp. 184–188. On page 188 of this paper there is a list of 9 references.

(45) Korvin-Kroukovsky, B. V., Savitsky, D., and Lehman, W. F., "Wetted Area and Center of Pressure of Planing Surfaces," Sherman M. Fairchild Fund Paper 244, Inst. Aero. Sci., originally published as ETT, Stevens, Rep. 360, Aug 1949. There is a list of 23 references on pp. 19–20.

(46) Bisplinghoff, R. L., and Doherty, C. S., "A Two-Dimensional Study of the Impact of Wedges on a Water Surface," Cont. NOa(s)-9921, Dept. Aero. Eng'g., MIT, 20 Mar 1950

(47) Murray, A. B., "The Hydrodynamics of Planing Hulls," SNAME, 1950, pp. 658–692. On p. 680 there is a list of 19 references.

(48) Savitsky, D., "Wetted Length and Center of Pressure of Vee-Step Planing Surfaces," ETT, Stevens, Rep. 378, Sep 1951, published by the Inst. Aero. Sci. as S. M. F. Fund Paper FF-6 of the same date. It lists 24 references on pp. 25–27.

(49) Clement, E. P., "The Analysis of Stepless Planing Hulls," SNAME, Ches. Sect., Apr 1951; abstracted in SNAME Member's Bull., Oct 1951, p. 15

(50) Kapryan, W. J., and Weinstein, I., "The Planing Characteristics of a Surface Having a Basic Angle of Dead Rise of 20 Deg and Horizontal Chine Flare," NACA Tech. Note 2804, Oct 1952

(51) Blanchard, U. J., "The Planing Characteristics of a Surface Having a Basic Angle of Dead Rise of 40 Deg and Horizontal Chine Flare," NACA Tech. Note 2842, Dec 1952

(52) Perry, B., "The Effect of Aspect Ratio on the Lift of Flat Planing Surfaces," Hydrodynamics Lab., CIT, Rep. E-24.5, Sep 1952. There is a list of 16 references on pp. 17–18.

(53) Knowler, H., "The Future of the Flying Boat," Fifth Louis Blériot Lecture, Assn. Française Ing. et Techn. de l'Aéronautique, Paris, 12 Mar 1952; abstracted in ASNE, Aug 1952, pp. 630–638; also in Engineering (London), 14 and 21 Mar 1952

(54) Chambliss, D. B., and Boyd, G. M., Jr., "The Planing Characteristics of Two V-Shaped Prismatic Surfaces Having Angles of Dead Rise of 20 Deg and 40 Deg," NACA Tech. Note 2876, Jan 1953

(55) Weinstein, I., and Kapryan, W. J., "The High-Speed Planing Characteristics of a Rectangular Flat Plate over a Wide Range of Trim and Wetted Length," NACA Tech. Note 2981, Jul 1953. Fig. 9(b) on p. 24, also pp. 5–6 of the text, show that there is a *depression* in the liquid surface just ahead of the pile-up, under the plate, at low trim angles. It is possible that this could be air drawn under the inclined surface, just as oil is drawn into a wedge-shaped gap in a plain bearing.

(56) Springston, G. B., Jr., and Sayre, C. L., Jr., "The Planing Characteristics of a V-Shaped Prismatic Surface with 50 Degrees Dead Rise," TMB Rep. 920, Feb 1955

(57) Clement, E. P., "Hull Form of Stepless Planing Boats," SNAME, Ches. Sect., 12 Jan 1955

(58) Kapryan, W. J., and Boyd, G. M., Jr., "Hydrodynamic Pressure Distribution Obtained During a Planing Investigation of Five Related Prismatic Surfaces," NACA Tech. Note 3477, Sep 1955

(59) Pournaras, U. A., and Sherman, P., "Model Test Results and Predicted EHP for a Round Bilge 40-Ft Aircraft Rescue Boat Design from Tests of (TMB) Model 4525," TMB Rep. 1002, Oct 1955.

53.9 Partial Bibliography on Hydrofoil-Supported Craft. A good, concise list of references on the development, characteristics, and performance of high-speed craft supported by hydrofoils is given by T. M. Buermann, P. Leehey, and J. J. Stilwell [SNAME, 1953, p. 264]. It is embodied in the following partial bibliography which contains additional references of less scientific but more general interest:

(1) Nutting, W. W., "The *HD-4*, a 70-Miler with Remarkable Possibilities," reprinted Smithsonian Report for 1919, Publn. 2595, Gov't. Print. Off., Washington, 1921

(2) Richardson, H. C., "The Trend of Flying Boat Development," ASNE, May 1926, Vol. XXXVIII, pp. 231–253. Historical data on "hydrovanes," now known as hydrofoils, are found on pp. 245–246.

(3) Guidoni, A., "Seaplanes, Fifteen Years of Naval Aviation," Jour. Roy. Aero. Soc., Jan 1928, Vol. 32, No. 205

(4) Keldysch, M. V., and Lavrent'ev, M. A., "On the Motion of an Aerofoil under the Surface of a Heavy Fluid, i.e., a Liquid," paper to ZAHI, Moscow, 1935; English Transl. by Science Transl. Serv., Cambridge, Mass., STS-75, Nov 1949

(5) Tietjens, O., "Das Tragflächenboot (The Hydrofoil Boat)," WRH, 1 Apr 1937, pp. 87–90; 10 Apr 1937, pp. 106–109. English transl. in TMB library.

(6) Weinig, F., "Zur Theorie des Unterwassertragflugels und der Gleitflache (On the Theory of Hydrofoils and Planing Surfaces)," Luftfahrtforschung, 20 Jun 1937, pp. 314–324. English transl. in NACA Tech. Memo 845, Jan 1938. On pp. 26–27 there are 11 references listed.

(7) Grunberg, V., "La Sustentation hydrodynamique par ailettes immergées: Essais d'un systéme sustenteur autostable (Hydrodynamic Support by Immersed Foils: Tests of a Self-Stabilizing Support System)," L'Aérotechnique, Jun 1937, 16th Yr., No. 174

(8) Coombes, L. P., and Davies, E. T. J., "Note on the Possibility of Fitting Hydrofoils to a Flying Boat Hull," Roy. Aircraft Estab., Farnborough, Rep. B. A. 1440, Nov 1937

(9) Kotchin, N. E., "On the Wave-Making Resistance and Lift of Bodies Submerged in Water," Trans. of the Conf. on the Theory of Wave Resist., USSR, Moscow, 1937; English transl. by A. I. (T) Air Ministry, R.T.P. 666, Mar 1938; SNAME T and R Bull. 1–8, Aug 1951

(10) Vladimirov, A., "Approximate Hydrodynamic Calculation of a Hydrofoil of Finite Span," ZAHI Rep. 311, Moscow, 1937; English transl., Br. Adm. Document, PG/53280/NID, May 1946

(11) "High Speed Craft: Some Comments on a Patent Specification Recently Filed from Dumbarton," SBSR, 2 May 1940, pp. 440–441. This article shows a proposed design of high-speed motorboat supported by a planing step or a hydrofoil forward and by a second hydrofoil aft, in which there is embodied a screw-propeller drive with a vertical shaft and bevel gears at both top and bottom. The steering rudders extend well down from the hull of the craft. This article mentions a type of boat evolved by J. Plum of the TMB staff.

(12) Adamson, G., and Van Patten, D., "Motor Torpedo Boats: A Technical Study," USNI, Jul 1940, pp. 976–996, esp. pp. 988–989, describing the Bell-Baldwin *HD-4*

(13) Sottorf, W., "Experimentale Untersuchungen zür Fräge des Wasserträgflügels (Experimental Examination of the Question of Hydrofoils)," Rep. 1319, Ger. Res. Est. for Aircraft, Inst. for Seaplane Develop., Hamburg, Dec 1940

(14) Benson, J. M., and Land, N. S., "An Investigation of Hydrofoils in the NACA Tank; I. Effect of Dihedral and Depth of Submersion," NACA Wartime Rep. L-758, Sep 1942

(15) Land, N. S., "Characteristics of an NACA 66, S-209 Section Hydrofoil at Several Depths," NACA Wartime Rep. L-757

(16) Ward, L. E., and Land, N. S., "Preliminary Tests in the NACA Tank to Investigate the Fundamental Characteristics of Hydrofoils," NACA Wartime Rep. L-766

(17) Durand, W. F., "Aerodynamic Theory," Vol. 2, Durand Reprinting Comm., 1943

(18) Abbott, I. H., von Doenhoff, A. E., and Stivers, L. S., Jr., "Summary of Airfoil Data," NACA Rep. 824, 1945

(19) Hook, C., "The Hydrofoil Boat for Ocean Travel," Trans. Liverpool Eng'g. Soc., Vol. LXIX, 1947–1948. In Fig. 3 on page 9 of this paper there are shown diagrammatic arrangements of a number of hydrofoil boats, captioned "Italian and German Types," said to have been taken from a patent by H. F. Schertel von Burtenbach, 1938.

(20) Rabl, S. S., "Pursuit of More Speed," Chesapeake Skipper, Apr 1950, pp. 12, 31, 32

(21) Hoerner, S. F., "Aerodynamic Drag," 1951

(22) Oetling, J. J., "The Possibilities of Hydrofoils," SNAME, North. Calif. Sect., 11 May 1951. Abstracted in SNAME Member's Bull., Oct 1951, p. 19.

(23) Kaemmerer, "Trag- und Dämpfungsflächenboote (Hydrofoil Motorboats)," Schiff u. Hafen, Apr 1952, pp. 121–122. This article gives a very brief resumé of the development work carried out on hydrofoil motor boats in Germany during World War II. The boats did not proceed beyond the experimental stage. A boat with an all-up weight of 100 t, powered by two 1,600-horse engines, attained a speed of 41 kt, while a second boat with a weight of 60 t was expected to reach 60 kt; the latter was, however, damaged before trials were run.

(24) Knowler, H., "The Future of the Flying Boat," ASNE, Aug 1952, p. 630

(25) Büller, K. J., "The Hydrofoil Boat," Hansa, 16 Aug 1952, p. 1090ff

(26) "Hydrofoil Boat *White Hawk*," The Motor Boat and Yachting, London, Sep 1952, p. 361

(27) "Modern Hydrofoil Boat Designed by H. F. Schertel," The Motor Boat and Yachting, London, Oct 1952, p. 414

(28) Sachsenberg, G., "On the Economy of the Traffic with Hydrofoil Speed Boats," Hansa, 1952, No. 30/31

(29) Schertel, H. F., "Tragflächenboote (Hydrofoil Supported Boats)," Handbuch der Werften, Band II, Schiffahrts-Verlag, Hansa, Hamburg, 1952, pp. 43–47. English translation available at the DTMB. For a photograph and description of a more modern 45-ft hydrofoil boat designed by Schertel (von Burtenbach) see The Motor Boat and Yachting, London, Oct 1952, p. 414.

(30) Büller, K. J., "Das Tragflügelboote (The Hydrofoil Boat)," STG, 1952, pp. 119–136

(31) Vertens, F., "German Contributions to the Develop-

ment of the Hydrofoil Speed Boat," Schiff u. Hafen, Mar 1953, p. 103

(32) Grupp, G. W., "Speedboats with Wings," Motor Boating, New York, Aug 1953, pp. 22–23

(33) "Water Wings Add Zip to Navy Craft," All Hands Mag., Bu. Nav. Pers., Oct 1953, pp. 14–16

(34) Buermann, T. M., Leehey, P., and Stilwell, J. J., "An Appraisal of Hydrofoil-Supported Craft," SNAME, 1953, pp. 242–279. This paper is abstracted briefly in the 14 Jan 1954 issue of SBSR, pp. 53–54.

(35) Coffee, C. W., Jr., and McKann, R. E., "Hydrodynamic Drag of 12- and 21-per cent Thick Surface-Piercing Struts," NACA Tech. Note 3092, Dec 1953. Covers tests at zero yaw angle, various depths, and various angles of rake. Two struts had NACA 661-012 sections and one an NACA 664-021 section.

(36) Warren, C. H. E., "A Theoretical Approach to the Design of Hydrofoils," Aero. Res. Counc., London, R and M 2836, Sep 1946, published 1953

(37) "Boats that Fly Atop the Water," Life, 27 Sep 1954, pp. 56–58, 60

(38) Imlay, F. H., "The Theoretical Dynamic Longitudinal Stability of a Constant-Lift Hydrofoil System," TMB Rep. 925, Dec 1954

(39) Miller, R. T., "Hydrofoil Craft," Yachting, Mar 1955, pp. 58–60, 127

(40) Büller, K., "New and Larger Hydrofoil Boats," European Shipbuilding, 1955, Vol. 4, pp. 5–8; abstracted in IME, Jul 1955, Vol. LXVII, pp. 102–103, with diagram of the *PT 20/54*, a Schertel-Sachsenberg craft, in its flying position. Brake-power to displacement ratios of the *Bremen* and *Messina* types, whose characteristics are given, are 59 and 55 horses per ton, respectively.

(41) "World's Fastest (Hydrofoil) Sailing Boat, *Monitor*," Ill. London News, 8 Oct 1955, p. 627; Yachting, Nov 1955, p. 71; SBSR, 17 Nov 1955, p. 637.

CHAPTER 54

Estimating the Air and Wind Resistance of Ships

54.1 Scope of This Chapter; Definitions. The general phenomena and the effects of the flow of air over the abovewater hull and the upper works of a ship are described in Secs. 26.15 and 26.16 of Volume I in purely qualitative fashion. The winds of nature, powerful enough to propel sailing vessels, produce sizable quantitative effects on mechanically driven ships, often of the order of tenths of the power and whole knots or more of speed. Reasonably accurate estimates or predictions of these effects are required, especially when analyzing ship-trial data [Eggert, E. F., EMB Rep. 264, Aug 1930; SNAME, 1932, pp. 17–44; 1933, pp. 243–295; Taylor, D. W., S and P, 1943, pp. 167–169].

Definitions applying to these phenomena and effects are given in Sec. 26.15, supplemented by Figs. 26.G and 26.H. It is most important to keep clear the distinction made there between the *wind drag* D_W, which always acts *downwind* from the relative wind direction, and the *wind resistance* R_{Wind}. The latter is the sum of the fore-and-aft components of both the wind drag and the wind lift, acting always along the principal ship axis, opposite to the direction of motion. This distinction is necessary because the wind forces are impressed on the ship separately from the hydrodynamic forces.

54.2 Increase of Wind Velocity with Height Above Water Surface. The boundary layer formed by the wind blowing over moderately long stretches of water is thick in proportion to the vertical dimensions of a ship hull, or even of its masts. The thickness δ(delta) may attain values greater than a thousand feet [Matveyev, R. T., Meteorologiya i Gidrologiya, No. 3, 1949, pp. 20–29; ASCIL Transl. 490]. Large wind velocities at high airplane altitudes are caused by movements of huge air masses and are not strictly a boundary-layer effect.

For the ordinary boundary layer in air or water the so-called reference velocity, represented by U_∞, is that at a great distance from the body or ship. Since this velocity is rarely known for the thick and high boundary layer in the atmosphere above a large water surface, it is customary to use as a reference, for ship-design and ship-operation purposes, some velocity that is easily measured. In the past, the reference velocity has often been considered to be that observed at a height of 50 ft above the water. However, there is no accepted standard height for measuring the wind velocity which is assumed to be acting on a boat or a ship as a whole. Nevertheless the wind velocities of interest to marine architects and ship operators are usually expressed as *multiples*, greater than 1.0, of whatever velocity near the surface is taken as the reference or the standard.

Theoretically, the air velocity over smooth water is zero at the water surface, as for a liquid flowing over a solid surface. Practically, even for model sail boats and sailing yachts having mast heights of 1 ft or less, the actual air velocities at measurable distances above the water surface are large. Taking all things into consideration, a reference height of 6 ft above the water surface is

considered logical and is used as the reference in this book.

The ship designer, naval architect, and ship operator then need a curve or table of multiples, to compare the wind velocity at other heights with that at 6 ft. The necessary data can be and have been derived from (1) theoretical considerations and from (2) observed simultaneous wind velocities at several heights above a reasonably level water surface.

Making use of boundary-layer theory it is possible to develop a simple formula which shows that the ratio of the wind velocities at two different heights above a solid, level surface should vary as the fifth root of the ratio of the heights [Experiment Tank Comm., Japan, "Abstract Notes and Data," 6th ICSTS, 1951, pp. 71–92]. Taking h_1 and h_2 as these heights, and W_1 and W_2 as the wind velocities at these heights,

$$\frac{W_2}{W_1} = \frac{\text{Wind velocity at height } h_2}{\text{Wind velocity at height } h_1} = \sqrt[5]{\frac{h_2}{h_1}} \qquad (54.i)$$

A discussion by D. Brunt, also based upon boundary-layer theory but making use of experimental observations to some extent, is given in his book "Physical and Dynamical Meteorology" [Cambridge (England), University Press, 1944, pp. 247–255]. Brunt is inclined to use a seventh-root velocity variation rather than a fifth-root variation, based upon the distribution in the 1/7-power velocity profile illustrated in the right-hand diagram of Fig. 5.K. It is apparent, from the discussion presented by Brunt, that the rate of wind variation with height is complex, depending upon a number of variables which could be evaluated only with difficulty in actual practice.

It is not a simple matter to find reliable experimental data known to have been taken over the water. Furthermore, the exact vertical location of the "Surface" observations used for reference are rarely stated. Presumably they are at least as high as a man sitting in a small boat. The low heights of interest to the ship designer, say several hundred feet, are in the category of micro-heights in the field of meteorology.

The only careful, systematic investigations made over the sea appear to be those of J. S. Hay, published in Porton Technical Paper 428 (unclassified) of 24 June 1954, issued by the Chemical Defense Experimental Establishment of the Ministry of Supply of Great Britain (copy in TMB library). Unfortunately, however, the observations covered a range of only 0.5 to 8 meters (1.64 ft to 26.248 ft) above the sea. Hay found that the local velocity U at any height h above the quiet water surface (represented by the symbol z in the paper) varied generally in accordance with the logarithmic formula

$$\frac{U}{U_{1.0}} = a \log_{10} h + b \qquad (54.ii)$$

where $U_{1.0}$ is the velocity at the reference height of 1 meter (3.28 ft), and a and b are numerical values tabulated by Hay for different wind and sea conditions.

The roughness of the sea surface, increasing with the wind velocity at the reference height, changes the type of viscous flow somewhat and with it the numbers a and b. Hay lists 8 references on page 16 of the report.

Because of the diminished relative roughness of the average water surface as compared to the average land surface, the speed of the wind for a given atmospheric disturbance is greater over water than over land. Likewise, the reduction in wind speed as the height is diminished, due to the increased wind friction over the land, is greater than over the water [Curry, M., "Yacht Racing," Scribner's, New York, 1948, p. 130]. For this reason, velocity observations made over land should not necessarily be taken as applying over water. However, even though it is known that they do not apply, it has been necessary to make some use of data taken over the land.

Based on available sources, listed in the next paragraph, the graphs of Fig. 54.A have been prepared. Briefly:

I. The solid-line graph A is based upon a combination of data from references (c) and (e) of the list which follows

II. The short-dash graph B at the left represents values derived from Eq. (54.1), based upon a wind velocity of 1 (unity) at 6 ft above the water level. It appears to represent the probable rate of variation over a reasonably smooth water surface as well, if not better, than most of the experimental data.

III. The long-dash graph C at the right of the figure represents the mean of the data from (b) of the following list, indicated by the small open circles.

The references consulted were:

(a) Schoeneich, "Der Windwiderstand bei Seeschiffen (The Wind Resistance of Oceangoing Ships)," Schiffbau, 22 Nov 1911, Vol. XIII, pp. 121–129.

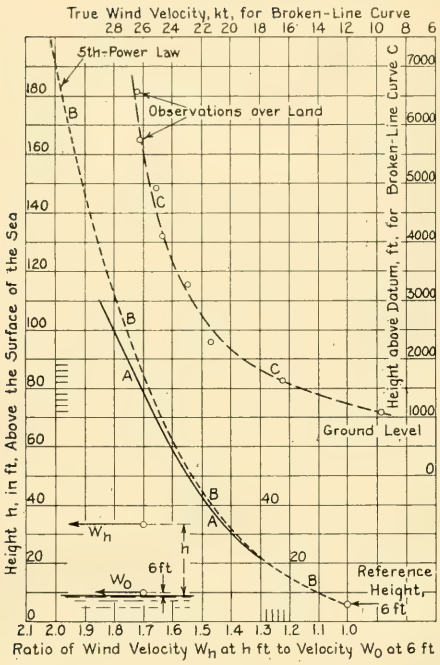

FIG. 54.A GRAPHS INDICATING VARIATION OF WIND VELOCITY WITH HEIGHT

Fig. 2 of this reference is a set of graphs of wind velocity with height, carried up to 43 meters per sec velocity and 60 meters height. The paper contains a set of rather complete wind-resistance calculations for the Atlantic liners *Mauretania* (old) and *Kaiserin Auguste Viktoria.*

(b) White, Margaret, "On the Velocity and Direction of the Wind Above Ground Level," Brit. Assn. Rep., 1912, pp. 420–422

(c) U. S. Chemical Warfare Service data, Edgewood Arsenal, Md., 1934, applying to variation of wind velocity with height over "open, unobstructed ground"

(d) Fox, Uffa, "Sail and Power," New York, 1937, p. 196

(e) Hanovich, I. G., Soloviev, U. I., and Churmack, D. A., "Korabelnie Dvizhitelni (Marine Propulsion Devices)," Moscow, 1949, BuShips Transl. 408, Mar 1951, p. 332

(f) Yachting, Jul 1950, p. 34, giving data taken at sea by a German oceanographic expedition, 1936

(g) "Trial Results of *Hakubasan Maru,*" Experiment Tank Committee, Japan, 1951, embodied in "Abstract Notes and Data," 6th ICSTS, pp. 71–92

(h) Köppen, Ringbuch der Luftfahrt, IDI; reprinted by Henschke, W., in "Schiffbautechnisches Handbuch (Shipbuilding and Ship Design Handbook)," Berlin, 1952, Fig. 17, p. 120. The mean curve given here, derived from experimental data, lies very close to the short-dash line B curve of Fig. 54.A, representing the fifth-power law.

Wind velocities W measured by an anemometer placed well above the hull might—and probably do—exceed those causing the actual wind resistance on a ship. Certainly an anemometer at deck level on a sailing yacht, whether a mechanical instrument or the nerves of the human face, is not a good indication of the wind velocity aloft. With wind effects varying as W^2, more must be known concerning the variation in wind velocities in the 0 to 200-ft range if wind drag and wind resistance are to be predicted with any degree of accuracy.

Probably because of the increase in boundary-layer thickness δ and in displacement thickness δ^*(delta star) with distance downwind, the direction of the wind at heights of interest to boats, yachts, and ships, is not truly horizontal. The wind-velocity vectors are inclined about 4 deg upward in the downwind direction [Curry, M., "Yacht Racing," Scribner's, New York, 1948, p. 131].

54.3 Flow Diagrams for Upper-Works Configurations. It is regrettable that there are available only a very few reasonably complete diagrams for the flow of air around the hull and upper works of a ship. There are fewer still of these diagrams for relative-wind directions other than directly ahead.

A series of five diagrams of this type, rather comprehensive but for ahead relative wind only, are published by H. N. Prins, in an article describing the hull features of the Dutch passenger liner *Oranje* [De Ingenieur, The Hague, Holland, 23 Jun 1939]. One of the diagrams, Plate II, is redrawn and reproduced as Fig. 68.L in Sec. 68.14.

There are a rather large number of smoke- and gas-flow photographs and diagrams to be found in the references listed in Sec. 68.15.

It is possible, in fact probable, that data exist for other upper-works configurations that would enable additional diagrams similar to Fig. 68.L to be drawn. Up to the time of writing (1955) these data have not been found.

54.4 General Formulas for the Wind Drag of Irregular Ship Hulls and Superstructures. Most of the older wind-drag data, published prior to the 1930's, apply to a *dimensional* relationship of the form

$$R_{\text{Wind}} = kA_A W_R^2 \qquad (54.\text{iii})$$

where R_{Wind} is the wind resistance, exerted in the direction of ship motion, A_A is the abovewater silhouette area of the ship (defined in Sec. 26.15), as viewed from astern, and W_R is the relative wind velocity, derived from the vectorial addition of the ship speed V and the true-wind velocity W_T. For what was supposed to be the worst case, the true wind was in those years assumed to be always from ahead.

The necessity for using data derived from aeronautical studies, many of them in wind tunnels, as well as data formerly expressed in other units of measurement, called definitely for non-dimensional wind-drag and wind-resistance formulas. On the basis that substantially all the drag of a ship hull and its upper works is a pressure effect, due to deflection and separation drags, the general equations for the wind drag D_W, with the latter always measured *in the same direction as the relative wind-velocity vector* W_R, are

$$D_W = C_{D(\text{Air})} \frac{\rho}{2} A_{\text{Proj}} W_R^2 \qquad (54.\text{iv})$$

$$= C_{D(\text{Air})} \frac{\rho}{2} A_A W_R^2$$

and

$$C_{D(\text{Air})} = \frac{D_W}{\frac{\rho}{2} A_A W_R^2} \qquad (54.\text{v})$$

Here the mass density ρ(rho) is, from Sec. X3.8 in Appendix 3, taken as 0.002378 slugs per ft^3, for "standard" air conditions at a temperature of 59 deg F, 15 deg C, and a sea-level pressure of 14.696 lb per in^2 or 2,116.2 lb per ft^2.

The area A_{Proj} or A_A is that of the abovewater silhouette of the hull or structure in question, when projected on a vertical plane normal to the direction of the *relative wind*. The velocity of that wind is W_R. For rough calculations it is assumed constant over the whole vertical span of the abovewater structure being blown upon.

For more refined estimates the structure should probably be considered as composed of two or more vertical layers, each with its own relative-wind velocity, dependent upon its average height above the water surface, employing the wind-velocity multiples of Fig. 54.A. In addition, each layer should be composed of a typical kind of structure, such as (1) hull, (2) upper works, and (3) spars and rigging, so that if appropriate a separate drag coefficient as well as a separate average relative-wind velocity W_R may be used

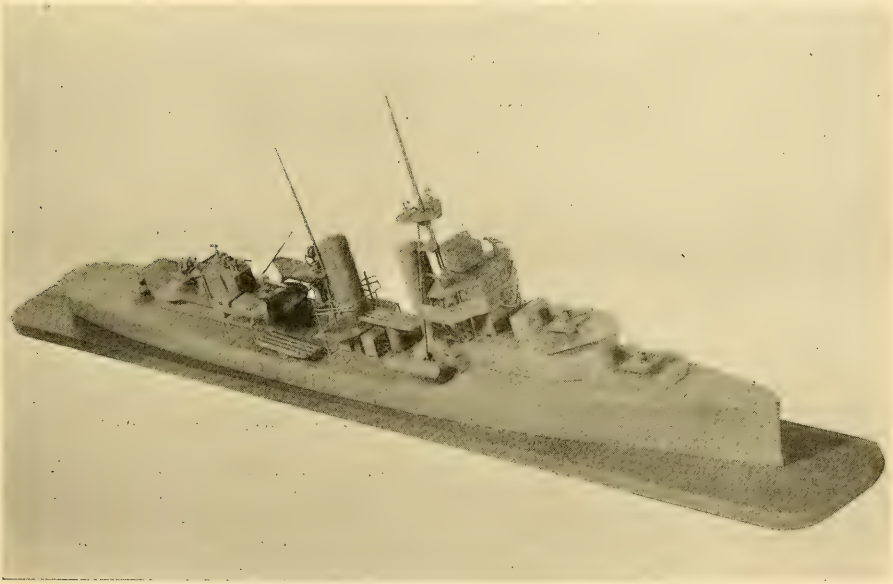

Fig. 54.B Typical Wind-Resistance Model

with each. G. S. Baker illustrates and uses this method in his book "Ship Efficiency and Economy" [1942, pp. 14–16], but for a slightly different purpose.

In still air, the relative-wind velocity W_R is that caused by the motion of the ship itself through the water, so that $W_R = V$. The *still-air resistance* is then

$$R_{SA} = C_{D(\mathrm{Air})}\frac{\rho}{2}A_A V^2 \qquad (54.\mathrm{vi})$$

As for the magnitude of this resistance, E. F. Eggert estimates it as from 2 to 4 per cent of the water resistance [TMB Rep. 264, Aug 1930, p. 1]. The first example of Sec. 54.10 indicates that for the ABC ship designed in Part 4 it is estimated as about 2.6 per cent of the bare-hull water resistance. Although it is not general practice to allow for still-air resistance in ship-powering estimates, this resistance is always with the ship, so to speak, unless the latter happens to run in a following natural wind having a velocity equal to its own speed.

For a relative wind compounded of ship motion and an ahead wind of gale force, the wind resistance can form a large percentage of the water resistance. For the second example of Sec. 54.10, assuming an ABC ship speed of 18.5 kt and a strong breeze of only 23 kt (true velocity), the wind resistance is 10.8 per cent of the bare-hull hydrodynamic resistance at that speed.

54.5 Notes on Wind-Resistance Models and Testing Techniques. The values of wind-drag coefficient $C_{D(\mathrm{Air})}$ now available for the estimation of the wind resistance of the hull and upper works of a ship of any size and type are derived almost exclusively from tests of special wind-resistance models, similar to that pictured in Fig. 54.B. These have been run in water and in air, sometimes in both. Despite the limitations in scope of the book imposed in Sec. I.5 of the Introduction to Volume I, a few notes are given here concerning the rather unusual techniques employed with these models.

When making tests with abovewater models to determine wind-drag coefficients, the models are:

(1) Mounted on the under side of a flat board or platform representing the water surface, and then towed inverted in a model basin. The under surface of the board is held at the water surface, with the model upside down in the water. The board, with the model, may be oriented in azimuth to represent relative wind impinging on the model at any bearing from right ahead to right astern.
(2) Made double, symmetrical about the designed waterline, embodying two abovewater hulls which are then towed submerged
(3) Mounted on the under surface of a flat platform and suspended, in inverted position, in a circulating-water channel.

When the test is conducted by procedure (3) it is possible to look up from underneath and watch the position and action of tufts attached to the abovewater hull and the upperworks. This is also possible in a wind tunnel but streamers of dye and ink injected into the slow-moving water of the channel show the flow to much better advantage than jets of gas or smoke injected into the fast-moving air of the wind tunnel.

There is little to represent boundary-layer development over the full-scale water surface under these conditions, causing a natural variation of velocity with vertical distance, because the mounting board is only several times as large as the planform area of the model. For the model test, therefore, the water (or wind) velocity is nearly constant over all parts of the model, from the lower part of the abovewater hull to the mast trucks.

Fig. 54.B illustrates what is known as a drawing-room model of a destroyer but it shows well the amount of detail which is customarily reproduced on wind-resistance models. The mounting board shown there is greatly enlarged for a wind-resistance test in water.

The experimental techniques developed to date do not simulate fully the actual ship conditions. This is not surprising because the full-scale conditions are not yet adequately known. However, the wind drags are usually not-too-large fractions of the total resistance to motion, and the available data appear to serve well for estimating purposes in the preliminary-design stage and for analysis and reduction of full-scale trial data.

54.6 Bibliography of Model Wind-Resistance Tests. There is given hereunder a partial list of published data relating to model wind-resistance tests. Other data undoubtedly exist but they have not yet been collected. In addition, the list contains references embodying shipboard observations on air drag and wind resistance and other references describing the use of these data in analyzing ship trials. The list follows:

(1) Peabody, C. H., "Experiments on the *Froude*," SNAME, 1911, Vol. 19, pp. 114–115
(2) Schoeneich, "Der Windwiderstand bei Seeschiffen (The Wind Resistance of Oceangoing Ships)," Schiffbau, 22 Nov 1911, pp. 121–129
(3) McEntee, W., "Notes from the Model Basin," SNAME, 1916, Vol. 24, p. 86, and Pls. 70, 71
(4) Smith, W. W., "Effect of Wind and Fouling Resistances on the U. S. S. *Neptune*," SNAME, 1917, Vol. 25, pp. 41–69
(5) Biles, H. J. R., "Notes on the Effect of Wind on Power and Speed," INA, 1927, Vol. LXIX, pp. 164–173
(6) Kempf, G., and Sottorf, W., "Probefahrtsmessungen (Ship-Trial Measurements)," WRH, 22 Jun 1928, pp. 232–236
(7) Hughes, G., "Model Experiments on the Wind Resistance of Ships," Engineering, 8 Aug 1930, p. 184
(8) Hughes, G., "Model Experiments on Wind Resistance of Ships," INA, 1930, Vol. LXXII, pp. 310–329 and Pls. XXXIII-XXXVI. This paper gives the results of wind-tunnel tests on abovewater models of the tanker *San Leandro*, the cargo vessel *Pacific Trader*, and the liner *Mauretania* (old).
(9) "The Effect of Wind on Ship Trials," EMB Rep. 264, Aug 1930
(10) "Test of Drawing Room Model of 10,000-Ton Light Cruisers (*Pensacola* and *Salt Lake City*, CL24, 25) in Water to Determine Forces Due to Wind," EMB Rep. 276, Dec 1930
(11) "Test of Drawing Room Model of U. S. Destroyer *Hamilton* in Water to Determine Forces due to Wind," TMB Rep. 312, Oct 1931
(12) Schoenherr, K. E., "On the Analysis of Ship Trial Data," SNAME, 1931, Vol. 39, pp. 281–301
(13) Pitre, A. S., "Trial Analysis Methods," SNAME, 1932, Vol. 40, pp. 17–44
(14) Baker, G. S., "Ship Design, Resistance, and Screw Propulsion," 1933, Vol. I, pp. 213–221
(15) Hughes, G., "The Effect of Wind on Ship Performance," INA, 1933, Vol. 75, pp. 97–121 and Pls. VIII-X
(16) "Test of Model of U. S. S. *Salinas* Inverted in Water to Determine Forces Due to Wind," TMB Rep. 345, Jan 1933
(17) Stevens, E. A., "Wind Resistance," ASNE, Feb. 1936, pp. 19–31; abstracted in SBSR, 2 Apr 1936, pp. 408–409
(18) Eshbach, O. W., "Handbook of Engineering Fundamentals," 1st ed., 1936, pp. 9–64 through 9–69, covering wind pressure on structures
(19) Malglaive, P. de, and Hardy, A. C., "The Transatlantic Liner of the Future," IME, 14 Dec 1937; abstracted in SBSR, 30 Dec 1937, pp. 811–818, esp. pp. 813, 817. The authors estimate that maximum streamlining on the *Lusitania* would have reduced the wind resistance only by the ratio of 0.17 to 0.12. Further, they estimate the still-air resistance as only 0.02 of the total hydrodynamic resistance; in a 30-kt head wind as only 0.08 of the total.
(20) Nolan, R. W., "Design of Stacks to Minimize Smoke Nuisance," SNAME, 1946, Vol. 54, pp. 42–82
(21) Van Lammeren, W. P. A., Troost, L., and Koning, J. G., RPSS, 1948, pp. 24–26, 69
(22) Kent, J. L., "The Design of Seakindly Ships," NECI, 1949–1950, Vol. 66, Part 8, pp. 417–442 and D159-D174
(23) Aertssen, G., "Sea Trials on a 9,500-ton Deadweight Motor Cargo Liner," joint INA-IME (Institute of Marine Engineers) mtg., 5 Apr 1955; abstracted in SBMEB, Jul 1955, p. 434. The author found that the adverse effects of wind and weather depended upon the power-displacement ratio; in other words, upon how hard the craft was being driven.
(24) A. J. W. Lap, in a published lecture on ship resistance, quotes extensively from Report 1 of the Japanese Shipbuilding Research Assn., 1954, in a discussion of the air resistances of ships and their superstructures [Int. Shipbldg. Prog., Sep 1955, Vol. 3, No. 25, pp. 509–513]
(25) Richter, E., "Strömmgsgünstige Formen von Schiffsaufbauten (Flow Around the Most Favorable Form of Ship Superstructures)," Schiff und Hafen, Jun 1955, pp. 351–356.

In addition to the tests on the wind-resistance models of the ships listed in the foregoing references and on Figs. 54.C, 54.D, and 54.E of Sec. 54.9, it is reported that tests have been made on models of several large tankers and of several floating drydocks. Up to the date of writing (1955) it has not been possible to locate and to present these data.

54.7 Drag Coefficients for Typical Abovewater Hulls and Upper Works. Modifying Eq. (54.iii) of Sec. 54.4 by applying it to the wind drag rather than the wind resistance, and adhering to the dimensional form,

$$D_W = kA_A W_R^2 \qquad (54.\text{vii})$$

When D_W is in lb, A_A is in ft^2, and W_R in kt, the value of k varies from 0.003 to 0.0056, for a relative-wind velocity from directly ahead. A round value for k, easily remembered, is 0.004.

R. Ellis quotes a dimensional coefficient k of 0.0055 for determining the wind drag of a moored, cruising-type sailing yacht, based upon wind velocities in hurricanes. He reckons the cross-sectional area A_A as the product of the maximum beam and the height of the cabin top above water [Yachting, Jun 1955, p. 60]. However, Ellis uses a wind velocity in mph; replacing this with a wind velocity in kt, the dimensional coefficient k should be increased by the factor $(1.15)^2$, or 1.3225. The coefficient k then becomes (0.0055)(1.3225) or 0.00727.

When D_W of Eq. (54.vii) is in kg, A_A is in m^2, and W_R in meters per sec, k is of the order of

0.045 to 0.063 for ship superstructures only [van Lammeren, W. P. A., Troost, L., and Koning, J. G., RPSS, 1948, p. 69].

On the basis of the foregoing, tests with above-water models towed upside down in basins give a 0-diml drag coefficient $C_{D(\mathrm{Air})}$ of the order of 0.85 to 1.2 or more. This agrees well with values for short, blunt-ended, 3-diml bodies [S and P, 1943, pp. 52, 159–160; RPSS, 1948, pp. 25, 69].

When the deck erections and upper works are not yet laid out, or are known only sketchily, it is possible to approximate the projected area of the abovewater silhouette, as seen from directly ahead, by E. F. Eggert's formula, $A_A = (0.5)B_X^2$. This assumes an average maximum effective height, above the water, of half the beam B_X. For the ABC ship of Part 4, with its tentative beam of 73 ft, the projected area by this rule works out as $(0.5)(73)^2 = 2{,}665$ ft^2. For a passenger-cargo ship it is probably on the small side.

The method of using the projected or silhouette area as the basis for the wind-resistance estimate, especially with the relative wind directly ahead, is open to some objection because it takes no account of the fore-and-aft position of the parts of this silhouette with respect to each other. A large deckhouse right forward, close to the bow and in the lee of the updrafts from the blunt bow, as on large Great Lakes freighters, probably causes less wind resistance than the same deckhouse farther aft. Further, on a large tanker, the forward house may be so far from the forecastle, and the after house so far from the forward house, that the shielding offered by each on the one astern is negligible, even with a relative wind from right ahead. Vessels with large fore-and-aft gaps or separations between major transverse areas therefore call for the use of coefficients in the high portions of the ranges listed previously in this section.

Table 54.a presents a number of dimensional wind-drag coefficients, taken from the material referenced there. In every case, so far as known, the coefficients given apply to wind forces generated by a *relative* wind of incident velocity W_R, blowing from directly ahead, where the relative-wind bearing angle θ(theta) is 0 deg.

When the mass density of the air is taken into account, and consistent units of measurement are used, the dimensional formula and the coefficients listed in Table 54.a give a range of values for $C_{D(\mathrm{Air})}$ in the 0-diml formula

$$D_W = C_{D(\mathrm{Air})} \frac{\rho}{2} A_A W_R^2 \qquad (54.\mathrm{iv})$$

which vary from 0.974 to 1.505. These are to be compared with the C_D's for flat plates of various aspect ratios, placed normal to the stream, which are listed in Fig. 55.B. When the coefficient $k = 0.004$ of the dimensional wind-drag Eq. (54.vii), employing units as listed at the beginning of this section, is converted for use in the 0-diml Eq. (54.iv), the value of $C_{D(\mathrm{Air})}$ works out as about 1.18.

54.8 Comments Concerning Wind-Friction Resistance of an Abovewater Hull. In Sec. 54.4 it is assumed that, because of the irregular shape of the abovewater portion of a ship, its wind drag is all pressure drag, varying as W_R^2. This is probably true for the general case, where the relative wind may blow from any bearing relative to the ship.

With the relative wind nearly ahead, a ship hull proper, excluding the upper works, resembles somewhat a train of streamlined cars behind a streamlined locomotive. In both cases the sur-

TABLE 54.a—APPROXIMATE WIND-DRAG COEFFICIENTS FOR VARIOUS TYPES OF SHIPS

Group I. Dimensional Values of k.

The values of k pertain to the formula $R_{\mathrm{Wind}} = kA_AW_R^2$, where R_{Wind} is in lb, A_A is in ft^2, projected normal to the wind, and W_R is in kt. Unless otherwise stated W_R is directly ahead.

Eggert, E. F.	$k = 0.004$ and A_A, if not known, is taken as $(B_X)^2/2$ [EMB Rep. 264, Aug 1930, p. 2]
Taylor, D. W.	$k = 0.004$ [S and P, 1943, pp. 51–52]
Chapman, C. F.	$k = 0.00454$ for an anchored motorboat [SSBH, 1951]
Chapman, C. F.	$k = 0.0051$ for an anchored sailboat, measuring A_A to top of deckhouse [SSBH, 1951]
Barnaby, K. C.	$k = 0.004$ but A_A is determined by adding to the projected area of the superstructure and upper works a diminished projected area of the hull proper, equal to that projected area times $0.45(C_B)$ [BNA, 1948, Art. 163, pp. 192–193]
Baker, G. S.	$k = 0.0033$ for an Atlantic liner and 0.004 for a cargo vessel, combined with a reduction factor which calls for using only about 0.3 of the actual projected *hull* area when computing the overall projected area A_A [SEE, 1942, pp. 14–16].

Group II. Non-Dimensional Values of $C_{D(\mathrm{Air})}$

See the text.

faces in contact with the air are large and long, many of the contours are reasonably uniform, and friction drag is no longer negligible. If the frontal area of such a ship hull is taken as equal to the maximum underwater area A_X, or even as $B(H)$, with an L/B ratio of say 7, the "wetted" abovewater area of the smooth side portions is of the order of $2L(H) = 2(7B)H = 14B(H)$. This proportion of wetted to frontal area is about the same as for a railway coach. Unfortunately, a reasonably accurate prediction of the friction drag for the coach must await more knowledge as to the actual air flow around it [Hoerner, S. F., AD, 1951, pp. 169–170]; the same is true of the ship hull.

54.9 Drag and Resistance with Wind on the Bow. For the reasons explained in Sec. 26.15 and illustrated in Fig. 26.I of Volume I, the relative wind blowing at an angle on the bow impinges separately on deck erections, stacks, and certain other elements of the upper works which normally benefit from shadowing when the relative wind is dead ahead or nearly so. Furthermore, a ship hull, lying at an effective angle of attack to the relative wind and acting as a short-span airfoil, cantilevered above the water surface, is creating an induced drag as well as the lift depicted in diagram C of Fig. 26.H. This induced drag, although not shown there, is additional to the pressure drag. It is measured as part of the wind drag and wind resistance when model tests are made, and is included in the coefficients set forth in this chapter.

As a result, the axial component R_{Wind} of the lift and drag forces due to the relative-wind velocity W_R at a range of relative-wind angles on the bow usually exceeds the value of the wind resistance R_{Wind} when the relative wind is from directly ahead. The ratio of these forces is expressed for convenience as k_θ. Then for any angle of relative wind θ, measured toward the right from ahead, $R_{\text{Wind}} = k_\theta D_W$, when D_W is measured at $\theta = 0$ deg. This is equivalent to

$$R_{\text{Wind}} \text{ at angle } \theta = k_\theta (R_{\text{Wind}} \text{ at } 0 \text{ deg}) \qquad (54.\text{viii})$$

The rates at which the coefficient k_θ vary with the direction of the relative wind for several ships of different types are illustrated in Figs. 54.C, 54.D, and 54.E. Two similar graphs, one for a cargo vessel with forecastle, centercastle, and poop, and the other for a passenger ship, are given by W. P. A. van Lammeren, L. Troost, and J. G. Koning [RPSS, 1948, Fig. 8, p. 25].

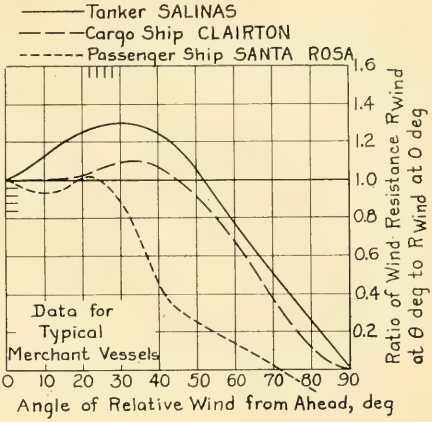

Fig. 54.C Graphs of k_θ for Three Merchant Ships

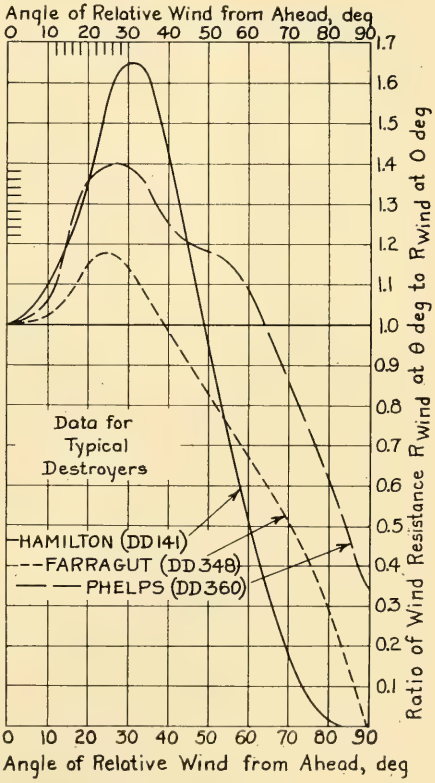

Fig. 54.D Graph of k_θ for Three Destroyers

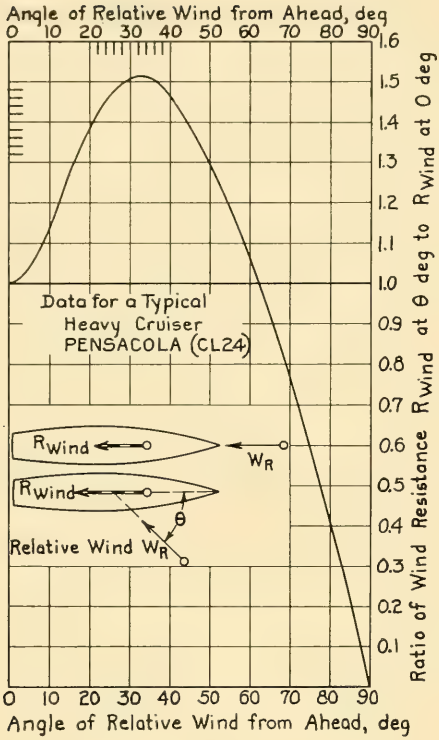

FIG. 54.E GRAPH OF k_θ FOR A HEAVY CRUISER

Three additional graphs are given by G. Hughes for a tanker, a cargo vessel, and a transatlantic liner [INA, 1930, pp. 321–324 and Pl. XXXVI].

These graphs are reproduced in SNAME, 1932, Fig. 14, p. 41. Additional graphs for an express cargo liner are given by G. Kempf in Fig. 7 on page 51 of this reference. A graph for the U. S. Maritime Administration *Mariner* class is published by V. L. Russo and E. K. Sullivan in SNAME, 1953, Fig. 45, page 212.

54.10 Prediction of Wind Resistance for ABC Ship of Part 4. As examples of the method by which the formulas and data of the preceding sections are employed in practice, the probable wind resistances of the ABC ship, designed in Part 4, are calculated for several design stages and conditions.

It is assumed first, that at an early stage in the preliminary design, before the abovewater body is drawn and the upper works are laid out, the still-air resistance is to be approximated for the trial speed of 20.5 kt. The transverse abovewater area A_A is taken, by Eggert's rule of thumb, as $(0.5)B_X^2$. With a beam of 73 ft, A_A becomes $0.5(73)^2 = 2{,}665$ ft^2. The dimensional Eq. (54.vii) is used for a first estimate, and k is taken as 0.004. Also, since there is no true or natural wind blowing, W_R is equal to V, and there is no variation of wind velocity with height, due to boundary-layer effect. Then

$$R_{SA} = D_W \text{ for this case}$$

$$= kA_AW_R^2 = 0.004(2{,}665)(20.5)^2 = 4{,}480 \text{ lb.}$$

Assuming a total hydrodynamic resistance R_T for the bare hull, from Chap. 66, as about 170,000 lb, the still-air resistance ratio is 4,480/170,000 = 0.0263. The bare-hull R_T value is used so that the still-air drag may be added as a percentage, like the overall appendage resistance, to predict the probable total trial resistance.

Next, consider the relative-wind resistance when $\theta = 0$ deg (wind ahead), the ship speed at sea is 18.5 kt, and the true wind velocity is 23 kt. The relative-wind speed is then $(18.5 + 23) = 41.5$ kt. Hence

$$R_{\text{Wind}} = kA_AW_R^2 = 0.004(2{,}665)(41.5)^2$$

$$= 18{,}360 \text{ lb.}$$

This represents a resistance augment, over that estimated for the bare hull at the trial speed of 20.5 kt, of (100)(18,360/170,000) or 10.8 per cent. It would be a much larger proportion of the total resistance at the 18.5-kt smooth-water ship speed of the problem given.

As a third approximation it is desired to estimate the wind resistance of the ABC ship, having abovewater hull and upper works of the general form shown in Figs. 66.O, 66.S, and 68.M, when conducting a full-speed run during standardization over the measured mile. Assume that the measured speed is 20.4 kt for a particular run, that the amemometer on top of the after pair of kingposts reads 41.5 kt, and that the wind direction indicator gives an angle of 22 deg on the port bow. The latter two readings are both for the relative wind, so it is not really necessary to know how fast the ship is going through the water to predict the wind resistance to be encountered.

From the dimensions on Fig. 54.F, corresponding to those on the three drawings mentioned, the silhouette area, looking from ahead, is estimated to be about 3,880 ft^2. This is nearly half

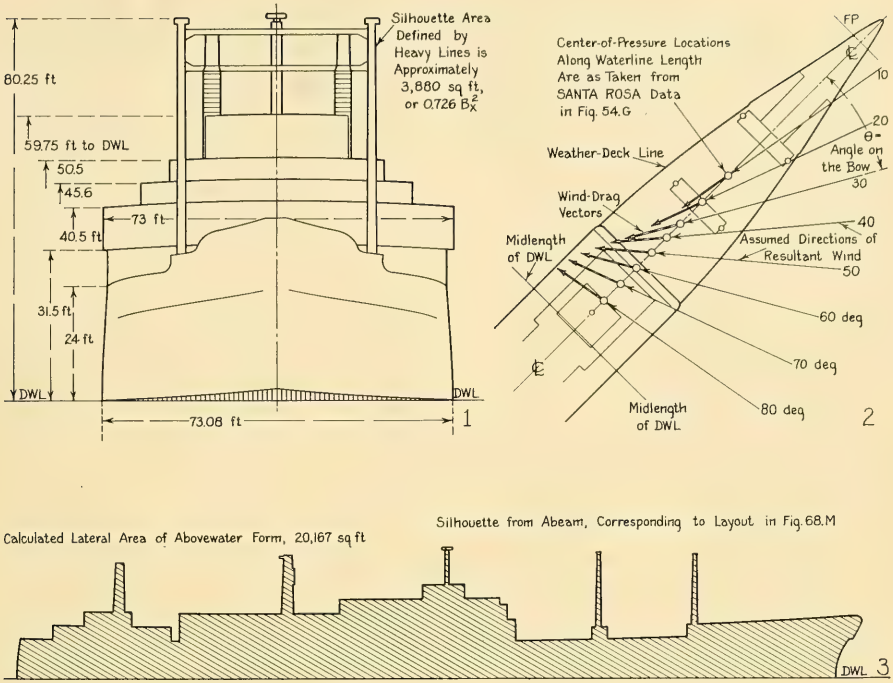

Fig. 54.F Wind-Resistance and Center-of-Pressure Layout for the ABC Ship of Part 4

again as large as the $A_A = (0.5)B_X^2$ value originally used. To keep the problem simple it is assumed that the relative-wind velocity over all this area is the same, eliminating any boundary-layer effect.

The value of k_θ is taken from the *Santa Rosa* short-dash curve of Fig. 54.C, for $\theta = 22$ deg, as approximately 1.15. Then, for $W_R = 41.5$ kt, Eq. (54.viii) gives

$$R_{\text{Wind}} = (k_\theta)k(A_A)W_R^2$$
$$= (1.15)(0.004)(3{,}880)(41.5)^2 = 30{,}739 \text{ lb.}$$

From Fig. 78.Nc of Part 4, the effective power P_E for the transom-stern design of ABC ship, predicted from model tests, is about 9,940 horses. For the water speed of 20.4 kt, equivalent to 34.45 ft per sec, the total resistance R_T, with appendages, works out as 9,940(550)/34.45 = 158,694 lb. The predicted wind resistance then represents an increase in the estimated total resistance at 20.4 kt of (100)(30,739)/158,694 or 19.4 per cent. Unless the machinery could develop more than its rated maximum power it is doubtful whether the ship could make 20.4 kt on the trial course against a 41.5-kt relative wind on the bow.

54.11 Magnitude of Wind Pressure. It is helpful at times to have an idea of the magnitude of the forces exerted by a natural wind on a flat plate or a flat surface normal to the wind direction. A number of authors have given tabulated data of this kind in the past, among them Dixon Kemp ["A Manual of Yacht and Boat Sailing," Cox, London, 3rd ed., 1882, p. 599, on which there is a table of wind-pressure intensity]. His values of normal pressure in lb per ft^2, for a range of wind velocity of 1 to 100 kt, corresponding to the complete range of the Beaufort scale from 1 to 12, were based upon a constant drag coefficient C_D of 1.87. It is now known that this drag coefficient varies from about 1.16 for a square plate with free edges to about 1.90 for an infinitely long strip, also with free edges.

The figures in Table 54.b are adapted from a table published more recently by K. C. Barnaby

TABLE 54.b—NOMINAL FORCE, VELOCITY, AND PRESSURE DUE TO NATURAL WINDS

The ram pressures are based on a ρ-value of 0.002378 slugs per ft³. The flat-plate pressures are based on a thin plate mounted in the open, with a separation zone on its leeward side.

Column 5 is calculated for a C_D of 1.16; column 6 for a C_D of 1.90.

The wind velocities correspond exactly to the Beaufort-scale numbers published in "Instructions for Keeping Ship's Deck Log," NavPers 15876 of July 1955, Bureau of Naval Personnel, U. S. Navy Department.

1	2	3	4	5	6
Nominal Force, Beaufort Scale	Description	Wind Velocity, kt	Ram Pressure, lb per ft²	Average Flat-Plate Drag, $b/h = 1.0$, lb per ft²	Average Flat-Plate Drag, $b/h = \infty$, lb per ft²
1	Light air	1–3	0.003 to 0.03	0.003 to 0.035	0.006 to 0.057
2	Light breeze	4–6	0.05 to 0.12	0.06 to 0.14	0.095 to 0.23
3	Gentle breeze	7–10	0.17 to 0.34	0.197 to 0.39	0.323 to 0.65
4	Moderate breeze	11–16	0.42 to 0.87	0.49 to 1.01	0.798 to 1.65
5	Fresh breeze	17–21	0.98 to 1.50	1.14 to 1.74	1.86 to 2.85
6	Strong breeze	22–27	1.63 to 2.40	1.89 to 2.78	3.10 to 4.56
7	Strong wind	28–33	2.6 to 3.7	3.02 to 4.29	4.94 to 7.03
8	Fresh gale	34–40	3.9 to 5.4	4.52 to 6.26	7.41 to 10.3
9	Strong gale	41–47	5.7 to 7.4	6.61 to 8.58	10.8 to 14.1
10	Whole gale	48–55	7.8 to 10.2	9.05 to 11.8	14.8 to 19.4
11	Storm	56–63	10.6 to 13.5	12.3 to 15.7	20.1 to 25.7
12	Hurricane	64–71	13.9 to 17.1	16.1 to 19.8	26.4 to 32.5
13		72–80	17.6 to 21.7	20.4 to 25.2	33.4 to 41.2
14		81–89	22.2 to 26.9	25.8 to 31.2	42.2 to 51.1
15		90–99	27.5 to 33.2	31.9 to 38.5	52.3 to 63.1
16		100–108	33.9 to 39.6	39.3 to 45.9	64.4 to 75.2
17		109–118	40.3 to 47.2	46.7 to 54.8	76.6 to 89.7

[BNA, 1948, p. 190]. The nominal wind force in column 1 is not a force in the strict sense of the word but a Beaufort-scale number used by mariners to indicate a range of velocity, set down in column 3. The wind velocities corresponding to the Beaufort-scale numbers in Table 54.b are taken from "Instructions for Keeping Ship's Deck Log," NavPers 15876 of July 1955, issued by the Bureau of Naval Personnel of the U. S. Navy Department. The ram or stagnation pressures in column 4 are those calculated by the expression $0.5\rho W_T^2$ where ρ is taken as 0.002378 slugs per ft³ for "standard" air and W_T is the velocity of the true or natural wind, in ft per sec.

The right-hand column of the referenced Barnaby table, not reproduced here, was calculated for a drag coefficient C_D of 1.18. Column 5 of Table 54.b is based upon a drag coefficient of 1.16, corresponding to that for a thin, flat plate of square outline and a length-breadth ratio of 1.0, normal to the wind, as in Fig. 55.B. The values in column 6 are for a thin, flat plate, standing in the open, with air access to the back, having a length-breadth or aspect ratio of infinity.

The reason why the flat-plate pressures are greater than the ram pressures is because there is a separation zone and a $-\Delta p$ region on the back of each plate, in addition to the $+\Delta p$ region on the front.

The wind drags listed in Table 54.b apply generally to wind screens and windbreaks on a ship, in much the same manner as to signboards ashore. Whether the drags are valid for deckhouse structures depends upon whether or not there is a separation zone on the leeward side of each house, the same as that behind a flat plate.

54.12 Location of Center of Wind Pressure. It is often convenient, and sometimes necessary, to know the approximate location of the point along the ship axis at which the total resultant wind force is applied. When combined in a suitable manner with the center of pressure for slow drift motion of the underwater hull, oriented on a selected heading, this would give the point at which the ship should be held by a single mooring, say, so as to remain in position on that heading.

Unfortunately, data on center of wind pressure are limited but Fig. 54.G contains five plots of the fore-and-aft CP positions for the wind-resistance

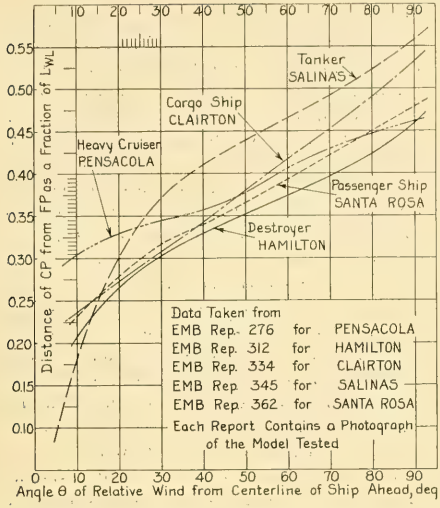

FIG. 54.G CENTER-OF-WIND-PRESSURE DATA FOR FIVE TYPICAL SHIPS
Theoretically, all graph values should be zero when $\theta = 0$

models of the five ships listed in the graphs of Figs. 54.C, 54.D, and 54.E. Schematic wind-drag force vectors for a few representative relative-wind directions are indicated on diagram 2 of Fig. 54.F. G. Hughes gives center-of-pressure data for three abovewater models tested in a wind tunnel [INA, 1930, p. 321 and Fig. 2 on Pl. XXXV; INA, 1933, Pl. VIII, Fig. 4], for values of θ from 0 to 180 deg.

54.13 Lateral Wind Drag. Ships underway are often subjected to strong relative winds from abeam, at an angle θ of approximately 90 deg, measured from ahead. Vessels anchored and at moorings, lying to the tide or moored at both ends in assigned positions, are subject to cross winds. Moreover, vessels often have to be berthed and unberthed when the true wind is about at right angles to their axes. The wind resistance under these conditions is nearly zero, but the wind drag may be very large.

The most extensive and probably the most reliable data as to lateral wind drag appear to be those of T. Thorpe and K. P. Farrell [INA, 1948, pp. 116–117]. These list transverse wind-drag loads for a wind velocity of 60 kt as ranging from 37.5 long tons for a large battleship to 7.85 long tons for a frigate or escort vessel. W. W. Smith, in reference (4) of Sec. 54.6, mentions a wind-resistance load of 22.6 long tons for a large collier with multiple derricks.

The value of the dimensional drag coefficient for a broadside relative wind is very nearly as large as for an end-on wind or for a flat plate having a length equal to that of the ship and a depth of twice the ship height (including the mirror image below the water surface). However, tests on models indicate a somewhat smaller drag coefficient for the broadside presentation.

For a *dimensional* expression of the form

$$D_W = k_B A_A W_R^2 \qquad (54.\text{viia})$$

the dimensional coefficient k_B for $\theta = 90$ deg has values ranging from 0.003 to 0.0042. In their analysis, and for practice, Thorpe and Farrell recommend a k_B of 0.004.

It is interesting to make an estimate of the wind drag exerted on the ABC ship of diagram 3 in Fig. 54.F when lying beam-to in a 60-kt storm wind. The silhouette area for $\theta = 90$ deg and for the ship at designed draft, estimated from Fig. 68.M and from diagram 3 of Fig. 54.F, is 20,167 ft^2. For a k-value of 0.0042, the maximum quoted by T. Thorpe and K. P. Farrell in Sec. 54.13, the lateral wind drag is

$$D_W = k_B A_A W_R^2 = 0.0042(20{,}167)(60)^2$$
$$= 304{,}925 \text{ lb.}$$

This is almost twice the ahead hydrodynamic resistance at the designed speed, as predicted by the model test. Under this lateral force the ship would, if left to itself, heel and drift downward, as described in subsequent sections.

54.14 Lateral Wind Moments and Angle of Heel. It is unfortunately possible for certain craft, especially when in a light or nearly light condition, with the relative wind about abeam, to be subjected to a wind-drag moment which exceeds the righting moment. The craft then capsizes. This can happen in areas of relatively smooth water, if a vessel is struck by a sudden high-velocity squall. In areas where waves already exist, the menace is obviously greater if the ship is perched broadside on a high wave crest, with a diminished metacentric stability, at the instant that it experiences the maximum force of the squall.

The heeling moment due to beam winds on full-scale vessels, about an axis in the waterplane, may be estimated by using a 0-diml formula

developed by the Bureau of Ships of the U. S. Navy Department. It is

$$K = C_K(0.5\rho)A_A h_A(\cos^2\phi)W_R^2 \qquad (54.\text{ix})$$

where C_K is the 0-diml heeling moment coefficient due to wind

A_A is the abovewater area for $\theta = 90$ deg, projected on the plane of symmetry, with the vessel upright

h_A is the height above the waterplane of the center of the area A_A with the vessel upright

ϕ(phi) is the angle of heel

W_R is the relative-wind velocity, assumed as directed abeam.

Model tests give a value of the product $C_K(0.5\rho)$ of about 0.00147, from which $C_K = 0.00147/(0.001189) = 1.236$. Entering the known or assumed values for a given situation, and assuming successive values of heel angle ϕ, increasing by 10 deg up to as great a range as desired, a curve of heeling moment on a basis of heel angle is plotted for a given wind velocity. Comparing this with the curve of righting moments in still water, the intersection gives the angle to which a ship will heel under the wind effect. Assuming a given maximum or allowable angle of heel, the righting moment for that angle may be set down as K in Eq. (54.ix) and the corresponding wind velocity be found.

This procedure is in the nature of a rough approximation because, like the example of the preceding section, it assumes a constant wind velocity over the whole lateral abovewater area. Further, it takes no account of second-order effects such as the downwind motion of the ship due to the lateral force exerted by the wind, or the fact that the ship is heeling away from the wind. For a sudden squall, it takes no account of the kinetic rolling energy in the ship when it reaches the *nominal* angle of equilibrium, which means that the ship would heel beyond the equilibrium angle. However, L. Gagnatto, as the result of a more rigorous analysis [ATMA, 1929, Vol. 33, pp. 53–74], finds that the rigorous method gives a maximum angle of heel sensibly less than that derived from the approximate method. A further analysis was carried out by Guntzberger and reported a few years later [ATMA, 1934, Vol. 38, pp. 341–355].

E. A. Wright has published a photograph, with accompanying notes, of a destroyer model undergoing a wind-resistance test (in a wind tunnel) when heeled [SNAME, 1946, Fig. 25, p. 393].

As an indication of the values to be expected under violent beam winds, a model of the World War I *Eagle* class patrol boats was floated in a shallow pan of water in a wind tunnel, where it was blown upon at various relative-wind bearings θ from 30 deg (on the bow) to 150 deg (on the quarter). The scale ratio was 48, the weight corresponded to the designed ship W of 480 t, and the full-scale $\overline{GM}$ simulated in the tests was 1.012 ft. This corresponded to $(1.012/26.23)B$ or $0.039B$. The dimensions and lines of the vessel are found on SNAME RD sheet 118.

At a full-scale wind velocity corresponding to 100 mph, 86.84 kt, by no means uncommon in hurricanes and typhoons, the maximum angle of heel was over 37 deg. Surprisingly, this occurred with the bow 130 deg away from the wind. The next greatest heel, 35 deg, was encountered with the bow 70 deg from the wind. With the wind abeam, or at bearings of 50 and 110 deg, the heel was less than 33 deg. The smallest heels, 20–22 deg, occurred when the bow was either 30 or 150 deg from the relative-wind direction [EMB Rep. 15, Jul 1920].

An interesting passage from this report is quoted as follows:

"3. The center of lateral resistance was previously determined by towing a larger but similar model of (an) *Eagle* boat sidewise and was found to be substantially at the water surface."

54.15 Estimated Drift and Leeway. It is difficult to estimate, in advance, just how fast a ship, without power and under given weather conditions, may be expected to drift under the action of wind alone. This is principally because ships vary in their attitudes to the wind when drifting, so the relative position of the ship axis and the wind direction must generally be assumed.

Granted that the ship drifts broadside to the wind, and that it is of normal form, a reasonable value of the 0-diml water-drag coefficient of its underwater body is 1.15. This is derived by assuming an actual L/H ratio of 20, but an effective ratio of 10, since at low speeds the ship behaves essentially as would its underwater hull, plus a superposed mirror image, drifting downwind in infinitely deep water. At these low speeds the effect of waves resulting from the broadside motion can be neglected. The drag coefficient C_D of a flat plate of these proportions is, from Fig. 55.B, about 1.5, but the ship has few sharp edges like the thin plate, especially under the

bottom. In any case, too high a value of C_D for the lateral water resistance represents an unsafe estimate, since the calculated rate of downwind drift is then smaller than is found on the ship.

The resistance to drift may be expressed by

$$\begin{aligned} R_{\text{Drift}} &= C_{D(\text{Water})}(0.5\rho_W)A_L(V_{\text{Drift}})^2 \\ &= C_{D(\text{Water})}(0.5\rho_W)L(H)(V_{\text{Drift}})^2 \end{aligned} \tag{54.x}$$

The force causing drift is the wind drag of the ship at the relative wind velocity W_R, expressed by

$$D_W = C_{D(\text{Air})}(0.5\rho_A)A_A W_R^2 \tag{54.iv}$$

The lateral wind force is calculated from the latter equation, substituted for the lateral resistance to drift R_{Drift} of Eq. (54.x), and this equation is then solved for the drifting speed V_{Drift}.

If the abovewater lateral projected area A_A is assumed equal to the underwater lateral area A_L, and C_D for wind drag is taken as 1.18, then for equal wind and drift drags

$$(1.18)\frac{\rho}{2}(\text{for air})W_R^2 = (1.15)\frac{\rho}{2}(\text{for water})(V_{\text{Drift}})^2$$

whence

$$\frac{V_{\text{Drift}}^2}{W_R^2} = \frac{1.18(0.001189)}{1.15(0.99525)}$$

or

$$\frac{V_{\text{Drift}}}{W_R} = 0.035$$

It is to be remembered that, since the ship is drifting downwind,

$$W_R = W_{\text{True}} - V_{\text{Drift}}.$$

54.16 Estimating the Forces on a Moored Ship. A brief discussion of the forces on a moored ship is included in Sec. 12.8. It is pointed out by T. Thorpe and K. P. Farrell [INA, 1948, p. 116] that a ship lying at a mooring is subject to forces due to wind, waves, and tidal current. Sec. 12.8 mentions that it is also subject to slope drag when the ship rides at anchor in an appreciable current, with the moored end higher than the free end. To the usual resistance forces derived from relative motion of the ship and the water there is added the drag of the non-rotating or non-operating propulsion device(s) due to the current flowing by them.

A ship with a normal proportion of its total bulk volume under water usually rides to the current rather than to the wind. This means that the wind may blow at any bearing relative to the ship, and that the greatest drag due to both current and wind may be expected when the ship is riding head to the current, with the wind about 30 deg on either bow. T. Thorpe and K. P. Farrell, in the reference cited, emphasize the effect of gusts and squalls, because the wind drag varies as the square of the maximum instantaneous velocity, assuming that it blows with this augmented velocity on the whole ship at once.

Wind-drag forces on groups of moored ships, lying alongside each other, are given by M. E. Long in TMB Report R-332 of December 1945, entitled "Wind Tunnel Tests to Determine Air Loads on Multiple-Ship Moorings for Destroyers of the DD692 Class."

The naval architect will require drag data on moored vessels only infrequently. No attempt is therefore made here to include, with or without adaptation, any of the tables, graphs, or diagrams given in the references.

54.17 Surface-Water Currents due to Natural Wind. A discussion of drift and leeway in particular, and of wind resistance in general, is not complete without some mention of the surface-water currents produced by a natural wind blowing over a body of water. Some data are available to relate the magnitude of this current to the wind velocity but without the necessary information as to the height above the water surface at which the velocity is measured.

E. F. Eggert states that this surface current, presumably more-or-less uniform for the draft of a surface ship of moderate size, has a magnitude of 0.015 times the wind velocity [EMB Rep. 264, Aug 1930, p. 1, based on data furnished by the U. S. Coast and Geodetic Survey]. C. O'D. Iselin states that on the average the surface water moves at about 3 per cent of the wind velocity. This is twice the value just quoted. Further, Iselin reports that the surface-water current moves in a direction about 30 deg to the right of the wind in the northern hemisphere (30 deg to the left below the equator) ["Oceanography and Naval Architecture," SNAME, New Engl. Sect., Jun 1954].

CHAPTER 55

The Calculation of Appendage Resistance

55.1 General. Chaps. 36 and 37 list and describe the use and effect of a considerable number of fixed and movable appendages, respectively, found on many types of surface vessels of normal form. Within the space available, this chapter endeavors to furnish data by which the resistances of the most common of these appendages are estimated or calculated. This is possible from several sources of information:

(a) Drag coefficients of submerged geometric bodies and shapes approximating those of the appendages
(b) Observed drag data for various ship appendages, generally from model tests
(c) Ranges of percentage of bare-hull resistance for appendages of normal size and form.

The drags listed in (b) are determined separately by towing a model and removing the appendages one by one. This involves some experience and knowledge as to just how much of each type of appendage to reproduce to small scale. This is especially true of representations of complicated objects such as handrails, antennas, and fittings on submarine models.

Screw propellers which are prevented from turning by casualty, or which are locked within the ship for other reasons, constitute a special kind of appendage, at least as far as drag is concerned. They represent a special case of the situation where the propeller rotates at other than a thrust-producing rate, and as such are discussed in Part 5 of Volume III.

There is a second engineering reason for calculating or predicting the resistance of appendages. This is to determine the hydrodynamic loads on the various parts of the appendage, so that these parts may be made sufficiently strong and rigid to meet all service requirements.

55.2 Scale-Effect Problems. A great deal has been written in the technical literature about the problems of assessing or determining the correct resistance of appendages when added to a towed or self-propelled model. An excellent resumé covering all aspects of this situation in which the ship designer is interested is presented by P. Mandel [SNAME, 1953, pp. 493–495]. Despite their efforts to solve the model-prediction problem, the techniques and prediction procedures of various model-testing establishments still vary rather widely.

The difficulty here is that almost all ship appendages are completely submerged, they do not make gravity waves, and hence dynamic similarity of flow is gauged by the Reynolds rather than by the Froude number. Only in exceptional cases, in model basins, can dynamic similarity on the R_n basis be achieved while the test of the model as a whole is being conducted on a Froude-number basis.

It may be assumed by the marine architect that, until these problems are resolved by the model-testing establishments, each one has good engineering reasons for its own procedure. Its predictions of appendage resistance will, in its own opinion, meet the needs of the ship designer, the shipbuilder, and the ship owner.

55.3 Customary Values and Proportions for Overall Ship Appendage Resistance. It is often necessary, as indicated in the latter part of Sec.

TABLE 55.a—PERCENTAGE INCREASES IN EFFECTIVE POWER P_E TO BE EXPECTED ON TRIALS OF THREE TYPES OF SHIP

The source of these data is given in the accompanying text.

Ship Type		Coaster	Tanker, single-screw	Passenger liner, twin-screw
Length,	ft	131.24	459.34	721.82
	meters	40	140	220
Trial speed,	kt	9.5	13	23
Roughness allowance	per cent in all cases	12	6	10
Air resistance, superstructures	per cent in all cases	2	3	4
Steering resistance	per cent in all cases	1	1	1
Bilge keels	per cent in all cases	1	2.5	2

66.9, to make a quick estimate of probable appendage drag before the appendages are designed or perhaps even before the ship lines are drawn. Such an estimate is possible only by knowing (or deciding) what appendages are involved and the type of ship to which they are to be fitted. The basis for estimate is then a percentage of the bare-hull resistance or effective power, based upon systematic data derived largely from model tests.

A few percentages of this kind, including other percentages as well, are given by W. P. A. van

TABLE 55.b—PERCENTAGE DECREASES WHEN SIX SERIES OF APPENDAGES ARE REMOVED IN SUCCESSION FROM A CRUISER MODEL

The values listed are percentages of the total bare-hull resistance of the model at the speed-length quotients given. The data are taken from tests of TMB model 3836.

	Name of Appendage Removed							
Speed-length quotient, T_q	Froude number, F_n	Steering rudder	Outboard double-arm struts	Inboard double-arm struts	Outboard intermediate strut and boss	Inboard intermediate strut and boss	Portion of bilge keels	Total
0.776	0.231	3.6	2.4	2.6	1.7	1.4	−0.5	11.2
1.046	0.311	3.5	1.8	3.7	1.3	0.9	1.0	12.2
1.319	0.593	1.9	2.4	1.5	1.4	0.9	1.6	9.7

TABLE 55.c—PERCENTAGE INCREASES OVER BARE-HULL RESISTANCE FOR ALL CUSTOMARY APPENDAGES, ACCORDING TO P. MANDEL

Speed-length quotient, $T_q = V/\sqrt{L}$	0.7	1.0	1.6
Froude number, $F_n = V/\sqrt{gL}$	0.208	0.298	0.476
Large, fast, quadruple-screw ships	10 to 16	10 to 16	
Small, fast, twin-screw ships	20 to 30	17 to 25	10 to 15
Small, medium-speed, twin-screw ships	12 to 30	10 to 23	
Large, medium-speed, twin-screw ships	8 to 14	8 to 14	
All single-screw ships	2 to 5	2 to 5	

Lammeren, L. Troost, and J. G. Koning [RPSS, 1948, p. 69]. They are reproduced in Table 55.a.

The graphs of Fig. 55.A show the increases in effective power P_E for a large destroyer when four types of appendage are added, one by one. The individual percentages may be obtained by the proper subtraction, on the basis that the resistance effects of the four appendage types are independent of each other.

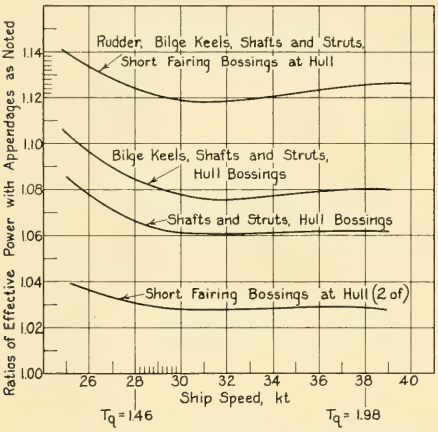

FIG. 55.A GRAPHS INDICATING PERCENTAGE INCREMENTS OF BARE-HULL RESISTANCE FOR FOUR SERIES OF APPENDAGES ON A DESTROYER

The graphs of Fig. 55.A indicate, for this model at least, that the percentage additions vary somewhat with the ship speed.

Table 55.b lists the percentage differences of total bare-hull resistance when a quadruple-screw cruiser model is run at three values of $T_q = V/\sqrt{L}$, with all appendages, and when six series of appendages are removed, one by one. Again the percentage differences are found to vary somewhat with the speed.

P. Mandel gives data on appendage resistance as a percentage of bare-hull resistance for five types of ship, at three speed-length quotients [SNAME, 1953, Table 8 on p. 494]. Table 55.c is adapted from the reference.

55.4 Classification of Appendages by Predominant Type of Drag. It is customary to treat the resistance of each ship appendage as predominantly friction or pressure drag. This avoids the complicated extrapolation method customarily used for the ship prediction.

An appendage is considered to add wetted surface and friction drag only if:

(a) Its greatest dimension lies in the direction of motion; in other words, it has a low aspect ratio
(b) Its surfaces lie in the general direction of flow when the ship motion is steady
(c) Its thickness, as a fraction of its length in the direction of flow, is small or negligible.

A roll-quenching keel is an excellent example for all the foregoing. Both long and short bossings for propeller shafts and large skegs are considered essentially as parts of the hull in that their wetted surfaces are added to that of the hull. Docking and resting keels are in the same category if their edges and endings are fair and they lie in the lines of flow. The friction drag R_F added by each is then proportional to its wetted area S. The discussion of Sec. 22.9 of Volume I indicates that there is as yet no definite rule for assessing the proper R_x for these appendages, and for determining the C_F value for each.

The appendage is presumed to add pressure drag only when one or more of the following conditions obtain:

(1) Its greatest dimension lies across the flow, and it has an appreciable or a high aspect ratio
(2) Its thickness, as a fraction of its length in the direction of flow, is about 0.1 or more
(3) Its fore-and-aft length is short, say not exceeding 0.02 the length of the ship. If wake velocities are neglected, V and ν(nu) are always the same, for both the appendages and the ship as a whole. This is equivalent to saying that R_x for the appendage is less than about $0.02R_n$ for the ship. The arm of the strut for an exposed shaft is an example falling within the limits of (1), (2), and (3).

Diving planes, short skegs, rudder support horns, strut hubs, exposed shafts, guards, fixed screw-propeller shrouding, and sound domes are among the appendages causing pressure drag only. A rudder, if forming a continuation of the ship hull or of a large skeg, may have its wetted area included in that of the main hull, with its drag assumed as entirely frictional. If separate from the hull, like an underhung spade rudder, its resistance is usually reckoned as a pressure drag only. W. P. A. van Lammeren, L. Troost, and J. G. Koning give 0-diml drag coefficients for seven types of rudders of varied section, all

having an aspect ratio of 2.5 [RPSS, 1948, Fig. 216, p. 326].

55.5 Lift, Drag, and Other Data for Typical Bodies Representing Appendages. Appendages are also classified by types or shape of body, on the basis that, if they resemble certain geometric forms, there are 0-diml drag coefficient data available in the literature by which their resistances may be approximated. The shapes in this category include symmetrical and asymmetrical airfoils, fuselages, and other parts of airplanes and airships, for which published drag data are rather extensive. For example, W. S. Diehl gives

Form of Body	Dimension Ratio	Reynolds Number	Drag Coefficient
Circular Flat Plate, Normal to Stream ($A_{Proj} = \frac{\pi}{4}D^2$)		$R_n = \frac{UD}{\nu} = >10^3$	$C_D = \frac{\text{Drag}}{0.5\rho A_{Pr} U^2} = 1.12$
Pair of Circular Discs in Tandem	$L/D = 0$	$>10^3$	1.12
	1		0.93
	2		1.04
	3		1.54
	$A_{Projected}$	is for One	Disc Only
Rectangular Plate, Normal to Stream	$\frac{b}{h} = 1$	$>10^3$	1.16
	5		1.20
	10		1.50
	∞		1.90
Circular Cylinder, Axis Parallel to Stream	$\frac{L}{D} = 0$	$>10^3$	1.12
	1		0.91
	2		0.85
	4		0.87
	7		0.99
Circular Cylinder, Axis Perpendicular to Stream	$L/D = 1$	10^5	0.63
	2		0.68
	5		0.74
	10		0.82
	20		0.90
	40		0.98
	∞		1.20
	$L/D = 5$	$>5(10^5)$	0.35
	∞		0.34
2-Diml Strut of Elliptic Section	$\frac{c}{t} = 3$	Abt. $6(10^4)$	0.20
2-Diml Streamlined Strut	$c/t = 2$	$>10^6$	0.20
	3		0.10
	5		0.06
	10		0.083
	20		0.094

FIG. 55.B DRAG-COEFFICIENT VALUES FOR A NUMBER OF WELL-KNOWN GEOMETRIC SHAPES

The velocity vector U indicates the direction of uniform flow in each case

Form of Body	Dimension Ratio	Reynolds Number	Drag Coefficient
Sphere of Diameter D		10^5	0.50
		$3(10^5)$	0.20
Hemisphere, Concave to Stream		$>10^3$	1.33
Hemisphere, Convex to Stream		$>10^3$	0.34
Ellipsoid, Major Axis ⊥ to Flow	$\frac{L}{D} = 0.75$	$<5(10^5)$	0.60
		$>5(10^5)$	0.21
Ellipsoid, Major Axis ∥ to Flow	$\frac{L}{D} = 1.8$	$>2(10^5)$	0.07
Model Airship Hull		$>2(10^5)$	0.05
Solid Cone (30 deg)			0.34
Solid Cone (60 deg)			0.51

FIG. 55.C DRAG-COEFFICIENT VALUES FOR A GROUP OF 3-DIML GEOMETRIC SHAPES

The velocity vector U indicates the direction of uniform flow in each case

drag and moment data on a great variety of these elements, as well as on seaplane and flying-boat hulls ["Tests on Aeronautical Fuselages and Hulls," NACA Rep. 236, 1926 reports, pp. 131–150]. S. F. Hoerner, in his book "Aerodynamic Drag," 1951, devotes his entire Chapter VIII, on pages 121–155, to the drag of aircraft components. He also gives a vast amount of 0-diml drag data, applicable to appendages in water, in other parts of the book.

Figs. 55.B and 55.C present the readily available geometric-shape data, with the values necessary for insertion in the 0-diml drag formula

$$D = C_D \frac{\rho}{2} A_{Proj} U^2$$

Here A_{Proj} may be $0.25\pi D^2$, $b(h)$, $L(D)$, or $b(t)$, as the case requires. These data are adapted from the following sources:

(a) "The Physics of Aviation," 1942, p. 75
(b) Van Lammeren, W. P. A., Troost, L., and Koning, J. G., RPSS, 1948, Fig. 26, p. 52
(c) Rouse, H., EH, 1950, Table 2, p. 126; also Fig. 90 on p. 124.

As an example of the application of these data, one may estimate the drag of the extensible sound-dome assembly shown in diagram 1 of Fig. 55.D in Sec. 55.7. This is on the basis of no hydrodynamic interference between neck and hull or between neck and head, and the absence of alternating circulation effects due to the vortex trail. It may be assumed that the ship speed is 12.3 kt, that the water is salt, at 59 deg F, and that no account is taken of variations in velocity across the boundary-layer thickness of the hull.

(1) For the neck, assume a diameter of 1.22 ft and a length below the hull of 3.22 ft. The L/D ratio is about 2.64 and the d-Reynolds number for 12.3 kt, or 20.77 ft per sec, is $Ud/\nu = (20.77)(1.22)(10^5)/1.2817 = 1.98$ million. This is greater than the value of $5(10^5)$ in the lower portion of the box of Fig. 55.B, devoted to the circular cylinder, with its axis normal to the flow. For this situation $C_D = 0.35$, hence

$$D \text{ (for neck)} = 0.35 \frac{1.9905}{2} [(3.22)(1.22)](20.77)^2$$
$$= 590.1 \text{ lb.}$$

(2) For the head, assume a diameter of 2.11 ft and a length of 1.72 ft. The L/D ratio is about 1.23 and the Reynolds number is $(20.77)(2.11)(10^5)/1.2817 = 3.419$ million. This is greater than the $5(10^5)$ referred to in the foregoing but much less than infinity. Hence

$$D \text{ (for head)} = 0.35 \frac{1.9905}{2} [(1.72)(2.11)](20.77)^2$$
$$= 545.3 \text{ lb.}$$

The total predicted drag is then $590.1 + 545.3 = 1{,}135.4$ lb.

A word may be said here about the drag of some of the bodies represented on Figs. 55.B and 55.C after the cavitating range has been reached. The drag coefficient $C_{D\sigma}$ for a cavitation number σ(sigma) is found to be related in fairly simple fashion to the non-cavitating drag coefficient, as described by P. Eisenberg [TMB Rep. 842, pp. 19–20], who gives values of the variables for a few well-known forms.

55.6 Allowances for Wake Velocities on Appendage Drag. With friction drag varying as a power of V in the range of 1.8 to 2.0, and pressure drag—excluding that from wavemaking—varying as V^2, it is important that a reasonably correct value be used for the relative water velocity in the prediction of appendage resistance. This means that it is necessary to estimate the probable actual velocity past the appendage (or its several parts) from the known or estimated flow pattern around the ship, considering wakes of all the kinds listed in Sec. 11.2 of Volume I and in Chap. 52. For instance, in the example concluding Sec. 55.5, if the shape of the ship and the sound-dome position in the ship were given, it could be estimated that for the 3.22-ft length of the neck the local velocity in the boundary layer would average only 0.78 of the ship speed. For the head, it could be predicted that, because of potential flow outside the boundary-layer cloak, the average velocity past the head would be 1.04 times the ship speed.

The modified drag, not calculated here, might not differ greatly from that derived in Sec. 55.5 but the moment of the drag, taken about the point of support at the hull, would be considerably greater. This is because the drag at various y-distances is proportional to the square of the local velocity U, which increases with the y-distance from the hull.

Some appendages lying abaft propulsion devices are acted upon by augmented velocities, to develop thrust-deduction forces. Because of the V^2 effect, the percentage increase in drag for a given condition is at least twice the percentage augment of velocity.

Those appendages (or parts of them) lying within separation zones might have drag values of the order of zero.

55.7 Shadowing Allowances for Appendages in Tandem. The shadowing allowance(s) for the downstream unit(s) of a system of similar appendages in tandem, like the fins or portions of a discontinuous roll-resisting keel, diagrammed in Fig. 36.M on page 553 of Volume I, or for any appendage lying downstream from another, indicated in diagram 2 of Fig. 55.D, depends upon:

(a) Whether or not the after unit is actually downstream from the leading one, having in mind the local direction of flow rather than the overall direction of motion. If directly in the wake of the upstream unit, the following one may benefit from positive wake velocities due to viscous flow or separation. If slightly to one side or the other it may suffer increased drag because of the augmented velocity $+\Delta U$ left in the water that passed around the leading unit.

(b) The shape of the bodies, particularly their

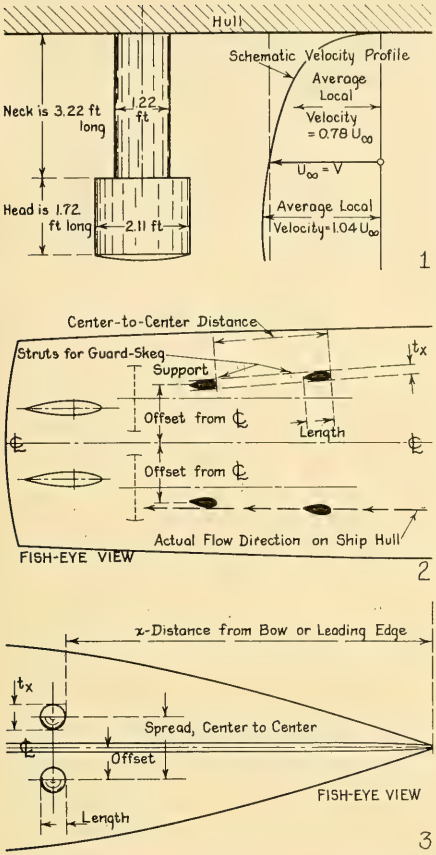

Fig. 55.D Definition Sketches for Appendages in Varying Flow, Appendages in Tandem, and Appendages Abreast

section shape if they are long and slender, with their axes roughly parallel. A leading unit of circular section generates a long separation zone abaft it, in which the drag of the following unit is diminished. On the other hand, a streamlined leading unit leaves in its wake a trail of augmented velocities, in which the drag of the following unit is increased.

(c) Whether the wake velocities from the leading unit, positive or negative as the case may be, are largely dissipated by the time the following unit comes along. This is, as a rule, a function of the ratio between the thickness and bluntness of the leading unit and the fore-and-aft distance to the following unit. For well-streamlined sections, normal to the flow, it may be the ratio between the section length and the fore-and-aft center-to-center spacing.

(d) Whether the trailing unit is so close to the leading unit as to modify the flow around the latter, over and above what it would be by itself in an infinite stream, and to change the drag of the leading unit. When placed close enough behind to lie in the separation zone of the leading unit, the following one may have *negative* drag, as discovered by G. Eiffel [Hoerner, S. F., AD, 1951, Fig. 7.1, p. 93].

Quantitative indications of what may be expected when the two appendages or units are in the form of struts are given by D. Biermann and W. H. Herrnstein, Jr., in NACA Report 468 of 1933, entitled "The Interference Between Struts in Various Combinations." Their conclusions, to be found on page 522, indicate that interference effects are to be expected if the leading and following units are closer than 5 section lengths to each other, center to center.

S. F. Hoerner also gives a considerable amount of interference drag data for airfoils (or hydrofoils), flat discs, strut sections, and cylinders in tandem [AD, 1951, pp. 83–84, 93–94]. A. Borden, D. B. Young, and W. M. Ellsworth, Jr., discuss the drag situation in "Hydrodynamic Induced Vibrations of Cylinders Towed in Various Combinations," TMB Report C-452, September 1951.

55.8 Modifications in Drag for Appendages Abreast. The general situation relative to adjacent appendages which must, to fulfill some special design requirement, be placed abreast each other, is depicted in diagram 3 of Fig. 55.D. Graphs indicating the single and combined drag of two 2-diml circular rods and of two 2-diml streamlined strut sections, placed abreast, are published by S. F. Hoerner [AD, 1951, Fig. 7.4, p. 95]. These show that, whenever practicable, the center-to-center transverse spread should be at least 4 times the maximum transverse section thickness t_X . For a spread of $2t_X$ (or $2D$) between the centers of a pair of circular cylinders of infinite length, the drag coefficient C_D of each cylinder is increased from its normal value of 1.2 to about 1.54.

55.9 The Drag of Exposed Rotating Shafts. An exposed rotating shaft, such as that driving a screw propeller, generates two kinds of friction

drag, in addition to a lift force by the Magnus Effect. The latter is described and discussed in Sec. 37.25 of Volume I and illustrated in Fig. 37.Q. The shaft also generates a pressure-drag force, to be described presently. Rotation of the shaft surface involves tangential friction and an increase in torque to keep it turning. The forward motion of the ship and shaft involves longitudinal friction, much the same as though the shaft were covered by a casing which did not rotate. A pressure drag, due to the oblique flow of water past the shaft, is exerted in the general plane of flow, at right angles to the shaft. This drag may or may not have a longitudinal component, depending upon the declivity and convergence—or divergence—of the shaft axis.

Taking the last item first, the shaft is considered as a fixed appendage in the form of a 2-diml circular cylinder, placed *normal* to a flow having an effective velocity equal to that component of the actual velocity perpendicular to the shaft axis and in the plane of that axis. In the absence of any better data, the actual streamline velocity may be taken as equal to the speed of the ship, and the direction of flow as parallel to the hull along an appropriate diagonal flowplane, indicated by surface (or preferably off-the-surface) flow markings, described in Chap. 52. This drag force will have a vertical or lifting component for most ship installations, possibly having a slight effect on the trim.

The exact nature of the axial and tangential components of the viscous flow around an exposed rotating shaft remain unknown in the present state of the art. It is customary, therefore, to neglect both friction-drag components on the shaft, unless the latter is excessively large and rotates at high speed, or unless it is so long that it has to be supported by two or more bearings, external to the hull.

To give an idea of the magnitudes involved, assume two shafts, each 12 inches in diameter, revolving at 400 rpm, and having an exposed length of 40 ft, lying at a mean angle of 8 deg to the lines of flow at a speed of 35 kt, equivalent to 59.11 ft per sec. The layout of P. Mandel [SNAME, 1953, Fig. 2, p. 466] shows the starboard shaft of a twin-screw arrangement of this kind. The tangential velocity at the surface of one shaft, due to rotation only (neglecting cross flow due to non-axiality), is $(12/12)\pi(400/60) = 20.95$ ft per sec. This is about one-third the forward speed of the ship and is about 2.5 times the cross-flow component due to non-axial flow at the shaft position, to be calculated presently.

Neglecting rotation and considering only the general flow in the vicinity, at an angle to the shaft, the axial component of velocity is [(59.11) cos 8 deg] or 58.53 ft per sec. The component normal to the shaft is [(59.11) sin 8 deg] or about 8.23 ft per sec. The C_D of a 2-diml circular cylinder of L/D ratio $40/1.00 = 40$ is, from Fig. 55.B, about 0.98. The normal force expected to be exerted on the shaft, neglecting the effect of rotation, is then

$$F = C_D \frac{\rho}{2} A_{\text{Proj}} U^2$$

$$= 0.98\left(\frac{1.9905}{2}\right)[(40)(1)](8.23)^2$$

$$= 2{,}640 \text{ lb, for the single shaft.}$$

The drag of locked screw propellers is discussed in Part 5 of Volume III.

55.10 Drag Data for Holes, Slots, and Gaps. What might be called reversed projections, in the form of recesses and holes, are considered here in the category of appendages, especially if they have physical dimensions corresponding to the appendages usually found on boats and ships. S. F. Hoerner has collected drag-coefficient data for holes and gaps, some based on a reference area equal to that of the opening in the fair surface and some based on the so-called frontal area of the downstream face [AD, 1951, pp. 55–56]. A stagnation point may be found here, as at Q in diagram C of Fig. 7.J, but if not it may be expected that some $+\Delta p$'s are developed on the downstream face.

Because of the rather complicated nature of the drag effects, the marine architect is referred directly to the Hoerner reference for such data as he may need.

The design of recesses to reduce their drag is discussed in Sec. 75.13.

55.11 Estimated Resistance of Discontinuities. The drag of any large discontinuity, invariably attached to a much larger body such as a ship hull, as distinguished from an appendage projecting well away from the hull, is dependent upon the flow pattern around it. The latter is, in turn, affected by the presence of the boundary layer on the large body, with its variation in local velocity across the boundary-layer thickness.

In aerodynamics the resistance of discontinuities of this type falls under the heading of interference

drag, as developed at the junction of two essentially dissimilar forms. Again the marine architect is referred directly to S. F. Hoerner's "Aerodynamic Drag," 1951, Chap. VII on pages 93–120, as embodying the essence of most of the known data in this field. Although written for the aeronautical engineer it should be intelligible to and useful for the marine architect who has read and is familiar with the previous chapters of the present book.

55.12 The Resistance of Large Appendages Considered as Parts of the Ship. Large appendages such as deep skegs and long bossings do not resemble bodies for which applicable and reliable pressure-drag data are available. Further, a skeg or bossing of a given shape may produce different flow, velocity, and pressure patterns, depending upon the form of the hull to which it is applied. There are companion interference effects here, both of the ship on the appendage and the appendage on the ship.

It is usually necessary to predict the drags of these large appendages by:

(1) Estimating the pressure drag from statistical percentage data, as in Sec. 55.3
(2) Taking account of the increased wetted area of the ship; that is, the external area of the appendage less the bare-hull area covered by it when applied. This involves an increased friction resistance R_F although, as explained in Secs. 22.9, 45.22, and 55.4, there are no acceptable rules for establishing the correct R_x values for these parts.
(3) Determining the drag from model tests, run with and without the appendage(s) in question.

55.13 The Calculation of Appendage Resistance for Submerged Vessels. The notes of the preceding sections of the present chapter apply to the calculation of the resistance of all appendages on submerged vessels, irrespective of their position relative to the hull. Those mounted on top of the hull will, upon occasion, break the water surface. In this case some pressure drag due to wavemaking, of an amount as yet undetermined, is added to the pressure drag due to forward motion. It may indeed be more necessary to predict this added drag as a design load on the appendage, rather than as an increment of resistance of the vessel as a whole, because this partly awash condition is not one for which resistance predictions are made.

The ratio of appendage resistance to the bare-hull resistance of a submersible is inherently larger than for a surface ship, notwithstanding the greater total bare-hull resistance of the *entire* vessel, including both the abovewater and the underwater portions in the surface condition. This is because of:

(a) The provision of diving planes, and possibly also of fixed stabilizers, and rope and cable guards, in addition to steering rudders
(b) The necessity for carrying one or more periscopes
(c) The high drag of radio, radar, and other antennas, and of the masts or supports for them
(d) The hull discontinuities embodied in large main-ballast flood-valve recesses or large flooding openings for the main-ballast tanks
(e) The provisions for normal handling of the vessel as a surface ship and for safety of the crew when working about the superstructure deck
(f) The provision of resting keels
(g) The work and expense involved in fairing and streamlining the abovewater portion of a vessel of the submersible type which is to spend only a small portion of its operating time submerged.

For a craft in the category of (g) preceding, the appendage resistance may well reach 80 or 90 or more per cent of the bare-hull resistance of the craft as a whole. For a true submarine which still requires steering rudder(s) and some kind of deck erection but must also carry diving planes, guards, and other excrescences, the appendage-resistance ratio submerged may be as high as 2.0 or 3.0. P. Mandel mentions that, in some cases [SNAME, 1953, p. 466], the appendages added to a submarine may cause the total drag to be 5 times that of the bare hull alone!

55.14 The Displacement of Appendages. The drag of an appendage is of course related to its size, although many other factors are involved. It may be of advantage to the marine architect, in the early stages of a preliminary design, to know the approximate size and volume of the average appendage, for ships of a rather wide variety of types.

Table 55.d gives some available information of this kind, in the form of individual weights of salt water displaced. From the data given, the percentages of the overall displacement can be calculated. While these data are by no means modern (Jan 1924) they may serve as the beginning of a more comprehensive and up-to-date compilation.

TABLE 55.d—Displacement of Appendages for U. S. Naval Vessels Prior to 1924

Name of Ship	Type of Ship	Designed $T_g = V/\sqrt{L}$	Displ., long tons	Number of		Type of Bilge Keel	Displacement in Long Tons of Salt Water									Remarks
				Props	Struts		Props	Shaft'g	Struts	Fairings, Short Bossings	Bilge Keels	Dock'g. Keels	Vert. Rudder	Shell Plating	Total	
Ramapo	Tanker	0.52	16,830	1		Plate	1.49				0.82		0.92	100.0	103.23	
Henderson	Transport	0.65	10,000	2	2	Plate	2.00	3.77	2.57	2.86	1.20		2.0	69.7	84.10	
Bridge	Supply ship	0.70	8,500	2	2	Plate	2.1	1.26	1.83	6.28	1.09		1.97	76.10	90.63	
Asheville	Gunboat	0.80	1,575	1		Solid	0.76				2.90		1.46	12.7	17.82	Prop value estimated
Tennessee	Battleship	0.86	32,300	4	4	Solid	2.9	6.1	6.8	8.0	15.4	40.1	incld.*	133.4	212.70	*Included with hull
Mayflower	Yacht	0.88	2,690	2	2	Solid	1.14	2.72	0.23		3.86	Bar keel	0.43	29.80	41.04	
	Fleet tug	1.041	1,000	1		Plate	0.57			0.28		2.86		5.12	9.00	
Widgeon	Minesweeper	1.045	950	1		Angle	0.60			0.87			incld.*	6.17	5.50	Fender, 0.50 Skeg, 0.49
Monocacy	River gunboat	1.045	190	2	2		0.29	0.77	0.01				(4)0.36	1.60	3.03	
Lexington	Aircraft carrier	1.165	39,137	4	4	Plate	8.00	4.69	14.73	35.26	1.43	37.9	incld.*	238.0	340.01	
V-1	Fleet submarine	1.165	2,119	2	2	Plate	0.74	2.14	0.84	Recess (−1.43)	0.36	3.26	3.22	24.6	35.16	Dbl'g. plt., 3.74 Fender, 0.77
Chester (old)	Scout cruiser	1.295	3,781.1	2	2	Solid	1.94	1.86	1.77	1.29	6.71		incld.*	28.85	42.42	
Omaha	Light cruiser	1.44	7,500	4	4	Plate	1.49	3.66	4.32	22.30	0.82	4.48	7.16	102.1	146.33	
Clemson	Destroyer	2.016	1,215	2	2	12″ I-beam	0.17	0.54	0.61	2.00	0.50		incld.*	14.0	17.82	

CHAPTER 56

Observed Resistance Data for Models and Ships

56.1 General Comments. This chapter gives information as to the availability in the technical literature of observed resistance data on models and ships of many types, particularly those tested as systematic or methodic series to determine the effect of certain variables. Accompanying notes indicate, where necessary, the location of the lines or body plans of the models or ships.

These data are supplemented by information concerning the resistance of unusual ship forms or of more-or-less standard forms run at unusual speeds.

Means are described for approximating the resistance of ships when their exact shape is not known, when they have not been tested at model scale at the speed desired, or when their displacements are different from the values for which data are available.

Some self-propulsion test data for typical vessels, plus references to other published data, are to be found in Chap. 60. In almost every case these give the predicted effective power P_E for the ship (or ship design) represented by the model.

56.2 Resistance Data from Tests of Models of Typical Ships. Attempts have been made from time to time, by interested individuals, to list, collect, and systematize the enormous mass of published data on the resistance tests of models. With so much time and energy devoted to this particular field, in the model basins of the world over the past seventy-five years, it is a pity that only a fraction of the existing test data are in a form usable for analysis and design, and in locations available to the naval architect and marine engineer.

The graphic data published by D. W. Taylor in the three editions of "The Speed and Power of Ships" contain, in one form or another, the resistance-speed curves of models representing many forms and types of ships, usually as parts of small groups or series. The period since World War II has brought a realization of the necessity for more systematic presentation of data of this kind, as witness the work of the Swedish State Model Basin and of the David Taylor Model Basin in reporting test data on numerous models of vessels of a given class. There is also a wider realization of the fact that, for analysis purposes on the part of a number of workers, the most comprehensive data on models and ships is none too complete.

A leader in this respect has been the Rome Model Basin. In the annual reports of this establishment ["Annali della Vasca Nazionale per le Esperienze di Architettura Navale"], of which Vols. I through XI are in the TMB library, there are included very complete data sheets and graphs giving the results of tests on selected ship models of a rather wide variety of types. As examples, there are included in Vol. X, published in 1941, test results for six models constructed to the order of various Italian firms. For these models there are given:

(a) Tables I and II, listing the principal dimensions, form coefficients, and other data for from one to five displacement and trim conditions on each model

(b) Tables III and IV, giving the observed drag R_T and speed V for the six models, at different displacements and trims, with water temperatures and other necessary data

(c) Tables V and VI, self-propulsion data for one model and model propeller
(d) Tables VII through XII, body plans, outboard profiles, details of appendages, and section-area curves for the six models
(e) Table XIII, drawing of the model propeller tested
(f) Tables XIV through XIX, curves of R_F, R_R, and expanded P_E for the six models
(g) Table XX, curves of self-propulsion data from the one model tested
(h) Table XXI, curves of C_T for the six models
(i) Tables XXII through XXIV, curves of C_F and C_T for the six models
(j) Tables XXV and XXVI, friction-resistance coefficients f in the dimensional formula $R_F = fSV^{1.825}$, for varied lengths of both model and ship
(k) Tables XXVII through XXIX, values of $\Delta^{1/6}$, $\Delta^{7/6}$, and $\Delta^{53/48}$ for all models.

There have been published, to the date of writing (1956), some 160 SNAME Resistance Data sheets. These carry complete descriptive and test data for the same number of models, representing a great variety of ship sizes and types. The observed resistance data are supplemented by predicted resistance data for geometrically similar ships of appropriate standard length, say 100 ft, 400 ft, or 1,000 ft. An example of the latter is the liner *Normandie*, RD sheet 39. Two sets of resistance data sheets are included in Sec. 78.16, made up for the model tests of (1) the ABC ship with the centerline skeg and transom stern, TMB model 4505, and (2) the ABC ship with the arch-type stern, TMB model 4505-1. The RD sheets for TMB model 4505 were also published in 7th ICSH, 1954 [SSPA Rep. 34, 1955, pp. 302–304].

There are available, to accompany the whole set of sheets:

I. Explanatory Notes for Resistance and Propulsion Data Sheets, SNAME Tech. and Res. Bull. 1–13, Jul 1953
II. Index to Model and Expanded Resistance Data Sheets Nos. 1–150, SNAME Tech. and Res. Bull. 1–14, Jul 1953
III. Summary Sheets, 7 in number, containing summarized data for RD sheets 1 through 160, and additional information needed for analysis.

A series of 29 data sheets containing the model-test data on that number of fishing-boat hulls, most of them run at several displacements, are published by Jan-Olof Traung on pages 281–310 of the book "Fishing Boats of the World," reviewed in the first part of Sec. 76.12. These sheets are similar to the SNAME RD sheets described elsewhere but contain less information per sheet.

There has recently been issued (November 1955), Part 1 of a group of "Fishing Boat Tank Tests," comprising data sheets on 150 models of fishing craft. Copies of this catalog may be obtained on application to the Fishing Boat Section, Technology Branch, Fisheries Division, Food and Agriculture Organization (FAO) of United Nations, Rome, Italy.

56.3 Systematic Resistance Data From Model Series; Taylor Standard Series with Contours of R_R/Δ. To make possible the calculation of the approximate residuary resistance of ships of widely varied shape and proportions, D. W. Taylor devised his now-famous Standard Series, with the thought that the residuary resistance of a ship could be predicted reasonably well from the measured resistance of a model *of the same proportions.*

Taylor's primary purpose was supplemented eventually by another, equally valuable if not equally important. This was the gradual but wide acceptance of the Taylor Standard Series residuary resistance as the yardstick for evaluating the worth of a particular shape of hull. This is done by comparing its *residuary resistance* to that of the Taylor Standard Series parent form of identical proportions. So outstanding was the shape of this parent form, derived from the hull of the British armored cruiser *Leviathan* [S and P, 1943, p. 181], that even a half-century later it is a definite mark of achievement to beat the Taylor Standard Series in that part of the speed range where optimum ship behavior is sought.

The parameters varied in the Taylor series, now known as the *proportions* of the models (and ships), were:

(a) Beam-draft ratio, B/H
(b) Displacement-length quotient, $\Delta/(0.010L)^3$, defined in Appx. 1
(c) Prismatic coefficient, C_P
(d) Speed-length quotient, $T_q = V/\sqrt{L}$, also defined in Appx. 1.

The parent form used by Taylor is described in Sec. 51.2. The lines and principal features of this form, together with eight curves of section areas

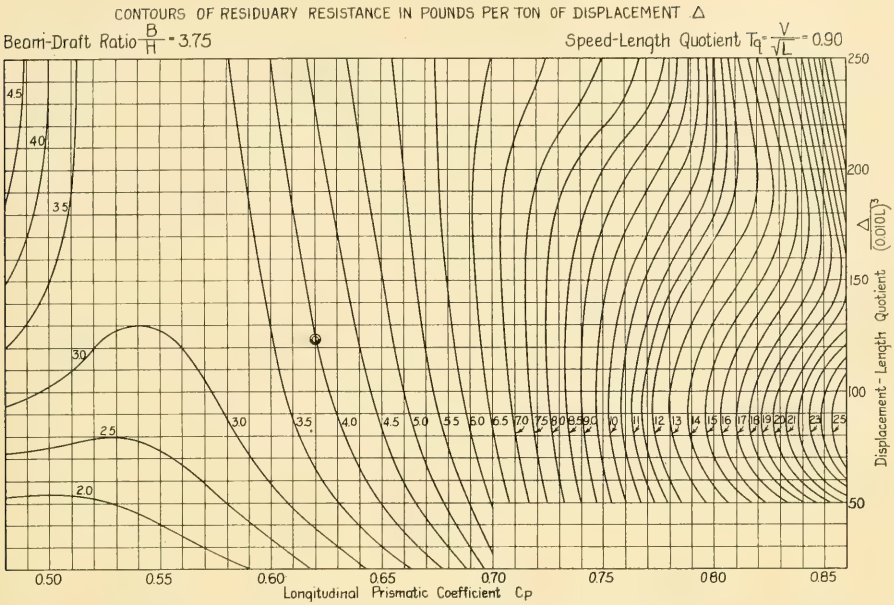

FIG. 56.A CONTOURS OF R_R/Δ FOR TAYLOR STANDARD SERIES MODELS HAVING A B/H OF 2.25, AT A T_q OF 0.90

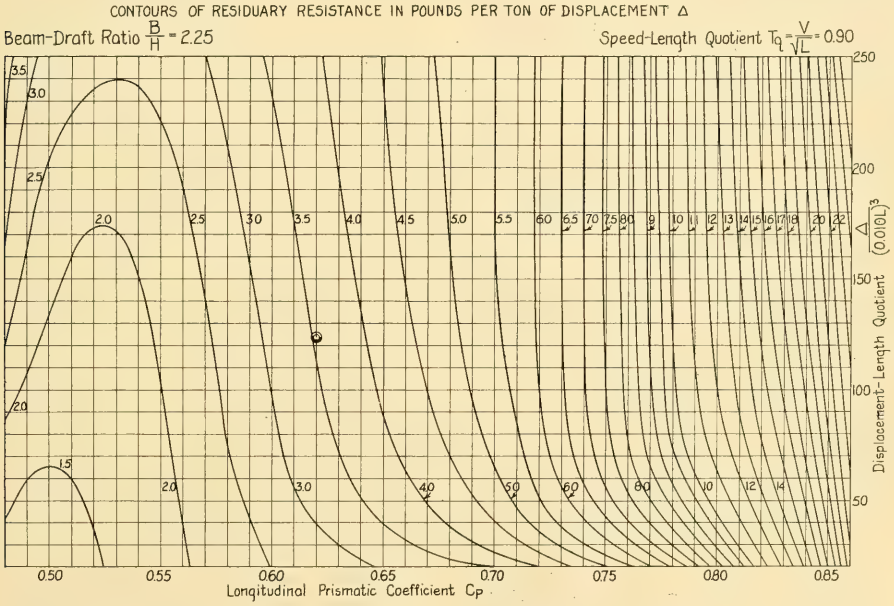

FIG. 56.B CONTOURS OF R_R/Δ FOR TAYLOR STANDARD SERIES MODELS HAVING A B/H OF 3.75, AT A T_q OF 0.90

for C_P values of 0.48 through 0.80, are shown in Fig. 51.A, based upon data from the following references:

(1) S and P, 1910, Vol. II, Figs. 79 and 80
(2) S and P, 1933, Figs. 70 and 71, p. 191
(3) PNA, 1939, Vol. II, Fig. 28, p. 92
(4) S and P, 1943, Figs. 184, 185, and 186, pp. 182–183.

The end results, in the form of contours of residuary resistance R_R in pounds per ton of displacement Δ for the given proportions, were published in the three editions of "The Speed and Power of Ships," as noted:

1910, Vol. II, Figs. 81 through 120, covering a range of T_q from 0.60 through 2.00, for two B/H ratios, namely 2.25 and 3.75, and for various ranges of displacement-length quotient and prismatic coefficient

1933, Figs. 72 through 111, pages 193 through 271, covering the same range of T_q , $\Delta/(0.010L)^3$, and C_P as for the 1910 edition

1943, Figs. 189 through 240, pages 189 through 240, covering a range of T_q of from 0.30 through 2.00, with the other variables remaining the same.

Two sets of contours from the latter reference are reproduced in Figs. 56.A and 56.B. They were selected to fit the ABC ship example of Sec. 57.6.

To use these contours, values of R_R/Δ are:

(a) Picked from two sheets for a B/H ratio of 2.25, (1) for a speed-length quotient just below that desired and (2) for a speed-length quotient just above it. The contours are entered with the C_P value along the horizontal scale and the $\Delta/(0.010L)^3$ value along the vertical scale.
(b) Picked from two sheets for a B/H ratio of 3.75, (1) for speed-length or Taylor quotients just below and (2) just above the desired value. These are the same T_q values as for (a) preceding.

The correct value of R_R/Δ is then found by linear interpolation first, between the B/H ratios of 2.25 and 3.75, and then between the two speed-length quotients.

To illustrate this procedure an example is worked out in Sec. 57.6 and Table 57.b for the transom-stern ABC ship having the preliminary characteristics listed as the fifth approximation in Table 66.e of Sec. 66.11.

56.4 Japanese Fishing-Vessel Standard Series. Because the Taylor Standard Series extended only to a maximum displacement-length quotient of 250, corresponding to a 0-diml fatness ratio $\nabla/(0.10L)^3$ of 250/28.51 or 8.77, it could not be used for predicting the performance of fat, chubby ship forms such as those of tugs, fishing vessels, and icebreakers. During the years 1946–1949 a group of Japanese, Atsushi Takagi, Takao Inui, and Shoichi Nakamura, undertook the testing of a standard fishing-vessel series covering 0-diml fatness ratios of from 6 through 15, corresponding to a range of Taylor displacement-length quotient of 171 through 428. The B/H values were 2.2 and 3.0, while the C_P values were 0.55, 0.60, 0.65, 0.70, and 0.75. The range of Froude number F_n was 0.16 to 0.38, corresponding to a T_q of 0.537 to 1.28.

Following their procedure of putting all parameters in 0-diml form, the Japanese plotted contours of specific residuary resistance C_w , where $C_w = R_W/(0.5\rho\nabla^{2/3}V^2)$. The data were published in final form in 1950 by the Fisheries Agency of Japan in a book entitled "Graphical Methods for Power Estimation of Fishing Boats."

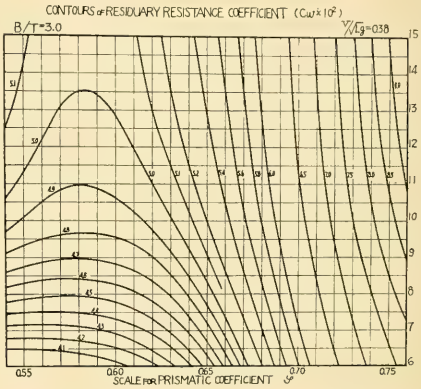

Fig. 56.C Typical Sheet of Contours of Residuary-Resistance Coefficient for Japanese Fishing-Vessel Series

Fig. 56.C is a reproduction of one of the contour sheets of this book, suitable for estimating the C_R values for the European fishing-boat model of J.-O. Traung, shown in Fig. 76.G. In this sheet the Japanese B/T, C_w , and ϕ(phi) expressions correspond to the B/H, C_R , and C_P expressions in the present book.

Unfortunately, the parent form selected for the Japanese fishing-boat series has too large a prismatic coefficient and gives a rather indifferent performance. It is possible to improve upon it in modern designs by as much as 10 per cent by lowering the C_P value from 0.70 to the order of 0.58. Furthermore, the models tested were not

more than 2.00 m or 6.56 ft in length; some of them were as short as 1.80 m, or 5.91 ft. There are no data to indicate the water temperatures at which these models were run nor what steps were taken, if any, to insure turbulent flow throughout.

Copies of these books, for those who wish to use the data, are to be found in:

(a) SNAME Headquarters in New York
(b) Bureau of Ships Technical Library, U. S. Navy Department
(c) Bureau of Ships Preliminary Design Section
(d) TMB Library.

56.5 Gertler Reworking of Taylor Standard Series Data of 1954, with Contours of C_R. When the American Towing Tank Conference decided in 1947 to adopt the Schoenherr friction-resistance formulation it was realized that this procedure would predict effective powers not directly comparable to those calculated from the original TSS contours mentioned and illustrated in Sec. 56.3.

The differences in the calculated effective powers result from two causes:

(a) The differences between the friction resistances obtained from the Schoenherr formulation and those from the old EMB 20-ft friction-plank results in the model range
(b) The differences between the friction resistances obtained from the Schoenherr formulation in the ship range and from the Tideman data used by D. W. Taylor [Schoenherr, K. E., SNAME, 1932, p. 285; PNA, 1939, Vol. II, Table 9, p. 114].

Item (a) is reflected as a difference in residuary resistance and thus requires that a lengthy correction to made to D. W. Taylor's R_R/Δ contours to render them comparable to modern data. Item (b) merely requires a substitution of the Schoenherr formulation with the appropriate roughness allowance to correspond to the Tideman data in the ship-prediction procedure.

In view of this situation, plus the fact that water temperatures and turbulence stimulation were not taken into account in the original TSS testing, it was decided at the David Taylor Model Basin to reanalyze the original test data on the Taylor Standard Series models. In the reanalysis, the methods and procedures employed were essentially the same as those currently used at Carderock. A total-resistance coefficient for the model was computed, from which an ATTC 1947 or Schoenherr friction-resistance coefficient was subtracted to give the residuary-resistance coefficient C_R.

The method of correcting for the effects of transition flow is based on the assumption that at low Froude numbers the specific residuary-resistance coefficient $C_R = R_R/(0.5\rho SV^2)$ is practically constant, as indicated in the left portion of Fig. 7.H. The original data showed that in general C_R decreased with decreasing speed so long as wavemaking resistance was important. There was then a short range of speed for which C_R remained constant, after which, as the speed was still further reduced, the coefficient again began to decrease. This latter decrease was attributed to transition flow, and was ignored. The practically constant value of the coefficient C_R is therefore used for all lower Taylor quotients T_q and Froude numbers, down to values of $T_q = 0.5$, $F_n = 0.149$.

Although this procedure is not rigorous, a number of recent tests of TMB 20-ft models which were towed with and without a turbulence-stimulating device indicate that in general turbulence stimulation results in no resistance change for models which experience only minor transition effects and those only at the lowest speeds. Good agreement was attained in most of these cases between the residuary-resistance coefficient curves from the unstimulated experiments, faired in the manner described, and those resulting from the tests with the turbulence-stimulating device. This seems to be especially true with forms having the TSS type of bow. Two 20-ft models of the Taylor parent form, having (longitudinal) prismatic coefficients C_P of 0.613 and 0.746, were tested at the Taylor Model Basin in 1951. In both cases it was found that turbulence stimulation was required only at low speeds. The procedure described in the foregoing gave reasonable agreement with the curves in the turbulent range [Todd, F. H., and Forest, F. X., SNAME, 1951, p. 678].

Corrections for restricted-channel effects in the Washington Basin were made by using the formulas given in TMB Report 460 entitled "Tests of a Model in Restricted Channels," by L. Landweber, dated May 1939, with the appropriate model and basin dimensions. This correction was in most cases small; even for the fullest model of the series it amounted to a decrease in resistance of only 2 per cent.

The results of the re-analysis of the Taylor Standard Series data, carried out by M. Gertler

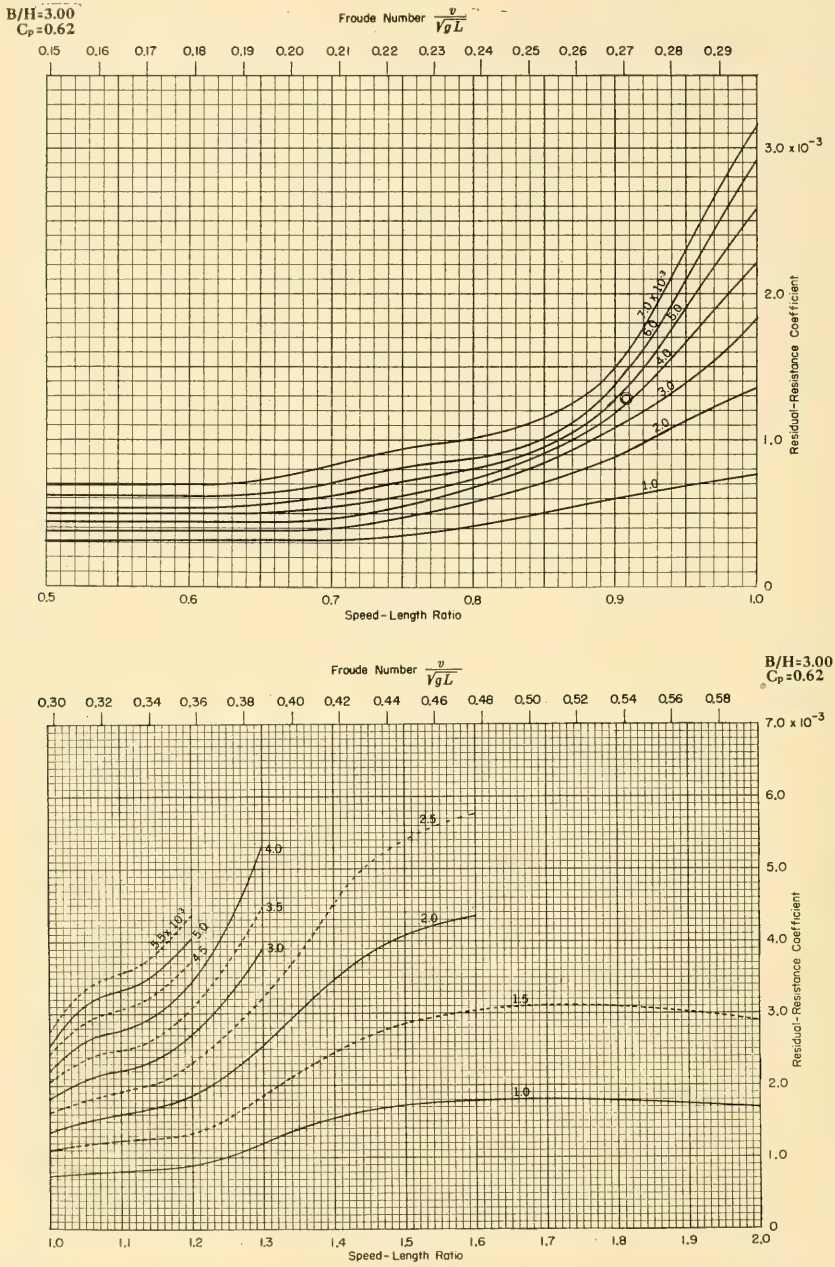

FIG. 56.D TYPICAL SET OF C_R CONTOURS FROM GERTLER REWORKING OF THE TAYLOR STANDARD SERIES DATA

and other members of the TMB staff, are given in a form which employs a completely 0-diml presentation [Gertler, M., "A Reanalysis of the Original Test Data for the Taylor Standard Series," TMB Rep. 806, Mar 1954, Govt. Print. Off., Washington]. The faired resistance data are given as curves of specific residuary-resistance coefficient C_R on a basis of both Taylor quotient $T_q = V/\sqrt{L}$ and Froude number $F_n = V/\sqrt{gL}$. Two of the major proportions used are, as before, the B/H ratio and the (longitudinal) prismatic coefficient C_P. The scope of the series has been enlarged to include a third B/H ratio of 3.00 in addition to the ratios of 2.25 and 3.75 published in the 1910, 1933, and 1943 editions of D. W. Taylor's "The Speed and Power of Ships." The intermediate values were obtained by interpolation, using the reworked data for the hitherto unpublished EMB Series 20 which had a B/H ratio of 2.92.

Instead of Taylor's dimensional displacement-length quotient the Gertler reworking makes use of the 0-diml volumetric coefficient $C_\nabla = \nabla/L_3$, expressed as a simple number times 10^{-3}. This number, without the 10^{-3} factor, is exactly the same as the ATTC fatness ratio $\nabla/(0.10L)^3$. The original Taylor wetted-surface coefficient $C_{WS} = S/\sqrt{\Delta L}$, which is dimensional, is replaced by the 0-diml $C_S = S/\sqrt{\nabla L}$.

These and the remaining steps in the reworking process are explained most comprehensively and meticulously by Gertler in the Preface and introductory portions of TMB Report 806, previously referenced.

The new presentation differs markedly from the original. Examining a pair of facing pages, reproduced as the two parts of Fig. 56.D, one sees the graphs of C_R for various volumetric coefficients $C_\nabla = \nabla/L^3$, or fatness ratios $\nabla/(0.10L)^3$, extending from the lowest speed-length quotient T_q of 0.5 to the highest value of 2.0. All the humps and hollows in the complete range of C_R, for any volumetric coefficient, are visible at a glance.

The pair of facing pages embodied in Fig. 56.D is used with another pair of pages, not reproduced here, to derive a preliminary estimate of the residuary resistance of the ABC ship, by the method described in Sec. 57.6 and illustrated in Table 57.c. The characteristic spot for the ABC ship values listed in that table is added to the figure.

Gertler's data have the disadvantage that the effect of variation of C_P on R_R/Δ is not readily apparent. By moving right and left across the page, the original Taylor contours show clearly the change in R_R/Δ for a change in C_P. However, in the range of T_q or F_n where friction resistance predominates, say below a T_q of 1.15, F_n of 0.342, the selection of C_P is *not* made on the basis of a minimum value of R_R/Δ. The effect of $\Delta/(0.010L)^3$ or $\nabla/(0.10L)^3$ on residuary resistance is shown well by both the Gertler reworking and the original Taylor Standard Series contours. The Gertler data have the advantage that, with three B/H ratios, interpolation is easier and more accurate. Indeed, for many B/H values close to 2.25, 3.00, and 3.75, and for a preliminary resistance estimate, interpolation for beam-draft ratio may be omitted entirely.

Although never stated in print in so many words it was felt by many that the R_R/Δ contours of the 1910, 1933, and 1943 editions of "The Speed and Power of Ships" were rather "heavily" faired, probably because in some regions there were not many spots with which to establish the proper contour positions on the diagrams. Comparisons of P_E for random models with the P_E values of the TSS models of the same proportions, corresponding to the EHP/Taylor EHP ratios of the SNAME Expanded Resistance Data sheets, when plotted on V or T_q, produced what are known as "angleworm" curves. Although many of these random models represented ships of superior and outstanding performance, their "angleworm" curves showed rapid and often violent plus and minus fluctuations in the values of [1 − EHP/Taylor EHP], on a basis of variation in the speed-length quotient T_q.

When the TSS data were reworked in 1948–1951, all "heavy" fairing was carefully avoided. Nevertheless, variations in the ratio of P_E to the reworked TSS P_E values still occur. If not angleworm in shape they are sinuous and irregular, and they are not always consistent with the variations of the original data. Additional comments on this feature are found in Sec. 57.6.

56.6 Resistance Data for Very Fat Ships. The lack of resistance data for ship forms of large 0-diml fatness ratio $\nabla/(0.10L)^3$, for which the Takagi Series described in Sec. 56.4 fills a partial need, led to the analysis of EMB and TMB test data for 44 fat models by R. F. P. Desel and J. T. Collins. The results are embodied in an MIT thesis submitted by them, dated 1952 [copy in the TMB library]. Although there were 13 tug models in the group, and 15 combinations of the

old U. S. Shipping Board parallel-middlebody bows, midship portions, and sterns [EMB Series 53, reported in S and P, 1943, pp. 70–72, 257–271], the models of the whole group forming the basis of this study were only loosely related. Some were tested in bare-hull condition, and others with various combinations of appendages. The B/H ratios varied irregularly but lay within the range of 2.0 to 3.0. The form coefficients were calculated on a basis of length on the waterline. Residuary resistances were derived by using the ATTC 1947

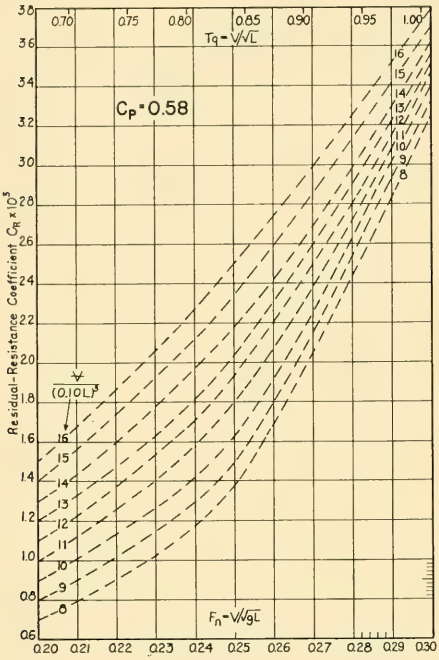

FIG. 56.E C_R DATA FOR FAT SHIPS, C_P = 0.58

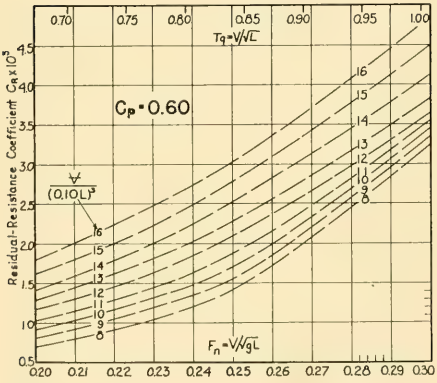

FIG. 56.F C_R DATA FOR FAT SHIPS, C_P = 0.60

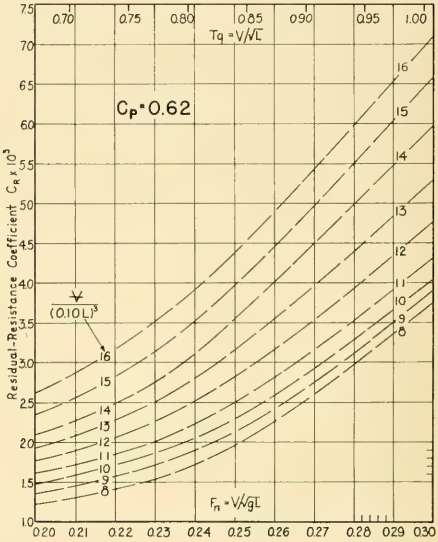

FIG. 56.G C_R DATA FOR FAT SHIPS, C_P = 0.62

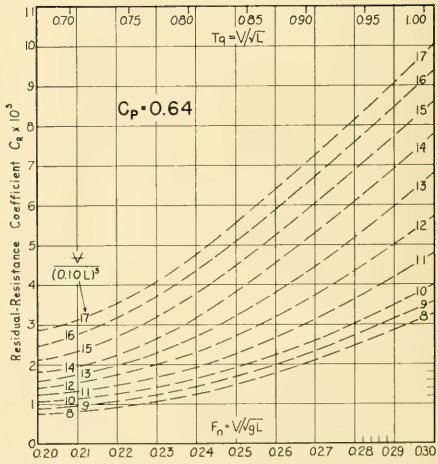

FIG. 56.H C_R DATA FOR FAT SHIPS, C_P = 0.64

friction formulation. Unfortunately, the speed range extended only from Froude numbers of 0.20 to 0.30, corresponding to T_q values of 0.672 to 1.007. Takagi's F_n range was from 0.16 to 0.38.

The thesis data thus derived are in the form of contours of fatness ratio $\forall/(0.10L)^3$ on a basis of C_R and C_P for eight equidifferent values of C_P, plotted on ten sheets for as many different F_n's. The cross-contours of fatness ratio, when plotted on C_R and F_n, for seven equidifferent values of C_P, appear in Figs. 56.E through 56.K. When thus presented they resemble those for the Gertler reworking of the Taylor Standard Series described in Sec. 56.5. The Desel-Collins data for $C_P = 0.72$ are omitted because this is much too large a C_P value for easy driving of a chubby, fat form.

Because of the unrelated forms and the rather severe fairing necessary to achieve a regular pattern of data it was not possible in this group of models to indicate the humps and hollows known to occur with change of speed and F_n. For this and other reasons the contours are shown as broken lines. Although lacking the reliability to be expected from tests of a comprehensive systematic series, these data nevertheless furnish an indication of residual resistance to be expected

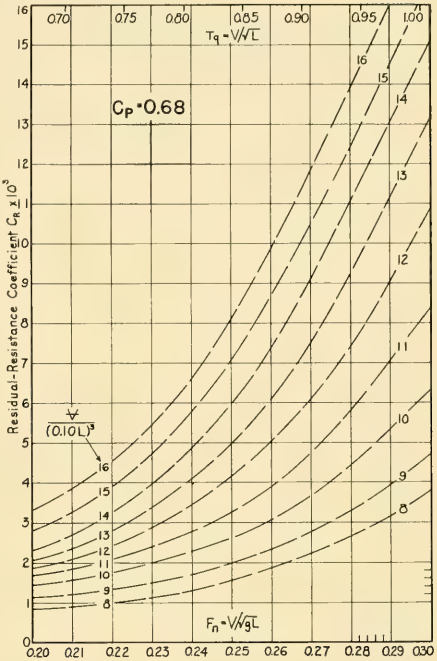

FIG. 56.J C_R DATA FOR FAT SHIPS, $C_P = 0.68$

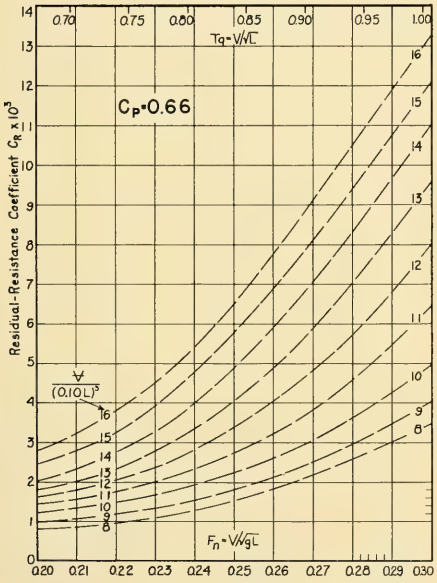

FIG. 56.I C_R DATA FOR FAT SHIPS, $C_P = 0.66$

in a region where few systematic model tests have been made.

Among the latter are tests of six fat models, expanded from the Taylor Standard Series, having displacement-length quotients of 300 and 400 (fatness ratios of 10.49 and 13.98, respectively), C_P values of 0.50, 0.60, and 0.70, and a B/H ratio of 2.25. Test data for these six bare-hull models are given in SNAME RD sheets 105 through 110 [ETT, Stevens, Rep. 279, Jan 1945]. Comparison of these latter data with the Desel-Collins contours indicates considerably lower—in some cases much lower—C_R values for the Taylor forms. This is due partly to the excellence of the TSS parent form and partly to the omission of all appendages on the Taylor models in the Stevens tests.

No examples are given for Figs. 56.E through 56.K because they are used in much the same way as the Gertler data in TMB Report 806.

H. H. Hagan, in a brief article entitled "The Powering of Ships" [SBSR, 7 Oct 1937, pp. 453–455] gives some information to serve as a

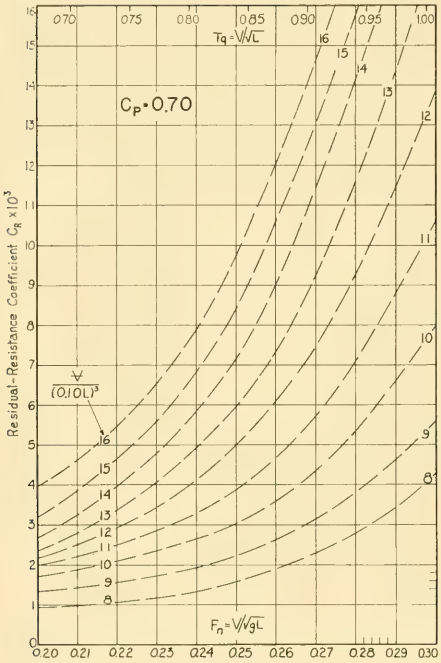

FIG. 56.K C_R DATA FOR FAT SHIPS, $C_P = 0.70$

guide in making resistance and power estimates for ships having displacement-length quotients in excess of those of the Taylor Standard Series. The data given are based upon the use of the Froude circular-constant system of notation.

56.7 Systematic Resistance Data for Parallel-Middlebody Variations. The first systematic model test data on the effect of varied amounts of parallel middlebody inserted between given entrances and runs were those published by W. Froude [INA, 1877, Vol. XVIII, pp. 77–97]. He plotted curves of residuary resistance R_R for constant speed V on a basis of length L_P of parallel middlebody, a procedure which has not been improved upon to this day. The low points in the R_R curves for a succession of speeds, or for a given speed, indicate the L_P values for minimum residuary resistance. These are not necessarily the values for minimum total resistance.

Data from tests of the 156 combinations of EMB Series 53, tested in 1931 for the U. S. Shipping Board and plotted on the Froude system, are published in:

(1) S and P, 1933, pp. 47, 67, 68, and Appendix D, pp. 299 through 327
(2) S and P, 1943, p. 50 and pp. 70 through 72; also Appendix D, pp. 255 through 271
(3) Brief extracts from these data are given by K. S. M. Davidson in PNA, 1939, Vol. II, pp. 67–69.

It is to be noted from the body plan of the parent form, given on page 257 of reference (2) above, that the Series 53 models had practically no bulb and were not patterned on the Taylor Standard Series lines.

The analysis of these parallel middlebody data, not completed for the 1933 and 1943 editions of "The Speed and Power of Ships," still remains to be done.

56.8 Resistance Data for Very Low Ship Speeds. Published data on ship resistance predicted from model tests rarely include the range all the way down to zero speed, yet it is often convenient to have some idea of the low-speed resistance, or at least to know how it varies with speed in this region.

The tables of C_F in SNAME Tech. and Res. Bull. 1–2 of March 1952, two small portions of which are reproduced as Tables 45.c and 45.d of Sec. 45.9, extend down to an R_n of 0.1 million, corresponding to a fore-and-aft space dimension of about 0.73 ft and a speed of 1 kt. The Taylor Standard Series contours [S and P, 1943] stop at a speed-length quotient T_q of 0.30, F_n value of about 0.089. The SNAME RD and ERD sheets carry down to a T_q and an F_n of about the same value.

A residuary resistance composed entirely of pressure resistance should vary as V^2 all the way to $V = 0$. However, plots of R_R/Δ on $V/\sqrt{L}$ for low speeds in the Taylor Standard Series show that it is the exception rather than the rule for the exponent of the curve of R_R on V to approximate 2. This is due partly to the extremely low resistances being measured but there appear to be evidences of viscous and other effects not entirely eliminated in the Froude model-testing procedure.

An approximation to the residuary resistance close to $V = 0$ is derived from a plot of R_R/Δ on $V/\sqrt{L}$ on log-log paper, somewhat similar to that of Fig. 30.B, for say three values of $V/\sqrt{L} =$ 0.40, 0.35, and 0.30. Extending the line in a generally straight direction downward gives an idea of the low value of R_R on T_q desired.

56.9 Rate of Variation of Model Residuary Resistance with Speed. For certain lines of analysis it is useful to know the rate at which the

residuary resistance of the hull of a model varies with speed in the equation $R_R = k(0.5\rho)SV^n$. This matter was investigated many years ago by D. Kemp [INA, 1883, pp. 124–125]. He stated that on the steam yacht *Oriental* the resistance (total in this case) varied as about V^2 in the low-speed range, but increased to about V^4 in a T_q range of 0.82 to 1.04, F_n of 0.244 to 0.310. It is known from measured ship-thrust data that R_F for hull surfaces of normal roughness varies as slightly less than the square of the ship speed, probably of the order of the 1.9 or 1.93 power. Although the absolute values of C_F cover a rather wide range, the rates of change of C_F with V, as indicated by a plot of C_F on R_n (with L and ν(nu) constant), are comparatively small. That portion of the hull drag due to deflection of the water, separation, and similar effects is assumed to vary as V^2. Unfortunately, since R_R includes these effects plus the drag due to wave-making, it is still difficult to break up what has hitherto been classed as residuary resistance into physical entities.

Analytic work on pressure drag due to wave-making, described in Chap. 50, indicates that what may be termed the V^2 component is only one of those acting. There are components of this drag which vary as the 4th, the 6th, the 8th, and higher powers of V. The expressions for these components are periodic in form, and they produce humps and hollows in the predicted ship-resistance curve, similar to those due to surface-wave interferences in model tests. It is to be expected, therefore, that graphs of pressure drag on a basis of speed will show rather pronounced irregularities.

D. W. Taylor made up graphs of this type for two groups of five models each, representing 400-ft ships. The two groups had C_P values of 0.56 and 0.64, respectively, and five different displacements, with ship values ranging from 1,920 to 11,520 tons. Using the formula $R_R = aV^n$ and plotting the velocity exponent n on a basis of ship speed, he obtained the curves shown in Fig. 54 on page 48 of S and P, 1943. For some of the models the residuary resistance varied at a rate exceeding the 11th power of the speed V. This diagram shows definite, rather narrow lanes embracing all the n values over certain speed ranges, despite the 1 to 6 variation in displacement-length quotients.

To determine whether there are systematic or characteristic patterns in the exponent n of the residuary-resistance formula $R_R = kV^n$, for the principal forms of ship hulls, there are plotted in Fig. 56.L the values of n from model test data on nine different vessels, as reported on the SNAME RD sheets listed hereunder:

RD sheet 39	Passenger ship	*Normandie*
56	Tanker	Tanker E [SNAME, 1948, pp. 368–369]
74	Tug	TCB Design TX-7
79	Cargo ship	U. S. Mar. Comm. *C-2* cargo vessel
92	Ore ship	*Wilfred Sykes*
96	Destroyer tender	U. S. S. *Dixie*
119	Destroyer	U. S. S. *Hamilton*
121	Heavy cruiser	U. S. S. *Pensacola*
	ABC ship of Part 4	Transom-stern design.

The residuary resistances for these models were calculated from the formula $R_R = C_R(0.5\rho)SV^2$, using the values of residuary resistance coefficient 10^3C_R listed on the RD sheets for a range of speed-length quotients. These were, in turn, calculated from the observed model resistance data and the ATTC 1947 friction formulation, as described in the SNAME Explanatory Notes accompanying the RD sheets, Technical and Research Bulletin 1–13, July 1953.

The ship wetted surfaces were obtained from the model wetted surfaces by multiplying by λ^2(lambda). The R_R values were plotted on log-log paper on a basis of T_q and F_n. The velocity exponents n were obtained by measuring the slopes of the R_R curves at even T_q values. This work is facilitated by the use of special log-log plotting sheets, available at the David Taylor Model Basin, which have a supplementary scale of slopes around the margin, to which a slope anywhere on the sheet is transferred by a set of parallel rulers.

A curve of R_R increasing with V on Fig. 56.L is associated with a finite positive value of n. If the resistance remains constant with increasing V, then $n = 0$, whereas if R decreases as V increases, which it does in certain speed ranges for planing and other craft, as shown on Fig. 53.D, n becomes negative. Large circles on the n-curves indicate the T_q for the designed speed along the curve for each ship.

The new velocity-exponent curves indicate that:

(a) The curves for various ship types by no means follow the same pattern, nor do they fall in lanes, as do D. W. Taylor's earlier data [S and P, 1943, p. 48]

(b) The n-value for the big ore ship reaches 5.75

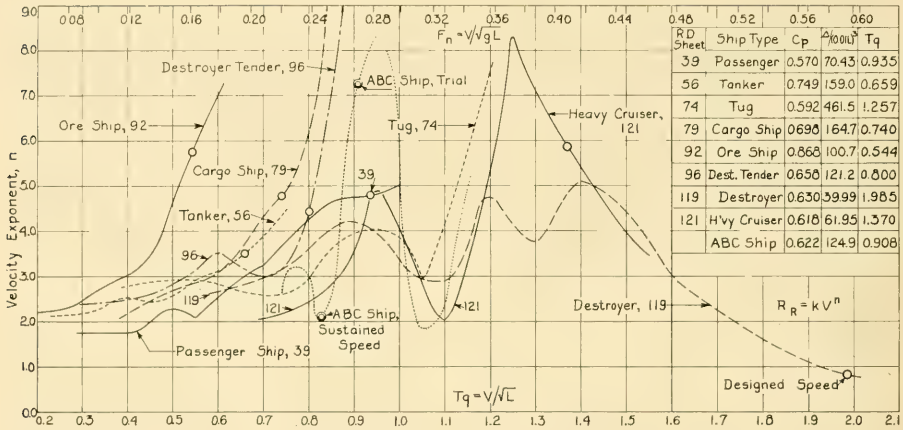

RD Sheet	Ship Type	C_p	$\Delta/100LJ^3$	T_q
39	Passenger	0.570	70.43	0.935
56	Tanker	0.749	159.0	0.659
74	Tug	0.592	461.5	1.257
79	Cargo Ship	0.698	164.7	0.740
92	Ore Ship	0.868	100.7	0.544
96	Dest. Tender	0.658	121.2	0.800
119	Destroyer	0.630	39.99	1.985
121	H'vy Cruiser	0.618	61.95	1.370
	ABC Ship	0.622	124.9	0.908

FIG. 56.L VARIATION OF SPEED EXPONENT IN RESIDUARY-RESISTANCE FORMULA $R_R = kV^n$ FOR NINE LARGE SHIPS

at the designed T_q of 0.544. This indicates that the large volume on a given length, characteristic of this ship, is carried at an unreasonably high price in wavemaking resistance. The n-value is only slightly over 3.0 at a T_q of 0.4. This reveals an acceptably low wavemaking drag for the lower speeds customary with this type when it was first developed into large sizes in the early 1900's.

(c) For actual ships which are driven hard, values of n exceeding 7.0, 8.0, and over are by no means unusual. High-speed ships may reach the greatest n-value at a speed less than the maximum, with a greatly diminished n at that speed, as for the heavy cruiser *Pensacola* and the destroyer *Hamilton* in Fig. 56.L. The following footnote by C. Rougeron is quoted from the U. S. Naval Institute Proceedings, February 1953, page 190:

"Actually, the speed-power ratio increases in a somewhat more complicated manner. In a recent French flotilla leader the 'direct' resistance is found to vary in proportion to the square of the speed at low speeds, to the 6th power of the speed in the vicinity of 28 knots; and only to the 1.35 power of the speed for speeds in the vicinity of 38 knots."

(d) Some planing craft show pronounced knuckles in the curve of R_R on V, with accompanying sudden drops in the value of n, as in Fig. 30.B. The data from which Fig. 53.D of Sec. 53.7 were plotted show no such sharp discontinuities but they do reveal that at several points the resistance levels out so that it varies with V at some power only slightly greater than 1.0.

(e) For high-speed planing craft it may be expected that, at T_q values near the maximum, n will be negative. This occurs for the PT boat in Fig. 53.D.

(f) There are irregularities in the n-curves unexplained on the basis of wave interference alone.

56.10 Variation of Total Resistance of Model and Ship with Speed-Length Quotient. It is useful at times for the designer to be able to find quickly the total resistance of a ship in some everyday terms such as pounds of total resistance per ton, expressed by R_T/Δ, at say the designed speed, when only the type of ship and the approximate Taylor quotient $T_q = V/\sqrt{L}$ or Froude number F_n are known. For example, the R_T/Δ value for a large, modern Great Lakes freighter at designed speed is about 2 lb per ton, that of an Atlantic liner is some 10 lb per ton, and that of a fast motorboat is of the order of 600 lb per ton. H. M. Barkla has published a log-log plot showing values of the ratio R_T/W on a base of T_q for eleven sailing-yacht and motorboat hulls, as listed on page 237 of his paper "High-Speed Sailing" [INA, 1951, Vol. 93]. The range of T_q is from 0.4 to 10 and of R_T/W from 0.004 to 0.3. Barkla's resistance-weight ratio is 1/2,240 times the ratio R_T/Δ, when the latter is expressed as pounds resistance per long ton of weight.

To provide data for a greater variety of water craft, both large and small, there have been plotted on Fig. 56.M the values of R_T/Δ, *at the designed speed,* of a considerable number of

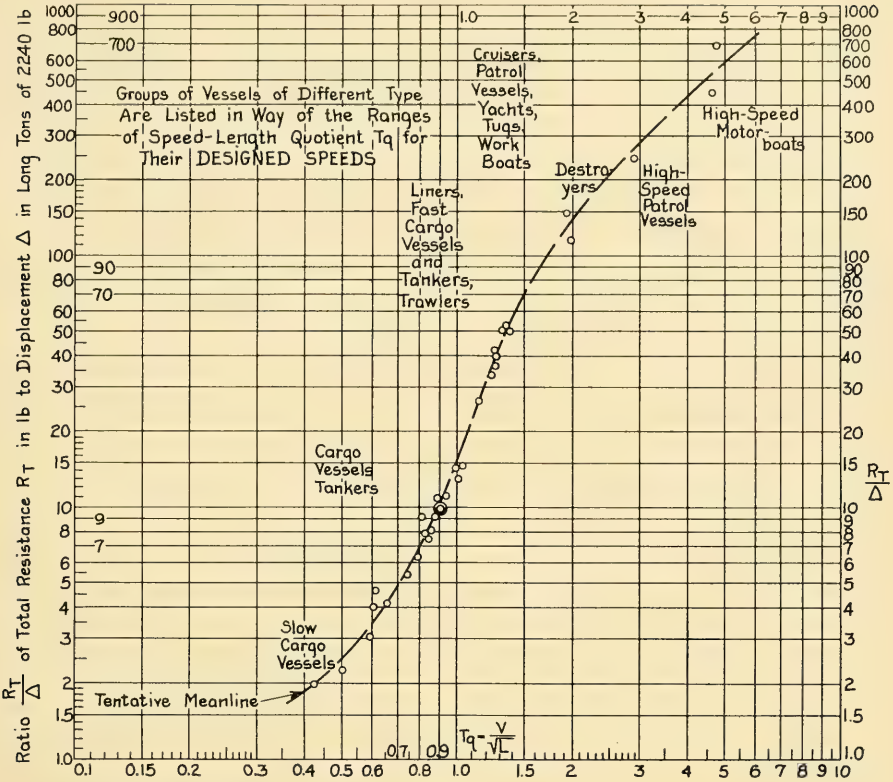

FIG. 56.M PLOT OF R_T/Δ ON T_q FOR MANY VESSELS AT THEIR DESIGNED SPEEDS

vessels of many types. The data indicated by the small circles on the figure are derived from calculated values of the total resistance of the ship, based upon model tests, at the speed listed in the general-information block on the respective SNAME RD sheets. Unfortunately, the model data on some sheets are for bare hull only; on other sheets they are for the hull plus simple appendages. This variation is considered not too important as the plot is intended for indicating approximate values only.

It is found that a single tentative meanline passes close to or through most of the designed-speed spots, regardless of the size or type of vessel or of the T_q at which it runs. For the higher T_q values there is considerable dispersion in the few available spots, especially as the vertical scale is logarithmic and the variations in per cent are considerably larger than the apparent variations on the figure. It is possible that a single meanline will not suffice in this region, especially in view of the large variations in characteristics of vessels running at the same T_q value. For instance, the upper circle at a T_q of about 1.93 represents a small patrol boat with a displacement-length quotient of 93.4, while the lower circle at a T_q of about 1.985 represents the destroyer *Hamilton*, with a displacement-length quotient of only 40. The plot of Fig. 56.M does, however, indicate regions of T_q where the data for certain classes of vessels are to be found.

It is probable that, as more model data are plotted in the upper right-hand corner of this graph, the final meanline will be considerably lower than the one now indicated, especially for high-speed craft of good to excellent performance.

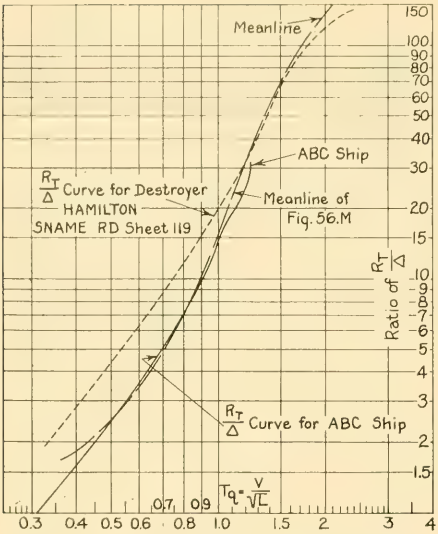

FIG. 56.N VARIATION OF R_T/Δ WITH SPEED-LENGTH QUOTIENT FOR TWO VESSELS

To determine whether the variations in R_T/Δ *for any one ship* follow the tentative meanline of Fig. 56.M for variations *in its own speed range*, a second plot in Fig. 56.N indicates the variation of R_T/Δ, on a base of T_q, for the destroyer *Hamilton* and for the transom-stern ABC ship designed in Part 4 of the book. At and not too far below the designed speeds of each vessel, at T_q values of roughly 1.9 for the *Hamilton* and 0.9 for the ABC ship, the agreement is fair for the former and remarkably good for the latter. This agreement covers both the slope and the position of the curves with respect to the tentative meanline of Fig. 56.M. Barkla also found, for the eleven boats mentioned by him in the reference cited earlier, that the total resistance-weight ratios for all of them plotted along S-shaped curves that lay remarkably close together.

It appears from the foregoing that a single meanline gives an acceptable quick approximation to the value of R_T/Δ for a wide range of T_q, regardless of the type of ship involved. Also that its slope affords a means of approximating the change in R_T/Δ to be expected for a given change in T_q at or near the designed speed.

It is manifest that additional data are needed for defining the meanline, either as a line or as a lane, in the region of Taylor quotient above 1.5.

56.11 Changes in Resistance with Changes of Trim and Displacement. It is customary, when towing a ship model, to observe the resistances at weight displacements other than the designed value W, say at $0.10W$ light and $0.10W$ heavy. Often a third set of resistances is measured at $0.20W$ light, all with zero trim. A fourth set of runs may be made in a so-called ballast condition, in which the ship is carrying a light load or cargo but is trimmed well by the stern to keep the stern propeller submerged. Despite the wealth of data on this subject known to be available at the David Taylor Model Basin, there has been no opportunity to analyze it and place it in readily usable form.

The designer is interested primarily in the effective and propeller powers at these light and heavy weights and trims. Further discussion of the corresponding prediction procedures is therefore found in Sec. 60.3, under the subject of ship-powering.

56.12 Measured Thrusts and Towing Pulls on Ships. Although thrustmeters were used on mechanically driven ships as long ago as 1845 [SNAME, 1934, p. 153], it is only within the past few decades that reliable and consistent thrust measurements on ships have become available. The measured net thrust, corrected for the axial component of the weight of all the rotating parts of the shaft systems, as described in the reference quoted and as discussed in Sec. 59.16, can be used directly for calculating the TD/Q ratio or the thrust coefficient K_T of the ship propeller. To obtain a measure of the actual ship resistance, these measured full-scale thrusts must be corrected by application of the thrust-deduction fraction t. Despite the possible existence of some scale effect in determining the value of t from self-propelled model tests the derived ship-resistance values may be taken as reasonably correct.

Ship thrust data measured in this way are available for a number of ships, as listed:

(a) U. S. S. *Pruitt*, destroyer; SNAME, 1921, pp. 14–32
(b) S. S. *Clairton* (1931 trials), cargo vessel; SNAME, 1932, pp. 17–44
(c) U. S. S. *Hamilton*, destroyer; SNAME, 1933, pp. 270–277
(d) M. S. *San Francisco*, combination passenger and cargo vessel; SNAME, 1936, pp. 195–227
(e) U. S. S. *YTB 500* and *YTB 502*, 100-ft harbor tugs; SNAME, 1948, p. 278 ff
(f) S. S. *Lucy Ashton*, ex-paddle steamer, driven by gas-jet engines, with the ship's own propulsion devices

removed; see the series of reports listed subsequently in this section.

The towing of ships, without their propulsion devices, to determine their full-scale resistances directly, has been a subject of active discussion among naval architects since about 1850. The thought that it constituted the only valid method of attack on ship-resistance and propulsion problems was, in fact, put forward in the late 1860's and early 1870's as one of the arguments against the proposals of W. Froude to establish the first model-testing basin. Froude, with his usual wisdom and thoroughness, tackled both the full-scale and the model problems. Under his supervision the hulk of H. M. S. *Greyhound*, less its propeller, was towed for resistance in the early 1870's but the results were somewhat disappointing, partly because of the excessive roughness (by modern standards) of the hull surface.

Since that time others have engaged in similar projects, using improved methods and instrumentation. The full-scale towing tests for which data have been published, including the *Greyhound* experiments, are listed hereunder:

(1) Froude, W., H. M. S. *Greyhound*, about 1874. Report published by Froude in the paper "On the Experiments with H. M. S. *Greyhound*," INA, 1874, pp. 36–73 and Pls. III-XIII. The towing-test data from the *Greyhound* experiments have been analyzed by A. M. Robb [INA, 1947, Vol. 89, pp. 6–15; abstracted in SBSR, 5 Jun 1947, pp. 568–571; also TNA, 1952, p. 449].

(2) Yarrow, A. F., British first-class torpedoboat, 100 ft long, 1883. Report published by Yarrow in the paper "Some Experiments to Test the Resistance of a First-Class Torpedo-Boat," INA, 1883, Vol. 24, pp. 111–117.

(3) Double-ended ferryboat *Cincinnati* (for New York harbor), 1896. Report published by F. L. DuBosque, SNAME, 1896, Vol. 4, pp. 93–104, esp. pp. 93–94.

(4) Yokota, A., Yamamoto, T., Shigemitsu, A., and Togino, S., hull of 40-ft steam launch, about 1929. Report embodied in the paper "Pressure Distribution Over the Surface of a Ship and its Effect on Resistance," Proc. World Eng'g. Congr., Tokyo, 1929, Vol. XXIX, Part 1, publ. in Tokyo in 1931. The steel steam launch forming the subject of these tests had an L_{PP} of 39.37 ft, an extreme beam of 9.79 ft, and a draft of about 3.99 ft. The tests included measuring the thrust at the thrust bearing during self-propelled tests. Further details from this paper and additional general data relative to the tests are given in Sec. 42.10. Data from tests of one-third scale models of the launch are mentioned also in Sec. 52.3.

(5) Hiraga, Y., hulk of Japanese destroyer *Yudachi*, about 1934. Reports published by Hiraga in the two papers "Experimental Investigations on the Resistance of Long Planks and Ships," INA, 1934, pp. 284–320 and Pls. XXVI-XXXIII, and "Experimental Investigations on the Frictional Resistance of Planks and Ship Models," Society of Naval Architects of Japan, Dec 1934, Vol. LV. The INA paper described and gave the results of towing tests on the destroyer *Yudachi*, on a so-called "plank ship," 77 ft long and 0.525 ft wide, as well as on a tug (unnamed), having a length of 114.83 ft and a displacement of 296.93 t. The displacement of the plank ship was 3.356 t; its L/B ratio was 147. Included in the towing test was a 26-ft model of the *Hashike* and of a 56-ft Vedette boat; see Pl. XXVI of the INA paper. Lines and other data of the 300-t twin-screw tug are given on Pl. XXXI of that paper.

(6) U. S. S. *YTB 502;* 100-ft, 1,000-horse single-screw harbor tug, early 1950's. This vessel was towed, with its propeller removed, by the U. S. S. *LSM 458*, the latter fitted with Kirsten rotating-blade propellers. Due to surging of the towed vessel, the presence of wake from the towing vessel, and other factors, the test data are not up to standard and have not as yet (1955) been fully analyzed.

(7) British Shipbuilding Research Association, *Lucy Ashton*, 1950–1951. This was an ex-paddlewheel steamer driven by abovewater gas-jet engines. The complete set of test reports follows:

(a) Denny, Sir M. E., "B. S. R. A. Resistance Experiments on the *Lucy Ashton*. Part I—Full-Scale Measurements," INA, 1951, Section on Int. Conf. Nav. Arch. Mar. Engrs., p. 40ff. The principal characteristics of the *Lucy Ashton* are:

L_{PP} = 190.5 ft	D = 7.177 ft (molded)
	C_B = 0.685
B = 21.0 ft (molded)	H = 5.0 ft, to bottom of hull proper
Δ = 390 t	S = 4,488 ft², incl. appendages
C_P = 0.705	C_M = 0.972.

(b) Conn, J. F. C., Lackenby, H., and Walker, W. P., "B.S.R.A. Resistance Experiments on the *Lucy Ashton*. Part II—The Ship-Model Correlation for the Naked-Hull Conditions," INA, 1953, p. 350ff. The first two parts were published as B.S.R.A. Rep. 107 in 1952.

(c) Lackenby, H., "B.S.R.A. Resistance Experiments on the *Lucy Ashton*. Part III—The Ship-Model Correlation for the Shaft-Appendage Conditions," INA, Apr 1955, Vol. 97, pp. 109–166

(d) Smith, S. L., "B.S.R.A. Resistance Experiments on the *Lucy Ashton*. Part IV—Miscellaneous Investigations and General Appraisal," INA, 1955.

(8) Nordström, H. F., hulk of Swedish destroyer *Wrangel*, about 1952. Report published as "Full-Scale Tests with the *Wrangel* and Comparative Model Tests," SSPA Rep. 27, 1953 (in English).

(9) Large-scale self-propelled model *D. C. Endert, Jr.*, representing a Victory ship; about 1953. Full-scale trials of a Victory ship were conducted by the Dutch in conjunction with tests of five model geosims, plus an independently powered 72-ft

model built of steel, named the *D. C. Endert, Jr.* One of the first installments of the published data on this project was prepared by W. P. A. van Lammeren, J. D. van Manen, and A. J. W. Lap, entitled "Scale-Effect Experiments on Victory Ships and Models. Part I, Analysis of the Resistance and Thrust Measurements on a Model Family and on the Model Boat *D. C. Endert, Jr.*," INA, Apr 1955, Vol. 97, pp. 167–245.

(10) French minesweeper *Aldebaran*, about 1954. The report of this work was published by R. Retali and S. Bindel in a paper entitled "Étude à la Mer de la Résistance à la Marche et de la Propulsion; Rapprochement avec le Modèle (Sea Trials to Determine Towing Resistance and Propulsion: Correlation with the Model)," ATMA, 1955. These trials involved towing the minesweeper *Aldebaran* with the minesweeper *Sirius* (a sister ship), with the two propellers of the *Aldebaran* removed and dummy hubs substituted. Otherwise the appendages on both vessels were the same, comprising roll-resisting keels, twin rudders, exposed twin propeller shafts, and twin supporting struts. Towline tensions were measured, both on the towing and on the towed vessels. Shaft torques were observed by torsion meter on the towing vessel but no propeller-thrust readings were taken.

The vessels were 140.95 ft long on the waterline, with a maximum waterline beam of 27.95 ft and a mean draft of about 7 ft. The displacement with appendages was 380 long tons.

(11) Šilović, S., and Fancev, M., "Measurements on M. V. *Rijeka*, with their Attempted Practical Application," INA Autumn meeting, 1955, in Yugoslavia; abstracted in SBMEB, Apr 1956, pp. 264–266.

CHAPTER 57

Estimate of Total Resistance for Surface and Submerged Ships

57.1 General. This chapter covers methods of estimating, calculating, and predicting full-scale resistance data for bodies or ships, intended to run on the surface or submerged, based upon available information. It does not discuss the extrapolation of model-test data to full scale for any specific ship design. Descriptions of this procedure, at least as utilized by members of the American Towing Tank Conference, are published in SNAME Technical and Research Bulletin 1–2, entitled "Uniform Procedure for the Calculation of Frictional Resistance and the Expansion of Model Test Data to Full Size," of March 1952. Details of the testing and extrapolating procedures, corresponding to those in general use in America, are described in Bureau of Construction and Repair Bulletin 7, entitled "The Prediction of Speed and Power of Ships by Methods in Use at the United States Experimental Model Basin, Washington," 1933.

This chapter also gives some information concerning the resistance of fully submerged bodies resembling submarines. These data may be found of benefit to the marine architect when he is called upon to approximate the drag of a non-ship form to be towed submerged.

57.2 Summary of Kinds of Ship Resistance. The various categories into which, in the present state of the art, the resistance of a ship to steady straight-line motion is divided, are listed in Secs. 12.1 and 12.10 of Volume I and defined in Secs. 12.2 through 12.7. This subdivision, based on the Froude theorem that the resistances due to tangential and to normal forces on the ship are for the most part independent and therefore can be segregated, is repeated here in Table 57.a for the convenience of the reader. However, the interactions listed in Secs. 12.1 and 12.10 are placed under a separate heading.

The following sections describe, in turn, various means of estimating these different kinds of resistance.

57.3 Ratios of Major Resistance Components. Useful ratios in analysis and design are the percentages of the friction and residuary resistances, according to the Froude subdivision, making up the total hull resistance. The solid line in Fig. 57.A, dividing the total R_T into friction R_F and residuary R_R over a T_q range of 0.4 to 2.0, is adapted from V. M. Lavrent'ev ["Marine Propulsion Devices," Moscow, 1949, Fig. 37, p. 85]. The same original diagram is published by G. E. Pavlenko ["Soprotivleniye Vody Dvizheniyu Sudov (The Resistance of Water to the Movement of Ships)," Moscow, 1953, Fig. 5, p. 16, covering a range of F_n from 0.1 through 0.6]. The broken line is based on data from the SNAME RD sheets for about twenty ships, more easily driven than those of the Taylor Standard Series. It includes a roughness allowance $(10^3)\Delta C_F$ of 0.4.

TABLE 57.a—CLASSIFICATION AND SUBDIVISION OF THE RESISTANCE OF A SHIP TO STEADY, STRAIGHT-AHEAD MOTION

I. Pressure Drag or Resistance, due to Normal Pressure on the Ship

(a) Deflection drag and closing thrust for the hull proper
(b) Deflection drag and closing thrust for the hull appendages
(c) Separation or eddying drag R_S and cavitation drag, for the hull proper and for the appendages
(d) Wavemaking drag R_W, for the hull proper and for such appendages as may be near enough to the surface to generate waves
(e) Drag due to the generation of spray roots and spray.

II. Friction or Tangential Resistance R_F on the Wetted Area. This is considered to be either:

(a) Tanvis resistance, varying as U or V to the first power
(b) Tanqua resistance, varying as U^2 or V^2
(c) Some unknown combination of (a) and (b), varying as an unknown (and probably varying) power of U or V between 1 and 2.
A different classification could be used here, embodying a subdivision into:
(c) Friction resistance on such hydrodynamically smooth surfaces, flat or curved, as may be incorporated in the ship
(d) Friction resistance due to roughness superposed on the hydrodynamically smooth surfaces, flat or curved.

III. Interactions between I. and II., as follows:

(a) Interaction effect of viscous or friction flow on the pressure resistance due to wavemaking, and the reverse, symbolized by R_{WF}
(b) Interaction effect of separation or eddying on the pressure resistance due to wavemaking, or the reverse, symbolized by R_{WS}
(c) Interaction effect of viscous or friction flow on the pressure resistance due to separation or eddying, or the reverse, symbolized by R_{SF}.

IV. Air and Wind Drag and Resistance, embodying:

(a) Still-air resistance R_{SA}, due to ship motion alone, with a true or natural wind of zero
(b) Wind drag D_W, exerted always downwind from the relative-wind direction. This drag has both transverse and axial components, due to aerodynamic lift and drag.
(c) Wind resistance R_{Wind}, composed of the net axial force imposed by the wind, acting opposite to the direction of ahead motion. The definitions of and distinctions between these terms are explained in Secs. 26.15 and 54.1 and illustrated in Figs. 26.G, 26.H, and 26.I.

V. Gravity Forces Acting on the Ship:

(a) Slope drag D_S, due to the inclination of the buoyancy-force vector to the weight-force vector, with a force component opposing motion
(b) Slope thrust T_S, similar to (a) preceding but with a force component assisting motion.

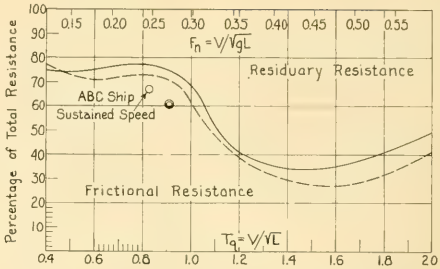

FIG. 57.A TYPICAL PERCENTAGES OF FRICTION AND RESIDUARY RESISTANCES FOR A RANGE OF SPEED-LENGTH QUOTIENTS

The significance of the two graphs is explained in the text

The circled spots are values for the ABC transom-stern ship designed in Part 4, for the sustained sea speed and trial speed, respectively.

Both curves are loci of division points for designed speeds at the various T_q and F_n values given. It is to be noted that the ratios of R_R to R_F vary rather widely over the speed-length range indicated. If ships are overdriven the percentage of R_R may be up to twice as great as that shown in the figure. If underdriven, it may be only two-thirds as large.

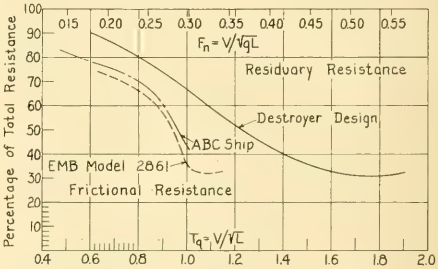

FIG. 57.B PERCENTAGES OF FRICTION AND RESIDUARY RESISTANCES FOR THREE SPECIFIC CASES

Fig. 57.B indicates, for an EMB research model, for the transom-stern ABC ship design, and for destroyers as a class, the variation of friction and residuary resistances throughout the intermediate and upper speed ranges of those ships. EMB model 2861 is the subject of the first model pressure-distribution tests made by E. F. Eggert [SNAME, 1935, pp. 139–150]. As expected, in the low-speed ranges before appreciable wavemaking begins, the total resistance in

each case is largely frictional. In the high-speed ranges, at and near designed-speed T_q values of 1.6, 1.7, or more, R_F is only slightly greater than $0.3R_T$.

57.4 Methods of Approximating the Total Resistance of a Ship. It is sometimes necessary to estimate the total resistance of a ship at a given speed, usually the designed speed, when nothing more is known of it than its principal dimensions and weight displacement. The ship in question may not even be designed or the one making the estimate may never have heard of it before. The ship has not been tested in model scale and there is no opportunity of doing so before the resistance estimate is required.

A crude approximation of the total resistance, for a speed V, is given directly by the formula

$$R_T = C_T(0.5\rho)SV^2 \tag{57.i}$$

where C_T is *estimated* for the T_q or F_n in question by reference to the full-scale values for one or more similar ships of nearly the same size, such as those listed in the SNAME RD Summary Sheets. The wetted area S is taken as the value for the similar ship or is derived by the C_S coefficient of Sec. 45.12. Care is required that the reference ship is of about the same length as the ship for which the total resistance is to be derived, so that for a given T_q or F_n the Reynolds number R_n and the specific total friction drag coefficient C_F are both nearly the same.

For example, in the early stages of the ABC design, described in Sec. 66.9, the total resistance is required to furnish a first approximation of the shaft power. Reference to the SNAME RD Summary Sheets indicates that the destroyer tender of RD sheet 96 closely resembles the ship being designed. The latter sheet indicates that the appendages are limited to a half-rudder only.

For the tender, at its designed speed of 20 kt, the value of the total specific resistance coefficient C_T is $3.023(10^{-3})$ and the wetted surface S is 46,509 ft^2. The designed speed V for the ABC ship is 20.5 kt, or 34.625 ft per sec; the numerical value of V^2 is 1,198.9. Then, for the ABC ship, on the assumption of the same C_T and the same S, and for roughly the same speed,

$$\begin{aligned} R_T &= C_T(0.5\rho)SV^2 \\ &= 3.023(10^{-3})(0.9905)(46{,}509)(1{,}198.9) \\ &= 166{,}960 \text{ lb.} \end{aligned}$$

This compares well, as a quick approximation, with the value of 171,830 lb derived in Sec. 66.9 by the use of the Schoenherr mean friction line and the Gertler reworked data of the Taylor Standard Series described in Sec. 56.5. Actually, for the destroyer tender, the C_T at 20.5 kt would be higher than the figure quoted.

One may, of course, pick a vessel from the SNAME RD and ERD sheets having proportions, shape, and form coefficients close to those selected for the vessel being designed. Reference to the appropriate SNAME ERD sheet gives directly the values of total resistance R_T, total resistance per ton of weight R_T/Δ, and P_E for a geosim vessel having a "standard" length of 100, 200, 400, or 1000 ft, as indicated on the sheet. The total resistance of the geosim ship of the length under design is then determined by correcting for the difference in friction resistance due to the differences in length and in speed between the reference ship and the "design" ship. This scheme, or a modification of it, has the advantage that curves of R_T and P_E can be constructed for a range of T_q or F_n considerably greater than will be encountered in practice. The full-scale data on the SNAME RD Summary Sheets are for the designed-speed spot only.

Another rapid method of approximating the total resistance for the designed-speed spot is to pick the value of R_T/Δ, at the proper T_q, from the meanline of Fig. 56.M. Multiplying this value by the weight displacement Δ gives R_T at once. For example, the R_T/Δ value for the ABC ship, at a T_q of 0.903, is 10.2 lb. Multiplying by 17,300 tons, the displacement at an early stage of the design, gives a total resistance of 176,400 lb. This compares with the 171,830 lb quoted earlier in the section.

It is customary, if time is available, to estimate separately the friction resistance R_F and the residuary resistance R_R by the methods of the two sections following, using model-test data from a parent form such as the Taylor Standard Series. They are added to give the total resistance R_T. This method enables the designer to draw curves of estimated R_F, R_T, and P_E for a very large range of Taylor quotient T_q or Froude number F_n.

Strictly speaking, the use of standard-series or reference data from models or ships of different shape, even though of the same dimensions and proportions and having exactly the same form coefficients, requires the use of a shape-correction

factor. For example, it has to be decided whether the shape contemplated for the design will have less (or more) resistance than the standard-series or reference hull of the same proportions. This is afforded, after a fashion, by the EHP/Taylor EHP or "angleworm-curve" ratios of the SNAME ERD sheets. However, with many such ratios at hand, it is still difficult to formulate anything approaching systematic rules for guidance in this matter. A bulb bow carried by the new design, if appropriate, will reduce its resistance below the Taylor Standard Series value. This is one reason why the resistance of the ABC transom-stern design, determined by model test, is less than the values calculated earlier in this section.

Most books on naval architecture give several formulas and methods for predicting the total resistance and effective power of ships in the design stage, perhaps before the lines are drawn and certainly before models are built and tested. For example, G. E. Pavlenko describes no less than eleven methods, dating from 1899 to the present, including Taylor's Standard Series, Ayre's method, and Doyère's method, for finding the resistance and effective power of merchant and naval vessels of different kinds ["Soprotivleniye Vody Dvizheniyu Sudov (The Resistance of Water to the Movement of Ships)," Moscow, 1953, pp. 305–379].

In all these cases, however, it is most important to note the limitations on each formula, graph, table, or method, as given in the text. If no limitations are mentioned, they should be sought in other references or directly from those who prepared and published them.

57.5 Ship Friction Resistance Calculation from Chapter 45. The methods used and the numbers required for a calculation of the ship friction resistance, including all types of roughness, are set forth in detail in Secs. 45.12 through 45.20. The method for calculating the wetted length and the wetted area S for planing hulls is discussed in Secs. 45.24 and 53.6.

The method of calculating the friction drag of a submerged submarine is essentially the same as for a surface ship, except for the inclusion of the *entire* outer area, surrounding what is described elsewhere as the bulk volume. The transverse curvature of the lower part of the hull of a submarine is, as a rule, relatively less than for the bilge corners on a large surface ship with flat or nearly flat floors. However, a submersible hull may have rather wide flat surfaces on top, to provide walking space on the superstructure deck. The transverse curvature along portions of the deck edges, even though they are rounded, is likely to be more severe than along the bilge corners of a surface vessel.

57.6 Residuary Resistance Prediction from Reference and Standard-Series Data. It is possible to approximate the residuary resistance of a surface ship, at a given speed V, or at a series of speeds, by assuming that it is the same as the residuary resistance R_R of a model having the same proportions. Data of this kind can be found in the SNAME RD sheets and similar sources. Continuing the discussion of Sec. 57.4, it is somewhat risky to rely on the proportions C_P, B/H, and $\Delta/(0.010L)^3$ (or $\nabla/(0.10L)^3$) as comprising the sole as well as the preponderant influences on residuary resistance, neglecting the shape factors entirely. What appear to be minor differences in shape or proportions often produce appreciable changes in resistance. These will not be explained, and can not be allowed for, until our present (1955) knowledge of ship hydrodynamics is considerably extended.

The calculation of values of R_R/Δ for a range of speeds and a given set of proportions, by assuming that these are the same as for a TSS "phantom" ship of exactly those proportions, takes it for granted that the shape of the proposed ship is as good as (and no better than) that of the TSS ship. This does not prevent a designer, however, from estimating that his proposed hull will have x per cent less or y per cent more residuary resistance than the TSS "phantom" hull. The difficulty here, as mentioned previously, is the lack of systematic and reliable data for selecting the x- and y-values.

The contours of R_R/Δ for the Taylor Standard Series are described in Sec. 56.3. Two sets of them, for $V/\sqrt{L} = 0.90$, are illustrated in Figs. 56.A and 56.B. These contours are intended to be used for ships having the same proportions C_P, B/H and displacement-length quotient $\Delta/(0.010L)^3$. The designer may apply, as x- and y-values, increments or decrements of R_R/Δ.

An illustrative example of the Taylor R_R/Δ method, for the fifth approximation of characteristics in the preliminary design of the transom-stern ABC ship described in Part 4, is given in Table 57.b. The basic data for this stage of the design are listed in the right-hand column of Table 66.e in Sec. 66.11. The proportions required

for this calculation are $C_P = 0.62$, $B/H = 2.808$, and $\Delta/(0.010L)^3 = 123.6$, while the value of T_q at the designed speed selected for this example is 0.908. The displacement is assumed here as 16,400 tons.

The linear interpolations described in Sec. 56.3 are set down in Table 57.b, adapted from D. W. Taylor's Table VIII-A [S and P, 1943, p. 63]. The characteristic spots drawn in Figs. 56.A and 56.B indicate the coordinates of $C_P = 0.62$ and $\Delta/(0.010L)^3 = 123.6$ for both B/H ratios (of 2.25 and 3.75, respectively), at a T_q of 0.90. The values of R_R/Δ for this speed-length quotient were picked from the originals of Figs. 56.A and 56.B, drawn to a scale over three times larger than that of the reproductions. Normally it is not possible to determine the values of R_R/Δ by inspection to more than three significant figures, indicated in Table 57.b for a T_q of 0.95.

The derived value of R_R/Δ of 4.014 lb per ton is then multiplied by the displacement Δ of 16,400 t to give the predicted total R_R of 65,829 lb, for the "phantom" TSS ship having the proportions of the ABC ship.

No allowance is made here for the difference between the salt-water specific gravity of 1.024 for all the TSS data and the specific gravity of 1.027 for the ABC ship.

The method of predicting the residuary resistance of a given ship from the "phantom" Taylor Standard Series ship having the same proportions is rather different when the Gertler reworked TSS data are employed. These are described in Sec. 56.5 and a sample calculation is set down in Table 57.c. The ship selected is the fifth approximation of the ABC design, listed in Table 66.e of Sec. 66.11, but the basic data now involve the wetted surface S and the fatness ratio $\nabla/(0.10L)^3$. These are, from Table 66.e, 44,759 ft^2 and 4.327, respectively. The mass density ρ is taken as 1.9905 slugs per ft^3 for "standard" salt water.

The volumetric coefficient ∇/L^3 of the Gertler

TABLE 57.b—Residuary-Resistance Prediction for ABC Ship From Taylor's R_R/Δ Contours

The characteristics and proportions listed correspond to those of the fifth approximation in Table 66.e in Sec. 66.11. The method illustrated here is adapted from D. W. Taylor's Table VIII-A in his "The Speed and Power of Ships," 1943, page 63. One particular pair of contours required here is reproduced in Figs. 56.A and 56.B.

The calculation is made for one speed only, 20.5 kt (the designed speed), at a T_q value of 0.908.

Length on waterline, $L = 510$ ft Beam, $B = 73$ ft

Displacement, $\Delta = 16{,}400$ t Draft, $H = 26$ ft

$$\frac{\Delta}{(0.010L)^3} = 123.6 \qquad C_P = 0.62 \qquad \frac{B}{H} = 2.808$$

$$\frac{B/H - 2.25}{1.50} = \frac{2.808 - 2.25}{1.50} = 0.372$$

1	2	3	4	5	6
$T_q = V/\sqrt{L}$	R_R/Δ from contours for $B/H = 3.75$	R_R/Δ from contours for $B/H = 2.25$	Difference; col. 2 minus col. 3	R_R/Δ correction for B/H ratio; col. 4 times $\frac{B/H - 2.25}{1.50}$	R_R/Δ for $B/H = 2.808$; col. 3 plus col. 5
0.90	3.998	3.503	0.495	0.184	3.687
0.95	5.95	5.60	0.35	0.13	5.73

Difference 2.043

$$\frac{T_q - 0.90}{0.05} = \frac{0.908 - 0.900}{0.05} = 0.16 \qquad 2.043(0.16) = 0.327$$

R_R/Δ at a T_q of 0.908 $= 3.687 + 0.327 = 4.014$ lb

$R_R = 4.014(16{,}400) = 65{,}829$ lb.

TABLE 57.c—Residuary-Resistance Prediction for ABC Ship From Gertler's C_R Contours

The characteristics and proportions listed correspond to those of the fifth approximation in Table 66.e of Sec. 66.11.

The C_R contours are given in TMB Report 806, "A Reanalysis of the Original Test Data for the Taylor Standard Series," by M. Gertler, March 1954. One particular pair of contours required here is reproduced in Fig. 56.D.

The calculation is made for one speed only, 20.5 kt (the designed speed), at a T_q value of 0.908.

Length on waterline, $L = 510$ ft
Displacement volume, $\forall = 574{,}000$ ft^3
Wetted surface, $S = 44{,}759$ ft^2
Beam, $B = 73$ ft
20.5 kt $\approx$ 34.62 ft per sec

Draft, $H = 26$ ft
$\forall/(0.10L)^3 = 4.327$
$B/H = 2.808$
$C_P = 0.62$
$0.5\rho = (0.5)(1.9905)$ slugs per ft^3 = 0.9953 slugs per ft$_3$

1	2	3	4	5	6
$T_q = V/\sqrt{L}$	C_R from contours for $B/H = 3.00$	C_R from contours for $B/H = 2.25$	Difference; col. 2 minus col. 3	C_R correction for B/H ratio; col. 4 times $\frac{B/H - 2.25}{0.75}$	C_R for $B/H = 2.808$; col. 3 plus col. 5
0.908	$1.278(10^{-3})$	$1.245(10^{-3})$	$0.033(10^{-3})$	$0.025(10^{-3})$	$1.270(10^{-3})$

$$\frac{\frac{B}{H} - 2.25}{0.75} = \frac{2.808 - 2.25}{0.75} = 0.743 \qquad 0.743(0.033) = 0.025$$

$$R_R = C_R(0.5)\rho S V^2 = 1.270(10^{-3})(0.9953)(44{,}759)(34.62)^2 = 67{,}630 \text{ lb.}$$

This is to be compared with the 65,829 lb derived in Table 57.b.

tables in TMB Report 806 is 1,000 times smaller than the 0-diml fatness ratio $\forall/(0.10L)^3$, so that the Gertler graphs are entered with the numerical value of this fatness ratio by neglecting the multiplier 10^{-3} marked on the graphs.

The fact that the residuary resistance as calculated by the Gertler C_R method is 2.7 per cent higher than that calculated from Taylor's R_R/Δ contours indicates that for certain combinations of proportions there are real differences between the original and the reworked TSS data. These differences have been explored by the Preliminary Design staff of the Bureau of Ships of the U. S. Navy Department for a considerable number of ship types, without revealing any systematic difference pattern. The magnitude of the differences, while not negligible, is small enough to permit a naval architect to use either method in the preliminary-design stage.

57.7 Telfer's Method of Predicting Ship Resistance. A method of extrapolating model test data to predict ship resistance was proposed and described by E. V. Telfer several decades ago [INA, 1927, Vol. 69, pp. 174–210; NECI, 1928–1929, Vol. 45, pp. 115–184]. Basically this scheme is simply a graphic one for effecting the extrapolation from model to ship data by the well-known Froude method [SNAME, 1932, p. 87], especially when the extrapolation is to be done, not from the test data on one but from the combined data on several geosim models of different scale ratios. Test data are available on a number of geosim families, each comprising three to six or more models. While the specific residuary resistance coefficients for selected T_q or F_n values are held constant, the specific friction resistance coefficients are modified in accordance with some accepted friction formulation such as the ATTC 1947 meanline. This is equivalent to drawing one line of a graph parallel to another line having a given position and slope.

Examples of Telfer extrapolations of this kind are found in:

(1) Telfer, E. V., "The Frictional Resistance of Ships," MENA, Oct 1922, pp. 387–390
(2) Telfer, E. V., "Notes on the Presentation of Ship Model Experiment Data," NECI, 1922–1923, Vol. XXXIX, pp. 221–299. Appendix 3 gives notes on the determination of the friction resistance by analysis of tests on ship-formed models of different length.
(3) Telfer, E. V., "Ship Resistance Similarity," INA, 1927, Vol. LXIX, pp. 174–190, 196–210, and Pls.

XIV-XVII. These plates contain several of the Telfer extrapolation diagrams.

(4) Horn, F., "Die Weiterentwicklung des Modellversuchsverfahrens zur Ermittlung des Schiffswiderstandes (The Further Development of Model Test Methods to Obtain Ship Resistance)," Schiffbau, 16 Nov 1927, pp. 504–510, esp. Fig. 1 on p. 507

(5) Telfer, E. V., "Frictional Resistance and Ship Resistance Similarity," NECI, 1928–1929, Vol. XLV, pp. 115–184

(6) SNAME, 1932, Fig. 13, p. 89, for three models of the U. S. S. *North Carolina* (old) series

(7) Van Lammeren, W. P. A., "Propulsion Scale Effect," NECI, 1939–1940, Vol. 51, p. 115ff

(8) Van Lammeren, W. P. A., Troost, L., and Koning, J. G., RPSS, 1948, pp. 39–40 and Fig. 13

(9) Telfer extrapolation diagrams have been prepared for the *Lucy Ashton* family of models; see the references listed under (7) in Sec. 56.12, esp. INA, 1953, Fig. 20 opp. p. 372 and Fig. 23 opp. p. 378; also INA, Apr 1955, Figs. 12 and 13 opp. p. 122

(10) Birkhoff, G., Korvin-Kroukovsky, B. V., and Kotik, J., "Theory of the Wave Resistance of Ships," SNAME, 1954, pp. 359–396, esp. Fig. 1 on p. 361

(11) Acevedo, M. L., Comments on Skin Friction and Turbulence Stimulation, 7th ICSH, 1954, SSPA Rep. 34, 1955, pp. 110–117, esp. p. 115

(12) Van Lammeren, W. P. A., van Manen, J. D., and Lap, A. J., "Scale Effect Experiments on Victory Ships and Models. Part I—Analysis of the Resistance and Thrust-Measurements on a Model Family and on the Model Boat *D. C. Endert, Jr.*," INA, Apr 1955, Vol. 97, Figs. 21 and 22 on pp. 184–185 and Fig. 25B on p. 232

(13) Sund, E., "On the Effects of Different Turbulence-Exciters on B.S.R.A. 0.75-Block Models Made to Various Scales," Norwegian Model Basin Rep. 11, Aug 1951. Figs. 1 through 11 on pp. 19–22 embody specific total resistance values, plotted on Reynolds number, for four models having scale ratios of 15, 22.5, 30, and 45.

(14) Pavlenko, G. E., "Soprotivleniye Vody Dvizheniyu Sudov (The Resistance of Water to the Movement of Ships)," Moscow, 1953, Fig. 154, p. 250. The diagram given is not exactly that of Telfer but the graphic method is the same, including the addition of a roughness allowance to the friction resistance for the ship.

The graphic procedure has several definite advantages. First, it is easy to visualize the agreement (or otherwise) of the several spots for model tests at a given T_q or F_n with the inclined extrapolation line for that speed-length ratio. The analysis is made still easier by plotting R_n on a log scale and C_T on a uniform scale because the extrapolation lines are then all straight (or very nearly so) and parallel, depending upon the friction formulation used. Indeed, analysis by any method other than a graphic one might be intricate and laborious. Second, as pointed out by G. Birkhoff, B. V. Korvin-Kroukovsky, and J. Kotik [SNAME, 1954, p. 361], it affords a plausible separation of the total specific resistance coefficient C_T into components, as well as an excellent visual representation of those components. Further, it visualizes the ship roughness allowance and illustrates rather forcibly the discrepancies which still exist because of inadequate model-testing techniques, lack of complete knowledge of scale effects, and similar factors.

The diagram of Fig. 57.C, deliberately drawn in schematic fashion, illustrates most of the features mentioned. The formula for the smooth, flat-plate, turbulent-flow friction line is assumed for simplicity to be an explicit function of C_F and log R_n, so the C_F line is straight when plotted on those coordinates. The horizontal gap between the model range and the ship range is deliberately closed to enable the features to be shown to better advantage. It is assumed that the average roughness allowance to be added to the friction line representing hydrodynamic smoothness is practically zero at the point B_1 and increases as indicated by the long-dash line B_1B_2, corresponding to the line CC on Fig. 45.E.

The vertical distance between C_1 and A_1, or between C_2 and B_1, is a measure of that portion of the total specific resistance C_T which corresponds to the separation drag, at speeds below which there is practically no wavemaking drag. However, as R_n increases toward the ship range, the line C_1C_2 is not extended straight to C_3, but beyond C_2 becomes parallel to B_1B_2, occupying the short-dash position C_2C_4.

At small values of R_n, in the small-model range, the boundary-layer thickness δ(delta) increases rapidly as the absolute model size diminishes. Even though stimulating devices on the small models render the flow completely turbulent the boundary-layer thickness is so large in proportion that the transverse velocity gradient at a given point along the run is smaller than it is at the corresponding point on the full-size ship or even on a model of normal size. This means, by reference to Fig. 7.B on page 124 of Volume I, that the port and starboard separation points on the small model are farther forward than on the large model or on the ship. The separation zone is thus wider and the separation drag is larger. Further, on the small model, there is a curvature effect, transverse in particular, which adds to the specific friction resistance C_F to be expected at that R_n. As a third item, listed on Fig. 57.C, the small

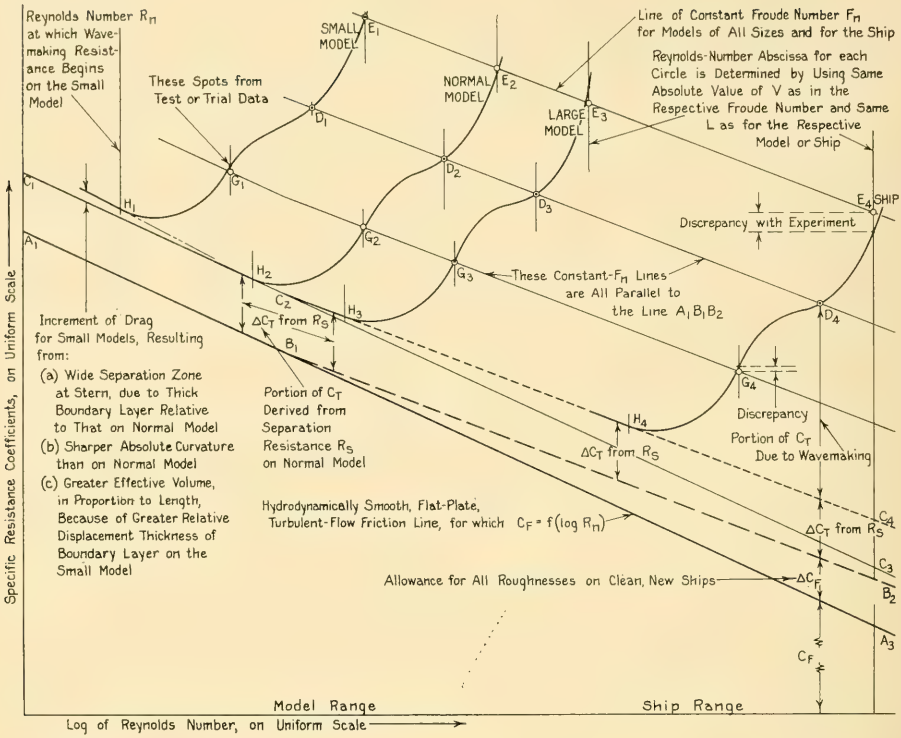

FIG. 57.C SCHEMATIC REPRESENTATION OF THE TELFER EXTRAPOLATION DIAGRAM TO ILLUSTRATE VARIOUS RESISTANCE FACTORS

model has a greater effective volume, in proportion to its length, because of the greater relative displacement thickness δ(delta) of its boundary layer. Because these three effects increase as the model size diminishes they give the impression, apparently not real, that the basic friction line should be steeper in this region.

If there are no effects other than those which have been enumerated, and if the wavemaking and other normal-pressure drags vary only as V^2 in the normal model and ship ranges, it should be possible to extend a line such as D_2D_3 by drawing it parallel to C_2C_4 . At a ship R_n corresponding to the F_n value for this line, the point D_4 should give the total specific resistance coefficient for the ship at the given F_n value. Similarly, other lines such as E_2E_3 could be drawn, so that the complete C_T curve $H_4G_4D_4$ for the ship would be predicted.

Rarely is it found in practice that points such as D_2 and D_3 both lie on a line parallel to $H_2H_3H_4C_4$. Almost certainly D_1 , D_2 , and D_3 do not, as may be noted by consulting the many diagrams in the references listed earlier in this section.

The accuracy and reliability of the Telfer method therefore rest heavily upon several factors, as yet not properly resolved:

(a) Exactly the proper degree of turbulence stimulation on small models to insure that the transition from laminar to turbulent flow, and the onset of separation, if any, occur at the *same relative positions* along the length as on the large model and on the ship

(b) The correct allowance for roughness of the full-scale ship surface. This is of course equally important, whether or not the Telfer method is employed.

(c) Wisdom, experience, and perhaps intuition to know how to draw a series of parallel extrapolation lines, in semi-log or any other known type of plotting, when the lines joining the corresponding spots for the different geosims are neither straight nor parallel.

Although it has been most useful for analysis, the Telfer method manifestly does not lend itself, in its present stage of development, to routine predictions of ship resistance, where the forces must be given in numbers of certain units.

57.8 Analytical and Mathematical Methods of Predicting Pressure Resistance. The use of pure analytical or mathematical procedures to calculate the pressure resistance of a body or ship due to wavemaking, as of 1955, is described in Chap. 50. This method has not yet progressed to the stage where a quantitative design prediction for a ship of normal form is a practical proposition. Furthermore, the pressure resistance due to eddying or separation can only be approximated, and the resistances due to the interactions listed in III of Table 57.a can not as yet be estimated by any known method.

57.9 An Approximation of Separation Drag. It is explained in Sec. 7.9 of Volume I that separation may occur, and cause added drag, abaft certain discontinuities in the forebody. Although explained, this drag unfortunately can not be estimated with any degree of assurance.

An estimate of the separation drag on the afterbody or run of a ship requires first an approximate delineation of those hull areas bounding the separation zone. Several methods for making this prediction are described in Sec. 46.3. Means of estimating the drag due to $-\Delta p$'s in separation zones are discussed in Sec. 46.5.

Some differential pressures have been observed at selected points on the transoms of certain square-stern models, but at the time of writing the data are incomplete and the results inconclusive.

57.10 Slope Resistance and Thrust. It may be assumed for a calculation of slope drag or thrust on a body or ship, described in Sec. 12.7, that the effective-slope angle in the equation D_S (or T_S) $= W \sin \theta$(theta) is that of the constant-pressure water subsurface passing through the center of buoyancy CB. If this subsurface is not plane (flat) along the ship length, its slope is measured at the CB position. If the subsurface slope is not known it may be assumed roughly equal to the surface slope. If, in turn, the latter can not be determined, the change of trim of the body or ship, reckoned from its attitude in level water at the same loading, may be used for the slope angle θ, provided account is taken of the change of trim caused by the ship's speed *through the water*.

It is reported that water will flow with a surface slope as small as 0.125 inch (0.0104 ft) to the statute mile. In this case sin θ is only $2(10^{-6})$. The slope drag of a 10,000-ton ship on such a slope is about 45 lb. The slopes of many navigable rivers are of the order of 5 to 8 ft to the statute mile, in which case sin θ may vary from 0.001 to 0.0015 [Durand, W. F., RPS, 1903, p. 119; Nowka, G., "New Knowledge on Ship Propulsion," 1944, BuShips Transl. 411, pp. 4–5]. The slope thrust on a 1,000-ton barge floating down such a river is from 1 to 1.5 ton, 2,240 to 3,360 lb, sufficient to give it a sizable differential downstream speed. This may be 3 or 4 kt over and above the river speed in the middle of the channel, sufficient to render it controllable by its own rudders.

For convenience, Table 57.d gives values (1) of the natural sine of the slope angle θ and (2) of the

TABLE 57.d—Slope Drag and Thrust Data for Varying Water-Surface Slopes

Drop in level, ft per 100 ft	Slope Angle θ, deg	Natural Sine of Slope Angle θ	Slope Drag or Thrust, lb per long ton of W
0.02	0.01	0.0002	0.45
0.04	0.02	0.0004	0.90
0.07	0.04	0.0007	1.57
0.1	0.06	0.001	2.24
0.2	0.11	0.002	4.48
0.3	0.17	0.003	6.72
0.4	0.23	0.004	8.96
0.5	0.29	0.005	11.20
0.6	0.34	0.006	13.44
0.7	0.40	0.007	15.68
0.8	0.46	0.008	17.92
0.9	0.52	0.009	20.16
1.0	0.58	0.010	22.40
2.0	1.15	0.020	44.80
3.0	1.73	0.030	67.20
4.0	2.29	0.040	89.6
5.0	2.86	0.0499	111.8
6.0	3.44	0.0599	134.2
7.0	4.00	0.0698	156.4
8.0	4.58	0.0798	178.8
9.0	5.15	0.0898	201.2
10.0	5.73	0.0996	223.1

slope drag D_S (or thrust T_S) in lb for a ship weight W of 1 long ton, covering a range of water-level drops per 100 ft horizontal distance varying from 0.02 to 10.0 ft. These correspond to a range of θ from 0.01 deg to 5.7 deg. The values so derived may then be related directly to the values of total resistance R_T per ton of weight displacement Δ, mentioned in the sections preceding. For example, the 100-ft version of the 944-t barge on SNAME RD sheet 141 has a value of R_T/Δ of 2.414 lb per ton at a speed V of 4.03 kt. If drifting down a river having a surface slope of about 0.12 ft per 100 ft, the slope thrust is sufficient to overcome the hydrodynamic drag for a 4.03-kt speed through the water. If steered properly the barge would go at least 4 kt downstream *through the water*. If the current velocity in way of the barge were say 3.5 kt, its speed past the banks or over the bed would be about 7.5 kt.

For the ABC ship of Part 4, ascending the river to Port Correo, it may be assumed that under certain flood conditions, with a river current of 4 kt in that portion of the channel section occupied by the ship, the drop in surface level is 0.1 ft per 100 ft. The corresponding slope drag from Table 57.d is 2.24 lb per long ton of weight displacement. Assuming a W value of 16,000 t at this stage of the voyage, the calculated slope drag is 35,840 lb. This is to be added to the ship's hydrodynamic drag. At the same time the current speed is subtracted from the ship's speed through the water, say 15 kt, to give a speed of 11 kt made good over the ground.

57.11 Ship Still-Air and Wind Resistance from Chapter 54. To all the resistances derived or mentioned in Secs. 57.5, 57.6, 57.9, and 57.10, where appropriate, there should be added the still-air or the wind resistance of the abovewater hull, of upper works, and of all projections from both. The ship creates a relative-wind speed W_R equal to its own trial speed V, even though there is no natural wind blowing over the trial course.

The significance of still-air resistance, wind drag, and wind resistance is described in Sec. 26.15 and illustrated in Figs. 26.G and 26.H. The methods of estimating and calculating them are described in Chap. 54.

57.12 Calculating the Overall Wetted Surface and Bulk Volume of a Submerged Object. A prediction of the pressure and friction drag of any submerged object, by any one of several methods, requires first a calculation of the *overall wetted surface* S_B and of the *bulk volume* $\forall_B$. The area S_B of a submarine is that *of the outer hull*, or of the pressure hull with outer tanks, plus that of the superstructure, deck erections, fairwaters, and all appendages except those in the "short" category defined in Sec. 45.12. The area S_B of a submerged object in general is the area bounding the portion which pushes the water aside as the object is self-propelled or dragged along.

The bulk volume $\forall_B$ is the entire volume within the wetted boundary, whether all of that volume is buoyant and weight-supporting or not. Any liquid in free-flooding spaces lying within the overall boundary is considered as solidified or frozen in place, so far as resistance to motion is concerned. For instance, the bulk volume of a whale with a mouth full of water includes the volume of that water because, for this example at least, it moves along with the animal. However, the overall wetted surface does not include that of the inside of its mouth, because there is no friction drag on that surface affecting the body motion.

The 0-diml bulk fatness ratio is defined as the ratio of the bulk volume $\forall_B$ or ∇_B to the quantity $(0.10L_{OA})^3$, where L_{OA} is the overall external length of the hull when submerged. Values of bulk fatness ratio, for submersibles and submarines of varied type and service, range from about 3.4 to 5.4, with values rising to 8.5 for craft intended for special service.

The overall maximum-section area A_X of a submerged body or submarine, as projected on the y-z plane, is measured to the same external boundary as the bulk volume. It is customary to take this area as the maximum transverse projected area or frontal area, even though the deck erections and fairwaters forming a part of this area lie in a different transverse plane than that of the maximum section of the main hull.

57.13 Drag Coefficients and Data for Submerged Bodies. There are many technical papers and reports in existence giving resistances, drag coefficients, and similar data for fully submerged bodies, most of them bodies of revolution intended to serve as basic shapes for airship hulls. Unfortunately, the validity of many of these data are questionable, because of:

(a) A practice of the 1900's, 1910's, and 1920's of testing models in wind tunnels at Reynolds numbers too small to produce flows that were dynamically similar to those expected on the

prototypes [Weinblum, G. P., TMB Rep. 758, May 1951, p. 1]

(b) Uncertainties as to the interference effects of supporting struts attached to the sides of the bodies, with their axes normal (or nearly so) to the body axis

(c) Towing models in water at inadequate submergence, and picking up wavemaking drag when the latter was supposed to be absent.

S. F. Hoerner abstracts most of the modern (1940–1950) drag data for streamlined bodies on pages 67–72 of his book "Aerodynamic Drag," published in 1951. Both Hoerner and W. S. Diehl give extensive drag data on a great variety of fuselage and hull shapes and components in the references listed in Sec. 55.5.

It is necessary in all these cases to differentiate clearly between published C_D values for total drag, including friction, and the C_D values for pressure drag only, often called "form drag" in the literature. Induced drag becomes a factor when the submerged bodies run at yaw or pitch angles and develop circulation around themselves because of this effective angle of attack.

57.14 Pressure Resistance of Submerged Bodies as a Function of Depth. Secs. 10.16 and 10.18 of Volume I emphasize that pressure resistance due to wavemaking remains a factor in the motion of a submerged body or simple ship, often of considerable importance, until the submergence is great enough to produce a flow pattern substantially similar to that at infinite depth. It is not possible to establish an arbitrary limit for this depth of submergence h, reckoned to the body axis, without taking into account the submergence-Froude number of Sec. 10.17, the ratio h/L_W , the L/D ratio, the form of the body or ship, and other factors. A square-bowed body obviously needs more depth to eliminate surface wavemaking than one with a tapering bow. A body or ship of normal L/D ratio, reasonably well streamlined and having a transverse section not drastically different from that of a circle, with no topside appendages or protuberances, is reasonably free of pressure drag due to wavemaking at a submergence, to its top, of three times its vertical diameter.

G. P. Weinblum tackles this problem for streamlined bodies of revolution in TMB Report 758, of May 1951, on an analytical and mathematical basis corresponding to that described in Chap. 50.

Sec. 7.2 points out that pressure drag due to separation decreases with depth because more external pressure is available to create a pressure gradient which will turn the water to follow the body slopes in the run. Of the quantitative nature of this effect around streamlined submerged bodies not much is known, except that at infinite depth there is sufficient pressure to turn the water around any corner, however sharp. This is on the basis that, if the water did not so turn in any region, a cavity or void would be left, in which the pressure would be substantially the vapor pressure of water. The decreasing-pressure gradient toward this cavity would then be very large, and would immediately generate sufficient lateral force to deflect the water and cause it to follow the surface. Although in practice there appears to be no actual void, the turning effect nevertheless remains.

A third factor enters here, primarily because it is necessary to rely upon model tests in air or water for practically all pressure-drag data. This is the interference effect of the struts or supports necessary to hold the model in the wind tunnel, in the water tunnel or channel, or in the model basin. If attached to the top, bottom, or sides of the body, the struts interfere with the flow pattern and change the velocity and pressure fields. If attached at the stern, a single longitudinal support or "sting" interferes with any separation zone that may exist there.

It is unfortunate that many of the published drag data on submerged bodies are to be taken with caution, because in these cases:

(1) The type, nature, shape, and position of the supporting struts are not described or shown in the test reports

(2) The depth of submergence of bodies tested in water is not known, nor are there any data of record concerning visible or measured wavemaking on the surface.

57.15 Resistance Due to Flow of Water Through Free-Flooding Spaces. The flow of water through the free-flooding spaces of both surface ships and submarines in straight-ahead motion is discussed in Sec. 20.9 of Volume I. There it is mentioned that free-flooding spaces which extend for a considerable distance forward and aft, so far that openings through the shell at the forward end lie in a $+\Delta p$ region while those at the after end are in a $-\Delta p$ region, may be expected to have longitudinal flow

through them. The action is much the same as the flow through a heat exchanger with its inlet forward and its discharge aft. The energy required to maintain this flow within the free-flooding spaces is necessarily taken from that developed by the propulsion device(s).

It is not possible at present (1955) to calculate this effect in terms of numbers; the designer must resort to large-scale model tests. However, one method of eliminating this waste of power is to fit (if practicable) transverse bulkheads within the free-flooding spaces so that little or no circulatory flow occurs in any one compartment. Another method is to so fashion the flooding (and venting) openings that entry and egress, and circulatory flow, is discouraged.

Eddying, with separation drag, is liable to occur around the edges of shell openings improperly formed. While this drag may be minute for any one opening it can assume sizable proportions for multiple openings, such as often occur by the hundreds in submarines.

CHAPTER 58

Running-Attitude and Ship-Motion Diagrams

58.1 General. The diagrams in this section, representing the in-motion trim attitude of models and ships of various proportions and shapes, supplement the general discussion in Chap. 29. These data are likewise related to the wave-profile data of Chap. 52, since the trim attitude for displacement-type hulls at sub-planing speeds is related directly to the wave profile.

58.2 Data for Predicting Sinkage and Change of Trim in Open, Deep Water. It is believed that most of the large model-testing establishments have a great amount of data on file relating to the change of level and trim of ship models undergoing test. Unfortunately, most of the published data apply to single ships or models, here and there, or to hull forms of unrelated and unsystematic proportions and shape. Examples of this are the data presented by D. W. Taylor [S and P, 1943], where in Figs. 21–25 on page 24 of the reference there are only trim indications and no numerical data, and where in Figs. 84–93 on page 73 there are given data on ten more-or-less unrelated models. W. P. A. van Lammeren, L. Troost, and J. G. Koning give change-of-trim data on only one model [RPSS, 1948, Fig. 38, p. 88]. J. L. Kent and R. S. Cutland present some change-of-trim data for models of high-speed ships [INA, 1935, Vol. 77, p. 81ff and Pls. XI, XII]. H. Lackenby shows the change of trim, for several different conditions, of the 190.5-ft *Lucy Ashton* and its 16-ft model, for a range of ship speeds from 6 to 15 kt [INA, Apr 1955, Vol. 97, Fig. 15 on p. 124].

The published data of D. W. Taylor on the ten models referenced have been incorporated in one set of graphs, embodied in Fig. 58.A. These endeavor to present the information in somewhat systematic fashion, although this is difficult when based on data from only ten models.

For the fifth approximation to the hydrodynamic features of the ABC ship of Part 4, covered in Sec. 66.11 and listed in Table 66.e, the C_P is 0.62 and the fatness ratio $\forall/(0.10L)^3$ is 4.327. To estimate the probable sinkage and trim from Fig. 58.A, at a T_q of 0.908, the 0-diml change of level of the bow is found by inspection and interpolation to be -0.46 per cent or $-0.0046L$. For the stern it is -0.145 per cent or $-0.00145L$. With a waterline L of 510 ft, these work out as -2.35 ft and -0.74 ft, respectively. The change of trim at 20.5 kt, by the bow, is $2.35 - 0.74$ or 1.61 ft, corresponding to an angle of $(1.61/510)/0.01745 = 0.181$ deg.

It is significant that, at the trial speed, the designed load draft at the FP, reckoned to the undisturbed water surface at a distance, increases from its nominal at-rest value of 26.00 ft to 28.35 ft, an augment of 9 per cent. What is more to the point, the freeboard at the FP *decreases* by 2.35 ft at the same speed, without any compensating advantages.

Published change-of-trim data on self-propelled models are almost nonexistent, possibly because experimenters thought that there would be little or no difference in level or attitude between the model when towed bare hull and when self-propelled with appendages. Figs. 58.B and 58.C, embodying the data for TMB models 4505 and 4505-1, representing the transom-stern and arch-stern variations of the ABC ship hull of Part 4, show that for this design at least the changes in level and attitude with speed are significantly different.

58.3 General Conclusions as to Changes of Level and Trim with Speed. Despite the handicaps enumerated in Sec. 58.2, it is possible to draw certain rather comprehensive conclusions from the available model-test data on change of

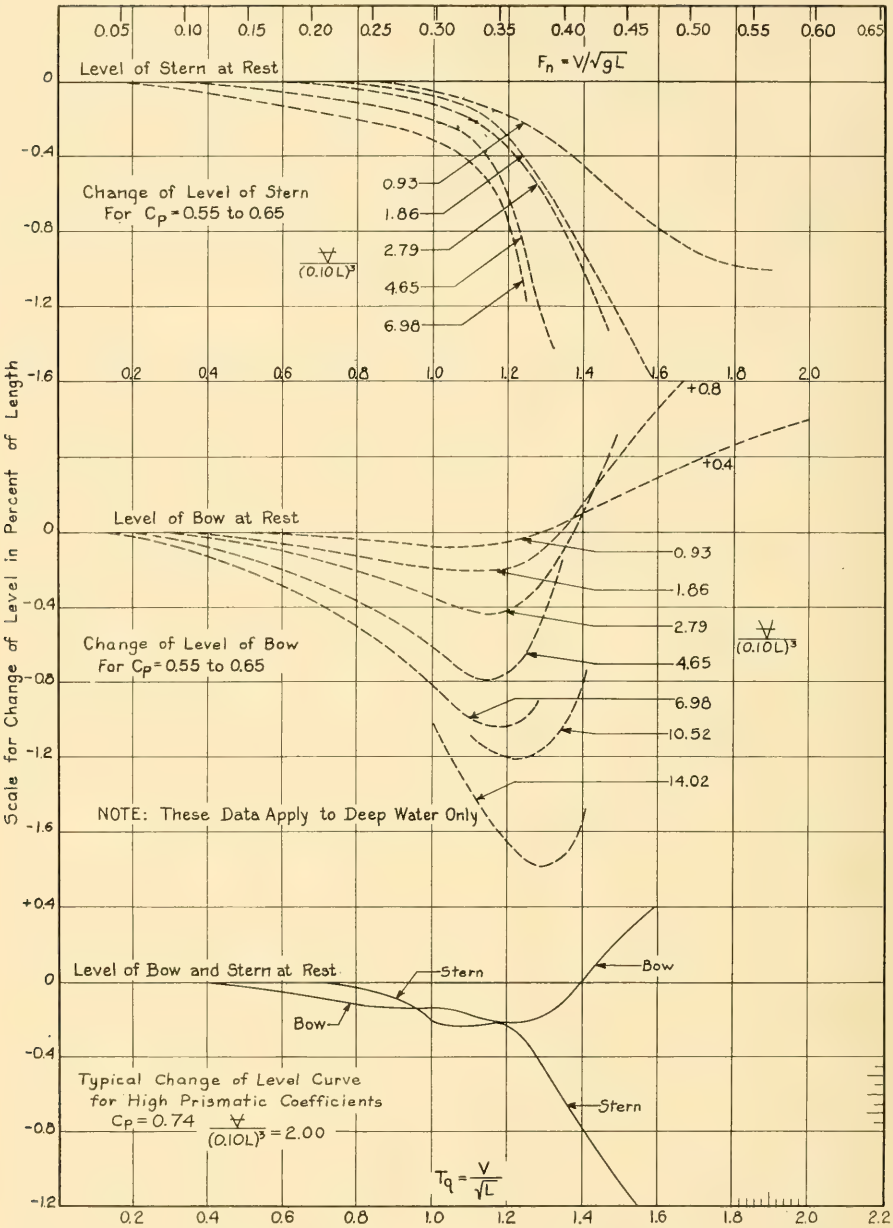

FIG. 58.A GRAPHS SUMMARIZING THE DATA OF D. W. TAYLOR FOR CHANGE OF TRIM IN DEEP WATER

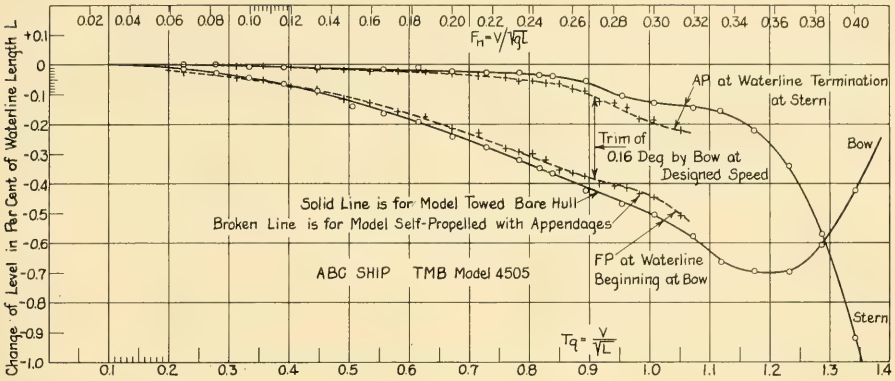

FIG. 58.B NON-DIMENSIONAL CHANGE-OF-TRIM DATA FOR TMB MODEL 4505, REPRESENTING TRANSOM-STERN ABC SHIP, WHEN TOWED BARE HULL AND WHEN SELF-PROPELLED

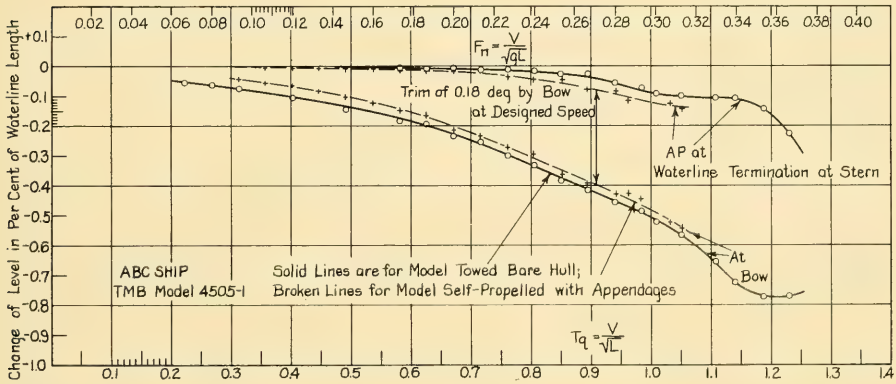

FIG. 58.C NON-DIMENSIONAL CHANGE-OF-TRIM DATA FOR TMB MODEL 4505-1, REPRESENTING ARCH-STERN ABC SHIP, WHEN TOWED BARE HULL AND WHEN SELF-PROPELLED

level and trim with speed. These are based upon the conclusions previously formulated by D. W. Taylor [S and P, 1943, pp. 72–74], taking account of test data on many models other than the ten listed on page 73 of the reference. So many variables enter the picture, however, that it is difficult, if not impossible to extend them over the entire range in which the marine architect is interested.

The modified conclusions, taken with the graphs of Fig. 58.A, enable reasonably precise predictions to be made for the running attitude of vessels not too different from the normal forms:

(1) For displacement-type vessels, supported primarily by buoyancy, the vertical forces developed by changes in hydrostatic pressure in the surface waterline region predominate over those due to Δp's resulting from hydrodynamic action (2) Vessels of the displacement type, having the waterline area concentrated near amidships, and large waterline areas for their length, drop bodily about in proportion to the fineness of their waterline endings and to their displacement-length quotient or fatness ratio. The drop is greater with *smaller* prismatic coefficients C_P because of the rather direct relationship between C_P and C_W , indicated in Fig. 66.H. For vessels having C_P values less than 0.65, with fine waterline endings and the waterline area well concentrated amidships, the bodily settlement and

the trim by the bow increase with the displacement-length quotient or fatness ratio.

(3) At low and moderate speeds, below a T_q of 1.0, F_n of 0.3, both bow and stern settle, the bow somewhat more than the stern, for the reasons given in Sec. 29.2 of Volume I

(4) Vessels having C_P values higher than 0.65, with full ends, level off at a T_q of 1.0 or just below. For T_q values in the range 1.0 to 1.2, there may be oscillations or perturbations in the trim values. At greater values of T_q the stern may be expected to drop much more than the bow.

(5) As the speed is increased beyond a T_q of 1.0, for vessels with C_P values of 0.65 and below, the bow settles more slowly. It reaches its lowest level at a T_q of from 1.05 to 1.30 (averaging about 1.15) and then rises rapidly. The bow reaches its at-rest level in a T_q range of 1.3 to 1.5, beyond which it continues to rise.

(6) The stern settles more and more rapidly beyond a T_q of about 1.1 or 1.2. Thereafter it settles much more rapidly than the bow rises, so that the ship as a whole continues to settle while the trim by the stern is rapidly increasing.

(7) At a T_q of about 1.7 to 1.8, the stern is settling less rapidly than the bow is rising, so that bodily settlement reaches its maximum. The stern does not change level much beyond a T_q of 2.0, while the bow always rises with increase of speed. As a result the vessel is rising bodily at speeds beyond a T_q of about 2.0.

(8) The center of gravity of *ordinary* (non-planing) vessels rarely rises to or above its original at-rest level at any practicable speed. Since the effect of the passage of the vessel is to depress the water immediately surrounding it, there may be an impression, at very high speeds, that the vessel does rise above its original level.

(9) Vessels of special form and planing craft, when driven to their designed high speeds, do rise bodily. Their behavior is described and illustrated in Sec. 29.3, on pages 415–417 of Volume I.

58.4 Data on Sinkage and Change of Trim in Shallow and Restricted Waters. The general subject of change of level and trim, at various speeds in shallow and restricted waters, is discussed in Secs. 18.7 and 35.7 of Volume I. Only sufficient information is given here to enable the marine architect to predict the sinkage and change of trim in confined waters in quantitative terms. These are important because of the extremely limited bed clearance with which large vessels transit certain canals, channels, and shoal areas, and the desire to maintain the highest practicable speed while doing so.

Fig. 35.D on page 530 of Volume I reproduces some trim data given by D. W. Taylor for a scout-cruiser model. Fig. 58.D indicates the 0-diml sinkage of bow and stern for three depth-draft ratios h/H over a wide range of speed-length quotient T_q and Froude number F_n. Paulus gives similar data for the German torpedoboat *S119* in

TABLE 58.a—Characteristics of Prototypes for Which Trim Data are Presented in Figs. 58.D and 58.E

Name of Vessel or Design Model number	Liberty EC2-G-AW2 TMB 3748-2	Victory VC2-S-AP3 TMB 3801	Tanker T2-SE-A1 TMB 3867	Inland Tanker T1-M-BT TMB 3886	D. W. Taylor's Scout Cruiser
Length, ft	427.3	445	510	311	412
Beam, ft	56.9	62	68	48.2	46.72
Draft, ft	27.7	28.5	30.2	19.19	17.35
Displacement, t	14,176	15,045	21,778	5,968	3,997.4
$\Delta/(0.010L)^3$	181.70	170.73	164.18	198.40	57.15
$\nabla/(0.10L)^3$	6.373	5.988	5.759	6.959	2.005
Prismatic Coefft., C_P	0.747	0.677	0.740	0.734	0.56(est.)
Midsection Coefft., C_M	0.98	0.98	0.98	0.98	
Block Coefft., C_B	0.735	0.669	0.722	0.726	
L/B ratio	7.51	7.18	7.50	6.45	8.82
B/H ratio	2.05	2.17	2.25	2.51	2.69
Midsection A_M, ft²	1,544.6	1,731.7	2,012.5	906.5	
$\sqrt{A_M}$, ft	39.30	41.61	44.86	30.11	
Model propeller	TMB 2869	TMB 2452	TMB 2864	TMB 2690	
Ship propeller D, ft	17.80	20.50	18.36	12.50	
Ship propeller P, ft	15.97	22.90	19.18	11.75	

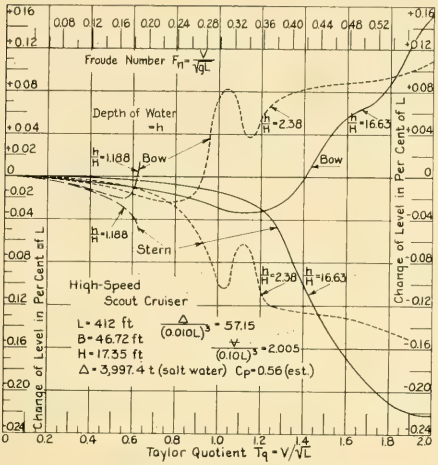

FIG. 58.D NON-DIMENSIONAL CHANGE-OF-TRIM DATA FOR HIGH-SPEED SCOUT CRUISER OF D. W. TAYLOR

reference (4) of Sec. 61.22. Other data are listed in Sec. 58.7.

It is obvious from the short-dash graphs for $h/H = 2.38$ in Fig. 58.D that the sinkage and change of level are greatly affected by the position of the vessel on the solitary wave which travels through the shallow water at the speed $c_C = \sqrt{gh}$. This critical speed can change rapidly with depth, as can the normal sinkage due to the Bernoulli contour system and the ship's Velox-wave system, so it must be remembered that a prediction of sinkage and trim for a nominal constant depth is that and no more.

For the prediction of the sinkage and change of trim in the cargo-vessel category, W. H. Norley has published rather complete data on the behavior of the models of four vessels in three depths of shallow water as well as in deep water [TMB Rep. 640, Feb 1948]. The graphs of Fig. 58.E give the 0-diml sinkage of both bow and stern for the four ship designs whose characteristics are listed in Table 58.a. The data represent self-propelled conditions for both models and ships.

An example of the use of these graphs, involving extrapolation to lower h/H values than those given, is worked out for the ABC ship of Part 4 in Sec. 72.8.

The data derived by Norley for full-bodied and blunt-ended vessels, as well as those derived by D. G. Davies in reference (12) of Sec. 58.7 for lake freighters having very high C_P values, reveal that at the low speed-length quotients customary in confined waters the ship trims by the bow, just as in deep water. This means that, if the initial keel or bottom slope is zero, and if the speed is too high, the ship touches the channel bed at its forward end.

58.5 Changes of Attitude and Trim of Ships with Fat Hulls. In former years, excessively fat and full forms like large scows, barges, and pontoons, could rarely be towed or propelled at speeds *through the water* high enough to change their attitude and trim, even in shallow and restricted areas. Sinkage and squat was therefore not much of a problem. With the advent of higher speeds and more powerful tugs and pushboats, the marine architect is left with little or no model data or full-scale observations for predicting the changes in *normal* bed clearance likely to be encountered by these craft in given areas. This situation is aggravated by the possibility of towing blunt-ended and full forms through regions where the water is shoaler than expected, and where the position of a craft upon a solitary wave will have a large effect upon the actual bed clearance.

In ETT, Stevens, Report 279 of January 1945 there are given on page 15 the change-of-level data for the two groups of models having displacement-length quotients $\Delta/(0.010L)^3$ of 300 and 400, and C_P values of 0.50, 0.60, and 0.70. The characteristics of these models are listed in the referenced report and in SNAME RD sheets 105–110.

58.6 Variation of Attitude and Position of Planing Craft with Speed and Other Factors. The matter of bodily rise of a planing craft above its position at rest, together with the changes in trim which occur throughout the whole speed range, are described and illustrated in Secs. 29.4 and 30.2 of Volume I. In fact, the sinkage and trim are related to the whole planing behavior. This, in turn, as brought out in Chap. 77, is a most important function of both weight and power.

Unfortunately, there are no known data by which the trim and vertical position of a planing craft may be estimated or predicted directly, corresponding to those in Fig. 58.A. Possibly there will never be a simple procedure for determining these values, because of the considerable number of parameters that are intimately

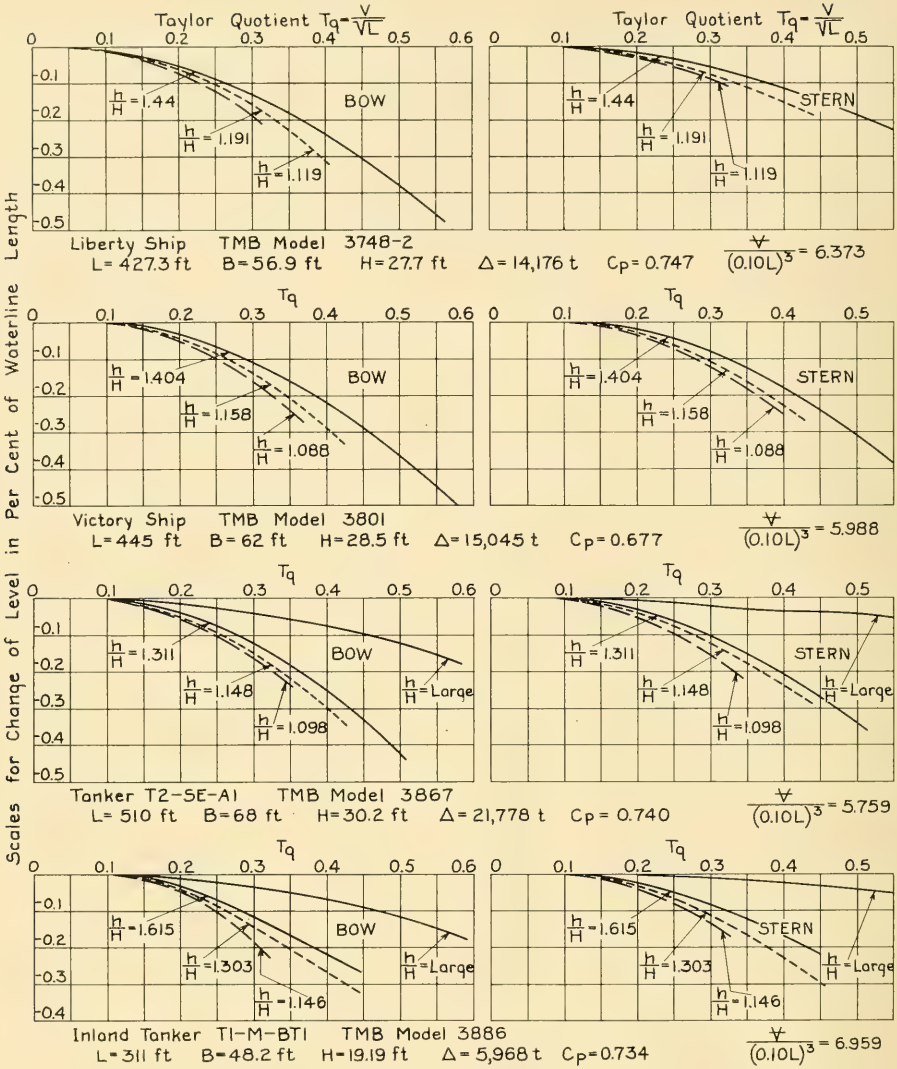

FIG. 58.E NON-DIMENSIONAL SINKAGE DATA FOR MODELS OF FOUR CARGO-SHIP TYPES, IN THREE OR FOUR DEPTHS WATER, WHEN SELF-PROPELLED

involved in the boat performance. One method now available to the marine architect is described and worked out for the ABC planing tender design in Sec. 77.27.

As a matter possibly of change in attitude and possibly of the peculiar flow and pressure effects due to limited bed clearance, it is significant that both the lift and the lift-drag ratio of a planing surface increase as the bed clearance and water depth diminish. However, these changes are not

appreciable until the water depth approaches or is less than the beam of the planing form. In view of the known performance of displacement-type vessels under similar circumstances it is not surprising that the drag and the trimming moment about the trailing edge of the planing form also increase with diminishing depth of water. Other features accompanying these changes are described by K. W. Christopher [NACA Tech. Note 3642, Apr 1956].

58.7 References to Published Data. As is the case with quantitative experimental or observed resistance data in shallow water, the greater part of the published information appears in the older technical literature. However, all of it together by no means covers the needs of the marine architect and ship operator of today (1955). Some of the available references follow:

(1) Yarrow, A. F., "Fast Torpedo Boats," Cassier's Mag., Jul 1897, Vol. XII, p. 294

(2) Anderson, M. A., and Gillmor, H. G., U. S. torpedoboats *Talbot* and *Gwin* (both old), ASNE, May 1898, Vol. X, pp. 493–501. These vessels were 99.5 ft long by 12 ft wide by 3.81 ft mean draft (2.1 ft forward and 5.54 ft aft). The change of trim at speeds of about 21 kt "amounted to about 41 inches (3.41 ft)." This corresponded to a T_q of $21/\sqrt{99.5} = 2.10$, $F_n = 0.625$, and a trim by the stern of about 1.95 deg.

The displacement was 45.75 tons and the displacement-length quotient 46.4. C_B was 0.413, C_X was 0.743, and C_W 0.659. From these data, C_P was 0.556.

(3) Gillmor, H. G., and Anderson, M. A., "The U. S. Torpedo Boat *Morris* (old)," ASNE, May 1898, Vol. X, pp. 502–508. For this vessel, L_{WL} was 138.5 ft, B_X was 15.0 ft, and H (mean) was 4.25 ft (2.75 ft forward and 5.75 ft aft). The trial displacement was 98 tons, with a displacement-length quotient of 36.88. C_B was 0.425, C_X was 0.755, and C_{WL} was 0.687. C_P , from the foregoing, was 0.563.

At a speed of 24 kt the change of trim was about 50 inches, or 4.17 ft. At this speed, $T_q = 24/\sqrt{138.5} = 2.04$; $F_n = 0.608$. The trim by the stern was about 1.72 deg.

On page 507 of the reference it says of the *Morris* that "she traveled on the back slope of a wave with a normal disturbance of the surface of the water."

(4) White, Sir W. H., MNA, 1900, pp. 466–467, 475–477. For the Yarrow 80-ft torpedoboat mentioned in this reference, at a T_q of 2.07, F_n of 0.616, the trim by the stern was about 2.5 deg.

(5) Durand, W. F., RPS, 1903, pp. 121–123

(6) Saunders, H. E., and Pitre, A. S., "Full-Scale Trials on a Destroyer," SNAME, 1933. Table 6 on p. 251 gives the trim data for the U. S. destroyer *Hamilton* (DD 141) for a range of speeds from 20 to 35.6 kt.

(7) Davidson, K. S. M., PNA, 1939, Vol. II, pp. 107–108

(8) Havelock, T. H., "Note on the Sinkage of a Ship at Low Speeds," Zeit. für Ang. Math. Mech., Aug 1939, pp. 202–205

(9) Taylor, D. W., S and P, 1943, Figs. 21–25, p. 24; Figs. 84–93, p. 73

(10) Van Lammeren, W. P. A., Troost, L., and Koning, J. G., RPSS, 1948, p. 88

(11) Sund, E., "On the Effects of Different Turbulence-Exciters on B.S.R.A. 0.75 Block Models Made to Various Scales," Norwegian Ship Model Basin Rep. 11, Aug 1951, esp. pp. 3, 4, 12, 13, and Fig. 12 on p. 23

(12) Davies, D. G., "Changes in Draft in Shoal Water," SNAME, Great Lakes Sect., Apr 1955; abstracted in SNAME Bull., Jul 1955, Vol. X, No. 2, p. 39.

CHAPTER 59

Predicting the Performance of Propulsion Devices

59.1 Relationship to Other Chapters. The form, use, behavior, and performance of many types of ship-propulsion devices are described in Chaps. 15, 16, and 17 of Part 1 and in Chaps. 32 and 33 of Part 2. A rather complete discussion of the aspects of efficiency of propulsion devices in general is found in Chap. 34. The application of data on and values of efficiency in the powering estimates for vessels is covered in Chap. 60. Notes, rules, and procedures for the design, utilization, and adaptation of the many forms of propulsion device to the many types of ships are described in Chaps. 69, 70, and 71 of Part 4. Cavitation and its effects, as applied to screw propellers in particular, are discussed in Chap. 47.

The present chapter endeavors to present, in concise but useful form, some of the quantitative information required by the marine architect who sets out to design a combination of ship and propulsion device. While a great deal of analytic work has been done along these lines, the designer who is called upon to fashion and proportion the propulsion device(s) for a particular ship is to a large extent forced to work ahead from the known performances of existing installations. Unfortunately, published data on the behavior of propulsion devices is often inadequate for purposes of prediction and design. Further, it is often unreliable in the sense that the quantitative data are not completely defined. For example, the source may state that the power developed to drive a single device is x horses, without specifying whether this is an indicated, brake, shaft, or propeller power.

59.2 Estimate of Propulsion-Device Efficiencies. The matters relating to and the factors governing the efficiency of various kinds of ship-propulsion devices are discussed at considerable length in Chap. 34. For the naval architect and marine engineer who wishes absolute or quantitative values of propulsion-device efficiency, there are the following:

(a) For screw propellers, the expected open-water efficiencies η_0(eta) and the probable range of efficiency for selected characteristics or for characteristics commonly used are found readily from the numerous groups of screw-propeller design charts listed in Sec. 70.4

(b) For other types of mechanical propulsion devices, acting directly on the water surrounding the ship, there are some published data on systematic series, such as the paddlewheel data referenced in Sec. 59.6, and some comparisons of efficiency to be found here and there in the technical literature. Two examples of these are the efficiency curves for (1) screw propellers within a fixed shrouding such as a Kort nozzle, (2) Voith-Schneider rotating-blade propellers, and (3) paddlewheels in the three sets of graphs of Figs. 34.M and 34.N. However, one serious shortcoming of data such as these is the lack of ade-

quate and precise definition for the information presented. Only rarely are the particular forms of propulsion device, corresponding to the efficiency curves, diagrammed or illustrated. The graphs or accompanying text do not always state whether the efficiencies are maxima, averages, or service values.

A rather large array of tabulated data derived from the self-propulsion tests of shallow-draft vessels with tunnel sterns is published by A. R. Mitchell [IESS, 1952–1953, Vol. 96, pp. 125–188]. These data do not, unfortunately, include values of the screw-propeller efficiencies but they do embody information on wake and thrust-deduction fractions and on propulsive coefficients.

H. Mueller has presented, for screw propellers of four different P/D ratios and for three variations of the current (1955) rotating-blade propeller, two sets of graphs showing variations with

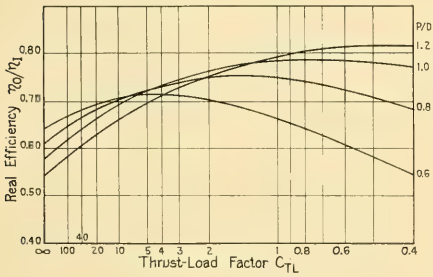

Fig. 59.A Values of Real Propeller Efficiency of Typical Screw Propellers for a Range of Pitch-Diameter Ratio and Thrust-Load Coefficient

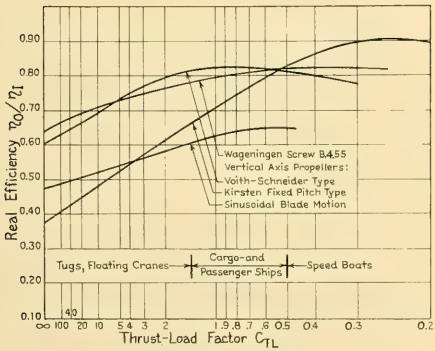

Fig. 59.B Values of Real Efficiency for a Screw Propeller and Several Rotating-Blade Propellers

thrust-load coefficient of what he calls "the degree of perfection" of these propellers [SNAME, 1955, pp. 4–30]. This is the ratio of the (open-water) propeller efficiency to the ideal efficiency, corresponding to what is defined in Sec. 34.4 of Volume I as the real efficiency, symbolized in the form $\eta_{\text{Real}} = \eta_0/\eta_I$. Figs. 59.A and 59.B, embodying these graphs, are adapted from Mueller's Figs. 6 and 7, respectively, of the reference cited.

59.3 Open-Water Test Data for Model Screw Propellers. For every model propeller characterized by the model-testing establishments of the world, involving models numbered in the thousands, the test results are available (in their archives) for a wide range of real-slip ratio s_R or advance coefficient J. As for making these data available to the profession at large, the characteristic curves plotted from the open-water observations on more-or-less unrelated propellers have been published in sporadic fashion, embodying probably not more than one per cent of the grand total. The availability of test data for related or series screw-propeller models is discussed in the section following.

The search for, and the systematic listing of the published source material for open-water test data on unrelated models is a formidable task. Much more of a task is the collection and presentation of these data in usable form, corresponding to the SNAME Propeller Data sheets. One set of these sheets, made up for TMB model propeller 2294, is reproduced in Figs. 78.Ma, 78.Mb, and 78.Mc of Part 4. The open-water characteristic curves for an 18-inch diameter TMB model propeller, tested as part of the ITTC program on comparative cavitation tests, are presented in Fig. 59.C. The arrangement of graphs in this figure is slightly different from the normal, represented by the diagram of Fig. 78.Mc, principally to keep the K_T and K_Q curves clear of each other.

A portion of the information relative to open-water test data which has come to the attention of the author in the preparation of the present volume is listed hereunder:

(1) Schmierschalski, H., "Ergebnisse systematischer Modellversuche mit hochtourigen flachgängigen Schraubenpropellern (Systematic Results of Model Tests with High-RPM, Low-Pitch Screw Propellers)," WRH, 7 Aug 1930, pp. 329–335. Logarithmic propeller charts, for area ratios of 0.42, 0.56, and 0.70, are given on pp. 333–335.

(2) TMB model propellers 1186–1187, 1188–1189, and 1190–1191; 3-bladed, built-up type, with modified

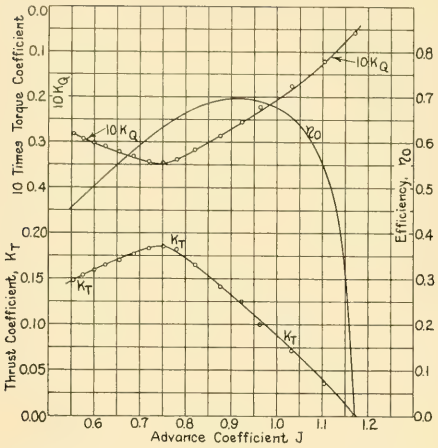

FIG. 59.C TYPICAL CHARACTERISTIC CURVES FOR A MODEL PROPELLER, DERIVED FROM A VARIABLE-PRESSURE WATER-TUNNEL TEST

ogival sections and elliptical outlines. Data are presented in SNAME, 1932, pp. 92, 102, 116.

(3) HSVA model propeller 1705, used to self-propel the Hamburg Basin model of the M. S. *San Francisco*; SNAME, 1936, Fig. 5, on p. 203. Unfortunately, no drawing of the model propeller is included in this reference.

(4) HSVA model propellers 1242 and 2003, having ogival-airfoil and double-symmetrical blade sections, respectively. Prototypes of these propellers were carried by the port and starboard shafts of the steamer *Tannenberg*, employed for special trials by the Hamburg Model Basin in 1938 ["Ergebnisse Naturgrosser Schraubenversuche auf Dampfer 'Tannenberg' (Results of Full-Scale Propeller Tests on the Steamer *Tannenberg*)," WRH, 15 Jun 1939, Vol. 20, No. 12. English version in TMB Transl. 91, Jul 1941]. Figs. 1 and 2 of the reference are drawings of the ship propellers and Figs. 4 and 3 give the characteristic curves for the open-water tests of the models.

(5) SSPA model propeller P6 for a fishing boat; the blades have airfoil sections.

D = 292.3 mm (11.55 in)	
P = 153.7 mm (6.05 in)	Z = 2 (adjustable)
P/D = 0.524	A_D/A_0 = 0.144

SSPA Rep 2, 1943, pp. 10–15, 30–32.

(6) Six 3-bladed propellers, adjustable; SSPA models P49, P50, P51, P52, P55, and P82. SSPA Rep. 4, 1945, pp. 8–13, 32–33.

(7) SSPA models P68, P69; SSPA Rep. 5, 1945, pp. 14–18

(8) SSPA model of identical 3-bladed propellers at each end of a double-ended ferryboat. Blades have double symmetrical sections.

D = 160 mm (6.31 in)	Z = 3
P = 155 mm (6.10 in)	A_E/A_0 = 0.42
P/D = 0.969	

SSPA Rep. 7, 1947; summary, and some table and figure legends in English.

(9) Fixed-pitch propeller, designed for and used on U. S. Navy tug *YTB 500*; SNAME, 1948, Fig. 5, p. 278. Four-bladed propeller with sections nearly symmetrical. D = 9.167 ft, P = 8.00 ft, P/D = 0.872. Mean-width ratio is 0.246 and A_D/A_0 = 0.525. Propeller is shown in Fig. 3 of the reference. Values of C_T and C_Q are in dimensional terms.

(10) SSPA model propeller, with airfoil and ogival blade sections.

D = 211.1 mm (8.31 in)	A_D/A_0 = 0.598
P = 200 mm (7.87 in)	Z = 4
P/D = 0.948	Rake = 12.8 deg

SSPA Rep. 13, 1949, pp. 10–11.

(11) Eight TMB model propellers, used to self-propel ten models of single-screw tankers; SNAME, 1948, pp. 360–379. The principal dimensions and characteristics of the full-scale propellers are given, together with the open-water curves, embodying dimensional values of C_T and C_Q . Unfortunately, no propeller numbers or drawings are included.

(12) TMB model screw propeller 2225; SNAME, 1951, Fig. 12, p. 637

(13) SSPA model propeller P156a for a coaster, with airfoil and ogival blade sections.

D = 208 mm (8.19 in)	Z = 3
P = 114 mm (4.49 in)	A_D/A_0 = 0.44
P/D = 0.55	Rake = 15 deg.

SSPA Rep. 24, 1953, pp. 40–43; includes propeller drawing.

(14) SSPA model propeller P160 for a coaster, with airfoil and ogival blade sections.

D = 260 mm (10.24 in)	Z = 4
P = 230 mm (9.06 in)	A_D/A_0 = 0.40
P/D = 0.89	Rake = 15.2 deg.

SSPA Rep. 24, 1953, pp. 40–43; includes propeller drawing.

(15) Characteristic curves derived from open-water tests of the several propellers used to drive the TMB Series 60 models and several associated models are given by J. B. Hadler, G. R. Stuntz, Jr., and P. C. Pien [SNAME, 1954, pp. 124–134, 152–156]. While this paper gives a drawing of only one propeller, TMB 3376, on page 124, drawings of the others are on file at the David Taylor Model Basin.

(16) SSPA model propellers P616, P617, P618, and P619. All propellers are 3-bladed, with developed-area ratios of 0.45, t_X/D ratios of 0.048, and rakes of 7.5 deg. The diameters and P/D ratios vary considerably. SSPA Rep. 35, 1955, pp. 12–15.

(17) Characteristic curves derived from open-water tests of the nine stock TMB propellers used to self-propel the ten tugboat models described by C. D. Roach [SNAME, 1954, Figs. 6(b) through 15(b),

pp. 601–619]. The C_Q and C_T plots in these figures embody dimensional data. This paper gives no drawings of any of the model propellers but all the TMB model numbers are included, and the drawings are on file at the David Taylor Model Basin.

59.4 Performance Data from Screw-Propeller Design Charts. The systematic data derived from the open-water tests of a multitude of series propellers, made in model basins all over the world, are published in the form of charts suitable for use in ship and propeller design. Thirteen kinds of screw-propeller-series charts are listed and described in Sec. 70.4. Comments on and comparisons of these charts are to be found in Sec. 70.5, while Sec. 70.6 describes and illustrates the procedure to be followed in making performance predictions from three of these chart types.

Other examples illustrating the manner in which screw-propeller performance is predicted from published propeller charts are found in Secs. 66.27 and 77.35, and in a paper "Propeller Coefficients and the Powering of Ships," by F. M. Lewis [SNAME, 1951, pp. 612–620].

The calculation of screw-propeller performance, by a method derived from analytic considerations, is covered by J. G. Hill in Appendix 2 of his 1949 SNAME paper, pages 161 and 162.

59.5 Performance Data on Paddlewheels and Sternwheels. In 1916 E. M. Bragg published a paper on "Feathering Paddle-Wheels" [SNAME, 1916, pp. 175–180, Pls. 90–98] in which he gave several sets of charts, intended to provide the designer with the same sort of information from systematic series as was included on the screw-propeller charts of that day. Unfortunately, these data are not readily applied by one who needs to design a modern paddlewheel.

To meet this need H. Volpich and I. C. Bridge undertook, in the early 1950's, to make systematic tests on a new series of models and to present the designer with tabulated and graphic information readily adaptable to his problems. The first installment of these data appeared in the paper "Paddle Wheels; Part I, Preliminary Model Experiments" [IESS, 1954–1955, Vol. 98, Part V, pp. 327–372]. It is understood that at the time of writing (1955) this systematic test program is still underway and that Part II of the report will appear in 1956. The data in this series of papers, taken with those of F. Gebers in reference (31) of Sec. 59.6, should go far toward filling, for the paddlewheel designer, the need which has been met by the availability of many design charts for the screw-propeller designer.

59.6 Bibliography on Paddlewheels. There appears to be no lengthy list of references appended to any of the better-known published papers and books on paddlewheel propulsion. The list given hereunder is by no means complete but it may serve the reader as a source of background information, as well as a source of experimental data and of information useful in design:

(1) Napier, J. R., "On the Effects of Superheated Steam and Oscillating Paddles on the Speed and Economy of Steamers," Trans. Inst. Engrs. Scot., 1863–1864, Vol. VII, pp. 86–102, Pls. V and VI. The "oscillating" paddles mentioned in the title of this paper are the feathering paddles of today. The table on p. 90 gives the principal paddlewheel and blade data for the steamers *Concordia* and *Berlin*. These vessels originally had radial wheels but were later altered to carry feathering wheels of smaller diameter and higher rate of rotation. On these feathering paddlewheels the blade spacing was only slightly greater than the blade width, the blade faces were flat, and the blades were apparently made of wood rather than iron.

(2) Rankine, J. W. M., "Shipbuilding: Theoretical and Practical," 1866, pp. 248, 251. Rankine refers to the preceding paper by J. R. Napier.

(3) Riehn, W., "Über die Wirkungsweise der Schaufelräder und der Schrauben bei Dampfschiffen (On the Operation of Paddlewheels and Propellers in Steamers)," Zeit. des Ver. Deutsch. Ing., 1884, Nos. 18–22

(4) Pollard, J., and Dudebout, A., "Théorie du Navire (Theory of the Ship)," 1894, Vol. IV, pp. 179–193

(5) Lovell, L. N., "American Sound and River Steamboats," Cassier's Magazine, Jul 1897, pp. 459, 482

(6) Durand, W. F., RPS, 1903, pp. 164–169, 198–203

(7) Paddle steamer *C. W. Morse*, Marine Engineering, Jun 1904, p. 279 ff

(8) Kaemmerer, W., "Raddampfer für die Anatolische Eisenbahn-Gesellschaft, erbaut von den Howaldtswerken in Kiel (Paddlewheel Steamer for the Anatolian Railways, built by the Howaldt Works, Kiel)," Zeit. des Ver. Deutsch. Ing., 12 Nov 1904, pp. 1725–1729. Figs. 9 and 10 on p. 1726 show the arrangement of a 4.5-meter (14.75-ft) outside diameter 8-bladed paddlewheel with the eccentric for the feathering mechanism centered ahead of and slightly *below* the wheel center.

(9) Hart, M., "Note sur le Changement des Roues des Paquebots *Le Nord* et la *Pas-de-Calais* (Note on the Alterations to the Paddlewheels of the Channel Steamers *Le Nord* and *Pas-de-Calais*)," ATMA, 1906, Vol. 17, pp. 169–186 and Pls. I through VIII

(10) Ward, C., "Shallow-Draught River Steamers," SNAME, 1909, Vol. 17, pp. 87–88

(11) Feathering paddlewheel, Schiffbau, 27 Dec 1911, pp. 210–211

(12) Teubert, O., "Binnenschiffahrt (Inland-Waters Ship

Operation)," Leipzig, 1912, Vol. I, pp. 224–442. A later edition of this book was published in 1932.

(13) "Experimental Towboats," House (of Representatives), 63rd Congress, 2nd Session, Document 857, 1914, Vol. 27. This report gives the results of many comparative tests run at the Univ. of Michigan, Ann Arbor, on models of radial and feathering paddlewheels, with many parameters varied. On p. 15 of the report there are listed ten conclusions drawn from an analysis of these paddlewheel tests.

(14) Bragg, E. M., "Feathering Paddle-Wheels," SNAME, 1916, pp. 175–180 and Pls. 90–98. It is believed that many of the data and charts of this report were based upon the work described in the preceding reference.

(15) Schaffran, K., "Modellversuche mit Schaufelrad-Propellern (Model Tests with Paddle Propulsion Devices)," STG, 1918, Vol. 19, pp. 475–520. Describes tests made on a number of models of feathering wheels, together with correlations with trials on several paddle steamers, the *Hugo Marcus* on the Elbe and the *Thommen* on the Danube.

The efficiencies of the model paddlewheels do not exceed 0.50 in any case.

Fig. 7 on p. 486 is a construction drawing of a pair of paddlewheels side by side on a single shaft, each pair with its own feathering mechanism.

(16) Sadler, H. C., and Kirby, F. E., "Design of Passenger Vessels for the Great Lakes," SNAME, 1925, pp. 101–108. Pl. 81 shows the design and dimensions of the feathering paddlewheels for the large vessels of the *Greater Detroit* class.

(17) Schoenherr, K. E., "Model Tests with Paddlewheels," EMB Rep. 176, Sep 1927. Gives curves of efficiency η_0 and characteristic curves for a number of variations of *radial* wheels only.

(18) Zilcher, R., "Leistung und Wirtschaftlichkeit von Flusschleppern verschiedener Antriebsart (Power and Economy of River Tugboats with Various Kinds of Propulsion)," WRH, 22 Dec 1927, pp. 556–561

(19) Baird, G., "Notes on the Development of Tug-Boat Machinery During the Past Forty-Six Years," NECI, 1935–1936, Vol. LII, pp. 89–102 and D19-D22. This paper depicts, on pp. 98–99, two tug paddlewheels of the feathering type, with 6 and 8 blades, respectively.

(20) Süberkrüb, F., "Der Radschiffsantrieb (Paddlewheel Ship Propulsion)," Schiffbau, 15 Mar 1939, pp. 115–119

(21) Gras, V., "Dieselelektrische Schaufelrad-Schlepper *Széchenyi* (Diesel Electric Paddle Tug *Széchenyi*)," WRH, 15 Aug 1939, pp. 247–256. Figs. 3, 4, and 15 on p. 250 show a direct electric-motor drive to the paddlewheel shafts. There are double paddles on each wheel, end to end.

(22) Blumerius, R., "Das Dieselradschiff (The Diesel Paddlewheel Ship)," Schiffbau, 15 Sep 1939, pp. 326–327; 15 Oct 1939, pp. 349–357. Fig. 21 on p. 354 gives the lines of the Danube River vessel *Stadt Wien*, which has a peg-top underwater midship section.

(23) Kretzschmar, F., "Einige Schiffbautechnische mitteilungen aus der Schweiz (Some Information about Shipbuilding Progress in Switzerland)," Schiff und Werft, 1 Mar 1943, pp. 74–77

(24) Gardner, J. H., "The Development of Steam Navigation on Long Island Sound," SNAME, HT, 1943, pp. 97–134.

(25) Helm, K., "Über den Heutigen Stand der Schaufelradfrage (On the Present Status of the Paddlewheel)," HSVA Rep. 881, 26 Jun 1944 (copy in TMB library). This report contains a treatise on paddlewheel developments and includes curves for paddlewheel design.

(26) "The *Bristol Queen*: A Modern Paddle Steamer," SBSR, 6 Mar 1947, pp. 224–227. The article gives photographs of the model feathering paddlewheels tested and of the self-propelled model of this vessel.

(27) Barr, G. E., "The History and Development of Machinery for Paddle Steamers," IESS, 20 Nov 1951, Vol. 95, Part 3, pp. 101–148. Paddlewheels are discussed on pp. 128–130, with numerous illustrations. There is a list of 7 references on pp. 138–139.

(28) Deetjen, R., "Erfahrungen mit einem speziellen Schaufelradantrieb für verkrautete Gewässer (Experience with a Special Paddlewheel for Use in Water with Weeds)," Schiff und Hafen, Mar 1952, pp. 80–81

(29) Henschke, W., "Schiffbautechnisches Handbuch (Shipbuilding and Ship Design Handbook)," Berlin, 1952, pp. 193–195

(30) Ostend-Dover Paddle Packet *Marie Henriette* of 1893, SBSR, 15 May 1952, p. 630

(31) Gebers, F., (with a contribution by F. Horn), "Das Schaufelrad im Modellversuch: Zwei Berichte der Schiffbautechnischen Versuchsanstalt, Wien (The Paddlewheel in Model Test: Two Reports of the Vienna Model Basin)," Vienna, Springer, 1952 (book in German).

(32) Krappinger, O., "Schaufelradberechnung (Paddlewheel Calculation)," Schiffstechnik, Aug 1954, pp. 30–36. This paper gives a number of graphs embodying the results of model tests, in a form useful to the designer. No translation known to be available in 1955.

(33) Volpich, H., and Bridge, I. C., "Paddle Wheels: Part I, Preliminary Model Experiments," IESS, 1954–1955, Vol. 98, Part 5, pp. 327–372. A bibliography of 8 items appears on p. 359, several of which are listed here.

The paper gives a brief general history of paddle propulsion and paddle research with a comment on the scarcity of experimental data for wheel design and analysis. Important deviations from the laws governing screw-propeller performance are noted and the purpose of the present investigation put forward. The apparatus used in testing two sizes of model wheel is described. The results of experiments with a radial and a feathering 9-float wheel at one immersion are given in detail for both wheel sizes and are discussed, together with methods of presentation. As the results are incomplete for design purposes, proposed future work is outlined; this will be published in a second paper.

Part II of this paper was presented to the IESS on 13 Mar 1956.
(34) "Quarter-Wheel Tugs for the Sudan," SBMEB, Dec 1955, pp. 705–706. This reference describes the six tugs of the *Tagoog* class, 125.5 ft long overall, 32.0 ft beam, and 3.0 ft draft, driven by a pair of radial-blade sternwheels, one on each quarter.

59.7 Test Results on Rotating-Blade Propellers. Many open-water tests of rotating-blade propellers, principally of the Kirsten-Boeing and the Voith-Schneider types, have been made by the old Experimental Model Basin and the David Taylor Model Basin at Washington, by the Netherlands Model Basin, and by other testing establishments. Unfortunately, the published results of these tests are rare. The most useful data, although not in the form of the usual characteristic curves, are those presented by Dr. Hans F. Mueller in his paper "Recent Developments in the Design and Application of the Vertical Axis Propeller" [SNAME, May 1955, pp. 4–30]. Two of his graphs are reproduced as Figs. 59.A and 59.B in this chapter.

Dr. Mueller advises the author [unpubl. ltr. to HES of 4 May 1955] that the publication of open-water test data on rotating-blade Voith-Schneider propellers, corresponding to those mentioned in Sec. 59.3 for screw propellers, were not made available in the technical literature for two reasons. First, those responsible for the development of these devices in the 1930's were hesitant to release the data until they had perfected a practical design of rotating-blade propeller which could compete with the best screw propeller. Second, a great deal of the open-water testing with models was done at the Netherlands Model Basin in Wageningen during the German occupation of that country in World War II. The latter data are in existence but have never been published.

Dr. Mueller points out that references (1) and (2) which follow may be of help to a designer employing this type of propulsion device. So far as known, these two references have not been translated into English.

(1) Mueller, H., and Helm, K., "Der Massstabeinfluss beim Voith-Schneider-Propeller (Scale Effect Encountered with the Voith-Schneider Propeller)," WRH, 15 Dec 1942, pp. 334–338
(2) Mueller, H., "Über das Zusammenarbeiten des Voith-Schneider-Propellers mit dem Schiff (On the Interaction of the Voith-Schneider Propeller and the Ship)," Schiff und Werft, Jun 1944, pp. 113–119.

A few other references, additional to those embodied in Secs. 15.13, 15.14, and 37.22, are:

(3) Kempf, G., and Helm, K., "Ergebnisse naturgrosser Schleppversuche mit dem Motorschiff 'Augsburg' (Results of Full-Scale Towing Tests on the Motorship *Augsburg*)," WRH, 15 Oct 1931, Vol. XII, pp. 347–348
(4) Betz, A., "Grundzätzliches zum Voith-Schneider-Propeller (Fundamentals of the Voith-Schneider Propeller)," HPSA, 1932, pp. 161–170
(5) Mueller, H. F., "Die Steuerkraefte des Voith-Schneider Propellers (The Steering Force of the Voith-Schneider Propeller)," WRH, 1 Jul 1938, pp. 202–204
(6) "Cycloidal Propulsion on Army Vessel (*Truman O. Olson*)," Naut. Gaz., Mar 1950, p. 25.

59.8 Available Performance Data on Hydraulic-Jet, Pump-Jet, and Gas-Jet Propulsion Devices. It is unusual, yet unfortunate, to find that in a search for performance data on hydraulic-jet propulsion to supplement the descriptions of Secs. 15.8, 32.5, and 34.13, most of the published data are largely historic. It is known that an English patent was granted to Toogood and Hayes, as far back as 1661 [Schoenherr, K. E., PNA, 1939, Vol. II, p. 122]; also that Benjamin Franklin made a proposal for jet propulsion of a boat in 1775. K. E. Schoenherr states, in the reference cited, that jet propulsion was actually applied by James Rumsey in 1782 to propel an 80-ft ferryboat between Washington and Alexandria, Va.

Most of the references on the older forms of jet propulsion might almost be termed ancient. The newer references are almost equally remote from the modern (1955) marine architect because most of them are in a classified status. Among the older references are:

(1) Brin, C. B., "On the Efficiency of Jet Propellers," INA, 1871, Vol. XII, pp. 128–149
(2) White, W. H., "The Water-Jet Propeller," MNA, 1882, pp. 532–538; MNA, 1900, p. 587ff. These references mention installations on the:
(a) *Waterwitch*, 1866
(b) Swedish torpedo boat, 1878
(c) British Admiralty torpedo boat, 1881
(d) German naval craft
(e) Hydromotor, Fleischer, 1879; Engineering, London, 9 Sep 1881
(f) American jet-propelled boat.
(3) "Verso la Soluzione del Problema del la Propulsion Idraulica (Toward a Solution of the Problem of Hydraulic Propulsion)," by Dr. Giacomo Büchi, Engineer, La Marina Italiana, Feb 1935, pp. 45–57. ONI, U. S. Navy, Transl. 76 (copy in TMB library).

One of the most systematic accounts is recorded by J. Pollard and A. Dudebout, in their "Théorie

du Navire" [1894, Vol. IV, p. 201], from which the following is translated. The comments in parentheses are those of the present author:

"379. Principal Examples of Turbine-Propulsors of the First Kind.

"As examples of the application to (ship) propulsion of the turbine-propulsors of the first kind (in which the water passes through the turbine radially), we will give them in chronological order:

"The *Enterprise*, built in 1853 by John Ruthven; this vessel was not successful and was (later) converted into a sailing ship

"The *Albert*, built the same year by Seydell at Stettin, ran successfully on the Oder for ten years

"The *Seraing II*, built about 1860 by Cockerill, at the same time as the identical ship *Seraing I*, fitted with articulated (feathering?) paddlewheels

"The *Jackdraw*, on which, in 1863, the British Admiralty attempted, but without success, an application of hydraulic propulsion

"The *Nautilus*, constructed in 1863 for the British Admiralty, which on trials on the Thames achieved a speed of 10 kt

"The English armed gunboat *Waterwitch*, built in the same year, successfully underwent comparative trials with the *Viper*, of the same type, fitted with twin screws

"The *Rival*, built in 1870 by the German Navy, proved a failure, due partly to an excess of draft over the predicted draft

"A torpedo boat with hydraulic propulsion, built in 1878 by the Swedish Government, to be tested comparatively with a ship of the same type fitted with two screws

"A torpedoboat of the second class, built by Thornycroft and Company in 1882, for the British Admiralty, and which was run through comparative trials with a similar ship having a single screw propeller

"Finally, a rescue or lifeboat recently (1894?) constructed by R. and H. Green of Blackwall (England), for the National Lifeboat Institution. It was fitted, by Thornycroft and Company, with an internal hydraulic propulsor, intended to prevent damage from shocks, beaching, or running foul of another ship."

A table on page 203 of this reference gives 20 items of technical data for the:

(a) *Waterwitch*

(b) *Viper*

(c) Two Swedish torpedoboats with hydraulic propulsion and with screw propellers

(d) Two Thornycroft torpedoboats, with hydraulic propulsion and with screw propellers.

A discussion by Pollard and Dudebout of the screw-turbine is to be found on pages 206–210 of the reference cited earlier in this section.

One of the few modern references describes a new ferryboat with so-called hydraulic-reaction propulsion, built by the Établissements Billiez [Nav. Ports Chant., Jul 1952, Vol. 3, p. 418 (in French)]. One pump on each side of the vessel takes in water through a converging conduit and discharges it through a valve which directs the flow either astern or ahead. The jets issuing from the vessel may be deflected so that they act as rudders. One jet may be reversed so that the boat turns on its axis; when both are reversed the stopping action is very powerful.

59.9 Performance Data on Controllable and Reversible Propellers. Open-water test data and performance characteristics of controllable and reversible propellers, defined and described in Sec. 32.19 of Volume I, are found only rarely in the technical literature. L. A. Rupp gives open-water characteristic curves derived from tests of a model representing the controllable propeller installed and tested on the U. S. Navy tug *YTB 502* [SNAME, 1948, pp. 278–279]. The graphs in Fig. 6 on page 279 of this reference embody characteristics for five different pitch settings of this propeller. The propeller itself, shown in Fig. 4 on page 277 of the reference, has the following features:

Number of blades, 4
Diameter, 9.50 ft
Pitch at $0.7R$, helix angle 20 deg, ahead position, 7.60 ft
Developed-area ratio, A_D/A_0, 0.502
Mean-width ratio, 0.268
Blade-thickness fraction, variable.

More extensive open-water data are given by W. B. Morgan in reporting the tests of a series of controllable propellers with 2, 3, 4, 5, and 6 blades [TMB Rep. 932, Nov 1954]. In this case three different hubs were used, to which the proper number of blades were clamped. The report includes a model propeller drawing, with five sets of characteristic curves for normal ahead operation. Morgan publishes, as Fig. 7 of his report, the open-water characteristic curves of the 4-bladed controllable propeller, TMB model 3227, when run in the astern direction, called "back driving."

L. C. Burrill discusses the "Latest Developments in Reversible Propellers" [IME and INA joint mtg., 1949, pp. J3-J32] as applying to three types developed in Europe but unfortunately he includes no open-water test data for models or full-scale prototypes of any of these propellers.

More recently, J. A. van Aken and K. Tasseron have published a paper entitled "Comparison Between the Open-Water Efficiency and Thrust of the Lips-Schelde Controllable-Pitch Propeller and those of Troost-Series Propellers" [Int. Shipbldg. Prog., 1955, Vol. 2, No. 5, pp. 30–40].

A contribution by R. F. P. Desel, entitled "Controllable Pitch Propellers in Ship Propulsion," appeared in Bureau of Ships Journal, April 1956, pages 2–6.

59.10 Performance of Miscellaneous Propulsion Devices. The general arrangement and method of operation of the Hotchkiss propeller are illustrated schematically in the diagram of Fig. 59.Da. A drawing showing the use of a Gill axial-flow propeller in a hydraulic propulsion device is reproduced in Fig. 59.Db.

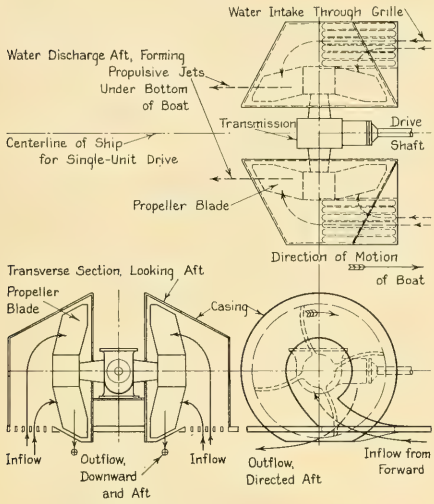

Fig. 59.Da Explanatory Diagram for the Hotchkiss Propeller

It has not been possible to find in the technical literature any published systematic performance data on these and other types of miscellaneous propulsion device, corresponding to the orthodox characteristic curves for screw propellers. The following may be mentioned as sources of reference information on the Hotchkiss propeller:

(1) Hotchkiss, D. V., "The Hotchkiss Internal Cone Propeller," The Shipbuilder, 1931, p. 180
(2) SBMEB, Apr 1937, p. 188. Illustrates "60-in Worm-Drive Cone Propellers for Wood Vessel." Also May 1937, p. 321, and Jul 1937, pp. 382–384.
(3) The Motorship, 1937–1938, p. 110
(4) A lifeboat fitted with Hotchkiss cone propellers is illustrated and described on pages 45–50 of the 13 January 1938 issue of Shipbuilding and Shipping Record. The following is quoted from pages 45–46:

> "The Hotchkiss system of propulsion consists of cones constructed of steel and provided with rotary impellers. One side of the cone is cut away, forming an aperture in contact with the water, which divides into inlet and outlet portions. As the impeller rotates, the centrifugal force of the water causes it to be projected tangentially from the larger end.

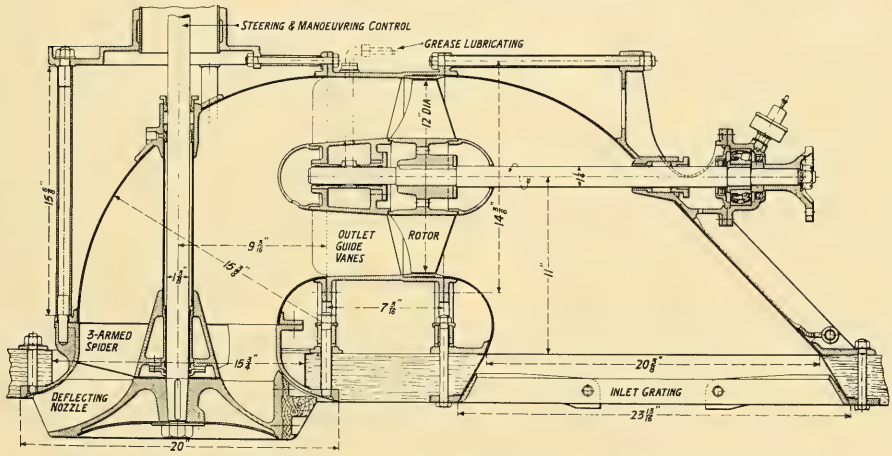

Fig. 59.Db Longitudinal Section Through a Hydraulic Propulsion Device Utilizing a Gill Axial-Flow Propeller

This drawing, reproduced from page 111 of the July 27, 1939 issue of Shipbuilding and Shipping Record, shows a Gill propeller (marked "rotor") with a close-fitting fixed shroud ring. In other installations the ring is attached to the blade tips and rotates with the propeller.

"Water is drawn in through about two-thirds of the length of the opening, measured from the smaller end. The water flows into the cone in the direction of rotation and the resultant spiral flow causes the water to leave the cone with increased velocity, thereby producing a reactive thrust which takes effect upon the internal surfaces of the cone."

(5) SBSR, 10 Feb 1938, p. 176; 2 May 1940, pp. 444–445. The latter reference contains rather detailed drawings of a 25-ft launch equipped with a double-cone propeller designed by Donald V. Hotchkiss for operation on the Irrawaddy River where floating debris and weeds are encountered. A grille is provided to exclude "objects which might damage the impellers if drawn into the intakes."

(6) Baader, J., "Cruceros y Lanchas Veloces (Cruisers and Fast Launches)," Buenos Aires, 1951; Fig. 175 on p. 221 illustrates a Hotchkiss propeller fitted in the side of a vessel

(7) On pages 358 and 359 of the September 1952 issue of The Motor Boat and Yachting there is an article, with drawings, about a small cone propeller installation suitable for dinghies. The following is quoted from page 358:

"Advantages of the system are that there is no projection outside the hull so that the draft of a craft using it is much reduced; the cone propeller can pass through weed beds, or over ropes or other obstructions without fouling, by reason of the self-clearing grids provided; installation is a simple matter and the cones can be installed in the most suitable part of the boat. A further important advantage is that the impeller can be employed to pump out the bilges, by providing piping connected to the small end of the cone."

For the Gill propeller, the available information is somewhat more scanty:

(a) Gill, J. H. W., "Der Hydraulische Schiffsantrieb für besondere Fahrtverhältnisse (The Hydraulic Ship Propulsion for Special Ship Operating Conditions)," Bull. Tech. du Bureau Veritas, 1921, p. 199

(b) The Shipbuilder, 1921, p. 24

(c) The Engineer, 1921, Vol. 1 of that year, pp. 140, 172

(d) MENA, 1923, p. 345

(e) SBSR, 19 Aug 1926, Vol. 28, pp. 202–204; 1939, Vol. 54, pp. 111–115.

59.11 Area Ratios, Blade Widths, and Blade-Helix Angles of Screw Propellers. The various blade-area ratios of a screw propeller are defined rather precisely in Sec. 32.8 of Volume I and in the "Explanatory Notes for Resistance and Propulsion Data Sheets," SNAME Technical and Research Bulletin 1–13, July 1953, page 16. The expanded-area ratio A_E/A_0, also known rather indefinitely as the blade-area ratio or the disc-area ratio, is the one employed almost exclusively in this book, particularly in the propeller-design discussion of Chap. 70 of the present volume.

It is often convenient, when laying out propeller apertures and edge clearances by the rules laid down in Sec. 67.24, to know the approximate maximum blade width for a screw propeller having Z blades and a specified (or approximate) expanded-area ratio A_E/A_0, or for a propeller having a given mean-width ratio c_M/D. The maximum width will depend to some extent upon the blade outline and shape but approximate values can be derived for blades of average shape, to permit establishing aperture and edge clearances in the preliminary-design stage. The broken-line graph of Fig. 59.E enables a designer to

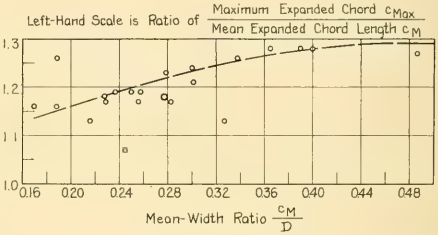

Fig. 59.E Graph for Estimating Maximum Expanded Chord Length from Mean-Width Ratio

estimate the maximum expanded chord length c_{Max} or the maximum blade width for a reasonable range of mean-width ratio c_M/D.

For example, the stock propeller (TMB 2294), used for the self-propulsion tests of the ABC transom-stern ship model, has a mean-width ratio of 0.238. From Fig. 59.E, the value of $c_{Max}/c_{Mean} = 1.19$, whence $c_{Max} = 1.19(0.238)D = 1.19(0.238)(20.0) = 5.66$ ft. The chord-length data on Fig. 78.Ma give a maximum length of 2.682 ft at the $0.7R$ for a 9.25-ft diameter. Stepping this up to the 20.0-ft diameter of the ultimate propeller design for the ABC ship gives a c_{Max} of 5.80 ft. This is only slightly greater than the value estimated from Fig. 59.E.

For the ABC propeller designed in Chap. 70, the actual value of c_{Max} at the $0.7R$, from Table 70.i, is 5.098 ft. From Fig. 59.E, for a c_M/D ratio of 0.229, derived in Sec. 70.31, the value of c_{Max}/c_{Mean} is 1.182 and $c_{Max} = (1.182)(0.229)(D) = (1.182)(0.229)(20.0) = 5.42$ ft. The estimated value is thus somewhat large. The forward aperture clearance of 4.7 ft, indicated in Fig. 66.Q, is somewhat less than the c_{Max} of 5.098 ft for the

propeller design of Chap. 70. It could and should be increased when making the revisions to the preliminary design described in Sec. 78.18.

In the event the mean-width ratio of a particular screw propeller is not known, it can be determined by the formula

$$\frac{c_{\text{Mean}}}{D} = \frac{\pi\left(\frac{A_E}{A_0}\right)}{2Z\left(1 - \frac{d}{D}\right)} \qquad (59.i)$$

Table 59.a lists the blade-helix angles ϕ(phi) for ten values of 0-diml ratio $x' = R/R_{\text{Max}}$ for EMB model propeller 2294, used as the stock propeller for the self-propulsion tests of the transom-stern ABC ship model, TMB 4505. A drawing of this propeller is reproduced in Fig. 78.L.

Table 59.b lists the blade-helix angles ϕ for a series of ten 0-diml radii x', and for five pitch-diameter ratios covering the range normally encountered in ship work. The pitch is assumed constant at all radii for this tabulation.

59.12 Pertinent Data on Flow Into Propulsion-Device Positions. The flow into the positions occupied by propulsion devices around a ship hull is discussed in and covered by various sections in Chaps. 17, 33, 52, 60, 67, and 69. The duplication and repetition involved are considered justified by the great importance of this phase of hydrodynamics as applied to ship design, and by the necessity for devoting increased thought and study to it in the future. The present section calls attention to a few particular features of this flow, and lists a number of sources of published material available for reference.

TABLE 59.a—Derivation of Blade-Helix Angles for TMB Model Propeller 2294

Fig. 78.L is a drawing of this propeller, used as the stock wheel for the self-propelled test of TMB Model 4505, representing the transom-stern design of the ABC ship of Part 4.

The helix angle is given for the tip section, even though the blade width there is zero.

$x' = R/R_{\text{Max}}$	Radius R, inches	$2\pi R$, inches	Local Pitch P, inches	$\text{Tan}\ \phi = \frac{P}{2\pi R}$	$\phi = \tan^{-1}\frac{P}{2\pi R}$
0.18	0.8687	5.458	8.587	1.5733	57°33′.3
0.3	1.448	9.098	8.907	0.9790	44°23′.5
0.4	1.930	12.127	9.155	0.7549	37°03′
0.5	2.413	15.161	9.355	0.6170	31°40′.5
0.6	2.896	18.196	9.465	0.5201	27°29′
0.7	3.378	21.225	9.478	0.4465	24°04′
0.8	3.861	24.259	9.478	0.3907	21°21′
0.9	4.343	27.288	9.478	0.3473	19°09′
0.95	4.585	28.808	9.478	0.3290	18°12′.5
1.00	4.826	30.323	9.478	0.3126	17°22′

TABLE 59.b—Tabulated Values of Helix or Blade Angle ϕ for Screw Propellers of Varied P/D Ratio

For these calculations it is assumed that the pitch P is constant at all radii.

	Pitch-Diameter Ratios				
$x' = R/R_{\text{Max}}$	1.4	1.2	1.0	0.8	0.6
0.1	77°21′	75°20′	72°33′	68°34′	62°22′
0.2	65°50′	62°22′	57°51′	51°51′	43°41′
0.3	56°03′	51°51′	46°42′	40°20′	32°29′
0.4	48°05′	43°41′	38°31′	32°29′	25°31′
0.5	41°43′	37°23′	32°29′	27°00′	20°54′
0.6	36°36′	32°29′	27°50′	23°00′	17°39′
0.7	32°29′	28°37′	24°27′	19°59′	15°16′
0.8	29°07′	25°31′	21°42′	17°39′	13°26′
0.9	26°21′	23°00′	19°29′	15°48′	11°59′
1.0	24°01′	20°54′	17°39′	14°17′	10°49′

One such feature applies to the element of a screw-propeller blade on which the instantaneous incident-velocity vector impinges in a plane not normal to the blade axis, corresponding to the non-axial flow situation described in Sec. 17.7 and depicted in diagram 1 of Fig. 17.D. It is again emphasized that for this case the *effective* velocity across the blade is the incident velocity U_R times the sine of the angle which that velocity vector makes with the blade axis, as projected on a plane passing through the base chord of the blade element and the blade axis. The situation here corresponds to that of the flow over an airplane wing with sweep-back. The effective velocity of the air stream, for generating lift, is the component of the speed vector lying normal to the blade axis, in a plane generally parallel to the wing. This is equal to the stream velocity times the cosine of the angle of sweepback [Collar, A. R., "Aeroelastic Problems at High Speed," Jour. Roy. Aero. Soc., Jan 1947, pp. 15–16].

Theoretically, this situation should apply also to a screw-propeller blade with skew-back, and to the converging flow of an inlet jet when approaching the propeller disc. In the former case, throughout most of the length of the blade, the local blade-axis direction is not normal to the tangent plane of the local incident flow. However, since the effect and the magnitude of sweep-back have not as yet (1955) been incorporated in any of the analysis or design phases for screw propellers, the effective velocity is assumed the same as the nominal incident velocity.

In the latter case, diagram 1 of Fig. 59.G of Sec. 59.13 indicates that for a thrust-load factor C_{TL} of 24, rarely reached in any kind of ship service, the convergence angle of the inflow jet, at the propeller tip, is about 19 deg. The cosine of this angle is 0.9455, but it must be remembered that the lift and the thrust for any blade element of thickness dR vary as the square of the incident velocity. The effective thrust on the tip blade element therefore appears to be reduced by the factor $(1 - \cos^2 \theta)$, where θ(theta) is the convergence angle. For the case mentioned this is $[1 - (0.9455)^2]$ or about 0.106.

Applying also to Fig. 59.G of Sec. 59.13, the graphs of Fig. 59.F indicate the ratios of the inflow-jet and outflow-jet diameters to the diameter of an imaginary actuator-disc propeller, for a range of thrust-load coefficient values up to 6.0. The data given are for positions $3D$ ahead of and $3D$ abaft the disc position, respectively.

Only in the case of *systematic* variations in inflow, occurring over most of the disc area, is it possible to predict their effect on propeller performance. For instance, general prerotation in the inflow jet, in a direction opposite to that of the propeller, results in a slower rate of rotation, a reduction in power absorbed, and (usually) an increase in efficiency for the generation of a given propeller thrust.

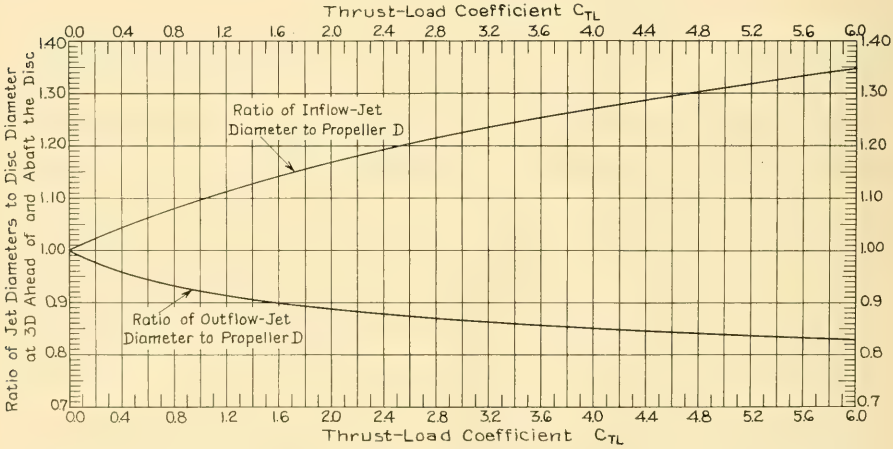

FIG. 59.F GRAPHS INDICATING RATIOS OF INFLOW- AND OUTFLOW-JET DIAMETERS TO DISC DIAMETER OF AN IDEAL SCREW PROPELLER

The following references may be found useful by the reader who wishes to pursue further the study of inflow to a screw propeller:

(1) Wood, R. McK., "Multiplane Interference Applied to Airscrew Theory," ARC, R and M 639, 1919–1920, Vol. 2, pp. 553–576

(2) Betz, A., "Development of the Inflow Theory of the Propeller," NACA Tech. Note 24, Nov 1920

(3) Betz, A., "The Theory of the Screw Propeller," NACA Tech. Note 83, Feb 1922

(4) Munk, M. M., "Notes on Propeller Design-III. The Aerodynamical Equations of the Propeller Blade Elements," NACA Tech. Note 95, May 1922

(5) Lock, C. N. H., and Bateman, H., "The Measurement of Airflow Round an Airscrew," ARC, R and M 1955, Nov 1924, pp. 385–399

(6) Weick, F. E., "Propeller Design: Practical Application of the Blade Element Theory-I," NACA Tech. Note 235, May 1926

(7) Weick, F. E., "Aircraft Propeller Design," McGraw-Hill, New York, 1930

(8) Helmbold, H. B., "Goldstein's Solution of the Problem of the Aircraft Propeller with a Finite Number of Blades," NACA Tech. Memo 652, Dec 1931

(9) Glauert, H., "Airplane Propellers," AT, Vol. IV, 1936.

59.13 Data on Induced Velocities and Differential Pressures. It is explained in Sec. 16.3 of Volume I that the induced flow and the contraction of the jet passing through the imaginary actuator disc representing a screw propeller are functions of the thrust-load factor C_{TL} at which the actuator is assumed to be working. The relative magnitude of the $-\Delta p$ ahead of the disc and the $+\Delta p$ abaft the disc for any given C_{TL} is similarly a function of that thrust-load factor, indicated by the graph of Fig. 16.B on page 249 of Volume I. Here, utilizing the Bernoulli Theorem, the ratio

$$\frac{-\Delta p}{+\Delta p} = \frac{3 + \sqrt{C_{TL} + 1}}{1 + 3\sqrt{C_{TL} + 1}} \qquad (59.ii)$$

At zero speed of advance, where C_{TL} has a nominal value of infinity, the ratio of $-\Delta p$ to $+\Delta p$ reaches its low limit of 0.333 [Troost, L., IME, Mar 1946, Vol. 58, p. 14].

Numerical values of the ratio of half the induced velocity far astern, $0.5U_I$, to the undisturbed

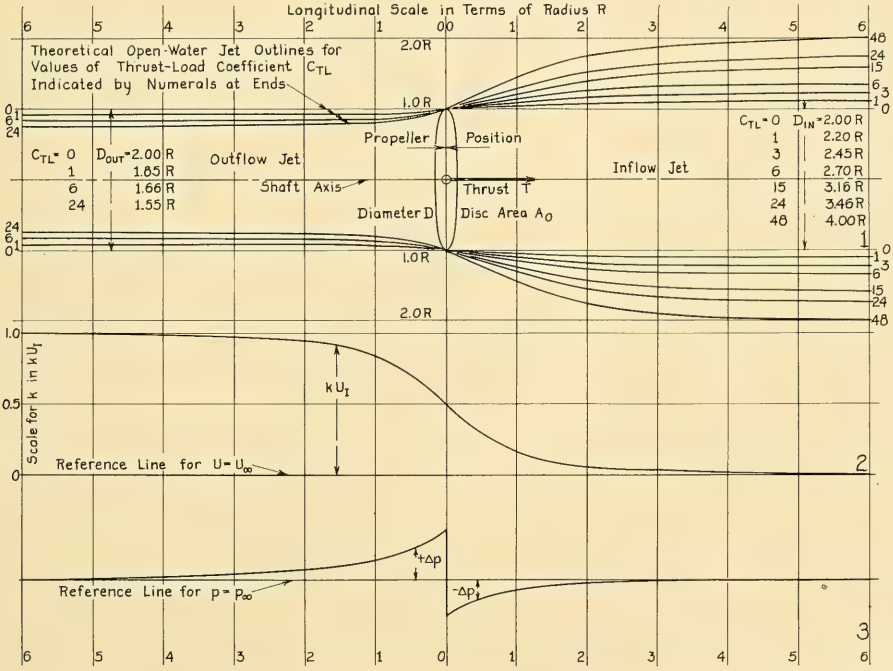

Fig. 59.G Theoretical Jet Outlines, Axial-Velocity Distribution, and Axial-Pressure Distribution for an Ideal Screw Propeller

stream velocity U_∞ at a distance, are listed in Table 34.a on page 508 of Volume I for a range of thrust-load factor C_{TL} of from 0.040 to 360.0. These ratios are indicated graphically in Figs. 34.D and 34.E on page 510 of that volume.

In diagram 1 of Fig. 59.G there are plotted, to scale, the longitudinal jet outlines for the liquid passing through an imaginary actuator disc from $6R$ or $3D$ ahead to $6R$ or $3D$ abaft the disc position, at varied thrust-load factors. If R is the radius of the actuator, Table 59.c gives the theoretical inflow and outflow jet radii for $3D$ ahead and $3D$ astern, respectively, for the seven values of C_{TL} indicated in Fig. 59.G. These are derived from the relationships

$$\frac{R_{\text{Inflow jet}}}{R} = \left(\frac{1}{\eta_I}\right)^{0.5} \qquad (59.\text{iiia})$$

and

$$\frac{R_{\text{Outflow jet}}}{R} = \left(\frac{1}{2 - \eta_I}\right)^{0.5} \qquad (59.\text{iiib})$$

for the $6R$- or $3D$-axial distance. For example, from Table 34.a, for a C_{TL} of 6.0, the ideal efficiency η_I is 0.549. Then

$$R_{\text{Inflow jet}} = R\left(\frac{1}{0.549}\right)^{0.5} = 1.35R$$

$$R_{\text{Outflow jet}} = R\left(\frac{1}{2 - 0.549}\right)^{0.5} = 0.83R.$$

Diagram 2 of Fig. 59.G illustrates graphically the rate of variation of $(U_\infty + kU_I)$ with axial distance ahead of and abaft the actuator disc. This rate is valid for any finite value of the thrust-load coefficient. Diagram 3 of the figure indicates a typical rate of variation of Δp with the same axial distance. In this case the differential-pres-

TABLE 59.c—INFLOW- AND OUTFLOW-JET DIAMETERS AT $6R$ AHEAD AND ASTERN OF AN IMAGINARY ACTUATOR DISC OF RADIUS R

The values tabulated are entirely theoretical, for an ideal liquid and no external interferences.

Thrust-load factor, C_{TL}	Ideal efficiency, η_I	Inflow-jet radius	Outflow-jet radius
0	1.000	$1.00R$	$1.00R$
1	0.828	$1.10R$	$0.924R$
3	0.667	$1.225R$	$0.866R$
6	0.549	$1.35R$	$0.830R$
15	0.400	$1.58R$	$0.791R$
24	0.333	$1.73R$	$0.775R$
48	0.250	$2.00R$	$0.756R$

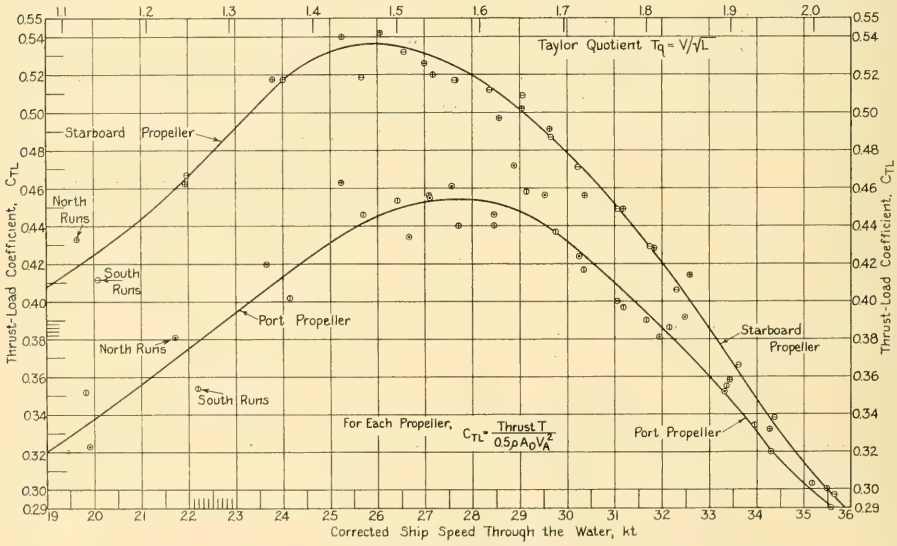

FIG. 59.H VARIATION OF THRUST-LOAD COEFFICIENT WITH SHIP SPEED AND SPEED-LENGTH QUOTIENT FOR DESTROYER *Hamilton* (DD141)

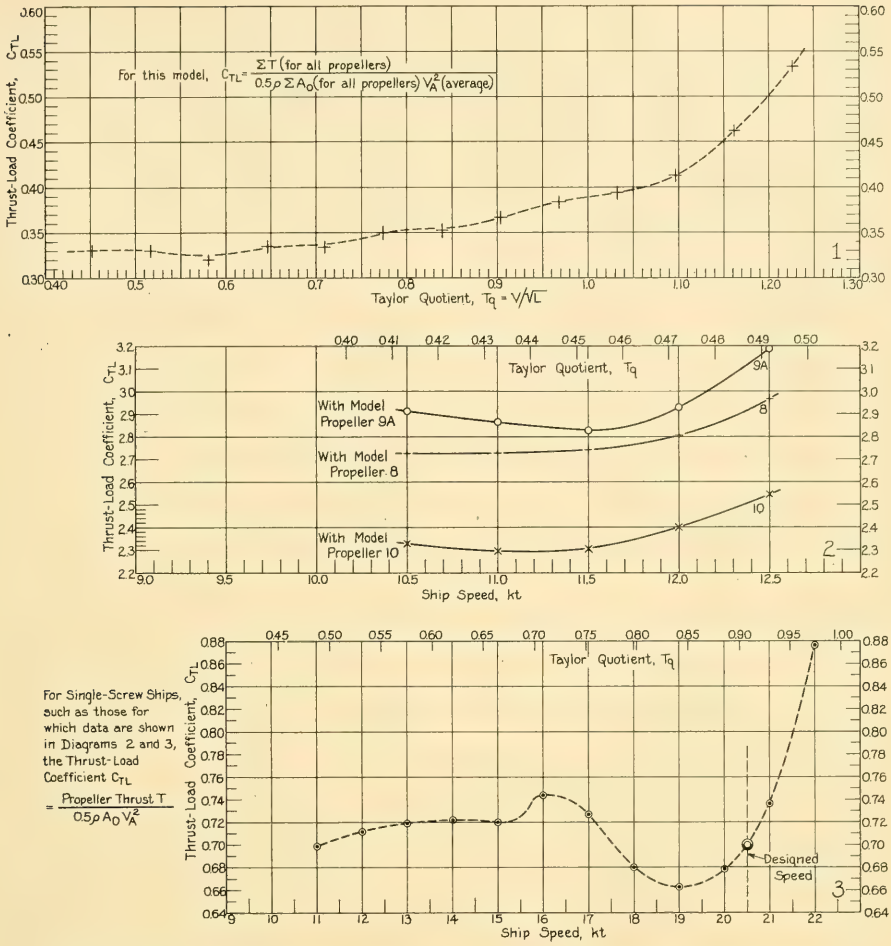

FIG. 59.1 VARIATION OF THRUST-LOAD COEFFICIENT WITH SHIP SPEED AND SPEED-LENGTH QUOTIENT FOR THREE MERCHANT-SHIP MODELS

sure curve is drawn for a C_{TL} value of 2.5, with a ratio $-\Delta p/+\Delta p$ of 0.737.

It is emphasized that the data presented in this section apply to perfect conditions in an ideal liquid, and that they conform only rarely to conditions encountered in practice.

Knowledge concerning the local values of the induced velocity, symbolized by kU_I, in the vicinity of the individual blades of an actual screw propeller behind a ship, would be extremely useful information. However, present developments (1955) permit only a direct determination of the hydrodynamic pitch angle β_I(beta), as in Secs. 59.17, 70.27, and 70.28, and this determination must often be made by trial-and-error methods.

59.14 The Thrust-Load Factor and Derived Data. As an indication of the manner in which the thrust loading on actual ships varies with speed throughout the normal running range,

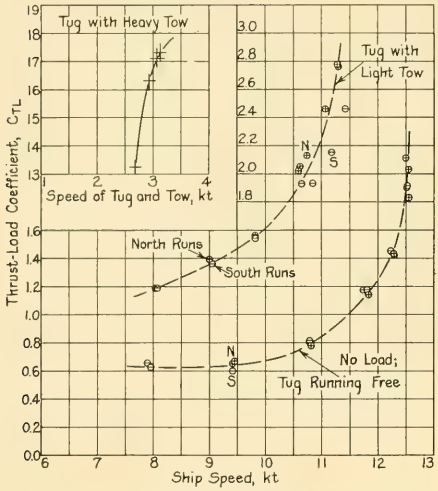

Fig. 59.J Variation of Thrust-Load Coefficient with Ship Speed for U. S. Navy Tug *YTB* 500, When Running Free and Under Two Towing Conditions

Figs. 59.H, 59.I, 59.J, and 59.K give plots of these values for a few vessels on which thrusts have been accurately measured during standardization and other trials, and for some selected models. The ship-trial data were taken from the following sources:

Fig. 59.H U. S. S. *Hamilton*. Trial of 9 May 1933; Tables 20 and 21 of pp. 274–277, SNAME, 1933. The speeds corrected by trial analysis were used for spacing the ordinates in this figure.

Fig. 59.J U. S. S. *YTB 500*. Trials of 1, 5, 13, 14, and 15 April 1948, using data in the Bureau of Ships (U. S. Navy Department) archives. The trials involved running free and with light and heavy tows.

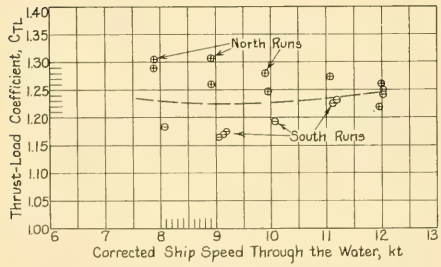

Fig. 59.K Variation of Thrust-Load Coefficient With Ship Speed for the S. S. *Clairton*

Fig. 59.K S. S. *Clairton*. Trials of 8 and 9 October 1931; SNAME, 1932, pp. 17–44. Corrected thrusts T are from Sheet I of Appendix 2 on p. 32; corrected ship speeds V through the water are from Part II of Appendix 1 on p. 31. The speeds of advance V_A were calculated from the corrected ship speeds V through the water by using wake fractions derived from a plot of those tabulated in Part I of Appendix 1 on p. 31.

There are included also data derived from the tests of three self-propelled models, as follows:

Fig. 59.I, diagram 1. Projected merchant ship design; data from TMB archives.

Fig. 59.I, diagram 2. Canadian lake freighter, L_{PP} = 647.25 ft, Ottawa model 95; National Research Council, Ottawa, Report MB-137 of 3 Jul 1951.

Fig. 59.I, diagram 3. ABC ship design, with transom stern, Fig. 78.Nb of Part 4.

Similar data can easily be plotted for any ship model from the results of the self-propelled tests.

When plotted on a basis of ship speed, or of speed-length quotient, the data reveal no definite pattern, except that the thrust-load coefficient may diminish with increase of speed in the ranges below the designed speed. For fine, fast hulls it may increase with speed, up to a T_q value of about 1.5 or 1.6. At this point the effect of the first trough of the ship's Velox-wave system is making itself felt, with a diminishing wake fraction w and an increasing ratio of speed of advance V_A to ship speed V. On a high-speed vessel, like the destroyer *Hamilton*, the wake fraction decreases toward zero, or may become actually negative, with an appreciable increase in the V_A/V ratio. With a given thrust the thrust-load coefficient decreases at a greater rate, because V_A is squared in the denominator of the expression for C_{TL}. However, in the case of the *Hamilton*, cavitation was encountered on the propellers at speeds in excess of 30 kt, so that other factors entered the picture.

In the case of the model of the transom-stern ABC ship, for which the C_{TL} data are plotted in diagram 3 of Fig. 59.I, there are rather sudden and unexplained changes in the range of 15–21 kt. These undoubtedly bear some relation to the changes in the values of w_T and t, indicated on Fig. 78.Nc, but the relationship is by no means clear. More data and a much more thorough analysis of this problem are required before the designer can attempt a prediction of the C_{TL} variation with speed for any given case.

59.15 Approximation of Screw-Propeller Thrust from Insufficient Data. It often becomes necessary, in the early stages of a ship design or in the

course of a conversion project, to estimate the screw-propeller thrust long before the propeller is selected or designed. Only the proposed ship speed may be known, or at most the power and rate of rotation of the engine.

A rule-of-thumb often used involves the dimensional relationship $T = kP_S$, where in English units T is in lb, P_S is in horses, and k varies from 30 on a tug exerting bollard pull at zero speed to a range of 10–15 for normal propulsion. For high-speed racing motorboats it may drop to 3 or less [Spencer, D. B., Pac. N. W. Sect., SNAME, 2 Feb 1951].

It is pointed out in Sec. 34.7 of Part 2 and Sec. 70.5 of Part 4 that there is a rather definite relationship between the thrust T and the torque Q developed by a screw propeller when working under any given set of relatively steady conditions. The torque to be exerted by a propelling plant is readily determined from assumed or known values of the shaft power and the angular rate of rotation n. The thrust may be estimated with equal facility by one or the other of the following 0-diml equations, depending upon the information available at the time of the estimate:

Thrust-torque factor

$$\frac{TD}{Q} = \text{a value derived from propeller charts}$$

$$= \left(\frac{K_T}{K_Q}\right) \text{ from open-water model propeller data.}$$

The latter relationship is easily derived from available plots, provided the pitch ratio and other principal characteristics of the propeller approximate those which will probably be used in the contemplated design. The TD/Q ratio varies only slowly with the real-slip ratio s_R or advance coefficient J. In any case the open-water data give appropriate values for any desired real-slip ratio or advance coefficient.

At a later stage in a ship design the propeller thrust is estimated from $T = R/(1 - t)$, where the hull resistance R and the thrust-deduction fraction t are estimated as described in Secs. 57.4 and 60.9, respectively, or are found from self-propelled model tests.

Using the ABC ship as an example for the successive stages of this estimate, the rule-of-thumb method, with k-values of 10 to 15 for normal propulsion, and for an estimated shaft power of 17,000 horses, gives a range of from (10) 17,000 = 170,000 lb to (15) 17,000 = 255,000 lb thrust.

Selecting a TD/Q value from the Prohaska logarithmic propeller chart in Fig. 70.B, by the method diagrammed in Fig. 70.A, gives the ratio $TD/Q = 5.8$ for a P/D ratio of 1.00. Again taking the power as 17,000 horses for this example, and the rate of rotation from Sec. 70.6 as 109.2 rpm or 1.82 rps, the expected torque at the designed speed is found by

$$Q = \frac{P_S}{2\pi n} = \frac{17{,}000(550)}{6.2832(1.82)} = 817{,}600 \text{ ft-lb.}$$

With a propeller diameter of 20 ft, the thrust prediction works out as

$$T = 5.8\left(\frac{Q}{D}\right) = 5.8\left(\frac{817{,}600}{20}\right) = 237{,}104 \text{ lb.}$$

From the open-water test data of the stock model propeller selected for the transom-stern, TMB 2294, presented in Fig. 78.Mc, the value of the fraction K_T/K_Q at a real-slip ratio of about 0.25, corresponding to a J-value of 0.735, is found to be

$$\frac{TD}{Q} = \frac{K_T}{K_Q} = \frac{0.148}{0.0265} = 5.58$$

Hence

$$T = 5.58\left(\frac{817{,}600}{20}\right) = 228{,}110 \text{ lb.}$$

From Sec. 70.6 the predicted propeller thrust, worked out at a later stage of the ABC ship design, is only about 193,500 lb. The thrust derived from the self-propelled model test, taken from Fig. 78.Nb for the 20.5-kt designed speed, is only 172,170 lb. The range of prediction covered by the preceding examples is rather large, but at least the estimated values are conservative.

59.16 Relation Between Thrust at the Propeller and at the Thrust Bearing. For a propeller-thrust estimate of the type described in the preceding section, it is usually assumed that the thrust bearing takes the whole propeller thrust. Actually, the thrust-bearing load equals the propeller thrust only when the friction effects in the bearings between the propeller and the forward end of all elements attached to and working with the shaft are neglected, *and* when the shaft declivity in the *running* condition is zero. Otherwise the thrust-bearing load equals the propeller thrust plus or minus an axial component of the weight of the propeller, shaft, and all engine

parts whose longitudinal position is fixed by the thrust bearing, depending upon whether the axial weight component is directed forward or aft. The axial friction effects in the various shaft and machinery bearings, with the parts rotating at any speed above very slow, may generally be neglected. The axial weight component is usually a secondary factor in the selection or design of a thrust bearing, but it is a factor of importance in the analysis of shipboard thrust measurements, where its magnitude is often appreciable, compared to the propeller thrust [SNAME, 1934, pp. 151–152].

Fig. 59.L, adapted from Figs. 13 and 14 on pages 151–152 of SNAME, 1934, illustrates diagrammatically several types of machinery, the weights of each to be included in the computation for the axial component, and the manner in which the various forces are combined at the thrust bearing. As further refinements, not always carried out in practice:

(1) The weight of the propeller and of those portions of the shafting completely surrounded by water may be reduced by the buoyant forces of the water on those parts

(2) Part of the measured thrust is due to the hydrostatic head over the section area of the shaft where it enters the hull stuffing box

(3) The $+\Delta p$'s exerted over the projected axial area of the hub abaft the blades, as well as the $-\Delta p$'s exerted over the forward exposed area of the hub, outside the shaft, are measured in model tests and reckoned in ship trials as part of the thrust exerted by the blades.

For high-speed vessels such as destroyers, in which the attitude changes materially from the at-rest to the running condition, the *actual* shaft declivity at any speed is a combination of that built into the ship (or that imposed by the particular loading condition) and the running trim at that speed. Assuming a change of trim from zero to full speed of 1.5 deg, not uncommon in these craft, the axial weight component of the rotating parts of one main propelling unit is changed by the sine of this angle, or some 2.6 per cent. This may amount to 3 per cent or more of the full-speed thrust [SNAME, 1933, pp. 268, 275, 277].

59.17 Estimates of Thrust and Torque Variation per Revolution for Screw Propellers. The reasons for the generation of thrust and torque variations on the blade of a screw propeller as it rotates, and for the application of offset forces and bending moments on the shaft, are described in Secs. 17.3 through 17.7, 17.12, and Sec. 33.13 in Volume I. The equalization of the thrust and

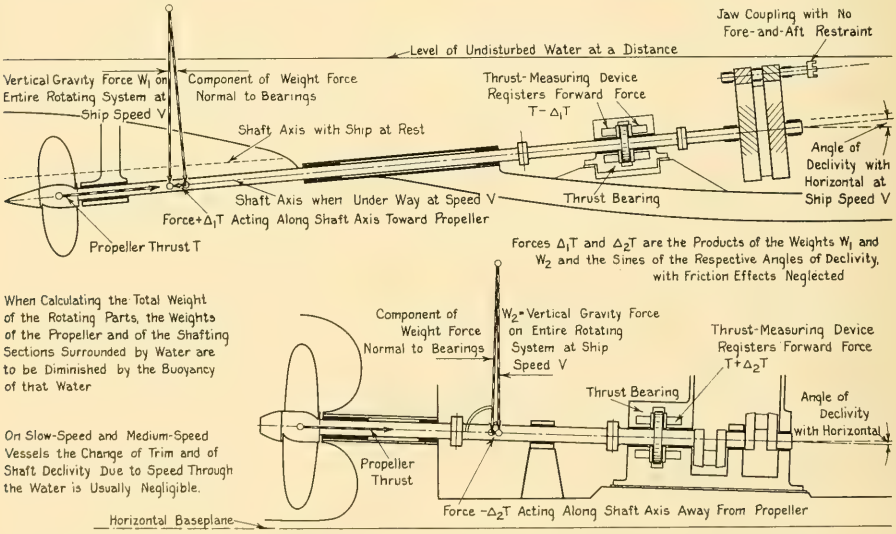

Fig. 59.L Weight and Force Diagrams Illustrating Relationship Between Propeller Thrust and Measured Axial Load on Thrustmeter

torque for all angular positions and the reduction of the bending moments is a design problem of long standing. Nevertheless, the advent of higher powers per shaft, especially on vessels carrying propellers abaft skegs, and the increasing emphasis on freedom from vibration, has made it necessary to devote much more intensive and thorough study to this project than was formerly the case. A great deal of clever experimentation, carried out in the period 1940–1955, has demonstrated that the variable forces and moments can be large enough not only to produce objectionable motion of the machinery parts and generate vibration in both hull and machinery but to account for actual breakage of the propeller shafts at sea.

Several decades ago R. J. Walker and S. S. Cook gave some data on wake and torque variations encountered on the single-screw tankers *San Florentino* and *San Fernando* [Mar. Eng'g., May 1921, p. 395]. They reported variations in torque ranging from a maximum of 1.35 times the mean, at a blade position of about 102 deg, to 0.59 times the mean at a position, for the same blade, of about 143 deg. Here the 12 o'clock position is taken as 0 deg, with angles increasing in a clockwise direction, looking forward, corresponding to diagram 1 of Fig. I.E. In the plane of symmetry at the disc position the wake fractions were found to vary from 0.536 at 6 o'clock in the tip circle to 0.627 at 12 o'clock in that circle. At 4:30 o'clock the wake fraction was 0.041; at 10:30 o'clock it was 0.255.

Diagrams of thrust and torque variations on a basis of angular position around the shaft axis, for the single blades of a 3-bladed screw propeller, and for the overall propeller, are given in Fig. 218 on page 281 of the Russian book "Korabelnye Dvizhiteli (Marine Propulsion Devices)," written by U. I. Soloviev and D. A. Churmack under the scientific supervision of I. G. Hanovich, Moscow, 1948. These page and figure numbers are the same in the Bureau of Ships (Navy Department) Translation 408 of this book, March 1951.

A paper by J. R. Kane and R. T. McGoldrick [SNAME, 1949, pp. 193–252] was devoted to an analysis of the longitudinal vibration of marine propulsion-shafting systems, resulting from variations in the thrust forces with angular position of the screw propeller. On pages 231–232 this paper lists 20 references.

More recently, N. H. Jasper and L. A. Rupp, in their paper "An Experimental and Theoretical Investigation of Propeller Shaft Failures" [SNAME, 1952, pp. 314–381], have given the wake-survey diagram of a single-screw ship, together with the calculated variations in propeller thrust, propeller torque, and other factors, on a base of angular position of the propeller. These are supplemented by measurements of the axial, torsional, and bending strains on the prototype propeller shaft. Figs. 59.M and 59.N are adapted from Figs. 33 and 34, respectively, of the paper. A list of 20 references is to be found on pages 364–365.

Supplementing the foregoing, E. P. Panagopulos and A. M. Nickerson, Jr., made further full-scale tests on a larger vessel. The results of this investigation were published by them in a paper entitled "Propeller-Shaft Stresses under Service Conditions—The S.S. *Chryssi* Investigation" [SNAME, 1954, pp. 199–241]. This paper is concerned largely with the bending stresses in the propeller shaft but Fig. 23 on page 227 is a graph showing the variation in the calculated thrust of one blade throughout a single complete revolution. The thrust varies from about 15,000 lb at the 9 o'clock position to 126,000 lb at 12:20 o'clock, to 42,000 lb at 4 o'clock, and to 123,000 lb at 6:36 o'clock.

A realistic look at this situation indicates definitely that an analytic procedure must be developed whereby the magnitudes, directions, and positions of the variable forces exerted by one

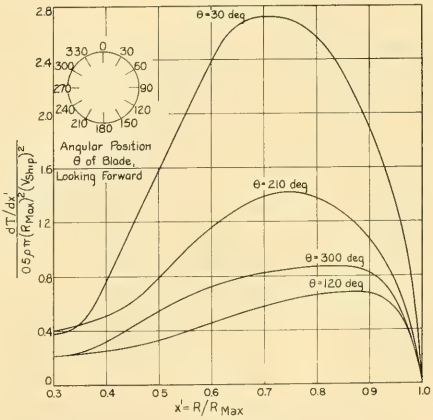

Fig. 59.M Variation of Thrust-Load Coefficient of a Screw Propeller with Dimensionless Radius, on a Basis of Dimensionless Radius, At Four Angular Positions

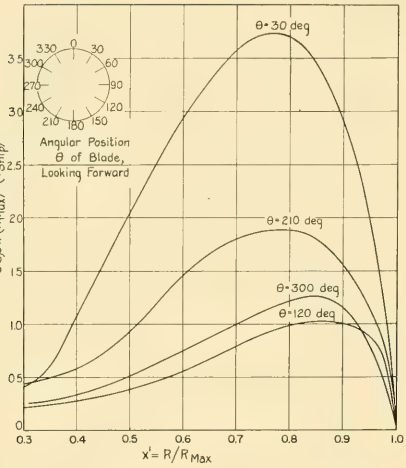

FIG. 59.N VARIATION OF MODIFIED TORQUE COEFFICIENT OF A SCREW PROPELLER WITH DIMENSIONLESS RADIUS, ON A BASIS OF DIMENSIONLESS RADIUS, AT FOUR ANGULAR POSITIONS

or by all the blades of a screw propeller can be predicted in the design stage. Its cost, for each new ship or for the first of a class, would be insignificant compared to breaking a shaft on a single-screw vessel, towing the ship home, and replacing both propeller and shaft.

It is explained in Sec. 17.6 of Volume I that the thrust and torque variations in question arise principally from non-uniform wake and irregular inflow velocity at the propeller. Techniques are available in many model basins whereby the actual velocities can be measured across propeller-disc positions (without the propeller working) and the wake velocities and fractions can be calculated.

At the present time there is no known precise method for calculating the thrust and torque variations directly from the wake-survey diagram. However, A. J. Tachmindji of the David Taylor Model Basin staff has calculated the vibratory forces from two wake-survey diagrams derived from a model of the Victory ship U.S.N.S. *Lt. James E. Robinson.*

These diagrams, reproduced in slightly modified form in Figs. 60.I and 60.J, are different from the others described and illustrated in Secs. 11.6, 11.7, and 60.6 in that they carry three sets of numerals at each observation point. The first set indicates the wake fraction, derived from the longitudinal component of velocity approaching the propeller-disc position. The second indicates the radial component of velocity, and the third the tangential component, all in fractions of the ship speed V. Since it is customary, in non-axial flow, to resolve the actual inflow velocity in a direction normal to the blade axis, indicated in diagram 2 of Fig. 17.C of Sec. 17.7 of Volume I, the radial component can be ignored in this analysis. However, the *radial* component is not to be confused with the *transverse* component of Figs. 11.E and 60.L. The latter corresponds to the vectorial addition of the radial and the tangential components.

In the referenced analysis and calculations, Tachmindji made use of the following assumptions:

(a) The instantaneous forces on a blade element are those of the steady state for the same velocity conditions

(b) The forces on a blade are not influenced by

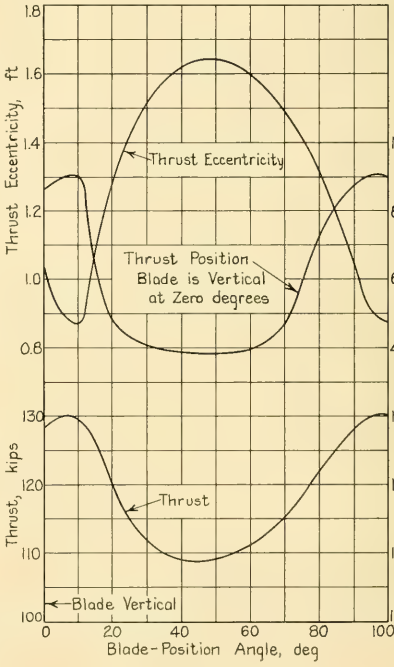

FIG. 59.O THRUST VARIATION FOR PART OF A PROPELLER REVOLUTION ON A VICTORY SHIP, U.S.N.S. *Lt. James E. Robinson,* Δ = 8,268 TONS

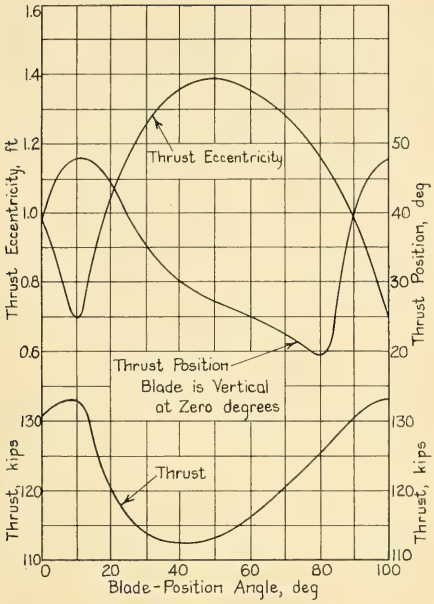

Fig. 59.P Thrust Variation on a Victory Ship Propeller, Δ = 11,606 Tons

the presence of adjacent ship structure or appendages.

The results of these calculations are published by H. R. Neifert and J. H. Robinson in "Further Results from the Society's Investigation of Tail-shaft Failures" [SNAME, 1955, pp. 495–550], where the authors give graphs showing various force and moment variations with angular blade position. Figs. 59.O and 59.P, adapted from Figs. 34 and 35, respectively, of the reference, show the variation in total thrust for the propeller; that is, the resultant of the thrust forces on all four blades. They also show the thrust eccentricity, corresponding to the offset from the propeller-shaft axis of the center of pressure CP of the total thrust load exerted axially forward on the entire projected blade area of the propeller. The third set of graphs indicates the angular position of this CP when a given blade is in any one angular position. Thus the horizontal scales at the bottom of each diagram apply to all three graphs on that diagram. For example, if in Fig. 59.O a blade is at 20 deg, the total instantaneous thrust of the whole propeller is just over 120,000 lb. The thrust eccentricity, or the offset of the CP from the shaft axis, is about 1.28 ft. The angular position of this CP, read from the upper right-hand vertical scale, is about 48 deg. In fact, regardless of the blade positions, it remains between 38 deg and 92 deg.

Fig. 59.O is calculated for a displacement of 8,268 tons, with a trim of 7.5 ft by the stern and a draft at the AP of 20.5 ft, not quite sufficient to cover the upper blade tips when the vessel is at rest. Fig. 59.P is calculated for a displacement of 11,606 tons with a trim of 3.83 ft by the stern and a draft at the AP of 24.50 ft. This places the propeller tips at the 12 o'clock position well below the surface in the at-rest condition.

Figs. 59.Q and 59.R, adapted from Figs. 36 and 37, respectively, of the Neifert and Robinson reference, show the corresponding variation in torque with angular position of the propeller, for the two displacements and trims listed in the preceding paragraph. They show also the magnitude of and variations in the upward vertical force resultant and the starboard transverse force resultant with angular position for the two displacements and trims.

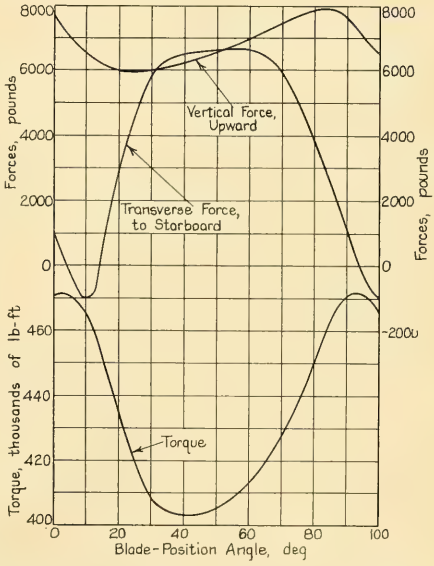

Fig. 59.Q Variation of Torque and Vertical and Horizontal Forces for Part of a Propeller Revolution on a Victory Ship, U.S.N.S. *Lt. James E. Robinson*, Δ = 8,268 Tons

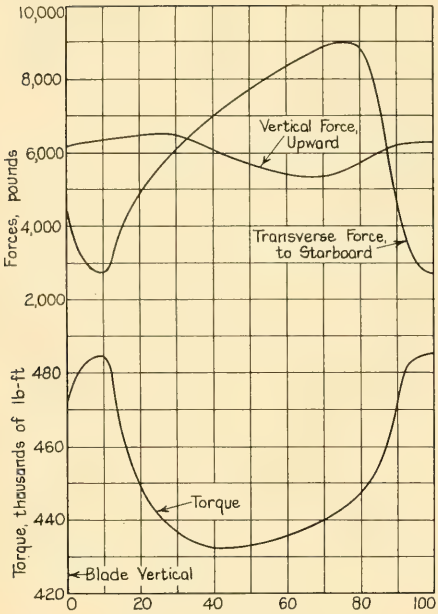

FIG. 59.R VARIATION OF TORQUE AND VERTICAL AND HORIZONTAL FORCES ON A VICTORY SHIP PROPELLER, Δ = 11,606 TONS

The effect of the simplifying assumptions on the calculations for these graphs creates some doubt as to the validity of the results, especially because of the first assumption of steady-state conditions. Currently (1956), Tachmindji is refining the method so that these assumptions will not have to be made. Nevertheless, because of the importance of this work in the design scheme, the unrefined method used by Tachmindji for the *Lt. James E. Robinson* calculation is outlined here.

To determine the thrust and torque characteristics for any blade section at a specific blade angle, there are several methods that can be employed. That of L. C. Burrill ["Calculation of Marine Propeller Performance Characteristics," NECI, 1943–1944, Vol. 60, pp. 269–294] is well adapted to this operation and was utilized by Tachmindji. It employs the circulation theory with suitable correction factors to relate experimental results with theory.

The steps involved in the Burrill method are as follows:

(1) The angle α_0(alpha) between the zero-lift line and the base-chord line is determined by the method of H. Glauert ["A Theory of Thin Airfoils," ARC, R and M 910, 1924–1925]. The angle α_0 is equal to $\alpha - \alpha_I$ and is usually negative for common hydrofoil sections, where the zero-lift line lies toward the back of the section from the base chord, as in Fig. 15.H.

(2) The advance angle β is calculated by using both the longitudinal wake fraction w_L and the tangential wake component w_T . The reasons for omitting the radial wake component are explained in a previous paragraph. Hence

$$\tan \beta = \frac{V(1 - w_L)}{2\pi Rn - Vw_T}$$

(3) Burrill's formulas and graphs enable the hydrodynamic angle of attack α_I to be determined as a function of β, β_I , and the geometry of the blade section. But since β_I can not be determined unless α_I is known or assumed, the calculation is one of successive approximations. Specifically, an effective angle of attack is assumed. Then, since $\beta_I + \alpha_I = \phi - \alpha_0$ (where, as indicated in (1) above, the zero-lift angle of attack α_0 is usually negative), β_I is known temporarily, and the calculation is carried out to determine α_I . The correct values of β_I and α_I are obtained when the assumed α_I equals the calculated α_I .

(4) The lift and drag of the blade section is then determined as a function of α_I , the relative velocity, the correction factors, and the geometry of the section.

(5) Knowing the lift and drag, the thrust and torque contributed by the blade section are then determined.

One calculation gives the thrust and torque of one blade radius at only one blade angle. In order to obtain the total thrust and torque it is necessary to calculate the thrust and torque at enough blade angles and blade sections so that they can be integrated to determine the total thrust and torque from one blade at any angle. The position angle θ of any one blade is assumed to be measured from the upward vertical or 12 o'clock point, in a clockwise direction when looking forward. Also

$T(x', \theta)$ is the thrust from the blade element at the 0-diml radius x' and the position angle θ

$Q(x', \theta)$ is the torque from the blade element at the 0-diml radius x' and the angle θ

$T_z(\theta)$ is the thrust per blade at the angle θ

$Q_Z(\theta)$ is the torque per blade at the angle θ
$F_Z(\theta)$ is the transverse tangential force per blade at the angle θ. Then

$$T_Z(\theta) = \int_{x'_{\text{Hub}}}^{1} T(x', \theta)\, dx'$$

$$Q_Z(\theta) = \int_{x'_{\text{Hub}}}^{1} Q(x', \theta)\, dx'$$

$$F_Z(\theta) = \int_{x'_{\text{Hub}}}^{1} \frac{Q(x', \theta)}{Rx'}\, dx'$$

If the total thrust for all blades at one blade angle is designated as $T(\theta)$, then

$$T(\theta) = \sum_{i=1}^{Z} T_Z\left(\theta + \frac{2\pi i}{Z}\right)$$

For a 4-bladed propeller, where $Z = 4$, the foregoing becomes

$$T(\theta) = T_Z\left(\theta + \frac{2\pi(1)}{4}\right) + T_Z\left(\theta + \frac{2\pi(2)}{4}\right) + T_Z\left(\theta + \frac{2\pi(3)}{4}\right) + T_Z\left(\theta + \frac{2\pi(4)}{4}\right)$$

The mean thrust is

$$T_{\text{Mean}} = \frac{1}{2\pi}\int_0^{2\pi} T(\theta)\, d\theta$$

Similarly, letting the total torque for all blades at any one blade angle be $Q(\theta)$, then

$$Q(\theta) = \sum_{i=1}^{Z} Q_Z\left(\theta + \frac{2\pi i}{Z}\right)$$

and

$$Q_{\text{Mean}} = \frac{1}{2\pi}\int_0^{2\pi} Q(\theta)\, d\theta$$

Setting $[F(\theta)]_h$ equal to the total horizontal transverse force of all blades at any one blade angle, and $[F(\theta)]_v$ equal to the total vertical transverse force of all blades at any one blade angle,

$$[F(\theta)]_h = \sum_{i=1}^{Z} F_Z\left(\theta + \frac{2\pi i}{Z}\right) \cos\left(\theta + \frac{2\pi i}{Z}\right)$$

$$[F(\theta)]_v = \sum_{i=1}^{Z} F_Z\left(\theta + \frac{2\pi i}{Z}\right) \sin\left(\theta + \frac{2\pi i}{Z}\right).$$

CHAPTER 60

Ship-Powering Data for Steady Ahead Motion

60.1 General. Although not always expressed in so many words, one aim of naval architects and marine engineers for the past century or more has been to find an adequate method of *calculating* directly the power necessary to drive a given ship at a given speed. By direct calculation is meant a determination of the ship power in the early stages of the design, directly from the data on paper, using whatever handbook or reference data that may be necessary, but without the building or testing of a model. The discussion in this chapter is limited generally to methods of direct estimate or calculation.

Chap. 57 describes methods of estimating the total hull resistance R_T of ship forms, making use of several different methods and various sources of test data. Certain of the powers used in ship design are derived readily from this resistance. Others, like the shaft power, can not be calculated directly nor can they be estimated easily.

It is emphasized here, as elsewhere in Parts 3 and 4 of the book, that the ship designer needs several different methods to give the required engineering answers. Choice as to the method selected, or as to which of several successive approximations is to be used, depends upon the time available for finding the answer, and the precision required in it. A rule-of-thumb procedure may be most appropriate for one situation yet highly unsuitable for another.

One caution against all methods of estimating and predicting ship power is that they shall be based on test and other data that are as comprehensive as possible. Limiting one's basic data to those for one kind and size of ship may be misleading or result in downright inaccuracies for borderline cases.

60.2 Estimation or Calculation of Effective and Friction Power. The derivation of towrope or effective power for a ship, when its resistance is found by the procedures described in Chaps. 56 and 57, involves only one simple step in multiplication, since $P_E = R_T V$. When the resistance is not known, either by estimate, calculation, or test, its value is by-passed, so to speak, by having the marine architect determine, in a single step, the probable effective power for a given ship form.

Many graphs and tables for finding the effective power for ships have been prepared and published over the years. It is difficult to assess their validity and usefulness because of uncertainty as to what basic data were used and how reliable these data were in the first place. In most cases, the graphs and tables cover vessels of one type only; possibly even of a small range of size or shape. For example, J. C. Robertson and H. H. Hagan, in their paper entitled "A Century of Coaster Design and Operation" [IESS, 1953–1954, Vol. 97, pp. 204–256, esp. Fig. 3 on pp. 212–213], give curves of brake power P_B for this type of

ship on a base of displacement weight W for various values of $T_q = V/\sqrt{L}$, where V is (apparently) the *trial speed* in kt. H. Volpich, in a discussion of this paper on pages 236–239 of the reference [also SBSR, 20 May 1954, pp. 634, 636], gives a nomogram (Fig. 12) for the power approximation of single-screw diesel-driven coasters embodying deadweight carrying capacity, ship length, brake power, and ship speed. It is useful for a quick and ready approximation to the power of a small ship.

J. L. Bates has published contours of constant effective power P_E for fast yachts having lengths in the range of 100 to 500 ft, speeds in the range of 10 to 20 kt, and the following ranges of form coefficient:

(a) Prismatic coefficient C_P from 0.62 to 0.66
(b) Displacement-length quotient $\Delta/(0.010L)^3$ from 40 to 45
(c) Maximum-section coefficient C_X from 0.75 to 0.83. These curves are to be found in MESA, September 1921, pages 678–680. Similar contours of constant effective power, for speeds in excess of 22 or 23 kt, are to be found in the 1920 edition of the Shipbuilding Cyclopedia [Simmons-Boardman, New York].

Contours of constant effective power for vessels of fine underbody, comprising yachts intended primarily for ocean cruising, coastal passenger vessels, gunboats, and certain seagoing tugs, are given by Bates in Figs. 3–5 on pages 681–683 of the MESA reference. The curves cover a C_P of 0.56, a range of displacement-length quotient of from 100 to 150, and a range of C_X of from 0.87 to 0.93. Representative vessels in the selected groups have, according to Bates, the characteristics listed in Table 60.a.

Here again it is noted that while the craft selected vary as to type they vary only little in those proportions affecting hydrodynamic resistance. A great many additional sets of contours would be needed to cover the whole ship-design field.

Bates' effective-power data are based upon test results from the Taylor Standard Series of models and from miscellaneous EMB models. While ship forms have changed somewhat since this analysis was made, the data should still serve for quick estimates of effective power for vessels of the proportions listed.

Since friction resistance for a ship is found by a direct calculation in any case, the friction power is derived invariably by the formula $P_F = R_F V$. The difficulties in determining the effects of roughness, described in Chap. 45, are of course reflected in a determination of the friction power. Numerical values of friction power are rarely employed in ship design but they are useful in illustrating the effects of changing the wetted area and of surface roughness.

60.3 Effect of Displacement and Trim Changes on Effective Power. Knowing the effective power P_E for the designed displacement and trim of a given vessel, usually as the result of a model test, it is often required to estimate the P_E for a somewhat different displacement of that vessel; possibly also for a different trim. Designer's and operator's requirements, besides calling for the effective-power variations corresponding to the usual 10 per cent light and heavy displacement, often extend to the so-called ballast condition, especially for cargo vessels. Here the weight displacement for a cargo-vessel design may approach half the designed value, and the trim by the stern of that vessel may be 0.3 or more of its designed draft.

As an aid in estimating these effective-power

TABLE 60.a—CHARACTERISTICS OF SELECTED VESSELS IN THE POWERING GROUPS OF J. L. BATES, 1920–1921

The references from which these data were taken are listed in the accompanying text.

Type	Length, ft	Displacement, long tons	Longitudinal Prismatic Coefficient, C_P	$\frac{\Delta}{\left(\frac{L}{100}\right)^3}$	$\frac{V}{\sqrt{L}}$
Passenger vessel	411	6,940	0.552	100	1.085
Intermediate type	520	17,470	0.576	124.3	0.832
Yacht	160	568	0.59	138.5	0.91
Yacht	210	950	0.59	102.8	1.31
Gunboat	221	1,371	0.584	127.1	1.075
Gunboat	225	1,575	0.565	138.5	0.8
Seagoing tug	180	950	0.578	163	1.05

changes without recourse to additional lengthy calculations or model tests, data have been analyzed from the tests of some two dozen models of ships of various types. The aim of this analysis is to determine the exponent n in the relationship

$$\frac{P_E \text{ for } (\Delta \pm \delta\Delta)}{P_E \text{ for } \Delta} = \left(\frac{\Delta \pm \delta\Delta}{\Delta}\right)^n = \left(\frac{\forall \pm \delta\forall}{\forall}\right)^n$$

$$\text{or } P_E \text{ for } (\Delta \pm \delta\Delta) = (P_E \text{ for } \Delta)\left(\frac{\Delta \pm \delta\Delta}{\Delta}\right)^n \qquad (60.\text{i})$$

It may be expected that these relationships will vary somewhat with speed-length quotient; possibly also with hydrodynamic ship proportions such as prismatic coefficient and fatness ratio.

Fig. 60.A gives a tentative mean line for a variation of n in Eq. (60.i) with T_q or F_n, as well as a lane in which the majority of n values may be expected to lie. They conform reasonably well for $\delta\Delta$, δW, or $\delta\forall$ values ranging from $+0.18$ to -0.40, and for large-trim as well as zero-trim changes accompanying the changes in displacement. The lane appears to be as valid for large $\delta\Delta$ or δW percentages as for small ones.

In general the exponent n is greater for a $+\delta\Delta$ or $+\delta W$ than for a $-\delta\Delta$ or $-\delta W$, especially when $T_q > 1.0$, $F_n > 0.30$.

The plotting of Fig. 60.A is based only indirectly on physical reasoning. The hulls which are less deeply immersed, more deeply immersed, or inclined with trim by the bow or stern, can only in exceptional cases be geosims of the designed underwater hull. Further, because of the different proportions in each case, the surface waterline changes, the wetted surface varies, and the flow pattern is different.

It is to be noted that, because of the arithmetic of the situation, the exponent n is extremely sensitive to changes in the power ratio. For example, for a displacement ratio $(\Delta - \delta\Delta)/\Delta$ of 0.9, and a power ratio $[(P_E \text{ for } 0.9\Delta)/(P_E \text{ for } \Delta)]$ of 0.9, the exponent $n = 1.0$. For the same displacement ratio and a power ratio of 1.0, the exponent $n = 0$, whereas for a power ratio of 0.81 the value of $n = 2$, since $1.0 = (0.9)^0$ and $0.81 = (0.9)^2$. Thus, while the possible selections of n for a given T_q from Fig. 60.A vary rather widely, the range of estimated P_E derived from them is rather small.

To avoid multiplying large numbers by factors very close to unity, which is the case when $\delta\Delta$ is small, and to avoid taking powers, the following formula can be used:

$$P_E = k\Delta^n$$

$$dP_E = kn\Delta^{n-1}\,d\Delta \quad \text{or} \quad \delta P_E = kn\Delta^{n-1}\,\delta\Delta$$

whence

$$\frac{\delta P_E}{P_E} = \frac{n(\delta\Delta)}{\Delta} \quad \text{and} \quad \delta P_E = P_E\left[\frac{n(\delta\Delta)}{\Delta}\right] \qquad (60.\text{ia})$$

For small percentage changes in the displacement Δ, Eq. (60.ia) is more accurate than Eq. (60.i) and easier to evaluate.

Take for example the ABC ship of Part 4, at a T_q of 0.9. Assume that the effective power P_E for the designed displacement and trim is 11,902 horses, equal to the estimated 10,820 horses of Sec. 66.9 plus 10 per cent for appendages and other factors. Assume also that n is selected from the mean line of Fig. 60.A as 0.72. Then for a partial-load displacement of 16,400 − 2,425 = 13,975 t, as listed in Table 66.f of Sec. 66.16,

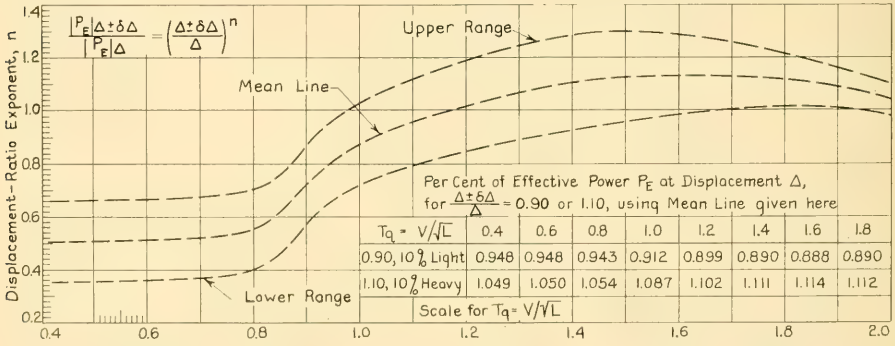

$T_q = V/\sqrt{L}$	0.4	0.6	0.8	1.0	1.2	1.4	1.6	1.8
0.90, 10% Light	0.948	0.948	0.943	0.912	0.899	0.890	0.888	0.890
1.10, 10% Heavy	1.049	1.050	1.054	1.087	1.102	1.111	1.114	1.112

FIG. 60.A GRAPHS FOR PREDICTING CHANGE IN EFFECTIVE POWER DUE TO A 10 PER CENT CHANGE IN DISPLACEMENT

representing a reduction $-\delta\Delta$ of 14.8 per cent from the designed value, the corresponding relationships are, from Eq. (60.i),

$$\frac{P_E \text{ for } (16{,}400 - 2{,}425) \text{ tons}}{P_E \text{ for } 16{,}400 \text{ tons}} = \left[\frac{(16{,}400 - 2{,}425)}{16{,}400}\right]^{0.72}$$

If $\Delta = 16{,}400$ tons is taken as 1.000Δ, and 2,425 tons as $\delta\Delta$ or 0.148Δ,

$$\frac{P_E \text{ for } (1.000 - 0.148)\Delta}{P_E \text{ for } 1.000\Delta} = \left[\frac{(1.000 - 0.148)}{1.000}\right]^{0.72} = 0.8911$$

This gives P_E for $0.852\Delta = 0.8911\ (11{,}902) = 10{,}606$ horses.

The reduction in effective power is only 10.9 per cent while the reduction in displacement is 14.8 per cent. This appears disappointing. It must be remembered, however, that if the displacement of the given vessel is increased by 14.8 per cent, a similar calculation indicates that the effective power of the ship is increased by only 10.45 per cent.

Using the incremental formula of Eq. (60.ia) without any exponents

$$\frac{\delta P_E}{P_E} = n\left(\frac{\delta\Delta}{\Delta}\right) = (0.72)(-0.148) = -0.1066$$

$$\delta P_E = -(0.1066)(11{,}902) = -1{,}269 \text{ horses.}$$

Then P_E for $0.852\Delta = 11{,}902 - 1{,}269 = 10{,}633$ horses. This is sufficiently accurate for engineering purposes in the design stage.

J. B. Hadler, G. R. Stuntz, Jr., and P. C. Pien have published not only effective power but shaft power, rpm, wake-fraction, thrust-deduction fraction, and other data for three of the five parent models of TMB Series 60, at both 60 and 80 per cent of the designed displacement [SNAME, 1954, Figs. 9, 10, and 11, pp. 137–139]. These may be compared with data at 100 per cent displacement in the same paper. Runs made at zero trim and at the usual trims by the stern for light and ballast conditions at each of these displacements indicated unexpectedly close agreement for all factors except the wake fraction. These data may

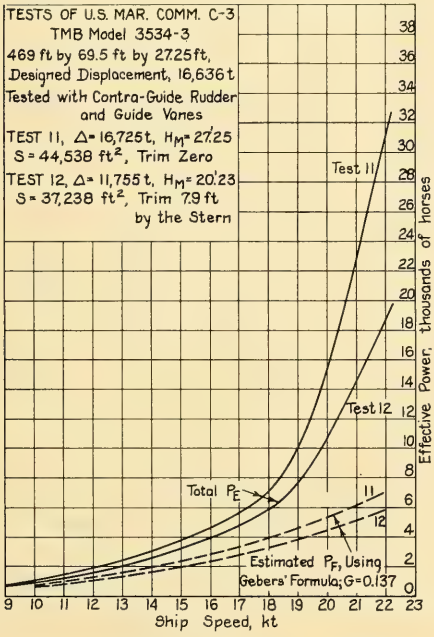

Fig. 60.B Variation of Effective and Friction Powers with Change in Displacement and Trim

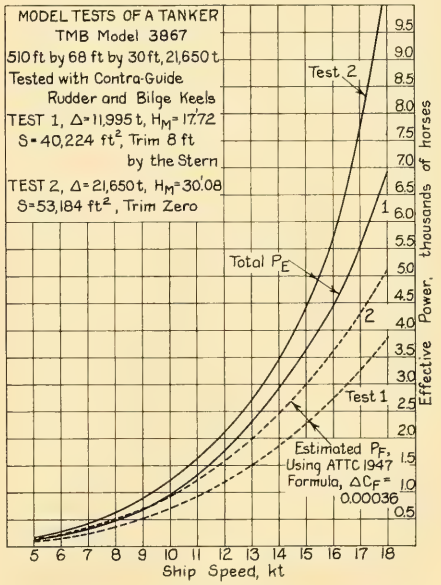

Fig. 60.C Variation of Effective and Friction Powers for a Tanker, Covering Full-Load and Ballast Conditions

be considered typical for medium and large single-screw vessels as a class.

There are in the archives of many ship-model testing establishments numerous sets of graphs similar to those of Figs. 60.B and 60.C. In these the effective powers, and sometimes the friction powers and other factors, are given for selected ship models when run at widely different displacements and trims. For cases similar to these, where the light displacements vary by some 30 and 45 per cent, respectively, from the heavy or normal-load displacements, the range is rather large for making estimates of effective-power changes by the graphs of Fig. 60.A.

60.4 Methods and Factors Involved in Predicting Shaft Power. The preliminary design of a ship can not proceed very far until the *shaft power* P_S needed to drive it at the designed speed is determined in some manner. It is customary to estimate or to predict this power by one or more of a series of methods, involving successive approximations. However, to afford a better understanding of the procedures underlying some of the early approximations, the later approximations are described first. The discussion here is limited primarily to screw propulsion.

The shaft power P_S is obtained directly from the effective power P_E by dividing the propulsive coefficient η_P(eta) into the latter. This is simple but estimating the proper value of η_P is not. From Eqs. (34.xv) and (34.xvi) of Sec. 34.7,

$$\eta_P = \eta_0(\eta_H)\eta_R = \eta_0\left(\frac{1-t}{1-w}\right)\eta_R$$

The value of η_0 is known for the working range of a considerable number of screw propellers suitable for driving a wide variety of ships. Published data can be supplemented by information obtained from model basins which have tested many propeller models. However, the working range of the advance coefficient J is also rather large, and η_0 may vary rather rapidly with J in that range. A J-value may be chosen, for a propeller not too heavily loaded, just under (less than) the J-value for maximum η_0 .

Estimating the hull efficiency η_H involves estimates of both the thrust-deduction fraction t and the wake fraction w. Methods of accomplishing this, in advance of or without self-propulsion tests of the ship model, are described presently in Secs. 60.8 and 60.9. Estimating the probable value of the relative rotative efficiency η_R is described in Sec. 60.10.

It is possible, with experience, to estimate the propulsive coefficient η_P directly, as is done for the first approximation to the shaft power of the ABC ship in Sec. 66.9 of Part 4. It is extremely difficult, however, to analyze this kind of experience and to set it down as a design rule. An attempt to do it is set down in Sec. 60.11.

A procedure for the preliminary estimate of the shaft power of merchant ships recently described by V. Minorsky [Int. Shipbldg. Prog., 1955, Vol. 2, No. 9, pp. 226–229] is in reality a dimensional version of the Telfer merit factor described in Sec. 34.10. It takes the form

$$\text{Powering factor} = \frac{V^{3.4}}{L^{1.2}P_S}$$

as compared to the 0-diml

$$\text{Telfer merit factor } M = \frac{\Delta V^3}{gLP_S} = \frac{WV^3}{gLP_S} \quad \text{(34.xxiv)}$$

The latter is assumed in Fig. 34.I on page 518 of Volume I to vary in some manner as F_n^2 , with further variations for better-than-average or less-than-average performance. The expression of V. Minorsky uses only a single average factor, which varies somewhat with block coefficient C_B and speed-length quotient $V/\sqrt{L}$.

G. Deparis, in his paper "Étude Comparative des Cargos; Puissance des Moteurs (Comparative Study of Cargo Vessels; Propelling-Plant Power)" [ATMA, 1955, Vol. 54, pp. 499–549], describes methods whereby "guestimates" may be made of propelling-plant power and speed on a basis of useful load, in an early stage of the preliminary design. The factors given are based upon a study of the characteristics of many ships, including undoubtedly the inefficient as well as the efficient ones.

J. E. Burkhardt discusses several methods of estimating ship power [ME, 1942, Vol. I, pp. 22–28] but all of them are covered in the present book, in one form or another. Descriptions of other methods of predicting shaft power are embodied in Secs. 60.13, 60.14, and 60.15.

60.5 Axial-Component Wake-Fraction Diagrams at Propulsion-Device Positions. Characteristics of the wake at propulsion-device positions are discussed in Chap. 11. Methods for indicating the situation graphically with respect to wake velocity and direction over the whole thrust-producing area are described there, specifically as applying to a screw propeller.

There is a great amount of published data on

wake, some of it listed subsequently in this section, in which only the fore-and-aft or direction-of-motion components of the actual wake velocities are indicated, as described in Sec. 11.4. The preponderance of these data might lead a marine architect to believe that this method of wake representation is adequate. The fore-and-aft actual-velocity components do indeed serve as the basis for the orthodox wake fraction in everyday use for powering estimates and for some analytic work. Nevertheless, it is important to realize that they tell only part of the story so far as flow at the propeller positions is concerned. The reasons for this are set down in Chap. 11 and in Sec. 60.7 following. The 3-diml representation of Fig. 11.F and of Figs. 60.D through 60.J in Sec. 60.6 of the present chapter gives a far more adequate, more accurate, and more useful indication of the flow situation in which the propeller must work.

Additional reasons for making use of a 3-diml wake diagram which shows the true water velocities, in both magnitude and direction, are brought out in Sec. 60.7.

It is true that the plotting of wake-survey diagrams in terms of contours of longitudinal-velocity components $V(1 - w)$ or of wake fraction w reveals certain features not well illustrated by the TMB 3-diml wake-vector diagrams of Figs. 11.F and 60.D through 60.K of Sec. 60.6. For example, the wake-contour diagram for TMB twin-skeg model 3898, published in SNAME, 1947, Fig. 32 on page 121, reveals the general pattern of wake irregularity more vividly than the 3-diml survey diagram of Fig. 22 of the reference, from which it was constructed.

A brief of sources embodying wake-survey diagrams with contour and other plots of local fore-and-aft velocity components or wake fractions is given here for the benefit of the reader:

(a) Calvert, G. A., "On the Measurement of Wake Currents," INA, 1893, Vol. XXXIV, pp. 61–67 and Pls. I, II, and III. Figs. 3, 4, and 5 on Pl. II are early wake-survey diagrams showing true wake speeds, in the lines of flow, as percentages of the ship speed. Calvert endeavored to account for the observed wake velocities by combining the wave wake with the viscous wake but a rather large discrepancy remained because he did not take into account the wake due to potential flow.

(b) Kempf, G., "The Wake of a Ship in Relation to that of its Model," SBSR, 14 Feb 1924, pp. 194–196. Describes wake wheels or vane wheels and gives results of model tests.

(c) Kempf, G., "Neue Betriebserfahrungen und Entwicklungen der Schiffbau-Versuchstechnik (New Experiences and Developments in the Technique of Ship Trials)," WRH, 1 Nov 1930, pp. 437–442, esp. Figs. 5, 5a, 8, and 9. English version in TMB Transl. 3, Dec 1930.

(d) Weitbrecht, H. M., "Mitstrom und Mitstromschrauben (Wake and Wake-Adapted Propellers)," WRH, 15 Dec 1930, pp. 505–507, esp. Figs. 6, 7, and 8

(e) Wake-fraction diagrams, indicating the variation in this fraction around a propeller tip circle, for sterns with V- and U-sections, are shown on page 254 of a paper by Dr.-Ing. E. Foerster entitled "Speed and Power of Ships" [MESA, May 1930]. These indicate a minimum wake fraction of about 0.42 for the U-shaped run and of about 0.18 for the V-shaped run. Similar diagrams, showing the variations in wake fractions around a screw-propeller disc behind different forms of bossing, are given at the bottom of pages 256 and 257 of the reference quoted.

(f) Weitbrecht, H. M., "Über Mitstrom und Mitstromschrauben (On Wake and Wake-Adapted Propellers)," STG, 1931, Vol. 32, pp. 117–133; also Figs. 23(a), 23(b), and 23(c) on p. 350, SNAME, 1950

(g) Kempf, G., Mitstrom und Mitstromschrauben (Wake and Wake-Adapted Propellers)," STG, 1931, pp. 134–152. This paper contains a considerable number of contour diagrams, showing longitudinal components of velocity and wake fractions, and other features. Fig. 25 on p. 793 of SNAME, 1955, is adapted from one of these diagrams.

(h) Baker, G. S., "Wake," NECI, 1934–1935, Vol. LI, pp. 303–320 and D137-D146. Shows wake-survey diagrams for a number of models.

(i) Yamagata, M., "Wake Measurement by a Working Propeller," 3rd ICSTS, Berlin, 1934, p. 67

(j) Yamagata, M., INA, 1934, pp. 286–396, esp. pp. 387–388 and Pl. XXXIX.

(k) Michel, F., "Strömungserregte Resonanzschwingungen (Resonant Vibration Caused by Flow)," WRH, 1 Feb 1939, pp. 29–31

(l) German twin-screw ship *Tannenberg*. Contours of equal fore-and-aft wake fraction are given by G. Kempf in WRH, 15 Jun 1939, pp. 167–174, especially pp. 170–171. An English version of this paper is found in TMB Transl. 91, Jul 1941, where the wake-survey and analysis diagrams appear on pages 10 and 11.

(m) Twin-skeg *Manhattan*, contours of equal longitudinal components of wake velocity abaft one skeg and for a considerable distance beyond; SNAME, 1947, Fig. 32, p. 121

(n) Troost, L., "The Effect of Shape of Entrance on Ship Propulsion," INA, 1949, pp. 169–170. Contours are given of equal wake fraction (axial component only) over the propeller disc of a small coaster, together with graphs showing the circumferential variation of the wake fraction for various radii.

(o) Harvald, S. A., "Wake of Merchant Ships," Danish Technical Press Copenhagen, 1950, esp. p. 80

(p) *Normandie*, transatlantic passenger liner. Two diagrams of the wake magnitudes abaft the outboard

bossings, made before and after alterations, are given by F. H. Todd, SNAME, 1949, Figs. 26 and 27, p. 234. These and other wake diagrams for the *Normandie* are published by F. Coqueret and P. Romano in SNAME, 1936, Figs. 1–4 on p. 135 and Figs. 9–10 on p. 139.

(q) Henschke, W., "Schiffbautechnisches Handbuch (Shipbuilding and Ship Design Handbook)," 1952, p. 132. Shows wake diagram for twin screws abaft bossings.

(r) Van Manen, J. D., Int. Shpbldg. Prog., 1955, Vol. 2, No. 8, pp. 162–163

(s) Kinoshita, M., and Ikada, S., Int. Shpbldg. Prog., 1955, Vol. 2, No. 9, Fig. 7, p. 237.

60.6 Three-Dimensional Wake-Survey Diagrams. If all the wake-velocity vectors are not parallel to the direction of motion but are generally parallel to each other and to one plane which contains the plane of the shaft, there exists what might be called simple non-axial flow. Such a flow might occur at a single-screw position under a wide, flat stern, sloping upward and aft at a nearly constant rate. Non-axial flow then occurs in the vertical plane, corresponding to that in diagram 2 of Fig. 17.C. Here, in the 12 o'clock blade position, the actual inflow-velocity magnitude is $U_A \sec \theta$(theta) while the effective velocity with respect to a blade element is U_A . It is the latter which is measured by a device that records or indicates only the fore-and-aft or direction-of-motion velocity components. For the special case considered, and for the 12 and 6 o'clock blade positions, the instrument indications are valid.

For other blade positions, however, such as those at or near 3 and 9 o'clock in the special situation considered, there is actually a large increase in incident or resultant velocity and effective angle of attack for the downward moving blade and a large decrease in both for the upward moving blade. Taking account of the induced velocities increases these differences. The fact that the lift varies as the square of the relative velocity at which the blade elements move still further increases the difference.

Typical 3-diml wake-survey diagrams on ship models, made with the TMB 13-orifice spherical-

TABLE 60.b—DATA ACCOMPANYING WAKE-SURVEY DIAGRAMS OF FIGS. 60.D THROUGH 60.H

All tests were made at the David Taylor Model Basin. The Taylor quotients are based on the ship lengths listed.

Model tested	TMB 3594	TMB 4358W-1	TMB 4358W-2	TMB 4358W-3	TMB 4414
Length of ship, ft	440	528	523.5	523	528
Draft, ft	18.13			27	27
Displacement, long tons	7,960	18,610	18,610	18,610	18,610
Speed, kt	18 for test	20	20	20	20
Taylor quotient T_q	0.86	0.87	0.87	0.87	0.87
Froude number F_n	0.256	0.259	0.259	0.259	0.259
Trim	zero	zero	zero	zero	zero
Propeller tip diameter, ft	12.76 (2 of)	22	22		22
Date of test	18 Sep 1939	12 Jan 1951	12 Feb 1951	3 Apr 1951	
Wake measured at	Prop. disc positions	1.11 ft for'd. of Sta. 20	5.0 ft for'd. of Sta. 20	4 ft for'd. of Sta. 20	Prop. disc position
Appendages	Not known	Bilge keels, rudder shoe, dummy hub, and fairwater	Bilge keels, dummy hub, and fairwater	Bilge keels, dummy hub, and fairwater	Not known

For details relating to TMB model 4414 (*not* 4144), see SNAME, 1954, Fig. 5, p. 402; Fig. 7, p. 404; and Fig. 11, p. 409. For those relating to TMB model 3594, see SNAME RD sheet 98.

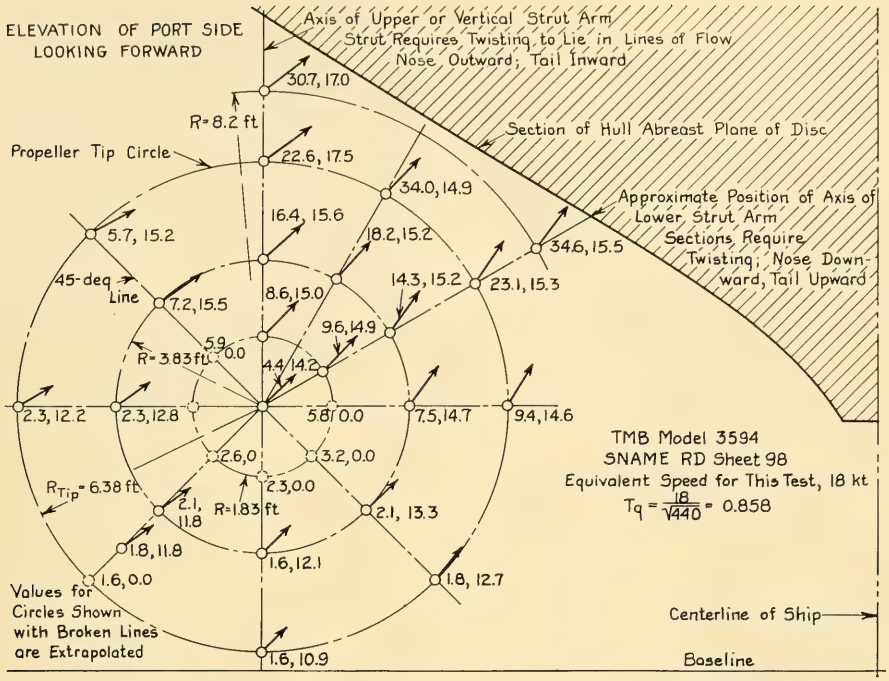

FIG. 60.D WAKE-SURVEY DIAGRAM FOR A TWIN-SCREW NAVAL VESSEL, U.S.S. *Terror*

head pitot tube, are reproduced in Fig. 11.F of Part 1 and Figs. 60.D through 60.J of the present section. The diagram of Fig. 60.D is for a wing propeller position on a twin-screw stern of normal form, while those of Figs. 60.E through 60.H are for single-screw sterns with centerline skegs, representing variations of the U. S. Maritime Administration *C4-S-1a* or *Mariner* class. Numerical data pertaining to these five are listed in Table 60.b. The diagrams of Figs. 60.I and 60.J, adapted from Figs. 32 and 33 of a paper by H. R. Neifert and J. H. Robinson [SNAME, 1955, pp. 525–526], are for the light and intermediate load conditions, respectively, of a model of the Victory ship *Lt. James E. Robinson*.

Fig. 60.K, for comparison, depicts the wake situation at the tail of a torpedo, in the form of a body of revolution but with two vertical and two horizontal fins *ahead* of the propeller positions.

Fig. 60.M of Sec. 60.7 is a wake-survey diagram for the propeller position on the transom-stern ABC ship which is designed and described in Part 4.

Diagrams such as those listed in the foregoing, which carry a multitude of survey points, may become cluttered up and confusing if they include the section lines for the portion of the afterbody or run just forward of the propeller position. These section lines, however, are important features in the wake analysis because they show the shape of the ship just ahead of the propeller position. For a comprehensive analysis they should be available on or with the wake-survey diagram, drawn preferably to the same scale.

Appended is a partial list of additional 3-diml wake-survey diagrams of the TMB type, as published in the technical literature:

(a) Twin-skeg *Manhattan* design; wake over propeller disc abaft skeg and for considerable distance beyond; SNAME, 1947, Fig. 22, p. 115
(b) U. S. Maritime Commission, *C-3* cargo vessel, TMB model 3534; SNAME, 1947, Fig. 45, p. 146
(c) U. S. Maritime Commission design for a transatlantic liner, TMB model 3917; SNAME, 1947, Fig. 58, p. 151
(d) U. S. Maritime Administration *Mariner* design, "closed stern," TMB Model 4358W-1; SNAME,

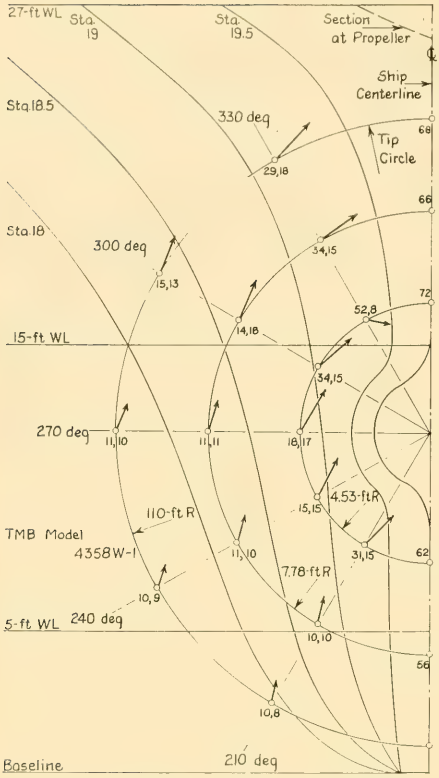

FIG. 60.E WAKE-SURVEY DIAGRAM FOR TMB MODEL 4358W-1, REPRESENTING A VARIATION OF THE *Mariner* CLASS HULL

1953, Fig. 17, p. 176. This diagram is the same as in Fig. 60.E.

(e) U. S. Maritime Administration, *Mariner* design, "open water" or "clear water" stern, TMB model 4358W-3; SNAME, 1953, Fig. 16, p. 126. This diagram is the same as in Fig. 60.G.

(f) Wake-survey data for a model of the *T-2* class tankers were published by N. H. Jasper and L. A. Rupp, SNAME, 1952, Fig. 25a, p. 347. Four afterbody sections at and adjacent to the stern are shown on this diagram.

60.7 Interpretation and Analysis of the TMB Three-Dimensional Wake Diagram. The method of plotting the projections of 3-diml incident-velocity vectors at propulsion-device positions, and of indicating the magnitude of the wake fractions and the transverse velocity components, is described in Sec. 11.6 and illustrated in the definition diagram of Fig. 11.E. Since it is most important to an interpretation and analysis of the 3-diml wake-survey diagram that the geometric relationships be clearly understood, the definition drawing is repeated here as Fig. 60.L.

The survey diagram is drawn on a sheet representing a transverse plane on the ship or model, passing through the longitudinal center of the propulsion device. For a model running at other than zero trim, and for a screw propeller mounted on a shaft having both declivity and convergence (or divergence), this plane is very nearly normal to the direction of motion. It is close enough to the plane of the disc, in both position and direction, to serve all engineering purposes. The various vectors drawn on this sheet represent simply the *projection upon it* of the incident velocity vectors

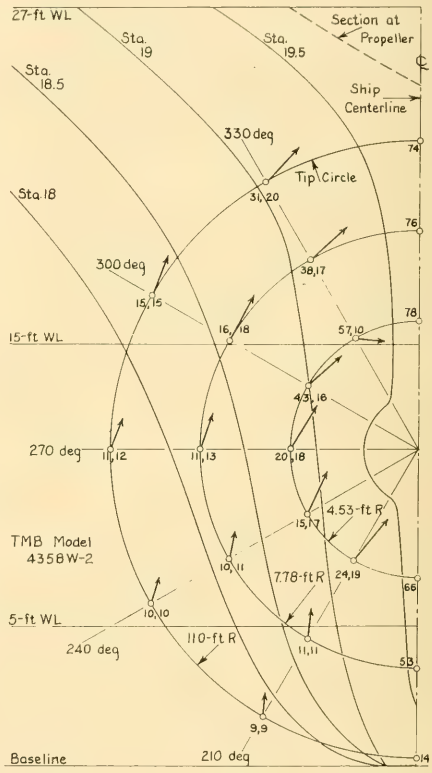

FIG. 60.F WAKE-SURVEY DIAGRAM FOR TMB MODEL 4358W-2, REPRESENTING A VARIATION OF THE *Mariner* CLASS HULL

of the water flowing through the disc position. Using the techniques available as of the date of writing (1955), the propulsion device is not working when the wake measurements are made, so there are no inflow and outflow jets and there is no race contraction.

The presence of what might be termed "intersecting" vector projections, of which there are both horizontal and vertical rows in the torpedo wake diagram of Fig. 60.K, means that the flowlines are converging at the base points of the vectors. The stream tubes meeting abaft the fins obviously can not cross each other, as do the vectors, although there may be some mixing due to flow irregularities. Rows of "intersecting" vectors of this kind are found abaft skeg and bossing terminations on ship models, and sometimes abaft shaft struts, if the measurements are sufficiently numerous.

Visual inspection of the wake-fraction numerals,

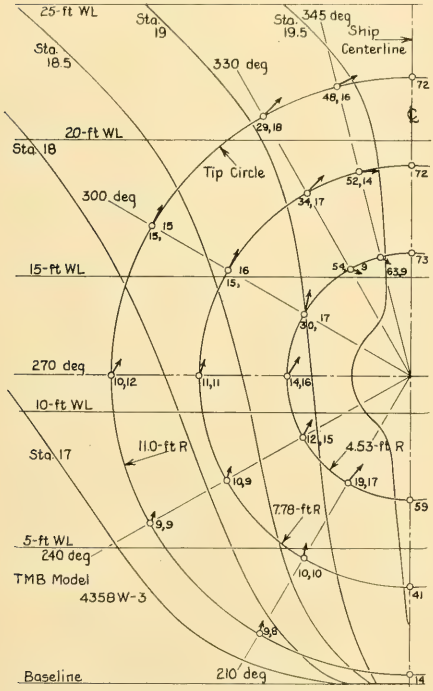

Fig. 60.G Wake-Survey Diagram for TMB Model 4358W-3, Representing a Variation of the *Mariner* Class Hull

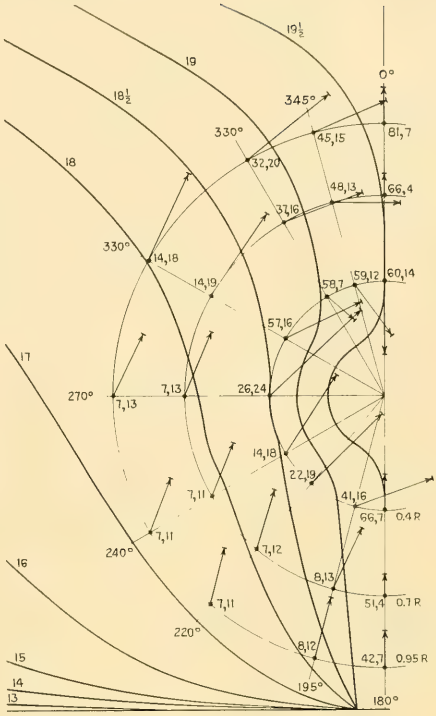

Fig. 60.H Wake-Survey Diagram for a Model Representing a Variation of the *Mariner* Class Hull

or the sketching of contours of equal wake fraction, indicates whether or not these values change in a reasonably uniform manner in all directions *across the disc.* It is to be expected that the numerical values of the wake fractions will increase progressively toward the adjacent hull, because of the retarded flow due to viscous wake within the boundary layer. Large or sudden changes in a transverse direction across the wake-survey plane are indications of longitudinal discontinuities in the flow; possibly also of partial separation or incipient eddies.

On rare occasions there are indications of longitudinal vortexes in a pattern of so-called "pinwheel" vector projections, appearing to have rotational components about a common center. This center may lie within or without the wake-survey field. A wake survey for the wall-sided ship of Fig. 25.F of Volume I would show such a

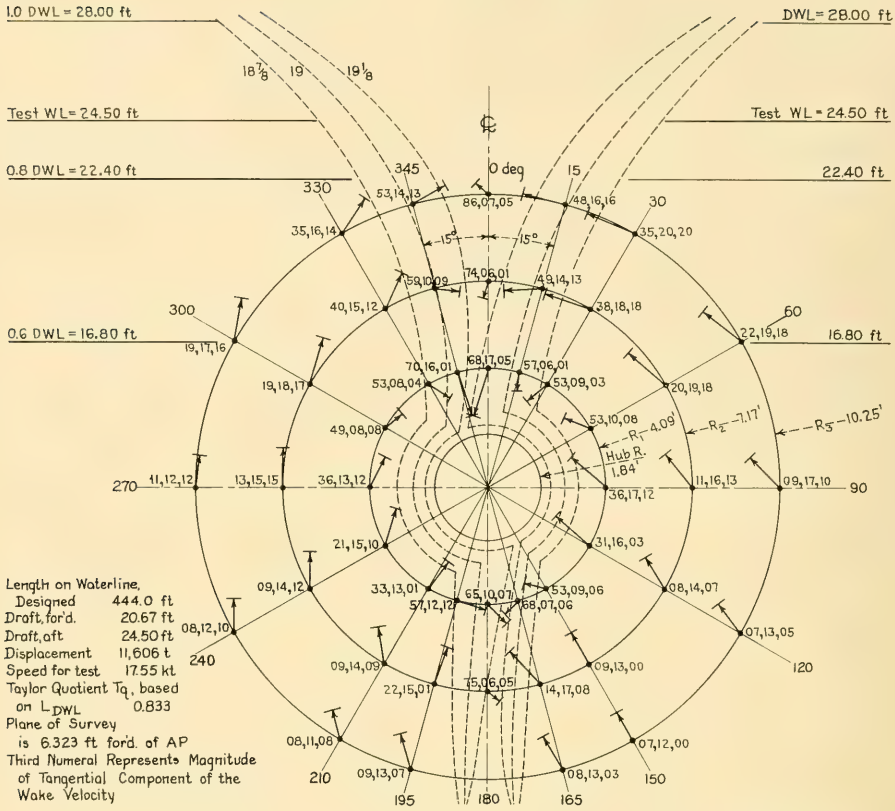

FIG. 60.I WAKE-SURVEY DIAGRAM FOR VICTORY SHIP, TMB MODEL 3801, AT 11,606 TONS DISPLACEMENT

pinwheel provided an adequate number of measurements were made. It would also show a characteristic feature of the presence of a longitudinal-axis vortex passing through the disc position of a screw-propeller. This vortex reveals itself by producing what may be called "opposite" transverse-velocity components, along any one radial line within the disc or at any one blade position. One or more of these components may indicate flow meeting the blade in its normal rotation while others *on the same blade* may indicate flow which follows the blade.

The magnitude of the tangential or rotational incident-velocity components around a circle of radius R in a screw-propeller disc, reckoned *normal to the blade axis* at any blade position, is a rough indication of the amount by which the blade is meeting or following the flow at that position. For example, in the diagram of Fig. 60.D, for TMB model 3594, the maximum meeting and following effects for an outward-turning propeller occur at 10:30 and at 4:30 o'clock, respectively. For the former, at the intermediate circle on the diagram, the wake fraction is 7.2 per cent and the transverse component 15.5 per cent, so that $\theta = \tan^{-1} 15.5/(100 - 7.2) =$ about 9.5 deg. The flow is meeting the blade. For the 4:30 o'clock position, $\theta = \tan^{-1} 13.3/(100 - 2.1) =$ about 7.7 deg. The flow is following the blade. At the 1:30 and 7:30 o'clock positions on that circle, the meeting and following effects are negligible. However, because of the radial components, the effective velocity over a blade element at 1:30 o'clock on that circle, with wake

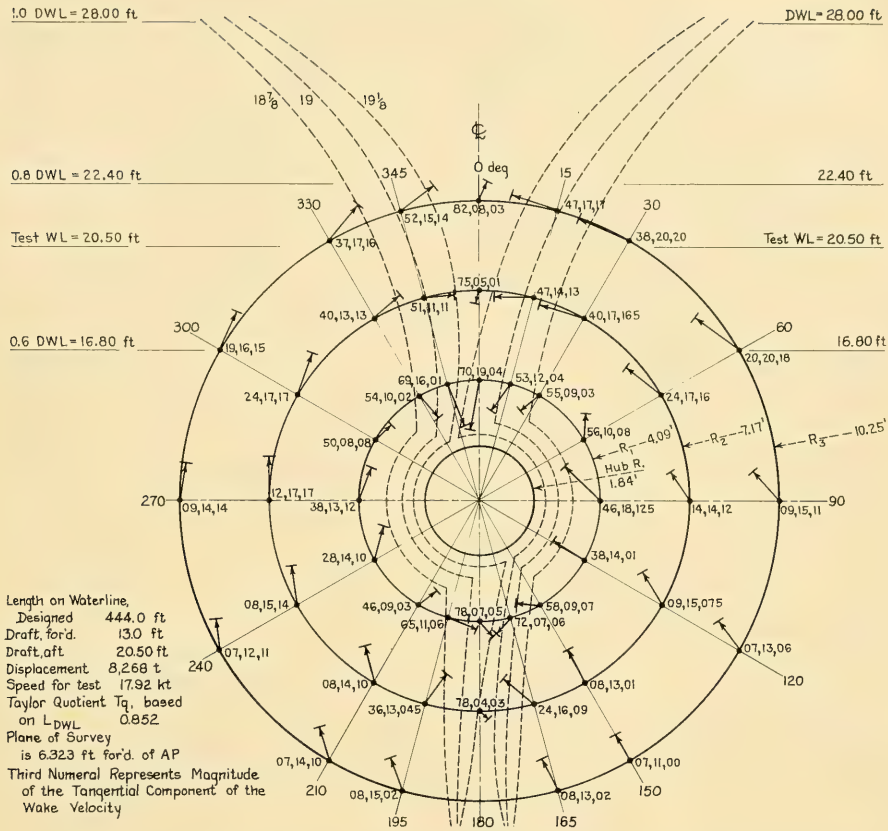

FIG. 60.J WAKE-SURVEY DIAGRAM FOR VICTORY SHIP, TMB MODEL 3801, AT 8,268 TONS DISPLACEMENT

fractions of 18.2 and 14.3 per cent in the vicinity, is only about $[100 - 0.5(18.2 + 14.3)] = 83.7$ per cent of the ship speed. Here the pitot head automatically takes account of the cosine of the angularity of flow.

The effect of the boundary layer is felt rather noticeably on the tip circle at the 1 o'clock position, where the wake fraction is 34 per cent.

Sec. 11.10 points out that no model-basin techniques in current routine use, and no graphic or tabular representations which have so far been developed, take account of variations in wake-velocity magnitudes and direction with time. If such variations exist, the current (1955) observation methods average them out. Unfortunately, the propulsion-device blades do not fail to take account of them. The result is that periodic forces are exerted on the blades, which when transmitted through the propulsion-device bearing usually produce vibration in the ship structure.

The foregoing is what may be termed a qualitative inspection and interpretation of wake-survey data. It lacks a set of specific rules, not yet formulated, to be used by the naval architect or marine engineer to discover flow features which need correction, such as those mentioned previously in this section. In the case of the liner *Normandie*, these features were revealed only by excessive vibration of the structure, which required withdrawing the vessel from service to rebuild the four bossings. In the case of certain large combatant vessels of the U. S. Navy,

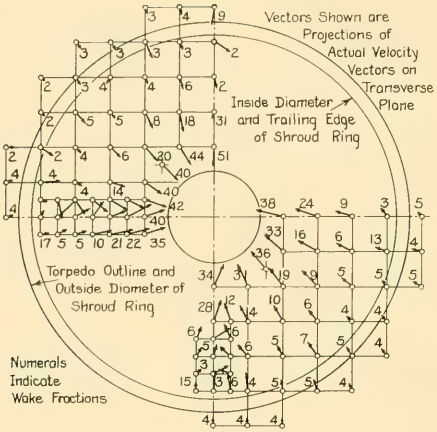

FIG. 60.K WAKE-SURVEY DIAGRAM FOR A TORPEDO WITH VERTICAL AND HORIZONTAL TAIL FINS

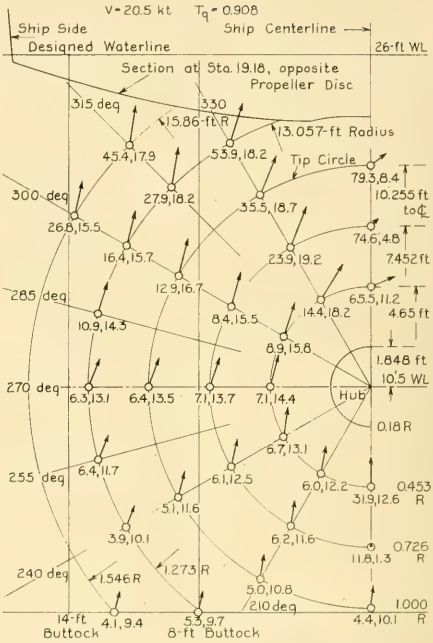

FIG. 60.M WAKE-SURVEY DIAGRAM FOR TRANSOM-STERN ABC SHIP, TMB MODEL 4505

these features were discovered during the construction period and corrected by hull changes before the vessels were launched.

There are a number of methods of quantitative analysis, by which magnitudes and variations of wake velocity are set down in graphic or tabular form. Several of these are illustrated in the references given in Sec. 60.5 for the plots of longitudinal wake-velocity or incident-velocity components. As described in Sec. 11.8, the analyses take account of either radial or circumferential variations when:

(1) A series of radii is selected and the circumferential values for each radius are averaged, or (2) A series of angular positions is selected and

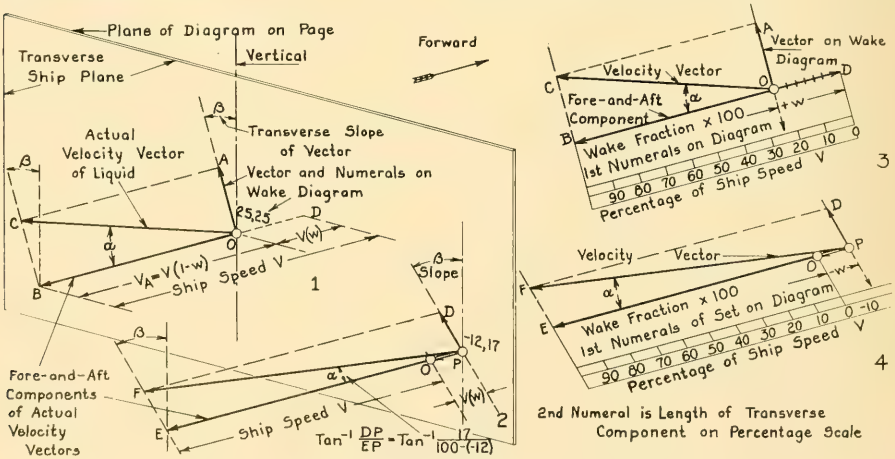

FIG. 60.L DEFINITION DIAGRAM FOR TMB 3-DIML WAKE-SURVEY DIAGRAMS

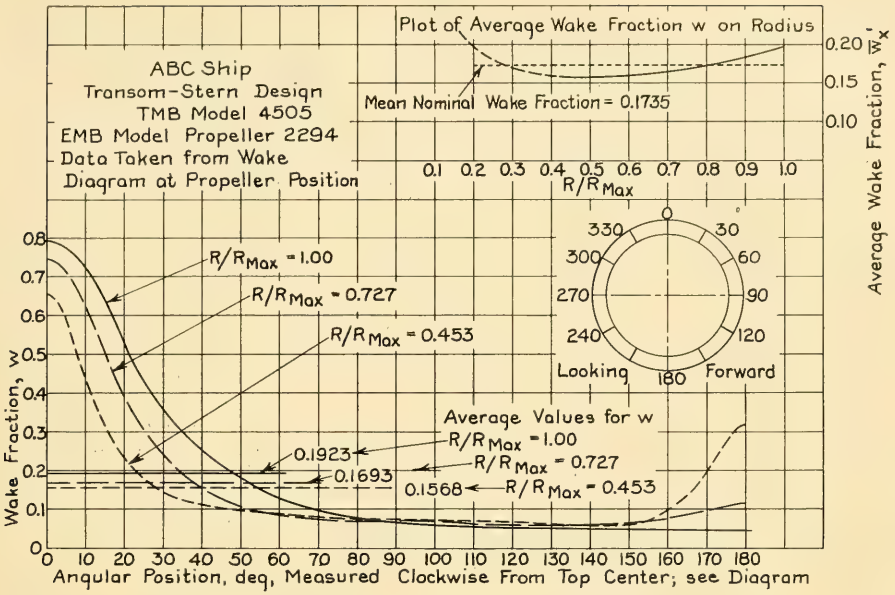

FIG. 60.N WAKE-ANALYSIS DIAGRAM FOR TRANSOM-STERN ABC SHIP, APPLYING TO FIG. 60.M

the radial variations for each position are averaged.

Fig. 60.M is a plot of the 3-diml wake survey for the transom-stern ABC ship of Part 4, made at the designed speed. Fig. 60.N is a graphic analysis of these data, prepared as a preliminary step to the design of a wake-adapted propeller for this vessel, described in Chap. 70. Values of wake fraction w are plotted in Fig. 60.N for three 0-diml radii, corresponding to $x' = R/R_{\text{Max}}$ of 1.00, 0.727, and 0.453, on a basis of angular position around the shaft axis. Averages for the complete revolution give

$x' = \dfrac{R}{R_{\text{Max}}}$ of 1.00	$w = 0.1923$
0.727	0.1693
0.453	0.1568

A plot of *radial* variation for wake fractions, when averaged around the entire circumference at each 0-diml radius, is given in the upper right-hand corner of the figure.

A somewhat more comprehensive method of analysis, probably representing more nearly the development of the future, is given by N. J. Brazell [SNAME, 1947, pp. 146–149], but the present author does not intend that these remarks shall be construed as an endorsement of all the detail steps and the calculation methods employed in that reference.

Finally, the model or ship propeller acts as an averaging or integrating instrument by taking account, degree by degree around a revolution, of the multitudinous variations in magnitude and direction of the incident-velocity vectors for the complete range of radius from hub to tip. However, because of the variations in direction as well as magnitude, involving changes in effective angle of attack, thrust, torque, blade loading, and the like, no direct analytic procedure has been devised for averaging actual wake velocities at a screw-propeller position.

By finding the speed of advance V_0 at which the same propeller, when tested in open water, produces the same torque (or thrust) as when run behind the model or ship, one assumes that the average speed of advance V_A "behind" is the same as the speed V_0 in the "open." Then knowing the speed V of the model or ship, the wake

fraction w is $(V - V_A)/V$. This is known in some quarters as the "analysis" wake fraction. That it can be considerably different from the arithmetic mean of the several wake fractions derived from a 3-diml wake-survey diagram, when averaged over a complete revolution of the propeller, is indicated by the short-dash horizontal line in the upper right-hand corner of Fig. 60.N. Here the mean nominal wake fraction, representing the arithmetic mean of the values of the average wake fraction for the nine 0-diml radii from 0.2 through 1.0, is 0.1735. For comparison, the wake fraction w_T (for thrust identity with the open-water test), for the transom-stern ABC model, when self-propelled at a speed corresponding to 20.5 kt, is 0.190, indicated on Figs. 78.Nb and 78.Nc.

This single value of the wake fraction, either estimated analytically or derived experimentally, is the value required for the shaft-power predictions of Secs. 60.4 and 60.14.

60.8 Estimating the Ship-Wake Fraction. The discussion in this section concerning the prediction of wake fractions for ship propulsion, as well as that in Sec. 60.9 for predicting thrust-deduction fractions, is limited strictly to procedures used in the early stages of a ship design, before any self-propelled model tests are run.

W. J. M. Rankine was among the first if not the first naval architect to establish a procedure for estimating the wake fraction for a ship propelled by a single screw. His method, published in his 1866 book "Shipbuilding: Theoretical and Practical," page 249, was based on the expanded length of a curved line drawn on the body plan of the ship in question. This curved line began at the center of the propeller and crossed the lines of successive sections forward of the propeller at right angles to those lines until it reached the maximum-section line. The ratio of the expanded length of this curved line to the length of the run was the approximate wake fraction desired.

Many other procedures for predicting the wake fraction in advance of model tests have been devised and used since then, as listed in the partial bibliography of Sec. 52.20. Among these procedures is one of D. W. Taylor, published in tabular form [S and P, 1933, Table XXV, p. 118; 1943, Table XXV, p. 121; PNA, 1939, Vol. II, Table 10 on p. 149]. The data in these tables, as well as the data mentioned subsequently in this section, were taken from special wake measurements on models or from wake-fraction values derived by model self-propulsion tests. Taylor's values are plotted in graphic form in diagram 1 of Fig. 60.O, together with more recent data from TMB model tests. They suffice for a rough estimate of w for the designed speed at an early stage of a preliminary design, despite the inconsistency of some of the values. Taylor's data, for both single-screw and twin-screw ships, are taken from S and P, 1943, Table XXV, page 121. Data from self-propelled tests of the 10 tanker models are from SNAME, 1948, pages 360–379; those for TMB Series 60, the tanker *Pennsylvania,* and the *Schuyler Otis Bland* are from SNAME, 1954.

J. Lefol in his paper entitled "Les Interactions entre la Carène et le Propulseur (Interactions Between the Hull and the Propeller)" [ATMA, 1947, Vol. 46, pp. 221–251], gives in Part VIII, on pages 235–236, nine formulas for wake fraction, taken from the published literature. Recently, in his discussion of the 1956 SNAME paper by F. H. Todd and P. C. Pien on the TMB Series 60 model tests, A. Q. Aquino proposes for single-screw vessels a formulation

$$w_T = (\text{A constant}) + \left[\frac{4B^2H(C_X)^{1.5}(C_{PVA})(C_{PA})}{\pi D^2 L(6.5 - 5.5C_{PVA})(3 - 2C_{PA})}\right] - k[f(\overline{LCB})]$$

where D is the propeller diameter.

A comprehensive summary of existing published data on wake at screw-propeller positions, as well as some not published, has been made by S. A. Harvald ["Wake of Merchant Ships," Danish Tech. Press, Copenhagen, 1950]. This is accompanied by a careful, studied analysis. The paper is replete with graphs and plots but unfortunately it lacks the flow and other diagrams that would have assisted the reader, and that might also have changed some of the author's ideas and conclusions. It is based solely on the longitudinal or axial component of the relative and the true-wake velocities, in the form of the customary speed of advance and Taylor wake fraction, and almost exclusively upon wake as affecting one or more stern screw propellers.

It is considered most significant that Harvald achieves his only major correlations with practice, and his only really consistent ones, when he uses predictions based on theoretical analyses. In the comparisons with empirical data, employing orthodox form coefficients and parameters, it becomes almost necessary at times to force

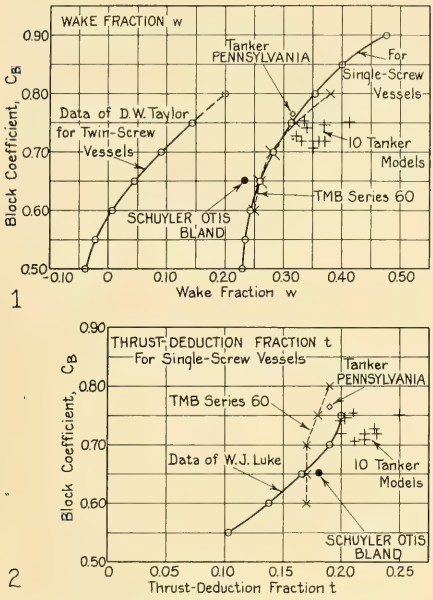

FIG. 60.O GRAPHS FOR D. W. TAYLOR'S PREDICTIONS OF WAKE FRACTION AND W. J. LUKE'S PREDICTION OF THRUST-DEDUCTION FRACTION

agreement. At their best, the relationships so established are complicated, confused, and often conflicting.

The use of the known features of the boundary layer abaft a flat plate accounts for most of the radial and tangential (peripheral) wake variations observed abaft normal forms of single-screw sterns. The derivation of the potential-flow wake abaft bodies formed by various combinations of sources and sinks in an ideal liquid gives a reasonably consistent picture of the potential-wake variations abaft ship forms of varying fullness, proportions, and size. B. V. Korvin-Kroukovsky uses this approach in his paper "On the Numerical Calculation of Wake Fraction and Thrust Deduction in a Propeller and Hull Interaction" [Int. Shipbldg. Prog., 1954, Vol. 1, No. 4, pp. 170–178]. However, an understanding of this paper requires a thorough knowledge of source-and-sink phenomena and stream functions, Lagally's theorem, friction resistance, and the various kinds of flow around bodies of revolution and ship-shaped forms.

In a still later paper S. A. Harvald carries on this analysis somewhat further ["Three-Dimensional Potential Flow and Potential Wake," Trans. Dan. Acad. Tech. Sci., 1954]. Applied Mechanics Reviews, May 1955, page 206, has this to say of it:

> "The Rankine bodies generated by various combinations of sources and sinks, situated at isolated points or distributed over lines and surfaces, are computed. The purpose of the work is to compute by this means the velocity field due to the ship's hull in the neighborhood of the propeller. Since the effect of the ship's boundary layer on the potential flow is neglected, the results should be only roughly applicable for this purpose."

There is as yet nothing approaching a formula or routine step-by-step procedure which a naval architect can use while his ship design is progressing.

Despite these intense analytical studies, S. A. Harvald comes to the conclusion, in the 1950 reference cited earlier in this section, that the empirical formula of K. E. Schoenherr [PNA, 1939, Vol. II, Eq. (110), p. 149] is, with slight modifications, the naval architect's best known method of predicting the wake fraction for a given design, when the hull shape has been delineated and the screw-propeller position(s) determined. The Schoenherr formula, without modifications but with standard symbols, as employed for single-screw vessels of normal or nearly normal design, is

$$w = 0.10 + 4.5\left(\frac{C_{PV}C_PB}{L}\right)\frac{1}{(7 - 6C_{PV})(2.8 - 1.8C_P)} + \frac{1}{2}\left[\frac{E}{H} - \frac{D}{B} - k'\,(Rake)\right] \qquad (60.ii)$$

where E is the height of the propeller axis above the baseplane at the disc position,

D is the propeller diameter,

$(Rake)$ is the rake angle of the propeller blade, measured in radians, and

k' is a coefficient that has values of:

(1) 0.3 for a normal stern
(2) 0.5 to 0.6 for a stern with aftfoot cut away.

This formula, despite its intricacy, is nondimensional. An example of its application, to the transom-stern single-screw ship designed in Part 4, is worked out presently.

K. E. Schoenherr gives a second set of formulas

[PNA, 1939, Vol. II, Eq. (112), p. 149], for twin-screw vessels with:

(a) Bossings and outward-turning propellers

$$w = 2(C_B)^5(1 - C_B) + 0.2 \cos^2\left(\frac{3\beta}{2}\right) - 0.02 \qquad (60.\text{iii})$$

where β(beta) is the slope of the bossing termination, measured in degrees

(b) Bossings and inward-turning propellers

$$w = 2(C_B)^5(1 - C_B) + 0.2 \cos^2 [\tfrac{3}{2}(90 - \beta)] + 0.2 \qquad (60.\text{iv})$$

(c) Propeller shafts supported by struts

$$w = 2(C_B)^5(1 - C_B) + 0.04 \qquad (60.\text{v})$$

For the single-screw ABC ship, the data required for the Schoenherr formula (60.ii) are, from the SNAME RD sheet of Figs. 78.Ja and 78.Jb and the drawings of Chaps. 66 and 67:

C_{PV}	= 0.822	E	= 10.5 ft
C_P	= 0.621	D	= 20.51 ft for the stock propeller used on TMB model 4505
B_X	= 73.08		
L	= 510		
H	= 26.163 ft	k'	= 0.6
		Rake	= 0.

Setting down the Schoenherr equation and substituting:

$$w = 0.10 + 4.5\left(\frac{C_{PV}C_PB}{L}\right)\frac{1}{(7 - 6C_{PV})(2.8 - 1.8C_P)} + \frac{1}{2}\left[\frac{E}{H} - \frac{D}{B} - k'\,(Rake)\right]$$

$$= 0.10 + 4.5\left[\frac{0.822(0.621)73.08}{510}\right] \cdot \frac{1}{[7 - 6(0.822)][2.8 - 1.8(0.621)]} + \frac{1}{2}\left[\frac{10.5}{26.163} - \frac{20.51}{73.08} - 0.6(0)\right]$$

$$= 0.255$$

This value of 0.255 for the 20.51-ft stock propeller compares with the value of about 0.24 from Fig. 60.O, where C_B is taken, from the fifth approximation in Table 66.e, as 0.593. As a matter of interest, the wake fraction determined from the model self-propulsion test with this propeller, at a speed corresponding to 20.5 kt, is 0.190; see Fig. 78.Nb. This is w_T, derived from thrust identity with the open-water test. The value of w_Q, derived from torque identity with that test, is 0.200.

For vessels with tunnel sterns, there are little or no published data on the wake fractions to be expected [Harvald, S. A., "Wake of Merchant Ships," 1950, p. 117]. For the arch-stern design of the ABC ship of Part 4, the self-propulsion curves of Fig. 78.I indicate a wake fraction w at the designed speed of only about 0.072.

In this connection it is of interest to note, from the statements of L. Troost, that:

> "Wake factors (based) on thrust identity depend on propeller loading (thrust-load coefficient). The more heavily loaded the propeller, the smaller is the wake factor we find [6th ICSTS, 1951 (SNAME, 1953), p. 143].',

The comments in parentheses are those of the present author.

60.9 Prediction of the Thrust-Deduction Fraction. It has been customary since the 1860's, when W. J. M. Rankine and W. Froude both worked on this problem [INA, 1865, pp. 13–39], to base predictions of the thrust-deduction fraction of screw-propelled vessels upon the estimate of the wake fraction [PNA, 1939, Vol. II, pp. 149–150]. So far as known this procedure has been limited generally to single-screw vessels. In any case, it gave little or no credit to efforts, put forward by D. W. Taylor and others, to decrease the thrust deduction by thinning the ship sections or "straightening" the surfaces of the hull and its appendages ahead of the propeller disc, so that less transverse area is acted upon by the $-\Delta p$'s ahead of the disc. These efforts were based upon the hope that the thrust-deduction fraction would be reduced at a greater rate than the wake fraction, so as to hold the hull efficiency to as high a value as possible.

W. J. Luke was among the earliest to give empirical values of the thrust-deduction fraction that were of practical use to the ship designer. D. W. Taylor and others quoted these values [S and P, 1933, p. 117; S and P, 1943, p. 120; PNA, 1939, Vol. II, Table 9, p. 148; RPSS, 1948, pp. 177–178]; they are plotted in diagram 2 of Fig. 60.O, together with more recent data from TMB model tests. They, like the wake-fraction graphs in diagram 1 of that figure, suffice for rough estimates in the preliminary-design stage of a ship of normal form.

C. H. Peabody, in his 1910 tests of the large,

independently powered model *Froude*, wisely included runs in which the single propeller was placed farther and farther abaft the sternpost, varying from its normal position to about $1.15D$ astern. Because of missing information it is not possible to analyze Peabody's test data in the manner presently to be described. Nevertheless, his Table I [SNAME, 1911, p. 95] indicates that at the highest speed reached by this craft, the thrust-deduction fraction t diminished from 0.35 to 0.077 for the range of propeller positions given.

In a paper "Vom Sog (Thrust Deduction)," H. M. Weitbrecht discussed the physical aspects of thrust deduction but pointed out that it was not then possible to predict the numerical value of the thrust deduction for a given ship form and propeller loading [Schiffbau, Schiffahrt, und Hafenbau, Jun 1938; English version in TMB Transl. 62 of Sep 1940].

K. E. Schoenherr and A. Q. Aquino, in the period 1930–1940, made a careful review of the existing literature on the ship-propeller interaction problem, undertook their own analysis, and supplemented it with plotted observations from the results of self-propelled tests on a great many models. Their work is described fully in TMB Report 470, published in March 1940. The following rules for estimating the thrust-deduction fraction, published by K. E. Schoenherr in 1939 [PNA, Vol. II, pp. 149–150], were developed from this project:

(1) For the thrust-deduction fraction of single-screw ships:

$$t = kw \qquad (60.\text{vi})$$

where k = 0.5 to 0.7 for vessels with streamlined or contra-rudders
= 0.7 to 0.9 for vessels with double-plate rudders with internal arms, attached to square rudder posts
= 0.9 to 1.05 for vessels with single-plate rudders and external arms

(2) For the thrust-deduction fraction of twin-screw ships, specifically:

(a) Ships with propellers and shafts carried by bossings

$$t = 0.25w + 0.14 \qquad (60.\text{vii})$$

(b) Ships with propellers and exposed shafts carried by struts

$$t = 0.70w + 0.06.$$

For the transom-stern, single-screw ABC ship designed in Part 4, the estimate of the wake and thrust-deduction fractions posed somewhat of a problem, because of the unorthodox stern shape and the lack of empirical data upon which to base predictions. With little information for guidance, with a screw propeller of diameter larger than normal, and with a tip clearance smaller than normal, it was guessed in Sec. 66.27 that the wake fraction w would be as high as 0.30 and the thrust deduction as low as 0.20. The corresponding hull efficiency η_H of 1.143 seemed reasonable.

When a stock propeller was selected to self-propel the model, by the procedure described in Sec. 70.6, the wake fraction derived by Eq. (60.ii) was 0.261, using dimensions and parameters corresponding to an early stage of the design. The thrust-deduction fraction was derived from Eq. (60.vi). The value of k for the latter was taken as 0.5, because of the contra-rudder shape proposed for the supporting horn and the underhung balance portion of the rudder. It seemed reasonable, further, to reduce the calculated value by 15 per cent, because of the very thin skeg to be placed ahead of the propeller. The predicted thrust-deduction fraction then worked out as

$$t = k(w)(1 - 0.15) = 0.5(0.261)(0.85) = 0.111$$

It was realized at the time that a thin skeg ahead of a single propeller was liable also to reduce the wake fraction. For a conservative estimate, without the 15 per cent reduction in t, the predicted hull efficiency η_H was

$$\frac{1 - t}{1 - w} = \frac{1 - 0.131}{1 - 0.261} = 1.176$$

It is brought out in (2) and (3) of Sec. 78.17 that the thrust-deduction and wake fractions derived from the model self-propulsion tests are appreciably different from those derived in these two sections.

B. V. Korvin-Kroukovsky gives the following equation from H. E. Dickmann for the estimated value of the thrust-deduction fraction:

$$t = (w_p)\frac{2}{1 + \sqrt{1 + C_{TL}}} = (w_p)\eta_I \qquad (60.\text{viii})$$

where w_p is the nominal potential-wake fraction and η_I is the ideal efficiency of the propeller. The problem here is to find the value of w_p, for which there is no simple solution.

An entirely different prediction procedure,

devised to take direct account of the factors which develop the thrust-deduction force, is based upon the rate of variation of $-\Delta p$ with fore-and-aft distance ahead of the propeller, and that of $+\Delta p$ abaft it. The assumption is made that these pressures vary with distance in very nearly the same manner as for a screw propeller working in open water or an airscrew working in open air, indicated by diagram 3 in Fig. 59.G. It is further assumed that, following D. W. Taylor's patent previously referenced, the $-\Delta p$'s are so small at 2 diameters ahead of the disc position that they can be neglected.

The method is based upon a summation of longitudinal forces exerted upon certain selected transverse sections of the ship, lying within an imaginary cylinder concentric with the propeller axis. This cylinder has the propeller diameter D, and extends both forward and aft from the disc position.

A similar imaginary cylinder in this position was shown by G. Kempf many years ago [STG, 1927, Vol. 28, p. 180]; also by E. F. Hewins as a method of determining the wake fraction w [Osbourne, A., "Modern Marine Engineer's Manual," 1943, Vol. II, p. 2311].

For the analysis described here, the transverse sections are at $2.0D$, $1.0D$, and $0.5D$ ahead of the disc position. A fourth section is taken through the maximum-area section of whatever rudder, rudder post, or horn combination lies abaft it. Any other transverse-section positions could be used if desired, and they could extend for more than $2D$ ahead of the disc position.

It is assumed that the $-\Delta p$ values at the three positions ahead have the relative multipliers or weights of 5, 2, and 1, respectively, indicated by the tabulation at the bottom of Fig. 67.V. The rudder section is given a multiplier or weight of 7 because it is usually closer than $0.5D$ to the disc and the $+\Delta p$'s in the outflow jet are greater numerically than the $-\Delta p$'s in the inflow jet for a screw propeller producing thrust. These multipliers are based upon the relative ordinate magnitudes of the $-\Delta p$ and $+\Delta p$ curves at the transverse sections selected. They are still somewhat arbitrary, and could be varied for a re-analysis.

Expanding the disc circles by amounts corresponding to the enlargement of area of the propeller inflow jet at the three selected forward disc positions is considered not justified. The same applies to contraction of the after disc circles. The jet area increases rather slowly immediately ahead of the propeller, even for the large thrust-load factors expected in the free-running operation of a normal ship with a not-to-large propeller, as indicated in diagram 1 of Fig. 59.G. The values of $-\Delta p$ are relatively so small, farther forward of the propeller, that the refinement of increasing the disc areas seems not justified by the approximate nature of the overall method. Moreover, the presence of the ship and its appendages, either ahead of or abaft the screw-propeller position, distorts the jets out of their normal axisymmetric shape. Little is known of what happens when they are so distorted, of the amount of hull surface covered by the water in them, and the differential pressures in that water.

The foregoing "cylinder" procedure assumes that the rudder always develops a thrust-deduction force in the form of a drag, acting opposite to the direction of motion, and that it always contributes to the thrust deduction. However, in the case of a contra-rudder, and some forms of streamlined rudder, each lying in a propeller outflow jet, it is known that the hydrofoil action on the rudder produces a forward component of lift which exceeds the drag. The rudder then exerts a thrust force on the ship, and helps to push it along. Theoretically, the *net* thrust force T_R exerted by the helping rudder, mentioned in Sec. 34.8 of Volume I, should be subtracted from the thrust-deduction force exerted on the hull or appendage ahead. This can only be done when the amount of this thrust force is better known.

In practice, the "cylinder" procedure involves the following steps:

I. On the afterbody lines plan of the ship lay off special stations at $0.5D$, $1.0D$, and $2.0D$ forward of the propeller-disc position. A fourth station is laid off through the maximum-thickness position of the rudder. Using the coordinates of these special stations, draw the corresponding sections on the body plan, as in Fig. 33.A of Part 2 in Volume I or in Fig. 67.V of Part 4. If a rudder horn is thicker than the rudder, or if any other appendage lies anywhere in the propeller outflow jet, draw a section (or sections) representing the *maximum* transverse thickness of the horn or appendage.

II. Draw on the body plan, over the section lines of the special stations, three circles, each representing the propeller-disc outline if moved suc-

cessively 0.5, 1.0, and 2.0 propeller diameters along the shaft, forward of the propeller position. Draw other circles for stations abaft the shaft, if necessary. If the shaft center is nearly or exactly parallel to the centerplane and the baseplane, only one circle is needed on a body plan showing the hull.

III. Mark carefully the outlines of the special stations lying within their respective projected disc circles. These outlines may be indicated by colored lines on the working plan, or the respective areas may be marked by different types of hatching, as in Fig. 33.A.

IV. With a planimeter, or by any other suitable means, determine the area of the propeller disc covered by the section of the hull and of the rudder (or horn or other appendage) at each of the special stations. In the same manner, determine the area of the propeller disc. As only the ratios of areas enter in this analysis the planimeter readings can be used directly, without converting them into absolute area units.

V. Multiply the area readings by suitable multiples, as indicated in the tabular portion of Fig. 67.V. Total the products and divide by the sum of the multiples, 15 in the case of the ABC ship, to obtain a weighted-average area reading. Divide the weighted area reading by the propeller-disc area reading to obtain the 0-diml area ratio.

VI. With this area ratio enter Fig. 60.P and pick off the estimated thrust-deduction fraction for the ship. The two graphs for this figure are still tentative, based as they are on the analysis of data from a rather limited number of model tests.

The procedure for estimating the thrust-deduction fraction for a rotating-blade propeller, and for designing the hull to keep the augment of resistance small, is essentially the same as for a screw propeller. Instead of the imaginary cylinder of circular section an imaginary rectangular tube is projected forward of—or abaft—the basket assembly of blades, for a distance equal to twice the blade length or to the diameter of the blade-axis circle, whichever is the greater.

All the foregoing indicates that determination of the thrust-deduction fraction in any given ship case is still largely empirical, and as highly uncertain. The problem is now (1955) being attacked along analytic lines, as it should have been years ago. It is hoped that this attack will

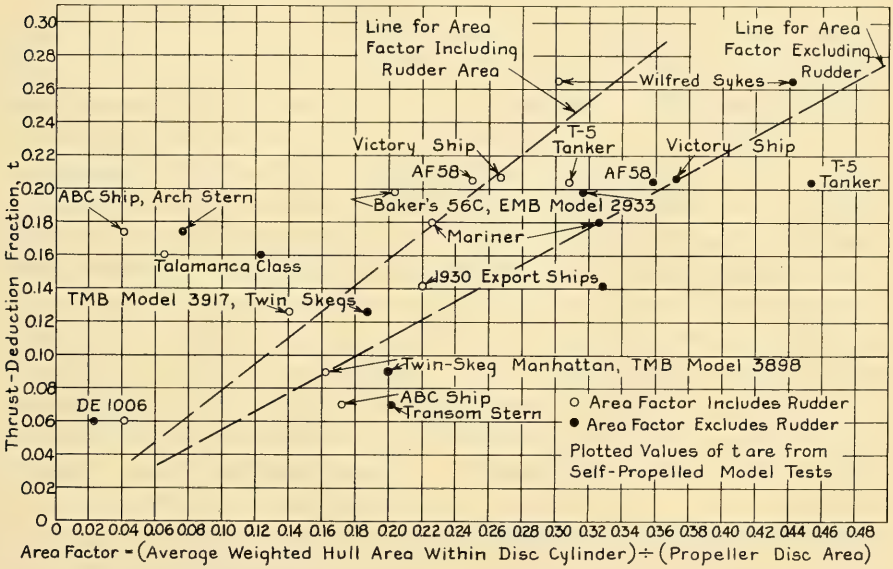

Fig. 60.P Graphs for Predicting Thrust-Deduction Fraction for Single-Screw Ships by the "Cylinder" Method

continue unceasingly until a logical and reliable prediction procedure is available.

60.10 Finding the Relative Rotative Efficiency. The physical and analytical basis for relative rotative or thrust-torque efficiency, as applied to a screw propeller working behind a model or ship, is described in Sec. 34.7 of Volume I. Further comments on this factor are embodied in Sec. 34.16.

It is necessary to estimate or predict the probable value of the relative rotative efficiency η_R when the expression $[\eta_0(\eta_H)\eta_R]$ is used to estimate the propulsive coefficient η_P. This prediction, however, is much more easily mentioned than made.

K. E. Schoenherr gives a few comments concerning this factor. In the absence of any more reliable and authoritative information these comments have acquired the nature of a prediction rule. He states that:

"The average values of the relative rotative efficiencies determined in the tests worked out to be 1.02 for the single-screw models and 0.985 for the twin-screw models.

"It should be emphasized that the foregoing formulas are valid only for merchant ships of normal form operating at speed-length (T_q) values below unity" [PNA, 1939, Vol. II, p. 150].

More recently L. C. Burrill and C. S. Yang have calculated the overall thrust and torque, including the K_T and K_Q values, for a group of screw propellers operating in certain assumed wake distributions over the propeller disc, corresponding to the conditions behind several hypothetical ships [INA, 1953, Vol. 95, pp. 437–460]. By calculating the same quantities for the same propellers working in a uniform flow, simulating open-water tests, they are able to predict the thrust-torque factors T_0D/Q_0 and TD/Q for the "open-water" and the "behind-ship" conditions, respectively. From the discussion of Sec. 34.7 in Volume I, the relative rotative efficiency is then

$$\eta_R = \left(\frac{Q_0}{T_0D}\right)\frac{TD}{Q}$$

where D is the propeller diameter, the same behind the ship as in open water.

As a result of their analysis Burrill and Yang conclude that:

"... the quantity designated relative-rotative-efficiency has a real meaning, in terms of the method of analysis usually adopted, and its value can be estimated by calculation, in the manner described in the paper [pp. 440–441 of the reference cited]. The numerical values obtained agree reasonably well with the experimental data" [INA, 1953, Vol. 95, pp. 446, par. 8(4)].

However, the calculations involved are laborious, at least with desk-type computers, and the values derived are generally in line with the empirical values previously used.

If a condition is assumed in which the torque Q behind the ship is the same as Q_0, then a value of η_R greater than unity indicates that the thrust T exerted by the propeller behind the ship is greater than T_0 in open water. The service conditions are such, therefore, as to make the propeller more efficient in pushing the ship than when it is just pulling itself along in open water.

Additional information concerning the values of η_R to be expected on single-screw ships is found in the following reports of self-propelled models:

(a) Ten tanker models; SNAME, 1948, Fig. 32, p. 416

(b) TMB Series 60 parent models and related models; SNAME, 1954, Figs. 12(a) and 12(b) on pp. 141–142. The values of η_R range from 1.04 to 1.01, with an average of about 1.02.

(c) Todd, F. H., and Pien, P. C., "Series 60—The Effect upon Resistance and Power of Variation in LCB Position," SNAME, 1956. Tables 18 through 22 list the relative rotative efficiency (as e_{rr} in that text) for a wide range of speeds on all the models tested.

For the reader who wishes to undertake some of this analysis on his own, the value of the relative rotative efficiency η_R is derived from the self-propelled test of a ship model by the following procedure. The case used as an example is that from the self-propelled test of TMB model 4505-1, representing the *arch-stern* design of the ABC ship undertaken in Chap. 67:

(1) The basic data are:

(a) The propeller diameter D, in this case 24.22 ft

(b) The wake fraction w, indicated on Fig. 78.I as 0.072 for 20.5 kt

(c) The thrust-deduction fraction t, taken from the same figure as 0.175

(d) The rate of propeller rotation n, of 90.1 rpm or 1.502 rps

(e) The propulsive coefficient η_P of 0.686

(f) The hull efficiency η_H is $(1 - t)/(1 - w)$ or $(1 - 0.175)/(1 - 0.072) = 0.889$.

The illustrative calculation is made for the designed speed only; this is 20.5 kt or 34.62 ft per sec. (2) The speed of advance V_A is the ship speed V times $(1 - w)$. In numbers, for the example cited, this is $V_A = 34.62(1 - 0.072) = 34.62(0.928) = 32.127$ ft per sec. Then

$$J = \frac{V_A}{nD} = \frac{32.127}{1.502(24.22)} = 0.883$$

(3) Consulting the characteristic curves for TMB model propeller 1986 used on the test in question, as shown in Fig. 78.H, the value of the real or working efficiency η_0 for a J-value of 0.883 is 0.750; this value is indicated by a note and an arrow on Fig. 78.H. From the general expression $\eta_P = \eta_0(\eta_H)\eta_R$, the relative rotative efficiency is

$$\eta_R = \frac{\eta_P}{\eta_0(\eta_H)} = \frac{0.686}{0.75(0.889)} = 1.029.$$

For the single-screw *transom-stern* ABC ship the self-propulsion model tests with a stock propeller, reported in Figs. 78.Na, 78.Nb, and 78.Nc, gave a propulsive coefficient η_P of 0.761 at the designed speed. For the advance ratio J at which the propeller operated in this test, the value of η_0 from the characteristic curves of Fig. 78.Mc was 0.685. The hull efficiency η_H, based on the thrust delivered by the model propeller, was 1.148. By the relationship between these four sets of η-values,

$$\eta_R = \frac{\eta_P}{\eta_0(\eta_H)} = \frac{0.761}{(0.685)(1.148)} = 0.968$$

This value is well below the one that would have been predicted by Schoenherr. Since it is less than 1.00, it works to the ship's disadvantage. There is no present explanation for it.

60.11 Determination of the Propulsive Coefficient. A great deal of guessing was involved in the estimates of propulsive coefficient η_P in the days before model basins made tests of self-propelled models. Since that time, naval architects and marine engineers have relied heavily upon the results of individual model tests to supply them with needed information as to the shaft power to be installed in the ship built from a particular design. The result is a dearth of systematic data by which to *predict* the correct propulsive coefficient for any given case. One might say that in the days when one had to make this estimate in order to power a ship there was insufficient background information to do it. When the designer no longer had to make it he did not trouble to analyze fully all the data available to him.

The situation was well described by K. C. Barnaby in the early 1940's ["The Coefficient of Propulsive Efficiency," INA, 1943, pp. 118–141] and it has not improved materially up to the time of writing (1955), despite publication of the data to be mentioned presently.

In tables published with his 1943 paper, Barnaby gave many values of η_P for a number of different types of ships, based primarily on a variation of η_P with $V/\sqrt{L}$ or Taylor quotient T_q. However, in his later book "Basic Naval Architecture" [1948, Art. 187, pp. 242–244], he presents these values on a basis of absolute ship length, but subdivided for single-screw, twin-screw, and quadruple-screw propulsion.

W. P. A. van Lammeren, L. Troost, and J. G. Koning present values of propulsive coefficient η_P for single-screw ships, for twin-screw ships, and for coasters (the latter presumably all single-screw vessels), based upon the rate of propeller rotation n [RPSS, 1948, pp. 284–288]. D. W. Taylor gives only general information on this subject and that of little help to the designer of a modern ship [S and P, 1943, p. 178].

Since the efficiency of propulsion depends upon a combination of the open-water or working propeller efficiency η_0, the hull efficiency η_H, and the relative rotative efficiency η_R, it should respond to variations in those efficiencies with the factors which control them. Among these may be mentioned:

(a) Type of propulsion device, whether open screw propeller, shrouded screw propeller, paddle-wheel, rotating-blade propeller, or their equivalents
(b) Relative position of ship and propulsion device, involving tip and aperture clearances, shape of hull near the propulsion devices, and other similar factors
(c) Thrust-load factor C_{TL}, which limits the ideal efficiency η_I and the 0.8-value of that efficiency, illustrated in Fig. 34.G
(d) Wake and thrust-deduction fractions, and the combination of the two
(e) Characteristics of the flow at the propulsion-device position(s), determining the relative rotative efficiency.

Consideration of (a) leads to the conclusion that entirely separate sets of prediction data are required for each type of propulsion device.

Figs. 34.M and 34.N give some not-too-recent values of η_0 for several types; Figs. 59.A and 59.B present more recent data on a few different types. In both series of diagrams the propeller efficiencies are based upon the thrust-load factor C_{TL} .

For a given ship resistance to be overcome, or a given propeller thrust to be produced, with constant wake and thrust-deduction fractions, the thrust-load factor C_{TL} increases and the actual propeller efficiency η_{Real} diminishes with decreasing diameter, while the rate of rotation n increases. This is because the thrust-load factor $C_{TL} = T/(0.5\rho A_0 V_A^2)$ increases as A_0 diminishes, the real or working efficiency η_0 decreases as C_{TL} increases, and η_P decreases with η_0 . Since the advance coefficient J usually decreases as η_0 decreases, indicated by Fig. 78.H, and since $n = V_A/(JD)$, a reduction in the thrust-producing area causes both J and D to diminish, and results in an appreciable increase in the rate of rotation n. The foregoing accounts for the moderate falling off of propulsive efficiency with increase of rpm, revealed by W. P. A. van Lammeren, L. Troost, and J. G. Koning [RPSS, 1948, Figs. 193 and 194, pp. 285–286].

The effect of the wake and thrust-deduction fractions, singly or in combination, is exceedingly complex, so much so that no general or detail rules have been formulated to predict their effect upon propulsive efficiency. Characteristics of the flow at the propulsion-device positions are related to the relative positions of the device and the hull. Not enough is known of these effects, both physically and analytically, to predict reliable and precise values of η_P in the preliminary- or contract-design stage.

Nevertheless, based upon the reasoning in the foregoing, upon data derived from the trials of many ships, and upon experience, a few prediction guides are set down:

(1) For ships driven by screw propellers, the number and consequently the position(s) of the wheels carried by each puts them in different categories so far as propulsive coefficients are concerned, indicated both by W. P. A. van Lammeren and by K. C. Barnaby in the latter's latest publication. This is elaborated upon in (5) following.

(2) For equally good hydrodynamic designs there is no reason why the propulsive coefficient η_P should vary with absolute ship or propeller sizes, provided the sizes are adequate to avoid scale effect

(3) A variation is to be expected with type of vessel because of the characteristically different hull shape, relative hull and propulsion-device position, and nature of flow at the propulsion device. A free-running, single-screw tug with a short, chubby hull and a propeller abaft it would be expected to have a different η_P than a long, slender, high-speed, single-screw patrol vessel with its propeller more or less under the hull.

(4) Within a single category as to number of propulsion devices and within a single type of device, assuming a constant thrust T and a constant wake fraction w, the value of η_P diminishes with a decrease in the thrust-producing area of the device, corresponding to the disc area A_0 of a screw propeller. The reasons for this are explained in a preceding paragraph.

(5) For a good hydrodynamic design of both ship and screw propeller, based upon data such as set forth in this book, the following values of propulsive coefficient η_P should be achieved, on the basis of a clean, new hull, at the designed speed:

(i) Single-screw vessels of the merchant and generally similar types, with speed-length quotients or fatness ratios in or near the design lane of Fig. 66.A . . . . . 0.82 to 0.72

(ii) Twin-screw vessels of modern (1955) merchant and similar types, having fatness ratios as in (i) preceding . . . . . 0.73 to 0.65

(iii) Triple-screw vessels; no adequate systematic data for vessels having three propellers nearly alike, or for vessels having larger center wheels absorbing more power than each of the wing wheels

(iv) Quadruple-screw vessels of the liner type . . . . . 0.65 to 0.60

(v) Single-screw tunnel or arch-stern vessels . . . . . 0.68 to 0.55

(vi) Double, triple, and quadruple-screw tunnel-stern vessels for operation in shallow and restricted waters . . . . . 0.60 to 0.45

(vii) For fat, chubby vessels such as tugs and fishing craft, propelled by single screws . . . . . 0.72 to 0.55, averaging about 0.65.

For speeds other than the designed value, the propulsive coefficient may vary rather widely [Barnaby, K. C., INA, 1943, pp. 118–141]. Below the designed speed, the value of η_P is usually greater than at the designed speed; at higher speeds, it is usually less. For the transom-

stern model of the ABC ship, as self-propelled, Fig. 78.Nc indicates a maximum η_P of about 0.78 at 15 kt for the ship, a value of 0.76 at the designed speed of 20.5 kt, and a diminished value of only 0.70 at about 22.4 kt, assuming that there is enough reserve of power to drive the ship that fast.

The designer is again reminded that the propulsive coefficient is to be regarded solely as a means of predicting a shaft power from an estimated or known effective power. It is not to be taken as a measure of merit in itself. A high value of η_P may be associated not only with a high value of effective power P_E but also with a high shaft power P_S . Thus a model test of design A may predict for speed V an effective power P_E of 7,200 horses, a shaft power P_S of 9,000 horses, and an $\eta_P = P_E/P_S$ of 0.80. For the same speed V, a test of design B, to meet exactly the same performance specifications, may predict an effective power P_E of 8,100 horses, a shaft power P_S of 10,000 horses, but an η_P of 0.81. Thus, a ship built to design B, having a greater η_P , would actually require a heavier and more expensive propelling plant, and more fuel to drive it, than a ship built to design A, with a lower η_P . This is the reason for stressing the use of a merit factor—and an estimating or predicting factor as well—which takes account of shaft power directly.

60.12 Data from Self-Propulsion Tests of Model Ships and Propellers. For the designer who is laying out a vessel not unlike many which have been run self-propelled in model scale in the past, there are available in the technical literature a considerable number of graphs which give model test data in the form used for many years by the Experimental Model Basin and the David Taylor Model Basin [Bu C and R Bull. 7, 1933, Fig. 8, p. 31]. Several of these graphs are reproduced as Figs. 60.Q through 60.T, of which Fig. 60.Q gives data for a U. S. Maritime Commission *C-2* design, and Fig. 60.R for a Great Lakes bulk ore carrier, the *Philip R. Clarke*. Others are listed hereunder, with the type or name of ship, or both, and with enough source information to locate them in the literature.

In many cases, including the figures listed, the graphs are not accompanied by the necessary information to understand, to analyze, or to make use of them fully. This pertinent information should include a body plan and enough of the adjacent part of the ship to show the propeller position(s) with respect to the hull and appendages, a model propeller drawing, a set of characteristic open-water test curves of the propeller(s), and perhaps a wake-survey diagram as well for each propeller position. This is one of the reasons for the rather comprehensive and elaborate form adopted for the SNAME Propeller Data and Self-Propulsion Data sheets, samples of which are reproduced in Figs. 78.Ma through 78.Nc.

I. Single-Screw Vessels

(a) High-speed cruisers of the U. S. S. *Wampanoag* and *Ammonoosuc* classes of 1867. Self-propulsion data derived from tests of EMB model 2569, with EMB model propeller 685, were published by James Swan [SNAME, 1927, Pl. 36]. This plate gives the principal dimensions only. The text of the paper is on pp. 43–54.

(b) Cargo ship, U. S. Mar. Comm. *C1-S-D1* design, with a reinforced-concrete hull of straight-element form. 350 ft by 54 ft by 26.25-ft draft; displacement 10,590 tons. Body plan shown in Fig. 76.C. Represented by TMB model 3754M. Prediction data from self-propulsion test 2, in ballast condition, at a displacement of 6,200 tons and a trim of 6 ft by the stern, are given in Fig. 60.S.

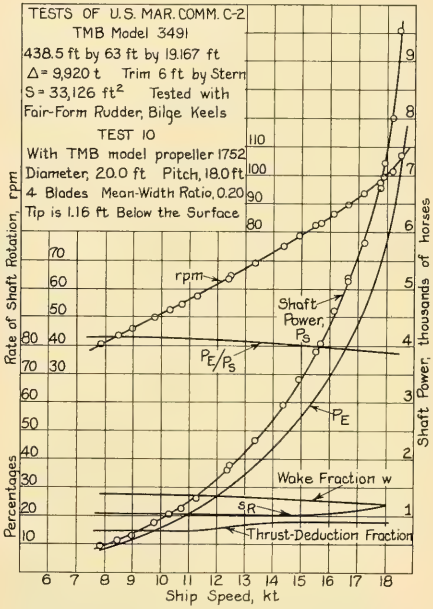

Fig. 60.Q Self-Propelled Model Test Curves for U. S. Maritime Commission *C-2* Design

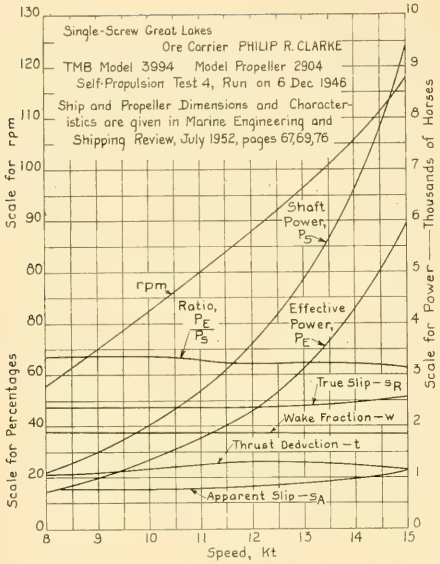

FIG. 60.R SELF-PROPELLED MODEL TEST CURVES FOR A GREAT LAKES ORE CARRIER

(c) Ten models of tanker hulls of somewhat varied shape but designed to meet the same basic specifications [Couch, R. B., and St. Denis, M., SNAME, 1948, pp. 360–379]

(d) U. S. Maritime Administration prototype ship *Schuyler Otis Bland*, curves of P_S , rpm, and η_P = ehp/shp only [Sullivan, E. K., and Scarborough, W. G., SNAME, 1952, Fig. 1, p. 472]. A more complete set of curves is given in SNAME, 1954, p. 155.

(e) TMB Series 60, embodying five parent forms of merchant vessels having block coefficients of 0.60, 0.65, 0.70, 0.75, and 0.80 [Hadler, J. B., Stuntz, G. R., Jr., and Pien, P. C., SNAME, 1954, pp. 121–178]

(f) *Mariner* class, speed and power curves from corrected trial data [SNAME, 1953, Fig. 6(a) on p. 111]; standardization trial data for two displacements, shaft power and rpm [SNAME, 1953, Fig. 31 on p. 148]

(g) Tanker *Pennsylvania* [SNAME, 1954, Fig. 21, pp. 156–157]

(h) Proposed coasters [SSPA Rep. 24, 1953, p. 43]. Designed speed 11 kt; to be achieved with either of two propellers, running at 175 and 360 rpm. Includes ship body plans and propeller drawings.

(i) Ten tug designs of a rather wide range of sizes and characteristics, from a 42-ft harbor tug to a 155-ft oceangoing tug [Roach, C. D., "Tugboat Design," SNAME, 1954, Figs. 6 through 15, pp. 600–618]. The hull lines are given but the propeller drawings are missing. The predictions from the self-propelled model data include all the derived curves for each design.

(j) German M. S. *San Francisco* [SNAME, 1936, Fig. 2 on p. 200; also SNAME, 1951, Fig. 10 on p. 140]

(k) Great Lakes bulk freighter *Wilfred Sykes*, in both full-load and ballast conditions [SNAME, Figs. 6 and 7, p. 75 and Figs. 8 and 9, p. 76].

II. Twin-Screw Vessels

(a) Armored cruisers, U. S. S. *Washington* class (old). Complete towing and self-propulsion data on three geosims published in SNAME, 1932, pp. 75–148, esp. pp. 93–96 and 99.

(b) Pacific liners *Mariposa* and *Monterey*. The published data include curves of model-test results for shaft power, effective power, propulsive coefficient, and rate of rotation, plus oil consumption per shaft horse per hour. Supplementing these curves are spots derived from the ship-trial data [SNAME, 1932, p. 349].

(c) New *Panama* class of passenger and cargo ships. The published data include results of towing and self-propelled model tests and open-water propeller curves. TMB model 3509 represents the ship and TMB models 1765 and 1766 the propellers. Full data are given, including the form coefficients [MESR, May 1939, pp. 210–211].

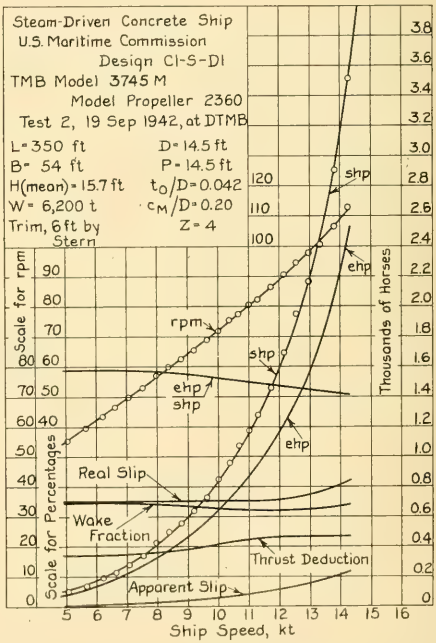

FIG. 60.S SELF-PROPELLED MODEL TEST CURVES FOR A STEAM-DRIVEN CONCRETE SHIP

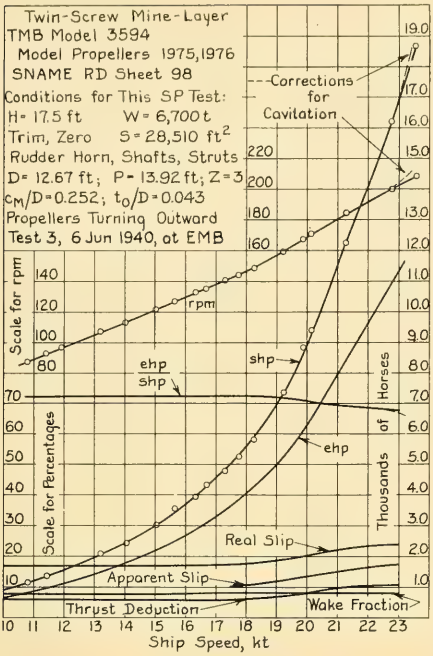

FIG. 60.T SELF-PROPELLED MODEL TEST CURVES FOR A TWIN-SCREW NAVAL VESSEL

(d) Minelayer U. S. S. *Terror* (CM5); EMB model 3594 and EMB model propellers 1975 and 1976. SNAME RD sheet 98. Fig. 60.T reproduces the self-propulsion data of Test 3, dated 6 Jun 1940.

(e) Medium-size Atlantic liner *America*; SNAME, 1940, pp. 9–49, esp. Fig. 2 on p. 11. The first portion of this paper was abstracted in SBMEB, Aug 1940, pp. 278–286; the self-propulsion data curves were published on p. 286. The tests were run on EMB model 3525 with EMB model propellers 1803 and 1804.

(f) Medium-size Atlantic liners *Constitution* and *Independence*. SNAME RD sheet 158; SNAME PD and SPD sheets not yet numbered (1955).

(g) Atlantic liner *Manhattan*, with normal V-type stern and bossings, as represented by EMB model 3041. A complete set of self-propulsion curves is given in Fig. 20 on p. 114 of SNAME, 1947. Table 3 on p. 113 gives complete general characteristics of this vessel.

(h) Twin-skeg *Manhattan* design, TMB model 3898. A complete set of self-propulsion curves is given in Fig. 21 on p. 114 of SNAME, 1947. Table 3 on p. 113 gives complete general characteristics for the hypothetical vessel represented by this model.

(i) Twin-screw tanker of extreme beam, Sun Shipbuilding and Dry Dock Company design, TMB model 3817, with normal form of stern. Self-propulsion curves are given by Fig. 15 on p. 110 of SNAME, 1947; general characteristics are in Table 1 on p. 109.

(j) Twin-skeg tanker of extreme beam, adapted from (i) preceding. TMB model 3821, for which complete self-propulsion curves are given in Fig. 16 on p. 110 of SNAME, 1947. The general characteristics of the prototype vessel are found in Table 1 on p. 109 of the reference.

(k) U. S. Maritime Administration 622-ft 23-kt design, TMB model 4424, ETT model 1448-1, for which complete self-propulsion data are given in SNAME, 1955, Fig. 4, p. 730. The body plan and characteristics of this vessel are given on pp. 728–729 of the reference.

III. Quadruple-Screw Vessels

(a) Large Atlantic liner S. S. *Normandie* (later U. S. S. *Lafayette*); SNAME RD sheet 39; also PD and SPD sheets, not yet numbered (1955).

The technique of predicting, from the test results on model ships and propellers, the shaft power, the rate of rotation of the propulsive device(s), and other factors in the full-scale ship performance has not yet (1955) been perfected so that scale effects are reliably eliminated. R. B. Couch has published a model-ship comparison, reproduced here in Table 60.c, in which the ratios of model prediction to ship performance are given for ten different ships [6th ICSTS, 1951, Table IV, pp. 146–147]. The comments which follow are adapted from those of Couch, as published on page 145 of the reference cited:

(1) The model-ship comparisons of Table 60.c are in general based on the identity of predicted and measured shaft power P_S . The model propulsion tests were run at the ship point of self-propulsion with all appendages fitted; in other words, the theoretical added friction on the model was compensated for by helping the model along. The ship-trial data were corrected to zero relative wind. Where thrustmeters were fitted the comparisons show close agreement on thrust in some instances. Uncorrected open-water propeller data were used throughout.

(2) A detailed analysis of the values tabulated is not available. It is hoped that such an analysis will shed further light on the scale-effect problem. However, certain trends may readily be noted:

(i) In all cases the rate of propeller rotation for the model is higher than for the ship

(ii) In nearly all cases the ship wake fractions are higher than those of the models

(iii) On the assumption of thrust-deduction

TABLE 60.c—PROPULSION FACTORS FOR SHIP AND MODEL FOR VARIOUS TYPES OF NAVAL AND COMMERCIAL VESSELS

Ship identification Type of vessel		Carrier A		Carrier A		Carrier B		Carrier C
Number of propellers		4		4		4		2
Paint coating		Zinc chromate		Hot plastic		Hot plastic		15 RC
Propeller location		Inbd	Outbd	Inbd	Outbd	Inbd	Outbd	
Wake fraction from (a) Thrust identity, w_T	Model	0.167	0.070	0.167	0.070	0.172	0.060	0.009
	Ship	0.197	0.062	0.228	0.113	0.295	0.102	0.059
(b) Torque identity, w_Q	Model	0.172	0.060	0.172	0.060	0.185	0.052	0.003
	Ship	0.220	0.064	0.245	0.117	0.333	0.125	0.050
Ratio of $(1 - w_{\text{Model}})/(1 - w_{\text{Ship}})$ (a) From thrust identity		1.037	0.992	1.079	1.048	1.175	1.046	1.053
(b) From torque identity		1.061	1.004	1.097	1.064	1.222	1.083	1.050
Ratio of n in rpm, for $\frac{\text{Model}}{\text{Ship}}$		1.020		1.038		1.032		1.030
Ratio of $\frac{C_T}{C_Q}$ for $\frac{\text{Model}}{\text{Ship}}$		0.994	1.015	1.013	1.013	0.946	1.035	0.977
Propeller efficiency behind ship, η_B	Model	0.677		0.703		0.690		0.640
	Ship	0.736		0.654		0.594		0.626
Relative rotative efficiency, η_R	Model	0.996		1.012		1.057		0.992
	Ship	1.088		0.975		0.932		0.956
Roughness allowance, ΔC_F		0.00055		0.00070		0.00095		0.00015
Model propeller	inches	7.00	7.467	7.00	7.467	7.316	7.30	5.565
diameter	feet	0.583	0.622	0.583	0.622	0.610	0.608	0.464

identity it follows that the ship hull efficiencies are also higher than the model values

(iv) The resistances used were those of the model when fitted with all appendages but without appendage scale-effect correction

(v) The roughness allowance figures given were obtained from the model-ship comparison, using the 1947 ATTC friction coefficients on the model and ship

(vi) On the average, the overall propulsive efficiency for the ship appears to be less than for the model.

(3) With the exception of the commercial vessels and Carrier C the ship-roughness values are in general relatively high; in these cases the wake fractions are also rather high for the ship. Closer agreement would be expected for new, clean, merchant vessels. Had thrustmeters been fitted to the merchant vessels and the wake fractions been computed for thrust identity, some differences would undoubtedly have been found but the general trends would have been about the same.

60.13 Merit Factors for Predicting Shaft Power. For making quick predictions of shaft power from a background of reference data, and for comparisons of ship performance, the Telfer merit factor described in Sec. 34.10 of Volume I is available in two forms, both producing the same 0-diml numerical values for a given set of basic data. These are, as listed under Eq. (34.xxiv),

$$M = \frac{\rho \forall V^3}{LP_S} \quad \text{and} \quad \frac{WV^3}{gLP_S}$$

Sec. 34.10 discusses a possible relationship between the Telfer merit factor M and the fatness ratio $\forall/(0.10L)^3$, which when plotted for mer-

TABLE 60.c—(Continued)

Ship identification Type of vessel		Cruiser D		Cruiser D		Cruiser E		Cruiser E	
Number of propellers		4		4		4		4	
Paint coating		Hot plastic		Zinc chromate		Hot plastic		Zinc chromate	
Propeller location		Inbd	Outbd	Inbd	Outbd	Inbd	Outbd	Inbd	Outbd
Wake fraction from	Model	0.038	0.010	0.048	0.010	0.053	0.020	0.046	0.006
(a) Thrust identity, w_T	Ship	0.088	0.069	0.077	0.069	0.078	0.075	0.089	0.048
(b) Torque identity, w_Q	Model	0.041	0.014	0.050	0.006	0.035	0.011	0.032	−0.006
	Ship	0.116	0.105	0.103	0.101	0.089	0.093	0.079	0.048
Ratio of $(1 - w_{\text{Model}})/(1 - w_{\text{Ship}})$									
(a) From thrust identity		1.055	1.063	1.032	1.064	1.027	1.059	1.047	1.045
(b) From torque identity		1.085	1.102	1.060	1.105	1.060	1.090	1.051	1.055
Ratio of n in rpm, for $\frac{\text{Model}}{\text{Ship}}$		1.045		1.031		1.027		1.022	
Ratio of $\frac{C_T}{C_Q}$ for $\frac{\text{Model}}{\text{Ship}}$		1.060	1.065	1.084	1.068	1.058	1.058	0.963	0.981
Propeller efficiency	Model	0.691		0.687		0.688		0.702	
behind ship, η_B	Ship	0.615		0.625		0.629		0.691	
Relative rotative	Model	0.955		1.000		1.008		1.038	
efficiency, η_R	Ship	0.915		0.915		0.938		1.020	
Roughness allowance, ΔC_F		0.00075		0.00040		0.00075		0.00015	
Model propeller	inches	6.867		6.867		6.514		6.514	
diameter	feet	0.572		0.572		0.543		0.543	

chant vessels of normal form is represented by a nearly straight meanline. It is almost certain that, for the general case, including vessels of large fatness ratio, there is no such simple relationship between these quantities. The plot would then reduce to a series of merit-factor groups for a number of ship types, each of which would lie within a relatively narrow range of fatness ratio. One such group would cover tankers, for example; another group tugs, and so on.

Regardless of the exact nature of the plot, a really useful diagram would give by inspection an average value of the merit factor M for a given type of ship or a certain minimum value which should be bettered in any new design.

When the quantities in Eq. (34.xxiv) are in the units generally employed by English-speaking marine architects the weight displacement W is in long tons of 2,240 lb, the ship speed is in kt, and the shaft power P_S is in English horses. Inserting the necessary factors in Eq. (34.xxiv) to suit the pound-foot-second system, it takes the dimensional form

$$M = \left[\frac{2{,}240(1.6889)^3}{550(32.174)}\right] \cdot \left[\frac{(W \text{ in tons})(V \text{ in kt})^3}{(L \text{ in ft})(P_S \text{ in horses})}\right] \qquad (34.\text{xxv})$$

$$= 0.61\,\frac{WV^3}{LP_S}$$

If the displacement weight is in kips of 1,000 lb, to avoid confusion as to the kind of tons employed, then

$$M = \left[\frac{1{,}000(1.6889)^3}{550(32.174)}\right]\left[\frac{(W \text{ in kips})(V \text{ in kt})^3}{(L \text{ in ft})(P_S \text{ in horses})}\right]$$

$$= 0.2723\,\frac{WV^3}{LP_S}$$

TABLE 60.c—(Continued)

Ship identification Type of vessel		4 Destroyers F-I	Destroyer J	Destroyer J	Liner K	Tanker L	Tanker M
Number of propellers		2	2	2	2	1	1
Paint coating		Zinc chromate	Vinyl resin	Vinyl resin (10 months out of dock)	Commercial	Commercial	Commercial
Propeller location							
Wake fraction from (a) Thrust identity, w_T	Model	−0.011	−0.005	−0.005	0.149	0.394	0.362
	Ship	0.019	0.025	0.036	—	—	—
(b) Torque identity, w_Q	Model	−0.011	−0.015	−0.015	0.156	0.390	0.348
	Ship	0.012	0.045	0.060	0.178	0.394	0.358
Ratio of $(1 - w_{\text{Model}})/(1 - w_{\text{Ship}})$ (a) From thrust identity		1.032	1.026	1.043	—	—	—
(b) From torque identity		1.024	1.063	1.080	1.025	1.006	1.016
Ratio of n in rpm, for $\frac{\text{Model}}{\text{Ship}}$		1.012	1.032	1.032	1.010	1.033	1.012
Ratio of $\frac{C_T}{C_Q}$ for $\frac{\text{Model}}{\text{Ship}}$		0.918	1.013	0.986	—	—	—
Propeller efficiency behind ship, η_B	Model	0.657	0.668	0.668	0.669	0.571	0.619
	Ship	0.661	0.620	0.627	—	—	—
Relative rotative efficiency, η_R	Model	0.969	0.988	0.988	0.952	1.028	1.024
	Ship	0.973	0.928	0.942	—	—	—
Roughness allowance, ΔC_F		0.00045	0.00050	0.00065	0.00040	0.00020	0.00030
Model propeller diameter	inches	7.805	7.805	7.805	7.20	10.00	9.517
	feet	0.650	0.650	0.650	0.600	0.833	0.793

Should the basic data be given in metric units, Eq. (34.xxv) is replaced by

$$M = \left[\frac{1{,}000(0.5148)^3}{75(9.806)}\right] \cdot \left[\frac{(W \text{ in metric tons})(V \text{ in kt})^3}{(L \text{ in meters})(P_S \text{ in metric horses})}\right]$$

whence $M = 0.1855$ times the second term.

It is emphasized that variations of the merit factor equations such as those listed produce exactly the same numerical values for consistent units in any system of measurement.

At an early stage in a preliminary design the displacement weight W and the speed V are generally known within rather close limits. There is either a limiting length L or a range of probable lengths from which the speed-length quotient T_q or the Froude number F_n is derived. Taking a selected or average merit factor M from Fig. 34.I for the value of F_n^2 at the designed speed, the estimated shaft power P_S is rapidly calculated from the equation

$$P_S = \left[\frac{0.61}{M}\right]\left[\frac{(W \text{ in tons})(V \text{ in kt})^3}{L \text{ in ft}}\right] \qquad (60.\text{ix})$$

This is done for the preliminary design of the ABC ship in Sec. 66.9, using a Telfer merit factor M of 9.5 and an F_n^2 of 0.0727. From the model tests made subsequently on the transom-stern ABC design, using the data reported in Sec. 78.16 for a ship speed corresponding to 20.5 kt, the Telfer merit factor M works out as

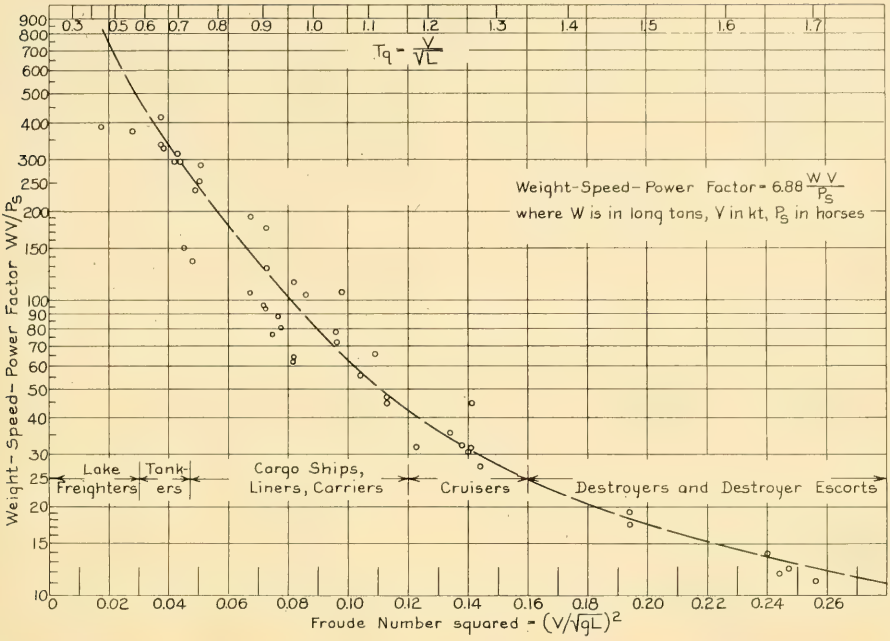

FIG. 60.U TENTATIVE MEANLINE FOR SELECTING THE WEIGHT-SPEED-POWER FACTOR FOR AN AVERAGE VESSEL

$$M = 0.61\,\frac{WV^3}{LP_S} = \frac{(16{,}573)(20.5)^3}{(510)(13{,}243)} = 12.895$$

This is nearly 36 per cent greater than the meanline value given by Fig. 34.I, indicating that the merit-factor method of estimation still requires considerable development.

An alternative merit factor makes use of a somewhat simpler 0-diml relationship in the form of

$$\text{Weight-Speed-Power Factor} = \frac{WV}{P_S} \qquad (60.x)$$

This is, in fact, the Telfer merit factor M divided by the Froude number squared, indicated as one of the terms in Eq. (34.xxiv) on page 517 of Volume I. When WV/P_S is plotted on a basis of F_n^2, as in Fig. 60.U, it indicates a dispersion for vessels of supposedly normal design as great as that evidenced in Fig. 34.I for the Telfer merit factor. Indeed, with a plot having a uniform instead of a log scale of ordinates, the dispersion in both would be much greater. It is apparently true that the propulsive merit of some vessels is vastly superior to that of others.

Using the tentative meanline of Fig. 60.U as an indicator for estimating the probable shaft power of an ABC ship design of average merit, the estimated power is worked out in Sec. 66.9.

60.14 Shaft-Power Estimates by the Ideal-Efficiency Method. A method of deriving the propulsive coefficient η_P from the ideal and real efficiencies of a screw propeller under a given thrust-load condition is described fully in Sec. 34.11 of Part 2, Volume I. An amplified version of that description is given here for the convenience of the reader. From the effective power and the propulsive coefficient the shaft power is found. This method also enables the designer to select a suitable P/D ratio for the propeller, and to approximate its rate of rotation n.

Assuming that this procedure is to be used in the early stages of a ship design, it is necessary to estimate or determine the total ship resistance R_T, and to select values of the wake and thrust-deduction fractions w and t, and of the relative rotative efficiency η_R, which appear reasonable for the design in question. The ship speed V is assumed to be known, as are the number of

propellers. If the propeller diameter D is not tentatively fixed, several solutions may be worked out, each for a different diameter.

The necessary formulas for this calculation are taken from Sec. 34.11:

$$V_A = V(1 - w) \qquad T = \frac{R_T}{1 - t}$$

$$P_E = R_T V = R_T\left(\frac{V_A}{1 - w}\right)$$

$$\eta_H = \frac{1 - t}{1 - w}$$

$$C_{TL} = \frac{2.546 P_E}{\rho D^2 V_A^3 \eta_H} \text{ in 0-diml form} \qquad (34.\text{xxvii})$$

$$C_{TL} = 290.68 \frac{P_E(\text{horses})}{\rho[D^2(\text{ft})][V_A^3(\text{kt})]\eta_H} \qquad (34.\text{xxviii})$$

in dimensional form.

When several propellers are to be used, D^2 is replaced by $\Sigma D^2 = D_1^2 + D_2^2 + D_3^2 + D_4^2$, as appropriate. The effective power P_E is always the total ship figure.

With the calculated 0-diml value of C_{TL}, the curves of Figs. 34.B, 34.C, or 34.E are entered and a value is found for the 0.8-ideal efficiency. This is taken to be the actual operating efficiency of the propeller, as yet not designed, and is equal to the open-water efficiency η_0 of some propeller at some advance ratio $J = V_A/(nD)$.

The position of the C_{TL} point along the 0.8-ideal-efficiency curve of Fig. 34.G indicates, by reference to the efficiency curves of the three Wageningen propellers, an approximate value of the pitch ratio P/D which may be expected to produce the most efficient propeller under the circumstances. Consulting the open-water characteristic curves of some "stock" propeller which has this pitch-diameter ratio, and entering the open-water efficiency curves with the η_0 value from the 0.8-ideal-efficiency curve, give at once the advance ratio $J = V_A/(nD)$. With the values of V_A and D previously used, the rate of rotation n is found. A nomogram for solving Eq. (34.xxviii) is embodied in ETT, Stevens, Technical Note 145; this facilitates working out a number of solutions for a different combination of assumptions.

A portion of this problem is worked out for an early design of the ABC ship in Sec. 66.27, sufficient only to derive a value of P_S. A somewhat more complete example is worked out here, using the basic values from the self-propulsion test of the ABC transom-stern model, to determine the agreement (or otherwise) with the self-propelled model predictions for the 20.5-kt trial speed. The basic conditions assumed are:

R_T = 160,120 lb, from Fig. 78.Nb
D = 20.51 ft, for stock propeller actually used, from Fig. 78.Ma
V = 20.5 kt ≈ 34.62 ft per sec
w_T = 0.190, from Fig. 78.Nb
t = 0.070, from Fig. 78.Nb; η_{HT} = 1.148
$V_A = V(1 - w)$ = 34.62(1 − 0.190) = 28.042 ft per sec
$T = R_T/(1 - t)$ = 160,120/(1 − 0.070) = 172,170 lb
$P_E = R_T V$ = 160,120(34.62) = 5,543,350 ft-lb per sec.

Then, from Eq. (34.xxvii),

$$C_{TL} = \frac{2.546 P_E}{\rho D^2 V_A^3 \eta_H}$$

$$= \frac{2.546(5{,}543{,}350)}{(1.9905)(20.51)^2(28.042)^3(1.148)}$$

$$= 0.666$$

It may be simpler and quicker for the user to calculate the thrust-load factor by

$$C_{TL} = \frac{T}{\frac{\rho}{2} A_0 V_A^2}$$

$$= \frac{172{,}170}{(0.99525)(20.51)^2(0.7854)(28.042)^2}$$

$$= 0.666$$

This is somewhat smaller than the 0.700 of diagram 3 of Fig. 59.I because the latter is calculated for a final-design wheel diameter of 20.0 ft.

From Table 34.a, or Fig. 34.B, the corresponding ideal efficiency η_I is 0.873 and the 0.8-ideal efficiency or real efficiency η_{Real} is 0.698. This is the working efficiency of the propeller at 20.5 kt. Consulting the open-water curves for the stock propeller in Fig. 78.Mc the advance coefficient J for η_0 = 0.698 is 0.769. Then $J = V_A/(nD)$, whence

$$n = \frac{V_A}{JD} = \frac{28.042}{(0.769)(20.51)}$$

$$= 1.778 \text{ rps or } 106.7 \text{ rpm.}$$

This compares with the value of 109.7 (or 1.826 rps) derived from the self-propelled model test; it indicates that the real or working efficiency of the propeller was somewhat less than 0.8 of its ideal efficiency.

Taking a J_T-value of 0.748, as determined by thrust identity from Fig. 78.Nb, the real efficiency η_{Real} or the open-water efficiency η_0 from Fig. 78.Mc is only 0.686. Assuming a value 1.02 for the relative rotative efficiency,

$$\eta_P = \eta_0(\eta_H)\eta_R = 0.686(1.148)(1.02) = 0.803$$

Since this is in excess of the $\eta_P = 0.761$ derived from Fig. 78.Nc, it indicates that the assumed relative rotative efficiency is too large. The last example of Sec. 60.10 shows that actually η_R was only 0.968. Using an η_P-value of 0.803 would have given a shaft power of

$$P_S = \frac{P_E}{\eta_P} = \frac{5{,}543{,}350}{(550)(0.803)} = 12{,}551 \text{ horses.}$$

This is less than the predicted shaft power of 13,243 horses from Fig. 78.Nb. It emphasizes the statement of D. W. Taylor, made several decades ago, that:

"It is better to underestimate relative rotative efficiency than to overestimate it. Underestimation results in a slightly larger propeller than overestimation" [SNAME, 1923, pp. 69–70].

60.15 Estimating Shaft Power for a Fouled- or Rough-Hull Condition. A recommended design procedure for building into a ship a sufficient speed margin to enable it to maintain an established schedule despite the handicaps of winds, waves, fouling, and other factors is described in Secs. 64.3, 65.3, and 69.9, and in Table 64.d, all in Part 4 of this volume. It should be possible eventually to predict the effect of each of these handicaps in quantitative terms, provided the conditions to be met are specified in some detail.

Considering the problem of fouling, or of serious deterioration of the paint coating on the underwater hull, the situation is presumably worst just before the end of a drydocking interval. As a check on the speed and power margins incorporated in the design, which are intended to be adequate all through this interval, it should be possible to estimate the propulsion performance in the foul-bottom as well as the clean-bottom condition.

One acceptable method is worked out here for the transom-stern hull of the ABC ship, designed in Part 4. The ship is assumed to be painted with a self-leveling (commercial) type of anti-fouling paint, to be 10 months out of dock, and to have an increase in specific resistance due to fouling of $\Delta_F C_F(10^3) = 1.25$, corresponding to the long-dash predicted ABC ship curve of Fig. 45.L. It is assumed that for half of the open-sea portion of a voyage under these circumstances, heavy weather has slowed the ship to an average of 17.7 kt. For the remaining half, therefore, in order to meet the sustained speed of 18.7 kt, the ship is called upon to average 19.7 kt. Can the ship do it, when fouled, with 95 per cent of its maximum designed power?

From Table 45.f of Sec. 45.18:

$\Delta_P C_F$ for the plating is taken as 0.0 since any roughness here is obscured by the deterioration of the anti-fouling paint coating and the presence of the fouling itself

$\Delta_S C_F$ for structural roughness is assumed as $0.1(10^{-3})$

$\Delta_C C_F$ for coating roughness is assumed as $0.1(10^{-3})$, covering deterioration of the paint

$\Delta_F C_F$ for fouling, from the long-dash line of Fig. 45.L, is taken as $1.25(10^{-3})$

Then $\Sigma\Delta C_F$ is $(0.0 + 0.1 + 0.1 + 1.25)(10^{-3}) = 1.45(10^{-3})$.

For the "make-up time" speed of 19.7 kt or 33.27 ft per sec, $T_q = 19.7/\sqrt{510} = 0.872$, $F_n = 0.26$. At this T_q, the specific residuary resistance coefficient C_R is, from Fig. 78.Jc, $0.94(10^{-3})$. The Reynolds number R_n for this ship speed, in standard salt water, from Table 45.b of Sec. 45.4, is 1,324 million, for which the specific friction resistance coefficient C_F from Table 45.d is $1.48(10^{-3})$. Then $C_T + C_F + \Sigma\Delta C_F = (0.94 + 1.48 + 1.45)(10^{-3}) = 3.87(10^{-3})$.

The wetted surface of the ship is, from Fig. 78.Ja, 69.85 times λ^2(lambda) for the ship or $(69.85)(650.25) = 45{,}420$ ft^2. Then for the fouled ship,

$$\begin{aligned} R_T &= C_T\left(\frac{\rho}{2}\right)SV^2 \\ &= (3.87)(10^{-3})\left(\frac{1.9905}{2}\right)(45{,}420)(33.27)^2 \\ &= 193{,}640 \text{ lb,} \end{aligned}$$

whence

$$P_E = R_T V = \frac{(193{,}640)(33.27)}{550} = 11{,}713 \text{ horses.}$$

For the fouled ship, at 19.7 kt, it is estimated

that the wake fraction w has increased from the 0.190 of Fig. 78.Nb to 0.210. The thickening of the boundary layer, and the increase of viscous-wake velocity due to fouling are assumed to have a greater effect on increasing w than the augmented C_{TL} has on reducing it, as described by L. Troost in Sec. 60.8. It is assumed further that the thrust-deduction fraction t has increased from 0.070 to 0.115, because of the greater thrust-load coefficient C_{TL} at which the propeller must operate. At this increased C_{TL} the inflow jet will have a somewhat larger diameter in way of the skeg, so that the $-\Delta p$'s will act on more of the stern area; this is another reason for increasing t.

For the clean ship, at 19.7 kt, η_H from Fig. 78.Nb is 1.148 but for the fouled ship it is

$$(\eta_H)_{\text{Foul}} = \frac{(1 - t)_{\text{Foul}}}{(1 - w)_{\text{Foul}}} = \frac{(1 - 0.115)}{(1 - 0.210)} = 1.120$$

The speed of advance V_A for 19.7 kt, fouled, is $V[(1 - w)_{\text{Foul}}] = 33.27(0.79) = 26.28$ ft per sec.

By interpolation from the values of $10^{-3}\ T$ from Fig. 78.Nb, the thrust T at 19.7 kt, for the clean ship, is 152,600 lb. Then for a ship carrying a propeller of 20.51-ft diameter, corresponding to the stock model propeller, $V_A = V(1 - w) = 33.27(1 - 0.190) = 26.95$ ft per sec, and

$$C_{TL} = \frac{T}{\frac{\rho}{2} A_0 V_A^2}$$

$$= \frac{152{,}600}{(0.99525)(20.51)^2(0.7854)(26.95)^2} = 0.639$$

For the fouled ship at 19.7 kt, $T = R_T/(1 - t) = 193{,}640/(1 - 0.115) = 218{,}800$ lb. Then

$$(C_{TL})_{\text{Foul}} = \frac{T_{\text{Foul}}}{\frac{\rho}{2} A_0[(V_A)_{\text{Foul}}]^2}$$

$$= \frac{218{,}800}{(0.99525)(20.51)^2(0.7854)(26.28)^2}$$

$$= 0.963$$

From a larger-scale version of Fig. 34.G or from Fig. 70.B, for a P/D ratio of 1.0, the value of the real efficiency η_{Real} for a C_{TL} of 0.639 is 0.717. For a C_{TL} of 0.963 on the fouled ship, and a P/D ratio of 1.00, the value of the real efficiency η_{Real} is 0.677. It is not possible to pick the latter value from the open-water characteristic curve of η_0 because the J-value and the rate of rotation n in the fouled condition are not known.

If the relative rotative efficiency η_R is assumed the same when the bottom is both clean and foul,

$$\frac{(\eta_P)_{\text{Foul}}}{\eta_P} = \frac{(\eta_0)_{\text{Foul}}(\eta_H)_{\text{Foul}}}{\eta_0 \eta_H}$$

$$= \frac{(0.677)(1.120)}{(0.717)(1.148)} = 0.921$$

R. W. L. Gawn states, on page 247 of his paper "Roughened Hull Surface" [NECI, 1941–1942, Vol. LVIII, pp. 245–272], that "Relative rotative efficiency is less when the surface is rough, . . . ," but he gives no numerical values.

Interpolating from the η_P = EHP/SHP values in Fig. 78.Nb, the value of η_P for the clean ship at 19.7 kt is 0.769. For the fouled ship at the same speed it is estimated to be 0.769(0.921) = 0.708. Hence

$$P_S = \frac{P_E}{\eta_P} = \frac{11{,}713}{0.708} = 16{,}540 \text{ horses.}$$

This is about 3,290 horses more, or about 25 per cent in excess of the 13,250 horses required to propel the clean ship at 20.5 kt, as predicted by the self-propelled model test. It is not much less than the whole clean-bottom power margin required to provide the speed differential from 18.7 kt (predicted P_S of 9,320 horses) to 20.5 kt (predicted P_S of about 13,250 horses), namely 3,930 horses. It corresponds to an average increase in shaft power P_S of only about 2.5 per cent per month, or about 0.08 per cent per day, yet when considered as an additional power expenditure it seems large.

For the designer who is to recommend a definite amount of shaft-power reserve to the owner, the situation definitely calls for an investigation of the use of hot plastic anti-fouling paint instead of the older type of self-leveling paint. From Table 45.f of Sec. 45.18:

$\Delta_P C_F$ for the plating is taking as 0.0, since any plating roughness is obscured by the hot-plastic paint coating and the fouling

$\Delta_S C_F$ for structural roughness is assumed to be $0.1(10^{-3})$, as before

$\Delta_C C_F$ to cover the initial roughness of the hot-plastic paint is taken as $0.5(10^{-3})$, from the left margin of Fig. 45.L

$\Delta_F C_F$ for fouling only, from the dot-dash line of Fig. 45.L, is $0.11(10^{-3})$.

Then $\Sigma\Delta C_F$ is $(0.0 + 0.1 + 0.5 + 0.11)(10^{-3}) = 0.71(10^{-3})$.

The values of C_R and C_F for the clean ship at 19.7 kt are $0.94(10^{-3})$ and $1.48(10^{-3})$, respectively,

as before. Then for the fouled ship $C_T = C_R + C_F + \Sigma\Delta C_F = (0.94 + 1.48 + 0.71)(10^{-3}) = 3.13(10^{-3})$. With a wetted surface of 45,420 ft^2, from the preceding example, the total resistance of the fouled ship is

$$R_T = C_T\left(\frac{\rho}{2}\right)SV^2$$

$$= 3.13(10^{-3})\left(\frac{1.9905}{2}\right)(45{,}420)(33.27)^2$$

$$= 156{,}610 \text{ lb},$$

whence

$$P_E = R_T V = \frac{(156{,}610)(33.27)}{550} = 9{,}474 \text{ horses.}$$

Since the ship with the hot-plastic coating is expected not to be as heavily fouled as with the self-leveling paint in the preceding example, it is estimated that the wake-fraction w is increased only from 0.190 to 0.200, and that the thrust-deduction fraction has gone up from 0.070 to only 0.100. For the clean ship, at 19.7 kt, η_H is 1.148 as before but for the fouled ship it is

$$(\eta_H)_{\text{Foul}} = \frac{(1 - t)_{\text{Foul}}}{(1 - w)_{\text{Foul}}} = \frac{(1 - 0.100)}{(1 - 0.200)} = 1.125$$

The speed of advance V_A for 19.7 kt, with the lighter fouling on the hot-plastic paint, is $V[(1 - w)_{\text{Foul}}] = 33.27(0.80) = 26.62$ ft per sec. For the fouled ship at 19.7 kt, $T = R_T/(1 - t) = 156{,}610/(1 - 0.10) = 174{,}010$ lb. Then

$$(C_{TL})_{\text{Foul}} = \frac{T_{\text{Foul}}}{\frac{\rho}{2} A_0[(V_A)_{\text{Foul}}]^2}$$

$$= \frac{174{,}010}{(0.99525)(20.51)^2(0.7854)(26.62)^2}$$

$$= 0.747$$

The thrust-load factor C_{TL} for the clean-bottom condition is 0.639, the same as for the preceding example. Similarly, η_{Real} for this factor is 0.717. For a C_{TL} of 0.747 on the fouled ship and a P/D ratio of 1.00, the value of η_{Real} is, from Fig. 34.G or Fig. 70.B, 0.703. Assuming as before that the relative rotative efficiency η_R is the same for both clean and foul bottom,

$$\frac{(\eta_P)_{\text{Foul}}}{\eta_P} = \frac{(\eta_0)_{\text{Foul}}(\eta_H)_{\text{Foul}}}{\eta_0\eta_H}$$

$$= \frac{(0.703)(1.125)}{(0.717)(1.148)} = 0.961$$

Interpolating from the η_P = EHP/SHP values in Fig. 78.Nb, the value of η_P for the clean ship at 19.7 kt is 0.769 as before. For the fouled ship at the same speed it is taken to be 0.769(0.961) = 0.739. Hence for the fouled ship with hot-plastic paint, at 19.7 kt,

$$P_S = \frac{P_E}{\eta_P} = \frac{9{,}474}{0.739} = 12{,}820 \text{ horses.}$$

This is less than the 13,250 horses required to drive the clean ship at 20.5 kt.

With a shaft power P_S of about 11,200 horses to drive the clean ship at 19.7 kt, from Fig. 78.Nb, an increase of 16,540 − 11,200 = 5,320 horses is required to overcome 10 months' fouling on the self-leveling paint, whereas an increase of only 12,820 − 11,200 = 1,620 horses suffices to overcome both the initial roughness of the hot-plastic paint and 10 months' fouling on that paint. Against this advantage must be placed the additional shaft power that would be required to drive the ship with hot-plastic paint, at all speeds, when just out of dock and for a few months thereafter. This and other powers can be calculated by the method described.

60.16 Increasing the Power and Speed of an Existing Ship. Marine architects are often called upon to increase the speed of a ship already built, either by improving its form and retaining its power plant, by changing its power plant and not its form, or by both.

In the matter of the power which can be delivered to and absorbed by a single screw propeller or other propulsion device, embodying a question which invariably arises whenever the matter of increased power is considered, it is to be remembered that shaft power is a function of both torque delivered to the propeller and the rate of rotation of the shaft. A given shaft can often be run at a higher rate of rotation at the same torque but only rarely can the same screw propeller be expected to absorb the increased power and to drive the ship efficiently at the increased rpm and ship speed.

It is conceivable that lengthening, fining, or otherwise altering an existing ship, designed for slow speed, may enable the altered ship to be driven at an increased speed with the same total resistance R_T or *effective* thrust $T(1 - t)$. The increased friction drag may be more than compensated for by the reduced pressure drag due to wavemaking and separation. However, the fact that the ship speed is increased, automatically raises the power by a corresponding amount,

even though no additional thrust is necessary to propel the ship at the increased speed.

Skeg and stern endings that are too blunt, ahead of a screw propeller, and insufficient clearances, may always be expected to generate vibratory forces and moments. At low speeds these may be of small magnitude and hence not objectionable. At higher speeds, however, a propeller developing increased thrust and absorbing greater power may generate vibratory forces and moments that are by no means acceptable. Air leakage from the surface may be initiated or augmented because of the greater $-\Delta p$'s in the blade fields. Cavitation may become a factor, at least in the region of the upper blades, because of the greater blade-section speeds, possible greater propeller diameter, and diminished depth of submergence of the blade sections in the upper blade positions. Fitting a propeller with wider blades, in an old aperture, actually diminishes the clearances, when they should be increased.

60.17 Powering for Two or More Distinct Operating Conditions. Exerting the maximum thrust at low towing speeds, combined with developing the greatest practicable free-running speed for shifting quickly from one operating area to the next, is mandatory for any tug worthy of the name. Economical propulsion at cruising speed, combined with efficient propulsion at high or top speed, is a design problem for any patrol vessel. Both economical and efficient propulsion, on the surface as well as submerged, is practically a "must" for every type of submersible, as well as some types of pure submarine.

Each of the foregoing is perhaps more of a design than a calculation problem, or perhaps more a problem of operation than of design. The operator and owner usually must decide how much one condition is to be favored over the other.

Sec. 67.15 mentions the proposals and actual installations of the past in which designers have attempted to meet the problem of driving a ship with one or two propellers under one operating condition and with two or more under another condition. This still involves running one set of wheels in both ranges, usually at different ship speeds and rates of rotation. It may be done by varying the pitch mechanically or accepting a reduction of efficiency in one or both conditions.

Permitting one or more propulsion devices to free-wheel while the others are driving means some added resistance due to the windmilling action of the free wheels. Furthermore, each shaft of a windmilling propeller, plus all those parts of the machinery which can not be unclutched from it, have to be lubricated continually during such an operation.

60.18 Backing Power from Self-Propelled Model Tests. A discussion of reversing and backing is included under maneuvering in Part 5 of Volume III. However, it is stated here that model-basin establishments equipped to conduct self-propulsion tests can carry out steady-state tests of this kind in the astern direction. Fig. 60.V embodies the results of such a test on EMB model 3594, representing the minelayer U. S. S. *Terror*. Fig. 60.T contains data for the ahead self-propulsion tests of this model at the same displacement and trim. It is to be noted that the thrust-deduction fraction in the backing condition is very large, as might be expected, and that the wake fraction is still positive. The propulsive coefficient is less than 0.40.

H. F. Nordström presents the test results and an analysis of the self-propelled experiments on models of fishing boats, in which astern thrust was achieved (1) by reversing the direction of rotation of the 2-bladed propellers when set for normal ahead running and (2) by angling the blades to give reverse pitch [SSPA Rep. 2, 1943; summary and some figure legends in English].

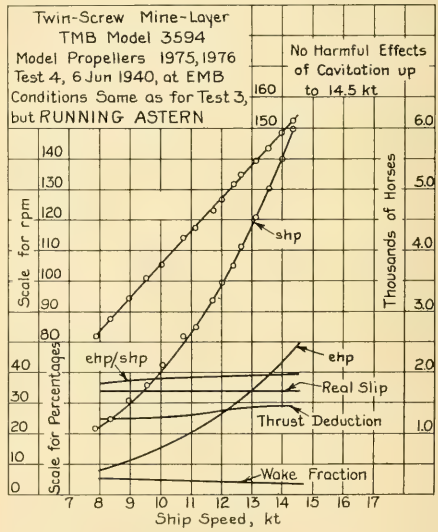

Fig. 60.V Backing-Test Data for a Twin-Screw Naval Vessel, from a Self-Propelled Model

CHAPTER 61

The Prediction of Ship Behavior in Confined Waters

61.1 General. The elements of the flow around a body or ship moving in shallow and restricted waters are described in Chap. 18. Aspects of the behavior of actual ships under these conditions are covered in Chap. 35. Some data on shallow-water waves are furnished in Secs. 48.15 and 48.16. Quantitative information on sinkage and change of trim in confined waters is given in Sec. 58.4.

The discussion in the present chapter is centered on the behavior, in shallow and restricted waters, of vessels intended primarily for operation in deep water. That in Chap. 72 is centered on the design of vessels intended to give the best possible performance in confined waters; their performance in deep water is usually a secondary consideration.

For hydrodynamic analysis and practical purposes *shallow water* is defined as an area of unlimited extent in a horizontal plane, of a depth that is generally uniform and equal to or less than that in which the *resistance* for a given speed is 1 per cent greater than in a deep-water area of the same unlimited extent.

Restricted water, applying generally to a horizontal plane, is defined as water of a reasonably uniform depth, deep or shallow, in which the lateral boundaries are sufficiently close to a vessel to increase its resistance for a given speed by 1 per cent or more. In this case, the percentage increase is considered to be due solely to the lateral restriction.

In the limiting case of water that is both shallow and restricted, known by the short term *confined water*, the combination of depth and width is such as to increase the open-sea deep-water resistance by 2 per cent or more. For this case, the limiting depth of shallow water for any ship is found from the diagram of Fig. 61.J. One way of determining the limiting width of restricted water is by calculating the least width for which the hydraulic radius R_H is diminished to an arbitrary ratio of 0.99 times the shallow-water depth, on the basis that for unlimited water the hydraulic radius R_H equals the depth h. This may, however, be much too severe a limitation for practical use. This requirement is, for example, practically never met in a model testing basin.

61.2 Typical Shallow-Water Resistance Data.

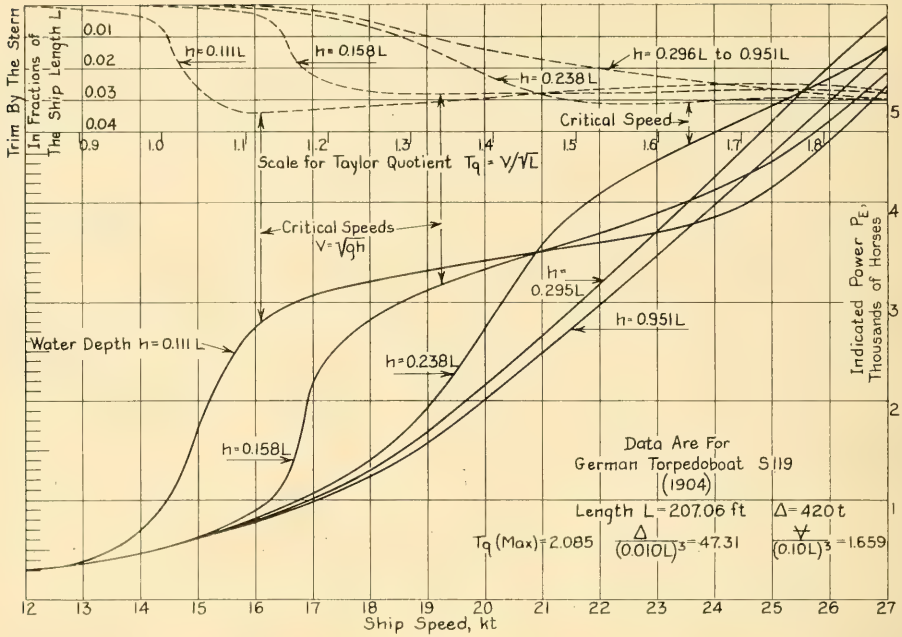

FIG. 61.A RESISTANCE AND TRIM DATA FOR A TORPEDOBOAT IN WATER OF VARIED DEPTH

There are, in the literature, a considerable number of typical graphs giving the variation of resistance and power with speed for ships running in shallow water. They are derived in part from tests on models and in part from ship trials. One set of curves, derived from a model test and illustrating the principal features, including the change of level at bow and stern, is reproduced in Fig. 35.D. Another set, derived from the trial results of a ship, is adapted from a set of graphs given by the German naval constructor Paulus in Fig. 2 on page 1872 of reference (4) in Sec. 61.22. The latter data are presented in Fig. 61.A. Others are to be found in the references cited in the list at the end of this section.

Paulus' data for the German torpedoboat *S119* reveal that the maximum trim by the stern occurs at a speed slightly less than that for which the increase in indicated power P_I (over the deep-water P_I) is a maximum. Also that the trim becomes less than the deep-water trim at a speed very slightly higher than that for which the shallow-water P_I drops below the deep-water P_I. The trims at the higher speeds, in all depths of water, are only slightly less than the maximum trims by the stern at the lesser (critical or near-critical) speeds. Unfortunately, Paulus does not give the lines or even the principal dimensions of torpedoboat *S119* forming the subject of his investigation.

Most of the model-test data referred to in the first paragraph of this section are suspected of giving resistances and powers that are too high, because of the restricting effect of the model-basin walls, added to the effect of the false bottom or other device used to simulate the shallow water. For example, in reference (34) of Sec. 61.22, where the shallow-water drag tests were intended to simulate behavior in open water of 13 meters depth, the hydraulic radius R_H works out as only about 9.5 m. For unlimited water of 13 m depth, R_H is also 13 m. A more classic example is W. Froude's full-scale towing tests on the *Greyhound* in the early 1870's, unquestionably made in water that was too shallow for the size of the vessel [Robb, A. M., TNA, 1952, p. 449].

61.3 The Quantitative Effect of Shallow Water on Ship Resistance and Speed in the Subcritical

Range. The quantitative effect of shallow water of unlimited extent on the resistance and speed of ships is expressed in at least three different ways, when the basis of comparison is a combination of resistance and speed in unlimited deep water:

(1) The effect of limited depth on ship speed at constant (or at a given) resistance
(2) The effect of limited depth upon resistance for a speed equal to a given deep-water speed
(3) Depths of water of unlimited extent beyond which there is no shallow-water effect on either resistance or speed.

The discussion in this section is limited to ship speeds less than the critical speed c_C of a wave of translation in water of the given depth h, where $c_C = (gh)^{0.5}$. Table 72.a of Sec. 72.3 lists values of c_C for a range of depths h from 2 through 40 ft.

The problem of the wavemaking resistance only in shallow water, and in confined waters as well, has been tackled on a purely analytical or theoretical basis by Sir Thomas H. Havelock, J. K. Lunde, and others. One of Lunde's contributions is his paper "On the Linearized Theory of Wave Resistance for Displacement Ships in Steady and Accelerated Motion" [SNAME, 1951], in which Part 2, on pages 50 through 60, applies directly to resistance due to wavemaking in shallow water of unlimited extent as well as in a canal. A more recent contribution is that of A. A. Kostyukov entitled "Resistance of Bodies in a Fluid to Motion near a Vertical Wall" (in Russian) [Dokladi Akad. Nauk, SSSR (N.S.) 99, 1954, pp. 349–352]. This paper is abstracted briefly in Applied Mechanics Reviews, December 1955, page 534, number 3846.

None of the existing (1955) analyses in the foregoing category is in a form to be readily useful to the marine architect. There have been a number of much more practical solutions proposed for this problem but many of them do not embody parameters which appear logical or scientific.

What appears to be the most satisfactory method of dealing quantitatively with these matters was developed some years ago in Germany by Otto Schlichting ["Schiffswiderstand auf beschränkter Wassertiefe; Widerstand von Seeschiffen auf flachem Wasser (Resistance of Seagoing Vessels in Shallow Water)," STG, 1934, Vol. 35, pp. 127–148; English version in EMB Transl. 56, Jan 1940; also van Lammeren, W. P. A., RPSS, 1948, p. 56]. This method has a partly theoretical and partly experimental basis. Some of its assumptions are open to question but it has the merit that it works, as an engineering solution to the shallow- and confined-water problems. It will undoubtedly give way in time to a more rigorous treatment but in the meantime it produces results in fair agreement with observed model and ship data.

The basis of O. Schlichting's method is illustrated graphically by Fig. 61.B, adapted from one of Schlichting's illustrations (Fig. 6 in the reference cited). The point A_1 represents the relationship between the total resistance $R_{T\infty}$ in unrestricted deep water and the corresponding ship speed V_∞ achieved with a given power. This may be assumed as the customary design point for a normal deep-water ship. Unless otherwise indicated, the subscript ∞ (infinity) in this chapter applies to the value of a designated quantity in water of infinite depth and width. The total resistance $R_{T\infty}$ is composed of the usual friction resistance $R_{F\infty}$ and a pressure resistance $R_{W\infty}$, which is assumed by Schlichting to be due entirely to wavemaking. These components are indicated at the right of the diagram.

The wavemaking resistance $R_{W\infty}$ is associated with a train of deep-water waves, belonging to the Velox system, whose speed is the same as the ship speed, so that the crests and the troughs occupy certain fixed positions relative to the ship. The fixed relationship between the wave length $L_{W\infty}$ and the speed c_∞ of these waves, assuming they are of trochoidal character and form, is given under (2) of Sec. 48.4. Squaring the equality given there,

$$c_\infty^2 = V_\infty^2 = \frac{gL_{W\infty}}{2\pi}$$

In shallow water the speed of a trochoidal wave of the *same length* $L_{W\infty}$ is less than V_∞. If c_h is this speed for a water depth h, the ratio between c_h in shallow water and c_∞ or V_∞ in deep water is, from Sec. 18.10 and Fig. 48.N of Sec. 48.15, expressed by

$$\frac{c_h}{V_\infty} = \left[\frac{(e^{4\pi h/L_W} - 1)}{(e^{4\pi h/L_W} + 1)}\right]^{0.5}$$

or (61.i)

$$\frac{c_h}{V_\infty} = \left\{\tanh\left(\frac{gh}{V_\infty^2}\right)\right\}^{0.5}$$

When the ship passes from deep water into shallow water of depth h, it can not make the

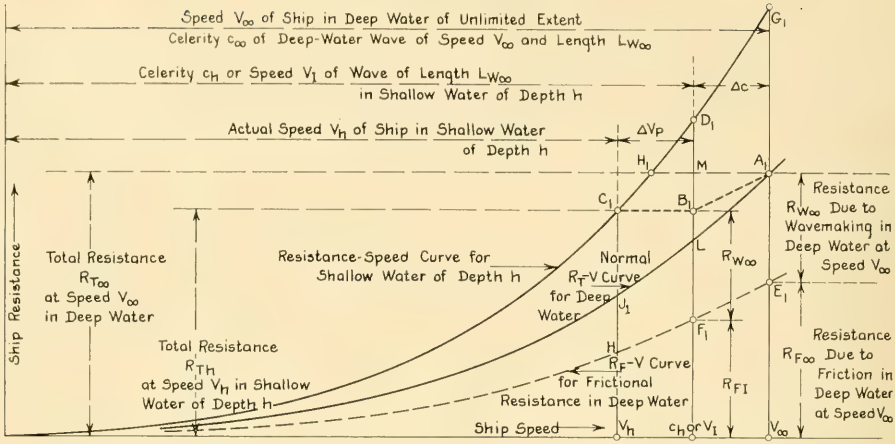

FIG. 61.B DEFINITION DIAGRAM FOR THE SHALLOW-WATER SPEED-RESISTANCE DETERMINATION OF O. SCHLICHTING

waves alongside it, of the Velox system, travel any faster than it does. The wave of translation or solitary wave which may go on ahead in a restricted channel does not enter into this discussion. Experience reveals that the crests and troughs of the Velox waves remain in essentially the same positions along the length of the ship as in deep water. However, the ship slows down by the ratio of the wave speeds in shallow and in deep water, given by the ratio c_h/V_∞ of Eq. (61.i). It may be assumed that, despite a change in profile due to increased wave height h_W in the shallow water, and other second-order changes, the pressure resistance $R_{W\infty}$ at the slower speed c_h is the same as it was at the speed V_∞ in deep water. Here, and in what follows, the subscript I applies to values at an intermediate speed $V_I = c_h$. Again it is assumed that wavemaking is responsible for all the pressure resistance.

The situation regarding resistance and ship speed is now represented graphically in Fig. 61.B by the point B_1. The pressure resistance $R_{W\infty}$ remains the same as at A_1, but the friction resistance is diminished from $R_{F\infty}$ to R_{FI}, that is, from its value at the point E_1 to its value at the point F_1. The total resistance at the speed V_I is diminished from $R_{T\infty}$ to R_{Th}, solely by the amount of this reduction. The ship speed is diminished from V_∞ to V_I.

A second effect now enters the picture. Because of the greater augment $+\Delta U$ of sternward velocity due to potential flow in the shallow water, especially in the limited space between the ship bottom and the water bed, explained in Sec. 18.2, the ship in shallow water has to move faster relative to the water which closely surrounds it. In other words, it must overcome a total resistance greater than R_{Th} to maintain the speed c_h or V_I. The resistance represented by the point B_1 in the figure is increased to that represented by the point D_1. Unfortunately, it is not possible to derive a simple expression for predicting or calculating this increase. Schlichting therefore assumes that the resistance R_{Th} remains the same as at the speed V_I but that the ship slows down until its total resistance again drops to R_{Th}. This involves a ship speed over the ground slower than V_I. The new reduced speed is V_h, represented by the point C_1 on the shallow-water resistance curve of the diagram of Fig. 61.B.

The amount of the first speed reduction Δc or, better, the ratio between the speed c_h and the unlimited deep-water speed V_∞, is determined solely from theoretical considerations, indicated by Eq. (61.i). The speed c_h or V_I is for convenience called here the *Schlichting intermediate speed* or the *shallow-water wave speed*. The ratio between this intermediate speed and the shallow-water ship speed V_h being sought, or the further speed reduction ΔV_P due to potential flow, is most difficult to determine theoretically. It is therefore derived from experiment data on models tested in shallow water. The sum of the constant wavemaking resistance $R_{W\infty}$ plus the friction

resistance R_{FI} at the intermediate speed V_I is applied as the resistance R_{Th} to the model shallow-water resistance-speed curve at the point C_1, giving the desired shallow-water speed V_h.

One feature of the diagram of Fig. 61.B is important. Since the abscissas represent wave velocities and ship speeds, and since the ratios between the several velocities and speeds are the items of primary interest, the horizontal scale may be laid off in values of what is known as the *critical-speed ratio* $(V_\infty/\sqrt{gh})$, $V_\infty/\sqrt{gL}$, the ship speed V, or even $(V_h/\sqrt{gL})$, as may be found most convenient, or in all of them together. The only requirement is that the water depth h and the ship length L remain constant in the problem, and that all the ratios be a function of V.

61.4 The Square-Draft to Water-Depth Ratio. O. Schlichting found that the ratio V_h/V_I is a function of a 0-diml parameter, namely the square root of the maximum section area A_X of the ship, divided by the water depth h. This appears logical because the increased potential-flow velocity under the ship, where most of the water flows in its passage around the hull, is a function of the space occupied by the ship. Although a ship of given maximum section area, corresponding generally to a ship of given overall size, may have a draft deeper than normal, with less bed clearance, this is compensated for by the fact that the beam is then less than normal. In this case more of the water flows around the sides, and less under the bottom. If the beam is very large in proportion to the draft, more water flows under the bottom but with the greater bed clearance there is then more room for it.

In any case the relationship developed by Schlichting appears to remain reasonably valid for ships of varied form as well as for all speeds below the *critical* speed of translation of a natural solitary wave in shallow water. It may be somewhat optimistic in predicting slightly too small a speed reduction for the general case, and it may be oversimplified, but it is acceptable until something better is worked out. The square root of the area of the maximum section, a linear dimension, is called for convenience the *square draft.* It is the draft of the equivalent ship having a square maximum section of the given area A_X, with a beam-draft ratio of 1.0. For shallow water of unlimited lateral extent the square draft $(A_X)^{0.5}$ is related to the water depth h. For restricted channels it is related to a linear dimension known as the hydraulic radius, symbolized

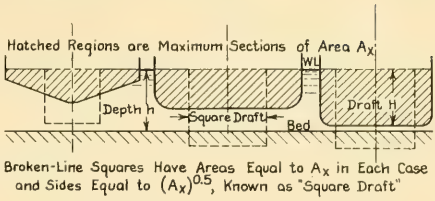

FIG. 61.C DEFINITION SKETCH FOR TERM "SQUARE DRAFT"

by R_H, described briefly in Sec. 18.11, and discussed further in Sec. 61.14.

Fig. 61.C indicates that, for broad, shallow vessels under which the bed clearance may often

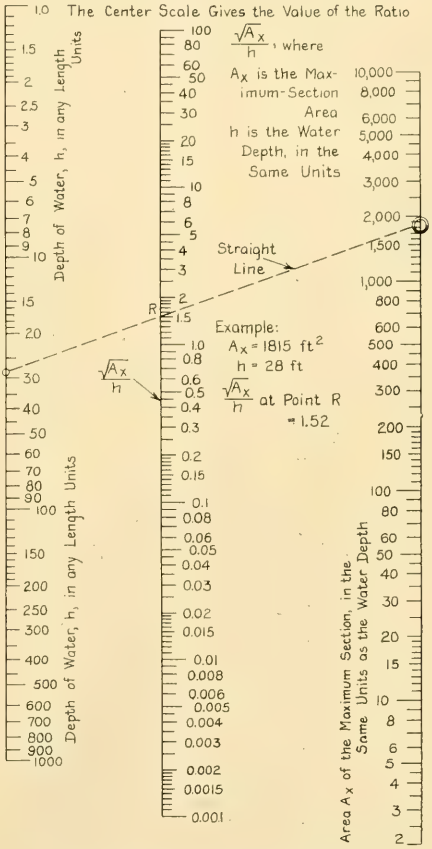

FIG. 61.D NOMOGRAM FOR DETERMINING SQUARE-DRAFT TO WATER-DEPTH RATIO

be measured only in inches, the value of the square draft may actually exceed the water depth. Fortunately, the relationships previously described continue to be reasonably valid under these conditions.

Fig. 61.D is a nomogram, designed and kindly furnished by Professor H. L. Seward, by which the value of the ratio $\sqrt{A_X}/h$ is determined by inspection when the values of A_X and h are known. This nomogram is applicable to any system of units provided h is expressed in a length unit and A_X in the same unit squared.

In shallow water of *unlimited extent* the hydraulic radius R_H equals the depth, so that $R_H = h$. The nomogram therefore gives values of $\sqrt{A_X}/R_H$ under these conditions.

61.5 Features Associated with the O. Schlichting Procedure. Several features of the Schlichting procedure require explanation and emphasis. If sufficient power is available, corresponding to the shallow-water resistance at the point G_1 in Fig. 61.B, and is applied to drive the vessel in the shallow water of depth h, it will run at the speed V_∞. This does not mean that it overruns the shallow-water Velox-system waves traveling at the speed V_I in the depth h but that it runs in waves which are the shallow-water counterparts of a deep-water Velox-wave system traveling at some faster speed $V_\infty + \Delta V_\infty$.

It is important to remember that the Schlichting procedure involves *resistances* rather than powers. To be sure, the effective power P_E is derived directly from R_T when V is known for any given condition but there is no simple method of estimating the shallow-water shaft power P_{SA} when the deep-water shaft power P_S is known.

The relationship $V_\infty/\sqrt{gh}$ controls the ratio V_I/V_∞, of intermediate speed to deep-water ship speed, independent of all reasonable absolute values of V_∞, *provided* the intermediate speeds remain well below the critical speed $c_C = \sqrt{gh}$. Similarly, the relationship $\sqrt{A_X}/h$ controls the ratio V_h/V_I, of shallow-water speed to intermediate speed, independent of the deep-water

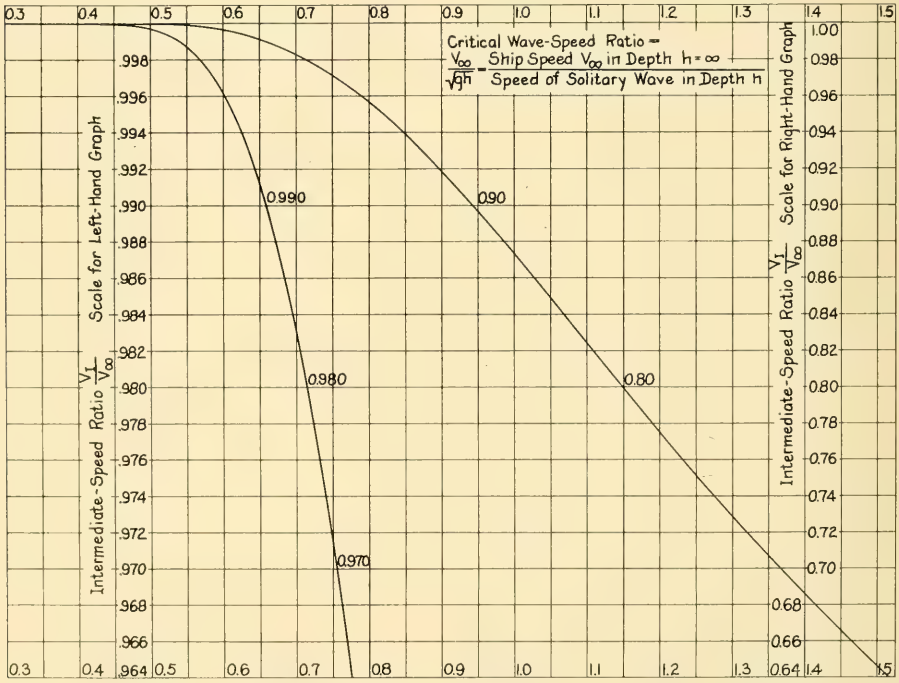

Fig. 61.E Graphs of Intermediate-Speed Ratio on a Base of Critical-Speed Ratio

speed V_∞ , again provided that the intermediate speed remains well below the critical.

Referring back to Fig. 61.B, the solution in the various cases presented in practice involves finding points such as G_1 and H_1 when the position of A_1 is known, or in finding the depths of water for which G_1 and H_1 lie at certain positions relative to A_1 .

This is not as easy as it looks or sounds because, first, there is not available, for a typical ship, a family of curves giving the resistances for a series of speeds, in waters of many different depths. Second, the pairs of points such as A_1 and C_1 in Fig. 61.B are not directly related to each other. Both the speed and the resistance are different for the two spots of a pair. When making calculations of the kind represented graphically by this figure it is generally necessary to plot two resistance-speed curves, one for shallow water of the given depth h and one for deep water, marking the companion spots A_1 and C_1 on each. Assuming that the water depth h is known, the plots are conveniently made at values of the critical-speed ratio $V_\infty/\sqrt{gh}$ (using a range of speeds V_∞), because it is then easier to determine the intermediate-speed position c_h or V_I for the point B_1 . A small range of the critical-speed ratio, embracing from three to five points, rather close together, is adequate if the problem is of limited application. If the water depth h is not known it may be convenient to plot the resistance curves on a basis of ship speed V or of Froude number F_n , depending upon the nature of the problem.

The ratio of the intermediate speed V_I to the deep-water speed V_∞ , called hereafter the *wave-speed ratio,* is determined by inspection from a theoretical curve giving V_I/V_∞ on a basis of critical-speed ratio $V_\infty/\sqrt{gh}$. Fig. 61.E shows two parts of such a curve; the shorter is a large-scale edition of a portion of the longer one, for easier reading in the lower critical-speed range. The nomogram of Fig. 61.F, also designed and generously furnished by Professor Seward, gives by inspection the value of the ratio $V_\infty/\sqrt{gh}$ when the deep-water speed V_∞ and the water depth h are known. There is a double scale for V_∞ , by which the right-hand line may be entered either in ft per sec or in kt.

The ratio of the shallow-water speed V_h in a depth h to the intermediate speed V_I , called hereafter the *potential-flow ratio,* is determined by inspection from experiment curves such as those

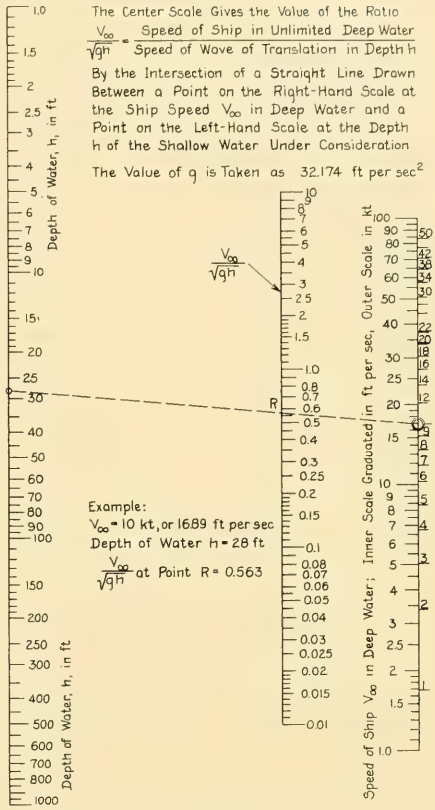

Fig. 61.F Nomogram for Determining Critical-Speed Ratio

of Fig. 61.G, in which the ratio V_h/V_I is plotted on a basis of the square-draft to water-depth ratio $\sqrt{A_X}/h$. The curve determined by Schlichting [STG, 1934, Fig. 9, p. 135; EMB Transl. 56, Jan 1940, Fig. 2, p. 3; EMB Rep. 460, May 1939, Fig. 9, p. 11] has been modified by:

(1) Decreasing slightly the potential-flow ratios V_h/V_I for small values of the square-draft to water-depth ratio. This was done to bring the potential-flow ratios in agreement with those determined by L. Landweber for restricted channels [EMB Rep. 460, May 1939, p. 11].

(2) Increasing the potential-flow ratios V_h/V_I rather markedly for the larger values of the square-draft to water-depth ratio because tests made in other model basins indicate conclusively that

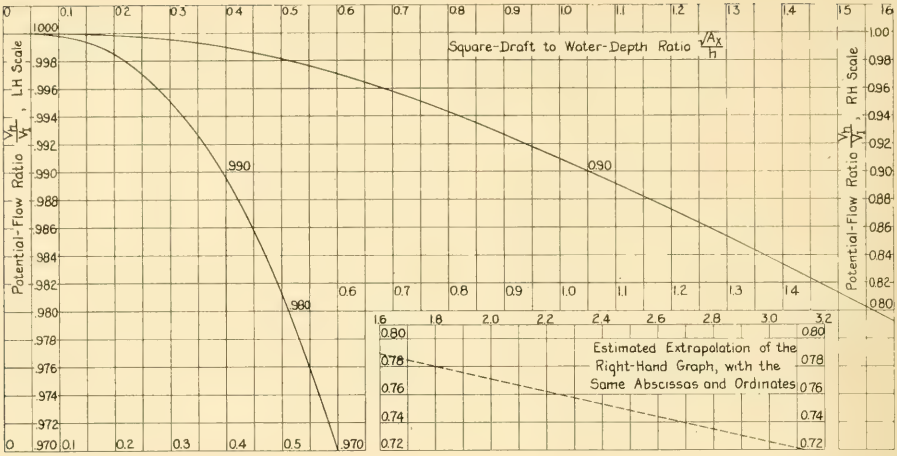

Fig. 61.G Graphs of Potential-Flow Ratio on a Base of Square-Draft to Water-Depth Ratio

there was some wall effect in Schlichting's shallow-water experiments

(3) Extending the graph derived by Landweber and mentioned in (1) preceding, which carried to a $\sqrt{A_X}/h$ ratio of only 1.6, to a value exceeding 3.0. This extension was made by plotting the available data on log-log paper and extrapolating the curve by eye. The portion so extrapolated is shown in broken lines in the lower right corner of Fig. 61.G.

The modified curves of Fig. 61.G are in two parts; the left-hand curve is a large-scale version of the corresponding portion of the larger right-hand one.

The Schlichting method takes no direct account of the slope drag involved in the shallow-water resistance problem, or of the change in attitude and slope drag when running from deep into shallow water. This drag becomes appreciable when approaching the critical speed, and it diminishes rapidly as this speed is exceeded. However, no method has been developed as yet for assessing the amount of slope drag under any given conditions. All that is known about it is that it represents an *increased* resistance.

Fig. 35.D of Sec. 35.6 demonstrates that in the case of the scout-cruiser model reported upon there, the maximum increase in shallow-water over deep-water resistance, as well as the maximum increase in trim by the stern, occur at a speed less than the critical speed or celerity c_G. Fig. 61.A of Sec. 61.2 shows definite trends in this direction. Whether this phenomenon is a function of slope drag, of the cross-sectional area of the water region in which the ship is moving, as brought out by O. Schlichting [TMB Transl. 56, p. 19], of other factors not yet evolved, or of some combination of these, is not yet certain.

The fact that there is little or no reduction in wave speed in shallow water until the ship speed reaches about half the critical speed, and that there is likewise a negligible speed reduction due to potential flow for small values of the square-draft to water-depth ratio is brought out more clearly in the examples which follow.

61.6 Practical Cases Involving a Given Depth of Water. Five cases, in two classes, appear to cover all normal shallow-water situations encountered in service:

(1) When the depth of shallow water is known or given:

Case 1a. To determine the reduced shallow-water speed for a given resistance when the deep-water speed and resistance are known

Case 1b. To determine the increased shallow-water resistance for a given speed when the deep-water resistance is known

Case 1c. To determine the deep-water speed and resistance when the shallow-water speed and resistance are measured.

(2) When the depth of shallow water is to be determined:

Case 2a. On the condition that the shallow-water resistance shall not exceed a given fraction of the deep-water resistance, say 1.02, for a given speed

Case 2b. On the condition that the shallow-water speed shall not fall below a given fraction of the deep-water speed, say 0.99, for a given resistance.

Cases 2a. and 2b. are discussed in Sec. 61.11.

A limiting case in the first class involves a determination of the reduction in speed for a specified depth when this reduction does not exceed 1 or 2 per cent at the most. A similar case in the second class involves a determination of the minimum depth at which the effects on speed and resistance shall be minor, say plus and minus 1 and 2 per cent, respectively.

Some problems encountered in practice start with the deep-water ship performance as a basis. Others require that the deep-water performance be predicted from the shallow-water behavior. In either case, the relationship between total and friction resistance with speed in deep water must still be known. These may be found:

(a) From the usual effective- and friction-power curves derived from tests of ship models
(b) By calculation from F_n and full-scale C_R, C_F, and C_T values on the SNAME RD Summary Sheets for vessels that are identical or nearly so
(c) By calculation from tests on standard series models or models of similar ships.

To draw curves of full-scale deep-water friction resistance and of total resistance, based on ship speed, such as those through $E_1 - H$ and through $A_1 - J_1$ of Fig. 61.B, respectively, requires at least three spots on each, and preferably five. To obtain these, it is necessary to work from the F_n and C_R values on the SNAME Expanded Resistance Data sheets rather than from the SNAME Summary Sheets. The tables which follow illustrate the principal steps in these calculations, as well as the derived values for each step. In all tables the ATTC 1947 or Schoenherr meanline has been used for calculating the friction resistance R_F, at a standard temperature of 59 deg F, 15 deg C, for standard salt water. The value of ΔC_F is taken as $0.4(10^{-3})$ in all cases.

There follow four practical examples illustrating a suitable procedure for problems falling under the several cases of the first class. The vessels selected are those for which SNAME Resistance Data sheets are available. The results would be about the same for other vessels having nearly identical resistance-speed curves.

61.7 Case 1a: To Find the Shallow-Water Speed from the Deep-Water Resistance-Speed Data. The first example, numbered 61.I for convenience, covers Case 1a of the preceding section. There, working from predicted deep-water data as to the speed and resistance of a ship, it is desired to determine the shallow-water speed, in a depth h, for the *same total resistance* R_T as in deep water. The region for which shallow-water data are desired is at and just below the designed speed of the vessel.

Example 61.I. The ship selected is the ore carrier covered by SNAME RD sheet 9, represented by TMB model 3818. The ship is 370 ft long by 64 ft beam by 17.5 ft draft, with a displacement of 8,850 long tons. The designed speed is 12.5 kt, for which $T_q = 0.65$, $F_n = 0.194$. The ship runs from deep water into a shallow estuary 24 ft deep. If the actual deep-water speed is 13 kt, slightly greater than the designed speed, what is the speed in the estuary with the same total resistance?

Briefly stated, the procedure is to construct a resistance-speed curve for the given depth of shallow water, and then to determine, from this curve, the ship speed at which R_{Th} is the same as for deep water. Referring to Fig. 61.B in Sec. 61.3, this requires:

(a) The construction of $(R_{T\infty} - V_\infty)$ and $(R_{F\infty} - V_\infty)$ curves for deep water, such as those through $A_1 - J_1$ and $E_1 - H$
(b) The determination of the positions of the points B_1 and C_1 for a series of selected points A_1
(c) Drawing an $(R_{Th} - V_h)$ curve through the C_1 spots
(d) Picking off the ship speed at H_1 for which R_{Th} equals $R_{T\infty}$. In detail, the V_I and V_h values are to be found for a series of V_∞ values. At each point A_1 a line A_1B_1 is to be drawn parallel to E_1F_1, giving the ordinates of B_1 and C_1.

The basic conditions for the ship and the water are first set up, and the numerical values derived from which the desired data are obtained. From the RD sheet mentioned, the maximum-section coefficient C_X of the ship is 0.9922 and the wetted surface S of the model is 87.82 ft². The scale ratio λ(lambda) of the model is 370/20.274 = 18.25, so that λ^2 is 333.06. The ship wetted surface is thus (87.82)(333.06) or 29,249 ft². This latter value may also be taken directly from the SNAME RD Summary Sheet listing this vessel. It is assumed that the deep-water and estuary surfaces are at sea level, where $g = 32.174$ ft per sec², and that both bodies are salt water at 59 deg F, where the mass density ρ(rho) = 1.9905 lb-sec² per ft⁴, and the kinematic viscosity ν(nu) = $1.2817(10^{-5})$ ft² per sec.

The area of the maximum section is 64(17.5)0.9922 = 1,111.3 ft². This is very close to the A_X of the model times λ^2, or 3.342(333.06) = 1,113.0 ft². The value of the

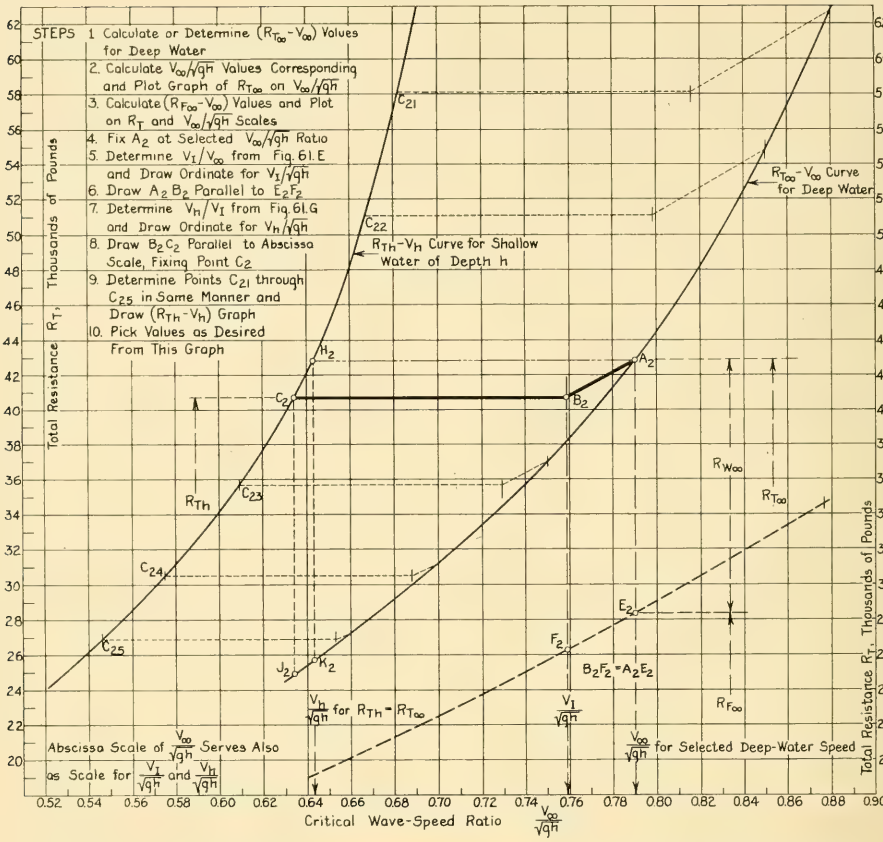

FIG. 61.H DIAGRAM ILLUSTRATING CONSTRUCTION OF A SHALLOW-WATER RESISTANCE-SPEED CURVE FROM A DEEP-WATER CURVE

square draft $\sqrt{A_X}$ is 33.34 ft, whence $\sqrt{A_X}/h$ is, by calculation or from Fig. 61.D, 1.389. Even with a bed clearance of 24 − 17.5 = 6.5 ft, the square draft is much larger than the actual water depth.

The value of the critical-speed ratio $V_\infty\sqrt{gh}$ for a speed of 13 kt, or 21.96 ft per sec, and a depth of 24 ft, is found from Fig. 61.F, or by calculation, to be 0.790. In this case a range of $V_\infty\sqrt{gh}$ of 0.60 to 0.90 appears to be ample for the abscissas of the points corresponding to A_1 and E_1 in Fig. 61.B. Instead of using a horizontal scale of ship speed V, as in Fig. 61.B, the abscissas of the new diagram for this case, reproduced as Fig 61.H, are plotted on a base of $V_\infty\sqrt{gh}$, to facilitate entry into the V_I/V_∞ curves of Fig. 61.E.

It is again pointed out that when the water depth h and the ship length L are fixed, as in this case, the $R_{F\infty}$ and $R_{T\infty}$ curves, whether plotted on a base of V_∞ , of $V_\infty/\sqrt{gh}$, or of $V_\infty/\sqrt{gL}$, have exactly the same shape, provided the horizontal scales are consistent. The horizontal scale to be used is therefore strictly a matter of convenience, provided it is based on a velocity.

The first step in the solution is to find the full-scale ship values of $R_{T\infty}$ and $R_{F\infty}$ for the range of values of $V_\infty/\sqrt{gh}$ from 0.60 through 0.90, so that the deep-water curves may be plotted. This is possible by using the values of $(10_3)C_R$ for a series of values of F_n for the speed range in question, available on SNAME ERD sheet 9 for a 400-ft ship. These particular values apply to a geometrically similar ship of any length.

The C_R values for a range of F_n from 0.1637 to 0.2233 are set down as the first line of entries in Table 61.a. A short calculation, as listed in the upper part of that table, indicates that this range of F_n gives a range of critical-speed ratio $V_\infty/\sqrt{gh}$ of from 0.6425 to 0.8765 for the given estuary depth of 24 ft. The method of working out the friction and the total deep-water resistances $R_{F\infty}$ and

$R_{T\infty}$ for these spots is indicated by the successive lines of Table 61.a. Plotting these values gives the curves through A_2–K_2 and through E_2–F_2 of Fig. 61.H.

The next step is to derive the values of $V_h/\sqrt{gh}$ for five (or more) selected values of $V_\infty/\sqrt{gh}$. These latter may correspond to the five F_n's of the first line of Table 61.a or, what is slightly easier for plotting, to certain principal abscissas on the diagram of Fig. 61.H. In this example the value of $V_\infty/\sqrt{gh}$ for the 13-kt speed happens to lie at one of these points, namely 0.790.

The method of determining the values of $V_h\sqrt{gh}$ for the selected values of $V_\infty/\sqrt{gh}$ is set down in Table 61.b. The V_I/V_∞ and V_h/V_I ratios give the values of the abscissas $V_\infty/\sqrt{gh}$ for the horizontal locations of the points B_2 and C_2 on Fig. 61.H, corresponding to the points B_1 and C_1 on Fig. 61.B. Determining the ordinates of a series of points such as B_2 and C_2 for a series of points such as A_2 enables the shallow-water total-resistance curve C_{21}–C_{25} to be laid down.

The value of the total resistance at the point B_2 on Fig. 61.H may be derived from that at a selected point A_2 by picking off the value $R_{T\infty}$ at A_2 and using the formula $R_{Th} = R_{T\infty} - R_{F\infty} + R_{FI}$. However, it is easier and quicker to draw the line A_2B_2 on the graph, parallel to the corresponding segment of the friction-resistance curve (that is, for the same range of $V_\infty/\sqrt{gh}$), and to mark the point B_2 at its intersection with the vertical line for the corresponding $V_I/\sqrt{gh}$ ratio. The ordinate of B_2 gives the ordinate of C_2 and value of R_{Th} for the corresponding point on the shallow-water curve. Through the six points such as C_{21} through C_{25} the shallow-water R_{Th}–V curve is drawn, remembering that the abscissas are really values of $V_\infty/\sqrt{gh}$. A horizontal line drawn from A_2, where $V_\infty/\sqrt{gh}$ is 0.790, representing the 13-kt ship speed, to the point H_2, gives the value $V_h/\sqrt{gh}$ of 0.643. Since $\sqrt{gh}$ is, from Table 61.a, equal to 27.79 ft per sec, V_h is (27.79)(0.643) or 17.87 ft per sec, equivalent to 10.58 kt. This is the answer desired. The speed reduction is (13 − 10.58)/13 = 2.42/13 or about 18.6 per cent.

Using the contours published by O. Schlichting [STG, 1934, Fig. 9; TMB Transl. 56, Fig. 9, p. 11; van Lammeren, W. P. A., RPSS, 1948, Fig. 30, p. 57] to determine the speed loss, $V_\infty/\sqrt{gh}$ is 0.790, $(V_\infty/\sqrt{gh})^2$ is 0.624, and $\sqrt{A_X}/h$ is 1.389. Entering with these arguments, the

TABLE 61.a—Calculation of Deep-Water Resistance-Speed Data for Example 61.I, Plotted on Fig. 61.H
Data marked with an asterisk (*) are taken from SNAME RD sheet 9. The value of ΔC_F is $0.4(10^{-3})$.

$F_n = V_\infty/\sqrt{gL}$*	0.1637	0.1786	0.1935	0.2084	0.2233
$\sqrt{gL} = 32.174(370)$ $= \sqrt{11{,}904.38}$	109.09	109.09	109.09	109.09	109.09
V_∞, ft per sec $\sqrt{gh} = \sqrt{32.174(24)} = 27.79$	17.858	19.483	21.109	22.734	24.360
$V_\infty/\sqrt{gh}$	0.6425	0.7010	0.7595	0.8180	0.8765
$(10^3)C_R$*	0.70	0.79	0.92	1.165	1.58
$0.5\rho S \doteq 0.9952(29{,}249)$	29,109	29,109	29,109	29,109	29,109
V_∞^2, ft² per sec²	318.91	379.59	445.59	516.83	593.41
$L/\nu = \dfrac{370}{1.2817(10^{-5})}$	$28.868(10^6)$	$28.868(10^6)$	$28.868(10^6)$	$28.868(10^6)$	$28.868(10^6)$
$R_n = [V_\infty L/\nu](10^{-6})$	515.5	562.4	609.4	656.3	703.2
$10^3(C_F)$ for ship	1.664	1.645	1.629	1.613	1.600
$10^3(C_F + \Delta C_F)$	2.064	2.045	2.029	2.013	2.000
$V_\infty^2(C_F + \Delta C_F)$	0.65823	0.77626	0.90410	1.04037	1.18682
$R_F = 0.5\rho SV_\infty^2(C_F + \Delta C_F)$, lb	19,160	22,596	26,317	30,284	34,547
$10^3(C_F + \Delta C_F + C_R)$	2.764	2.835	2.949	3.178	3.580
$V_\infty^2(C_F + \Delta C_F + C_R)$	0.88147	1.07614	1.31404	1.64248	2.1244
$R_T = 0.5\rho SV_\infty^2(C_F + \Delta C_F + C_R)$, lb	25,659	31,325	38,250	47,811	61,840

TABLE 61.b—DERIVATION OF VALUES OF $V_h/\sqrt{gh}$ FROM SELECTED VALUES OF CRITICAL-SPEED RATIO $V_\infty/\sqrt{gh}$

Selected values of $V_\infty/\sqrt{gh}$	0.660	0.700	0.750	0.790	0.800	0.850	0.880
V_I/V_∞ ratio from graph of Fig. 61.E	0.990	0.983	0.972	0.960	0.957	0.939	0.927
$V_I/\sqrt{gh}$ ratio, by multiplication	0.653	0.688	0.729	0.758	0.766	0.798	0.816
V_h/V_I ratio, from graph of Fig. 61.G, for $\sqrt{A_X}/h = 1.389$	0.836	0.836	0.836	0.836	0.836	0.836	0.836
$V_h/\sqrt{gh}$ ratio, by multiplication	0.546	0.575	0.609	0.634	0.640	0.667	0.682

speed loss determined by inspection is about 20.3 per cent. This discrepancy, although not a major one, is due undoubtedly to Schlichting's use of data for unlimited shallow water which were observed in a model basin of rather limited width.

As a matter of interest, the total resistance in deep water at 10.58 kt, represented by the point K_2, is about 25,750 lb. That at the same speed in the 24-ft depth, represented by the point H_2, is about 42,800 lb, some 166 per cent of the deep-water resistance.

Only a short segment of the shallow-water $(R_{Th} - V)$ curve is required for this problem. However, it is well to plot a considerable portion of it, so that other shallow-water problems which arise in the design stage of a ship, or in an analysis of its trials, may readily be solved.

61.8 Case 1b: To Find the Shallow-Water Resistance from the Deep-Water Resistance-Speed Data. Determining the shallow-water resistance R_{Th} for any speed, assuming a given depth of water h, and a knowledge of the deep-water $(R_{T\infty} - V_\infty)$ data, is equivalent to drawing a set of $(R_T - V)$ curves for both conditions and comparing the total-resistance values at any selected ship speed V. This is exactly what was done in Case 1a of Sec. 61.7, when a curve of total resistance R_T on a base of critical-speed ratio $V_\infty/\sqrt{gh}$ was calculated for deep water, and a curve of total resistance in water of depth h was constructed from it. The segment C_2J_2 of Fig. 61.H represents the increase in total resistance at a critical-speed ratio corresponding to the horizontal position of those points. The segment H_2K_2 is the ΔR_T for a critical-speed ratio corresponding to the abscissa of both H_2 and K_2, as calculated at the end of the preceding section.

When the depth h is fixed or known, the actual ship speeds may be determined by multiplying each of the critical-speed ratios by the factor $\sqrt{gh}$ and then converting the ft-per-sec values thus obtained (if English units are used) to kt. Alternatively, a scale of kt may be calculated and added along the lower edge of Fig. 61.H.

61.9 Case 1c: To Find the Deep-Water Speed and Resistance When the Shallow-Water Speed and Resistance are Measured. Assume that a ship is, by force of circumstances, required to run trials in shallow water of a known depth h. Assume further that it is possible, by a means not stated, to measure the total ship resistance R_{Th} at the depth h, as well as the speed V_h, for the range of speeds covered by the trials. It is desired to know the corresponding deep-water total resistances $R_{T\infty}$ and speeds V_∞; or, in effect, to construct an $(R_{T\infty} - V_\infty)$ curve from the known $(R_{Th} - V_h)$ curve.

The procedure described here is roughly the reverse of that for Case 1a in Sec. 61.7. Referring again to Fig. 61.B, the method involves starting from a known shallow-water curve containing points such as C_1 and H_1 and constructing a deep-water curve having a series of points such as A_1.

Since the depth h is specified, it is best to construct a graph similar to that in Fig. 61.I on a base of $V/\sqrt{gh}$.

The ratio $\sqrt{A_X}/h$ and the value of $V_h/\sqrt{gh}$ (for any given spot such as C_3) are first determined by calculation. The ratio V_h/V_I is then picked from the experiment curves of Fig. 61.G. Dividing this ratio into $V_h/\sqrt{gh}$ gives $V_I/\sqrt{gh}$. The ordinate passing through the point B_3 of Fig. 61.I is then erected at this value and the horizontal line C_3B_3 is drawn. The intermediate speed is V_I, equal to V_h divided by the V_h/V_I ratio.

The friction resistance R_{FI} for the intermediate speed V_I is next calculated or determined; this is represented on the base of $V/\sqrt{gh}$ by the ordinate to the point F_3. In order to find the slope

of the friction-resistance curve in the region between $V_I/\sqrt{gh}$ and $V_\infty/\sqrt{gh}$ it is necessary to calculate R_F for a speed somewhat higher than V_I so that the point E_3 may be plotted. It is well, in fact, to calculate R_F for a series of ship speeds, say the ones corresponding to the F_n values in the speed range under consideration on SNAME ERD sheet 2. This is done in Table 61.c for the example set up subsequently in this section, and the results are plotted in the long-dash lines of Fig. 61.I.

The problem is now to find the speed V_∞ for which the intermediate speed V_I is the correct one for the specified depth. It is known, first, that V_∞ is definitely greater but probably not too much larger than V_I ; also that the value $V_\infty/\sqrt{gh}$ is greater than $V_I/\sqrt{gh}$ by exactly the same ratio. Entering the theoretical curve of Fig. 61.E with the known ratio $V_I/\sqrt{gh}$, a value of V_∞ and a ratio of V_I/V_∞ are selected for trial at a value of $V_\infty/\sqrt{gh}$ somewhat larger numerically than the given $V_I/\sqrt{gh}$. If the wave-speed ratio V_I/V_∞ , applied to the tentative deep-water speed V_∞ , gives a ship speed V_I equal numerically to the intermediate speed previously determined from the potential-flow ratio, then the tentative speed V_∞ , and the critical-speed ratio $V_\infty/\sqrt{gh}$, are the correct ones. Otherwise, the process is repeated until the intermediate speeds and the speed ratios are numerically the same.

Having found the proper value of $V_\infty/\sqrt{gh}$ and the speed V_∞ , erect this ordinate on Fig. 61.I; it is the one on which A_3 is located. Then through B_3 draw a line parallel to F_3E_3 , meeting the $V_\infty/\sqrt{gh}$ ordinate at A_3 . This is one point on the desired $(R_{T\infty} - V_\infty)$ curve. The remaining points are located in the same way.

With the $(R_{T\infty} - V_\infty)$ curve as derived in this manner there may be plotted for comparison and reference the deep-water resistance-speed curve as predicted from model tests or as calculated from standard series or other data. An example of this case follows.

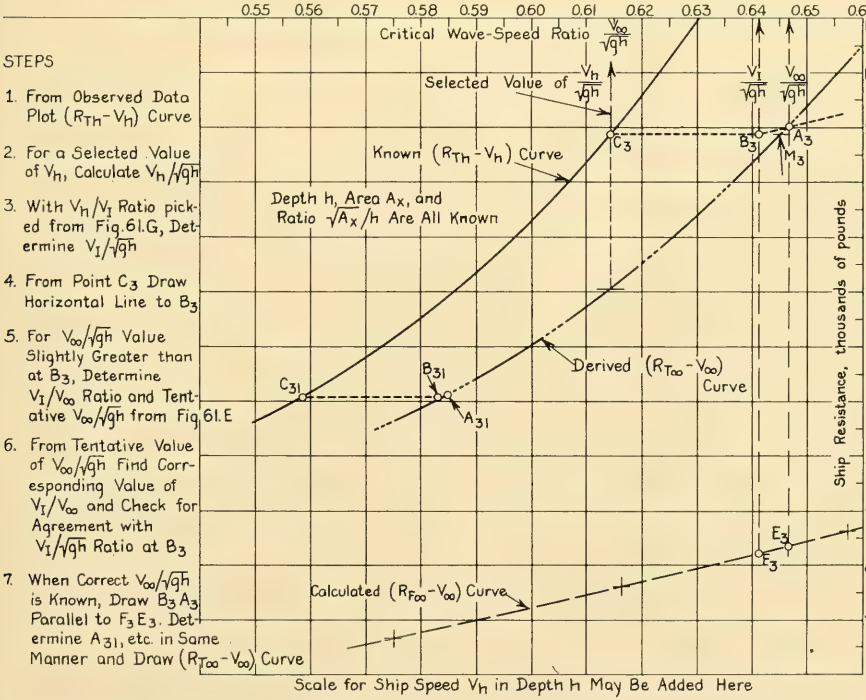

FIG. 61.I CONSTRUCTION OF A DEEP-WATER RESISTANCE-SPEED CURVE FROM A KNOWN SHALLOW-WATER CURVE

TABLE 61.c—CALCULATION OF SHIP FRICTION RESISTANCE FOR CASE 1.c

The data marked with asterisks (*) are from SNAME RD sheet 2.

$V/\sqrt{gL}$ or Froude number F_n*		0.2084	0.2233	0.2382
$\sqrt{gL} = \sqrt{32.174(487.5)}$		125.2	125.2	125.2
V, corresponding ship speed	ft per sec	26.09	27.96	29.82
$\sqrt{gh} = \sqrt{32.174(64)}$	ft per sec	45.37	45.37	45.37
$V/\sqrt{gh} = V/45.37$		0.5750	0.6163	0.6573
$(0.5\rho)S = 0.9952(51{,}047)$		50,802	50,802	50,802
V^2	ft² per sec²	680.69	781.76	889.23
$L/\nu = 487.5/[1.2817(10^{-5})]$	sec per ft	$38.035(10^6)$	$38.035(10^6)$	$38.035(10^6)$
$R_n = VL/\nu$	millions	992.33	1,063.46	1,134.20
$(10^3)C_F$ for ship, SNAME T and R Bull. 1-2		1.532	1.519	1.508
Add $(10^3)\Delta C_F$ of 0.4		1.932	1.919	1.908
$V^2(C_F + \Delta C_F)$		1,315.09	1,500.2	1,696.65
$R_F = (0.5\rho)SV^2(C_F + \Delta C_F)$	lb	66,809	76,213	86,193

Example 61.II. The vessel selected is a tanker of 20,584 long tons displacement, 487.5 ft in length by 68 ft beam by 29.87 ft draft, forming the subject of SNAME RD sheet 2. It was tested as TMB model 3617. It is designed to run at a speed of 16.5 kt in deep water. If the curve of total resistance on ship speed, as determined by trials run in unrestricted (unlimited) shallow water having an average depth of 64 ft, is given by the curve through the points C_{3I} and C_3 of Fig. 61.I, find the corresponding curve for deep water. The trials were conducted in standard salt water, at sea level, having a temperature of 59 deg F.

From data on the SNAME RD sheet, the value of C_X is 0.9803. Hence $A_X = 0.9803(68)29.87 = 1{,}991.15$ ft². Using the model A_X of 3.353 ft² times λ^2 (= 594.14), this comes out as 1,992.15 ft². The square draft $\sqrt{A_X}$ is 44.63 ft, whence $\sqrt{A_X}/h$ is 44.63/64 = 0.6973. The wetted surface S is, from the SNAME RD Summary Sheets, 51,047 ft².

The method of calculating the ship friction resistance R_F for three selected values of F_n from SNAME ERD sheet 2 follows that previously listed in Table 61.a, except that the total-resistance calculation of the latter is omitted. Plotting the R_F values on a basis of $V/\sqrt{gh}$ gives the long-dash curve through the points F_3 and E_3 of Fig. 61.I.

The solid curve through C_{3I} and C_3 is plotted from the R_{Th} and the V_h data observed on the trial. Although designed for only 16.5 kt in deep water the vessel in question had sufficient margin of power to make 16.5 kt in shallow water, at a total resistance of 158,900 lb, corresponding to point C_3. It is desired to know the deep-water speed V_∞ which would be achieved at a total resistance $R_{T\infty}$ equal to the measured R_{Th} at the speed V_h in shallow water. Better, it is desired to plot a $(R_{T\infty} - V_\infty)$ curve for a range of normal operating speeds from the $(R_{Th} - V_h)$ data observed on the trials.

Starting first with the 16.5-kt point at C_3, the value of $V_h/\sqrt{gh}$ is 0.6143. The position of the ordinate of the point B_3, opposite C_3 and at the same value of R_{Th}, is determined from the $V_I/\sqrt{gh}$ ratio. This is found by entering the graph of Fig. 61.G with the known ratio of square draft to water depth, where for this ship $\sqrt{A_X}/h$ is derived in the upper lines of Table 61.d. The V_h/V_I ratio is found to be 0.958, whereupon $V_I/\sqrt{gh}$ is $(V_h/\sqrt{gh})/(V_h/V_I)$ or 0.6143/0.958 = 0.6412. The point B_3 is plotted upon this ordinate and a horizontal broken line drawn from C_3 to B_3 on Fig. 61.I.

The method of arriving at a correct value of $V_\infty/\sqrt{gh}$, as described earlier in this section, is illustrated by the steps listed in the lower portion of Table 61.d. Erecting an ordinate at $V_\infty/\sqrt{gh} = 0.6467$ and drawing a broken line through B_3 parallel to that portion of the friction-resistance curve directly below it produces the intersection A_3. This is one point on the desired $(R_{T\infty} - V_\infty)$ curve. The data for another point are derived in the right-hand column of Table 61.d.

The speed V_∞ which would have been made in deep water at the *same* total resistance R_{Th} as in shallow water is found by extending the horizontal line C_3B_3 in Fig. 61.I until it intersects the $(R_{T\infty} - V_\infty)$ curve at the point M_3. With a value of $V_\infty/\sqrt{gh} = 0.6451$ at this point, Table 61.d indicates that the deep-water speed sought is 17.33 kt. This is 0.83 kt more than the speed made in shallow water.

TABLE 61.d—CALCULATION OF TWO SPOTS ON DEEP-WATER SPEED-RESISTANCE CURVE FROM KNOWN SHALLOW-WATER SPEED-RESISTANCE CURVE

Selected V_h for ship	kt	16.5	15.0
V_h	ft per sec	27.87	25.34
$gh = (32.174)(64)$		2,059.14	2,059.14
$\sqrt{gh}$	ft per sec	45.37	45.37
$V_h/\sqrt{gh}$		0.6143	0.5585
$\sqrt{A_X} = \sqrt{1{,}991.15}$	ft	44.63	44.63
$\sqrt{A_X}/h = 44.63/64$		0.6973	0.6973
V_h/V_I from Fig. 61.G		0.958	0.958
$V_I/\sqrt{gh} = (V_h/\sqrt{gh})/(V_h/V_I)$		0.6412	0.583
First estimate of $V_\infty/\sqrt{gh}$		0.648	0.585
First value of V_I/V_∞ from Fig. 61.E		0.9913	0.9971
$V_I/\sqrt{gh}$, by multiplication		0.6424	0.5833
Second estimate of $V_\infty/\sqrt{gh}$		0.646	0.5845
Second value of V_I/V_∞ from Fig. 61.E		0.9915	0.9971
$V_I/\sqrt{gh}$, by multiplication		0.6405	0.5828
Interpolated value of $V_\infty/\sqrt{gh}$		0.6467	0.5847
$V_\infty/\sqrt{gh}$ for same R_{Th} as in depth h		0.6451	0.5837
$V_\infty = (V_\infty/\sqrt{gh})\ (\sqrt{gh})$	ft per sec	29.27	26.48
	kt	17.33	15.68
Difference, $V_\infty - V_h$	kt	0.83	0.68

61.10 Limiting Case of 2 Per Cent Speed Reduction in Water of a Given Depth. For the limiting case in the first class, when the speed reduction in shallow water is limited to say 2 per cent of the speed V_∞ in deep water, a simplified procedure is justified. The points A_1 and B_1 of Fig. 61.B are then so close together that $R_{T\infty}$ is sensibly equal to R_{Th}. The shallow-water speed V_h may be found from V_∞ simply by multiplying together the two ratios V_h/V_I and V_I/V_∞.

Examination of Fig. 61.E reveals that the ratio V_I/V_∞ is practically 1.0 for all values of the critical-speed ratio $V_\infty/\sqrt{gh}$ from 0.0 through 0.4, and that it diminishes very slowly for values of that ratio through 0.7, where V_I/V_∞ is 0.983. From Fig. 61.G it appears that the ratio V_h/V_I is practically 1.0 for all values of the square-draft to water-depth ratio $\sqrt{A_X}/h$ from 0.0 through about 0.12. At a $\sqrt{A_X}/h$ ratio of 0.5 the potential-flow ratio V_h/V_I has diminished only to 0.9812. Each of these reductions is less than 2 per cent.

Combinations of values of V_h/V_I and V_I/V_∞ which, when multiplied together, produce a ratio of $V_h/V_\infty = 0.98$, representing a 2 per cent reduction in speed, are plotted as the graph ABCDE on Fig. 61.J. These are on a base of $\sqrt{A_X}/h$ for the potential-flow ratio V_h/V_I and of $V_\infty/\sqrt{gh}$ for the intermediate-speed ratio V_I/V_∞. Four additional graphs, similarly constructed, cover combinations which give speed

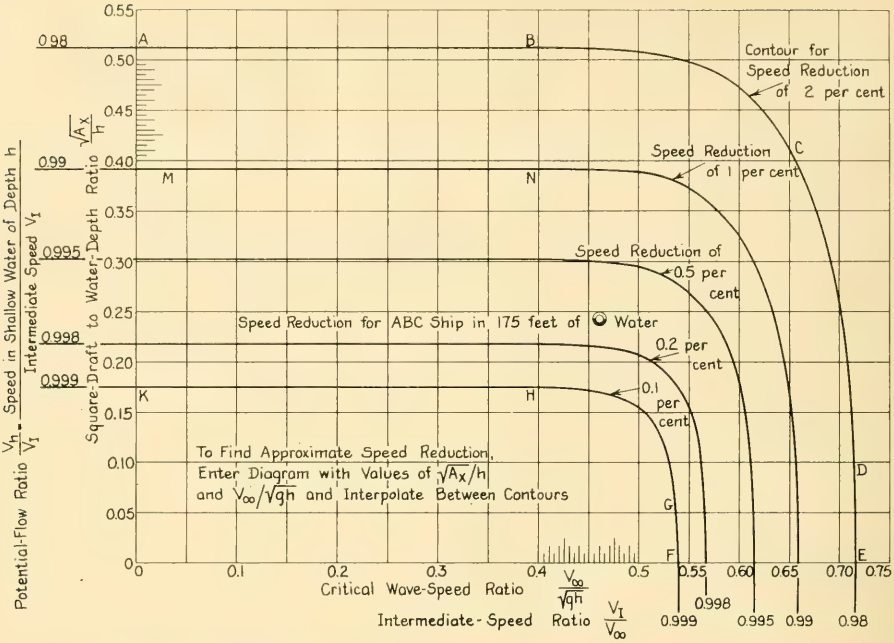

FIG. 61.J GRAPHS FOR DETERMINING THE LIMITING WATER DEPTHS FOR VARIOUS SMALL SPEED REDUCTIONS

reductions of 1.0, 0.5, 0.2, and 0.1 per cent, respectively.

While the statement of this example, and of others in this chapter, gives the impression of straining at small quantities, the principal purpose of the example is to illustrate the method. A secondary purpose is to carry the calculations to a limit beyond which they would probably never go in practice.

From the 2 per cent curve of Fig. 61.J it appears that at critical-speed ratios $V_\infty/\sqrt{gh}$ below 0.4, in the region AB, only the square-draft to water-depth ratio $\sqrt{A_X}/h$ influences the speed reduction. At the higher critical-speed ratios, but at values of $\sqrt{A_X}/h$ below about 0.1, in the region DE, only the critical-speed ratio $V_\infty/\sqrt{gh}$ affects the speed reduction. At greater values of both ratios, in the region BCD, both have an effect in diminishing the speed.

Example 61.III. To show how this family of graphs is used, take the case of the ABC ship designed in Part 4, for which A_X is 1,815 ft² and $\sqrt{A_X}$ is 42.6 ft. The limiting depth at which the ship can run slowly, with a reduction of only 1 per cent in speed, is found from the value of $\sqrt{A_X}/h$ at M on Fig. 61.J, namely 0.393. The limiting depth h is therefore $h = \sqrt{A_X}/0.393 = 42.6/0.393 = 108.4$ ft. For this depth the critical-speed ratio can not exceed 0.4, represented by the point N. The limiting ship speed $V_\infty = 0.4\sqrt{gh} = 0.4\ [32.174(108.4)]^{0.5} = 23.62$ ft per sec, equivalent to 13.98 kt. Water deeper than 108.4 ft must therefore be found in order to run a valid sea trial at 20.5 kt.

Assume that a region having a depth h of 175 ft is tentatively selected. The square-draft to water-depth ratio is then $42.6/175 = 0.243$ and the critical-speed ratio is $[(20.5)(1.6889)]/\sqrt{32.174(175)} = 0.461$. Entering Fig. 61.J with these values a point is found (marked by the distinctive circle) at which the predicted speed reduction is only about 0.3 per cent. This is well within the 1 per cent limit. The 175-ft depth is therefore adequate.

61.11 Cases 2a and 2b: To Find the Limiting Depth for a 2 Per Cent Increase in Resistance. Turning to Cases 2a and 2b of the second class of Sec. 61.6, involving a determination of the limiting depth of unrestricted shallow water in which the resistance for a given speed is increased by say 2 per cent, or at which the speed for a given resistance is diminished by say 1 per cent, a simplified and approximate procedure is again justified. Water depths in navigable waters are

almost never uniform, so that when a limiting depth is determined, someone must decide whether it is to be looked upon as a mean or as a minimum depth.

For slow and intermediate-speed ships of normal or full form, having a relatively large maximum-section area, the limiting depth h is almost certain to be large enough to make the limiting critical-speed ratio $V_\infty/\sqrt{gh}$, as well as the ratio $\sqrt{A_X}/h$, rather small, as they are in the region HK of Fig. 61.J. Indeed, the first may be so small as to make the wave-speed ratio V_I/V_∞ practically unity; see the first example following. On the other hand, for a fine, fast ship running at higher critical-speed ratios, the depth h is so great in proportion to the square draft $\sqrt{A_X}$ that the value of the potential-flow ratio V_h/V_I may be practically 1.00, as in the region FG of Fig. 61.J; see the second example following. The ratio V_I/V_∞ then becomes the sole factor in determining the depth.

The approximate method described here gives quickly the limiting depth of unrestricted shallow water in which a ship must run to insure that its shallow-water total resistance R_{Th} does not exceed 1.02 times its deep-water total resistance $R_{T\infty}$. The basis of this method is that the resistance varies as a certain—but undetermined—power of the speed in any narrow speed range or at any selected speed. As a rough average it may be assumed that $R \cong kV^2$, in which case $dR \cong 2kV(dV)$. For any small range in which k and V may be assumed constant, a 2 per cent increase in resistance is therefore reflected by a 1 per cent increase in speed. This is the basis for the statement that at the limiting depth the shallow-water speed V_h shall be not less than 0.99 times the deep-water speed V_∞ for the given deep-water resistance $R_{T\infty}$.

Since the speed reduction may be due to a decreased Velox-wave speed or to augmented potential flow around the ship both factors must be considered. As the first depends upon the critical-speed ratio $V_\infty/\sqrt{gh}$ and the second upon the square-draft to water-depth ratio $\sqrt{A_X}/h$, they can not easily be put upon a common basis except to say that for any given conditions the value of h to be determined must be the same for both.

The speed reduction due to either factor manifestly can not exceed 0.01. From Fig. 61.E the value of the critical-speed ratio $V_\infty/\sqrt{gh}$ can not exceed 0.658, for which $V_I/V_\infty = 0.99$. From Fig. 61.G the square-draft to water-depth ratio $\sqrt{A_X}/h$ can not exceed 0.393, where $V_h/V_I = 0.99$. Below a critical-speed ratio of 0.40 the intermediate speed V_I is practically equal to the deep-water speed V_∞ so that this part of the theoretical curve need not be considered. Below a square-draft to water-depth ratio of 0.1 the shallow-water

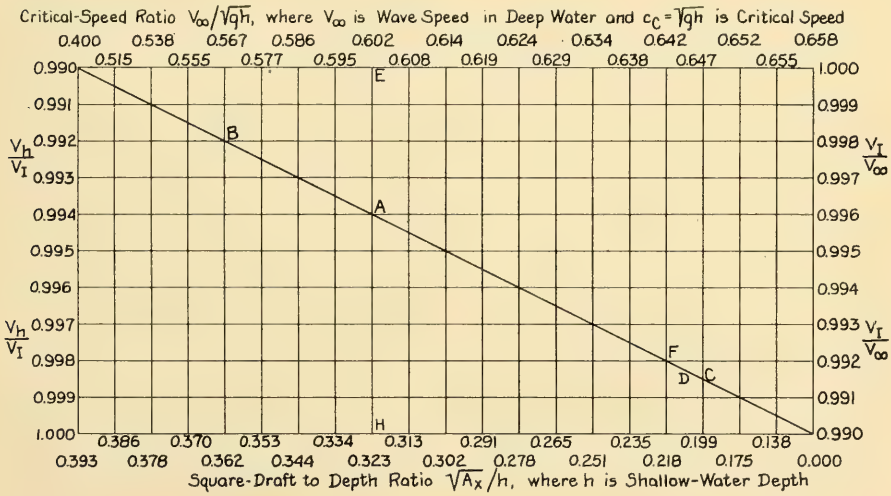

FIG. 61.K DIAGRAM FOR DETERMINING THE LIMITING WATER DEPTH FOR A SPEED REDUCTION OF 1 PER CENT

speed V_h is practically equal to the intermediate speed V_I. In the ranges of critical-speed ratio and square-draft to water-depth ratio between those mentioned the *sum* of the speed reductions due to both causes can not exceed 0.01 for the depth to be determined. This is on the basis that for small values of these differences, not exceeding 0.01, they may be determined accurately either by addition of the differences or by multiplication of the corresponding speed ratios. For example, $0.99(0.99) = 0.9801$ while $\{1.0 - [(1.00 - 0.99) + (1.00 - 0.99)]\} = 0.9800$.

Fig. 61.K is a diagram for use in calculating the required limiting depth. Unfortunately, until further developed, it involves a trial-and-error procedure. At and beyond the left end of the diagram the speed reduction of 0.01 is assumed to be due entirely to augmented potential flow while at and beyond the right end it is due entirely to reduced wave speed in the shallow water. Between the ends both effects occur, and they are additive, as for EA + AH = EH. Here EA is the speed reduction due to wave speed, corresponding to the right-hand scale, while AH is that due to potential flow, corresponding to the left-hand scale. The values of each are taken from the theoretical and experimental curves of Figs. 61.E and 61.G for a critical-speed ratio of 0.602 (top scale) and a square-draft to water-depth ratio of 0.323 (bottom scale).

The method of using the diagram is explained in the examples which follow. The nomograms of Figs. 61.D and 61.F may be entered for ready determination of the values $\sqrt{A_X}/h$ and $V_\infty/\sqrt{gh}$, or these values may be calculated, as in Examples 61.IV, 61.V, and 61.VI.

To take care of the situation on low-speed and high-speed ships, where the total resistance may vary at less or more than the square of the speed, additional diagrams of this type may be constructed from the data on Figs. 61.E and 61.G, for overall speed ratios correspondingly greater or less than 0.99.

Example 61.IV. For the sake of simplicity, since only the deep-water speed and the square-draft enter into the problem, it is assumed that the vessel selected for this example has a maximum-section area of 1,600 ft², with a square draft of 40.00 ft. It is desired to find the limiting depth of water, at sea level, in which the resistance does not exceed 1.02 times the deep-water resistance at speeds of 10, 20, and 30 kt. These speeds are equivalent to 16.89, 33.78, and 50.67 ft per sec, respectively; $g = 32.174$ ft per sec², $\sqrt{g} = 5.672$.

For the lowest speed of 10 kt assume first that the potential-flow effect limits the depth of water. At the extreme left of Fig. 61.K, where $V_h/V_I = 0.990$, the square-draft to water-depth ratio $\sqrt{A_X}/h$ is 0.393, whence the limiting depth h is $40.00/0.393 = 101.8$ ft. Assuming on the other hand that all the speed reduction is due to wave effect, for an intermediate-speed ratio V_I/V_∞ of 0.990 the critical-speed ratio $V_\infty/\sqrt{gh}$ is 0.658. Then

$$\frac{V_\infty}{\sqrt{gh}} = 0.658, \quad \text{whence} \quad \sqrt{h} = \frac{V_\infty}{0.658\sqrt{g}}$$

or

$$h = \frac{V_\infty^2}{(0.658)^2 g} = \frac{(16.889)^2}{(0.433)(32.174)}$$
$$= 20.5 \text{ ft.}$$

For any square-draft to water-depth ratio less than the lowest value 0.393 at the extreme left of the diagram of Fig. 61.K, the limiting depth is greater than 101.8 ft, whereas the common value for h is somewhere between that value and 20.5 ft. The critical-speed ratio $V_\infty/\sqrt{gh}$ is therefore smaller than 0.658. In fact, it may be smaller than 0.400, at the left end of the diagram. For a value of $V_\infty/\sqrt{gh} = 0.4$,

$$h = \frac{V_\infty^2}{(0.4)^2 g} = \frac{285.27}{(0.16)(32.174)} = 55.4 \text{ ft.}$$

The fact that it is not possible, within the limits of the diagram, to achieve a common value for h indicates that the potential-flow effect is the determining one while the wave-speed effect is zero. The required depth is therefore 101.8 ft.

For the 20-kt speed assume, as a starter, that the point A represents the operating condition. Here the square-draft to water-depth ratio is 0.323, and the depth determined from that ratio is $40/0.323 = 123.8$ ft. The corresponding critical-speed ratio is 0.602 and the depth derived from it is

$$h = \frac{V_\infty^2}{(0.602)^2 g} = \frac{(33.78)^2}{(0.36)(32.174)} = 98.4 \text{ ft.}$$

It is obvious that the first depth is slightly too large and that the square-draft to water-depth ratio should therefore be larger than 0.323. Assume a value of 0.362, at the point B. This gives a depth h of $40/0.362 = 110.5$ ft. The corresponding critical-speed ratio of 0.567 gives a depth of

$$h = \frac{(33.78)^2}{(0.567)^2 g} = 110.3 \text{ ft.}$$

The estimate of the position of B was excellent in this case, so that no further computation is necessary.

For the 30-kt speed, assume the point C where the square-draft to water-depth ratio is 0.199 and the critical-speed ratio is 0.647. Then $h = 40/0.199 = 201.0$ ft, and

$$h = \frac{(50.67)^2}{(0.647)^2 g} = 190.6 \text{ ft.}$$

Making another calculation for the point D, where the square-draft to water-depth ratio is about 0.209, gives a limiting depth h of $40/0.209 = 191.4$ ft. Using the critical-speed ratio of 0.645, the depth is

$$h = \frac{2{,}567.4}{(0.645)^2 g} = 191.8 \text{ ft.}$$

The limiting depth required is therefore approximately 192 ft.

To determine the limiting depth at which the shallow-water effects become negligible, for all practical purposes, it may be assumed that this depth corresponds to a condition where the shallow-water resistance does not exceed 1.005 of the deep-water resistance. As the resistance may again be assumed, for a first approximation, to vary between the square and the cube of the ship's speed, an increase in resistance of 0.005 corresponds to an increase in speed of the order of about 0.002. Similarly, limiting the resistance in shallow water to that encountered in deep water involves a speed reduction to the order of $0.998V_\infty$ in the shallow water whose depth is to be determined.

If the product of the V_h/V_I and the V_I/V_∞ ratios is to exceed 0.998, the values of both ratios must be close to 1.000. Assuming that the value of the V_h/V_I speed ratio must exceed 0.998, examination of the corresponding curves of Fig. 61.K shows that the value of $\sqrt{A_X}/h$ must be less than about 0.218, regardless of the size of the ship. Furthermore, the percentage of critical velocity must be less than 0.567, regardless of the speed. This is equivalent to shrinking the diagram of Fig. 61.K to the point where the vertical limits on both end scales are 0.998 and 1.000. Two values of the limiting depth h are first derived from the two relationships given. If they are not nearly the same the depth h is determined by trial and error as before.

Example 61.V. The data for this example are taken from SNAME RD sheet 39; TMB model 3796. A liner of 62,660 tons displacement, 962 ft long by 117.8 ft beam by 34.39 ft draft, having a C_X of 0.981, is expected to run at a speed of 32 kt. What is the limiting depth of unrestricted shallow water in which the speed with a given deep-water resistance does not drop below $0.998V_\infty$? No account is taken of other ship-performance factors such as possible vibration.

The maximum-section area A_X of the ship is 117.8 (34.39)0.981 = 3,974 ft². The square draft $\sqrt{A_X}$ is 63.03 ft. The speed of 32 kt is equivalent to 54.05 ft per sec. The value of g is taken as 32.174 ft per sec².

By the potential-flow criterion alone (point F on Fig. 61.K), the ratio $\sqrt{A_X}/h$ is 0.218 and the limiting depth is 63.03/0.218 = 289.1 ft.

By the critical-speed criterion alone (point B on Fig. 61.K), the value of $V_\infty/\sqrt{gh}$ is 0.567 and the limiting depth is

$$h = \frac{V_\infty^2}{(0.567)^2 g} = \frac{2{,}921.4}{(0.3215)(32.174)} = 282.4 \text{ ft.}$$

These two values of h are close enough so that the larger of the two may be assumed as the limiting one. In this case it might be well to set the minimum depth as 290 ft.

Example 61.VI. At the opposite extreme, assume a motorboat having a maximum section area A_X of 6.25 ft², running at 9.5 kt, or 16.05 ft per sec. What is the limiting depth of unrestricted shallow water in which the speed with a given deep-water resistance does not drop below $0.998V_\infty$? The value of g is taken as 32.174 ft per sec².

As a starter, consider that the overall velocity ratio $V_h/V_\infty = 0.998$ is made up of the two ratios $V_h/V_I = 0.9997$ and $V_I/V_\infty = 0.9982$. These values are admittedly arbitrary but with a little experience they can be estimated rather closely. Then from Fig. 61.K, at a V_h/V_I ratio of 0.9997, the square-draft to water-depth ratio $\sqrt{A_X}/h$ is 0.115. Hence, transposing,

$$h_1 = \frac{\sqrt{A_X}}{0.115} = \frac{\sqrt{6.25}}{0.115} = 21.7 \text{ ft.}$$

For a V_I/V_∞ ratio of 0.9982, the critical-speed ratio $V_\infty/\sqrt{gh}$ from Fig. 61.K is 0.563. Again transposing,

$$h_2 = \frac{V_\infty^2}{g(0.563)^2} = \frac{(16.05)^2}{(32.174)(0.563)^2} = 25.3 \text{ ft.}$$

The potential-flow effect is so small here that the square-draft to water-depth ratio is somewhat indeterminate. Nevertheless, it is apparent that, because of the greater depth required to produce the assumed wave-speed ratio, the latter factor is also the determining one in this case. The minimum depth is therefore of the order of 25 or 26 ft.

61.12 D. W. Taylor's Criterion for the Limiting Depth of Water for Ship Trials. A simple formula is given by D. W. Taylor for the minimum depth of water h involving "no increase of resistance" [S and P, 1943, p. 79]. This is the dimensional expression: Minimum depth = 10 (draft H) $(V/\sqrt{L})$, where the depth h, the draft H, and the length L are in ft, and the speed V is in kt. Taylor gives the following limitations for this formula:

"1. To vessels not of abnormal form or proportions up to a block coefficient C_B of 0.65
2. For speeds for which $V/\sqrt{L}$ is not greater than 0.9
3. The formula may be of use beyond the limits indicated above, but in such cases (it) needs to be applied with caution and discretion."

Despite these limits, expressly stated, this formula has been used rather widely for estimating minimum depths of water in which to conduct ship trials.

Taylor's formula as it stands is not consistent dimensionally, for the reasons given in Appendix

2 of Volume I. It can be made so, as explained there, by substituting $3.367F_n$ for the Taylor quotient $V/\sqrt{L}$, whereupon it becomes

$$h_{\text{Min}} = 33.67(H)F_n \qquad (61.\text{ii})$$

Applying this formula to the liner of Example 61.V, where the draft H is 34.39 ft and the Froude number F_n at the designed speed of 32 kt is $54.05/\sqrt{32.174(962)} = 0.307$, the predicted value of $h_{\text{Min}} = 33.67(34.39)(0.307) = 355.5$ ft. This is compared to a limiting depth of 290 ft for a $\Delta R_{T\infty}$ of 0.4 per cent, as derived in Sec. 61.11, Example 61.V. Taylor's formula is therefore conservative or perhaps on the safe side.

61.13 Predicted Shallow-Water Resistance by Inspection. The procedures described in Secs. 61.5 through 61.11 for determining quantitatively the effect of shallow water on ship speed and resistance in the subcritical range are somewhat tedious, and are not well suited to making the on-the-spot estimates often required. Furthermore, they give no indication, not even approximate, as to what may be expected in the supercritical range, which may easily be reached under certain conditions in practice.

A means of making predictions as to relative speeds and resistances in shallow and deep water by inspection serves a certain purpose in design procedure, although it is admittedly neither adequate, accurate, or reliable. The simplified procedure of Sec. 61.10 and Fig. 61.J could be extended to cover *speed* reductions from 2 per cent up to 5 per cent, and possibly up to 10 per cent, provided the differences between the shallow-

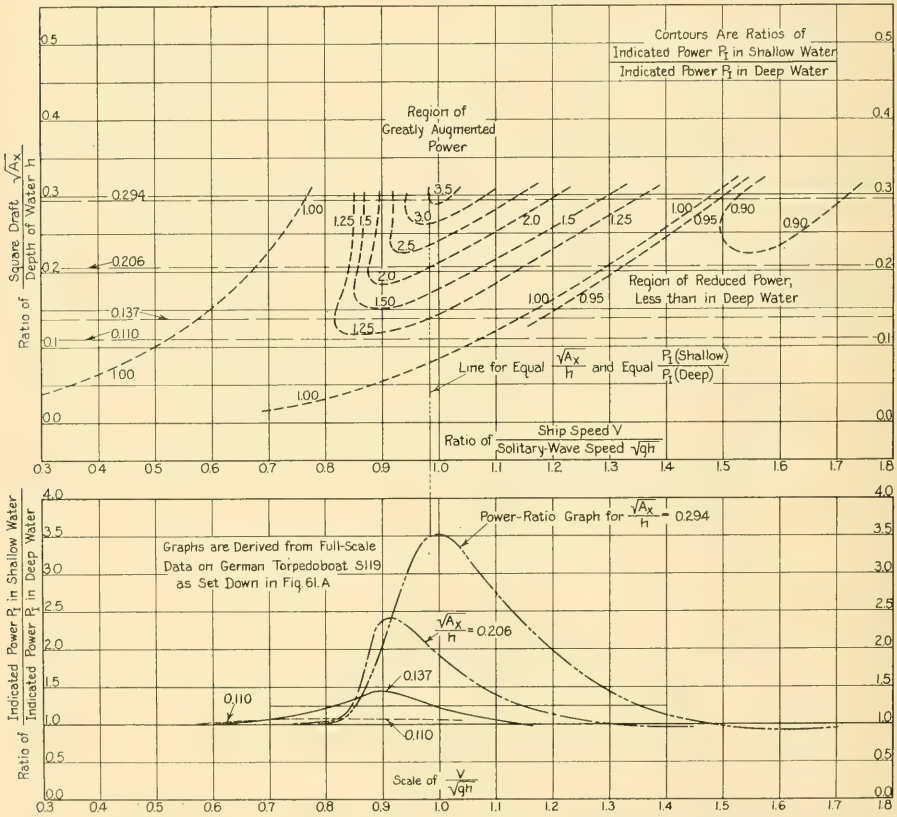

Fig. 61.L One Set of Graphs for Determining Increases in Shallow-Water Total Resistance by Inspection

water and deep-water total resistances at points such as C_1 and A_1 on Fig. 61.B could be neglected.

For estimates of the change in total *resistance* at the same speed, when moving from deep to shallow water, the problem is considerably more difficult, since the answer depends upon the slopes of the graphs of R_T on V in the region being investigated.

Because of the lack of reliable methods for transforming increased total resistance in shallow water to terms of increased *power*, discussed in Sec. 61.16 following, there is some merit in a prediction method by inspection which endeavors to predict the increased power directly. Even though a ship is rarely pushed in shallow water to speeds which would be considered normal if the water were deep, it is helpful to know approximately how much power would be required under these circumstances.

A graph suitable for such a purpose is the partial diagram at the top of Fig. 61.L, having contours of the ratio (shallow-water power)/(deep-water power) plotted on appropriate arguments. Following the procedure developed by O. Schlichting, these are $\sqrt{A_X}/h$ and $V/\sqrt{gh}$, where V is a given speed, in either deep or shallow water, and $\sqrt{gh}$ is the solitary-wave speed in water of depth h.

The contours in Fig. 61.L are indicated as tentative, since they are derived from isolated data observed on one series of ship trials, that of the German torpedoboat *S119*; see reference (4) of Sec. 61.22. These data are recorded graphically in Fig. 61.A. They are reduced, in the lower diagram of Fig. 61.L, to graphs indicating the ratios of indicated power P_I in shallow water to P_I in deep water, for four depths of shallow water, on a basis of the ratio $V/\sqrt{gh}$, the same as for the upper diagram in that figure. It is assumed for this reduction that a depth of water h equal to $0.951L$, indicated in Fig. 61.A, represents deep water. It is further assumed that the prismatic coefficient C_P of this vessel is 0.64, from which A_X is calculated to be 45.5 ft^2 and $\sqrt{A_X}$ is 6.75 ft. The four graphs of the lower diagram of Fig. 61.L therefore represent indicated-power ratios at $\sqrt{A_X}/h$ values of 0.110, 0.137, 0.206, and 0.294.

Reduction of full-scale ship data in similar fashion, from the references of Sec. 61.22, gives contours which are extremely difficult, if not impossible to reconcile with those of Fig. 61.L, so much so that they are not included here. In most

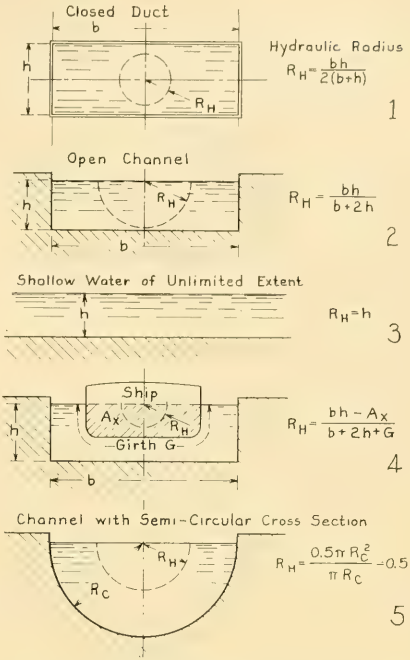

FIG. 61.M DEFINITION SKETCHES FOR HYDRAULIC RADIUS

of these cases the value of A_X has to be estimated, as was done for the *S119*. Available data from model tests are, by the method of analysis described, out of line with the ship data and with each other. It seems clear at this stage (1956) that all the pertinent variables in the confined-water situation have not been taken into account.

61.14 Calculating and Using the Hydraulic Radius of Channels. As is explained presently, predictions of the effect of the sides and the bed of channels upon ship resistance make use of the characteristic channel dimension known as the *hydraulic radius*, rather than the water depth h used for shallow-water predictions. For a closed duct with no solid body inside it this is the ratio, described in Sec. 18.11, of the transverse duct or flow area to the wetted perimeter of the duct. This situation is depicted at 1 in Fig. 61.M, where b, h, and R_H are all drawn to the same scale, and R_H has the dimensions of a length. An open channel with no ship in it, as in diagram 2, has wetted perimeter on only the bottom and the

two sides. With the same water area as the duct, its R_H is larger. For an open channel with a ship, as at 4, R_H is the ratio of (1) the cross-section area of the water in the channel to (2) the wetted perimeter of the *solid boundaries* of both channel and ship. In shallow water of infinite width, when $b \to \infty$, the depth h, the ship girth G, and the ship section area A_X become negligible with respect to the water-area and width factors. The hydraulic radius R_H then becomes equal to the depth h, as at 3 in the figure. For a rectangular canal this is expressed in symbols as:

$$R_H = \frac{bh - A_X}{b + 2h + G}\Bigg]_{\substack{b \text{ is large} \\ \text{compared to} \\ \text{other factors}}} = \frac{bh}{b} = h \tag{61.iii}$$

Assuming a waterway with horizontal bottom and vertical sides, not occupied by a ship, the hydraulic radius is related to the water depth h in the following manner:

Width b in terms of h	1	2	3	10	20	50	100	200
R_H in terms of h	0.33	0.50	0.60	0.833	0.909	0.962	0.980	0.990

For open channels of non-rectangular and irregular sections, with ships in them, the hydraulic radii are determined by exactly the same procedure, governed by the same rule. Example 61.VII, in the next section, illustrates the method.

Studies made in connection with the preparation of Fig. 61.L, combined with analyses undertaken (in 1956) subsequent to those reported in the remaining sections of this chapter, indicate rather definitely that shallow-water effects cannot be correlated on the basis of the single "transverse" parameter $\sqrt{A_X}/h$, nor can confined-water effects be correlated solely on a basis of $\sqrt{A_X}/R_H$. This applies particularly to effects associated with the *potential-flow* ratio of Sec. 61.5, between the shallow-water speed V_h and the Schlichting intermediate speed V_I. Analyses of the blocking effect of model basins upon the ship models towed in them indicate that the interference effects are negligible even when, because of the limited width of the basin, the hydraulic radius of its section is not much more than half of its actual depth. By this criterion, the basin is by no means the equivalent of unlimited deep water of the same depth. Nevertheless, it serves as such, apparently because of the very large bed clearance under the largest (and widest) flat-bottomed model that is towed in it. Since more of the water goes under the bottom of a model with a large B/H ratio than with a small one, the effect of small bed clearance becomes greater as the B/H ratio increases. Unfortunately, not enough is known of these and other effects to take account of them quantitatively at the present time.

61.15 Estimating the Effect of Lateral Restrictions in Shallow Water in the Subcritical Range. Since the speed of a wave of translation in a restricted channel depends only on the depth of the channel, it appears plausible to assume that O. Schlichting's theoretical assumption concerning the equality of pressure resistance due to wavemaking at the speed V_∞ and V_I remains valid for these restricted channels. The second assumption of Schlichting concerning the speed correction due to the potential flow around the ship hull requires modification to take account of the width of the channel. The relationship developed by L. Landweber [TMB Rep. 460, May 1939, p. 10] involves, instead of the depth of water h as before, the hydraulic radius. The necessity for taking full account of the lateral restrictions is emphasized by the following comments, quoted from a discussion by F. Rayner on page 114 of a paper by A. F. Yarrow [INA, 1903]:

> "... one of the greatest difficulties in towing on inland waters is the friction between the boats and the sides and bottom of the water way. I have myself seen, on some of the narrow canals, steam barges almost stationary when going through what are called, in canal language, "bridge holes," where you get the minimum width, and consequently enormous friction; as soon as the boat gets away from the bridge, she shoots ahead."

The ratio $\sqrt{A_X}/h$, relating the square draft to the water depth, then becomes $\sqrt{A_X}/R_H$, relating the square draft to the hydraulic radius. The fact that Landweber used, in the reference cited, a value twice as large as that defined here was compensated for by his use of a factor 2 in the ratio of square draft to hydraulic radius.

When the substitution of R_H for h is made, the potential-flow ratio V_h/V_I for confined waters becomes a function of $\sqrt{A_X}/R_H$ for the restricted channels. A procedure corresponding exactly to the Schlichting method described in Sec. 61.5 can then be employed. This means that Fig. 61.G serves for making the numerical calculations as before, provided the user remembers that the upper scale is a square-draft to hydraulic-radius ratio.

From the theoretical curves of Fig. 61.E and the experimental curves of Fig. 61.G the speed and the resistance of a ship in a restricted channel can then be computed when its deep-water speed and resistance are known. The procedure to be followed is the same as for computing shallow-water resistance; several examples follow.

Example 61.VII. Take the case of the 370-ft shallow-water ship of Example 61.I preceding, moving in the channel depicted at 1 in Fig. 61.N. The essential model and ship data are given on SNAME RD sheet 9, covering TMB model 3818. What would be the actual ship speed at a resistance equal to that for 8 kt in deep water? The ship has a maximum section area A_X of 1,111.3 ft² and the water is at sea level, with a temperature of 80 deg F. The value of the square draft $\sqrt{A_X}$ is 33.34 ft. The value of g is 32.174 ft per sec².

The section area of the water around the ship, using the values in diagram 1 of the figure, is

$$A_{\text{Channel less ship}} = [(250)(35)] + \frac{(35)^2}{2} + \left[(60.6)\left(\frac{35}{2}\right)\right] - 1{,}111.3 = 9{,}311.7 \text{ ft}^2.$$

The wetted perimeter, including that of the ship, is

$$P = 250 + 35 \text{ cosec } (45 \text{ deg}) + 35 \text{ cosec } (30 \text{ deg}) + 98 = 467.5 \text{ ft}.$$

The hydraulic radius is then 9,311.7/467.5 = 19.92 ft, only a little more than half the channel depth. The $\sqrt{A_X}/R_H$ ratio is 33.34/19.92 or 1.67.

The equivalent "rectangular" depth h_{Eq} of the channel is the section area *without the ship*, divided by the surface width, or (9,311.7 + 1,111.3)/(250 + 35 + 60.6) = 10,423/345.6 = 30.16 ft.

The value of V_∞ is 8 kt or 13.51 ft per sec. Then

$$\frac{V_\infty}{\sqrt{gh_{\text{Eq}}}} = \frac{13.51}{\sqrt{32.174(30.16)}} = 0.43.$$

From the theoretical curve of Fig. 61.E, the corresponding value of the intermediate speed ratio V_I/V_∞ is 1.00 and $V_I = V_\infty$. Hence all the speed reduction is due to potential flow. Since the points corresponding to A_1 and B_1 of Fig. 61.B coincide, the friction resistance does not come into the picture, nor is it necessary to construct any deep-water and restricted-channel resistance curves.

Entering the extrapolated broken-line portion of the curve of Fig. 61.G for a square-draft to hydraulic-radius ratio of 1.67, the value of the potential-flow ratio V_h/V_I is 0.783. Since $V_I = V_\infty$ in this case, $V_h = 0.783V_\infty = 0.783(13.51) = 10.6$ ft per sec or 6.28 kt. This is the required speed.

It is pointed out in Eq. (61.iii) of Sec. 61.14 that when the channel width b becomes large in proportion to the channel depth h, as when a shallow river widens into a shallow estuary, the term $2h$ in the expression for the hydraulic radius drops out, leaving simply the quotient bh/b, whereupon the hydraulic radius R_H becomes equal to the depth h.

The question now arises, what constitutes unrestricted shallow water? This is difficult to answer explicitly because it depends upon the maximum-section area of the ship being considered with the water and upon the square-draft to hydraulic-radius ratio. Put in another way, the effect of using the ratio $\sqrt{A_X}/R_H$ instead of the ratio $\sqrt{A_X}/h$, where h is the restricted-water depth, depends to some extent upon the position of the ratio point along the graph of Fig. 61.G. At small values of the ratio $\sqrt{A_X}/h$, toward the left end of the diagram, the potential-flow speed ratio V_h/V_I changes very little with change in water depth. In any case, one or two calculations involving the hydraulic radius, along the lines of Example 61.VII, should clear up the matter readily. When the channel width becomes from 100 to 200 times the depth, the table in Sec. 61.14 indicates that the restricted channel has become the practical equivalent of open, unlimited shallow water.

61.16 Lack of Reliable Data on Power and Propulsion-Device Performance. No satisfactory method has yet been developed for estimating the increase in shaft or propeller power, the change in rate of propulsion-device rotation, or the variations in other propulsion factors due to shallow and restricted waters. E. A. Wright touches briefly on these matters [SNAME, 1946, Fig. 10, p. 381]. The present unsatisfactory situation is due partly to the limitations imposed by various kinds of propelling machinery on the combinations of rotational speeds, torques, and powers developed by them. The usual ship-performance data are rarely of much help because, for example, the throttle setting may be held

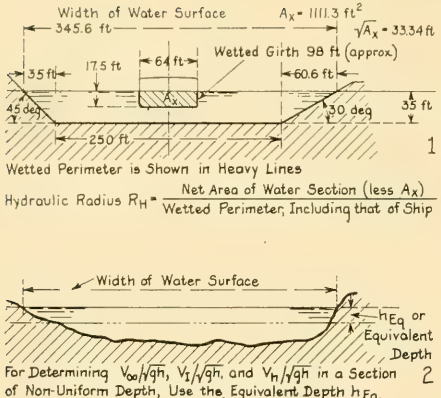

FIG. 61.N EXPLANATORY AND ILLUSTRATIVE SKETCHES FOR EQUIVALENT DEPTHS AND HYDRAULIC RADII OF RESTRICTED CHANNELS

constant and *all other* variables allowed to change. The water depths may fluctuate widely with ship location in the shallow area or along the channel; the resistances and perhaps the speeds fluctuate with them.

Unless a ship is designed for special service in confined waters, only rarely does it have any great reserve of power to match the increase in resistance in the shallower channel depths and narrower widths, assuming that it is advisable or permissible to maintain the deep-water speed. If it is so designed, the limiting conditions become the basis of the design, and the operator gets whatever improved performance he can from the ship in deeper and more open water.

When the ship speed is reduced because of the diminished velocity of the Velox-wave system in shallow water, the speed of the ship through the surrounding water—in other words, its *relative speed*—is correspondingly reduced because the water stands still, generally speaking, while the wave moves by. This is the reason why the friction resistance is reduced when the ship slows from its deep-water speed to its intermediate speed.

The ship resistance R_T is reduced by this decrement in R_F, represented by the ordinate MB_1 in Fig. 61.B, but not by as much as it would be for a corresponding speed reduction in deep water. Thus point B_1 in the figure is higher than point L. For the intermediate speed V_I, therefore, the shallow-water power, $R_{Th}(V_I)$, is greater than it would be for the same speed in deep water. The rate of rotation drops by a ratio somewhat greater than V_I/V_∞, assuming the wake fraction w constant, because of the greater resistance that must be overcome and the greater thrust to be developed. Furthermore, as the thrust loading at point B_1 is greater than it would be at point L, the propeller efficiency drops slightly, still further increasing the power at the point L.

As the ship speed diminishes from the intermediate value V_I to the shallow-water value V_h, with no change in total resistance, the effective power P_E diminishes, as do the thrust T and the speed of advance V_A, unless the augmented backflow occurs in a region occupied by the propulsion device(s). From here on, the data are scanty and the analysis is nearly nonexistent.

At a sufficiently low value of $V_\infty/\sqrt{gh}$, the ship speed is reduced solely because of the ratio $\sqrt{A_X}/h$. The speed drops from V_∞ to V_h but the resistance remains the same. All the water ahead of the ship has to get around astern, it must flow backward in this process, and the backward flow is much faster close to the ship. The ship thus has to move against what amounts to a contrary current in the channel, so that the lost of speed is equal to the effective velocity of this counter current. Assuming that the ship moves through the water close around it with the same relative speed, the shaft power and rate of rotation of the propulsion device(s) should remain substantially the same as at the speed V_∞ in deep water.

61.17 Data on Confined-Water Operation at

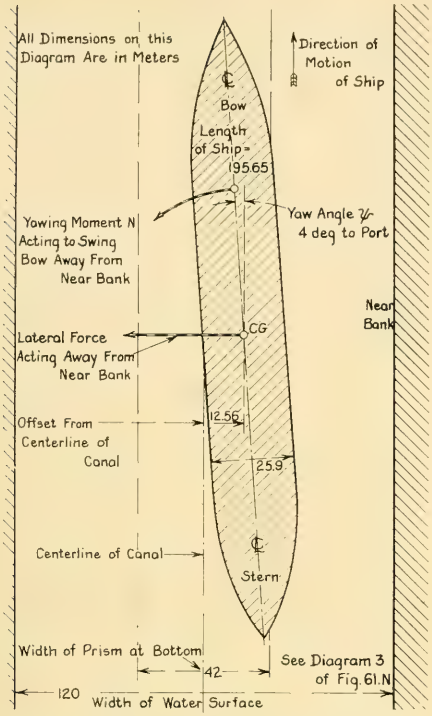

Fig. 61.O Diagram of R. Brard's Full-Scale Prototype of Model 111 in Full-Scale Suez-Canal Section

Supercritical Speeds. If supercritical speeds are reached, as they can be on many fine, fast vessels in shallow-water areas where there are no limitations on squat, on the eroding action of waves along the banks, and on interferences with other craft, the shaft power at certain speed-length quotients may fall below the value required in deep, unlimited water. In Sec. 29.7 of Volume I it is explained that a following vessel riding on the front of a transverse wave created by a leading vessel is able to keep station at reduced shaft power and with a reduced rate of rotation of its propulsion device(s). In actual cases, following destroyers have been able to hold position with a 20 per cent reduction in rpm.

Data relating to the resistance, speed, and change of trim of a heavy cruiser model running at a supercritical speed in a model channel are given by E. A. Wright [SNAME, 1946, Fig. 29, p. 396]. Similar data are to be found in some of the references of Sec. 61.22.

61.18 Data on Offset Running Positions and Steering in a Channel. Few published quantitative data are available on the offset running of a ship between canal walls, or alongside a single wall, as depicted in Figs. 18.G and 18.H and described in the accompanying text of Secs. 18.5 and 18.6 of Volume I; see also Fig. 61.O. The two outstanding sources appear to be:

(1) Garthune, R. S., Rosenberg, B., Cafiero, D., and Olson, C. R., "The Performance of Model Ships in Restricted Channels in Relation to the Design of a Ship Canal," TMB Report 601, August 1948. Section 4 of this report covers the behavior of models in central and offset positions, in varied depths of channel, both towed and self-propelled, and with different rudder angles. During many of these tests the ship model was stationary in a current of moving water. Yawing moments, lateral forces, and rudder angles to maintain equilibrium conditions are given in terms of the other variables.

(2) Brard, R., "Maneuvering of Ships," SNAME, 1951, pp. 229–257. This paper reports the results of tests on three ship models in a model channel representing the Suez Canal [SNAME, 1951, pp. 232–242]. Graphs of lift, drag, and yawing moment coefficient, C_y, C_x, and C_n, respectively, are supplemented in Figs. 10 and 11 of the reference by graphs of lateral forces and turning moments for a rather wide range of yaw angles in three different lateral positions, first on the canal centerline and then offset by 0.15 and 0.30 of the 42-meter bottom width of the full-scale canal section. The ship beam was 25.9 meters or 25.9/42 = 0.617 of that width, and its draft was 10.4/13 or 0.8 of the canal depth.

From Brard's Fig. 10 on page 241 of the reference the lateral force on the ship represented by Paris model 111 was, at the maximum offset, found to be zero at about 1.2 deg yaw angle away from the near bank. From Brard's Fig. 11 on page 242 the value of the turning-moment coefficient C_n at this yaw angle was about 0.075, acting to swing the bow away from the near bank. A rudder angle applied toward the bank, to counteract this yawing moment away from it, would set up a lateral force to push the ship away from the bank. Equilibrium would therefore be achieved at a yaw angle less than 1.2 deg.

This is the reason why, to get the ship away from the near bank and back into the center of the channel, rudder angle is applied *toward the near bank!*

61.19 Prediction of Ship Resistance in Canal Locks. The force required to push or pull a close-fitting ship into or out of a lock, discussed

in Sec. 35.12, is estimated by methods derived from model tests [EMB Rep. 189, Mar 1928].

It is shown in the references cited that the augmented lock resistance R_L may be related to the open-water resistance R_0 by the equation

$$\frac{R_L}{R_0} - 1 = kn^2 \qquad \text{(61.iv)}$$

where n is the ratio of the maximum-section area A_X to the transverse clearance area between the ship maximum section and the lock boundaries. The coefficient k is a number which has been found by experiment to vary from 6.2 to 20 and over but whose average value may be taken as about 11. Eq. (61.iv), shown graphically in Fig. 61.P, should predict R_L/R_0 within plus and

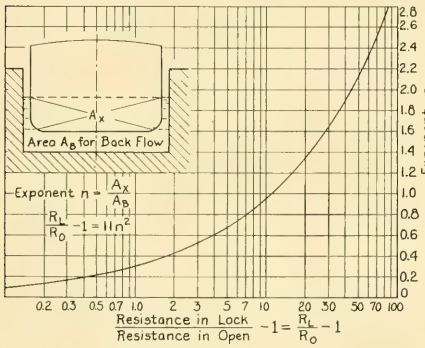

Fig. 61.P Graph for Determining Added Resistance of Ships When Transiting Canal Locks

minus 25 per cent for entrance and exit speeds not exceeding 3 kt, as applied to ships having lengths of 600 ft or more. The model tests covered ranges of n from about 0.2 or less to 2.82. It is perfectly feasible, however, to transit ships with clearances so small that n is approximately 8 to 10.

61.20 Unexplained Anomalies in Shallow and Restricted Water Performance. It has been the experience of most analysts and experimenters on ship behavior in confined waters that no sooner have they found a rule which appears to predict performance reasonably well than a case crops up which upsets all their calculations. This indicates definitely one thing: There are certain actions and effects not yet known and taken into account, involving phenomena not now observed.

The following extract is from page 6 of TMB Report 640, February 1948, by W. H. Norley:

"There is some indication, from a study of the sinkage curves, that the sinkage may vary with the beam-draft ratio of the ship. It is recommended that a systematic investigation with models in shallow water be made, the only variable being the beam-draft ratio, to obtain further information on sinkage."

Very slight unevenness in a solid basin floor, such as in the TMB shallow-water basin, combined with bed clearances approaching zero, make it almost impossible to obtain accurate shallow-water resistance data with models. Bed irregularities in ship operating areas may have similar effects on full-scale resistance and power. Unknown current magnitudes and directions at the several depths over an irregular bed may also influence ship behavior in an unpredictable manner.

Until it is known what to observe, careful experimenters will record all the data which can conceivably have any bearing whatever on the result, when they conduct ship trials in shallow and restricted waters.

As an indication of some of the unexplained anomalies which now exist, there are listed hereunder some data given to the author in January 1949 by the then Captain Arleigh A. Burke, USN, based upon his experience as commanding Officer of the light cruiser U. S. S. *Huntington* (CL107):

(1) When operating in the shallow waters of the River Plate, with depths varying from 26 to 35 ft, draft of the ship about 25 ft, it was possible to achieve a ship speed of about 15 kt by making revolutions for about 19 kt in deep water. However, when increasing the rate of propeller rotation above this value, it was stated that the ship actually ran *more slowly* than 15 kt.

(2) It was found difficult to move the ship sideways in shallow water. This included attempts to move the bow and the stern separately as well as to move the ship bodily in crab fashion, by the motion known as sidling.

(3) When passing through the Suez Canal the ship would keep herself more or less in the center of the channel without any appreciable steering. If she sheered slowly toward one bank a positive differential pressure would build up on the bank side of the bow and push the bow back toward midchannel. Having swung so that the bow was headed away from the shore the ship would work herself out from the near bank.

61.21 Summary of Shallow- and Restricted-Water Effects. Summarizing the effects of

shallow and restricted waters upon ship performance, as described and explained in Chaps. 18 and 35 of Volume I and in the preceding sections of this chapter, the following items appear in qualitative terms:

(a) The draft below the still-water surface is increased because of the deeper sinkage of the ship in the intensified Bernoulli contour system
(b) The changes of trim are augmented because of the intensified Velox-wave system
(c) The overall sinkage and trim is a function of the position and slope of the ship on the surface of a solitary wave of translation which may be traveling near the ship
(d) The pressure drag or resistance is increased because of the constrictions imposed on the ship velocity and pressure fields by the rigid boundaries
(e) The slope drag or slope thrust encountered is a function of the slope and the position of the ship with respect to the solitary wave of translation
(f) The slope drag may be sufficient, when it changes sign and becomes a slope thrust, to cause a *decrease* in total drag with an *increase* in speed, at a point just above the critical speed
(g) The friction drag is increased, partly by the augmented rearward motion of the water past the ship and partly by the thinning of the boundary layer, with consequent increase in velocity gradient in the laminar sublayer, when the clearances between the ship and the rigid boundaries become small
(h) The ship vibration is generally intensified and magnified in shallow water.

61.22 Partial Bibliography on the Effects of Confined Waters on Models and Ships. A partial list of references follows on shallow- and restricted-water effects and on the behavior of ships in confined waters:

(1) White, Sir William H., "Notes on Recent Experience with Some of H. M. Ships," INA, 1892, pp. 160–186
(2) Rasmussen, A., "The Influence of the Depth of Water upon the Speed of Ships," Engineering, London, 7 Sep 1894. This article is reprinted in (5) following, pp. 18–20.
(3) Laubeuf, M., "Influence de la Profondeur de l'Eau sur la Vitesse des Navires (Influence of the Depth of Water on the Speed of Ships)," ATMA, 1897, Vol. 8, pp. 207–213. A partial translation is available at the DTMB.
(4) Paulus, Naval Constr., "Versuche zur Ermittlung des Einflusses der Wassertiefe auf die Geschwindigkeit der Torpedoboote (Tests of the Effect of Water Depth on the Speed of Torpedoboats)," Zeit. der Ver. Deutsch. Ing., 10 Dec 1904, pp. 1870–1878. This paper contains records of trials of the German torpedoboat *S119*, including wave-profile and change-of-trim diagrams for a series of speeds.
(5) Rasmussen, A., "Some Steam Trials of Danish Ships," INA, 1899, pp. 12–26 and Pl. V, describing tests on the Danish torpedoboats *Makrelen* and *Söbjörnen*
(6) Rota, G., "On the Influence of Depth of Water on the Resistance of Ships," INA, 1900, pp. 239–248, giving the results of tests on Italian torpedoboat models
(7) White, Sir William H., MNA, 1900, pp. 469–470
(8) Haack, M., "Nouvelles Récherches sur la Résistance des Carènes et le Fonctionnement des Bateaux (New Investigations on the Resistance of Hulls and the Functioning of Ships)," ATMA, 1900, Vol. 11, pp. 41–48. This is a discussion of shallow-water performance, based upon the published data of Captain Rasmussen and General Rota, in INA for 1899 and 1900, respectively.
(9) Schütte, J., "Neuere Versuche über Schiffswiderstand in freiem Wasser (New Experiments on Ship Resistance in Open Water)," Proc. Ninth Int. Shipping Congr., Düsseldorf, 1902
(10) Durand, W. F., RPS, 1903, pp. 110–119. Covers the "Increase of Resistance Due to Shallow Water or to the Influence of Banks and Shoals."
(11) Popper, S., INA, 1905, Part I, pp. 199–201 and Pls. L-LIII
(12) Yarrow, H.; report on the trials of a Yarrow-built destroyer, INA, 1905, Part II, pp. 339–343, 349–358, and Pls. LXXIX-LXXXI
(13) Marriner, W. W., INA, 1905, Part II, pp. 344–358 and Pls. LXXXII, LXXXIII
(14) Watts, Sir Philip, INA, 1908, pp. 69–70
(15) Watts, Sir Philip, INA, 1909, pp. 176–178 and Pls. XV and XVI, reporting on trials of the British destroyer *Cossack*. The pertinent data for the two measured-mile courses on which this vessel was run are:

(a) Skelmorlie mile, depth h = 240 ft, critical wave speed = 87.8 ft per sec or about 52 kt
(b) Maplins mile, depth h = 45 ft, critical wave speed = 38.05 ft per sec or about 22.5 kt

(16) Sadler, H. C., "The Resistance of Some Merchant Ship Types in Shallow Water," SNAME, 1911, pp. 83–86
(17) Baker, G. S., and Kent, J. L., "Effect of Form and Size on the Resistance of Ships," INA, 1913, Part II, pp. 37–60 and Pls. III, IV. Fig. 5 on Pl. IV shows a 2-diml ship-shaped forebody in a uniform stream parallel to the longitudinal axis, and gives streamlines for the flow of the water around this forebody and between two parallel boundaries. The forebody was "shaped" by combining 2-diml line sources and sinks with a uniform stream parallel to the ship axis.
(18) Taylor, D. W., "Relative Resistances of Some Models with Block Coefficient Constant and Other Coefficients Varied," SNAME, 1913, pp. 1–8,

esp. pp. 2–6 and Pls. 8–11, covering tests made in shallow water

(19) Havelock, T. H., "Effect of Shallow Water on Wave Resistance," Proc. Roy. Soc., London, 1922

(20) Heckscher, E., "Beziehungen zwischen Antriebskraft und Geschwindigkeit bei verschiedenen Fahrwassertiefen (Relation Between Propulsion and Speed at Different Water Depths)," WRH, 22 Sep 1929, pp. 368–370

(21) Lock, C. N. H., and Johansen, F. C., "Wind Tunnel Interference on Streamlined Bodies," ARC, R and M 1451, 1933

(22) Baker, G. S., SD, 1933, Vol. I, pp. 193–209

(23) Kreitner, J., "Über den Schiffswiderstand auf Beschränktem Wasser (Concerning Ship Resistance in Restricted Waters)," WRH, 1934, Vol. XV, pp. 77–82. English transl. in BuShips (U. S. Navy Dept.) Transl. 389, Sep 1950.

(24) Heiser, H. M., "The Effect of Shallow Water upon the Resistance of Ships," USNI, Vol. 64, May 1938, pp. 709–713. This is a restatement of the data mentioned by D. W. Taylor in S and P, 1943, pp. 74–81 from W. H. White, INA, 1892, Rasmussen (1899), Rota (1900), and Watts (1908 and 1909). The author gives Taylor's dimensional formula $h_{\text{Min}} = 10H(V/\sqrt{L})$; see the comments on this formula in Sec. 61.12.

(25) Schmidt, W., and Blank, H., "Geschwindigkeitsänderung von Schiffen auf Flachem Wasser (Speed Changes for Ships in Shallow Water)," Schiffbau, 15 Mar 1938, Vol. 39, pp. 100–103. Part of this paper is an analysis of the shallow-water data given by Rasmussen, Paulus, and Watts, in references (4), (5), and (15), for the *S119*, *Makrelen*, *Söbjörnen*, and *Cossack*.

(26) Schmidt, W., and Blank, H., "Schiffsgeschwindigkeit in Kanälen (Ship's Speed in Canals)," Zeit. des Ver. Deutsch. Ing., 2 Jul 1938, Vol. 82, pp. 794–796

(27) Tupper, K. F., "Contribution to the Question of the Effect of the Basin Walls on Ship Model Tests," Proc. Fifth Int. Congr. Appl. Mech., 1939, pp. 509–512

(28) Helm, K., "Tiefen- und Breiteneinflüsse von Kanälen auf den Schiffswiderstand (Influence of Depth and Breadth of Channels on Ship Resistance)," WRH, 1 Sep 1939, pp. 277–278; also HSPA, Part II, Oldenbourg, Berlin, 1940, pp. 144–171. A list of 7 references appears on the last page. There is an English abstract of this paper on pages 224–226 of the referenced HSPA volume.

(29) Comstock, J. P., and Hancock, C. H., "The Effect of Size of Towing Tank on Model Resistance," SNAME, 1942, pp. 149–197

(30) Taylor, D. W., S and P, 1943, pp. 74–81

(31) Wright, E. A., SNAME, 1946, Fig. 29 on p. 396. Describes model tests conducted in a restricted channel at Newport News, with models towed at both subcritical and supercritical speeds.

(32) Van Lammeren, W. P. A., Troost, L., and Koning, J. G., RPSS, 1948, pp. 17–19, 56–60, 74–76

(33) Lunde, J. K., "On the Linearized Theory of Wave Resistance for Displacement Ships in Steady and Accelerated Motion," SNAME, 1951, pp. 25–85, esp. pp. 50–60 for a discussion of shallow-water conditions

(34) Brard, R., "Maneuvering of Ships in Deep Water, in Shallow Water, and in Canals," SNAME, 1951, pp. 229–257, esp. Figs. 4, 5, and 6 on pp. 237–238

(35) Robb, A. M., TNA, 1952, pp. 444–449

(36) Schuster, S., "Investigations of Flow and Drag Conditions of Ships in Motion in Water of Limited Depth and Width," STG, 1952, Vol. 46, pp. 244–288 (in German). The following review of this paper by T. P. Torda is quoted from Appl. Mech. Rev., Apr 1955, Rev. 1239, p. 180:

"An extensive discussion of existing literature and theories is given. The problems of limited depth, and ship motion is channels of limited width, are discussed in the light of various theories and experiments. In particular, the results of model experiments are discussed. The theories of wave form and wave propagation are extended and hydraulic considerations are discussed. In concluding the paper, author notes that the problems of limited depth and limited width of water are different and cannot be treated by a uniform theory. Author recommends the use of the nomogram developed in the paper for the treatment of actual problems of ship motion in limited waters. Discussions of the paper by F. Horn, G. Weinblum, W. Graff, R. O. Schlichting, H. Dickmann, and Klindwort are given, together with the reply of author."

(37) A list of 27 references, some of them quoted in the foregoing, is given by G. S. Baker on pages 124–125 of his paper "The Effect of Shallow Water on the Movement of a Ship," INA, Apr 1952, pp. 110–125.

CHAPTER 62

Estimating the Added Mass of Water Around a Ship in Unsteady Motion

62.1 General. In Sec. 3.4 of Volume I there is explained the concept of the added mass of the entrained liquid surrounding a body or ship in unsteady motion. In a recent paper, K. Wendel gives a superb exposition of this concept in both physical and mathematical terms [STG, 1950, Vol. 44, pp. 207–255. English version in TMB Transl. 260 of Jul 1956]. Moreover, his discussion is extended to cover the accelerative-force and pressure features not treated in Sec. 3.4 or in the present chapter, as well as other modes of motion. It should be possible for the reader who is familiar with the preceding portions of Parts 1, 2, and 3 of this book to follow Wendel's development intelligently, and to derive great benefit from it, even though some of the details are passed over. His description of the derivation of added liquid masses for ships which are heaving and rolling, with and without bilge keels, applies to the discussion of wavegoing in Part 6 of Volume III.

The effect of the added mass of entrained liquid around a body in unsteady motion, in a relationship of (1) the forces applied to the body, and (2) the resulting body accelerations, is often called the inertia effect. The added mass itself is sometimes called the accession of inertia for the body. In other quarters it is called the hydrodynamic mass. Similarly, the 0-diml coefficients relating the added mass of liquid to the mass of the body, called here the added-mass (or added mass moment of inertia) coefficients, are often called the inertia (or moment of inertia) coefficients. These important definitions are discussed further in Sec. 62.2.

For the treatment in Parts 5 and 6 of Volume III of ship motions in maneuvering and wavegoing, both of which involve unsteady motions, the added mass of the entrained water almost always enters as a sizable factor. In general, the added masses are of the same order of magnitude as the ships themselves. For the design of a new ship, or for estimating the performance of an existing one, numerical values must be known or estimated. Knowledge of the quantitative effects of the entrained water in adding to the mass is also necessary in a study of body and ship vibration in liquids, discussed at some length in Sec. 20.11 of Volume I and in subsequent sections of this chapter.

It is indicated in Sec. 3.4 that the magnitude of the added mass is determined normally from a knowledge of the kinetic energy in the velocity field around the body for a given mode of motion. This energy, in turn, is calculated from an expression defining the velocity potential throughout the field around the body.

For practically every case cited throughout the present chapter, where the added-mass coefficient is derived by analytic instead of by empirical methods, the value is calculated on the basis of the following assumptions:

(1) The potential theory is valid for the case in hand. This means that the body is completely surrounded by an ideal liquid of great extent in all directions, in which only potential flow takes place. This liquid is without viscosity, therefore no boundary layer exists.

(2) The flow pattern and the added mass of

entrained liquid are constant, independent of the frequency or the amplitude of unsteady motion

(3) There are no discontinuities in the liquid surrounding the body or ship, which means that no separation or cavitation exists

(4) There are no damping forces or moments acting on the body or ship, because of the lack of viscosity in the liquid

(5) For those modes of unsteady motion which do not involve directly the speed of the body or ship along its major axis, the added mass of the entrained liquid is independent of this speed

(6) For a body floating on water, in a state of equilibrium, the kinetic energy and the added-liquid mass are assumed to be half of the respective values for a fully and deeply submerged "double body" composed of the underwater form plus its mirror image above the free surface of the liquid

(7) For some of the analytic procedures developed to determine the kinetic energy in the liquid surrounding the underwater hull of a surface ship, such as the 1929 method of F. M. Lewis, described in Sec. 62.3, it is assumed that the ship has vertical or wall sides all around at the surface waterline. This means that there is no discontinuity in the "double body" at the surface-waterline level.

(8) So far as the 3-diml effects of finite length and tapering ends on the added mass of entrained liquid are concerned, the effects on the underwater hull of a surface ship are assumed to be half of those on an elliptic ellipsoid having the same proportions of length, beam, and draft.

No great study is required to realize that in practice, with ships and their parts, practically none of these assumptions are truly valid. When the ships and appendages are moving through a real liquid like water, they are surrounded by boundary layers, but the viscous effects appear to be minor except for very small bodies. There is increasing evidence that the added-liquid masses around a vibrating or oscillating body change with frequency and amplitude of vibration, especially at the higher frequencies. This means that the motion is not that of a body in an ideal liquid, surrounded only by potential flow. E. Schadlofsky, in reference (14) of Sec. 62.8, went so far as to say that for these reasons it was hopeless to attempt an added-mass determination by analytic methods. At high frequencies and large amplitudes there may easily be cavitation, especially in regions where $-\Delta p$'s exist because of normal ship motions. Further, as R. Brähmig points out [TMB Transl. 118, Nov 1943, pp. 2–3]:

> "Whereas the calculated hydrodynamic (added) mass depends only on shape (of the body), its value may vary with flow conditions in a real, eddying medium. A satisfactory agreement of the calculated result with the mass increase in the actual flow is therefore possible only when the flow patterns of the two differing phenomena are identical."

There is damping of some sort in practically all unsteady motion; certainly in all ship vibration. Assumption (6) requires that the flow pattern around the actual underwater ship form be half of that around the "double body." It neglects the free-surface and gravity effects, whatever they may be, and the dissipation of energy by waves generated around the sides of the ship and moving away from it.

Despite all these drawbacks and disadvantages the data derived from potential theory have been most useful. In many cases the simplifying assumptions have only minor influences, and in most cases one can be reasonably certain that the effect of factors not allowed for are definitely additive or subtractive.

It is again emphasized here, as is pointed out in Sec. 3.4 and illustrated in Fig. 3.F, that the added mass of the liquid set in motion during acceleration or deceleration is primarily a function of the mode of motion of the body or ship. That mode must be known or assumed before one sets out to estimate or to calculate the added-mass effect. For example, in the case of an ellipsoid of revolution, the field kinetic energies and added-liquid masses are by no means the same for (1) translational motion in a given plane parallel to the major axis and (2) bending or flexural vibration, with two nodes and three loops, in the same plane. For a 2-diml body of rectangular section they are not the same for translational motion in a plane parallel to the long sides as for that type of motion in a plane parallel to the short sides.

The latter difference is illustrated quantitatively for the floating box of unit length and rectangular section of Fig. 62.A of Sec. 62.2, having a beam $2a$ and a draft a. The added-liquid mass for up-and-down unsteady motion is $0.76\rho\pi a^2$, while for right-and-left sidling motion the added-liquid mass is $0.25\rho\pi a^2$.

The mass of the floating box, for unit length, is $2\rho a^2$. Therefore the virtual mass of both box

and entrained liquid, for unit length and for up-and-down unsteady motion, is $m_B + m_L = 2\rho a^2 + 0.76\rho\pi a^2 = (2 + 0.76\pi)\rho a^2$. The virtual-mass coefficient, from Sec. 3.4, is $(m_B + m_L)/m_B$ or

$$C_{VM} = \frac{(2 + 0.76\pi)\rho a^2}{2\rho a^2} = \frac{2 + 2.388}{2} = 2.19$$

The corresponding added-mass coefficient is simply m_L/m_B or

$$C_{AM} = \frac{0.76\rho\pi a^2}{2\rho a^2} = \frac{2.388}{2} = 1.19$$

This coefficient is always, by the definitions of this book, equal to $(C_{VM} - 1.0)$.

62.2 Added-Liquid Masses for Some Geometric Shapes and for Selected Modes of Motion. It is stated in Secs. 3.4 and 3.5 of Volume I that the added mass of the entrained liquid around a body in unsteady motion, symbolized by m_L, is determined by the combination of size, volume, shape, and mode of motion of the body and the mass density ρ of the surrounding liquid. The mass density of the body, symbolized by m_B, is the ratio of its own mass to the mass of the volume of liquid that it displaces. *In the general case* the added liquid mass m_L has no relation to the body mass m_B.

If the body is a 1-ft cube of cork its mass is small; if it is a 1-ft cube of lead, its mass is large. However, for a given mode of motion in each case, in a given liquid, the added mass of entrained liquid for each cube would be exactly the same. There is not much point, therefore, in relating these cork and lead body masses to a given added mass of some liquid surrounding them, for example water, while they execute this unsteady motion.

If, however, the submerged 1-ft cube is of heavy wood, so that its weight is exactly equal to that of a 1-ft cube of the adjacent water—in other words, if the cube is *buoyant*—then the ratio m_L/m_B becomes most useful in ship design. It is called the *added-mass coefficient*, symbolized by C_{AM}. The ratio $(m_L + m_B)/m_B$ for a buoyant body is called in this book the *virtual-mass coefficient*, symbolized by C_{VM}. In some quarters the latter name is applied to the former ratio, and added-liquid mass is called virtual mass. In other quarters the added mass is called the hydrodynamic mass. It is most important, therefore, in any discussion of this kind, that the marine architect know exactly what is meant in every case.

It is equally important that he know what is meant by inertia coefficients, mentioned in Sec. 62.1. In most technical books and papers the inertia coefficients, linear and angular, correspond to the added-mass coefficients described in the foregoing, for translational and rotational motion, respectively. Sometimes other names, or additional names, are applied to them to indicate the exact mode of motion.

It is customary, although writers are by no means always specific in this matter, to base the inertia coefficients on the mass (or mass moment of inertia) of a buoyant body which has the same mass as the identical volume of liquid would have. This is always the case for the added-mass coefficient defined here. A. F. Zahm, for one, puts the matter this way:

> "Each inertia coefficient therefore is a ratio of the body's apparent inertia, due to the field fluid, to the like inertia of the displaced fluid moving as a solid" [NACA Rep. 323, 1929, Part V, p. 437].

In this case the last four words are the important ones, because the mass density for the solid body is then the same as for the liquid displaced by it. This method breaks down for the infinitely thin flat plate which has finite added liquid mass for unsteady motion normal to its plane but zero buoyant or displaced volume. However, it serves very well for all practical purposes.

The foregoing is a necessary preliminary to a discussion of the added masses of a variety of geometric shapes and of ship hulls because of the presence, in the technical literature on this subject, of certain form, shape, and proportion coefficients involving added mass. These can easily be confused with the added-mass coefficients and the inertia coefficients for buoyant bodies, in which the displaced-liquid mass equals the body mass. The text endeavors to make the distinction clear as each of these form coefficients is encountered.

As a means toward this end, the lead of K. Wendel is followed in stressing the added-liquid masses themselves instead of the added-mass or inertia coefficients. These added-liquid masses and added-liquid weights are the numerical values required by the marine architect; the coefficients are convenient tools with which to make early estimates, and the necessary tools with which to conduct analytic investigations.

There are a considerable number of geometric shapes or bodies for which velocity potentials

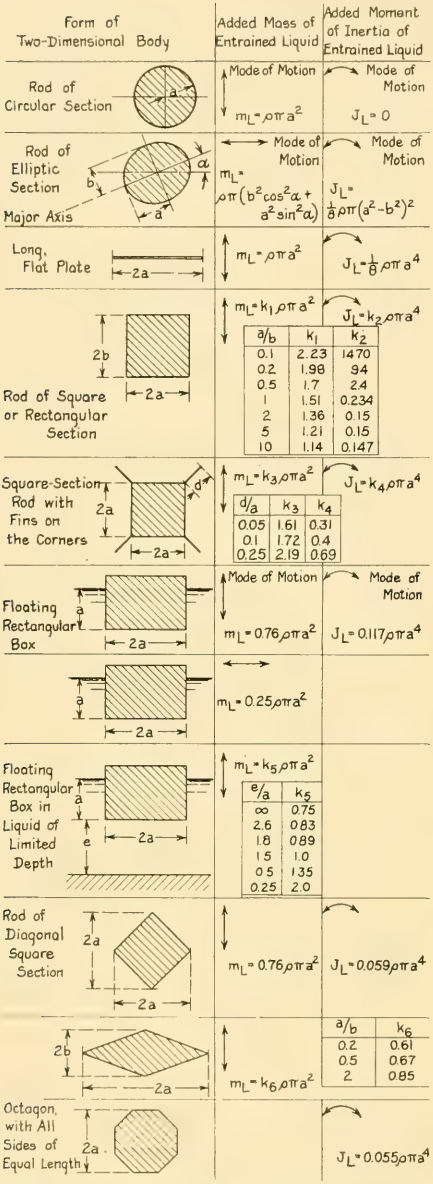

FIG. 62.A ADDED-LIQUID-MASS VALUES FOR SOME TWO-DIMENSIONAL GEOMETRIC SHAPES IN UNSTEADY MOTION
All values given are for unit lengths normal to the page. The respective modes of motion are indicated by the double-headed arrows.

and stream functions can be set up, applying to simple modes of body motion. Of these bodies the 2-diml elliptic-section cylinder, depicted near the top of Fig. 62.A, is a well-known example. The velocity-potential expressions make it possible to calculate, *for an ideal liquid*, the total amount of kinetic energy involved in the intricate particle motion around such a body, out to infinity distance, when it moves in one of the given modes of unsteady motion. The result is a function involving the square of the body velocity U_B and the first power of the mass density ρ of the liquid, no matter what the shape of the body or the direction in which it is moving with respect to its own axis. From the kinetic-energy function the added mass of the entrained liquid for the corresponding mode of motion is readily determined, as indicated in Sec. 3.4. In general, the added mass of the entrained liquid can be calculated for the motion of any body for which a velocity potential and a stream function can be set up and for which the kinetic energy in the flow can be derived.

Fig. 62.A contains diagrams of a number of 2-diml geometric shapes, it indicates one or more modes of motion for each, and it gives the added-mass values in terms of the mass density ρ of the surrounding liquid and the physical dimensions of the bodies. Most of the data in this figure were derived from those given by K. Wendel [STG, 1950, Vol. 44, pp. 207–255; English version in TMB Transl. 260, Jul 1956]; those for the general case of the 2-diml elliptic-section cylinder are from L. M. Milne-Thomson [TH, 1950, p. 239]. Except as indicated in the diagrams, all the values listed are for bodies submerged at a considerable depth in an infinite expanse of liquid, so that at infinite distances from the moving bodies the particle motions are all zero. In a practical sense, therefore, the diagrams apply only to certain appendages on a surface ship having a roughly geometric shape, lying well below the surface, and to fully submerged submarine vessels.

Fig. 62.B gives corresponding added-liquid-mass data for a series of 3-diml geometric bodies, and for circular and elliptic discs, derived from data on standard reference works on hydrodynamics by Sir Horace Lamb and L. M. Milne-Thomson.

A considerable number of references dealing with the added mass of entrained liquid around bodies of various types is listed on pages 100 and 101 of the book "Hydrodynamics," prepared and published by the National Research Council,

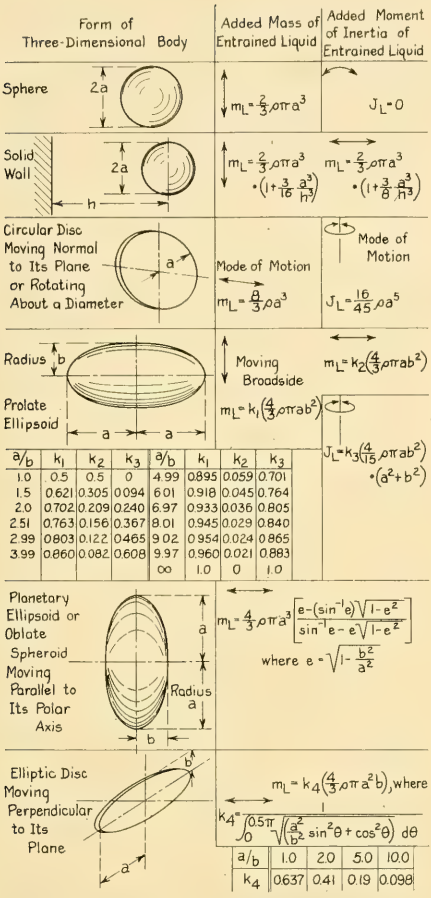

a/b	k_1	k_2	k_3	a/b	k_1	k_2	k_3
1.0	0.5	0.5	0	4.99	0.895	0.059	0.701
1.5	0.621	0.305	0.094	6.01	0.918	0.045	0.764
2.0	0.702	0.209	0.240	6.97	0.933	0.036	0.805
2.51	0.763	0.156	0.367	8.01	0.945	0.029	0.840
2.99	0.803	0.122	0.465	9.02	0.954	0.024	0.865
3.99	0.860	0.082	0.608	9.97	0.960	0.021	0.883
				∞	1.0	0	1.0

a/b	1.0	2.0	5.0	10.0
k_4	0.637	0.41	0.19	0.098

FIG. 62.B ADDED-LIQUID-MASS VALUES FOR SOME THREE-DIMENSIONAL GEOMETRIC SHAPES IN UNSTEADY MOTION

The respective modes of motion are indicated by the double-headed arrows.

Washington, 1932. Formulas giving the inertia coefficients of a variety of 2-diml and 3-diml shapes developed from the general or elliptic ellipsoid having semiaxes a, b, and c, and enabling the added masses (and added mass moments of inertia) of entrained liquid to be calculated for translational motion along, and for rotational motion about the three major axes, are given by A. F. Zahm [NACA Rep. 323, 1929, Part V, Table VIII, p. 445].

G. P. Weinblum and M. St. Denis present, in graphic form, values of the three linear and the three angular inertia coefficients for the elliptic ellipsoid, again for translational motion along, or for rotational motion about the three principal axes. These data cover a range of ratios between the semiaxes a, b, and c corresponding to the proportions of normal ships [SNAME, 1950, Figs. 6–11, pp. 189–190]. For use with added-mass values for the general ellipsoid, the body mass m_B of a *buoyant* ellipsoid in a liquid of mass density ρ is $(4/3)\pi\rho abc$.

As set down in the SNAME paper and in the list to follow, each of these linear (and angular) inertia coefficients represents the ratio between (1) the added-liquid mass (or mass moment of inertia) about the complete elliptic ellipsoid to (2) the mass (or the mass moment of inertia) of the complete ellipsoid along or about the axis specified, when it has the same mass density as the displaced liquid. For a half-ellipsoid representing the underwater body of a surface ship, these added-mass (or added mass moment of inertia) values are all halved but the ratios and the coefficients remain the same.

It is interesting to note that, in some cases, the mass of half of an elliptic ellipsoid is remarkably close to the mass of the water displaced by the underwater hull of a ship of the same principal dimensions. For example, in the case of the ABC ship designed in Part 4, a half-ellipsoid having the same proportions and size as the ship has the following dimensions:

Semimajor (longitudinal) axis $a = L/2 = 510/2 = 255$ ft, from Table 66.e.

Semiminor (transverse) axis $b = B_X/2 = 73/2 = 36.5$ ft

Semiminor (vertical) axis $c = H$ (*not* $H/2$) $= 26$ ft.

The half-volume of this ellipsoid is $(0.5)(4/3)\pi abc$. The weight of the buoyant half-ellipsoid is, in lb, the half-volume times ρ times g. Hence the weight displacement of the half-ellipsoid in salt water at sea level is

$$W(\text{long tons}) = \left(\frac{1}{2}\right)\left(\frac{4}{3}\right)\frac{\pi\rho g(abc)}{2{,}240}$$

$$= \left(\frac{1}{2}\right)\left(\frac{4}{3}\right)\frac{3.1416(1.9905)32.174(255)36.5(26)}{2{,}240}$$

$$= 14{,}490 \text{ t}.$$

The weight displacement of the ship is 16,400 t.

The block coefficient C_B of an elliptic ellipsoid (or of half such an ellipsoid) is $[(4/3)\pi abc]/(8abc) = \pi/6 = 0.5236$. The block coefficient C_B of the fifth approximation to the preliminary design of the ABC ship is, from Table 66.e, 0.593.

The mass moment of inertia of the liquid displaced by the buoyant elliptic ellipsoid is:

For rotation about the x-x or a-axis,

$$\tfrac{4}{15}\pi\rho abc(b^2 + c^2)$$

For rotation about the y-y or b-axis,

$$\tfrac{4}{15}\pi\rho abc(a^2 + c^2)$$

For rotation about the z-z or c-axis,

$$\tfrac{4}{15}\pi\rho abc(a^2 + b^2).$$

The British Shipbuilding Research Association has collected, and S. L. Smith has published added-mass data for prolate spheroids, for bodies of other shapes, and for surface ships having a rather wide range of Ⓜ or $L/\nabla^{1/3}$ values [INA, 1955, pp. 525–561, esp. Fig. 12 on p. 542]. The data are for axial or surging motion, either acceleration or deceleration, parallel to the axis of symmetry of the body or the principal axis of the ship. Fig. 62.C is adapted from the reference, with an added scale of fatness ratio $\nabla/(0.10L)^3$. The spots on the original graph, indicating the source and kind of data, are not reproduced here. It is assumed that all the surface-ship data are for hulls without propulsion devices of any kind.

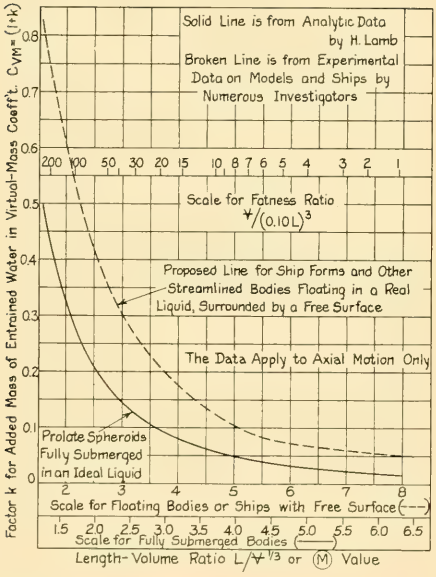

Fig. 62.C Added-Liquid-Mass Data for Submerged Prolate Spheroids, and for Other Floating Streamlined Bodies and Ship Forms

This figure has been adapted from one published in INA, 1955, Fig. 12, p. 542.

L. Landweber and A. Winzer have computed, by potential theory, the added-mass coefficients C_{AM} for a series of streamlined bodies of revolution having fore-and-aft asymmetry [ETT, Stevens, Rep. 572, Jun 1955]. The typical body, shown diagrammatically in Fig. 62.D, has its x-axis

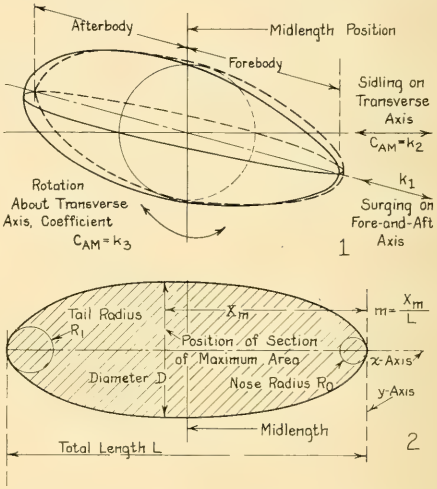

Fig. 62.D Definition Sketch of Body of Revolution of L. Landweber and A. Winzer, with Fore-and-Aft Asymmetry

coinciding with the axis of revolution. In this case, however, the y-axis lies at $x = 0$, that is, at the nose. With L as the length of the body, and D its maximum diameter, the nondimensional coordinates become $x' = x/L$ and $y' = y/D$. Of the seven body characteristics, using notation corresponding to that employed elsewhere in this book:

m is the 0-diml abscissa occurring at $y' = 0.5$. In other words, $m = x/L$ where $y = D/2$.

R_0' is the 0-diml radius of curvature at the nose. It is equal to R_0L/D^2, where R_0 is the absolute radius of curvature at the nose.

TABLE 62.a—Body Characteristics and Added Liquid-Mass Coefficients for a Series of 31 Forms

Body No.	Body Characteristics						Added-Mass Coefficients		
	L/D	m	R_0'	R_1'	C_P	Fatness ratio, $\mathcal{V}/(0.10L)^3$	k_1	k_2	k_3
1	4	0.40	0.50	0.10	0.65	31.91	0.0866	0.854	0.598
2	5	0.40	0.50	0.10	0.65	20.43	0.0629	0.889	0.693
3	6	0.40	0.50	0.10	0.65	14.18	0.0480	0.913	0.757
4	7	0.40	0.50	0.10	0.65	10.42	0.0381	0.930	0.802
5	8	0.40	0.50	0.10	0.65	7.977	0.0310	0.942	0.835
6	10	0.40	0.50	0.10	0.65	5.106	0.0219	0.958	0.880
7	7	0.36	0.50	0.10	0.65	10.42	0.0385	0.929	0.800
8	7	0.44	0.50	0.10	0.65	10.42	0.0378	0.930	0.803
9	7	0.48	0.50	0.10	0.65	10.42	0.0375	0.931	0.805
10	7	0.52	0.50	0.10	0.65	10.42	0.0374	0.931	0.805
11	7	0.40	0.50	0.10	0.55	8.816	0.0404	0.927	0.814
12	7	0.40	0.50	0.10	0.60	9.617	0.0382	0.930	0.810
13	7	0.40	0.50	0.10	0.70	11.22	0.0395	0.928	0.791
14	7	0.40	0.00	0.10	0.65	10.42	0.0399	0.927	0.795
15	7	0.40	0.30	0.10	0.65	10.42	0.0384	0.929	0.801
16	7	0.40	0.70	0.10	0.65	10.42	0.0383	0.929	0.801
17	7	0.40	1.00	0.10	0.65	10.42	0.0394	0.928	0.796
18	7	0.40	0.50	0.00	0.65	10.42	0.0389	0.928	0.798
19	7	0.40	0.50	0.05	0.65	10.42	0.0385	0.929	0.800
20	7	0.40	0.50	0.15	0.65	10.42	0.0377	0.930	0.803
21	7	0.40	0.50	0.20	0.65	10.42	0.0374	0.931	0.804
22	5	0.40	0.50	0.10	0.60	18.85	0.0632	0.889	0.704
23	5	0.40	0.50	0.10	0.55	17.28	0.0670	0.885	0.710
24	7	0.34	0.50	0.10	0.65	10.42	0.0387	0.929	0.799
25	7	0.40	0.50	0.30	0.65	10.42	0.0369	0.923	0.806
26	7	0.40	0.50	0.40	0.65	10.42	0.0365	0.932	0.808
27	7	0.40	0.50	0.50	0.65	10.42	0.0363	0.933	0.809
28	6	0.36	0.50	0.00	0.55	12.00	0.0527	0.907	0.762
29	7	0.36	0.50	0.00	0.55	8.816	0.0417	0.924	0.805
30	8	0.36	0.50	0.00	0.55	6.750	0.0340	0.937	0.838
31	10	0.40	0.50	0.00	0.60	4.712	0.0224	0.958	0.882

R_1' is the 0-diml radius of curvature at the tail. It is R_1L/D^2, where R_1 is the absolute radius of curvature at the tail.

C_P is the prismatic coefficient, $= \mathcal{V}/[\pi(0.5D)^2L]$

k_1 is the added-mass coefficient C_{AM} for unsteady longitudinal or surging motion, parallel to the x-axis

k_2 is the added-mass coefficient C_{AM} for unsteady lateral or sidling motion, parallel to the y-axis.

k_3 is the added mass moment of inertia coefficient C_{AM} for rotation in pitch, nose up and nose down, about the horizontal transverse axis at midlength.

The shape of the fore-and-aft meridian section is defined by a sixth-degree polynomial.

Table 62.a gives the numerical results of the work of Landweber and Winzer, for a series of 31 bodies of revolution of varied characteristics.

62.3 Comparison of a Vibrating Ship with a Vibrating Geometric Shape. The deeply submerged submarine is approximated reasonably well by the general (elliptic) ellipsoids described in Sec. 62.2 or by the family of bodies of revolution with fore-and-aft asymmetry listed in Table 62.a.

The surface ship floating in equilibrium, with its hull partly immersed and partly exposed, when subjected to unsteady motion in any one of its six degrees of freedom, is surrounded by a flow pattern which is by no means well known, except possibly for the case of straight-ahead motion. Figs. 20.G, 20.H, and 20.I of Volume I indicate, in frankly schematic fashion, the probable

general nature of the flow pattern for vertical and lateral unsteady motions, corresponding to 2-noded vibration in vertical and horizontal planes. The problem is how to estimate or to derive numerical values for the added mass of entrained liquid, or for the added mass moment of inertia, around an actual surface-ship hull in unsteady motion in any or all of its degrees of freedom.

The problem of most frequent application, and at least of major interest, is that of finding the added- or virtual-mass coefficients for a ship in vibration. This involves a separate—and additional—group of degrees of freedom. Many years ago H. W. Nicholls found that, for a rectangular-section model vibrating vertically, the added-mass coefficient was approximated by

$$C_{AM} = 0.37\frac{B}{H} + 0.20 \qquad (62.i)$$

where B was the beam and H the draft of the model. For the model which he used, C_{AM} worked out as 0.78. For a triangular-section model he found it to be 0.70 [TMB Rep. 395, Feb 1935, p. 9].

Much later it was stated by F. H. Todd [SNAME, 1947, Vol. 55, p. 160] that, for vertical vibration only:

"In calculations on the natural frequency of ship hulls (in 2-noded vibration), the total virtual mass of the hull and water together varies from 2 to 4 times the ship displacement. The variation is linear with beam-draft ratio, and is given approximately by the line

$$\text{Virtual inertia factor} = \frac{1}{3}\left(\frac{B}{H}\right) + 1.2$$

The virtual inertia factor is defined as the ratio of (displacement + entrained water) to displacement."

Here the virtual inertia factor corresponds to the virtual-mass coefficient C_{VM} . The added-mass coefficient C_{AM} is $C_{VM} - 1.0$ or

$$C_{AM} = \frac{1}{3}\left(\frac{B}{H}\right) + 0.2 \qquad (62.ii)$$

where 0.2 is the viscous-resistance or damping factor.

For the ABC ship of Part 4, the added-mass coefficient approximated by this method would be

$$C_{AM} = \frac{1}{3}\left(\frac{73}{26}\right) + 0.2 = 0.936 + 0.2 = 1.136$$

For the *Gopher Mariner* at the heavy displacement [SNAME, 1955, pp. 436–494, esp. pp. 451, 473], at a mean draft of 24.42 ft, the corresponding value by this method is

$$C_{AM} = \frac{1}{3}\left(\frac{76}{24.42}\right) + 0.2 = 1.037 + 0.2 = 1.237$$

However, the data from Table 1 of TMB Report 1022, of May 1956, based on the 1929 method of F. M. Lewis and the reduction factor of J. L. Taylor for 2-noded bending of an ellipsoid [SNAME, 1955, p. 471], give a C_{AM} of only 0.978 for 2-noded vertical vibration.

Supplementing the foregoing, an excellent summary of the adaptation of knowledge concerning the added mass of the entrained water to ship-vibration problems was given by F. H. Todd in 1947 [SBMEB, May, Jun, Jul, 1947, Vol. 54, pp. 307–312, 358–362, 400–403, respectively; ASNE, Feb 1948, pp. 86–110, esp. pp. 101–104].

The use of a straight-line function embodying the B/H ratio as a means of determining the added-liquid mass for vertical vibration, despite its unexpected applicability to many types of ship, can at best be considered only a first approximation, to be used in an early stage of the design when the hull form is not yet known. Moreover, it takes no account of the fore-and-aft distribution of the added mass of entrained liquid, other than to assume that it is the same as on all other ships for which reliable data are available.

A somewhat different method, for use after the ship is structurally complete but before it is placed in commission, is perhaps more applicable to ship appendages than to hulls proper. It involves a comparison of the resonant frequency of the appendage structure in air with the resonant frequency of the same structure in water. The structure can be set in motion by a vibration generator, first when the ship is on the building ways or in the building dock, with the appendage surrounded by air. It is again vibrated when the vessel is in the water, with the vibration generator (above the water) imparting its periodic forces through some kind of flexible connection with the appendage.

Then

$$C_{VM} = \frac{(f_{\text{in Air}})^2}{(f_{\text{in Water}})^2},$$

or (62.iii)

$$C_{AM} = \frac{(f_{\text{in Air}})^2}{(f_{\text{in Water}})^2} - 1$$

Because of the second powers involved, this method requires a very careful measurement of both frequencies.

A second method, of much more general application, is to develop procedures whereby the added-liquid masses (and mass moments of inertia) can be derived from the known values for geometric shapes, as outlined in Sec. 62.2 and as listed on Figs. 62.A and 62.B. For many of the geometric shapes for which the velocity potentials, kinetic energies of the surrounding flow, and added-liquid masses are known, the lower halves resemble roughly the underwater forms of ships having the same size and proportions. For 2-diml bodies, this resemblance applies to the immersed transverse sections of the surface ships under investigation; for 3-diml bodies it applies to the whole underwater hull, as described for the half-ellipsoid and the ABC ship of Part 4 in the preceding section. It is then assumed that the added mass of the liquid surrounding the immersed section or hull of the ship is one-half of the value calculated for the whole geometric section or geometric form far below the surface. For example, if $2a$ is taken equal to $2b$ in the case of the submerged rod of rectangular section, in Fig. 62.A, its lower half is identical to that of the floating rectangular box in the same figure, which has a draft of a and a beam of $2a$. For $2a = 2b$ of the first case the added liquid mass m_L for the up-and-down motion is $1.51\rho\pi a^2$; for the second case it is $0.76\pi\rho a^2$.

It is rare that any surface ship, except possibly an old canal boat or a special barge, has a constant transverse section, or one that could be termed average for the entire length. Manifestly, the shape of the actual transverse sections, and the distribution of this shape along the ship length, determine the flow pattern at different stations, the kinetic energy in the surrounding unsteady flow, and the added mass of the liquid. Further, the boat, barge, or ship has a finite length, with

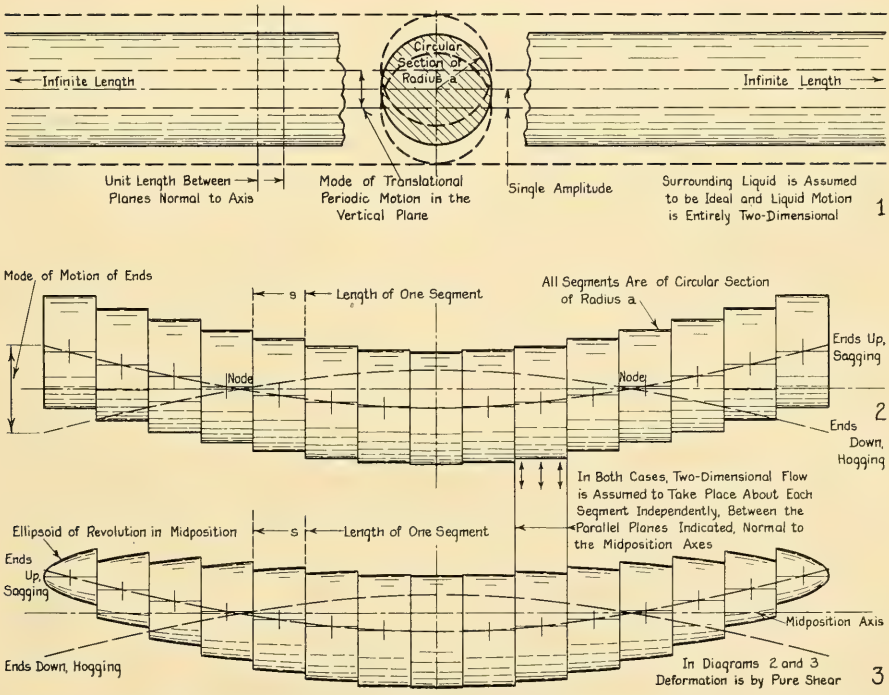

FIG. 62.E FIRST STAGE IN TRANSFORMATION OF OSCILLATING CYLINDRICAL BAR TO SHIP STRUCTURE IN 2-NODED VERTICAL VIBRATION

ends; almost invariably it tapers toward those ends, so that 3-diml flow is involved.

At the time of writing (1956), the general procedure whereby the underwater hull of a surface ship is compared to one or more geometric forms to determine the added mass of entrained liquid has undergone about a quarter-century of development, applying to one particular degree of freedom. This mode of motion, as mentioned previously, is in addition to the usual six degrees of freedom in that it embodies periodic bending or flexure in a vertical plane, usually with two nodes and three loops or antinodes, such as that encountered in the fundamental resonant vibration of a ship hull in the vertical plane. The processes in this development, which should be understood clearly by the marine architect who undertakes to calculate and to use intelligently the added-mass values for his ship design, are outlined here in a combination of diagrams and words.

Diagram 1 in Fig. 62.E illustrates a circular-section bar of radius a, with its axis horizontal. The bar is oscillating vertically (actually in the plane of the page) in a pure translational mode, embodying rising and dropping for equal distances above and below its normal position. It is assumed that the rod is buoyant, having the same mass density as the surrounding liquid, and that at this stage it is deeply submerged in an ideal, non-viscous liquid. For such a 2-diml body, a section of which is pictured at the top of Fig. 62.A and in diagram 1 of Fig. 62.E, the added-liquid mass *per unit length* is $\pi\rho a^2$, where ρ is the mass density of the buoyant rod *and* of the surrounding liquid. All the unsteady flow in this liquid takes place in vertical planes bounding unit lengths, normal to the horizontal midposition axis of the rod.

The rod is next cut off to a given length L, with free or exposed ends. It is then made to vibrate in the vertical plane (that of the page) with two nodes, at its fundamental frequency in the surrounding liquid, taking both the rod mass and the added-liquid mass into account. The problem of predicting the fundamental frequency in advance then resolves itself into one of finding the numerical value of the added-liquid mass for this mode of motion. This may be tackled in two ways; they are described separately in the paragraphs which follow.

For the first method it is assumed that the rod, although a single solid entity so far as its elastic characteristics are concerned, is made up of a number of separate but adjacent length segments in the form of thick circular discs, indicated in diagram 2 of Fig. 62.E. The unsteady flow around each of these circular discs is assumed to take place in vertical planes normal to the straight or midposition axis of the rod, so that for each segment the added-liquid mass is $\pi\rho a^2$ times the length s of the segment. Although the discs near the ends move up and down with a greater amplitude, and a greater velocity, than the discs at the center, the added-liquid mass *for each segment* is not changed because of this situation, at least not for the low frequencies involved here. However, since there are no imaginary planes beyond the end segments to insure pure 2-diml flow there, it is obviously not acceptable to multiply the added-liquid mass for each disc by the number of discs and to say that this is the added-liquid mass for the whole flexing or bending bar. One reason is that the bar in diagram 2 is deformed in pure shear rather than in pure bending, or in a combination of the two. Another reason is that the flow near the exposed ends is certainly 3-diml in character.

F. M. Lewis, who developed this method in 1929, utilized as a solution for the second portion of this problem a longitudinal reduction factor. This represented the ratio between (1) the added-liquid mass around an ellipsoid of revolution in vertical vibration and (2) the added-liquid mass around a circular bar undergoing pure shear deflection, having the same length L as the bar in diagram 2 of the figure but in effect forming part of an infinitely long circular rod. For his solution, embodied in SNAME, 1929, pages 6–11, Lewis assumed that the 3-diml circular-section ellipsoid also deformed in pure shear. This meant that the flow around any section took place between vertical planes normal to the horizontal, straight midposition of the ellipsoid, represented in diagram 3 of Fig. 62.E. He thus obtained a reduction factor $J_{2\text{-Node}}$ which he applied to the added-liquid mass around *each* of the circular segments, from one end of the bar to the other. The reason for doing this, instead of applying $J_{2\text{-Node}}$ to the whole added liquid mass, appears presently. The reason for not summing up the varied added-liquid masses for the segments of radius a, a_1, a_2, a_3 $\cdots$ of the ellipsoid of diagram 3 is also explained presently.

To make this elongated and pointed ellipsoid resemble the underwater hull of a surface ship

more closely, its numerous length segments, separated by adjacent vertical planes, could each be made semielliptic in transverse shape. They could be given proportions corresponding to the ratio [(beam)/(section draft)] of the several sections along the length of the ship in question. The sections forward, for example, could have their major axes vertical; those amidships could have them horizontal. This modification, however, would not assist in the solution being sought since the added-liquid mass around any 2-diml elliptic shape having a unit length and a major axis of length $2a$, for unsteady motion normal to that axis, is $\pi\rho a^2$, the same as for a circle of radius a or diameter $2a$. This relationship is indicated in the several elliptic sections of Fig. 62.F. The added mass of the liquid surrounding

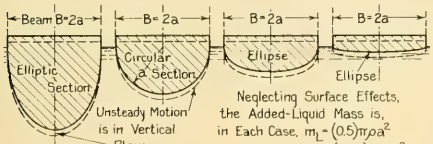

Fig. 62.F Series of Elliptic Body Sections, All Having the Same Added Liquid Mass Per Unit Length

an elliptic section in an ideal fluid is a function of one variable only, namely the square of the beam, reckoned at right angles to the direction of motion. For a section of unit length and beam B_X, either semicircular or semielliptic in shape, the added mass m_L is $(0.5)\rho(\pi/4)B_X^2$ or $0.125\rho\pi B_X^2$.

It would be an advantage, if it could be done, to modify the shape of the horizontal plane through the major axis of the geometric body so that it would have the same beam, at given 0-diml proportions of its length from the nose, as does the designed waterline of the ship. However, this again is not a satisfactory procedure because to determine the longitudinal reduction factor for such a body, non-ellipsoidal in shape, and usually with fore-and-aft asymmetry, would require a determination of the added mass by a lengthy and laborious procedure corresponding to that employed by L. Landweber and A. Winzer, and described in the latter part of Sec. 62.2.

F. M. Lewis worked out a clever alternative scheme whereby the added mass of an underwater ship hull can be approximated by a much simpler and more straightforward procedure. For this method, the representative body is composed of a series of constant-section, vertical segments, say about 20 in number, separated by vertical planes representing the equally spaced stations set up when making the lines drawing of the ship for which the added-mass data are desired. Each constant-section segment has the correct designed-waterline beam B at its appropriate station, at midlength of the segment. However, instead of using elliptic section shapes, Lewis found that by employing conformal transformation, described briefly in Sec. 41.11, he could obtain the added-liquid-mass values for transverse section shapes which resembled closely those found on ships, including rectangles with square corners and V-shapes with sharp keels. Diagrams showing these shapes were published by Lewis in Plates 2 and 3 of his SNAME, 1929 paper and were reproduced by K. Wendel in Fig. 10 of his STG, 1950 paper; they also appear on pages 21 and 23 of TMB Translation 260, July 1956, and in Figs. 186(a) through 186(g) and Fig. 187, on page 320 of the book "The Design of Merchant Ships," by J. C. A. Schokker, E. M. Neuerburg, and E. J. Vossnack [H. Stam, Haarlem, 1953].

To make these section shapes more adaptable for comparison with transverse sections on ships, Lewis employed eight separate proportions for the circumscribing rectangles bounding them. These proportions, symbolized by H in his paper and represented actually by the ratio [(half-beam)/(section draft)], for one side only of a symmetrical ship, varied from 0.2 to 2.0. In the referenced paper by Wendel and in TMB Translation 260 the eight circumscribing rectangles have a half-beam of a and a section draft of b.

It is most important to remember, in this connection, that the section draft corresponds to the ship draft (vertical distance between DWL and baseline) *only* if the section in question extends all the way to the baseplane; otherwise it is the vertical distance from the DWL to the bottom of the section in question. For a transom-stern section, this section draft may be only 0.1 the ship draft. The referenced publications are unfortunately not specific on this point but the principal features are shown in diagram 4 of Fig. 62.G.

Instead of tabulating the added-liquid masses for these 2-diml section segments of unit length, Lewis set up a relationship in which they were referred to *half of the added-liquid mass* for a segment having a circular section of radius a

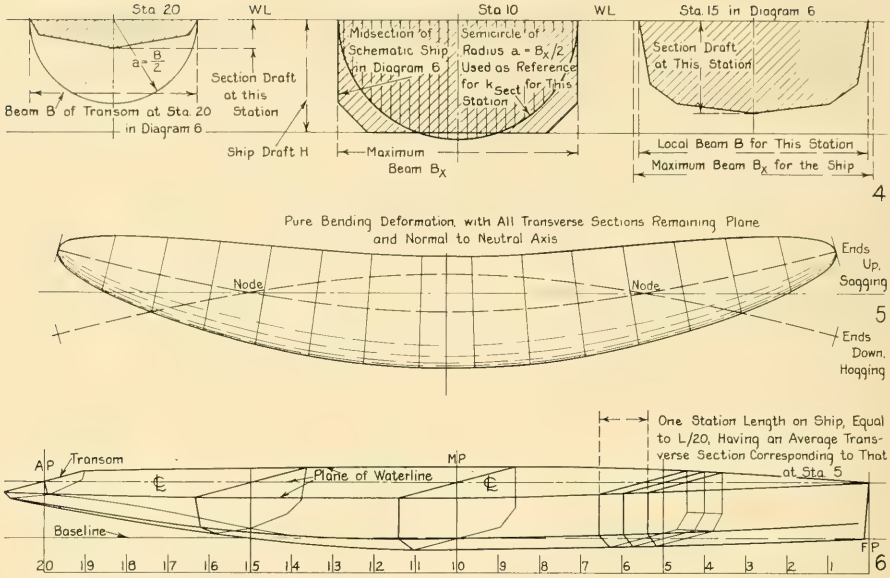

FIG. 62.G SECOND STAGE IN TRANSFORMATION OF OSCILLATING CYLINDRICAL BAR TO SHIP STRUCTURE IN 2-NODED VERTICAL VIBRATION

and unit length. He used this quantity as a reference because, in the process of setting up the relationship, the deeply submerged 2-diml circular-section segment of Fig. 62.A is brought to the surface so as to float with a waterline corresponding to its horizontal diameter. If the top half of the circular-section segment is removed, the lower half of semicircular section is still buoyant, because its mass is $0.5\pi\rho a^2$ per unit length and the mass of the displaced water is exactly the same.

Lewis' relationship is in the form of a "coefficient" C, defined as follows:

$$C_{\text{Lewis}} = \frac{\text{Added-liquid mass for a ship-shaped segment of unit length, beam } B\text{, and section draft to bottom of section}}{\text{Half of the added-liquid mass for a circular-section segment of unit length, radius } a \text{ or beam } B = 2a}$$

This, incidentally, although called "the inertia coefficient for that (ship) section" by Lewis, is not a true inertia coefficient in accordance with modern general usage. It might be distantly related to such a coefficient but only because the ship-shaped section of Lewis is transformed from a circle.

Because C. W. Prohaska also has a relationship of this kind, supported by different analytical and experimental data, and also designated as C, it appears wise to substitute for the symbols C_{Lewis} and C_{Prohaska} a k-symbol corresponding to those listed in various places in Figs. 62.A and 62.B. A suitable symbol appears to be k_{Sect} which, for 2-diml flow in a translational mode, is exactly the same as C_{Lewis} above. For a rectangular ship section having a [(beam)/(section draft)] ratio of 2.0, with square corners at the bilges, k_{Sect} is 1.512 (given as 1.51 in the referenced figures). The value of k_{Sect} for rectangles of other proportions are given in a graph by F. M. Lewis and K. Wendel [SNAME, 1929, Pl. 4 at top; TMB Transl. 260, Jul 1956, Fig. 21 on p. 34]. For a ship section of semicircular shape having a B/H ratio of 2.0, k_{Sect} is 1.00, since in this case the added mass of the ship section corresponds to the added mass of the semicircular section used as the reference.

It is now possible to determine the added-liquid mass per unit length of a ship section corresponding to one of the shapes depicted by

Lewis, and having approximately the correct ratio [(beam)/(section draft)] of the ship section under consideration. Introducing the shape factor k_{Sect},

Added mass of ship-shaped section of unit length

$$= k_{\text{Sect}}(\tfrac{1}{2})\pi\rho a^2 = k_{\text{Sect}}(\tfrac{1}{8})\pi\rho B^2$$

and

Added weight of added mass of liquid surrounding ship-shaped section of unit length

$$= k_{\text{Sect}}(\tfrac{1}{8})\pi\rho(g)B^2 \qquad (62.\text{iv})$$

where the beam B is that at midlength of the constant-section segment in question; in other words, the local beam.

F. H. Todd made it unnecessary to compare the shape of the given ship sections with the transformations of F. M. Lewis by publishing, in reference (24) of Sec. 62.8, a graph which gave the shape factor direct from known values of the ratio [(beam)/(section draft)] and the section coefficient estimated from the body plan.

C. W. Prohaska modified the diagram somewhat so that the abscissas were values of the ratio [(beam)/(section draft)] for the section in question and the ordinates were values of the section coefficient [ATMA, 1947, Vol. 46, Fig. 24 on p. 196; TMB Rep. 739, Oct 1953, Fig. 1 on p. 14; SNAME, 1955, Fig. 34 on p. 471]. In all three references cited the ordinates were labeled β(beta), which is the alternative ITTC symbol for midship-section coefficient. This is misleading because the section coefficient has a value of β only at the midship or maximum section. The present author has further modified the Prohaska graphs by substituting the shape factor k_{Sect} for the "coefficient" C. In their new form the graphs are reproduced here as Fig. 62.H; the method of defining the section coefficient is clearly illustrated in diagram 4 of Fig. 62.G.

It is to be noted that for a section coefficient of 0.7854, corresponding to that of a semicircle, the value of k_{Sect} is constant for all values of the ratio [(beam)/(section draft)]. When the latter ratio is 1.0, the ship section is a semicircle and the shape factor k_{Sect} is 1.00. When the [(beam)/(section draft)] ratio has values other than 1.0, the ship sections having shape factors k_{Sect} of 1.00 are all ellipses, because their added-liquid masses are, from Fig. 62.F, the same as for a semicircular segment of unit length having the same beam.

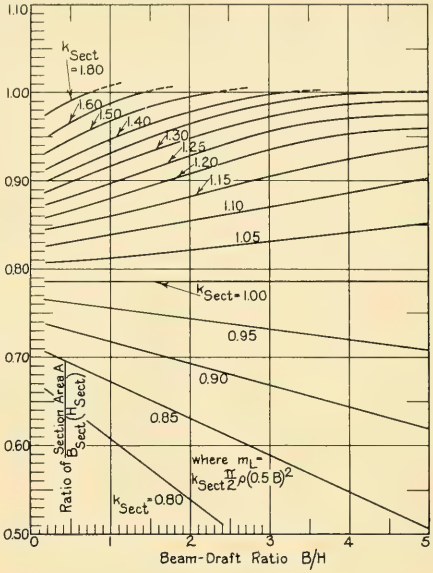

Fig. 62.H C. W. Prohaska's Graphs for Determining Section-Shape Factors by Inspection

Prohaska has supplemented the k_{Sect}-values for the ship-shaped sections of F. M. Lewis by values for other more intricate sections, resembling those of ships with bossings and other projecting appendages [ATMA, 1947, Figs. 16, 17, 18, pp. 191–192]. These section shapes and shape factors are also derived by conformal transformation.

The added mass of the entrained liquid around the transverse sections of a ship vibrating vertically, calculated by the methods just described, is still valid only for the flow around each 2-diml segment, where the segment motion and the surrounding flow are confined between two vertical planes at the ends of the segment. This situation is represented by diagrams 1 and 2 in Fig. 62.E, drawn for a cylindrical bar and for an ellipsoid of revolution, respectively. It is now necessary to apply to the added mass around this segment a *longitudinal reduction factor* to compensate for the 3-diml nature of the actual flow, equal or corresponding to Lewis' factor $J_{2-\text{Node}}$ mentioned earlier in this section. Because of the use of the standard sysbol J for mass or polar moment of inertia, the 3-diml reduction factor is symbolized by R. However, concerning a factor R derived for an ellipsoid of revolution and applied to a

ship form, Wendel has this to say [TMB Transl. 260, pp. 13–14]:

"It is true that this kind of approximation must be considered as somewhat rough since it takes into account neither the specific shape of the displacement body nor the width-depth ratio; nevertheless a better approximation which, no doubt, would also be more complicated, seems to be unnecessary so long as we confine ourselves to slender bodies."

Plate 4 of Lewis' 1929 SNAME paper gives values of the following reduction factors for an ellipsoid of revolution, covering a range of L/B_X or L/D ratio of from 3 to 18:

R_1 for heaving motion or pure translation in a vertical plane. This is the same set of values as given by C. W. Prohaska, in his graph marked "Lamb" [ATMA, 1947, Fig. 25, p. 197], where the small diagram indicates this type of motion.

R_2 for rotational motion in a vertical plane, presumably about a transverse axis at midlength and middepth

R_3 for 2-noded flexure, with deformation occurring by shear deflection only; this latter feature is important to remember

R_4 for 3-noded flexure, with deformation occurring by shear deflection only; this again is important to remember.

Fig. 62.I is a graph giving numerical values of these four factors.

For the 2-noded flexure by pure shear, represented by diagrams 2 and 3 in Fig. 62.E and by diagram 6 in Fig. 62.G, the added *weight* of entrained liquid for each transverse segment is multiplied by the Lewis reduction factor R_3. The weights for all the segments are then superposed upon the weights of the masses composing the structure, machinery, cargo, and other parts of the ship, applying the weight ordinates at the proper points or stations along the diagram which

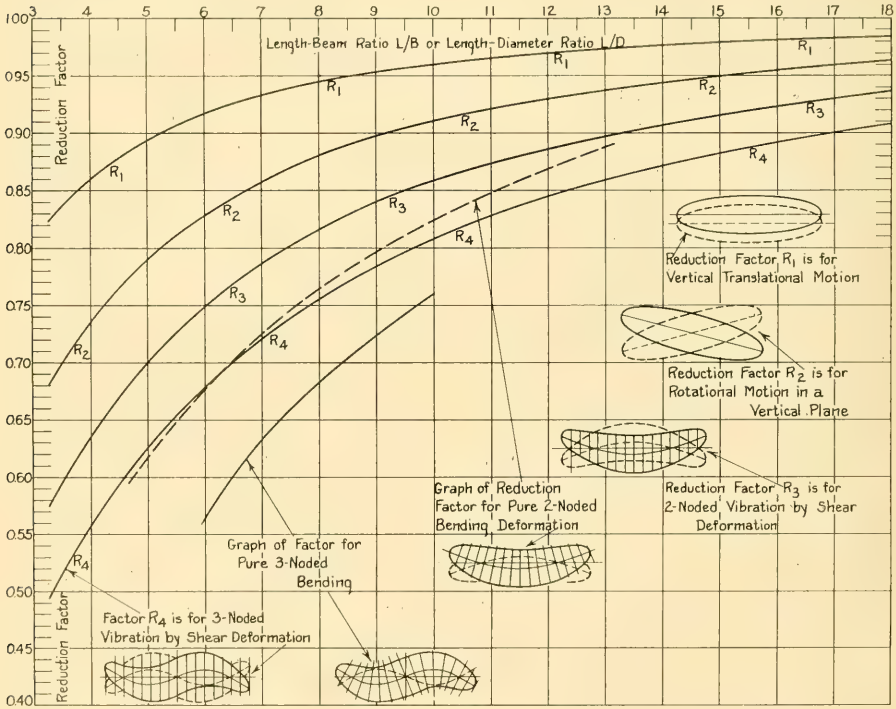

Fig. 62.I Graphs of Reduction Factors R of F. M. Lewis and J. L. Taylor for Three-Dimensional Flow

represents the length of the ship; see Fig. 37 on page 472 of SNAME, 1955.

It now becomes necessary to return to a consideration of the second method for determining the added mass of the entrained liquid around the circular rod of diagram 2 in Fig. 62.E, when *flexing* in 2-noded vertical vibration. F. M. Lewis adopted the schematic method shown in that diagram because he felt that the possible error involved in assuming pure shear deflection, rather than bending deflection, was less than the error involved in shifting from the ellipsoid of revolution (or its lower half) to the actual underwater hull of a ship, at least for the proportions corresponding to those of a ship. However, in 1930 J. Lockwood Taylor published the values of a reduction factor for an ellipsoid of revolution, vibrating vertically in an ideal liquid with 2 nodes and 3 loops, by considering pure bending deflection rather than pure shear deflection. This means that, as indicated in diagram 5 of Fig. 62.G, the transverse planes separating the several segments remain normal to the bent axis of the ellipsoid. The segments are thus thin on the concave side and thick on the convex side, as they are in a simple bent beam. Taylor found reduction-factor values as much as 8 per cent below those of Lewis.

A graph of J. L. Taylor's factor for 2-noded pure bending is published by C. W. Prohaska [ATMA, 1947, Fig. 25, p. 197]; also by R. T. McGoldrick and V. L. Russo [SNAME, 1955, Fig. 35, p. 471]; it appears in TMB Report 739, October 1953, Fig. 2 on page 14. It is presented here, along with those of Lewis, in Fig. 62.I, supplemented by Taylor's values for 3-noded bending vibration of an ellipsoid, given on page 170 of his 1930 INA paper, reference (9) of Sec. 62.8. Prohaska's diagram indicates graphically that the reduction factors are for an ellipsoid flexing in 2-noded vibration; those of TMB Report 739 and of the 1955 SNAME reference do not.

Since the ship may be assumed to bend more nearly like a simple beam when vibrating vertically, at least in the lower modes of vibration, with 2, 3, and possibly 4 nodes, and since the data of J. L. Taylor for an ellipsoid vibrating in this manner are available, it is present practice (1956) to use Taylor's (smaller) reduction factor for 2-noded vibration rather than that of Lewis. Many years ago E. B. Moullin pointed out that Lewis' added-mass values had to be reduced by 10 per cent [INA, 1930, p. 179]. It is not clear whether he had in mind what has later come to be the difference between Lewis' reduction factor for pure shear and J. L. Taylor's reduction factor for pure bending, or some other effect. In any case, a recent re-analysis of model and ship vibration data indicates that the method of F. M. Lewis, combined with the reduction factor of J. L. Taylor for 3-diml flow, give values of the added weight of the entrained water around a vibrating ship which are still too high, at least for 2- and 3-noded vertical vibration [McGoldrick, R. T., and Russo, V. L., SNAME, 1955, p. 490]. Further study and analysis are required before additional refinements in these prediction methods can be attempted.

A comparison of the procedures followed by F. M. Lewis, C. W. Prohaska, K. Wendel, and others in predicting the added mass of the entrained liquid about the underwater hull of a ship, vibrating vertically in its fundamental 2-noded or 3-noded frequency, indicates a number of discrepancies with the assumptions of Sec. 62.1 which are not discussed there:

(1) Although the limiting conditions set up for the conformal transformation appear to take account of the free-surface effects, as do the electric analogies set up by J. J. Koch, it is by no means clear that these cover adequately the situation for ship-shaped sections, even in an ideal liquid having mass but no viscosity. For example, most of the ship sections developed by Lewis and mentioned in the reference have vertical sides at the waterline although most of those developed by Prohaska do not. There is a question whether full compensation has been made in the analytic process for the flare or tumble home to be found on actual ships in this region. K. Wendel comments that in Koch's experiment "··· it is possible to satisfy the boundary condition only approximately; ···" [TMB Transl. 260, p. 34].

(2) The analytic method described takes it for granted that the ship, built to the shape shown by the lines, has boundaries that remain rigid locally, even though the ship flexes as a whole. It is perfectly possible, and indeed quite probable, that some flat or nearly flat areas of hull plating, lying generally normal to the direction of vibratory motion, "give" or yield or deflect under the external accelerative pressures and forces by amounts of the same order of magnitude as the hull deformations. Carried to the limit, one would

expect a ship with a soft-rubber hull boundary to set up only trifling amounts of kinetic flow in the surrounding water. The added mass of entrained liquid would then be extremely small.

(3) It has been assumed by many analysts and experimenters that the added-liquid mass in vertical vibration for typical ship sections was independent of both frequency and amplitude for the lower modes of vibration, with two and three nodes. Nevertheless, the model experiments of H. Holstein, described in reference (25) of Sec. 62.8, indicate a large variation in shape factor k_{Sect} when the frequency and amplitude are varied, even in a range of frequency encountered on ships. Graphs indicating these variations, and the discrepancy with theory for a ship section approximately rectangular, are included in Fig. 32 of the Wendel reference [STG, 1950; TMB Transl. 260, p. 44].

Rather than to work out the problem of predicting the added mass of entrained water around the hull of the ABC ship of Part 4 in 2-noded vertical vibration as an example of the method described in this section, there is given hereunder a summary of the steps, with brief comments for each step:

I. The ship is divided into 21 length segments, 19 of them having a full station length of 510/20 = 25.5 ft, and the two end segments having a half-length of 25.5/2 = 12.75 ft. The fore-and-aft centers of all but the two end segments fall on the station locations, 1 through 19. For all the 21 sections, 0 through 20, it is assumed that the section shape on the body plan is representative of the entire segment length pertaining to that station.

II. List the whole waterline beams B and the section drafts (not necessarily the ship draft) for the 21 stations. Compute the 21 ratios [(beam B)/(section draft)].

III. Estimate the value of the fullness or section coefficient for each section, by inspection or by some simple method. If there are any concave portions in the section outlines, fill them out by straight tangents before determining the section coefficient.

IV. Using the graphs of Fig. 62.H, determine the shape factor k_{Sect} for each section. These factors may be checked by entering the half-body diagrams of F. M. Lewis [SNAME, 1929, Pls. 2, 3; STG, 1950, Fig. 10; TMB Transl. 260, Jul 1956, Fig. 10 on p. 23] with the proper ratio of [(beam B)/(section draft)] and selecting by inspection a section shape approximating that for the ship. The shape factor k_{Sect} is then the "coefficient" C of Lewis. The half-body diagrams of C. W. Prohaska may also be used in the same way [ATMA, 1947, Figs. 16, 17, 18 on pp. 191–193; SBMEB, Nov 1947, Fig. 11, p. 593]. Prohaska's "coefficient" C is also the same as k_{Sect}.

V. Select the proper reduction factor R of J. L. Taylor from the indicated graph of Fig. 62.I, for the L/B_X ratio of the ship.

VI. Determine the added-liquid weight per unit of ship length for each station by

$$m_L(g) = (k_{\text{Sect}})(R)(0.125)\pi\rho(g)B^2 \qquad (62.\text{v})$$

The shape factor k_{Sect} is usually different for each station but the reduction factor R is the same for all stations.

VII. Multiply the added-liquid weight per unit length by the length of each of the 21 segments. Apply the weights thus found to the weight curve for the ship, at the proper stations.

J. C. A. Schokker, E. M. Neuerburg, and E. J. Vossnack give a somewhat-too-brief summary of the available methods for estimating or calculating the added mass of the entrained water for the vertical mode of ship vibration on pages 319–321 of their book "The Design of Merchant Ships" [H. Stam, Haarlem, 1953]. On page 340, in Fig. 222, they give a nomogram, apparently first published by C. W. Prohaska [ATMA, 1947, Fig. 29, p. 201], for approximating, in vertical vibration, the ratio of (1) the mass of the entrained water to (2) the mass of the ship, taking account of the midship-section coefficient C_M, the beam-draft ratio B/H, the length-beam ratio L/B_X, the ratio of the water depth to draft h/H, and the block coefficient C_B. This ratio is also found by a rather complicated formula in Section 131 on page 326. Neither the nomogram nor the equation suffice, however, for determining the longitudinal distribution of the added mass of the entrained water. These authors list 32 references on pages 341–342 of their book.

62.4 The Change of Added Mass Near a Large Boundary. All the comments in the foregoing are based upon the motion of a body or ship at a great distance from any rigid or unyielding boundary which would interfere with the flow pattern of an ideal liquid. The air-liquid interface or free surface of a body of water represents a boundary which is, in a practical sense, both flexible and yielding.

If a rigid boundary is introduced under a decelerating ship, as when it runs suddenly into shallow water, the kinetic energy in the unsteady flow around the ship is increased, probably because the particles are no longer free to follow a minimum-energy pattern. Hence, the added mass of the entrained water begins to increase appreciably by the time the bed clearance under the ship has diminished to less than its mean draft. This is in accordance with the results derived analytically by H. Lamb, L. M. Milne-Thomson, and others, which indicate that the added mass of entrained liquid increases as a solid boundary of infinite extent is approached.

If the decelerating body suddenly approaches a limiting vertical boundary of limited extent but of large proportions compared to itself, such as a small tug which surges up to a large ship at too high a speed, or an exercise torpedo which runs into the side of a hull, the analytic study indicates that the added mass of the water around the smaller decelerating body should also increase. However, it is reported that in one of the few known cases where this theorem has been applied in practice, the observed data indicated that the added mass of the smaller body was reduced, so that it became easier to stop within a given distance or time interval. The smaller body had the general form of an ellipsoid of revolution and it was approaching the larger body by a sidling motion. It is entirely possible that other factors were present in the latter case and were not taken into account.

62.5 Estimating the Added-Mass Coefficients of Vibrating Ships in Confined Waters. The effect of shallow water upon a vibrating ship is discussed in Sec. 35.13 of Volume I; Fig. 35.G illustrates schematically the flow around the sections of a ship form in vertical vibration. Sec. 35.14 explains that ship vibration, particularly in the vertical direction, is greatly magnified in shallow water. This is also discussed by F. M. Lewis in a paper "Ship Vibration" [Proc. World Eng'g. Cong., Tokyo, 1929, Vol. XXIX, Part 1, publ. in 1931, pp. 203–204]. T. W. Bunyan states that the various critical vibration frequencies and amplitudes, in a transverse direction, are also affected by restricted waters such as the Suez Canal [IME, Apr 1955, Vol. LXVII, p. 100].

F. M. Lewis, in the reference cited, states that from physical reasoning and analytic study the inertial effect of the added mass of entrained water is greater in shallow water than in deep water. Despite verification of the foregoing by the experiments of J. J. Koch and C. W. Prohaska, to be mentioned presently, and the full-scale tests by R. T. McGoldrick on the Great Lakes ore carrier *E. J. Kulas* [TMB Rep. 762, Jun 1951, esp. Table 1 on p. 4 and p. 11], F. H. Todd and W. J. Marwood report that, for one ship case at least, the opposite result was found [NECI, 1947–1948, Vol. 64, p. D127].

Assuming an increase in added-liquid mass in shallow water, the direct result of the increase in total mass is to decrease the natural frequency of the ship, so that resonant vibration in a frequency range below that of the exciting forces at the operating speed in deep water might occur within that lowered range in shallow water. For example, the blade frequency for the single-screw drive of the ABC transom-stern ship of Part 4 at the designed speed in deep water, is, from Fig. 78.Nb, $Z(\text{rpm}) = 4(109.7) = 438.8$ cycles per min. The sixth-moded vertical vibration of the hull, which for certain reasons might be objectionable, is assumed to occur at 380 cycles per min. At the sustained speed of 18.7 kt, this is still well below the blade frequency at that reduced speed, likewise in deep water. However, when running in the river below Port Correo the propeller rpm might be reduced to say 81, and the blade frequency to 324 cpm. The shallow-water effect on the added-liquid mass might be great enough to lower the sixth-moded resonant frequency from 380 to 324 cpm. Not only would this be exactly in the running range but there would be an enormous magnification effect with the nominal bed clearance of only 4 ft under the ship. K. Wendel mentions a case similar to this on page 71 of TMB Translation 260, July 1956. The problem of the naval architect is to determine, and if possible to predict in advance, the magnitude and effect of the changes such as this in added mass, frequency, and amplitude.

The specific information known to be available concerning the effect of shallow water on the added mass of the water around a ship, when vibrating vertically, is limited to the experimental data of:

(1) Koch, J. J., "Eine experimentelle Method zur Bestimmung der reduzierten Masse des mitschwingenden Wassers bei Schiffsschwingungen (Experimental Method for Determining the Virtual Mass for Oscillations of Ships)," Ing.-Arch., 1933, Vol. IV, Part 2, pp. 103–109;

English version in TMB Transl. 225, May 1949
(2) Prohaska, C. W., "Vibration Verticales du Navire (Vertical Vibrations of the Ship)," ATMA, 1947, Vol. 46, pp. 171–219; abstracted in English in SBMEB, Oct 1947, pp. 542–546 and Nov 1947, pp. 593–599; complete English translation (unpublished in 1956) available in TMB library. A list of 21 references appears on pp. 214–215 of the original paper.
(3) Prohaska, C. W., discussion of paper entitled "Ship Vibration," by F. H. Todd and W. J. Marwood, NECI, 1947–1948, Vol. 64, pp. D119-D123, plus authors' reply on p. D127
(4) Marwood, W. J., and Johnson, A. J., "Vibration Tests on an Up-River Collier with Special Reference to the Influence of Depth of Water," NECI, 1953–1954, Vol. 70, pp. 193–216, D103-D110.

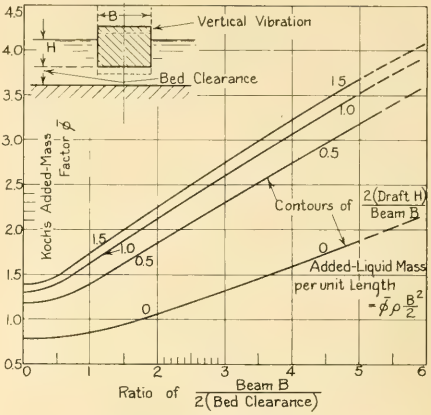

FIG. 62.J ADDED-LIQUID-MASS DATA OF KOCH FOR A RECTANGULAR-SECTION SURFACE SHIP, VIBRATING VERTICALLY IN SHALLOW WATER

Koch's data in (1) were obtained by tests in a 2-diml electrolytic tank, using the methods described in Sec. 42.13. The tank represented a horizontal half of a rectangular-section channel, with half of the underwater body of a rectangular-section ship in the center of the channel. The half-breadth of the channel was about 7 times the half-beam of the ship. This was considered by Koch to be the equivalent of a channel of infinite width.

Figs. 62.J and 62.K, adapted from Figs. 8 and 11 of the Koch reference, give data for determining the added mass of the entrained liquid around a floating 2-diml body of rectangular section, for a combination of variables involving the beam B, the draft H, and the bed clearance h-H (in the notation of the present book) between the bottom of the ship and the bed of the channel. Fig. 62.J gives these data for vertical vibration; Fig. 62.K for horizontal vibration.

For one who studies the papers of either Koch or Prohaska, it is important to remember that the "added mass factor" $\bar{\phi}$ (phi bar) of Koch's paper (TMB Transl. 225) and the "coefficient" C of Prohaska's paper, although non-dimensional in both cases, are based upon the masses of two different transverse shapes of underwater body. This factor and this coefficient are therefore only shape factors for the bodies in question, to be defined presently. They are not true added-mass or inertia coefficients.

The reference body of Koch is a buoyant one

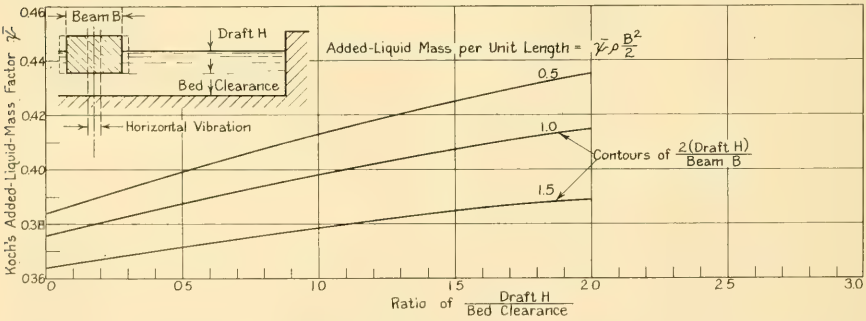

FIG. 62.K ADDED-LIQUID-MASS DATA OF KOCH FOR A RECTANGULAR-SECTION SURFACE SHIP, VIBRATING HORIZONTALLY IN SHALLOW WATER

of *constant* rectangular section having a beam B ($2b$ in his paper), a draft H of half the beam, and a unit length. Its body mass m_B is therefore $\rho(B)(B/2)(1.0) = \rho B^2/2$ per unit length; in Koch's notation it is $2\rho b^2$. Therefore, to obtain the added mass m_L of entrained liquid for a buoyant rectangular-section body of beam B, applying to any given combination of the variables listed in the second paragraph preceding, it is necessary to multiply Koch's "added mass factor" $\bar{\phi}$ by $\rho B^2/2$. Then for the given rectangular-section body of beam B, the added-liquid mass $m_L = \bar{\phi}\rho B^2/2$ per unit length.

The reference body of Prohaska is a buoyant one of semicircular section having a flat, horizontal top and a curved under side, with a beam B ($2b$ in the paper), a draft H of half the beam (b in the paper), and a unit length. Its body mass m_B is therefore $\rho(\pi/8)B^2$ per unit length; in Prohaska's notation it is $0.5\pi\rho b^2$. Hence, to obtain the added mass m_L for a floating body having a beam B and any type of constant section within the limits of Prohaska's tests, depicted in his Fig. 19, and for any combination of the variables listed by Prohaska (section coefficient β and depth-draft ratio T/d), it is necessary to multiply his "coefficient" C by $0.125\pi\rho B^2$. Thus for the given body of beam B, the added liquid mass $m_L = C(0.125)\pi\rho B^2$ per unit length.

The reference body of Prohaska has a semicircular section which can be inscribed within the rectangular section of Koch. Therefore, it has a mass m_B which is $\pi/4$ times that of Koch, from which it follows that Prohaska's $C = 4\bar{\phi}/\pi$ or Koch's $\bar{\phi} = \pi C/4$.

The data of C. W. Prohaska, set down in (2) preceding, were obtained with 2-diml (constant-section) models of limited length and of varied section shape and fullness, moved bodily up and down in a tank of water, with their longitudinal axes parallel to the water surface. The water depth h was varied by altering the position of an adjustable bottom. It was found that V-type transverse sections always gave greater added-mass coefficients than U-type sections, and that the m_L-values for hollow sections were approximately the same as for sections which had the hollows filled out by drawing tangents between the projecting points.

Fig. 62.L, adapted from one of the several shallow-water graphs given by Prohaska, namely Fig. 32 on page 204 of the 1947 ATMA paper, summarizes in diagram 1 the shape-factor or Prohaska "coefficient" C data in terms of (1) the section coefficient, based on the local beam

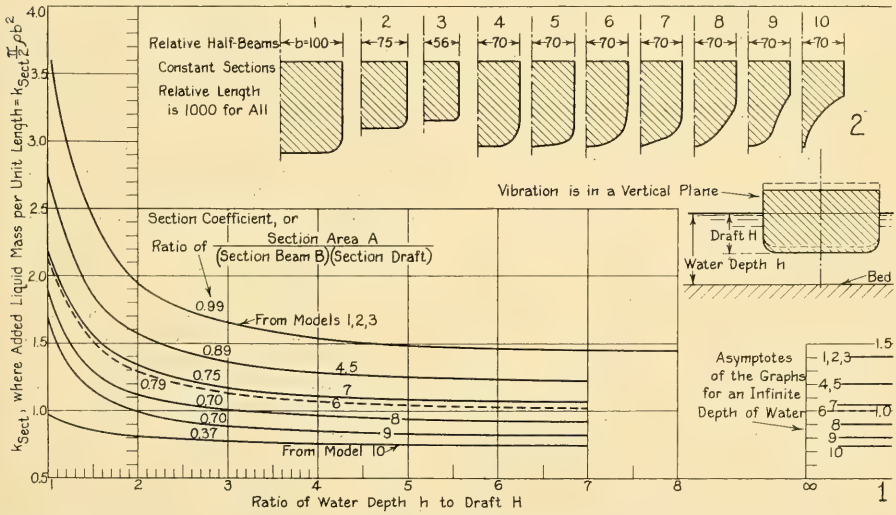

FIG. 62.L ADDED-LIQUID-MASS DATA OF C. W. PROHASKA FOR A SURFACE SHIP WITH NORMAL SECTIONS, VIBRATING VERTICALLY IN SHALLOW WATER

B and the section draft, and (2) the ratio h/H, relating the depth of water to the ship draft.

Koch's shallow-water shape factors $\bar{\phi}$ apply to rectangular sections only, so to use them for a ship one would have to assume a constant section for the entire length. Prohaska's shallow-water shape factors apply to sections of varying fullness, from 0.99 to 0.37, so that a calculation could be made for a ship with somewhat tapering ends by using segments of diminishing section coefficient toward the ends.

Applying the data of Koch and Prohaska to the vertical-vibration problem of the ABC ship of Part 4, transiting the 30-ft river between Port Correo and the sea, the basic data are:

Draft, $H = 26$ ft
Depth of water, $h = 30$ ft
Bed clearance, $h - H = 4$ ft
Ratio of draft to half-beam, $2H/B_X = 52/73 = 0.71$

Maximum-section coefficient, $C_X = 0.956$
Ratio of depth of water to draft, $h/H = 30/26 = 1.15$
Ratio of half-beam to bed clearance, $B_X/[2(h - H)] = 73/[2(4)] = 9.1$

Applying these data to Koch's graph with ITTC notation, Fig. 62.J, they fall far beyond the limits of the graph. Applying the equivalent ratios to Koch's *original* graph, Fig. 8 of reference (1) at the beginning of this section, and extrapolating roughly, $\bar{\phi}$ appears to have a value of about 5.0 for a ship having a constant rectangular section throughout. Since Koch's $\bar{\phi} = m_L/(\rho B_X^2/2)$, the added-liquid mass is of the order of

$$m_L = (0.5)\bar{\phi}\rho B_X^2 = (0.5)(5.0)\rho B_X^2$$
$$= 2.5\rho B_X^2 \text{ per unit length.}$$

From Prohaska's original data, reproduced in diagram 1 of Fig. 62.L, his "coefficient" C is about 2.9 for a ship having a *constant* section coefficient of 0.956. The added-liquid mass is therefore of the order of

$$m_L = \mathrm{C}\frac{\pi}{2}\rho\frac{B_X^2}{4} = (2.9)(0.125)\pi\rho B_X^2$$
$$= 1.14\rho B_X^2 \text{ per unit length.}$$

The *weight* of the added-liquid mass is $g(m_L)$ in each case.

This is a rather large discrepancy but the comparison is hardly fair to the data of Koch because, as indicated in Fig. 62.J of the present section, as well as in Fig. 31 on page 203 of Prohaska's ATMA, 1947 paper, Koch's experiments do not cover such a small depth-of-water to draft ratio.

62.6 Estimating the Added-Mass Coefficients for Vibrating Propulsion Devices. Data on the added mass of entrained water surrounding the thrust-producing blades of any type of mechanically driven propulsion device are required for predicting the vibration characteristics of the component parts or of the entire mechanical propelling system.

For a propulsion device like a paddlewheel, with blades generally normal to their direction of motion relative to the surrounding water, the added mass of entrained liquid may be approximated by the known m_L for a submerged flat plate of rectangular outline, in unsteady motion in a direction normal to its surface. For this case, the added mass is given in Fig. 62.A for the rectangular flat plate having dimensions of $2a$ and $2b$. However, the paddlewheel case is by no means simple because all the submerged blades create surface waves, and one or two or more blades are always partly in and partly out of the water. So far as known, no engineering rule has been developed for estimating the added mass m_L of paddlewheels or sternwheels.

The rotating-blade propeller presents a much different case because the several blades usually (except in maneuvering) lie at only a small angle (the attack angle) relative to their direction of motion through the surrounding water. However, what is wanted in this case is the added mass for a mode of motion which is tangential to the spindle circle at each spindle position. This quantity depends upon the pitch ratio and the exact type of blade motion. Moreover, it changes with the position of a blade on the blade orbit or spindle circle. It can be assumed roughly as one-half the added liquid mass for the blade, reckoned for a mode of motion normal to the projected area of the blade [Mueller, H. F., unpubl. ltr. to HES, 6 Jul 1956]. This liquid mass, added to the mass of the blade and summed up for all the blades, plus the mass of the supporting and actuating machinery, gives the polar moment of inertia of the whole assembly about the axis of propeller (not blade) rotation.

For the screw propeller the marine architect is interested in the added-liquid masses and the corresponding added mass moments of inertia

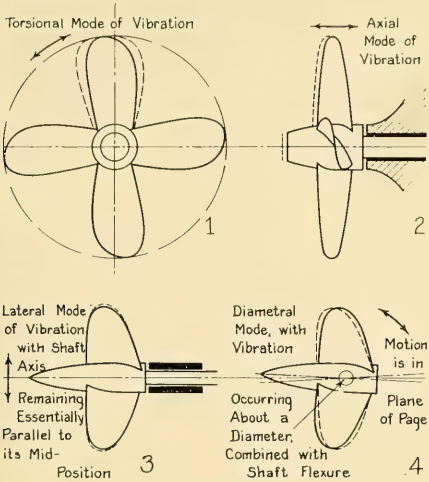

FIG. 62.M MODES OF MOTION OF A VIBRATING SCREW PROPELLER ON A SHIP

for four modes of motion illustrated schematically in Fig. 62.M:

(1) Torsional or rotational, about the propeller-shaft axis, as in diagram 1, assuming that the latter remains essentially straight
(2) Axial, parallel to or along that axis, indicated in diagram 2
(3) Lateral, corresponding to the sidewise motion of a propeller shaft in a loose bearing next to the propeller, as in diagram 3. This also includes a motion due to sidewise bending of the propeller shaft at the propeller, in which the propeller moves only in a direction parallel to the normal disc plane, without diametral rotation.
(4) Diametral rotation, as in diagram 4, corresponding to angular motion of the propeller out of the normal plane of its own disc, due to bending or whirling of the propeller shaft about some selected diametral axis in the propeller.

There are indications that the depth of immersion of a screw propeller is a factor in all four modes, because of the "relieving" effect of a free surface close to the vibrating blades.

To determine the value of the added mass moment of inertia for the torsional mode of (1) preceding, a number of tests have been made with model propellers, among them those of R. T. McGoldrick, described in TMB Report 307 of July 1931. These tests comprised a set of torsional-vibration experiments on a group of brass model propellers, 16 inches in diameter, conducted in both air and water at the U. S. Experimental Model Basin. The P/D values ranged from 0.60 to 2.00. However, these tests produced only the general conclusions that:

(a) For a fixed amplitude and frequency the effect (on the polar moment of inertia J) varies directly with the blade-width ratio, and with the pitch ratio. In other words, J increases as both c_M/D and P/D increase.
(b) For a given propeller the effect (on the polar moment of inertia J) increases with frequency and amplitude
(c) In order to determine the per cent increase in (polar) moment of inertia in any given case, the amplitude and frequency of the propeller (vibration) must be approximately known.

Some years later R. Brähmig made an analytic study of the torsional-vibration problem of screw propellers, listed as reference (29) of Sec. 62.8. He considered variations in frequency and amplitude as affecting the added mass of the entrained liquid, and gave a full statement of the similitude conditions and scale effect involved in the model experiment technique. Results are quoted in his paper for torsional-vibration tests on flat circular discs but none for model screw propellers in the same mode. However, Table 2 of this reference lists rotational-amplitude and frequency data for the propellers of three ships.

As a rule, the amount of rotation amplitude and the frequency in water are almost never known with any reasonable certainty for a ship, and the effect of the surrounding water on the polar moment of inertia varies widely as indicated in TMB Report 307. It was therefore decided, by those working in this field, that the only practical interim answer was to accept a percentage increase in the polar moment of inertia of the propeller mass in air, regardless of the pitch ratio, the mean-width ratio, the ratio of hub diameter to overall diameter, and all other factors. For this mode of vibration, the effect of an abnormally large or small hub is possibly less pronounced because of the small radii involved. However, the sine of the geometric blade angle is large at the radii near the hub.

Based on these tests, an overall mean of 25 to 30 per cent increase in J, due to the added mass of the entrained water, was used for many years; this is the value given by J. R. Kane and R. T.

McGoldrick on pages 199 and 200 of SNAME, 1949. Subsequent experience has indicated a single average value of 25 per cent increase in J due to added-liquid mass for the pure torsional mode of motion [Garibaldi, R. J., "Procedure for Torsional Vibration Analysis of Multimass Systems," BuShips, Navy Dept., Unclassified Res. and Dev. Rep. 371-V-19, 15 Dec 1953, p. 6].

For the axial mode of vibration the situation is rather complicated, since the blade sections usually lie at rather large angles to each direction of motion, forward and aft, and the blade width is a major factor. Kane and McGoldrick explain it in most readable terms on pages 199 and 200 of their paper "Longitudinal Vibration of Marine Propulsion Shafting Systems" [SNAME, 1949]. For axial vibration they recommend that, as an approximate estimate, the added liquid mass m_L be taken as 40 to 60 per cent of the propeller mass m_{Prop}. Further experience on their part indicates a single value of 60 per cent. In other quarters, a value of 50 per cent "is normally used" [E. F. Noonan, BuShips, Navy Dept., unpubl. memo to HES of 15 Jun 1956].

Kane and McGoldrick also give a dimensional equation having a semianalytic basis, of the following form:

m_L for the axial mode of motion, in lb,

$$= k \frac{1}{\left[0.23\left(\frac{P}{D} \text{ at } 0.67R_{\text{Max}}\right)^2 + 1\right]} \cdot (Z)(0.010D \text{ in inches})^3\left(\frac{c_M}{D}\right)^2 \qquad (62.\text{vi})$$

where k has an empirical value of about 9,100.

This formula is converted to 0-diml form by inserting the weight density w of the water in which the propeller is working. Incorporating the constant $k = 9{,}100$, and eliminating the units of measurement for the diameter D, the 0-diml equation then becomes

m_L for the axial mode of motion

$$= 0.245w \frac{1}{\left[0.23\left(\frac{P}{D} \text{ at } 0.67R_{\text{Max}}\right)^2 + 1\right]} \cdot (Z)(D)^3\left(\frac{c_M}{D}\right)^2 \qquad (62.\text{vii})$$

For the ABC transom-stern ship of Part 4, having a final design of propeller shown in Fig. 70.O, the P/D ratio at $0.67R_{\text{Max}}$ is 1.199, $Z = 4$, $D = 20$ ft, and the mean-width ratio $c_M/D = 0.229$. Then for salt water having a weight density w of 64.0 lb per ft^3, the added mass m_L for the axial mode is, by substitution in Eq. (62.vii),

$$m_L = 0.245(64.0) \frac{1}{[0.23(1.199)^2 + 1]} \cdot (4)(20.0)^3(0.229)^2$$

$$= 19{,}790 \text{ lb.}$$

The estimated weight of this propeller in manganese bronze is 40,750 lb, which gives an m_L/m_{Prop} ratio of only 48.6 per cent.

For the lateral mode of vibration, depicted in diagram 3 of Fig. 62.M, no analytic solution or test data appear to be available in published form. A percentage increase of 10 in the propeller mass is recommended by R. T. McGoldrick (Conf. of 7 Jun 1956).

For the diametral mode of motion, diagrammed at 4 in Fig. 62.M, McGoldrick recommends a percentage increase of 50 in the mass moment of inertia, in air, of the propeller for the same mode of motion about the same axis, due to the moment of the added mass of the entrained water.

62.7 Added-Mass Data for Water Surrounding Ship Skegs and Appendages. Fins, deep keels, fixed stabilizers, and thin skegs of moderate to large area are subject to lateral vibration when excited by mechanical or hydrodynamic forces. The frequency of resonant vibration must be clear of any exciting-force frequency, especially for a periodic force of large magnitude, if magnification of the resonant vibration is to be avoided. The graphs in EMB Report R-22 of April 1940, describing full-scale vibration tests of one of the twin skegs of the battleship *Washington* (BB55), illustrate the mode of vibration and the resonance variations with frequency for a ship structure of this kind.

When a large, thin, vibrating appendage with moderately sharp edges is surrounded by water, the kinetic energy in the velocity field is high. This means a large added mass of entrained liquid. Indeed, the added-mass coefficient C_{AM} may easily reach 2, 3, or 4. For a thin-plate structure like a sailing-yacht centerboard, it may exceed 6 or 8. Not only must the magnitude of this mass be known to predict the resonant frequency when in water, but the frequency is often drastically lowered, so that it lies in an undesirable position, within the range of exciting-force frequencies.

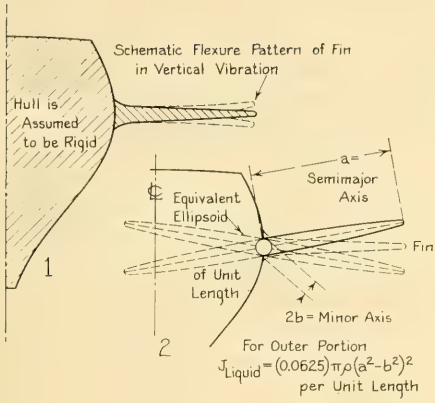

Fig. 62.N Method of Estimating the Added Liquid Mass for a Large, Thin, Cantilever Structure in Lateral Vibration

Cantilever structures, comprising a category which embodies most of the appendages listed, sway with a motion somewhat resembling that of a tree in a gusty wind, illustrated schematically in Fig. 62.N. The root of the cantilever is relatively rigid, so that most of the motion occurs near the tip, as with the *Washington* skeg mentioned previously. In the absence of a specific analytic solution covering this case, a reasonable approximation is achieved by assuming that the cantilever has a semielliptic section and that it is hinged to the hull at its midlength, at a point corresponding to the root attachment of the cantilever. This produces a motion, approximately normal to the plane of the thin appendage, which is greater than that of the cantilever structure near the root but less at the tip. Experience indicates that the kinetic energies and added masses in the two cases are of the same order of magnitude.

From the second diagram at the top of Fig. 62.A a 2-diml elliptic-section cylinder in unsteady oscillatory motion about an axis at its center has an added mass moment of inertia J_L of $(0.125)\pi\rho(a^2 - b^2)^2$ per unit length, where a is half the semimajor axis and b is half the semiminor one.

As an example of this method, take the case of the thin, vertical centerline skeg under the transom stern of the ABC ship of Part 4, for which sections are indicated in Fig. 66.P and a profile in Fig. 66.Q. This skeg is of variable depth, below the hull, but it may be assumed from Fig. 66.Q to have an average depth, normal to the centerline buttock in the vicinity, of about 16.5 ft. This is the semimajor axis of an equivalent semielliptic section. The semiminor axis is estimated from Fig. 66.P as 2.5 ft. Then, for standard salt water at 59 deg F, 15 deg C, and for half of the elliptic section, the moment of inertia of the added-liquid mass, about the point of attachment of the skeg to the hull, is

$$\begin{aligned} J_L &= (0.0625)\pi\rho(a^2 - b^2)^2 \\ &= 0.0625(3.1416)1.9905[(16.5)^2 - (2.5)^2]^2 \\ &= 27{,}654 \text{ slug-ft}^2 \text{ per ft length,} \end{aligned}$$

the latter reckoned generally parallel to the centerline buttock in the vicinity.

62.8 Partial Bibliography on Added-Mass and Damping Effects. There are listed here a number of references in the technical literature relating to the added or entrained masses around bodies, ships, and typical forms of interest to the marine architect. This list includes the references mentioned throughout the present chapter.

An excellent historical summary of the development of means for evaluating and taking account of the added mass of entrained water around a vibrating ship is given by R. T. McGoldrick in the introduction and text of TMB Report 395, issued in February 1935. The bibliography on page 30 lists most of the early papers of importance, beginning with that of Otto Schlick in INA, 1884.

A bibliography on vibration, containing 73 references, was collected by the SNAME Hull Structure Committee and published as part of the work on Project S-7 in SNAME Bulletin, January 1952, pages 14–15. A supplementary list of 30 references was published in SNAME Bulletin, October 1952, page 27.

References pertaining to added-liquid mass effects, published subsequent to 1924, include:

(1) Nicholls, H. W., "Vibration of Ships," INA, 1924 pp. 141–163
(2) Taylor, J. L., "Ship Vibration Periods," NECI, 1927–1928, Vol. 44, pp. 143–176
(3) Cole, A. P., "The Natural Periods of Vibration of Ships," IESS, 1928–1929, Vol. LXXII, pp. 43–86
(4) Kempf, G., and Helm, K., "Auslaufmessungen am Schiff und am Modell Dampfer *Hamburg* (Retardation Measurements on the Ship and on the Model of the Steamer *Hamburg*)," WRH, 7 Sep 1928, pp. 336–340. These authors found a virtual-mass coefficient for retardation and straight-ahead

motion of from 1.06 for small vessels to 1.04 for large vessels.

(5) Lewis, F. M., "The Inertia of the Water Surrounding a Vibrating Ship," SNAME, 1929, Vol. 37, pp. 1–20 and Pls. 1–5

(6) Lewis, F. M., "Ship Vibration," Proc. World Eng'g. Cong., Tokyo, 1929, Vol. XXIX, Shipbldg. and Mar. Eng'g., Part 1 (published in 1931), pp. 193–212, esp. the discussion on Water Effects on pp. 203–204. There are 42 references listed on pp. 209–210.

(7) Taylor, J. L., "Some Hydrodynamical Inertia Coefficients," Phil. Mag., Jan-Jun 1930, Vol. IX, Series 7, pp. 161–183

(8) Abell, T. B., "A Note on the Direct Measurement of the Virtual Mass of Ship Models," INA, 1930, LXXII, pp. 303–309

(9) Taylor, J. L., "Vibration of Ships," INA, 1930, Vol. LXXII, pp. 162–196, esp. pp. 163–164 and Appx. A, pp. 169–170

(10) Browne, A. D., Moullin, E. B., and Perkins, A. J., "The Added Mass of Prisms Floating in Water," Proc. Camb. Phil. Soc., 1930, Vol. XXVI, pp. 258–272. A brief quotation from p. 263 of this reference is given on p. 299, Sec. 20.11 of Volume I.

(11) Moullin, E. B., "Some Vibration Problems in Naval Architecture," Proc. Third Int. Cong. Appl. Mech., Stockholm, 1930, Vol. III, pp. 28–30

(12) "Effect of Entrained Water in the Mass Moment of Inertia of Ship Propellers," EMB Rep. 307, Jul 1931

(13) Todd, F. H., "Some Measurements of Ship Vibration," NECI, 1931–1932, Vol. 48, p. 65ff

(14) Schadlofsky, E., "Über Rechnung und Messung der Elastichen Eigenschwingungen von Schiffskörpern (The Calculation and Measurement of Elastic Natural Frequencies of Ship Hulls)," STG, 1932, Vol. 33, pp. 280–325. English version in EMB Rep. 382 of Jun 1934, also bearing the number EMB Transl. 7. To this report belongs EMB Supplement to Report 382, containing a translation of the discussion on the Schadlofsky paper, pp. 326–335 of the original reference.

(15) Koch, J. J., "Eine experimentelle Method zur Bestimmung der reduzierten Masse des mitschwingenden Wassers bei Schiffsschwingungen (Experimental Method for Determining the Virtual Mass for Oscillations of Ships)," Ing.-Arch., 1933, Vol. IV, Part 2, pp. 103–109; English version in TMB Transl. 225, May 1949

(16) Todd, F. H., "Ship Vibration—A Comparison of Measured with Calculated Frequencies," NECI, 1932–1933, Vol. 49, p. 259ff

(17) Dimpker, A., "Über Schwingende Körper an der Oberfläche des Wassers (On Vibrating Bodies on the Surface of the Water)," WRH, 15 Jan 1934, Vol. 15, pp. 15–19

(18) Lundberg, S., "Vibrationsforeteelser (Vibration Measurement)," Tekniska Samfundets Handlinger, Göteborg, 1934, No. 4; also "Einige Untersuchungen über schiffsschwingungen (Some Investigations of Ship Oscillations)," WRH, 1 Oct 1936, pp. 295–299

(19) Burrill, L. C., "Ship Vibration: Simple Methods of Estimating Critical Frequencies," NECI, 1934–1935, Vol. 51, pp. 259–276

(20) Conn, J. F. C., "Backing of Propellers," IESS, 1934–1935, Vol. 78, pp. 27–83. The author states, on p. 57, that W. Froude found from the *Greyhound* experiments a virtual-mass coefficient, for straight-ahead motion, of from 1.16 at the light displacement to 1.20 at the heavy displacement.

(21) McGoldrick, R. T., "A Study of Ship Hull Vibration," EMB Rep. 395, Feb 1935. Describes and analyzes tests made by the EMB staff on the U. S. destroyer *Hamilton* (DD141) and on two structural models. Pages 9–11 discuss the "Correction for Effect of the Surrounding Water." Pages 30–32 of this report carry a list of 29 references.

(22) Guntzberger, H., "Effet Amortisseur de l'Hélice sur les Oscillations de Torsion des Lignes d'Arbres (Buffer Effect of the Propeller on the Torsional Vibrations of Line Shafting)," ATMA, 1935, Vol. 39, pp. 251–259. The author finds an augmentation of polar moment of inertia of 60 per cent of the corresponding polar moment of mass of a steel screw propeller. He mentions the fact that an augmentation percentage of 25 is generally used, as listed in Sec. 62.6 of the present book.

(23) Lewis, F. M., "Propeller Vibration," SNAME, 1935, Vol. 43, pp. 252–285

(24) Todd, F. H., "Vibration in Ships," Tekniska Samfundets Handlinger, Göteborg, 1935, No. 5, pp. 125–151 (in English)

(25) Holstein, H., "Untersuchungen an einem Tauchschwingungen ausführenden Quader (Investigation of the Heaving Oscillations of a Parallelepiped)," WRH, 1 Dec 1936, pp. 385–389

(26) Lewis, F. M., "Propeller Vibration," SNAME, 1936, Vol. 44, pp. 501–519

(27) Sezawa, K., and Watanabe, W., "The Vibration Damping of a Ship in her Moving State," Zōsen Kiōkai (The Society of Naval Architects of Japan), Dec 1938, Vol. LXIII. This reference describes experiments made to determine the added mass of liquid surrounding hinged plates.

(28) Baumann, H., "Trägheitsmoment und Dämpfung belasteter Schiffsschrauben (Damping and Moment of Inertia of Loaded Ship Propellers)," WRH, 15 Aug 1939, Vol. 20, pp. 260–261

(29) Brähmig, R., "Die Experimentelle Bestimmung des Hydrodynamischen Massenzuwachses bei Schwingkörpern (Experimental Determination of the Hydrodynamic Increase in Mass in Oscillating Bodies)," Schiffbau, 1 Jun 1940 and 15 Jun 1940; English version in TMB Transl. 118, Nov 1943. This paper carries a list of 34 references.

(30) Prohaska, C. W., "Lodrette Skibssvingninger med 2 Knuder (Longitudinal Ship Vibration with 2 Nodes)," Thesis, Kobenhavn, 1941

(31) Havelock, T. H., "The Damping of the Heaving and Pitching Motion of a Ship," London, Edinburgh, and Dublin Phil. Mag. and Jour. Sci., 1942, Vol. 33

(32) Lewis, F. M., "Dynamic Effects," ME, 1944, Vol. II, pp. 139–140. Contains a long list of references on

"Vibration of Ships," some of which apply to the present chapter.

(33) Horne, L. R., "Stopping of Ships," NECI, 1944–1945, Vol. 61, p. 311ff

(34) Havelock, T. H., "Notes on the Theory of Heaving and Pitching," INA, 1945, Vol. 87, pp. 109–122, esp. pp. 109–110 discussing the added mass of entrained water for ship forms. For heaving, Havelock gives a C_{AM} of 0.8 to 1.0; for pitching he gives 0.4 to 0.5.

(35) Lamb, Sir Horace, "Hydrodynamics," 1945, 6th ed. The table of contents and the index, between them, list the following pages, among others, for data on added- and virtual-mass coefficients, as well as for data on the body masses themselves:

Inertia coefficients, of a circular cylinder, 77
circular disc, 137
of an elliptic cylinder, 85, 88
of a sphere, 124
of two spheres, 130
of an ellipsoid, 153, 155
general, 166
in cases of symmetry, 172.

(36) Prohaska, C. W., "Vibrations Verticales du Navire (Vertical Vibrations of a Ship)," ATMA, 1947, Vol. 46, pp. 171–219. Discussion of the added mass of the entrained water is found on pp. 189–205. On pages 214 and 215 there is a list of 21 references. Abstracted in English in SBMEB, Oct 1947, pp. 542–546 and Nov 1947, pp. 593–599. Complete English translation, as yet unpublished (1956), at the David Taylor Model Basin.

(37) Todd, F. H., "The Fundamentals of Ship Vibration," SBMEB, May, Jun, Jul, 1947, Vol. 54, pp. 307–312, 358–362, 400–403, respectively

(38) Todd, F. H., and Marwood, W. J., "Ship Vibration," NECI, 1947–1948, Vol. 64, pp. 193–210, D113-D128

(39) John, F., "On the Motion of Floating Bodies," Communications on Pure and Applied Mathematics, Mar 1949, Vol. II, No. 1

(40) Ursell, F., "On the Heaving Motion of a Circular Cylinder on the Surface of a Fluid," Quart. Jour. Mech. and Appl. Math., Jun 1949, Vol. II, Part 2

(41) Kane, J. R., and McGoldrick, R. T., "Londitudinal Vibrations of Marine Propulsion-Shafting Systems," SNAME, 1949, pp. 193–252, esp. pp. 199–200

(42) May, A., and Woodhull, J. C., "The Virtual Mass of a Sphere Entering Water Vertically," NOL memo 10636, 3 Mar 1950; ONR project NR-062-024; copy in BuShips, Navy Dept., library. See also Nat'l. Res. Council, U. S., Bull. 84, 1932, p. 97.

(43) Wendel, K., "Hydrodynamische Massen und Hydrodynamische Massenträgheitsmomente (Hydrodynamic Masses and Hydrodynamic Mass Moments of Inertia of Entrained Water)," STG, 1950, Vol. 44, pp. 207–255. English version in TMB Transl. 260, Jul 1956. A bibliography of 27 items appears on p. 252 of the original; pp. 73–74 of the translation.

(44) Weinblum, G., and St. Denis, M., "On the Motions of Ships at Sea," SNAME, 1950, pp. 184–248, esp. pp. 189–192 on Inertia Forces and Free-Surface Effects

(45) McGoldrick, R. T., "Determination of Hull Critical Frequencies on the Ore Carrier S. S. *E. J. Kulas* by Means of a Vibration Generator," TMB Rep. 762, Jun 1951. In an appendix to this report, pp. 18–19, E. H. Kennard describes a method for estimating the added mass of entrained water around a ship for any mode of vertical vibration.

(46) Wendel, K., and Boie, C., "Experimentelle Bestimmung der Hydrodynamischen Masse an ganz und Teilweise getauchten Körpern (Experimental Determination of Hydrodynamic Masses on Totally and Partly Immersed Bodies)," Hansa, 8 Dec 1951, Vol. 88, pp. 1788–1790

(47) Weinblum, G., "Über Hydrodynamische Massen (On Hydrodynamic Masses)," Schiff und Hafen, Dec 1951, pp. 422–427 (in German)

(48) Weinblum, G. P., "On Hydrodynamic Masses," TMB Rep. 809, Apr 1952

(49) Havelock, Sir Thomas H., "Ship Vibrations: The Virtual Inertia of a Spheroid in Shallow Water," INA, 1953, Vol. 95, pp. 1–9. On page 7 there is a list of 7 references.

(50) Marwood, W. J., and Johnson, A. J., "Vibration Tests of an Up-River Collier with Special Reference to the Influence of Depth of Water," NECI, 1953–1954, Vol. 70, pp. 193–216

(51) McGoldrick, R. T., Gleyzal, A. N., Hess, R. L., and Hess, G. K., Jr., "Recent Developments in the Theory of Ship Vibration," TMB Rep. 739, Oct 1953, esp. pp. 13–15

(52) Grim, O., "Calculation of Hydrodynamic Forces Caused by Oscillation of Ship Hulls," STG, 1953, Vol. 47, pp. 277–299 (in German)

(53) McGoldrick, R. T., "Comparison Between Theoretically and Experimentally Determined Natural Frequencies and Modes of Vibration of Ships," TMB Rep. 906, Aug 1954, esp. pp. 9, 14

(54) Havelock, Sir Thomas H., "Waves Due to a Floating Sphere Making Periodic Heaving Oscillations," Proc. Roy. Soc., Series A, Jul 1955, Vol. 231, pp. 1–7; see Appl. Mech. Rev., Feb 1956, No. 504, pp. 74–75.

PART 4

Hydrodynamics Applied to the Design of a Ship

CHAPTER 63

Basic Factors in Ship Design

63.1 Definition of Ship Design. One who fashions a ship in this modern age of specialization can not be satisfied simply that it floats, moves itself through the water, and carries passengers or cargo over the water from one place to another. It must meet certain definite requirements; indeed, it must almost certainly do some things better than any other ship which can be built to meet those requirements. This superiority can be developed in the evolution of the design, in the use of the most suitable materials, or in the application of the best workmanship throughout. It can be developed by a combination of all three, but it is in the evolution of the design in general, and the hydrodynamic design in particular, that we are concerned here.

Design, for the naval architect and marine engineer, may be defined as the art of fashioning a ship by an intelligent and logical selection of those features of form, size, proportions, and arrangement which are open to his choice, in combination with those features which are imposed upon him by circumstances beyond his control.

Design is largely a matter of thinking and planning. This requires, above all, knowledge, intelligence, and understanding. One can have any one or two of these qualities, but without the third his ship-designing ability lacks that something which will make his designs uniformly successful. Knowledge can be gained from books and many other sources of engineering information. Intelligence may be brought out by a process of uncovering that which is innate in any architect and engineer. Understanding must be learned, and often the hard way.

Understanding, in general, means a comprehension of all problems and relationships and phenomena. Specifically, to the one dealing with problems of hydrodynamics, it means comprehension in its fullest sense of the elements and the intricacies of liquid flow, and of the means of dealing with and predicting the characteristics of this flow.

63.2 Application and Scope of Part 4. It is hoped that a study as well as a reading of the first three parts of the book has given the ship designer a generous share of the knowledge, intelligence, and understanding needed to fashion the form and features of a complicated modern ship. As his knowledge increases, so will his intelligence and his understanding. He will realize that he can grasp the meaning of those manifestations of nature that may long have remained a mystery to him, and that he can comprehend the whys and wherefores of so many kinds of flow and action phenomena that were formerly bewildering and meaningless.

This fourth part of the book therefore undertakes to outline the procedure whereby the information set down in Parts 1, 2, and 3 may be utilized in the hydrodynamic aspects of ship design. After taking up various phases of the procedure, in a manner paralleling those followed

in the preceding chapters, it gives a practical example of the design of a modern ship. It stresses the specified limitations and requirements, the free or open choices available to the designer, and the compromises that are unavoidable in anything put together by one man to satisfy the conflicting wishes of other men.

No ship design can be carried very far without considering the primary features involving hydrostatics. Among these are displacement and trim, metacentric stability, floodability, subdivision, and damage control. They are treated extensively in textbooks and other references [PNA, 1939, Vol. I], and require no further elaboration here. They are brought in as necessary, without detail consideration, in the ship-design example which follows.

That phase of ship stability generally known as dynamic stability but defined here as *dynamic metacentric stability* is, however, very definitely a problem involving ship and liquid motion. It is accordingly included in Part 6 of Volume III, under the chapters relating to wavegoing characteristics.

63.3 General Assumptions as to Propelling Machinery. With a few exceptions which are noted at the proper places, there is no need to consider the type of propelling machinery in any phase of the hydrodynamic design. It is taken for granted here that the machinery is adapted to the most efficient rate of rotation for the selected type of propulsion device, although too often the reverse is true. For propelling the ship, the propulsion device can be driven by a turbine, a reciprocating engine, an electric or hydraulic motor, or a hand crank, as long as the desired torque is applied, the requisite rate of rotation is attained, or the necessary power is delivered.

An exception to this rule is the case of the ship, mounting two or more propdevs on opposite sides of the centerplane, which is called upon to make frequent turns and maneuvers at relatively high speeds and powers. Here the port and starboard propdevs operate in liquid streams moving at different velocities with respect to the ship. The type of propulsion machinery almost certainly affects the rates of rotation and the powers delivered and absorbed on the two sides. Another exception is the case of the ship which must maneuver rapidly, and in which the maneuverability is in direct proportion to the promptness with which the propelling machinery responds to its own controls.

There are cases also where the type or form of the propelling machinery affects the declivity and the parallelism or divergence of the screw-propeller shafts, just as the position of the machinery almost invariably determines the position of one end of the propeller shaft. On some high-powered vessels, the necessary clearances for machinery inside the vessel may prevent shaping or fining the hull where this procedure would otherwise be desirable.

The matter of locating the propelling machinery in the stern or in other fore-and-aft positions is really not one for discussion in this book, except that:

(a) The location of the machinery aft may affect the shape of the stern and the position of the shaft carrying a screw propeller, because of the clearances required inside the vessel
(b) The machinery weight assists in trimming the vessel by the stern and pushing the screw propeller down under water.

The matter of the absolute speed of the ship, and of its actual size, is usually determined by economic, military, or other considerations beyond the control of the designer. He must, however, be prepared to predict the results of variations in these factors, and of each upon the other, so that when a final design decision must be reached, it can be based upon sound and accurate premises.

63.4 The Fundamental Requirements for Every Ship. Every ship designer, no matter how logical and realistic he may be, needs to get back to first principles every so often in his search for the best way to make nature serve him. He need not think it in the least beneath his dignity or intelligence to write down, in a few lines, as did the renowned Rankine many years ago [STP, 1866], the following simple requirements for every ship:

(a) To float on or in water
(b) To move itself or to be moved with handiness, in any manner desired
(c) To transport passengers or cargo, or other useful load, from one place to another
(d) To steer and to turn, in all kinds of waters
(e) To be safe, strong, and comfortable in waves
(f) To travel or to be towed swiftly and economically, under control at all times
(g) To remain afloat and upright when not too severely damaged.

He needs, furthermore, courage and confidence to strike out boldly for the principal goal by the shortest and most direct route, using first principles he has learned and adhering almost religiously to fundamentals. It was this procedure which produced the remarkably successful group of large landing craft in World War II, with little or no experience to fall back upon and the fate of nations at stake.

63.5 Design as a Compromise. A designer must, at least in the early stages, forget about compromises in a really new and pioneering project. In the first place, he is by no means certain that compromises must be made. He may be surprised to find that a certain stern shape, odd but seemingly necessary, makes him a gift of improved maneuvering and increased deck space as well as more efficient propulsion.

If compromises must later be admitted, it is a comfort to remember that much of ship design and construction is a compromise. This applies equally to roughing out a dugout canoe from the best available tree, or keeping the propeller tips of a twin-screw ship inside the projected deck line at the stern. However, if the effects of all the possible variables are known, the designer can choose with wisdom the final size, shape, or form of each of his elements when he makes his compromise. In this way he attains the maximum benefits from the selected combination of all of them.

Let the compromises be made with professional honesty, sound logic, and good judgment. Let them be known to all and admitted by all. Let them be based upon sturdy reasoning, and let them be tempered by a knowledge and an experienced consideration of all the causes, effects, and consequences.

63.6 The Essence of Design. British naval architects have an old saying, with respect to the shape and form of a ship, that what looks right is right. This invariably brings an immediate rejoinder about who is doing the looking; manifestly not just anybody, but one with an experienced and practical eye. The eye that has deliberately been trained becomes accustomed to look not only for efficiency and utility but for beauty, symmetry, and harmony as really essential features of design. It looks, above all, for simplicity and for the feeling of effortless ease that nature puts into many of her most dynamic moods and manifestations.

A good ship, like a good person, is not necessarily the largest, strongest, or fastest that can be fashioned, regardless of the other features, but the one in which the best combination of elements produces the most useful, harmonious, and satisfying whole.

63.7 The Design Schedule for a Ship. This book treats only of the hydrodynamic aspects of ship design, and carries some of these aspects only through the preliminary-design stage. It is difficult, therefore, to visualize the immense amount of thought and planning that has to be put into the design of a ship to achieve the best possible results. According to Ambrose Hunter ". . . it can be truthfully said that it takes every bit as long to design a successful modern trawler as to build one . . ." ["The Art of Trawler Planning," Ship and Boat Builder and Naval Architect, London, Feb 1953, p. 259]. What is true for a trawler is true for any vessel, large or small.

63.8 The Field for Future Improvements in Design. It is natural for the naval architect and marine engineer who is blessed with enterprise and ingenuity to strive for improvements in his work. It is human for him to wish to excel and to surpass the work of others. Remembering that nothing was ever done so well that it could not be done better, he continually entertains the hope that by his improved understanding of basic phenomena he can look forward, as his creations take form and life, to greater efficiency and higher performance. As certain machines appear to be reaching their peak efficiencies and certain engineers or scientists are loudly proclaiming that nothing in the way of radical advances can be hoped for, other engineers and scientists are opening up new lines of attack which often extend the practicable limits by leaps and bounds. This was the case with the piston-type engine and the screw propeller for airplanes when the jet-type engine appeared upon the scene. It is often said that the screw propeller for ship propulsion is about to reach its limit of performance, whereupon propellers of increased capacity and improved efficiency under certain working conditions appear in successful service.

It is well in ship design as in any other work not to be bound by preconceived ideas of what is possible or by the accomplishments of one's self and others in the past. A designer who is prepared, or in fact is eager to offer novel and improved solutions to old or new design problems, based upon comprehensive knowledge of fundamental physical laws and the confidence bred of successful

thinking and experience, usually succeeds in finding some ship owner or ship operator who is willing to back his engineering judgment.

In this quest for improvement the designer does well to heed the caution expressed by G. Nowka in his "New Knowledge on Ship Propulsion" of 1944 [BuShips Transl. 411, Apr 1951] when he says "The principal guiding rule in shipbuilding must read: *Do not interfere with the laws of hydrodynamics.*"

Put in another way this means: Do not try to tell the water what it has got to do or to *make* it do something which you desire. It will do what it wants to do, and that only, in accordance with the laws of its behavior.

Another excellent guiding rule for future hydrodynamic ship design, formulated by a ship operator on a basis of economics and experience, says that:

> "Good hydrodynamic features incorporated into the design of a ship cost nothing originally but afford benefits to the owner and operator which last forever" [Lowery, R., SNAME Spring Meeting, 1956, in comments on Vincent paper].

CHAPTER 64

Formulation of the Design Specifications Involving Hydrodynamics

64.1 General. The hydrodynamic design project carried through this part of the book involves a combination passenger and cargo vessel, because the requirements for such a craft are relatively severe. This vessel is intended to travel between the hypothetical cities of Port Amalo, Port Bacine, and Port Correo, leading to the simple project name *ABC Design.*

Any working example of this kind is but one of a multitude which can be presented to a marine architect. Chap. 76 in this part therefore discusses variations from big-ship rules, applying to the design of special hull forms and special-purpose craft. It considers only the problems peculiar to the majority of special designs and not treated adequately or at all in the ABC design.

In an effort to cover the hydrodynamic design field for small craft as well as for large ships, Chap. 77 contains a working example of a design for a motor tender for the ABC ship.

64.2 The First Task of the Designer. Complete success in a design project is only achieved after careful formulation of the purposes and aims of the project. Once formulated, these aims are kept continually in view and constantly in mind. There is no better way of doing this than to write them on paper, to look at them frequently, and to think about them all the time.

It is considered in many quarters that a ship owner or operator can be relied upon to formulate his own requirements and that these will suffice for the design of the ship. He, however, is taking only his view of the picture, whereas the designer must look at it from many angles. Furthermore, the owner is often so familiar with his own requirements that it does not occur to him to pass them on to the designer as peculiarities. The designer must think of the right questions to ask, then ask plenty of them, interpret offhand comments, and perhaps find out for himself by riding on and watching the operation of a similar vessel [Simpson, D. S., SNAME, 1951, p. 558]. This is why the designer must in effect prepare his own picture and plan to survey it from all angles.

Setting down the ends to be achieved is often not as simple and straightforward a task as appears at first sight. Some designers are fortunate enough to come by it naturally but most have to learn it the hard way, and without any good text or adequate reference works available for study.

This chapter is by no means a course in writing specifications but all the simple rules involved in preparing the hydrodynamic and related features of a ship specification are set down here, supplemented by a few of the more complicated but equally necessary rules. It covers the development of fairly complete specifications for the general and the hydrodynamic features of the ABC ship design which is to be prepared as the illustrative example.

It is not possible to work up a set of coherent design requirements by neglecting or omitting any considerations whatever of hydrostatics, metacentric stability, strength, engineering, cargo handling, and accommodations such as passenger quarters and crew's berthing and messing. However, only enough of the foregoing features are brought in to make the design specifications hold together, with major accent on those features having to do with hydrodynamics and ship motions.

64.3 Statement of the Principal Design Requirements. Even though they may already have been partially or completely drafted by someone else, it is wise for the designer to restate the design requirements in his own language. When properly worded, these emphasize the limitations

and conditions imposed by the owner or operator. The latter may have overlooked certain features, seemingly unimportant in appearance but vitally essential in design, in his version of the specifications. The ship designer must, moreover, be prepared to present to the ship owner-operator adequate engineering data upon which the latter can make certain design choices within his province. The data and facts are to be collected, developed, and presented by the designer in the form of clear, concise digests, setting forth the advantages and disadvantages, the premiums and the penalties associated with each choice. The owner-operator can then feel that he is making logical, intelligent selections from a reasonable number of design alternatives.

For instance, can the designer build up a case for wide bilge or roll-resisting keels forward that project beyond the side at the designed waterline, on the basis of augmented roll- and pitch-quenching characteristics? Will the owner-operator accept a projection of the rudder beyond the extreme stern overhang for the sake of improved flow to the propeller and reduction of vibration?

One's views as to what features of the ship are important and controlling often depend upon his position in the overall setup. A limitation on length, for example, may be only an expression of well-hardened opinion on the part of an operator who thinks that it should be possible to get everything he wants in a ship of a certain size. It may be, on the other hand, a vital restriction to the designer if he is endeavoring to squeeze out a small margin of speed or power.

The salient features of a muddled and verbose specification may need to be brought out so as to keep them alive and vivid before a designing staff. These and other reasons may well justify the extra time spent on highlighting essentials and generally reworking the specifications furnished by someone else.

The guiding principle in the preparation or revision of design requirements, first, last, and always, is to keep the language direct, straightforward, and simple. Stress the specific but informal treatment. Start off by setting down, in plain language and short words, just what the ship is required to do; just what mission it is to fulfill. A ship which ultimately does not carry out its appointed mission is to be reckoned not a success, no matter how efficiently it may meet one or more secondary requirements.

The combination passenger and cargo vessel for the Port Amalo—Port Bacine—Port Correo route was selected as one likely to present the most varied and numerous ship-design problems for consideration in this part of the book. The mission of a hypothetical vessel of this type, operating in an imaginary part of the world, is rather easily roughed out. The result is given in Table 64.a. This mission, as with the requirements to follow, is intended to emphasize the size, form, power, speed, and other design features having to do primarily with hydrodynamics. It would be amplified considerably when considering the ship as a whole.

TABLE 64.a—PARTIAL DESIGN SPECIFICATIONS FOR A COMBINATION PASSENGER AND CARGO VESSEL

MISSION

The vessel described in these specifications is intended to be used for:

(1) The transportation of passengers to and from Port Amalo, Port Bacine, and Port Correo, making the outbound trip from Port Amalo in that order and the homeward trip in reverse order
(2) The transportation of liquid bulk cargo from Port Correo to Port Amalo, and of high-class package cargo back and forth between Port Amalo, Port Bacine, and Port Correo.*

The service to be rendered requires:

(3) The safe and comfortable transportation of the passengers on a rigid, year-round schedule, established well in advance, regardless of local and seasonal weather conditions
(4) The storage and transportation of the high-class package cargo safe from damage by the elements or from violent and jerky ship motion
(5) Performance of the required transportation as efficiently and economically as the present state of the art permits
(6) Safe and rapid handling and berthing of the vessel *under its own power* at Ports Bacine and Correo.

*The "liquid bulk cargo" mentioned in (2) preceding is not necessarily composed of heavy oil or its products. However, G. A. Veres has recently (1955) proposed the carrying of passengers on high-speed tankers [SBSR, 23 Jun 1955, p. 797; 7 Jul 1955, p. 5].

The next step is to write out the principal duties which the ship is to fulfill, and the principal requirements which *must* be met. If there are compulsory or mandatory limitations, include them by all means. Do not clutter up these major features of the specifications with details of lesser importance, or with superlatives intended to emphasize them.

The first items to set down are those involving

size and displacement volume. The ship hull must have enough bulk volume to contain all that is to be put inside it, both below and above water. It must have enough displacement volume to float itself when carrying a high-weight-density cargo which does not fill its holds. List these volumes and weights as a preliminary to estimating and determining the total weight, bulk volume, and principal dimensions of the ship, but do not attempt to fix the latter features at this stage.

Whatever the custom and procedure may be elsewhere for determining the overall size of the ship, it is assumed here, for the sake of working up a well-proportioned design, that there is no major limitation on size and dimensions except for:

(a) The general requirement (5) of Table 64.a for the greatest performance from the least ship
(b) A specific draft limitation for passage of a canal and a river during the voyage.

TABLE 64.b—Considerations of Size and Displacement Volume

The ship shall be able to:

(7) Carry a liquid-bulk cargo of 4,000 t (of 2,240 lb) from Port Correo to Port Amalo on each trip, for which liquid the weight density will not exceed 42 ft^3 per ton of 2,240 lb [Wormald, J., "The Carriage of Edible Oil and Similar Cargoes," IME, Apr 1956, Vol. LXVIII, pp. 65–91]
(8) Carry a total weight of package cargo not exceeding 3,000 t back and forth between all ports, requiring a net or usable storage space not less than 300,000 ft^3
(9) Load and unload package cargo at Port Bacine, both coming and going, without disturbing any through package cargo
(10) Carry sufficient fuel to permit bunkering at Port Correo and making the round trip to Port Amalo and return, on the basis of the rigid all-year schedule specified in the foregoing, plus a 15 per cent reserve-fuel capacity. The weight density of the fuel will not exceed 42 ft^3 per ton.
(11) Carry sufficient fresh water and consumable stores, stocking up at Port Amalo and replenishing upon return, to permit making the round trip to and from Port Correo
(12) Devote a volume of 400,000 ft^3 of enclosed space exclusively to passenger service
(13) Make a safe and expeditious passage, under its own power, of the 25-mi ship canal leading to Port Amalo, which has a minimum depth of 28 ft
(14) Negotiate without assistance the 204-mi passage of the fresh-water river from Port Correo to the sea, on the basis of a minimum depth of 30 ft in the navigable area
(15) The size and weight of the ship shall be a minimum consistent with these and subsequent performance requirements.

The outcome of this procedure, for the ship selected as the example, is contained in Table 64.b.

A speed requirement is not yet in the picture. Indeed, before beginning consideration of it there is prepared a summary of the meteorologic and oceanographic conditions which the vessel is to encounter. Table 64.c contains the summary for this design problem. If these conditions vary during the operating season, as is usually the case, they are carefully analyzed and evaluated.

TABLE 64.c—Meteorologic and Oceanographic Conditions

(16) Full account shall be taken, as important factors in the design, of the meteorologic and oceanographic conditions in the regions in which the ship is to operate. The average latitude over the whole voyage is 20 deg. Surface winds, along the fringes of the hurricane belt between Port Amalo and Port Bacine, may be expected to blow from any direction at velocities up to 90 kt. These are accompanied by ocean waves corresponding to a fetch of at least 500 mi
(17) Tidal currents in the long ship canal leading to Port Amalo may reach 0.5 kt. In the river between the sea and Port Correo the combined tidal and river current may reach 2.75 kt, flowing downstream.
(18) Water temperatures in the fresh-water river at and below Port Correo range from 75 to 80 deg F; those in Ports Amalo and Bacine range from 60 to 75 deg F. It shall be possible to deliver the maximum designed or rated power of the propelling machinery with a sea-water temperature of 75 deg F. Water temperatures in the open sea average about 68 deg F.
(19) Fouling is a factor to be reckoned with at all seasons of the year while the vessel is at sea. Fouling may stop temporarily while the vessel is in the ship canal leading to Port Amalo and in the fresh-water river leading to Port Correo but the roughnesses already accumulated will not disappear.

Hurricanes of major proportions may be expected to occur along part of the route during only some three months of the year. However, unexpected and troublesome storms, with large steep waves, often are encountered for a month and a half or two months before and after the hurricane season, overlapping the seasons of heavy passenger travel. Full account of these adverse conditions therefore is taken when laying out the design. With the rather careful modern plotting and hour-by-hour reporting of storm centers to be expected in the worst areas, it may be possible for the ship, with an ample reserve of speed, to save time by running around the storms rather than remaining on course and slowing down to go through them.

Although heavy marine fouling is the rule in

certain warm, salt-water portions of the route, the vessel is traversing the open sea and exposed to fouling for only a fraction of the voyage time, averaging probably not more than 0.6 of that time. Furthermore, the relatively high speed at which it is expected to travel prevents this menace from becoming more than a normal factor in powering.

The dock-to-dock schedule which the owner-operator has laid out is divided into a canal-and-river schedule and an open-sea schedule by applying the allowable navigational speed of 10 kt in the ship canal in and out of Port Amalo and a reasonably safe speed through the river in and out of Port Correo. After docking and maneuvering time at all ports is taken into account, the buoy-to-buoy schedule comes out of the remaining time and distance by simple arithmetic. For this sea schedule the *average speed* made good in open water, at either full load or any intermediate displacement and corresponding trim, in fair weather or foul, with smooth or rough bottom, works out as a minimum of 18.7 kt.

This is a week-in, week-out performance speed and not a design figure. The ship must be capable of an augmented sea speed to guarantee making the average sustained speed of 18.7 kt under the handicaps of wind, weather, waves, currents, and fouling. The manner of accomplishing this is explained under Design and Performance Allowances in Sec. 65.3 and under Powering Allowances in Sec. 69.9. Suffice it to say here that the analysis thus made indicates the necessity for the ship to be capable, in smooth water, with clean bottom, at full designed load and in zero natural wind, of making at least 20.5 kt. Other considerations of easy steaming, freedom from wear and tear, long intervals between major machinery overhauls, and general dependability of both materiel and personnel, discussed in Sec. 69.9, require that the 20.5-kt speed be accomplished by the development of *only 95 per cent* of the maximum designed power.

Summarizing this analysis and working in a few related supplementary features produces the speed and wavegoing requirements of Table 64.d. Restrictions against pounding, slamming, and lurching, against being pooped in a following sea, and against carrying away gear on deck are not listed separately because they are implicit in items (3) and (4) of the mission, set forth in Table 64.a.

Before going further into the speed and propulsion specifications, the maneuvering requirements are considered because they may bear some relation to the number and position of propellers to be installed. An analysis of maneuvering, in turn, calls for a statement of the restricted-water characteristics of various parts of the vessel's route, somewhat similar to that of the meteorologic and oceanographic conditions affecting wavegoing. The principal features are set down in items (27) through (29) of Table 64.e. The canal bend at Mile 20 is diagrammed in Fig. 64.A, which contains also the estimated tracks of large vessels proceeding in both directions, with their limiting offset positions in the canal. The essentials of the maneuvering situation at Port Bacine are copied from the chart in Fig. 64.B, with the *estimated* ship tracks and positions

TABLE 64.d—SPEED AND WAVEGOING

(20) The average or *sustained sea speed* made good in each deep-water, open-sea portion of the voyage, in any or all service displacements and under corresponding trim conditions, in any weather, and with any reasonable amount of bottom roughening and fouling, shall be at least 18.7 kt

(21) The augmented sea speed, to achieve the sustained speed, is set tentatively at 20.5 kt. This is to be made in smooth, deep water, with clean bottom, in zero natural wind, and at any and all service displacement and trim conditions.

(22) Whatever the augmented sea speed, it shall be attained by the use of not more than 95 per cent of the maximum designed power of the propelling machinery

(23) In general, the ship and machinery shall operate at maximum efficiency under conditions (21) and (22)

(24) The ship may have to slow temporarily in heavy weather to 65 per cent of its average sea speed of 18.7 kt; this is 12.16 kt. If so, the schedule *must* be met by a corresponding increase in the speed in good weather. The estimated reduction in speed for constant thrust equivalent to a smooth-water speed of 20.5 kt shall not exceed 45 per cent when running into a head sea, at an angle of encounter of 180 deg, through regular waves having lengths L_W of from 0.8 to 1.5 the ship length L, and heights h_W not exceeding $0.55\sqrt{L_W}$. (The speed reduction from 20.5 kt to 12.16 kt is 40.7 per cent). Water ballast, preferably fresh water, may be admitted to groups of empty liquid cargo tanks as desired to establish satisfactory propeller submersion and to provide added ship mass on the outward voyage from Port Amalo, when the liquid bulk cargo is not on board.

(25) The ship shall be as free of resonant pitching in the waves to be encountered as may be compatible with other requirements

(26) A reasonable expenditure of weight or power, or both, to secure *effective* roll-quenching is acceptable to the owner. Effective quenching is defined as diminishing the roll angle to 0.25 (one-quarter) of its natural value.

TABLE 64.e—MANEUVERING

The restricted waters forming part of the route and the required ship operation in them are described as follows:

(27) Directly upon leaving its berth at Port Amalo the vessel must make a 180-deg turn in close quarters but tugs are available and will be used

(28) The ship canal leading from Port Amalo to the sea has a length of 25 mi and a minimum depth of 28 ft. For 16 mi of its length the bottom prism width varies between 400 and 475 ft. Banks and bed of the restricted channel are of hard sand and gravel. At Mile 20 in this restricted portion there is a circular-arc bend, with short transition sections at the ends, having a total change in direction of 50 deg and an inside radius of 3,800 ft; see Fig. 64.A. The bottom width at midlength of this bend is 500 ft and the depth is 32 ft.

(29) Port Correo is at the head of ocean navigation on a long, wide, fresh-water river, 204 mi from the sea, with a minimum and fairly constant depth of 30 ft in the dry season and a soft mud bottom. Large trees and other flood debris are often encountered floating in the river.

(30) Adequate steering and maneuvering characteristics shall be provided for traveling in the ship canal leading from the sea to Port Amalo, on the basis of meeting other large ships in this canal. It is not necessary to meet these ships in the bend at Mile 20. Similar requirements are established for the passage of the river leading from the sea to Port Correo.

(31) It shall be possible to berth the vessel at Port Bacine, under its own power, in a slip terminated by U-shaped walls of solid masonry, 100 ft apart in the clear at the head of the slip and extending for a distance of 160 ft therefrom. An open-work wooden pier prolongs one of these walls for a distance of 450 ft, indicated in Fig. 64.B. The vessel must, under its own power, make a 50- or 60-deg turn after backing out of the slip and prior to proceeding out of the channel to sea. The clearance to the opposite side of the navigable area, measured from the extreme end of the wooden pier and in line with it, is 1,500 ft.

Specifically, when running at any practicable displacement and trim, the ship shall be capable of:

(32) Executing the transient portions of a turn, swinging first away from and then back into a straight course, involving changes of heading of from 25 to 30 deg for each maneuver, and gaining or losing an offset of 400 ft, perpendicular to the approach path, in a curved run of 2,100 ft. This shall be accomplished in a canal prism having a depth of 32 ft and a bottom width of 400 to 500 ft, at speeds of from 6 to 8 kt, and with not more than one-third the maximum rudder angle.

(33) Swinging bow to port and stern to starboard, and vice versa, when operating the propulsion device(s) in an astern direction, with negligible wind and in water having a depth-draft ratio not exceeding 1.5, or a maximum depth of 40 ft. It shall be possible to execute this maneuver from a standing start or from a straight approach path when moving astern at a speed not exceeding 13 kt.

(34) Executing a 180-deg turn within a tactical diameter of 3,000 ft in deep water, with full rudder angle and at an approach speed of 19 kt

(35) When turning in accordance with (34), the angle of heel shall be limited to 10 deg. A maximum angle not exceeding 8 deg is preferred.

(36) At an ahead speed of 20.5 kt, on a straight course, it shall be possible to execute a crash-back maneuver and to stop dead in the water with a head reach not exceeding 6 ship lengths

(37) The machinery shall be capable of developing an astern torque of 80 per cent of the rated ahead torque, and an astern rate of rotation of 50 per cent of the ahead rate, with the ship stationary in the water, as at the end of a crash-back maneuver

(38) If left to itself when running ahead in smooth water, with no perceptible swinging motion and the rudder stationary at zero angle, the ship shall not deviate progressively from its original course. In other

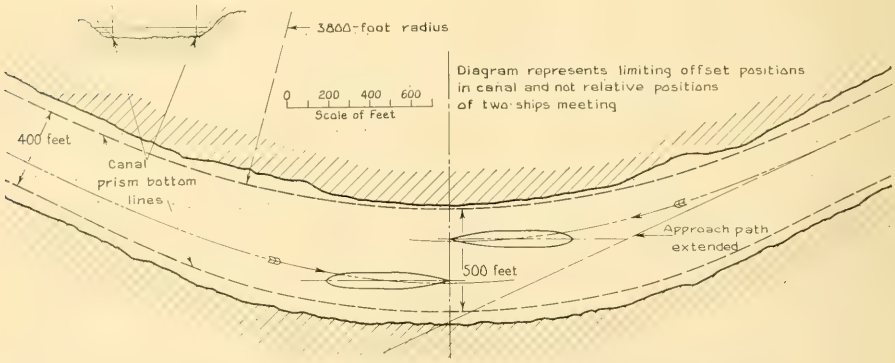

FIG. 64.A SCALE DIAGRAM OF 50-DEG BEND IN CANAL LEADING FROM PORT AMALO TO THE SEA

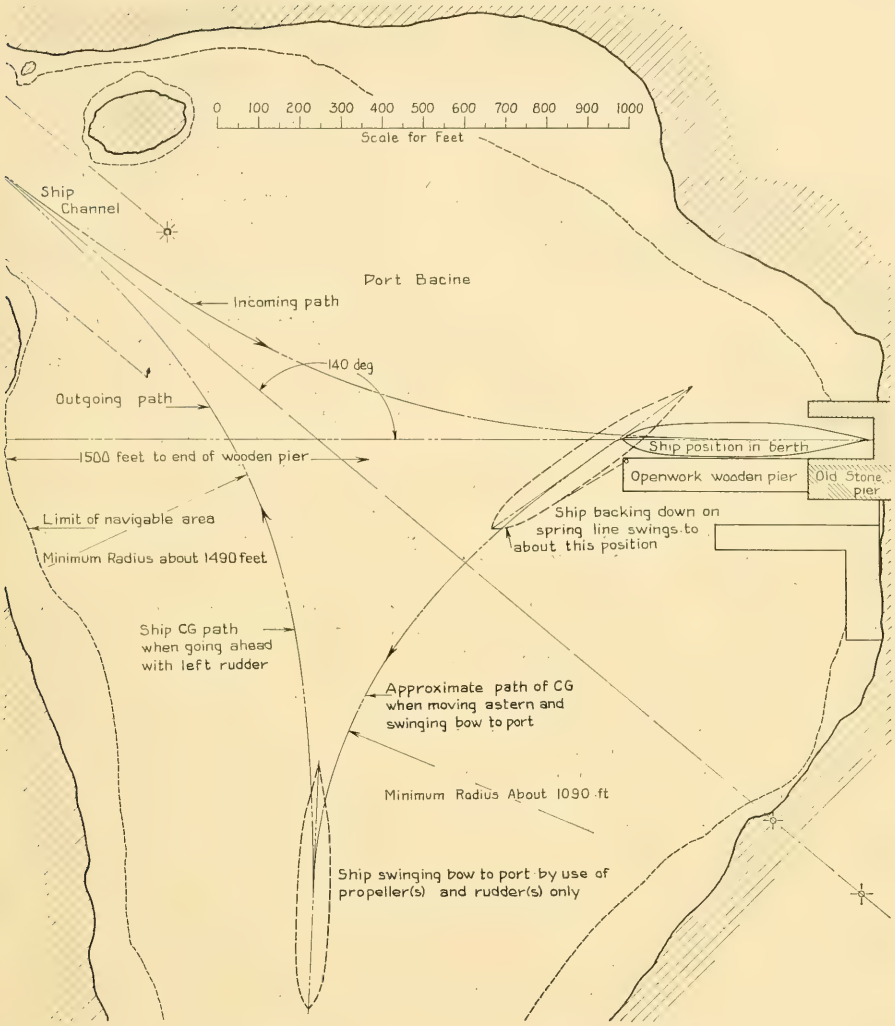

Fig. 64.B Proposed Maneuvering Diagram for ABC Ship in Port Bacine

words, the ship shall possess dynamic stability of route.

(39) A limiting small rudder angle not exceeding 3 deg shall suffice for good manual steering in smooth, deep water and negligible wind, at all speeds over one-half of the sustained speed, with right or left variations in yaw not to exceed 2.0 deg. This shall include all displacement and trim conditions likely in open-sea running.

(40) A rudder angle not exceeding 7.5 deg shall suffice for steady, straight-course running in straightaway reaches of the canal at Port Amalo and the river at Port Correo, with from 3 to 4 ft channel-bed clearance under the ship

(41) The ship shall be controllable when underway in heavy weather at whatever speeds and courses can be maintained in that weather.

added. These are based upon entering the ship head-on, directly from the sea entrance, and upon swinging the ship by a considerable amount, when backing out of the slip, by working on a spring line attached to the outer end of the pier.

Translating the ship maneuvers of Figs. 64.A and 64.B into specific maneuvering requirements gives the items listed as (32) and (33) in Table 64.e. Because of lack of authentic information on the astern maneuvering characteristics of ships, the requirements in (33) are left rather general in character. The requirements in (34) and (36) are intended to insure that the vessel can be maneuvered handily in an emergency.

Rather exceptional controllability as regards steering is called for, because of the more than 450 miles of restricted-water traveling that is required of the vessel on each voyage.

Power is not a factor in these restricted waters because the speeds are limited by wave wash on the banks, the presence of other vessels close by, and the excessive sinkage at the stern that would be encountered at the higher speeds.

64.4 Absolute Size as a Factor in Maneuvering Requirements. Maneuvering requirements, involving steering, turning, stopping, backing, and the equivalent, form a sadly neglected part of the specifications for all types and sizes of water craft. Increasing emphasis has been placed, and will continue to be placed, upon the safety of life and of vessels at sea. It has been necessary in past emergencies, and it will be more necessary in future ones, for all types of craft to undertake turning and other maneuvers which will confuse those who are dropping or firing missiles from the air. It may be expected, therefore, that maneuvering requirements will appear with increasing frequency in ship specifications. The insertion of specific numbers, making the requirements more definite, will certainly follow.

When selecting definite numbers for maneuvering requirements it is to be remembered that these can not be based, for small craft as well as large ships, entirely upon some linear dimension such as the length. Things happen much faster on a small vessel than on a large one. The rate of motion on a small craft, for geometrically similar maneuvers, increases directly as the square root of its linear ratio to the large craft. As long as human beings with more-or-less fixed reaction times operate the craft, it is necessary to take account of these factors. Thinking and giving piloting orders for a ship transiting a canal is a far cry from the same procedure for a self-propelled model in a miniature channel, with a time rate possibly five or six times as fast.

Consider a modern 25-ft pilot model of a large planing boat. The pilot model might well run at 33 kt, with a T_q of 6.6, while the 81-ft full-scale craft makes 60 kt at the same T_q . The former covers its own length in 0.45 sec whereas the latter requires 0.80 sec. With a linear scale ratio of 3.24, the time ratio is $(3.24)^{0.5}$ or 1.8 times as fast for the pilot model. Other things being equal, the 25-ft craft turns in a circle over 3 times as tight as the 81-ft one, and so on.

As the absolute size increases, on the other hand, the proportion between (1) the time for a disturbance to manifest itself and (2) a human perception or an automatic-control time increases rather rapidly.

On small craft, often with large powers relative to their size, too-rapid maneuvering can inconvenience or injure personnel and result in damage to materiel. On large ships, demands for improved maneuvering performance can run rapidly at times into increased weight, complication, and cost.

64.5 Tabulation of the Secondary Requirements. When all the principal requirements have been set down, and it is known what the ship

TABLE 64.f—DESIRABLE FEATURES INVOLVING HYDRODYNAMICS AND FORM

Insofar as practicable, consistent with the principal requirements of the design, the ship shall:

(42) Possess a square moment of area coefficient of the designed waterline, about the longitudinal axis, not less than 0.55

(43) Take in and discharge water for heat enchangers at points *not below* the 1-ft waterline, reckoned from the baseplane

(44) Be prepared to anchor with two bower anchors in the river leading from Port Correo to the sea, in currents up to 2.3 kt

(45) Discharge the products of combustion, from whatever source, at such a point and in such a manner that they will not form a nuisance to either crew or passengers

(46) Be free of spray and high-speed local air currents so that in "outdoors" weather, passengers shall not be inconvenienced in their enjoyment of the sun, sky, and sea

(47) Provide internal heavy-weather access to all spaces in which personnel are required during cruising at sea

(48) Have no vulnerable projections outside the main hull within the first 150 ft of the length, from the keel up to the 35-ft waterline, which might be damaged by the old stone pier at Port Bacine; also have no projections below the fair line of the bottom of the main hull.

must do, the next step is to put down what the owner or operator would *like* to have the ship do. This involves listing the secondary or desirable features of the specifications. These afford the designer an idea of the preferences involved, and the relative importance of each. As such, they furnish a valuable guide in working up many elements of the design. It is wise to list all features of this kind, even though at first thought they may seem only remotely related or distinctly unrelated to the hydrodynamics of the problem. A statement prepared along these lines may have the form of that presented in Table 64.f. The relationship of certain of these features to the hydrodynamic design becomes apparent as the design proceeds.

TABLE 64.g—FEATURES NOT OTHERWISE CLASSIFIED

(49) Freedom from vibration and noise, while not a must, is a most desirable end to be achieved. In any case, the estimated frequencies of periodic hydrodynamic forces shall be reported to the builder at least two months before the vessel's first sea trials.

(50) It is expected that, by the time the vessel is put into service, the harbor regulations will prohibit the discharge of sanitary drains into the water areas at all three ports, the canal, and the fresh-water river

(51) The *maximum* layover times at the three ports may be assumed as follows:

Port Amalo, 3 days; Port Bacine, 24 hours; Port Correo, 2.83 days (68 hr).

With the desirable features it is well to include limitations, restrictions, and other specifications of a so-called negative nature. In other words, the specifications should describe clearly and definitely any and all things that the ship should *not* do or should *not* have. The features listed under (49) and (50) of Table 64.g belong in this category.

The specifications in this stage are terminated by a group of items, not conveniently classified. Three of them appear in Table 64.g.

The problem of working over these requirements until they are mutually consistent and are in numerical, coefficient, or other form, ready to apply to the detail design, is taken up in the chapter following.

The liquid capacity called for in these specifications not only permits the ship to carry liquid cargo on the particular run or in the particular service for which it is designed but enables it to carry any other liquid cargo which may be involved in some unexpected service of the future. In the existing state of world industrialization it appears that for the life of this vessel liquids of some kind or other will always be useful and profitable cargo. Furthermore, the provision of this tankage in the after part of the hull makes it possible to utilize water ballast to insure adequate propeller submersion and freedom from slamming and pounding when running in waves at relatively light-load conditions.

CHAPTER 65

General Problems of the Ship Designer

65.1 Interpretation of Ready-Made Design Requirements. It is possible for the hapless ship designer to be confronted with a set of preposterous requirements and specifications, not of his own formulation. On first reading these may seem to call for achieving the impossible. After an anxious time the designer may be relieved, but nevertheless bewildered, to find that he is not expected to meet them, but only to be awed by their severity. He may, on the contrary, find that they have both claws and teeth, and that he is expected to accomplish what no one before him has done. It is most important, therefore, that when a set of requirements and specifications is handed to him, the designer assess them carefully and that he determine in advance how they are to be interpreted.

However, it is assumed here that the ship requirements are laid down in all sincerity and that they are expected to be observed in the same fashion, both as to their spirit and their letter. If there is in them any semblance of reaching for the moon, the reaching is clearly indicated and there is good reason for it. A case in point is the superlative deep-water and open-sea performance required of the ABC design, which in many respects is a limited-draft river vessel. If parts of the requirements are intended primarily for information and guidance rather than strict compliance, they in turn are clearly so marked.

65.2 Departures from the Letter of the Specifications. Notwithstanding the most conscientious effort, it is rarely possible to comply with every letter of the complete design requirements and performance specifications for a ship. Some compromises must always be made to produce the design and some relaxation of the specifications be accepted. The burden of accepting these compromises rests with the owner or operator for whom the ship is being designed. A decision concerning a modification or relaxation of the specifications can only be made intelligently on the basis of reasonably accurate and reliable information concerning the price which the owner or operator must pay for this change, either in money or in speed, power, endurance, and performance.

It is a duty of the ship designer to offer constructive suggestions, propose compromises, or put forth alternative solutions in all cases of conflict between the original requirements and specifications. This procedure applies as well to conflicts between these requirements and the capabilities of construction materials, machinery, and equipment in the present state of the art. For example, vertical or wall sides are indicated for the bow sections of a fast or high-speed ship in way of the bow-wave crest. To accomplish this may require a rather sharp reentrant curve in the bow section lines above the top of this wave crest. This spoils, in a way, the gently flaring V-sections which may have been drawn in forward above the water line for good wavegoing performance. The designer therefore prepares to estimate the increase in smooth-water resistance and power due to the use of fair V-sections *and* to predict the possible adverse effects of somewhat hollow V-sections when pitching or plowing into head seas. Similarly, he is prepared to give figures relating to the change in resistance and power, and the modification in roll-quenching characteristics, for proposed variations in the bilge-keel length.

65.3 Design and Performance Allowances. Whether or not they are written specifically into the requirements, a ship designer must, by

interpretation or direct discussion with the owner-operator, arrive at a schedule of allowances or performance factors which is to be followed throughout the course of the design. Granting that the designer's estimates are invariably correct and his calculations precise, he is truly a prophet if he can predict the combinations of overload, overspeed, and other operating conditions to be encountered in the life of the ship. If the ship takes these in its stride, he is praised for having designed a good one. If not, he is liable to be blamed because the ship can not take a little extra once in a while. Indeed, the mark of a superlative designer may be as much in the margins, allowances, and design factors which, in his knowledge, intelligence, and engineering intuition, he inserts here and there as in the balance which he achieves in the overall design.

It is difficult to give rules for these allowances. The more performance that is being squeezed out of a design, the smaller the allowances must necessarily be and the greater the knowledge of the forces and other factors involved. In a high-speed racing motorboat, for example, they approach zero. In an icebreaker they can and should be large.

Emphasis is laid on the primary function of the vessel, and the allowances favor the continued and reliable performance of that function. A ferryboat running on a published timetable, year in and year out, with many people relying on its schedule, is given a generous power and speed allowance, provided economy is not sacrificed. A tug can always use extra power, to meet the increasing demands of progress as the vessel puts in more and more years of service.

The less accurately some quantity can be determined the greater allowance a designer is generally forced to place upon it. The less real proof he has of the validity of some estimate or prediction, or the less confidence he has in it, the greater must be his allowance.

The mission of the ABC ship requires, from Table 64.a, adherence to a "rigid, year-round schedule, established well in advance, regardless of local and seasonal weather conditions." The owner-operator is emphatic in pointing out that this means what it says. The study forming the basis of the speed requirements of Table 64.d indicates a minimum average or *sustained speed* of 18.7 kt to achieve the mission. How is this best attained when there are so many unknown factors?

It is well at this point to discuss briefly the expression "sustained speed." This term often is used but seldom defined, perhaps because to sustain a speed in one area or on one run means something quite different from sustaining it on another run. For the ABC ship it means both parts of the one-way run, as well as the voyage as a whole. For the general case, the ability of a ship to make a given sustained speed means that it has, in self-contained fashion, whatever it takes in the way of allowances and margins to *average* this speed over any run, in spite of:

(a) Wind, waves, and weather
(b) Roughness drag due to deterioration of the paint or other coating and that due to fouling of any and all kinds
(c) Improper trim or attitude for the speed range, due to causes beyond control of the ship personnel
(d) Temporary slowdowns or stoppages due to inadequacies of or casualties to personnel or materiel
(e) Loss of capacity, power, or efficiency because of deterioration, delayed overhaul, and general wear and tear
(f) Low quality of fuel
(g) Any combination of the foregoing and any other adverse influences.

To average a given sustained speed on a run, come what may, means that a ship has to possess a reserve capacity or ability of some kind. This not only is to make up for lost time but to keep going regardless of the circumstances, short of hurricanes, typhoons, and the like. No ship can be designed to cope with extreme emergencies. The reserve is designed into and built into the ship, in the form of allowances. The design allowance is based upon 100 per cent functioning of all personnel and materiel. The performance allowance takes care of incomplete functioning, as set forth in (d), (e), and (f) preceding.

There are several ways of making these allowances. The most logical and undoubtedly the preferred one is for the designer to modify the owner-operator requirements for his own use and then to design as closely as practicable to those modifications. It is thus possible, when the vessel is completed, to check the actual design from the observed performance, and to use the information thus confirmed for future designs. For example, instead of calling for 15 per cent extra shaft power, or some other amount picked from operating data to insure that the sustained speed

is achieved, the designer adds a definite allowance to that speed. This may be, say, one-third of the power margin, on the basis that the shaft power varies about as V^3. The speed allowance is then +5 per cent. He proceeds to design the ship closely to this augmented speed.

When the trials are run it is usually as easy, or perhaps easier, to measure the 15 per cent extra power as the 5 per cent extra speed. However, with a speed margin that can be reliably predicted, and with a ship fashioned and built for the augmented speed, the designer is in a better position to promise the given sustained speed than if he crowds extra power into a ship built only for that speed. Other reasons for designing-in a speed margin rather than a power margin are set forth in Part 6 of Volume III under wavegoing.

E. V. Lewis points out that with the large powers and high smooth-water speeds of many modern (1956) vessels it becomes increasingly difficult to maintain high average speeds in certain rough-water areas such as the North Atlantic [SBSR, 30 Aug 1956, p. 277]. It may be expected, however, that increased emphasis on wavegoing characteristics and further progress in wavegoing design will increase the rough-water speeds so that, when it is sufficiently important, a high sustained speed can be achieved in any service.

For the preliminary hydrodynamic design of the ABC ship, or for any other design in which a speed rather than a power allowance is to be incorporated, the selection or determination of that allowance requires careful study, combined with intelligence, judgment, and wisdom. There are considerations of sea routes to be followed, times of arrival and departure during the day, reliability in maintaining the sailing schedule, economics, and many others which need not be entered into or elaborated upon here.

On the basis that heavy weather slows the ship to say 0.7 times its sustained speed for a certain portion of an open-sea run, simple arithmetic indicates what the augmented sea speed must be to bring the average up to the sustained speed. A similar procedure can be applied to the speed effects of bottom roughening and fouling or to an assumed compulsory slowing of the propelling plant for any given length of time. The contingency in which the delays occur unexpectedly at the very end of a run is met by speeding up for good measure in the early part of the run. This matter is discussed by R. K. Craig, when describing the service performance of a passenger liner with engines aft [SBMEB, Dec 1955, p. 693].

The speed allowance of 1.8 kt for the ABC ship, from 18.7 to 20.5 kt, or roughly 10 per cent, as specified tentatively in Table 64.d and as incorporated in Table 65.a with other design and performance allowances, is intended to serve only as an example of the procedure involved.

TABLE 65.a—ABC Ship: Design and Performance Allowances

Performance Item	Owner-Operator Requirements	Augmented Requirements of Designer
Displacement and draft	Not to exceed about 25 ft in Port Amalo canal	Maximum of 26 ft at Port Correo with +0.04 margin on fixed hull and machinery weights
Hull-volume margin	400 t of consumable stores loaded at Port Amalo and not on board at Port Correo, under full-load conditions	
Speed margin	Sufficient to average 18.7 kt at sea on any and all parts of run, under any specified loading condition	20.5 kt under trial conditions at full load
Power margin		P_S necessary to make 20.5 kt
Allowance for fouling, bad weather, and the like		Average 18.7 kt when clean at not more than 0.80 P_S max under any load condition
Performance allowance		20.5 kt under trial conditions at 0.95 P_S max designed
Propeller rotative speed	Not specified	Within 0.015 of rated n at 0.95 P_S max
Tactical diameter at 19 kt	3,000 ft	0.9 (3,000) = 2,700 ft

However, design to the 20.5-kt requirement means that this can be made the trial speed, under ideal trial conditions. Both the design and the ship can be proved on trial, leaving the owner-operator with the assurance that the ship has an adequate margin of both power and speed. The general method followed here for the ABC ship has been used for the design of merchant-type naval auxiliaries for the U. S. Navy for twenty years or more. It has been found eminently successful, for services of varied nature, in most of the oceans of the world.

65.4 Basis for the Selection of Ship Dimensions. At a very early stage in the design of a ship, or perhaps before that design is really begun, it is necessary to determine the basis for the selection of the principal ship dimensions. These include, not only the customary linear length, beam, depth, and draft but the volume, displacement, and weight; possibly even the general shape of the ship. Almost invariably it must be decided whether:

(a) The ship is to be designed on a weight-carrying basis
(b) The design is to be on a volumetric basis, to provide space
(c) Inflexible limits are to be imposed on certain dimensions, such as for a ship which must fit inside certain piers at a terminal or which must pass through locks in a canal.

The displacement of ships carrying cargoes of high weight densities or specific gravities is as a rule fixed by the weight of the cargo or load to be carried plus the weight of hull and machinery, fuel, consumable stores, and margin. The underwater hull must possess sufficient volume to support the total weight in water of the specified density. When ships are to carry bulky but not particularly heavy cargoes such as railway cars, trucks, automobiles, and other vehicles it is generally possible to carry much of this cargo volume above the designed waterline. Due regard is of course given to metacentric stability and other requirements. In designs of this kind, a large if not the greater part of the useful enclosed volume of the ship is above water, leaving only enough volume in the underwater hull to carry the total weight.

In the case of submarines it is necessary to crowd within the pressure hull everything which can not be entirely or partly surrounded by water when the vessel is submerged or running on the surface. The volume of the pressure hull, plus the volume of all structure, fittings, and equipment lying in the water when the submarine is submerged, determines the displacement or total weight of the vessel for water of the specified density. This volume displacement is substantially the same for the vessel under any running condition, in water of a given specific gravity, because the scale weight of the ship remains substantially the same. If fuel is consumed it is replaced by an equivalent weight of water, and so on. It is possible, however, to vary the amount and percentage of reserve buoyancy in a submarine design by varying the shape and volume of the outer hull, since the main-ballast tanks between the two are empty in surface condition and filled with water when submerged. For submerged propulsion all this volume, plus all the water volume in the free-flooding spaces, has to be taken into account, just as if it were frozen into ice and carried along with the ship. This is the *bulk volume* of the submarine.

Because of available space around and depth under the ship when docking and maneuvering, of limited first cost, of adequate metacentric stability, or of some factor not remotely related to hydrodynamic design it often becomes necessary to impose some definite or arbitrary limits upon the principal linear dimensions for a given weight or volumetric capacity. This is where the designer's troubles really begin.

65.5 Determination of the General Hull Features. The general hull features of a new ship design can be determined in either of two ways. One can start figuratively in the air—or better, in the water—with only the operating requirements, and fashion the ship out of the blue. Alternatively, one can expand or contract the hull "of a known vessel of good performance" [Ellis, J. J., Froude, R. E., INA, 1892, p. 211] and thus obtain a first approximation to a new vessel which will fulfill those requirements.

It is theoretically possible for an experienced ship designer, working to a given set of specifications, to select a type of hull, to determine its general shape, to define its proportions, and to make a tentative decision to embody in it some special or unusual feature by working only from available reference libraries, including his own. It has often been done, and most successfully, despite the many indefinite and unpredictable elements which come into the picture. Indeed, it is often much better to start with a clean sheet,

as it were, because then the design problems are visualized more clearly and they may be solved in the most simple and direct manner.

Using an alternative procedure, it is often possible to work up a new hull design as a variant or as a development of a previous design which has proved itself in the same service and which may be taken as a sort of parent form. This procedure is facilitated by reference to the rather comprehensive data now in existence on the behavior of a multitude of ships and their models, such as the SNAME Resistance Data sheets 1 through 160. The quantitative information required to set up a design and to carry it through the successive steps must necessarily be derived from model and ship performance data which are known to be accurate and reliable. When in doubt, the data are to be used with caution or, if possible, only after a check and double check.

The parent-form-copying or development procedure manifestly forms an unsound or at least an uncertain basis for the design of a ship to meet totally new and unexpected requirements. A certain amount of improvement results from successive developments of a given parent design but more real progress is often made by starting out afresh. Remember that the ship being copied or modified was designed not yesterday but several years ago. Its designer would be the first to admit that much has been learned since then. If starting out today, even he would not reproduce the design exactly.

65.6 Limits for Wavegoing Conditions to be Encountered. To develop intelligently a good ship design for wavegoing requires the establishment, if practicable, of some sort of limits for the wavegoing conditions to be encountered, more precise than those of Table 64.d. Will most of the waves be shorter or longer than the ship, or about the same length? Will they be long and regular, or short, steep, and confused? This can be done on the basis of:

(a) Existing knowledge of weather and waves along the specified route in the various seasons of the year, based on some sort of statistical analysis of extensive data
(b) Selection from the statistical data of the characteristics and pattern of the predominant wave, or the features of the one which is likely to prove the most troublesome
(c) An arbitrary declaration that the ship shall give its best performance in a specified type of sea, and a deliberate acceptance of whatever performance is obtained in other types of seas.

Obviously, the design problem is materially simplified if the ship is to operate on only one run and to travel only in certain areas, especially if the sea conditions in those areas are reasonably consistent and predictable.

65.7 The Bracketing Design Technique. In a pioneering design, for which the basic physical phenomena are somewhat uncertain and the results of past experience are limited or nonexistent, it frequently becomes necessary for a designer to reach far into an unknown and untrodden field. He must commit himself and others to the acceptance of risks or the expenditure of funds which under normal circumstances could not be justified as good engineering. In this predicament he desperately needs any kind of assurance, no matter what its source or reliability. Fortunately, there is one means by which a ship designer can extricate himself from a situation such as this—a method which has been found useful and successful in many other lines of endeavor.

The essence of this method is to determine the extreme limits of position in the unknown field, then to fix a position between these limits by any simple convenient method which appears suitable. The region in which the unknown solution is to be found lies somewhere between the two limits and is thus bracketed by them. The position of the region with respect to the limits, in other words the spotting of the region where the solution probably lies, involves a process of arithmetic averaging or of estimating by a sort of mean proportional of the limits.

A design problem of this kind developed with the shaping of the alternative arch-type or tunnel stern for the ABC ship, described in Sec. 67.16. It was considered most important that the maximum fore-and-aft slope of the roof of the tunnel be as large as possible, yet not so large as to result in irregular flow or separation along the tunnel roof. There was ample full-scale evidence that on large ships with twin skegs, tunnel slopes of 8 to 9 deg were satisfactory, with the roof submerged a moderate amount below the at-rest waterline. There was evidence on some special models that a centerplane slope of 30 deg, at the same degree of submergence but on a convex body surface and not in a concave tunnel roof, was free from separation. It seemed reasonable to

halve the 30-deg slope of the special models, giving 15 deg, but at the same time it appeared risky to double the ship slopes, involving values as high as 16 to 18 deg. Nevertheless, this procedure narrowed the choice from somewhere in the wide range of 21 deg, between 30 and 9 deg, to the much smaller range of 3 deg, between 18 and 15 deg. On the basis that no ship would be built with an arch stern unless a model was first thoroughly tested, the maximum tunnel slope was set at 18 deg. Subsequent flow tests on the model showed no separation or harmful flow of any kind.

65.8 Adherence to Design Details in Construction. Although all features of ship construction are outside the scope of this book it is considered rather important to point out that, no matter how good the ship design, it requires a thorough and intensive follow-through, from beginning to end of the building period. Only in this way can a designer insure that the continual pressure to cut corners in production does not affect the service performance and reliability of the vessel. In the event of failure or casualty the blame is liable to fall as much on the designer as on the builder.

Nowhere is this follow-through more necessary and important than in the shaping, assembly, and finishing of the underwater hull surface and appendages. The most carefully calculated and cavitation-free rudder or strut shape is of no avail unless the form indicated on the plans is faithfully reproduced on the ship. Indeed, a projecting welding bead, transverse to the flow in a high-velocity region near the surface, can and has produced cavitation, noise, and vibration of plate panels. Not only that, it has produced erosion, first of the paint coating and then of the plate metal itself.

65.9 Guaranteeing the Performance of a New Ship Design. Finally, the ship designer must, upon the completion of a design, execute what is in effect a guarantee of its performance. Where the application of hydrodynamics is concerned, as in this book, the guarantee relates to propulsion, maneuvering, wavegoing, and all other normal and special operations taken for granted or specifically mentioned in the original requirements.

A designer who has, to his own satisfaction, embodied sufficient allowances to meet the various specifications need have little fear that at the conclusion of his work the ship will fail or be found lacking in any element of its behavior. Only too often, unfortunately, the designer's hand is forced in that he is required to make disturbing compromises or to embody features against which he is warned by his better judgment or his engineering instinct. Under these circumstances he must go to some pains and often to great lengths to assure himself that his estimates and predictions are reliable.

CHAPTER 66

Steps in the Preliminary Design

66.1 General Considerations. There are as many ways of executing the hydrodynamic design of a ship, at least in its preliminary stages, as there are ship designers. Each of them is particularly suited to the knowledge, experience, background, and ability of the designer so that each has its particular merits. An example of such an alternative method is given by E. E. Bustard in his paper "Preliminary Calculations in Ship Design" [NECI, 1940–1941, Vol. LVII, pp. 179–206 and D49–D62]. A presentation such as that set down here is of necessity limited to a single method, or at most, to two such methods. These are based logically upon a consideration of flow phenomena, paralleling that followed in Parts 1 and 2 of the book. Since knowledge of the hydrodynamic phenomena pertaining to interactions between all portions of the ship is not yet complete, part of the preliminary-design work must be accomplished by empirical methods based upon ship-model tests, ship-trial data, and past experience.

As a means of illustrating the procedures and steps involved in the application of hydrodynamic principles and knowledge to ship design, the preliminary layout and a portion of the final design of the ABC vessel, whose requirements and specifications were formulated in Chap. 64, is carried through in this and succeeding chapters. This craft is of the merchant type and is largely orthodox in character, with elements similar to those found on many past and current designs of ships. A number of unusual features are included, partly to give character to the design and partly to permit application of much of the hydrodynamic knowledge and many of the procedures previously set down.

66.2 Analysis of the Hydrodynamic Requirements. Before beginning the preliminary design it is well to analyze some of the specifications and requirements formulated in Sec. 64.3. Portions of them require conversion into terms directly applicable to the hydrodynamic design, resulting in quantities which can be used as

TABLE 66.a—Restricted-Channel and Open-Sea Data

Sector of Voyage	One-Way Distance, naut. mi	Total Voyage Distance, naut. mi	Depth, min., ft	Width, min., ft	Hydraulic Radius, R_H, ft, approx.
Port Amalo ship canal, restricted portion	16	32	28; 32 at bend	400; 500 at bend	20.0
Port Amalo ship canal, wide portion	9	18	28; 30 or more in spots	1,000 to 3,500	21.4 to 29.8
Port Amalo buoy to Port Bacine buoy, open sea	1,122	2,244	225	Unlimited	Equal to depth
Port Bacine to sea buoy (4 times per voyage)	1 abt.	5 abt.	45	1,500	over 40
Port Bacine sea buoy to Port Correo river mouth	1,384	2,768	Very large	Unlimited	Equal to depth
River mouth to Port Correo	204	408	30	1,200 to 15,000	26.7 min.
Total mileage per voyage		5,475			

parameters or which can be introduced directly into formulas, tables, and graphs.

First there is required a computation of the distances to be traveled at each of several speeds, and the times involved in steaming at those speeds. Here and elsewhere in the book, the distances are in nautical miles. From Port Amalo to Port Bacine, dock to dock, is 1,148 mi by the best route, of which 25 mi is in the Port Amalo ship canal and an insignificant portion, 1 mi or so, in Port Bacine Harbor. Of the 25 mi in the canal, the 16 mi at the Port Amalo end is in a restricted channel. From Port Bacine to Port Correo, dock to dock, is 1,589 mi by the approved track, of which 204 mi is in the large, fresh-water river. The distances, water depths, channel widths, and hydraulic channel radii R_H are given in Table 66.a. The values of R_H, derived by the method of Sec. 61.14, are somewhat variable because of the irregular configuration of the beds and banks of the several restricted waterways.

Adverse and favorable currents are investigated from the appropriate Sailing Directions. Their directions and velocities are listed for reference in Table 66.b.

The Sailing Directions specify a maximum speed of 8 kt for any large vessel in the restricted-channel portion of the Port Amalo ship canal, and advise a speed of not to exceed 10 kt in the remaining wide portion of the canal. No limiting

TABLE 66.b—Tidal and Water Data for Route of the ABC Ship

Sector of Voyage	Tidal Current		Rise and Fall of Tide	Kind and Temperature of Water
	Direction	Velocity, kt		
Port Amalo to the sea, through ship canal	Irregular	0.5 max.	Negligible	Salt, 60 to 70 deg F
Port Bacine	Ebb and flood	0.2 max.	Plus and minus 2 ft	Salt, 60 to 75 deg F
Port Correo to the sea, through long river	Downstream	1.5 min.; 2.75 max.	Plus 6 ft for flood conditions	Fresh, 75 to 80 deg F
Open sea	Irregular	Negligible	Not important	Salt, 68 deg F

speed is specified in the river leading out from Port Correo and no safe speed can be predicted until the size and shape of the vessel is known. Past experience with smaller vessels, however, indicates that this may be limited to 13 or 14 kt, reckoned as *speed through the water* rather than speed over the ground.

The layover, standby, and maneuvering times are then set down, in hours, as in the upper part of Table 66.c, starting with the beginning of a voyage at Port Amalo. Opposite these are marked the estimated average fuel-consumption rates for the periods given, intended to cover all auxiliary as well as propelling-plant loads. These rates are expressed as fractions of the fuel-consumption rate at the maximum designed power. Multiplying these average fractions by the hours during which fuel is burned at the corresponding rate gives the corresponding hours during which the consumption would be the same if the vessel were steaming at maximum designed power.

The elapsed times for the underway sectors are then calculated, as shown in the lower part of Table 66.c. In the open sea, it is assumed that the fuel consumption for each hour is that corresponding to the designed maximum power, despite the fact that the actual speed is generally less, averaging 18.7 kt as compared to 20.5 kt or slightly more, and that the elapsed time is longer. This extra fuel, calculated as necessary but not

TABLE 66.c—FUEL CONSUMPTION RATES FOR VOYAGE COMPONENTS

The expression *rated fuel* signifies the rate of fuel consumption at maximum designed power, all services in operation.

Name of Operation	Times, hr	Estimated fraction of rated fuel	Rated fuel-hr
MANEUVERING AND STOPPED			
Port Amalo, warming up and maneuvering in harbor	2	0.10	0.20
slowing down, discharging pilot, and so forth	1	0.05	0.05
Port Bacine, slowing down, warping to dock	1	0.15	0.15
layover, maximum	24	0.08	1.92
backing out from dock, maneuvering	1	0.35	0.35
Port Correo, docking and standby	1	0.10	0.10
layover, maximum	68	0.06	4.08
backing out and turning	1	0.40	0.40
Port Bacine, as above, total, return portion of voyage	26	0.093	2.42
Port Amalo ship canal, picking up pilot, slowing, docking	2	0.20	0.40
Port Amalo, layover, maximum	72	0.05	3.60
Totals	199 hr		13.67 rated fuel-hr
UNDERWAY			
Port Amalo ship canal, 16 mi at 8 kt	2	0.20	0.40
9 mi at 10 kt	1	0.25	0.25
Port Amalo to Port Bacine, sea sector, 1,122 mi at 18.7 kt	60	1.00	60.00
Port Bacine to Port Correo, sea sector, 1,384 mi at 18.7 kt	74	1.00	74.00
River mouth to Port Correo, 204 mi at 11.5 kt over the ground*	18	0.22	3.96
Port Correo to river mouth, 204 mi at 15.5 kt over the ground**	13	0.22	2.86
Port Correo to Port Bacine, sea sector, thence to Port Amalo, sea sector, as above	134	1.00	134.00
Port Amalo ship canal, as above	3		0.65
Total	305 hr		276.12 rated fuel-hr
Grand Total	504 hr or 21 days		289.79 rated fuel-hr

*14 kt less 2.75 kt for adverse current is 11.25 kt;
13 kt less 1.5 kt for the same is 11.5 kt

**14 kt plus 1.5 kt favorable current is 15.5 kt;
13 kt plus 2.75 kt favorable current is 15.75 kt

intended to be burned except in an emergency, constitutes the reserve fuel supply. Whether it equals or exceeds the 15 per cent required by item (10) of Table 64.b remains to be seen as the design progresses. If the ship is slowed by heavy weather it is nevertheless assumed that the fuel-consumption rate remains the same as for maximum designed power and for a speed slightly in excess of 20.5 kt in good weather. The fuel consumption when traveling in the shallow and restricted portions of the route is estimated only roughly for the present.

66.3 Probable Variable-Weight Conditions. Although the variable weights are not, strictly speaking, a part of the hydrodynamic-design picture, they do affect it in that they govern the displacement and trim and hence the volume and shape of the underwater hull in the several operating conditions. They also, with the respective specific gravities of the water, vitally affect the bed clearances that will obtain in the shallow and restricted portions of the route. In Table 66.d there are set down seven conditions, out of perhaps a dozen or more to be expected in the course of a routine voyage, as an indication of the range of displacement that might be encountered. The amount of fuel to be carried is still a rough guess, but the variations in total displacement are far greater than any possible variation in the fuel capacity.

It is to be noted from Tables 64.b and 66.d that since the bunkering for the whole voyage is done at Port Correo and the replenishment of all consumable stores at the other end of the line, the full load for which storage space must be provided is never on board at any one time. It is estimated that of the 700 t of fresh water, supplies, stores, and other consumables which can be carried, only 400 t is left on board at Port Correo, when the full amounts of fuel, liquid cargo, and package cargo are assumed to be loaded. As indicated in the first line of Table 66.d, this represents the *maximum service load.*

66.4 First Weight Estimate. The first step in the preliminary design is to determine the approximate weight of the ship with its cargo, the displacement volume required to support this weight, and the approximate linear dimensions. The following items of the weight estimate, all in tons of 2,240 lb, are known from the requirements of Table 64.b:

(a) Liquid bulk cargo . . . . . 4,000 t
(b) Package cargo . . . . . 3,000 t

Guesses of other major weight items are based on the background experience of the ship designer and such reference data as he may have. These items are deliberately set down here without reference to any handbook or other information, to make the example as general as possible. They are:

TABLE 66.d—First Statement of Variable-Weight Conditions, ABC Ship
All weights are in long tons of 2,240 lb or 2.24 kips of 1,000 lb.

Load Condition	Bulk Liquid Cargo, t	Package Cargo, t	Fuel, t	Consumable Stores, t	Total Variable Weights Aboard, t	Variation from Designed-Load Condition, t
Designed maximum service load, leaving Port Correo	4,000	3,000	2,200	400*	9,600	None
Arriving Port Amalo	4,000	3,000	1,200	100	8,300	−1,300
After unloading cargo, Port Amalo	0	0	1,100	50, min.	1,150	−8,450
Leaving Port Amalo in hurricane season, Condition H_1	2,000 as ballast	3,000	1,100	700	6,800	−2,800
Leaving Port Amalo, expecting heavy weather, Condition H_2	3,000 as ballast	1,000, partial cargo	1,100	700	5,800	−3,800
Arriving Port Correo, good weather	1,000 as ballast	3,000	150, reserve	400*	4,500	−5,050
After unloading, Port Correo	0	0	150, reserve	375	525	−9,075

*Somewhat less than half of the 700 t loaded at Port Amalo has been consumed

(c) Hull and fittings	6,400 t
(d) Propelling machinery	800 t
(e) Fuel, including reserve	2,200 t
(f) Consumable supplies and stores in heaviest condition	400 t
(g) Tentative margin, about 3 per cent of the total	500 t
Estimated weight displacement, (a) through (g)	17,300 t
In kips of 1,000 lb,	38,752

The corresponding displacement volume, at a round figure of 35 ft^3 per ton of salt water, is 605,500 ft^3.

Another way of arriving at the estimated weight displacement is to base the hull, machinery, and other fixed weights on a percentage of the total. The useful load is, including the fuel:

(1) Liquid bulk cargo	4,000 t
(2) Package cargo	3,000 t
(3) Fuel, including reserve	2,200 t
(4) Total amount of fresh water, supplies, and consumable stores for which storage is to be provided on board	700 t
Total	9,900 t

A combination passenger and cargo vessel of this type should be able to carry 0.55 of its weight as useful load, leaving 0.45 of the displacement as the ship weight. Using the first displacement estimate of 17,300 t and this ratio of 0.55, the useful load is 9,515 t, only slightly smaller than the 9,900 t listed in the paragraph preceding. Actually, of the latter amount, only 9,600 t is on board in the designed maximum service-load condition, as when loaded at Port Correo. This is because 300 t of item (4) preceding is consumed on the way from Port Amalo.

The ship-weight portion of the total, 45 per cent, is 7,785 t, which is somewhat larger than the sum of 6,400 t for hull weight and 800 t for machinery, items (c) and (d) of the previous tabulation. A small-scale graph of the ratio of useful load (actually deadweight) to total design displacement, for large passenger vessels and Atlantic liners, is plotted by C. R. Nevitt on a basis of speed-length quotient $V/\sqrt{L}$ or Taylor quotient T_q, within the range of 0.70 to 1.05 [SNAME, 1945, Fig. 1, p. 316]. More recent plots for selecting this and many other ratios and parameters, based upon data from certain general types of recent American ships, are given in convenient form by Nevitt [ASNE, May 1950, pp. 303–324]. However, in common with many other graphic aids of this kind, there is nothing in the reference to indicate the basis on which the original designer selected a certain ratio or parameter for a ship represented by a given spot on a diagram. Furthermore, one does not know whether the ship represented by that spot was easily driven or otherwise. This latter situation is remedied partly by taking data from the SNAME Resistance Data sheets. These give in most cases the predicted effective power for a ship of standard length with respect to that for a Taylor Standard Series ship of the same length.

66.5 First Approximation to Principal Dimensions; The Waterline Length and Fatness Ratio. The next logical step is to estimate roughly the length of the ship. As pointed out in Sec. 24.2, this length for the ABC ship is on the waterline, at a draft corresponding to the designed maximum service load at which a speed of 20.5 kt is to be achieved in smooth water. A tentative length may be taken from plots of empirical data such as those of Nevitt [ASNE, May 1950, Figs. 7, 8, 9, pp. 308–309], or it may be read by inspection from the analysis summaries of the SNAME RD sheets for combination passenger and cargo ships of about 17,500 tons displacement, and designed speeds of the order of 18.7 to 20.5 kt. The former plots give an L_{PP} of about 480 to 500 ft for normal ships and 500 to 520 ft for fine ships. This corresponds to an L_{DWL} range of about 500 to 535 ft. The latter tabulation gives a somewhat less definite value for L_{DWL} of the order of 500 ft.

A first guess at the minimum length is 500 ft. For this length the Taylor quotient $T_q = V/\sqrt{L}$ is $20.5/\sqrt{500} = 0.917$. The Froude number F_n is T_q (0.2978) = 0.273, and the displacement-length quotient $\Delta/(0.010L)^3 = 17{,}300/(5)^3 = 138.4$. The 0-diml fatness ratio $V/(0.10L)^3$ is $605{,}500/(50)^3 = 4.84$.

The question now arises, How do these parameters fit together to insure a ship easily driven? Is the length too small for the displacement and the required speed? Is the ship too fat for its speed? Considering hydrodynamics only, ship length is a matter of providing the easy longitudinal curvature necessary to permit an underwater body of the requisite volume to be driven easily and efficiently at the specified speed. In selecting the length, however, several other hydrodynamic factors enter:

(a) The proper relationship of speed and length so that a hump in the hull-resistance curve is avoided

(b) A suitable balance between the added friction drag on a too-long hull, with its extra wetted area, and the added pressure drag on a too-short one, with its sharper longitudinal curvature.

G. S. Baker gives a dimensional formula for determining the length L_{PP} between perpendiculars, namely

$$L_{PP} = 24\left(\frac{V}{2 + V}\right)^2 \Delta^{1/3} \qquad (66.i)$$

where L_{PP} is in ft, V is "the speed (in kt) for average fine weather at sea," and Δ is in long tons [NECI, 1942–1943, Vol. 59, p. 29]. Taking first the sustained speed V of 18.7 kt for the ABC ship, and the estimated displacement Δ of 17,300 t, Eq. (66.i) gives

$$L_{PP} = 24\left(\frac{18.7}{20.7}\right)^2 (17{,}300)^{1/3} = 506.5 \text{ ft.}$$

Using for V the trial speed of 20.5 kt,

$$L_{PP} = 24\left(\frac{20.5}{22.5}\right)^2 (17{,}300)^{1/3} = 515.3 \text{ ft.}$$

Baker's formula is put into nearly dimensionless form by substituting $\forall$ for Δ, and changing the numerical coefficient accordingly. However, Baker's definition for V remains somewhat indefinite, and the ratio of L_{PP} to L_{DWL} depends upon the type of stern. Using a specific volume of 34.977 ft^3 per long ton for salt water, (Eq. 66.i) becomes

$$L_{PP} = 24\left(\frac{V}{2 + V}\right)^2 \frac{\forall^{1/3}}{(34.977)^{1/3}}$$

or

$$L_{PP} = 7.3388\left(\frac{V}{2 + V}\right)^2 \forall^{1/3} \qquad (66.ii)$$

For the trial speed of 20.5 kt, Eq. (66.ii) gives

$$L_{PP} = 7.3388\left(\frac{20.5}{22.5}\right)^2 (605{,}500)^{1/3} = 515.4 \text{ ft.}$$

A slight discrepancy in length is expected here because the volume of 605,500 ft^3 was calculated by assuming a specific volume of 35 ft^3 per ton instead of the standard figure of 34.977 ft^3 per ton.

If all the governing factors could be known, properly weighed, and taken into account there would undoubtedly be found a most efficient length for each such set of conditions. Many designers are hesitant about exceeding that length, even though they do not know what it is. However, the excellent performance of many ships in the past, after a lengthening process which involved an increase of from 11 or less to 30 or more per cent of their original waterline length, is an indication that too long a hull is by no means the handicap that has been anticipated in the past [Mar. Eng., 7 Jul 1954, pp. 66–67, 81].

A preliminary study of the wavegoing situation, elaborated upon in Part 6 of Vol. III, indicates that the greatest speed reduction is to be expected when the ratio of wave length L_W to ship length L_{WL} is from 0.8 to 1.0. Also, a study of available data such as those in H.O. 602, 1947, reveals that the maximum wave lengths to be expected in the ocean areas traversed by the ABC ship are of the order of 385 ft. For a ship length of 515 ft, the ratio L_W/L_{WL} is 385/515 or 0.747. This is rather close for comfort to the low limit of 0.8, but at least it does not lie within the range 0.8 to 1.0.

A somewhat different line of attack on the length problem, still empirical and admittedly taking account of quiet-water performance only, is based upon data collected from the following sources, among others:

(1) Bates, J. L., Shipbuilding Encyclopedia, 1920, p. 200
(2) Liddell, E., NECI, 1934–1935, Vol. 51, pp. D45–D46
(3) Nevitt, C. R., SNAME, 1945, Fig. 2, p. 316
(4) Van Lammeren, W. P. A., RPSS, 1948, Fig. 39a, p. 89
(5) Thayer, E., SNAME, 1948, Fig. 29, p. 409
(6) Vincent, S. A., unpubl. ltrs. to HES, Sep 1947, Oct 1952
(7) SNAME Resistance Data sheets.

These data, for merchant and combatant vessels of orthodox form which have given good performance, cover a wide range of Taylor quotient, fatness ratio or displacement-length quotient, and longitudinal prismatic coefficient C_P. They have been checked and supplemented by comparison with the proportions of models listed on the SNAME RD sheets which have bettered Taylor Standard Series performance at and near the designed speeds. The result is two pairs of empirical curves on Fig. 66.A which bound two design lanes.

The upper pair defines the limits of displacement-length quotient $\Delta/(0.010L)^3$ and 0-diml fatness ratio $\forall/(0.10L)^3$ on a base of T_q and F_n for good practice and normal designs. The lower pair defines the limits of C_P in the same way. However, the values for good designs may well

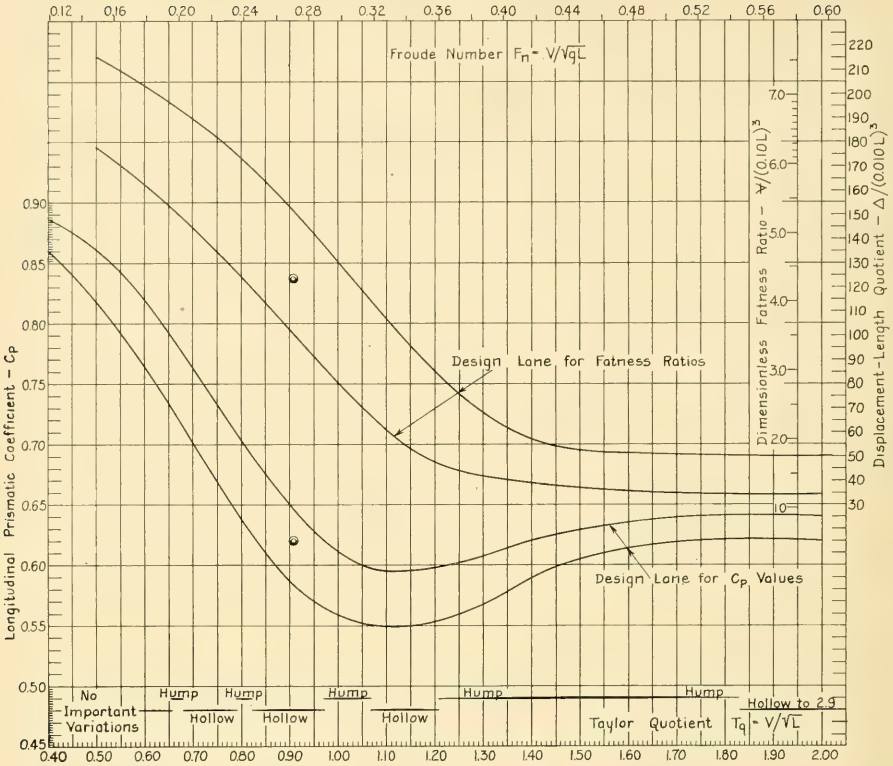

FIG. 66.A DESIGN LANES OF PRISMATIC COEFFICIENT, DISPLACEMENT-LENGTH QUOTIENT, AND FATNESS RATIO

The design lane for fatness ratios should have one or more upper branches for tugs, fishing vessels, patrol boats, and similar craft in the T_q range of about 1.00 and above. However, these lanes are not well defined and are not shown here.

The design lanes of Fig. 66.H, and those of Fig. 66.J through 66.N, embody the prismatic coefficient C_P as one of the principal parameters. The C_P values on the referenced graphs apply generally to the region of $T_q = 0.4$ through $T_q = 1.20$ of the "Design Lane for C_P Values" of the present figure; in other words, to the left-hand branch only.

fall outside these lanes when special requirements are being met. For example, the fatness ratios for icebreakers lie far above the upper design lane of Fig. 66.A, as do those of tugs and fishing vessels. This ratio, as well as the C_P , may lie above the lane for any ship which has a limitation on maximum length or in which some important advantage is gained by using the shortest practicable length.

Considering the ABC ship, for which there is no such limitation, and consulting the upper lane of Fig. 66.A with the fatness ratio 4.84 for the guessed length of 500 ft, the fatness ratio is found rather close to the upper limit for the T_q of 0.917. This 500-ft length may be, therefore, somewhat short for the load to be carried and the speed to be made. It is well, as the next operation, to select a length that may be slightly too long. This reduces the value of T_q and increases that of C_P . Repeating the operation for an L_{DWL} of 525 ft, close to the values given by the Baker formula, results in a T_q of $20.5/\sqrt{525} = 0.895$, a displacement-length quotient of 17,300/144.70 = 119.6, and a fatness ratio of 605,500/144,700 = 4.185. This spot is well inside the upper lane of Fig. 66.A.

Repeating the operation for a 515-ft length gives a T_q of 20.5/22.69 = 0.903, a displacement-length quotient of 17,300/136.59 = 126.7, and a fatness ratio of 605,500/136,590 = 4.433. This

point plots almost in the middle of the upper lane; the 515-ft length is apparently about right. At least it seems so at this stage. A ship longer than 525 ft on the designed waterline need not be considered until other features are investigated for these three lengths. Although a still greater length involves additional wetted surface there may be other good reasons for using it.

The significance of the special spots found on this and succeeding diagrams is explained subsequently in the chapter.

At the bottom of Fig. 66.A there appears a subdivision worked out by D. W. Taylor [S and P, 1943, p. 48] which indicates the position of humps and hollows in the curves of residuary resistance for a large range of T_q values. Reference to this subdivision indicates that the three T_q's for the tentative lengths of 500, 515, and 525 ft all lie in the middle of a hollow, slight but definite, for vessels of normal form. Here R_R is slightly less than it would be for a smooth curve of mean or "natural" values of R_R on V [Davidson, K. S. M., PNA, 1939, Vol. II, p. 70]. This is explained in Sec. 10.14.

Fig. 66.B, adapted from Taylor's shaded length-speed diagram [S and P, 1943, Fig. 55, p. 48], gives for ready reference a set of dimensional values in English units by which the hollow-hump positions for any ship length and any speed are found by inspection.

66.6 The Longitudinal Prismatic Coefficient. The prismatic-coefficient design lane of Fig. 66.A, especially at the low-speed end, does *not* give the optimum C_P for a given T_q or F_n, such as may be obtained from the Taylor Standard Series contours of R_R/Δ, because in that region the friction resistance is generally the major part of the total resistance. For example, the original contours of R_R/Δ for the Taylor Standard Series [S and P, 1943, pp. 201, 227] for a T_q value of 0.90 and a $\Delta/(0.010L)^3$ range of 138.4 for the 500-ft length to 119.6 for the 525-ft

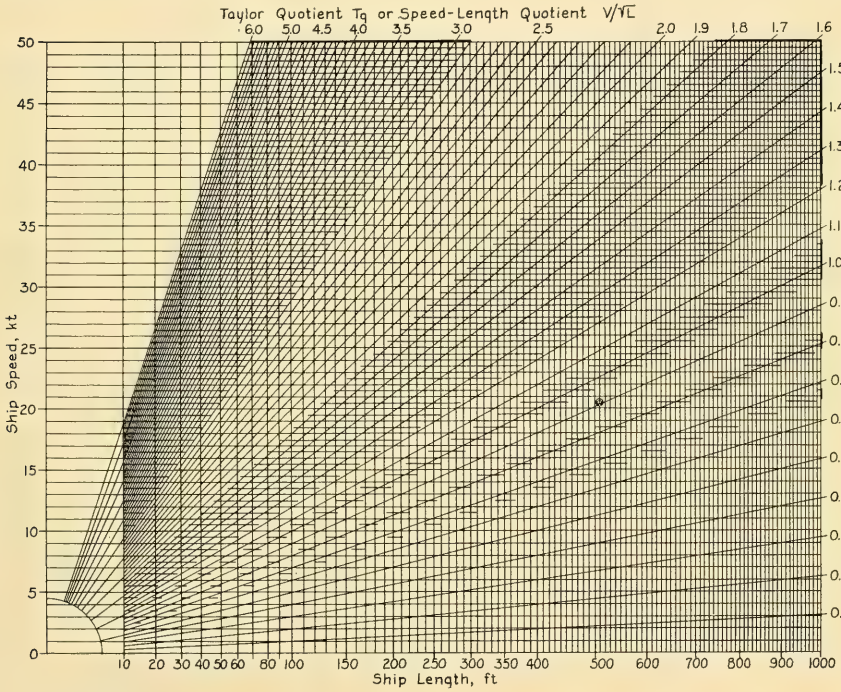

Fig. 66.B Diagram Illustrating Positions of Humps and Hollows in Residuary-Resistance Curves, in Terms of Ship Length and Speed

length, show that the minimum value of R_R/Δ occurs at a C_P of about 0.52 for a B/H of 2.25, and at a C_P of 0.54 for a B/H of 3.75. These values are considerably less than the average C_P value of 0.62 given by the lower design lane of Fig. 66.A. This is because the longer and more pointed forms, with the lower C_P values of 0.52 to 0.54, have too much wetted area and friction resistance for the specified displacement volume.

Similarly, the design lane of Fig. 66.A, in the higher ranges of T_q, gives values of C_P which are lower than those indicated by the regions of lowest residuary resistance per ton ratio, R_R/Δ, in the TSS contours. This is because the lane is positioned to suit high-speed vessels like destroyers which have to drive easily at cruising speeds that are much lower than the designed speeds. For a vessel designed to run always at high speeds, or for a vessel with sufficient nuclear fuel to eliminate the cruising-radius problem, at least so far as fuel only is concerned, the optimum C_P for a T_q of 2.00 would be in the range of 0.65 to 0.70 or more, depending upon the fatness ratio, as indicated by the TSS contours.

Restrictions on length and other factors often require a C_P somewhat higher than the best figures.

The middle of the lower lane gives values of C_P from about 0.614 for the short 500-ft ship to about 0.624 for the long 525-ft ship. A good value of C_P, at least at this stage, appears to be about 0.62.

A number of formulas, most of them for straight lines, have been developed to approximate the steep part of the "roller coaster" C_P lane of Fig. 66.A in the restricted region of T_q between 0.50 and 0.90. These ignore the need for design information applying to vessels in other speed-length ranges.

Beyond the left end of the lower lane, with T_q and F_n approaching zero and with wavemaking practically nonexistent, the C_P may approach a very high value as an asymptote, probably of the order of 0.90 to 0.95 or more. This means that craft which are not required to travel fast can approach a rectangular box shape, as illustrated in Fig. 66.C and as explained under barge design in Part 5 of Volume III.

It is again emphasized that the fatness ratio or prismatic coefficient for every ship need by no means lie within the lanes of Fig. 66.A, or that other parameters need conform to corresponding graphs to follow in this chapter. Special cases

Fig. 66.C A Speed-Length Quotient of Nearly Zero and a Prismatic Coefficient Approaching 1.00

A horse-propelled cargo carrier on the Erie Canal in 1916. Photograph by the author.

and requirements call for special designs. The lanes are simply to give the designer an idea of the range of values for a vessel of normal form that drives easily.

66.7 The Maximum-Section Coefficient; The Draft and Beam. There is little in the way of reliable information, empirical or otherwise, from which to select a tentative maximum-section coefficient C_X for any point in the complete range to T_q or F_n. This is equally true, for that matter, in a range of any other parameter [Taylor, D. W., S and P, 1943, Fig. 70, pp. 63–64]. This may be, for the reason stated in Sec. 24.10, that variations of C_X in themselves have little effect upon hull resistance. However, the branched design lane of Fig. 66.D gives an indication of the general region in which a good C_X is to be found, for approximately the same ranges of T_q and F_n as in Fig. 66.A.

The limiting optimum value of C_X is 1.00 at a T_q of 0.0, as for a square- or rectangular-section hull which rarely has to move. When it does move, hull drag is usually no problem. The ratio C_X may well be made greater than 1.0, in fact up to 1.1 or more, if there are practical reasons for doing so, such as adding blisters for underwater-explosion protection. As $V/\sqrt{L}$ increases, the design lane widens until at a T_q of 1.05, F_n of about 0.31, the value of C_X for good design lies between 1.00 and 0.90. At still higher T_q and F_n values, two classes of vessels are distinguished:

(1) Those intended for high speeds, where beam is sacrificed to keep down the longitudinal waterline curvature and to reduce resistance due to wavemaking but remains adequate for the service;

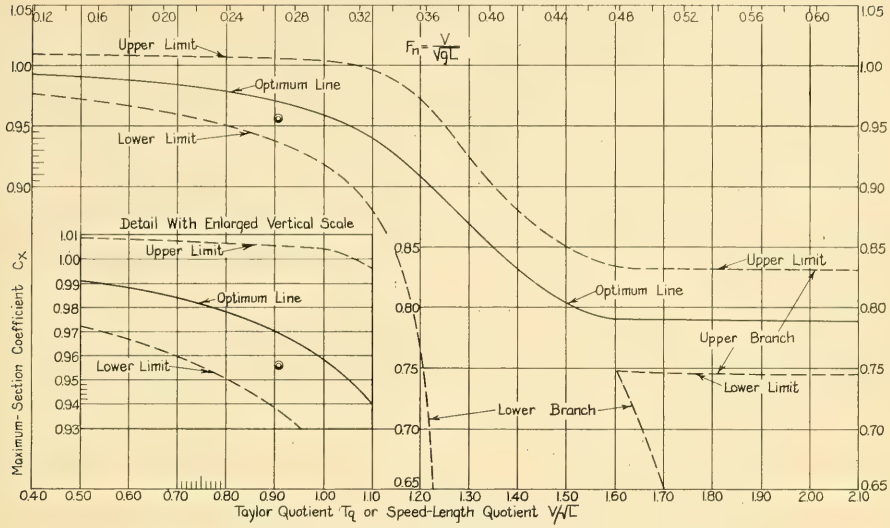

FIG. 66.D GRAPH FOR NORMAL VALUES OF MAXIMUM-SECTION COEFFICIENT C_X

they are indicated by the upper branch of the C_X lane

(2) Those designed to travel fast for their length, but for which a relatively large beam is a necessity, to afford stability, internal volume, deck space, and the like. They are indicated by the lower branch of the lane. Examples are fishing vessels, ferryboats, tugs, minesweepers, yachts, and small freight vessels. In fact, for these types the C_X values may drop well below the lower limits of the plot of Fig. 66.D, approaching 0.50 or 0.40 [Simpson, D. S., SNAME, 1951, p. 569]. The branch lane for these low values contains no optimum line, because there appears to be little or nothing systematic about the C_X values in this region.

If the ship is required to have the largest practicable volume for a given set of principal dimensions, as for cargo vessels which must pass through locks, the midsection is made as full as operating clearances permit. This may give a C_X of 0.995 or more, used on Great Lakes freighters. Since practically all vessels are drydocked or hauled out periodically, certain clearances may be required for these operations.

The best structural connection between the bottom and the side along the middle portion of a ship hull calls for a curved plate at the corner. However, these corners have been formed by what may be termed large-scale chamfering, using two chines with about 45-deg angles, as in the straight-element section shape sketched at 1 in Fig. 27.A. On vessels built for some European rivers and on towed steel barges built a half-century ago for service on the Erie Canal, the lower hull corners are made by structural angles, applied *outside* the side and bottom plating, with a bilge radius of practically zero [Nixon, L., SNAME, 1896, p. 20 and Pl. 19].

Since the ABC ship is to give good performance in the shallow and restricted waters of the Port Amalo canal and the river below Port Correo, there must be plenty of room for the water to pass around the ship, especially under it. This means that the maximum-section coefficient C_X, or the midsection coefficient C_M, should not exceed about 0.96, on the basis of a midsection of normal form. With a displacement volume of 605,500 ft^3 and a waterline length of 515 ft, for the middle-length ship of the three mentioned in Sec. 66.5, the maximum-section area A_X for a prismatic coefficient C_P of 0.62 is

$$A_X = \frac{\nabla}{L(C_P)} = \frac{605{,}500}{515(0.62)} = 1{,}896 \text{ ft}^2.$$

The minimum depth of channel out of Port Amalo is 28 ft but between one-third and one-half

of the fuel will have been consumed by then, bringing the ship up in the water by the order of a foot or so. The ship drops to a deeper draft in the fresh water of the river at Port Correo, and ample clearance must be left over the river bed, which has a minimum depth of 30 ft. It appears necessary, at least at this stage of the design, to limit the draft in salt water to a maximum of 26 ft. This draft then corresponds to the maximum designed service load being carried when leaving Port Correo. From Table 66.d, first line, and from the first weight estimate, the consumable-store weight is only 400 t at this time, compared to the 700 t which the ship must carry when fully stocked at Port Amalo.

For the 515-ft ship the beam B_X at the maximum-area section is then

$$B_X = \frac{A_X}{C_X(H_X)} = \frac{1{,}896}{(0.96)26} = 75.96 \text{ ft.}$$

This is quite large for a seagoing ship only 515 ft long. The length-beam ratio is small, namely 515/75.96 = 6.78. The beam-draft ratio is rather large, equal to 75.96/26 = 2.92. The latter ratio is not too large but it increases as fuel is consumed during the voyage.

The large beam will undoubtedly give all the square moment of area required in the designed waterplane for transverse metacentric stability. Indeed, it may give too much for easy rolling. Almost certainly it will involve additional pressure resistance from wavemaking, due to the correspondingly large waterline slopes and the pressure disturbances set up around the wide ship. This matter is brought up again, a little later in the design.

Working through the procedure described, for a ship 525 ft long on the waterline, with a C_P of 0.62,

$$A_X = \frac{\forall}{L(C_P)} = \frac{605{,}500}{525(0.62)} = 1{,}860 \text{ ft}^2$$

$$B_X = \frac{A_X}{C_X(H_X)} = \frac{1{,}860}{(0.96)26} = 74.52 \text{ ft}$$

$$L/B_X = \frac{525}{74.52} = 7.05 \quad B_X/H_X = \frac{74.52}{26} = 2.866$$

This 525-ft length gives considerably better pro-

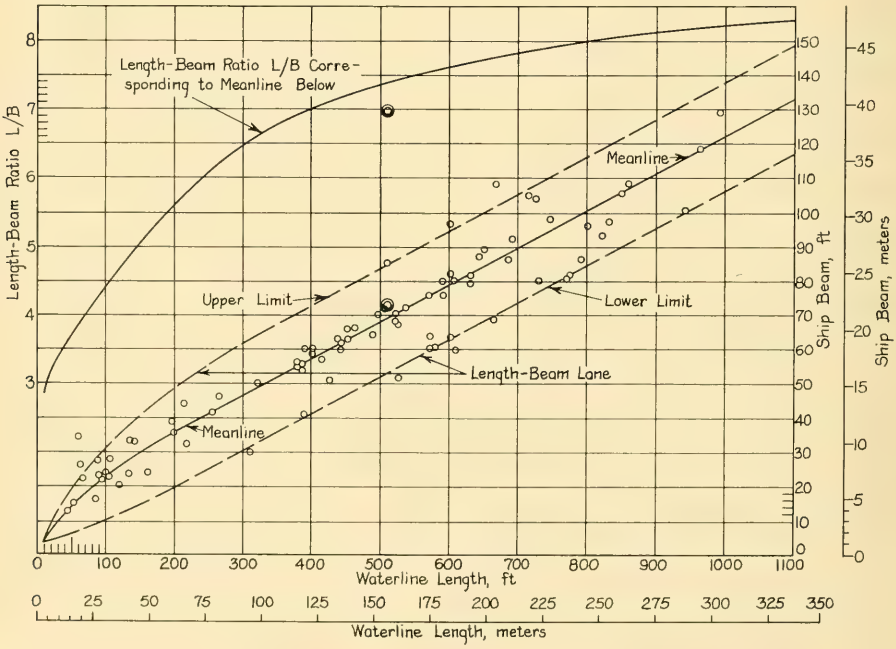

Fig. 66.E Plot of Length-Beam Ratio and Beam on Ship Length

portions for a ship of the speed and service required, although the beam is still large.

Supplementing the discussion in Sec. 24.11, Fig. 66.E gives a range of absolute beams on a basis of absolute lengths, based on data from many successful ships, for which a great number of the spots are shown. The meanline indicated is rather an average location for most of the ship values than one drawn through the center of the lane marked by the upper and lower ranges of absolute beam on absolute length. Also indicated is a curve of 0-diml L/B ratios corresponding to the meanline.

Some modern craft built for speed with manual propulsion only, among them canoes, sculls, and racing shells, retain the high L/B ratios characteristic of dugout and American Indian canoes for many centuries past. However, there has been an increasing demand through the years for utility, for inherent stability not always possessed by the canoe with a man (or men) standing up in it, for still more utility with top hamper, and finally for greater all-around safety. This has broadened the beam of boats and small ships gradually, without too much regard for the effect of the small L/B ratio on propulsion. If metacentric stability, maneuvering, and other features are more important than propulsion, the design has to favor them.

For the ABC design the beams given in the preceding paragraphs are slightly greater than those shown by the meanline but they are well within the lane.

The block coefficient for the 525-ft vessel works out as

$$C_B = \frac{\nabla}{L(B_X)H_X} = \frac{605{,}500}{525(74.52)26} = 0.595+$$

This checks, as it should, with

$$C_B = C_P(C_X) = 0.62(0.96) = 0.595+$$

For the three waterline lengths of 500, 515, and 525 ft, and for a constant C_P of 0.62, the proportions and dimensions already worked out and some of those remaining to be derived are indicated for convenience in Table 66.e, in Sec. 66.11.

66.8 First Estimate of Hull Volume. It is advisable at this point to make a rough volumetric check of the vessel to insure that everything can be accommodated within the hull, above as well as below water. It is now necessary to include the *full* weight and volume of consumables and other items to be carried during any part of the voyage. Using the data from Table 64.b and the same subdivision as in the first weight estimate of Sec. 66.4:

(a) Liquid bulk cargo, 4,000 t at 42 ft^3 per t	168,000 ft^3
(b) Package cargo, 3,000 t at 100 ft^3 per t	300,000 ft^3
(c) Hull structure, on a basis of 4.5 ft^3 per t for 6,400 t of hull steel, fittings, and other construction materials, *plus* 4 times that volume for the waste space around it	144,000 ft^3
(d) Estimate for propelling and other machinery . . . . . (This is very large compared to the figures given by G. G. Sharp [SNAME, 1947, p. 462] but in view of the unorthodox features being considered for an alternative stern, with the propelling machinery aft, it is not reduced at this stage)	300,000 ft^3
(e) Fuel, 2,200 t at 42 ft^3 per t . .	92,400 ft^3
(f) Fresh water, lubricating oil, supplies, and other consumable stores, 700 t at 100 ft^3 per t .	70,000 ft^3
(g) Accommodations for officers and crew, estimated	100,000 ft^3
(h) Passenger quarters and service .	400,000 ft^3
(i) Non-usable space	100,000 ft^3
Total volume	1,674,400 ft^3

The foregoing does not include an allowance for keeping hatchways clear, to facilitate access to the cargo, nor for the volume of expansion trunks over the liquid-cargo tanks.

The volume listed is about 2.77 times the tentative underwater displacement volume of 605,500 ft^3 but it includes practically all deck erections. For a combined passenger and freight vessel, it appears somewhat large but perhaps not too large at this stage of the design.

66.9 First Approximation to Shaft Power. Before making a second weight estimate it is necessary to approximate the propelling power, so as to determine more accurately the machinery weights and the fuel capacity.

The first rough estimate of shaft power P_S is derived from the assembled data on merit factors in Secs. 34.10 and 60.13. The first of these,

the Telfer merit factor M, is represented by values of $WV^3/(gLP_S)$ for a range of Froude numbers squared. Taking the 515-ft or middle length of ABC ship as the example, for which F_n^2 is 0.0727, the broken meanline of Fig. 34.I gives a tentative merit factor M of about 9.5. Using the dimensional Eq. (34.xxv) of Sec. 34.10,

$$P_S = 0.61\frac{WV^3}{L(M)} = 0.61\frac{(17{,}300)(20.5)^3}{(515)(9.5)}$$

$$= 18{,}582 \text{ horses.}$$

Since the 20.5-kt speed is to be made at 0.95 of maximum designed power, by item (22) of Table 64.d, this power is 18,582/0.95 = 19,560 horses.

Using the alternative weight-speed-power factor WV/P_S of Fig. 60.U, for an F_n^2 of 0.0727, the broken meanline gives a value of about 125. Then, with the dimensional formula on Fig. 60.U,

$$P_S = 6.88\frac{17{,}300(20.5)}{125} = 19{,}520 \text{ horses.}$$

The designed maximum power estimate is then 19,520/0.95 = 20,550 horses.

It is emphasized that, when making estimates from the meanlines, one assumes that a ship of modern design is to perform no better than the average of a number of older ships. Further, since the merit-factor ordinates of both Figs. 34.I and 60.U are logarithmic, a value picked among the spots for the better ships may easily be from 20 to 40 per cent better than the average. This means estimated powers of from 20 to 40 per cent below those calculated in the preceding paragraphs.

The third estimate is made by the use of the ATTC 1947 or Schoenherr friction line, the ATTC 1947 roughness allowance ΔC_F of $0.4(10^{-3})$, and the Taylor Standard Series data as reworked by M. Gertler [TMB Rep. 806, Govt. Print. Off., Wash., Mar 1954].

At this point it is necessary to take account of the average temperature of the sea water in which the ship is to run, specified in item (18) of Table 64.c. For this temperature, 68 deg F, the value of the mass density ρ(rho) of salt water, from Table X3.e, is 1.9882 slugs per ft^3. The kinematic viscosity ν(nu), from Table X3.h, is $1.1372(10^{-5})$ ft^2 per sec. The former is 0.99884 times the value of ρ = 1.9905 slugs per ft^3 for the standard condition of temperature 59 deg F, while the latter is 0.88726 times the value of $\nu = 1.2817(10^{-5})$ ft^2 per sec for the same standard temperature. The former ratio is sufficiently close to 1.000 for all preliminary-design purposes. The latter ratio is some 11 per cent less than 1.000, but its effect on C_F at the large ship Reynolds numbers is small. Since the effect of the 68-deg kinematic viscosity is to diminish the calculated friction resistance, its use is somewhat questionable in a preliminary design. For these reasons, and because the "standard" values of ρ and ν for 59 deg F are easily remembered, the latter are employed throughout Part 4 of the book.

Entering the large-scale portion of Fig. 45.H with a C_X of 0.96 and a B/H of 2.92 for the 515-ft ship, the wetted-surface coefficient C_S is found to be 2.618. The first approximation to the wetted area is then $C_S\sqrt{\nabla L} = 2.618\sqrt{605{,}500(515)} = 46{,}231$ ft^2. From Table 45.b the Reynolds number R_n is about 1391 million for the 515-ft length, for the 20.5-kt speed of 34.62 ft per sec, and for a kinematic viscosity ν in "standard" salt water of $1.2817(10^{-5})$ ft^2 per sec. From Table 45.d the value of C_F is $1.470(10^{-3})$. Adding a roughness allowance ΔC_F of $0.4(10^{-3})$ for a clean, new ship of as-yet-undetermined shape or surface condition, gives $C_F + \Delta C_F = 1.870(10^{-3})$.

Entering the appropriate graph of the B/H = 3.00 group of the reworked Taylor Standard Series contours, reproduced in Fig. 56.D of Sec. 56.5, for $C_P = 0.62$, $T_q = 0.903$, $F_n = 0.268$, and $\nabla/(0.10L)^3 = 4.433$, the value of C_R is found to be $1.25(10^{-3})$. Entering the B/H = 2.25 group with the same values, C_R is $1.21(10^{-3})$. Since B/H is actually 2.92, C_R is found by linear interpolation to be approximately $1.246(10^{-3})$. At the 20.5-kt speed, therefore, the specific friction resistance is considerably more than half of the total resistance, namely $1.870(10^{-3})$ as compared to $(1.870 + 1.246)10^{-3} = 3.116(10^{-3})$. The amount of wetted surface is therefore something to be watched carefully in the design.

The total drag R_T of the bare underwater hull is estimated from Eq. (45.ii) of Sec. 45.7, namely $R_T = (\rho/2)V^2S(C_R + C_F + \Delta C_F) = qS(1.246 + 1.470 + 0.4)10^{-3}$, where for the first approximation ρ is taken as 1.9905 slugs per ft^3 for salt water. Then $R_T = 0.99525(34.62)^2(46{,}231)3.116(10^{-3}) = 171{,}830$ lb, whence

$$P_E = \frac{R_TV}{550} = \frac{171{,}830(34.62)}{550} = 10{,}816 \text{ horses.}$$

A round figure is 10,820 horses.

As a check calculation by Taylor's original method [S and P, 1943, pp. 59–60], the friction resistance per ton of displacement is found by

taking first the dimensional wetted-surface coefficient C_{WS} from Fig. 20 on page 22 of the reference. With $B/H = 2.92$ and $C_X = 0.96$, the value of C_{WS} is, as nearly as can be determined, 15.02. For a 515-ft ship the length-correction factor α(alpha) is 0.997, taken from the diagram at the right of Fig. 188 on page 188 of the reference. Then for a $\Delta/(0.010L)^3$ quotient of 126.7 and a T_q of 0.903, the friction resistance per ton of displacement for a ship having a C_{WS} of 15.4, from the plot of Fig. 188, is 6.1 lb. For the 515-ft ship with a C_{WS} of 15.02, and an α of 0.997,

$$R_F = 6.1\,\frac{(15.02)}{(15.4)}\,(0.997) = 5.932 \text{ lb per t.}$$

For the C_P of 0.62, the displacement-length quotient of 126.7, the B/H ratio of 2.25, and the T_q of 0.90, the value of R_R/Δ is, from page 201, 3.55 lb. For a B/H ratio of 2.92, it is, by linear interpolation between $B/H = 2.25$ and $B/H = 3.75$, 3.75 lb. Similarly, for $T_q = 0.95$, R_R/Δ is 5.779 lb. Again interpolating linearly for $T_q = 0.903$, R_R/Δ is 3.872 lb for the parameters given.

The bare-hull resistance R_T is then

$$\left(\frac{R_F}{\Delta} + \frac{R_R}{\Delta}\right)\Delta = (5.932 + 3.872)17{,}300$$

$$= 169{,}610 \text{ lb.}$$

The agreement with 171,830 lb as found by the third method is within 1.3 per cent and is good enough at this stage of the design.

Another quick method for approximating the total bare-hull resistance R_T of the ship is to use the graph of Fig. 56.M, comprising values of R_T/Δ plotted on T_q over a wide range of relative speeds. It applies to any type of vessel from a lake freighter up to a high-speed patrol craft. Entering Fig. 56.M with a T_q of 0.903, corresponding to the designed speed of 20.5 kt of the ABC ship, the value of R_T/Δ is 10.2 lb per long ton. With an estimated displacement of 17,300 tons, this gives a bare-hull resistance R_T of 176,400 lb. This is 2.66 per cent higher than the resistance estimated by the third method described, but is at least on the high side for the present.

If the vessel is to be driven by a single screw, the ship requirements appear to call for no appendages except a single rudder and a pair of roll-resisting keels. A rudder having an area of $0.02(LH)$ would have a projected blade area of about $0.02(515)26 = 268$ ft^2, and a surface area of something over 536 ft^2. A pair of roll-resisting keels 200 ft long and 3 ft wide would have a total wetted area of about $2(200)3(2) = 2{,}400$ ft^2. The hull area covered up by the bases of roll-resisting keels of triangular section would average about 1 ft wide by 2(200) ft long, or say 400 ft^2. The total added area for rudder and keels is then $536 + 2{,}400 - 400 = 2{,}536$ ft^2, which is $2{,}536/(46{,}231) = 0.055$, or 5.5 per cent of the bare-hull area. On the basis of additional wetted area alone, this is not more than 6 per cent of the friction resistance, which in turn is only about 62 per cent of the total. The increase in total drag is therefore of the order of 4 per cent. However, it seems wise at this stage to double this effect and allow about 8 per cent of the total resistance for the final appendage drag. Since the requirement of item (26) of Table 64.d states that "A reasonable expenditure of weight or power, or both, to secure *effective* roll-quenching" is acceptable to the owner, it may be considered advisable, at a later stage of the design, to make the roll-resisting keels even larger than indicated here.

In the absence of any better information, an additional 2 per cent is included to cover the drag of the condenser scoop and the circulating-water discharge, making 10 per cent in all.

So far as can be determined at this time there is sufficient allowance for fouling in the 1.8-kt difference between the 18.7-kt scheduled speed for the whole voyage and the 20.5-kt trial speed under clean-bottom smooth-water conditions.

The tabulated data at the end of Sec. 60.11 give a range of propulsive coefficient of 0.82 to 0.72 for clean, new, single-screw ships of modern hydrodynamic design. It seems reasonable to assume that a value of η_P as high as 0.74 can be achieved for a single-screw ABC ship, even though the design is not yet worked out. Using an appendage-and-scoop factor of 0.10 for added resistance, and a propulsive coefficient of 0.74, a first approximation to the shaft power is $(10{,}820)(1.10)/0.74 = 16{,}084$ horses.

Item (22) of Table 64.d states that the sustained sea speed of 20.5 kt shall be attained by the use of not more than 0.95 of the maximum designed power. The latter is therefore $16{,}084/0.95 = 16{,}930$ horses. This is considerably less than the first and second estimates of 19,560 and 20,550 horses, but all are within the capabilities of a modern single-shaft plant and a single propeller.

Again it is emphasized that all these estimates are for average performance, with generous

allowances such as doubling the estimated appendage resistance.

Further, it is assumed in all the foregoing that the resistance of the final ABC hull will not exceed that of the Taylor Standard Series hull of the same proportions and weight displacement. This is certainly the end to be sought; in fact, the designer should look forward to bettering the TSS performance. In this connection the following is quoted from a discussion by S. A. Vincent [SNAME, 1948, p. 403], where the comments in parentheses are those of the present author:

> ". . . few vessels having prismatic coefficients from about 0.72 to 0.75 are as good as the (Taylor) Standard Series models at designed speeds suitable for the prismatic coefficient (see Fig. 66.A). At higher or lower speeds for this particular range of vessels and also for vessels having prismatic coefficients beyond this range, the resistance for good forms is below that of the Standard Series, often considerably below . . . the designer would do well to have the Standard Series form in mind when drawing the lines of vessels having prismatic coefficients between about 0.72 and 0.75."

In the event that the hull shape developed for the ABC ship should prove more resistful than the Taylor Standard Series, it is possible to apply a contra-guide ending to the single centerline skeg, and to use a contra rudder. These together should regain a certain amount of power lost in driving the hull itself. At this stage it appears that a bulb bow might be beneficial. If so, a still greater amount of power could be regained.

66.10 Second Estimate of Principal Weights. The most uncertain weight items in the first rough estimate of Sec. 66.4 were those of the hull, the propelling machinery, and the fuel. In accordance with the conclusions of Sec. 69.2 the ABC design is to be worked up on the basis of a single propeller.

The best available information, at the time of writing (1955), for a *complete* single-screw steam power plant in the range of 16,000 to 17,000 horses is 165 lb per horse. The total estimated propelling-plant weight at this stage is then 16,930(165) = 2,793.5 kips or 1,247.1 t; say 1,250 t. This is 450 t, or 56.3 per cent more than the 800 t of the original estimate, an indication of the surprises that often turn up in operations of this kind.

From Table 66.c in Sec. 66.2 the estimated fuel to be burned per voyage corresponds to that for approximately 290 hours of steady steaming at maximum designed power. A steam plant of this size, also at the time of writing, should be able to produce full power at a fuel rate of 0.58 lb per horse per hr; certainly on 0.6 lb [Barnaby, K. C., INA, 1950, p. J8]. An estimated allowance for the hotel load, for full atmosphere control, including dehumidification, and for other items not covered by the hydrodynamic specifications, is 0.1 lb per horse per hr, making a total of 0.70 lb for all purposes.

As a check on the first item, W. I. H. Budd and O. Praznik show a fuel rate of slightly under 0.575 lb of oil per horse per hour for all purposes [SNAME, 1948, Fig. 1, p. 472]. This apparently does not include fuel for the hotel services.

Concerning the second item it is probably more logical to determine the fuel rate for services on a basis of the total personnel on board per day at sea or in port. However, as the rates in question are being used solely for a design example rather than for an actual ship they need not be more than roughly representative of good practice at the time of writing.

The fuel consumption per voyage is then estimated as 290(16,930)(0.70) = 3,437 kips or 1,534.4 t. A round figure is 1,550 t. This is 650 t less than that allowed for in the first weight estimate, and 200 t more than enough to compensate for the 450 t of additional propelling-machinery weight in the second estimate.

A further check on proportions of hull-and-fittings weights to total weight with all useful load, on the basis of riveted seams and welded butts in the shell plating, a three-compartment standard for floodability, the possible use of a special type of single-screw stern, and the judicious use of light alloys for topside weights, indicates that the hull proper with fittings should weigh about 35 per cent of the loaded ship. The original hull weight of 6,400 t may be reduced at this stage to about 5,960 t. The original margin of 500 t, just under 3 per cent, may safely be cut to 330 t, just about 2 per cent.

A second weight estimate looks about as follows:

(a)	Liquid bulk cargo	4,000 t
(b)	Package cargo	3,000 t
(c)	Hull and fittings	5,960 t
(d)	Propelling machinery	1,250 t
(e)	Fuel, including reserve	1,550 t
(f)	Fresh water, supplies, and the like .	400 t
(g)	Weight margin	330 t
	Estimated total weight displacement	16,490 t

The corresponding displacement volume at the nominal figure of 35 ft^3 per ton of salt water is 577,150 ft^3.

It is again pointed out that the percentages, unit weights, fuel rates, and other values and relationships in these weight estimates may not agree with those used by some reader-designers nor may they continue to be reasonable figures in the light of technical developments in the next few decades. They are intended only as numbers in an example and they in no way affect the procedures in the hydrodynamic design of the vessel carried through here.

66.11 Second Approximation to Principal Dimensions and Proportions. The second estimate brings the weight displacement down by 810 t from the 17,300 t of the first estimate. On this basis alone the ship can be made smaller; for one thing, the beam can be reduced from the order of 75 ft to a more reasonable figure. It is to be remembered, however, that the volumes to be accommodated within the hull and deck erections remain substantially the same, and that in the first estimate of volume the hull appeared to be none too large.

Further, since it is customary to reckon the

TABLE 66.e—Tentative Hydrodynamic Features of Several Vessels of Different Lengths

For the fourth and fifth approximations, 90 t has been deducted from the hull weights for the shell plating, to give the molded displacement.

Approximation		First	Second	Third	Fourth	Fifth
Item	Units					
L Length, waterline	ft	500	515	525	515	510
L^3 times 10^{-6}	ft^3	125	136.59	144.70	136.59	132.65
$\sqrt{L}$	$ft^{1/2}$	22.36	22.69	22.91	22.69	22.583
a. Liquid cargo	t	4,000	4,000	4,000	4,000	4,000
b. Package cargo	t	3,000	3,000	3,000	3,000	3,000
c. Hull and fittings	t	6,400	6,400	6,400	5,870	5,870
d. Propelling mach.	t	800	800	800	1,250	1,250
e. Fuel	t	2,200	2,200	2,200	1,550	1,550
f. Consumables	t	400	400	400	400	400
g. Margin	t	500	500	500	330	330
Total W	t	17,300	17,300	17,300	16,400	16,400
$\forall$ at 35 ft^3 per t	ft^3	605,500	605,500	605,500	574,000	574,000
V Speed, trial	kt	20.5	20.5	20.5	20.5	20.5
V	ft/sec	34.62	34.62	34.62	34.62	34.62
$T_g = V/\sqrt{L}$		0.917	0.903	0.895	0.903	0.908
$F_n = V/\sqrt{gL}$		0.273	0.269	0.267	0.269	0.271
$\Delta/(0.010L)^3$	t/ft^3	138.4	126.7	119.6	120.1	123.6
$\forall/(0.10L)^3$		4.84	4.433	4.185	4.202	4.327
C_P		0.62	0.62	0.62	0.62	0.62
C_X		0.96	0.96	0.96	0.935	0.956
C_B		0.595	0.595	0.595	0.579	0.5
A_X	ft^2	1,953	1,896	1,860	1,798	1,815
B_X	ft	78.25	75.96	74.52	74	73
H	ft	26	26	26	26	26
B/H		3.01	2.92	2.87	2.85	2.808
L/B		6.39	6.78	7.05	6.96	6.986
C_S			2.618			2.616
S	ft^2		46,231			44,759
C_W						0.719
$\overline{LCB}/L$						0.507
$\overline{LMA}/L$						0.515
Per cent of parallel WL						0
Per cent of parallel middlebody						0

principal dimensions and to calculate the form coefficients to the molded form, as explained in Sec. 66.21, it is possible to consider about 90 t of the displacement as helping to support the weight of the shell plating and appendages. The volume of the molded hull, to the outside of the frames, is therefore smaller by about 90(35) = 3,150 ft^3. Specifically, it is 577,150 ft^3 less 3,150 ft^3, or 574,000 ft^3.

Considering for the moment the middle tentative length of 515 ft, with its T_q of 0.903, the displacement-length quotient for a weight W of 16,490 − 90 = 16,400 t is 16,400/136.591 or 120.1. The 0-diml fatness ratio is 574,000/136,591 or 4.202. This is just below the middle of the upper lane of Fig. 66.A, so the 515-ft length still appears appropriate.

The maximum section area A_X for a C_P of 0.62 is

$$A_X = \frac{\forall}{L(C_P)} = \frac{574{,}000}{515(0.62)} = 1{,}798 \text{ ft}^2 .$$

Reducing the beam to 74 ft gives

$$C_X = \frac{A_X}{B_X(H_X)} = \frac{1{,}798}{74(26)} = 0.9345$$

This maximum-section coefficient appears, from Fig. 66.D, to be somewhat on the low side. Using a beam of 73 ft,

$$C_X = \frac{A_X}{B_X(H_X)} = \frac{1{,}798}{73(26)} = 0.947$$

This is still somewhat low. It is possible that, with some 800 t off the original displacement, the length is a little longer than need be. Taking a reduced length of 510 ft, and retaining $C_P = 0.62$,

$$A_X = \frac{\forall}{L(C_P)} = \frac{574{,}000}{510(0.62)} = 1{,}815 \text{ ft}^2$$

whence

$$C_X = \frac{1{,}815}{73(26)} = 0.9563,$$

which is satisfactory at this stage.

These new dimensions give an L/B ratio of 510/73 or 6.986 and a B/H ratio of 73/26 or 2.808. The block coefficient C_B is (0.62)0.956 or about 0.593. The Taylor quotient T_q is 20.5/22.583 = 0.908, the displacement-length quotient is 16,400/132.651 = 123.63, and the 0-diml fatness ratio is 574,000/132,651 = 4.327. As a convenient check at this point the graphs of Fig. 66.E indicate a mean L/B ratio of about 7.4 for a vessel 510 ft long.

For convenient reference the data derived in the foregoing for the tentative lengths of 500,515, 525, and 510 ft, plus a few additional items to be derived, are listed in Table 66.e.

66.12 Selection of Hull Shape. Up to this point the preliminary design has involved only principal dimensions and proportions. It is now necessary to think of the *shape* which the vessel's hull is to take. While it is admitted that the Taylor Standard Series shape, derived from a twin-screw cruiser of the early 1900's, is not necessarily adaptable to any vessel designed in subsequent years, especially one with a single screw, it is without question a good shape from the standpoint of easy driving.

Other good shapes, excellent ones, have been developed through the years, shapes which no designer need hesitate to copy if they serve his purpose. He is cautioned, however, not to attempt "breeding" better ship lines by *averaging* good existing lines; this has been tried and definitely found wanting.

It is extremely difficult in the present state of the art, especially without benefit of model tests, to predict the effect of shape changes in a parent form. Nevertheless, it is considered far preferable to modify a given good shape to meet the designer's needs than to make up a new shape by adding a good stern to a good but unrelated bow, or by any process of averaging. These matters are discussed in greater detail in Sec. 66.24.

66.13 Layout of Maximum-Section Contour. The tentative value of C_X as selected from Fig. 66.D determines whether the maximum-section contour is to be rectangular, following closely the lines for limiting beam and draft, whether it is to be well cut away, as in a keel type of sailing yacht, or whether it is to take some intermediate form.

If it is desired, in fashioning the form, to place as much displacement as possible amidships, the use of a hard bilge and a relatively "square" section need not interfere materially with the flow except to increase the transverse velocity gradient and the local friction resistance around the sharp bilge.

In a vessel which is to run at not more than medium or fast speed in deep water, there is no reason why the bottom can not be perfectly flat over a considerable area. The floor lines at the midsection need not be raised unless this is required for drainage of the tanks and spaces lying just above this bottom, or for some other practical purpose.

Excessive transverse metacentric stability developing in the course of the design is relieved by narrowing the surface waterline and working tumble home into the midsection or into the section of maximum area for a considerable distance below the DWL, possibly half way down to the baseplane. Increased displacement volume and carrying capacity is achieved by working an underwater bulge into this section below the designed waterplane. If the vessel already has adequate metacentric stability, this bulge need not increase the waterline beam.

As a check on the tentative value of C_X for the ABC design at this stage a maximum-section contour is drawn. This requires that the rise of floor, if any, be established. It gives an idea of the roll-resisting characteristics of the section, leading in turn to an estimate of the bilge-keel width which is required and that which can be allowed.

To meet the requirements of the ABC design it is decided tentatively that:

(a) There is to be some rise of floor, to provide for internal tank drainage and to give more room for water moving aft under the ship in the shallow waters to be traversed
(b) The side of the ship in way of the designed waterline is to be given a slight tumble home if possible but in any case is not to have an outward flare in that region
(c) There should be room to fit roll-resisting keels which are at least 3 ft wide amidships, to help counteract the effect of the shallow draft and the wide beam.

A rise of floor of 1.0 ft is tentatively selected. With a half-beam amidships of 36.5 ft and a half-siding of say 1.5 ft, this gives a floor slope of 1.0/35.0 = 0.0286, corresponding to slightly over 1.6 deg. The rise-of-floor to beam ratio is $\overline{RF}/B_X$ = 1.0/73 = 0.0137.

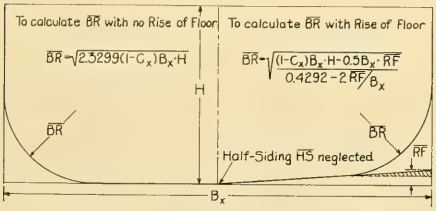

Fig. 66.F Formulas for Computing Bilge Radius $\overline{BR}$

Assuming for a starter that the floor line and the ship's side are both straight, and that the bilge contour is a circular arc, the appropriate formula of Fig. 66.F enables the bilge radius $\overline{BR}$ to be readily calculated. For the ABC ship this comes out as 10.76 ft, equal to $0.1474B_X$, for an A_X value of 1,815 ft^2 and a C_X of 0.9563. Taking a half-siding of 1.5 ft, a molded half-beam of 36.5 ft, and a molded draft of 26 ft, one-half of the maximum section is laid out as in Fig. 66.G.

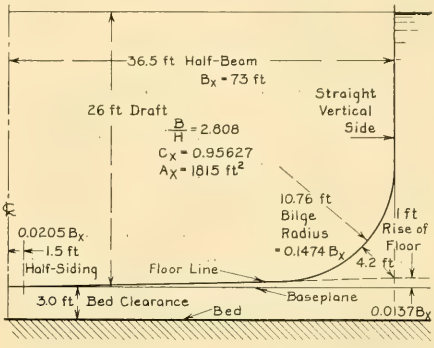

Fig. 66.G Half of Maximum-Section Contour for ABC Design

A heavy bed line is drawn in at h = 29 ft. The rise of floor and the slack bilge appear to provide ample room for backflow under and around the ship in the shallow and restricted areas of the river and the canal but of course the large corner radius detracts from the inherent roll-resisting characteristics of the hull. However, there is room enough for roll-resisting keels at least 4 ft wide amidships, if desired, without having them project below the floor line extended or beyond the extreme beam.

The first conflict between requirements now appears in graphic form. With the fairly large B/H ratio of 2.8, the large ratio of $\overline{BR}/B_X$ = 0.1474, and a value of $\overline{BM}$ that is certain to be large, there are indications of heavy rolling ahead, hence the need for deep roll-resisting keels. The compromise thus indicated between restricted-water and wavegoing needs may not be the best one but it will be allowed to stand for the time being. At least the restricted waters must be traversed twice every voyage while waves that produce deep rolling may or may not be encountered on every trip.

66.14 First Estimate Relating to Metacentric Stability. Before the preliminary design proceeds too far it is well to know the general situation relating to transverse metacentric stability. While this can not be determined accurately until the waterline shape is fixed, the waterplane coefficient C_W and other characteristics of the waterline generally are determined, in turn, by the metacentric-stability requirements.

In years gone by the value of C_W was approximated by the use of a ratio between (1) the prismatic coefficient C_P and (2) the waterplane coefficient C_W, known as the *relation coefficient,* symbolized by C_Y. This ratio was found to be more nearly constant than other ratios among the various form coefficients and was used for estimating C_W before the lines were drawn [Barnaby, K. C., BNA, 1948, p. 24].

Based upon the satisfactory service performance of a large number of merchant vessels, from small cargo ships to large liners, with data kindly furnished by the U. S. Maritime Administration, the diagrams of Fig. 66.H have been prepared. They give acceptable relationships between (1) the prismatic coefficient C_P and the waterplane coefficient C_W, corresponding to the relation coefficient just described, and between (2) C_W and the transverse inertia coefficient C_{IT}.

To use the diagram, start with the value of C_P, say 0.62 for the ABC ship, then cross horizontally to the lower diagonal line. The abscissa of this first intersection gives a good average value of C_W, in this case 0.713. Then go up this ordinate to the upper diagonal line, whereupon the ordinate of the second intersection gives the value of C_{IT}, approximately 0.561 for the ABC design. Because of certain differences in normal-form ships with different numbers of propellers there is one diagram for single-screw vessels and another for twin- and multiple-screw vessels. Using the values picked for the single-screw ABC design, the square moment of area of the waterplane works out as $I = [B_X^3(L)C_{IT}]/12 = [73^3(510)0.561]/12 = 9{,}275{,}150$ ft^4. The metacentric radius BM, equal to $I/\forall$, is 9,275,150/574,000 or 16.16 ft.

Long experience demonstrates that a reasonable value of transverse metacentric height to satisfy both comfort and safety requirements is about $0.06B_X$ [Niedermair, J. C., SNAME, 1936, pp. 419–420; INA, 1951, p. 144]. For the 73-ft beam of the ABC ship this gives GM = (0.06)73 or 4.38 ft.

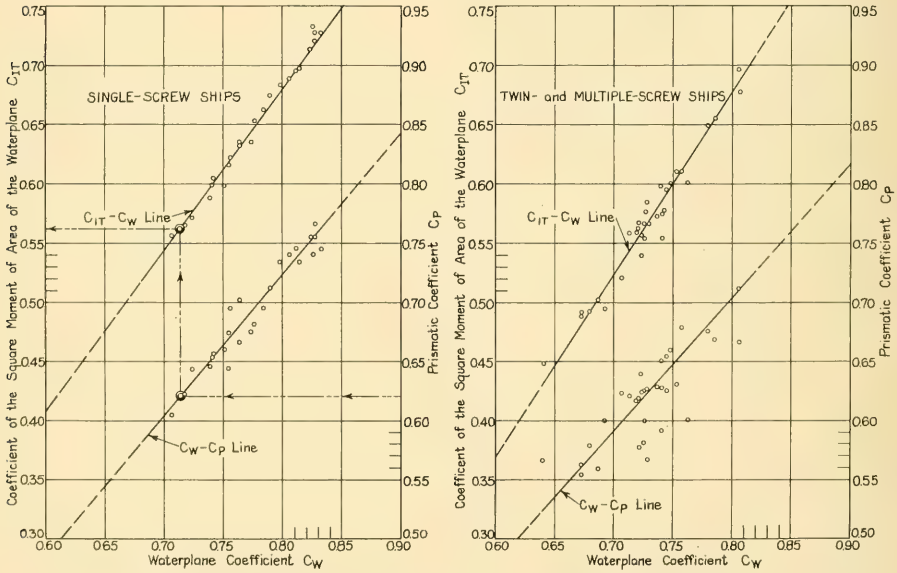

Fig. 66.H Data for Selecting Waterplane Coefficient and Transverse Moment-of-Area Coefficient for Given Prismatic Coefficients

The height $\overline{KB}$ of the center of buoyancy CB above the baseline is determined at this stage by the Normand formula, often known as the Morrish formula [Normand, J.-A., "Formules Approximatives de Construction Navale (Approximate Formulas for Naval Architecture)," Paris, Arthus Bertrand, 1870; Pollard, J., and Dudebout, A., "Théorie du Navire," 1890, Vol. I, p. 113; SNAME, 1893, p. 29]

$$\overline{KB} = H - \frac{1}{3}\left(\frac{H}{2} + \frac{\forall}{A_W}\right)$$

or (66.iii)

$$H - \overline{KB} = \frac{1}{3}\left(\frac{H}{2} + \frac{\forall}{A_W}\right)$$

For the ABC design at this stage H is 26 ft, $\forall$ is 574,000 ft^3, and $A_W = 510(73)0.713 = 26{,}545$ ft^2, whence $\forall/A_W = 574{,}000/26{,}545 = 21.62$.

Then $\overline{KB} = 26 - 1/3(13 + 21.62) = 14.46$ ft,

$$\overline{KM} = \overline{KB} + \overline{BM} = 14.46 + 16.16 = 30.62 \text{ ft},$$

$$\overline{KG} = \overline{KM} - \overline{GM} = 30.62 - 4.38 = 26.24 \text{ ft}.$$

This means that, with the assumptions made, the CG of the fully loaded vessel lies very nearly in the designed waterline. It should easily be possible to keep the CG below this limit, even with a fairly large abovewater hull and with the sizable upper works required for passenger quarters. On the other hand, the CG is not so high as to produce undesirable rolling features [Vedeler, G., INA, 1925, p. 166]. It is, in fact, somewhat lower in proportion than is customary for ocean liners [de Vito, E., INA, 1952, Table VIII; partial abstract in SBSR, 13 Nov 1952, pp. 642–643].

The expression KB^2/H is available as a rough check on the value of $\overline{BM}$, where k varies from 0.08 to 0.10 [Attwood, E. L., and Pengelly, H. S., pp. 111, 476]. For a rectangular box hull, $\overline{BM} = 0.083B^2/H$. For the ABC design, where B is at present 73 ft and H is 26 ft, $\overline{BM}$ = (say)$0.08(73)^2/26 = 16.40$ ft, compared to the value of 16.16 ft determined previously.

A complete preliminary design requires, at this or at a slightly later stage, an estimate of the vertical and horizontal CG position as determined by the weights [PNA, 1939, Vol. I, pp. 102–103], including if possible a check from the known values for a somewhat similar ship. It requires also an estimate of the transverse metacentric stability for the light as well as the loaded condition; possibly also for one or more intermediate loading conditions. As these are not directly a part of the hydrodynamic design they are omitted here.

The range of stability and the heeling or righting energy pertaining to dynamic metacentric stability are approximated, according to Sec. 68.6, when the abovewater hull has been roughed out.

66.15 First Sketch of Designed Waterline Shape. The next step in determining the shape of the vessel is to lay out the designed waterline. The diagrams of Fig. 24.G illustrate some historic yet highly instructive waterline shapes. Fig. 51.C depicts the actual designed-waterline shapes for six typical vessels in several speed-length groups. The B/B_X values for many other waterline shapes are to be found on the SNAME Resistance Data sheets.

Because of the effect of the waterline slopes forward upon surface wavemaking and of the waterline slopes aft upon separation, the shape of the waterplane depends upon the speed-length quotient T_q or F_n at which the vessel is to run. Since the relative speed of the ABC ship is rather high, with a T_q of 0.908 and an F_n of 0.270, a small waterline slope at the stem and an easy waterline in the entrance are indicated, to keep down the pressure resistance R_P due to wavemaking. With the small length-beam ratio of 6.986, and the likelihood of using a bulb bow, a considerable degree of hollowness in the entrance waterlines is a certainty. Taking into account the speed ratios listed and the C_P of 0.62, S. A. Vincent's data of 1930 [MESA, Mar 1930, Fig. 5, p. 139; revised unofficially to 1952] indicate something between a very hollow and a moderately hollow entrance waterline.

A study of nominal WL entrance slopes i_E for easily driven hulls, plus available reference data on the subject, produced the graphs of Fig. 66.I.

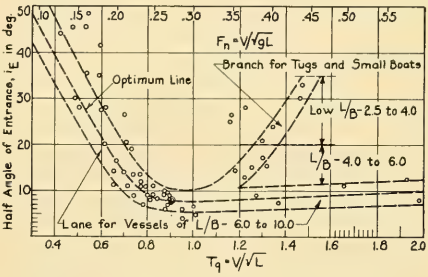

Fig. 66.I Graph of Design Values for Waterline Slope i_E at Entrance

These exclude the shapes of stems made blunt for construction or functional purposes only. Past practice, and good performance as well, indicated by the spots in the region of $T_q = 0.4$ to 0.75, has embodied—and justified, in a way—the use of large i_E values in these low-speed ranges. Further study of the large deflection drag undoubtedly associated with these blunt stems, plus consideration of the equally large wavegoing drag in head seas, calls for a reduction in these slopes, if practicable. The design lane in Fig. 66.I is therefore lower than one laid out to fence in most of the spots.

Because of the lower L/B ratio of short vessels, explained in Sec. 66.7 and indicated graphically in Fig. 66.E, their i_E values are necessarily larger. Fig. 66.I contains therefore a branched design lane for vessels of low L/B but high $V/\sqrt{L}$ ratios. The lane for vessels of $L/B = 6.0$ to 10.0 rises slightly at high T_q's because of the straight or slightly convex designed-waterline shapes used in the forebodies of these craft. For the ABC waterline entrance an i_E value of 7 or 8 deg appears suitable for the present, until the whole waterline is laid out and its characteristics are checked with various requirements.

Hydrodynamically, and for easy driving, any parallel waterlines at and near the surface are to be avoided, for the reasons given in Secs. 4.7 and 24.13. If parallel middlebody is used, parallel waterlines of course come with them. When vessels are built on slips or in docks of limited width, or when they have to pass through canal locks, some parallel waterline is inevitable, even without parallel middlebody. The lane on Fig. 66.J is an indication of what has been found acceptable in the past on vessels with varying C_P. Judging by this the ABC ship could have a parallel portion of the DWL up to about $0.22L$, but to keep the longitudinal waterline curvature more nearly constant a value of $0.0L$ is selected. This is also within the lane.

The fore-and-aft position of the *maximum* designed waterline beam B_{WX}, which may or may not be opposite the maximum-area section, is determined by the position of the latter to some extent. Nevertheless, for easy-driving ships these positions are well related to the C_P value, and hence are shown logically on different diagrams. Fig. 66.K gives a lane of good positions for a large range of C_P values. When there is any parallel waterline, the indicated position along the ship length is for the midlength of that

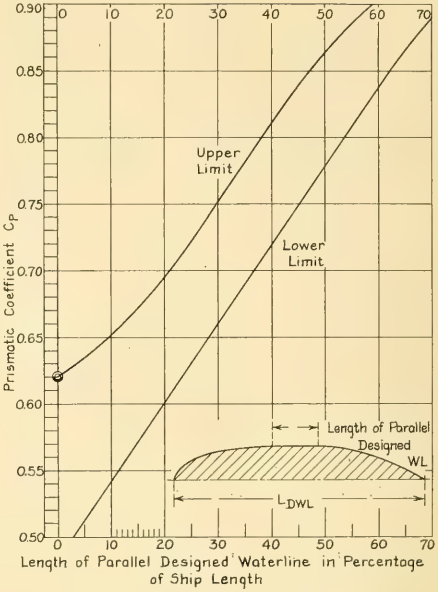

Fig. 66.J Design Lane for Percentage of Parallel Waterline

portion. On the ABC design the optimum position appears to be about $0.54L$; the exact position is not too important. It will probably depend upon subsequent adjustment of the DWL to achieve nearly constant curvature.

Inspection of the many waterline endings and run slopes i_R on the available SNAME RD sheets, for ships of normal form and with canoe or whaleboat sterns, together with those shown in Figs. 23.A, 24.G, and 51.C, indicates the extreme difficulty of shaping such a stern with a slope i_R of 15 deg or less. Even the TSS parent form, EMB model 632, with a C_W of only 0.66 and an L/B ratio of 6.85, has a run slope at the stern as high as 22 deg; see Fig. 24.G. One solution, and the one adopted here for the ABC afterbody, is to use an immersed-transom stern, along the lines described in Sec. 23.2 and illustrated in Fig. 23.A. A conservative preliminary figure for a not-too-wide transom beam B_U on the ABC ship is $0.3B_X$. This may have to be increased later to keep the run slopes down to the order of 12 or 13 deg.

Despite difficulties encountered with the wavegoing performance of certain full-stern vessels

of the past [Thompson, R. C., NECI, 1935–1936, pp. 216–217], no such problems have presented themselves with the multitude of full-stern and transom-stern vessels of the U. S. Navy built from the middle 1930's to the present. Since the transom stern proposed here is on the small side as transom sterns go, it is considered acceptable for this preliminary design.

It is now possible to sketch a tentative designed waterline for the ABC ship on the basis of the following:

(a) Length, 510 ft
(b) Slope at stem, 7 to 8 deg
(c) Entrance offsets from S. A. Vincent [MESA, Mar 1930, Fig. 5, p. 139], for T_q = 0.8 to 0.85, with hollow portion
(d) No parallel waterline
(e) Slope at stern, 13 deg, maximum
(f) Beam, maximum, 73 ft
(g) Position of B_{WX}, 0.54L, or 275.4 ft abaft FP
(h) Nearly constant curvature amidships
(i) $C_W = 0.713$; $A_W = 510(73)0.713 = 26{,}545$ ft^2

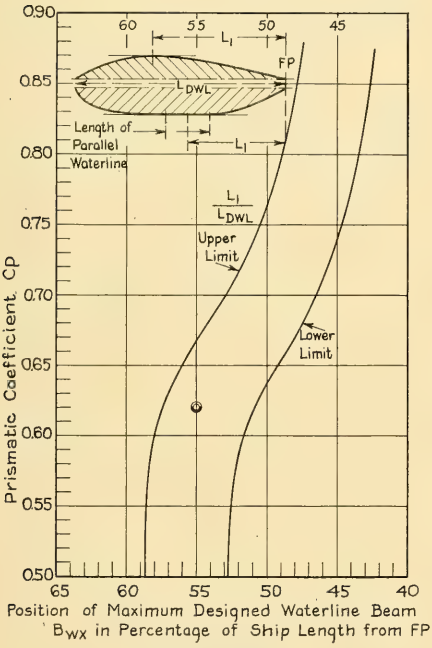

Fig. 66.K Fore-and-Aft Position of Maximum Waterline Beam B_{WX}

(j) Transom width $B_U = 0.3(B_X) = 21.9$ ft
(k) Transom radius in planform, tentative, 0.10L, or say 50 ft.

Several attempts produce a result that meets the requirements fairly closely. The preliminary sketches are not illustrated here but the final designed waterline shape appears in Fig. 67.A. A preliminary check of the curvature, by the graphic method described in Chap. 49, indicates that the early contours could stand some smoothing. However, before making another try at the designed waterline it is well to see how other parts of the underwater form work out.

66.16 Estimated Draft Variations. It is useful at this stage, as an aid in developing other features of the underwater body, to have some idea of the variations in draft to be encountered in the several variable-weight conditions. The first statement of these conditions, given in Table 66.d of Sec. 66.3, requires modification because of the changes in fuel weights. The second variable-weight statement appears in Table 66.f.

The *tons per foot* immersion for the designed-waterline dimensions tentatively selected are approximately 26,545/35 or 758.4 tons per ft, equivalent to about 63.2 tons per in. This value diminishes as the load decreases and the ship comes up in the water. The change is allowed for in a rough way by reducing the 758 tons per foot progressively to a guessed value of 725 tons per ft at the lighter drafts. On this basis the drafts corresponding to the entries in Table 66.f are about as set down in Table 66.g. These show that when the vessel is returning to Port Amalo through the canal it is some 975 t lighter than the designed maximum service displacement. When leaving Port Amalo it may be from 2,400 to 3,400 t lighter or even more, depending upon the liquid ballast carried. This decreases the mean draft by from 3.26 to 4.63 ft. It may be expected to reduce the maximum draft, with the stern down to keep the propeller under water, by at least 1.0 ft. The minimum bed clearance under the middle of the ship in the Port Amalo canal is then 28 − (26 − 3.26) = 5.26 ft, which is undoubtedly more than enough for the limiting speeds of 8 and 10 kt. The designed draft of the vessel might possibly be increased from 26 to 27 ft, but then the bed clearance in the river when leaving Port Correo would be 3 ft minus the fresh-water sinkage correction, or about 2.35 ft. This is smaller than the 3 ft indicated in Fig. 66.G.

TABLE 66.f—SECOND STATEMENT OF VARIABLE-WEIGHT CONDITIONS

This table, at the present stage of the design, supersedes Table 66.d.

Load Condition	Liquid Cargo, t	Package Cargo, t	Fuel, t	Consumable Stores, t	Total Aboard, t	Variation from Designed Condition, t
Designed maximum service, leaving Port Correo	4,000	3,000	1,550 (full capacity)	400	8,950	0
Arriving Port Amalo	4,000	3,000	875	100	7,975	−975
After unloading cargo, Port Amalo	0	0	875	50, min.	925	−8,025
Leaving Port Amalo in hurricane season, Condition H_1	2,000 as ballast	3,000	825	700	6,525	−2,425
Leaving Port Amalo expecting heavy weather, Condition H_2	3,000 as ballast	1,000 partial cargo	825	700	5,525	−3,425
Arriving Port Correo	1,000 as ballast	3,000	150 reserve	400	4,550	−4,400
After unloading, Port Correo	0	0	150 reserve	375	525	−8,425

It appears too small for the proposed river speeds of 13 and 14 kt.

A conference with the owners and operators at this point reveals that they have in mind amending the original requirements to call for taking on board, during certain seasons of the year, a substantial amount of the consumable food stores at Port Correo rather than at Port Amalo. This would increase the designed maximum displacement by the same amount and put the ship deeper in the water than the original 26.65-ft mean draft when starting down the fresh-water river. It is decided, therefore, not to increase the salt-water draft beyond 26 ft for the molded displacement of 16,400 t.

It is possible to estimate the moment to alter trim per unit value and the change of displacement per unit change of trim by the stern, using established methods [Owen, W. S., PNA, 1939, Vol. I, pp. 42–43]. However, such an estimate is not worth while at this stage because the underwater hull is not yet roughed out. The method of allowing for changes in trim for this particular design is described in some detail in Sec. 66.32.

Unloading all cargo at the same time at Port Amalo lightens the vessel by some 8,025 t, indicated in Tables 66.f and 66.g, while the same procedure at Port Correo reduces its displacement by some 8,425 t. These conditions correspond to mean draft reductions of the order of 11.07 to 11.62 ft. Although it is not done here, the transverse metacentric stability at these light loads must be carefully checked in a complete preliminary design.

66.17 Sketching the Section-Area Curve; The Maximum-Area Position. Sketching a preliminary section-area curve involves first a fullness ratio for the curve equal to the prismatic coefficient C_P selected. For the ABC design, this is 0.62. The section-area curves of the Taylor Standard Series [Taylor, D. W., S and P, 1943, p. 182], reproduced in Fig. 51.A, are good average curves. They are quite satisfactory for preliminary guides, with the limitations that the section of maximum area is at the midstation, there is no parallel middlebody, and the areas near the stern apply to a twin-screw vessel of normal form. References giving other sets of typical section-area curves for single-screw vessels, covering a rather wide range of C_P values, are listed in Sec. 51.6.

Working over the guide curve for the appropriate C_P requires preliminary selection of certain parameters, as follows:

(a) Position of the section of maximum area along the length, expressed as LMA and reckoned as a fraction of the length L abaft the FP, for the prismatic coefficient C_P that matches the Froude number or Taylor quotient corresponding to the designed speed

TABLE 66.g—First Statement of Variable Draft

The variations from the designed maximum service load are taken from the last column of Table 66.f. The sinkage value for fresh water is reckoned constant, at its maximum value.

Load Condition	Variation from designed load, t	Estimated tons per foot immersion	Estimated mean draft, ft
Designed maximum service, in salt water	0	758	26.0
Sinkage in fresh water, ft			0.65
Leaving Port Correo	0		26.65
Arriving Port Amalo	−975	750	24.7
After unloading at Port Amalo	−8,025	725	14.93
Leaving Port Amalo in hurricane season, Condition H_1	−2,425	745	22.74
Leaving Port Amalo, expecting heavy weather, Condition H_2	−3,425	740	21.37
Arriving at mouth of river below Port Correo, salt water	−4,400	735	20.01
Sinkage in fresh water, ft			0.65
Arriving at Port Correo	−4,400		20.66
After unloading at Port Correo, fresh water	−8,425	725	14.38 + 0.65 = 15.03

(b) Extent (L_P/L) and position of any parallel middlebody to be used. Normally the midlength of the parallel middlebody is at the fore-and-aft position selected for the maximum-area section.

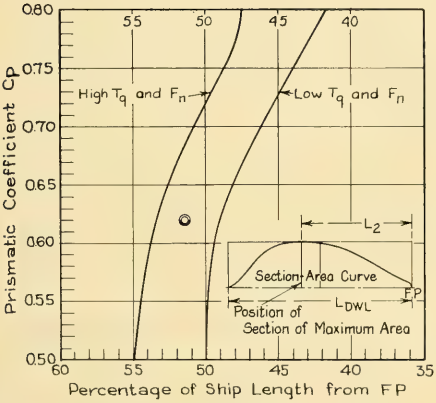

Fig. 66.L Longitudinal Position of Section of Maximum Area $\overline{LMA}$, or of Midlength of Parallel Middlebody

(c) Forward-perpendicular area ratio f_E and terminal value t_E of any bulb bow to be incorporated

(d) Area ratio f_R of any submerged transom to be embodied in the design.

In 1930 S. A. Vincent published a design lane giving the best location for the position of the section of maximum area, or for midlength of the parallel middlebody, in a range of T_q values less than 1.00, $F_n < 0.298$ [MESA, Mar 1930, p. 135]. This has since been revised with his assistance. Fig. 66.L gives the new lane, widened at low C_P's and narrowed at high C_P's. As for other lanes of this type, a designer need not remain between the fences if there are good and sufficient reasons for going outside.

For the ABC ship, with a C_P of 0.62, an optimum position of the maximum-area section is about $0.015L$ abaft midlength of the DWL. The value of $\overline{LMA}$ is then $0.515L$.

66.18 Parallel Middlebody. The next step is to determine whether or not any parallel middlebody is to be incorporated in the hull. If so, its extent (amount) and fore-and-aft position are

to be determined. Unfortunately, the results of the parallel-middlebody series of models developed by D. W. Taylor, reported in the 1943 edition of his book "The Speed and Power of Ships," pages 70–72 and 257–271, have not been analyzed and put in suitable design form. It is therefore necessary to use an empirical design curve. Taking as a basis Taylor's original 1910 diagram [the same as S and P, 1943, Fig. 83, p. 71], his data have been supplemented by parallel-middlebody percentages (L_P/L) for ship models on the SNAME RD sheets whose performance was equal to or better than that of the TSS model of the same proportions. When suitably extended to cover higher and lower values of C_P, the new plot of Fig. 66.M reveals that these ship data lie in a rather narrow lane running diagonally across the diagram. Since C_P and T_q (or F_n) are, for easily driven ships, related by the lower design lane of Fig. 66.A, the data recently analyzed are therefore plotted in Fig. 66.M on a basis of C_P only. The new design lane gives directly the proper ratio of L_P to L_{DWL}.

D. W. Taylor's original diagram [S and P, 1943, Fig. 83, p. 71], as well as Fig. 66.M, reveal that:

(a) Inserting parallel middlebody of length L_P is a definite advantage at low T_q and F_n values. For a given C_P it adds displacement amidships and allows finer ends. It also gives rectangular passenger and cargo spaces and may result in reduced building costs.

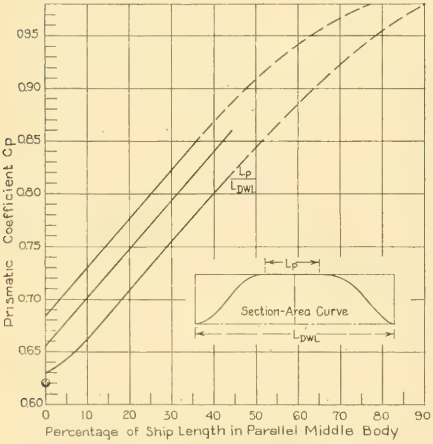

FIG. 66.M DESIGN LANE FOR PERCENTAGE OF PARALLEL MIDDLEBODY

(b) The ratio L_P/L, as it affects resistance, is insensitive to changes in the fatness ratio $\forall/(0.10L)^3$ or the displacement-length quotient $\Delta/(0.010L)^3$

(c) For a given T_q and C_P there is an optimum ratio of L_P/L. This optimum may be departed from materially without much increase in resistance. However, it is to be remembered that *excessive* amounts of parallel middlebody produce undesirable shoulders in both the section-area curve and the near-surface waterlines. They make the entrance too blunt and thus affect the resistance adversely. The design problem becomes one of balancing the return in increased displacement volume and the ease of construction against the price of added resistance and fuel consumption. At C_P values of 0.80 or higher the demand for carrying capacity on a given set of overall dimensions usually outweighs any endeavor to achieve the best hydrodynamic performance.

(d) Length of entrance L_E and run L_R are closely related to and should be considered with L_P, both as to magnitude and position of the latter. The fore-and-aft position of the midlength of the parallel middlebody is given by the value of LMA, the same as for the longitudinal position of the section of maximum area.

(e) Practical variations in L_P/L in a given case have little effect on the wetted surface and friction resistance

(f) The ratio L_P/L has a controlling effect on the ship's transverse wave pattern, for the reasons given in Sec. 25.10

(g) Hard spots or shoulders at the ends of the L_P are to be carefully avoided. These shoulders initiate their own wave systems and increase resistance.

Comparing Fig. 66.J, for percentage of parallel waterline, with Fig. 66.M for percentage of parallel middlebody, the values indicated on the former are always greater than those on the latter for any ship or normal form with tapered ends. The design lanes of these two graphs narrow in width with increasing C_P. Both vanish at the terminal point of $C_P = 1.00$, where the parallel waterline and the parallel middlebody both extend the entire length of the body or ship.

For the ABC design, with its C_P of 0.62, the amount of parallel middlebody given by Fig. 66.M is definitely zero. Assuming that in another design a certain amount of parallel middlebody is advantageous, this uniform section is, as indi-

cated in a preceding paragraph, placed with its midlength at the selected fore-and-aft position LMA of the section of maximum area.

66.19 Bulb-Bow Parameters. Considering next the forward end of the ship, it is determined first whether a bulb bow is advisable as a means of saving pressure resistance. This is governed largely by the ratio of the speed to the length at the point where maximum performance is desired. The greatest saving is in the region of a T_q of 1.0; it tapers off down to a T_q of about 0.75 or less and it diminishes at T_q values up to 1.5 or more. Inspection of F. H. Todd's Table 5 [IME, Feb 1945, p. 18], as well as of Fig. 67.D in Sec. 67.6, reveals that for the speed-length quotient of 0.908, corresponding to the trial speed of the ABC ship, a bulb bow is indicated.

It is to be borne in mind that this ship, for probably the greater part of its time at sea, will run at a speed closer to 18.7 kt than 20.5 kt. In other words, the T_q for the majority of service hours will approximate only $18.7/\sqrt{510} = 0.828$, $F_n = 0.247$. At this lower speed the bulb may show up to less advantage. Furthermore, a smaller f_E is called for than at the higher T_q of 0.908, in the ratio of about 0.07 to 0.08 or more.

The bulb parameters may be worked out by D. W. Taylor's method [S and P, 1943, pp. 65–70, 243–254]. However, it is pointed out in some detail in Sec. 67.6, where this procedure is illustrated, that it is rarely possible to utilize all of the optimum section area in a bulb, because of interferences with bower anchors and possible under-the-bulb slamming.

There is one other factor to be considered. In the lighter-load conditions on the ABC ship it is comtemplated that liquid cargo or water ballast in the tanks aft will be used to bring the stern down and to give the propeller adequate tip submergence. At these varied trims by the stern the bulb at the bow will be nearer the surface and will emerge at less angles of pitch than at full load.

If the proposed under-the-bottom anchor installation described in Sec. 68.11 does not work out, it may be necessary at a later design stage to fit bower anchors in the orthodox side locations. This consideration alone points to the wisdom of using, for the ABC design, a considerably smaller bulb area f_E than that indicated by the full-speed, full-load conditions. The value of $f_E = 0.02$ from the broken line of Fig. 67.D, representing installations of the past, is hardly enough to make a bulb worth while. An intermediate value of $f_E = 0.06$ lies within the optimum range, and it affords ample room for the bottom anchor contemplated, although it is somewhat lower than the optimum for the proportions of this vessel.

From the upper diagram of Fig. 67.D a value of $t_E = 0.9$ is tentatively selected for the designed range of T_q of from 0.828 to 0.908.

The detail design of the bulb is worked out in Sec. 67.6.

66.20 Transom-Stern Parameters. For an estimate of the immersed-transom area and the value of f_R it is assumed first that the transom is definitely to clear at the designed speed of 20.5 kt. In other words, at this speed the entire transom area is to be exposed to the air. On the assumption described in Sec. 67.20 that the corresponding Froude number, using the immersed-transom depth H_U as the length dimension, is limited to 5.0, this immersed depth works out as follows:

$$F_t = 5.0 = V/\sqrt{gH_U},$$

whence

$$g(H_U) = \left[\frac{20.5(1.6889)}{5.0}\right]^2$$

or

$$H_U = \frac{1}{32.2}(6.925)^2 = 1.49 \text{ ft}.$$

Taking the transom width previously agreed upon of $(0.3)73 = 21.9$ ft and a constant depth of 1.5 ft, the immersed-transom area at rest would have a maximum value of about 33 ft^2. The terminal value f_R is about $33/1{,}815 = 0.018$. A tentative value of $f_R = 0.02$ seems reasonable when first sketching the section-area or A-curve. Certainly it will not be larger than this.

Further details of immersed-transom design are given in Sec. 67.20.

66.21 The Preliminary Section-Area Curve. With the data thus assembled it is possible to lay down, in the standard 1:4 box described in Sec. 24.12, a tentative section-area curve for the ABC design. The typical A-curve on S. A. Vincent's 1930 data for a C_P of 0.60 [MESA, Mar 1930, Fig. 4, p. 138] is ticked in with dots on the plot. This is checked from the cross curves of W. P. A. van Lammeren [RPSS, Fig. 42, p. 92], from those of F. H. Todd for the TMB Series 60 [SNAME, 1953, pp. 516–589], or from similar sources, provided the curves lend themselves to vessels with bulb bows.

The position of the section of maximum area is marked as $0.515L$ from the FP. The tentative value of $f_E = 0.06$ is laid off at the FP and a tangent to the section-area curve at the FP is drawn by working backward the formula in Sec. 24.12. Since f_E is 0.06, the intercept ② is $1.00 - 0.06 = 0.94$. Multiplying 0.94 by 0.9, which is the tentative value of t_E, gives the intercept ④ as 0.846. Adding 0.846 to 0.06 indicates that the tangent at the FP intersects the midlength ordinate at a value of A/A_X of 0.906. Although the corresponding values are slightly different for the final section-area curve, Fig. 67.W illustrates the intercepts mentioned. The value of f_R is laid off as 0.02 but there are insufficient data to indicate a good terminal value of t_R. This preliminary A-curve is omitted for lack of space but the final curve is depicted in Fig. 67.W.

Integrating the preliminary curve numerically gives an underwater hull volume of 572,050 ft^3 and a C_P of 0.618. Both values are a little small when compared to the previous figures of 574,000 ft^3 and 0.62, but before modifying the curve it is well to see what the underwater form looks like when other requirements are applied. The first A-curve appears sufficiently fair to permit swelling or shrinking it here and there, but it must first be found where these volume changes are of most benefit to the ship. A discontinuity in the A-curve is to be expected at the stern, where the single-skeg area drops rather suddenly to zero.

In this connection it is to be remembered that ship sections, body plans, and waterlines, are customarily laid off to the molded dimensions of a ship. For a metal vessel this is to the outside of the framing and the inside of the plating. Furthermore, the rudder, roll-resisting keels, propeller, exposed shafting, and other appendages displace considerable quantities of water and thus help to support themselves. The volume occupied by the plating of a steel vessel is assumed equivalent to about 0.0075 times the molded volume if in-and-out strakes are employed. It is about 0.005 times that volume if the plating is flush, as in a welded vessel [Robb, A. M., TNA, 1952, p. 77]. The volumes occupied by the appendages are readily computed when they are roughed out.

For the ABC ship it may be assumed at this stage that the shell is to be rather fully welded and nearly all flush. Taking a value of 0.0055∇, the corresponding volume is $(0.0055)(574{,}000) =$ 3,157 ft^3 and the weight is $3{,}157/35 = 90.2$ t; say 90 t. This leaves a molded displacement of 16,400 t or 574,000 ft^3 as the end point in working up the final A-curve and the underwater hull form.

66.22 Longitudinal Position of the Center of Buoyancy. As an indication of the fore-and-aft position where the CG must lie, an integration of the preliminary section-area curve shows that the value of $\overline{\text{LCB}}$ is about 0.506 or $0.507L$, reckoned abaft the FP. This position is slightly abaft the midwidth of the lane in Fig. 66.N.

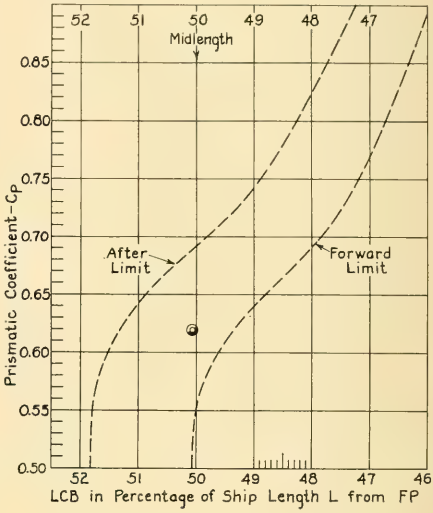

FIG. 66.N USUAL LONGITUDINAL POSITION OF CENTER OF BUOYANCY $\overline{\text{LCB}}$

Incidentally, this diagram differs slightly from that of Fig. 24.H in its extension to higher values of C_P. In view of the uncertainty in the position of the limits, the lanes in both figures are bounded by broken lines.

On most of the plots in this chapter, beginning with Fig. 66.A and ending with Fig. 66.N, there are spots formed by a pair of concentric circles with the lower half of the intervening space blacked in. These indicate the values of the several coefficients and parameters corresponding to the *completed* preliminary design of the ABC ship. They are the same as those listed for the fifth approximation in Table 66.e of Sec. 66.11.

66.23 Preparation of Small-Scale Profiles and Sections. The time has now come to see what the proposed ship is to look like. It is possible to

do this by sketching freehand on paper with light-blue cross-section lines, producing the result depicted in Fig. 66.O. Small profiles, sections, and deck plans, plus a midship section, bow and stern profiles, and a stern elevation to larger scale, suffice for this purpose. The first such sketches for the ABC design were drawn to a scale of 80 ft = 1 in. For a complete preliminary design these sketches would be supplemented by an inboard profile and several additional deck plans, drawn to a considerably larger scale.

The maximum-section contour of Fig. 66. G and the preliminary designed waterline form the bases of these sketches. A tentative freeboard amidships of 23 ft is selected and then checked as described in Sec. 66.30. A sheer line is drawn in, more or less by eye, with the low point of the deck well aft of amidships and with a sheer forward that looks right, to be checked later as outlined in Sec. 68.4.

A curved raking stem and a bulb that projects slightly forward of the FP complete the small-scale bow profile. At the stern the immersed-transom depth of 1.5 ft is laid off below the designed waterline and a stern profile raking slightly forward is added above it. The square transom is indicated as fading out above the waterline to a rounded main-deck planform at the stern.

The wide, somewhat shallow underwater form calls for rather drastic narrowing aft if proper flow to both top and bottom blades of a single propeller is to be achieved. A pronounced cutting up of the stern might give a reasonably good performance with twin screws; a twin-skeg form of stern almost certainly would. However, the use of two separate propelling plants for an output of the order of 16,000–20,000 horses involves increases in space, cost, weight, operating personnel, and so on. For the reasons elaborated upon in Sec. 69.2, it appears not justifiable.

The efficient, economic transportation required by item (5) of the mission, in Table 64.a, calls for high propeller and propulsive efficiency. One method of gaining the former is to use a screw propeller of the largest practicable disc area and diameter.

For the current style (1955) in single-screw merchant vessels having canoe or whaleboat (cruiser) sterns, a good rule for the propeller diameter D is to keep it less than $0.7H$ at the designed-load condition. This insures reasonable submergence at drafts not too much smaller than the maximum, and as good submergence as can

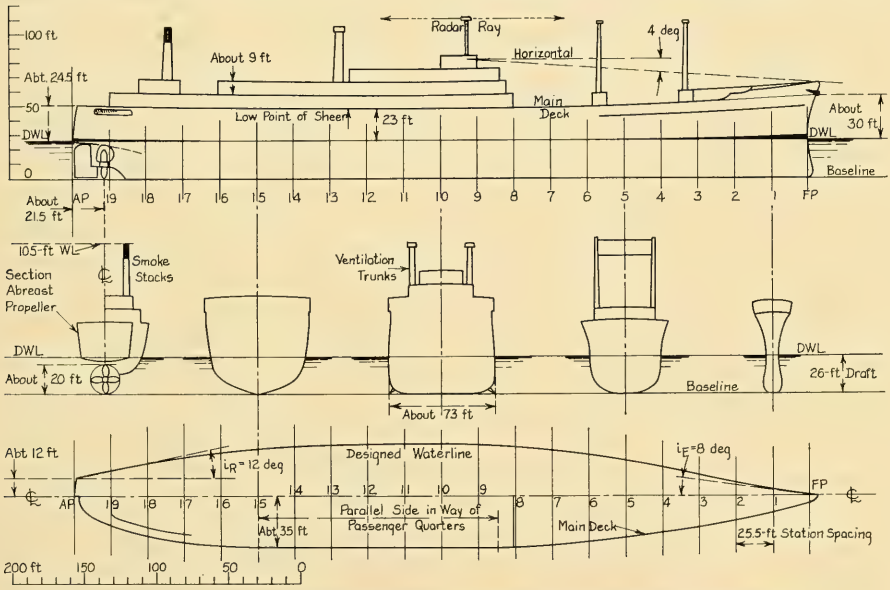

Fig. 66.O Sketches of Outboard Profile, Main Deck and Waterline, and Sections

be expected in wavegoing. With a draft H of 26 ft, this gives a limiting diameter of 18.2 ft. For better-than-average efficiency the propeller should be considerably larger, with a diameter of the order of 20 ft. The latter size is selected for the ABC ship, as the basis for further sketching.

It is soon found that, even by working reverse curvature into the buttocks ahead of the transom, it is difficult to make room for such a large propeller on the centerline. The situation is eased somewhat by eliminating the rudder shoe, carrying a semi-balanced rudder on a fixed horn, and dropping the propeller disc almost down to the baseplane. However, when enough fore-and-aft room is left for the rudder, the horn, and the propeller aperture abaft the upper blades, the propeller-disc position is rather far forward, where the buttocks are definitely curving downward. Flattening the under side of the main hull to fair into the transom leaves a sort of shelf of considerable extent just above the wheel. The latter is thus shielded exceptionally well from air leakage but it is difficult to provide a large tip clearance at the top center.

An adaptation of the twin-skeg stern with a single propeller mounted in the tunnel *between* the skegs offers advantages which appear to warrant the development of a preliminary-design variation along these lines. This arrangement eliminates many of the usual difficulties in single-screw sterns by:

(a) Removing from the vicinity of the centerline the lower apex of the V-sections in the skeg ending, the rudder shoe, and other obstructions which normally have to be accommodated abreast the propeller on the centerline

(b) Moving the propeller farther aft, where there is more vertical clearance between the baseplane and the buttocks, by shortening the fore-and-aft length of the rudders. There would be twin rudders behind the two skegs instead of a single rudder.

(c) Providing room for a propeller of greatly increased diameter because of the much smaller tip clearance needed inside the tunnel.

Further developments of this alternative stern, called an arch form, are described in Sec. 67.16. It becomes apparent, as the small-scale afterbody sketches proceed, that it may require different widths and shapes of the designed waterline in the run than the transom stern.

66.24 Molding a New Underwater Form. Within the framework of the selected ratios, proportions, coefficients, and parameters, plus the general shape tentatively selected in the preceding sections, it is now required to fashion a good underwater form. So far as propulsion is concerned, it should have the smallest practicable shaft power which will drive it at the designed maximum speed and meet the remaining specification requirements. It may or may not have a low total hull resistance, but it must embody a machinery plant that represents the minimum in first cost and in operating expenses consistent with durability and reliability.

The creation of such a shape, as the best final solution of a most complex flow and resistance problem in hydrodynamics, is probably as much a matter of unconscious understanding and of inspiration as of the straightforward use of all available hydrodynamic knowledge. The selection of a good underwater form as a guide is contingent upon the availability of a store of information on ship forms, contained in the designer's own files or in those available to him, in the technical literature, in the SNAME RD sheets, and in similar sources. It is equally contingent upon the availability, among those data, of a form resembling the one wanted, and on a certain amount of knowledge and good judgment, mixed with experience, when working over that form.

Many good shapes have been developed through a long process of intelligent refinement, as witness the Taylor Standard Series. For the ABC design being carried through here the Taylor Standard Series form has too low a maximum-section coefficient, 0.923 as compared to a range of 0.955 to 0.96, it has too low a waterplane coefficient, 0.66 as compared to at least 0.71, and it does not have a bulb bow. Further, as the TSS parent is essentially a twin-screw form, it appears not suitable for the single-screw project in hand, even though the B/H ratio of 2.92 is close to the ABC beam-draft ratio of 2.808. The TMB Series 60, block 0.60 parent form, having a C_P of 0.614, has too full a maximum section ($C_X = 0.977$) for the easy shallow-water driving required of the ABC ship, too small a B/H ratio (2.50), too much parallel waterline (15 per cent), and no bulb bow. Rather than to follow some other well-developed form of good performance, or to use it as a guide, a large-scale body plan for the new ship is roughed out on a clean sheet, both literally and figuratively, on

the basis of present hydrodynamic knowledge.

The guiding principles in this procedure are based upon an understanding of the water flow around a ship-shaped form, and the effects of this flow. One such principle is based upon the fact that, for the underwater hull of a surface vessel which varies not too widely from the normal, the upper layers of water met by the ship pass around the sides of the entrance while the lower layers pass under the bottom. This feature is illustrated by Figs. 4.O, 22.E, 24.L, 25.G, 66.R, and a number of diagrams in Chap. 52. In the run, the water which has passed around the sides rises rather rapidly toward the surface, so that toward the stern the water flowing over the hull is largely that which has come up from under the bottom. The shortest paths from the bow to the stern are, *in general*, those which cross the section lines at right angles, indicated by the position of flowlines when projected on the midsection and shown in a body plan. However, it is not always possible for the water to flow in this fashion under a more-or-less flat free surface and around a hull which must meet requirements other than those of minimum resistance.

Since neither the section shapes nor the flowline positions for an entirely new hull are known at the outset, this means that both have to be worked in simultaneously, as for the flowlines (streamlines) and the equipotential lines of a flow net, described in Sec. 2.20.

Compliance with this shortest-path rule, conformity to the general flow pattern described in the references listed, and consideration of curvature changes along the flowlines, calls for V-shaped sections in both the entrance and the run. Consideration of pressure resistance due to wavemaking, and of the height of the bow-wave crest in particular, calls for vertical-sided entrance sections in way of the bow-wave crest. A bulb bow does not work well into V-shaped bow sections, nor is it easy to fashion a deep forefoot from them, where the bulb must be. These considerations, coupled with the division of flow described in (1) of the following paragraph, indicate that U-shaped bow sections are to be preferred to V-shaped sections, for this ship at least.

Specifically, a few more detailed rules may be formulated for guidance in shaping the hull of the ABC design, with its B/H ratio of about 2.8 and its T_c of about 0.9. These should be part of a comprehensive set for a large range of B/H values, hull shapes, and speed-length quotients but making up this set is a formidable task not yet completed. The present additional rules are:

(1) Along the region of the designed waterline, extending below that line for the order of 0.20 to $0.25H$ at the bow, $0.9H$ amidships, and $0.10H$ at the stern, the water flows primarily around the sides. The position of the dividing line at the stem between the side and the bottom water depends also upon the height of the wave crest at the bow and the change of level at the bow when underway.

(2) To minimize surface wavemaking the changes in longitudinal curvature along the flowlines in this belt, as well as the curvature itself, should be a minimum. This embraces the *number* of curvature changes between bow and stern; the lowest possible number is two.

(3) Changes in curvature in the side-water region indicated in (1), at successively deeper depths below the designed waterline, should if practicable be offset longitudinally, and should not occur at any one transverse station. The reason for this is explained in Sec. 4.8 and the accompanying Fig. 4.I

(4) In the region at the stem below about 0.20 to $0.25H$, measured downward from the designed waterline, the water flows outward but then swings downward rather rapidly, to pass under the bottom inside the turn of the bilge, below about 0.9 to $1.0H$

(5) The twisting of the stream tubes accompanying this turning of the flow, depicted in Fig. 4.P, should be accomplished as easily and as gradually as practicable. Some remarks by D. W. Taylor, made many years ago [SNAME, 1907, p. 11], are still pertinent at this point; comments in parentheses are those of the present author:

"... this work shows the importance of an easy bilge, tolerably well forward, that is to say, at about one-quarter the length of the ship from the bow. The water is trying hard to get under the bottom, and if you have a shape such that it is difficult to get around the sections, you have a ship that is harder to drive. Some of our analyses of model trials appear to indicate that at about the point where the water wants to go under the ship, you ought not to have (a) full section—not over eighty-five per cent coefficient of fullness (section coefficient) at the outside."

(6) If the ship has a deep centerline skeg under the stern the stream tubes passing out from under the bottom must twist back again through nearly 90 deg as they approach the skeg ending. Assuming a single propeller carried by the centerline skeg the flow should, somehow or

other, be brought nearly parallel to the shaft axis as it passes into the propeller disc.

(7) The same as for the side-water paths, the changes in curvature along the bottom-water paths should be a minimum, both in number and magnitude. This means easy and gradual longitudinal slopes in the actual flowplanes, with small magnitudes of curvature.

So much for the general rules, to be kept in mind as sketching of the sections progresses.

The layout of the maximum-area section, taken from Fig. 66.G, forms the basis for the body plan. The station offsets of the tentative designed waterline are laid off along the 26-ft designed waterline trace on this plan and are numbered accordingly. Short vertical lines are sketched in through these points in the entrance, to serve as zero-flare references for the section lines where they cross the designed waterline.

The bulb-bow section at the FP is drawn first, following the rules of Sec. 67.6. A tentative section at Sta. 5 is then sketched in at the forward quarterpoint. Its section coefficient is taken from a curve of section coefficient based on ship length, similar to Fig. 67.I of Sec. 67.10. The section outline is tangent to the floor line at the bottom and to the vertical reference line at the DWL; a large radius or easy sweep is used below about $0.3H$. This is the region where the bottom water does its greatest twisting and where particular care is required to insure easy flowlines. Except for the designed-waterline region it is probably the most important part of the hull, at least in the entrance, and the part that has the greatest influence upon pressure resistance. Before easing the section at Sta. 5 too much, the area is measured and checked with the forward-quarter ordinate at Sta. 5 on the preliminary section-area curve. Section 5 is reshaped as necessary to give the proper area and section coefficient; see Sec. 67.10. This may involve a possible widening of the DWL. By the use of the bilge diagonal for fairing, or several waterlines, or both, it is fairly simple to sketch in the remaining entrance sections, meeting the designed waterline along the short vertical reference lines, including inside them the areas given by the preliminary section-area curve, and conforming to the section-coefficient curve. The abovewater portions of the section lines in the entrance are reserved for the time being.

Turning to the afterbody a tentative transom outline at the AP is next sketched, following the rules of Sec. 67.20. Since the afterbody is to terminate in nearly horizontal shelf-like sections approximating the form of the immersed portion of the transom it is evident that any centerline skeg must of necessity be relatively thin. This skeg will, in fact, form a sort of major appendage to be added under the main hull. The next step is therefore to sketch in, on a separate large-scale stern profile, the centerline or half-siding buttock, the one meeting the bottom of the transom and representing roughly the top of the skeg. There must be room at about the after quarterpoint, or possibly at one-fifth of the length from the stern, for a large-diameter motor or gear on the main shaft, low down in the vessel. The half-siding buttock therefore must start no farther aft than the after quarterpoint and must rise rather rapidly to meet the bottom of the transom. Indeed, if reverse curvature (concave downward) is to be worked into the after end of this buttock, as is desirable, the latter must rise at a rather steep angle forward of the concave portion. One must be prepared to bring it upward at a slope approaching closely the critical angle for separation at a submergence of about $0.7H$. It is known that the owners will require one or more model tests as a check on the performance of the underwater hull. It appears, therefore, that a centerline or half-siding buttock slope as steep as 17 or 18 deg may be risked at this stage of the design. Laying this buttock down to a large scale on what will eventually be the stern profile gives a series of heights for the termination at the centerline of all main-hull sections in the run.

Taking the after quarterpoint at Sta. 15 as a sort of midpoint in the run, an easy curve is swept in between the designed-waterline intercept and the half siding at the baseline. The lower or inboard portion of this section is made somewhat flat and the upper portion is given a slight outward flare at the DWL. The area at Sta. 15 is then measured and checked with the A-curve, whereupon the section is readjusted as necessary.

Sections between Stas. 10 and 15 are rather easily drawn, following the general procedure for the sections between Stas. 5 and 10. A section line is drawn first to meet the centerline buttock, as if there were to be no skeg; see the broken lines at Stas. 16 through 18.5 in Fig. 66.P. The skeg is then drawn in separately. However, the stations abaft 15 include the skeg as a part of the main hull, so some little sketching and re-

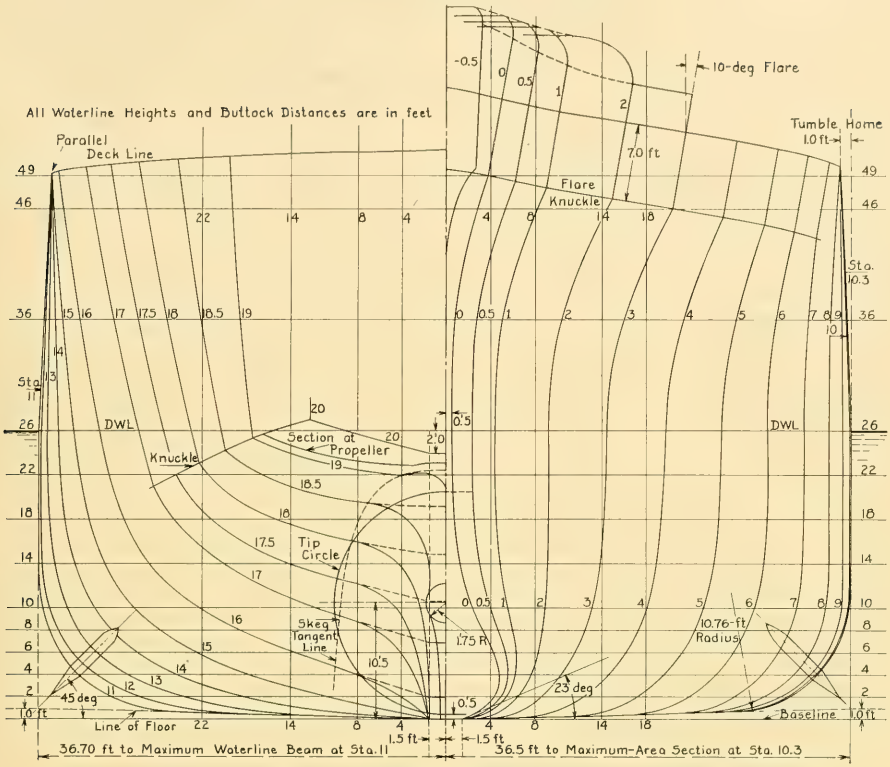

FIG. 66.P BODY PLAN OF ABC SHIP WITH SINGLE-SKEG TRANSOM STERN

adjustment is necessary to bring their areas into conformity with the tentative A-curve. As the skeg area diminishes to zero at the forward end of the propeller aperture, leaving only the main hull abaft that point, a discontinuity in the A-curve appears there.

Holding the waterline (level-line) slopes in the upper part of the skeg termination to a value not exceeding 15 deg involves a considerable amount of drawing and erasing. It requires the use of transverse fillets with rather small radii where the upper end of the skeg ending merges into the hull. However, these small fillets offer no particular disadvantage provided the resulting flow is generally parallel to the fore-and-aft line of fillets and does not cross it.

The body plan for the single-skeg transom stern is reproduced in its final form in Fig. 66.P.

The question of "clubbing" the lower part of the centerline skeg is discussed in Sec. 67.23. Since the aftfoot is to be cut away on the ABC design, working a club into the remainder of the skeg, just above the keel, would leave it rather far forward of the propeller to be effective.

66.25 Bow and Stern Profiles. To finish roughing in the centerline skeg the position and shape of its termination are added to a large-scale stern profile. This is done by starting at the transom termination—the location of the AP—and working forward. With a single skeg and a single screw, a single rudder is indicated. It should have some mechanical clearance ahead of the transom; 2 ft appears adequate at this stage.

To meet the maneuvering conditions in Port Bacine the rudder needs to have ample area. By the first approximation of Sec. 74.6 this area is say $0.02(L)H = 0.02(510)26 = 265.2$ ft^2. Assuming for the moment that the rudder height is

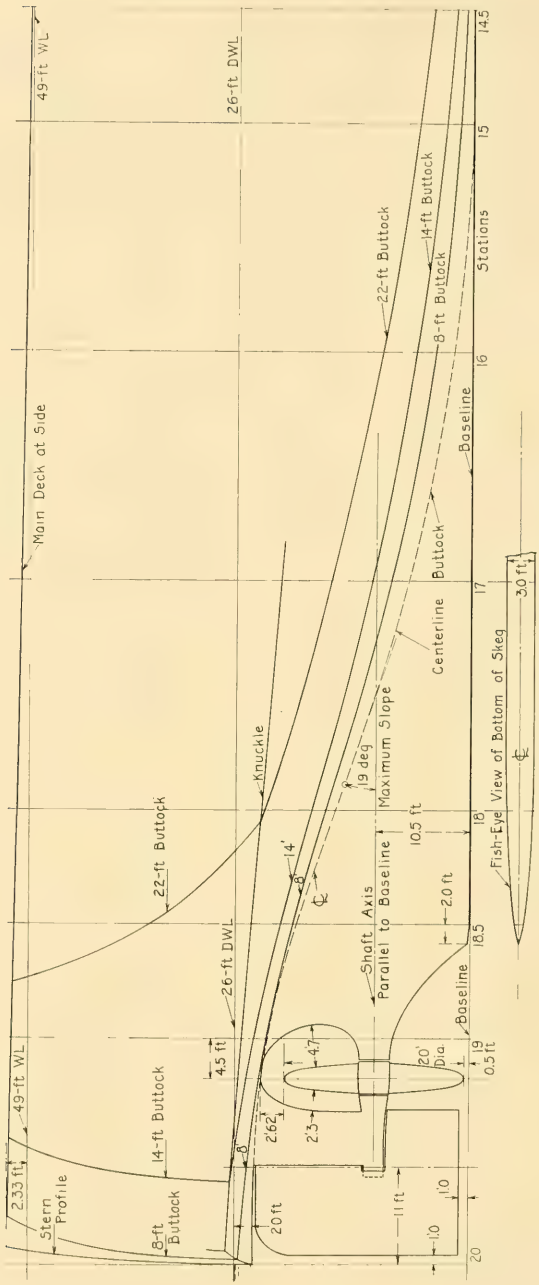

Fig. 66.Q Profile of Transom Stern with Single Skeg

about $0.7H$, or 18.2 ft, its fore-and-aft length is roughly 14.5 or 15 ft. With a clearance of 2 ft between the leading edge of the rudder and the after edges of the propeller blades, the after end of the propeller hub is of the order of 19 ft forward of the AP. Estimating the propeller hub as about 4 ft long, the plane of the propeller disc is about 21 ft forward of the AP.

At this disc position the height of the tentative half-siding buttock, already laid down, is about 23 ft above the baseline. When the aftfoot is cut away to save wetted surface and improve maneuvering, the propeller should have at least 0.5 ft clearance above the baseplane. With a tip clearance at the hull of about 2.4 ft, a rather small figure for a large wheel with a shelf-type stern above it, the relative tip or hull clearance for a 20-ft propeller works out as $0.12D$. It is doubtful whether a larger screw could be accommodated under this type of stern, on a draft of 26 ft.

The propeller tip circle is now drawn in on the body plan, and a rough outline of the propeller side projection added to the stern profile. Making the aperture clearance ahead of the upper blades at least $0.2D$ or 4 ft, rather larger than customary [ME, 1942, Vol. I, p. 275], terminates the upper aperture some 26.5 or 27 ft forward of the AP. This is the position into which the upper part of the skeg is to be faired. After the rudder is increased in area, and other small changes are made, the resulting stern profile is as delineated in Fig. 66.Q. The worked-out example in Sec. 59.11, combined with the design rules for propeller apertures in Sec. 67.24, and with the characteristics of the screw propellers found suitable for this design, indicate that the aperture forward of the upper blades is still somewhat small.

Details affecting the bow profile are covered in Secs. 67.4 and 68.7.

Before proceeding any further with the lines it is well (1) to insure that the wetted surface is not becoming too large in proportion to the size of the ship, and (2) to make a second check of the probable shaft power for a propeller D_{Max} of 20 ft. These are done in the sections following.

66.26 Analysis of the Wetted Surface. The wetted surface, by the estimate of Sec. 66.9, is to involve an expenditure of well over half the maximum designed power in overcoming friction. As a check it is useful to consider D. W. Taylor's broad conclusions on this subject [S and P, 1943, pp. 22–23]. They are adapted here to an analysis of the ABC design but they apply to any usual type and form of ship:

(a) For a given volume or weight displacement the wetted surface varies mainly with length, very nearly as $L^{0.5}$. At this stage it appears that the 510-ft length of the ABC ship is not too great in relation to other dimensions or with respect to the ship's mission.
(b) For a given displacement and length the wetted surface varies little within the permissible limits of beam and draft in service. With a B/H ratio of 2.808 and a C_X value of 0.956 for the ABC hull, reference to Fig. 45.H indicates that the wetted-surface coefficient C_S is in a region close to the minimum for normal vessels.
(c) For a given displacement and dimensions, the wetted surface is affected very little by minor variations of hull shape. The ABC sections are neither the extremely full ones which, according to Taylor, are somewhat prejudicial to low S, nor are they the extremely fine ones which are markedly prejudicial.
(d) After length, the most powerful controllable factors affecting wetted surface are the forefoot, the aftfoot or deadwood, and the appendages.

The parts listed in (d) have large surfaces compared to their volumes. For the ABC design the presence of the bulb bow should more than repay its extra wetted surface. It is proposed to cut the aftfoot away by an undetermined amount. The rudder, with its large surface in proportion to its volume, is necessary. The fixed horn to support it, if given a twisted or contra-form to recover energy in the propeller outflow jet, should likewise pay its way. The roll-resisting keels, not a part of the main hull, are considered in Sec. 73.18.

There is some added surface under the transom stern of the ABC ship. It is hoped that the extra friction drag of this surface may be overcompensated by the energy recovered in straightening (leveling) the flowlines of the water leaving the stern.

66.27 Second Approximation to Shaft Power. Making use of the thrust-load factor method for powering described in Sec. 60.14, the results for the ABC ship are as follows. From Sec. 66.9 the resistance R for the bare hull is estimated, in round figures, as 172,000 lb. An increase of 10 per cent for appendages gives an estimated final hull drag of 189,200 lb. The corresponding propeller thrust T for an estimated thrust-deduction

fraction t of 0.20 is 189,000/(1 − 0.20) = 236,500 lb.

The disc area A_0 of the 20-ft propeller is 314.16 ft^2. For an estimated wake fraction w of 0.30, the speed of advance V_A is 20.5(1 − 0.3) = 14.35 kt or 24.24 ft per sec. The ram-pressure load over the disc area is then $(0.5)\rho A_0 V_A^2 = qA_0 = 0.9953(314.16)(24.24)^2 = 183{,}725$ lb. The thrust-load coefficient C_{TL} is $T/qA_0 = 236{,}500/183{,}725 = 1.287$. The corresponding real efficiency, taken as $0.8\eta_I$ from Fig. 34.B, is 0.636. This is η_0 for the working condition of the propeller.

The hull efficiency η_H is $(1 - t)/(1 - w) = (1 - 0.2)/(1 - 0.3) = 0.8/0.7 = 1.143$. Assuming a relative rotative efficiency η_R of 1.02, the derived value of $\eta_P = \eta_0(\eta_H)\eta_R = 0.636(1.143)1.02 = 0.7415$. This is remarkably close to the value of $\eta_P = 0.74$ assumed in Sec. 66.9.

Until something further is known about the new hull shape and its probable performance, the latest derived power and machinery-weight figures from Secs. 66.9 and 66.10 are allowed to stand, namely 16,930 horses and 1,250 tons.

66.28 Sketching of Wave Profile and Probable Flowlines. The Standard-Series procedure developed by Taylor was an effort to predict, in advance of or without a model test, the probable effective power required to drive the bare hull of a ship of given proportions. This procedure omitted any means of judging the effects of changes in shape for fixed proportions. One method of accomplishing this is an analysis of the flow diagrams around a model of the selected shape. However, to employ this method for predictions, in advance of model tests, it must be possible to draw a lines-of-flow diagram from a rough set of lines, such as those of the ABC design at this stage.

Unfortunately, neither the method of analysis or the techniques of drawing the lines of flow in advance have been worked out. Nevertheless, the latter is attempted here, on the basis of the principles set forth in the sections preceding, and with the background of the diagrams in Chap. 52. If it is possible only to tell whether or not a form has objectionable features the prediction procedure is well worth while. In any case the experience gained will go far toward working out the unknown methods and techniques.

The first step is to start with the wave profile because the surface contour along the side affects the flow pattern below it. This effect extends all the way to the bilge if the Velox system waves are relatively deep.

It is observed from Figs. 52.I and 52.J that the height of the bow-wave crest is a function of the Froude number F_n or the speed-length quotient T_q and of the waterline slope i_E in the entrance. The bow-wave crest height (not necessarily the spray of the bow roll) becomes noticeable at a T_q of 0.5, F_n of about 0.15; at this low limit a small or a large waterline slope in the entrance appears not to have too great an effect, one way or the other.

Using the procedure described in Sec. 52.5, the bow-wave crest height for the ABC ship is calculated as 7.17 ft. This is measured from the plane of the undisturbed water level at a great distance from the ship. To find how far this crest may climb up the side of the ship there must be added the predicted sinkage or change of level of the bow. The graphs of Fig. 58.A give this change of level as $-0.0046L$ or $-0.0046(510) = -2.35$ ft. At the stern the change is about $-0.00145L$, corresponding to $-0.00145(510)$ or about -0.74 ft.

The predicted lag of the bow-wave crest, worked out in Sec. 52.5, is 13.86 ft. This is at about $0.027L$ abaft the FP, where the sinkage of the bow, by linear interpolation between -2.35 ft and -0.74 ft, is about 0.05 ft less than at the bow. The bow-wave crest may then be expected to rise up the side by (7.17 + 2.35 − 0.05) ft or 9.47 ft, indicated in Fig. 66.R.

It is almost certain that the effect of the bulb bow on the ABC ship is to lower the crest height predicted by the referenced formulas. However, no quantitative data are available, so this lowering is not taken into account. Since a small waterline-entrance slope and a bulb bow generally go hand in hand, it is probable that a substantial reduction in height occurs on vessels having these features.

When there is any flare whatever in the section lines lying inside a bow-wave crest, the wave profile rises higher on the ship's side than it would have if the section lines had been vertical.

The bow-wave crest heights as predicted for the ship and as observed on the model are intended to be independent of any thin spray roots extending above the crest line.

The graphs of Fig. 52.H and the procedure illustrated in Sec. 52.5 produce a predicted stern-wave height for the ABC design of 5.32 ft. This is for a normal form of stern, probably of the canoe

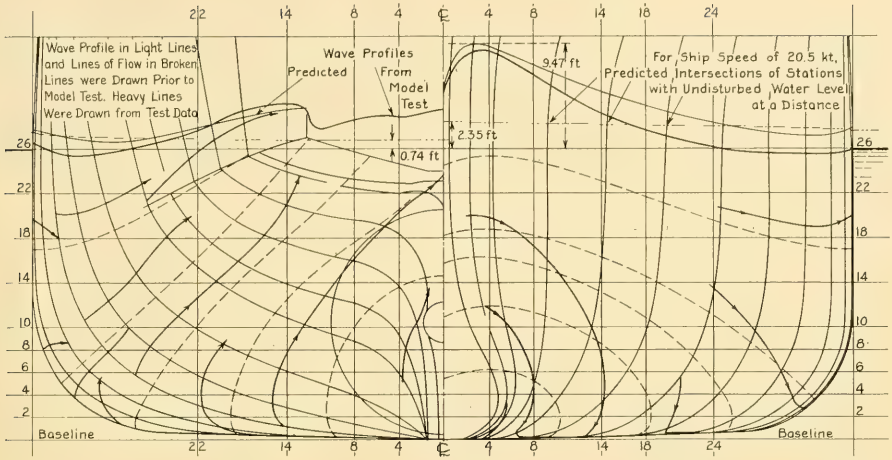

Fig. 66.R Predicted and Observed Wave Profiles and Flowlines for Bow and Single-Skeg Transom Stern

or whaleboat type; there are no known data to indicate what the stern-wave height would be for a transom-stern hull. Since the water closes in at a much slower rate along the small waterline slopes ahead of the transom, one might estimate a wave height above the surface of the undisturbed water at a distance of something less than 2/3 the predicted amount for a normal stern, say 3.55 ft.

The stern-wave crest may be expected to climb up the side of the ship at the outboard corner of the transom by this amount plus the stern sinkage of 0.74 ft, or about 4.29 ft.

The data listed in Sec. 52.6 indicate that a ship corresponding to the ABC design, running in a range of T_q values from 0.828 to 0.908 (from 18.7 to 20.5 kt), F_n of 0.247 to 0.270, is accompanied by transverse waves of the Velox system about half as long as the ship. At 20.5 kt there is a first crest about $0.027L$ abaft the FP, a second crest at about amidships, and a third crest at or near the stern. As a matter of interest, the length of a trochoidal wave at the 20.5-kt speed of the ABC ship is, from Table 48.d and the accompanying formulas, 234.3 ft. This is roughly $0.46L$. The general pattern for these and other speed ranges, on cargo-ship models, is shown in Figs. 52.I and 52.J.

Furthermore, it is known that when the T_q value coincides with the position of one of the hollows along the lower edges of Fig. 66.A there is a prominent wave crest at the stern. When it coincides with a hump, there may be a wave hollow at the stern, or a crest of greatly diminished height.

The *exact* shape of the accompanying wave profile is manifestly a function of the shape of the hull and of certain distinctive features, some known and some unknown. If a ship waterline has pronounced shoulders, not necessarily as sharp as those of the parallel-sided, wedge-ended form of Fig. 10.F, secondary wave systems are generated. Their transverse Velox waves combine with those of other systems to form a rather complex pattern. A predicted wave profile for the ABC hull with a single-skeg transom stern is sketched in light lines in Fig. 66.R *before* any test runs are made on a model.

To predict the flowline positions it is estimated that the dividing point on the stem, between the water passing around the side and that under the bottom, is relatively high, because of the large B/H ratio and the expected drop of the bow of about 2.4 ft. A figure of $0.3H$ or 7.8 ft below the DWL appears about right; this is at the 18.2-ft WL. The flowlines sketched in the forebody resemble those of diagram 3 in Fig. 4.O, and of the many illustrated in Chap. 52.

It is to be expected that the wave profile, representing a constant-pressure upper boundary, will influence the shape of the flowlines passing around the side, perhaps down to the 10-ft waterline or below.

The flowlines under the nearly flat bottom, not

shown in Fig. 66.R, may be expected to diverge slightly with distance as they move aft. Under a run that is roughly flat, or of a shallow V-shape, the flowlines lie generally along the buttocks, parallel to the centerplane of the vessel. When the buttocks terminate at a knuckle under water, as at Stas. 18 to 20 in Fig. 66.R, the flowlines lying somewhat parallel to the buttocks may be expected to leave the ship surface at the knuckle.

The predicted flowlines are indicated in light broken lines on the body plan of Fig. 66.R. The actual flowlines, determined from a test of a 20-ft model, using chemicals on the model surface, are shown in heavy full lines in the figure. The wave profile marked along the side of the model is indicated also by a heavy full line.

66.29 Comparison with a Ship Form of Good Performance. It is still possible, with a given set of principal proportions and form coefficients, to vary the underwater shape within rather wide limits, and to obtain perhaps wider variations in the resistance for a given F_n . Existing forms, often several of them, are therefore wisely used as guidance or as a means of keeping one from getting too far afield. Certainly a well-tried parent form or a ship form which has a high merit coefficient and which has proved itself in service can be employed as:

(1) A starter for laying down a set of lines
(2) A sort of running comparison as the hull shaping proceeds
(3) A reference, after model tests have been made, for judging the performance of the new form.

If future progress is to be made, however, past or existing forms should not be too slavishly copied unless one knows rather accurately just what features are responsible for their good (or bad) performance. The designers of these forms would be the first to admit that they could unquestionably be improved with further thought and effort.

Following a series of model tests, comparisons may be made of the effective powers of a new design with the effective powers of the TSS ship of the same proportions. This comparison for the ABC hull, comprising the transom stern designed in this chapter and an alternative arch stern described in Sec. 67.16, is to be found in Sec. 78.16 and Figs. 78.J and 78.K.

66.30 Abovewater Hull Proportions for Strength and Wavegoing. The ABC ship requires, as do many others, rather large internal volumes for accommodating the passengers and crew and for carrying the machinery and cargo. The ratio of total hull and superstructure volume to underwater hull volume of 2.77, derived previously in Sec. 66.8, is therefore somewhat large. It appears that the abovewater hull will stand rather high out of the water. A flush-deck type of ship is indicated, as in Fig. 66.O, possibly with a short forecastle to give added freeboard and hull depth at the stem, and with so-called tonnage openings below the main deck near the stern.

Taking for a starter a minimum freeboard of 23 ft at the lowest point of the deck at the side, the hull depth D is $26 + 23 = 49$ ft. By the criteria of C. R. Nevitt [ASNE, May 1950, pp. 318–319] and others, it appears that the 49-ft depth and the L/D ratio of 10.4 lie within a good design range for a length L of 510 ft and a draft H of 26 ft. The ratio of draft H to depth D is $26/49 = 0.531$. The depth from the keel to the top of the highest superstructure, when related to the beam, is approximately

$$[26 + 23 + 3(9)]/73 = 76/73 = 1.041.$$

Based upon Atlantic-liner practice [de Vito, E., INA, 1952; partial abstract in SBSR, 13 Nov 1952, pp. 642–643] this ratio could be as high as 1.16 or 1.20. In any case, it is assumed that the necessary preliminary strength calculations, not gone into here, show the assumed hull depth of 49 ft to be adequate for a static wave whose height is $1.1\sqrt{L}$, or $1.1\sqrt{510} = 24.84$ ft [Niedermair, J. C., "Ship Motions," ASNE, Feb 1952, p. 14]. Fig. 48.E in Sec. 48.7 embodies a graph of these heights for various wave lengths.

The ship appears to have adequate freeboard throughout, of the order of $0.045L$ or more, when the abovewater hull is made large enough for the volumetric capacity and for the required depth of ship girder. A detailed study of the abovewater hull, taking all necessary factors into consideration, is given in Chap. 68. A further study of its ability to meet all wavegoing service requirements is deferred to Part 6 in Volume III.

However, it is possible at this stage to make the first estimate of its natural rolling period. For this estimate the added mass of the surrounding water is not taken into account, partly because it is not known, and partly because the actual period is then longer than the estimated one. As a result, the ship should be somewhat more comfortable than predicted.

Using the standard formula [PNA, 1939, Vol. II, p. 11, Eq. (22)] and assuming different values for the gyradius k and the transverse metacentric height $\overline{GM}$.

$$T = \frac{2\pi k}{\sqrt{g\,\overline{GM}}}$$

(1) For a $\overline{GM}$ of $0.06B_X$ or 4.38 ft,

(a) When $k = 0.25B_X$ or 18.25 ft, $T = 9.65$ sec, for a complete roll. This is somewhat too small for the comfort of passengers and the safety of package cargo.

(b) When $k = 0.30B_X$ or 21.9 ft, $T = 11.58$ sec. This is still rather short for comfort, on a rolling ship, but not too short as to be disturbing at this stage.

(2) For a $\overline{GM}$ of $0.04B_X$ or 2.92 ft,

(a) When $k = 0.25B_X$ or 18.25 ft, $T = 11.82$ sec

(b) When $k = 0.30B_X$ or 21.9 ft, $T = 14.19$ sec.

It is apparent that, with the large beam, the lowest permissible $\overline{GM}$ will produce the most comfortable ship.

66.31 First Longitudinal Weight and Buoyancy Balance. Before completing this first stage of the preliminary design it is necessary to determine approximately whether, for the designed maximum service-load condition:

(a) The ship has reasonable longitudinal balance, with the CG in nearly the same transverse plane as the CB

(b) The volumes of the various parts of the ship, as well as of the passenger quarters and cargo spaces, can be contained within the total volume of the hull and superstructure. This requires a re-check of the hull volume estimate of Sec. 66.8.

(c) There is sufficient room within the hull structure for certain large items such as reduction gears or motors on the propeller shaft

(d) The hull volume is so large as to be objectionable from the standpoint of ship handling in a strong wind.

A body plan on a much larger scale than the small sketches of Fig. 66.O is now available in Fig. 66.P for an adequate estimate of the areas, volumes, and moments to be used in this operation. Further, it is assumed that the abovewater hull has already been roughed out, as in the upper part of Fig. 66.P, and that a rough outline has been made of the upper works (superstructure). It is now possible to sketch in the principal subdivisions between passenger and crew accommodations, package-cargo space, liquid-cargo tanks, fuel-oil tanks, and machinery spaces. These are indicated by the hatched areas on the profile of Fig. 66.S.

A rough integration of these volumes, allowing 5 per cent for ship structure in the dry spaces, gives the tentative volumes of Table 66.h. For comparison there are listed also the required volumes of Sec. 66.8.

It is next necessary to determine whether the

TABLE 66.h—SECOND ESTIMATE OF VOLUMES FOR ABC DESIGN

Item	Required Weight, t	Required Volume, ft³	Estimated Volume, less Structure, ft³	Comments
Liquid bulk cargo	4,000	168,000	180,140	Somewhat larger than necessary, but permits shifting volume and weight to obtain required $\overline{LCG}$
Package cargo	3,000	300,000	308,030	
Propelling machinery	1,250	300,000	293,900	May require some of liquid cargo space. Includes no space above main deck.
Fuel oil	1,550	65,100	82,560	Additional volume permits cofferdams not shown in Fig. 66.S
Consumables	700	70,000	65,930	Can take some space from fuel oil or use some double-bottom space
Officers and crew		100,000 (est.)	34,020	Deficiency accepted for time being
Passenger quarters		400,000	402,970	

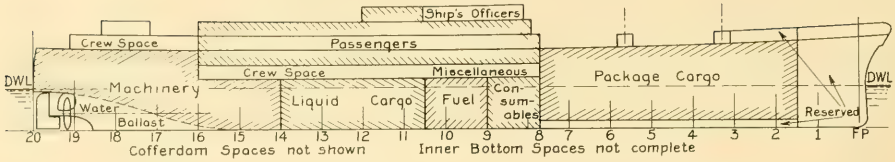

FIG. 66.S TENTATIVE DISTRIBUTION OF PRINCIPAL VOLUMES IN THE ABC DESIGN

ship trims properly with the principal weights in the locations indicated. Selecting approximate centers of gravity for each of the items the longitudinal weight balance comes out as indicated at the bottom of Table 66.i.

This tentative balance for the designed-load condition is necessarily crude. The volume and location of the package-cargo spaces, the tankage, the machinery spaces, and other items on Fig. 66.S are still only approximate. Since these matters involve static problems only, not directly related to the hydrodynamic design, they are followed only to the point of checking the trim in two of the variable-weight conditions, described in Sec. 66.32.

However, an important hydrodynamic-design rule, for these as well as for the later stages described in Chap. 67, is well kept in mind: If, after developing what is considered to be an easily driven hull shape, the CG is found to be offset from the CB of that shape, do not change the shape to bring the CB to the CG position. Rather, rearrange the internal spaces, volumes, and weights to bring the CG to the CB position of the low-resistance hull.

66.32 Propeller Submersion and Trim in Variable-Load Conditions. Having found reasonable agreement in the $\overline{\text{LCG}}$ and $\overline{\text{LCB}}$ values for the weight balance in the designed-load condition, at the 26-ft draft in salt water, there remains to consider the situation when:

(1) The vessel is only partly loaded, as when leaving Port Amalo in the hurricane season, condition H_1 of Table 66.f of Sec. 66.16

(2) When arriving at the river mouth below Port

TABLE 66.i—FIRST LONGITUDINAL WEIGHT BALANCE

Moment arms are in terms of station spacing, 25.5 ft. Moments are taken about the midlength at the DWL, Sta. 10.

Item	Weight, tons	Arm forward	Moment forward	Arm aft	Moment aft
Liquid cargo	4,000			−2.25	−9,000
Package cargo	3,000	+5	+15,000		
Hull and fittings	5,870			−0.333	−1,955
Propelling machinery	1,250			−6	−7,500
Fuel oil	1,550	+0.25	+388		
Consumables (part load)	400	+1.63	+652		
Margin (at $\overline{\text{LCG}}$)	330	0	0	0	0
Total	16,400	For'd.	16,040	Aft	−18,455 16,040 −2,415

$$\frac{-2{,}415}{16{,}400} = 0.1473 \text{ station-length abaft Sta. 10}$$

The tentative CG position is at Sta. 10.1473 so that $\overline{\text{LCG}}$ is 0.5074 L. Since the tentative $\overline{\text{LCB}}$ is 0.506 L, it should not be difficult to bring the CG forward by 0.0014 L or about 0.71 ft.

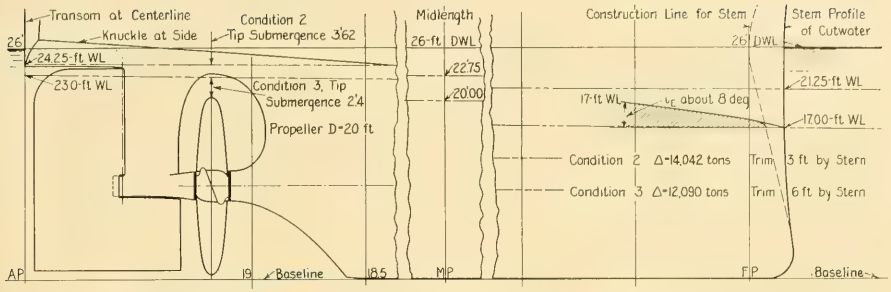

Fig. 66.T Selected Inclined Waterlines for the Two Principal Variable-Weight Conditions

Correo. Table 66.g indicates that the estimated mean drafts under these two conditions are 22.74 and 20.01 ft, respectively. For round numbers assume that these are 22.75 ft and 20.00 ft, involving reductions in the 26.0-ft mean draft of 3.25 ft and 6.00 ft.

It is useful to have an idea of the changes in trim for a given internal arrangement of the principal weights. It is necessary at some stage of the preliminary design to check on the transverse metacentric stability for these two loading conditions. However, the most important hydrodynamic feature is to keep the propellers well under water, with a reasonable tip submergence and as good shielding from air leakage as can be obtained.

The procedure followed in the ABC design is first to establish two drafts aft, corresponding to the two variable-weight conditions, which will insure air-free flow to the propeller. Following this, the internal weights are so arranged that the centers of gravity in the two loading conditions coincide with the CB's for the displacements and stern drafts selected. A check is then made to insure that, if a bulb bow is used, as in the present case, it will not be too close to the water surface for open-sea running. The stern draft for the heavier condition, 16,400 t − 2,425 t = 13,975 t, is made 24.25 ft, to place the bottom of the transom at the AP a few inches under water in the at-rest condition. The stern draft for the lighter condition, 16,400 t − 4,400 t = 12,000 t, is selected as 23.0 ft, which gives a tip submergence at the propeller disc of just under 2.5 ft. Fig. 66.T illustrates these features. While this submergence is admittedly small, both absolutely and relatively, the propeller is running at a considerably smaller thrust-load factor at this light displacement. Furthermore, the stern-wave crest at 20.5 kt should be sufficient to fill all the volume between the at-rest waterplane and the under side of the hull just forward of the transom.

Projecting the traces of the two waterlines

TABLE 66.j—Weight, Buoyancy, and Stability Data for Two Variable-Weight Conditions of the ABC Ship

The figures given apply to the molded shape and dimensions of the transom-stern underwater hull, for which the weight displacement, molded, in standard salt water is 16,400 tons.

Mean draft, ft	22.75	20.00
Tons less than designed weight, from Table 66.g	2,425	4,400
Weight displacement, nominal, t	13,975	12,000
Trim by the stern, selected, ft	3.0	6.0
Volume displacement, from molded lines, ft³	491,147	422,900
Corresponding weight, at 35.977 ft³ per ton, t	14,042	12,090
Tons less than designed weight, actual	2,358	4,310
$\overline{LCB}$, in fraction of L from FP	0.508	0.513
Coefficient of square moment of area C_{IT} of WL about x-axis	0.512	0.503
Calculated $\overline{BM}$, ft	17.37	19.80
Inclined waterplane area, ft²	26,220	25,670
$\overline{KB}$, estimated, from Normand formula, Sec. 66.14, ft	12.72	11.18
$\overline{KM}$, derived, ft	30.09	30.98
$\overline{KG}$, estimated, ft	27.00	27.50
$\overline{GM}$, probable, ft	3.09	3.48

TABLE 66.k—LONGITUDINAL WEIGHT BALANCE FOR 20-FT MEAN DRAFT, 6-FT TRIM BY THE STERN

From Table 66.j, $\overline{LCB}$ is 0.513 L from the FP. This corresponds to a CG location at Sta. 10.26, or 0.26 station-length abaft Sta. 10. With a weight displacement of 12,090 tons, from Table 66.j, the corresponding after moment, in terms of tons times station lengths, is −0.26 (12,090) = −3,143.4.

Item	Weight, tons	Arm forward	Moment forward	Arm aft	Moment aft
Water ballast, after peak tanks	910			−7.0	−6,370
Water ballast in liquid-cargo tanks	180			−3.6	648
Package cargo	3,000	+5	15,000		
Hull and fittings	5,870			−0.333	−1,955
Propelling machinery	1,250			−6	−7,500
Fuel oil	150	+0.25	38		
Consumables	400	+1.3	520		
Margin (at 0.5075 L)	330			−0.15	−50
Total	12,090		+15,558		−16,523

Even with a very large capacity assumed for the after peak tanks this still lacks 2,178 station-tons of being sufficient after moment to bring the CG to Sta. 10.26 and to give the ship a trim of 6 ft by the stern.

forward to the midlength drafts of 22.75 and 20.00 ft, as on Fig. 66.T, gives drafts at the FP of the ABC ship of 21.25 and 17.00 ft, respectively. The entrance at the 17-ft WL has an i_E of only 8 deg, and the widest portion of the bulb is some 13 ft below the at-rest waterline at the bow. This should be sufficient for good average performance in the open sea.

Working over the body plan of Fig. 66.P up to the two inclined waterplanes in question gives the weight, buoyancy, and stability values listed in Table 66.j. It is to be noted that the weight reductions for the displacements corresponding to the two inclined waterlines of Fig. 66.T are 2,358 t and 4,310 t, as compared to the reductions of 2,275 t and 4,400 t from Table 66.g. The assumed variable-weight conditions are only approximations, so the displacement reductions as derived from the inclined waterlines are used for the remainder of the analysis.

The problem is now one of internal arrangement, to insure that the CG's for the two variable-weight conditions can be brought to the calculated CB positions. Since the $\overline{LCG}$ for the lighter condition appears to be the most difficult to achieve, Table 66.k is made up to find what can be done with the internal layout of Fig. 66.S.

Only by crowding a very large volume of water into the after peak tanks, involving some wing tanks abreast the machinery space not previously contemplated, is it possible to obtain an after moment at all. This value still lacks 2,178 station-tons, or 55,539 ft-tons, of the necessary amount to trim the ship the required distance by the stern.

Another difficulty arises because of the large hogging moment imposed on the ship by the full capacity of package cargo forward, the heavy water ballast way aft, and the nearly empty liquid-cargo tanks near amidships.

Regardless of the problems facing the designer at this point, problems not directly involving hydrodynamics which are not worked out here, the method of attack for efficient propulsion in the variable-load conditions is considered basically sound. In this connection there are quoted the suggestions of N. H. Jasper and L. A. Rupp for new ship designs [SNAME, 1952]:

Page 344. "(e) Give greater consideration to providing increased volume in after-ballast tanks of cargo vessels to maintain a fully submerged propeller, if practicable."

Page 354. "5. *Ships should be operated at a condition of trim which will insure immersion of the*

propeller. In the design stage, consideration should be given to increasing the capacity of the after ballast tanks of cargo vessels to permit fully submerged propeller operation."

66.33 First Approximation of Steering, Maneuvering, and Shallow-Water Behavior. It is difficult to obtain an idea of the steering, maneuvering, and shallow-water characteristics of the hull as roughed out at this early stage of the design. Nevertheless, something should be known of them before the preliminary design proceeds much further.

Good steerability, as pointed out in Part 5 of Volume III, is largely a matter of avoiding excessive dynamic instability of route and providing sufficient swinging moment through the use of the rudder. The former is largely a function of the amount and position of the fixed and movable fin area at the stern, comprising the rudder, horn, skeg, and the like. It may depend somewhat on the shape and proportions of the hull. In the ABC design there is considerable latitude in the rudder and skeg areas, especially because the aftfoot is to be cut away by a "suitable" amount. The swinging moment is a function first, of the shape and area of the rudder, and second, the magnitude of the lateral forces which may be expected on a rudder horn, if fitted, and on the adjacent portions of the main hull. The amount of the swinging moment, in turn, depends on the ease—or difficulty—with which the ship is swung to a drift angle that generates sufficient inward lift to balance the centrifugal force.

The ABC ship must traverse rather considerable distances with relatively small clearances under the bottom. Time lost in these inland waters means just as many hours to make up as the same time lost in the open sea. Furthermore, the maximum speed in the long, fresh-water river, especially on the downstream trip with the ship heavily loaded, may be limited as much by the ability to steer the ship and to turn it around bends in the river as by the action of the shallow and restricted waters in augmenting the resistance or causing unfavorable changes in its running attitude.

The turns in the river leading from Port Correo and in the canal leading to Port Amalo are known to be of sufficiently large radius to enable the average cargo vessel to negotiate them without difficulty. However, the ABC design is expected to average nearly as high a speed in these waters, at least in the river below Port Correo, as many cargo vessels make in the open sea. Furthermore, traveling at these higher speeds means more rapid response of the ship for an equal degree of safety.

Considering the single-screw, centerline-skeg design of stern depicted in Figs. 66.P, 66.Q, and 67.R, the single rudder is directly behind the propeller, where it works in the outflow jet. It is far enough abaft the propeller to take advantage of some augmented outflow-jet velocity abaft the disc. It is as close as possible to the stern so that the arm of its swinging moment is large. There is good opportunity to tailor the movable and the fixed areas to suit all the steering requirements. Adequate and possibly superior steering may therefore be predicted at this stage, leaving the detailed design until later.

Considering next the maneuvering requirements, Fig. 64.B indicates that when backing out of the slip at Port Bacine the ship must turn with a minimum radius of about 1,090 ft. When going ahead, out of the harbor, the minimum radius is about 1,490 ft. The latter represents a steady-turning diameter of 2(1,490)/510, or a little over 5.8 lengths. This must be accomplished at a relatively slow speed since the ship is at a standstill at the inner end of the "Y" in the harbor. When backing, the steady-turning radius is equivalent to about 2(1,090)/510, or some 4.27 lengths, likewise at a relatively slow speed.

It is manifest without making any calculations that the ship's propeller will have to supplement the normal rudder forces to create the necessary swinging moments for making these turns. Indeed, it is possible that both the ahead and the astern turns must be effected more by swinging the ship on its vertical axis than by changing its heading through fore-and-aft motion. Normally, this situation would point up the need of twin screws. However, as the turns are to be made in a counter-clockwise direction, bow to port and stern to starboard, in which a vessel with a single right-handed propeller normally swings, it is possible that the necessary augmentation can be obtained with a single propeller.

66.34 Preparation of Alternative Preliminary Designs. Often the ship for which the design is being prepared is a large or important one. Possibly a number of vessels are to be built to the same design, or major decisions may depend upon the performance of one ship. Wisdom then dictates that several studies be made in the pre-

liminary-design stage or that alternative designs be carried along far enough to indicate their relative merit in meeting the established requirements and specifications. In a sense, this is only a part of good planning, which pays handsome dividends in any kind of endeavor. The phenomenal success of the transatlantic Cunarders *Lusitania* and *Mauretania* (old), designed in the early 1900's, was due directly to the extraordinary amount of study and preparation carried out along many different lines before their plans were completed.

The preparation of multiple design studies permits an excellent degree of bracketing for the final design by extending these studies deliberately into regions beyond those contemplated for the actual ship. Rather surprising results, exceeding those possible by following conventional lines, are often unearthed or revealed in this manner.

There are facilities available in practically all maritime countries for exhaustive testing of ship models under a wide range of conditions, at a cost that is small in proportion to the ship cost. There is little excuse for embarking on a major shipbuilding project without comparative tests, on model scale, of several different hull forms. For the proposed 4-day American superliner of the early 1930's, T. E. Ferris built 22 models and tested no less than 14 of them [SNAME, 1931, pp. 314–315]. For the transatlantic liner *America* of the late 1930's, the Newport News shipyard alone tested approximately 50 models, although these were small ones and some of them involved changes in the principal dimensions [SNAME, 1940, p. 10].

66.35 Laying Out Other Types of Hulls. It is intended that the discussion and the design diagrams in the preceding sections of this chapter cover the preliminary hydrodynamic design of ships within a rather wide range of proportions. This range extends as far as the limits of the coefficients and parameters of the various graphs. Since most of the plots are based upon 0-diml variables, the range of size extends all the way from boats to liners. The design of the round-bottom motor tender for the ABC ship, carried through in Chap. 77, reveals much the same procedure as for the larger vessel.

For special-service vessels, certain proportions and functions are exaggerated at the expense of resistance, propulsion, and other characteristics normally considered important. Chap. 76 discusses these variations for a rather wide variety of hull forms.

66.36 Effect of Unrelated Factors Upon the Hydrodynamic Design. The requirements for the ABC design in Chap. 64 were deliberately set up, as should be the case for every boat or ship, to give the designer as much freedom as possible to shape and proportion the hull. This applies to the parts both above and below water, in an effort to produce the maximum of performance so far as all phases of water flow and ship motion are concerned. At the least, he should have latitude in establishing the one feature which may be found most critical when developing the design. If, for example, rather severe limits are imposed on the layout of a high-speed ship in everything except the length, the designer still can do a great deal by adjusting the length and by fixing the shape and proportions of his vessel to meet the exacting requirements imposed upon him.

More often than not, however, the designer is forced to employ his strongest arguments to obtain the latitude he needs in such a principal feature. All too frequently he is stymied and must make the best of a situation which he realizes from the beginning is crowding him against the wall. Faced with a reluctance on the part of the ship owner or operator to make the ship longer than a set figure, confronted with the forces of nature in shortening the roll of a ship which is too wide, or recognizing the limitations of channels which the ship must traverse, he is driven to fuller forms than he would otherwise select or to the incorporation of features which his better judgment tells him to avoid.

Often, too, through no fault of anyone in particular, factors not even distantly related to hydrodynamic features are given priority over them. Whether the water flow is of paramount importance or not it is still governed by certain physical laws. The designer must get this knowledge, then use it to minimize the harmful effects of unrelated factors, and to assess these effects when they can be minimized no further.

It goes without saying that many considerations other than the ones discussed in this chapter enter into a determination of the weight and volume displacements, the principal dimensions, the proportions, the shape, and the general arrangement which mark the end of a preliminary ship design. One of these, and a most important

one for merchant vessels, is cargo handling, especially of the package rather than the bulk type. It is most ably and interestingly discussed by F. G. Ebel in "Notes on Cargo Handling" [SNAME Member's Bull., Feb 1954, pp. 19–27]. Another one is cargo stowage, particularly for vessels with box-shaped holds, discussed in Sec. 76.5.

In practice, a dozen or perhaps two dozen combinations may be worked up as indicated in this chapter before the most promising of them are carried along further in greater detail.

CHAPTER 67

Detail Design of the Underwater Hull

67.1 General. Based upon the preliminary ship layout described in Chap. 66, the hydrodynamic design proceeds with the fashioning of the individual parts, making decisions as to certain secondary form characteristics, such as the more definite determination of the waterlines, section lines, and diagonals, and the shaping of the hull ahead of and adjacent to the positions of the propulsion devices.

The factors considered here are those which govern smooth-water performance. Whether they may be expected also to result in good behavior during maneuvering and wavegoing, and possibly also during operations in shallow and restricted waters, is considered in Parts 5 and 6 of Volume III and in Chap. 72, respectively, together with particular features which have to do primarily with those special operations.

The matter of smoothness of the hull and minor fairings is covered in Chap. 75; only the major features are discussed here.

In this attack on the design problem the size and shape of each part is selected on the basis of its anticipated action in one or more of the fundamental types of flow around it. The whole design is then modified or adjusted on the basis of the interactions which may be expected, employing the best available thought and knowledge on the subject.

67.2 Shape of Vessel Near Designed Waterplane. The principal features governing the shape of the designed waterline for a given speed-length quotient T_q or F_n are discussed in Sec. 66.15, together with a presentation of empirical methods for making a selection of good DWL parameters.

Some consideration is required of possible modifications to the nominal at-rest designed-waterplane shape due to the ship's own waves. If the changes in surface level due to wavemaking at the selected T_q are appreciable, and if the sections near the waterplane have sloping sides, the shape of the waterplane *at the actual wave profile* may change enough to alter the expected performance. For example, a rather full canoe or whaleboat stern, well tapered in way of the at-rest waterplane but flaring to a wide deck above, may possess a considerably greater slope than the designer intended along the raised surface of the stern-wave crest, with consequent undesirable separation. A heavy flare above the entrance waterline, by humping up the bow-wave

crest, may neutralize much of the benefit gained in careful shaping of the at-rest waterline at the designed draft.

It is mentioned previously, but the caution is worth repeating, that too much hollowness abaft the bow, resulting from an effort to fine the bow waterlines to an extreme, may involve an excessive and undesirable slope in front of the forward shoulder.

For the transom-stern ABC ship laid out in Chap. 66 the first sketches of the designed waterline are modified to suit the development of the underwater hull described in detail in this chapter. The *final* waterline shape, with its parameters and 0-diml offsets, is drawn in the lower diagram of Fig. 67.A. That of the arch-stern alternative design, described in Sec. 67.16, is drawn in the upper diagram of the figure.

For a stern shape which is wide and essentially flat on its under side, like that of a scow, the horizontal waterlines at the stern close in toward the centerplane at steep slopes with that plane. For a truly flat stern with no rise of floor in the sections this waterline slope i_R reaches 90 deg. However, in cases of this kind, the flow upward and aft under the stern is primarily along the buttocks, or at least more upward than inward. If so, the waterline slopes lose their significance. Fig. 67.B reveals very steep slopes for the near-surface waterlines at the stern of the ABC ship, faired rather abruptly into the centerline-skeg waterlines. However, inspection of Fig. 66.Q shows easy buttock slopes in this region; Fig. 66.R indicates that the actual flow under the stern is more or less along these buttocks.

The surface waterplane has a definite function, not only in minimizing a surface-wave disturbance, but in providing sufficient square moment of area to insure the necessary transverse metacentric stability. As a rule, the best way to change the metacentric height is to change the maximum beam, assuming that this can be done. Certainly, it is to be preferred to pulling the designed waterline in and out, here and there. This nibbling and padding usually changes the moment of area only slightly but it may have major adverse effects upon the propulsion characteristics of the underwater form. On the other hand, so much attention can be devoted to the hydrodynamic features of the designed waterline that its stability features are overlooked.

Exactly this happened in the course of the preliminary design of the ABC ship. It was

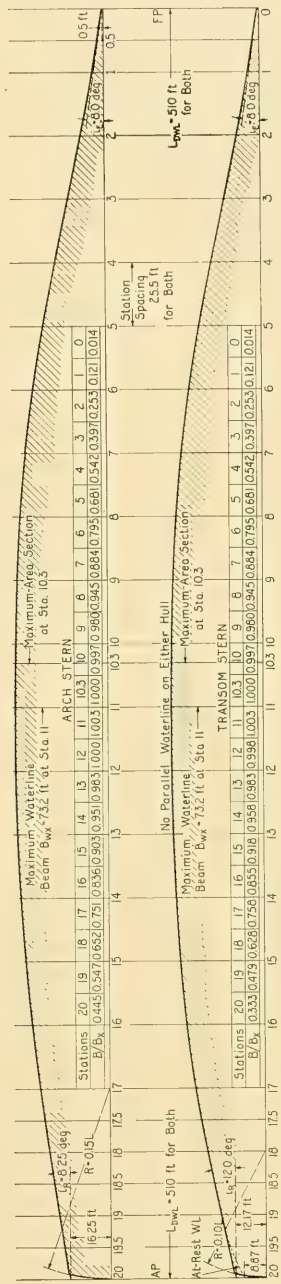

Fig. 67.A Designed Waterlines for Transom Stern and Arch Stern of the ABC Ship

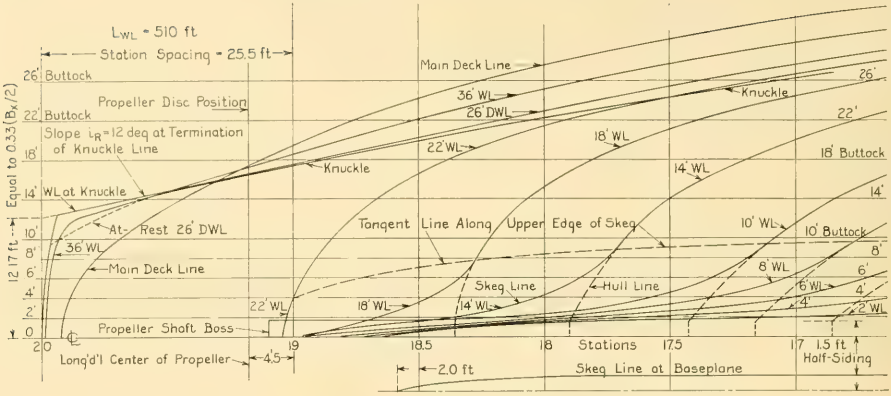

Fig. 67.B After Portions of Afterbody Waterlines for the Transom-Stern ABC Ship

considered that, by reason of the wide waterplane aft, in way of the transom, shown in the lower diagram of Fig. 67.A, enough square moment of area would be gained there to more than compensate for the rather drastic narrowing of the whole hull in the entrance. A check of the designed-waterline I_T value, which should have been made before, actually was made *after* the lines had been sent to the model basin. It revealed a C_{IT} of only slightly over 0.52 whereas the preferred value was 0.561 and the required value, from item (42) of Table 64.f, was 0.55. A proposal to remedy this situation is discussed in Sec. 78.18.

67.3 Waterline Curvature Plots. A designed waterline is to be checked for uniformity of curvature before it is considered acceptable and before it is used as a basis for shaping the remainder of the hull. Secs. 49.10 through 49.14 describe approximate and precise methods, both graphical and mathematical, of accomplishing this operation.

The 0-diml curvature plots for the designed waterlines of the ABC transom-stern, single-skeg ship, as well as for the alternative arch-type stern described in Sec. 67.16, are given in the lower diagram of Fig. 67.C. The upper diagram gives corresponding plots for the Taylor Standard Series parent form, EMB model 632 (modified), and for a merchant ship of good performance. All three indicate certain correct features, so far as they are known, for a good designed-waterline shape:

(a) Not-too-violent changes in curvature with x-distance along the length. As an indication of how suddenly this 0-diml curvature can change, a straight line tangent to a circle of diameter B_{WX} involves a sudden change of 0-diml curvature of from 0 to 114.6.

(b) No great extremes of concave or convex curvature at any point along the length

(c) A curvature plot with the minimum of longitudinal waviness. Generally such waviness indicates poor fairing or inaccurate drawing of the waterline.

(d) A curvature plot with rather long portions of constant or nearly constant curvature, as for the TSS waterline, provided there are no abrupt changes at the ends of these portions.

67.4 Underwater Hull Profile. The bow profile under water is determined from the desired section and waterline shapes at the bow, extending from the baseline up to the designed waterline, rather than from an effort to achieve a particular profile that supposedly has merit. In other words, the bow profile is determined in a sort of automatic fashion, just as if one whittled a wooden model to the desired section shapes forward and then cut away the model on each side until the waterlines met the centerplane. Developed in this way a ship bow with wall-sided sections all the way to the stem terminates in a plumb stem. One with pure triangular V-sections terminates in a straight raked profile passing through the lower vertexes of these sections.

For many ships which operate in shallow waters, temporary grounding forward is a not unusual occurrence. It may be advisable on these craft to cut up the forefoot and thus remove

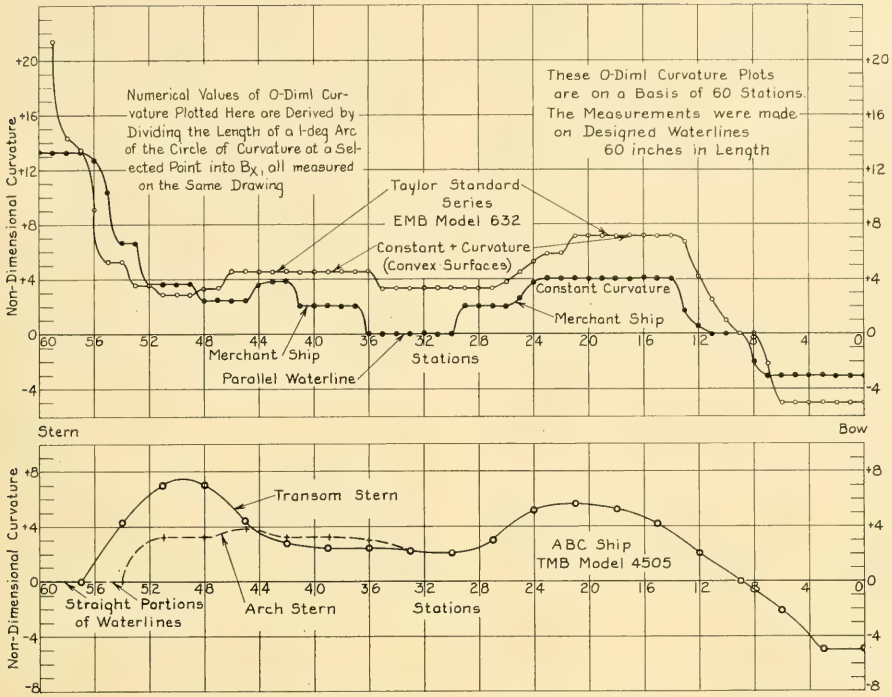

FIG. 67.C NON-DIMENSIONAL CURVATURE PLOTS OF DESIGNED WATERLINES FOR THREE SHIPS

that part of the ship which is most vulnerable to damage when taking the ground. Also, as described in Sec. 25.5, a small amount of friction and pressure resistance often may be saved by trimming up the forefoot slightly, in addition to saving some wetted surface.

There may be merit in shifting progressively aft the forward waterline beginnings with depth below the surface, as explained in Sec. 4.8 and illustrated in Fig. 4.I. This is especially true if the waterline entrances are blunt. This bow shape, embodying a heavily raked underwater profile resembling the Maier bow, saves some wetted surface and may result in a slight reduction of pressure drag. There is reason to believe, however, that better performance is achieved, at least at some T_q values, by fining all the waterlines and carrying them nearly to the FP.

The bow profile of the ABC design is the result of combining a bulb bow of slightly ram form, extending forward of the FP, with a sharp cutwater. The former is described in Sec. 67.6 and illustrated in Fig. 67.E. The latter is described in Sec. 73.3 and illustrated in Fig. 73.B.

The stern profile below water is influenced largely by the number and type of stern propulsion devices selected and their tentative positions, especially if there is a single propdev on or near the centerplane. For a screw propeller, the combination of proper hydrodynamic position with the type, shape, and position of the steering rudder(s) leaves little of the stern profile to be delineated to suit the engineering sense of the individual designer. Furthermore, that portion of the stern profile just below the DWL must be considered in conjunction with a larger portion lying above the DWL. In fact, the stern profile is usually so dependent upon other considerations having to do with skeg endings, propeller clearances and apertures, transom forms, and similar features that it seems wise to discuss these features in detail in those parts of the book devoted particularly to them. The ABC design is no exception in this respect.

67.5 Stem Shape at Various Waterlines. For minimum pressure resistance and reduction in size of the bow-wave crest, and for the elimination of spray and feather, the horizontal sections at the stem of a vessel, just above and just below the surface waterline, are made as sharp as possible. Theoretically, they are formed by continuations of the entrance and bow waterlines, with whatever hollowness the latter may have, when carried forward to their normal intersections in the plane of symmetry of the vessel.

The hull structure of a wooden or metal vessel inside the extremely thin, tapering stem dictated by these hydrodynamic considerations is difficult and expensive to fabricate. A simple solution is to cut the structure back and terminate the stem in a blunt or large-radius section, sometimes with a radius of 1 ft or more, producing the circular-arc beginnings depicted in Fig. 25.A. The resulting bow feather is then accepted.

A circular-arc leading edge, because of the sharp change in curvature at the point where it joins the nearly straight side of the entrance, is susceptible to both separation and cavitation. On a high-speed vessel, therefore, the planforms at various levels of the stem, especially near the surface waterline, are made elliptical, with a gradual change in curvature and an easy transition into the side.

Blunt stems build up relatively high dynamic resistance below the waterline, which adds directly to the pressure resistance of the ship. The blunt nose of a submerged bow bulb, and the bluntness in the horizontal sections of the stem for some distance above it, are accepted for the sake of the benefit they afford in other respects. They also enable the ship length to be kept to a minimum.

Both the hydrodynamic and the structural problems described in the foregoing, at least on a metal vessel, are solved by adding an appendage in the form of a sharp, narrow cutwater. That designed for the ABC ship is described in Sec. 73.3 and illustrated in Fig. 73.B.

With modern fabrication and erection methods there is no excuse for lapping the shell plating on the outside of the stem to form a discontinuity, diagrammed at D in Fig. 7.J. Indeed, there is a definite disadvantage to this construction on a high-speed vessel because of the cavitation that takes place abaft the discontinuity in the regions of low hydrostatic pressure, near the surface. This may be accompanied by possible erosion of the shell plating. It is certain to tear or pound off the paint coating. Harmful cavitation, setting up erosion, causing noise, and inducing vibration and panting of the plating has in fact occurred abaft projecting welding beads on high-speed vessels where flush shell plates were attached to a rabbeted stem casting. Any measurable stem radius, fair or not, is liable to cause separation at the surface and cavitation farther down, if pushed to speeds of the order of 40 or 50 kt.

67.6 Design of a Bulb Bow. The purpose of the bulb bow, explained in Sec. 25.3, is to reduce the height of the bow-wave crest and the magnitude of the pressure resistance caused by it. This does not mean that the blunt surface waterlines producing the high crest are to be retained just because there is to be a bulb to cut down the high waves caused by them. By moving some of the displacement volume from the region of the surface to well below it, into the bulb, it is possible to fine the surface waterlines. Both the finer lines and the presence of the bulb act to improve the hydrodynamic performance of the ship. It may be said, therefore, that in general the design of a proper bulb bow involves also a definite fining of the surface and near-surface regions in the entrance.

When a normal form of bow is converted to a bulb form, good design procedure based on hydrodynamics requires that the displacement volume in the bulb be removed from a surface-waterline region immediately abaft the stem, say from the FP back to about 0.15 or 0.20 of the waterline length. This reduces the angle of entrance and the amount that the surface water is pushed sideward in the vicinity of the first bow-wave crest. Normally it need not and should not be removed from the surface and near-surface waterlines in the vicinity of the forward shoulder.

When a relatively large bulb is fitted, displacement volume is also removed from the lower outer corners of the sections at and ahead of the forward quarter point, for a region extending from about 0.15L to 0.40 or 0.45L, depending upon the shape of the original hull and the amount of volume to be shifted.

The manner in which both these changes are made is well described and illustrated by E. S. Dillon and E. V. Lewis in Figs. 7 through 11 of their paper "Ships with Bulbous Bows in Smooth Water and in Waves" [SNAME, 1955, pp. 726–766].

The following is quoted from page 731 of the

referenced paper, with additions in parentheses by the present author:

"... displacement gained in the larger bulbs was removed from the parent form in the region of the design(ed) waterline so as to progressively fine the angle of entrance as bulb size increased. Some displacement also was transferred from the shoulder near the turn of the bilge into the larger bulbs while at the same time the design(ed) waterline was filled out almost imperceptibly at the (forward) shoulder to recover transverse waterplane inertia which had been lost by fining the angle of entrance. This latter step, while perhaps not best from pure resistance point of view, was nevertheless essential in maintaining stability characteristics constant for the design throughout the range of bulb sizes."

When considering a bulb bow for a new design it is first necessary to determine whether the speed range is appropriate to its use. D. W. Taylor's analysis [S and P, 1943, p. 69] indicates a low limit of the order of $T_q = 0.7$, $F_n = 0.208$, but at this low speed the optimum terminal value t_E is close to zero, which is almost out of the question for a ship section-area curve. E. M. Bragg's tests and analysis, in the same reference, indicate a low limit of the order of $T_q = 0.80$, $F_n = 0.238$. The bulb appears to be most useful in the vicinity of $T_q = 1.0$.

An attempt to reconcile the model-test data of E. F. Eggert, E. M. Bragg, and A. F. Lindblad, and to evolve systematic values of the design parameters f_E and t_E from them, has so far proved unsuccessful. The design values actually used on a considerable number of vessels whose performance bettered or equaled that of the Taylor Standard Series have been plotted therefore on a basis of speed-length quotient. From these plots the tentative design lanes of Fig. 67.D were derived. They indicate, for T_q, a low limit of 0.70, $F_n = 0.208$, and a high limit of 1.50, $F_n = 0.447$.

Those who use them as interim guides until better rules are developed should recognize the following shortcomings:

(a) The f_E values do not increase indefinitely with T_q beyond the range of $T_q = 1.5$ shown in the diagram. They almost certainly diminish to zero at some upper limit of T_q around 1.9 or 2.0.
(b) The proper value of f_E appears to depend upon C_P and the displacement-length quotient $\Delta/(0.010L)^3$ or the fatness ratio $\forall/(0.10L)^3$, but the various model-test data show conflicting trends. It is probable that the best value of f_E increases with both C_P and the fatness ratio.

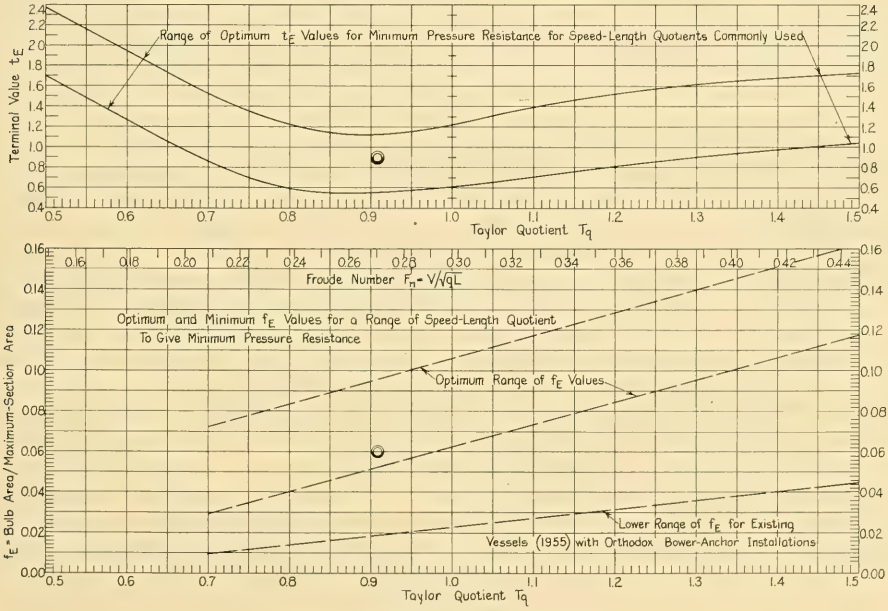

FIG. 67.D DESIGN DATA FOR BULB BOWS

(c) The upper and lower limits of C_P and fatness ratio for which bulb bows give beneficial results are not yet determined
(d) It is possible that the best value of t_E depends upon factors other than T_q but if so no definite trends are yet apparent. Selecting the proper value of t_E appears, however, to be less important than using the proper value of f_E .

A rather surprising feature of the lower or f_E diagram of Fig. 67.D is that, for a large number of existing vessels of good propulsion performance, the bow bulb-area-ratio f_E is rarely more than half the optimum value, although in one case it approaches and in another case it exceeds the optimum. These low values are traceable partly to conservatism, partly to lack of precise knowledge of the behavior of bow bulbs at sea, but mostly to possible damage from bower anchors, dropped from the orthodox stowage positions high in the vessel and close to the stem.

The design rules laid down by W. C. S. Wigley in the summary of his classic paper "The Theory of the Bulbous Bow and Its Practical Application" [NECI, 1935–1936, Vol. LII, p. 65], can hardly be improved upon today, twenty years later. They are set down here, with the present author's comments in parentheses, and with only minor changes to comply with the nomenclature in this book:

(1) The useful speed range of a (ship with a) bulb is generally from $T_q = V/\sqrt{L}$ of 0.8 to 1.9 (somewhat different from that of Fig. 67.D)
(2) The worse the wavemaking of the hull itself is, the more gain is to be expected with the bulb, and vice versa
(3) Unless the lines (forward) are extremely hollow the best position of the bulb is with its (longitudinal) center at the bow, that is, with its nose projecting forward of the hull
(4) The bulb should extend as low as possible consistent with fairness in the lines of the hull
(5) The bulb should be as short longitudinally and as wide laterally as possible, again having regard to the fairness of the lines
(6) The top of the bulb should not approach too near to the water surface. As a working rule it is suggested that the submergence of the highest part of the bulb should be not less than its own total thickness (measured transversely).

Moving the bulb well forward of the FP produced excellent results on pre-World War I battleships of the U.S. Navy, from the *Delaware* class of 1910 to the *Arizona* class of about 1915. An even greater forward projection is embodied in the recent French liners *Flandre* and *Antilles* [SBSR, 24 Jul 1952, pp. 115–117].

A bulb of extremely large f_E ratio, very low, very wide, and very flat on the bottom, was the "platypus" forefoot of EMB model 3383, developed and tested by E. F. Eggert in the late 1930's [SNAME, 1939, pp. 303–330].

67.7 Laying Out the Bulb for the ABC Ship. For the ABC design, projecting the bulb forward of the construction FP by the length of a cutwater such as mentioned in Sec. 67.5 makes it possible to provide a nearly plumb external profile below water, as drawn in Fig. 67.E. There is no particular virtue in this plumb profile as such, except possibly as a matter of appearance. Likewise there is none in the ram-bow profile that would accompany a bulb bow forward of the FP, except to get the bulb into that forward position, relative to the waterline.

Extending the bulb below the baseplane is generally out of the question in practice, although it might be done on vessels designed to meet particular requirements, or it might be extended below the baseplane as a special appendage.

Taking the ABC ship as an example of the design procedure, the fitting of a bulb bow on this vessel was settled, at least tentatively, in Sec. 66.19. It was decided to use, pending a further check, a section-area intercept f_E of 0.06 and a terminal value of $t_E = 0.9$ at the FP. These values are indicated by special spots on Fig. 67.D. It remains to be seen whether a value of t as small as 0.9 will fit the final section-area curve.

Assuming for the moment that the bulb can be worked physically into the ship, a brief calculation is made to determine how much pressure resistance is likely to be saved by it. Taking values of R_R/Δ in lb per ton from Figs. 241 through 244 of D. W. Taylor's S and P, 1943, a curve of residuary resistance in pounds per ton of displacement is plotted in Fig. 67.F for the fine ship of series A. This has a C_P of 0.60, a displacement-length quotient $\Delta/(0.010L)^3$ of 60, and a B/H of 3.35. Four R_R/Δ values, for T_q's of 0.559, 0.783, 1.006, and 1.118, enable this curve to be located reasonably well, especially for the region of $T_q = 0.8$ to 0.9. Reference to Figs. 248 through 252 of S and P, 1943 edition, enables a second curve of residuary resistance in pounds per ton displacement to be plotted for the fat ship of

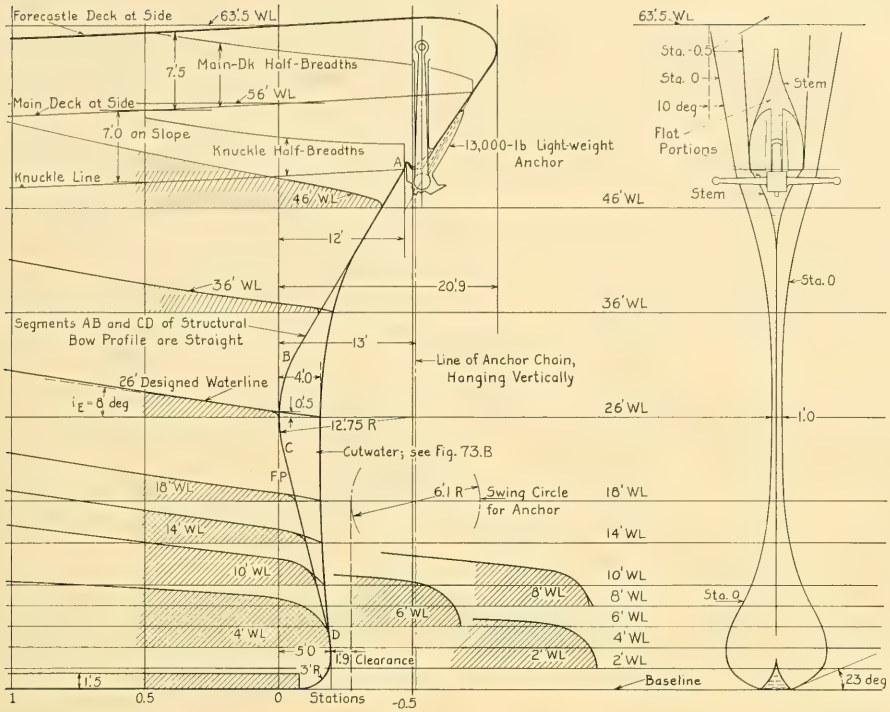

Fig. 67.E Bow Profile, Bulb Bow, and Cutwater for ABC Ship

series B, for which C_P is 0.65, the displacement-length quotient is 150, and the B/H ratio is 3.20.

The next step is to determine the residuary resistances of two vessels without bulbs, having parent forms identical with those of the Taylor Standard Series, and proportions as given in the preceding paragraph. In Table 67.a this derivation is set down in tabular form. The four points corresponding to the R_R/Δ values calculated for the series A and series B ships without bulbs, at T_q values of 0.8 and 0.9, are indicated as such on the plot of Fig. 67.F. The R_R/Δ values to be saved by fitting bulb bows to the two ships are indicated by the vertical intercepts between the four points just mentioned and the curves for the corresponding ships with bulbs.

Reducing these intercepts to percentages of R_R/Δ of the parent-form ships without bulbs, as in Table 67.b, the savings to be expected are of the order of 11 to 18 per cent at a T_q of 0.8 and 14 to 18 per cent at a T_q of 0.9. This is certainly enough to justify fitting a bulb bow to the ABC design, even for the sustained speed of 18.7 kt, where $T_q = 0.828$.

J. M. Ferguson has very recently (August 1955) prepared an analysis of D. W. Taylor's test data by which it is possible to determine by inspection the saving in *total* (not residuary) resistance by using the best values of the terminal value t and the FP area ratio f, or other combinations of t and f, without making the special calculations just described. Ferguson's data are unpublished but they are on file in the TMB library.

The ABC bulb bow is to extend forward of the FP, hence the area corresponding to f_E is measured at that station. If the bulb were rounded into the FP, the area would be that at the plane of the forward perpendicular lying within the bulb surfaces when extended to that station, disregarding the rounding.

Since the bulb volume should be as far below the designed waterline as possible the bottoms of

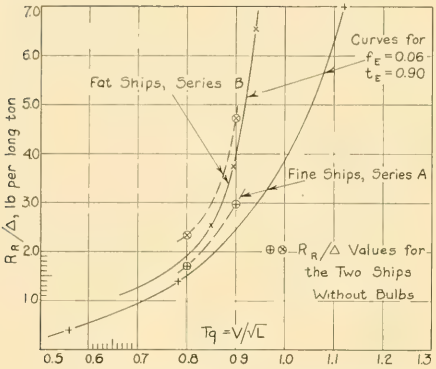

FIG. 67.F COMPARISON OF RESIDUARY-RESISTANCE-PER-TON VALUES FOR NORMAL AND BULB BOWS

all the bulb sections intersect the baseline. A good shape for the bulb section, extending all the way up to the DWL, and lying in or projected upon the transverse plane of the FP, is that of a decanter. As a starter in laying out this section, first draw two short vertical lines at the DWL, at the half-beams selected for the stem, and then lay off the keel half-siding on each side of the baseline. From the outer edges of the keel draw two short floor lines at a suitable rise-of-floor angle. This may, for a ship to run in the open sea, range from 20 to 45 deg, depending upon the contemplated width of the bulb proper. The aim is to prevent objectionable pounding and slamming under the bulb.

If the bulb section were made triangular, with its apex at the DWL and with a zero rise of floor, its width at the bottom would be that of the section area at Sta. 0 divided by half the draft. Two diagonal lines are drawn, one of which is marked DC in Fig. 67.G, diagram 1, representing the two sides of this triangle. With a diameter which is of the order of one-eighth greater than the total bottom width of the triangle, draw a construction circle tangent to the baseline. Using the half-beam at the DWL, the keel half-siding, the floor lines, the straight-sided triangle, and the construction circle as guide lines, sketch in a decanter shape, as is done in diagram 1 of Fig. 67.G for the ABC ship. The f_E value here is 0.06. It is found that, in general, the bulb section passes close to the upper intersection of the triangle and the construction circle, and that its maximum beam is about that of the circle.

Adhering strictly to Wigley's criterion (6), quoted earlier in this section, that the submergence of the top of the bulb be not less than its maximum breadth, the construction circle for any bulb

TABLE 67.a—DERIVATION OF R_R/Δ VALUES FOR TWO TSS SHIPS WITHOUT BULB BOWS

The data presented here are taken from the TSS contours of R_R/Δ given by D. W. Taylor in S and P, 1943. The derived values of R_R/Δ are plotted on Fig. 67.F.

FINE SHIP, Series A

$C_P = 0.60$ $\Delta/(0.010L)^3 = 60.0$ $B/H = 3.35$

T_q	R_R/Δ for $B/H = 3.75$	R_R/Δ for $B/H = 2.25$	Diff.	$M_1 \times$ Diff.	R_R/Δ for $B/H = 3.35$
0.8	1.73	1.63	0.10	0.073	1.703
0.9	3.05	2.80	0.25	0.182	2.982

$$\text{Multiplier} = M_1 = \frac{3.35-2.25}{3.75-2.25} = 0.733$$

FAT SHIP, Series B

$C_P = 0.65$ $\Delta/(0.010L)^3 = 150.0$ $B/H = 3.20$

T_q	R_R/Δ for $B/H = 3.75$	R_R/Δ for $B/H = 2.25$	Diff.	$M_1 \times$ Diff.	R_R/Δ for $B/H = 3.20$
0.80	2.53	2.02	0.51	0.323	2.343
0.90	5.00	4.27	0.73	0.462	4.732

$$\text{Multiplier} = M_1 = \frac{3.20-2.25}{3.75-2.25} = 0.633$$

should have a diameter not much greater than half the draft. If this design rule is followed, the area ratio f_E of a bulb laid out in accordance with these rules is limited to a maximum of about 0.10, indicated in diagram 2 of Fig. 67.G. If larger ratios are desired the upper part of the bulb must approach the surface closer or the lower part must assume more of a triangular or platypus form, with a diminished rise of floor. A bulb with an area ratio $f_E = 0.135$, on a vessel of relatively shallow draft, where $B/H = 3.07$, is shown by E. S. Dillon and E. V. Lewis [SNAME, 1955, Fig. 9, p. 735]. The construction circle for this bulb has a diameter of from 0.7 to $0.8H$, depending upon how it is used.

To simplify construction, with the rather heavy plating called for in this region, the sides of the bulb are if possible made developable surfaces, described in Sec. 27.1. The lower part of the bulb may be the surface of a cone, not necessarily a circular one, whose vertex lies well ahead of the FP. The following is copied from D. W. Taylor [S and P, 1943, p. 69]:

"The ingenious naval architect will have no difficulty in devising bulbous forms where little or no furnacing of the structural plating is necessary."

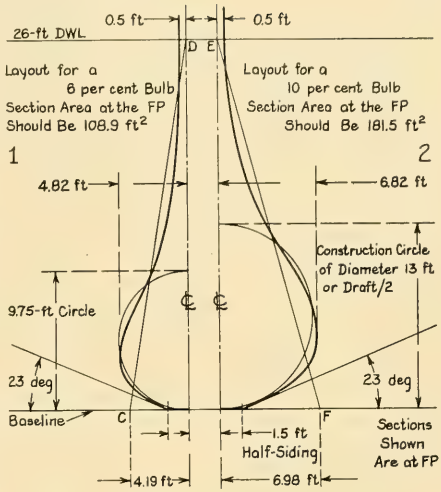

Fig. 67.G Layout Diagram for a Bulb-Bow Section

Sketching in a section similar to that of the FP, at about Sta. 1 or 2, corresponding in area to either or both of those intercepts on the section-area curve and fairing generally with the bulb

TABLE 67.b—Predicted Improvement in Residuary Resistance Due to Bulb Bow

The value of T_q for the ABC ship at 18.7 kt is $18.7/\sqrt{510} = 0.828$.

		R_R/Δ	Saving in Residuary Resistance with Bulb
At $T_q = 0.80$			
Fine ship, without bulb		1.703	$\frac{0.193}{1.703} = 0.113$ or 11.3%
with bulb		1.510	
	Diff.	0.193	
Fat ship, without bulb		2.343	$\frac{0.423}{2.343} = 0.181$ or 18.1%
with bulb		1.920	
	Diff.	0.423	
At $T_q = 0.90$			
Fine ship, without bulb		2.982	$\frac{0.542}{2.982} = 0.182$ or 18.2%
with bulb		2.440	
	Diff.	0.542	
Fat ship, without bulb		4.732	$\frac{0.672}{4.732} = 0.142$ or 14.2%
with bulb		4.060	
	Diff.	0.672	

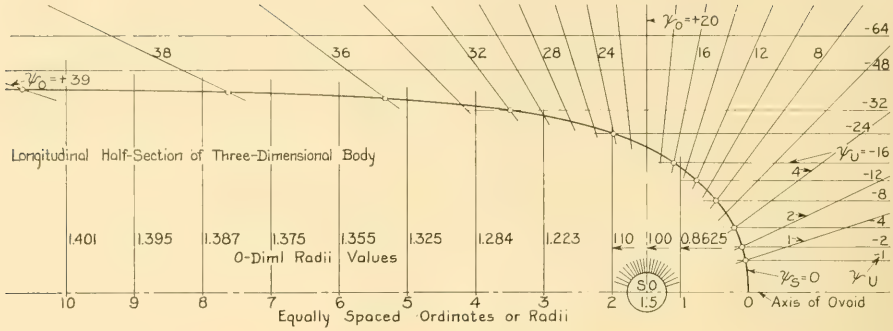

Fig. 67.H Construction of a 3-Diml, Single-Ended Rankine Ovoid for a Bulb Bow

sections at the FP, gives an approximation of the slenderness of the bulb cone and the position of its apex forward of the FP.

If some variation from a developable conical shape is acceptable, the waterlines through the maximum transverse thickness of the bulb may approximate the shape of a single-ended Rankine ovoid generated by a single 3-diml source placed in a uniform stream. Fig. 67.H illustrates the method of graphic construction, described in Chap. 43, and shows the shape of an axial section through one-half of such a form. The proportions are varied by changing the source strength relative to that of the uniform stream.

The lower profile of an ovoid bulb could be delineated in the same way except for the practical requirement of a flat keel extending well forward for docking support. Having this in mind it is convenient to terminate the lower profile in a radius tangent to the base plane, say of the order of $0.10H$ [SNAME, 1930, Pl. 41], or it may be about equal to the mean radius of the extreme nose of the Rankine form. For the ABC design the dimension adopted is 3.5 ft; this means that the straight keel for docking extends forward to the FP.

The matter of shaping the bottom of the bulb to avoid pounding and slamming during wave-going is discussed further in Part 6 of Volume III.

If the bulb remains normally well submerged in service, as it might in inland waters, where pounding or slamming is rarely if ever encountered, the bulb sections may be made rather definitely triangular, with a fairly flat bottom [Eggert, E. F., SNAME, 1939, pp. 303–330; Lindblad, A. F., "Experiments with Bulbous Bows," SSPA Rep. 3, 1944, p. 7]. This puts the centroid of the bulb area even farther below the DWL, with its accompanying advantages. It is still possible to work developable surfaces into the bottom and the sides of this triangular bulb.

67.8 Check on Bulb Cavitation. In the past there has been no definite low limit of draft, in smooth water at least, at which it is not advisable to fit a bulb at the bow. Even for high-speed light-draft vessels intended to run in large waves, bulb bows have been used to advantage. An example is the pre-World War II Italian cruiser *Pola*, having a standard displacement of 10,000 t, a length of approximately 600 ft, a beam of 67.7 ft, a draft of 19.5 ft, and a B/H ratio of 3.47. At a speed of 33.9 kt, T_q for this vessel is 1.38; F_n is about 0.41. A close-up bow view of the *Pola* is published in Schiffbau [1 Mar 1933, p. 89]. Other examples are the heavy cruisers U.S.S. *Pensacola* and U.S.S. *Salt Lake City*, described on SNAME RD sheet 121, with f_E values of 0.083; see also Fig. 52.Kc.

For the first time, so far as known, cavitation was recently (1954) observed on each side of the bulb of another light-draft high-speed vessel somewhat resembling the *Pola*. In smooth water the two cavities were plainly visible from the forecastle head.

This new development definitely calls for elliptic or pointed rather than circular beginnings of the waterlines well below the DWL. The shape of the waterline at each draft, and possibly also the shape of some other characteristic line, must therefore be one for which cavitation will not occur at the cavitation number σ(sigma) actually encountered on the ship at designed draft in smooth water. This check was not made for the bulb design of the ABC ship since the observations

described in the preceding paragraph were reported long after the completion of the underwater hull design and the construction and tests of the ABC model.

When calculating the cavitation number for the ship it is well to be conservative and to omit the allowances for increased head above the various parts of the bulb due to the bow-wave crest or to sinkage at the bow. The transient cavitation which occurs along the sides of the bulb during wavegoing, when the bulb rises toward the surface, may be accepted.

Incidentally, it is not possible to observe either the separation or the cavitation on a routine model test because the Reynolds number R_x or R_d at the stem is too low to produce a flow dynamically similar to that on the ship, and because, with full atmospheric pressure above the basin water, the model cavitation number is much higher than in the full scale.

Assuming for the ABC ship that at some light-load displacement and trim the depth of water h to the axis or widest part of the bulb, reckoned from the at-rest WL, is only 13.5 ft, that the head h_A corresponding to the atmospheric pressure is 33 ft, and that the head due to the vapor pressure of water, h_V, is 0.5 ft, the total static head at the axis of the bulb is represented by $(h + h_A - h_V) = (13.5 + 33 - 0.5) = 46.0$ ft. Assuming also that the speed is 20.5 kt, or 34.62 ft per sec, the velocity head $h_U = V^2/2g = (34.62)^2/(64.348) = 18.63$ ft. Then $\sigma = 46.0/18.63 = 2.47$. This value is far in excess, numerically, of the cavitation number $\sigma = 0.50$ at which cavitation occurs on the hemispherical head of a body of revolution, from diagram 1 of Fig. 47.E. Indeed, it is in excess of that at which cavitation occurs on a blunt head [Rouse, H., and McNown, J. S., "Cavitation and Pressure Distribution: Head Forms at Zero Angle of Yaw," State Univ. Iowa, Studies in Eng'g., Bull. 32, 1948, pp. 54, 65]. No cavitation in smooth-water running need be expected around the bulb bow of the ABC ship.

The cavitation number σ, corresponding to conditions on this or any other ship, is found quickly by the use of the monogram of Fig. 47.B, by entering it with the total head in ft and the ship speed in kt.

67.9 Selection of Section Shapes in Entrance and Run. The first decision with respect to section shapes in the entrance and the run is whether they shall be of predominantly U- or V-shape. If the vessel is to give its best performance under conditions which make a bulb bow of advantage, the entrance sections in the forward fifth- or quarter-length are necessarily of U-form. They begin with an hour-glass shape at the bulb, considering the abovewater sections as well, and work aft into a more or less straight side, which may be vertical or flared outward.

Following this rule, the sections in the forebody of the ABC ship are of predominantly U-form. That portion of the entrance lying inside the estimated position of the bow-wave crest is made sensibly vertical so as not to accentuate the crest with outward-sloping section lines above the DWL, with a consequent increase in pressure drag due to wavemaking.

An easy path for the curved and twisting flowlines around the lower portion of the entrance is achieved by working as large radii as possible into the lower "corners" of the U-sections in way of the forward quarter. This is illustrated for the ABC design in Figs. 66.P and 66.R. It is shown more prominently in the TSS body plan in Fig. 51.A. It has been possible to reduce bare-hull resistance by the order of 8 per cent in a bulb-bow model solely by cutting away the lower outer corners of the sections abaft the bulb and relocating the displacement volume upward by filling out the waterlines of the same sections. At the suggestion of S. A. Vincent, this was done with the first set of forebody lines of the ABC ship. Following the model tests of the hull shown in Fig. 66.P it is believed that the form would benefit by a further change of the same kind.

If deep or shallow V-sections are to be used in the entrance, the section shapes follow a fairly regular pattern from the stem to the main body of the hull forward of amidships, with their lower outer corners well rounded. The relatively small differences between V-shaped and U-shaped sections are well illustrated by G. Vedeler, in a diagram embodying alternative hull designs for a given set of specifications [6th ICSTS, 1951, pp. 169–170].

The design of cutaway dory-type bows with pronounced V-sections, as in the Maierform, in icebreakers, and in vessels like the old pilot boat *New York*, is discussed under these special forms in Chap. 76.

The shape of sections in the run is determined largely by the tentative shape selected for the designed waterline and by the positions selected for the propulsion devices. The latter is a major

factor, because the section shapes largely govern the nature of the flow to these devices. Near the stern a secondary factor may be the tentative rudder position(s). For normal-form sterns the fitting of twin or multiple screws calls for sections of predominantly V-shape. For single screws a V-shape merging into a U-shape helps to provide a greater degree of equality in the vertical distribution of wake velocity, and possibly also a higher average wake fraction than a V-shape. With the latter it is almost impossible to obtain anything but blunt endings in the upper part of a centerline skeg.

It is to be recalled, when sketching in the run sections, that most of the water passing the run comes up from under the bottom. Put in another way, the water coming up from underneath the ship covers a greater surface area of the run, as projected on the body plan, than the water coming around the sides. The importance of good shaping in the run was appreciated many decades ago and its need could well be brought to the attention of naval architects every few years. The following extract is taken from pages 16 and 17 of a thesis by Mr. H. de B. Parsons entitled "Ship Design and a Systematic Method of Construction," submitted in partial fulfillment of a B.Sc. degree at the Stevens Institute of Technology, Hoboken, N. J., in 1884:

> "This eddy resistance, produced by an 'unfairness' in the run, is a fault common to many boats otherwise well designed. The run is the most important part of the ship, as well as the most difficult to design, and should, therefore, receive very attentive study. If it is not given a shape, capable of letting the water close in naturally and smoothly under the stern, the negative pressure of the water against that part of the ship, will be lessened, or, what amounts to the same thing, the direct head resistance will be increased, thus producing a decided loss in efficiency."

With the relatively large B/H ratio of 2.80 in the ABC ship, and a transom at the stern, the section lines in the run fall into a pattern which resembles more nearly the orthodox twin-screw rather than the single-screw hull. This shape of run does not lend itself to deep U-sections in the portion leading to the propeller. For this reason, and to hold the thrust-deduction forces to a minimum, the centerline skeg was made as thin as practicable, having due regard to accessibility and lateral stiffness. It was then added to the main hull as a sort of appendage, indicated by

TABLE 67.c—DATA ON SECTION COEFFICIENTS IN THE ENTRANCE FOR TYPICAL MERCHANT SHIPS

Name or Number of Ship	Max.-Sect. Coefft., C_X	Minimum Value of Sect. Coefft.	Ratio of $\frac{L_E}{L}$	Per cent of L abaft FP for lowest value	Ratio of Sect. Coefft. at that point to C_X
Passenger liner *America*, H = 32.5 ft	0.977	0.820	0.500	24.0	0.839
Seaplane tender, EMB model 3412	0.986	0.88	0.500	43.0	0.892
Passenger-cargo, *Yarmouth*	0.933	0.73	0.500	38.0	0.782
Passenger-cargo, *Talamanca*	0.980	0.85	0.510	25.5	0.867
Superliner Model 17, EMB 3045-1, Mar. Eng'g., Feb 1932	0.995	0.85	0.500	42.0	0.854
Superliner Model 22, EMB 3077-1, Mar. Eng'g., Feb 1932	0.988	0.72	0.515	30.1	0.729
Passenger, *Mariposa* (1932)	0.990	0.82	0.477	19.9	0.828
Passenger-cargo, Ferris design	0.962	0.76	0.41	30.5	0.790
Passenger, *Malolo*	0.977	0.67	0.500	24.0	0.686
U. S. Transport *Heywood*	0.955	0.78	0.500	23.0	0.817
Passenger, *Great Northern*	0.947	0.78	0.51	29.4	0.824

the broken section lines and the skeg tangent line in the afterbody of Fig. 66.P.

To preserve a nearly constant waterline slope at the stern, in the *actual* wave profile at trial speed, the waterlines just above the 26-ft DWL terminate in a vertical knuckle at the outer lower corner of the transom. With a sharp *horizontal* knuckle at Sta. 20 it seems preferable to carry the latter knuckle forward until it fades out between Stas. 16 and 17.

67.10 Variation of Section Coefficient Along the Length. One means of knowing whether the lower corners of the sections ahead of and at the forward quarterpoint are cut away sufficiently is to plot the section coefficients on a base of ship length. It is indicated in Fig. 24.I that a normal form of this curve passes through the given value of C_X at the maximum-area section, diminishes slowly toward the FP, and rapidly toward the AP. Because of the parallel middlebody worked into some ships it is also necessary to consider the shape of the forward portion of the section-coefficient curve with respect to the entrance length L_E rather than the ship length L.

Many years ago D. W. Taylor emphasized the importance of easy curvature in the section lines at about the forward quarterpoint. He stated then—and it appears to be true by present knowledge—that "at about the point where the water wants to go under the ship, you ought not to have a full section—not over 85 per cent coefficient of fullness at the outside" [SNAME, 1907, p. 11]. While a section coefficient of 0.85 at the forward quarterpoint (0.25L abaft the FP), represents a good design for easily driven vessels, it can and does rise and fall with the value of C_X. It is perhaps better to say that the lowest value of the section coefficient in the entrance should fall within the range of 0.25 to 0.45L_E from the FP. Within this interval of length it should have a value of the order of 0.80 to 0.90 of the C_X value. These ranges are taken from the data of Table 67.c, for the position and value of the minimum section coefficient in the entrance of a number of merchant ships and designs, and from unpublished data on a rather wide variety of combatant vessels.

Fig. 67.I is a plot of the section coefficient for the ABC ship with both the single-skeg transom stern and the twin-skeg arch stern. The shape of the curve is typical for a vessel of this type. For this ship, with a C_X of 0.956, the minimum value of the section coefficient is 0.873. It occurs at 0.165L, or 0.320L_E, abaft the FP. The ratio of

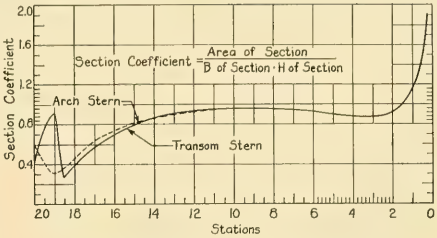

Fig. 67.I Plot of Section Coefficient for ABC Ship with Alternative Sterns

the section coefficient at that point to C_X is 0.873/0.956 = 0.913, which is somewhat higher than it should be. A reworking of the lines at and near the forward quarterpoint, mentioned in Sec. 67.9, would bring down this value. Curves similar to those of Fig. 67.I, for many other vessels of varying sizes and types, may be calculated and plotted from the tabulated B/B_X and A/A_X data and from the profiles shown on the SNAME Resistance Data sheets.

For a ship with a bulb bow the section coefficients reach a value of 1.00 somewhere between 0.05 and 0.10L. Forward of this point they rise rapidly to an extremely large value, perhaps 10 or more, just abaft the FP.

If the designed waterline in way of the forward quarterpoint is relatively full, with section lines which flare out from below the DWL, the section coefficients can be low even though the curvature at the lower corner is relatively sharp. This is why the section coefficient remains only a partial indication of easy flowlines around and under the bottom. It needs supplementing or replacing by a measure of flowline curvature or the equivalent.

67.11 Hull Shape Along the Bilge Diagonal. It was customary at one time to make use of a bilge-diagonal coefficient C_{BD}, corresponding to the fullness ratio of the hull in a diagonal plane through (1) the intersection of the DWL plane with the centerplane and (2) the intersection of the floor line at the maximum section and the half-beam line at that section, sketched in Fig. 25.H. The bilge diagonal is still used for fairing purposes but it is rarely used as a modern design feature, probably because the water flow almost never follows its trace in the forebody and only rarely in the afterbody.

67.12 Side Blisters or Bulges. There are few, if any existing design rules, formulated or unformulated, for the hydrodynamic design of

blisters or bulges on a ship. Sec. 76.9 discusses the design of ship hulls with discontinuous sections and includes a number of design rules. Certain of these are applicable also to ships with blisters and bulges.

Manifestly, the addition of a blister to the main hull or the swelling of a bulge on the boundary of it comprises an integral part of the volume which must be pushed through the water. The form coefficients and parameters of the ship carrying them apply therefore to its *outside* dimensions, shape, and surface. A ship already built, to which a bulge or blister of large size is applied, becomes in fact a new ship, with new proportions, new parameters, new hull coefficients, and a different shape.

Assuming that the transverse section contours of a bulged form are fair, the discussions of Secs. 24.10 and 25.8 show that neither the maximum-section shape nor its fullness coefficient C_X have an appreciable effect on the ship resistance. This means that the bulge can be shaped and positioned to suit other requirements. If it comes at the designed waterline, of course, it almost certainly changes the B_X/H ratio, the angles of waterline slope in the entrance and run, the waterplane coefficient C_W , the transverse moment of area coefficient C_{IT} , and other parameters. If it comes below the DWL it changes only the fatness ratios $\Delta/(0.010L)^3$ and $\forall/(0.10L)^3$. There is considerable latitude in these values for a good design.

67.13 General Arrangement of Single-Screw Stern. The counter or fantail type of stern, with its relatively thin and deep centerline skeg, its rather long fore-and-aft abovewater overhang, and its wide upper decks, came down through the sailing ships of the Middle and Modern Ages. It persisted as the normal form of stern for mechanically driven vessels until the 1930's and beyond. In the two decades preceding the time of writing (1955) it has, for reasons still rather obscure, largely been replaced as the normal single-screw stern by the whaleboat or canoe (cruiser) type. The latter has the practical advantage that it is probably less costly and less difficult to build, that it affords better protection to the rudder and propeller, and that, lacking projections and discontinuities, it is not likely to give trouble in a following sea. Hydrodynamically, it usually offers better shielding of the propeller against air leakage and, because of the greater waterline length, it should result in smaller surface waterline slopes at the stern. Rarely, however, are these small enough to avoid separation at the DWL.

What is really important is the underwater hull shape forward of the propeller, as it effects flow to the wheel, and the augment of resistance due to the reduced-pressure field in the inflow jet. What is equally important, not only for propulsion but for propeller maintenance, is that the single wheel be kept well submerged in all operating conditions. With the large powers now being put into single screws, of the order of 20,000 horses or more, and the likelihood of still greater single-shaft powers in the future, as ship speeds increase, it is imperative that the waterline slopes ahead of the propeller aperture be such as positively to avoid any liability of separation.

At the level of the 0.7 to 0.9 radius on a propeller blade in the 12 o'clock position, the skeg waterline slopes just ahead of the aperture should not exceed 15 deg for near-surface levels, or 18 to 20 deg for levels that are *always* well below the surface in smooth-water running. This slope is to be carried aft, as close as practicable to the aperture, eliminating blunt endings on sternposts or stern weldments, forgings, or castings. The terminal radii should be no greater than necessary to prevent corrosion on thin sections, say 0.1 ft or less on large vessels.

The aftfoot may be cut up in profile to meet maneuvering requirements, to form what is sometimes called a clear-water stern, provided dynamic stability of route is assured, and the necessary docking support remains along the centerline keel. If it is known that the flow is aft and upward in the cutaway region the level lines in the skeg termination may be rather blunt. It is the hull slope along the actual flowline that counts, below as well as above the shaft axis.

In some tugs the aftfoot is cut away, as in a clear-water stern, to afford greater maneuverability but the keel bar and the sternpost are extended aft and downward, respectively, to carry a rudder shoe and to act as a guard for both propeller and rudder ["Kort Nozzle Tug *Maamal*," SBSR, 20 Nov 1952, p. 676].

Freedom from objectionable stern vibration in service is often a requirement that ranks in importance with efficient propulsion. Meeting this demand means, in addition to a fine skeg ending ahead of the propeller, an adequate aperture clearance ahead of the sweep lines of the propeller blades. This must be enough to keep down to acceptable limits the periodic lateral forces on the skeg as each blade, with its circulation pattern

and pressure field, passes through the aperture. An adequate and proper aperture clearance, although undoubtedly a function of the pressure distribution around the adjacent blade elements, can not be defined within close limits on the basis of present knowledge. This matter is discussed further in Secs. 67.23 and 67.24.

A modern form of whaleboat or canoe stern for single-screw merchant vessels of normal design is represented by the sterns of the five TMB Series 60 parent forms for block coefficients from 0.60 through 0.80. The typical stern profile is illustrated in a diagram published by F. H. Todd [SNAME, 1953, Fig. 28, p. 562]. The adaptation to a particular propeller is delineated by J. B. Hadler, G. R. Stuntz, Jr., and P. C. Pien [SNAME, 1954, Fig. 2, p. 123].

In a modification of the normal single-screw stern, such as that laid out for the ABC design in Figs. 66.P and 66.Q, the transom leads forward to a sort of shelf, worked at about the level of the top of the propeller aperture and the top of the rudder. One purpose of this shelf is to protect the propeller from air leakage as long as the shelf is submerged. Another is to permit fining of the upper portion of the skeg ending ahead of the upper propeller blades by making the skeg more of an appendage than a part of the main hull. The arrangement then resembles that of each side skeg in a twin-skeg design, discussed in Sec. 67.21 and in the technical literature [SNAME, 1947, pp. 97–169]. However, it is not as easy as might be expected, with this arrangement, to obtain the requisite fining of the upper levels of the skeg ending while giving the skeg an ample degree of lateral stiffness.

The profile drawing of Fig. 66.Q is an elevation of the aftermost quarter-length, drawn in orthodox fashion. The centerline buttock is included as a sort of construction line, indicating the profile shape of the after main-hull sections on the basis that the thin centerline skeg is treated as an appendage. The transom-stern body plan, Fig. 66.P, indicates this feature in the form of broken-line continuations of the sections at Stas. 16 through 18.5, carried through to the centerline without taking account of the skeg.

The aperture clearance forward of the upper blades is made exceptionally large and the aftfoot of the skeg is cut away to save wetted surface and to improve maneuvering. It is to be noted that whereas the centerline buttock is horizontal for about 11 ft forward of the AP, it was found not possible to level out the lateral buttocks in the same way without decreasing the slopes of the lower transom edges or losing displacement

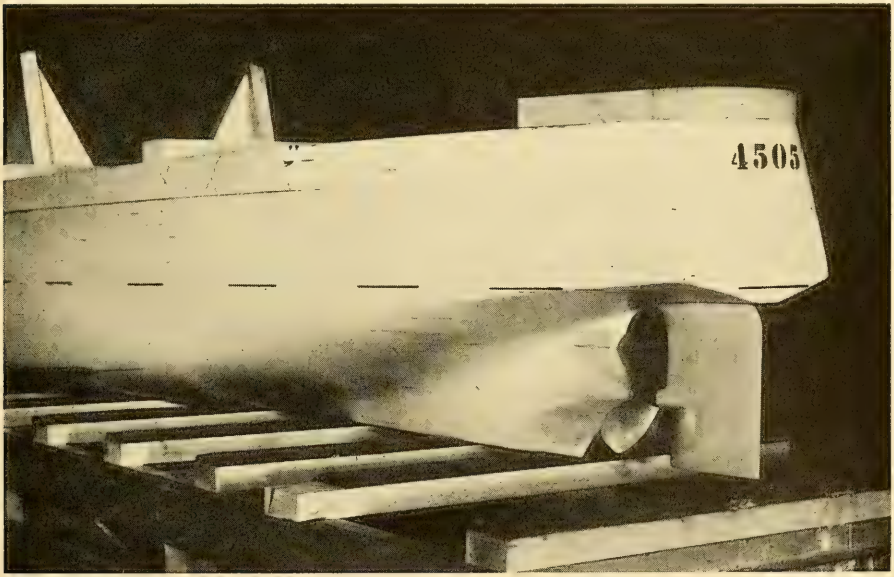

Fig. 67.J Port Quarter View of Transom-Stern Model for ABC Ship

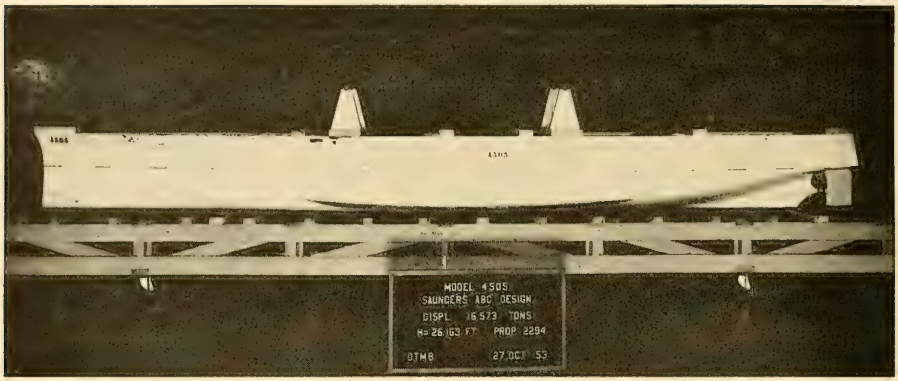

Fig. 67.K Profile View of Transom-Stern Model for ABC Ship

volume by hollowing the main portion of the hull at and forward of the propeller position.

The upper after corner of the rudder is rounded off to provide a moderate gap below the free-water surface and to avoid breakdown of the rudder at large angles.

These features are pictured in photographs of TMB model 4505, representing the transom-stern ABC ship, reproduced here as Figs. 67.J and 67.K.

A further modification of this shelf or transom design, particularly for a high-speed craft, limits the single centerline skeg to a sort of vertical bossing which terminates just below the shaft. Carrying this design one step further cuts the bossing back to a short length of fairing where the shaft emerges from the hull and supports the propeller bearing by a single-arm or double-arm strut, with intermediate struts as may be necessary.

67.14 Stern Forms for Twin- and Quadruple-Screw Vessels. The Taylor Standard Series stern, delineated in Fig. 51.A [S and P, 1943, Figs. 185 and 186, pp. 182–183], was adapted from the British twin-screw armored cruisers of the 1895–1905 era but it still represents an excellent basic form for twin-screw hulls of today. It is adaptable to several types and shapes of single centerline rudder, including the spade or underhung rudder, as well as to rather wide variations in profile. It may be used with open struts to support the twin shafts or twin bossings may be superposed on it.

Lack of space precludes the insertion of sections in which a second alternative stern, with twin screws, could be designed for the ABC ship, as an additional example of hydrodynamic design procedure. However, a twin-screw stern (excluding bossings) usually poses fewer shaping problems and interferences, and it may be expected to have less bare-hull resistance than an equally good single-screw stern.

Save for the cases where quadruple screws are carried underneath a flat-bottomed or transom-stern hull, with the shafts supported by struts, or for the cases where two of the four quadruple screws are carried by deep skegs, the design of a normal form of quadruple-screw stern follows that of the normal twin-screw stern rather closely. The inboard propellers are placed in about the same positions as for twin screws. The outboard propellers are mounted farther forward and farther from the centerline, usually far enough so that their discs are clear of the inboard propeller discs when both sets are projected on the plane of the maximum section. Whether the four propellers project far beyond the abovewater sides of the hull, as on the light cruisers of the (U.S.) *Omaha* class of the 1920's, or whether they lie entirely below the hull as on a wide transom-stern design, is more a matter of the general hull shape than of the underwater hull design. Rarely, if ever, is the hull shape modified for the outboard propellers, except as may be necessary to accommodate machinery parts inside. The four shafts are carried in bossings, in open struts, or in any desired combination of the two.

The positioning of screw propellers relative to the hull, especially the matter of tip clearances, is discussed further in Secs. 67.24 and 69.3.

67.15 Notes on Three- and Five-Screw Installations. Although triple screws are, at the time of writing (1955), not favored for modern ship designs, there have been many successful installations in the past. Notable among these were the U. S. cruisers *Columbia* and *Minneapolis* of the 1890's, many early turbine-driven vessels of the 1900's, the passenger vessels *Great Northern* and *Northern Pacific* of 1914, and the many cruisers and large German capital ships of the World War I and World War II periods. An excellent photograph of the Cunard liner *Carmania*, fitted with triple 3-bladed propellers, is shown on Plate 161, SNAME, 1905. A photograph of the *Columbia* in dock, showing the three 3-bladed built-up propellers, is published in Cassier's Magazine [Feb 1896, p. 325]. The triple-screw arrangements on the Argentine battleships *Moreno* and *Rivadavia* are illustrated in Schiffbau [11 Oct 1911, p. 19]. There was a proposed triple-screw World War II German destroyer of the *Z-51* class, with internal-combustion engine drive [ASNE, Feb 1948, pl. opp. p. 30]. There were four engines of 10,000 horses each coupled to the center shaft and one each of 10,000 horses to the two wing shafts. The center propeller was of course much larger than the two others. The vessel was to carry a large centerline spade rudder and smaller offset twin rudders.

The triple-screw stern, despite its use on many medium and large vessels in the past, presents difficulties with propelling machinery and propeller design. The hull shape in way of the center skeg or center portion ahead of a middle screw is vastly different from the shape ahead of the wing screws, even when the latter are carried by bossings. The friction wakes, the angularity of the flows, and the uniformity of water speeds over the discs will not be the same for the center and the wing propellers. Although not strictly necessary, it is almost never possible to make the center propeller absorb the same power at the same rate of rotation as the wing propellers.

Many designers have been disillusioned by attractive proposals to use the center propeller solely for intermediate-speed and cruising purposes, only to find in service that:

(1) There were practical difficulties in uncoupling the wing shafts and permitting their propellers to free-wheel while cruising

(2) There were many problems in designing a center propelling plant which would operate economically and efficiently at both cruising speed and at full speed.

While attractive from the point of reducing the number of propelling plants and propulsion devices on a high-power ship, triple screws may have to be associated with something rather new and different in the way of ship sterns to realize their full possibilities.

It is not beyond the bounds of probability that with further increases in ship power it may be found advisable to fit five screw propellers on a ship. A stern design for such a vessel appears to involve many problems of both the triple-screw and the quadruple-screw stern. Because of this and other reasons it has not, so far as known, been attempted on more than model scale.

67.16 The Arch Type of Single-Screw Stern. With the increased reliability, decreased weight and space, and reduced fuel consumption of the larger sizes of modern ship propelling plants it becomes increasingly desirable to take advantage of the inherent simplicity and lower first cost of single-screw propelling machinery, to say nothing of its higher propulsive coefficient. Propeller design has progressed to the point where powers much higher than those delivered to single wheels in the past can be absorbed at reasonably low rotational speeds. If the rate of rotation is sufficiently increased, if the propeller is made large enough, and if it is kept adequately submerged, the shaft power of 50,000 horses mentioned elsewhere may be achieved in the not distant future.

Much higher propulsive coefficients can be and have been obtained with single-screw than with twin- or multiple-screw propulsion but these are predicated upon advantageous flow conditions at the propeller disc. Good flow is obtained with relatively long and thin vertical skegs ahead of the propeller, giving reasonably high hull efficiencies [$\eta_H = (1 - t)/(1 - w)$] at the propeller position without excessive circumferential variation and without objectionable separation or eddying.

As the size of vessels in this category increases, so does the beam-draft ratio, because the draft is more severely limited by depths in the waterways of the world than the beam is limited by berthing and docking facilities. The progressive increase in beam, over the years, due largely to damage-control requirements, has meant increased difficulty in fining the waterlines forward

to keep down pressure resistance due to wave-making. It is perhaps even harder to draw in the lines aft so they merge into a long and relatively narrow skeg ahead of the single propeller. Unless the stern is deliberately made wide and flat, incorporating a feature not well adapted to vessels which must operate with a great variation in draft aft, the demand for fine lines at both ends of a medium-speed or fast vessel cuts severely into the waterplane area necessary for transverse metacentric stability. All things considered, it is difficult to fine the designed waterline ending in a single-screw ship of normal form without encountering separation and accepting the drag which comes with it. To avoid surface separation completely means limiting the waterline slopes to a value not exceeding about 12 or 13 deg. With beams continuing to increase, this situation is slowly becoming worse. Something needs to be done about it.

The termination and the slopes of waterlines forward of a single-screw propeller aperture have on many occasions in the past been relatively blunt and heavy, with no consistently objectionable effects. This was principally because the powers absorbed by individual propeller blades were small and the transient forces and moments produced when these blades swung through regions of highly variable wake were also small. With higher and higher blade loadings the periodic forces and moments likewise increase, so that turning out a design with greater power than a previous design, or re-engining a ship to accomplish the same purpose, is by no means as simple as making the propeller shaft a little larger and mounting a new propeller to absorb the increased power.

In the orthodox single-screw stern the propeller is in the same vertical plane as the:

(a) Arch structure over the aperture
(b) Rudder
(c) Rudder horn, if fitted
(d) Sternpost
(e) Rudder post
(f) Shoe projecting from the heel of the ship to carry the lower rudder pintle.

Any attempt to increase the propeller diameter, to provide more tip clearance, or to leave more vertical clearance in the aperture, runs head on into the situation that many other parts must also be accommodated in the centerplane.

By shifting the fixed parts into different vertical planes where each has all the space it needs, dividing the one large rudder into two smaller ones, and hanging each of them behind an offset skeg, much more room is left for a single propeller on the centerline. Furthermore, in a wide ship it is far easier to work gentle slopes into the sides of twin skegs, especially in their upper portions where they join the hull, than into a single centerline skeg. If a single propeller is mounted in a sort of tunnel between the offset skegs with an arch-shaped roof overhead it can have a diameter 20 to 25 per cent larger than would otherwise be possible. The fact that the tip clearance in this tunnel can be made sensibly constant for more than half-way around the propeller disc means that this clearance can be very small. It can indeed be vastly smaller than is thought necessary on an orthodox single-screw installation to keep vibration down within reasonable limits. This leaves still more room to swing a larger wheel.

For the ABC design, a propeller-disc diameter of 24 ft was selected as one which would always remain submerged; that is, as one for which the wheel could be kept submerged during the several variable-load conditions by the use of liquid cargo or salt-water ballast in the after peak tanks, coupled with the filling of the tunnel by a solid inflow jet. The tip clearance of 1 ft was estimated to be a reasonable value, considering that it would be constant over at least half the circumference. It was not too small to bring the blade-tip fields too close to the hull and not too large to lose the benefit of whatever boundary layer existed on the inside of the arch.

This reasoning was based upon satisfactory clearances of the order of 0.25 ft for propellers of one-third the diameter on tunnel-stern push-boats. In fact, since only mechanical clearance is required, the tip clearance on a 24-ft wheel might be reduced to less than 0.5 ft, assuming flush hull plating abreast the propeller, truly concentric with its axis.

For a 20 per cent increase in propeller diameter over that for the transom-stern design, from 20 to 24 ft, the disc area is increased 44 per cent. The thrust-load coefficient is reduced 30.5 per cent ($1.00/1.44 = 69.5$) by this change alone. A comparison of the propulsive efficiencies of the 20-ft propeller with the single centerline skeg and of the 24-ft propeller with the arch stern is given in Sec. 78.15.

The afterbody plan of Fig. 67.L shows how the

tunnel between the side skegs is widened slightly with distance forward of the propeller in an endeavor to allow for the increased area of the inflow jet with that distance. The tunnel is necessarily deep in that portion of the length normally occupied by a single centerline skeg because of the need for providing docking support in that region.

At the time the first modern twin-skeg sterns were developed, an easy slope of the tunnel roof was considered an important feature, so much so that the maximum value was limited to 8 or 9 deg. It is now known that separation does not occur at these small slopes, even at the free-water surface. Well below the surface, where much more hydrostatic pressure and pressure gradient is available to change the water direction, the slopes can be considerably greater than the 12- or 13-deg surface limit. For the ABC design, it was believed safe to increase the maximum slope to about 18 deg, provided the tunnel areas ahead of the propeller were kept large enough. In fact, unpublished model test data on the twin-skeg *Manhattan* hull form [SNAME, 1947, p. 116] indicated a definite thinning of the boundary layer in way of the longitudinal bottom convexity at the forward end of the tunnel, with fairly high transverse velocity gradients at the hull surface. This is an additional guard against separation farther aft along the sloping roof of the tunnel. Incorporating these features into an alternative arch-type stern for the ABC ship produced the body plan of Fig. 67.L and the stern profile of Fig. 67.M.

The resulting stern arrangement is not unlike one proposed in 1874 by Robert Griffiths [INA, 1874, pp. 165–178 and Pl. XXIV, Fig. 3a]. He, too, was concerned about adequate flow of water to the screw propeller.

The profile drawing in Fig. 67.M shows the starboard skeg, looking from outboard, with the starboard rudder. The centerline buttock resembles in shape that of the transom stern, depicted in Fig. 66.Q, except that in this case the transom immersion at this buttock is only 0.5 ft, it extends horizontally up to the propeller position, and it does not fair into the keel until Sta. 14.5. The maximum buttock slope, at about Sta. 17.35,

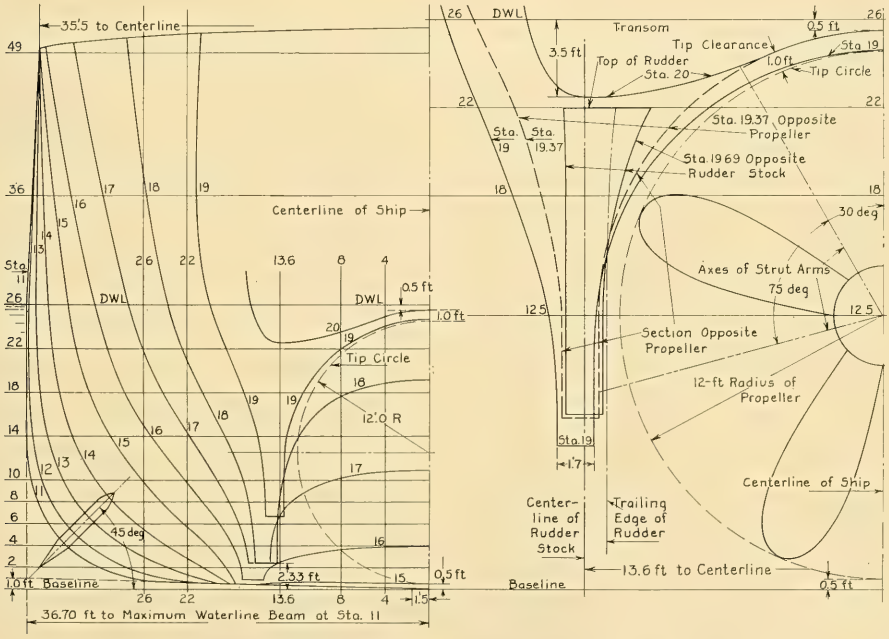

Fig. 67.L Afterbody Plan of Arch-Type Stern for ABC Ship

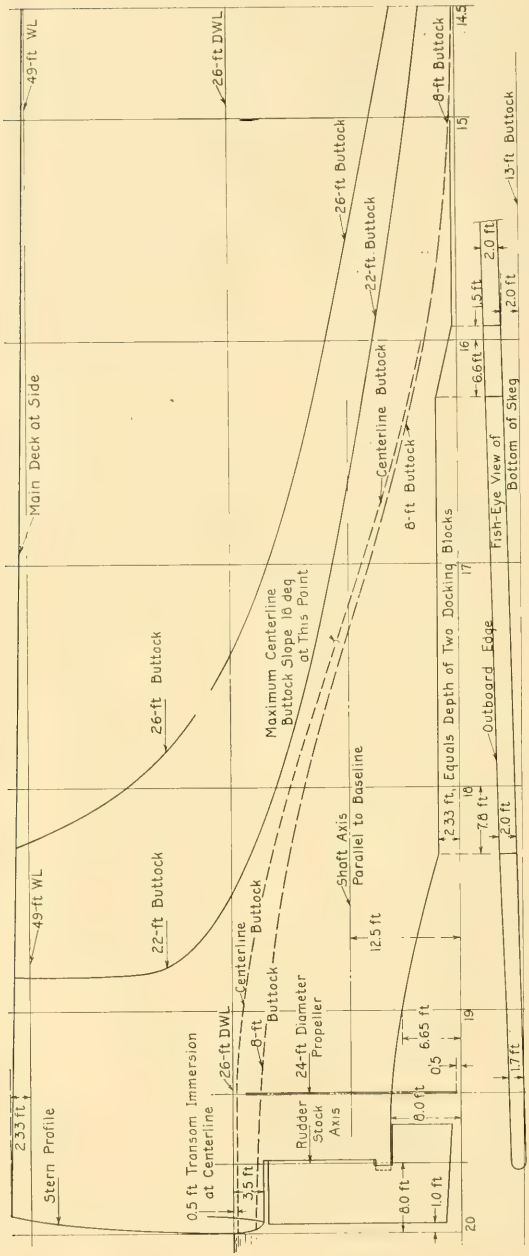

Fig. 67.M Afterbody Profile and Partial Fish-Eye View of Arch-Type Stern for ABC Ship

is 18 deg. This is about twice the maximum slope previously recommended for tunnels between skegs [SNAME, 1947, Rule 9, p. 130] but it is made deliberately steeper in an attempt to slow up the water passing through the tunnel and increase the positive wake velocity at the propeller position.

The aftfoot on each skeg is cut away, not so deeply as in the transom-stern design but extending farther forward. To eliminate unnecessary wetted surface, to improve maneuvering characteristics, and to insure a better flow of water into the forward end of the tunnel between the skegs, the lower edge of each is cut up for a considerable distance to a height of 2.33 ft (28 in), above the baseplane, equal to the depth of two docking blocks. This horizontal skeg foot is 2 ft wide and extends from about Sta. 16.25 to Sta. 18.3. Between Stas. 15 and 16 there is another flat horizontal region at the bottom of each skeg, lying at a distance above the baseplane corresponding to the rise of floor at about the 16-ft buttock. The fish-eye view in the lower part of Fig. 67.M indicates the manner in which the skegs converge slightly with distance, from their forward to their after ends. Transverse sections at the stations in the vicinity of the propeller position are shown to large scale in the right-hand diagram of Fig. 67.L.

The twin rudders, lying close to the projected tip circle on either side, resemble somewhat the curved-blade, tilted-stock twin rudders of the Thornycroft destroyers of a half-century ago [INA, 1908, Pl. IV, Fig. 6]. The tops of the rudders are depressed 4 ft below the DWL to guard against air leakage and possible rudder breakdown on turns, with the ship heeling and diminishing the submergence of the top of the rudder on the high side.

To avoid awkward fairing in the vicinity of the rudder head the transom contour is dropped at the sides to 3.5 ft below the DWL, on the basis that some separation drag due to non-clearing of this deep portion is preferable to irregular eddying above the top of the rudder. Outboard of the skegs the section lines fall naturally into a V-pattern corresponding to that of a narrow ship with centerline skegs such as would be obtained by removing the center portion between the 14-ft buttocks and bringing the two outboard sides together.

The forebody of the arch-stern design is exactly the same as that of the transom-stern design back to Sta. 11, corresponding to $0.55L$.

67.17 Flow Analysis for the Arch Type of Stern. Although it may involve some duplication of material in the preceding section, there is given here a brief analysis of flow conditions under the arch type of stern. This analysis serves also as an indication of the study that should be given to a novel design of this kind in the preliminary-design stage.

What is termed here the arch stern for deep-water vessels is distinguished from the tunnel stern found on craft intended to operate in shallow water, described in Sec. 25.19, by the fact that, in the former, the tunnel roof never extends above the designed waterline. Design rules for tunnel sterns with roofs elevated above the water surface are contained in Sec. 72.13.

There has been no difficulty in keeping the centerline tunnel full of water on ships with twin skegs when proportioned as outlined previously [SNAME, 1947, pp. 130–131]. Perhaps this is because in a twin-skeg design, with propellers carried by each skeg, only a part of the tunnel area is occupied by propeller discs. In the present case the propeller disc occupies nearly all of the tunnel area at the propeller position. In a single-tunnel or arch type of single-screw stern, the selection and proportioning of the tunnel area, starting from its forward end, therefore needs great care. The propeller inflow jet, contracting in area as it moves toward the propeller, practically fills the tunnel. Too small a tunnel could be highly detrimental to propulsion. In fact, there were indications when an alternative arch stern for the ABC ship was being planned, that tunnel-stern towboats and pushboats suffered from excessive thrust-deduction forces, apparently as a result of constrictions in the tunnels ahead of the propellers. It was felt that this could possibly be avoided in the ABC ship by keeping the tunnel roof well up in the region just ahead of the wheel.

To diminish the tunnel-roof slopes on the ABC design to values smaller than those indicated in Fig. 67.M would involve loss of valuable displacement volume, shifting part of the propelling machinery farther ahead, a longer exposed propeller shaft, and a further widening of the forward or entrance portion of the tunnel. Any net increase in resistance, such as that caused by thrust deduction, is of course only justified if the

gain in power from the expected high average wake drops the propeller or shaft power below the value to be expected with an orthodox type of stern. It is recalled in this connection that, practically without exception, the model tests of normal-form sterns and twin-skeg sterns, on a comparative basis, showed higher effective powers but lower propeller or shaft powers for the twin-skeg form.

By retaining the high tunnel slopes, at values which would just avoid separation or $-\Delta p$'s along the roof of the arch, it was hoped to create artificially a forward wake current over most of the tunnel area. This is exactly what is accomplished by a bulb at the bottom of a skeg ending, sketched in Fig. 25.L. It appeared, furthermore, that the wake velocities within the arch should be higher than they were in the original twin-skeg tunnels of the late 1930's and the early 1940's [SNAME, 1947, pp. 97–169]. These velocities should also be considerably more uniform across the tunnel area because of its circular section, without the inside corners of the earlier tunnels on twin-skeg ships. Furthermore, by having the propeller disc fill nearly all of the tunnel area it should be possible to take advantage of the forward wake velocities in *all* the water passing through it. However, as the tunnel does not cover all the propeller disc in the ABC design, it was expected that below the shaft axis the wake velocities would be appreciably lower than those above the axis.

Fig. 67.N View from Aft of Arch-Stern Assembly on ABC Ship Model

In relatively slow-speed tunnel-stern pushboats and towboats built to operate in shallow waters there appears to be no great difficulty in getting water through a narrow bed clearance under the vessel, into the tunnel(s), and thence aft to the propeller(s). However, this does not necessarily assure the designer that this flow is adequate in a deep-water vessel with the same type of stern, which has to traverse shallow waters occasionally, like the ABC ship. What saves the situation here is the necessity for the deep-water vessel to slow down if the bed clearance is small, else it squats and its stern drags on the channel bed.

Finally, it is realized that the increased disc area and improved flow pattern expected with this arch type of single-screw stern, pictured in Fig. 67.N, are offset to some extent by the adverse effect of the items listed hereunder, based on a comparison with a single-screw stern of normal form:

(a) Increased wetted surface of the side skegs. This has been reduced somewhat by cutting up the skegs 2.33 ft, the height of two docking blocks.
(b) Necessity for a shaft strut within the arch to support the propeller bearing
(c) Drag of the exposed propeller shaft and of a short fairing or bossing at its forward end
(d) Necessity for two rudders, neither of which lies in the propeller outflow jet
(e) Probable necessity for placing, farther forward than in a normal single-skeg stern, that part of the propelling machinery directly attached to the shaft, because of the reduced rate of rotation associated with the larger propeller and the larger main gear.

Despite these initial disadvantages, the ABC type of arch stern was considered by several experienced naval architects who examined it to have sufficient promise to justify the building and testing of a model. In the present state of the art, this is the best that can be done with any new design.

67.18 Design of Hull and Appendage Combinations. Very frequently the final design of that portion of a ship hull adjacent to a fixed or movable appendage is only possible after the

detail design of the appendage itself is completed. This is particularly true at the stern of a vessel, in the vicinity of a screw propeller and a rudder. A suitable procedure to be followed here is well illustrated by the first design of the arch-type stern for the ABC ship. It involved a closely spaced pair of skegs and rudders, a large screw propeller with exceptionally small tip clearance, an exposed propeller shaft, a propeller-bearing housing *abaft* the propeller, supported by multiple strut arms, and a contra-propeller effect in the strut arms. After this arch-type stern was completely designed it was found that an installation very similar to it had been embodied in the Dravo pushboat *Pioneer* nearly two decades before, even including the twist in the strut arms [SBSR, 14 Mar 1935, pp. 291–293]. The general arrangement of these appendages, as built into and tested on the self-propelled model of the ABC vessel, is illustrated in Figs. 73.F, 73.H, and 74.L in Chaps. 73 and 74 on fixed and movable appendages, respectively.

Supporting a propeller bearing within the centerline tunnel requires either a V-strut of the usual type ahead of the propeller or a strut of special type abaft it. Since the tunnel is partly obstructed by a short bossing where the shaft comes out of the hull and a length of exposed rotating shafting, sketched in Fig. 67.O, a V-strut ahead of the propeller would only add to the obstructing effect. Standard strut arms, because of their isolated positions and short fore-and-aft lengths, are not suitable as deflectors to impart reversed rotation to the flow in the inflow jet; see the discussion of the contra-propeller in Sec. 36.9. The arch-stern arrangement permits moving the propeller well aft, into a nearly horizontal portion of the tunnel, but at the expense of getting the rudders too near the propeller to take advantage of the augmented outflow velocity, described in Sec. 33.21. However, there is no obvious reason, except perhaps an instinctive one, for maintaining this fore-and-aft distance, expecially as the rudders do not lie *within* the outflow jet.

Moving the propeller bearing with its supporting struts abaft the propeller clears the tunnel of this obstruction and makes it possible to use the strut arms as vanes for taking out the rotation in the outflow jet and developing an additional thrust, in the manner of a contra-rudder. Furthermore, by using three and possibly four arms, curved to straighten the flow in the outflow jet, these arms can have long, thin sections while at the same time they provide adequate support for the bearing housing. One or two arms, generally vertical, take the weight of the propeller and the after half of the exposed shaft while the two side arms steady the bearing laterally. The arms are so spaced as to encounter the blade-pressure fields at random or in succession rather than simultaneously, indicated in Fig. 67.P. The arms are thin and of relatively large chord, to give good hydrodynamic performance. The multiple-strut and bearing-housing combination can possibly be assembled in place and welded into the ship, if considered advisable, as an integral part of the structure.

To remove the propeller in such a setup it is necessary either to split the propeller-bearing housing and drop the lower half or to provide a separate section of exposed shafting. Removal of such a section enables the propeller to be pulled forward a short distance, far enough to get the shaft extension out of the after bearing. Normally the first scheme is objectionable because with the standard method of propeller attachment of

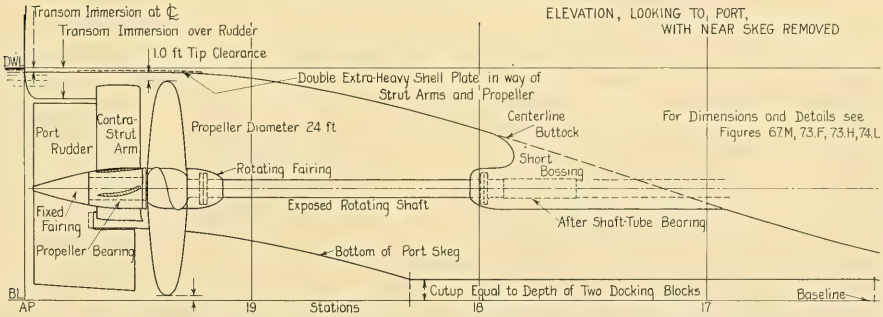

Fig. 67.O Arch Stern Underwater Profile of ABC Ship, with Near-Side Skeg Removed

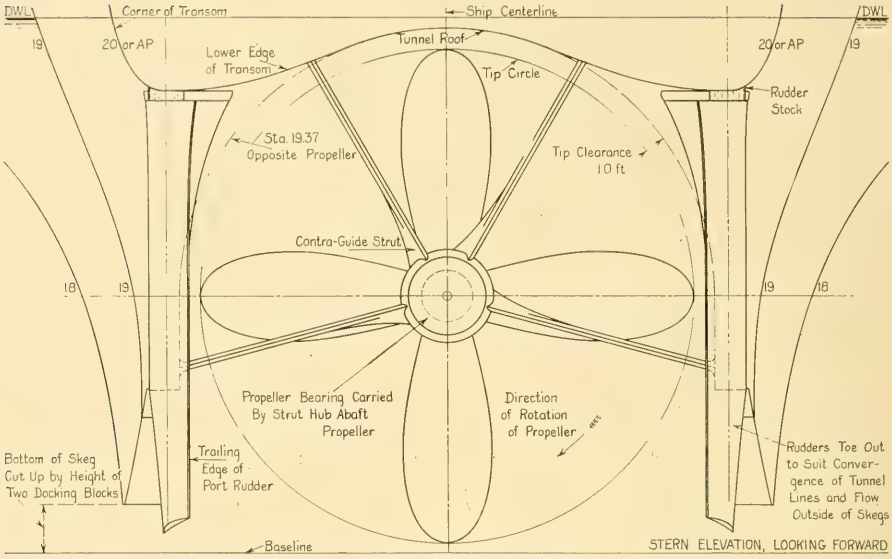

FIG. 67.P ABC ARCH-TYPE STERN ARRANGEMENT, ELEVATION FROM AFT

taper, keys, and nut, the shaft extension must have a diameter smaller than the root of the threads for the nut. To obtain sufficient area in the propeller bearing the journal becomes so long that it is no longer stiff enough to remain straight. This is aggravated by the additional length required for the propeller nut. The load is then far from uniform on the propeller-bearing material, with unequal and excessive wear.

The obvious solution is to:

(1) Attach the after end of the exposed propeller shaft directly to the forward end of the propeller with a pair of bolted flanges sufficiently substantial to take the bending and torsion loads and to withstand the torsional vibrations in the rotating system. These flanges are indicated in broken lines in Fig. 67.O and in full lines in Fig. 74.L.
(2) Fashion the propeller journal integral with the propeller hub ahead of it. The journal can then be made any size and shape desired.

Structural plans for this type of stern should call for a wide transverse belt of double-extra-heavy plating abreast the 24-ft propeller and the 4-armed strut, extending approximately from the bottom of the port skeg to the bottom of the starboard skeg. Except for the forward end near the top, this belt is cylindrical in shape, concentric about the propeller-shaft axis. The purpose of this heavy plating is to:

(a) Provide a permanently fair surface outboard of the propeller tips, so as to hold the small tip clearance constant throughout the life of the vessel
(b) Maintain a fair surface under the action of the rotating pressure fields at the blade tips. With correspondingly heavy transverse framing inside, local forces are distributed over the whole stern structure, instead of being permitted to deform the structure in their immediate vicinity. The thickness of this belt, at least double that of the adjacent shell plating, combined with its transverse curvature, renders it free from panting without excessive local stiffening.
(c) Serve as a strong connection for the hull ends of the four strut arms. These ends, approximately straight fore and aft, are intended to be passed through slots in the heavy belt plate and welded to the internal framing as well as to the belt plate. Fig. 73.F of Sec. 73.8 gives typical longitudinal and transverse sections through the belt plate, showing its attachment to the two upper strut arms.

67.19 Comments on Design of an Unsymmetrical Single-Screw Stern. The function of a

contra-guide stern or skeg ending, described in Sec. 25.16 and discussed in greater detail in Sec. 67.22, is to change the direction of the water flowing past the skeg ending so as to *meet* the rotating propeller blades in the vicinity of the 12 o'clock and the 6 o'clock positions. The skeg is deliberately twisted away from the centerplane of the ship, for a half-propeller diameter or more ahead of its termination, to cause the water to flow to the propeller in the desired contrary direction. This unsymmetrical construction more than pays for its added resistance by the resulting increase of incident velocity on the blade elements, the increased effective angle of attack, and the higher efficiency of propulsion.

The flow of water on a ship with a more-or-less normal stern, carrying a right-handed propeller, is generally upward and aft under the stern. It *meets* the downward-swinging blades in the 2, 3 and 4 o'clock positions. However, the water flowing aft and upward on the port side of the single skeg *follows* rather than meets the blades in the 8, 9, and 10 o'clock positions. The problem now confronting the marine architect is to increase the propulsive efficiency of a single-screw vessel still further, possibly as much as 3 or 4 per cent, by changing the direction of the water on the port side so that it flows downward and meets the upward-swinging blades. If this full change can not be made, because of prohibitive drag and other reasons, it may at least be possible to diminish the upward angle of flow on the port side.

There is no structural, machinery, or hydrodynamic reason why the stern of a single-screw vessel with a single centerline skeg need be symmetrical if there is a distinct advantage to be gained by making it decidedly unsymmetrical, much more so than the present contra-guide stern. Indeed, there is no reason why, if the ship is to benefit by the change, the axis of the single propeller need be in the centerplane or even exactly parallel to it.

There are cases on record of tanker models in which the flow near the end of a centerline skeg carrying a single propeller is directed *downward* as it meets the propeller. This may be due to deflection from the under side of a separation zone below the water surface and above the propeller, or to downward flow on the insides of two large longitudinal-axis vortexes coming off the bilges, somewhat larger than the one diagrammed in Fig. 25.F. Unfortunately in these cases the downward deflection occurred on *both* sides of the skeg so the propeller did not benefit from it any more than it benefits from the normal upward flow on both sides.

It should not be necessary deliberately to create a separation zone on the port side of the ship to deflect the flow downward on that side. Bulging the stern out to fill the space which would be occupied by such a zone means that, on a ship of limited length, there would be another separation zone abaft the bulge, with its added drag. It is not yet known how to accomplish this downward deflection of water on the port side without using up all or more of the energy to be gained by the change but there is undoubtedly some way of doing it.

Any asymmetry in the stern in a scheme of this kind has no appreciable effect upon maintaining the upright position of the ship. Likewise it should have no effect in steering or turning; indeed, such a change might improve the steering characteristics because of the present need for carrying 2 or 3 deg of right rudder on a single-screw ship with a right-handed propeller.

67.20 Proportions and Characteristics of an Immersed-Transom Stern. There is little reason, at least as far as resistance, speed, and power are concerned, for the use of an immersed-transom stern unless, at some speed below the designed value, the water clears the transom and leaves its entire after surface exposed to atmospheric pressure. Present knowledge indicates that this speed depends mostly on the immersed depth of the transom at its lowest point, and partly upon the buttock slopes just ahead of the lower edge of the transom. As described in Sec. 25.14, a so-called "transom" or submergence Froude number F_h may be set up, having as its length dimension the greatest immersed draft H_U of the transom below the at-rest waterline. For reasonably flat buttock slopes at the stern, indicated as i_B in Fig. 25.I, F_h may be as small as 5, possibly as small as 4. Table 67.d gives a set of immersed-transom drafts and corresponding speeds, for a g value of 32.174 ft per sec^2, at which the Froude number F_h equals 5.0.

In general, the immersed-transom draft H_U is selected upon the basis of the lowest speed at which economical operation is desired, particularly when this speed lies below that at which the underwater portion of the transom is completely exposed to the air. The lower this speed, the shallower should be the immersed portion of the

TABLE 67.d—IMMERSED-TRANSOM DRAFTS H_U AND CORRESPONDING SPEEDS FOR A TRANSOM-SUBMERGENCE FROUDE NUMBER F_h OF 5.0

Here $V/\sqrt{gH_U} = 5.0$. The draft H_U is measured in the at-rest condition. The value of g is taken as 32.174 ft per sec².

Speed V, kt	Speed V, ft per sec	H_U, ft	Speed V, kt	Speed V, ft per sec	H_U, ft
6	10.134	0.128	34	57.426	4.103
8	13.512	0.227	36	60.804	4.596
10	16.890	0.355	38	64.182	5.124
12	20.268	0.511	40	67.560	5.673
14	23.646	0.695	42	70.938	6.538
16	27.024	0.908	44	74.316	6.863
18	30.402	1.149	46	77.694	7.506
20	33.780	1.418	48	81.072	8.167
22	37.158	1.717	50	84.450	8.866
24	40.536	2.043	52	87.828	9.594
26	43.914	2.398	54	91.206	10.340
28	47.292	2.780	56	94.584	11.126
30	50.670	3.189	58	97.962	11.928
32	54.048	3.632	60	101.340	12.770

transom. If the ship powers in this range are of little or no importance, the immersion can be deeper if there are other reasons for making it so. If only high-speed operation is of importance, in the range of T_q from about 1.1 or 1.2 to 4.0 or more, F_n from 0.33 or 0.36 to 1.19 or more, the draft H_U at the transom may be a quarter or more of the draft of the ship. If reasons other than water flow and resistance predominate, such as on a floating whale factory with an immersed-stern ramp, the lower transom edge is placed as deep as may be necessary.

The transom need only be wide enough to prevent separation of flow along the sides of the ship at the waterline. If a transom stern is adopted to achieve useful hull volume and deck space at the stern, it is made as wide as need be. A normal transom stern may therefore have a width of 0.8, 0.9, or more of the maximum waterline beam B_{WX} of the vessel.

It was at one time considered that the immersed-transom area ratio A_U/A_X was the principal parameter in the selection and design of a stern of this type. On the basis that the transom must clear before its benefits are fully realized it is obvious that, for a given area ratio, the immersed draft can change greatly, depending upon the transom waterline beam B_U or the *transverse* section slopes at or near its lower edge. Since the latter two parameters apparently have no direct effect upon either the performance or the design, provided the beam is great enough to prevent separation at the waterline ahead of the transom, the effect of the transom-area ratio is questionable. To be sure, this ratio appears as f_R on the section-area curve, an example of which is given in the lower diagram of Fig. 24.F, but the significance of this ratio, as well as the terminal value t_R at the AP, remains to be discovered. On high-speed craft the immersed-transom area ratio may be made 0.15 or more, depending upon the desired shape of the buttocks aft.

The exact transverse *shape* of the submerged transom is not too important, except as it affects the immersed draft H_U . It can have a vee or a rectangular shape to suit the lines of the run, it can have square or rounded corners in a transverse plane to correspond to the lines forward of it, and it can have flare or tumble-home at the sides. Likewise, the planform can be varied throughout rather wide limits from a flat transverse to a V-shape or to a curved shape. So far as known, it is not even necessary that the planform curvature below the designed waterline remain convex to the hull.

Rounding off the bottom edges of the transom, sketched in Fig. 67.Q, and the more-or-less vertical corners at the sides, in the region below the full-speed wave profile, is sometimes done to ease construction or improve appearance. Although there is definitely an increased drag due to the fringing separation zones at the forward ends of these rounded corners the increase is rarely measurable. Rounding the vertical

corners is probably less objectionable than rounding the lower edges.

The transom bottom slope i_S , measured in a transverse plane, is related to slamming and as such is discussed in Part 6 of Volume III.

Before the shaping of the transom stern of the single-skeg ABC ship was completed, in the course of preparing the body plan of Fig. 66.P, the transom depth was increased from the original 1.5 ft to 2.0 ft. This gave more slope to the lower transom section lines and decreased the probability of pounding or slamming under the stern.

The planform of the ABC transom stern at the DWL is made slightly convex, with a radius of $0.10L$, partly to facilitate angling the vessel into a short berth, not much greater than its length, and partly for the sake of appearance. The transom width at the DWL, projected to the plane of the AP, is $0.33B_X$.

The transom of the ABC arch-type stern, sections of which appear in Figs. 67.L and 67.P, is deliberately made deeper at the outer corners than the depth which will clear at 20.5 kt in order to avoid the most troublesome problem of fairing the upper parts of the two skeg endings, under the hull. Some separation is certain to exist in either case. It is considered far preferable to fair the hull directly into the upper portions of the two rudders, and to accept eddying abaft the deep sides of the transom, than to permit separation farther forward, nearer the propeller and possibly interfering with rudder action.

The transom planform of this vessel is made slightly convex, with a radius of $0.15L$. The transom width at the DWL, projected to the plane of the AP, is $0.445B_X$.

In profile, the shape of the transom is generally determined as a matter of appearance and construction. In all vessels which may upon occasion be required to run astern at considerable speeds,

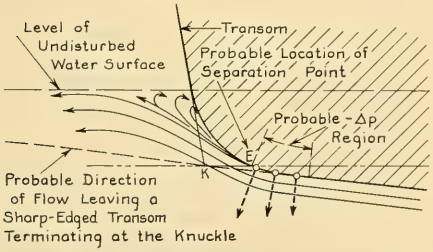

Fig. 67.Q Diagram of Probable Flow Under Rounded Transom Edge

the matter of throwing spray or meeting waves is one to be given consideration. A square, vertical transom should apparently be avoided for this reason, yet large vessels with a stern termination of this type have reported no difficulties in service.

Taken by and large, the transom stern of the German World War II destroyers of the *Narvik* class, portrayed in Fig. 67.R, is commended as

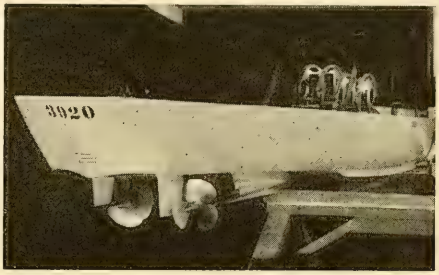

Fig. 67.R Transon Stern on Model of German Destroyers of *Narvik* Class

embodying all desirable hydrodynamic features and offering a pleasing and ship-shape appearance without expensive or complicated construction.

67.21 The Design of a Multiple-Skeg Stern. Design rules for multiple-skeg sterns are available in rather complete form in the technical literature [SNAME, 1947, pp. 130–132]. The historical examples in that reference are supplemented by a quadruple-screw design for English channel service by John Dudgeon [INA, 1873, pp. 88–95 and Pl. VIII]. The hull form illustrated in the latter reference comprises two skegs, with two screws inboard and two screws outboard of them. The tunnel between the skegs extends all the way to the bow. So far as known, no craft of this type was ever built.

For the design of multiple skegs on a modern craft the rules in the SNAME 1947 reference are considered adequate, when supplemented by the following:

(1) Consider the use of twin skegs or multiple skegs only on afterbody forms which lend themselves to this arrangement, or on which beneficial results may be expected. This includes wide ships, or ones with large B/H ratios, where it is difficult to close the waterlines in to the centerplane without large slopes. In general, the afterbody should have a prismatic coefficient C_P of 0.60 or larger.

(2) Incorporate a forebody which would be employed with a normal form of stern
(3) Do not hesitate to use twin or multiple skegs under a transom or shelf-type stern
(4) Do not be concerned about asymmetry between the inboard and outboard sides of skegs carrying screw propellers if the water flow or propeller performance is improved thereby
(5) Give serious consideration to the use of twin or multiple rudders. If maneuvering qualities are important, twin rudders are placed abaft twin propellers.
(6) Work out an arrangement whereby the rudders, propellers, and shafting can be disassembled or removed with the least interference between themselves or from other parts
(7) For rudders mounted in propeller races, keep them far enough from the propellers to permit removing the propellers without disturbing the rudders other than turning them to a convenient angle
(8) If the afterbody of the ship is especially wide and full, and the ship is to have three or four propellers, consider spreading the skegs far apart, and carrying the outboard or wing propellers in the skegs. The inner propeller(s) may be placed in the tunnel between the skegs, with the shaft(s) for the inner propeller(s) carried by double-arm struts of the erect V-type.

Study of flow phenomena since the publication of the 1947 reference indicates that the former limiting slopes for the tunnel roof may be approximately doubled, making them 16 to 18 deg, but probably with an accompanying increase in thrust-deduction fraction. The flow pattern should be checked, however, by taking the usual flowlines around the skegs and inside the tunnel in a model basin, *and* by observation of tufts in a circulating-water channel. The thrust-deduction values require checking by a self-propelled model test.

If tests on a model with chemical indicators or tufts show irregular flow within the tunnel or water crossing underneath the skeg in the design as completed, the skegs may be shifted sideways until a satisfactory flow pattern is obtained. If twin skegs of full depth interfere with maneuvering they may be cut away in profile in the manner of a clear-water single-skeg stern.

67.22 Design Notes for the Contra-Guide Skeg Ending. These design notes apply to contra-guide features in a *vertical* skeg termination ahead of a screw propeller. The unsymmetrical termination usually extends both above and below the propeller axis, but this is not necessary. The plane of the termination passes through, or lies close to the shaft axis. The purpose of the contra-guide feature is, as explained in Sec. 25.16, to leave as little as possible of the rotational or tangential component of velocity in the *outflow* jet of the propeller. Before proceeding with the design of a contra-guide skeg ending, it should be known whether a contra-rudder is to be fitted abaft the propeller to accomplish part of this purpose.

The design problem consists of:

(a) Determination of the true deflection angle θ_S abaft any unsymmetrical skeg ending. This is a general problem involving the flow about the trailing edge of any body when circulation is not present, discussed in Sec. 36.3.
(b) Subdivision into a series of subproblems, one each for a series of horizontal planes passing through the termination of selected radii on the propeller. It is customary to subdivide the propeller radius R into tenths or twentieths, indicated on the propeller drawing of Fig. 70.O. If the exact or final propeller diameter D is not known at the time, the skeg ending may be intersected by horizontal planes passing through the waterlines used for delineating the remainder of the hull.
(c) Selection of the actual angle θ_S to which the flow into various radii of the propeller shall be deflected. This flow is directed always to *meet* the propeller blades when rotating in the ahead direction.
(d) Selection of the offsets of the deflector terminations from the ship centerplane or from the construction plane of the skeg, to give the angles selected in (c)
(e) Avoidance of separation on those sides of the deflectors having the steeper waterline slopes.

Reference books on the design of hydraulic machinery, including propeller-type pumps, appear to give little or no specific information on the actual design of guide vanes ahead of impellers.

One of the early patents on this device [U. S. 1,500,073, by Hans Haas, 1 July 1924], states that the deflector shape "has proved to be specially suitable" when the product of (1) the rotational velocity component imparted to the water opposite any propeller radius *and* (2) that propeller radius formed (3) a constant quantity

for the entire radial extent of the deflectors. This means roughly that the natural sine of the deflection angle θ_S imparted to the water abaft the skeg termination at any selected point, times the propeller radius R at that point, is constant, or that the natural sine of the deflection angle varies inversely as the radius.

A. Betz of Göttingen in his paper "Zur Theorie der Leitapparate für Propeller" ["The Theory of Guide Vanes Applied to the Propeller," NACA Tech. Memo 909, Sep 1939], makes the basic assumption that the tangential velocity component in the outflow jet, due to induced velocity, varies inversely as the radius from the propeller axis. This corresponds to the variation mentioned in the Haas patent. Unfortunately, the Betz paper does not tell how to design the vanes. The outline of a proposed method follows.

Consider first the determination of the correct or effective deflection angle for any given unsymmetrical skeg ending. Obviously, from reference to Fig. 67.S, there is no single flow in the

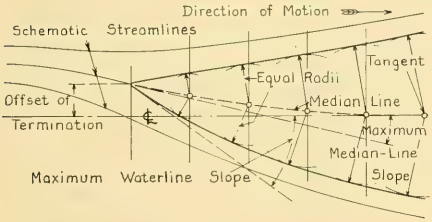

Fig. 67.S Method of Laying Out Skeg Waterline from Median Line

region abaft the ending where the propeller works but a confluence of two flows. There is little reason to believe that the flow over the convex side, having the greatest slope to the longitudinal axis, is the predominant one. There is ample evidence that the effective flow abaft the trailing edge of a hydrofoil surrounded by circulation moves more nearly in the direction of the concave or straight side. However, the circulation around the whole ship hull in a horizontal plane, due to the slight asymmetry in question, is surely very small. Whereas the flow abaft a thick airfoil or hydrofoil producing lift is predominantly in the direction of that passing along the face or $+\Delta p$ side of the foil, as is indicated by many published flow photographs, this is unlikely to be the case here. If it were, the prerotation which could be given to a screw-propeller inflow jet would be rather moderate. If, on the other hand, what is desired is to lessen the angle of flow by which water in the inflow jet follows the blades, described in Sec. 33.12, then even small slopes on the concave or pressure side of a skeg ending or bossing termination can be most effective.

For design purposes it is sufficiently precise to assume that, as indicated in Fig. 67.S, the direction of flow at a small distance abaft the trailing edge of a skeg corresponds to the direction of a tangent to or extension of the *median line* of the skeg ending at that edge. A "small" distance is assumed to be from 0.5 to 0.9 times the width of a blade on the propeller. If the aperture clearance is greater than 0.9 times a blade width, the direction of flow expressed by the speed-of-advance vector U_A is assumed to be more nearly a prolongation of the $+\Delta p$ or concave side of the unsymmetrical skeg ending.

Actually, the amount of prerotation to be imparted ahead of the disc by the design being worked out depends upon:

(1) The tangential component of induced velocity which is to be imparted by the blade element at any radius. This in turn is a function of the effective or hydrodynamic angle of attack α_I of that element, the strength of the circulation there, and the magnitude of the induced velocity U_I far astern.

(2) Whether enough rotation is to be put in ahead of the disc to give zero resultant rotation abaft the disc, or whether some contra-guide feature, such as a contra-rudder, is to be fitted abaft the propeller, to take out the remainder of the rotation in that region.

It is often necessary to design the appendages, at least for a model test, before the propeller design is worked out, so that the values in item (1) may have to be estimated or taken from data on some other design. It is a difficult design problem to achieve the first step listed in item (2). It may be said, therefore, that in the present state of the art a skeg ending should not be called upon to compensate for lack of a contra-guide device abaft the propeller.

It is not possible without more extended knowledge of the intricate flow which takes place between a skeg ending and a screw propeller to state definitely the parameters and the relationships which should govern the variation of median-line slope θ_S with radial distance from the pro-

peller axis. Were these relationships available it would still be necessary to substitute in them some data assumed for the propeller proposed but not finally selected. It appears sufficient, therefore, to state that the skeg ending slope θ_S should vary with propeller radius at some rate less than the geometric blade angle ϕ of the proposed propeller. Table 59.b lists these angles for tenths of blade radii and a rather wide range of P/D ratios. A good working rule, admittedly an engineering compromise without theoretical foundation until the analytic and experimental development is carried further, is to vary the offset termination with propeller radius as $\sin^2 \phi$. The θ_S is then left to adjust itself by proper fairing of the skeg ending into the offset termination. A table listing the variation of ϕ and $\sin^2 \phi$ with R, for a P/D ratio of 0.98, is given in Fig. 67.T, described later in this section.

Practical considerations, both structural and hydrodynamic, usually limit the maximum offset of the trailing edge to somewhat less than the half-diameter of the propeller-bearing boss. It is not wise to work too large a hunk of metal into a cast stern frame where the deflected portion joins the boss. Too small a reentrant angle on the inside of the deflected portion of the skeg or stern frame encircling the propeller shaft bearing is not conducive to good flow.

The geometric blade angle ϕ still has an appreciable value at the tip of any propeller; it is about 10.8 deg for a P/D ratio of 0.6. Similarly, the induced velocity $k_1 U_I$ generated at the tip has a small but appreciable axial component. Even when the $\sin^2 \phi$ relationship is used, the skeg-ending slope θ_S is a little more than zero opposite the blade tips. The reason for using the $\sin^2 \phi$ function is to avoid offsets which are too large opposite the tips; this is brought out more clearly in Sec. 74.16, in connection with the design of a contra-rudder. Further, if the propeller blades are already heavily loaded at the tips, it is not wise to load them further. On the other hand, A. Betz makes the point ["Zur Theorie der Leitapparate für Propeller (The Theory of Contra-Vanes Applied to the Propeller)," Ing. Archiv, 1938, Vol. 9, pp. 435–452; English transl. in NACA Tech. Memo 909, Sep 1939, p. 13] that efficiency is gained by carrying the twist to distances far beyond the propeller radius. This means that a skeg ending need not terminate top and bottom with symmetrical waterlines.

It is found, in most cases, that when a fair median line is laid out, as in Fig. 67.T, and skeg section lines are drawn on either side by the equal-radii construction shown, there is a slight hollow on the side of the skeg having the smaller curvature. This is arbitrarily filled in to produce a fair surface.

By the requirements of Table 64.a, item (5),

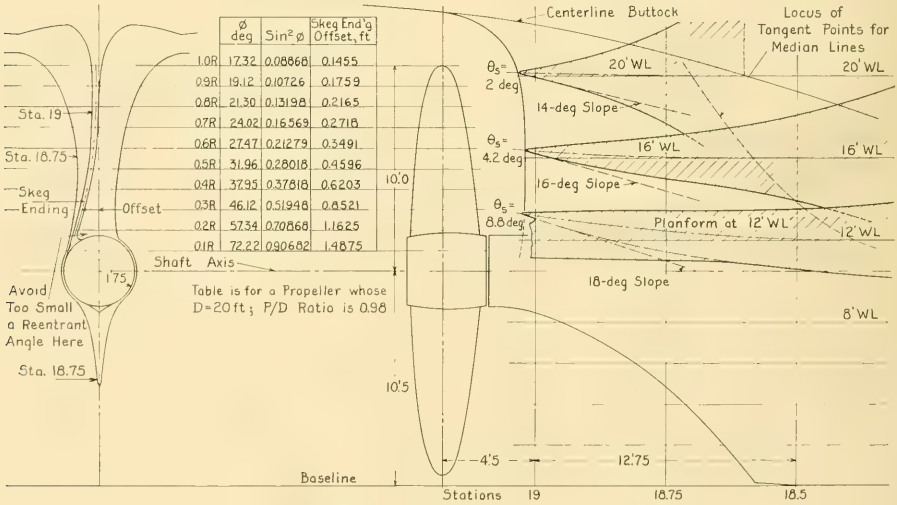

	ø deg	$\sin^2$ ø	Skeg End'g Offset, ft
1.0R	17.32	0.08868	0.1455
0.9R	19.12	0.10726	0.1759
0.8R	21.30	0.13198	0.2165
0.7R	24.02	0.16569	0.2718
0.6R	27.47	0.21279	0.3491
0.5R	31.96	0.28018	0.4596
0.4R	37.95	0.37818	0.6203
0.3R	46.12	0.51948	0.8521
0.2R	57.34	0.70868	1.1625
0.1R	72.22	0.90682	1.4875

Fig. 67.T Design of Contra-Guide Skeg Ending for ABC Transom-Stern Ship

the propulsion of the ABC vessel is to be effected as economically as the present state of the art permits. A twisting of the skeg ending to give a contra effect is therefore indicated for the single-skeg transom stern. The skeg waterlines above the shaft are fined to reduce the thrust deduction and it would be easy to work a considerable degree of deflection into that structure. However, above the shaft axis the aperture clearance is deliberately made large, so that the benefit to be derived from prerotation is doubtful. Further, the lower part of the skeg, below the shaft axis, is cut away so far that any deflection effect would be lost on the propeller. A contra-shape is to be worked into the fixed rudder horn, above the shaft axis, and there appears to be room for enough shaping of the horn to remove much of the jet rotation. Taking all factors into consideration, therefore, it is decided *not* to provide a contra-guide skeg ending for the transom-stern afterbody.

Nevertheless, as an example of the rules given herein, a contra-guide ending is laid out for the upper half only of the single skeg of the ABC ship, producing the form shown in Fig. 67.T. This embodies a more nearly vertical profile above the shaft, with less aperture clearance than for the symmetrical skeg ending.

The radius of the propeller bearing boss shown in Fig. 66.P, the body plan of the transom-stern design, is 1.75 ft. The maximum offset value, at a starting level of $x' = 0.1$ or $R = 0.1R_{\text{Max}}$ above the propeller-shaft axis, is taken as 0.85 times the boss radius, or 0.85(1.75 ft) = 1.4875 ft. Assuming a constant P/D ratio of 0.98 for the propeller, the blade angle ϕ at $0.1R$ is 72.225 deg and $\sin^2 \phi$ is 0.90682. This is a sort of reference value corresponding to the $x' = 0.1$ offset of 1.4875 ft. For example, at $x' = 0.7$, ϕ is 24.019 deg and $\sin^2 \phi$ is 0.16569. Then the offset at $x' = 0.7$ is (0.16569/0.90682)1.4875 ft = 0.2718 ft, as listed in the table on Fig. 67.T. At $x' = 1.0$, where ϕ is 17.325 deg, $\sin^2 \phi$ is 0.08868 and the offset is (0.08868/0.90682)1.4875 ft = 0.1455 ft.

The slope of the median line bisecting the angle between the *terminal* portions of the level waterlines on each side of the skeg ending is limited to the order of 0.175. This corresponds to just under 10 deg, as reckoned from the ship centerplane or the construction plane of the skeg. These limits are admittedly rather arbitrary, to comply with the requirements of the paragraph following. The median-line slope varies from this maximum value just beyond the radius of the propeller-bearing boss to a much smaller value at 1.0 or 1.1 times the propeller radius.

Since no separation, or semblance thereof, must occur in way of the inside of the skeg deflector, especially in front of the upper propeller blades, there is another practical limit to which the trailing portion may be bent. The slope of any waterline through the offset portion of the skeg ending, assuming this waterline to be generally in the plane of flow, should under normal circumstances not exceed 18 deg or, at the most, 20 deg, especially at the shallow drafts. This is admittedly a rather indefinite rule which requires amplifying and checking from actual ship designs known to be successful. Values which are definitely out of bounds can be determined from vessels where separation, vibration, and air leakage are known to exist. For the ABC ship, Fig. 67.T, it is possible to hold the maximum median-line slope at the 12-ft WL, at about $x' = 0.16$, to some 8.8 deg, with a maximum slope on the convex side of 18 deg at the same level.

The use of a contra-guide skeg ending is approached with caution when the waterlines (or flowlines) leading up to the forward edge of the propeller aperture in a skeg have a slope already approaching the limit beyond which separation may be expected at that level, indicated in Sec. 46.2. Superposing the deflector shape upon a symmetrical skeg ending diminishes the waterline slope on one side but greatly increases it on the opposite side.

The augmented slope on the outer or convex side, away from the deflection, may easily become greater than the critical slope for separation. Since the blunter waterlines are generally to be found above the shaft axis, it is wise, under these circumstances, to limit the deflecting portion of the skeg to the region *below* the shaft boss, leaving the upper portion symmetrical, with equal waterline slopes on each side.

In view of the limited pressure, and the low pressure gradient available on the convex side of a twisted skeg or stern, the water on that side is not easily changed in direction. This means that a relatively long time, coupled with a relatively long distance, of the order of 0.5 to 1.0 times the propeller diameter, may be required to impart to it any appreciable transverse component of velocity without risking separation. To take care of this situation, the asymmetrical slopes of the contra-ending are to merge gradually into the symmetrical waterline slopes ahead of them.

Generally no part of the median line is straight until it merges into the centerplane or the skeg construction plane. It may have a parabolic or other suitable shape. If it is expected that the ship will, in some service conditions, run with a portion of the contra-guide skeg ending exposed to the air, the terminal median-line slope at the free surface should not exceed about 3 deg. In any case, it is wise to work gentle slopes into any twisted skeg ending, consistent with achieving the desired prerotation of the inflow jet. If the owner and builder are to go to the trouble and expense of twisting such a skeg ending, the twisting can at least be done properly.

For twin-skeg endings, assuming outward-turning propellers, the twisting involves deflection of the lower portions of the skegs in an *outward* direction. This is inadvisable if it produces markedly *expanding* tunnel sides, specifically cautioned against in Sec. 67.21. On the other hand, one way to increase the efficiency of twin-skeg propulsion is to slow down the water in the lower after portion of the tunnel. Good design therefore indicates as much expansion in tunnel area in this region as is thought to be consistent with regular flow, to be confirmed by thorough tests in a circulating-water channel with the propellers driving. Any adverse or detrimental flow conditions pertaining to the twisted skeg endings will certainly show up when the flow pattern in this region is determined. This is specially recommended if the skeg endings have full lines, with large waterline slopes, and if contra-guide features are incorporated in them.

Indeed, a necessary step in the design of any contra-guide skeg ending, as it is for a deflection-type bossing and a contra-rudder, is a flow test in a circulating-water channel, using tufts, dye, or the equivalent, to check freedom from separation, irregular or cross flow, and any other questionable features.

Design rules for deflection-type bossings, usually more nearly horizontal than vertical, are given in Sec. 73.10.

Some notes applying to the incorporation of contra-guide features and contra-rudders in auxiliary sailing yachts and propeller-driven small boats are presented by F. A. Fenger [Rudder, Jan 1954, pp. 76–79].

67.23 Shaping the Hull Adjacent to Propulsion-Device Positions; Hull, Skeg, and Bossing Endings. One guiding principle in shaping a hull form to produce efficient operation of a selected propulsion device is that the inflow jet contracts in lateral dimensions and area as it approaches the device, normal to the flow direction. Further, this contraction continues in the outflow jet for an appreciable distance downstream from the device. These axial distances are of the order of at least one diameter in the case of a screw propeller; of the blade length, measured transversely, in the case of a paddle-wheel; and of the "basket" diameter in the case of a rotating-blade propeller. The contraction ratio, as pointed out in Sec. 16.3, is a function of the thrust-load factor C_{TL}. Since the thrust, the propeller-disc area, and the speed of advance are known reasonably well at this stage of the design the outlines of the inflow and outflow jets for open-water operation can be visualized by reference to Fig. 59.G.

A second guiding principle is that the hull should produce, in the region selected for the propulsion device, a flow of water which results in the most efficient and most uniform loading of the blades. For example, the swept volume of a rotating-blade propeller and a paddlewheel includes the whole thickness of the boundary layer next to the hull, as portrayed in diagrams 1 and 2 of Fig. 11.C, plus a region of potential flow outside the blades. This is not particularly objectionable, however, where the mechanism is able to take it. Furthermore, the sum of the overloading forces for all the immersed blades, as created within the boundary layer, remains nearly constant throughout each revolution of the device.

A third principle, really a corollary of the second, is that unavoidable local loading of the blades, one at a time, with the resulting unequal loading of the whole device, is to be reduced to a minimum. This occurs particularly when the tip or the outer portion of a single screw-propeller blade passes through the region of high wake velocity in a ship boundary layer or behind a zone of separation.

The commendable progress of the last two decades, in which screw-propeller blade shapes have been brought into close conformity with the drawings, is at the time of writing (1955) beginning to be matched by general refinements in sternpost, skeg, and bossing terminations at the forward edges of propeller apertures. The fact that individual propeller shaft struts had to be as thin as possible made it relatively easy to specify and to obtain sharp terminations at their trailing edges. Since the advent of cast-steel

sternposts and bossing or spectacle frames the square and blunt endings of forged-steel stern frames have largely disappeared. However, the slopes are too steep and the trailing edges of sternpost castings are in general still much too blunt to eliminate objectionable separation and eddying behind them. Also there is no more excuse to lap shell plating on the outside of a sternpost than to lap it on the outside of a stem. The effect is different but it is an objectionable discontinuity just the same.

The projecting portions of Thermit welds used to join several cast or forged sections of a sternpost—or a stem—need not be left for reinforcement. They can and should be trimmed off to conform to the shape of the adjacent parts. Likewise, butt welds can and should have the external reinforcements removed.

The slope angles on the trailing edges of skegs and other major parts should be 15 deg or less, reckoned from the known or the predicted direction of water flow. Drawings of these trailing edges should call for smoothnesses and tolerances of the same order as those required on shaft struts.

Despite all that is said here and elsewhere about the fining of skeg endings ahead of a screw propeller, experience indicates that some deliberate thickening of the skeg ending ahead of its termination increases the wake fraction at the disc position. It is particularly beneficial *below* the shaft axis in a normal form of single-screw stern, where the average wake fraction is usually much smaller than above the axis. The greatest thickening can be applied at the bottom, just above the keel, where the upward and aft flow of the water eliminates most of the boundary-layer wake. For this reason the thickening of such a skeg ending is called *clubbing*. However, the design of a club ending or bulbous skeg, illustrated in Fig. 25.L, is a ticklish procedure. If the thickening is carried too far, it may do more harm in producing vibration than help in improving propulsion [Williams, E. B., Thornton, K. C., Douglas, W. R., and Miedlich, P., SNAME, 1950, p. 78]. No design rules have as yet been formulated for this feature.

As a means of reducing the interference from a skeg ahead of a screw propeller the designer may shorten the skeg drastically, expose the propeller shaft, and support the propeller bearing by a V-strut just ahead of the wheel. This arrangement has been in use for many years on motorboats and larger vessels, such as on the center shafts of the German "schnellboote" or high-speed S-boats of World War II. Its use undoubtedly diminishes the wake fraction at the propeller but it may diminish the thrust-deduction fraction by a greater amount, and it may reduce the periodic vibratory forces from the propeller.

As a rule, the profiles of major hull and skeg endings are not too important except as they affect aperture clearances, discussed at length in the section following.

67.24 Aperture and Tip Clearances for Propulsion Devices. The lift load per unit area on the blades of any moderately loaded screw propeller, corresponding to the weight loading per unit of wing area on an airplane, lies within rather narrow limits, say 8 to 13 lb per in^2. Furthermore, the section shapes within the region of heaviest loading, say from 0.5 to 0.95R, are quite similar for both narrow and wide blades of a modern screw propeller. On this basis the circulation patterns and the pressure fields around all screw-propeller blade elements in the given radius range may be taken as roughly similar, using the expanded-chord length as a reference dimension. Based on these assumptions, the pattern of corresponding streamlines and isobars is roughly proportional in size to the chord length or blade width. Very approximately, therefore, at least for a not-too-wide range of thrust loading, a point in space one blade width from a blade element on one propeller is subject to the same pressure as a point in the same corresponding position, one blade width distant from a blade element on another propeller. This is an absolute rather than a relative value because, ahead of the propeller at least, the reduced pressure can not drop below the vapor pressure of water.

The foregoing argument may be a reason for specifying propeller-aperture clearances, defined in Sec. 33.3 and indicated in Fig. 33.D as "upper aft," "upper forward," and so on, in the form of absolute dimensions for a certain range of propeller diameters or ship sizes [ME, 1942, Vol. I, Table 1, p. 275; van Lammeren, W. P. A., RPSS, 1948, Fig. 73, pp. 127, 278]. It may be a reason even for specifying these edge clearances as functions of the propeller diameter [Ayre, Sir Amos L., INA, 1951, pp. 145–148]. It appears, however, that the propeller-aperture clearances are logically a function of the maximum blade width of the propeller.

In general, the aperture clearance *ahead* of the propeller, at the 0.7R, should be *equal to or*

greater than the expanded chord length of the widest element or section. It is pointed out in Sec. 33.3, and diagrammed in Fig. 33.E, that the clearance abaft the wheel, at the $0.7R$, may be less than that ahead. However, it should not be small enough to interfere with the circulation flow around the blade elements, or to bring the trailing edge of the blade through a region of large $+\Delta p$ ahead of a blunt rudder post or equivalent. A good rule is to make the after edge clearances, both upper and lower, as marked on Fig. 33.D, not less than the maximum thickness of whatever hull element or fixed or movable appendage may lie abaft the propeller.

It is well to note that the application of the rules given here require prior knowledge of the maximum blade width of the propeller which it to run in the aperture being designed. Also that most of the propeller charts employed to work out the preliminary design of a wheel, following Sec. 70.6, do not give the ship designer the blade-width data for the optimum propeller. He is then required to use the maximum expanded-chord width for that series propeller which best meets the needs for the preliminary design.

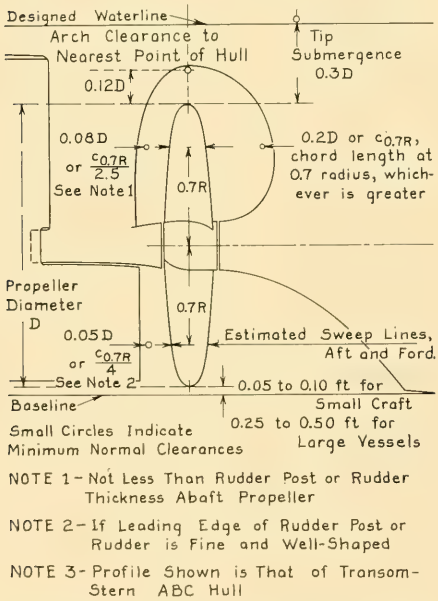

FIG. 67.U ELEVATION OF RUDDER HORN, PROPELLER APERTURE, AND SKEG ENDING FOR ABC TRANSOM STERN

Taking the 4-bladed Wageningen B.4.40 series, for example, the note in small print at the right of Table 8 on page 204 of the Dutch book "Resistance, Propulsion, and Steering of Ships" [RPSS, 1948] states that the (expanded maximum) blade-element length at $0.6R_{\text{Max}}$ is $0.2187D$. For the after aperture clearance, specified as not less than the thickness of the fixed or movable appendage lying abaft it, the designer is required to rough out these parts; this is, in fact, part of the preliminary stern design.

A general guide at this point as to the loading on the individual blades and the aperture clearances necessary is the value of the thrust-load factor C_{TL} on the propeller. If of the order of 1, the clearances may be somewhat on the low side. If 2 or greater, the clearances must be larger to avoid vibration.

Fig. 67.U is a diagram which indicates, by the small circles and the rules set down, aperture clearances which are in general acceptable, for a screw propeller not too heavily loaded. The contours give the actual clearances worked into the preliminary transom-stern design for the ABC ship.

Rules similar to those for single-screw propeller-aperture clearances govern for the edge clearances at the termination of bossings, multiple skegs, and the like, indicated in Fig. 33.B of Sec. 33.3, with the proviso that this clearance, at any propeller radius, should be not less than the expanded chord length of the blade at that radius.

It is difficult, with present knowledge, to formulate a rule for determining the hull tip clearance of a screw propeller, illustrated in Figs. 33.B and 33.C. In fact, probably no one rule or group of rules could cover all cases to be encountered in ship design. Two features, not entirely independent, are involved here. First, the propeller blade tip should not be subjected to brief passage through a region of high wake velocity where the lift and drag forces on its elements are suddenly increased. Second, assuming uniform, non-axial flow, a blade tip should not swing close enough to the hull to cause a sudden large force on the shell plating or an adjacent appendage due to the pressure field around the blade or beyond the tip.

Keeping the blade tips clear of high-wake regions is a matter of:

(a) Boundary-layer thickness, a function principally of absolute ship speed, of fore-and-aft

or x-distance from the stem, of transverse hull curvature, and of hull roughness

(b) Boundary-layer velocity profile, which is a function of hull roughness, transverse curvature, and other factors. For example, a tip clearance which may be greater than the boundary-layer thickness δ(delta) when the ship has a clean bottom, freshly painted, may be much less than δ when the bottom has been severely roughened by barnacles and other marine growth.

(c) The shape of hull endings, of skeg and bossing terminations, and of objects ahead of the propeller which may produce near-separation.

Keeping the hull clear of the most intense part of the blade-pressure field beyond the tip involves much more knowledge of this field than exists at present. For a given thrust loading it appears, however, to be a direct function of the circulation distribution at the tip. The assumption that this distribution is roughly similar for all screw propellers leads to one of the rules in present use, which gives the hull tip clearance as a function of the propeller diameter. Since the thrust loading among different types of ships varies rather widely, however, this latter factor can no longer be neglected. Furthermore, the circulation is increased and the pressure field is greatly intensified when the tip swings through a high-wake portion of the boundary layer. Both the factors mentioned therefore require careful thought and study when establishing hull tip clearances.

The shape of the ship sections opposite a screw-propeller position, whether concave and generally concentric with the propeller axis or convex to that axis, is an important feature, although it is not yet known how this effect is related to or combined with that of tip clearance.

The volume of the adjacent hull or appendage is at times a controlling factor.

Blade tips often pass an appendage or a part of the hull which occupies only a small area and a small radial distance in the plane of the disc. Examples are the shoe at the bottom of a sternpost to carry a lower rudder bearing or a rope and cable guard on a submarine. Only mechanical clearance is then necessary, say 0.10 to 0.50 ft, depending upon the size of the vessel. If the appendage is liable to be bent toward the propeller axis in service, as for the cable guard of the submarine, this clearance may be increased by say twice the dimension of the appendage, measured radially from the propeller axis. Another example is the V-shaped portion of the hull, sometimes rather narrow, lying above the arch of the propeller aperture in a single-screw stern of the canoe or whaleboat (cruiser) type. The volume is small and the obstruction occupies only a small part of the circumference around the tip circle.

An adjacent structure of considerable area, lying generally in a longitudinal plane passing through or close to the propeller axis, calls for greater tip clearance even though it is thin. A larger area is exposed to the pressure fields beyond the tips as the blades pass by. The tip clearance for such a structure could possibly be as small as $0.1D$ or less for a lightly loaded propeller, C_{TL} of the order of 1.0, yet as large as $0.2D$ or more for a heavily loaded one, with a C_{TL} of the order of 3.0.

An adjacent expanse of hull plating, generally flat in shape and more or less normal to the plane of the propeller disc, calls for an ample tip clearance, following the reasoning of Sec. 33.3 and of the preceding paragraphs. A logical and comprehensive rule has not yet been developed for calculating a minimum or a desirable tip clearance under these conditions. Incidentally, this clearance is measured transversely, in the early stages of a design, between the propeller disc or tip circle and the hull section directly abreast it. When it is known whether or not the propeller is to be raked, and when the slope of the adjacent hull surface can be determined, the minimum clearance is measured from the tip circle of the swept volume *normal* to the hull, as in diagrams 1 and 3 of Fig. 33.B.

The recommended method for selecting screw-propeller tip clearance abreast a generally flat fore-and-aft structure is to determine first, from Fig. 45.C or from Eq. (5.viii), the *nominal* thickness of the turbulent boundary layer at the x-distance from the bow selected for the propeller position. The *sustained* speed is the one used for this estimate because it gives the greatest value of δ. The boundary-layer thickness thus derived is only a rough approximation for large values of x, but it is at least an approximation.

It is also estimated, from the turbulent-flow velocity profiles of Fig. 5.K, that the friction-wake velocities in the outer half-thickness of the boundary layer are less than about 0.1 the ship velocity V. At the same time it is known that the boundary-layer thickness is increased by fouling of the hull surface, as in Fig. 22.H. It seems wise, therefore, to fix the hull tip clearance at a value at least as

great as 0.7 times the nominal boundary-layer thickness δ(delta).

For the ABC transom-stern design, at an estimated x-distance of 489 ft, δ is 2.8 ft from Fig. 45.I, and 0.7δ is 1.96 ft. From Fig. 66.Q the tip clearance at the top of the wheel, arrived at indirectly, is 2.62 ft. This should take care of a certain amount of thickening of the boundary layer under the stern due to fouling, for which there are no rules at present (1955).

Since so little is known concerning the effect of hull shape and curvature on this nominal thickness δ, wake measurements are made on a model at the proposed propeller position(s), extending from a point inboard as close to the hull as may be experimentally practicable, to a region outboard, at least $0.1R$ beyond the far side of the propeller disc(s).

The nominal boundary-layer thickness δ on the short model is greater in proportion to the scale ratio than the nominal thickness on the ship, described in Sec. 6.8 and illustrated in Fig. 6.E. This is compensated for by the inevitable thickening of the ship boundary layer when the hull surface is roughened by fouling. The propeller tip circle should, if practicable, be kept outside the boundary-layer region on the model where the wake fraction is 0.25 or more, reckoned preferably by the pitot-tube survey method illustrated in Sec. 60.6.

Where tip and edge clearances are both involved, as for the wing propeller of a twin-screw vessel with long bossings, and where vibration is to be minimized, the combination of theory, model tests, and experience all indicate that fore-and-aft edge clearance is more important than transverse tip clearance. In other words, it is better to move the propeller aft and to cut away the bossing termination as far as possible, than to move the propeller outward, away from the hull [Tomalin, P. G., SNAME, 1953, p. 592].

67.25 Baseplane and Propeller-Disc Clearances. The baseplane clearance for a screw propeller is determined by the service operating conditions, by considerations of drydocking, and possibly by the fact that the ship may rest on the bottom at certain wharves when the tide is out, as in the Thames at London. For a propeller unprotected by a shoe, say on a twin-screw craft, the baseplane clearance may vary from a minimum of 0.2 ft on small vessels to 0.5 or 0.7 ft on large ones [van Lammeren, W. P. A., RPSS, 1948, p. 279].

For certain vessels whose maximum or extreme draft is appreciably less than the channel or river depths where they are to operate, the baseplane clearance may be negative. The propeller disc then extends below the baseplane for a distance limited only by the height of the blocks when the vessel is drydocked or hauled out. Only rarely should this exceed 4 ft; probably 5 ft is a maximum.

When propellers are mounted abreast each other or nearly so their disc clearances may, if necessary, be reduced to mechanical values only, say $0.05D$, regardless of the direction of their relative rotation. Indeed, the large 19.5-ft twin screws of the old Atlantic liners *Teutonic* and *Majestic*, built in 1889, had a *negative* disc clearance of 5.5 ft [Maginnis, A. J., "The Atlantic Ferry," London, 1892, pp. 186–187; Cassier's Mag., Jan 1897, p. 231; Barnaby, S. W., "Marine propellers," 1900, pp. 64–65]. The port propeller disc was placed 6.25 ft ahead of the starboard disc and the tips of each wheel swung *beyond* the centerplane, to the opposite side of the vessel, through a large aperture in the centerline skeg. Contemporaneous accounts of the behavior of these passenger liners, at that time the largest on the Atlantic, make no mention of vibration or other disturbances caused by these overlapping propellers, possibly because of their large diameter and relatively light thrust loading.

When adjacent propellers are offset by appreciable fore-and-aft distances, as on quadruple-screw vessels of normal form, great care is required in establishing the disc clearance between the outboard and inboard wheels, reckoned by the projection of their discs on a transverse plane. The general direction of flow in way of these offset propellers is first approximated by analytic methods or determined by flow tests on a model, preferably in a circulating-water channel. Following this, it is necessary to sketch in the probable boundaries of the inflow and outflow jets of each propeller, doing this on a plane passing approximately through the propeller shaft axes and normal to the hull plating in the vicinity. On the principle that, at designed speed, the general direction of flow through the outflow and inflow jets is not modified appreciably by angular differences between the flow direction and the shaft axes, the propeller jets should be resketched to follow the general ship flow. They do not, in general, follow the shaft axes. When so modified the outflow jet of the forward propeller theoret-

ically should be clear of the disc of the after propeller. This means that if the general ship flow runs parallel to the ship centerline there can be nominal overlap of the propeller discs, with a small negative disc clearance, because of the contraction in the outflow jet of the forward propeller. In the *Omaha* class of quadruple-screw light cruisers of the U. S. Navy, designed in about 1919, there was negative disc clearance of this kind but the vessels ran successfully for many years without vibration troubles. Similar difficulties reported on other quadruple-screw vessels with offset wing propellers having positive disc clearances are believed due to excessive elasticity of the thrust-bearing foundations within the ship.

When a vessel with offset propellers turns with a drift angle, the propeller outflow jets change shape, rather drastically if the turn is a tight one. Undoubtedly in these cases the outflow jet of the forward or wing propeller on the outside of the turn passes through the disc of the inboard propeller. Two propellers on the same side of the ship can almost never be given sufficient disc clearances to avoid this interference.

67.26 Adequate Propeller-Tip Submergence. As a general rule the greater the tip submergence the better, until it reaches a value equal approximately to the propeller radius R. This is the standard or minimum tip submergence used for open-water propeller tests in model basins. There is no need of increasing it further unless to eliminate or reduce cavitation, or to insure adequate submergence when the ship is pitching heavily during wavegoing.

The tip submergence required for any load or operating condition, indicated in Figs. 33.B, 33.C, and 33.D, is a function of the:

(a) Thrust-load factor at which the propeller is intended to work. The greater the value of C_{TL}, the greater the submergence needs to be.

(b) Advance ratio or slip ratio, related to (a)

(c) Radial distribution of circulation along the propeller blade, particularly near the tip. Large $-\Delta p$ values near the tip call for a water layer of appreciable thickness over the propeller.

(d) Amount of shielding from air leakage which can be expected from the hull at the running attitude of the ship

(e) Increased (or decreased) nominal tip submergence due to a wave crest (or trough) over the propeller position.

Numerical values or ratios are not available for estimating the proper or minimum tip submergence as functions of (a) and (b). It is known only that the greater the thrust loading, the greater the advance ratio, and the greater the circulation near the blade tips, the greater is the $-\Delta p$ on the back of the blade tips and the thicker must be the superposed water layer to prevent air leakage. Regions of high wake velocity close to the water surface augment (a), (b), and (c) locally and call for good shielding.

If the hull shape is such as effectively to shield the propeller from air leakage, say in the form of a wide transom stern over a single wheel, the nominal tip submergence can be small, approaching zero. In fact, under the tunnel stern on a shallow-draft vessel the tip submergence is definitely negative.

For the thrust loadings and advance ratios on low- and medium-powered ships having propellers of adequate diameter, the increase in water depth due to the wave crest which forms at the stern when running at designed speed is usually sufficient to shield the wheel. Under these conditions, the nominal tip submergence may also be small.

When maneuvering rapidly, such as during crash-backs, the pressure differentials around the upper blade tips become extremely large. Shielding by the hull, as in tugs, is the only effective preventive against air leakage.

The degree of submergence—or emergence—expected during wavegoing is considered subsequently in Part 6 of Volume III, together with its effect on propeller performance.

67.27 Design for Minimum Thrust Deduction. The manner in which a thrust-deduction force is exerted on a hull, either inside the limits of the inflow jet ahead of the propeller or inside those of the outflow jet astern of it, leads to the conclusion that the transverse projected areas within these jet limits should be a minimum. This is accomplished for a skeg carrying a screw propeller by keeping the skeg as thin as possible for at least 2 diameters ahead of the wheel, within the limits of an imaginary cylindrical surface projected from the screw disc along the propeller axis, described previously in Sec. 33.2 and illustrated in Fig. 33.A. A large bossing carrying a wing propeller is likewise as thin as possible consistent with stiffness as a shaft support. For a tunnel within which a screw propeller is mounted the roof of the tunnel is not to drop too sharply

in the 2-diameter regions just ahead of and just abaft the disc. Fig. 67.M indicates that this condition is not met in the ABC arch-stern design.

A single-screw stern having an exceptionally thin skeg, with the after part *cut entirely away*, leaving the propeller supported by a projecting stern tube, is illustrated and described by H. Waas [STG, 1952, Fig. 9, p. 209, and Fig. 18, p. 214]. If found practicable in any particular case this is one way to reduce thrust-deduction and lateral vibratory forces at the same time. If the after end of the stern tube needs support, it can be provided by a V-shaped strut assembly.

Paddlewheels mounted abreast parallel waterlines or in way of the maximum waterline beam are admirably placed for eliminating practically all resistance-augment forces. In fact, it is quite possible, with a pair of paddlewheels amidships, for the $-\Delta p$ field to extend forward into the entrance and the $+\Delta p$ field back into the run. The differential pressures then generate thrust forces in the *ahead* direction and the thrust-deduction fraction is negative. It is unwise, however, to rely upon this unless it is confirmed by a model test.

The reduced-pressure field ahead of a sternwheel extends forward of the point of immersion of the foremost blade for a distance estimated as twice the maximum depth of blade immersion, or dip, as it is called. For this and other reasons, set forth in Sec. 72.11, the buttock endings of a sternwheel vessel are given an easy slope, and possibly reverse curvature, below the level of the wave profile at designed speed.

The first approximation of the resistance augment to be expected at the designed speed is found by the transverse-area method, described in Sec. 60.9. The method of performing this operation for the transom-stern ABC design is illustrated in Fig. 67.V.

67.28 The Final Section-Area Curve. When all principal parts of the underwater hull, excluding the appendages, are worked out sufficiently to indicate the distribution of volume

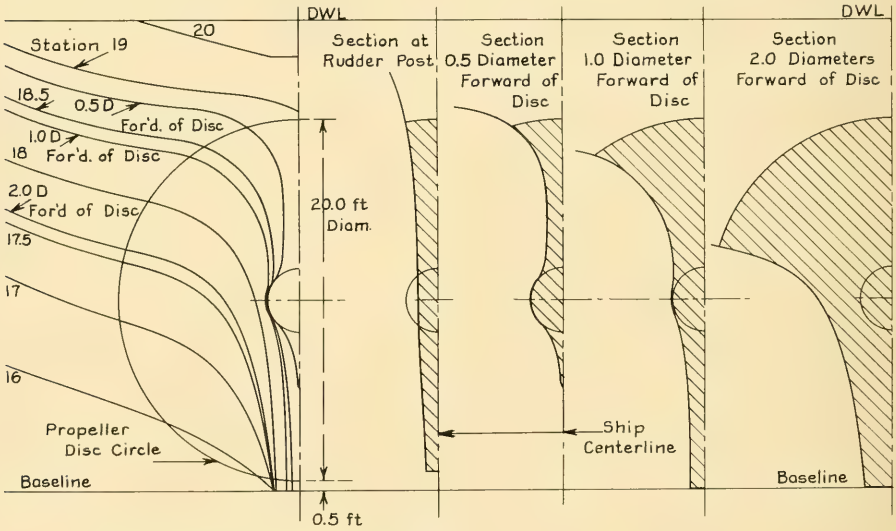

Station	Area Reading by Planimeter	Multiple	Area times Multiple
Rudder	138	7	966
0.5 D For'd	103	5	515
1.0 D For'd	248	2	496
2.0 D For'd	578	1	578
Prop Disc	988	Σ=15	Σ=2555

Weighted Area $= \frac{2555}{15} = 170.33$

Area Factor $= \frac{170.33}{988} = 0.172$

Predicted Value of t, from Fig. 60.P, is 0.135

Fig. 67.V Weighted-Area Diagram for ABC Transom Stern, for Prediction of Thrust-Deduction Fraction

throughout the ship length, a revised section-area curve is drawn. The areas are determined for at least 20 sections, the A/A_X values calculated, and a fair curve passed through the 21 ordinates. A bulb bow calls for fairing to a designated f_E value at the FP; a transom stern to an f_R value at the AP. A discontinuity of sorts is to be expected opposite a skeg ending, especially at the forward end of a propeller aperture. The final A-curves for the ABC ship, covering both types of stern, are drawn in Fig. 67.W.

Except for the regions known to be discontinuous the eye should detect no unevenness in the curve, nor should it appear when using a batten. However, the eye is often deceived by the presence of other lines in the vicinity, even those in the coordinate network. Hence the 0-diml curvature for at least 20 and preferably 40 stations along its length is determined by one or more of the methods described in Chap. 49 and is plotted to the same base as the section-area curve. Fig. 67.X shows a 0-diml curvature plot of the A-curve of Fig. 67.W for the ABC design with the transom type of stern, as well as similar plots for the Taylor Standard Series model, EMB 632 (modified), and for a merchant ship of good performance.

Integrating the section-area curve, by whatever procedure may be appropriate [PNA, 1939, Vol. I, pp. 13–27], gives:

(a) By its fullness coefficient, the corresponding prismatic coefficient C_P . For the ABC ship this should be within 0.01 or less of the selected value of 0.62.
(b) The molded underwater volume, without appendages, up to the designed waterline. This should correspond to the ABC ship displacement weight of 16,400 t for standard salt water.
(c) An accurate determination of $\overline{\text{LCB}}$, with respect to the FP, for reference and comparison purposes.

This revised A-curve may be considered as final if the analysis brings out no objectionable features or irregularities in it, if the values of C_P and $\forall$ are reasonably close to those selected, and if final fairing of the lines to a large scale indicates no appreciable changes in the amount or distribution of volume.

67.29 Modification of Normal Design Procedure for a Hull with Keel Drag. It often becomes necessary, for reasons of propulsive coefficient, rotative speed of the propelling plant,

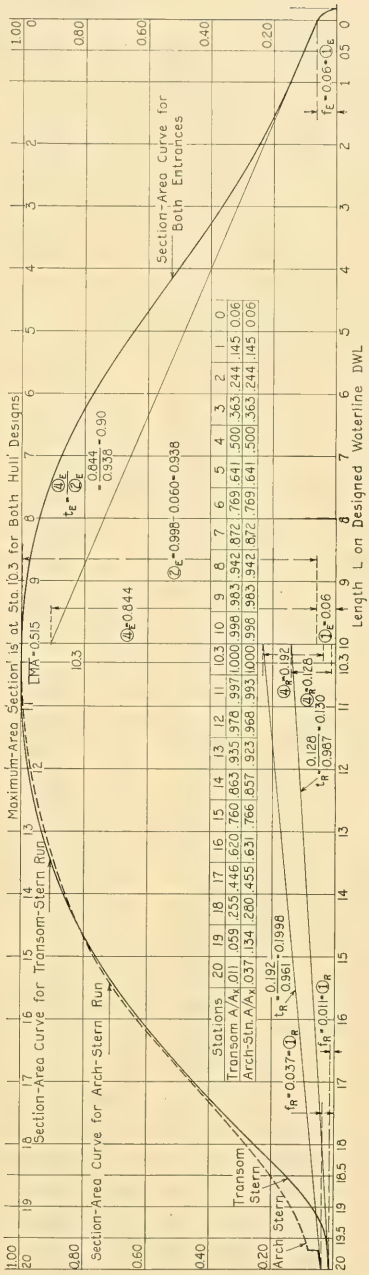

Fig. 67.W Section-Area Curves for Transom-Stern and Arch-Stern ABC Designs

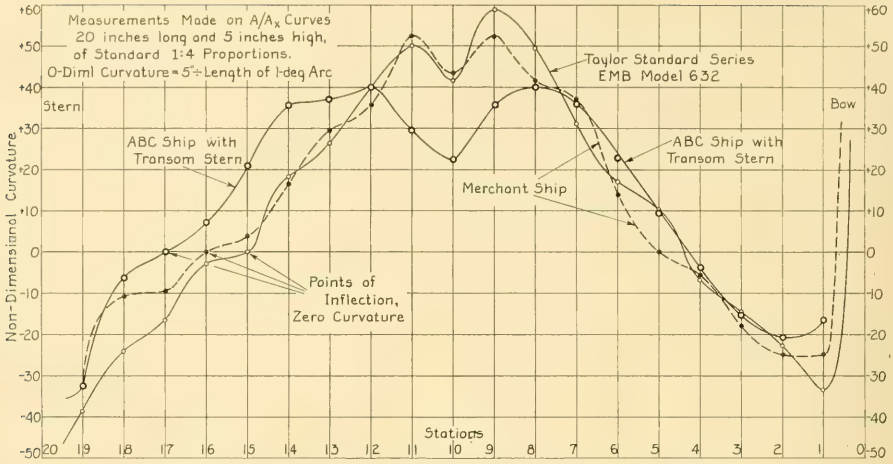

FIG. 67.X NON-DIMENSIONAL CURVATURE PLOTS OF THREE SECTION-AREA CURVES

towing power, or maneuverability, to fit a screw propeller or other propulsion device which has an appreciably greater diameter than the draft of the hull, as worked out in the preliminary design. As it is not good to have the propeller tips constantly breaking surface, a projection of the propeller disc below the baseplane is accepted. This can be done, without protection for the lower tips, on a vessel like a destroyer which only rarely runs in water that is shallow relative to its extreme draft. The propeller blades in their lower positions can be protected against fouling with ropes or cables by a drooping skeg bar or a depressed extension of the keel. For substantial protection by the hull, in the case of ships which travel regularly in relatively shallow water, the keel line is inclined downward and aft until it passes below the propeller disc. At the same time the keel line is usually lifted under the entrance so that the mean draft remains about the same as for a design with propellers of normal diameter.

It is brought out in Sec. 66.32 that any ship in ballast or light-load condition should be trimmed sufficiently by the stern to keep the propeller well submerged. While such a vessel may run for a large portion of its operating time with a sizable trim aft, the situation is by no means the same as for a ship which is designed to run continuously in a corresponding attitude and to deliver its best performance under these conditions.

The keel drag necessary for propeller protection is often very large. There are cases of light-displacement passenger steamers in which the drag is equal to the mean draft, with a draft forward of only about one-third of the maximum draft aft.

A hull with keel drag may be laid down by constructing first a normal form with zero drag and then tilting all the waterlines, closing them up vertically at the FP and opening them out at the AP. This transformation is of course accompanied by a major shift aft of both the LMA and the LCB. Since the volume of the afterbody increases in this operation, there is no particular problem in shifting the CG aft to give the vessel the desired trim.

Another method of design is to rough out a hull of essentially normal form and then to stretch the centerline skeg vertically until the aftfoot is as deep as desired. There is no need for cutting up the forefoot to correspond unless it is required for fairing or unless a long, straight keel is wanted for drydocking.

If the designed keel drag does not exceed about 0.1 of the mean draft, the difference between the performance of a vessel designed specifically for this drag and of one designed for zero drag and trimmed a corresponding amount by the stern should be small or negligible, of the order of 2 or 3 per cent. The performance with drag may be better, due to finer waterline slopes in the entrance, increased immersion or submergence of the

propeller, or other causes. On the other hand it may be worse because of increased drag due to separation behind fuller waterlines at the stern.

If the keel drag is limited to small amounts it may easily become more of a nuisance in laying out or building the ship than a help in its service performance.

67.30 Underwater Exhaust for Propelling Machinery. A passenger-carrying vessel having propelling machinery that produces gaseous products of combustion and that is intended to run at all times with the propeller(s) fully submerged offers a favorable opportunity for installation of underwater gas exhaust. This is especially true if the gas-producing portion of the propelling machinery can be placed close to the stern, and if the draft aft is reasonably constant.

On the basis that an alternative vertical gas outlet is provided in the form of a tall post or slender stack, to care for lighting off, port operation, low-speed running, maneuvering, and emergencies, it may be assumed that the duct area required for underwater exhaust need be no greater than that for vertical exhaust at full power. This takes no account of the possible condensation of steam in the exhaust gases or the use of stack-gas cooling as a margin against too high velocity of the combustion gases in the ducts leading to the underwater stern outlet.

To insure that the gases are discharged into the separation zone deliberately formed abaft the stern, within the variations in draft which will occur there, a high-level as well as a low-level gas outlet is required. Both may be connected to the gas discharge lines which should enter the high-level outlet box from the top, to prevent entry of sea water back into the gas line. Escape of gas from the high-level outlet when running at the shallower draft at the stern is prevented by a combined gravity- and buoyancy-operated flap valve which closes when it is above the waterline but opens when it is submerged.

On the basis of limiting slopes of 15 deg for separation at the light- and deep-draft waterlines of a vessel of about the size of the ABC ship but having a canoe stern, the separation zone is estimated to extend from the AP to points at least 20 ft forward on either side. Assuming a depth of 2 ft for each outlet screen, one-third of the length of the separation zone on the two sides is ample to provide the necessary outlet area. The estimated back pressure is of the order of zero, or it may be slightly negative, due to the $-\Delta p$ in the separation zone. Further model and full-scale experiments are necessary to verify this point.

When underway in smooth water the stern-wave crest may rise above the at-rest designed waterline by an amount estimated as from 2.5 ft to 4.0 ft, depending upon the stern shape and other circumstances. It may be necessary to provide several levels in the outlet boxes so that one may be selected which best suits any given operating condition.

When the ship is pitching in waves so that the selected underwater gas outlet for the mean draft is alternately submerged and exposed, it may be necessary to lock the flap valves closed in the outlet boxes and to resort to vertical stack-gas discharge.

67.31 General Notes on Water Flow as Applied to Hull Design. At the risk of boring the reader with duplication it can not be too strongly recommended that the flow pattern and the wake diagram at the positions proposed for any type of propulsion device be adequately investigated and recorded on a model by chemical or physical means, by strings or tufts, and by spherical-ended pitot tube. These data should be given great weight when finally fixing the form of the ship and its appendages adjacent to the propeller positions and when establishing the propeller clearances.

It may be taken as an axiom, in the detail design of the underwater hulls of ships and their appendages, that separation and cavitation and all other forms of discontinuity in a liquid, whenever and wherever occurring, are detrimental to good performance. As such they are to be carefully and systematically minimized or avoided altogether.

CHAPTER 68

Layout of the Abovewater Form

68.1 General Design Features, Exclusive of Wavegoing. Were it not for wavegoing requirements the abovewater portions of a ship down to the ship-wave profile at designed speed could be given a strictly utilitarian shape. This shape might even be found adequate to meet damage-control and floodability requirements. Actually it is done with many ferryboats, day-service passenger vessels for inland waters, river and harbor craft, and canal boats. Since the abovewater shape of the average seagoing vessel is so intimately related to wavegoing, a considerable part of the discussion pertaining to it is found in Part 6 of Volume III. The design rules in this chapter therefore apply principally to ships of all types operating in protected waters, as well as to those features covered by the general service of every vessel.

68.2 Reserve-Buoyancy Requirements. Reserve buoyancy in the form of intact or watertight volume of the main hull above the designed waterplane, a rather important feature of submersible and submarine vessels, is rarely set down as a design item for a surface ship. It is not to be found in the requirements of Chap. 64 for the ABC ship. It appears partly as the customary specification for minimum freeboard to some specified deck, when the ship is designed to remain afloat with one, two, or three compartments flooded. It also appears as a requirement for an adequate range of transverse metacentric stability, although rarely stated in so many words. Wavegoing requirements are not forgotten but they generally take the form of a minimum freeboard, just mentioned, plus a rise of the weather-deck line forward and aft in the form of sheer.

For the heeling and change-of-trim conditions to be expected in service, assuming that the situations represented by them are essentially static, a certain margin of buoyancy or freeboard is necessary, particularly in the form of a limiting distance above the heeled waterplane. This takes care, among other things, of the overshoot action accompanying a relatively sudden list, or of incidental waves. The margin may take the form of a corresponding distance above the waterplane when trimmed, to give protection against the water in the crests of waves made by the ship's own motion or by passing vessels. Certain types of craft acquire temporary and unexpected lists, like the heel of a tug when a heavy towline tension is exerted transversely or the heel of a small day-service passenger vessel when a great many passengers crowd suddenly to one rail or the other. All craft may at times be subject to unsymmetrical loading and may have to run at the corresponding lists or trims for uncomfortably long periods.

The reserve-buoyancy volume could well be reckoned, not from the designed waterplane with the vessel at rest, but from the actual wave profile when the ship is running at its designed speed. For example, both the buoyant volume and the reserve-buoyancy volume of a small, fast tug have an appreciably different shape in way of the surface when the tug is running free than when it is pulling and standing almost still. It can be argued that a vessel will never be

running at its designed speed when it needs all its reserve buoyancy. The answer to this is that one never knows what a ship may have to do during its lifetime, nor what kind of rough handling and severe treatment it may receive when trying to do its best.

A logical and practical specification, supplementng that of floodability and range of transverse metacentric stability, calls for a minimum reserve-buoyancy volume, expressed as a percentage of the displacement volume below the designed waterplane. A minimum of 25 per cent for a new vessel is a reasonable and not particularly exacting requirement. Reserve-buoyancy ratios for a number of submarines, of the vintage of 1901 through 1918, are given by E. Dodero [Ann. Rep., Rome Model Basin, 1941, Vol. X, pp. 95–107]. These vary from 0.112 through 0.467, averaging 0.252. The watertight closures of a surface ship are by no means as secure as are those of a submarine, so these values represent some sort of minimum for the average surface vessel. For the latter, a maximum of 0.35 or more is not too much. This, with freeboard and other requirements, should insure that hatches and other vulnerable hull openings are reasonably out of reach of the destructive action of solid, green water [Goodall, F. C., "Whaleback Steamers," INA, 1892, pp. 192–193].

Even though the hull may be extended farther upward than reserve-buoyancy requirements demand, such as the deck of a ferryboat which must match the top of a landing platform at various stages of the tide, it may not be necessary to build an intact or watertight hull all the way up.

One item taken care of in floodability calculations but often overlooked on small vessels for which these calculations are not made is the matter of the *fore-and-aft position* of the reserve buoyancy. If a craft is bilged and flooded aft it does little good to have a great volume of reserve buoyancy forward. On many fishing vessels, especially tuna clippers, the freeboard aft is deliberately low to facilitate getting fish in over the side. It has to be recognized that the safety of these craft is equally jeopardized by the absence of adequate reserve buoyancy there [Hanson, H. C., "The Tuna Clipper of the Pacific," SNAME, Spring Meet'g., 1954, p. 6].

68.3 Freeboard and Sheer for Protected Waters. Any craft which produces bow and stern wave crests of appreciable height when underway in protected waters, such as a free-running tug, needs a certain amount of freeboard regardless of that embodied in the reserve-buoyancy requirements. If it may be called upon during its lifetime to operate when trimmed heavily by the bow or the stern it needs still more. The position and shape of the sheer line with reference to the designed waterline is then controlled largely by the wave-profile, trim, and reserve-buoyancy requirements.

The craft may have a curved sheer line, as for a seagoing vessel, or it may have a straight weather-deck line if the freeboard everywhere exceeds the minimum. However, there is an optical illusion involved in looking at any vessel with a straight deck line throughout its length which makes it appear that the hull is hogged slightly. When appearance is a consideration, it is desirable to incorporate some curvature in the deck or hull line at the side, with the bow normally higher than the stern and the stern higher than some position near or slightly abaft amidships.

If there are practical reasons for straight deck lines throughout a considerable part of the length, it is possible to retain the sheered appearance by adding sheer only at the bow, or in the forebody. By the clever and artistic use of curved bulwark lines, combined with the slight depression in the deck edge at the side due to camber, or even of curved painted lines on the hull, it is possible to avoid entirely the appearance of hogging while holding a perfectly straight deck line at the centerplane.

"It was generally found best for appearance' sake to fix the lowest point of the freeboard about one-fifth to one-seventh of the ship's length abaft amidships; and to give rather quicker curvature aft so as to prevent the tangent to the sheer line falling below the horizontal when the ship had the maximum trim by the stern" [Narbeth, J. H., INA, 1942, pp. 144–145].

68.4 Freeboard and Sheer for General Service. Concerning freeboard requirements for general service, it may be well at this point to review the object of freeboard, and its functions. These were well expressed some seventy years ago in the following terms:

"Perhaps the most important of these are: to limit the ship's load; to provide a reserve of buoyancy, both as a margin against leakage and as lifting power in a sea way; to assist in securing a sufficient range of stability; to provide a suitable height of working platform, and to protect the vessel from deck damage" [West, H. H., INA, 1883, Vol. 24, p. 205].

It is mentioned, in the discussion of reserve buoyancy in Sec. 68.2, that a certain *minimum* freeboard of the intact hull amidships, or at the lowest point of the sheer line, is more often than not regulated by law. This takes into account considerations of the range of transverse metacentric stability, floodability and damage control, rolling and righting energy, classification and insurance rules, and the like, which need not be gone into here. All these and other features are discussed by H. F. Norton in Chapter II and by J. F. Macmillan and J. P. Comstock in Chapter V of PNA, 1939, Vol. I. Normally the minimum freeboard based upon the considerations set forth therein is sufficient to meet the wavegoing requirements for the service of any particular ship. However, the freeboard may be and often is determined by the difference between the hull-girder depth D necessary for strength and rigidity, and the draft H. This is the basis for selection of the freeboard of the ABC ship amidships, explained in Sec. 66.30.

To this freeboard there must be added sheer at the bow, and generally also at the stern, if the vessel is not to be inundated when pitching at sea. As a rule, the lower the minimum freeboard the higher must be the sheer forward. The freeboard for wavegoing, discussed more fully under design for wavegoing in Part 6 of Volume III, is therefore usually measured at the bow rather than amidships, although the freeboard for good wavegoing is sometimes reckoned at 0.3 the length from the FP, or at 0.1 that length. The latter procedure is based upon the reasoning that the most objectionable water comes over the side at those positions.

Fig. 68.A is a diagram for selecting a value of the freeboard at the forward perpendicular in the preliminary-design stage. Its scale of abscissas is dimensional, for the reason that the average steepness ratio of natural waves increases as the wave length decreases. In other words, short waves are steeper than long waves. For a short craft like a fishing boat the ratio of freeboard forward to length must be large while for a large liner this ratio can be diminished considerably. The heavy curved line of the figure is intended to indicate this relationship. It is broken because its position is still tentative. In general, the ships with ratios above the line have proved to be good-to-excellent sea boats in service. Many of those below the line are definitely lacking in freeboard forward.

The minimum freeboard forward (and aft) is also determined by a combination of minimum freeboard amidships and a sheer height forward

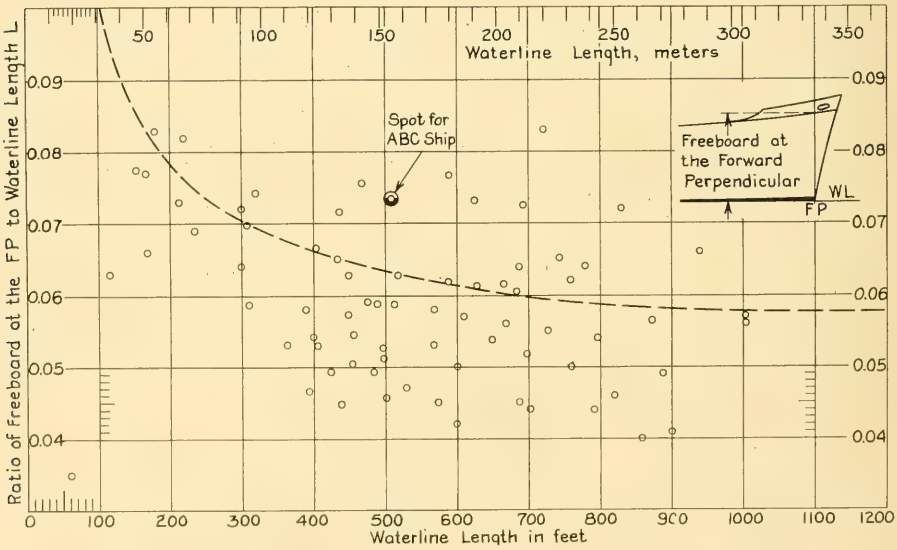

Fig. 68.A Tentative Freeboard Ratio for Ships Traversing the Open Sea

TABLE 68.a—Sheer Heights in Fractions of Waterline Length

Source and Reference	At Bow	At Stern	Low point of sheer from FP
Rankine, W. J. M., "Shipbuilding: Theoretical and Practical," 1866, p. 100, taken from plans of actual vessels			
Great sheer	0.033 L	0.017 L	
Medium sheer	0.02 L	0.01 L	
Small sheer	0.01 L	0.0 L	
Simpson's handbook, 1919, p. 50	0.0167 L	0.0055 L	
Maximum allowable German sheer, 1921, Mar. Eng'g., Apr 1921, p. 309	0.0292 L		
Proposed British standard sheer for flush-deck vessels, Mar. Eng'g., Apr 1921, p. 309		0.0131 L	
American Bureau of Shipping, PNA, 1939, Vol. I, pp. 66–67	0.0167 L +1.67 ft	0.0083 L +0.83 ft	Amidships
Talamanca, combination passenger and freight vessel	0.0186 L	0.0093 L	
Enern, whale catcher	0.0714 L	0.0262 L	0.5928 L
Southern Soldier, whale catcher	0.1175 L		

(and aft) to be added to this value. The ratio of sheer heights forward and aft to ship length, set down in Table 68.a, indicate little change in the past century for normal designs of merchant vessels but a great spread for vessels of even the same type. D. Arnott gives a diagram containing six different standard sheer lines for a 400-ft vessel, with ordinates in inches [Mar. Eng'g., Apr 1921, Fig. 4, p. 309]. All these lines have their low points at about 0.53L from the FP. The highest of them in the forebody is marked "Maximum Allowable German Sheer," and has a value of 140 in, or 0.0292L, at the FP. The highest in the afterbody is marked "Proposed British Standard Sheer (flush deck vessel)" with a value of about 63 in, or 0.0131L, at the AP.

The great spread of values in the data of Table 68.a also applies to the data upon which the tentative line of Fig. 68.A was drawn. A better shape and position for this line must await further hydrodynamic analysis and confirmation from reliable ship performance data.

The ratio of (1) freeboard at the bow to (2) length is found rarely to exceed 0.08 to 0.09. If the ratio of freeboard amidships to length reaches the range of 0.08 to 0.09, sheer forward is no longer necessary for wavegoing. Regardless of the freeboard amidships, a relatively high bow is built into special vessels like whale catchers, where personnel have to man stations at the forecastle head. Fig. 68.B is a recent excellent example of this type, the *Enern*, built for whaling in the rough waters of the Antarctic [MENA, Mar 1953, pp. 114–119]. Another is the Japanese whale catcher *Konan Maru 11*, with a very high gunner's platform at the bow [The Motor Ship, London, Oct 1954, p. 301; SBSR, 23 Sep 1954, p. 403].

If steep deck slopes are objectionable, sheer and freeboard are easily gained in large increments by the addition of a forecastle or poop on top of a deck with normal slope and sheer. This is carried to the extreme in lightships by adding a complete deck, so that the freeboard-amidships-to-length ratio may approach or exceed a value of 0.10.

As might be expected, a ship which is still safe with a low freeboard, like a tanker loaded with cargo having a specific gravity less than water, or a tuna boat on which heavy fish have to be yanked over the side by manpower, needs and profits by more sheer than the normal amount. In fact, long experience with vessels performing different duties indicates the need for at least four or possibly five kinds of sheer profile. Schematic diagrams of parabolic profiles, set down in

Fig. 68.C, apply to types of vessels in the following services:

(1) Low- and intermediate-speed merchant types, low point of sheer at or close to amidships, $0.50L$ from FP, sheer at stern about 0.5 of sheer at bow. In average heavy-weather areas the wave speeds are greater than the speeds of these slow vessels. For a considerable part of their running time they are being overtaken by seas, hence the need for rather large sheer at the stern.

(2) Medium-speed passenger and cargo ships and intermediate liners, low point of sheer at about 0.575 to $0.625L$, sheer at stern about 0.33 of sheer at bow. These vessels, running at speeds higher than those in (1) preceding, spend less of their time being overtaken by following seas. Furthermore, they often have more than the minimum freeboard in order to have internal space for accommodations. However, at the higher speeds, they pitch more than the slower vessels. With their finer entrances the pitching axis is farther aft.

(3) Large medium- and high-speed liners, low point of sheer at about 0.65 to $0.75L$, sheer at stern about 0.2 of sheer at bow. To obtain internal volume and superior wavegoing performance the freeboard is usually exceptionally high. This means that the pitching depth at the stem and at the stern are adequate without using great sheer. The latter may, in fact, be governed more by appearance than by wavegoing, or by the necessity for rapid shedding of the water that may come aboard.

(4) Tankers, trawlers, fishing vessels, and other low-freeboard craft, low point of sheer at from 0.5 to $0.65L$, sheer at stern about 0.7 of sheer at bow. An alternative straight-element profile for tankers is indicated in broken lines. There are inclined straight lines at the bow and stern and about half a ship length of straight sheer amidships, parallel to the baseline. Most of the tankers are in the same category as the intermediate-speed merchant cargo types, running for a large percentage of the time in overtaking seas. However, at these speeds they require more sheer aft than the cargo vessels because their average freeboard is less. The trawlers and fishing vessels heave to or creep along at slow speeds on all courses and in all weathers so that they are overtaken by waves to about the same degree as other ships encounter them.

(5) Tug and similar types, lowest point of deck profile at about 0.65 to $0.8L$, sheer at stern about 0.4 of sheer at bow. Ocean-going tugs may require from 1.5 to 2.0 times as much sheer forward as harbor tugs. To prevent the excessive heels mentioned in Sec. 68.2 it is necessary that the towing bitts of tugs be kept close to the water. This means that the low point of the profile is well aft, in the vicinity of the bitts, and that the sheer aft is the minimum permissible by standards of safety which have been proved in everyday service.

For sailing yachts the low point of the sheer line is usually much farther aft than for any other type. It can be as far aft as 0.75 times the overall length from the bow.

All the sheer curves in Fig. 68.C are arcs of second-order parabolas, $x^2 = -az$, where z is directed keelward for + values. Their axes are vertical and their vertexes are at the low points indicated by circles. The forward and after arcs belong to different parabolas but they can belong to the same one if the low-point position and the forward and after sheers correspond. New sheer lines are easily drawn by taking constant percentages of the ordinates shown in the figure, as illustrated for the sheer line of the ABC design.

If construction costs are a factor, any part or all of the sheer line may be straight, as shown in

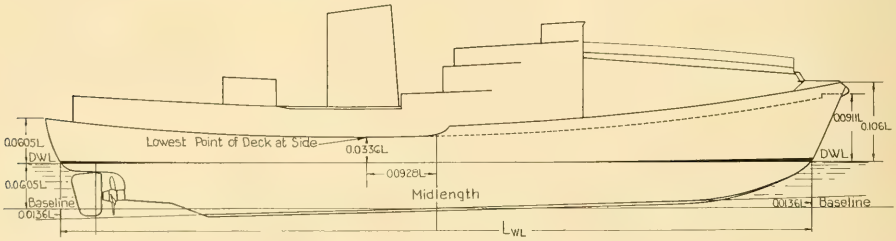

Fig. 68.B Typical 0-Diml Freeboard Ratios for a Whale Catcher

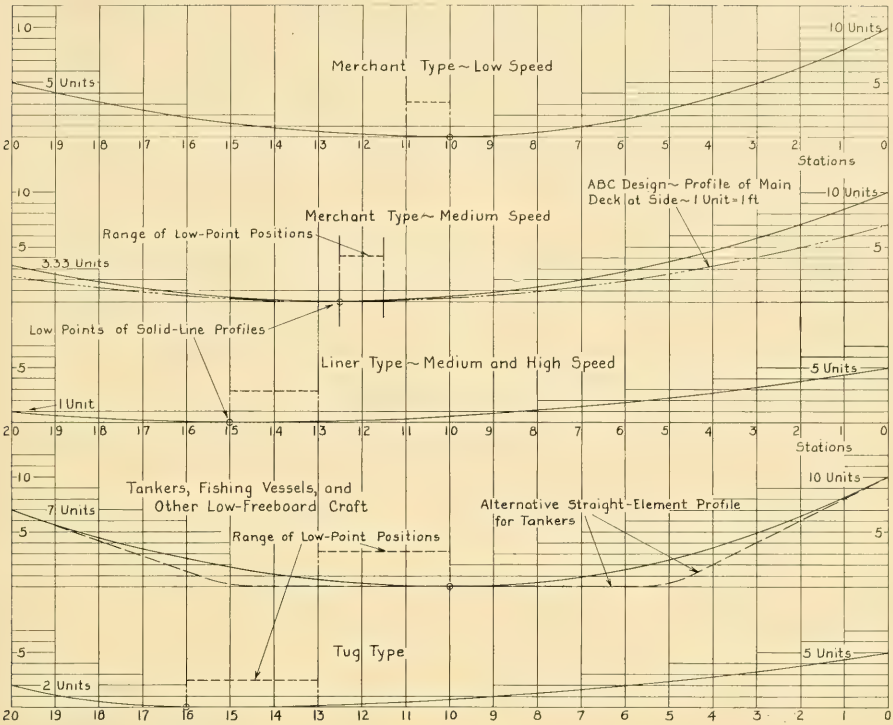

Fig. 68.C Non-Dimensional Sheer Lines for Five Classes of Vessel

broken lines for the tankers, provided the freeboard and the pitching depths forward and aft, described in Part 6 of Volume III, are adequate.

A factor to be considered on all craft which are required to travel in waves in ballast condition, when trimmed well by the stern, is that there should still be some residual sheer with respect to the at-rest water surface when in this attitude. Changes of trim due to loading alone may at times reach 3 deg, corresponding to a slope of 0.0524.

68.5 Design of Abovewater Section Shapes; Tumble Home; Compound Flare. The shape of the abovewater sections of a seagoing ship is governed partly by functional and utilitarian reasons and partly by wavegoing requirements. Design details pertaining to the latter are given in Part 6 of Volume III. Factors of importance in the former are:

(a) Large deck area at the ends as well as amidships, for carrying bulky cargo items such as miscellaneous vehicles, trucks and trailers, airplanes being ferried, small yachts, boats, and the like

(b) Large abovewater volume within the hull, for accommodating passengers or for storing low-density cargo or supplies

(c) Small deck area and small abovewater volume, for reducing top weights and lowering the CG

(d) Recessed or tumble-home sides, for clearing the abovewater portions of docks and other ships, especially when the ship is subject to roll from low swells or list from cargo handling and when adequate facilities are not available for keeping the ship breasted off.

The combination of continuously curved surface and near-surface waterlines with parallel level lines in way of the passenger accommodations well above the DWL is embodied to an almost exaggerated extent in the Netherlands passenger

liner *Oranje* of 1939 [Prins, H. N., and Ijsselmuiden, A. H., De Ingenieur, The Hague, Holland, 23 Jun 1939, p. 50; 30 Jun 1939, p. 74; WRH, 15 Oct 1939, pp. 316–323; TMB Transl. 128, Nov 1939]. The tumble home amidships is 8.75 ft in a height of about four decks above the DWL, for a waterline beam of 83.5 ft. This is so extreme that the lifeboats can not be launched clear of the ship's side.

Tumble home is not called for by the particular requirements of the ABC ship. It is incorporated, however, in the body plans of Figs. 66.P and 67.L, in an effort to provide parallel sides and constant beam in that portion of the ship set aside for passenger accommodations. Laying out, building, and equipping staterooms and similar rooms is greatly simplified if the region has parallel straight sides, practically zero sheer, and no deck camber, corresponding to a building on shore [Watsuji, H., SBSR, 2 Aug 1934, p. 118].

Tumble home is usually, but not necessarily confined to the abovewater hull. It may be extended below the DWL in order to achieve a reduction in C_{IT} , to modify the rolling characteristics in some respect, or to take care of a slight list when the vessel is in light condition [SNAME, 1905, Pl. 119].

It is often desired, for wavegoing, to incorporate flare in the abovewater sections forward for a considerable distance above the DWL. To avoid the excessive top weights and volumes involved by carrying that flare all the way to the weather deck, a compound-flare section of the type sketched at E in Fig. 26.B is useful.

Compound flare built into the bows of British cruisers for the past forty years has proved its worth in service. More recently it has been worked into the cargo vessels of the British *Windsor* class, both forward and aft [MESR, Jul 1952, pp. 89–90]. It is often of advantage, with no appreciable impairment of wavegoing behavior, to widen the deck below the weather deck so as to get more useful room there. This is because internal space lying above a ship's side with excessive flare is difficult to utilize.

The following method of working a compound flare into the abovewater entrance is adapted from that employed by the Naval Construction Department of the British Admiralty and is published with the kind permission of the Director of Naval Construction, Sir Victor G. Shepheard:

(a) The shape and position of the weather deck at the side is determined from operational and other requirements and is faired in the usual way, in all three planes. The section lines forward are faired into this deck edge and completed as though there were to be no compound flare.

(b) A fair knuckle line is then drawn on the outboard profile (sheer drawing) in the position desired for the lower edge of the diminished-flare region. Its vertical position, shape, and curvature depend upon the position of the internal decks below the weather deck, the anchor-stowage positions selected, and other factors. The line of the knuckle runs more-or-less parallel to the weather deck, or at a slope to it, either up aft or down aft, depending partly on appearance and the aesthetic sense of the designer.

(c) At two selected stations, about 1/3 and 2/3 the length of the knuckle from the bow, two level lines are drawn on the body plan, representing the height of the knuckle line at those stations, as taken from the outboard profile

(d) Two partial-section lines are projected down on the body plan from the weather deck edge, at the stations in question, to the knuckle level lines at those stations, giving the knuckle half-breadths. A suitable flare slope above the knuckle is about 80 deg (with reference to the horizontal). It is not necessary that the flare slope be constant for all stations; appearance and room inside the ship may determine this.

(e) Laying out the knuckle half-breadths at the two selected stations, and the fore-and-aft position of the knuckle line at the stem, a fair line is drawn on the half-breadth plan, giving the half-breadths of the knuckle at all stations along its length

(f) Level lines for the remaining stations are then added to the body plan, whereupon the knuckle half-breadths for these stations are laid off on them

(g) With the points thus determined the knuckle line projection is completed on the body plan, and the straight section-line segments above the knuckle are drawn in between the weather deck and the knuckle

(h) The original section lines below the knuckle are now flared out in easy curves to meet the knuckle intersections at the respective stations, after which the section-line segments above and below the knuckle, and the knuckle itself, are check-faired

(i) Adjustments may be necessary if the resulting flare below the knuckle is too great to avoid objectionable pounding or slamming

(j) For structural reasons the knuckle should be well clear of all deck edges along the shell.

The knuckle and the compound flare in the forebody sections of the ABC ship, delineated in Fig. 66.P, are laid out by the procedure described. The knuckle at Sta. −0.5 lies slightly above the knuckle line because of discontinuities in way of the single centerline bower-anchor position.

For vessels carrying wing screw propellers it may upon occasion seem wise to afford lateral protection to the propellers by widening the abovewater hull above them, rather than by fitting abovewater propeller guards.

68.6 Check of Range of Stability and Dynamic Metacentric Stability. At this stage in the preliminary design, if not before, a check is made to insure that:

(1) The range of positive metacentric stability, in a transverse plane and for the static case only, is adequate for the service expected of the vessel. This operation is particularly important for a vessel of special shape, such as sketched subsequently in diagram 1 of Fig. 68.K in Sec. 68.12. The method of accomplishing this is set forth in many text and reference books on naval architecture [PNA, 1939, Vol. I, p. 135].

(b) The vessel possesses adequate dynamic metacentric stability in a transverse plane; in other words, it has sufficient stored-up righting energy to more than absorb the dynamic rolling energy [Vincent, S. A., PNA, 1939, Vol. I, pp. 135–136]. This matter is discussed further under wavegoing in Part 6 of Volume III.

68.7 Abovewater Profile and Deck Details. The abovewater profiles of a ship, like the section shapes, are governed partly by the necessity of meeting certain wavegoing requirements and partly by utilitarian needs. They may result from fairing the sections into the ends, or from a desire to achieve a certain appearance. Centerline anchor stowages at the bow and stern, propeller-aperture clearances for single-screw vessels, and other features usually play a part more important than hydrodynamics [Coqueret, F., and Romano, P., SNAME, 1936, pp. 131–132].

In the main, however, the abovewater profile should, like the underwater profile described in Sec. 67.4, be a sort of automatic result of first determining the ship form desired, in transverse planes, and then carrying the hull surfaces forward and aft, in fair shapes, until they meet at the centerplane. This is what happened when the flaring, slightly concave abovewater entrance sections of the fast sailing ships of the 1840's were carried forward to produce what is now known as the clipper bow, pictured at 1 and 2 in Fig. 26.D.

It is regular shipyard practice to camber a straight stem to compensate for the optical illusion of concavity inherent in a perfectly straight stem bar [Baier, L. A., unpubl. ltr. to HES, 4 Aug 1950].

Profiles and planforms for transom sterns are discussed and illustrated in Sec. 67.20.

For the ABC ship the planform of the main deck is made elliptical at the stern, solely as a matter of appearance. Some additional abovewater volume and deck space are achieved by carrying the transom all the way up to the main deck, as has been done on many U. S. warships, but at the expense of some additional weight and an unquestionably heavy, clumsy appearance at the stern.

The forebody portions of the ABC transom and arch sterns, above the DWL, are exactly alike back to Sta. 11. However, the afterbody portion of the ABC arch-type stern above the DWL is slightly different from that of the transom-stern ship because of the greater waterline beam at the AP. The main deck planform and the uppermost level lines are rounded in the same way, except to a larger radius.

68.8 Selection of Deck Camber. A normal degree of circular-arc or parabolic camber in a weather deck, with a rise at the centerline amounting to say 0.020 or $0.025B_X$ for the widest part of the ship (0.25 inch per foot of beam corresponds to $0.0208B_X$), is some help in shedding water during wavegoing but it is hardly to be classed as a quick-unloading device for a boarding sea in an emergency. Constructions for circular and parabolic arcs are illustrated at 1 and 2 in Fig. 68.D; also by G. de Rooij in "Practical Shipbuilding" [1953, Figs. 329a and 329b, p. 133].

No one camber shape among a number that are available has any particular hydrodynamic superiority or significance. The camber may be appropriate, therefore, to the drafting as well as to the shipfitting and fabricating procedures. For this reason a fixed camber curve may be used for all widths of deck along the length. The curvature or slope need be sufficient only to insure that, within the life of the ship, there will be *no depressions* in the deck at any small heel angle because of ill-formed or buckled plates or minor service damage.

Flat, straight decks are admittedly economical

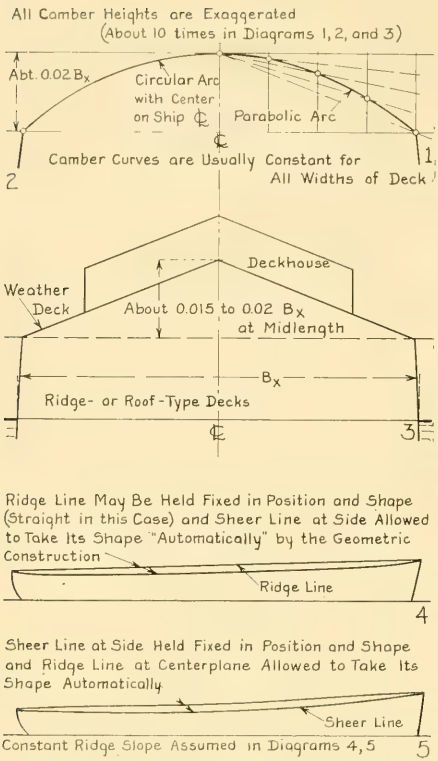

FIG. 68.D STRAIGHT AND CURVED DECK CAMBER LINES

in the drafting, shipfitting, and fabricating stages but no ship deck, certainly not one of metal, ever finishes flat nor does it remain flat. It always bends downward under its own weight, if not under compression loads due to riveting and welding. Generally there are more plating buckles downward than there are upward. Here is a case where the greater stiffness of an aluminum deck plate of equal or slightly less weight might be a distinct advantage.

Ridge-type decks, like the low ridge roof of a house, illustrated at 3 in Fig. 68.D, are composed of two flat surfaces each lying at a small angle to the horizontal, only large enough to insure drainage in service, and joined in a low knuckle at the centerline. This knuckle is a straight line if the ridge surfaces are flat [Dawson, A. J., SNAME, 1950, Fig. 10, p. 13]. However, the knuckle can be curved, with a sheer incorporated in it, leaving the deck-beam lines composed of two straight elements, lying at a constant angle to each other. The ridge surfaces are then developable cylinders of very large radius.

In fact, if a circular or parabolic arc of *constant shape* is employed for the deck-beam lines on a cambered deck, and if the intersections of the deck-beam lines with the centerplane lie on a straight line fore and aft, as at 4 in Fig. 68.D, the whole deck is a developable cylindrical surface. If the deck line at the center or at the side follows a curved sheer, corresponding to 5 in the figure, the departure from true cylindrical form, for any one plate, is usually insignificant.

A ridge-type deck, having the same rise at the centerline, possesses considerably more slope amidships and less slope at the sides of the vessel than a camber with a circular arc or even with a parabolic arc. Whether this represents an advantage for the straight-element deck in shedding water is debatable, especially as at one angle of list the high side has no slope at all.

68.9 Bulwarks and Breakwaters. Bulwarks, either partial or full, are appropriate for both large and small vessels when it is desired to:

(a) Afford some protection along a deck edge against wind and spray blowing across the deck
(b) Prevent marginal waves and crests from slopping over onto the deck
(c) Retain on board loose gear, small items of deck cargo, fish dumped from nets, and the like.

If the owner desires or permits, bulwarks may be added solely for the sake of appearance, as when carrying a graceful sheer line along a straight deck edge.

While bulwarks can hold back some marginal water from coming over a deck edge they can and do keep on deck large menacing weights of water which need to be unloaded quickly, before the next sea comes aboard. Freeing slots along the lower edge of the bulwarks, or hinged-cover freeing ports in the bulwarks, are provided for this purpose but the average head to make water run through them rapidly is rather low. Furthermore, the port edges are usually sharp and the orifice coefficient is also low.

It is customary to provide a port opening of 0.1 the bulwark area and to limit the bulwark height to 5 ft [Lovett, W. J., "Applied Naval Architecture," 1920, p. 174]. This rule takes no account of the width of the vessel and the volume of water trapped between bulwarks of a given height, apparently on the theory that for a given

angle of heel, the greater part of the water on a wide ship spills over the top of the bulwarks.

To require that a deckload of water, up to the top of the bulwarks, should run off completely within the interval of one pitching cycle would practically require taking away the bulwarks altogether. It is therefore necessary to assume that some roll angle or pitch angle, or both, will unload most of the water over the bulwark rail. To get rid of the rest of the water in one pitching or rolling period it appears that the freeing-port area should be more nearly 0.2 the bulwark area. Furthermore, this freeing-port area should be provided *abreast* the volume which needs to be emptied if the vessel ships a deckload of solid water.

Bulwarks at the extreme bow can serve as an effective increase in freeboard in that region, over and above that provided by the intact hull. If not extended too far aft, say to not farther than the point where the local beam exceeds $0.5B_X$, it should be possible to leave them solid, without freeing ports or slots.

Breakwaters require positioning and shaping so that the maximum water is deflected for the minimum of splash or spray over the top. This calls for a deflecting surface which is never—or rarely ever—normal to the onrushing water and which does not form an objectionable spray-thrower for water in quantities greater than the breakwater is designed to handle. The water deflected from the forward side should have no upward component, and as great an outward component as possible, to throw it toward the gunwale and get it off the deck. Fig. 68.E illustrates, at 3 and 4, two alternative methods of accomplishing this. The function of the horizontal lip along the top of the barrier is to throw moderate quantities of water back forward but to permit large quantities to pass over the breakwater without too violent obstruction.

The breakwater on a forecastle is usually of V-shape in plan, with its vertex forward and with diagonal sides extending practically to the deck edges. The planform angles may vary from 45 to 60 deg with the centerline, indicated at 1 and 2 on Fig. 68.E. The height at the center, where the water can not run off the deck freely, should be higher than at the sides. A breakwater having an elliptic or parabolic planform, with the sharp curvature forward, is shown for an early German "schnellboote" (high-speed boat) in Schiffbau [26 Oct-2 Nov 1921, Fig. 4, p. 114]. There may be two breakwaters in tandem, separated by an appreciable fore-and-aft distance, so that the water spilling over one is trapped by the second. A set of tandem breakwaters of concave section is fitted on the French battleship *Jean Bart* [The Ill. London News, 9 Apr 1955, p. 661].

A breakwater of any type requires adequate bracing against the hydrodynamic forces. These are not accurately or even roughly known but their order of magnitude may be estimated by assuming a dynamic load imposed by solid water striking the breakwater at a certain velocity. For a head sea, or an angle of encounter α(alpha) of 180 deg, this is compounded of (1) the speed V which it is estimated the ship can make in heavy weather and (2) the orbital velocity U_{Orb} of the crest of a wave which breaks over the forecastle and strikes the breakwater. While, strictly speaking, the dynamic pressure is that due to the component of $(V + U_{Orb})$ normal to the breakwater, there is little assurance that the deck load of water sliding aft on the forecastle will strike the breakwater from ahead. The blow may just as well come from the side, striking against one face for

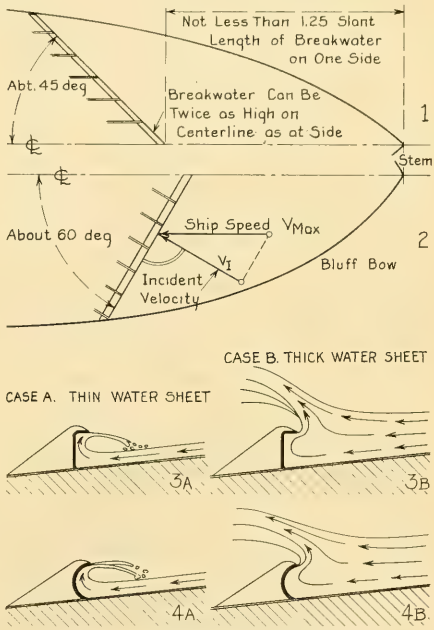

Fig. 68.E Design Sketches for Forecastle Breakwaters

its whole length. Only one such impact is necessary to tear loose a breakwater that is not sufficiently strong or sturdy. It appears unwise, therefore, to use for the design any striking velocity less than the sustained speed V plus the orbital velocity U_{Orb}.

The force on the breakwater, exerted parallel to the deck, may be taken as that developed by a uniformly distributed ram pressure $q = 0.5\rho(V + U_{\text{Orb}})^2$ acting over the whole area of the face. When an obstruction of this kind deflects onrushing water back upon itself there is usually a doubling of the impact load. This is compensated for in the present instance by the fact that a stream of water only half as high as the breakwater can be reversed in direction by the action of the deflectors shown in Fig. 68.E. A deeper layer of water is only deflected upward, with a ram pressure corresponding to $(V + U_{\text{Orb}})$ and a force on the breakwater that is not doubled. Fitting the breakwater at an angle of from 45 to 60 deg to the ship centerline, indicated in the figure, deflects water outward and helps to reduce the impact load on the structure for seas coming from directly ahead.

For the ABC design, it may be assumed that the ship can maintain 18.7 kt in a sea made up of regular waves 800 ft long with an angle of encounter α of 180 deg. If these waves have a steepness ratio as great as 1/20 the orbital velocity in the crests is, from Table 48.e, approximately 10 ft per sec. The nominal striking velocity is then 31.6 ft per sec (equivalent to 18.7 kt) plus 10 ft per sec or say 42 ft per sec. Taking a round value of 1.00 for 0.5ρ in salt water, the ram pressure is approximately $1.00(42)^2$ or 1,764 lb per ft^2. This is just over 12 lb per in^2. The ultimate-load factor for an installation of this kind, where it is particularly important that it not be torn loose or that leaks should not be started in the forecastle deck, should be at least 5 times the calculated load.

If it is desired to expend only a moderate amount of weight on a breakwater, the generation of excessive ram and dynamic pressures on it is prevented by cutting holes in it. These are of moderate size, at about midheight. The holes permit the breakwater to catch and shed small amounts of water but relieve the load on it when large quantities of solid water come rushing against the breakwater structure [SBMEB, Jan 1954, p. 43]. In this respect it resembles the dive brakes of certain airplanes, in the form of flaps rather well perforated with holes.

68.10 Design of Anchor Recesses. Protruding stockless anchors are unsightly and they are abominable spray-throwers. They represent definite collision hazards in that such an anchor can tear open the whole side of another ship, when the bumping or sliding damage might otherwise be slight.

It is reported that on the German World War II battleships *Bismarck* and *Tirpitz* the anchors were hauled, not into orthodox external hawsepipes or anchor recesses but up onto the main deck. There they lay flat, suitably secured. When it was desired to anchor, they were apparently pushed over the side by mechanical gear. This left the sides of the bow entirely clear of any major projections or recesses, and eliminated the throwing of spray from that cause.

On the German World War II cruiser *Prinz*

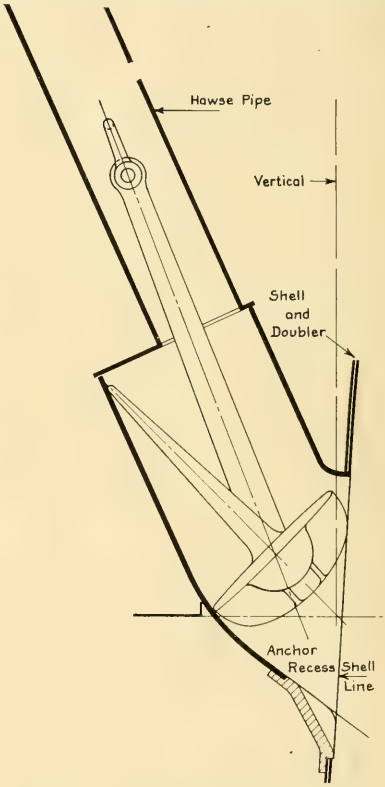

Fig. 68.F Anchor Recess as Used on Great Lakes Freighters

Eugen the spare anchor was stowed in a centerline hawsepipe well up in the clipper bow but there were no hawsepipes as such for the port and starboard bower anchors. They were drawn up, practically on top of the weather deck, onto shelves built into the side and the deck at the gunwale, where the anchors lay nearly horizontal. An arch piece over the stock held the anchor in position and kept the chain from jumping out of the shelf. However, because of the acute angle between the stock and the deck line a projecting bolster was necessary. These bolsters and the anchors could still throw some spray. Similar stowages have been provided on certain classes of small combatant vessels of the U. S. Navy during the 1940's and 1950's.

Recesses of varied types have been worked into ships in the past to house stockless anchors, many of which are still unsightly and are objectionable spray-throwers. A proper anchor recess should really house the anchor, not only within the fair line of the side but, so far as practicable, within the hull plating itself, leaving only enough opening to pass the anchor when the flukes are in line with the stock. Recesses for stockless anchors may properly be fitted on vessels as small as 100-ft harbor tugs [AM, Apr 1953, p. 21].

Anchor recessing is accomplished on the Great Lakes by the general arrangement shown in Figs. 68.F and 68.G, in successful use there for the past four or five decades. The "backroom" required for this scheme is made available in lake freighters by the extremely blunt waterlines in the vicinity of the recess and the hawsepipe, with horizontal slopes of the order of 40 or 45 deg. On the British battleship *Vanguard*, completed in the late 1940's, the external surfaces of the anchors form a remarkably fair continuation of the adjacent ship's side [Ill. London News, 18 Sep 1954, p. 473]. On some British passenger liners of the same era, among them the *Himalaya*, the anchor recess opening is not much larger than the crown and tripping lugs of the anchor, corresponding to the small openings on the Great Lakes freighters.

On bows of relatively fine form, completely recessed stockless anchors can be fitted by offsetting the port and starboard anchors in some convenient fashion, and by bringing the chain for each bower anchor up on the *opposite* side of the vessel. This arrangement gives space for each anchor recess about equivalent to the full width of the bow instead of limiting it to a space on its

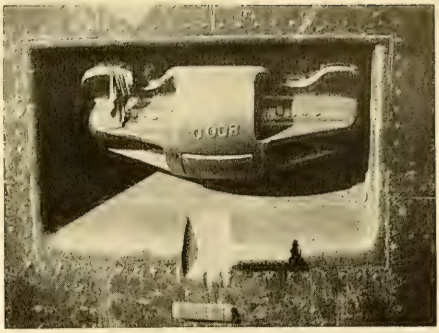

Fig 68.G Anchor Housed in Recess, Great Lakes Freighter

Photograph by courtesy of the Great Lakes Engineering Works

respective side of the centerplane. Crossed recessed anchors were used successfully on the 3,000-ton U. S. Navy submarines *Argonaut*, *Nautilus*, and *Narwhal* in the 1920's, and may have been used elsewhere.

Wherever an anchor chain under load changes direction on a ship, at least three consecutive links should bear on some fixed bolster or structure. Since the chain can lead in a great range or directions in service this poses a problem, whether the chain comes out of a hawsepipe recessed in a pocket or whether it runs over an external bolster. The designer must also remember that there is little to be gained by pulling the anchor up into a recess and then adding, *outside* the fair plating surface, a tripping plate or bolster that will throw nearly as much spray as the anchor itself.

It is also a problem to provide an external bolster large enough, let alone the lower corner of a recess within the hull plating, for a bower anchor which must drop clear of a sizable bulb at the forefoot.

Considering specifically the ABC design, with an abovewater bow shape shown on Fig. 67.E, there is sufficient beam at the level of either the main or the forecastle deck to permit full recessing of stockless anchors in the usual way. This would involve crossed chains, however, leading the starboard anchor chain to the port wildcat and vice versa. As the vessel is not to be required to moor with two anchors and a single chain in normal service, there appears to be no objection to protecting the anchor windlass from the weather by mounting it on the main deck under cover.

However, the width of the abovewater body at the hawsepipes is so narrow, as compared to the width of the bulb bow under them, that a dropping anchor is sure to strike the shell plating at the bulb.

It is therefore proposed that the ABC ground tackle consist of:

(a) One heavy under-the-bottom anchor, housed and handled as outlined in Sec. 68.11

(b) One abovewater bower anchor housed in a centerline hawsepipe in the stem, with its flukes drawn up tightly against the projecting bow, above the crown and forward of the hawsepipe.

68.11 Proposed Under-the-Bottom Anchor Installation for Ships with Bulb Bows. Since an anchor is always used under water it seems absurd to hoist and carry it above water, unless possibly to clear turns of chain which are wrapped around it accidentally. Under-the-bottom anchors were installed on the famous ironclad *Monitor* and on several British-built vessels of the 1860's. They have frequently been proposed through the years for ships that could not house them conveniently above the water; one such was the "great mushroom anchor" to be hung under the semi-globular naval battery *Cerberus* [SNAME, 1904, Pls. 7, 18½]. A combination of underwater mushroom anchor and abovewater stockless anchor was in use for many years on U. S. submarines in the early part of this century [Nimitz, C. W., USNI, Dec 1912, pl. facing p. 1200]. G. de Rooij shows an under-the-bottom anchor for modern submarines ["Practical Shipbuilding," 1953, Fig. 611, p. 264].

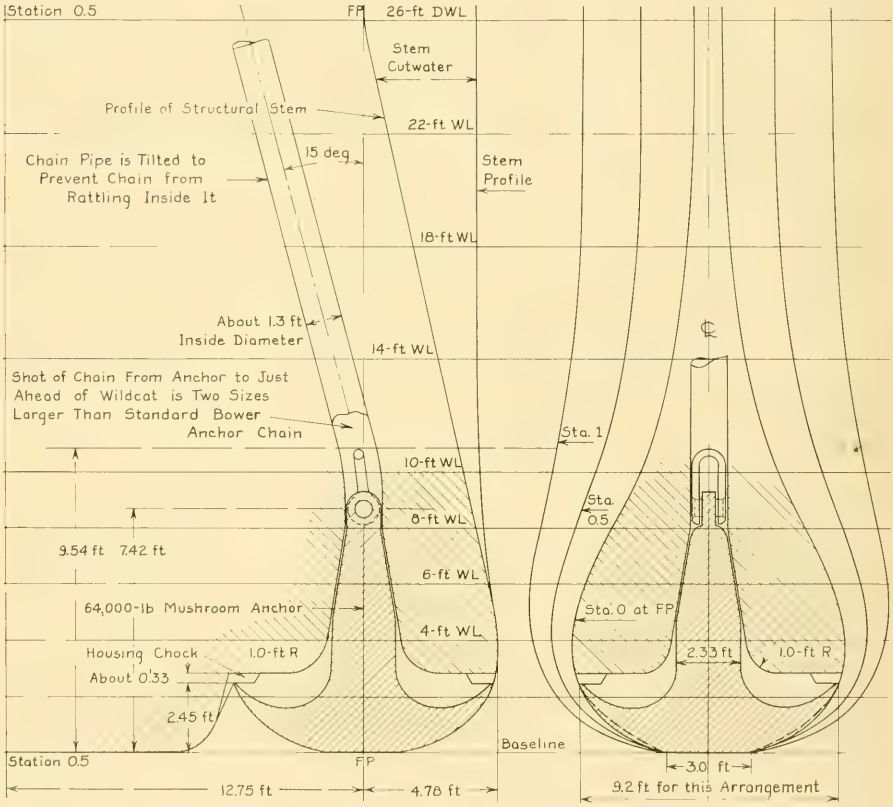

Fig. 68.H Proposed Housing for Mushroom Anchor in a Bow Bulb

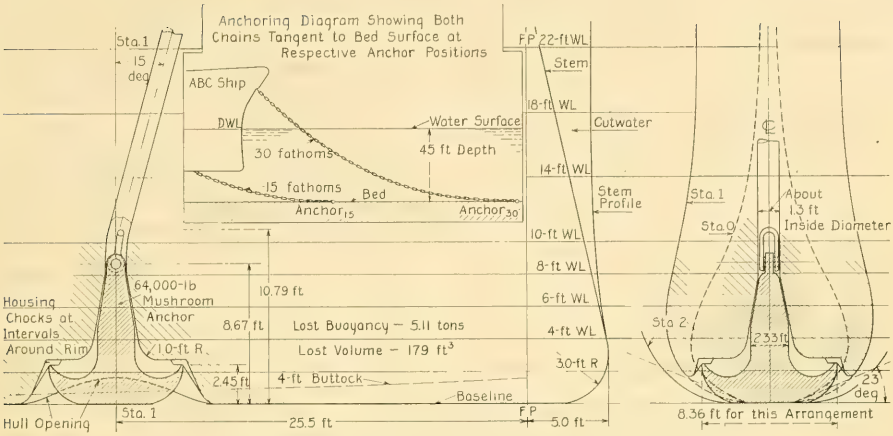

Fig. 68.I Proposed Under-the-Bottom Mushroom Anchor for ABC Ship

The ABC proposal involves:

(a) One 13,000-lb centerline bower anchor above water, of the U. S. Navy lightweight type, known as an LWT anchor, housed in the manner shown by Fig. 67.E

(b) One extra-heavy centerline mushroom anchor, below water, housed within and dropping out of the bulb at the keel, indicated in Fig. 68.H.

The mushroom anchor is proposed because it is more free of fouling by the chain than any other type, and because it houses reliably and firmly, out of sight, in a hawsepipe of simple shape and sturdy construction. Above the mushroom anchor and to a point just under the wildcat, at the main deck level, Fig. 68.H shows a length of chain several sizes heavier than the regular anchor chain. This is to insure that no breakage occurs in a section which is not easily accessible when the ship is afloat. The heavier chain next to the anchor also increases its holding power. Both chains going over the wildcats are of the standard size for this vessel.

An alternative arrangement for housing the bottom anchor farther aft is shown in Fig. 68.I. If the anchor windlass is to be kept well forward, it is necessary to move the hawsepipe as far aft as the vicinity of Station 1, at about $0.05L$, in order to house the anchor completely above the baseplane and to provide a slope of 15 deg in the hawsepipe leading from the anchor recess to the wildcat. A slope of this order is necessary to prevent the chain from rattling and banging in the chainpipe with the ship underway. Indidentally, this arrangement provides a full half-turn of chain around a horizontal wildcat, possibly 1 or 2 links more than is customary on bow-anchor windlasses of the orthodox type.

One great advantage of anchoring through a keel-line hawsepipe is that a much flatter "lie" of the anchor and chain is obtained, with a much shorter scope of chain, illustrated by the box diagram of Fig. 68.I, than if the chain is led from a hawsepipe many feet above the surface. This is especially true in the shallow water of rivers, estuaries, and harbors, where the ship occupies a much smaller mooring circle. On the ABC ship the difference in level of the hawsepipe openings is some 50 ft, or well over 8 fathoms, indicated in the small-scale diagram of Fig. 68.I. The heavy chain pendant next to the mushroom anchor, some 46 ft or over 6.5 fathoms long, is of great assistance here. These factors combined might permit reducing the weight of the mushroom anchor, which must be normally at least 2.5 times as heavy as a stockless anchor for the same holding power in firm ground. It is, furthermore, far easier to obtain a three-link bearing for the chain leading out of the morning-glory-shaped bottom anchor recess than out of any known shape of abovewater hawsepipe and bolster. Lastly, the anchor and hawsepipe are mounted much lower in the vessel than is customary, helping to lower the CG.

It is recognized that the under-the-bottom anchor scheme for the ABC ship has several disadvantages of major proportions:

(1) Greater weight of mushroom anchor, conservatively estimated as 64,000 lb, compared to 22,500 lb for a stockless anchor, or 13,000 lb for an LWT anchor. Slightly greater weight of chain, due to the extra-heavy 6.5-fathom shot just above the anchor.

(2) Greater power required in the anchor windlass to hoist the heavier anchor and adjacent shot of heavy chain. Inasmuch as the holding power calculated for the ABC ship is 160,000 lb, a standard windlass might be adequate for the purpose if not required to hoist both anchors simultaneously.

(3) Greater hawsepipe and chainpipe weights

(4) Lost buoyancy due to water around anchor and chain in hawsepipe and lower part of chainpipe, amounting to about 5 tons in the ABC design. Sufficient volume is left above the cup of the anchor to clear stones, clay, and mud caught in the cup, as well as to permit the anchor to drop clear in the river below Port Correo, where there may be less than 4 ft bed clearance above the mud.

(5) Difficulty of buoying the bottom anchor when dropped

(6) Impossibility, except in clear tropical waters in daylight, of noting the direction in which the anchor chain leads from the hawsepipe. However, with a bottom anchor and a short scope, this information is not really necessary.

Although the proposed under-the-bottom anchor installation has by no means proved itself sufficiently to warrant working it into the design of a ship to be built, it is carried through here as part of the ABC preliminary design because it permits the use of a moderate bulb and a forecastle that is not too wide and blunt.

68.12 Knuckles and Other Longitudinal Discontinuities. Flaring sides, projections, recesses, and other discontinuities of considerable fore-and-aft extent often have to be worked into the above-water form to meet service or utilitarian needs. For smooth-water conditions, with relatively small waves, these discontinuities have little or no adverse effect provided they are kept clear of the ship-wave profile along the free surface under any conditions of load, trim, heel, and speed likely to be encountered. Even for wavegoing, the external knuckle of the compound-flare type of section proves quite acceptable.

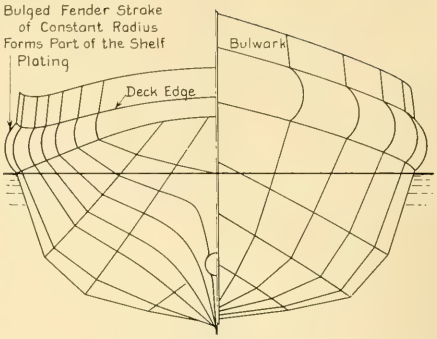

Fig. 68.J Bulged Fender Strake for a Small Vessel

The projecting edges of thick fenders or fender strakes require chamfering in a transverse plane to prevent their hanging up on similar projections along docks, especially when the tide level rises and falls. This chamfering should also be sufficient to prevent the fender from throwing objectionable spray, although the offending surfaces need to be nearly vertical to eliminate all spray.

A neat solution to the problem of the above-water fender is offered by the heavy, bulged fender strake of Fig. 68.J, forming a part of the main hull. In addition to satisfying all the hydrodynamic requirements this construction has great inherent stiffness as a fender because of its shape and it requires no care and preservation in service, other than that afforded to the hull proper. The ship designer is cautioned, however, not to place a bulge of this kind where the water can climb up around its convex surfaces in normal running.

Reentrant discontinuities or coves, near the designed waterline, are to be avoided where

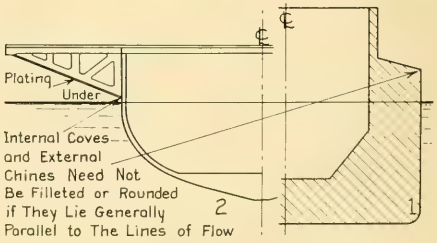

Fig. 68.K Projecting Blisters and Sponsons

practicable but not necessarily shunned. Reentrant angles in these coves, typified by the long cove at the bottom of the set-back trunk of diagram 1 in Fig. 68.K, and by the long junctions of hull and sponsons in the ferryboat section at 2 in Fig. 68.K, and in SNAME RD sheet 84, can approach 90 deg provided this small angle is necessary for other reasons. Little extra drag is encountered if these coves are under water in some load condition provided the corners follow the temporary flowlines reasonably well.

Keeping abovewater discontinuities out of the reach of waves at sea is well-nigh impossible. The smaller the change in direction as the water strikes the discontinuities the less spray they throw and the smaller are the hydrodynamic forces exerted on them.

68.13 Transverse Discontinuities. Any longitudinal discontinuity which runs for a considerable distance along the ship is also a transverse discontinuity. The latter is distinguished here as one which involves a projection—or a recess—from the fair section lines in the vicinity which is large compared with its fore-and-aft length. A good example is an old-fashioned gun sponson on a combatant vessel, protruding from the ship's side like a bay window to obtain a line of fire along the side. Projections or recesses of this type, if kept clear of the ship-wave profile, need no special consideration from a hydrodynamic standpoint for ships which travel in relatively smooth water, surrounded only by their own waves.

The use of isolated transverse braces or supports for overhanging portions of the abovewater hull or upper works, even when nominally clear of the wave profile, is not encouraged. Under some unusual and unlooked-for circumstances these transverse members are liable to become fouled by floating debris, ice, or breasting floats (camels).

Abovewater projections may be fitted, as on whaling factory ships [SBSR, 5 Dec 1946, pp. 625–635], to increase the deck space locally, to serve as large-area fenders for protection of the underwater hull when other vessels lie alongside in the open sea, and for other purposes.

68.14 Shaping and Positioning of Superstructure and Upper Works. Several major considerations enter into the design of that portion of any ship lying above the main hull. Every deck erection, every spar or post, every protuberance of whatever kind has a utilitarian purpose. Even wind screens and shelters have to be provided for passengers, especially on high-speed ships [Currie, Sir William, SBMEB, Jul 1955, p. 435]. Some of these purposes are served only in port, some only at sea, and some are used almost all the time. Aside from the effect of these upper works on weight, cost, and transverse metacentric stability, practically all of them involve some air drag and produce some wind resistance. To overcome this, extra power must be provided or exerted, or speed must be sacrificed.

"The model of the (old) *Mauretania* required an increase of 20 per cent in power to drive the structure added to represent deck houses" [Barry, R. E., Mar. Eng'g., Sep 1921, p. 690].

Regardless of the type of vessel or the service expected of it, any owner and operator may be expected to affirm that convenience of access, availability of outside light and air, comfort of the passengers, and the needs of the crew are to take precedence over the reduction of wind resistance of the upper works. Put in another way, he will unquestionably be found reluctant to sacrifice utility, passenger comfort, and other factors having to do with the handling and operation of the vessel for the sake solely of reducing its wind resistance. Nor will he generally find it a paying proposition to spend a great deal of money and effort to diminish the wind resistance, at no sacrifice in other features, unless some outstanding improvement is to be gained.

Tests at the Case School of Applied Science, on 33-in wind-tunnel models of the Atlantic liner *Manhattan*, showed that by completely streamlining the whole ship—in other words, by treating both hull and upper works as a unit—the wind resistance with the relative wind ahead was reduced approximately 84 per cent, compared to the *Manhattan* as built. This was for a ship speed of 20 kt, a true wind speed of 23.2 kt, and a relative wind speed of 43.2 kt. The modification involved an entirely different concept of a passenger ship, with everyone completely housed at all times, but it indicates what can be done if all other considerations are disregarded.

This effort shows how easy it is to lose sight of the fact that so-called streamlining of individual deckhouses and other erections above the hull by no means insures that it will be easier for the crew to make their way about the upper works under storm conditions. Structures of fair form, when blown upon in a direction approximating

that for which they were shaped, rarely have sizable regions of reduced velocity or separation around them. They create few eddies in which a person can stand, as is possible in the lee of a square corner on a deckhouse, and fewer calm areas in which a passenger can sit in comfort.

"The wind velocity over the open decks (with an excessively streamlined superstructure), even in quite mild conditions, can be such as to render intolerable any attempts to walk or sit out!" [Hind, J. A., SBSR 14 Jul 1955, p. 37].

To pass around a streamlined structure in a gale requires bucking a wind of ferocious velocity; this becomes a struggle if one is heavily clothed. Nevertheless, certain things can be done to reduce the air drag without sacrificing any functional features of the upper works.

First, it is possible, even in rather small vessels, to provide complete internal access from living quarters to operating stations for all officers and crew. Indeed, this is now general practice on large vessels and may be taken for granted in any modern new design. If the same provision is made for unusual operating conditions and for manning emergency stations it is possible to eliminate the necessity for crew members to move around outside the upper works in bad weather. The diagram for composition of air velocities around a ship, indicated at C in Fig. 26.H, shows that the ratio between the true-wind velocity W_T and the ship velocity V has an appreciable effect upon the bearing angle of the relative-wind velocity W_R at the ship. For winds normally encountered in good weather at sea, with velocities not exceeding 20 kt, this relative-wind angle increases, for a wind nominally on the beam, from 45 deg abaft the bow at 20 kt to about 59 deg abaft the bow for 12 kt. For winds of strong-gale force, say 60 kt, the difference between the relative-wind angles for a nominal beam wind is still appreciable, of the order of 71.5 to 80.5 deg abaft the bow for 20 and 12 kt, respectively. Streamlining a deckhouse which can not swivel into the wind like a weathervane but which is shaped to give minimum air drag with the true and relative winds both dead ahead appears somewhat absurd.

A deckhouse not extending all the way to the sides or to the ends of a surface ship hull and not having any overhanging deck at its top level, may be considered as relatively sheltered from the wind if it has a height not exceeding 0.12 or 0.15 times the beam of the ship and if it lies an equal distance back of the side of the ship. This is because of the separation zones behind the sharp corners at the deck edges and the reduced velocities in way of the miscellaneous small obstructions on the deck. Unit air pressures on the exposed sides of deck erections increase with their height above the main hull and likewise with the absolute size of the areas subjected to ram pressure from the wind. For a wind velocity of 60 kt, or 101.33 ft per sec, with an air temperature of 59 deg F, the ram pressure q due to wind in a stagnation area is $(0.5)(0.00238)(101.33)^2$ or 12.22 lb per ft^2. For a 30-kt ship steaming into a 60-kt wind, developing a relative velocity of 90 kt, or 152.00 ft per sec, the corresponding ram pressure is 27.49 lb per ft^2.

Shaping the deck erections for least wind drag is based upon a relative-wind direction of about 30 deg on either bow, because it is at about this angle that the wind blows separately on the several structures spread along the length of the vessel. This is also the angle, indicated by the diagrams of Sec. 54.9, at which the fore-and-aft wind resistance R_{Wind} becomes a maximum. The beneficial effects of housing uptakes, ventilators, mast and instrument foundations, and the like, within deck erections necessary for some other purpose, are not to be overlooked. Objects which can not be so enclosed often lie in the lee of larger objects (inside the separation and eddying region behind them), at the 30-deg relative-wind angle, and so do not require any streamlining for themselves. It is not to be forgotten, however, that swirling backflows into these regions, where $-\Delta p$'s exist, may take with them smoke, soot, and foul gases discharged from poorly placed openings.

As an indication of what may be expected in the way of air flow about a great variety of deck erections and upward projections from the hull and superstructure, for a relative wind from ahead, Fig. 68.L shows the velocity vectors in both elevation and plan view around the hull and upper works of a large ship. Diagrams 1 and 2 of this drawing were adapted from a series of five detailed diagrams published by H. N. Prins, in an article describing the hull features of the Dutch passenger liner *Oranje* [De Ingenieur, The Hague, Holland, 23 Jun 1939, Pl. II and p.W. 56]. The comprehensive data were taken from wind-tunnel tests, made on a specially constructed model of the vessel, complete to the last detail. Unfortunately, they cover only the wind-ahead

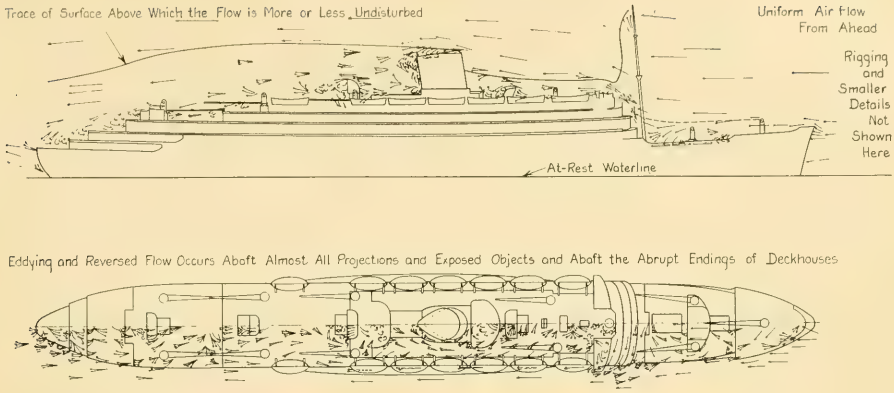

Fig. 68.L Air-Flow Pattern Over a Passenger Ship, from a Model Test

condition but they illustrate vividly the back flow, the eddies, and the extreme irregularity of the air flow in general.

For the many smaller ships, and some large ones [Swedish tanker *Oceanus*, SBSR, 2 Dec 1954, p. 736; The Motor Ship, London, Dec 1954, pp. 374–375], on which the deckhouses and other deck erections (except possibly for a raised forecastle) are all the way aft, there is a possible major shift of the center of pressure of the hull and upper works which may affect maneuverability in a high wind. Apparently this offers no real problem in operation, aside from learning initially how the ship behaves and controlling it accordingly.

It is customary, for many ship designs, to build a simple, inexpensive model, usually called a drafting-room model, embodying the hull above the DWL and all the principal deck erections and exposed parts in their proper shapes, sizes, and locations. Fig. 54.B shows such a model. It is an easy task, for which techniques are well developed [Nolan, R. W., SNAME, 1946, pp. 46–60], to mount this model in a large wind tunnel at various angles to the relative wind and to determine the nature of the flow over and around it. A light thread or tuft, carried by a thin wand which is manipulated by hand and placed at selected points, indicates instantly the type of flow to be expected there. Multiple tufts of contrasting color, attached to the model at many points, are readily photographed for record, at any test condition. Indeed, such a model may be tested in the open provided a platform or deck is available, over which a uniform wind is blowing. A long fish pole, carrying the roving thread or tuft, enables the experimenter to stand far enough from the model so that his body does not interfere with the uniform air flow near the model.

Sir Victor G. Shepheard describes the results of wind-tunnel tests made at the NPL, Teddington, upon such a model of the British Royal Yacht *Britannia* [INA, 7 Apr 1954, pp. 11–13]. In this case white smoke filaments were used, which were found to photograph satisfactorily.

It is possible to make exactly the same type of flow test on an upside-down model of the upper works attached to a large horizontal surface board and suspended in the water of a circulating-water channel. Jets of water from a suitable pump are caused to issue from the stacks at a velocity having the proper ratio to that of the overall stream, corresponding to the relative-wind velocity. Colored dye injected into the water streams from the stacks gives a true and vivid indication of the paths of the exhaust gases on the full-scale ship, complete with swirls, eddies, and the like.

Methods for calculating the air drag and wind resistance of ship hulls, upper works, and deck erections are given in Chap. 54.

68.15 Design of Facilities for Abovewater Smoke and Gas Discharge. Since World War II, a considerable amount of research and development on methods of keeping combustion and objectionable exhaust gases and soot clear of passenger and operating spaces on ships has revealed that:

(a) These gases must be discharged into regions of relatively smooth and regular flow, rather than into flow containing large-scale eddies. The discharge must be above and outside of separation zones, else the gases are scattered widely in regions of low velocity or are drawn back and downward by the reversed flow and the eddies.

(b) Stacks of large diameter, width, and horizontal area create their own separation zones, into which the escaping gases are drawn, thence to find their way to the decks below

(c) Raising the stack top to a great height, projecting far above the top of the turbulent region, will not of itself prove satisfactory because of the soot and dirt that falls upon the ship at relative wind velocities approaching zero [Smith, W. W., SNAME, 1946, pp. 76–77]

(d) To insure that gases issuing from a stack top in the open are projected far enough into the regular flow to prevent their mixing with the turbulent flow behind the stack or over the ship it is necessary that the stack-gas velocity S, approximately vertical, be at least as great as the relative-wind velocity W_R in the open. The velocity S may have to be 1.5 or $2.0W_R$ if the volume of stack gas is not large. For the worst *general service* conditions the maximum relative-wind velocity W_R may be taken as 40 kt, so that for no contamination the stack-gas velocity should exceed 65 ft per sec if there are adjacent turbulent areas. For fine, fast, high-powered ships the actual relative wind velocity may reach 60 or 65 kt, corresponding to 100 or 110 ft per sec, under conditions when the decks and upper works should still be smoke- and gas-free.

(e) It may under some circumstances be possible to project the objectionable gases into the tip vortex of a long, thin stack shaped like a symmetrical airfoil. If caught in such a vortex the gases remain there reasonably well, at least until they are downwind far enough to be clear of the ship.

(f) For fast ships in which the relative wind is generally in the forward quadrant a shield around the forward side of the stack opening or a partial elbow directing the combustion gases aft as well as upward, long used on French men-of-war and built into the German cruiser *Prinz Eugen* and other naval vessels, is a simple means of retaining some of the upward component of stack-gas velocity in an effort to keep the gases clear of the turbulent region. This shield or elbow, however, is properly placed *at the forward edge of the gas opening*, and *not* at the forward edge of a stack structure that may be larger than the opening.

(g) If, for reasons of appearance, tall chimney-shaped stacks are not acceptable, combustion and exhaust gases may be discharged from the after upper corner of a stack casing, as on the liners *Constitution* and *Independence* (1950–1951).

Supplementing (a) preceding, wind-tunnel tests on ship models reveal that set-backs or steps in the forward surface of a multi-deck superstructure give the equivalent of a streamlined forward face if the set-back slope through the upper edges of the various vertical surfaces is not more than 30 deg with the horizontal. If the slope is as great as 60 deg, the turbulent separation region above the uppermost deck is about as high and as large as if the superstructure face were a solid vertical wall, with a 90-deg slope. Furthermore, performance on the ship is found to be somewhat better than the model tests predict [Acker, H. G., SNAME, New Engl. Sect., Oct 1951, p. 5].

For the reader who wishes to pursue the subject further the following references are quoted:

(1) Durand, W. F., AT, Julius Springer, 1936, Vol. III, p. 165

(2) Valensi, J., "Méthode des fillets de fumée (maquettes d'avions, ailes d'avions) (Method of Smoke Filaments using Models of Airplanes and Airplane Wings)," Publ. Sci. et Tech. du Ministère de l'Air, 1938, No. 128, pp. 11–16

(3) Sherlock, R. H., and Stalker, E. A., "A Study of Flow Phenomena in the Wake of Smokestacks," Univ. Mich. Res. Bull. 29, Mar 1941

(4) Ijsselmuiden, A. H., "Machine- en electrische installatie van het m.s. '*Oranje*' (Machinery and Electrical Installation of the Motorship *Oranje*)," De Ingenieur, 7 Jul 1939, p. 79. In Figs. 27, 28, and 29 on this page, there are given three diagrams of stack arrangements tested, apparently in a wind tunnel. For each of the diagrams there is sketched the type of flow found to issue from and to lie above and abaft the stack.

(5) Squire, H. B., and Troucer, J., "Round Jets in a General Stream," ARC, R and M 1974, 1944

(6) Nolan, R. W., "Design of Stacks to Minimize Smoke Nuisance," SNAME, 1946, pp. 42–82

(7) Sharp, G. G., "Design of Modern Ships," SNAME, 1947, pp. 462–466

(8) Valensi, J., and Guillonde, L., "Sur les Formes de Carénage de Cheminées de Navires Propres à Éviter le Rabattement des Fumées (On the Shaping of Stacks of Ships Intended to Prevent the Settling of Smoke over the Decks)," ATMA, 1948, Vol. 47, p. 173

(9) Eustaze, S., "Le Rabattement des Fumées sur les Ponts d'un Navire; Essais sur Modèles et Dispositions Pratiques (The Settling of Smoke over the Decks of a Ship; Tests on Models and Practical Arrangements)," ATMA, 1951, pp. 285–307

(10) Ower, E., and Burge, C. H., "Funnel Design and Smoke Abatement," INA, 1950, Vol. 92, pp. J19–J37; also ASNE, Aug 1951, p. 704. Seven references are listed on p. 730 of this latter article.
(11) Acker, H. G., "Stack Design to Avoid Smoke Nuisance," SNAME, New England Sect., Oct 1951
(12) Valensi, J., "Sur un Moyen Propre à Éviter le Rabattement des Fumées sur les Ponts des Navires (On a Good Method of Getting Rid of the Smoke Settling on the Decks of Ships)," Bull. Tech. du Veritas, Mar 1952
(13) Thieme, H., "A Contribution to Funnel Aerodynamics," Schiff und Hafen, Nov 1952, p. 453
(14) Richter, E., "Neuzeitliche Schornsteinformen (New Forms of Stacks)," Schiffstechnik, Aug 1954, pp. 36–44
(15) Craig, R. K., "Passenger Liner with Engines Aft," IME, Dec 1955, Vol. LXVII, Figs. 21 and 22, pp. 446–447; abstracted in SBMEB, Dec 1955, pp. 689–693.

The obvious advantages of placing the propelling machinery as far aft as practicable in the ABC design are augmented by moving the exhaust fan or smoke discharge aft with it, where the gas may be projected upward through one or two tall, slender stacks.

The superstructure for housing the passengers and the public spaces is a unit placed well aft to clear the forward deck for the handling of package cargo and to be close to the pitching axis. The derrick posts forward are to be in pairs, so it appears logical and architecturally consistent to carry this scheme aft by mounting two tall inlet-and-exhaust-air shafts over the superstructure and placing two steeple-type smoke stacks well aft, one over each steam generator. An estimate of the extent of the turbulent region over the ship is sketched in Fig. 68.M with a moderate true wind of 25 kt from ahead, on the basis of H. G. Acker's estimate that the thickness of the turbulent zone over the top of the superstructure is of the order of 0.8 the height of a stepped-front superstructure above the main hull. Combined with a ship speed of 20 kt, the relative-wind velocity is 45 kt, or about 76 fps.

The stack gases from each of two modern 8,500-horse steam generators should require a circular outlet not more than 3.0 ft in diameter for a gas velocity S of the order of 55 to 75 ft per sec [MacMillan, D. C., SNAME, 1946, p. 68; Sharp, G. G., SNAME, 1947, p. 465; Sullivan, E. K., and Scarborough, W. G., SNAME, 1952, pp. 488–490]. The top of each stack casing could then have a width of say 3.5 or 4.0 ft with a fore-and-aft length of 5 ft. This leaves room for a safety-valve escape pipe and for a damper and its mechanism to keep the stack-gas velocity high at reduced powers, as when running in the Port Amalo canal and the river below Port Correo. To give the structure rigidity *without* the use of heavy scantlings or stays, the bottom width is of the order of 5 ft. The bottom length is increased to some 8 ft to give the profile the appearance of sturdiness. The aft edge is raked downward and aft like the transom profile. The streamlined casing, in the form of a round-cornered rectangle at the top, converts to a square-cornered rectangular shape just above the fidley. This is to provide a rigid foundation where the ends and sides of the stack casing attach to the transverse beams and fore-and-aft carlines directly below them.

If it were considered that an *underwater* smoke discharge, into the $-\Delta p$ region of the separation zone, along the lower edge of the transom, could be worked out in the course of the design of the vessel, the position of the steam generators well aft would lend itself admirably to this arrangement.

"Necessity, if not reason, has provided another flourish. Large steamships now expel their waste gases through giant chimneys surmounted by all manner of strange devices. To prevent these unpleasant vapours obstinately returning to spotless decks below, invention has run riot in providing amusing, if not always elegant or effective, headgear for funnels. Angels' wings, admirals' caps, upturned pudding bowls, skeleton triplanes—all of these and other fancies now proudly sail the oceans in the cause of science and clean decks. What shall we see tomorrow? Perhaps someone may get rid of those obnoxious fumes somewhere else? Why not through the stern?" [SBSR, 1 Apr 1954, p. 401].

Some excellent comments relative to the disposal of the products of combustion, made by

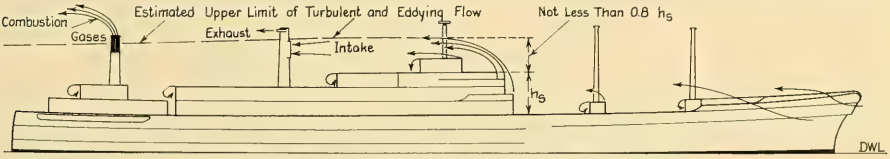

Fig. 68.M Estimated Air-Flow Pattern Over the ABC Ship

John Johnson two decades ago, are still worthy of serious consideration by the ship designer [Thomas Lowe Gray lecture, IME, 10 Jan 1936; SBSR, 16 Jan 1936, p. 74].

68.16 Reducing the Wind Drag of the Masts, Spars, and Rigging. Tall, raked masts on a self-propelled vessel are undoubtedly relics of sailing-ship days. They serve well for the flying of flags, the carrying of navigation lights, and the working of long derrick booms. Nevertheless, with their attendant rigging they are subject to heavy loads when rolling and they represent wind resistance out of all proportion to their usefulness. A tall vertical pole or post, properly attached to the ship structure and without benefit of stays, can mount a radar antenna, hold up one end of a radio antenna, support a crow's nest, carry a range or masthead light, and serve as an air intake or exhaust, all at the same time. It can not easily be streamlined for flow on all bearings in which high relative winds are encountered but its wind drag is at least justified by the number of functions which it performs simultaneously.

Masts intended to be used as ventilators appeared as far back as 1860 on the steamer *Ly-ee-Moon* [SBSR, 9 Nov 1939, p. 507]. It is possible that these in turn were relics of the early smoke stacks which were extremely tall in order to obtain good natural draft.

Self-supporting masts and derrick posts, with all stays eliminated to reduce wind drag, interference, and expense, are coming rather rapidly into use [SBSR, 8 Oct 1953, pp. 484–485; MENA, Dec 1953, p. 53; SBSR, 24 Jun 1954, pp. 800–801]. On the liner *Orsova* the running rigging for the derricks is carried entirely *inside* the posts [SBSR, 20 May 1954, p. 645].

68.17 Consideration of Increased Draft Through the Years. Before leaving the preliminary design of the abovewater body as finished it is to be remembered that, as the result of a continual series of modifications and changes in the course of its life, most of which act to increase the weight, the ship sinks slowly but steadily deeper in the water. This is specially true for a combatant vessel or for a merchant vessel which is likely to be converted to a naval auxiliary in time of emergency. A heavy or pronounced flare or a sharp knuckle may in this way be brought too close to the designed waterline. A flat counter may be lowered to the point where it is subject to frequent sea slap and slamming from underneath. A transom stern may have its immersed draft increased to the point where the transom does not clear at the designed speed. Finally, a propeller designed for the original displacement may be heavily overloaded at a later one, when the average draft has increased.

68.18 Preparation of Hull Lines for Model Tests. It is recalled that the design rules for screw-propeller apertures and clearances embodied in Sec. 67.24 are in many cases based upon propeller-blade widths, upon the thicknesses of rudder posts, and so on. To determine whether there is room for the propulsion devices on the outside and, in the proper places, for the propelling machinery within the ship, it is necessary to run through a preliminary design of these devices, in the manner outlined in Chaps. 67, 69, 70, and 71.

Before attempting to delineate the whole ship hull on a single drawing, the fixed and movable appendages need to be roughed out and checked for position, shape, and dimensions. This procedure is described in Chaps. 73 and 74. Furthermore, the hull-and-appendage combination requires design attention and checking to insure that shallow-water maneuvering, wavegoing, and other requirements are met. These matters are covered in Chap. 72 and in Parts 5 and 6 of Volume III. Simultaneously the preliminary design needs working over for arrangement, volumes, capacities, strength, metacentric stability, damage control, and other non-hydrodynamic requirements.

With this work accomplished, and with the shape and principal features of the underwater and abovewater hulls, propulsion devices, and appendages worked out, a set of lines for the hull as a whole is drawn. This is in no sense a set of lines to which the ship is to be built. For the hydrodynamic design, its principal function is to guide the building of a model or models for towing, self-propulsion, maneuvering, shallow-water, wavegoing, and other tests.

The preparation of lines to embody all the features developed in the foregoing sections is largely a matter of drafting, except as mathematical processes such as those discussed in Chap. 49 may be used to calculate the offsets for drawing (and fairing) these lines.

A high degree of precision at this stage is not called for. The lines should be to a sufficiently large scale, not only for construction of the model, but for a fairly detailed design of all the appendages which are eventually to be added to it.

CHAPTER 69

The General Design of the Propulsion Devices

69.1 Introductory Comment. There are considered in this chapter only those features which are common to the design of all mechanical ship-propulsion devices which act on the water. Discussions of specific devices such as screw propellers, paddlewheels, rotating-blade propellers, and the like, are found in the two chapters following. The systematic treatment of these design features does not necessarily follow the order in which the characteristics for any one type of propulsion device are worked out or selected in actual practice.

69.2 Type and Number of Propulsion Devices. Only rarely can lines be sketched for the form of a new ship without first making a tentative decision as to the type, number, and position of the propulsion devices. Too often these features are determined by the types, sizes, and powers of the propelling units available; admittedly this procedure is inescapable at times. It is proper to remember, however, that the propulsion devices are installed to drive the ship. The function of the propelling machinery is to drive these devices at rates and powers which result in the highest efficiency and the greatest economy for both. Generally speaking, therefore, the type, number, and position of the propulsion devices are determined directly from the ship requirements. The corresponding features of the machinery are selected to suit the devices.

So many considerations, most of them conflicting, enter into the selection of the propulsion-device characteristics that it is difficult to set down the procedure in systematic form. The outline given here may serve until something better is developed, remembering first, last, and always that no propulsion device, whatever its type and position, can be expected to perform well in a region of poor flow.

The *type* is selected first, on the basis of:

(1) Operating requirements, including limiting draft of vessel and available depth of water

(2) Maximum ship speed and total power required to be absorbed by the device(s)

(3) Best general position in the vessel, considering the latter's type, functions, and duty

(4) Amount of wavegoing anticipated, with consequent change of position of the instantaneous water surface with reference to the region in which thrust is being produced, such as the disc of a screw propeller

(5) Type of propelling plant available or desired. This boils down generally to the rate of rotation of the output shaft on the last machinery unit, just ahead of the propulsion device. In the past, slow-speed engines drove screw propellers through multiplying gears, and in the present, high-speed engines drive paddlewheels through reduction gears. Therefore there need be few limitations in this respect.

(6) Facilities available for repair or replacement of the propulsion devices and their parts in the areas where the ship is to operate, either by the ship's force or by repair crews

(7) Frequency with which the propulsion devices

are to be used, such as those on a self-propelled floating crane.

Concerning the *number* of propulsion devices, the following considerations govern:

(a) Available depth of water in operating areas, limiting extreme draft, probable draft of hull of vessel, and approximate beam-draft ratio of hull. This item involves factors such as adequate tip submergence to prevent air leakage to submerged devices, adequate hydrostatic head to prevent cavitation, most efficient blade lengths, and permissible extension, if any, below the baseplane. It may be necessary, for some of these reasons, to fit a larger number of small-diameter or small-size propulsion devices, or a fewer number of large-diameter ones.
(b) Special operating requirements such as those for maneuvering in restricted waters and emergency stops. Wing propellers provide appreciable swinging moments by going ahead on one and backing on the other.
(c) Probability of large exciting forces and excessive hull vibration if large powers are concentrated in too few propulsion devices. As of 1955, the largest power applied to the propeller of a single-screw vessel, the tanker *W. Alton Jones*, is about 22,000 horses [Mar. Eng'g., Nov 1955, p. 119]. However, powers of the order of 50,000 horses are being developed by the individual propellers of quadruple-screw installations, and these may eventually be reached by the propellers of fast, single-screw ships. K. E. Schoenherr pointed out some years ago that it was then "possible to design propellers to transmit 50,000 horsepower on one shaft and to obtain propulsion efficiency of as high as 80 per cent on single-screw ships" [SNAME, Phila. Sect., 21 Feb 1947].
(d) Interference likely to be caused with internal arrangements in the vessel by the presence of one, two, or more shafts, including their shaft alleys or tunnels
(e) Efficiency of propulsion. One large propulsion device, if there is room for it and if good inflow is indicated, almost invariably proves more efficient than two or more small ones, reckoning efficiency here on the basis of the least propeller or shaft power for a given weight displacement and length of the ship.
(f) Reliability and safety aspects of the entire engine-shaft-propulsion-device combination
(g) A good general rule is to use no more propulsion devices than the special requirements of the design demand, and no more than the number for which good working positions can be found.

69.3 Positions and Limiting Dimensions. The matter of how far to keep the thrust-producing areas away from the hull and its boundary layer, or how close to bring them to the hull, is discussed for screw propellers in Secs. 67.23 through 67.25 and for paddlewheels and other devices in Chap. 71.

The selection of the particular *position* of the propulsion device(s) in any ship takes into account:

(1) The nature of the flow into the possible positions, considering wake fraction, uniformity of inflow velocity, non-axiality, and absence of excessive turbulence
(2) The possibility of fitting contra-flow or contra-guide devices adjacent to the propulsion device(s)
(3) Freedom from entrained air coming along the hull from forward, leakage air coming from the free surface, and eddies in or trailing abaft separation zones
(4) The tip submergence considered necessary in view of the specified loading and anticipated wavegoing conditions
(5) Permissible depression of the blade tips below the baseplane. Usually this can not exceed about 4 or 5 ft, the height of the keel blocks in the average drydock.
(6) Available propelling-machinery positions within the hull.

Each design case is considered on its own merits, taking account of all the items listed in this section and in Sec. 69.2. It is difficult to set down rules which apply even in the majority of cases, especially when the relative importance of the several controlling items often is not known in advance. N. J. Brazell has given some good ideas in a paper entitled "The Positioning of Propellers and Shafts" [ASNE, Feb 1948, pp. 32–48]. On the motor vessels *Brunshausen* and *Brunsbüttel* the single propeller is mounted about 9 ft abaft a clear-water stern post, in an effort to improve propulsive efficiency and to reduce vibration [SBSR, 12 Jan 1956, p. 38; MENA, Jan 1956, p. 28; both references embody photographs of the stern].

The result of an analysis by H. Dickmann [Ingenieur-Archiv, 1938, p. 452], set down briefly by K. E. Schoenherr [PNA, 1939, Vol. II, p. 145], is that:

". . . for best efficiency of propulsion the screw propeller should be located in a high friction wake, a negative or low positive streamline (potential-flow) wake and in the crest of a wave."

The condition that the propeller work in a negative or low positive potential or streamline wake is that which obtains generally in a normal form of ship if the hull is assumed to be expanded to include the displacement thickness δ^*(delta star) of the boundary layer. With run lines of easy slope, such an expanded form has only a moderate positive streamline wake fraction due to potential flow.

To achieve the highest practicable negative streamline wake fraction, propellers could be mounted on outriggers abreast the section of maximum area, occupying about the same position as paddlewheels. Here the speed of advance becomes greater than the ship speed. Because there is no ship forward of the side propellers, the thrust-deduction fraction becomes practically zero. High negative-wake fractions are actually to be found inside Kort nozzles and other types of fixed propeller shrouding.

When some form of hydraulic jet propulsion is employed, requiring large volumes of water to be taken within the hull boundaries and discharged from internal ducts, the positions and shapes of the inflow and the outflow openings become almost a part of the main hull design. These features, of which relatively little is known, are indeed worthy of more attention than is normally devoted to the position of a screw propeller and the shape of the hull in its vicinity. Following the practice on jet-propelled aircraft, the ram action of the water flowing toward the hull is utilized to force water into the inlet and to keep it moving against the friction and pressure resistance encountered within the internal ducts. This is accomplished, where practicable, by an inlet opening facing directly forward or forward and outward.

As for the *limiting dimensions* of propulsion devices, it is obvious that there are practical limits dictated by good all-around engineering, good mechanical design, and economic operation of the vessel which are in conflict with hydrodynamic requirements for the ultimate in propulsion-device efficiency. To increase the latter means increasing the thrust-producing area and lowering the thrust-load coefficient C_{TL} but at the expense of increased volume occupied by and increased weight of the propulsion device and the propelling machinery. It is probable that the designer of ship-propulsion devices always has been faced and always will be faced with the fact that existing fabrication and shipping facilities for these devices are too small. Nevertheless, larger facilities have always been built in the past and they will continue to be made available in the future. There is no reason why the propulsion-device designer should be bound by existing facilities if he can produce a better or more efficient ship.

Since most propulsion devices rotate, there are problems of gearing and transmission, which may govern the rate of rotation and through it may influence the size of the propulsion device, the thrust-load coefficient, and the hydrodynamic efficiency. Furthermore, the necessity for mechanical protection of the propulsion device against damage by external objects, and for shielding it against air leakage, as is done for a screw propeller by the main hull of a single-screw tug, may call for a diameter smaller than would otherwise be used.

The required thrust-producing area A_0 of any type of propulsion device being considered is readily calculated from the ship resistance R_T and the speed V. After estimating or assuming values of the wake and thrust-deduction fractions w and t and selecting a thrust-load factor C_{TL} which will give a good value of the real efficiency $(0.8\eta_I)$, the values are substituted in the formula

$$T = \frac{R_T}{1 - t} = \frac{C_{TL}}{\frac{\rho}{2} A_0 V_A^2} = \frac{C_{TL}}{\frac{\rho}{2} A_0 [V(1 - w)]^2}$$

whence

$$A_0 = \frac{2C_{TL}(1 - t)}{\rho R_T [V(1 - w)]^2}$$

E. Burtner gives a simple dimensional formula for determining quickly the diameter of a screw propeller in the course of a preliminary design [ASNE, Aug 1953, pp. 545–548]. This formula appears to give reasonable values for both 3- and 4-bladed wheels and for a rather wide range of expanded-area ratio. It is

$$D \text{ (in ft)} = \frac{[P_S \text{ (in horses)}]^{0.2}}{(\text{rpm})^{0.6}} \qquad (69.i)$$

On page 547 of the reference Burtner includes a small-scale nomogram for finding any one of the three values quickly when the other two are known. For example, assuming for the ABC ship

that P_s is 16,000 horses and D is 20 ft, the estimated rpm are about 118. The rates of rotation derived by the use of several propeller charts in Sec. 70.6 vary from about 104 to about 110 rpm.

69.4 Effect of Type and Design of Propelling Machinery. The general design of propulsion devices is never dissociated entirely from the type and design of propelling machinery because these units or systems are, always figuratively and generally literally, at opposite ends of the same shaft. Nevertheless it may not be amiss to point out in this book that the greatest freedom of choice for the design, construction, *and* position in the ship for both the propulsion-device and the propelling-plant systems is afforded by a suitable combination of the following elements:

(a) A type of power-generating plant which need not be located in the ship in some specific region, dictated by the position of the propulsion device(s), but which can be placed where it best satisfies ship operating conditions. It should not be forced into a certain—and not always desirable—position because the propulsion-device design requires compliance with a completely different set of conditions, nor should it be such that it will fit into only one position in the ship.

(b) A completely flexible power-transmission system by which a power-generating plant or driving member can be connected to a driven member on the propulsion-device shaft with freedom of direction of rotation, direction of shaft axes, relative position in the vessel, and distance between the two. Freedom of this type is afforded by electric-wiring or piping systems.

(c) A propulsion-drive unit which is small, light, compact, and adaptable as to location, requiring a minimum of maintenance

(d) A propulsion-drive speed changer which permits use of the optimum speeds for both the propulsion-drive unit and the propulsion device.

At the time of writing (1955) these requirements are met for a wide range of powers by the following units grouped in one machinery plant. The important matters of space, weight, and cost are not disregarded but are for the moment considered secondary to flexibility. The specific mention here of an installation resembling an electric-drive plant is intended solely as an example and not as indicating the best or the ultimate achievement to fulfill the requirements of the preceding paragraph. Such an installation comprises:

(1) An electric generating plant, driven by a steam, internal-combustion, or gas-turbine engine, or a plant of some type unknown at present but which may be found feasible in the future. This plant is to be in units of sizes and powers which lend themselves readily to manufacture, to installation in the most advantageous position(s) in the ship, to economical and efficient operation, and to progressive maintenance.

(2) An electric transmission system, either AC or DC, with the necessary safety and control devices

(3) A reasonably high-speed rugged electric motor or motors, suitably cooled and protected from dirt, moisture, spray, and liquid. The modern railway traction motor fulfills all these requirements.

(4) Speed-changing gearing of the single- or double-reduction or epicyclic type, utilizing wherever practicable the so-called flexible construction which provides uniform load distribution along the gear faces and consequent maximum loading on the teeth.

Practically all the elements required by the foregoing, although some of them in limited powers only, are available and have proved themselves in severe service afloat [Lisle, T. O., Motorship, New York, Mar 1953, p. 36], often where weight and space are at a great premium. It is to be hoped, for the sake of the ship designer who is keenly interested in the hydrodynamics of his propulsion device(s), that active development along these lines will continue.

69.5 Number and Position of the Engines. Paralleling the comment in items (a) through (g) of Sec. 69.2, on the number of propulsion devices, it may be said that:

(a) A single machinery unit is lighter, more compact in total volume occupied, more cheaply and easily installed and maintained, and cheaper to run than several units of the same total power. Aside from only one engine there is only one thrust bearing, one line shaft, one propeller or stern-tube shaft, and one set of shaft bearings and hull stuffing boxes. The space and weight of the fuel saved may be devoted to other useful items.

(b) A single unit requires fewer operating personnel. This in turn reduces the space and weight devoted to crew accommodations and required for crew's stores.

(c) Modern machinery may not yet be sufficiently

reliable so as never to require any reserve propelling unit(s) to bring the vessel home in the event of casualty. It is, however, vastly more reliable than was the machinery of a former age, which saw a shift to twin-screw machinery largely to provide this measure of safety.

The position of the propelling machinery in the vessel is of interest in the hydrodynamic design principally because it:

(d) Affects the declivity and the horizontal angle(s) of the propeller shaft(s), as well as the shape and positions of the shaft struts or bossings external to the main hull
(e) Affects the size and shape of the hull in way of large motors, gears, condensers, or other machinery parts which need certain clearances from the hull structure
(f) Concerns the readiness with which the screw propellers *are kept submerged in all operating conditions.* This item is considered *most important* [Rupp, L. A., and Jasper, N. H., SNAME, 1952, pp. 352, 354].
(g) Affects the disposition of the products of combustion and the air resistance of stacks, standpipes, or other deck erections
(h) Controls the possibilities and the methods of underwater gas exhaust.

Assuming that the ABC ship is to be driven by screw propellers at the stern, the following line of reasoning was employed when determining the proper number. With the tentative beam-draft proportions of the first combinations of Table 66.e of Sec. 66.11, varying from 78.25:26 to 74:26, it appears easy to fit twin screws. However, the propellers are there to drive the ship, not necessarily to make it easy to design or construct. On the basis of requirement (5) of Table 64.a, for "Performance of the required transportation as efficiently and economically as the present state of the art permits," a single screw is definitely indicated. The resultant saving in fuel and corresponding increase in other useful items should be of the order of 3 per cent. It is agreed, however, between the designer and the future owner and operator, that a preliminary design with twin screws is to be worked up if time and opportunity permit.

The layout selected for the ABC design calls for the machinery units to be placed as far aft as practicable, following in some measure the designs of the combination passenger and cargo vessels *San Francisco* (old) and *Maui* of the early and middle 1910's, running between San Francisco and Honolulu. Two later Matson liners, designed primarily for carrying cargo, and having the single-screw machinery installed way aft, were the *Manulani* and the *Manukai* [MESA, Sep 1921, pp. 707–708]. This arrangement, incidentally, was adopted as far back as the period 1843–1845 in the American auxiliary sailing ships *Commodore Preble* and *Bangor* [Bradlee, F. B. C., "Steam Navigation in New England," Salem, 1920] and in the *Edith* and the *Massachusetts*, built for R. B. Forbes [American Neptune, Jan 1941, Pls. 2, 5]. A much later version is the Shaw-Savill liner *Southern Cross*, a pure passenger ship, with a single mast and single stack, far aft [Ill. London News, 19 Dec 1953, p. 1020; MENA, Dec 1953, p. 569; SBSR, Int. Des. and Equip. No., 1954, pp. 3–4]. In Europe an after machinery position was first used on the English coastal collier *John Bowes* in 1852 [Bowen, F. C., SBSR, 30 Sep 1937, pp. 421–422]. It is no longer necessary, as on the latter vessel, to put the machinery and the smoke stack "right aft," out of the way of the fore-and-aft sails on three masts. Nevertheless, the other reasons for placing the machinery in the stern are as valid today as they were in 1845, 1852, and again in 1892, when the steamer *Turret* was built in this fashion. These reasons, stated at the time by F. C. Goodall [INA, 1892, pp. 194–195] and later by G. C. V. Holmes ["Ancient and Modern Ships," 1906, Part II, p. 120] are summarized here from those authors:

(1) When the ship is without cargo it helps her to trim by the stern, and thus gives good immersion to the propeller
(2) Water or fuel tanks may be fitted in the after part of the vessel, to help submerge the propeller, as shown on Plate XXIII of the Goodall paper of 1892. This is now standard on all Great Lakes vessels, and is incorporated in the ABC design.
(3) The main shaft is shorter and lighter, with fewer bearings to watch and lubricate
(4) The hold space occupied by the shaft tunnel is saved
(5) Using the most valuable part of the hull, the rectangular section amidships, greatly facilitates the stowage of cargo [SBMEB, Jan 1953, p. 4]
(6) Less useful volume is lost, around the machinery components, if they are placed in the after part of the vessel.

A subsequent commentary is equally applicable:

"... of the ship in a big swell pitching, the bow and stern moving through many feet and the amidships movement only angular, and this space occupied by the engine, and the engine was never seasick ..." [Lord Brabazon, SBSR, 23 Oct 1952, p. 555].

Comments on machinery-aft positions were made by G. Gravier, concerning the performance of the passenger steamer *El Djezäir* [SBSR, 23 Sep 1954, p. 397], and by A. C. Hardy [SBSR, 7 Oct 1954, p. 465].

More recently E. C. B. Corlett has made a further study of the advantages and disadvantages of installing machinery aft, based upon modern conditions. He also discusses the question of placing the navigating bridge and all the crew accommodation aft [The Motor Ship, London, Feb 1955, pp. 483–485; IME, Jun 1955, Vol. LXVII, pp. 84–85].

69.6 Use of Systematic Wake Variations. It has been said [author unknown] that "The more uniform the wake, the simpler does it become to design an efficient propeller." Fortunately, because of the practicability of changing the size, form, and attitude of the blade sections along a length or a radius, it is only needful that this uniformity be maintained for the complete travel path of any given blade section. For a screw propeller this calls for circumferential uniformity in the wake fraction at any radius.

When examining wake diagrams such as those in Chap. 60 the procedure is to look for systematic variations which permit the propulsion device to be adapted locally to them. The next step is to determine the correct or proper average wake characteristics in the regions where the variations from this average are the smallest.

When contemplating the design of a paddle-wheel, for instance, it is known that, apart from a consideration of ship-wave effects, the wake velocities near the ship hull are positive because of the viscous flow in the boundary layer alongside. Farther from the ship, outside the boundary layer, these velocities are negative because of the accelerated regions of potential flow abreast the ship, indicated in the velocity profiles of diagram C of Fig. 6.B. Theoretically, the paddle blade elements away from the ship should travel faster than those next to the ship. However, this is not feasible in a shipboard installation and it might not be advantageous hydrodynamically for other reasons. The blade load per unit area next to the ship is therefore larger than at a distance from the ship. Were it necessary to equalize the blade loads per unit length for any reason this could be done by narrowing the blade at its inner end and widening it at its outer end.

For practical and mechanical reasons, it is advantageous to have the greatest blade load nearest to the point where the torque is delivered to the wheel. The increased loading at the inner end of a paddlewheel blade, or at the hull end of a Kirsten-Boeing rotating-propeller blade, is accordingly accepted. The rotating blades of a Voith-Schneider propeller develop thrust on opposite sides during any one revolution. It is possible to take advantage of the velocity variation in and beyond the boundary layer by local changes in the width but not in the section of a blade.

69.7 Rate and Direction of Rotation of Propulsion Devices. Rather extensive comment concerning the rate of rotation of screw propellers is given by J. E. Burkhardt [ME, 1942, Vol. I, pp. 28–35]. These remarks, coupled with the discussion of Sec. 70.10 on the rate of rotation of screw propellers as an element in design, is sufficiently general so that no further comment is needed here about other propulsion devices. The matter of selecting a rate of rotation that will not cause vibration of the ship structure or of its major parts in resonance with the shaft or blade frequencies is discussed briefly in Sec. 69.15.

The selection of the direction of rotation of these devices for a new ship design usually depends upon the relative importance of the propulsive efficiency to be achieved and the maneuvering and other qualities desired. For small craft it may also depend upon the availability of propelling plants developing the necessary individual shaft powers and which rotate in the directions desired, left-hand or right-hand. For the smaller vessels, where one may have to use available stock machinery, rotation in a desired direction may be too expensive because of necessary modifications or may involve the carrying of too many spare parts on a craft equipped with engines rotating to both hands. In large vessels practically all propelling plants, at least in the design stage, can be made to operate in either direction.

The interposition of reduction or multiplying gears may or may not change an engine direction to the desired propeller direction. Nevertheless, it is generally possible, even in the construction stage, to obtain a desired direction of rotation of the propulsion-device shaft if there are sufficient advantages to be gained thereby.

Assuming that the latter is the case, a systematic variation in the flow at the position of the propulsion device is looked for, one which will give a superior efficiency or perhaps a larger absolute thrust for a particular direction of rotation. This matter is discussed in Secs. 33.4 and 33.6. If the upward component of flow on the outboard side of a twin skeg is larger than on the inboard side, outward-turning screw propellers are indicated so that the outer blades moving downward may "meet" the water flowing upward to them. If for some special reason the reverse is the case, as with the outside water flowing horizontally and the inside water upward through a tunnel, inward-turning propellers are found more efficient. If circumstances limit the design of long deflection-type bossings or asymmetrical skegs to a particular diversion of the surrounding water the screw-propeller rotation is selected to take advantage of it, provided of course that other design requirements are met.

Considering hydrodynamics only there are very few reasons why any propulsion device of a single- or multiple-unit installation may not rotate in the direction which best produces the desired performance of that unit by itself. This is on the basis that the outflow jet from any one device does not pass through the disc or thrust-producing area of another device, and that the resulting unbalanced torque applied by the propelling plants to the hull, discussed in Sec. 69.13, lies within acceptable limits.

It is customary for large vessels, but by no means necessary for all vessels, that screw propellers be rotated in the following directions:

(a) Twin screws, in opposite directions, especially if the flow patterns are decidedly of opposite hands, symmetrical with the centerplane
(b) Surface propellers or those which run for much of the time with part or all of their upper blades out of water, *must* rotate in opposite directions in pairs if the large lateral forces produced by them are to be balanced
(c) Triple screws embody wing propellers rotating in opposite directions. The center propeller rotates in the most suitable and convenient direction, especially if under some conditions the vessel is to be propelled entirely by the center propeller, with the wing propellers free-wheeling.
(d) Quadruple screws rotate, in pairs, in opposite directions on opposite sides of the ship.

69.8 Design to Equalize or to Apportion the Powers of Multiple Propellers.

As soon as it is decided to use multiple propulsion devices, two or more in number, the designer begins to think about the problem of equalizing the powers absorbed by all of them. This corresponds to the proper proportioning of the powers, regardless of the number of propulsion devices, to the designed powers of the propelling units which are to drive them. The large quadruple-screw liner *Empress of Britain* of the early 1930's was propelled by two large inboard screws plus two smaller outboard ones. All four were to be used in transocean service but for around-the-world cruising the outboard screws were to be removed entirely, leaving the ship to be driven by the inboard propellers only. These were capable of absorbing two-thirds of the total power and were the only ones which could be reversed.

Proper design procedure involves consideration and, if possible, control of the following items at each propulsion-device position:

(a) Boundary-layer thickness and velocity profile, for both clean- and foul-bottom conditions
(b) Retardation or possible reversal of flow behind blunt bossing or skeg endings, involving wake fractions with large positive values, possibly exceeding 1.0
(c) General and local direction of flow through propeller discs or other thrust-producing areas, plus wake-survey data. This is a case where consideration of only the axial component of flow is definitely not adequate.
(d) Non-axiality of flow, due not only to the shape of the adjacent hull but to the necessity for placing shafts to suit the engines inside and the propulsion devices outside
(e) Possibility of an outflow jet from a propulsion device ahead finding its way into the inflow jet of one abaft it
(f) Rate of rotation of the various propulsion devices when absorbing the designed powers. The propeller torque may be so large that the engine delivers rated torque at less than the designed rate of rotation, preventing the development of full rated power. On the other hand, the speed of advance may be so high that the engine reaches its rated rpm when developing less than the rated torque.
(g) Necessity for accurate correlation of torque and rate of rotation to achieve full rated powers for internal-combustion engines driving (single or) multiple propellers.

The available data relating to power equalization and proportioning and to correlation of torque and rate of rotation on existing merchant ships or on self-propelled models of them are by no means extensive. J. M. Labberton in a paper entitled "A Method for Determining Proper Pitch for the Inboard and Outboard Propellers on a Four-Screw Ship" [ASNE, Nov 1937, pp. 576–584], discusses this question and gives the following data for the old *Mauretania*, taken during the trials of 1907:

	Port Outer	Port Inner	Star. Inner	Star. Outer
Rate of rotation, rpm	187.3	186.6	188.6	188.6
Shaft power, horses	17,350	20,650	20,650	18,600

All four propellers had a diameter of 17 ft and a pitch of 15.75 ft. In this case the rates of rotation were as uniform as could be hoped for in such a large new ship but the inner propellers were absorbing some 53.5 per cent of the total power, or about 15 per cent more than the outer propellers.

The designer may find that he has only limited freedom in shaping the hull and placing the propulsion devices. After he has done what he can in positioning these devices properly and working out the adjacent appendages he is able to make use of existing model-testing techniques which indicate and record the flow velocities and directions at the propeller positions, both at the hull and appendage surfaces and at distances from them. It is possible, for example, to make a wake survey at an after propeller position with a model propeller working in a position ahead. Facilities have been developed but are not yet in general use in model basins, whereby a wake survey is made just ahead of a working propeller.

From these data it is possible to estimate rather closely the wake magnitude and distribution at each propeller position. An estimate of the individual thrust-deduction fractions is, however, still difficult. Before a model is self-propelled it should be possible to determine what variations in propeller design are necessary to compensate for hull features not under the control of the designer. One or more series of self-propelled tests, possibly with a change in propeller design in between, should insure reasonably close equalization or apportioning of the full-scale shaft powers, and correlation of the torque-rpm values.

69.9 Powering Allowances. A doctrine involving design and performance allowances, applying to the hydrodynamic features of a new ship whose principal characteristics are being formulated, is set down in Sec. 65.3. The emphasis in that section, repeated subsequently in the present one, is concentrated on the outstanding advantages to be gained by designing a speed margin rather than a power margin into the ship. This means that the ship hull is shaped to be driven efficiently at a speed greater than the sustained speed when developing its maximum power. The alternative method, practiced in some quarters, is to design the ship hull for the sustained speed and then to add a large power allowance. This might be acceptable if the problem were only one of overcoming increased resistances due to heavy weather and to fouling. However, it results in overdriving and poor performance at the augmented speeds necessary for a ship which, running on a definite schedule, has to make up time after a spell of bad weather.

Good design of the propelling plant of any water craft calls for a reserve of power (1) to meet emergencies, (2) to enable the plant to keep running and to deliver a sort of average power with minor casualties, and (3) to permit it to run much of the time at less than maximum rating. With pressures, loads, and other factors reduced, wear and tear is usually diminished and the periods between overhauls is increased.

Almost every plant is capable of developing an emergency overload power for a few minutes, perhaps for a few hours, if it becomes a matter of saving life or the ship. Since this may result in slight but permanent damage to the machinery, it is not considered in the customary powering calculation. The *maximum designed shaft power* is therefore that "for which the propulsion machinery is designed to operate continuously" [SNAME, Stand'n. Trials Code, 1949, p. 11]. For powering a boat or ship, the machinery reserve is reckoned below this level.

In general, the reserve of power is a function of the length of time that operation at maximum designed power is required. For a racing motorboat which may run at full throttle only a few hours between engine overhauls, but which must then do its utmost, the reserve is practically zero. If the game is considered worth the candle, so to speak, the emergency power is called upon, in which case the reserve is negative. The other extreme is a boat or ship which operates under a wide range of conditions and which stops for repairs only when it will no longer run. The

reserve may then be as much as 0.3, 0.4, or 0.5 of the maximum designed power.

Notwithstanding that the word "designed" implies that the machinery is able to develop its maximum power continuously, a full measure of reliable everyday operation, over most of its life, is assured by limiting the maximum designed speed to that which is developed by say 0.95 of the maximum designed power [Burkhardt, J. E., ME, 1942, Vol. I, p. 28]. It is usually assumed that this speed is to be achieved at the full-load or other specified draft, in smooth, deep water of the given specific gravity, in fair weather (little or no wind), and with a clean bottom. In other words, it represents a trial speed at 0.95 of the maximum designed power, with a so-called machinery reserve of 5 per cent.

Actually, a ship design starts with the designed sea speed or service speed, determined from the schedule which the ship is to maintain, or from a study of economic and other reasons. For the ABC design this operation was completed by the owner and operator before the design requirements were formulated. To compensate for slowing down in heavy weather a reserve of speed above the designed sea speed is necessary. This is achieved either by one or by a combination of the following:

(a) Specifying it as an *increment* of speed, resulting in the 1.8-kt differential of the ABC design (the difference between 20.5 and 18.7 kt)
(b) Calling for a *percentage* increase in speed over the designed sea speed, varying from about 8 to 15 per cent
(c) Requiring a percentage increase in power over that necessary to drive the ship at the designed sea speed under trial conditions, usually from 20 to 30 per cent or more.

When taking account of small percentages the question arises as to the point in the ship at which the maximum designed power of the machinery is to be delivered; also as to the kind of power represented by it, whether indicated, brake, shaft, or propeller power. There are different means employed to measure power, and there is still some uncertainty as to just where along the line, from the heat-to-work conversion point to the propeller, the power is to be measured. It is most important, therefore, that the hull and propeller designers know exactly where this point is, and what is transmitted there. In fact, there are many good reasons for rating the propeller, not in terms of the power absorbed (in horses) but in terms of the torque required to turn it and the thrust achieved at the thrust bearing, all at a specified rate of rotation [Smith, E. H., IESS, 1954–1955, Vol. 98, Part 3, pp. 127–128]. The losses encountered in transmission between the thrust bearing and the propulsion device are then to be estimated or predicted by the propeller designer in cooperation with the machinery designer.

As has often been done in the past, the designer may wish to add a reserve of power over and above that necessary for the sustained speed to be achieved under trial conditions in good weather, following the method of (c) preceding. He may add an average percentage to this power, using a figure taken from good practice, or he may wish to base his reserve on an analysis of the particular situation involved. At least four, and sometimes six or more factors enter into the percentage increase applied to the power predicted for sustained speed in good weather and with clean bottom. These factors, with their customary percentages, are:

(1) Weather, involving an increase in power to maintain speed against head winds and seas or to make up time lost by slowing in waves	8 to 15
(2) Fouling by marine organisms or other roughness	6 to 20 or more
(3) *Increase* with age of structural and propeller roughness and of displacement (in some vessels)	2 to 5
(4) Machinery reserve, to care for minor casualties, inefficient handling, fuel under standard quality, normal wear and tear, and slow deterioration in performance with length of service	4 to 6
(5) Still-air and normal wind resistance of ship	2 to 4
(6) Scale effect between model and ship (may be plus or minus)	1 to 3 or 4
(7) Cavitation loss in high-powered vessels	0 to 10 or more.

All these factors, if taken into account, may total from 23 to 54 per cent or more, depending upon their individual signs and values. It is customary to omit some and to emphasize others, particularly the increase for fouling. The total increase in power, over that required to maintain the sustained sea speed under trial conditions, is

then of the order of 20 to 30 per cent [ME, 1942, Vol. I, p. 28; Troost, L., SNAME, 1953, p. 576].

It is to be noted that item (6) of the tabulation above does *not* include a sort of average allowance for appendages, as is customary in some quarters. This is taken care of by the model-testing establishment, on the basis of the kind, number, shape, size, and location of the appendages, relative to the hull and to each other.

When estimating and applying the power percentages to the predictions derived from model tests it is most important to insure that an allowance corresponding to one or more of the foregoing factors has not already been worked into the model-basin predictions. In America it is customary to omit all the allowances listed except the $\Sigma(\Delta C_F)$ for plating, structural, and coating roughnesses to be expected on a clean, new vessel under trial conditions; see Sec. 45.18.

It is generally necessary, at some stage in the formulation of requirements or in the preliminary design, to know the speed-power relationships when some or all of these increases in resistance and power are in effect. For example, when the bottom is dirty the wake fraction becomes greater and the thrust loading of the propeller is increased. It must also be decided at what power the propelling plant is to operate at maximum efficiency. At a later stage the detail propeller design calls for an estimate of the propulsion factors at what might be termed the propeller-design point, to be explained presently.

Model-testing techniques [C and R Bull. 7, 1933, p. 32] permit running a self-propelled model under conditions in which the model propellers develop thrust under or over that necessary to push the model through the water. The auxiliary towing or retarding force is adjusted to provide the equivalent of underwater body resistance, additional drag due to roughness of the hull surface, and any overload that may be expected on the ship due to fouling, adverse weather, and the like. This procedure admittedly does not change the velocity profile, the thickness, and other features of the boundary layer corresponding to the effects of the roughnesses which produce the additional drag but it does increase the model propeller thrust loading. Any desired thrust overload can be applied to the model or runs can be made with varying overload to give predictions for any estimated power increase at a given speed. One method successfully used for many years predicts ship and propeller operating conditions at the designed trial speed but with a power increase of 12.5 per cent above that required for trial conditions. This 12.5 per cent increase is a sort of selected average between clean-bottom trial conditions with no adverse forces acting on the ship and a 25 per cent increase to be expected toward the end of the docking interval, with some adverse weather and other overloads thrown in.

Data derived from this procedure are definitely to be preferred, for predicting service performance and for design of the ship propellers, to data derived from driving a smooth model faster than the sustained speed by the use of the maximum power that it is proposed to put in the ship.

It is pointed out in Sec. 65.3, and it is again emphasized in a discussion of speed reduction in wavegoing in Part 6 of Volume III, that a ship is in much better position to maintain a high sustained speed if it has a speed margin designed into it rather than a power margin designed into the propelling machinery alone. The speed margin may be a percentage above the sustained speed or it may be a speed increment, as mentioned in (a) and (b) preceding. It may be determined by a graphic method such as that described in Sec. 69.10. Whatever the method employed to determine the speed margin, the designer has more assurance of achieving the extra speed required to make up for lost time if the ship is fashioned to make that extra speed easily.

69.10 Graphic Representation of Powering Allowances and Reserves. Assuming a no-overload condition for the ship, involving only the unavoidable plating, structural, and coating roughnesses to be expected in the clean, new condition, a typical speed-power curve is as indicated by AGB in Fig. 69.A. If the clean, new ship were run at the maximum designed power P_{Max}, under perfect trial conditions, the speed-power point would be at B and the speed would be V_{Max}. If the power were limited to 0.95 of the maximum designed value, the speed-power point would be at G and the speed would be V_{Trial}.

Running the vessel at the power P_{Max} with k_1 per cent of increased resistance due to adverse effects, along the curve DG_1C marked "AVERAGE OVERLOAD" on the figure, gives the speed-power point C for a speed somewhat less than the trial speed V_{Trial}. The ship can now run at this speed with maximum designed power P_{Max} or it can run at a reduced speed V_2 with

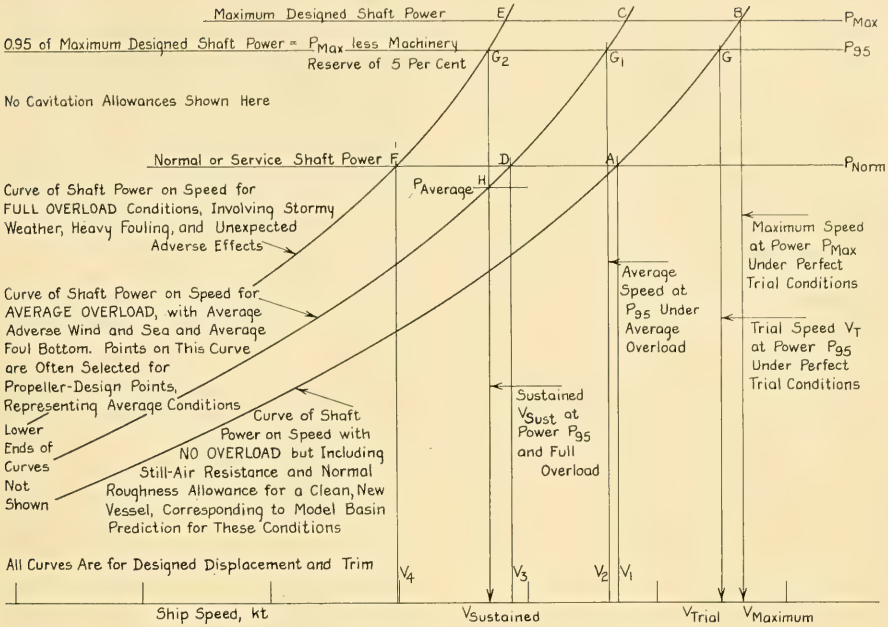

Fig. 69.A Explanatory Diagram for Powering Allowances in a Large Vessel

95 per cent of maximum power. Under what might be termed "FULL OVERLOAD" conditions, corresponding to the curve FG_2E, and utilizing only 95 per cent of the designed maximum power, the ship is able to maintain a sustained speed V_{Sust}, at the speed-power point G_2.

If the ship is really to sustain this speed for long periods it must be capable of running faster than V_{Sust} part of the time. Assuming full-overload conditions all the time this is not possible by Fig. 69.A unless the power is increased above P_{95} (and above P_{Max} as well). Rather than to do this it is assumed, and logically so, that the sustained speed is to be achieved under average-overload conditions, along the curve DG_1C in the figure. This means that with a sort of average power, represented by the ordinate of the point H, the ship has a reserve of power represented by the ordinate HG_2. With this reserve, extending up to P_{95} at the point G_1, it is capable of achieving the speed V_2. This speed is somewhat less than V_{Trial}, but as long as the speed margin $(V_2 - V_{Sust})$ is greater than the possible speed reduction $(V_3 - V_4)$ to be anticipated over any lengthy period, the ship is assured of maintaining the sustained speed and of keeping up with its schedule.

Unfortunately in practice the designer rarely if ever knows the precise location of the average-overload or the full-overload speed-power curves on his plot, despite the availability of procedures such as those in Secs. 45.22 and 60.15. He is reasonably certain in the design stage of the no-overload, speed-power curve AGB, with its values of V_{Max} and V_{Trial}. He knows, furthermore, that the speed-power values along the curve AGB can be checked by carefully conducted ship trials. He also knows the required sustained speed. He may therefore select a speed V_1 such that the speed margin $(V_1 - V_{Sust})$ is sufficient in his opinion, and in the judgment of the owner and operator, to make good the sustained speed. From the no-overload curve of the figure, this speed V_1 then corresponds to the point A, also easily determined in advance with reasonable accuracy and subject to confirmation on trial. The corresponding power is P_{Norm}, which with an average overload should give a speed V_3, slightly in excess of the sustained speed or at least not less than that speed. For most ship

designs, P_{Max} is about 1.25 or 1.30 times P_{Norm}.

One means of making this procedure more precise is to have the self-propelled model run with an estimated average overload, say 1.25 times the no-overload ship resistance, as mentioned in the preceding section. Then curve DG_1C as well as curve AGB is obtained and the speeds V_2 and V_3 are predicted reasonably well.

The next problem, equally as important as the establishment of these speed-power-overload relationships, is selecting the condition for which the propeller is to be designed. First, it must be capable of absorbing the power P_{Max} at some rate of rotation n which can be achieved by the engine when delivering that power. Second, it must operate efficiently at either P_{95} or P_{Norm}, whichever the owner and operator thinks most important, and at a ship speed corresponding to the selected power and to an overload condition at which the owner and operator wishes the ship to do its best. This is usually but not necessarily the power for which the propelling plant is designed to run most efficiently and economically. At the power, ship speed, and overload condition selected the rate of rotation of the propeller and the propelling plant must also correspond.

In general, the propeller-design point may be taken as G_1 in Fig. 69.A. If so, a check is made to insure that the propeller efficiency does not fall off appreciably at the points D and H. This is one reason why some propeller designers are reluctant to work a propeller near the peak of its efficiency curve, for fear that at the lower loadings and real-slip values the so-called working point will pass over the maximum-efficiency hump and slide down the steep side of the η-curve.

If internal-combustion propelling machinery is utilized the maximum power P_{Max} can be developed only at the exact rpm for which the engine is designed. This rate of rotation must in turn correspond to a certain ship speed for that power. If maximum efficiency at a sustained speed corresponding to full overload is desired, the speed-power point G_2 should be the propeller-design point. Although F is also a point on the full-overload speed-power curve it may not represent the power developed by the internal-combustion engine at a rate of propeller rotation corresponding to the speed V_4. However, if the engine-propeller combination can drive the ship at full overload at the speed corresponding to the point G_2 it almost certainly can, with some lesser power, maintain the slower speed at F. If a higher speed is aimed for, at maximum designed power corresponding to an average overload at the point C, the speed-power and the propeller-design points are then represented by that point.

It is again emphasized that speed-power points such as G_2 or C are only achieved accidentally on a ship, when the overload from all causes happens to be either the average or the full value assumed by the designer. It is therefore not possible to check these points on an actual ship by full-scale tests. On the other hand, the speed-power points B, G, and A are easily reached and checked under planned trial conditions. It is therefore logical to embody one of these points, say G, as one of the design requirements and to call for a check of it as a ship-contract stipulation.

This is essentially what was done in Table 64.d and Sec. 66.9 for the ABC design, when the trial speed of 20.5 kt was required at a power expenditure of $0.95P_{Max}$, corresponding to the point G on Fig. 69.A. To prevent the problem from becoming too complicated, especially as overload values are not accurately known, the ABC propeller is also designed in Chap. 70 for the speed-power point G. The data from the model self-propulsion test, without overload, correspond to that point. The additional shaft power from P_{95} to P_{Max} is taken care of by the machinery designer.

Under other circumstances the propeller could be designed equally well for the points G_1 or G_2, depending upon advance knowledge as to overloads, the type of machinery to be installed, the judgment of the designer, and the wishes of the owner and operator.

69.11 Selection of Feathering, Adjustable, Reversible, or Controllable Features. Feathering features on paddlewheels form an integral part of the design of these devices. As such they are discussed in Secs. 71.6 and 71.7.

Feathering and folding propellers are fitted almost exclusively on sailing yachts with auxiliary power, as a means of reducing the drag of the stationary propeller. Notes relative to their use are found in Sec. 71.13.

Adjustable screw propellers, described briefly in Sec. 32.19, carry blades whose position relative to the hub can be changed only when the adjusting mechanism is out of water. They permit pitch changes in the event that the ship resistance in service is found not to agree with that predicted in the design stage. Altering the pitch in this manner is one means of insuring that internal-

combustion engines can run at the proper rate of rotation to develop their maximum power. It may also be found in service that fouling rates, with consequent increased friction powers, are higher than those contemplated during the design.

The foregoing advantages, including the very practical one of replacing a damaged blade, are balanced against the slightly diminished efficiency resulting from the larger hub and from unfairness around the blade attachments. This matter is discussed at length in Sec. 70.43.

Reversible propellers, in which the blades swivel and the shaft continues to rotate in the same direction, eliminate reverse gears and reversing mechanism in the propelling plant. This is only done at the expense of mechanical complication in the shaft and the propeller, increased diameter and bulk of the propeller hub, and certain hydrodynamic disadvantages described in Sec. 32.19. However, if reversibility of thrust is the primary object, the latter are not too important. The problems are then primarily ones of engineering rather than hydrodynamics.

So many extraneous problems enter into a decision to use controllable propellers that no attempt is made to give them here. The designer may with benefit study the references listed in Sec. 32.19 and repeated here for convenience:

(a) McEntee, W., SNAME, 1927, pp. 87–91, and Pls. 43–47
(b) Gutsche, F., Zeit. d. Ver. Deutsch. Ing., 15 Sep 1934, p. 1073
(c) Ackeret, J., Escher-Wyss Bull., May-Jun 1935, p. 63
(d) Fea, L., Ann. Rep. Rome Model Basin, 1938, Vol. VII, pp. 74–89
(e) Rupp, L. A., "Controllable-Pitch Propellers," SNAME, 1948, pp. 272–358
(f) Burrill, L. C., "Latest Developments in Reversible Propellers," IME, 1949, Vol. LXI, pp. 1–11; INA, 1949, Vol. 91, pp. J3–J32
(g) Nichols, H. J., "An Hydraulically Controlled C-P Propeller System," Motorship, New York, May 1949, pp. 22–23, 44–46
(h) Baader, J., "Cruceros y Lanchas Veloces (Cruisers and Fast Launches)," Buenos Aires, 1951, p. 209
(i) Doell, H. A., "What is the Controllable-Pitch Propeller?" Mar. Eng'g., Aug 1953, pp. 71–76
(j) Van Aken, J. A., and Tasseron, K., "Comparison Between the Open-Water Efficiency and Thrust of the Lips-Schelde Controllable-Pitch Propeller and those of Troost-Series Propellers," Int. Shipbldg. Prog., 1955, Vol. 2, No. 5, pp. 30–40.

A word of caution is included: Do not expect that it will be found worth while to install a controllable propeller solely to enable the propeller to run at the proper pitch for any given loading condition [Rupp, L. A., SNAME, 1948, p. 273].

The problems involved in the detailed design of controllable propellers are so specialized and so complex that no attempt is made to present any of them in this chapter. It may be assumed that organizations which have produced successful service installations are in much better positions to design controllable propellers than is the ship designer.

The fairing caps of the hubs of many controllable propellers contain essential parts of the blade-shifting mechanism and are as long if not longer than the propeller hub proper. It may be necessary to cut a notch in the leading edge of an all-movable rudder blade to clear the hub cap [Mar. Eng'g., Feb 1953, p. 1; Jan 1955, p. 104].

69.12 Propulsion Devices to be Used with Contra-Vanes, Contra-Guide Sterns, and Contra-Rudders. In general, as described in Secs. 33.12, 36.8, 36.9, and 37.16, it is immaterial whether rotation is introduced in the inflow jet of a screw propeller and taken out by that propeller or whether the rotation produced by the propeller is taken out by a contra-rudder or equivalent device placed in the outflow jet. However, for a given average resultant water velocity at the blade elements, the angular speed of the propeller is usually slightly less if some rotation is imparted to the inflow jet ahead of it. Actually, as far as the design of the propeller is concerned, it may be proceeded with on the basis of no prerotation, following which an adjustment may be made to determine the probable angular speed for a given torque and thrust.

Good propulsion-device design, and good ship design as well, calls for a thrust-producing device which inherently leaves as little systematic disturbance as possible in its wake, and which requires the least amount of predeflection or prerotation in the inflow jet.

69.13 Disadvantages of Unbalanced Propulsion-Device Torque. On semi-planing and planing craft carrying multiple propellers below the hull in such position that the flow to both the port and starboard sides of each propeller is substantially the same, there are numerous practical reasons for selecting and installing main engines and propellers which rotate in the same direction. However, this arrangement has the disadvantage that, because of the rotation in the propeller outflow jets or races abaft the propellers, there may be a resultant asymmetrical lateral force from the rudder(s). It may be difficult to find

the neutral angle for each and this angle may change with speed. An effect of this kind is more pronounced when the rudders lie within the propeller outflow jets. Furthermore, there is a cumulative torque reaction from all the engines which results in an appreciable listing or heeling moment and an ever-present heel at moderate to high speeds.

This heeling moment due to torque should be counteracted, not by a fixed moment, as of ballast or machinery asymmetry, but by a torque which varies generally as the engine torque, increasing gradually with speed and power. This is best accomplished by applying a hydrodynamic torque which automatically increases with speed. For right-hand engines and propellers, a positive heeling moment is required, acting to produce a starboard heel. On some V-bottom planing craft [Bureau of Ships Bull. of Inform. 32, 1 Oct 1948] the chine spray strip is modified to slope its lower edge downward and outward, giving it a negative dihedral angle with the bottom of the boat. The water moving out transversely from under the boat is deflected sharply downward, and an upward force results from this change of direction.

The hydrodynamic compensating torque is also produced by a well-cambered hydrofoil placed in an offset position in the propeller outflow jet, so as to develop a lift force forming a torque opposite to that of the propeller. Fig. 73.P illustrates and Sec. 73.21 describes a pair of twisted hydrofoils in the form of a cross, placed in the outflow jet of a single screw propeller to accomplish this purpose.

69.14 Propulsion-Device Design to Meet Maneuvering Requirements. The design of ship hulls to meet maneuvering requirements is discussed in Part 5 of Volume III. There are presented here a few features relative to the type, position, and size of the propulsion devices when maneuvering is a major consideration. For stopping and running astern, some design comments and pertinent references are given by J. E. Burkhardt [ME, 1942, Vol. I, pp. 35–38]. Fortunately there are available sufficient data from tests of model propellers running astern, listed in the references of Part 5, to enable the designer to check the ability of a propeller to produce a specified thrust for astern operation. There are also available in Sec. 60.18 the results of backing tests on one self-propelled model.

While it is true that ships can be and have been steered by changing the rates of rotation of wing propellers carried by them, the turning moments are usually too small to be of any considerable benefit in rapid maneuvering. Indeed, if any drastic change is to be made in a vessel's turning path it is necessary to *reverse* the wing propeller(s) on the inside of the turn. It is doubtful if any vessel carrying screw propellers can have its turning characteristics materially improved by any practicable positioning of the wing screws or wing shafts at a large distance from the centerplane.

Despite the overwhelming percentage of time during which any ship is employed in ahead operation, the requirements for developing astern thrust and for maneuvering may and often do influence the design of the propulsion device(s). For example, on a paddle tug with independent wheels, frequently employed in backing and turning, the paddle blades are properly straight rather than curved in section. They should, furthermore, enter and leave the water vertically, if this is feasible without too much complication. An icebreaker which needs powerful astern thrusts to fulfill its mission may advantageously have screw propellers with blade sections nearly or completely symmetrical, as for the screw propellers of the double-ended ferryboat.

By and large any special requirements for starting, stopping, and turning are fulfilled by propulsion devices with large thrust-producing areas. The larger these areas the better, since for a given speed of advance V_A the thrust depends upon the thrust-load factor and ultimately upon the disc area.

69.15 Relation of Propulsion-Device and Hull-Vibration Frequencies. A discussion of machinery and hull vibration as such is definitely outside the scope of this book. Nevertheless, it is pointed out here that the rate of rotation of the propulsion devices, whatever their type, should not be fixed until a study has been made of the probable vibration characteristics of the hull and propelling machinery under various loading conditions [Lewis, F. M., ME, 1944, Vol. II, pp. 130–137; Kane, J. R., and McGoldrick, R. T., SNAME, 1949, pp. 193–252]. This insures that the propulsion-device rpm or the blade frequencies $n(Z)$ do not coincide with a 2-noded or 3-noded hull frequency in vertical or horizontal flexure, so that a slight mechanical or hydrodynamic unbalance is magnified over the whole ship. Strictly speaking, the torsional hull frequencies should also be estimated and compared with the proposed shaft rpm.

It is usually easy to design or to alter local structures or small parts of the ship to keep their resonant frequencies out of the range of propdev rpm or blade frequencies at speeds where the exciting forces are high. However, to make material changes in these characteristics of the hull proper, or of large parts of it, is often well-nigh impossible.

Probable torsional and longitudinal resonant frequencies of the propulsion-device-shaft-gear-turbine (or motor) system are likewise estimated, to insure that they do not fall within the range of shaft or blade frequencies at or near service power or maximum designed power [Sullivan, E. K., and Scarborough, W. G., SNAME, New Engl. Sect., Apr 1952].

CHAPTER 70

Screw-Propeller Design

70.1 General Considerations. The design of screw propellers for ships, as developed at the time of writing (1955), embodies so many facets that nothing short of an entirely separate volume, or book, can do it justice. Only in this way can there be presented to the naval architect and marine engineer all the useful and usable information on this subject, including rules for propeller design. G. S. Baker approached this two decades ago [SD, 1933, Vol. II, pp. 1–68], and the Russians made it a reality in 1949, when they published two comprehensive books on marine propulsion and marine-propeller design.

The design data and procedures are now so numerous and so well laid down as almost to justify the often-heard facetious remark: Designing a good propeller is easy; one has to work only to design a poor one. Nevertheless, cavitation at low speeds, cavitation erosion, unbalance in power between inboard and outboard screws, and too large or too small propeller diameters still turn up in the most unexpected places. Screw-propeller design procedure, in all its phases, is by no means adequate or perfected.

Because of the large volume of existing literature, the discussion in this chapter carefully

avoids major duplication and appreciable overlaps with published material in books, papers, and reports, especially those readily available to the average marine architect. The major portion of the chapter is devoted to a description of the short method of Dr. H. W. E. Lerbs for the design of a screw propeller, based on the circulation theory. Accompanying a step-by-step description of this method, a sample calculation is carried along for a propeller to be used with the transom-stern design of ABC ship, the hull of which is laid out in Chaps. 66, 67, and 68. This description, incidentally, is believed to be among the first based on this theory by which *all* the elements in the design are derived by a continuous, straightforward procedure. This makes it suitable for a designer with little or no background or experience, save the knowledge of flow and circulation and its application to the ship and screw-propeller combination, to be found in Chaps. 14–17 and 32–34 of Volume I of this book.

The symbols, terms, and definitions employed in this chapter conform to those listed in Appendix 1 of this volume. They are described in SNAME Technical and Research Bulletin 1–13, containing "Explanatory Notes for Resistance and Propulsion Data Sheets," July, 1953, and illustrated in Figs. 32.F, 32.G, and 32.H of Secs. 32.8 and 32.9.

70.2 Design Requirements for a Screw Propeller. It is possible that one reason for the shortcomings in the numerous design methods and procedures, including those discussed in Sec. 70.3, is a partial lack of appreciation of the basic requirements to be met and of the practical needs of the ship owner and operator. Perhaps even more basic are what might be termed the practical needs of the ship itself.

For example, as long ago as 1938 a propeller designer, F. McAlister, when discussing the results of a symposium on marine propellers [NECI, 1937–1938, Vol. LIV, pp. D141–D142], declared that, as reported in SBSR, 6 October 1938, page 415, "none of the papers in the symposium tabulated the *qualities required* (the italics are those of the present author) for full-sized propellers for ships under service conditions. He suggested that from the purchaser's point of view these requirements were:

"(I) That the (new) propeller must be of the highest possible efficiency—say 10 per cent (or more) higher efficiency than the average existing propeller

"(II) Must not sing or be unduly noisy

"(III) Must not vibrate or must eliminate whatever vibration may be due to the existing propeller

"(IV) Must not erode, or at least must be better in this respect than the existing propeller

"(V) Must be of sufficient strength and first-class workmanship to ensure a long life free from trouble.

"The information given in the papers gave no guidance in these directions. It might be the case that these 'purchaser's' requirements can be met in exceptional cases, but it is surely a serious reflection on ordinary practice to suggest that propellers as now fitted are, on the average, 10 per cent less efficient than they might be."

70.3 Comments on Available Design Methods and Procedures. It is expected, when many minds work on a problem in the atmosphere of a democratic way of life, there will be many lines of attack and many partial or complete answers. This is as it should be, because different kinds of answers are required for different situations. Furthermore, the problem—screw-propeller design in particular—is so complex that no single line of attack can do more than make a rather narrow path through the entire region to be covered.

The procedures now in use among naval architects and marine engineers vary from the heavily theoretical to the intensely practical, but fortunately each is useful in some particular situation. An engineer may select a propeller diameter and pitch by some simple formula or nomogram and order a propeller out of a catalog, or he and his assistants may toil for several months, calculating a propeller design for which no ready rules or precedents are available. The day is past, or nearly so, when the marine engineer sketched his propeller freehand in the foundryman's notebook, penciling in the few principal dimensions.

It is well to recognize, therefore, that a group of several of these methods has its place in the scheme of things, even in a so-called advanced age. For example, in the design of the underwater hull of the ABC ship, begun in Chap. 66, one of the principal aims is to swing as large a propeller as possible. Since the limit of ideal efficiency described in Sec. 34.2 increases as the thrust loading decreases, and the latter decreases as the propeller diameter increases, it works out that the larger the propeller, the greater the propeller efficiency, all other things being favorable. The tentative diameter of 20 ft, on a 26-ft draft, is based on a propeller somewhat larger

than that given by the rule of thumb, $D < 0.7H$, equal in this case to 0.7(26) or 18.2 ft.

When, at a later stage of the design, after the resistance of the hull had been estimated, together with the wake and thrust-deduction fractions, it was possible to calculate the thrust-load factor and to know that it was low, as desired. When the shaft power was estimated, it was found from several propeller-design charts that a 20-ft propeller would absorb it when running at a reasonable rate of rotation.

At a still later stage, when it was necessary to pick a suitable stock propeller for the model self-propulsion test, the P/D ratio and other principal characteristics were determined approximately by several established methods, called chart methods, mentioned presently and described in Sec. 70.5.

For the latter part of the preliminary design of the ABC ship, a final design of screw propeller for a second series of model tests (not conducted) was carried through by the Lerbs short method, based upon the circulation theory, described in Secs. 70.21 through 70.38.

These several methods are mentioned to show that the approximations, estimates, and calculations required at different stages of a ship and propeller design call for different procedures. Some call these 5-sec, 5-min, 5-hr, and 5-day procedures, depending upon how soon the answer is wanted. The precision of each is of the same order as the time required. Others call them the 1st, 2nd, 3rd, and 4th approximations. The important fact is to realize that the first approximation is based upon the application of one single rule of thumb; the last one upon all the scientific and engineering information available. All of them have their logical functions in the design of any one propeller.

In general, neglecting the thumb rules, the various procedures fall into two groups:

(1) Those based upon systematic experimental data, derived from tests of model propellers in methodical series, with uniformly varying parameters and characteristics. The data, when checked and analyzed, are put in the form of graphs, diagrams, or charts, whence the name *chart design*.
(2) Those based upon the application of hydrodynamic theories and knowledge of flow, embodying such gap-fillers and correction factors (derived usually from experimental data) as are required to compensate for lack of accurate and adequate knowledge here and there.

The first group labors under the disadvantage that it applies only to propellers with the same number of blades, blade shape, section shape, and so on, as the propellers of the series tested. The second is deficient in that factual knowledge concerning the nature of the physical water flow around a propeller and the applicable hydrodynamic theories, as well as the necessary confirmations of the latter, lag rather far behind the necessity for knowledge to give the practical answers.

The chart method tells only what happens to the overall forces and moments on a propeller which someone has already fashioned, whether it be well fashioned or not. The analytic method leads gradually but surely to a better understanding of the physics of the problem, which governs the forces and moments, and hence to an indication of just how a screw propeller should be fashioned to give the desired results.

70.4 Requirements for, Availability of, and Listing of Propeller-Series Charts. It should be recognized at the outset that any chart or analytic procedure may, and probably will take a different form, depending upon the characteristics that are given or fixed and those which are to be derived. For the purpose of this book, one procedure only of each kind is described, embodying freedom of choice for the designer in that primary characteristic which should, for the best performance, permit him the greatest leeway. For example, in the hull design of the ABC ship, roughed out in Chap. 66, the weights to be carried by the ship are specified, as is the speed, leaving the length free for selection of the optimum dimension.

For the propeller designs to be worked out as examples in this chapter, the power to be absorbed is governed by that required for driving the hull at the designed speed. It is anticipated that the best screw propeller will be that having the greatest practicable diameter, so the hull in the vicinity of the propeller position is designed with this in view. Strictly speaking, this means that the propeller diameter is fixed at the beginning of its design, but at a figure which should produce a most efficient wheel. The rate of rotation, the pitch-diameter ratio, and other factors remain to be selected so as to give high propulsive efficiency in service. In other circumstances the propeller power and rate of rotation might be fixed, with the best diameter to be found.

Regardless of the primary characteristics given

and to be derived, a good screw-propeller data sheet or design chart meets the following requirements, listed in the order of their importance:

(a) As for any graph of its kind, it should "... show at a glance the variation of the most important dependent variables with the independent variable" [Schoenherr, K. E., SNAME, 1951, p. 629]
(b) The range of the sheet or chart should cover all propulsion conditions that may reasonably be expected
(c) The most important variable to be derived from each sheet should appear in the formulas applicable to that sheet in its first power and should occupy the principal position in the formula or chart
(d) The primary numerical design values to be taken from the chart should require little or no interpolation between curves to give the precise engineering answer
(e) The primary variable on at least one sheet of a group should be the pitch/diameter ratio
(f) The chart should be readily entered and the desired values found without effort, confusion, or misunderstanding. It is better to have separate charts than to embody too many features on one chart. In other words, a propeller design chart "should possess graphical simplicity, permitting ease of reading and interpolating" [Kane, J. R., SNAME, 1951, p. 626].
(g) All chart parameters should be dimensionless, with dimensions in any system of units to be derived by simple substitution and calculation
(h) The chart should be no larger than necessary for the precision required in ship and propeller design but large enough for easy visual selection of the data desired
(i) Nomograms should be embodied, wherever practicable, for determining the values of chart parameters and certain physical quantities
(j) With at least three variables given, the chart should yield all the data for the preliminary design of a screw propeller, specifically:

(1) Diameter, pitch, and pitch-diameter ratio
(2) Number of blades (considering propeller efficiency only), expanded-area ratio, mean-width ratio, and blade-thickness fraction
(3) Blade shape (outline) and blade-section shape
(4) Hub-diameter ratio
(5) Maximum or actual open-water efficiency or both
(6) Possibility and effect of cavitation, perhaps by auxiliary charts.

(k) There should be sufficient charts in a group to permit a propeller designer to enter them with given values of any of the primary variables
(l) Future chart groups should embody the approved symbols adopted by the International Towing Tank Conference.

Propeller-series charts must necessarily be adaptable to the several variations of the design problem actually encountered. These depend upon which factors are known or given and which are unknown. K. E. Schoenherr has set down this situation in systematic fashion, from which the following is adapted [PNA, 1939, Vol. II, p. 159]:

First, Preliminary Design.
(i) Given the designed ship speed V, the corresponding effective power P_E or total resistance R_T, and the propeller diameter D. Required to find the propeller pitch P and the rate of rotation n (in rpm) for the best propeller efficiency.
(ii) Given the designed ship speed V, the corresponding effective power P_E, and the rate of rotation n of the propeller shaft. Required to find the propeller pitch P and diameter D for the best efficiency.
Second, Final Design. Given the curve of effective power P_E as a function of ship speed V, the propeller diameter D, the rate of rotation n (in rpm) and the engine output in horses, at the designed rpm, as delivered to the propeller shaft. Required to find the propeller pitch P, the propeller efficiency η_0, and the ship speed V obtainable under the given conditions.
Third, Analysis. Given the propeller dimensions, the ship speed V, the shaft power P_S, the propeller thrust T, and the rate of rotation n, in rpm. Required to find the fractions s_R for real slip, w for wake, and t for thrust deduction.

A considerable number of chart groups are now available, in one form or another, to the propeller designer. These are listed hereunder, as an adaptation of a listing and a description by F. M. Lewis [SNAME, 1951, pp. 612–613]:

(I) Charts of R. E. Froude; also known as the series charts of R. W. L. Gawn [Froude, R. E., INA, 1892, pp. 292–294; INA, 1908, pp. 185–204; Baker, G. S., SD, 1933, Vol. II, Fig. 14 and pp. 41–44; Gawn, R. W. L., INA, 1937, pp. 159–187; van Lammeren, W. P. A., RPSS, 1948, pp. 251–256].

The coefficients are, in Baker's notation:

Slip constant $X = \dfrac{N(P/D)D}{V_1}$, where N is in rpm, D in ft, and V_1 ($= V_A$) is the speed of advance in kt

Diameter constant

$$Y = \frac{H}{D^2 V_1^3}\left[\frac{P/D}{(P/D) + 21}\right]\left(\frac{1}{B}\right),$$

where H is the thrust power in horses, V_1 the speed of advance in kt, P and D are in ft, and B is a thrust factor for the blade type, actually an arbitrary function of blade-area ratio. The latter is presumably the ratio A_D/A_0. Cross curves of the diameter constant Y and the revolution constant X^2Y are plotted on a grid of X, Y, and η(eta). The developed-area ratio A_D/A_0 of Gawn's series propellers extended up to 1.10. The method of using the R. E. Froude-Gawn charts is explained by W. P. A. van Lammeren in detail in the reference cited.

(II) Charts of D. W. Taylor [S and P, 1943, pp. 99–102, 109–112, 275–292]. The basic coefficients are:

δ (delta) $= \dfrac{Nd}{V_A}$, where N is in rpm, d is the diameter in ft, and V_A is the speed of advance in kt

$B_P = \dfrac{NP^{0.5}}{V_A^{2.5}}$, where P is the propeller power in horses. The number of blades is generally added as a subscript to the basic coefficient, such as B_{P3}.

$B_U = \dfrac{NU^{0.5}}{V_A^{2.5}}$, where U is the thrust power in horses.

Cross curves of δ and efficiency e are plotted on a grid of P/D as ordinate and B_P or B_U as abscissas. Other chart forms are used with the coefficients:

$C_U = a\dfrac{U}{d^2\left(\dfrac{pN}{1000}\right)^3}$, where a is the pitch ratio p/d, U is the thrust power in horses, d is the diameter, and p is the pitch, both the latter in ft

$A_U = \dfrac{1000aU}{d^2V_A^3}$, where the symbols are as described previously for the Taylor charts.

These coefficients and charts, as given in the reference quoted, are for model propellers tested in fresh water. Since the coefficients are dimensional they do not produce ship-design data for salt water unless a correction is made for the differences in mass density [Kane, J. R., SNAME, 1951, pp. 625–626]. D. W. Taylor's statement that "... marine propellers work in water of practically constant density ..." [S and P, 1943, p. 100] is too sweeping. Many ships operate in fresh water only, and others in water that varies from fully fresh to fully salt.

A table of values of $V_A^{2.5}$, for a range of V_A in kt from 5 to 50, is given by L. P. Smith [ASNE, Nov 1935, p. 562].

(III) Charts of K. Schaffran. First published in German in "Systematische Propellerversuche (Systematic Propeller Experiments)," Strauss, Berlin, 1916. Later published in English in what was virtually a treatise on the subject, entitled "The Influence of Propeller Revolutions Upon the Propulsive Efficiency of Merchant Ships," NECI, 1923–1924, Vol. XL, pp. 254–320 and Pls. II–XII. Some of these data were published subsequently in WRH, 15 Nov 1934, Vol. 15, pp. 324–327; see also W. P. A. van Lammeren, RPSS, 1948, pp. 191–196.

The coefficients are:

Slip constant $C_s = \dfrac{nD}{V_E} = \dfrac{nD}{V_A}$, where n is the rate of rotation in rps, D is the diameter, and V_E (or V_A) is the speed of advance, all in consistent units

Revolutions-torque constant $C_{mn} = n\sqrt[3]{\dfrac{M}{V_E^5}}$, where M is the torque

Diameter-torque constant $C_{dm} = \dfrac{1}{D}\sqrt[3]{\dfrac{M}{V_E^2}}$

Diameter-thrust constant $C_d = \dfrac{\sqrt{S}}{DV_E}$, where S is the thrust

Revolution-thrust constant $C_n = \dfrac{n\sqrt{S}}{V_E^2}$

The basic grids are C_s on C_d and C_s on C_n.

(IV) Charts of W. Schmidt ["Zusammenfassende Darstellung von Schraubenversuchen (Summarized Description of Propeller Experiments);" this is a pamphlet published by Zeit. des Ver. Deutsch Ing., in 1926; copy in TMB library. See also a paper entitled "Vorausberechnung der Günstigsten Schiffsschraube (Calculation of the Most Favorable Ship Propeller)," by H. Völker; abstracted by W. Hinterthan in WRH, 1 Dec 1939,

pp. 368–370]. Schmidt's presentation was based upon the model-test data of K. Schaffran.

The coefficients are J ($= V_A/nD$ by standard notation) and:

① $\dfrac{\text{PHP}}{\rho n^3 D^5}$

② $\dfrac{\text{PHP}n^2}{\rho V_E^5}$

③ $\dfrac{\text{PHP}}{\rho D^2 V_E^3}$, where PHP is the propeller power in horses, $V_E = V_A$ is the speed of advance in kt, and D is the propeller diameter in ft.

There is another set of coefficients in which the propeller power is replaced by the thrust power. Cross curves of P/D ratio and e ($= \eta_0$ in standard notation) are plotted on a logarithmic grid of J and coefficient ① of the preceding list. The other coefficients are determined by inclined logarithmic scales.

(V) Charts of K. E. Schoenherr [PNA, 1939, Vol. II, pp. 158–168].

The principal coefficients, all dimensionless, are:

Thrust coefficient $K_t = \dfrac{T}{\rho n^2 d^4}$

Torque coefficient $K_q = \dfrac{Q}{\rho n^2 d^5}$, where K_t and K_q correspond to the standard K_T and K_Q, and d is the propeller diameter

Efficiency $e = \dfrac{K_t}{K_q}\left(\dfrac{J}{2\pi}\right)$

The values of K_t, K_q, and efficiency e are plotted to a base of J.

(VI) Charts of L. Troost and W. P. A. van Lammeren [RPSS, 1948, pp. 196–223]. These are based upon a so-called A-series of model propellers, copied from G. S. Baker, in which rather narrow blades and airfoil sections give good performance but are suitable only for lightly loaded propellers, outside the cavitating range; and a so-called B-series, in which wider blades are able to carry greater thrust loadings, the losses from cavitation are small, and the propellers are generally free from singing.

The basic coefficients are:

$\delta = \dfrac{ND}{V_a}$, where N is the rate of rotation in rpm, D is the propeller diameter in ft, and V_a ($= V_A$) is the speed of advance in kt

$B_p = \dfrac{NP^{0.5}}{V_a^{2.5}}$, where P is the propeller power in English horses

$A_p = \dfrac{1000\left(\dfrac{H_0}{D}\right)P}{D^2 V_a^3}$, where H_0 is the pitch in ft

$C_p = \dfrac{\left(\dfrac{H_0}{D}\right)P}{D^2\left(\dfrac{PN}{1000}\right)^3}$

$B_u = \dfrac{NU^{0.5}}{V_a^{2.5}}$, where U is the thrust power in English horses

$\eta_p = \dfrac{K_s}{K_m}\left(\dfrac{\Lambda}{2\pi}\right)$, where K_s is the 0-diml thrust coefficient, K_m the 0-diml torque coefficient, Λ(lambda) the advance coefficient V_E/nD, and η_p the propeller efficiency.

The contours are δ and η_p on a grid of H_0/D ratio and B_p, A_p on a grid of the same kind, C_p on the same kind, and B_u on the same kind.

(VII) Charts of L. Troost ["Open Water Test Series with Modern Propeller Forms, Part 3, Two-Bladed and Five-Bladed Propellers," NECI, 1950–1951, Vol. 67, Part 3, pp. 89–130].

This is a later system developed by Troost, known as the continental or "μ(mu)-σ(sigma)" system. The principal relationships are:

$$\mu = n\sqrt{\frac{\rho D^5}{Q}} = \frac{1}{\sqrt{K_Q}} \qquad \sigma = \frac{TD}{2\pi Q} = \frac{K_T}{2\pi K_Q}$$

$$\phi = V_A\sqrt{\frac{\rho D^3}{Q}} = \frac{J}{\sqrt{K_Q}}$$

Cross curves of P/D, $e(\eta_0)$, and ϕ(phi) are plotted on a grid of μ and σ.

(VIII) Charts of Newport News Shipbuilding and Dry Dock Company. These are described briefly and one of them is illustrated in a discussion by J. R. Kane [SNAME, 1951, pp. 626–627; also p. 629].

The coefficients are J and:

$B = n\sqrt{\dfrac{550\ \text{PHP}}{\rho V_A^5}}$, to be used when n is limited

$\Delta = D\sqrt{\dfrac{\rho V_A^3}{550\ \text{PHP}}}$, to be used when D is limited, where PHP is the propeller power in English horses.

Cross curves of P/D are plotted on grids of J, e (= efficiency η_0), and B or Δ(delta).

(IX) Charts of H. H. W. Keith (formerly professor of naval architecture at MIT). These were carefully drawn to about 7.25 in by 7.25 in, but were never published. They involve two coefficients:

$C_R = \dfrac{NU^{0.5}}{V_A^{2.5}}$ (this is identical with D. W. Taylor's B_U)

$C_D = \dfrac{U^{0.5}}{DV_A^{1.5}}$

where N is the rate of rotation in rpm, U is the thrust power in English horses, D is the propeller diameter in ft, and V_A is the speed of advance in kt.

The values of C_R and e (= efficiency η_0) are plotted on a grid of C_D and P/D. The latter scale is uniform and exceptionally large. Photostats of these charts are in the TMB library.

(X) Charts of J. G. Hill [SNAME, 1951, pp. 631–633]. The principal coefficients are:

$$C_P = \frac{2\pi Qn}{\frac{\rho}{8}\pi D^2 V^3}$$

$$C_S = \frac{T}{\frac{\rho}{8}\pi D^2 V^2}$$

where V is the speed of advance (V_A in ITTC notation) and all other symbols are standard. The propeller efficiency η_0 (not so marked) is shown by contours on the two sets of diagrams. To render them more compact they are plotted as the square roots of C_P and C_S on a base of J in each case.

(XI) Charts of C. W. Prohaska. These are logarithmic-type diagrams based upon the earlier charts of G. Eiffel and W. Schmidt. They embody both the dimensional coefficients of D. W. Taylor and a group of corresponding 0-diml coefficients, with double inclined logarithmic scales. Examples of these charts are given in Figs. 70.A and 70.B to follow, and they are described in Secs. 70.5 and 70.6.

(XII) Charts of F. M. Lewis [SNAME, 1951, pp. 612–615 and 618–620]. The principal coefficients are:

Thrust coefficient $K_T = \dfrac{T}{\rho n^2 D^4}$

Torque coefficient $K_Q = \dfrac{Q}{\rho n^2 D^5}$

Loading coefficient $K_U = \dfrac{T}{\rho D^2 V_A^2}$

Efficiency $e(= \eta_0) = \dfrac{K_T}{K_Q}\cdot\dfrac{J}{2\pi}$.

These charts give contours of the 0-diml coefficients K_T, K_Q, K_U, and e (= efficiency η_0), as listed in the foregoing, on a basis of J and P/D, using data from the Wageningen B.3 and B.4 series of model propellers. A number of examples in the reference cited show how these charts are used.

(XIII) Charts of W. E. Fermann, formerly of the General Motors Corporation, developed specifcally for towing and similar situations where the values of the advance coefficient are extremely low. These charts are in four groups:

Design coefficient $S_D = V_A[\rho d^2/P_S]^{1/3}$ as abscissas and pitch-diameter ratio $a = p/d$ as ordinates (uniform scale), with contours of propeller efficiency e_P and advance coefficient $J = 101.33V_A/(N_P d)$, and a reference line of $e_{P(\mathrm{Max})}$ with S_D constant

Design coefficient $S_N = V_A[\rho/(P_S N_P^2)]^{1/5}$ as abscissas and pitch-diameter ratio $a = p/d$ as ordinates (uniform scale), with contours of e_P and $J = 101.33V_A/(N_P d)$, and a line of $e_{P(\mathrm{Max})}$ with S_N constant

Design coefficient $E_D = V_A[\rho d^2/P_U]^{1/3}$ as abscissas and pitch-diameter ratio $a = p/d$ as ordinates (uniform scale), with contours of e_P and $J = 101.33V_A/(N_P d)$ and a line of $e_{P(\mathrm{Max})}$ with E_D constant

Design coefficient $E_N = V_A[\rho/(P_U N_P^2)]^{1/5}$ as abscissas and pitch-diameter ratio $a = p/d$ as ordinates (uniform scale), with contours of e_P and $J = 101.33V_A/(N_P d)$ and a line of $e_{P(\mathrm{Max})}$ with E_N constant.

Here V_A is the speed of advance in kt, P_S is the shaft power (per shaft) in horses, N_P is the propeller rpm, d the propeller diameter in ft, p the propeller pitch in ft, and ρ the mass density of the water.

As mentioned previously, Fermann's charts are particularly valuable for the design of propellers for tugs and for towing purposes which operate at low speeds of advance and high thrust-load factors. For many of these problems the range of D. W. Taylor's charts is entirely inadequate. The Fermann charts have not been published or circulated but a set is available in the TMB library.

So far as known, the design methods and charts developed by C. W. Dyson ["Screw Propellers," Simmons-Boardman, New York, 1924] are no longer used by propeller designers.

70.5 Comments on and Comparison of Propeller-Series Charts. Some or all of the propeller-series charts listed in Sec. 70.4 possess certain disadvantages, rendering them less than convenient for the use of the propeller designer:

(a) The parent series of models possesses characteristics known to be inferior to those of later designs. Specifically, they have ogival root sections, blade outlines without skew-back, blade root sections that are too thin, and so on. This is no fault of the chart makers but a feature inherent in their age.
(b) It is necessary to interpolate between irregularly curved lines to find the proper P/D ratio. The basic series diagrams or B_P and B_U charts of D. W. Taylor [S and P, 1943, pp. 275–292] are admirable in this respect, with their uniform scales of pitch-diameter ratio, closely subdivided.
(c) It is necessary to make preliminary calculations or tabulations, to draw an auxiliary curve on the chart, and to locate its intersections with certain chart curves before determining the value of the parameter desired
(d) The charts as reproduced in the literature are too small and too crowded with lines for everyday work. This situation may be remedied in some cases by procuring large-scale prints of the charts from the originators.
(e) They are not usable for small values of the advance coefficient J or large values of the real slip ratio s_R, as for problems involving towing. The Fermann charts are in effect inversions of many of the standard charts, in that the parameter values corresponding to low advance coefficients and extra-large real-slip ratios are at the working ends.

Considering the rather varied amount of propeller information useful in the preliminary design of a ship, where backing, maneuvering, and operations other than propulsion must be considered, the so-called logarithmic type of propeller chart has much to recommend it. This is on the basis that the designer does not object to a rather concentrated serving of technical information, all on one piece of paper.

The logarithmic method of presentation, as far as can be learned, was originated by Gustav Eiffel in France and later developed by Wilhelm Schmidt in Germany, indicated by the following references to Eiffel's work:

(1) "Nouvelles Récherches sur la Résistance de l'Air et l'Aviation (New Research on Air Resistance and Aviation)," Paris, 1914
(2) "Travaux Exécutés Pendant la Guerre, 1915–1918 (Projects Completed During the War, 1915–1918)," Paris, 1919
(3) "L'Étude sur l'Hélice Aeriénne (A Study of the Airscrew)," Paris, 1920.

The most modern and the most useful, as well as the most comprehensive logarithmic presentation is that of C. W. Prohaska, of the Institute of Technology of Denmark, in Copenhagen. Many of these diagrams are based upon test data from the Wageningen series of propellers developed by L. Troost but there are others in the group based upon tests of single propellers. One such diagram is presented in Fig. 70.A.

This diagram contains the usual propeller characteristic curves of torque coefficient K_Q, thrust coefficient K_T, and open-water efficiency η_0, all non-dimensional. The abscissas, embodying two separate scales, are 0-diml values of the advance coefficient J and dimensional values (in English units) of the Taylor advance coefficient δ. The ordinates are a series of simple numbers, ranging from 0.006 to 1.0, for the 0-diml coefficients and for the efficiency fractions. Both horizontal and vertical scales are logarithmic.

There are 4 diagonal scales on the diagram, 3 double and 1 single. The upper scales of each of the three pairs represent the dimensional values of the factors A, B_U, and B_P of D. W. Taylor's notation, respectively. The mathematical expressions for each of these, in English units of tons, feet, horses, and knots, are listed in a column in the upper left-hand corner of the diagram. The lower scales of each pair represent the 0-diml thrust-load factor C_{TL}, and the basic 0-diml factors b_T and b_Q of Prohaska, respectively. The fourth single scale gives values of the 0-diml fraction TD/Q.

The original Prohaska charts, such as those from which Figs. 70.A and 70.B are adapted, carry additional scales showing the values of K_Q, K_T, and η_0 for $J = 0$, and the values of J for $K_Q = 0$ and $K_T = 0$. These limit scales are omitted from the reproductions to avoid excessive complication.

The values on the three curves of K_Q, K_T, and

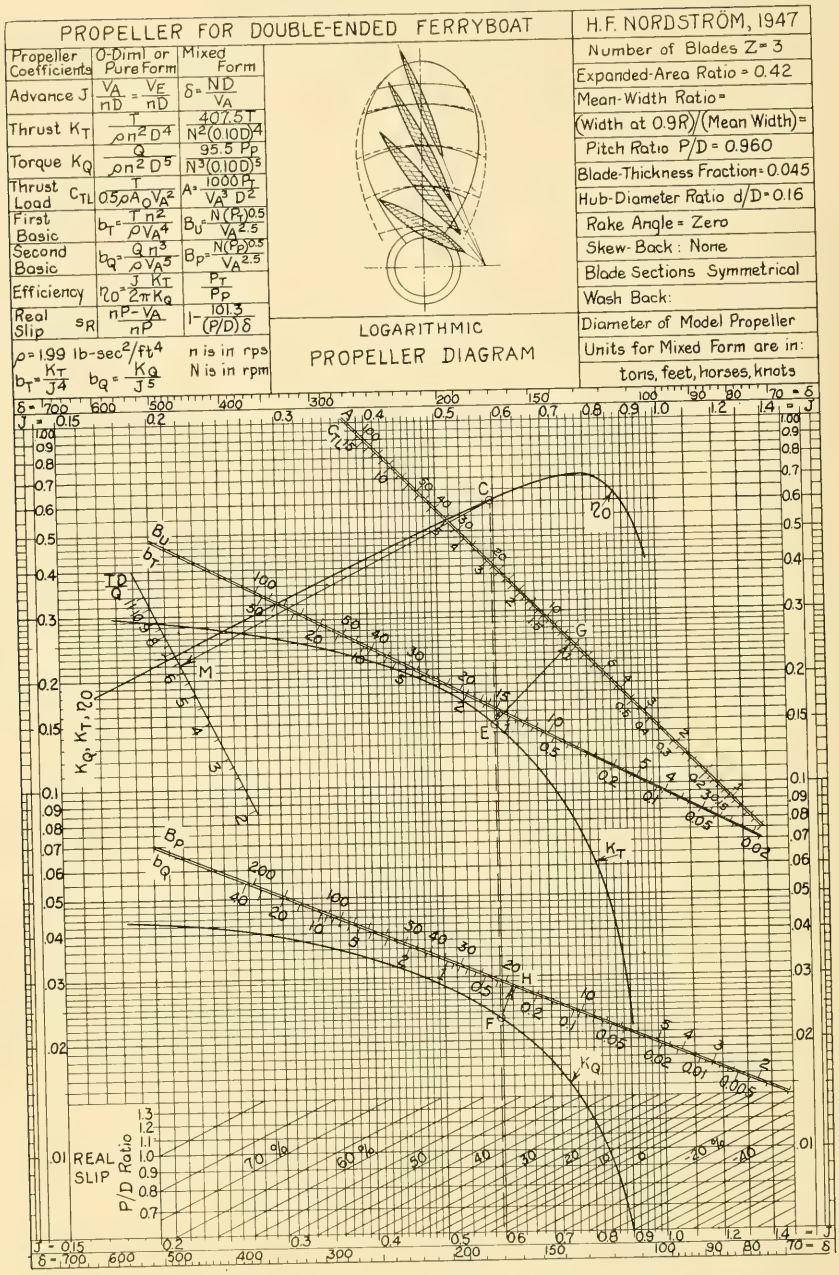

Fig. 70.A Logarithmic Chart of C. W. Prohaska for a Single Screw Propeller

η_0 of Fig. 70.A are related to each other by a vertical ordinate intersecting all three of them at the particular advance coefficient J (or δ) at which the propeller is operating. Such an ordinate is drawn in broken lines on the figure through the points C, E, and F. Corresponding values on the three double and one single inclined scales are determined by dropping perpendiculars on them from the three intersecting points C, E, and F, indicated in the diagram. A single perpendicular CM is dropped from the η_0-curve intersection to the scale of TD/Q. Two perpendiculars are dropped from the point E on the K_T curve, one to the double scale of first basic coefficient and the other, EG, to the double scale of thrust-load coefficient. A single perpendicular is dropped from the point F at the K_Q-curve intersection to the point H on the double scale for the second basic coefficient. By having the two scales of each pair opposite each other at the feet of the perpendiculars EG, FH, and the second short perpendicular from E, it is convenient to pick off either dimensional or non-dimensional values, or to enter the diagram with these values.

Assume that a symmetrical-section propeller such as that depicted on Fig. 70.A is to be used and that the 0-diml thrust-load factor C_{TL} is 1.065. The scale of C_{TL} is entered at the point G and a line GE is drawn perpendicular to that scale until it intersects the K_T-curve at E. The ordinate CEF is erected through the point E and the 0-diml J value is read from either the top or the bottom scale as 0.596. If the speed of advance V_A and the propeller diameter D are known, the rate of rotation is obtained directly from the relationship $n = V_A/(JD)$. The actual working efficiency at the point C on the η_0 curve is read off from the side scale as 0.61.

The 0-diml value of the second basic coefficient b_Q is determined by dropping a perpendicular from F to the inclined scale at H, whereupon the 0-diml value of b_Q is read off as 0.313. With the values of mass density ρ, speed of advance V_A, and rate of rotation n all known, the torque Q is determined from the b_Q formula given on the diagram. The power P_P which will be absorbed by the propeller is calculated from the derived values of n and Q.

If the rate of rotation n is given and the power P_P is known, corresponding to the situation in Sec. 59.15, the torque Q is derived by direct calculation. The thrust T is found either from the value of TD/Q at the intersection M, or from the first basic coefficient b_T at the intersection near E.

By and large, the use of any particular series chart for the preliminary design of a screw propeller gives essentially the same kind of answer. This is on the basis that the test data for the model propellers from which the charts were constructed did not suffer from scale or surface effects, that the observed data are accurate and carefully plotted, and that the use of dimensional expressions does not omit important factors or introduce unknown errors. For example, since model propellers are almost invariably tested in fresh water, the derived data are also for fresh water. A mass-density factor ρ(rho) which is omitted for convenience or simplification, as was done by D. W. Taylor, may make a 2 or 3 per cent difference in ship-propeller data calculated for salt water [Kane, J. R., SNAME, 1951, p. 626; Schoenherr, K. E., SNAME, 1951, p. 628].

A comparison of five kinds of propeller-series charts then in use was made some two decades ago by H. F. D. Davis [ASNE, Feb 1932, pp. 8–24]. The discrepancies between the five sets of preliminary-design characteristics worked out from the charts was rather more than would now be acceptable. It must be remembered, however, that the parent propellers all had rather different characteristics, especially with regard to mean-width ratio and blade-thickness fraction. Unfortunately, a more modern comparison is not available, worked out in the same detail. Some rather general comments are to be found in the discussion of a recent paper by F. M. Lewis [SNAME, 1951, pp. 621–641].

For a beginner in the field, it is bewildering to find so many kinds of charts, all ostensibly for the same purpose, but actually varied to suit the type of initial data and the nature of the answer desired by several groups of people, experienced in these procedures. It is likewise most confusing to find different symbols on each kind of chart, with some expressions dimensional and others non-dimensional. After trying them all, or all that are available, he is in better position to decide which meets his own particular needs, either for analysis or for practical design.

It is characteristic of any and all propeller-series chart-design procedures that the numerical values required for the full-scale ship are obtained only by estimating the wake fraction w and the thrust-deduction fraction t. The V_0 of the open-water test corresponds only to V_A on the ship, whence $V = V_A/(1 - w)$, and the thrust T

required of the ship propeller is greater than the predicted total ship resistance R_T by the ratio $1/(1 - t)$. Further, the propeller efficiency η_B behind the ship is greater (or less) than the open-water efficiency η_0 by the relative rotative efficiency η_R. These three unknown factors may be estimated from analyses of trial data on similar ships [Davis, H. F. D., ASNE, Aug 1932, pp. 332–352; Schoenherr, K. E., PNA, 1939, Vol. II, Chap. III] or, as is usually the case, they may be determined from tests of a self-propelled model.

70.6 Preliminary-Design Procedure, Employing Series Charts. For the screw-propeller-design procedure set down in this book several of the series charts are utilized in the preliminary-design stage, particularly for determining the characteristics and for selecting a suitable stock propeller to be used in the first self-propulsion tests of the ABC ship models. This is not to be taken as an indication that series charts are suitable for making only first approximations in the early stages of a ship design. In fact, by far the greater number of propellers designed in practice and manufactured for ships are worked up from these charts, insofar as the propeller features can be determined from them.

The references of Sec. 70.4 in which the various propeller-series charts are published usually describe in considerable detail the procedure to be followed for the particular problem at hand. In many cases they also contain examples worked out to illustrate these procedures.

As examples of the methods of using propeller-series charts there are given here the steps employed and the calculations made for the preliminary design of a propeller for the transom-stern ABC ship, leading to the selection of a stock propeller for self-propulsion tests of the first model.

The following three methods were used:

(1) That of K. E. Schoenherr, based upon tests of EMB series propellers, as set down in PNA, 1939, Vol. II, pp. 158–168, including propeller-design charts 1 through 4
(2) That of F. M. Lewis, based upon tests of Wageningen B-series propellers, as described in SNAME, 1951, Vol. 59, pp. 618–620
(3) That of C. W. Prohaska, based upon logarithmic charts embodying the test data of the Wageningen B series of model propellers.

Certain data were taken as basic for all three methods, using a propeller diameter D of 20 ft, derived in Chaps. 66 and 67. The designed ship speed, for which the propeller is to give optimum performance, is 20.5 kt. The ship resistance at this speed is estimated in Sec. 66.9 as 171,830 lb, or say 172,000 lb. The corresponding effective power P_E is 10,827 horses. The wake fraction w is estimated from Eq. (60.ii) in Sec. 60.8 as 0.261. This figure is different from the 0.255 worked out as the illustrative example in that section because it is calculated at an early stage of the design, using preliminary dimensions and parameters instead of the final ABC values inserted in the illustrative example.

The thrust-deduction fraction t is estimated by the method described in Sec. 60.9, applying a 15 per cent reduction to the value derived from Eq. (60.vi) because of the very thin skeg contemplated ahead of the propeller. This gives a predicted value for t of 0.111.

To keep the propeller loading as low as possible, consistent with good performance, four (4) blades are to be used. This means that the blade width and blade thickness can be small, with a resulting rather high efficiency. The mean-width ratio c_M/D is taken tentatively in the range of 0.20 to 0.25. The blade-thickness fraction t_0/D is assumed to be of the order of 0.04 to 0.05. These values are typical for 4-bladed propellers [PNA, 1939, Vol. II, p. 157] and are considered reasonable for the first approximation. Since adequate clearance is allowed in the design of the propeller aperture on the transom-stern ABC ship, and since the skeg ahead of the propeller is relatively thin, the inclination of the streamlines in the inflow jet with reference to the propeller axis should not be unduly large. There appears to be no need, therefore, of raking the blades, especially as they would then have to be thicker to withstand the offset centrifugal forces.

The Prohaska preliminary-design procedure is described and illustrated first. Prohaska's propeller-design chart, as contrasted to the propeller-data chart of Fig. 70.A, is somewhat more intricate and is used in a somewhat different manner. Fig. 70.B, adapted from one of these charts, contains five sets of K_Q graphs, five K_T graphs, and five η_0 graphs, one each for a given P/D ratio, plus the four sets of diagonal scales of Fig. 70.A. In addition there are three maximum-efficiency graphs for use when:

(i) The thrust-load coefficient C_{TL} or the factor A is known

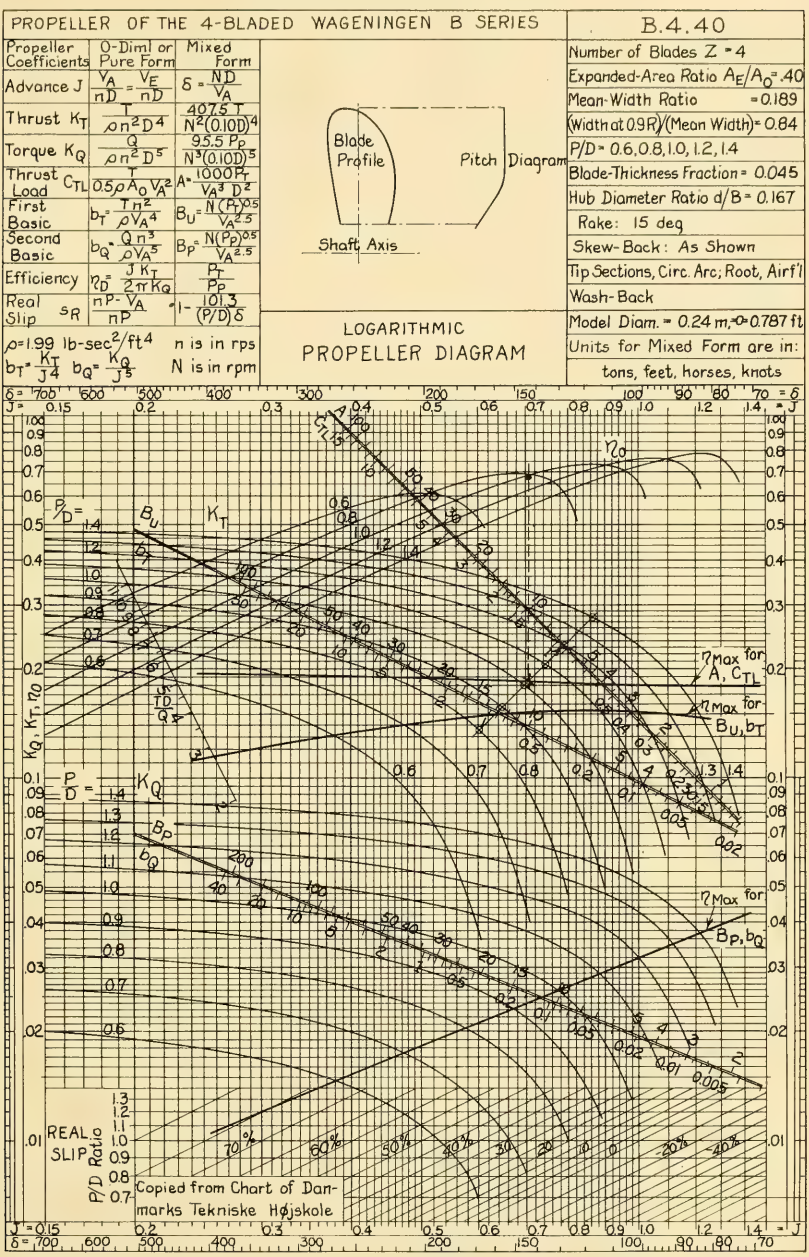

FIG. 70.B LOGARITHMIC CHART OF C. W. PROHASKA FOR FIVE PROPELLERS, WAGENINGEN B.4.40 SERIES

(ii) The basic factors b_T or B_U are known
(iii) The basic factors b_Q or B_P are known.

For the study on the ABC ship, the propeller diagram for the B.4.40 series is selected. This series number indicates that the propeller has four (4) blades and that its expanded-area ratio A_E/A_0 is 0.40. The mean-width ratio is only 0.189, from the information block in the upper right corner, but this group of propellers appears to correspond most nearly to that desired.

The first step is to find the thrust-load coefficient C_{TL}, using the expression $C_{TL} = T/(0.5\rho A_0 V_A^2)$. The thrust T is obtained by dividing the total resistance R_T of 172,000 lb by $(1 - t) = 0.889$; it is found to be 193,476 lb. The speed of advance V_A is the ship speed, 20.5 kt, times $[(1 - w) = 0.739]$, or 15.15 kt. The thrust-load coefficient then becomes

$$C_{TL} = \frac{193{,}476}{(0.5)(1.9905)(0.7854)(20)^2[(1.6889)15.15]^2} = 0.945.$$

Prohaska's chart, Fig. 70.B, is entered on the lower of the pair of upper right-hand diagonals, marked C_{TL}. Draw a perpendicular to this line at the value of $C_{TL} = 0.945$, marked on the diagram by an arrowhead. Where this perpendicular crosses the graph marked "η_{Max} for C_{TL}," interpolate for the correct value of P/D from the series of five K_T curves for various P/D ratios. The optimum P/D value corresponding to the crossing marked with an "x" on the diagram is 1.02.

From this crossing draw a vertical line to the top of the diagram. Where this line cuts the series of η_0 efficiency curves, at a point corresponding to a P/D of 1.02, marked by a small solid circle, read the corresponding efficiency value η_0. From the scales at the right or left the open-water efficiency is 0.68.

Continuing up the vertical line to the lower horizontal scale at the top, the value of the advance coefficient J is read off as 0.703. From the relationship $J = V_0/(nD)$ or $n = V_0/(JD)$, calculate the rpm as follows:

$$n = \frac{V_0}{JD} = \frac{V_A}{JD} = \frac{1.6889(15.15)60}{(0.703)20} = 109.2 \text{ rpm}.$$

If this rate of rotation appears to be not suitable, for some reason or other, it may be necessary to sacrifice some propeller efficiency for a desired rate which is faster or slower. The amount so sacrificed is determined by following the procedure described, except that instead of picking η_0 and J values for the crossing of the C_{TL} perpendicular and the graph of "η_{Max} for C_{TL} or A," they are picked for the crossings of that perpendicular with the several K_T graphs for a range of P/D values. The latter crossings are marked by small open circles. The values derived for the complete range of P/D available on the chart are listed in Table 70.a.

TABLE 70.a—VARIATION OF EFFICIENCY WITH RATE OF ROTATION AND P/D RATIO

The data listed here are for the Wageningen B.4.40 series propellers from Prohaska's logarithmic chart, Fig. 70.B.

Thrust-load Coeff. C_{TL}	Pitch-Diameter Ratio P/D	Advance Coeff. J	Propeller Efficiency η_0	Rate of Rotation rpm
0.945	0.8	0.601	0.675	127.7
0.945	0.9	0.648	0.675	118.4
0.945	1.0	0.695	0.680	110.4
0.945	1.1	0.747	0.675	102.8
0.945	1.2	0.790	0.670	97.2

The efficiency drops off only one point at the most, from 0.680 to 0.670, for a rather wide range of P/D ratio and rate of rotation. As a matter of interest, H. F. Mueller's data in Fig. 59.A show that for a C_{TL} of 0.945, as used here, the P/D ratio for maximum efficiency could be as high as 1.2. The expected propeller efficiency would be η_I (from Table 34.a) = 0.835 times $(\eta_0/\eta_I = 0.794)$ or 0.663.

To determine whether the blade shapes, areas, and sections of the B.4.40 series are the best, the propeller designer is required to go through the same steps for the Wageningen B.4.55 series. A check for the ABC ship, not given here, revealed that with its wider blades the B.4.55 series is considerably less efficient.

Using Schoenherr's charts, the problem is that represented by category 1.(a) [PNA, 1939, Vol. II, p. 159]. As before, the designed ship speed V is 20.5 kt, the effective power P_E is 10,827 horses, and the propeller diameter D is 20 ft. From Schoenherr's Chart 1, Fig. 20, on pages 160 and 161 of the reference,

$$K_{td} = \frac{58.913}{(\text{sp.gr.})(1 - t)(1 - w)^2} \cdot \frac{P_E}{V^3 D^2}$$

$$= \frac{58.913}{1.027(0.889)(0.739)^2} \cdot \frac{10{,}827}{(20.5)^3(20)^2}$$

$$= 0.371245 = 0.371$$

Then Schoenherr's $K_t = K_{td}(J)^2$. For a range of values of the advance coefficient J from 0.60 to 0.80, the calculated values of K_t are listed in Table 70.b. The parabola corresponding to these

TABLE 70.b—DATA FOR PLOTTING AUXILIARY CURVE ON SCHOENHERR CHART

From the text, $K_{td} = 0.371245 = 0.371$.

Advance Coefficient J	J^2	$K_t = K_{td}J^2$
0.60	0.3600	0.1336
0.65	0.4225	0.1569
0.70	0.4900	0.1819
0.75	0.5625	0.2088
0.80	0.6400	0.2376

values is then drawn lightly in pencil on Chart 1. At the intersection of this pencil parabola with the heavy broken line marked "e_{Max} (or η_{Max}) for K_{td} Const." the following optimum values are picked off:

$$J = 0.748 \qquad \eta_0 = 0.683.$$
$$P/D = 1.02$$

Since rpm $= V_A(60)/(JD)$, where $J = 0.748$, the rate of rotation is found to be 102.6 rpm. Except for the slower rate of rotation, the pitch-diameter ratio and the efficiency are close to those obtained from the Prohaska chart for the Wageningen B.4.40 series. The latter have a mean-width ratio of 0.189 and a blade-thickness fraction of 0.045. The EMB propellers upon which Schoenherr's Chart 1 is based have a mean-width ratio of 0.20 and a blade-thickness fraction of 0.05. The difference in rate of rotation is undoubtedly due to the airfoil blade sections of the Wageningen propellers and the ogival sections of the EMB propellers, with zero-lift lines at different angles to the base chords, where the nominal pitch is measured.

Since the mean-width ratio of the ABC ship propeller may exceed 0.20, Schoenherr's Chart 2 is used to obtain an alternative solution for a mean-width ratio of 0.25 and a blade-thickness fraction of 0.05. This gives the values:

$$J = 0.740 \qquad \eta_0 = 0.673$$
$$P/D = 1.02 \qquad \text{rpm (by calculation)} = 103.7$$

The narrower-blade propeller appears to be the better of the two.

Using the Lewis charts for the same given values, and following the procedure described [SNAME, 1951, pp. 614–615 and Type 3, pp. 619–620], it is noted that Lewis' coefficient K_U is the same as Schoenherr's K_{td}, except that the wake fraction used is that derived from what is known as thrust identity only. Lewis' K_U, defined as $T/(\rho D^2 V_A^2)$, has the form of a thrust-load coefficient; it is equal to $(\pi/8)C_{TL}$. Taking Lewis' published chart for the Wageningen B.4.55 series propellers, and drawing a curved line lightly in pencil for a constant value of $K_U = 0.371$, the corresponding values of the parameters sought are as listed in Table 70.c. From this table the best values appear to be:

$$J = 0.702 \qquad \eta_0 = 0.665$$
$$P/D = 1.00 \qquad \text{rpm (by calculation)} = 109.3$$

TABLE 70.c—DATA FOR PLOTTING AUXILIARY CURVE ON LEWIS CHART

Here Lewis' K_U = Schoenherr's $K_{td} = 0.371245 = 0.371$.

Pitch-Diameter Ratio	Advance Coefficient, J	Rate of Rotation, rpm	Efficiency, η_0
0.80	0.596	128.8	0.64
0.90	0.649	118.3	0.655
1.00	0.702	109.3	0.665
1.10	0.750	102.3	0.660

Except for the lower efficiency, because of the too-wide blades of this series, the values are very nearly equal to those obtained from the Prohaska chart.

The stock model propeller for the ABC ship model should thus have the following characteristics:

(a) The ship to model scale ratio λ (lambda) is 25.5
(b) $D_{\text{Model}} = D_{\text{Ship}}/\lambda = 20/25.5 = 0.7843$ ft or 9.412 in
(c) The P/D ratio is about 1.00 or 1.02
(d) The mean-width ratio should be about 0.20
(e) The blade-thickness fraction is about 0.045 to 0.050
(f) The proper expanded-area ratio A_E/A_0 is about 0.40.

The actual selection of the stock model propeller is discussed in Sec. 78.4.

Subsequent to the selection of this propeller, J. D. van Manen published a paper in which he

gave graphs and rules for finding the developed-area ratio of a screw propeller in the preliminary-design stage ["Recent Data on Cavitation Criteria," Inter. Shipbldg. Progr., 1954, Vol. 1, No. 1, pp. 39–47]. The following values pertaining to the ABC transom-stern design were used to calculate the ratio A_D/A_0 by the procedure on page 45 of the reference:

Thrust to be delivered by the propeller in salt water, 193,476 lb
Rate of rotation n (assumed), 109 rpm or 1.817 rps
Speed of advance V_A or V_E, 15.15 kt or 25.59 ft per sec
Number of blades Z, 4
Submergence of propeller axis below at-rest waterline, 15.5 ft
Assumed height of stern-wave crest above at-rest WL, 1 ft
Assumed vapor-pressure head e, 1 ft
Atmospheric-pressure head, 33 ft
Value of pressure head $(p_\infty - e)/w$, 48.5 ft.

The derived values were:

Diameter D, 19.75 ft
Mean pitch-diameter ratio P/D, 0.952
Cavitation number σ_0 at a value of $R/R_{\text{Max}} = 0.8$, in the 12 o'clock position, 4.01
Developed-area ratio A_D/A_0, 0.532.

By one of the alternative calculation methods given by van Manen the value of A_D/A_0 (his F_a/F) is 0.546. The developed-area ratio is sufficiently close to the expanded-area ratio, at least for not-too-wide blades, so that no distinction need be made between them.

The diameter is thus slightly smaller than that assumed in the calculations preceding, and the pitch-diameter ratio is some 5 or 6 per cent less, but the area ratio is considerably larger. However, the final design computations for the ABC propeller, at the end of Sec. 70.31, give a ratio A_E/A_0 of 0.478, indicating reasonable agreement with the foregoing.

70.7 Modification of Series-Chart Procedure for Other Design Problems. For preliminary designs in which the propeller is required to have good backing performance, as for tugs and ferryboats, there are few propeller-series charts available. The stopping and backing situation is discussed rather fully in Part 5 of Volume III of this book. Suitable propeller-design features are well set forth by W. P. A. van Lammeren [RPSS, 1948, pp. 259–260], based upon the following references:

(a) Kempf, G., HSPA, 1940, Vol. II, p. 46
(b) Conn, J. F. C., IESS, 1934–1935, Vol. 78, p. 27
(c) Gebers, F., Schiffbau, 1933, p. 235
(d) Robertson, J. C., MESA, 1929, p. 102.

The only comprehensive data available on the characteristics of model propellers for what might be termed full backing conditions are those given by H. F. Nordström in "Screw Propeller Characteristics" [SSPA Rep. 9, 1948]. In this report Nordström presents the results of tests on nine 4-bladed model propellers, with P/D ratios varying from 0 to 1.6, over a range of advance coefficient J from $+2.0$ to -2.0.

The problem of designing screw propellers intended to run normally in the partly immersed condition is discussed under surface propellers in Sec. 71.10.

70.8 Preliminary Comments on Propeller-Design Features. Strictly speaking, any propeller series chart intended for analysis and design purposes is valid only for other propellers having the same geometric shape and physical characteristics. For example, systematic data based on tests of model propellers having small solid hubs do not represent the expected performance of full-scale propellers with larger built-up hubs. In the case of almost every new design it is necessary to depart from the parent propeller in some physical respect. The designer must have at least some indication of the effect of these changes upon the predicted performance of the new design.

A few of the principal propeller features have to be decided upon before the preliminary design is begun; they are the given quantities, so to speak. Others can be determined after the principal characteristics are known, such as the exact shape of the blade profile or the rake.

An alternative method is to work up a series of preliminary designs with the given quantities varied systematically, and then to select the best of the series for further development toward a final design. This is done by K. E. Schoenherr for four different propellers, to determine the effect of varying D and n [PNA, 1939, Vol. II, Table 18, p. 172]. If series charts are used, the time involved for each design is so small that this should almost be considered as routine procedure.

Rather than to burden the description of the series-chart method in Secs. 70.5 and 70.6 or the

Lerbs short method in Secs. 70.21 through 70.38 with paragraphs involving considerations of engineering instead of analysis for hydrodynamics, there are given here some brief comments on the selection of certain physical features as governed by the problem in hand.

70.9 Selection of Propeller Diameter. In both the series-chart and the Lerbs short-cut examples worked out in this chapter the propeller diameter is selected in advance. If there are operational or other limitations on diameter, the designer has little or no freedom of choice. He must do the best that is possible under the circumstances, but with a clear understanding on the part of everyone concerned that it is not the best that could be done if he were free of these limitations.

If he has freedom of choice as to diameter, he proceeds on the basis that the propeller is the most important unit in its part of the ship, and that it can have whatever diameter best fits it for the task to be performed. If propulsive efficiency is not a primary requirement then almost any available propeller can be used and only the sketchiest of design procedures is necessary.

Sec. 34.2 describes and illustrates the reasons why screw propellers with the largest diameter and the lowest thrust loading may be expected to work at the highest real efficiency. Some years ago K. E. Schoenherr said ". . . in general, that propeller is the best choice which has the largest diameter admissible in the propeller aperture" [PNA, 1939, Vol. II, p. 166]. F. M. Lewis removed the latter restriction by saying that "In nearly all cases of modern ships the optimum diameter will be the largest that is practical, . . ." [SNAME, 1951, p. 619]. If the ship hull is designed to accommodate the propeller, rather than the other way around, the latter will be properly guarded against air leakage from the surface, against racing at sea, against rotating through a region of excessively high wake, and against all other ills to which a large propeller is supposed to be subject.

The principal aim in the preliminary design of the ABC hull was to swing the largest possible single propeller. This was the reason for developing the arch type of stern, which permitted a propeller diameter D of 24 ft on a draft of only 26 ft. The arch recess afforded effective shielding from air leakage and (it was hoped) equally effective protection against racing when the ship is pitching. The reason for using the large propeller was to keep the thrust-load coefficient low and to obtain a wheel that would work in a region of the highest possible ideal and real efficiencies, the latter represented by a value of about $0.8\eta_I$. Another reason was that pointed out by E. K. Sullivan and W. G. Scarborough in their paper on "Machinery Design of the *Schuyler Otis Bland*" [SNAME, 1952, pp. 467–503]. There (on page 474) they stated that, as a result of their studies, "the largest propeller that could be accommodated would have the least total annual operating cost."

Objections against large casting and shipping sizes and weights can be overcome by developments in detachable blades and welded assemblies described in Sec. 70.43. It is assumed in the foregoing that the rate of rotation n of the propeller shaft can be and is adjusted to suit the optimum diameter. If not, n becomes a given quantity and D is one of those to be found by the design procedure.

Means of determining the proper diameter, and comments on optimum screw-propeller diameters, are given by:

(1) Schoenherr, K. E., PNA, 1939, Vol. II, pp. 159, 165, 170, 172
(2) Van Lammeren, W. P. A., RPSS, 1948, pp. 232–233
(3) Lewis, F. M., SNAME, 1951, pp. 619–620
(4) Van Manen, J. D., and Troost, L., SNAME, 1952, pp. 446–448
(5) Edstrand, H., "Model Tests on the Optimum Diameter for Propellers," SSPA Rep. 22, 1953 (in English).

If the propeller power and the ship speed are low, the friction and pressure drag of the blades becomes large in proportion to the thrust. Some efficiency *may be* gained by reducing the propeller diameter below the optimum given by the orthodox design procedures. However, the designer is cautioned against any reduction of this kind for higher powers and higher speeds, where it may result in an actual loss of efficiency. The arguments against this are set forth by H. Edstrand, in reference (5) preceding, especially pages 24–27 and Figs. 13 and 14. His diagrams illustrate clearly the reasons for decreasing D in one case and holding it in another.

70.10 Determining the Rate of Rotation. Closely related to the selection of propeller diameter is a determination of the proper rate of rotation. On the basis that the propeller designer has the same freedom of choice as for propeller diameter, and that optimum propulsive performance is desired, the rate of rotation n should be

that which gives the maximum propeller efficiency η_0 under the trial or designed-load conditions specified.

While the design procedures described by examples in this chapter give n as a part of the solution, several practical requirements are to be met before this value can be approved, as it were. The first involves the ability of the selected or probable type of propelling machinery to deliver the required torque and power at the specified rate of rotation. This situation is discussed at some length by J. E. Burkhardt [ME, 1942, Vol. I, pp. 28–33]. It is assumed here that no problems are presented because of the type of engine and of the reduction gear or transmission system employed.

K. E. Schoenherr illustrates a procedure whereby the effect on propeller efficiency η_0 of varying n, P/D, and certain other variables is readily determined [PNA, 1939, Vol. II, p. 172 and Tables 19, 20].

Finally, the vibration characteristics of the ship, the engine, the shafting, and the machinery foundations must be considered when selecting the rate of rotation. However, this is primarily a matter of the number of blades, and as such is discussed in Sec. 70.12.

70.11 The Proper Pitch-Diameter Ratio; Pitch Variation with Radius. Assuming that the rate of rotation for the designed maximum or other specified power is fixed, or that it is to lie within certain limits, the pitch of the propeller is the next factor which logically evolves, since for zero real slip the effective pitch is the average speed of advance divided by the rate of rotation. However, for analysis and ship-design purposes the pitch-diameter ratio is found to be a preferable parameter.

In Sec. 34.15 the effects on propeller efficiency of too high and too low a P/D ratio are described and illustrated. In practically all propeller-series design charts it is possible to pick a P/D ratio which gives the maximum propeller efficiency η_0 for a given set of working conditions. In Fig. 70.B, for example, it is noted that there is a curve of optimum efficiency $\eta_{0(\mathrm{Max})}$ for thrust-load factor C_{TL}. A line normal to the inclined double scale for C_{TL} and A cuts the heavy line for $\eta_{0(\mathrm{Max})}$ at the best J-value. Interpolation between the values of K_T for the various pitch-diameter ratios, along the normal line mentioned, gives the optimum P/D values. A point vertically above this intersection, on the curves of efficiency η for the selected P/D ratio (interpolated if necessary), gives the working efficiency η to be expected.

When propulsion is by a piston-type internal-combustion engine in which the mean effective pressure in the cylinders is limited to a maximum value, it becomes necessary, as pointed out in Sec. 69.8, to match the rate of rotation and the torque very carefully in order to achieve the maximum or rated brake power. In other words, if the full power of the engine is to be utilized, delivered at a certain rate of rotation and at none other, the power absorbed by the propeller connected to it has to be exactly the same, neglecting transmission losses. It is most important, therefore, that after the engine is selected both the pitch and the diameter of the propeller be correct for the shaft power and rate of rotation available.

Experience through the past several decades indicates that inaccurate predictions almost always err on the side of designing a propeller which absorbs too much power at the specified rate of rotation. If slowed down to match the power of the engine, the rate of rotation is usually less than for maximum engine power. The common remedy is to cut off the blade tips; this enables the engine to run up to rated speed (and power) but often spoils the shape of a useful part of the propeller.

There is a great deal of discussion in the literature on screw propellers concerning the wisdom or the necessity of attempting to match the pitch at each radius with the average wake velocity at that radius. This matching is undertaken on the basis that the blade element at each radius should work at an effective angle of attack that is efficient for that radius. Obviously, some elements should not be underloaded while others are overloaded, by any reasonable method of reckoning. Furthermore, overloading the extreme blade tips involves excessive tip-vortex losses.

Three situations are to be considered here, in which there may be:

(I) An appreciable variation of wake velocity (or wake fraction) with radius from the propeller axis, combined with a reasonably uniform wake velocity around the circumference at any radius. This situation occurs abaft most bodies of revolution, like torpedoes, when the propeller axis coincides with the body axis.

(II) Some consistent variation of wake velocity with radius from the propeller axis, but in which

the magnitude of wake velocity around the circumference at any radius is highly irregular. This is the case in the disc position of a single screw carried abaft a centerline skeg on a ship of normal form.

(III) A possibility or probability of cavitation, or perhaps a certainty of it if the effective angles of attack of the blade elements at each radius are not kept within certain limiting values. Although cavitation is not normally to be expected in the upper blade positions of the propeller of a single-screw ship, it can and probably does occur if the vessel is fast and if it is driven hard in a loading condition where the at-rest tip submergence is small, approaching zero.

Good propeller design to meet situation (I) unquestionably calls for a radial variation in pitch corresponding generally to the radial variation in wake velocity, so that a given distribution of thrust with radius fraction is achieved. It has been the aim of many inventors and ship designers to incorporate a stern bulb around a single-screw propeller axis which would produce a high average wake velocity as well as one which was reasonably uniform around a circumference at each radius. However, because of the predominantly upward component of flow under the sterns of most ships, this desirable end has so far not been attained.

L. C. Burrill and C. S. Yang made a comprehensive theoretical study of many situations, involving both uniform and non-uniform wake velocities over the propeller disc, for a series of screw propellers having a great many types of variation of pitch with radius [INA, 1953, pp. 437–460]. In fact, they cover analytically most of the situations that would be encountered in a wide variety of ship designs. They arrived at certain general conclusions concerning radial pitch variation which appear to cover most phases of situations (II) and (III) preceding that a ship designer might be likely to encounter. Items (1) through (4), listed hereunder, are quoted verbatim from page 446 of the Burrill and Yang reference:

"(1) From the point of view of overall efficiency, and apart from any consideration of cavitation or flow breakdown, there appears to be no material advantage to be gained from the adoption of a radial variation of pitch, both in a uniform stream and in a variable wake-stream

"(2) In particular, it seems that there is no special advantage to be gained from the application of the various alternative methods of design, based on the principle of minimum-energy loss, which have been examined, as any gain which might be achieved in the ideal or hydrodynamic efficiency by the adoption of these procedures is very small, and is overshadowed by the effects of blade-efficiency (i.e., section-drag losses, etc.) introduced by the changes in angles of incidence where the wake concentration is high

"(3) On the other hand, the above results suggest that no special loss in efficiency is to be expected from the adoption of moderate pitch variations which are favourable from the point of view of cavitation or flow breakdown, and this leaves the designer considerable freedom in the matter of adopting such alternative pitch-variation lines from root to tip of the blades as might be considered desirable from this point of view

"(4) It appears that the quantity designated relative-rotative-efficiency has a real meaning, in terms of the methods of analysis usually adopted, and its value can be estimated by calculation, in the manner described in the paper. The numerical values obtained agree reasonably well with the experimental data."

In the example of propeller design by the circulation theory carried through in detail in Secs. 70.21 through 70.38 of this chapter a propeller is worked up by the Lerbs short method for the single-screw transom-stern design of the ABC ship. It may be argued that, by the Burrill-Yang criteria, the variations in wake velocity and wake fraction for this case, indicated by Figs. 60.M and 60.N, are not sufficient to justify the design of a wake-adapted propeller. Furthermore, cavitation is not expected to be a problem in the propulsion of this vessel. Nevertheless, the Lerbs 1954 design procedure is carried through on the basis that both of these features do require special attention. This renders the design solution more general in character and makes it fully applicable, as described, for a situation where radial wake variation and the possibility of cavitation should definitely be taken into account.

If large ship propellers could be and were purchased from stock, there might be some reason for omitting a propeller-design calculation that requires more than one or two man-days. For a large ship, expensive to run as well as to build, requiring a custom wheel, so to speak, there is every reason why a propeller-design procedure should take account of all the possibilities and should take advantage of all the latest developments in the art.

70.12 Choice of Number of Blades. The choice of the number of blades is one of the first decisions to be made in the design of a screw propeller. As an aid in reaching this decision, two or more preliminary designs may be worked up as a sort of series, each with a different number of blades. The final selection is usually based on a

consideration of the natural frequencies of vibration of the hull, the machinery foundations, the propelling plant, and the propulsion system [Kane, J. R., and McGoldrick, R. T., SNAME, 1949, Vol. 57, pp. 193–252]. The number of blades which best avoids these frequencies or their major harmonics in the operating speed range is chosen [Brehme, H., Schiff und Hafen, Nov 1954; abstracted in English in MENA, Aug 1955, pp. 318–321].

In some cases restrictions on propeller diameter, or the need for large blade area, coupled with high power requirements, indicate the use of 5 or even 6 blades. Also this number of blades may be necessary to keep resonant frequencies outside of the operating speed range. Two-bladed propellers are used on sailing ships with auxiliary power, as they offer the least resistance when housed abaft the skeg in the sailing condition.

For twin- or multiple-screw ships, a 4-bladed propeller can be of smaller diameter than a 3-bladed propeller for the same power. This means that smaller bossings and struts can be used to maintain the same hull tip clearance. Usually, the reduction in appendage resistance more than compensates for the small loss in propeller efficiency when using four blades. As in single-screw ships, propeller efficiency is usually a secondary consideration in the choice of the number of blades. First, there is little variation in efficiency between 3- and 4-bladed propellers and second, vibration considerations will again be the controlling factor, especially for ships of moderate to high power. In many cases other factors, such as type of engine, number of cylinders, and the like, enter into the choice of the number of blades.

Further discussions of the proper number of blades to be used for a screw propeller are given by:

(a) G. S. Baker, SD, 1933, Vol. II, pp. 49–50
(b) R. H. Tingey, ME, 1942, Vol. I, pp. 277–278
(c) D. W. Taylor, S and P, 1943, pp. 143–144
(d) W. P. A. van Lammeren, RPSS, 1948, pp. 225–226.

Although it appears absurd from the point of balancing and of reduction of bending moments on the propeller shaft, there are some appreciable advantages in the use of a single-bladed propeller. These are discussed by S. Sassi [Ann. Rep. Rome Model Basin, 1938, Vol. VII, pp. 95–99]. There is reported the case of a ship which normally traveled at 10.5 kt at 70 rpm but which, with all blades except one broken off, made 7 kt at about 85 rpm [SBSR, 6 Mar 1924, p. 289].

It is interesting to note that screw-propeller designers, even in the earliest days of development of this device, considered that they had some latitude in the number of blades and usually exercised it.

70.13 Use of Raked Blades. Due to the contraction of the inflow jet ahead of the propeller, the water enters the propeller disc at a slight inward angle, depicted in Fig. 32.M. A slight rake aft places the blades normal to the flow, with a gain in efficiency. On the other hand, rake causes an increase in the bending stresses in the blade due to the fact that the centrifugal force is offset from the blade root. In heavily loaded or high-speed propellers this latter factor is usually the controlling one in limiting rake. Rakes of over 15 deg are seldom used in any ship or propeller design.

Forward rakes are rarely seen. Sir Charles Parsons at one time advocated a forward rake of 1 in 10 for very thin propeller blades on the high-speed experimental vessel *Turbinia*. His idea was that an axial component of the centrifugal force on them would act in an after direction and help balance the thrust forces acting forward [Burrill, L. C., IME, 1951, Vol. LXIII, p. 15].

In some ship designs, where the maximum volume must be crowded into a given length, the hull profile is not only carried well aft toward the propeller position(s) but the waterlines have large slopes in this region. Blades may then be raked aft to augment the fore-and-aft clearances between the propeller sweep line and the forward edge of the aperture opening, if the vessel has a single screw, or between the sweep line and the hull, bossings, skegs, or struts if it has multiple screws. W. P. A. van Lammeren [RPSS, 1948, p. 229] gives the following *limits* (not design or optimum values) for rake:

(a) With moderately loaded screws for merchant vessels, 6 to 10 deg for single-screw ships, and 8 to 12 deg for twin-screw ships
(b) With heavily loaded, fast-running screws for warships generally no rake is used.

When running under load a propeller blade actually bends forward. This may be as much as 0.10 or 0.12 ft at the tip of a destroyer propeller. Thus if it is desired to run at the designed speed with no rake it would be wise to design the propeller with a little rake aft to allow for this bending effect.

If proper attention is given to the details of

the stern arrangement in the design stage, allowing ample clearances in all directions, little or no rake is required. There is usually no excuse to be forced to excessive angles of rake in order to obtain proper aperture clearances.

70.14 Propeller-Hub Diameter; Hub Fairing. Some general comments on hub-diameter ratios d/D are given here. More detailed comments are to be found in Sec. 70.43, under a discussion of the mechanical construction of screw propellers.

It is rarely possible to consider hydrodynamics alone in a discussion of hub shape and diameter for a screw propeller, especially for one at the stern of a hull. Obviously the blades must be attached to some sort of hub or enlargement on the shaft, which can not have too small a diameter. Further, the geometric pitch angle ϕ(phi) becomes very large as the radius R is diminished toward zero; too large, in fact, to make any blade lift effective in producing useful thrust. Finally, there is no point in making the hub much smaller than the diameter of the housing for the propeller shaft bearing just ahead of it.

There have been recurring proposals, over the past century or more, for propeller hubs having diameters of one-third or more of the propeller diameters. Some early ship propellers were built in this way. While it is true that the root sections of a normal screw propeller do relatively little work as a rule, at least they permit the water to pass through, which a large solid hub would not do.

From considerations of strength and mechanical attachment, both of the hub to the shaft and the blades to the hub, the diameter of the propeller hub depends partly upon the diameter of the shaft and partly upon the widths of the blade sections at the root, where they join the hub. It usually varies between $0.16D$ and $0.20D$ for solid propellers. For controllable or built-up propellers the diameter of the hub may be as large as 0.28 or $0.30D$, with a possible maximum of $0.25D$ for a propeller having blades that are demountable but not adjustable [ME, 1942, Vol. I, Fig. 2, p. 269]. It is pointed out in Sec. 70.43 that a loss of efficiency of from 1 to 1.5 *points* may be expected if a built-up rather than an integral hub is used; for example, a drop in η from 0.685 to 0.675 or 0.670.

To avoid separation and cavitation abaft the hub, a fairing cap is usually fitted at the after end. This cap also covers the propeller nut. In many cases the hub fairing cap does not rotate but is attached to the fixed part of the rudder, the rudder horn, or the rudder itself, as described in Sec. 74.15 and illustrated in Figs. 66.Q and 74.K.

It is customary and convenient, as well as good design, to shape the propeller hub and its cap as a fair, tapering continuation of the barrel or boss just forward of the propeller which houses the propeller bearing. This means that the end of the propeller hub next to the bearing has a diameter about equal to that of the bearing barrel. The end away from that barrel has a reduced diameter, as small as is consistent with the necessary mechanical strength and rigidity for the type of attachment of the hub to the shaft.

In the case of built-up propellers with adjustable or demountable blades it is rarely possible to make the hub diameter as small as the bearing barrel so that the fair surface of revolution between the latter and the end of the hub cap has a bulge in it in the vicinity of the disc plane.

In a speed range where the smaller, pointed end of a propeller fairing cap is covered with a hub vortex or swirl core, sometimes having a diameter half as great as that of the cap at its larger end, the portion of the cap within the core is obviously serving no useful purpose. It is possible, in some cases, to eliminate the swirl core or hub vortex entirely by cutting the cap off square at about two-thirds or three-quarters of its length from the after end. The separation drag which occurs abaft this blunt end is almost certain to be less in magnitude than the drag resulting from the presence of vapor pressure only inside a swirl core of somewhat smaller diameter. If the pressure is low enough and other conditions are favorable, the swirl core may persist, even abaft a blunt or square ending ["All Hands," Bu. Nav. Pers., U. S. Navy Dept., Feb 1953, pp. 18–19].

It appears unlikely, on a fast or high-speed ship, that any reasonable slope at the pointed end of a fairing cap will eliminate the swirl core or hub vortex entirely. Certainly the small slopes of 8 and 10 up to 20 deg (with reference to the shaft axis), previously used on the fairing caps of the fastest vessels, such as the World War II German cruiser *Prinz Eugen*, are inadequate for this purpose.

Swirl cores abaft the fairing caps of model propellers have been observed and photographed in model basins, variable-pressure water tunnels, and circulating-water channels. However, because

of the known and unknown scale effects, it is not yet safe to make full-scale predictions from a model experiment. Swirl cores and hub vortexes have been and can be observed on ships through special glass viewing ports installed in proper locations in the shell.

70.15 Determination of Expanded-Area Ratio; Choice of Blade Profile. For design purposes in this book the blade area of a propeller corresponds to the *expanded* area of all the blades. This is usually expressed as the ratio of the expanded area A_E to the disc area A_0. As a means of arriving at the blade outline or profile, use is made of the mean-width ratio, represented by the ratio of the average expanded chord length c_M of one blade to the propeller diameter D. The high and low limits for these ratios, in recent and current propeller design, are given by K. E. Schoenherr and W. P. A. van Lammeren [PNA, 1939, Vol. II, p. 157; RPSS, 1948, p. 227]:

Propellers for	Expanded-Area Ratio	Mean-Width Ratio
Any type of vessel	Rarely less than 0.35 to 0.40	
Cargo ships, 4-bladed		0.20 to 0.25
Cruisers and destroyers, 3-bladed	1.00 to 1.10	0.45 to 0.50 or more

The total expanded area of the Z blades of a propeller must be:

(1) Large enough, when combined with the differential pressures $+\Delta p$ and $-\Delta p$, to develop the lift and thrust forces required

(2) Small enough to avoid excessive blade surface and resulting large friction drag [van Lammeren, W. P. A., RPSS, 1948, pp. 226–227]

(3) Large enough to develop the required thrust at high blade velocities (and possibly also low hydrostatic pressures) without objectionable cavitation

(4) Large enough to satisfy the requirements for retardation in the case of emergency stops or sudden reversals

(5) Large enough so that the blade elements at the several radii have sufficient section modulus to give the blades the necessary strength and rigidity.

Unfortunately, propeller-series charts do not give direct answers as to the proper expanded-area (or developed-area) or mean-width ratios. They indicate only that a new propeller with the area ratio of the parent model(s) may be expected to give the performance indicated by the chart. Variations from the parent values have in the past usually been left to the experience and judgment of the designer, with little to rely upon if he does not have that kind of experience.

Only recently there have appeared a new series of graphs and a procedure based upon cavitation characteristics of the models of certain propeller series, devised by J. D. van Manen, whereby values of the proper developed-area ratio may be determined [Inter. Shipbldg. Progr., 1954, Vol. 1, No. 1, pp. 39–47]. Data derived by this method are presented at the end of Sec. 70.6.

In the example of the Lerbs' method of designing a wake-adapted propeller by the circulation theory, described in Secs. 70.21 through 70.38, in which cavitation is definitely to be avoided, the chord widths of the sections at the outer radii are selected to give $-\Delta p$ values which will not drop the pressure on the back below the vapor pressure of water. The chord lengths of the sections at the root are fixed by a combination of the amount of metal required and a thickness ratio t_X/c that is not too large. With chord lengths fixed for the inner and outer radii, and a fair profile drawn around them, the expanded area is more or less fixed, and with it the ratios A_E/A_0 and t_X/c.

Despite the large variety of blade-profile types illustrated in Fig. 32.L there are few established design rules for the choice of the best or most appropriate profile for any given case. The profile is narrow or wide, depending upon the expanded area required. It is skewed if it is desired to spread the pressure field developed by one blade over a sizable sector of the disc circle. The expanded profile has a certain minimum width if the propeller is to be free of cavitation. Within the limits of normal shape, any profile may be selected, without a detrimental effect upon performance, which meets any other requirements for the propeller design in hand.

Comments in the literature on blade outline are to be found in:

(a) Van Lammeren, W. P. A., RPSS, 1948, pp. 226–227
(b) Schoenherr, K. E., PNA, 1939, Vol. II, pp. 157, 162. On page 157, 1st col., there is given a formula (119) which produces a practical form of expanded blade outline that is generally elliptical in shape. Although not stated there, this is for a propeller not subject to cavitation.

Comments concerning proper blade widths are given in Sec. 70.17.

70.16 Selecting and Applying Skew-Back. The hydrodynamic reasons for applying skew-back to screw-propeller blades are explained in Sec. 32.15. Repeated briefly, skew-back is used to prevent certain corresponding points on the blade sections at every radius, or at a group of adjacent radii, from passing simultaneously through a region of high wake velocity directly abaft a skeg ending, a bossing termination, or a large strut. The necessity for skew-back in the design of a surface propeller is perhaps somewhat easier to understand. Here it is not desirable that the entire length of the leading edge of a blade, or an appreciable portion of that edge, should swing downward and strike the water surface at the same instant.

The actual application of skew-back is handicapped, however, because it is not yet known just what part of a blade element requires to be offset successively, in time or in angular position, from the high-wake region. This part is probably not the leading edge, nor the trailing edge, nor the locus of the midlengths of the expanded elements. It is possibly the locus of the centers of pressure of the elements, possibly the locus of the points of maximum thickness, or better still the locus of points opposite a certain part of the pressure field of each element, as yet not known. Lacking this information, the locus of the positions of maximum blade-element thickness is probably the best but, as explained presently, the use of this line is neither convenient nor practical.

Little is yet known about the rate at which the backward offset of the selected skew-back line should change with blade radius or, in other words, what should be its shape, defined in Sec. 32.15. Manifestly, the basic reference line or plane for establishing skew-back is the position of the region of maximum wake velocity, at or near its intersection with the plane of the propeller disc. For a vertical, symmetrical, center-plane skeg ending this is the vertical plane through the propeller axis. For a contra-guide skeg ending the locus of the maximum-wake positions in the plane of the disc is not known

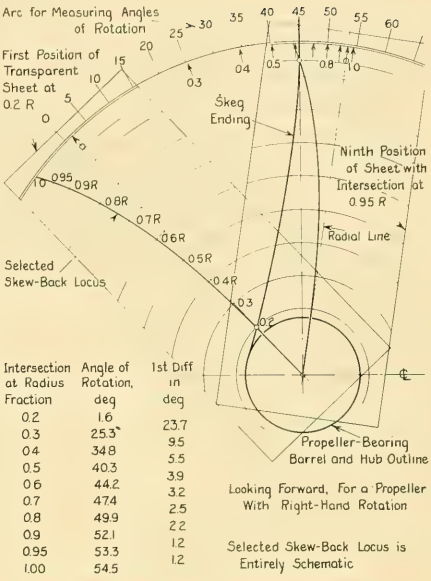

Intersection at Radius Fraction	Angle of Rotation, deg	1st Diff in deg
0.2	1.6	23.7
0.3	25.3	9.5
0.4	34.8	5.5
0.5	40.3	3.9
0.6	44.2	3.2
0.7	47.4	2.5
0.8	49.9	2.2
0.9	52.1	1.2
0.95	53.3	1.2
1.00	54.5	

FIG. 70.C GRAPHICAL METHOD FOR CHECKING SKEW-BACK LINE

exactly, because of the oblique flow occurring in the fore-and-aft clearance space between the skeg ending and the propeller disc.

Lacking better data, such as a comprehensive wake survey would give, it appears satisfactory to assume that the basic or reference trace for skew-back is that of the actual skeg ending, projected axially aft to the propeller disc. Such a line appears on Fig. 70.C, showing the elevation from aft of the upper half of a skeg ending with contra-guide features.

Summarizing, the trace serving as the basic reference, when establishing skew-back, may be:

(a) Straight in the disc plane, as for a symmetrical skeg ending or bossing termination
(b) Curved in the disc plane, as for a contra-guide skeg ending
(c) Curved, with modifications, as when the deflected flow abaft a contra-guide ending is projected back to the plane of the propeller disc, or to some other position.

The locus of the propeller may be:

(d) Straight in the disc plane, along a radius, as in the elliptical-outline blades with ogival sections of a half-century ago

(e) Straight in the disc plane, not coinciding with a radius, from the hub radius to the tip radius
(f) Curved, usually with a sweep-back toward the tip that is opposite to the direction of rotation.

Whatever the shape of the locus on the propeller which is *not* to pass simultaneously across the basic reference trace abaft the hull ending, the former is drawn on a sheet of thin transparent material to the same scale as the reference trace. In Fig. 70.C the transparent material is shown as rectangular in outline and the selected-skew-back locus is drawn in its proper position with reference to a straight radial line tangent to the locus at the hub radius. To the transparent sheet there are added concentric circles at $0.2R$, $0.3R$, and so on. A pin is inserted through both the transparent overlay and the under sheet upon which the skeg ending is drawn, at the propeller-shaft axis, so that the overlay may be rotated to simulate the rotation of the propeller. An arc is added on the under sheet, just outside the tip circle in the figure, to indicate the angular amount by which the overlay is rotated from an assumed zero position.

The overlay is turned in the direction of propeller rotation until the locus on it crosses the basic reference trace at some selected fraction of the maximum radius, say at $0.2R$. The angular position of the overlay is then noted, following which it is turned until the locus crosses the reference trace at the next selected radius fraction, say $0.3R$. The angular position is again noted. By taking the angles between successive angular positions, set down as first differences in the table on Fig. 70.C, it is possible to determine at a glance whether the successive differences between a group of adjacent angles are small or appreciable, or whether they are equal or unequal. A group of equal and appreciable differences indicates successive crossings of the locus and the reference trace at equidifferent angular and time intervals. A group of zero differences indicates a simultaneous crossing over the corresponding portion of the blade radius. This simultaneous crossing is almost invariably to be avoided.

A limited study of propellers with swept-back blades that have performed well in service indicates that successive crossings of the *leading edge* are spaced at more nearly uniform angular intervals than the crossings of any other known locus. Therefore, until a better locus is found it appears acceptable to take the *leading edge of the projected outline* as the one whose radial segments should swing *successively* and *uniformly* into the high-wake region.

It is not feasible, however, by any method as yet known, to fashion a suitable projected-blade outline, with fair root-to-tip characteristics, by working from the leading edge. Experience indicates that the locus of the midlengths of the *expanded* blade sections is the most suitable construction line in which to introduce the skew-back. This midlength locus, to which are applied the half-chord expanded lengths of the forebodies of the blade sections at the various radii, is then adjusted in shape until the leading edge resulting from this construction gives the desired equidifferent angular intersections. This is determined by the method diagrammed in Fig. 70.C, substituting the leading edge for the purely schematic rotating locus shown there. At or near the tip it is expected that the angular differences will increase because of the large-radius curves used to form the tip profile. The midlength locus is preferred over the locus of the chordwise positions of the maximum thickness of each section because the former is usually made tangent to the pitch reference line at the hub and it has less curvature at the outer radii.

Until more is known concerning the controlling locus, it appears wise, if possible, to give definite angular separation at the successive radii to both the midlength-of-chord locus and to the position-of-maximum-section locus. In addition, both should be fair from root to tip of the blade, as should the leading and trailing edges.

Good values for the skew-back at the tip, measured as indicated in Fig. 70.O of Sec. 70.36 and by Fig. 78.L, lie between 20 to 25 per cent of the maximum chord length c_{Max} of the blade.

The designer is cautioned, on a moderately or heavily loaded propeller at least, *never* to apply an appreciable amount of skew to a screw-propeller blade in a forward or ahead direction, for the reasons given in Sec. 70.44.

For a given maximum thickness t_X at each section, a blade with large sweep-back has a smaller thickness ratio t_X/c because the lengths of the sections are usually greater in the circumferential direction of flow across the blade than they would be in a blade with no sweep-back. This thinness is generally a help in deferring cavitation.

Theoretically the dynamic ram pressure built up on the extreme leading edge of a fast-running

propeller is large, and its harmful effect can be reduced by skew-back, but the angle made by the leading edge with the radius has to be large to make much difference here.

70.17 Design Considerations Governing Blade Width. The matter of proper blade width for a screw propeller, usually expressed as the mean-width ratio c_M/D, follows rather closely after the discussion of expanded-area ratio in Sec. 70.15. If the designer has no preconceived ideas regarding the blade width he usually encounters difficulty in this phase of the problem. A partial solution is to adopt the blade width, or approximately that value, of the series model propeller which appears to give the best performance from the chart-design procedure. For example, W. P. A. van Lammeren gives [RPSS, 1948, pp. 204, 214] the chord length of the widest section for one series in terms of the propeller diameter D. J. G. Hill includes some brief instructions [SNAME, 1949, p. 152].

Assuming that the blade width and outline are selected, the next step is a check to determine whether the blade area is sufficient to avoid cavitation, using one of the available cavitation diagrams:

(a) L. C. Burrill, RPSS, 1948, Fig. 123a, p. 186
(b) Wageningen Model Basin, RPSS, 1948, Fig. 123a, p. 186
(c) J. D. van Manen and L. Troost, SNAME, 1952, Fig. 14, p. 455
(d) J. D. van Manen, Int. Shipbldg. Prog., 1954, Vol. 1, No. 1, pp. 39–47
(e) H. W. E. Lerbs' data in PNA, Vol. II, Figs. 30 and 31, pp. 179, 181
(f) W. P. A. van Lammeren's chart in 6th ICSTS, 1951, Fig. 30, p. 94, reproduced with some modifications of detail in Fig. 47.G of the present volume.

Two examples illustrate how this is done, both for the 20-ft propeller of the ABC transom-stern ship:

(1) Cavitation check with Lerbs' data, using the symbols given in Figs. 30 and 31 of the reference, with a rate of rotation of 110 rpm and a depth to the shaft axis of 15.5 ft.

$$A_E/A_0 = 0.40,$$

$$A_E = 0.40(A_0) = 0.40\pi(10)^2 = 125.66 \text{ ft}^2$$

$$n = 110 \text{ rpm or } 1.8333 \text{ rps}$$

$$p_{\text{Static}} = p_s = p_0 - p_e$$

$$= 14.7(144) + 15.5(62.43)(1.027) - 52$$

$$p_s = 2{,}116 + 994 - 52 = 3{,}058 \text{ lb per ft}^2$$

$$K_c = \frac{p_s A_E}{\rho n^2 d^4} = \frac{3{,}058(125.66)}{1.9905(1.8333)^2(20)^4}$$

$$= \frac{384{,}268}{1{,}070{,}410} = 0.359$$

For a speed of advance of 15.15 kt or 25.59 ft per sec,

$$J = \frac{V_A}{nd} = \frac{25.59}{(1.8333)(20)} = 0.698.$$

For a p/d ratio of 1.0 this point falls well within the region of no cavitation.

(2) Cavitation check by the van Lammeren method, employing his symbols:

$p_0 - p_e = p_s = 3{,}058$ lb per ft^2, from (1) preceding

$$\sigma_0 = \frac{p_0 - p_e}{0.5\rho V_A^2} = \frac{3{,}058}{0.99525(25.59)^2} = \frac{3{,}058}{651.7} = 4.69$$

$$\text{Factor} = \sigma_0(F_a/F_0)p = 4.69(0.4)(1.0) = 1.87$$

$$J/p = \frac{0.698}{1.0} = 0.698$$

Using these factors, the plot of Fig. 47.G indicates that they are in the region of no cavitation.

One feature concerning blade width, rarely discussed in the literature, is that of its effect upon the periodic vibratory forces excited in or on the adjacent ship structure. Assuming the same shape of $-\Delta p$ (and $+\Delta p$) chordwise pressure-distribution curve on both wide and narrow blades delivering equal thrust, the mean $-\Delta p$ (or $+\Delta p$) on the wide blade is smaller and the pressure peaks are less pronounced. It follows that, for a given rate of rotation, the periodic forces exerted by the wide-blade pressure fields should be smaller in magnitude and longer in duration. Both features favor the wide-blade propeller in lessening the vibratory forces on the ship carrying it.

70.18 Selection of Type of Blade Section. The selection of the proper type and proportions of the blade sections is important. These may be different for the inner, the intermediate, and the outer radii. What is more important, perhaps, is that the type, shape, and proportions of the blade sections be suited to the work to be performed.

Of the blade-section types illustrated in Fig. 32.K, the single-ended and double-ended symmetrical sections are employed primarily on propellers intended to give good stopping and backing performance, and to run astern for long periods, as on a double-ended ferryboat.

Airfoil sections with what is known as lifted leading and trailing edges, set back from a base chord passing through the main portion of the face, are necessary in way of the roots and the inner radii to obtain good flow through the regions where the blades are close together; see the blade-spacing diagrams at the lower left-hand corners of Figs. 70.O and 78.L. If the leading edges are not lifted sufficiently, cavitation and erosion are liable to occur on the faces, close abaft those edges.

There are many types of airfoil section suitable for screw propellers. Some of the most satisfactory forms are those developed by the National Advisory Committee for Aeronautics, based upon the principle of superposing the ordinates of a symmetrical hydrofoil upon a curved or cambered meanline, with or without minor modifications here and there. The merits of these NACA sections and the advantages of using them are described in detail by I. H. Abbott, A. E. von Doenhoff, and L. S. Stivers, Jr., in NACA Report 824, issued in 1945, and entitled "Summary of Airfoil Data." The manner in which these sections are developed for a particular case is described in Sec. 70.31.

70.19 Shaping of Blade Edges and Root Fillets. In former years many propeller drawings did not specify the detailed shapes for the blade edges but this procedure is no longer compatible with good design. One method of doing this, for sections with circular noses and tails and setback as well, is shown by W. P. A. van Lammeren [RPSS, 1948, Fig. 126, p. 190].

The leading edge of a blade must be thick enough to:

(a) Withstand the impact of small objects without nicking or deforming the blade edge permanently
(b) Avoid local cavitation, either on the face or back, when the angle of attack changes from its predicted value; that is, when the direction of the incident velocity shifts with respect to the blade. This change can occur throughout one revolution because of local circumferential variations in the wake velocity or it can occur for the whole propeller because of changes in displacement, in ship resistance, and in thrust loading over the disc area.
(c) Render the blade section reasonably invulnerable to changes in the angle of attack, due to variations in the local speed of advance, in the direction of flow, and other factors.

Both leading and trailing edges must be thin enough to:

(d) Eliminate excessive dynamic pressures along the leading edge because of the relatively large velocity with which the blade passes through the water. This is particularly true for the sections at the outer radii. Although screw propellers are rarely designed for partial immersion, there are large dynamic pressures due to impact when the exposed blade portions strike the water surface.
(e) Eliminate losses due to separation drag at the trailing edge
(f) Prevent the formation and shedding of eddies and the lateral vibration which causes noise and singing.

For the leading-edge shape, a circular arc is simple and satisfactory. This is achieved as indicated in the axial view of Fig. 70.O by bringing the face and back section outlines in to tangent points on a small circle. For the trailing edges much smaller circular arcs are used. If, however, the blade sections are rather thick at the extremity of the run, they are given a chisel shape, illustrated by Fig. 70.P in Sec. 70.46.

It is possible that some full or rounded form of edge at the blade tip may be found which will diminish the intensity of the tip vortexes by increasing the diameter of the vortex cores.

In the working drawing of a final propeller the exact shapes of the leading and trailing edges and of the tip edge are to be shown by an adequate number of large-scale details, such as those given by R. H. Tingey [ME, 1942, Vol. I, Fig. 6, p. 280, Detail "A"]. W. Henschke gives a tip radius (in thickness) of $0.0015D$ and a trailing edge radius of $0.008c$ ["Schiffbau Technisches Handbuch," 1952, p. 145].

The root fillets, also lacking details in days gone by, are now of the constant-stress shape diagrammed by R. H. Tingey in Fig. 16 on page 292 of "Marine Engineering" [Vol. I, 1942]. This produces a form resembling that given by nature to the bottom of a tree, where the trunk joins the roots and where large bending moments are to be resisted.

70.20 Partial Bibliography on Screw-Propeller Design. Although they are not all quoted in this and other chapters relating to screw propellers, there is given here a *partial* bibliography of the principal references on the design of screw propellers for ships, most of them dating from about

1939. A few applicable references covering airscrew design are included.

A very complete bibliography containing 227 items, listing references in the literature for some 50 or 60 years prior to 1939, is given by K. E. Schoenherr [PNA, 1939, Vol. II, pp. 187–194]. Another extensive bibliography with 191 items, many of them duplicating the PNA items but extending only to the year 1942, is given by W. P. A. van Lammeren [RPSS, 1948, pp. 295–301].

The references in the appended list appear generally in chronological order, without any attempt at grouping or classification. They do not duplicate the references in Sec. 70.4, listing the literature concerning propeller-series charts for analysis and design purposes.

(1) Betz, A., "Schraubenpropeller mit geringstem Energieverlust (Screw Propeller with Minimum Loss of Energy)," with an Appendix by L. Prandtl, Nachr. der Kön. Gesellschaft der Wissenschaften zu Göttingen, Math-Phys., 1919, p. 193

(2) Betz, A., "Eine Erweiterung der Schraubenstrahl-Theorie (An Expansion of the Screw-Race Theory)," Zeitschrift für Flugtechnik und Motorluftschiffahrt, 1920

(3) Helmbold, H. B., "Zur Aerodynamik der Treibschraube (On the Aerodynamics of the Screw Developing Thrust)," Zeitschrift für Flugtechnik und Motorluftschiffahrt, 1924, pp. 150 and 170

(4) Bienen, Th., and von Kármán, Th., "Zur Theorie der Luftschrauben (On the Theory of the Airscrew)," Zeit. des Ver. Deutsch. Ing., 1924, p. 1237; Vol. 68, Nos. 48, 51; Vol. 69, No. 25

(5) Bienen, Th., "Die gunstigste Schubverteilung für die Luftschraube bei Berucksichtigung des Profilwiderstandes (The Most Favorable Thrust Distribution for the Airscrew)," Zeitschrift für Flugtechnik und Motorluftschiffahrt, 1925, p. 209

(6) Helmbold, H. B., "Die Betz-Prandtlsche Wirbeltheorie der Treibschraube und ihre Ausgestaltung zum Technischen Berechnungsverfahren (The Betz-Prandtl Vortex Theory and its Development into a Technical Calculation Method)," WRH, 9 Dec 1926, pp. 565–569; 22 Dec 1926, pp. 588–595. English version in EMB Transl. 15, Feb 1936.

(7) Horn, F., "Versuche mit Tragflügel-Schiffsschrauben (Tests with Airfoil-Section Ship Propellers)," STG, 1927, Vol. 28, pp. 342–446

(8) Slocum, S. E., "Practical Application of Modern Hydrodynamics to Marine Propulsion," ASNE, Feb 1927, pp. 1–38

(9) Helmbold, H. B., "Nachstromschrauben (Wake-Adapted Propellers)," WRH, 7 Dec 1927, pp. 528–531

(10) Helmbold, H. B., and Lerbs, H., "Modellversuche zur Nachprüfung der Treibschrauben-Wirbeltheorie (Model Tests to Verify the Vortex Theory for a Propeller Producing Thrust)," WRH, 7 Sep 1927, pp. 347–350

(11) Prandtl, L., and Betz, A., "Vier Abhlandlungen zur Hydrodynamik und Aerodynamik (Four Treatises on Hydrodynamics and Aerodynamics)," Göttingen, 1927

(12) Helmbold, H. B., "Über den Vortriebswirkungsgrad (On Propulsive Efficiency)," WRH, 22 Apr 1928, p. 151

(13) Goldstein, S., "On the Vortex Theory of Screw Propellers," Proc. Roy. Soc., London, Series A, 1929, Vol. 123, pp. 440–465

(14) Weick, F. E., "Aircraft Propeller Design," McGraw-Hill, New York, 1930

(15) Lerbs, H. W. E., "Kurventafeln zur Berechnung Starkbelasteter Freifahrtschrauben nach der Tragflügeltheorie (Graphs for Calculation of Heavily Loaded Open-Water Screw Propellers According to Airfoil Theory)," HSVA Rep. 101; WRH, 1 Feb 1933, pp. 29–31

(16) Gutsche, F., "Versuche an Propellerblattschnitten (Tests on Propeller Blade Sections)," Schiffbau, 1 Aug 1933, pp. 267–270; 15 Aug 1933, pp. 286–289; 1 Sep 1933, pp. 303–306

(17) Kempf, G., and Foerster, E., "Hydromechanische Probleme des Schiffsantriebs (Hydrodynamic Problems of Ship Propulsion)," Teil II, Oldenbourg, Munich and Berlin, 1940. This book contains a number of papers relating to ship propellers, with summaries in English.

(18) Helmbold, H. B., "Uber den Einfluss der Strahlkontraktion auf die Wirkungsweise breitflügeliger Schraubenpropeller (Schiffsschrauben) (On the Influence of the Race Contraction and its Effect on Broad-Bladed Screw Propellers (Ship Screws))," WRH, 15 Nov 1933, pp. 319–324

(19) Chartier, C., "Sur le Champ Hydrodynamique autour d'une Hélice à Trois Pales (On the Hydrodynamic Field Around a Screw Propeller with Three Blades)," CR, Acad. Sci., Paris, 1933, Vol. 196, p. 1642

(20) Gutsche, F., "Verstellpropeller (Variable-Pitch Propeller)," Zeit. des Ver. Deutsch. Ingr., 1934, Vol. 78, p. 1073; mentioned in NECI, 1937–1938, Vol. LIV, p. D212. In the latter reference Gutsche tells about a series of propeller charts giving T, Q, and η and going down to zero speed or 100 per cent slip.

(21) Schoenherr, K. E., "Recent Developments in Propeller Design," SNAME, 1934, Vol. 42, pp. 90–127

(22) Smith, L. P., "Quick Approximation for Preliminary Propeller Design," ASNE, Nov 1935, pp. 557–568

(23) Durand, W. F., "Aerodynamic Theory," Vol. IV, Division L, written by H. Glauert, Springer, Berlin, 1936

(24) Chartier, C., "Champ Hydrodynamique autour d'une Hélice Marine Triple Propulsive (Hydrodynamic Field Around a 3-Bladed Screw Propeller)," CR, Acad. Sci., Paris, 1936, Vol. 203, p. 1232

(25) Gutsche, F., "Die Entwicklung der Schiffsschraube in Licht der Neuzeitlichen Strömungslehre (The Development of the Ship Propeller in the Light of Modern Flow Theory)," Zeit. des Ver. Deutsch. Ing., 26 Jun 1937, pp. 745–753. A partial translation

of this paper is given in ETT Stevens Note 202 of 12 Oct 1952.

(26) Lösch, F., "Uber die Berechnung des induzierten Wirkungsgrades stark belasteter Luftschrauben unendlicher Blattzahl (On the Calculation of the Induced Efficiency of Heavily Loaded Airscrews of Infinite Blade Number)," Luftfahrtforschung, Jul 1938, Vol. 15, No. 7. English version in NACA Tech. Memo 884, Jan 1939.

(27) At the session of the North-East Coast Institution of Engineers and Shipbuilders for 1937–1938 there was held a "Symposium on Propellers," at which the following ten papers were presented. These papers are published in NECI, 1937–1938, Vol. LIV, pp. 237–414, with the discussions on pp. D133–D222. The paper titles and authors are:

(a) Baker, G. S., "The Qualities of a Propeller Alone and Behind a Ship"
(b) Horn, F., "Measurement of Wake"
(c) Allan, J. F., "Aerofoil Sections in Screw Propellers"
(d) Duncan, W. J., "Torsion and Torsional Oscillation of Blades"
(e) Gawn, R. W. L., "Effect of Shaft Brackets on Propeller Performance"
(f) Troost, L., "Open-Water Test Series with Modern Propeller Forms"
(g) Kent, J. L., "Propeller Performance in Rough Water"
(h) Kempf, G., "Further Model Tests on Immersion of Propellers, Effect of Wake and Viscosity"
(i) Benson, F. W., "Propellers for Tugs and Trawlers"
(j) Yamagata, M., "Model Experiments on the Optimum Diameter of the Propellers of a Single-Screw Ship."

(28) Troost, L., "Open-Water Test Series with Modern Propeller Forms," NECI, 1937–1938, Vol. LIV, pp. 321–326 and D185–D192. This paper covers the tests of the 4-bladed narrow-tip A.4.40 Wageningen series, the B.4.40, and the B.4.55 series. These had 15-deg rake and airfoil sections at all radii.

(29) Troost, L., "Open-Water Test Series with Modern Propeller Forms, Part 2, Three-Bladed Propellers," NECI, 1939–1940, Vol. LVI, pp. 91–95 and D41–D48. This second paper by Troost covers the tests of 3-bladed propellers of the B.3.35 and B.3.50 Wageningen series, also having 15-deg rake and airfoil sections at all radii.

(30) Troost, L., "Open-Water Test Series with Modern Propeller Forms, Part 3, Two-Bladed and Five-Bladed Propellers, Extension of the Three- and Four-Bladed B Series," NECI, 1950–1951, Vol. 67, Part 3, pp. 89–130; discussion in Part 5, pp. D45–D50; author's closure in Part 6, pp. D51–D54

(31) Kramer, K. N., "Induzierte Wirkungsgrade von Best-Luftschrauben endlicher Blattzahl (Induced Efficiencies of Optimum Airscrews with a Finite Number of Blades)," Luftfahrtforschung, Jul 1938, Vol. 15. An English translation of this paper appears in NACA Tech. Memo 884, Jan 1939.

(32) Gutsche, F., "Einfluss der Gitterstellung auf die Eigenschaften der im Schiffsschrauben Entwurf benutzten Blattschnitte (Influence of the Stagger on the Functioning of the Blade Sections Used in Ship-Screw Design)," STG, 1938, Vol. 39, pp. 125–175

(33) Schoenherr, K. E., "Propulsion and Propellers," PNA, 1939, Vol. II, Chap. III. This chapter, on pp. 187–194, lists 227 items of reference.

(34) Flugel, G., "Die günstigste Schubverteilung bei Propellern (The Optimum Thrust Distribution in Propellers)," Schiffbau, Schiffahrt und Hafenbau, 15 Apr 1940, pp. 108–112; 15 Sep 1940, pp. 250–253; 15 Oct 1940, p. 272

(35) Gutsche, F., "Versuche an umlaufenden Flügelschnitten mit abgerissener Strömung (Experiments on Rotating Airfoils in the Stalling Condition)," STG, 1940, Vol. 41, pp. 188–226

(36) Tingey, R. H., "Propellers and Shafting," ME, 1942, Vol. I, pp. 267–304

(37) Lerbs, H. W. E., "Der Stand der Forschung über den Schiffspropeller im Hinblick auf die Technische Berechnung (The Present Status of Theoretical Research on Ship Propellers with Respect to its Technical Application)," WRH, 15 Feb 1942, pp. 57–62; TMB Transl. 243, Jan 1952

(38) Burrill, L. C., "Developments in Propeller Design and Manufacture for Merchant Ships," IME, Aug 1943, pp. 148–169. This is a comprehensive but concise paper of general interest, covering many phases on the subject. On pp. 13–14 the author gives a list of 24 recommended references.

(39) Burrill, L. C., "Calculation of Marine Propeller Performance Characteristics," NECI, 1943–1944, Vol. 60, pp. 269–294 and Pls. 8–11. Design is normally based upon the model-test data of D. W. Taylor. The circulation or vortex theory is utilized to develop improvements not incorporated in existing series. A mean camber line is selected and the blade sections are superposed on it.

(40) Baker, G. S., "Fundamentals of the Screw Propeller," IME, Jan 1944

(41) Ludwieg, H., and Ginzel, I., "Zur Theorie der Breitblattschraube (On the Theory of the Broad-Bladed Screw Propeller)," Aerodynamische Versuchsanstalt, Göttingen, Rep 44/A/08, UM 3097, 1944

(42) Guilloton, R., "Considerations sur les Hélices (A Discussion of Screw Propellers)," Publications Scientifiques et Techniques de la Direction des Industries Aeronautiques, Paris, 1944

(43) Abbott, I. H., von Doenhoff, A. E., and Stivers, L. S., Jr., "Summary of Airfoil Data," NACA Rep 824, 1945

(44) Strassel, H., "Camber Corrections for Screw Profiles," MAP Völkenrode, MAP-VG 90-T, 1946

(45) Schoenherr, K. E., "Propellers," SNAME, Phila. Sect., 21 Feb 1947. There is an abstract of this paper on pages 17 and 18 of the SNAME Member's Bulletin for May 1947.

(46) Weissinger, J., "The Lift Distribution of Swept-Back Wings," Zentrale für Wissenschaftliches Berichtswesen, 1942, No. 1553. There is an English translation of this paper in NACA Tech. Memo 1120, Mar 1947.

(47) Burrill, L. C., "On Propeller Theory," IESS, Mar

1947, Vol. 90, pp. 449–488; Jun 1947, pp. 489–501. On pp. 475–476 there is a bibliography of 27 items.

(48) Van Lammeren, W. P. A., Troost, L., and Koning, J. G., "Resistance, Propulsion and Steering of Ships," 1948, Chap. II, Propulsion. This chapter has a huge bibliography of 191 items on propellers and propulsion.

(49a) Glauert, H., "The Elements of Aerofoil and Airscrew Theory," Cambridge, England, 2nd ed., 1948

(49b) Weinig, F., "Aerodynamik der Luftschraube (The Aerodynamics of the Airscrew)," Berlin, 1940

(50) Loftin, L. K., Jr., "Theoretical and Experimental Data for a Number of NACA 6A-Series Airfoil Sections," NACA Rep. 903, 1948

(51) Lerbs, H. W. E., "The Applied Theory of Free-Running Ship Propellers," AEW Rep. 42/48, Nov 1948

(52) Burrill, L. C., "Propeller Design and Propeller Theory," read on 11 May 1948 before the Shipbuilding Group of Dansk Ingeniorforening; published by Teknisk Forlag A/S Dansk Ingenioforenings Forlag, 1949. (In English)

(53) Hill, J. G., "The Design of Propellers," SNAME, 1949, pp. 143–192

(54) Kane, J. R., and McGoldrick, R. T., "Longitudinal Vibrations of Marine Propulsion-Shafting Systems," SNAME, 1949, pp. 193–252

(55) Guilloton, R., "The Calculation of Ship Screws," INA, 1949, Vol. 91, pp. 1–26

(56) Lerbs, H. W. E., "An Approximate Theory of Heavily Loaded Free-Running Propellers in the Optimum Condition," SNAME, 1950, Vol. 58, pp. 137–183

(57) Lewis, F. M., "Propeller Coefficients and the Powering of Ships," SNAME, 1951, pp. 612–641

(58) Lerbs, H. W. E., "On the Effects of Scale and Roughness on Free-Running Propellers," ASNE, Feb 1951, pp. 58–94. On pp. 93–94 the author gives a list of 15 references.

(59) Ginzel, I., "Influence of Blade Shape and of Circulation Distribution on the Camber Correction Factor," Admiralty Research Lab., ACSIL/ADM/52/46, Oct 1951

(60) Burrill, L. C., "Sir Charles Parsons and Cavitation," Parsons Memorial Lecture, IME, 1951, Vol. LXIII, pp. 1–19

(61) Okeil, M. E., "The Optimum Loading of a Marine Propeller," INA, Jul 1952, pp. 162–178. This represents a study under the supervision of L. C. Burrill, based upon the circulation or vortex theory of the screw propeller. Most of the references on pages 177 and 178 are included in this bibliography.

(62) Ginzel, I., "Theory of the Broad-Bladed Propeller," Admiralty Research Lab., Jun 1952

(63) Gawn, R. W. L., "Effect of Pitch and Blade Width on Propeller Performance," INA, 29 Sep 1952, Vol. 94, pp. 316–317; SBSR, 16 Oct 1952, p. 496 and pp. 509–511. Describes open-water tests of 37 model propellers in a systematic series. All the propellers are 20 inches in diameter, are 3-bladed, and have ogival blade sections with elliptic blade outlines and no skew-back or rake. The series covers a range of P/D ratio from 0.4 to 2.0 and of developed-area ratio A_D/A_0 from 0.2 to 1.1. The data are plotted in chart form.

(64) Lerbs, H. W. E., "Moderately Loaded Propellers with a Finite Number of Blades and an Arbitrary Distribution of Circulation," SNAME, 1952, pp. 73–123

(65) Van Manen, J. D., and Troost, L., "The Design of Ship Screws of Optimum Diameter for an Unequal Velocity Field," SNAME, 1952, pp. 442–468

(66) Burrill, L. C., and Yang, C. S., "The Effect of Radial Pitch Variation on the Performance of a Marine Propeller," INA, 1953, pp. 437–460

(67) Hannan, T. E., "Principles and Design of the Marine Screw Propeller," Ship and Boat Builder, Part 1, Jan 1953, pp. 221–227; Part 2, Feb 1953, pp. 263–270; Part 3, Mar 1953, pp. 306–311; Part 4, Apr 1953, pp. 347–353

(68) Lerbs, H. W. E., "The Loss of Energy of a Propeller in a Locally Varying Wake Field," TMB Rep. 862, Nov 1953

(69) Edstrand, H., "Model Tests on the Optimum Diameter for Propellers," SSPA Rep. 22, 1953

(70) Berggren, R. E., and Graham, D. J., "Effects of Leading Edge Radius and Maximum Thickness Chords; Ratio on the Variation with Mach Number of the Aerodynamic Characteristics of Several Thin NACA Airfoil Sections," NACA Tech. Note 3172, 14 Apr 1954

(71) Lerbs, H. W. E., "Propeller Pitch Correction Arising From Lifting Surface Effect," TMB Rep. 942, Feb 1955

(72) Silverleaf, A., and O'Brien, T. P., "Some Effects of Blade-Section Shape on Model Screw Performance," NECI, 1955. Abstracted in SBSR, 10 Feb 1955, pp. 172, 174.

(73) Van Manen, J. D., and van Lammeren, W. P. A., "The Design of Wake-Adapted Screws and their Behavior Behind the Ship," IESS, 1955, Vol. 98, Part 6

(74) Burrill, L. C., "Considérations sur le Diamètre Optimum des Hélices (Considerations Governing the Optimum Diameter of Ship Propellers)," ATMA, 1955, Vol. 54, pp. 231–261

(75) Burrill, L. C., "The Optimum Diameter of Marine Propellers: A New Design Approach," NECI, Nov 1955, Vol. 72, Part 2, pp. 57–82; abstracted in SBMEB, Apr 1956, pp. 267–271

(76) "Propeller Design and Performance Calculations," SBSR, 5 Jan 1956, pp. 9–10.

For the reader's benefit, there are some 17 additional references, closely related to this subject, given by J. G. Hill [SNAME, 1949, p. 170].

70.21 Design of a Wake-Adapted Propeller by the Circulation Theory. Propeller design by the chart method is analogous to the design of a hull by working from a series such as the TMB Series 60, or by virtually copying a previous design having the proportions desired, combined with a good performance. However, there comes a time

when the design requirements are so unusual, or the situation is so special, that there is no existing design from which to work. New waters must be traversed, so to speak, which are not only unfamiliar but for which there are few reliable sailing directions. One such situation occurs when cavitation is to be expected—and avoided. Another occurs when wake surveys show an unusual distribution of velocity at the propeller position, or when it is desired to take full advantage of a more-or-less normal wake variation. A third might arise if it were desired to eliminate all possibility of tip-vortex cavitation cores, requiring the blades to be almost completely unloaded at their tips.

For problems of this kind, and for developments of the future leading to appreciable improvements in propeller performance, it is necessary to fall back upon an analytic method. This in turn must be based on the fundamental hydrodynamics of the problem, in this case the theory of circulation as applied to a screw propeller. There are to be found in the literature at least six papers dealing with this subject and making use of the successive developments of the theory up to the time each paper was prepared and published. These are:

(1) Schoenherr, K. E., "Propeller Design by the Betz-Prandtl-Helmbold Circulation Theory," PNA, 1939, Vol. II, Chap. III, Sec. 10, Art. 3, pp. 168–170
(2) Van Lammeren, W. P. A., "Design of a Wake-Adapted Screw by Means of the Circulation Theory," RPSS, 1948, Chap. II, Secs. 138–140, pp. 248–250
(3) Hill, J. G., "The Design of Propellers," SNAME, 1949, pp. 143–192
(4) Van Manen, J. D., and Troost, L., "The Design of Ship Screws of Optimum Diameter for an Unequal Velocity Field," SNAME, 1952, Vol. 60, pp. 442–468
(5) Van Manen, J. D., and van Lammeren, W. P. A., "The Design of Wake-Adapted Screws and their Bahaviour Behind the Ship," IESS, 1954–1955, Vol. 98, pp. 463–482
(6) Eckhardt, M. K., and Morgan, W. B., "A Propeller Design Method," SNAME, 1955, pp. 325–374.

For the design of what is called a *wake-adapted* propeller, the procedure is to employ the fundamental hydrodynamic concepts of circulation set forth in Chap. 14. At the present stage of the art it is necessary to call upon certain semi-analytic and experimental sources for information which will enable a propeller designer to start with his requirements and end with a screw-propeller design. To do this, the designer need have only the knowledge that is set down in Volumes I and II of this book.

In most discussions of the design of wake-adapted propellers by the circulation theory, there are gaps and omissions which make it practically impossible for anyone except an expert in the field to carry through a design by the methods described. The sections to follow in this chapter give a complete and continuous story for a new method, recently (1954) developed by Dr. H. W. E. Lerbs of the David Taylor Model Basin staff. It is a short-cut method based on the theory he described completely in his paper "Moderately Loaded Propellers with a Finite Number of Blades and an Arbitrary Distribution of Circulation" [SNAME, 1952, pp. 73–123].

No attempt is made to give here a theoretical explanation of the principles involved. There are quoted only the formulas actually employed, accompanied by a written and tabular explanation of their use.

Lerbs' short-cut method was chosen for several reasons:

(i) It has not been published before in this form and thus offers a new approach to the problem

(ii) It produces the answer rather directly and involves a minimum of reliance on intuition, background, and previous propeller-design experience

(iii) It gives promise of becoming an excellent method of rational design for a wide variety of screw propellers

(iv) It is backed up by Lerbs' theoretical papers and is based on sound hydrodynamic principles

(v) Design calculations using this short method were checked by parallel calculations with Lerbs' rigorous method, described in his referenced paper. The results gave satisfactory agreement.

Lerbs' theory for moderately loaded, wake-adapted propellers is based on the assumption that the induced-velocity components of the second and higher degree can be neglected. In the development of the short-cut method two additional assumptions are made; first, that the induced velocity is always perpendicular to the resultant relative velocity and second, that the Goldstein function may be applied, relating the behavior of a propeller with a finite number of blades to that of one with an infinite number of blades.

The propeller design is carried out in this chapter along the following lines. The terms listed are defined and described as the discussion proceeds:

(a) Determine the number of blades, the propeller diameter, the hub diameter, the rake, if any, and the rate of rotation
(b) Calculate the required thrust-load coefficients and advance coefficients
(c) Determine the ideal efficiency with jet rotation from Kramer's charts
(d) By successive approximations, calculate the hydrodynamic pitch angle and the thrust distribution over the blade which allows the propeller to develop the required thrust
(e) Determine the lift-coefficient product, apply the lifting-surface correction to the hydrodynamic pitch angle, and calculate the hydrodynamic pitch distribution
(f) From strength considerations determine the blade-thickness fraction and the maximum-blade-thickness distribution
(g) Choose the type of meanline and thickness form to be used for the blade sections
(h) Using cavitation criteria, determine the maximum camber of the meanline and the chord lengths of the blade sections from appropriate charts
(i) Fair the blade outline and determine the final chord lengths, camber ratios, and lift coefficients
(j) Apply the curvature correction to the camber ratio
(k) Correct for viscous flow by adding an angle of attack at the various blade sections. Calculate the final pitch distribution.
(l) Determine the amount of skew-back, if any
(m) Draw the propeller
(n) Calculate the final propeller efficiency corresponding to the design conditions.

Owing to the intricacy of all existing design methods for screw propellers, based upon the vortex or circulation theory, it is necessary to employ a number of special symbols. For the Lerbs method described and illustrated in the sections following, all the special symbols, additional to the standard symbols listed in Appendix 1, are defined when they are first used. Nevertheless, these special symbols are listed here in one place, with brief titles for each:

$(C_{TL})_S$	Thrust-load coefficient based upon the ship speed V instead of upon the usual speed of advance V_A
i	Tangent of one half the angle of rake of a screw-propeller blade, based upon the notation of D. W. Taylor [S and P, 1943, p. 134]
k	Ludwieg-Ginzel curvature correction, applied to the camber ratio
m_{X0}	Maximum section camber, corrected
S_e	Allowable stress in a propeller blade, based upon the notation of D. W. Taylor [S and P, 1943, p. 137]
T_I	Non-viscous thrust, as in a perfect liquid
x'	Ratio of local radius R to tip radius R_{Max} of propeller
$\bar{w}_{x'}$	Average local wake fraction
$w_{x'}$	Average local wake fraction, corrected to match the effective wake
β_{IC}(beta)	Corrected hydrodynamic pitch angle
ϵ (epsilon)	Drag-lift ratio of an airfoil or blade section
η_K(eta)	Kramer's ideal efficiency, with jet rotation
λ (lambda)	Absolute advance coefficient, equal to $V_A/(\pi nD)$
λ_S	Absolute advance coefficient, based upon ship speed V instead of speed of advance V_A
μ(mu)	Viscous-flow correction
σ_S (sigma)	Cavitation number based upon ship speed V instead of the resultant incident velocity V_R on a blade section.

70.22 ABC Ship Propeller Designed by Lerbs' 1954 Method. As a help in understanding Lerbs' method, and as a practical illustration of its use, a screw propeller is designed here for the transom-stern ABC ship. The design is based upon the wake survey diagrammed in Fig. 60.M.

Although cavitation is not expected on this ship, and the wake-velocity distribution is in no way unusual, the design procedure is carried through as though these two features presented real problems.

When selecting the model propeller to be used in the self-propulsion model tests of the transom-stern ABC ship designed in this part of the book, an estimated propeller thrust of 193,476 lb was used. This led to the conclusion presented in Secs. 70.6 and 78.4 that the stock model propeller should have a P/D ratio of 1.02, four blades of moderate width, and airfoil sections along the inner radii. The calculated rate of rotation was 109.2 rpm at the designed ship speed of 20.5 kt. The corresponding advance coefficient J was 0.703, and an open-water efficiency of 68.0 per

cent was expected. That this estimate was fairly accurate is shown by the recorded rpm of 109.7 at 20.5 kt in the model self-propulsion test. However, using the resistance of the ship with appendages, obtained from the resistance test of TMB model 4505, and a thrust-deduction fraction of 0.07 at 20.5 kt, obtained from the self-propulsion test with TMB model propeller 2294, a revised thrust is calculated.

$V = 20.5$ kt; $P_E = 10{,}078$ horses, from model-resistance test; thrust-deduction fraction $t = 0.07$

$$R_T = \frac{550P_E}{V} = \frac{550(10{,}078)}{1.6889(20.5)} = 160{,}098 \text{ lb}$$

$$T = \frac{R_T}{1 - t} = \frac{160{,}098}{0.93} = 172{,}148 \text{ lb.}$$

The predicted thrust required to drive the ship is much less than the estimated thrust. This means that a new combination of P/D ratio and rate of rotation n might give a higher propeller efficiency than the combination used in selecting the model stock propeller, based on the higher thrust.

Consulting Prohaska's logarithmic charts for Wageningen Series B.4.40 and B.4.55 model propellers, one of which is reproduced as Fig. 70.B, and entering with the thrust-load coefficient C_{TL} of 0.709, based on the lower thrust value and an effective wake fraction of 0.195 from the self-propulsion test, the following optimum characteristics are determined:

$$P/D = 1.2 \qquad J = 0.86$$

$$n = 1.620 \text{ rps or } 97.2 \text{ rpm} \qquad \eta_0 = 0.72$$

The open-water propeller efficiency obtained from the self-propulsion test with the stock propeller at the designed speed was roughly 68 per cent. This means that there is a possible gain of about 4 per cent in propeller efficiency, with a corresponding increase in the propulsive coefficient. A new propeller design for the ABC ship is thus definitely indicated.

70.23 Choice of the Number of Blades for the ABC Design. General comments concerning the number of blades to be used in a screw-propeller design are embodied in Sec. 70.12. Those in this section are limited to the final design of propeller for the transom-stern ABC ship.

This vessel, with the afterbody profile of Fig. 66.Q, supplemented by Fig. 67.U, is designed with what is known as a clear-water stern. As might be expected, and as is revealed in Fig. 60.M, there is a high-wake-velocity region near the top of the propeller circle, where the propeller passes the skeg ending and cuts through the boundary layer beneath the transom. Cutting back the lower portion of the skeg should have reduced the magnitude of the wake velocities in the lower half of the propeller circle. Nevertheless a localized region of moderate positive wake velocities remains in the neighborhood of the 6 o'clock position. With such a wake configuration, it is advisable to use a propeller with an even number of blades, to minimize the unbalance in thrust between the blades in the 12 o'clock and 6 o'clock positions and to reduce the periodic bending of the propeller shaft in a vertical plane. A 4-bladed propeller is the logical choice, as has been found from long experience with single-skeg single-screw ships, unless a subsequent analysis indicates that a 6-bladed propeller is needed to place the blade frequency (n times Z) in a certain range.

Ample edge clearance is allowed in the propeller aperture of the ABC transom-stern design, between the end of the skeg and the propeller sweep line, to keep vibratory forces to a minimum.

70.24 Determination of Rake for the ABC Propeller. The propeller aperture and stern arrangement of the transom-stern ABC ship are designed so that no rake is required. There is some contraction in the inflow jet, to be sure, as for any screw propeller, but this is not augmented greatly at the disc position because the lines of the skeg ending ahead of it are deliberately made fine. The rake angle is set at 0 deg for the design carried through here but it could have been set at any angle up to about 5 deg if the designer wished to take advantage of the inflow contraction.

70.25 Propeller-Disc and Hub Diameters. The transom stern of the ABC ship was designed to accommodate the largest practicable propeller diameter on the given draft of 26 ft. This was done to obtain the greatest possible propulsive coefficient, on the basis that the machinery could be designed to produce the required shaft power at whatever rate of rotation appeared best for the propeller. The maximum propeller-disc diameter resulting from this procedure was 20 ft. The diameter of the propeller is thus considered fixed at the outset of the design. The rate of rotation n in rpm and the P/D ratio are now to be chosen to give the maximum propeller and propulsive efficiency.

For a design situation where the diameter is not fixed, it is necessary to determine the optimum

value of D by the use of existing propeller-design charts, subject to the comments given earlier in Sec. 70.9, or by model experiment.

On the ABC ship, no shaft calculations were made for the transom-stern design, so the hub diameter was assumed as $0.18D$, the same as for the stock model propeller. The hub is faired into the rudder horn as shown in Figs. 66.Q, 67.U, and 74.K.

70.26 Calculating the Thrust-Load Factors and the Advance Coefficients. With some of the primary characteristics fixed it is possible to start the design of the wake-adapted propeller by Lerbs' short method. For the ABC propeller-design problem only the thrust T, the ship speed V, and the maximum propeller diameter D are fixed. The rate of rotation n is to be chosen to give maximum efficiency. In many design cases there will be limitations on rpm as well, due to restrictions on the size of reduction gears or by a requirement for a given rate of rotation at a given power with a direct-drive diesel engine. In these cases, the designer accepts the limitations and attempts to attain the maximum propeller efficiency possible, even though it is less than the optimum.

For the ABC ship a rate of rotation to give maximum propeller efficiency was chosen in Sec. 70.22, on the basis of the Wageningen Series propeller data as laid down on Prohaska's logarithmic charts. These indicated an η_0 of 0.72 for an n of 1.620 rps or 97.2 rpm.

For Lerbs' short method it is best to work on a thrust basis. Because of the assumptions involved in this method, described in Sec. 70.21, corresponding formulas on a power basis do not yield equally good results. When using the rigorous method described by Lerbs in his referenced paper on moderately loaded propellers, either a thrust basis or a power basis can be employed. Thus if the designer is limited to a given power plant, he must convert the shaft power to effective power P_E and this P_E to thrust. In the design of the ABC ship, there is no maximum limitation on shaft power, so the design is started by using the thrust obtained from the model resistance test with appendages, calculated in Sec. 70.22.

The following data are known:

Diameter, $D_{\text{Max}} = 20$ ft Radius $R_{\text{Max}} = 10$ ft

$$A_0 = \pi R_{\text{Max}}^2 = 314.16 \text{ ft}^2$$

Designed ship speed $V = 20.5$ kt $= 34.622$ ft per sec

$P_E = 10{,}078$ horses, from model resistance test

Thrust $T = 172{,}148$ lb

Thrust-deduction fraction $t = 0.07$; $1 - t = 0.93$; from model self-propulsion test for 20.5 kt

Effective wake fraction $w = 0.195$; $1 - w = 0.805$; from model self-propulsion test for 20.5 kt

Rate of rotation $n = 1.620$ rps or 97.2 rpm; from Sec. 70.22

Number of blades $Z = 4$

Average local wake fraction at the various radii, $w_{x'}$, from the wake survey on TMB model 4505, derived by the method described subsequently in this section

$\rho = 1.9905$ slugs per ft^3 for salt water at 59 deg F

$0.5\rho = 0.99525$ slugs per ft^3.

The next step is to calculate the thrust-load coefficients and advance coefficients. The initial calculations are all based on non-viscous flow. It is therefore necessary to convert the thrust calculated from the model test to a non-viscous thrust. A good approximation for this is given by the following relationship, which was determined by considering the viscous forces on a blade element:

$$T_I = 1.03T$$

where T is the customary thrust in viscous flow and T_I is the thrust in non-viscous flow.

$$T_I = 1.03(172{,}148) = 177{,}312 \text{ lb}$$

Speed of advance $V_A = V(1 - w) = 34.622(0.805) = 27.871$ ft per sec

Thrust-load coefficient

$$C_{TL} = \frac{T_I}{(0.5\rho)A_0V_A^2} = \frac{T_I}{(0.5\rho)\pi(R_{\text{Max}})^2V_A^2}$$

$$= \frac{177{,}312}{0.99525(314.16)(27.871)^2} = 0.7300$$

The thrust-load coefficient based on ship speed is

$$(C_{TL})_S = \frac{T_I}{(0.5\rho)A_0V^2}$$

$$= \frac{177{,}312}{0.99525(314.16)(34.622)^2} = 0.4731$$

The absolute advance coefficient J_{Abs} or

$$\lambda = \frac{V_A}{\pi nD} = \frac{27.871}{(3.14)(1.620)(20)} = 0.2738$$

The absolute advance coefficient based on ship speed

$$\lambda_S = \frac{V}{\pi nD} = \frac{34.622}{(3.14)(1.620)(20)} = 0.3401$$

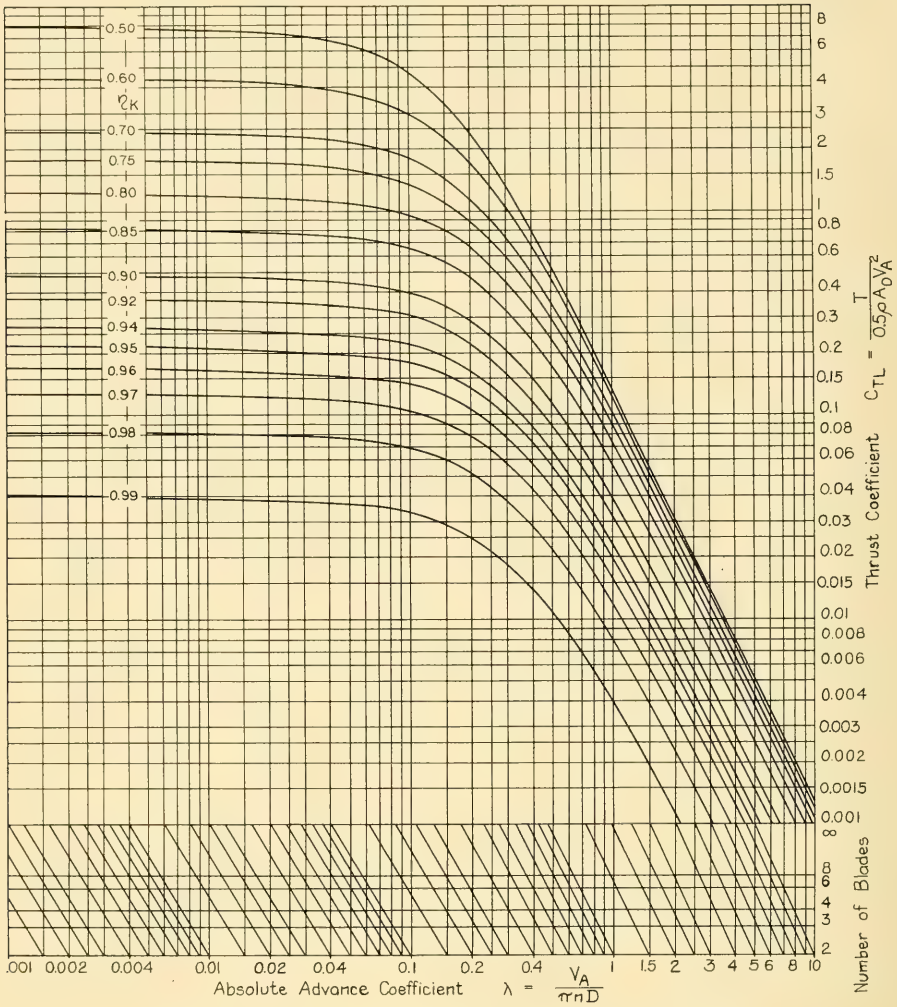

Fig. 70.D Kramer's Contours of Ideal Efficiency η_K with Jet Rotation

Using the calculated values of $C_{TL} = 0.730$ and $\lambda = 0.2738$, enter Fig. 70.D, a chart prepared by Kramer [see reference (31) in Sec. 70.20], and determine the *ideal efficiency with jet rotation* η_K. This ideal efficiency η_K differs from the η_I described in Sec. 34.2 in that it considers the effect of both the axial and rotational components of the induced velocity. The better-known ideal efficiency η_I, derived from the momentum theorem, considers only the axial component of the induced velocity.

To get a good value it is best to plot a curve of η_K on a basis of C_{TL}. Enter Fig. 70.D with λ along the bottom scale, in this case 0.2738, follow the diagonal line up to the number of blades Z, then move vertically to the several curves of η_K in the vicinity of the thrust-load coefficient $C_{TL} = 0.730$ previously calculated. The final

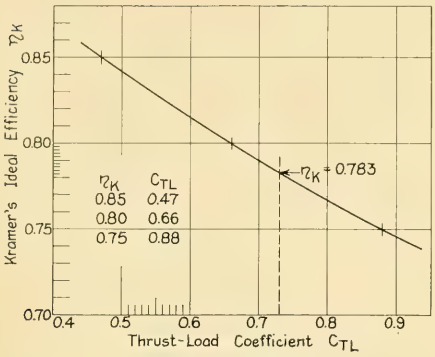

FIG. 70.E VARIATION OF IDEAL EFFICIENCY η_K WITH THRUST-LOAD COEFFICIENT

determination of η_K for the exact C_{TL} is shown in Fig. 70.E. Thus $\eta_K = 0.783$ for $C_{TL} = 0.730$.

70.27 First Approximation of the Hydrodynamic Pitch Angle and the Radial Thrust Distribution. The next step is to calculate the hydrodynamic pitch angle β_I, using the following formula, which represents Lerbs' approximate optimum condition for a wake-adapted propeller:

$$\tan \beta_I = \frac{\lambda}{x'} \cdot \frac{1}{\eta_K} \left[\frac{1 - w_{x'}}{1 - w} \right]^{1/2} \qquad (70.i)$$

Here x' is the ratio of the local radius R to the tip radius R_{Max} of the propeller, namely $x' = R/R_{\text{Max}}$, and $w_{x'}$ is the corrected average wake at each radius, to be explained presently.

The *average* local wake fraction $\bar{w}_{x'}$ at each 0-diml radius, obtained from the wake survey, is shown in Fig. 60.N. It is found that the average wake fraction over the propeller-disc position obtained by pitot-tube measurements with the model propeller not mounted, called the *nominal wake fraction,* rarely agrees with the wake fraction obtained from the model self-propulsion test at the same speed, known as the *effective wake fraction.* This is a common occurrence in model testing. It indicates that the action of the propeller and the presence of the rudder have a definite influence on the wake velocities. For the ABC ship, the nominal wake fraction over the propeller disc, obtained from the wake survey and shown in Fig. 60.N, is 0.1735 at 20.5 kt, as compared to the effective wake fraction of 0.195 from the model self-propulsion test. To compensate for this difference, the local wake fraction at each radius is multiplied by the ratio of (1) the effective wake from the self-propulsion test to (2) the nominal wake from the pitot-tube survey. The method thus makes use of the wake-fraction distribution found by the wake study, with the numerical values modified so that its average over the propeller is the same as that derived from the self-propulsion test. In the ABC propeller design, the local nominal wake fraction at each radius is increased by the factor

$$\frac{0.195}{0.1735} = 1.1239 \text{ or } w_{x'} = 1.1239\, \bar{w}_{x'}.$$

TABLE 70.d—CALCULATION OF HYDRODYNAMIC PITCH ANGLE

Col. A	Col. B	Col. C	Col. D	Col. E	Col. F	Col. G	Col. H	Col. I	Col. J
$x' = R/R_{\text{Max}}$	λ/x'	$\lambda/x'(1/\eta_K)$	$\bar{w}_{x'}$	$w_{x'}$	$1 - w_{x'}$	$\frac{1 - w_{x'}}{1-w}$	$\left[\frac{1-w_{x'}}{1-w}\right]^{1/2}$	$\tan \beta_I$	β_I
0.2	1.3690	1.7483	0.196	0.220	0.780	0.969	0.9844	1.7210	59°51′
0.3	0.9127	1.1656	0.169	0.190	0.810	1.006	1.0030	1.1691	49°28′
0.4	0.6845	0.8742	0.158	0.178	0.822	1.021	1.0104	0.8833	41°27′
0.5	0.5476	0.6992	0.157	0.176	0.824	1.024	1.0119	0.7076	35°17′
0.6	0.4563	0.5827	0.159	0.179	0.821	1.020	1.0100	0.5885	30°29′
0.7	0.3911	0.4995	0.164	0.184	0.816	1.014	1.0070	0.5030	26°42′
0.8	0.3422	0.4370	0.170	0.191	0.809	1.005	1.0025	0.4381	23°39.5′
0.9	0.3042	0.3885	0.182	0.205	0.795	0.988	0.9940	0.3862	21°07′
0.95	0.2882	0.3681	0.188	0.211	0.789	0.980	0.9899	0.3644	21°01′

Col. B = λ/x, where $\lambda = 0.2738$
Col. C = (Col. B) $(1/\eta_K)$ where $\eta_K = 0.783$
Col. D; $\bar{w}_{x'}$ is obtained from Fig. 60.N, which was determined from the wake survey with the pitot tube
Col. E; $w_{x'} = 1.1239\bar{w}_{x'}$
Col. F = 1 − Col. E
Col. G = Col. F/(1 − w), where (1 − w) = 0.805 at the designed speed, obtained from self-propulsion test
Col. H = (Col. G)$^{1/2}$
Col. I Using Eq. (70.i) = (Col. C) (Col. H)
Col. J From standard tables

The calculation of β_I from Eq. (70.i) is shown in Table 70.d.

The next step is to calculate a thrust-load coefficient $d(C_{TL})_S$, at each radius, based on the ship's speed, using the formulas to be given presently. These values, when integrated over the whole radius, should give a thrust-load coefficient which is close to the desired coefficient, $(C_{TL})_S$, calculated earlier in Sec. 70.26. If the values are not close, within 1 or 2 per cent, then it is necessary to make additional approximations by modifying the hydrodynamic pitch angle β_I until the required accuracy is obtained.

The formulas necessary for executing this step are:

$$\tan \beta = \frac{V_A}{\omega R} = \frac{\lambda_S}{x'}(1 - w_{x'}) \qquad (70.\text{ii})$$

$$\frac{U_{IT}}{V_A} = \frac{2 \sin \beta_I \sin (\beta_I - \beta)}{\sin \beta} \qquad (70.\text{iii})$$

$$\frac{U_{IT}}{V} = \frac{U_{IT}}{V_A}(1 - w_{x'}) \qquad (70.\text{iv})$$

$$d(C_{TL})_S = 4\left(x'\mathrm{K}\frac{U_{IT}}{V}\right)\left[\frac{x'}{\lambda_S} - \frac{1}{2}\left(\frac{U_{IT}}{V}\right)\right] dx' \qquad (70.\text{va})$$

$$(C_{TL})_S = 4\int_{x'_{\text{Hub}}}^{1}\left(x'\mathrm{K}\frac{U_{IT}}{V}\right)\left[\frac{x'}{\lambda_S} - \frac{1}{2}\left(\frac{U_{IT}}{V}\right)\right] dx' \qquad (70.\text{vb})$$

where β is the advance angle

U_{IT} is the tangential component of the induced velocity

K(kappa; capital) represents what is known as the Goldstein factor.

Most of the relationships in the preceding paragraphs and several which appear in subsequent sections can be determined directly from the basic propeller-blade-section velocity diagram which is shown in Fig. 70.F.

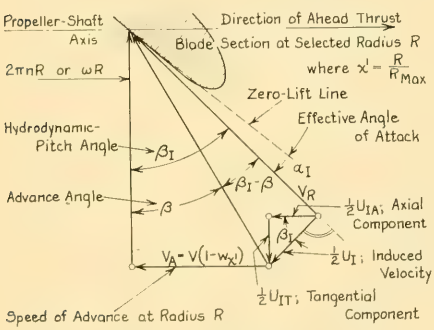

Fig. 70.F Definition Diagram for Velocity Vectors at a Blade Element

The calculations for the first approximation are given in Table 70.e. In Col. O of this table the Goldstein factor K is introduced to take into account the effect of a finite number of blades, since the fundamental theory is based upon an infinite number. Fig. 70.G shows curves of this factor for 4 blades and for various 0-diml radii, plotted on a base of $1/\lambda_I$, where $\lambda_I = x' \tan \beta_I$. Somewhat similar curves are given by J. G. Hill for 3, 4, and 8 blades [SNAME, 1949, Figs. 19, 20, 21, pp. 159–160]. For 5 or 7 blades it is necessary to interpolate between the adjacent even-blade values. This introduces a slight error but it is the best that can be done at present. The Goldstein factor K, as shown by the curves of Fig. 70.G, is calculated with certain simplifying approximations, which introduce small inaccuracies near the hub and tip sections. For this reason, new and more accurate Goldstein factors have been calculated on the TMB Univac for 3, 4, 5, and 6 blades. They are tabulated and published as graphs in TMB Report 1034 of March 1956; the graphs also appear as Figs. 1–3 on pages 326–329 of SNAME, 1955. The resultant changes in K entail slight changes of η_R in Fig. 70.D, not taken care of here.

When calculating $(C_{TL})_S$ in Col. V of Table 70.e, the small thrust developed between the $0.2R$ and the hub at $0.18R$ is neglected. At the most this would introduce only a very small error. Actually, it is negligible because this area of the blade contributes little or nothing to the thrust when the root fillets are added.

The $(C_{TL})_S$ calculated by using Eqs. (70.ii), (70.iii), (70.iv), and (70.v), as shown in Table 70.e, is 0.452 as compared to the desired value of 0.473. This is 4.4 per cent low, which is too large a discrepancy. It means that a second approximation must be made by modifying the hydrodynamic pitch angle β_I .

70.28 Second Approximation of β_I and the Radial Thrust Distribution. When modifying β_I , it is found that a 1 per cent increase in $\tan \beta_I$ causes approximately a 5 per cent increase in $(C_{TL})_S$, and vice versa. The new $\tan \beta_I$ is thus given by the formula

$$\text{2nd approx. } \tan \beta_I = \frac{\text{1st approx. } \tan \beta_I}{1 + \frac{1}{5}\left[\frac{\Delta(C_{TL})_S}{(C_{TL})_S}\right]} \qquad (70.\text{vi})$$

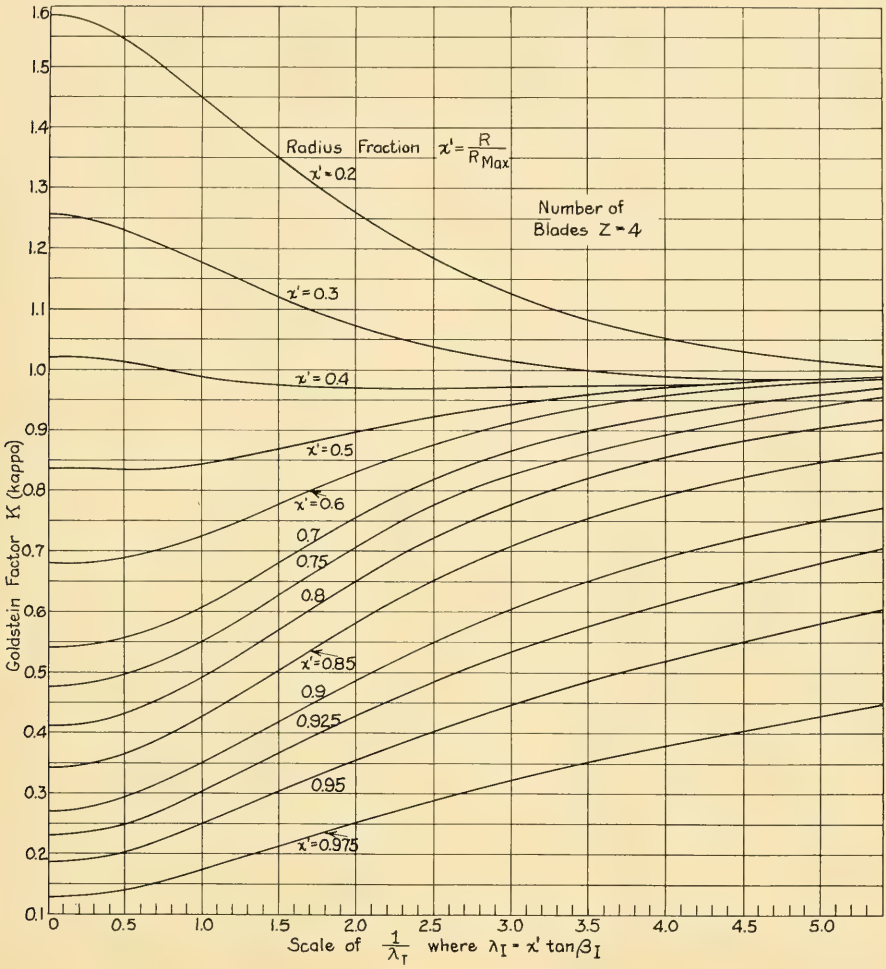

FIG. 70.G PLOT OF GOLDSTEIN FACTOR K(KAPPA) FOR A SCREW PROPELLER WITH 4 BLADES

where $\Delta(C_{TL})_S$ = 1st Approx. $(C_{TL})_S$ − Desired $(C_{TL})_S = 0.452 - 0.473 = -0.021$.

$$\text{2nd approx. } \tan\beta_I = \frac{\text{1st approx. } \tan\beta_I}{1 - \frac{1}{5}\left(\frac{0.021}{0.473}\right)}$$

$$= 1.0089\ (\text{1st approx. } \tan\beta_I).$$

The calculations for the second approximation are shown in Table 70.f. This repeats the operations in Table 70.e but with a new $\tan\beta_I$.

By the second approximation a $(C_{TL})_S$ of 0.470 is obtained, compared to the desired value of 0.473. This is only 0.63 per cent low, and is well within the required range of accuracy. It is usually found that two approximations of this kind are sufficient.

The final thrust distribution along the 0-diml radius is shown in Fig. 70.H, plotted from the data in Cols. A and T of Table 70.f.

70.29 Determination of the Lift-Coefficient Product and the Hydrodynamic Pitch-Diameter

TABLE 70.e—First Approximation of β_I and $(C_{TL})_S$

Col. A $x' = R/R_{Max}$	Col. B β_I	Col. C λ_S/x'	Col. D $\tan\beta$	Col. E β	Col. F $\beta_I - \beta$	Col. G $\sin\beta_I$	Col. H $\sin(\beta_I - \beta)$	Col. I $\sin\beta$	Col. J U_{IT}/V_A	Col. K U_{IT}/V	Col. L $\frac{1}{2}U_{IT}/V$	Col. M λ_I	Col. N $1/\lambda_I$	Col. O K (kappa)	Col. P $x'K$	Col. Q $x'KU_{IT}/V$	Col. R x'/λ_S	Col. S $x'/\lambda_S - \frac{1}{2}U_{IT}/V$	Col. T $\frac{d(C_{TL})_S}{4}$	Col. U SM	Col. V Product
0.2	59°51′	1.701	1.3265	52°59′	6°52′	0.8647	0.1196	0.7985	0.2590	0.2020	0.1010	0.3442	2.905	1.134	0.2268	0.04581	0.588	0.4870	0.0223	1	0.0223
0.3	49°28′	1.134	0.9184	42°34′	6°54′	0.7600	0.1201	0.6764	0.2699	0.2186	0.1093	0.3507	2.851	1.022	0.3066	0.06702	0.882	0.7727	0.0518	4	0.2072
0.4	41°27′	0.8503	0.6989	34°57′	6°30′	0.6620	0.1132	0.5729	0.2616	0.2150	0.1075	0.3533	2.830	0.972	0.3888	0.08359	1.176	1.068	0.0893	2	0.1786
0.5	35°17′	0.6803	0.5606	29°17′	6°0′	0.5776	0.1045	0.4891	0.2468	0.2034	0.1017	0.3538	2.860	0.936	0.4680	0.09519	1.470	1.368	0.1302	4	0.5208
0.6	30°29′	0.5669	0.4654	24°57.5′	5°31.5′	0.5072	0.09628	0.4219	0.2315	0.1901	0.0950	0.3531	2.832	0.904	0.5424	0.1031	1.764	1.669	0.1721	2	0.3442
0.7	26°42′	0.4859	0.3965	21°38′	5°06′	0.4493	0.08889	0.3687	0.2166	0.1767	0.0884	0.3521	2.840	0.852	0.5964	0.1054	2.058	1.970	0.2076	4	0.8304
0.8	23°39.5′	0.4252	0.3440	19°0′	4°39.5′	0.4013	0.08122	0.3256	0.2002	0.1620	0.0810	0.3505	2.853	0.762	0.6096	0.09876	2.352	2.271	0.2243	2	0.4486
0.9	21°07′	0.3779	0.3004	16°43′	4°24′	0.3603	0.07672	0.2876	0.1922	0.1528	0.0764	0.3476	2.877	0.593	0.5337	0.08155	2.646	2.570	0.2096	4	0.8384
0.95	21°01′	0.3580	0.2825	15°47′	4°14′	0.3423	0.07382	0.2720	0.1858	0.1466	0.0733	0.3462	2.889	0.438	0.4161	0.06100	2.793	2.720	0.1659		
																			0	1	0

Column B; β_I from Col. J, Table 70.d
Col. C $= \lambda_S/$(Col. A), where $\lambda_S = 0.34013$
Col. D Using Eq. (70.ii) = (Col. C) (Col. F, Table 70.d)
Col. E From standard tables
Col. F = Col. B − Col. E
Col. G From standard tables
Col. H From standard tables
Col. I From standard tables
Col. J Using Eq. (70.iii)
Col. K Using Eq. (70.iv), $(1 - w_{x'})$ from Col. F, Table 70.d

Col. L = ½(Col. K)
Col. M; $\lambda_I = x' \tan\beta_I$; $\tan\beta_I$ from Col. I, Table 70.d
Col. N = 1/Col. M
Col. O K is the Goldstein factor from Fig. 70.G
Col. P = (Col. A) (Col. O)
Col. Q = (Col. K) (Col. P)
Col. R = 1/Col. C
Col. S = Col. R − Col. L
Col. T Using Eq. (70.v) = (Col. Q) (Col. S)
Col. U Simpson's multipliers
Col. V = (Col. T) (Col. U)

$$(C_{TL})_S = \frac{\Sigma 3.3905 \quad \frac{4(3.3905)}{30}}{}$$

$$(C_{TL})_S = 0.4521$$

TABLE 70.f—Second Approximation of β_I and $(C_{TL})_S$

Col. A $x' = R/R_{Max}$	Col. B New $\tan\beta_I$	Col. C β_I	Col. D $\beta_I - \beta$	Col. E $\sin\beta_I$	Col. F $\sin(\beta_I - \beta)$	Col. G $\sin\beta$	Col. H U_{IT}/V_A	Col. I U_{IT}/V	Col. J $\frac{1}{2}U_{IT}/V$	Col. K λ_I	Col. L $1/\lambda_I$	Col. M K	Col. N $x'K$	Col. O $x'KU_{IT}/V$	Col. P $x'/\lambda_S - \frac{1}{2}U_{IT}/V$	Col. Q $\frac{d(C_{TL})_S}{4}$	Col. R SM	Col. S Product	Col. T $d(C_{TL})_S$
0.2	1.7363	60°04′	7°05′	0.8666	0.1233	0.7985	0.2676	0.2087	0.1044	0.3473	2.879	1.136	0.2272	0.04742	0.4836	0.0229	1	0.0229	0.0916
0.3	1.1795	49°42.5′	7°08.5′	0.7627	0.1242	0.6764	0.2801	0.2269	0.1134	0.3539	2.826	1.023	0.3069	0.06964	0.7686	0.0535	4	0.2140	0.2140
0.4	0.8912	41°42.5′	6°45.5′	0.6653	0.1176	0.5729	0.2731	0.2245	0.1122	0.3565	2.805	0.971	0.3884	0.08720	1.064	0.0928	2	0.1856	0.3712
0.5	0.7139	35°31.5′	6°14.5′	0.5810	0.1087	0.4891	0.2582	0.2128	0.1064	0.3570	2.801	0.935	0.4675	0.09948	1.364	0.1357	4	0.5428	0.5428
0.6	0.5937	30°42′	5°44.5′	0.5105	0.1000	0.4219	0.2420	0.1987	0.0994	0.3562	2.807	0.902	0.5412	0.1075	1.665	0.1789	2	0.3578	0.7156
0.7	0.5075	26°54.5′	5°16.5′	0.4525	0.0918	0.3687	0.2253	0.1838	0.0919	0.3552	2.815	0.850	0.5950	0.1094	1.966	0.2151	4	0.8604	0.8604
0.8	0.4420	23°51′	4°51′	0.4034	0.0846	0.3256	0.2096	0.1696	0.0848	0.3536	2.828	0.760	0.6080	0.1031	2.267	0.2337	2	0.4674	0.9348
0.9	0.3896	21°17′	4°34′	0.3630	0.0796	0.2876	0.2009	0.1597	0.0798	0.3506	2.852	0.590	0.5310	0.08480	2.566	0.2176	4	0.8704	0.8704
0.95	0.3676	20°11′	4°24′	0.3450	0.0767	0.2720	0.1946	0.1535	0.0768	0.3492	2.864	0.437	0.4152	0.06373	2.716	0.1731			0.6924
																0	1	0	

Col. B Using Eq. (70.vi) = 1.0089 $\tan\beta_I$; $\tan\beta_I$ from Col. I, Table 70.d
Col. C From standard tables
Col. D = Col. C − (Col. E, Table 70.e)
Col. E From standard tables
Col. F From standard tables
Col. G Col. I, Table 70.e
Col. H Using Eq. (70.iii)
Col. I Using Eq. (70.iv), $(1 - w_{x'})$ from Col. F, Table 70.d
Col. J = ½ Col. I
Col. K; $\lambda_I = x' \tan\beta_I$ = (Col. A) (Col. B)

Col. L = 1/Col. K
Col. M Goldstein factor from Fig. 70.G
Col. N = (Col. A) (Col. M)
Col. O = (Col. I) (Col. N)
Col. P = (Col. R, Table 70.e) − Col. J
Col. Q Using Eq. (70.v) = (Col. O) (Col. P)
Col. R Simpson's multipliers
Col. S = (Col. Q) (Col. R)
Col. T = 4(Col. Q)

$$(C_{TL})_S = \frac{\Sigma 3.5213 \quad \frac{4(3.5213)}{30}}{} = 0.4695$$

or 0.470

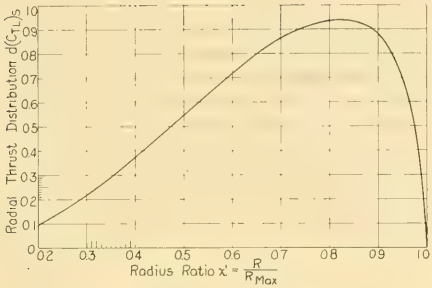

FIG. 70.H VARIATION WITH RADIUS FRACTION OF THRUST-LOAD COEFFICIENT BASED ON SHIP SPEED

Ratio. Having found the values of the hydrodynamic pitch angles β_I and the radial thrust loading which allow the propeller to develop the required total thrust, it is possible to proceed with the next phase of the calculation. This consists of finding the lift-coefficient product $C_L(c/D)$, applying the lifting-surface correction factor, and calculating the corrected hydrodynamic P/D ratio. The lift-coefficient product is determined from the following formula:

$$C_L(c/D) = \frac{4\pi}{Z}(x'\mathrm{K}) \sin \beta_I \tan(\beta_I - \beta) \qquad (70.\text{vii})$$

where c is the chord length of the blade sections and C_L is the lift-coefficient of the blade section at each radius.

Next, using the tangential induced-velocity ratio U_{IT}/V found in Table 70.f of the previous section, it is possible to compute the lifting-surface correction factor. This factor is needed because the propeller-design problem is a boundary-value problem, which at present is not amenable to exact solution. This solution would lead to a curvature of the flow which is different at the different stations along the chord length. The curvature correction by Ludwieg and Ginzel, introduced later in Sec. 70.33 and applied to the camber ratio, takes into account only the curvature at the midlength of the section. This flow curvature requires a corresponding additional curvature of the section to maintain its properties. The additional change of curvature over the chord length requires for its correction the addition of an angle of attack. This angle of attack has been determined by Lerbs on a basis of Weissinger's simplified lifting-surface theory [NACA Tech. Memo 1120, Mar 1947]. Even in the framework of this simplified theory, the calculation of the additional angle of attack is rather laborious. Fortunately, a sufficiently close approximation is obtained by using the expression:

$$\frac{\tan \beta_{IC}}{\tan \beta_I} = 1 + \frac{1}{2}\left[\frac{U_{IT}}{V} \cdot \frac{\lambda_S}{x'}\right] \qquad (70.\text{viii})$$

where $\tan \beta_{IC}$ is the corrected hydrodynamic pitch angle [Lerbs, H. W. E., "Propeller Pitch Correction Arising From Lifting-Surface Effect," TMB Rep. 942, Feb 1955].

Design experience indicates that, for destroyer-type propellers, 0.75 times the term inside the bracket of Eq. (70.viii) gives a better pitch

TABLE 70.g—DETERMINATION OF LIFT-COEFFICIENT PRODUCT, LIFTING-SURFACE CORRECTION, AND HYDRODYNAMIC PITCH-DIAMETER RATIO

Col. A	Col. B	Col. C	Col. D	Col. E	Col. F	Col. G	Col. H
x'	$\sin \beta_I$	$\tan(\beta_I - \beta)$	$\frac{4\pi x'\mathrm{K}}{Z}$	$C_L\left(\frac{c}{D}\right)$	$1 + \frac{1}{2}U_{IT}\lambda_S/Vx'$	$\tan \beta_{IC}$	P/D
0.2	0.8666	0.1243	0.7138	0.07687	1.1776	2.0447	1.285
0.3	0.7627	0.1253	0.9642	0.09214	1.1286	1.3312	1.255
0.4	0.6653	0.1185	1.220	0.09618	1.0954	0.9762	1.227
0.5	0.5810	0.1094	1.469	0.09336	1.0724	0.7656	1.203
0.6	0.5105	0.1005	1.700	0.08721	1.0563	0.6271	1.182
0.7	0.4525	0.09233	1.869	0.07810	1.0447	0.5302	1.166
0.8	0.4034	0.08485	1.910	0.06538	1.0361	0.4580	1.151
0.9	0.3630	0.07987	1.668	0.04835	1.0302	0.4014	1.135
0.95	0.3450	0.07695	1.304	0.03462	1.0275	0.3777	1.127

Col. B From Col. E, Table 70.f
Col. C From standard tables, using $(\beta_I - \beta)$ from Col. D, Table 70.f
Col. D = $[4\pi$ (Col. N, Table 70.f)$]/Z$
Col. E Using Eq. (70.vii) = (Col. B)(Col. C)(Col. D)
Col. F Lifting-surface correction factor
= 1 + (Col. J, Table 70.f) (Col. C, Table 70.e)
Col. G Using Eq. (70.viii) = (Col. F)(Col. B, Table 70.f)
Col. H Using Eq. (70.ix) = π(Col. A)(Col. G)

distribution than the fraction 1/2 shown there.

The calculations for the lift-coefficient product and the lifting-surface correction are given in Table 70.g.

Having applied the lifting-surface correction factor to the hydrodynamic pitch angle, it is possible to calculate the initial hydrodynamic P/D ratio for each 0-diml radius by the formula

$$(P/D)_{x'} = \pi x' \tan \phi \qquad (70.\text{ix})$$

where ϕ(phi) is the pitch angle and is equal to β_{IC} at this stage of the design. This calculation is also shown in Table 70.g. A plot of the P/D ratios is given by the lower curve of Fig. 70.I. The upper curve in this figure is explained later.

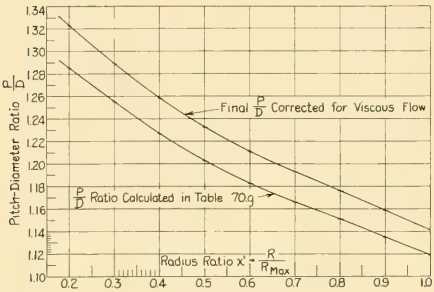

Fig. 70.I Plots of Pitch-Diameter Ratio on Radius Fraction

70.30 Finding the Blade-Thickness Distribution. The next step is to make an estimate of the blade-thickness distribution along the radius. This is based on a simplified strength calculation given by Eq. (70.x) which follows. The first term of this equation represents the compressive stress, the second term shows the increase in the compressive stress due to the centrifugal-force effect, and the right-hand side of the equation is the allowable stress.

$$\frac{C_1 P_S}{4.123 n D^3 \left(\frac{t_0}{D}\right)^3} + \frac{D n^2 i \phi_4}{12{,}788\left(\frac{t_0}{D}\right)} = S_C + \frac{D^2 n^2}{12{,}788} \qquad (70.\text{x})$$

where C_1 is a coefficient depending upon the P/D ratio at the $0.7R$. It is obtained from Fig. 70.J [RPSS, 1948, Fig. 180, p. 270; S and P, 1943, Fig. 161, p. 138]

P_S is the shaft power *per blade*

n is the rate of rotation in rpm

t_0/D is the blade-thickness fraction

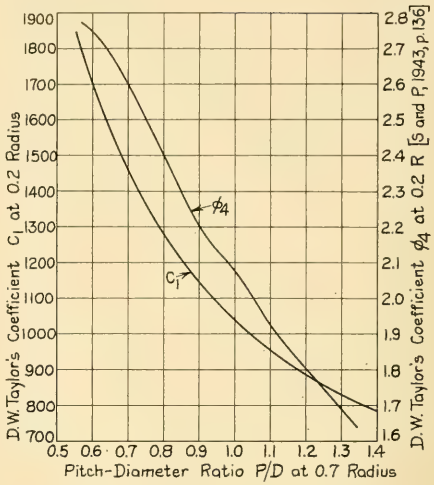

Fig. 70.J Graphs of D. W. Taylor's C_1 and ϕ_4 on Pitch-Diameter Ratio at $0.7R_{Max}$

D is the propeller diameter in ft

i is the tangent of one-half the angle of rake

ϕ_4 is a coefficient depending upon P/D at $0.7R$, obtained from Fig. 70.J [RPSS, 1948, Table 22, p. 270].

S_C is the maximum allowable stress. For manganese bronze, S_C is 6,000–7,000 psi for merchant ships or other ships that cruise near their maximum power. It is 13,000 psi for warships or other vessels that operate at full power only infrequently.

Eq. (70.x) is usually solved by assuming values of t_0/D. A plot is made of the values of the left side of the equation on a basis of t_0/D. The required t_0/D is found where the curve crosses the line given by the right-hand side of the equation.

For the ABC design, the second term of Eq. (70.x), showing the centrifugal-force effect, becomes zero since the rake angle is zero. The equation is thus directly solvable for t_0/D.

$$P_S = \frac{13{,}250}{Z} = \frac{13{,}250}{4} = 3{,}312.5 \text{ horses}$$

$$n = 97.2 \text{ rpm} \qquad D = 20 \text{ ft}$$

$$i = 0 \qquad (P/D)_{0.7R} = 1.166$$

$$C_1 = 908 \text{ from Fig. 70.F} \qquad S_C = 6{,}000 \text{ psi}$$

Substituting in Eq. (70.x)

$$\frac{(908)(3{,}312.5)}{(4.123)(97.2)(20)^3(t_0/D)^3} + 0 = 6{,}000 + \frac{(20)^2(97.2)^2}{12{,}788}$$

whence $t_0/D = 0.053$.

The radial distribution of the maximum thickness of the blade elements is obtained from the following equation, given by J. D. van Manen and L. Troost ["The Design of Ship Screws," SNAME, 1952, Fig. 11, p. 453]:

$$\frac{t_X}{D} = \frac{t_{\text{Tip}}}{D} + f\left(\frac{t_0}{D} - \frac{t_{\text{Tip}}}{D}\right) \qquad (70.\text{xi})$$

where t_X/D is the ratio of the maximum blade-section thickness to the diameter at any 0-diml radius x' and t_{Tip}/D is assumed as 0.003, a typical value.

Values of f for the various radii are:

$x' = R/R_{\text{Max}}$	0.2	0.3	0.4	0.5
f	0.788	0.665	0.551	0.443

0.6	0.7	0.8	0.9	1.00
0.344	0.251	0.162	0.079	0

The calculations for t_X/D values are made in accordance with Eq. (70.xi) and the values are set down in Col. B of Table 70.h.

Any method of strength calculation may be used in this phase, as long as the required t_X/D ratio at each radius is obtained. A designer is by no means restricted to using the formula shown in this section. The strength of the propeller is related definitely to the design problem, but is independent of the fundamental propeller theory.

70.31 Blade-Section Shaping by Cavitation Criteria. It is now possible, by using cavitation criteria, to determine the camber m_X of the meanline, the chord length c, and the lift coefficient of each blade element. This is done by the use of charts; Fig. 70.K is one of them.

To use these charts it is first necessary to decide on the blade-section shape. Modern airfoil shapes are found as satisfactory as any. They are obtained by superposing a given set of thickness ordinates on a given meanline. What happens, in effect, is that a selected airfoil section, with a straight base chord through its midwidth, is bent until this base chord becomes the selected curved meanline. In this way, all cambered airfoil sections are transformed from symmetrical sections.

The same shape is used for all blade sections from the root to the tip. Good blade sections are obtained with the NACA 16, 66, 64A, and 65A thickness forms. These, in combination with one of the meanlines recommended in the following paragraph, give airfoil sections which have low drag-lift ratios and uniform distribution of pressure along the chord length. For the latter reason they have favorable cavitation characteristics. The four recommended thickness forms are listed in the order of preference, although there is little difference among them. The NACA 66 form has zero thickness at the trailing edge; therefore, for use on marine screw propellers it must be modified slightly to give finite thickness at that edge. The other thickness distributions can be used directly without modification. The NACA 16 thickness form has performance characteristics similar to those of the TMB EPH section. The latter is a combination of an ellipse at the nose, two parabolas along the two sides, and a hyperbola at the tail; it derives its name from the first letters of these three types of curve. It is an efficient thickness form but unfortunately there is no EPH design chart available, corresponding to those for the NACA sections. A propeller designer should use it with caution because the eddying abaft its trailing edge might cause the blade to flutter or to sing. Additional comments on thickness forms are made in Sec. 70.34.

Meanlines commonly used with the thickness forms listed are the circular-arc and the so-called a = 1.0, a = 0.8, and a = 0.8 (modified) meanline. The "a" meanlines have uniform chordwise pressure distribution from the leading edge to the point designated by a = x/c, where x is a distance from the leading edge. From this point to the trailing edge the load decreases linearly. The a = 0.8 (modified) meanline has slight curvature in the decreasing portion of the load curve. Because of this pressure distribution the "a" meanlines have good cavitation characteristics. Also when combined with a given thickness form they give blade sections with less hollow on the face than if the same thickness form were used with the circular-arc meanline. The a = 0.8 (modified) meanline is usually associated with the NACA 6A-series airfoils. Complete data for the NACA 16 and 66 thickness forms and the a = 1.0 and a = 0.8 meanlines are given in NACA Report 824, 1945. The data for the NACA 64A and 65A thickness forms and the a = 0.8 (modified) meanline are given in NACA Report 903, 1948. The exact process for combining a meanline and a thickness distribution to obtain an airfoil section

TABLE 70.h—Thickness Distribution, Chord Length, and Lift Coefficient

Col. A $x' = R/R_{Max}$	Col. B t_X/D	Col. C $C_L\left(\frac{c}{t_X}\right)$	Col. D $\cos(\beta_I - \beta)$	Col. E $1 - w_{x'}$	Col. F $\frac{(1 - w_{x'})}{\cos(\beta_I - \beta)}$	Col. G $\frac{V}{V_R}$	Col. H $\left(\frac{V}{V_R}\right)^2$	Col. I $x'wR_{Max}$ lb per ft²	Col. J $p_\infty - e - x'wR_{Max}$ lb per ft²	Col. K σ_S	Col. L σ	Col. M 0.85σ	Col. N t_X/c	Col. O m_X/c	Col. P t_X ft	Col. Q c ft	Col. R C_L
0.2	0.0424	1.813	0.9924	0.780	0.7741	1.0315	1.064	128	2930	2.456	2.613	2.221	0.2000	.....	0.848	4.240	0.3626
0.3	0.0362	2.545	0.9922	0.810	0.8037	0.8416	0.7082	192	2866	2.402	1.701	1.446	.....	.....	0.724	.....	.....
0.4	0.0306	3.143	0.9930	0.822	0.8162	0.7019	0.4926	256	2802	2.349	1.157	0.984	.....	.....	0.612	.....	.....
0.5	0.0252	3.705	0.9941	0.824	0.8291	0.5971	0.3565	320	2738	2.295	0.8182	0.695	0.1250	0.0320	0.504	4.032	0.4631
0.6	0.0202	4.317	0.9950	0.821	0.8169	0.5165	0.2668	384	2674	2.241	0.5979	0.508	0.0870	0.0270	0.404	4.644	0.3755
0.7	0.0156	5.006	0.9957	0.816	0.8125	0.4538	0.2059	448	2610	2.188	0.4505	0.383	0.0612	0.0228	0.312	5.098	0.3064
0.8	0.0111	5.890	0.9964	0.809	0.8106	0.4039	0.1631	512	2546	2.134	0.3480	0.296	0.0439	0.0194	0.222	5.057	0.2586
0.9	0.0070	6.907	0.9968	0.795	0.7924	0.3630	0.1318	576	2482	2.080	0.2742	0.233	0.0319	0.0167	0.140	4.389	0.2203
0.95	0.0050	6.924	0.9970	0.789	0.7866	0.3458	0.1195	608	2450	2.054	0.2454	0.209	0.0285	0.0152	0.100	3.509	0.1973
1.0	0.0030														0.060		

Col. B Using Eq. (70.xi)
Col. C = (Col. E, Table 70.g)/Col. B
Col. D From standard tables. $(\beta_I - \beta)$ from Col. D, Table 70.f
Col. E $(1 - w_{x'})$ from Col. F, Table 70.d
Col. F = (Col. D) (Col. E)
Col. G Using Eq. (70.xii) = (Col. G, Table 70.f)/Col. F
Col. H = (Col. G)²
Col. I Reduction in head = x' (64.043) 10, in lb per ft², where 10 = $D/2$
Col. J = 3,058 − Col. I, in lb per ft²

Col. K Using Eq. (70.xiii) = Col. J/0.5ρV^2 = Col. J/0.5 (1.9905) (34.622)² = Col. J/1,193
Col. L Using Eq. (70.xiv) = (Col. H) (Col. K)
Col. M = 0.85 (Col. L)
Col. N From Fig. 70.K, entering with Col. C and Col. M
Col. O From Fig. 70.K, entering with Col. C and Col. M
Col. P = (D) (Col. B) = 20 (Col. B)
Col. Q = Col. P/Col. N
Col. R = (Col. C) (Col. N)

TABLE 70.i—Faired Chord c, C_L, t_X/c, m_X/c, and Corrected P/D Ratio

Col. A $x' = R/R_{Max}$	Col. B Faired c, ft	Col. C Faired t_X/c	Col. D Faired C_L	Col. E Faired m_X/c	Col. F k_1 for $\lambda = 0.4$ $(A_E/A_0)_3 = 1.0$	Col. G k_2 for $(A_E/A_0)_3 = 0.358$ $\lambda = 0.274$	Col. H k_3 for	Col. I k	Col. J $\frac{m_{X0}}{c}$	Col. K m_{X0} ft	Col. L β_{IC} degrees	Col. M α_1 degrees	Col. N $\beta_{IC} + \alpha_1$	Col. O $\tan(B_{IC} + \alpha_1)$	Col. P P/D	Col. Q P, ft
0.2	4.240	0.2000	0.3626	0.0224	0.858	1.17	1.05	1.054	0.0213	0.0903	63.94	0.65	64.59	2.1050	1.323	26.46
0.3	4.470	0.1620	0.4123	0.0265	0.746	1.19	1.05	0.932	0.0284	0.1269	53.09	0.74	53.83	1.3678	1.289	25.78
0.4	4.690	0.1305	0.4102	0.0276	0.643	1.20	1.05	0.811	0.0340	0.1595	44.31	0.74	45.05	1.0018	1.259	25.18
0.5	4.865	0.1036	0.3838	0.0269	0.550	1.23	1.05	0.710	0.0379	0.1844	37.44	0.69	38.13	0.7849	1.233	24.66
0.6	5.010	0.0806	0.3480	0.0252	0.469	1.27	1.05	0.626	0.0403	0.2019	32.09	0.63	32.72	0.6425	1.211	24.22
0.7	5.098	0.0612	0.3064	0.0228	0.406	1.33	1.05	0.567	0.0402	0.2049	27.93	0.55	28.48	0.5425	1.193	23.86
0.8	5.057	0.0439	0.2586	0.0194	0.365	1.40	1.05	0.537	0.0361	0.1826	24.61	0.47	25.08	0.4680	1.176	23.52
0.9	4.389	0.0319	0.2203	0.0167	0.340	1.50	1.05	0.536	0.0312	0.1369	21.87	0.40	22.27	0.4095	1.158	23.16
0.95	3.509	0.0285	0.1973	0.0152	0.331	1.55	1.05	0.539	0.0282	0.0990	20.71	0.36	21.07	0.3853	1.150	23.00

Col. B From Fig. 70.L
Col. C = (Col. P, Table 70.h)/Col. B
Col. D = (Col. C, Table 70.h) (Col. C)
Col. E From Fig. 70.K and Fig. 70.M
Col. F From Fig. 70.N, Diagram 1
Col. G From Fig. 70.N, Diagram 2
Col. H From Fig. 70.N, Diagram 3
Col. I; $k = k_1k_2k_3$ = (Col. F) (Col. G) (Col. H)

Col. J Using Eq. (70.xvi) = (Col. E)/Col. I
Col. K = (Col. B) (Col. J)
Col. L From standard tables, using $\tan\beta_{IC}$ from Col. G, Table 70.g
Col. M; $\alpha_1 = 1.8C_L$ = 1.8 (Col. D) in degrees
Col. N = Col. L + Col. M
Col. O From standard tables
Col. P; $P/D = \pi x' \tan(\beta_{IC} + \alpha_1) = \pi x'$ (Col. O)
Col. Q = 20 (Col. P)

is explained in detail in NACA Report 824, 1945, pages 3–4.

The chart in Fig. 70.K was constructed for Kármán-Trefftz blade sections. This type of section, obtained by a conformal transformation from a circle, has a circular-arc face, a circular-arc back, and a circular-arc meanline. Fig. 70.K can be used, with only a slight sacrifice in accuracy, for a circular-arc meanline in combination with various thickness forms, such as the NACA 16 or the 60–69 series. It can not be used, however, for any other meanlines. In the design of the propeller for the ABC ship the circular-arc meanline is adopted because, at the time of writing (early 1955), the chart shown in Fig. 70.K was the only one available. Similar charts for the following combinations of thickness forms and meanlines are under construction at the David Taylor Model Basin:

Thickness Form	Meanline
NACA 16	a = 1.0
NACA 16	a = 0.8
NACA 65A	a = 1.0
NACA 65A	a = 0.8 (modified)
NACA TMB Modification	a = 0.8

The fifth form listed embodies an NACA 66 nose and a parabolic tail, developed by the David Taylor Model Basin to eliminate the objectionable thin trailing edge mentioned earlier in this section.

The design chart corresponding to the blade section selected, in this case the chart reproduced in Fig. 70.K for Kármán-Trefftz sections, is entered with the cavitation number σ(sigma) and the product $C_L(c/t_X)$. The latter product is obtained at each radius by dividing $C_L(c/D)$ by t_X/D; the value of each of these terms has already been determined for the ABC propeller. The cavitation number σ is calculated by the formulas:

$$\frac{V}{V_R} = \frac{\sin\beta}{(1 - w_{x'})[\cos(\beta_I - \beta)]} \tag{70.xii}$$

$$\sigma_S = \frac{p_\infty - e - x'(R_{\text{Max}})w}{0.5\rho V^2} \tag{70.xiii}$$

$$\sigma = \frac{p_\infty - e - x'(R_{\text{Max}})w}{0.5\rho V^2}\left(\frac{V}{V_R}\right)^2 = \sigma_S\left(\frac{V}{V_R}\right)^2 \tag{70.xiv}$$

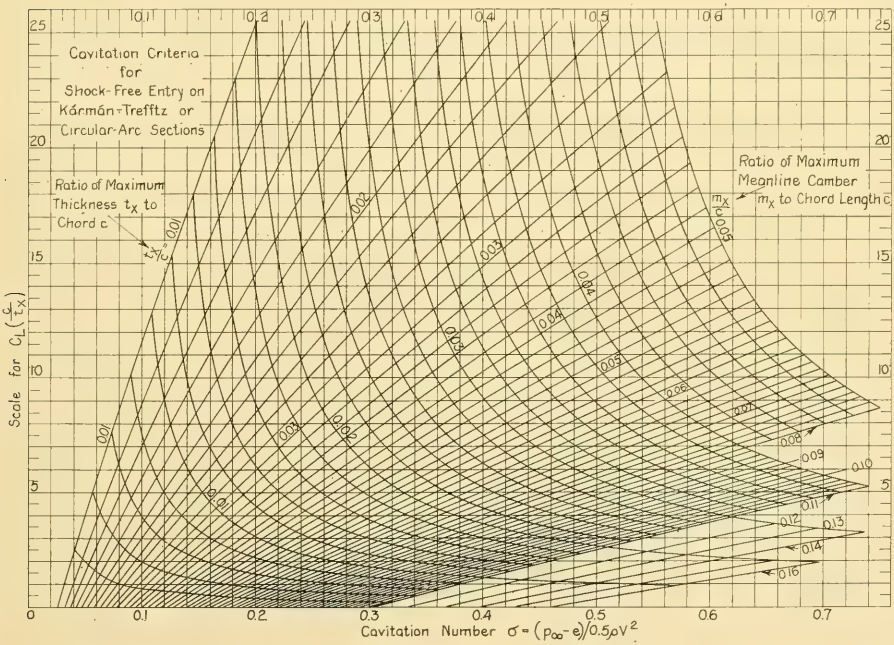

Fig. 70.K Diagram of Cavitation Criteria for Circular-Arc Camber Lines and Blade Sections

where V_R is the resultant velocity approaching the blade element

σ_S is the cavitation number at each blade element, with the blade in the upper vertical or 12 o'clock position, *based on the ship speed* V

σ is the cavitation number, based on the resultant velocity V_R

p_∞ is the static pressure at the shaft axis, or the atmospheric pressure plus the hydrostatic pressure with the ship at rest

e is the vapor pressure of salt water at an average service temperature, taken here as 0.36 psi or 52 lb per ft^2

$x'(R_{\text{Max}})w$ is a term to correct the cavitation number to each blade element, with the blade in the upper vertical or 12 o'clock position

w is the specific weight of standard salt water = 64.043 lb per ft^3

x' is the 0-diml ratio R/R_{Max} .

For the ABC ship the shaft centerline is 15.5 ft below the designed waterline. The wave crest or hollow due to the wave profile at the designed speed is ignored in these calculations. In the ABC ship, the positive wave height resulting from the crest at the stern adds a slight margin of safety against cavitation.

$$p_\infty = 14.7(144) + 15.5(64.043) = 3{,}110 \text{ lb per ft}^2$$
$$p_\infty - e = 3{,}110 - 52 = 3{,}058 \text{ lb per ft}^2$$

The remaining calculations for cavitation numbers and for the maximum-camber ratio m_X/c, the chord length c, and the lift coefficients of the blade elements at the various radii are shown in Table 70.h.

When entering Fig. 70.K to pick the ratios m_X/c and t_X/c, the value of σ is reduced by 15 per cent, as shown in Col. M of Table 70.h. It is customary to do this for all merchant ships as a safety factor to guard against intermittent cavitation which may arise from the non-uniformity of the wake in a peripheral direction. For ships in which there are highly concentrated wakes, such as those behind a bossing or a large strut, the reduction should be as much as 20 per cent. For high-speed, high-powered vessels with fast-running propellers, where it is almost impossible to avoid cavitation, no reduction in σ is made.

There are additional limiting factors in the propeller design which must be considered at this time. First, the blade-thickness ratio t_X/c at the hub section or at the $0.2R$ section should not exceed values of 0.16 for destroyer-type propellers, and 0.18 to 0.20 for merchant-ship propellers. Above these limiting values, the drag-to-lift ratio of a blade section begins to rise rapidly. Second, the lift-coefficient C_L for any blade section should not exceed about 0.6. Values greater than this give propellers with poor stopping and backing characteristics and increase the liability of air leakage from the surface.

Using the values of 0.85σ and $C_L(c/t_X)$, calculated in Tables 70.h and Fig. 70.K, the blade-thickness ratios t_X/c and camber ratios m_X/c are found only for the 0.5 to 0.95 radii. The inner radii are off the chart, which means that cavitation is of little or no concern at these blade sections. In this case, a limiting value of t_X/c of 0.20, mentioned in the preceding paragraph, is assumed at the $0.2R$ section. The $0.2R$ chord length is then calculated. This length, together with those determined from Fig. 70.K, are laid down on a sketch and a smooth expanded blade outline is drawn. The result is illustrated in Fig. 70.L. The expanded blade lengths are, for the time being, laid out symmetrical to the radial disc line. The method of introducing skew-back is described later.

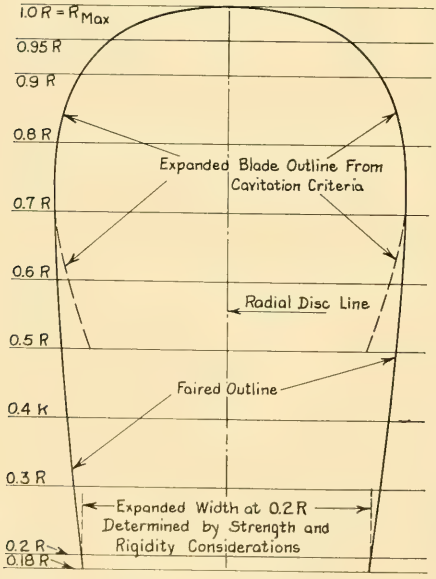

Fig. 70.L Expanded Blade Outlines with Minimum Widths for Cavitation Prevention

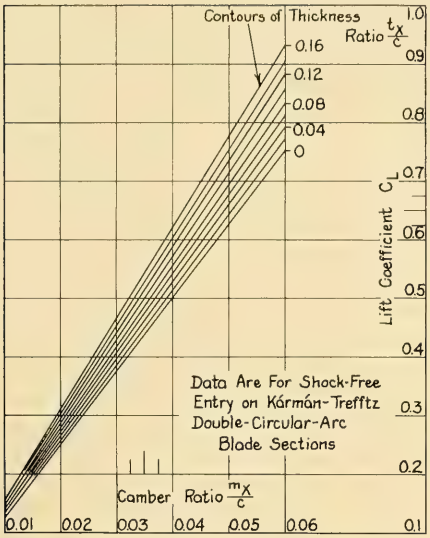

Fig. 70.M Camber-Ratio Chart for Circular-Arc Blade Sections

The faired chord lengths at $0.5R$ and $0.6R$ are greater than required to avoid cavitation. The chord lengths from the $0.7R$ to the tip are exactly as determined by the cavitation criteria. The final chord lengths for all radii are tabulated in Col. B of Table 70.i. The corresponding values of t_X/c and C_L are shown in Col. C and Col. D of that table. The final maximum-camber ratios m_X/c are obtained from Fig. 70.K. For those sections which do not fall within the limits of this graph, Fig. 70.M is used. As explained earlier in this section for Fig. 70.K, the graphs of Fig. 70.M were prepared for use with the Kármán-Trefftz blade sections and the circular-arc meanline. Fig. 70.M also can be used to give an approximate solution for the circular-arc meanline in combination with other thickness distributions. The maximum camber ratios for all radii are shown in Col. E of Table 70.i. With the faired chord lengths from Fig. 70.L, the expanded-area ratio A_E/A_0 is calculated to be 0.478. Multiplying the disc area A_0, 314.16 ft^2, by the fraction 0.478 gives the absolute expanded area, 150.17 ft^2. Dividing this area by the number of blades Z, then by the blade length, 8.2 ft, and then by the diameter D, gives the mean-width ratio $c_M/D = 0.229$.

70.32 Procedure When Cavitation is Not Involved. In many cases, cavitation is of no concern for the propeller under design and the cavitation number σ, or 0.85σ, is completely off the chart of Fig. 70.K. It is then necessary to use some other means to arrive at the blade outline and chord lengths. The usual procedure is to select these features from one of the standard screw-propeller series such as the Wageningen or TMB series. With this procedure a suitable expanded-area ratio A_E/A_0 is needed. A good first estimate of the ratio A_E/A_0 is made by using one of the cavitation diagrams of L. C. Burrill, of the Wageningen Model Basin, or of J. D. van Manen and L. Troost [RPSS, Fig. 123a, p. 186; SNAME, 1952, Vol. 60, Fig. 14, p. 455]. The referenced diagrams give the projected blade area A_P. This can be converted to the expanded area A_E with sufficient accuracy by using the following formula [RPSS, 1948, Formula 167, p. 177]:

$$A_P/A_E = 1.067 - 0.229(P/D) \qquad (70.\text{xv})$$

where P/D is the pitch-diameter ratio at $0.7R$.

The value of the developed-area ratio A_D/A_0 may be estimated by a procedure devised by J. D. van Manen [Int. Shipbldg. Progr., 1954, Vol. 1, No. 1, pp. 39–47] and described in Sec. 70.6.

Using the expanded-area ratio thus obtained, and one of the standard-screw series, calculate the values of c, t_X/c, and C_L. These values are then checked to determine whether the limiting conditions explained previously in Sec. 70.31 are met, i.e., whether $C_L < 0.60$ at all blade sections, and whether t_X/c at the hub is < 0.16 to 0.20, depending upon the type of propeller. If these conditions are not met, a new expanded-area ratio is assumed and new calculations are made. By trial and error a suitable blade area and width are finally achieved.

70.33 Corrections for Flow Curvature and Viscous Flow. Returning to the ABC propeller design, with the maximum camber ratio m_X/c determined from the faired blade outline, it is possible to apply the curvature-correction factor discussed in Sec. 70.29. This factor is obtained from the curves of Fig. 70.N, following the steps outlined on that figure. It is used in the following equation:

$$\frac{m_{X0}}{c} = \frac{1}{k}\left(\frac{m_X}{c}\right) \qquad (70.\text{xvi})$$

where m_{X0}/c is the corrected maximum camber ratio

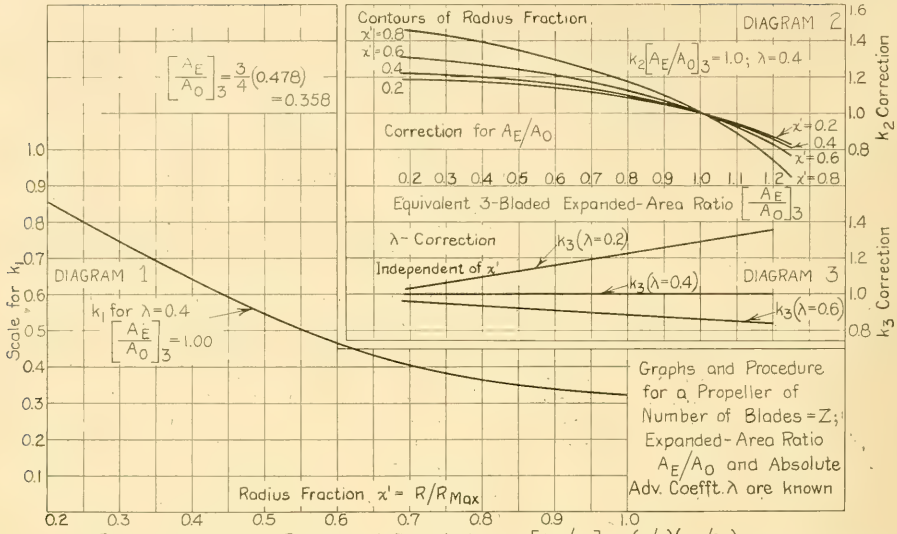

1. Reduce to 3-Bladed Propeller of Equivalent Area $[A_E/A_0]_3 = (3/Z)(A_E/A_0)$
2. Read k_1 for $\lambda = 0.4$ and $[A_E/A_0]_3 = 1.00$ from Curve of Diagram 1 for the Series of Values of x'
3. Read Correction Factor k_2 for Equivalent $(A_E/A_0)_3$, in this case 0.358, and for x' Values from Diag. 2
4. Read Correction Factor k_3 for Proper λ from Diagram 3
5. Multiply k_1, k_2, and k_3 to Obtain Final Correction Factor for Use in Eq. (70.xvi)

Fig. 70.N Graphs for Flow-Curvature Corrections

k is the correction for the curvature of the propeller flow.

The application of this correction and the calculation of maximum camber are shown in Table 70.i on page 622.

All the calculations made thus far are for a non-viscous liquid. In order to compensate for the decrease in lift which occurs in actual water, a small viscous-flow correction angle is added to the hydrodynamic pitch angle at each section. This correction depends upon the meanline. For a symmetric meanline, as embodied in the circular-arc or a = 1.0 sections, the correction is given by the following equation:

$$\alpha_1 = C_L \frac{(1 - \mu)}{0.1097} \qquad \text{(70.xvii)}$$

where α_1 is the added viscous-flow correction angle, in deg

μ is the viscous-flow factor.

In this equation 0.1097 is the slope of the lift curve for infinite aspect ratio; in other words, the increase in lift for an increase of 1 deg in angle of attack. The viscous-flow factor can be taken as follows:

(a) For a circular-arc meanline, $\mu = 0.80$
(b) For an a = 1.0 meanline, $\mu = 0.74$
(c) For an a = 0.8 meanline, μ is approximately 1.0, so that α_1 becomes zero.

For the ABC design, using a circular-arc meanline, this viscous-flow correction is simplified to

$$\alpha_1 \cong 1.8 C_L \text{ (in deg)}$$

The hydrodynamic pitch angle β_{IC} is then increased by α_1 and a new and final P/D ratio is calculated, using Eq. (70.ix). The pitch angle ϕ is now equal to $\beta_{IC} + \alpha_1$. These calculations are shown in Table 70.i. The final P/D values are listed in Col. P of Table 70.i and are plotted as the upper line on Fig. 70.I in Sec. 70.29.

Attention is called to the fact that the pitch distribution shown in the upper curve of Fig. 70.I is not typical for a normal single-screw merchant ship of the 1950's. The ABC ship has a transom stern and an unusually thin skeg; the latter probably contributes most to the unusual local wake variation shown in Fig. 60.M. The wake fraction for a normal single-screw ship is low at the tip, increasing rapidly to high values near

the hub. A wake-adapted screw for the latter type of wake variation has a pitch distribution with the P/D ratio increasing toward the tip. Just the opposite is obtained in the ABC design.

70.34 Final Blade-Section Shapes for the ABC Design by Lerbs' Method. The ABC ship propeller, designed here, has hollow blade faces in the outer sections and a mussel shape in the outer radii, similar to many German designs of World War II. Hollow-face sections are unusual for merchant-ship propellers at the time of writing (1955) but if they improve the cavitation performance of a propeller they are worth while. Taking advantage of modern production methods, hollow sections are only slightly if any more difficult to manufacture. By use of the a = 1.0 or a = 0.8 meanlines, the hollow in this case could probably be reduced or eliminated. Since the charts used in this design, shown in Figs. 70.K and 70.M, were not available for the a = 1.0 and a = 0.8 meanlines in combination with suitable thickness forms, the circular-arc meanline was employed and the hollow sections accepted. The design procedure is the same regardless of what meanline or design chart is used.

The propeller designer is cautioned, however, that screw propellers with hollow-face sections do not perform well when backing; some do not even meet normal needs for routine ship maneuvering. Whether they would in the case of the ABC ship is not determined here. For this and other reasons some propeller designers prefer to use airfoil sections at the inner radii and circular-back sections with straight faces (orthodox ogival shapes) for the outer radii.

In many cases the hollow can be removed by reducing the camber ratio m_{X0}/c until it is no more than $0.5t_X/c$, where t_X/c is the blade-thickness ratio. The loss in lift due to reduction in camber is then compensated for by the addition of an angle of attack α_2 . The pitch angle ϕ becomes $\beta_{IC} + \alpha_1 + \alpha_2$.

The added angle of attack needed to compensate the lift for any reduction in camber ratio depends on the meanline. For a circular-arc meanline, the correction is given by Eq. (70.xviii). This formula, when used with a = 1.0 or a = 0.8 meanlines, introduces only a small error.

$$\alpha_2 = 2(57.3)k\left[\Delta\left(\frac{m_{X0}}{c}\right)\right] \qquad \text{(70.xviii)}$$

where α_2 is the added angle of attack in deg

k is the curvature correction

$[\Delta(m_{X0}/c)]$ is the reduction in camber ratio.

This procedure was tried for the ABC design, but it resulted in an unfair pitch distribution and was considered unacceptable. It is more or less a trial-and-error method, i.e., the camber is reduced, an angle of attack added, and the pitch distribution checked. These three items are then adjusted until satisfactory relationships are obtained. Since the ABC ship propeller is an unusual case, the hollow-face sections are accepted rather than to adopt flat sections with an unfair pitch distribution. In the normal merchant ship, hollow sections can be avoided, if desired, by using one of the other recommended meanlines, and by adjustment of the angle of attack and camber ratio as necessary.

Hollow-face sections, as obtained in this design, undoubtedly will have satisfactory cavitation performance. However, when these sections have thin leading edges, as they would with the NACA 16 thickness forms, they are sensitive to changes in angle of attack, which occur in any wake field due to non-uniformity of flow into the propeller. A blunter leading edge reduces this sensitivity. For this reason, the NACA 65A thickness form [NACA Rep. 903, 1948, pp. 6–7] is used for the ABC ship propeller. It gives the desired leading-edge thickness with only a slight loss in the cavitation characteristics along the rest of the chord length. If the blade sections have no hollow then the NACA 16 thickness forms are better.

The NACA 65A thickness form with the circular-arc meanline gives airfoil sections which are curved near the trailing edge. The back or $-\Delta p$ side is convex to the flow, and there is a concavity on the face or $+\Delta p$ side. Again this can be avoided by using the a = 0.8 (modified) meanline, in which case the trailing-edge surfaces are straight lines.

Undoubtedly more desirable blade sections will be obtained with the new design charts, similar to Fig. 70.K, in course of preparation when the ABC project was underway [Eckhardt, M. K., and Morgan, W. B., "A Propeller Design Method," SNAME, 1955, pp. 334–338]. However, the main purpose of this chapter is to outline a method of propeller design. Availability of the new charts will not change the method.

70.35 Introducing Skew-Back in the ABC Blade Profile. Sec. 70.16 states that a good

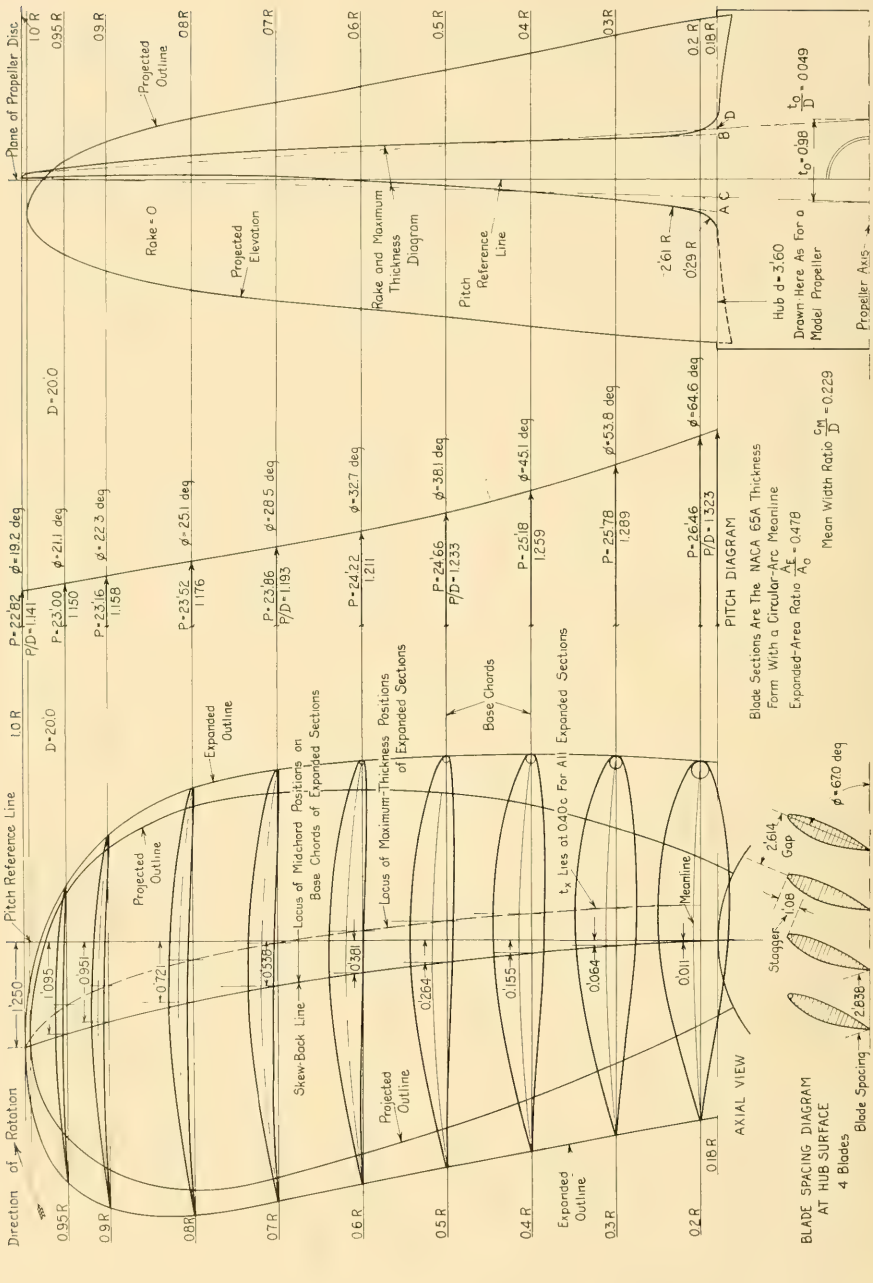

FIG. 70.0 DRAWING OF PROPELLER DESIGNED FOR THE ABC TRANSOM-STERN SHIP

range of values of the skew-back at the tip is from 0.20 to $0.25c_{\text{Max}}$. For the ABC propeller, the tip skew-back is taken as $0.245c_{\text{Max}}$ or 1.25 ft. An easy curve, representing the locus of the midlengths of the blade-section chords, is then drawn for the skew-back line, starting at the extreme-tip section and approaching the pitch reference line as a tangent at the hub. The expanded outline is laid out, half a chord length on each side of the skew-back line. From this the projected outline is drawn, explained in Secs. 32.9 and 32.10 and illustrated in Fig. 32.I. With the *projected outline* sketched in, the angular variation of the leading edge as each blade section passes the vertical plane through the 12 o'clock propeller position is checked. The interval between sections for the ABC ship propeller, drawn in Fig. 70.O of Sec. 70.36, is as follows:

$0.2R$——
1.5 deg
$0.3R$——
2.1 deg
$0.4R$——
2.4 deg
$0.5R$——
2.8 deg
$0.6R$——
2.7 deg
$0.7R$——
2.7 deg
$0.8R$——
4.4 deg
$0.9R$——

This shows a fairly regular interval and is considered satisfactory. It may be necessary at times to draw several skew-back lines before a satisfactory angular interval is obtained.

Several schemes were tried to achieve this. It was finally concluded, as related in Sec. 70.16, that the locus of the midlengths of the expanded blade sections represents the most convenient construction line. It is almost impossible to start with an arbitrary projected outline and finish with fair contours in the expanded outline.

70.36 Drawing the Propeller. All unknowns have been calculated or determined so it is now possible to delineate the propeller. The final drawing of the ABC design, following the arrangement and details laid down in Fig. 32.F of Volume I or on the SNAME PD sheet of Fig. 78.L, is shown in Fig. 70.O. A large propeller having the same general blade shape and the same characteristics, except that it has constant rather than variable pitch, is illustrated in a photograph published by The Marine Engineer and Naval Architect [Aug 1954, p. 300].

One point needs explanation. The required blade-thickness fraction t_0/D is 0.053 as calculated from the strength considerations. The blade-thickness fraction shown on Fig. 70.O is only 0.049.

The axis thickness t_0 on Fig. 70.O has been determined graphically by conventional practice [SNAME, Tech. and Res. Bull. 1–13, Jul 1953, p. 22]. As can be seen from Fig. 70.O, this convention gives a blade-thickness fraction that is not truly representative of the thickness at the hub. Thus the actual t_X, equal to AB in Fig. 70.O, is greater than CD, indicated by the construction lines for determining t_0. The propeller actually has the correct thickness required by strength considerations, and t_0/D would equal 0.053 if the face and back lines were straight. However, for the sake of uniformity, the conventional method for finding t_0 graphically should always be followed.

70.37 Calculating the Expected Propeller Efficiency. The final step in the design, by Lerbs' short method, is to calculate the expected propeller efficiency. This is given by the following relationship:

$$\eta_0 = \eta_K \frac{1 - 2\lambda_I\epsilon}{\left[1 + \left(\frac{2}{3}\right)\frac{\epsilon}{\lambda_I}\right]} \qquad (70.\text{xix})$$

where η_0 is the propeller efficiency

η_K is the ideal efficiency with jet rotation and is equal to 0.783, from Fig. 70.E

ϵ(epsilon) is the drag-lift ratio of a blade section or airfoil.

A close approximation of ϵ is given by:

$$\epsilon \cong \frac{0.008}{C_L \text{ at } 0.7R} = \frac{0.008}{0.3064} = 0.0261$$

C_L is obtained from Col. D, Table 70.i.

$\lambda_I = x' \tan\beta_{IC}$ at $0.7R$, where $\tan\beta_{IC}$ is obtained from Col. G, Table 70.g.

$$\lambda_I = 0.7(0.5302) = 0.3711$$

$$\eta_0 = 0.783\left[\frac{1 - 2(0.3711)(0.0261)}{1 + \left(\frac{2}{3}\right)\left(\frac{0.0261}{0.3711}\right)}\right]$$

$$= (0.783)(0.9367) = 0.733$$

$$\eta_0 = 73.3 \text{ per cent.}$$

By way of comparison, as discussed in Sec. 70.22, Prohaska's logarithmic chart for the Wageningen propeller series B.4.40, Fig. 70.B, indicates a P/D ratio of 1.2 and a propeller efficiency η_0 of 0.72. The same parameters as calculated by Lerbs' short method are P/D = 1.193 at the 0.7 radius and η_0 = 0.733. This shows satisfactory agreement with a good standard propeller series.

70.38 Summary of Design Steps for Lerbs' Short Method; Schoenherr's Combination. Summarizing the procedure of Secs. 70.21 through 70.37:

(1) Determine the number of blades Z, the rake, the propeller diameter D, the hub diameter d, and the rate of rotation n

(2) Calculate the thrust-load coefficient C_{TL}, the coefficient $(C_{TL})_S$, and the absolute advance coefficients λ and λ_S

(3) Determine the ideal efficiency with jet rotation η_K from Fig. 70.D

(4) With successive approximations, determine the hydrodynamic pitch angle β_I, and the thrust distribution over the blades which will allow the propeller to develop the required thrust; use Eqs. (70.i) through (70.vi) and Fig. 70.G

(5) Determine the lift-coefficient product $C_L(c/D)$, apply the lifting-surface correction, and calculate the hydrodynamic pitch-diameter ratio P/D for each blade section; use Eqs. (70.vii) through (70.ix)

(6) From strength considerations, calculate the blade-thickness fraction t_0/D, and the maximum-blade-thickness distribution ratio t_X/c; use Eqs. (70.x) and (70.xi) and Fig. 70.J

(7) Choose the type of meanline and thickness form to be used for the blade sections

(8) Using cavitation criteria, determine the maximum camber of the meanline m_X, the chord lengths c of the blade sections, and the lift coefficients C_L of the sections; use Eqs. (70.xii) through (70.xiv) and Fig. 70.K

(9) Draw and fair the blade outline and determine the final chord lengths, maximum cambers, and lift coefficients; use Fig. 70.M if necessary

(10) Apply the curvature correction to the camber ratio; use Eq. (70.xvi) and Fig. 70.N

(11) Apply the viscous-flow correction and calculate the final pitch distribution; use Eqs. (70.xvii) and (70.ix)

(12) Determine the amount of skew-back and lay out the skew-back line

(13) Draw the propeller

(14) Calculate the final propeller efficiency; use Eq. (70.xix).

The Lerbs 1954 method, described here, is considered neither too long nor too intricate for the final design of a screw propeller to go on an important or costly ship, especially as it gives the designer more flexibility in taking account of unusual conditions than a method based solely on empirical or experimental data. The calculations proper can be made by anyone who knows arithmetic, algebra, logarithms, and elementary trigonometry. The several correction factors involved in this procedure, some of them semi-empirical, will disappear with increasing knowledge. The analytic framework of this method should serve well for the insertion of results of future research and the presentation of additional useful data for the propeller designer, especially when more is known of the flow in and around the propeller position.

K. E. Schoenherr has recently [SNAME, 1955, p. 366] outlined a logical, workable combination of the propeller-design chart and analytic method embodying the following steps, adapted from the reference:

(a) The problem is first solved by the use of design charts and the methods described in PNA, Vol. II, Chap. III

(b) The method of Th. Theodorsen in his book "Theory of Propellers" [McGraw-Hill, New York, 1948] is then applied to obtain the lift-grading curve

(c) The blade area, blade width, and blade-thickness distribution are chosen to keep the propeller out of cavitation, to meet strength requirements, and to give good thickness ratios

(d) Lift-coefficient curves for the sections are calculated, if not already available, by the method of L. C. Burrill, explained in reference (39) of Sec. 70.20

(e) The angle of attack is read from the lift-coefficient curves and the final pitch distribution is obtained by smoothing out the calculated results

(f) The effective pitch obtained from the foregoing calculations is compared with the pitch obtained from the design chart as a check on the accuracy of the solution.

According to Schoenherr, "... variable wake can be introduced readily" into this design procedure.

70.39 Avoiding Air Leakage with Inadequate Submersion. For a designed-speed and a designed-load condition, assuming no severe limits imposed by the projected service of the vessel, a tip submergence so inadequate as to permit drawing air is a matter of ship rather than propeller design. Nevertheless, limitations are often imposed, and ships do have to propel themselves with reasonable efficiency at drafts (and tip submergences) less than the designed amounts.

The operation of propellers under these conditions is described in the references of Sec. 71.10 and is well summarized by W. P. A. van Lammeren [RPSS, 1948, pp. 262–263]. From this reference it "... appears that screws having blades with wide tips and circular-back sections are more likely to be free from air-drawing."

70.40 Design Comments on Propellers for the Supercavitating Range. If the cavitation noise, erosion, and vibration are not serious, a certain amount of either bubble or sheet cavitation, or both, may be tolerated on heavily loaded screw propellers, *provided* this loading represents the maximum that may be encountered under any condition of service. This is somewhat analogous to loading a boat to the gunwales *if it is known* that the boat is to encounter no waves.

When pushing screw propellers to their limit of ultimate performance, involving large $-\Delta p$'s, large real-slip ratios, and high velocities over the backs of the blades, it becomes necessary, at least in the present state of the art, to accept sheet cavitation in the running range, and heavy cavitation at that. This is the case with high-speed and ultra-high-speed planing craft, particularly racing motorboats.

It is described previously, in Sec. 23.12, that the practical limit of intensity of the $-\Delta p$ on the suction side of the blade, from which most of the lift and thrust are derived, occurs at the vapor pressure of water. As the cavitation number is lowered, sheet cavitation covers more and more of the back of each blade. The thrust falls off rapidly and the rate of rotation increases, so that the propeller serves no longer as a suitable or efficient driving mechanism for the ship which carries it.

However, if the propelling machinery is able to turn it fast enough, a rather unexpected situation develops. When finally the whole back area is uncovered and exposed to vapor pressure in the cavity a further increase in the rate of rotation usually results in a slowly *increasing* thrust. This is shown by L. P. Smith for several models of ship propellers, where, after reaching low points in the thrust curves due to cavitation, the thrust begins to rise steadily as the rate of rotation is increased [ASME, Jul 1937, Vol. 59, pp. 409–431, esp. pp. 415–419 and Figs. 6, 7, and 11]. It is also shown by R. W. L. Gawn for a pair of motor torpedoboat propellers [NECI, 1948–1949, Vol. 65, Fig. 14, p. 370], where at an advance coefficient J of about 0.62 to 0.67, the values of K_T begin to increase after reaching their minimum values. In fact, for one propeller, the K_T value at $J = 0.6$ is as high as at $J = 0.75$ and at $J = 0.83$, with a minimum value at $J = 0.67$.

Under the conditions described, not only is the pressure over the whole suction side of the blade then reduced nearly to zero absolute, representing the limit for service conditions, but the friction resistance on the back of the blade is eliminated, because moving water no longer touches it. Under these conditions the propeller is *fully cavitating*, and is said to be running in the *supercavitating range*. The flow over the blade then resembles that of the right-hand diagram in Fig. 23.I.

There has been some theoretical work done in Russia on the supercavitating propeller but, so far as known, the only published references translated into English at the date of writing (1955) are:

(1) Posdunine, V. L., "On the Working of Supercavitating Screw Propellers," INA, 1944, pp. 138–149

(2) Posdunine, V. L., "Problems in Ship-Propeller Design," Soviet Science, Feb 1941; English transl. in SBMEB, Feb 1946, pp. 69–70

(3) Epshteyn, L. A., "On the Action of the Ideal Supercavitating Propeller," Inzhenerniy Sbornik, 1951, Vol. IX. This paper lists five previous Russian references, published in the period 1943–1945.

Posdunine, in his 1944 paper, speaks of experimental proof for his claim to reasonably high thrust and efficiency in the supercavitating range. Despite his assurance that these data would be forthcoming they appear never to have been published in English.

In the discussion of Posdunine's 1944 paper by F. H. Todd, on p. 144, there are given the results of variable-pressure water-tunnel tests at the NPL, Teddington, on a screw propeller, when extended into the supercavitating range.

One feature of the design problem, upon which much more remains to be done, is that of preventing the flow, when altered by the sheet cavity over the back of one blade, from adversely affecting the pressure on the face of the following blade. This is done by:

(a) Reducing the number of blades and the blade overlap (when viewed generally normal to the blade surface) to a minimum

(b) Keeping the slip ratio low, with a reasonably low angle of attack on each blade

(c) Increasing the pitch-diameter ratio, to increase the gap between blades.

The slip ratio can only be held down by loading the propeller lightly. This may be achieved by increasing the disc area or the expanded blade area, but is best accomplished in the case of the supercavitating propeller by reducing the ship resistance and the propeller thrust to the lowest possible values. At the high speeds in question, this is only possible with planing craft in which the resistance varies as some power of the speed less than the square, possibly even less than the first power; see Fig. 53.D.

Not more than three blades, and not too wide blades at that, should be used on a propeller working for the most part in the heavily cavitating or supercavitating range. Two-bladed propellers are preferred. Pitch-diameter ratios should probably exceed 1.4, and may run as high as 2.0 or more.

If it is known that a propeller will cavitate fully throughout the running range, its blade sections may be of triangular shape, with blunt or square trailing edges. The blade speed is so extremely high, and the static pressure usually so low that the water can not possibly close in behind even a fair blade section. Wedge-shaped propeller blade sections for supercavitating propellers are discussed by G. Rabbeno [Ann. Rep. Rome Model Basin, 1938, Vol. VII, p. 91]. The stiffness—and strength—of the blade may be concentrated in the metal near the trailing edge, enabling the leading edge and the blade section to be considerably finer than normal. Comments on supercavitating flow past foils and struts, applicable to the propeller-design problem, are given by M. P. Tulin ["Cavitation in Hydrodynamics," NPL, Oct 1955, paper 16; SBSR, 3 Nov 1955, pp. 570-571].

For the ultra-high-speed screw propeller which provides the dynamic lift for holding up the stern of a very fast planing craft, with the propeller shaft, the struts, and the propeller hub normally out of water, it is important that there be a stabilizing influence to hold the stern of the boat at its proper level. One solution is to set up a compensating downward vertical force known as the "antilift." This force exceeds the dynamic upward lift created by the lower blades if the propeller rides too high but it is less than the upward lift if the propeller rides too low. Means of incorporating this feature in a propeller design are described in considerable detail by E. C. B. Corlett [The Motor Boat and Yachting, Sep 1954, pp. 387–388].

70.41 Design of Bow Propellers, Coupled and Free-Running. Bow propellers are either driven by independent engines, at a speed suitable to the needs of the moment, or they are, in the case of many double-ended ferryboats, coupled to the engine and the stern propeller by a straight-through shaft. Icebreakers with bow propellers are in the first category, along with the larger ferryboats, where fuel economy is important.

Icebreakers and other vessels with bow propellers are usually required to back hard upon occasion, or to run in the opposite direction. The bow propeller then becomes the stern one. Under these conditions symmetrical sections are employed, with straight meanlines. Actually, since the propellers rotate in opposite directions at different times, the sections are elliptical or lens-shaped, symmetrical on each side of the midchord position, similar to those of Fig. 70.A [S and P, 1943, Fig. 153, p. 132, Type 3]. What might be termed double-symmetrical blades of this kind, running in the open, give identical performance when rotating one way or the other.

70.42 Open-Water and Self-Propelled Model Tests. No existing propeller-design procedure is sufficiently comprehensive and reliable to give an *accurate* prediction of the open-water performance of a screw propeller built to a particular design, either on model or full scale. When the new propeller design is only slightly different from that of a propeller which has already been tested it would appear that the designer could be reasonably certain of predicting its performance. Nevertheless, minor changes which seem insignificant often produce appreciable differences in performance. One never knows when this will happen.

It seems wise, therefore, in the case of a new propeller design, to build a model and to test it, (1) in open water, (2) in a variable-pressure water tunnel, and (3) in a self-propelled model of the ship for which it is designed. Unfortunately, it was not possible to do this for the wake-adapted propeller designed in Secs. 70.21 through 70.37, nor to include the test data in Chap. 78.

70.43 Mechanical Construction; Type of Hub; Shaping and Finish of Blades. The mechanical design and the details of construction of screw propellers, of both the solid and the built-up types, have become rather well standardized in the past century. They are described and illustrated by R. H. Tingey [ME, 1942, Vol. I, pp. 267–293, esp. pp. 291–293] and by the authors of up-to-date handbooks on marine engineering.

The choice of whether a particular design of propeller is to be of the solid or built-up type is usually made by the owner and operator, often based upon considerations far removed from hydrodynamics. The marine architect is called upon only to state how much reduction in efficiency is involved if the wheel is built up. This depends upon the ultimate size and shape of the hub, including the flanges at the roots of the blades, the fairing of the bolts and nuts for these flanges, the fairing of the whole hub into the hull, and other features. The probable reduction in efficiency on the ship, mentioned in Sec. 70.14, is of the order of 2 or 3 per cent. If a solid propeller has an efficiency η_0 of 0.70 the equivalent built-up propeller may have an η_0 of $(0.70)(0.97) = 0.679$. In what are known as *points*, often used by marine engineers to indicate a change in percentage numerals, this is a reduction of $(70 - 67.9) = 2.1$ points.

As a means of reducing this loss and retaining the demountable-blade advantage, there are several possibilities which call for comment:

(1) The built-up propeller *without* adjustable features. In the orthodox design, followed for many decades, the base or bolting flange of each blade is circular. This permits some adjustment in geometric pitch when the blade is bolted firmly in place on the hub. However, if the blade is shifted in this process, the shift must be a *constant angle* $d\phi$ for all blade sections. This is by no means equivalent to a constant change in linear pitch P, or even to a constant percentage change in P, because $P = 2\pi R \tan \phi$ and the distance $2\pi R$ changes with radius. The great number of solid propellers in use indicates a small need for the adjustable feature and for changing pitch in service. By eliminating the adjustment in angle, and with it the need for the circular base flange on each blade, it is possible to make the blades *detachable* or demountable without greatly increasing the size of the hub.

(2) It appears almost certain that in the not-distant future there will be developed a strong, not-too-expensive, corrosion-resisting, weldable ferrous alloy for propeller blades which will permit the separate blades of a screw propeller to be cast individually with specially shaped root palms and welded to a steel hub, or to an enlargement on a short stub shaft. An arrangement diagram of the latter scheme, for the arch-stern ABC ship, is sketched in Fig. 74.L.

(3) The availability of a strong, rigid, ferrous alloy will, among other things:

(a) Enable the larger propellers, whose shipment is expensive and inconvenient, to have their hubs and blades assembled by welding at the yard where the ship is built. Annealing of the welds is possible by induction heating.

(b) Eliminate the trouble, expense, and vulnerability of tapered fits, keyways, keys, screw threads, and nuts necessary to attach the present propellers to their shafts. Bolted flanges are much simpler and more reliable.

(c) Eliminate the need for galvanic-action protectors in the neighborhood of bronze propellers, with their never-ending added drag and continual expense

(d) By the use of plated chromium or some other material, such as on the stub shaft projecting abaft the ABC ship propeller in Fig. 74.L, eliminate the need for bronze bearing sleeves on steel shafts.

Constant pressure and attention applied to the manufacture of more accurate propellers for the past two or three decades, that is, propellers conforming more nearly to the design drawings, has produced valuable results. Tolerances of plus or minus 1/4 per cent in mean face pitch over a blade, and of plus and minus 1/2 per cent in local pitch variation, are now being approached or exceeded. Blade thicknesses in important positions are being specified and measured. This is excellent as far as it goes, but it still leaves as unspecified the *shape* of the entire back or $-\Delta p$ surface of the blade. However, there is a growing appreciation of the importance of back shape among owners and operators as well as among propeller designers. Lack of suitable equipment to make measurements on large propellers, both during manufacture and inspection, is delaying progress along this line.

Edge shapes of propeller blades are important. These require delineation on the drawings by large-scale details or by geometric dimensions,

described in Sec. 70.19. They are rather easily checked by small full-scale templates.

Considering that the surfaces of a screw-propeller blade almost always travel through the water faster than the ship, and the surfaces of the outer portions often several times as fast, the blade surfaces should be as smooth as modern tools and techniques can make them. Indeed, in keeping with the necessity for smaller roughness tolerances on a large ship than on its model, to make the two surfaces hydrodynamically smooth, the full-scale propeller surface should actually be smoother than that of its model.

In particular, no lifting holes should be drilled through the blades, contrary to the design shown by R. H. Tingey [ME, 1942, Vol. I, Fig. 1, p. 268], nor should nicks and bent-over portions of the edges be permitted to remain after the first opportunity to repair them. It often happens that, if the dock trials are run with the ship's own propellers in place, pieces of wire rope and other debris which have been dropped overboard at a fitting-out dock may be picked up by the propellers, with damaging effects. If a ship's propellers have been so menaced, it is wise to have all blade edges examined by a diver after the vessel is in clear water, before it is permitted to undertake standardization and acceptance trials.

In this connection the following is quoted from the Conclusions of the Sixth International Conference of Ship Tank Superintendents, 1951, page 10:

"6. The Conference re-emphasizes Decision 2 of the 1948 Conference on this subject, which stated that 'It is necessary that the model propellers should be made to a high degree of precision and in all published work the measured tolerances and the quality of the surface finish should be stated.'"

How to keep this ship-propeller surface smooth, even on the "stainless" metals which are essentially resistant to corrosion and erosion, is still a problem, but one for metallurgists rather than marine engineers.

70.44 Blade Strength and Deformation. On many if not most screw propellers it is necessary to shape the root sections, and possibly also some others, to give the necessary strength and rigidity to the blades. On icebreakers and iceships, structural considerations may outweigh those of hydrodynamics. However, it is not possible in this book to devote space to this feature, other than has already been done in Secs. 70.19 and 70.30.

Rather complete procedures for determining blade thicknesses adequate for strength and rigidity, and for calculating stresses in the blade material, are found in the following references:

(a) Schoenherr, K. E., SNAME, 1934, pp. 113–114
(b) Schoenherr, K. E., PNA, 1939, Vol. II, p. 157
(c) Taylor, D. W., S and P, 1943, Chap. 29.3, pp. 127–141
(d) Tingey, R. H., ME, 1942, Vol. I, pp. 281–291
(e) Van Lammeren, W. P. A., RPSS, 1948, pp. 269–273
(f) Hecking, J., "Strength of Propellers: Analysis Made in Connection with Classification Rules at the American Bureau of Shipping," MESA, Oct 1921, pp. 762–767.

It may very well be that elastic deformation under heavy load of the blades of a nearly perfect "static" design will modify rather appreciably the shape and the performance contemplated by the designer. This is a manifestation of hydroelasticity, described in Sec. 21.5 and mentioned in Sec. 70.13. Furthermore, this deformation may take place periodically and in varying amounts as a blade rotates through a complete revolution, leading to blade vibration and other objectionable results.

It is interesting to note in this connection the comments made by Dixon Kemp in the late 1890's in his treatise on yacht design ["Yacht Architecture," Cox, London, 1897, 3rd ed., p. 284]:

"There would seem to be some advantage if the blades are elastic, and bend whilst revolving, especially in the case of small vessels; and Messrs. Yarrow have recorded a case within their experience of torpedo boat propulsion where, by submitting a thin elastic blade for a perfectly rigid one, the speed was altered from 17½ knots to 19 knots."

It is unfortunate that no record has yet been found of the shape and materials of these thin, elastic blades, nor an explanation of their superior performance.

To return to a consideration of modern wheels, the propeller designer is advised to sketch a so-called deformation diagram of his propeller, in which the estimated deformations under thrust load are greatly exaggerated for emphasis. The aim is to delineate the shape of the propeller blade under load and to determine changes in pitch at various radii. Procedures for constructing these diagrams are as yet not well formulated but a few hints may be helpful for guidance:

(a) The thrust forces are exerted roughly normal to the line joining the nose and tail of each section. The drag force may be neglected because it acts generally in line with the chord of each section.
(b) At the effective angles of attack normally

encountered, and with hydrofoil or airfoil section shapes, the lift force may be expected to act at a point between 0.25c and 0.40c abaft the nose of each section

(c) The bending forward (in the direction of thrust) of cantilevered screw-propeller blades due to thrust load is usually not diminished as the designed thrust-load factor decreases because the blades are made thinner in an effort to increase the efficiency

(d) The centrifugal forces acting on raked blades are functions only of the amount of *actual* rake, taking deformation into account, the radii of the sections involved, and the rate of rotation ω(omega).

The deformation of heavily loaded screw-propeller blades is best counteracted, not by thickening the blades but by using materials of the highest practicable modulus of elasticity. The nickel-copper alloys and the corrosion-resisting chromium-iron alloys are considerably superior to the best bronzes in this respect, although accurate data as to elastic moduluses are often difficult to obtain.

Screw-propeller blades which have long, thin trailing overhangs such as those of the weedproof type shown in diagram 12 of Fig. 32.L and those fitted on the liner *Normandie* in the early 1940's, almost certainly suffer some bending of the overhang in an ahead direction. This reduces the geometric pitch angle ϕ, straightens out the mean-line, and diminishes the blade camber in that region. The net effect is to reduce not only the local but the overall lift of the blade sections at those radii. A slight additional camber of the overhung portions may well be introduced to overcome this deformation and to make all the blade area work effectively.

On a propeller which is loaded moderately or heavily, the blades are *never* skewed to an appreciable extent in the forward or ahead direction. Were this done, the centers of pressure on the outer elements, lying near the forward quarter- or third-points of these elements, would be much farther ahead of the torsion axis in the root sections of the blade than they are abaft that axis in a blade swept or skewed normally aft. This would mean a greater twisting moment forward, and a greater *increase* in the geometric pitch angle ϕ than the reduction in that angle when the blades are swept back. This increment $\Delta\phi$ increases the effective angle of attack α_I, increases the lift on the outer elements, and increases the twist deformation. The effective angle of attack α_I thereupon becomes still greater. A vicious cycle continues until the vessel speeds up to match the increased thrust, the engine slows down because of the increased torque, or the blade takes a permanent set in twist.

A sequence of events of this kind is encountered when a heavily loaded propeller with swept-back blades has its direction of rotation reversed, as during a crash-back maneuver. The greatly disturbed condition of the water around it probably saves the propeller but at least one case is on record where blades have been bent in a sudden high-power reversal.

70.45 Propeller Materials and Coatings to Resist Erosion. One of the most satisfactory materials now known for use in screw propellers which must resist corrosion, erosion, and impact from sand, ice, and the like is an alloy composed of approximately 14 per cent chromium and 86 per cent iron. This alloy is capable of heat treatment to give yield points of the order of 70,000 lb per in^2. As for other iron alloys, the yield point is fairly definite; this is not the case for the bronzes and brasses containing large quantities of copper. The proper kinds of corrosion-resisting irons and steels have proved in practice their ability to withstand severe usage on vessels which must work in the ice.

A corrosion-resistant alloy of austenitic characteristics was employed by the Germans some years ago for the propellers of destroyers and similar naval vessels. This is an alloy containing 22 per cent chromium and 11 per cent nickel, with most of the remainder composed of iron. Screw propellers of this alloy require special casting techniques, special cutting tools, and tedious machining procedures but once fabricated they stand up well in service. Examples are the two corrosion-resisting steel propellers removed from the German destroyer *Z37* and now (1954) on exhibition at the Engineering Experiment Station at Annapolis, Maryland.

Some comments on cavitation erosion and means of preventing it on marine propellers and other appendages are given by S. F. Dorey [Jour. Inst. Metals, Great Britain, Jul 1954; ASNE, Feb 1955, pp. 94–96]. On page 95 of the latter reference appears the following, modified slightly for emphasis:

"A reasonable assessment of the erosion-resistance of an alloy is given by the product of (1) the surface Brinell

hardness number and (2) the erosion-fatigue resistance expressed in tons per in^2 for 50 million cycles of reverse bending. The more highly resistant alloys have values in excess of 800, and in descending order of merit they include:

(a) Austenitic stainless steels
(b) Aluminum bronzes, with or without nickel additions
(c) Low-nickel stainless steels
(d) Silicon monel
(e) Monel metal
(f) High-tensile bronze
(g) Turbadium bronze.

"Below 800 are placed the normal:

(h) Manganese bronzes
(i) Silicon bronzes
(j) Phosphor bronzes
(k) Gun metals
(l) Cast irons
(m) Aluminum alloys.

"This does not imply that the manganese bronzes which have given such good servide have poor resistance, but they are used purely as a basis of comparison."

Designs and techniques have been evolved, and are in use on the blades of propeller-type turbines in hydroelectric plants [ASNE, Nov 1946, pp. 547–549; Maritime Reporter, 1 Mar 1955, p. 17], whereby a thin corrosion-resisting steel cladding is applied to a cast-steel blade by welding, either in the form of a multitude of welding beads from corrosion-resistant rod or a thin sheet of rolled corrosion-resisting metal.

It is entirely possible that some form of plastic coating may be evolved which will protect a blade from minor mechanical damage. This coating might resist the action of sand and mud, prevent corrosion, resist erosion by cavitation, and serve as an insulating layer over a copper alloy so that no galvanic-action protectors would be needed on the adjacent steel surfaces of the hull and the appendages. To make such a coating reliable and successful, however, will undoubtedly call for a special application procedure, involving the following operations:

(1) Heating the entire propeller in an oven for a considerable period, to drive out all the moisture in the interstices between the metallic crystals
(2) Subjecting the heated propeller to an almost complete vacuum, to pull out not only all the moisture but all the gases to be found within the metallic structure
(3) Application of a sealing compound while the propeller is still heated and under a vacuum, to fill up all the internal crevices and pockets where gases or moisture might otherwise collect
(4) Application and curing of a durable plastic coating to all the external surfaces except those which have to be in metal-to-metal contact with the propeller shaft.

It is believed that the blistering and other difficulties with plastic and similar propeller coatings in the past have arisen from the presence of moisture and gases within the metal proper, underneath the coating. The procedure outlined in the foregoing is similar to that which was found necessary and which has been employed successfully for many years in vacuum-impregnating the wound coils of electric motors and other electric devices.

70.46 Prevention of Singing and Vibration. It is assumed in Sec. 23.7 that the singing of propeller blades is due to the alternating circulation component around a blade section, and the periodic variation in lift, accompanying the shedding of alternate vortexes in a vortex street or trail. It is possible to relate the frequency of lateral vibration with the blade velocity, the Strouhal number S_n, and the Reynolds number R_n *provided* the diameter or transverse dimension of the vibrating (and eddy-creating) body is known. This transverse dimension corresponds generally with the thickness t in Fig. 70.P,

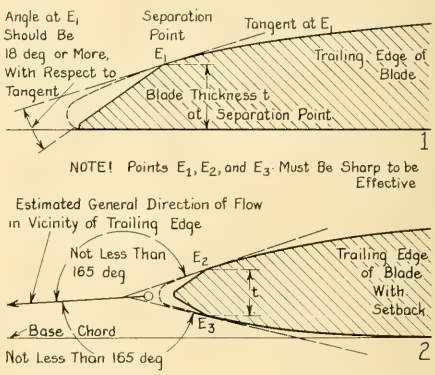

FIG. 70.P SKETCH OF CHISEL TYPE OF TRAILING EDGE
To eliminate singing effectively it is most important that the corners at E_1, E_2, and E_3 be *sharp*, to create definite, fixed separation points there.

roughly abreast the average position of the separation points E on one or both sides of the blade. If the trailing edge of the section were approximately semi-circular it would be easy to estimate the value of t, but difficult to confirm it.

For a complex shape of trailing edge, as in the figure, the effective thickness is both difficult to estimate and to confirm. A means of making a tentative prediction is given by F. Kito [Zōsen Kōkai, Japan, May 1948, No. 277; also Abstract Notes and Data for 6th ICSTS, 1951, pp. 41–42 (in English)].

From Sec. 2.22 the Strouhal number is

$$S_n = \frac{fD}{U}, \text{ or } f = S_n\left(\frac{U}{D}\right) = S_n \frac{V_{\text{Blade}}}{t} \qquad (70.\text{xx})$$

Here f is the vibration frequency, lying within the audible range to produce singing, generally above 10 per sec and below 10,000 or 12,000 per sec. Practically, the highest audible frequency of a singing propeller is about 700 to 1,200 cycles per sec. The velocity U is the blade velocity V_{Blade}, obtained by combining vectorially the rotational velocity $2\pi nR$ with the advance velocity V_A. The blade velocity varies with radius R, with rate of propeller rotation n, and with ship speed V. The maximum occurs at or near the tip at full designed speed; the minimum at some smaller combination of the three variables. As a low limit it should be satisfactory to use $R = 0.4R_{\text{Max}}$, $n = 0.5n_{\text{Max}}$, and $V = 0.5V_{\text{Max}}$.

The blade-section Reynolds numbers R_n are calculated for these two extremes, and from the graph at the left in Fig. 46.G the corresponding limiting values of S_n are found. The value of t for the limiting radii is then estimated and from Eq. (70.xx) the frequency f is calculated. If f lies within the audible range, objectionable singing is possible. An example illustrating this procedure is worked out in Sec. 46.9.

If singing is thought probable, or if it is actually occurring, it is almost invariably prevented or eliminated by the use of the so-called chisel edge, sketched in heavy lines in Fig. 70.P. Provided there is no large slope well ahead of the trailing edge where separation might begin, the two corners thus formed comprise two definite and *fixed* separation points at the upstream end of a narrow separation zone between them. The eddy pattern in this zone remains sensibly steady, to the extent that any eddy pattern can do so. At least, the circulation around the blade does not vary periodically, with a frequency in the audible range, nor does it fluctuate in magnitude at any such frequency.

Other methods of providing fixed separation points along the trailing edges of propeller blades, to prevent singing, are shown by J. A. van Aken [European Shipbldg., 1955, Vol. 4, Fig. 3, p. 31].

The singing propeller is discussed briefly by F. M. Lewis [ME, 1944, Vol. II, p. 131]. A partial list of references relating to singing propellers is given in Sec. 46.10.

CHAPTER 71

The Design of Miscellaneous Propulsion Devices

71.1 General Considerations. The screw propeller is now so widely employed for propulsion in water that almost any other type of device is unusual by comparison. Likewise, in a program of research, experiment, and development that is in keeping with the total number of propulsion devices employed, a very large proportion has been devoted to screw propellers. As a result, the design of other types has suffered rather severely. In fact, in most books of this kind the discussions of other propulsion devices are limited to brief mentions only. Design notes and rules for these miscellaneous devices are notable by their absence. This situation is not easily nor quickly remedied, hence the notes and comments for these devices, in this chapter, are by no means as comprehensive, definite, and helpful as they should be.

Although the title does not so indicate it, this chapter treats also of certain design aspects when screw propellers and other propulsion devices are intended to work in unusual positions. Examples of this are under-the-bottom screw propellers, tandem propellers, and contra-rotating propellers.

The order of subjects in this chapter follows in general those of Chaps. 15 and 32 in Volume I.

Data for predicting the performance of propulsion devices of all types, or references to those data in the literature, are given in Chap. 59.

71.2 Design Features of Paddletrack Propulsion. Paddletrack propulsion is mentioned briefly in Sec. 15.4, described in Sec. 32.2, and illustrated in Fig. 32.A.

Very little analytic work has been done on paddletracks and there has been only a moderate amount of *systematic* experimentation on model and full scale. Correlation of the large number of specific tests, on both self-propelled models and full-scale craft, made in the United States during the period 1940–1955, is difficult and time consuming, so much so that it may not be undertaken or completed for an indefinite period.

The hydrodynamic design requirements for reasonably efficient paddletrack propulsion in the water have been pushed rather far in the background by the need for closely spaced cleats which will insure adequate traction and support on the ground. It so happens that almost any kind of deep cleat gives some measure of propulsion in the water (or in liquid mud) but only certain cleat designs provide substantial support and withstand severe usage over any type of ground, including submerged rocks, reefs, and concrete roads.

For the reasons given, no attempt is made here to furnish design notes or criteria for paddletrack propulsion.

71.3 Notes on the Hydrodynamics of Paddlewheel Design. It is reported that S. W. Barnaby, in his treatise on propeller design of 1885, stated that "As a propelling instrument the paddle is not inferior to the screw and some of the best recorded performances have been obtained with it." Screw-propeller performances have improved since then but so have those of the paddlewheel, especially of the feathering type.

There are many rivers in the so-called navigable areas of the world in which the depth of water is of the order of 2 or 3 ft only, and in which trees, logs, and all manner of debris, floating and waterlogged, are constantly encountered. Under these conditions paddlewheel or sternwheel propulsion is almost a necessity [Hobson, C. A., "Sternwheel Vessels for River Work," Ship and Boat Builder and Naval Architect, London, May 1953, pp. 371–377].

Paddlewheels are still to be considered for pleasure steamers, tugs, and other craft plying on the smooth, shallow waters of lakes, estuaries, and rivers, where draft restrictions prevent the use of screw propellers large enough to give high or even moderate efficiencies. If the paddles are separately driven, as on many European tugs, the maneuverability can not be approached by any other type of propulsion except multiple rotating-blade propellers diagrammed in Fig. 37.P.

The low rate of rotation n of paddlewheels does not match the high n of most modern propulsive machinery, but the current and future developments in reduction gearing and flexible couplings give promise of adequate means for utilizing both, while retaining their individual advantages.

Although the paddlewheel does not retain the prominence it once enjoyed, it is still reckoned as one of the standard ship-propulsion devices, for which design data should be available. For this reason, and because the paddlewheel data in the literature are rather scanty and widely scattered, some space is devoted here to a more-or-less systematic presentation of them.

Judged on the basis of the rotating-blade propeller and the screw propeller with a Kort nozzle, both reasonably acceptable as shallow-water propulsion devices, the efficiency curves of Figs. 34.M and 34.N reveal the paddlewheel as a rather poor third. If, however, corresponding curves were added for screw propellers working under tunnel sterns, as alternatives for shallow-water propulsion, it would be found that they too had low efficiencies. In fact, it is believed that the latter will average about 0.4 at reasonable thrust-load values, and that these efficiencies will rarely approach or exceed 0.5 in actual service. Provided, therefore, that the thrust-load factor of a paddlewheel design can be kept between 1.0 and 0.5 or below, it need not suffer from the handicap of low propulsive efficiency for its particular applications.

The action and geometry of the feathering paddlewheel, a type which is almost universally used when the propulsive efficiency is important, are described in Sec. 32.3 and illustrated in Fig. 32.B. The text and drawings include definitions of the various hydrodynamical and mechanical terms. Diagram 2 of Fig. 15.G indicates that the effective thrust-producing area of a pair of side paddlewheels, equivalent to the disc area A_0 of a screw propeller, is equal to the combined (transverse) length $2s$ of the blades of both wheels times the maximum immersion of their lower edges, known as the *dip*. The dip ratio is the dip, measured to the at-rest WL, divided by the blade width or height h.

Based upon the principle that the most efficient propulsion takes place when the least $+\Delta U$ value is imparted to the greatest mass of liquid, the blades of an efficient paddlewheel should have the greatest area (transverse length times radial width or height) consistent with a balanced wheel-and-ship design. Plunging the blade into the water and lifting it out again constitutes unwanted and undesirable motion and involves wasted energy in the water. The blades are therefore as long, parallel to the water surface, as their positions and as operating requirements permit. In other words, blade area is achieved preferably with blade length measured transversely, rather than with radial width or height. Theoretically, since the ships on which modern paddlewheels are fitted encounter waves only on rare occasions, there are apparently no limits to the transverse length of blade except those imposed by mechanical and structural considerations. When the blade length becomes excessive, with undue twisting of the blade on a feathering wheel, two separate paddlewheels, side by side, are mounted on each side of the vessel and keyed to the port and starboard ends of a single shaft, with a separate feathering mechanism for each of the four assemblies. However, if the blades are too large and the thrust loading is too small, too great a proportion of the work is expended in blade friction through vertical motion, and there is too much churning through plunging each blade into the water and lifting it out again. Like a screw propeller, the paddlewheel can have too much blade area for its own good.

The volume swept through by an immersed blade is partly boundary layer, with an average U less than the ship speed V, and partly a potential-flow region where the average U is almost

certainly greater than V. Since so little is known of these velocities for the paddlewheel positions on ships, especially as the wheels extend outward from one-third to one-half the beam, it is customary to assume that the speed of advance V_A and the ship speed V are the same.

There has been in the past some difference of opinion among commentators and designers with regard to the radius at which the tangential velocity of a paddlewheel blade is to be measured, for the purpose of determining the slip ratios. By some this velocity is measured at a radius corresponding to the distance from the wheel center to the bottom of a blade in its lowest position. Twice this radius is roughly the overall wheel diameter, leaving out of account the angularity of feathering blades as they swing around the circle and the presence of external rings serving as guards and as ties between the arms. "The actual slips can only be determined by careful analysis of the path of the paddles at given speeds of boat and wheels" [Taylor, S., SNAME, 1908, p. 245; Stevens, E. A., Jr., SNAME, 1908, p. 246]. It appears customary, however, to measure the tangential blade velocity at the midheights of the blades for a radial wheel, and at these positions or at the trunnion centers for a feathering wheel [SNAME, 1926, p. 187]. The difference usually is not appreciable. Fig. 32.B indicates that the circle corresponding to these trunnion positions is in this book called the *blade circle*. The tangential velocity of this circle is represented by the symbol $V°$ (vee circle).

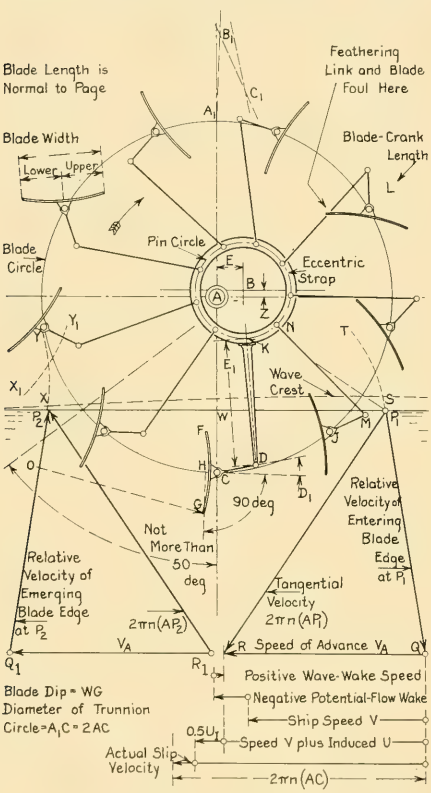

Fig. 71.A Definition and Design Sketch for Feathering Paddlewheels

For the wheel shown here, the trunnions are placed at midheights of the blades.

The vector diagram in the lower right corner of Fig. 71.A indicates all the velocities known to be acting in the case of a paddlewheel drive, with their correct ahead or astern directions. Their magnitudes in this diagram are, however, purely schematic. They will remain so until more data are made available, covering the flow across the entire width of a paddlewheel (length of a blade), from its inboard to its outboard end. When the curved paths of the blades and the waves on the surface of the adjacent water are taken into account, the velocities are not all horizontal, nor do they remain the same in various parts of the field swept by the blades. In the past, as previously described, this situation has been simplified at one stroke by assuming that $V_A = V$. The apparent-slip ratio is then

$$s_A = \frac{V \text{ of blade circle} - V_A}{V \text{ of blade circle}}$$

$$= \frac{V \text{ of blade circle} - V \text{ of ship}}{V \text{ of blade circle}} = \frac{V° - V}{V°}$$

For radial wheels the ratio s_A ranges from 0.2 to 0.3. For feathering wheels on ships of relatively fine form it varies from 0.1 to 0.2, averaging about 0.15. E. M. Bragg gives values of s_A for nine passenger ships, ranging from 0.146 to 0.223, when reckoned on a basis of the tangential speed of the midheight of the (feathering) blades [SNAME, 1916, Pl. 90]. For paddlewheel tugs O. Teubert gives a range of s_A values from 0.3 to 0.5 ["Binnenschiffahrt (Inland-Waters Ship Operation)," 1912, p. 445]. For operation in shallow and restricted waters, Teubert adds 0.1 to all the apparent-slip ratios mentioned.

71.4 Calculating the Blade and Wheel Proportions and Dimensions. Each side paddlewheel may be assumed to act on a quantity of water moving within the bounds of a horizontal stream tube of rectangular cross section, corresponding to the length s and the height h of one blade. The water speed in the outflow portion of the tube may be assumed equal to the tangential blade-circle speed $V°$. The volume of water so acted upon per unit time is

$$\frac{V}{t} = Q = s(h)(V \text{ of blade circle}) = s(h)V° \quad (71.\text{i})$$

The mass of the water passing through the tube in unit time is ρ(rho) times the quantity rate in Eq. (71.i). The increased velocity imparted to it by the blade is (V of blade circle $-$ V of ship) or $(V° - V)$. Assuming that all the blades encountering water on each side can be replaced by one effective blade on that side, the thrust exerted is then

$$T(\text{per effective blade}) = \rho(s)hV°(V° - V) \quad (71.\text{ii})$$

When the thrust-deduction fraction is taken as 0.0, the thrust T exerted by the two effective blades of the two side paddlewheels equals the total resistance R_T of the ship. Then

$$R_T = 2[T(\text{per effective blade})]$$
$$= 2\rho(s)hV°(V° - V)$$

The effective area of a blade on each wheel, of length s and height h, is

$$(s)h = \frac{R_T}{2\rho V°(V° - V)} \quad (71.\text{iii})$$

As a practical example, assume that the ABC ship of Chaps. 64 and 66 is to be driven by two paddlewheels instead of by a single screw propeller. Also that the total hull resistance R_T for a given condition at $V = 20.5$ kt or 34.62 ft per sec is 176,400 lb, derived in Sec. 66.9 from the meanline of Fig. 56.M. Assume also that the apparent-slip ratio s_A is 0.16, and that the thrust-deduction fraction t is 0.0, so that $R_T = T$. Then

$$s_A = \frac{V° - V}{V°} = 0.16,$$

whence $(V° - V) = 0.16V°$ and $V° = 1.191V$

$$= 41.2 \text{ ft per sec.}$$

The so-called slip velocity is $(V° - V) = 6.58$ ft per sec. Then

$$(s)h = \frac{R_T}{2\rho V°(V° - V)}$$
$$= \frac{176{,}400}{2(1.9905)(41.2)(6.58)} = 163.4 \text{ ft}^2.$$

For a check, consider the Long Island Sound passenger steamer *Commonwealth*, for which trial data are given by E. M. Bragg [SNAME, 1916, Pl. 90]. This vessel is selected from among the nine listed in the table because it has the greatest engine power and a speed of 20 kt, close to the 20.5-kt speed of the ABC ship. With an indicated power P_I of 12,000 horses for the 20-kt speed, and an assumed overall mechanical efficiency of 0.92, the shaft power P_S is 11,040 horses. With a propulsive coefficient η_P of 0.5, also assumed, the effective power P_E is 5,520 horses. At 20 kt or 33.78 ft per sec the total resistance R_T is 5,520(550)/33.78 = 89,876 lb. A third unknown is filled in by assuming that the thrust-deduction fraction is 0.0, so that the thrust T is also 89,876 lb.

The diameter over the blades of the *Commonwealth* wheel is 31.0 ft. With a blade width of 5.0 ft, the diameter measured to the midheights of the blades is 26.0 ft. At full power the wheel ran 29.8 rpm or 0.497 rps. The tangential velocity at tne midheight circle, taken for the moment as the blade circle, is $\pi(26)0.497 = 40.59$ ft per sec. The value of $(V° - V)$ is then $40.59 - 33.78 = 6.81$ ft per sec. The apparent-slip ratio s_A is 6.81/40.59 = 0.1677, which agrees closely with Bragg's tabulated value of 0.167.

Substituting in Eq. (71.iii) to obtain the effective area of a blade

$$(s)h = \frac{T}{2\rho V°(V° - V)}$$
$$= \frac{89{,}876}{3.981(40.59)(6.81)} = 81.67 \text{ ft}^2.$$

The blades on this vessel were actually 14.5 ft long by 5.0 ft wide, with an area of 72.5 ft^2 per blade. This gives a reasonable correlation with the calculated value, considering the assumptions that had to be made and the simplifications involved in the formulas used, to be explained presently. The thrust per unit area of each blade works out at 89,876/[(2)72.5] = 619.8 lb per ft^2.

To continue with the design example for the proposed paddlewheels to drive the ABC ship, it is first necessary to decide whether the calculated effective area per blade of 163.4 ft^2 is to be reduced by some factor which brings the simplified

calculation of Eq. (71.iii) into agreement with corresponding values calculated from observed ship data. There are several difficulties here. The published data available to the analyst lack one or more of the important values necessary for a logical calculation. The simple formula of Eq. (71.iii) takes no account of velocities induced by adjacent blades, spillover around the edges of the blades, motion of the blades in a loop-shaped path as worked out in the early years of paddlewheel propulsion [S and P, 1943, Figs. 168 and 169, p. 149], and changes in the elevation and shape of the water surface in way of the blades. Furthermore, it assumes that not several but only one blade at a time, on each paddlewheel, is acting upon the water. The rectangular area of the stream tube in which momentum is being imparted to the water, when so derived, is undoubtedly larger than the rectangular area of one blade. It may be more nearly the area of the thrust-producing segment indicated by the hatched rectangles on each side of diagram 2 of Fig. 15.G.

Purely as a means of working out a numerical example it is assumed here that a reduction factor may be applied to the calculated blade area, because of the conditions described in the preceding paragraph. This factor is established arbitrarily for the moment as 0.90. The necessary area per blade on the ABC paddlewheel is then only $163.4(0.9) = 147.06$ ft^2. A better reduction factor may be taken when it is found. For paddle tugs it is possible that no reduction in calculated effective area should be made.

The next step is to select the proportions of the blades. The narrower and shallower they are, the smaller can be the wheel diameter and the higher its rate of rotation, but at the expense of shaft and paddlewheel length and overall beam of the vessel. The deeper and shorter the blades, the less can be the wheel width and the overall beam but at the expense of greater wheel diameter and a slower rate of rotation. The slower the rate of rotation the larger and heavier is the propelling machinery.

The average value of length-height ratio s/h of a blade in Bragg's referenced table is slightly in excess of 3.0, with a maximum blade width for the nine vessels listed of 5.0 ft. Assuming a blade width of 6.5 ft for the ABC ship, developing nearly twice the power of the fastest vessel tabulated there, the blade length is about 22.6 ft and the length-height ratio is just under 3.5.

This length is within the limit given by D. W. Taylor [S and P, 1943, p. 150], who states that good practice requires the blades for a *seagoing* vessel to be no longer than one-third the beam. A blade length of $0.4B$ is a good figure for any type of smooth-water ship; a maximum value for any design, except paddlewheel tugs, is $0.5B$.

The average pitch ratio, illustrated in Fig. 32.B and defined as the circumferential distance between adjacent trunnions of a feathering paddlewheel divided by the blade height, is of the order of 1.5 for the most modern designs in the Bragg table. This gives a circumferential spacing on the trunnion circle, assumed for the moment as equal in diameter to the circle passing through the midheights of the blades, of $1.5(6.5) = 9.75$ ft. Taking 10 blades as a starter, the circumference of the ABC trunnion circle is $9.75(10) = 97.5$ ft; its diameter is $97.5/\pi = 31.03$ ft.

The outside diameter of the paddlewheel, assuming no circumferential rings external to the blades, is approximately $31.03 + 6.5 = 37.53$ ft, giving a blade-height ratio of $6.5/37.53 = 0.1733$. This is somewhat larger than the largest value of 0.168 (for the *Tashmoo*) in Bragg's table. It could be reduced by using 11 blades instead of 10 but with the selected pitch ratio of 1.5, this would increase the overall wheel diameter to about 40.7 ft. The blades could be narrowed to 6.0 ft, giving a blade-circle diameter of $[11(6.0)1.5]/\pi = 31.5$ ft and a blade-height ratio of only $6.0/(31.5 + 6.0) = 0.16$. However, this would increase the blade length to $147.06/0.6 = 24.5$ ft. While still of the order of one-third of the beam of 73 ft for the ABC ship, the length-height ratio of each blade is 4.09, which is considerably too large for actuation by one feathering crank at one end.

71.5 Alternative Methods of Determining Paddlewheel Blade Area. Other methods of calculating the effective area per blade, such as that described by D. W. Taylor [S and P, 1943, p. 150], are based upon the same combination of the engine power (possibly determined previously by the owner or operator), the ship speed, the slip ratio, the wheel diameter, and the rate of rotation. Taking the formula given by Taylor

$$A = K\frac{P}{V^3} \qquad (71.\text{iv})$$

where A is the area of two blades, in ft^2, one on each side of the ship

K is a coefficient depending primarily upon the apparent-slip ratio and secondarily upon

many other factors. For apparent-slip ratios ranging from 0.10 to 0.30, $K = [212.5 - 375(s_A)]$

P is the shaft or indicated power; unfortunately a rather loose definition

V is the ship speed in kt.

Assuming for the bare-hull ABC ship an effective power of 10,816 horses, from Sec. 66.9, and a propulsive coefficient η_P of as high as 0.55 for a modern design, the value of P for Eq. (71.iv) is about 19,660 horses. That of K, for an assumed apparent-slip ratio of 0.16, is $[212.5 - 375(0.16)] = 152.5$. Substituting in Eq. (71.iv)

$$A = K\frac{P}{V^3} = 152.5\frac{19{,}660}{(20.5)^3} = 347.9 \text{ ft}^2.$$

The effective blade area on each side of the vessel is half of this value or 173.9 ft^2. This is a somewhat larger area per blade than the value of 163.4 ft^2 calculated by Eq. (71.iii) but the discrepancy is perhaps not too large, considering the assumptions made.

The additional formulas given by W. F. Durand [RPS, 1903, pp. 198–201] and by O. Teubert ["Binnenschiffahrt," 1912, p. 446] are dimensional, as is the formula given by D. W. Taylor. They require in addition an estimate of the wheel diameter and the rate of rotation, or both.

Another method of approximating a suitable blade area, if complete and reliable reference data were available, is to make use of the thrust-load coefficient and to work backward to find the equivalent thrust-producing area A_0 by the following formulas, assuming as before that $V_A = V$:

$$C_{TL} = \frac{T}{0.5\rho A_0 V_A^2} = \frac{T}{0.5\rho(\text{equivalent } A_0)V^2}$$

Equivalent area A_0, for both sides,

$$= \frac{T}{C_{TL}(0.5\rho)V^2}$$

For example, taking the total resistance R_T of the *Commonwealth*, derived earlier in this section as 89,876 lb, and assuming that it equals the thrust T of both paddlewheels, with a thrust-deduction fraction t of 0.0, it is possible to derive the thrust-load factor C_{TL} for this vessel. The speed is 20 kt, or 33.78 ft per sec. The apparent dip of the blades, so called by Bragg because it is measured to the at-rest WL, is 7.58 ft and the length of each blade is 14.5 ft, so that $A_0 = 2(7.58)14.5 = 219.82$ ft^2. Then

$$C_{TL} = \frac{T}{0.5\rho A_0 V^2}$$

$$= \frac{89{,}876}{0.9953(219.82)1{,}141.1} = 0.3599, \text{ say } 0.36$$

Assuming the same value of C_{TL} for the ABC ship at a speed of 20.5 kt or 34.62 ft per sec, and using the value of $R_T = T = 176{,}400$ lb mentioned earlier,

Equivalent area

$$A_0 = \frac{T}{C_{TL}(0.5\rho)V^2}$$

$$= \frac{176{,}400}{0.36(0.9953)1{,}198.5} = 410.8 \text{ ft}^2.$$

This is the estimated thrust-producing area on both sides of the vessel; on one side it is 205.4 ft^2. With a tentative dip ratio of 1.35, the estimated area of one blade is $205.4/1.35 = 152.1$ ft^2. This value is only slightly larger than the estimated area of 147.06 ft^2, derived previously in this section by using the momentum method, with a reduction factor of 0.9.

The usefulness of the C_{TL} method obviously depends upon knowledge as to proper thrust-load coefficients for design purposes. For instance, the value of C_{TL} for the *Tashmoo* from Bragg's table, using a mechanical efficiency of 0.9 and a propulsive efficiency of 0.55, is only 0.26 as compared to the 0.36 of the *Commonwealth*. For a paddle tug, pulling heavy loads at slow speeds of advance, the thrust-load coefficient might reach or exceed 10 times these values.

71.6 Relation of Paddlewheel Diameter and Position to Ship Hull Design. Taking account of general design considerations, the selection of paddlewheel diameter is one rather closely related to the overall ship design, because it concerns the:

(a) Space which can be allowed for the wheel boxes or recesses
(b) Overall beam of the vessel, measured to the guards outside of the wheels
(c) Type of engine, and of reduction gear if fitted
(d) Rate of rotation n of the paddlewheel drive
(e) Speed of the vessel
(f) Probable values of wake fraction w and real-slip ratio s_R.

In general, the greater the wheel diameter the more efficient is its propulsive action. With a larger diameter the blades enter and leave the water more nearly tangential to the resultant-

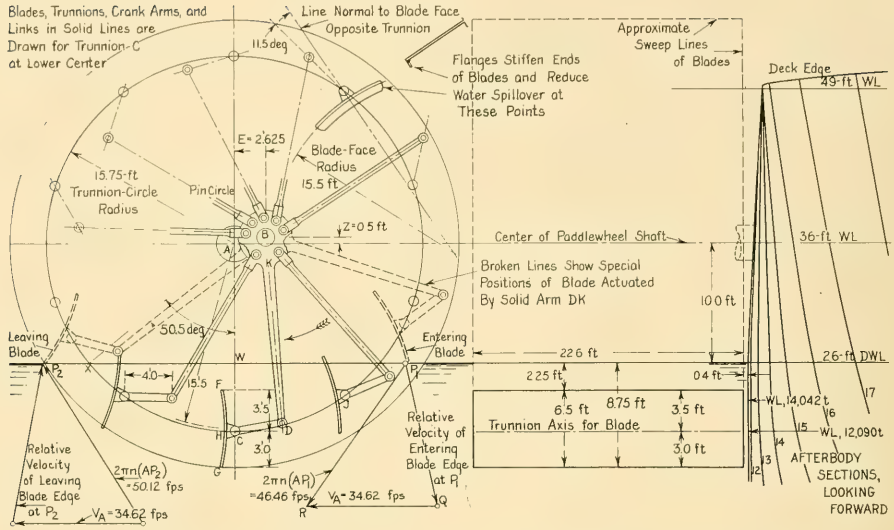

FIG. 71.B LAYOUT ACCOMPANYING EXAMPLE OF A FEATHERING PADDLEWHEEL DESIGN FOR THE ABC SHIP

velocity vector, indicated in the left-hand diagram of Fig. 32.B and in the layout elevation of Fig. 71.B, for a greater part of their width. There are also more blades acting simultaneously, with a lighter loading on each and smaller losses from induced effects. Furthermore, the submerged blades move more nearly parallel to the straight-aft direction in which the water is to be accelerated by them.

The correct fore-and-aft position of paddlewheels, important for efficiency if the wave profile has marked crests and troughs, is governed by the position of the wave crests along the ship when running at the speed for which the best propulsion performance is desired. This feature is much more important for a vessel running in shallow water than in deep water. To take advantage of the wave wake the wave crest should be approximately under the wheel center. This position can sometimes be estimated for a new design, and it may be predicted by comparison with an existing design if the hulls have the same shape. Wave profiles for some paddle steamers are shown in Sec. 52.2; references are given there for other published profiles. The wave profile is quickly and reliably determined, however, from a model test.

From the wave profile of the ABC transom-stern ship, given on the SNAME RD sheet in Fig. 78.Ja, it appears that the best fore-and-aft position for a pair of paddlewheels on that vessel is at about Sta. 11. This happens to coincide very nearly with the position of maximum waterline beam.

The next problem is to determine the vertical position of the paddlewheel shaft center with respect to the designed waterline. The selection of the dip ratio, or the decision as to how far the bottom of the deepest blade is to drop below the at-rest waterline at the designed draft, may hinge on practical rather than hydrodynamic reasons. It depends upon the wheel diameter, how many blades are to be in the water at any one time, whether feathering is employed or not, and the maximum variation in anticipated draft for which propulsion is to be reasonably efficient. For a shallow-water vessel, the greatest submergence depth of the bottom of a blade should be slightly less than the draft. Consideration of these and other factors, for vessels of various types, results in blade immersions varying from only some 0.7 of the height to immersions of 1.4, 1.5, or more of the blade height. D. W. Taylor points out that the dip ratio may reach 2.0 for a very long, narrow blade on a large wheel, without loss of efficiency [S and P, 1943, p. 150].

Another relationship between the wheel diameter and the blade dip involves the angular

length of arc of the blade circle, passing through the blade trunnions, which is immersed in the designed-draft condition. For a paddlewheel to run at a medium rate of rotation, or perhaps above average, say not more than $n = 35$ rpm or 0.58 rps, this arc should extend for about 50 deg forward and aft of the lower center position, or a total of 100 deg. For a fast-running paddlewheel of less than average diameter, with normal dip, the arc on either side of lower center may be 55 deg or more, corresponding to a total of 110 deg.

For use in selecting a final dip ratio for the ABC ship, in the designed-load condition at which the paddlewheels are to give their best performance, Bragg's table has values of apparent dip ratio, measured to the at-rest waterline, varying from 1.27 to 1.52. The ABC value of 1.35, selected tentatively in Sec. 71.5, combined with a blade height of 6.5 ft, gives a dip of 8.76 ft. With a diameter of 37.53 ft and a radius of 18.77 ft, the wheel center lies $18.77 - 8.76 = 10.01$ ft above the at-rest water level. The circle passing through the midheights of the blades, with a radius of $18.77 - 3.25 = 15.52$ ft, therefore strikes the at-rest water surface at an angle ahead of the lower center of $\cos^{-1}(10.01/15.52) = 49.8$ deg. This is acceptable, and the dip ratio of 1.35 may be considered as fixed.

With an apparent-slip ratio of 0.16 the value of $V° = 41.2$ ft per sec, from Sec. 71.4. Dividing this value by the blade-circle circumference of 97.5 ft gives a rate of rotation n of 0.4225 rps or 25.35 rpm.

It is now possible to sketch a layout of the proposed paddlewheel alongside the transom-stern ABC ship, about as indicated in Fig. 71.B. Rounding out the dimensions to get rid of the small decimal fractions, the paddlewheel center is placed 10.0 ft above the DWL, or at the 36-ft WL. The external wheel diameter is nominally 37.5 ft, but for a wheel of the feathering type the volume swept through by the outer edges of the blades is not a true cylinder. Nominally, the outside wheel diameter is twice the distance from the wheel axis to the bottom of the blade at the lower center or 6 o'clock position, corresponding to twice the distance AG in Fig. 71.B.

The maximum waterline beam lies very close to Sta. 11, and a mechanical clearance of 0.4 ft between the hull and the inner ends of the blades appears to be adequate. With blades 22.6 ft long, their outer ends lie 23 ft from the widest portion of the ship's side (including the shell plating). The feathering mechanism is to be *outside* the wheel, with the eccentric pin carried by a fore-and-aft guard forming the lower edge of the paddlewheel box. If there is an outer shaft bearing carried by this guard the feathering links must be pinned to an eccentric strap around the shaft, and possibly also around the bearing. The mechanism then resembles that sketched in Figs. 32.B and 71.A.

Although the dip appears large when drawn in the elevation from aft of Fig. 71.B, the markers showing the WL elevations at Sta. 11 for the two variable-load conditions of Sec. 66.32 and Fig. 66.T indicate that the dip is actually too small for those lighter displacements.

Some paddlewheels are designed so that both the radial width or height and the radial position of the blades may be changed without too much difficulty and expense after the ship is built. A certain measure of adjustment is desirable if the draft at the wheel axis is to change more-or-less permanently during the life of the vessel. It would be very much better, of course, if the vertical position of the paddlewheel axis could be changed as well.

71.7 Design Notes on Paddlewheel Details and Mechanism. The next phase of the design involves an analysis of the dimensions, ratios, proportions, and other features to insure that those tentatively established in Sec. 71.6 will produce a good overall mechanical and hydrodynamic design. This involves a more careful consideration of the features selected rather arbitrarily in Secs. 71.5 and 71.6.

Clearance between inboard paddle ends and the fixed hull is generally limited to the minimum permissible mechanical value, say from 0.2 ft on small vessels to 0.5 ft on large ones. The value of 0.4 ft indicated in Fig. 71.B is rather small but not too small. Every fraction of a foot added here adds to the overhang of the shaft.

The blade-spacing or pitch ratio, defined as the circular-arc distance CJ over the blade width FG in Fig. 71.A, should preferably be about 2.0 times the blade depth, to avoid interference between blades. However, this calls for very large wheel diameters. Practical limitations on weight and space are usually such as to reduce this ratio to as low as 1.6 or 1.5. If the dip ratio WG/FG of that figure is made about 1.2 to 1.5 the combination of pitch ratio with dip ratio and a reasonable blade-circle diameter gives a total immersed-blade area of from 2.0 to 2.5 times the area of one blade, irrespective of the angular

position of the wheel. The pitch ratio of 1.5 and blade spacing of 9.75 ft previously adopted for the ABC wheel appear not too small.

The average position of the center of pressure CP on each moving blade, in the course of its travel through the water, is somewhat below its geometric center, possibly only 0.4 times the blade width from the bottom. It is customary to place the blade trunnion at a point somewhat below the midheight point H in Fig. 71.A. This means that the blade-circle or trunnion-circle diameter is somewhat greater than twice the radius to the midheights of the lowest blade, at the 6 o'clock position. For the nine vessels listed in Bragg's table, reference (14) of Sec. 59.6, this diameter ratio varies from 1.00 to 1.04. The ratio of the height of trunnion above the lower edge of the blade in the 6 o'clock position to the blade height varies from 0.40 to 0.50. For the ABC ship of Fig. 71.B it is taken as 3.0/6.5 = 0.462. Thus in the elevation from starboard, at the left of Fig. 71.B, GH is 3.0 ft and HF is 3.5 ft. The trunnion circle passing through H has a diameter of 2(AH) = 2(AG − GH) = 2(18.75 − 3.0) = 31.5 ft.

Having determined the trunnion-circle diameter, the blade width, and the blade spacing, the number of blades becomes approximately π times the trunnion-circle diameter divided by the blade spacing, CJ in Fig. 71.B, to the nearest whole number. There is no particular advantage in using an odd or even number of blades but the minimum practical number is about 6, preferably not less than 7, although paddlewheels have been built with only 5 blades. The number 10, selected for the ABC ship in Sec. 71.4, is a good average value from the Bragg table.

There is undoubtedly an advantage in mounting the port and starboard paddlewheels on their shafts at an offset or phase angle corresponding to half the angular distance between adjacent blade trunnions, so as to have the water entry of the port blades taking place midway between those of the starboard blades. This would depend, however, on the torsional-vibration characteristics of the paddlewheel shaft.

Even with feathering blades, it is almost never possible to use a wheel diameter (or trunnion-circle diameter) large enough to cause the blade edges to enter and leave the water in a direction parallel to the resultant-velocity vectors at those points. For instance, in Fig. 71.A the lower edge of the entering blade TS is almost exactly tangent to the resultant-velocity vector P_1Q on the forward side of the wheel. However, on the after side, the leaving edge of the blade X_1Y_1 is far from tangent or parallel to the vector Q_1P_2. The blade would have to shift angularly about its trunnion to the position XY to comply with this condition. Furthermore, if one wishes to make a comprehensive analysis, the position of the wave profile, the direction of flow within the wave, and the known component velocities of Fig. 71.A all require to be taken into account.

The practical solution is to make the lower edge of an *entering* blade meet the water surface with the blade tangent to the resultant velocity vector. Curving the blade radially, with its concave and $+\Delta p$ side aft, helps to accomplish this. However, this very curvature can be said to impart a greater upward component of velocity when the blade leaves the water than would be the case if its surface were flat. The major source of noise and vibratory forces in a paddlewheel drive appears to be the periodic impact of the *entering* blades. This involves a sufficiently heavy blow, for example, to render a paddle vessel audible before it appears around a bend in a river. It is important, therefore, to favor this condition and to provide as nearly shock-free entrance as possible at this point. It is the excessive lifting of the water as the blade leaves the surface which raises the high crest abaft most paddlewheels, pictured in Fig. 73.J, and which makes it possible to use a fixed contra-vane abaft the wheel to such good advantage.

There is no fixed value, nor are there very definite limits, for the radius of curvature of the blade faces. This may be as large as 1.5 times the blade-circle radius, AC in Fig. 71.A, or as small as 1.0 times that radius. The latter ratio is used in the layout of Fig. 71.B, where it is taken as 15.5 ft.

If feathering wheels are fitted to a double-ended ferryboat or other craft which must run equally well in either direction the blades are made flat rather than curved. The feathering mechanism can be so designed that they enter and leave the water at about the same angles when going astern as when going ahead.

To provide plenty of leverage for the unbalanced forces acting on the entering and leaving blades the lengths of the crank arms are made from 0.5 to 0.7 times the blade width. This length is 4.0 ft, or 0.615 times the blade width of 6.5 ft, for the layout of Fig. 71.B.

Whereas most elementary diagrams of paddlewheels show the crank arms at right angles to the base chord of the concave blades [S and P, 1943, Fig. 170, p. 150], these arms are sometimes set as much as 15 deg or more, up or down, from the normal positions. Using an up angle, as in the ABC ship layout and as indicated at D_1 in Fig. 71.A, results in a larger angle between the feathering link and the crank when the lower edge of the entering blade touches the water.

There is one fixed arm on the orthodox feathering hub or eccentric which serves to turn it as the wheel rotates. The drag links connecting this hub or eccentric to the crank arms of the blades are attached to the hub by pins spaced uniformly around its periphery. These lie on what is known as the pin circle. The result is different angular positions of the several blades when each successive blade trunnion passes through the lower center (the position C in Fig. 71.A). In other words, if the wheel of Fig. 71.A is rotated by one blade space, the angular positions of the several blades will be different than shown there. This is because the eccentric strap does not move by an angular amount of [360/(number of blades)] deg about its own center when the wheel proper rotates through this distance, due to the angularity of the fixed arm on the eccentric strap and the blade crank to which it is pinned. Thus, as the wheel rotates, each blade enters and leaves the water at slightly different angles from all the other blades. The smaller the pin circle on the hub or eccentric, as shown in Fig. 71.B, the smaller is the variation. It is one of the reasons for mounting the feathering mechanism on the *outside* of a paddlewheel which does not have an outboard bearing [ATMA, 1906, Vol. 17, Pls. V and VI]. The other reason is that the eccentricity E and the vertical offset Z of the center B of the rotating hub can be shifted readily after the ship is built and placed in service, in case it is found desirable to shift the blade angles with respect to the at-rest water surface. A large strap, rotating on a fixed eccentric around the inboard shaft bearing of the paddlewheel, involves more lubrication problems and does not lend itself to shifting its position at a later date.

In many elementary treatises on paddlewheels it is stated that the use of a feathering mechanism effectively doubles the wheel diameter. In other words, the blades are supposed to move as though they were part of a radial wheel having a center at or near the point A_1 in Fig. 71.A, where the base chord GF of the lowest blade intersects the top of the blade circle. Actually, for the wheel shown, the base chord for the blade section at J passes through C_1 ; the base chord ST, when extended, passes through B_1 . That through X_1Y_1 passes through still another point, and these points would all change position for new blades in corresponding positions if the wheel rotated one blade space.

If the pin-circle radius were zero, such as would be the case if all the inner ends of the feathering links were pivoted at the eccentric or hub center B, the locus of the outer ends of these links, corresponding to the points D and M in Fig. 71.A, would be a true circle with its center at B. For this simplified special case, the problem of finding the proper position for B (relative to A) such that the entering and leaving blades would have the proper attitude for the conditions selected is still not easy, because of the curvature of the blades. When the pin-circle radius is finite, there are as many solutions as there are number of blades, depending upon the position around the circle of the fixed arm KD actuating the feathering mechanism.

The problem is partly simplified by using the fixed arm to position the entering and leaving blades, as is done in the left diagram of Fig. 71.B. Even so, the problem remains one of trial and error because the designer does not know the radius AP_1 , and the tangential-velocity vector P_1R, until the linkage is sketched in for a given position of B and for given values of the other parameters involved. Having arrived at a reasonable solution for the entering blade, the position of the leaving blade is then sketched. It may be far out of proper position, farther than indicated at the extreme left of Fig. 71.B.

A new solution is worked out, perhaps taking account this time of the wave profile in the vicinity, omitted from Fig. 71.B. Bragg's referenced table reveals that good designers by no means arrive at the same answers, but it may very well be that they are trying to achieve a slightly different result each time.

There is undoubtedly a best geometric relationship between the eccentricity E of a feathering paddlewheel, the trunnion-circle diameter AC of Fig. 71.B, and the blade-crank length CD. For the French paddlewheels illustrated by M. Hart [ATMA, 1906, Pl. V], E is 0.5 meter, D is 5.660 meters and the blade-crank length is 0.8 meter. For the Anatolian paddler of reference (8)

of Sec. 59.6, E is 0.24 meter, D is 3.56 meters and L(blade-crank length) is 0.36 meter. The eccentricity ratio is $0.5/0.8 = 0.625$ in the first case and $0.24/0.36 = 0.667$ in the second. The eccentricity ratios of the more recent vessels of Bragg's table vary from 0.584 to 0.69. That of the ABC paddlewheel in Fig. 71.B is $2.625/4.0 = 0.656$.

It is possible, by raising the eccentric center B above the level of the wheel axis A, to:

(1) Help bring the leaving blade more nearly tangent to the resultant-velocity vector on the after side

(2) Avoid or reduce the mechanical interference between a blade and the feathering link which operates it, on the forward side of the wheel. In diagram 1 of Fig. 32.B, the nearly horizontal feathering link on the forward side just clears the upper edge of its blade. The same is true in Fig. 71.A but, for the next blade above, the feathering link actually fouls the inner edge of the blade. A similar situation in practice is met either by making the feathering links of rectangular section and bending them so as to clear the blades [Teubert, O., "Binnenschiffahrt," 1912, p. 444], or by notching the inner edges of the blades to clear the links [Hart, M., ATMA, 1906, Vol. 17, Pls. V and VI].

With the usual feathering mechanism, having an eccentric center forward of the shaft center, the feathering links are in compression, especially when the blades are entering or leaving the water. The links can not, therefore, be too slender for their length without risk of buckling. J. Scott Russell proposed a variation of the usual geometric arrangement whereby the eccentric center (B in Fig. 71.A) lies *abaft* the wheel axis. The blade cranks are thus on the after or $+\Delta p$ sides of the blades, and the feathering links are, when loaded heavily, always in tension.

71.8 Variations from Normal Paddlewheel Design. Where damaging debris is frequently encountered and repairs to blades must be made on the spot or locally, often by the ship's force, radial blades are used, bolted to the wheel arms. The blades can be shifted in or out, radially, to suit a more-or-less permanent change in draft or trim. They can be varied in width, or shifted radially, to permit the wheel torque and speed to be varied so as to obtain the maximum engine power with the greatest ship speed or towline tension. The radial blades are simple and cheap and they produce thrust but they are not particularly efficient. They impart useless upward and downward components of motion to the water [Teubert, O., "Binnenschiffahrt," 1912, Figs. 305, 306, p. 441; S and P, 1943, Figs. 168, 169, p. 149] and they leave a great deal of energy in a series of short, steep waves trailing astern.

Wheels with flat, smooth blades geared to a shaft so as always to stand with their heights truly *vertical*, and with annular support rings always above the waterline, as devised by Georg Fricke of Lembruch, Germany, have proved excellent for propulsion in calm waters, grown thick with grasses and weeds. The blades press the weeds down vertically and do not become foul [Deetjen, R., Schiff und Hafen, Mar 1952, pp. 80–81; this German article is abstracted in SBSR, 8 May 1952, p. 579].

A partial list of references in the technical literature on paddlewheels, relating to both model and full-scale devices, is to be found in Sec. 59.6.

It should be clear from the foregoing that, whatever its place in the scheme of things propulsive, the analysis and design of a paddlewheel represents a marvelous exercise in practical hydrodynamics and practical machine design. Not only does the paddlewheel need an extension of the motion analysis published by M. Hart [ATMA, 1906, Vol. 17, Pls. II and III] but the experience gained in such an analysis would be invaluable when analyzing the action of other propulsion devices and in preparing systematic rules for their design.

71.9 Design Notes for Hydraulic-Jet and Pump-Jet Propulsion. Methods of achieving what is often termed hydraulic propulsion are described in Sec. 15.8 and elaborated upon in Sec. 32.5. The efficiencies of the principal systems are discussed in Sec. 34.13. In Sec. 59.8 there is given a list of the principal references on this subject, both historical and technical. Some of them are valuable in design as indicating the pitfalls to be avoided.

It is pointed out in Sec. 15.8, and it is again emphasized here that the air, gas, or water jet employed for propulsion may, like that from the airscrew, be discharged into the atmosphere above the water. An example of this is the Russian shallow-draft river launch propelled by twin water jets and pictured in The Illustrated London News [11 Dec 1954, p. 1070].

Hydraulic-jet propulsion lends itself to craft for special duty, where the outside of the hull must

be kept clear of protuberances or where some similar characteristic is more important than the downright efficiency of propulsion. In most lifeboat installations (those operating from life-saving stations ashore) the jet ducts can not protrude beyond the fair hull line, and a considerable sacrifice in propulsive efficiency is accepted. If, as may be expected for these craft, good backing qualities are required, the pump must be of the axial-flow or propeller type unless flap valves in the ducts are employed.

Maneuverability and steering as well as propulsion are achieved with a pivoted jet, arranged to discharge water in any relative direction desired. As with a steering propeller, however, it is mandatory to incorporate a low-friction thrust bearing in the swiveling head, because all the propulsive thrust is exerted through this swiveling connection between the jet elbow and the boat, indicated in Fig. 71.C. If the friction is large

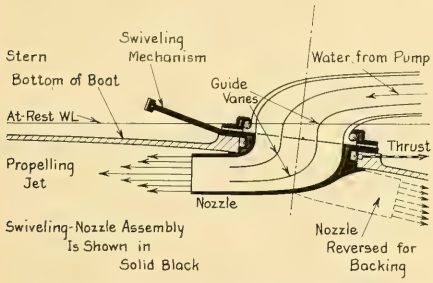

Fig. 71.C Schematic Arrangement of Reversible Jet-Propulsion Device for a Small Boat

in this large-diameter bearing, often incorporating a watertight stuffing box as well, the craft can not even be steered.

When working up the design of one of these systems the procedure divides itself naturally into several steps:

(1) Determination of the quantity-rate or amount of water per unit time to be handled, the area(s) of the jet(s), and the amount of increased velocity to be imparted to this mass of water to produce the thrust required

(2) Working out the method whereby this quantity-rate is to be taken in and led to the pump or impeller which is to impart the augment of pressure and velocity to it

(3) The fashioning of the ducts and passages, for both the inlet and the outlet water, so that the hydraulic losses will be a minimum

(4) Estimating or calculating the rating of the pump or impeller and the power necessary to drive it.

There have been many recent successful developments of guide-vane assemblies by which the flow of water can be changed in direction abruptly yet efficiently. Relatively sharp turns can now be worked into the ducts of the hydraulic propulsion setup without excessive hydraulic losses. This gives the designer considerable latitude in leading a stream of water around inside a vessel. Practically all modern circulating-water channels and variable-pressure water tunnels for the testing of model propellers under cavitating conditions embody corner guide vanes of this type. Up-to-date design rules and criteria have been worked out by the St. Anthony Falls Hydraulic Laboratory in Minneapolis, Minnesota. In fact, it is possible by employing a large rotary valve with vanes to "switch" the water from one duct to another or to reverse its direction.

Centrifugal pumps of good design show efficiencies of well over 0.80 and reaching 0.90 at the rated output. Propeller-type or axial-flow impeller pumps with fixed blades should do at least as well [Rouse, H., EH, 1950, Chap. XIII]. Design and performance data on hydraulic pumps of various kinds are given by J. W. Daily in the reference cited and by G. F. Wislicenus [FMTM, 1947].

Supercharging of the pump, to increase the ambient pressure and to delay or prevent cavitation of the blades, may be accomplished by making use of the ram or dynamic pressure built up at the duct inlet by the motion of the craft through the water. This is also used to help force the required quantity of water through the duct toward the pump, against the friction resistance of the walls.

The hull of a craft designed for reasonably efficient propulsion with fixed ducts requires special forming in way of the jet intakes and discharges, whether these openings are at the bow or stern or along the hull. The design of any installation of importance should be checked at least by flow tests on a small model and preferably by performance tests and pressure measurements on a larger model.

The curved-vane diffusers and the various other means adopted by hydraulic engineers to

raise the operating efficiencies of propeller-type pumps can all be applied to the propulsion of a ship, *if* the hull has a shape which lends itself to the building in of the necessary ducts or jet boundaries. It is hardly to be expected that a form of underwater hull which, over many decades, has evolved into one suited to the screw propeller will be found readily adaptable for the efficient use of fixed propeller shrouding, propeller-type pump-jets, or hydraulic jets. Experience with the Kort nozzle, described in Sec. 36.19, indicates that it is not easily fitted to a vessel of normal form.

The same basic hydrodynamic laws and relationships are used for the design of axial-flow impeller pumps with casings as for open-stream ship propellers but the attack on the problem is quite different. The available engineering data are in such form as to apply only to the design of each class of devices by itself. For this discussion they are known as impellers and propellers, respectively.

The quantity rate of flow $Q = \forall t = AUt$, inside the solid casing boundaries of cross-section area A, must remain the same from inlet to outlet, hence it is used as a basic quantity in the impeller-pump design. If ΔU is the increase in velocity imparted by the impeller from the casing inlet to the casing outlet, the impeller thrust T is, from Newton's second law of motion,

$$T = \int_Q \rho(\Delta U)\, dQ = \rho Q(\Delta U) \qquad (71.\text{v})$$

This is the same as Eq. (71.ii) of Sec. 71.4 and of Eq. (34.xxix) of Sec. 34.13.

Assuming that the inlet velocity is the difference between the ship speed V and the wake speed V_W *at the inlet position*, reckoned here the same as the speed of advance V_A at a propeller position, then $V_{\text{Inlet}} = V_A = V - V_W$. The increase in velocity ΔU through the casing and impeller is taken as a fraction of the inlet velocity V_A. Also $Q = T/(\rho\Delta U)$. The pressure or pumping head h_P then required of the impeller is equal to the increase in kinetic energy of the water passing through the pump, or

$$h_P = \frac{1}{2g}\left[(V_A + \Delta V)^2 - V_A^2\right]$$
$$= \frac{V_A^2}{2g}\left[2\frac{\Delta V}{V_A} + \frac{(\Delta V)^2}{V_A^2}\right] \qquad (71.\text{vi})$$

From here on the design problem becomes lengthy and complicated, to be solved by methods developed by hydraulic engineers for the design of ducts and pump impellers rather than by those worked up by marine engineers for propulsion devices working in the open. Unfortunately, the design data on hydraulic-jet propulsion apparatus are relatively meager, particularly because there has been little in the way of logical, progressive, modern development except on classified projects for combatant vessels and new weapons. It should be kept in mind always, however, that efficient hydraulic-jet propulsion requires the largest practicable diameter of jet and the smallest relative velocity of jet water, reckoned with respect to the surrounding undisturbed water.

It is proposed in Sec. 34.13, and repeated here, that the whole jet-propulsion system be designed on an energy or work basis, rather than on a pressure and force basis, as is customary for screw propellers.

71.10 The Design of Surface Propellers. There are no systematic data, so far as known, for the design of surface screw propellers. These are deliberately intended to run with only partial immersion, either because of draft limitations or because of the lift force that is to be obtained from them, described in Sec. 33.11. A few references pertaining to this particular design phase are:

(a) Smith-Keary, E. M., "The Effect of Immersion on Propellers," NECI, 1931–1932, Vol. XLVIII, pp. 26–44 and D1–D17
(b) Kempf, G., "Immersion of Propellers," NECI, 1933–1934, Vol. L, pp. 225–248 and D123–D138
(c) Kempf, G., "The Influence of Viscosity on Thrust and Torque of a Propeller Working Near the Surface," INA, 1934, pp. 321–326 and Pl. XXXIV
(d) De Santis, R., "The Effect of Inclination, Immersion, and Scale on Propellers in Open Water," INA, 1934, pp. 380–385 and Pls. XXXVI–XXXVIII
(e) Baker, G. S., "The Qualities of a Propeller Alone and Behind a Ship," NECI, 1937–1938, Vol. LIV, pp. 239–250 and D135–D146.

General comments and design data on "Partially Immersed Propellers" are given by W. P. A. van Lammeren, L. Troost, and J. G. Koning [RPSS, 1948, pp. 262–263].

Some practical pointers for the design of surface propellers on high-speed racing motorboats are published by E. C. B. Corlett in "Trends in Very High Speed Craft" [The Motor Boat and Yachting, Sep 1954, pp. 386–388].

The thrust-load factor for a surface propeller is of course based upon the fractional disc area

which is expected to be immersed when the propeller is operating, indicated by diagram 7 of Fig. 15.G.

The unbalanced blade-disc forces from the immersed and working blades, depicted in diagram 1 of Fig. 33.K, are usually balanced by introducing equal and opposite forces from a second propeller rotating in the opposite direction. If these forces are desired or needed to give the craft angular acceleration when turning, and if the turning is always in the same direction, as in a motorboat which always makes left-hand turns during a race, they are balanced by a lateral force produced by a constant rudder angle when straight running is desired.

Since there are certain to be air holes instead of cavitation pockets on the forward or reduced-pressure sides of the partly immersed blades, the available thrust is low, as is the maximum propeller efficiency. Conservative design calls for the use of an efficiency not greater than half or two-thirds that of the same propeller working fully submerged.

At the average draft and running condition to be expected in service, the hub of a surface propeller should be just clear of or just touching the water on its under side. This may eliminate the necessity of a watertight stuffing box for the shaft. It will certainly free the propeller of friction resistance on the hub surface.

A cover or guard is almost a necessity over the upper blades of a surface propeller, partly for safety and partly to keep down the showers of spray and geysers of water which would otherwise be thrown up at the stern.

71.11 Asymmetric Propulsion. It is often convenient to offset the propulsion device from the centerplane of a vessel, especially in auxiliary yachts where an aperture for a centerline propeller adds to the sailing resistance and detracts from the efficiency of the steering rudder [Baader, J., "Cruceros y Lanchas Veloces (Cruisers and Fast Launches)," Buenos Aires, 1951, Fig. 203, p. 255 and Fig. 205, p. 256. The situation is similar to that of a crippled multiple-screw ship driven by one wing propeller, with all other propellers missing.

Moment calculations, supported by service experience with damaged vessels, indicate that if the rudder area is sufficiently large and if the offset of the thrust line from the center of gravity does not exceed 15 per cent of the maximum beam, the asymmetric moment of thrust is only of secondary importance in steering and possibly also in turning. For a sailing yacht, this may require carrying some small compensating rudder angle. As the mechanical propulsion is an auxiliary drive at the best, the helm handicap can be accepted for larger benefits which may be derived when sailing.

A rather comprehensive article entitled "A Propeller for the Auxiliary," with several illustrations of asymmetric drives for sailing yachts, is published by M. E. Williams [Yachting, Feb 1955, pp. 54–55, 114]. This article reveals that asymmetric drives and auxiliary drives, the latter discussed in Sec. 71.13, both require the same serious consideration of flow in their vicinity as is given to the propeller position on a much larger vessel.

71.12 Feathering and Folding Propellers. The proper design of all vessels with two or more means of propulsion, such as the sailing yacht with auxiliary power, requires that the propulsion devices of one system be not a hindrance when those of the other system are being used. The problem of the effect of screw-propeller resistance on the sailing speed of a yacht is discussed by K. S. M. Davidson and D. S. Connelly ["If We Hadn't Been Dragging That Propeller," Yachting, May 1940, p. 68]. Permitting one propulsion device to free-wheel or to coast, if it will, is one answer but not always the best one.

In the early days of steam as an auxiliary power in sailing ships this problem was usually solved by fitting a 2-bladed propeller and placing its blade axes vertical when it was stopped. The sternposts on those ships were so wide that the two blades, if not the hub, could lie neatly in the "shadow" of the post, within the eddies of the separation zone directly abaft the post. Other solutions of this problem are to feather the propeller blades, as is done on modern aircraft, to fold them, or to house the propeller in some suitable manner. J. Scott Russell mentioned feathering propeller blades nearly a century ago [MSNA, 1865, p. 474].

A *feathering propeller* is defined as one whose thrust-producing blades can be turned on their own axes so that the blade sections are generally parallel to the direction of motion. An under-the-bottom rotating-blade propeller would be feathered, for example, by rotating each blade on its spindle axis so that all the leading edges would face directly forward.

A *folding propeller* is one in which the thrust-

producing blades are hinged so that their axes are swung into positions generally parallel to the direction of motion. In a 2-bladed folding screw propeller each blade folds aft so that its blade axis is sensibly parallel to the shaft axis, with a frontal area considerably smaller than that of a feathered propeller. Both feathering and folding propellers are illustrated by J. Baader on page 210 of his book "Cruceros y Lanchas Veloces (Cruisers and Fast Launches)" [Buenos Aires, 1951].

A 2-bladed screw propeller with *folding* blades, for sailing vessels with auxiliary power, arranged to swing aft and form a continuation of the propeller hub, was proposed and illustrated by Henry Claughton in the early 1870's [INA, 1873, pp. 52–55 and Pl. IV]. The folding was accomplished by a rod which slid lenghwise within the hollow propeller shaft. The inventor claimed, and rightly so, that the folding propeller was superior to the feathering one because the blades of the latter always have some objectionable twist, no matter what the angle at which they are feathered. At the time of writing (1955) folding screw propellers are available in diameters of the order of 1 or 2 ft. They are reported to have a drag only 0.1 that of a solid propeller when it is not rotating [Ship and Boat Builder and Naval Architect, London, May 1953, p. 378].

An adaptation of the "shadowing" 2-bladed propeller, lying in the eddies behind a wide sternpost, is what may be called the housing propeller. This device, pulled in axially with its shaft and held snugly against the hull, was proposed a half-century ago for large vessels [Hamilton, J., INA, 1903, pp. 233–235 and Pls. XXX, XXXI; De Rusett, E. W., INA, 1903, p. 237]. In the 2-bladed form, and with the feathering feature developed in recent years, it is possible to swing the blades nearly fore and aft. They can then, when the propeller and shaft are pulled inward, be drawn into a relatively narrow groove left for this purpose in the end of a skeg supporting the shaft. Provided the mechanical problems can be worked out, this affords one solution for a 2-bladed bow propeller on an icebreaker, mentioned later in Sec. 76.26. Here the propeller is either very useful if it can be run or it is a nuisance if left extended, depending entirely upon the ice conditions.

71.13 Auxiliary Propulsion for Sailing Yachts. There is only one answer to the question often asked by yachtsmen: Where is a good place to put a permanent propeller, to serve as auxiliary propulsion on a sailing craft? There is no good place. In almost any position the propeller is a nuisance for sailing and a misfit for propulsion. To be honest, there is not even a least objectionable place. All locations have disadvantages, from the point of view of both sailing and propulsive efficiency. Even the temporary outboard propeller, hung over the stern or the side, has its drawbacks.

The usual position and arrangement, embodying a centerline propeller working in an aperture cut partly from the sternpost or the after end of the keel and partly from the rudder, is depicted in diagram 2 of Fig. 71.D. To be sure, the propeller outflow jet impinges on the rudder but a sailing craft has a rudder adequate for controllability at low speeds, regardless of the method of propulsion. The propeller aperture, small compared to the boat profile, almost necessarily has thick boundaries. If the craft is of wood, the edges of the opening are liable to be very thick compared to the propeller diameter. As much fairing as

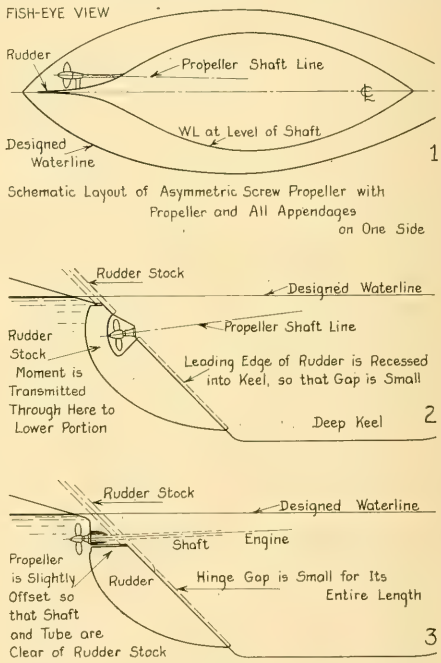

Fig. 71.D Auxiliary Propulsion Arrangements for Yachts

practicable on the forward and after edges is indicated, to prevent separation behind the forward side of the aperture, to keep the wake velocities from being irregular, and to minimize the augmentation of resistance on the after side of the aperture. A 2-bladed propeller lies generally within the aperture when mechanical propulsion is not required, *provided* there is a blade-position marking inside the vessel, and there is some way to place and hold the shaft in the proper angular position. The aperture detracts from the steering and maneuvering characteristics of the vessel but as the rudder is generally large enough for control at speeds much less than that at which the propeller drives the craft, it remains adequate for the purpose.

A propeller may be mounted *above* the top of the rudder with a short exposed drive shaft and a short single-arm strut [Rudder, Mar 1954, p. 37; May 1954, p. 78]. The propeller shaft must be offset slightly from the centerline to clear the rudder stock.

A somewhat more ship-shape installation, based on both the mechanical and the hydrodynamic features involved, is to drop the upper end of the rudder and leave, in its stead, a fixed portion of the after end of the fin keel under the hull. The propeller shaft passes through this fixed portion and the propeller is mounted abaft it. The arrangement permits a reasonably sharp fin-keel ending ahead of the propeller, with fillets between keel and hull which taper to zero at the extreme after end, about as indicated at 3 in Fig. 71.D [Yachting, May 1951, p. 62; Rudder, Apr 1954, p. 37]. Again, however, the propeller and its shaft must be offset slightly from the centerline, to permit the shaft tube and the rudder-stock casing to clear each other. The propeller bossing in the fixed fin above the top of the rudder then has an offset termination similar to those of certain bossings and multiple skegs in large ships but with the disadvantage that in the smaller craft the flow may cross the swelling for the shaft at a slightly greater angle.

A yacht in which the mechanical propulsion is of the same order of importance as the sail is that known as the motor sailer. A most useful discussion of the propulsion and design problems of this class is given by D. Phillips-Birt [Rudder, May 1955, pp. 12–15, 46–55].

J. Baader devotes a whole chapter to the auxiliary propulsion of the sailing yacht ["Cruceros y Lanchas Veloces", Buenos Aires, 1951, pp. 249–256 (in Spanish)]. In this chapter he gives three design graphs for the auxiliary powering of these yachts.

71.14 Vertical Drive for Screw Propellers; Under-the-Bottom Propellers. The combination of a screw propeller mounted on a short horizontal shaft and driven by bevel gears from a vertical shaft is known everywhere in the form of the familiar outboard-motor propulsion unit. However, design features which can be accepted for units in which the power in horses rarely exceeds one or two hundred are not always workable in larger units, such as are likely to be utilized in the future. On all the modern portable installations there is a horizontal barrier or "anti-cavitation" plate to prevent air in the separation zone abaft the casing which carries the vertical drive shaft from working down the after edge of the casing into the propeller disc. This plate must be considerably larger and must extend farther aft when a more powerful propeller is used. Indeed, the vertical casing sections will themselves require lengthening and fining. Efficient and reliable water-excluding and lubrication devices and systems are called for if the vertical drives are to transmit powers in thousands of horses instead of hundreds, and if they are to run continually for days on end.

Besides being retractable by hinging or swinging, as in the customary outboard-motor assembly, vertical-drive propeller systems lend themselves to packaging in self-contained units. These may be installed in vertical recesses or wells and removed when desired, similar to the *Sea Otter* installations of World War II. The propellers at the lower ends of the assemblies may project below the baseplane, or below a flat, cut-up portion of the vessel at the stern, similar to that for the usual type of rotating-blade propeller installation. Large-diameter 2-bladed propellers may be passed through small-diameter wells or small openings by keeping the blades vertical. In the early days of steam it was possible to lift the 2-bladed propeller up on deck through a well in the hull at the stern. A modern installation, proposed for an oceanographic research vessel, is shown in Fig. 33.J.

A partly sectioned isometric view of a modern outboard-propulsion unit in package form, designed to swing the propeller upward by mechanical means, is shown by A. C. Hardy ["Modern Marine Engineering," London, 1955, Vol. II, p. 154].

Flow to under-the-bottom propellers, working below vertical wells which house retractable or removable units, is practically axial but it may suffer from non-uniformity because of the presence of the boundary layer. If the propellers are actually below the baseplane, and in a region where the ship bottom is sensibly flat, parallel to the direction of motion, there should be little augment of resistance due to the pressure fields created by the propellers. Although thrust-deduction forces were observed on the *Sea Otter* model, this is believed due to the fact that the closures at the bottoms of the vertical wells in the models were not watertight. The $-\Delta p$ and $+\Delta p$ fields set up by each propeller extended up into the lower portion of each well, where small forces acting aft, opposite to the direction of motion, were developed on both the forward and after walls of the well.

71.15 Design of Devices to Produce Transverse and Vertical Thrust. For docking, mooring, and shifting berth, in areas where the port facilities are not adequate, it frequently becomes necessary for a ship to sidle or to change its heading. This usually happens when it is not possible to shift an appreciable distance either ahead or astern, certainly not far enough to create the offset or make the change in heading by the ordinary operations of maneuvering. This offset or change in heading requires the application of a more-or-less static force at one or both ends of the vessel, in a direction approximately perpendicular to its centerplane and in line with the shift in position desired.

Normally these forces are applied by tugs pushing and pulling or by ropes between fixed objects and the ship, connected to capstans or winches. When neither the tugs nor the fixed objects are available, and when the offsets and changes of heading are required to be performed frequently as a routine part of a vessel's operation, this may be accomplished by fitting separate auxiliary propellers which apply thrust in a transverse direction [SBSR, 20 Nov 1952, pp. 659–660].

The simplest installation of this kind is the straight-through type illustrated schematically in Fig. 71.E. A substantial shroud ring encircles the propeller to carry the gear teeth. The increase in diameter—and area—at the propeller position enables a larger and more efficient wheel to be used, and partly compensates for the area occupied by the shaft and its bearings, or by a bevel-gear mechanism if a different type of drive is employed. The problem here is keeping the gears small enough so that the area occupied by the gear casing is not excessive. A straight-through installation of this general type is found in the Canadian ferry *Princess of Vancouver*, except that the water is moved transversely through a duct of rectangular section by a Voith-Schneider propeller [Ill. London News, 19 Mar 1955, p. 516; MENA, Mar 1955, p. 112].

If sufficient beam is available at the position selected for the transverse propeller or thrust-producing device it may be advisable to use a vertical-shaft propeller in a Z-shaped passage having offset openings to port and to starboard. Fig. 71.F is a schematic arrangement for such an installation. It removes from the water passage the bevel-gear box which would be required for a straight-through transverse duct, with a drive shaft entering at right angles to its axis. The two sets of corner vanes are placed in the two elliptical intersections of the circular ducts, where the increased area compensates for the flow restrictions imposed by the multiple vanes.

The propeller shaft, shown vertical in the figure, may lead in any desired direction to the drive motor, permitting the latter to be placed in the most convenient and protected position in the ship. The Z-shaped duct remains in the transverse plane through the drive shaft but this plane may be either vertical or horizontal or may lie at any convenient angle.

To prevent separation of the inflowing water at points such as E_1 and E_2 in Fig. 71.F the

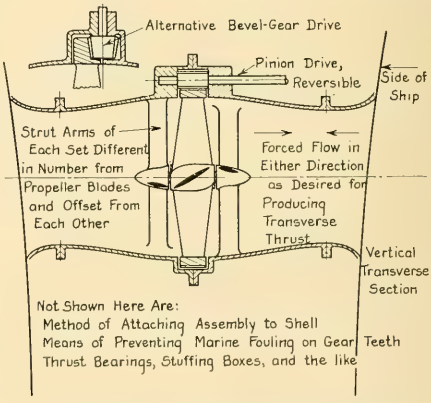

Fig. 71.E Schematic Arrangement of Auxiliary Propeller for Exerting Transverse Thrust

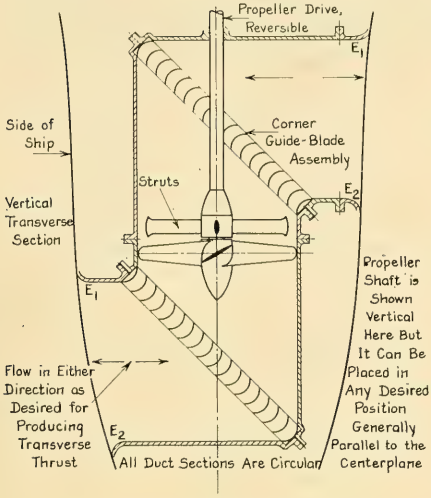

FIG. 71.F SCHEMATIC ARRANGEMENT OF VERTICAL-DRIVE SCREW PROPELLER FOR EXERTING TRANSVERSE THRUST

entrances are rounded, say to a radius of 0.1 or more of the duct diameter. There should be enough hydrostatic head above the uppermost duct to prevent drawing air from the surface.

The efficiency of a propeller-type device to produce transverse thrust is measured, not by the usual ratio of output to input but by whether or not the device works. This depends upon the lateral thrust developed. The thrust in turn depends first upon the diameter of the propeller and the rate at which momentum is imparted to the water in a transverse direction. It depends also upon the length and shape of the transverse duct, because of the friction and pumping-pressure losses in the water being forced through it.

If the two openings of the transverse duct lie in regions where there is much slope to the waterlines, there is liable to be some slight but definite effect of these discontinuities when the vessel is underway. It is generally not possible to close the openings when they are not in use so that when the vessel yaws or turns there may be some transverse flow of water through the duct. This may cause windmilling of the propeller unless it is locked.

The best positions for propellers producing transverse thrust are in the forefoot and in the aftfoot. These are usually thin, so the ducts may be short. They are well removed from the center of gravity of the ship, so the turning moments are large.

Any large transverse opening, such as for a transverse propeller, cut through the thin skeg of a ship just ahead of an unbalanced rudder at its after end, may or may not be detrimental to turning. The opening permits leakage of $+\Delta p$ built up by the rudder on the inside of a turn. If the vessel is turning at a large drift angle, there may be cross flow through the duct from the outside to the inside of the turn. Furthermore, if the propeller is not locked by non-overhauling drive gears or a brake, it may windmill under these conditions.

71.16 Design Features of Tandem and Contra-Rotating Propellers. Normally, it is not good design to place propulsion devices of any kind in tandem, even when they are as far away as the bow and stern propellers of a double-ended ferryboat. If, under unusual circumstances, it becomes necessary or desirable to absorb a relatively large amount of power by a propulsion-device combination occupying a limited disc or thrust-producing area, it is possible to achieve reasonable efficiency by driving the propulsion devices separately. This enables each to run at a proper advance coefficient $J = V_A/(nD)$, depending upon the speed of advance at its own position. Still better is a type of drive which automatically adjusts its rate of rotation so that its propulsion device absorbs a pre-determined power.

For tandem screw propellers, described in Sec. 32.20, a device which has possibilities for certain applications is a sort of contra-propeller interposed between the leading and following units of a pair of tandem propellers [Schmierschalski, H., WRH, 1 Sep 1939, pp. 278–279; HSPA, Vol. II, 1940, pp. 79–102, with English summary on pp. 217–218]. This star-shaped set of guide vanes, with or without a fixed shrouding around the outside, is intended to recover the rotational energy in the outflow jet of the leading propeller and to impart enough pre-rotation to the inflow jet of the following propeller so that the rotational energy in the final outflow jet is very nearly zero. The mechanical problems involved in placing a fixed appendage of this kind between two tandem screw propellers on the same shaft have not, so far as known, been tackled except on model scale.

It is customary, although not necessary, to

place the discs of contra-rotating propellers close to each other, spacing them along the shaft axis at only a small fraction of the propeller diameter, just sufficient for the hubs and the blades to clear each other. The following propeller is made slightly smaller in diameter than the leading propeller because of the contraction in the outflow jet from the latter.

If both propellers of a pair rotate oppositely at the same rate, the pitch of the after wheel is made slightly greater to produce generally the same thrust, torque, and power as the forward one. There is no reason, however, why both propellers need rotate at the same rate if other rates or ratios are preferable.

For contra-rotating propellers such as those mounted on the afterbody of a torpedo, where the flow is definitely converging toward the shaft axis as it approaches the leading propeller, both propellers of the group can be raked aft to advantage, provided centrifugal-force and other factors are properly taken care of.

The design of contra-rotating propellers poses a problem discussed in Sec. 67.22 for the contra-guide skeg ending. It is to find the exact direction of the flow in the outflow jet from the leading propeller as it meets the leading edges of the blades of the following propeller. This is a matter partly of determining the direction at which the flow leaves the trailing edges of the forward wheel and partly of the amount of induced velocity imparted to it by that wheel, at a distance astern represented by the forward sweep line of the after wheel.

There are two published design procedures available:

(1) Lerbs, H. W., "Contra-Rotating Optimum Propellers Operating in a Radially Non-Uniform Wake," TMB Rep. 941, May 1955. On page 22 there is a list of 6 references. In general, this method takes account of the effects arising from the difference of the wakes at the propeller discs and from the contraction of the race between them. The design procedure is outlined by steps but no example is given.

(2) Van Manen, J. D., and Sentić, A., "Contra-Rotating Propellers," INA, Apr 1956; SBSR, 3 May 1956, pp. 302–303; SBMEB, Jul 1956, pp. 462–463; Int. Shipbldg. Prog., Sep 1956, Vol. 3, No. 25, pp. 459–473. Eight references are given and a numerical example is included.

H. W. Lerbs observes that contra-rotating pairs of propellers are efficient only for large P/D ratios, say more than 1.2; that is, when the tangential components of the induced velocities are large. Normally, large P/D ratios accompany small thrust-load factors C_{TL}.

71.17 Design Notes Relative to Rotating-Blade Propellers. The functioning of the rotating-blade propeller is described and illustrated in Sec. 15.13 and Figs. 15.I, 15.J, and 15.K. Its use for steering and maneuvering as well as propulsion is discussed in Sec. 37.22 and illustrated by the diagrams of Figs. 33.H, 37.O, and 37.P. References to test results on propellers of this type are given in Sec. 59.7. Additional references in the technical literature are:

(1) Mueller, H., "Schiffsmodellversuche im Strömungsgerinne (Ship Model Tests in a Flowing-Water Channel)," Schiffbau, Schiffahrt, und Hafenbau, 1936, Vol. 37, pp. 168–173, 206

(2) Mueller, H., "Einfluss des Hohlsogs auf das Arbeiten des Voith-Schneider-Propellers (Influence of Cavitation on the Working of the Voith-Schneider Propeller)," Zeit. des Ver. Deutsch. Ing., 1938, Vol. 82, pp. 566–568

(3) Fuller, W. E., "A Radical Departure in the Conventional Tugboat Design, and a New Use for Cycloidal Propulsion," ASNE, Aug 1953, pp. 639–645

(4) "German Craft with Voith-Schneider Propellers," SBSR, 23 Sep 1954, pp. 409–413

(5) "Voith-Schneider Propulsion;" booklet of 23 pages prepared and published by the J. M. Voith Company of Heidenheim, Germany (in English). Copy in TMB library.

It is desired again to emphasize that this type of propulsion device can be employed to produce thrust in any direction within any selected plane of rotation, whether horizontal, vertical, or inclined. Diagram 2 of Fig. 33.H illustrates schematically a rotating-blade propeller fitted to a submarine with its axis horizontal, or nearly so, and its plane of rotation generally vertical and parallel to the plane of symmetry.

A suitable thrust-load factor C_{TL} for a rotating-blade propeller, expressed by $C_{TL} = T/(0.5\rho A_0 V_A^2)$, is based upon an area equivalent to A_0 which is rectangular in shape. It represents the maximum transverse section through what is known as the basket or barrel formed by the blades, having a height equal to the blade length and a width equal to the diameter of the pitch circle. This corresponds to the hatched area of diagram 6 of Fig. 15.G. In practice, the proportions of this rectangle remain sensibly constant, having a ratio of pitch-circle diameter to blade length of about 1.5 to 1.75. W. Henschke gives a sketch and a table of principal dimensions of Voith-Schneider propellers, taken from "Schiff-

baukalender," 1935 ["Schiffbautechnisches Handbuch (Ship Design and Shipbuilding Handbook)," Berlin, 1952, p. 192]. For this series of sizes the ratio of (basket or barrel diameter)/(blade length) has a constant value of 1.67.

The nominal thrust-producing area of a rotating-blade propeller may, and generally does occupy more area normal to the direction of motion than a screw propeller; sometimes more than twice as much. The thrust-load factor is therefore, like that of the paddlewheel, much less than for a screw propeller to do essentially the same work. Diagram 2 of Fig. 34.M and the graphs of Fig. 34.N show that, below a C_{TL} value of about 2.2, the efficiency of a Voith-Schneider propeller may be expected to exceed the 0.8-ideal-efficiency value of a screw propeller.

The thrust-producing area adjoins the hull at its upper or inner end, without the tip clearance associated with a screw propeller. The wake fraction at the propeller position is therefore almost certain to be higher—and more variable as well—than for a screw propeller *in the same position.* There are no published formulas or systematic data available for a prediction of the wake fraction.

Similarly, the thrust-deduction fraction is not readily determined from orthodox or routine reference data. The area of the propeller inflow jet is larger, because of the larger equivalent A_0, but the $-\Delta p$'s are usually of smaller intensity. It is probable that, with a stern cut away sufficiently to provide easy flow to an under-the-bottom propeller, in a direction generally normal to the blade axes, the thrust-deduction fraction will be lower than for a normal-form stern with a screw propeller.

An efficient design and installation of a rotating-blade propeller calls for blades that are sufficiently narrow to eliminate interference between them and sufficiently long to provide adequate area for the thrust to be delivered. There must be sufficient submersion of the whole assembly to avoid harmful cavitation in way of the upper ends of the blades. While the presence of the large flat under surface of the hull above the propeller minimizes air leakage to the $-\Delta p$ regions, it is difficult to prevent detrimental cavitation at high blade loadings.

The arrangement shown in Fig. 71.G is in general similar to that of the stern of the turbo-electric motorship *Helgoland* of 1939, at that time "the largest seagoing vessel yet fitted with Voith-Schneider propulsion" [SBSR, 21 Dec 1939, pp. 644–645]. This vessel had a length between perpendiculars of 328 ft, a beam of about 43.5 ft, and a speed of 17 kt. The rotating-blade propellers were each designed to absorb a shaft power of 2,000 horses, with electric driving motors mounted directly on the propeller casings.

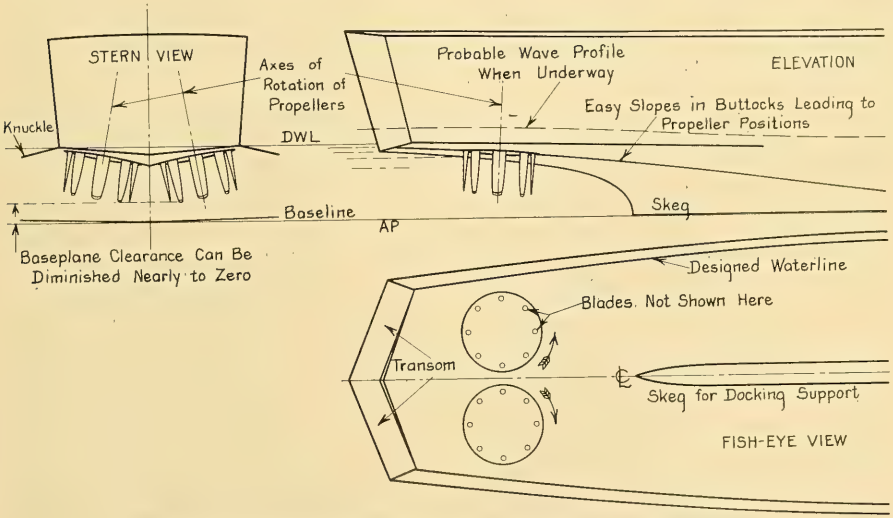

Fig. 71.G Arrangement of Twin Rotating-Blade Propellers at the Stern

The rotating-blade propeller lends itself particularly well to craft which must hold position against wind, tidal-current, and other forces when stationary or nearly so. It is reported [SBSR, 12 Mar 1953, p. 342], in an article on "German Small Craft," that:

"The Voith-Schneider propeller has proved of particular value in applications where large athwartships thrusts are required. It has therefore been fitted for buoy lifting and laying vessels which have to be operated in particularly difficult waters."

The article is accompanied by the outboard profile of a small lighthouse tender with a long, sloping, cut-up stern and two Voith-Schneider propellers, one well out on each side, set with their axes pointing upward and inward. The blade tips are well above the baseplane. However, the tops of the blades come rather close, perhaps too close, to the water surface.

The large diameter of the rotating assembly of a propeller of this type lends itself equally to a high gear reduction from a high-speed engine or motor or to a low-speed motor drive. The angular speed of the propeller is usually not a major design problem.

On the other hand, the rotating-blade propeller, of whatever type, has been plagued from the beginning of its development by the unavoidable complication and relative vulnerability of the internal mechanical gear. With half a dozen or more blades to position, not only for straight-ahead steady running but for changing the pitch and changing the direction of the resultant thrust, the mechanical-design problem is difficult at the best [Mueller, H. F., "Recent Developments in the Design and Application of the Vertical Axis Propeller," SNAME, 1955, pp. 4–30]. Simplifications have been effected to make the parts more sturdy, but these changes have, more often than not, involved some reduction of the hydrodynamic efficiency. By dint of excellent engineering the rotating-blade propeller continues to run. It is possible that some of the developments which have brought a greatly increased measure of reliability to the controllable propeller may do the same for the most useful rotating-blade device.

71.18 Airscrew Propulsion. An early type of "skimming boat" with airscrew propulsion, apparently intended for work in extremely shallow water, was designed and built by Yarrow of Glasgow about 1921 [Mar. Eng'g., Jul 1921, p. 538]. An air-rescue task is clearly indicated, since the wide, flat-bottomed craft was capable of a speed of 50 miles per hour. A later type is shown by D. Nicolson [NECI, 1937–1938, Vol. LIV, Fig. 5, p. 117]. Sea sleds or inverted V-bottom craft driven by airscrews are illustrated in Motor Boating [New York, Jan 1946, p. 112]. Two types of high-speed boats driven by airscrews are shown by J. Baader, in a chapter in which he gives design instructions and data for the powering of this type of craft ["Cruceros y Lanchas Veloces (Cruisers and Fast Launches)," Buenos Aires, 1951, pp. 222–224].

Propulsion by airscrew(s) is selected when:

(a) Weeds, grasses, and other marine growths are so profuse and thick that hydrodynamic propulsion by weedproof screw propellers, or by sculling propellers, paddlewheels, and similar devices is out of the question

(b) The hull and the engine are so high above the water surface, as in a hydrofoil-supported craft, that it is undesirable or inconvenient to transmit the power to a propeller under water

(c) It is necessary to eliminate the noise and other disturbance made under water by mechanical propulsion devices. This may be mandatory for certain fishing operations.

(d) It is desired to measure the hull resistance of a craft, free of all hydrodynamic propulsion effects.

To compensate for the down-pitch moment of the airscrew thrust, at a large relative height above the line of action of the water-resistance forces, any small boat carrying an airscrew must have a large hydrodynamic moment resisting the thrust moment. This is one reason for the use of sled-type craft of rectangular cross section, resembling the floats of early seaplanes.

Airscrew propulsion is exceedingly inefficient—indeed, it is almost ineffective—when the speed of advance is low, as it would be for even a small swamp boat plowing through a heavy growth of weeds. Air flow through the propeller then resembles that depicted in Figs. 16.K and 16.L, when momentum is imparted to only a small mass of "new" air in any given interval of time or given distance of forward travel. The propulsive efficiency mounts rapidly as the speed of advance increases in proportion to the velocity of the outflow jet of the propeller. For this type of drive, therefore, the resistance of the craft to be driven should be low and the resulting speed high.

CHAPTER 72

Design Features Applicable to Shallow and Restricted Waters

72.1 General. The elements of the flow about a body or ship in shallow and restricted waters are discussed in Chap. 18; the behavior of actual ships under the same conditions is described in Chap. 35. Formulas, graphs, and procedures for predicting or estimating the behavior of ships in confined waters are set down in Chap. 61.

The design comments, suggestions, and rules given here apply primarily and rather exclusively to craft which operate more or less continually in water that is shallow with reference to the linear dimensions of the vessel. One rule of thumb for all speed ranges is that a shallow depth is one which is less than the beam of the vessel. Perhaps a better one is that a shallow depth is less than twice the draft. Another rule, for the subcritical range only, is that the depth is less than the so-called *square draft*; in other words, less than the square root of the maximum-section area, or $\sqrt{A_X}$. To be sure, many such shallow-water vessels are required to traverse deep spots now and then but at some sacrifice in performance, if need be, to insure the best shallow-water behavior.

For design and operational purposes, craft intended to run in shallow and restricted waters are divided into four categories:

(1) Self-propelled, fine-lined craft having a shallow-water speed V_h that is close to but always less than the critical speed c_C for the nominal or average depth h. The speed V_h may always be less than the critical speed c_C for the shallowest part of the route. These craft usually carry passengers and moderate amounts of freight.

(2) Self-propelled, full-bodied craft of moderate speed, where V_h does not exceed about $0.7c_C$, for the carrying of the maximum amount of cargo on a given set of limiting dimensions

(3) Non-self-propelled barges, lighters, and scows

(4) Self-propelled pushboats and towboats, for which the free-running shallow-water speed V_h may exceed the critical speed c_C.

Design notes and rules for the latter two groups are given in Part 5 of Volume III. For the second group, carrying capacity is usually of far greater importance than efficiency of propulsion or hydrodynamic performance. Bottoms are flat and of large area, lying at the limiting-draft level. Waterlines are full and sides are vertical or nearly so, except perhaps in way of the inflow jets to screw propellers. The hydrodynamic design features in this chapter are therefore limited generally to vessels in the first category preceding.

Design notes previously published for particular types and for shallow-water vessels as a class may be found in the following references:

(a) Ward, C., "Shallow-Draught River Steamers," SNAME, 1909, Vol. 17, pp. 79–108

(b) Wilson, R. C., "Construction and Operation of Western River Steamers," SNAME, 1913, Vol. 21, pp. 59–65

(c) Baker, G. S., "Ship Design, Resistance and Screw Propulsion," 1933, Vol. I, pp. 209–212; Vol. II, Chap. XXVI, pp. 136–142
(d) Mitchell, A. R., "Shallow Draught Ships," INA, Jul 1952, pp. 145–153
(e) Mitchell, A. R., "Tunnel Type Vessels," IESS, 1952–1953, Vol. 96, pp. 125–188.

72.2 Reference Data on River, Canal, and Channel Slopes and Currents. The free surfaces of all flowing rivers, tidal estuaries, open channels, and canals in which horizontal currents flow, have some slope with reference to the horizontal. Data on the surface slopes of all the principal rivers in the United States, subdivided into river regions where the slopes change rapidly or where there are reliable data, are given in both tabular and graphic form in a paper by H. Gannett entitled "Water-Supply and Irrigation Papers of the U. S. Geological Survey, No. 44, Profiles of Rivers in the United States," U. S. Geological Survey, Washington, 1901.

Nothing in this paper indicates the slopes which might occur during flood conditions, or those which might obtain in short reaches of the order of 1 mile in length. The construction of dams in many of the rivers since 1901 has of course changed the situation materially. The slopes cover a rather wide range, as indicated hereunder:

Location	*Drop in ft per geographical mile of 5,280 ft*
Sacramento River	3.0, maximum
Missouri River	1.0 average; varies from 0.7 to 1.3
Platte River	Averages 5.0 or 6.0
Colorado River	Two steepest slopes are 22.0 and 31.2, corresponding to natural tangents of 0.00417 and 0.00591; remainder are 6.0 to 8.0.

G. Nowka gives the surface slopes of some European rivers as about 1 in 1000 ["New Knowledge on Ship Propulsion," 1944, BuShips Transl. 411]. Here the slope thrust is sufficient to produce a speed which gives steerageway to a non-self-propelled barge when drifting downstream. This is equivalent to a 5.28-ft drop per geographical mile or a 6.08-ft drop per nautical mile.

The steepest reaches in any large navigable river of the world are in the Yangtze in China, where the river rises some 600 ft in the 1000 miles between its mouth and the city of Chungking. Certain sections when in flood have free surfaces so steep that the currents in the navigable channels reach velocities of 12 to 14 kt.

The method of calculating the drag and thrust due to the declivity of the surface upon which a ship or body is floating is described in Sec. 57.10.

72.3 Economical and Practical Speeds in Shallow and Restricted Waters. Decisions as to the designed speeds for shallow-water vessels are properly made by the prospective owners and operators, on a basis of many factors other than hydrodynamics. However, the designer may be called upon to give information and advice on this matter. He is therefore required to have some knowledge of the factors involved and some quantitative data for reference.

The first things to know about the shallow-water and restricted-water regions in which the ship is to run are the depth, bottom contours, channel dimensions, water-section outlines, current directions, current velocities, and local current irregularities. This may be greatly complicated by variations in these factors due to flood and tidal conditions. These in turn depend upon the weather as well as the seasons and the rotation of the earth.

It is not adequate to depend upon average values of the water factors previously listed, either as averages of distance or of time. It is necessary to assume extremes as well, if ship operation is to be maintained on schedule. Further, disaster may, and usually does lurk around the corner of the one operating situation that has not been investigated properly and for which preparations have not been made.

First, a reasonably uniform depth h is determined for a certain section of the route, under given conditions. The next step is to find the speed of the solitary wave in that depth, so that the ratio of a given shallow-water ship speed V_h to the critical wave speed c_c may be known. As an aid in relating contemplated ship speeds to the solitary-wave speed for any depth, Table 72.a gives the latter speed for a considerable range of depths to be encountered in practice.

The values given in this table are for still-water conditions, with no current. When the water in an estuary, river, or channel is flowing in one direction or the other, the solitary wave speed of Table 72.a is still valid when reckoned with reference to a point *fixed in the water*. When a ship is overtaking a solitary wave, therefore, it makes no essential difference whether the ship is moving with the current or against it. The important factors are the wave speed and the ship speed, both reckoned through the water.

It is emphasized, however, that the critical

speed of the solitary wave or wave of translation can and does change rapidly with the depth of water and the configuration of the bed. Since the wave itself is short, a change in depth that is relatively short in the direction of motion changes the speed of advance of the wave rather suddenly. For instance, in passing over a narrow rock ledge its speed is changed in proportion to the clear depth over the ledge. It may be more than disconcerting to the pilot of a ship moving at just below the critical speed in the deeper water to find the solitary wave suddenly dropping back and raising the bow of his vessel.

The contours of Fig. 61.L indicate the regions of both the critical-speed ratio $V_h/\sqrt{gh}$ and the square-draft to depth ratio $\sqrt{A_X}/h$, where the total shallow-water resistance R_{Th} is only slightly greater than the total deep-water resistance R_T, as well as the regions where the ratio of these two values mounts rapidly. If the square-draft to depth ratio $\sqrt{A_X}/h$ is low, the point where the resistance begins to increase rapidly is at about $0.8\sqrt{gh}$ or $0.8c_G$.

This corresponds to a speed, in ft per sec, of about $4.54\sqrt{h}$, when the depth h is in ft. In kt, the value is about $2.69\sqrt{h}$. In metric units, the limit is, in meters per sec, about $2.5\sqrt{h}$ when h is in meters; in kt, it is about $1.29\sqrt{h}$ when h is in meters [Kempf, G., "Wirtschaftliche Geschwindigkeiten bei Fahrt auf flachem Wasser (Economical Speeds When Running in Shallow Waters)," WRH, 7 Dec 1923, pp. 601–602; SBSR, 5 Jun 1924, pp. 671–672].

TABLE 72.a—SOLITARY-WAVE SPEEDS FOR A RANGE OF UNIFORM SHALLOW-WATER DEPTHS

The celerity c of the solitary wave or wave of translation is related to the depth h by the formula $c = \sqrt{gh}$, where g is the acceleration of gravity. In English units g is taken as 32.174 ft per sec². For this table, 1 kt is 1.6889 ft per sec.

Water depth h, ft	Celerity c, ft per sec	Celerity c, kt
2	8.02	4.75
3	9.82	5.81
4	11.34	6.71
5	12.68	7.51
6	13.89	8.22
7	15.01	8.89
8	16.04	9.50
9	17.01	10.07
10	17.94	10.62
12	19.65	11.63
14	21.22	12.56
16	22.69	13.43
18	24.07	14.25
20	25.37	15.02
22	26.61	15.76
24	27.79	16.45
26	28.92	17.12
28	30.01	17.77
30	31.07	18.40
35	33.56	19.87
40	35.87	21.24

In the reference cited Kempf makes the statement that the *maximum increase in resistance* has been found to occur at a critical-speed ratio V_h/c_G of about 0.927. Examination of the graphs of Figs. 35.D and 61.A reveals that, despite somewhat erratic data, this ratio is perhaps on the high side. A better practical ratio of the shallow-water ship speed to the critical speed is about 0.9. The critical-wave speed ratio at which the highest *percentage increase* of the ratio [(total resistance in water of depth h)/(total resistance in deep water)] occurs is slightly lower still.

It is true that in the 1820's, and possibly for a century before that time, horse-drawn canal boats traveled at supercritical speeds, taking advantage of the reduction in resistance gained thereby. However, the canals of those days were shallow affairs, probably not more than 5 or 6 ft deep, so that a towing speed of 8 mph lay in the supercritical range. With the deeper depths of modern inland waterways, of 10 ft or more, traveling at supercritical speed involves traffic and other risks. Furthermore, with a long string of barges it is not possible to have all of them ride simultaneously on the face of a solitary wave.

72.4 Design for Reduction of Confined-Water Drag, Sinkage, and Squat. If the deductions made by Otto Schlichting and described in Secs. 61.3, 61.4, and 61.5 are correct, two major factors—and only two—are responsible for the changes in resistance and speed which occur between deep-water and confined-water conditions. The first is the increased pressure drag from the augmented surface wavemaking. The second is the increased friction drag from the augmented water velocities in the backflow under and along the hull. The remedy for the first is to use a hull that has small pressure drag due to wavemaking to begin with. That for the second is, if practicable, to provide more room for the water to get around the ship and thus to reduce the backflow velocity.

Cutting away the lower outer corners or the

diagonal bulges of the maximum section is one means of reducing the effect of the second factor. A better one, because most of the flow passes the ship under the bottom, is raising the floors or decreasing the draft. This gives more flow area between the ship and the stream bed.

Fortunately, these are equally good solutions to the handicap imposed by lateral boundaries close aboard. It is seldom that the beam or the waterline width of the sections can be appreciably reduced because of the need for deck space, for large metacentric stability, or for lateral room within the hull. In any case, the possible reductions in waterline beam or overall hull width are usually of inconsequential amount, except as they may affect the behavior of the ship in a tight-fitting lock.

The best and, in fact, the only known method of reducing the sinkage and squat found troublesome at high speeds is to increase the backflow area and the bed clearance. On the basis that a given restricted channel can not be made wider and deeper the solution is to make the vessel shallower and the maximum-area section smaller. There are no formulas or systematic data available for predicting the sinkage and squat under confined-water conditions but Sec. 58.4 contains some sinkage and change-of-trim values for a few vessels in shallow water. Sec. 58.7 lists references in which other data of this kind, derived from model tests, may be found.

The importance of this feature is emphasized in the extract from a letter of F. A. Munroe, Jr., Marine Director, Panama Canal Company (of unknown date), published on page 74 of "Marine Engineering" for January 1955:

> "A minimum of 5 feet of water under the keel is considered essential to guard against the squatting effect of a large body moving in a restricted channel and the seiche in the Cut created by the drawing of water at the Pedro Miguel Locks end of the Cut."

72.5 Transverse Dimensions and Section Shapes for Shallow-Water Running. The combination of water depth h and speed V_h to be achieved is almost invariably fixed before the design of a shallow-water ship is undertaken. This leaves the designer, if he has some freedom with the length, the choice of the area A_X and the shape of the maximum section and the overall draft H in relation to the water depth h. Within reasonable limits, the hull most easily driven at the relatively high speeds often required of these vessels, where wavemaking in shallow water is a factor, is one having a low fatness ratio, $\forall/(0.10L)^3$, of the order of not more than 3.0. Sometimes this ratio is as low as 1.4 or 1.5, corresponding to displacement-length quotients $\Delta/(0.010L)^3$ of from 40 to 43. If the overall size is limited, if power is cheap, and if useful load is crowded on, the designer may have to fill the waterway section with all the ship that can be pushed through it, regardless of the square-draft to depth ratio $\sqrt{A_X}/h$.

One way to reduce the maximum-section area A_X is to reduce the draft, but practical considerations may set a minimum limit. There must be enough displacement volume to carry the weight of the vessel and its useful load. There must also be enough hull depth to give it structural strength and rigidity. Too large a beam-draft ratio is not advantageous for propulsion because it increases the waterline slopes at the bow and stern for a given displacement volume. However, if propulsive efficiency is not a major factor, there is no hydrodynamic limit to the beam of a craft intended for restricted-channel operation. Obviously, it must be necessary for two such craft to meet or pass each other in the same channel, or for a single vessel to pass through a lock. If the craft is sufficiently shallow to afford a sizable clearance under the bottom for the passage of displaced water, it may well be that a vessel with a large beam-draft ratio and a small draft is actually easier to handle and less liable to run foul of the banks or of other craft than one which has less beam but also less bed clearance.

The most efficient solution, considering all phases of the water flow around the hull, is to embody a large rise of floor in the midship or the maximum-area section, together with a large bilge radius. The use of floor slopes as high as 10, 15, or 20 deg in the transverse sections acts to increase the draft but this is more of a nominal than an actual increase because of the limited width of the deep-keel portion. If the waterway bed is soft or yielding, occasional encounter of this deep-keel portion with that bed does nothing more than rub off the paint.

The maximum draft may be limited severely by some especially shallow part of the operating area. The necessary displacement volume is then achieved only by using a nearly flat floor and a relatively large maximum-section coefficient C_X, possibly 0.9 or more. When this occurs, it may be necessary to hold to the relatively flat floor lines for only a limited length amidships.

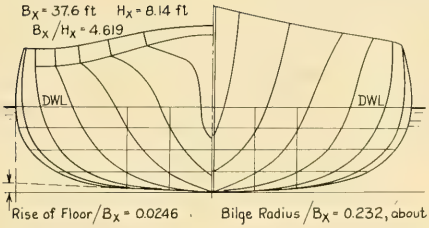

FIG. 72.A BODY PLAN OF DETROIT RIVER STEAMER *Tashmoo*

Along the greater part of the ship length, there is still adequate room to pass the displaced water underneath the bottom. This was done in the design of the Hudson River paddlewheel steamer *Mary Powell*, with a rather flat floor [Int. Mar. Eng'g., May 1920, pp. 406–407], and in the design of the large Lake Erie paddlewheel steamer *Greater Detroit*, to be described presently.

72.6 Typical Shallow-Water Vessels. It is helpful here to examine the forms and other data or some fast shallow-water vessels with slender hulls,—vessels which have given many decades of splendid and even superior performance. The fact that some of these craft were designed and built nearly a century ago is supplemented by the amazing realization that their performance is still good by the standards of today (1955). Many of them, therefore, appear to be perfectly valid bases for a modern, systematic analysis of design for a fast, shallow-water vessel.

Among these vessels are mentioned:

(a) The famous Hudson River steamer *Mary Powell*, designed and built in 1861, when naval architecture in the United States was only emerging from the practical stage. The designed waterline of the run of this vessel is illustrated in diagram B of Fig. 24.G. The complete lines are to be found in "International Marine Engineering" for May 1920, pages 406 and 407; see also a paper by B. F. Isherwood in the Journal of The Franklin Institute, July 1879, Vol. 78, pages 18–27. A model of this vessel, EMB 530, was made and tested at the old Experimental Model Basin at Washington. The results were reported upon most favorably by D. W. Taylor.

(b) Detroit River excursion steamer *Tashmoo*, the body plan of which is reproduced in Fig. 72.A [SNAME, 1901, pp. 1–12; Pl. 3 contains the complete lines of both the *Tashmoo* and the *City of Erie*; also SNAME, HT, 1943, pp. 383–386]

(c) The Lake Erie steamer *City of Erie*, the body plan of which is given in Fig. 72.B. It was, like the *Tashmoo*, designed by Frank E. Kirby, who specialized in lake and river steamers. Its famous race with that vessel in 1901, in the relatively shallow waters of Lake Erie, is still remembered [SNAME, 1901, pp. 1–12].

(d) Hudson River steamer *New York*, the body plan of which is reproduced in Fig. 72.C [SNAME,

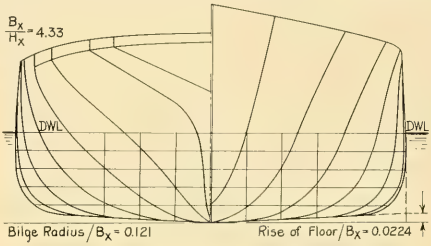

FIG. 72.B BODY PLAN OF LAKE ERIE STEAMER *City of Erie*

1906, pp. 31–40 and Pls. 14 and 15]. A model of this vessel, EMB 529, was made and tested at the old Experimental Model Basin at Washington. This and the two vessels preceding are listed in the table of E. M. Bragg [SNAME, 1916, Pl. 90].

(e) Hudson River steamer *Hendrik Hudson*, designed by J. W. Millard and Brothers, New York [Mason, C. J., MESA, Feb 1930, pp. 100, 104]

(f) Lake Erie steamer *Greater Detroit* (sister vessel *Greater Buffalo*), designed by Frank E.

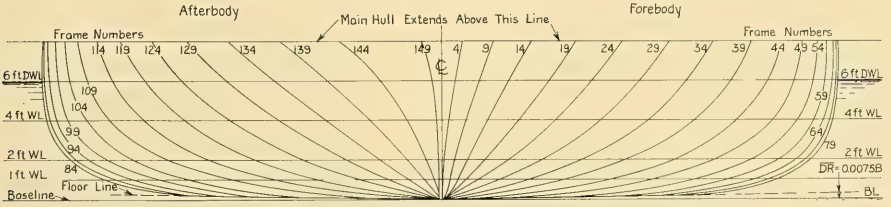

FIG. 72.C BODY PLAN OF HUDSON RIVER STEAMER *New York*

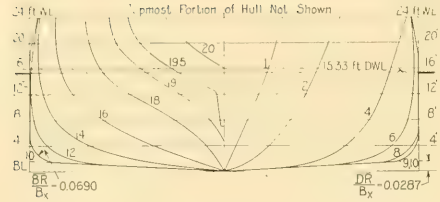

FIG. 72.D BODY PLAN OF LAKE ERIE STEAMER *Greater Detroit*

Kirby in conjunction with H. C. Sadler [SNAME, 1925, pp. 101–108 and Pls. 64–83]. Fig. 72.D is a body plan of this vessel, adapted from the reference. Earlier vessels of this general type are described and illustrated elsewhere [SNAME, HT, 1943, pp. 377–378, 382].

Some dimensions and form data on these vessels, unfortunately not complete and not too reliable because of conflicting published figures, are given in Table 72.b. Additional data on some of these vessels, pertaining principally to their feathering paddlewheels, is given by E. M. Bragg [SNAME, 1916, Pl. 90].

Steam navigation on Long Island Sound, in the period from 1850 to 1910, resulted in the development of fast vessels driven by side paddlewheels, resembling the general design of the *Greater Detroit* [SNAME, HT, 1943, pp. 97–134]. However, although they were of relatively shallow draft, these vessels appear not to have been designed to run in particularly shallow water. They are not further described here as having design features useful for shallow-water craft.

The design of shallow-water vessels for inland waterways in Europe is discussed by G. Lauterbach in "Schiffbautechnisches Handbuch (Shipbuilding and Ship Design Handbook)," Berlin, 1952, pages 613–635.

Possibly because high-speed vessels built for service in confined waters have been considered as specialized craft, factual data on the hulls of these and other ships are rather hard to find in the technical literature. For large vessels at least, pages printed nearly a century ago contain much more information than those of recent years. One outstanding article in the latter category treats largely of the machinery and speaks only briefly of the hull [SNAME, HT, 1943, pp. 97–134]. Most of the published data are lacking the customary hull coefficients, or the essential information by which these data can be calculated. If the length is given the displacement may not be, and vice versa.

TABLE 72.b DIMENSIONS AND FORM DATA FOR AMERICAN RIVER STEAMERS OF THE PERIOD 1870–1940
All the vessels in this table were driven by side paddlewheels.

Name of Ship	*Mary Powell*	*Tashmoo*	*New York*	*Hendrik Hudson*	*Greater Detroit*
When built	1869	1900		1906	1923 (about)
Designed speed, kt	16.66	18.9	18.75	20	18.3
Length on waterline, ft	284 (290?)	302.9	329.6	400	530
Beam, extreme, ft	34	37.6	40		58
Draft, maximum, ft	6.0	13.6 (?)	6	9 (aft)	15.33
Depth, ft	9.33				
Displacement, long t	890 (881?)	1,170	1,240	1,972	9,220 (short)
Displacement-length quotient of Taylor	39.28	42.1	37.7	30.8	61.9
Fatness ratio, $\nabla/(0.10L)^3$	1.38	1.473 (est.)	1.322 (est.)	1.08 (est.)	2.17 (est.)
A_X, ft²	198.5		216		
S, wetted surface, ft²	7,953		11,250		
Coefficient, block, C_B	0.506		0.548		
prismatic, C_P	0.520				
max. sect., C_X	0.973		0.90		
Speed-length quotient, T_q	0.98	1.086	1.033	1.00	0.794
Wheel diameter, outside, ft	31 (extreme)	22.43	29.83	24.0	37.42
Rate of rotation, n, revs. per sec	0.36	0.667	0.465	0.692	0.52
Power, indicated, P_I	1,745	3,400	5,975 (est.)	6,000	10,500
Length-beam ratio	8.529	8.05	8.24		9.14
Beam-draft ratio	5.67		6.67	4.4 (aft)	3.803
Parallel middlebody, per cent of L					5.0

TABLE 72.c—DIMENSIONS, RATIOS, AND PROPORTIONS FOR AMERICAN RIVER STEAMERS OF THE PERIOD 1850–1870

The dimensions marked by asterisks (*) are those listed by J. Scott Russell [MSNA, 1865, Vol. I, p. 666]. The remaining ratios and coefficients are derived from the published dimensions.

L^*, ft	B^*, ft	H^*, ft	A_X^*, ft²	L/B	B/H	L/H	C_X
244	31	4.5	126	7.87	6.89	54.2	0.903
280	35	5.5	175	8.00	6.36	50.9	0.909
322	38	7.5	245	8.47	5.07	42.9	0.860
325	45	10.5	375	7.22	4.29	30.9	0.794
330	40	6.0	220	8.25	6.67	55.0	0.917
360	42	5.0	200	8.57	8.40	72.0	0.952
245	31	3.0	90	7.90	10.33	81.7	0.968
260	29	400	110	8.97	7.25	65.0	0.948
260	38	4.0	150	6.84	9.50	65.0	0.987
240	39	4.0	155	6.15	9.75	60.0	0.994
225	38	4.5	150	5.92	8.44	50.0	0.877

To make up partly for this dearth of published data on large shallow-water vessels in the category under discussion there are given in Table 72.c some dimensions of shallow-draft river steamers plying on the eastern and western rivers of North America prior to 1870. These and other data, published by Normal Scott Russell and John Scott Russell, are verging on the ancient, or at least the historical, for a book on modern ship design. Nevertheless, they form a considerable part of the published systematic data and they indicate the range of ratios and proportions within which successful shallow-water designs may be evolved.

Normal Scott Russell, in his paper "On American River Steamers" [INA, 1861, Vol. II, pp. 105–127 and Pls. IX through XIV], gives on pages 126 and 127 some dimensions of the *Commonwealth* (old), designed and built for operation on Long Island Sound, and the *Memphis*, for operation on the Mississippi River. On page 127 there are two tables of data, one for the "Best Boats on Eastern Waters," and the other for the "Best Boats on Western Waters." The first lists nine vessels, with 14 entries per vessel; the second lists seven vessels, with 14 entries per vessel. J. Scott Russell gives the following data for the *City of New York* (not to be confused with the *New York* of Table 72.b) [MSNA, 1865, Vol. I, pp. 664–665; Vol. II, Pl. 164]:

$L_{WL} = 300$ ft $\quad P_I = 1{,}800$ horses

$B = 40$ ft $\quad A_X = 288$ ft²

$H = 8.25$ ft $\quad C_X = 0.873$

$L/B = 7.5 \quad V = 20$ mph $= 17.4$ kt

$B/H = 4.85 \quad T_q = V/\sqrt{L} = 1.005.$

Lines and body plans for ships driven by sternwheels, as distinguished from side paddle-wheels, are to be found in:

(1) Ward, C. E., "Shallow-Draught River Steamers," SNAME, 1909; lines for a dredge tender are drawn on Pl. 30

(2) 156-ft stern-wheel towboat, Chief of Engineers, War Department, SNAME, 1925, Pls. 45–46

(3) Giroux, C. H., "Performance Tests on Diesel-Electric Stern-Wheel Towboats," SNAME, 1926, pp. 185–202, esp. Pls. 87, 88, and 101

(4) Brodie, J. S., "Modern River Towboats," body plan of "Refined Type of Sternwheeler with Scow Bow and Stern and Rudder Recesses," SNAME, 1936, p. 359.

72.7 Length, Longitudinal Curvature, and Wetted Surface. No ship which is designed to make real speed in shallow water should be crowded into too short a length or have blunt ends. The limited depth of water accentuates the crests and hollows in the wave pattern. The Velox-wave heights should not, if it is avoidable, be accentuated further by full ends and sharp curvature. When the crests of these waves are superposed on a solitary wave of translation the steepness becomes large and the trim excessive.

For minimum overall resistance, a long, fine hull is advisable, with the greatest length and the least beam permitted by the design specifications. This reduces the longitudinal curvature of waterlines and diagonals and decreases the wave-making. The chart of Fig. 66.B, showing the regions at which humps in the resistance curve can be avoided, *does not apply here* because the speeds for a given wave length are less in shallow water than in the deep water for which the chart is drawn.

Added length involves extra wetted surface,

which acts to increase the friction resistance, especially with a high backflow velocity. However, the gain from a small square-draft to water-depth ratio $\sqrt{A_X}/h$ is likely to be greater than the loss from the increased wetted area. A ratio of $\sqrt{A_X}/h$ less than 1.05, as shown by the curve of Fig. 61.G, produces a speed loss from augmented potential flow of less than 10 per cent, while a ratio below 0.375 is responsible for a speed loss of only 1 per cent.

If the length is limited, increase the beam but hold a small draft. The additional bed clearance provided for normal flow under the bottom should more than compensate for the greater waterline slopes associated with the wide beam.

It is comforting to know that, in general, a form of hull suitable for confined waters is found to give good performance in water of any extent and depth, especially for low values of C_P and of fatness ratio $\forall/(0.10L)^3$. Thus a vessel designed to do well in the shallow portion of a route of varying depth is by no means at a disadvantage when operating in the deep portion of the route.

72.8 Modifications to Normal Forms for Shallow-Water Operation. For the vessel which runs mostly in deep water but also has to perform well in shallow and confined waters the concessions to the shallow-water requirements depend upon the relative importance of ship performance in one and in the other. A good example of this situation is the ABC ship, for which the design requirements are set forth in Chap. 64.

Considering the features of this vessel as regards its operation in the canal leading from Port Amalo to the sea, and in the river below Port Correo, it is noted from Table 72.a that for the 28-ft depth of the former the speed of the wave of translation is 17.77 kt. For the 30-ft depth of the latter the critical speed is 18.40 kt. Both are well over the speeds contemplated in those portions of the route, hence the ship will be running in the subcritical range in both cases.

The matter of providing room for the backflow under and around the ship is handled in Sec. 66.13, when laying out the contour of the maximum-area section.

A reserve of power is almost always available to overcome the augmented resistance in confined waters, because the deep-water speed at any draft and trim is in excess of that permitted by local regulations when traversing confined-water areas.

For the 10-kt ABC ship speed in the Port Amalo canal, T_q is $10/\sqrt{510} = 0.443$; at a draft of 26 ft, the value of depth h/draft $H = 28/26 = 1.08$. From Fig. 58.E, using the *T-2* tanker as a basis, the estimated sinkage is $0.0043L$ at the bow and $0.004L$ at the stern; or 2.19 ft and 2.04 ft, respectively. It is necessary to extrapolate the graphs to obtain these values.

For the 14-kt speed (through the water) in the river below Port Correo, T_q is $14/\sqrt{510} = 0.62$; at a draft of 26.5 ft in the fresh water, the value of $h/H = 30/26.5 = 1.13$. The estimated sinkage at the bow is $0.0068L$ or 3.47 ft; at the stern it is $0.0062L$, or 3.16 ft. A much greater extrapolation is required here, in Fig. 58.E, than for the Port Amalo canal estimate.

The C_P value of the *T-2* tanker is 0.74 compared to 0.62 for the ABC ship, and the fatness ratio is 5.76 compared to 4.327. Despite the greater beam of the ABC ship, it appears that the estimated sinkages could all be reduced to about 0.8 of the values given. Even so, the nominal 2-ft bed clearance in the Port Amalo canal is reduced to only $2.0 - 1.75 = 0.25$ ft; in the river below Port Correo it is only $3.5 - 2.78 = 0.72$ ft. These are small but probably representative of modern medium-speed operations in shallow-water areas.

72.9 The Adaptation of Straight-Element Design to Shallow-Water Vessels. A vessel required to operate in confined waters, with restrictions to flow imposed by channel bed and boundaries, should logically receive more than the usual amount of careful hull shaping. It needs everything that can be done to improve the flow around the hull. Nevertheless, the bed and side clearances for most of these vessels approach zero in some part of their operating areas; often in many parts of those areas.

The practical impossibility of shaping the hull to compensate for more than a fraction of these handicaps makes it good design, as well as good engineering, to take this opportunity of incorporating straight-element features in the underwater form. A judicious use of chines, coves, and developable surfaces affords a surprising degree of flexibility to the designer, as is evidenced by the Hillman shallow-water pushboat. A body plan of a craft of this type, 115 ft long by 27 ft beam, is reproduced in Fig. 72.E. Its outboard profile, less numerous details, is drawn in Fig. 72.F. While this vessel was designed primarily for pushing, the general shape should serve well

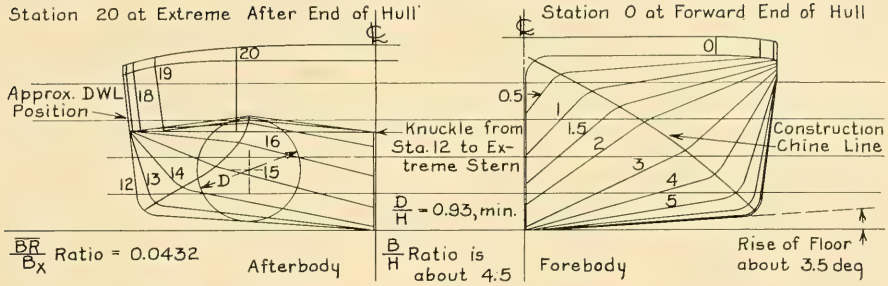

Fig. 72.E Body Plan of Hillman Pushboat with Straight-Element Frame Sections

for any other type of shallow-water vessel running at moderate speed.

The reentrant angles in the forebody sections forward of Sta. 2.5 prevent the flare from becoming excessive in way of the bow wave. At the same time they provide support for a wide deck with its pushing pads (or for passenger accommodations or cargo). Forward of and abaft Sta. 2.5 the section lines lie approximately normal to the lines of flow as the water from ahead passes under the vessel. In the afterbody, the extension of the nearly vertical side down to a long horizontal knuckle, lying at an appreciable distance below the DWL, prevents leakage of air to the propeller region, well inboard from the side. The craft depicted in Figs. 72.E and 72.F was in addition fitted with two Kort nozzles, shown in outline only in the latter figure, which served as additional shields against air leakage. Although it was not possible to arrange for a flow test of a model of this vessel in the TMB circulating-water channel, it appears that the water flow along the afterbody would likewise move easily under the section lines shown.

72.10 Bow Shaping. Shaping the bow and the entrance is a much more difficult operation on a shallow-water craft with a B/H ratio of from 4 or 5 to 10 than on a deep-water vessel, with a ratio of 2.5 to 3.5. The large beam-draft ratio, coupled with the usual requirements for wide decks in a vessel which must carry most of its useful load above the main hull, produces the large flares in the entrance shown on the body plans of Figs. 72.A through 72.E.

If the length is not restricted, the designed waterline slopes in the entrance and run can be made acceptably small, despite a large maximum beam. This helps greatly to counteract the effect of heavy flare in the entrance sections. The entrance slope of the DWL for the *Mary Powell* was only about 6.5 deg; that of the *New York* about 5 deg. The maximum run slopes were 13.8 deg and 15.5 deg, respectively.

A scow, sled, or spoon bow lets most of the water flow easily under the bottom but when the bed clearance is reduced nearly to nothing, the bow must also let it flow easily around the sides. Further, something approaching the shape of a vertical skeg is required forward on a vessel with this type of entrance to provide a stabilizing or fulcrum effect for assistance in steering and turning. This is the reason for the V-shaped forefoot of the Hillman design of Fig. 72.E. A. R. Mitchell recommends that on full-bodied craft of this type the slope of the DWL forward be *not less than* 28 deg, because at a lesser angle more of the water flows around the sides and not under the bottom [INA, Jul 1952, p. 148].

He further recommends that to facilitate this under-the-bottom flow ". . . stem in profile should

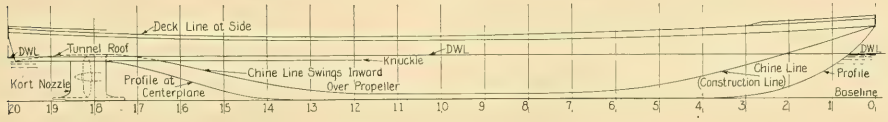

Fig. 72.F Outboard Profile of Hillman Pushboat

Both Figs. 72.E and 72.F are adapted from drawings kindly furnished by the Hillman Barge and Construction Company of Pittsburgh

be swept aft as gently as possible below the load waterline; the buttocks forward should be very easy and the bilges rounded" [INA, Jul 1952, p. 148]. This is done in the Hillman pushboat previously referenced, as depicted in the profile of Fig. 72.F. The forefoot is cut away in similar fashion on the *Mary Powell* and the *New York*, indicated by the lines drawings in the references cited for those vessels.

72.11 Slope and Curvature of Buttocks. In the slow- and moderate-speed ranges, on a wide, shallow craft, most if not very nearly all of the flow passes under the bottom. The buttock slopes and curvatures therefore demand the same attention as the waterlines near the surface in a deep-water ship design. This calls for easy transitions where the forward buttocks or forelines curve downward and aft and under the bottom. Examples of these are found in the keel profile and the chine line at the bow of the Hillman design of Fig. 72.F.

For drafts of the order of 8 to 6 ft or less, it is well to hold the buttock slopes under the run to a maximum of 15 deg with the horizontal; a maximum of 12 or 13 deg is better.

Apparently to save time and labor and to facilitate fabrication and erection, the buttocks under the run of small shallow-draft vessels often have a sharp knuckle where they leave the baseplane. Abaft this knuckle they are straight, with constant slope. If they are given reverse curvature, so as to slope downward and aft behind the propeller position, there is a second sharp knuckle where this change is made. It is pointed out repeatedly in Parts 1 and 2 of Volume I that water resists this sudden change in direction, often with objectionable consequences. It is usually found, furthermore, that with some planning and some alteration of the structural plans, it is just as easy to provide a good path for the water flow as to make a poor one.

72.12 Adequate Flow of Water to the Propulsion Devices. The provision of means whereby water may have free and easy entry to the propulsion devices is much more important in a shallow-water than in a deep-water design. The use of side paddlewheels eliminates the necessity of shaping the hull locally to suit some particular kind of device, especially to insure good flow to it. In fact, this problem almost solves itself, except for the proper fore-and-aft position of the wheels along the hull to bring them in the crest of a transverse Velox wave for the speed of most efficient propulsion. Further comments concerning this feature are included in Sec. 71.6.

When limitations on overall beam prevent the use of side wheels, the paddlewheels can always be placed at the stern. Here they may be either in the form of a pair, one on each quarter with the drive mechanism in between, or there may be only a single wheel, extending all the way across the ship. In either case it is by no means easy to provide the necessary displacement volume at the stern and at the same time to embody the reverse curvature in the buttocks under the run which will project the inflow to the stern paddlewheels in a direction that is roughly horizontal.

The after termination of the hull, just ahead of the stern wheel(s), should not present a surface against which the outflow jet, when the wheels are going astern, can be reflected aft from the hull. If an appreciable part of it is so reflected, an engine order for astern rotation is liable to be followed by an *ahead* motion of the ship!

If rotating-blade propellers with vertical axes are fitted at the stern, or at both bow and stern, one or both ends are cut up toward a flat bottom region in the vicinity of each propeller. This prevents the blade tips from extending below the keel. The blades are approximately vertical and the water coming from under the ship meets them in a nearly horizontal direction. It may be found advisable to fit several of these propellers abreast because the draft limitations are certain to restrict the lengths of the blades.

A shallow-water craft of normal form, to be driven by screw propellers, generally requires at least two screws if the draft is limited and the speed is high enough to call for large powers. In addition, twin screws are useful if not mandatory to overcome the sluggish maneuvering qualities of any vessel under which the bed clearance is small. To prevent any undue reduction in propeller diameter and disc area, with its loss of efficiency and maneuvering power, designers of years gone by resorted to arrangements which are still used to advantage if the situation demands:

(a) Make the tip submergence slightly negative, with the tips normally out of water, on the basis that they will have adequate submergence in the stern-wave crest. This is only feasible if there is to be such a crest at the propeller position and if the propellers are to be lightly loaded.

(b) Place the propellers under a wide torpedoboat

stern, with its lower surface lying very slightly below the DWL, and with a small tip clearance under this surface. N. G. Herreshoff and others built many successful craft to this design.

(c) Use surface propellers for extremely small drafts. This scheme, of course, does not increase the thrust-producing area in proportion to the increase in diameter.

(d) Employ a tunnel-stern design, with at-rest tip submergences ranging from a small positive to a large negative value.

72.13 The Design of a Tunnel Stern. The tops or roofs of the tunnels described in Sec. 25.20 and diagrammed in Fig. 25.M may lie below the designed waterline or extend above it. The design rules given here apply generally to a tunnel whose roof extends *above* the DWL.

When laying out a tunnel stern, whether for one or for multiple screw propellers, it is first decided how much of the propeller disc and the upper blades can be out of water. It is believed that a tunnel system can be designed to function properly even if the shaft axis lies *above* the DWL, as for a surface propeller. This extreme may be considered necessary to permit removing a propeller through an access hatch above, provided the vessel can not be trimmed by the bow for this purpose. However, it is preferable to place the axis at least $0.10D$ below the DWL, where D is the propeller diameter. This keeps the propeller bearing always lubricated (if this is a practical item), keeps the tunnel entirely full of water, and prevents cutting too much out of the hull for the tunnel slopes forward and aft.

The hull tip clearances need be only large enough to insure against mechanical rubbing under all conceivable circumstances and to pass any foreign material that may be in the water without jamming it between the propeller tips and the hull. A tip clearance of 0.04 times the propeller diameter appears to be ample, both mechanically and hydrodynamically. The small tip clearances necessary to insure that the highest part of the tunnel runs full of water may be a partial insurance against excessive tip-vortex losses, particularly when the slip ratio is large.

The next major step is to determine the maximum permissible fore-and-aft slope of the tunnel top, forward of the wheel. Although described in Sec. 25.20, it is well to emphasize here the effect on propulsion of the roof slopes, both forward of and abaft the wheel. In the words of a renowned designer and builder of these craft, A. F. Yarrow ["The Screw as a Means of Propulsion for Shallow Draught Vessels," INA, 1903, p. 107]:

> "There will be an increased resistance to the forward motion of the vessel, due to the action of the screw in reducing the pressure of water at the inclined part of the tunnel forward of the propeller, and this increased resistance is common, more or less, to all screw ships, but it is probably proportionately greater in this class of vessel than in those where the propeller in in the usual position. There is also a loss of efficiency due to the resistance of the inclined surface of the tunnel aft of the propeller."

The region of maximum slope, at about half height of the tunnel, is usually not far below the DWL, where the hydrostatic pressure is small. Good design *to prevent separation* calls for a maximum roof slope, in a vertical plane through the shaft, not exceeding 14 or 15 deg. A. R. Mitchell recommends a limit of 12 deg in fast vessels and 15 deg in slow ones [INA, Jul 1952, p. 148]. This is on the basis of a negligible change of trim when underway.

However, limiting the roof slope to avoid separation is only part of the story, on the basis that propulsive efficiency is a design factor of sufficient importance so that it can not be disregarded completely. A value of η_P(eta) superior to those achieved in the past, even though it is not comparable to that of a large deep-water vessel, is possible only by rather drastic leveling of the tunnel-roof slopes, both forward of and abaft the propeller position. These may have to be of the order of 6 to 10 deg, instead of 12 or 15 to 18 deg. The Hillman design of Figs. 72.E and 72.F achieves this and more. Moving the tunnel boundaries farther forward of and abaft the propeller position reduces the displacement volume aft so that the stern portion of the hull becomes not much more than a cover over the propeller inflow and outflow jets.

There are major structural problems involved in stiffening and supporting a long stern overhang with a buoyancy that is small compared with its size and weight. One solution is to raise the deck aft and increase the girder depth, as was done by the Dravo Corporation for the 200-ft pushboats *A. D. Haynes II* and *Valley Transporter* [Maritime Reporter, 15 Dec 1955, p. 11].

Another important reason for small fore-and-aft slopes in the roof of a tunnel over a screw propeller is to provide as great an astern thrust as possible with a given shaft power and a given

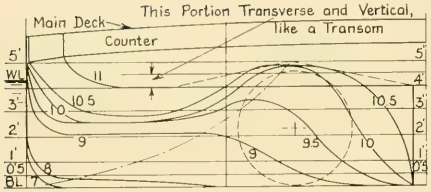

Fig. 72.G Afterbody Plan of Twin-Screw Vessel with Oblique Tunnels

overall disc area of the propeller(s). All shallow-draft self-propelled vessels are required to do a great deal of maneuvering. Furthermore, they maneuver under the handicap of sluggish response because of the limited bed clearance and the obstructions to under-the-bottom flow within that clearance. A configuration of the bottom of the hull and the tunnel roof which facilitates flow from aft is therefore almost as important as a configuration providing good flow from ahead. The slope of the roof abaft the wheel may have to be reduced to the order of 5 deg, if the backing characteristics are sufficiently important.

Contraction of the inflow jet to the propeller is allowed for by flaring the sides and widening the tunnel from aft forward, in much the same manner as the tunnel between twin skegs is widened. The same effect is achieved by progressively increasing the radius of the tunnel roof, also from aft forward.

It is customary to drop the elevated tunnel roof abaft the propeller position until at the extreme stern it meets or falls just below the at-rest water level. This prevents air from being drawn into the tunnel when the propeller rotates astern. It also keeps debris from floating into the tunnel from aft when the vessel is at rest. Unfortunately, this shape also gives rise to an added thrust-deduction force which detracts from the propelling power, described in Sec. 25.20 and earlier in the present section. The length required for an easy slope abaft the propeller positions may be as much as 0.15 or 0.18L; that for a 14-deg maximum slope forward as much as 0.23 to 0.25L.

For vessels having two or more screw propellers, it is customary to provide a separate tunnel for each propeller. If the vessels are to run in regions where there is enough bed clearance to permit a good flow of water to the propellers *from under the bottom*, it appears best for the tunnel recesses ahead of the propeller positions to be parallel to the ship centerline. The tunnels may, with propeller shaft axes, even diverge slightly with distance aft. It often happens, on the other hand, that the bed clearance is extremely small, so small in fact that the propellers can not be fed adequately with water from underneath. One solution is to draw it in from the sides, from the open regions abreast the hull, using oblique, converging recesses that are tunnels in name only. These oblique tunnels were developed at least as early as 1938 and were said to have performed well in service, when the conditions were favorable to their use.

Figs. 72.G and 72.H, adapted from model lines published by A. R. Mitchell ["Tunnel Type Vessels," IESS, 1952–1953, Vol. 96, Fig. 9, p. 141], illustrate one form of oblique tunnel for a twin-screw shallow-draft vessel. This proved its superiority in self-propelled model tests over a vessel with parallel tunnels, when run in shallow water. Fig. 24 on page 165 of the IESS reference is a photograph of half the afterbody of a model built to this design. The same photograph is reproduced in INA, July 1952, Fig. 10, facing page 148. Results of the tests are described rather fully on pages 143 through 150 of the Mitchell reference.

For a tunnel-stern towboat, built without oblique tunnels, on which the flow to the propellers was inadequate because of limited bed clearance under the hull in shallow water, L. A. Baier and J. Ormondroyd effected a solution by building a large-diameter duct through the hull for each propeller. This duct took in water forward, above the baseplane, and discharged it downward and aft through the tunnel roof ahead of the propeller [Third Midwestern Conf. on Fluid Mech., Univ. of Minn., Jun 1953, pp. 406, 411].

H. Waas shows a twin-screw shallow-draft river craft with propellers far outboard, each housed in a tunnel that fits the tip circles closely but is of limited circumferential extent. A partly underhung, balanced rudder is fitted abaft the skeg endings just outboard of the wheels. The propellers are carried by struts forward of them [STG, 1952, Figs. 16, 17, p. 213].

If the exposed positions of the blade tips of the propellers can be accepted, there is no reason why the tunnel in which they work can not extend abaft the propeller in a direction nearly horizontal. The elevated portion of the outflow jet, acted upon by gravity forces, falls at a certain

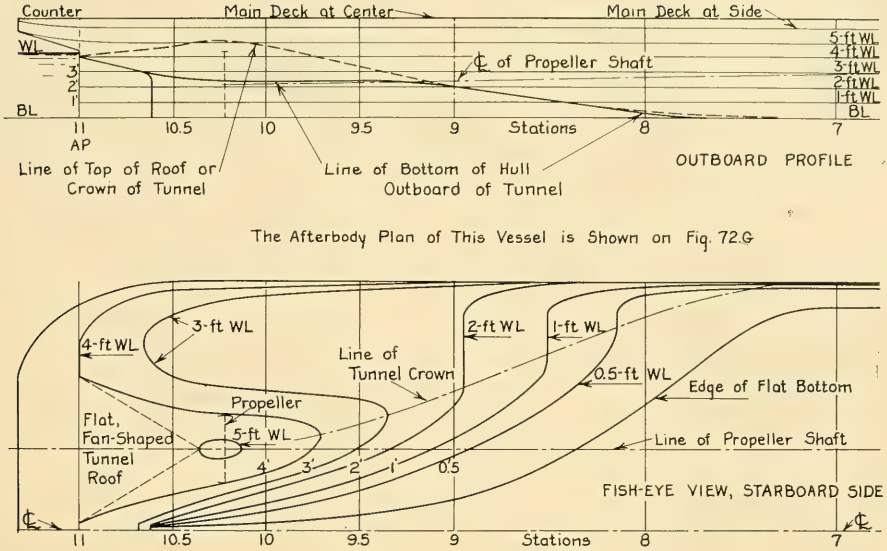

Fig. 72.H Outboard Profile and Fish-Eye View of Vessel with an Oblique Tunnel

rate; in addition, the jet contracts aft. The top of the tunnel can be bent downward slightly to take care of these two effects. It is easy for the propeller, when rotating ahead and accelerating the vessel in that direction, to sweep the air out of the tunnel and to fill it completely with water. However, keeping debris out of the propeller and keeping air out of the disc when going astern, as mentioned previously, require a closure for the after end. Indeed, if the after end is not closed in some way the craft may not go astern at all. Making this closure by dropping the tunnel roof is not always the best solution, especially when there are large changes of draft aft. This difficulty is overcome by a simple yet effective hinged flap, introduced by A. F. Yarrow in the early 1900's, which may be lowered to close the after end of the tunnel. Fig. 72.I shows schematically the arrangement of a device of this kind.

The flap forms the upper part of the tunnel ending, either close abaft the propeller or at a short distance from it. The raising and lowering may be done mechanically or automatically; in the latter case the force exerted by the outflow jet holds the flap at the proper angle. The flap is sealed along its sides. Its lower edge is a fraction of a foot below the at-rest waterline, with the vessel in the light condition, so as to exclude air when the propeller is starting. When underway the flap levels out; its after end usually rises above the waterline. A good tunnel seal is maintained in all conditions of loading. The resistance is lowered because of the reduced inclination of the tunnel roof abaft the propeller. Going astern, the automatic flap is forced down onto a sill, which is set at the lowest point of flap travel. This maintains the seal in the tunnel and the propeller continues to work in solid water [Mitchell, A. R., IESS, 1952–1953, Vol. 96, p. 183].

When the change in draft aft is small, for various service conditions, tunnel endings with

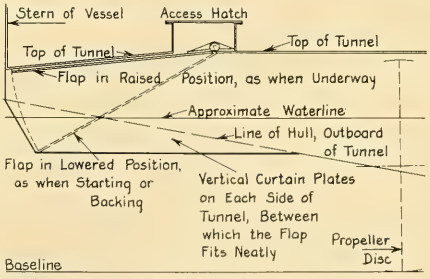

Fig. 72.I Arrangement Sketch of a Hinged Flap Closing the After End of a Propeller Tunnel

small down slope give satisfactory performance and avoid the added complications of the automatic flap. C. E. Ward pointed out, many years ago, that the design of a tunnel-stern craft should be such as to enable the vessel to pivot longitudinally about the fore-and-aft position of the propeller(s) as the loading changes [SNAME, 1909, p. 100]. In other words, the draft at the propeller position should remain more or less constant with changes in the displacement volume and the trim. If, instead, the draft at the stern can be kept nearly constant, the tunnel remains closed at its after end to the same degree and a tunnel flap is not necessary.

One problem in twin- or multiple-screw tunnel sterns, where a propeller is mounted so close to the side that the hull plating forms virtually one side of the tunnel, is that air is liable to be drawn into the inflow jet because of the reduced pressure there. When the ship or tunnel side does not project far enough below the actual waterline to form an adequate pressure barrier, air is sucked under and into the propeller. Large chunks of air striking the propeller produce objectionable noise and vibration. L. A. Baier and J. Ormondroyd report that "vicious stern vibration" on a twin-screw towboat, resulting from air leakage of this kind, was corrected by adding vertical streamlined fins outboard of the propellers [Third Midwestern Conf. on Fluid Mech., Univ. of Minn., Jun 1953, p. 406].

The necessary thrust-producing area A_0 is not easily obtained with a single screw propeller whose diameter is limited by a shallow draft. Tunnel-stern craft are, therefore, usually designed to be driven by two, three, or four screw propellers. There is, however, the case of the tunnel-stern tugs built for Yukon River service in 1898, with six screw propellers, each 3.33 ft in diameter, on a total beam of only 32 ft [Mar. Eng'g., Jun 1898; ASNE, Aug 1898, Vol. X, pp. 740–745; Ward, C. E., SNAME, 1909, pp. 105–106].

72.14 Hull Surfaces Abreast Screw Propellers. The hull surface in way of the small tip clearance provided under the roof of a tunnel should be flush, free of seam laps and butts, and preferably without projecting rivet points and welding heads; in other words, as fair and smooth as good workmanship can make it. The finished tunnel illustrated by A. R. Mitchell [IESS, 1952–1953, Vol. 96, Fig. 15 on p. 155; INA, Jul 1952, Fig. 6 opp. p. 147], with its protruding strut-arm pads, doublers, and hoisting eyes, is an example of what not to do. The hoisting fittings can be of the recessed type, similar to those illustrated in Fig. 75.F. The doublers can be converted to thick, single-layer shell plate and the strut-arm connections can be entirely within the hull.

The strake or ring of plating abreast the wheel is preferably made heavier than the rest, as illustrated for the arch type of stern of the ABC ship in Figs. 67.O and 73.F. It is to be held in position securely by substantial internal framing. Careful fitting of any access hatch over the propeller is necessary to insure a flush surface in the roof. Bolts, nuts, and other securing devices for this hatch are to be kept clear of the tunnel surface. The curved under surfaces of all tunnels, both ahead of and abaft the propeller positions, are to be fair, with sufficient stiffness to remain so and to avoid panting and vibration.

The Germans have proposed for small tunnel-stern craft that the portion of the tunnel roof directly over the screw propeller be made of resilient instead of stiff material. In other words, rubber rather than steel [STG, 1952, Figs. 6 and 7, pp. 207–208]. There is a structural advantage, and possibly a lessening of the vibratory forces if the hull boundary in way of the propeller tips yields with the pressure variations in the blade fields. The effect of a yielding boundary on the continuity and other characteristics of the water flow is not known well enough to justify the use of a resilient boundary as more than an experiment.

72.15 Powering of Tunnel-Stern Craft. The naval architect and marine engineer designing a self-propelled shallow-draft vessel with screw propellers must face the fact that, in the present state of the art, enclosing any appreciable sector of the tip circle within a tunnel recess reduces both the propulsive coefficient η_P and the effective propeller thrust $T(1 - t)$ at low speed. This is undoubtedly because of excessive thrust-deduction forces on the tunnel roof(s) for relatively long distances ahead of and abaft the disc positions. In any case, available published data, principally those of A. R. Mitchell [IESS, 1952–1953, Vol. 96, pp. 125–188], reveal that rarely if ever is it safe to employ a value of η_P for speed and power predictions greater than 0.50. Indeed, Mitchell goes so far as to state that:

> "Generally speaking, it is most unwise to guarantee a specific speed when the depth of water under the keel is less than the draught of the vessel" [INA, Jul 1952, p. 152].

In this connection it is to be noted from Figs. 72.E and 72.F that whereas the Hillman boat depicted there carries a pair of screw propellers having a diameter large in proportion to the draft, there is only a vestige of a tunnel in the afterbody plan. Further, the down slope abaft the propeller position is rather small. This craft is reported to perform excellently in all respects, and the principal reason given is the free flow of water to the wheels [E. W. Easter, unpubl. ltr. of 2 Feb 1951 to HES].

72.16 Handling of the Vibration Problem in Shallow Water. Secs. 35.13 and 35.14 describe the manner in which vibration of the ship hull and its many smaller elements is manifested in motion of the water and is magnified in a shallow-water region. The only known method of avoiding these objectionable effects is to eliminate the vibratory forces at their source. The periodic forces generated by the blades of various propulsion devices are reduced, as explained in Sec. 33.15, first by reducing the thrust loading, using larger thrust-producing areas and lower slip ratios; then by cutting down the high loading in certain regions, such as those of high wake.

When water can not flow freely to a propulsion-device position from one direction, because of confined-water limitations, good design dictates that means be provided whereby it can come in from another direction. This is the reasoning behind the oblique tunnels described in Sec. 72.13. However, it can not always be assumed, without the confirmation of flow tests with geometrically similar boundaries, that the water will follow man-made paths, no matter how attractive they may appear to the eye.

72.17 Partial Bibliography on Tunnel-Stern Vessels. There is a vast technical literature on self-propelled shallow-water craft with tunnel sterns but unfortunately much of it is superficial and descriptive. The partial bibliography of this section lists some of the older technical references and most of the modern ones, omitting many of those containing general descriptions only:

(1) Thornycroft, Sir John, "Steamers for Shallow Rivers," Cassier's Magazine, Marine Number, Jul-Aug 1897, Vol. XII

(2) The twin-screw river gunboat H.M.S. *Sheikh* is described briefly in ASNE, Feb 1898, Vol. X, p. 230

(3) Notes concerning the "light-draught gunboats" *Heron* and *Jackdaw*, built for the British Navy, are to be found in ASNE, Feb 1898, Vol. X, pp. 227–228 and May 1898, pp. 556–559. These vessels are 100 ft long by 20 ft wide by 2 ft draft. Twin screws 3.41 ft in diameter are fitted in twin tunnel recesses. The speed is 10.5 mph or 9.13 kt.

(4) Brief notes on "light-draught steamers," specifically the *Melik* and the *Sultan*, are to be found in ASNE, May 1898, Vol. X, pp. 509–510; also ASNE, Aug 1898, Vol. X, pp. 783–785

(5) Ward, C. E., "Speed and Power Trials of a Light-Draught Steam Launch," ASNE, Feb 1898, Vol. X, pp. 183–192. This was a tunnel-stern, single-screw craft, 66.5 ft by 10.5 ft by 4 ft depth, with a draft of 1.83 to 2.0 ft and a weight of 12.03 tons. The propeller had a diameter of 2.5 ft. The art of designing these craft would have advanced much more rapidly than it did if all trial results had been published in as complete a form as given here.

(6) De Berlhe, B., "Note sur la Construction et l'Échantillonnage des Navires Destinés à la Navigation Intérieure (Note on the Construction and Inspection of Ships for Inland Waters)," ATMA, 1903, Vol. 14, pp. 298–300. This paper contains drawings of eight types of tunnel sterns for shallow-draft ships.

(7) Yarrow, A. F., "The Screw as a Means of Propulsion for Shallow Draught Vessels," INA, 1903, pp. 106–117

(8) Ward, C. E., "Shallow-Draught River Steamers," SNAME, 1909, pp. 79–106 and Pls. 23–86; especially pp. 96–101

(9) Teubert, O., "Die Binnenschiffahrt (Ship Operation on Inland Waterways)," Leipzig, 1912, Vol. I, pp. 476–481. A second edition, not much different from the first, appeared in 1932.

(10) Wilson R. C., "Construction and Operation of Western River Steamers," SNAME, 1913, pp. 59–66

(11) "Mississippi-Warrior River Towboats," Mar. Eng'g., Jun 1921, pp. 432–437. This article describes and illustrates the vessels of the *Natchez* class, 200 ft long by 40 ft beam by 10 ft depth, with a draft of 6.5 to 7 ft. There are two propellers operating in tunnels, with a tip emergence at rest of about $0.37D$. Each propeller has four blades, with $D = 9.33$ ft and $P = 8.5$ ft.

(12) "Experimental Towboats," House (of Representatives), 63rd Congress, 2nd Session, Document 857, 1914, Vol. 27. This is the full report of a most comprehensive investigation, both in America and abroad, to determine the best type of shallow-water towboat and towed barges for inland waters. It gives the results of a multitude of model tests on vessel forms for paddlewheel and screw-propeller drive and of comparative tests on models of radial and feathering paddlewheels.

(13) "Experimental Towboats," House (of Representatives) 67th Congress, 1st Session, Document 108, 1922, Vol. 9. This report, of 194 pages, describes the full-scale trials made as a result of the recommendations in House Document 857. Since so many different experiments were tried by modifying at least three different existing craft, the results were inconclusive, as could have been expected before they were begun.

(14) McEntee, W., "Model Experiments with River

Towboats—Stern-Wheel and Tunnel Propeller Types Compared," SNAME, 1925, pp. 63–66 and Pls. 44 through 60; also pp. 83–90

(15) Foerster, E., and Stapel, G., "Der Dreischraubenschlepper *Direktor Schlüter* (The Triple-Screw Tug *Director Schlüter*)," WRH, 22 Feb 1929, pp. 59–61. Shows a tug for inland waters with three screws abreast in three tunnels.

(16) Hinz, M., and Lang, H., "Der Dreischrauben-Motorschlepper *Amsterdam* (The Triple-Screw Motor Tug *Amsterdam*)," WRH, 7 Feb 1930, pp. 43–48. Shows body plan and stern lines of a shallow-water tug having three screws abreast in three tunnels.

(17) Brodie, J. S., "Modern River Towboats," SNAME, 1936, pp. 350–388

(18) Dawson, A. J., "Power of Shallow-Draft River Towboats," SNAME, 1937, pp. 145–159

(19) Tunnel-stern towboat *St. Louis Socony*, MESR, Apr 1939, p. 172. A profile of this craft shows a 10-deg slope to the tunnel roof forward of the propeller and an 11.2-deg slope in the after portion. The tunnel roof embodies sharp transverse knuckles with no rounding.

(20) Edwards, V. B., and Cole, F. C., "Water Transportation on Inland Rivers," SNAME, HT, 1943, pp. 400–422, esp. p. 412

(21) "Standardized River Towboats," AM, Oct 1948, pp. 36–39. This article shows stern and bow photographs and an outboard profile on a vessel carrying 4 flanking rudders, 2 steering rudders, a single-tunnel stern, and a single propeller inside a Kort nozzle.

(22) Dawson, A. J., "The Development and Economic Potential of Inland Waterways Transportation," First Pan-Amer. Eng. Conf., Rio de Janeiro, 15–24 Jul 1949, esp. pp. 5–21

(23) Alaskan river boat, Rudder, Aug 1951, p. 41. This vessel has a length of 64.5 ft, a beam of 17.33 ft, and a draft of only 1.0 ft, with a tunnel stern. With a brake power of 165 horses it is designed to make 11 kt.

(24) Mitchell, A. R., "Shallow Draught Ships," INA, Jul 1952, pp. 142–153

(25) Mitchell, A. R., "Tunnel Type Vessels," IESS, 1952–1953, Vol. 96, pp. 125–188. This is a comprehensive, instructive, and informative paper, well supplied with model- and ship-test data and generously illustrated with drawings and photographs.

(26) Jastram, H., "Ein Neuer Schiffstyp mit Grossraumtunnel (A New Ship Type with an Enlarged Tunnel)," STG, 1954, Vol. 48, pp. 154–164.

CHAPTER 73

The Design of the Fixed Appendages

73.1 General Rules for Design of Fixed Objects in a Stream. In view of the close relation which certain of the fixed appendages bear to other parts of the hull, comments applying to particular design features of these appendages are to be found here and there among the chapters of Part 4. Some duplication is considered justified for the sake of assembling all the appendage-design information in one place.

Intelligent positioning and shaping of the fixed appendages can be executed only on the basis of a careful prediction of water flow around the ship hull, based upon detailed knowledge derived from appropriate tests of models or full-scale investigations on ships of similar form. This requirement applies not only to the flow next to the hull surface but at some distance from it, depending upon the projection of each appendage beyond the hull. It applies also to abovewater appendages which may frequently be immersed or submerged during wavegoing.

Flow in the vicinity of a propulsion device producing thrust is influenced to a certain extent by the induced flow resulting from circulation around the blades. The magnitude of this induced flow varies with the thrust produced but the change in flow direction depends upon the relationship of the induced-flow and the ship-flow vectors. When designing appendages that are to be mounted near these propulsion devices the resultant flow needs to be studied carefully.

The types and numbers of fixed appendages which can be applied to all kinds of ships are almost legion. The discussion in this chapter is therefore limited to the principal or important types, in each of which the hydrodynamic characteristics are essentially the same. It is hoped that whatever the nature or shape of the unusual appendage, it can be linked to one or more of the foregoing types for purposes of design. Failing this, its design can be worked out on the basis of its function and a study of the probable flow around it, with check tests in a circulating-water channel.

73.2 The Design of Leading and Trailing Edges. The less the slope of the sides of the entrance of a streamlined 2-diml body, or of the nose of a 3-diml body, the less is the deflection of the flow and the magnitude of the $+\Delta p$ in this region. However, there are other design features to be considered:

(a) The entrance slopes are made small *only* when the direction of flow is exactly known, and when

it is so constant in service that cavitation or separation does not occur on one side or the other of the nose

(b) Lengthening the long nose or entrance increases the wetted area and the friction drag

(c) Thinning the entrance or nose renders it vulnerable to damage and susceptible to corrosion. There is also the possibility of cavitation if the body runs at an appreciable yaw angle.

(d) A limber entrance is easily set in vibration by periodic external disturbances.

At a free-water surface, a leading edge can rarely be too thin to reduce resistance, spray, and feather, provided it is strong enough to resist random side loads and has enough lateral stiffness to hold itself firm against lateral vibration. A thin leading edge projecting through the surface is vulnerable to damage by floating debris.

As the depth below the free surface increases, the leading edge can be thickened, if there are advantages to be gained thereby. However, this is to be done with caution, having in mind the following:

(1) There is ample hydrostatic or pumping pressure available to make the liquid close in around the body abaft the nose

(2) A semi-circular leading edge joined to the two parallel or slightly flaring sides of a 2-diml body, or a hemispherical nose on a 3-diml body, is *not* a good form. It is susceptible to cavitation and separation abaft the head portion [Rouse, H., and McNown, J. S., "Cavitation and Pressure Distribution," State Univ. Iowa Studies in Eng'g., Bull. 32, 1948]. The head should be elliptical, as diagrammed in the upper part of Fig. 73.A, with diminishing slope *and* curvature at the junction of the head and the straight or nearly straight sides abaft it.

(3) If the variation in yaw angle or angle of attack is not too large, the leading edge may be pointed, using separate circular arcs, somewhat like the nose of a projectile. The ogival head is then merged into an elliptical shoulder.

(4) Increased wetted surface on a pointed nose may cause more drag than increased pressure resistance on a blunt one

(5) Length may be a major objection, for some reason or other, requiring a deliberate shortening at the expense of nose shape.

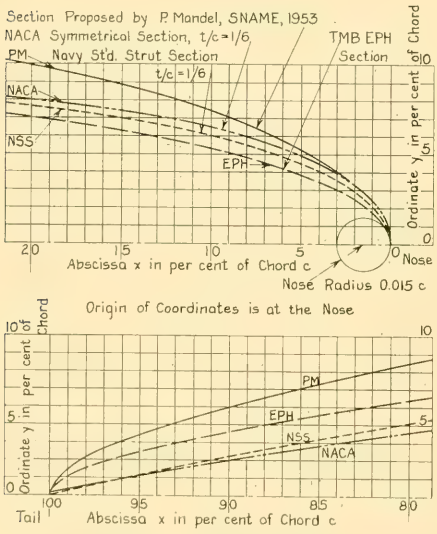

Fig. 73.A Leading and Trailing Edges of Several Strut and Hydrofoil Sections

It is explained subsequently, in a discussion of rudders as movable appendages, that sharp leading edges should be avoided on those parts of a ship which may from time to time encounter appreciable components of cross flow. The latter components are those developed at the stern of a vessel when it is sweeping around on a turn. In view of the much smaller magnitude of cross flow at the bow or in the forebody of a vessel it is rarely necessary to anticipate a relative flow there other than from directly ahead. For this reason the stem may be made as sharp as is consistent with practical considerations in building the vessel.

All that is said elsewhere about the trailing edges of sternposts, skeg endings, bossing terminations, and contra-guide sterns applies equally to the after edges of appendages of smaller absolute size. In particular, the endings should be thin enough not to generate harmful vortex trails, with alternating lateral forces on the appendage.

73.3 The Stem Cutwater. On a metal ship it is useful to employ a curved stem plate or casting, roomy enough for internal fabrication or assembly. However, if the ship runs at medium or high speeds, the blunt stem throws a high feather of spray, which may be objectionable, and it generates some unnecessary pressure drag. Both problems are solved by adding a sharp cutwater to the stem as an appendage. This reduces the

waterline slope at the stem nearly to zero and smooths out local discontinuities at the same time. In fact, shell plating may be applied to the outside of a stem without a rabbet if faired by such a device. The slope of a cutwater, in a horizontal plane, need rarely average less than 5 deg, or about 1 in 12. Usually, a slope of 6 or 7 deg, or about 1 in 10 or 1 in 8, is small enough. The radius at the extreme leading end may be 0.04 ft or less. The waterline section at the extreme nose is elliptic rather than circular.

A design lending itself to modern fabricating methods, and adaptable to a bulb bow, is sketched for the ABC ship in Fig. 73.B. The space inside the false stem or cutwater is filled with a light-weight, water-excluding, and rust-resisting material such as a foamed-in-place resin. This prevents the nearly flat sides from panting under the pressure variations they are likely to encounter at high speed and takes care of maintenance for an indefinite period.

The sharp, "soft" cutwater is obviously not adaptable to a vessel which must, during a turn-around, have its nose pushed up against a pier or quay. For a ship with bower anchors in side hawsepipes, the cutwater is made sturdy enough to withstand the pull of a chain crossing the bow.

The wetted surface of a stem cutwater is a continuation of that of the main hull. It is therefore added to the latter as an appendage and its surface taken into account when calculating friction drag. Since it lies directly behind the leading edge, where the local specific friction resistance coefficient C_{LF} has its highest value, the cutwater surface should be exceptionally smooth.

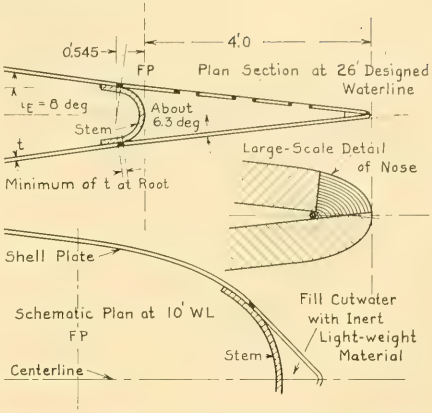

Fig. 73.B Design of Cutwater for the ABC Ship

73.4 Selection of Struts or Bossings. The designer may find useful a summary of the advantages and disadvantages of both struts and bossings, so that all phases of the selection problem

TABLE 73.a Comparison of Design, Construction, and Operation Features of Shaft Struts and Bossings

ADVANTAGES

Struts

Lighter overall weight
Less volume and weight displacement
More precise alignment with flow
Smaller shadowing effect of appendages projecting from hull
Less overall first cost
Less liability of vibration due to periodic forces exerted on hull by propeller

Bossings

Access to more shafting and shaft bearings without docking
Protection of shafting and bearings (except propeller bearing) from foreign matter, wear, corrosion, incidental damage, and major damage from striking piles, buoys, and chains
Some degree of pitch damping and steadying effect in a following sea
Appreciable reduction in shaft power due to deflection or contra-guide features, if employed
Greater average wake fraction at propeller positions

DISADVANTAGES

Struts

Inadequate protection of exposed shafting from corrosion or from damage to corrosion-resisting coating or covering
Less protection of shaft and propeller bearings from foreign matter, wear, and striking large objects such as buoys and their mooring chains
Greater liability of cavitation ahead of propeller, with erosion and corrosion of strut arms

Bossings

Greater overall weight
Probably greater overall first cost
Greater liability of irregular flow abaft bossing terminations
Greater periodic vibratory forces exerted on hull by propeller
Reduction of maneuverability and turning characteristics

may be studied and the merits of each may be assessed for every new design as it arises.

Whatever the advantages of bossings for any particular application, there is a low limit to a bossing size unless the latter is to be closed up completely from the outside. The workmen who have to get inside of these bossings for fabrication, erection, riveting, or welding are of more-or-less fixed size, as are those who must take care of repairs and maintenance for the life of the vessel. For these reasons bossings are little used on small vessels.

Table 73.a summarizes the advantages and disadvantages inherent in the great majority of strut and bossing installations. The comments apply to single-screw and triple-screw ships as well as to the arrangements customary on twin- and quadruple-screw vessels.

It is difficult to make any general statements concerning reductions in shaft power to be achieved by the use of either shaft struts or bossings in any particular case, assuming that alternative designs benefit from the same amount of study, experimentation, and development [Mandel, P., SNAME, 1953, pp. 466–468]. The designer of a large or important vessel, or one which is to serve as the lead ship for quantity production, is believed justified in carrying alternative strut and bossing designs through to the model stage at least.

73.5 Strut Design for Exposed Rotating Shafts. If the weight displacement of large bulky bossings is undesirable, propeller shafts are left exposed, carried by water-lubricated bearings supported from the hull by double arms set in the form of a Vee. For certain applications, single arms have been employed, especially when they are short and can be given adequate rigidity. Parsons used a number of them successfully on the three shafts of the *Turbinia* in the 1890's [SNAME, 1947, Fig. 10, p. 105]. However, more modern experience, with larger sizes and higher shaft powers, indicates that when the single arms are longer than the maximum strut-hub diameter they suffer from:

(a) Lack of lateral stiffness
(b) Possibility of resonant lateral vibration as a cantilever weighted at the outboard end
(c) Excessive lateral loading by Magnus Effect on the shaft, or hydrodynamic lift due to cross flow when turning, or both. Fractures of modern single-arm struts in service, due to transverse lift produced by cross flow when turning, to vibration, and to other causes, indicate the wisdom of avoiding them unless the arms are shorter than the limit given.

The proper or best shape of the strut-arm section has been the subject of long and careful study, based upon structural as well as hydrodynamic considerations. The differences in drag between the various shapes of long-established usage are small, even in proportion to the total appendage resistance. It is probably more important that the strut arm as installed conform closely to some specified shape, worked out by a long development process, than that the shape be of a particular kind or have special characteristics. The section delineated by D. W. Taylor, used in U. S. Naval vessels for many decades past, could have been shorter for the same thickness, with a c/t_X ratio of 6.0 instead of 7.5. This would have involved cutting off only the tail; in fact, this portion often disappeared anyway as a result of erosion, pitting, or rusting in service.

Excellent replacements are the:

(a) EPH or Ellipse-Parabola-Hyperbola section developed by the David Taylor Model Basin during World War II. This has a trailing edge sufficiently blunt to get rid of the previous difficulties with fabrication and corrosion of the slim Navy Standard strut. It is not so blunt as to cause objectionable separation and eddy buffeting of the trailing portion in the absolute sizes normally used for shaft struts.
(b) Section proposed by P. Mandel [SNAME, 1953, pp. 468–469], with a c/t_X ratio of 4.3.

The comparative proportions and shapes of the three sections mentioned, plus an NACA symmetrical section, are shown graphically in Fig. 73.C. The abscissas and ordinates for constructing the section outlines accurately are tabulated by Mandel [SNAME, 1953, Fig. 3, p. 468]. Many other characteristics are described by him, together with design considerations involving both structural and hydrodynamic features.

Of far more importance than the shape of the strut-arm section is the placing of this section in the local direction of flow so that in service it runs with no yaw angle or angle of attack. It is true that the local direction of flow changes with yaw during steering, with rate of swing during turning, and with ship position during wavegoing. It may also change with displacement, draft, and trim. Nevertheless, it probably remains constant within a degree or so at all normal operating speeds in

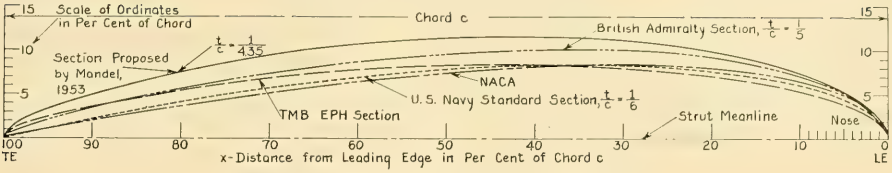

Fig. 73.C Half-Sections of Five Strut Shapes

straight-ahead motion on a given course. It seems reasonable to assume that the ship is running in this fashion for about 98 per cent of its operating time.

The proper angle can be estimated after a fashion, using data for flow around the stern as given in various chapters. Nevertheless, good design requires an experimental determination on a model with special apparatus. It is preferred, because of the influence of induced velocity in the water passing into a propeller disc, that the strut-arm section angles be determined while the adjacent propeller is delivering normal thrust. This can be done, along the lengths of the two struts of a pair, by apparatus described and illustrated by H. F. Nordström [SSPA Rep. 32, 1954, Figs. 22 and 23, pp. 30–31].

Twisting the strut arms to suit the angle of flow is usually an inconvenience when the struts are built, but failure to align the strut sections with the flow, especially ahead of a propeller disc, only invites trouble by setting up disturbances in the inflow jet.

Whether a strut with two or more arms lies ahead of or abaft a screw propeller, it is well to avoid a strut-vee angle (see Fig. 36.B) which is nearly or exactly the same as the angle between two blades which may be passing the arms simultaneously. A convenient example in this respect is the four-arm strut abaft the 4-bladed propeller of the arch-stern ABC ship, described in Secs. 73.7 and 73.8 and illustrated in Fig. 73.F of Sec. 73.8. When looking forward on this vessel, consider the radial position of the lower port strut arm as zero angle. With spacings of 75, 60, and 75 deg between the three pairs of arms, reckoned in a clockwise direction, the angular positions are tabulated as follows:

Strut Arms	3-Bladed Propeller	4-Bladed Propeller	5-Bladed Propeller
0	0	0	0
75	120	90	72
135	240	180	144
210	360	270	216

Should a 5-bladed wheel be fitted at a later time on this vessel, the angular "stagger" is rather small. With one blade opposite the port lower strut arm the next blade is only 3 deg ahead of the port upper arm, the second blade 9 deg behind the starboard upper arm, and the fourth blade 6 deg behind the lower starboard arm.

The matter of whether the strut-arm axes lie close to the propeller-shaft axis (radial type) or whether they are spread so as to pass close to the mean radius of the strut hub (tangential type), is often determined from a structural rather than a hydrodynamic standpoint [Roop, W. P., "The Strength of Propeller Shaft Struts," SNAME, 1926, pp. 119–137 and Pls. 44–52]. Considering the flow of water through the strut position there is probably little to choose between the two. The tangential arms are well spread at the hub but they usually involve reentrant angles alongside the barrel considerably smaller than 90 deg. Radial arms give good attachments for supporting the shaft but the passage between the arms at the hub surface may be somewhat constricted if the strut-vee angle is small. To avoid blocking effects due to closeness of the arms at the hub there should be an open space at the barrel surface equal to at least 3 times the maximum strut-arm thickness, indicated at 2 in Fig. 73.D. Better still, a clearance circle may be drawn between the arms equal to the maximum outside diameter of the hub, as at 1 in the figure. Strut-vee angles larger than 60 deg represent good solutions of all requirements but it frequently becomes necessary to decrease this angle to the order of 45 deg. This should be a minimum value, to afford adequate rigidity to the assembly.

Fairing the hub ends of the strut arms into the strut hub or barrel is probably more a matter of structural continuity than of easing the flow around these junctions. A fillet radius at the barrel equal to or exceeding the maximum strut-arm thickness appears to be adequate for good flow, even at the apex of a transverse reentrant angle. However, the strut arms at their juncture

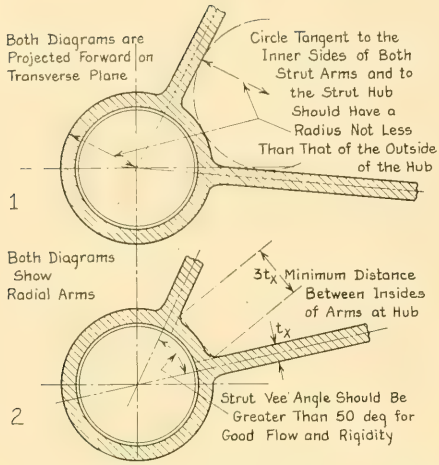

Fig. 73.D Hydrodynamic Requirements for Strut-Arm Positions at the Strut Hub

with the strut hub are lengthened with large-radius fillets forward and aft, principally to give stability of position to the strut hub.

At the hull ends of the strut arms, provided these go *through* into the hull, no fairing is necessary if they stand normal to the shell or nearly so. When the transverse reentrant angle at the shell becomes 70 deg or less, a fillet is introduced by some convenient method. The fillet radius increases as the reentrant angle becomes smaller. It is often possible to bend the strut arm and have it enter the hull nearly normal to the shell.

Struts are attached to the hull by external palms only when no other method can be used. The palm endings are sloped and faired so that a section through them, in the direction of flow, approximates that of one side of a standard (or acceptable) strut section.

Normally it is not necessary, for hydrodynamic reasons only, to increase the length or the fineness of a strut-arm section where it attaches to the strut hub or to the shell. If fairing is required on the sides of the section, for structural or other reasons, a longer termination is automatically necessary if the section fineness is to be maintained.

Under no circumstances should an upper strut arm join the hull at a point above the free-water surface if propulsion performance at a displacement and trim corresponding to the position of that surface is considered of major importance. A hole in the water is certain to form at the free surface abaft the strut, because of the low hydrostatic pressure there. The minutest degree of separation abaft the tail of the section is almost certain to provide a reduced-pressure passage for air, extending from the hole at the surface all the way down to the propeller hub. Here the air passes into the propeller disc in the manner illustrated by Fig. 23.D, reduces the thrust, and creates noise and vibration.

If it ever becomes necessary to carry or to rig a strut section which must come to the surface, a flat subsurface plate resembling those in Figs. 7.E and 36.O is attached to it just below the surface and in the line of flow. This plate prevents air from leaking down through the bottom of the hole in the water, just abaft the strut. An extra-long fairing is necessary above this plate if the strut is not to create excessively large waves at the surface or to throw inordinate amounts of spray.

It is customary to place the strut-arm axes in transverse planes, that is, square to the baseplane. It may often be better to rake or tilt them out of these planes if they can be shortened thereby, if their axes can be placed more nearly normal to the direction of water flow, or if better attachments can be made to the hull structure. The angle of rake or sweep-back can be as large as 30 deg with the transverse plane. If piercing the free surface is unavoidable it is best to rake the strut down and forward. This creates less separation than when raked down and aft, as explained in Sec. 36.17 and illustrated at 5 in Fig. 36.O.

73.6 Strut-Arm Section Shapes for Ultra-High Speeds. For planing craft which operate at high speeds and for ultra-high-speed racing motorboats the exposed propeller shafts are invariably carried by single-arm or V-type struts. The submergence of these struts is small because of the relatively small draft, hence the cavitation index is correspondingly low. At the high speeds at which they travel it is impossible to make a strut section sufficiently long to be free of cavitation over its after portion. It is the practice therefore to utilize only the forward portions of these sections, making the entrances fine and narrow, and terminating them in square or boat-tail endings in the manner illustrated in Fig. 73.E. They then resemble the transom stern on a fast motorboat. Single struts having blunt ends may be placed forward of the propeller provided there is an exposed sloping shaft ahead of the strut.

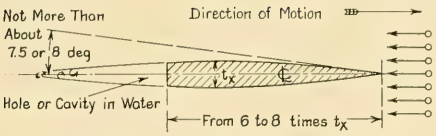

Fig. 73.E Boat-Tail Strut-Arm Section for High Speed

The open ditch made by the shaft may be large enough so that the water clears the strut arm altogether.

It is often possible to place a fixed single-arm strut abaft the propeller and to use it as the forward or fixed portion of a compound rudder. The forward edge of the rudder blade is close behind or is mounted inside the after edge of the strut arm.

73.7 Appendages for the Arch-Stern ABC Design. Sec. 67.16 describes the general considerations governing the design of appendages at the after end of the ABC ship with the arch-type stern, as well as some of the details. A few additional notes are added here to cover certain features illustrated subsequently in the following drawings:

(1) Contra-struts abaft propellers, Fig. 73.F of Sec. 73.8
(2) Short bossings for propeller shafts, Fig. 73.H of Sec. 73.9
(3) Large propeller, built up by welding, with flange connections to shaft, and twin rudders abaft twin skegs, Fig. 74.L of Sec. 74.15.

The arrangement developed for the first preliminary design and indicated schematically in Figs. 73.F and 74.L embodies:

(a) An integral forward bolting flange, propeller hub, and after shaft or propeller journal of steel, eliminating all taper fits, keys, threads, propeller nuts, and the like
(b) An after shaft or propeller journal which is short and of large diameter, with adequate stiffness to prevent bending and to insure reasonably uniform loading of the bearing surface
(c) Separate propeller blades, bolted to the shaft-hub-journal combination with circular flanges, studs, and nuts in the orthodox fashion for a built-up adjustable propeller
(d) As an alternative to (c), separate propeller blades which are removable but not adjustable. Eliminating the pitch-changing feature and the necessity for circular blade flanges may make the built-up propeller more simple and sturdy, with a smaller hub diameter.
(e) As an alternative to (c) or (d), separate blades of alloy or corrosion-resisting steel. These may be solid or, as in an Italian proposal, may be of hollow cellular construction, with welded parts of steel plate [SBSR, 1 Oct 1953, p. 459]. Each blade may have its own root palm or flange, welded to the steel hub and to the adjacent palms, or the blades may be welded to short stubs, made integral with the hub, illustrated for the quadruple-arm strut hub in Fig. 73.F.
(f) A propeller-bearing sleeve which is mounted in its housing at an angle approximating that of the slope of the propeller journal when all parts are in place
(g) A propeller-bearing sleeve which is withdrawn aft from its housing, to afford ample clearance for the propeller journal when installing the propeller assembly or removing it from the ship
(h) A propeller journal surface of heavy chrome plating with a ground finish, thus eliminating a bronze sleeve which might cause corrosion of the propeller journal and the hub
(i) A strut hub of cast steel with the usual internal circumferential lands for carrying the shaft-bearing sleeve. To the outside of this hub are cast four short arms, curved in contra-fashion to permit the inner or shaft ends of the strut arms, fabricated from heavy rolled plate, to be butt-welded to them. The fillets at the forward and after ends of the strut-arm connections at the hub are incorporated entirely in the short arms, cast integral with the hub.
(j) A readily removable exposed rotating propeller shaft, attached by bolted flanges to the flanged propeller hub at its after end and to the flanged stern-tube shaft at its forward end
(k) A rotating shell forward of the propeller to cover the bolted flange and to serve as a fairing into the propeller hub
(l) A fixed conical cap of suitable shape and proportions abaft the propeller-bearing housing or strut hub, forming the after end of the streamlined assembly comprising the rotating shell, the propeller hub, the strut hub, and the tail fairing
(m) A suitable means of inducing adequate water flow through the propeller bearing for lubrication and cooling. A flared rope guard at the forward end of the strut-bearing hub and a large hole in the after end of the fixed fairing cap, opening into what would be a separation zone or a swirl core abaft the hole, should be sufficient for this purpose.

73.8 Layout of Contra-Struts Abaft Propellers. If the propeller bearing and the barrel carrying it are both mounted abaft the propeller, as in the ABC arch-stern design, the procedure for laying out contra-struts to hold the bearing barrel or strut hub follows in general that described in Sec. 74.16 for a contra-rudder. There is, however, a much smaller background of experience for struts as to acceptable limits for median-line angles, twist offsets, and the like.

In the design of the ABC arch-stern struts, it was evident at an early stage that, because of the large barrel radius, 2.25 ft, a reference value of 0.85 times this radius at $0.1R_{\text{Max}}$ of the propeller was much too large, in that the median-line slopes at the leading edges of the struts became excessive. Falling back upon the designer's judgment, as must often be done, this ratio was halved. The basic offset is therefore (0.85/2) 2.25 ft or 0.9562 ft, listed at the bottom of the table on Fig. 73.F. Even so, the median-line slope of the leading edge at $0.2R_{\text{Max}}$ is 32.5 deg, although this could be reduced somewhat by changing the shape of the median line. The remaining offsets are determined by using the $\sin^2 \phi$ relationship described in Sec. 67.22. Details of the resulting design of contra-strut and hub assembly, with a heavy belt plate in the shell abreast the propeller and strut arms, are drawn in Fig. 73.F.

A considerable number of references relating to contra-propellers and guide vanes, both forward of and abaft a screw propeller, are listed by W. P. A. van Lammeren [RPSS, 1948, References 136 and 137 on pp. 299–300].

73.9 The Design of Bossings Around Propeller Shafts. The first step in the design of any bossing, whether long or short, or of the straight (fairing) or deflection type, is to position the screw propellers to be carried by it. This matter is covered in Secs. 67.23 and 69.3. When

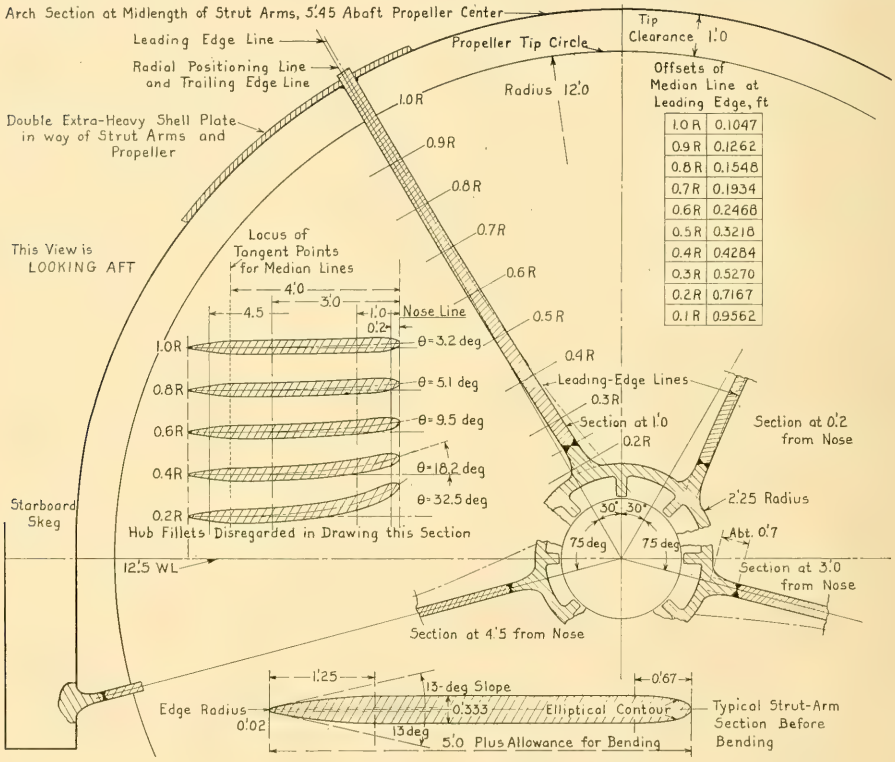

Offsets of Median Line at Leading Edge, ft	
1.0 R	0.1047
0.9 R	0.1262
0.8 R	0.1548
0.7 R	0.1934
0.6 R	0.2468
0.5 R	0.3218
0.4 R	0.4284
0.3 R	0.5270
0.2 R	0.7167
0.1 R	0.9562

FIG. 73.F LAYOUT OF QUADRUPLE STRUT ARMS AND HUB FOR ABC ARCH-STERN SHIP

the rate of propeller rotation is known and the propeller power is fixed within rather narrow limits, the size of shafting, bearings, and other mechanical parts to be housed by the bossings are determined within equally close limits. In combination with the room needed for internal access, these features fix the minimum size of certain parts.

The second step is to settle upon the exact nature and function of the bossing. Is it to be of the short or the long type? Is it solely for fairing and for protection of the shafting and bearings? Is it to be of the deflection type, possibly with an auxiliary support strut for the propeller bearing, as in diagram 3 of Fig. 36.H? It may be that, under a broad, flat stern, the bossing is to be called upon to serve as a docking keel as well as a bossing.

The third step is to find the direction of flow at and near the hull surface in the region to be occupied by the bossing. If of the long type, the bossing is in reality an extension of the watertight hull. It is not an external appendage which can be modified later, if and when desired.

Because of the length and the appreciable volume of a long-type bossing, the flow around it when in place may be significantly different than that indicated around the bare model when the initial flow tests are made. For instance, suppose that the principal plane of the bossing has been placed over the trace of a flowline observed on the model hull without the bossing. The water which formerly flowed easily along the hull surface is now displaced by the bossing volume. It has to flow somewhere else, and in so doing it may take a route that is not conducive to good flow or good propulsion. A second flow check on the model is therefore indicated, to be followed by wake observations in the propeller-disc position abaft the bossing, including records of the directions of the velocity vectors. A further check is called for on the uniformity of flow as it leaves the upper and lower surfaces of the bossing.

If a long bossing is not properly shaped and positioned, the flow around it may contain large corkscrew vortexes. It may develop a combination of longitudinal and transverse eddies which cause the flow at a given point abaft the bossing to fluctuate with time. An unsteady flow of this kind is detected on a model only with instruments which are sensitive to these variations.

On high-speed vessels, especially those of light draft, where the head of water over the bossing is necessarily small, model tests of proposed installations have even revealed an extensive *uncovering* of the upper surface of the bossing, exposing parts of the upper blades of a propeller carried by it.

That portion of a bossing of any type which encloses a propeller shaft is fixed at its after end by the position of the propeller bearing. At its forward end some latitude in position with respect to the emerging shaft is permissible. This depends upon the size of the bossing at that end, the position of the propelling machinery, and other internal arrangements. If the bossing is for fairing and shaft protection only the bossing termination slope β(beta) and the traces of the bossing body along the hull are established in such manner that flow takes place around it with the least possible interference. It is often difficult to estimate the local directions and traces of this flow along the hull. Lines of flow taken on a model, especially with a temporary rod in place to represent the bare propeller shaft, are most helpful at this stage. Better still are flow directions, indicated by flags or vanes at a distance from the hull equal to the mean projection of the bossing at each station.

It is customary first to sketch the bossing shape on the body plan by stations, sections, or frames. These are supplemented by the traces of bossing flowplanes, flat or slightly curved, passed through the bossing at varying distances from the adjacent main hull. The traces correspond generally to intersections of the stream surfaces in the boundary and adjacent layers, diagrammed in Figs. 36.D and 36.H. The transverse slope of a bossing, intended for fairing only, is approximately normal to the slopes of the section lines in the vicinity. This reduces the wetted area to a minimum and avoids reentrant angles less than 90 deg. Proposals have been made in the past, requiring such rigid adherence to this rule that the bossing plane is curved in transversely, so as to remain normal to the section lines as the latter become steeper with distance aft, toward the propeller [Völker, WRH, 1 Jun 1934, pp. 131–132].

When selecting the transverse slope it is well to make sure that no part of the bossing lies close to the free surface of the water in any operating condition, if efficient propulsion and freedom from vibration is desired.

Section shapes for the bossings of twin-screw vessels are to be found in the following:

(a) Sadler, H. C., "The Effect of Bossing Upon Resistance," IESS, 1908–1909, Vol. LII, pp. 147–159 and Pl. IX. Discusses effect of large and small termination angle β.

(b) Simpson, G., "The Naval Constructor," New York and London, 4th ed., 1919, p. 59
(c) Baker, G. S., SD, 1933, Vol. I, Fig. 7, p. 14
(d) Hughes, G., "Model Experiments on Twin-Screw Propulsion, Part I", INA, 1936, pp. 145–158 and Pls. XVI-XX. Four bossings with very small termination angles β are shown on Pl. XVII.
(e) Eggert, E. F., SNAME, 1939, Fig. 52, p. 329, shows the bossing sections of EMB model 3383, stern 3-S_2
(f) Van Lammeren, W. P. A., Troost, L., and Koning, J. G., RPSS, 1948, Fig. 54, p. 99
(g) Baker, G. S., INA, 1952, Fig. 13, p. 109. This shows a bossing symmetrical about the bossing plane, with a termination slope angle of 21 deg.
(h) De Rooij, G., "Practical Shipbuilding," 1953, Fig. 252b on p. 105; Fig. 561 on p. 241; Figs. 562 and 563 on p. 242.

When shaping the bossing termination, the propeller deserves all the edge clearance which can be afforded ahead of it, consistent with proper support of the propeller bearing and adequate rigidity of the bossing structure.

The actual termination, inboard of the barrel portion around the propeller bearing, deserves as much attention with respect to fining as the termination of a shaft strut. This is much more, incidentally, than has often been accorded it in the past. The sections through the bossing termination in Fig. 73.G, developed by the Newport News Shipbuilding and Dry Dock Company for the S. S. *Talamanca* and class, indicate what can and should be done in this respect. They afford the propeller full opportunity for doing its best in the water trailing abaft the bossing. It is not surprising that the vessels to which these bossings are fitted have given over two decades of successful and satisfactory service. It is adequate proof that large apertures, small slopes in the bossing flowplanes, and sharp trailing edges are compatible with strength, rigidity, and ease of fabrication.

The cantilever rigidity of the heavy frame carrying the propeller shaft bearing must certainly be adequate. Nevertheless, some ships have carried excessively blunt terminations in the past which spoke only too eloquently of a structural design that almost crowded out the hydrodynamic design.

The designer must decide whether the cylindrical or conical barrel which houses the shaft and the propeller bearing should attach to the bossing tangentially or radially. It is possible to favor structural, mechanical, and other considerations provided the flow over the entire bossing surface is free from eddies, crossovers, and abrupt changes. For example, if the plane of the bossing termination is offset from the shaft axis, as in Figs. 36.D and 73.G, the reentrant angle at the bearing hub should be not less than 90 deg. Further, the bossing surface on the "full" side need not project much beyond the bearing hub.

The design rules set down in the foregoing for long, straight bossings at the stern apply also to those which might be fitted for twin bow propellers on an icebreaker, or for bow and stern propellers on a ferryboat.

Short bossings are used primarily to fair an

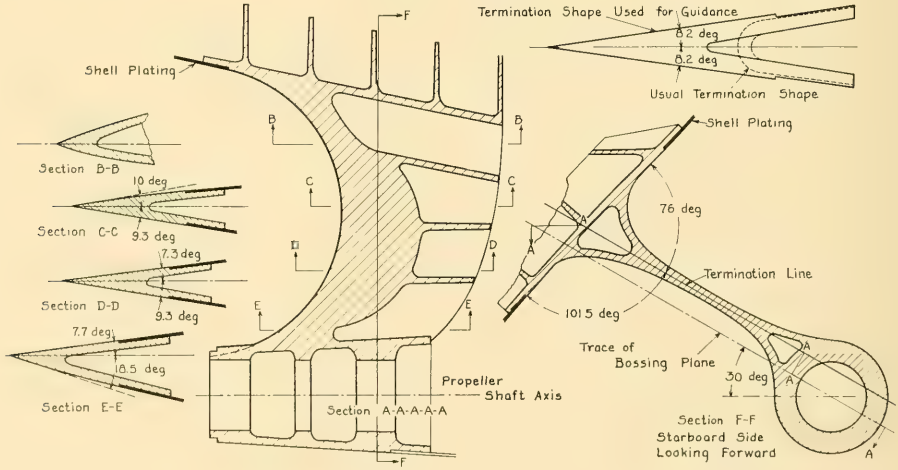

FIG. 73.G TWIN-SCREW BOSSING TERMINATION CASTING FOR S. S. *Talamanca* AND CLASS

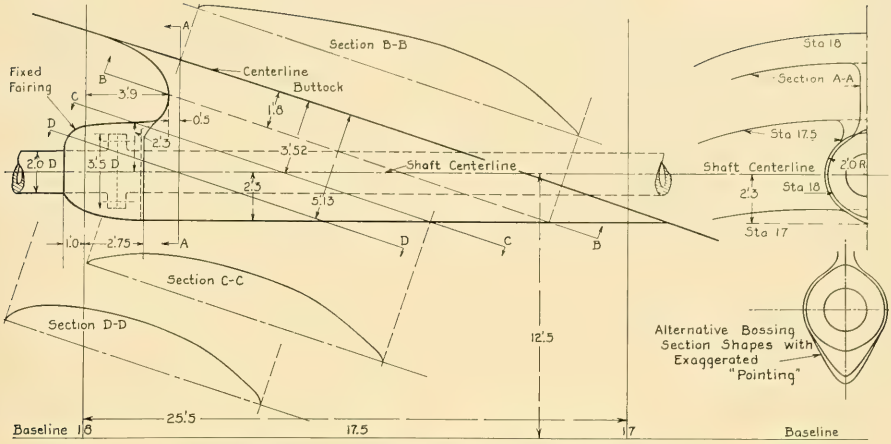

Fig. 73.H Shape of Short Bossing for ABC Arch-Stern Ship

exposed propeller shaft where it emerges from the hull, described in Sec. 75.10. The design rules are essentially the same as for long bossings, except that deflection or contra-guide endings are never incorporated in them because the endings are too far from the propellers. A short bossing is often required to provide a fairing around a coupling or flange which connects the section of an exposed propeller shaft to the stern-tube shaft just ahead of it. Were it not for this, the fairing could well be limited to a projection from the main hull on the inboard side only, filling in the space where eddies would otherwise form and leaving only mechanical clearance next to the shaft.

On either long or short bossings some pressure drag can be saved, for an insignificant increase in wetted surface, by "pointing" the outer or upstream surface of the bossing upon which the flow impinges. To the customary circular transverse shape or section of the outer barrel of such a bossing there is added a triangular or Gothic-arch portion, about as shown in the two end views of Fig. 73.H, depicting the short-bossing design for the arch-stern ABC ship. A moderate amount of pointing results in marked fining of the leading ends of the traces of the bossing flowplanes lying generally parallel to the hull in that vicinity, indicated by Sections B-B, C-C, and D-D of the figure. The locus of the "points" of the added triangle or arch, when projected on the body plan, lies parallel to the flowlines in that region. At a distance from the hull these lines are not necessarily parallel to those marked by flow indicators directly on the hull. This modification adds slightly to the stabilizing-fin area but the effect is small.

An example of a fixed appendage producing somewhat similar effects is a bar of pointed or arch shape, mounted in an inclined position under the exposed rotating shaft of a high-speed motorboat. It creates an air- or vapor-filled separation zone in the form of an inclined ditch, within which the propeller shaft revolves with negligible liquid friction [H. B. Greening patent application].

On most short bossings the flow crosses the bossing barrel around the shaft bearing at a considerable angle. A fining of the trailing ends of the bossing flowplane traces is achieved by continuing the bossing termination along the leeward or downstream side of the barrel. This modification, along with the pointed arch, is incorporated in the short bossing of the ABC arch stern, drawn in Fig. 73.H.

To save weight and displacement, exposed propeller shafts are sometimes run through the shell plating simply by cutting a clearance opening in the plating. The stern-tube bearing and the fittings pertaining to it are then installed entirely within the fair lines of the hull. The recess thus presented, filled as it is with the shaft and with partly inert water, presents no sensible interference to the flow. A small fairing may be fitted inboard and astern of the protruding shaft, mentioned in a preceding paragraph of this section and illustrated in Fig. 75.I of Sec. 75.10. Separa-

tion and eddying at this point are avoided at the expense of an insignificant increase in volume displacement, weight, and wetted surface.

73.10 Design Rules for Deflection-Type or Contra-Guide Bossings. Ship designers have been reluctant to use deflection-type or contra-guide bossings on vessels with wing propellers because of the uncertainty as to just how much twist can be used and just how it can be worked into them. They fear that this twist may cause eddying, introduce vibration, and do more ultimate harm than good to the propulsion characteristics and behavior of the vessel as a whole. True, a deflection-type bossing, even though designed only to reduce the unfavorable component of flow as it enters the propeller disc, requires much greater care in shaping than the fairing type of long bossing. Further, it calls for more thorough checking by model tests. Separation of flow may well occur with careless or improper design, leading to ensuing vibration and other troubles.

As with a contra-guide skeg ending the twist is imparted in a direction contrary to the rotation of the propeller blades when running ahead. If the wing propellers are definitely to turn outward, and the stern is of normal form, the bossing termination lies at a small slope β with the horizontal. With inward-turning propellers the slope is larger than for a bossing of the fairing type. Indeed, the termination may approach a vertical position, with a slope of 70 or 80 deg or more.

The amount of twist which can be imparted is a function of the fore-and-aft length of the bossing and of the smallness of the reentrant angle against the shell, on the reduced-pressure side of the bossing, convex to the flow. Fig. 36.H illustrates these features as applied successfully to the U. S. destroyer *Worden* (DD 352), where the reentrant angle on top of the bossing was much smaller than normal. It is true that separation generally occurs alongside a surface when the slope of that surface with the direction of motion exceeds a limiting angle. However, a twist imparted to the water by a *long* bossing with easy curves may possibly act to diminish this critical slope by changing the general direction of flow at its after end.

When designing a contra-guide bossing it is kept constantly in mind that the water is being forcibly deflected on the straight or concave side and *must* follow the bossing-flowplane curvature there. It is only constrained to follow the convex side by the conversion of some kinetic energy into sufficient potential energy and pressure, with an adequate pressure gradient, to accelerate it inward toward the bossing surface, at right angles to the latter.

In the present state of knowledge, it is perhaps well to limit the angle between the convex side of a deflection-type bossing and the corresponding side of a fairing bossing for the same ship design to a maximum of about 8 or 10 deg. It is also well to limit the reentrant angle at the after end of a deflection-type bossing to a minimum of some 60 or 65 deg, reckoned from the adjacent hull surface.

When the designer has done his best on paper he may try his hand in modeling clay. The bossing so developed is added to the model and run for flow directions. This may be in a model basin but, if at all possible, the flow should be observed in a circulating-water channel. A flow test and a wake survey, including measurements of velocity magnitude and direction in the propeller disc, are much more necessary for a deflection-type bossing than for one of the fairing type.

The designer who is looking—and hoping—for a real reduction in shaft power, of the order of 5 or 10 per cent, such as that achieved on the U.S.S. *Worden*, should not be discouraged when a first attempt at laying out a deflection-type bossing produces erratic flow around the propeller position. It may produce no reduction in shaft power at all. Indeed, the design knowledge relating to this type of bossing is still so limited that only by accident could a designer expect to arrive at the proper shape and proportions on the first trial. Modified bossings are rather easily applied to a model and more easily checked for flow in a tuft test in a circulating-water channel. In fact, it can be stated as an inflexible rule that no contra-guide bossing should be incorporated in a ship design and in the construction drawings without the most complete flow investigation on a model, both with and without the propeller working. This involves measuring on the model, if it is practicable, the transient variations in torque and thrust as each propeller blade passes through a complete revolution. At some time in the future it should involve measurements of the periodic pressure fluctuations and force variations on the bossing and adjacent hull.

73.11 Vertical Bossings as Docking Keels. For vessels which are wide aft in proportion to their immersed depth, with rather flat stern

sections and cut-up profiles, the angle β of the bossing termination often works out as close to 90 deg. In other words, the bossing stands nearly vertical. It is usually difficult to provide adequate docking support for the sterns of these vessels. A logical procedure is to use the vertical bossing as a support keel, since a high degree of strength and rigidity is required in it to support the shaft and propeller. Fig. 36.E of Sec. 36.7 indicates that little or nothing need be sacrificed in the way of form to provide the necessary flat surface on the bottom of such an appendage. A bossing designed to act also as a docking keel should have a slope such that the line of action of the support force from the docking blocks, at midwidth of the flat under surface of the bossing, remains *within* the bossing until it enters the main hull.

The fact that the propeller blades project below the docking support surface and that the blocks under the bossing(s) have to be built up higher than the remainder may be taken care of by modern (1955) drydocking procedures.

73.12 Design Notes on Fixed Screw-Propeller Shrouding; The Kort Nozzle. Certain screw-propeller installations involving fixed shrouding are described in Sec. 32.5 and illustrated in Figs. 32.D and 32.E. Propeller nozzles in general and Kort nozzles in particular are described in Sec. 36.19 and diagrammed in Fig. 36.P.

The detail design of Kort and other fixed nozzles is intricate and specialized, so much so that it can not be described adequately in the space available here. Instead, there are given a number of recent references which contain the best description of this procedure available in the literature:

(1) Gutsche, F., "Fortschritte in der Entwicklung des Binnenschiffs mit Eigenem Antrieb (Progress in the Development of Self-Propelled Ships for Inland Waters)," Zeit. des Ver. Deutsch. Ing., 1935, p. 1155

(2) Büchi, G., "Possibilità di Recupero Della Scia ed Esperienze sul Mantello d'Elica (Possibility of Exploiting the Wake and Experiments with Propeller Shrouding)," Ann. Rep. Rome Model Basin (in TMB library), 1936, Vol. VI, pp. 91–98

(3) Gutsche, F., "Einflusz der Gitterstellung auf die Eigenschaften der in Schiffsschraubenentwurf benutzten Blattschnitte (Influence of the Cascade Position on the Characteristics of the Blade Sections Used in the Design of Ship Screws)," Mitteilungen der Preuzischen Versuchsanstalt für Wasserbau und Schiffbau, Berlin, 1938, No. 34; see also STG, 1938, p. 125

(4) Roscher, E. K., "Wirtschaftliche und wissenschaftliche Bedeutung unmantelter Schiffsschrauben (Economic and Scientific Importance of Shrouded Ship Propellers)," STG, 1939, pp. 150–167

(5) Dickmann, H. E., "Grundlagen zur Theorie Ringförmiger Tragflügel (Fundamentals of the Theory of Ring-Shaped Airfoils)," Ing.-Archiv, 1940, p. 36

(6) Riddell, A. M., "The Theory and Practice of the Kort Nozzle System of Propulsion," INA, 1942, pp. 87–114

(7) Some design notes given by W. P. A. van Lammeren, RPSS, 1948, p. 267

(8) Amtsberg, H., "Entwurfs- und Berechnungsverfahren für Kortdüsen (Design and Calculation Methods for Kort Nozzles)," Arbeitsblatt 5/1950/01 der KdT, Berlin, 1950

(9) Horn, F., "Teil A (Part A)," "Theoretische Grundlagen und grundsätzlicher Aufbau des Entwurfsverfahrens (Basic Theory and Design Fundamentals)," STG, 1950, Vol. 44, pp. 141–169, with a list of 8 references on p. 169 (in German)

(10) Amtsberg, H., "Teil B (Part B)," "Praktisches Auswahlverfahren für Optimale Düsensysteme (Practical Selection Method to Determine Optimum Nozzle Systems)," STG, 1950, Vol. 44, pp. 170–206 (in German)

(11) An excellent summary of these two papers is given (in German) and a most workable design procedure, with examples, is found in "Handbuch der Werften (Construction Handbook)," published by Hansa in Hamburg, 1952, pp. 67–88. On page 88 there is a bibliography of 14 items.

(12) An NACA 4415 section is recommended for a Kort nozzle by F. Horn and H. Amtsberg; it is shown by W. Henschke, in "Schiffbau Technisches Handbuch (Shipbuilding and Ship Design Handbook)," 1952, pp. 165–166. The nozzle section and the sketch of Fig. 73.I is adapted from Fig. 44 on p. 167 of the Henschke reference.

(13) "Triple-Screw Ohio River Tugboat *John J. Rowe*," SBSR, 17 Nov 1955, p. 641. The three propellers of this craft, 7.67 ft in diameter, are each enclosed in Kort nozzles, with a steering rudder abaft each

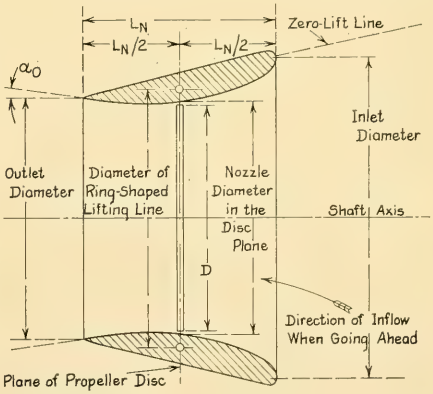

FIG. 73.I DEFINITION-DESIGN SKETCH FOR KORT NOZZLE

propeller. The reference embodies a stern view of the vessel on the ways, showing the propellers, nozzles, and rudders. There are six flanking rudders in addition to the three steering rudders. The craft has a length of 164 ft, a beam of 44 ft, a depth of 10 ft, and a draft of 6.5 ft.

(14) Roscher, E. K., "Kort Nozzle Propulsion of Ships," Shipbuilding, 1955, Vol. I, p. 84 ff; abstracted in IME, Apr 1956, Vol. LXVIII, pp. 105–106

(15) Van Manen, J. D., "Recent Research on Propellers in Nozzles," SNAME, New York Sect., 30 Oct 1956.

For design purposes the Horn and Amtsberg references of 1950 are the most useful and valuable.

Although it does not contain design rules as such the marine architect who sets out to study the advisability of using fixed shroudings with screw propellers will require reference to the paper "Open-Water Test Series with Propellers in Nozzles," by J. D. van Manen [Inter. Shipbldg. Prog., 1954, Vol. 1, No. 2, pp. 83–108].

D. S. Simpson has the following to say concerning this type of installation:

"The Kort nozzle, now almost universally used on the river towboats, has (made) a definite contribution to all vessels used principally for towing, although it shows little change in free route performance. Experiments indicate that the hull must be designed for it as nozzles added to existing (hull) designs have not given the expected improvement in towing power" [SNAME, 1951, p. 560].

A very real problem associated with the provision of fixed shrouding is building the necessary rigidity into it and attaching it firmly to the hull. This applies equally to the design of shrouding intended for mechanical protection only and to that installed for improving the efficiency of propulsion. The shape of the shrouding is so foreign to that of a normal ship that when added as an appendage it never appears to belong to the ship. To obtain an integrated design it may eventually be necessary to design a whole new type of afterbody.

If the shrouding or nozzle is part of the initial design, a stern with a shallow transverse arch and gently sloping buttocks over the propeller is indicated. The under side of the arch then forms the top of the nozzle opening. The nozzle proper benefits by two hull attachments, each as long as the nozzle, and spread laterally by the width of the arch.

The application of a nozzle-shaped fixed shrouding or enclosing duct to an existing ship is best limited to propeller positions abaft large skegs or to those underneath wide, rather flat sterns. Here a reasonable amount of rigid structural anchorage is available at or near the top of the shrouding. Although a distance equal to the fore-and-aft length of the shrouding is available for this attachment, the real need is for width of anchorage, to hold the shrouding concentric with the propeller-tip circle.

While a horizontal strut connection or tie to the bottom of a large ship skeg carrying a nozzle-enclosed propeller is not mandatory, it is greatly to be preferred. It can not be very deep, otherwise it would extend below the baseplane. Likewise, it can not be very wide or it would interfere with the contraction of the inflow jet to the lower part of the propeller disc. Nevertheless, it is a tie to a relatively rigid portion of the ship structure and as such it should be utilized to the utmost.

73.13 Shaping and Positioning of Contra-Vanes Abaft Paddlewheels. The action of contra-vanes forward of and abaft paddlewheels and sternwheels is described in Sec. 32.4 and illustrated in Fig. 32.C. These vanes are fixed appendages applied solely to improve the efficiency of propulsion.

So far as known, the only model experiments on and full-scale trials of either leading or trailing contra-vanes were those made under the supervision of F. Süberkrüb ["Vergleichende Modellversuche mit Süberkrüb Leitflächen an einem freifahrenden Schaufelrad, Teil II (Comparative Model Experiments with Süberkrüb Guide Plates On a Free-Running Paddlewheel, Part 2)," HSVA Rep. 321, 3 Mar 1936 (in German), copy in TMB library; "Neue Verbesserungen in der Hydromechanik des Radantriebs (New Improvements in the Hydromechanics of Paddlewheel Propulsion)," WRH, 15 Sep 1941, pp. 269–271]. The notes in this section are based partly on these data and partly on the general hydrodynamic knowledge set forth elsewhere in the book.

Considering first the forward or leading vane, it is pointed out in Sec. 71.6 that a side paddlewheel is best positioned so that a wave crest lies about opposite the point where the blades enter the water on the forward side of the wheel. If the leading contra-vane is placed under this crest, the water flows to it in a direction nearly horizontal. As a hydrofoil, cambered to deflect the water slightly downward, its lift is exerted in a direction close to the vertical. There is very little or no thrust component of this lift force; as the lift is otherwise not useful it should be kept to a minimum. The entrance of the contra-vane is

therefore placed so that the meanline at the nose is parallel to the streamlines of the incident flow. For a leading contra-vane ahead of a stern wheel, as in diagram 2 of Fig. 32.C, it is necessary to determine the flow direction at the nose position by some kind of ship or model test.

M. Hart has published two diagrams which show the resultant-velocity vectors, with reference to a stream of undisturbed water flowing past the side of the ship, of the upper and lower edges of the blades in a series of immersion positions [ATMA, 1906, Vol. 17, p. 179 and Pls. II, III]. These do not take account of the velocities induced by the blades, for which no comprehensive, reliable data can be found. It is considered, therefore, that the run or after portion of the leading vane can best be shaped with its *upper surface* parallel to a tangent to the sweep circle of the outer blade edges at that point. There should be enough clearance between this upper surface and the outer blade edges to pass any floating debris that may be drawn down below the surface.

The trailing edge of the forward contra-vane should lie at about the level of the blade trunnions, perhaps slightly below the midwidths of the blades in their lowest positions. As for chord length fore and aft, this can be of the order of 1.5 to 2.0 times the blade width on the paddlewheel or sternwheel, for both leading and trailing vanes.

For the after or trailing vane, the predominant flow is that which forms the high, steep wave just abaft the wheel. This is indicated in Fig. 73.J, adapted from the Süberkrüb reference mentioned earlier in the section. The contra-vane is best placed where the flow vector at the subsurface level of the vane has its steepest slope. In the layout of the figure it is possible to keep the vane above the at-rest waterline, although a position under other wave-slope conditions might be as low as the lowest trunnion level of the blades. The lower surface of the run portion of the trailing contra-vane, just ahead of the trailing edge, should conform generally to the flow within the wave crest at that position and level.

Since the lift of the after vane has a forward thrust component, this curved-section hydrofoil should have a high lift and a low drag. The meanlines of both leading and trailing vanes will have a rather large camber for their chord lengths.

The contra-vanes may be made reasonably thin if supported at say two intermediate transverse points as well as at the ends. Their curved section shape gives them inherent stiffness, as for a blade of the wheel itself.

Were a vessel fitted with contra-vanes to run in waves these devices would be subject to impact or slamming. They would have to be designed to withstand an impact load much larger than the lift load. The equivalent static load would probably be of the order of 2,000 lb per sq ft or more. This is about 4 times the uniform propelling load applied to the blades of a paddlewheel.

Side paddlewheels are in themselves rather effective roll-quenching devices. The contra-vanes are much more effective for this purpose, but even without impact they may require support for vertical forces far greater than those imposed

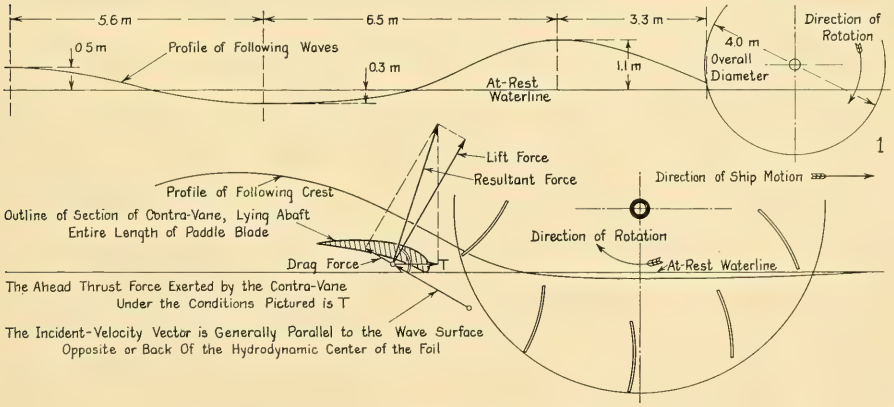

Fig. 73.J Proposed Contra-Vane Arrangement of F. Süberkrüb

upon them when acting ouly to change the direction of flow.

Limited hydrostatic pressure on the upper surfaces of the guide vanes makes cavitation, separation, and air leakage a problem. The situation is aggravated because the considerable transverse length of the contra-vanes requires for their support a series of vertical plates which project up through the free-water surface. Despite all that may be said to their advantage, contra-vanes are in the category of the short vanes of the contra-propeller described in Sec. 36.9, with most of the disadvantages enumerated there.

If the friction drag of both sets of contra-vanes is considered too much a handicap, the forward set can be omitted, since it is probably the least effective of the two.

The smaller the wheel diameter, the greater the dip, the greater the immersion arc of the trunnion circle, and the greater the angle (with the horizontal) which the blades enter and leave the waves, the more useful should be the contra-vane installation.

73.14 Design Features of Supporting Horns for Rudders; Partial Skegs. Rudders of the balanced, partly underhung, compound or flap type require a fixed support in the form of a horn or partial skeg ahead of the hinge or stock axis. This support may take a great variety of shapes, depending upon the single or multiple functions for which it is designed. It may be a structural support only, it may be intended to exert large lateral forces by pressures induced from a movable tail, it may have to serve as a vertical stabilizing fin, and it may have contra-features built in. Profiles of representative shapes are sketched or illustrated in Figs. 21.B, 24.C, 26.E, 28.A, 33.B, 37.A, 37.D and 37.J of Volume I, and in Figs. 74.K, 74.N, and 75.E of this volume.

The profile of a horn or partial skeg is determined by the structural support it is intended to give, the location of internal members to which it can be anchored, and the amount of vertical projected area desired in it. Few rules can be given for laying out these profiles. It can only be pointed out that structural skegs or horns usually require a long base on the hull or a long extension into the hull.

Hydrodynamic considerations should never be permitted to squeeze the upper and the lower bearings of any rudder-and-horn assembly so close together vertically that the lateral forces on these bearings become excessively large. Such a distorted design requires, as a rule, long (high) bearings, having length/diameter ratios so large that it is almost impossible to obtain uniform pressure over the whole bearing length because of bending or deformation of the parts. As a consequence, the bearings wear unevenly and excessively, leaving the rudder free to vibrate. Since the rudder is already in a region of disturbed flow the resulting slackness may cause pounding, with more wear and still more vibration.

Partial skegs intended as restoring-moment stabilizers benefit from large aspect ratios and relatively narrow tips. Those intended as damping-moment stabilizers have a moderate to large area in combination with the attached movable rudder. Skegs intended to be self-clearing when encountering ropes, cables, and nets, such as those on submarines, require their leading edges to be set at rather small angles to the direction of ship motion. These are not necessarily small with respect to the direction of local water flow. The outer or lower ends of horns or partial skegs, especially if they are long in a fore-and-aft direction, should lie generally parallel to the adjacent flow except for such appendages of this nature as are utilized for docking or resting purposes.

Structural skegs intended only for docking or resting can be integral parts of the hull or additions on the bottom. If the latter, it is simpler to omit the fairings along the edges where the skeg sides join the hull; this is acceptable if the conditions mentioned in Sec. 75.5 are satisfied. It is generally the case for a partial centerline skeg. If the skegs are built as integral parts of the hull it is simpler and better to fair them easily into the hull surfaces and to provide generous means of access from the inside. Incidentally, it is desirable although by no means necessary that skegs which have docking functions should terminate with their lower surfaces on the base-plane or at the level of the bottom of the keel. However, to save displacement, wetted surface, and vertical fin area in the lateral plane, they can be cut up from the keel plane by the heights of one, two, or three tiers of docking blocks, generally 14, 28, and 42 inches, respectively.

The fineness of the leading edge on any horn or projecting skeg is determined by the range of directions from which the local flow may impinge upon it under normal operating conditions. In other words, the horizontal section has sufficient thickness abaft the leading edge so that separation

and cavitation are not liable to occur alongside it except for short periods. For example, the horn supporting the rudder under a ship with a broad, flat stern runs normally at angles of attack varying from zero to a few degrees on either side. However, when the stern swings around and skids over the water in a turn, the angle of attack on this fixed appendage may rise initially to 15 or 20 deg. The angle of attack is, as explained in Sec. 36.10, applied in the wrong direction to facilitate the turn.

Separation is almost certain to occur on the inside of the turn. Cavitation may occur as well, if the top of the horn is sufficiently close to the water surface. By making the leading edge of the horn reasonably blunt this separation or cavitation is at least confined to a limited region. It would otherwise, on a thin section with a sharp entrance, extend all the way forward to the leading edge. The skeg section is usually combined with the rudder section to make a streamlined whole. Section shapes found satisfactory on high-speed vessels are similar to the strut sections diagrammed in Fig. 73.C. Their coordinates are given by P. Mandel [SNAME, 1953, Fig. 3, p. 468].

Horns supporting rudder tails and forming compound or flap-type combinations require special shaping and recessing for the tail. This is to give the minimum clearance and pressure-leakage area between the fixed and movable portions, for the reasons stated in Sec. 37.3. It is easily and simply achieved by providing one or more fixed lugs on the inside of the rudder recess, directly forward of the stock axis. If the forward edge of the movable tail of the rudder is finished to form a surface concentric with the axis, the mechanical clearance between this surface and the fixed lug may be quite small. The manner in which this may be accomplished is illustrated in Fig. 73.K.

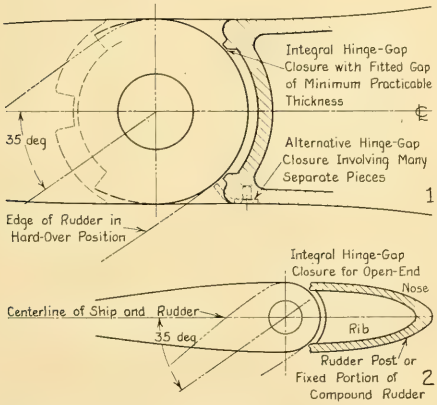

Fig. 73.K Hinge-Gap Closures for two Types of Rudder

73.15 Selecting the Position, Type, and Number of the Roll-Resisting Keels. The first step in the design of roll-resisting keels is to determine whether or not they are actually needed. If required, what are the operating conditions, and what are the keels called upon to do? It is pointed out in Sec. 36.13 that the discontinuous or multi-fin type of keel is advantageous only when the vessel is moving through the water. A continuous or solid type is indicated if roll-quenching characteristics are required at low or creeping speeds or when at anchor.

Assuming that the continuous type of keel is selected, the next step is to determine its general proportions, dimensions, and location on the hull. The total area is to some extent governed by the degree of roll damping expected or demanded and the inherent roll-quenching characteristics of the underwater form. A hull shape approaching a circular form, as on some submarines, requires a high degree of quenching from the keels, compared to the rolling moments applied by surface waves. A hull with nearly square sections in the middle-body calls for a smaller degree of quenching moment. Practically all roll-resisting keels involve some increase in appendage resistance.

The best transverse location for the keels is on the corners of the bulge between side and bottom or at positions having the greatest radius from the rolling axis. The position must insure practically if not definitely continuous submergence under all operating conditions. If the rolling axis is not known from model or full-scale tests, it may be assumed at the intersection of the centerplane and the waterplane, or at a parallel line through the center of gravity CG for the particular weight distribution assumed.

A. Caldwell ["Steam Tug Design," 1946, p. 42] states that "the bilge keels will answer their purpose most effectively if placed at that point on the shell which is farthest from the metacenter." He does not explain his reasoning in this matter.

A first approximation to the midsection position is obtained by drawing on the body plan a diagonal from the rolling axis to the point where the

diagonal offset on the midsection is a maximum. There is a further condition that the diagonal should make an angle with the tangent to the shell at the diagonal intersection which is at least 80 deg. The angle that counts is the one at the shell, not with the horizontal.

For negligible pressure resistance and minimum friction resistance, the keel should lie along the lines of flow in its region. It forms in effect a diagonal stream surface, parallel to the lines of flow at the ship hull and for the entire width of the keel away from the hull. These lines of flow, especially on a fast or a high-speed ship, change position and shape with speed because of the influence of the surface-wave profile. A trace conforming to the flow at one particular speed is therefore selected. This is generally the service speed or the highest speed at which the ship is to run for the greater part of its time in service.

For slow-speed vessels with nearly square sections in the middlebody, it may be assumed that the flow is approximately parallel to the bilge corner for the region where the bilge-diagonal offset is 0.9 or more of the maximum bilge-diagonal intercept amidships. It is vastly preferable, however, to check a proposed trace with surface lines of flow on a model. It is still better to double-check the position with tufts or flags mounted on pins and extending for at least 0.9 the maximum width of the bilge keel from the hull.

Occasionally it happens that when laying out a trace from the optimum position amidships, the keel leads up too close to the free-water surface or down too close to the floor line or the baseplane. One portion of the keel may then be terminated when it moves out of optimum position and another portion started in an offset position, reckoned girthwise, where it may be placed to better advantage for performing its function. The keel endings at this offset may, in fact, overlap longitudinally by the length of the taper on each keel but no overlap is preferred, shown in the lower profile of Fig. 73.L. There may, of course, be a fore-and-aft gap of any desired length between them. In general, the *girthwise offset* should be at least 1.5 times and preferably 2 times the full width of each keel near the gap, shown by the middle diagram of Fig. 73.L.

For ships of such full sections that working clearance is not available for keels in way of the midship bulge, the roll-resisting keel may be omitted there. Separate shorter keels are then laid out, forward and aft, where the clearance is adequate. Such a design is illustrated in the upper profile of Fig. 73.L.

For a vessel with a large but exceptionally slack midsection, and a limit to the width of the excrescences that can be applied to it, such as a motor lifeboat, it is possible to fit two roll-resisting keels abreast on each side of the hull. In such a layout the spread between the adjacent keels is made at least 6 times the maximum width of each keel to insure its proper functioning. On the Dutch liner *Oranje* of the late 1930's, which was built with discontinuous bilge keels of the picket-fence type, a second partial row of such keels was added below the main row [WRH, 15 Jan 1939, p. 21]. The transverse spacing was, with justification, less than that prescribed in the foregoing for solid bilge keels abreast.

73.16 Bilge-Keel Extent, Area, and Other Features. Because of its greater lever arm, and possibly also because of its width with reference to the thickness of the boundary layer, a keel on a sharp bulge, designed to give a certain degree of roll-quenching, may be relatively narrow. It must be wider, however, as the bulge radius is increased.

Having determined the girthwise position of the roll-resisting keel, a point is selected on the exterior portion of the diagonal, indicated at K

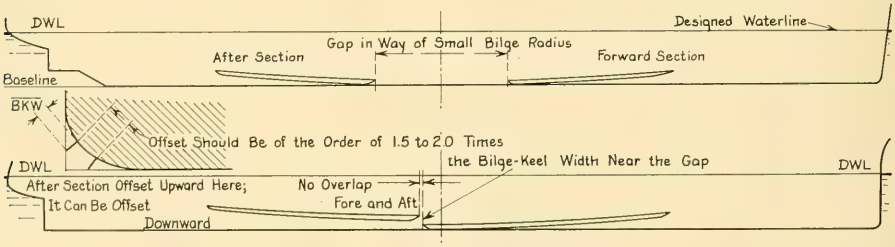

Fig. 73.L Bilge-Keel Arrangements With Gap and Offset Amidships

on Fig. 73.M, where the included angle between the two adjacent tangents to the hull is 100 to 120 degrees. The distance between the point K and the hull gives an acceptable hydrodynamic as well as practical width for the keel. For a perfectly square-cornered bilge this gives, as it should, a width of zero. The maximum width is for a semi-circular midsection, where it is 0.302 $(B/2)$ for a 100-deg angle and $0.154(B/2)$ for a 120-deg angle.

The length of the keel is determined partly by the area required, assuming that the average width has already been determined, and partly by the length of that portion of the ship for which an adequate lever arm for the keel can be obtained. When the transverse sections have narrowed or contracted so that the lever arm, R_K, as measured by the distance OB on Fig. 73.M, becomes less than a certain fraction of the lever arm at the maximum bilge-diagonal offset, the keel is terminated. Since the effectiveness of the keel varies about as R_K^3, there is little to be gained by making the minimum R_K less than about 0.8 the maximum. At this point $(0.8)^3 = 0.512$. For vessels of rather full midsection, say $C_X > 0.90$, this fraction may be kept larger than 0.85. For vessels of slack section, where $C_X < 0.90$, a minimum value of 0.75 might be justified.

The midplane of the roll-resisting keel may change angle with the horizontal, at a gradual and moderate rate from amidships to either end, as may seem appropriate when considering the flow of water in its vicinity, at a distance from the shell. Use of the "tangent rule" set down at the beginning of this section produces a narrow keel alongside the sharp-bulged sections of a form and a very wide keel alongside the narrow or slack sections. For the same total area, however, a more efficient keel is obtained by making it as wide as possible amidships and keeping it of approximately constant width. This is because the additional width amidships has a much greater lever arm than at the ends of the keel.

All too frequently the maximum width or the amidships width of a roll-resisting keel is limited by working clearances around the keel edges. This prevents damage when lying alongside quay walls and when entering graving docks. The clearances are expressed generally as (1) a distance inboard of the point of extreme beam at any section and (2) a clearance above the baseplane throughout the length. The latter is desirable when hauling bilge blocks, especially when the

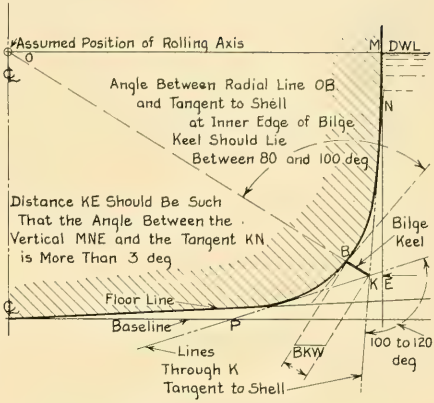

Fig. 73.M Bilge-Keel Design Diagram at Midsection

bilge-block bearers slope slightly downward toward the centerline of the dock. In some cases it may be necessary to provide this clearance above the floor line rather than above the baseplane. In fact, this requirement may be expected for all vessels which are to have bilge blocks hauled under them when drydocking. To obtain the required clearance it is often necessary to shave off the bilge-keel width amidships.

The forward and after ends of the keels are tapered *gradually* to practically zero width. A gradual taper occupies a length at least 3 times the keel width, with a maximum slope of about 40 deg. For any leading edge lying forward of about $0.5L$ from the FP, the taper should occupy at least 5 times the keel width, with a maximum slope of 20 deg for medium-speed and 10 deg for high-speed ships. This taper avoids fouling or catching ropes and cables on the ends and eliminates sharp structural discontinuities where the keels terminate.

It is possible that ships with sections projecting beyond the limits of waterline beam, where $C_X > 1.0$, hardly need roll-resisting keels at all. A flat, shallow raft with a deep fixed keel, having a C_X approaching 0.0, likewise needs no additional appendage because of the powerful roll-damping effect of the keel. Yachts, with deep fixed keels, no bilge keels, and values of C_X less than 0.5 behave much like the raft, except for the additional steadying effect of their sails. Of all the intermediate forms, the craft which needs the maximum roll damping is one having a B/H

ratio of 2.0, a semi-circular maximum section, a C_X of $\pi/4$ or 0.785, and a rolling axis in the waterplane, at the center of the circular-arc section.

A design curve or lane to give suitable values of the roll-resisting keel area A_K with relation to some other suitable term should therefore have a maximum at a C_X value of about 0.785, corresponding to a semi-circular midsection, and two minimums at values of C_X approximating 1.0 and 0.0. P. Mandel has given such a design lane for the range of C_X from 0.7 to 1.0 [SNAME, 1953, Fig. 25, p. 492], based upon the ratio $10A_K/(LH)$, where A_K is the bilge-keel area on one side of the vessel. The graph should in fact diminish toward zero at C_X values of 0.4 or less, corresponding to those of deep-keel yachts.

73.17 Structural Considerations in Bilge-Keel Design. The published literature and reference books on the structural design and construction of ships overlook many of the important features of bilge-keel design. Some of these are closely related to hydrodynamics and are accordingly discussed briefly here.

The roll-resisting keels are in effect principal longitudinal members of the ship structure, resembling stringers. As such they must diminish gradually in section so that the shell connection at any point may carry the increment of shear load applied at that point. In other words, the keel and the hull must stretch and compress together. The securing angles attaching the keel to the shell should project well beyond the end of the keel proper, about as diagrammed in Fig. 73.N of Sec. 73.18.

If the roll-resisting keels extend forward to the vicinity of the quarter point, and if they rise to points above the baseline greater than about 0.3 the draft in any operating condition, the forward ends require strengthening against wave slap and water impact.

The transverse shape of a roll-resisting keel should remain relatively sharp and pointed at its outer edge. If it needs lateral stiffening, such as is often afforded by a half-round bar, this is best provided by an outer-edge flange such as that on an I-beam with the outer flange trimmed down. This construction gives increased damping

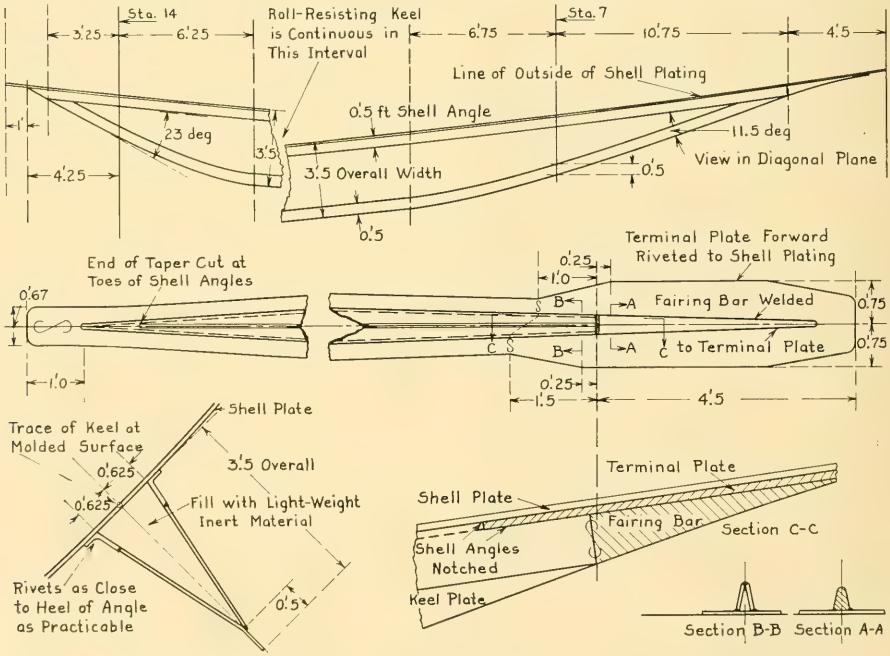

Fig. 73.N Structural Layout for Roll-Resisting Keels for the ABC Ship

with some increase in friction resistance. It requires a rather careful preliminary flow study on a model, to insure that not only the keel proper but the outer flange lie in the streamlines. A flange on the free edge should not carry around the tapered portion at the ends but should itself be tapered to zero where the width-tapering of the keel begins.

A triangular keel section affords immeasurably greater structural rigidity than a thick flat section. It is preferred where weight and displacement considerations permit. The section can take the form of an acute-angled triangle with a peak angle of not more than 15 deg, without any sacrifice of damping qualities. On large vessels expected to roll heavily the base of the triangular section of a roll-resisting keel may be as great as 0.4 or more of the keel width.

Bilge keels are heavily loaded in an alternating cycle. The extreme forward end is partly unsupported unless it is brought to a rather long, sharp point. All in all, the normal bilge keel requires a special structural attachment to render it secure for long periods of hard service. Indeed, the forward sections of roll-resisting keels on fast and high-speed vessels could well be built of heavier scantlings than the rest.

The attachment of the base of the keel to the hull should be stronger than that of the sides or projecting portions of the keel to the base. This insures that if the keel is overloaded in any way, the shell connections will remain intact.

73.18 Design of Roll-Resisting Keels for the ABC Ship. The roll-resisting keel traces for the ABC ship, shown on Fig. 66.P, were determined by flow tests on the model, using pivoted flags which projected from the hull for a distance corresponding to some 3 ft on the ship. From the straightness of the traces as projected on the midsection plane it might appear that they were simply drawn as diagonals on the body plan. It so happens that the flow on either side of the bilge-keel positions straightens itself, as it were, in these regions. This does not always occur, as evidenced by the wavy keel traces on the *Mariner* class, reported by V. L. Russo and E. K. Sullivan [SNAME, 1953, Fig. 18, p. 127]. Were the crests and troughs of the Velox waves more pronounced along the side of the ABC ship, the bilge-keel trace might well be affected by them.

The slack bilge of this ship was laid out to permit the attachment of wide roll-resisting keels, for the reasons given in Sec. 66.13. The maximum keel width of 3.5 ft, or about $0.0477B_X$, still leaves a clearance of about a foot above the floor line and a foot inside the side of the ship.

The bilge-keel area was governed in this case only by the rules in the sections preceding and by the endeavor to obtain as much bilge-keel area as possible without sacrificing other features. The keels were carried forward and aft, as shown in Fig. 66.P, to points where they were considered as no longer paying their way. The *effective* length is some 7 stations (Sta. 7 to Sta. 14); this is equivalent to 178.5 ft or 0.35 times the waterline length.

The taper at the forward ends was made about 18 ft long, shown in Fig. 73.N, or over 5 times the depth, exclusive of the structural terminal plate and fairing bar. That at the after end was made some 10 ft long, or about 3 times the depth.

The width of the triangular keel at the base is 1.5 ft, or 0.43 times its maximum depth. The hydrodynamic loads imposed in quenching roll are transferred to the hull as a combination of shear loads and normal loads. The latter pull in and out on the shell in line with the side plates of the triangular structure. Any offset members in this structure, such as side plates of the keel riveted to shell angles, are almost certain to develop high bending moments and eventually to become loose. It is for this reason that the shell angle should be very heavy. The rivets which hold this angle to the shell are placed as close as possible to the force-application lines in the side plates. This means as close as they can be driven to the bosom of the bar.

73.19 Design of Docking, Drift-Resisting, and Resting Keels. The best design procedure for docking keels, on a large, heavy ship where considerable off-center support is mandatory, is to make them unnecessary by working the desired flat supporting surface into the bottom of the ship itself. In regions where direct support is required and the normal faired lines lie somewhat above the blocking level at the baseplane, the bottom of the ship is brought down deliberately to the level of the tops of the docking blocks. Figs. 67.L and 67.M for the arch-stern ABC design indicate, in the regions near the baseplane at Stas. 14 and 15, how this is done. Although in this ship the hull terminates at the after quarter-point in a flat surface coinciding with the floor line, the shape would be essentially the same if brought down to the baseplane. In many ships this modification involves only a surprisingly

small change in form, even when the docking support is offset from the centerplane. The resulting discontinuities are moderate, distorting the flow only slightly and involving little or no added drag. Obviously, at the ends of a ship with the usual deep forefoot and aftfoot the major support area is under the centerline keel. Such a keel is kept down to baseplane level for as great a proportion of the length as possible, consistent with good flow and drag and with the required maneuvering characteristics. In a normal design the flat keel should lie in the baseplane for at least 0.8 of the waterline length, although in special cases this ratio may diminish to 0.7, 0.6, or less [Clark, L., ATMA, 1900, p. 361]. For the transom-stern ABC hull this ratio is 0.925, indicated in Figs. 66.Q and 66.T, even though the aftfoot is cut away. For the arch-stern ABC design, centerline support is provided for 0.75 times the length plus two rows of side support, under the skegs, each for about $0.15L_{WL}$.

If the hull proper can not be brought down to the level of the baseplane for docking support, the next best procedure is to raise part of the docking-keel level above the flat-keel level. In any one area this can be done by adding standard layers of material, say 4 in or 14 in thick, to the tops of the regular docking blocks. A ship of moderate draft usually has ample clearance over the raised blocking in a dock, even when some compartments are damaged and flooded. The designer may cut out the unwanted or undesirable portion of a deep keel or skeg without sacrificing blocking support by raising the bottom or support surface parallel to itself by a multiple of the blocking thickness. Figs. 67.M and 67.O show that under the two offset skegs of the ABC arch-stern design, the level is raised 28 in, or 2.33 ft. Support by keel and skegs is thus provided over 0.913 of the waterline length.

Blocking-support areas in a small ship should preferably be at least 6 in wide. In a large ship 2 ft is the minimum, but 3 or 4 ft is preferred.

An excellent drift-resisting keel for metal-hulled vessels is a centerline box keel placed underneath the main hull. An appendage of this kind was fitted to the single-hull type of submarines built by the Electric Boat Company during the period 1900–1925. This keel was used as a duct for pumping out water tanks along the length of the hull, as well as a means of holding fixed ballast. It was made of two heavy channels with their flanges facing outward. They were riveted to the circular pressure hull through their upper flanges and a heavy horizontal closing plate was bolted to their lower flanges. The bosoms of the two channels, on the outside, were filled with blocks of lead bolted in place as more-or-less permanent ballast. These centerline box keels were rugged enough to serve as resting keels when the ship lay on the bottom or as support keels when it was docked.

There is no practicable limit to the depth of a drift-resisting keel provided it is sufficiently sturdy to take its share of the load when docking. The keel is designed to be of watertight construction, with one bottom plate and two side plates, the latter attached to the flat keel plate. If the keel is long relative to the vessel it becomes in effect one of the longitudinal strength members. As such the side plates are attached to the hull in a manner to prevent transverse cracking of both the side plates and the adjacent shell plates. A flanged plate or a channel is used for the bottom member so as to bring the fore-and-aft welds above the lower outboard corners and relieve them of concentrated loads during docking.

Not only the knuckles or lower corners of the keel but the upper corners should be as sharp as practicable, with reentrant angles not less than 90 or 100 deg. The junction of the drift-resisting keel and the hull should *not* be filleted as is the case of the keep keel on a sailing yacht. The outside and inside corners mentioned are deliberately introduced to offer the maximum of dynamic resistance on the advancing side of the keel and the maximum of pressure resistance due to separation on the retreating side of the keel when drifting or sidling.

The inside of the keel may be filled with (1) some lightweight water-excluding material blown into place, with (2) some inert ballast which will not accelerate corrosion of the metal, or with (3) an inert gas.

The fine, deep sections of some fishing vessels, resembling those of a deep-keel yacht, have excellent inherent drift-resisting as well as roll-damping characteristics. Body plans and lines are shown in an article reporting NPL tests with models, entitled "Experiments with Herring Drifters" [SBSR, 28 Jul 1938, pp. 103–106].

Whether any centerline drift-resisting keel provides sufficient roll quenching to permit elimination of the roll-resisting keels is open to question. This depends upon the shape of the transverse section and the length of the lever arm of the

centerline keel from the rolling axis. It appears well established, however, that any downward projection on the centerplane, for a normal beam-draft ratio, has a beneficial effect in quenching roll.

For vessels of nearly rectangular section and large beam-draft ratio, say 4 or more, two drift-resisting keels fitted at the lower corners of the hull serve also as roll-resisting and as docking keels. In this case, the lateral spread is made large, at least 8 times the keel depth, to avoid interference and to make both keels fully effective when subjected to transverse flow.

Resting keels on a submarine may or may not project below the keel, depending upon the design requirements. They need not even be flat on the bottom, if there is an advantage in a special shape.

The sides of docking and resting keels flare outward above the support surface, and they meet the hull so that the reentrant angle is greater than 90 deg. This feature is illustrated in Figs. 36.N and 73.O.

Docking and resting keels offer the minimum of resistance when they follow the flowlines under the bottom. This means that under a flat-bottomed ship they should diverge slightly from forward aft, indicated by the directions of the under-the-bottom flowlines of Fig. 52.V. This divergence is of no particular consequence in a dock equipped to take vessels of large horizontal area which may have these keels. A ship with a rather large rise of floor may have well-curved flowlines; the docking or resting keels preferably follow them.

The direction of flow toward and away from docking and resting keels is known rather accurately from model tests and remains fixed for all steady-state straight-line travel. For this reason the ends are invariably fined on both sides of the keel. The bottom surface is carried out to a point, to give the maximum support surface, then may be cut up rather sharply, as shown at 6 in Fig. 73.O.

Notches, deep and wide enough to permit making their boundaries securely watertight, may be worked into the upper portions of deep keels. These help in the venting of air bubbles which find their way under and inside the keels and which might work their way up into injection openings. The venting openings are necessary in submarines which have main-ballast flood valves or flooding openings below them. Excess air from the blowing of these tanks can not be trapped below the keels.

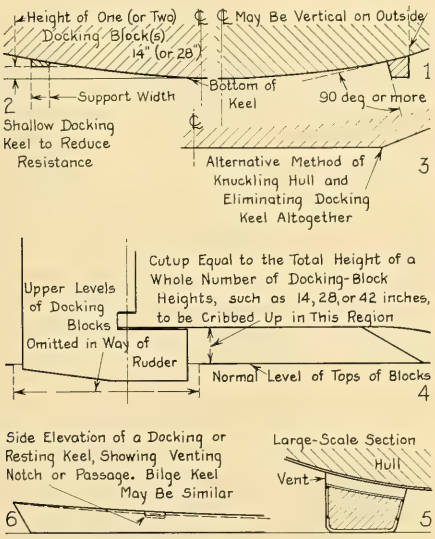

Fig. 73.O Design Sketches for Docking Keels

73.20 The Design of Fixed Stabilizing Skegs or Fins. The design of fixed skegs or fins intended primarily to act as stabilizing surfaces, excluding in this case stabilization against roll, is based upon:

(1) The damping forces and moments required to be exerted by them in the angular motions of pitch and yaw. Damping of the translatory motions of heaving, surging, and sidling is seldom necessary and is excluded here.

(2) The hydrodynamic lift exerted by these surfaces, and the corresponding restoring moments developed by them, when the ship axis departs from the normal straight-ahead motion axis and the surfaces run at a finite angle of attack. This may be an angle of either yaw or pitch. Good design requires that the fins or skegs be placed in a region of relatively smooth flow, as distinguished from a region of eddying in a separation zone. In general, the lift force developed by them should be zero for the normal attitude and normal operating condition of the vessel.

In airplanes the disposable weights usually are too small to permit achieving equilibrium by moving them forward and aft. Stabilizer surfaces with adjustable angle of attack are often provided in the tail to produce compensating moments for maintaining trim balance. In submarines provision is made in the liquid trimming system for

changing quickly the longitudinal compensating moments. It is not feasible in these vessels to provide hydrodynamic moment compensation because of the increased drag, weight, and mechanical complication of an adjustable stabilizer. There is the further important fact that the submarine may be running slowly or be stopped when trim compensation is required.

The trailing end of a ship hull, together with such rudders or planes as may be attached to it, possesses a definite but unknown stabilizing property. Actually, damping in pitch and yaw results from the swinging of both ends of the hull about the corresponding axis, but restoring moments are expected only from the after part. For angular damping the area of all movable rudders, planes, and fins mounted normal to the direction of local motion is added to the area of the fixed portions. For the most effective dynamic damping from these surfaces they are mounted as close as possible to the hull, to prevent unnecessary leakage from the $+\Delta p$ to the $-\Delta p$ sides.

Just how much fixed and movable stabilizing surface is demanded for stability of route is not a matter for ready calculation or reliable prediction, especially if the hull under design is of essentially different shape from that of a hull which has been satisfactorily stabilized in the past. This matter is discussed further under Maneuvering in Part 5 of Volume III.

To insure zero restoring force or moment on fixed stabilizers when none is desired, they must be placed exactly in the lines of flow. For a surface vessel these lines are only by accident or coincidence parallel to the axis of the ship or its direction of motion. For a stabilizing fin or skeg placed in the outflow jet of a screw propeller, the water follows the hull-flow pattern when the vessel is self-propelled rather than the direction of the propeller axis. If the stabilizers are near the surface the flow directions almost certainly change with speed because of the change in profile of the Velox wave system. This calls for the selection of a given speed at which the lines of flow are to be paralleled. In the case of submersibles which must perform well on the surface as well as below it this procedure is further complicated by the possible existence of different lines of flow for the surface and submerged conditions. Usually, however, the critical conditions for which fixed stabilizers are required occur during submerged running. When well below the surface the flow pattern does not change materially for small variations from the normal running attitude.

Considering only the restoring forces and moments produced by hydrofoil lift at an angle of attack, stabilizing fins and skegs act more efficiently as their aspect ratio is increased. However, there are practical limits to the distances which these appendages may project beyond the hull or to which they may approach certain other boundaries such as the baseplane or the planes defining extreme half-beams. A reduction in the aspect ratio must be accepted if the stabilizer area is large. This is not a disadvantage because a surface short in the direction of motion and long in a direction normal to it has low dynamic damping. Taking all factors into account, the best fore-and-aft length for such a skeg or fin appears to be approximately equal to its extension from the hull. If the hull is relatively large in area at the point of attachment, compared to the size of the stabilizer, the *effective* aspect ratio is of the order of 2.0, for the reasons given in Sec. 14.11.

It is difficult to formulate design rules for the different but common form of stabilizing or "fulcrum fin" required on any flat-bottomed boat to provide a pivot point for the rudder moment. On a small centerboard sailboat, the board is raised or lowered to give the required area. For the balsa rafts of the Incas, exemplified by the *Kon-Tiki* of T. Heyerdahl, thin planks pushed down vertically between the fore-and-aft logs at selected positions served as multiple stabilizers. This gave the "rafters" a great freedom for adjustment and relieved the builder of the burden of selecting a fixed—and proper—set of positions when the raft was put together.

On a high-speed motorboat carrying a fulcrum fin, a trial-and-error process of positioning is indicated, at gradually increasing speeds, or else a miniature centerboard may be used, mechanically operated from the driver's seat. J. Baader shows the shape, relative size, and position of this forward or fulcrum fin for a number of successful motorboats ["Cruceros y Lanchas Veloces (Cruisers and Fast Launches)," Buenos Aires, 1951, pp. 115, 119, 322–325, 341].

Fixed stabilizers and skegs, especially on submarines, may often be called upon for complementary functions such as propeller guards and docking supports for the stern. In this case their outer edges may be reinforced with shallow flanges similar to those described for the roll-resisting keels in Sec. 73.17. These flanges must

be placed in the lines of flow, but the proper position is easily determined from a tuft test.

73.21 Design of Torque-Compensating Fins. So far as known, there are no finished designs or working shipboard installations of devices intended to counteract the effect of the unsymmetrical propelling-plant torque, described in Sec. 33.19.

The approximate heel angle resulting from unbalanced propeller torque is readily determined by entering the righting-moment curve of the ship with the propeller torque Q. In this case it is assumed that the righting moments are not altered due to forward motion of the vessel. Any such effect is usually of the second order of magnitude.

As the first stage in such a study it is proposed that this be accomplished by fitting abaft the screw propeller a fixed fin traversing some convenient diameter of the outflow jet. This fin, like the well-known contra-rudder described in Sec. 37.16, is twisted on opposite sides of the shaft axis to develop thrust while extracting rotational energy from the outflow jet. It thus combines a torque-compensating device with a means of improving the propulsive efficiency. The counterbalancing torque produced by this device is a function of the velocity of flow over it, just as the propeller torque is a function of the resultant velocity at an average blade element. The counterbalancing torque thus increases with ship speed and rate of rotation, to match the increasing propeller torque throughout the ship speed range.

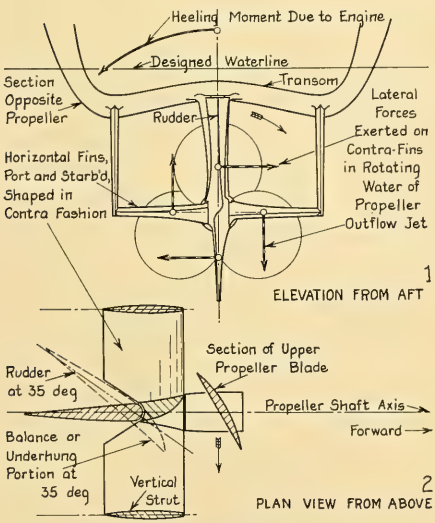

Fig. 73.P Proposed Scheme for Counteracting Unsymmetric Engine Torque

To provide the necessary compensating torque from one diametral fin, the contra-effect could be somewhat larger than is customary for a contra-rudder. Methods of developing the twisted shape for the latter are described in Sec. 74.16.

A set of torque-compensating fins, each having three or more radial arms, symmetrical with respect to the shaft axis, could be used if convenient in place of the single fin with two arms. The problem here, as with the two-arm assembly, is to support the contra-fins in their proper positions without increasing the appendage resistance by a disproportionate amount. Fig. 73.P is a sketch of such a device, with a vertical fin worked into a compound-type contra-rudder assembly. A horizontal fin is supported at the center by the rudder post and at its outer ends by two vertical struts. An upward component of flow abaft the single propeller might require a tilting of the horizontal arm, downward and forward.

Sec. 69.13 describes a method of using unsymmetric spray strips on a high-speed planing craft to achieve a measure of dynamic reaction to unbalanced engine torque.

73.22 Fixed Guards and Fenders. Projections from the fair surface of the hull in the form of fixed guards or fenders are of two types, those primarily vertical and those which lie generally parallel to the direction of motion. Of the first type are guards for external scupper and drainage leads or, occasionally, for operating gear which must be external to the shell. Of the second type are fenders and projecting fender strakes, extending over considerable portions of the length but covering limited portions of a transverse section.

The vertical projections are an abomination from every point of view and are to be avoided wherever practicable. They throw spray at all except the lowest speeds and they cause pressure resistance and separation drag, with holes in the water behind them. They cover up shell surfaces liable to heavy corrosion and they are vulnerable to damage from other craft or heavy objects lying alongside.

Longitudinal fenders, regardless of type of section or construction, must often be placed at

the positions of maximum waterline or extreme beam. These positions may vary vertically, or girthwise, from station to station on a ship, so the fenders can seldom be led along the lines of flow to insure minimum drag. Perhaps this is just as well, because most of them lie near the free-water surface. Here the lines of flow under the waves of the Velox system change with speed and with position along the length. Moderate amounts of rolling and pitching also change the direction of the resultant flow accordingly.

Considering structural, fabrication, first-cost, and maintenance factors, as well as hydrodynamics, nothing can equal or surpass the heavy fender strake which forms an integral part of the shell plating. It involves practically no increase in drag. It eliminates all discontinuities in the fair form of the hull except the strake edges. It takes care of all problems of leaky connections, unseen corrosion, spray throwing, and the like. It serves best when acting as the outer boundary of an irregular hull section, with some transverse curvature for stiffness, diagrammed at 1 in Fig. 73.Q. It is adequate, never-

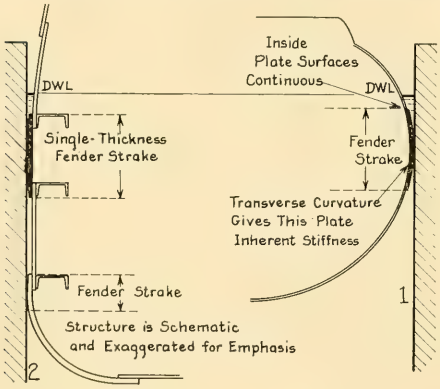

FIG. 73.Q FORMS OF HEAVY FENDER STRAKES

theless, with possibly some slight increase in weight, for vertical ship sides against vertical walls, sketched at 2 in the figure.

A heavy fender strake of this type is *always* made an outside strake. If the seams are riveted or if they are welded a strake is easily removed from the outside for repair or replacement. A fender strake of this kind, standing vertical at the maximum beam of an underwater bulge, is shown by J. L. Bates and I. J. Wanless [SNAME, 1946, Fig. 14, p. 332]. Diagram 2 of Fig. 73.Q is a schematic sketch of a similar fender strake.

When placing propeller guards it is necessary to take account of the wave profile aft, plus the the usual disturbed-surface layer covering it, in the deepest draft-aft condition, to insure that these guards remain out of water and do not throw spray.

A rather large-scale drawing of a bow rudder and its close-fitting guard, designed for a cross-channel steamer, is published in The Shipbuilder [(now SBMEB) Jan-Jun 1914, Vol. X, p. 36]. Another one is given by G. de Rooij ["Practical Shipbuilding," 1953, Fig. 495, p. 203]. Twin weed skegs outboard of the twin propellers of a 63-ft motorboat are shown in (American) Motorship, April 1948, page 34.

73.23 Design to Avoid Vibration of Appendages. Means of predicting and avoiding the singing of screw propellers are outlined in Secs. 23.7 and 70.46. It is equally important that those parts of the main ship hull and those appendages in the vicinity of the propulsion device(s) be designed to have certain natural periods of vibration in water. These should be different from the exciting frequency of the blades or other principal parts of the propulsion device(s). There are techniques available, similar to those described in TMB Report R-22 of April 1940, whereby the natural frequencies of the parts of appendages in question may be determined on existing ships, or on new ships *prior to the first sea trial.* This involves the local attachment of small vibration generators in watertight casings, or the excitation of the appendages in their natural modes, also in water, by connecting the generators and the appendages with long struts.

Long, slender, and well-streamlined appendages like strut arms nevertheless require checking for their susceptibility to resonant vibration. Under operating conditions they may be followed by a vortex street or trail. Existing data (1955) are far from adequate as to the eddymaking characteristics of elongated sections, especially in the yawed attitudes to be found during turning and wavegoing.

A few general rules may be laid down as a help to the designer in this respect:

(1) A vortex street or trail may be shed from any section, yawed or otherwise, on which there are opposite separation points, and on which these separation points may shift forward or aft

along the section outline without encountering abrupt discontinuities. One such section is a thin ellipse; another is a strut section with an elliptic trailing edge.

(2) The probable angle of non-axial flow for any appendage section may be estimated from:

(a) The nominal non-axiality of the flow, considering the type of ship motion

(b) The position of the appendage on the ship

(c) The flow-obstructing or flow-straightening features in the vicinity.

For example, an appendage far removed from the estimated position of the pivoting point in a tight turn has a *nominal* degree of non-axial flow that is far greater than the average drift angle of the ship, measured at the CG. On the other hand, if the appendage is in a tunnel, or directly abaft a long skeg, it is protected, in a way, from this cross flow.

An example of the method of estimating the vibratory characteristics of a typical streamlined appendage in the form of a long strut arm is given in Sec. 46.9.

73.24 Design of Water Inlet and Discharge Openings Through the Shell. This section treats only of the design of inlet and discharge openings for circulating water to the main propelling machinery or to pumping plants large in comparison to that machinery, such as in a fireboat. The design of secondary openings for taking water into and discharging it from the hull of a ship represents no particular problem that does not occur with the major openings. The comments and illustrations of Secs. 8.6, 8.7, and 36.20 apply to all these openings in a general way. For the discussion of the present section it is convenient to assume axes of reference fixed in the ship. The surrounding water is then considered as a stream flowing past a stationary opening in the hull.

The kinetic energy in the boundary layer may be utilized for forcing water through internal piping and heat exchangers of one kind or another whenever there is sufficient velocity head for conversion into the requisite pressure head. In this case the available velocity head is that corresponding to flow in the boundary layer along the shell. This may be taken as 0.5 the nominal ship speed for preliminary estimates, less the head corresponding to the desired velocity through the internal system. In practice, it is found that there is no particular advantage in using the scoop type of injection unless the speed of the ship equals or exceeds 20 kt in service. In this case the determining figure appears not to be the speed-length quotient or the Froude number but the absolute speed of the ship.

The longitudinal position of the main injection is fixed within rather narrow limits by the position of the internal heat exchangers. There is some latitude in transverse position to suit service conditions, with the proviso that the injection *must always remain submerged* under the most severe kinds of wavegoing. For an icebreaker the logical position for the injection is under the bottom, clear of as much ice as possible. For a vessel to operate in shallow water it should not be too near the bottom, otherwise it may be in the mud. For vessels which may be required to operate in waves in a relatively light condition, especially at light or shallow draft forward, there are problems other than that of picking up water with the scoop. Air bubbles are entrained by wave action or impacts under the forefoot, but it is probable that they follow fairly definite paths under the bottom.

Water injections are to be kept clear of these paths, using model tests to determine the air-bubble routes. Particularly, injections should not be installed close below roll-resisting keels, docking and resting keels, or other longitudinal appendages beneath which air is liable to be trapped.

When considering the use of a condenser-scoop installation, or when selecting the type, the price to be paid in resistance—and effective power—always involves a combination of the scoop inlet *and* the discharge. Since it is the discharge which often creates the hydraulic (suction) head necessary to draw water through the condensers, this is the element of the pair which may be expected to develop the greater resistance.

Regardless of the merits of any one hydrodynamic design of inlet scoop or discharge outlet there is always the problem of finding room for these fittings in the bottom or the lower corners of the ship under or alongside the machinery spaces. When room is assigned there is the matter of cutting into main structural members. Finally, the large piping has to be led to and from the condenser(s), and space must be made available for a stand-by power-driven circulating pump for maneuvering.

In Sir Charles Parsons' *Turbinia* of 1897 there were two condensers with circulating water fed to them in series from two scoops, one on each

side of the vessel. Each scoop was fitted with a flap so that one could act as a discharge while the other was acting as an inlet. By throwing over both flaps, the water direction was reversed and any foreign matter choking the tubes was drawn overboard. At a later stage in the life of the vessel an overboard discharge was fitted in the crossover between the after ends of the condensers so that both scoops could take in water simultaneously and pass it through the condensers in parallel [INA, 1897, p. 233; ASNE, May 1897, p. 376].

In the flush-lip inlets of the Schmidt type, in which there is no scoop or external projection as such, it is no small matter to guard against the entrance of large fish and foreign objects into the heat exchangers. Longitudinal bars must be fitted across the scoop entrance, spaced perhaps 0.3 ft apart. They need rigidity to serve as guards and to prevent lateral vibration. They must have bolted end connections for ready removal. The flow must be maintained around them in the desired quantity. The bars and their end connections must make so little disturbance that air is not pulled out of solution in the water and passed along to the heat exchanger. For all types of inlet it seems best to mount the guard bars or guide vanes in a single, integral streamlined assembly which can be held in place by recessed bolts and removed as a unit.

There is great merit in a type of inlet and discharge, hydrodynamically efficient, which can lead into and out of the machinery spaces in a transverse plane, making a rather sharp angle with the shell, up to 90 deg. Such a design, developed in Italy, employs a generally rectangular opening with a moderately projecting lip. A set of sharply curved guide vanes, as used in all modern water tunnels and channels, changes the direction of the water. The guide vanes serve also as strainer bars to prevent the entry of large fish, blocks of ice, and other foreign objects.

Besides having an efficiency and a resistance apparently comparable to scoops of the Schmidt design, the Italian arrangement of Lattanzi and Bellante [Italian patent 404,551 of 18 Jun 1943; Bureau of Ships, Navy Dept., Transl. 529. Also Orlando, M., Ann. Rep Rome Model Basin, 1940, Vol. X] has the advantage of superior flow, especially the absence of vortexes within the inlet diffuser. Although it has not, so far as known, been tested as a discharge outlet there is no reason why it should not work equally well in either direction, as did the similar scoops and discharges in destroyers and other vessels of the World War I period.

Despite the known workability of flush inlet scoops there is also much to be said for a scoop—and a discharge—which project sufficiently from the ship's side to take advantage of the greater velocity in the boundary layer at a small distance from the shell. The right-hand upper diagram of Fig. 73.R is an attempt to sketch a device which may produce the desired result. In an orthodox form of flush scoop the slowly moving water entering on the forward side, combined with the faster moving water entering on the after side, often creates an eddy with backflow just abaft the forward surface of the diffuser. The guide-vane arrangement should be such as to pick up an appreciable "belt" of water at the inside of the

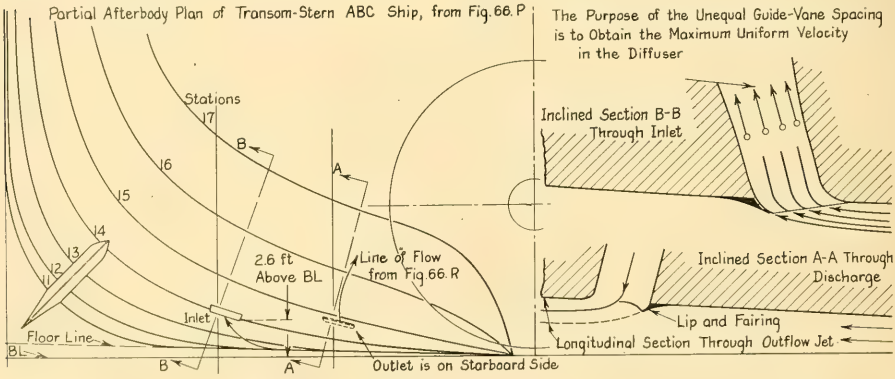

Fig. 73.R Main-Injection and Discharge Layout for Transom-Stern ABC Ship

boundary layer and accelerate it *inside* the scoop. The after guide vanes should pick up a smaller quantity of water in the more rapidly moving intermediate layers and slow it down inside the scoop. The aim is that at the entrance to the diffuser the water shall be moving regularly at more-or-less uniform velocity, indicated by the four velocity vectors of Fig. 73.R.

On high-speed vessels, and probably on medium-speed craft as well, the roll-resisting keels along the bilge corners act to collect the air bubbles passing under the ship and to shoot them out in two streams from the after inboard sides of the bilge keels. This phenomenon is particularly noticeable in a circulating-water channel when air bubbles are circulating with the water. The regions in the vicinity of the flowlines emanating from the trailing edges of the bilge keels should therefore be kept clear of injection or inlet openings through the shell, to prevent accumulations of air in the water sides or cooling jackets of heat-exchanger systems.

The position shown in the left diagram of Fig. 73.R for the circulating-water inlet to the main condenser of the ABC ship is well clear of this air-collecting region on the port side.

Openings in the hull for the *discharge* of water from internal machinery may be located with relative freedom to suit the internal arrangements. In fact, they need not even be below the water surface under all conditions of operation. It is logical to lead water out through the hull in the same manner as it was brought in, by inverting the scoop section and directing it into the boundary layer at a small angle to the flow there. To be sure, if structural, mechanical, or space considerations demand it, water can be discharged into the boundary layer at any angle up to 90 deg with the flow, diagrammed in Figs. 8.G and 8.H. Rarely, however, is there not sufficient room to provide a short elbow with multiple turning vanes for changing the flow direction mechanically instead of producing a hydrodynamic disturbance in the boundary layer. If the elbow is considered too elaborate, and involves too large a hole in the shell, fairing pieces can always be fitted, corresponding to those in the referenced sketches.

73.25 Partial Bibliography on Condenser Scoops. Research on inlets of the scoop type, for taking water into condensers and other large heat exchangers, has continued steadily if not rapidly for the past half-century or more. Appended is a list of references giving partial coverage for the reader who wishes to pursue this subject further:

(1) Schmidt, H. F., "Theoretical and Experimental Study of Condenser Scoops," ASNE, Feb. 1930, Vol. XLII, pp. 1–38. Comprises a basic treatment, beginning with hydrodynamic fundamentals.

(2) Hanzlik, H. J., "Condenser Scoops in Marine Installations," ASNE, May 1931, pp. 250–264

(3) Schmidt, H. F., and Cox, O. L., "Test on a One-Quarter Scale Model Scoop on the U.S.S. *Welborn C. Wood* and Preparatory Laboratory Experiments," ASNE, Aug 1931, Vol. XLIII, pp. 435–466. Fig. 5 opposite p. 437 shows the inlet flow in the plane of the shell. Fig. 13 on p. 445 gives variations in pressure and velocity, as measured on the U.S.S. *Raleigh* (CL 7), for the first 14 inches out from the shell, in way of the inlet-scoop position.

(4) Weske, J. R., "Investigation of the Action of Condenser Scoops Based upon Model Tests," ASNE, May 1939, Vol. 51, pp. 191–213. Discusses discharge as well as inlet performance.

The arguments and explanations in the six references which follow afford a useful insight into the practical features of the flow into inlet scoops for internal heat exchangers:

(5) Schmidt, H. F., "Some Notes on E.H.P. Calculations and Propeller Characteristics," ASNE, Nov 1933, Vol. XLV, pp. 528–533. This brief paper discusses the influence, on the effective power required to drive the ship, of taking in cooling water for condensers through inlet scoops, utilizing the forward motion of the ship. The author points out that this increment has to be added to the power predicted by tests of a self-propelled model.

(6) Schade, H. A., "Discussion of Notes on E.H.P. Calculations," ASNE, Nov 1933, Vol. XLV, pp. 534–535. This is a discussion of the preceding reference (5).

(7) Schmidt, H. F., "Further Discussions on Notes on EHP Calculations," ASNE, Feb 1934, Vol. XLVI, pp. 107–109. This is in turn a reply to reference (6).

(8) Schade, H. A., "Discussion of Mr. Schmidt's Reply," ASNE, Feb 1934, Vol. XLVI, pp. 110–111

(9) Schmidt, H. F., "Reply to Discussion by Lt. H. A. Schade," ASNE, May 1934, Vol. XLVI, pp. 251–253. This article contains a photograph showing flowlines into an inclined inlet without lip.

(10) Schmidt, H. F., "A Criterion for Scoop Cavitation," ASNE, Aug 1934, Vol. XLVI, pp. 352–356. Facing p. 353 of this reference there is a photograph showing the lines of flow into the model of a lipless inlet scoop of the Schmidt type.

(11) "Comparative Tests of Condenser Scoops," EMB Rep. 384, Jul 1934. Describes tests run on EMB model 3293, representing the DD 364–379 class of destroyers of the U.S. Navy.

(12) Rabbeno, G., "Appunti Preliminari sulle Variazioni per Reciproca Influenza nelle Potenze Assorbita dalla Circolazione Refrigerante e dalla Propulsione

velle Turbonavi Veloci (Preliminary Notes on Variations, due to Reciprocal Influence, in the Power Absorbed by the Cooling (Condensing) Water and by the Propulsion Plant in High-Speed Turbine-Driven Ships), Ann. Rep. Rome Model Basin (in TMB library), 1936, Vol. VI, pp. 67–76

(13) Orlando, M., "La Circolazione ai Condensatori nel Naviglio Veloce (The Circulation in the Condensers of High-Speed Ships)," Ann. Rep. Rome Model Basin (in TMB library), 1936, Vol. VI, pp. 76–90

(14) Reilly, J. R., and Hewins, E. F., "Condenser Scoop Design," SNAME, 1940, pp. 277–293; 301–304. This is an excellent, comprehensive, detailed discussion of the problem of designing inlet and discharge scoops, with a great deal of experimental and design data and an example worked out for a pair of inlet and outlet scoops. The text is supplemented by numerous flow diagrams.

(15) TMB Report R-43 of September 1941 entitled "The Effect of the Flow of Water Through Condenser Scoops on the Resistance of a Destroyer Model."

(16) A theoretical discussion of the water flow into scoops of various shapes, in which flow nets have been prepared by conformal and Schwartz-Christoffel transformations, is given by C. Igonet in ATMA, 1945, Vol. 44, pp. 447–466. So far as known no translation is available.

(17) BuShips Translation 529, of article entitled "Esperienze Aerodinamiche su Modelli di Bocche di Presa per l'Acqua di Raffreddamento dei Condensatori Marini (Aerodynamic Tests on Models of Intake Scoops for Cooling Water of Marine Condensers)," by Dr. B. Lattanzi and Dr. E. Bellante, Aerodynamic Laboratory of Guidonia, 26 Jul 1941

(18) Frick, C. W., Davis, W. F., Randall, L. M., and Mossman, E. A., "Experimental Investigation of NACA Submerged Duct Entrances," NACA Rep. ACR A5I20, Oct 1945

(19) Breslin, J. P., and Ellsworth, W. M., Jr., "Progress Report: Research on Main Injection Scoops and Overboard Discharges," TMB Rep. 793, Sep 1951

(20) Spannhake, W., "Comments and Calculations on the Problem of the Condenser Scoop," TMB Rep 790, Oct 1951.

Pertinent design notes on discharge openings are given by E. P. Worthen, with a drawing of the device used on the *Mariner* class of the 1950's [SNAME, 1953, Fig. 43, p. 201].

73.26 Design and Installation of Galvanic-Action Protectors. It can not be expected that carefully shaped bossing and skeg terminations, strut arms and hubs, rudder posts, and other fixed appendages will give creditable hydrodynamic performance if cluttered up with excrescences in the form of galvanic-action protectors, studs, nuts, and what not. It appears probable that these protectors will have to be fitted for some time to come. Their installation should call for a measure of design and construction effort comparable to that devoted to the bossing, strut, and propeller design. The use of partly recessed zinc plates, socket-head cap bolts, shoulder nuts, and similar devices is one step toward improvement, indicated in Fig. 73.S.

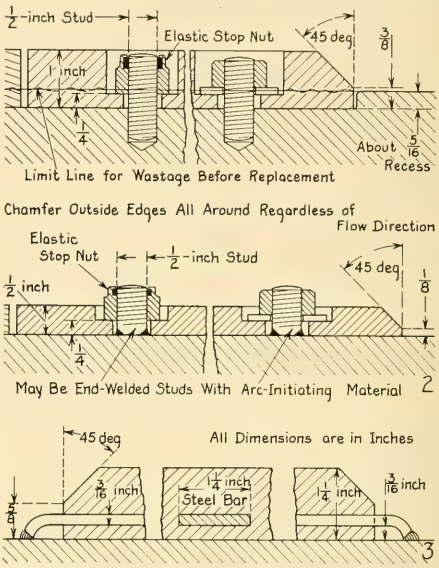

Fig. 73.S Proposed Fairing and Attachment of Galvanic-Action Protectors

Certainly there appears little excuse, in an age which prides itself on its technologic achievements, for the addition of fully protruding protectors on any ship which spends a reasonable proportion of its life underway.

In areas of the waters of the world where corrosion of the steel hull plating is exceptionally severe, this corrosion is often reduced to small proportions by bolting rows of plates or blocks of anodic materials directly to the shell plating [Kurr, G. W., "Check Costly Hull Corrosion," Mar. Eng'g., Nov 1954, pp. 57–60, also p. 12]. The added drag of these excrescences is undoubtedly large. However, it might well be less than the added friction drag of the loose bottom paint and the severely pitted plating surfaces which would be encountered without the anodic protectors.

Other methods involving external devices in the form of appendages, temporary or permanent,

are described by H. F. Harvey Jr., and O. J. Streever [SNAME, 1953, pp. 431–463]; also by D. P. Graham, F. E. Cook, and H. S. Preiser in their paper "Cathodic Protection in the U. S. Navy; Research-Development-Design" [SNAME, Nov 1956].

73.27 Design Notes for Locating Echo-Ranging and Sound Gear on Merchant Vessels. A good underwater sound installation for transmitting and receiving, whether of the fixed or retractable type, involves a neat combination of acoustic and mechanical engineering, hydrodynamics, and naval architecture. Aside from the purely acoustic features involved, the most important single factor in an efficient design is to shape the sound head or sound dome so that it is free from cavitation and separation. It must also be placed under the ship in a position where it is clear of air entrained in the streams which flow past it.

A sound head may be in the form of a streamlined body of revolution, resembling the hull form of a stubby true submarine vessel or an airship. When carried by a post or strut, it forms an assembly which is usually retractable. Such a form is reasonably free from flow noises but it does not lend itself to swinging bodily in azimuth for horizontal search. Furthermore, when yawed slightly it is no longer a streamlined body. A vertical, streamlined 2-diml enclosure, with the sound head rotating inside it, can rarely be made long enough to be entirely free of separation, air bubbles, and possible cavitation along its after or trailing portion.

A fore-and-aft location of the sound gear at a distance abaft the stem of about $0.15V^2$, where V is in kt and the x-distance is in ft, appears to be as satisfactory as any. More important, however, than both shape and fore-and-aft position may be the sound-head distance below the hull. A deep projection keeps the sound head always under water when the vessel is pitching. Further, it is below the boundary layer and beneath the streams of air bubbles entrained at the bow, near the free surface, and flowing aft under the hull. This usually requires that the head be extensible and retractable.

For the ABC ship at say 20 kt, the distance abaft the stem would be $0.15(20)^2$ or 60 ft, corresponding to about Sta. 2.35. At a distance of 4 ft below the keel the head should be well below the most disturbed portion of the boundary layer. For a fishing trawler traveling at say 10 kt, the head could be at a distance of $0.15(10)^2$ or 15 ft from the bow. If also placed 4 ft below the keel it should be in a good listening position and should remain submerged unless the vessel is pitching deeply.

CHAPTER 74

The Design of the Movable Appendages and Control Surfaces

74.1 General. This chapter undertakes to set forth design notes for the movable appendages whose use and effect are described in Chap. 37. Most of these are control surfaces of one kind or another, such as rudders and diving planes. The fact that maneuvering in general, and the prediction of the effect of control surfaces in particular are discussed in Part 5 of Volume III means that the design rules of this chapter lack some of the numerical values to be found in other chapters of this part.

Specifically, the methods of predicting the effects of given control surfaces and of estimating the torques on their spindles or stocks are not described here but are included in Part 5. Only an outline is given, in Sec. 74.7, of an improved method for determining the proper areas for control surfaces. The detailed procedure is unfinished at the time of writing (1955).

74.2 Positioning Rudders and Planes. Other things being equal, rudders and diving planes are best placed where the swinging and diving (or rising) moments of the forces exerted by them are the greatest. This usually means placing them at the greatest practicable horizontal distances from the CG.

The magnitude of the induced velocity in the outflow jet increases with distance downstream from a screw propeller, explained in Sec. 16.3. Its beneficial effect upon the resultant velocity past a rudder increases the transverse force developed by the rudder when the latter is mounted well abaft the propeller. This is explained in Sec. 33.21 but a slightly different version is added here.

From the diagram of Fig. 16.A, the area of the outflow jet in an ideal liquid diminishes directly as $(U + kU_I)$ increases. The outflow-jet diameter diminishes as $A^{0.5}$ while the lift increases as $(U + kU_I)^2$ or as A^{-2}. Therefore, the transverse force on that portion of a control surface lying within the jet should increase as $A^{-1.5}$. This means that the increased outflow-jet velocity at a distance abaft the disc more than compensates for the reduction in the area of the control surface covered by the jet.

For this reason, confirmed by model tests, the best relative position of the rudder, when it lies within an outflow jet, is with its leading edge from 0.75 to 1.00 times the propeller diameter D abaft the plane of the disc [van Lammeren, W. P. A., RPSS, 1948, p. 336]. Fig. 74.A illustrates sche-

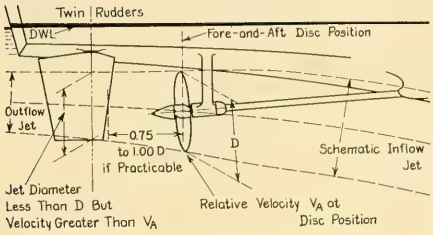

Fig. 74.A Diagram Illustrating Augment of Outflow-Jet Velocity at a Rudder Position

matically an installation of this kind. This rule also applies to the fore-and-aft positioning of a single rudder between the outflow jets of two screw propellers, provided the jets are close enough so that they impinge upon it at reasonable rudder angles, say 20 deg or more. Indeed, for single-screw ships, where rudder effect alone is considered, it is well to keep the leading edge of the rudder well abaft the propeller if this can conveniently be done.

Some useful information relative to flow at the centerline rudder position on a model, as affected by the boundary layer, by the outflow jets from adjacent screw propellers, and by the lateral motion of the stern during a turn, is given by W. G. Surber, Jr. ["An Investigation of the Flow in the Region of the Rudder of a Free-Turning Model of a Multiple-Screw Ship," TMB Rep. 998, Oct 1955]. It has not been possible to unearth corresponding data from tests of single- and twin-screw models.

On vessels where maneuverability and rudder effect is an important requirement, the movable blades of rudders are placed well below the surface or their upper portions are protected in some other effective way from partial breakdown due to leakage of air from the surface. The blade lengths at the top, near the surface, may be made shorter than at the bottom. The upper after corner of a rudder may be cut back, as was done for the transom-stern ABC ship; see Fig. 74.K of Sec. 74.15. The effects of heel, wave action, change of trim, and other factors which obtain during turning are not to be lost sight of in checking for possible air leakage to the reduced-pressure side of the rudder during that maneuver.

The trailing edge of a steering rudder should not be placed too near the lower corner of an immersed transom. When the speed is high enough to expose the whole after surface of the transom, down to the lower corner, air may "jump" to the reduced-pressure side of the rudder. This occurs when the gap between the transom corner and rudder is small enough or the pressure differential large enough. The resulting air leakage greatly reduces the rudder force on a turn. For the "lifting" rudders described in Sec. 37.18, air leakage of this kind is necessary to the success of the arrangement, but for a ship not carrying them, air finding its way to a rudder is definitely detrimental. Testing techniques are now available in the larger model basins whereby this air leakage can be photographed and detected on a free-running model during a turn. The air leakage could be prevented in a transom-stern design by extending the bottom beyond the transom plane as a thin horizontal lip. However, this might introduce difficulties when backing or when running in an overtaking sea.

Rudders and planes hung wholly or partly on the after ends of horns, skegs, fins, and keels are most effective as lateral-force-producing devices when coupled closely to those fixed members. This does not necessarily mean that they give rapid response when angled quickly, as discussed in Sec. 74.18. Special devices to prevent leakage of differential pressure through the hinge are very much worth while; some of them are described in Secs. 73.14 and 74.14 and illustrated in Fig. 73.K.

A rudder or plane should definitely be kept clear of a swirl core or hub-vortex cavity, described in Sec. 23.14 and illustrated in Figs. 23.K and 23.L. This usually forms abaft the hub or fairing cap of a screw propeller on a fast or high-speed ship but there are evidences that it may appear at a moderate speed. The cavity is likely to be so large that the portion of a rudder against which it strikes is totally ineffective. The rudder structure in its wake is subject to pitting, erosion, and hammering, which may result in fracture of the parts and tearing off of the portion under attack. A rudder on a fast but not high-speed ship, subject to damage of this kind, is shown by V. L. Russo and E. K. Sullivan [SNAME, 1953, pp. 124–125]. Another such rudder, on a slower ship, is illustrated in Marine Engineering, New York, October 1954, page 44. It is known that in some cases, such as following a sharp turn, the swirl core or hub vortex shifts around on the fairing cap. In other words, it does not always trail from the exact point or tail of the cap. A good rule, therefore, is to keep clear of a possible swirl core

having a diameter as large as that of the hub, and following the direction of the streamlines for the ship flow in the vicinity.

Wherever practicable, it should be possible to remove propellers, dismantle propeller shafts, and examine propeller bearings without disturbing or removing rudders or diving planes mounted near them.

It is not necessary that the axes of offset rudders be exactly vertical or that those of multiple rudders be parallel, if their hydrodynamic performance can be improved thereby. Mechanical simplicity in the steering gear need not be a determining factor in cases of this kind.

With regard to the placing of rudders in regions of good flow, where they can do what is expected of them, the design rule embodied by W. J. M. Rankine on page 95 of his 1866 treatise on "Shipbuilding: Theoretical and Practical" is as applicable today as the day it was written:

> "It is also necessary that the rudder should be immersed, not in a mass of eddies dragging behind the ship, but amongst particles of water whose motion, relatively to the ship, consists in a steady flow astern. Hence the same fairness and fineness of the water-lines and buttock-lines of the afterbody which are essential to speed and economy of power are essential to good steering also."

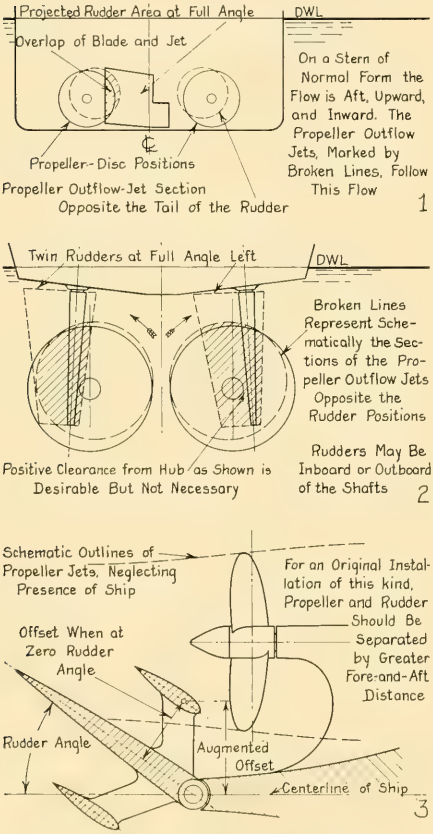

FIG. 74.B POSITIONS OF MULTIPLE RUDDERS WITH RESPECT TO OUTFLOW JETS

74.3 Single or Multiple Rudders? In a normal form of twin-screw stern a single rudder hung between two propellers usually angles far enough so that a considerable portion of the trailing area of its blade swings into the projected disc area of one or the other of the propellers. This is true even though account is taken of the customary inward and upward shifts of the twin-screw propeller outflow jets, conforming to the general direction of flow in the vicinity, and to the contraction in those jets. Diagram 1 of Fig. 74.B illustrates schematically the situation described.

A single rudder is sometimes placed between two screw propellers which lie so far apart transversely that the rudder blade *does not swing appreciably* into the outflow jet of either at its extreme range of angle. Although not always lacking in steering and turning action, such a rudder is liable not to function adequately, no matter what its area.

It is possible that the single rudder, if lying in a "strong" flow having a small positive or a slight negative wake velocity, produces the desired lateral force. The same rudder, lying in a "weak" flow, with a large positive wake velocity and a small speed of advance, is inadequate to maneuver the ship. Smaller twin rudders, lying close to or within the outflow jets, are indicated for situations of this kind. Here again, depicted by diagram 2 of Fig. 74.B, account is taken of whatever lateral or vertical displacement, or both, results from the fact that the propeller outflow jet contracts and that it follows the direction of flow under the hull.

Efforts to achieve the same effect with so-called biplane or triplane rudders, when a single blade is found inadequate, may be disappointing. Multi-blade rudders, operated by a single stock and steering gear, are usually used. These represent a simpler alteration than fitting twin rudders

abaft the propellers. In the event multiple blades are used, the wing or offset blades should lie abaft the stock axis of the main blade, so that when swung at an angle the wing blades move *farther* from the centerplane, indicated in diagram 3 of Fig. 74.B. Otherwise, as the wing rudder elements are swung to achieve large angles of attack they move *toward* the centerline by $(1 - \cos \delta)$ times their offset distance. In effect, the wing blades back away from the outflow jets they are supposed to utilize.

All modern ships, merchant or combatant, may be required to dodge abovewater and underwater missiles in a future emergency. For a ship requiring a high degree of maneuverability every offset screw propeller whose axis lies within a reasonable distance of the centerline, say not more than one-quarter of the beam, should have a rudder behind it. *Every* propulsion device on a submarine should have a diving plane in its outflow jet.

A multiple-skeg stern logically embodies a rudder behind every skeg carrying a screw propeller, whether a high degree of maneuverability is specifically called for or not. On the alternative arch stern of the ABC ship, with its single large propeller between two skegs, it is logical to hang a rudder on the after end of each skeg. Fig. 74.K of Sec. 74.15 shows how this is done.

When shifting from a single rudder to twin rudders in a design, without other major changes in the hull, it is good practice to give each twin rudder a blade area of about 0.6 to 0.7 the area of the single rudder. This is justified by the increase in turning effort achieved with the larger total area. It is realized that the total weight of twin rudders, supports, and steering gear, based on only 0.5 the area of a single rudder, is almost certainly greater than for a single rudder. In other words, if the increased weight of double rudders is accepted, it is good design to make it really worth while by increasing the rudder effect at the same time. However, this should not be carried so far that the turns made by the vessel are excessively sharp and the ship speed in the turn is so greatly reduced that its maneuvering characteristics are impaired.

The minimum transverse distance between the stock axes of the blades of multiple rudders is, if practicable, made equal to or greater than the *maximum* blade length of each rudder, measured fore and aft, so that the pressure field of one will not interfere too much with that of the other, when they are fully angled.

A shallow-draft pushboat, with limited rudder depth, and with need for steering and maneuvering the entire push as well as itself, requires multiple rudders to achieve the necessary lateral forces and turning moments. For maneuvering in extremely shallow water, when the bed clearance is measured in inches rather than in feet, and when traveling in swift, turbulent currents, the craft requires multiple rudders for itself alone, to say nothing of the need for maneuvering when other craft are being pushed.

In many river craft propelled by sternwheels, the rudders are placed ahead of rather than abaft the propulsion devices. Here they do not work in an outflow jet of augmented velocity, so that the equivalent effect is achieved only by fitting multiple rudders of larger total area. The limited draft is also a factor here. Sometimes the multiplication of rudder area ahead of the sternwheels on these vessels is not sufficient. To make up for it, one or two "monkey rudders" are hung on a frame abaft the wheels, to take advantage of the increased velocity in the outflow jet.

74.4 Shaping the Rudder and the Adjacent Portion of the Ship. Fortunately, the designer often has considerable freedom in shaping the stern profile of a ship, and in the contour and position of the rudder(s). Further, he is often permitted to work up alternative stern arrangements; in these he can forget tradition and strive for maximum performance. For example, in a single-screw stern departing somewhat from the normal form it may be found possible to work in a sort of flat or shallow-V shelf, well submerged at load draft, over the top of a spade-type rudder. If so, the vessel benefits from:

(a) An increase in the rudder aspect ratio and the lift coefficient for a limited range of rudder angle. This is due to the close fit and the negligible differential-pressure leakage between the hull and the top of the rudder. To keep the horizontal gap small, at the top of the rudder, bolted palms for connecting the blade to the stock may be placed somewhat below the extreme top of the rudder. The recesses for assembling the bolts may be closed by cover plates.

(b) Providing the equivalent of a surface plate to prevent undue air leakage from the surface and breakdown of the rudder action when the $-\Delta p$'s are large

(c) Providing an excellent internal support for the thrust bearing, tiller, and steering gear.

In case the V-shape of the stern is only moderately shallow, and the sides rise at an appreciable angle from the edges of the flat over the rudder, there is an opportunity to derive some lateral pressure on and some swinging moment directly *from the hull itself*. This is because the hull is near the top of the rudder and because of the close fit there. At the designed speed, the crest of the stern wave is expected to cover a sizable area of the hull above the rudder, as projected on the centerplane, in addition to that which lies below the at-rest waterline. This increases the area over which Δp's are exerted.

A spade rudder may be tapered (reduced in fore-and-aft length) toward the bottom to:

(1) Increase the aspect ratio
(2) Reduce the strength of the tip vortex at the bottom when exerting heavy lifts and lateral forces
(3) Thin the lower part and reduce its drag
(4) Diminish the bending moment at the head of the rudder.

Sometimes the possibility of air leakage to the top of a spade rudder can not be prevented. It is then wise to reduce rudder area at the top, shortening the rudder and moving its contour line farther from the adjacent water surface. The area thus removed from the top of the blade is shifted to the bottom, well below the surface, possibly making the rudder longer at the bottom than at the top. A change like this was found successful two decades ago in the design of the U.S.S. *Farragut*, a destroyer of the DD348 class.

A centerline rudder on a twin- or multiple-screw stern produces the greatest lateral forces when it follows as closely as possible the contour of the stern. There should be the minimum leakage area between the rudder and the adjacent portions of the ship upon which the rudder pressure fields act. The lower the horizontal joint between hull and rudder, the greater the hull areas above it, projected upon the centerplane, which are acted upon by these pressure fields. Whether this enables the use of a smaller rudder depends upon many other factors.

A rudder hung from a skeg along its *entire* leading edge, and preferably fitting the hull closely along its top, has the advantage that it is developing the maximum turning moment on the hull. While it is completely unbalanced it can be made smaller (shorter or narrower) than a rudder not so closely fitted. The torques upon its stock, and those to be exerted by the steering gear, are thus decreased. Nevertheless, such a design is logical only when the vessel is intended almost exclusively for ahead operation, as in sailing craft. It is an advantage if backing is only incidental and if there are no specific requirements about handling the rudder during backing or when moving astern.

The horn or compound-type rudder, illustrated at 5 in Fig. 37.D, is not in the foregoing category. Actually, its effective aspect ratio is usually rather small.

For an isolated rudder, not attached to a deep skeg or keel, or to a horn, too high an aspect ratio is to be avoided because of the breakdown in hydrofoil flow—and in lift—which occurs at relatively small rudder angles [van Lammeren, W. P. A., RPSS, 1948, p. 323]. High nominal aspect ratios in single rudders, say up to 3.5 or 4.0, can be accepted if the rudder lies partly or wholly within the outflow jet of a propeller. The fact that the rudder is benefiting from the augmented outflow velocity may make it unnecessary, in combination with these high aspect ratios, to use rudder angles beyond the stalling value of 20 or 25 deg.

Long experience with spade and horn-type rudders and horizontal diving planes, on bodies as well as on ships, indicates that for maneuvering (rather than for steering only) a control surface which is approximately square is as serviceable as any. This is because the breakdown or stalling point is deferred to larger angles. A greater total lift or lateral force can be achieved, greater maximum control-surface angles can be used, and the bending and torque moments in the stock are more nearly balanced.

Wherever practicable, a rudder deliberately placed in an outflow jet to take advantage of the induced velocity should span the whole jet close to a diameter. Excessive underhang in spade rudders, clearances to withdraw propeller shafts, and the presence of swirl-core cavitation may interfere. In this case spanning a portion of the jet is of course much better than missing it altogether.

When one or more operative conditions of a vessel involve large changes in draft in the vicinity of the rudder, the actual immersed rudder area must be proved satisfactory for all conditions. As a rule, both hull and rudder come out of the water simultaneously so that the smaller immersed area of the rudder suffices to control what is left of the hull in the water. However, adequate performance in such a situation can by no means

be taken for granted. A separate calculation or model test is called for to cover this condition.

An L-shaped or J-shaped rudder hung behind a thin hull or skeg should not have an excessively long forward balance portion, indicated in diagrams 1 and 2 of Fig. 74.Ca. When such a rudder is swung hard-over, say to the right, the forward end of the balance portion swings to the left or to port. The region of $+\Delta p$ on the ahead or starboard side of the balance then lies under the port side of the skeg. In normal circumstances a large $-\Delta p$ is being developed here to augment the transverse force to port. Although, so far as known, no specific studies have been made on this point it appears that the presence of the $+\Delta p$ and $-\Delta p$ regions so near each other is detrimental to maneuvering.

R. E. Barry reports a situation similar to this on a French cruiser, as indicating a rudder shape and position to be avoided in practice ["Random Notes by an Old Seaman," Mar. Eng.'g., Feb 1921, p. 137 and Figs. 8, 9]. This vessel had a

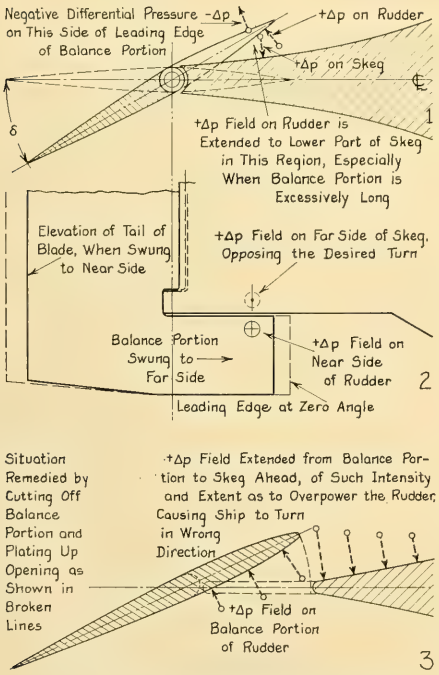

Fig. 74.Ca Effect of Pressure Field Exerted by the Balance Portion of a Rudder

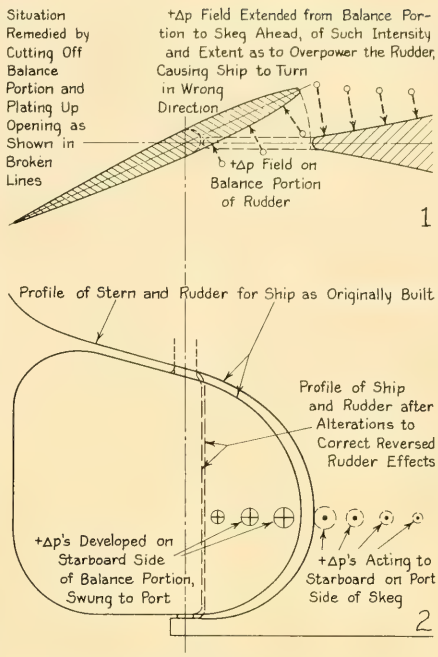

Fig. 74.Cb Example of Reversed Rudder Action Due to Pressure Field Exerted by the Balance Portion of a Rudder

balanced rudder swinging in a close-fitting aperture, sketched at 1 and 2 in Fig. 74.Cb. When steering it was found that the ship swung in the *opposite* direction to that in which the rudder was angled. According to Barry this showed "... that the banked up pressure on the side (indicated by the four right-hand vectors in diagram 2 of the figure) was greater than on the rudder. When the balance was cut off and the aperture plated up, the vessel steered satisfactorily."

A situation such as that described in the preceding paragraphs is avoided if there is an aperture of appreciable area forward of the rudder blade. A rudder and stern embodying this arrangement are diagrammed at 4 in Fig. 74.D. Actually, to obtain the *rapid response* to rudder action discussed in Sec. 74.18, the aperture ahead of the rudder is made rather large compared to the blade area, indicated by diagram 3 of Fig. 74.D.

A small aperture, fitted on some older vessels abreast the tips of wing propellers and sketched in diagram 2 of the figure, is too small to afford a

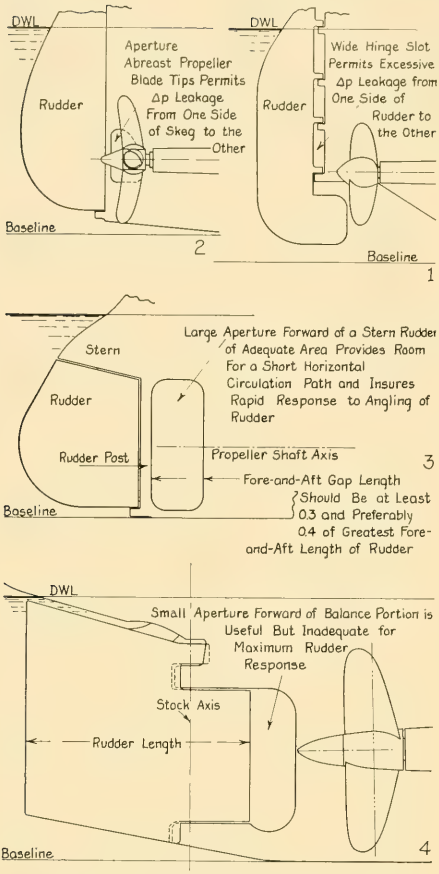

Fig. 74.D Apertures and Gaps Ahead of Ship Rudders

good circulation path for the water. It is too large as a leakage gap. It probably does more harm in steering than the benefit it affords in reducing propeller vibration.

Diagram 1 of Fig. 74.D illustrates a design, rather common in years gone by, in which the provision of working clearances for removal of the pintles and their bearings, and for lifting out the whole rudder, was apparently more important than ease of steering. The large leakage gap detracts from the usefulness of the rudder and diminishes the lateral force built up on the adjacent hull by the angled rudder.

Rounding the outline or profile corners of rudders is by no means a necessity, provided fair flow is reasonably certain around the rudder at all rudder angles and under all operating conditions.

For practical reasons, such as to provide bottom clearance when docking, it is often necessary to terminate the bottom of a rudder in a horizontal plane parallel to and just above the baseplane. When such a rudder is mounted under the stern of a ship, it may lie in a region of flow having an appreciable upward component of velocity, indicated in Fig. 25.K. The after ends of the lower rudder sections then project into the flow lines, as does the aftfoot in that figure. If a reduction of area at the bottom can be made up by an increase elsewhere on the blade, the after lower edge of the rudder may be cut up or the bottom of it may be sloped to conform to the flow lines in this region. These changes should save some pressure drag during the greater portion of the time, when the rudder is serving only to steer the vessel.

It is good design to shape a close-coupled rudder (at either bow or stern) as a continuation of the adjacent hull surface. Nevertheless, this procedure can become detrimental if the adjacent hull is full and the thickness ratio of the rudder becomes large or if the sides of the rudder have much slope [Denny, M. E., IESS, 1934–1935, Vol. 78, p. 411]. In any case, the free or swinging edge of the rudder, the one that is downstream when the rudder is steering, should generally be tapered to a reasonable thickness and not terminated bluntly.

Wherever and whenever practicable the leading edge of a rudder is recessed into a groove in the trailing edge of the horn, the skeg, or the keel supporting it. This is partly for fairing but mostly for closing the hinge gap against detrimental leakage. Further steps to close the gap are described in Sec. 74.14 and illustrated in Fig. 73.K of Sec. 73.14.

The fact that positive clearance above the baseline for the foot of the rudder is often mandatory should never deter the naval architect from extending it below the baseline if the needs of the situation require it. The rudders of many Chinese junks slide along a diagonal axis, parallel to that of the stock, so that they extend well below the baseplane when at sea. The portable rudders of small sailboats almost invariably project below the baseplane when they are shipped. The successful use of fixed rudders projecting below the baseplane on many vessels,

operating in shallow as well as deep waters, proves that they do not suffer frequent or serious damage, as might be supposed. Furthermore, provided these operations are planned in advance, they do not represent serious inconveniences when drydocking or hauling out.

A variety of types and shapes of rudder, hull, and aperture are shown by K. E. Schoenherr [PNA, 1939, Vol. II, pp. 224–226]. Of these, however, the single-plate rudder of his Fig. 15 is practically obsolete, except for inexpensive installations on small vessels. L. Troost, J. G. Koning, and W. P. A. van Lammeren show a larger variety, including the screw-propeller position(s) for each type and shape [RPSS, 1948, pp. 331–338]. G. de Verdière and V. Audren describe the results of model tests on still other rudder shapes and arrangements [ATMA, 1951, Vol. 50, pp. 491–514].

74.5 Design Procedure for Conflicting Steering Requirements. It is as necessary to know the range of speeds for which optimum steering is required as it is to know the speed for optimum performance of the hull or the propulsion device(s). In this respect the sailing craft poses the most difficult design problem. It must steer and maneuver well throughout the entire range, from the greatest speed of which it is capable down to practically zero speed.

It is interesting to note the manner in which this is achieved, especially for vessels with flap-type rudders hung directly on the main hull. If the vessel is relatively small, say less than 100 ft in waterline length, the underwater hull is cut away sharply at both ends and the remaining portion is short compared to the overall size of the vessel. The horizontal circulation path around it is short, so that the response to rudder angle is good at any speed. The rudder is hung directly on the skeg or deep keel, so that steering is adequate and reliable even at slow speeds.

For the large sailing ship the slow-speed steering is equally good, but the underwater hull is much longer in comparison, and the response is slower. In this case, however, the response should be more deliberate. It gives the crew the extra time necessary to trim the sails and perform other duties connected with the sailing evolutions. It would be dangerous, in many cases, to permit the vessel to swing too rapidly.

The mechanically propelled vessel poses a different problem. The shape and position of a rudder, and its relation with respect to the adjacent hull, is not necessarily the same when quick response at moderate power is required as it is when the vessel is called upon to steer well, with the propulsion device rotating very slowly or actually stopped. Since both requirements are often included, and understandably so, the solution in such a case appears to embody two separate features:

(1) A large tail section of the rudder blade lying directly abaft a sizable portion of the hull, or abaft a horn or skeg of appreciable area compared to that of the tail, with the smallest practicable hinge gap
(2) A sizable foil portion having ample clearances ahead of and abaft it, to provide room for the rapid setting up of the circulation needed to produce immediate steering response.

The designs of the rudders for both the transom-stern and arch-stern hulls of the ABC ship were carried out with these features in mind. A better all-around solution is probably to use one or more spade rudders of generous area, provided these can be accommodated in the design.

74.6 First Approximation to Control-Surface Area. The discussion in this section is limited to rudders mounted in the vertical plane, or nearly so. Diving planes of submarines and other control surfaces are omitted because of the widely varying requirements for different types of service. Although the rudders of mechanically driven vessels have developed through the years in the almost complete absence of specific steering or maneuvering requirements, the resulting rudder parameters and hull-rudder proportions lie within not too wide a range.

Based solely upon the ratio of the rudder area A_R to the lateral area A_L of the ship, or to the product of the length L and the draft H, the relative size of steering rudders has increased gradually but steadily during the past half-century. In fact many ships built in the 1900's or 1910's had to have their rudders increased in area, often by as much as 20 or 30 per cent, indicated by the listing in Table 74.a. A rudder of given area, working in a propeller-outflow jet, gives greater lateral forces as the propeller power is increased, and may even provide better maneuverability at a higher speed. The shift to proportionately larger rudders appears to be a sign of unconscious but actual stepping-up of maneuverability requirements. It may be expected that this intensifying process will continue, and that

TABLE 74.a ORIGINAL AND INCREASED RUDDER-AREA DATA ON U. S. NAVAL AUXILIARIES OF THE 1900–1920 PERIOD

All the vessels listed had single rudders. So far as known, the areas apply to the *movable* rudder blades only.

Ship	USN desig. (old)	Type	Speed, kt	Number of propellers	Original		Increased	
					Rudder area, ft²	Per cent rudder area to longl. plane	Rudder area, ft²	Per cent rudder area to longl. plane
Neptune	AC8	collier	12.93	2	173.25	1.19	224	1.54
Orion	AC11	collier	14.47	2	173.25	1.26	224	1.63
Proteus	AC9	collier	14.67	2	172.4	1.30	215	1.61
Jupiter	—	collier	—	2	180	1.30	224	1.62
Kanawha	AO1	tanker	14.25	2	—	1.48	—	—
Bridge	AF1	store ship	14.0	2	145.3	1.77	—	—
Henderson	AP1	transport	14.0	2	160.6	1.77	—	—
Lebanon	—	auxiliary	8.5	1	—	1.34	—	1.55
Arctic	AF7	store ship	11	1	—	1.36	—	1.53
Rappahannock	AF6	store ship	11.5	1	149.0	1.23	175	1.44

in the future rudders will be made progressively larger, more effective, or more efficient. In an era when combatant vessels are not the only ones which have to confuse those who are dropping or firing missiles from the air this is a logical development.

W. P. A. van Lammeren, L. Troost, and J. G. Koning in 1948, and P. Mandel in 1953, gave some rudder-area data which furnish a good first approximation for the rudder-blade sizes on modern vessels of a variety of types [RPSS, 1948, Table 13, p. 343; SNAME, 1953, Table 3, p. 482]. The ratios of Table 74.b have been adapted from these tables, utilizing for guidance certain unpublished data from other vessels. Conforming to the definitions of Sec. 37.2 the rudder area in each case is taken to be that of the movable blade only.

There are practical and scientific difficulties in working with tables of the kind represented by 74.a and 74.b, even when making a first approximation to the required rudder-blade area:

(1) The published data imply, but do not state that all the ships (for which the tabulated percentages are given) possessed adequate or satisfactory steering and maneuvering qualities
(2) Although they may indicate the length-depth ratio of the rudder blade, they make no mention whatever of its position with respect to the hull or to fixed appendages in its vicinity. They attempt no estimate of the probable proportion of transverse force exerted by the movable rudder blade and by the adjacent hull or appendage.
(3) They take little or no account of the cutup or cutaway at one or both ends of the hull. In many cases this can be of small amount but can have a relatively large effect.
(4) If the tables mention other factors, or give data on them, it is found difficult to correlate these factors with the reported steering or turning performance.

The projection of the propeller discs below the main hull, mentioned by P. Mandel [SNAME, 1953, p. 481] and diagrammed by him in Table 3 on page 482 of that reference, is an important feature in maneuvering. However, it could be represented in a more logical and comprehensive manner than that given in the reference. In turning, the detrimental effect of the projecting propeller blades is not related directly to the outline of the maximum section but with respect to the cross flows under the hull *at the propeller positions*. This cross flow has not been studied systematically and it is not easy to establish a suitable criterion for the propeller-blade projection.

Until something better is developed, one may use the area of the propeller disc(s) below a horizontal line drawn tangent to the under side of the main hull or other large appendage at or close to the fore-and-aft position of the propeller disc(s). While the propeller blades on the inside

of the turn are somewhat shielded from cross flow by the ship ahead of them, those on the outside of the turn are exposed to a greater degree of cross flow. One may say that, for a first approximation, an average of these effects forms a good estimate.

The total absence of diagrams showing the rudder profiles, the ship or large-appendage profiles, and the relative positions of the movable rudder blades and the adjacent ship render all published data of the kind shown in the references cited previously in this section as something less than useful. In fact, it appears that only by taking account of these features, which govern the proportion of (1) the transverse force on the rudder to (2) the total transverse force on the end of the ship, can the major inconsistencies of the published tables be cleared up.

It is possible that further analytic study should be given to a method, little-used in modern naval architecture, of proportioning the movable-blade area of the rudder to the midsection area of the ship. Quoting from W. J. M. Rankine in 1866 [STP]: "That eminent shipbuilder, the late Mr. John Wood, made the breadth of the rudder 1/8th of that of the ship." This meant that, with a depth of rudder about equal to the draft, the rudder length was about 0.125 times the midsection beam. This method of selecting the proper rudder area is given by A. Caldwell in his book on "Steam Tug Design" [London, Jul 1946]. It is still used by aeronautical engineers in proportioning the rudders of dirigibles.

TABLE 74.b—RATIOS OF RUDDER-BLADE AREA A_R TO LENGTH-DRAFT PRODUCT (LH) FOR MERCHANT-TYPE VESSELS

The rudder area is considered to be that of the *movable* blade only. The proportions given are for ships with single rudders.

Type of Ship	$(10^2)A_R/(LH)$
Liners, large, fast and high-speed	1.6–1.8
Passenger and cargo ships, large, medium-speed	1.6–2.0
Tankers, large, fast and medium-speed	1.7–2.1
Passenger and cargo ships, small, slow-speed	1.7–2.3
Cargo ships, fast	1.8–2.0
River steamers, fast	1.7–2.0
Cargo ships, normal, medium-speed	1.7–2.5
Auxiliary vessels for national defense	1.9–2.4
Cargo ships, small; coasters	2.0–2.3
Cross-channel ships, required to maneuver in harbors	2.0–2.2
Sailing ships, large	2.0–2.5
Ferryboats for harbors, fishing vessels	2.5–4.0
Tugs, towboats	3.0–4.0
Work boats, small	4.0–5.0
Inland waterways craft, for confined waters	4.0–8.0

Based upon the data in the references listed earlier in this section and upon the ratios given in Tables 74.a and 74.b, a few general rules are formulated for use in the preliminary design stage of a ship:

(a) A rudder, to be fully effective, must lie in a region of flow which is free of greatly reduced velocity, eddies, and reversed flow

(b) No mechanically propelled vessel, regardless of type, should have a ratio of rudder area A_R to rectangular underwater area $L(H)$ smaller than 1.6 per cent. A minimum of 1.7 per cent might be better; the 1953 table of P. Mandel shows a minimum of 1.9 per cent.

(c) The percentage of rudder-blade area overlapping the propeller outflow jet at the rudder position should be as large as practicable. This is especially true for vessels operating at a T_q value less than 1.0 and for flows past the rudder which are suspected of being "weak," with large positive wake velocities and small speeds of rudder advance. It is possible, as stated previously in Sec. 74.3, that a "strong" flow, with a large speed of rudder advance and a small overlap, has more beneficial effect than large overlap of the same rudder in a "weak" flow.

(d) The percentage of cutaway area and the ratios of cutaway length to ship length lie within rather narrow limits for the average vessel. If the cutaways are adequate, the exact ratios *appear* not to be major factors in its maneuverability.

(e) Twin rudders for large ships may have a combined blade area as great as $0.03L(H)$. A baseplane clearance of 0.5 ft appears to be adequate for any deep-water vessel, regardless of size.

(f) When adequate draft is available and multiple rudders are used, the aspect ratio is made rather large, to give the greatest coverage across an outflow jet or the maximum pressure abaft a skeg.

74.7 Determining the Proper Areas of Various Control Surfaces. There is outlined in this section a new procedure for determining, as a second or third approximation, the required area of the movable blade of a control surface. The method as described here applies to a steering rudder in a vertical plane but it is essentially the same for a control surface mounted on a surface ship or submarine in any other plane.

A suitable and adequate rudder-design method should produce, to meet a given set of steering and maneuvering requirements, the proper type of rudder, the rudder-blade area, the proportions and shape of the blade, and the maximum rudder angle. To meet unusual operating conditions it should also produce the rate of angling or laying the rudder and other design features. Looking at the rudder-design problem in its larger aspects, it should also be coordinated with what might be termed the maneuvering design of the hull as a whole.

Because the project is still incomplete, the description which follows is simply a statement of the various steps involved, with some comments on each. The project has not been carried through to the point where a numerical answer, acceptable by engineering standards, can be obtained by it for a given situation. Presenting an outline only is considered justified because of the need for thought and study on this design problem along new and logical lines.

The starting point is a careful analysis of the steering and maneuvering requirements of the vessel for which the rudder is to be designed. These are preferably expressed in numerical terms somewhat more specific than those for the ABC ship in Table 64.e, items (27) through (41), especially items (28), (30) to (32), and (34). If requirements for maneuvering have not been laid down by the owner or operator they are prescribed for the ship under study by the designer himself, based upon his own experience in the operation of similar types and sizes of ships.

The rudder and other gear required for maneuvering, like the hull and the propelling machinery necessary for propulsion, must as a rule be designed to meet the most severe operating condition. It is usually the case, although it may not be taken for granted, that the lesser requirements are then satisfied as a matter of course.

Just what constitutes the most severe maneuvering requirement for a ship—the one calling for the largest rudder area at the optimum or specified rudder angle—can by no means be determined by inspection of the owner's and operator's specifications. For the average vessel, however, it is more important to change direction quickly and decisively in an emergency maneuver, to avoid collision with obstructions or with another ship, than it is to make a subsequent turn at a given radius or speed. In other words, the rudder is more valuable for sheering the vessel off its original course in the shortest possible time and distance than for guiding it precisely around a steady turn with a large change of course. The situation is somewhat similar to that specified in item (32) of Table 64.e where, to make a canal turn properly, the vessel must accomplish an offset of 400 ft from the approach path extended in a curved arc of 2,100 ft, at a specified speed and rudder angle. It is exactly the same as that faced by a diving submarine. In an emergency, the submarine must get under the water surface and point its nose downward in the shortest possible time and distance from the dive or "execute" point.

To be sure, every ship must be able to change its course at will, to reverse its direction of swing, and to follow a tortuous path, but there is reason to believe that the initial sheering maneuver is the most demanding and the most important. This means that, with the vessel proceeding at steady speed on a straight approach path when a sharp turn is ordered, the rudder must be angled to its full amount very rapidly and a certain maximum swinging moment N, to be discussed presently, must be applied by it to the ship.

The sheering maneuver at the beginning of a turn is a logical as well as a practical assumption with which to guide the rudder design because:

(a) The forces and moments exerted on a ship in the first few seconds of this transient stage largely determine how rapidly, and in what ahead distance, the vessel can clear its approach path extended, change its heading, and sheer off to one side or the other

(b) For an analytic solution, the velocity magnitude and direction of the water flowing toward the rudder when beginning a turn may be assumed to be substantially the same as it was a few instants before, when the ship was proceeding along the approach path with zero rudder angle, in a steady-state condition. With this simplification, only the effect of the angled rudder need be evaluated just after the initial point of the turn.

(c) Once the ship is in the turn, the determination of the swinging moment produced by the rudder and the moment produced by the ship itself, acting as a hydrofoil with an angle of attack, becomes exceedingly complex. This is true for an experimental as well as an analytical attack on the design problem.

(d) As an incidental argument, it is possible in many model basins to measure the transverse

force exerted on a ship model abreast a rudder position when the rudder is angled and the model is constrained to move in what amounts to a straight continuation of the approach path. This serves as some sort of check for a particular preliminary design of rudder rather than as an aid in the course of the design.

The sheering maneuver must be defined in specific terms if it is to form part of the maneuvering specifications of a ship or if it is to serve as the controlling factor in a rudder design. These terms should include the rate of change of heading following an order to turn and the shift of position of the CG laterally from the approach path, in the positive or negative direction of the y_0-motion axis. All these should be on a basis of time and of advance in the x_0-direction.

The complete solution outlined in the first sentence of the second paragraph of this section involves too many answers to render itself workable with present techniques (1955). It is necessary at this stage to assume reasonable, tentative values or conditions for some of the answers, namely:

(1) The general dimensions, size, and shape of the ship hull, as well as certain of its maneuvering characteristics
(2) The fore-and-aft position of the rudder and rudder stock along the hull axis. The assumed swinging axis of the vessel may be taken at its CG. The distance from the CG to the rudder-stock position is the moment arm of the lateral rudder force, although, strictly speaking, this distance should be measured to the instantaneous center of pressure CP of the rudder blade.
(3) The type (or types) of rudder to be worked into the design problem. Alternative preliminary designs may be required for alternative rudder types (and shapes).
(4) Some idea of the shape of the rudder blade and of its position with respect to the adjacent hull or the nearby fixed appendages
(5) The maximum swinging moment N to be applied to the hull under the most severe maneuvering requirement. This is a major feature, which should be derived rather than assumed, by a process to be discussed shortly.

The situation is as sketched in Fig. 74.E. Dividing the swinging moment N by the moment arm a of the rudder gives the transverse force F_L required to be exerted *on both the rudder blade and the ship* at and near the rudder-stock position.

The designer then determines, by estimate from empirical data and possibly later by calculation, the proportion of this lateral force F_L which he may reasonably expect to be exerted on the hull and the fixed appendages. This portion is indicated as F_H in the figure. The remainder of the transverse force is that to be exerted on the movable rudder blade when fully angled. This is normal to the ship axis, indicated as F_R . With an assumed maximum rudder angle δ(delta), an effective angle of attack of the rudder equal to it, an assumed aspect ratio, and an average value of lift coefficient for hydrofoils suitable as rudders, the problem is worked backward and the hydrofoil or blade area is approximated. The calculation is repeated for as many different ship speeds, or as many different initial assumptions, as may be desired.

Of the data listed under (1) through (5) preceding, the determination of the maximum swinging moment N poses by far the most difficult problem. The method of finding it for any particular design situation is not yet worked out but the following factors require consideration:

(i) The maneuvering characteristics of the hull proper, without the rudder(s). Carried to the limit with respect to rapid change of heading, a ship in the form of a circular tub would require only enough tangential force at its surface to overcome the polar inertia and the friction resistance. Carried to the opposite limit for rapid lateral change in position, a long slender craft requires rather extreme measures in the way of applied forces and moments to accomplish the offset from the extended approach path which is required for a sheering maneuver.
(ii) The polar moment of inertia of the ship about the vertical swinging axis for the particular loading condition specified
(iii) The added inertia of the entrained water for the superposition of the swinging mode of motion, when the ship starts to turn
(iv) The steady speed of the ship along the approach path

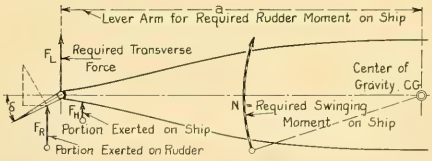

Fig. 74.E Diagram of Rudder and Ship Forces and Moments

(v) The possible effect of shallow or restricted water, if operation in confined areas is involved.

The process of deriving the swinging moment may be largely empirical until the method is further developed. Eventually it should be determined by a relation analytically derived.

On the basis that the sheering maneuver described previously in this section calls for the greatest swinging moment and rudder effect, the analytic method appears to involve:

1. Laying out a series of successive positions, at equidifferent time intervals, with respect to the point where the emergency turn order is given, known as the "execute" point, and the approach path extended. There is a considerable backlog of this information, published and unpublished, with which to approximate or to bracket the required data for a number of ship types.
2. Finding the initial angular acceleration α(alpha) required to make the ship occupy these positions while moving forward in the initial portion of a turn. In fact, it is possible that the necessary data may be obtained on board ship from simultaneous course and rudder-angle measurements, made by recorders now available.

By calculating or estimating the polar moment of inertia J_S of the ship for swinging motion, including the added inertia of the water, the required swinging moment N is given by

$$N = J_S\alpha \tag{74.i}$$

The value of N may well be found to vary with approach speed so that the designer is called upon to work out a series of solutions if the speed range is large.

On the basis that the total lateral force F_L of Fig. 74.E is determined, and that the sheering maneuver occupies the predominant role, the next step is to determine, in terms of numbers, the fractional part of this force that is exerted on the hull. In the present state of the art the fraction F_H/F_L , alluded to previously and called here the *hull-force fraction*, can at best only be estimated. A correct estimate must be based upon knowledge of the pressure field exerted by the angled rudder in its vicinity. Available data on this feature are rare; they are neither analyzed nor published. It might be more realistic, therefore, to say that for the present the hull-force fraction is only guessed. It may be of the order of 1/4, 1/3, or 1/2, leaving 3/4, 2/3, or 1/2 of the total lateral force F_L to be developed by the rudder blade.

If a dynamometer is available to carry a model rudder and to measure the lateral force on its stock, the *rudder-force fraction* F_R/F_L may be determined during the test of a constrained ship model, run straight ahead with angled rudder under a towing carriage in a model basin. The model can and should be self-propelled during this test.

Following a determination or an estimate of the transverse force component F_R on the rudder, the designer proceeds to apply the laws of the hydrofoil and to calculate how much area A_H is required to produce a lift equal to this force. As previously mentioned, the problem is simplified for the case being described by assuming that the effective angle of attack α_I of the rudder as a hydrofoil is equal to the mechanical rudder angle δ. However, it is still necessary to know the relative water speed past the rudder, corresponding to the rudder's speed of advance, especially as this speed enters the lift-force formula to the second power. The potential-, friction-, and wave-wake velocities must all be taken into account, *plus* the negative-wake velocity due to the augmented velocity in the outflow jet of any propulsion device lying ahead of the rudder.

A two-part rudder composed of a tail and an underhung foil is illustrated for the general case in diagram 5 of Fig. 37.D and for the transom stern of the ABC ship in Fig. 74.K of Sec. 74.15. For such a rudder it is undoubtedly not valid to assume that each part (tail and foil) generates its own lift independently, by its own set of rules or by its physical action alone. Nevertheless, this approximate procedure must be used until something better is developed.

In addition to the assumed kinds and nominal aspect ratios of the various hydrofoil elements of the rudder blade, the effective angle of attack, and the speed of advance, mentioned earlier in the section, the designer now knows or has estimated the total lift force F_R required of the rudder. Assuming a sort of standard type of hydrofoil or flap section for each part, it is possible for him to estimate the lift coefficients and to determine with reasonable accuracy the area necessary to exert the required lift force on each part. Graphs giving some of the necessary data are found in Figs. 44.A through 44.D. Other data are to be found in the references listed in Secs. 44.3, 44.4, and 44.5.

The sum of the areas thus derived may be equal

to, but will usually differ from the total movable area tentatively assumed when the blade was first sketched. Adjustments are made to the area or shape or aspect ratio, one or all, and a second hydrofoil calculation is made, similar to the first.

For the case of the compound or flap-type rudder the exact value of the ratio of the movable-blade lateral force F_R to the hull lateral force F_H, and the exact value of the lift coefficients used to calculate the movable-blade force, depend upon the tightness assumed for the hinge closure. Unfortunately the effect of actual hinge gaps and hinge leakage is not yet assessed in the full scale. Data from aeronautical tests require some analysis before they are applicable to the ship problem.

Similar comment applies to the assessment of the effects of horizontal gaps between parts of the rudder and the hull, and a determination of the proper effective aspect ratio for each part of the rudder. Certain useful data derived from tests of low-aspect-ratio hydrofoils are included in Sec. 44.3.

In the event that the maximum turning moment is required in a steady turn, to meet certain operational needs, the physical action on both rudder and ship is no longer simple or well known. The design procedure is not yet outlined and may not be for some time to come.

As an indication of the absolute magnitude of the moments required to maneuver a ship there are available the results of model tests in which the rudder was angled by various amounts while the model was constrained to travel in steady, straight-ahead motion. This corresponds, as previously described, to the few moments after a signal to turn is given but before a ship has time to change direction from its straight approach path. Among these tests are some conducted by G. H. Bottomley at the NPL, Teddington ["Maneuvering of Single-Screw Ships: The Effect of Rudder Proportions on Maneuvering and Propulsive Efficiency," Inst. Civ. Engrs., London, 1935, No. 175]. The model represented a ship having the following characteristics:

L_{PP}, 400 ft	C_P, 0.70
B, 52 ft	CG assumed at midlength between perpendiculars
H, 23 ft	CG to rudder stock, about 200 ft
Δ, 9,400 t	Area A_R of standard rudder, 144 ft^2
V, 14 kt	$A_R/[L(H)] = 0.016$.
P_E, 2,200 horses	
P_S, 3,160 horses	

The model was run with the usual fixed rudder post of rectangular section ahead of the rudder, then with four fixed fins of uniform thickness added abaft the post (and ahead of the rudder), representing full-scale lengths of 0, 2.08, 4.16, and 6.25 ft. The combined full-scale fin-and-rudder area was always 144 ft^2, indicated in Fig. 1 of the reference. The area of a fairing of varied width added ahead of the rudder post, as well as the area of the post itself, was not included in the nominal fin-and-rudder area.

On the basis of these test data Bottomley then calculated the fore-and-aft length of four hypothetical rudders which, when placed behind the four fins mentioned, would give the same initial ship-turning moment at small rudder angles (5 deg) as the original rudder (called R_4) when mounted abaft the rectangular-section rudder post. If four rudders of these lengths had been mounted abaft the four fins mentioned, horizontal sections through the assemblies would have appeared as sketched in Fig. 74.F. Assuming that

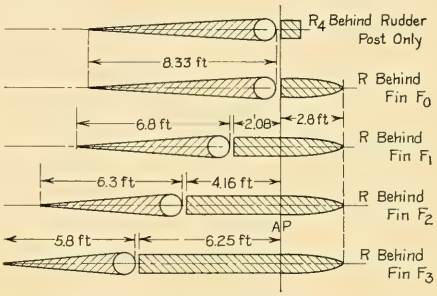

Fig. 74.F Rudder-Fin Assemblies of G. H. Bottomley

By calculation, all five of these assemblies give the same initial ship-turning moment for small rudder angles of the order of 5 deg.

Bottomley's calculations were correct, and that the scale effects in the model tests were insignificant, each of the five assemblies appearing in the figure would give an initial turning moment of 2,400 ft-tons on the ship used as the basis of the tests, reckoned about the CG.

The values of this moment at rudder angles of 15 and 35 deg are given in Table 74.c, copied from the Bottomley reference, together with the torques that would have been required to hold the rudders in those positions. Considered as a design reference, the tabulated ship-turning moments are

TABLE 74.c Ship-Turning Moments and Rudder Torques for a 400-ft Ship

Adapted from G. H. Bottomley, "Maneuvering of Single-Screw Ships," ICE, London, 1935, No. 175, Appx. I, p. 19. The rudders and fins listed in the two left-hand columns are illustrated diagrammatically in Fig. 74.F.

Rudder type	Abaft fin of type	Length of rudder, ft	Area of movable rudder, ft²	Ship-turning moment, ton-ft			Torque on rudder head, ton-ft			Percentage reduction in rudder torque		
				Rudder Angle						Rudder Angle		
				5°	15°	35°	5°	15°	35°	5°	15°	35°
R_4	Rudder post only	8.33	144	2,400	7,200	13,600	19	67	172	—	—	—
R	F_0	8.33	144	2,400	7,800	17,300	17	56	179	+10	+16	−4
R	F_1	6.80	118	2,400	7,700	15,400	12	40	115	+37	+40	+33
R	F_2	6.30	109	2,400	7,600	14,600	10	34	98	+46	+49	+43
R	F_3	5.8	100	2,400	7,500	13,600	9	29	83	+53	+57	+52

low because the value of $A_R/[L(H)] = 0.016$ is low for a modern vessel (1955).

K. E. Schoenherr has plotted some of Bottomley's test data in grahic form [PNA, 1939, Vol. II, Fig. 13, p. 209]. Fig. 8 on page 13 of the Bottomley reference indicates that a long cruiser-stern profile lying close above the full-length rudder gives a larger ship-turning moment than with the same rudder and other profiles. Undoubtedly much of this moment is being exerted on the hull proper above the rudder.

It is realized that the procedure suggested earlier in this section requires considerable development, to say nothing of practical use, before it is ready for application in general ship design. It is of interest to know that this method, greatly simplified, was used with success when designing the diving planes of the large 3,000-ton U. S. submarines of the 1920's. While the shape of the main hull adjacent to the movable planes was such that little if any vertical force was exerted on the hull, the planes were sized and fashioned by requiring that they were to hold the vessel level at a given depth with a given resultant vertical force, either in excess weight or in excess buoyancy.

The method outlined here is elaborated upon in Part 5 of Volume III of this book.

74.8 Positioning the Stock Axis Relative to the Blade; Degree of Balance. In general a control surface, working in relatively open water, develops the same lift or lateral force—and drag—for a given angle of attack regardless of the fore-and-aft position of the stock and axis relative to the blade. The torque increases rapidly, however, as the stock axis is shifted away from the center of pressure. For rudders, planes, and fins which must be rather closely coupled to a hull there remains a considerable range of positions for the stock axis to suit the available actuating torque or to meet other requirements.

Any rudder steered by a hand tiller must trail; in other words, the center of pressure CP must always be abaft the stock axis. There must be a positive rudder torque, at any angle and in any condition, which acts to restore the rudder to zero angle. Examples are tiller-operated rudders on small sailboats or yachts. The rudder must of itself swing into line with the flow when going ahead. For steering, it must be held forcibly in position at any other rudder angle. A mechanically operated rudder designed for hand steering must also trail, especially when there is no holding mechanism at the control end of the gear. This corresponds to steering an automotive vehicle in which the steering gear returns to zero—or nearly so—if the hands are taken off the wheel.

If a hand steering gear is used for emergencies only it is still necessary that the torque be small enough for manual operation. A large ship rudder requires many hands to move it, using the emergency gear, and may involve danger to the steersmen if the rudder is overbalanced and takes charge. Indeed, it may at times be imperative to let nature bring the rudder back to a small or to zero angle when the man or mechanical power to move it are not available.

Even though a hand steering mechanism is

non-overhauling the effort or the time required to take off rudder angle in an emergency may be too great to justify letting the CP move ahead of the stock axis under any condition. If the rudder torque becomes excessively large, the fore-and-aft length of the blade—and the actuating moment required to turn it—must be decreased and the aspect ratio increased, as was done on the large hand-steered sailing ships. This can, of course, also be done on ships which are mechanically steered.

With certain types of hydraulic steering gears it is possible for an overbalanced rudder to take charge in an emergency and swing rapidly to its hard-over position, causing the ship to circle out of control as long as it is moving ahead.

The necessity for going astern on mechanically propelled vessels, and for much backing and maneuvering on special-service vessels, often calls for the least practicable steering rudder torque, whether the craft are steered by power or by hand. This generally requires that the center of pressure CP when going ahead be forward of the stock axis so that the CP when going astern will not be too far from that axis. Shifting the stock axis aft on the blade takes care of this situation but involves the additional disadvantage of possible rudder instability and chatter at zero angle, especially with slackness in the gear, and a tiresome job of steering if the gear is of the overhauling type. The relative position of the two CP's and the axis, for all service conditions, is therefore determined by the most important service operating requirements.

The following design rules govern the degree of balance on rudders for steering and turning. They are predicated upon reasonably uniform flow over the whole rudder blade:

(1) The rudder definitely should trail at all angles on any craft:

(a) Designed for hand steering, and for pleasure only

(b) Designed for hand steering, and where, for efficiency and safety, the rudder effort must be "felt." Examples are racing sailboats and motorboats.

(c) Steered by one man who must also attend to other duties, such as a lone fisherman.

(2) The rudder is best made slightly underbalanced at small angles for ahead operation at service speed on any vessel:

(a) Designed to run for long periods with small rudder angle, with a premium on steering effort and power, and wear and tear on the steering mechanism

(b) Where a reduced rudder-angle rate may be accepted for astern operation

(c) Which may have to maintain speed ahead in the event of a casualty to the power steering gear which leaves the rudder free to swing.

(3) The rudder may be slightly overbalanced at small angles for ahead operation at service speed:

(a) When the friction in the mechanical or emergency gear is enough to prevent the rudder from taking charge if power is lost and from swinging to the hard-over position.

(4) The rudder may be overbalanced for angles not more than one-third of the maximum and appreciably overbalanced for the small angles used for steering:

(a) On special-service vessels called upon for much backing and maneuvering, or for hard-over rudder shifts at the maximum rate, when it is an advantage to have the ahead and astern rudder torques equalized as far as practicable, with neither of them very large

(b) On vessels provided with reasonably reliable power-operated auxiliary or emergency steering gears.

Non-uniform flow over the control-surface blade, whose general effects are described in Sec. 37.7, may influence the balance situation; at least the possibility or probability of this flow requires consideration in the design stage. The nature of the flow may control the distribution of balance area along the stock axis, generally normal to the adjacent hull, and the position of this area relative to the retarded water in boundary layers or to the accelerated water in propeller-outflow jets.

For example, a spade rudder blade is often made shorter (in the direction of flow) at the bottom, well below the hull, than close to the hull, in order to reduce the stock bending moment. This means that the balance portion is longer (fore and aft) near the hull than below it. In fact, the length of the balance portion compared to the blade length, defined as the *length-balance ratio* in Sec. 37.2, may be greater near the hull than the *area-balance ratio*. At the bottom of the rudder it may be less. With the long portion of

the blade working in the boundary layer and the short portion in a propeller outflow jet, the balance ratios within the jet largely determine the actual rudder balance and are the ones to be given primary consideration in the design.

If a partly underhung rudder is laid out with a balance portion so long that, at or near the hard-over position, the forward end of this portion swings into a propeller-outflow jet, the negative torque thus created appreciably affects the balance situation as determined on a uniform-flow basis.

In some cases a balance portion lies only in one-half of a screw-propeller outflow jet, or mostly in that jet. It is then acted upon by water having a tangential component of velocity due to rotation imparted by the propeller, primarily in one direction. A balance performance predicted for uniform or for axial flow may require appreciable modification because of this tangential or rotary flow, quite apart from any consideration of the neutral angle of the rudder. Special studies or model tests are required to insure proper design. The same may apply to the design of offset rudders encountering inward-and-aft flow at the stern.

Numerical balance ratios, either of area or of length, have meaning only when applied to control surfaces of given section and shape in a given type of flow. They can be distinctly misleading when comparisons are made between dissimilar rudders. It is the position of the CP with respect to the axis for each condition which counts. In other words, the degree of balance is determined by the actual rudder torque and not by the balance ratio. The CP position requires careful determination when the torques are large or when definite over- or underbalance is being sought.

The foregoing general design procedure applies also to the positioning of the stock axes for diving planes, active fins, and other control surfaces.

Data for estimating control-surface torques for a degree of balance and for a blade shape tentatively selected are given by:

(a) Darnell, R. C., "Hydrodynamic Characteristics of Twelve Symmetrical Hydrofoils," EMB Rep. 341, Nov 1932
(b) Schoenherr, K. E., PNA, 1939, Vol. II, pp. 204–210. Chap. 44 of the present volume gives adaptations of some of Schoenherr's diagrams.
(c) Van Lammeren, W. P. A., RPSS, 1948, pp. 319–332
(d) Hagen, G. R., "Rudder Design Data ... Obtained from Tests on Five Model Rudders," TMB Rep. C–125, Jun 1948
(e) Hagen, G. R., "Effects of Variations in Thickness-Chord Ratio of Rudders in a Slipstream," TMB Rep. C–487, Jan 1952.

Additional design data are given in Part 5 of Volume III.

74.9 Selection and Proportion of Chordwise Sections. Considering solely the development of lift or lateral force, there are situations—unfortunately not yet fully predictable—for which a thick, flat-plate blade attached at the ship or hull end to a cylindrical stock is the best rudder section to use. Certainly nothing much more elaborate than such a plate, rounded at the leading edge and fined at the trailing edge, is justified for many small boats.

A rudder on a large ship, however, gets a free ride, as it were, for a good part of the time that the ship is in operation, since steering rarely involves a continuous rudder motion. In this case high lift is only one of several factors; easy flow and low resistance carry considerable weight when a rudder-blade section is chosen. As a consequence, the overall advantages of fitting streamlined rudders are so outstanding that their use is taken for granted wherever this type of construction is at all feasible. The exact section shape is not too important provided certain basic principles are borne in mind:

(a) The leading edge is to be neither too sharp, so that it produces discontinuous flow when the angle of attack is large, nor too blunt, so as to develop excessively high dynamic pressures at the nose
(b) The section at the leading edge is made elliptical in shape, *not* semicircular, for the reasons given in Secs. 36.3 and 67.5. If cavitation is not expected at zero or neutral angle, it should be deferred, at least for the small angles encountered when steering.
(c) The curvature in the entrance or leading portion is easy, diminishing gradually from the nose to the region of maximum thickness, complying with instructions in the last paragraph of Sec. 49.8
(d) The section outline or contour along any streamline is fair, without jogs, buckles, welding creases and upset lines, or other discontinuities across the streamlines
(e) The extreme trailing portion is no thicker than it need be for structural purposes. It is well tapered, terminating in an edge that is only thick enough to withstand nicking and corrosion.

For a ship on which the rudder is required to produce good steering and maneuvering but behind which the rudder region is filled with slowly moving water, the usual symmetrical hydrofoil section, tapering in the run, is not adequate to give prompt rudder response. The rudder section may then be carried aft from the stock axis at full thickness, with a square ending, or the sides may even be splayed outward toward the trailing edge. This section shape gives the necessary lift forces at small rudder angles for adequate steering in the manner described in Sec. 37.17 and illustrated in Fig. 37.L.

There appear to be no design rules, or even rules of thumb, to use for guidance in the selection or delineation of splayed or fish-tail rudder sections. In most cases these sections are employed to compensate for extreme eddying or backflow. As the poor flow conditions should not exist in the first place there is little point in conducting systematic research to find out how to correct them by using unusual rudder sections rather than by reshaping the run of the hull.

Whatever the shape of the trailing edge of a rudder (or diving plane) section, whether inside a propulsion-device outflow jet or not, it should be such that there is *never* any doubt in the mind of the water as to just where it is going to separate from the section. If the trailing edge can not be fine, narrow enough so that the eddies abaft it are insignificant, it should be cut off square, or even splayed like the split tail of a weathervane. It is never to be rounded enough to permit the separation points on either side to shift backward and forward, with consequent eddy buffeting, rattling, vibration, and perhaps even more serious consequences. This is one reason for not using a TMB EPH section, with its rounded section at the trailing edge. This section can, if desired, be terminated in a double-chisel shape, depicted in diagram 2 of Fig. 70.P.

It is doubtful whether any rudder section suitable for practical use can be kept free of separation and cavitation at extremely large *effective* angles of attack, of the order of 30 to 35 deg. These are always encountered when a rudder is swung rapidly to a hard-over position while the ship is moving on a straight course or perhaps is swinging in the opposite direction. The probable maximum effective angle of attack after the ship has started swinging, at a rate approximately half of that in a steady turn, has to be estimated, using the best known procedure. A nose shape is selected for which the lift coefficient C_L is still increasing at this attack angle.

The maximum thickness of a rudder section, occurring almost invariably abreast the stock axis, and the variation of this thickness along the depth of the rudder, is generally a matter of structural design. As such it is not covered here. When the blades of rudders and planes are made removable from the stock it may be necessary to increase the thickness ratio t_x/c at the support ends of spade rudders and cantilevered diving planes to a maximum of 0.25. However, this large thickness should not be carried too far along the blade. Normally, the thickness ratio t_x/c does not exceed 0.20 or 0.167 at the stock end of the rudder. Toward the free, unsupported end of a cantilevered rudder or plane, where the required section modulus is diminishing rapidly, the thickness ratio can be reduced considerably. The value of t_x/c is usually only about 1/6 of that at the stock end.

The sections of a close-coupled simple rudder, or of the close-coupled portion of a compound rudder, form a continuation of the hull, skeg, or fin to which it is attached. There should be no enlargement and no more discontinuity at the hinged joint than is required to give the rudder clearance to swing from one side to the other.

Tests of various rudder sections at the David Taylor Model Basin indicate that a simple section shape composed of a semi-circular nose and perfectly straight sides, tapering to zero thickness at the trailing edge, possesses lift-drag ratios superior to those of the NACA sections suitable for rudders. The thickness ratios t_x/c were 0.15 and less. Further, the breakdown or stalling point is delayed to a greater angle and the maximum lift is increased. So far as known, no confirmation of these features in full scale is available at the time of writing (1955). It is possible that the use of a short elliptic nose to prevent cavitation there would not detract from the advantages of the section.

The straight-sided shape of these sections, or of sections similar to them, may be found valuable in a study of dynamic stability of route, discussed in detail in Part 5 of Volume III. The convex side of a rudder, exposed to the angled flow on the "outside" of a ship in a yaw, may set up undesirable $-\Delta p$'s acting to increase the yaw. Straight rudder sides of the proper shape would develop $+\Delta p$'s, acting to reduce the yaw angle.

74.10 Structural Control-Surface Design as

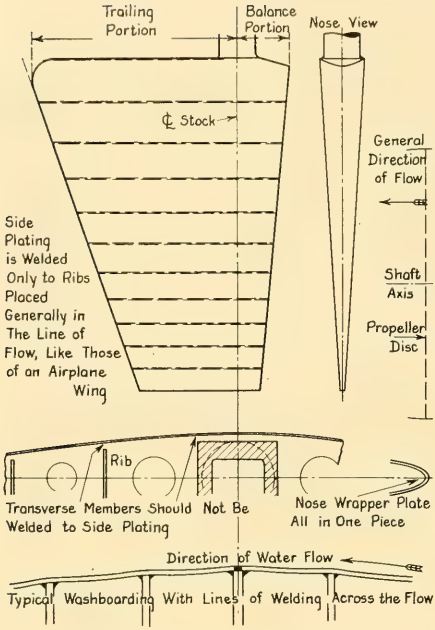

FIG. 74.G RUDDER STRUCTURE WITH ONE SYSTEM OF WELDS PARALLEL TO THE FLOW

Affected by Hydrodynamics. Any control surface, especially on a high-speed vessel, requires a structural design and a fabrication procedure which will insure that the selected control-surface section, along the line of flow, is achieved in the building of the ship and is maintained in service. The finished boundary plating on a structure that is hollow, as are most control surfaces, must be fair and smooth, without wrinkles or bulges. Further, it must be so stiffened that it maintains its fairness and shape while subjected to many different kinds of loading,—steady, intermittent, and alternating. This is one reason why the thin coverings of airplane wings and control surfaces are attached to ribs or stiffeners which lie in the direction of flow.

Indeed, the process of welding a rudder assembly may introduce discontinuities in the surface before the ship is completed. Internal stiffening members attached to the boundary plates by inside welds produce ridges in those plates because of shrinkage of the weld metal when cooling. If the internal stiffeners are placed generally normal to the flow, welding gives the boundary plates a washboard effect, illustrated schematically in the lowest diagram of Fig. 74.G. The boundary plates of a rudder or a diving plane should be attached primarily to internal structural members which run fore and aft, parallel to the streamlines of the liquid flowing over it, as in the topmost diagram of Fig. 74.G. This is especially true if the control surface lies within the outflow jet of a screw propeller or other propulsion device.

If practicable, there should be no joints, welding beads, or the like, transverse to the flow, anywhere in the entrance of the control surface. This is achieved by wrapping a single plate around the nose and both sides of the entrance, and attaching it to the frame only by fastenings parallel to the flow. These fastenings are spaced as closely as practicable, normal to the flow, so as to make the plating relatively rigid, with little likelihood of panting or bending between supports and of failure through fatigue.

74.11 Design Notes for Motorboat Rudders. The general principles for the design of the rudders

TABLE 74.d—RATIO OF RUDDER AREA TO LATERAL-PLANE AREA FOR MOTORBOATS AND SIMILAR CRAFT

The data listed here are translated from the book of J. Baader entitled "Cruceros y Lanchas Veloces (Cruisers and Fast Launches)," Buenos Aires, 1951, pages 333 and 335. The percentages of Group III include, for each case, the total projected area of the two rudders.

On pages 334 and 337 of the reference Baader gives profiles of thirteen launches, motorboats, and motor yachts, showing the relative positions and comparative sizes of screw propellers and rudders for these craft.

	$(10^2)A_R/L(H)$
I. Boats with One Screw Propeller and One Rudder	
Minimum surface for good steering	2
Normal surface for steering and maneuvering	2.5
Ideal surface for steering and maneuvering	3
Best surface for going astern	4 to 5
Maximum surface for special cases	10
II. Boats with Two Screw Propellers and One Rudder (between them)	
Minimum surface for steering	2.5
Normal surface for steering and maneuvering	3
Best surface for maneuvering conditions	4 to 5
III. Boats with Two Screw Propellers and Two Rudders	
Minimum surface for steering	2
Minimum surface for steering and maneuvering	2.5
Advisable surface for steering and maneuvering	3
Best surface for going astern	4 to 5

of mechanically powered small boats embody those of Sec. 74.8 relative to balance and trailing, plus the increased relative rudder area indicated for small craft in Tables 74.b and 74.d. Whereas formerly many of these rudders were operated by hand, some of them now have power gear, and a few of them automatic steering.

For craft which run at speed-length or Taylor quotients T_q of 3 or more, $F_n > 0.89$, the rudder forces and moments are large compared to other forces and moments. This applies to heeling as well as swinging moments, so that whether or not a boat banks properly (inward) on a turn may depend as much on the rudder as on the hull. As the T_q and the absolute speeds reach higher values it is increasingly important that the rudder be of the proper size and shape.

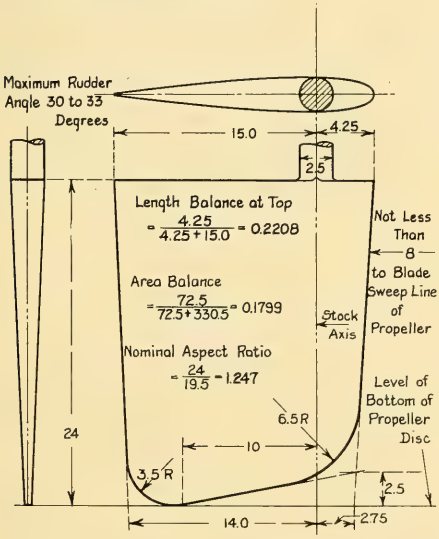

FIG. 74.H MOTORBOAT RUDDER WITH STREAMLINED SECTIONS

Fig. 74.H indicates the outline and principal dimensions of a type of streamlined rudder developed by Elliott Gardner for a 45.5-ft air rescue boat, based upon systematic full-scale tests and experience extending back to 1925. It is reported to be suitable for all speeds from 5 to 50 mph, or 4.3 to 43.4 kt.

Fig. 74.I is a more modern rudder of somewhat similar design, intended for use on a 52-ft air rescue boat, but having parallel sides in the run

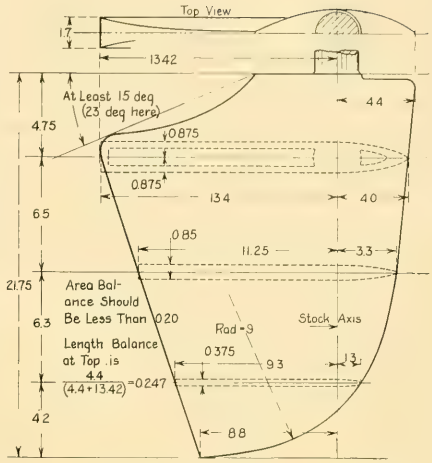

FIG. 74.I BLUNT-ENDED PARALLEL-SIDED MOTORBOAT RUDDER

The numerals may represent any units of measurement or serve as relative proportions.

or tail portion and a wide, square trailing edge. It is cut away at the after upper corner because:

(a) The $+\Delta p$ built up on the *ahead* side of the upper after corner of an angled rudder with a horizontal top, indicated in Fig. 74.H, exerts a lift force under the stern and depresses the bow. While this is an advantage in straight-away running, it is liable to cause the bow to trip in a turn [Grenfell, T., "Some Notes on Steering of High Speed Planing Hulls," SNAME, Pac. Northwest Sect., 27 Sep 1952; abstracted in SNAME Bull., Jan 1953, p. 35].

(b) The portion removed permits a more-or-less solid stream of water to pass over the angled rudder, close under the hull. This acts as a shield to prevent air leakage to the astern or $-\Delta p$ side of the rudder. Whether cut away or not, it is preferable to place the rudder so that it lies completely *under* the hull at any angle, to obtain the maximum shielding effect from air leakage.

The nominal aspect ratio of the horizontal-top rudder of Fig. 74.H is 1.247 whereas that of the more modern design in Fig. 74.I is 1.224.

The design of rudders for high-speed motorboats of the planing type, especially those which travel at values of the Taylor quotient $T_q = V/\sqrt{L}$ in excess of 5, is based largely upon experiment

and experience. A generous portion of both is made available to the profession in a paper entitled "Some Notes on Steering on High-Speed Planing Hulls," by T. Grenfell, previously referenced in this section. Grenfell recommends that the aspect ratio of rudders for these ultra-high-speed craft be of the order of 2, making them twice as deep as they are long.

74.12 Design of Close-Coupled and Compound Rudders. Any close-coupled simple rudder is in reality a compound rudder, but its effect is not easy to predict because the greater part of the quantitative data in existence are for flap-type hydrofoils of rather different proportions. However, sufficient information has been obtained from special model tests [Abell, T. B., INA, 1936, pp. 137–144 and Pl. XV; van Lammeren, W. P. A., RPSS, 1948, pp. 327–328] to enable a fairly reliable estimate to be made of the part of the total transverse force exerted by the movable rudder and the part exerted on the fixed or ship structure adjacent to the rudder. Part 5 of Volume III contains a series of diagrams from which these fractional parts can be estimated for any probable rudder arrangement. From that point on the design follows the procedure described in the sections preceding.

The indications from a series of rudder and stern profiles and corresponding graphs of ship turning moment given by W. P. A. van Lammeren [RPSS, 1948, Fig. 221, p. 331] are that none of the fixed fins or posts shown there contribute much additional force to that exerted by the movable rudder blade.

When designing a compound-type control surface, or one with a movable blade carrying a flap, it is well to limit the angle of the movable portion, or the flap, to the order of 20 deg either way, especially if the length of the movable portion or flap is less than 0.4 of the chord length of the whole section [NACA Rep. WRL-419, Jan 1944]. This eliminates any possibility of stall. However, if the whole control surface is of low aspect ratio, or if the movable portion is very large compared to the whole, it is possible that the movable portion or flap may remain effective up to angles of 35 deg either way.

74.13 Conditions Calling for Tubular Rudders. When steering in shallow, fast flowing rivers, prompt rudder action at just the right moment may mean the difference between a safe passage and disaster. For this type of service no single-blade or multi-blade rudder is adequate. If swinging or steering propellers can not be used, one or more tubular or box rudders or swinging Kort nozzles may be employed, arranged so as to change the direction of the whole propeller-outflow jet. Fig. 74.J illustrates an experimental rudder of this type.

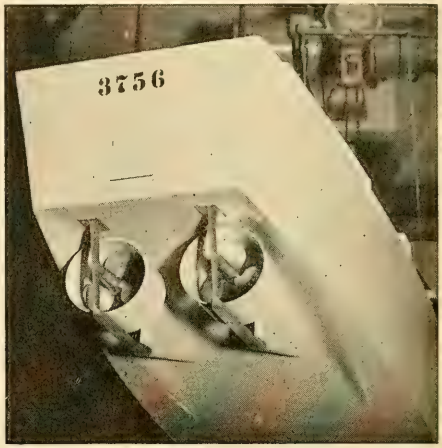

Fig. 74.J A Pair of Tubular, Swiveling Rudders

For proper mechanical clearance the stock axis must pass close to or through the plane of the propeller disc. Even then a constant small tip clearance is not possible unless the tubular rudder has a shape abreast the propeller that is approximately spherical. Against the efficacy of a proper design of tubular rudder must be balanced the liability of bending the tube on rocks or debris in the stream bed and jamming the propeller inside it.

74.14 Closures for Rudder Hinge Gaps. Sec. 37.3 and diagram 9 of Fig. 37.D illustrate the manner in which differential-pressure leakage can take place between the $+\Delta p$ and $-\Delta p$ sides of a rudder-and-support assembly, even when the clearances are reasonably small. On old sailing ships it was customary to keep this gap as small as easy movement of the wooden parts would permit. Clearance spaces left for lifting the rudders far enough to get the pintles out of the gudgeons were covered by filling plates [Barry, R. E., Mar. Eng'g., Sep 1921, p. 689]. In general, plates or other closures should be fitted on the fixed portion of the post-and-blade assembly. This is the reason for the fixed lugs on the sternpost shown by Fig. 73.K of Sec. 73.14.

For an excellent discussion of the hydrodynamic and other problems associated with the closing (or narrowing) of vertical and horizontal gaps the reader is referred to P. Mandel [SNAME, 1953, p. 489, under "Rudders—Gap and Horizontal Break"]. S. F. Hoerner gives useful information concerning the relative drag of various across-the-flow gap configurations between a symmetrical-section airfoil and its trailing-edge flap, together with notes on the effect of the airfoil thickness and flap thickness at the hinge [AD, 1951, pp. 57–58]. These data apply directly, for straight-ahead running, to ship rudders hung abaft thin skegs or rudder horns.

74.15 Rudder Designs for Alternative Sterns of ABC Ship. The estimates of area for the rudder designs of the ABC ship, described in this section, are based only on the first approximation of Sec. 74.6, and not upon the more logical procedure outlined in Sec. 74.7. Furthermore, the designs of the rudders themselves are carried only far enough in this section to produce control devices which would have about the same resistance (certainly no less) than could be expected of the final refined rudder designs for the two alternative ABC ship sterns.

When roughing in the stern profile of the ABC ship with transom, described in the first part of Sec. 66.25, a first approximation for the area of the *movable* blade of a single centerline rudder was $0.02(L)H$, or 265.2 ft^2. From Table 74.b this is a high-limit value for large, medium-speed passenger and cargo ships. The selection of the maximum value in the table was based upon the need for excellent steering and turning qualities in the Port Amalo canal and when maneuvering out of the harbor at Port Bacine, indicated in Figs. 64.A and 64.B.

Based upon the use of a clear-water aftfoot and no rudder shoe, the rudder had to be partly or completely underhung. To avoid placing the single rudder in the paths of the hub vortexes from the single propeller ahead, it was decided to embody a partly underhung rudder and to carry it by a horn which extended far enough below the hull to include a fixed fairing abaft the propeller hub. A foil of generous area placed below the horn, with a short circulation path and plenty of clearance for the circulatory flow, would provide the quick response necessary for steering the ship in the Port Amalo canal and in the river below Port Correo.

Small-scale sketches indicated that, with a transom submergence of 2 ft and a baseplane clearance of 0.5 ft for the foot of the rudder, the portion of the blade abaft the stock axis could be at least 22 ft high by 10 ft long, with a projected area of about 220 ft^2. Adding say 25 per cent for the balance portion of the foil ahead of the stock gave a tentative total area of $220 + 55 = 275$ ft^2, which appeared ample. With the balance portion extending from 0.5 ft above the baseplane to about 1.5 ft below the shaft axis (at the 10.5-ft WL), its height was 8.5 ft, giving a tentative fore-and-aft length of $55/8.5 = 6.5$ ft. The length balance was then $6.5/(10 + 6.5) = 0.394$. This value seemed rather large but not too large for a rudder which must be angled without requiring an excessive torque when going astern.

With a clear-water skeg ending and a baseplane clearance of 0.5 ft for the propeller, the baseplane clearance of 0.5 ft for the rudder appeared somewhat small to the owner and operator. It was therefore increased to 1.0 ft. The upper after corner of the tail of the blade was also cut away to provide a greater gap and more protection against air leakage below the edge of the transom. The three lower corners were left square. The shape and dimensions of the blade when sketched at the conclusion of the preliminary design of the transom-stern hull appear in Fig. 74.K. It has a total area of 273 ft^2, or 0.0206 of the product $L(H) = 510(26)$ at the designed draft.

The lateral area of the fixed horn as sketched in the figure is about 89 ft^2, or roughly 24 per cent of the combined area of blade and horn. Because of its closeness to the blade it appears that the differential pressures set up on the fixed horn will add materially to the lateral force exerted by the blade when the latter is angled.

For the arch-stern ABC hull described in Sec. 67.16 and illustrated in Figs. 67.L and 67.M, there was little in the way of design data for guidance, by which to select a ratio of rudder-blade area to the product of the waterline length and draft. The stern was laid out so that, at a reasonably small rudder angle, either the port or the starboard blade would swing into the projection of the propeller disc. Fig. 67.P indicates that the trailing edges of both rudders, at zero angle, lie close to this projection. The contraction in the outflow jet is assumed small because the stock axes lie only about $0.33D$ abaft the disc position.

It was estimated that an increase of at least 25 per cent over the blade area of a rudder lying

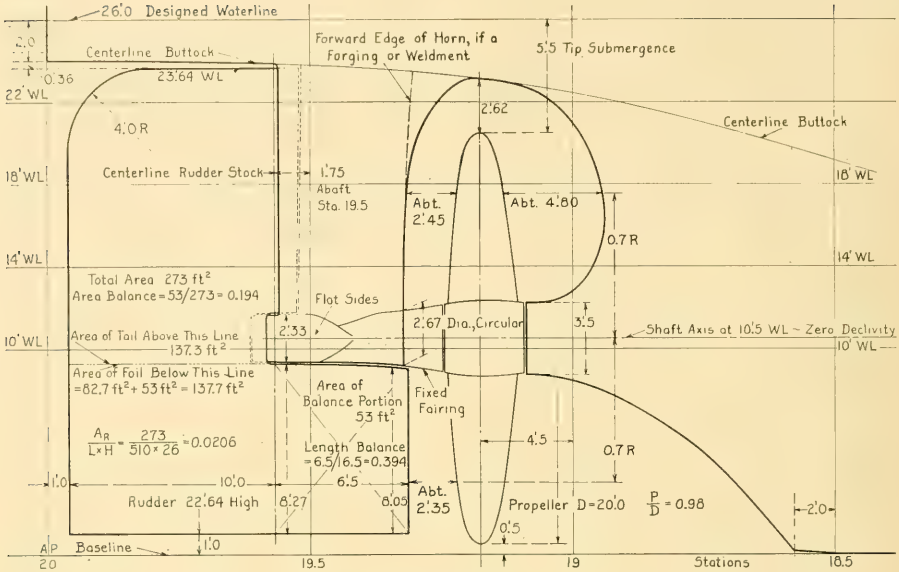

Fig. 74.K Details of Aftfoot, Propeller Aperture, Rudder Support, and Rudder for ABC Transom-Stern Ship

abaft a single propeller would be required to give the arch-stern ship as good maneuvering characteristics as the alternative transom-stern ship. The adverse effect of the increased lateral area of the twin skegs would, it was believed, be offset by the increased lateral force which the twin rudders would, acting as flaps, generate on the portions of the fixed skegs just ahead of them. Further, the addition of an underhung foil on each rudder would provide the quick steering and turning response needed for running in the confined waters at each end of the ship route. When finally sketched, as in Fig. 74.L, the total movable-blade area of both rudders was 346.74 ft². This was 346.74/13,260 or 0.0261 of the product $L(H)$, an increase of 26 per cent over the same ratio for the single, centerline-rudder design of the transom-stern ship.

These twin rudders are in effect only the trailing edges of the two arch-stern skegs. Each is arranged to swing about a vertical axis 8 ft forward of what would be the skeg ending and each carries an underhung foil extending below the bottom of the skeg termination. The rather unusual horizontal sections of the tail portions of these rudders arise from a deliberate continuation of the *inside* skeg waterlines close to the anticipated flowlines in the tunnel. The convergence of the outside waterlines is such as to terminate the skegs and rudders in trailing edges that lie as close as possible to the outflow jet of the propeller. The resulting thick and unsymmetrical sections leave some uncertainty as to the hydrodynamic behavior of the hinged tail portions, when acting as flaps hinged to the main skegs. In view of the lack of information about them, a series of maneuvering tests with a model is definitely indicated before the arch-stern design is carried beyond this preliminary stage.

The selection of the proper thickness ratios and the horizontal section shapes for the single, streamlined rudder of the transom-stern ship involves no such limitations as those just described for the arch-stern design. To be sure, the thickness ratio for the single rudder is to some extent governed by the thickness of the fixed horn which is necessary to afford adequate rigidity to the lower rudder bearing. This is a matter of structural analysis and calculation and as such it is outside the scope of the book. The thicknesses indicated on Fig. 74.N of Sec. 74.17 are estimates only, based upon similar installa-

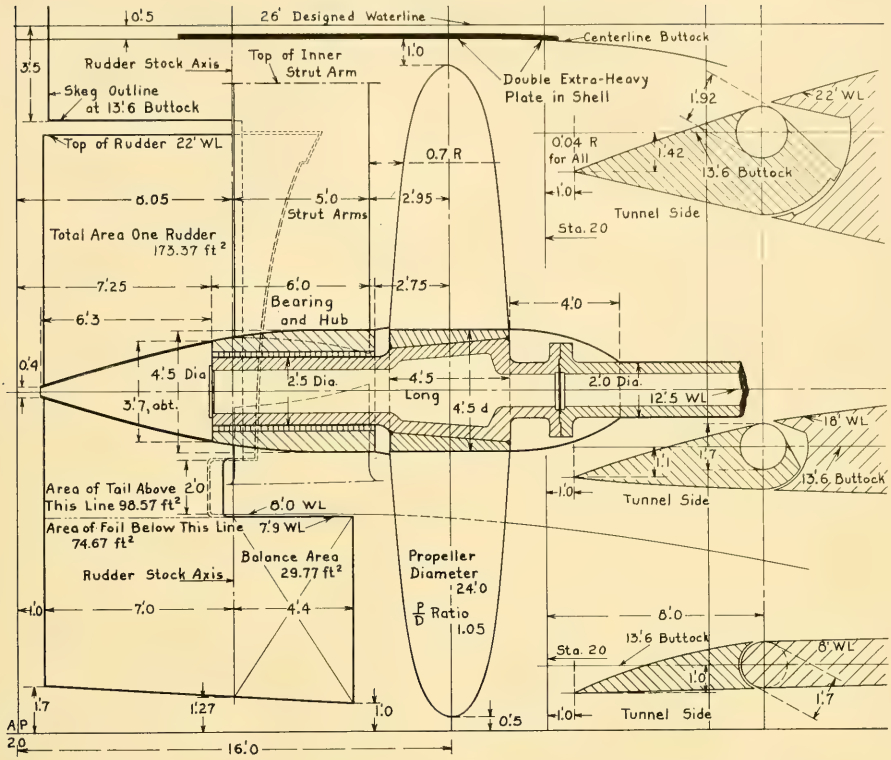

Fig. 74.L Vertical Centerplane Section Through Shaft, Propeller, and Strut-Bearing Support of ABC Arch-Stern Design

tions with fixed horns of somewhat less relative depth.

Before the time came to sketch the streamlined rudder for the transom-stern ABC ship it was decided to use a form of contra-rudder. A fair-form rudder with a flat meanline plane, even when designed as a unit with the fixed horn, involves design problems which are adequately covered by P. Mandel [SNAME, 1953, pp. 474–490] and by others listed at the end of Sec. 74.8. They are not further discussed here. The layouts of the contra-rudder and the contra-guide horn, as applying to the ABC transom-stern design, are described in Secs. 74.16 and 74.17 which follow.

74.16 Design Notes for a Contra-Rudder. Strictly speaking, the contra-flow feature on a rudder is not a functional part of the rudder as a control surface but is an energy-recovering and a thrust-producing device. In fact, it need not be movable, as is the rudder. Typical horizontal sections for a compound rudder with contra-features in the fixed portion only, and in both the fixed and movable portions, are shown by W. P. A. van Lammeren [RPSS, 1948, Fig. 55, diagrams e and f, respectively, p. 100]. However, as a rudder is required with normal screw propulsion, the friction drag of a separate fixed surface is eliminated by incorporating the contra-flow feature in the rudder. For the design of this feature, the rudder is considered to remain at its zero or neutral angle.

The design problem consists of:

(a) Establishing a series of horizontal planes above and below the propeller axis, described for the contra-guide skeg ending in Sec. 67.22, for

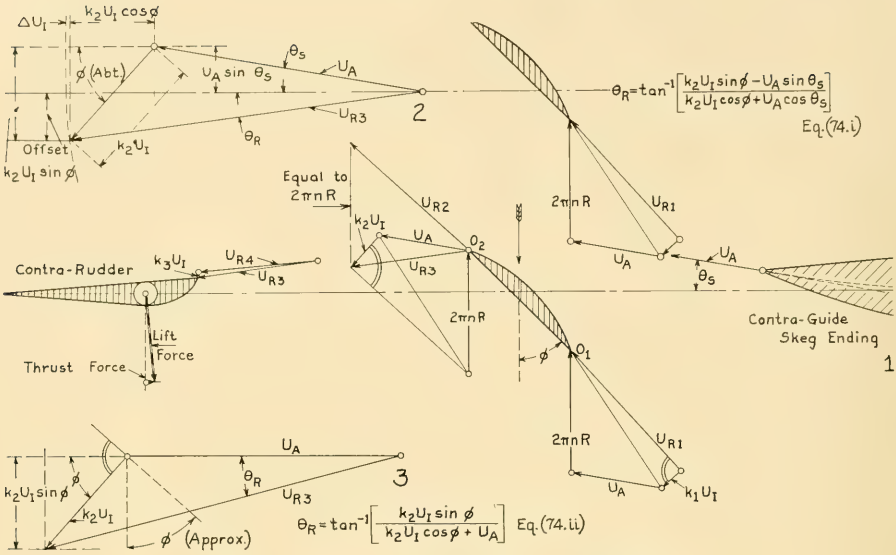

FIG. 74.M VECTOR DIAGRAM FOR DESIGN OF CONTRA-RUDDER

which separate velocity diagrams and rudder sections are to be drawn

(b) Estimating the magnitude of the induced velocity U_I at each propeller radius, as well as the factors k_1, k_2, and k_3 in Fig. 74.M. These data are required to determine the resultant velocity vector U_{R3} for the given radius at the fore-and-aft location selected for the leading edge of the contra-rudder. The latter position is usually determined by the aperture clearance provided abaft the wheel.

(c) Drawing velocity diagrams similar to those in Fig. 74.M, assuming that a contra-guide skeg ending, if one is to be used, is already designed

(d) Estimating the magnitude of the induced velocity to be set up by the contra-rudder hydrofoil section itself, of which half may be expected to develop ahead of the leading edge of the contra-rudder. It is of interest to note that the flow due to circulation through the aperture between a propeller blade and a contra-rudder blade is in the *same* direction for both, namely forward in the direction of motion of the propeller blade. In many cases the velocities induced by the rudder are small and may be neglected in the design.

(e) Selecting a curve for the leading edges of the hydrofoil sections of the rudder blade at the various levels or propeller radii, as projected on a transverse plane. The offsets of these edges are then laid off at each level. This matter is discussed in detail in a paragraph following.

(f) Calculating (or estimating) a minimum thickness for the contra-rudder. This involves the calculated diameter of the stock or main vertical structural member necessary to carry the side loads expected. These in turn have to be estimated rather roughly until more of the rudder is laid out. If the contra-rudder is to be of the compound type, with a fixed forward portion, a certain stiffness is required for this latter member.

(g) Selecting a hydrofoil section thick enough to meet the needs of (f), combined with proper fore-and-aft position of the maximum thickness t_x

(h) Calculating the lift on the selected section at the nominal angle of attack indicated by the velocity diagram for the propeller radius in question. From these data a second approximation to the loading curve on the stock is found, by which the stock scantlings are checked. Although the lateral thrust loads are in opposite directions above and below the shaft axis the bending moments and shear loads are heavy in the vicinity of that axis.

(i) Adjusting the several hydrofoil shapes and positions so that a 3-diml body based upon them is fair with respect to its traces in a series of

vertical transverse planes between the leading and the trailing edges of the rudder.

The steps listed in the foregoing require some explanation, given here in the same order as (a) through (i).

The velocity diagrams of Fig. 37.K, for a contra-rudder installation only, are supplemented by those of Fig. 74.M, for an installation of both contra-guide skeg ending *and* contra-rudder. In the latter diagrams the incident flows on the propeller are shown for two adjacent blade sections, unrolled into the flat. This is an aid in visualizing the flow leaving the skeg ending, represented by the vector U_A, and that forming one of the components of incident flow on a blade section at the same level.

It is customary to show the flow meeting a moving-blade element with reference to axes *in that element.* The vector U_A is therefore combined with the rotational vector $2\pi nR$ and with the induced-velocity vector k_1U_I to give the incident-velocity vector U_{R1}. When the flow leaves the moving blade along U_{R2} it is again referred back to axes fixed in the ship by combining it with the rotational vector $2\pi nR$, but in a reverse direction. This is equivalent to combining the inflow vector U_A with the induced-velocity vector at the trailing edge of the blade element, the latter equal to k_2U_I. The flow meeting the hydrofoil section of the rudder is then represented *nominally* by the vector U_{R3}.

It is now required to select a section shape for the contra-rudder, and a nominal angle of incidence with respect to the ship centerplane, which will insure smooth flow around the rudder with a reasonable lift force and forward-thrust component. What is wanted first is the value of the angle θ_R which the vector U_{R3} makes with the ship axis. Second, the amount of offset of the leading edge of the contra-rudder section is to be determined.

If the fraction k_2 is estimated (or determined in some manner) it is possible to derive θ_R by a graphic construction such as that in diagram 2 of Fig. 74.M. The velocity induced by the hydrofoil section of the rudder, shown as k_3U_I in the small-scale diagram 1 of the figure, is omitted from the large-scale diagram 1 to avoid confusion. It is also assumed, for the sake of simplicity but without appreciable error, that the induced-velocity vectors k_1U_I and k_2U_I lie normal to the base chord of the blade section, at the geometric blade angles ϕ marked in the diagram. The nominal value of the obliquity θ_R of the velocity vector U_{R3}, incident on the rudder section, may be calculated by Eq. (74.i), set down in the upper RH corner of the figure.

For a contra-guide skeg ending designed as in Sec. 67.22, the angle θ_S is known for any blade radius or level. If the skeg ending is symmetrical, as in Fig. 37.K, the expression for θ_R reduces to that of Eq. (74.ii), alongside the large-scale diagram 3 of Fig. 74.M. The value of U_I is always small with respect to U_A, and k_2 is always less than 1.00, because the full value of U_I is developed only far astern. Eq. (74.ii) therefore reduces to $\theta_R = \tan^{-1}(C \sin \phi)$. Here C, representing k_2U_I/U_A, is a small fraction, say 0.15. For any normal propeller the geometric blade angle ϕ seldom exceeds 65 deg at the hub surface, hence $C \sin \phi$ has a maximum value of about 0.135. The angle θ_R then has a maximum value of about 8 deg, where $\theta_R = \sin \theta_R = \tan \theta_R$, approximately.

Actually, it is possible to derive the average value and direction of U_A only from model tests or very special ship tests. Further, U_A is almost never constant along the upper or the lower blade radii, either in magnitude or direction, nor does the mean upper value of U_A equal the mean lower one. As a consequence, and because of the varying circulation at different blade radii, the maximum induced velocity U_I is almost never the same for all radii, nor is it known precisely at any radius. To cap all the foregoing, the factors k_1 and k_2 are not well known. While values reasonably close to the actual ones could undoubtedly be substituted in the expressions for θ_R in Fig. 74.M, there are practical factors which require a more realistic approach to this design problem.

It is recalled that for the design of a contra-guide skeg ending discussed in Sec. 67.22 the value of θ_R derived analytically for points opposite the outer propeller radii are small but they are still too large for practical use. Employed here, they would produce a rudder which had no straight or symmetrical sections whatever. Whether this much of a departure from the orthodox streamlined rudder would be the best device for steering a straight course for long periods could only be determined by successive full-scale installations on the *same* vessel. The doubt expressed in the foregoing is heightened by the fact that it is also rarely possible to use hydrofoil sections which deliver the water directly astern with the rudder at zero angle. The large camber necessary to

accomplish this imposes lift loads which increase the thickness ratio and make it more difficult to lay out hydrofoil sections of suitable shape.

With these considerations in mind a compromise solution employing a leading-edge offset on the rudder varying as $\sin^2 \phi$, utilized previously for the design of the contra-guide skeg ending discussed in Sec. 67.22, is employed here for the contra-rudder as well. The offset taken as a reference may be based, as before, on a value of about 0.85 times the propeller hub radius $d/2$ opposite the 0.1 propeller radius. A graph for selecting the angle which the median line at the leading edge of a fixed contra-propeller blade is to make with the fore-and-aft plane is given by R. Wagner [STG, 1929, Fig. 44, p. 224]. This graph could be used as well for the leading edge of a contra-rudder, whether this edge were the fixed portion of a compound rudder or the leading edge of a balanced rudder. It calls for an angle of 45 deg at $0.13R$ (of the propeller), 19 deg at $0.48R$, and 9 deg at $0.80R$.

Whatever rule is used, some asymmetry in the form of leading-edge angle does and should remain abaft the propeller-blade tips, as for the contra-guide skeg ending, at vertical distances above and below the shaft axis equal to the propeller radius R_{Max}.

A transition is necessary from the maximum twist toward the trailing edge of the propeller blades at the 12 o'clock position to the maximum twist in the opposite direction (but also toward the trailing edges) at the 6 o'clock position. This should be made gradually, *not abruptly*, across the "shadow" of the propeller hub. In fact, one good way to make it is to use a cylindrical propeller hub and to work a large hub fairing into the contra-rudder in this region. By this means abrupt and harmful discontinuities in the rudder structure abaft the hub are avoided. A variation of this method is to work a bulb into the rudder at the transition point, extending well aft on the rudder [Maritime Reporter, 1 Feb 1954, p. 23].

If all the rotation is to be taken out of the propeller-outflow jet, the median lines of the trailing edges of the contra-rudder sections should be parallel to the mean plane of the rudder in its zero or neutral position. It may possibly be better to make the face, on the $+\Delta p$ side of the trailing edge, parallel to this mean plane. Also, if an appreciable forward component of the lift or lateral force on the rudder is to be realized as thrust, it is advantageous to place the base chord of each of the rudder sections at an appreciable angle to the mean plane of the rudder blade. All this may require that, not only must the leading edge be directed and offset one way from this plane, but the trailing edge must be offset the other way. The transition takes the form of a crossover from one side to the other, abaft the propeller hub, in both the leading and trailing edges, but in opposite directions. As a means of avoiding sharp corners and coves along which the water must flow, and of structural discontinuities in the rudder as well, an easy transition is also called for when the trailing edges are offset from the mean plane of the blade.

In one of the earliest descriptions of the contra-propeller, for installation abaft a screw, R. Wagner mentions that: "A particularly good result is obtained by shaping the trailing edges of the blades eccentrically to the hub center" [transl. of Schiffbau, 14 Feb 1912, pp. 365–366]. He does not, unfortunately, give specific reasons for this statement. The diagram accompanying the reference has the trailing-edge offset marked by a symbol, not mentioned in the text. Incorporating this offset gives the designer somewhat more freedom in shaping the vane or blade which is to convert some of the rotational energy into thrust, and places the base chord at a greater angle to the ship axis. If other conditions are right, a somewhat greater forward-thrust component is derived from a given lift force.

For the single rudder of the ABC transom-stern ship it is decided not to incorporate any offset in that part of the blade lying abaft the rudder stock or in its trailing edge. When, as described in Sec. 74.17, a contra-shape is incorporated in the fixed horn ahead of the rudder stock, there will be an appreciable lift force acting to starboard on the unsymmetrical hydrofoil assembly composed of this horn and the tail of the rudder. Combined with the Hovgaard Effect, described in Sec. 33.17, there will be a continual lateral force acting to push the stern to starboard when the ship is going ahead. This swinging effect can be counteracted only by giving a contra-shape to the underhung foil and exerting a hydrofoil lift force to port. The preponderance of force to starboard may still require carrying more than the usual amount of right rudder to maintain a straight course. This is another reason for not working a contra-guide ending into the upper portion only of the centerline skeg ending. It too would exert a lateral force to starboard and

augment the right rudder to be carried to maintain a straight course.

The design of the contra-shaped movable foil follows the design of the contra-shaped fixed horn or skeg above it, described in Sec. 74.17. Normally, the thickness ratio of the foil sections in a partly underhung rudder diminish rather rapidly from the lower bearing to the bottom of the rudder, until at the lower edge this ratio may be of the order of 0.03. The high value of about 0.115 for the section at the 2-ft WL for the foil shown in Fig. 74.N of Sec. 74.17 is due to:

(1) The short vertical height of the foil, because the fixed horn is extended below the propeller shaft axis
(2) The uncertainty involved in drastic thinning of a contra-section, expecially in a rudder of this type.

Thinning the lower-edge sections represents no problems, provided it is determined that the contra-performance can be maintained. If the lower sections are left thick, a flow test might indicate the advisability of sloping the lower edge of the foil down and forward, with a baseplane clearance of say 0.5 ft at the forward end and 1.5 ft at the after end.

The compensating force exerted to port by the contra-shaped foil is probably augmented by holding the trailing edge of the foil on the centerplane; that is, by not offsetting it to port, as is customary in contra-rudders. The foil then works at a greater effective angle of attack in the outflow-jet water which, below the shaft axis, is directed aft and to port behind a right-hand wheel. Rather than to offset only the trailing edge of the tail, above the shaft axis, and to introduce a discontinuity in the rudder structure, the entire portion of the blade abaft the stock axis is made symmetrical.

Finally, when the rudder is designed, and a model is built, the flow is checked in a circulating-water channel with tufts attached to various parts of the rudder. One test should be made with the propeller working, and another with the rudder at an angle. Unfortunately, it was not possible to do this with the model of the transom-stern ABC design.

Entirely aside from the increase in propulsive coefficient which may be achieved by a contra-rudder on any ship, which should be from 4 to 6 per cent under average conditions, there is a decided advantage on a high-powered, moderate-speed ship in bending the leading edge of a rudder, contra-fashion, instead of using a simple streamlined affair, with the base chords of all sections parallel to each other. In the rotary cross flow of the outflow jet the contra-flow shape acts to reduce cavitation, pitting, erosion, buffeting, vibration, and noise. An example of a severely pitted *Mariner* class rudder, not so shaped, is given by W. G. Allen and E. K. Sullivan [SNAME, 1954, Fig. 25, p. 541]. T. W. Bunyan illustrates the pitting which occurred on a combination of thin rudder post and a rudder hung directly abaft it, lying in the outflow jet of a single, centerline propeller. Both were streamlined but were entirely symmetrical about the vertical plane through the propeller axis [IME, Apr 1955, Vol. LXVII, No. 4, p. 105].

74.17 Design of a Contra-Horn for the ABC Transom-Stern Ship. For the transom-stern ABC ship whose stern profile is shown in Fig. 74.K, the rudder horn or small skeg abaft the propeller extends below the shaft axis so that a fixed dummy fairing for the propeller hub may be carried by it. For ease in removing the shaft nut and the propeller on the actual ship, this fairing is made removable.

In view of the appreciable fore-and-aft length of the fixed rudder horn it is found possible to incorporate all of the twist and camber of a contra-guide device in the portion above the propeller axis. As explained in Sec. 74.16, this leaves the tail sections of the movable blade entirely symmetrical. Below the propeller axis, all the twist and camber is incorporated in the balance portion of the rudder foil, forward of the rudder-stock axis, also described in that section.

In the original layout of the propeller-hub fairing at the lower end of the rudder horn it appeared that the diameter of this fairing at its juncture with the horn would be 3.0 ft, with a radius of 1.5 ft. As a basis for calculating the offsets for the twist at the leading edge of this horn, the offset at $0.1R_{\text{Max}}$ above the propeller axis was taken as 0.85 times 1.5 ft or 1.275 ft. The remaining offsets, calculated by the $\sin^2 \phi$ rule described in Sec. 67.22, are tabulated on Fig. 74.N. The offsets below the shaft axis, to be embodied in the leading edge of the foil, are the same as those above that axis, for the same radii.

When TMB model propeller 2294 was selected from stock to drive the transom-stern model, it was necessary to reduce the hub-fairing diameter at its junction with the horn from 3.0 ft to 2.67

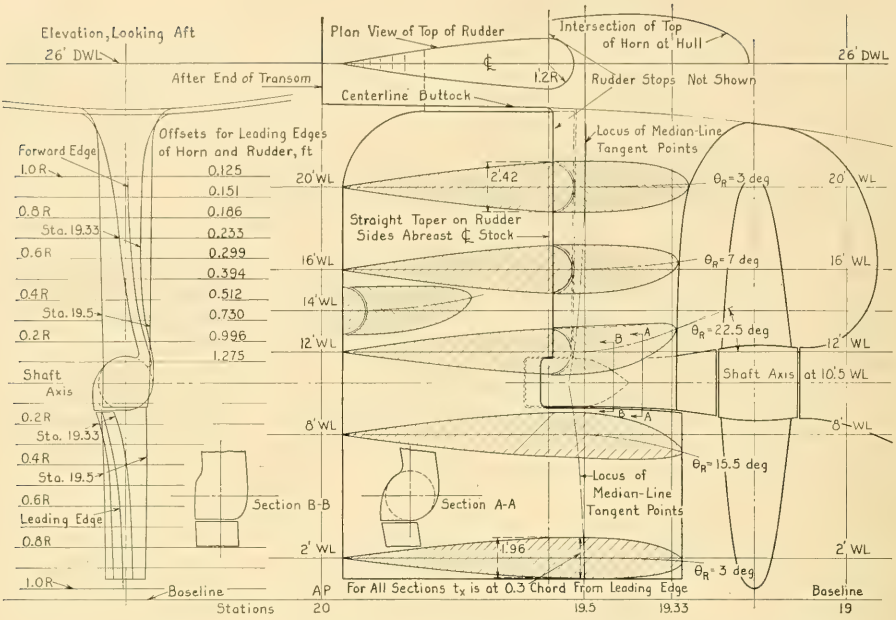

Fig. 74.N Arrangement and Details of a Contra-Horn and Rudder for ABC Transom-Stern Ship

ft. However, the leading-edge offsets of the horn above the shaft axis and the balance portion of the rudder foil below it were left unchanged. This necessitated a short length of reverse curvature (inward) just above the hub fairing, shown in the end elevation at the left of Fig. 74.N.

The maximum median-line slope at the leading edge of the contra-fairing on the horn, just above the hub fairing, is 22.5 deg. This is considered acceptable because of the large angle θ_R with which the water leaves the propeller-blade elements in this region. Separation is not a problem here provided the incident flow from the blade elements at the root strikes the leading edge of the horn at about this angle.

The fixed horn and the tail of the rudder (when at zero angle) are considered as a single assembly when laying out the section outlines for the horn. The thickness ratio at each level is governed by (1) the profiles of the rudder and horn, which establish the chord length c, and (2) by the necessary thickness for the horn, to give it structural stiffness. The latter determines the value of t_X . No section designations or sets of coordinates are specified or recommended here because there are a considerable number of good ones from which the designer may choose [Mandel, P., SNAME, 1953, pp. 486–488].

An important feature of section outlines for compound rudders, similar to the one shown in Fig. 74.N, is the shape of the extreme nose. This statement holds even though contra-guide sections are worked into the forward or fixed portion. A shape too nearly circular leads to cavitation or separation along the sides of the section, a little abaft the nose, especially if the radius is large. A nose that is too pointed may also be subject to cavitation or separation on the "lee" side, when there is no contra-shape and when the angled flow from a propeller ahead strikes the leading edge of the rudder at a large angle with the meanline plane through the rudder. A practical example of this is described in the last paragraph of Sec. 74.16.

M. Kinoshita and S. Okada show the results of measurements on models made by M. Yamagata, in which the flow just below the propeller hub makes an angle of over 50 deg with the meanline plane of the rudder [Int. Shipbldg. Prog., 1955, Vol. 2, No. 9, Fig. 8, p. 238]. It is clear that, as

these Japanese authors point out, much more knowledge is needed concerning the details of flow abaft an actual screw propeller before the designer is able to shape properly the leading edge of a rudder horn or a balanced rudder.

74.18 Design for Rapid Response to Rudder Action. The development of a given lift or normal force when angled is only one of the things which a rudder or other control surface is called upon to do. It must also do this rapidly, so as to provide quick response on the part of the ship. An excellent example is the control surface in the form of an active roll-resisting fin. This has only 10 sec at the most in which to shift its position from hard over one way to hard over the other and to produce a useful force and rolling moment before it has to shift position back again. Another example is the rudder of a ship traversing a canal, for which rapid response is much more important than the simple ability to steer or to turn one way or the other.

The shorter the circulation path around a rudder the smaller is the mass of water to be set in motion and the sooner are the circulation and lift established. A hydrofoil which is called upon to exert a normal force rapidly should be short in the direction of motion and have reasonably large clearances or apertures both ahead and astern. A short, high spade rudder is the best answer to this design problem. A balanced rudder hung on a small horn, short in the fore-and-aft direction, is the next best.

For a simple, balanced rudder or a flap-type, unbalanced rudder at the stern of a twin- or multiple-screw ship (or at the stern of a ship driven by side paddlewheels), the clearance for circulation in a horizontal plane around the rudder is provided by an aperture forward of the rudder. This resembles the aperture in which a propeller would be fitted if the ship had only a single screw. Two such apertures are sketched in diagrams 3 and 4 of Fig. 74.D. An equivalent aperture of large area lies ahead of the underhung foil portion of the rudder in diagram 5 of Fig. 37.D.

74.19 Utilization of Automatic Flap-Type Rudders and Diving Planes. There appears to be a definite application in the field of control surfaces for the hinged hydrofoil with automatic flap, depicted in diagram 2 of Fig. 14.U. This device is called here, for want of a better name, the *automatic flap-type* rudder or diving plane. There is incorporated in it some simple leverage or equivalent mechanism to apply positive flap angle as the main control surface is angled. Both the control-surface angle and the flap or tab angle are in the same direction, whether the rudder is right or left, or the plane is at rise or dive. The flap action always increases the lift of, and the lateral force on the control surface.

This device has been utilized successfully for a number of years on the active fins of the Denny-Brown roll-stabilization gear, referenced in Sec. 37.9. The linkage for applying flap angle automatically is outside the watertight hull of the vessel but in view of its extreme simplicity it has operated well in service.

Although no designs have been prepared, or installations made, so far as known, it should be possible to substitute this device for almost any rudder or diving-plane installation which fits closely against a fixed portion of the hull. The simple Denny-Brown linkage or its equivalent may be used for operating the flap.

For a control surface subject to severe pounding or slamming when in waves, the flap may have to be restricted to only a portion of the rudder height or the diving-plane width. The total impact forces on the flap may then be small enough to be withstood by the automatic angling mechanism.

74.20 Design Notes for Bow Rudders; Rudders for Maneuvering Astern. It is pointed out in Sec. 37.11, supplemented by Fig. 37.G, that a bow rudder produces decidedly inferior steering action with the ship going ahead. Bow rudders are fitted, therefore, primarily on vessels required to back for appreciable distances. Under these conditions, the bow rudder becomes a stern steering rudder, in the normal sense of the term.

If it were sufficiently important to pay for the additional complication and the added steersman, a bow rudder might justify itself on a long, fast, slender craft, operating in shallow and restricted waters. With such a rudder it might be possible to move the ship sideways, or to hold it against wind and other effects. It would act in this case much as the bow planes on a submarine; in other words, not as a turning mechanism but as a transverse-force-producing device.

The bow rudder, as a rule, has no induced velocity to augment its effect, but neither does it suffer from a reduced speed of advance because of friction wake.

The fitting of a bow rudder requires a forefoot that is rather full in profile and thin in section. There is little to be gained by mounting the stock

in the forward portion of the rudder. Usually there is not adequate room for the stock and its bearings if this is done. The hull is so thick at the after end of the aperture that it is not possible to take advantage of a balance portion abaft the stock, where the flow would be very disturbed. The customary solution is to mount the stock at the extreme after end, with or without a pintle and bearing at the keel level. A rudder of this type is shown by G. de Rooij ["Practical Shipbuilding," 1953, Fig. 495, p. 203].

74.21 General Design Rules for Bow and Stern Diving Planes. Bow and stern diving planes on submarines suffer from certain design limitations which should be but are not yet overcome:

(a) The bow planes, almost invariably required to rig in or house within the fair hull lines, are not easily supported when given great span and a large aspect ratio. Furthermore, their inner ends can rarely lie close against the hull, with a small gap throughout the complete range of rise and dive angles.
(b) The port and starboard stern planes, placed across the propeller-outflow jet(s), can almost never lie with their inner ends close against the hull, or close to each other, principally because of the triangular gap necessary to swing the steering rudder between them. It, too, must lie within or close to the outflow jet(s).
(c) To produce the maximum possible vertical forces for a given weight and size of installation the planes are often worked far beyond the normal breakdown range of a symmetrical hydrofoil.

An effective compromise to meet all these conditions calls for an aspect ratio of approximately 1.0, with no cantilever or image effect. In other words, the diving planes are made roughly square in planform. It is assumed that they do not benefit in lift by being close to the hull or to some large vertical surface.

The non-housing diving planes of a submarine are so near the surface, when the vessel is not awash or submerged, that in a heavy sea they are subject to severe impact in the form of wave slap. This applies to both bow and stern planes. A good design requirement, admittedly formulated on a not-too-scientific basis, is that these planes shall withstand as a working load an impact pressure of 1,000 lb per ft^2 over their entire horizontal area.

A somewhat similar but possibly less drastic requirement could be imposed on rudder installations in which any part of the rudder rises above the water surface during wavegoing.

74.22 Contra-Features for Diving Planes. Whether placed in the outflow jets of propellers or not the diving planes of submarines rarely work in flows that are symmetrical about the mean plane of the blades. First, the flow in any vertical plane is rarely symmetrical with respect to the submarine axis. Second, it is rarely possible to locate the diving planes in symmetrical positions relative to that axis. The flow at any plane position usually has some vertical component of velocity. The neutral plane angle must be adjusted accordingly or the leading edge of the plane must be bent or twisted to point into the direction of flow. This bending, similar to that at the leading edge of a contra-rudder, prevents the center of pressure from lying too far forward of the plane axis.

A pair of diving planes, placed in a symmetrical position abaft the propeller of a single-screw submarine and twisted, contra-fashion, serves to:

(1) Recover rotational energy in the outflow jet and convert it to useful thrust
(2) Compensate partly for the unbalanced reaction exerted by the submarine propelling plant, in the manner described by Sec. 73.21.

74.23 Setting Neutral Control-Surface Angles. When rudders are offset from the vertical plane of symmetry, either as parts of single-rudder or multiple-rudder installations, the water almost never flows past them in a direction parallel to that plane, with the ship moving straight ahead at a steady speed. To achieve equal turning effects, right and left, with equal amounts of right and left rudder angle, each rudder must be placed carefully at zero angle in its neutral position. This adjustment is made for the condition when the propulsion devices are working; all other conditions are assumed to be normal.

The neutral position is determined with relative ease in a self-propelled model test by any one of several methods. However, if there is a possibility either of laminar flow or of separation on the rudder, due to its form or to the shape of the hull in the vicinity, there may be some scale effect, because of unexpected shifts in the transition or separation points. If so, the model predictions are uncertain when applied to the ship.

It is difficult if not impossible to determine

neutral rudder positions on a full-scale vessel. The friction forces in the steering gear and rudder stock are large in proportion to the hydrodynamic torque on the stock at small rudder angles. The torques due to friction may even exceed those due to water flow around the rudder. Furthermore, unless it is known definitely that the rudder will trail if left to itself, one is reluctant to disconnect the tiller or bypass the steering gear with the vessel traveling at the speed for which the correct neutral position is required.

It oftens happens that a neutral position which gives zero torque on the stock of an offset rudder is not the one which results in minimum resistance or shaft power. Either the ship designer or the owner and operator must then decide whether the neutral setting is to be for minimum rudder torque or minimum overall resistance.

For multiple rudders operated by a single steering gear, with tillers connected by drag links, it is sometimes possible to fit a temporary link for the early sea trials and to replace it by a permanent link having the proper length.

74.24 Selection of Swinging Propellers for Steering and Maneuvering. Swinging propellers, described in Sec. 37.22, form perhaps the simplest and most efficient of steering and maneuvering devices. In fact, any propeller, large or small, driven through the medium of a shaft that is approximately vertical, lends itself admirably to this means of steering. The complete propeller thrust, albeit somewhat modified by a large degree of non-axial flow when the propeller is first swung to a large angle, remains available as an oblique force. A large force component normal to the ship axis serves as the equivalent of the transverse force which would otherwise be exerted by a rudder. The mechanical steering mechanism for a large or high-powered installation must be non-overhauling, otherwise the torque reaction from the vertical shaft takes charge and swings the propeller when steering or turning is not desired.

Efficient propulsion, combined with the swinging motion of the horizontal shaft and the propeller, require that the inflow jet of water to the angled propeller does not encounter undue interference from parts of the hull ahead of it. Unless the speed of advance is small the axis of the inflow jet follows the predominant flow in the vicinity instead of the angled propeller axis.

If the vertical drive shaft and its housing do not project from underneath a portion of the stern which is continually submerged, a horizontal subsurface plate is required on the housing at some point below the water surface to prevent leakage of air from the atmosphere to the propeller. A so-called "anti-cavitation" plate of this kind, although usually much too small, is embodied in the vertical-shaft housings of all outboard-motor installations.

If the propeller disc lies entirely below the keel, a steering propeller lends itself to use as a tractor propeller at the bow. It may operate either singly or in combination with one or more other steering propellers at the stern. A bow steering propeller, however, is rarely able to take advantage of any wake velocity due either to viscous or potential flow. Instead of swinging aft and upward, like an outboard motor installation when shallow water is suddenly encountered, it must usually swing outward and upward.

For auxiliary propulsion as well as steering there is available the so-called "active" or Pleuger rudder developed in the early 1950's in Germany [Hansa, 16 Jul 1952, Vol. 89, p. 918; also p. 921]. This device, comprising a submersible electric motor driving an auxiliary propeller and swinging about a vertical axis like a rudder, is described at some length in Sec. 37.22. At the time of writing (1955) it is available in limited powers only, not exceeding several hundred horses.

CHAPTER 75

The Problem of Hull Smoothness and Fairing

75.1 General Considerations; Definitions. Smoothness as related to hydrodynamics is a physical characteristic of the underwater surfaces of a vessel, regardless of the size, configuration, or location of those surfaces. It applies to the hull, the propulsion devices, the control surfaces, and all appendages, hence is properly considered as a general item applicable to all the external ship elements. Fairing, fillets, transition pieces, fillers, and their equivalents likewise apply to all the external ship elements, hence it is appropriate to consider them here as a class.

Smoothness, as used in this chapter, denotes the absence of small irregularities of the kind associated with rough or flaked paint coatings, rust, pits, rivet points, and welding beads. It indicates also that a surface has the proper curvature and that it is free of waviness such as is often encountered at and between internal frames or stiffening members. It takes for granted the structural discontinuities inherent in the use of lapped seams and butts, raised strakes, doublers, and other irregularities involved in applying the shell plating in relatively small pieces. *Fairing,* aside from its frequent use as a general term, applies principally to portions of generous radius, expressed in multiples of the shell-plating thickness, worked into or applied to various parts to insure easy water flow around them. *Fillets* are defined as the roundings worked into coves or internal corners or castings, weldments, and other structural members, as well as the transition pieces added to bridge gaps and discontinuities in the hull and its appendages.

In general, smoothness is sought and required in an effort to avoid unnecessary power losses due to excess friction resistance. Its possible effect in reducing underwater noise is not discussed here, although that may become a factor in fishing and other operations of the future.

Fairings, fillets, and fillers are applied primarily to avoid high dynamic pressures, cavitation, or separation. In some cases these discontinuities in the flow create undesirable disturbances ahead of propulsion devices and control surfaces. In almost every case the occurrence of high Δp's, separation, or cavitation increases the drag of the appendage. It is pointed out elsewhere that the added drag at each appendage may be insignificant compared to the total drag of the ship. Nevertheless, the cumulative effect may be considerable, sufficient to neutralize the improvement gained from some special design of hull or propulsion device.

The increased drags due to dynamic pressure, cavitation, and separation are pressure effects and as such vary as the square of the relative velocity of water flow. The effects of inadequate fairing and filleting therefore increase rapidly with the speed of the vessel. What may be accepted as a negligible increment of pressure drag on a slow or medium-speed cargo vessel for the sake of economy of construction becomes a matter of inefficient propulsion on a high-speed liner, where an increment of first cost is easily justified by a saving in fuel over many years of operation.

75.2 The Importance of Smoothness and Fairing. Nature goes to considerable pains to work fairings into many of her creatures. Man can hardly do less if he is far-sighted and looking for improvements. A close study of many natural structures reveals the hitherto little-recognized

fact that many fairings are indeed not excrescences but parts of the structure and important parts at that. A tree is so shaped just above its point of attachment to the ground that the stresses in the wood of its trunk are very nearly constant with height when the tree bends with the wind as a cantilever beam. This is almost identical with the most modern type of fairing at the roots of screw-propeller blades, employing a constant-stress transition shape where the blades join the hub. The fairing of the afterbody of a whale or a porpoise into its horizontal flukes is an admirable combination of hydrodynamic streamlining, rapid and effective change of cross-section area and shape, arrangement of muscles for manipulating the flukes as propulsion devices, and muscular flexing of the flukes as control surfaces.

Plates bounding the ship hull are intended to be flat or gently curved, as the case may be, when they are incorporated in the design and delineated on the drawings. Only rarely is any unfairness allowed for when calculating the strength or the rigidity of a ship structure. Why, then, does the ship not deserve equally honest treatment when it is built? Even the uninitiated realize instinctively that the underwater hull of a vessel must be fair to insure efficient propulsion. Why then should the vessel be penalized throughout its life because of unfairness resulting from a few days of improper work during its construction? Increases in friction resistance due to roughness, of the order of 30, 40, 50, and up to 100 per cent of the smooth, flat-plate R_F , are being encountered on large, fast, modern vessels. This fact should be adequate proof that something drastic needs to be done. Fairness and smoothness are essential parts of a ship. An attitude on the part of all concerned which recognizes that these are not something to be applied, like a coat of paint, just prior to launching will go far toward solving this problem for the designer.

75.3 Specific Smoothness Problems on the Shell Plating. In the matter of the greatest practicable smoothness of the shell in the finished ship, at least four areas deserve attention:

(1) The extreme bow, and a belt abaft it, up to say 0.2 or 0.3L from the FP. This is because the local specific friction resistance C_{LF} is very high for the small x-distance and the low R_x in this region, indicated by Fig. 45.E.

(2) The region directly in front of inlet scoops for condensers and other heat exchangers, so that the relative liquid velocities in the inner portions of the boundary layers will be high. This applies to a belt about 2 or 3 times the inlet width and perhaps 10 times its length.

(3) The afterbody, say from about 0.6 to 0.7L to the extreme stern. Fig. 75.A is an adaptation of

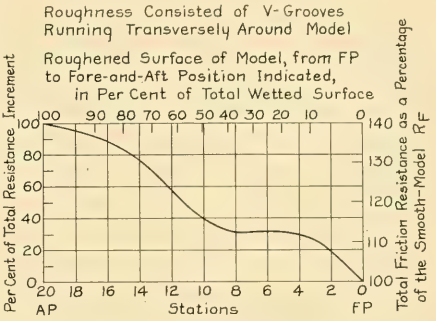

Fig. 75.A Variation of Friction Drag Due to Roughness Along the Ship Length

model-test data published by G. Kempf [HSPA, 1932, Fig. 7, p. 81], indicating the variation of friction-resistance augment, up to 140 per cent of the smooth, flat-plate total, when a model was roughened by cutting V-grooves around it for various percentages of its length.

(4) The region immediately ahead (within 1 or 2 diameters) of a propulsion device, when the water leaving this surface flows directly into the device

(5) The examples of Sec. 45.15 indicate that the greater the absolute speed of the ship, the smaller is the permissible roughness to achieve a hydrodynamically smooth surface.

The foregoing states, in effect, that the only part of the hull which need not be smooth is that around amidships. However, if any favoring is possible, or practicable, it is well to know where attention to smoothing is most worth while. These comments apply equally, if not primarily, to structural roughnesses, many of which can be prevented or eliminated in the design and drafting stage.

The rounded or peaked points of countersunk rivets should project from the fair outer surface of the shell by not more than the amounts indicated in diagrams 1 and 2 of Fig. 75.B. This is sufficient to insure tight rivets and to allow for reasonable corrosion of the point in service. Welding beads, regardless of their orientation

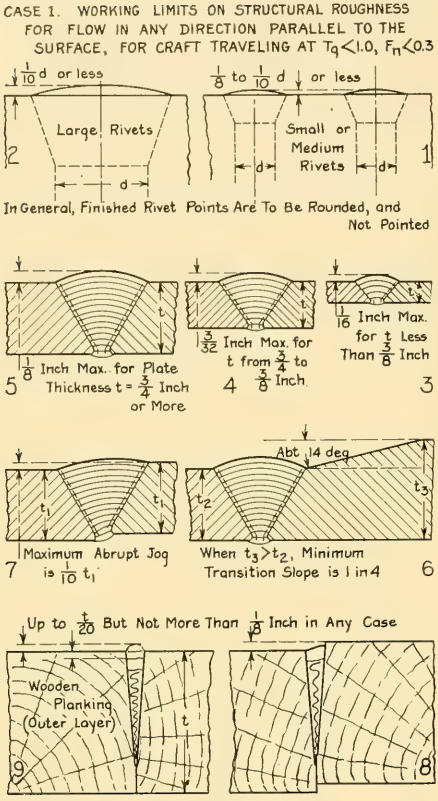

FIG. 75.B WORKING LIMITS ON STRUCTURAL ROUGHNESS, FLOW PARALLEL TO THE SURFACE, CASE 1

with respect to the prevailing flow, should not project from the fair surface by more than the limits indicated in diagrams 3, 4, and 5 of Fig. 75.B.

When prefabricated sections of a ship are welded together, they are found sometimes not to fit properly. The alignment at the shell, considering smoothness only and not structural continuity, should conform to the limits indicated in diagram 7 of the figure. When the abutting plates are of unequal thickness, and the excess is on the outside, the length of the transition taper is to be not less than 4 and preferably 6 times the difference in thickness; see diagram 6 of Fig. 75.B. Corresponding smoothness and offset limits for the adjacent planks and the calking of wooden boats are depicted in diagrams 8 and 9.

If riveted butts normal to the flow are to be lapped, the exposed plate edges should face forward on slow-speed ships. Here the separation drag abaft plate edges facing aft is greater than the dynamic-pressure drag against edges facing forward. When faced forward the exposed plate edges are to be chamfered as indicated at 1 in Fig. 75.C.

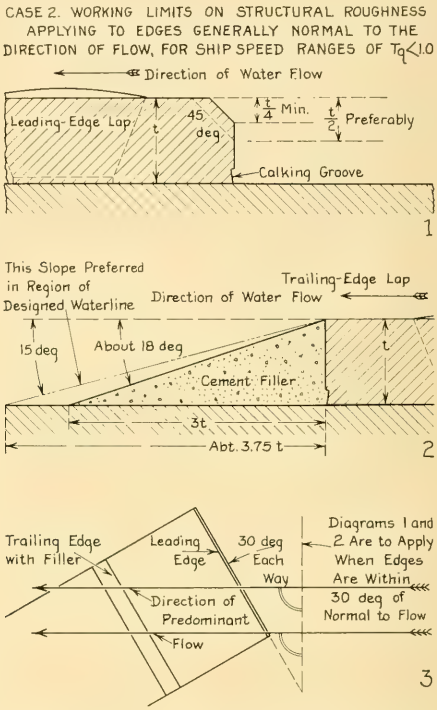

FIG. 75.C WORKING LIMITS ON STRUCTURAL ROUGHNESS, CASE 2

For ships of higher speed, with limits as yet undetermined, the pressure drag on forward edges exceeds the separation drag on after surfaces. In this case, the exposed edges are best faced aft. If a reasonable degree of smoothness is also required, a cement filler or a rivet cement is applied in the region abaft the exposed trailing edge, diagrammed at 2 in Fig. 75.C.

An exposed plate edge is considered "transverse" if it lies within 30 deg of a line normal to the adjacent water flow, indicated at 3 in the figure. In some quarters, however, chamfering

and filling of exposed edges is called for if they lie within 70 deg of the normal to the flow.

In fact, it is good design, and probably worth while from the point of view of fuel saving during the life of a vessel, to chamfer exposed corners or to add filler along exposed edges, indicated in Fig. 75.D, even though these edges lie generally

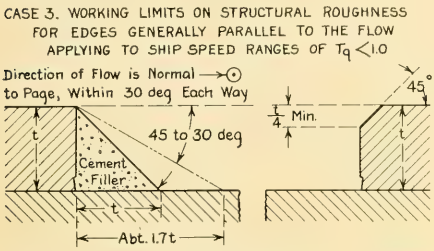

Fig. 75.D Working Limits on Structural Roughness, Case 3

parallel to the flow. The exact flow directions all over a ship surface are not known too well, despite the advances of recent years in the techniques of observing and recording flow around a model. The pitching, rolling, and heaving motions of a ship in waves, even though not violent, add motion components which change the flow directions relative to the ship surface.

This is not the place to discuss the matter of applying shell plates on a metal ship to produce a hull surface that is fair and without waviness, as contemplated by the lines drawing. It is a proper design procedure, however, to emphasize the necessity for accomplishing this if the construction phases of shipbuilding are to keep pace with the design phases.

Riveted flush seams and butts, with a single strap inside, lack the rigidity and the reliability of lapped riveted joints, despite the lack of symmetry of both, because of the stretchable butt strap in between. Sad experiences with oil leakage in the single-strapped butts of the bottoms of numerous vessels proves that this method of achieving external smoothness is structurally unsound. The remedy for it in riveted construction, namely double butt straps, is structurally good but hydrodynamically "unsmooth." Welded butts are the real answer, especially for large, high-powered, or important vessels which run at T_q values in excess of 1.0, and of which a high propulsive performance is demanded.

On yachts, where glistening appearance may be a more important factor than easy water flow, and where expense is usually not an item to be considered, the outer surfaces of metal hulls are often freed of their projections by hand grinding. The depressions are then leveled and the whole surface given a high degree of fairness by troweling on a cement or filler which adheres firmly to the metal for long periods without repair or attention. On certain large ships the coves associated with riveted lapped seams and butts have been filled by applying the same type of cement. The filler is tapered off to zero thickness at a distance from the cove equal to 4 or 5 plate thicknesses, somewhat as shown in Figs. 75.C and 75.D. This filler is heavier than water so that the additional displacement volume of the filled coves is less than the corresponding weight. In other words, the filler does not carry its own weight. The extra displacement weight, coupled with the extra expense, possibly may be justified only in a ship running at a T_q greater than about 1.0 or 1.1, $F_n > 0.3$ or 0.33, or in case there is only a small margin of power for a specified minimum speed.

Unfortunately, the smoothest metal shell surface can be well-nigh ruined by the application of poor anticorrosive or antifouling coatings. When the antifouling coating contains a self-leveling agent like varnish or enamel, and when this dries hard, the minor projections are minimized by the self-smoothing action of the coating around them. This thins the freely flowing material over the projections and thickens it over the hollows.

For the reasons explained in Sec. 5.21, the roughnesses which project through the laminar sublayer are primarily responsible for the roughness drag. The laminar sublayer thickness δ_L(delta) is, as indicated by the formulas of Fig. 5.R and those of Sec. 45.10 on pages 104–105 of the present volume, a function of the kinematic viscosity ν(nu) of the water, of the x-distance from the bow of the ship, and of the speed V of the ship. This speed, or the relative velocity U_∞ of the undisturbed water, is by far the most important factor. It is the reason why rough or gravelly surfaces on large, fast ships generate large friction resistances, even when the roughness heights are minute with respect to the ship size.

The ABC ship under design in this part of the book is in what may be called the fast-speed class, with a Taylor quotient T_q of 0.908 and an F_n of about 0.27. It is worth while, therefore, to eliminate all irregularities in the plating which come into

contact with the water during normal running. This calls for all underwater butts to be flush. All seams, if lapped and riveted, are to be as nearly as practicable parallel to the lines of flow in their respective regions. This is especially the case in the leading 0.2 or 0.3 of the length and in the after half or two-thirds of the run. If this can not be accomplished the seams in these regions, lying at angles greater than about 30 deg to the flow, should be faired with a suitable filler compound as described earlier in this section. In fact, for the leading 0.2 of the length, flush welded plating throughout promises the best possible service performance.

75.4 The Utilization of Casting or Welding Fillets. The working of generous fillets into the coves or inside corners of castings for hull components is almost mandatory as a matter of good foundry practice. Furthermore, many inside corners occur where thin sections meet heavy sections. Proper gradation in the distribution of material calls for transition regions that are improved by the use of large-radius corners. Four pairs of corners filleted in this manner are shown around the strut hub in Fig. 73.F.

When large appendages and structural parts which form a portion of the outer hull are made up as weldments, good design precludes the use of masses of welding beads in inside corners. Certainly not enough beads can be added to produce the equivalent of the generous-radius fillets in a large casting. If fillets in weldments are really necessary, for hydrodynamic reasons, they should be worked into the adjacent structural parts, more or less independent of the welding. It may be necessary either to machine the fillets into the weldment or to modify the design so that excessive weld metal need not be deposited. An example of this design is illustrated in Fig. 73.F, where stubs for attaching the strut arms are incorporated in the strut-hub casting. The fillets are cast integral with the stub arms and the hub.

75.5 Inside Corners Requiring Negligible Fillets. As background information for the design features discussed in this section, the principal characteristics of flow about longitudinal discontinuities are described in Secs. 8.2, 27.8, and 28.2, particularly that encountered around long chines and coves. It is not possible to assess quantitatively the effect of these longitudinal discontinuities by any method yet developed, or to give design rules with numbers.

When flow takes place past two fixed intersecting surfaces with a reentrant angle not less than about 80 deg, *and* the flow is generally parallel to the intersection of these surfaces, no fillet is required, for hydrodynamic reasons at least, along the cove thus formed. The water in this case does its own fairing, explained in Sec. 6.7 and illustrated in diagram B of Fig. 6.D. Common examples of intersections of this type are to be found where shaft struts enter the hull, diagrammed in Fig. 36.B for a pair of V-struts and in Fig. 73.F for the ABC arch-stern ship. Similar intersections occur where small skegs, horns, and the like project below the main hull. A not-so-common example, but one of much greater size, is the long right-angled cove formed where a large deck erection, such as a conning-tower fairwater, rises from the flat superstructure or upper deck of a submarine. The longest and the most common pair of coves are those to be found alongside a single-plate type of roll-resisting keel. Both reentrant angles are of the order of 90 deg, yet the sharp cove at the intersection with the hull appears not to develop excess resistance or to interfere with the keel performance.

For reentrant angles of less than 80 deg, good design is a matter partly of judgment and partly of circumstances. There is a blocking effect at the inside corner, and this effect increases rapidly as the acute angle becomes smaller. On the one hand, the water can do its own blocking and slowing down. On the other, a fairing can be added to the inside corner, *provided* the leading and trailing ends of the fairing can themselves be faired.

In the case of movable appendages attached to or projecting from a hull, such as rudders fitting close under the stern, or diving planes with small hull clearances, it is not practicable, nor is it necessary, to fit fairings. A similar case is that of the retractable sound dome which, when in use, is lowered bodily below the keel of a ship through a hole only slightly larger than the planform of the dome. If no separation or eddying is to be expected abreast or behind the dome, there is no particular need for fairing the 90-deg inside corner where the dome meets the hull. Taking account of the variation in translational velocity under the keel, due to the boundary layer, does not change the situation or require any means of improving the flow along the inside corners.

75.6 The Fairing of Appendages in General. Supplementing the foregoing, there are given here a few design notes applicable to the fairing

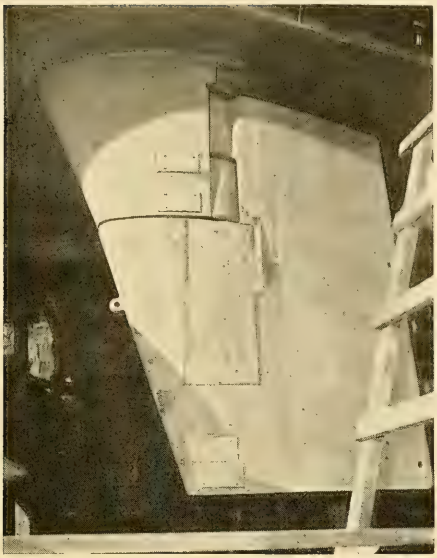

Fig. 75.E Roughnesses and Discontinuities on a Rudder Horn and Rudder

of appendages in general. Specific problems are discussed in the sections following.

There is no excuse, from the point of view of hydrodynamics and propulsion, and little reason from the structural standpoint, for fitting external strut-arm pads with their bases projecting beyond the fair surface of the ship. This is especially true in an age which is blessed with welding and other improved methods of attaching structural parts to each other. At times the pads must be mounted external to the shell, as on some wooden vessels. The projecting edges are then relieved with a large radius on the forward edge and along the sides, supplemented by a long taper on the after side of the pad.

There appears to be no more excuse for leaving exposed the heads and nuts of bolts connecting the palms of rudder stocks and rudders, considering the infrequency with which they are disturbed or removed. Certainly it is incongruous to smooth and fair everything else in the vicinity but to leave a half-dozen or dozen of these sharp-cornered fastenings projecting into the flow [SBSR, 27 May 1954, p. 10 of Advt]. In the same fashion it is inconsistent to shape a strut or a rudder section to some very special streamlined form and then to plaster it with thick plates of zinc which must make the water wonder what the naval architect or shipbuilder expects of it. Fig. 75.E is a good illustration of what not to do in the way of roughening the surface of a horn and a rudder lying in the outflow jet of a propeller.

75.7 Recessed Lifting and Mooring Fittings. It is frequently the practice to apply a veritable multitude of external padeyes, clips with lifting eyes, and eyebolts to the shell plating in the run. These permit the easy and quick attachment of lifting devices and tackle for the handling of propeller blades, rudders, exposed shafts, and other demountable underwater parts when in dock. The practice is by no means limited to small vessels, or to those of slow and medium speed. Many, if not most of the fittings are under water at the designed-load draft, particularly when the stern-wave crest is taken into account. Individually, the pressure drag resulting from each of these fittings is small, but collectively they present a formidable impediment to the motion of the ship. Furthermore, many of them throw spray when underway. They give anything but a neat, trim appearance to a run which is supposed to embody everything that the naval architect and the shipbuilder have learned about streamlining in the past several decades.

The handling of aircraft on flight decks that must remain smooth, and the tight fits of air-

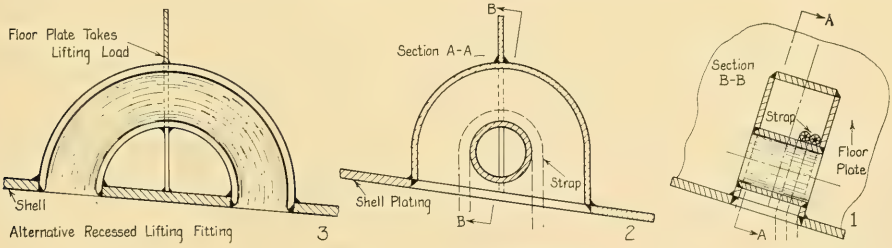

Fig. 75.F Recessed Lifting Fittings

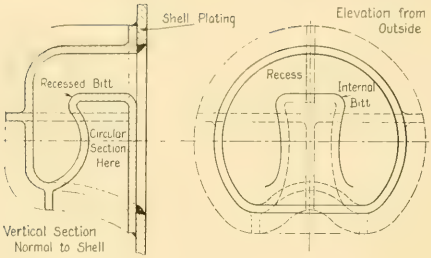

Fig. 75.G Recessed Mooring Bitt

craft-carrier hulls in canal locks have led to the development of a number of recessed fittings for lashing, lifting, and mooring. Two types of simple, welded, recessed lifting fittings are diagrammed in Fig. 75.F, adaptable to any position or slope of shell plating. A single recessed bitt or Dutch dolphin is depicted in Fig. 75.G. A strap is easily passed through the lifting fittings and an eye is quickly thrown over or lifted off the bitt. While designed as an abovewater installation this dolphin may be used in positions which are under water at some load conditions.

75.8 Fairing the Enlargements Around Exposed Propeller Shafts. The hubs of shaft struts, the external or exposed couplings of the propeller shafts passing through them, and the hubs of the propellers carried by these shafts require fairings as units. In other words, the leading fairing, the enlarged strut-hub body, the propeller hub, and the trailing fairing are treated as parts of a single body. They should, theoretically, form a continuous streamlined surface for a considerable length along the shaft axis. One solution for the fairing of such an assembly is represented by the design of these parts on the wing shafts of the World War II German cruiser *Prinz Eugen*, illustrated in Fig. 75.H. The fact that the maximum diameter of the integrated fairing combination is considerably larger than that of the strut hub is not to be taken as an indication of good or recommended design. This shape was adopted for many German men-of-war of the 1930's and 1940's. Its use can be justified, at least partly, by the following line of reasoning.

The best flow to the root sections of the blades of a screw propeller, where the interference effects are large and uniform flow is a useful factor, is obtained when the structure surrounding the propeller shaft bearing and the strut hub is absolutely fair for a rather long distance ahead of the propeller hub. This requirement is met in the assembly drawn at 1 in Fig. 75.H. Not the least important part of this continuous fair form is the easy curve at the forward end, where the diameter of the assembly has to increase from the diameter of the shaft to one nearly three times as large. The slight decrease in diameter from the forward end of the assembly back through the propeller hub conforms to the pattern of the flow lines in the inflow jet and contributes a slight inward component of velocity which partly compensates for the centrifugal force due to induced rotation in the jet at the propeller. When a propeller is located abaft a large skeg or long bossing this reduction of radius through the propeller hub is a natural consequence of the tapering form of the skeg or bossing. It is natural in cases of this kind to give the propeller blades a reasonable amount of rake but the designer of the *Prinz Eugen* propellers did not see fit to do so.

Good design for minimum resistance and easy water flow calls for the use of curved profiles from leading to trailing edge of this or an equivalent assembly. There should be no sharp discontinuities such as are sometimes encountered when the leading fairing in front of a cylindrical strut hub is made of straight conical form. If such an assembly can be expected to remain completely submerged under all except the most severe pitching conditions in waves, the maximum diameter may be at the propeller hub. If a large diameter is not required there for other reasons it may be in the strut hub, as in the German design illustrated. Manifestly, the farther aft

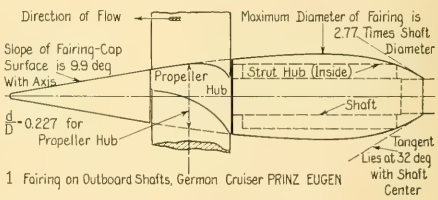

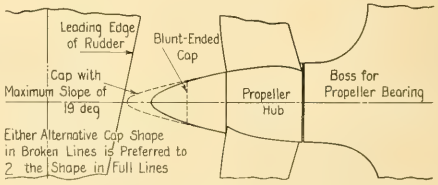

Fig. 75.H Fairings for Strut and Propeller Hubs

that this maximum diameter occurs in the assembly the greater must be the slope of the fairing abaft it, unless a blunt-ended cap is used.

For high-speed ships, a propeller hub fairing long enough to eliminate entirely the swirl core described in Sec. 23.14 and illustrated in Fig. 23.K would probably have to extend for one or more propeller diameters abaft the hub. This is on the basis that the core is generated entirely by the water set in rotation by friction around the hub. In practice, such an appendage is out of the question, especially as the propeller hub fairing must also clear any rudder placed in the outflow jet. There are two compromises available here. One is to give the profile of the propeller hub fairing a range of slope angles from about 15 deg to a maximum of about 22 deg, terminating the fairing in an ogival form having a radius of about 0.1 the radius of its larger end. Variations of such a form are drawn in full and broken lines at 2 in Fig. 75.H. The other compromise, on the basis that the swirl core is in reality the combined vortex of the several blade-root vortexes, is to terminate the fairing in a square end at about 0.7 to 0.5 the propeller hub diameter d. This is also shown on Fig. 75.H.

Further comments on propeller-hub fairings and caps are given in Sec. 70.14.

Exposed sleeve-type couplings on a propeller shaft are partly faired by trimming off the ends of the sleeves themselves. This has the added advantage of a gradual transition in the combined rigidity of the sleeve and the shaft. The result is a stress concentration in the shaft of diminished magnitude at the ends of the sleeve.

A flange-type shaft coupling exposed to the water all around may be enclosed in a substantial casing of fair form, about as illustrated in Figs. 73.H and 74.L. If the fairing rotates with the shaft as in the latter figure, it may be filled with wax or other preservative to protect the mechanical parts of the coupling. If it is stationary, as in Fig. 73.H, it can be "pointed" slightly on the upstream side and given a streamlined tail of sorts on the downstream side, following the general shape of the short bossing diagrammed in that figure. So far as known, it makes little hydrodynamic difference whether the transition from the stationary to the rotating parts, and vice versa, occurs in a parallel or cylindrical portion of the enlargement, or at its beginning or ending, next to the shaft surface. Gaps required for working clearances between fixed fairings and rotating shafts need not be large and these discontinuities need have no detrimental effects.

The ends of non-ferrous journal sleeves shrunk onto steel shafts generally lie within other fairings. If not, they may abut rubber or other protective coverings around the portion of the shaft which would otherwise be exposed to sea water. In any case they are relatively thin and need little or no fairing of their own.

The fairing of intermediate strut hubs follows the general lines suggested in other paragraphs of this section, as does the fairing of propeller hubs abaft skegs or bossings.

Water-lubricated shaft bearings require a continual longitudinal circulation of liquid through the bearing when the ship is underway. An opening around a rotating shaft and just inside a fixed leading-edge fairing of oval or ogival shape is in a region of $+\Delta p$, sufficient to force the water through. Any $-\Delta p$ occurring abaft a trailing fairwater helps to draw water aft through the bearing. The fairing ahead of a shaft-bearing hub may rotate with the shaft, as does the propeller hub of the arch-stern ABC ship in Fig. 74.L. A bell-mouthed strip around the bearing hub, shown in that figure, then serves as a scoop for the lubricating and cooling water. A hole in the center of the fixed fairing abaft the bearing hub serves to draw the water out of the after end.

75.9 The Fairing of Propeller Hubs in Front of Simple or Compound Rudders. For a propeller placed immediately ahead of a simple or compound-type rudder, or ahead of a rudder hung on a fixed rudder post, the propeller hub is faired neatly by a swelling of the fixed portion, by a projection extending forward from the post, or by both. A rudder of the balanced type, with its stock axis intersecting or lying close to the propeller shaft axis, can be notched moderately on its forward edge, cutting into the balance portion, to provide clearance for a conical or ogival propeller fairing cap of reasonable length.

One form of fixed fairing for a propeller hub, easily worked into a deep horn or into the fixed portion of a compound-type rudder, is embodied in the transom-stern design of the ABC ship, illustrated in Figs. 66.Q, 67.U, 74.K, and 74.N. Rope and cable guards to protect the opening between the rotating propeller hub and the fixed fairing, as well as removable sections of the latter to facilitate taking off the propeller shaft nut and the propeller, are readily incorporated in a fixed fairing of this type.

When the propeller shaft bearing is placed *abaft* the propeller, as is done on many high-speed motorboats and on the arch-stern design of the ABC ship, this bearing may be carried by a partial skeg, a deep horn, or a fixed rudder post, extending down abaft the wheel. The rudder is usually mounted as a hinged flap along its after edge. The fairing assembly is then composed of the following parts, reckoned from forward:

(1) Leading fairing, rotating with the shaft and the propeller hub
(2) Propeller hub
(3) Propeller shaft bearing housing with rope guard and water scoop on leading end
(4) Fairing for bearing housing, which may extend aft into the flap or moving portion of the rudder.

On the ABC ship, with twin rudders, a fixed fairing is mounted abaft the strut barrel or hub supporting the propeller bearing, indicated in Fig. 74.L.

75.10 The Fairing of Exposed Shafts at Emergence Points. Exposed shafts which emerge, as do most of them, at small angles with the adjacent hull surface represent a problem in fairing. The simplest and the cheapest method is to omit the fairing altogether, build a watertight recess within the hull, up to the after stern-tube bearing, and pass the rotating shaft out through a clearance hole in the shell plating.

A reasonable amount of fairing, with no increase in displacement volume and little added cost and weight, is achieved by adding a pair of removable shaped plates to enclose a free-flooding space between the hull and the shaft. These extend for a short distance abaft the hull opening, indicated at 1 in Fig. 75.I. If there is no enlargement or flange on the shaft which must be drawn past the fairing, the complication of bolting on a non-watertight fairing which must be removed frequently for examination of the hull underneath is obviated by extending the framing locally and incorporating the fairing plate into the shell proper, in the manner shown at 2 in Fig. 75.I. On a large or medium-size vessel the free-flooding

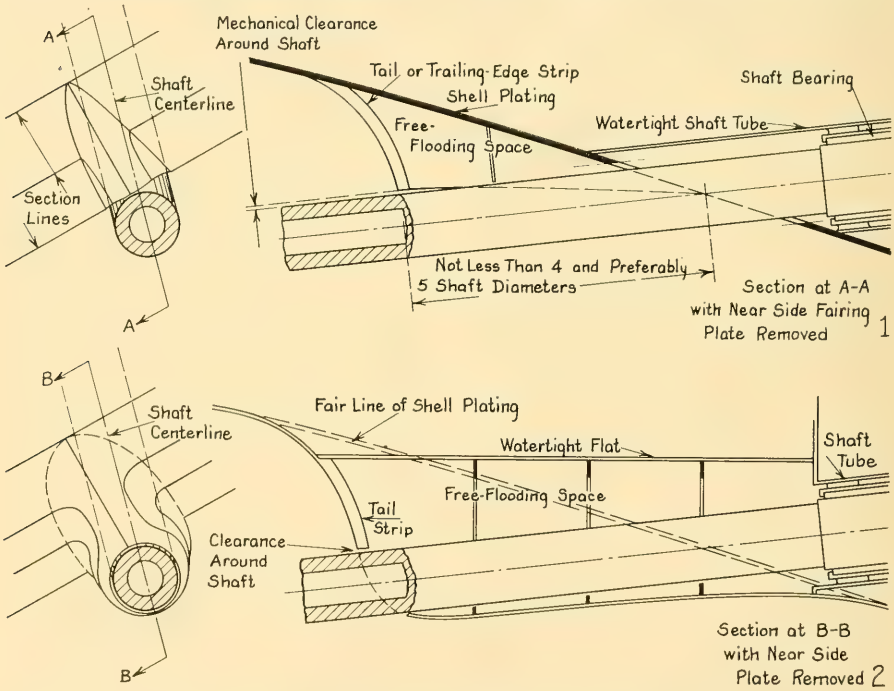

Fig. 75.I Two Types of Hull Fairing Around Exposed Propeller Shafts

space is inspected by entering the hole through which the shaft is withdrawn.

The best method of fairing at this point, and one which may eliminate an intermediate strut otherwise required, is to build a short bossing out from the hull, terminating in a single-arm strut member carrying a shaft bearing. An excellent fairing of this type was incorporated in the Bath-designed World War I destroyers of the U. S. Navy. Despite the small clearances around the shaft tube within the ship, it is preferable that a short bossing of this type be made completely watertight and an integral part of the hull.

Design notes and rules covering these short bossings are given in Sec. 73.9.

75.11 The Termination of Skegs and Bossings. The endings of short skegs and short bossings are subject to separation drag if the slopes of the surfaces of these appendages exceed certain angles *with the flowlines*. So far as known, the critical values of these angles depend primarily upon the hydrostatic pressure. They are of the order of 13 to 14 deg at the surface and perhaps 20 deg at a submergence depth of 20 ft or more; see also Sec. 46.2.

The terminations of deep skegs on single-screw vessels, of large skegs on multiple-screw vessels, and of long bossings usually lie immediately ahead of the propellers. Their terminations must be fine else the eddying and other disturbances created behind them are carried directly into the propeller discs without an opportunity for smoothing out the flow. The square, blunt sternposts of cheaply built cargo vessels are particular offenders in this respect, despite the slow speed of both the ship and the propeller. Indeed, it is only because of this slow speed that unfair surfaces of this kind can be tolerated.

The flexibility afforded by modern knowledge and techniques in the casting of structural members or in the assembly of these members as weldments makes available to the ship designer a ready means of fining the terminations of skegs and bossings. Indeed, a shining example of excellent bossing terminations, even by modern standards, was designed and built into the S.S. *Talamanca* class by the Newport News shipyard in about 1930. Fig. 73.G is traced from some of the Newport News drawings, with the permission of the Newport News Shipbuilding and Dry Dock Company.

Sufficient rigidity can rarely be incorporated in a heavy terminal member to prevent lateral deflection or vibration of a large skeg or bossing. Since the adjacent shell plating and the framing contribute a large portion of the actual rigidity there is no reason why their scantlings can not be increased to permit fining of the skeg or bossing ending as required for easy flow into the propeller position. Actually, the optimum solution of this particular design problem is *not* necessarily to stiffen the structure unduly but to shape it in such a manner that the periodic and transient forces acting upon it are diminished.

The matter of shaping the endings of skegs and bossings in profile to provide the necessary aperture clearances is discussed in Secs. 67.23 and 67.24.

75.12 Precautions Against Air Entrainment. The phenomenon of air entrainment and its detrimental effects are discussed in Sec. 20.10. This section mentions methods of eliminating the formation and the trapping of air bubbles around the underwater hull, as well as they are known in the present state of the art.

The most direct cause of trouble on a merchant ship is the multitude of air bubbles which pass over the shell diaphragm of a fathometer or echo-sounder, usually installed in a horizontal position under the bottom. The bubbles interfere with the sonic pressure waves emanating from and impinging upon such a diaphragm so that depth readings are not satisfactory. For smooth-water operation at deep or load draft the best position for such a diaphragm is well forward, say in the first 0.1 or 0.15 of the length. This is ahead of the point where the flowlines from the stem, in the vicinity of the bow-wave crest, pass down under the ship. The flow diagrams of Chap. 52 illustrate this feature for a great variety of hull shapes. For operation in waves, especially when the forefoot emerges, or for operation in ballast or light-load condition, there is practically no diaphragm position on the sides or under the bottom which is entirely free of air interference or air blanketing.

Design rules for guarding against problems of air entrainment are limited by present knowledge to the following:

(a) Avoid projections on the hull which face downward and which can trap air when the bow drops during pitching. A downward-facing ledge as narrow as the thickness of a projecting shell plate is sufficient to take some air bubbles down with it. Projecting edges of fenders are worse in

this respect because they extend farther from the ship's side.

(b) Avoid any semblance of a flat bottom forward beneath which air may be caught and buried under the hull when the forefoot emerges and then plunges heavily during wavegoing. The air is carried aft from this region, along the bottom of the ship, by the relative motion of the water.

(c) Wherever practicable, the water-injection openings on the under side of a ship are to be kept free of streams of air bubbles. Usually, these are trapped by the ship waves in smooth-water operation and carried along under the ship in more-or-less well-traveled routes. The routes can be determined reasonably well in a circulating-water channel by injecting a small stream of air at any point around the bow where water appears to be falling on itself (as in a breaking bow-wave crest) and tracing the route of the bubbles visually or photographically.

Venting holes in keels, for the escape of air trapped below them, are described in Sec. 73.19 and illustrated in Fig. 73.O.

Air leakage to rudders, propellers, and the like is prevented by overhanging portions of the stern, by Jenney fins, and by similar devices, described elsewhere in the book.

75.13 Design Notes for Shallow Recesses. A shallow recess, illustrated at 1 in Fig. 75.J, is defined here as one which has a depth $-h$ below the fair solid surface less than either its breadth b across the flow or its length e in the direction of flow. It has a closed bottom, so there is no auxiliary liquid flow into or out of it.

Judging principally by results of flow tests for inlet openings in the shell, such as condenser scoops, any shallow recess of appreciable length in the direction of flow may be expected to have a stagnation point on its downstream face, illustrated at Q in diagram C of Fig. 7.J and at Q in diagram 2 of Fig. 75.J. The presence of ram pressure on such a surface, facing forward, means large $+\Delta p$'s and added drag. Other features of the flow are discussed in Sec. 8.3.

W. Froude found in the early 1870's, when experimenting with a pressure speed log for ships [Brit. Assn. Rep., 1874, p. 256], that if a circular pipe as small as 0.04 ft in diameter was fitted square to and terminated flush with a flat surface parallel to the direction of liquid flow, there was developed a small $+\Delta p$ within the mouth of the pipe, amounting to about 0.04 of the ram pressure $q = 0.5\rho U_\infty^2$. This $+\Delta p$ would undoubtedly have been larger for an opening longer in the direction of flow. In any case it would be sufficient to start a flow into the opening if a circuit for the liquid were provided.

In the design of closed-bottom recesses to create minimum drag, one obvious solution is to offset the downstream edge inward, away from the water flow, depicted at 3 in Fig. 75.J. S. F. Hoerner indicates that a setback at this edge equal to 8 per cent of the depth of the downstream face, when combined with a square, flush corner at the upstream edge of the recess, reduces the overall drag by an appreciable amount [AD, 1951, Fig. 4.22, p. 56]. Relieving the downstream edge in this manner, for a hull opening, involves special shaping of the shell plating and possibly local trimming of framing members. This is an expensive item on any kind of metal hull. If the recesses are few, and the openings large, as for the hopper-door recesses under a dredge, it may be worth while to incorporate this setback in the downstream edge of each of them. It is not recom-

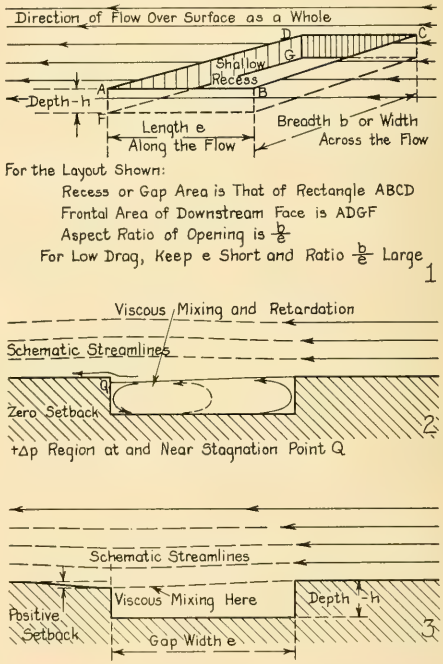

Fig. 75.J Definition and Flow Sketches for Shallow Recesses

mended that the shell at the leading edge of the opening or recess be bulged outward solely to move the stagnation point and the $+\Delta p$'s outward from the forward-facing surface at the trailing edge. In any case, *do not* chamfer, relieve, or set back the *leading edge* of the recess. According to Hoerner, this approximately doubles the drag of a recess with upstream and downstream edges both flush and square.

The effect of depth-width or length-depth ratios of shallow recesses, and of setback as well, is rather intricately bound up with boundary-layer thickness and velocity profile in way of the recess; possibly also with the position of the recess on the hull. The best design rule here is the common-sense one, which is to make the recess as shallow as operating and service conditions permit. If the recess is large and the trailing edge can be set back to reduce the area exposed to $+\Delta p$'s, by all means do it.

As for the effects of what might be termed aspect ratio for the openings of recesses, Hoerner states that the "flow jumps easily" across a wide, short gap, lying across the stream. It "penetrates deeply into the longitudinal groove" formed by a gap lying with its long dimension parallel to the stream, or within 10 deg of the parallel direction [AD, 1951, p. 56]. Because of the "much higher drag" in the latter case, the designer should, if practicable, place a recess with its shortest dimension parallel to the flow.

75.14 Practical Problems in Achieving Underwater Smoothness and Fairness on a Ship. In the matter of hull smoothness and fairing, the problem of the conscientious ship designer resembles closely that of the executive who must carefully apportion his time and energy. The executive's solution is not to pass over all the details but to know which details are of sufficient importance to justify his attention. Similarly, the ship designer must know which roughnesses require smoothing, how much time and trouble to devote to fairing, and what will be the effect of neglect to incorporate the necessary smoothing or fairing procedures. An excellent guide in this respect is the group of data on the drag of surface irregularities assembled by S. F. Hoerner [AD, 1951, pp. 49–54].

By and large, it is not difficult to achieve the smoothness called for by specification requirements or to design proper fairings. Indeed, it is often easier, if the job is planned properly from the start, to make a ship or its parts fair, well adapted to easy water flow around them, than to make them abrupt or irregular. The difficulty arises, first, in making good engineering compromises between initial cost and maintenance on the one hand and improved service performance on the other hand. The second difficulty is convincing all those concerned with the design and building of the ship that the refinements apparently justified by improved service performance are really worth while. All too often, it is feared, the designer and the shipbuilder look upon efforts to provide smoothness and to incorporate fairings as either outright compromises or trivial details not worthy of their attention. In too many cases the shipbuilder looks upon these efforts as nuisances and the ship owner as additional means of draining his pocketbook.

In yachts, sleek appearance above water is almost more important than smoothness under water. Several centuries of experience with them prove that when the designer and builder and the artisans realize the importance of smoothness, it is achieved at no great increase in cost and time. New tools are designed, new techniques are developed, and new procedures utilized which make it relatively easy to smooth up the yacht hull when it is known *in advance* that it must be smooth. What has been done with yachts can be accomplished with merchant and other vessels. The designers and builders take pride in the increased speeds of modern ships. They will take pride in their smoothness as soon as they and all others concerned are convinced that the necessity for smoothness increases as the *square* of that increased speed.

CHAPTER 76

The Design of Special Hull Forms and Special-Purpose Craft

76.1 Classification of Special Hull Forms and Special-Purpose Craft. The design procedure outlined in the previous chapters of Part 4 applies generally to all types of craft which float on or in the water and which are either self-propelled or towed. However, the design rules presented in those chapters are intended mainly for medium and large general-purpose ships of not-too-extreme form. Design of small craft is taken up in Chap. 77 following. The operating requirements for other types of water craft, of which there are legion, call for vessels especially designed to meet them. They involve unusual design problems, many of which do not occur elsewhere.

Fortunately, the possible variations in the hydrodynamic features entering into the solution of these design problems are by no means as great as the many kinds and variations of water craft involved. These features may first be related to the various kinds of liquid flow, as is done in Part 1 of the book. The features are then adapted to the flow, following which various typical combinations of hull and propulsion devices are considered. It is thus possible to treat, in more or less systematic fashion, the particular design problems associated with the multitudinous hull forms and special-purpose craft that are continually being placed before the "general practice" ship and propeller designer.

The variety of special-purpose craft may be expected to increase in the future as long as specialization in the transportation field continues. However, the types and the details of liquid flow around these craft will increase only as man's knowledge of hydrodynamics increases, and as active use is made of this knowledge.

Although the designer of large vessels may for

the moment not be interested in special-service craft, it may be useful for him and give him valuable ideas to read through the various requirements and the design comments and rules in this chapter.

With these thoughts in mind, the unusual forms and types now in general use throughout the world are classified in Table 76.a, as an aid in orienting the reader's mind to the discussions which follow.

Design features applicable to shallow and restricted waters, without regard to vessel type,

TABLE 76.a—Classification of Special Hull Forms and Special-Purpose Craft

To make this table complete and comprehensive, special types of vessels are included whose design is not discussed in this chapter.

Hull Proportions and Features	General Characteristics	Ship Types
Fine and slender	Small resistance, small displacement-length quotient, small power	High-speed launches and yachts Racing shells
Long, narrow, blunt-ended	Large carrying capacity for limiting transverse dimensions	Great Lakes ore carriers and tankers
Straight-element and discontinuous-section forms	Ease, rapidity, and low cost of construction. Existing hulls supplemented by blisters.	Various, both large and small
Fat and chubby	Small size, handiness, maneuverability	Tugs, pushboats Fireboats Fishing vessels Dredges
Shallow-water, self-propelled	Small draft	Pushboats Towboats
Box-shaped, towed	Large carrying capacity and metacentric stability, large resistance	Barges, lighters, scows, floats
Box-shaped, self-propelled	Large carrying capacity, unusual cargo or installations	Lighters, derricks Floating drydocks Damaged ships
Load-supporting, moored	Large carrying capacity, floatability and stability in swift currents	Bridge pontoons
Wind power	Freedom from mechanical installations and fuel	Sailing craft and yachts
Asymmetric hulls		Aircraft carriers, sailing canoes
Multiple-hulled craft	Large metacentric stability, small resistance	Catamarans, trimarans
Planing craft	High speed with limited power	Motorboats, speedboats Racing motorboats
Double-direction	Efficient operation in either direction without turning	Ferryboats
Icebreaking	Large power, resistance against crushing, maneuverability	Icebreakers, iceships
Land and water	Ability to travel in liquid, on solid, or in any intermediate medium	Amphibian, mud craft
Beaching	Beaching and backing off, load carrying	Landing craft, river craft, coastal vessels in remote areas
Underwater		Submarines

as well as certain important features of self-propelled craft intended to operate in confined waters, are discussed in Chap. 72.

Special features in the design of tugs, towboats, pushboats, and self-propelled lighters, as well as non-self-propelled barges, scows, and floats, are covered in Part 5 of Volume III, under the general subject of Towing.

76.2 The Design of Fine, Slender Hulls; Canoes, Racing Shells, and Fast Launches. As long as watercraft are required to be propelled by manpower and as long as men have to handle or carry them there will remain a demand for a craft of small resistance and small weight compared to its speed and carrying capacity. Such a demand is met by the birchbark canoe of the American Indian and the kayak of the Eskimo. Canoes of greater fineness but also of greater weight, dug out of single logs or built up of large parts, are still in existence and still used by many peoples of the world. These are driven by as many as a hundred paddlers each [Ill. London News, 9 Jul 1955, p. 81]. It is entirely probable that many of these fine-ended designs evolved from a desire to minimize water disturbance and noise when hunting. For the craft paddled by one or two persons, a reduction of resistance—and thrust—is far more personal and important than if there is an engine available to drive it.

Dixon Kemp, in his book "A Manual of Yacht and Boat Sailing" [Cox, London, 3rd ed., 1882], devotes Chap. XXVI, on pages 374–381, to "Canoeing." It contains drawings and rather detailed descriptions of a considerable number of British and American canoes. A story and excellent photographs of canoes and kayaks built by the natives of northwestern North America are found on pages 77–79 of the February 1917 issue of the Pacific Marine Review.

Some historical and technical data on the canoes of America are given by H. I. Chapelle ["American Small Sailing Craft," Norton, New York, 1951, pp. 36–38]. Design features of the modern light-weight canoe, the small-boat version of the long, slender ship, and still popular as a pleasure craft, are discussed and presented by R. P. Beebe [Rudder, Jan 1954, pp. 49–53, 82]. This article illustrates five typical canoe midsections.

The ultimate in fineness and reduction of both friction and pressure resistance is achieved by

TABLE 76.b—Comparative Form and Performance Data for Two Types of Manually Propelled Craft and One Mechanically Propelled Vessel

These data are taken from published information by F. H. Alexander (see the reference quoted in the text) and by K. C. Barnaby [INA, 1950, p. J13].

The circular-constant parameters are those of R. E. Froude; see Appendix 1.

For comparison with the 8-oared shell, a single-oared shell is about 1 ft wide, and weighs about 28.5 lb, without crew.

Item	8-oared Racing Shell	Whaleboat, 10 oars	Cross-channel Steamer
1. Length on LWL, ft	62.0	28.0	320.0
2. Beam, extreme, ft	2.0	6.85	40.0
3. Draft, ft (estimated)	0.5		
4. Displacement, tons, with crew	0.81	1.70	1,850
5. $\forall$ (estimated), ft^3	28.4	59.5	64,750
6. Wetted surface, ft^2	109.5	133	12,510
7. Speed, kt	10.0	6.7	22.75
8. Speed, ft per sec	17.0	11.33	38.4
9. Value of Ⓜ	20.2	7.17	7.97
10. Value of Ⓢ	11.78	8.73	7.76
11. Value of Ⓚ	6.025	3.58	3.78
12. Value of Ⓛ	1.34	1.34	1.34
13. Value of $V/\sqrt{L}$	1.27	1.27	1.27
14. Value of $\Delta/\left(\frac{L}{100}\right)^3$, tons for 100-ft length	3.5	77.5	56.5
15. Resistance, lb	77	81	87,300
16. Resistance, plus still-air D_{SA}, lb	90.0		
17. Resistance per ton of displacement, lb	95.0	47.6	47.2
18. Resistance ratio, Friction/Total	0.95	0.51	0.40
19. Value of Ⓒ	1.162	1.662	1.469

TABLE 76.c—DATA ON FAST LAUNCHES AND TORPEDOBOATS PRIOR TO 1905

Launches	Torpedoboats	Designer	Length on WL, ft	Displ. in running condition with crew and fuel	Power, horses	Speed, kt	T_q	Total Weight in lb per horse
XPDNC		Herreshoff	42.2	3,250 lb	75	23.0	3.541	43.4
Napier (twin-screw)		Yarrow	40	7,170 lb	150	25.98	4.108	47.8
Dixie		Crane	40	5,160 lb	150	26	4.111	34.4
Veritas		Gielow	56	12,000 lb	283	23.2	3.100	42.4
Panhard		Electric Launch Co.	39.91	3,621 lb	70	23	3.640	51.7
Vingt-et-Un II		Crane	38.75	3,850 lb	75	22	3.534	51.4
	Normand torpedoboat		157	168 t	3,920	29.15	2.326	96
	Yarrow torpedoboat		152.7	144 t	2,000	25	2.023	161.5
	Herreshoff torpedoboat		175.5	165 t	3,200	28.6	2.158	115.5
	Thornycroft torpedoboat destroyer		244	420 t	8,000	29	1.857	117.5

the well-known racing scull or shell. This is designed and built for rowing by one, two, four, or eight persons. Of no strictly utilitarian purpose, except to provide exercise in the open air and athletic competition, the racing shell apparently has achieved the ultimate in hydrodynamic development entirely by cut-and-try methods. Principal dimensions and form data for an 8-oared shell of some decades back, published by F. H. Alexander ["The Propulsive Efficiency of Rowing," INA, 1927, pp. 228–244 and Pl. XXV; abstracted in SBSR, 21 Jul 1927, pp. 76–77], are set down in Table 76.b, to be found on page 229 of the reference. Of interest are the comparative data on a 10-oared whaleboat and a cross-channel steamer. The high value of R_T/Δ of 95 lb per ton for the racing shell is rather remarkable, although not too far out of line with the data in Fig. 56.M. Also to be noted is the fact that the friction resistance for the racing shell may be as high as 95 per cent of the total.

Attempts to reduce the friction resistance by reducing the wetted surface, using a shorter length and a greater beam, gave no reduction in resistance [EMB Rep. 117 of Aug 1925 and EMB Rep. 283 of Feb 1931]. The fact that the smaller R_n accompanying the shorter length increases the value of C_F was possibly overlooked in this investigation. A transom stern was tried on model scale, likewise with no improvement. With their extremely fine bows, and with clean, polished hull surfaces, it is possible that the racing shell benefits from some laminar flow at and abaft the bow.

However, a shape of these extreme proportions, having L/B ratios of 25, 30, or more, in which the human propelling machinery is not part of the craft proper, is obviously of limited application. In fact, the craft, with its crew, does not even have positive metacentric stability. On any narrow hull of this kind the oars must be kept out and the craft balanced by holding them in the water.

There is a possibility that concentrated loading in long, flexible craft of this type may, because of sagging, change the form and the hydrodynamic characteristics in the operating condition.

A comprehensive treatment of the hydrodynamic aspects of racing-shell design is given in EMB Report 117, published in August 1925. Informative in this respect is an article of about that time in the Scientific American [Jun 1925, pp. 369–370].

Considering fast launches and torpedoboats as two other types of craft with fine, slender hulls, some interesting data on vessels of the vintage of 1905 and earlier are given by C. H. Crane [SNAME, 1905, p. 369]. The technical information in Table 76.c, adapted from the Crane reference, contains calculated values of T_q which

are of interest to a designer. These craft did not plane in a strict sense, despite the T_q values of 4.0 or more. Midsections of some of them are shown in Plate 190 of the reference. Deck plans and waterline planforms are drawn on Plates 191 and 192, while photographs of some of the boats underway are reproduced on Plates 193–197.

Other successful yachts and launches of this type were designed and built by N. G. Herreshoff. A few of them are described and illustrated by L. F. Herreshoff [Yachting, Sep 1950, pp. 26–27].

While these vessels had shapes no longer considered stylish or efficient, they represented, and still represent the furthest point reached in the development of fine-ended displacement-type craft. Their shapes are almost necessary for hulls which are not permitted to create large surface disturbances when moving rapidly ["Speed Without Fuss," The Motor Boat and Yachting, Sep 1956, p. 423]. These shapes may very well become useful for certain requirements not yet presented to the naval architect. Speaking of the future, the requirements of the early years of mechanical propulsion for a craft which could be driven swiftly yet easily and smoothly, such as a pleasure launch or yacht, may be expected to continue as long as mechanical propulsion is utilized. When another cycle of human behavior rolls around, the former demand for a *quiet* craft, gliding gracefully yet rapidly, may well be repeated.

Jet and rocket propulsion may, in the years ahead, be applied to slender displacement forms for certain particular duties rather than to the skimming and planing forms now associated with high speeds over the water. Pounding and slamming on planing craft, even in small waves, may well set a limit on the ultimate speed at which their hulls will hold together.

Except for the additional wetted surface unavoidable with large L/B or L/H ratios, and the extra friction resistance involved, the optimum shape for a hull, to reduce the pressure resistance due to wavemaking and separation to a minimum, is one which is definitely fine and slender. The L/B ratio may then exceed 10 and even approach 15. This is not easy to accomplish in a small craft, which needs space for the crew, passengers, propelling machinery, and some useful load but must have metacentric stability as well.

A satisfactory compromise between length-beam ratio and absolute length is determined by the speed-length quotient T_q or the Froude number F_n at which the craft is expected to make its maximum speed. The lengths and proportions which were developed through the years when this was the predominant type for small, high-speed craft are given by C. H. Crane [SNAME, 1904, pp. 321–326; 1905, p. 369]. Some of them are listed in Table 76.c. The B/H ratio is frequently amenable to some variation but it is only rarely, if at all, that the propulsion performance can be improved by departing from the proportions listed in the table.

With the length-beam and beam-draft proportions likely to be found the optimum, the draft may become a small proportion of the length; so small, in fact, that it is difficult to provide sufficient rudder area in an efficient shape of blade except by projecting it well below the baseplane.

With the large L/B ratios mentioned here it is easy to keep the waterline run slopes below 11 or 12 deg and thus to eliminate all possibility of separation at the stern. Attempts to save resistance by cutting off the stern and its wetted surface are rarely successful unless the transom so formed is kept out of water at all speeds. Working reverse curvature into the buttocks and terminating them tangent to the at-rest WL is good design provided the occasional wave slap under the stern can be accepted. However, any curvature of the stern buttocks, convex downward, develops $-\Delta p$'s under them and drags the stern down, with all the disadvantages of excessive trim by the stern.

Special problems are involved in the design of high-speed craft running at so-called "interference" speeds in the range of $T_q = 1.3$ to 1.8, $F_n = 0.39$ to 0.54, where a practically continuous resistance hump is shown by Fig. 66.B. The design problems involved are discussed at some length by E. Rolland, on the basis of designs of former years by N. G. Herreshoff and E. W. Graef [ATMA, 1951, Vol. 50, pp. 443–462; an English translation of this paper is available at the David Taylor Model Basin].

76.3 Ultra-High-Speed Displacement Types. Despite the insistent modern demand for ultra-high-speed ships to carry cargoes or other useful loads, reckoned by the hundreds or the thousands of tons, relatively little thorough and systematic investigation has been devoted to the displacement type of hull driven at speed-length or Taylor quotients T_q exceeding 2.0 or 2.2, F_n greater than about 0.60 or 0.66.

The 100-ft *Turbinia* of C. A. Parsons made 34 kt in the 1890's, and the 100-ft steam yacht

Arrow, designed by C. D. Mosher, reached the unprecedented speed of 45 kt a few years later. For displacement-type vessels to reach T_q values of 3.4 and 4.5 was remarkable, and still is, but the useful loads carried by each were extremely small.

An early form of the German schnellboote (fast boat), a displacement-type craft intended to maintain high speed on the high seas in heavy weather, is described and illustrated in Schiffbau [26 Oct-2 Nov 1921, pp. 112–116]. A set of small-scale lines of this round-bottom craft is included in the article. During World War II the Germans built and operated a considerable number of these so-called S-boats of a later version [Rupp, L. A., NavTechMisEu Rep. 338–45 of 23 Aug 1945; Büller, K., Handbuch der Werften, 1952, pp. 37–42]. The David Taylor Model Basin made numerous tests following World War II of TMB model 3993 representing some of these craft [TMB Rep. 628 of Jan 1948 and other reports].

Although by no means cargo carriers in the accepted sense of the term these craft did carry an appreciable useful load, and they performed admirably in such rough-water areas as the English Channel and the North Sea. They may well serve as the starting point for the development of larger and faster versions, carrying larger proportions of useful weight.

76.4 Long, Narrow, Blunt-Ended Vessels; Great Lakes Cargo Carriers. Limitations on beam and draft imposed by canal locks, drydocks, pier facilities at loading and unloading ports, and shallow water along the route produce a ship form that is abnormally elongated, especially if the carrying capacity is high. The result is a series of widely varying types, among which may be listed the American (freight) car float, the self-propelled cargo-carrier of the Erie and other American canals, the river steamer and its towed barges of the large European rivers, and the bulk-cargo carrier of the American Great Lakes. Only the self-propelled craft are considered here; the others are discussed in Part 5 of Volume III.

In the past, these limitations have produced box-like or block-shaped vessels, with the ends whittled off just enough to make them manageable in the confined waters in which they operated or to enable them to be self-propelled with some reasonable degree of efficiency. The Great Lakes freighter has benefited from a great deal of attention, devoted both to its construction as well as its design. It is perhaps not strange, in view of the low speeds at which these vessels formerly traveled, that the emphasis has been on capacity and cargo handling rather than on hydrodynamics. R. Curr gives the lines of a Great Lakes bulk ore carrier of a half-century ago [SNAME, 1908, Pl. 87]. Fig. 76.A shows the lines of a World War II design of some 40 years later, similar to the design covered by SNAME Resistance Data sheet 90.

J. J. Henry gives a considerable amount of statistical and other data on Great Lakes bulk ore vessels in his paper "Modern Ore Carriers" [SNAME, 1955, pp. 92–95], but here again the emphasis is on features other than hydrodynamics. Table 76.d lists five more vessel types and supplies supplementary information on hull proportions and features and form coefficients. Discrepancies between the two tables are due generally to lack of precise definition of the terms listed.

The bibliography of 24 items at the end of the Henry paper, a number of which apply to ocean-going vessels with few draft and beam limitations, is supplemented by the references which follow:

(1) Babcock, W. I., "Longitudinal Bending Moments of Certain Lake Steamers," SNAME, 1905, pp. 187–207 and Pls. 119–133. This paper, although primarily structural, gives principal dimensions of the *Victory* and the *Elbert H. Gary*.

(2) Sadler, H. C., and Lindblad, A., "Stresses on Vessels of the Great Lakes Due to Waves of Varying Lengths and Heights," SNAME, 1922, pp. 77–82. The text and Pl. 13 contain some data relating to hydrodynamic design.

(3) Lindblad, A. F., "Some Features Affecting the Economy of the Lake Freighters," SNAME, 1923, pp. 37–49 and Pl. 9

(4) Cross, A. W., SNAME, 1928, pp. 51–62 and Pls. 41–51. The paper is built around a description of the steamer *Harry Coulby*, having an L_{WL} of 615.2 ft, a B of 65 ft, a displacement of 19,092 long tons and a speed of 11.3 kt.

(5) Fisher, C. R., and Kennedy, A., Jr., "Turbine Electric Drive as Applied on the Great Lakes Cargo Ships," SNAME, 1928, pp. 235–248 and Pls. 135–138. This paper on propelling machinery gives a considerable amount of hull design and ship performance data on the steamer *Carl D. Bradley*.

(6) Workman, J. C., "Shipping on the Great Lakes," SNAME, HT, 1943, pp. 363–376

(7) Baier, L. A., "The Great Lakes Bulk Cargo Carrier; Design and Power," SNAME, Great Lakes Sect., 1947, Vol. 55, pp. 385–390. On p. 390 of this paper the author gives a list of 25 references pertaining to the Great Lakes bulk cargo carrier.

(8) Mathews, S. T., "Resistance and Propulsion Tests on a Model of a Lake Freighter," Div. Mech. Eng., Nat. Res. Council, Ottawa, Rep. MB-137, 3 Jul 1951

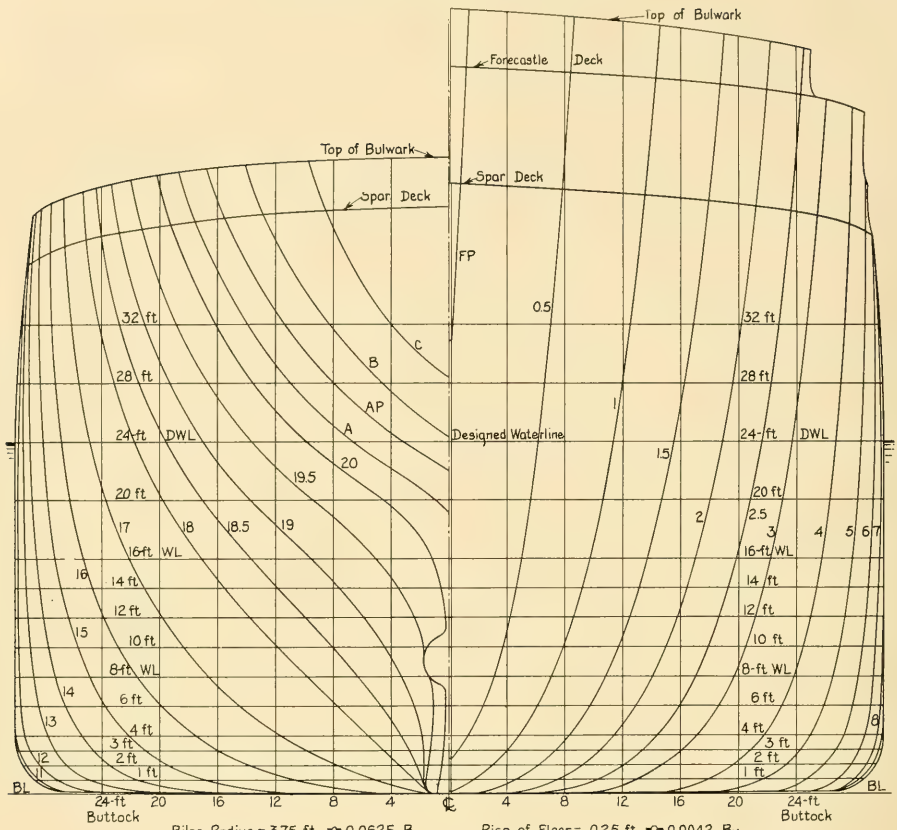

Bilge Radius = 3.75 ft, ⇥ 0.0625 B_X Rise of Floor = 0.25 ft, ⇥ 0.0042 B_X
Tumble Home = 0.75 ft, ⇥ 0.0125 B_X Length of Parallel Middlebody = 330 ft, ⇥ 0.542 L_{WL}
Position of Maximum-Area Section at Midlength of Middlebody, = 0.478 L_{WL} from FP
Length of Entrance = 126 ft, ⇥ 0.207 L_{WL} Length of Run = 139 ft, ⇥ 0.228 L_{WL} i_E of Entrance = 45.7 deg; i_R = 37.4 deg
Length Overall = 620.0 ft Length Between Perpendiculars = 605.0 ft Length on Keel = 595.0 ft Length on 24-ft DWL = 609.0 ft
Beam, Molded = 60.0 ft Depth, Molded = 35.0 ft

FIG. 76.A BODY PLAN, U. S. MARITIME COMMISSION DESIGN *L6-S-A1* OF GREAT LAKES FREIGHTER

(9) Schaeffner, C. R., "C4 Conversion to Great Lakes Ore Carrier *Tom M. Girdler*," SNAME, Gulf Sect., 19 Oct 1951; abstracted in SNAME Member's Bull., Jan 1952, p. 20

(10) Cowles, W. C., "New Ore Carrier *Philip R. Clarke*," MESR, Jul 1952, pp. 62–81; also MESR, Dec 1952, p. 72

(11) Zuehlke, A. J., and Rankin, G. F., "Largest Lakes Self-Unloader, the *John G. Munson*, Goes into Service," MESR, Oct 1952, pp. 50–63; also MESR, Dec 1952

(12) "Steamer *Edward B. Greene* Becomes the New Cleveland-Cliffs Flagship," MESR, Nov 1952, pp. 38–50

(13) "Conversion Job, King Size (*Joseph H. Thompson*)," Naut. Gaz., Nov 1952, pp. 16–19, 30. This article describes the conversion of the *C4-S-B2* vessel *Marine Robin*, utilizing only the after portion.

(14) "600-Foot Lakes Ore Carriers Built in East Coast Shipyard," Mar. Eng'g., Jan 1953, pp. 36–47; describes the first vessel of the *Johnstown* class

(15) "The 690-Foot *Ernest T. Weir*," Mar. Eng.'g., Apr 1954, pp. 36–46; also Mar. Eng'g., Dec 1954, p. 60

(16) Downer, H. C., "Ore Carrier *Richard M. Marshall*," Mar. Eng'g., Jun 1954, pp. 44–60

(17) "Largest on the Lakes (steamer *George M. Humphrey*)," Maritime Reporter, 15 Nov 1954, p. 27

(18) De Rooij, G., "Practical Shipbuilding," 1953, Figs. 799 and 800 on p. 373.

The following SNAME RD sheets apply to vessels of the Great Lakes bulk ore-carrier type, and refer to the loaded condition:

Sheet number	Length, ft	Beam, ft	Draft, ft	Displ., long t	Speed, kt
90	609.2	59.8	24.0	21,536	10.4
92	661.2	70.0	25.5	29,112	14.0
128	487.7	51.2	20.5	12,630	13.0
129	595.7	51.2	20.5	15,862	13.0
130	647.2	67.0	24.0	25,430	12.0

There are a number of additional references, covering the years 1897 to the present, to be found under the subject headings "Great Lakes" and "Lake Vessels" in the SNAME Index to Transactions, 1893 to 1943, and in the latest editions of the SNAME Yearbook.

Discussing design features, the transverse limitations determine the dimensions and possibly also the shape of the midsection. This usually is wall-sided and flat-bottomed, with C_X values of 0.99 or more. If the vessels are to run on inland waters, as is generally the case when such severe beam and draft limitations exist, roll-resisting keels are dispensed with. The lower-corner radii of the midsection are made as small as the designer and operator dare to use, or as the canal locks will permit. Small-radius corners give a ship section rather good inherent roll-damping characteristics, so the bilge keels may not be missed.

With 50 per cent or more of the length in parallel middlebody, as is the case on most of these vessels, there is usually an appreciable saving in construction costs because of this factor. However, to achieve the greatest benefit from this feature, the constant-area section amidships should have a straight sheer line, with constant depth. For the average inland or protected waters, it should be sufficient to add sheer at the ends only, as in the alternative straight-element profile for tankers of Fig. 68.C.

With the beam and draft fixed arbitrarily, and the length established approximately by the carrying capacity, it appears at first sight that the relatively large wetted surface resulting from this combination must be accepted. This is likely to be up to 10 per cent greater than for a ship of normal form. The ratio of friction resistance to total resistance is therefore large, of the order of 0.6 or more. Because of their length and the extent of shallow water they must generally traverse, these vessels run at relatively low values of T_q, of the order of 0.4 to 0.55, F_n of 0.12 to 0.164.

It must also be recognized in the design of these vessels that many of them run in shallow-water regions, in the form of dredged channels or rock cuts, in which the *nominal* bed clearance is reckoned in small fractions of a foot. On a large Great Lakes freighter, for example, the square-draft to depth-of-water ratio $\sqrt{A_X}/h$ may reach the value of $\sqrt{1700}/25.2$ or 1.62. The sinkage at even a relatively low speed may be equal to this nominal clearance so that the ship actually scrapes along over the bottom. It seems not possible to relieve this situation by any drastic reduction in C_X without cutting into the useful load. The alternative operating solutions are to load to a lesser draft, or to slow down in areas of extreme shallow water.

In the past the trend of design for vessels of this type has been to keep the block coefficient high and to carry the maximum amount of useful load within the limiting length, beam, and draft. High resistance and high power were not frowned upon by the operators if large cargoes could be carried. However, for vessels like Great Lakes ore carriers which run in deep as well as shallow water, and where the total amount of cargo carried per vessel during the ice-free season is the principal operating criterion, there may be a better solution. Increasing the speed by fining the ends and carrying several more whole cargoes per season may more than make up for less tonnage per cargo [Telfer, E. V., SNAME, 1951, p. 222]. It is possible, as Telfer points out, that a modified form of bulb bow might have a useful application at the low T_q values at which these ships usually run. It is certain—indeed it is proved by several conversions—that fining the stern and paying attention to the flow to the propeller in the run will produce an appreciable gain in *average* speed with little or no increase in engine or propeller power. In fact, if the continuous development of the Great Lakes bulk carrier over the past century [Baier, L. A., SNAME, 1947, pp. 385–390; SNAME, HT, 1943, pp. 365–375] is projected into the future, it indicates an improvement in form and an increase in speed with no reduction in long-time carrying capacity, that will continue to improve its usefulness.

Fig. 76.B pictures the stern of a recent (1954) Great Lakes ore carrier, designed by the American Ship Building Company of Cleveland, Ohio, in which a definite improvement was made in the form of the run ahead of the propeller.

TABLE 76.d—Dimensions, Proportions, and Form Data for Great Lakes Bulk-Cargo Carriers

All dimensions are in feet to the proper power. All powers are in English horses. All weights and displacements are, so far as can be learned, in long tons of 2,240 lb but the displacement weights to given waterlines are usually for fresh water. All vessels are single-screw, and all propellers are 4-bladed, unless otherwise stated.

Since the lines of these vessels were not available it was not possible to recalculate the form coefficients to the waterline length instead of to the calculation length used by the designers.

Name of Vessel	*Harry Coulby*	*Governor Miller*	*Benjamin Fairless*	*Sewell Avery*	*Wilfred Sykes*	*Tom M. Girdler*	*Cliffs Victory*	*John G. Munson*	*Philip R. Clarke*	*Johnstown*	*Joseph H. Thompson*	*Ernest T. Weir*	*Richard M. Marshall*	*George M. Humphrey*
When Built	1927	1938	1942	1942	1950	1951	1951	1952	1952	1952	1952	1953	1954	1954
Principal Dimensions and Characteristics Length overall, L_{OA}	630.75	610.75	639.5	620	678.0	602.5	620.25	666.25	647	626.1	714.1	690	643.7	710.0
Length bet. perps., L_{PP}	607	593.81	622.75	605	666.0	585	600.96	640	629.25	611	696.0	670.25	628.83	690.0
Waterline length at load draft, L_{WL}	615.2			609.2	661.2								634.3	
Length for calculation of form coeffs., L	607	586*	614**	595**	650.0**	585	600.96	640	620**	600**	696.0	661.0	617.5**	678.0
Beam, molded	65	60	67	59.8	70.0	71.5	62	72	70	70	71.5	70	67.0	75
Depth, molded	33	32.5	35	35	37.0	35	38	36	36	37	38.5	37	35	37.5
Draft, maximum, molded	20	22.14	24	24	25.5	24.25	25.96	25	24.89	24.5	26.1	25.54	24.6	25.5
Displ., total, to max. draft, fresh water, long tons	19,092	18,940	24,115	20,980	28,510	21,170	20,599	27,570	26,400	24,745	29,058	28,830	24,870	31,650
Light ship weight	5,092	4,725	5,850	5,020	6,810	6,400	5,626	7,806	6,025	6,306	7,465	6,882	6,130	7,246
Deadweight, total	14,000	14,215	18,265	15,960	21,700	14,770	14,973	19,764	20,375	18,439	21,593	21,948	18,740	24,404
Displ.-length quotient, $\Delta/(0.010L)^3$	85.1	93.9	104.1	99.7	103	104	94.6	105.1	110.7	114.5	86.0	99.0	103.8	101
Fatness ratio, 0-diml, $\forall/(0.10L)^3$	3.06	3.38	3.75	3.59	3.71	3.74	3.41	3.78	3.98	4.2	3.10	3.57	3.74	3.64
$\overline{LCB}$				0.484	0.4928				0.4917	0.4890	0.466		0.4841	

Proportions and Form Coefficients														
Length-beam ratio, L/B	9.35	9.77	9.16	9.96	9.29	8.18	9.69	8.89	8.86	8.57	9.73	9.44	9.22	9.04
Beam-draft ratio, B/H	3.25	2.71	2.79	2.49	2.75	2.95	2.39	2.88	2.81	2.86	2.73	2.74	2.73	2.94
Entrance length				126.7	140				130	144			125.1	
Run length				152.3	162				159	180			154.1	
Run-entrance ratio				1.203	1.157				1.223	1.25			1.23	
Parallel-body length				330.2	348				331	276			349.6	
Per cent parallel body				55.5	53.5				53.4	46.0			56.6	
Block coefficient	0.867	0.872	0.871	0.855	0.875	0.745	0.764	0.859	0.873	0.860	0.804	0.873	0.868	0.873
Prismatic coefficient		0.881	0.878	0.863	0.882	0.760	0.774		0.881	0.868	0.809	0.880	0.875	0.880
Midsection coefficient		0.992	0.993	0.991	0.992	0.981	0.987		0.991	0.991	0.994	0.992	0.991	0.992
Waterplane coefficient				0.908	0.930				0.933		0.858			
Vertical prismatic coefficient				0.942	0.941				0.935					
Half-angle of entrance, deg				44	47.5					44.5				
Wetted surface, bare hull				57,870	71,110								62,861	
Wetted-surface coefficient, $C_{WS} = S/\sqrt{\Delta L}$				16.12	16.30								15.80	

TABLE 76.d—*Concluded*

Name of Vessel	*Harry Coulby*	*Governor Miller*	*Benjamin Fairless*	*Sewell Avery*	*Wilfred Sykes*	*Tom M. Girdler*	*Cliffs Victory*	*John G. Munson*	*Philip R. Clarke*	*Johnstown*	*Joseph H. Thompson*	*Ernest T. Weir*	*Richard M. Marshall*	*George M. Humphrey*
Power and Speed: Propulsion Devices														
Shaft power	3,000#	2,000	4,000	2,500#	7,000	9,000	8,500	7,000	7,000	7,000	9,000	7,000	5,000	8,500
Designed speed, mph	13.0		14	12.5	16	19	20	16.25	16.3	16	18	16	16.3	16.5
Designed speed, kt	11.3		12.2	10.8	13.9	16.5	17.4	14.1	14.2	13.9	15.6	13.9	14.2	14.3
Taylor quotient, $V/\sqrt{L}$	0.459		0.492	0.443	0.545	0.673	0.709	0.558	0.570	0.568	0.592	0.537	0.572	0.550
Rate of rotation, rpm	95	90	90	80	100	85	85	104	108	115	104	108	107	103.3
Propeller diameter		15.5	17.5	16.5	18.5	21.67	20.5		17.5	18.0##	19.0	17.5	17.884	19.5##
Propeller pitch		14.5	16(max)	15.5	16.27	21.67	22.75		15.15	13.0	18.27	15.15	13.67	15.66
Mean-width ratio				0.230	0.246				0.320					
Blade-thickness fraction				0.0442	0.0495				0.0524				0.0585	

* Length to stern frame
** Keel length
# Indicated power in horses
5-bladed propellers

Fig. 76.B Great Lakes Ore Carrier *George M. Humphrey* in Building Dock

Photograph by Denny C. Harris, Cleveland, Ohio. The 5-bladed propeller is of built-up construction. Note the fine skeg ending up under the stern. The aperture on the centerline at the stern is the hawsepipe for the stern anchor.

Summarizing the hull-design problem resolves itself into:

(a) Achieving the required carrying capacity with the minimum length and wetted surface
(b) Holding the sinkage down to the minimum practicable value
(c) Shaping the ends to keep down the pressure resistance due to wavemaking, separation, and the like.

The wavemaking pressure resistance, at a limiting T_q of, say 0.7, can never be a large part of the whole unless the bow is deliberately made too blunt. On the other hand, the separation drag can be excessive. These hulls are therefore in the class where the major part of the fining needs to be done at the stern. The demands of the owners and operators for the highest possible ratio of useful load to total displacement, in the full-load condition, is generally such that the stern can not be fined sufficiently to eliminate all separation, even at depths as low as the axis of a single propeller. Not only is the separation drag kept large by this limitation but the possibilities of air leakage to the propeller, with its consequent loss of power, vibration, and noise are aggravated.

It appears that a not-too-wide transom stern, with an immersion in the load condition of only a foot or so, might be a partial answer to this problem. The transom shelf can be wide enough to guard against air leakage to the propellers and it can be used to make up the displacement volume lost by fining the skeg forward of the

single propeller. On ships of the maximum length permitted by turning basins and pier facilities, all this length could be put into the waterline.

76.5 The Design of Dry-Cargo Vessels with Box-Shaped Holds. Somewhat similar to the long, narrow, blunt-ended vessel, and to the canal boat, and not unlike the box-shaped watercraft of Sec. 76.15, is the vessel which is required to house rectangular, box-shaped, dry-cargo spaces within the boundary of a ship-shaped hull. In some respects the design problem resembles that of a newsprint carrier in which the storage space is required, almost literally, to be larger than the dimensions of the outer shell!

Vessels of the rectangular- or box-hold type include:

(a) Seatrains, in which railway cars are stowed on tracks at levels from the bottom of the holds to and including the upper deck [Burrill, L. C., "The Design and Construction of the Rail-Car Carrying Steamship *Seatrain*," NECI, 1929–1930, Vol. XLVI, pp. 179–204 and Pls. VI, VII; MESR, Aug 1952, front cover]

(b) Cargo-container craft, in which the cargo consists almost exclusively of metal shipping containers in the form of cubes and parallelepipeds. For these vessels the cargo, when loaded and unloaded, as well as when transported, may be stowed instead on pallet boards suitable for handling by fork-lift trucks. The combination of pallet and material carried by it is usually of box shape.

(c) So-called trailer ships, in which the cargo consists of the box or body portions of trailer trucks, minus the tractor portions [Mar. Eng'g., Apr 1954, pp. 48–49, 60; Jan 1955, pp. 57–58, 74].

These ships are designed on the principle that all holds are to be truly rectangular, with flat floors or decks and vertical sides and bulkheads. The boundaries are all to be flush on the hold side and to stand at right angles to each other. Actually, instead of designing a ship hull of normal form and arranging cargo holds inside it, the holds are laid out first and the ship envelope is drawn around them.

The hydrodynamic design problem becomes one of fashioning such an envelope so that it has the greatest practicable fullness coefficient but is not too difficult to drive. The box-shaped holds can not be raised appreciably to help with the hull shape because of the consequent loss of volume and the raising of the center of gravity of the cargo. No design rules are available for developing an acceptable underwater form under these conditions except the general principles of achieving reasonably good flow around all parts of the hull and a reasonably uniform pressure distribution. The comments in Chaps. 8, 27, and 28 relative to the flow around and the behavior of straight-element and discontinuous-section forms are of value here.

Achieving practically a rectangular maximum transverse section presents no problem because successful ships are now built with C_X values of 0.99 or more. By using a flat inner bottom and placing a vertical wing-tank bulkhead inboard of the shell on each side, the transverse section of the hold is completely rectangular.

To obtain the greatest length of this full rectangular section, the cargo holds must occupy *all* of the fullest portions of the length, leaving the tapered portions at the ends to accommodate the propelling and auxiliary machinery and miscellaneous equipment.

It is by no means necessary to break up or interfere with the best hold space by the installation of a midship deckhouse, as has been the practice on tankers and ocean-going ore ships for many decades. The whole central portion of the vessel may be kept clear for hatches, cargo-handling gear, and deck loads, if desired, by moving the machinery and accommodations all the way aft. This was done on the large Swedish tanker *Oceanus* [SBSR, 16 Dec 1954, p. 20 of advt.; Motor Ship, London, Jan 1955, p. 460] and is shown by J. J. Henry in his "Artist's (and presumably Naval Architect's) Conception of a Modern Ore Carrier" [SNAME, 1955, p. 57].

76.6 The Design of Straight-Element Hulls. Other than to obtain the special V-bottom shapes for high-speed motorboats and other planing craft, the straight-element form defined in Sec. 27.1 is used to facilitate hull construction. This involves not only reductions in cost, time, and effort but in the amount and kind of fabricating equipment required. Depending upon the structure of the boat or ship the transverse frame members may be made up of straight segments around the periphery, the planking or shell plating may be made developable, embodying single curvature only, or there may be a combination of both. If ease of construction is a predominating factor, the shape of the underwater hull, and perhaps also that of the abovewater hull, must conform to the limitations of the

amateur or inexperienced builder, to the lack of equipment in small plants, or to the necessity for rapid and economical fabrication and erection.

It is often convenient to replace the sharp corners of polygonal sections with rounded corners but in this case the corners lying along any diagonal must generally be of fixed radius if rapid production methods are employed.

The principal design requirement for straight-element hulls is that the chines (and coves) shall lie in the adjacent lines of flow in such a manner that water does not cross these external discontinuities.

The principles set forth in Chaps. 4, 27, and 52, concerning the manner in which water flows around a ship, are employed to estimate the direction which the water may be expected to take. It is well to remember that, if the beam-draft ratio is large, most of the flow goes under the bottom.

In the present state of the art it is not always easy to predict the flow around hulls of unusual shape. Fortunately, it is possible, even with small models, to check the flow directions experimentally on a straight-element form, so that the designer can obtain an idea of the flow pattern while the hull form is still sufficiently "plastic" to be changed readily.

For the best performance a cove line is not placed where the water flowing around the ship is required to cross it. Fortunately, this is considerably less important than for a similar crossing of a projecting chine, because of the sensibly inert water carried along in the cove and the usually shallow depth of the reentrant portion.

If a chine extends above the designed waterline in the entrance, it is generally necessary that the slope of the chine, when projected on the centerplane with the craft at rest and reckoned with respect to the at-rest WL, be reasonably large, to insure upward dynamic lift when pitching and encountering waves and to throw spray clear of the hull. A suitable range of angles of slope for exposed forward chines of planing craft, applicable to all straight-element forms, has not as yet been laid down. However, a series of chine shapes and positions, based partly on the intended service and partly upon the maximum T_q and F_n at which the craft is to run, is shown in Fig. 77.I.

The minimum number of chines is one at each diagonal bulge, as in the hull of the well-known flat-bottomed skiff, punt, or dory. In this case the chine angle approaches 90 deg but as the relative speeds are low the chine line can depart from the lines of flow to facilitate construction.

For a sailing yacht which is almost never upright when moving through the water, the shape of the underwater hull varies with the angle of heel, as do the lines of flow for that particular heel. The flow may also vary for the speed or range of speed corresponding to that heel, because of the considerable wavemaking. Nevertheless, it is to be expected that, by simple flow tests or other means, a chine line may be found which fits all these flow positions rather well.

The maximum number of chines (or coves) which can be worked longitudinally into a hull is limited only by the number of strakes desired to meet construction requirements. As many as five chines on each side have been employed successfully in some hulls, illustrated by the body plans of Figs. 27.B and 68.J. As the projecting corners in multiple-chine sections approach 180 deg there is less need for placing them exactly in the lines of flow. The chine positions therefore can favor the lines of plating or the type of framing to be used.

Frame sections which are nominally straight may be given a slight outward bow or camber, corresponding to the camber in a weather deck. This is not enough to involve forming or furnacing. Metal plating applied to slightly bowed frames lies flatter, or perhaps one should say with less waviness, than if held to perfectly straight frame lines [Baier, L. A., unpubl. ltr. to HES of 4 Aug 1950].

The degree to which a hull surface may vary from one which is exactly of single curvature depends upon the size of the surface in question compared to the size or the area or the shape of the sheet or plate of which that surface is to be made. A wooden plank may be bent, twisted, and sprung out of its natural shape, fastened to the frame of a boat, and left in its sprung shape for years provided it is not too wide or too thick for the shape to be impressed upon it. A wide sheet or plate of metal may often be pulled and stretched to make it conform slightly to a second degree of curvature. A wide sheet of plywood, assembled in the flat, may not respond to such treatment without definite and detrimental cracking.

If the straight-element form facilitates construction in any particular case, it is equally advantageous to incorporate it into the above-

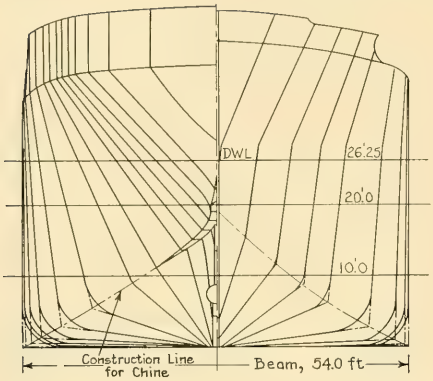

FIG. 76.C BODY PLAN OF WORLD WAR II CONCRETE-HULL STEAMER, U. S. MARITIME COMMISSION DESIGN *C1–S–D1*

water body. Indeed, the use of straight sides, either plumb or sloping slightly, is standard on many ships in which straight elements are not otherwise employed.

The elements of greatest practical benefit are the straight and level sheer line, utilizing a section of constant depth, and the straight or ridge-type deck-beam lines described in Chap. 68.

Examples of straight-element ship forms which have been designed and constructed in the past are described and illustrated in the following:

(1) U.S. Navy landing craft LCI (L). The original body plan is shown by E. A. Wright, SNAME, 1946, Fig. 14, p. 384.

(2) World War II concrete steamer, U.S. Maritime Commission, *C1-S-D1* design, TMB model 3745M. A body plan of this ship is reproduced, by courtesy of the U.S. Maritime Administration, in Fig. 76.C. Table 76.e gives the dimensions and form data for this design.

(3) World War I patrol boat, *Eagle* class, SNAME RD sheet 118

(4) Ferryboat *John J. Walsh*, 1938; HT, SNAME, 1943, p. 174

(5) Ferryboat *Coquivacoa*, 1938; SNAME, HT, 1943, p. 179. This vessel has a flat bottom and straight-V sections.

(6) Detroit Diesel Engine Division, GMC Report MID 2–21 on 47.5-ft Double-Chine Work Boat, no date but about 1947. See SNAME RD sheets 102 and 104.

(7) Motor canal boats with flat bottoms and straight segments of section lines, SBSR, 17 Jan 1935, p. 64

(8) Small, light-displacement sailing yacht, with single chines and transom stern, Yachting, May 1950, p. 60

(9) Small Thames tugs with chamfered chine and hull surfaces that are presumably developable, SBSR, 3 Jun 1954, p. 703.

TABLE 76.e—HULL-FORM PARAMETERS AND PROPORTIONS FOR WORLD WAR II CONCRETE STEAMER

This craft, of the U. S. Maritime Commission *C1-S-D1* design, had transverse sections made up of straight lines joined by short arcs.

Length between perps.	L_{PP}	350 ft
Length on waterline	L_{WL}	357.3 ft
Length overall	L_{OA}	366.33 ft
Beam	B	54 ft
Draft, loaded	H	26.25 ft
Depth of hull	D	35 ft
Displacement	Δ	10,950 t
Speed	V	10 kt
Speed-length quotient	T_q	0.529
Displacement-length quotient	$\Delta/(0.010L)^3$	240
Beam-draft ratio	B/H	2.057
Coefficient, prismatic	C_P	0.767
Coefficient, maximum section	C_X	0.988

76.7 Partial Bibliography on Straight-Element Ship Designs. A list of the principal references on this subject, but by no means a complete list, is given here for the benefit of a ship designer working up a straight-element form:

(1) Taylor, D. W., "Some Experiments with Models Having Radical Variations of After Sections," SNAME, 1914, p. 61ff

(2) McEntee, W., "Cargo Ship Lines of Simple Form," SNAME, 1917, pp. 101–107 and Pls. 20–26; also Int. Mar. Eng'g., Jan 1918, p. 19

(3) McAleer, J. A., "Straight Lined and Fabricated Ships," Int. Mar. Eng'g., Apr 1918, p. 234

(4) Bion, C. W., "A System for the Design of Ships with Straight-Lined Sections," Int. Mar. Eng'g., Jun 1918, pp. 335–338

(5) Sadler, H. C., and Yamamoto, T., "Experiments on Simplified Ship Forms," SNAME, 1918, p. 157

(6) Baker, G. S., and Kent, J. L., IESS, 1918–1919, Vol. LXII, p. 216

(7) "A Cubist Ship (S. S. *Newton*)," Mar. Eng'g., Feb 1921, pp. 119–120. The stern of this vessel terminates in a rather narrow square transom of triangular section, with its apex at the bottom.

(8) Thomas, J. B., "The Powering of Ships," London, 1921, pp. 276, 278, 287

(9) Wrobbel, J. F. K., "Model Experiments on Rhine Ships," SBSR, 3 Apr 1924, pp. 398–400

(10) Robb, A. M., "Straight-Frame Ships," IESS, 1924–1925, Vol. LXVIII, p. 313

(11) Hay, M. F., "The Maierform of Hull Construction," INA, 1931, pp. 30–51

(12) Baker, G. S., "Ship Design, Resistance and Screw Propulsion," 1933, Vol. I, pp. 85–87, 115–118. There are illustrated here the lines of a standard "N" type ship of World War I.

(13) Edward, J., and Todd, F. H., "Steam Drifters: Tank and Sea Tests," IESS, 1938–1939, Vol. LXXXII, pp. 51–107

(14) Johnson, Eads, "Ferryboats," SNAME, HT, 1943, pp. 172, 174, 179

(15) Stephens, E. O., "Thames (Dumb) Barges," INA, 1945, pp. 170–184

(16) Holt, W. J., "Admiralty Type Motor Fishing Vessels," INA, 1946, pp. 295–307

(17) Wright, E. A., "A Pattern for Research in Naval Architecture," SNAME, 1946, p. 374, particularly LCI (L) original body plan in Fig. 14 on p. 384

(18) Aitken, R. L., "Special Wartime Prefabrication Methods Employed in the Construction of Small Vessels," IESS, 1947, Vol. 90, pp. 246–288, 322–344. Gives many diagrams of small vessels with straight frame segments.

(19) Emerson, A., "Experiment Work on Merchant Ship Models During the War," NECI, 1947–1948, Vol. 64, pp. 289–332, esp. p. 320

(20) Van Lammeren, W. P. A., Troost, L., and Koning, J. G., RPSS, 1948, p. 110

(21) Thiel, P., Jr., Johnson, R. W., and Ward, L. W., "The Resistance and Wake of Nine Double-Chine Simplified Hull Forms," Univ. Michigan Thesis, May 1948. The introduction gives a list of straight-element-form vessels built and in service.

(22) During World War II a considerable number of small cargo vessels, 173 to 176 ft long, were built with straight-element sections and double chines along the bilges. One such vessel is shown in the National Geographic Magazine, Jul 1948, p. 88.

(23) Bayard, N., "Stock Sloop," The Rudder, Feb 1950, p. 44. This craft has 4-sided polygonal frames, from keel to gunwale. It is not known whether the hull surfaces are developable.

(24) Simpson, D. S., "Small Craft, Construction and Design," SNAME, 1951, pp. 554–611, esp. Fig. 21 on p. 580. On page 558 the author comments that:

"As the size increases (above 50 or 60 ft) there would appear to be an excellent field for the double-chine hull form, especially for vessels that operate under varying displacement and trim conditions and in rough waters. There is little difference from the molded (rounded) form in hull characteristics but the double chine with its straight frames and warped (developable) shell surfaces can be built with much less equipment and at a considerable saving in cost."

(25) Williamson, B., SNAME, 1950, Fig. 19, p. 21 shows double-chine corner endings on barges. The developability of these surfaces is not known.

(26) Examples of straight-element barge and lighter hulls, with resistance data, are to be found on SNAME RD sheets listed hereunder:

Sheet number	Type of vessel
38	LST
40	Landing craft—LSI (L)
44	Landing craft
99, 138	Oil barges
131	Oceangoing barge, 200-ft
132, 133, 136, 139	Harbor barges
134, 140, 141	Barges
135	Pier barge, 150-ft
137	Nesting barge, 77-ft
148	Car float, 285-ft

(27) Other straight-element forms are illustrated in Figs. 27.B, 27.C, 68.J, and 72.E of this book

(28) Pavlenko, G. E., "Soprotivleniye Vody Dvizheniyu Sudov (The Resistance of Water to the Movement of Ships)," Moscow, 1953, Figs. 328–336, pp. 441–443; also Figs. 337–339, pp. 446–447. Nothing is known of the performance of the straight-element forms represented by the body plans of the figures cited.

(29) Thames barge tug *Jaycee*, 62 ft in overall length, 16 ft in beam, and drawing 7.5 ft, has straight-line frame sections illustrated in SBSR, Int. Des. and Equip. No., 1955, p. 69

(30) Some proposed British cargo-ship designs with double chines at the turn of the bilge and other straight-element features are shown by E. C. B. Corlett [SBMEB, Nov 1955, pp. 639–641].

76.8 Drawing Ship Lines with Developable Surfaces. The principles and the geometry of developable surfaces for boats were, so far as known, first enunciated by C. P. Burgess in reference (a) listed hereunder. The graphic procedures for delineating developable surfaces were devised by G. Hartman and others within the next decade, including methods of drawing the customary ship lines in 3-angle or orthogonal projection, when the boundaries are developable surfaces.

The principal known references are:

(a) Burgess, C. P., "Developable Surfaces for Plywood Boats," The Rudder, Feb 1940, pp. 34–35

(b) Hartman, G., "Developing a Plywood Design," Motor Boating, Jan 1945, pp. 82–84, 140

(c) Hartman, G., "Designing a Sailboat to Use Plywood," Motor Boating, Jan 1946, pp. 67–69, 218

(d) Werback, C. E., "More About 'Developable' Surfaces," The Rudder, Mar 1945, pp. 30–31, 147

(e) Losee, L. K., "Developable Surfaces: Their Properties and Delineation as Applied to the Shells of Vessels," unpublished manuscript dated 7 Feb 1947.

As an aid in the shaping of a boat having completely developable surfaces, Fig. 76.D incorporates all the data shown by Hartman in Fig. 4 of reference (b), with all the original and some supplementary markings. The systematic procedure outlined hereunder is adapted from the instructions published by Hartman in that reference:

(1) The principal dimensions and proportions of the boat to be designed are assumed to be selected in advance. These are, for the example given here, expressed in terms of the chine length L_C and the chine beam B_C.

(2) In general, the surfaces may be flat, cylindrical, or conical; in this example, only conical surfaces are employed

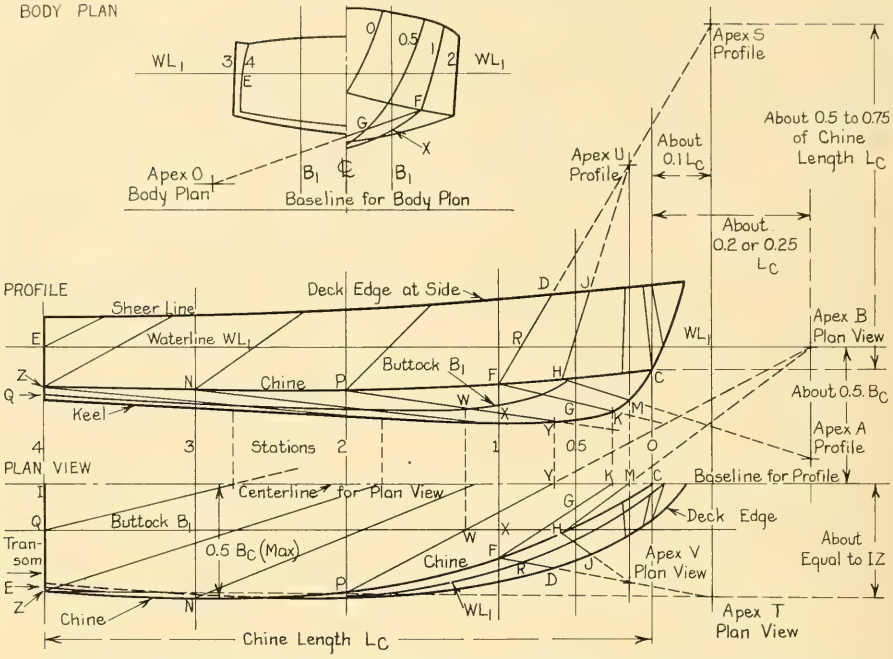

FIG. 76.D DIAGRAM ILLUSTRATING LAYOUT OF DEVELOPABLE SURFACES FOR A SMALL V-BOTTOM BOAT

(3) First establish arbitrarily the deck edge at side or sheer profile, the chine profile, the baseline in the profile, and the chine planform by drawing them in the customary manner for orthogonal projection. It is necessary to draw the sheer profile of the deck in approximately its proper relation with respect to the chine profile. In the example given by Hartman and utilized here, the baseline in the profile happens to coincide with the centerline in the plan view. It is required to find the deck edge in plan, the keel profile, and the stem profile, and to make the orthodox lines drawing with section lines and buttocks.

(4) For laying out the side, place the apex S in the profile at a height of about 0.5 to 0.75 times the chine (or overall) length L_C above the chine beginning C at the stem, and slightly forward of that beginning (0.1 L_C in the figure)

(5) Place apex T in the plan (opposite apex S and in the plane of the projection of that apex in the plan view) at a distance from the centerline, *on the same side* as the plan view to be drawn, approximately equal to the length of the half-chine beam IZ at the transom

(6) To get the proper rounding and fullness of the forward deck, the apex U in the profile, for the forward portion of the side, is to be lower and farther aft than the apex S in the profile. Its position is fixed presently.

(7) Apex A in the profile, for the conical bottom surface, is located about 0.2 or 0.25 L_C ahead of the chine beginning C. Its vertical position below the chine beginning determines the depth of the forefoot and the rise of floor in the forward sections.

(8) Apex B in the plan is located opposite apex A and *across the centerline* from that side of the bottom to be drawn. It is positioned laterally at about the distance 0.5 B_C from the centerline.

(9) Divide the chine length L_C into a convenient number of equidifferent station lengths; there are four such lengths in Fig. 76.D

(10) Draw a side generatrix from the point F along the chine profile at Sta. 1 by laying down a straight line from F to the apex S. This intersects the sheer line already drawn at D in the profile.

(11) Lay down the plan view of this generatrix by drawing a straight line from F in the plan view to apex T

(12) Project the point D in the profile downward to the latter generatrix FT, intersecting it at D. This is one point in the plan view of the deck edge at the side. FD in the profile and FD in the plan view are two projections of the same straight line in the side of the boat at the forward quarter.
(13) Starting similarly with points P, N, and Z in the chine profile, find the plan contour of the deck edge at the side abaft the point D in the plan.
(14) To get the fullness of side required at the bow a shorter and fuller cone is used. This transition is made by having the first element of the new cone *coincide* with the last element of the old cone; for example, FDU and FDS in the profile. This means that the apex U in the profile *must* lie on the generatrix FDS. Apex V is laid down on the generatrix FDT opposite apex U.
(15) From a selected point H in the chine profile forward, draw HJ on a straight generatrix toward the bow-profile apex U. This straight line intersects the sheer line at J in the profile.
(16) From the point H on the chine in the plan view, opposite H in the profile, draw a straight line to apex V
(17) Project J in the profile downward to the generatrix HV, which it intersects at J in the plan view. This is another point along the deck edge in the plan.
(18) Continue in this manner until sufficient points in the forward deck edge are available to permit drawing this line for the entire length
(19) As an aid in delineating the deck edge aft in the plan view a waterline WL_1 is drawn through the hull in the profile, parallel to the baseline. By establishing the approximate outline of the transom, half of which is indicated in the body plan, it is possible to lay down the point E on the plan view and to determine another point along the deck edge aft, lying on the generatrix ET. Another way to do this is to extend the chine for a station or two abaft the transom and follow the regular procedure.
(20) To determine the keel profile, first draw a line in the plan view from F on the chine to apex B in the plan, intersecting the centerline at K
(21) In the profile, draw a line from F on the chine to apex A. Project K in the plan upward to its intersection K in the profile with the generatrix FA. Point K is one point on the keel profile.
(22) Draw a line from another point H on the chine in the plan view to apex B; it intersects the centerline at the point M
(23) Draw a line from H on the chine in the profile to apex A. Project the point M in the plan upward until it intersects the generatrix HA at M in the profile. This is another point on the keel profile. Continue in this manner until all points along the keel profile are determined.
(24) To assist in delineating the after portion of the bottom and to help in preparing the lines drawing later, draw a buttock B_1 at about 0.4 times the half-chine beam $B_c/2$ (or draw several of them). Then draw the generatrix QB and proceed as before.

To draw the buttock B_1 in the profile:

(25) The generatrix PYB in the plan view intersects the buttock B_1 at the point W. Project this point upward, intersecting the (same) generatrix PYA in the profile at W. This is one point on the desired buttock. The remaining points are drawn in the same manner.
(26) To draw the waterline WL_1 in the plan view, the generatrix FDS in the profile intersects this waterline at the point R. Project R downward until it intersects the (same) generatrix FDT in the point R of the plan view. This is one point on the desired waterline. Continue in the same manner to find remaining points.
(27) To draw the customary body plan, it is possible to lay down the projections of the deck edge, the chine, and the keel on a transverse plane, using the station offsets of the other two views
(28) Draw apex O on the body plan, using the transverse offset of apex B in the plan and the vertical height of apex A in the profile. The transverse projections of the two apexes for the side are drawn in the same manner but they are not shown in Fig. 76.D.
(29) From the known point F on the body plan, where the chine crosses Sta. 1, draw a generatrix to the apex O. The point G where this generatrix FGO crosses the section line for Sta. 0.5 is then found by stepping off (1) the offset from G in the plan view to the centerline or (2) the height from the baseline to G in the profile, along the line FGO. Sufficient points for drawing this and all the other section lines are found by continuing this operation. The section lines, when drawn, are found to have the usual shape for a developable surface, slightly convex outward.

When the process is finished the boat may not have the shape that the designer intended. He

may then shift the various apex positions and go through the delineation process all over again. Even the most experienced designers of small craft with developable surfaces find this necessary, but with practice it is possible to perceive when the developed shape is departing from that visualized, and to correct it before too much work is put into an undesired delineation.

In the example described, the chine is used as a directrix for both the bottom and the side. Only two cones were used for the side but three, four, or more could have been used to give the side a greater tumble home aft or for other reasons. Five cones, four above the side and one below it, are employed for the 23-ft high-speed boat drawn in Fig. I on page 30 of the Werback reference cited. In fact, the apex can continue to shift from one generatrix to the next, following a continuous curve in space, *provided* that the apex always remains clear of (outside of) the portion of developed surface that is to be worked into the boat.

Reduced to their utmost simplicity, portions of developable surfaces can be flat or cylindrical. In these cases, the traces of given generatrixes are parallel to each other in all three views of an orthogonal projection.

Considering the importance of the bottom shape in a V-section craft with chines, both the keel line and the chine may be established at the outset and used as a pair of directrixes. The procedure in this case, somewhat more involved than that described, is covered in an unpublished paper by L. K. Losee, reference (e) listed at the beginning of this section. Mr. Losee is, at the time of writing (1955), on the staff of the Bureau of Ships of the U. S. Navy Department.

76.9 Design of Discontinuous-Section Forms; Blisters and Bulges. Chap. 28 explains that it is frequently convenient to incorporate discontinuities in the transverse sections of an underwater hull, either to simplify construction or to take care of some special situation which arises after the vessel is built. The ship which has a blister added to the outside of its hull, as in Fig. 76.E, whether it is a vessel which needs torpedo protection or more beam and displacement, or a submarine which needs external ballast tanks attached to its pressure hull [USNI, Feb 1955, p. 159], calls for the use of design principles that are essentially the same.

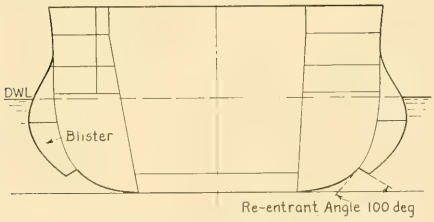

Fig. 76.E Midsection of World War II German Cruiser *Prinz Eugen* with Blisters

Actually, if certain basic principles are followed, rather amazing discontinuities of this type, in the way of saddle tanks, thick fender strakes, and the like, can be worked into underwater sections without incurring too much friction or pressure resistance. These principles may be stated as follows:

(a) The chine lines are to be so placed that the water, when flowing around the ship at the speed and under the conditions considered most important, follows but does not have to cross them

(b) When there are "offset" surfaces between chines and coves, illustrated in diagram 3 of Fig. 76.F, which are of appreciable area *when projected on a vertical transverse plane,* it appears wise to make the projected areas facing aft about equal to those facing forward, even though the actual offset surfaces do parallel the lines of flow. For example, in the body plans of the German submarine *U-111* in Figs. 28.B and 28.C, the projected area of the offset surfaces between the chines and the coves in the forebody is of the same order of magnitude as the area of those in the afterbody. There is no known hydrodynamic justification for this rule; only the engineering intuition of the author.

(c) The lower offset surfaces of discontinuous sections, if near the water surface, are shaped to parallel the general surface-wave profile at the selected speed. Otherwise they will lie at angles to the streamlines and may produce areas of separation.

(d) It is desirable to limit the sides or offset surfaces of a cove, at least those lying perpendicular or nearly so to each other, to the minimum practicable widths. This can frequently be accomplished by sloping or cutting away the edge of the projecting portion beyond the region where a right-angled connection is required for structural reasons, indicated in diagrams 1 and 2 of Fig. 76.F.

(e) The reentrant angle at the bottom of a cove should be as large as practicable; in no case

should this angle, measured on the water side, be less than 90 deg. If the reentrant angle of a cove is much larger than 120 deg and approaches 180 deg, the position and direction of the cove, with reference to the adjacent streamlines, is not too important.

(f) The discontinuities should fade out at the ends and merge gently into the fair form of the hull

(g) Shell openings on ducts or pipes leading into the hull proper are best kept clear from the region close underneath the offsets in discontinuous sections. This is particularly true where both sides of the cove slope upward, forming a possible trap for air. Such a cove in the entrance may easily collect air coming down from the region of the bow-wave crest. The length of the discontinuity may be so great that this air is not readily carried along and released in the run, where the cove slopes upward.

Although they represent longitudinal discontinuities of relatively small transverse section, *bulged fender strakes* may be classed with small bulges and blisters. Discussing structural matters for a moment, the combination of simplicity of construction, ease of upkeep, and greater efficiency dictates the use of heavy, *single-thickness* fender strakes, conforming to the adjacent hull shape or bulge, instead of built-up external fenders. They may lie below the surface waterline on submarines, as at 3 in Fig. 36.N and at 1 in Fig. 73.Q, or at or near the waterline on tugs, sketched in Fig. 68.J. Diagrams 4 and 5 of Fig. 76.F illustrate several types of bulged fender strakes, not including one of circular-arc section. These may be worked in as part of the hull plating, either above or below water, and in a flat or curved side.

Blistered fender strakes should involve not-too-small reentrant angles where they join the main hull plating. As far as practicable they should follow the actual lines of flow as modified by surface waves, especially at that speed for a given ship at which low resistance is considered important. If bulged fender strakes must of necessity be placed at the waterline the disturbance to surface wave action must be accepted.

It should be possible, when blister sections are sketched in, to lay down suitable cove traces which will, when the blister is in place, lie very nearly along the resultant lines of flow. This is particularly true if the blister, as it should, fairs reasonably well into the original hull and does not make an awkward bump upon it.

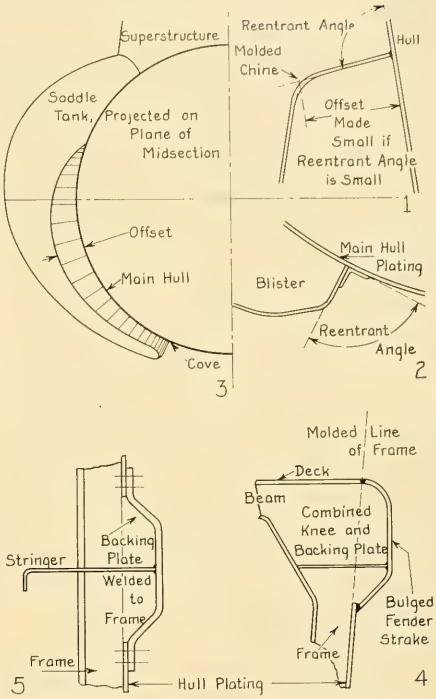

Fig. 76.F Design Details for Discontinuous Sections

When designing a blister to be added to an existing ship, for which the lines of flow are available, these may be used for guidance in laying out the coves, chines, knuckles, and other longitudinal discontinuities. It must be expected, however, that the addition of a blister of relatively large volume may change the flow pattern around the combination. A check test is called for at an early design stage to insure that the flow around the ship-and-blister assembly is satisfactory.

A special case arises when external blisters are added locally—and usually temporarily—in the form of boxes, pontoons, and the like to give added buoyancy, or transverse metacentric stability, or both, to a hull which must be floated through a region of exceptionally shallow water, or which must be held upright when lifted to a draft corresponding to that acceptable for the shallow-water area [MESR, Jun 1952, p. 53; Oct 1954, p. 58].

It is sometimes necessary to tow a vessel thus

supported, either before or after entering the shallow water, through a region of deep water. The towline tension for such an operation must be approximated and the protuberances, with their connections to the main hull, must be able to withstand the forces and moments due to waves and to the motion of the buoyed-up hull in waves. No systematic design data are available for use in situations of this kind but the problem is one readily and simply handled by a model basin which possesses a model of the ship to which the protuberances are to be attached.

76.10 Vessels with Fat Hull Forms. Length of hull, which is an asset when striving for speed and propulsive efficiency, becomes somewhat of a liability when first cost, compactness, hull stiffness, maneuverability, and habitability are important factors. This is especially true for craft which are small compared to the minimum sizes for berths, lockers, passageways, and access for the crew. Sailing yachts, tugs, small fishing craft, work boats, and similar vessels are, more often than not, fat and chubby. Icebreakers are larger vessels in this category. Their displacement-length quotients run up to 500 or more, with 0-diml fatness ratios of 17.5 and above. Their length-beam ratios are invariably small, generally less than 5 and sometimes as small as 3.

Figs. 66.D and 66.I indicate that separate design lanes, or branches of regular lanes, are needed for these craft. The two lanes of Fig. 66.A each have branches of this kind. They are omitted from the latter figure partly to avoid complication and partly because insufficient data have been collected to locate them properly. In general, data for existing craft in the fat and chubby category are widely scattered.

It is unfortunate that the Taylor Standard Series was not extended to embody fat forms having displacement-length quotients $\Delta/(0.010L)^3$ in excess of 250, corresponding to a fatness ratio $\forall/(0.10L)^3$ of 8.77. Partly to fill this gap there are given in Sec. 56.6 the results of an analysis of miscellaneous model-test data on fat forms made by R. F. P. Desel and J. T. Collins.

76.11 Requirements and Design Notes for Fishing Vessels. Fishing vessels of all types and sizes are characterized by the requirement that they must "keep the sea and work on it, all the year around, and in all weathers" [Simpson, D. S., SNAME, 1951, p. 561]. Large or small, they are essentially robust, ocean-going craft, whether they work five miles off a wintry, rock-bound coast or, like whale catchers, they travel from Norway to the Antarctic and back again for every whaling season.

It is pointed out by Ambrose Hunter ["The Art of Trawler Planning," Ship and Boat Builder and Naval Architect, London, Feb 1953, pp. 259–260] that fishing vessels in general:

(I) Are similar to tugs in that they have to tow fishing gear, nets, and trawls, yet have to possess a high free-running speed
(II) Are akin to lightships in that they spend more time stopped at sea than any other type
(III) Are like sailing yachts in their resistance to drifting, ease of handling, and extreme maneuverability.

Specific hydrodynamic requirements adapted from D. S. Simpson [SNAME, 1951, p. 561] and R. F. Symonds [SNAME, 1947, pp. 381, 384] include the following, together with appropriate comments concerning design:

(1) Adequate metacentric stability, both static and dynamic, for all conditions of loading, including the top weight of a coating of ice over everything above water. This coating may amount to 20 tons or more. Metacentric stability is outside the scope of this book; see PNA, 1939, Vol. 1, Chap. III, pp. 99–137, and other standard references.
(2) Moderate change of trim between extreme operating conditions, such as when entering and leaving the fishing grounds
(3) More than adequate or above-average wave-going ability, at all speeds which can be maintained in the heaviest weather. These design features are covered in Part 6 of Volume III.
(4) Easy motion to provide a good working platform in reasonably rough water, over a range of speeds where fishing gear can be handled. The design comments of (3) preceding apply here as well.
(5) Reasonably dry decks, accepting spray but no breaking seas or solid water, over the range of speeds mentioned in (4), so that fishing can proceed even in bad weather. The design comments of item (3) apply.
(6) Extra-large freeing ports or freeing slots in the bulwarks, screened to hold men, gear, and fish but not water
(7) Ability to slow down or to heave to while retaining steering control, so that the vessel can be held in any desired position in wind and waves

(8) Sufficient submergence of the propeller and rudder, under wavegoing conditions, to give them a hold on the water and to render the vessel fully manageable

(9) Minimum of drifting when broadside or nearly so to the wind and sea, as when hauling in gear and nets from abeam. The effect of drift-resisting keels is discussed in Sec. 36.15; some design rules for them are included in Sec. 73.19. The drift-resisting effect of a deep hull, like that of the pilot boat *New York* illustrated in Fig. 36.K, is appreciable.

(10) Positive stability of route under all load conditions; this is discussed in detail in Part 5 of Volume III

(11) Ample speed for running to and from the fishing grounds. This feature is rather closely related to the provision of a reasonably high free-running speed for tugs. It is one reason why fishing vessels, like tugs, are invariably over-powered for their size.

While nothing is said in the foregoing about minimum resistance and shaft power to meet the several requirements, there is no more excuse for unnecessary resistance and little more excuse for unneeded power in a fishing vessel than in a craft of any other type.

With respect to fishing vessels as a class, Jan-Olof Traung has come to the following conclusions concerning the effect of form parameters on resistance, based upon analyses of tests on a considerable number of models [Int. Fishing Boat Congr., Paris and Miami, Oct-Nov, 1953, "Outline to a Catalog of Fishing Boat Tank Tests"]:

(a) The displacement-length ratio is of little importance. In other words, it can be as high as required for other reasons.

(b) Enlarging the beam does not increase resistance

(c) The center of buoyancy should be well aft. It is possible that the position of the maximum-area section should also be abaft midlength.

(d) Differences in the block coefficient C_B, below 0.55, have little or no influence

(e) The prismatic coefficient C_P is of great importance, with an optimum value of about 0.575

(f) Transom sterns act to reduce resistance

(g) The half-angle of entrance, or the waterline slope i_E in this region, should be low

(h) Parallel middlebody and sharp shoulders are to be avoided. Fig. 76.G illustrates the lines of one of Traung's models.

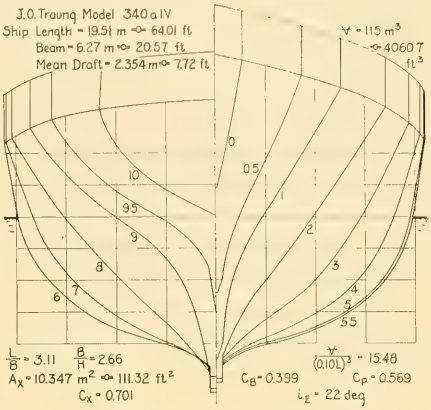

FIG 76.G BODY PLAN, EUROPEAN FISHING BOAT, J.-O. TRAUNG'S MODEL 340a

Data from the Japanese fishing-vessel standard series are referenced and summarized in Sec. 56.4.

The multiplicity of longitudinal fender bars fitted on some steel trawlers to prevent damage to the shell plating by heavy fishing gear banging along the side is probably more objectionable from a maintenance standpoint than for the added resistance which they cause. A construction much to be preferred from all points of view is described and illustrated in Sec. 73.22 and Figs. 73.Q and 76.F. It embodies heavier shell plating and a complete absence of all applied appendages in the form of fender bars, fender shapes, and fender strips.

A combination of controllable propeller and swinging tubular rudder or Kort nozzle, designed for astern as well as ahead propulsion, is an excellent combination for a fishing craft. Such a combination, designed by the Swedish naval architect Jan-Olof Traung, is illustrated and described in Motorship, New York, Jun 1950, pages 42 through 44.

76.12 Partial Modern Bibliography on Fishing Vessels. The modern literature on the design and construction of fishing vessels, say for the period following the year 1930, is very extensive. This is not surprising because, although the average fishing vessel is less than 100 or 125 ft in length, the number of types and kinds is incredibly large.

An insight into the great breadth of this field and the variety in it is afforded by a reading of the excellent recent book entitled "Illustrations

of Japanese Fishing Boats." Although published by the Fisheries Agency of Japan, in 1952, the man primarily responsible for it is Atsushi Takagi, Chief of the Fishing Boat Section of the Fisheries Agency. Among other information the book contains the following:

(a) Summary tables of the Japanese fishing fleets by types of vessels and kinds of engines, made up of some 23 or 24 categories
(b) Tabulated characteristics of 42 typical vessels, from whale factory ships to fisheries training boats, giving general information, principal dimensions, capacities, form coefficients, and related data for light- and full-load condition, as well as full-scale trial data; 37 entries for each vessel
(c) Forty photographs of typical fishing vessels, both large and small
(d) Technical data on 50 typical fishing vessels, comprising general arrangement plans, lines drawings, displacement and other curves, machinery and piping arrangements, fishing gear arrangements, refrigeration installations, and the like. The data presented are not the same for all vessels. The largest vessel has 15 plates of data; the least important vessels 3 and 4 plates.
(e) All dimensions are in the metric system.

A more recent informative book, of international scope, is "Fishing Boats of the World," edited by Jan-Olof Traung and published by Fishing News, London, 1955, through A. J. Heighway Publications, Ltd., Ludgate House, 107 Fleet St., London, E.C.4. The following explanatory paragraph is copied from the letter forwarding the first of these books from the Food and Agriculture Organization of the United Nations:

"It is important to emphasise that 'Fishing Boats of the World' is not meant to be a book on naval architecture. It is a book dealing with that part of fishing boat design which is missing from all textbooks on naval architecture, and it is so written and presented that everyone concerned with building fishing boats can find its illustrations and information of practical value. It is not suggested that the book contains information about every type of fishing boat, but it does provide a comprehensive survey of a great number of boats, from beach landing craft to modern trawlers and factory ships."

The specific references which follow are listed for convenience under the headings:

Historical and General
Model Tests
Design and Construction
Small Vessels
Tuna Clippers
Trawlers and Sealers
Whale Catchers
Fisheries Research and Exploration Vessels.

Historical and General

(1) Owen, G., "Outstanding New England Types of Fishing Boats, Whalers, and Yachts," SNAME, HT, 1943, pp. 145–151, 163–164
(2) "Ships and Sailing Albums," Book 4, Kalmbach Publishing Co., 1027 No. Seventh St., Milwaukee 3, Wis. Describes New England fishing schooners.
(3) Cunningham, D. B., "Notes on Trawl Fishing," IESS, 1948–1949, Vol. 92, pp. 260–330
(4) Hardy, A. C., "Seafood Ships," Crosby, Lockwood & Son, Ltd., 20 Tudor St., London, E.C.4., 1947
(5) Symonds, R. F., and Trowbridge, H. O., "The Development of Beam Trawling in the North Atlantic," SNAME, 1947, pp. 359–384
(6) "A Review of the British Fishing Industry," Continental Daily Mail, London, Apr 1952
(7) D. S. Simpson gives 8 references to papers and articles on fishing and fishing-boat design in SNAME, 1951, p. 582
(8) There are many references to be found under the heading "Fishing Vessels" in the Engineering Index Summaries of the SNAME Member's Bulletins, dating from 1946 to the present
(9) Many journals publish news on current trends in fishing-boat design and construction. General-arrangement drawings of new fishing boats can normally be found in every issue of the following journals:
Yachting Magazine, 205 East 42nd Street, New York 17, N.Y.
The Rudder, 9 Murray Street, New York 7, N.Y.
"Fishing Gazette," Fishing Gazette Publishing Corporation, 461 Eight Ave., New York, N.Y.
"Pacific Motor Boat," Miller Freeman Publications, Inc., 71 Columbia St., Seattle 4, Washington.
(10) Articles about fishing boats, but with fewer drawings, are published in:
"Atlantic Fisherman," Atlantic Fisherman, Inc., Goffstown, New Hampshire
"Pacific Fisherman," Miller Freeman Publications, Inc., 71 Columbia St., Seattle 4, Washington.
(11) The U.S. Government Fish and Wildlife Service publishes the monthly "Commercial Fisheries Review." This is obtainable by writing to the Service at the U.S. Department of the Interior, Washington 25, D.C.

Model Tests

(12) Nordström, H. F., "Försök med Fiskebåtsmodeller (Tests with Fishing Boat Models)," SSPA Rep. 2, 1943; English summary on pp. 30–32 and 5 references on p. 29
(13) Traung, Jan-Olof, "Några Erfarenheter Från Tankförsök med Fiskebåter (Some Experiences of Tank Tests with Fishing Boats)," Unda Maris, Göteborg Yearbook of the Nautical Museum, 1947–1948. The paper carries a summary in English on pp.

65–68 but there is a complete English version in BSRA Transl. 58. A very comprehensive paper, with a list of 40 references on pp. 62–63.

(14) Traung, Jan-Olof, "Skärpning av Fiskebåtars Förskepp (Finer Entrances for Fishing Boat Hulls)," Göteborg Yearbook, 1948; translated by the BSRA

(15) Traung, Jan-Olof, "Svenska Tankförsök med Fiskebåtsmodeller (Swedish Tank Tests with Fishing Boat Models)," Norwegian Shipping News, 1949, No. 9; translated by the BSRA

(16) There are SNAME RD sheets for fishing vessels available as indicated hereunder. Some form coefficients and proportions are listed under "TRL" on page 35 of SNAME Tech. and Res. Bull. 1–14, Jul 1953:

Sheet number	Type	Length, ft	Beam, ft	Draft, ft	Speed, kt
111	Trawler	130	28.5	12.5	13
123	Trawler	110.5	22.48	10.69	11
125	Trawler	144.4	27.1	12.8	11.5
126	Trawler	227.5	38.55	17.18	12
127	Trawler	59.2	16.96	5.12	10
142	Trawler	119.8	25.67	11.0	12.5
157	Trawler	124.7	24.6	11.48	11.5

Design and Construction

(17) Taylor, A. R., "Fishing Vessel Design," INA, 1943, pp. 95–103

(18) Spanner, E. F., "Seaworthiness and Stability of Trawlers and Drifters," Joint mtg. INA and IESS, 24 Sep 1946. Abstracted in SBSR, 26 Sep 1946, pp. 354–356; 3 Oct 1946, pp. 381–382.

(19) Holt, W. J., "Admiralty Type Motor Fishing Vessels," INA, 12 Apr 1946, pp. 295–307

(20) "New Type of Motor Fishing Vessels for the Herring Industry Board," SBSR, 5 Jun 1947, pp. 566–567. Lines drawings are given of two 65-ft experimental herring drifters, based on previous model experiments.

(21) Smith, R. A., "Scantlings for Small Wooden Vessels," SNAME, Pac. Northwest Sect., 26 Aug 1950

(22) Simpson, D. S., "Small Craft, Construction and Design," SNAME, 1951, pp. 554–611, esp. pp. 561–564 on the trawler, and drawings on pp. 564–569, 571, 574–579, 581

(23) Traung, Jan-Olof, "Improvement of Fishing Vessels," FAO Fishing Bulletin, Jan/Feb and Mar/Apr 1951, Food and Agricultural Organization of the U.N., International Documents Service, 2960 Broadway, New York, N.Y.

(24) Henschke, W., "Schiffbautechnisches Handbuch (Shipbuilding and Ship Design Handbook)," 1952, Section on "Fishing-Vessel Design," pp. 592–613

(25a) Traung, Jan-Olof, "Fisheries and Naval Architecture," FAO Fisheries Bulletin, 1955, Vol. VIII, No. 4 (in English), FAO, United Nations, Rome.

(25b) A good review of current literature on fishing-vessel design and construction throughout the world is given in the FAO World Fisheries Abstracts, published by the FAO Headquarters in Rome.

Small Vessels

(26) "Modern Development of the Herring Drifter," SBSR, 30 Apr 1942, pp. 468–470. Gives outlines of profiles, with freeboard and sheer, as well as body plan.

(27) "*Arcturus*–Shrimp Trawler with New Idea," Motorship, New York, Jul 1947, pp. 26–28, 30. Length 108 ft, beam 25 ft, and designed draft 7 ft.

(28) Dyer, J. M., "The Development of the Columbia River Gill-Net Boat," SNAME, Pac. Northwest Sect., Oct 1947

(29) "Presenting a Group of Fishing Vessels Powered by GM-Diesels," Diesel Times, Mar 1948, pp. 7–8. Shows several 60- and 65-ft vessels with large transom sterns.

(30) Nickum, G. C., "Pacific Coast Fish Processing Vessels," SNAME, Pac. Northwest Sect., 9 Dec 1949

(31) Robison, D., "Diesel Draggers," Diesel Prog., Apr 1950, pp. 56–57

(32) Mann, C. F. A., "Twin Steel Diesel Shrimpers," Diesel Prog., Jan 1951, p. 47. These vessels are 54 ft long by 16 ft beam by 6 ft depth, with wide transom sterns.

(33) Goodrich, J. F., "The Fishing, Processing Vessel *Deep Sea*," SNAME, Pac. Northwest Sect., 27 Apr 1951

(34) Granberg, W. J., "Northwest Yards Launch Fishing Craft," Diesel Prog., May 1951, pp. 44–45.

Tuna Clippers

(35) Snyder, G., "Stability of Tuna Clippers," SNAME, Pac. Northwest Sect., 3 May 1946

(36) Mann, C. F. A., "*Sun Traveler*—A 121-Foot Tuna Clipper for San Diego," Diesel Prog., Mar 1948, p. 52

(37) "Tuna purse seiner *Santa Helena*," Diesel Prog., Jun 1948, pp. 41–42

(38) Mann, C. F. A., "New Baby Tuna-Clipper *Conqueror*," Diesel Prog., Feb 1949, pp. 30–31

(39) Petrich, J. F., "The Tuna Clipper," SNAME, North. Calif. Sect., 31 Mar 1949

(40) Pugh, M. D., "The Tuna Clipper *Carol Virginia*," Motorship, New York, May 1949, pp. 18–19

(41) Mann, C. F. A., "Tuna Clipper *Mermaid*," Diesel Prog., Sep 1949, pp. 42–45

(42) Mann, C. F. A., "*Mary E. Petrich* World's Largest," Diesel Prog., Oct 1949, pp. 40–41. Describes and illustrates tuna clipper with an overall length of 150 ft, a beam of 34 ft, a depth of 16 ft, and a maximum speed of 13.75 kt.

(43) Mann, C. F. A., "Tuna Clipper *Hortensia-Bertin*," Diesel Prog., May 1950, pp. 54–55

(44) Barbour, H. J., "*Marilyn Rose*, Pacific's Newest Tuna Clipper," Diesel Prog., Sep 1950, pp. 46–47

(45) Mann, C. F. A., "A Temporary Lull in Tuna Clippers Ends with Diesel Powered *Modego*," Diesel Prog., Jan 1951, p. 53

(46) Hanson, H. C., "The Tuna Clipper of the Pacific," SNAME, 1954 Spring Meeting. This is a well-illustrated and informative paper; see also SNAME 1954, pp. 30–42. For the 130-ft vessel whose

curves of form are given in Fig. 11, the following data have been worked out for a 17-ft draft:

L = 130 ft	B/H ratio = 1.76	$\Delta/(0.010L)^3$ = 494
B = 30 ft	Δ = 1,085 long tons	$V/(0.10L)^{\frac{1}{2}}$ = 17.32
D = 17 ft	C_B = 0.648	V = 11.7 mi per hr ≈ 10.16 kt
L/B ratio = 4.33	C_P = 0.732	C_W = 0.88 C_X = 0.88.

Trawlers and Sealers

(47) Symonds, R. F., and Trowbridge, H. O., "The Development of Beam Trawling in the North Atlantic," SNAME, 1947, pp. 359–384, esp. pp. 371–384 on Trawler Design

(48) Shearing, Douglas, "152-foot Trawlers for French Fishing Industry," Diesel Prog., Feb 1948, p. 56, with photograph of trawler *Clair de Lune*. Single propeller is variable pitch, with D of 8.83 ft, P of 6.175 ft, and 4 blades. Speed is 11 kt with n of 200/60 = 3.33 rps.

(49) Diesel-engined Sealer (*Terra Nove*) on Maiden Voyage, Diesel Prog., Feb 1948. L_{OA} is 140 ft, B is 28 ft, and D is 14 ft. Speed is 9 kt.

(50) French fishing trawler *Saint Joan*, Proc. Am. Merch. Mar. Conf., 1949, p. 292. A photograph shows rather well the form of the hull amidships and the form of the run, with the single propeller and rudder.

(51) Diesel trawler *Gudrun*, Diesel Times, Oct 1949, pp. 1–2. Length is 115 ft and beam 23 ft.

(52) "A Powerful Motor Trawler," SBSR, 31 Jan 1952, p. 139. This vessel has a length of 185 ft, a beam of 30.5 ft, a depth of 16 ft, and a speed of 13.63 kt.

(53) Jaeger, H. E., "Large Trawlers," INA, Apr 1954; abstracted in the May 1954 issue of The Motor Ship, London, pp. 62–63.

Whale Catchers

(54) Matthews, L. H., "South Georgia: The British Empire's Subantarctic Outpost," 1931, pp. 123, 125–126

(55) Granberg, W. J., "Diesels go Whaling," Diesel Prog., Dec 1949, pp. 34–35. Describes wooden vessels, 115 to 140 ft long, for North Pacific whaling.

(56) Norway's New Whale-Catcher Ships, Nautical Gazette, Jan 1951. Mentions a 16-kt speed with a brake power P_B of 2,400 horses.

(57) Whale catcher *Setter II*, SBSR, Feb 1952, p. 55. This vessel has an L_{OA} of 177.5 ft, an L_{PP} of 160 ft, a depth D of 17.5 ft, and a mean draft, fully loaded, of about 15.6 ft, including a bar keel about 0.62 ft deep. The displacement corresponding is 1,080 long tons. The trial speed is 15.3 kt, and the vessel has a single screw.

(58) Shearing, Douglas, "The Whaler *Enern*," Diesel Prog., Sep 1953, pp. 36–37. This vessel has an L_{OA} of 210 ft, an L_{PP} of 186.5 ft, a B of 33 ft, and a D of 18.33 ft. The brake power of the single engine is 2,700 horses; n is 225 rpm or 3.75 rps, and the speed V is 16–17 kt.

Fisheries Research and Exploration Vessels

(59) Hanson, H. C., "The Conversion of Pacific Fisheries Exploration Vessel," SNAME, Pac. Northwest Sect., Oct 1947

(60) Mann, C. F. A., "Diesel Ship *John N. Cobb*," Diesel Prog., Apr 1950, pp. 40–41.

76.13 Fireboats or Firefloats. Fireboats as a class are among the earliest of mobile special-service vessels, dating in the Americas from the 1870's. In Europe these vessels are normally called firefloats. It is probable that neither the vessels themselves nor the class will ever be large, yet the type is interesting for the complex problems it poses in naval architecture and marine engineering.

The service requirements involving hydrodynamics, listed hereunder, are adapted from a paper by A. D. Stevens [SNAME, 1922, pp. 137–141 and Pls. 44–52], from a group of excellent articles in Motorship [New York, May 1950, pages 17–57], and from a more recent paper by D. S. Simpson [SNAME, 1951, pp. 564–568]. They are set down more or less in the order of their importance:

(a) Instant availability and prompt arrival at the fire. This involves free-running speeds of 11 to 14 kt, in the present stage of development, depending upon how far the craft has to travel from its station.

(b) Extreme maneuverability, involving a high degree of handiness, rapid response, and ability to move in almost any direction. In particular, the boat must be able to steer and maneuver when backing.

(c) Ability to stay put in the position and at the heading desired, under the reaction forces exerted at the discharge nozzles

(d) Stiffness sufficient to give only a moderate list, say not in excess of 6 deg, when all fire-fighting nozzles are directed horizontally and abeam, and discharging at full capacity

(e) Flexibility of drive for propulsion and for pumping. The greater part of the power should be available for taking the vessel to the fire; an equally large portion should then be available for pumping water.

(f) Freedom from clogging of the fire-pump suctions if the boat has to operate in water depths only slightly exceeding its draft. These suctions must also remain clear of ice and debris floating at or near the surface.

(g) Ability to push or pull on vessels in an emergency, like a tug. This involves propulsion devices with large disc areas or equivalent-disc areas A_0. In terms of screw propellers this means

that they are neither too small nor too heavily loaded when running free.

(h) Too much attention need not be paid to a hull of minimum free-running resistance, if other more important features are thereby improved. As a rule, the pumping requirements call for plenty of power so that a not-too-high hull drag may be accepted if it leads to a better all-around firefighting craft.

(i) Harbor icebreaking features, if called for; see Sec. 76.26 following.

To achieve maneuverability and handiness in and around scenes of possible fires:

(1) The craft should not be too large. Depending upon the pumping capacity required, lengths of 70 to 80 to 90 ft are adequate. Lengths of 110 and 120 ft are approaching the extreme; 125 ft is possibly the maximum [Parsons, H. de B., SNAME, 1896, p. 49].

(2) The length-beam ratio should not exceed 5.0. Preferably it should lie between 4.0 and 4.5.

(3) The sides should have continuous curvature, as for a tug, to enable the heading to be changed readily when the vessel is alongside a pier or another ship. The ends should be well rounded, to prevent the craft from jamming itself between piles and the like.

(4) The draft should be a minimum consistent with other characteristics

(5) There should be no excessive keel drag or filling out of the lateral plane at either end

(6) The rudders should always be so placed as to lie in the propeller outflow jets.

The reaction forces at the discharge nozzles or monitors, illustrated pictorially in Fig. 76.H and indicated numerically by the example given later in this section, can be very large. They are counteracted by one or more of the following procedures or devices:

(7) Constantly moving the fireboat or holding it on a certain heading with its propulsion device(s) turning over. This may involve a corresponding shift of the water streams to keep them playing on a desired spot of the fire.

(8) Passive drift-resisting keels, described in Sec. 36.15, or the equivalent. These are a help at times but they are not adequate for all possible situations.

(9) The provision of one or more swinging or rotating-blade propellers. This method, however,

Fig. 76.H Honolulu Fireboat *Abner T. Longley* With Jets in Action
Photograph by Lawrence Barber, Portland, Oregon

necessitates either an accepted projection of the swinging propellers and rotating blades below the hull or cutups in the hull forward and aft to accommodate these devices. There is generally not room within the vessel, nor would there always be room under it, for retractable propellers of any kind. The cutups involve an increase in thrust deduction and a loss of efficiency but there are several successful applications of this kind. A ferryboat installation, equally applicable to a fireboat, is that on the Virginia ferry *Northampton*, where a Voith-Schneider rotating-blade propeller under the bow supplements the twin propellers at the stern [Motorship, New York, New York, Aug 1950, pp. 26–27, 43].

(10) It may at times be possible to turn a few of the jets in the opposite direction, to balance some of the reactions from the firefighting jets

(11) Concentrating the monitors near midlength of the vessel avoids the turning or swinging moments set up when monitors near the ends are playing.

An arrangement of underwater reaction jets might be thought more efficient for holding the fireboat in position because these would impart momentum to some of the surrounding water in the same direction as the jet. It is to be remembered, however, that neither force nor pressure is communicated backward through a liquid jet, at least not for distances more than a few times the jet diameter. The reaction force is all developed when accelerating the water *in the nozzle*, so the force is made no greater by playing the jet against some fixed obstacle nearby or by directing it into the water. When the nozzle reactions are used to augment the propulsive thrust to get the fireboat free of a hot spot in an emergency, playing the jets horizontally into the air gives the greatest reaction.

One important feature of fireboat design involving hydrodynamics has to do with the efficiency of the monitor nozzles. This is measured by the percentage of the total quantity flow of water that can be delivered per unit time *at the greatest possible distance from the nozzle*, reckoned on the basis of the quantity rate passing through the nozzle. A jet which disintegrates on its way to the fire or which has a short trajectory is inefficient. Breaking up of the jet in the air, as well as failure of the water to "carry," is a function of the turbulence existing in the water upon its entrance into the large end of the nozzle. Low turbulence, a more "solid" jet, and projection of more water to a greater distance is achieved by slowing down, straightening out, and quieting the water immediately ahead of the nozzle. There is insufficient information available in connection with Fig. 76.H to indicate how far the five jets are carrying in that case. Nevertheless, the photograph clearly reveals that a considerable amount of water is dissipated in the form of spray and would probably never reach a fire into which the jets were directed. The reader who is interested in this aspect of fireboat design may consult a paper by H. Rouse, J. W. Howe, and D. E. Metzler, entitled "Experimental Investigation of Fire Monitors and Nozzles" [ASCE, 1952, Vol. 117, pp. 1147–1188]. Improved designs recommended for nozzles and monitors are shown in Fig. 3(c), Table 1, and Fig. 21 on pages 1152, 1172, and 1174, respectively, of the reference cited, and in Fig. 76.I of the present section.

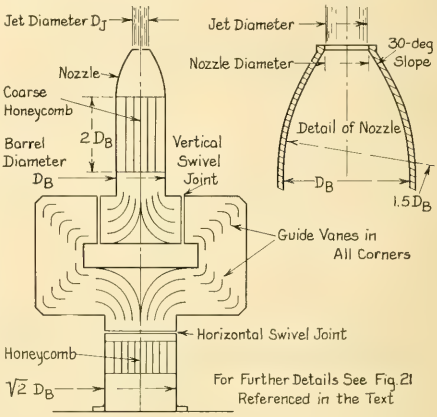

Fig. 76.I Improved Design of Fixed Fire-Fighting Monitor Recommended by the Iowa Institute of Hydraulic Research

In the design recommended by the IIHR and illustrated here, there are two honeycombs for removing turbulence, one in the stand and another in the barrel. Flow in the 90-deg corners is facilitated by the guide vanes shown. The nozzle is simpler than, and superior in performance to orthodox designs.

To obtain an idea of the reaction exerted by the vertical swiveling part of a monitor, comprising a nozzle fed from a horizontal 90-deg branch on each side, assume that the barrel fed by these

branches is of 6-in diameter, and that the nozzle orifice, slightly larger than 2 in, produces a 2-in diameter jet. As the same water passes through both, $V_{\text{Jet}} = (6^2/2^2)V_{\text{Barrel}} = 9V_B$. From the energy equation [Rouse, H., EH, 1950, pp. 65–66]

$$\frac{V_B^2}{2g} + \frac{p_B}{w} = \frac{V_J^2}{2g} = \frac{(9V_B)^2}{2g} \qquad (76.i)$$

Assume further that the acceleration of gravity g is 32.174 ft per sec^2, that the salt water being pumped has a specific weight w of 64 lb per ft^3, and that the pumping pressure in the barrel is 150 psi. Then

$$V_B = \sqrt{\frac{2gp_B}{w(9^2 - 1)}} = \sqrt{\frac{64.35(150)144}{64(80)}} = 16.5 \text{ fps}$$

whence $V_J = 9(16.5) = 148.5$ fps. As the feeding branches come into the barrel at right angles, ΔV is also 148.5 fps, reckoned in the jet direction.

Then F_m, the force on the vertical-swiveling nozzle assembly, is

$$F_m = \rho Q \Delta V$$
$$= 1.9905\left[\frac{148.5\pi(1)^2}{144}\right]148.5 = 958 \text{ lb.}$$

The horizontal reaction on the fireboat is, roughly, the nozzle-assembly reaction times the cosine of the angle of elevation of the nozzle above the horizontal. The *transverse* reaction on the boat is the horizontal reaction times the sine of the angle which the nozzle makes with the boat centerline.

It is sometimes necessary to hold a fireboat reasonably stationary in space in a tidal current or flowing river. The propulsion devices turning over slowly furnish the necessary force to breast the current but there remains the problem of holding the craft transversely against the water-jet reaction forces if the monitors are playing at right angles to the current direction.

An expert boat handler can possible yaw the fireboat slightly toward the direction of the fire and balance the transverse yawing force against the combined nozzle reaction forces. However, the design situation here is exactly comparable to one frequently met with in submarines, where it is necessary to hold the vessel at about zero trim and at a given depth against relatively large amounts of positive or negative buoyancy. For negative buoyancy this is done by giving the bow planes a slight rise angle and the stern planes a slight dive angle; in this position the leading edges of both sets of planes point upward and both are exerting positive lift. By adjusting the angles, the moment of these lift forces balances the moment of the negative buoyancy.

Tipping the submarine over on its side, in imagination, produces the fireboat equipped with both bow rudder and stern rudder. Swinging the leading edges of both rudders toward the fire produces a lateral force to counteract the nozzle reaction force. It is to be remembered, however, that the lift produced by the bow rudder, without the benefit of a propeller outflow jet, varies directly as the first power of the rudder angle and as the square of the water velocity past it. A 4-kt current might easily give the required lateral force forward, with not too great a rudder angle, whereas this might be difficult to obtain, with a large rudder angle, in a 1-kt current.

Appended is a brief list of references relating to fireboats, supplementing those mentioned at the beginning of this section:

(i) Parsons, H. de B., "Fire-Boats," Cassier's Mag., May 1896, pp. 28–45. This article carries a considerable amount of historical data and many illustrations.

(ii) Parsons, H. de B., "American Fire-Boats," SNAME, 1896, pp. 49–64. Tables I, II, and III give detailed data on 24 fireboats dating from 1875 through 1895.

(iii) West, C. C., "Centrifugal-Pump Fire-Boats," SNAME, 1908, pp. 211–228 and Pls. 116–121

(iv) Seattle Fireboat *Alki*, Diesel Prog., Mar 1949, p. 43

(v) Robison, D., "Milwaukee's New Fire Boat *Deluge*," Diesel Prog., Oct 1949, pp. 24–25. The overall length is 96.58 ft, the waterline length is 93 ft, and the molded beam is 23 ft, with a draft of 6.75 ft.

(vi) Houston Fireboat *Captain Crotty*, MESR, Dec 1952, pp. 86, 112

(vii) New Fireboat *John D. McKean* for New York City, Mar. Eng'g., Feb 1953, pp. 79–80; Sep 1954, pp. 54–58; SBSR, Int. Des. and Equip. No., 1955, pp. 68–69. The L_{OA} is 128.75 ft, the L_{WL} 125 ft, the B 30 ft, the D 14.25 ft, and the H_{Max} is 9.25 ft; there are 2 screws.

(viii) "The World's Fire-Fighting Boats," SBSR, Int. Des. Equip. No., 1956, pp. 61–65.

76.14 Distinguishing Design Features of Self-Propelled Dredges. A self-propelled suction dredge, while digging, is an example of a ship acted upon by other than hydrodynamic (and aerodynamic) forces. This is because practically all of them draw up the bed material through one or more *drag pipes*, inclined aft and downward.

Each of these pipes has a scraper of some sort at its lower end and a large mouth adjacent to it through which the bed material is carried by suction, suspended in a powerful stream of water. At its upper end, possibly also at other points along its length, the drag pipe is hinged or swiveled about a horizontal, transverse axis. The scraper and the pipe may thus be lowered to the desired depth when digging or drawn up above the baseplane (and the waterplane) when the dredge is running free.

Self-propelled dredges may have two drag pipes, one outboard on either side, or a single pipe, lowered through a long center well. A diesel-electric twin-screw hopper dredge of the latter type, having a length of 290 ft and a beam of 58 ft, is illustrated in the technical literature [SBSR, 8 May 1952, p. 48; also 9 Apr 1953, p. 42].

Most large model-basin establishments have tested models of self-propelled dredges (for example, TMB models 3132, 3175, 3597, 3633, and 3779), and some of them have made resistance tests of drag-pipe assemblies at various attitudes and speeds. Unfortunately, however, much of this information is so specialized that it has not found its way into the technical and reference literature. The drag encountered by the scraper units depends upon the nature of the bottom, the depth of cut being made, and other factors.

The ahead resistance and the lateral forces occasioned by the mouth of the drag pipe when scraping on the bottom, and the hydrodynamic resistance of the inclined drag pipe(s) moving ahead through the water, are not exactly comparable to the towline tension on a tug or to the wind force on a sailboat. Nevertheless, the drag-pipe resistances and scraper forces call for increased propeller thrust and they may interfere with steering.

A self-propelled dredge usually scrapes or dredges in shallow water, with a small bed clearance. Furthermore, it necessarily scrapes at slow speed, so that more than the usual rudder effect is required to keep it under control and moving in the desired lanes. This means that the rudder(s) must be of greater-than-normal blade area and that they must be placed in the outflow jets of propellers, to provide the necessary lateral forces at low speeds.

Aside from the ground and hydrodynamic resistances of the drag pipes and their gear, the principal resistance components peculiar to self-propelled dredges are the pressure drags developed by the discontinuities in the bottom, in the form of large recesses under the hopper doors. If the doors, opening downward, are not to swing below the baseplane the recesses are unavoidably deep. The greater the hopper capacity of the dredge the more recesses there are.

Hopper-door recesses in the bottoms of self-propelled dredges of a half-century ago are illustrated by T. M. Cornbrooks [SNAME, 1908, Pl. 140], where one port and one starboard row is indicated. Each recess is 4.42 ft wide and about 3 ft deep vertically. There are 6-in by 6-in by 5/8-in angles all around the lower edge of each recess, projecting both into the recess and below the bottom of the ship. The two rows of recesses are slightly over 6 ft apart, measured to their inboard edges. Recesses in later designs of dredges are similar, indicated by the lines drawings of SNAME RD sheet 103 and of ETT Stevens Technical Memorandum 100.

The whole subject of hopper-door recesses in the bottom is discussed in Chap. VIII, pages 213–250, of the Scheffauer reference listed near the end of this section. Several conical dump valves of a new type are illustrated in this reference. They practically eliminate the large hopper-door recesses and the hydrodynamic resistance generated by them.

Most self-propelled suction dredges, with their limited draft and large underwater volume, have large B/H ratios. That of the 247-ft hopper dredge described in SNAME RD sheet 103 is 3.08, at load draft. For other vessels of this type it is 4.5 or more. At reduced draft, as when returning from the dumping ground to the dredging area, the B/H ratios are considerably larger.

This type of hull definitely calls for a twin- or multiple-skeg stern [SNAME, 1947, pp. 97–169]. It is much easier to shape a twin-screw stern of large beam and small draft with double skegs than with a normal form. Further, there is every reason to anticipate a better flow around the twin skegs, although the resistance may suffer because of the increased wetted area. Certainly it is far simpler to hang twin rudders abaft twin skegs carrying propellers than to mount them under a normal-form stern of generally V-shape.

As an indication of the percentage of time during which a self-propelled seagoing suction dredge is running to and from the dumping grounds, T. M. Cornbrooks shows that for a working period of about 7.5 days, during which time the dredge made 44 complete round trips, it was outward

bound to the dumping ground and inward bound to the dredging area, traveling like a normal vessel, for about 31 per cent of the total time [SNAME, 1908, p. 249].

Since the dumping ground must of necessity be some deepwater area where the refuse will not interfere with navigation in the future, and since it may be rather well out to sea, self-propelled dredges must possess a reasonable amount of freeboard, sheer, and reserve buoyancy.

A brief list of references, limited almost exclusively to seagoing, self-propelled dredges of the hopper type, follows:

(1) Robinson, A. W., "Hydraulic Dredging," Cassier's Mag., Nov 1896, pp. 37–47

(2) Cornbrooks, T. M., "Sea-Going Suction Dredges," SNAME, 1908, pp. 247–249 and Pls. 140–146

(3) "The United States Suction Dredge *New Orleans*," Scientific American, 1 Jun 1912, front cover and p. 494. This vessel had a single centerline drag pipe, with water jets on the scoop to help break up the mud in the river bed.

(4) Styer, W. D., "Hydraulic Seagoing Hopper Dredges," SNAME, 1924, pp. 28–48

(5) Vaughn, H. B., Jr., "Seagoing Hydraulic Hopper Dredges," SNAME, 1941, pp. 262–299

(6) Barakovsky, V., "The Dredgers," Schip en Werf, 10 and 24 Jan 1947

(7) Frech, F. F., "Design and Construction of Seagoing Hopper Dredges with Special Reference to *Essayons*," SNAME, Phila. Sect., 27 Apr 1949. Abstracted in the publication Motorship, New York, issue of Sep 1949, beginning on p. 38. See also MESR, Dec. 1952, pp. 74–75, and Mar. Eng'g., Mar 1954, pp. 48–57.

(8) McCarthy, E. W., "Hopper Dredge (*Ciudad de Barranquilla*) for Government of Colombia," Naut. Gaz., Mar 1950, pp. 14–15, 37. This is a twin-screw dredge having a hopper capacity of 1,000 cu yd, an overall length of 240.5 ft and a speed of 11 kt.

(9) The general features of six shallow-water self-propelled twin-screw hopper-type dredges are described and illustrated in Diesel Times, Apr 1951. This article also describes the seagoing, self-propelled, twin-screw hopper dredge *Pacific*, built in 1937, as well as the self-propelled hopper dredge *Sandpiper*, built in Montreal and used on the Lake Maracaibo Bar in Venezuela.

(10) Low, D. W., "Considering Dredging Craft," IESS, 1951–1952, Vol. 95, Part 6, pp. 438–484, esp. pp. 463–474; also Part 7, pp. 485–491. Paper is concerned only with self-propelled dredges. There are no diagrams of hopper recesses or doors but there are discussions of them on pp. 472, 483.

(11) French suction dredger *Charles Belleville*, MENA, May 1952, p. 221

L_{OA} 309 ft	D 19.75 ft
L_{BP} 291 ft	H 13.83 ft in fresh water
B_E 49.25 ft	Hopper capacity is 35,310 ft^3

There are two 27.5-inch diameter suction pipes, one on each side, with swivel joints *below* the waterline. The pipes are 72 ft long and the vessel can dredge in water up to 50 ft deep. There are twin spade rudders and 9 hopper doors under the bottom.

(12) Scheffauer, F. C. (editor-in-chief), "The Hopper Dredge; Its History, Development and Operation," Off. of Chief of Engineers, U.S. Army, Washington, Gov't. Print. Off., 1954. An extensive bibliography is given on pages 375–376 of this reference. The following is taken from the Preface on page ix, as applying to this book:

"It is not a manual by the use of which a novice may design a dredge, but rather a guide for the use of those who may be engaged in the construction and operation of plant of this character."

76.15 Self-Propelled Box-Shaped Vessels. There is a constant demand for a craft which has the carrying capacity of the customary barge, lighter, or scow but which is able to move itself from place to place without the services of a tug. Very often an equally important requirement is that the craft be simple, cheaply or rapidly built, or both, with hull boundaries having easy curvature or else none at all. The ultimate in this respect was probably reached by the so-called "rhino ferries" of World War II, built up in the field by bolting together standard steel boxes having the form of rectangular parallelepipeds.

The requirements for this group treat the propulsion characteristics as being definitely secondary to the load-carrying characteristics, yet they are of little practical use unless they can be self-propelled. The answer to this problem is to accept the square corners and the flat sides and to push or pull them, or both, by outboard drives with propellers whose discs lie below the bottom plane of the box. Swinging these propellers about a vertical axis solves the problem of steering, backing, sidling, and maneuvering, all at once. Lifting them up about a horizontal axis solves the shallow-water, repair, and maintenance problem. The complete power plants, in packaged units that float, are inserted in niches or slots provided for them in the box assemblies, or are attached temporarily in any convenient manner.

A power unit with a rotating-blade propeller might be used to propel a box-shaped craft, except that the vertical blades projecting below the plane of the bottom of the box would be vulnerable in shallow water.

76.16 Self-Propelled Floating Drydocks. A floating drydock which can propel itself in the open sea at a reasonable speed when nominally unloaded, which can maneuver after a fashion,

FIG. 76.J AERIAL VIEW OF U. S. NAVY *ARD* TYPE FLOATING DRYDOCK

Official U. S. Navy photograph. The gate which closes the stern is hinged horizontally along its lower edge. Screw propellers, if fitted for self-propulsion, would be close to the extreme stern and just inboard of the outside of the dock.

and which can control itself when hove to in heavy weather, has all the principal attributes of a ship, and is so classified here. Basically, it resembles a single-ended car ferry or a "seatrain" in its ability to accommodate a bulky, heavy cargo, with the disadvantage that the "cargo" is generally all in one package, extending below the water as well as above it. The self-propelled floating drydock also may be considered as a partly submersible ship with a large, U-shaped,

open docking recess and a tail gate, or as a single-section floating drydock with a ship bow and the same tail gate.

The question of whether any floating drydock should be self-propelled is not at issue here. These notes are included for the benefit of a designer who may be called upon to lay out a self-propelled craft of this type, whatever its service or purpose may be. As a rule, he will be called upon to work on a craft which is not suitable for self-propulsion but must be made so by his resourcefulness or ingenuity.

An early form of self-propelled floating drydock with Ruthven hydraulic propulsion was illustrated by Vice-Admiral Sir E. Belcher many years ago [INA, 1870, pp. 197–211 and Fig. 2, Pl. I]. It seemed logical at that time to use hydraulic jet propulsion since the dock had to be equipped with pumps in any case to handle the water in its various compartments. A similar type of drydock, proposed by G. B. Rennie [INA, 1883, Vol. XXIV, p. 225ff] was intended to be propelled by six hydraulic jets on each side, indicated on Plate XV of the reference.

A similar dock with one screw propeller outboard at each after corner was proposed by L. Clark in a somewhat later paper, supplemented by some comments of W. Froude [INA, 1877, Vol. XVIII, Pl. XIV, Figs. 2 and 3; also discussion on p. 196]. Froude reminded the author (Clark) that:

> "If you put a screw close to a ship, cut off without any run at all, the propulsive effect of the screw becomes absolutely *nil*."

A ship-shaped, floating drydock (*ARD 1*), capable of handling a destroyer of the middle 1930's, was designed by the Bureau of Yards and Docks of the Navy Department and built for the U. S. Navy in 1934. This dock was designed to accommodate propelling machinery and propellers for self-propulsion but was never so fitted. It had an overall length of 393 ft, a beam of 60 ft, and a depth of 33 ft, with a maximum draft when flooded of 30 ft. Bow and stern views of this dock were published at that time and later [SBSR, 23 Aug 1934, p. 200; Motorship, New York, Apr 1950, p. 27; Mar. Eng'g., Apr 1954, p. 110, shows a stern view of the larger *ARD 8*, L_{OA} = 486 ft, B = 72 ft].

A bow aerial view of an *ARD* floating dock appears on the front cover of Bureau of Ships Journal for April 1953. A stern aerial view is reproduced in Fig. 76.J. The positions originally intended for the propellers of *ARD 1* were under the after outer corners of the stern, slightly forward of the tail gate.

A not-too-blunt bow, illustrated in the Bureau of Ships Journal photograph, is a necessity if a drydock or any craft of this general shape is to be self-propelled at a reasonable speed without an inordinately large propelling power. Assuming a 420-ft waterline length and an upper limit of speed of 10 kt, T_q is $10/\sqrt{420} = 0.488$, F_n = about 0.145. From Fig. 66.I the optimum waterline entrance slope is 32 deg but since the graph is relatively steep in this region the slope could be raised to 40 deg or more if other more important requirements forced this change.

A floating drydock requires considerably more bed clearance, or water under it, than the ships being docked. Since the dock is often moored close inshore, generally in areas not useful for operating ships, the overall draft must be kept to a minimum. This complicates the problem of where to put the propulsion devices while retaining a reasonable degree of efficiency in their operation.

A multiple-arch type of stern, similar to the single-arch stern described in Sec. 67.16, appears to offer the best promise of good propulsive efficiency while maintaining the stiffness necessary in the floor structure of any floating drydock. Such a stern would have a profile corresponding approximately to that for the single-arch ABC stern shown in Figs. 67.M and 67.O. The propellers could be large compared to the light draft, as their upper tips could extend above the WL. They would be protected excellently all around, and they could even be made accessible for inspection and repairs by flooding the forward dock tanks. The multiple skegs should give excellent stability of route, and the multiple rudders abaft them equally good maneuvering characteristics.

The design of a ship-shaped floating drydock for towing only, embodying skegs or rudders or both at the stern, is discussed in Part 5 of Volume III, under the design of towed craft.

76.17 Design of Temporary Bows for Emergency Running and Towing. A design problem akin to that of shaping a bow for a self-propelled floating drydock is laying out a temporary bow on a ship which has lost its own bow. Towing or pushing a vessel terminated at its forward end only by a flat watertight bulkhead is an extremely precarious operation. A danger-

ously heavy load can be built up on the immersed area of such a bulkhead by dynamic action of the water, even at low speeds. Indeed, a vessel with only a portion of its bow caved in, but with a hole by which the dynamic pressure *at that point* is transmitted to the boundaries of the flooded portion, can develop high dynamic loads on those boundaries, indicated by diagram 1 of Fig. 76.K.

A vessel damaged in this manner can and should be towed with the undamaged end foremost, even to the extent of towing stern first, without benefit of the steering effect of a rudder at the trailing end. A photograph of a large tanker without a bow, being towed in this manner, is reproduced in Shipbuilding and Shipping Record [5 Jun 1947, p. 559]. Under these conditions the propeller is permitted to free-wheel, if practicable. A combination of square leading and trailing ends, such as might be encountered on a transom-stern destroyer with its bow broken off, may result in some yawing or weaving during a towing operation. However, if the damaged vessel is towed with its good end foremost, the holding bulkhead should remain intact and the ship should stay afloat.

If the bow is damaged or missing, and it is desired to bring the vessel home *under its own power*, a rather blunt false bow is found adequate. Straight sides and an entrance slope of 45 deg, sketched at 4 in Fig. 76.K, should suffice for reasonably rapid travel. If head seas are likely to be encountered, a rake to the false bow sides—any amount that is found practicable up to 15 deg or so—pays for itself in easing the impact loads on the flat surfaces. Because of the flat sides on the temporary bow, it can be expected that the wavegoing loads on the hull, at reduced speed, will be at least as large as on the undamaged vessel at normal speed.

With a well-constructed false bow of the type illustrated in diagrams 3 and 4 of Fig. 76.K and in reasonably smooth water, it should be possible to make at least one-third the speed to be expected with the undamaged vessel. In fact, vessels have made ocean crossings under their own power with false bows very much blunter than the one depicted in diagrams 3 and 4 of the figure. One such ship was the U.S.S. *Selfridge* (DD 357), which had its bow blown off in the South Pacific during World War II. Fig. 76.L shows the vessel in a floating dry dock with the false bow completed. A photograph of the vessel under way in this condition is reproduced in the Bureau of Ships (U. S. Navy Department) Journal for May 1953, page 12.

76.18 Floats for Pontoon Bridges. A variation of the box-shaped, load-carrying barge or lighter is the moored float intended to support

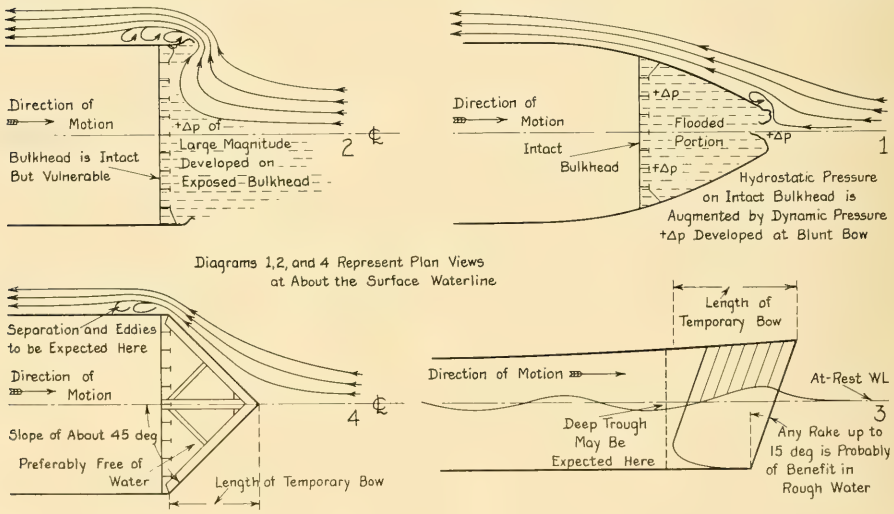

Fig. 76.K Schematic Design for Temporary Bows of Damaged Vessels

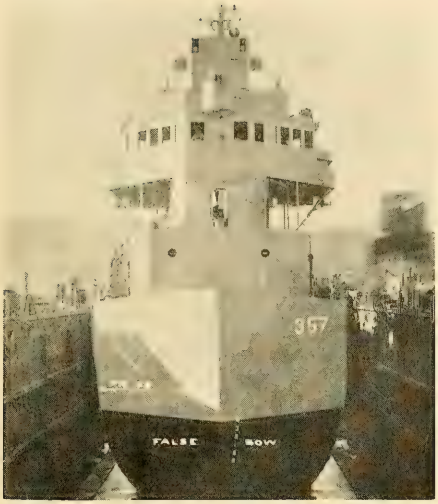

FIG. 76.L TEMPORARY BOW FITTED TO U. S. S. *Selfridge* (DD 357)

Official U. S. Navy photograph. The waterline slopes of this particular bow are very large, much larger than are recommended for a craft required to make a transocean crossing under its own power.

large fixed weights over water, in the manner of pontoons for temporary bridges. In general these pontoons must carry their loads in swift streams or rivers, on the surface of which wind waves of considerable height and magnitude are often formed. The problem here is not exactly comparable to that of a towed craft carrying the same weight at the same speed, equal to the velocity of the river current, because the pontoon may not be entirely free to trim. Furthermore, the pontoon is usually anchored by a cable or chain which leads downward at a considerable angle and exerts an appreciable downward component of force at the bow.

For almost any river, the current velocity at the center exceeds the mean current speed, because of the retarded flow in the boundary layers along the sides and over the bed. In a swift river the wavemaking drag may exceed the friction drag. Since the downstream pull on each pontoon varies as the second power at least of the current velocity, and possibly as some higher power, the increase of current velocity from any source whatever is not to be regarded lightly. The overall drag is an important factor because it affects the type, strength, and arrangement of the mooring gear. In the case of rivers at flood stage, the pontoon may lie at an angle to the current even though when moored at a normal stage it may have been in line with the current.

For floats or pontoons which are open and undecked, adapted for nesting inside each other in transit, adequate freeboard possesses an importance only slightly less than that of low drag. If the floats are moored in relatively shallow water, the bow-wave crests are augmented. Furthermore, when floats are placed close to each other along the bridge, the water flows at augmented speed between them, with a consequent dropping of the water level there. Even though the wave crests at bow and stern may be high, each float drops bodily in the water, as does the simple ship in diagram 1 of Fig. 29.B.

76.19 Yacht-Design Requirements; Some Aspects of Sailing-Yacht Design. Yachts, defined as craft intended for pleasure, recreational, competitive, or ceremonial purposes only, may be classified first by size:

(1) Large, exceeding 100 or 125 ft in overall length. For hydrodynamic design purposes these are essentially displacement-type ships.
(2) Medium, over 50 ft in overall length of hull proper but not exceeding 125 ft
(3) Small, under 50 ft in overall length of hull.

By type and method of propulsion they may be classified as:

(a) Displacement-type, mechanical propulsion only, including water jets. These are usually designed by the rules applying to larger vessels.
(b) Semi-planing type, mechanical propulsion only, including airscrews and water jets
(c) Planing type, mechanical propulsion only, including airscrews, water jets, gas jets, rockets, and the like
(d) Sailing yachts with auxiliary mechanical propulsion
(e) Sailing yachts without mechanical power.

The design notes in Chaps. 66 through 75 of this part should suffice for the hull and propdev design of the large and medium yachts with mechanical propulsion. The semi-planing and planing craft of groups (b) and (c) preceding are classed as motorboats, for which design procedures and rules are set down in Chap. 77. Some features of sailing-yacht design are discussed subsequently in this section.

Leaving aside for the moment the sailing yacht

which is intended purely for racing, certain general and detail requirements apply to all yachts:

(i) Appearance is usually a major item, if not the principal one. To be a true yacht, a craft must look like a pleasure rather than a utility craft. Styles, tastes, and fashions vary with individuals and change with time. No one but the owner can say whether he wants a 3-kt houseboat to look like a Roman chariot, or whether he wants a 40-kt speedboat to look like an airplane.

(ii) Accommodations for engaging in manifold activities, even on a small craft. At first sight, this and the preceding item appear far removed from hydrodynamics but they involve freeboard, sheer, air and wind resistance of the hull and upper works, and other features having to do with maneuvering and wavegoing.

(iii) Speed in smooth water, coupled with endurance and fuel capacity at some specified speed

(iv) Ability to travel safely, and not too uncomfortably in waves, to ride out storms when hove to, and to negotiate passages through inlets and rivers with currents, tide rips, and choppy water

(v) Useful load-carrying capacity, generally on a usable-volume rather than a weight-carrying basis. This item is closely related to that of accommodations.

(vi) Maneuverability, like other items to follow, is usually not specified by the prospective owner but can never be overlooked by the naval architect. This includes the ability to handle the craft, usually with a very large part of its volume out of water, in high winds blowing from unfavorable directions.

(vii) Practically any yacht which expects to run in open water should have adequate metacentric height for a large range of stability. For the sailing yacht there should be a positive righting moment at 80 deg angle of heel. This means a reasonable width of deck on the lee side, high watertight coamings, self-bailing cockpits, and no internal ballast which can shift when rolling or when heeled to the extreme angle.

(viii) A distribution of weights as nearly amidships as possible, to keep down the polar moment of inertia of the whole craft about the pitching axis

(ix) For the sailing yacht, the maximum practicable performance as to speed, freedom from leeway, and steering with the craft running at an angle of heel, when the underwater body is definitely and drastically asymmetric about any longitudinal axis

(x) As is customary for all other sets of requirements in the book, items not related to hydrodynamics are omitted.

The renowned yacht designer and builder Nat G. Herreshoff laid great emphasis on quiet smooth running in all his craft, and devoted much time and attention to achieving this end. While most of the noise made by mechanically propelled craft comes from the main *and auxiliary* machinery, much of the vibration and rough running may well have a hydrodynamic origin. No specific design rules are given here for insuring quiet smooth operation in a yacht. It is pointed out only that these features are by no means negligible in a craft intended for pleasure, rest, and relaxation.

A sailing yacht usually receives its greatest driving force and makes its highest speed when running at a large angle of heel. It is the aim of the designer, and it is often possible, so to shape the hull as greatly to increase its effective length in the heeled position. This in turn, acts to decrease the speed-length or Taylor quotient or the Froude number and to make the vessel drive more easily as the propelling thrust is increased. Most sailing yachts, when driven hard, reach Taylor quotients of 1.2 to 1.3, corresponding to a Velox wave length (from bow-wave crest to first crest following) somewhat greater than the waterline length at rest, with zero heel.

To illustrate some of these features, Fig. 76.M is a body plan of a one-design sailing yacht, having a waterline length of 32.0 ft, kindly furnished by Olin J. Stephens, II, of the firm of

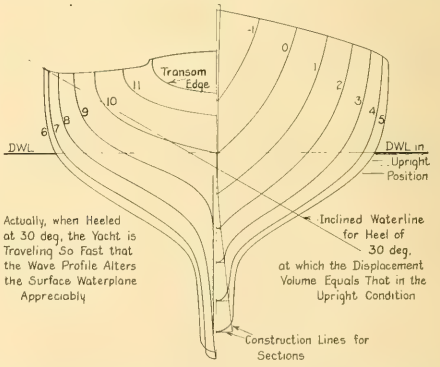

FIG. 76.M BODY PLAN OF SAILING YACHT WITH INCLINED WATERLINE

Sparkman and Stephens, Inc. On this body plan there is drawn an inclined waterline for a heel of 30 deg, when the main deck edge touches the water on the low side, for the condition in which the inclined volume $\forall$ equals the upright volume $\forall$.

Diagram 2 of Fig. 76.N gives a half-waterline shape with the yacht upright; diagram 1 shows the whole waterline shape in the inclined position just described. This shape, corresponding to the intersection of the hull with the level of the undisturbed water *at rest*, is definitely unsymmetric, even about a diagonal line drawn from the stem to the extreme after end of the inclined waterline. For this particular yacht, the inclined WL has very nearly the same length as the upright WL, when measured parallel to the ship axis. If measured along the diagonal broken line in diagram 1 of Fig. 76.N it is about 1.012 times the upright WL length.

The foregoing analysis applies to the static case only, with the water surface undisturbed by any waves whatever. The dynamic situation when sailing is far different, even in smooth water. At their top speeds these craft generate a very pronounced Velox-wave system, with high crests at bow and stern and a deep trough amidships. The immersed length of the inclined waterline is then considerably longer than that shown in diagram 1 of Fig. 76.N, and its shape is probably much different. There is a similar difference between the at-rest inclined section-area curve and the corresponding A-curve when underway. This difference may be greater than between the upright and inclined A-curves of diagrams 4 and 3, respectively, of Fig. 76.N.

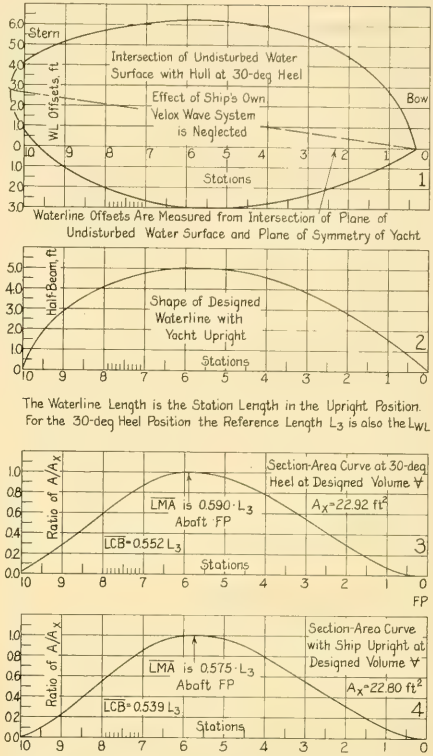

Fig. 76.N Inclined and Upright Waterplanes of Sailing Yacht of Fig. 76.M, with Corresponding A-Curves

While considerable research has been and is being carried on relative to the overall resistance and propulsion aspects of sailing-yacht design and performance, this should be extended to cover the wave profiles and lines of flow at various angles of heel. Put in another way, attention should be focused as much on the flow patterns around the hull when underway as on its form coefficients, section-area curves, and other parameters. All too often the latter apply only to the upright condition, with the vessel at rest. In the few modern books on sailing-yacht design there is little discussion of the hull characteristics in the inclined condition [Skene, N. L., "Elements of Yacht Design," 5th ed., 1944, Fig. 45, p. 75]. Sec. 29.8 mentions a much older paper by R. C. Allen covering some phases of this subject ["Naval Science," 1875, Vol. 4, pp. 89–93]. A. B. Murray cites the case of two six-meter yachts where the difference between the upright and the heeled performance was an important factor in the racing abilities of the respective craft [Yachting, Dec 1946, p. 60]. In his words, ". . . although *Jack* had lower resistance with zero heel angle, her resistance in a heeled-over, close-hauled attitude was higher than *Jill's*."

In fact, it is probable that too little attention has been given to the inclining forces and moments, involving wind forces high up on the sails and rudder forces low down on the hull. There is an appreciable down-pitch moment, comparable to that encountered in motorboats driven by airscrews, due to the high position (on the sails) of the line of application of the thrust compared

to the center of resistance of the underwater hull.

Many sailing yachts have transom sterns. On these craft, where the propulsive power is limited to that which can be derived from the wind, the shape and position of the transom may be of greater relative importance than on a high-speed motor yacht or a destroyer. At slow speeds the transom must definitely be kept out of water, to avoid the separation drag abaft it. At higher speeds it may be possible to accept the added drag, especially if some of the deflection drag behind the bow-wave crest can thereby be eliminated.

Several new ratios appear in the design of sailing yachts. Among them may be mentioned the *ballast ratio* and the *sail-area to wetted-surface ratio*. In its simplest terms, the ballast ratio is the ratio of the total weight of ballast, both inside and outside (portable and fixed in the keel), to the total scale weight of the yacht. It ranges from 0.25 to 0.35 or more, depending upon the beam and other factors. There are rather elaborate ways of defining ballast, by modern racing rules, but the scheme remains the same.

The sail-area to wetted-surface ratio applies primarily to small sailboats which run fast enough to generate large dynamic lifts and which approach planing speeds, although it is also a factor in the design of purely displacement types. It has probably been assumed by some yacht designers that the hull resistance of a sailboat in the semi-planing range is due largely to friction, so that speed and actual wetted area are the major factors. They are indeed factors but it is doubtful that they are the major ones. They are certainly not the only factors.

D. Phillips-Birt presents a discussion which, though applied to a sail-and-power craft called a motor sailer, embodies a number of useful comments on sailing-yacht design in general [Rudder, May 1955, pp. 12–15, 46–55].

As an indication of the type of unpublished data available on sailing-yacht design, and of those to be expected in the not distant future, the following is quoted from an article by A. B. Murray of the Experimental Towing Tank, Stevens Institute of Technology [Yachting, Dec 1946, pp. 62, 110]:

"However, a system of correlation has been worked up which provides a useful yardstick of performance for sailing yachts of all sizes. Upright resistance, speed-made-good, leeway angle, stability, and balance are put into coefficient forms which eliminate the effect of differences in length and displacement. Upright resistances of the full size boat for a few selected fixed speed-length ratios are divided by the displacement in tons. The resulting ratios are of the same order of magnitude for all lengths of boats, tending to be smaller as the boat length is increased. Plots of the ratios against load water line make a convenient chart for comparison of hull resistance. Similar coefficients are worked up for other performance characteristics. For instance, an excellent basis on which to compare performance to windward is obtained if close-hauled speed-made-good is divided by $\sqrt{L}$ for a few fixed values of true wind speed. By similar methods, stability, leeway angles, and balance may be compared. Charts of all these characteristics have been prepared for a large number of Tank tested boats. These charts give immediately a means for evaluating a new design, besides indicating performance trends.

"Another step was taken when a method was set up to compare three important characteristics on the basis of hull alone without effect of sails or center of gravity position. This compares hull resistance, leeway angles and longitudinal center of lateral resistance for three heel angles at a standard speed and stability which are functions of boat length. By separating hull characteristics from the sail power, a more critical analysis may be made of the problem."

76.20 Brief Bibliography on Sailing-Yacht Design. While no attempt has been made to collect all the published and unpublished references relating to the design of sailing yachts the reader may find the following brief bibliography useful and interesting from a historical and general information standpoint:

(1) Harvey, J., "On the Construction and Building of Yachts," INA, 1878, Vol. 19, pp. 150–158
(2) Kemp, Dixon, "A Manual of Yacht and Boat Sailing," Cox, London, 3rd ed., 1882
(3) Kemp, Dixon, "Fifty Years of Yacht Building," INA, 1887, Vol. 28, pp. 232–246
(4) Nixon, L., "Yachts in America and England," SNAME, 1894, pp. 261–277
(5) Kemp, Dixon, "Yacht Architecture: A Treatise on the Laws which Govern the Resistance of Bodies Moving in Water; Propulsion by Steam and Sail; Yacht Designing; and Yacht Building," Horace Cox, London, 3rd ed., 1897. This is a veritable treatise on naval architecture in most of its phases.
(6) Crane, C. H., "Some Thoughts on the Design of Modern Steam Yachts," SNAME, 1903, pp. 57–65
(7) Erismann, M. C., "The Effect of the Universal Rule in Recent Yachts," SNAME, 1906, pp. 223–241
(8) Warner, E. P., and Ober, S., "The Aerodynamics of Yacht Sails," SNAME, 1925, pp. 207–232 and Pls. 133–146
(9) Fox, Uffa, "Sailing, Seamanship, and Yacht Construction," 1934
(10) Baier, L. A., INA, 1934, pp. 107–108. Gives a brief discussion of form variations for sailing yachts.
(11) Stephens, W. P., "Yacht Measurement," SNAME, 1935, pp. 7–42

(12) Burgess, C. P., "The America's Cup Defenders," SNAME, 1935, pp. 43–70
(13) Nevins, H. B., "On the Building of a Yacht," Yachting, Mar, Apr, May 1935
(14) Davidson, K. S. M., "Some Experimental Studies of the Sailing Yacht," SNAME, 1936, Vol. 44, pp. 288–344. There is a bibliography on pp. 303–304, 312.
(15) Davidson, K. S. M., "Model Tests of Sailing Yachts," The Rudder, Aug 1937, pp. 14–15, 56, 58
(16) Fox, Uffa, "Thoughts on Yachts and Yachting," 1939
(17) Stephens, W. P., "Traditions and Memories of American Yachting," 1942
(18) Owen, G., "Outstanding New England Types of Fishing Boats, Whalers, and Yachts," SNAME, HT, 1943, pp. 151–164
(19) Skene, N. L., "Elements of Yacht Design," Dodd-Mead, New York, 1944
(20) Herreshoff, L. F., "The Common Sense of Yacht Design," The Rudder Publishing Co., New York, 1945. In two volumes.
(21) Aupetit, A., "Essais de Yachts (Tests on Yachts)," ATMA, Jun 1946, Vol. 45, pp. 433–452
(22) Murray, A. B., "Towing Tank Developments," Yachting, Dec 1946, pp. 60–62, 110, 112. Abstracted in SBSR, 9 Jan 1947, p. 37. Devotes a considerable amount of discussion to sailing yacht design problems which have been or should be investigated by tests of models.
(23) "Symposium on Sailing Yacht Design," SNAME, New Engl. Sect., 18 May 1948; see SNAME, 1948, p. 90
(24) Barnaby, K. C., BNA, 1954, 2nd ed., pp. 244–256, Arts. 165–169 as follows:
(165) Sail Propulsion
(166) The *Gimcrack* Sail Coefficients
(167) Sail Plans
(168) Centre of Effort and "Lead"
(169) Sail Area and Power to Carry Sail
(25) Barnaby, K. C., "Progress in Marine Propulsion, 1910–1950," INA, 1950, pp. J14–J15
(26) Chapelle, H. I., "American Small Sailing Craft; Their Design, Development and Construction," Norton, New York, 1951
(27) Barkla, H. M., "High-Speed Sailing," INA, 1951, Vol. 93, pp. 235–257. This is one of the few papers in the technical literature which tackles the problem of yacht design on a fundamental, analytic basis.
(28) Douty, J. F., "History of Chesapeake Bay Sailing Vessels," SNAME, Ches. Sect., 29 Nov 1951
(29) Morwood, John, "Sailing Aerodynamics," Morwood, 123, Cheriton Rd., Folkestone, Kent, 1953
(30) Denes, Gabor, "Yacht Research," The Motor Boat and Yachting, Dec 1954, pp. 524–525
(31) Yacht Research Council of Great Britain. Photographs of experimental work shown in The Illustrated London News, 4 Dec 1954, p. 1009.
(32) Chapelle, H. I., "The Search for Speed under Sail: An Outline of the Development of Yacht Design in America Until the 20th Century," a series of several articles beginning in the Feb 1955 issue of Yachting, pp. 58–61, 94–98. Part II appears in the Mar 1955 issue, pp. 71–75, and Part III in the Apr 1955 issue, pp. 66–70, 112, 114.
(33) Davidson, K. S. M., "The Mechanics of Sailing Ships and Yachts," Surveys in Mechanics, edited by G. K. Batchelor and R. M. Davies, Cambridge University Press, 1956, pp. 431–475. There is a list of 17 references on p. 475.
(34) Allan, J. F., Doust, D. J., and Ware, B. E., "Yacht Testing," INA, 11 Oct 1956
(35) Scheel, H., "It's Beam That Makes the Boat Go," Yachting, Jan 1957, pp. 146–147, 285
(36) Crane, C. H., "What Limits Speed Under Sail?" Yachting, Mar 1957, pp. 53–56, 100, 102.

76.21 Asymmetric Hull Forms. Although practical applications of the asymmetric hull are rare, for ships which are built to travel upright, they do exist. When a marine architect sets out to design a vessel which has an underwater hull of different breadth and shape on the port and starboard sides of the construction centerplane, he wants to be sure that his unusual creation will be acceptable and serviceable.

Among the asymmetric-hull craft which have performed exceedingly well, not only for years but for centuries, there may be mentioned:

(a) The sailing yacht and the sailing vessel. Although almost invariably designed to have symmetry about the centerplane when at rest, they always present an asymmetric form to the water when heeled and propelled at any appreciable speed by the wind.
(b) The sailing canoes of Oceania. These employ asymmetric hulls to eliminate centerboards, leeboards, and similar devices, as described in Sec. 24.21 and illustrated in Fig. 24.M. They make use of outriggers to give them the required degree of metacentric stability under sail.
(c) The gondolas of the canals and lagoons of Venice, described briefly in Sec. 24.21
(d) The individual hulls of catamarans are usually asymmetric about their own construction centerlines.

Several other cases present themselves in practice:

(e) The long, slender ship which becomes slightly bent due to collision or other major damage. When the expense of straightening it appears exorbitant, the marine architect may be called upon for an opinion as to whether it really needs straightening or not.
(f) Ships to ferry, to tend, or to house operating aircraft, such as airplane tenders and aircraft

carriers, in which the various installations and the weights can not be balanced transversely
(g) Ships for special operations which have elaborate and expensive apparatus installed on one side only.

The degree of asymmetry designed into a hull is measured conveniently by the following:

(i) The port and starboard partial beams, measured in the same way as for the half-beam on a normal symmetrical vessel
(ii) The percentage of the maximum beam by which the center of buoyancy CB is shifted from its normal centerplane position. This is measured by the transverse distance between the CB and a vertical longitudinal plane through the construction centerline, as compared to the maximum beam.
(iii) The percentage of the total displacement volume which is shifted from one side of the hull to the other, relative to the vertical longitudinal plane through the construction centerline. For example, if 53.7 per cent of the underwater volume lies on one side of that plane and 46.3 per cent on the other side, the percentage of asymmetry in volume is $(53.7 - 46.3)/2$ or 3.7 per cent.

The numerous form coefficients based upon ratios of various areas and volumes to the areas or volumes of the circumscribing rectangles or parallelepipeds are calculated in the same manner for the asymmetric as for the symmetric ship.

A few notes may be set down for the design of asymmetric hulls which are to be built that way, based upon the usual demand for reasonable if not minimum power, maximum speed, and acceptable maneuverability of the asymmetric vessel, corresponding to those for one that is symmetrical:

(1) The CG is to be found in the same vertical plane as the CB, offset from the construction centerplane toward the wide side, with the vessel upright and carrying the designed load
(2) The CB and the CG should, whenever practicable, have essentially the same offset for load conditions lighter than the designed, to insure that the ship remains upright at all drafts and trims
(3) Based upon a construction centerplane that passes through the hull terminations at the bow and stern, the propulsion devices are usually, but not necessarily mounted symmetrical to that plane
(4) On the assumption that both the friction and the pressure resistance are exerted in a vertical longitudinal plane through the center of buoyancy, which appears reasonable, but that the resultant propelling thrust is exerted along the construction centerline, there is a constant moment due to these forces alone which acts to swing the ship toward the wide side. Unless the length-beam ratio is less than 5 or 6, this constant turning moment is likely to be of small consequence although it will *always* be of the same sign. It is wise to augment the steering control for a ship of this type over that provided for a normal design. The augment may equal but need not exceed the percentage by which the center of buoyancy is offset, described in (ii) preceding.

76.22 Design Problems in Multiple-Hulled Craft. It sometimes happens that a large beam can be accepted for the purpose of carrying objects which are bulky and awkward to handle but relatively light in weight. It may be possible to improve the metacentric stability or load distribution in a craft by utilizing two or more widely spaced but narrow hulls instead of one wide hull. The term *catamaran* is in this book restricted to craft which have two hulls of approximately equal size. An outrigger canoe is considered to have one main hull only; the outrigger is a form of auxiliary-displacement device corresponding somewhat to the wing-tip float of a flying boat or seaplane. A craft having one main hull and one supplementary hull abreast on either side is known as a *trimaran*. The side hulls may be of approximately the same size or they may be smaller than the main hull.

In view of the many possible uses for towed or self-propelled craft with multiple hulls no attempt is made to set down their requirements here.

The crux of a suitable design of water craft in which two separate hulls must move along easily, side by side, is the shaping of the region between the two hulls. Only rarely can the hulls be made sufficiently short and narrow, compared to their spread, that they may be considered as independent bodies, hydrodynamically speaking. If they are slim enough to produce relatively narrow velocity and pressure fields, they may still be long enough to cause interferences between the surface-wave patterns between the hulls, as shown in Fig. 76.O. The diverging crests of the *inside* Velox wave systems will meet each other and be reflected on or about the construction centerplane, just as if there were a thin plate mounted vertically between the hulls in that plane.

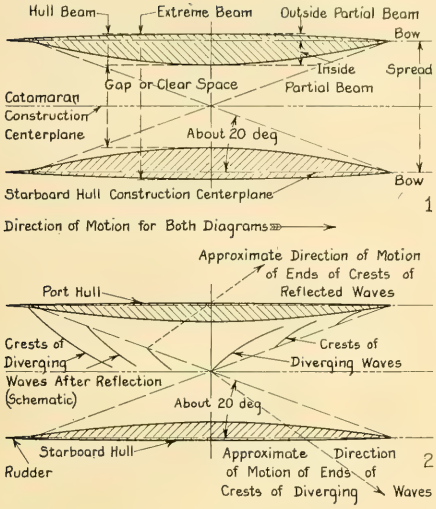

FIG. 76.O DEFINITION AND DESIGN SKETCHES FOR CATAMARANS

Thus instead of the inside crests of the Velox system from the port hull traveling across toward the stern of the starboard hull they are reflected on the construction centerplane of the catamaran and travel back toward the stern of the port hull, whose bow generated them.

Considering the small projected area of each hull against which a stern-wave crest could push it is perhaps wise, if possible, to have this reflected crest just clear the stern. Assuming that, as illustrated in Fig. 10.B, the crest lines diverge at an angle of about 20 deg to the construction centerplane of each hull, Fig. 76.O indicates that the spread between the hulls should be at least the waterline length times the natural tangent of 20 deg, or about $0.364L_{WL}$.

The waterline beam of each hull, port plus starboard, depends greatly upon the amount of weight that must be carried on a given length, and upon the permissible draft. It may vary from about $0.06L_{WL}$ on a sailing catamaran designed to reach a Taylor quotient T_q of 3 or 3.5, to $0.12L_{WL}$, $0.15L_{WL}$, or more on a craft for more utilitarian purposes.

If the catamaran is sail-propelled, the lee hull is immersed more deeply when underway than when at rest, and the weather hull less deeply. Despite the seemingly large spread between the hulls, the craft heels somewhat to leeward under sail. If poorly handled it may even capsize. This means that the burden of preventing leeway falls on the leeward hull. Like the flying proa or the sailing canoe of Oceania, described and illustrated in Sec. 24.21 and Fig. 24.M, the leeward hull should therefore be flat (or nearly so) on the outside and *cambered in planform on the inside.* This means that whatever speeding up of water occurs in the venturi section between the two hulls is an advantage. It increases the magnitude of the $-\Delta p$'s on the windward side of the lee hull, which rides deeper in the water than the windward hull. On the other hand, the clear space between hulls must not be too small, else a blocking effect takes place there. With a catamaran assembly of the type shown in Fig. 76.O, the clear space between them should be not less than 3 or 3.5 times the maximum waterline beam of each hull.

If the catamaran is mechanically propelled the planforms of the hulls are apparently not too important provided the speed-length quotient T_q is not too large. Each hull may be symmetrical about its own centerplane, or each may be flat on the inside, as best suits other features.

Because of the ever-present difficulty of obtaining sufficient usable and protected volume within the hulls of a catamaran, these hulls may be flared rather sharply above the waterline, especially on their insides.

Bracing the two hulls against twisting in waves is a structural problem but determining the loads and forces involved is one of hydrodynamics. Unfortunately no method has yet been devised for calculating their values.

Catamaran hulls with flat bottoms, if properly shaped, can be relied upon to produce some dynamic lift, as in a planing craft. However, the aspect ratio is usually too small to permit the bottom of such a hull to act as an efficient planing surface.

It is sometimes reported that the "tunnel" formed by the inboard surfaces of two catamaran hulls and the under surface of a large, horizontal deck structure joining them has a special shape. It is intended that the blocking effect of the air trapped in this tunnel will provide a $+\Delta p$ under the deck and lift the assembly partly out of the water. Something of this kind might take place at values of $T_q = 5$ or more, but even then it is most uncertain.

G. H. Duggan designed and built an unusual form of sailing yacht, the *Dominion* of 1898, in

which two canoe-shaped hulls were combined with a shallow scow type of hull. A small body plan of this craft, accompanied by a photograph of it under sail, is published in Yachting [Dec 1946, p. 72]. In this case, however, the designer did not have to concern himself too much with air flow between the hulls because at its higher speeds the craft sailed at a large angle of heel, with only the leeward "canoe" in the water.

Sec. 25.23 contains a number of references to catamarans and trimarans in the modern (1955) technical literature. Older literature goes back at least as far as Dixon Kemp's "A Manual of Yacht and Boat Sailing" of 1882 [Cox, London, 3rd ed.]. In Chap. XXVI of this book, pages 348–356, entitled "Double Boats," Kemp describes and illustrates a number of catamarans, including several built by N. G. Herreshoff in 1876 and the years following. C. Grasemann and G. W. P. McLachlan mention two ships designed for English Channel service, each having twin hulls. The *Castalia,* built by the Thames Ironworks Company in 1874, had two half hulls with the inboard sides vertical. The *Express,* a more successful venture, built by Messrs. Andrew Leslie and Company at Hebburn-on-Tyne in 1878, had two complete hulls ["English Channel Packet Boats," Syren and Shipping Ltd., London, 1939].

C. J. Wickwire describes the 35-ft catamaran designed and built by D. and A. Locke of Detroit, based upon careful design studies supplemented by model tests [Lakeland Yachting, Jul 1953, pp. 28, 40–41]. The extreme beam is 12 ft; the individual hulls, flat on their outboard sides and cambered on their inboard sides, each have a beam of 4.5 ft. Certain notes relating to modern practice which may be found useful in the design of catamarans are embodied in a paper by R. F. Turner entitled "Catamarans, Past, Present and Future" [SNAME, Pearl Harbor Sect., 13 Sep 1955; abstracted in SNAME Bull., Oct 1955, pp. 31–32].

76.23 Requirements for and References on Ferryboats. While most double-ended vessels, whether self-propelled or not, are intended for the short-haul transportation of people, creatures, and objects as ferryboats, their use is not necessarily restricted to this type of service. They are therefore considered here primarily as vessels which must operate equally well in either direction. There are, to be sure, many one-direction car and train ferries, running on longer routes, which load over the bow or stern and which in most cases have to back for relatively long distances out of or into their slips. The latter are definitely special-service vessels.

Because they are intended to fill such a great variety of needs it is difficult to formulate general requirements for the hydrodynamic design of ferryboats. A few of these, covering their special features, follow.

For double-ended vessels:

(1) Limiting length, maximum beam, and draft, for existing or contemplated slips
(2) Ability to start and stop promptly, at large values of acceleration and deceleration, for cutting down the running time, for maneuvering, and for emergency stopping
(3) Excellent steering and maneuvering characteristics. Most ferries are required to cross tidal currents at large angles. Furthermore, most of them cross the normal routes of water traffic nearly at right angles.
(4) Great metacentric stability because all the useful load is above the main deck and it is well to limit the list when the vehicle loads are not symmetric or when the passengers all rush to one side. This happens usually when the vessel is carrying only part of its full load [SNAME, 1926, pp. 228–229].
(5) Large flare in the abovewater body for increasing the metacentric stability as the load displacement and the draft increase [MESR, Mar 1939, p. 109]
(6) An unnecessarily large transverse metacentric height is to be avoided because it does not permit the vessel to yield and to roll readily when it strikes the "racks" on either side when entering its slip [Stevens, E. A., SNAME, 1896, p. 100]
(7) Large *longitudinal* metacentric stability, to prevent the ends from being depressed unduly when the weights are concentrated there, in loading or unloading [DuBosque, F. L., SNAME, 1896, pp. 95–96]
(8) Large deck overhangs, sponsons, and the like, because the useful load is one of volume rather than of weight. At the same time the overhangs must be kept clear of wind waves and the ship's own waves.

For single-ended vessels:

(9) No excessive flare under the car-deck or vehicle-deck level, to cause pounding and slamming when wavegoing
(10) If required to back into, or out of long

slips, adequate steering ability when running in either direction

(11) If intended to run in the open sea, enough freeboard at the open end(s) of the car or vehicle deck, or enough protection for that deck, at both ends, to keep menacing quantities of water off of it.

M. E. Denny, in a paper "A Diesel-Electric Paddle Ferry-boat" [IESS, 1934–1935, Vol. 78, pp. 381–412], went to some pains to list the specific design requirements which may be expected for such a craft. Supplementary requirements are given by F. L. DuBosque and E. A. Stevens in two papers describing screw-propelled ferryboats for New York harbor [SNAME, 1896, pp. 93–104 and Pls. 32–35; SNAME, 1893, p. 192].

Other useful references on this subject are:

(a) Stevens, E. A., "Some Thoughts on the Design of New York Ferryboats," SNAME, 1893, pp. 192–209 and Pls. 46, 57

(b) DuBosque, F. L., "Speed Trials of a Screw-Propelled Ferryboat," SNAME, 1896, pp. 93–104 and Pls. 32–35

(c) Stevens, E. A., and Paulding, C. P., "Progressive Trails of Screw Ferryboat *Edgewater*," SNAME, 1902, pp. 15–21 and Pls. 1–3. The following quotations are taken in full from this reference, p. 15: "The following is the approximate performance of several vessels of this class at about that speed:

Name	W. L. Length, ft	Displ., tons	Block Coeff.	Slip, per cent	Admty. Coeff.
Bremen	217	900	0.34	16	154
Cincinnati	200	952	0.42	18.5	133
Netherlands	203	825	0.36	18.5	144
Edgewater	173	687	0.42	14.5	173

"The above data are close approximations only."

P. 17.

"Dimensions of *Edgewater*:

Length on water-line	173 ft
Beam on water-line	34 ft
Draught to base on trial	9 ft, 6 5/8 in
Displacement to base on trial	687 tons
Wetted surface to base on trial	5,764 square ft
Propellers—diameter	8 ft
Pitch, bow	10.03 ft
stern	10.19 ft
Projected area, each	26.4 square ft."

(d) Stevens, E. A., "Progressive Trials of Screw Ferryboat *Bremen*," SNAME, 1903, pp. 1–14

(e) Stevens, E. A., "Some Problems in Ferry Boat Propulsion," SNAME, 1905, pp. 1–7 and Pls. 1–4

(f) DuBosque, F. L., "A Fire-proof Ferry-boat," SNAME, 1906, pp. 7–29. The table on pp. 11–12 gives principal dimensions of ferryboat *Hammonton*.

(g) Olsen, H. M., "Danish State Railway Ferries," IESS, 1908–1909, Vol. LII, pp. 180–193 and Pls. X–XIV. This paper describes and illustrates the ferries *Helsingborg*, *Storebaelt*, and *Prins Christian*. Table I on p. 191 lists the principal dimensions and particulars of 22 Danish ferries; there are 12 entries per vessel.

(h) Wyckoff, C. D. S., MESA, Oct 1921, pp. 750–751. This article describes and illustrates the diesel-electric ferryboat *Poughkeepsie*, which has its bow and stern propellers carried at the ends of a fin keel extending below the hull; see also SNAME, HT, 1943, Fig. 6, p. 170.

(i) The Boston Harbor ferryboats *Lieut. Flaherty* and *Ralph J. Columbo* are described and illustrated in MESA, Nov 1921, pp. 826–830. The vessels are 174 ft long overall and 57 ft wide over the guards, with a hull beam of 40 ft. The hull depth is 15.33 ft and the service draft 9 ft. The two propellers, attached to two shafts bolted together amidships, have a diameter of 7.5 ft and a pitch of 10.5 ft.

(j) Kennedy, A., Jr., and Smith F. V., "Electric Propulsion for Double-Ended Ferryboats," Amer. Inst. Elect. Engr., Pac. Coast Conv., Sep 1925. The general conclusions arrived at in this paper are reprinted in SNAME, 1926, pp. 225–226].

(k) Gross, C. F., and Green, C., "Some Considerations in Design of Ferryboats," SNAME, 1926, pp. 217–248 and Pls. 119–130. Pl. 128 is a midship section of the San Francisco Bay ferryboat *Hayward*.

(l) Mitchell, E. H., "The Design and Propulsion of Fast Double-Ended Screw Vessels," INA, 1928, pp. 88–102 and Pl. X

(m) Ferry *Lymington* with Voith-Schneider propulsion, SBSR, 14 Apr 1938, p. 495; also 5 May 1938, pp. 590–591

(n) Johnson, Eads, "Ferryboats," SNAME, HT, 1943, pp. 165–196, 378–380, 386–387

(o) Nordström, H. F., and Freimanis, E., "Modeliförsök med en Färja (Model Experiments with a Ferry)," SSPA, Rep. 7, 1947. Summary in English.

(p) Motorship, New York, Aug 1950, pp. 15–29, 36–43

(q) S. S. *Vacationland*, Diesel Prog., Aug 1950, pp. 33–35; also Apr 1952, pp. 42–45

(r) SNAME RD sheets 27, 84, 100, and 150

(s) Ferryboat *Pvt. Joseph F. Merrell*, MESR, Feb 1952, p. 61, showing wave profile; also Dec 1952, p. 85. This vessel is 290 ft overall by 277.5 ft on the 14.25-ft WL, by 69 ft over guards by 49 ft beam of hull at 14.25-ft draft. Propeller D = 20 ft and draft is 13.17 ft in normal operating condition.

(t) Great Lakes carferries *Spartan* and *Badger*, Mar. Eng'g., Mar 1953, pp. 42–57

L_{OA} = 410.5 ft	C_B = 0.656
B = 59.5 ft	P_S = 7,000 horses, normal
D = 24.0 ft	V = 18 mph or 15.66 kt
H = 18.5 ft	Twin screws
Δ = 8,860 t	

(u) Ferry *Carabobo* for Venezuela, Mar. Eng'g., Dec 1953, p. 76; Dec 1954, p. 73

L_{OA} = 162 ft	D = 12 ft
L_{PP} = 161.67 ft	H = 8 ft
B = 42 ft	Δ = 850 t

(v) San Diego-Coronado ferry *Crown City*, Mar. Eng'g., Apr 1954, pp. 58–59; Dec 1954, p. 79

L_{OA} = 242.13 ft	B of hull = 46 ft
L_{PP} = 230 ft	D = 17.25 ft
B over guards = 65.13 ft	H approx. = 11.5 ft
	Δ = 995 t

(w) Lengthened ferry *Princess Anne*, Mar. Eng'g., Jul 1954, pp. 66–67, 81. After conversion,

L_{OA} = 350 ft	B over guards = 59 ft
L_{PP} = 340 ft	D = 19.1 ft
	H = 10.5 ft.

(x) Ferry *Cameron*, Mar. Eng'g., Aug 1954, p. 63

(y) Automobile and passenger ferry *Evergreen State*; see Mar. Eng'g., Jan 1955, p. 70; Diesel Progr., Mar 1955, pp. 40–41; Diesel Times, Nov 1955, p. 7. Said to be one of the largest ferries of its type in the world, with a length of 310.17 ft, a beam of 73.17 ft over the guards, a beam of 53.5 ft at the waterline, and a depth of 23.25 ft. At a draft of 15.0 ft it displaces 2,022 tons. There is a diesel-electric drive to separate shafts and single 10.5-ft diameter propellers at each end of the vessel. The power which can be applied to *each* propeller is about 3,000 horses; 10 per cent of this is delivered to that propeller which is at the bow on any one run and 90 per cent to that at the stern. The trial speed is 15 kt at 171 rpm.

(z) De Rooij, "Practical Shipbuilding," 1953, Figs. 801 and 802 on pp. 374–375.

76.24 Characteristics of Propelling Plant and Propulsion Devices for Double-Ended Vessels. When simplicity of propelling plant is a primary requirement, as usually occurs on ferryboats designed for short runs, both end screw propellers are coupled firmly to the same shaft so that they run at identical rates of rotation. This means, as described in Sec. 33.8, that neither propeller runs at an efficient advance coefficient, and the propulsive coefficient is likewise low. This situation was described admirably by F. L. DuBosque, well over a half-century ago, and it has improved little, if any, since that time:

"The usual speed of this boat in ferry service is 11 miles per hour, and at this speed it requires 20 per cent more power to propel the boat with two screws than with one screw pushing, and 69 per cent more power to propel the boat with the screw at the bow than at the stern. If the same power could be put into one screw at the stern as is used by the two screws, the speed would be increased from 11 miles to 11.53 miles per hour. It is clear, therefore, that the bow screw is inefficient. When under way, it thrust a column of water against the bow of the boat at a velocity equal to the slip ratio of the screw, and considerable power is absorbed through friction of the blade surface; but a ferryboat's bow becomes its stern at each succeeding trip, and it is therefore impossible to dispense with the forward screw" [SNAME, 1896, pp. 94–95].

If both propellers must exert thrust simultaneously to accelerate the craft at the high rates required for short runs, or to drive it at the required speed, the type of propelling machinery is preferably such as to permit varying the rates of rotation and delivering the maximum power to each propeller. This is done by:

(1) Providing a separate prime mover for each propeller, connected by separate shafts

(2) Utilizing an electric, hydraulic, or other type of drive in which individual motors on each propeller shaft are driven from a central generating plant. This is not too difficult even though separate dynamos (generators) and pumps are not installed for each motor.

(3) Uncoupling the bow propeller and permitting it to free-wheel, while the vessel is driven entirely by the stern propeller. This is possible only if either propeller can deliver the necessary power. It is not as uneconomical as it seems because of the higher wake fraction and greater propulsive efficiency for the stern propeller. To be sure, it requires the fitting of some kind of clutch, fluid coupling, or free-wheeling device between the prime mover and each propeller.

Model tests with ferryboats having all three methods of propulsion, carried out in the Swedish State Model Basin at Göteborg, are described in:

(a) Nordström, H. F., and Freimanis, E., "Modellförsök med en Färja (Model Experiments with a Ferry)," SSPA Rep. 7, 1947. Summary in English.

(b) Nordström, H. F., and Edstrand, H., "Propulsion Problems Connected with Ferries," SSPA Rep. 17, 1951. Entirely in English.

For a ferryboat which travels bow first on its runs, which enters its slips either bow first or stern first, and which is handicapped by narrow slip clearance, cross winds, loose ice, and the like, an admirable solution is to employ an under-the-bottom rotating-blade propeller at the bow. This may supplement one or two rotating-blade propellers or screw propellers at the stern. The bow propeller augments propulsive power when desired, provides powerful lateral forces and steering effects at the bow, and creates a backward flow of water at the head of the ship when entering a slip, so as to clear out debris and ice [Virginia ferry *Northampton*, Motorship, New York, Aug 1950, pp. 26–27, 43]. The principal drawback to this arrangement is that, if the rotating-blade propellers are not retractable, and are not used to help propel the vessel, they must *always* be idled when underway.

Brief design rules for feathering paddlewheels on a double-ended ferryboat are given in Sec. 71.7.

It is emphasized in Part 5 of Volume III, under the discussion of retardation and acceleration, that to be able to start and stop properly, the propulsion devices of a ferryboat must have a thrust-producing area, equal or equivalent to A_0 in Fig. 15.G, that is large in comparison to the size of the vessel. If driven by screw propellers these must have a relatively large blade area as well as a large diameter. Sometimes the necessary blade area can be achieved only by increasing the propeller diameter [DuBosque, F. L., SNAME, 1896, p. 103].

76.25 Design Notes for Ferryboat Hulls and Appendages. The relatively large metacentric height required for a ferryboat calls for a large designed waterline, in all loading conditions, with respect to its displacement volume. Because the cargo to be carried is one of volume rather than of weight, the length and beam are also large with respect to the displacement volume. This means a small maximum-section coefficient and a rather large beam-draft ratio.

It may be expected that with its large waterline area, small maximum-section coefficient, and relatively shallow draft the ratio of the wetted surface S of a ferryboat hull to the factor $\sqrt{\nabla L}$ will be large. This means a large wetted-surface coefficient C_S , perhaps so large as to be off the scale of the graph in Fig. 45.G.

Rather clever shaping of the waterlines is called for to achieve a fineness at the ends which will avoid undue pressure resistance because of wave-making forward and excessive pressure resistance due to separation aft, yet which will provide the square moment of area about the pitching axis called for by (7) of Sec. 76.23. If this can not be accomplished, it is usually the hull resistance which has to suffer. Fig. 76.P is a plot of half of the designed waterline of the ferryboat *Cincinnati*, described in reference (b) of Sec. 76.23 preceding. A complete set of lines for a double-ended ferryboat taken from Het Schip, issue of February 1929, is reproduced to small scale by W. P. A. van Lammeren, L. Troost, and J. G. Koning [RPSS, 1948, Fig. 195, p. 289].

Because thrust deduction is developed both abaft the bow propeller and forward of the stern propeller, it is important if both work simultaneously that the hull be fined as much as practicable abaft and ahead of these propellers. This fining should extend for at least 2 and preferably 3 propeller diameters abaft and ahead of the respective propeller discs. Actually, the form of hull adjacent to screw-propeller positions and the propeller clearances are determined for *each* end propeller, by the rules of Secs. 67.23 and 67.24, on the basis that that propeller pushes from the stern. The resulting design should be entirely adequate for a propeller which pulls from ahead.

The combination of length to afford adequate space on deck, large waterline area for metacentric stability, and fining of the ends results in a block coefficient C_B that is extremely low compared to its value for the average cargo vessel. The first table accompanying reference (c) of Sec. 76.23 shows a range of C_B from 0.34 to 0.42.

Because of the full waterline endings, described elsewhere in this section, and of the large speed-length quotients at which modern ferryboats run, the heights of the bow- and stern-wave crests are factors to be reckoned with in design. The necessary clearances must be provided above the wave profile and under the sponsons or supports for the deck overhang, as well as the necessary freeboard for normal running. In addition, there must be some assurance that a heavily loaded vessel will not take water over the main deck when encountering or passing through

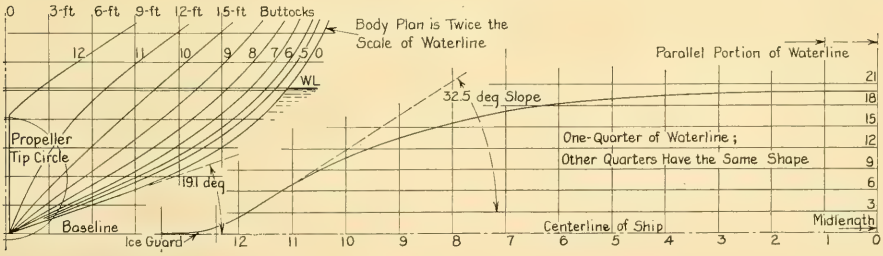

Fig. 76.P Half-Body Plan and Half-Waterline for New York Ferryboat *Cincinnati*

high waves made by another vessel [Naut. Gaz., Feb 1951, p. 28; MESR, Feb 1952, p. 61; MESR, Dec 1952, p. 85; Mar. Eng'g., 1954, p. 12]. In this case the encountered wave is superposed on the ship's bow wave. Running over shoal spots and meeting the unexpected waves which often come along at inopportune times can greatly reduce the nominal main-hull freeboard above these crests. Solid water over the large deck areas at the ends can be disastrous.

Double-ended and double-direction craft are invariably fitted with double steering rudders. Because of the excessive torque imposed on a bow rudder if it is allowed to swing and to take part in the steering action, to say nothing of its inefficiency as a steering device, for the reasons explained and illustrated in Sec. 37.11 and Fig. 37.G, it is preferable to lock the rudder mechanically at the end which happens to be the bow. The steering control to that rudder is disconnected or de-energized, a centering pin is dropped into the top of the rudder, and the vessel is steered only with the rudder at the after or trailing end. For this reason, each rudder is required to provide the entire control necessary for maneuverability of the vessel.

Even though located in a propeller outflow jet, as it should be, the rudder(s) of a ferryboat should be relatively large, to enable it to dodge traffic, to maneuver promptly in a fog, to enter and leave its berth in a cross tidal current, and to turn around, if need be.

Ice guards and rope guards are often fitted ahead of bow rudders and abaft stern ones. If these extend continuously around the outer rudder profile, from the hull above to the rudder shoe below, they form effective rope guards [Graemer, L., Schiffbau, 11 Oct 1911, Fig. 4, p. 4, and Pls. 1–2; WRH, 15 Dec 1939, p. 381]. However, if they are bent inward accidentally, even only slightly, they foul the rudder and prevent its swinging. They have one advantage that they create a separation zone of sorts in which the larger part of the rudder blade lies, so that excessive torque is not applied continually on a rudder at the leading end of the vessel. Conversely, they may vibrate transversely because of alternate eddies shed abaft them. It is therefore best to make such a guard, if fitted, a sort of prolongation of the sides of the rudder blade.

There is much to be said in favor of supporting a long, wide deck overhang on each side of a ferryboat with a plated-in sponson. It affords additional buoyancy and righting moment in an emergency, it eliminates fouling of a long row of strut supports by waves and foreign objects, and it gives a far cleaner appearance to the craft as a whole. Some notes and sketches relative to these sponsons are found in Sec. 68.12 and Fig. 68.K. An admirable view of the hull of the ferryboat *Evergreen State*, embodying this feature, is published in Diesel Times, November 1955, page 3.

The hulls of many ferryboats lend themselves to the use of straight-element forms. A few of this kind, to be found on ferryboats in service, are illustrated in SNAME, HT, 1943, Figs. 9, 11, and 20 on pages 172, 174, and 179, respectively.

76.26 Special Problems of Icebreakers and Iceships. An *icebreaker* is a special-service vessel capable of breaking up and making its way through heavy floe ice, pack ice, and solid sea ice. It makes navigable lanes for other vessels as well as for itself. Indeed, it may be called upon to tow other vessels through these lanes, or to push on another icebreaker ahead of it when the going gets particularly rough. Its primary duty, involving great power on a limited length and exceptional sturdiness, is such that it can carry very little useful load, either in weight or volume, other than that required for its own services. Like a tug, it is often called upon to deliver maximum forward (and astern) thrust at or near zero speed. This thrust, furthermore, is required to overcome forces other than its own hydrodynamic resistance, just as its structure is required to withstand forces other than those imposed upon it in wavegoing.

An *iceship* is a vessel designed and constructed for, or adapted to traveling in heavily iced waters without the necessity for breaking solid ice and making its own water lane. It is intended to be capable only of withstanding ice impact and traversing an ice field which has previously been broken up by an icebreaker or by natural causes such as wind and swell. As a rule, the iceship is of more-or-less normal form, although it may have a Maier bow, intended to ride up on and break through not-too-thick ice. Its hull plating is thick at the waterline belt, at least, and its framing is heavily reinforced. It is, in fact, designed and constructed for carrying cargo or for some other *primary* mission. Its ability to make its way through and to withstand not-too-heavy ice is purely secondary ["Ships for Arctic

Use" (designations T-AKD-1 and T-AK270), Maritime Reporter, 15 Sep 1955, pp. 11–13].

No specific requirements other than the general functions listed in the two paragraphs preceding are given for icebreakers and iceships because the service varies rather widely. A vessel suitable for breaking a lane and convoying large vessels through the Northwest Passage, for example, is entirely unsuitable for clearing out a small harbor and working around slips. The details of ship handling in various kinds of ice are mentioned in a number of the references of Sec. 76.27 following, but are given in more methodic fashion in the 1948 Edition of the British Antarctic Pilot, Chap. I, pages 42–54, under "Ice Navigation."

While the process of bucking ice is in no sense a hydrodynamic action there are major hydrodynamic problems involved. Considering the solution of these problems and the selection of design features for an icebreaker (not an iceship) in somewhat the same order as in Chaps. 64 through 68 for a surface ship, the appended list supplements one previously given by D. R. Simonson ["Bow Characteristics for Ice Breaking," ASNE, 1936, Vol. 48, pp. 249–254]:

(1) Waterline length
(2) Normal displacement
(3) Length-beam and beam-draft ratios
(4) Engine power
(5) Thrust available from the propeller(s) at low speeds
(6) Transverse section shape
(7) Number and position of propellers
(8) Forebody shape
(9) Appendages.

These items have to be balanced against carrying capacity, steering and maneuvering qualities, allowable draft, and economical power.

The length is limited to the practicable minimum so that the vessel can work to advantage in open-water spaces of small size. The waterline length and the weight are also important because they largely determine the downward icebreaking force which can be exerted at the bow when the latter is pushed up on the ice and the vessel lifts forward, usually by an angle less than 5 deg.

Although there are limited authentic data for analysis it appears obvious from a consideration of the mechanics involved, presented by D. R. Simonson in the reference cited, and by R. Runeberg in references (2) and (5) of Sec. 76.27, that the smaller vessels are not intended to break ice as thick as required for the larger ones.

More important than the length of an icebreaker is its length-beam ratio, which must be small for superior maneuverability in driving through leads in the ice. When forcing its way into a harbor or inlet the ship must go around corners, or must back and fill and turn to clear an open space for other vessels. The icebreaker may even have to back up or turn around to free convoyed vessels that have become stuck in the ice behind it [Sokol, A. E., USNI, May 1951, p. 482].

Fortunately, the very large beam relative to the length needed for this purpose is also required to clear a lane wide enough for a convoy following behind. This lane can not always be straight, so the corners must be cut off for longer vessels in the rear.

A study of beam-draft data for a large number of icebreakers (and designs), reveals rather wide variations with weight displacement. Considering only those vessels whose performance is known to be good or excellent, optimum values of L/B ratio with weight W (or Δ) may be taken from the vicinity of the curved broken line in Fig. 76.Q. This ratio increases from about 3.6 in small vessels to 4.5 in the largest vessels of this type.

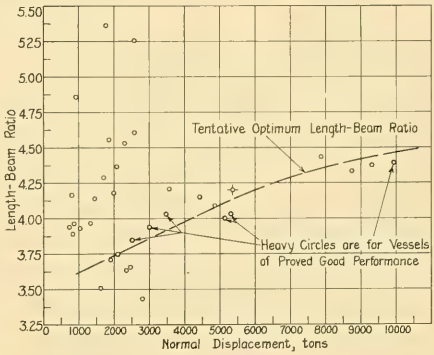

Fig. 76.Q Plot of Length-Beam Ratios for Icebreakers

A similar study of B/H ratio on waterline length reveals no clear optimum value, possibly because the load conditions are rather variable, and possibly because the draft needs to be as large as practicable to allow the use of large-

diameter propellers with tip submergences great enough to clear surface ice.

With these small L/B ratios and relatively deep drafts it is natural that the block coefficients should be low and the displacement-length quotients or fatness ratios high. The C_B values are of the order of 0.5 and the 0-diml fatness ratios range from 8 or less to about 15.

Like a tug, the icebreaker has waterlines, both above and below the DWL, which are well curved throughout. These enable it to follow desirable leads or to extricate itself when temporarily caught.

The ship often has to back off, stop, and gain the maximum possible speed ahead in a short distance so that its momentum can be added to the thrust forces to push the ship's bow up over the ice. This means an ample reserve of power and propellers that are large enough to develop very high thrust values. In certain kinds of ice the friction of a thick pack may exceed the water friction around the hull, especially at low speeds.

On the basis that it is usually desirable to break the ice without too much charging or ramming, the thrust to keep the ship going at low speeds in ice (say 3 kt) and at high real-slip ratios or J-values is a function of the propeller-disc area, the propeller power, and the overall efficiency of the power plant. At low speeds, this efficiency is only from 10 to 25 per cent. Simonson (in the reference quoted) gives an approximation of 1 (long) ton of thrust from the propeller(s) per 100 horses of indicated power in the engines.

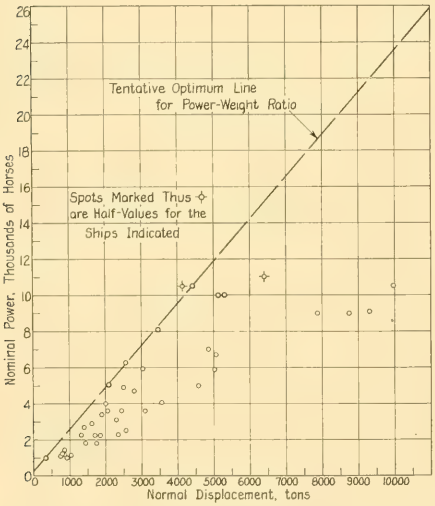

Fig. 76.R Plot of Power-Displacement Ratios for Icebreakers

When Scotch boilers and reciprocating engines furnished the only available propelling power, their large volume and heavy weight made it possible to get only limited indicated power within an icebreaker hull. This is believed the reason why the data of Fig. 76.R show powers much less than those considered necessary by modern standards, represented by the sloping design line. The latter indicates roughly a dimensional ratio of about 2.35 horses delivered at the propeller(s) for each (long) ton of weight displacement, although a ratio of 2.5 is not unduly high. The former should give an unspecified but adequate free-running speed for any icebreaker, regardless of its duties in ice-free waters.

The transverse sections necessary in an icebreaker to prevent crushing of the ship structure as a whole by pack ice put under pressure over large areas are peg-top in form. They taper inward and downward rather sharply from a level above the designed waterplane, following Colin Archer's design for the famous Norwegian polar expedition ship, the *Fram*, first used by F. Nansen and later by R. Amundsen [Nansen, F., "Farthest North," Harper, New York, 1897, Vol. I, pp. 57–71. On the plate opp. p. 60 there are an inboard profile, a deck plan, and two sections of the *Fram*]. Archer designed this hull in the form of a vertical wedge which, when subjected to lateral pressure from large floes of moving ice, causes the vessel to be lifted bodily and hence to avoid crushing of the hull and ultimate destruction. The close resemblance between the midsection of the *Fram*, designed over 60 years ago, that of R. E. Peary's *Roosevelt*, designed in the early 1900's [Mar. Eng'g., May 1905, p. 193; Zeit. des Ver. Deutsch. Ing., 8 Jul 1905, p. 1135; Scientific American, 15 Jul 1905, pp. 47–48], the midsection of the U. S. Coast Guard icebreakers of the *Northwind* class [Johnson, H. F., SNAME, 1946, pp. 112–151], and the body plans of many other icebreakers, old and new, are proof of Archer's excellent reasoning and designing ability.

R. Runeberg [ICE, 1900, p. 122] gives examples of early icebreakers (prior to 1900) with transverse section slopes at the vicinity of the DWL of from 79 to 90 deg. He says that there is no need to make the slope less than 79 deg and that

a slope of 85 deg should suffice for "all ordinary ice-breakers." H. F. Johnson, in 1946, says that the slopes for the flaring sides of the midship section should be between 70 and 80 deg.

A pronounced tumble home above the DWL is desirable to prevent the fouling of top hamper when working around other vessels. One other feature of the abovewater body not to be overlooked at this point is the minimum freeboard when heavily loaded. Entirely aside from wave-going requirements, a reasonable amount of hull extending above the ice level is required to insure that, if held fast in the ice, the ship is not overwhelmed by overriding floes and pressure ridges rising above the water level. Nansen's *Fram*, although undamaged by lateral squeezing in its drift over the Arctic Ocean in 1893–1896, nevertheless was nearly overwhelmed and sunk by ice coming in six feet deep over the rail on 3–7 January 1895 [Nansen, F., "Farthest North," 1897, Vol. II, pp. 47–60].

The early, heavily powered steel icebreakers of the 1890's and 1900's were almost invariably equipped with bow propellers, as were many of those of later years. This was on the theory that, after the breaker's bow had ridden up over a thick ice layer and broken it into chunks, partly by impact and partly by sheer weight, the inflow current to the bow propeller(s) would draw the ice down under the ship. The outflow current would push it aft under the ship, leaving the bow free to break more ice.

It may be well to remember, however, that when F. E. Kirby of Detroit introduced the first bow propeller on the icebreaking car ferry *St. Ignace* for the Straits of Mackinac in 1888 [Runeberg, R., ICE, 1900, Vol. CXL, pp. 109–129], it was to perform an entirely different function. Faced with the problem of getting a ship through ice that was piled in layers all the way down to the channel bed, Kirby held the icebreaker's bow to the ice with a powerful stern propeller while the bow propeller, *going astern*, forced a current of water into the ice mass ahead to loosen it. When some of it was loosened, the bow propeller was set to drive ahead, whereupon the inflow current produced by it drew loose ice from the mass and pushed it aft. After the ship advanced until it was again stalled, the process was repeated. Following Kirby's success, bow propellers were fitted to many icebreakers, whether faced with the same operational problems or not. This is another example of the importance of knowing why things are done when new ships are designed.

It has since been found that when the ice is thin enough to be broken up and drawn down under the bow by the inflow current from the bow propeller, without damaging the propeller, then the latter is of great assistance. When a thick layer of heavy snow lies on top of a relatively thin layer of sea ice the abovewater bow banks the snow up in front of it until finally the ship can no longer force its way through. The procedure then is to break up the ice by small increments and to suck both ice and snow down and under the ship, finally ejecting it behind. A bow propeller or propellers are of great assistance here as well. If the ice is so heavy that as the ship rides up on it the bow propeller is struck by huge blocks, these blows are liable, not only to bend or break the propeller blades but to bend the shaft or to dislodge the thrust bearing inside the ship.

The meaning of the foregoing is that, under conditions which may change from day to day, the ship needs a bow propeller or propellers or else it is encumbered by them. Although the mechanical problems seem almost insurmountable, especially for such heavy-duty machinery, it may nevertheless be possible at some time in the future to develop a housing bow propeller for an icebreaker. This might be a 2-bladed affair, made controllable and reversible from within, with nearly flat blades having thick symmetrical sections. When not in use the blades could be feathered fore and aft and the whole propeller drawn backward into a shallow recess in a lower vertical portion of the stem. This would support the blades and hub against the impact of heavy blocks of ice striking from ahead. When desired for use the bow propeller with its shaft could be pushed forward a short distance by an internal hydraulic or equivalent mechanism. With the blades then turned to the desired angle, the propeller would be instantly available for pulling the ship ahead, sucking blocks of ice down clear of the upper part of the bow, or helping to back the ship out of a jam in the ice.

While the thrust deduction due to positive differential pressures $+\Delta p$ abaft the bow propeller of an icebreaker is of no more than secondary consideration, the free passage of broken ice through and abaft the wheel calls for the same fining of the hull behind the propeller as would be the case were it used for normal propulsion.

Indeed, the bow propellers of the ferryboat and of the icebreaker, although installed for entirely different normal functions, involve many of the same hydrodynamic principles in their action. The ferryboat bow propeller often comes in handy for clearing loose ice out of the head of its slip.

For the designer faced with the problem of considering one or two bow propellers, or of designing an icebreaker with them, a most useful document is SSPA Report 20 by H. F. Nordström, H. Edstrand, and H. Lindgren, entitled "Model Tests with Icebreakers." It was published in 1952 and is entirely in English.

Whether a bow propeller is fitted or not, D. R. Simonson mentions in the reference cited earlier in this section that it is often necessary to fill out what would be the forefoot, just above the baseline, in order to obtain sufficient displacement volume forward. The resulting bow profile corresponds somewhat to that of an icebreaker with a bow propeller. The vertical stem portion extending for a distance above the keel performs another useful service in that it prevents a vessel with a constant slope of about 30 deg in the bow profile from riding up so far on a deep accumulation of ice cakes that it can not be backed off. The vertical portion of the stem acts also as a cutter to loosen up the lower layers of ice in deep windrows. Fig. 76.S shows the vertical portion of the stem abaft a bow propeller position. This portion should be retained, as previously noted, even without a bow propeller. The peg-top underwater sections, the tumble home above the waterline, and the massive bossings are also well shown in the figure.

The forward buttocks should be sloped as much or more than the bow profile, extending back to the section of maximum beam, so that the whole forward part of the ship acts effectively to break ice. The characteristics of the forebody should be duplicated as much as possible in the afterbody since the vessel will be required to break ice when backing.

The following is quoted from page 254 of the Simonson reference:

> "It is desirable to work the same angles into the buttocks of the fore body to obtain equalization of lifting forces when the ice carries past the bow without breaking clear of the hull. As for the frame sections, they should show a marked flare at the waterline to relieve the crushing force of the ice."

It is obvious that vessels having V-shaped midship and other sections similar to those of icebreakers, with their large bulge radius, possess little in the way of roll-damping characteristics. Without roll-quenching devices of some kind they roll deeply and heavily, to the great detriment of their habitability. When the beam-draft

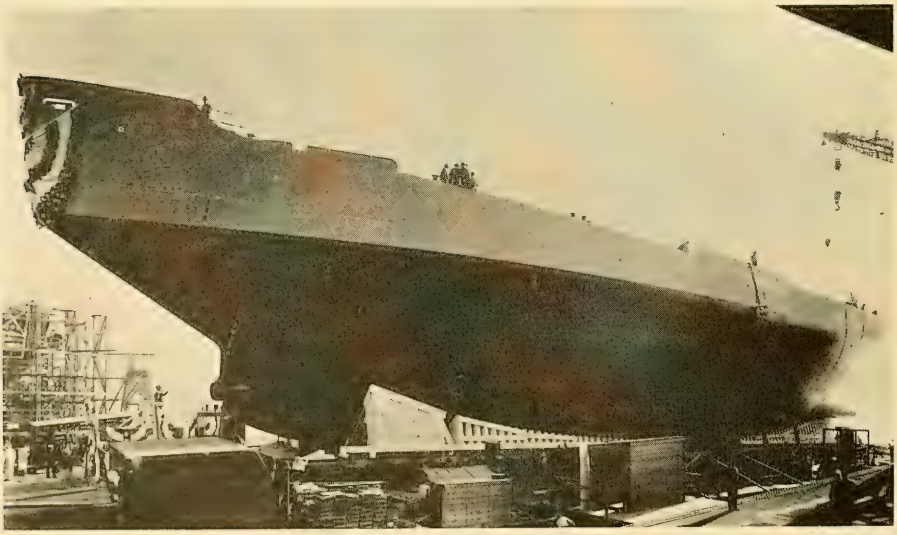

Fig. 76.S Bow Quarter View of Hull of an Icebreaker of the *Wind* Class

ratio is moderately large they also roll sharply unless the polar moment of inertia about the fore-and-aft rolling axis is large.

The usual type of roll-resisting keel is vulnerable in the ice. Any type of retractable projection is almost as vulnerable. Plate-type keels, as distinguished from those of triangular section, may be added at the start of each voyage and used to quench roll until such time as they are bent over or stripped off by the ice.

Most icebreakers carry fuel and other liquids in certain wing tanks connected by pumps. Shifting these liquids from one side to the other produces enough heeling moment to rock the vessel and help free it from the ice. If sufficient power and weight could be spared to make this shift in the order of half the natural rolling period, the active roll-quenching tanks thus formed would go far toward making the icebreaker a more livable ship in the open sea.

Protection against large blocks of ice striking a single propeller at the stern is afforded by fitting one or more fins, generally horizontal, ahead of the propeller, projecting on each side from the centerline skeg [M. S. *Kista Dan*, SBSR, 19 Jun 1952, pp. 778–779; 25 Dec 1952, p. 831; M. S. *Theta*, The Motor Ship, London, Jan 1954, p. 458]. Since the flow of water along such a skeg is aft and upward, the fins should lie in the natural streamlines, as determined from model lines of flow and as checked by tufts or equivalent methods. A "ladder" of three or four fins, one above the other, parallel to the shaft line and extending forward for perhaps a propeller diameter, might have a beneficial propulsion effect in producing more nearly axial flow in ice-free water. Such a layout, however, requires careful checking in the design stage, preferably on a model in a circulating-water channel. The trailing edges of all such fins require fining to avoid separation and eddying ahead of the wheel.

Rudders of icebreakers and iceships are invariably completely submerged. They are protected after a fashion by horns, preferably integral with the hull, projecting downward *beyond* the rudders and below their tops, so as to break up the ice when going ahead *or astern* and prevent blocks from wedging themselves between the top of the rudder and the hull. To meet the exacting maneuverability requirements they should be larger than normal but are often just the opposite, to make them less vulnerable to damage from the ice.

Underwater inlets and discharges for the cooling water of heat exchangers are often shut off by ice cakes resting across the openings or by broken ice lodged in the strainers. It is customary to provide a water box inside the shell to which the circulating lines can be connected. Water discharged into this box is cooled by contact with the shell before it is used over again. Similar water boxes are fitted on vessels required to operate in very shallow water where the outboard connections could be plugged temporarily and where the system could be filled with mud, silt, or sand.

Published model-test data on icebreaker hulls are rather meager. There is available to the designer SSPA Report 20, published in 1952 by H. F. Nordström, H. Estrand, and H. Lindgren, entitled "Model Tests with Icebreakers." This is abstracted in SBSR of 5 June 1952, pages 726–728; the Swedish report is, however, entirely in English.

76.27 Tabulated Data and References on Icebreakers. The first tabulation of dimensions, characteristics, and other data on icebreakers was made by R. Runeberg in references (2) and (5) of the list in the latter part of this section. These data are contained in a single table on page 285 of reference (2), published in 1889; otherwise the small tables of data are somewhat scattered throughout both references.

The first really comprehensive tabulation appears to be that of H. F. Johnson [SNAME, 1946, pp. 112–151]. A large 3-page table on pages 114–116 contains 44 entries for 39 icebreakers and iceships. In the same year (1946) I. V. Vinogradov published in Moscow a Russian book entitled "Vessels for Arctic Navigation (Icebreakers)," which has a rather complete list of tabulated data on pages 22–23 and 26–34. The ships described in these tables date from 1871 to 1938. The book appears to cover the theoretical and analytical aspects of icebreaker design rather well, and it contains a great deal of miscellaneous tabulated data. At the time of writing (1955) only the table of contents has been translated into English. The Library of Congress number is VM451.V5.

Table 76.f contains some dimensions, proportions, and characteristics of modern icebreakers, supplementing the 1946 list of H. F. Johnson. These data were gathered from published sources so they are incomplete and in many cases inconsistent. This is due partly to a lack of strict definitions of displacements, powers, and other

TABLE 76.f—DIMENSIONS, PROPORTIONS,

All dimensions are, unless otherwise stated, in ft to the proper power. All powers are in English

GENERAL Name of Vessel	*Holger Dansk*	*D'Iberville*	*Labrador*	*Thule*
When built	1942	1953	1953	1953
Where built	Odense Staal-skibsvaerft	Lauzon, Quebec	Sorel, Quebec	
Nationality	Danish	Canadian	Canadian	Swedish
Remarks		Iceship		
PRINCIPAL DIMENSIONS AND CHARACTERISTICS Length, overall, ft	226.0	310.8	296	204
Length bet. perps., ft		288	250	
Waterline length at given draft, ft	210.3	300 (est.)	250	187
Beam, maximum, ft	55.5	66.5	63.8	52.6
Beam, waterline, ft	53.4	64.5	61.0	49.9
Depth, molded, to weather deck, ft	24.5	40.0	37.8	
Draft, normal, ft	17.8	30.42	27.5	17.6
Draft, maximum, ft	19.5		29.0	
Displ., normal, t	3,040	9,930		2,100
Displ., maximum, t			6,400	
Ice-belt plating, thickness, in	3/4 to 7/8		1-5/8	
Frame spacing, ft	1.46			
Ballast pumps, capacity, t per hr	800			
Capacity of trimming or heeling tanks, t				
PROPORTIONS AND FORM COEFFICIENTS Length-beam ratio, for waterline	3.94	4.46	4.10	3.75
Beam-draft ratio for normal displ.	3.00	2.15	2.22	2.83
Block coeff., C_B	0.520	0.590	0.534	0.534
Prismatic coeff., C_P	0.634			
Maximum-section coeff., C_X	0.82			
Waterplane coeff., C_W	0.73			
Half-angle of entrance, deg	43.5			

AND FORM DATA FOR ICEBREAKERS

horses. All weights and displacements are, so far as can be learned, in long tons of 2,240 lb.

Elbjorn	*Voima*	*General San Martin*	*Glacier*	*Kapetan Belousov*	Unnamed
1953	1953	1953	1955	1954	1958 (est.)
		Seebeck	Pascagoula	Helsinki	Helsinki
Danish	Finnish	Argentine	USA	Russian	Russian
		Research and supply vessel			To be built (1956)
167.5	274	277.8	309.6	273	390
		242.8	290.0	265	
	254.3	252.5	290.0		363.4
	63.6	62.3	74.0	63.8	80.4
39.3	61.4	61.0	72.5	63.0	
	31.2	32.3	38.0	31.1	
16.2	21.0	21.3	25.75	23.67	31.2
1,400	4,415			5,360	12,800
			8,300		
				6,400(?)	
	107			5.5° list in 1.5 min	
	4.15	4.14	4.00	4.20	4.52**
2.43	2.92	2.86	2.82	2.74	2.58**
	0.482		0.537	0.489	0.507 (est.)

**Based on maximum beam.

TABLE 76.f—

PROPORTIONS AND FORM COEFFICIENTS—(*Continued*) Name of Vessel	*Holger Dansk*	*D'Iberville*	*Labrador*	*Thule*
Flare amidships at WL, deg	16			
Displ.-length quotient	326	369 (est.)	410*	321
Fatness ratio, 0-diml	11.4	12.9 (est.)	14.4*	11.2
$\overline{\text{LCB}}$				
PROPELLING MACHINERY Number of primary units		$P_I = 2 \times 5{,}400$, diesel-elect.	$P_B = 6 \times 2{,}000$, diesel-elect.	$P_B = 3 \times 1{,}600$, diesel-elect.
PROPULSION DEVICES Number of shafts, total	3	2	2	3
for'd.	1			1
aft	2	2	2	2
Shaft power, horses, total normal		10,800	10,000	5,040
forced	6,610	15,120		5,550
Shaft power, horses, bow normal				1,680
forced	2,120			
Shaft power, horses, stern normal	4,080	10,800	10,000	3,360
forced	4,490	15,120		
Rate of rotation, bow props, rpm	141			180
stern props, rpm	123	145		145
SPEED AND RADIUS Speed, specified, kt	15	16		
Cruising radius, mi		12,000		
Taylor quotient, T_q	1.034	0.924		

(*Continued*)

Elbjorn	*Voima*	*General San Martin*	*Glacier*	*Kapetan Belousov*	Unnamed
			20		
	269		341*	288	268**
	9.4		11.9*	8.2	7.6**
	$P_B = 6 \times 2{,}000$, diesel-elect.	4 diesel-elect.	$P_B = 10 \times 2{,}400$, diesel-elect.	6 diesel-elect.	$P_B = 8 \times 3{,}250$, diesel-elect.
2	4	2	2	4	3
1	2			2	
1	2	2	2	2	3
2,700	10,500	6,500	21,000	10,500	22,000
3,375		7,100			
900	3,500/7,000				
1,125					
1,800	7,000/3,500	6,500	21,000		
2,250		7,100			
200	180			180	
160	120	138		120	330
					19
					20,000
					0.997

* Based on maximum displacement
** Based on maximum beam

terms and partly to incomplete descriptions of the terms for which numerical quantities are given. In any case, the new tables provide a framework for filling in missing data in the future.

In a number of cases new icebreakers have been built to replace old ones and have been given exactly the same names.

There follows a selected list of references on ice, icebreakers, and iceships, giving what are believed to be the principal sources of information. Except for the Vinogradov book of 1946 and the Schiffbau references, these are all in English.

(1) "Bibliography on Ice of the Northern Hemisphere," H. O. Publ. 240, Hydrographic Office, U.S. Navy, 1945

(2) Runeberg, R., "On Steamers for Winter Navigation and Ice-breaking," ICE, 1888-1889, Vol. XCVII, Part III, pp. 277–301 and Pls. 3–5. These plates show arrangement plans and lines drawings for the ships *Express*, *Bryderen*, *"Ice Boat No. 2,"* (driven by paddles!) and a projected steamer for the Finland Government. It seems incredible but this reference appears to be the first one in the technical literature on this subject. Runeberg tackles the design problems involved in icebreaking from an analytic point of view and develops formulas covering the various operations under:

Ice-breaking by a continually progressing steamer
Ice-breaking power of a steamer when charging
Effect produced by the continued working of the engine
Frictional resistance caused by change of motion
Displacement of metacenter (vertically).

These sections are followed by discussions entitled "Details of Construction" and "Particulars of Some Ice-Breaking Steamers." Among the latter are the *Express*, *Isbrytaren*, *Oland*, *Bryderen*, *Em. Z. Svitzer*, *Starkodder*, *Ice-Boat No. 2*, and a proposed steamer for the Finland Government.

Runeberg's comments and conclusions in this reference are somewhat modified by those in a later ICE article by him, dated 30 Jan 1900, reference (5) hereunder.

(3) Cassier's Magazine, Jul 1897, Vol. XII, p. 326, shows the stern view of a vessel in a drydock at Newport News. From all indications this ship is an icebreaker. In any case it has a very large beam, a considerable amount of tumble home all around, and is fitted with two huge 4-bladed propellers with fan-shaped blades. The propellers are of the built-up type with securing bolts or nuts that project prominently from the hubs. It is believed to be Russian.

(4a) A "gigantic Russian ice crusher" is mentioned in ASNE, Aug 1898, Vol. X, pp. 917–918; also ASNE, Nov 1898, Vol. X, pp. 1222–1223. According to the latter reference this vessel was launched on 29 Oct 1898. It is 305 ft long and 71 ft beam, with a depth of 42.5 ft. When fully loaded, the draft is 25 ft, and the corresponding displacement 2,000 t. However, the displacement given is much too small for the dimensions. Although not specifically named in the reference, this vessel appears to be the *Ermack*.

There are three propellers aft and one propeller forward, driven by four engines having a combined (indicated?) power of 10,000 horses. It is believed to have been designed by Admiral Makarov.

On page 1223 it states that "The stern of the ice breaker is cut to form a recess, into which the stem of another vessel can be securely lashed, and thus obtain the utmost protection from her powerful consort."

(4b) Swan, H. F., "Ice-Breakers," INA, 1899, Vol. 41, pp. 325–332 and Pls. LIX-LXII; tells about the *Ermack* and the Finnish icebreaker *Sampo*

(5) Runeberg, R., "Steamers for Winter Navigation and Ice-breaking," ICE, 1900, Vol. CXL, Sect. I, pp. 109–129 and Pl. 4. The plate embodies an arrangement plan and lines drawing of the *Aegir*, complete lines drawings of the *St. Marie* and *Sampo*, and forebody lines drawings of twelve icebreaking vessels, built between 1871 and 1896. Runeberg discusses the bow propeller, which was apparently introduced by F. E. Kirby on the Straits of Mackinac ferry *St. Ignace* in 1888.

(6) "Icebreakers for the Port of Stockholm," the Shipbuilder (now SBMEB), Jan-Jun 1914, Vol. X, pp. 55–57. L_{OA} = 200 ft, L_{PP} = 188 ft, B_X = 55.75 ft, D = 21.5 ft. The ship has one large stern propeller plus one smaller bow propeller; also there is some drag in the keel.

(7) The Russian icebreakers *Sviatogor* and *Alexander* are illustrated in Schiffbau, 11 Feb 1920, pp. 402–403; also in Engineer, London, 26 Dec 1919. Some details are:

Sviatogor	*Alexander*
3 screws, all aft	2 stern screws, 1 bow screw
L_{OA} 99.2 m = 325.48 ft	L_{OA} 85.64 m = 280.98 ft
L_{WL} 90.52 m = 297.0 ft	L_{WL} 83.20 m = 272.98 ft
B 21.64 m = 71.0 ft	B 19.45 m = 63.81 ft.

The midsections of these vessels, shown on page 404 of the Schiffbau reference, are of the typical pegtop shape, with a large tumble home above the DWL.

(8) Flodin, J., "Ice Breakers," Mar. Eng'g., Sep 1920, pp. 707–712

(9) Kari, A., "The Design of Ice-Breakers," SBSR, 22 Dec 1921, pp. 802–804. Some of the information given in this article is included in Mr. Kari's book entitled "Design and Cost Estimating of Merchant and Passenger Ships." The reference discusses static and dynamic icebreaking, length, length-beam and length-depth ratios, and gives various formulas useful for design and for predicting the performance of a ship designed elsewhere.

(10) "Swedish Ice Breaker of 2,450 Tons Displacement and 6,000 I.H.P.," SBSR, 12 Mar 1925, p. 310

(11) "(Russian) Ice Breaker *Krisjamis Valdemar*," The Shipbuilder, Jul 1925; abstracted in ASNE, Aug

1925, pp. 611–612; SBSR, 4 Mar 1926, pp. 247–251. A small sketch showing the general hull shape and the principal dimensions of this vessel is found in WRH, 22 Jan 1929, Fig. 9, p. 30.

(12) Judaschke, F., "Konstruktionsbedingungen fur die in Eisgang und Eisbrechdienst zu verwendenden Schiffe (Construction Specifications for Ships Going Through Ice and in Ice-Breaking Service)," WRH, 22 Jan 1929, Vol. 10, pp. 27–31 (in German). Comments in English on this article are to be found in Marine Engineer, Mar 1929, p. 116.

(13) Icebreaker *R. B. McLean*, for the Hudson Bay Railway of the Canadian Government, MESA, Nov 1930, p. 610. The displacement is 5,034 t, the L_{BP} is 260 ft, the B 60 ft, D 31 ft, H 19.5 ft. Indicated power 2 times 3,250 horses.

(14) Hammar, H. G., "The Construction of Cargo Vessels Intended for Winter Traffic and Navigation in Ice," SBMEB, Mar 1931, p. 175

(15) Halldin, G., "Federal Icebreaker *Ymer*," Teknisk Tidskrift, Stockholm, Part I, Jan 1932; Part II, Feb 1932

(16) "Diesel-Electric Ice-Breaker *Ymer*," SBSR, 25 Aug 1932, pp. 175–177

(17) Christofferson, V., and Ericson, N., "The Federal Ice Breaker *Ymer's* Machinery Installation, with Particular Attention to the Main Plant," Part VIII, Stockholm, Aug 1932, following ref. (15)

(18) Christofferson, V., and Ericson, N., "Federal Ice Breaker *Ymer's* Machinery Equipment, with Special Emphasis on the Propelling Machinery," Part IX, Stockholm, Sep 1932

(19) "Ice Breaker *Ymer* (9,000 B.H.P. Machinery)," Motorship, Jan 1933, p. 366

(20) "Ice-Breaker *Goeta Lejon*," SBMEB, Feb 1933, p. 91

(21) "Ice Breaker *Ymer*" for Swedish Government, Motorship, London, Apr 1933, pp. 7–14; also MESA, May 1933, pp. 165–167

(22) "Japanese Ice Breaker *Soya Maru*," MESA, May 1933, pp. 162–164, 182. Gives particulars, trial data, and photographs.

(23) Holmberg, G., "Federal Ice Breaker *Ymer's* Trial Runs," Teknisk Tidskrift, Stockholm, Jan 1934

(24) Gouljaeff, N., "Ice Breakers," SBMEB, Mar 1935, pp. 143–150. Gives a bibliography of information on icebreaker design.

(25) Simonson, D. R., "Bow Characteristics for Ice Breaking," ASNE, 1936, pp. 249–254

(26) Hunnewell, F. A., "U.S. Coast Guard Cutters," SNAME, 1937, pp. 81–114. Describes cutters *Escanaba*, *Algonquin*, and *Raritan* (110-ft harbor cutter).

(27) Mendl, W. V., "Ice Breakers," SBMEB, Oct 1938, pp. 543–544. Gives formula for thickness of ice that can be broken.

(28) "The *Sisu*, A Diesel-Electric Ice Breaker," Motor Ship, London, Apr 1939, pp. 22–24. Finnish icebreaker. Gives particulars of vessel, with arrangement plan and photographs.

(29) Macy, R. H., "Icebreakers," USNI, 1940, Vol. 66, pp. 669–674

(30) Smith, R. Munro, "The Design of Icebreakers," SBSR, 6 Feb 1941, pp. 127–128. This gives general particulars for a typical icebreaker, suggests length-beam and beam-draft ratios, and gives a formula for thickness of ice that can be broken.

(31) "Icebreakers," SBSR, 20 Nov 1941, pp. 481–484, 491

(32) "The Ice-breaker *Ernest LaPointe*," SBMEB, Jan 1942, pp. 13–18. This is a twin-screw ice-breaking and channel-surveying vessel built in Canada for the Canadian Department of Transport.

(33) Wasmund, J. A., "Coast Guard Ice-Breaking Vessels," MESR, Dec 1944, pp. 184–186. Includes discussions of hull construction, bow propellers, propulsion motors, speed control, and power requirements.

(34) "Ice-Breaker Design," MESR, Apr 1945, pp. 142–145. Includes a history of icebreaking vessels and gives particulars of various icebreakers.

(35) "Coast Guard's Diesel Powered Ice-Breakers," Motorship, London, Jun 1945, pp. 562–566, 604

(36) Johnson, H. F., "Development of Ice-Breaking Vessels for the U.S. Coast Guard," SNAME, 1946, Vol. 54, pp. 112–151. A very complete paper, summarizing development to date and describing the design of modern icebreakers.

(37) Vinogradov, I. V., "Vessels for Arctic Navigation (Icebreakers)," Moscow, 1946 (in Russian)

(38) Outboard profile of Swedish icebreaker with diesel drive, having controllable twin propellers aft and one small screw propeller forward, is shown in AM, Jul 1948, p. 26

(39) Thiele, E. H., "Machinery Installation of the *Wind* Class Coast Guard Icebreakers," ASME, 29 Nov–3 Dec 1948, No. 48–A–111

(40) Finnish Government Icebreaker *Into*, with 12,000 B.H.P. Machinery," Motor Ship, London, Aug 1950, pp. 166–167. Includes particulars of vessel, discussion of machinery, profile and arrangement plans. Ship has two bow and two stern propellers, with a motor power of 4 times 3,500 horses.

(41) Kassell, B. M., "Russia's Icebreakers," ASNE, Feb 1951, pp. 137–152

(42) "A Motorship for Arctic Waters (*Kista Dan*)," SBSR, 19 Jun 1952; pp. 829–831

L_{OA} = 212.88 ft	H, as cargo vessel = 18.083 ft
L_{PP} = 185 ft	V = 12 kt
B, molded = 36.75 ft	Deadweight capacity as a cargo vessel (iceship) = 1,200 tons

(43) De Rooij (pronounced Rooy), G., "Practical Shipbuilding," H. Stam, Harlem, Holland, 1953, Fig. 16 on p. 19, Art. 208 on p. 372, and Fig. 798

(44) Article on icebreakers in The Shipping World, 30 Jun 1954, Vol. 130, pp. 655–657. Abstracted in IME, Jan 1955, Vol. LXVII, pp. 13–14. These references give data on the *Thule*, *Elbjorn*, and *Voima*.

(45) "Ships Against Ice," Bureau of Ships Journal, Navy Dept., Aug 1954, pp. 2–6

(46) Canadian Icebreaker *Labrador*, MENA, Aug 1954, pp. 293–294. Gives general particulars and an outboard profile.

(47) One of six *icebreaking cargo vessels* for Russia, being built in Holland, is illustrated and described in

MENA, Aug 1954, pp. 288–290. These vessels have a single screw driven by a 7,000-horse electric motor turning at 150 rpm.

L_{OA} = 425 ft B = 61.58 ft H = 27.63 ft
L_{PP} = 387 ft D = 36.79 ft Deadweight capacity at this draft = 6,500 tons. V = 15 kt. These vessels have a profile resembling almost exactly that of a regular icebreaker.

(48) "Ingalls Launches Most Powerful Icebreaker," Mar. Eng'g., Oct 1954, p. 58

(49) "The Twin-Screw Diesel-Electric Ship *General San Martin*; an Ice-breaking, Research and Supply Vessel for the Argentine," SBMEB, Feb 1955, pp. 108–109; also The Motor Ship, London, Jan 1955, p. 432, and MENA, Dec 1954, pp. 480–481. The last reference contains photographs of the bow and stern of the vessel in the building dock and a photograph of the completed ship under way.

(50) "Diesel-Engined Soviet Icebreakers," The Motor Ship, London, Feb 1955, p. 503. Illustrates and describes the three vessels of the *Kapetan Belousov* class, as well as the two 12,840-t icebreakers now on order (1955). Abstracted, with outboard profile, in IME, Jun 1955, Vol. LXVII, pp. 86–87; see also SBSR, 6 Sep 1956, pp. 313–315.

(51) "Icebreaker with 12,000-B.H.P. Machinery," The Motor Ship, London, Dec 1956, p. 362

L_{OA}, 273 ft	H, mean 22.33 ft
L_{WL}, 260 ft	Δ, 4,950 t
B_{EX}, 63.75 ft	P_B(normal), 10,500 horses.

76.28 Hydrodynamic Design Features of Amphibians. It may be expected that the future will find more and more peacetime uses for a good combination of water craft and land vehicle, notwithstanding that its development to date is due largely to its wartime usefulness. Indeed, the first successful "alligator" of Donald Roebling was used originally in 1933, in the otherwise impenetrable expanse of the Florida Everglades, for rescuing hurricane victims and downed aviators. During the recent war its descendants served as means of carrying medical supplies and even as mobile hospitals. Refitted World War II DUKW's are already serving as combination fireboats, rescue, and salvage craft, equally useful on dry land and in the water [Rudder, Aug 1952, pp. 24–25]. There is no reason why they should not be useful as ship-to-shore package and personnel carriers in out-of-the-way places where ships must anchor off and where there are no shore facilities.

For these duties an amphibian must:

(a) Run in and on any kind of liquid or solid medium, from fresh and salt water to dry land, or any combination of these two. There is no permissible "holiday" for travel in mud. If it is soft enough it acts as a liquid; if hard enough, as a solid.

(b) Have an adequate reserve-buoyancy ratio, not only for wavegoing but for the bank requirement of (f) following. This is more important in an amphibian than in a surface vessel because the former can rarely be ship-shaped or have much of a weather deck.

(c) Maintain the reserve-buoyancy ratio throughout the design and construction period. This means that the total scale weight can not exceed the weight of the lightest water displaced by the buoyant volume up to the safe working waterline. Judging by some bitter experiences of the past, it means that an ample weight margin *must* be included in the preliminary design.

(d) Possess adequate freeboard to guard against water from the crests of its Velox waves. With a blunt bow and full form, these crests may be high.

(e) Limit its water speed to 1/3, 1/4, or possibly a smaller ratio of its maximum land speed

(f) Be able to drop down or run up a bank having a slope of at least 30 deg with the horizontal, both below and above the water surface.

An amphibian, in the form of a wheeled or tracked vehicle which can propel itself along the surface of the water, or of a boat which can run on dry land with wheels, tracks, or the equivalent, can hardly be expected to have a high degree of propulsive efficiency when running in either medium. If the primary object of the design is to produce a load- or passenger-carrying vehicle, a watertight body to give it flotation may be a clumsy encumbrance. Shaping this body to ease the water flow around it and at the same time to incorporate a pair of paddletracks, one or more screw propellers, or a paddlewheel involves compromises which must be worked out for each particular case. Applying wheels or tracks to an object designed primarily as a water craft is no less of a special problem. Fig. 76.T shows how clumsy such a craft can look and still perform well as an amphibian.

This is not the place to advance arguments for or against the use of wheels or tracks for traveling on land, through sand and mud, or over submerged reefs. There might be some reason for discussing the relative merits of propellers and paddletracks if the form of the craft were in any way standardized. It may, nevertheless, not be amiss to list briefly the advantages, disadvantages, and precautions to be observed in adapting and

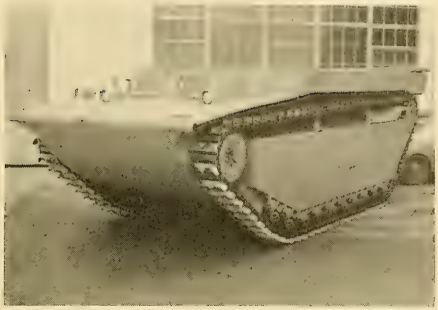

FIG. 76.T ONE TYPE OF TRACKED AMPHIBIAN
Official U. S. Navy photograph. Note the M-shaped paddles or cleats on the two moving tracks and the relatively close spacing of these paddles along the tracks.

employing one of the several possible methods of water propulsion:

(1) The paddletrack has the advantage that the same mechanical installation is utilized for running on both the water and the land, including propulsion as well as maneuvering. If it is sufficiently strong and durable it is satisfactory for extended land travel but not for high speeds ashore unless it can somehow be rubberized. Balancing this present shortcoming is the great advantage that the track furnishes the only known adequate and acceptable propulsion in the complete range of media from clear water to hard ground, comprising silt, sand, vegetable growths, and mud of all possible consistencies.

(2) The screw propeller is adapted only for use in media having the consistency of water. Undoubtedly, it is the most efficient of the propulsion devices, and capable of producing the highest speeds at which craft of this kind can travel in water. The propeller can be housed and at the same time protected in a tunnel under the stern of the craft, similar to that on a shallow-draft vessel. An adaptation of the outboard or swinging propeller is possible. It is even practicable to provide, as John Ericsson did for the American auxiliary sailing ship *Massachusetts* in 1845, a propeller carried by an arm swinging in a transverse plane [Isherwood, B. F., "Engineering Precedents for Steam Machinery," Vol. II, pp. 213–220]. When working it is swung down so that the propeller is below or at least abaft the hull. When not working it is swung up, well clear of the ground and inside the frontal or transverse projected area of the vehicle. The screw propeller will give good performance provided water can flow easily to it, either from the side or under the bottom.

(3) The central paddlewheel is specially adapted to divided-hull craft of the catamaran type. It is simple mechanically, is easily constructed, maintained, and repaired, and is reasonably efficient for shallow-water craft. It is admittedly bulky, cumbersome, and heavy for the power delivered.

(4) The sternwheel is indicated only for raft-like craft designed for traveling in extremely shallow water

(5) A water jet to propel a heavy, resistful amphibian is, with its ducts, likely to occupy more space than can be devoted to it. Such a device might serve for a lighter craft.

(6) The amphibian driven by a paddlewheel of some kind or by one or more screw propellers needs a good rudder. Probably it needs more than one to approach the maneuverability of the tracked vehicle, which can change its track speeds or even go astern on one track while going ahead on the other. Rudders in amphibians propelled by paddlewheels or screw propellers are almost of necessity placed in the outflow jets from those propulsion devices.

(7) Despite its clumsy form, maneuverability of an amphibian may not be too difficult to achieve because the length-beam ratio of such a contrivance is usually about 3 or 4 and rarely exceeds 5.

Despite the fact that an amphibian is of no practical use unless it can travel in water, it is possible that whatever water-propulsion device is fitted to it may have to play a secondary role to the land-propulsion gear. Because of the variety of possible configurations, not much can be said as to design for water propulsion except to emphasize that the water must have a reasonably good path to flow to whatever propdev is fitted. Because of the interference effects described in Sec. 32.2, the cleats on moving paddletracks always give the best performance when they are spaced as far apart as the considerations of ground or land travel permit.

Although the water-excluding portion of an amphibian may look more like a covered wagon than a boat or ship, the law of Archimedes still applies. The craft sinks in the water until the weight of water displaced equals its scale weight.

Because of the relatively high bow-wave crest and deep following trough created by the amphibian body when running at moderate speed,

and because it has a prow which resembles that of a scow more than that of a boat, the provision of adequate freeboard at the running attitude is particularly important. This is almost impossible to calculate and there is little background of empirical data for reference. Towing and simple self-propulsion tests of small-scale models are definitely indicated. Fortunately, when the drag is almost wholly due to pressure and when the wavemaking aspects are to be studied, tests can be accomplished in any of the small model basins.

76.29 Vessels Designed for Beaching. It is reported that the Chinese junk became, in the course of its long development, a rather more than passable landing craft because of the almost total lack of piers and wharves along the traffic routes. In fact, it is supposed that the ancient use of a non-watertight forepeak and a watertight collision bulkhead at its after end stemmed from the hopelessness of keeping tight the hull seams around the stem with constant beaching. While the shallow-draft sternwheel river steamers of America were not designed expressly for beaching they were eminently adapted for tying up along the river banks and handling cargo whenever the occasion demanded and wherever there was a bank suitable for the purpose. Like the amphibian, therefore, the first craft designed for transferring cargo directly to a bank or beach were engaged in peaceful pursuits. The need for peacetime landing craft may be expected to continue as long as shore facilities lag behind human needs.

Requirements for vessels to carry heavy, bulky, and expensive cargo for landing directly on the beach must state the:

(a) Minimum slope of beach wherever a landing needs to be made

(b) Minimum depth for keeping one end of the craft waterborne or, conversely, the distance within which the ship shall approach the water's edge at the beach

(c) Range of tide or water level to be expected at and during the landing

(d) Strength and direction of tidal and other currents at the bank or beach

(e) Wind waves and surf to be encountered

(f) Percentage (approximate) of the useful load which can be devoted to changing the trim of the craft to accommodate the depth and slope of the beach

(g) Relative importance of landing on a beach as compared to maintaining speed and wavegoing in the open sea.

The foregoing requirements are in addition to those for a ship of normal design which lands at a pier or quay.

The conflicting requirements of (1) acceptable wavegoing behavior for ocean voyages and (2) shallow draft with trim by the stern for landing may be met by the same procedure as for ships in ballast and for tankers traveling light, that is, by the use of liquid (water) ballast. This can be pumped out just before landing at the beach or it can be shifted aft to give the desired trim.

A much worse problem is not so easily solved by the compromises often encountered in ship design. This involves the almost inevitable use of a broad, flat, shallow bow, adapted to landing on broad, sand beaches but wholly unsuited for wavegoing. The only reasonable solution to this impasse appears to be the use of liquid ballast, liquid fuel, or liquid cargo in the forward part of the vessel.

The bow is, by this means, pushed down as far as possible, in an effort to keep the flat portion always under water, so that slamming does not occur there. The liquid is shifted aft when approaching the beach, to lighten the vessel forward and to accommodate the slope of the beach.

Proposals are made from time to time for a landing craft to be fitted with bow propellers and to run in waves with the deep end forward. This sounds attractive but has the disadvantage of a high thrust-deduction fraction for screw propellers positioned ahead of the hull, as well as inadequate submergence and racing because of the large amplitude of pitch at the bow when traveling in waves.

A form well adapted to operation in reasonably rough water and to running in toward shore through heavy swells and surf is one having a flattened W-section, similar to a pair of inverted-vee hulls, like two sea sleds placed side by side. Three projecting keels may be fitted under it to act somewhat as longitudinal stabilizing fins and to resist slewing, yawing, and broaching. In addition, the three keels provide great lateral stability when beached, to say nothing of an excellent distribution of the beaching load. Under certain circumstances the absence of flat, horizontal surfaces under the bow might defer or eliminate slamming. Under other sea conditions, especially

FIG. 76.U LANDING CRAFT WITH INVERTED V-BOTTOM AT STERN

Official U. S. Navy photograph. The small auxiliary rudder forward of the strut is for control when backing. The hole in the rudder permits withdrawing of the propeller shaft without unshipping the rudder.

if driven hard, the W-sections forward might produce large accelerations and decelerations, as does the sea sled. The under side of the stern of a landing craft with a single inverted vee of small slope is illustrated in Fig. 76.U.

Although it has to date (1955) been used on small vessels only, there is a great advantage in having hydraulic jet propulsion available under the bottom when getting off a bank or beach. By directing the jet forward, toward the region where the bow is aground, it is extremely useful for washing away the sand or soil and freeing the vessel easily.

General arrangement drawings and principal dimensions of landing and beaching craft of intermediate size (LCF and LCT) are given by G. de Rooij ["Practical Shipbuilding," 1953, Figs. 791 and 792 on pp. 368–369]. Model test data for four models of landing craft are found on SNAME RD sheets 38, 40, 43, and 44.

76.30 Some Hydrodynamic Design Problems Common to All Submarines. There are no books, and there is little technical literature, which discuss the *design* of submarine vessels [Hay, M. F., "The Design of Submarines," SNAME, 1909, pp. 233–255]. The hydrodynamic design alone involves matters of diving and surfacing, dynamic equilibrium, speed and propulsion, maneuvering, and wavegoing, both surface and submerged. Diving and surfacing involve in turn the flooding, venting, and blowing of the main ballast tanks which provide the reserve buoyancy of the submarine when it is on the surface.

It is impossible, within the space allotted in this book, to do more than describe briefly certain special problems encountered in this hydrodynamic design, having to do primarily with operation submerged. One seldom finds these problems discussed scientifically in any kind of literature. A statement of them, with their present solutions (or lack of solutions), should not only broaden the outlook of the marine architect engaged in the design of surface vessels but also give him a more penetrating insight into the influence of hydrodynamics on the design of all kinds and sizes of water craft.

I. *Requirements.* It might be thought strange, were it not for so many other missing ship-operation requirements, that no basic requirements for submarine vessels have ever been formulated and published. Those which follow are sketchy but they may at least serve as the groundwork for development in the future. They are based upon a possible, even though seemingly remote utilization of the submarine vessel for peaceful purposes. No attempt is made to go into detail or to insert numbers in these requirements:

(a) Submerge and emerge, while stationary or under way, when initially on the surface or submerged. This may or may not have to be accomplished within a given interval from the "execute" signal, starting from a given set of conditions as regards ballast water carried and percentage of reserve buoyancy.

(b) Run submerged at a given nominal depth, throughout the complete speed range, without varying up or down more than a given amount from that depth

(c) Run submerged, throughout a given speed range, without exceeding specified trim angles (by the bow or stern) for the series of speeds

(d) Maintain a given depth, within specified limits, when the excess of static weight or buoyancy reaches a certain limiting amount, generally a percentage of the total weight or buoyancy, at all submerged speeds above a certain minimum

(e) Hold a given depth and maintain a level fore-and-aft attitude, within not-too-close limits, when underway submerged at a very slow speed, less than a certain maximum. This is the operation known as *hovering.* The speed is so low that dynamic control is rather weak.

(f) Change depth, either up or down, within a given elapsed time from level running at the original depth to level running at the new depth,

within certain limits of speed, diving-plane angles, fore-and-aft inclination of the vessel, and excess static weight or buoyancy

(g) Change course in a horizontal direction when submerged, from the small angles involved in normal steering to turns of 180 deg or more

(h) Possess good wavegoing performance as a surface vessel, including reasonable safeguards for personnel who may be on deck at sea, when the craft is either stopped or underway

(i) Provide adequate freeboard in the surface condition, for access hatches leading to the pressure hull which may be open when underway or at anchor

(j) Rest on the bottom for appreciable periods, and possibly travel along the bottom.

II. *Physical Arrangement.* To serve as a background for a discussion of hydrodynamic design problems of a submarine there must be some knowledge of the principal physical features of this type of vessel. It is possible but not likely that a further half-century of development will modify somewhat the physical arrangements of the modern (1955) design. One such design, relatively modern, is shown by G. de Rooij ["Practical Shipbuilding," 1953, Fig. 42 on p. 29 and Fig. 788 in the back of the book. A brief description is given in Sec. 203 on page 368].

The submarine which is also required to give a good account of itself on the surface, called a submersible in this book, possesses two rather distinct hulls, taking into consideration the underwater and the abovewater portions as units performing distinctly different functions. The always-buoyant *inner* or *pressure hull* is of a form best adapted to resist external hydrostatic pressure, with practically no regard for the ease with which it could, as an independent unit, be driven through or along the surface of the water. The *outer hull* is a ship-shaped envelope built around the inner or pressure hull, designed to minimize resistance of the combination for surface propulsion and to provide spaces between the hulls for water-ballast tanks and fuel tanks.

The portion of the outer hull lying below the waterplane in surface condition, indicated in diagram 2 of Fig. 37.C and in the schematic section of Fig. 76.V, fulfills exactly the same function for a submarine as for a surface vessel. It is generally designed in the same manner, with necessarily more regard for machinery clearance, access between hulls, and special fittings. Similarly, the underwater hull design is tied into the abovewater design to insure acceptable wavegoing performance, the same as for the surface ship. While it is perfectly possible for a properly sealed submarine to plow *through* surface waves instead of riding over them, it suffers from much the same retardation as would a surface vessel under similar circumstances.

Most of the space between the inner and the outer hulls is devoted to the provision of added buoyancy when the vessel is on the surface. In this condition the water-excluding volume of the outer hull up to the surface waterline, in what is known as diving trim at full buoyancy, is equal to the water-excluding volume of the inner hull plus all its external appendages. The result is that, when the vessel is on the surface, the inner hull and its appendages are raised above the level of the surrounding water by a volume equal to that of the main-ballast tanks, between the inner and outer hulls and below the surface waterline. This main-ballast-tank volume divided by the inner or pressure-hull volume is thus the reserve-buoyancy ratio in the surface condition.

It is customary, on double-hulled submersibles, for the main-ballast tanks to extend above the surface waterline in diving trim. In fact, this is usually necessary, to provide adequate initial metacentric stability and a safe range of positive stability. The volume of the main-ballast tanks above the surface waterline adds to the reserve-buoyancy volume of the pressure hull and of all water-displacing appendages and objects above the waterplane. The vertical hatching of Fig. 76.V indicates this volume in schematic fashion.

A rather complete general discussion of these features, including the matters of equilibrium of static forces and of metacentric stability discussed subsequently in this section, is given by A. I. McKee [Bu C and R, Tech. Bull. 8–29, Nov 1929; also "Development of Submarines in the U.S.," SNAME, HT, 1943, pp. 344–355].

When the craft submerges, sea water must be admitted to the main-ballast tanks to destroy the buoyancy which lifted the pressure hull above the water in the surface condition. For a vessel having a water-excluding displacement when submerged of say 3,000 tons, the weight of water to be admitted to the main-ballast tanks may exceed 1,000 tons. Furthermore, to permit flooding with this water, the air in the main-ballast tanks must be vented to the atmosphere.

Admitting this much water and venting an

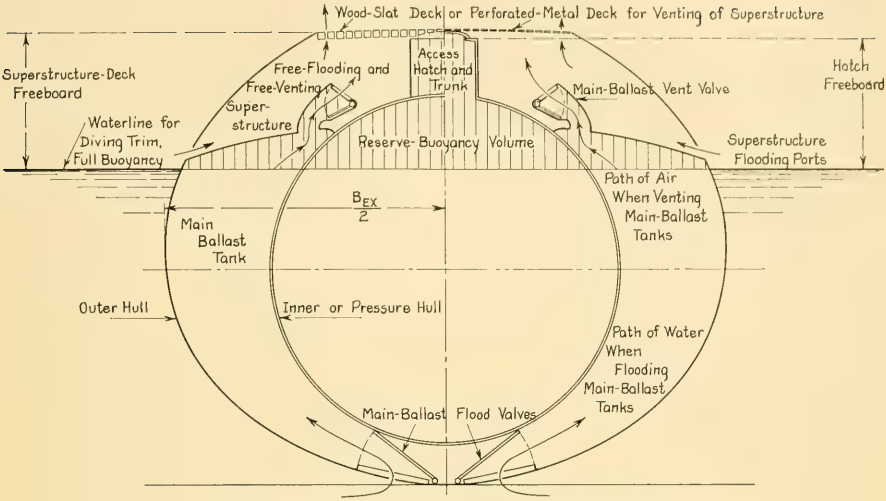

Fig. 76.V Schematic Section of Double-Hulled Submersible Showing Main-Ballast Flooding and Venting Arrangements and Buoyant Volumes

equal volume of air, while at the same time exercising control of the flooding and venting among a number of separate tanks, involves a rather elaborate system of large flood valves in the lower part of the outer hull and correspondingly large vent valves along the tops of the main-ballast tanks, indicated schematically in Fig. 76.V.

Somewhat similar water-handling systems are required for taking aboard, pumping out, and shifting what is known as variable-ballast water within the pressure-proof boundaries of the submarine. The admission, discharge, and transfer of water serve as compensation for the expenditure of useful weights such as food, stores, and lubricating oil; for the taking aboard of additional useful weights; and for the moving of these weights fore and aft and transversely within the pressure-proof boundaries to suit the mission of the vessel.

Because a submarine is not burdened with vulnerable deck hatches and rarely requires personnel to work on deck at sea, except possibly for a limited region amidships, its freeboard to the superstructure deck can be much lower than that of a surface vessel. With this low freeboard it is expected that solid water will be taken aboard. Several expedients are adopted for unloading this water expeditiously. The topside is given a large tumble home and the deck edges are often well rounded into the side, so that the beam of the flat or cambered deck is rarely more than 0.7 of the maximum beam at the surface waterplane. The deck forward, excluding the rounded turtleback on each side, may be not more than 0.5 times the beam at the corresponding section. The perforations and slots in the deck, placed there to provide rapid venting of the free-flooding superstructure volume, afford a means of sluicing away the deck load of water before it slides aft during an up pitch and dashes against the deck erections amidships.

The freeboard at the extreme stern may be diminished to zero, so far as wavegoing characteristics are concerned. If, however, the surface speed is high enough to produce a crest of appreciable height on the stern wave, the outer hull should be carried up at least to the top of this crest, with the vessel in running trim.

The flooding ports or openings along the lower edges of the superstructure volume, just above the surface waterline, represent an unsolved problem as far as combining rapid flooding of the superstructure with minimum drag along the surface waterline is concerned. A continuous flooding slot along the lower edge of the superstructure, used at various times, is not an acceptable solution because of the relatively large

quantities of stationary water which can enter there. When these are picked up and accelerated by transverse structural members and other parts housed within the superstructure a useless loss of energy is involved.

The volume of water occupying certain small free-flooding spaces below the surface waterplane, rarely to be found on surface craft, is considered as a part of the ship weight which must be carried along. Outside water must be displaced around these spaces the same as around the other parts of the hull. In one respect these several volumes of water are treated as though they were blocks of ice, frozen in place. If the free-flooding spaces have external openings in regions where there is a pressure gradient on the outside of the hull, a flow of water through the spaces takes place because of this pressure gradient. Energy expended in setting up and maintaining this flow, generally of an eddying character and invariably undesirable, is energy lost so far as the propulsion of the submarine is concerned.

III. *Equilibrium of Static and Dynamic Forces.* In a surface vessel, nature takes care of the balance between the hydrostatic weight and buoyancy forces by adjusting the latter so as to equal the weight force imposed by the crew. If the weight is increased by loading something aboard, the vessel sinks to provide the additional buoyancy. In a submerged submarine the buoyancy force is usually fixed by the total volume of the water-excluding structure and external parts, combined with the density of the surrounding water. The crew then has to make the necessary internal adjustments in the weight force, by admitting or expelling or shifting variable-ballast water, if equilibrium is to be maintained.

While it is possible for the primary static forces of weight W and buoyancy B to be balanced by taking in or pushing out variable-ballast water, this is the exception rather than the rule in submerged operation. It is rarely possible to achieve an exact balance of primary hydrostatic forces, and moment as well, when underway beneath the surface. In addition there are vertical dynamic forces and moments generated when the vessel is underway by the lack of symmetry of the outer hull about any longitudinal horizontal plane, by the presence of deck erections and appendages, and by small inclinations of the fore-and-aft axis to the direction of motion. Combined, these render the equalization of weight W and buoyancy B a matter of hydrodynamics as well as hydrostatics.

Admitting and expelling variable-ballast water in suitable quantities and at the proper locations as the submarine is moving can take care of the preponderant hydrostatic inequalities between W and B. However, the hydrodynamic inequalities usually vary in magnitude with ship speed. They, as well as the undetermined (W-B) values, are normally compensated by vertical forces derived from hydrofoil action of the diving planes.

It is found that an amazing variety of submarine forms are afforded adequate control in rising and diving by the usual arrangement of bow and stern planes.

IV. *Metacentric and Pendulum Stability.* The problem of adequate metacentric stability when in the so-called "awash" condition, during either diving or surfacing, undoubtedly involves a time element to a small degree, and hence partakes of the nature of hydrodynamics. There are free surfaces in most if not all of the main-ballast tanks at some time or other during flooding or blowing. Each tank is in communication with the sea and only indirectly with its companion tank on the opposite side of the vessel. For this reason it is necessary to reckon a loss of $\overline{BM}$ corresponding only to the square moment of area of the free surface in each tank about its own fore-and-aft axis, and not about the longitudinal axis of the vessel. As a practical matter the time element enters particularly in the blowing-down operation while surfacing. This requires some minutes, during which time the loose water in each main-ballast tank is in direct communication with the sea through the flood valves at the bottom of the tank. There must be sufficient control over the compressed air delivered to the main-ballast tanks on the two sides to hold the vessel in a sort of average upright position, even when acted upon by a heavy beam sea, with water surging up and down in the tanks.

For a consideration of the forces and moments involved in maneuvering submerged it is necessary to realize that the submarine in that condition has no effective or intact surface-waterline area (and no loose water), so that $\overline{BM} = 0$ and the metacenter M coincides with the center of buoyancy CB. What holds the submerged submarine upright is the fact that the center of

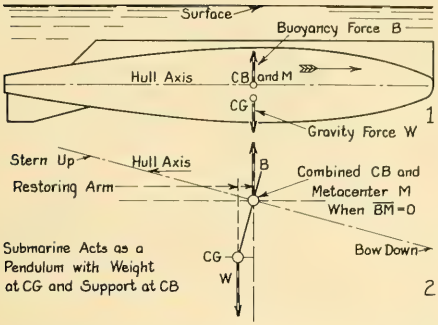

FIG. 76.W SKETCH ILLUSTRATING PENDULUM STABILITY OF SUBMERGED SUBMARINE IN PLANE OF SYMMETRY

gravity CG lies *always* below the combined center of buoyancy and metacenter. This gives the vessel what is known as *pendulum stability*, with G always below M, illustrated in Fig. 76.W. Any moment of weight forward or aft of the submerged CB causes the vessel to trim in that direction until the center of gravity is directly underneath the center of buoyancy. A small offset may result in a large trim angle unless the necessary correction is made to the CG position. When the vessel is inclined submerged by some external moment, either in heel or in trim, there is always a pendulum-type restoring moment acting to level it off at an equilibrium attitude. When underway, this moment is superposed on the hydrodynamic moments.

V. *Hull Shape and Propulsion.* The question is repeatedly raised, when submarine shape and propulsion is discussed, why the submarine designer should not take advantage of the developments of nature, involving a process of evolution extending through untold millenniums. He is questioned as to why he does not copy some sort of aquatic fish or mammal, such as the shark or the porpoise, or even the whale. These creatures are known to be, for their size, capable of prodigious speeds, exceeding 20 kt in spurts for the porpoise and the whale. They make these speeds, at least in the case of the porpoise, with what seems to be effortless ease.

The achievements of fish and aquatic mammals, in the matter of propulsion and maneuvering and related operations, have been the subject of scientific, engineering, and physiological study for three-quarters of a century or more. Research along these lines is continuing, steadily if slowly. A few features already learned from them are discussed in Sec. 15.6 and illustrated in Fig. 15.C under flexible-fin propulsion.

However, in an effort to copy features that will be helpful in submarine design, two obstacles present themselves. They have not yet been surmounted.

The first is that, while the general mechanism of fish propulsion is known, man has not discovered the exact method by which the fish or the sea mammal achieves its highest speeds or swims rapidly for long periods of time. Manifestly, these methods must be known and understood before they can be copied or utilized. For example, it is asserted that, in order to maintain a speed of 20 or 25 kt while converting food energy into propulsion energy and motion at the highest rate known to man, a porpoise would have to consume his entire weight in small fish every half hour. It seems certain that the animal does not do this, at least while traveling continually at such high speed. It is also asserted that a pigeon, if as inefficient as some man-made airplanes, would have to carry along an internal-combustion engine with a power of several horses, in order to make its known speed through the air.

The second is that for the great majority of creatures in this category, propulsion is based inherently upon flexure of the body as a whole, in addition to motion of the fins, tail, and flukes. Certainly, swimming at the high relative speeds desired always involves body undulations. Man has not yet invented a submarine structure which can withstand great hydrostatic pressures and house a powerful propelling plant, while at the same time possessing great flexibility and capable of generating S-shaped undulations which travel along its length.

Actually, because of their varying environment and their different needs, fish and mammals are often rather poorly streamlined by modern hydrodynamic and aeronautic standards. If it becomes necessary, on a submarine, to depart from a good streamline shape, that of some fish or mammal could be accepted.

VI. *Maneuvering Submerged.* The term maneuvering, as used here, involves:

(1) Transient and steady motions in a straight line parallel to the submarine axis
(2) Steering and turning in a plane that is horizontal or nearly so

(3) Rising, diving, and depth-keeping in a vertical plane.

The bulk shape and bulk volume of the vessel are involved in each case, as contrasted to a smaller underwater volume for the surface ship. If submerged to a depth h of the order of several times its hull height $\hbar$, the effect of the free surface above it is negligible. This situation is contrasted with that of the surface ship, surrounded by an air-water interface upon which gravity waves can be formed.

Heel when turning, usually only an inconvenience on a surface vessel, can introduce vertical forces and moments on a submarine which affect its trim attitude and perhaps its depth of submergence. Unless the submarine carries a topside rudder of the type described in Sec. 37.14 and illustrated in diagram 2 of Fig. 37.C, the same steering rudder that "handles" the normal lateral area on the surface must, for horizontal steering and turning submerged, "handle" the greater lateral area of the entire bulk of the submarine.

One feature related to both speed and propulsion and to maneuvering requires mention. Unlike a surface vessel the speed and propulsion requirements for a submerged submarine can not be dissociated from those of trim and attitude. In other words, it is useless for a submarine to be able to travel at a certain speed submerged unless the vessel can be held at the desired attitude and depth at that speed.

76.31 Lightships or Light Vessels. The design of a lightship or a light vessel, whether manned or unattended when on station, represents some extremely interesting problems in hydrodynamics, which have benefited from only sporadic scientific study in the past. A few of these are discussed here, in rather limited scope.

Stated briefly, the requirements for a lightship are for a vessel that shall:

(1) Display the necessary lights or other identification, send out both abovewater and underwater sonic signals, transmit radio signals, and perform similar functions. These are best accomplished when the vessel is upright and at zero trim although they must be carried out under all ship-motion conditions.

(2) Remain afloat and operable and on station, invariably an exposed one, regardless of the state of the sea and of the wind and weather. In fact, the worse the conditions, the more necessary it is that the vessel maintain its charted position.

(3) Exert the minimum pull, consistent with other characteristics, on its mooring cable or line, when subjected to wind, or current, or both

(4) Be free of violent or undesirable yawing under the influence of wind or waves or both

(5) Reduce the motions of rolling, pitching, and heaving to a minimum consistent with other requirements and the wavegoing conditions to be encountered. This is to reduce fatigue of personnel and wear and tear on equipment, whether the vessel is manned or unmanned.

(6) Be able to propel itself at reasonable speed and to maneuver, if the vessel is of this type.

The lightship is in a class with the life-saving boat discussed in Sec. 76.32 with respect to its ability to remain on station, completely operative except for its propulsion plant, when all other vessels of its size (and larger) are required to seek shelter in port.

Its freeboard coefficient or freeboard-to-length ratio is much greater than that of any other type of craft except a life-saving boat. Similarly, the reserve-buoyancy ratio is very large, perhaps even larger than that of the latter craft.

Lightships may have much more than the usual amount of sheer, especially forward, unless the vessel has one more deck height, for its whole length, than would be customary in other vessels of its size.

While low resistance in a lightship when moored in a seaway is one of the major requirements, some of it may be sacrificed to permit the use of special features furthering the vessel's mission. One such feature is a set of extremely wide roll-resisting keels, possibly stayed by auxiliary struts extending from near the outer edges of the keel to the adjacent hull [SBSR, 17 Jan 1935, p. 66]. Another would be an effective pitch-damping device, provided a successful one could be devised for this type of vessel. Indeed, anything which assists in damping any part of the wavegoing motion is a useful feature, whether the craft is manned or unattended.

Self-propulsion, if provided, is almost never a primary feature, but the drag exerted by the stationary propeller in a current should be held to the minimum practicable amount.

In only a very few cases does the technical literature contain reasonably complete principal dimensions, hull parameters, form coefficients, and other characteristics of lightships. Table 76.g

TABLE 76.g—PRINCIPAL DIMENSIONS AND CHARACTERISTICS OF LIGHTSHIPS

Name	*Puffin*	U.S.L.V. 43	*Ruytingen*	U.S.L.V. 74	U.S.L.V. 94	*Alarm*	*Lurcher No. 2*
Date	1887	1881	1891		1912		
Source	SNAME, 1913, p. 108	SNAME, 1913, p. 108			SNAME, 1913, pp. 97–118	Shipbldr., Jan–Jun, 1914, pp. 295–296	
L_{OA}, ft	101.5	110.75	30m (98.43 ft)	118	135.75		128.0
L_{PP}, ft	93.5				112.92		
L_{WL}, ft						104	112.0
B, molded, ft	20.75	25.67	7.82m (25.65 ft)	28.5	29	24	30.5
D, ft	11.92	11.5		14.7	15.33	15	21.4
H, ft					12.75	10.67, mean	
Δ, tons		191 t, gross	338	495	660		
L_{WL}/B ratio	4.77, abt.	4.1, abt.	more than 3.82	4.0, abt.	4.3, abt.	4.34	
B/H ratio					2.28	2.25	
C_P					0.5*		
C_B					0.43*		
C_W					0.79		
C_X					0.67		
$\overline{GM}$, ft					1.42 to 0.75		
Moorings	1.875-in chain						7,000-lb anchor; 1.875-in chain

* The C_B, C_P, and C_X values for the full-load condition are not consistent but they are the ones given in the diagram of displacement and other curves

embodies the rather meager information of this type which could be collected for six lightship designs dating from 1881 through about 1914. Additional information and data, on old as well as modern vessels, are to be found in the brief list of references which follows:

(a) Body plan of *Elbe* lightship, with a B/H ratio of 25.25/12.46 = 2.03, and a rise of floor of 24 deg, is shown in Schiffbau, 26 Jun 1912, pp. 715–722, Pl. 3

(b) Idle, G., "The Effect of Bilge Keels on the Rolling of Lightships," INA, 1912, pp. 103–123 and Pls. IX–XI. Figs. 10–13 on Pl. X illustrate by flowlines the assumed motion of the water around the ship hull and around the bilge keels when rolling.

(c) Cook, G. C., "The Evolution of the Lightship," SNAME, 1913, pp. 97–118 and Pls. 52–63. Gives considerable historical data. Shows arrangement plans, body plan, and lines of self-propelled U.S. Lightship 94. Principal dimensions and hull coefficients are listed in Table 76.g. The wedges of immersion and emersion are intended to be nearly equal. The bilges are very slack. The full-load displacement at 18.58-ft draft is about 1,072 t. Static stability is a maximum at about 60 deg, and very large at 100 deg. The roll-resisting keels are of triangular section, 1.5 ft wide. See also The Shipbuilder (now SBMEB), Jan-Jun 1914, Vol. X, pp. 215–220.

(d) Cooper, F. E., Liverpool Eng. Soc., Mar 1914; also The Shipbuilder (now SBMEB), Jan-Jun 1914, Vol. X, pp. 295–296. Describes the non-self-propelled light vessel *Alarm*, whose dimensions are listed in Table 76.g. The bilge keels extend for $0.6L$ and are about 1.2 ft wide.

(e) New *Lurcher No. 2* Lightship, Diesel Prog., Mar 192, p. 59

(f) New *Overfalls* Lightship, Mar. Eng'g., Apr 1953, p. 45

(g) New *Ambrose* Lightship, Mar. Eng'g., Sep 1953, p. 85

(h) Lightship *Kish Bank*, illustrated in SBSR, 27 Jan 1955, p. 36, has a centerline hawsepipe just above the DWL for mooring on station plus a regular hawsepipe on each bow with port and starboard bower anchors and separate chains. The Motor Boat and Yachting, Aug 1954, p. 357, shows a photograph indicating extreme local sheer at the bow.

(i) Light vessel *Osprey*, SBMEB, Jun 1955, pp. 417–418; SBSR, 30 Jun 1955, p. 841. This non-self-propelled ship has an overall length of 136.42 ft and a beam of 25 ft, with "exceptionally large bilge keels." The mooring is by 1.75-in chain, attached to a 4-ton mushroom anchor, with port and starboard 1.5-ton anchors in reserve.

(j) De Rooij, G., "Practical Shipbuilding," 1953, Figs. 793 and 794 and Sec. 206 on pp. 369, 373.

76.32 Life-Saving or Rescue Boats. The life-saving or rescue boats discussed in this section are the self-propelled craft which are based on shore stations, or on large station ships afloat. They exclude the lifeboats carried by passenger and other vessels, intended only to remain afloat and stay together on the scene until the rescued personnel can be taken aboard another vessel. Despite improved methods of removing personnel from vessels in distress it appears that life-saving boats operating from home or shore stations will be required for many years to come.

Presumably general design requirements exist for these craft but none have been located in the technical literature, especially none that relate directly to hydrodynamics. The following specifications appear to meet these needs:

(1) The craft shall be able to operate in the open sea or to stand by in practically any weather, no matter how severe

(2) The boat shall be self-righting without crew, when rolled to any angle of heel up to 180 deg

(3) It shall be virtually unsinkable; in other words, it shall remain afloat, even when moderately damaged

(4) The reserve-buoyancy ratio, with crew only, shall be exceptionally large, preferably of the order of 2 or 3. The wind resistance inherent in this large abovewater volume is accepted. With all the rescued personnel which can crowd aboard, the reserve-buoyancy ratio shall be not less than 1.0.

(5) There shall be a covered deck at both ends, of arched or turbleback form, designed to relieve itself of water and spray which comes aboard well before the craft is subjected to a succeeding load of water

(6) All cockpits and depressions in the weather deck shall be self-bailing, with the boat carrying its crew and the maximum number of rescued personnel

(7) The free-running speed, without passengers but with crew and full fuel and stores, shall be sufficient to reach a disaster scene expeditiously. It shall be not less than 10 kt, in smooth water and no wind, and preferably 12 kt or higher.

(8) The propulsion devices shall be housed, preferably, within the overall fair surface of the hull. In any case it shall be possible to operate them in shallow water, with the boat just aground, or when directly alongside a larger vessel.

(9) The fore-and-aft position of the propulsion devices shall be such that they continue to produce thrust when running under heavy pitching conditions

(10) The draft shall be the minimum compatible with other requirements listed

(11) The type and position of the rudder(s) shall be such that steering or maneuvering control of the boat is maintained at all times, regardless of the state of the sea.

It is clear from item (1) preceding that these boats represent very nearly the ultimate in the wavegoing performance required of any vessel at sea. It might almost be said that life-saving boats should float and remain upright when all other craft sink or turn bottom side up. To achieve requirements (1) and (4) they are distinguished by very large freeboard at the bow and stern, usually very nearly equal at both ends, by a very large sheer, and by a very large volume of abovewater reserve buoyancy, often in the form of closed compartments intended for buoyancy only.

The self-righting requirement (2) means that the boat should have positive transverse metacentric or positive pendulum stability when inclined to *any position in roll.* It should not only right itself from heel angles between 90 and 180 deg but should be capable of rolling completely over (360 deg), without serious damage, if caught by a breaking beam sea.

Cockpits and other depressions exposed to the weather are rendered self-bailing by making them watertight, with freeing slots passing out through the sides or down through the bottom. Some water enters through these slots when the boat pitches and rolls but the amount is small, usually only enough to cause slippery footing or to freeze into objectionable ice in cold weather.

On certain life-saving boats of older design, which were not required to be self-righting, it was customary to fit one or two projecting appendages, resembling roll-resisting keels, along the bulge on each side. These were slotted so that, in the event the boat turned bottom side up, the survivors could use them as hand rails. In fact these appendages were wide enough to serve rather well as roll-resisting keels, despite the hand holes cut through them. There is no reason why a self-righting rescue boat could not be fitted with one or two pairs of roll-resisting keels, to improve the wavegoing performance and to serve as fenders or guards for the lower portions of the hull.

To meet specification (7), propulsion may be by ducted propellers, approaching pure hydraulic-jet propulsion, or by screw propellers working in tunnels of suitable shape. Hotchkiss propellers, with impellers entirely inside the hull, are often employed. Any type of propeller or impeller taking suction from the bottom of the boat must be able to work in water-mud or water-sand mixtures.

A Gill screw propeller, fitted inside an internal duct, taking suction through a grating and discharging through a rotable "deflecting nozzle," is sometimes used for a lifeboat installation [SBSR, 27 Jul 1939, pp. 111, 113]. Figs. 59.Da and 59.Db show the general arrangement and method of operation of the Hotchkiss and Gill propellers, respectively.

It is pointed out in reference (o) of the attached list that rescue-boat speeds of the past, usually not exceeding 8.5 kt, are no longer considered adequate. Speeds up to 20 kt, to be incorporated in German life-saving boats under design at the time of writing (1955), will call for a rather drastic modification in the double-ended form which has been standard since the days when all these craft were propelled by oars. Transom sterns of moderate width are indicated for speed-length quotients exceeding about 1.2 or 1.3. It is possible that the high-speed, round-bottom, transom-stern patrol boat of small size, already developed into a craft capable of withstanding extremely heavy weather, may be found suitable for life-saving boats meeting the requirements listed at the beginning of this section.

Appended is a brief list of references relating to life-saving or rescue boats. Although by no means complete it will give the reader some idea of the design problems involved:

(a) Reynolds, O., "On Methods of Investigating the Qualities of Lifeboats," Manchester Literary and Philosophical Society, 14 Dec 1886, in which Professor Reynolds advocated the use of models

(b) Corbett, J., "Experiments with Lifeboat Models," INA, 1890, pp. 263–283 and Pls. XIV and XV. Reserve-buoyancy ratio of craft in the period 1862–1890 varied from about 0.75 to 2.1.

(c) Barnett, J. R., "Motor Lifeboats of the Royal National Lifeboat Institution," INA, 1910, pp. 112–119 and 129–139; also Pl. X. This paper contains the principal lifeboat requirements, expressed in somewhat general terms.

(d) Everett, H. A., "Stability of Lifeboats," SNAME, 1913, pp. 133–143 and Pls. 73–82. While this paper applies to lifeboats as carried on larger vessels, it contain interesting information for the designer making a study of life-saving craft.

(e) Barnett, J. R., "Recent Developments in Motor Life-boats," INA, 1922, pp. 283–290 and Pls. XIX-XXII

(f) Barnett, J. R., "Motor Life-boats of the Royal National Life-boat Institution," INA, 1929, pp. 225–236 and Pls. XXIII and XXIV

(g) Motor lifeboat *Insulinde*, Zeit. des Ver. Deutsch. Ing., 13 Apr 1929, pp. 499–503; WRH, 22 Apr 1930, pp. 165–166

(h) Ghiradi, L., "Moyens de sauvetage modernes (Modern Methods of Lifesaving)," ATMA, 1932, Vol. 36, pp. 83–104

(i) "Improved Design of Royal National Lifeboat Institution Lifeboats," SBSR, 15 May 1947, pp. 482–483

(j) "The German Lifeboat Service," SBSR, 5 Jun 1947, pp. 556–557

(k) Self-righting, non-sinkable Coast Guard lifeboat is illustrated in USNI, Dec 1948, p. 1552

(l) Attwood, E. L., Pengelly, H. S., and Sims, A. J., "Theoretical Naval Architecture," 1953, pp. 181–183

(m) "German Lifesaving 'Cruisers'," SBSR, 13 Jan 1955, pp. 41–43. This well-illustrated paper describes the newest types of German lifesaving "cruisers" for rescue work. These craft are "of a larger, faster, and more powerful type than previously used."

The *Bremen* is a converted steel hull having an overall length of 57.42 ft, a beam of 13.75 ft, and draft of 4.58 ft. The brake power is 2 times 120 horses; the top speed is 11 kt.

The first of the larger boats built expressly for rescue work is the *Helgoland*. It has an overall length of 73.75 ft, a beam of 17.75 ft, and a draft of 4.75 ft. The brake power is 2 times 300 horses and the designed top speed is 20 kt.

Each of these rescue craft carries a smaller or "daughter" boat in an inclined trough set in the stern, enabling the smaller boat to be launched and hauled aboard at will. The "daughter" boat is 16.42 ft long and 6.5 ft wide.

Although the righting arms are large when the boats are inclined to 90 deg, apparently neither of them are intended to withstand rolling completely over and righting themselves, as for the smaller lifeboats.

The two propellers of the *Bremen* are carried in side tunnels. There is one balanced rudder abaft each propeller with its lower pintle carried by a skeg bar which serves as a guard for both propeller and rudder. Between the port and starboard skeg bars there is mounted a horizontal hydrofoil which serves as a trim-control device to depress the stern of the larger craft when it is desired to launch or to take aboard the smaller one.

(n) A further discussion of British and German lifeboats for sea-rescue work, of the period 1954–1955, is given by G. Wood in SBSR, Int. Des. and Equip. No., 1955, pp. 67–68. The new British *Coverack* class are 42.5 ft long, with twin screws driven by diesel engines, having a range of 238 miles at 8.38 kt.

(o) "The Future of the R.N.L.I. Lifeboat," SBSR, 30 Jun 1955, pp. 828–829. This article discusses a number of requirements and features for lifeboat design and indicates the probable future trends for British lifeboats in particular and all lifeboats in general.

(p) "Fast German Rescue Ship (*Herman Apelt*)," SBSR, 25 Aug. 1955, p. 259 (illustration). Length, 66 ft; beam, 15 ft; speed, 17 kt.

(q) "A New Watson Class R.N.L.I. Lifeboat," The Motor Boat and Yachting, Feb 1956, pp. 62–63.

76.33 Special-Purpose Craft of the Future. No one can predict the uses, not now dreamed of, to which water craft will be put in the future. It is certain, however, that the creation of new forms or the adaptation of existing forms to these uses is to be done most efficiently by the application of hydrodynamic knowledge, as has been the aim in this book.

CHAPTER 77

The Preliminary Hydrodynamic Design of a Motorboat

77.1 Scope of This Chapter. A motorboat is defined in this chapter as a mechanically propelled craft having a length of about 110 ft (33.5 meters) or less, running at a Taylor quotient T_q greater than 1.0, $F_n > 0.3$, and of a general type which may or may not include the fishing vessels and yachts of Secs. 76.11 and 76.19. The treatment here is limited to craft driven by screw propellers. The motorboats may be supported wholly or in part by water buoyancy or by dynamic lift on the hull proper. In other words, they may be of the displacement, the semi-planing, or the full-planing type. Hydrofoil-supported craft are in a separate category, discussed in Chap. 31 and partially covered by the limited bibliography of Sec. 53.9.

As introductory material for notes on the design of a planing hull, Chap. 13 discusses basic planing phenomena and Chap. 30 the behavior of actual planing craft. Some quantitative data on dynamic lift and planing and a rather lengthy set of references are given in Chap. 53. Notes for guidance in determining whether a craft designed to meet a given set of requirements is to be of the displacement type, or whether it is to be a semi-planing or a full-planing form, are found in Sec. 77.10 of the present chapter.

One aim of this chapter is to collect and correlate certain small-craft performance and design information applicable to motorboats in general, supplementing the large-ship data set down in earlier chapters. Sec. 77.41 contains a partial bibliography relating to small-craft, yacht, and motorboat design. It is to be hoped that, in the

not distant future, an enterprising small-boat designer will present a much more extensive summary and digest of all available and useful information, as N. L. Skene did some years ago in his book "Elements of Yacht Design," and as D. S. Simpson and P. G. Tomalin did more recently [SNAME, 1951, pp. 554–611; 1953, pp. 590–634].

Manifestly, it is not possible to compress into this chapter, with its illustrative examples, all the essentials and fundamentals that have appeared in each of several books on the design of motorboats, listed in the bibliography of Sec. 77.41, to say nothing of the valuable information in the multitude of technical papers and articles on this subject. It endeavors only to cover certain hydrodynamic features of motorboat design in a manner similar to the coverage of the principal features of large-ship design in Chaps. 64 through 68. It stresses the differences in characteristics and procedures necessitated by the difference in size, as well as by the presence of a major supporting force other than buoyancy in the form of dynamic lift.

As an illustration of the use of the data presented and the procedures described, there are included in the chapter the preliminary hydrodynamic designs of two motorboats, to two alternative specifications. One involves a fast semi-planing hull and the other a high-speed full-planing hull.

77.2 General Considerations Relating to Motorboat Design. For water craft of all kinds there is little difference in behavior with size if care is taken to maintain dynamic similarity of flow. This is done when a self-propelled free-running model, or a pilot model large enough to carry one or more persons, is built as part of the development work on a large project. Dynamic similarity of flow is not fully realized if model tests include towing of the model of a mechanically propelled craft but exclude self-propulsion tests of that model, when driven by a small-scale replica of its propulsion device. This matter is discussed further in Sec. 77.40. Since similarity of flow is almost never completely achieved, as when endeavoring to run simultaneously at the same values of the Froude number *and* of the Reynolds number for both model and ship, similarity is maintained for that flow which is considered the most important. This is the basis of the whole technique of ship-model testing.

Considering vessels of the displacement type, for which the speeds are usually restricted to T_q values less than 2.0 or 2.5, $F_n < 0.60$ or 0.74, the comments as to water flow and ship behavior of Chaps. 24, 25, and 26 of Part 2 are valid regardless of size, at least for all craft large enough to carry an adult human. Except for certain limitations on small craft because of the accommodations which have to be provided for human beings of nearly constant dimensions, the design rules and considerations set forth in Chaps. 66, 67, and 68 of Part 4 apply to small craft as well as to large ones. W. F. Durand pointed out as long ago as 1907, in his book "Motor Boats; A Thoroughly Scientific Discussion of Their Design, Construction, and Operation" [Int. Mar. Eng'g., London and New York, 1907, Library of Congress number VM341.D9] that:

> ". . . the selection of principal dimensions, hull coefficients and parameters, underwater form, and the size and form of appendages is handled in almost exactly the same way as for a large vessel."

The principal difference—and unfortunately also a principal difficulty—lies in estimating the total weight of the finished small craft, especially if it is of some new type. There is another difference, discussed in Part 6 of Volume III under Wavegoing, in that the short wind and ship waves to be met by a motorboat or motor cruiser are considerably steeper than the long waves having the same ratio of wave length to ship length for a large vessel.

The motorboat has wavegoing adventures, even in waters that are considered sheltered. Velox waves from passing vessels of larger size or greater speed are steep and sometimes troublesome, as are the waves stirred up in shallow areas by sudden squalls and storms. As a rule, the slowing down of motorboats in shallow and restricted waters is taken for granted, so that no special hull shapes are required for these conditions.

Motorboats of the *semi-planing type* represent a considerably more difficult design problem than those of the displacement type. The change of trim when underway becomes a major design parameter and the necessity for an accurate estimate of the weight becomes much more acute. Moreover, there is a rather wide variety of possible hull shapes from which the proper choice has to be made. It must be admitted that in the past these problems have not had the benefit of the systematic empirical and practical study, to say nothing of the scientific and analytic research

that has been devoted to the design of larger ships. Until this time comes, the hydrodynamic and other aspects of semi-planing motorboat design will not be adequately covered, in reference books or elsewhere.

In the design procedure for a *full-planing craft* it is necessary to emphasize the large and numerous differences between the design problems for a displacement craft, set forth in Chaps. 66, 67, and 68, and those applying to a planing motorboat:

(1) In the first place, the total resistance in pounds per long ton of displacement, R_T/Δ or R_T/W, is higher than for a displacement-type craft, often by two orders of magnitude. Whereas R_T/W for a tanker may be 4 or 5, for a liner 10 or 12, and for a destroyer or similar high-speed craft up to 130 or 150, the R_T/W value for a motorboat with a T_q of 5 or 6 is 700 or 800, indicated clearly by Fig. 56.M. The latter figure represents a ratio of say 750 to 2,240, or roughly one-third of the total weight.

(2) In the second place, the buoyancy force corresponds to practically the entire weight of a displacement-type vessel, whereas for a planing craft it may be not more than one-third or perhaps only one-thirteenth of the total weight. The remainder is dynamic lift.

(3) The shape of the bottom of a displacement-type craft usually affects only its pressure resistance but may and often does have an effect upon maneuvering and wavegoing. In a planing craft the bottom shape affects its ability to plane at all, its behavior when planing, its pitching and porpoising characteristics, its wavegoing behavior and its slamming loads, as well as its controllability, stability of route, and heel when steering and turning.

(4) For a destroyer or similar high-speed vessel running on the after side of its own bow wave the slope drag may be as much as $0.015W$, corresponding to say 30 or 35 lb per long ton. On a motorboat, before planing is reached, it may be as high as $0.10W$ or more, corresponding to say 225 lb per ton.

(5) The actual wetted surface of a planing craft diminishes rapidly as the speed increases, until at designed speed it may be only one-third or less of the at-rest value

(6) The still-air resistance of a large ship is rarely a large percentage of the hydrodynamic resistance but in an ultra-high speed motorboat it may approach that resistance in value, and be accompanied by large vertical forces. Furthermore, the abovewater volume and exposed area of a motorboat increase with the speed, as the craft rises out of the water.

The planing-boat design problem is not only vastly different from that of the displacement-type craft but is vastly more intricate, with interrelationships and interactions of major effect. In perhaps no other branch of water-craft design is there so great a dependence of each design feature upon all the others. A 10 per cent increase in displacement of a vessel supported only by buoyancy means that it sinks somewhat deeper in the water and runs at slightly reduced speed but it retains essentially the same underwater form and gives about the same performance. A 10 per cent increase in weight of a planing craft may prevent it from planing at all, and from reaching more than half of its designed full speed. A slight change in shape of the bottom surface which supports the craft when planing may not only prevent its planing but double its running trim by the stern. Another slight change in bottom shape, hardly large enough to be noticeable, may lift it to planing position but may render it actually dangerous to handle at high speed.

The planing-craft designer must accordingly reconcile himself to learning, and understanding, what amounts almost to an entirely new science and art. Fortunately for him, dynamic lift and other planing phenomena have also called for intensive study and experimentation on the part of aeronautical engineers and aerodynamicists who have been designing seaplanes and flying boats for the past half-century. Many more minds and hands were concentrated on the problem than would have been the case if the naval architect had had to go it alone.

The attainment of superior hydrodynamic performance is perhaps of greater importance in small pleasure craft than in small utility craft. A person who builds or buys a boat and runs it for sheer enjoyment expects to have fun and not trouble. He is in a position, as when buying an automobile, to pick and choose, and to be satisfied with nothing but the best.

For the same reasons, appearance may likewise be more of a factor than it is on a larger vessel, although as a rule not more important than performance in the water. Even a racing yacht must have pleasing lines. A skipper who is proud of her racing record must also be proud of her

appearance. He must like to look at her as well as to sail her.

Many modern motorboats, and small sailing yachts as well, are of the V-bottom, hard-chine type, as contrasted with the round-bottom craft discussed in earlier chapters of Part 4. The fast, hard-chine, full-planing craft may have stepless hulls or hulls with double or multiple steps. In the former, there is a single bottom surface generating dynamic lift, terminating in a single transverse edge at the stern. In the latter there are two or more separate lift-generating surfaces, each with its own sharp downstream edge. In some cases the sharp, deep edges of steps may run in diagonal directions, both fore-and-aft and transversely.

77.3 Special Design Features for Small-Craft Hulls. The design of small-craft hulls under about 110 ft (or 33.5 m) in length requires particular emphasis on certain features of lesser relative importance on large vessels. Among these are:

(1) The normal size of a human adult and the more-or-less fixed deck heights, headroom, berth and bunk sizes, messing spaces, seating room, passages, access areas, and stowage facilities resulting therefrom. A skiff, for example, must have enough stability so that a man can stand up in it without risk of capsizing. A motorboat can not have bunks smaller than a given minimum size.

(2) The diminution in transverse metacentric stability with scale as the vessel becomes smaller, especially when certain factors or parameters remain constant. This is the reason why, when sailing *in the same wind*, a model yacht has to have a much larger and heavier ballast keel in proportion to its hull than the full-scale prototype.

(3) The increased space required for handling and stowing relatively larger items of equipment on deck. A dinghy carried for safety purposes is much larger in proportion than a lifeboat on a larger vessel.

(4) The proportionately larger area of hull and upper works on a small craft, because the fixed deck height is large with respect to the hull size

(5) The increased inconvenience from spray with everything closer to the water, with higher relative speeds, and with heavier impact loads from slamming at those speeds

(6) The relatively larger $T_q = V/\sqrt{L}$ or F_n values at which most small craft run. Anything less than 6 kt is likely to be unacceptable in any pure power boat and more is generally needed. For this reason the values of T_q for non-planing craft rise from a minimum of 1.3 to a maximum of 1.5 or more, F_n in excess of 0.45 [Phillips-Birt, D., The Motor Boat and Yachting, Apr 1953, p. 158].

(7) The larger change of trim for small craft at their designed speed. Vision ahead, and fairly close aboard, must be maintained at all trim angles to be encountered in the speed range.

(8) The increased importance of aerodynamic loads with high absolute motorboat speeds, and the effects of natural winds on high abovewater structures

(9) The types of hull construction and building procedures are of considerably greater variety than for large vessels. This is of importance to the hydrodynamic problem because of the possibility that the finished weight may exceed the estimated weight. If so, the calculated or predicted dynamic lift is not sufficient to raise or to trim the boat to the position or attitude where its hydrodynamic resistance is matched by the power and thrust available.

The considerations of Sec. 77.2 combine with the special features mentioned in this section to render the preliminary design of a motorboat of the semi-planing or full-planing type exceedingly complex as compared with that of a large displacement-type vessel. W. P. Walker describes the situation admirably by saying that:

> ". . . (he) considers it one of the paradoxes of his profession that the smaller the ship the greater are the problems associated with its design, . . ." [IESS, 1948–1949, Vol. 92, p. 304].

The large number of successful displacement-type, semi-planing, and planing boats in service proves that they can be designed. However, the embarrassingly frequent poor performers and downright failures leave most designers with a distinct sense of uncertainty in the behavior of their next product if it is different from what has already been built and run.

The published design comments and notes suffer to some extent from this uncertainty, as well as from the lack of a straightforward procedure or sequence of operations by which one can actually design a boat. However, they can be greatly improved if experienced designers are able to find time and are willing to write down, systematically and in detail, the most reliable

and useful information in their possession. These data, when made available to the profession at large, will surely lead to improvement and progress.

The present effort is to be looked upon, therefore, as only a beginning in the application of hydrodynamics to the design of small craft.

77.4 Design Notes for Displacement-Type Motorboats. There has been a major change in what may be termed the "normal" form of the motorboat in the course of a half-century. The fine, slender launches of the 1900's and the 1910's have become the much fatter transom-stern forms of the 1930's, 1940's, and 1950's. This major change in shape has left the marine architect with little save his own resources in the design of a displacement-type motorboat. W. F. Durand's design procedure of 1907, embodied in the book referenced in the first part of Sec. 77.2, differed but little from that of a liner of about the same proportions. Indeed, the analysis undertaken for the preparation of Chaps. 66, 67, and 68 still leaves the marine architect with unfinished spaces and missing design lanes on the following:

(a) Fig. 66.A; the design lane for fatness ratios should have an upward branch, not indicated on that plot, for relatively high values of $\forall/(0.10L)^3$ in the range of T_q above 1.0
(b) Fig. 66.D shows the upper portion only of a lower branch into which the value of the maximum-section coefficient C_X drops rapidly for yachts, tugs, fishing craft, and other small vessels. This is because of the need for large deck space, for wide beam to give metacentric stability, for a deep keel with which to resist drifting, or for other reasons.
(c) Fig. 66.E illustrates the manner in which the beam B_X diminishes to a limiting or minimum average value of about 2 or 3 ft as the vessel length diminishes to zero
(d) Fig. 66.I; because of the wider beam of small vessels the waterline slopes at the entrance branch off into a lane of their own, for the present not too well defined.

A graph given by D. Phillips-Birt ["The Design of Small Power Craft," The Motor Boat and Yachting, London, Apr 1953, pp. 158–162] for the selection of prismatic coefficient C_P on a basis of a given $T_q = V/\sqrt{L}$ lies well above the design lane of Fig. 66.A for large vessels. This is undoubtedly due to the need in small craft of finding space for all that must be carried, including the people on board. The ends have to be filled out more than on a large ship, where spaces for man and his requirements are more readily provided.

Some additional design information which applies to certain kinds of motorboats and small craft, together with applicable references, is given in Secs. 76.2 and 76.3.

77.5 Semi-Planing and Planing Small Craft. It is difficult to define a semi-planing craft, or to limit, by a description in words, the range of variables within which a small craft of this type is best located, as it were. Until something more appropriate is devised, a semi-planing craft is assumed to be one intermediate between a displacement type and a true- or full-planing type, without specifying the speed range too closely. Put in another way, the craft is of the semi-planing type when:

(1) The dynamic lift becomes appreciable with respect to the weight of the boat, say more than 5 per cent of the latter. It may, in fact, become the controlling factor in its design and performance.
(2) The total resistance R_T becomes more than 10 or 15 per cent of the total weight W
(3) The craft trims by the stern at its designed speed and the center of gravity CG at this speed is at least as high with reference to the undisturbed water surface as when the boat is at rest
(4) Roughly, the speed range lies between T_q values of 2.0 and 3.0, F_n between 0.60 and 0.89. This corresponds to the upper part of the intermediate range of Fig. 29.D.

A somewhat more practical way of defining a semi-planing craft is to say that it is the round-bottom version of a high-speed planing craft, more suitable than the latter for moderate weight-carrying purposes and for continuous operation in heavy weather.

The length used in semi-planing craft design is the waterline length of the vessel when at rest, with the loads on board specified for the designed condition, the same as for a displacement-type vessel. The change of level or of trim that occurs when running at designed speed or below is not taken into account here.

The craft is of the full-planing type when:

(a) The dynamic lift is the controlling factor in its design and performance
(b) The total resistance R_T rises above 10 to 15 per cent of the total weight W to a range of from 25 to 75 per cent or more of that weight

(c) The CG at the planing speed rises *above* its position when the craft is at rest, reckoned with respect to the level of the undisturbed water surface

(d) The designed-speed range lies *above* T_q values of 2.5 or 3.0, $F_n > 0.74$ or 0.89. This corresponds to the range given in (1) of Sec. 30.2, subject to the qualification given there.

A fifth criterion for differentiating a semi-planing from a full-planing type of boat is that used at the Experimental Towing Tank, Stevens Institute of Technology. It is based on the fact that the full-planing type is always built with chines at the outer edges of the bottom. Here a full-planing condition is defined as that in which the water breaks away cleanly from the chine for the entire length of the boat. No water curls up over the chine and wets either the sides or the transom.

A sixth criterion is that given in (3) of Sec. 30.2, illustrated graphically in Fig. 30.B. This defines the full-planing speed as that at which there is a sharp reduction of the exponent n in the formula $R_T = kV^n$.

The length used for planing-craft design purposes varies. It may be:

(i) The chine length L_C, projected upon the baseplane

(ii) The waterline length L_{WL} at normal load and trim when the craft is at rest

(iii) The overall length L_{OA}.

This matter is discussed further in subsequent sections.

77.6 Operating Requirements for Planing Forms. There are a number of operating requirements peculiar to all planing forms which call for consideration ahead of the particular requirements of the owner and operator. The former are in addition to the normal requirements for speed, maneuverability, good wavegoing behavior, and adequate stability, the same as for any other small craft. The items listed and discussed here are adapted from those previously published by C. R. Teller [Motor Boating, New York, Ann. Show Number (Jan), 1952, pp. 66–68, 247–249]:

(1) At less than planing speed, that is, when running as a displacement-type boat, the planing craft must be as seaworthy as the best displacement boat. Otherwise it is no seagoing vessel.

(2) The speed at which the craft passes the hump-resistance region and begins to plane must be low. It should be no higher than the speed at which a displacement-type hull of the same approximate size begins to require an inordinate amount of power.

(3) To achieve successful wavegoing performance a planing hull must plane at a speed so far below the cruising range that in a seaway it will maintain its planing characteristics. If the craft is involuntarily slowed to below that speed it should at once regain its planing position upon an increase in speed. This factor is of the most vital importance. For example, if a planing hull must travel at 14 kt to reach planing speed and if it has a sustained cruising speed of only 16 kt, the adverse effect of only a small or moderate sea will suffice to slow the craft down to below the planing speed of 14 kt. It will struggle along, alternately planing and falling back below hump speed. Such a craft is, in the words of Teller, "neither a successful planing boat nor an honest displacement boat."

(4) If the planing craft is deliberately throttled to below planing speed, it must have as good wavegoing performance as the best displacement-type hull. Otherwise, if the planing boat experiences power-plant failure in a gale or has to be slowed because of fog or any other cause, it is no longer a seagoing vessel.

(5) The planing hull must be as free from pounding and slamming as the best displacement-type hull of the same size, *running at the same speed.* Otherwise it is no seagoing vessel.

(6) Finally, the true planing craft is not a weight-carrying vessel, in the sense of a cargo ship. Its use should be restricted to carrying special equipment, certain types of cargo in an emergency, or so-called premium loads, where the expense involved in transportation is justified by the saving in time. An aircraft rescue boat is an excellent example illustrating these features. Indeed, the planing craft may well be regarded more nearly as a seaplane or flying boat than as an ordinary boat. If the flying boat is overloaded it can not and will not take off from the water. If the planing craft is overloaded it likewise will not take off and plane.

77.7 General Notes on the Powering of Small Craft. The general subject of powering for motorboats and other small craft is touched upon here briefly, as a preliminary discussion of quantitative power estimates in Secs. 77.14 and 77.26.

The designed or minimum speeds for which motorboats are powered are usually those to be

made in quiet water, either fresh or salt as specified, with a clean, smooth, new bottom, and with the propelling machinery delivering its rated power or some specified fraction thereof, corresponding to the 0.95 factor of Sec. 69.9.

It is important for the naval architect as well as for the marine engineer to realize that because of the limit on mean effective pressure in the cylinders, any reciprocating internal-combustion engine can produce its rated power only at a certain rate of rotation. At a lesser rotating speed, the power is less. Furthermore, it may not be possible for the engine to deliver its rated power at a higher rotating speed than that for which it is designed or adjusted. This makes it most important that the small-craft propeller be one which, at a desired boat speed, absorbs exactly the engine output, less the transmission and shafting losses. More power absorption means that the engine and propeller both have to speed up to make the powers match, if indeed this can be done.

It is customary to overpower the modern motorboat, just as a modern tug or fishing vessel is overpowered, but not for exactly the same reasons. Motorboat overpowering resembles more nearly, in fact, the gross overpowering of the modern (1955) passenger automobile. Engine life is longer and wear and tear is less at reduced powers. The engine power actually required for the greater part of the time is delivered reliably even though the engine may be somewhat out of adjustment or the fuel may not be up to standard.

For these reasons, and others not mentioned, powering allowances are as necessary for a small craft as for a large one. It is customary for these to cover the power needed for:

(a) Increase in weight due to thorough wetting of the boat structure, if of wood, corresponding to a period of at least six months in the water and in the weather, covering at least two seasons

(b) Unavoidable increases in weight with time in service, because of adding new equipment. Demands for increased carrying capacity, over and above design requirements, are not in this category. Logically, they must be paid for separately, either in increased power or reduced speed.

(c) Roughening of the bottom surface because of rusting, pitting, oxidizing, flaking, peeling, uneven calking, and fouling by marine organisms

(d) Reduction of propelling-machinery efficiency and output because of wear and tear, low grades of fuel, and excessive time between overhauls

(e) Damage to blades of propulsion devices from numerous causes, probably of more frequent occurrence on small craft than on large ones.

77.8 Principal Requirements for a Preliminary Design Study. The craft selected as the running example in this chapter is a small motor tender for the ABC ship designed in Chaps. 64 through 68. The first step in the preliminary hydrodynamic design of this motorboat is to outline the mission of the craft; in other words, to state what it is required to do. After consultation with the owners and operators of the large vessel, this is set down in items (1) and (2) of Table 77.a. It is followed

TABLE 77.a—MOTOR TENDER FOR ABC SHIP; PRINCIPAL HYDRODYNAMIC AND OTHER REQUIREMENTS

MISSION—The craft described in these specifications is to:

(1) Serve as a power launch for and to be carried on board the ABC ship whose requirements are set forth in Tables 64.a through 64.g

(2) Serve as an all-weather tender for the ferrying of personnel, incidental packages, and miscellaneous portable articles from ship to shore and vice versa, under special conditions where the ship must anchor or lie-to.

WEIGHT AND SIZE LIMITATIONS—To permit hoisting it on board the ABC ship the boat is to:

(3) Have a gross hoisting weight not exceeding 25,000 lb, including a full supply of fuel, other consumables, parts, tools, and two crew members, the latter assumed to weigh 350 lb. Hoisting is to be by a single hook on the ship.

(4) Be capable of stowage, in a secure position for travel at sea, on the weather deck either forward of or abaft the passenger accommodations

(5) Have an overall length not exceeding 40 ft.

CARRYING CAPACITY AND ACCOMMODATIONS —The tender is to:

(6) Be capable of carrying one of the following items, or any reasonable combination of all three, not exceeding 3,000 lb in weight:

(a) Twelve passengers plus a maximum crew of four

(b) Cargo in packages or luggage, in total weight not to exceed 2,300 lb and in total volume not to exceed 125 ft^3, plus a maximum crew of four

(c) Eight passengers and a maximum crew of four, plus one litter patient

(7) Provide protection from rain, wind, spray, and sun for all passengers and cargo.

SPEED AND ENDURANCE—The craft shall be able to:

(8) Achieve a speed of:

(a) 18 kt in smooth water with a half-load of fuel, a crew of two, and two passengers and their personal baggage

(b) 14 kt in smooth water with a full load of fuel and cargo.

(9) Run at full power for six hr without replenishing fuel.

TABLE 77.a—(Continued)

SAFETY—The following requirements apply:

(10) The fuel used in the power plant shall be diesel fuel or its equivalent; no type of gasoline or equally volatile fuel is permitted
(11) The tender shall remain afloat and upright if completely swamped, with crew, passengers, and cargo on board. The cargo may be considered as 50 per cent permeable, and the special flotation volume as fully intact.
(12) Drinking water and emergency rations for sixteen persons for two days are to be carried
(13) Safety and operational equipment as required by regulations of the U. S. Coast Guard for operation in semi-protected ocean waters.

OTHER REQUIREMENTS

(14) It shall be possible to warm up and run the power plant for a short period before the boat is hoisted out
(15) The boat shall preferably bank inward on turns in normal steering
(16) The craft shall possess adequate steering control in either head or following seas
(17) It shall not pound or slam excessively, so as to risk injury to the boat structure or to the crew and passengers, when running in rough water at speeds in excess of 10 kt
(18) The design and construction shall be rugged and substantial, suitable for hard service and reliable operation in salt water.

by requirements for weight, carrying capacity, speed, endurance, safety, and other features, embodied in items (3) through (18). Still other items may develop as the design proceeds.

The prospective operators wish an alternative design prepared for a craft to meet substantially the same general requirements as in Table 77.a but to run at a higher maximum speed with less carrying capacity. The detail requirements are set down in Table 77.b.

It is noted that complete freedom is left to the designer with respect to the following, for both the principal and the alternative designs:

(a) Type of hull, whether displacement, semi-planing, or full-planing. However, a conference with the prospective operators of the ABC ship brings out that reliability of operation, all-weather behavior, and load-carrying performance of the craft are considered of paramount importance. Speed can be sacrificed if need be.
(b) Hull proportions, principally the L/B ratio but more important still, for actual stowage on the ship, the maximum beam
(c) Hull draft or limiting draft
(d) General shape and appearance of hull
(e) Power plant and power
(f) Number of propellers
(g) Materials of construction
(h) Method of attaching the single-ring hoisting sling.

77.9 Analysis of the Principal Requirements. Before starting the design proper it is well to analyze the requirements, in terms of the background already gained in the preliminary design of the ABC ship. The overall length of 40 ft is fixed for both the principal and the alternative designs. To achieve the load- and volume-carrying capacities required, it is almost a certainty that the stern will have to be of the transom type. From an examination of the published data for other motorboats an average length for the waterline at rest may be estimated as 37 or 38 ft; the lower value is on the safe side. Its square root is 6.083. Based upon the speeds in item (8) of Table 77.a and item (b) of Table 77.b, the T_q and F_n values are:

Speed 14 kt
$T_q = 14/6.083 = 2.30$
$F_n = 2.30(0.2978) = 0.685$

Speed 18 kt
$T_q = 18/6.083 = 2.96$
$F_n = 2.96(0.2978) = 0.881$

Speed 24 kt
$T_q = 24/6.083 = 3.95$
$F_n = 3.95(0.2978) = 1.176.$

Nothing is said in the specifications about running trim; that is, change of trim when underway. Excessive trim by the stern, resulting either from placing the useful load too far aft, or

TABLE 77.b—MOTOR TENDER FOR ABC SHIP; REQUIREMENTS FOR ALTERNATIVE HIGH-SPEED DESIGN

An alternative design of motor tender is to be prepared having the general requirements of items (1) through (14) plus (18) of Table 77.a, modified by the following:

(a) Carrying capacity of six passengers plus a crew of two, all having an average weight of 170 lb per person, plus a cargo of packages or luggage weighing not in excess of 900 lb and having a volume not in excess of 50 ft^3, plus a two-thirds load of fuel
(b) Speed, 24 kt minimum, in quiet water, with the load of item (a)
(c) Run at full power for two hr without refueling
(d) The boat shall bank inward on turns when running in the planing range
(e) The craft shall possess adequate steering control in either head or following seas
(f) It shall not pound or slam excessively, so as to risk injury to the boat structure or to the crew and passengers, when running in rough water in the planing range
(g) The craft shall not porpoise at any operating speed.

from too much squat, increases the power unnecessarily and leads to impaired maneuvering and wavegoing. On the other hand, the craft with only the crew on board, but with full fuel, should not trim unduly by the bow. Better still, it should not trim by the bow at all.

Since the steering is to be entirely by hand, the rudder(s) must trail under all running conditions.

Freedom from pounding and slamming in both designs calls for V-sections in the lower forebody, with appreciable rise of floor. The speeds in all cases approach those for planing, especially at light loads, hence the buttock lines aft should be straight or only very slightly convex downward.

77.10 Tentative Selection of the Type and Proportions of the Hull. For the principal design it appears practicable to shape one hull that will run well at both 14 and 18 kt. However, the total weight displacements will be different for these two speeds because of the different useful loads of items (8)(a) and (8)(b) of Table 77.a. The underwater portions of the hull will thus be somewhat different in the two conditions, especially if the trim changes between loadings. It is expected, nevertheless, that the 18-kt condition will be the controlling one in the principal design. The 24-kt craft, to run definitely in the planing range, is destined to have an entirely different hull.

From Sec. 77.9, the T_q value for an 18-kt design of 37-ft length is below 3.0. If the whole available length of 40 ft overall is used, the WL length will be about 39 ft and the T_q value 2.88. A semi-planing type of hull is tentatively indicated. This, combined with the important requirement for excellent wavegoing performance, points to a round-bottom hull as the preferred shape. For the faster 24-kt boat, running at a T_q of the order of 4.0, well within the planing range, a hard-chine, V-bottom hull is called for. These will hereafter be called, for convenience, the round-bottom boat and the V-bottom or full-planing boat.

On a basis of quiet-water resistance, D. De Groot says that "the upper limit for the advantageous use of the U-form (round bottom) lies . . . somewhere about $V/\sqrt{L} = 3.25$" [Int. Shipbldg. Progr., 1955, Vol. 2, No. 6, p. 70]. Fig. 77.A is adapted from De Groot's diagram, showing the round-bottom and V-bottom regions in graphic form. However, the dividing line in his plot corresponds to a T_q of about 3.13; this was not changed in the adaptation. The 18-kt 37-ft combination for the ABC tender lies slightly inside the round-bottom region in the figure.

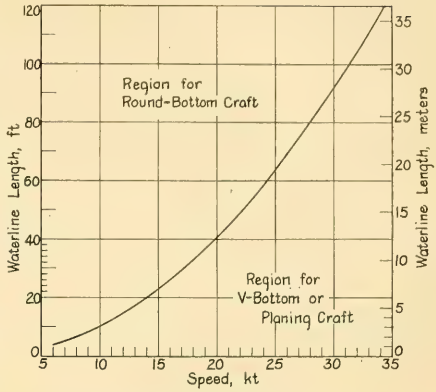

Fig. 77.A Ranges of Size and Speed for Round-Bottom and V-Bottom Craft

Adapted from the data of D. De Groot, referenced in the text.

Because the design of a planing craft represents what might be termed the general case, embodying practically all the variables to be encountered in laying out and selecting parameters for small craft, it is described first. This is not to make the problem more difficult but to avoid introducing entirely new features into the story at points which would break up the reader's line of thought. The round-bottom design procedure then becomes one of simplifying that for the general case.

77.11 First Space Layout of the 24-Knot Planing Hull. The first actual step in the design of the ABC tender, as for any motorboat, is to determine about how large the boat has to be to meet the design requirements. This is done by making a series of sketches to a convenient scale, usually free-hand on ruled or light-lined coordinate paper, showing proposed internal-space layouts. Sec. 77.3 points out that these craft are relatively small in proportion to a human and his accommodations afloat. They must, therefore, almost invariably be designed on a volume basis rather than a weight-carrying basis. The size of the boat is determined, not so much from those dimensions which will, with a normal form, give enough volume displacement to float the weight to be carried as from the positions of the boat-shaped boundaries which will enclose the various spaces and units needed to meet the specification requirements. Several separate space studies are

desirable, perhaps a dozen or more, especially when the designer is allowed some latitude in arranging the various principal units, the accommodations, and the service facilities.

For craft over 25 ft or 30 ft in length the preliminary space layouts may involve two or more deck plans, one for the weather deck and another for the space below deck. A boat-shaped hull sketched around these spaces affords a rough idea of the principal dimensions such as overall length, beam, and depth of hull. Profiles based on these hull sketches indicate the positions and sizes of houses or other erections projecting above the weather deck. Having the general size and shape, or perhaps one might say the minimum size and shape, the designer proceeds to incorporate certain other features in the sketches such as minimum freeboard and sheer, freeboard at or near the bow, and profiles of the bow and stern. He shows crew and passengers, as well as "cargo" in the present case, in their proper or proposed positions.

Even though the powers and sizes of the engine(s) are not yet known, the spaces for propelling machinery and auxiliaries can be roughed in, leaving them oversize in case of doubt. The hull structure usually presents no problem at this stage, unless fire or subdivision bulkheads are required. The buoyancy tanks or compartments for flotation in an emergency can usually be worked into spaces not useful for anything else. Their volumes should, if practicable, be so placed that the swamped boat is supported at or about zero trim.

Fig. 77.B was drawn from the last of several layout and arrangement sketches made for the ABC planing-type tender. These indicated that a craft 40 ft in overall length, with an estimated displacement weight of 25,000 lb, was somewhat larger than necessary. A smaller boat, 35 ft in overall length and 32 ft long on the waterline, appeared to be sufficiently roomy but with an estimated weight of 18,000 lb its displacement-length quotient of 245 was too high. The boat shown in the figure, with a waterline length of 35 ft, provides room enough to meet the requirements of Table 77.b and is not too heavy for its length. The layout is nevertheless considered purely preliminary. Its sole purpose is to show that the spaces called for by the specifications can be fitted into a craft of the minimum dimensions represented by the sketch. It does not necessarily represent the best arrangement possible within the limitations established by the owner and operator.

77.12 First Weight Estimate; Weight-Estimating Procedure. The second step in the design of the planing-type craft is to make a preliminary weight estimate of the complete boat, in operating condition and with the full useful load on board.

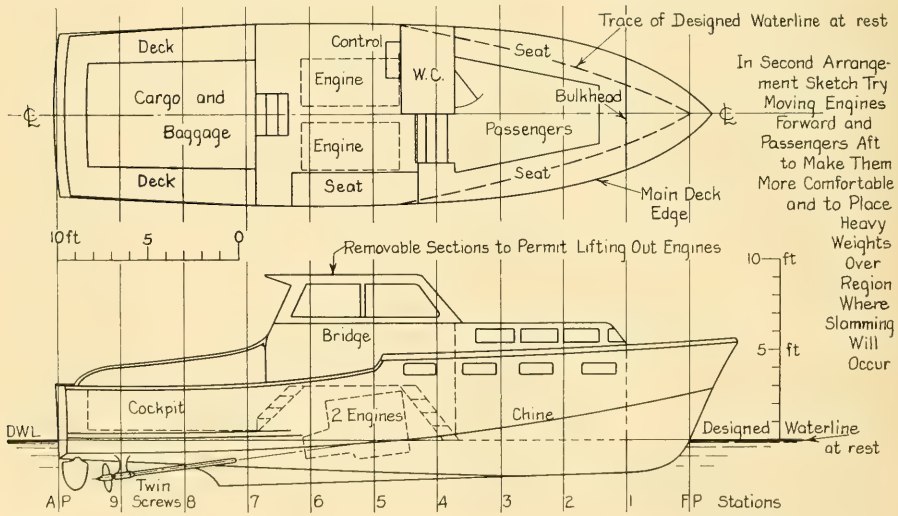

Fig. 77.B Sketch of Tentative Space Layout for V-Bottom Tender for ABC Ship

This may be handled in several ways. All of them, like that used for the ABC ship in Sec. 66.4, involve weight estimates for a craft which is still in a distinctly nebulous state. To make this situation more difficult, reliable published information as to the weight percentages of the various groups and detailed information as to the actual scale weights for motorboats are much scarcer than corresponding data for large vessels. A start in this direction has recently been made by E. Monk ["Weight and the Motor Boat," Yachting, Jan 1955, pp. 118–120]. The graphic data presented by Monk, comprising a relationship between waterline length at rest and total weight for wooden pleasure boats, are embodied in the lower broken-line curve of Fig. 77.C. The full-line

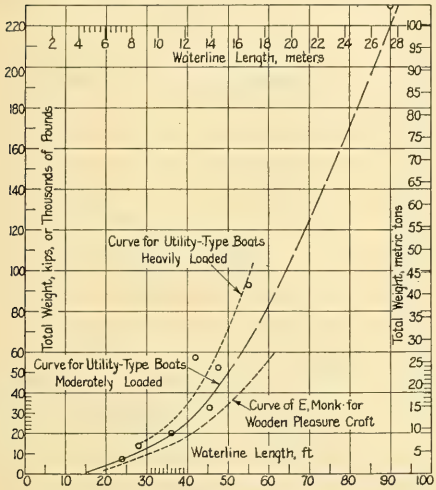

Fig. 77.C Relation Between Weight and Waterline Length of Two Types of Small Craft

portion of the middle graph, with a tentative extension in long dashes, is based upon data from about a dozen motorboats of the moderately loaded type for which the total weights are known. Because of the spread in some of these data, indicated by the small circles in the figure, a third tentative meanline for boats of the heavily loaded type is shown by short dashes. It is almost certain that any graph of this type will consist of a family of curves, representing boats designed for widely different missions.

When total weights of motorboats are given in the technical literature, they are rarely accompanied by a statement of the corresponding loading condition(s). Lacking accurate and adequate sources, the designer is usually forced to create his own or to obtain access, by one means or another, to data that remain unpublished.

For the ABC tender, assuming that it is to be built of wood (or of a material having an equivalent weight), and that it has a waterline length as short as 35 ft, Monk's broken-line curve of Fig. 77.C indicates that it will weigh at least 17,000 lb. It will certainly be heavier than a pure pleasure craft, and probably not much lighter than a moderately loaded utility boat. To be on the safe side, the designer should assume a weight not less than 18,000 lb. Incidentally, the two lower graphs of this figure reveal that, for the permissible maximum waterline length of about 39 ft, the total weight should be less than the 25,000-lb limit of Table 77.a.

It is emphasized here, and this emphasis will be repeated several times in the sections to follow, that the preliminary weight estimate, and the revisions to it, can make or break a small-craft design. If the total weight is estimated correctly, the boat should perform as predicted. If the weight is underestimated, the boat almost certainly will fail to meet expectations.

A rule-of-thumb check on the weight estimate serves as a sort of maximum limit for a boat that is expected to give good planing performance. This says that the displacement-length quotient $\Delta/(0.010L)^3$ should not exceed 200, and that it should be lower if possible. For a total weight of 18,000 lb, or 8.04 t, and a waterline length as short as 35 ft, the displacement-length quotient is $8.04/(0.35)^3 = 187.5$. For the moment this requirement is therefore met.

With what appears to be a reasonable total weight the next step is to make a first approximation of the power required to drive the ABC planing-type tender at 24 kt, so that the machinery and fuel weights can be predicted. From the calculations described subsequently in Sec. 77.14 the brake power is of the order of 430 horses. On the basis of using two diesel engines, giving a better arrangement of machinery space and facilitating engine removal and overhaul, the total estimated machinery weight, including all liquids in the systems, is 5,300 lb. The details of this estimate are taken from returned weights of actual installations, as furnished by the engine manufacturers.

Considering the fuel weight, the owner's re-

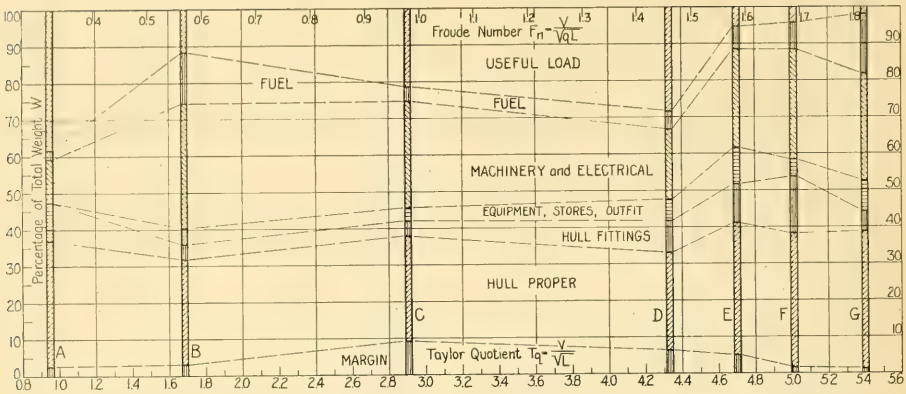

FIG. 77.D PERCENTAGE DISTRIBUTION OF PRINCIPAL WEIGHTS FOR SEVEN MODERATE- TO HIGH-SPEED CRAFT

quirement in item (c) of Table 77.b calls for a 2-hr supply at full power. Under these conditions the fuel rate for the two 215-horse engines proposed is about 0.5 lb per brake horse per hr, so that 430 lb of fuel is required for both engines for a 2-hr run. Since the owner has had no previous service experience with a tender of this kind, it seems wise at this stage to allow for a considerably enlarged fuel capacity, say about twice that actually required. With an assumed weight of 6.2 lb per gal, 860 lb of fuel amounts to 860/6.2 = 138.7, or say 140 gal. A further study of the probable service required of this tender reveals that, despite the increased capacity, it may be necessary under some circumstances to return to the parent ship for refueling before the day's work is done. There may be times when this will be extremely inconvenient, so another 50 gal is added to the fuel capacity for good measure, bringing the total capacity to 190 gal, or 1,178 lb.

The weights reasonably well known at this stage are:

(1) Useful load, from owner's requirements, six passengers at 170 lb plus 900 lb of packages, 1,920 lb
(2) Weight of engines, ready to run, 5,300 lb
(3) Fuel; although the owner requires only two-thirds capacity on board for the designed speed, the full capacity is listed here, 1,178 lb
(4) Crew, two persons at 170 lb, 340 lb.

The known weights total 8,738 lb, leaving 18,000 − 8,738 = 9,262 lb for the weight groups still to be considered.

One method of making a preliminary weight estimate of the remainder, with the craft not yet roughed out in the form of lines or structural drawings from which weights can be calculated, is to use a weight-percentage diagram such as that of Fig. 77.D. Here the percentages of seven weight groups, making up a total of 100 per cent for the complete boat, are plotted on a basis of Taylor quotient T_q (and F_n) for seven different planing craft for which reasonably reliable data are available. Only a general pattern of weight distribution is apparent for any of the boat types, because of great differences in the operating functions of the various craft, listed in Table 77.c. For the ABC planing-form tender, with an assumed WL length of 35 ft, the Taylor quotient $T_q = 24/\sqrt{35} = 4.05$. The only reference craft of Fig. 77.D with a T_q of about this value is the 24-ft personnel boat, designation D of the table and the figure. Here the combined total of useful load, fuel, and machinery (including electrical items) is 52.5 per cent, working down from the top in Fig. 77.D. For the craft being designed the corresponding percentage is 8,738/18,000 = 48.5, leaving 51.5 per cent for the hull, hull fittings, equipment and stores, electrical and electronics gear, and margin.

What appears at this stage to be a reasonable subdivision of the 51.5 per cent is:

(a) Hull, 28 per cent or 5,040 lb
(b) Hull fittings, 9 per cent or 1,620 lb. This must include the hoisting slings if they are built in and carried as part of the boat structure.

TABLE 77.c—WEIGHT DISTRIBUTION FOR DIFFERENT MOTORBOAT TYPES

The data in this table supplement those set down graphically in Fig. 77.D. The Taylor quotients listed are based upon the waterline length, where this is known.

Function of boat	Designation	Nominal length, ft	Full-load weight, lb	Position of CG abaft the mid-length, ft	T_q, Max.	Type of Hull
Aircraft refueling (tug type)	A	42 (L_{WL} = 40.0, about)	57,552	2.62	0.95	Round-bottom
Utility, wooden hull	B	57 (L_{WL} = 55.0)	93,172	—	1.686	Round-bottom
Personnel (ferrying)	C	28 (L_{WL} = 26.67)	14,040	—	2.905	V-bottom
Plane personnel (ferrying)	D	24 (L_{WL} = 22.42)	7,400	2.24	4.33	V-bottom
Aircraft rescue	E	36 (L_{WL} = 35.0)	20,210	3.20	4.7	V-bottom
Aircraft rescue	F	45.5 (L_{WL} = 43.3)	32,600	3.47	5.013	V-bottom
Rescue	G	52 (L_{WL} = 47.5)	52,406	4.55	5.4	V-bottom

(c) Equipment and stores, 6 per cent or 1,080 lb

(d) Electrical and electronics gear, 1.4 per cent or 252 lb

(e) Margin, 7 per cent or 1,260 lb.

The estimated percentages or weights, or both, are checked by the designer with those for planing craft of somewhat similar type, size, and speed range which he is able to gather from any sources whatever. The reliability of these data must be determined or assessed by the designer using them. In some few cases it may be possible to make direct weight estimates of certain items, such as electronics gear, by deciding just what is to be put into the boat.

It appears from Fig. 77.D that the machinery weight of 5,300 lb, with its percentage of 29.4, may be on the high side. On the other hand, the hull percentage of 28 may be low. Good engineering practice indicates that in this preliminary stage the margin of 7 per cent is low; 10 per cent would be much better. A second weight estimate is definitely in order, before the design is too far advanced.

77.13 Second Weight Estimate. For a revised estimate, somewhat more care is exercised in arriving at reasonable figures. As is the case for the full-scale ABC ship designed in the earlier chapters of this part, the weight figures given are *purely illustrative* and are not intended to serve as a rigid guide for any actual motor boat design. The weights, powers, and even the types of engine will change as the art of engineering advances, but a good weight-estimating procedure remains essentially the same.

First, there are set down the weights specified by the owner and operator, because these can be rigidly controlled for the boat trials. These are:

Useful load, 6 passengers and 2 crew at 170 lb per person,	1,360 lb
Cargo and baggage,	900 lb.

The largest weight group under the designer's control is that of the hull. For a fast planing boat which is to travel at a T_q of the order of 4.00, and for a hull which has to be lifted by a crane or derrick twice every time it is used, a percentage of 33, based on the total boat weight, is probably as small as should be considered.

The next largest weight group is that of the machinery. Two diesel engines, similar to the GM HN-10 model, are capable of delivering a *total* brake power of 330 to 450 horses, depending upon the injectors used. The first estimate of the

brake power required is about 430 horses. When rigged for direct drive and fitted with hydraulically operated clutches, with all lubricating oil carried in the engine sumps, the weight is 2,650 lb per engine or 5,300 lb total. This includes all liquids in the engines and the piping systems. It is the same as was used for the first estimate.

With an increase in the ratio of hull weight to total weight of from 0.28 to 0.33, it is clear that too much additional fuel can not be carried if the percentage of margin is also to be increased. The fuel is therefore limited to the 140 gal necessary to run both engines at full power for 4 hr. Its weight is 140(6.2) = 868 lb.

Hull fittings usually account for an unreasonably large proportion of the total weight for small boats because many of these parts are of standard size and constant weight for a rather wide range of boat sizes. A good value for a twin-screw planing boat of 35-ft waterline length seems to be about 8 per cent of the total.

The planing boat under design is a tender, therefore many usual items of equipment are not required. For example, no bunks or mattresses are needed. Stores can be held to a minimum and only a small quantity of drinking water need be carried. A low percentage of weight assigned to the stores group, say only 3.0 per cent of the total, appears adequate.

The customary amount of electrical and electronic equipment is called for. This is estimated as 800 lb.

To avoid overweight, the most common fault of planing motorboats, an ample margin is mandatory. At this stage a good 10 per cent of the total of the preceding groups is none too much, or about 9.5 per cent of the resulting total.

A summary of the groups of the second weight estimate follows:

Hull = 0.33(18,000) =	5,940 lb
Hull fittings = 0.08(18,000) =	1,440 lb
Equipment, stores, outfit, water = 0.03(18,000) =	540 lb
Machinery, diesel, wet =	5,300 lb
Electrical, estimated =	800 lb
Fuel, 140 gal at 6.2 lb per gal =	868 lb
Passengers and crew =	1,360 lb
Cargo and baggage =	900 lb
Total	17,148 lb

Adding a margin of 9.5 per cent of the total weight the latter is 17,148/0.905 = 18,948 lb. In round numbers this is 19,000 lb or 8.482 long tons.

At no stage of the design or construction should the weight of the boat exceed this figure. Any reduction under this limit is a definite advantage. A revision of the displacement-length quotient gives

$$\frac{W \text{ (or } \Delta)}{(0.010L)^3} = \frac{8.482}{(0.35)^3} = 197.8$$

The design limit of 200 for this quotient is approached closely but not exceeded.

E. Monk publishes a weight distribution for an average cruising motorboat, in percentage form similar to Fig. 77.D, without giving an average value or range of T_q [Yachting, Jan 1955, p. 118]. He also gives, in the same reference, a breakdown of the hull structural weights only, for average V-bottom and round-bottom cruisers.

D. S. Simpson gives a simple and convenient method for estimating the preliminary values of eleven weight groups for a trawler design [SNAME, 1951, p. 561]. For the weight of the hull and its joiner work, the estimate is based upon the product of the ship length L, the beam B, and the hull depth D, all expressed in feet, times selected coefficients which give the weights in long tons. For the deckhouses, their weight is based upon their volume times another coefficient. The weight of gear and equipment, and of ballast, is based upon the length L in ft times a selected coefficient to convert it into tons. The particular coefficients for these dimensional expressions are derived only from a rather voluminous collection of data, combined with a generous amount of background and experience. They work at present with little in the way of method and system; they would work much better if some additional time and study could be devoted to them.

When the motorboat (or small-craft) design is more completely worked out an overall direct estimate of weights is made, by the method described in Sec. 77.39.

77.14 First Approximation to Shaft and Brake Power. The first, and perhaps the second and third approximations as well, to the shaft power of a surface ship are made by suitable methods which give the designer an idea directly of the shaft power necessary to drive a given size and type of ship at the required speed. The first part of Sec. 66.9 contains examples of two methods employed in the preliminary design of the ABC ship.

For the designer of a motorboat, on which the proportion of propelling-machinery weight is much greater than on a normal type of displace-

ment vessel, it is imperative to know, very early in the design, about how much shaft (or brake) power is called for and the approximate weight of this machinery. Perhaps because it has been customary to make direct power estimates in the past, as distinguished from indirect estimates based upon effective power and propulsive coefficient, there are more shaft (or brake) power estimating procedures available to the motorboat designer than to the one who undertakes to design a large ship. Unfortunately, these many methods usually give as many different answers, and sometimes the answers vary widely among each other. Moreover, the observed data upon which these procedures are based also vary in reliability, principally because of the lack of proper instrumentation and techniques whereby shaft powers for small craft may be measured accurately on trial. In the late 1920's and early 1930's Sir Charles Ross undertook a lengthy research project in an effort to measure the brake power of small-boat internal-combustion engines by recording the rate of rotation and measuring the rate of fuel consumption with extreme care. Unfortunately the project was never finished nor were the results of the work written up for publication. The designer is therefore left with the hope that when a given engine is put into a boat it will deliver the same brake power at the output shaft at rated rpm that it did when it ran on the factory test stand.

One of the simplest direct estimates of brake power is the table and the dimensional "K" formula of K. C. Barnaby [BNA, 1954, Table 40

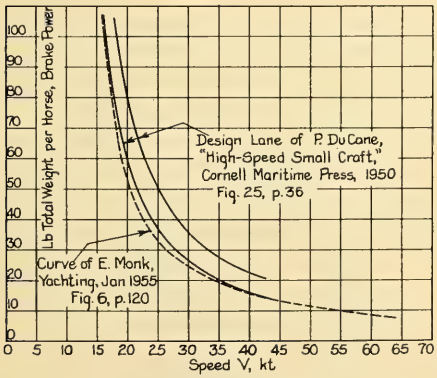

Fig. 77.E Relationship of Speed to Brake Power for Small Craft

TABLE 77.d—Values of the K. C. Barnaby Powering Coefficient K_1 in Equation (77.i)

The values set down here are from a table published by K. C. Barnaby ["Basic Naval Architecture," Hutchinson's, London, 2nd ed., 1954, p. 310].

Waterline length, ft	Type of Hull and Limits of Speed-Length Quotient T_q		
	Round-bottom, transom, and very flat stern	V-chine, stepless	Multiple steps
	T_q 2.5 to 3.5	T_q 2.75 to 4.5	T_q 3.5 to 6.5
20	2.25	2.75	3.6
25	2.4	2.9	3.8
30	2.6	3.10	3.96
35	2.8	3.4	4.15
40	3.05	3.65	4.3
45	3.24	3.85	4.48
50	3.34	4.0	4.6

on p. 310 and Figs. 132, 133 on pp. 449–450]. Although Figs. 132 and 133 cover lengths of 20 to 50 ft, the speed V extends only to 17 kt, so that for the 18-kt as well as the 24-kt ABC tenders it is necessary to use Table 40 and Barnaby's formula

$$V = K_1\sqrt{\frac{P_B}{\Delta}} \text{ or } P_B = \Delta\,\frac{V^2}{K_1^2} \text{ or } P_B = \frac{WV^2}{K_1^2} \qquad (77.i)$$

where Δ is the weight in long tons and K_1 is found from Table 77.d, adapted from the Barnaby reference just cited.

Another simple powering estimate gives the dimensional ratio W/P_B of weight to brake power as a function of the absolute speed V, but without the use of a length parameter. Fig. 77.E embodies two graphs by P. Du Cane and one by E. Monk, adapted from the references cited in the figure. The two lines given by Du Cane are intended to be the boundaries of a design lane lying between them. It is obvious from these graphs that the weight of boat per unit of shaft or brake power, or the amount of shaft or brake power per unit weight of boat, each of them often quoted in the literature, vary widely with the designed speed.

Although the legend of P. G. Tomalin's "Nomogram for Speed and Power" [SNAME, 1953, Fig. 8, p. 601] states that it applies to planing hulls, experience indicates that the power predictions given by it are too low except for values

of the Taylor quotient T_q less than 2.0. This is below the planing range for most motorboats.

C. E. Werback has developed still another dimensional relation, derived originally by G. F. Crouch, of the following form:

$$V(\text{kt}) = C\,\frac{\sqrt[4]{L_{WL}\,(\text{ft})}}{\sqrt{\dfrac{W\,(\text{lb})}{P_S\,(\text{horses})}}} \qquad (77.\text{ii})$$

Transposed for deriving the shaft power in terms of the other quantities it becomes

$$P_S\,(\text{horses}) = \frac{W\,(\text{lb})\;V^2\,(\text{kt})}{C^2\sqrt{L_{WL}\,(\text{ft})}} \qquad (77.\text{iia})$$

Analysis of this method indicates that a family of curves for various displacement-length quotients $W/(0.010L)^3$ is required for taking off proper values of the coefficient C. However, on the basis that displacement-length quotients for good planing craft are of the order of 200 or slightly less, Fig. 77.F gives a graph for selecting

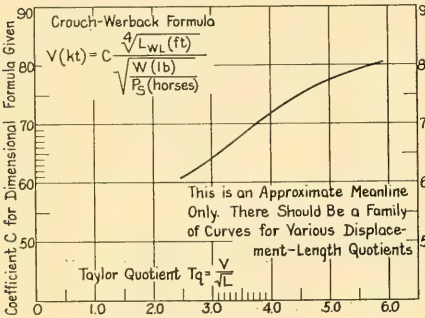

Fig. 77.F Crouch-Werback Formula and Graph for Relating Shaft Power to Length, Speed, and Weight

C at T_q values greater than 2.5 and not exceeding 6.0.

D. Phillips-Birt gives a dimensional formula exactly the same as K. C. Barnaby's (Eq. 77.i) for relating the brake power P_B, the total weight W, and the speed V ["The Design of Seagoing Planing Boats," The Motor Boat and Yachting, Jan 1954, p. 29]. This takes the alternative forms

$$V(\text{kt}) = K_2\sqrt{\frac{P_B\,(\text{horses})}{W\,(\text{long tons})}} \qquad (77.\text{iii})$$

$$P_B\,(\text{horses}) = \frac{V^2W}{K_2^2} \qquad (77.\text{iiia})$$

where the coefficient K_2 is taken from a table given by Phillips-Birt, reproduced here as Table 77.e.

N. L. Skene uses a formula almost exactly the same as Eqs. (77.i) and (77.iii), with the alternative forms

$$\frac{C}{V\,(\text{mph})} = \sqrt{\frac{W\,(\text{lb})}{P_B\,(\text{horses})}} \qquad (77.\text{iv})$$

$$P_B\,(\text{horses}) = \frac{W\,(\text{lb})\;V^2\,(\text{mph})}{C^2} \qquad (77.\text{iva})$$

The values of Skene's coefficient C range from:

(a) 180 to 185 for high-speed runabouts
(b) 190 to 205 for multiple-step or shingled hydroplanes
(c) 210 for single-step hydroplanes of good design
(d) 220 for small sea sleds to 270 for the largest and most efficient sleds
(e) 240 to 250 for small, three-point hydroplanes ["Elements of Yacht Design," New York, 1944, p. 222].

A value of $C = 185$ appears appropriate for the ABC tender.

Five of the methods listed give first approximations to the shaft power as follows, based upon an estimated weight, at this stage, of 19,000 lb or 8.482 tons, a speed of 24 kt, a waterline length L_{WL} of 35 ft, a T_q of 4.056, and an F_n of 1.208:

I. Method of K. C. Barnaby, Table 77.d. With a boat of the V-chine, stepless type, 35 ft long, and $V/\sqrt{L} = 4.056$, K_1 is 3.4. Then

$$P_B = \Delta\,\frac{V^2}{K_1^2} = 8.482\,\frac{(24)^2}{(3.4)^2} = 422.6 \text{ horses.}$$

II. Method of P. Du Cane, Fig. 77.E. The ratio of (W in lb)/(P_B in horses) is estimated conservatively at 43. Then

$$P_B = (W \text{ in lb})/43 = 19{,}000/43 = 442 \text{ horses.}$$

III. Method of Crouch-Werback, where C is taken as 72 from Fig. 77.F, and Eq. (77.iia) is

$$P_S\,(\text{horses}) = \frac{W\,(\text{lb})\;V^2\,(\text{kt})}{C^2\sqrt{L_{WL}\,(\text{ft})}}$$

$$= \frac{19{,}000(24)^2}{(72)^2\sqrt{35}} = 356.9.$$

From this the brake power P_B is estimated as 356.9/0.95 or 375.7 horses.

TABLE 77.e—VALUES OF THE PHILLIPS-BIRT POWERING COEFFICIENT K_2 IN EQUATION (77.iii)

The values set down here are taken from a table published by D. Phillips-Birt [The Motor Boat and Yachting, Jan 1954, p. 29].

	Length of boat, ft						
	16	20	25	30	40	50	60
Very efficient planing forms with small rise of floor	2.8	3.0	3.25	3.48	3.95	4.40	4.90
Good modern (1954) V-bottom boats	2.5	2.65	2.90	3.15	3.60	4.10	4.55
Old-fashioned, narrow, V-bottom boats	2.35	2.55	2.75	3.00	3.50	3.95	4.40
Round-bilge boats	2.10	2.33	2.45	2.60	3.00	3.40	3.80

IV. Method of D. Phillips-Birt, Eq. (77.iiia), where K_2 from Table 77.e is 3.38. Then

$$P_B \text{ (horses)} = \frac{V^2 \text{ (kt) } W \text{ (long tons)}}{K_2^2}$$

$$= \frac{(24)^2(8.482)}{(3.38)^2} = 427.7.$$

V. Method of N. L. Skene, where $C = 185$ and Eq. (77.iva) is

$$P_B \text{ (horses)} = \frac{W \text{ (lb) } V^2 \text{ (mph)}}{C^2}$$

$$= \frac{19{,}000(27.6)^2}{(185)^2} = 422.9.$$

The results from three of the four methods are surprisingly consistent, considering that only the speed, weight, and waterline length enter as variables. They indicate a brake power of about 430 horses, for which two HN–10 diesel engines with large injectors appear ample. They should be able to deliver, at full throttle, a total of 2 times 225 or 450 horses at rated brake power.

A more accurate power estimate, at a later stage in the design, is described in Sec. 77.26.

As a check on the foregoing one may use the dimensional formula of F. L. Marran and H. R. Shaw, derived from an analysis of full-scale data on many motor-driven small craft ["Motor Boat Powering," The Rudder, Jun 1950, pp. 16–17, 48]

$$V = \frac{242.5}{\left[\dfrac{W}{P_B}\right]^{0.699}} + M_L \qquad (77.\text{v})$$

Here V is the predicted speed in kt, W is the scale weight of the boat in lb, P_B is the total rated brake power of all engines, and M_L is a length correction factor, for which the authors give a table and a graph in the reference cited. For the ABC full-planing tender, where W is 19,000 lb, P_B is 430 horses, and M_L for a 35-ft length is 7.10,

$$V = \frac{242.5}{\left(\dfrac{19{,}000}{430}\right)^{0.699}} + 7.1 = 24.2 \text{ kt}.$$

The agreement, for this 24-kt design at least, is remarkably good.

77.15 Selecting the Hull Features; Section Shapes. Whether the 24-kt speed can be achieved with the engines selected is principally a matter of keeping the total weight within the limit of 19,000 lb. To be sure, the form of the hull chosen for the planing craft under design has an appreciable effect upon its performance, especially as to dryness, controllability, and behavior in waves, but the overall weight still remains the controlling factor in its smooth-water speed. This weight can not be estimated more closely until the hull is shaped, the lines drawn, structural features determined, and arrangement drawings prepared.

Considering first the type of section to be used, there are four basic forebody or entrance types, diagrammed in Fig. 77.G. The concave section at 2, with a relatively low chine and small rise of floor, gives excellent smooth-water performance. The wetted area at planing speed is usually a minimum because the water is thrown abruptly off the chine with little or no wetting of the sides. Craft with these sections usually run at a favorable trim with a desirable shape of planing surface presented to the water. The result is a form with minimum smooth-water resistance, having high speeds at low powers and full planing behavior at low speed-length quotients. However, the concave lower sections are unsuitable for wavegoing. In

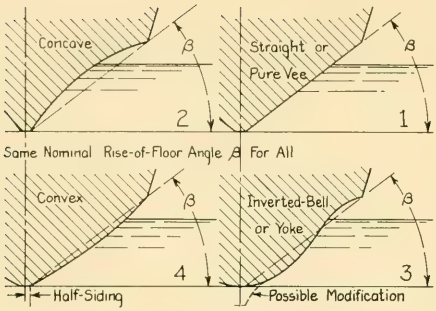

FIG. 77.G FOUR TYPES OF TYPICAL FOREBODY SECTIONS FOR PLANING CRAFT

rough water there is heavy pounding and slamming, accompanied by either a reduction in speed or a risk of damage to the boat and injury to the personnel.

Better performance in rough water is obtained by raising the chine forward and increasing the rise of floor but this change increases the resistance and involves a sacrifice of smooth-water speed. Running into a wind, the concave forward section keeps the boat dry because the water is thrown to the side with little spray and disturbance. In heavy weather, entrance sections which are fine as well as concave result in heavy pitching. They give little reserve buoyancy and they are still subject to pounding and slamming.

Boats with convex sections, sketched at 4 in Fig. 77.G, and of a type to be found in developable bottoms, have higher smooth-water resistances than those with concave sections. The water climbs up the side more easily and does not separate cleanly from the chine, resulting in greater wetted area. This type of section is much better for wavegoing because, like the round-bottom form, it presents a constantly decreasing flare to the oncoming (and upcoming) water as the bow pitches down. Pounding and slamming are reduced considerably or avoided altogether. The convex section builds up reserve buoyancy and acts to ease the pitching motion. As might be expected, boats with convex sections will not plane as rapidly or as readily as those with concave sections.

Convex sections throw considerably more spray and make the boat wetter in a wind. The fitting of spray strips, described in Sec. 77.20, largely overcomes these disadvantages. Convex sections forward give more internal volume than concave sections. This is often an important design consideration.

Straight entrance sections, depicted at 1 in Fig. 77.F, have many of the disadvantages of both the concave and convex types with few of their advantages. Straight segments are often used in sections near the stern where the rise of floor is a minimum and there is little difference between the various section types. In regions of high rise-of-floor angle, they are used only for ease of construction.

The yoke or inverted-bell section, drawn at 3 in the figure, offers a good compromise. It gives the excellent wavegoing performance of the round-bottom entrance but retains the sharp angle at the chine to throw the water off cleanly, thus holding down the wetted area. It provides adequate reserve buoyancy, an ample rise of floor, and a constantly diminishing flare with vertical distance above the base, to prevent slamming and pounding. By using a high chine forward, the entrance sections are kept fine enough to avoid too great a hook at the chine corner where water could be trapped in a slam. The rounded portion near the centerline acts to deflect the water under the bottom and give reasonably quick planing with good flow lines. Bell-shaped sections produce less spray than the pure convex type. They have the disadvantage that they are more difficult to construct, they involve slightly higher building costs, and they can not be worked into developable surfaces. They have slightly greater resistance in smooth water than the low-chine concave sections, due to the greater wetted surface, but probably less resistance than pure convex sections.

77.16 Rise-of-Floor Magnitude and Variation. The rise of floor or deadrise, expressed as a section-slope angle β(beta), is an important characteristic of a planing boat. In fact, its choice influences many other features of the underwater and above-water hulls. From pure planing and dynamic-lift considerations the smaller the rise-of-floor angle the better; in other words, the barn-door type of inclined flat surface is the best load-carrying device. As the rise-of-floor angle of the bottom increases, the resistance increases and the dynamic lift diminishes.

In the case of racing motorboats of the stepless type, having a continuous bottom terminating in the transom edge, this bottom is often made practically flat. At other times it has a shape approximating that of an inverted deck with a

small camber. Excessive slamming and pounding in waves are accepted in the effort to reach the ultimate in speed. At Froude numbers of 4.5 or 4.8, Taylor quotients of 15 or 16, the minimum pressure and friction drag are achieved with the minimum of bottom surface in contact with the water. The spray, like the pounding, is taken for granted as an unavoidable characteristic of ultra-high-speed performance. If the craft jumps completely out of water because of impact with the crests of waves, this too is accepted providing the stabilizing fin, the lower blades of the propeller, and the rudder can be kept reasonably well in the water.

Obviously, a planing boat with a flat bottom does not make a satisfactory boat for all-around service. High rise of floor is necessary forward for wavegoing and for low resistance at speeds below planing. Some rise-of-floor angle is necessary in the bottom aft to provide dynamic stability of route and proper steering qualities, although the angle required at the extreme stern is small. Thus most planing boats are built with what is known as a twisted or warped bottom, with a decreasing rise-of-floor angle from forward aft. D. Phillips-Birt gives the following typical values for these angles:

Amidships, 14 to 18 deg, flattening along the run to 2.5 to 4 deg at the stern [The Motor Boat and Yachting, Jan 1954, p. 28; "Motor Yacht and Boat Design," London, 1953, p. 148].

G. A. Guins states, in the paper listed as reference (16) of Sec. 77.41, that the minimum rise-of-floor angle found necessary for satisfactory longitudinal stability is 7 deg, together with a long tapering skeg.

Some planing boats are built with an untwisted bottom, embodying a constant rise-of-floor angle from amidships to the stern. Compared to the warped bottom, the constant-slope bottom usually gives less rise of floor amidships and more at the stern. The untwisted bottom has the lower smooth-water resistance of the two, but its use may lead easily to other unfavorable characteristics such as poor location of the center of buoyancy or bad steering qualities. Most small-boat designers seem to find it easier to obtain good planing-boat performance with the twisted bottom than with the constant-slope type.

77.17 Chine Shape, Proportions, and Dimensions. Inasmuch as the sensibly flat bottom of a planing craft, within the boundaries of the chine, produces practically all the dynamic lift, there are valid hydrodynamic reasons for devoting to the chine the attention it has received since the early 1950's at the hands of E. P. Clement ["The Analysis of Stepless Planing Hulls," SNAME, Ches. Sect., 3 May 1951; "Hull Form of Stepless Planing Boats," SNAME, Ches. Sect., 12 Jan 1955]. In his 1955 paper Clement approaches the planing-boat design problem by using the chine length L_C, the chine beam B_C, the chine projected area A_C, the chine planform shape, and certain loading factors on the chine area as the fundamental design parameters. However, the lack of comprehensive and reliable full-scale performance data renders this scheme something less than adequate at the present time (1956). For convenience, Clement has embodied the data of the referenced 1951 and 1955 reports in a new report entitled "Analyzing the Stepless Planing Boat" [TMB Rep. 1093, Nov 1956].

Nevertheless, the maximum chine beam $B_{C(\mathrm{Max})}$ serves as an excellent starting point for determining the proper transverse dimensions of a planing craft. Good design graphs of what appears to be a maximum chine beam on a basis of waterline length, although the author does not mention either of them specifically, are given by D. Phillips-Birt ["Motor Yacht and Boat Design," London, 1953, Fig. 51, p. 147]. The graphs of Fig. 77.H are adapted from curves 1 and 2 of the reference cited. Ratios of $L_{WL}/B_{C(\mathrm{Max})}$ between 3 and 4 are typical of modern planing craft. In fact, many of the smaller boats, 20 to 25 ft in length, have ratios less than 3. For the ABC tender of 35-ft waterline length a maximum beam at the chine of about 10 ft is indicated. The fore-and-aft position of the point of maximum chine beam should lie in the range of 0.55 to $0.65L_{WL}$ abaft the FP.

If good planing is desired the chine beam is kept full to the stern, with a value at the transom ranging from 0.80 to 0.90 of $B_{C(\mathrm{Max})}$. A wide stern is also beneficial to steering when planing. However, in rough weather, especially in a following sea, too wide a stern may cause broaching or sudden sheering from one side to the other. This condition is aggravated if the craft is running below planing speed. To improve wavegoing behavior and steering under these conditions, it is advisable to tuck in the sides at the stern to say 0.65 to 0.75 of the maximum beam at the chine. Acceptable chine planforms, at least for larger planing craft, are shown by E. P. Clement ["Hull Form of Stepless Planing Craft," SNAME, Ches.

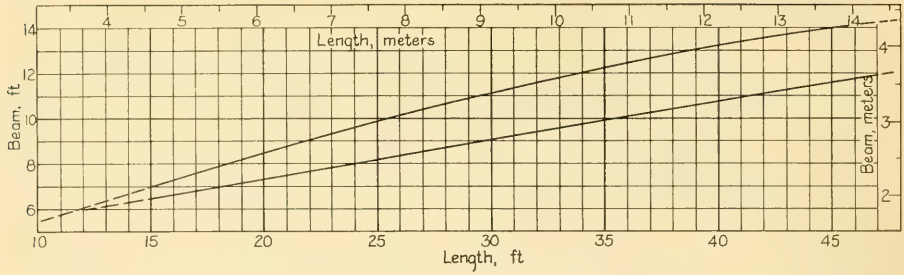

The Upper Curve Represents Good Practice for Planing Craft as of 1953. The Lower Curve is for High-Speed Planing Hulls [Phillips-Birt, D., "Motor Yacht and Boat Design," Coles, London, 1953, p. 147]

FIG. 77.H RELATIONSHIP OF LENGTH TO BEAM FOR PLANING CRAFT IN GENERAL AND HIGH-SPEED PLANING HULLS IN PARTICULAR

Sect., 12 Jan 1955, Pl. 5]. Two other chine planforms are shown in SNAME RD sheets 116 and 147.

The shape and position of the chine line in elevation (as projected on the centerplane) have a certain influence upon the shape which can be or is given to the transverse sections. Conversely, the shape given to the sections has a large effect upon the curvature and position of the chine, with respect to the at-rest waterplane. Little information is available in the literature, at least so far as actual or optimum characteristics are concerned, relative to the height of the chine above or below the designed waterline, its shape and curvature, the amount of chine exposed when the vessel is at rest, and so on. To correct this situation in some degree the graph of Fig. 77.I shows the position in profile of the chine line for some representative planing craft. The chine-line elevations are laid down on a constant length of at-rest waterline, divided into 10 equal station spaces, numbered from forward aft. The height of the chine above or below the designed waterline is given in per cent of the L_{WL} .

The following comments are furnished concerning the behavior of the boats represented in the diagram:

A. Luders 18-ft tender. A very satisfactory little craft. When planing it rides high on its extreme after end, with its forefoot out of water. A cross breeze acts to blow the bow off course, making it necessary to meet the puffs with the helm. With such a high chine forward the volume abreast it is considerably reduced. Large weights must be concentrated aft. This produces a planing hull which rides high but it reduces the pay-load capacity. It is suitable principally for small boats.

B. Huckins 33-ft pleasure cruiser. These hulls have consistently run at high speeds. They have excellent planing qualities and are safe in heavy weather.

C. U. S. Coast Guard 40-ft utility boat. This craft has good rough-water behavior but is somewhat wetter amidships than a similar boat with a round bottom.

D. Motor torpedoboat, L_{WL} = 66.5 ft. This craft has low resistance and excellent performance in smooth water but it pounds very heavily in rough water.

E. EMB Series 50 parent form. This was designed many years ago and is not a particularly good planing hull. It pounds in rough water.

F. U.S.S. *PT 8*. A good performer in rough water but has high quiet-water resistance. Undoubtedly its form could be improved by better section shapes.

G. German S-boat of World War II; chine elevation not shown in Fig. 77.I. The V-bottom design of these craft was 112 ft long on the at-rest waterline and at 42 kt the T_q was 3.97. The chine crossed the DWL at Sta. 2.58. Its elevation at the FP, Sta. O, was $+0.0375L_{WL}$; at the AP, Sta. 10, it was $-0.017L_{WL}$ [U. S. Naval Technical Mission in Europe Rep. 338–45 of Aug 1945 (copy in TMB library)].

From the foregoing it appears that the planing boats with records of good performance, especially in rough water, have relatively high chines forward. This of course means that the forward sections can be and are made finer, with large rise-of-floor angles. Considering these factors and

other hydrodynamic reasons, the following general design rules are given, based on a 10-station waterline length and the craft at rest at the designed load and trim:

(1) The chine height at Sta.0, above the designed waterline at rest, should be at least $0.06L_{WL}$. If the design is for a small pleasure boat the chine can be higher, up to $0.13L_{WL}$ above the designed waterline, because the pay load is small and the lost internal volume is relatively unimportant. If it so happens that pay-load capacity is important then a low chine height may be necessary to get additional internal volume, at a sacrifice of rough-water performance.

(2) Large boats can operate satisfactorily with less chine height forward than can small boats, because the small, steep waves usually encountered have less influence on the rough-water performance of the larger craft

(3) The chine should lie above the at-rest waterline from Sta. 0 at the FP to a point somewhere between Sta. 3 and Sta. 5

(4) The chine line should be straight from Sta. 6 or 7 to the stern. There should be no concave curvature in this region.

(5) The chine line from Sta. 6 or 7 to the stern should be parallel to or have only a slight slope upward and forward with respect to the at-rest waterline. Large slopes are to be avoided.

(6) The chine depth at Sta. 10 should be about $0.010L_{WL}$ to $0.030L_{WL}$ below the designed waterline

(7) If the boat is intended for smooth-water operation only, a lower chine height forward can be used. Indeed, if smooth-water speed is important, a lower chine height is desirable in that region.

(8) Spray strips of the general form shown in Fig. 30.A should be fitted along the chine, especially at the forward sections and preferably along the entire length. This matter is discussed more fully in Sec. 77.20.

77.18 Buttock Shapes; The Mean Buttock. The buttock shapes in the bottom of a planing craft are so important that some repetition is justified in emphasizing them. With the straight floor segments customary in V-bottom planing

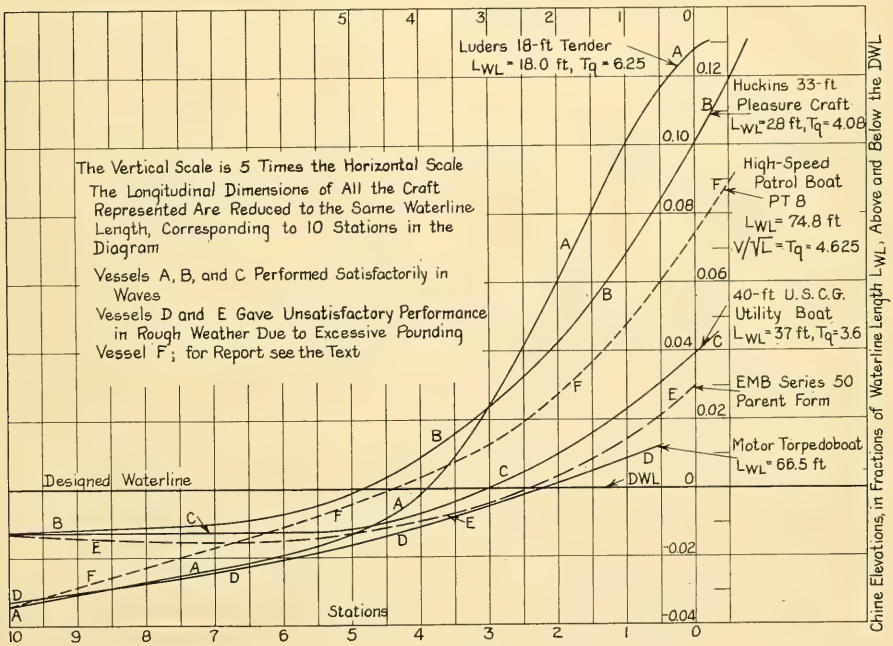

FIG. 77.I DIMENSIONLESS CHINE-ELEVATION DIAGRAMS FOR SIX TYPES AND SIZES OF PLANING CRAFT

boats the fore-and-aft shapes of the buttocks are largely determined by the shape of the chine, when projected on the centerplane. This is true particularly in the afterbody.

The shape and position of the buttock at about one-quarter beam on each side of the centerline, often called the *mean buttock*, is used by some as one of the characteristic parameters of a planing craft [Clement, E. P., "Hull Form of Stepless Planing Craft," SNAME, Ches. Sect., 12 Jan 1955, pp. 2–3].

Straight buttocks in the wetted region, where the dynamic pressures are generated, reduce or avoid negative differential pressures under the afterbody. These in turn act to prevent bottom suction and excessive trim by the stern.

The effect of concavity in the buttocks under the afterbody, reckoned with reference to the water underneath, is described in the section following.

Convex buttock lines under the afterbody act to develop $-\Delta p$'s, but the convexity is sometimes unavoidable. Successful planing boats have been and can be designed with slightly convex buttock lines in the run, but they require careful attention to other features of the design, such as the center-of-gravity location, because of the negative lift generated under the bottom.

It is mentioned previously in item (4) of Sec. 77.17, it is to be discussed in item (1) of Sec. 77.19, and the designer is cautioned here that slight downward hooks in the buttocks near the stern are to be used with caution. They often produce erratic and sometimes even dangerous performance.

77.19 Trim Angle and Center-of-Gravity Position; Use of Trim-Control Devices. Theoretical and practical considerations relating to the running trim of a planing craft are rather thoroughly discussed by A. B. Murray [SNAME, 1950, pp. 658–692]. It is customary, in analytic and design work, to express the trim in degrees; this is the form employed in the present chapter. It would be preferable, if the full-scale data for it could be readily derived, to express the trim as a linear distance over the boat length, as is done for large vessels. Measuring the sinkage or rise at the bow and stern would give the naval architect a direct measure of the amount by which the center of gravity shifts its vertical position.

For most planing boats, the ideal planing angle for least smooth-water resistance lies between 4 to 6 deg by the stern. This much trim often results in discomfort to passengers and an unattractive appearance when viewed from outside the boat. It may actually interfere with the steersman's vision from the control station. Moreover, the possibility of porpoising is greater with the larger trim angles. As a practical compromise the running-trim angle of a planing craft is usually kept below 2 or 3 deg; the greater resistance and lower speed inherent in this lesser trim are accepted. Limiting the trim to these small angles requires that the center-of-gravity position be farther forward than would otherwise be the case. This in turn acts to prevent porpoising.

There are many advantages in level running aside from those just mentioned, when the force and moment to achieve the smaller trim angle are applied by a trim-control device external to the planing under surface of the hull proper. The slope drag—called by some the induced drag, and illustrated in Fig. 53.A—is diminished, the load-carrying ability of the boat is greatly increased, and it usually behaves better in waves. Trim-control devices to accomplish this are discussed in Secs. 30.11 and 37.24 but the principal kinds are listed here for the convenience of the designer:

(1) A wedge or "shingle" applied to the under side of the bottom at its extreme after end, or a controllable flap hinged to the bottom in such manner that it forms a downward "hook" of variable angle at the extreme after ends of the buttocks terminating on it. The thickness of such a wedge, and the angle it makes with the bottom on the full-scale boat, still require to be determined by cut-and-try methods. The wedge must be applied with caution because too much wedge action and vertical lift at the extreme stern are liable to have a disastrous effect upon the steering, especially in a following sea.

(2) The controllable flap, with its variable "hook" angle, probably requires for best performance something better than a simple mechanical device which holds it rigidly in any selected position. A yielding device, loaded with a gas or with liquid, similar to the Plum stabilizer mentioned in (3) following, should improve the performance of both the boat and the trim-control device when in waves.

(3) The Plum stabilizer, whose action is explained briefly in Sec. 37.24. This was developed and described many years ago [Motor Boating, Mar 1928, pp. 16–17, 54, 134] and has benefited by a

great amount of development by the inventor, John Plum, in the period 1945–1955. From the first, however, it produced amazing increases in the capabilities of a planing craft as compared with boat performance without trim control.

(4) Surface propellers, such as those fitted to sea sleds, and propellers on ultra-high-speed racing motorboats which become surface propellers at high speed, exert an upward lift at the disc position which acts as a trim-control device. In fact, some planing craft with surface propellers are not able to get through the hump speed and to plane without their help.

(5) It is possible that some form of auxiliary subsurface hydrofoil may be found useful in the future for trim control but no practical device of this kind is as yet developed.

Because of its rather specialized nature, no trim-control device is considered for the ABC planing-form tender, and it is not discussed further here.

Lacking the trimming effect of a trim-control device, of surface propellers, or of an auxiliary hydrofoil, and neglecting for the moment the effect of buoyancy, it is apparent that the fore-and-aft position of the center of gravity CG of a full-planing craft must lie close to the center of pressure CP of the dynamic lift on the wetted area of the bottom. There is no direct, practical method now available (1955) for determining this CP position on an actual boat. It must be estimated, therefore, with reference to some part of the planform, on a basis of experimental data from models. The chine planform, projected on the baseplane, is the logical element to use, and the center of area of this element is the logical reference point in it. Unfortunately, the chine area has not been in use long enough, or to a sufficient extent among planing-craft designers, to build up a fund of reference data indicating optimum relative fore-and-aft positions of the center of the chine area and of the CG. E. P. Clement gives some performance data for several types of motorboats with the CG abaft the center of chine area A_C by from 2.1 to 11.1 per cent of the chine length L_C ["Hull Form of Stepless Planing Boats," SNAME, Ches. Sect., 12 Jan 1955, Pls. 6–8, 10]. On Plate 9 of the reference Clement gives a plot of CG positions expressed in the manner described, related to the ratio $A_C/\nabla^{2/3}$, based on data from half a dozen models of large planing boats.

In the absence of more extensive chine data it has been customary to indicate the fore-and-aft CG position as a fraction of the WL length from Sta. 0 at the waterline beginning or from the extreme stern. The chine planforms of all single-step planing craft terminate at the transom, and the chine planforms approximate a shape that is rather well standardized. Referring the CG to the at-rest WL termination is therefore a reasonable engineering procedure.

The $\overline{\text{LCG}}$ values for the two test conditions reported by Clement on Plate 6 of the reference cited are $0.537L_{WL}$ and $0.567L_{WL}$, respectively. C. W. Spooner, Jr., in reference (26) of Sec. 77.41, states that the value of $\overline{\text{LCB}}$ (and presumably also of $\overline{\text{LCG}}$) varies from about $0.53L_{WL}$ at a T_q of 1.5 to $0.58L_{WL}$ at or above a T_q of 3.0. He reports that successful high-speed designs have had the CB as far aft as $0.68L_{WL}$, with engines in the stern and V-drives to the propellers.

Moving the CG forward reduces the running trim and lessens the risk of porpoising but at the expense of increase in wetted length and wetted area. The effect on the total resistance depends upon the variation of friction and pressure resistance with trim angle, indicated by graphs similar to those in Fig. 77.O of Sec. 77.26. At low trims the total resistance usually increases but this is not to be taken for granted by any means, as witness the beneficial effect of trim-control devices.

77.20 Spray Strips. The form, position, and function of spray strips are well described and generously illustrated by R. Ashton [ETT Tech. Memo 99, Feb 1949]. These devices, probably first employed on multi-engine seaplanes and flying boats to keep spray out of the offset propellers, are excellent illustrations of the more-or-less major hydrodynamic effects produced by minor, if not almost insignificant physical features.

Spray strips are most important along the forward portion of the boat. However, it is usually beneficial to fit them for the full length. They can be used to advantage on all hulls, round-bottom as well as V-bottom with chine, except perhaps for forms with concave sections and low chines which have extremely sharp chine corners. On certain round-bottom craft they can also be used as fender strakes.

Spray strips usually result in a slight increase in resistance at low and cruising speeds. However, their many beneficial effects outweigh this slight disadvantage. They:

(a) Decrease resistance at planing speeds
(b) Deflect spray roots and random water sharply off the sides
(c) Reduce spray throwing
(d) Provide a positive lift in the forward part of the boat which helps counteract any diving moment
(e) Reduce, in round-bottom boats, the large bow wave which at full speed sometimes climbs high up the side toward the deck edge. The spray root and spray accompanying this wave can be troublesome at times.

FIG. 77.Ja MODEL OF LARGE V-BOTTOM CRAFT RUNNING WITHOUT SPRAY STRIPS

The displacement-length quotient $\Delta/(0.010L)^3$ for this hull is 80. It is being towed here at a T_q of 3.5. The spray root climbs up the side and the spray rises higher than the deck.

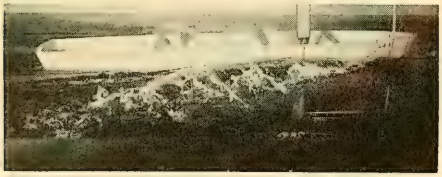

FIG. 77.Jb MODEL OF FIG. 77.Ja RUNNING WITH SPRAY STRIPS

The spray roots and the spray are thrown to either side, well clear of the hull. The speed-length quotient T_q is the same as for Fig. 77.Ja but the bow is lifted slightly higher.

The photographs, Figs. 77.Ja and 77.Jb, reproduced from the Ashton report referenced at the beginning of this section by the permission of the Experimental Towing Tank, Stevens Institute of Technology, offer an excellent pictorial means of comparing spray formation on a planing-hull model, with and without spray strips. There are many other pairs of photographs in the Ashton report which give similar comparisons for both models and full-scale motorboats, and which show the beneficial effect of the spray strips.

The Appendix to the referenced ETT report by R. Ashton contains design comments from three "highly capable and well-known designers," supplemented by design sketches on page 27. Fortunately for the designer, spray strips are in the nature of appendages which can be adjusted in form and position to produce the best effect without either major or minor changes in the hull.

77.21 Stem Shape. Up to a speed-length quotient T_q of 2.0, F_n of 0.60, the stem of a displacement or semi-planing type of boat should be nearly plumb. This takes advantage of all the waterline length possible, without increasing the hull weight to provide an overhang. For a higher T_q and F_n , the forefoot should be cut away, starting above the waterline, to get the bow wave under the boat as much as possible and to lessen sheering in a seaway [Spooner, C. W., Jr., "Speed and Power of Motorboats," unpublished manuscript dated Oct 1950 (in TMB library)].

For pleasure craft of all three types discussed in this chapter the matter of appearance is not to be overlooked. There is some objection, from this standpoint, to a stem which rakes downward and forward under any trim or running condition. To prevent this, the stem must have a rake downward and aft, when at rest, of at least 6 deg, and possibly as much as 7 or 8 deg.

77.22 Deep Keel and Skeg; Other Appendages. Most motorboats carry a centerline keel that is rather deep, compared to the flatness of the bottom. This keel terminates aft in a skeg through which passes the shaft tube and shaft for an engine and propeller that happen to be located on the centerline. Examples are the small planing motorboat of Fig. 30.A and the larger round-bottom utility boat of Sec. 77.33 and Fig. 77.T. Besides acting as a support and fairing for the centerline shaft the skeg serves as a deep vertical fin which gives the boat dynamic stability of route and facilitates steering by serving as a sort of fulcrum about which the rudder moment is applied. For high-speed racing motorboats this skeg is reduced to a small, thin metal fin, generally forward of midlength, which also serves as a fulcrum about which the swinging moment exerted by the rudder is applied.

There are no known rules for positioning and shaping this skeg, unless it is desired to have it extend far enough below the keel to serve as mechanical protection ahead of the propeller. Many such skegs are included on published drawings of motorboats but a designer consulting these drawings rarely knows whether the skegs shown in them are good or otherwise.

Rudders for motorboats are discussed in Sec. 74.11. Comments upon the fairing of external pads for the attachment of strut arms to wooden motorboat hulls are given in Sec. 75.6.

77.23 Interdependence of Hull-Design Features. The principal hull-design features of a planing craft are much more dependent upon each other than are those of a displacement-type vessel, just as the latter are much more intimately tied together than are the corresponding features of an airplane. For a planing craft the beam, the chine height, the rise of floor, and the type of sections are all related and must go hand in hand in fashioning the boat.

A proper design procedure involves selecting the desirable features pertaining to each individual parameter, and then working out a compromise to produce the nearest approach to the desired overall performance that can be estimated during the preliminary design. Often several different types of section may be used to advantage along the length of a boat. Yoke sections forward easily transform into convex or straight sections aft. Concave sections are often employed forward to obtain good planing characteristics, transforming into convex sections amidships and aft where space is needed for the machinery plant and for tanks to carry liquids. Convex forward sections lend themselves to an easy transformation to straight sections where the rise of floor is small.

Still greater compromises are made when selecting features favorable to both seakindliness and planing. In many boats the seakindly round-hull form is used in the entrance, transforming into the hard-chine efficient planing hull in the run. The reverse of this is sometimes encountered, but there appears to be no advantage in such an arrangement [Phillips-Birt, D., The Motor Boat and Yachting, Jan 1954, p. 27].

77.24 Layout of the Lines for the ABC Planing-Type Tender. With the comments of the preceding sections as a background the designer is now ready to lay down a tentative set of lines. He must anticipate that this set may be only the first of a half dozen or more, in his search for a shape that best meets the design requirements. For this reason it is well to start with a scale just large enough to permit measuring lengths, areas, angles, and slopes with reasonable accuracy.

The first line to draw is a waterline for the profile and the bow and stern elevations. The designer is advised to work to this waterline as a sort of fixed reference plane, the same as for a larger ship. Even though, as described presently, it may be necessary later on to change slightly the water-surface level on the hull to effect a balance between weight and buoyancy rather than to draw a new set of lines, the original waterline (or waterplane) serves a definite purpose in establishing dimensions, proportions, and parameters while the size and shape of the hull are being worked out.

Using the planing-type ABC tender as an example, it is assumed as a starter that all the requirements can be met on a WL length of 35 ft. A horizontal waterline of this dimension is drawn to a convenient scale, with Sta. 0 at the FP or waterline beginning and Sta. 10 at the AP or waterline ending. The latter is also the transom position on the centerline. The shape of the hull is to be based, but only generally at this stage, upon the arrangement sketch of Fig. 77.B.

The next step is to fix the shape of the chine and to position it vertically with respect to the DWL. A tentative chine line is drawn according to the rules previously discussed:

(a) Chine height at the FP. Because of the good wavegoing performance desired the chine height at the FP is made greater than the value of $0.06L_{WL}$ previously mentioned in item (1) of Sec. 77.17. This allows finer sections forward with less probability of slamming and pounding. A chine height of $0.073L_{WL}$ appears adequate.
(b) Chine height at the AP. A tentative value is $-0.021L_{WL}$.
(c) Straight chine line from Sta. 7 aft, for the aftermost 0.3 of the length
(d) Chine, as projected on the centerplane, crosses the DWL between Stas. 4 and 5.

The plan view of the chine is then laid out on the basis of the preliminary arrangement sketch of Fig. 77.B. As a rule, the maximum chine beam should lie within the range of 0.55 to $0.65L_{WL}$ abaft the FP. For the ABC tender it is placed at Sta. 6, or at $0.60L_{WL}$ abaft the FP. The maximum chine beam is tentatively selected as 10 ft, which gives a ratio L_{WL}/B_C of 3.5. This is typical for a modern high-speed planing craft, for which the ratio L_{WL}/B_C varies from 3.0 to 3.6. The beam at the transom ending is made about 0.9 the maximum beam, or 9 ft. Subsequent fairing of the lines and working over the design produces a $B_{C(\mathrm{Max})}$ of 10.04 ft and a chine beam at the transom of 8.96 ft.

In this design a wide stern is chosen because

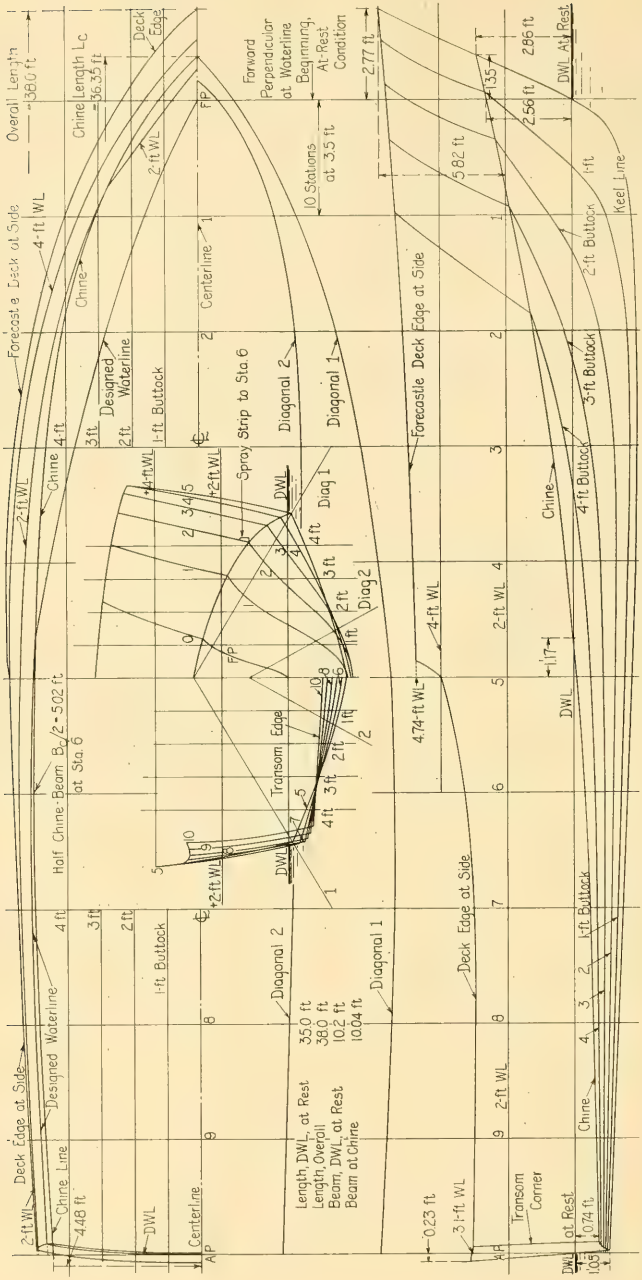

Fig. 77.K Lines Drawing for Planing-Type ABC Tender

the boat will operate most of the time in sheltered harbors or rivers. In addition, it improves the steering when planing.

A tentative keel line is next drawn in the elevation. It is so placed with reference to the chine as to give a rise-of-floor angle amidships in the range of 14 to 18 deg. At the stern the range is from 1 to 4 deg. If constant rise-of-floor angle aft is desired, with no twist in the afterbody bottom, the angle may be of the order of 6 to 9 deg. The lines of two motorboats of good performance published by L. Lord ["Naval Architecture of Planing Hulls," 1946], in Fig. 41 on page 89 and Fig. 43 on page 92, have constant rise-of-floor angles of 5.8 deg and 9.2 deg, respectively. Those of one planing boat whose lines are published by D. D. Beach [The Rudder, Jan 1954, p. 38] average about 8.3 deg.

The sections are next sketched in. For the ABC tender, sections of inverted-bell shape are suitable forward, fairing into slightly convex sections in the run. As previously mentioned, these sections give volume forward but still allow the water and spray to break off cleanly at the chine. They will probably result in slightly greater resistance in smooth water, but should give improved wavegoing performance. Sections with slightly convex bottom segments are favored aft, as they provide more hull volume and allow lower mounting of the engines.

When the sections are sketched in, a tentative check is made of the volume of the hull up to the designed waterline at rest. When this was first done for the ABC tender the volume was found to be smaller than that corresponding to a weight of 19,000 lb of salt water. It would have been necessary to increase the draft about 0.5 ft to support the estimated boat weight. This was unacceptable as it lowered the chine too far and it altered the wavegoing characteristics intended for the forward sections.

Increasing the volume required the following changes:

(1) The chine submergence at the AP was increased to $0.0275L_{WL}$ or 0.962 ft . The revised chine crossed the DWL between Sta. 3 and Sta. 4. It was still a straight line from Sta. 7 to the stern at Sta. 10.

(2) The depth of the keel below the DWL was increased slightly

(3) The chine forward remained at the same position with respect to the DWL.

The net effect was to decrease the rise-of-floor angles in the run of the boat. Every effort was made to keep the buttock lines straight in the run, especially abaft Sta. 7.

The sections were then redrawn with the same general characteristics, and the new hull volume was calculated. The volume below the DWL was found to be slightly more than needed, but a uniform decrease in draft of about 0.21 ft along the whole length gave the correct volume. A lifting of the whole boat in this manner is usually found acceptable, because all the changes in the hull characteristics are favorable. The revised chine height at the FP is $+0.0731L_{WL}$ and at the AP it is $-0.0211L_{WL}$. The relocated chine crosses the new designed waterline between Stas. 4 and 5.

Next, the fore-and-aft position of the center of buoyancy CB is determined, and a check is made with available data such as those presented at the end of Sec. 77.19 to determine whether the CB lies within a range of CG position found acceptable for good planing-boat design. If the CB is not less than $0.55L_{WL}$ or more than $0.65L_{WL}$ from the FP, the CG can probably be placed within that range so that the craft will float at the draft and in the attitude desired when at rest. If the CB is as far forward as $0.45L_{WL}$ from the FP, or as far aft as $0.70L_{WL}$, the hull will have to be reshaped to correct this condition. The craft is liable to porpoise if the at-rest CB—and the CG—are too far aft.

After making the necessary shifts in the section and other lines, and checking the volumes and CG positions, the lines are faired and drawn, including the abovewater body to the main-deck edge. The final result for the ABC planing-form tender is shown in Fig. 77.K. The section-area or A/A_X curve is drawn in Fig. 77.L, in the usual 1:4 box. This is supplemented by the B/B_{WX} curve, drawn so that the half-beam $B_{WX}/2$ is equal to one-fourth the waterline length L_{WL} .

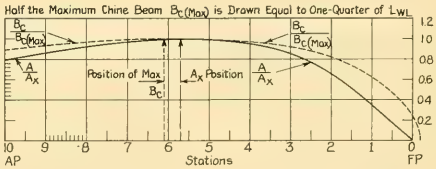

Fig. 77.L Dimensionless Waterline-Offset and Section-Area Curves for Planing Tender of ABC Ship

77.25 Design Check on a Basis of Chine Dimensions. Despite the logical nature of the procedure and the various design data given in Sec. 77.17, based upon the chine dimensions, proportions, and position, there are insufficient background and reference data to enable a new planing craft to be laid out on a basis solely of the chine dimensions and characteristics. It is nevertheless useful at this point to ascertain how the characteristics already determined for the ABC tender compare with the available chine data plotted by E. P. Clement ["Hull Form of Stepless Planing Boats," SNAME, Ches. Sect., 12 Jan 1955; also TMB Rep. 1093, Nov 1956].

There are listed in Table 77.f the principal dimensions and characteristics of the ABC planing-form tender, derived by the methods described in the sections preceding. Included in the table are some of the ratios used as parameters by Clement, based upon the actual dimensions of the craft whose lines are depicted in Fig. 77.K.

As a check of these dimensions and ratios with the data given by Clement in the reference cited, Figs. 77.M and 77.N have been adapted from his Plates 12 and 13, with necessary changes to standard notation. Using the tentative total weight of 19,000 lb for the full-planing tender, Fig. 77.M is entered along the bottom scale and a value of the ratio L_C/B_C of 3.86 is taken from the meanline shown. With a fore-and-aft chine length L_C of 36.35 ft from Table 77.f, the mean chine beam $B_C = 36.35/3.86 = 9.417$ ft.

With the L_C/B_C ratio of 3.86, Fig. 77.N is entered along the bottom scale and a ratio of $A_C/\forall^{2/3}$ of 0.3 is taken from the meanline. The value of $\forall^{2/3}$ from Table 77.f is 44.484 ft^2; A_C is found to be 413.7 ft^2. This is considerably larger than the projected area of the chine, 334.6 ft^2, of the actual boat of Fig. 77.K. If this larger value of A_C is divided by the actual chine length, the mean chine beam B_C is found to be 413.7/36.65 or 11.29 ft. If, on the other hand, this larger area is used in combination with the L_C/B_C ratio of 3.86, the fore-and-aft chine length comes out as 39.96 ft.

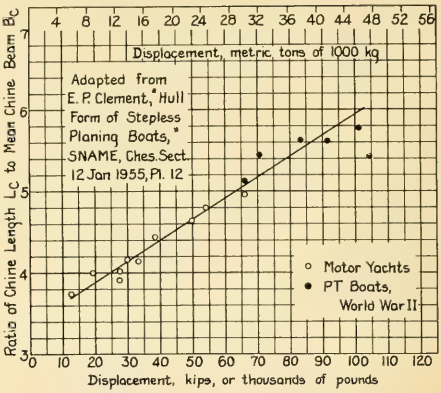

FIG. 77.M VARIATION OF CHINE RATIO L_C/B_C WITH DISPLACEMENT

The dimension L_C is the projected length of the chine and B_C is the mean width of the projected chine planform. The displacement corresponds to the buoyancy volume with the boat at rest. The solid line represents a tentative meanline for the data plotted here.

TABLE 77.f CHINE CHARACTERISTICS AND OTHER FEATURES OF PROPOSED FULL-PLANING TENDER FOR ABC SHIP

The principal dimensions, characteristics, and other data listed here are for the craft whose lines are shown in Fig. 77.K.

$L_{OA} = 38.0$ ft
$L_{WL} = 35.0$ ft
L_C of chine $= 36.35$ ft
$W = 19{,}000$ lb
$\Delta = 8.482$ long tons
$T_q = V/\sqrt{L} = 24/\sqrt{35}$
$= 4.057$
$\Delta/(0.010L)^3 = 197.8$

$\forall = 296.7$ ft^3 in standard salt water
$A_X = 10.56$ ft^2
$L_E = 0.57L_{WL}$, from FP to section of maximum area

A_W of at-rest waterline $= 281.9$ ft^2
A_C of chine, projected, $= 334.6$ ft^2
$\forall^{1/3} = 6.6696$ ft
$\forall^{2/3} = 44.484$ ft^2

Ratios Based upon the Chine Dimensions:
$A_C/\forall^{2/3} = 334.6/44.484 = 7.522$ $\qquad L_C/B_C = 36.35/9.205 = 3.949$
B_C mean, over chines, $= A_C/L_C = 334.6/36.35 = 9.205$ ft
Ratio of Weight W/(Brake Power P_B at designed speed) $= 19{,}000/430$(est.) $= 44.19$
Weight W/(Brake Power P_B) $= 19{,}000/450$ (to be installed) $= 42.22$
Center of projected area of chine, A_C, lies at $0.532L_{WL}$ abaft the FP
Rise of floor at midlength of $L_{WL} = 18.25$ deg; at AP $= 3.75$ deg
$\overline{\text{LCB}} = 0.594L_{WL}$ or 20.79 ft abaft the FP
$\overline{\text{LCG}}$ is assumed to be in the same fore-and-aft position, corresponding to 3.29 ft abaft midlength of the designed waterline or 14.21 ft forward of the AP.

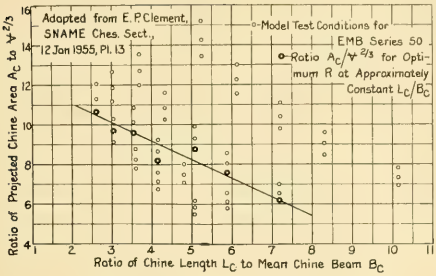

FIG. 77.N VARIATION OF CHINE-AREA RATIO $A_C/\nabla^{2/3}$ FOR OPTIMUM RESISTANCE, ON A BASE OF CHINE RATIO L_C/B_C

The solid line represents a combination of ratios indicating minimum resistance, based upon the available data. For the EMB Series 50 the LCG was at $0.011L_C$ abaft the center of area of the projected chine planform, at zero deg initial trim.

A moderately loaded utility-type planing boat about 40 ft long would, by reference to Fig. 77.C, probably weigh in the vicinity of 23,000 lb. This would involve a length greater than the proposed 35 ft to meet other optimum design conditions. An increase in the mean chine beam from the 9.205 ft of the actual craft to the 11.29 ft derived in the preceding paragraph would likewise involve a heavier boat. On the basis that a full-planing craft of modern design produces somewhat more dynamic lift for a given overall resistance than the planing forms of EMB Series 50, no attempt is made here to increase the chine area and the chine dimensions of the boat under design to correspond to the meanline values given by Clement's graphs of Fig. 77.M and 77.N.

77.26 Second Estimate of Shaft Power, Based Upon Effective Power. With a body plan of the 24-kt, full-planing type of ABC tender laid down and the principal dimensions and parameters selected, the next design step is to make a second estimate of the shaft power. The method employed here is that described by A. B. Murray ["The Hydrodynamics of Planing Hulls," SNAME, 1950, pp. 658–692], based upon the factors and relationships discussed in Secs. 53.2 through 53.7. It embodies a calculation of friction, residuary, and total resistance based upon flat-plate values of specific friction coefficient and upon wetted-surface and resistance data derived from experiments on model planing hulls and surfaces.

This will be recognized as one of the methods used for predicting the power of the ABC ship itself, in Chap. 66. Nevertheless, the indirect Froude procedure, when applied to the powering of motorboats, lacks an equivalent degree of reliability because of the unknown effect of the propulsion devices in changing the trim (and the resistance) and because data on propulsive coefficients η_P(eta) for motorboats are extremely scarce. Adequate apparatus and proved techniques for the self-propulsion of motorboat models are almost nonexistent, as are reliable data on the brake or shaft powers required to drive full-scale craft. To make the situation still more uncertain for the designer, little is known, in specific values, of the effect of the propulsion devices on the running trim of any particular boat. This change of trim when self-propelled, beneficial or otherwise, can change the resistance by a large percentage. Applying an estimated propulsive coefficient to so variable a factor would normally not be recommended. It serves here, for the present, because nothing better is available. In a way, it serves also for the future on the basis that the development of techniques for predicting motorboat performance will follow the same lines as for larger vessels.

An example of the method recommended by Murray in the reference cited early in this section, developed by the staff of the Experimental Towing Tank at the Stevens Institute of Technology, is given by him on pages 668–671 of his paper. This is based on a tentative planing-boat design and is carried through in comprehensive, step-by-step fashion.

The data required for calculating the total resistance and the effective power of the full-planing type of ABC tender, using the method described by Murray, are taken from the sections preceding and from the dimensioned lines drawing of this tender in Fig. 77.K. Summarizing, these are:

Weight W = 19,000 lb

Chine beam B_C at midlength of the designed waterline, Sta. 5, = 9.96 ft

Chine beam at the transom, Sta. 10, = 0.9(9.96) = 8.96 ft

Rise-of-floor angle at midlength, Sta. 5, = 18.25 deg

Rise-of-floor angle at the transom, Sta. 10, = 3.75 deg.

For the after portion of the underwater body, which makes up most of the planing surface at

the designed speed, the afterbody mean chine beam is 9.46 ft, slightly less than B_C. Strictly speaking, Murray's data are not applicable to the present case, because they are derived from models with a constant rise-of-floor angle β. However, they are used here by taking as the reference angle β the mean of the rise-of-floor angles at the midlength section and at the transom. This is 0.5 (18.25 + 3.75) or 11 deg.

The speed coefficient, based on the mean chine beam of the afterbody, is

$$C_V = \frac{V}{\sqrt{gB_C}} = \frac{24(1.6889)}{\sqrt{32.174(9.46)}} = 2.324 \quad (77.\text{vi})$$

The load coefficient, also based on the afterbody mean chine beam, is expressed as C_Δ in Murray's referenced paper but is represented by C_{LD} in the ATTC notation. It is

$$C_{LD} = \frac{W}{wB_C^3} = \frac{19{,}000}{64.043(9.46)^3} = 0.3504 \quad (77.\text{vii})$$

The dynamic-lift coefficient, assuming a constant rise-of-floor angle of β, is

$$(C_{DL})_\beta = \frac{L}{0.5\rho V^2 B^2} = \frac{2C_{LD}}{C_V^2}$$

$$= \frac{2(0.3504)}{(2.324)^2} = 0.1298 \quad (77.\text{viii})$$

This is on the basis that the entire weight W of the boat is supported by dynamic lift. Data so derived are certainly on the conservative side.

The dynamic-lift coefficient $(C_{DL})_0$ for a rise-of-floor angle of $\beta = 0$ is required for the resistance calculations. To determine it, enter the lower part of Fig. 53.B in Sec. 53.4 with the average rise-of-floor angle β of 11 deg and the value $(C_{DL})_\beta$ of 0.1298. The derived value of $(C_{DL})_0 = 0.155$.

The sum of the friction resistance R_F and the residuary resistance R_R is the total drag force opposing motion, represented as the sum of the forces I and J in Fig. 13.C. However, as it is not always practicable or possible to determine

TABLE 77.g—Resistance Calculation for Full-Planing Tender Hull of Fig. 77.K by Murray's Planing-Surface Data

The data referenced in the heading of this table are found in Fig. 53.B, Sec. 53.4.

Col. A	Col. B	Col. C	Col. D	Col. E	Col. F	Col. G	Col. H	Col. I	Col. J	Col. K	Col. L	Col. M	Col. N	Col. O	Col. P
Trim angle, deg, θ	$\theta^{1.1}$	$\frac{(C_{LD})_0}{\theta^{1.1}}$	Ratio of wetted length to B_C, λ	Mean wetted length, ft, L_{WS}	$L_{WS}(B_C)$	Wetted surface, ft², $S = \frac{L_{WS}(B_C)}{\cos\beta}$	$10^6 R_n$	Schoenherr friction coeff., $10^3 C_F$	$10^3\Delta C_P = 0.40$; $10^3 C_P + 10^3\Delta C_F$	θ, deg	S times $10^3(C_F + \Delta C_F)$	R_F, lb	tan θ	R_R, lb	R_T, lb
2	2.14	0.0724	5.00	47.3	447.4	455.8	149.6	1.960	2.360	2	1075.7	1760	0.0349	663	2423
3	3.35	0.0463	3.62	34.2	323.5	329.6	108.2	2.050	2.450	3	807.5	1321	0.0524	996	2317
4	4.59	0.0338	2.77	26.2	247.8	252.4	82.87	2.128	2.528	4	638.1	1044	0.0699	1328	2372
5	5.87	0.0264	2.20	20.8	196.8	200.5	65.79	2.199	2.599	5	521.1	852	0.0875	1662	2514
6	7.18	0.0216	1.77	16.7	158.0	161.0	52.82	2.270	2.670	6	429.9	703	0.1051	1997	2700
7	8.50	0.0182	1.46	13.8	130.5	132.9	43.65	2.335	2.735	7	363.5	595	0.1228	2333	2928

Col. B—From small table, Fig. 53.B of Sec. 53.4, top part

Col. C—$(C_{LD})_0$ from lower part of Fig. 53.B. Enter with $\beta = 11°$, $(C_{LD})_\beta = 0.1298$

Col. D—λ, ratio of wetted length L_{WS} to beam B_C; $\lambda = L_{WS}/B_C$. From curves of Fig. 53.B, top part

Col. E—[(Col. D)(B_C)]; $L_{WS} = \lambda B_C$

Col. F—[(Col. E)(B_C)]

Col. G—$S = (L_{WS})B_C/\cos\beta$

Col. H—$R_n = VL_{WS}/\nu = \frac{1.6889(24)L_{WS}}{1.287(10^{-6})} = 3.1630(10^6)L_{WS}$

Col. I—From tables, SNAME Tech. and Res. Bull. 1–2

Col. L—[(Col. G)(Col. J)]

Col. M—$R_F = 0.5\rho V^2 S[10^3 C_F + 10^3(\Delta C_F)] = 0.5(1.9905)[1.6889(24)]^2 S[10^3 C_F + 10^3(\Delta C_F)]$
$= 1635.7$ (Col. L)

Col. N—From standard tables

Col. O—$R_R = L \tan\theta = \Delta \tan\theta$

Col. P—$R_T = R_R + R_F =$ Col. M + Col. O.

TABLE 77.h—Calculation for Center-of-Pressure Location for Full-Planing Hull of Fig. 77.K by Murray's Planing Surface Data

The data referenced in the heading of this table are found in Fig. 53.C, Sec. 53.5.

Col. A	Col. B	Col. C	Col. D	Col. E	Fol. F	Col. G
θ, deg	L_{WS}	λ	λ^n	K	$K\lambda^n$	CP forward of AP, ft
2	47.3	5.00	0.77	0.89	0.685	32.4
3	34.2	3.62	0.82	0.835	0.685	23.4
4	26.2	2.77	0.85	0.79	0.672	17.6
5	20.8	2.20	0.88	0.76	0.669	13.9
6	16.7	1.77	0.92	0.735	0.676	11.3
7	13.8	1.46	0.94	0.72	0.677	9.35

Cols. B and C—From previous calculations of Table 77.g
Col. D—From lower part of Fig. 53.C
Col. E—K from upper part of Fig. 53.C
Col. F—[(Col. D)(Col. E)]
Col. G—CP/L_{WS} = $K\lambda^n$; CP = (Col. F)(Col. B).

the magnitude of the normal force F on the bottom, and as the minor hydrodynamic forces H are not well known at this time (1955), it is necessary to substitute for the expression $[F \sin \theta + (E + H) \cos \theta]$ the equivalent expression found in most of the technical literature, namely $(L \tan \theta + R_F \sec \theta)$. Here $R_R = L \tan \theta = W \tan \theta$. The friction drag R_F would normally be augmented by the factor sec θ but since θ is usually small, probably not exceeding 6 or 7 deg, with a value of sec θ not more than about 1.0075, it is customary to omit this factor. The friction resistance R_F is then added directly to the residuary resistance R_R to give the total resistance R_T.

The complete calculations, by Murray's method, of the friction, residuary, and total resistances of the ABC planing tender, for a series of trim angles at the designed speed of 24 kt, are set down in Table 77.g. Entering the lower diagram of Fig. 53.C in Sec. 53.5 with the appropriate data, the position of the center of pressure CP ahead of Sta. 10 at the transom (or the AP) is calculated by the method illustrated in Table 77.h.

It is to be noted that in Col. E of Table 77.g the mean wetted length L_{WS} comes out as considerably longer than the waterline length L_{WL} for a trim angle θ of 2 deg. However, this seems not to affect the validity of the final results.

It is possible that the full ATTC 1947 ΔC_F allowance for full-scale roughness of $0.4(10^{-3})$, indicated in Col. J of Table 77.g, is not justified for a high-speed motorboat of this kind. As a tender for the ABC ship it will be in the water and subject to fouling and deterioration of the bottom coating for only a small percentage of the time. Again, however, the use of the full allowance in the preliminary-design stage leads to a conservative estimate of the engine power.

The various resistance and center-of-pressure values derived in Tables 77.g and 77.h are plotted on a base of trim angle θ in Fig. 77.O. Murray's curves of minimum (total) resistance per pound of displacement for planing hulls [SNAME, 1950, Fig. 21, p. 677] afford a check of sorts on the values derived in the foregoing. From Table 77.f the displacement-length quotient of the ABC

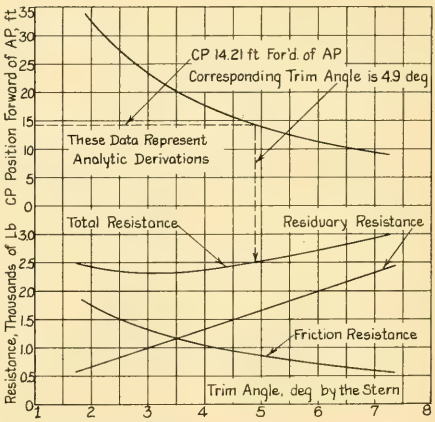

Fig. 77.O Predicted Resistance Components and Trim Angle for Planing Tender of ABC Ship

tender is 197.8 and the T_q at designed speed is 4.057. From the referenced graph the minimum resistance per pound of weight for a displacement-length quotient of 160 to 180 is 0.123 lb, corresponding to a resistance of 2,377 lb for a displacement of 19,000 lb. From Fig. 77.O the minimum resistance predicted, at a trim angle θ of 3.25 deg, is 2,320 lb.

The $\overline{\text{LCB}}$ of the boat at rest is found, by routine methods, to be approximately $0.594L_{WL}$ abaft the FP. By Table 77.f, the center of the projected chine area is found to be $0.532L_{WL}$ abaft the FP. The CB thus lies at slightly more than 6 per cent of L_{WL} abaft the centroid of the chine area. This is close to an average value as indicated by E. P. Clement ["Hull Form of Stepless Planing Boats," SNAME, Ches. Sect., 12 Jan 1955, Pl. 9].

It may be assumed that the CG of the boat laid out in Figs. 77.B and 77.K lies directly above the center of buoyancy CB when the craft is at rest. Then $\overline{\text{LCG}} = 0.594L_{WL} = 0.594(35) = 20.79$ ft abaft the FP, or 14.21 ft forward of the AP at the transom. To run at a steady trim the CP position on the bottom must lie approximately under the CG position in the hull. From the upper graph of Fig. 77.O, the running trim for this CG position is found to be about 4.9 deg by the stern. At this trim the total resistance R_T from the lower set of graphs of that figure is 2,500 lb.

The resistance data given by Murray take no account of the still-air drag of the hull and upper works above the DWL. To predict this value for the ABC tender, it is necessary to estimate the transverse projected area above water. A rough calculation from Fig. 77.B gives 60.2 ft^2. For the still-air drag the designer may use the dimensional formula $D_{SA} = 0.004A_AV^2$ [S and P, 1943, p. 52], where D is in lb and V is in kt. Substituting, $D_{SA} = 0.004\ (60.2)\ (24)^2 = 138.7$ lb. Other coefficients for this formula are given in Sec. 54.7.

Based upon the rule given by H. F. Nordström [SSPA Rep. 19, 1951, p. 15], the resistance of well streamlined appendages for a twin-screw motorboat need not exceed 7 per cent of the bare-hull total resistance. An estimated value is then $0.07(2{,}500) = 175$ lb. Still-air drag and wind resistance for motorboats are discussed further in Sec. 77.37.

The total resistance $R_T + D_{SA} + R_{\text{App}} = 2{,}500 + 138.7 + 175 = 2{,}813.7$ lb. The effective power is then $2{,}813.7(24)1.6889/550$, or about 207 horses. Assuming a propulsive coefficient η_P of 0.50 in the absence of a better value, the shaft power P_S (or better, the propeller power P_P) is $P_E/\eta_P = 207/0.50 = 414$ horses. With a transmission loss of say 5 per cent in the shafting and bearings, the brake power P_B required to be delivered by the engines is $414/0.95 = 436$ horses.

This independent estimate compares well with the first approximations to the shaft power in Sec. 77.14, where it was found that two engines, each delivering a brake power of 225 horses, would be adequate for the purpose.

K. C. Barnaby gives a few average values of the propulsive coefficient η_P as applying to craft in the category being considered here [INA, 1943, Appx. 1, p. 126]:

(a) 25-ft motorboats, average η_P is about 0.58
(b) 50-ft motorboats, average η_P is about 0.59.

Barnaby's book "Basic Naval Architecture" [1954, Art. 191, Fig. 100, p. 306] contains a graph of average η_P values which indicates a propulsive coefficient of only about 0.45 for single-screw craft 50 ft long. Since this graph extends to lengths of 1,000 ft it may not be intended to cover motorboats.

77.27 Running Attitude and Fore-and-Aft Position of the Heavy Weights. To visualize the situation at this stage relative to the probable position of the proposed craft with reference to the surrounding water and its running attitude when planing, the designer proceeds to predict certain features. Among these are the change in elevation of the center of gravity CG with speed, the fore-and-aft position of the center of pressure CP and of the CG, the dimensions and shape of the wetted bottom surface, the position of the probable impact area in waves, and the best positions for the heavy weights in the boat.

There are at least two methods of determining the vertical position of the boat when underway at full speed with respect to the level of the surrounding undisturbed water. One is to make use of a diagram such as that given by A. B. Murray in Fig. 2 on page 658 of his referenced paper, or in Fig. 29.D of Volume I of the present book, for a full-planing craft of about the same size and shape. Although Murray's diagram referenced in this case is for 40-ft V-bottom motorboats it should serve reasonably well for the ABC tender, which is 35 ft on the waterline and 38 ft overall. At the designed speed of 24 kt, equivalent to 27.6 mph, the rise of the center of gravity above its at-rest position is approximately 0.7 ft, or

0.0175 of the 40-ft length. For a craft 38 ft long the rise of the CG would be about 0.67 ft.

Another method is to lay out an elevation or profile of the boat at its designed speed and in its predicted position and attitude with respect to the undisturbed smooth water into which it is advancing. One detailed method of accomplishing this is described in the paragraphs which follow.

With the CG and the CP tentatively located by the procedures of Sec. 77.26 in a transverse plane 14.21 ft forward of the AP, the corresponding running attitude is 4.9 deg by the stern. The mean wetted length L_{WS} at this trim angle is, by interpolation from Col. B of Table 77.h, 21.4 ft.

According to B. V. Korvin-Kroukovsky, D. Savitsky, and W. F. Lehman [ETT, Stevens, Rep. 360, Aug 1939, Fig. 15, p. 36] the forward edges of the wetted area of a planing craft when underway are defined by the bases of the spray roots under the bottom. These extend generally in two straight lines from a point on the keel to points abaft this on either chine. When the wetted area on one side of the hull is projected on the centerplane the point of intersection of the spray-root base with the chine lies somewhat above the level of the undisturbed water surface. This situation is illustrated schematically in the small figure published by A. B. Murray as a part of Fig. 10 on page 665 of his paper "The Hydrodynamics of Planing Hulls" [SNAME, 1950]. The mean wetted length L_{WS}, measured generally parallel to the mean buttock at the quarter-beam, is the arithmetic mean of the wetted length of the keel and the wetted length along the chine. The difference between these two lengths, indicated as L_1 in ETT, Stevens, Report 360, is estimated by Eq. (17) on page 14 of that report, namely

$$L_1 = \frac{(\text{planing surface beam}) \tan \beta}{\pi \tan \theta} \qquad (77.\text{ix})$$

It is probable that this length is a function of the local rather than of the average chine beam and rise-of-floor angle. For the ABC planing tender these are taken as the local chine beam at Sta. 5, equal to 9.96 ft, and the local rise-of-floor angle at midlength, equal to 18.25 deg. Then, for a trim θ of 4.9 deg,

$$L_1 = \frac{(9.96)(0.3298)}{3.1416(0.0857)} = 1.22(9.96) = 12.2 \text{ ft.}$$

On the basis of perfectly flat V-shaped bottom surfaces, with constant angle β and no twist, the wetted length of the keel should equal the mean wetted length L_{WS} plus half the length L_1. For the ABC tender this is 21.4 ft plus 6.1 ft or 27.5 ft. This wetted keel length is laid off along the keel, forward from the AP, terminating at the point K in Fig. 77.P. The wetted chine length is 21.4 ft less 6.1 ft or 15.3 ft. This distance is laid off along the chine, also forward of the AP, terminating at the point C. The diagonal broken line KC in the figure forms the locus of the spray-root bases on each side. Taking for granted that the water breaks off cleanly along the chines, and that the transom clears to its lower edge, the wetted area lies entirely under the after portion of the V-bottom, indicated by the hatched area in the figure.

The point K is placed at the level of the surrounding undisturbed water, and the craft is trimmed 4.9 deg by the stern. Its profile is then drawn in, picturing the position and attitude of the hull with respect to the undisturbed water level. Fig. 77.P is this profile for the ABC full-planing tender, with dimensions and explanatory notes.

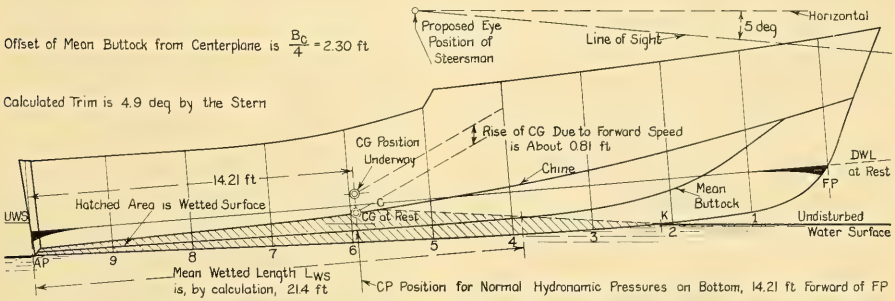

FIG. 77.P DIAGRAM SHOWING PREDICTED RUNNING POSITION AND ATTITUDE OF PLANING TENDER AT FULL SPEED

Assuming a suitable vertical position of the CG, in this case 0.5 ft above the DWL, the at-rest and underway CG positions are placed on the drawing, in a transverse plane 14.21 ft forward of the AP. Scaling the rise of the CG due to the forward speed of 24 kt from the original of Fig. 77.P gives 0.81 ft, as compared to the 0.67 ft derived from the Murray reference earlier in the section.

Two other features now require some consideration. The first is the question of whether or not the steersman at the control station can see ahead over the bow in this running attitude. Fig. 77.P indicates that with the stem carried all the way up to the forward deck line, vision in a horizontal direction is just possible from the proposed control station. In order to see clearly to a point on the water surface some 90 ft ahead of the steersman, his line of sight would have to be depressed about 5 deg, indicated by a broken line in the figure. Clear vision at this angle would necessitate rounding the stem head and using some reverse sheer forward.

The second matter is one of appearance. A planing boat running at full speed with a trim of the order of 5 deg by the stern seems to be struggling along, as though it could not quite get through its hump speed. The same boat, running at the same speed but with a trim of only some 2 deg, gives that delightful impression of smooth, effortless running which is the aim of every motorboat designer and builder and the hope of every owner and operator. Few among those who ride or watch seem to realize, or to be concerned, that the resistance and power may be less at 5 deg than at 2 deg trim by the stern. If level running becomes of more importance than efficiency of propulsion, a trim-control device of some kind is clearly indicated, as described in Secs. 36.26 and 37.24.

The next step is to estimate, possibly from a diagram such as Fig. 77.P, about where the impact area will be under the bottom when the craft runs at high speed through relatively short waves. If this area is well forward of the CG the boat receives an up-pitch moment as it strikes every crest. If, however, the impact forces are applied more or less underneath one of the heavy weight groups such as the propelling machinery, the result of slamming on wave crests is limited generally to a compression of the structure between the engine bearers and the bottom of the boat, with an effective reduction in pitching moment.

Despite the fact that this item has received little attention in the technical literature, John Plum and others who have produced high-speed planing craft which give reasonably satisfactory behavior under these severe conditions maintain that the proper adjustment of the fore-and-aft location of the heavy weight groups, *and* the control of the proper trim angle, are more important factors in superior wavegoing performance than any particular or special shape of the hull. To give the naval architect a more reliable background in this respect and to furnish him with better design rules, an intensive and thorough study of the effect of weight location and trim control should be carried out at the earliest opportunity.

77.28 First Space Layout of the 18-Knot Round-Bottom Hull. For the round-bottom type of semi-planing motorboat selected tentatively in Sec. 77.10 as the one best suited for the 18-kt speed, the requirements of Table 77.a indicate that the craft must make this speed with a half-load of fuel and a crew of two, as well as two passengers and their personal baggage. It must, however, be able to accommodate, at the slower speed of 14 kt, any of the items listed in (6) of Table 77.a and to run for 6 hr at full power. In short, it must have power enough for the 18-kt load and speed, but room enough for the 14-kt load.

Sketching a preliminary arrangement indicates, as it did for the full-planing boat, that a hull 40 ft long is unnecessarily large and that the weight limit of 25,000 lb need not even be approached. A second arrangement sketch, reproduced in Fig. 77.Q, reveals that a transom-stern hull of 35-ft waterline length is ample to contain the necessary spaces and volumes without crowding.

For this length the Taylor quotient T_q at 14 kt is 2.366, $F_n = 0.705$. For 18 kt it is 3.042, $F_n = 0.906$. From the utility-boat curve of Fig. 77.C, the total weight should be not in excess of 18,000 lb or 8.036 tons. Using the Phillips-Birt Eq. (77.iiia) of Sec. 77.14, the 14-kt speed, and the proper value of K_2 from Table 77.e,

$$P_B \text{ (horses)} = \frac{V^2 \text{ (kt) } W \text{ (long tons)}}{K_2^2}$$

$$= \frac{(14)^2(8.036)}{(2.80)^2} = 201.$$

It is to be remembered that at the 18-kt speed the useful load (and the total weight) will be considerably less than 8.04 t. It appears for the moment that *one* of the HN-10 diesel engines

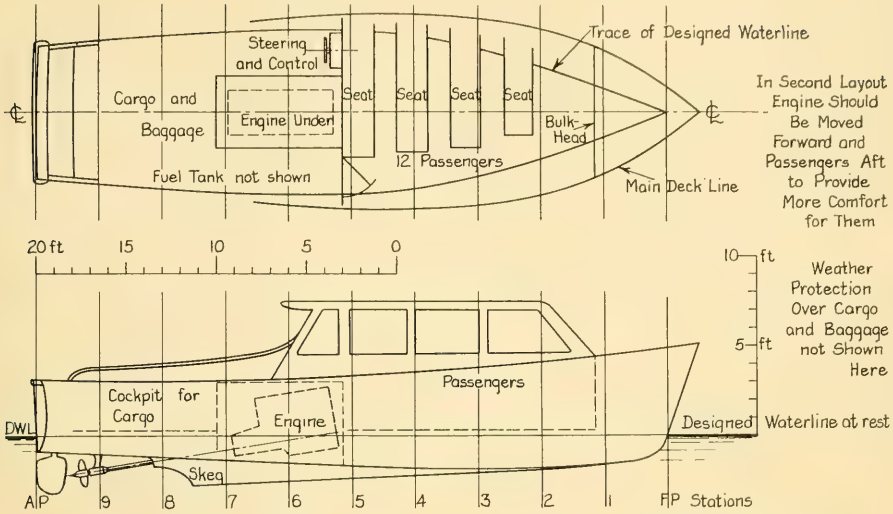

FIG. 77.Q SKETCH OF TENTATIVE SPACE LAYOUT FOR ROUND-BOTTOM TENDER FOR ABC SHIP

mentioned in Secs. 77.13 and 77.14 for installation in the 24-kt planing tender, with a maximum brake power of 225 horses, may be sufficient for the round-bottom tender. At least, it will be used for a first weight estimate.

77.29 First Weight Estimate for the 18-Knot Hull. A first weight estimate is made by using a few known weights plus reasonable percentages (from Fig. 77.D) of the estimated gross weight of 18,000 lb. These are, in lb:

	18-kt hull	14-kt hull
(1) Pay load, including crew	1,000	3,000
(2) Diesel engine, one HN-10 or the equivalent, including water and oil in the engine	2,650	2,650
(3) Fuel for 6 hr at full power, reckoned as 0.5 lb per brake horse per hr	338 (half capacity)	675
(4) Hull weight; a slightly greater percentage than for the V-bottom, hard-chine form, say 34 per cent	6,120	6,120
(5) Hull fittings, say 6 per cent	1,080	1,080
(6) Equipment and stores, say 3 per cent	540	540
(7) Electrical, say 3.3 per cent	594	594
(8) Margin, about 7 or 8 per cent	1,200	1,440
Total	13,582 lb	16,099 lb

In round figures these become 13,600 and 16,100 lb, or 6.071 and 7.187 t, respectively.

77.30 First Power Estimate for the 18-Knot and 14-Knot Conditions. The first power estimates for the round-bottom tender are made by five separate direct methods, some of which are the same as those employed in Sec. 77.14 for the full-planing tender.

I. Employing first the K. C. Barnaby formula of Eq. (77.i) with $K_1 = 2.80$ from Table 77.d for a 35-ft round-bottom boat, the brake power estimates for the two speed conditions are:

(a) For the 18-kt boat

$$P_B = \frac{V^2W}{K_1^2} = \frac{(18)^2(6.071)}{(2.80)^2} = 251 \text{ horses}$$

(b) For the 14-kt boat

$$P_B = \frac{V^2W}{K_1^2} = \frac{(14)^2(7.187)}{(2.80)^2} = 180 \text{ horses.}$$

II. Using the Phillips-Birt Eq. (77.iiia), with $K_2 = 2.80$ from Table 77.e for a 35-ft round-bottom boat, the brake-power estimates for the two speed conditions are exactly the same as for the K. C. Barnaby formula in I. preceding.

III. Using the Crouch-Werback Eq. (77.iia) of Sec. 77.14 for the 18-kt boat only, as it is not valid for $T_a < 2.5$, and taking C as 64.7 from Fig. 77.F,

$$P_S = \frac{W\text{ (lb) } V^2\text{ (kt)}}{C^2\sqrt{L_{WL}\text{ (ft)}}}$$

$$= \frac{13{,}600(18)^2}{(64.7)^2\sqrt{35}} = 178 \text{ horses.}$$

Assuming a transmission loss of 5 per cent, the necessary brake power is 178/0.95 = 187 horses.

IV. Skene's Eq. (77.iva) of Sec. 77.14 does not apply to round-bottom forms. Instead he gives a graph of the dimensional ratio $P/W^{7/6}$ on a base of $T_q = V/\sqrt{L}$, where P is in horses (presumably of brake power) and W is in tons ["Elements of Yacht Design," New York, 1944, Fig. 147, p. 295].

(a) For the 18-kt boat, where W is 6.071 t, $W^{7/6}$ is 8.20. For $T_q = 3.042$, the value of $P/W^{7/6}$ from Skene's graph is 25. Then $P = 25(8.20) = 205$ horses.

(b) For the 14-kt boat, where W is 7.187 t, $W^{7/6} = 9.98$. For $T_q = 2.366$, the value of $P/W^{7/6}$ is 13. Then $P = 13(9.98) = 130$ horses. This seems very low.

V. The nomogram of P. G. Tomalin [SNAME, 1953, Fig. 7, p. 600, for displacement-type vessels] gives:

(a) For the 18-kt boat, weighing 13,582 lb, a predicted shaft power P_S of 195 horses. Then $P_B = 195/0.95 = 205$ horses.

(b) For the 14-kt boat, weighing 16,099 lb, a predicted shaft power P_S of 165 horses. Then $P_B = 165/0.95 = 174$ horses.

The chart of H. F. Nordström for determining effective power P_E , Fig. 48 of SSPA Report 19, 1951, is a good one for craft of this type but unfortunately it does not extend far enough for either the 18-kt or the 14-kt designs considered here.

From the foregoing it is manifest that the 18-kt light-load condition is the one which controls the amount of engine power required. Of the empirical estimates, that of the Crouch-Werback formula is only 187 horses, and is decidedly low. Those of the Skene graph and of the Tomalin nomogram are identical and low, but to a lesser degree. The identical predictions of the K. C. Barnaby and Phillips-Birt formulas, 251 horses, are higher than the average by a greater amount. Despite these variations, it appears safe at this stage to make use of one HN-10 engine or its equivalent, with a rated brake power P_B of 225 horses.

All the foregoing estimates are based upon the brake power P_B at the engine coupling, and upon the designed (maximum) speed V and weight W of the *complete* boat.

77.31 Selecting the 18-Knot Hull Shape and Characteristics. The round-bottom design discussed in these sections is intended to run at two speeds, at different displacements. The high-speed light-load condition is found to control the engine power to be installed but for the selection of hull features the heavy-load condition is used. For the ABC ship itself, where the hull at its designed full-load displacement could have been shaped to run well at either the sustained speed or the maximum speed, it was considered better design to fashion it for the higher speed. Although it was known that the ship would run for much of the time at reduced load and draft, the design was laid out for full load and full draft.

Here, however, it is not possible to install enough power to reach the higher speed at the heavier load condition. This limitation would apply, at least with modern (1955) reciprocating, internal-combustion power plants, to all semi-planing as well as full-planing craft. It is considered good boat design, therefore, to shape the hull for the heavier load condition and the deeper draft.

Although the alternative design of the ABC tender, running in the lower range of speeds, is to have a round bottom it is nevertheless of the semi-planing type. For this reason, as well as to give it adequate metacentric stability and to provide a better internal arrangement, a wide-beam hull is again favored.

As a first guess, a maximum waterline beam of 10 ft is selected. It is placed at Sta. 6 or at $0.60L_{WL}$ from the FP. At the 14- to 18-kt speeds at which this craft will run, a narrower stern is favored than for the 24-kt full-planing hull. Following seas are more of a problem in steering the slower craft and the liability of broaching is greater. The transom width is tentatively selected as only $0.75B_X$ or 7.5 ft. A waterline is then sketched in, avoiding any hollow in the entrance portion.

D. Phillips-Birt recommends certain optimum prismatic coefficients for small craft in the range of T_q from 1.3 to 1.8 ["The Design of Small Power Craft," The Motor Boat and Yachting, Apr 1953, p. 160]. While the lowest T_q value for this version of the ABC tender is 2.366 for 14 kt, Phillips-Birt's value of $C_P = 0.69$ is used as a starter. For an L_{WL} of 35 ft and a weight displacement of 7.187 t, the underwater volume $\forall$ is 251.4 ft^3 and the maximum-section area is

$$A_X = \frac{\forall}{C_P(L_{WL})} = \frac{251.4}{(0.69)(35)} = 10.4 \text{ ft}^2.$$

This area is about the same as for the 24-kt planing-type tender, the beam is about the same, and the length is exactly the same. The keel profile of the 24-kt boat in Fig. 77.K, at the bottom of the hull proper, is therefore used as a guide in drawing a similar profile for the round-bottom craft. The depth at the fore-and-aft position of the section of maximum area is selected as 1.65 ft, about the same as for the faster boat.

There is no general or special rule concerning the longitudinal position of the maximum-area section for a boat of this type. To afford a clean run toward the transom it should, however, not lie abaft the midlength of the waterline. It is preferably placed slightly forward of that point. For the design in question it is taken at $0.47L_{WL}$ from the FP.

Any small-craft designer welcomes the opportunity to study the hull shapes fashioned by others, even though he may have little intention of following or copying any of them. Sources of a considerable amount of these data are listed here for convenience:

(a) Nordström, H. F., "Some Tests with Models of Small Vessels," SSPA Rep. 19, 1951. This publication gives the body plans of many round-bottom forms, together with their section-area curves and tabulated model-test data. Text is in English.

(b) Baader, J., "Cruceros y Lanchas Veloces," Buenos Aires,1951. The text is in Spanish, as yet untranslated (1957), but the lines drawings are understood by any naval architect.

(c) Beach, D. D., "Power Boat Form," The Rudder, Jan 1954, pp. 38–43, 90. The author gives lines drawings of seven modern hull forms, with the practical and the hydrodynamic reasons for their various features and characteristics.

(d) Literally hundreds of lines drawings of modern motorboats are to be found on the pages of yachting and motorboating magazines, most of them mentioned in the references of Sec. 77.41.

It is extremely unfortunate that, with such a wealth of published data at hand, a motorboat designer renders himself vulnerable by rarely knowing whether the shape he is using for guidance is a good one or not. In other words, he seldom knows a fraction as much about the good or bad performance of a boat as he knows about its physical shape and other features from the published lines, arrangement drawings, photographs, and descriptions. As an example of what should be done with published material, D. S. Simpson includes a sketchy body plan of a round-bottom motorboat, but gives rather full comments on the behavior of the actual craft in service [SNAME, 1950, pp. 681–682]. Information of this kind is extremely valuable but almost equally rare.

77.32 Layout of the Lines for the ABC Round-Bottom Tender. Laying out the underwater lines for the semi-planing motor tender being designed here calls for following the general principles set forth in previous sections for this operation on full-planing craft. Fashioning the abovewater hull is based upon considerations of wavegoing, good vision from the control platform and other operating requirements, convenience of the passengers and crew and, last but not least, appearance.

Specifically, the first three steps involve roughing in the maximum-section contour, laying out a designed waterline, and sketching a preliminary section-area curve, much as they did for the large ABC ship design in Chap. 66. Summarizing from Sec. 77.31:

(a) The maximum waterline beam B_{WX} is 10.0 ft. Its fore-and-aft position is $0.60L_{WL}$ from the FP.
(b) The half-siding at the bow may be taken tentatively as 0.05 ft
(c) The designed waterline beam at the transom (or at the AP) is 7.5 ft
(d) The maximum-section area is 10.4 ft^2
(e) The value of $\overline{\text{LMA}}$ is $0.47L_{WL}$, reckoned from the FP
(f) The keel profile of the 24-kt full-planing tender, at the bottom of the hull proper, is to be used as a guide.

The first layout of the maximum-area section (actually taken at the position of B_{WX}) indicated that the initial beam of 10 ft was too large and that the keel line used for guidance lay too near the at-rest waterplane. The floor lines in the bottom had too small a rise to insure reasonable freedom from pounding. The bottom slope was in fact smaller than for the corresponding sections of the full-planing form. Unfortunately there appears to be no set of minimum values to be used as a design criterion for selecting a proper rise-of-floor angle for this type of boat.

The combination of wide beam and shallow underwater body produced an extremely sharp curvature at the turn of the bilge. Indeed, the maximum-area section had the appearance of one taken from a hard-chine hull in which the chines had simply been rounded off. For the second layout the beam was decreased and the keel line was lowered.

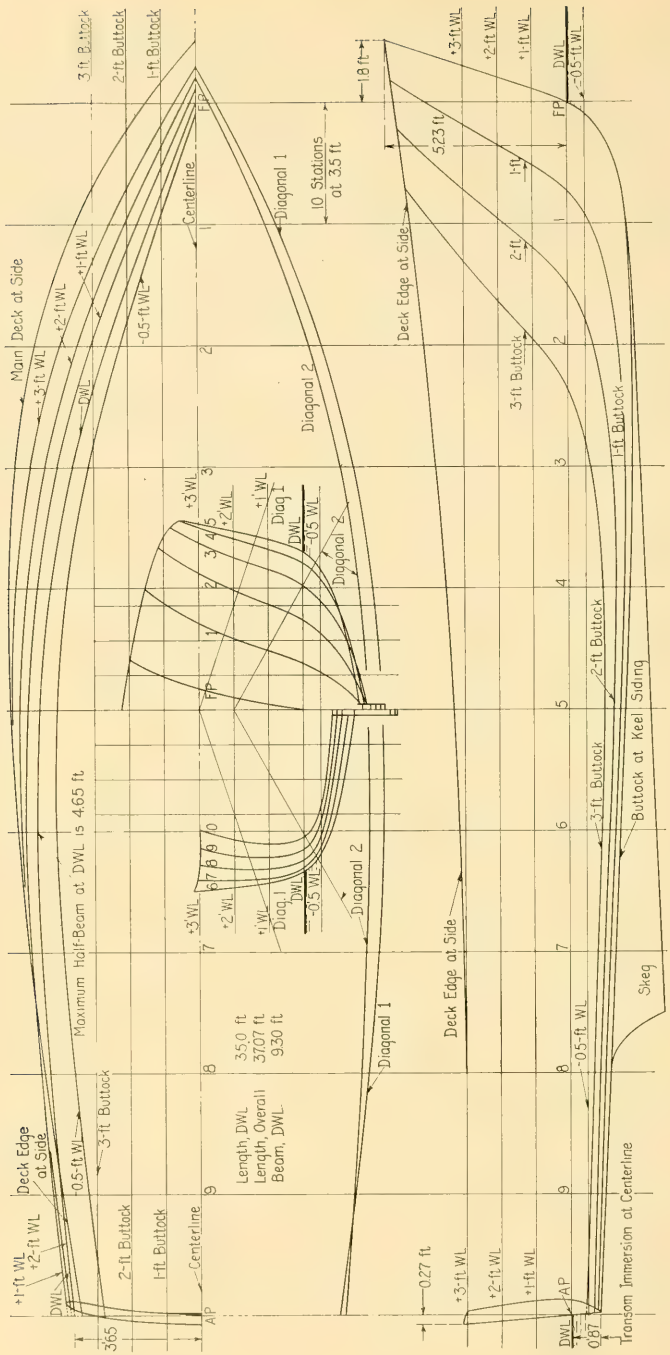

Fig. 77.R Lines Drawing for Round-Bottom ABC Tender

Sketching a tentative designed waterline through the three points given in the summary presented no problem, but there is no way of knowing whether it is a good one until the sections are drawn. Before this can be done, there has to be a tentative section-area curve from which to work.

Before sketching such a curve for a normal form of motorboat it is necessary to fix its termination at the AP. Here again there are few design rules for selecting an immersed-transom area A_U but the immersed draft H_U should not exceed the values given in Table 67.d. For a speed of 18 kt, it is about 1.15 ft; for 14 kt, about 0.695 ft. Probably it should not exceed 1.0 ft in the present case. With a transom beam B_U of 7.5 ft and an average draft of say 0.6 ft, the value of A_U is 4.5 ft^2 and A_U/A_X is 0.43. A section-area curve is sketched in roughly through the three known points and a check on the probable volume is obtained. It should be about 6.07 (35) or 212.5 ft^3.

Many of the descriptive articles listed in Secs. 77.31 and 77.41 include section-area curves with the hull lines. These may be used by the designer as guides.

Starting again with a new and deeper keel profile, an assumed designed waterline, and a tentative section-area curve, sketching of the sections at the various stations may proceed. When drawing these sections a distinct effort is made to keep the buttocks in the run as straight as possible. Even though the craft is not intended to plane at the designed load, this shape may be relied upon to encourage planing at the higher speeds, under loads (total weights) that are somewhat lighter than those specified.

When the section areas correspond roughly to the section-area curve ordinates, and the rise of floor of each appears to be adequate to prevent pounding, with convex sections in the entrance and not-too-sharp transverse bilge curvature, the designer may proceed to add the abovewater body.

The main deck edge at the side is drawn to give a moderate flare in the forward sections, a slight flare in the midship sections, and some tumble home in the stern sections. Unless deck space is required in service, the extremely wide decks seen in many motorboat designs do little but add weight and require exaggerated flare in the forward sections. The latter may, in turn, easily lead to dangerous slamming when waves strike under this overhang.

For the ABC round-bottom tender the stem is made more nearly plumb than that of the planing tender. This provides a greater waterline length on a given overall length, with lower resistance at the speeds below planing.

Upon completion of the shaping and fairing for this craft, involving the preparation of two successive sets of lines, it was found that the volume under the tentative waterline at rest was slightly greater than that required by the heavy-load W of 16,100 lb of salt water. Rather than to draw a third set of lines the designed waterline was lowered to give the correct volume. The final faired lines are reproduced in Fig. 77.R.

All the revised characteristics and parameters were checked to make sure that they were satisfactory. They are listed in Table 77.i.

A final section-area curve of the usual 1:4 proportions, and a curve of B/B_{WX} ratio, are laid down in Fig. 77.S, together with the fore-and-aft

TABLE 77.i—HULL CHARACTERISTICS AND OTHER FEATURES OF PROPOSED ROUND-BOTTOM TENDER FOR ABC SHIP

The principal dimensions, characteristics, and other data listed here are for the craft whose lines are shown in Fig. 77.R.

L_{OA} = 37.07 ft
L_{WL} = 35.0 ft
B_X = 9.04 ft
W = 16,100 lb
Δ = 7.188 long tons
$\Delta/(0.010L)^3$ = 167.6

B_{WX} = 9.3 ft
B_U of transom = 7.3 ft
$\forall$ = 251.4 ft^3 in standard salt water
A_X = 10.6 ft^2
A_W of at-rest waterline = 250.9 ft^2
H_U of transom = 0.87 ft at rest

SPEED DATA

V = 14 kt at full load; $T_q = V/\sqrt{L}$ = 2.366
V = 18 kt at light load; $T_q = V/\sqrt{L}$ = 3.042

HULL PARAMETERS

$\overline{LCB}$ = 0.530L_{WL} from the FP
C_P = 251.4/(35)(10.6) = 0.678
L/B_{WX} = 35/9.30 = 3.763
B_U = 0.785 B_{WX}
i_E of entrance = 21 deg; i_R of run, at transom corner, = 5.75 deg.

C_X = 10.6/9.04(1.7) = 0.690
C_W = 250.9/35(9.04) = 0.793

$\overline{LMA}$ = 0.47L

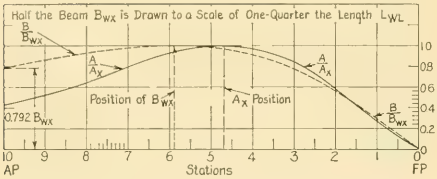

FIG. 77.S DIMENSIONLESS WATERLINE-OFFSET AND SECTION-AREA CURVES FOR ROUND-BOTTOM TENDER OF ABC SHIP

positions of the maximum ordinates of each. This completes the preliminary hydrodynamic design of the ABC round-bottom tender, as worked out in this chapter.

77.33 Example of a Modern Round-Bottom Utility-Boat Design. An example of a round-bottom design for a motorboat somewhat larger than that of the ABC tender is the 50-ft open utility boat designed recently (1954) by C. E. Werback. Fig. 77.T is a body plan of this craft and Table 77.j lists its characteristics for the light- and full-load conditions.

TABLE 77.j—DIMENSIONS AND OTHER DATA FOR THE 50-FT ROUND-BOTTOM UTILITY BOAT OF FIG. 77.T

Light displacement, 24,500 lb = 10.937 t
Speed, 13.5 kt
Full-load displacement, 48,000 lb = 21.784 t
Speed, 10.5 kt
L_{OA} = 50.02 ft L_{WL} = 48.0 ft
B_E (over guards) = 14.48 ft B_{WX} = 12.02 ft
Freeboard at FP above DWL = 6.2 ft
Freeboard amidships = 4.1 ft
Freeboard at AP = 4.02 ft
Draft to bottom of skeg = 3.92 ft
Radius at full power = 145 miles
Brake power, one 165-horse diesel engine
Fuel, 170 gallons
At 13.5 kt, $T_q = V/\sqrt{L} = 1.950$
At 10.5 kt, $T_q = V/\sqrt{L} = 1.517$
$\Delta/(0.010L)^3$ at full load = 21.78/0.1106 = 197.2
Ratio of (lb/P_B) at full load = 48,800/165 = 296.0 lb per horse.

This craft has buttock lines that are very nearly straight in the region from Sta. 8 to Sta. 12, or for the aftermost third of the length. The minimum rise-of-floor angle at Sta. 4, one-third of the length from the bow, exceeds 8 deg. The ratio of transom beam to maximum waterline beam is rather large for a round-bottom boat but in this case it provides additional room within the hull.

77.34 Design for a Motorboat of Limited Draft. For a motorboat of normal design, the extreme draft is often determined by the size and vertical position of the propeller(s) and rudder(s). The bottom of the skeg or rudder shoe may be the lowest projection but if so it is lower than the bottom of the propeller tip circle to give protection to the latter.

When the draft is limited by operating conditions, or when it is desired to give the propellers some protection, they may be recessed upward into one or more tunnels just as they are in larger tunnel-stern shallow-draft vessels. Usually, however, there is insufficient length to drop the tunnel roof down to the plane of the designed waterline abaft the wheel, so the after end of the upper portion of the tunnel is exposed.

In certain speed-length ranges, particularly just below hump speed, the change of trim and squat for most motorboat forms is large. Shallow water exaggerates this situation because of the increased steepness of the waves, generated either by the boat's own motion or by natural winds. It must not be expected, therefore, that a boat which has a draft of x ft when at rest may be able to run, under a variety of conditions, in water of x ft depth without scraping along or striking on the bottom.

When working up the characteristics of a shallow-draft motorboat the designer may, with what appears to be a reasonable first weight estimate, convert this weight to volume of the liquid in which the craft is to run. Then on the basis of a tentative waterline area and shape, he may determine the mean draft necessary to give the displaced volume, assuming first that this draft is constant under the entire waterline area. As a first approximation, the maximum draft of the hull proper may be taken as equal to 3 times the mean draft. Additional draft needed to provide dynamic stability of route, or mechanical

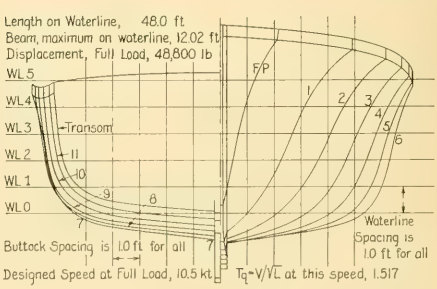

FIG. 77.T BODY PLAN OF 50-FOOT UTILITY BOAT

protection to the propeller(s) and rudder(s), is added to the hull draft.

This estimate, plus a preliminary layout of the propeller(s) and rudder(s), and an estimate of the sinkage at the stern, indicates roughly whether the limiting-draft conditions can be met.

Because of the small immersion of its surface propellers and the small trim by the stern at which it runs, a sea-sled type of motorboat may be admirably suited to operation in waters of limited depth. A 75-ft cruising yacht of the sea-sled type, in which the extreme draft is of the order of only 3.5 ft, is illustrated in the literature [Yachting, Apr 1950, p. 62].

77.35 Estimate of Screw-Propeller Characteristics. For the selection of preliminary screw-propeller characteristics for a motorboat, use is made here of a nomogram developed by W. E. Fermann, issued by the Marine Division of the Federal-Mogul Corporation, and used since 1943 by the Bureau of Ships of the U. S. Navy Department. The diagram is reproduced as Fig. 77.U. On the facing page there are instructions for its use, supplemented by an example worked out for the 24-kt planing type of ABC tender.

Use of this Fermann nomogram requires that three of the principal quantities be known:

(a) The speed of advance V_A of the propeller, expressed as miles per hour, where 1 kt = 1.15 mph. The value of V_A is reckoned as 0.90 the speed V of the boat for a single-screw craft with a fine run and 0.95 times that speed for twin-screw craft, whether of the planing or round-bottom types. P. G. Tomalin gives a special nomogram for determining the factor $(1 - w)$ [SNAME, 1953, p. 602].

(b) The shaft power P_S delivered *at each propeller*. This may be taken as 0.95 times the rated brake power P_B of the engine connected to that propeller. The instructions accompanying the Fermann chart state that the shaft power is equal to the brake power times the efficiency of transmission to the propeller times a barometric modifier times a sustained-load factor. The product of the last three factors is given as an average of 0.90 for gasoline engines and 0.85 for diesel engines.

(c) The rate of rotation in rpm *at which the propeller turns*. This is equal to the engine rpm for direct drive.

Taking the twin-screw 24-kt planing type ABC tender as an example:

(1) The speed of advance V_A is 0.95 (24) kt. In the units required for the chart, Fig. 77.U, this is 0.95(24)(1.15) = 24.84 mph.

(2) The shaft power, considered here as the power delivered directly to the propeller, is 207 horses per shaft, from the calculation at the end of Sec. 77.26. On the basis that the engine is rated for sea-level operation the barometric modifier of (b) preceding is 1.00, for a boat to be operated always at sea level. Strictly speaking, since the 24 kt is a maximum trial speed and not a sustained speed, the sustained-load factor should also be 1.00. However, it seems wise, as in the case of the ABC ship described in Chap. 69, to limit the power at designed speed to about 0.96 of the maximum. Allowing for transmission losses of the order of 3 per cent and taking the nearest round figure, the shaft power delivered at each propeller is assumed to be 210 horses.

(3) The engines are designed to run at 2,500 rpm at rated full power.

Only when special performance justifies the cost is it possible to install a custom-made motorboat propeller, conforming to a design drawn up in accordance with big-ship methods such as described in Chap. 70. Normally, a propeller is selected from stock, having the desired number of blades, diameter, pitch, and mean-width ratio.

77.36 Propeller Tip Clearances; Hull Vibration. For a craft of the displacement type the propeller-tip clearance need be no more than the nominal turbulent boundary-layer thickness δ (delta), determined for an x-distance equal to that from the stem to the propeller position and for a speed V equal to the highest boat speed expected. Using the ABC round-bottom tender as an example, the x-distance to the propeller is about 33 ft. At a speed of say 14 kt or 23.65 ft per sec in standard salt water, R_x from Table 45.b is about 60 (10^6). Assuming that the flow is fully turbulent and interpolating between the graphs of Fig. 45.C, the value of δ at the propeller is about 0.3 ft. The data plotted there are for fresh water but the values would not change materially for salt water.

For a planing craft, the R_x length is somewhat shortened because of the diminished wetted length along the keel. For the ABC planing tender, running at 24 kt or 40.53 ft per sec, the mean wetted length is just under 22 ft, giving an R_x of about 66 (10^6) in salt water and a δ at the propeller position (from Fig. 45.C) of the order of

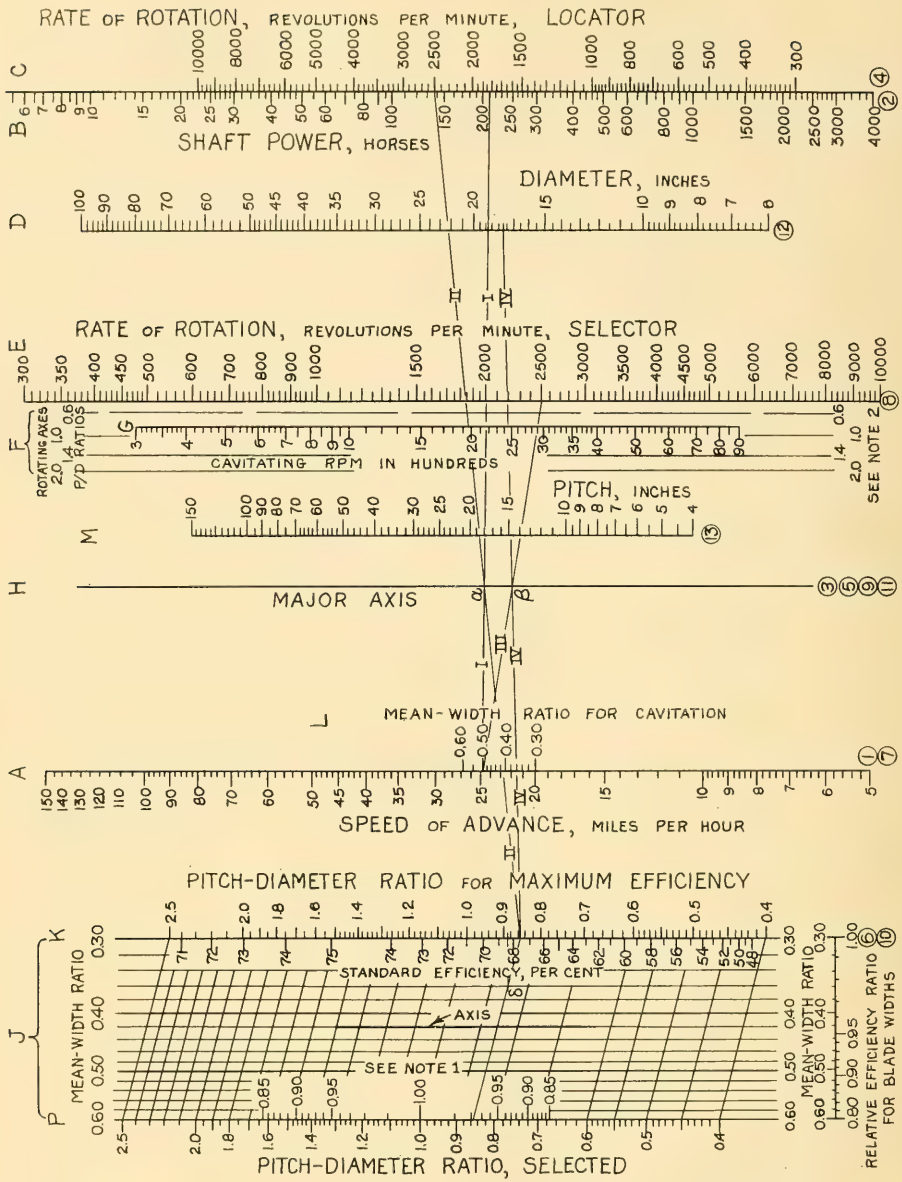

NOTE 1 – SCALE INDICATES RELATIVE EFFICIENCY RATIO WITH VARIATION IN P/D RATIO

NOTE 2 – IF FIRST DIAMETER IS NOT SATISFACTORY, ROTATE STRAIGHTEDGE ABOUT P/D AXIS UNDER SCALE F UNTIL A SUITABLE DIAMETER AND PITCH ARE FOUND

FIG. 77.U MULTIPLE NOMOGRAM OF W. E. FERMANN FOR DETERMINING CHARACTERISTICS OF MOTORBOAT PROPELLERS

Operations on Chart

Op. I. Connect the speed of advance, scale A, by a straight line with the shaft power in horses, scale B; mark the intersection on the major axis H. [This intersection is marked α for convenience when working out the example for the ABC planing-hull tender]. Referring to the numerals in circles at the bottom of the chart, the line extends from ① to ②, with the intersection α at ③.

Op. II. Connect the rate of rotation in rpm, scale C, with the intersection α on the major axis H; extend this line (marked II on the chart) to the scale K; mark the pitch-diameter ratio there. This is ④ through ⑤ to ⑥.

Op. III. Connect the speed of advance, scale A, with the rate of rotation in rpm, scale E; mark the intersection β on the major axis H. This is ⑦ to ⑧, marking the intersection at ⑨.

Op. IV. Connect the pitch-diameter ratio (Op. II) with the intersection β on the major axis H; extend this line and read the diameter and the pitch from scales D and M, respectively. This is ⑩ through β on ⑪ to ⑫ and ⑬. The readings on scales D and M give the diameter D and the pitch P of a 3-bladed propeller of maximum efficiency, for a mean-width ratio of 0.3. For a 2-bladed propeller, increase the diameter by 5 per cent. For a 4-bladed propeller, decrease the diameter by 6 per cent.

If the diameter must be reduced, return to Op. IV, then rotate the straight edge about its intersection with the proper pitch-ratio line of scale F. Read a suitable new diameter D and a new pitch P on scales D and M.

Check for Cavitation

In Op. IV, namely ⑩ through the intersection β at ⑪ to ⑫ and ⑬, check the intersection of this line with the "Cavitating rpm" of scale G. If the "Cavitating rpm" value is lower than the rate of rotation of the propeller in rpm, increase the diameter (and the pitch) or the blade area. This is done as follows:

Op. V (not shown graphically in the figure). On Grid J connect the derived pitch-diameter ratio (Op. II) on scale K with the same value on scale P. Mark the intersection of this line with the "mean-width ratio" to be tried. Then extend a horizontal line from this intersection to scale K, obtaining a new pitch-diameter ratio.

Op. VI. Connect this new pitch-diameter ratio with the major-axis intersection β (Op. III; number ⑨). Read the new diameter D and pitch P from scales D and M. Mark a new intersection with the "Cavitating rpm" of scale G.

Op. VII. Connect the intersection with scale G (Op. VI) with the 0.30 mean-width ratio point on scale L. Mark the intersection γ(gamma) of this line with the major axis H.

Op. VIII. Connect the new mean-width ratio, scale L, with the major-axis intersection γ (Op. VII) and project the line to scale G; then read the new "Cavitating rpm."

Repeat V, VI, VII, and VIII, if necessary, trying another mean-width ratio.

As an example of the method of using the Fermann multiple nomogram, there is worked out the example for one propeller of the planing-type tender for the ABC ship.

The basic data for one engine-shaft-propeller combination, given in the text, are as follows:

(i) The boat speed is 24 kt and the assumed speed of advance is 24(0.9) = 21.6 kt. This corresponds to 24.8 mph.
(ii) Shaft power or, strictly speaking, the propeller power, is 210 horses
(iii) Rate of rotation of engine at its rated brake power of 225 horses is 2,500 rpm.

Starting with Op. I, the point on scale A for the speed of advance of 24.8 mph is connected by the straight line marked "I" with the point on scale B for the required shaft power of 210 horses. The major-axis intersection on scale H is at α.

For Op. II the point on the rate-of-rotation scale C for 2,500 rpm is connected by a straight line marked "II" with intersection α on the major axis H. This straight line is extended to scale K, where the pitch-diameter ratio for maximum efficiency is found to be 0.852.

The point on the speed-of-advance scale A for 24.8 mph is connected by a straight line marked "III" with the point on the rate-of-rotation scale E for 2,500 rpm. This line intersects the major axis at the point β.

The point on scale K for a P/D ratio of 0.852 is connected by a straight line marked "IV" with the intersection β on the major axis. This line is then extended to the diameter scale D to indicate a diameter of 17.7 inches. The crossing of the straight line "IV" with the pitch scale M indicates a pitch of about 14.8 inches. The ratio of 14.8 to 17.7 gives a P/D ratio of 0.836. This discrepancy from the 0.852 value found in Op. II is due apparently to local warpage of the print from which the drawing of Fig. 77.U was made.

In a check for cavitation it is noted that the straight line "IV" crosses the "Cavitating rpm" scale G at about 2,450 rpm. This is less than the rated rpm of 2,500 so that the diameter or the blade area needs to be increased. To avoid increasing the non-axiality of the flow, it is preferable to hold the propeller diameter and enlarge the blade area. As a trial the mean-width ratio is increased from 0.30 to 0.36.

The first step is to connect the point for the P/D ratio of 0.852 on scale K with the same point on scale P. The point where this diagonal straight line crosses the vertical line under J for a mean-width ratio of 0.36 is marked δ. A horizontal line is drawn through the intersection δ, meeting the scale K at a P/D value of 0.88. This is the new pitch-diameter ratio of Op. V.

The point for the new P/D ratio is connected with the intersection β on the major axis and the straight line is extended to the scales D and M (this line is omitted in the figure to avoid confusion). The new diameter D is 16.75 inches and the new pitch P is 14.6 inches. The straight line for this Op. VI crosses scale G at a value of 2,530 rpm. This "Cavitating rpm" intersection is then connected to the 0.30 mean-width ratio point on scale L. The intersection of this line with the major axis H is identified as γ. It is omitted from the figure.

For Op. VIII a line is drawn from the new mean-width ratio value of 0.36 on scale L, through the intersection γ to meet scale G, where the new value of the "Cavitating rpm" is read off as 2,790. This is more than 10 per cent above the shaft rpm of 2,500 and is therefore acceptable.

Tentatively, therefore, each of the two propellers for the planing-type ABC tender will be 3-bladed, with a diameter of approximately 16.75 inches, a pitch of about 14.6 inches, and a mean-width ratio of 0.36.

0.2 ft. Here the x-distance involved is slightly less than the mean wetted length, because the propeller is to be forward of the transom.

Without any more than instinctive or intuitive knowledge of viscous flow, boundary layers, or wake velocities, N. G. Herreshoff built many successful high-speed launches, yachts, and torpedoboats in the half-century between 1870 and 1920 with extremely small tip clearances [Herreshoff, L. Francis, "N. G. Herreshoff and Some of the Yachts He Designed," The Rudder, Mar 1950, pp. 33–35; Sep 1950, pp. 26–27, 56–58]. He was fully as conscious as are modern marine architects of the advantages of smooth running and the need for holding vibration to a minimum. There is some question, therefore, as to whether radial or hull tip clearance is an important feature in a small craft [Tomalin, P. G., SNAME, 1953, p. 611].

The structural scale effect, which causes a small structure of a given material to be more rigid than a geometrically similar large one *of the same material*, may render the hull less susceptible to vibration than on a large vessel. Nevertheless, it seems wise on any small craft, regardless of size, not to reduce the tip clearance below 0.083 ft (1 inch) or, at the most, 0.0625 ft ($\frac{3}{4}$ inch) [Lakeland Yachting, May 1952, p. 20].

On all small boats built for pleasure purposes, and on most utility craft as well, comfortable riding and freedom from vibration acquire an importance comparable to that on large vessels. P. G. Tomalin has discussed this matter at some length [SNAME, 1953, pp. 610–613] so that it is considered necessary only to reference it here.

77.37 Still-Air Drag and Wind Resistance. It is mentioned in item (6) of Sec. 77.2 that in an ultra-high-speed motorboat the still-air resistance may approach the hydrodynamic resistance in magnitude. In any type of motorboat, with by far the greater part of its total volume above the water surface, neither the still-air drag D_{SA} nor the wind resistance R_{Wind} is ever a negligible or an inconsiderable part of the total resistance. If it is not a major factor in resistance and powering at cruising speeds it can still become important for maneuvering. When the drag in a beam wind creates a swinging moment that, for example, always causes the craft to fall off and swing downwind, the crew may have difficulty holding it in a hove-to position, head to both wind and sea.

Proper design of the upper works on a motorboat, with the center of its "sail" area in the proper fore-and-aft position, is usually more important than on a large vessel.

Chap. 54 contains sufficient information for an estimate of the still-air drag of the hull and deck erections of a small craft. Sec. 77.26 contains a computation of this drag for the planing-type of ABC tender.

77.38 Design of Control Surfaces and Appendages. The principal control surfaces and appendages on a motorboat or other self-propelled small craft are:

(1) Deep keel or skeg, or a combination of the two
(2) Vertical stabilizing fin on an ultra-high-speed craft, to provide a sort of fulcrum about which the rudder moment can act. Many types of these are shown by J. Baader on pages 115, 119, 322–325, and 341 of the reference listed under (4).
(3) Propeller shaft(s), usually exposed
(4) Shaft struts for supporting propeller bearings. These may be either forward of or abaft the propeller. On ultra-high-speed craft the propeller bearing is sometimes carried by a swivel fitting on the rudder [Baader, J., "Cruceros y Lanchas Veloces (Cruisers and Fast Launches)," Buenos Aires, 1951, Fig. 104, p. 130].
(5) Steering rudder(s)
(6) Inlet scoops for cooling water to the propelling machinery; see Fig. 34 on page 42 of the Baader reference just cited.

The deep keels or skegs act partly as stabilizing fins to give the craft stability of route, they prevent skidding and sideslipping, and they probably add some roll-quenching effect [Fig. 265 on p. 328 of the Baader reference listed in (4) preceding]. Practically, they serve as partial housings for centerline propeller shafts and as a protection for the hull when grounding. There appear to be few design notes or rules in the literature other than those given by D. Phillips-Birt ["Motor Yacht and Boat Design," 1953, pp. 65–66].

Exposed propeller shafts in a high-speed craft of shallow draft are a constant source of hydrodynamic difficulty. The drag normally encountered on such an appendage is aggravated by the ditch or hole in the water made by it, where the ambient pressure is too small to develop a pressure gradient which will cause the water to close in abaft the shaft. Further, the ditch, hole, or separation zone extends aft into and through the propeller disc. The only design solution here,

short of eliminating the shaft altogether or raising it out of the water at speed, is to make it as small as possible in diameter.

Because the shaft struts of motorboats are usually short, and because they gain in relative rigidity with decrease in size, due to the structural scale effect, it is frequently possible to make them of the single-arm type [Phillips-Birt, D., "Motor Yacht and Boat Design," 1953, p. 124; Baader, J., "Cruceros y Lanchas Veloces (Cruisers and Fast Launches)," Buenos Aires, 1951, Fig. 47, p. 60].

Design notes for motorboat rudders are discussed in Sec. 74.11. Additional notes are given by D. Phillips-Birt on pages 67 and 68 of the reference just cited.

77.39 Third Weight Estimate. Having settled on the general arrangement and equipment and the principal details of hull, machinery, and appendages of a motorboat design, it is now possible to make a more reliable estimate of the weights, using smaller parts and groups than those listed in Secs. 77.13 and 77.29. Moreover, when this stage of the preliminary hydrodynamic design is reached, detailed arrangement layouts and sketches of the framing and structure will have been started. These will include rough drawings of the revised internal arrangements, drawn to a scale considerably larger than those of Figs. 77.B and 77.Q, as well as framing layouts showing the tentative scantlings, sizes, positions, and characteristics of many of the principal parts of the hull and some of the details.

It is now time to determine, for example, whether the hull proper of the round-bottom ABC tender is liable to weigh more than the 34 per cent of the total weight allowed for it in Sec. 77.29. The slings for hoisting the ABC tenders, if carried partly rigged in the boats, involve weights not normally included under hull fittings. Indeed, the hulls themselves may require strengthening to take the constant wear and tear of hoisting them in and out of the parent ship.

The third weight estimate involves a more-or-less detailed listing of all the principal parts in each group, and a calculation of the weight of each. Instead of the 8 items of Secs. 77.13 and 77.29, there should be more nearly 80. Even 180 items are not too many at this stage. As an excellent example, the weight calculations for a U. S. Navy 52-ft rescue boat, with direct drive, embodied 24 separate weight groups for the light-load condition, 30 groups for the hoisting-load conditions, and 31 groups for the full-load condition. Prepared by the Chris-Craft Corporation for the Bureau of Ships of the U. S. Navy Department, the entries for the light-load condition alone occupied 56 tabulated sheets.

Of the large weight groups, the machinery is usually the heaviest. Indeed, the fuel weight itself may be appreciable. Only rarely is a motorboat designed unless there is a propelling plant ready to put into it. The engine and its attached components usually have been built, tested, and weighed, so that the designer knows just what figure to set down for the units furnished by the machinery manufacturer. The fuel has a weight density that is known within close limits, so that when the fuel capacity is fixed, the designer can set down a second fixed figure for the fuel weight.

The largest single remaining weight group is that of the hull structure, including fastenings but excluding hull fittings. As the largest unknown item it deserves the most attention in the weight estimates. Lacking reliable information concerning previous construction or faced with a novel design for which weight data probably do not exist, the designer can:

(a) Calculate the area of the hull boundaries, both below and above water, then multiply this area by an average weight of hull planking or plating, framing, and reinforcing
(b) Follow the same procedure for the weather deck, if of appreciable area, and for internal bulkheads, flats, and platforms
(c) Calculate the weight of the deckhouses and deck erections
(d) Estimate the weight of what might be termed hull trim, such as guard rails, fenders, rubbing rails, spray strips, chafing pieces, doublers, and foundations for main and auxiliary machinery.

By a somewhat different procedure, the designer may:

(e) Rough out the structure by drawing the usual midship section, with its scantlings, supplemented by several other typical sections, showing the structure at those points in some detail
(f) Calculate the weight of all the parts in each typical section and draw a weight curve on a basis of length. The area under this curve represents the hull weight.

Certain features are of great importance in the final weight estimate; first, that they be included and second, that the estimated weights assigned to them be adequate. To enumerate and explain:

(1) If the hull is built of wood, it inevitably absorbs a certain amount of moisture as soon as it is launched, no matter how well it is protected by paints and similar coatings. This is called *soakage*. The moisture can be absorbed above the waterline from rain and spray, as well as below that line, from routine immersion. It adds directly to the weight of the boat as built.

(2) Woods of the same kind and grade vary rather widely in weight, even if of the same moisture content. A boat is more likely to be built of heavy pieces than light ones, unless a deliberate selection is made. Wooden boats constructed to the same drawings, by the same builder, have been known to vary plus and minus 10 per cent in weight in the course of a building program extending over a year or more.

(3) For a design that is different from one for which adequate weight data are available, or for one that is novel, no naval architect can estimate accurately, in advance, the weight of the various parts, nor can he list all the parts that the builder (or he) will put into the boat by the time it is finished

(4) The owner, operator, crew, and others are certain to add weights which were never contemplated or allowed for in the design. When the performance of the boat suffers as a result, the designer is usually the one who has to take the initial blame.

(5) New technologic developments bring into being certain items of equipment, such as radar, which may not have been in existence or even thought of when the design was completed. It is for this reason that numerous combatant vessels have been designed with margins to take care of increases in weight throughout most of the life of the vessel.

The element of soakage in a wooden hull needs much more emphasis than has been given to it in the past. It is perhaps safe to say that many small-boat designers and builders have an utterly unrealistic attitude concerning the amount (weight) of moisture which a wooden hull can and does absorb when afloat and exposed to the elements. It has long been recognized that even the best of paint and enamel coverings will not prevent this absorption. It is perhaps not so well known that a plastic coating on one surface only will not prevent absorption through the other. The astounding weight reductions recorded by drying and weighing a small sailboat hull, where the weight ranged from 375 lb wet to 275 lb dry, are vividly presented by C. C. Walcutt [Yachting, May 1955, pp. 64–65, 108–110].

The number of motorboat designs of the past for which the total weights have been underestimated is no less than appalling. The finished weight has been known to exceed the weight estimate by 10 per cent or more, and the speed to be 10 per cent below the predicted value, solely because of overweight. Despite the time, labor, and expense involved, correct motorboat design procedure calls for the making of a *detailed* weight estimate. This is possible as soon as the design of the hull arrangements and hull structure is essentially complete, the list of fittings and equipment is made, and decisions have been rendered as to just what gear the boat is to carry.

77.40 Self-Propelled Tests for Models with Dynamic Lift. An exception to the procedure set down in Sec. I.5 of the Introduction to Volume I is justified here to emphasize the necessity for the self-propulsion of models of craft in which the forces or moments generated by the propulsion devices are likely to be large compared to those generated by buoyancy or dynamic lift. The various velocity and pressure fields and forces set up by the propulsion devices are of such magnitude in proportion to the other forces acting that they can not be neglected in an endeavor to determine the resistance and running attitude of the full-scale craft. For high-speed vessels this running attitude is most important because the slope drag is large in proportion to the hydrodynamic drag.

A never-to-be-forgotten example of the inadequacy of the towed model test alone is that of the sea sled described in Sec. 30.13. Indeed, the lift force produced by the surface propellers at the stern of a craft of this type may be so necessary to reduce the trim and the overall resistance that unless the propellers are running fast enough to produce this force the craft may become nearly inoperable. It may, in effect, have only two speeds, full speed or stop, with an inability to run satisfactorily or efficiently when slowed down.

It was for many decades the practice, when stepping up the observed resistance of models of full-planing craft, to ignore the friction resistance entirely. The total observed resistance was multiplied by the cube of the scale ratio, with the usual allowance for water density, to predict the resistance of the prototype. This was on the basis that the wetted surface diminished appreciably

when planing, and possibly also on the assumption that the surfaces of any type of planing craft would always be smooth. It is now found far preferable, and far more accurate, to expand the observed data to full scale in the same manner as for a large, displacement-type vessel [Peters, S. A., SNAME, 1950, p. 682].

"Furthermore, there is need for the development of equipment and techniques for self-propelling models of planing craft, if guesswork is to be eliminated from estimating engine power requirements, and maneuvering characteristics" [Curry, J. F., SNAME, 1950, p. 688].

77.41 Partial Bibliography on Motorboats. Sec. 53.8 gives a partial list of references on planing surfaces, dynamic lift, and planing craft. The emphasis here is on the analytical and empirical aspects of predicting performance rather than on the practical aspects of design.

A few references from Sec. 53.8 are repeated here, but for the most part the items listed in the present section contain design notes and information of direct practical use. Furthermore, the references apply to displacement craft and to round-bottom motorboats of the semi-planing type, as well as to full-planing boats of many kinds.

(1) Crane, C. H., "High Speed Gasoline Launches," SNAME, 1904, Vol. 12, pp. 321–325. Pl. 94 of this paper gives speed-rpm, speed-slip, speed-power, and other curves of the launch *Vingt-et-Un II*, designed by Crane. See also Yachting, Jan 1952, p. 62.

(2) Crane, C. H., "Problems in Connection with High-Speed Launches," SNAME, 1905, pp. 365–373 and Pls. 190–197. The first three of these plates give midsection shapes, outboard profiles, waterlines, and deck plans of a number of small torpedoboats and fast launches of that time.

(3) Durand, W. F., "Motor Boats; A Thoroughly Scientific Discussion of their Design, Construction, and Operation," International Marine Engineering, London and New York, 1907, L. C. No. VM 341.D9

(4) Luders, A. E., Sr., "Model Experiments and Speed Trials of 60-ft Motor Cruiser *Kathmar II*," SNAME, 1913, Vol. 21, pp. 177–180 and Pls. 110–112

(5) Gamon, T. A., "Model Experiments on Express Cruisers of Deadrise Type; For High Speed-Length Ratio Deadrise Type Proves Superior to Round Bilge Model—Resistance of Appendages Investigated," Inter. Mar. Eng'g., Aug 1918, pp. 473–476

(6) Smith, R. Munro, "The Design and Construction of Small Craft," published by The Technical Section, Association of Engineer and Shipbuilding Draughtsmen, 96, St. George's Square, Westminster, London, 1924. A considerable number of reproductions of this book have been distributed in the United States.

(7) Nicolson, D., "Design and Construction of High-Speed Motor Boats," INA, 1927, Vol. LXIX, pp. 121–143 and Pls. X and XI

(8) Richardson, H. C., "Aircraft Float Design," Ronald Press, New York, 1928

(9) McKenzie, Ian L., "The Powering of High-Speed Motor Yachts," SBSR, 16 May 1935, pp. 554–557

(10) Nicolson, D., "High-Speed Motor Craft," NECI, 1937–1938, Vol. LIV, pp. 98–118 and Pls. I and II; also pp. D25–D32; abstracted in SBSR, 13 Jan 1938, pp. 39–40. This paper is devoted to a description of the design and construction of ultra-high-speed motorboats having lengths of from 22 to 75 ft and Taylor quotients T_q of from 6.97 to 3.94. The single graph of power-weight ratio on a base of speed in kt begins at 35 horses per pound and 35 kt and extends up to over 150 kt.

(11) Hadeler, W., "Motortorpedoboote-Schnellboote (Motor Torpedoboats-High-Speed Boats)," Zeit. d. Ver. Deutsch. Ing., 12 Aug 1939, pp. 917–924. An English version of this paper is given in TMB Transl. 88, Jan 1940.

(12) Miller, R. T., Johnson, V. D., and Towne, S. R., "The Design of a High-Speed Torpedo Boat," Thesis, Webb Inst. Nav. Arch., New York, Apr 1940

(13) Skene, N. L., "Elements of Yacht Design," New York, 1944. While much of this book is devoted to the design of sailing yachts, there is a considerable amount of information relating directly to the design of motorboats and small powered craft. This is especially true of Chap. XV on Resistance, pp. 181–209, Chap. XVI on The Hydroplane, pp. 210–223, and Chap. XVII on Screw Propellers, pp. 224–240.

(14) Lord, L., "Elementary Considerations of Planing Hull Design," SNAME, Phila. Sect., 18 Oct 1946

(15) Lord, L., "Naval Architecture of Planing Hulls," Cornell Maritime Press, New York, 1946

(16) Guins, G. A., "The Design of Pleasure Planing Craft from Model Studies," SNAME, Pac. Northwest Sect., 13 Sep 1947; abstracted in SNAME Member's Bull., Jan 1948, p. 18. Author found by tests on small models that the best value of the ratio [(average waterline length)/(average waterline beam)] is 2.63 for work in rough water. Range of boat sizes is not given. Best rise-of-floor angle "for spray deflection and soft riding" found to be 38.5 deg at FP and 21 deg at $0.3L$ from FP. Minimum rise-of-floor angle for satisfactory longitudinal stability is 7 deg.

(17) Baier, L. A., "Power-Length-Speed," AM, New York, May 1948, pp. 34–35. Covers relatively slow-speed work craft of lengths from 40 to 100 ft, speeds of 9 to 12 kt, weight displacement 50 to 300 t.

(18) Thiel, P., Jr., Johnson, R. W., and Ward, L. W., "The Resistance and Wake of Nine Double-Chine Simplified Hull Forms," Thesis, Dept. Nav. Arch. and Mar. Eng'g., Univ. Mich., Ann Arbor, May 1948. The models forming the subject of this thesis have certain characteristics of motorboats.

(19) Peters, S. A., "Development of the Motor Torpedo Boat," SNAME, Ches. Sect., 3 Nov 1948. Abstracted in SNAME Member's Bull., Jan 1949, p. 21.

(20) "Tests of Twenty Related Models of V-Bottom Motor Boats, EMB Series 50," TMB Rep. R-47, Revised Edition, Mar 1949. This report was originally number 170 in the ETT series, issued on 28 Oct 1941, under the authorship of K. S. M. Davidson and A. Suarez. Unfortunately, the parent form chosen for this series has a chine that is considered too low forward, by modern standards. There are indications that the observed resistances are too low, because of laminar flow on many of the models. The data are plotted as contours of total model resistance per lb of displacement, or R_T/W, as contours of running trim angle in deg of model wetted surface, and of other factors.

(21) Locke, F. W. S., Jr., "An Empirical Study of Low Aspect Ratio Lifting Surfaces with Particular Regard to Planing Craft," Jour. Aero. Sci., Mar 1949, Vol. 16, No. 3, pp. 184–188

(22) Ashton, R., "Effect of Spray Strips on Various Power-Boat Designs," ETT, Stevens, Tech. Memo. 99, Feb 1949. This report is generously illustrated with excellent photographs of both models and full-scale motorboats, showing the spray formations very clearly. The appendix contains useful design comments, with sketches—a rather unusual feature for a report of this kind.

(23) Korvin-Kroukovsky, B. V., Savitsky, D., and Lehman, W. F., "Wetted Area and Center of Pressure of Planing Surfaces," ETT, Stevens, Rep. 360, Aug 1949. This is the Sherman M. Fairchild Publication Fund Paper 229, issued by the Inst. Aero. Sci., New York, N. Y.

(24) Du Cane, P., "High-Speed Small Craft," Cornell Maritime Press, 1950. This book embodies, in 21 chapters, informative comment and design data on hulls, machinery, equipment, operation, and trials, in the size range up to 130 ft in length and in the speed range above 15 kt.

(25) Herreshoff, L. Francis, "N. G. Herreshoff and Some of the Boats He Designed," The Rudder. This comprises a series of articles, subdivided into about 12 chapters, which ran more or less regularly through the years 1949 and 1950.

(26) Spooner, C. W., Jr., "Speed and Power of Motor-Boats up to a Speed-Length Ratio of Three," unpubl. manuscript dated Oct 1950; available in the TMB library

(27) Murray, A. B., "The Hydrodynamics of Planing Hulls," SNAME, 1950, pp. 658–692. This is a most informative and useful paper for the practical naval architect. There is a bibliography of 19 items on p. 680.

(28) Clement, E. P., "The Analysis of Stepless Planing Hulls," SNAME, Ches. Sect., 3 May 1951

(29) Baader, J., "Cruceros y Lanchas Veloces; Su Dinamica, Propulsion y Navegacion (Cruisers and Fast Launches; Their Hydrodynamics, Propulsion, and Operation)," Buenos Aires, 1951 (in Spanish). This appears to be by far the most comprehensive book on the subject of motorboats and sailing craft, of small to moderate size, that has ever been published. It includes a considerable amount of information on naval architecture in general and some data on hydrodynamics in particular. It is generously illustrated, with drawings and graphs that are nothing less than superb.

(30) Latimer, J. P., "Characteristics of Coast Guard Powered Boats," SNAME, Ches. Sect., 13 Oct 1951. Abstracted in SNAME Member's Bull., Jan 1952, p. 18. This paper describes and gives drawings and photographs of a rather wide variety of sizes and types of motorboats, from 18 to 52 ft in length. Most of the paper is devoted to a description of the USCG 40-ft utility boat, embodying three variations.

(31) Nordström, H. F., "Some Tests with Models of Small Vessels," SSPA Rep. 19, 1951 (in English). Data are given, with body plans and graphs, embodying test results on 27 different models of round-bottom and V-bottom boats (with chines). On pages 15 and 16 the report gives data as to the resistance of appendages and the probable values of propulsive coefficient.

(32) Simpson, D. S., "Small Craft, Construction and Design," SNAME, 1951, pp. 554–582. This paper is devoted mostly to the larger craft in the small-vessel group, although many of the excellent design comments in it apply to the motorboat group as well.

(33) Savitsky, D., "Wetted Length and Center of Pressure of Vee-Step Planing Surfaces," Inst. Aero. Sci., Sep 1951, S. M. F. Fund Paper No. FF-6. This report also carries ETT, Stevens, number 378. It lists 24 references on pp. 25–27.

(34) Grenfell, T., "Some Notes on Steering of High-Speed Planing Hulls," SNAME, Pac. Northwest Sect., 27 Sep 1952; abstracted in SNAME Member's Bull., Jan 1953, p. 35

(35) Phillips-Birt, D., "Motor Yacht and Boat Design," W. and J. MacKay and Co., Ltd., Chatham, England, 1953. A splendid addition to the scant literature on the problems and compromises of power boat design. There are chapters on size, speed, behavior, accommodation, appearance, stability, construction, hull form, powering, propellers, planing boats, and examples in design. American distributor, J. de Gräff, Inc., 64 W. 23rd St., New York 10, N. Y.

(36) Phillips-Birt, D., "The Design of Small Power Craft; Design Problems to be Solved by the Naval Architect," The Motor Boat and Yachting, London, Apr 1953, pp. 158–162. This excellent article, like all the papers and books of this author, gives an incredible amount of general information in a small space. This reference covers, in addition to general comments, the following:

Design requirements
Speed and power
Power and hull proportions
Hull form
Principles of engine installation
Seaworthiness and stability.

(37) Tomalin, P. G., "Marine Engineering as Applied to Small Vessels," SNAME, 1953, pp. 590–634. This paper gives a number of nomograms and other data useful for the designer of small craft.

(38) "Boats Today," Universal Motor Company, con-

taining detailed designs and descriptions of 101 interesting boats created by 53 American and Canadian naval architects, Oshkosh, Wis., 1953

(39) Shaw, P. S., National Research Council of Canada Reports as follows:

MB-162, "Results of Tests on a Model of a 27-ft Motor Cutter," 6 Nov 1953
MB-164, "Results of Tests on a Model of a 27-ft Whaler," Nov 1953
MB-172, "Results of Tests on a Model of a 27-ft Landing Craft, with Preliminary Propeller Dimensions," 25 May 1954
MB-173, "Full Scale Trials on the RCN 27-ft Motor Seaboat," 4 Jun 1954

(40) Phillips-Birt, D., "The Design of Sea-Going Planing Boats; A Discussion of the Different Types and Their Characteristics," The Motor Boat and Yachting, Jan 1954, pp. 26–31. This article gives a large amount of technical information and some design rules, all in an amazingly small space. The following subjects are covered:

Planing
Round bilge or chine?
Displacement and shape of section
Beam
The planing angle
Calculating the power required
Stepped hulls.

(41) Beach, D. D., "Power Boat Form," The Rudder, Jan 1954, pp. 38–43, 90. This is an excellent resumé of seven typical modern powerboat forms, represented by lines drawings in each case, with the hydrodynamic and practical reasons for their various features and characteristics.

(42) Jacobs, W. R., "Comparison of Hull Resistance for 'Standard Series' Ships, V-Bottom Motorboats and Flying Boats," ETT Stevens Tech. Memo. 71, Apr 1954

(43) Phannemiller, G. M., "Modern Design and Construction Methods as Applied to 95-Ft Patrol Boats," SNAME, 1954, pp. 643–687. Figs. 2–5 on p. 644 give four body plans and bow profiles considered in the design of these boats.

(44) Corlett, E. C. B., "Trends in Very High-Speed Craft, Part 1," The Motor Boat and Yachting, Sep 1954, pp. 386–388; Part 2, Oct 1954, pp. 446–447

(45) Mason, J., "The Complete Book of Small Boats," Bobbs-Merrill, Indianapolis, 1954

(46) Monk, E., "Weight and the Motor Boat," Yachting, Jan 1955, pp. 118–120. The author gives typical percentages for 10 weight groups in the hull only of V-bottom and round-bottom hulls, as well as percentages for 12 groups in the total weight of an "average cruiser."

(47) Clement, E. P., "Hull Form of Stepless Planing Boats," SNAME, Ches. Sect., 12 Jan 1955

(48) De Groot, D., "Resistance and Propulsion of Motor-Boats," Inter. Shipbldg. Prog., 1955, Vol. 2, No. 6, pp. 61–80. There are 9 references on page 77 of this paper.

(49) Phillips-Birt, D., "Small Craft-Stability and Seakindliness," SBSR, 28 Jul 1955, p. 110. Says that Fairmile B-class rolled uncomfortably with L = 112.0 ft, B = 18.25 ft, L/B = 6.14, and $\overline{GM}$ = 1.75 ft. Later D-class was very much better with L = 110.0 ft, B = 21 ft, L/B = 5.24; "very much lower weights and greater GM." The following is copied from the reference:

"Unusually stiff small craft have natural rolling periods as short as 3½ seconds, and 5 to 6 seconds is usual. This means that under a wide range of seagoing conditions, the wave period will exceed that of the boat. The period of a 100-ft wave is about 4½ seconds; that of a 250-ft wave is 7 seconds. In beam seas these will also be the periods of encounter, while in quartering seas the period of encounter will be greater, by amounts depending on the ship's speed and course.

"While the period of encounter is longer than the boat's natural rolling periods, small craft tend to roll in the period of the waves. They are, more often than large vessels, in the condition of forced rolling, their motions governed by the prevailing sea rather than their hull form."

(50) "Design Features of Fast Patrol Boats," The Motor Ship, London, Aug 1955, pp. 208–209. The principal dimensions and characteristics are:

L_{OA} = 71.375 ft
L_{WL} = 67.0 ft
B, molded = 19.0 ft
B, overall = 19.833 ft
D, molded, amidships = 10.21 ft
H, extreme, = 6.083 ft
L/B = 67/19 = 3.526.

These craft are driven by twin screws and twin engines of 2,500 horses (shaft power) each. The weight of each engine (presumably dry) and its reverse gear is 10,500 lb.

These craft are of the V-bottom type, with hard chines and slightly hollow floor sections. The chine line crosses the DWL at about 0.30L from the forward WL termination.

(51) SNAME RD sheet 116, covering a 74.81-ft by 13.22-ft by 3.17-ft, 40-kt, PT boat, TMB model 3592-1

(52) SNAME RD sheet 147, covering a 30.18-ft by 8.54-ft by 1.34-ft, 26-kt, twin-screw pleasure cruiser, ETT model 917

(53) " 'The Motor Boat and Yachting' Manual," London, Temple Press, 1955

(54) Stoltz, J., "Fundamental Design of Stepless Planing Hulls," Motor Boating, New York, Feb-Jun 1956. This is a comprehensive paper which appeared after the writing of the present chapter had been completed. On page 54 of the June 1956 issue there is given an outline of the design procedure for stepless planing craft, in 26 operations. Reprints of the five parts of this paper may be obtained from Motor Boating, 572 Madison Ave., New York 22, N.Y.

(55) Clement, E. P., "Analyzing the Stepless Planing Boat," TMB Report 1093, Nov 1956.

CHAPTER 78

Model-Testing Program for a Large Ship

78.1 Preliminary. Progress of the hydrodynamic design, on paper, is suspended when:

(a) As many features have been developed, and as much of the behavior has been predicted, as the state of the art permits, working from reference books and data only
(b) The design has been narrowed to say two alternatives, for which an evaluation on paper indicates no preference
(c) The design is so novel that predictions of its probable performance can not be made on a basis of existing data or experience.

This is the stage at which to make towing and self-propelled model tests. Few ships, especially of an untried design, can be built so quickly and cheaply that some time and expense devoted to model testing is not worth while. During World War II a model test worked into a total preliminary-design period of less than one week made it possible to eliminate one propeller, one shaft, and one propelling plant from what had originally been a triple-screw layout. For a vessel of the size of the ABC ship, and for a design with its unusual features, a series of tests embracing everything within the capacity of the modern model basin establishment is considered well justified. It is both good naval architecture and good advance insurance. Such a program, laid out in this chapter, was actually carried through for the ABC design at the David Taylor Model Basin before this volume was completed, except for the tests relating to maneuvering and wavegoing.

Many marine architects are not familiar with the capabilities of an up-to-date ship-model testing plant and do not realize how much assistance can be rendered in confirming or modifying a ship design. A typical test schedule is therefore described in some detail.

78.2 Model-Test Data Desired for a Major-Ship Design. The specific model-test data listed here are intended to confirm, or otherwise, the corresponding data predicted in the course of the preliminary hydrodynamic design, worked up in the preceding chapters of Part 4. These cover, briefly:

(a) Resistance of the hull, first without appendages (bare hull), and then with them
(b) Sinkage and trim of the hull; this may be measured on the hull either when it is bare or with appendages
(c) Wave profile and flow pattern around the hull, first without appendages, to determine the traces of the roll-resisting keels and to check other features; later with appendages and with the propeller(s) working
(d) Wake vectors or flow directions at positions selected for the arms of struts to support propeller bearings, as a guide to orienting or twisting these arms into the lines of flow
(e) Wake vectors at the propeller position(s), with struts, bossings, or other appendages in place ahead of the propeller(s)

(f) Shaft power required to drive the hull with all appendages, rate of rotation of the propeller(s), and other self-propulsion factors, first with stock propellers(s), and then with propeller(s) designed especially for the hull
(g) Open-water and cavitation data on propeller(s) designed specially for the hull
(h) Determination of the proper neutral angles for multiple rudders; observation of dynamic stability of route and maneuvering characteristics, with a free-running model; controllability when backing
(i) Wavegoing performance of the hull, when meeting waves from ahead and being overtaken by waves from astern
(j) Shallow-water and restricted-channel behavior
(k) Nature and magnitude of the periodic vibration forces imposed on the hull by the propeller.

It is not always possible or advisable to conduct all these tests or to make them in the order given. For example, the preliminary design of roll-resisting keels should not be completed nor the keels be fitted to the model until after lines-of-flow observations on the bare hull indicate their proper positions. In the case of hull designs with offset skegs and tunnels it should be known from the flow tests that there is no cross flow under the skegs, eddying alongside them, or separation and eddying in the tunnel before shafts and struts are fitted and self-propulsion tests are made.

78.3 Model-Test Notes for Preliminary ABC Designs. Rather than to give the preliminary notes and to describe a detailed model-test schedule in general terms, applicable to any case, the data prepared for model tests of the preliminary designs of the ABC ship are quoted in full in this section and in the sections following. The wording is such as might be embodied in a request for a complete set of model tests.

There are two separate ABC hull forms to be tested. Each has the same forebody, forward of Sta. 10, but a different afterbody. These are designated for convenience as:

(1) Transom-stern, single-skeg; called transom stern for short
(2) Arch- or tunnel-stern, with double skegs; called arch stern for short.

Two separate models may be made or one bow may be bolted to either of two sterns. So far as can be determined at present, model tests at displacements less than about 0.8 the designed displacement will not be called for. The minimum model weight for the partly loaded condition, approximately 1,650 lb for a 20-ft model, should be sufficient to care for the necessary midship bulkheads and connecting bolts; see the last paragraph of Sec. 78.5.

The models may be made of wood or wax provided they will be suitable for the entire test schedule.

As is customary at model-testing establishments, the models are to be built to the molded lines shown on the drawings, with no allowances for shell plating.

The appendages, only a part of which are shown on the drawings available at this stage, are expected to consist of:

(a) Cutwater applied to the forward edge of the stem. This is considered in the nature of an appendage and is not to be in place during the bare-hull tests. (Actually it was in place on the ABC model bow).
(b) Roll-resisting keels, of shape, size, transverse position, and fore-and-aft extent to be determined only after lines of flow have been taken for both hull shapes. In view of the contemplated width of the roll-resisting keels, 3.5 ft on the ship and 0.1373 ft on the model, it is desired that the keel trace on the hull be determined by flags or vanes at a distance from the hull as well as by lines of flow on the hull. These traces should extend at least from Sta. 6 to Sta. 14.
(c) Rudder horn and single rudder for the transom-stern design. These latter are to have a contra-shape, designed to recover rotational losses in the propeller outflow jet, but they are to be omitted in their entirety from the bare-hull transom-stern model. Drawings showing these appendages are to follow.
(d) Double rudders for the arch-stern model. The double rudders and the skegs on this model are to be adapted for maneuvering tests to be conducted subsequently, involving movable blades with stocks that can be turned from the deck. Only the unbalanced tails of these rudder blades, above the level of the lower edges of the skegs, are to be fitted to the bare hull; these may be in dummy form. The balanced foils below the lower edges of the skegs are to be added subsequently as appendages, or else the dummy upper portions are to be removed and the movable maneuvering rudders fitted.
(e) Bottom anchor and recess

(f) Cooling water intake scoop and discharge for main condenser are not to be reproduced.

The principal dimensions, form coefficients, ratios, and design parameters for the ABC ship, at this stage of the design, are listed for the information and convenience of the Model Basin staff in Table 78.a. A set of drawings ultimately furnished the Model Basin, with their corresponding figure numbers, is listed in Table 78.b.

A few words of explanation are inserted at this point for the benefit of the reader who may have noted slight numerical discrepancies here and there in the tabulated data and in the text. For example, the bare-hull volumes and displacements for the transom-stern and arch-stern ABC designs, as listed in Table 78.a, differ slightly from those in Table 78.c. Any one who has designed a ship, or a house, or a machine, appreciates that the design is constantly developing, with almost continual changes in dimensions and characteristics. To make the illustrative examples in Part 4 more realistic, the numerical data are taken directly from the work sheets of the author and his assistant, at appropriate stages in the design. The reader will, it is hoped, understand if not all these discrepancies are specifically accounted for.

TABLE 78.a—Principal Dimensions, Ratios, and Coefficients for the ABC Design

These data apply to the design at the point where model tests are requested. They are modified slightly in the SNAME RD sheets. The figures given apply to the bare hull, molded, at the stage in the design when they were first furnished to the Taylor Model Basin.

Dimensions, Ratios, and Coefficients	Transom-Stern Assembly	Arch-Stern Assembly
L_{WL}	510 ft	510 ft
B_X	73 ft	73 ft
H	26 ft	26 ft
$\forall$	575,847 ft^3	579,642 ft^3
Δ	16,464 tons at 34.977 ft^3 per t	16,572 tons at 34.977 ft^3 per t
A_X	1,815 ft^2	1,815 ft^2
Speed V	20.5 kt	20.5 kt
$V/\sqrt{L}$	0.9078	0.9078
L/B_X	6.986	6.986
B_X/H	2.808	2.808
$\Delta/(0.010L)^3$	123.76	124.58
$\forall/(0.10L)^3$	4.341	4.370
C_P	0.622	0.626
C_X	0.956	0.956
C_W	0.719	0.724
C_B	0.595	0.599
C_{PV}	0.828	0.827
C_{IT}	0.529	0.529
$\overline{\text{LCB}}$	0.507	0.511
$\overline{\text{LCF}}$	0.550	0.554
$\overline{\text{LMA}}$	0.515	0.515
f_E	0.06	0.06
t_E	0.855	0.855
i_E	8.0 deg	8.0 deg

TABLE 78.b—List of Drawings Furnished to the Model Basin in Connection With the Model-Test Program for the ABC Ship

Figure in Part 4	Title
66.P	Body Plan with Single-Skeg Transom Stern
66.Q	Profile of Transom Stern with Single Skeg
67.A	Designed Waterlines for Transom Stern and Arch Stern
67.B	After Portions of Afterbody Waterlines for the Transom-Stern Hull
67.E	Bow Profile, Bulb Bow, and Cutwater
67.L	Afterbody Plan of Arch-Type Stern
67.M	Afterbody Profile and Partial Fish-Eye View of Arch-Type Stern
67.W	Section-Area Curves for Transom-Stern and Arch-Stern Designs
73.B	Design of Cutwater
73.F	Layout of Quadruple Strut Arms and Hub for the Arch-Stern Ship
73.N	Structural Layout for Roll-Resisting Keels
74.K	Details of Aftfoot, Propeller Aperture, Rudder Support, and Rudder for Transom-Stern Hull
74.L	Vertical Centerplane Section Through Shaft, Propeller, and Strut Bearing Support of Arch-Stern Design
74.N	Arrangement and Details of a Contra-Horn and Rudder for Transom-Stern Hull

78.4 Use of Stock Model Propellers for First Self-Propulsion Tests. Considerable time is saved, to say nothing of expense, if the first self-propelled tests of a model are conducted with an available model propeller. At the time of undertaking the tests of the models for the ABC ship (1953), the David Taylor Model Basin had a stock of well over 3,000 propellers suitable for use with ship models of conventional sizes. Other large model basins performing self-propelled tests are similarly equipped. Model propellers, unlike towing model hulls, are almost never thrown away. Model basin staffs have sufficient index information to enable the selection of a model propeller on a basis of diameter, pitch-diameter ratio, number of blades, mean-width ratio, blade-thickness fraction, type of blade section, and so on.

While tests with a stock propeller furnish only an approximation to the shaft power and rate of rotation for a range of ship speeds, they serve to confine the range of the probable wake and thrust-deduction fractions within rather narrow limits. With average values inside these limits it is possible to recalculate the shaft power and rate of rotation for a propeller other than the stock model by the short method described in Secs. 70.21 through 70.38. The propeller designer is able to undertake a final design with far more assurance than if he were forced to approximate the wake and thrust-deduction fractions and other design factors by less precise methods.

Since there are two propeller diameters represented in the alternative ABC designs, 20 and 24 ft, it is necessary to determine the availability of two stock wheels which have the same scale ratio as the two models.

Assuming that the ship models are to have an L_{WL} of 20 ft, ample for the testing of a preliminary design if the propellers are sufficiently large, the scale ratio λ(lambda) is $510/20 = 25.5$. This gives values of $\lambda^{0.5}$ of 5.0498, λ^2 of 650.25, and λ^3 of 16,581.4. Dividing the propeller diameters by 25.5 gives 0.7843 ft, or 9.412 in, for the 20-ft wheel and 0.9412 ft, or 11.294 in., for the 24-ft wheel. The first preliminary propeller design by the chart method, similar to that described in Sec. 70.6, indicates optimum P/D ratios of 0.975 and 1.045, respectively. (A later calculation, quoted in full in Sec. 70.6, gave an optimum P/D ratio for the transom-stern wheel of 1.02). With 4-bladed propellers the blade width need not be large nor the thickness great. Reasonably modern blade sections, of airfoil type near the hub and ogival type near the tips, are available in stock, as are propellers with small or zero rake.

An examination of the TMB stock list reveals two right-hand 4-bladed propellers having the following characteristics:

Item	*TMB 2294*	*TMB 1986*
Diameter of model propeller, in	9.652	11.40
Full-scale diameter for λ of 25.5, ft	20.5	24.22
Pitch-diameter ratio	0.98	1.05
Mean-width ratio	0.238	0.213
Blade-thickness fraction	0.038	0.047

The corresponding full-scale diameters are slightly larger than contemplated in the hull design. However, as it appears that the 20-ft wheel for the transom-stern hull is on the small side, and as further study of the tunnel stern indicates that the tip clearance may to advantage be less than the 1.0 ft originally planned, these two propellers are considered suitable for the preliminary self-propulsion tests. The larger wheel has a rake of approximately 6 deg aft, but some brief sketching indicates that this is small enough not to interfere with its performance ahead of the four strut arms. It appears, therefore, that a standard waterline model length of 20 ft can be used. The scale ratio λ is then fixed at 25.5.

In view of the relatively large wake velocities to be expected around the inside of the tunnel in the arch-stern design, a reduced pitch for the outer blade sections of the propeller is definitely indicated. This prevents overloading the tip regions and the formation of strong tip vortexes. Since TMB model propeller 1986 was designed for a single-screw vessel with normal stern and has constant pitch for 0.5 to 1.0 R, it will be rather heavily loaded in that region when run under the arch-stern model.

78.5 Displacement and Draft Conditions. The ABC models are to be run at a relatively advanced stage of the preliminary design, when it is known what appendages are to be carried and their sizes and shapes are rather well determined. Their total volume is readily calculated, as is the additional volume below the 26-ft DWL due to the shell plating. It is decided therefore to run *all tests* in the designed-load condition at a model weight corresponding to the *total* finished ship weight, with plating and all appendages, when floating at the designed waterline in salt water having a specific volume of 34.977 ft^3 per long ton of 2,240 lb, at 59 deg F, 15 deg C.

Since each model is to be built to the molded lines of the respective hull design, is to have no representation of plating, and is to carry no appendages in the bare-hull condition, it may be expected to float slightly deeper than the designed draft when ballasted to the total weight prescribed. There are several reasons for this apparently illogical procedure:

(1) Tolerances and unavoidable errors in fairing the preliminary lines, in making the early volume calculations, and in shaping the model render it almost a coincidence when the model floats at *exactly* the correct draft

(2) The change in draft due to the added volume of the shell plating and normal appendages is usually insignificant. For the two ABC hulls, the change is less than 2 inches on the ship.

TABLE 78.c—WEIGHT AND VOLUME DATA FOR MODEL RESISTANCE TESTS

All resistance tests in the designed-load condition are to be run at zero trim fore and aft.

All figures given are subject to minor changes as the designs proceed but will be made firm before the first model resistance tests are run.

Item	Transom-stern hull	Arch-stern hull
Volume of molded hull, ft³	575,754	579,457
Volume, additional, occupied by shell plating, ft³	2,802	2,811
Volume, additional, of appendages, ft³ (propellers not included), as follows:		
Bilge keels	750	750
Rudder blade and horn	534	
Rudder blade tails abaft skegs (2 of)		257
Rudder foils below skegs (2 of)		134
Cutwater at stem	21	21
Total, ft³	579,861	583,430
Volume lost in bottom anchor recess, ft³	179	179
Net volume to 26-ft DWL	579,682 ft³	583,251 ft³
Corresponding weight displacement in standard salt water, 34.977 ft³ per long ton, 59 deg F	16,573 t	16,675 t

NOTE:—The following data are given for information and comparison only:

Item	Transom-stern hull	Arch-stern hull
Bare-hull weight displacement	16,461 t	16,567 t
Shell plating and appendages	112 t	108 t

(3) It is preferable, when testing to determine the drag effects of the appendages, not to change both the form and the weight of the model at the same time. For the two ABC hulls the weight change is of the order of 0.7 per cent.

(4) Long experience indicates that the test results are more consistent if the *weight* of the model is kept constant for both bare-hull and all-appendage (including plating) conditions.

The calculated volume and weight data for the two alternative designs, following the procedure described, are listed in Table 78.c.

From Sec. 66.32 and Fig. 66.T, the weight displacement at the light-load Condition 3 is 12,090 tons. The model weight for this condition, taking $\lambda^3 = 16{,}581$, is $(12{,}090)(2{,}240)/16{,}581 = 1{,}633$ lb. Deducting the weight of ballast necessary to trim the model by the stern to a 23-ft draft at the AP for the ship, it is believed that this leaves sufficient structural weight for a two-part wax model of block coefficient about 0.60, with midship transverse bulkheads and connecting bolts.

78.6 Resistance Tests. Bare-hull resistance tests are first to be run on the models of both designs. After observation and photographing of the wave profiles, lines of flow over the hull, and flow details around the stern, as specified for the bare hulls in the sections following, resistance tests are to be run with both models when fitted with all appendages.

The range of speed for all resistance tests listed in the foregoing and for the self-propulsion tests listed subsequently is from approximately 0.3 to at least 1.1 times the expected smooth-and-deep-water speed at 0.95 of maximum designed power,

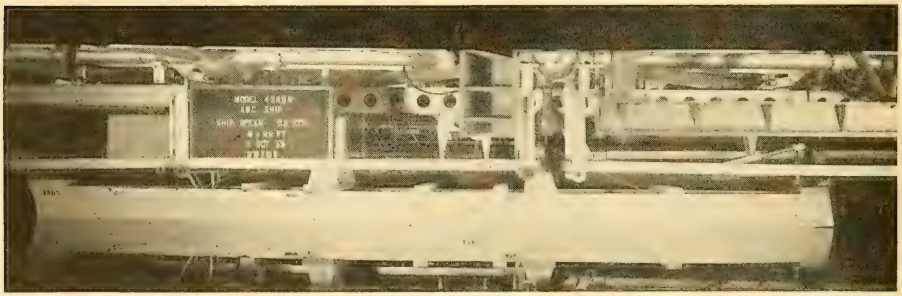

FIG. 78.A TMB MODEL 4505 FLOATING AT DESIGNED DRAFT AND TRIM

In this photograph, and in others of this chapter, the original exposures were made with the bow of the model facing toward the left, in unconventional fashion. They have not been reversed, left for right, because of the numbering and lettering that would likewise have been reversed.

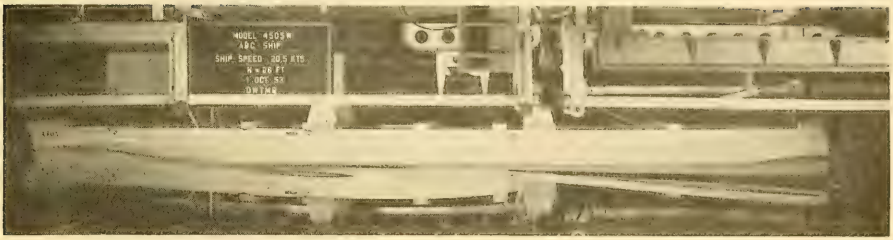

Fig. 78.B TMB Model 4505 at a Speed Corresponding to 20.5 kt for the Ship
The subscript "W" following the TMB model number on the legend signifies that the model is made of wax.

namely 20.5 kt. This range corresponds to about 6 through 22.5 kt for the ship; 1.18 through 4.46 kt for the model. The reason for the emphasis on the low-speed range is to:

(1) Determine the deep-water resistance corresponding to the low speeds necessary for the ABC ship in the canal leading to Port Amalo and in the river leading to Port Correo
(2) Determine rather accurately, in the bare-hull condition, the separation drag in the range below that at which wavemaking occurs.

Even though stimulation may be considered necessary by the David Taylor Model Basin to insure turbulent flow over practically the entire area of the model hulls it is desired that, if practicable, some resistance measurements be made in the low-speed range without turbulence stimulation of any kind.

The shell plating at both ends of the ABC ship is to be welded, with butts and laps both flush. For the remainder of the length the strakes of plating are to be raised and sunken, with welded butts and riveted seams. All excrescences are to be kept to a minimum, and fairing is to be careful and thorough. A type of bottom coating is to be used that is either self-leveling or inherently smooth. It is believed, therefore, that a roughness allowance ΔC_F of $0.30(10^{-3})$, to be applied to the ATTC 1947 or Schoenherr friction values, is ample to represent the new, clean-bottom condition of the ship.

The usual photographs of both models under the towing carriage are to be taken, at zero speed and at speeds corresponding to 20.5 kt for the ship, 4.06 kt for the model, first when run bare hull, without the cutwater, and then when run with all appendages.

Figs. 78.A and 78.B are reproductions of the photos of the transom-stern model, at zero speed and at a speed corresponding to the ship trial speed of 20.5 kt. The lower carriage platform furnishes a reference for estimating visually the sinkage and trim (by the bow) when underway.

78.7 Wave Profiles and Lines of Flow. Wave profiles and lines of flow are to be taken on both models, bare-hull condition, at a speed corresponding to 20.5 kt for the ship, 4.06 kt for the model. The wave profile is to include the profile across the transom. (See Fig. 66.R).

For all resistance and self-propulsion tests the model speeds are to be noted at which the transom clears; in other words, when the entire area of the transom is exposed to the air. Undoubtedly this will be different for the two types of stern. If necessary to determine this clearing speed the model is to be run faster than that corresponding to 22.5 kt. (See Sec. 78.19).

It is desired that the lines-of-flow observations

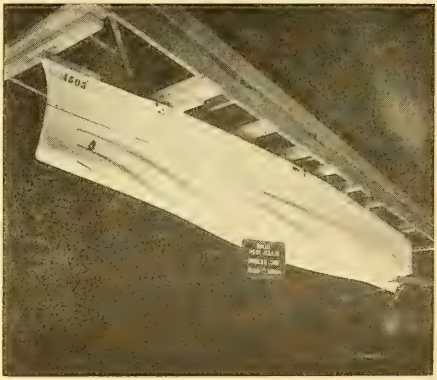

Fig. 78.C Bow-Quarter View of Transom-Stern Model Showing Lines of Flow by Chemical Means
The photograph is inverted to afford better visualization of the flow.

Fig. 78.D Stern-Quarter View of Transom-Stern Model of ABC Ship, Showing Lines of Flow by Chemical Means

at the hull surface include practically the entire length of the model. The lines should begin as far forward as Sta. 1 if practicable, but in any case not farther aft than Sta. 2. They should extend all the way to the stern.

Fitting-room photographs are to be taken of the hull to show, as graphically as possible, the lines of flow resulting from these tests. The usual projection of the flowlines on the transverse plane is also to be made on a body plan.

For determining the proper positions for the roll-resisting keels, flag indicators are to be mounted along the bilges on the model, extending from the side for a distance equivalent to about 3 ft for the ship.

Figs. 78.C and 78.D are bow and stern views of TMB model 4505, inverted from the positions as photographed, showing the surface lines of flow as revealed by a chemical indicator. The traces derived from the model, when measured, are those shown in the heavy lines of Fig. 66.R in Sec. 66.28. Fig. 78.C shows clearly how the water at the sides of the bow sections sweeps around and flows along under the bottom. The upward-and-aft flow alongside the centerline skeg is indicated clearly in Fig. 78.D.

78.8 Flow Observations with Tufts; Sinkage and Trim; Wake Vectors. Before any appendages are added to the arch-type stern, flow observations between and around the skegs are to be made in the circulating-water channel, using tufts attached to the model. It is particularly desired to learn whether there is any evidence of separation along the roof of the tunnel or of cross flow under the bottoms of the skegs.

Flow observations with tufts are to be made on both models in the circulating-water channel when driven at the model point of self-propulsion by the stock propeller. Still flash photographs suitable for reproduction are to be taken from alongside and from underneath both sterns. These are to be supplemented by motion-picture photographs if any unusual flow conditions are encountered.

It should be possible to swing the double rudders of the arch-stern model to observe the change in flow with rudder angle.

Sinkage and trim measurements are to be taken at the FP and AP on both models through the complete range of speeds covered in the tests. These data are to be recorded when both the bare-hull and the with-appendages resistance tests are run. The bare-hull data are required for comparison with published data on sinkage and trim. The data with appendages are to enable the full-scale thrust measurements on the ship to be corrected for the weight component of the shaft, propeller, gear, and other rotating parts [SNAME, 1934, pp. 151–152]; see also Sec. 59.16.

The wake vectors at the propeller-disc positions are to be determined for both types of sterns. In view of the small hull clearance under the transom stern and the still smaller tip clearance inside the tunnel of the arch stern, consideration is to be given to the use of the 5-orifice spherical-ended pitot tube, with its smaller head, for determining the wake vectors, in place of the 13-orifice tube with the larger head. In any case, the head should not be so large as to interfere with or modify the flow it is intended to measure.

For the transom-stern model the wake observations are to be extended outward to cover a half-beam at least as wide as that of the ship section

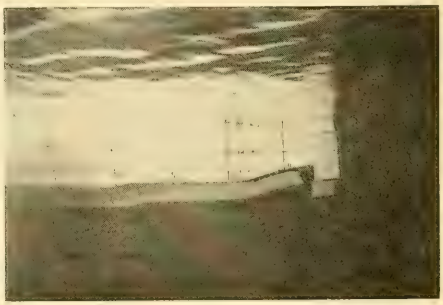

Fig. 78.E Underwater Profile of Arch-Stern Model, TMB 4505-1, in Circulating-Water Channel

The dark irregular streaks represent flow positions of tufts of dark yarn attached to the model surface.

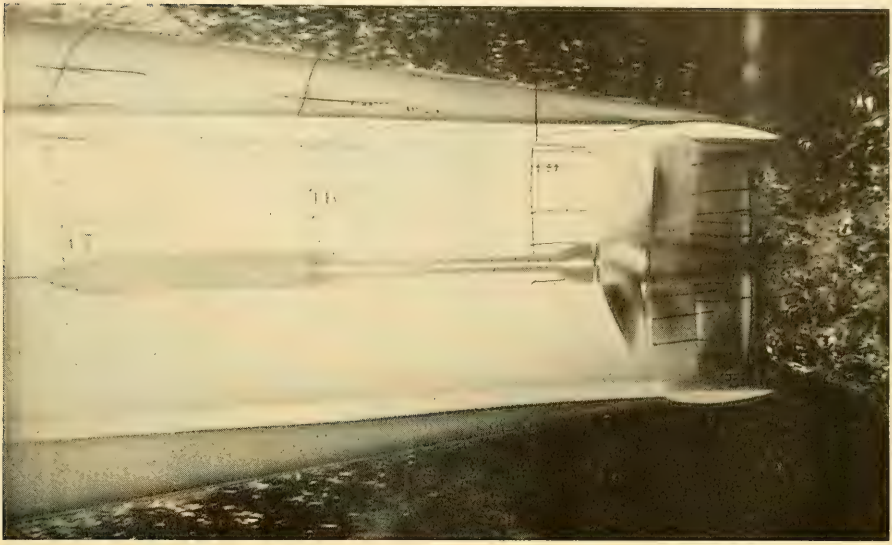

FIG. 78.F FISH-EYE VIEW OF ARCH-STERN MODEL IN CIRCULATING-WATER CHANNEL
Some cross flow is visible under the flat bottom of the side skegs.

abreast the propeller disc. (This was not fully accomplished; see Fig. 60.M).

Actually, the transom-stern model was not checked for flow in the circulating-water channel because of the good flow pattern indicated on the bare-hull model. The TMB work schedule was such that the circulating-water test of the arch-stern model was not made until all appendages were fitted and the model was self-propelled. Figs. 78.E and 78.F are through-the-water photographs of the after portion of the ABC arch-stern model, TMB 4505–1, taken in the TMB circulating-water channel. Other than a slight cross flow under the flat bottoms of the skegs, the water passes easily and regularly through the tunnel and around the skegs.

Sinkage and trim data on the transom-stern model with appendages, when both towed and self-propelled, are plotted in Fig. 58.B. Wake-survey data are plotted in Fig. 60.M and analyzed in Fig. 60.N.

78.9 Self-Propelled Tests. Self-propulsion tests are to be run on both models, carrying all appendages except the condenser intake and discharge, using stock propellers TMB 2294 and 1986, over the range of speed specified for the resistance tests. The displacements are to be as indicated in Table 78.c. It is not necessary to make SP tests with the stock propellers in the partly loaded condition.

It is desired that the D_f correction [Bu C and R Bull. 7, 1933, pp. 37–38] for all self-propulsion tests allow for a roughness of the clean, new ship corresponding to a ΔC_F of $0.30(10^{-3})$, as applied to the ATTC 1947 or Schoenherr friction values. No overload tests are required.

When the results of the foregoing tests have been worked up and evaluated, a new propeller will be designed and built for the most promising of the alternative designs. A new set of self-propulsion tests is to be run, over the range of speeds specified for the resistance tests:

(1) At the full-load displacement, draft, and trim condition
(2) At the partly loaded conditions, with displacement, draft, and trim by the stern to be as specified subsequently.

Fitting-room photographs are to be taken of the sterns and after quarters of both models to show the shape of the hull and arrangement of appendages.

The new propeller for the transom-stern ABC ship is designed in Chap. 70 by the Lerbs short method. A new model was not built to this design.

The stern appendages on the transom-stern

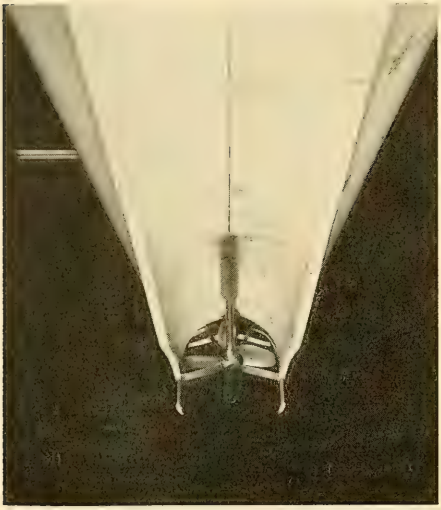

Fig. 78.G Fish-Eye View of Arch-Stern Model 4505-1, Looking Up and Aft, With All Appendages in Place

model are shown in Fig. 67.J of Sec. 67.13; those on the arch-stern model in Fig. 78.G.

78.10 Open-Water Propeller Tests. It is assumed that for the stock propellers listed in Sec. 78.4, the open-water propeller-test data are available.

The new model propeller intended to be designed and built specially for the selected ABC hull design is to be characterized in open water, following the standard procedure of the David Taylor Model Basin.

The predictions indicate that both the special 20-ft and the 24-ft (ship size) propellers should be free of cavitation if the bottom of the transom is kept in the water in the one case and the tunnel is kept full of water in the other. There appears to be no need of conducting cavitation tests on a model propeller designed for either type of hull.

If assistance can be furnished from the Design Office for the purpose, the new propeller is to be measured and checked, and some quantitative values obtained for its surface finish.

The new model propeller was designed but not built, hence there are no test data for it.

78.11 Neutral Rudder Angle and Maneuvering Tests. Tests are to be conducted with the arch-stern model to determine the neutral angle for the double rudders and to obtain certain turning characteristics. This model, if it represents the selected design for the ABC hull, is to be self-propelled with the new model propeller; otherwise with the stock propeller. The weight displacement, draft, trim, and the like are to be for the designed-load condition with appendages, as set down in Table 78.c.

The neutral rudder angle for each rudder is to be determined by a special test, first on the basis of the optimum steering characteristics when running ahead, and then on the basis of good steering and minimum propeller power for driving the ship in straight-ahead motion. Rudder angles for maneuvering tests are to be reckoned from these neutral angles.

Free-running maneuvering tests are to be carried out in the equivalent of deep water, to determine:

(a) The complete turning path through a 180-deg turn, including advance, transfer, and tactical diameter, at an approach speed of between 19.5 and 20 kt, model speed between 3.86 and 3.96 kt, with rudders at 35 deg; see item (34) of Table 64.e
(b) The maximum angle of heel when turning as in (a).

Because of the interval elapsing between the publication of Volume II and Volume III, the latter covering the subject of maneuvering, none of the tests listed here were made on either model.

78.12 Controllability Tests in Shallow Water. Controllability tests are to be carried out for the arch-stern model, under the designed-load condition described in Table 78.c, with the model propelling motor and the steering-gear motor arranged for distant manual control. If it so happens that these tests can be conducted in shallow water, when the model is ready, the depth is to correspond to a full-scale depth of 40 ft, model depth 1.78 ft. Otherwise, the tests are to be conducted in the shallowest depth available.

The model shall then:

(1) Execute a crash-back maneuver. From a straight approach path at a speed corresponding to 20.5 kt, 4.06 kt for the model, the propelling motor is to be reversed within 3 sec, about 15 sec for the ship, and an astern torque applied, as nearly as practicable equal to 0.8 of the ahead torque for 20.5 kt. The rate of propeller rotation astern is to be, as nearly as practicable, not in excess of 0.5 of the ahead rate for 20.5 kt. Obser-

vations are to be made of the successive ship position, torque, thrust if practicable, rate of rotation, and other pertinent data.

(2) Be left to itself, when running ahead at a speed corresponding to 20.5 kt, with neutral rudder angle and no perceptible swing, to determine whether or not the model deviates progressively from its course, as it would if it had dynamic instability of route.

(3) Be run ahead in a speed range corresponding to 10.25 to 20.5 kt for the ship, 2.03 to 4.06 kt for the model, to determine its general steering characteristics. Maximum rudder angle and maximum yaw, if practicable, are to be observed but no special instrumentation need be provided for this test.

(4) Be run astern at speeds varying from 0 to 8 kt for the ship, 0 to 1.58 kt for the model, to demonstrate that it will turn as directed by the rudder(s). The rate of propeller rotation is not limited for this test.

78.13 Wavegoing Model Tests. A wavegoing model at least 6 or 7 ft long is to be constructed to the hull shape which proves superior (to have the lower propeller power) in the self-propelled tests. This model is to be fitted with all *principal* erections above the main deck level, in block form, as well as with the following appendages:

(a) Cutwater
(b) Rudder horn on the transom-stern model
(c) Rudder(s)
(d) Bower or abovewater anchor. The hull in the vicinity of this anchor is to be represented rather closely to scale.

The model is to be so weighted that the longitudinal radius of gyration is about $0.23L$, reckoned about an assumed $\overline{\text{LCG}}$ of $0.505L$ from the FP. If possible without special instrumentation, an estimate is to be made of the natural pitching period of the model in quiet water, for angles not exceeding plus and minus 10 deg. The natural rolling period of the model, for an initial heel of the order of 30 deg, is likewise to be determined in quiet water.

The model is to be towed through simple regular waves by a gravity dynamometer, loaded to give a constant pull as required to tow the model at a speed corresponding to 20.5 kt for the ship in smooth, deep water. The waves are to vary in length from 0.5 to $2.5L$, 255 ft to 1,275 ft full scale. The wave height of *each system* is to be:

(a) $0.55\sqrt{L_W}$, corresponding to an $h_W = 12.42$ ft for $L_W = 510$ ft
(b) $L_W/30$, corresponding to an $h_W = 17$ ft for $L_W = 510$ ft
(c) Such other proportion as may appear advisable and be agreed upon before starting the tests. The angle of encounter is to be 180 deg (ship heading directly upsea), but a few runs are to be made at angles of encounter of 0 deg (following or overtaking sea).

Still photographs are to be made of the model at extreme up- and down-pitch positions, in regular waves of a length which produce the worst ship behavior.

78.14 Vibratory Forces Induced by the Propeller. In view of the unusual forms of the alternative sterns for the ABC ship, as well as the small tip clearances contemplated, it would be extremely useful to have some indication of the propeller-excited vibratory forces to be expected on the hull. However, at the time of writing (1955) the instrumentation for this purpose is still being developed by the David Taylor Model Basin under SNAME Technical and Research Project H-8. When it is available, vibration tests can be included in a model test program.

78.15 Reporting and Presenting Model-Test Data. Except for the notes concerning reproductions of the model-test data, this section is written generally in the wording that would be employed in requesting this work of a large-model-basin establishment.

It is planned that SNAME Resistance Data, Propeller Data, and Self-Propulsion Data sheets will be made up (by the Design Office; in this case, the author and his assistant) for the tests of both models and of the special model propeller built for the selected model.

Sufficient data are to be observed and recorded to enable the results to be presented in the form described for the items following. The data listed are to be presented separately for each model and model propeller:

(1) Curves of effective power P_E and friction power P_F, both bare hull and with appendages, for the fully loaded and partly loaded conditions, including calculated values of the wetted surface S for each condition. The value of ΔC_F, as previously stated in Sec. 78.6, is to be taken as $0.30(10^{-3})$. (Curves of effective power P_E for both models of the ABC ship are given in Fig. 78.Nc on page 892 and in Fig. 78.I).

(2) Curves of effective power P_E calculated for the Taylor Standard Series model of identical proportions, using the ATTC 1947 friction data, with a ΔC_F equal to that for the actual models, and the reworked TSS data of M. Gertler (this work is to be done by the Design Office). The TSS curve is to cover the full-load condition only. (These curves are not plotted but "angleworm" curves giving the ratio (EHP/Taylor EHP) are found in Figs. 78.Jc and 78.Kc on pages 882, 885).

(3) Body plan showing lines of flow in entrance and run, wave profile, location of separation zones if determined, and other flow details. (Reproductions of the transom-stern plan are given in Figs. 52.U and 66.R).

(4) Photographs of pertinent features of the flow tests with tufts. (See Figs. 78.E and 78.F of Sec. 78.8).

(5) Curves of sinkage of bow and stern, at the FP and the AP, plotted as fractions of the length L on a base of both T_q $(= V/\sqrt{L})$ and F_n. (These are plotted for the ABC transom-stern hull in Fig. 58.B and for the arch-stern hull in Fig. 58.C, for both the towed and the self-propulsion conditions. A discussion of the differences is included in Sec. 58.2).

(6) Transverse section at the propeller position (in the plane of the propeller disc), with wake vectors and components indicated diagrammatically. (Fig. 60.M is adapted from the TMB diagram).

(7) Curves of shaft power P_S (or propeller power P_P), effective power P_E, rate of propeller rotation n, ratio of P_E/P_S (or P_E/P_P), thrust-deduction fraction t, wake fraction w, and real-slip ratio s_R, for each model when driven by (1) the stock propeller, and (2) the propeller of special design. (These are reproduced in Fig. 78.I for the arch-stern model and in Fig. 78.Nc for the transom-stern model, when driven by the stock propellers only).

(8) Open-water characteristic curves of η_0, K_T, and $10K_Q$, on a base of advance number J, for the propeller of special design. (See Fig. 78.H for TMB propeller 1986 and Fig. 78.Mc for TMB propeller 2294. The propeller designed in Chap. 70 was not tested as a model).

(9) Plot of successive positions of ship during a 270-deg turn at a specified speed (between 19.5 and 20 kt for the ship) and with a 35-deg rudder angle. (This test was not carried out).

(10) Controllability in shallow water. (No test was made on either ABC model).

(11) Plot of wavegoing-speed ratio on ratio of

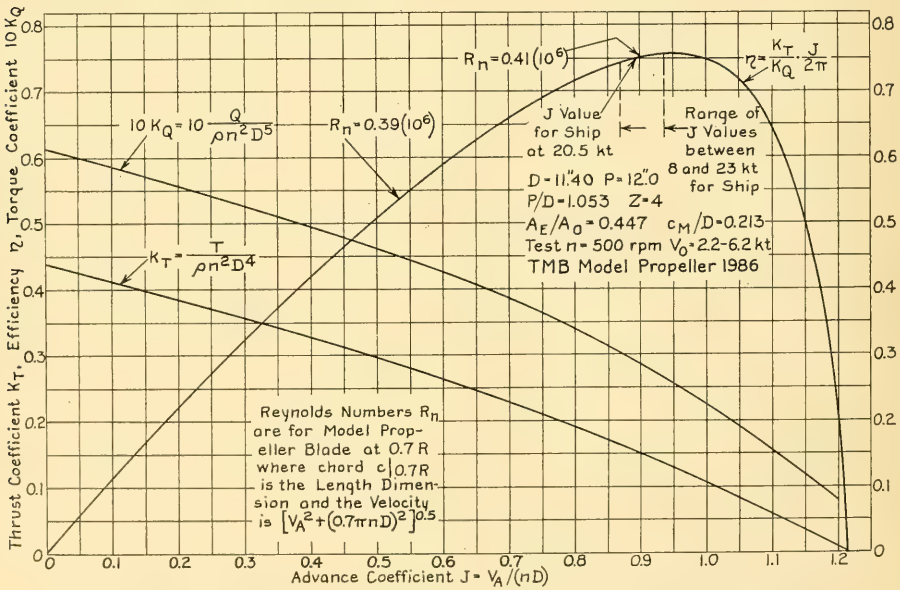

FIG. 78.H CHARACTERISTIC CURVES OF TMB MODEL PROPELLER 1986, DERIVED FROM OPEN-WATER TESTS

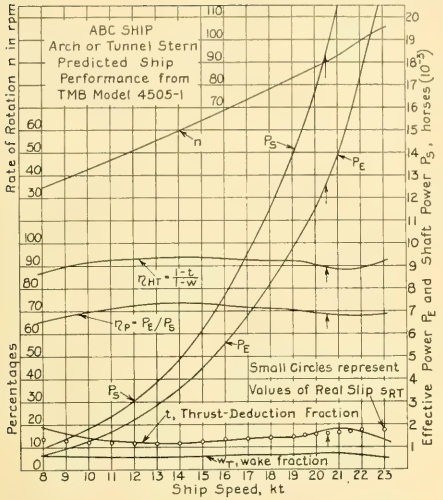

FIG. 78.I PLOT OF DATA FROM SELF-PROPELLED TEST OF ARCH-STERN ABC SHIP

L_W/L_{Ship}, based on 20.5 kt as a reference smooth-water speed for the ship, when towing at constant thrust through simple, regular waves having varied lengths. (No wavegoing model was made of either ABC design).

(12) Photographs showing ship behavior at extreme up- and down-pitch positions, in waves of the most unfavorable length (when the ship is wettest). (No test).

78.16 Test Results for Models of the ABC Ship. The data derived from the tests of TMB models 4505 and 4505–1 are reported here by preparing and reproducing sets of SNAME RD, PD, and SPD sheets, of the type in use at the date of calculation (1954). These sets are complete except for the drawing of TMB model propeller 1986, used on the arch-stern model, and for the body plans and profiles of the ends, to be found in Chaps. 66 and 67.

An index to the respective figure numbers and sheet titles follows:

Figs. 78.Ja and 78.Jb	SNAME Resistance Data sheets for TMB model 4505, representing ABC transom-stern design
Figs. 78.Jb and 78.Jc	SNAME Expanded Resistance Data sheets for TMB model 4505, for 400-ft length
Figs. 78.Ka and 78.Kb	SNAME Resistance Data sheets for TMB model 4505–1, representing ABC arch-stern ship
Figs. 78.Kb and 78.Kc	SNAME Expanded Resistance Data sheet for TMB model 4505–1, for 400-ft length
Fig. 78.L	EMB model propeller 2294
Figs. 78.Ma and 78.Mb and 78.Mc	SNAME Propeller Data sheets for EMB model 2294 (cavitation test not made)
Figs. 78.Na and 78.Nb and 78.Nc	SNAME Self-Propulsion Data sheets for TMB model 4505 (transom-stern design) driven by EMB model propeller 2294.

Model propellers 1986 and 2294 were built at the old Experimental Model Basin in Washington but were transferred in 1940 to the David Taylor Model Basin. The identifying abbreviations "EMB" and "TMB" are therefore interchangeable.

A much more comprehensive and detailed account of the model testing on this project has been prepared by Commander E. R. Meyer, USN, who participated in the testing. This has been issued as TMB Report 1006, February 1957.

The reader will note that some of the symbols on the RD, PD, and SPD sheets of Figs. 78.J through 78.N are not those approved by the ATTC and ITTC, and do not conform to those listed in Appendix 1. This is because the SNAME data-collection program on models was begun several years before approval of the now-standard symbols. It has been considered preferable to retain certain older symbols and abbreviations, such as EHP, e, and the like, in order to present the data consistently on all sheets. The reader should have no difficulty in making the transition to modern standards.

78.17 Comments on Model Tests and Analysis of Data. During all ABC model tests more readings were taken, and over a wider speed range, than is customary for the usual merchant-vessel hull form. The procedure was first to cover the entire range with about ten readings. The speed range was then run through a second and third time, using about the same number of readings at intermediate speeds. After complete coverage was obtained in this manner, additional runs were made to recheck certain spots or to fill in critical sections of the resistance curve where rapid changes were occurring.

This method of testing, as contrasted to running once through the speed range in the usual progressive manner, from low to high values, can be expected to give more scatter in the test spots. On the other hand, it gives more validity to the test results. It is considered remarkable that all the test spots for each of the ABC models, obtained during a day's running, fell into a smooth pattern.

MODEL RESISTANCE DATA

SHIP 510'x 73.08'x 26'.163, 16573 TON LABORATORY TMB WATER TEMP. 70° F λ 25.5
S.S. PASSENGER CARGO, 20.5 KNOTS BASIN DEEP WATER WATER COND. STILL (.9727) $\lambda^{1/2}$ 5.0498
MODEL NO. 4505 BASIN SIZE 963'x 51'x 22' MODEL MATERIAL WAX λ^2 650.25
APPENDAGES STEM CUTWATER MODEL LENGTH 20.0 MODEL FINISH WAX λ^3 16,581
REMARKS TEST 2 DATE 1 OCT. 53 TURBULENCE NONE

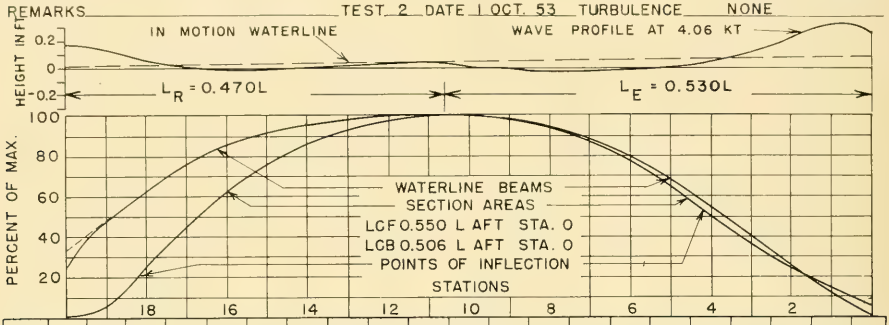

A/Ax	.011	.058	.253	.450	.622	.761	.861	.935	.979	.999	.998	.980	.942	.872	.770	.643	.501	.363	.243	.144	.059
B/Bx	.243	.479	.628	.759	.857	.918	.957	.983	.999	1.003	.997	.980	.943	.882	.794	.679	.542	.396	.252	.121	.013
BD/BD[illegible]	.069	.156	.353	.513	.625	.714	.781	.834	.872	.897	.902	.893	.867	.814	.737	.636	.518	.387	.253	.121	.013
dA/dL	0	2.95	4.08	3.72	3.11	2.40	1.76	1.18	.64	.16	.21	.57	1.06	1.75	2.33	2.72	2.81	2.61	2.17	1.84	1.57

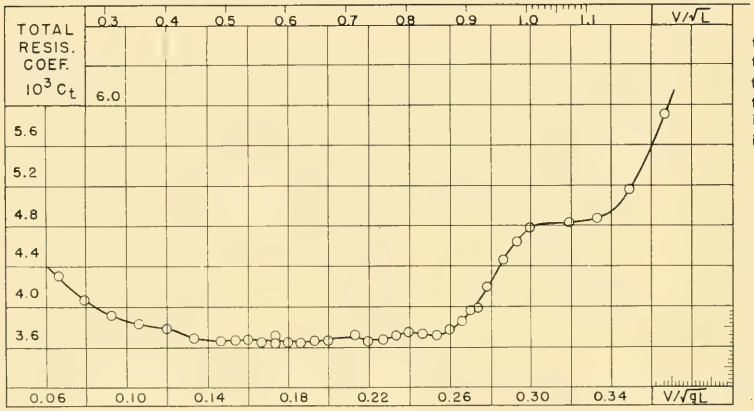

f_E 0.059
f_R 0.011
t_E 0.900
t_R 0.130
i_E 8°
i_R 12°

L 20.0 FT.
B_X 2.866 FT.
H 1.026 FT.
TRIM 0 FT.
D 2177 LBS. F.W.
Δ 0.9997 TONS S.W.
∇ 34.967 FT.^{3}
S 69.85 FT.^{2}
OBL. CORR. NO
A_X 2.7922 FT.^{2}
A_W 41.076 FT.^{2}

V_{kts}	R_t	$10^3 C_t$	$V/\sqrt{gL}$	$R_n \times 10^{-6}$	V_{kts}	R_t	$10^3 C_t$	$V/\sqrt{gL}$	$R_n \times 10^{-6}$	V_{kts}	R_t	$10^3 C_t$	$V/\sqrt{gL}$	$R_n \times 10^{-6}$
1.0	0.83	4.303	.0666	3.201	2.70	5.14	3.658	.1797	8.643	3.99	11.85	3.859	.2656	12.77
1.20	1.13	4.068	.0799	3.841	2.80	5.52	3.650	.1864	8.963	4.06	12.60	3.964	.2703	13.16
1.395	1.47	3.916	.0929	4.466	2.90	5.96	3.674	.1931	9.283	4.11	13.00	3.990	.2736	13.16
1.59	1.87	3.835	.1058	5.090	3.00	6.38	3.675	.1997	9.603	4.19	14.20	4.193	.2785	13.41
1.795	2.35	3.781	.1195	5.746	3.20	7.35	3.721	.2130	10.24	4.305	15.75	4.407	.2866	13.78
2.00	2.85	3.694	.1331	6.402	3.30	7.70	3.666	.2197	10.56	4.40	17.35	4.646	.2929	14.09
2.20	3.42	3.663	.1464	7.042	3.40	8.20	3.678	.2263	10.88	4.50	18.70	4.788	.2995	14.41
2.30	3.75	3.675	.1531	7.363	3.50	8.78	3.716	.2330	11.20	4.80	21.45	4.827	.3194	15.37
2.40	4.05	3.645	.1598	7.683	3.595	9.33	3.744	.2393	11.51	5.00	23.50	4.873	.3328	16.01
2.50	4.41	3.658	.1664	8.003	3.70	9.85	3.730	.2463	11.84	5.25	27.40	5.154	.3495	16.81
2.60	4.85	3.720	.1731	8.323	3.80	10.35	3.716	.2530	12.16	5.51	34.60	5.908	.3668	17.64
2.60	4.75	3.643	.1731	8.323	3.90	11.09	3.780	.2596	12.48					

ρ 1.9362 LBS. SEC.^{2}/FT.^{4}
ν 1.0552 $\times 10^{-5}$ FT.^{2}/SEC.

BASED ON L_{WL}

L_{WL} L_{BP}/L_{WL}
$\Delta/(0.0101L)^3$
$\nabla/(0.100L)^3$
L/B_X $L/\nabla^{1/3}$
C_B C_P C_W
LCF LWL AFT STA. 0
LCB LWL AFT STA. 0
$S/\sqrt{\Delta L}$

FIG. 78.Ja SNAME RD SHEET FOR TRANSOM-STERN TMB MODEL 4505

RATIOS AND COEFFICIENTS

L/B_X	6.978	C_P	0.621	C_W	0.717	A_X/A_M	1.002	MAX. IMB/B_X	1.003
B_X/H	2.793	C_X	0.950	C_{PV}	0.822	B_X/B_M	1.0028	MAX. WLB/B_X	1.003
$\Delta/(0.01OL)^3$	124.96	C_{PF}	0.601	C_{PA}	0.643	H_X/H_M	1.000	C_{IT}	0.528
$\nabla/(0.10OL)^3$	4.371	C_{WF}	0.612	C_{WA}	0.825	BKW/B_X	0.048	C_{IL}	0.449
$L/\nabla^{1/3}$	6.116	C_{PVF}	0.932	C_{PVA}	0.740	BR/B_X	0.147	T_q	0.908
$S/\nabla^{2/3}$	6.532	C_{PE}	0.623	C_{PR}	0.619	DR/B_X	0.014		
$S/\sqrt{\Delta L}$	15.62	C_{WE}	0.633	C_{WR}	0.812	HS/B_X	0.021		
C_B	0.589	C_{PVE}	0.935	C_{PVR}	0.724	KB/H	0.557		

EXPANDED RESISTANCE DATA

DIMENSIONS FOR 400 FT. LENGTH

L 400.0 FT.	Δ 7997.7 TONS S.W.	T 59 °F		FRICTION BASIS
B_X 57.32 FT.	∇ 279,740 FT.^{3}	ρ 1.9905 LBS SEC^2/FT.^{4}		SCHOENHERR - SCHOENHERR
H 20.52 FT.	S 27,940 FT.^{2}	ν 1.2817x10^{-5} FT.^{2}/SEC.		ROUGHNESS ALLOWANCE
TRIM 0 FT.				0.30

REMARKS

$V/\sqrt{gL}$	.06	.08	.10	.12	.14	.16	.18	.20	.22	.24
$V/\sqrt{L}$	.202	.269	.336	.403	.470	.537	.605	.672	.739	.806
(K)	.525	.701	.876	1.052	1.226	1.402	1.578	1.753	1.928	2.103
V kts	4.04	5.38	6.72	8.06	9.40	10.74	12.10	13.44	14.78	16.12
$10^{-6}R_n$	213	283	354	425	496	567	637	708	779	850
$10^3 C_f$	1.868	1.798	1.746	1.705	1.672	1.643	1.620	1.599	1.579	1.562
$10^3 C_r$	0.820	0.618	0.540	0.560	0.540	0.590	0.658	0.735	0.765	0.870
$10^3 \Delta C_f$	0.300	0.300	0.300	0.300	0.300	0.300	0.300	0.300	0.300	0.300
$10^3 C_t$	2.988	2.716	2.586	2.565	2.512	2.533	2.578	2.634	2.644	2.732
$10^3 C_t\ S/\nabla^{2/3}$	19.52	17.74	16.89	16.75	16.41	16.55	16.84	17.21	17.27	17.85
(C) 400	0.778	0.707	0.673	0.667	0.654	0.659	0.671	0.686	0.688	0.711
R	3869	6235	9264	13218	17608	23179	29943	37743	45821	56317
R/Δ	0.48	0.78	1.16	1.65	2.20	2.90	3.74	4.72	5.73	7.04
EHP	48	103	191	327	508	764	1112	1557	2079	2787
TAYLOR EHP		95	185	310	475	720	1040	1460	2010	2750
EHP/TAYLOR EHP		1.084	1.032	1.055	1.069	1.061	1.069	1.066	1.034	1.013

$V/\sqrt{gL}$	.26	.28	.30	.32	.34	.36				
$V/\sqrt{L}$	.873	.941	1.008	1.075	1.142	1.209				
(K)	2.279	2.454	2.629	2.805	2.980	3.155				
V kts	17.46	18.82	20.16	21.50	22.84	24.18				
$10^{-6}R_n$	921	991	1062	1133	1204	1275				
$10^3 C_f$	1.547	1.533	1.520	1.508	1.497	1.486				
$10^3 C_r$	0.950	1.410	2.025	2.090	2.235	2.840				
$10^3 \Delta C_f$	0.300	0.300	0.300	0.300	0.300	0.300				
$10^3 C_t$	2.797	3.243	3.845	3.898	4.032	4.626				
$10^3 C_t\ S/\nabla^{2/3}$	18.27	21.18	25.12	25.46	26.34	30.22				
(C) 400	0.728	0.844	1.001	1.014	1.049	1.204				
R	67643	91122	123970	142940	166860	214560				
R/Δ	8.46	11.39	15.50	17.87	20.86	26.83				
EHP	3626	5265	7674	9436	11701	15929				
TAYLOR EHP	3710	5400	8400	10750	13750	18500				
EHP/TAYLOR EHP	0.977	0.975	0.914	0.878	0.851	0.861				

FIG. 78.Jb SNAME ERD SHEET FOR TRANSOM-STERN TMB MODEL 4505

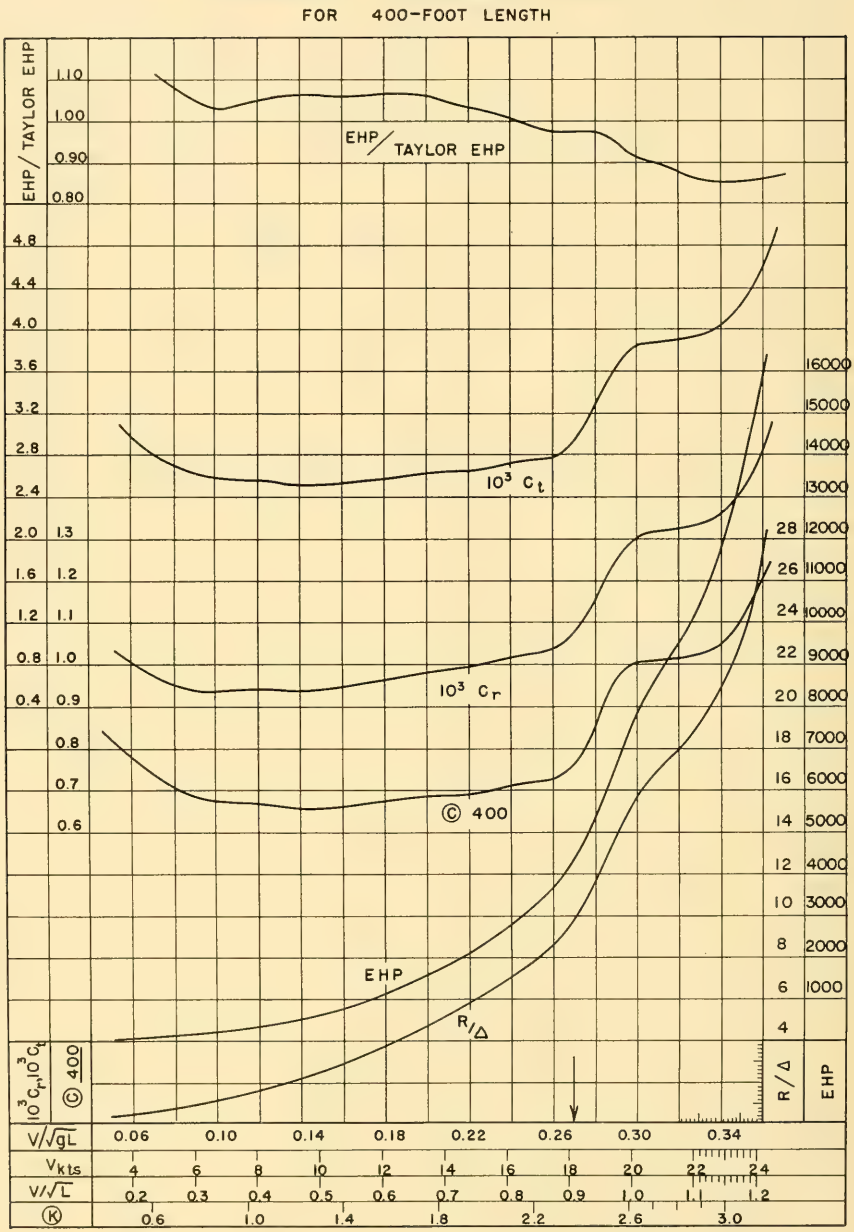

FIG. 78.Jc SNAME EXPANDED RESISTANCE CURVES FOR TMB MODEL 4505

MODEL RESISTANCE DATA

SHIP 510' 73'.08 26'.086, 16,675 ton LABORATORY TMB WATER TEMP. 66 λ 25.5
S.S. Passenger Cargo, 20.5 knot BASIN Deep Water WATER COND. Still (.9732) $\lambda^{1/2}$ 5.0498
MODEL NO. 4505-1 BASIN SIZE 963' 51' 22' MODEL MATERIAL Wax λ^2 650.25
APPENDAGES Half Rudders, Stem Cutwater MODEL LENGTH 20'.0 MODEL FINISH Wax λ^3 16,581
REMARKS Arch Stern TEST 6 DATE 30 Oct. 53 TURBULENCE None

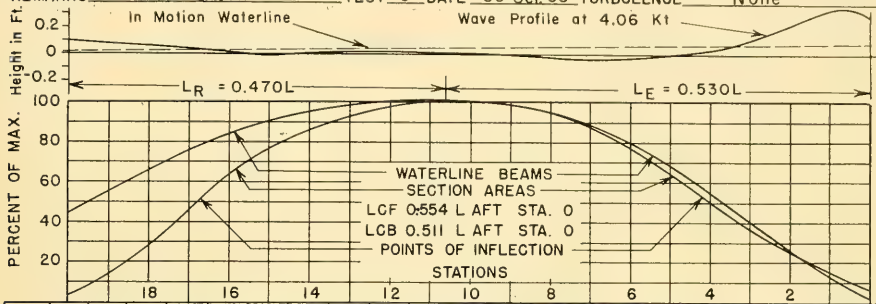

A/A$_X$	.038	.135	.277	.450	.631	.764	.858	.927	.974	.999	.998	.980	.942	.872	.770	.643	.501	.363	.243	.144	.059
B/B$_X$	.444	.549	.651	.752	.836	.902	.950	.983	1.000	1.003	.997	.980	.943	.882	.794	.679	.542	.396	.252	.121	.013
BD/BDI	.021	.438	.499	.561	.588	.692	.763	.821	.867	.897	.902	.893	.867	.814	.737	.636	.518	.387	.253	.121	.013
dA/dL	1.42	2.40	3.17	3.70	3.12	2.23	1.63	1.17	0.72	0.23	0.21	0.57	1.06	1.75	2.33	2.72	2.81	2.61	2.17	1.84	1.57

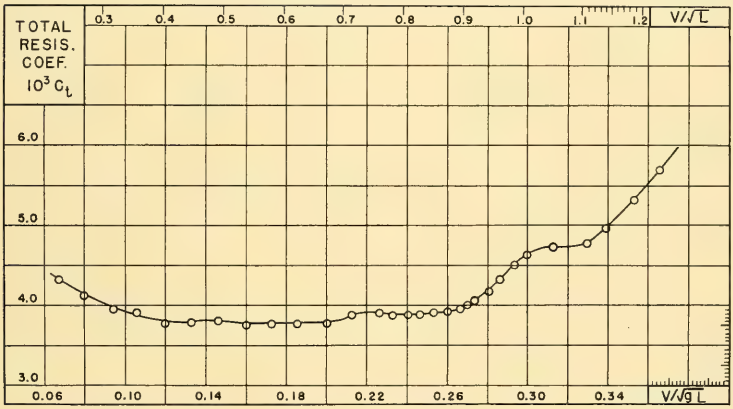

f_E 0.059
f_R 0.038
t_E 0.900
t_R 0.200
i_E 8°
i_R 8.25°

L 20.0 FT.
B_X 2.866 FT.
H 1.023 FT.
TRIM 0 FT.
D 2190.4 LBS. F.W.
Δ 1.0054 TONS S.W.
∇ 35.166 FT.^{3}
S 74.466 FT.^{2}
OBL. CORR. NO
A_X 27.92 FT.^{2}
A_W 41.437 FT.^{2}

V_{kts}	R_t	$10^3 C_t$	$V/\sqrt{gL}$	$R_n \times 10^{-6}$	V_{kts}	R_t	$10^3 C_t$	$V/\sqrt{gL}$	$R_n \times 10^{-6}$	V_{kts}	R_t	$10^3 C_t$	$V/\sqrt{gL}$	$R_n \times 10^{-6}$
1.00	0.89	4.326	.067	3.034	3.40	9.28	3.902	.226	10.32	4.40	17.95	4.507	.293	13.35
1.20	1.22	4.118	.080	3.641	3.50	9.76	3.873	.233	10.62	4.505	19.35	4.634	.300	13.67
1.405	1.60	3.940	.094	4.263	3.60	10.35	3.882	.240	10.92	4.70	21.50	4.731	.313	14.26
1.595	2.04	3.898	.106	4.839	3.70	10.98	3.899	.246	11.23	4.95	24.00	4.761	.330	15.02
1.80	2.51	3.766	.120	5.461	3.80	11.57	3.895	.253	11.53	5.10	26.48	4.949	.339	15.47
2.00	3.12	3.791	.133	6.068	3.90	12.28	3.924	.260	11.83	5.31	30.80	5.310	.353	16.11
2.20	3.79	3.806	.146	6.675	4.00	12.93	3.928	.266	12.14	5.50	35.35	5.680	.366	16.69
2.40	4.46	3.764	.160	7.282	4.06	13.60	4.010	.270	12.32					
2.60	5.23	3.761	.173	7.888	4.06	13.57	4.001	.270	12.32					
2.80	6.10	3.782	.186	8.495	4.10	14.02	4.054	.273	12.44					
3.00	7.02	3.791	.200	9.102	4.20	15.13	4.169	.280	12.74					
3.205	8.20	3.880	.213	9.724	4.30	16.45	4.324	.286	13.05					

ρ 1.9371 LBS. SEC^2/FT.^{4}
ν 1.1133 $\times 10^{-5}$ FT.^{2}/SEC.

BASED ON L_{WL}
L_{WL} ____ L_{BP}/L_{WL} ____
$\Delta/(0.01 L)^3$ ____
$\nabla/(0.01 L)^3$ ____
L/B_X ____ $L/\nabla^{1/3}$ ____
C_B ____ C_P ____ C_W ____
LCF ____ LWL AFT STA. 0
LCB ____ LWL AFT STA. 0
$S/\sqrt{\Delta L}$ ____

FIG. 78.Ka SNAME RD SHEET FOR ARCH-STERN TMB MODEL 4505-1

RATIOS AND COEFFICIENTS

L/B_X	6.978	C_P	0.627	C_W	0.723	A_X/A_M	1.002	MAX. IMB/B_X	1.003		
B_X/H	2.802	C_X	0.952	C_{PV}	0.825	B_X/B_M	1.0028	MAX. WLB/B_X	1.003		
$\Delta/(0.01OL)^3$	125.68	C_{PF}	0.601	C_{PA}	0.655	H_X/H_M	1.000	C_{IT}	0.528		
$\nabla/(0.100L)^3$	4.396	C_{WF}	0.612	C_{WA}	0.838	BKW/B_X	0.048	C_{IL}	0.462		
$L/\nabla^{1/3}$	6.105	C_{PVF}	0.935	C_{PVA}	0.744	BR/B_X	0.147	T_q	0.908		
$S/\nabla^{2/3}$	6.938	C_{PE}	0.623	C_{PR}	0.631	DR/B_X	0.014				
$S/\sqrt{\Delta L}$	16.61	C_{WE}	0.633	C_{WR}	0.827	HS/B_X	0.021				
C_B	0.597	C_{PVE}	0.938	C_{PVR}	0.727	$\overline{KB}/H$	0.557				

EXPANDED RESISTANCE DATA

DIMENSIONS FOR 400 FT. LENGTH

L 400 FT.	Δ 8043.2 TONS S.W.	T 59 °F	FRICTION BASIS	Schoenherr - Schoenherr
B_X 57.32 FT.	∇ 281,328 FT.^{3}	ρ 1.9905 LBS SEC^2/FT.^{4}		
H 20.46 FT.	S 29,786 FT.^{2}	ν 1.2817 x 10^{-5} FT.^{2}/SEC.	ROUGHNESS ALLOWANCE	0.30
TRIM 0 FT.				

REMARKS

$V/\sqrt{gL}$	.06	.08	.10	.12	.14	.16	.18	.20	.22	.24
$V/\sqrt{L}$	.202	.269	.336	.403	.470	.537	.605	.672	.739	.806
Ⓚ	.525	.700	.876	1.051	1.226	1.401	1.576	1.751	1.926	2.101
V kts	4.04	5.38	6.72	8.06	9.40	10.74	12.10	13.44	14.78	16.12
$10^{-6}R_n$	213	283	354	425	496	567	637	708	779	850
$10^3 C_f$	1.868	1.798	1.746	1.705	1.672	1.643	1.620	1.599	1.579	1.562
$10^3 C_r$	0.790	0.642	0.545	0.565	0.645	0.680	0.740	0.830	0.965	0.990
$10^3 \Delta C_f$	0.300	0.300	0.300	0.300	0.300	0.300	0.300	0.300	0.300	0.300
$10^3 C_t$	2.958	2.740	2.591	2.570	2.617	2.623	2.660	2.729	2.844	2.852
$10^3 C_t\ S/\nabla^{2/3}$	20.52	19.01	17.98	17.83	18.16	18.20	18.46	18.93	19.73	19.79
Ⓒ 400	0.818	0.757	0.716	0.710	0.723	0.725	0.735	0.754	0.786	0.788
R	3830	6290	9282	13244	18344	24002	30895	39105	49285	58791
R/Δ	0.48	0.78	1.15	1.65	2.28	2.98	3.84	4.86	6.13	7.31
EHP	48	104	192	328	530	791	1148	1614	2237	2910
TAYLOR EHP		95	190	320	510	765	1100	1535	2125	2860
EHP/TAYLOR EHP		1.094	1.011	1.025	1.039	1.034	1.044	1.051	1.053	1.018

$V/\sqrt{gL}$	.26	.28	.30	.32	.34	.36				
$V/\sqrt{L}$	.873	.941	1.008	1.075	1.142	1.209				
Ⓚ	2.277	2.452	2.627	2.802	2.977	3.152				
V kts	17.46	18.82	20.16	21.50	22.84	24.18				
$10^{-6}R_n$	921	991	1062	1133	1204	1275				
$10^3 C_f$	1.547	1.533	1.520	1.508	1.497	1.486				
$10^3 C_r$	1.050	1.360	1.850	1.980	2.210	2.790				
$10^3 \Delta C_f$	0.300	0.300	0.300	0.300	0.300	0.300				
$10^3 C_t$	2.897	3.193	3.670	3.788	4.007	4.576				
$10^3 C_t\ S/\nabla^{2/3}$	20.10	22.15	25.46	26.28	27.80	31.75				
Ⓒ 400	0.801	0.882	1.014	1.047	1.108	1.265				
R	70061	89716	118330	138910	165830	212240				
R/Δ	8.71	11.15	14.71	17.27	20.62	26.39				
EHP	3756	5184	7324	9170	11629	15757				
TAYLOR EHP	3870	5720	8850	11670	14550	19150				
EHP/TAYLOR EHP	0.973	0.906	0.828	0.786	0.799	0.823				

FIG. 78.Kb SNAME ERD SHEET FOR ARCH-STERN MODEL 4505-1

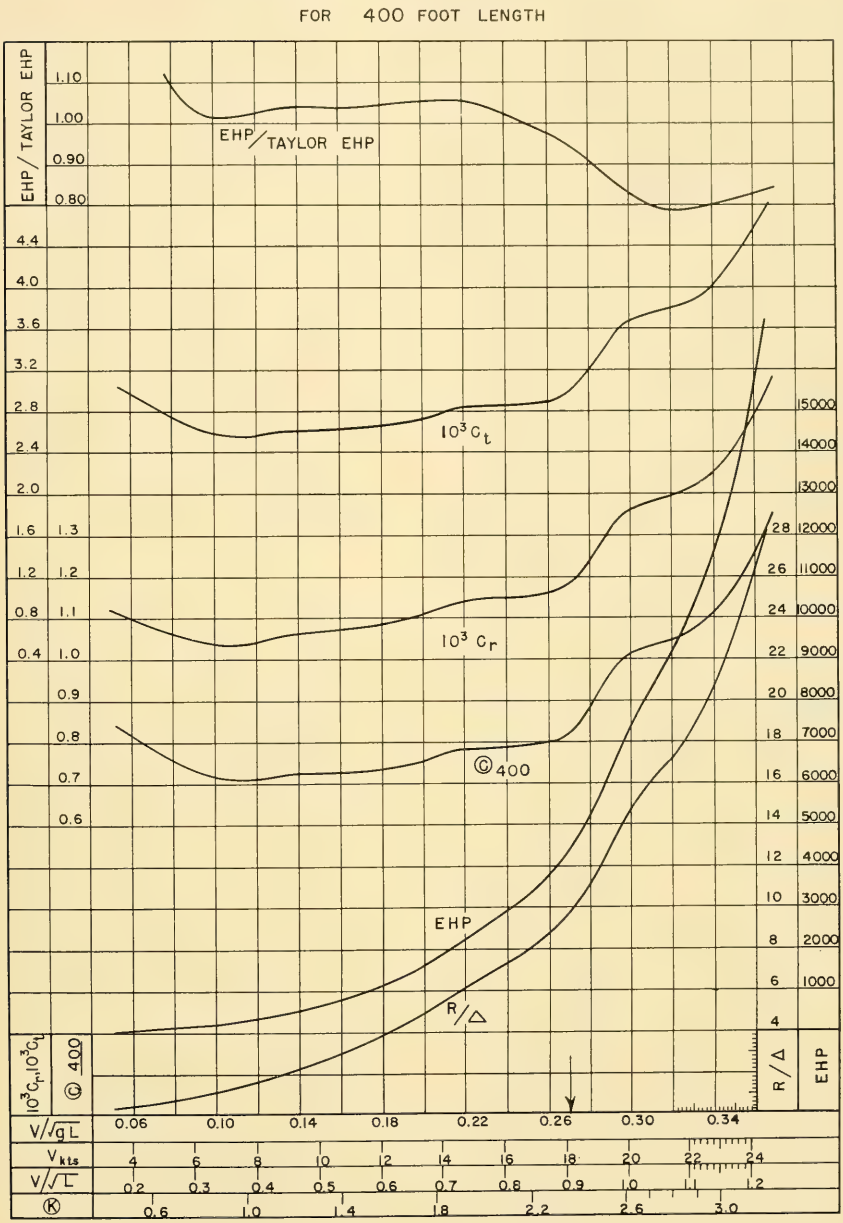

FIG. 78.Kc SNAME EXPANDED RESISTANCE CURVES FOR TMB MODEL 4505-1

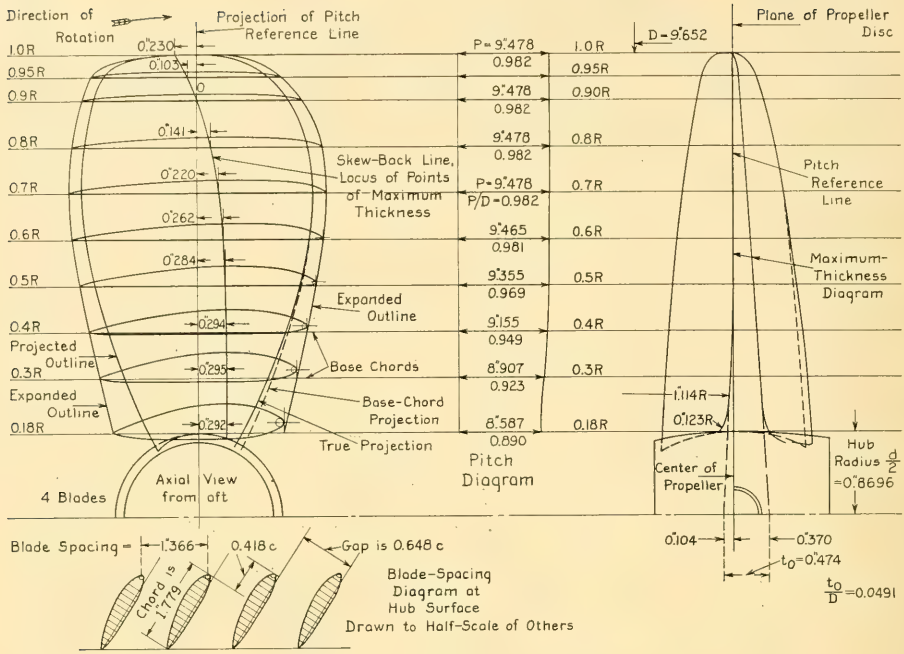

FIG. 78.L EMB MODEL PROPELLER 2294

Fig. 78.O is a plot of the observed total resistances R_T for the transom-stern model, TMB 4505, both with and without turbulence stimulation. Apparently, stimulation is not required on this model, nor do the stimulating devices (short studs) have any effect on the measured resistance. Included in the diagram is a plot of the dimensional ratio R_T/V^2, where R_T is in lb and V is in kt. It is customary at the David Taylor Model Basin to make this as a check while the resistance testing is in progress.

It was noted and commented on by the TMB staff members responsible for testing these models that their performance during the test runs was uniformly excellent. When measuring resistance, the models settled down quickly, allowing rapid adjustment of the pan weights. Once the correct weight was established there was little oscillation of the resistance scriber from the zero line. In the self-propulsion tests the actual D_{f0} weights used on the pan agreed very closely with the calculated D_f values, resulting in remarkably low ΔD_f corrections [C and R Bull. 7, 1933, pp. 37–38].

This consistency and reliability, for both models, is believed to be due directly to the fact that separation around the hull is limited to the region abaft the transom and that the separation points at the water surface always lie exactly at the outer corners of the transom. On a form having waterline slopes both less and greater than the critical slope for separation, the separation points may and undoubtedly do lie at slightly different positions for each run at the same speed. The positions depend upon the "history" of the viscous flow, on a distance basis, reckoned from the bow of the model back to the points in question. The separation points may not remain fixed during the constant-speed portion of a run, and they may not be opposite each other, on the two sides of the model.

The chemically traced flowlines on the surface of the transom-stern model, depicted in Figs. 78.C and 78.D of Sec. 78.7, reveal definite flow patterns. There appears to be no uncertainty on the part of the water as to the paths that it is to follow. There are no excessively wide, dark traces indicating undesirable slowing up in any region.

PROPELLER DESIGN DATA

DIAMETER, D 9.25 ft PITCH, P AT 0.70 R 9.08 ft P/D 0.982

NO. BLADES, Z 4 ROTATION RIGHT HAND DESIGNED rpm 200

HUB DIAMETER, d 1.667 ft d/D 0.180 c_m/D 0.238 t_0/D 0.0491

RAKE ANGLE 0 deg NATURAL TANGENT 0

REMARKS DESIGNED ORIGINALLY FOR SALVAGE VESSEL, U.S. NAVY

MODEL PROPELLER CHARACTERISTICS

PROPELLER NO. 2294 LABORATORY EMB DIAMETER, D 9.652 in

TEST V_0 2.08 to 5.50 kt TEST n_0 11.29 to 11.14 rps h_{axis}/D 1.088

DISC AREA, A_0 73.169 in^2 EXP. AREA, A_E 36.364 in^2 PROJ. AREA, A_P 30.994 in^2

EXP. AREA RATIO 0.497 PROJ. AREA RATIO 0.424

REMARKS ABC SHIP DATA D = 20.51 ft, d = 3.696 ft, P = 20.13 ft, rpm = 115

BLADE-SECTION DIMENSIONS AND RATIOS

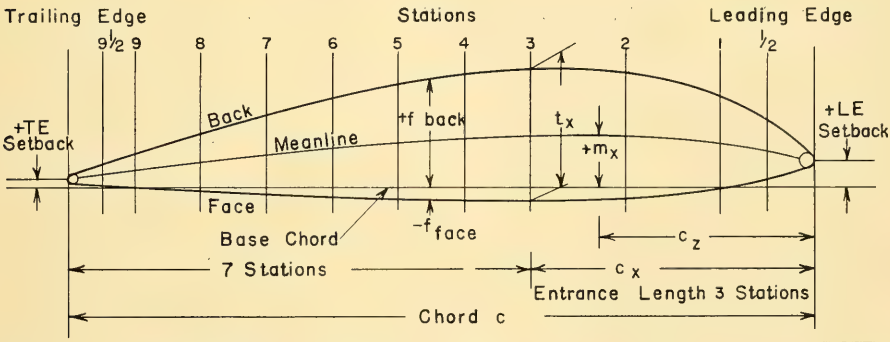

SECT	Chord c	Max Thickns t_x	Max Camber m_x	$\frac{t_x}{c}$	$\frac{m_x}{c}$	$\frac{c_x}{c}$	$\frac{c_z}{c}$	$\frac{c}{D}$	R_{TE}	TE Setback	LE Setback	R_{LE}	
HUB	1.779	.3713	.1248	.209	.0701	.336	.336	.184	.0109	.0717	.113	.0380	
0.3R	2.040	.3043	.1183	.149	.0580	.355	.355	.211	.00948	.0434	.0861	.0296	
0.4R	2.263	2496	.1126	.110	.0498	.370	.370	.234	.00835	.0205	.0635	.0226	
0.5R	2.466	.2043	.1022	.0829	.0414	.385	.385	.255	.00722	.00722	.0400	.0157	
0.6R	2.612	.1713	.08565	.0656	.0328	.400	.400	.271	.00609	.00609	.0174	.00870	
0.7R	2.682	.1383	.06913	.0516	.0258	.418	.418	.278	.00543	.00543	.00543	.00543	
0.8R	2.609	.1052	.05261	.0403	.0202	.444	.444	.270	.00543	.00543	.00543	.00543	
0.9R	2.290	.0722	.03609	.0315	.0158	.475	.475	.237	.00543	.00543	.00543	.00543	
0.95R	1.990	.0557	.02783	.0280	.0140	.491	.491	.206	.00543	.00543	.00543	.00543	

FIG. 78.Ma SNAME PD SHEET FOR EMB MODEL PROPELLER 2294

OPEN-WATER TEST DATA

BASIN EMB SIZE 470' x 42'.7 x 14'.7 TEST NO 1 DATE 7 APR. 1942

WATER T 60 deg F ρ 1.9383 lb-sec^2/ft^4 ν 1.2109 x10^{-5} ft^2/sec

FOR V_O = 4.06 kt and n_O = 10.58 rps, R_n at 0.7 R = 0.368 x10^6

V_O	n_O	T_O	Q_O	J	K_T	$10K_Q$	η_O	V_O	n_O	T_O	Q_O	J	K_T	$10K_Q$	η_O
0	5.773	11.84	1.325	0	.439	.611	0	4.68	10.91	6.84	1.200	.901	.071	.154	.658
0	6.560	15.24	1.696	0	.438	.606	0	4.73	10.69	5.74	1.067	.929	.062	.143	.640
2.08	11.29	30.84	3.783	.386	.299	.456	.403	4.91	10.64	3.39	0.800	.969	.037	.108	.526
2.23	11.48	30.94	3.825	.407	.289	.445	.421	5.20	10.72	1.44	0.567	1.018	.016	.076	.332
2.61	11.77	29.74	3.750	.466	.265	.415	.473	5.50	11.14	0.44	0.467	1.037	.004	.058	.125
2.88	11.59	26.74	3.442	.522	.246	.393	.519								
3.13	11.18	22.34	2.917	.588	.220	.358	.575								
3.30	11.00	19.54	2.583	.630	.199	.327	.610								
3.48	10.76	16.54	2.242	.679	.176	.297	.641								
3.60	10.62	14.74	2.021	.712	.161	.275	.665								
3.65	10.49	13.74	1.900	.731	.154	.265	.676								
3.87	10.46	11.94	1.700	.777	.135	.239	.699								
4.06	10.58	10.69	1.563	.806	.118	.214	.707								
4.35	10.72	9.24	1.438	.852	.099	.192	.701								

SECT	Ordinates	BLADE-SECTION STATIONS											Ordinates	SECT
		9 1/2	9	8	7	6	5	4	3	2	1	1/2		
HUB	f_b	.0600	.0922	.149	.202	.246	.283	.303	.310	.297	.247	.203	f_b	HUB
	f_f	-.0174	-.0322	-.0504	-.0591	-.0609	-.0609	-.0609	-.0609	-.0496	-.0052	.0348	f_f	
0.3R	f_b	.0565	.0843	.133	.177	.217	.246	.265	.270	.260	.218	.178	f_b	0.3R
	f_f	-.0148	-.0252	-.0339	-.0339	-.0339	-.0339	-.0339	-.0339	-.0339	-.0156	.0156	f_f	
0.4R	f_b	.0504	.0757	.119	158	.190	.216	.233	.237	.231	.194	.157	f_b	0.4R
	f_f	-.0087	-.0122	-.0122	-.0122	-.0122	-.0122	-.0122	-.0122	-.0122	-.0113	.0061	f_f	
0.5R	f_b	.045	.066	.103	.137	.165	.186	.200	.204	.200	.170	.134	f_b	0.5R
	f_f	0	0	0	0	0	0	0	0	0	0	.0017	f_f	
0.6R	f_b	.0435	.0591	.0870	.114	.137	.156	.168	.171	.166	.142	.109	f_b	0.6R
	f_f	0	0	0	0	0	0	0	0	0	0	0	f_f	
0.7R	f_b	.0400	.0539	.0756	.0957	.113	.126	.136	.138	.136	.116	.0878	f_b	0.7R
	f_f	0	0	0	0	0	0	0	0	0	0	0	f_f	
0.8R	f_b	.0339	.0443	.0583	.0722	.0852	.0957	.103	.105	.102	.0887	.0704	f_b	0.8R
	f_f	0	0	0	0	0	0	0	0	0	0	0	f_f	
0.9R	f_b	.0296	.0374	.0461	.0591	.0608	.0661	.0704	.0722	.0713	.0617	.0513	f_b	0.9R
	f_f	0	0	0	0	0	0	0	0	0	0	0	f_f	
0.95R	f_b	.0278	.0365	.0417	.0470	.0504	.0539	.0548	.0557	.0548	.0478	.0417	f_b	0.95R
	f_f	0	0	0	0	0	0	0	0	0	0	0	f_f	

FIG. 78.Mb OPEN-WATER TEST DATA FOR EMB MODEL PROPELLER 2294

CAVITATION TEST DATA

TUNNEL _____ TUNNEL JET _____ TEST NO. _____ DATE _____

WATER T _____ deg F VAPOR PRESSURE, e _____ lbs/ft^2 ρ _____ lb-sec^2/ft^4

AIR CONTENT _____ METHOD OF MEASUREMENT _____

V_o	P_{Abs}	n	T	Q	K_T	$10K_Q$	σ_v	V_o	P_{Abs}	n	T	Q	K_T	$10K_Q$	σ_v

OPEN-WATER CHARACTERISTICS AND CAVITATION CURVES

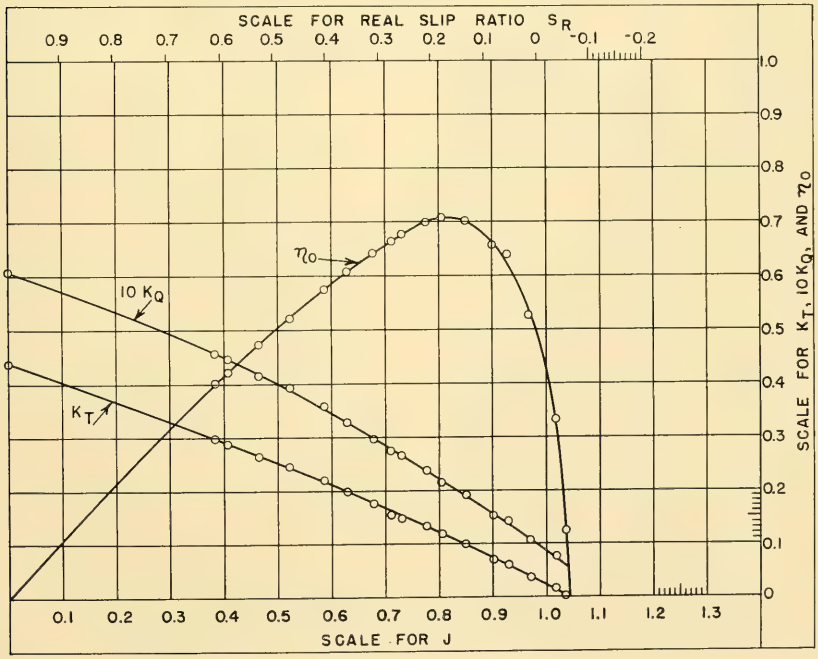

FIG. 78.Mc OPEN-WATER CHARACTERISTICS FOR EMB MODEL PROPELLER 2294

SELF-PROPELLED MODEL DATA

SHIP 510' x 73.08' x 26.163, 16573 T LABORATORY T.M.B. RESISTANCE DATA SHEET ____
S.S. PASSENGER CARGO, 20.5 KT BASIN DEEP WATER PROP. DATA SHEET ____
MODEL NUMBER 4505 BASIN SIZE 963' x 51' x 22' TURB. STIM. NONE
APPENDAGES RUDDER, MODEL LENGTH 20.'0 ft WATER TEMP. 66 deg F
BILGE KEELS, STEM CUTWATER MODEL DISPL. 2177 lb,FW ρ 1.9371 lb-sec^2/ft^4
MODEL TRIM 0 ft ν 1.1133 x10^{-5} ft^2/sec
FRICTION FORMULATION SCHOENHERR - SCHOENHERR $10^3 \Delta C_F$ 0.3
WETTED SURFACE, WITH APPENDAGES 74.608 ft^2

		INBOARD	OUTBOARD
REMARKS	PROPELLER(S) NO(S)	TMB 2294	
n_0 AND n ARE REVOLUTIONS	DIAMETERS	9.652 in	in
IN 101.33 FT.	PITCHES	9.475 in	in
	ROTATION	RH	

MODEL-SELF-PROPELLED TEST RESULTS

V	D_f	D_{fo}	R_I	EXPERIMENTAL DATA						CORRECTED RESULTS					
				INBOARDS			OUTBOARDS			INBOARDS			OUTBOARDS		
				T_0	Q_0	n_0	T_0	Q_0	n_0	T_0	Q_0	n_0	T_0	Q_0	n_0
2.20	1.25	1.24	2.396	2.87	.396	132.6				2.86	.395	132.5			
2.39	1.44	1.45	2.874	3.35	.474	130.8				3.36	.475	130.9			
2.60	1.67	1.65	3.450	3.82	.550	132.7				3.80	.547	132.5			
2.80	1.90	1.92	4.001	4.70	.627	131.9				4.72	.630	132.0			
3.00	2.14	2.15	4.586	5.22	.729	132.3				5.23	.730	132.4			
3.20	2.39	2.44	5.414	6.55	.834	132.9				6.60	.840	133.1			
3.40	2.66	2.75	6.228	6.55	.941	133.6				6.64	.952	134.0			
3.50	2.80	2.80	6.618	7.25	1.017	134.5				7.25	1.017	134.5			
3.60	2.91	2.93	7.009	7.30	1.093	135.0				7.32	1.096	135.1			
3.70	3.08	3.05	7.396	8.25	1.152	134.4				8.22	1.148	134.3			
3.80	3.21	3.15	7.804	8.28	1.217	134.5				8.22	1.179	134.3			
3.90	3.38	3.47	8.305	9.05	1.273	135.2				9.14	1.284	135.5			
4.06	3.62	3.48	9.385	10.00	1.475	136.9				9.86	1.457	136.5			
4.10	3.68	3.95	9.736	10.55	1.482	136.6				10.82	1.516	137.4			
4.20	3.86	3.83	10.921	11.75	1.702	139.4				11.72	1.697	139.4			
4.30	4.00	4.05	12.013	13.20	1.896	142.1				13.25	1.902	142.2			
4.395	4.16	4.23	13.372	16.00	2.107	144.2				16.07	2.114	144.3			
4.50	4.33	4.36	14.646	18.05	2.267	145.4				18.08	2.270	145.4			

FIG. 78.Na SNAME SPD SHEET FOR TRANSOM-STERN TMB MODEL 4505, OBSERVED DATA

	V	11	12	13	14	15	16	17	18	19	20	20.5	21	22
	$10^3(C_F+\Delta C_F)$	1.889	1.873	1.857	1.843	1.829	1.817	1.807	1.796	1.785	1.777	1.771	1.768	1.759
	$10^{-3}R_F$	31.480	37.145	43.222	49.750	56.677	64.062	71.922	80.143	88.747	97.895	102.44	107.38	117.25
	$10^{-3}R$	39.972	48.421	57.424	66.837	76.517	89.994	103.98	116.98	130.33	147.67	160.12	176.66	217.94
CENTER OR INBOARD SHAFTS	$10^{-3}T$	45.945	55.657	66.005	76.824	87.951	103.44	115.28	125.79	140.14	158.79	172.17	190.16	248.22
	$10^{-3}Q$	170.70	201.71	233.82	269.27	305.38	356.06	409.21	461.18	515.40	585.82	634.03	701.21	877.15
	rpm	56.9	62.1	67.3	72.4	77.8	83.5	89.3	95.0	100.1	106.0	109.7	113.9	123.8
	t	.130	.130	.130	.130	.130	.130	.098	.070	.070	.070	.070	.071	.122
	w_T	.220	.220	.220	.220	.220	.220	.216	.200	.190	.190	.190	.190	.205
	V_{AT}	8.58	9.36	10.14	10.92	11.70	12.48	13.33	14.40	15.39	16.20	16.60	17.01	17.82
	J_{RT}	.745	.745	.745	.745	.742	.739	.737	.749	.760	.755	.748	.738	.698
	J_{RQ}	.732	.736	.741	.746	.748	.749	.752	.751	.750	.746	.738	.729	.701
	s_{RT}	.241	.241	.242	.241	.243	.248	.249	.237	.226	.231	.238	.248	.276
	s_{RQ}	.254	.250	.245	.240	.237	.237	.234	.235	.236	.241	.248	.258	.286
	$1-w_T$	.780	.780	.780	.780	.780	.780	.784	.800	.810	.810	.810	.810	.795
	$1-w_Q$	.766	.771	.776	.781	.786	.791	.800	.802	.800	.800	.800	.800	.798
	η_{HT}	1.115	1.115	1.115	1.115	1.115	1.115	1.151	1.163	1.148	1.148	1.148	1.147	1.104
	η_{RT}	.957	.980	1.003	1.014	1.025	1.030	1.000	.971	.976	.971	.968	.961	.985
	η_{OT}	.684	.684	.684	.684	.682	.680	.678	.686	.691	.688	.685	.679	.655
	K_T	.148	.148	.148	.148	.149	.150	.152	.146	.141	.144	.147	.151	.169
	$10K_Q$	.267	.264	.261	.258	.257	.256	.253	.254	.255	.258	.262	.268	.285
OUTBOARD SHAFTS	$10^{-3}T$													
	$10^{-3}Q$													
	rpm													
	t													
	w													
	V_{AT}													
	J_{RT}													
	J_{RQ}													
	s_{RT}													
	s_{RQ}													
	$1-w_T$													
	$1-w_Q$													
	η_{HT}													
	η_{RT}													
	η_{OT}													
	K_T													
	$10K_Q$													
	EHP/SHP	.730	.748	.765	.774	.779	.781	.780	.775	.774	.767	.761	.749	.712
	EHP	1350	1784	2292	2873	3524	4421	5427	6465	7603	9068	10078	11390	14721
	SHP	1849	2385	2996	3712	4524	5661	6958	8342	9823	11823	13243	15207	20676

FIG. 78.Nb SNAME SPD SHEET FOR TRANSOM-STERN TMB MODEL 4505, DERIVED DATA

FULL-SCALE SHIP AND WATER CHARACTERISTICS; DATA AND CURVES

L 510 ft S 48514 ft^2 ρ 1.9905 $lb\text{-}sec^2/ft^4$

B_x 73.08 ft λ 25.5 ν 1.2817 $\times 10^{-5}$ ft^2/sec

H 26.193 ft $T_q = V/\sqrt{L}$ 0.908 AT 20.5 kt R_n 1378 $\times 10^6$

Δ 16573 t, SW, OF 34.977 ft^3/t T 59 deg F F_n 0.270

FULL-SCALE PROPELLER DATA

INBOARD DIAM. 20.510 ft
PITCH 20.134 ft
A_O 330.39 ft^2
A_P 139.96 ft^2
A_E 164.21 ft^2
OUTBOARD DIAM. ft
PITCH ft
A_O ft^2
A_P ft^2
A_E ft^2

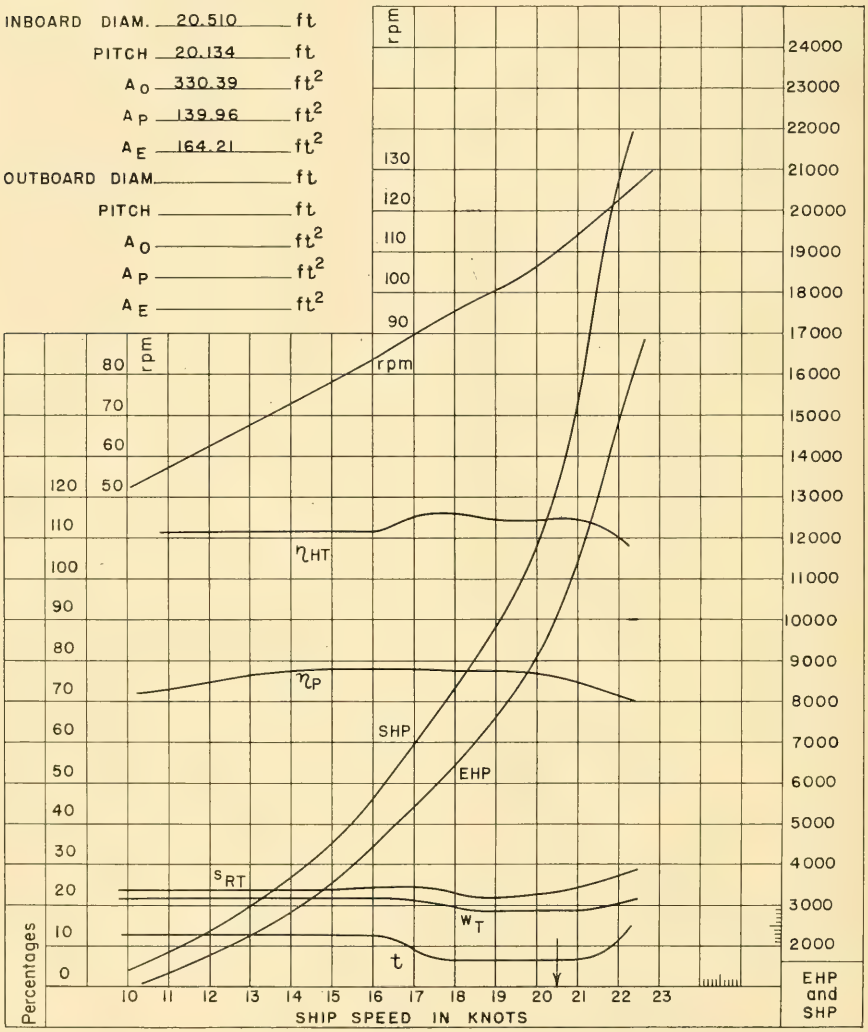

FIG. 78.Nc FULL-SCALE SHIP AND WATER CHARACTERISTICS FOR TRANSOM-STERN MODEL 4505 WHEN SELF-PROPELLED

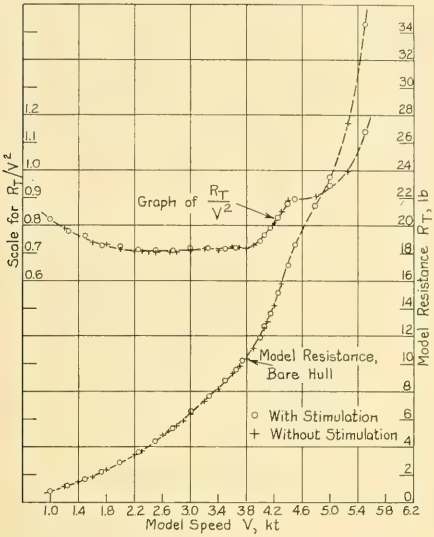

FIG. 78.O PLOT OF TOTAL RESISTANCE R_T AND OF RATIO R_T/V^2 FOR TMB MODEL 4505

The off-surface vanes mounted along the bilges likewise showed no uncertainty as to the proper water direction. The bilge-keel traces deduced from them are remarkedly fair.

Taking first the transom-stern design, represented by TMB model 4505, and analyzing the speed-power differences between the values calculated on paper and those predicted from the model tests, certain features stand out:

(1) It was both conservative and optimistic to estimate, as was done in Sec. 66.9, that the resistance would be no lower and no higher than that of the Taylor Standard Series hull of the same proportions. In the first place, it was difficult to assess the effect of the transom in advance. In the second place, it was known that a sizable bulb was to be used at the bow but it was questionable whether this bulb would be beneficial at the low T_q of 0.908. Actually, the effective power P_E is about 3.5 or 4 per cent *lower* than the TSS effective power at that T_q .

(2) The wake fraction w of 0.30 used for the transom-stern hull in the shaft-power estimate of Sec. 66.27 was derived from the best available data on the self-propulsion of single-screw models. It was admittedly optismistic; indeed, since a value of only 0.190 was achieved in the model self-propulsion test, the estimate was unduly optimistic. The calculation of Sec. 60.8, using K. E. Schoenherr's formula [PNA, 1939, Vol. II, p. 149], was not made until after the hull form had been completely fashioned and a stock propeller had been selected for the first SP tests. Even then, the predicted value of w was 0.255, considerably higher than the test value of 0.190 from Figs. 78.Nb and 78.Nc.

(3) The estimated thrust-deduction fraction t of 0.20, used in Sec. 66.27, is close to the value of 0.30(0.7) = 0.21, derived by Eq. (60.vi) from K. E. Schoenherr's simple formulas [PNA, 1939, Vol. II, pp. 149–150] on the basis of using a streamlined rudder. When the transom-stern ABC hull had been fully shaped, and it was known that a contra-rudder was to be fitted, a smaller value of t was selected. Taking the coefficient 0.5 listed for contra-rudders in Sec. 60.9, the new t-value would have been 0.255(0.5) = 0.128. Utilizing the stern shape of the hull by the method illustrated in Fig. 67.V, and taking account of the rudder, the predicted thrust-deduction fraction from the upper graph of Fig. 60.P was 0.135. There appeared to be little justification for anticipating a low t-value of 0.07, as was actually derived from the self-propulsion tests. Nevertheless, the hull efficiency η_H of 1.161, estimated by using a wake fraction of 0.255 and a thrust-deduction fraction of 0.135, is remarkably close to the value of 1.148 derived from the self-propelled model-test data of Fig. 78.Nb. The hull efficiency of 1.143, estimated at an early stage of the design and set down in Sec. 66.27, is likewise remarkably close to both these figures.

(4) The estimated P_E/P_S ratio or η_P value of about 0.74 of Secs. 66.9 and 66.27 was admittedly somewhat random and even more hopeful. The higher η_P of 0.761 from the model tests may be due to the care with which the afterbody and skeg were shaped, in an effort to achieve good flow to the wheel. On the other hand, it may be ascribed to the use of:

(a) The contra-fashioning of the rudder-support skeg and the rudder, which had not yet been decided upon when the power estimates of Secs. 66.9 and 66.27 were made

(b) A propeller diameter somewhat larger than the average. A diameter of 0.7 the draft, one of the simple rules, would have been 0.7(26) = 18.2 ft, whereas the corresponding diameter was 20.51 ft for the stock propeller used.

(c) A centerline skeg that was unusually thin and narrow, in a deliberate effort to cut down the thrust deduction.

A designer may well question the usefulness or the validity of an estimating procedure, recommended for use in the paper stage of a preliminary design, which says (in Sec. 66.27) that 16,930 horses will be required at the shaft at the designed speed while the test results of a self-propelled model, from Fig. 78.Nb, indicate that the shaft power need not exceed 13,250 horses. Allowing say 2 per cent for the resistance of a scoop not fitted to the model, and for power to drive the circulating water through the condenser of the main propelling plant, the model prediction corresponds to a reduction of some 19 per cent in the estimated power. Conversely, the calculation represents an increase of about 25 per cent in the shaft power predicted by the self-propelled model test. It must be remembered, however, that little or nothing was known of the shape or details of the hull when the first and larger estimate was undertaken.

Actually, a third approximation or estimate of the shaft power should have been made for the transom-stern ABC ship after the lines had been drawn, the appendages designed, and the stock propeller selected. This could have been done while the model was being built. With data available as listed hereunder, the procedure and results are outlined briefly in the following:

(i) When the manner of plating the hull has been decided, the roughness allowance ΔC_F (for the clean, new hull) of $0.4(10^{-3})$ of Sec. 66.9 is reduced to the value of $0.3(10^{-3})$ of Sec. 78.6. This means that $C_F + \Delta C_F$ is $(1.470 + 0.3)(10^{-3}) = 1.770(10^{-3})$. Adding the value of C_R of $1.246(10^{-3})$ from Sec. 66.9, C_T is $(1.246 + 1.770)(10^{-3}) = 3.016(10^{-3})$. Then

$$\begin{aligned} R_T &= (\rho/2)V^2SC_T \\ &= (0.99525)(34.62)^2(46{,}231)(3.016)(10^{-3}) \\ &= 166{,}322 \text{ lb.} \end{aligned}$$

(ii) With the appendages designed, and with no condenser scoops to be added or cooling water to be circulated in the model, there is no longer any reason for doubling the calculated appendage-resistance increase of 4 per cent or for adding the full scoop resistance, as was done in Sec. 66.9. The augment of resistance for the appendages is then taken as 5 instead of 10 per cent.

(iii) Applying the 1.05-factor from (ii) to the R_T of (i) preceding,

$$R_{T(\text{App})} = (1.05)(166{,}322) = 174{,}638 \text{ lb.}$$

(iv) The thrust-deduction fraction t, using the area factor 0.172 from Fig. 67.V and entering the upper graph of Fig. 60.P, is 0.135. This procedure takes account of the presence of the rudder in each case. The estimated value of the propeller thrust T is

$$174{,}638/(1 - 0.135) = 174{,}638/0.865 = 201{,}894 \text{ lb.}$$

(v) The wake fraction w predicted from the Schoenherr formula, using Eq. (60.ii) and the ship and propeller dimensions at this stage, is 0.254. The speed of advance at 20.5 kt is $20.5(1 - 0.254) = 20.5(0.746) = 15.29$ kt or 25.82 ft per sec.

(vi) The ram-pressure load over the disc area of the 20-ft ship propeller is $(\rho/2)A_0V_A^2 = qA_0 = 0.99525(25.82)^2(0.7854)(20)^2 = 208{,}609$ lb.

(vii) With a thrust T from (iv) preceding of 201,894 lb, the thrust-load factor $C_{TL} = T/(qA_0) = 201{,}894/208{,}609 = 0.968$. This is somewhat less than the value of 1.287 predicted in Sec. 66.27. It means that the real efficiency of the propeller will be somewhat higher than previously estimated.

(viii) The rate of rotation of the ship propeller is not known at the stage at which this approximation is made. It is therefore assumed that its real efficiency will be $0.8\eta_I$, based upon the reasoning of Sec. 34.4. Consulting Fig. 34.B with the C_{TL} value of 0.968, the predicted real efficiency η_0 is 0.665.

(ix) With a w-value of 0.254 and a t-value of 0.135, the corresponding η_H is $(1 - t)/(1 - w) = (1 - 0.135)/(1 - 0.254) = 0.865/0.746 = 1.160$. Assuming an η_R-value of 1.02 from K. E. Schoenherr [PNA, 1939, Vol. II, p. 150], the estimated propulsive coefficient η_P is $\eta_0(\eta_H)\eta_R = 0.665(1.160)1.02 = 0.787$.

(x) The predicted shaft power is $R_{T(\text{App})}V/(550)(0.787) = 174{,}638(34.62)/432.85 = 13{,}968$ horses.

This is only 5.5 per cent greater than the P_S of 13,243 horses derived from the model self-propulsion test. The η_P of that test, at 20.5 kt, was 0.761 and the η_R only 0.968. The real efficiency of the stock propeller used was 0.685 instead of the 0.665 predicted by the estimate of (viii) preceding.

Values of the propulsive coefficient η_P derived from the self-propelled test of the ABC transom-stern model, for a range of ship speed from 9 to 23 kt, are plotted in Fig. 78.P. For comparison

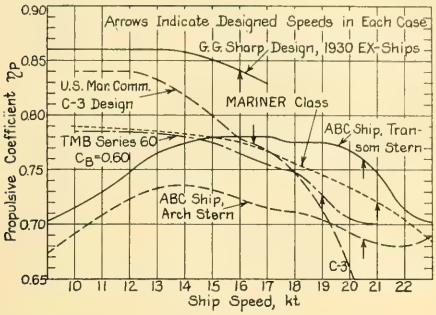

FIG. 78.P COMPARISON OF PROPULSIVE COEFFICIENT η_P FOR MODELS OF ABC SHIP AND OTHER DESIGNS

there are plotted similar values for the ABC arch-stern model, for the TMB Series 60 model having a C_B of 0.60, and for three types of merchant vessels of outstanding performance, from the period 1930–1955.

Incidentally, the Telfer merit factor of Eq. (34.xxv) of Sec. 34.10 of Volume I, based upon the model predictions from tests of the transom-stern model, is

$$M = 0.61 \frac{W(\text{long tons})V^3(\text{kt})}{L(\text{ft})P_S(\text{horses})}$$

$$= 0.61 \frac{16{,}573(20.5)^3}{510(13{,}243)}$$

$$= 12.895$$

For a T_q of 0.908, an F_n of 0.2704, and an F_n^2 of 0.07312, this value is well above the meanline of Fig. 34.I, from which a value of about 9.5 was used for the first shaft power approximation of Sec. 66.9.

To return to an analysis of the behavior of the transom-stern ABC model, a reduction in calculated shaft power of the magnitude indicated in the foregoing is comforting from the point of view of first cost and operation. However, it means to the designer that a new weight estimate is in order, with machinery and fuel weights, as well as overall displacement, that are appreciably diminished. For a project that is being done thoroughly it may even mean a revision of the preliminary design and the running of additional model tests, on the basis that a revised hull of slightly smaller volume will be as efficient as the first hull.

However, before any radical steps are taken, the following items are to be considered:

(I) The procedure for running the model self-propulsion test does not take full account of the increased roughness effect to be encountered on the ship as compared to that on the model, even when the ship hull is clean and new

(II) A re-reading of the items previously listed in this section indicates that all the differences between the original calculated or estimated performance of the ship and the actual performance of the model are in favor of the ship design as represented by the model.

In other words, practically everything that has been done to develop the ship, from the time that it had principal dimensions and proportions only, has made it better than the "phantom" ship of the Taylor Standard Series form having the same proportions. To assume that all these favorable factors will carry over into the full-scale ship on trial, and at the magnitudes indicated by the model test, is expecting a great deal.

Just how much of the indicated reduction in shaft power can be carried into the next stage of the preliminary design should perhaps be determined only after the model is modified as described in Sec. 78.18, and after the modified model is tested self-propelled with the new propeller designed in Chap. 70.

The lower graph of Fig. 78.Q reveals that for the transom-stern ABC design the increase of resistance for appendages, over most of the speed range, averages about 5 per cent. This corresponds to the estimate made earlier in the present section. However, in the vicinity of 22 kt ship speed, the effective power with all appendages is *lower* than the effective power in the bare-hull condition! Since the ship will probably never run at this speed, except at light load when the immersed hull has a different effective shape, the reason for this anomaly is somewhat of an academic matter. The variations with speed in the ratio of (1) effective power with appendages to (2) bare-hull effective power shown by Fig. 78.Q indicate that the appendage resistance is probably related to wavemaking around the ship. Further than this it has not been possible to account for the unusual feature described.

It is considerably more difficult to analyze the performance of the arch-stern design, TMB model 4505–1, because of its unusual hull shape and the almost total lack of reference data for such a form. Despite the drastic change in shape of the run from the normal transom stern, and an

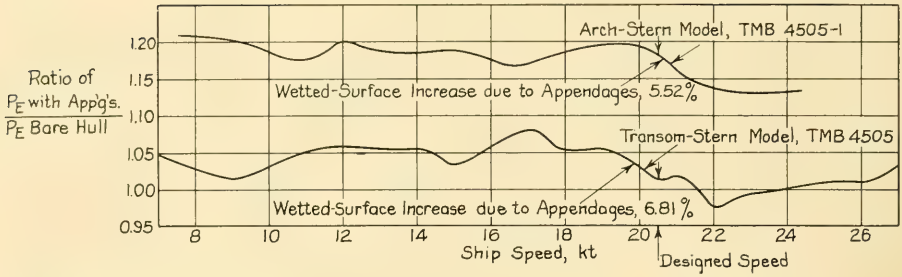

Fig. 78.Q Ratios of Effective Powers, With and Without Appendages, for Transom-Stern and Arch-Stern ABC Designs

increase of bare-hull wetted surface of 5.8 per cent over that of the bare transom-stern hull, the effective power P_E at designed speed is about 2 per cent *lower* than that of a Taylor Standard Series hull of the same proportions. This superiority increases rapidly with speed above the trial speed of 20.5 kt, even more so than for the transom-stern hull.

Although the several appendages were designed with great care, the increase in resistance of 18 per cent due to them appears high. However, in this case the wetted areas of the exposed shaft, the strut hub, and the quadruple strut arms are not added to the bare-hull wetted area. Consequently, the pressure drag of these parts is certain to show up as a large augment of the specific residuary resistance C_R. Subsequent discussion with designers of tunnel-stern shallow-water craft reveals that appendage resistances in this type of vessel are consistently high.

When making propeller calculations preparatory to selecting the stock propeller, mentioned in Secs. 70.6 and 78.4, values of the probable wake and thrust-deduction fractions were determined by the Schoenherr formulas used for the transom-stern design. On this basis, admittedly inadequate but the only one available, the values derived for the arch stern were 0.273 for the wake fraction and 0.164 for the thrust-deduction fraction.

For the designed or trial speed of 20.5 kt, the arch-stern self-propelled data from Fig. 78.I are:

Shaft power, 18,300 horses
Effective power, 12,500 horses
Propulsive coefficient $\eta_P = P_E/P_S = 0.686$
Wake fraction, 0.072
Thrust-deduction fraction, 0.175
Hull efficiency $\eta_H = (1 - 0.175)/(1 - 0.072) = 0.889$.

The expected high wake inside the arch did not exist. In fact, the w-value derived from the self-propulsion test was only slightly more than one-quarter of the estimated value. The thrust-deduction fraction was slightly higher than the anticipated value of 0.164. It was known that large thrust-deduction forces would be generated by the four strut arms lying in the outflow jet of the propeller, but it was hoped that these would be partly or wholly compensated by the contra-effect on these arms. It is possible that there were appreciable upward components of velocity in the flow passing the two horizontal arms. This would have increased the appendage resistance as well as the thrust-deduction forces.

Nevertheless, the propulsive coefficient of over 0.68 is extremely high for this type of stern, where values of 0.50 are considered very good.

Analysis indicates that the real or working efficiency η_0 of the large-diameter 24.22-ft propeller at the designed speed of 20.5 kt is about 0.750. This is higher by 6.5 points, or 9.5 per cent, than the η_0 for the 20.51-ft wheel of TMB model 4505 of the transom-stern ship.

78.18 Proposed Changes in Final Design of ABC Ship. In the normal course of a building program for a multi-million dollar ship the design and model-testing procedure described in Part 4 represents only the early stages of the development prior to the completion of the contract plans. Nevertheless, the designer who has carried the ship along this far is convinced that, given a little more time, he can modify and improve upon it considerably. A few such improvements are outlined here for the ABC ship.

In the first place, the designed waterlines of both alternative hulls have values of transverse square moment of area I_T that are certainly on

the low side. Furthermore, the change of direction of the water flowing around and under the forward sections, forward of the quarterpoint at Sta. 5, is more abrupt than it should be. The almost obvious step is to widen the designed waterline still further in way of Stas. 3 and 4, following an earlier change, and to trim away the hull lower down in this region. This gives a better path to the water. The change is reflected in a lowering of the minimum value of the section coefficient ahead of the forward quarterpoint. Sec. 67.10 calls attention to the fact that this is rather high for good design.

At this stage, a few details need to be watched but not necessarily corrected. One such relates to the midships portion of the designed waterline of the ABC ship. In the final fairing of the lines preparatory to making the model the maximum section fell at Sta. 10.6 or 0.530L rather than at Sta. 10.3 or 0.515L. The beam at this section (Sta. 10.6) faired to a value of 73.33 ft rather than 73.0 ft. As the $\overline{\text{LMA}}$ of 0.530L still fell within the design lane of Fig. 66.L (it lies to the left of the double circle in that figure), and as the ship was to have a transom stern which made it easier to obtain small waterline slopes in the run, this value was accepted. The slightly larger beam was also accepted as the waterline curvature plot with this beam proved to have most of the desirable features. The final dimensions and coefficients of the ABC ships as built into the models are given in the SNAME RD sheets of Figs. 78.J and 78.K.

After the bilge-keel trace for the forebody had been determined on the model it developed that the combination of bilge-keel width shown on Fig. 73.N and the bilge-keel trace caused the outer edge of the keel to project beyond the DWL in the upright position from Sta. 8 forward to about Sta. 6.5. The requirements of item (48) in Table 64.f call for no projections beyond the fair line of the hull for the first 150 ft from the stem. Sta. 6.5 is about 166 ft from the FP. However, for ease in handling, the hull shape should embody one of the following modifications:

(a) Determine whether the widening of the DWL in the entrance, proposed earlier in this section, would bring the present keels within the DWL limits. If not,

(b) Taper the forward end of the keels to a greater extent and reduce the width back to at least Sta. 8

(c) Retain the same leading-end taper but shorten the keels, moving the leading ends aft from Sta. 6.4 to about Sta. 7.5.

The principal question is, what to do to improve the hydrodynamic performance of either or both of the alternative designs? The basis for this step is to find out just what gives them the performance they now have. What is it, for example, that causes the thrust-deduction fraction t of the transom-stern form to drop from a constant value of 0.125 or 0.13 in the intermediate-speed range to a remarkably low value of 0.07 in the normal running range of 18 to 20.5 or 21 kt? With a nearly constant wake fraction and propulsive coefficient the hull efficiency rises but the relative rotative efficiency η_R drops. There is a slight hump in the C_R curve of the 400-ft ship in Fig. 78.Jc at a T_q of 0.68, probably because at this speed the ship is only some 2.5 Velox wave lengths long. There is a smaller but sharper hump at a T_q of about 0.83. For the 510-ft ABC ship the corresponding speeds are 15.4 and 18.7 kt. From Fig. 78.Nc it is noted that these humps occur somewhat beyond the *ends* of the transition portions in the t and η_{HT} curves [where $\eta_{HT} = \eta_H = (1 - t)/(1 - w)$]. Beyond 21 kt for the ABC ship, at a T_q of about 0.93, when the ship length is approaching 1.5 wave lengths, the propulsive efficiency falls off, as it does in most ships above the designed speed. However, the superiority over the Taylor Standard Series hull, in respect to resistance and effective power, increases in this range.

A search for improvement obviously calls for a careful determination and rather close study of the wave profiles and flow patterns around the hull and into the propeller at the 16- and 18-kt speeds, perhaps also at the 21-kt speed.

The fact that, despite an increased wetted-surface area of 5.8 per cent, the resistance of the arch-stern bare hull drops below that of the transom-stern bare hull at 28 kt, where the T_q is about 1.240, is well worth looking into. The remarkably low resistance of both hulls in the 23- to 25-kt range indicates that these forms might well find application to shorter, high-speed vessels.

On the basis that, of the two alternative sterns, the transom-stern arrangement has selected itself, so to speak, the owner-operator now has two choices. Either he may:

(1) Hold the speeds originally called for, adhere to the schedule already set up, and reduce the

engine power by a substantial amount, of the order of 15 or more per cent, or he may

(2) Step up the schedule, retain the engine power originally estimated, and increase the ship speeds, both sustained and trial.

The background for this decision involves hydrodynamics in only a small way but it is useful to discuss that small influence. Consulting the speed-power curves of the transom-stern design in Fig. 78.Nc, and assuming no scale effect between model and ship, it is safe to assume that the ship can make 21.1 kt with a shaft power of 16,000 horses, retaining the former limit of 0.95 times the maximum designed shaft power. Stepping up the sustained speed to 19.5 kt, at which about 10,750 horses are required for deep-water, clean-bottom conditions, means that this speed can be achieved with a power expenditure of only 67.2 per cent of the 0.95-maximum limit. This is still conservative planning.

At the 21.1-kt speed the P_E/P_S ratio drops to 0.75, and the hull efficiency η_{HT} to 1.14, with only small changes in the t and w values. At the 19.2-kt speed these factors have about the same values as at 18.7 kt. In other words, the ship is still running efficiently, in the higher range, so far as speed and power are concerned. The rpm's increase from 110 to 114 at the higher trial speed but this permits smaller and lighter gears than were originally involved. To be sure, the sustained speed is increased only 0.8 kt, an increase of but slightly over 4 per cent from 18.7 kt. This may not be sufficient to make the increased power economically worth while.

The history of mechanically driven vessels, extending back for more than a century and a half, is replete with instances of re-engining at greater powers. Some of this may have been due to increases in load and in displacement. Much of it was undoubtedly to reduce fuel consumption by the use of more efficient machinery. Not a little was carried out to increase the sustained speed, so as to keep pace with newer ships. The economic features are not discussed here, but the ship that benefits the most by this re-engining is the one which has a speed margin designed into the hull in the first place. It is a good sign, in a way, that the ABC ship is a better performer at higher speeds than at the speed for which it was designed.

78.19 Comments on Illustrative Preliminary-Design Procedures of Part 4. The illustrative examples worked into Part 4 of the book, comprising the large ABC ship of the early chapters and the motor-driven tenders of Chap. 77, are carried only far enough to demonstrate the use of the various graphs, diagrams, and rules embodied in the text. The limited treatment in these chapters is by no means to be taken as an indication that the preliminary hydrodynamic design for an actual ship can or should be limited to that set down in this volume. Problems of maneuvering and of wavegoing are discussed more fully in Volume III, Parts 5 and 6, respectively.

For example, considering first the features commented upon in the present chapter, relating to the ship itself:

(1) It is apparent from the position of the wave profile observed on the transom-stern model and drawn on the afterbody portion of Fig. 66.R that the transom did not clear at the designed speed, despite previous indications to the contrary. In fact, it did not clear fully until the speed was far in excess of any speed that the ship could reasonably have attained. The reason appeared to be the large upward component of flow in the water just below the lower edge of the transom. Nevertheless, with a resistance some 4 per cent less than that of a Taylor Standard Series model of the same proportions there appeared to be no reason for changing the existing transom stern without the benefit of a further extended study. In any further development of this design, studies of the separation drag abaft the transom, mentioned in (2) of Sec. 78.6, should be pursued.

(2) The so-called neutral positions of the two lower (horizontal) strut arms in the arch-stern design should have been established *before* the design of the quadruple strut-arm and hub assembly was finished and this appendage was added to the model. The small-scale assembly could readily have been constructed to permit changing these positions on the self-propelled model, or some special means could have been provided whereby the flow in this region could have been observed in greater detail during the circulating-water-channel test.

(3) No attempt is made in Part 4 of the book to calculate or estimate the power that would be required to move the necessary amount of cooling water through the main condenser at the designed ship speed.

Considering next a few of the ship features mentioned in the early chapters of this part, and not worked out adequately there:

(i) Further studies should be made of the internal arrangements, supplementing the discussion in Sec. 66.32, to enable the vessel to float at the intermediate-load waterlines indicated in Fig. 66.T. These should be combined with studies of the effect of the variable weights, in each of the proposed arrangements, upon the bending moments imposed on the hull structure.

(ii) Estimates should be made of the effective and shaft powers and probable speeds in the variable-load conditions, for both deep and shallow water

(iii) The sinkage of the bow at designed speed, indicated on Figs. 58.B and 66.R, is rather large. The widening of the designed waterline forward, as proposed in the first part of Sec. 78.18, should improve this situation.

(iv) A study, much more comprehensive than that of Sec. 60.15, should be made of the effect of fouling on the total resistance, on the wake and thrust-deduction fractions, the propeller thrust, and the propeller (or shaft) power.

There was no time or opportunity to design, lay out, and test a third alternative stern for twin-screw propulsion of the ABC ship, as mentioned in Sec. 69.5 on page 571.

With respect to the preliminary hydrodynamic designs of the two small motor-driven tenders for the ABC ship, serving as the illustrative designs in Chap. 77, the treatment given there is likewise abbreviated. For a well-rounded project, even of this limited scope, a number of additional items should be considered:

(a) A determination, by the best methods available, of the lowest speed at which the 24-kt V-bottom hull would actually plane, when carrying the specified load. This would indicate whether the craft could still run in the planing range if slowed by wind and sea, as mentioned in (3) of Sec. 77.6.

(b) For the examples cited, involving motorboats which are to be in the water only for the hours in which they are required to run, the additional weight due to water soakage is not a problem. Nevertheless, this item must be considered for motorboat designs in general.

(c) It is possible that for a motorboat, on which the propelling machinery receives much less care than on a large vessel, the reduction from maximum rated power to maximum sustained usable power should be considerably larger than 5 per cent of the former, as recommended for large vessels

(d) For the particular illustrative examples described, a comprehensive preliminary design should include a check on the fore-and-aft trim with full fuel and crew but with no cargo or passengers

(e) An adequate preliminary design for a full-planing boat should include an estimate of the vertical forces and pitching moments to be expected from propulsion devices carried at the stern

(f) Definite steps should be taken to reduce the running trim of a 35- or 40-ft motorboat which, as indicated in the early stage of the preliminary design for the ABC tender, is as great as 5 deg. The trim limit in this respect probably should diminish as the absolute size of the boat increases.

APPENDIX 1

Symbols and Their Titles

X1.1 General. This appendix lists all the symbols employed in the text of Volume II except for a few used and described or defined locally and not having general application. It is identical, except for one or two deletions, a few additions, and minor modifications in titles, to the list of symbols and their titles in Sec. X1.5 of Appendix 1 of Volume I, pages 597–611.

Notes relating to prior approval of these symbols, subscripts for use with them, the method of indexing, and abbreviations accompanying them are found in Secs. X1.1, X1.2, X1.3, and X1.4 on pages 596–597 of Volume I and need not be repeated here.

It is expected that a much more comprehensive list of symbols and terms, with complete definitions, in the form of a "Nomenclature for Hydrodynamics as Applied to Ship Design," will appear eventually as an SNAME publication. In the meantime, use can be made of the definitions in SNAME Technical and Research Bulletin 1–12, "Explanatory Notes for Resistance and Propulsion Data Sheets," July 1953.

The Greek Alphabet.

Α	α	alpha	(ăl′fȧ)	*Α*	*α*
Β	β	beta	(bā′tȧ; bē′tȧ?)	*Β*	*β*
Γ	γ	gamma	(găm′ȧ)	*Γ*	*γ*
Δ	δ	delta	(dĕl′tȧ)	*Δ*	*δ*
Ε	ε	epsilon	(ĕp′sĭ lŏn)	*Ε*	*ε*
Ζ	ζ	zeta	(zā′tȧ; zē′tȧ?)	*Ζ*	*ζ*
Η	η	eta	(ā′tȧ; ē′tȧ)	*Η*	*η*
Θ	θ	theta	(thā′tȧ; thē′tȧ)	*Θ*	*ϑ*
Ι	ι	iota	(ī ō′tȧ)	*Ι*	*ι*
Κ	κ	kappa	(kăp′ȧ)	*Κ*	*κ*
Λ	λ	lambda	(lăm′dȧ)	*Λ*	*λ*
Μ	μ	mu	(mū; mōō; mü)	*Μ*	*μ*
Ν	ν	nu	(nū; nü)	*Ν*	*ν*
Ξ	ξ	ksi	(zĭ; kse̅)	*Ξ*	*ξ*
Ο	ο	omicron	(ŏm′ĭ krŏn; omĭ′; om′ĭ kroṅ)	*Ο*	*ο*
Π	π	pi	(pĭ; pē)	*Π*	*π*
Ρ	ρ	rho	(rō)	*Ρ*	*ϱ*
Σ	σ	sigma	(sĭg′mȧ)	*Σ*	*σ*
Τ	τ	tau	(tou)	*Τ*	*τ*
Υ	υ	upsilon	(ūp′sĭ lŏn)	*Υ*	*υ*
Φ	φ	phi	(fĭ; fe̅)	*Φ*	*φ*
Χ	χ	chi	(kĭ; kē; kē ~ chē)	*Χ*	*χ*
Ψ	ψ	psi	(sĭ; pse̅)	*Ψ*	*ψ*
Ω	ω	omega	(ō mē′gȧ; ō′mĕ gȧ; ô mĕg′ȧ)	*Ω*	*ω*

X1.2 List of Symbols and Titles.

a—Acceleration, linear

a—Air-content ratio or relative air content

a—Vortex spacing, transverse, in a vortex street or trail

A—Area in general; a projected area; area of a transverse section of a body or ship, projected on the transverse y-z plane

A_y—Area, maximum centerplane, of a submerged body or ship, projected on the x-z or centerline plane; not to be confused with A_L, the lateral area of the underwater body of a surface ship

A_z—Area, maximum horizontal, of a submerged body or ship, projected on the x-y or baseplane; not to be confused with A_W, the waterplane area of a surface ship

A_A—Area, abovewater, projected, at any selected bearing or viewing angle

A_B—Area, projected, of bow diving planes of a submarine

A_C—Area, projected chine, of a planing craft

A_D—Area, developed blade, of a screw propeller, outside the boss or hub

A_E—Area, expanded blade, of a screw propeller, outside the boss or hub

A_H—Area of any hydrofoil, projected on a plane through the base chords, meanlines, or equivalent lines

A_L—Area, lateral, of the underwater body of a surface ship; not to be confused with A_y, the *maximum* centerplane area of a submerged body or ship, projected on the x-z or centerplane

A_M—Area, midlength or midsection, of a ship, midway between the forward and after perpendiculars

A_0—Area, disc, of a screw propeller

A_P—Area, projected blade, of a screw propeller, outside the boss or hub

A_P, A_U—Propeller coefficients of D. W. Taylor, dimensional in character. When T is in lb, Q is in lb-ft, n is revolutions per sec, V_A is in ft per sec, and P and D are in ft, $A_P = (P/D)(55.033C_Q)/(1 - s_R)^3$ and $A_U = (P/D)(8.7587C_T)/(1 - s_R)^2$ [Taylor, D. W., S and P, 1943, p. 101; PNA, 1939, Vol. II, p. 141].

A_R—Area, projected, of a rudder or other vertical movable control surface, lying generally parallel to the ship centerplane

A_S—Area, projected, of stern diving planes of a submarine

A_U—Area, immersed transom, projected on a transverse plane; this does not necessarily correspond to that embodied in the *after perpendicular* area ratio f_R of D. W. Taylor

A_W—Area, waterplane, of a ship floating on the surface; not to be confused with A_x

A_X—Area, maximum transverse section, of the underwater body of a ship floating on the surface; for a submerged body or ship such as a submarine, the *maximum* area as projected on the transverse y-z plane, preferably indicated in the latter case as A_x, using a lower-case subscript

A_{WA}—Area, waterplane, of afterbody

A_{WE}—Area, waterplane, of entrance

A_{WF}—Area, waterplane, of forebody

A_{WR}—Area, waterplane, of run

A/A_X—Section-area ratio, referred to the section of maximum area

A_D/A_0—Developed-area ratio of a screw propeller

A_E/A_0—Expanded-area ratio of a screw propeller

$A_L/(LH_M)$—Lateral-area ratio of a surface ship

A_P/A_0—Projected-area ratio of a screw propeller

A_U/A_X—Immersed-transom-area ratio, referred to the section of maximum area A_X. If the transom is at the AP, this is the value of f at the AP.

dA/dL—Rate of change of section area with length along the ship

dA/dx—Rate of change of section area with distance along the x-axis of a ship, when referred to cartesian coordinates

b—Breadth or width in general

b—Span of a hydrofoil, tip to tip, or support to tip when cantilevered

b—Vortex spacing, longitudinal, in a vortex street or trail

B—Beam at the designed waterline, at any designated station

B—Buoyancy force on a body or ship, whether the body is in equilibrium with the gravity force or not

B_n—Boussinesq number, expressed as $U/\sqrt{gR_H}$ or $V/\sqrt{gR_H}$

B_C—Beam at the chine, at any designated station, for a V-bottom planing craft

$B_{C(\mathrm{Max})}$—Beam at the chine, maximum, wherever occurring on a planing craft

B_E—Beam, extreme, *wherever* it occurs on the main hull, above or below the designed waterline

B_M—Beam, designed waterline, at midlength between perpendiculars

B_P, B_U—Basic propeller design variables of D. W. Taylor, dimensional in character. When T is in lb, Q is in lb-ft, n is in revolutions per sec, V_A is in ft per sec, and P and D are in ft,

$$B_P = (D/P)(23.772\sqrt{C_Q})/(1 - s_R)^{2.5}$$

and

$$B_U = (D/P)(9.4835\sqrt{C_T})/(1 - s_R)^2$$

B_U—Beam, designed waterline, of the immersed transom

B_X—Beam, designed waterline, at the section of maximum area

B_{IX}—Beam, maximum, of the immersed or underwater body, *wherever* it occurs

B_{WX}—Beam, maximum, at designed waterline, *wherever* it occurs along the length

b^2/A_{Proj}—Aspect ratio of a hydrofoil of any kind; also b^2/A_H

B/B_X—Ratio of the designed waterline beam at any section to the designed waterline beam at the section of maximum area

B_X/H_M—Ratio, beam-draft, based on the *mean* draft H_M; B_X/d is the alternative form

B_X/H_X—Ratio, beam-draft, at the section of maximum area; B_X/d_X is the alternative form

c—Celerity or velocity of a wave with respect to the undisturbed liquid in which it occurs, $= \sqrt{gL_W/(2\pi)}$

c—Chord length of an airfoil or hydrofoil, such as an expanded propeller-blade section, a rudder blade, a fin, or other device; alternative symbol l

c_h—Shallow-water wave speed, in depth h

c_C—Critical wave speed or velocity in shallow water of depth h, $= \sqrt{gh}$

c_E—Celerity of an elastic or compression wave in any medium

c_M—Chord length, mean or average, of a hydrofoil, or of the expanded blade sections of a screw propeller outside the hub

c_R—Chord length, root, of a cantilevered hydrofoil; also the chord length at midspan of a symmetrical-planform hydrofoil

c_T—Chord length, tip, of a hydrofoil

c_X—Distance from the leading edge to the point of maximum thickness of a hydrofoil section, measured parallel to the base chord

c_Z—Distance from the leading edge to the position of maximum camber of the meanline of a hydrofoil section

C—Cross force, *normal to both* the direction of motion or resultant liquid flow and the direction of lift

C_A—Coefficient, Admiralty; the value of the dimensional expression $\Delta^{2/3}V^3/P_I$(or $\Delta^{2/3}V^3/P_S$), where Δ is the weight displacement in tons of salt water

C_B—Coefficient, block, $= \forall/(LB_XH_X)$; alternative symbol δ(delta)

C_C—Coefficient, cross-force, $= C/(qA_L)$; see NOTE under C_D

C_D—Coefficient, drag, $= D/(0.5\rho AU_R^2) = D/(qA)$

NOTE:—In the mathematical expression for this coefficient, as for many others in the list, it is possible to use D and R, U and V interchangeably. It is also possible, for special work, to substitute for A any expression having the same dimensions, such as (BH), L^2, B^2, and H^2, provided this is explicitly stated. The symbol q for ram pressure signifies $0.5\rho U_R^2$ or $0.5\rho V_R^2$.

C_F—Coefficient, mean or average specific friction drag, $= D_F/(qS)$; see NOTE under C_D

C_J—Coefficient of reduction, of a rudder or control surface; the ratio of the actual torque on a ship rudder stock to the torque calculated for the same rudder angle and relative speed in open water

C_K—Coefficient, rolling moment, $= K/(qAL)$; see NOTE under C_D

C_L—Coefficient, lift, $= L/(0.5\rho A_HU_R^2) = L/(qA_H)$; see NOTE under C_D

C_M—Coefficient, midlength section, $= A_M/(B_MH_M)$; alternative symbol β(beta)

C_M—Coefficient, pitching moment, $= M/(qAL)$; see NOTE under C_D

C_N—Coefficient, yawing moment, $= N/(qAL)$; see NOTE under C_D

C_P—Coefficient, prismatic, longitudinal, $= \forall/(LA_X)$; alternative symbol ϕ(phi)

C_P, C_U—Coefficients, propeller, of D. W. Taylor, dimensional in character. When T is in lb, Q is in lb-ft, n is in revolutions per sec, and P and D are in ft:

$$C_P = 52.889(P/D)C_Q\ ;$$

$$C_U = 8.4175(P/D)(1 - s_R)C_T$$

[Taylor, D. W., S and P, 1943, p. 101; PNA, 1939, Vol. II, p. 141].

C_Q—Coefficient, torque, $= Q/(n^2D^2P^3)$. This coefficient is dimensional and is becoming obsolete.

C_R—Coefficient, residuary drag or resistance, $= R_R/(qS) = C_T - C_F$; see NOTE under C_D

C_S—Coefficient, wetted-surface, dimensionless, $= S/\sqrt{\forall L} = S/\sqrt{\nabla L}$

C_T—Coefficient, total drag or resistance, $= R_T/(qS) = C_F + C_R$; see NOTE under C_D . In this particular case, the use of the wetted surface S is arbitrarily taken as the standard; the use of any other value equivalent to (length)^2 is covered by a special note.

C_T—Coefficient, thrust, $= T/(n^2D^2P^2)$. This coefficient is dimensional and is becoming obsolete.

C_V—Coefficient, speed, usually of a planing craft, $= V/\sqrt{gB}$; preferably called the b-Froude or beam-Froude number

C_W—Coefficient, load, of a planing craft, $= W/(wB^3)$; the symbol C_{LD} is preferred

C_W—Coefficient, designed waterplane, $= A_W/(LB_X)$; alternative symbol α(alpha)

C_X—Coefficient, maximum section, $= A_X/(B_XH_X)$

C_Y—Coefficient, relation, $= C_P/C_W$

C_τ—Coefficient, shearing stress, in viscous flow, $= \tau/q$

C_{AM}—Coefficient, added mass, of entrained water around a body or ship, as related to the ship mass

C_{BD}—Coefficient, bilge diagonal; ratio of the area inside a bilge diagonal to the area $[L(\overline{\mathrm{BDI}})]$

C_{CP}—Coefficient, center of pressure, for a hydrofoil; ratio of (the distance from the leading edge to CP) to (the chord length c)

C_{DL}—Coefficient, dynamic lift, of a planing craft, $= W/(qB^2) = 2(C_{LD})/C_V^2$

C_{IL}—Coefficient of square moment of area of waterplane for pitch, $= I_L/[(L^3B_X)/12] = I_L/(0.083L^3B_X)$

C_{IT}—Coefficient of square moment of area of

waterplane for roll, $= I_T/[(B_X^3L)/12] = I_T/(0.083B_X^3L)$

C_{LA}—Coefficient, lateral area, $= A_L/(LH_M)$

C_{LD}—Coefficient, load, of a planing craft, $= W/(wB^3)$; alternative symbol is C_W but the former is preferred

C_{LF}—Coefficient, *local* specific friction drag, as distinguished from C_F, the mean or average coefficient

C_{PA}—Coefficient, prismatic, afterbody, $= \forall_A/(L_AA_M)$

C_{PE}—Coefficient, prismatic, entrance, $= \forall_E/(L_EA_X)$

C_{PF}—Coefficient, prismatic, forebody, $= \forall_F/(L_FA_M)$

C_{PR}—Coefficient, prismatic, run, $= \forall_R/(L_RA_X)$

C_{PV}—Coefficient, prismatic, vertical, $= \forall/(A_WH_X) = C_B/C_W = (C_PC_X)/C_W$; alternative symbol ϕ_V

C_{TL}—Coefficient, thrust-load, $= T/(0.5\rho A_0V_A^2)$; see NOTE under C_D

C_{VM}—Coefficient, virtual mass, in transient flow or motion conditions; the ratio of the mass of the body or ship *and* the surrounding entrained water to the mass of the body or ship. This coefficient, equal to 1.0 plus the coefficient of added mass C_{AM}, is always greater than unity.

C_{WA}—Coefficient, waterplane, afterbody, $= A_{WA}/(L_AB_M)$

C_{WE}—Coefficient, waterplane, entrance, $= A_{WE}/(L_EB_X)$

C_{WF}—Coefficient, waterplane, forebody, $= A_{WF}/(L_FB_M)$

C_{WR}—Coefficient, waterplane, run $= A_{WR}/(L_RB_X)$

C_{WS}—Coefficient, wetted surface, of D. W. Taylor, $= S/\sqrt{\Delta L}$, where Δ is the displacement in tons of 2,240 lb of salt water of sp.gr. 1.024 (35.075 ft^3 per ton) and L is the mean immersed length in ft

C_{PVA}—Coefficient, prismatic, vertical, afterbody, $= \forall_A/(A_{WA}H)$, where H is the draft at midlength of the afterbody

C_{PVE}—Coefficient, prismatic, vertical, entrance, $= \forall_E/(A_{WE}H)$, where H is the draft at midlength of the entrance

C_{PVF}—Coefficient, prismatic, vertical, forebody, $= \forall_F/(A_{WF}H)$, where H is the draft at midlength of the forebody

C_{PVR}—Coefficient, prismatic, vertical, run, $= \forall_R/(A_{WR}H)$, where H is the draft at midlength of the run

c_M/D—Mean-width ratio of the blades of a screw propeller

c_T/c_R—Taper ratio of a cantilevered hydrofoil

d—Diameter, boss or hub, of a screw propeller

d—Draft of a floating body or ship; alternative symbols H and T; H is preferred

d_X—Draft of a floating body or ship at the section of maximum area; alternative symbols H_X and T_X

D—Depth, molded, of a ship hull

D—Diameter in general; diameter of a body of revolution or of a propulsion device

D—Drag, as a force opposing motion in a liquid

D_f—Towing force applied to a ship model during a test at the ship point of self-propulsion

D_B—Diameter, blade-circle, of a paddlewheel

D_E—Drag, separation, due to differential pressures in a separation zone

D_F—Drag, friction

D_H—Drag, hydrodynamic

D_I—Drag, induced

D_P—Drag, pressure

D_R—Drag, residuary, $= D_T - D_F$

D_S—Drag, slope, of a floating body on an inclined liquid surface

D_T—Drag, total; the sum of the friction, pressure, separation, and all other types of drags due to relative liquid motion

D_W—Drag, wind; the *downwind* force exerted by the relative wind on a body or ship, to be distinguished from the axial component R_{Wind}

D_{ST}—Diameter of steady-turning path

D_{Tact}—Diameter, tactical

d/D—Boss or hub diameter fraction of a screw propeller

ΔC_F—Roughness allowance, specific, for a body or ship, to be added to the smooth, flat-plate, turbulent-flow specific friction resistance coefficient

dn, Δn—Streamline spacing or stream-tube width, normal (transverse) to the direction of flow

Δp—Differential pressure increase or decrease, finite

ΔR—Augmentation of resistance due to pressure effects from a propulsion device

ds, Δs—Equipotential-line spacing, along the direction of flow

$\pm\Delta U$—Differential velocity increase or decrease, finite

e—Base of Napierian or natural logarithms; for example, $\log_e$

e—Vapor pressure of water

E—Energy; work

E_n—Euler number or pressure coefficient $= p/q = (p - p_\infty)/q = \Delta p/q$

f—Camber of an airfoil or hydrofoil (6th ICSTS symbol); also m for meanline camber

f—Frequency; eddy frequency in a vortex street or trail

f—Friction coefficient of a surface in water, according to W. Froude, in the equation $R_F = fSV^n$; this is dimensional

f—A function

f—Ordinates, back and face, of an airfoil or hydrofoil

f—Ratio of the section area at an end perpendicular to the section area at midlength. This is D. W. Taylor's "f" [S and P, 1943, p. 65].

f_E—Ratio of the section area A at the FP to the section area A_M at midlength

f_G—A function applying to a group of geometrically similar bodies or ships

f_R—Ratio of the section area A at the AP to the section area A_M at midlength. The ratio A_U/A_M is equal to f_R only if the immersed transom lies at the AP.

F—Force in general

F—Freeboard

F_n—Froude number; in general, $= U/\sqrt{gL} = V/\sqrt{gL}$

F_b—b-Froude number; specifically, the beam Froude number of a planing craft $= V/\sqrt{gB} = U/\sqrt{gB}$

F_h—Submergence-Froude number, where h is the depth of submergence, $= U/\sqrt{gh} = V/\sqrt{gh}$

F_D—Blade-disc force of a screw propeller, exerted tangentially in the plane of the disc at the radius R of the CP of any given blade, so that $Q = F_D R$ for that blade

F_D—Damping force

F_I—Inertia force

$F_\forall$—$\forall$-Froude number; specifically, the volume Froude number,

$$= V/\sqrt{g\forall^{1/3}} = U/\sqrt{g\forall^{1/3}} = V/\sqrt{g\nabla^{1/3}}$$

g—Acceleration due to gravity $= w/\rho$

G—Girth, linear, measured generally from the DWL

h—Depth in general; depth of submergence of a body or ship, such as a submarine

h—Head, hydrostatic, hydraulic, or potential; height or depth of liquid

h_P—Head, pressure, due to pumping, $= p_P/w$, as distinguished from head due to gravity

h_T—Head, total, including hydrostatic h, pumping h_P, and velocity h_U; the same as the Head, total, Bernoulli, symbol H

h_U—Head, velocity, $= U^2/(2g)$

h_V—Head, vapor, of a liquid

h_W—Height of a wave from trough to crest

h_∞—Head of liquid in an undisturbed stream of infinite extent

$\hbar$(pronounced hull height)—Hull height of a submerged body or submarine, top to bottom, or deck to keel

h_W/L_W—Steepness ratio of a wave

H—Head, total, Bernoulli, $= [U^2/(2g)] + p/w + h$; the same as the Head, total, symbol h_T

H—Draft of a floating body or ship; alternative symbols d and T

H—Shape factor of a boundary-layer velocity profile, $= \delta^*/\theta$, where θ is momentum thickness

H_A—Draft, aft; generally measured at the after perpendicular

H_D—Drag, keel, as a vertical distance, representing a difference in drafts at the forward and after perpendiculars when the keel line is extended to those perpendiculars

H_E—Draft, extreme, wherever occurring along the length

H_F—Draft, forward; generally measured at the forward perpendicular

H_M—Draft, mean, at midlength

H_U—Draft, immersed transom

H_X—Draft at section of maximum area; alternative symbols d_X and T_X

$\hbar/B$—Hull-height to beam ratio of a body

$\hbar/L$—Hull-height to length ratio of a body

H_D/L—Slope of keel, in a ship with a designed drag; keel-drag ratio

i—Slope of a line defining a form, with reference to a specified or selected axis or plane; may be expressed as an angle in degrees or as a natural tangent

i_B—Slope, bowline or buttock, with reference to baseplane

i_D—Slope, diagonal, with reference to intersection of a diagonal plane and the centerplane

i_E—Slope, waterline, in entrance, with reference to centerplane, neglecting local shape at the stem; alternative symbol $(1/2)\alpha_E$

i_F—Slope of floor (bottom of ship), with reference to baseplane

i_R—Slope, waterline, in run, with reference to centerplane

i_S—Slope, section line, with reference to baseplane; this slope becomes greater than 90 deg in way of a tumble home

i_W—Slope, waterline, general

I—Square moment of area of a plane surface about an axis in that plane

I_L—Square moment of area of a waterplane about the transverse axis through CF, for pitching motion

I_T—Square moment of area of a waterplane about the longitudinal axis through CF, for rolling motion

I_W—Square moment of area of a free-water surface, with axes defined for each case

I_{xx}—Square moment of area of a plane surface through an axis x-x in that plane

J—Advance coefficient, number, or ratio, $= U_A/(nD) = V_A/(nD)$; $V_E/(nD)$ is the alternative expression

J—Moment of inertia of the mass of a body or ship; this is a true moment of inertia as compared to the square moment of area of a plane surface denoted by I

J_L—Moment of inertia of a body or ship for pitching motion, about an axis transverse to the plane of symmetry

J_T—Moment of inertia of a body or ship for rolling motion, about a longitudinal axis

J_x, J_y, J_z—Moments of inertia about the x-, y-, and z-body axes, respectively

J_{xx}—Moment of inertia of the mass of a body about an axis x-x

J_{Abs}, λ(lambda)—Absolute advance coefficient, number, or ratio, $= U_A/(\pi nD) = V_A/(\pi nD) = V_E/(\pi nD)$

k—Constant of capillarity (6th ICSTS symbol)

k—Fractional value, at any point in a propulsion device, of the ultimate induced velocity U_I far astern

k—Radius of gyration

k—Surface roughness height, average; hill height above a smooth reference surface

k_x, k_y, k_z—Radii of gyration about the x-, y-, and z-body axes, respectively

K—Bulk modulus of elasticity of a liquid

K—Rolling moment about longitudinal x-axis

K_Q—Torque coefficient, non-dimensional, $= Q/(\rho n^2 D^5)$

K_S—Equivalent sand roughness; requires also a surface or area density factor and other relationships, not yet worked out for the general case

K_T—Thrust coefficient, non-dimensional, $= T/(\rho n^2 D^4)$

K_T/K_Q—Thrust-torque factor $= TD/Q$

l—Chord length of an airfoil or hydrofoil; alternative symbol c

L—Length, the principal longitudinal dimension of a ship; any characteristic length, specified in detail; for special study, the length on the surface waterline WL of the immersed form of a ship, at any draft and trim

L—Lift as a force, when generated by a combination of circulation and uniform flow or by a deflected flow

L_A—Length, afterbody, $= L/2$

L_C—Length, projected, of the area bounded by the chine of a planing craft

L_D—Lift, dynamic, due to planing action

L_E—Length, entrance, from FP to section of maximum area or to forward end of parallel middlebody

L_F—Length, forebody, $= L/2$

L_H—Lift, hydrodynamic

L_M—Length of model, as distinguished from ship length L_S

L_P—Length, parallel middlebody, of constant shape and area

L_R—Length, run, from section of maximum area or after end of parallel middlebody to WL termination or other designated point

L_S—Length of ship, as distinguished from model length L_M

L_W—Length of a surface gravity wave from crest to crest or trough to trough

L_{EF}—Length, effective, for hydrodynamic analysis, as defined locally

L_{OA}—Length, overall or extreme, wherever occurring on the main hull, in a direction parallel to the longitudinal axis

L_{PP}—Length between perpendiculars (6th ICSTS symbol)

L_{WS}—Length, mean wetted, of a planing craft

L_{WL}—Length, on any given waterline

L_{DWL}—Length, on designed waterline

L/B_X—Length-beam ratio; beam-fineness ratio, greater than unity

L/D—Lift-drag ratio

L/D—Length-depth ratio; depth-fineness ratio, greater than unity

L/D—Length-diameter or fineness ratio of a body of revolution, greater than unity

L/h—Length to hull-height ratio of a submerged body

m—Camber ordinates of the meanline of an airfoil or hydrofoil section, reckoned from the base chord

m—Mass in general, $= W/g$; mass of a body or ship, $= \Delta/g$

m—Metacentric height, $= \overline{GM}$, for use in mathematical formulas

m—Strength of a source or sink, such that the total volume of liquid per unit time flowing from a 2-dimensional source of unit depth is $2\pi m$ and from a 3-dimensional source is $4\pi m$

m_X—Camber ordinate, maximum, of the meanline of a hydrofoil or blade section, reckoned from the base chord

M—Merit factor of E. V. Telfer, described in Secs. 34.10 and 60.13

M—Moment, pitching or trimming, about the y- or transverse body axis

M_n—Mach or Cauchy number, for relating the speed of a body around which flow is being studied to the speed of elastic waves in the surrounding liquid

M_{CS}—Moment exerted by a control surface about a principal axis of a body or ship

m_X/c—Camber ratio of a hydrofoil

n—Index or exponent in general

n—Rate of angular rotation, speed, or velocity, generally expressed as revolutions per unit time; alternative symbol ω(omega), generally expressed as radians per unit time

n—Tuning factor; ratio of natural period T of ship motion to period of encounter T_E of waves

n_0—Angular rate of rotation of a propulsion device in open water

Δn—Streamline spacing or stream-tube width, normal to the direction of liquid motion

N—Moment, yawing, about deck-to-keel or z-axis

O—Friction coefficient of a surface in water, according to R. E. Froude

$\otimes$—Amidships in general

$\otimes_{PP}$—Amidships, defined as the midlength between perpendiculars

$\otimes_{WL}$—Amidships, defined as the midlength on waterline; alternative $\otimes_{DWL}$

p—Angular velocity in roll about the x- or longitudinal body axis

p—A pressure intensity in general; any force per unit area

p_A—Pressure, atmospheric

p_C—Pressure, bubble or cavity

p_H—Pressure, hydrostatic

p_I—Pressure, impact

p_0—Pressure, ambient; see also p_{AH} and p_∞

p_P—Pressure, pumping

p_{AH}—Pressure, ambient, $= (p_A + p_H)$ = sum of atmospheric and hydrostatic pressures; see also p_∞

p_{Abs}—Pressure, absolute

p_∞—Pressure, ambient, of the liquid in an undisturbed stream, at a great distance from a body or ship; this is an absolute pressure unless otherwise indicated

$\pm\Delta p$—Pressure, differential, positive or negative, reckoned from the ambient pressure p_∞

P—Pitch in general; pitch of a propulsion device

P—Power in general

P_n—Planing number, $= D_T/L_D$

P_B—Power, brake

P_E—Power, effective or towrope, $= RV$

P_F—Power, friction

P_I—Power, indicated

P_P—Power, propeller, $= 2\pi Qn$; formerly known as delivered power

P_S—Power, shaft, $= 2\pi Qn$ plus shaft friction power

P_T—Power, thrust, $= TV_A = TV_E$

P_{EF}—Pitch, effective, when exerting zero net thrust

P/D—Pitch ratio of a propulsion device

q—Angular velocity in pitch about the y- or transverse body axis

q—Dynamic pressure at a stagnation point Q; ram pressure, expressed by $(0.5\rho U^2)$ or $(0.5\rho V^2)$

Q—Quantity rate of flow of a liquid, in terms of volume per unit time, where $Q = \mathcal{V}/t$; output of a source or input of a sink

Q—Torque, specifically, torque applied *at* a propulsion device

Q_0—Torque of a propulsion device in open water

Q_S—Spindle moment or torque, on a controllable propeller

Q_{CS}—Control-surface hinge or stock torque, exerted about the stock axis

r—Angular velocity in swing or yaw about the deck-to-keel or z-axis

r, R—A radius in general

R—Resistance, as a force, opposing motion in a liquid; alternative D for drag

R_n—Reynolds number in general, $= UL/\nu = VL/\nu$

R_b—Reynolds number for propeller-blade sections where the velocity term is the nominal liquid velocity past the blade section and the space term is the expanded chord length at $0.7R$. Here $V_{\text{Blade}} = \{V_A^2 + [2\pi n(0.7R)]^2\}^{0.5}$ and $R_b = [(c_{0.7R})(V_{\text{Blade}})]/\nu$.

R_d—d-Reynolds number, with the diameter or width D as the space term, $= UD/\nu = VD/\nu$

R_x—x-Reynolds number, with distance x abaft the leading edge as the space term, $= Ux/\nu = Vx/\nu$

R_δ—δ-Reynolds number, with boundary-layer thickness δ(delta) as the space term, $= U\delta/\nu = V\delta/\nu$

R_C—Radius of curvature of path or turning circle

R_F—Resistance to motion, friction

R_H—Radius, hydraulic, of a channel; the area of liquid in a transverse plane divided by the wetted perimeter

R_I—Resistance, ideal, of a model run at the ship self-propulsion point, $= R_T - D_f$

R_P—Resistance, pressure, due to forces acting normal to a surface

R_R—Resistance, residuary, $= R_T - R_F$

R_S—Orbit radius of the circular motion of a surface particle in a gravity wave

R_S—Resistance, separation

R_T—Resistance, total, of a body or ship to motion; the sum of the friction, pressure, separation, and all other types of resistance due to relative liquid motion

R_W—Resistance due to gravity wavemaking

R_{Wind}—Resistance, wind; the *axial* component of the force exerted by the relative wind on a body or ship, along its x-axis; to be distinguished from the *downwind* drag D_W

R_{RC}—Radius of the rolling circle of a trochoidal wave

R_{SA}—Resistance, still-air; the wind resistance due to ship speed alone through still air

s—Space or distance in general, along a straight line or curved arc

s—Specific gravity of a liquid, non-dimensional, represented by the ratio {[Weight (or mass) of a given volume of the liquid]/[Weight (or mass) of the same volume of pure water]}

s_A—Slip ratio, apparent, $= 1 - [V/(nP)]$

s_R—Slip ratio, real or true, $= 1 - [V_A/(nP)] = 1 - [V_E/(nP)]$

Δs—Equipotential-line spacing, equal to Δn, measured in the direction of liquid motion

S—Surface area in general; surface, wetted

S—Velocity, discharge, of stack or exhaust gases

S_n—Strouhal number, in general

S_l—l-Strouhal number, based upon length L as the significant dimension, $= fL/U$, where f is the frequency of eddies shed behind a body and forming a vortex street or trail

S_d—d-Strouhal number, based upon diameter D as the significant dimension, $= fD/U$

S_B—Surface, wetted, surrounding the bulk volume of a body or ship

$S/\sqrt{\Delta L}$—Wetted-surface coefficient of D. W. Taylor, where Δ is the weight displacement in tons of salt water, as defined under $\Delta/(0.010L)^3$; the same as C_{WS}

$S/\sqrt{\mathcal{V}L}$—Wetted-surface coefficient, non-dimensional; the same as C_S

$S/\mathcal{V}^{2/3}$—Wetted-surface to (volume$^{2/3}$) ratio

t—Temperature in general

t—Terminal ratio of D. W. Taylor, as applied to the shape of a section-area curve; see t_E and t_R

t—Thickness in general; thickness of an airfoil or hydrofoil section

t—Thrust-deduction fraction, $= (T - R_T)/T$

t—Time in general

t_E—Terminal ratio of D. W. Taylor, as applied to the section-area curve at the FP [S and P, 1943, p. 65]

t_0—Thickness of a screw-propeller blade, projected to the shaft axis; see SNAME Tech. and Res. Bull. 1–13, 1953, p. 22

t_R—Terminal ratio of D. W. Taylor, as applied to the section-area curve at the AP, in the same manner as for t_E

t_X—Maximum thickness of any selected hydrofoil section

T—Draft of a floating body or ship; alternative symbols H and d

T—Thrust; usually ahead thrust; specifically, thrust developed by a propulsion device

T—Time or period of a complete cycle; natural period of oscillatory ship motion of any kind

T_q—Taylor quotient, $= V/\sqrt{L}$, where V is in kt and L in ft; this is dimensional

$\mathcal{T}$(pronounced toll)—Towline tension in general

$\mathcal{T}_x$, $\mathcal{T}_y$, $\mathcal{T}_z$—Components of towline tension relative to the x-, y-, and z-axes, respectively, of a body or ship

T_E—Period of encounter of waves, referred to a ship or other point

T_E—Thrust, effective, exerted on a ship by a propulsion device, $= T(1 - t)$

T_H—Period of heave

T_0—Thrust of a propulsion device in open water

T_P—Period of pitch

T_R—Period of roll

T_S—Thrust, slope, exerted by gravity on a floating body on an inclined liquid surface

T_W—Period of a gravity wave

t_X/c, t_X/l—Thickness ratio of a hydrofoil section

t_0/D—Blade-thickness fraction of a screw propeller

u—Velocity, linear component of, in direction of longitudinal or x-axis of a body or ship

U, V—Velocity or speed in general; specifically, velocity of the liquid U or speed of the body or ship V, irrespective of units of measurement

U_A, V_A, V_E—Velocity or axial speed of advance of a propulsion device, reckoned in the direction of motion of the device, $= U - U_W = V - V_W = U(1 - w) = V(1 - w)$

U_I—Velocity, induced, at a great distance astern of a finite-length hydrofoil with circulation

U_R, V_R—Velocity or speed, resultant, of the flow approaching a hydrofoil, taking account of induced velocity

U_S—Relative impact or striking velocity

U_T—Velocity or speed, tip, of the blades of a propulsion device, $= \pi nD$

U_W, V_W—Velocity or speed, wake, resulting from all causes acting around a body or ship, reckoned in the direction of motion

U_{IA}—Velocity, induced, axial; the axial component of the induced velocity at a selected point in a propeller jet with rotation

U_{IT}—Velocity, induced, tangential; the tangential component of the induced velocity at a selected point in a propeller jet with rotation

U_∞, V_∞—Velocity of the liquid in the undisturbed part of a stream or at a great distance from a body or ship

U_τ—Velocity, shear, in viscous flow, defined by $\sqrt{\tau_0/\rho}$

U_{Orb} or U_O—Orbital velocity of a surface particle in a gravity wave

v—Velocity, linear component of, in direction of transverse or y-axis of a body or ship, positive to starboard

V, U—Speed or velocity in general; specifically, speed of the body or ship V or velocity of the liquid U, irrespective of units of measurement

V_h—Speed of ship in water of depth h

$V°$ (V of blade circle)—Velocity, nominal tangential, of the blades of a paddlewheel, measured at midheight of the blades for a radial wheel and at the blade-trunnion circle for a feathering wheel

V_A, V_E, U_A—Speed or velocity of advance of a propulsion device, reckoned in the direction of motion of the device, $= V(1 - w) = U(1 - w)$

V_I—Schlichting intermediate speed, for analysis of shallow-water performance

V_M—Speed of model, as distinguished from ship speed V_S

V_0—Speed of advance of a propulsion device in open water; speed of a ship along the approach path just prior to entry into a turn

V_R, U_R—Speed or velocity, resultant, of the flow approaching a hydrofoil

V_S—Speed of ship, as distinguished from model speed V_M

V_S—Velocity of sound in a medium

V_T—Towing speed of a tug

V_{ST}—Speed, steady-turning

V_W, U_W—Speed or velocity, wake, resulting from all causes acting around a body or ship, reckoned in the direction of motion

V_∞, U_∞—Speed of the liquid in the undisturbed part of a stream at a great distance from a body or ship

$\forall$ (pronounced vol)—Volume; displacement volume of a body or ship; alternative symbol ∇ (also pronounced vol)

$\forall_A$—Volume, afterbody, of a ship

$\forall_B$—Volume, bulk, as of a submerged submarine

$\forall_E$—Volume, entrance, of a ship

$\forall_F$—Volume, forebody

$\forall_P$—Volume, parallel middlebody

$\forall_R$—Volume, run

$\forall/(0.10L)^3$ or $\nabla/(0.10L)^3$—Fatness or (volume-0.1 length) ratio. This is preferred to a length/volume ratio because it increases as the fatness increases, the same as the displacement-length quotient of D. W. Taylor.

$V/\sqrt{L}$—Taylor quotient T_q or speed-length quotient, where V is in kt and L in ft; this is dimensional

w—Velocity, linear component of, in direction of the z-axis of a ship, from deck to keel

w—Wake fraction of Taylor, $= (V - V_A)/V = (V - V_E)/V$

w—Weight density, or weight per unit volume, $= W/\mathcal{V} = \rho g$

w_F—Wake fraction, Froude, $= (V - V_A)/V_A$

w_Q—Wake fraction, determined from torque identity

w_T—Wake fraction, determined from thrust identity

W—Weight in general; displacement weight; weight or gravity force; scale weight of a body or ship, where $W = mg$

W—Wind velocity

W_n—Weber number, relating to surface tension, $= U^2L/\kappa$(kappa) $= U^2D/\kappa$; see NOTE under C_D

W_R—Wind velocity, relative to ship

W_T—Wind velocity, true, over the earth's surface; sometimes called the natural-wind velocity

W_{SA}—Wind velocity, still-air, caused solely by the motion of a ship in still air

x—Longitudinal body axis, positive forward

x'—Radius ratio, 0-diml, of a screw propeller, $= R/R_{\text{Max}}$

x_0—Motion axis, reckoned usually in an ahead direction, tangent to the sea surface

X—Component of hydrodynamic force on a body or ship along its longitudinal or x-axis

y—Normal distance, perpendicular to the surface, to any point in the boundary layer of a viscous liquid

y—Transverse body axis, positive to starboard

y_0—Motion axis, reckoned usually to starboard or to the right of the x_0-axis

Y—Component of hydrodynamic force on a body or ship along its transverse or y-axis

z—Vertical body axis, positive from deck to keel

z_C—Shaft convergence, expressed as an angle or slope with reference to the centerplane, after projection on the baseplane

z_D—Shaft declivity, expressed as an angle or slope with reference to the baseplane, after projection on the centerplane

z_0—Motion axis

Δz—Sinkage of a body or ship when moving on the surface of a liquid

Z—Component of hydrodynamic force on a body or ship along its keelward or z-axis

Z—Number of blades in a propulsion device

α(alpha)—Acceleration, angular

α—Angle of attack of a hydrofoil, geometric

α—Angle of encounter of waves, between the direction of wave travel and the direction of ship motion. For a head sea, $\alpha = 180$ deg.

α—Designed waterplane coefficient; alternative symbol C_W

α—Ratio, linear or scale, full-size body or ship to model, greater than unity; alternative symbol λ(lambda)

α_A—Nominal angle of incidence on a control surface

$(1/2)\alpha_E$—Angle of entrance, half, neglecting local shape at the stem; alternative symbol i_E

α_I—Angle of attack of a hydrofoil, hydrodynamic, measured from the attitude or position of zero lift to the direction of the resultant velocity, taking induced velocity into account

α_N—Angle, neutral, between the zero-lift position of a control surface and the body or ship axes

α_0—Angle of attack of a hydrofoil, zero-lift; alternative symbol α_Z

α_S—Angle of attack of a hydrofoil, stalling

α_Z—Angle of attack of a hydrofoil, zero-lift; alternative symbol α_0

α_{CR}—Angle of attack of a hydrofoil, critical

β(beta)—Advance angle for a propeller-blade element, $= \tan^{-1}[V_A/(2\pi nR)]$ for the radius R

β—Angle of bossing termination, extreme after edge, with reference to the baseplane; slope of floor i_F or "deadrise" in a planing craft; angle of obliquity for a flat surface impacting a liquid

β—Angle of drift in turning

β—Coefficient, midlength section; alternative symbol C_M

β_I—Hydrodynamic pitch angle of a screw-propeller blade section at any radius R, taking induced velocity into account

γ(gamma)—Projected angle of roll

γ—Dihedral angle, measured from the axis of a hydrofoil to a normal erected on the plane of symmetry

Γ(gamma, capital)—Circulation, strength of, around a hydrofoil or body

δ(delta)—Angular displacement of a control surface from its neutral position

δ—Coefficient, block; alternative symbol C_B

δ—Thickness of a boundary layer in viscous flow

δ—Advance ratio of D. W. Taylor, $= nD/V_A$. When n is expressed in rpm, D in ft, and V_A in kt, as was done by Taylor, this ratio is dimensional and equal to $101.33/J$

δ_B—Angle, bow plane, with reference to ship axis

δ_L—Thickness of the laminar sublayer of a viscous boundary layer

δ_N—Angle, neutral, of a control surface

δ_P—Angle, diving plane or horizontal control surface, with reference to body or ship axis

δ_R—Angle, rudder, with reference to ship axis

δ_S—Angle, stern plane, with reference to ship axis

δ^*(delta star)—Displacement thickness of a boundary layer,

$$= \int_0^\delta \left(1 - \frac{U}{U_\infty}\right) dy$$

Δ(delta, small capital)—An increment or decrement; see also the combination symbols listed under the letter D

ΔC_F(using small capital delta)—Increment of specific friction resistance due to surface roughness and other factors

Δ(delta, large capital)—Displacement weight or scale weight, in tons of salt water (see item following); gravity load on the water for a planing craft

$\Delta/(0.010L)^3$ or $\Delta/(L/100)^3$—Displacement-length quotient of D. W. Taylor for salt water having a sp.gr. of 1.024 at 59 deg F or 15 deg C, equivalent to 63.863 lb per ft^3 or 35.075 ft^3 per ton of 2,240 lb, and for a length L in ft; this is dimensional and is equal to the displacement, in English long tons, of a geometrically similar ship 100 ft long

∇(pronounced vol)—Volume; displacement volume of a body or ship; alternative symbol $\mathcal{V}$ (also pronounced vol)

∇_B—Volume, bulk; alternative symbol $\mathcal{V}_B$

ϵ(epsilon)—Angle of downwash or sidewash

ϵ—Drag-lift ratio of a blade section or hydrofoil

ζ(zeta)—Slope of the surface of a gravity wave, reckoned with respect to the horizontal

η(eta)—Angle, vertical path, between the horizontal plane and the velocity vector of the motion of the CG of a ship

η—Efficiency, general

η—Elevation, surface, of a wave, with reference to a plane, usually the still-water level

η_B, η_E—Efficiency, propeller, behind ship $= \eta_O\eta_R$

η_G—Efficiency, gearing

η_H—Efficiency, hull, $= (1 - t)/(1 - w) = P_E/P_T$

η_I—Efficiency, ideal

η_K—Efficiency, ideal, with jet rotation

η_M—Efficiency, mechanical

η_O—Efficiency, propeller, in open water, $= (K_T/K_Q)[J/(2\pi)] = (T_0V_0)/(2\pi n_0Q_0)$

η_P—Efficiency, propulsive $= P_E/P_P = \eta_O\eta_H\eta_R$

η_R—Efficiency, relative rotative, $= \eta_B/\eta_O = \eta_E/\eta_O$

η_S—Efficiency, shafting

θ(theta)—An angle in general

θ—Angle of pitch or trim in a ship, with reference to the designed or normal attitude in the fore-and-aft plane. Its natural tangent is the algebraic difference of the changes in elevation of the designed waterline at the end perpendiculars, divided by the length L.

θ—Momentum thickness of boundary layer

$$= \int_0^\delta \frac{U}{U_\infty}\left(1 - \frac{U}{U_\infty}\right) dy$$

θ_R—Slope, with reference to the ship centerplane, of the incident flow on a contra-rudder

θ_S—Slope, with reference to the ship centerplane, of the median line of a contra-guide skeg ending

κ(kappa)—Coefficient of kinematic capillarity $= k/\rho$, where k is the constant of capillarity

K—Goldstein factor in propeller design, to take account of the number of blades

λ(lambda)—Angle, leeway, or of leeway

λ, J_{Abs}—Coefficient, absolute advance, $= V_A/(\pi nD) = V_E/(\pi nD)$

λ—Ratio, linear or scale, full-size body or ship to model, generally expressed as a number greater than unity; for example, 20th scale or 1:20 model; alternative symbol α(alpha)

μ(mu)—Magnification factor in resonant motion

μ—Strength of a doublet, or close-coupled source and sink

μ—Viscosity, coefficient of dynamic, $= \tau(\text{tau})/(dU/dy)$

ν(nu)—Kinematic viscosity, coefficient of, $= \mu/\rho$

ξ(ksi)—Angle, tab, with reference to the control surface on which it is mounted

ρ(rho)—Mass density, or mass per unit volume, $= m/\mathcal{V} = w/g$

σ(sigma)—Cavitation index, $= (p_{\text{Abs}} - e)/q$

σ_N—Cavitation index based on angular velocity, for propeller tests, $= (p_{\text{Abs}} - e)/(0.5\rho n^2D^2)$

σ_U, σ_V—Cavitation index based on liquid

velocity, for propeller tests, $= (p_{Abs} - e)/(0.5\rho V_A^2)$

σ—Surface tension

σ_1, σ_2, etc.—Indexes of dynamic stability of route

σ_{CR}—Cavitation index or number, critical

Σ(sigma, large capital)—Sum, summation

τ(tau)—Shear, intensity of internal, in the viscous flow of a liquid, proportional to (dU/dy); shearing stress

τ_0—Shear intensity in a viscous liquid at a solid-surface boundary

ϕ(phi)—Angle, geometric pitch or helix, of a screw-propeller blade at any radius

ϕ—Angle of heel, list, or roll, reckoned about the longitudinal ship axis

ϕ—Potential function such as a velocity potential, where $u = \partial\phi/\partial x$, $v = \partial\phi/\partial y$, $w = \partial\phi/\partial z$

ϕ—Coefficient, prismatic, $= \forall/(LA_X)$; alternative symbol C_P

ϕ_V—Coefficient, prismatic, vertical; alternative symbol C_{PV}

ψ(psi)—Angle of yaw

ψ—Current or stream function

ψ_0—Radial stream function for a source

ψ_K—Radial stream function for a sink

ψ_S—Stream function for the flow around a stream form

ω(omega)—Angular speed or velocity, generally expressed as radians per unit time; alternative symbol n, generally expressed as revolutions per unit time

Ω(omega, capital)—Gravity potential, due to the earth's gravity force.

X1.3 Abbreviations for Positions and Conditions.

C—Center

E—Separation point on a body in a stream, where the relative flow velocity becomes zero at the body surface in the process of reversing direction

K—Any point along the intersection of the baseplane with the plane of symmetry

N—Neutral or ambient-pressure point on a body in a stream, where $U = U_\infty$ and $p = p_\infty$

O—Origin of coordinates

Q—Stagnation point on a body in a stream, where the relative flow velocity is zero and the dynamic pressure equals the ram pressure q

AP—After perpendicular, designed

CA—Center of area

CB—Center of buoyancy of a body or ship

CE—Center of effort, as for the wind blowing on a sail

CF—Center of flotation; geometric or moment center of the surface waterplane area A_W

CG—Center of gravity or center of mass of a body or ship

CM, CM_T, M—Metacenter, for transverse inclination

CM_L, M_L—Metacenter, for longitudinal inclination

CP—Center of pressure of hydrodynamic forces on a body

CS—Static center; center of resultant of weight W and buoyancy B

CCF—Center of cross forces applied normal to the direction of motion of the CG *and* normal to the direction of lift

CLA—Center of lateral area of the underwater body, as projected on the plane of symmetry

CLP—Center of lateral pressure; not necessarily at the center of lateral area

CWL—Construction waterline, as a position only

0-diml—Non-dimensional, as applied to physical expressions; also as applied to flow having characteristics variable in one dimension only

2-diml—Two-dimensional, as applied to flow, shape, and the like

3-diml—Three-dimensional, as applied to flow, shape, and the like

DWL—Designed waterline, as a position only

FP—Forward perpendicular, designed

LE—Leading edge

MP—Mid perpendicular

PP—Between perpendiculars; pivoting point

SK—Sink, as a drain for radial flow

SO—Source, as a source of radial flow

TE—Trailing edge

TP—Towing point or towed point

WL—Waterline in general; free-surface waterline in any condition, undisturbed by waves; this may or may not be at the DWL

Sp.gr.—Specific gravity.

X1.4 Abbreviations for Physical Concepts Having Scalar Dimensions. The superposed bar or vinculum over the groups of letters in this section indicate that they represent scalar quantities, measurable in orthodox units.

$\overline{BD}$—Bilge-diagonal offset, at any station, measured on the diagonal plane from the centerline intersection to the hull surface

$\overline{BG}$—Pendulum stability height, as of a submarine, when the surface waterplane area is negligible and CM coincides with CB

$\overline{BM}$, $\overline{BM}_T$—Metacentric radius for transverse inclination

$\overline{BM}_L$—Metacentric radius for longitudinal inclination

$\overline{BR}$—Bilge radius at section of maximum area

$\overline{BDI}$—Bilge-diagonal intercept, measured between (1) the intersection of the bilge diagonal with the centerline at the designed waterline and (2) the intersection of this diagonal with the floor line, when extended to the vertical at $B_X/2$

$\overline{BKW}$—Bilge-keel width, measured at midlength or wherever this width is a maximum

$\overline{BD}/\overline{BDI}$—Ratio, bilge-diagonal offset to bilge-diagonal intercept, at any station

$\overline{BKW}/B_X$—Ratio, bilge-keel width to designed waterline beam at the section of maximum area; $\overline{BKW}$ is measured at midlength because it is usually greatest there

$\overline{BR}/B_X$—Ratio, bilge radius to designed waterline beam, at the section of maximum area

$\overline{DR}$—Deadrise; see last part of definition for $\overline{RF}$

$\overline{GM}$, $\overline{GM}_T$—Metacentric height, transverse, from CG to CM, for transverse inclination

$\overline{GM}_L$—Metacentric height, longitudinal, from CG to CM_L, for longitudinal inclination

$\overline{HS}$—Half siding at flat keel, wherever it is a maximum

$\overline{HS}/B_X$—Ratio of the greatest half-siding at flat keel, wherever it occurs, to the beam at the section of maximum area

$\overline{KB}$—Center of buoyancy above baseplane

$\overline{KG}$—Center of gravity above baseplane

$\overline{KM}$, $\overline{KM}_T$—Distance of metacenter above baseplane for transverse inclination

$\overline{KM}_L$—Distance of metacenter above baseplane for longitudinal inclination

$\overline{KS}$—Sheer height at side, minimum, above baseplane

$\overline{KB}/H$—Ratio of height of center of buoyancy above baseplane to draft

$\overline{LCB}$—Longitudinal center of buoyancy abaft FP, in fraction of L; alternative L_{CB}

$\overline{LCF}$—Longitudinal center of flotation abaft FP, in fraction of L; alternative L_{CF}

$\overline{LCG}$—Longitudinal center of gravity abaft FP, in fraction of L; alternative L_{CG}

$\overline{LMA}$—Longitudinal position of section of maximum area abaft FP, in fraction of L; alternative L_{MA}. If a vessel has parallel middlebody, this position is taken as the midlength of the middlebody.

$\overline{MCT}$—Moment to change trim, followed by appropriate unit

$\overline{PWL}$—Length of the parallel or straight-sided portion of the designed waterline

$\overline{RF}$—Rise of floor at shell at section of maximum area, reckoned as a height above the baseplane when projected to $B_X/2$; also called "deadrise" and abbreviated $\overline{DR}$

$\overline{RF}/B_X$—Ratio, rise of floor to beam.

X1.5 Abbreviations for Units of Measurement. For convenience these abbreviations are placed in natural groups involving length, area, volume, weight, pressure, power, time, and the like, rather than in alphabetic order.

The same abbreviation applies to both the plural and singular of the word(s) it represents. Periods are not inserted after any abbreviation or part thereof.

Trigonometric abbreviations are well known and are not listed here.

Length	*Area*
in—inch	sq in, in^2—square inch
ft—foot	sq ft, ft^2—square foot
yd—yard	sq yd, yd^2—square yard
fm—fathom	sq mi, mi^2—square mile
mi—mile; nautical mile unless otherwise indicated	
mm—millimeter	sq mm, mm^2—square millimeter
cm—centimeter	sq cm, cm^2—square centimeter
m—meter	sq m, m^2—square meter
km—kilometer	sq km, km^2—square kilometer

Volume

cu in, in^3—cubic inch
cu mm, mm^3—cubic millimeter
cu ft, ft^3—cubic foot
cu cm, cm^3—cubic centimeter
cu yd, yd^3—cubic yard
cu m, m^3—cubic meter
gal, U.S.—gallon
gal, Imp.—gallon, Imperial, equal to 1.201 U.S. gal
bbl—barrel

Weight

oz—ounce	kip—a thousand pounds
lb—pound	kg—kilogram

t—ton (to be further specified)

Pressure

lb in^2, psi, psig—pounds per square inch; above atmospheric or gage pressure, unless otherwise specified
lb ft^2, psf—pounds per square foot
psia—pounds per square inch, absolute
atm—atmospheres of pressure, in units of roughly 14.7 lb in^2
kg cm^2—kilograms per sq cm, in units of roughly 14.2 lb in^2

Moment or *Torque*

in-lb—inch-pound
ft-lb—foot-pound
kg-m—kilogram-meter

Angles and *Arcs*

deg—degrees of arc
rad—radians, $360/(2\pi)$

Power

h—horse, a unit of power, in English units unless otherwise specified
hp—horsepower
bhp—brake power, in English horses
ehp—effective power, in English horses
ihp—indicated power, in English horses
php—propeller power, in English horses
shp—shaft power, in English horses

Time and *Rate*

μs—micro second, one millionth of a second
ms—millisecond
sec—second
min—minute
hr—hour
fps or ft per sec—foot (feet) per second
fpm or ft per min—foot (feet) per minute
cfs—cubic foot per second
cfm—cubic foot per minute
cms—cubic meter per second
cps—cycles per second
gpm—gallon per minute
hz—hertz, frequency of 1 cycle per second
rps—revolutions per second
rpm—revolutions per minute
mph—miles (generally geographical) per hour
mps—meters per second
kt—knot, one nautical mile per hour

Temperature

deg—degree
deg C—degree Centigrade
deg F—degree Fahrenheit.

X1.6 Circular Constant Notation. The several symbols of the circular constant notation of R. E. Froude and G. S. Baker are listed here, with the non-dimensional formulas which express their values as multipliers of well-known 0-diml numbers. Following these are the dimensional forms, as applied to English units of measurement.

It is important that consistent units be employed in the formulas listed hereunder, as well as in all other pure formulas, containing physical concepts only. For example, in the English system of measurement, units should be lb, ft, and sec. The same value of g should be used for all the expressions.

Ⓜ Length-Displacement Constant. The ratio of the length L of the ship to the length of the side of a cube having the same volume of displacement $\forall$ or ∇ as the ship.

$$Ⓜ = \frac{L}{\forall^{1/3}} = \frac{L}{\nabla^{1/3}}$$

Ⓚ Speed-Displacement Constant. The ratio of the speed V of the ship to the speed of a wave with a length equal to half the length of the side of a cube having the same volume of displacement $\forall$ or ∇ as the ship.

$$Ⓚ = \frac{V}{\sqrt{\frac{g}{2\pi}\frac{1}{2}\forall^{1/3}}} = \frac{V}{\forall^{1/6}}\sqrt{\frac{4\pi}{g}}$$

$$= \sqrt{4\pi}\,\frac{V}{\sqrt{g\forall^{1/3}}} = 3.545F_{\forall}$$

Ⓒ Resistance Constant. One thousand times the ratio of the resistance R to the displacement weight W, divided by the square of the speed-displacement constant Ⓚ. Here $W = w\forall$.

$$Ⓒ = \frac{1000R}{W}\frac{\forall^{1/3}}{V^2}\frac{g}{4\pi} = \frac{1000R}{w\forall}\frac{\forall^{1/3}}{V^2}\frac{g}{4\pi}$$

$$= \frac{1000}{8\pi}\frac{R}{\frac{1}{2}\rho\forall^{2/3}V^2} = 39.79C_T\frac{S}{\forall^{2/3}}$$

where C_T is the total specific resistance coefficient based on $\forall^{2/3}$ as the reference dimension.

Ⓛ Speed-Length Constant. The ratio of the speed V of the ship to the speed of a gravity wave of length equal to half the length L of the ship.

$$Ⓛ = \frac{V}{\sqrt{\frac{g}{4\pi}\frac{L}{2}}} = \sqrt{4\pi}\left(\frac{V}{\sqrt{gL}}\right) = 3.545F_n$$

Ⓟ Speed-Prismatic-Length Constant. The ratio of the speed V of the ship to the speed of a wave

of length $C_P(L)$, where C_P is the prismatic coefficient of the ship and L is the ship length.

$$Ⓟ = \frac{V}{\sqrt{\frac{g(LC_P)}{2\pi}}} = \sqrt{\frac{2\pi}{C_P}}\,\frac{V}{\sqrt{gL}}$$

$$= 2.5066\,\frac{F_n}{\sqrt{C_P}} = \frac{Ⓛ}{\sqrt{2C_P}}$$

Ⓢ Wetted-Surface Constant. The ratio of the ship wetted surface S to the area of one face of a cube having the same volume displacement $\forall$ or ∇ as the ship.

$$Ⓢ = \frac{S}{\forall^{2/3}} = \frac{S}{\nabla^{2/3}}$$

There are given hereunder the familiar *dimensional* expressions for the several circular constants, where L is in ft, Δ is in long tons of 2,240 lb, V is in kt, S is in ft^2, and P_E is in English horses:

$$Ⓜ = 0.3057\,\frac{L}{\Delta^{1/3}}$$

$$Ⓚ = 0.5834\,\frac{V}{\Delta^{1/6}}$$

$$Ⓒ = 427.1\,\frac{P_E}{\Delta^{2/3}V^3}$$

$$Ⓛ = 1.055\,\frac{V}{\sqrt{L}}$$

$$Ⓟ = 0.746\,\frac{V}{\sqrt{C_P(L)}}$$

$$Ⓢ = 0.0935\,\frac{S}{\Delta^{2/3}}$$

There is no Appendix 2 in this volume.

APPENDIX 3

Mechanical Properties of Water, Air, and Other Media

X3.1 General. There are many published sources of information concerning the mechanical properties of water, air, and other common fluids. The tabulated values in these sources, while often differing within the range of significant figures shown, are all sufficiently precise for the usual problems in engineering design.

Nevertheless it is disconcerting, to a student or especially to an engineer, when shifting from one field to another, say in a time of national emergency when everyone is harassed, to encounter a group of different values for what is apparently a standard state of some medium. Furthermore, certain ratios in everyday use in naval architecture are by no means consistent when derived in several different ways. To clarify this situation for the marine architect a set of so-called "standard" values has been evolved, for both fresh and salt water. They are described and tabulated in the sections which follow. A set of standard values for air already exists.

While the five significant figures embodied in these "standard" water values are by no means necessary in making first and second approximations or in the early stages of a ship design, they lend themselves to the desk-machine calculation now almost universal in the later stages of a ship design, or in the preparation of technical reports.

X3.2 Reference Data for Weights, Volumes, and Mass Densities of "Standard" Fresh and Salt Water. The so-called standard unit weights, mass densities, temperatures, and specific gravities in use for many years by naval architects and by model basins, at least in America, were selected for the most part because they were round numbers, easy to remember, and easy to use. Indeed, if they approximated 1.0, they were often thrown away. That they were anything but consistent among themselves was not too important, because the deviations involved were generally of smaller magnitude than the overall precision of measurement of the various operations.

They began with the use of the round numbers 35 ft^3 per ton for sea water and 36 ft^3 per ton for fresh water. These gave values of 64.000 lb per ft^3 for salt water and 62.222 lb per ft^3 for fresh water, based on long tons of 2,240 lb. Incidentally, because some seas in the world contain fresh water in their upper levels, the term "salt water" is used in this book; it also stands in better contrast to "fresh water."

When round numbers were used, the specific gravity of salt water on a basis of fresh water came out as 36/35, or 1.0286. Since this was larger than the ratio existing in most parts of the oceans, the U. S. Experimental Model Basin, half a century ago, adopted a smaller value of 1.024. The origin of this figure is not known but it was embodied in all the calculations of the 1910 edition of D. W. Taylor's "The Speed and Power

TABLE X3.a—Reference Data for Standard Water

All data are for a water temperature of 59 deg F or 15 deg C and a latitude of 45 deg. All logarithms are to the base of 10.

Title	Standard English Units	Values	Log_{10}
Mass density, ρ, salt water, sea level	slugs per cubic ft	1.9905	0.29896
Mass density, ρ, fresh water, sea level	slugs per cubic ft	1.9384	0.28744
Weight per cubic ft, w, salt water, sea level	lb	64.043	1.80647
Weight per cubic ft, w, fresh water, sea level	lb	62.366	1.79495
Cubic ft per long ton, 2,240 lb of salt water at sea level	cubic ft	34.977	1.54378
Cubic ft per long ton, 2,240 lb of fresh water at sea level	cubic ft	35.917	1.55530
Acceleration of gravity, g, at sea level, latitude 45 deg	ft per sec^2	32.174	1.50751
Standard specific gravity, salt water, sea level	dimensionless	1.027	0.01157

Supplementing the foregoing, the head of standard salt water corresponding to a pressure intensity of 1.00 psi is 144/64.043 = 2.2485 ft. A head of 1.00 ft is equivalent to a pressure intensity of 64.043/144 = 0.4447 psi.

The head of standard fresh water corresponding to a pressure intensity of 1.00 psi is 144/62.366 = 2.309 ft. Conversely, a head of 1.00 ft is equivalent to a pressure intensity of 62.366/144 = 0.4331 psi.

of Ships." In the meantime, ship designers retained the round numbers of 36 and 35 previously described.

As model-basin practice became more refined and as the use of Reynolds number and other non-dimensional ratios increased, there arose a need for accurate values of the mass density ρ(rho) for salt water and fresh water, represented by the ratio of the weight density or weight per unit volume w divided by the acceleration of gravity g. The round numbers for the ratios 64/32.17 and 62.22/32.17 were taken by many as 1.99 and 1.94, respectively. Others took 2.0 as a round number for 1.99 and 1.0 as a round number for 0.5ρ. The ratio of 1.99 to 1.94 is 1.026, which corresponds to the sea-water specific-gravity figure used in Europe for many years.

The need for adopting a single reference temperature for comparing the results of model tests and for working up predictions of ship performance has led to the adoption of an international or ITTC standard, which is 59 deg F, 15 deg C. This is a reasonable engineering average for the waters of the world although somewhat low for model-basin water in general. The latter averages about 68 deg F, or 20 deg C. Ocean temperatures range from about 86 deg F, 30 deg C, in the tropics to about 28 deg F, −2.2 deg C, in the polar regions. Temperatures in the open water of the Great Lakes average about 47 deg F in the seasons open to navigation. To permit ship machinery to operate with reasonable efficiency anywhere in the world a maximum injection-water temperature of about 75 deg F, 24 deg C, should be used.

The standard reference temperature for water is intended to be used only for analysis or comparison work. It is employed for making predictions only when no other temperature is pertinent or is specified. If a ship is designed to run primarily in the polar regions or in the tropics, the values corresponding to the respective sea

TABLE X3.b—Supplementary Data on Water

Characteristics of ocean water of D. W. Taylor and the U. S. Experimental Model Basin, at a temperature of 50 deg F, 10 deg C, as embodied in the 1910, 1933, and 1943 editions of "The Speed and Power of Ships" and other publications.

Title	Standard English Units	Values	Log_{10}
Specific gravity, ocean water	dimensionless	1.024	0.01030
Cubic ft per long ton of 2,240 lb	cubic ft	35.075	1.54500
Weight per cubic ft, w	lb	63.863	1.80525
Mass density, ρ	slugs per cubic ft	1.9849	0.29774

TABLE X3.c—STANDARD CHARACTERISTICS OF THE WATER USED IN SEVERAL MODEL BASINS IN NORTH AMERICA

The basin water is assumed to be at an average temperature of 68 deg F, 20 deg C.

Title	Sea Level	David Taylor Model Basin, Carderock*	Great Lakes Level (Ann Arbor)	Ottawa, Canada
Weight per cubic ft, w, lb	62.311	62.274	62.287	62.4
Mass density, ρ, slugs per ft^3	1.9367	1.9367	1.9367	1.9379
Cubic ft per long ton	35.948	35.970	35.926	35.898
Acceleration of gravity, g, ft per sec^2	32.174	32.155	32.162	32.2

*Taken from TMB Hydromechanics Work Instruction 20–25 of 3 Apr 1950.

temperatures expected in service are used. If, however, these service temperatures are not known or are not specified in advance, all ship powers derived from model tests are worked up for "standard" salt water or fresh lake and river water at 59 deg F.

The adoption of this standard temperature made it possible to prepare standard reference data for water, to be employed in all model-basin and ship-design work. For establishing these data, the following general principles were laid down:

(a) The ratios between the several sets of values should be consistent

(b) The "standard" values should be as close as practicable to the actual average physical values

(c) Round numbers would not be necessary, with modern desk-type calculating machines available everywhere

(d) New "standard" values should be extended to five (5) significant figures, to achieve consistency, not only for sea level but for all other levels

(e) The data would cover most of the model and ship activities in America if calculated for sea level and for Great Lakes level. Similar calculations for other lake levels could be made as desired.

Table X3.a lists the reference data described in the preceding paragraphs. For reference purposes there are given in Table X3.b the corre-

TABLE X3.d—MASS DENSITY OF FRESH WATER, EMBODYING VARIATION WITH TEMPERATURE

The values are in English engineering units of slugs per ft^3. They correspond to those adopted by the American Towing Tank Conference in 1939 and published in SNAME, 1939, p. 416. To convert them to pounds weight, multiply by the local acceleration of gravity g.

Temperature, deg F	Mass Density, ρ	Temperature, deg, F	Mass Density, ρ	Temperature, deg F	Mass Density, ρ
32	1.9399	52	1.9394	70	1.9362
34	1.9400	54	1.9392	72	1.9358
36	1.9401	56	1.9389	74	1.9352
38	1.9401	58	1.9386	76	1.9347
40	1.9401	59	1.9384	78	1.9342
42	1.9401	60	1.9383	80	1.9336
44	1.9400	62	1.9379	82	1.9330
46	1.9399	64	1.9375	84	1.9324
48	1.9398	66	1.9371	86	1.9317
50	1.9396	68	1.9367		

There are given hereunder the gravity constants, or values of the acceleration of gravity g, in ft per sec^2, for sea level at six values of latitude. These data apply also to Table X3.e.

15 deg	25 deg	35 deg	45 deg	55 deg	65 deg
32.101	32.120	32.145	32.174	32.203	32.229

TABLE X3.e—MASS DENSITY OF SALT WATER, 3.5 PER CENT SALINITY, EMBODYING VARIATION WITH TEMPERATURE

The values given are in English engineering units of slugs per ft³. They correspond to those adopted by the American Towing Tank Conference in 1939 and published in SNAME, 1939, p. 416. To convert them to pounds weight, multiply by the local acceleration of gravity g.

Temperature, deg F	Mass Density, ρ	Temperature, deg F	Mass Density, ρ	Temperature, deg F	Mass Density, ρ
32	1.9947	52	1.9921	70	1.9876
34	1.9946	54	1.9917	72	1.9870
36	1.9944	56	1.9912	74	1.9864
38	1.9942	58	1.9908	76	1.9858
40	1.9940	59	1.9905	78	1.9851
42	1.9937	60	1.9903	80	1.9844
44	1.9934	62	1.9898	82	1.9837
46	1.9931	64	1.9893	84	1.9830
48	1.9928	66	1.9888	86	1.9823
50	1.9924	68	1.9882		

sponding data for salt water of specific gravity 1.024, as used by D. W. Taylor in his books and by the Experimental Model Basin [C and R Bull. 7, 1933, pp. 18–19].

Table X3.c lists the data used by several model-testing establishments in North America for model-basin water at a temperature of 68 deg F, 20 deg C.

X3.3 Mass-Density Values of Fresh and Salt Water, in English and Metric Engineering Units. Values of the mass density ρ of both fresh and standard salt water, as adopted by the American Towing Tank Conference in 1939 and published in SNAME, 1939, page 416, are presented in Tables X3.d and X3.e, respectively. The values for salt water are derived from experiments with actual ocean water as contrasted with previous tables based on sodium-chloride solutions [SNAME, 1939, p. 418]. The ρ-values are in English engineering units of slugs per ft³ and cover a range of temperature, 32 deg F through 86 deg F, nearly as large as that encountered in the various waters of the world.

The slug of mass in the English system is the mass to which an acceleration of one ft per sec² would be given by the application of a one-pound force at a given point on the earth. To convert the values of mass to those of weight at any point, multiply by the acceleration of gravity g at that point. The values of g at sea level, for

TABLE X3.f—MASS DENSITY OF FRESH WATER, EMBODYING VARIATION WITH TEMPERATURE

The values given are in metric engineering units of slugs per meter³.

Temperature, deg C	Mass Density, ρ	Temperature, deg C	Mass Density, ρ	Temperature, deg C	Mass Density ρ
0.00	101.95	11.11	101.93	21.11	101.76
1.11	101.96	12.22	101.91	22.22	101.74
2.22	101.96	13.33	101.90	23.33	101.70
3.33	101.96	14.44	101.88	24.44	101.68
4 44	101.96	15.00	101.87	25.56	101.65
5.55	101.96	15.56	101.87	26.67	101.62
6.67	101.96	16.67	101.85	27.78	101.59
7.78	101.95	17.78	101.83	28.89	101.56
8.89	101.94	18.89	101.80	30.00	101.52
10.00	101.94	20.00	101.78		

There are given hereunder the gravity constants or values of the acceleration of gravity g, in centimeters per sec², for sea level at six values of latitude. These data apply also to Table X3.g.

15 deg	25 deg	35 deg	45 deg	55 deg	65 deg
978.428	979.004	979.780	980.665	981.551	982.332

TABLE X3.g—MASS DENSITY OF SALT WATER, 3.5 PER CENT SALINITY, EMBODYING VARIATION WITH TEMPERATURE

The values given are in metric engineering units of slugs per meter³.

Temperature, deg C	Mass Density, ρ	Temperature, deg C	Mass Density, ρ	Temperature, deg C	Mass Density, ρ
0.00	104.83	11.11	104.69	21.11	104.46
1.11	104.83	12.22	104.67	22.22	104.43
2.22	104.82	13.33	104.65	23.33	104.40
3.33	104.81	14.44	104.63	24.44	104.36
4.44	104.79	15.00	104.61	25.56	104.33
5.55	104.78	15.56	104.60	26.67	104.29
6.67	104.76	16.67	104.57	27.78	104.25
7.78	104.75	17.78	104.55	28.89	104.22
8.89	104.73	18.89	104.52	30.00	104.18
10.00	104.71	20.00	104.49		

TABLE X3.h—KINEMATIC VISCOSITY OF FRESH AND SALT WATER, IN ENGLISH ENGINEERING UNITS

The values listed are for $(10^6)\nu$ in ft² per sec. The salinity of the salt water is 3.5 per cent. The fifth significant figures in this table are somewhat doubtful.

Fresh Water	Temperature, T, deg F	Salt Water	Fresh Water	Temperature, T, deg F	Salt Water
1.9291	32		1.1937	61	1.2470
1.8922	33		1.1769	62	1.2303
1.8565	34		1.1605	63	1.2139
1.8219	35		1.1444	64	1.1979
			1.1287	65	1.1822
1.7883	36				
1.7558	37		1.1133	66	1.1669
1.7242	38		1.0983	67	1.1519
1.6935	39		1.0836	68	1.1372
1.6638	40		1.0692	69	1.1229
			1.0552	70	1.1088
1.6349	41	1.6846			
1.6068	42	1.6568	1.0414	71	1.0951
1.5795	43	1.6298	1.0279	72	1.0816
1.5530	44	1.6035	1.0147	73	1.0684
1.5272	45	1.5780	1.0018	74	1.0554
			0.98918	75	1.0427
1.5021	46	1.5531			
1.4776	47	1.5289	0.97680	76	1.0303
1.4538	48	1.5053	0.96466	77	1.0181
1.4306	49	1.4823	0.95276	78	1.0062
1.4080	50	1.4599	0.94111	79	0.99447
			0.92969	80	0.98299
1.3860	51	1.4381	0.91850	81	0.97172
1.3646	52	1.4168	0.90752	82	0.96067
1.3437	53	1.3961	0.89676	83	0.94982
1.3233	54	1.3758	0.88621	84	0.93917
1.3034	55	1.3561	0.87586	85	0.92873
1.2840	56	1.3368	0.86570	86	0.91847
1.2651	57	1.3180			
1.2466	58	1.2996			
1.2285	59	1.2817			
1.2109	60	1.2641			

TABLE X3.i—KINEMATIC VISCOSITY OF FRESH AND SALT WATER, IN METRIC ENGINEERING UNITS

The values listed are for $(10^6)\nu$ in meters^2 per sec. The salinity of the salt water is 3.5 per cent. The fifth significant figures in this table are somewhat doubtful.

Fresh Water	Temperature, T, deg C	Salt Water	Fresh Water	Temperature, T, deg C	Salt Water
1.5189	5.00	1.5650	1.0632	17.88	1.1129
1.4928	5.55	1.5392	1.0486	18.33	1.0983
1.4674	6.11	1.5141	1.0343	18.89	1.0841
1.4428	6.67	1.4897	1.0204	19.44	1.0701
1.4188	7.22	1.4660	1.0067	20.00	1.0565
1.3955	7.78	1.4429	0.9933	20.56	1.0432
1.3727	8.33	1.4204	0.9803	21.11	1.0301
1.3506	8.89	1.3985	0.9675	21.67	1.0174
1.3291	9.44	1.3771	0.9549	22.22	1.0048
1.3081	10.00	1.3563	0.9427	22.78	0.9926
1.2876	10.56	1.3360	0.9307	23.33	0.9805
1.2678	11.11	1.3162	0.9190	23.89	0.9687
1.2483	11.67	1.2970	0.9075	24.44	0.9572
1.2294	12.22	1.2782	0.8962	25.00	0.9458
1.2109	12.78	1.2599	0.8851	25.56	0.9348
1.1929	13.33	1.2419	0.8743	26.11	0.9239
1.1753	13.89	1.2245	0.8637	26.67	0.9132
1.1581	14.44	1.2074	0.8533	27.22	0.9028
1.1413	15.00	1.1907	0.8431	27.78	0.8925
1.1250	15.56	1.1744	0.8331	28.33	0.8824
1.1090	16.11	1.1585	0.8233	28.89	0.8725
1.0934	16.67	1.1430	0.8137	29.44	0.8628
1.0781	17.22	1.1277	0.8043	30.00	0.8533

six values of latitude, are given as part of Table X3.d on page 917.

For calculation of the acceleration of gravity at any point, H. Rouse gives, for English engineering units, the empirical relationship

$$g(\text{in ft per sec}^2) = 32.1721 - 0.08211 \cos 2\phi - 0.3h(10^{-5})$$

where ϕ(phi) is the latitude in deg and h is the elevation in ft above mean sea level at that latitude [EMF, 1946, Eq. (233), p. 358].

Tables X3.f and X3.g present the values of mass density ρ for fresh and salt water, respectively, in metric engineering units, for the convenience of those using this system.

The slug of mass in the metric system is the mass to which an acceleration of one meter per sec^2 would be given by the application of a one-kilogram force at a given point on the earth. Values of the acceleration of gravity g at sea level, for six values of latitude, are given as part of Table X3.f on page 918.

X3.4 Kinematic-Viscosity Values of Fresh and Salt Water, in English and Metric Engineering Units. Values of the kinematic viscosity ν(nu) for both fresh and salt water, expressed in English engineering units, are set down in Table X3.h. These values, based on sources available in September 1939, were adopted in that year by the American Towing Tank Conference and published in SNAME, 1939, page 417.

The fifth significant figures in this table are doubtful.

The English values of Table X3.h were later converted to metric engineering units by H. F. Nordström and other members of the SSPA staff in Göteborg and published in SSPA Report 18, 1951, page 6. These metric values are set down for convenience in Table X3.i.

X3.5 Other Mechanical Properties of Fresh and Salt Water at Atmospheric Pressure; Dynamic Viscosity and Surface Tension. Tables X3.d through X3.i preceding list the mass density ρ and the kinematic viscosity ν of fresh and salt water in a limited range of temperature, such as is encountered in the oceans of the world.

TABLE X3.j—MECHANICAL PROPERTIES OF FRESH WATER AT ATMOSPHERIC PRESSURE

The data in this table, expressed in English engineering units, are taken from H. Rouse [EMF, 1946, p. 364].

Temperature, T		Mass Density, ρ, slugs per ft^3	Weight Density, w, lb per ft^3	Dynamic Viscosity, μ, lb-sec per ft^2	Kinematic Viscosity, ν, ft^2 per sec	Surface Tension, σ, lb per ft
deg F	deg C					
32	0	1.94	62.4	$3.75(10^{-5})$	$1.93(10^{-5})$	0.00518
40	4.4	1.94	62.4	3.24	1.67	0.00514
50	10.0	1.94	62.4	2.74	1.41	0.00508
60	15.6	1.94	62.4	2.34	1.21	0.00503
70	21.1	1.94	62.3	$2.04(10^{-5})$	$1.05(10^{-5})$	0.00497
80	26.7	1.93	62.2	1.80	0.930	0.00492
90	32.2	1.93	62.1	1.59	0.823	0.00486
100	37.8	1.93	62.0	1.42	0.736	0.00479
120	48.9	1.92	61.7	$1.17(10^{-5})$	$0.610(10^{-5})$	0.00466
150	65.6	1.90	61.2	0.906	0.476	0.00446
180	82.2	1.88	60.6	0.726	0.385	0.00426
212	100	1.86	59.8	0.594	0.319	0.00403

Table X3.j lists these and other data, for fresh water, to a smaller number of significant figures but over a much larger range of temperature. The ρ and ν data are supplemented by data on specific weight w, dynamic viscosity μ(mu), and surface tension σ(sigma), taken from the reference cited in the table.

Because of the lack of complete information, the data on salt water in Table X3.k are somewhat sketchy, although derived from various sources. The dynamic-viscosity values were taken from the book "The Oceans: Their Physics, Chemistry, and General Biology," by H. U. Sverdrup, M. W. Johnson, and R. H. Fleming, Prentice-Hall, Inc., New York, 1942, page 69. These authors do not give tables for the variation of surface tension with temperature but they state, on page 70, that it "is slightly greater than that of pure (fresh) water at the same temperature."

X3.6 Data on Change of State of Fresh and Salt Water. Table X3.l lists vapor-pressure or change-of-state data for fresh water for the full range of temperature from freezing to boiling. These vapor-pressure data vary slightly from those listed in Table 47.a of Sec. 47.3, but since the change-of-state pressures appear to change with air content and other factors, the data for pure water serve only as a sort of engineering reference.

The freezing point of pure fresh water is 32 deg F, 0 deg C. The effect of impurities and the

TABLE X3.k—MECHANICAL PROPERTIES OF SALT WATER AT SEA LEVEL AND ATMOSPHERIC PRESSURE

In general, the water whose characteristics are listed here is of 3.5 per cent salinity.

Temperature, T		Mass Density, ρ, slugs per ft^3	Weight Density, w, lb per ft^3	Dynamic Viscosity, μ, c.g.s. units	Kinematic Viscosity, ν, ft^2 per sec	Surface Tension, σ, lb per ft
deg F	deg C					
28	−2.2	——	——	——	——	——
32	0	1.995	64.18	$18.9(10^{-3})$	——	(see text)
40	4.4	1.994	64.15	16.4	——	——
50	10.0	1.992	64.10	13.9	$1.46(10^{-5})$	——
60	15.6	1.990	64.04	12.1	1.26	——
70	21.1	1.988	63.95	10.6	1.11	——
80	26.7	1.984	63.85	$9.3(10^{-3})$	0.983	——
90	32.2	——	——	——	——	——
100	37.8	——	——	——	——	——

TABLE X3.l—DATA ON CHANGE OF STATE OF FRESH AND SALT WATER

The data on vapor pressure of fresh water are taken from H. Rouse [EMF, 1946, Table XI, p. 364]. The note concerning the vapor pressure of sea water is taken from page 67 of the book "The Oceans: Their Physics, Chemistry, and General Biology," by H. U. Sverdrup, M. W. Johnson, and R. H. Fleming, 1942. Table 29 on page 116 of the reference, not reproduced here, lists the "maximum vapor tension in millibars" over water of 3.5 per cent salinity for a range of temperature from −2 deg C to 32 deg C.

Temperature, T		Vapor Pressure, e, psia	
deg F	deg C	Fresh Water	Salt Water
32	0	0.08	"Sea water within the normal range of concentration has a vapor pressure about 98 per cent of that of pure water at the same temperature, and in most cases it is not necessary to consider the effect of salinity, since variations in the temperature of the surface waters have a much greater effect upon the vapor pressure."
40	4.4	0.11	
50	10.0	0.17	
59	15.0	0.25	
60	15.6	0.26	
70	21.1	0.36	
80	26.7	0.51	
90	32.2	0.70	
100	37.8	0.96	
120	48.9	1.0	
150	65.6	3.7	
180	82.2	7.5	
212	100.0	14.7	

presence of other solutions is to lower it slightly.

The freezing point of salt water having a salinity of about 35 parts per thousand, corresponding to 3.5 per cent, is from −1.9 deg C to perhaps −3 deg C; probably it is close to −2 deg C. The last figure corresponds to about 28.5 deg F.

X3.7 Elastic Characteristics of Water and Other Common Liquids. The bulk modulus of elasticity of a liquid, also called the volume modulus of compressibility, represented by the symbol K, is defined as the ratio of the change in pressure to the volumetric strain [Binder, R. C., "Fluid Mechanics," 1947, p. 160], or as "the ratio of a differential unit compressive stress to the relative reduction in volume which the stress produces" [Rouse, H., EMF, 1946, p. 328]. Expressed in symbols,

$$K = \frac{\Delta p}{-\dfrac{\Delta \mathcal{V}}{\mathcal{V}}} = -\frac{\Delta p}{\dfrac{\Delta \mathcal{V}}{\mathcal{V}}}$$

The value of K in English engineering units is of the order of 300,000 psi.

According to H. Rouse [EMF, 1946, p. 363] the values of the bulk modulus K given in Table X3.m, which apply to its elastic characteristics at atmospheric pressure, increase by about 2 per cent for each 1,000 lb per sq in rise in pressure intensity. H. U. Sverdrup, M. W. Johnson, and R. H. Fleming, on page 69 of the reference cited in the two preceding sections, indicate a reduction in mean compressibility, in bars, of from 4,659 at 0 deg C, at the surface, to 4,009 at about 10,000 meters, or a depth of over 32,000 ft. The values listed in Table X3.m for salt water are based upon a 9 per cent increase in elastic modulus under average conditions [Rouse, H., EMF, 1946, p. 363].

The speed of sound c in any medium is the square root of the quotient of the bulk modulus of elasticity K and the mass density ρ. In symbols it is $c = \sqrt{K/\rho}$. For salt water at 59 deg F, 15 deg C, this is $\sqrt{339{,}000(144)/1.9905} = 4{,}954$ ft per sec, approx.

The following is quoted from page 363 of the Rouse reference:

"If the nominal value of E (the symbol K is used here) for fresh water is taken as 300,000 pounds per square inch, corresponding values for other common liquids will be as follows:

Salt water,	330,000 (This is a 10 per cent increase)
Glycerine,	630,000
Mercury,	3,800,000
Oil	180,000 to 270,000 pounds per square inch."

X3.8 Mechanical Properties of Air and Exhaust Gases at Atmospheric Pressure and at Sea Level. There appear to be some slight variations

in the mechanical properties of air at atmospheric pressure and at sea level, depending upon what source is consulted. A. H. Shapiro, in Volume I of his book "Compressible Fluid Flow," 1953, pages 612–613, gives the following principal data, to which supplementary data have been added:

Height above sea level, h	0 ft
Temperature, T	59 deg F, 15 deg C
Speed of sound, c	1,117 ft per sec
Pressure, p	2,116.2 lb per ft^2
	$\approx$ 14.696 psi
	$\approx$ 29.91 inches of Hg
	$\approx$ 759.7 mm. of Hg
Mass density, ρ	0.002378 slugs per ft^3
Weight density, w	0.0765 lb per ft^3
Coefficient of viscosity, μ	3.719(10^{-7}) slugs per ft-sec
Kinematic viscosity, ν	1.564(10^{-4}) ft^2 per sec.

Corresponding data for air, over a range of temperature from 0 deg F to 200 deg F, are listed in Table X3.n.

For possible use in wind-resistance calculations, as well as for the design of stacks and other outlets to carry exhaust gases and products of combustion free of the working and living spaces on a ship, Table X3.o gives the mechanical properties of a typical combustion gas for a rather wide range of temperature.

TABLE X3.m—Bulk Modulus of Elasticity of Fresh and Salt Water at Atmospheric Pressure

The data are taken from H. Rouse [EMF, 1946, p. 364], except that the value of K for fresh water at 100 deg F is increased to 332,000 to agree with a faired curve of these values. The K-value for 59 deg F, 15 deg C, is interpolated from this curve.

Temperature, T		Elastic Modulus, K, psi	
deg F	deg C	Fresh water	Salt water
32	0	289,000	315,000
40	4.4	296,000	323,000
50	10	305,000	332,000
59	15	311,500	339,000
60	15.6	312,000	340,000
70	21.1	319,000	348,000
80	26.7	325,000	354,000
90	32.2	329,000	358,000
100	37.8	332,000*?	362,000*?
120	48.9	333,000?	363,000?
150	65.6	328,000?	358,000?
180	82.2	318,000?	347,000?
212	100	303,000?	330,000?

*The numbers marked with interrogation points are doubtful.

TABLE X3.n—Mechanical Properties of Air at Atmospheric Pressure

The data given here are taken from H. Rouse [EMF, 1946, Appendix, Table X, p. 363], with a change to ITTC 1951 symbols.

Temperature, T, deg F	Mass Density, ρ, slugs per ft^3	Weight Density, w, lb per ft^3	Dynamic Viscosity, μ, lb-sec per ft^2	Kinematic Viscosity, ν, ft^2 per sec
0	0.00268	0.0862	3.38(10^{-7})	1.26(10^{-4})
20	0.00257	0.0827	3.50	1.36
40	0.00247	0.0794	3.62	1.46
60	0.00237	0.0763	3.74	1.58
80	0.00228	0.0735	3.85(10^{-7})	1.69(10^{-4})
100	0.00220	0.0709	3.96	1.80
120	0.00215	0.0684	4.07	1.89
150	0.00204	0.0651	4.23	2.07
200	0.00187	0.0601	4.49(10^{-7})	2.40(10^{-4})

TABLE X3.o—Mechanical Properties of Stack and Exhaust Gases

The composition of the typical gas is described in the text.

Temperature, T, deg F	Volume Density, ft^3 per lb	Weight Density, w, lb per ft^3	Mass Density, ρ, slugs per ft^3
200	163.7	6.11(10^{-3})	1.97(10^{-4})
225	170.0	5.89	1.90
250	176.1	5.68	1.83
275	182.3	5.49	1.77
300	188.5	5.31	1.71
325	194.7	5.14	1.65
350	200.9	4.98	1.60
375	207.1	4.83(10^{-3})	1.55(10^{-4})
400	213.3	4.69	1.51
425	219.5	4.56	1.47
450	225.7	4.43	1.43
475	231.9	4.31	1.39
500	238.1	4.20	1.35
525	244.3	4.09	1.32
550	250.5	3.99(10^{-3})	1.28(10^{-4})
575	256.7	3.90	1.25
600	262.9	3.80	1.22
625	269.1	3.72	1.20
650	275.3	3.63	1.17
675	281.5	3.55	1.14
700	287.7	3.48	1.12

TABLE X3.p—DENSITY CHARACTERISTICS OF COMMON LIQUIDS AND GASES UNDER ATMOSPHERIC PRESSURE AT 60 DEG F

The data in these tables are adapted from those given by H. Rouse [EMF, 1946, Appendix, Tables VII, p. 357, and VII, p. 358].

LIQUIDS UNDER ATMOSPHERIC PRESSURE AT 60 DEG F

Liquid	Mass Density, ρ, slugs per ft^3	Weight Density, w, lb per ft^3	Liquid	Mass Density, ρ, slugs per ft^3	Weight Density, w, lb per ft^3
Alcohol, ethyl	1.53	49.3	Mercury	26.3	847
Benzene	1.71	54.9	Oil		
Brine (20% NaCl)	2.23	71.6	lubricating	1.65–1.70	53–55
Carbon tetrachloride	3.09	99.5	crude	1.65–1.80	53–58
Gasoline	1.28–1.34	41–43	fuel	1.80–1.90	58–61
Glycerine	2.45	78.8	Water		
Kerosene	1.51–1.59	49–51	fresh	1.94	62.4
			salt	1.99	64.0

GASES UNDER ATMOSPHERIC PRESSURE AT 60 DEG F

Gas	Mass Density, ρ, slugs per ft^3	Weight Density, w, lb per ft^3	Gas Constant, R ft per deg F	Adiabatic Constant, k
Acetylene	0.00215	0.0693	59.3	1.26
Air	0.00237	0.0763	53.3	1.40
Ammonia	0.00141	0.0455	89.5	1.31
Carbon dioxide	0.00363	0.117	34.9	1.28
Helium	0.000329	0.0106	386.0	1.66
Hydrogen	0.000165	0.00531	767.0	1.40
Methane (natural gas)	0.00132	0.0424	96.3	1.32
Oxygen	0.00262	0.0844	48.3	1.40
Nitrogen	0.00229	0.0739	55.1	1.40
Sulfur dioxide	0.00537	0.173	23.6	1.26

The typical gas used for the calculation of this table has the following constituents, by volume:

CO_2, 13 per cent	N, 75.5 per cent
H_2O, 9 per cent	O_2, 2.5 per cent.

The gas constant R for this mixture is 52.5 ft per deg F, as compared to a gas constant of 53.3 for atmospheric air, hence their behavior at any given temperature is about the same.

X3.9 Mechanical Properties of Other Liquids and Gases. The naval architect and marine engineer, in the course of the hydrodynamic design of a ship, may have to deal only infrequently with liquids and gases other than those referred to in the preceding sections of this appendix. Nevertheless, it is useful to have the characteristics of these other media readily available in numerical terms.

Table X3.p, embodying data adapted from H. Rouse [EMF, 1946], gives the density characteristics of a number of common liquids and gases under atmospheric pressure at 60 deg F, 15.6 deg C.

Rouse also gives in graphic form the viscosity characteristics of common gases and liquids encountered in engineering work [EMF, 1946], as follows:

Fig. 194, page 360 of Appendix, dynamic viscosity versus temperature for common gases and liquids

Fig. 195, page 361 of Appendix, dynamic viscosity versus temperature for typical grades of oil

Fig. 196, page 362 of Appendix, kinematic viscosity versus temperature for common fluids.

X3.10 Chemical Constituents of Sea Water. Forty-nine elements are known to exist in sea water; probably there are others. The most important of these, generally the ones which occur in the largest amounts per unit volume, are:

(a) Chlorine
(b) Sodium
(c) Magnesium
(d) Sulphur
(e) Calcium
(f) Potassium
(g) Bromine
(h) Strontium
(i) Boron
(j) Silicon

These and the remaining data in this section are taken from the extensive information assembled by H. U. Sverdrup, M. W. Johnson, and R. H. Fleming in "The Oceans: Their Physics, Chemistry, and General Biology" [Prentice-Hall, Inc., New York, 1942].

Although the chemical compounds in sea water appear to be present in proportions that are remarkably constant, it is difficult to isolate and measure them by present methods of analysis. Table 35 on page 173 of the reference lists these constituents in two groups:

I.	Chloride, Cl^-	18.98 parts per thousand
	Sulphate, $SO_4^=$	2.65
	Bicarbonate, HCO_3^-	0.14
	Bromide, Br^-	0.065
	Fluoride, F^-	0.0013
	Boric acid, H_3BO_3	0.026 parts per thousand.
II.	Sodium, Na^+	10.57 parts per thousand
	Magnesium, Mg^{++}	1.272
	Calcium, Ca^{++}	0.400
	Potassium, K^+	0.380
	Strontium, Sr^{++}	0.0133 parts per thousand.

Adding up the exact figures in the original table, the total is roughly 34.48 parts per thousand.

It is possible that by the time the sea water, with these constituents plus its dissolved air and gases, is mixed up with shipboard machinery in the form of steam generators, condensers, evaporators, heat exchangers, and the like, some of the constituents are altered. This may be the reason why the analysis which follows does not agree in certain respects with the data presented in the book referenced previously:

"Sea water contains about 3.5 percent of dissolved solids by weight, as follows:

$NaCl$, or sodium chloride (common salt), 2.72 percent
$MgCl_2$, or magnesium chloride, 0.38 percent
$MgSO_4$, or magnesium sulphate, 0.17 percent
$CaCO_3$, or calcium carbonate, 0.01 percent
$MgBr$, or magnesium bromide, 0.01 percent.

"Of these, the magnesium chloride is most objectionable because it breaks down, forming hydrochloric acid, $MgCl_2 + 2H_2O = 2HCl + Mg(OH)_2$. Other acids formed from these solids are: Carbonic, sulphuric, and nitric. These can be neutralized by compounding properly with alkali" [MESR, Nov 1949, p. 75].

Just because calcium sulphate, calcium carbonate, and magnesium hydroxide are found in the scale on evaporators may not mean that these compounds were present in the sea water being evaporated, in just that form [Brush, C. E., and Browning, R. C., "Notes on Prevention of Scale in Evaporators," SNAME, Ches. Sect., 21 Jan 1949].

X3.11 List of Pertinent References. References consulted in the preparation of the tables and groups of data in this appendix are listed hereunder:

(1) Rouse, H., EMF, 1946, Appendix, pp. 357–365
(2) Rouse, H., (editor), EH, 1950, Appendix, pp. 1004–1012
(3) Rouse, H., and Howe, J. W., BMF, 1953, Appendix, pp. 231–238
(4) Eshbach, O. W., (editor), "Handbook of Engineering Fundamentals," Wiley, New York, 1st ed., 1936
(5) "Landolt-Börnstein: Physikalich-Chemische Tabellen (Chemical-Physical Tables)," edited by W. A. Roth and K. Scheel, Julius Springer, Berlin, 1923–1936
(6) "Smithsonian Physical Tables," Smithsonian Institution, Washington, ninth revised edition, Vol. 88, 1954
(7) "International Critical Tables," McGraw-Hill, New York
(8) "Handbook of Chemistry and Physics," Chemical Rubber Publishing Company, Cleveland
(9) Sverdrup, H. U., Johnson, M. W., and Fleming, R. H., "The Oceans: Their Physics, Chemistry, and General Biology," Prentice-Hall, Inc., New York, 1942.

APPENDIX 4

Useful Data for Analysis and Comparison

X4.1 General. Hydrodynamic analysis and design can rarely proceed very far without getting into the realm of numbers, for expressing magnitudes and intensities of one kind or another.

The recent phenomenal growth in the availability of tabular material [Luke, Y. L., "Numerical Analysis," Appl. Mech. Rev., Aug 1955, p. 310], prepared and published for the scientist and the engineer in general, should find its counterpart in an expansion of similar material for the naval architect and marine engineer. This appendix, taken in conjunction with Appendix 3, is considered a minor but appreciable beginning for both hydrodynamicist and marine architect.

X4.2 Customary Units of Measurement in the English System. It is customary, although not universal, to express the magnitudes of all important physical terms or concepts in units of some system of measurement. The units of the English engineering system, listed in Table X4.a, are used in this book unless indicated otherwise for a particular case.

The "consistent" units of the English system are normally the pound, the foot, and the second.

X4.3 Ratios Between English Units of Measurement; Standard Values. Most of the ratios between units used to express given concepts are simple numbers, learned in elementary school. Examples applying to the length concept are 1 yd = 3 ft and 1 mile = 5,280 ft. However, certain other relationships are not so simple, nor do they always remain fixed. One such ratio is the number of degrees in a radian, represented by $360/2\pi = 57.2956$, usually abbreviated to 57.3. Another familiar example is the number of feet in a nautical mile. This ratio has had a

TABLE X4.a—CUSTOMARY UNITS OF MEASUREMENT IN THE ENGLISH SYSTEM

Symbol	Term	Abbreviations for units of measurement
L, B, H, h, s	Dimensions and distances	in, ft, yd, fm, mi
V	Ship speed (a knot is a speed of one nautical mile per hour)	kt, ft per sec, mi per hr
A	Area	sq in, in^2; sq ft, ft^2
$\forall$, ∇	Volume	cu ft, ft^3
α, δ, etc.	Angles	deg, radians
t	Time	sec, min, hr
U	Linear velocity, when used generally	ft per sec, mph, kt
ω(omega)	Angular velocity	radians per sec
a	Linear acceleration	ft per sec squared, ft per sec^2
α(alpha)	Angular acceleration	radians per sec squared, radians per sec^2
F	Force	lb
M	Moment	lb-ft
W, Δ	Weights, displacements Larger units are kips of 1,000 lb, short tons of 2,000 lb, and long tons of 2,240 lb	lb
m	Mass	slug
I	Square moment of area	ft^4
J	Polar moment of inertia	slug-ft^2

TABLE X4.b—Corresponding Values of Speed, in Four Different Units

The number of significant figures is limited to those used in rapid engineering calculations.

Ft per sec	Meters per sec	Kt	Miles per hr	Ft per sec	Meters per sec	Kt	Miles per hr
1.69	0.52	1	1.15	86.14	26.25	51	58.73
3.38	1.03	2	2.30	87.83	26.77	52	59.88
5.07	1.55	3	3.45	89.52	27.28	53	61.03
6.76	2.06	4	4.61	91.21	27.80	54	62.18
8.44	2.57	5	5.76	92.90	28.31	55	63.34
10.13	3.09	6	6.91	94.58	28.83	56	64.49
11.82	3.60	7	8.06	96.27	29.34	57	65.64
13.51	4.12	8	9.21	97.96	29.86	58	66.79
15.20	4.63	9	10.36	99.65	30.37	59	67.94
16.89	5.15	10	11.52	101.34	30.89	60	69.09
18.58	5.66	11	12.67	103.03	31.40	61	70.25
20.27	6.18	12	13.82	104.72	31.92	62	71.40
21.96	6.69	13	14.97	106.41	32.43	63	72.55
23.65	7.21	14	16.12	108.10	32.95	64	73.70
25.34	7.72	15	17.27	109.78	33.46	65	74.85
27.02	8.24	16	18.43	111.47	33.97	66	76.00
28.71	8.75	17	19.58	113.16	34.49	67	77.16
30.40	9.27	18	20.73	114.85	35.00	68	78.31
32.09	9.78	19	21.88	116.54	35.52	69	79.46
33.78	10.30	20	23.03	118.23	36.03	70	80.61
35.47	10.81	21	24.18	119.92	36.55	71	81.76
37.16	11.33	22	25.33	121.61	37.06	72	82.91
38.85	11.84	23	26.49	123.30	37.58	73	84.06
40.54	12.36	24	27.64	124.99	38.10	74	85.22
42.22	12.87	25	28.79	126.68	38.61	75	86.37
43.91	13.38	26	29.94	128.36	39.12	76	87.52
45.60	13.90	27	31.09	130.05	39.64	77	88.67
47.29	14.41	28	32.24	131.74	40.15	78	89.82
48.98	14.93	29	33.40	133.43	40.67	79	90.97
50.67	15.44	30	34.55	135.12	41.18	80	92.13
52.36	15.96	31	35.70	136.81	41.70	81	93.28
54.05	16.47	32	36.85	138.50	42.21	82	94.43
55.74	16.99	33	38.00	140.19	42.73	83	95.58
57.43	17.50	34	39.15	141.88	43.24	84	96.73
59.12	18.02	35	40.30	143.56	43.75	85	97.88
60.80	18.53	36	41.46	145.25	44.27	86	99.04
62.49	19.05	37	42.61	146.94	44.79	87	100.19
64.18	19.56	38	43.76	148.63	45.30	88	101.34
65.87	20.08	39	44.91	150.32	45.82	89	102.49
67.56	20.59	40	46.06	152.01	46.33	90	103.64
69.25	21.11	41	47.21	153.70	46.85	91	104.79
70.94	21.62	42	48.37	155.39	47.36	92	105.94
72.63	22.14	43	49.52	157.08	47.88	93	107.10
74.32	22.65	44	50.67	158.77	48.39	94	108.25
76.00	23.16	45	51.82	160.46	48.91	95	109.40
77.69	23.68	46	52.97	162.14	49.42	96	110.55
79.38	24.19	47	54.12	163.83	49.93	97	111.70
81.07	24.71	48	55.28	165.52	50.45	98	112.85
82.76	25.22	49	56.43	167.21	50.96	99	114.01
84.45	25.74	50	57.58	168.90	51.48	100	115.16

TABLE X4.c—CORRESPONDING VALUES OF TAYLOR OR SPEED-LENGTH QUOTIENT AND FROUDE NUMBER

For this tabulation the corresponding values have been taken as $V/\sqrt{gL} = 0.2978V/\sqrt{L}$ and $V/\sqrt{L} = 3.358V/\sqrt{gL}$

$T_q = V/\sqrt{L}$	$F_n = V\sqrt{gL}$	$T_q = V/\sqrt{L}$	$F_n = V/\sqrt{gL}$	$T_q = V/\sqrt{L}$	$F_n = V/\sqrt{gL}$	$T_q = V/\sqrt{L}$	$F_n = V/\sqrt{gL}$
0.30	0.0893	1.05	0.3127	1.80	0.5360	2.70	0.8041
0.35	0.1042	1.10	0.3276	1.85	0.5509	2.80	0.8338
0.40	0.1191	1.15	0.3425	1.90	0.5658	2.90	0.8636
0.45	0.1340	1.20	0.3574	1.95	0.5807	3.00	0.8934
0.50	0.1489	1.25	0.3722	2.00	0.5956	3.20	0.9530
0.55	0.1638	1.30	0.3871	2.05	0.6105	3.40	1.0125
0.60	0.1787	1.35	0.4020	2.10	0.6254	3.60	1.0721
0.65	0.1936	1.40	0.4169	2.15	0.6403	3.80	1.1316
0.70	0.2085	1.45	0.4318	2.20	0.6552	4.00	1.1912
0.75	0.2234	1.50	0.4467	2.25	0.6701	4.20	1.2508
0.80	0.2382	1.55	0.4616	2.30	0.6849	4.40	1.3103
0.85	0.2531	1.60	0.4748	2.35	0.6998	4.60	1.3699
0.90	0.2680	1.65	0.4914	2.40	0.7147	4.80	1.4294
0.95	0.2829	1.70	0.5063	2.50	0.7445	5.00	1.4890
1.00	0.2978	1.75	0.5211	2.60	0.7743	5.20	1.5486

number of values in the past, varying from 6080 to 6080.3 ft. Only recently a new international ratio has been adopted, to be given presently. Still another example is the ratio between speed in knots and speed in miles per hour; the latter value is still used for motorboats in many quarters.

In 1954 a new International Nautical Mile was adopted by the Defense Department of the United States. This has a length of 6,076.10333 ft or 1,852 meters, indicating a conversion ratio of 3.280833 ft per meter, or 39.3699996 in per meter. The U. S. legal conversion ratio is 39.370000 in per meter. A speed of 1 International Nautical Mile per hour is equivalent to a speed of 1.6878 ft per sec, 1.15077 geographical or statute mi per hr, and 0.51444 meter per sec.

However, when the calculations embodied in the text of Volume II of the present book were made, prior to 1954, the nautical mile approved for use in the U. S. Navy had a length of 6,080.20 ft. This corresponds to a speed of 1.6889 ft per sec, 0.51478 meter per sec, and 1.1516 mi per hr. These values were used throughout Parts 3 and 4, expecially in the conversion diagrams of Figs. X4.A through X4.F of Sec. X4.4. Other ratios between English units of measurement are indicated on those diagrams.

A list of corresponding values of speeds, in ft per sec, meters per sec, kt, and mi per hr, from 1 through 100 kt, is given in Table X4.b. These figures, carried to only two significant figures beyond the decimal point, were kindly furnished

LENGTH

Multiply Number of by → / to Obtain ↓	Centimeters	Feet	Inches	Kilometers	Nautical Miles	Meters	Geographic Miles	Millimeters
Centimeters	1	30.480	2.5400	10^5	$1.8532 \cdot (10^5)$	100	$1.6093 \cdot (10^5)$	0.1
Feet	$3.2808 \cdot (10^{-2})$	1	$8.3333 \cdot (10^{-2})$	3280.8	6080.2	3.2808	5280	$3.2808 \cdot (10^{-3})$
Inches	0.39370	12	1	$3.9370 \cdot (10^4)$	$7.2962 \cdot (10^4)$	39.370	$6.3360 \cdot (10^4)$	$3.9370 \cdot (10^{-2})$
Kilometers	10^{-5}	$3.0480 \cdot (10^{-4})$	$2.5400 \cdot (10^{-5})$	1	1.8532	0.001	1.6093	10^{-6}
Nautical Miles		$1.6447 \cdot (10^{-4})$		0.53959	1	$5.3959 \cdot (10^{-4})$	0.86839	
Meters	0.01	0.30480	$2.5400 \cdot (10^{-2})$	1000	1853.2	1	1609.3	0.001
Geographic Miles	$6.2137 \cdot (10^{-6})$	1.8939 $\cdot (10^{-4})$	$1.5782 \cdot (10^{-5})$	0.62137	1.1516	$6.2137 \cdot (10^{-4})$	1	$6.2137 \cdot (10^{-7})$
Millimeters	10	304.80	25.400	10^6		1000		1

FIG. X4.A CONVERSION FACTORS FOR LENGTH, ADAPTED FROM O. W. ESHBACH

VOLUME

Multiply Number of by → / to Obtain ↓	Cubic feet	Cubic inches	Cubic meters	Gallons (U.S. Liquid)	Liters	Barrels (U.S. Liquid)
Cubic feet	1	$5.7870 \cdot (10^{-4})$	35.315	0.13368	$3.5315 \cdot (10^{-2})$	5.6146
Cubic inches	1728	1	$6.1024 \cdot (10^4)$	231.0	61.024	
Cubic meters	$2.8317 \cdot (10^{-2})$	$1.6387 \cdot (10^{-5})$	1	$3.7854 \cdot (10^{-3})$	0.001	0.15899
Gallons (U.S. Liquid)	7.4805	$4.3290 \cdot (10^{-3})$	264.17	1	0.26417	42.0
Liters	28.317	$1.6387 \cdot (10^{-2})$	1000.0	3.7855	1	158.99
Barrel (U.S. Liquid)	0.17811		6.2899	$2.3810 \cdot (10^{-2})$	$6.2899 \cdot (10^{-3})$	1

FIG. X4.B CONVERSION FACTORS FOR VOLUME

TABLE X4.c—Continued

$F_n = V/\sqrt{gL}$	$T_q = V/\sqrt{L}$	$F_n = V/\sqrt{gL}$	$T_q = V/\sqrt{L}$	$F_n = V/\sqrt{gL}$	$T_q = V/\sqrt{L}$	$F_n = V/\sqrt{gL}$	$T_q = V/\sqrt{L}$
0.03	0.1007	0.21	0.7052	0.39	1.3096	0.90	3.0222
0.04	0.1343	0.22	0.7388	0.40	1.3432	1.00	3.358
0.05	0.1679	0.23	0.7723	0.42	1.4103	1.10	3.6938
0.06	0.2015	0.24	0.8059	0.44	1.4775	1.20	4.0296
0.07	0.2351	0.25	0.8395	0.46	1.5447	1.30	4.3654
0.08	0.2686	0.26	0.8731	0.48	1.6118	1.40	4.7012
0.09	0.3022	0.27	0.9066	0.50	1.6790	1.50	5.0370
0.10	0.3358	0.28	0.9402	0.52	1.7461	1.60	5.3720
0.11	0.3694	0.29	0.9738	0.54	1.8133	1.70	5.7086
0.12	0.4030	0.30	1.0074	0.56	1.8805		
0.13	0.4365	0.31	1.0410	0.58	1.9476		
0.14	0.4701	0.32	1.0745	0.60	2.0148		
0.15	0.5037	0.33	1.1081	0.62	2.0820		
0.16	0.5373	0.34	1.1417	0.64	2.1491		
0.17	0.5709	0.35	1.1753	0.66	2.2163		
0.18	0.6044	0.36	1.2089	0.68	2.2834		
0.19	0.6380	0.37	1.2424	0.70	2.3506		
0.20	0.6716	0.38	1.2760	0.80	2.6864		

by the David Taylor Model Basin from data assembled for towing-carriage design.

X4.4 Conversion Ratios, English-Metric and Metric-English. Conversion factors for English-metric and metric-English calculations, as well as ratios between certain units in the English and metric systems, are given in Figs. X4.A through X4.F for length, volume, linear velocity, weight, pressure, and power, respectively. These diagrams follow the general scheme of those published in a "Handbook of Engineering Fundamentals," edited by O. W. Eshbach, Wiley, New York, second edition, 1952, pages 1–148 through 1–159.

Fig. X4.G contains five sets of English-metric and metric-English conversion graphs, reproduced from "Problems of Polar Research," edited by W. L. G. Joerg [American Geogr. Soc., Sp. Publ. 7, 1928, p. 458], from which values within certain ranges may be picked off by inspection.

Other standard English-metric conversion ratios are:

(a) The U. S. legal yard is 3600/3937 meter

(b) The U. S. legal pound mass is 0.453592 kg

(c) The acceleration of gravity, corresponding to 32.174 ft per sec^2, is 9.80665 meters per sec^2.

LINEAR VELOCITY

Multiply Number of by → / to Obtain ↓	Centimeters per second	Feet per second	Kilometers per hour	Knots	Meters per second	Miles per hour
Centimeters per second	1	30.480	27.778	51.478	100	44.704
Feet per second	$3.2808 \cdot (10^{-2})$	1	0.91133	1.6889	3.2808	1.4667
Kilometers per hour	0.036	1.0973	1	1.8532	3.60	1.6093
Knots	$1.9425 \cdot (10^{-2})$	0.59209	0.53959	1	1.9425	0.86838
Meters per second	0.01	0.30480	0.27778	0.51478	1	0.44704
Miles per hour	$2.2369 \cdot (10^{-2})$	0.68182	0.62137	1.1516	2.2369	1

Fig. X4.C Conversion factors for Linear Velocity

WEIGHT

Multiply Number of by → / to Obtain ↓	Kilograms	Pounds avoirdupois	Kips, thousands of pounds	Tons, long	Tons, short	Tons, metric
Kilograms	1	0.45359	453.59	1016.0	907.19	1000
Pounds avoirdupois	2.2046	1	1000	2240	2000	2204.6
Kips, thousands of lb	$2.2046 \cdot (10^{-3})$	0.001	1	2.240	2	2.2046
Tons, long	$9.8420 \cdot (10^{-4})$	$4.4643 \cdot (10^{-4})$	0.44643	1	0.89286	0.98420
Tons, short	$1.1023 \cdot (10^{-3})$	$5.000 \cdot (10^{-4})$	0.500	1.120	1	1.1023
Tons, metric	0.001	$4.5359 \cdot (10^{-4})$	0.45359	1.0160	0.90719	1

Fig. X4.D Conversion Factors for Weight

TABLE X4.d—Corresponding Values of Displacement-Length Quotient and 0-Diml Fatness Ratio
The conversion factors used here are described in Sec. X4.5.

$\frac{\Delta}{(0.010L)^3}$	$\frac{\forall}{(0.10L)^3}$	$\frac{\Delta}{(0.010L)^3}$	$\frac{\forall}{(0.10L)^3}$	$\frac{\forall}{(0.10L)^3}$	$\frac{\Delta}{(0.010L)^3}$	$\frac{\forall}{(0.10L)^3}$	$\frac{\Delta}{(0.010L)^3}$
20	0.7015	260	9.1195	0.5	14.255	12.5	356.38
30	1.0523	270	9.4703	1.0	28.510	13.0	370.63
40	1.4030	280	9.8210	1.5	42.765	13.5	384.89
50	1.7538	290	10.172	2.0	57.021	14.0	399.14
60	2.1045	300	10.523	2.5	71.276	14.5	413.40
70	2.4553	310	10.873	3.0	85.531	15.0	427.65
80	2.8060	320	11.224	3.5	99.786	15.5	441.91
90	3.1568	330	11.575	4.0	114.04	16.0	456.16
100	3.5075	340	11.926	4.5	128.30	16.5	470.42
110	3.8583	350	12.276	5.0	142.55	17.0	484.68
120	4.2090	360	12.627	5.5	156.81	17.5	498.93
130	4.5598	370	12.978	6.0	171.06	18.0	513.19
140	4.9105	380	13.329	6.5	185.32		
150	5.2613	390	13.679	7.0	199.57		
160	5.6120	400	14.030	7.5	213.83		
170	5.9628	410	14.381	8.0	228.08		
180	6.3135	420	14.732	8.5	242.34		
190	6.6643	430	15.082	9.0	256.59		
200	7.0150	440	15.433	9.5	270.85		
210	7.3658	450	15.784	10.0	285.10		
220	7.7165	460	16.135	10.5	299.36		
230	8.0673	470	16.485	11.0	313.61		
240	8.4180	480	16.836	11.5	327.87		
250	8.7688	490	17.187	12.0	342.12		
		500	17.538				

A recent book by O. T. Zimmerman and I. Lavine, entitled "Conversion Factors and Tables, Second Edition," published by the Industrial Research Service, Inc., of Dover, N. H., in 1955 "... provides an accurate source of fundamental physical relationships as well as several thousand useful constants for the conversion of units" [Appl. Mech. Rev., Oct 1955, p. 412, rev. 2955].

X4.5 Ratios of Ship Parameters and Coefficients. The ratios between certain well-known ship parameters and coefficients have

PRESSURE

Multiply Number of by → / to Obtain ↓	Atmospheres	Centimeters of mercury at 0 deg C	Inches of mercury at 0 deg C	Inches of water at 15 deg C	Feet of water at 15 deg C	Kilograms per square meter	Pounds per square inch
Atmospheres	1	$1.3158 \cdot (10^{-2})$	$3.3421 \cdot (10^{-2})$	$2.4559 \cdot (10^{-3})$	$2.9471 \cdot (10^{-2})$	$9.6785 \cdot (10^{-5})$	$6.8046 \cdot (10^{-2})$
Centimeters of Hg at 0 deg C	76 0	1	2.5400	0.18665	2.2398	$7.3556 \cdot (10^{-3})$	5 1715
Inches of Hg at 0 deg C	29.921	0.39370	1	$7.3483 \cdot (10^{-2})$	0.88179	$2.8959 \cdot (10^{-3})$	2.0360
Inches of H_2O at 15 deg C	407.18	5.3576	13.609	1	12.00	$3.9409 \cdot (10^{-2})$	27.707
Feet of H_2O at 15 deg C	33.932	0.44647	1.1341	$8.3333 \cdot (10^{-2})$	1	$3.2841 \cdot (10^{-3})$	2.3090
Kilograms per square meter	$1 0332 \cdot (10^{4})$	135.95	345 31	25.374	304.49	1	703.07
Pounds per square inch	14.696	0.19337	0.49116	$3.6092 \cdot (10^{-2})$	0.43310	$1.4223 \cdot (10^{-3})$	1

Fig. X4.E Conversion Factors for Pressure

POWER

Multiply Number of by → / to Obtain ↓	Foot-pounds per minute	Foot-pounds per minute	Horses (English)	Kilowatts	Horses, metric (cheval-vapeur)	British thermal units (BTU) per minute
Foot-pounds per minute	1	60	3.300 $\cdot (10^{4})$	4.4267 $\cdot (10^{4})$	3.2548 $\cdot (10^{4})$	778.26
Foot-pounds per second	$1.6667 \cdot (10^{-2})$	1	550	737.78	542.47	12.971
Horses (English)	$3.0303 \cdot (10^{-5})$	$1.8182 \cdot (10^{-3})$	1	1.3414	0.98630	$2.3584 \cdot (10^{-2})$
Kilowatts	$2.2590 \cdot (10^{-5})$	$1.3554 \cdot (10^{-3})$	0.74547	1	0.73526	$1.7581 \cdot (10^{-2})$
Horses, metric (cheval-vapeur)	$3.0724 \cdot (10^{-5})$	$1.8434 \cdot (10^{-3})$	1.0139	1.3601	1	$2.3911 \cdot (10^{-2})$
BTU's per minute	1.2849 $\cdot (10^{-3})$	7.7094 $\cdot (10^{-2})$	42.402	56.879	41.821	1

Fig. X4.F Conversion Factors for Power, Adapted from O. W. Eshbach

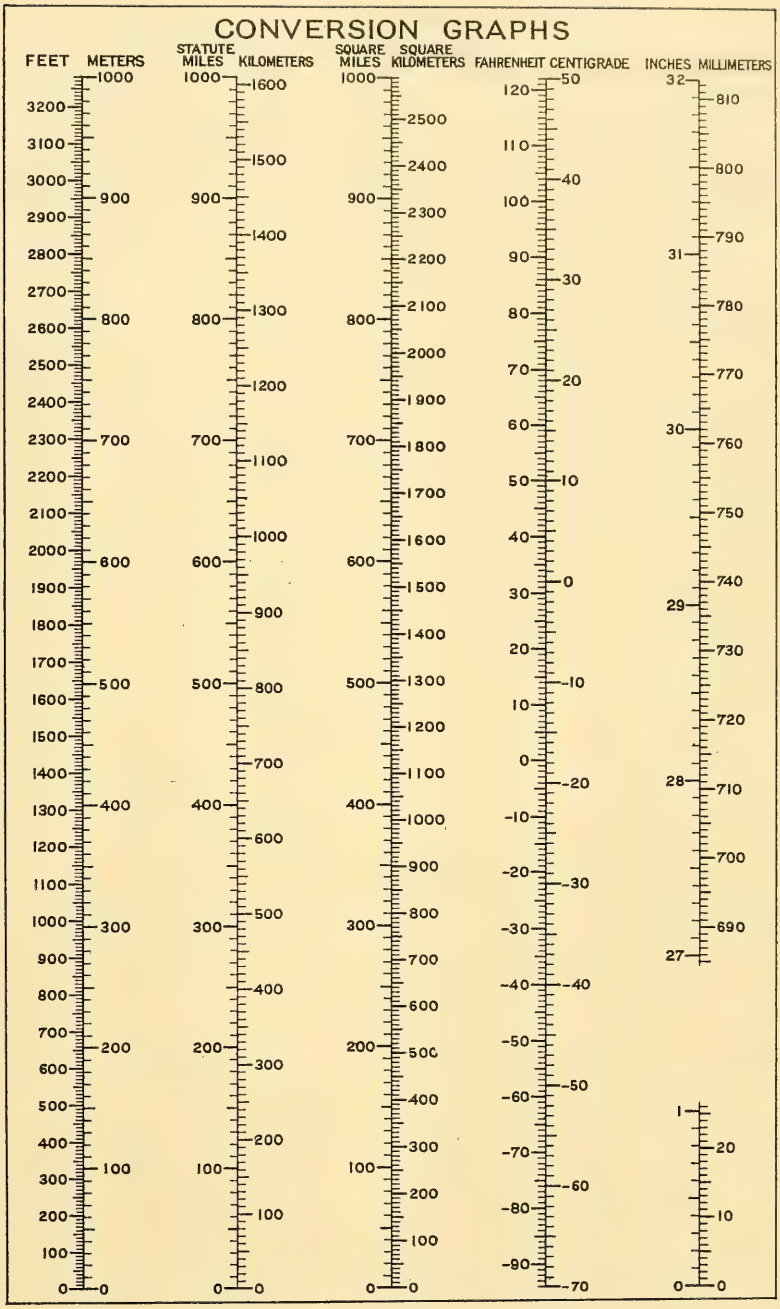

Fig. X4.G Conversion Graphs of W. L. G. Joerg

definite values whether they are dimensional or dimensionless. When the concepts forming parts of dimensional parameters are given certain accepted values it is then possible to express their relationships to the dimensionless values, for any given system of measurement. There are tabulated in this section certain ratios which occur frequently in the treatment of hydrodynamic problems in ship design.

One such ratio in everyday use is that between the Taylor quotient T_q and the Froude number F_n. By definition and accepted practice, $T_q = V/\sqrt{L}$, where V is in kt and L in ft; by consistent units, $F_n = V/\sqrt{gL}$, where V is in ft per sec, g in ft per sec^2, and L in ft. The ratio between T_q and F_n depends upon the "standard" value assumed for the acceleration of gravity g and the length of a nautical mile. At a latitude of 45 deg and at sea level, g is taken as 32.174 ft per sec^2. For this book, 1 nautical mile is 6080.20 ft. Then

$$F_n = \frac{V\ (\text{ft per sec})}{\sqrt{gL}} = \frac{1.6889V\ (\text{kt})}{\sqrt{32.174L\ (\text{ft})}}$$

$$= 0.2978\,\frac{V\ (\text{kt})}{\sqrt{L\ (\text{ft})}} = 0.2978T_q$$

or

$$T_q = \frac{F_n}{0.2978} = 3.358F_n$$

For rule-of-thumb work, $F_n = 0.3T_q$ and $T_q = 10F_n/3$.

Corresponding values of the pair T_q and F_n, and the pair F_n and T_q are listed in Table X4.c, for a range sufficient to cover all design problems for boats and ships, small and large.

Another conversion that needs to be made often is the one between D. W. Taylor's displacement-length quotient $\Delta/(0.010L)^3$ and the 0-diml fatness ratio $\forall/(0.10L)^3$. A conversion factor has to be fixed here because of Taylor's use of a specific gravity for salt water of 1.024, corresponding to a volume of 35.075 ft^3 per long ton. For converting from the displacement-length quotient to the 0-diml fatness ratio, the former is multiplied by 0.035075 or divided by 28.510. To obtain values of the displacement-length quotient from the 0-diml fatness ratio, multiply the latter by 28.510 or divide it by 0.035075.

Table X4.d lists corresponding values of these two quantities.

X4.6 Frequently Used Numbers, Their Powers, and Logarithms. The numbers frequently used in hydrodynamic ship-design problems, together with their frequently used powers and with logarithms of these numbers to the base 10, are listed hereunder in a form to make them readily available for calculation purposes.

For certain special numbers the grouping is in accordance with the general subjects discussed in Parts 1 and 2.

LENGTHS AND AREAS

12,	$\log_{10} = 1.07918$
144,	$\log_{10} = 2.15836$
1,728,	$\log_{10} = 3.23754$
3.281 ft per meter,	$\log_{10} = 0.51601$

SPEEDS AND VELOCITIES

1.6889 ft per sec for 1 kt, in this book,	$\log_{10} = 0.22760$
1.467 ft per sec for 1 mph,	$\log_{10} = 0.16643$
1.6878 ft per sec for international knot, 1954,	$\log_{10} = 0.22732$
$\frac{1}{1.6889} = 0.5921$,	$\log_{10} = 9.77240$
$(1.6889)^2 = 2.8524$,	$\log_{10} = 0.45521$

ACCELERATIONS

$g = 32.174$ ft per sec^2	$\log_{10} = 1.50751$
$\sqrt{32.174} = 5.6722$,	$\log_{10} = 0.75375$
$\frac{1}{\sqrt{32.174}} = 0.17630$,	$\log_{10} = 9.24625$

KINEMATIC VISCOSITY

When ν(nu) $= 1.2285(10^{-5})$, then

$$\frac{1}{1.2285(10^{-5})} = 0.8140(10^5)$$

When $\nu = 1.2817(10^{-5})$, then

$$\frac{1}{1.2817(10^{-5})} = 0.7802(10^5)$$

WAVE ACTION

$$\sqrt{\frac{g}{2\pi}} = \sqrt{\frac{32.174}{2\pi}} = 2.2629 \text{ English units}$$

$$\sqrt{\frac{g}{2\pi}} = \sqrt{\frac{9.80665}{6.2832}} = 1.2493 \text{ metric units}$$

$$\sqrt{2\pi} = 2.50663$$

$$\frac{1}{\sqrt{2\pi}} = 0.39894.$$

Personal-Name Index

In the case of persons having a great many actual entries in this volume, only the most important are included.

With a few exceptions, the names of people mentioned in the Acknowledgements section of this volume, beginning on page v, are not duplicated in this index.

Ship-Name Index

In addition to the ship names occurring in the text, there are listed here a few class names, such as "Export Line ships," to cover cases where individual ship names are not given.

In many cases the pages listed in this index contain only references to the subject of the abbreviated index entry, and not the subject itself. For example, under *Allegheny* in the column below, page 233 of this volume does not embody a reproduction of the body plan but tells where it may be found.

Subject Index

General. Appendix 1 of this volume contains an alphabetical list of symbols, letter groups, and abbreviations, with their short titles. These features are therefore omitted from the subject index.

Rules Followed in Making up this Index. All principal words in the part headings, chapter headings, section headings, and text—and in some cases the figure captions and table headings—are included in the subject index. In general, this takes in nouns and adjectives but not verbs, adverbs, prepositions, and articles.

Abbreviations. To make the entries as descriptive and useful as possible, yet to keep them concise, abbreviations or short forms are employed, where necessary, for words that are familiar and frequently used. Plurals are formed by adding the customary "s" and "es" to the shortened nouns.

Examples are the following:

Abbrev	for abbreviation	est	for estimate	rev	for revolution
approx	approximate or approximation		estimated	screwprop	screw propeller
			estimating	sec	section
asymm	asymmetry or asymmetrical	long'l	longitudinal	spec	specification
		man'g	maneuvering	stereo	stereoscopic
bet	between	max	maximum	subm	submarine
coeff	coefficient	prelim	preliminary		submerged
calc	calculating	prop	propeller	surf	surface
	calculation	propdev	propulsion device	symm	symmetrical
circ	circulating	press	pressure	transv	transverse
corresp	corresponding	ref	reference	unsymm	unsymmetrical
def	definition	req't	requirement	var	variation
descr	description	rel	related	vel	velocity
diam	diameter		relative (to)	vert	vertical
diml	dimensional		relating or	vol	volume
distr	distribution		relation	WL	waterline
eff'cy	efficiency	resist	resistance	DWL	designed waterline
		restr	restricted		
			restriction